

Underground Space

the 4th Dimension of Metropolises

Editors:
Jiří Barták
Ivan Hrdina
Georgij Romancov
Jaromír Zlámal

Volume 1

UNDERGROUND SPACE – THE 4th DIMENSION OF METROPOLISES



BALKEMA – Proceedings and Monographs
in Engineering, Water and Earth Sciences

PROCEEDINGS OF THE 33rd ITA-AITES WORLD TUNNEL CONGRESS,
PRAGUE, CZECH REPUBLIC 5–10 MAY 2007

Underground Space – the 4th Dimension of Metropolises

Edited by

Jiří Barták
Czech Technical University, Prague

Ivan Hrdina
METROSTAV a. s.

Georgij Romancov
METROPROJEKT Praha a. s.

Jaromír Zlámal
POHL cz, a. s.

VOLUME 1


Taylor & Francis
Taylor & Francis Group
LONDON / LEIDEN / NEW YORK / PHILADELPHIA / SINGAPORE

CRC Press
Taylor & Francis Group
6000 Broken Sound Parkway NW, Suite 300
Boca Raton, FL 33487-2742

© 2007 by Taylor & Francis Group, LLC
CRC Press is an imprint of Taylor & Francis Group, an Informa business

No claim to original U.S. Government works
Version Date: 20120518

International Standard Book Number-13: 978-0-415-88967-4 (eBook - PDF)

This book contains information obtained from authentic and highly regarded sources. Reasonable efforts have been made to publish reliable data and information, but the author and publisher cannot assume responsibility for the validity of all materials or the consequences of their use. The authors and publishers have attempted to trace the copyright holders of all material reproduced in this publication and apologize to copyright holders if permission to publish in this form has not been obtained. If any copyright material has not been acknowledged please write and let us know so we may rectify in any future reprint.

Except as permitted under U.S. Copyright Law, no part of this book may be reprinted, reproduced, transmitted, or utilized in any form by any electronic, mechanical, or other means, now known or hereafter invented, including photocopying, microfilming, and recording, or in any information storage or retrieval system, without written permission from the publishers.

For permission to photocopy or use material electronically from this work, please access www.copyright.com (http://www.copyright.com/) or contact the Copyright Clearance Center, Inc. (CCC), 222 Rosewood Drive, Danvers, MA 01923, 978-750-8400. CCC is a not-for-profit organization that provides licenses and registration for a variety of users. For organizations that have been granted a photocopy license by the CCC, a separate system of payment has been arranged.

Trademark Notice: Product or corporate names may be trademarks or registered trademarks, and are used only for identification and explanation without intent to infringe.

Visit the Taylor & Francis Web site at
http://www.taylorandfrancis.com

and the CRC Press Web site at
http://www.crcpress.com

Underground Space – the 4th Dimension of Metropolises – Barták, Hrdina, Romancov & Zlámal (eds)
© 2007 Taylor & Francis Group, London, ISBN 978-0-415-40807-3

Table of contents

Preface XXV

Organisation XXVII

Volume 1

Section 1: Underground city design, planning of underground constructions

Largest transportation system – Metro and road in the same tunnel 3
V.M. Abramson & S.Yu. Loubotski

Anchor recovery under extreme conditions in downtown Leipzig, Germany 7
L. Babendererde & P. Elsner

Construction of Metro IV.C2 Ládví – Letňany in Prague 13
V. Bartoň, M. Kochánek, V. Valeš & J. Kutil

Planning for Canada's first bored road tunnel in over 40 years Kicking Horse Canyon Project 19
D. Brox, S. Bean, P. Branco & T. Coulter

Preparation of Metro's A line extension in Prague 27
V. Cigánek & J. Růžička

Preparation of Metro's new D line in Prague 33
V. Cigánek & J. Růžička

The Turecký Vrch railway tunnel 39
M. Dávid, J. Mára & J. Korejčík

Collectors – System approach to the regeneration of technical infrastructure in the city of Prague 45
F. Dvořák & M. Hradecký

Years of planning and implementation: Two major urban tunneling projects in Los Angeles, California, USA 51
M.A. Elioff, B.W. Miya & J.H. Albino

Geological and geotechnical conditions in underground structures design of Rome subway: The B-Line extension 59
R. Enrione, A. Eusebio, L. Soldo, R. Funiciello & L. Solimene

Ontologies, thesauruses and information systems for tunnels 65
N. Faure

Building the underground infrastructure of Lausanne's new m2 metro line 69
F. Gaj & M. Badoux

Metro Santiago – Building an urban tunneling industry from the ground up 75
A.R.A. Gomes, M. Böfer & P. Muñoz

The slivenec tunnel on the Prague city ring road 81
O. Hasík & K. Závora

Portals – The architecture visible in cities and landscape 87
O. Hasík & P. Šourek

Study of the ship lift structure at the Slapy Dam 91
M. Jakoubek, J. Kuňák & P. Uher

Design of the District Heating Tunnel in Copenhagen 97
T. Kasper, C. Edvardsen & M. Faurschou

Excavation connecting the underground ventilation station and the underground expressway tunnels 103
Y. Konishi, I. Kamegaya, A. Ueda & Y. Imanaka

Prague – Beroun, new railway connection 111
D. Krása, J. Růžička & O. Hasík

Underground high-speed railway – The phenomenon of urbanistic development in Prague 117
E. Kyllar

Railway line Prague centre – Ruzyně airport 125
J. Martinec & P. Zobal

The Trans Hudson Express (THE) Tunnel 131
N. Munfah & A.D. Silber

CTA Block 37 Tunnel Connection in downtown Chicago 137
V. Nasri & P. Razgha

Construction of a large underground station under a station in operation 143
T. Niibori, Y. Seki, T. Sato, T. Yamada & T. Fujiwara

The next step: The Very Long Tunnel (VLT) 149
H. Ostlid, W.C. Grantz, J. Saveur & B. Jakobsen

Planning and construction of major infrastructure works in Croatia 155
J. Radic, P. Djukan & Z. Zderic

The Dulles Corridor Metrorail Project – Tunneling aspects of the Metrorail extension to Washington, DC Dulles International Airport Phase I and Phase II 161
J. Rudolf, V. Gall & K. Zeidler

Experience from architectural design and Build of the underground space 167
P. Šafránek

Study on underground space planning of Shanghai EXPO 2010 173
H.H. Zhu, P. Li, X. Wang, F.L. Peng & Y.S. Li

Section 2: Geotechnical survey and improvement of ground mass

Part 2.1 Geotechnical survey

The impact of puncturing support on the expansion of seismic effects during blasting activities in tunnels 179
H. Antičević, Z. Ester & M. Dobrilović

Two different concepts of geotechnical survey and monitoring in exploration galleries for tunnels in Prague – Lahovská exploration gallery and Blanka exploration gallery 191
R. Chmelař & B. Březina

Inverse analysis on measurements realized during a tunnel excavation 197
S. Eclaircy-Caudron, D. Dias & R. Kastner

Prediction of the ground conditions ahead the TBM face in the tunnels of Guadarrama (Spain), using geophysical methods and in situ testing 203
J.M. Galera, S. Pescador, A. Rodríguez & M. Torres

Risk analysis of soil transition in tunnel works 209
Q.F. Hu & H.W. Huang

Feasible Boulder treatment methods for soft ground shielded TBM 217
W.W. Jee & S.-G. Ha

Reasons of swelling of miocene clays near Třebovice in Bohemia 223
F. Kresta

Geophysics method used to recognize the boundary between different deposits 227
R. Kuszyk & M. Superczyńska

Geotechnical exploration for the Dobrovského Tunnel in Brno 231
J. Pavlík, D. Rupp & L. Klímek

Design and construction of a large underground cavern in Atlanta, Georgia, USA 237
T.W. Pennington, R.F. Cook, D.P. Richards & G. Barnes

Development of in-situ tunnel-ahead detection system using electromagnetic wave 243
H.H. Ryu, G.C. Cho, Y.J. Sim, G.H. Lee & J.K. Lee

A modified design of a large section tunnel as an auxiliary spillway along large faults 249
Y.W. Shin, I.K. Lee, T.S. Park, H.S. Choi, S.C. Park, J.K. Kim, M.S. Lee, K.H. Shin & B.H. Han

Geotechnical control during the excavation of the tunnel of Guadarrama 255
I. Tardáguila, B. Celada, J.M. Galera

Assessment of rock mass properties using machine performance data from roadheaders 261
K. Tsukamoto, H. Hamada & S. Ebisu

Deep tunnelling in hardrock with large diameter TBM: What's up? An experience from the Gotthard Base Tunnel 267
I. Vicenzi, S. Pedrazzini, A. Ferrari, G. Gubler & O. Böckli

Laboratory tests for EPB tunnelling soil conditioning 273
R. Vinai, D. Peila, C. Oggeri & S. Pelizza

3D geo-modeling for spillway tunnel construction in the complex fault region 279
W.S. Yoon, U. Jeong, B.H. Han, K.H. Shin, S.S. Lee & Y.K. Kim

Dilatometer tests in deep boreholes in investigation for Brenner base tunnel 283
M. Zalesky, Ch. Bühler, U. Burger & M. John

Part 2.2 Improvement of ground mass

The dimensioning of tunnel face reinforcement 289
G. Anagnostou & K. Serafeimidis

Cost-effective pre-injection with rapid hardening microcement and colloidal silica for water ingress reduction and stabilisation of adverse conditions in a headrace tunnel 297
A.K. Bahadur, K.G. Holter & A. Pengelly

Experimental investigation on backfill grouting deformation characteristics of shield tunnel in sand 303
Y.-w. Han, W. Zhu, X.-c. Zhong & R. Jia

Advances in synthetic injection technology, do they improve tunnel construction productivity? 307
W. Kay, T. Yang

Injection techniques used at the old workings and karst voids abandonment under the built-up residential areas in the Urals 311
A.B. Kondratov

Instabilities at the Messochora tunnel, Greece: Ground improvement and safety evaluation based on observational data 315
V. Kontogianni & Y. Thanopoulos

Rock bolt integrity evaluation in tunnelling using ultrasonic NDT techniques 321
J.S. Lee, H.J. Kim, I.M. Lee, S.I. Han & Y.J. Lee

Jet-grouting in underground construction 327
A.G. Malinin & P.A. Malinin

Modelling of ground freezing in tunnelling 331
E. Pimentel, A. Sres & G. Anagnostou

Performance evaluation of ground improvement by electrical resistivity tomography 337
T. Shimizu, K. Narumoto & S. Ebisu

Reinforcing Effects around tunnel face by crown & face reinfored 345
J.H. Shin, S.H. Choi & S.B. Woo & Y.K. Choi

Laboratory testing of chemical grouting effects in rocks 353
K. Souček, L. Staš, R. Šňupárek & I. Kroutilová

Section 3: Research, development and design of underground constructions in built-up areas

Deformation computation based on numerical modelling for urban NATM tunnelling 359
M.Z.A. Elrehim

Numerical analysis of TBM road tunnels under Suez Canal at Port Said 367
A. Abu-Krisha

Numerical modeling of face stability for TBM tunneling 373
A.A. Krisha

Impact of the face anchoring on the stability of underground working 377
J. Aldorf, E. Hrubešová & L. Duris

Bentonite and grout flow around a TBM 383
A. Bezuijen

Volume changes in grout used to fill up the tail void 389
A. Bezuijen & W.H. van der Zon

Laboratory tests on compensation grouting, the influence of grout bleeding 395
A. Bezuijen, M.P.M. Sanders, D. den Hamer & A.F. van Tol

Software solutions for sensitivity studies in design of tunnels 403
E. Bieth, L. Chantron & P. Roure

Safety problems of underground structures in the design 409
N. Bulychev, N. Fotieva & A. Levchenko

Stability and deformations in large-scale underground constructions 415
A. Butovič

Particular design for nuclear long term interim storage 421
N. Dias, J. Triclot, H. Lagrave & E. Breton

Design and construction of a tunnel using the technology for controlling muck flow in the cutting chamber of an earth pressure balance shield of large cross section 427
H. Dobashi, M. Matsuda, K. Matsubara & A. Kitayama

Estimation of front-end stability using field displacement 435
R.M. Faure, J.F. Thimus, F. Demoulin & S. Delvaux

Influence of soil grouting on the shallow tunnel linings stress state in urban areas 439
N. Fotieva, N. Bulychev, S. Antziferov, A. Sammal & P. Deev

Analyses of underground structures crossing an active fault in Coronado, California 445
T. Gregor, B. Garrod & D. Young

Numerical modeling of tunnel excavation and lining under high initial stresses and high underground water pressures at Jinping Mountain 451
W. Chen & H.-N. Ruan

Simulation of failure around a circular tunnel using a bonded particle model 457
D.S. Cheon, C. Park, S. Jeon & Y.-S. Jeong

Deformation prediction for tunnels at PiccEx junction in London Heathrow – An engineering approach 463
J. Jäger & A. Stärk

Improved design method for 2-arch tunnel 469
W.G. Jeon, K.-H. Jeong, J.H. Lee, H.-H. Ahn & S.-W. Lee

Evaluation of strength parameters for the single shell tunnel in Korea 475
K.H. Joon, L.S. Ho, S.H. Seong & B.G. Jin

Measurements and seismic effects of vibrations caused by urban tunneling 481
Z. Kaláb & J. Knejzlík

Design method considering construction loads during shield tunneling using a three-dimensional FEM analysis model 487
K. Kasuga, N. Kawada, A. Shiratori, N. Fukai & M. Saitou

Development of a new center-cut method: SAV-cut (Stage Advance V-cut) 493
D. Kim, S. Noh, S. Lee, B. Park & S. Jeon

A study of the invert tunnel's behavior in a weathered-rock using laboratory model test and numerical analysis 501
K.J. Kim, S.Y. Koh, S.Y. Choo, C.S. Hong & D.J. Hwang

Design and installation waterproofing system for access shafts of service tunnels on Palm Jumeirah Island 507
M.K. Kundu, M.E. Ryjevski & D.G. Solter

Seismic behavior of Tubular Roof & Trench Method (T.R.&T) by numerical analysis 513
C.-w. Kwak, I.-j. Park, S.-h. Kim & J.-y. Kim

A laboratory test for determination of the optimum installation number of face bolts 519
K.W. Seo, S.W. Lee, T. Domon & K. Nishimura

Development of tunnel drainage system using drain board 523
G.P. Lee, H.S. Shin, G.J. Bae & S.W. Lee

The effects of tunnelling on an adjacent single pile 527
C.J. Lee, S.H. Jun, N.J. Yoo & G.W. Kim

Loads on the center pillar of two-arch tunnel under the influence of discontinuity planes in the ground 533
S.D. Lee, G.W. Byun, B.J. Oh & I.W. Lee

A case study of tunnel excavation adjacent to a steep slope 539
S.-C. Lee, L.-B. Chiou & G.-F. Lin

Subsurface settlement profiles above shallow and deep model tunnels at large ground loss 545
Y.-J. Lee & C.S. Yoo

Application of digital image processing in tunnel excavation 553
L. Biao, Q.W-ge, L. Yang & Wei, Hong-chun

Recent development of tunneling techniques in Taiwan 559
H.S. Liu, P.C. Hou & C.T. Chang

Construction method of connecting tunnel in a shield-driven tunnel 567
J. Liu, F. Zhang & H. Kong

Closely constructing influence forecast of hydraulic tunnel under-cross existing railway tunnel 571
G. Lun, Q. Wen-ge & W. Fei

Monitoring of the state of pipes in sewage networks as an element of adapting such networks to the technical demands of modern, urban subterranean infrastructure 577
C. Madryas & B. Przybyła

Investigation behavior of vertical shaft under loadings of intake tower at first filling of Doosti Dam 583
D. Massoud

Membrane waterproofing – Activation of the grouting system and its re-sealing ability 589
R. Matzner & M. Grossmann

Geomechanical studies for a road tunnel in volcanic formations 595
A.T. Menezes, F.M. Varela, L. Ribeiro e Sousa & F. Moura

Large-scale model tests for the verification of Braced Rib Arch Method for shallow overburden tunnel 603
S.M. Na, S.H. Moon, S.P. Lee, S.H. Cho & S.D. Lee

An investigation into the effects of Shiraz metro tunnels on the stability of Ghadir bridge 609
I. Namazi, R. Rahmannejad, M.A.E. Farsangi & H. Jamshidi

Extension of the Underground Space Information Management System: Road tunnel maintenance 613
Y. Ohnishi, P.A. Bruines, T. Nakai, M. Ryu, T. Katou & K. Tsujimori

Performance of pile due to tunneling-induced soil movements 619
C.W. Ong, C.F. Leung, K.Y. Yong & Y.K. Chow

The continual load development measurement of the central concrete pillar in the Valík tunnels 625
J. Pacovský, J. Svoboda Jun. & R. Vašíček

The Josef underground educational facility project 631
J. Pacovský, J. Svoboda Jun. & R. Vašíček

Displacements estimate due twin tunnel excavation under low overburden 635
E.A. Palma Filho, A.C. Zingano, J.C. Koppe & J.F.C.L. Costa

Parametric study of displacements on sequential and full-face tunnel excavation 639
S. Papakonstantinou & W. Schubert

Characteristics of the ice-ring with phase change of water to ice for LNG underground storage 645
C. Park, D.S. Cheon, S.K. Chung, H.D. Lim, Y.J. Park & S.D. Lee

Underground exploitation of a granite mine by large voids: stability aspects 651
D. Peila, S. Pelizza & C. Guardini

Analysis of input parameters of the rock mass 661
J. Pruška

Study on neighboring construction of three parallel shield tunnels in soft ground by centrifugal model test 667
W. Qiu, Y. Zheng, S. Li, R. Wu & H. Guo

The effect of advance rate on shield loading in squeezing ground 673
M. Ramoni & G. Anagnostou

Benefits and life-cycle costs of underground projects 679
J. Reilly & H. Parker

New York Second Avenue Subway – Initial support design of shallow rock caverns 685
K. Rossler & C. Stone

Laboratory and numerical investigation of tunnel reinforced with face bolts 693
K.W. Seo, T. Domon & K. Nishimura

Non-linear FE analysis of a grouted pipe-roofing reinforcement applied to a tunnel portal area 697
H.S. Shin, G.J. Bae, D.G. Kim & S.W. Lee

An enhanced pre & post processing techniques for three dimensional tunnel analysis: Tunnel Modelling Wizard 705
J.H. Shin, J.H. Moon & D.S. Shin

Design parameter determination for modeling of pre-reinforced zones in a tunnel 713
K.I. Song, G.C. Cho, S.R. Lee & J.H. Lee

Computer aided hierarchical ground characterization for underground structures 721
A. Steiner & W. Schubert

Developments of structural performance assessment for sewer liners 727
C. Madryas & A. Szot

Experimental verification of final tunnel lining performance 733
P. Šourek & J.L. Vítek

Stability analysis and excavation schemes of large-span highway tunnel under complex geological conditions 739
J.S. Tang, S.Y. Liu, L.Y. Tong & C.H. Shen

Introductory tunnel design – Lining types and selection: A case history of large span soft ground tunnel design 745
B.F. Townsend & C.R. Speers

Effectiveness of zonal ground mass pre-stressing round an opening at grouting 751
K. Vojtasík & J. Aldorf

Geotechnical model for pipe roof supports in tunneling 755
G.M. Volkmann & W. Schubert

Model analysis of pre-lining methods used in tunnel construction 761
V. Vrba & J. Barták

L-Surf – Large scale underground research facility for safety and security 767
V. Wetzig

New high-speed railway lines Stuttgart 21 and Wendlingen-Ulm -approximately 100 km of tunnels 771
W. Wittke

Estimation of multi-well dewatering induced pile foundation settlement in phreatic zones 779
Y. Xiang, S. Chen & C. Yu

Estimation of rock load for the design of 2-arch tunnel lining 785
K. You, M. Sagong & J.S. Lee

An analytical solution of shield tunnel based on force method 791
X. You, Z. Zhang & Y. Li

Expert system for D&B tunnel construction 799
C.W. Yu & J.C. Chern

Progress of drill and blast tunnelling efficiency with relation to excavation time and costs 805
S. Zare & A. Bruland

Analysis of the ultimate states of the underground tunnel lining 811
J. Zlámal

Author Index 817

Volume 2

Section 4: Urban tunnelling and its monitoring: conventional and mechanized tunnelling

Part 4.1 Monitoring

Redesign and monitoring of a portal structure in built-up area 827
E. Akis, Z. Etkesen, T. Solak, R. Mucukgil, E. Durukan & M. Unver

The influence of vibrations and noice on the housing development on the cover of the Mrazovka tunnel in Prague during tunnel driving and its putting into service 833
L. Bartoš & L. Bartoš

Advanced online monitoring for urban tunneling projects 837
N. Benecke, P. Althaus & U. Kalz

Geotechnical monitoring of the Valik tunnel construction near Pilsen 841
R. Bernard

The use of guide lines in tunnelling 847
G. Cassani & L. Mancinelli

Rio de janeiro subway – Challenges of the access tunnel to the cantagalo station 851
A.A. Coutinho, M.A.L. Rocha, L.E. Sozio & W. Bilfinger

Prediction of subsidence during tunnel construction 857
K. Grossauer, R. Leitner, W. Schubert & P. Sellner

Monitoring of ground massif using TR-GEO georadars while drifting tunnels 863
S.V. Izyumov & I.I. Goltsman

Application of tunnel information system for construction supported by international cooperation 867
C.Y. Kim, K.Y. Kim, Y.Z. Lee, S.W. Hong, S.H. Baek, K.W. Seo, W. Schubert & Y.S. Seo

Influence of water back rise on tunnels and surface 871
M. Kolečkář, J. Němeček & I. Zemánek

Geotechnical support of construction and operation of the Underground and transport tunnels 877
N.I. Kulagin & K.P. Bezrodny

Influence of the primary support stiffness on the surface subsidence during tunnel construction 883
J. Likar & M. Venta

Deformation behavior of west Mao mountain highway tunnel in gravel deposits layers during excavation 889
L.Y. Tong, S.Y. Liu, C.H. Shen & L.M Liu

EPB-Tunnelling control and monitoring in a urban environment: The experience of the "Nodo di Bologna" construction (Italian High Speed Railway system) 895
V. Marchionni & V. Guglielmetti

Monitoring of structures and environment under construction and service of underground transportation projects in Russia 903
V. E. Merkin, S.N. Vlasov

Geotechnical monitoring of the excavation exploratory galleries for the Dobrovského tunnel in Brno 907
D. Rupp, J. Pavlík & L. Klímek

An optimised monitoring of critical buildings adjacent to tunnel construction in urban area 913
S.H. Shin, C.Y. Kim, K.Y. Kim, K.S. Jue & S.W. Hong

Monitoring during the construction of a shallow urban tunnel and counter measures 917
T. Solak, Z. Etkesen, A. Sirin & T. Düzgün

Longitudinal surface settlements induced by EPB tunneling in Bangkok Clay 921
S. Suwansawat

Tunnel excavation by controlling water pressure in the ground with unevenly distributed water bearing strata 927
H. Takahara, J. Yorita, Y. Tuzuki & H. Takahashi

Prognosis of underground structures deterioration based on in-situ measurements 933
M. Vaníček, I. Vaníček, J. Pruška, M. Bubeníček, D. Jirásko & K. Soga

Interaction between tunnelling and groundwater – its impact on tunnel behavior and ground settlement 939
C.S. Yoo, S.B. Kim, Y.J. Lee, S.H. Kim & H.T. Kim

Part 4.2 Conventional tunnelling

Integrated design and construction of Klashnice tunnels 947
P. Anagnosti & D. Lukich

Tunneling in an urban critical area – A case study 953
J.M. Carvalho, A.T. Cavalheiro & P. Teixeira

Construction of city service tunnel in Ostrava without preliminary protection of surface 961
K. Franczyk & K. Dolinek

Aspects of urban tunneling within the project of Sitina tunnel 965
M. Frankovský, T. Aoki, S. Choma, V. Chomová & V. Kotrík

New Austrian Tunneling Method: Directly under an expressway on weak silt 971
K. Fujimoto, J. Yorita, Y. Sasaki, N. Yamaki & M. Okamura

The Prague new connection tunnels 977
M. Gramblička, D. Cyroň & M. Chyba

Development of rock fracturing method, and application of EG-Slitter method to the tunnel 983
T. Hara, M. Okamura, T. Kimura & K. Ishiyama

The Sir Adam Beck II intake tunnels – homage to the builders 987
D. Heath & C. Murdock

Královopolský Tunnel in Brno, CZ 995
V. Horák, J. Pechman & J. Rožek

Planning and design of the A3 Hindhead tunnel, Surrey, UK 1001
T.J. Ireland, T.A. Rock & P. Hoyland

Geotechnical investigations and construction conditions for the tunnel “Strazevica” on E-75 motorway near Belgrade 1009
B. Jelisavac, S. Jotic, S. Savic, V. Vujanic, M. Roljic, M. Jotic & S. Milenkovic

The construction of tunnel “Lipak” within the framework of E-75 motorway on Belgrade city bypass stretch 1015
S. Jotic, S. Savic, M. Jotic & V. Vujanic

Settlement control during the construction of urban tunnels by NATM Construction of Kitayama tunnel on national highway 455 1021
T. Komatsu, H. Kitamura, K. Matsubara & T. Sakurai

Highways in the Czech Republic in terms of tunnel construction 1027
P. Laušman

Urban tunneling under existing structure 1031
H.S. Lee, K.S. Jue, D.Y. Kim, W.H. Jung & Y.N. Lee

Large double adjoined binocular tunnels in shallow and soft ground – Shoji tunnel project 1037
M. Mori, M. Nakano, K. Shirakawa, M. Koike & M. Iwano

Stability estimation method and analysis for pillar considering the reinforcement during twin-tunnel excavation 1045
S. Park, S.W. Yoon & J.S. Hwang

Design and construction of the longest road tunnel with eight-lane in China 1049
H.F. Qu, H.H. Zhu, Y.C. Cai & X.Y. Zhuang

Experiences from driving dual-rail tunnels on Prague metro's IV.C2 route 1055
J. Růžička, M. Kochánek & V. Valeš

Development of grade separation structures with small cross-sections 1063
M. Shimizu, A. Watanabe, T. Genjyun, M. Kurisu, Y. Hagihara, T. Maeda & H. Watanabe

Civil tunnelling with electronic blasting systems – Early experience from Korea 1071
Y.-S. Song & D. Kay

Blanka tunnel complex in Prague 1079
P. Šourek, L. Šajtar, F. Polák, J. Dvořák, A. Butovič & M. Hadrava

Study on the behavior of an ultra-large section tunnel project in unconsolidated ground-Design and construction of the Minoh toll road tunnel 1085
K. Taketomo, Y. Mitarashi, H. Shiokawa, S. Nishimura & K. Konishi

Large deformations in squeezing ground in the Saint-Martin La Porte gallery along the Lyon-Turin base tunnel 1093
J. Triclot, M. Rettighieri & G. Barla

Geotechnical conditions, methods, and issues of building the transportation tunnels in the wider area of Belgrade 1099
V. Vujanic, M. Jotic, S. Milenkovic, J. Josipovic & B. Jelisavac

Construction of major trunk road tunnels in Moscow 1105
B.I. Yatskov, A.M. Zemelman, S.N. Vlasov & I.S. Bubman

Selecting auxiliary construction methods for NATM tunnel excavation in urban areas 1111
J. Yorita, Y. Sasaki, N. Yamaki & M. Okamura

Part 4.3 Mechanizing tunnelling

Construction update and TBM Excavation Seymour Capilano Twin Tunnels Project, Vancouver, Canada 1119
D. Brox, D. Phelps, B. Garrod, T. Morrison & A. Saltis

Stress–strain soil behavior during tunneling in soft ground: Experimental study on 1g-earth pressure balanced shield model 1125
D. Branque, C. Boutin & H.V. Doan

Conquering the construction challenges of the arrowhead tunnels 1133
B. Fulcher, J. Bednarski, M. Bell & W. Burger

Ground loss control in EPB TBM tunnel excavation 1141
M.C. Gatti & G. Cassani

City-Tunnel Leipzig, a challenge for the shield drive 1147
W. Glitsch & T. Maidl

Integral studies on mechanical functions of mudding agents and the properties of muddified soils in the EPB shield tunneling technology 1153
T. Hanamura, J. Kurose, Y. Aono & H. Okubo

North-South Urban Light Railway Cologne – A challenge for planning and construction – Technical solutions for the accomplishment of the upcoming tasks concerning the tunnels 1161
D. Handke & L. Tempel

The latest technology in mechanized tunnelling – the design of the world's largest EPB and slurry shield TBMs 1169
M. Herrenknecht & K. Bäppler

Compressed air work with tunnel boring machines 1175
M. Herrenknecht & K. Bäppler

Stormwater management and road tunnel (SMART) 1183
G. Klados, Y.H. Kok, D.R. Parks & D.T. Tavender

Wienerwaldtunnel – a challenging tunneling project 1191
H. Köhler

The construction of shield tunnel crossing right under Shinkansen station 1197
A. Kojima, T. Inoue, A. Sano, M. Shimizu & S. Suematsu

Non-circular full face tunnel boring machines – 21st century challenge 1205
M. Krčík

Toulouse Metro Lot 2: soil conditioning in difficult ground conditions 1211
A. Martinotto & L. Langmaack

Upper bound solutions for tunnel face stability considering seepage and strength increase with depth 1217
J.K. Park, J.T. Blackburn & J.-H. Ahn

Gotthard Base Tunnel: Work progress at the five construction sections 1223
M. Rehbock-Sander & A. Gerdes

Innovative design and construction in sydney's newest underground rail line 1229
J.J. Rozek

Evaluation of the effects of shield tunneling on the historical Sio-Se-Pol bridge piles 1235
H.S. Nejad, H.H. Hosseini & R.R. Nejad

Review of the project Uetliberg tunnel 1241
A. Sala

Completion of a trans-Tokyo Bay long-distance undersea shield tunnel 1247
S. Shirai, T. Takeuchi, S. Kurosaki, M. Takebayashi & T. Tomidokoro

Behavior of the shield studied with 3D geological structure models 1253
M. Sugimoto, H. Sasao, Y. Ootsuka, T. Ogawa, K. Harada & E. Kondo

Lining response of twin tunnels affected by EPB shield operation 1261
S. Suwansawat

A86-West Paris ring road-a Bi-mode TBM 1267
J.L. Toris

RandstadRail Rotterdam – Experiences with tunnelling in difficult ground conditions 1275
D.C. van Zanten, D. Handke & M.C. Braam

Section 5: Underground constructions executed from surface in built-up areas

Analysis of long-term deformations of an earth-covered tunnel 1283
J. Barták

Underpinning of live MRT piers for Singapore's new Circle Line Interchange Station 1289
T.F. Lim, B.S.C. Tan, K. Kozo, W.A. Chang & C. Rintu

Design and construction of a cofferdam for a sub-sea tunnel on The Palm Jumeirah, Dubai 1297
J.S. Gahir, A. Mochizuki, N.O. Othman & M.A. Qamzi

Flood protection of Prague Metro after the 2002 flood 1303
M. Jakoubek

Underpinning using Pipe-roof 1309
K. Kazutaka & S. Takaaki

Mathematical modelling of arch-shaped cut-and-cover structures 1315
K. Kunc, J. Pruška & J. Barták

Numerical modelling of the interference between underground structures and aquifers in urban environment. The Turin subway – Line 1 1323
G. Ricci, R. Enrione, A. Eusebio & R. Crova

Application of corrugated structural plates to a cut & cover tunnel 1331
Y.W. Shin, W.R. Yu, B.S. Chun & K.Y. Kim

Evaluation of the stability of anchored diaphragm wall basing on acceptance tests of anchors 1335
A.S. Lewandowska & M.M. Czajewska

London Heathrow Terminal 5 – Construction and monitoring of Piccadilly Extension Junction 1341
A. Stärk & J. Jäger

Effect of moving load to foundation excavation support configuration 1347
C. Xiuwen, L. Yuanfang, Q. Ying, L. Chi, C. Guanghuang, W. Shuping, C. Zhoupin & H. Zhangjun

Section 6: Concrete in underground construction

Part 6.1 Sprayed concrete

Finite element analyze single shell lining based on contact mechanics 1355
J. Zhang, W. Qiu & H. Zhang

The development of early-high-strength shotcrete and the evaluation of improved tunnel support system 1361
H. Kanazawa, T. Nishi, T. Kiuchi, S. Nishizaki & Y. Furuto

Study on a strength characteristic and a quality control of the high-quality shotcrete which aimed at single-shell structure of a tunnel lining 1369
T. Tosaka, T. Asakura, T. Abe, Y. Ito & M. Suenaga

Applications of a shotcrete robot for creating an immediate comparability of mix designs 1377
M. Thewes & G. Vollmann

Sprayed concrete for primary tunnel lining 1383
P. Polák, D. Cyroň, J. Vlašimský & V. Mika

Concrete and shotcrete with crushed aggregates: Experience from the AlpTransit construction site Mitholz 1389
R. Weiss

Certification of shotcrete nozzlemen around the world 1395
C. Larive & K. Gremillon

Robotic application of a unique sprayable membrane for the waterproofing of a subsea tunnel 1401
S.L. Lamhauge, K.G. Holter & C. Ziegler

Part 6.2 Cast in situ and precast concrete

Study on cracks control of tunnel lining concrete at an early age 1409
H. Takayama, M. Nonomura, Y. Masuda, T. Nakayama, M. Takahashi & Y. Kojima

A study on fire resistant segment using short fiber resin 1417
S. Seki, T. Goto, T. Morita, Y. Hayashi & T. Nakagawa

Basic studies on Earthquake-resistance of tunnel linings 1423
H. Miyabayashi, T. Tosaka, A. Isogai, K. Yashiro & T. Aruga

A study on the seismic design methods for precast concrete lining (PCL) 1431
D.-H. Lee, Y.-T. Choi, D.-H. Kim & B.-W. Jo

Design of inner lining at the Gotthard Base Tunnel, approach for the evaluation of loads, the different types of lining 1439
R. Stadelmann, A. Pfeffer & Z.Q. Wei

Final lining of the Valík Tunnel on D5 express highway – the vault construction 1445
Z. Vozárik & J. Svoboda

Development in pre-cast concrete segmental circular tunnel linings 1451
Y.K. Vimalanathan

Design of replaceable structural lining segments 1457
W. Qiu, J. Zhang & D. Li

Structural behavior of SFRC tunnel segments during TBM operations 1461
R. Burgers, J. Walraven, G.A. Plizzari & G. Tiberti

Development of damage detection method on the tunnel lining from the laser scanning data 1469
J.-S. Yoon, M. Sagong & J.S. Lee

The MASW method for testing tunnel lining integrity 1475
R.-M. Faure, G. Lefebvre, M. Karray & G. Hémond

Design of the strengthening of tunnel linings under localized pressures 1481
A.R. Marí & C. Molins

DeCo Grout – Innovative grout to cope with rock deformations in TBM tunnelling 1487
B. Billig, B. Ebsen, C. Gipperich, A. Schaab & M. Wulff

Immersed tunnels state-of-the-art 1493
L.C.F. Ingerslev

Immersed tunnels continue to meet the challenges of water crossings 1499
W.C. Grantz, V. Tanal, L.C.F. Ingerslev, J.-N. Wang & D.P. Richards

Case study for the deterioration of lining in vehicular tunnel based on ventilation system 1505
J.H. Choo, H.S. Ryu, Y.S. Shin & S.R. Ahn

Březno tunnel shaft 1509
E. Stehlík, J. Heřt & T. Parák

Repair and reinforcement of damaged tunnel by Acid Mine Drainage (A.M.D.) 1513
Y.-S. Lee, T.-k. Yoon, Y.-S. Shin & J.-J. Han

Section 7: Distribution and management of risks and accidents during tunnelling

Data management for highly mechanized shield tunnelling in the construction of the line 9 metro Barcelona 1521
C. Deulofeu, H. Schwarz, U. Maidl & M. Comulada

Tunneling in water-bearing unconsolidated ground according to specifications for auxiliary methods revised to reflect varying soil conditions – Constructions in the north work section of the Takaoka tunnel on the Hokuriku-Shinkansen railway line 1527
F. Furukawa, Y. Hino, H. Inoue, H.Inoue, K. Asari & J. Yorita

Use of risk management plan for urban mechanized tunnelling projects: From the establishment of the method to the successful practice 1535
P. Grasso, E. Chiriotti, S. Xu & N. Kazilis

Risk analysis and evaluation considering geotechnical stability and environmental effect in tunnel design 1541
D.-H. Kim, C.-R. Choi, S.-J. Oh, Y.-G. Kim & J.-K. Park

Third party safety issues in international urban tunnelling 1549
G. Lance, J. Anderson & D. Lamont

Risk management in connection with execution of underground structures and surface development securing 1555
A.J. Lossmann & B.V. Motyčka

Contracting issues for conventional tunnelling 1559
N. Munfah

Development and application of the new TBM risk management system 1565
K. Murakami, M. Murayama, K. Terada, Y. Fuke, Y. Miyajima & K. Aoki

Risk assessment of discharge due to tunnel excavation using simplified seepage analysis system (SWING) 1573
Y. Ohnishi, H. Ohtsu, K. Takahashi & T. Yasuda

Driving of shallow tunnel in uncertain geological boundary conditions – a case history 1579
R. Pöttler, F. Thum & W. Jöbstl

Geotechnical risk management for tunneling beneath open water 1585
D.P. Richards & B. Nilsen

Impact of a geological incident on the construction of a land sewer outfall in Ferrol, northwest Spain 1591
J.L.S. Fernández, B.A. Álvarez & I.P. de Vera Moreno

Sub-sea microtunnel by pipe jacking method – construction challenges 1597
S.S. Ahmed, S. Alfaour & M.Al Ghanem

Geotechnical safety management on site 1603
W. Schubert

NATM tunnelling at Dulles Airport 1609
E. Stehlík & M. Srb

Risk management of the construction of tunnels using Tunnel Boring Machines (TBMs) 1613
A.H. Thomas & J.P. Banyai

Assessment of ecological safety in the process of underground development on the example of a big Russian city 1619
V. Umnov & N. Vorozheykina

Managing risk – successful project delivery, underground infrastructure for Terminal 5 Heathrow Airport, UK 1623
O.I. Williams

Development and application of process-oriented shield tunneling risk management system 1629
T. Xuan, W. Huiming & B. Chow

Evaluation of tunnel behavior and decision making of counter measures in weak zones 1633
H. Yagi, M. Hashimoto, Y. Yoshida, K. Tamamura & A. Uneda

The measures for preventing acid rock drainage through the results of acid rock drainage assessment and contamination transport numerical analysis 1641
Y.-Il. Yoo, J.-B. Oh, D.-H. Lee, J.-G. Kim & H.-P. Chun

State of the art tunnelling technologies 1647
Ž. Žderić, G. Pervan & Đ. Radić

Author Index 1653

Volume 3

Section 8: Tunnel equipment: fire and operational safety

Part 8.1 Safety equipment

Safety analysis of the Branisko tunnel ventilation 1663
M. Bettelini, M. Bakoš & N. Seifert

Safety doors in the world's longest tunnel under the Gotthard: Outstanding requirements and performance. Feed-back from the bidding phase and results from the testing phase on selected prototypes 1671
D. Fabbri, C. Strassl & S. Peggs

Mechanical equipment in long, high-speed rail tunnels – Specification and operational experience of doors, cabinets, containers and other elements in the Loetschberg Base Line 1677
R. Haldimann, S. Nyfeler & P. Reinke

Study on the behavior of smoke from a train fire based on the track gradients in railroad tunnels equipped with a forced ventilation system 1687
D.-H. Kim, Y.-J. Jang & J.-J. Moon

An experimental study on the tunnel pressurization for smoke control 1693
H.S.A. Lee, I.S.B. Oh, K.C.C. Lee, W.K. Kim & W.J. Kim

Effectiveness of critical velocity method for evacuation environment in a railroad tunnel at fire situation 1699
S.-C. Lee, S.-H. Lee & J.-H. Lee

Numerical simulation in effect of compartmentalization with Water Screen (WS) in a tunnel fire 1705
M. Murakami, H. Kurioka, O. Imazeki, H. Kuwana & R. Amano

Road tunnel equipment 1711
M. Novák, V. Misárek & D. Benda

Site ventilation of a long deep tunnel: The lot Bodio of the Gotthard base tunnel 1717
M. Oberaigner & F. Romerio

Ventilation of cross-passages in long rail tunnels: Requirements and possible solutions with a passive or an active ventilation system for the Gotthard base tunnel 1721
D. Portmann, P. Reinke, B. Hagenah & A. Busslinger

Fire test in the Mrázovka tunnel and its impact on the ventilation control systems in tunnels Mrázovka and Blanka 1727
J. Pořízek, M. Hanfová & L. Šajtar

Optimization of tunnel system based on ITS architecture 1733
P. Přibyl

Increasing industrial safety and climatic conditions by the use of spray nozzles 1739
A. Rudolf, O. Gloth & P. Schürmann

Towards tunnel facility management: Applying asset management to the operation and maintenance of tunnels within infrastructure networks 1745
J. Ruiter

International tunnel control system – introduction and experiences from realization 1749
J. Řehák

System of traffic control on Prague inner city ring 1755
J. Štefan

Facility management methods for an improved serviceability of traffic tunnels and their application to tunnel drainage problems 1759
M. Thewes, F. Heimbecher & G. Vollmann

Part 8.2 Fire protection measurement

Fire protection concept for the Ceneri base tunnel 1767
S. Čufer

Newest issues of integrated road urban tunnel fire protection system 1773
N.F. Davydkin & S.N. Vlasov

Creation of advanced technologies in the generation of electrically safe flows of finely dispersed water for fire protection of underground installations 1779
A.S. Chirko, A.V. Karpyshev & M.D. Segal

Modeling of blasts and fires accidents in tunnels 1783
A.S. Chirko, P. Efremov, V.E. Fortov, V.V. Golub & A.V. Zibarov

Fire test to characterize fire-induced damage of concrete lining in NATM tunnel 1787
S.-W. Choi, S.-H. Chang, G,-J, Bae, J.-W. Kwon

Large scale fire tests with different railway overhead systems – experience by the test center 1793
S. J. Seirer, V. Wetzig

The research on countermeasure of fireproofing and rescue for long highway tunnel 1799
Y.-D. Wang, Y.-X. Xia & N.-B. Deng

Experimental study on mechanical behaviors of tunnel lining under and after fire scenarios 1805
Z.G. Yan & H.H. Zhu

Part 8.3 Risk analysis

Risk analysis of the Branisko tunnel 1813
M. Bakoš, N. Seifert & M. Bettelini

ITA-Committee on operational safety of underground facilities – COSUF: Role and Objectives 1819
A. Haack

Optimisation of road tunnel safety based on risk analysis 1827
M. Holický, J. Smolík & L. Šajtar

Austrian Risk Analysis for road tunnels development of a new method for the Risk Assessment of road tunnels 1835
B. Kohl, K. Botschek & R. Hörhan

Safety requirements of the 53 kilometer railway tunnel through the Alps between Italy and France 1841
J.E. Nieuwenhuis, F.Q. Ambrunaz, E. Verbesselt, E. Boisguerin, P. Piepers & A. van der Giessen

Operational safety of road tunnels: Safety reviews of tunnel projects and existing tunnels 1849
N. Seifert & R. Siegenthaler

Experiences and (in)effective application of QRA for assessing tunnel safety in the Netherlands 1853
C.J. Soons, J.W. Bosch, P.H.A.J.M. van Gelder & J.K. Vrijling

Emergency egress provisions and their guidelines 1861
M. Vasilovska & M. Reedman

Section 9: Historical underground constructions; maintenance and reconstruction of underground constructions

Geotechnical recent issues in relation to past mining activities at urban area of historical mining towns in Slovakia 1871
V. Bauer, E. Sombathy & M. Stavnikovič

Results of the excavation works in upgrading the Frejus railway tunnel 1879
P. Grasso, M. Pescara, F. Valdemarin & G. Beccaria

Monitoring and evaluation after repair and reinforcement of damaged 3-lane Freeway Tunnel located within fault Influenced zone 1885
J.-S. Hou, D.-J. Tseng & Y.-H. Lee

Environmentally friendly subway construction in the overcrowded city of Tokyo 1891
K. Irie & S. Nishibayashi

Reliability assessment, repair, and replacement of historic water tunnels and their contribution to California's sustainability 1897
J. Kaneshiro, F. Kintzer, M.L. Piek, R. Yoshimura, D. Van Horsen, G. Korbin, K. Lovelie, J. Carfrae, R. McManus & C. Ovalle

Study on maintenance planning for tunnels by risk management system 1907
S. Konishi, K. Kuribayashi, K. Sudou, K. Kamemura, M. Hori & C. Hatakenaka

Reconstruction of the Jablunkov tunnels 1913
J. Korejčík & J. Růžička

Upgrading old masonry interceptor sewers to modern sewerage standards 1919
C. Madryas, A. Szot & L. Wysocki

The old railway tunnel of Mainz – A design and construction concept for the expansion of two approx. 150 year old tunnels in urban areas 1925
Th. Marcher, G. Braun & F. Jiricny

Analytical investigation of damaged tunnel linings by the action of excessive earth pressure 1931
H. Mashimo

Historical damages of tunnels in Japan and case studies of damaged railway tunnels in the Mid Niigata Prefecture Earthquakes 1937
M. Shimizu, T. Suzuki, S. Kato, Y. Kojima, K. Yashiro & T. Asakura

Close underpass of ancient tunnels: Methodology and results 1945
A. Sorlini, G. Amoretti & F. Zannoni

Advanced methods for tunnel assessment 1949
G.R. Sulibhavi & W.A. Parks

"Lokve" tunnel rehabilitation – experiences and applied solutions 1955
Z. Tomanović

The ring method application to the Prague Metro construction 1959
P. Vozárik

Value Preservation of underground infrastructure through focused conceptional planning 1963
N. Winkler & A.W. Ackermann

Diagnosis and repair of a subway tunnel 75 years old 1969
T. Yamamoto & S. Matsukawa

Author index 1975

This page intentionally left blank

Underground Space – the 4th Dimension of Metropolises – Barták, Hrdina, Romancov & Zlámal (eds)
© 2007 Taylor & Francis Group, London, ISBN 978-0-415-40807-3

Preface

The Czech Tunnelling Committee ITA/AITES – as organizer of the 33rd World Tunnel Congress 2007 in Prague – has been elected by the ITA member countries three years ago. We have been very honoured by their confidence and grateful to the ITA for its support.

The ITA annual congresses and meetings have become premier events in the international tunnelling and underground construction calendar.

The theme of the WTC 2007 "Underground Space – the 4th Dimension of Metropolises" has been chosen as we feel it to be still more and more topical regarding the permanent growth of concentration of the world population into metropolises and megacities. The underground offers the hope of help to solving of related problems.

Hundreds of potential participants and interested companies and institutions from all over the world had been invited to submit their papers and contribute to the development of underground construction. The response to free paper submission was very impressive and many of the accepted papers contained new information and demonstrated further growth in the significance of our industrial branch. We would like to reaffirm our appreciation to all our colleagues for their great willingness to share knowledge and for their continued support.

The Proceedings of the ITA-AITES WTC 2007 – the book and the CD-ROM – present the full papers accepted by the Scientific Council of the Congress. Authors submitted 382 abstracts which were reviewed and 316 full papers were selected for publication. The published papers have been grouped into 9 sections – main discussion topics of the Congress.

This page intentionally left blank

Underground Space – the 4th Dimension of Metropolises – Barták, Hrdina, Romancov & Zlámal (eds)
© 2007 Taylor & Francis Group, London, ISBN 978-0-415-40807-3

Organisation

The following groups have been closely involved in the organization of the Congress:

INTERNATIONAL ADVISORY COMMITTEE:

Chairman: Zdeněk D. EISENSTEIN (Canada)
Members: André ASSIS (Brazil)
Jean-Paul GODARD (France)
Gyula GRESHIK (Hungary)
Wojciech GRODECKI (Poland)
Alfred HAACK (Germany)
Jindřich HESS (Czech Republic)
Martin KNIGHTS (United Kingdom)
Koichi ONO (Japan)
Harvey PARKER (USA)
Sebastiano PELIZZA (Italy)
Sergey N. VLASOV (Russia)
Harald WAGNER (Austria)
Jian ZHAO (Switzerland)

ORGANIZING COMMITTEE:

Chairman: Georgij Romancov
Members: Josef Aldorf, Jiří Barták, Claude Berenguier (ITA-AITES Secretary General), Eva Bundová, Josef Dvořák, Matouš Hilar, Ivan Hrdina, Miroslav Kadlec, Štefan Kovalčik (Slovakia), Jana Lepičová, Libor Mařík, Karel Matzner, Petr Mičunek, Miloslav Novotný, Stanislav Sikora, Jiři Smolík, Petr Vozárik

SCIENTIFIC COUNCIL:

Chairman: Jiří Barták
Secretary: Karel Matzner
Members: Josef Aldorf, Radko Bucek, František Dvořák, Josef Dvořák, Otakar Hasík, Matouš Hillar, Miroslav Kolečkář, Václav Krch, Bernhard Maidl (Germany), Libor Mařík, Jaroslav Pacovský, Jiří Pavlík, Pavel Polák, Jan Pruška, Pavel Přibyl, Alexandr Rozsypal, Jiří Smolík, Martin Srb, Ermín Stehlík, Ludvík Šajtar, Richard Šňupárek, Jan Vítek, Petr Vozárik, Jaromír Zlámal

ITA-AITES 2007 OFFICIAL WTC ORGANIZERS:
CZECH TUNNELLING COMMITTEE ITA/AITES
GUARANT INTERNATIONAL, spol. s r. o.
AGENTURA BONUS

The editors would like to acknowledge the great effort expended by all these colleagues and friends in the organization of the ITA-AITES 2007 Congress in Prague.
Jiří Barták – Ivan Hrdina – Georgij Romancov – Jaromír Zlámal

This page intentionally left blank

Section 1
Underground city design planning of underground constructions

This page intentionally left blank

Underground Space – the 4th Dimension of Metropolises – Barták, Hrdina, Romancov & Zlámal (eds)
© 2007 Taylor & Francis Group, London, ISBN 978-0-415-40807-3

Largest transportation system – Metro and road in the same tunnel

V.M. Abramson & S.Yu. Loubotski
Sistema GALS OJSC, Russia

ABSTRACT: Brief description of design and construction features of a unique project, Serebrianoborsky tunnels, is presented in the article. The project comprises three tunnels, each 1514 m long, including two 14.2 m diameter transport tunnels, one 6.3 m diameter service tunnel and five cross drifts connecting these tunnels. The tunnels are built using Herrenknecht TBMs with shields of respective diameters operating according to the bentonite face hydraulic support technology. The design was awarded prize of International Exhibition of Innovations in Brussels.

In accordance with the new Moscow Master Plan, extensive trunk street/road development program is underway in the city.

A trend seems to evolve for new trunk roads to be laid in tunnels crossing the whole city districts and leaving intact both the habitat and surface buildings, man-made structures and architectural monuments; it means that there appear long trunk road urban tunnels. This is particularly important for such a complex urban body as Moscow where the historically formed ring/radial trunk street system makes it insistent to create a transportation system capable of providing for both perfect traffic control and links between peripheral districts and the centre.

On the basis of the Master Plan, a new radial transportation corridor, Krasnopresnenski Avenue, is being formed in Moscow, the corridor making it possible both to create a new trunk road in the western sector of the capital and to provide conditions for road users to comfortably pass from the city center to the "Baltiya" Moscow – Riga Federal Highway.

The first "Baltiya" Moscow – Riga Federal Highway section joining the Moscow Ring Road (MKAD) was completed in 1996. However, the highway could not enter the city owing to the fact that the alignment crossed two protection zones: the Serebryany Bor forest park and the Krylatskoye dwelling and nature territory. Construction of a surface road could infringe ecological situation of the region since it would have been inevitable to cut trees in the Serebriany Bor forest, to demolish some important dwelling buildings and to disturb natural landscape.

At present, the Moscow – Riga trunk road is linked with the city centre through MKAD and its interchanges at Roubliovskoye and Volokolamskoye Chaussees resulting in essential superfluous run and additional traffic load at MKAD section between these interchanges.

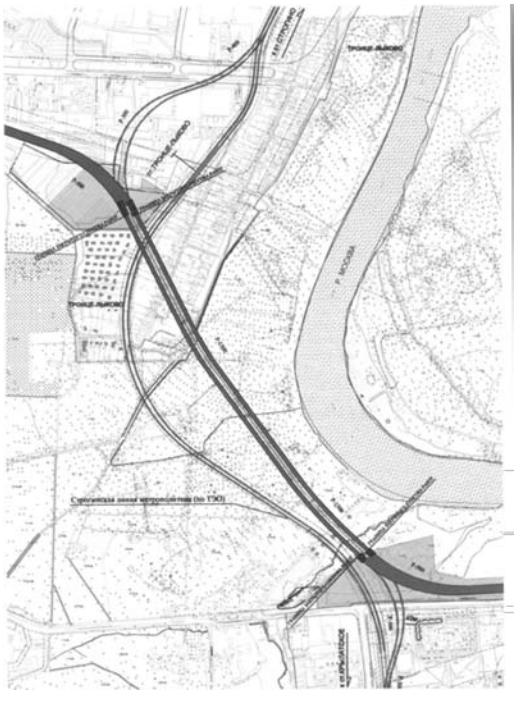


Figure 1. Tunnel site with approaches combined with Stroguinskaya metro line.

Besides, the Stroguinskaya metro line from Krylatskoye Station to Stroguino Station linking household areas of this region with the city centre is currently under construction along an alignment close to that of the proposed tunnels (Figure 1).

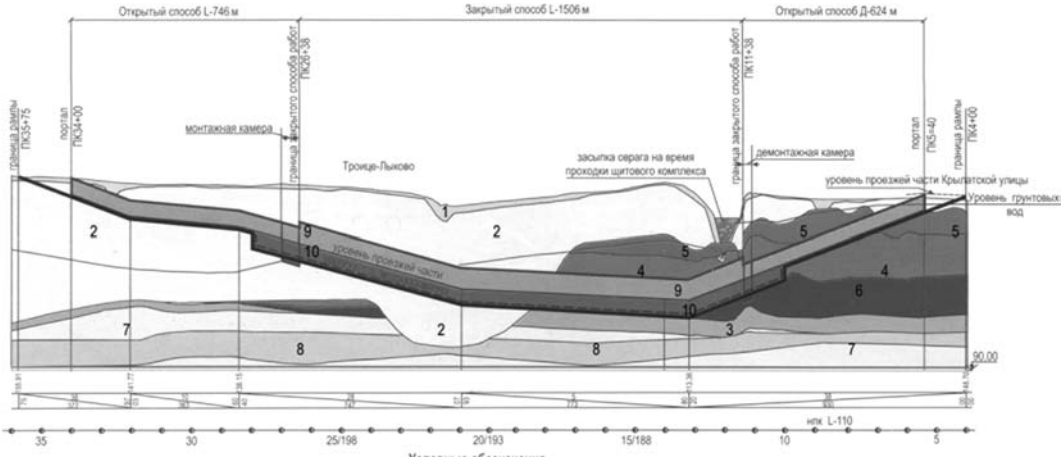


Figure 2. Longitudinal profile of tunnel section with approaches combined with Stroguinskaya metro line. 1 – filled-in soils: sand, sandy-loam, unconsolidated loam with brick and concrete breakage; 2 – wet and water-saturated alluvial and aqua-glacial sand of various grain size with layers of sandy-loam and loam, locally with gravel and boulders; 3 – tough-plastic and semi-hard (occasionally hard) Jurassic clay; 4 – semi-hard (occasionally hard) Jurassic clay; 5 – water-saturated chalk sand and sandy-loam, soft loam with sandy-loam layers; 6 – tough-plastic and semi-hard Jurassic loam, water-saturated sandy-loam; 7 – medium-hard and hard fractured and badly fractured water-saturated coal limestone; 8 – hard and semi-hard coal clay and clayey marl; 9 – road right-of-way; 10 – metro right-of-way.

Thus, serious problems that arose in the prestigious North-West region of Moscow were to be urgently solved to improve transportation conditions of the city.

Metroguiprotrans designers could find the solution having proposed basically new engineering and construction approach consisting in laying two 14.2 m diameter tunnel barrels under the whole protection and household zone, each tunnel accommodating two transportation modes: road for 3 traffic lanes in the upper level and metro tracks in the lower one. This approach was patented and awarded with a prize of International Exhibition of Innovations held in Brussels in 2003; at present, such world-first "dual-purpose" tunnel barrels are being built at the section where alignments of Krasnopresnenski Avenue and Stroguinskaya line of Moscow Metro coincide.

Construction site is located at the second and the third right flood land terraces of the Moskva River, absolute elevations of the graded surface varying from 145 to 155 m.

Geological composition of the region is represented with deposits of the Quaternary, Cretaceous, Jurassic and Coal periods.

The Quaternary deposits encountered at many sites are represented with technogenic as well as with alluvial and aqua-glacial soils, presumably those of sandy and sandy-loam types.

There are several ground water tables along the alignment including Jurassic, Ratmir and Souvorov water-bearing layers.

The free ground water table is measured at absolute elevations from 126 to 130 m. Thickness of the layers vary from 12 to 30 m. Permeability factor varies from 4 to 15 m/day (Figure 2).

Implementation of this project has become possible owing to the fact that principally new Herrenknecht tunnel boring machines were used, the machines operating with combined hydraulic and air face support 14.2 m diameter shields at depths providing for complete safety of the city habitat independently of geological and hydrological conditions. It made possible to successfully complete driving all Krasnopresnenski Avenue tunnels (Figure 3).

The Krasnopresnenski Avenue tunnel section thus consists of three tunnels – two 14 m diameter 1514 m long transport tunnels and one 6 m diameter 1514 m long service tunnel located between the transport ones (Figure 4). The service tunnel is used to accommodate utilities, to perform ventilation functions and, in case of emergency, to provide for evacuation of the passengers and for unhampered approach of fire and rescue teams to the site of emergency. Cross drifts connecting the three tunnels are made every 250 m to provide for the approach. Total length of the transport tunnels including the ramp sections makes 2550 m, two 1514 m long tunnels having been driven in closed techniques using one tunnel boring machine. The following construction sequence was used: first the left transport tunnel, then the service tunnel (while driving the service tunnel, the main TBM was dismantled, transported to the base ground and reassembled to drive the

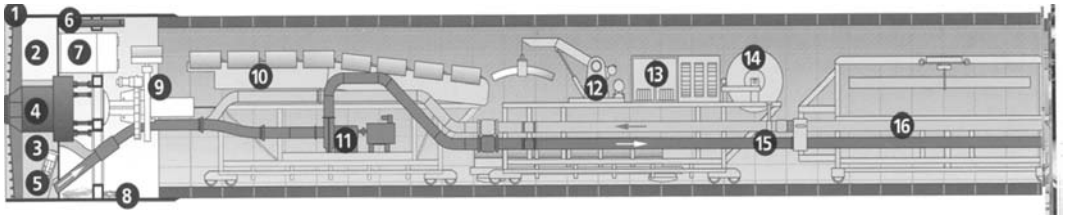


Figure 3. Mixshield design. 1 – cutterhead; 2 – air cushion; 3 – bentonite suspension; 4 – drive; 5 – stone crusher; 6 – cylinder; 7 – decompression chamber; 8 – navigation cylinder; 9 – segment erector; 10 – segment transporter; 11 – muck pump; 12 – segment lifting crane; 13 – power shield; 14 – cable drum; 15 – muck removal pipeline; 16 – feeding pipeline.

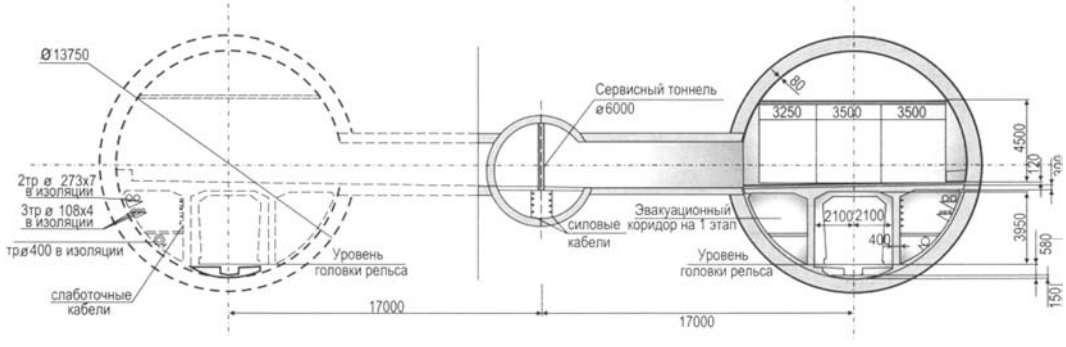


Figure 4. Cross-sections of Serebryanoborsky Tunnels.

right transport tunnel); the right tunnel was the last to be driven. In order to provide for the tunnels to be built, a 9.2 m^2 base ground was arranged with start shafts for all the tunnels, building for all separation equipment, storage ground for lining segments, compressor room and utilities.

In order to be able to drive all three tunnels from the same base ground, a 6.3 m diameter TBM of the same type as TBM for the main tunnels. Reinforced concrete segments for lining rings were manufactured at an updated plant in Moscow in accordance with design prepared by Metroguiprotrans OJSC specialists. Rings for the main tunnels are as wide as 2 m, each consisting of 8 main segments and a locking one.

The left tunnel driving commenced in May 2004. At present, all the three tunnels are driven, while construction of the cross drifts and the roadway as well as installation of technological equipment is underway. Average and maximum advance rates of the main TBM made 200 m and 250 m per month respectively. Owing to strict adherence to the design face support hydraulic pressure values, surface settlement in the course of driving were brought to minimum and did not exceed 10–12 mm.

At two thirds of the alignment, the tunnels pass through water-saturated sand soils and through clay soils at the remaining third. Given the difficult ground conditions, the cross drifts are built using special soil stabilization forestalling methods. The techniques used for each drift differ depending on particular soil properties. Horizontal jet-grouting, cement grouting, stabilization with various materials and soil freezing are used.

In order to provide for the required air quality and safety parameters in the tunnels in case of fire, forced feeding and extraction ventilation and powerful smoke-removal systems are installed. Each tunnel is ventilated with respective individual systems. The tunnels are built according to the highest fire-safety requirements; the whole inner surface of each tunnel is protected with special cover capable of withstanding open fire action within 3 hours.

Completion of this tremendous project scheduled for December 2007 will finalize creation of the direct transport communication between the “Baltiya” expressway and the centre of Moscow resulting in mitigation for the traffic-overloaded Volokolamskoye and Roubliovskoye Chaussees. Besides, 1.5 km long metro line will be built.

Tunneling practice will get enriched with one of the world most important underground structures, a complex of combined road and metro systems making it possible for major cities to more efficiently solve their transportation problems.

This page intentionally left blank

Underground Space – the 4th Dimension of Metropolises – Barták, Hrdina & Romancov (eds)
© 2007 Taylor & Francis Group, London, ISBN 978-0-415-40807-3

Anchor recovery under extreme conditions in downtown Leipzig, Germany

Dipl.-Ing. Lars Babendererde & Dipl.-Ing. Philipp Elsner
Babendererde Ingenieure GmbH, Bad Schwartau, Germany

ABSTRACT: In the inner city of Leipzig, Germany, the London, U.K. based AMEC group, an international infrastructure specialist, faced the problem that old cable anchors from the construction pit of a multiplex shopping centre built by AMEC in 1999/2000 had to be recovered from under existing buildings. The anchors were finally recovered by a pile borer and a slurry wall excavator in a first stage and by pipe jacking under compressed air along the anchor axes in a second stage.

1 INTRODUCTION

In the years 1999 and 2000 the British AMEC group, represented by its Leipzig office, built and afterwards managed the multiplex centre "Petersbogen", which is in the heart of the inner city of Leipzig. The centre is comprised of shops, restaurants, a cinema, a casino and the judicial branch of the Leipzig University. The complex is four (4) stories high and has four (4) basement levels of which the first is a shopping area, whereas the others are used for underground parking and building utilities.

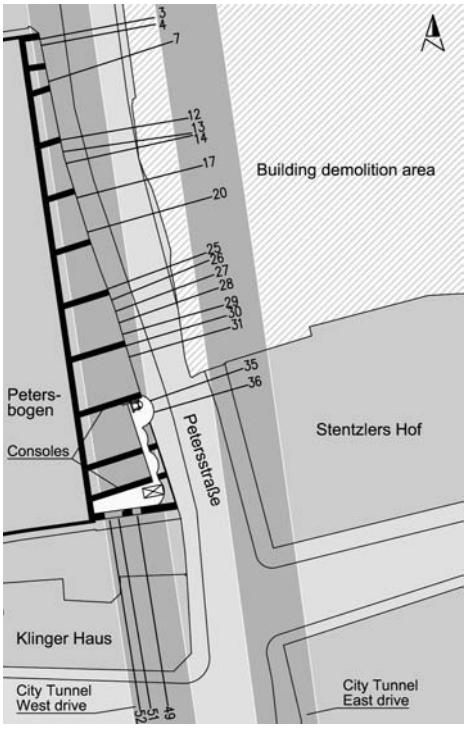


Figure 1. General layout.

During the design phase of the building AMEC had to consider that a future underground railway line, the so-called "City Tunnel Leipzig" consisting of two tubes, would pass in a shallow alignment under the property of the Petersbogen's southeast corner. As part of the building permit AMEC had to guarantee that no permanent installations would be positioned within the future tunnel cross sections.

Due to the high ground water level with permeable layers of soil on top of impermeable ones, a water tight construction pit was planned, enclosed by deep slurry walls reaching into the impermeable layers. In the slurry walls, steel beams were positioned to stabilise the free standing part of the wall. In order to reduce wall movement and the steel beam cross section two layers of cable anchors were planned by the designer. The anchor geometry accounted for limitations from the tunnel.

2 THE TROUBLE STARTED

In 1999, the contractor for the construction pit began the work as designed and tendered. Soon after the work began he ran into remnants of foundation from former buildings, which had been announced in the tender documents. Due to excavation problems the contractor changed the building pit design to three rows of anchors. But now the bottom layer was ending right in the future City Tunnel cross section.

The contractor promised to get the anchors back out of the ground by explosive recovery. This meant small ductwork would be interlaced within the cables of the anchors, so that the grout bulb could be loaded

with explosives in the form of a cortex. Through the explosion, the grout bulb would then be cracked, making the steel cables easy to pull out of the ground. Also, a back-up method was offered.

The work continued according to the alternative plan. Unfortunately, when time came to recover the anchors, the contractor found that he could not fill some of the ductworks with any cortex and others could only be filled with a smaller and less effective cortex than planned. The result was that the contractor failed to recover 43% of the anchors. As if that wasn't enough, the alternative recovery method with the hollow drill rods also failed.

The contractor tried several other recovery methods. First, he tried to loosen the bedding of the anchors in the soil with the help of jet grouting lances. After that, he tried to destroy the grout bulbs with large amount of explosives which were detonated in extra boreholes bored parallel to the anchors. Even the pulling technique was varied from pulling all cables of an anchor at once to pulling only single cables or smaller groups. But all methods failed.

Finally, the construction schedule became so pressing on AMEC that the regular construction works had to continue.

3 A NEW ATTEMPT

At this stage AMEC requested Babendererde Ingenieure to prepare new solutions for the anchor recovery. As specialists for TBM tunnelling, the first solution was to check whether the slurry TBMs of the City Tunnel could simply drive through the cable anchors. This idea was quickly abolished due to unpredictable high risks and costs.

It was then investigated what would be necessary to recover the anchors from inside of the TBMs. Although it was technically feasible, the costs were enormous and unacceptable for AMEC.

The third alternative was to construct small, hand driven ducts, secured with fibre reinforced shotcrete under compressed air. Starting from within the basement level of the Petersbogen, miners would have to dig a tunnel towards the critical zone of the anchors and then, from one anchor to the next, to cut away the sections within the City Tunnel alignment. The shotcrete ducts would have been no match for the TBMs, which were equipped for mixed face conditions comprising cohesive and non cohesive soils with stones and layers of hard, abrasive quartzite.

After the preparation of this solution the client suddenly learned that a building opposite to the Petersbogen, under which 15 of the 20 remaining anchors were lying, was about to be demolished to make space for a new department store.

New options were considered. The final solution was to pull the anchors out of the ground with the help

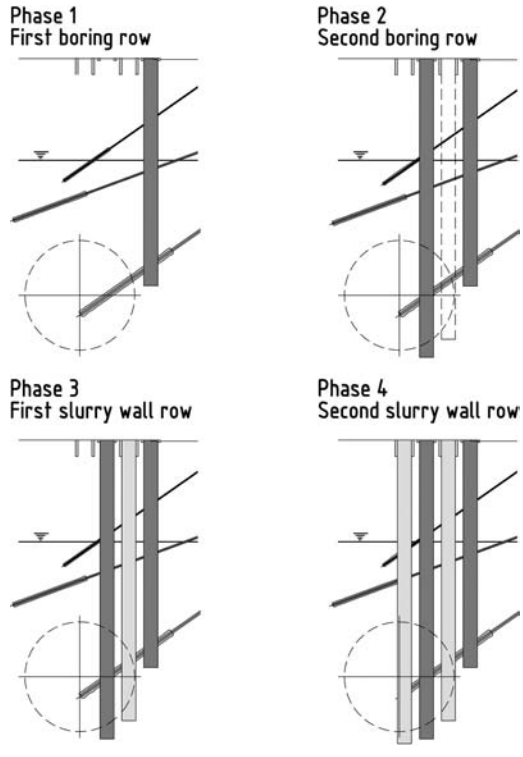


Figure 2. Working steps for recovery from above ground.

of pile borers and slurry wall excavators which were already available due to required site preparations for the new department store. So in the summer 2004 a 75t pile borer and a 120t slurry wall excavator were driven to Leipzig to dig for cable anchor pieces with a maximum weight of 30 kg.

4 GOING FISHING

The final plan was to cut the anchors with a pile borer ID 1,2 m. Two (2) rows of cuts were foreseen. The first row was supposed to cut each anchor into two (2) sections, one (1) within the tunnel and one outside of the tunnel. The second row was supposed to cut the sections within the tunnel into two (2) sections of equal size ranging between 3 and 4 m in average length. The bore holes were to be filled with a one-phase boring suspension which hardened after a while to form an artificial soil of similar strength compared to the natural soil in this area.

Then the slurry wall excavator would perform two (2) rows of excavation to pull out the remaining sections of the cable anchors. The trenches were to be stabilized by the same suspension which was already being used for the borings.



Figure 3. Construction site.

5 RECOVERY FROM ABOVE

The excavation works were no problem for the pile borer and the trench excavator. The pile borer cut even through anchors with nine (9) steel cables without any recognisable evidence for the driver. Thus, every single bucket of excavated material from the ground had to be closely observed while pulled above ground and dumped into the bucket of waiting wheel loader. Often cables of an anchor were obviously hanging in the teeth of the boring bucket. In general, the cable sections were between 60 and 120 cm long and heavily twisted because of the boring rotation. Yet some cable sections also were squeezed into the bucket and were spotted during the dumping onto the wheel loader bucket. The emptying of the wheel loader was also closely observed. Some cables were disintegrated to single wires and it was often only during the last dumping from the wheel loader that such wires were found.

Time and again a “hit” on an anchor was indicated by steel cable sections hanging from the boring bucket. Then, in the next one or two buckets coming up, more pieces from that hit were found. Nevertheless, it also happened that just a few distorted wires were the only indication of a successful hit.

The important task of the Supervising Engineer in this stage was to explicitly map, record and photograph every single finding, and then identify which anchor was cut. The mapping was used to get a closer idea where exactly each anchor was lying to verify the positions of the following slurry wall excavations. If one considers that there were two (2) more layers of cable anchors above the one searched for and that through the deviations of the anchors and the borings alike sometimes anchors were found where none had been expected, the identification became a big puzzle which finally was solved.

After all findings had been interpreted, the excavation with the slurry wall excavator began. Whilst watching and searching through the excavated material during the borings was often tedious work, now the big hits were being made. As planned, the trench excavator easily pulled out the remaining sections of the cable anchors.

Up to 4 m long sections were brought to the surface in one piece. As the locations of the anchors were quite well known through the borings, it could even be predicted at which position and depth anchors should be found. The job advanced well and was finished within the tight and unmodifiable time frame which was given to AMEC by their neighbour and his construction works.



Figure 4. Anchor section under slurry wall excavator.



Figure 5. Recovered and cleaned anchor section.

6 FIVE TO GO

After the successful recovery of the first 15 anchors there were still five (5) to get out. All five (5) anchors were located in the southeast corner of the shopping centre. Anchor no. 35 and 36 extended to the east. They were 19 m long, bored at an angle of 35° and had a 9.5 m long grout bulb each. The anchors were perpendicular to the City Tunnel axis and the last approximately 4.5 m of the grout bulbs were directly within City Tunnel east drive cross section. The intersection between the anchors and the tunnel was under one of the neighbour's buildings, the so-called "Stenzlers Hof".

The other three anchors no. 49, 51 and 52 extended to the south. They were 32 m long, bored at an angle of 35° as well and had a 11.5 m long grout bulb each. The anchors were parallel to the City Tunnel west drive crossing it from the top to the bottom at a length of about 15 m. Due to their length, the anchors' grout bulb started shortly under the tunnel's invert. Also in this case the intersection between the anchors and the tunnel was situated under a listed building, the so-called "Klinger Haus".

Again, as previously mentioned, a recovery from above was impossible as the important sections of the anchors were covered by buildings. So the designer, as well as the client, accepted that the only solution left was to recover the anchors from underground, although it was unclear at this moment how, and from where, this should be done. The deepest parts of the anchors to recover were about 25 m below the surface and 17 m below the ground water table.

Digging down from the Petersstraße was impossible. It is the main shopping street in Leipzig. The compensation alone to shop owners due to construction work in front of their shops would have been enormous. In addition, any work from within the basements of the buildings above the anchors was impossible. The rooms were too small for any sensible operation and they were occupied by the tenants. Therefore, the only possible solution was to start from somewhere within the property of the client, which was the Petersbogen building.

The anchor heads were lying roughly at a depth at the middle of the third basement level and 1 m below the ground water level. Fortunately, the construction of the building in the southeast corner was different from the rest of it. In general, the building had four basement levels. But in the area of the later City Tunnel the client had been allowed to build only two basement levels, thus the third and fourth basement levels had to be reduced in their expansion. In order to keep the future tunnel free from massive loads from the overhanging building part, it was constructed on huge reinforced concrete consoles which were attached to the side walls of the third and fourth basement levels.

As a result of the special construction, the five anchors ended actually under the Petersbogen building. Due to the fact we decided to cut an opening into the slab of the parking level in the southeast corner and dig tunnels under the cover of the slab to reach the anchor heads. Then micro tunnels could be launched, one for each anchor.

With the help of 1.2 m ID pipes driven under 35° downwards over each anchor, the anchors could be dug out and cut to pieces parallel to the jacking progress. The excavation had to be performed by hand, by a man sitting in the head of the pipe. Since pipes would end in the City Tunnel cross section, a pipe material had to be selected which later would mean no harm to the TBMs of the City Tunnel.

The decision was made to use CC-GRP (centrifugally cast glass fiber reinforced plastics) pipes made by HOBAS. A Slurry TBM with discs is able to cut through such pipes when it comes upon them in the ground. Nevertheless, any steel elements permanently installed in the pipes were forbidden.

For steering and as protection for the first pipe's face, a mini steel shield was necessary although it had to be dismantled and carried back out of the pipe of each tunnel drive.

The biggest challenge and impact during excavation was coming from the ground water. The ground water table was equal to the level of the slab. It was impossible to lower it by pumping with mainly sands to excavate through, buildings all around and the deepest anchor sections being at 17 m below the ground water table. Under the given boundary conditions, ground freezing was also impossible. Therefore the only option left was excavation under compressed air. A service room, in the very south-east corner of the second basement level, was chosen as the entry point to the tunnels.

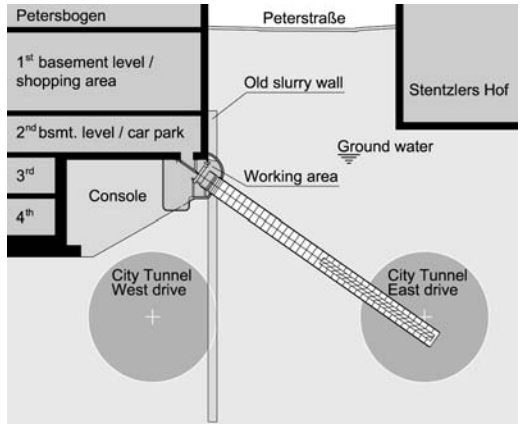


Figure 6. Recovery from underground.

The decision was made to cut a hole $3.0 \times 1.5\,m^2$ into the floor and excavate downwards from there. The service room walls consisted of reinforced concrete and it had just one door. The door had to be taken out and an air lock was connected to the opening. Static calculations confirmed that the walls would withstand 1.8 bar inner air pressure.

7 SITE INSTALLATION

After a short tender phase with a hand picked group of candidates site installation began in December 2005. The winning bidder Gildemeister GmbH & Co. KG from Berlin, Germany, started to alter the service room of the parking level. The hole was cut into the floor, a rented air lock was installed to the door opening and a serial of core drillings was set through the upper working chamber wall to enable installation of all the required utility lines needed in the working chamber. A rail system from the parking area through the air lock into the upper working chamber for hand pushed lorries and a rail crane under the ceiling completed the preparations in the building. Meanwhile outside of the building, the compressed air stations, a medical air lock, stores and accommodations were installed in an area next to the Petersbogen. This area was held free by AMEC for future expansions of the shopping centre.

8 RECOVERY FROM UNDERGROUND

In January 2006 the compressed air works began. The south working chamber along anchors 49, 51 and 52 was excavated between the first two consoles under complete cover of the slab of the second basement level. The east wall of the chamber, which was the only one open to the in-situ soil beneath the basement levels, was secured with an arch of reinforced shotcrete. Then openings were cut into the first console at the positions of anchors 49 to 52 in preparation of the pipe jacking. After that, an opening was cut into the second console to dig a tunnel towards anchors 35 and 36, where the north working chamber was excavated.



Figure 7. Air lock in underground car park.

Meanwhile, the contractor transported a custom made jacking frame to the position of anchor 52 and installed it between the two consoles. He then installed the mini-shield.

After a learning period, the overall excavation speed became faster than expected with exception of tunnelling through a quartzite layer, which was time consuming and which each of the five tunnels had to pass through. The pipe jacking got underway with 40 cm long pipes because longer pipes could not pass through the air lock. Soil transport was carried out with a small lorry going up and down the pipe. The sand and silt was taken from the face with a small blade. Hand-held core drills were used to drill holes into the quartzite rock and a hydraulic splitter was used to break it.

Parallel to the excavation, the anchor became visible more and more and it was regularly cut every 40 cm parallel to the laying of a new pipe.

After the intended depth of the tunnel was reached, the mini shield had to be dismantled and transported up to the working chamber again. The tunnel was cleared of all installations and finally filled with artificial soil. Afterwards, the jacking frame was moved to anchor 51



Figure 8. Jacking station for anchor 51.



Figure 9. Excavation in the head of the pipe.



Figure 10. Anchor in the face.

and modified to fit to the new position and then the working cycle started again. One after another, anchors 51, 49, 36 and 35 were recovered.

9 COMPRESSED AIR PROBLEMS

It was obvious that the air pressure had to be increased concurrent with the increasing depth of the excavation. It was discovered during the excavation of anchor 52 that losses of compressed air were much higher than expected and finally they exceeded the capacity of the compressor stations.

Extensive sealing efforts became necessary. The working chambers were sprayed completely on all surfaces with a water reacting polymer, forming a rubber-like inliner. The ring gap around the jacking pipes (the shield had a small over-cut) was filled with bentonite, and the pipe joints were sealed with a custom made rubber gasket. Together, these measures significantly stopped the air losses enough to continue excavation.

10 IMPACT ON THE NEIGHBOURHOOD

The excavation continued with hardly any affect on the neighbourhood given that the setup of the construction site was in an empty building pit, as well as in the basement of the Petersbogen. Only the compressed air was responsible for some excitement during the middle of the construction. It is normal when compressed air is pressed into the ground that it tries to rise to the surface. In open areas the air dissipates over a wide area, but in this case, in the heart of the city with only buildings and bitumen paved sidewalks and roads, the air concentrated around only the few escape points available. This time it was on a 50 m long strip along the curbstone of the Petersstraße. One night after some heavy rain, unexpectedly a lot of bubbles became visible. The police was called on the scene three (3) times in 24 hours (once, every shift) looking for gas leaks.

An additional point where the air exited was on the opposite side of the Petersstraße, in the basement of the Stentzlers Hof. The air was coming in through a joint in the foundation slab. Together with the air, a small amount of water was pressed in as the slab was only marginally above the ground water level. It took a few words of reassurance to convince the owner that there was no danger to his property.

11 END OF WORKS

Finally, by the end of May 2006, the last anchor was recovered and the working chambers were all filled with artificial soil. Not only had all anchors been recovered, but it was also revealed by in depth investigations of all anchor pieces that design and execution faults on the explosive recovery were the reason why that method failed for 43% of the anchors. The ductwork had been designed at the lower limit of the theoretical required cross section.

Nevertheless, it is the opinion of the authors that the explosive recovery is a capable method, which was demonstrated successfully at another construction site in Berlin, Germany, where 175 cable anchors were recovered. In Leipzig, if the design had simply chosen larger ductwork, accounting for the importance of the recovery, and the realisation that sometimes an increase of effort is necessary, explosive recovery could have worked as well.

12 CONCLUSIONS

In the inner City of Leipzig, Germany, 20 cable anchors had to be recovered. Dependent on the individual boundary conditions two different, innovative recovery methods were designed and successfully executed with hardly any influence on the public life around the construction sites: the recovery with pile borers and slurry wall excavators from above the ground and the excavation with the help of pipe jacking tunnels starting under an existing building. Both methods proved successful and it was even possible to find out why the intended recovery by explosions in the grout bulbs failed.

Underground Space – the 4th Dimension of Metropolises – Barták, Hrdina & Romancov (eds)
© 2007 Taylor & Francis Group, London, ISBN 978-0-415-40807-3

Construction of Metro IV.C2 Ládví – Letňany in Prague

V. Bartoň, M. Kochánek & V. Valeš
METROPROJEKT Praha, Prague, The Czech Republic

J. Kutil
IDS, Prague, The Czech Republic

ABSTRACT: The construction of another leg of Prague Metro's C line is currently in progress. The extension with the length totalling 3.9 km is designed as an underground Metro route with 3 stations in open foundation pits. The technology of building the sections between stations is subject to the geological composition of the area. Under the layer of made-up ground, argillaceous earths and arenaceous marls there are layers of sand rocks and clay stones, the characteristics of which allow building part of the sections between stations by tunnelling technologies. For the most favourable sections the project authors suggest driven dual-rail tunnels of a closed profile with the floor arch of the stope area of 58–66 sq. metres. For the other sections they suggest using single-rail tunnels or sections in open foundation pits. The conceptual design of the stations is based on the latest trends used in the construction of the section put into operation in 2004. The Stříškov station is designed as a single-nave hall. The bearing structure of the glass areas is designed from steel. The common hall area integrates the vestibule and platforms. The height of the station's interior consists of three functional levels, i.e. the platform level, the mezzanine level and the ambient ground level – the ground floor. All the three publicly accessible levels form a lockable area, which is only available to the public when the Metro operates. The Prosek station is designed as a classic monolithic reinforced-concrete building with three operational levels – the level below the platform, the platform and the vestibule (underground). The structure is designed with steel columns located between rails. The Letňany station is designed as a monolithic reinforced-concrete frame with a variable width of three plus one fields. The platform area features a simple frame with an opening for direct lighting. The station consists of three storeys, with two stories at the platform. A single-storey structure of a side-track building, with two rows of columns, is adjacent to the station.

1 INTRODUCTION

The underground is the main backbone system of the Prague transport skeleton. The new routes improve the transport serviceability of the localities, create new development areas and increase the value of areas around the new stations. The implemented extension of line C from the Ládví station onwards will bring about all these advantages. The transport situation will improve not only in Prosek and Letňany, but also in the whole north-eastern area of Prague. There will be a large bus terminus station at the Letňany station, and a park-and-ride yard (P + R), which is highly needed in this part of the city.

In relation to the completed 1st stage of the 4th operating section of underground line C (section Holešovice railway station – Ládví), the construction of its extension commenced in 2004 in the direction of Prosek and Letňany, with a long-term municipal transport terminal station in the area of the Prague exhibition ground in Letňany. The track is laid under the ground in a relatively shallow depth, the stations are performed by cut and covered method, the tunnels are partly driven and partly performed by cut and covered method and they are mostly double-tracked. The construction is located in Prague 8, 9 and 18, i.e. in the cadastral districts of Kobylisy, Libeň, Prosek, Střížkov, Vysočany and Letňany.

As every similar project of metro line, even this one includes a number of interesting structural solutions from the field of tunneling, concrete construction and architectural ideas that, according to our opinion, are worth attention.

The investor of the project is Dopravní podnik hl.m. Prahy a.s. (a public transport operator), represented by the contracting authority, Inženýring dopravních staveb a.s.

The building permit documentation, tender documentation and the detailed design documentation have been elaborated by METROPROJEKT Praha a.s.

2 CONSTRUCTION OF THE UNDERGROUND AS A PART OF THE PRAGUE TRANSPORT INFRASTRUCTURE DEVELOPMENT

2.1 *Principles of the transport-urban solution*

The track leads from the existing terminus Ládví to the Střížkov station, which will serve the locality of Prosek, and the remaining part of the locality will be served by the Prosek station. A temporary park-and-ride yard with 203 parking places is designed at the Střížkov station. At the new terminus in Letňany, which has two vestibules, a bus terminal station is designed with a large parking area and a park-and-ride yard with 683 parking places next to the northern vestibule. Both these vestibules meet requirements for future connecting to the planned Prague exhibition ground.

2.2 *Basic data on the construction*

Length of construction IV.C2 4599 m Maximum longitudinal gradient of the track 3,95% Minimum horizontal radius of the track rails 500 m Number of stations 3.

1. Střížkov – an excavated station with a side platform and a single vestibule incorporated into the station hall. The level of the platform is 5.6 m under the surface level,
2. Prosek – an excavated station with a side platform and a single underground vestibule connected to underpasses under Vysočanská and Prosecká Sts. The level of the platform is 10.6 m under the ground,
3. Letňany – a long-term terminus, excavated, with an island platform connected to 2 underground vestibules. The level of the platform is 10.3 m under the landscaped surrounding ground.

3 STRUCTURAL AND ARCHITECTONIC DESIGN OF THE STATIONS

3.1 *Střížkov station*

The Střížkov station is a wayside excavated station with side platforms, located at the crossroads of Vysočanská and Teplická Sts. Along with the track section in the direction of the Prosek station it represents a part of track IV.C2, where the underground track level is closest to the surface.

It is an open hall room and thank to a light steel structure of the roofing it enables maximum glazing of the peripheral jacket of the station and thus lightening of the station hall by daylight, which makes it look like an overground station, although both the platforms are deeper compared to the surroundings ground. By opening of one sidewall into the opened excavated atrium, the station is in a direct visual contact with the external space and enables future level connecting with a shopping centre connected directly to the atrium room. On the other side, the station is connected to an underpass under Vysočanská St., enabling comfortable disability access to both platform edges. The internal room of the public part of the station is vertically divided into three functional levels, i.e. the platform level, the counterlevel and the level corresponding to the surrounding ground. The operating-technical part of the station is located under the ground, the underpass under Vysočanská street and the structure of the intermediate ceiling over the platform including the flooring of the foot-bridges are made of cast-in-situ reinforced concrete.

The supporting structure of the glazed roof of the station consists of two slanted steel arches decussating each other with a box cross section of a changeable height. They are fixed in massive concrete foundation

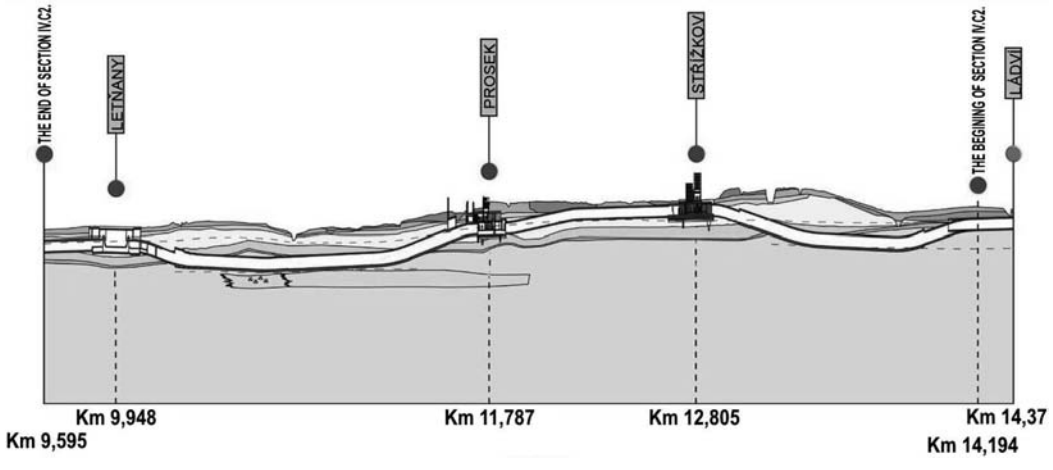


Figure 1. Longitudinal profile of metro IV.C2.

blocks hidden in the underground parts of the station. Four rows of tow bars suspended on the arches hold the roof structure. The main central box girder consists of two plain-web components, interconnected in the lower and upper parts with a framed girder. The girder is equipped with a number of transverse ribs – beams of changeable height. Ribs are interconnected by horizontal steel plate girder of circular shape on the side of the roof . The roof periphery is supported by steel socketed stanchions of "Y" shape with a changeable cross section. The glazed peripheral jacket is connected to these stanchions.

The total length of the Střížkov station structure is 228 m and the steel roofing structure with a ground plan shaped like a lens is 130 m long and its greatest width is 42 m.

3.2 *Prosek station*

The Prosek station is a wayside excavated station with side platforms, located at the crossroads of Prosecká and Vysočanská. Given a greater depth of the underground (the platform level is 10.6 m under the ground), the station is fully covered under the ground, with square glazes skylights designed in the steel structure in the area of the vestibule and the connecting shopping passages enabling partial lighting of the interior of the station by daylight. The street level is reached by the

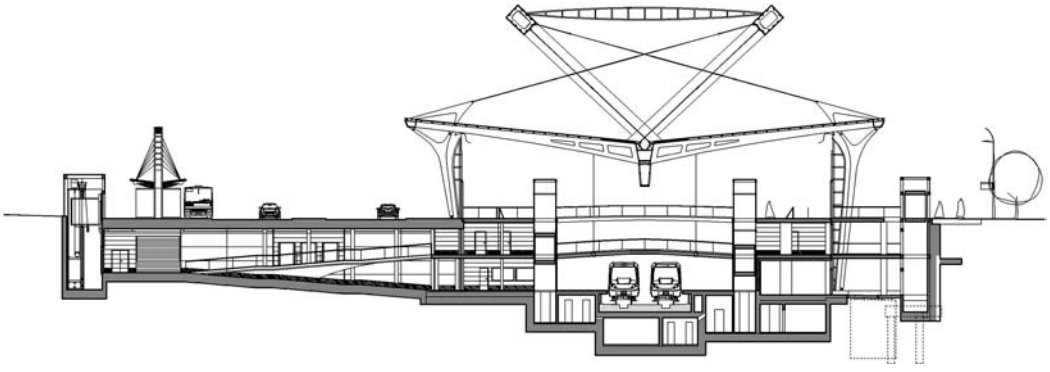


Figure 2. Cross section of the Střížkov station.



Figure 3. Design of the Střížkov station.

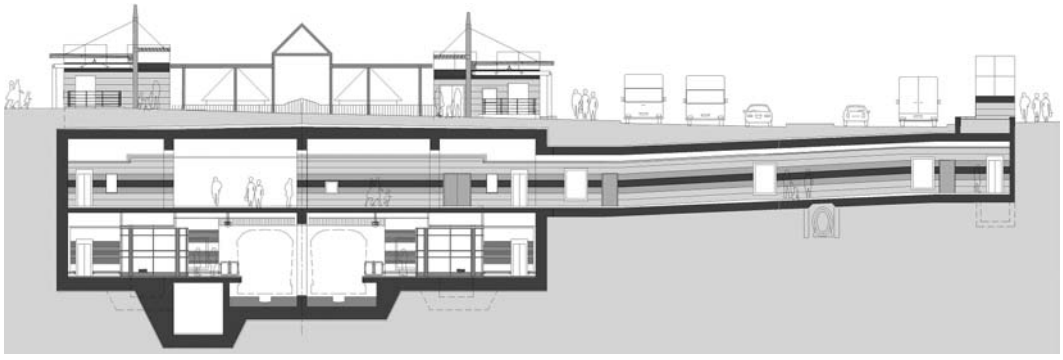


Figure 4. Cross section of the Prosek station.

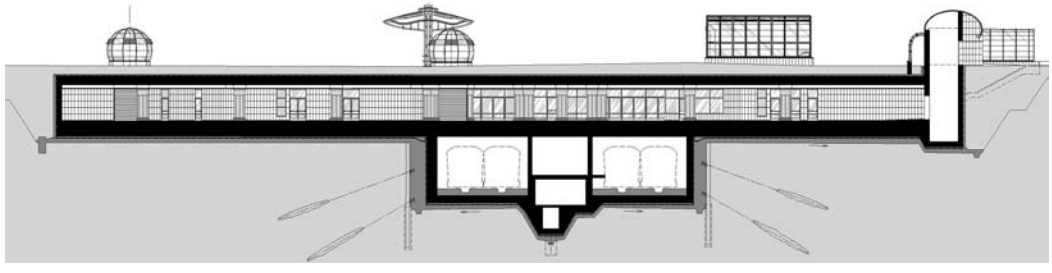


Figure 5. Cross section of the Letňany station.

skylights and exits with staircases and lifts for immobile people. The supporting structure of the station in the cross section consists of a closed cast-in-situ reinforced concrete frame with various internal divisions. The basic internal element of the internal division is a series of columns along the whole length of the station in the centre between the underground rails. The basic module interval of the columns in the longitudinal direction is 7.0 m. In terms of height, the structure of the station in the area of the platform and the technical-operating room is divided into three levels: the platform level, the level under the platform and the level of the vestibule with connected shopping passages and underpasses. In the remaining areas the division is into 2 height levels, i.e. the foundation slab under the underground rails and the intermediate ceiling at the level of the vestibule. A part of the underpasses with exits reaching beyond the ground plan of the station is naturally only at a height of one floor. The total length of the station structure is 210 m, the width ranges between 10–24 m. The height in the parts with three levels is 14.0 m and in parts with two internal levels it reaches 10 m.

3.3 *Letňany station*

The Letňany station is a long-term terminus located north of Kbelská St. and it should be a part of the entrance room of the future Prague exhibition ground replacing the existing temporary halls. The station is excavated with an island platform connected to 2 underground vestibules with exits ascending over the ground level. The platform level is 10.3 m under the landscaped surrounding ground.

The structure of the station in the cross section consists of a closed cast-in-situ reinforced concrete frame with an angular foundation slab in a constant width of 24.8 m in the whole station and a shunting track, i.e. a total length of 416.0 m. In the related part towards the Prosek station in a length of 176 m, the width of the structure continuously decreases to 16.4 m in the place of connection to the driven single-track tunnels. In the area of the platform the frame structure of the station is dipteral with a number of columns located in the axis of the platform in an interval of 6.4 m in the longitudinal direction. As regards the height, this part of the structure is divided by an intermediate ceiling at the level of the platform into the technological part under the platform with headroom of 2.3 m. The hall of the platform itself has a headroom of 8.35 m with a reinforced longitudinal girder over a number of columns and it will be covered by a lower ceiling lowered by 600 mm. Outside the platform space, the structure of the platform is prevailingly divided by longitudinal walls or wall pillars (in the shunting track) into a three-wing structure and in terms of height it is divided into three

levels – the level under the platform, the level of the platform and the level of the vestibules. The total height of the closed frame of the station is 12.65 m, in the section of the shunting track and excavated tunnels in front of the station the structure is single-floored, height of 6.8 m.

4 TRACK TUNNELS

The design of the track tunnels related to the construction of the underground IV. C2 was based on the effort to construct two-track tunnels in the maximum possible extent. A great advantage of this design in the case of station tunnelled two-track tunnels consists in larger profiles of the tunnel, which makes it possible, especially if the New Austrian Tunnelling Method is used (NATM), to introduce high-performance station tunnelling techniques enabling flexible changing of the machines in the working face. This is reflected in increased speed of tunnelling, resulting in costs reduction of the tunnel construction.

A great benefit of this conception is mainly experienced in the excavated track tunnel between the Střížkov and Prosek stations. The pit excavated for the construction of the tunnel has a width of approx. 12 m. For the construction of 2 two-track tunnels connected to the station with island platforms, it would be 20.5 m i.e. 70% greater volume of excavation work. The aforementioned reasons had an essential impact on the design of the Střížkov and Prosek stations, which are designed with side platforms. On the contrary, as regards the long-term terminus in Letňany, the island platform is advisable for operating reasons.

Base inter-axial distance of the tracks in the cut two-track tunnel is 3.7 m and in the excavated two-track tunnel 3.6 m. This distance determines the diameter of the cross section of the proposed tunnels. In the sections aligning to the stations, the inter-axial distance of the tracks usually continually increases, and thus the cross section of the tunnels also increases in relation to the layouts of the station.

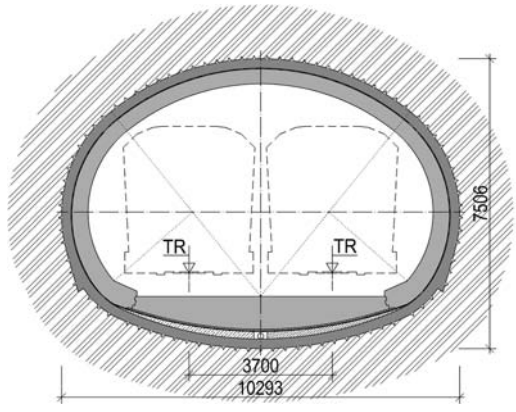


Figure 6. Cross section of the double-track driven tunnel.

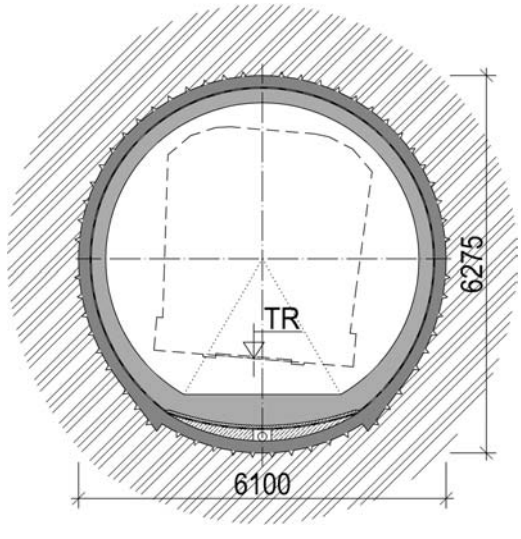


Figure 7. Cross section of the single-track driven tunnel.

4.1 *Driven track tunnels*

A double-track tunnel was constructed here in the section of Ládví – Střížkov (975) m and in the section of Prosek – Letňany (1,280 m). The double-track tunnel was connected to two single-track driven tunnels in the direction of the Letňany station (length of 2×63 m). All cross sections of the double-track tunnels have a closed oval shape with stope surface of approx. 64 m^2. The tunnelling employed the NATM technologies – the tunnel was tunnelled by a primary lining of air-placed concrete with a thickness of 200–350 mm (based on the quality of the rock massif) reinforced by steel mesh combined with bar rock anchors. The tunnels were prevailingly tunnelled by horizontal division of the stope into a calotte and the lower part of the tunnel. In exceptional cases in a short section below the residential areas with thin hanging layer, the stope was also divided vertically. Following the completion of the tunnelling, waterproofing using a PVC foil, thickness of 3.0 mm, was installed on the front of the lining and the secondary lining was concreted using cast-in-situ reinforced concrete. This lining was made in 10-m strips so that the tunnel bottom was concreted at the first stage and the vault was concreted in a moving formwork at the second stage. The minimum clear width of the double-track tunnel is 8.9 m, the minimum clear height is 5.5 m and the minimum thickness of the internal steel-concrete lining is 400 mm.

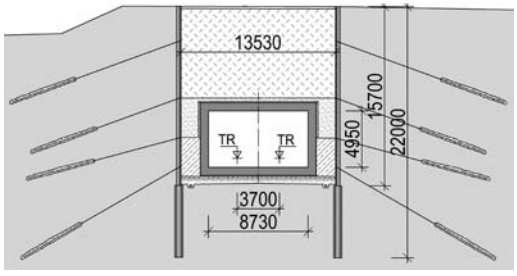


Figure 8. Cross section of the double-track excavated tunnel.

4.2 *Excavated track tunnels*

In construction of metro IV.C2 the two-track excavated tunnels are implemented of total length of 1251 m, of which in the Ládví – Střížkov section of 337 m, in the Střížkov – Prosek section of 772 m and in the Prosek – Letňany section of 142 m. Single-track excavated tunnels are not intended for the track. The double-track excavated tunnel has a minimum clear width of 8.4 m and a clear height of 4.95 m. From the structural point the simple closed frames of cast-in-situ reinforced concrete are designed. The thickness of the slabs and walls ranges from 700 to 800 mm, according to respective hydrogeological conditions. The tunnels were made in 12 m strips. On the inside, the tunnel is fitted with closed waterproofing PVC foil, min. thickness 2 mm with underlayers and protective layers. The tunnels were made in open excavation pit, secured with anchored strutted sheeting or pile timbering. The depth of the excavation pit ranges from 9.0 to 17.0 m. The backfill is performed to reach the original ground level above the tunnel roof.

Underground Space – the 4th Dimension of Metropolises – Barták, Hrdina & Romancov (eds)
© 2007 Taylor & Francis Group, London, ISBN 978-0-415-40807-3

Planning for Canada's first bored road tunnel in over 40 years Kicking Horse Canyon Project

Dean Brox
Hatch Mott MacDonald, Vancouver, B.C. Canada

Steve Bean, Paulo Branco
Thurber Engineering Limited, Victoria, B.C./Mississauga, ON, Canada

Terry Coulter
Coulter Consulting Limited, Victoria, B.C. Canada

ABSTRACT: The Kicking Horse Canyon Project (KHCP) involves upgrading approximately 26 kilometers of the Trans-Canada Highway in BC from the town of Golden to the western boundary of Yoho National Park to a modern four-lane standard. The KHCP is being undertaken in three Phases. Phase 1 comprised the replacement of the Yoho Bridge which was completed in 2004. Phase 2 comprises the replacement of the Park Bridge and grading work that is currently under construction, and Phase 3 comprises upgrading of the remaining stretches from the Yoho Bridge to Golden and the Brake Check to the Yoho Park Boundary. The preliminary design for the Phase 3 West section between Yoho Bridge and Golden is currently in progress and is evaluating new highway alignments through the steepest terrain section of the canyon that include two to three short (<1 km) tunnels as well as one alignment that includes a nearly 2.9 km tunnel that would be the longest bored road tunnel in North America. If constructed, the tunnel requirements for the highway improvement will represent the first major road tunnels in Canada in over 40 years. The preliminary design for the road tunnels comprises twin tube, 2-lane road tunnels. The road tunnels would be constructed within mixed sedimentary bedrock comprising limestones, dolostones, and shales with rock strengths varying from 30 MPa to 240 MPa. State-of-the-art road tunnel fire, life and safety requirements following NFPA requirements have been adopted given the increasing awareness for road tunnel safety measures. Comprehensive geotechnical site investigations have been completed as part of preliminary design studies. Portal location and tunnel design and constructability issues have been evaluated as part of the preliminary design work and are presented.

1 INTRODUCTION

The Kicking Horse Canyon Project (KHCP) involves upgrading approximately 26 kilometers of the Trans-Canada Highway in B.C. from the town of Golden to the western boundary of Yoho National Park to a modern four-lane standard. Due to the rugged nature of the canyon section and the requirements of the BC Ministry of Transportation this upgrading has required the consideration of tunnels as part of the preliminary stage of the project.

The KHCP is being undertaken in three phases. Phase 1 comprised the replacement of the Yoho Bridge which was completed in 2004. Phase 2 comprises the replacement of the Park Bridge and a major through cut in rock to a depth of 80 m that is currently under construction and planned for completion in late 2007, and Phase 3 comprises upgrading of the remaining stretch westwards from the Yoho Bridge to Golden and east of Phase 2.

The preliminary design for the Phase 3 section has evaluated several new highway alignments through the canyon that include two to three short (<1 km) tunnels as well as one alignment that includes a nearly 2.9 km tunnel. The construction for the Phase 3 section may commence in 2008/2009 and both traditional Design-Bid-Build and Design-Build-Finance-Operate (DBFO) contract approaches are being considered.

Both contract approaches have been implemented to date on past and current works. If constructed, the tunnel requirements for the highway upgrading represent the first major road tunnels in Canada in over 40 years since the construction of tunnels along the Trans-Canada Highway in the Fraser River Canyon. Most notably, the nearly 2.9 km tunnel option would be the longest road tunnel in North America.



Figure 1. Kicking Horse Canyon circa 1920's.



Figure 2. Kicking Horse Canyon.

Figure 1 shows a historical photograph of the highway through the canyon section.

2 PROJECT LOCATION

The Kicking Horse Canyon Project is located immediately east of the town of Golden, B.C. which is over 700 km northeast of Vancouver, B.C. and over 250 km west of Calgary, Alberta within the East Kootenay region of B.C. The section of the highway improvement project comprises 26 km of existing 2-lane highway from the town of Golden to the west gate of Yoho National Park. The Kicking Horse Canyon comprises a fairly narrow and winding canyon with maximum relief of nearly 500 m exhibiting very steep rock slopes as shown in Figure 2.

The elevation of canyon section of the alignment is approximately 1000 m and the main canyon section of the project is generally trending east-west with the Kicking Horse River flowing westwards through the canyon. The main CP Rail line is present along the lower slopes of the canyon and mostly along the northern side of the canyon below the existing

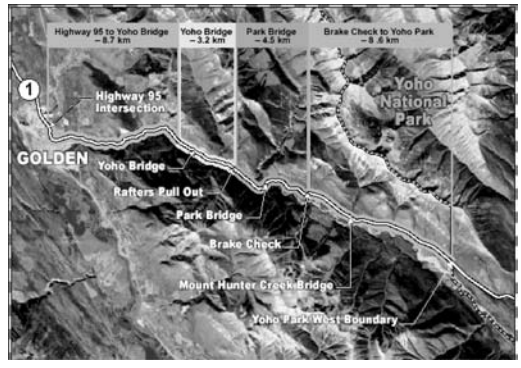


Figure 3. Project location and works phases.

highway. Figure 2 illustrates the project location and Phases of the project.

3 ROAD TUNNEL ALIGNMENT OPTIONS

Several studies have been completed since the early 1990's to identify highway improvement solutions for the Kicking Horse Canyon Project. The work from some of these studies identified several highway alignments along both the north and south sides through the canyon section. Recent preliminary work including terrain and natural hazard studies have indicated that a major ancient landslide is present along the south side of the canyon thereby precluding a highway alignment on the south side.

The remaining alignments along the north side of the canyon were evaluated further in terms of natural hazards and constructability in terms of maintaining the existing highway during construction. Following further work to date there exist two preferred alignment options referred to as the NB-2 and NC-2 alignments as shown in Figure 4.

The NB-2 alignment comprises a single, approximately 2.9 km tunnel that deviates northwards below a sharp ridge known as Frenchman's Ridge, passes under Dart Creek valley, a 400 m wide U-shaped hanging glacial valley, and continues eastward below the Black Wall Bluffs. The west portal is sited near the grade of the existing highway and the east portal is sited about 20 m below grade and at a sharp bend of the existing highway. Figure 3 shows the NB-2 alignment. The maximum cover along the NB-2 alignment is about 300 m below the Black Wall Bluffs. The minimum cover along the NB-2 alignment occurs within the Dart Creek valley and is under investigation at the time of writing.

The NC-2 alignment comprises three, short tunnels with lengths of about 555 m, 565 m and 565 m respectively for a total tunnel length of about 1685 m.

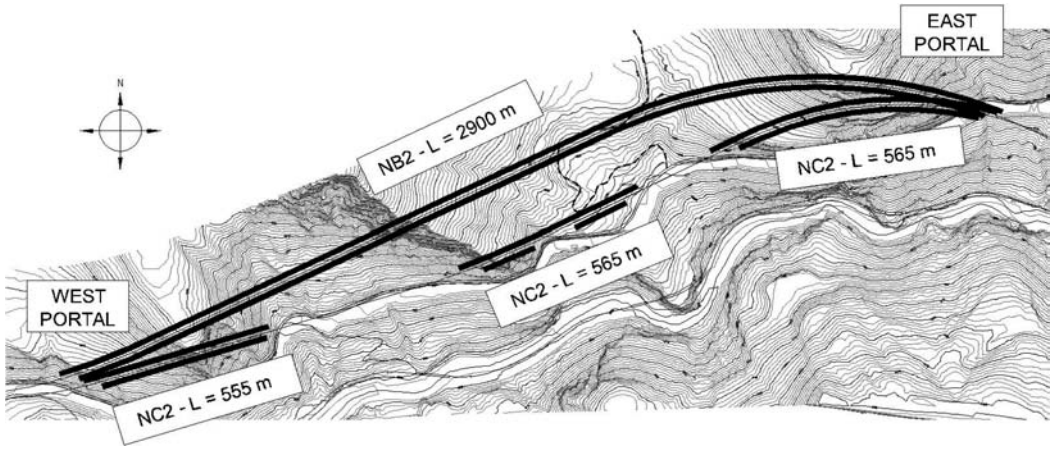


Figure 4. Road tunnel alignments.

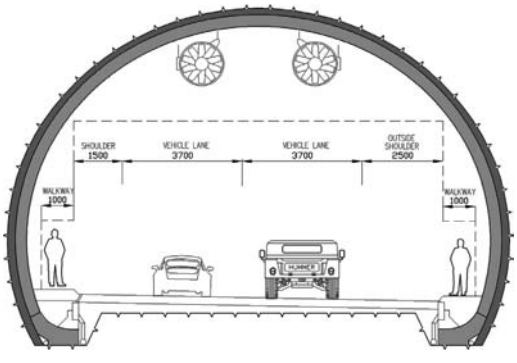


Figure 5. Large tunnel cross section.

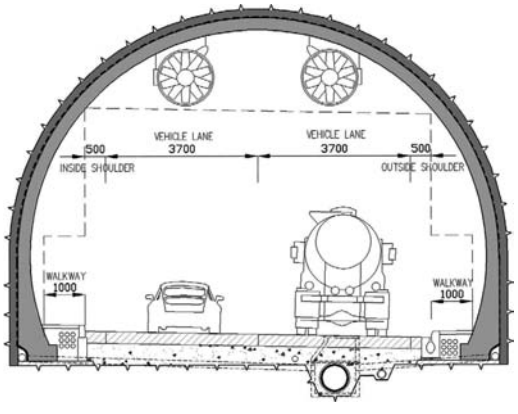


Figure 6. Small tunnel cross section.

The NC-2 alignment deviates not as much northwards as the NB-2 alignment but rather cuts through the series of bluffs/ridges along the canyon. The six portals required for the NC-2 alignment are sited both above and below grade of the existing highway.

With the development of possible new alignments through the canyon section it has been recognized that it is necessary to address the requirements of the external stakeholders. These requirements include maintaining access for CP Rail and river rafting businesses operating from upstream of the canyon, and to allow safe passage through the canyon for bi-cyclists. These requirements indicate that at least one lane of the existing highway will have to be maintained.

4 ROAD TUNNEL CROSS SECTION

Tunnel cross-section geometry was evaluated during the early stages of the preliminary design in recognition of the potential cost sensitivity and traffic safety requirements. As it was recognized that no tunnel roadway geometry criteria for road tunnels neither in Canada nor elsewhere in the world, a review of tunnel roadway geometry was undertaken and three options were developed for safety and costing consideration. The original tunnel cross sections varied from 115 m^2 to 127 m^2 and were based on lane widths of 3.7 m, walkways on both sides of 1.0 m, and varying shoulder widths of 1.5 m, 1.75 m, and 2.5 m, the largest allowing for emergency vehicle access (Figure 5). The initial tunnel cross section options were based on adopting large sized tunnels rather than minimized size tunnels similar to those in Europe. Cost comparison of these initial cross sections did not indicate significant cost increases for the largest size tunnel of 127 m^2. Smaller tunnel cross section options (90 m^2) have also been developed based on minimum shoulder dimensions for consideration based on acceptable international practice (Figure 6).



Figure 7. Geotechnical drilling by helicopter.

5 GEOTECHNICAL INVESTIGATIONS

Comprehensive geotechnical site investigations have been completed as part of the preliminary design work for both tunnel alignments. Historical geotechnical investigations have been completed throughout the canyon dating as far back as 1985. The recent fieldwork has comprised seismic refraction surveys at all portal locations as well as across the Dart Creek valley, over 1900 m of rotary core drilling, point load strength testing, in situ packer permeability testing, and laboratory rock strength and abrasivity testing. Piezometers have been installed in many of the boreholes completed along the tunnel alignments.

Access to some of the boreholes at portal locations and along the tunnel alignments was difficult and was only accomplished by helicopter. All boreholes were drilled vertically and the deepest borehole completed was about 250 m along the Black Wall Bluffs. Figure 7 illustrates drilling of one of the deepest boreholes from the upper reaches of the Black Wall Bluffs by helicopter assistance.

6 TUNNELLING CONDITIONS

6.1 *Site geology*

The geology along the proposed tunnel alignments comprises sedimentary bedrock of the McKay Group and the lower part of the Glenogle Formation that has been subjected to eastward thrust faulting and folding with overturning. The McKay Group of rocks comprises five main sub-units (COMk2 to COMk6) that can be characterized as shaley limestones (odd numbered sub-units) and dolomitized limestones (even numbered sub-units). These five sub-units are present along the western and central sections of the alignment. The shaley limestones are finely laminated whereas the dolomitized limestones appear to be more massive in nature. The lower part of the Glenogle Formation can be described as a mixed slate/shale/dolomitic siltstone with finely laminated dolomitic beds.

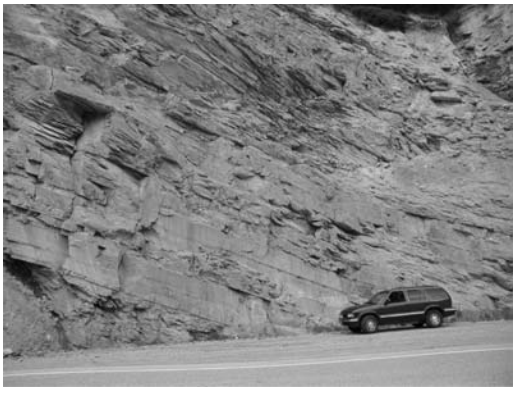


Figure 8. Existing rock cut.

Extensive bedrock outcrops are present in massive sub-vertical rock cuts formed by the original highway construction and appear along almost the entire tunnel alignments. Figure 8 shows a typical large rock cut of bedded limestone along the central section of the tunnel alignments.

6.2 *Rock strength and abrasivity*

Numerous point load strength index tests and uniaxial compressive strength (UCS) test were completed on the drill core. The rock strength of the shaley and dolomitized limestones generally varies from 15 MPa to 100 MPa with an average strength of about 60 MPa. The rock strength of the dolomitic shales and siltstones generally varies from 20 MPa to 240 MPa with an average strength of about 100 MPa. Figures 9 and 10 illustrate the variation of rock strength based on UCS lab testing results of the limestones and shales respectively. Rock abrasivity was evaluated based on CERCHAR Testing. CERCHAR Abrasivity Index (CAI) values for the limestones indicated values generally ranging from 0.8 to 2.4 characterizing the rock as slightly to non-abrasive. CAI values for the shales indicated values generally ranging from 2.0 to 4.0 characterizing the rock as very abrasive.

6.3 *Rock fracturing*

Rock fractures are pervasive within the limestone and siltstone/shale bedrock in the form of bedding and sub-vertical fractures that can be identified from both

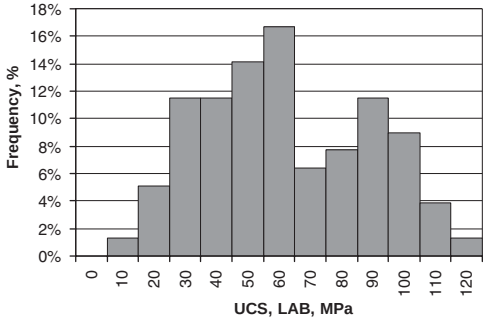


Figure 9. Rock strength – limestones.

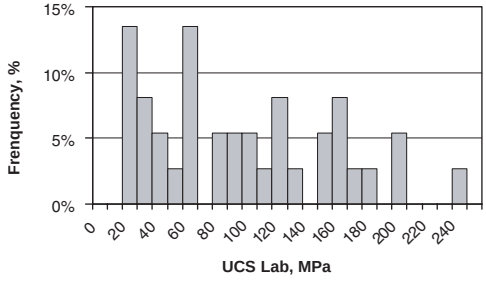


Figure 10. Rock strength – shales.

drillcore and surface outcrops. The dip of the bedding within both the limestones and shales typically ranges from 15 to 20 degrees. The dip direction of the bedding is northeasterly for the limestone and northerly for the shales. The main sub-vertical fractures sets are prominent as orthogonal fractures and are generally oriented both perpendicular and sub-parallel to the strike of the bedding. Bedding fractures are typically very smooth and planar. Figures 11 and 12 illustrate stereonets of the rock fractures within the limestones and shales respectively.

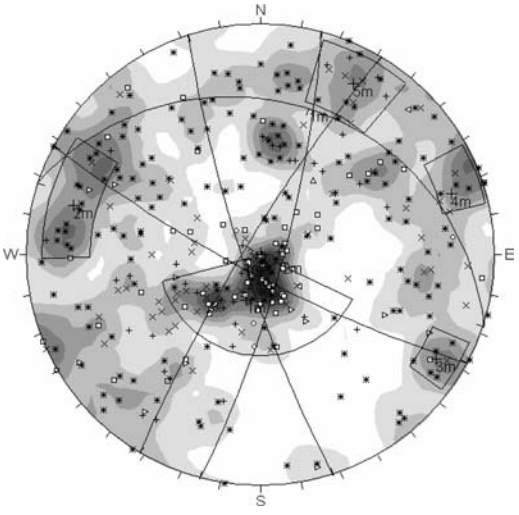


Figure 11. Rock fractures – limestones.

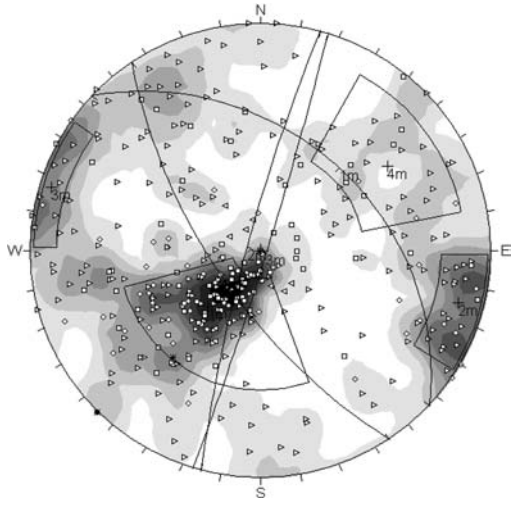


Figure 12. Rock fractures – shales.

6.4 *Major fault/shear zones*

The geology along the tunnel alignments has been intruded by both sub-vertical and sub-horizontal thrust type faults. Sub-vertical fault/shears have been mapped from outcrops below the tunnel alignment along the CP Rail right-of-way and are expected to be present across the tunnel alignments. The most distinct sub-vertical faults are referred to as the West, Middle and Dart Creek Faults. The thicknesses of the West and Middle Faults are inferred to be no more than 10 m while the Dart Creek Fault is inferred to be as much as 20 m in thickness.

The most prominent major fault/shear feature along the tunnel alignments is referred to as the Black Wall Bluffs Fault. This fault zone is a thrust fault that is clearly visible in a sub-vertical rock cut at the western edge of the Black Wall Bluffs. This zone is comprised of highly distorted siltstone and shale bedrock as shown in Figure 13 and is currently inferred to be undulating in nature and may also be present near the east portal. The overall orientation of this fault is inferred to be dipping less than 20 degrees towards the northeast. The fault is present in the exposed rock cut over a vertical height of about 15 m and may have an overall thickness as much as 25 m based on a limited number of borehole intersections from targeted drilling. It is noted that complete recovery of this fault was obtained in one of the boreholes that were targeted.



Figure 13. Black Wall Bluffs Fault exposure.

Interpretation of the possible length of intersection of this major fault with the proposed tunnels has been made based on a 3D geological model using surface outcrop and borehole data. Results from the model suggest that the length of the intersection of this fault with the tunnel could be as much as 250 m extending over much of the eastern portion of the tunnel alignment. The geotechnical relevance of this fault zone in terms of construction cost is not considered to be significant enough to justify modification of the tunnel alignment to reduce this intersection length versus the possible increased costs associated with higher capacity tunnel support that may or may not be necessary.

6.5 *Groundwater conditions*

The groundwater table is inferred to be at a shallow depth below surface along the tunnel alignments. A limited number of packer permeability tests were completed in the dolomitized limestones along the Dart Creek valley section of the tunnl alignments. These tests indicated rock mass permeability of this generally massive bedded bedrock is in the order of 5×10^{-7} m/s to 5×10^{-10} m/s. Given the relatively low cover along the alignments, the magnitude of groundwater inflows from most of the bedrock is not expected to be significant. Significant groundwater inflows can however be expected from the identified sub-vertical faults at Dart Creek valley and possibly from the Black Wall Bluffs Fault.

Artesian groundwater conditions are indicated from two boreholes completed into bedrock in Dart Creek. These conditions are inferred to represent groundwater flow under pressure either along the top of bedrock in the Dart Creek valley or within the extensive thickness of glacial overburden in which the Dart Creek stream course has disappeared and then re-appears at a location on the north side of the existing highway. These artesian groundwater conditions may pose problems for surface excavation in the overburden at Dart Creek but are not expected to have any influence on tunnel excavation in bedrock below Dart Creek valley.

7 FIRE, LIFE AND SAFETY DESIGN ISSUES

The fire, life and safety design requirements for road tunnels is currently undergoing significant changes and improvements as a result of the recent series of significant fires within major road tunnels in Europe. No such requirements are established for road tunnels in Canada as a code of practice and therefore the current approach for the proposed tunnel options is to adopt those standards set out by the National Fire Protection Agency (NFPA) of the United States that are considered to represent state-of-the-art industry practice. These standards set out requirements for the maximum spacing of pedestrian cross passages, fire suppression, communications, lighting, ventilation, and operations monitoring. In Europe, there currently exist a number of research groups dedicated to establishing a suggested code of practice for fire, life and safety requirements for road tunnels. The cost of the fire, life, and safety requirements for road tunnels is a significant portion of the overall construction costs. Significant costs are also associated with providing a tunnel operations center and operations monitoring and maintenance.

8 CONSTRUCTABILITY ISSUES

8.1 *Tunnel excavation and support*

The stability of the tunnels will be predominantly influenced by the formation of potentially unstable rock wedges formed along the crown and haunches due to the presence of the pervasive bedding in conjunction with orthogonally oriented sub-vertical fractures. Large bedding slabs can be expected to form and be unstable, requiring regular support for stability and safety.

Owing to the generally strong and bedded nature of most of the bedrock it is expected that the tunnels can be excavated by a standard 2-stage top heading and bench approach or even possibly full face method depending on the final size of the tunnels. Conventional tunnel support measures comprising pattern rock bolts with mesh and shotcrete are expected to provide adequate support for the majority of the tunnels. Enhanced tunnel support measures comprising lattice girders in conjunction with mesh and shotcrete and possibly supplemented with forepoling or self-boring anchors may be necessary at the intersection of major fault zones such as the Black Wall Bluffs Fault.

Kinematic and numerical analyses have been competed to assess excavation stability in terms of the

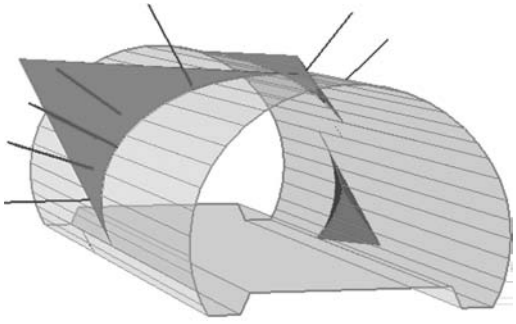


Figure 14. Typical large unstable wedge.

maximum size of potentially unstable wedges formed around the tunnels and any potential for overstressing to confirm the adequacy of conventional tunnel support requirements. Figure 14 shows an example of a large unstable wedge that may form along the sidewall of the proposed tunnels that would be required to be supported using pattern rock bolts during excavation.

8.2 *Portal excavation*

The proposed portal locations are sited in very close proximity to the existing highway. Bedrock is present at very shallow depth for most of the portals for the NC-2 alignment and the west portal for the NB-2 alignment. The main challenge for excavation of the portals in rock will be controlled blasting and management of traffic due to the close proximity of the existing highway.

In comparison, mixed overburden materials are present to a depth greater than 10 m at the east portal of both alignments. The nature of these materials is not well defined but is believed to comprise loose side-cast material from the construction of the original highway.

The east portal is sited below the existing highway and presents a challenge for excavation and support in order to prevent any impact to the existing highway. An initial portal layout was developed based on commencing tunnel excavation in bedrock for minimum tunnel costs that requires significant excavation into the existing highway as shown in Figure 15.

A preferred alternative to this layout has been developed based on commencing tunnel excavation as soon as possible with minimum cover through overburden material as shown in Figure 16.

This alternative layout provides an appropriate buffer from the existing highway however would require specialized tunnel support measures including some form of pre-support such as forepoling or self-boring anchors at a higher cost for the initial section of tunnel.

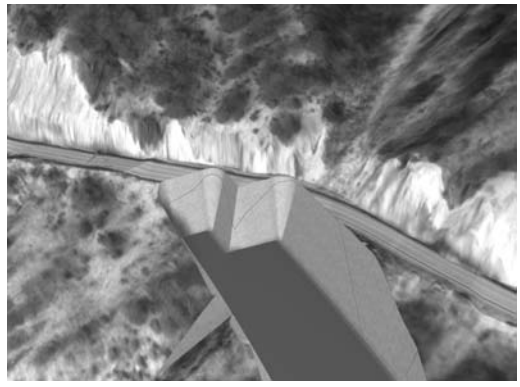


Figure 15. East portal excavation in rock.

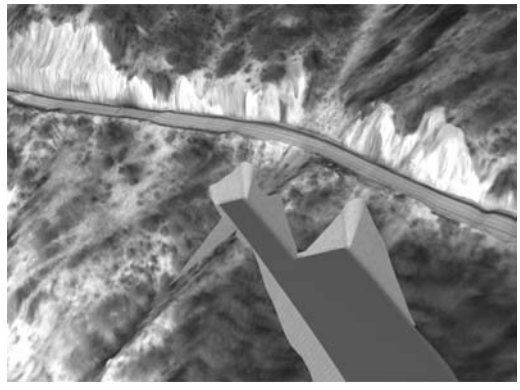


Figure 16. East portal excavation in overburden.

A portal excavation layout for the east portal that does not impact the existing highway also provides the benefit that the highway serves as an avalanche and rockfall catchment bench during operations. The east portal is located immediately adjacent to hazardous avalanche chutes that would otherwise require some form of protection-shed structure at the east portal.

8.3 *Dart creek intermediate access tunnel*

Owing to the expected relatively large portal excavations required to be formed prior to tunnel excavation, it has been recognized that the low cover section of the Dart Creek valley offers an opportunity for the construction of an intermediate access tunnel and laydown area that provides great benefits to the project. In addition to independent access for tunnel excavation, the intermediate access tunnel prevents any need for muck haulage along the existing highway to the designated spoil disposal site in the Dart Creek valley. Also, the intermediate access tunnel may be used for permanent emergency access during operations from



Figure 17. Dart Creek intermediate access tunnel/laydown/spoil site.

a tunnel control center that is currently proposed to be located near the access tunnel at Dart Creek.

The proposed intermediate access tunnel would be constructed entirely in bedrock after surface excavation and the establishment of an appropriate laydown area located immediately north of the highway in Dart Creek as shown in Figure 17.

ACKNOWLEDGEMENTS

The authors gratefully acknowledge the permission of the BC Ministry of Transportation to publish this paper. The Owner's Engineer Team for the preliminary design work comprises Focus Corporation, UMA-AECOM, Hatch Mott MacDonald, and Thurber Engineering Ltd., along with several specialist consultants. Geophysical surveys were completed by Frontier Geoscience of Vancouver. Geotechnical drilling was completed by Sea to Sky Drilling of Burnaby, BC. Laboratory testing was completed by Thurber Engineering Ltd. and packer permeability testing was completed by Golder Associates of Burnaby, BC. Abrasivity testing was completed by SubTerra in Seattle, USA.

Underground Space – the 4th Dimension of Metropolises – Barták, Hrdina & Romancov (eds)
© 2007 Taylor & Francis Group, London, ISBN 978-0-415-40807-3

Preparation of metro's a line extension in Prague

V. Cigánek & J. Růžička
METROPROJEKT Praha, Prague, The Czech Republic

ABSTRACT: Metro network is the backbone of the public transport system of any large city and, from this point of view, a further development of this system is a substantial question and one of the priorities. The current Metro network in Prague consists of three lines: A, B and C, with 53 stations and the total line length of approximately 54 km. There is a dedicated depot for each line (in Hostivař, Zličín and Kačerov). One of the primarily monitored construction projects in the Metro network is currently the extension of Metro's A line westwards. Given the overall extent of the project, it is envisaged that the project will be divided into stages: – The operation section of the A line, from Dejvická to Motol; the newly considered extension westwards to the area of the Petřiny housing estate and to the Motol Teaching Hospital; operation length of 6.0 km, 4 stations. If required, this operation section can be flexibly shortened so that it will terminate at Petřiny. (operation length of 4.5 km, 3 stations), – The continuing operation section Motol – Prague Ruzyně Airport (the north branch), operation length of approximately 7 km, 4 stations. A study work is currently in progress to check the construction and technical feasibility of the route designed in this way (the penetration through the Prague Ruzyně Airport in the lane of railway transport, new station layout, etc.). The implementation of this route, if any, directly depends on how it will be actually needed in relation to the transport from and to Prague Ruzyně by rail, – South branch – Motol – Zličín, operation length of 5.0 km, 3 stations. The Motol – Bílá hora section is identical with the route of the above-mentioned north branch of the line, further continuing to the Řepy housing estate and the Zličín station (approximately 3.8 km). In this regard, the line can be branched at Bílá hora. This south branch is only viewed as a prospective development of the Metro network in this quadrant of the city.

1 INTRODUCTION

An extension of the Metro Line A is planned to generally improve the quality of the City's northwest sector traffic service by capacitive rail traffic. The improvement should become evident by a total reduction of bus lines in this area of Prague. In combination with the so far considered railway connection, a possibility to achieve a tranfer terminal in the area of Dlouhá Míle and Ruzyně Airport via a new track has been considered, having no impact on the railway fixed under the Prague Capital's City Plan. At the same time, a plan to remove the existing Metro Line A terminus from the Dejvická station to a more suitable and less exposed location, in terms of town planning, towards the outskirts of the Town, has been considered.

2 GENERAL DESIGN PRINCIPLES

Within the context to the new facts, the planned solution represents a basic change of the concept of the Metro Line leading to the area of Dědina housing estate, then actually directly to the Dlouhá Míle terminal and, finally, to the Ruzyně Airport alone. At the same time, an effort has been maintained to keep the advantages of the initial solution, enabling the basic route to branche in the area of Bílá Hora to Řepy housing estate and Zličín terminus. It is possible to consider the priority of the selected direction of routes' leading according to specific needs in given time. In light of progress of the line construction, the possibility to terminate its phase in the Petřiny station has been moved to the Motol station.

An expected final option of the solution is to lead the line from the existing Dejvická station in the track Červený Vrch – Veleslavín – Petřiny – Motol – Bílá Hora – Dědina – Dlouhá Míle – Ruzyně Airport with a possibility of branching behind the Bílá Hora station to Řepy – Zličín direction with a linkage to Zličín Depot of the Line B. A subject matter to modify the line via Ruzyně Old Airport with a possibility to insert another station into such area was verified as a consequence of reaction on Metro routing in a new track led through Prague Airport area of interest.

In terms of train traffic operation, railcards for train set turning and deposition are dislocated en route within the context of the particular stations, taking

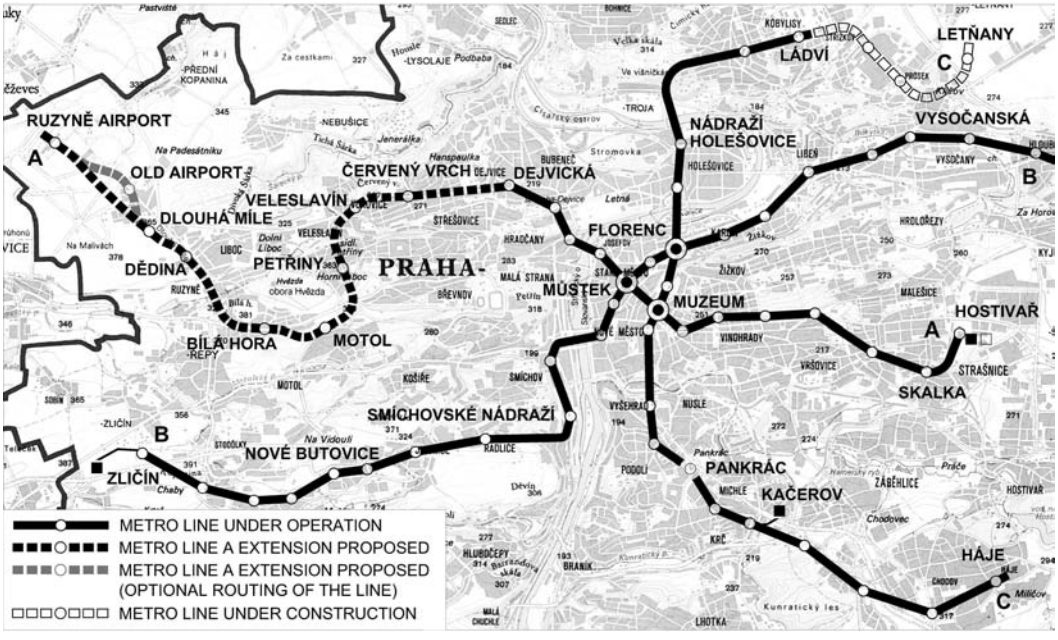


Figure 1. Section of the Prague Metro network.

into account a possibility to put the Line into service step by step as well as traffic organization during extraordinary operation situations and variability of service train rides to provide the maintenance during regular night exclusions. The railcard for set turning and deposition is projected in the Ruzyně Airport Terminal station as well as in the Motol and Bílá Hora Phases terminal stations. Such arrangement enables train turnings up to ca. 5 km down the Line.

According to standards, the following description of the Line's final solution was compiled down the stationing direction, i.e. from Ruzyně Airport to Dejvická stations. On the basic level of knowledge, it discusses the designed issue in terms of specific stations and sections between the stations.

2.1 *The Ruzyně Airport station*

The Ruzyně Airport station is a driven single-nave station with a central platform in depth of 20.9 m below ground surface. Its location, height position and links to the area comply with the Airport's development plans and expected railway terminus of the railway line Airport – Town Centre. At the same time metro terminus location accepts possibility of further extension of railway line under the new Sever II Airport Terminal's building and expand the stop by including another rail with a platform on the northern side.

The station is designed as terminus on a long-term basis, having a rail arrangement to enable turning and depositions of train sets. Therefore, siding and stabling rails in a four-rail arrangement are designed behind the station. The station tunnel including coherent the siding and stabling rails is regarded as a cavern with cross section of the excavation area of about 220 m^2 in length of 450 m. The cavern shall be driven by NRTM with a vertical and horizontal excavation segmentation of the stope. It will be partially driven in Jurassic rocks (calotte) and partially in Upper Palaeozoic and Proterozoic rocks. Two single-track tunnels 2310 m long will connect terminus with the station Dlouhá Míle. The tunnels will be largely driven in Upper Palaeozoic and Proterozoic rocks. They will rise to Jurassic formations solely in the neighbourhood of the Dlouhá Míle station. The tunnels will be performed by TBM with mounted reinforced lining. An open building pit for the Dědina station and adjacent tunnels will be used for deployment of TBM complex. Total length of the open building pit will be 450 m. The sequence of the works has to enable passing of TBM through the Dlouhá Míle station.

2.2 *The Dlouhá Míle station*

In terms of its location, the Dlouhá Míle station is fixed to have a direct linkage to the stop included in the Airport and Town Centre railway connection, similarly as the Ruzyně Airport station. The main importance of the station generally lies in an option to form a quality traffic terminal, especially for transfers from

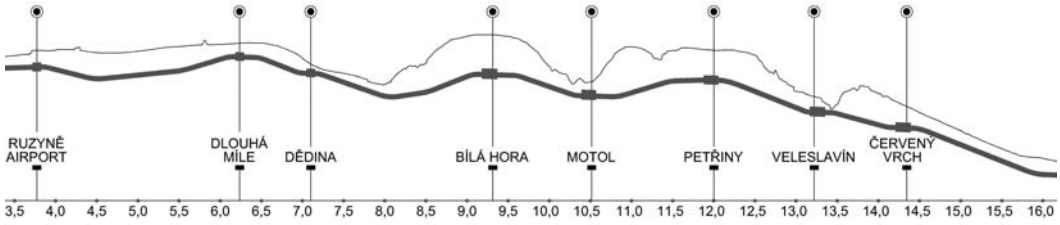


Figure 2. Exaggerated longitudinal profile metro line A extension.

long distance bus lines and regional bus transports. The junction also comprises a capacity parking (P + R System), located in a close linkage to the Metro and railway station on its eastern side.

The station is designed as driven station with a platform 17.3 m under the ground surface across under the projected railway stop. In this way a direct interconnection of the Metro station central platform to both railway stop departure edges is ensured, serving as departure edges of coherent bus transport as well. A direct exit from the Metro station to the surface via lift systems ended in the P + R parking premises is designed in the south part of the station.

The Dlouhá Míle station including the section of rail crossover behind the station is regarded as a cavern with a cross section of ca. 220 m^2. The excavation is regarded by use of NRTM with a vertical as well as horizontal segmentation, similarly as in the Ruzyně Airport. It will be driven in Jurassic formations. Two single-track tunnels 620 m long towards the Dědina station will follow the cavern. Again, TBM is considered concerning the tunnel excavation. As mentioned above, it is considered that the TBM will be deployed at the Dědina station. The track tunnels will be largely driven in Jurassic rocks, however, they will dip into Ordovic layer environment in front of station Dědina.

2.3 *The Old Airport station – an optional routing of the line*

The direction of the above described general routing of the Line is re-arranged in the section between Ruzyně Airport and Dlouhá Míle stations in order to be possible to insert another metro station near the Old Ruzyně Airport. Driven one nave station was proposed with a platform in depth of 12.2 m below ground surface. Distances between the station's centre and Ruzyně Airport/Dlouhá Míle stations make 1710 m, eventually 917. Total prolongation of the Line using this option then makes ca. 150 m.

The building pit premises of the driven Old Airport station would be utilized to deploy TBM to excavate single-track tunnels both in direction to the Ruzyně Airport and Dlouhá Míle stations and then to the Dědina station, where the pit may be utilize either to dismount the TBMs or turn and subsequent reverse excavation. In this option, the track tunnel will rise up to the environment of Jurassic formations ca. 500 m before the Old Airport station, in which they will be driven up to the Dlouhá Míle station.

2.4 *The Dědina station*

The Dědina station is designed as a driven one nave station with a central platform in approximated depth of 12.2 m below ground surface. It is located northwest from the Krnovská – Vlastina Streets crossing. The distance between the station's centre and a following The Bílá Hora station is 2211 m.

Beyond the Dědina station, the line sharply slopes down to Ruzyně area to safely undergo the existing residential area. Then it grades up to Bílá Hora, to the following station. The maximum longitudinal gradient is 39.5%. The line routes through Litovice Brook flood plain in this section. Saturated quaternary sediments in the area where the proposed Metro single-track tunnels undergo the bed of the brook have approximate thickness of 8 to 10 m. The metro vertical alignment is designed approximately 8 m under the base of the mantle formations. The bedrock here is formed by Ordovic slates of Letná strata. It is possible to excavate the designed single-track tunnels by TBMs in such rock environment and to warrant very small gradients of the existing Ruzyně low-floor residential area as well. The TBM will be deployed in the section of the open building pit beyond the Dědina station and will be dismounted either in the cavern of the driven one nave station Bílá Hora or as long as the station is passed in the area near to stabling rails before the Motol station.

2.5 *The Bílá Hora station*

The Bílá Hora station is situated transversally under Karlovarská Street between Karlovarská – K Motolu and Karlovarská – Turnova crossings. The station is driven with a platform in depth of 49.2 m below ground surface. One underground vestibule situated under the centre of the existing tramway line loop is considered. A thickness of the quaternary mantle formations

moves in the range of 2 to 6 m. The rock overburden of the station is largely formed by Jurassic formation sediments. The stratum is about 35 m high. However, the station itself is situated to Ordovic strata. It is possible to project any type of driven station including the most sophisticated one nave station under such given geological conditions.

The line continues through driven single-track tunnels to the area near to the Motol Hospital's northern entrance, where a metro station of the same name is located. The section has a maximum longitudinal gradient of 34.6%, and is approximately 1100 m long.

2.6 *The Motol station*

The Motol station is located north of Kukulova Street in the service area near of the Motol Hospital area's northern entrance. The station is orientated in east-west direction with a single vestibule accessible from the west front of the platform. A subway under Kukulova Street follows the vestibule. The station is designed as shallow driven station with a platform in depth of 18.1 m below ground surface. Concerning the projected vertical and horizontal alignment of the track, the station is situated in very unfavourable geological conditions. A slumping gradient at the edge of the Jurassic plate is in the overburden of the station. The bedrock where the station would be executed is formed by Ordovic strata. It would be suitable to consider that the station should be driven, preferably consisting of two separate tunnels with a sufficient rock intermediate pillar, interconnected by transversal corridors followed by the access to the station.

Due to the expected phasing of the works the station is equipped as a temporary terminus with a rail yard for set turning as well as deposition during the phase. Three-rail arrangement beyond the station (against the direction of stationing) is expected. Within a context of standard requirements, the direction and height design of turning rails is different from the track rails of the future status. A rectification of the section will be necessary if the line will continue in future.

The line turns to the north via a left-oriented curve beyond the Motol station and is led to the Petřiny station. The driven single-track tunnels are 1085 m long.

2.7 *The Petřiny station*

The Petřiny station is situated under Brunclíkova Street with a centre approximately in a prolongation of Fajmanové Street. The station is designed as a driven one nave station with a platform in depth of 36.5 m below ground surface. It has a single underground vestivule located before a crossing with Na Petřinách Street. A subway with exits on both sides of the Na Petřinách Street including exits to rearranged tramway platforms follows the vestibule. Eventually, a long direct section and track tunnel gradient conditions in direction to the Motol station allow to execute the station as a temporary terminal as well (in frame of phasing of the works). Siding and stabling rails a four-rail arrangement are designed concerning the station. Due to operation and technological reasons, such arrangement is completed by two single rail junctions (before and beyond the station), allowing to achieve a maximum operation's versatility.

A thickness of mantle formations moves around 2 m. There is a bulky Jurassic formation strata of app. thickness 18 m and a bedrock, in which a cavern of the station including shunt rails will be driven, is formed by Ordovic rocks. A thickness of rock missive's overburden without the mantle formations will move around 26 m. The line turns to the northeast via a curve beyond the station and is led to the Veleslavín station. The section has a maximum longitudinal gradient of 39.5%, and the driven single-track tunnels are 1110 m long.

2.8 *The Veleslavín station*

The Veleslavín station with a centre approximately under Evropská Street is situated in the area between the existing ČD line (the Veleslavín Railway Station) and eastern section of K Červenému vrchu Street. The station is designed as shallowly driven with a platform in depth of 19.4 m below ground surface. It has a single underground vestibule situated between the ČD line and Evropská – Kladenská Streets crossing. The location of the station, vestibule and individual exits is designed to allow direct linkages to a temporary bus terminal during the phase and at the same time to respond in advance to the planned modernization of the existing ČD line without any need for reconstruction.

The projected routing direction and height of the line and given geological conditions allow designers to propose a construction of a two naves driven station with a row of bearing pillars in the axle of the station, on which a reinforced girder supporting inside footing of station tunnel vaults is placed. Such station's design allows a sectioning progress of the station's construction even in less convenient geological conditions and a low height of the overburden. To ease a dispersal of passengers from escalators to the area of the driven part of the station, the driven part situated under Evropská Street may be combined with the excavated section to the Petřiny station, where the exit escalators will be placed and the structure will have no internal supports.

In direction to the Červený Vrch station, excavated track tunnels will follow the driven part of the station between which a technological part of the station may be placed. The line then continues as driven up to the Červený Vrch station. There is a maximum gradient 26.9% in the section.

Table 1. Basic information on the line.

	Final status	Motol phase
Construction length of the projected section	12.793 7 km	5.663 8 km
Operational length of the projected section	12.7 km	6.0 km
Number of the stations	8	4

Table 2. Basic Information on the stations.

Station name	Station type	Platform depth under ground surface, m	Distance between stations, m
Ruzyně Airport	driven	20.9	
			2465
Dlouhá Míle	driven	17.3	
			866
Dědina	cut and cover	12.2	
			2211
Bílá Hora	driven	49.2	
			1202
Motol	driven	18.1	
			1485
Petřiny	driven	36.5	
			1220
Veleslavín	driven	19.4	
			1125
Červený Vrch	driven	26.7	
			2175
Dejvická	existing		

2.9 *The Červený Vrch station*

The Červený Vrch station is situated under Evropská Street, in the area between Evropská – Arabská and Evropská – Horoměřická Streets crossings. The station is designed as driven one nave station with a single excavated vestibule. The platform's depth under ground surface is 26.7 m in the centre of the station. The rock environment around the station is formed by Skalec quartzites with a thickness in the overburden of the station between 13 and 22 m.

Table 3. Basic information on line's optional routing.

	Final status	Motol phase
Construction length of the projected section	12.946 4 km	5.663 8 km
Operational length of the projected section	12.9 km	6.0 km
Number of the stations	9	4
Prolongation of optional route	153 m	

Table 4. Basic information on the stations (Line's Optional Routing)

Station name	Station type	Platform depth under ground surface, m	Distance between stations, m
Ruzyně Airport	driven	20.9	
			1701
Old Airport	cut and cover	12.2	
			917
Dlouhá Míle	driven	17.3	

The vestibule accessible from the eastern front of the station is situated to the crossing with Horoměřická Street with a linkage to considered small terminal of town and suburban bus lines, destined especially from Nebušice, Jenerálka and Horoměřice areas. A subway under Evropská Street follows the hall, allowing a direct transfer to the existing tramway line on Evropská Street as well.

Beyond the Červený Vrch station this Metro Line continues via two one-rail track tunnels 1835 long and ends in shunt rails of the existing Dejvická terminus station on the Prague's Metro Line A. The track tunnels decline in a maximum gradient of 39.5% in direction to the Dejvická station. They will be largely mined in quaternary soils and below the underground water level. A tunnel construction by use of excavating machines is considered with regard to geological conditions and considerably big length of the Line's section.

This page intentionally left blank

Underground Space – the 4th Dimension of Metropolises – Barták, Hrdina & Romancov (eds)
© 2007 Taylor & Francis Group, London, ISBN 978-0-415-40807-3

Preparation of Metro's new D Line in Prague

V. Cigánek & J. Růžička
METROPROJEKT Praha, Prague, The Czech Republic

ABSTRACT: Metro network is the backbone of the public transport system of any large city and, from this point of view, a further development of this system is a substantial question and one of the priorities. The current Metro network in Prague consists of three lines: A, B and C, with 53 stations and the total line length of approximately 54 km. There is a dedicated depot for each line (in Hostivař, Zličín and Kačerov). One of the primarily monitored construction projects in the Metro network is currently the construction of the new fourth Metro line, line D. The operation length of its first planned operation section is 10.2 km with 10 stations. Given the overall extent of the project, it is envisaged that the project will be internally divided into two or three operation sections, which will directly follow one another. The implementation of Metro's new D line has been monitored for a long time and gradually stabilized into the current form. The D line, located in the southern sector of the city, is a completely new rail transport element, thus reacting to the current completely inconvenient situation when buses are used as the means of public transport there. What is more, the buses mostly transport the passengers to Metro's C line (the Kačerov station) and partly also to the B line (the Smíchovské nádraží station). The transport characteristics of the D line are different from those of the currently operated Metro lines because surveys show that the D line traffic will be much lower than that of the other Metro lines. The use of a new light system is being considered for the Prague Metro, its new D line, in view of the above-mentioned facts and the worldwide trends of the overall modernization of rail transport systems. The 'light Metro' is viewed as the base of a new transport system, which will serve the city and can also penetrate into the region.

1 INTRODUCTION

The Line D is the fourth diameter in the Prague metro network. Its objective is to provide radial transit to the centre from the areas of Krč, Lhotka, Libuš, Nové Dvory, Písnice and the development territories on the southern edge of Prague.

The first operational section of the Line D should partially improve the operational situation on the Line C. By opening the Line D to traffic, a portion of the traffic load will be transferred from the Line C to the Line D, thus the train occupancy on the operating Line C will be partially reduced.

The main benefit of the first operational section of Line D must, however, be sought for in the replacement of the extensive bus traffic leading along Vídeňská Street, and a decrease in the high passenger traffic intensity at the Kačerov metro station. At the same time we can expect that the passenger interchange volume at the Muzeum station will also be diminished.

Not negligible advantage is also elimination of operational vulnerability of the Line C on the Nusle Bridge, as well as the development of a new metro line from the southern region of the city to the city centre. The pre-stressed reinforced concrete structure of the Nusle Bridge is threatened in the long term by the effects of stray currents, and by the fact that the need for overall reconstruction of the bridge in the future cannot be excluded.

A section of the metro network with the three operating lines A, B and C and the Line I D under preparation, is shown in Fig. 1. The Line C is shown including its section IV C2 Ládví – Letňany, which is under construction with the completion scheduled for the middle of next year.

2 BASIC DATA

- Region: the City of Prague
- Employer: Municipality of Prague
- User: Dopravní podnik hlavního města Prahy (a passenger transport authority)
- Construction period: commencement after 2008

3 ROUTE DESCRIPTION

The basic range, or the sphere of service provided by this section of the Line D marked as I D is currently understood to cover an area from Písnice to the Hlavní

Nádraží station. Variants to the solution are focused specially on the vehicle category and corrections in the details of the horizontal and, above all, vertical alignment associated with the selected vehicle category. At the same time, the issue of compatibility with the other kinds of rail transit existing in the PID (Prague integrated transit system), is under consideration, from the aspect of possible utilization of the system in a regional scale.

The above-mentioned extent of the line differs from the expectations of the planning department of the City of Prague. It roughly represents unification of the originally discussed two operational sections of this line (the section I D from Náměstí Míru to Nové Dvory and section II D from Nové Dvory to Písnice), with an extension comprising one interstation section toward the south (a part of the originally discussed section III D) to the Hlavní Nádraží metro station. The internal division of the project and of both the process of opening the Line I D to traffic into phases has not been stabilized unambiguously; it will be a subject of further design preparation.

A total of 10 metro stations have been included into the design of the first operational section of the Line D, i.e. the Hlavní Nádraží, Náměstí Míru, (the crossing with the Line A), Náměstí Bratří Synků, Pankrác, (the crossing with the Line C), Olbrachtova, Nádraží Krč, Nemocnice Krč, Nové Dvory, Libuš and Písnice stations.

It will be possible to design 60–100 m long trains for the Line D, considering the transport demand. The line will be serviced by a new depot in Písnice with a planned capacity of 20 trains 100 m long.

The newest documentation prepared by METROPROJEKT Praha a.s. in 2004 in two variants agrees with the positions of stations and general horizontal alignment of this line determined by previous studies.

The dissected topography of Prague, the considerable differences in elevations of individual valleys and terraces above them (e.g. the Vltava River valley, Nusle valley, Pankrác terrace, Krč valley, Nové Dvory and Libuš terraces, etc.) puts heavy demands on the design of the alignment for lines using traditional rail systems. Within the scope of rail systems used for urban mass, traditional heavy metro rail lines with their standard design parameters (horizontal curve diameter $R \geq 500$ m, rising gradient up to 40‰, stations on straight line or up to a radius $R \geq 800$ m) are especially difficult to accommodate to Prague terrain configuration. This often results in stations placed at great depths, with demanding access roads, time losses for passengers, and significant operational costs, incurred namely due to escalators (see Fig. 2).

With respect to the above problems and because of the fact that the order had specified neither a particular system nor a vehicle, the following basic design parameters of a light rail mass transit system were formulated at the beginning of the work on the design:

Horizontal curves on a running track: in general $R \geq 305$ m (80 km/hour)

Horizontal curves at a station: min $R = 300$ m (at max. platform length of 100 m)

Maximum rising gradient on a running track: 60‰

Maximum rising gradient at a station: 15‰



Figure 1. Section of the Prague Metro network.

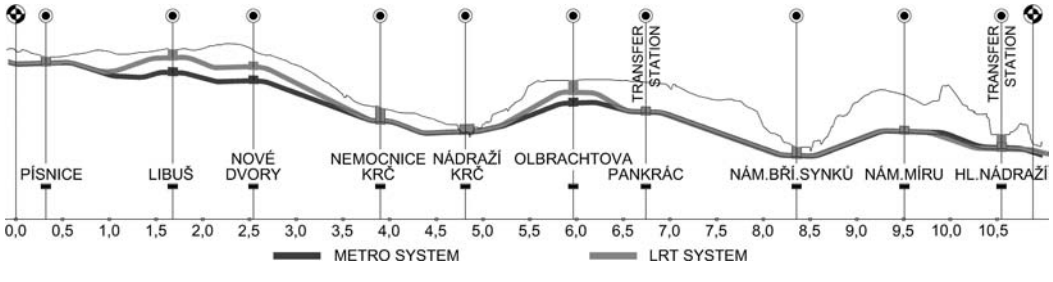


Figure 2. Exaggerated longitudinal profile metro line I.D of the Variant 1 and 2.

3.1 *The variant 1*

The variant 1 represents the conception of the Line D as a "traditional metro" in the meaning of the principles developed by the planning department of the City of Prague, excepting the overall extent of the Line I D and the route deviation from the originally intended Zálesí station to the Nemocnice Krč station. The operational length of this variant amounts to 10.2 km.

3.2 *The variant 2*

The variant 2 deals with a light rail mass transit concept. Regarding the horizontal alignment, it keeps the horizontal alignment designed for the traditional metro (Variant 1), but individual stations are closer to the surface, as allowed by local conditions. The Zálesí station is, similarly as in the variant 1, replaced by the Nemocnice Krč station. The Hlavní Nádraží station is situated in a position set off in the northwest direction to the close vicinity of railway areas. The operational length of this variant of the route is also of 10.2 km.

It must be added for the sake of completeness that also legislative issues will probably have to be solved should the light rail system or another similar system be introduced. The technical level of today produced trains eliminates differences between metro cars and tramway cars. The LRT or light metro conception has been used for rather a long time. Those trains are capable of safe operation in the conditions of tramlines while providing travelling comfort of traditional metro. No explicit regulations exist currently for this track conception. The main issues are the spatial arrangement of railway structures and geometrical configuration of rails; the current regulations valid for tramlines allow more economic alignment, differing clearance profiles for the tramline and metro, and other aspects. The Ministry of Transport, the Department of Railway Tracks and Railway Transport, are not preparing any regulation for the light metro or LRT. It would certainly by possible to start from regulations used in other EU member countries.

4 DESCRIPTION OF THE VARIANT 1 STATIONS AND ROUTE SECTIONS

4.1 *The Písnice station*

The Písnice station is very important both for the overall line D and the southern sector, but also, above all, for the onward transport services operating outside the agglomeration. This is because the station will become a large traffic terminal for buses and for car traffic. At the same time, the station is probably to be a three-rail terminal. Running rails continue further as a connecting track to the planned depot for the Line D in Písnice. This arrangement is suitable in the case of the Line D definitively terminating at this location. This cut and cover station, which is designed to have an intermediate platform and two surface concourses, is at a depth of 8.3 m under the ground surface. Connecting route section creates two single-track tunnels. The length of these tunnels is 1258 m.

4.2 *The Libuš station*

The position of the Libuš station is designed in compliance with the principles of the town planning scheme. It is in the neighbourhood of Novodvorská Street, across the Libuš residential area and its servicing facilities centre. The station is designed as a mined single-span structure, at a depth of about 25 m under the ground surface, with one at-grade concourse oriented toward the south, toward a pedestrian subway under Novodvorská Street.Route section in direction to the station Nové Dvory is formed by two single-track tunnels as well. The total length of these tunnels is 763 m.

4.3 *The Nové Dvory station*

This station is designed as a mined station, the top of rail (TR) about 34 m under the ground surface, with two concourses. It is of an underground, mined, single-span, two-concourse type, capable of functioning as a terminus. The northern, main concourse is connected to Durychova Street, which is a place where a transfer link to onward means of transport is provided. The southern concourse is oriented toward Chýnovská Street. It is designed as an at-grade structure, which will be easy to incorporate to the new urban structure in the future. Next part of metro line is formed by driven double-track tunnel except part of line adjacent to the stations with central platforms. The total length of this section is 1259 m.

4.4 *The Nemocnice Krč station*

The station is designed as a cut-and-cover structure, with an intermediate platform connected at the ends with concourses via vertical roads. Both concourses are designed as lightweight glazed pyramid-shaped pavilions. The station is 13–15.5 m deep under the surface. There are two short single-tract driven tunnels at the station. Next part is formed by double-track tunnel which is 550 metres long. Small thickness of overburden does not allow to perform driven double-track tunnel under the street Nad Havlem. For this reason 282 m of special single-track tunnels combination was designed in front of metro station Nádraží Krč.

4.5 *The Nádraží Krč station*

This is the only at-grade station on this line. It has side platforms and two at-grade concourses. It is built partially on a bridge structure spanning Kunratice Brook between the "Southern Connection" expressway and

the area of the railway station Prague – Krč. Despite the fact that the station is likely to be the least exploited station of the Line D in terms of the volume of passenger traffic, its undisputed significance lies in the unquestionable importance of the transfer to railway in the context of the development of the Prague integrated transit system and gradual implementation of an interval urban railway traffic system.

The other, not less important town design aspect of the Nádraží Krč station is the fact that owing to the pair of opposite at-grade concourses and connected pedestrian subways (the northern subway is under the "Southern Connection" expressway, and the southern under the station yard) the metro station allows the interconnection of the area found north of the Southern Connection, the grassed areas around an original manor-house and along a stream, and areas south of the railway station, which are today completely isolated from each other. In this way the metro station will make the green areas accessible for pedestrians, thus it will help to overcome the existing urban barriers formed by a couple of nearly parallel line traffic structures. A glazed steel structure of the platform and connected concourses will provide a pleasant contrast with the other underground metro stations. Daylight penetrating to the platform, the possibility to watch surrounding greenery and immediately adjoining water surfaces from the metro car interior, as well as the night illumination of the grounds, should represent architectural aspects for overall cultivation of this, today "forgotten" corner of Prague. Behind the station there is a double track tunnel perform by cut and cover method Length of this section is 283 m. Section from street V Podzámčí to the Station Olbrachtova is formed by double-track tunnel. Length of this section is 872 m.

4.6 *The Olbrachtova station*

This is a mined single-vault station with a pair of side platforms. It is situated under Na Strži Street, with the top of rail (TR) level about 26 m under the ground surface. The only at-grade vestinbule hall is placed to the free space of the south-western quarter of the intersection of Jeremenkova, Olbrachtova and Na Strži Streets. Route section between Olbrachtova and Pankrác stations is formed by double-track tunnel. Rail connection to metro line C is inserted into this section. Rail branching forced itself the enlargement of tunnel cross section.

4.7 *The Pankrác station*

This single-vault mined station with side platforms and the TR level about 33 m under the ground surface is situated in the close vicinity of the cut-and-cover station existing on the Line C, in an area delimited on one side by the intersection of Na Pankráci and Na Strži Streets. The construction will create a passenger interchange node comprising the station on the Line C and the station on the Line D. Nearly the whole route section between Pankrác and Náměstí Bratří Synků is formed by double-track tunnel. Merely a short part in front of the Náměstí Bratří Synků station is formed by single-track tunnels. Access gallery length of 450 m enabling transport of tunneling equipment was designed in this section. This gallery will be exploited as a ventilation shaft in the final stage.

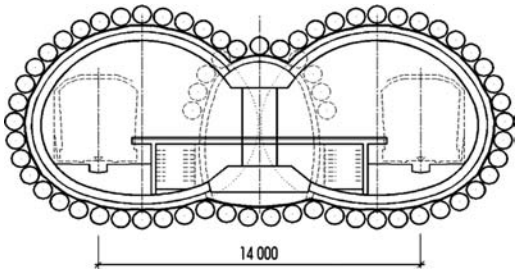


Figure 3. Cross section through the mined part of the Náměstí Bratří Synků station.

4.8 *The Náměstí Bratří Synků station*

This is a structure where combined techniques are to be utilised. The 30 m long part of the station that is situated at a shallow depth under existing buildings is an atypical double-vault mined structure with load bearing pillars in the centre of the platform. The station is situated to the flood plain of Botič Brook, and a major portion of the tunnel profile will extend into saturated fluvial sediments. A special microtunnelling technique is therefore being under consideration, i.e. a continuous canopy consisting of micro-tunnels installed along the profile of the future station tunnel to stabilize the subsequent partial excavation faces. The other part is situated outside the building. It is a large-span cut-and-cover structure with 2 rows of internal columns. The TR level is about 11 m under the ground surface. The station has side platforms and two concourses. The southern at-grade concourse is situated directly to the space of Bratří Synků Square.

Behind the northern part of this station short section of single-track tunnels was designed. Tunnelling of under Botič brook bed will be complicated for geological conditions which are very unfavourable. Water-bearing sediments of Botič valley wold and adjacent houses pose many problems for tunneling technology. Next part of route will be performed in open building pit. Remaining part of section between Náměstí Bratří Synků and Náměstí Míru stations form double-track tunnel and two single-track tunnels close to Náměstí Míru station.

Table 1. Basic information on the stations.

Station name	Station type	Platform depth under ground surface Variant 1 (2), m	Distance between stations, m
Písnice	cut-and-cover	8.3	
			1358
Libuš	driven*	25.0 (12.0)	
			863
Nové Dvory	driven	34.0 (19.0)	
			1359
Nemocnice Krč	cut-and-cover	13.0–15.5	
			910
Nádraží Krč	at-grade		
			1155
Olbrachtova	driven*	26.0 (14.0)	
			777
Pankrác	driven	33.0	
			1613
Nám. bratří Synků	combined	11.0	
			1153
Náměstí Míru	driven	40.0	
			1040
Hlavní nádraží	under the protective structure	15.0	

*Variant 2 allows cut-and-cover design for the stations.

4.9 *The Náměstí Míru station*

The Náměstí Míru station with the TR level at a depth of roughly 40 m under the ground surface is designed as a mined single-vault station with an intermediate platform, with direct transfer to the Line A, and with two concourses situated towards the points where Sázavská Street meets Vinohradská Avenue and Francouzská Street respectively. This design allows direct transfer from the Line D and Line A to all tramlines in the given area. The barrier-free access from the ground level to the platform of the Line D is provided by vertical lifts with their entrances in Korunní Avenue. The platforms on the lines D and A are also interconnected by a lift. Two single-track tunnels length of 940 m continue to the Hlavní nádraží station.

4.10 *The Hlavní Nádraží station*

One of the deciding traffic structures important for the whole city, which significantly affects the possibilities of making use of the area of reconstruction existing in the south-western quarter of the intersection of Seifertova and Italská Streets, is also the planned metro Line D, or the metro station Hlavní Nádraží. This station will be built under an inverted U-shaped protective structure. This structure will allow both the commercial buildings that are to be built in advance of the metro to be founded, and the metro station to be constructed subsequently inside this space. The client for the above ground part of the project will take care of technical feasibility of execution of openings in the protective structure required for the passage of vertical routes leading from the station (the northern concourse) and for the access ramps built for metro construction purposes.

Three driven single-track tunnels of stabling siding are part of this station.

5 DESCRIPTION OF THE VARIANT 2

The basic principle of this variant is the effort to get the light metro alignment as close to the surface as possible. The aim of utilization of smaller vehicles is to achieve a smaller clearance profile, steeper longitudinal gradients along the route (accommodation of the alignment to the terrain configuration so that the project is cheaper) and possibly automatic operation.

The spatial design of the stations is identical with the design used in the variant 1, although the stations are placed closer to the ground surface, to a position that is allowed by the maximum longitudinal gradient possible in the framework of the given terrain configuration. Regarding the Náměstí Míru and Náměstí Bratří Synků stations, even the elevation remains the same as the elevation used in the variant 1. The reason is that the Náměstí Bratří Synků station cannot be closer to the surface because of the existing structures in the underground space, and the priority for the Náměstí Míru station is to have short transfer relationships to the existing station on the Line A.

In general, from the aspect of the horizontal alignment designed in the variant 2, it can be stated that the alignment copies the trace of the variant 1, which means that the design parameters are fully compatible with a traditional metro system. Regarding the gradients, for the reason of virtual invariability of the elevation of the stations within the section Pankrác – Hlavní Nádraží, the route gradient is left identical with that designed in the variant 1. It is therefore again fully compatible with the traditional metro. Gradients over 40‰ are designed for the section Nové Dvory – Pankrác. This solution gets the Nové Dvory station closer to the ground surface approximately by 14 m (TR – 19 m, the station remains to be mined, three-vault type) and the Olbrachtova station roughly by 12 m (TR – 14 m, cut-and-cover design). The risen station Nové Dvory allowed also the Libuš station to get closer to the surface (TR – 12 m, cut-and-cover design). Conception of technical solution of track tunnels is the same as in variant 1.

This page intentionally left blank

Underground Space – the 4th Dimension of Metropolises – Barták, Hrdina & Romancov (eds)
© 2007 Taylor & Francis Group, London, ISBN 978-0-415-40807-3

The Turecký Vrch railway tunnel

M. Dávid, J. Mára, J. Korejčík
Metroprojekt Praha, Prague, The Czech Republic

ABSTRACT: The project of the modernisation of main railway corridors is in progress in Slovakia. The project includes the railway route Nové Mesto nad Váhom – Púchov. This route leads through a rugged country, which, in the Turecký Vrch section, is listed as a protected landscape area. Authors of the design studied several variants. The straightened alignment, and environmental reasons in particular eventually contributed to their preference to the tunnel variant over an up to 40 m deep side-hill cut leading along the entire length of the hill side. The mined double-rail tunnel is 1,775 m long, with the length of the mined section amounting to 1,740 m. The cut-and-cover sections total 35 m. The maximum overburden depth is 100 m. Complicated geological conditions, verified by an exploration gallery, were the reason why the authors of the design selected the New Austrian Tunnelling Method, which allows a flexible response to changes expected in geological conditions. The lining of the mined tunnel consists of two shells with an intermediate waterproofing membrane covering the vault and side walls. The tunnel profile is designed with regard to train aerodynamics, for the speed of 160 km/h (prospectively 200 km/h).

INTRODUCTION

At present, the railway line curves round the side of Turecký Vrch (Turecký Hill) in close proximity to a national road and the Biskupice canal. The current conditions in the narrow basin do not allow changes in the alignment which are required for increasing the speed limit over the track. This is why a new alignment has to be designed, with the best variant containing a mined double-rail tunnel. This variant provides the best solution to the conflict between the interest in protecting the Turecký Hill protected landscape area and the interest in the space for the modernisation of the railway line. The alignment passing through Turecký Hill begins in an extremely confined space in front of the entrance (southern) portal, where the railway line, the I/61 national road and a protective embankment of the Biskupice canal run in parallel with each other. It leaves the exit portal on the northern side via a right-hand curve, designed to minimise the work in the unfavourable environment of secondary loess. The portal proper can be built in a minimised construction trench.

The double-track railway tunnel is designed for the UIC C clearance profile, with firm trackbed and the track-centre distance of 4200 mm, on two R 2000 m and 1995 m reverse curves and a tangent section, and on minimum longitudinal gradients of 3.5‰ and 4‰; this design satisfies the speed up to 200 km/h. The clearance profile is unified for the entire length of the tunnel, with the exception of two contact-line tensioning chambers with an enlarged profile, which are approximately in the middle of the tunnel. The primary excavation support with a variable thickness of the lining will provide protection for a time sufficient for application of the waterproofing system and subsequent erection of the permanent secondary cast-in-situ reinforced concrete lining. Revetment walls are designed for both portal sections to allow the construction of the cut-and-cover tunnel blocks with a minimised impact on the surrounding protected landscape area. Natural and unforced incorporation of the portals into the landscape will be achieved by utilisation of free stone from a local quarry.

1 GEOLOGICAL CONDITIONS

The Turecký Hill massif consist mainly of carbonate rock layers and, partly, from the north, Quaternary sediments. The tunnel overburden depth varies from a minimum of about 3 m at the southern mined portal to approximately 100 m.

The northern (exit) portal and the about 80 m long initial section of the tunnel will be built in a complex of Quaternary sediments of aeolian and diluvial origin, which are represented mostly by strata of yellow to yellow-grey secondary loess. In the initial 40 m long section, the thickness of the series of strata is expected to cover the entire height of the tunnel cross section combined with polygenetic sediments consisting of brown-coloured aeolian-diluvial sandy shales. These sediments are frequently mixed with diluvial debris, which have an underlier consisting of about

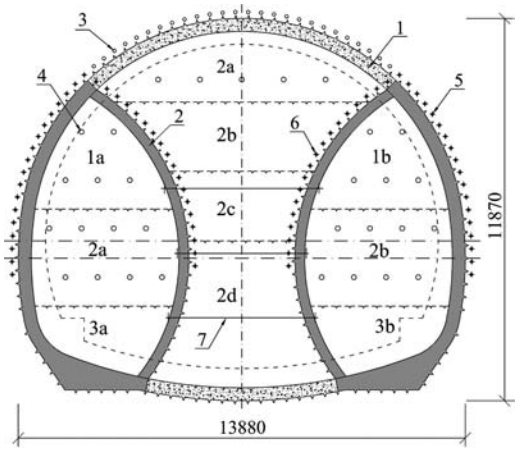


Figure 1. The cross section for the excavation through the Quaternary sediments. 1-Primary lining 400 mm thick, 2-Temporary lining 300 mm thick, 3-ø 108/16 tube micropiles or self-drilling micropiles injected with cement grout, 4-FACE SUPPORT: GRP anchors injected with cement grout, 5-Side drifts: GRP forepoles, 6-Side drifts: GRP self-drilling forepoles, 7-Tie rods.

2 m thick layer of Neogene claystone and sandy clay; the bedrock consists of dolomites weathered to the depth of about 2 m. The tunnel overburden is about 10 m to 15 m thick. An increased amount of diluvial debris mixed with loam, larger cobles and boulders is expected in the following 20 m long section, where the overburden thickness will increase to 25 m. In the remaining 20 m long section, the tunnel bottom will probably pass through the weathered bedrock, which will gradually rise to cover the entire tunnel cross section. The overburden will be 30 m to 35 m thick.

The other tunnel section, which is 60 m long, will be driven through a rock mass consisting of dolomite layers in the invert and bench, overlaid by a series of limestone layers in the excavation crown. Apart from several dip faults, there will also be effects of weathering encountered in this section; karst phenomena cannot be excluded in this section.

The rock massif through which the 1600 m long tunnelled sections will pass consists of Mesozoic series of layers of carbonate rocks (dolomites and limestone). Based on the results of surveys, we can state that the Mesozoic massif of Turecký Hill and mainly the dolomite series of strata are intensely tectonically disturbed. The blocks of carbonate rock are not affected by a more significant process of deep weathering. A larger depth of weathering may be bound to the faults; the weathering depth can be expected to vary between several meters and first tens of metres. Apart from sinkholes, the karst phenomena will even be present in subsurface parts of the massif. They will be mainly bound to the zones or more intense fracturing and loosening of the rock mass, or to the zones of tectonic failures and open faults. The carbonate massif is expected outside the zones of tectonic faults and rock loosening should be water saturated to a minimum degree. Despite the nearly continuous covering by impervious aeolian sediments, loess and secondary loess, ground water is supplied to the undisturbed blocks of the massif nearly exclusively through infiltration of precipitation. No significant impact on the existing regime of surface water or underground water due to the tunnel construction is expected.

2 THE DOUBLE-TRACK MINED TUNNEL

2.1 *Tunnel excavation*

The main proportion of the excavation is expected to be performed from the northern portal, only a smaller part will be driven from the southern portal. The reason is the large volume of earthmoving and large extent of the support of the construction trench required at the southern portal, problems with dump location in the vicinity of this portal, and the necessity for solving the crossing of the large-volume muck transport with the existing operating railway line. The drill-and-blast technique (controlled blasting) is expected to be utilised for breaking the competent rock. Soil and fractured rock mass will be disintegrated mechanically by excavators or even heavy impact breakers.

The New Austrian Tunnelling Method (the NATM) is designed to be utilised, with the primary support consisting of C 16/20 sprayed concrete, welded mesh, rock bolts, lattice girders and spiles. Based on the engineering geological survey, the following excavation support classes are anticipated: 2, 3, 4, 5a1 and 5a2 in the rock environment and 5b1 a 5b2 in the environment consisting of Quaternary sediments (a soil environment).

In terms of complexity and the geological conditions encountered, the tunnel being designed is categorised as geotechnical category 3, which belongs among the most difficult in the field of tunnel construction. The poor quality of the rock massif is a result of the existence of discontinuities, weathering, proximity of significant faults and possibility of occurrence of karst phenomena. The above-mentioned difficulties adversely affect not only the process of breaking the rock by the drill-and-blast technique, but also the process of the rock massif deformation lasting until a new state of equilibrium is reached. It will, therefore, be necessary, even with respect to the size of the excavated cross sections, to divide the excavation face in both directions, horizontal and vertical.

The excavated cross section for the soil environment (an 80 m long drive) is 13.9 m wide and 11.9 m high; the excavated cross-section area is 137.2 m^2. The

tunnel profile is closed by an invert and is divided into two side-wall partial excavation faces and a central partial excavation face. The partial excavation faces are sub-divided into top headings and cores with bottoms. When both side-wall excavation sequences are finished, the excavation of the central pillar will start. When the entire soil environment tunnel excavation section is completed, the invert will be cast in parallel with the construction of the central tunnel drain and toe drains. When the required strength of the invert concrete is reached, a temporary roadway will be constructed and the tunnel excavation through the rock massif (toward the southern portal) will start. The primary lining thickness of 400 mm is designed for this environment, while the temporary lining of the central pillar excavation will be 300 mm thick. The tunnel length is divided into three sections differing in terms of the method of the crown support. The stability in the first section will be provided by a two-tier canopy of ø108/16 × 25 m long grouted pre-support tubes, which will be installed from the portal excavation trench. The second section, where the crown is found in relatively cohesive soil, will utilise a canopy consisting of fans of grouted self-drilling or driven spiles 6 m long, with 5 m overlaps. The third section lies at the soil/rock massif interface, where layers of little cohesive soil and debris may occur. For this reason, the canopy designed for this section consists of fans of ø108/16 × 10 m long grouted pre-support tubes with 5 m overlaps. All of the partial faces will be protected by a layer of shotcrete. The stability of the faces will be provided by glass fibre reinforced plastic anchors (a 40/5 mm GRP band grouted with cement mortar). Effectiveness and the necessity for these anchors will be verified in the first section of the excavation.

The excavated cross section of the tunnel driven in the rock environment (a 1660 m long drive) is 13.1 m to 13.7 m wide and 10.3 m to 11.4 m high. The cross-section area ranges from 105.1 m^2 to 129.7 m^2. A horizontal excavation sequence consisting of the top heading (the maximum height of 6.8 m) and the bench with the bottom is designed for the whole length of this section. This sequence meets the requirements for keeping the excavation face stable, as well as for accessibility and sufficient room for usual tunnelling equipment. The thickness of the primary lining is designed at 150 mm to 300 mm.

There are two 11 m long contact-line tensioning chambers with the excavated cross-section area of 194.4 m^2 designed at chainage 103.325 and 103.425. The enlargement to the profile designed for the chambers will be carried out subsequently when the entire tunnel length excavation is completed with the basic cross section maintained. The enlargement work will start in the top heading, then the remaining part of the profile will be enlarged. The chambers are provided with an invert and 400 mm-thick primary lining. There will be safety recesses on both sides of the tunnel, at intervals of 20 m.

Based on mathematical modelling, we expect that deformations of the primary lining in the crown in the support classes 2 to 4 will be up to 50 mm, in the class 5A up to 80 mm and in the class 5B up to 150 mm. There are no buildings inside the settlement trough. Contingent increased settlement cases pose no threat to the surrounding area; they are only a problem in terms of the tunnelling work.

2.2 *The final lining and tunnel equipment*

The final lining of the mined double-track tunnel will be constructed using travelling tunnel formwork. The casting will be divided into two phases: the invert or strip foundation casting and casting of the vault and side-walls. The casting blocks will be 10 m long. A minimum 2 m wide and 2.2 m high (measured from the walkway surface) safety recess is located in every other block. The recess contains an inspection shaft built on the drainage, and a manhole on the cable duct. Cable chambers for installation of the contact-line tensioning equipment will be cast in two phases, identically with the entire tunnel.

The internal radius of the final C25/30 reinforced concrete lining is 6.1 m. There are several variants of the lining designed, depending on the excavation support class and foundation conditions. The thickness of the lining reaches 300 mm to 400 mm. The reinforcement consists of lattice arches combined with welded mesh or strap pieces if necessary. The major part of the tunnel is founded on strip foundation; the 600 mm thick invert is designed only for the portal blocks and the section driven through soil. In both above-mentioned cases, tie-up reinforcement is designed. Blinding concrete and infill concrete is of the C 16/20 and C 8/10 grade. The intermediate waterproofing system is of the umbrella type, i.e. covering only the vault and side walls and ending at the level of the toe drains.

The central tunnel drainage duct consisting of a 500 mm-diameter PE pipe is embedded in the tunnel bed between the two rails. Toe drains consisting of 200 mm-diameter flat-bottom PVC drainage pipes are on both sides, behind the outer surface of the final lining. The toe drains pass through inspection manholes built in the safety recesses; transverse drains lead from each manhole to manholes on the central drainage duct. Both drainage pipelines are embedded in porous concrete, at a gradient identical with that of the railway track. They terminate in a pair of interconnected shafts, from which water flows to fire protection reservoirs.

Walkways about 900 mm wide are designed on either side of the tunnel. There are steel handrails installed at a height of 1.1 m above the pavements; the lines of the handrails are broken at the safety recesses. There is a 12-way PE cable duct embedded in the

walkways. The cable duct is cut in the safety recesses by manholes containing outlets for electrical equipment (tunnel illumination, sockets, switches). The dry fire main (a 110 mm-diameter PE pipeline), which is fed with water from the fire protection reservoirs, is found under both walkways. A hydrant valve is installed in the inspection manhole in each safety recess. Both branches of the dry fire main are interconnected every 100 m; the connecting pipelines are terminated by outlet valves installed in shafts on the central drainage duct to make emptying of the fire main possible.

The numbers of all tunnel blocks, safety recesses and escape routes and their distance from the closest portal or the escape gallery entrance will be marked in the tunnel. There are oblique guide-strips interconnecting the neighbouring safety recesses designed with the aim of facilitation of safe movement and search for a shelter in the tunnel. The marking will be painted on the internal surface of the final lining. Sign tables will be imprinted into the concrete surface during the casting.

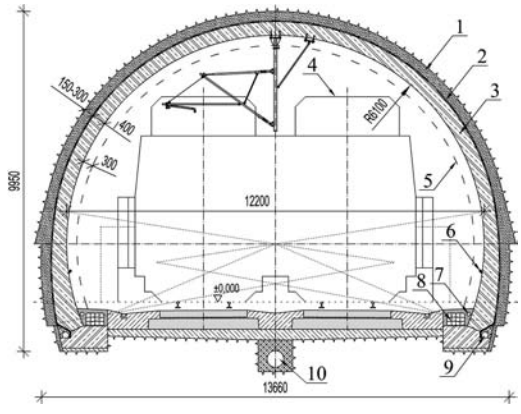


Figure 2. Typical tunnel cross section 1-primary lining C16/20 shotcrete, 2-waterproofing layers, 3-secondary lining C25/30 reinforced concrete, 4-safety margin, 5-clearance envelope, 6-steel handrail, 7-fire main, 8-cable duct, 9-drainage behind outer surface, 10-central drainage duct.

3 THE NORTHERN (EXIT) PORTAL

The exit portal is located in a deep erosion furrow in the northern slope of Turecký Hill. The terrain surface in front of the portal will be cut to comply with requirements of a mustering area for the fire rescue service equipment and emergency vehicles, including an access road with a bridge over Bošáčka stream. This area will be supported by retaining walls and provided with a handrail above the stream. There will be a small building housing a standby power unit and the tunnel equipment control elements there, and a fire protection reservoir, which is built in an excavation box lined with secant pile walls. The reservoir is fed with water from the stream, and also with the water from the tunnel drainage treated by means of a downflow baffle. The water from the reservoir flows again to the stream, via a safety overflow. The exit portal area is at a distance approximately of 100 m west of the existing railway track.

The construction of the cut-and-cover tunnel and a permanent revetment wall requires a 24 m × 32 m construction trench to be excavated and provided with temporary support. The rock massif in the area of the trench consists of a complex system of Quaternary sediments (see Geological conditions – the northern portal), which extends approximately 4 m under the tunnel structure. The water table is found roughly 7 m under the structure. The vertical walls of the construction trench will be supported by a system of vertical micropiles (ø152/18 tubes) provided with a layer of C20/25 sprayed concrete with welded mesh. The walls will be anchored at six anchoring tiers by 24 m to 30 m long stranded anchors (10 m-long roots). The tops of the micropiles are covered by anchored reinforced concrete capping pieces; in the lower tiers, the anchors pass through steel wallers. The anchoring of the reinforced concrete capping pieces skirting the terrain is permanent. There are parapet walls built on the top of the capping pieces, and gutters diverting rainwater flowing down the slope outside the portal area are laid behind the parapet walls. A pile wall which will be built from the level of 1.6 m above the top of rail will extend the northern micropile wall (parallel with the railway track), thus the maximum depth of the excavation will reach 18 m. The former pile wall consists of 1.20 m-diameter, 12.3 m long piles. The toe of each reinforced concrete pile is keyed into weathered dolomites; each pile is extended by means of three pieces of 8 m long micropiles (ø108/16 tubes). The top of each pile is anchored by a 34 m long temporary stranded anchor (a 10 m long root). The opposite southern pile wall, with the length equal to the length of the cut-and-cover tunnel, will consist of the same type of piles, 10.2 m long, with the tops at the level 0.5 m under the top of rail. The piles are again extended by micropiles; the tops are not anchored. The two opposite pile walls built along the cut-and-cover section will be braced against each other under the invert by an 800 mm thick vaulted reinforced concrete slab. The entire above-mentioned structural system is designed to transfer the load to the competent bedrock. In addition, a protective 500 mm thick reinforced concrete transition slab will be cast between the portal and railway bridge, which is designed to eliminate the differential settlement existing in this section.

The construction of the final lining in the cut-and-cover sections will start only when the casting of the adjacent blocks of the mined tunnels has been completed. The same travelling form is planned to be used

for both the mined and cut-and-cover tunnel sections; formwork for moulding of the outer surface will be added in the cut-and-cover section. The cut-and-cover portal block is 10 m long; it is provided with the invert. The front end of the portal block is vertical. The thickness of the upper vault lining of 550 mm is uniform; the invert is 800 mm thick; tie-up reinforcement will be used. The tunnel equipment is identical with that used in the mined section.

A final reinforced concrete revetment wall (C 25/30) lining the excavation box will be built in parallel to the railway track in front of the entrance portal and perpendicularly to the track behind the portal. The walls provide permanent support to the slope in the environment consisting of Quaternary sediments which are liable to sliding. The walls are supported with permanent 34 m long stranded anchors installed in three tiers. An unreinforced concrete block originates around the portal block of the mined tunnel. The block is found between the revetment walls. Its surface, inclining at 5:1, is clad in natural stone obtained from a local quarry to be properly incorporated into the landscape.

4 THE SOUTHERN (ENTRANCE) PORTAL

The new alignment declines from the existing route toward the entrance portal at a very acute angle, and it runs along a side-hill cut in rock, which gradually grows in the depth. The slope of the cutting reposing at 40° to 60° is stabilised. The new alignment is at a 1 m distance only from the original route at the beginning of the cut; the distance reaches 16 m at the end. A temporary relocation of the track shifting the rails approximately 3 m from the existing track in the direction from the hill side is designed for the period of the works to allow enlargement of the site facility in front of the portal and increase the safety of operations during the course of the construction. The portal is located in a distinct erosion furrow in the eastern slope of the massif, which consists chiefly of carbonate series of strata containing the Wetterstein Limestone and, in the top layers, Quaternary sediments. A hard surfaced area for mustering of the fire rescue service and an access road with a bridge over the Biskupice canal will be provided in front of the portal. There will be a small building on the edge of this area, which will house a standby power unit and the tunnel equipment control elements. A cut-and-cover fire protection reservoir (partially covered with the backfill of the portal block) will be built beside the portal. The reservoir is supplied with rainwater collected in the erosion furrow and flowing via a trough and a storm-water inlet, and water from the tunnel drainage treated by means of a downflow baffle. The safety overflow is provided via an old culvert leading to the Biskupice canal.

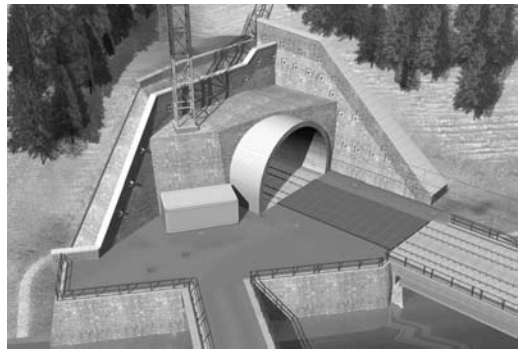


Figure 3. The northern (exit) portal.

The entrance portal is part of the cut-and-cover tunnel section; it is built in a 25 m long excavation box, which is located in a side-hill cut with the rock wall about 17 m high and is an extension of the side-hill cut excavated in front of the portal. The vertical walls of the excavation box will be supported by micropiles (ø152/18 tubes) and C 16/20 sprayed concrete with welded mesh. The tops of the micropiles will be fixed in a reinforced concrete capping piece, which will be anchored with 6 m to 8 m long pre-stressed stranded steel rock anchors. The lower tier of anchors will pass through steel wallers. A canopy consisting of horizontal ø108/16 × 25 m long grouted pre-support tubes will be constructed at the front end of the excavation box to stabilise the excavation at the beginning of the tunnel drive, where the overburden will be very shallow and its transverse gradient is very steep.

The final lining of the cut-and-cover tunnel is constructed in the same way as in the case of the exit portal. Two cut-and-cover tunnel blocks have the invert. The front end of the portal block is slanted and provided with a flange preventing rainwater from flowing over the edge. The final liners of the vault and invert are 550 mm and 600 mm thick respectively. The tie-up reinforcement system is designed. The tunnel equipment is identical with the equipment used in the mined section. The backfill of the cut-and-cover tunnel plus the portal will be carried out approximately at a slope angle identical with that of the original slope. The stability of the slope will be improved by spreading a layer of natural stone.

The side of the 120 m long side-hill cut excavated in front of the portal will be supported by a revetment wall parallel with the rails; the height of the wall will increase in the direction toward the portal. The lower part of the wall will consist of one or two levels of a 500 mm thick masonry wall built using free stone selected in a local quarry. The wall is inclined at 5:1, and the individual levels are separated by a berm. The upper part of the revetment wall, which is separated by a berm lined with a handrail, is clad in grass pavers

laid at a 70° incline. The total thickness of the structure amounts to 600 mm. In both above-mentioned cases, the surface of the side-hill cut is supported by shotcrete with welded mesh tied to the surface with anchors. Grass pavers will stabilised, if necessary, using 4 m to 6 m long corrosion-protected rockbolts. The part clad in natural stone will be stabilised by an anchoring system using the above-mentioned rockbolts. The berm is not designed for the lower part of the 10 m long section of the masonry revetment wall found just before the portal so that sufficient space is available in front of the portal.

5 THE ESCAPE GALLERY

The escape route, which is designed in compliance with the fire safety concept and results of the risk analysis, leads via a 244.7 m long transverse gallery driven on a 0.5% downward gradient from the tunnel and ends on the surface in the location of a former bridge over the railway track. The escape gallery has a horseshoe shaped profile. It will be driven by the NATM, with the support consisting of C 16/20 sprayed concrete primary lining, welded mesh, rock bolts, lattice arches and spiles. Based on the engineering geological survey, the design specifies 2 excavation support classes: class 2 and class 3.

The casting of the gallery lining is expected to be divided into two phases, the bottom and the vault plus side walls. The 120 mm thick bottom will be cast using C 25/30 concrete reinforced with welded mesh combined with tie-up reinforcement. The drainage sub-base will be made from porous concrete. The round vault with the inner radius of 1.65 m and the side walls will be made of C25/30 reinforced concrete with the minimum thickness of 200 mm. The main reinforcement elements are lattice girders and welded mesh. The intermediate waterproofing membrane covers the vault and side walls, and ends at the bottom in the longitudinal toe drainage.

A 17 m long air lock chamber is provided in the part of the gallery adjacent to the tunnel. It is separated from the tunnel by a 2.2 m wide fire resistant door, and from the escape gallery by a 2.2 m wide steel door. The air lock is positively pressurised by a forced ventilation system independent of the escape gallery ventilation system to prevent smoke entry from the tunnel to the escape gallery.

The rock wall created on the surface in the location of the escape gallery mouth is supported by a 300 mm thick retaining wall provided with side wings.

6 CONCLUSION

The process of underground construction significantly differs from the other construction branches due to the specific nature, limited knowledge of geological conditions, often unpredictable circumstances, dependence on the means and methods of construction, and significant construction risks. The application of the NATM makes the construction process as well as the completed structure safe through the observational method and thorough geomonitoring. Geology is the factor which affects the complexity, technique and duration of construction. It is best visible at the northern portal where the Quaternary sediments represented by secondary loess significantly complicate the work on the excavation box, tunnel excavation and erection of the final lining. The most serious complication will be the task to excavate the side-hill cut in rock in the constrained conditions existing at the southern portal, in close proximity to the existing railway track, which will be in service throughout the construction period. Despite all problems, the design tries to respect the character of the natural forest-steppe environment in the protected landscape area of Turecký Hill.

Regarding the construction organisation, the construction time could be shortened if necessary by implementation of additional one or two points of attack in the middle of the tunnel, at the end of the escape gallery, which would be driven and provided with primary lining in advance. This solution would, however, require widening of the access road to the escape gallery and possibly even enlargement of the gallery cross section according to the tunnelling equipment used.

The detailed design for the Turecký Hill tunnel was issued in 2005. In Slovakia, it is a kind of a “pilot design” developed within the framework of the “Upgrade of Railway Lines of the Slovak Republic to speeds up to 160 km/h”, prospectively 200 km/h. The completion of the Turecký Vrch tunnel will add an important section to the quality and fast link between Bratislava, the Slovak capital, and Žilina, a centre of northwestern Slovakia. The tunnel construction is expected to start in 2007.

Underground Space – the 4th Dimension of Metropolises – Barták, Hrdina & Romancov (eds)
© 2007 Taylor & Francis Group, London, ISBN 978-0-415-40807-3

Collectors – System approach to the regeneration of technical infrastructure in the city of Prague

F. Dvořák & M. Hradecký
INGUTIS Ltd., Prague, The Czech Republic

ABSTRACT: Collectors represent a new element in the quality of distribution and regeneration of technical infrastructure, which in a long-term perspective enables its inspection and maintenance as well as the increase in capacity without negatively affecting the environment. For their successful spatial integration into the city, it is necessary to asses closely a set of limiting factors. These factors not only include the geological conditions, but also the existing buildings, technical infrastructure, traffic and city operation. New collector ducts generate an open system, which enables their further expansion. Their concept must respect the principles of underground urbanism and requires consistent coordination with other underground structures in the area with respect to land-use planning.

1 INTRODUCTION

Historical centre of Prague, the capital city of the Czech Republic is a collection of substantial cultural, architectural and urban values that developed over the last centuries. Its high significance is proved by the registration of the Prague historical reserve among the city zones that are protected by the UNESCO organization. However, an increasing number of the city's and country's social and cultural activities is based in the centre, which creates a great demand for traffic and technical infrastructure with prevailing citywide character. Every activity is dependent upon the infrastructure's full functionality and sufficient capacity.

For attractiveness of the city centre and development of its operation and service and due to the lack of surface space, a new resource for further development of the city is the underground. Many linear and solitary structures of various functional uses are situated in the underground. These involve a complex solution for technical infrastructure regeneration in terms of aggregation of two or more underground service ducts into collectors.

2 COLLECTORS – PRINCIPLES AND REASONS

2.1 *Structures' characteristics and their reasons*

For more than 30 years, laying of pipes and cables is being designed into underground man-sized ducts, mainly in new residential areas in the suburbs of Prague. This way of underground services laying has a significant and substantial role in the regeneration and development of technical infrastructure within the Prague historical reserve. Existing cable and especially pipe service ducts are often old and considerably defective, very often with reduced or exceeded lifetime. Moreover, with increasing demands on the city development, their capacity becomes insufficient.

A gradually updated plan of collectorisation of the municipality is being created for the purpose of land-use planning. According to this plan, an open system of collector ducts is being created. This system enables further expansion into other parts of town and branching-off into adjacent streets. Therefore, this is not only a local solution of technical infrastructure laying or realignment but a system solution of problems with technical infrastructure in city centres.

2.2 *Advantages of building collectors*

Advantages that result from laying of underground services into collectors are stated in the following notes. The advantages are from a long-term perspective obvious especially for consumption collectors that immediately supply particular surface buildings:

- Main aspect represents an easy inspection and maintenance of inbuilt utility lines without an impact on the surface, as well as the safety of the operation of the utility lines secured by a system of control measurements and centralized control of operation from one control centre.
- Increase in lifetime of utility lines by diminishing the negative effects of ground environment (corrosion, stray currents, dynamic effects of traffic etc.).

This relates to economical operation and a reduction in losses during faster search for damaged utility lines.
- Elimination of surface excavations for all subsequent maintenance and repair works on the utility lines. This results in a cut-down in traffic limitations as well as environmental impact.
- Possibility of easy increase in capacity of particular medium by laying a utility line of a greater size or even a change of a medium.

3 INITIALIZATION OF BUILDING COLLECTORS

The impulse for building collectors is a need for an analysis of possible solutions for sets of problems linked to the development of the surface and the underground of the city centre. Assessments of present conditions and prognosis of the future development are monitored in areas involving city territory and surface buildings, technical and traffic infrastructure and environment.

3.1 *Development of city territory and surface buildings*

This area includes assessment of complex development of a city zone or reconstruction of a city block. This also involves territorial preparations of locally situationally defined large solitary structures. A dispositional utilization of underground levels including the solution for regeneration of underground services must form an integral part of the historical district's land-use plan.

3.2 *Condition and development of underground services*

A Large amount of cable and pipe utility lines is in dissatisfactory state. Pipe ducts that are 80–100 years old can be considered in emergency conditions and over their lifetime limit. Outflow of water into subsoil is a common occurrence. However, even for relatively newer utility lines, negative effects of ground environment (humidity, corrosion, stray currents, dynamic effects of traffic etc.) contribute to shortening of lifetime. With the problem of lifetime and technical condition also comes the problem of insufficient capacity of existing utility lines for their extensive use as well as absence of sufficient reserve for their perspective development.

As an alternative to laying utility lines into the ground and persistent excavation works, a system of collector network has been under development in Prague since 1985.

3.3 *Traffic infrastructure solution*

Due to constantly rising traffic demands in the city centre, new solutions that enable both road capacity increase and solutions for present problem sites are being searched for. Conception of rail and non-rail traffic must respect specifics of the historical city centre and conditions of the city historical reserve, which limits the increase of traffic in the centre. A motivation for solving the problems of utility lines is also the modernization of tram tracks (including solutions for traffic narrows, which are very common in the city centre).

One of the solutions is the use of city underground levels, which are mainly used by linear structures (metro, road tunnels). This incites the need for solutions for exposed traffic junctions by building overpasses and underground garages. This usually incites the need for realignment of great number of utility lines (preferably into matched structures – collectors).

3.4 *Environment*

Construction works that relate to utility lines constantly disturb the environment of the city centre. These construction works are either intended (during expansion or renovation of utility lines) or unintended (during emergency). They always cause a negative impact on the city. Therefore, collectors represent an alternative solution for utility lines regeneration.

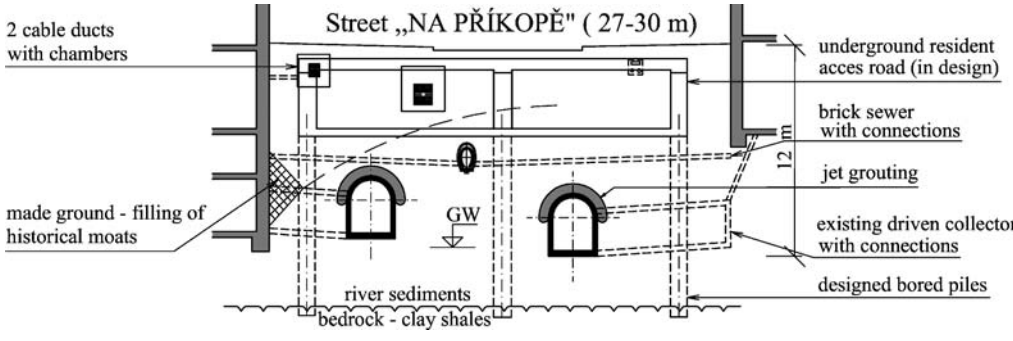


Figure 1. Prikopy Collector – prerequisite for utility lines realignment and possible future execution of an underground road.

Their execution represents a short-term environmental impact. Long-term positive effects will appear during their operation over the whole lifetime period.

4 CATEGORISATION OF COLLECTORS AND THEIR APPLICATION IN PRAGUE CENTER

4.1 *Philosophy of development of collectors in Prague*

A concept for systematic approach in collector network generation that represents a system solution for underground services in the centre of Prague was executed in a land-use planning documentation called "General plan of collectorisation in central Prague". The first concept was published in 1982 and covered a broader territory of the centre with an estimated development timescale of few decades. It was updated several times during the subsequent years to reflect new standards in the concept of the city and underground services development. The extent of collectorised territory was then partly modified to cover the area of "The Prague Historical Reserve". The last study, which specified the changes in the land-use plan, was completed in 2005. Its purpose is to include the main supply 2nd category collector ducts (see below) into the land-use plan – a basis for area development.

At present, the total length of operational collector ducts in Prague is more than 90 km. Out of this length, almost 18 km of operational collector ducts of both further described categories are in the historical centre. Other collectors are being constructed or are in an advanced phase of designing. The rest of about 80% of underground reinforced concrete collectors represent structures in new residential areas in the suburbs of Prague.

A Collector Control Centre at Senovazne Square is a part of the system and is the only control centre in the network. Constant operational monitoring and control of the branched collector system of the whole Prague (centre and suburbs) is performed there.

4.2 *Collector types*

Collectors are divided into two separate, but technologically connected systems according to their functional purpose. Besides the below stated character of inbuilt utility lines, both systems differ in situational and depth level positioning as well as cross section, which results in differentiation of applied construction technologies caused by geological conditions:

– 2nd category collectors – supply – essential distribution of utility lines of city-wide character in greater depths and wider territory with surface outlets in limited number of locations and blocks of houses. These ducts are intended to transport media into individual city zones. They lead straight and if possible in bedrock. Branch ducts, which end in shafts in duct crossings, connect deep technical chambers on 2nd category collectors with 3rd category collectors.
– 3rd category collectors – consumption – direct supply of adjacent buildings with particular media. Their situational and depth level positioning is close to place of consumption – adjacent buildings. They therefore usually lead on city owned land. Connection into the buildings is done by a side collector and then by borings for pipes and cables into basements of the buildings. Depth level of the collector, as close to the surface as possible, significantly affects the choice of suitable construction technologies. Influence of construction works on this type of collectors is highly notable on the surrounding area – especially on buildings and utility lines. This usually invokes big geotechnical challenges like acceptable deformation and the effect of driving on the surrounding area.

5 ASPECTS OF COLLECTORS' SITUATION INTO THE CITY

A complex assessment of all limiting aspects of collector construction as well as all specific conditions according to the characteristics of the place and structure is necessary for spatial situation of the underground structure into cramped situational and depth level conditions of the city centre.

5.1 *Surface structures*

Existing surface and underground structures represent a basic input for the solution. Definition of extent of surface structures in relation to public land is necessary for positioning collectors and all their structures, which are in contact with the surface.

For ducts in smaller depths, underground parts which stick out from facades into the area of the public

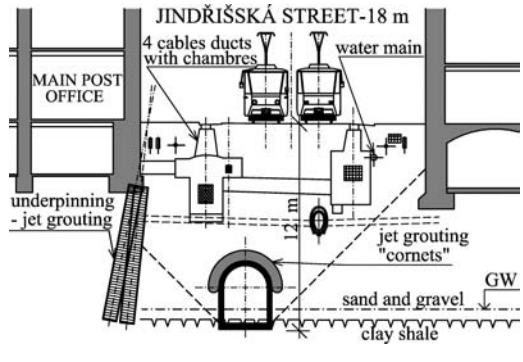


Figure 2. Design of most driven 3rd category collectors in the centre of Prague, under the level of sewer ducts.

land are crucial, as well as all underground premises of other structures. Unknown remains of filled and unfilled underground spaces and relicts of former area redevelopment are crucial, too. Logical demands for historical monuments preservation and archaeological research are respected when situating collectors in the town historical reserve.

From a geotechnical point of view, the character and quality of adjacent surface structures is crucial, as well as their static and constructive systems. Static securing of the structures before start of construction might be necessary.

5.2 *Existing underground services*

Utility lines are an issue for all underground structures in Prague. Search for pipe and cable utility lines of all owners in the area is crucial, as well as definition of inviolable ones (cannot be realigned), possibly realignable and realignable without problems. The inviolable utility lines of citywide character include trunk sewers, large pipelines and telecommunication cables matched into cable ducts with frequent chambers.

It is usually impossible to respect normative protective zones of all utility lines in the city centre. It is therefore necessary to adopt all protective and securing measures before and during the construction.

Another factor which comes into play is the demand by utility lines owners for full functionality of their existing lines during realignment. Therefore, the new realigned utility lines must be built in a different place.

Acceptable levelling of underground collectors is an issue as well. This is significantly limited by levelling of other media (especially sewers and cable ducts).

Levelling of sewer tubing (including sewer connection inlets) in depths of 6–7 m under the surface divides the subsoil into two levels.

This affects the possible levelling of the collector, either above or below the sewer.

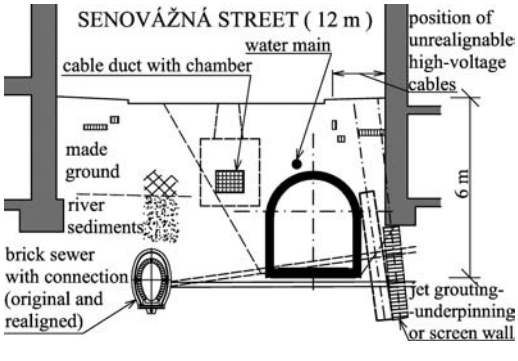


Figure 3. 3rd category collector whose execution brought up difficulties with utility lines and adjacent buildings supporting.

The collector must not be situated in the protective zone of the sewer and affect the structures of the sewer. The levelling is therefore possible either above the sewer (4–5.5 m under the surface) or below the structures of the sewer. Levels between 10–14 m below the surface are most common for collectors in the centre. Their least statically suitable levelling is due to execution in cohesionless soils, which are partly saturated. Position below the level of footing bottoms of most buildings demands complex static measures for securing the overburden and the adjacent structures.

5.3 *Traffic and city operation*

Traffic and city operation represents the third basic requirement for incorporation of collectors into the city. This is a very delicate problem not only during the concept phase but also during the execution phase of the collector, when it usually affects the public. Minimization of local negative effects on the operation of the city (its traffic and supply) and their duration is therefore demanded. Basic demand is functionality of traffic and rail mass transport. Construction works in protective zones of the metro are subject to special reviews and execution procedures. There is a strict requirement for structural and static inviolability of all metro structures.

Compromise solutions for possible temporary traffic replacements, which are acceptable by traffic and city authorities, are being searched for during the documentation reviews as well as solutions for construction site traffic (including acquisition of public land for construction site installations).

Enabling access to existing buildings and commercial objects in them (possibly by an alternative entrance) represents another measure during the construction works. Fulfilling of this demand is usually bound to applied construction technology, work processes and phasing.

In some cases, construction works on the collector might closely relate to works on a traffic structure. For example a parallel alignment of a collector and a traffic tunnel or underground collector and a tram track.

5.4 *Possibilities of execution*

Selection of possible application of specific technologies for collector execution depends on spatial resources of the site, geological conditions and assessment of impact of the works on the vicinity. Cut and cover technology and pre-cast constructions are mainly used for collectors in the new residential zones in the suburbs.

On the other hand, in town centres, feasibility of execution of cut and cover linear structures is restricted to entrance shafts in crossings and branching of collector ducts, as the effect of construction works on the city operation and environment is substantial in the centre.

Underground tunnels for particular collector ducts are driven from these shafts, which represent initial structures. Differentiation of used technologies, procedures and supporting measures is determined by the collector category and therefore its levelling (depth under the surface).

3rd category collectors are designed in small depths. They therefore require large amount of additional measures for stability securing and safety of boring, as well as static supporting of adjacent structures and underground services. 2nd category collectors are driven deeper, usually in bedrock, which is, if possible, unaffected by weathering.

5.5 *Collector preparation specifics*

This issue is also important for incorporation of collectors into the city. Public benefit of these structures is not that obvious, when all the utility lines situated in the ground are still functional. Moreover, expansion of the metro is more appreciable by the public and city authorities.

Specifics of preparation mainly result from great amount of parties to an action during the documentation reviewing at every level of administrative action. Property ownership matters of adjacent buildings are difficult. This incites the need for permits of all the owners (mainly for connections into their buildings). Present standard practice of the construction process creates harder relations between the involved partners. Demands for responsibility for damage done to others' property and the environment are applied consequentially. Complex evaluation of the present state of all structures before the start of works is necessary for further negotiations about damage caused during execution of the collector. This is performed by monitoring of present state of the buildings and sewer ducts as well as geotechnical monitoring during the execution performed on the surface as well as in the underground.

6 GEOTECHNICAL PROBLEMATICS OF DESIGN AND EXECUTION

6.1 *Solving geotechnical tasks*

For incorporation of a collector into the city, in addition to the above stated spatial aspects, it is necessary to work out a geotechnical analysis of static behaviour of the structure and its effect on the surrounding environment. It is necessary to review the process of execution of the collector during all construction phases as well as effect of the structure during the whole life time. Solving the geotechnical tasks, is therefore one of the limiting factors of the conceptual solution in which both limit states (ultimate, serviceability) must be respected.

The effect of construction works on the progression of strains in bedrock and the creation of subsidence zone is monitored with respect to safety system "collector structure – bedrock environment – buildings and underground services". Disposition, design, technology and process of execution, as well as a set of measures as a part of advanced works or driving of the collector arise from analysis of acceptable strains of surface structures and utility lines in overburden.

Consistent evaluation of static aspects of possible levelling of the collector is an integral part of these analyses. This was closely described in the categorization paragraph.

6.2 *Rock conditions*

Local geological conditions are a basic input data for geotechnical analysis. Their complexity in the centre of Prague is not only caused by historical development and broken morphology, but also by lithological evolution of rock environment and tectonic deformation of bedrock. Another factor is the erosion caused by the Vltava River. Two characteristic units can be defined in the geological profile – bedrock and quaternary sediments. Bedrock is situated in depth between 12 and 15 m under the surface level, in areas with terraced levels, the depths drop down to 6 m.

Bedrock usually consists of Ordovician shale of various compositions (clay, sand, silt) with insets of solid layers of sandstone and quartzite. Differentiation of separate layers of shale causes big differences in physical and mechanical characteristics, as well as in weathering processes resistance.

Overburden layers of quaternary terraced sediments are formed by clayey sands and sands with gravel, which turn into gravels at the base of the quaternary. Specifics of the made-up ground result from their variable thickness and composition affected by anthropogenic processes. Known and unknown underground spaces from former buildings are common. Usual thickness varies between 3 and 4 m, in places with filled moats up to 6–7 m. Made-up ground is relatively compact, with common archaeological findings.

6.3 *Hydrological conditions*

Hydrological conditions are another important input, which directly affects the phases of the concept and execution of the collector. Groundwater table, which creates a continuous level in a permeable environment of gravelous sand and especially gravel, runs approximately between 10 and 12.5 m below the surface in a depth range depending on the terrain morphology.

Thickness of saturated layer varies between 1 and 5 m depending on the shape of the bedrock. Groundwater level and its changes over time depend upon the water level in the Vltava River. It was necessary to revalue the levels of groundwater used for designing collectors after the floods in 2002 and to raise the

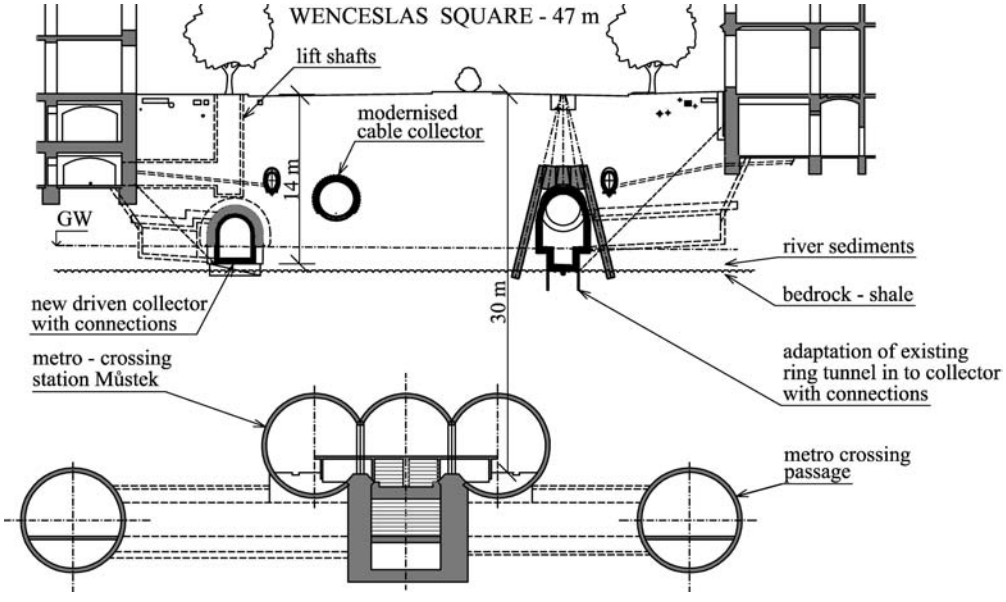


Figure 4. Further development of collectors in Prague – Collector at Wenceslas Square. Current execution of a new duct and proposed difficult adaptation of a present duct into a collector with connections into all adjacent buildings.

values of cent-year's flood level. Analyses of environment permeability, yield of water inflows and groundwater chemistry are necessary for determining the effect of the construction works on the area. A basic task is monitoring the behaviour of groundwater and its acceptable changes with respect to existing buildings.

7 COLLECTORS A UNDERGROUND URBANISM

Underground space has a great value in cramped conditions of the city centre for possibility of its utilization for purposes, which can't be placed on the surface or which would significantly affect the environment. There is therefore a necessary demand for systematic solution of proposed and planned underground structures including urban plans for underground utilization. Plans for utility lines development are an integral part of these solutions. Open system of collectors with the possibility of expansion is an appropriate solution in the centre of Prague.

Consistent coordination of all structures including qualified prognoses of future solutions and procedures is necessary, so that the planned structure isn't limited or restrained by previous inappropriate actions. The aim is to eliminate spontaneity and collisions in the underground utilization and to establish a system, similar to the existing system of urban plans of the surface. In case of collector network, this mainly means defining the levelling and solving collisions with metro and main utility lines of citywide character.

This also involves a sense of permanent value of all underground structures and their difficult dismantling. These financially demanding structures (usually with long pay-off period) are designed for long time operation (in terms of decades). Complex conception of the task of spatial incorporation of the structure demands a multidisciplinary approach of all participants.

8 PROGNOSIS OF FURTHER DEVELOPMENT

Development of collectorisation in Prague will continue. More than 3 km of consumption collectors are being built or prepared. Expansion of deep supply collectors (including an underground crossing of the Vltava river) in total length of more than 3.2 km is being prepared at the same time.

Operating collectors, as well as collectors in preparation, contribute to valuation of existing facilities in the area, improvement of operation of the city and its environment within the historical centre. Therefore, it is important to include the system of collectors among the components forming the city.

Underground Space – the 4th Dimension of Metropolises – Barták, Hrdina, Romancov & Zlámal (eds)
© 2007 Taylor & Francis Group, London, ISBN 978-0-415-40807-3

Years of planning and implementation: Two major urban tunneling projects in Los Angeles, California, USA

M.A. Elioff & B.W. Miya
Parsons Brinckerhoff, Los Angeles, California, USA

J.H. Albino
Stanford University, Palo Alto, California, USA

ABSTRACT: One of the world's major metropolitan areas, Los Angeles, California, has seen construction of over 80 km (50 miles) of large diameter tunnels for subway, wastewater, and water supply over the last 25 years. Two of these tunneling projects, the East Central Interceptor Sewer (ECIS), and the Los Angeles Metro Gold Line Eastside Extension (MGLEE) are examined to describe the 15 to 20 year durations of planning, design, and construction of the tunnels and to provide an overview for future planning and scheduling in urban settings. Aspects of the projects contributing to the complexity and schedule are discussed, including; identification of need and initial planning, the environmental processes, design and changes in technology, impacts of public perceptions on tunneling, protection of property, funding, and changes in all of the above over the duration of the project. The two projects are very different in terms of ultimate use. The complex process planning and design for tunneling in urban areas, however, are similar.

1 TUNNELS IN LOS ANGELES – OVERVIEW

Over 80 km of large diameter tunnels have been constructed in Los Angeles, California (USA) over the past 20 years for transportation and water projects. Project duration, including construction, planning, and design can be well over about 15 years for these tunnel projects in urban areas. In this paper the Metropolitan Transportation Authority's (Metro) Gold Line Eastside Extension (MGLEE), and the City of Los Angeles' East Central Interceptor Sewer (ECIS) are described.

The recently complete ECIS project involved over 18 km of Earth Pressure Balanced (EPB) driven tunnel using four TBMs through a densely populated area of central Los Angeles. The MGLEE tunnels are under construction as of September 2006 and represent 4.3 km of underground construction within a 10 km light rail project, also in a densely populated urban area of East Los Angeles. Two EPB TBMs are being used to drive the MGLEE tunnels.

Both tunnel projects are successful in terms of tunneling performance. Although the two projects are very different in terms of ultimate use; the complex process of tunneling in urban areas in the United States is similar. The following provides short summaries of project history for use in future planning of urban tunneling projects. As these two projects were constructed along the same approximate timeline (over 15 years), we also present some of the relationships between the projects; for example, changes in technology and local perceptions of tunneling. Other projects in Los Angeles are presented supporting case history.

2 METRO GOLD LINE EASTSIDE EXTENSION

The MGLEE tunnels have been in planning, design, and construction for over 20 years. Figure 1, Project Timelines, illustrates the overall schedules. The MGLEE project will extend the existing Metro Gold Line Light Rail (LRT) presently in operation from Pasadena to Union Station in downtown Los Angeles. MGLEE includes the construction of a dual track system, in three cross-sections: Aerial (3 bridges), tunnel (2.7 km) and at-Grade (7.1 km). The underground segment was placed under narrower sections of 1st Street in the older Boyle Heights neighborhood of East Los Angeles. Underground structures include two portals, cut-and-cover sections adjacent to portals, twin-bored tunnels (6.7 m diameter), and two stations.

Upon completion, the LRT will extend the Metro Rail system, currently comprised about 118 km of

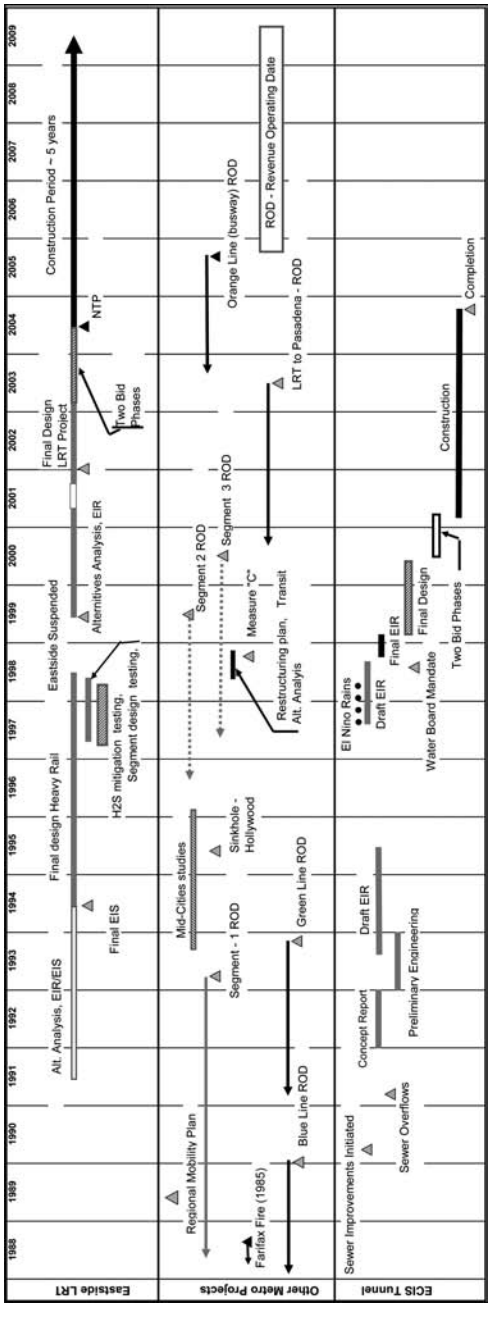


Figure 1. Project timelines.

urban rail and 22 km of busway. Figure 2, Metro Rail Systems, Existing and Planned, illustrates the MGLEE alignment relative to the subway system, and previously planned Metro segments. The existing

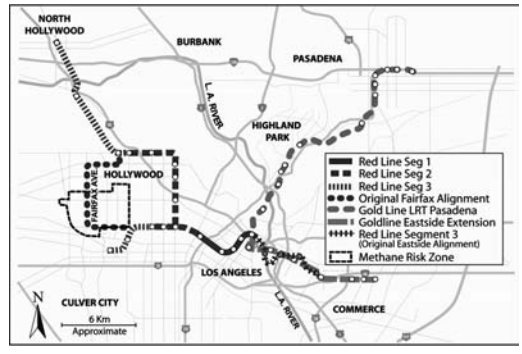


Figure 2. Metro Rail Systems, existing and planned (Blue and Green Line LRTs not shown).

Metro system includes three LRT lines (Blue, Green and Gold), the first becoming operational in 1990).

2.1 *Planning and environmental issues*

To understand some of the planning issues for the MGLEE project, a brief history of Metro Rail is presented. After two failed ballot measures in 1968 and 1974, Los Angeles County voters approved Proposition A in 1980, which authorized a half-cent sales tax to build the regional rail transit system. The Draft Environmental Impact Statement (EIS) concluded that a Rapid Transit System (ultimately heavy rail) would provide a high-capacity system for the regional core. The final EIS (1983) presented a 30 km subway from downtown Los Angeles west along Wilshire Blvd., and north on Fairfax Ave. (USDOT 2002). A methane explosion occurred in 1985 under a building in the Fairfax area, and subsequent studies recommended that "methane zones" be created in Los Angeles, requiring building code changes for construction in these areas. Tunneling was deemed unsafe, and Metro began studying alternative alignments to avoid the methane zone along Wilshire Blvd.

Metro re-aligned the subway or "Red Line" system to avoid the methane zone, and began design and construction of the system in three Major Operating Segments (1, 2 and 3) for funding purposes and to deliver completed operating segments in series. Segment 3 originally included plans for an Eastside Extension of the Redline Subway, a Mid-City Extension, and a Northern route. Of these Segments-3 routes, only the northern extension has been completed to date. The Mid-City Extension began planning to circumvent the methane zone.

Planning for the Eastside began in 1989 – with a Regional Mobility plan that formally identified the need for major rail transit improvements in the region and Metro's and the adoption of the 30-year Integrated Transportation Plan (Metro 1994).

Environmental Phases for projects in the USA were established after the National Environmental Policy Act (NEPA) became federal law in 1970. NEPA requires that alternatives be evaluated and subjected to public review. The preferred alternative(s) are carried forward for further environmental review during preparation of Draft and Final Environmental Impact Statements (EIS), with public comments addressed during the Draft phase. The state of California has similar requirements under the California Environmental Quality Act (CEQA), resulting in preparation of an Environmental Impact Report (EIR).

In April 1993, Metro and the Federal Transportation Authority (FTA) completed the Alternatives Analyses evaluate the Eastside Options. The preferred alignment would use heavy rail technology and continue Red Line Segment-1 from Union Station approximately 11 km east in two phases, the first being a 6.4 km tunneled segment. The Final EIS/EIR was completed in 1994 and final engineering began in early 1995, nearly in parallel with the Mid-City Extension.

2.2 *Design and technology Red Line Eastside extension*

Los Angeles geology presents some additional tunneling "constraints," namely seismic conditions and the presence of naturally occurring subsurface gas. Both conditions require additional provisions for design, construction, and final operations.

For all Red Line segments, a "two-pass" tunnel lining system was developed to include a "high-density polyethylene" (HDPE) water and gas barrier. Underground stations were also constructed using the HDPE barriers to "wrap" all underground structures. Open face shields were used for all soft-ground tunnels, as this was the traditional tunneling method used in Los Angeles, and most of the tunnel reaches were above groundwater.

Initial design for the Eastside Red Line tunnels included new challenges for Metro – given construction issues on prior tunnels – as well as discovery of new seismic feature and subsurface contamination, in addition to the overall seismic and naturally occurring gas conditions.

2.2.1 *Tunnels*

Final tunnel design began just as the Metro Red Line System construction had suffered from some highly publicized events: ground surface settlement of up to 30 mm was experienced along Hollywood Blvd's "Walk of Fame," (1994) and a sinkhole (1995) also in Hollywood, occurred during the enlarging of a Segment 2 tunnel to correct tunnel alignment.

Much of the planned Eastside subway length was non-linear, and meant that tunnel reaches were often under commercial and residential properties – as well as city streets. Tunneling risks were "elevated" due to recent experiences and the added potential property impacts.

In part due to publicized events, Metro commissioned an expert Tunnel Advisory Panel to assess tunneling conditions in Los Angeles with respect to world-wide experience. The Panel concluded in November 1995 that compared to world-wide experience, geologic conditions in Los Angeles were generally more favorable, the cost of tunneling relatively low, and tunneling performance, based on surface settlements, was "slightly better." The panel recommended consideration of EPB TBMs for future projects (Eisenstein et. al., 1995).

Designers were already recommending pressure-face TBMs, and slurry TBMs exclusively, for the Mid-City alignment. In Mid-City, additional geotechnical investigations were evaluating subsurface gas conditions – which were found to be as high as those in the methane zone, and with the addition of high hydrogen sulfide (H2S) levels. Studies for Mid-City concluded that not only should the gas-bearing formations be avoided, but also recommended consideration of ground pre-treatment, such as use of an oxidizing agent, and that tunnel construction should proceed using slurry TBMs to further contain gases in pipelines until they could be treated at the surface.

The studies on the Mid-City segment became applicable to the Eastside Extension, as ground contamination was found in an industrial area west of the Los Angeles River. H_2S and methane were present which lead to specification of slurry machines for this reach only. For other reaches, the Contractor would be given an option for pressure-face technology (EPB or slurry). Soil-gas studies for the Eastside included pre-treatment of the ground.

Use of pressure-face TBMs would also reduce the potential for surface settlement – as compared to open shield methods. Given that the alignment was not consistently within the public right-of-way, many buildings would be directly over the tunnels. Designers evaluated over 200 structures near or over the tunnel and developed a comprehensive compaction grouting program for additional building protection.

2.2.2 *Linings*

In addition to precautions taken for tunnel construction in gassy ground, tunnel final liners had to be "gas-proof." The traditional two-pass system with expanded initial liners would not be acceptable with the use of pressure-face machines, since effective use of pressure-face tunneling also requires gasketed segments and grouting immediately after the rings are assembled. No precedent for one-pass liners in gassy ground was found, and Metro undertook further studies in 1997–98 to develop a one-pass liner with additional gas sealing properties.

This one pass liner consisted of a double-gasketed segment with convex radial joints – principally to "flex" during earthquakes so that the tunnel remained sealed from gas. A six-month, full scale, laboratory testing was conducted, at the University of Illinois, to evaluate tunnel structural capacity under seismic and ground loadings. Tests of gas leakage through gaskets were also performed. For another level of redundancy against potential gas intrusion, the final liner design also included a slightly oversized tunnel – about 15 cm on the radius, to allow for future placement of HDPE and additional concrete to secure it. As for the existing operating portions of the subway, Eastside Extension design called for continuous gas detection in the operating tunnels and additional emergency ventilation.

2.2.3 *Fault crossing*

During geotechnical explorations for the tunnel in 1996, geologists postulated that an escarpment (approximately 13 m rise in the ground surface over 200 m) actually represented a potentially active buried thrust fault. (A buried thrust fault ruptures at depth, and causes surface deformation (bending) but not an abrupt offset). Extensive geotechnical investigations were carried-out to estimate recurrence intervals and deformations – should a seismic event along this feature occur – and develop design criteria. Neither the tunnel nor the thrust fault are linear features, and the tunnel crossed the fault in three locations. At two locations, Metro designed a more flexible steel liner to accommodate movement.

2.3 *Politics and public perceptions*

Legislation, both federal and local, has impacted Metro System overall, and stopped the Red Line Eastside Extension as it was going to construction.

Overall system delays occurred after the methane explosion investigation in 1985, when the Los Angeles congressional representative amended the subway's funding bill to contain the provisions that tunnels would not be constructed in the methane zone. (A reversal of this legislation – given new technology (for example pressure-face TBMs), was approved 30 years later in September 2006).

Mainly due to some publicized events, including those briefly described in section 2.2.1, along with an economic recession, and the perception of construction cost over-runs, local legislation was passed by Los Angeles County voters in 1998, prohibiting use of local funds (the half-cent sales tax) on subway construction.

After discussions on funding and tunneling safety, Metro conducted a "re-structuring plan" and a "Regional Transit Alternatives Analysis" to evaluate available funding and fixed guideway alternatives to heavy rail for the three transit corridors – including the Eastside. The Alternatives Analysis and environmental process was repeated 1999–2002, with the preferred alternative for final design being light rail technology (LRT), for the most part at-grade, with a 2.7 km of tunnel and two underground stations. The LRT project, The Metro Gold Line Eastside Extensions (MGLEE) would extend an existing LRT, the Metro Gold line, from Union Station to East Los Angeles.

2.3.1 *Final design MGLEE*

The new alignment had some tunneling advantages in that it became aerial or at-grade west of the Los Angeles River and thus avoided highly contaminated areas. Much of the previous tunnel design could be used (pressure-face TBM specifications, double gaskets, etc.) with adjustments for LRT tunnel diameter. On the other hand, the relationship between the tunnel alignment and the escarpment changed, and additional geotechnical investigations were undertaken to evaluate station design, where one station was nearly parallel to the feature.

Final design included assessment of construction contract form and packaging, with consideration of bidder qualifications, possible incentives for performance, and use of the Design-Build (DB) contracting methods. Ultimately, the project was let in three contracts: an underground segment (station excavations and tunnels, by Design Bid Build (DBB)), the at-grade portion (including final station structures), and a bridge. The at-grade/station finish contract was DB. The underground contract was advertised first and separately, but was re-bid months later concurrently with the DB contract. Initial bid to award duration was over 18 months.

2.4 *Right-of-Way, permits and third party items*

The LRT tunnels were aligned more closely with the public streets, however, the street alignments, had some abrupt changes that could not be accommodated with TBM tunneling radii.

This along with some shallower reaches led to design of a grouting program for about 30 structures. Thus, in addition to property acquisition for the station sites, subsurface easement for the tunnels, and construction easements for grouting had to be obtained. Over 30 properties needed to be researched for title and negotiations with property owners etc.

2.5 *Funding*

Transit funds in the United States typically consist of Federal, state, and local money – and much competition between public agencies for available funds. To receive the funds, agencies must comply with various conditions; e.g. completion of Alternatives Analyses and the EIR, which involves a significant

public comment element. The MGLEE went through this process twice for the environmental documents, and was finally granted $490.7 million from the US Department of Transportation, or slightly over half of the estimated $899 million required for the project. Of this, approximately $200 million was estimated for the underground (DBB) portion of the project. The construction of both contracts was awarded to a Joint Venture (JV) of Washington Group, Obayashi and Shimmick, with the tunnels subcontracted to Traylor Brothers and Frontier Kemper JV.

2.6 *Construction*

Construction of the MGLEE project began in July 2004 with tunneling beginning in February 2006. At this writing, underground stations have been excavated and tunnel construction is about 70 percent complete. The EPB technology has performed better than expectations, as measured ground settlement has not exceeded 1.0 cm.

3 EAST CENTRAL INTERCEPTOR SEWER

ECIS is an 18.4 km, 4.7 m excavated diameter sewer that increases Los Angeles' wastewater infrastructure capacity. Construction was recently completed, and the new sewer was placed into full operation in August 2004. From any perspective, the project is considered highly successful. There were few construction impacts to the community, costs were within budget, and schedule slippage was managed. Nevertheless, the total duration from concept to completion was over 15 years.

The tunnel alignment runs west from the Los Angeles River east of Downtown, and generally stays under east-west oriented streets until it turns south onto La Cienega Boulevard. Finally, it turns west under the Baldwin Hills and connects to an existing Sewer in Culver City. Figure 3 shows the ECIS with respect to the Metro Rail System.

3.1 *Planning and environmental processes*

The City completed various planning studies for ECIS, including an Alternative Alignment analysis and an initial draft environmental impact report in the early 1990's. Opposition to the project from various neighborhood associations – objecting to construction disruption and potential sewer odors – caused the project to be placed on hold in 1995. The initial Environmental Impact Report was never completed.

"El Nino" rainstorms in the 1997–98 winter season caused the city's sewer system to overflow and major sewage spills. The State of California Regional

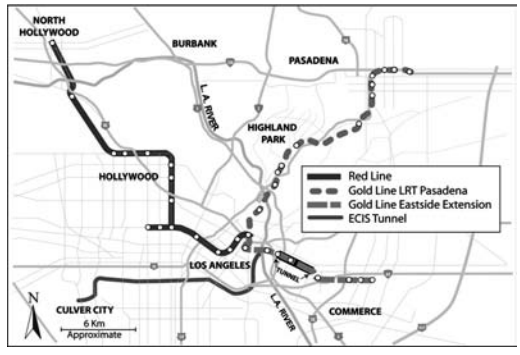


Figure 3. ECIS and existing Metro Rail Systems.

Water Quality Control Board took action and mandated the completion of the ECIS and six other sewer projects within a tight time schedule. Fines were established for exceeding the scheduled completion milestones.

A second EIR addressed concerns raised during the first Draft EIR. For this process, the City emphasized having community leaders endorse the project. There was still considerable community opposition to the project, but the City Council approved the Final EIR in November 1998. (City of Los Angeles, 1998).

The decision to tunnel the entire 18 km as opposed to using cut and cover methods was made during this planning and environmental documentation phase. An outcome was that drop structures had to be designed to divert flows from the existing collector sewers into the new ECIS pipe. The existing collector sewers averaged in depth around 7.6 m, and the invert for the ECIS tunnel averaged about 20 m.

3.2 *Design and technology*

The final design began in 1999 and took approximately 18 months to complete. There were several significant technical challenges for tunneling including minimizing ground settlement. This specific issue drove the City to specify pressure-face (EPB or slurry) TBMs. Discussions among designers and the City's Board of Consultants transpired as open shield technology could still be considered appropriate for much of the tunnel's reach, and cost savings might be realized. Ground was mostly very dense sand with clays and silts, above the water table, and generally considered ideal for the open shield. In addition, given the relatively small diameter, at over 15 m depth in many reaches, meant that predicted settlements would be within the 20 mm allowable presented in EIR. Ultimately, given the Metro experience and the raised public awareness of tunneling risks, pressure-face machines were specified.

3.3 *Bid and award of the tunnel contract*

Given this first use of pressure-face TBMs in Los Angeles, The City implemented a contractor prequalification process to ensure that only experienced tunnel contractors would be allowed to bid.

The project went to bid twice due to issues related to these prequalifications. In the first bid period, advertising began in March 2000. The second bid package advertised in September 2000 and was awarded to Kenny/Shea/Traylor/Frontier-Kemper, JV for $240.4 million in January 2001.

3.4 *Politics and public perception*

As described above for the MGLEE project, during the mid 1990's, there was a high level of public apprehension concerning tunneling in Los Angeles.

During this time, the City had investigated alternative construction methods including open trench construction, which initially appeared more cost-effective and would impose less tunneling risk. The advantages and disadvantages were raised with the community during the Environmental phase. The process resulted in demonstrating that the advantages of tunnel construction greatly outweighed the impacts caused by open trench methods. Public comments during the process also resulted in a change of alignment for the final design.

3.5 *Right-of-Way and protection of property*

Acquisition of shaft sites, laydown areas, temporary easements, and subsurface easements was a critical activity. The intent was to locate the ECIS under public right-of-way, but there were areas along the alignment where the sewer had to cross under private properties. For the 18 km tunnel, over 1,000 real estate transactions were performed including title searches, appraisals, negotiations, purchases, construction easements, and subsurface easements, and starting eminent domain proceedings.

This effort took over 18 months to complete, running in parallel with final design, as the Environmental Process requires that no real estate transactions be made until the Final EIR has been adopted.

3.6 *Construction of ECIS project*

The original construction schedule estimate was 3.5 years. During construction, there were several unforeseen events. These resulted in seeking a contract extension to avoid fines for late completion. The milestone date to place ECIS into service was changed from November 30, 2003 to August 30, 2004. Major unforeseen events impacting schedule included:

- Discovery of a Native American grinding stone
- Re-sequencing work at a work site to allow access to four homes
- Additional precautionary permeation grouting at selected locations
- Complex real estate transactions for acquisition of one shaft site
- Slower tunneling excavation rates

3.7 *Funding*

The project costs were paid through the City's Sewer Construction and Maintenance Fund, and a State of California Revolving Fund that loans to water agencies.

Documentation required by the State for loan eligibility included:

- A Value Engineering study
- Minority/Women/Other Business Enterprise quarterly reports
- The City's water conservation plan
- Draft revenue program
- Project performance certification after one year of operation

3.8 *Changes in the duration of the project*

To offset the delays caused by the unforeseen events, various activities were accelerated. Some of these included:

- Awarding the contract before all right-of-way was acquired: The City assumed a risk of property not being available
- Specifying a fourth TBM
- Acquisition of additional land for a second pipe laying operation
- A 6-day workweek with two 10-hour shifts
- Change to a prefabricated pipe at one drop structure – in lieu of a concrete cast-in-place option

4 CONCLUSIONS

For tunnel projects in urban areas to be built in a reasonable time frame, planners and designers must expect and plan mitigations for interruptions in the project schedule due to environmental issues, funding, and the bid process as well as develop technical solutions for design. From these examples alone, we see that major changes are not uncommon as a result of the Environmental Studies and public comment.

Planning, design and construction of major infrastructure projects in urban environments requires many years and is costly. In planning, the agency must also use demand projections that look 50 to 100 years into the future to maximize the value to the public. The examples presented here are a clear indication of

the long-term effort associated with providing a very much needed improvements to the communities they serve.

REFERENCES

City of Los Angeles, 1998, North Outfall Sewer-East Central Interceptor Sewer, Draft EIR, S1-38.

Eisenstein, Dan, et. al, 1995, Los Angeles County Metro Rail Project: Report on Tunneling Feasibility and Performance: 1–4.

Los Angeles County Metropolitan Transportation Authority (Metro), 2004, Final Environmental Impact Report, Los Angeles Eastside Corridor, S1-37.

US Department of Transportation (USDOT), Federal Transit Administration, 2002, Record of Decision; Los Angeles Eastside Corridor.

This page intentionally left blank

Underground Space – the 4th Dimension of Metropolises – Barták, Hrdina, Romancov & Zlámal (eds)
© 2007 Taylor & Francis Group, London, ISBN 978-0-415-40807-3

Geological and geotechnical conditions in underground structures design of Rome subway: the B-Line extension

R. Enrione, A. Eusebio & L. Soldo
Geodata S.p.A., Turin, Italy

R. Funiciello
Universitá degli Studi Roma Tre, Rome, Italy

L. Solimene
Comune di Roma – Dipartimento VII, Rome, Italy

ABSTRACT: Underground works, in complex urban areas, can present prominent levels of risk connected with various ambits: low overburden, buildings facing the line, interference with acquifers, soil of poor geotechnical characteristics, presence of man-made cavities. The knowledge of the geological – technical context is the first and inevitable stage of study, for the development of an underground construction project, by which it is possible to achieve a high level of sensibility about the underground space and to propose mitigation measures for the risks associated, both during the construction phase and during exploitation. The case of Rome subway B-line extension is presented, where a rigorous procedure, involving geotechnical investigations and consecutive phases of study, has been applied both for the preliminary design and for the construction phase (PAT – Protocol for Advancement of Tunnel excavation). The illustrated approach has been consolidated from the experience of many similar completed projects, and has become a standard practice.

1 THE WORK AND THE TRANSPORTATION SYSTEM OF ROME

1.1 *The "Mobility System" of Rome*

The transportation planning of a city like Rome presents a high level of complexity and requires the choice of strict planning tools.

The "Mobility System", drawn up and approved by the local administration, is the reference programmatic document, in which the different existing transportation networks, the actions for their development and updating find a rational placement and harmonization.

According to the "Mobility System", the subway network proves to be a necessary means of transport, which is able to connect, in a rather short time, the highly populated areas of the suburbs to the city center. This aim is being further developed, as shown in the ambitious enlargement plan (Fig. 1).

1.2 *The subway B-line extension*

The B-line extension project coherently fits in the above described mobility scenario, enabling the old line to settle close to the existing ring-road highway (Grande Raccordo Anulare, GRA) and thus representing an important nodal exchange (Fig. 2).

The B-line extension includes 3 km of new line, 3 intermediate stations and a new depot. In this way, the San Basilio, Torraccia and the new Casal Monastero districts will be served for the first time, with the view of a contextual requalification of their urban and social context and also installing new services.

From a technical point of view, the new metropolitan section will be realized entirely underground, with excavation between retaining structures and below the cover slab (top-down method). This will allow the surface conditions to be restored quickly, limiting the disturbance to the public to a relatively short time and ensuring the separation of underground works from ordinary daily activities.

1.3 *The assignment*

The engineering services, necessary to the preliminary and definitive design of B-line extension, has been assigned by the local administration (Comune di Roma) to the group of companies composed of C. Lotti & Associati, Geodata, Siteco and A2G.

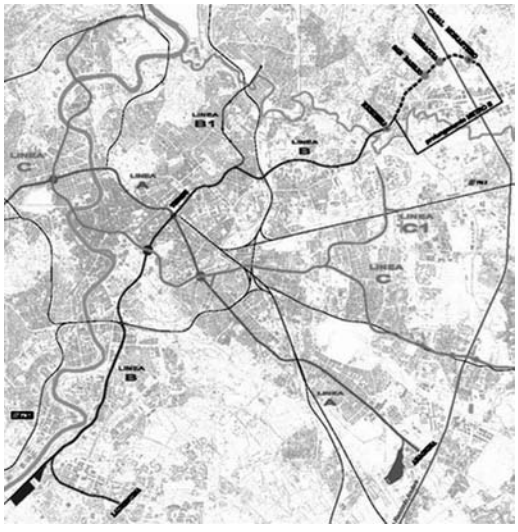


Figure 1. The subway network enlargement plan and the location of the B-line extension.



Figure 2. The B-line extension design in the Casal Monastero area.

2 TERRITORIAL CONTEXT, POSSIBLE DIFFICULTIES AND BASIC PHILOSOPHY

The project of the new subway section had to face many difficulties, connected to the insertion of the works in the already complex territorial context of reference, due to specific technical uncertainties, which were pointed out since the very first planning stages, as being associated with an initial level of high risk.

More specifically, the major difficulties were proved to be directly or indirectly connected to the geological-technical context that consequently assume high priority on the design agenda, even before specific studies and geotechnical investigation took place.



Figure 3. Collapse of a cavity in Rome (Via Bricci).

The most important uncertainties, directly connected to geological-technical context, are the following:

- type of soil intercepted by the excavation, with highly variable level of cementation and poor geotechnical characteristics;
- presence of an unconfined aquifer at the tunnel level and possibly other deeper aquifers, even in pressure;
- verified presence of man-made cavities in the site, single or complex ones, also of big size (Fig. 3).

The most significant aspect indirectly connected to the geological-geotechnical context is the presence of many buildings along or facing the line of the work.

It is therefore clear that the full knowledge of the geological-technical context is an indispensable prerequisite for the design. This is not only for normative reasons or design completeness (as often required today), but also for the management and mitigation of the risks during construction.

This is especially effective if performed since the very first steps of a project, that is since the Preliminary Design, when specific studies and geotechnical exploration can be successfully used to reduce uncertainties while work's structural designing can be directed at best.

This process will ensure the most effective definition of:

- risks connected to the construction, with reference to the design;
- functional level provided by the line;
- resulting economical and financial schedule.

The value of this approach can further increase once extended to the construction phase by a constant monitoring of the excavation parameters and by the analysis of the work's actual conditions (PAT Method: Protocol for Advancement of Tunnel excavation, Grasso et al. 2002a,b). These are strategic activities for the risk management and its mitigation, as they ensure a

real-time comparison between the design scenario and that encountered during construction.

The B-line extension of Rome subway, designed with a deep awareness of the above described philosophy, well illustrates the Geodata's methodological approach.

3 THE METHODOLOGICAL APPROACH

The methodological approach followed for the design of the B-line extension is based on a well defined succession of phases; each phase was established on the results of the previous one. In this way a sequential "cascade" process was introduced, by which the activities of every single phase proved to be efficiently rationalised (in terms of quantity, typology and costs) as systematically addressed by the issues of the prior phase (Fig. 4).

The process, by favouring a constant comparison with the Owner, benefited from the contributions of the whole project management team, thus permitting a better definition and management of risks.

In the following pages the method outline will be described and subsequently account will be given of the level of knowledge that has been reached by its application.

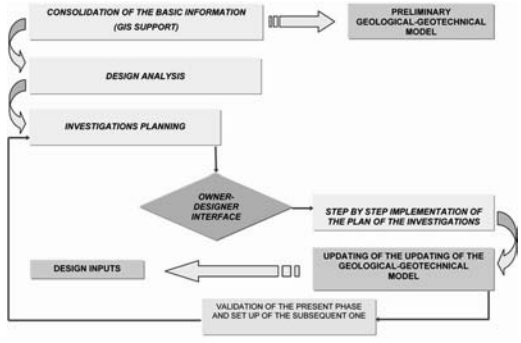


Figure 4. Methodological process flow-chart.

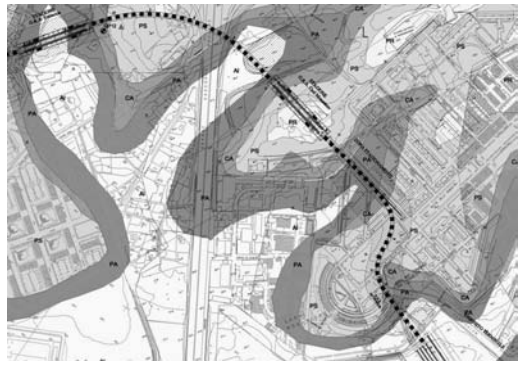


Figure 5. Extract of the Geological Map: actual alluvial deposit (hatched bright zone) and volcanic sequence (hatched grey-scale zone).

3.1 *Consolidation of basic information and preliminary geological-geotechnical model*

The first phase of the process is the collection of all the information and data concerning the geological-geotechnical context, that were available since the Preliminary Design started off. They are: general bibliography, available stratigraphic evidences, technical studies and previous design documentation (in particular, Feasibility Design). This first phase proved to be a strategic one, because it led to an immediate awareness of the context in a very short time.

Technical and reconnaissance surveys were also performed, so that the gathered information could be set in its proper context and the knowledge of the "geo" scenario could be further investigated in a rational way, minimizing the impact on the urban activities and reducing time-cost for the geotechnical exploration.

A platform of GIS (Geographic Information System) was prepared for ground data filing, consultation and real-time updating.

It should be noted that in complex areas, such as Rome, with buried channels and erosion forms, complex lateral eterophies between alluvial and volcanic sediments, etc. reliance must be placed on engineering geological interpretation of available information, prediction on the basis of known geological relationships and careful interpolation and extrapolation of data.

For this reason inside the investigations for the design of Line B the value of the geological surveying phase and the presence in the geological and geotechnical design team of specialist in Structural Geology and Sedimentology were emphasized: also in urban areas, with limited rock and soil outcrops the "geological survey" (improved in this environment with trenches, shafts and other indirect data) made it possible a correct interpretation of the results obtained from the deep investigations. At the end of the first phase a preliminary geological-technical model was defined, substantially represented by a geological map (Fig. 5) and by the corresponding profile along the axis of the work.

3.2 *The project and the plan of site investigation*

After the "geo" context was defined, even if preliminary, the design phase started off; its development took into account the potential risks that had emerged in the previous stage. The hypothesis of the project was since the beginning aimed at reducing risks of the construction phase.

In parallel, once the uncertainty margins of the "geo" context were determined, a specific investigation plan was developed and validated by the Owner; it included different steps: geophysical (Stage I) and geotechnical ones (stages II and III).

3.3 *Update of the geological-geotechnical model*

Once the investigation steps I and II were performed, a first update of the geological-technical model followed, based on which significant design indications to manage risks were given.

4 PRELIMINARY GEOLOGICAL-GEOTECHNICAL MODEL

In the following paragraphs the results of consolidation of the basic information will be showed, with reference to the geological-technical investigations. The analysis of every ambit of study ended up with the characterization of the difficulties connected to the construction, on which the subsequent investigation steps was planned.

4.1 *The geological scenario*

The area of interest is located inside the Thyrrhenian margin of Apennines. Its complex geomorphic, stratigraphic and structural elements can be traced back to the geodynamic evolutionary characters of the Apennines chain of the late Pliocenic-Quaternary period (Ventriglia, 2000).

Above the oldest carbonate levels, not relevant for the design, terrigenous sandy-clayey sediments of Pliocene can systematically be found (Argille di Monte Vaticano, Marne Vaticane, Argille azzurre). These units act as substrate of reference for the subsequent elements. Over them, pre-volcanic alluvial deposits occur (Unità di Santa Cecilia), consisting of gravel, clay and sand, organized in complex stratigraphic relationship.

The pyroclastic sequence that follows is of a later age and is linked to the past explosive volcanic activities, which are characterized by old altered tuffs (from Unità di Tor de Cenci to Successione di Sacrofano), pozzolane (Pozzolane Rosse) and lithoid tuff (Tufo Lionato). Finally one can find the actual alluvial sediment and the more recent man-made filling, often remarkably thick.

Considering the complexity of the stratigraphic features, a geophysical and geotechnical investigation was necessary to reorganize the geological elements concerning the project.

4.2 *Geomorphology and underground cavities*

The area is characterized by the presence of river Aniene's right tributaries, which flow in relatively deep



Figure 6. Cavities found along the line with buildings above (Pietralata area).

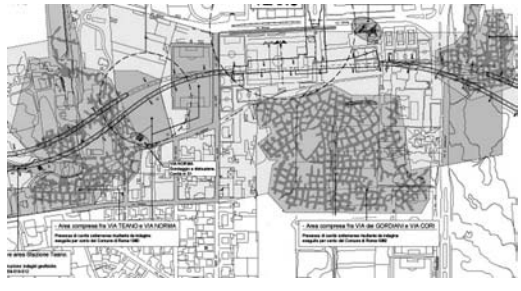


Figure 7. Map of cavities surveyed (hatched grey zone) and risk of being intercepted.

flat valleys, whose sides have often been changed by extraction activities. Old or current instability phenomena are not visible, neither along vertical caves faces, because of the good technical characteristics of the volcanic soils.

In the concerned area underground cavities can occur; they can be caused by the extraction of lithoid tuff (Tufo Lionato) and Pozzolane Rosse, especially in the areas of S. Basilio and Casal Monastero, where the great thickness of the volcanic units favoured the extractions (Fig. 6).

Single and isolated cavities can also be found everywhere, especially inside the pyroclastic sequence; they were generally excavated to function as a well or water storage tank.

Since the beginning, the identification and mapping of man-made cavities proved to be a necessary step, both for technical (difficult realization of support works and excavations) and for safety reasons (buildings near the excavation areas, underground utilities networks, etc.). This activity was performed through surveys, within the planned site investigations, systematically integrated with the GIS platform (Fig. 7).

4.3 *Geotechnical and hydrogeological issues*

The involved lithologies show a high degree of heterogeneity in terms of mechanical characteristics and cementation, in particular:

- pre-volcanic alluvial sediments show prevalent silty granulometry, low density and high water content; occasionally cemented levels. Generally they present poor mechanical characteristics (both resistance and deformability);
- pyroclastic sequence shows a stratified aspect, with alternation of altered (incoherent, mechanically poor) and competent (lithoid tuff) levels;
- actual alluvial deposits show clayey-silty granulometry, good plasticity and high deformability;
- man-made fills present a highly variable granulometry, with incoherent behaviour.

Some potential, major, construction consequences derive from this complexity: for example, the presence of lithoid levels makes difficult the excavation with traditional tools, as well as the possible escape of bentonite-slurry used for the excavation of retaining walls.

A detailed geotechnical investigation was therefore necessary, in order to examine every encountered lythology, both in situ and in laboratory.

The potential hydrogeological problems can be related to underground water at the level of the design (interference with excavations and supporting works, dam effect, hydraulic overpressure); possible deterioration of the setting by underground cavities.

To manage risks at best, all the drillings were provided with stand-pipe and Casagrande type piezometers, for a continuous monitoring of piezometric levels.

5 THE SITE INVESTIGATIONS

5.1 *Step I – The geophysical investigations*

The first step of investigation was performed by combining geophysical surveys of georadar and geoelectrical methods, developed along work's longitudinal axis; the results were reciprocally merged for a better resolution. Site calibration by the selected methods was conducted, accomplished by two field-tests focused on searching for man-made cavity.

Geoelectrical tomography (multi-electrod with spacing <3 m) highlighted resistivity values of 50–200 Ωm for the top layers (pyroclastic sequence) and lower values for the deeper layers, 5–50 Ωm (prevolcanic alluvial deposit, completely saturated). No significant cavity was detected.

Two resistivity anomalies were identified in the prevolcanic alluvial layer (400–600 Ωm): subsequently tested with boreholes, they turned out to be portions of a very loose soil, partially washed out by groundwater flow (Fig. 8).

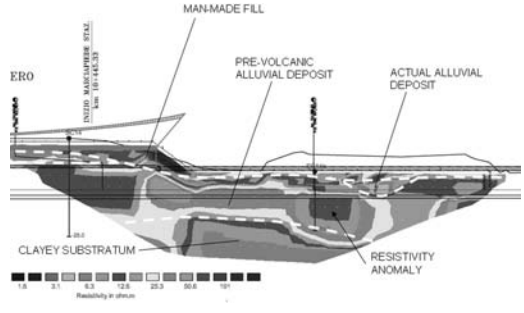


Figure 8. Geophysical section with resistivity anomaly identified, subsequently investigated with test boring.

A multi-array georadar survey was then carried out, for a multiple frequency scanning of the underground context. At first, frequencies at 100–200–600 MHz were adopted, with a lower penetration but higher resolution. Later, an ultra-low frequency antenna was used (25 MHz) for not build-up area only, where no disturbance-factors should be present for the radio signal. Its maximum penetration reached 10 m.

On the whole, the georadar survey has highlighted a complex network of underground utilities as well as the stratification of the upper portion of the pyroclastic sequence.

5.2 *Step II – Geotechnical investigaion*

According to the findings of the previous step, a first geotechnical investigation was conducted, with core borings and laboratory tests: geophysical anomalies was directly explored as well as the most interesting areas.

In total, 27 test boreholes were drilled, all of which provided with piezometers (open stand-pipe or Casagrande stand-pipe, occasionally coupled in the same borehole, for simultaneous logs of different aquifers).

SPTs, Lefranc, Lugeon and pressiometer tests were systematically performed in the boreholes, for a better definition of the geological and hydrogeological context.

5 piezocone tests (CPTUs) were carried out on the alluvial deposits.

Ultimately, for archaeological reasons, 9 additional borings were drilled around the presumed-ancient building of Casal Monastero.

6 UPDATING OF THE GEOLOGICAL-TECHNICAL MODEL OF REFERENCE

At the end of the process the preliminary geological-technical context (Fig. 9) was updated (Fig. 10).

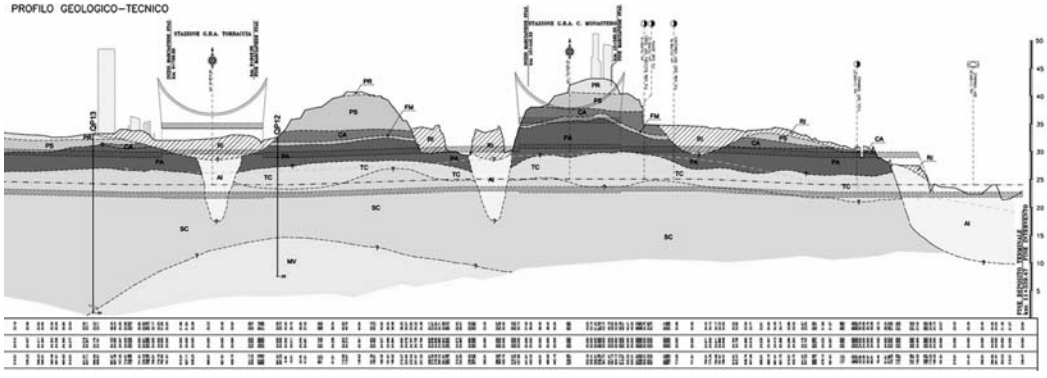


Figure 9. Profile of the preliminary geological-technical model.

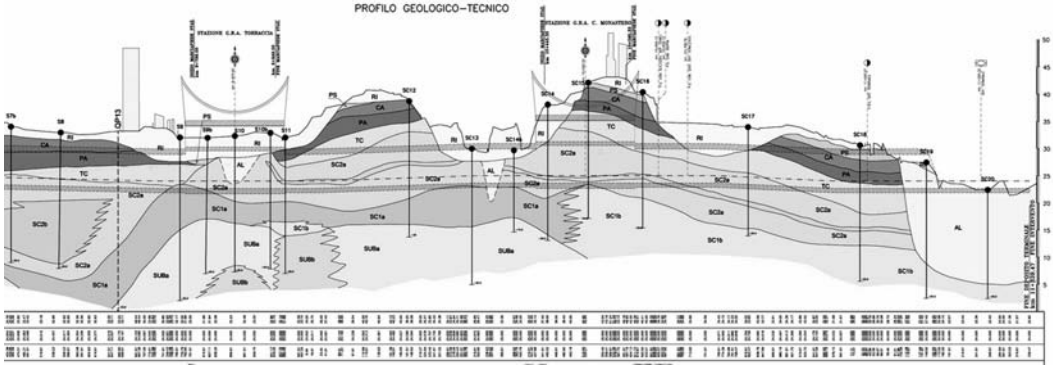


Figure 10. Profile of the updated geological-technical model.

The higher level of details permitted a considerable reduction of the uncertainty margin as well as risks associated with the construction of the subway extension.

In parallel, the GIS archive was kept up to date, with a final reconstruction of the geological-technical model, through 3D rendering.

7 CONCLUSIONS

The proposed method has shown how a rigorous protocol of study, rationally developed, could permit a timely identification of the critical aspects for the design, the further studies and management of these critical aspects in the design process, till the selection of the most appropriate typological solutions for minimizing the connected risks. This has been implemented step by step, with an easy-to-follow-again methodology, both by the Owner and by the Designer.

The whole process was followed by the continuous development of the geological-geotechnical model in GIS environment. This activity will proceed in the further design stages and will be completely accomplished in the construction phase, with the implementation of the PAT protocol that will en-sure the management of risks and any unforeseen situations through the most efficient counter-measures, predefined in the design stage.

REFERENCES

Funiciello, R. & Giordano, G. 2005. Carta geologica del Comune di Roma.

Grasso, P., Chiriotti, & Xu, S. 2002. Riduzione e condivisione dei rischi residui associati allo scavo di un tunnel meccanizzato in ambito urbano attraverso l'uso di un protocollo di avanzamento. *Convegno Nazionale di Geotecnica, L'Aquila*.

Grasso, P., Mahtab, M.H., Kalamaras, G.S. & Einstein, H.H. 2002. On the Development of a Risk Management Plan for Tunnelling. *28th ITA General Assembly and World Tunnel Congress, Sydney*.

Ventriglia, U. 2000. Geologia del territorio del Comune di Roma.

Underground Space – the 4th Dimension of Metropolises – Barták, Hrdina, Romancov & Zlámal (eds)
© 2007 Taylor & Francis Group, London, ISBN 978-0-415-40807-3

Ontologies, thesauruses and information systems for tunnels

N. Faure
SOLEM France, Archamps, France

ABSTRACT: Usefulness of glossaries has not to be proven in the tunnel conception environment. However, glossaries are limited to simple lexical information; semantical information could be interesting to add for multiple uses.

Ontologies allow this addition, along with reuse and easy implementation in a computer system. This paper aims at showing what is an ontology and how it could be built for the tunnelling community. By the tunnelling community, too, for one of the main backdrafts of "classical" information systems ontologies are their high level of technicity. Some ways of avoiding this problem are proposed.

As an illustration, ontology-driven projects are presented with their application and first results. One of the most promising of these projects, more precisely described, combines rule-based knowledge representation and ontology to allow expert-supervised and semi-automatic compliance of a tunnel project to a set of norms or recommendations.

1 INTRODUCTION

This paper deals with some considerations about knowledge management for tunnels. It features at first some elements about terminological knowledge and existing tools, as it is true that "knowledge representation begins with words" (Sowa, 2001), then it unfolds some considerations about the adaptation to other tools (ontologies) for the tunneling community.

What is presented here is a point of view built from the early experience given by various existing or under development projects of knowledge representation and management for the tunneling community. These projects are intended to give tunneling experts and specialists assistance during the course of a tunnel-related work (types of said works varying with individual projects). They are mainly computer systems conceived to be complementary with existing computer tools (which deal mainly with graphics and mechanical calculus).

2 A VARIETY OF TOOLS

When it comes to collecting words, one think to indexes (a collection of words) or glossaries (an index, associated with definitions). But there are more tools than just indexes and glossaries. Let's have a quick look at them:

– a **taxonomy** is some kind of index, organised along some hierarchical guidelines. Taxonomies are often built along the specialisation/generalisation guideline (specialisation: from rock to metamorphic rock to granite; generalisation: the other way – from granite to rock). This induces some limited semantics, even if this can be constrained to the terminological field with the hyponymy/hyperonymy relations (narrower/broader term). Taxonomies can vary, however: they have often one type of relation only, but may also feature other relations – meronymy (part-of relations) is often chosen. In our example, Rock has a narrower term, Granite, which has some components (Quartz, Mica, Feldspar).
– taxonomy introduces some semantics, but do not take well into account the alternative uses for some words (polysemia). This is where the **thesaurus** intervenes, which features, as in a glossary, definitions, and as in a taxonomy, hierarchical relations; but also similarity relations ("see also", "related terms") – which can be used for figuring polysemia, but for other information retrieval goals as well (e.g. finding Music from Rock).
– thesaurus deal not only with terminology (defined here as the collection of terms and their meaning), but dabble also with semantics (defined here as the relationships between various meaning of one word – or group of words). The step beyond is **ontology**. Originally borrowed from philosophy (where the term stands for "the study of what is in being"), ontology has been used in the information systems field from the early nineties. To most people, ontologies are gigantic thesauruses, and indeed they are, but they are more systematic than thesauruses: they depict the knowledge domain,

while the thesaurus is limited to information retrieval.

The next part of this paper expands this last point and describes ontologies, in their diversity and in their uses.

3 ELEMENTS ABOUT ONTOLOGIES

A quick explanation of what is an ontology could be its most famous definition, given by Gruber (1993):

"An ontology is the specification of a conceptualization".

In other words, and at greater length, ontologies rise from another problematic entirely than thesauruses: the matter with ontologies is: "how to describe synthetically the knowledge about things?" The second thought behind this one being, of course: "and use this knowledge for some computer-assisted task". So, conceptualization is a set of objects and constraints between these objects which represent what is known about the field these objects belong to. But, as the whole thing is about knowledge, and knowledge does not belong to the physical world, but is rather applied to it for understanding, these objects are concepts. And as concepts are fundamentally ideas, something of the mind, they are expressed by words. (There is need here for a lot more theoretical explanation, but this should be quite off-topic).

It explains, then, why thesauruses and ontologies look strangely familiar: they are both made of words and relations; it explains also why they are essentially different.

But then, there is the specification part.

3.1 *Models and concepts*

Building a structure for concepts, terminological considerations being irrelevant, is another matter entirely than building some reference structure for general ideas (although this is a quite arduous task, either). This is where models come.

Models are, simply put, some "strategy of irrelevance", which means that it is the result of a choice of objects and relations relevant in a given context, and the deliberate exclusion of every other.

This way, models are everywhere. The "simple" glossary begins with a simple model, for it has a theme, it concentrates on a set of words relevant for a domain; and our geotechnical thesaurus can be rid of the junction between Rock and Music, and Music itself – as Music is irrelevant in a geotechnical context. This is called a "domain", a field of knowledge. The ontologies we discuss here are domain ontologies (some ontologies are deemed global, but their use and "tuning" is very uneasy).

Conceptualization, then, is also a modeling, and as such do not differ greatly from the simple models except that it is formally specified (although this is sometimes discussed). Which means that a simple, natural-language definition of a concept is not sufficient for this concept to be formal: it needs more depth, a definition relatively to other concepts, and a sign (say, a word) exclusively attached to it.

As a result, the concept appears as a category: the set of all things in being that matches its definition. This definition being itself a set of attributes, which are, in turn, concepts of their own right elsewhere in the ontology. This is an old logical approach, but it works quite well with the object-oriented languages of computer science and their logical counterparts (currently, the OWL language is becoming popular for building web-based ontologies).

What does all this imply for tunneling?

3.2 *An ontology of tunnelling*

From what have been said about ontologies, we can conclude rightly that an ontology is essentially context-dependent, or at least model-dependent.

Research has recently evolved towards a multi-modeling conception of ontologies, which means that multiple models can co-exist in an ontology. This is done, more or less, with what can be called "point of view" approaches: for example, one point of view sees the road as a surface where traffic evolves according various parameters, another sees the same road as a concrete layer upon a compacted patch of soil, in which water infiltration has to be minimal. For the same concept "road", attributes and distribution of these attributes is different – modeling is different.

This could be an interesting way of building ontologies in such a diversified field as tunnels-related activities (even considering narrower ontologies such as tunnel construction, tunnel maintenance, safety in tunnels, etc…).

However, much of these point of view approaches still depend on a broader model – extremely arduous and painstaking to obtain in the case of geotechnics, as it needs a broad consensus and a formal definition of every item (which, due to the probabilistic nature of everything soil-related, is quite impossible to obtain).

It should therefore be interesting to build a specific model for each tunnel case, from a knowledge base or another kind of existing data, but without relying on a previous, global model.

That is the point of the RAMCESH project and affiliate projects, led by the SOLEM France society.

3.3 *Induction rather than deduction*

More in line with case-based reasoning (CBR), a new approach for building ontologies is considered: a global formal model is not the starting point, but the end of ontology building, resulting from the

combination of various specific, rather incomplete, models.

These incomplete models ("pieces" of models) are fairly common in the geotechnical literature: observations of some precise material behavior, general consideration about a technical implementation, etc…

These pieces of models, represented in some proper formalism (which should be quite simple and manageable by other than computer scientists), are then combined according to some project considerations in a broader piece of model, and so on until a coherent and rather exhaustive model is attained.

Of course, this type of combinational model has the risk of being not so exhaustive, for every piece of the ideal project model does not exist in the literature, or rather in the knowledge base built from the literature.

But remember: this is a computer-assisted system that we discuss here, not a computer-based tunnel project builder. This approach needs domain specialists and experts for more than supervision, but also for exploitation of the results. And better for them to "fill the blanks" in a model than to build this model from scratch.

In the RAMCESH project, those pieces of models are named "knowledge grains" and use informal concepts; the concepts gaining increased formality by being combined with other grains.

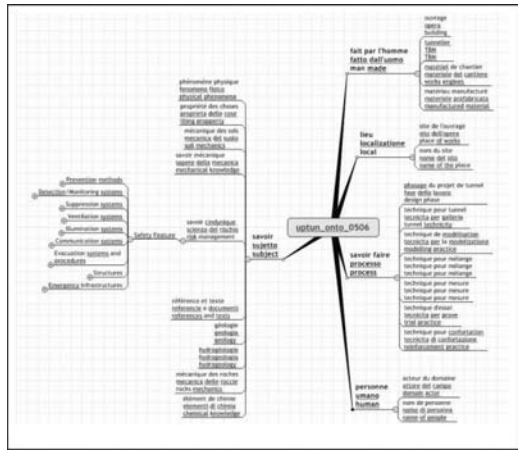


Figure 1. An overview of top-level UPTUN-Onto concetualization.

4 ONTOLOGY: TUNNEL-RELATED USES

The general use for ontologies is communication (Uschold & Gruninger, 1996): communication between people, systems and/or organizations.

For example, ontologies are at the center of what is called the Semantic Web, which aim is to allow "intelligent research" among the Internet – or more specialized networks. The ontologies used or planned in the tunneling community have this same aim.

The CONFEC7 project, for example, is aimed at building an ontology from the normative knowledge contained in the Eurocode 7 (the new European norm about geotechnical calculus); from this point on, every geotechnical project (expressed in an appropriate formalism) can be easily reviewed according to this knowledge, and estimated compliant or not to the norm.

UPTUN is an European Community project focused on the upgrading of safety in tunnels. One of its parts uses an ontology, which describes the various security systems and the way they interact. According to some user-provided data (through various forms describing intended safety modifications), it describes the way safety evolves in a tunnel.

Aforementioned RAMCESH project (from which CONFEC7 project is derived) focus is to give specialists the opportunity to develop their tunneling projects according to some literature-supported specific theories, then to automatically compare the way they have conceived the project with other projects, stored in memory or conceived by other specialists.

Other uses considered in these projects and others include tendering (roughly, estimating prices and delays from the description of a tunneling project) or day-to-day survey of field works and panel of optimized choices according to the results. More documents-oriented applications are possible, too, as the automated indexation of documents (this is a direct semantic web application), but they only indirectly imply tunnels.

One subject of difficulty when building such tunneling ontologies is that it is quite time-consuming for experts to build ontologies. And as tunnel experts are required to build tunnels and not ontologies, this is a major problem. To address it, the general choice made in the tunnels-related ontologies projects mentioned before has been to develop network solutions and sequential procedures to allow various experts to implement the system easily, and not necessarily during long working sessions.

This choice is also related with some conclusions drawn from the expert systems experience for tunneling activities of the eighties-nineties: the implication of the domain experts in the implementation of such knowledge-based systems must be maximal (Magnan, 1992). Formulation and, foremost, use of knowledge must be an expert domain prerogative: the reasoning process of such systems must be expert-driven, not computer-driven (hence, the computer-assisted bias mentioned in chapter 3.3).

This leads to such approaches as UPTUN-Onto or the RAMCESH ontology construction system,

oriented to increased user-friendliness, for the ontology user and builder is the tunnel expert.

One more important point about ontologies when oriented toward such a large and international community is that they have an edge regarding multilingual possibilities. Being conceptually modeled, ontologies are virtually language-independent, i.e. concepts and their relations are the same, only their designation change. This point is discussed in the case of cultural facts, but for the main part, tunneling ontology (featuring physical concepts) should be culturally independent.

Computer-wise, ontologies are fairly portable, as they rely on current and easily accessible technologies, mainly XML and XML-related languages and formalisms (RDF, RDFS, . . .). Therefore, it should not be a technical burden to any organization's computer division to deploy such systems.

5 CONCLUSION

The few applied experiments – that we know of – of ontology development for tunneling uses have shown some merits and drawbacks. Merits concern the very nature of ontologies: terminological and conceptual models in a same portable system, high adaptability to network and distributed contributions, modularity in modeling process. Drawbacks are often directed to the computer-system dimension of ontologies: languages and logical approaches far too uncommon for the tunneling engineer and high degree of formalism required where it is not always possible.

However, these drawbacks can be dealt with, as illustrated in this paper with some current projects and theories.

In fine, ontologies are quite adaptable to the tunneling environment and community; regarding the past trials of glossaries and indexes for the domain, it would certainly be profitable to build such reusable models, for both terminological and conceptual motives.

REFERENCES

Faure, N., *Représentation des connaissances géotechniques*, Proc. Conf. Inforsid 2006

Gruber, T. *A Translation Approach to Portable Ontology Specifications*. Knowledge Acquisition, 1993

Khoury, G., Majorana, C., *European action on fire safety in tunnels*, World Tunneling, 2004

Magnan, JP., *CESSOL: Bilan du Développement d'un Système-expert*, in Geotechnique et Informatique, Proc. Int. Conf. on Geotechnics and Computers, Presses de l'École Nationale des Ponts et Chaussées, Paris, 1992

Magnan, JP., *L'organisation du travail en géotechnique: développement, normalisation et artisanat*, Lettre de la Géotechnique 26 et 27, Société Internationale de la Mécanique des Sols et de la Géotechnique, 2002

Sowa, J., *Knowledge Representation*, Brooks/Cole, 2001

UPTUN Project, www.uptun.net

Uschold, M., Grüninger M., *Ontologies: Principles, Methods and Applications*. Knowledge Engineering Review, 1996

Underground Space – the 4th Dimension of Metropolises – Barták, Hrdina, Romancov & Zlámal (eds)
© 2007 Taylor & Francis Group, London, ISBN 978-0-415-40807-3

Building the underground infrastructure of Lausanne's new m2 metro line

F. Gaj & M. Badoux
Métro Lausanne – Ouchy SA

ABSTRACT: A new subway line is under construction in the city of Lausanne, on the shores of Lake Geneva in Western Switzerland. Called "*projet m2*", it is designed for an annual capacity of 25 millions passengers and is scheduled to open in late 2008. It will offer a new "urban elevator" to a city characterized by its steep slopes. The trains of the new fully automatic "driverless" transportation system will feature rubber tires allowing them to climb slopes averaging 6% and reaching up to 12%. It will be the first automatic metro to cope with such steep gradients. About half of the 450 mios Euro project budget will be spent on the 6 km long new infrastructure. It includes approximately 2.9 km of new tunnels, 2 km of new cut-and-cover tunnels, 0.5 km of old tunnels to be renovated and 14 stations. The construction of six separate tunnels in parallel was required to respect the very tight construction schedule and to respond to the varying geological conditions. The engineers and contractors face difficult technical and logistical challenges as these tunnels are excavated at low depth in a dense urban environment. This article will give an overview of the complexity of the project, including different excavation techniques, as well as the point of view of the Client regarding its role in the project managing process.

1 SUSTAINABLE DEVELOPMENT

A new subway line of Switzerland is being built in Lausanne, Switzerland. With a population of about 250'000, Lausanne is a relatively small city for a fully automatic subway system. The ambitious project, named *projet m2* aims at boosting public transportation in a city characterized by a difficult topography and a growing traffic problem. The project received broad public support in November 2002, when the local state population accepted the proposed project funding (overall budget of 450 mio €). Construction work started in spring 2004 and commercial service is scheduled for the second half of 2008. Key project data are presented in table 1.

Covering a distance of approx. 6 km (fig. 3), the m2 line will link the Geneva Lake shore at 373 m.a.s.l. with the suburb of Eplinges at 711 m.a.s.l. (i.e. 338 m higher, which explains the origin of the "urban elevator" expression). Fourteen stations will be distributed along the alignment.

6 km in 20 minutes
1 train every 3 minutes in the central portion
6,600 persons per hour
25 millions persons per year
37,000 jobs at less than 300 m from any metro station
6,000 cars "removed" from the city center

Figure 1. *projet m2* performances.

2 TUNNELLING CHALLENGES

From the "tunneling" point of view, the *projet m*^{2} has been characterized by some challenges requiring the engineers and contractors best performance.

Although most of the m^2 tunnels are at a "standard" low depth of 15–25 m in a relatively good rock (the swiss "molasse", composed by an alternance of sandstone and marls), some segments are very shallow and, sometimes, in weak water saturated soils (sands and gravels).

The most interesting examples are:

- Saint-Laurent tunnel: excavation beneath the traditional masonry bridge "Grand-Pont" (fig. 2).
- Langallerie tunnel: excavation through sands, gravels and silts, 3–4 m under the foundations of Rue Langallerie buildings (fig. 4).
- Viret tunnel: excavation at less than 1m beneath the foundations of the Rue Madeleine buildings (fig. 5).
- Bugnon tunnel: excavation through sands, gravels and silts, less then 1 m beneath an existing tunnel connecting two buildings of a large hospital.

Two others objects are worth mentioning.

The first one is the construction of a new bridge (Pont St-Martin) through the piles and abutments of an existing century old masonry and steel bridge (Pont Bessières, fig. 6).

Due to topography of the city, a bridge was necessary to connect two areas separated by a deep valley.



Figure 2. Saint-Laurent tunnel. Note the passage under the 19th century "Grand-Pont" masonry bridge.

Instead of creating a completely new bridge that would have difficulty to integrate in the urban environment, the designers chose boldly to place the new bridge just below an existing one (fig. 6). The technique adopted to excavate through the piles of the existing bridge (with no interruption of bridge traffic) is a mix of structural engineering and underground technology consisting in:

1. reinforcement of the piles by longitudinal and transversal pre-stressed cables and passive anchors in order to bring confinement to the remaining pile material around the void to be created;
2. umbrella forepoling to reinforce and protect the crown of the void to be created;
3. excavation of the masonry by hydraulic hammer through;
4. construction of a reinforced concrete frame.

Another interesting object is the retrofit of the existing LO tunnel. This ancient masonry tunnel was built in the 19th century for Europe's first cablecar which linked the Geneva Lake with the city center. In order to adapt this tunnel to the new metro alignment, the foundation of the tunnel needed to be lowered 5 m with respect to the original level. Obviously, this had to be done without damaging the tunnel structure and the above-standing buildings.

The solution chosen by the engineers is (fig. 7):

1. execution of a triple curtain of sub-vertical jet-grouting columns on both sides of the tunnel to provide vertical underpinning of the foundations;
2. first 2 m high excavation;
3. execution of 45° inclined jet-grouting reinforced "anchor-columns", in order to improve the adjacent ground and to provide horizontal support;
4. repetition of steps 2 and 3 down to the bottom;
5. casting of the new foundation and walls and installation of horizontal metallic props at mid-height.

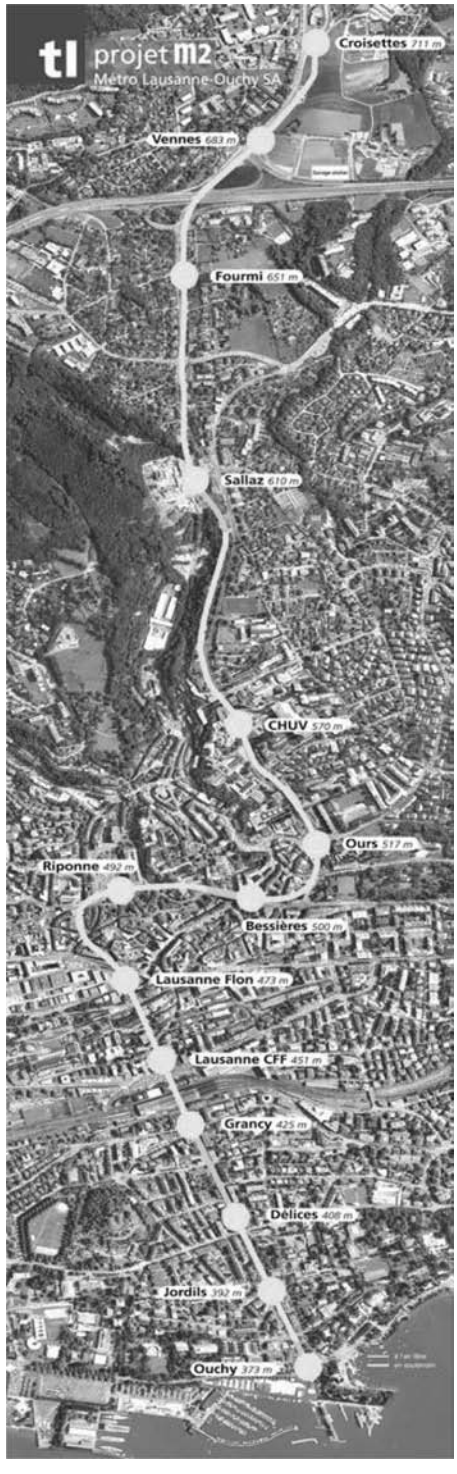


Figure 3. *projet m2*.

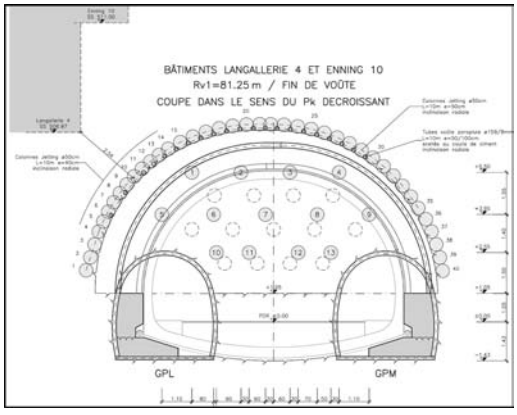


Figure 4. Transversal section of Langallerie tunnel. Note the jet-grouting columns, the side drifts and the proximity to buildings foundations.

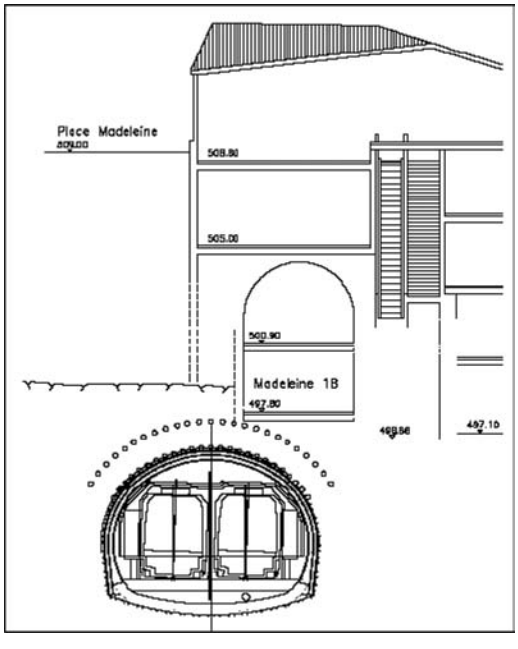


Figure 5. Transversal section of Viret tunnel. Note the umbrella forepoling and the proximity to building foundations.

Different consolidation techniques were used in order to ensure structural safety and settlement control during the construction of tunnels. They include:

– Umbrella forepoling for tunnel crown pre-reinforcement;
– Fiberglass nailing of the tunnel front;
– Jet-grouting, both subvertical and subhorizontal;



Figure 6. Construction of the Pont St-Martin below the Pont Bessières.

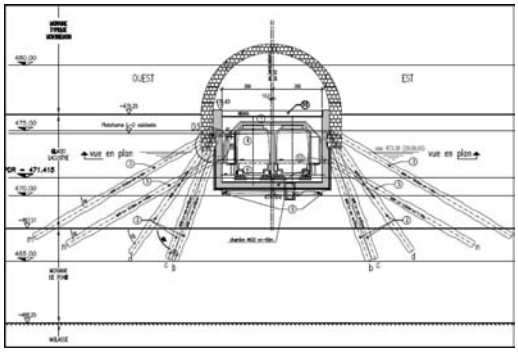


Figure 7. Transversal section of the LO tunnel. Note the existing masonry structure and the jet-grouting columns for underpinning and consolidation.

– Cement grout injections by means of "tubes a manchettes" (non-return valves fitted tubes) for ground improvement.

2.1 *The Saint-Laurent tunnel accident*

The project was unfortunately marred by a serious construction accident.

Late afternoon on February 22, 2005, the front of the Saint-Laurent tunnel collapsed. A large volume (approx. 1500 m^3) of mud flowed into the tunnel, when an unexpected pocket of water saturated sands and gravels was encountered, thus creating a sinkhole that reached the surface 15 m above.

The sinkhole formed under a main square of Lausanne's downtown historic shopping district (Place St-Laurent) and partially under the foundations of a multi-story building (fig. 8). Thanks to Santa Barbara nobody was hurt and the accident only caused material damage.



Figure 8. View of Place Saint-Laurent after the Saint-Laurent tunnel accident. Note the large sinkhole, which extends partially under the building.

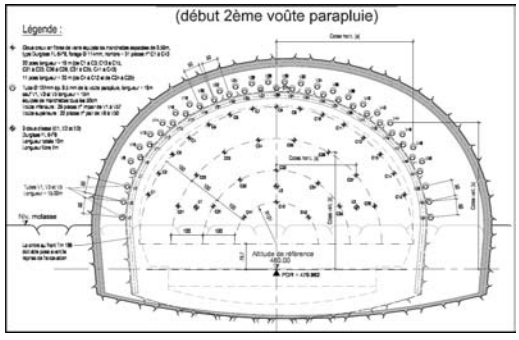


Figure 9. Consolidation measures throughout the critical zone of the St-Laurent tunnel. Note the large number of boreholes for umbrella and injections.

At the moment of writing this article, two inquiries are on-going to determine the causes and responsibilities of the accident, thus no comments on this subject can be made.

The response to the accident required prompt and decisive action by all the parties involved (Besides the engineer and contractor, this includes the Owner and the local political authorities and administrations).

Within two days, countermeasures were taken to stabilize the situation and avoid the progression of the sinkhole which threatened to cause the collapse of adjacent buildings. These measures include:

- Stabilization of the sinkhole walls with shotcrete.
- Further stabilization of the sinkhole with sprayed liquid nitrogen applied in order to freeze the soil at the bottom of the sinkhole and reduce the erosion induced by water circulation.
- Creation of a wall of piles bored from the surface into the tunnel. This wall acted as a "plug" by blocking the flow of material from the sinkhole into the tunnel.
- Filling of the sinkhole with porous material.

Ten days after the accident, the sinkhole was completely filled and the crisis was over. Further measures were taken in the following weeks and months in order to finish the tunnel on time in spite of the accident. Despite its strong emotional impact, the accident did not stop or delay the construction project.

(In retrospect, it is noteworthy for the profession to note that the successful management of the crisis contributed very significantly to reduce the damage to the credibility and image of the *projet m2* resulting from the accident).

After the accident, it was determined that a 35 m long zone of soft and partially disturbed soil between the collapsed tunnel front and a molasse rock formation required special excavation techniques. It was decided to open a new excavation front from the northern adit in order to excavate this critical zone "from the rear".

The following measures were implemented for the excavation of this critical passage (fig. 9):

- Crown pre-reinforcement by means of a double umbrella heavy forepoling, made by metallic tubes and grout injections through singles "manchettes"
- Front pre-reinforcement by means of fiberglass nails coupled with grout injections through singles "manchettes".

The consolidation works and the excavation of the critical zone lasted 7 months. More than 500 m^3 of cement grout were injected (pressure between 3 and 5 bars) into the soil to improve its geotechnical characteristics.

3 PROJECT CHALLENGES

From the Owner's point of view, the challenges of the project include technical and non-technical issues, such as:

- Being a subway project, *projet m2* is mostly built underground. Project optimization measures brought the portion of the new line which is underground to 90%. This implies much construction work at low depth in an urban environment and the associated level of uncertainty and potential for "bad surprises". Planning and managing underground excavation and civil works always entails a certain level of risks. (The *projet m2* is no exception, as it suffered by the serious tunnel accident described above).

  Managing this "underground risk" is a classic application of modern risk management thinking. Since "risk zero" is – unfortunately – an unreasonable objective, the stakeholders of underground construction project must be ready to work on measures to limit the probability of negative events and

on measures to reduce their consequences if they occur.

– The civil engineering infrastructure of the project is built by 8 consortia of construction companies working simultaneously on 10 to 12 worksites with 4 sets of engineering firms (fig. 11). The Owner must be in position to manage and coordinate different companies and contracts. Strong presence is required to counter the natural tendency of each individual structure project to "take its own" technical or planning course.
– Because the worksites are located in the urban environment of the city center, special care and emphasis are required on the relationship with the neighbors, public and city services. More than 200 mios € shall be spent in 3 years and a half on the construction side of the project. With such a high rate of worksite production in a relatively small city, it is crucial to control the project impact on the surroundings and the city.

4 THE CLIENT'S TEAM ROLE

The overall project management is provided by the Métro Lausanne–Ouchy SA, a company managed by the public transport authority of Lausanne. Although the engineering services are delegated, as usual, to different consultant companies, the Client has put in place a team specifically assembled to manage the project.

(This section presents "lessons learned" of Owner's representatives on the role of the Owner's team. The authors are fully aware that these comments are nothing new and/or that their relevance to projects conducted in different conditions and context is uncertain).

The client's team is not there to substitute the resident engineers, but to aid and support them in dealing with the strategic issues and specific problems. The tasks of the Client representatives include:

– to support, back up and control the resident engineer in his design and management tasks;
– to coordinate the different lots in order to have consistent application of the generic performance requirements across the project;
– to keep a constant pressure on the resident engineers and contractors, in order to reduce the risk of cost overrun and delays;
– to support the resident engineers for contractors' claims management;
– to centralize information and defend/promote the project toward the public and authorities.

In the end, the primary role of the Client's team is to ensure that the planning and the budget are respected and without compromising on the safety and quality requirements.

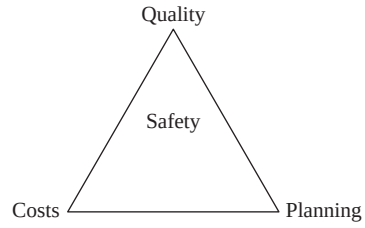


Figure 10. Multi-dimensional approach applied to *projet m2*.

Lots	Engineers	Contractors
2000	**SDIA** *SD Ingénierie, CETP* *Giacomini & Jolliet* *Catella, Hauenstein &* *Ehrensperger*	**CTC 2000** *Batigroup* *Marti et Perrin Frères* *Bertholet & Mathis*
1900		**ATV** **Association Tunnel Vennes** *Infra Tunnel, Bernasconi*
2100	**EMCH & BERGER + LUSCHER**	**JPF Construction SA**
1700	**SDIA** *SD Ingénierie, CETP* *Giacomini & Jolliet* *Catella, Hauenstein &* *Ehrensperger*	**MABAT 1700** *Marti, Batigroup*
1600		**RAM** - *Rusconi, Martin, ADV*
1500	**GEB** *Emch & Berger* *GEOS, DIC* *Architram* *Inst. Géotechnique*	**Consortium Lot 1500 - CHUV** *JPF, Induni, Evéquoz et Gétra*
1400		**Groupement 1400** *PraderLosinger, Losinger Construction,* *Frutiger Vaud, Murer, Déneriaz Sion*
1300	**GEMEL** *GVH Tramelan SA,* *Géotest, Architram* *Fellrath & Bosso SA*	**APB - Association Pont Bessières** *Losinger Construction, Frutiger Vaud*
1200	**GIT-LEB** *Piguet & associés* *CSD-Monod* *Tschumi-Merlini*	**AOC** **Association Ouchy-Croisettes** *Dénériaz, Zschokke Locher* *Grisoni Zaugg, Zschokke* *Walo Bertschinger*
1100		
1030	**SDIA** *SD Ingénierie* *CETP* *Giacomini & Jolliet* *Catella, Hauenstein &* *Ehrensperger*	
1020		**Consortium Lot 1020** *JPF, Frutiger Vaud*
1010		**Consortium RAM** *Rusconi-Martin-ADV*

Figure 11. Overview of *projet m2* engineers and contractors JV.

Since the beginning of construction, the Owner's team has tried to pursue with the Engineers and Contractors a sustained search for solutions in terms of technique, planning and budget. It is clear to all that on a large public construction project, the Owner has to do more then record decisions and events and process payments. He has a central role to play in assisting and guiding the project partners in this optimization effort. He is best positioned to arbitrate between conflicting demands.

Without interfering with safety aspects of the projects for which the specialist engineers and contractors are responsible, he can foster a project culture in which design, problem-solving and decision making explicitly happen in the quality-planning-costs triangle (fig. 10).

One-dimensional problems are the exception; it is usually beneficial to try to explicitly address problems in the three-dimensional. Optimization is about having the best combination of all three. Identifying and evaluating possible trade-offs is difficult, but it is often the key to finding the "best" solution, i.e. to optimization.

Owners' representatives have to be pragmatic and remind themselves and their partners the simple message that: "*The people who finance the whole project does not want the best technical solution at an unreasonable price and unacceptable delay. The people want a reasonable solution at the lowest possible price and in the shortest possible time*".

This is illustrated in fig. 10 with a triangle bringing together the three key elements of project management. Meeting technical requirements (in terms of quality, performance et durability), controlling costs and respecting schedules cannot be dissociated. It is not enough to "have one or the other". Of course, safety considerations must be treated differently because they include non-negotiable elements. But if safety requirements are clearly identified, there is usually a range of solutions to a given problem which respect them and optimization in the quality-planning-costs triangle still applies.

5 SUMMARY AND CONCLUDING REMARKS

Two and half years after beginning of civil works, the construction of the *projet m2* new infrastructure generally progresses according to plan. In spite of a serious tunneling accident described above, the construction project is on time. At this point:

- eight new tunnels have been broken through;
- two 19th century tunnels have been retrofitted;
- more than 1 km of new cut-and-cover trenches have been built;
- two new bridges have been completed.

As any large infrastructure project in an urban environment, especially when underground work is required, the *projet m2* presented interesting and unique technical challenges. Two examples involving the retrofitting of traditional existing structures of traditional masonry construction are described above:

- the construction of a new reinforced concrete bridge through the masonry piles of an existing bridge;
- The underpinning of the lining foundations of a 19th century old tunnel in order to lower its ground slab.

But technical successes are not enough. Unlike scientists who can often focus on technical aspects of their work, our task as engineers has to integrate a broad, and sometimes contradictory, set of requirements and considerations. In particular, the successful completion of large projects – such as *projet m2* – requires the project partners to constantly think and optimize in the quality-planning-costs triangle. In the eyes of an Owner's representative, this approach is as important as meeting the technical challenges. The Owner must therefore foster a project culture and environment where this optimization can happen. Most engineers know that this is part of their responsibility toward the entities they serve and respond well to this challenge.

REFERENCES

Perret, A., Maurer, D., Badoux, M. 2004. Le volet génie civil du m2. *Lausanne Underground. Tracés 22. Bulletin téchnique de la Suisse Romande.* Lausanne

Badoux, M., Gaj, F., Perret, A. 2005. Le projet m2 – Présentation générale. *Construction des tunnels à Lausanne: m2, Tridel, Glion. Réunion de printemps, 14 avril 2005, Lausanne. Publication de la Société Suisse de Mécanique des Sols et des Roches*

GEMEL JV 2003–2006. Design documentation

GIT-LEB JV 2003–2006. Design documentation

SDIA JV 2003–2006. Design documentation

EMCH & BERGER 2003–2006. Design documentation

Badoux, M. 2006. Bilan à mi-parcours. *Tracés 19. Bulletin téchnique de la Suisse Romande.* Lausanne

Underground Space – the 4th Dimension of Metropolises – Barták, Hrdina & Romancov (eds)
© 2007 Taylor & Francis Group, London, ISBN 978-0-415-40807-3

Metro Santiago – Building an urban tunneling industry from the ground up

Alexandre R.A. Gomes & Martin Böfer
Geoconsult Latinoamerica Ltda., Santiago, Chile

Pablo Muñoz
Metro de Santiago, Santiago, Chile

ABSTRACT: Santiago's Metro construction started in the early 70s with the use of extensive cut-&-cover tunnel methods. This type of construction was further used in the 80s, causing major disruptions in the urban surface and strong public opposition. This situation and Metro S.A. key decision to seek for fastest, more efficient and less disruptive construction alternatives, lead to the first mined tunnel experiment under a public Park in 1994. That successful trial tunnel demonstrated the feasibility and benefits of mined tunneling and bestowed Metro S.A. the required confidence to give priority to mined construction in its future projects. Following this decision, and boosted by the continuous and massive array of new subway projects developed in the following decade, a brand-new urban tunneling culture and industry surged in Santiago de Chile. This paper presents this historical evolution, addressing the most relevant landmarks along this way so far.

1 INTRODUCTION

In the early year 2000, the Santiago's subway network was comprised of not more than 40 km and 46 stations with only about half percent of its network being of underground construction, mainly with cut & cover boxes. Nowadays, with the additional 17.5 km of new line extensions planned to be completed in 2009, the subway network will have shown a considerable expansion reaching a total length of 104.5 km and 108 stations, with over 60 km of mined tunnels and more than 70 underground stations.

This lapse of time has seen not only the subway network increase more than twofold but also the establishment, from the ground up, of a whole new urban tunneling industry in Chile. Matter of fact, previously to this period, mined tunneling proficiency in Chile was mainly coming from the construction of rock tunnels for the energy and mining sectors and there was no expertise at all in urban tunneling and soft ground.

Relying mainly on local contractors and designers, fed by a continuous know-how transfer from international tunneling consultants, a remarkably rapid evolution occurred in various aspects of tunnel design and construction, enabling in a short period the development of technical- and very cost-effective solutions for urban mined tunneling in the mostly favorable ground conditions of Santiago de Chile.



Figure 1. Metro system map.

2 SANTIAGO'S SUBWAY HISTORICAL EVOLUTION

2.1 *The early years – 70s and 80s*

Santiago's subway construction began in the early 70s with Lines 1 and 2. Construction was mainly of



Figure 2. Metro construction in the 70–80s – C&C method.

cut- & -cover type with some sections at grade. Cut & cover boxes were built either within sloped or braced excavations. Braced diaphragm walls were also applied at some sections.

This method was further used in the 80s. However, aside from the massive utilities relocation work required, the large construction periods and traffic and surface disruptions, these methods became slowly unacceptable to the community expectations, requiring Metro S.A. to search for less disruptive construction methods (Mercado, C. et al, 2004).

2.2 *The first mined tunnel trial*

In 1994, Metro S.A. ventured to carry out the first mined tunnel experiment, under the public Baquedano Park, during the construction of the first L5 extension. Excavation of the single-tube, double track running tunnel was carried out with full face and the provision of a large central supporting core. Equipment were standard back-hoe excavators.

Design was carried out by local consultant joint venture Ingendesa/ARA. The tunnel presented a horseshoe shape without invert and was excavated in sequential rounds of 0.8 m–1.0 m with a timely differed installation of a double shotcrete lining, 55 cm thick, reinforced with wire-mesh and lattice girders. It is relevant to mention that, at this time, shotcrete technology was poorly known in Chile and only the dry method basics were know from the mining sector experience.

During the construction of this tunnel, monitoring of deformations was carried out only in specific locations and the guarantee of tunnel stability was provided only by the thick shotcrete lining. Ground conditions were favorable, with the typical Santiago's subsoil consisting in quaternary sediments of gravel from the Mapocho and Maipo river basins, the so called "Ripio de Santiago", which presents excellent geomechanical characteristics and are very suitable for tunneling



Figure 3. View excavation and support – First mined tunnel.

(average values at tunnel springline: $\gamma = 22\,\mathrm{kN/m^3}$; $c' = 40$ Kpa; $\phi' = 45°$; $E' = 300$ Mpa; $ko' = 0.3$). The ground water table is variable, but in general is located well below the tunnels at a depth of 70–80 m.

2.3 *Mined tunnels go downtown*

The 2.8 km second line 5 extension to the west was planned to run through a densely built up area in the city center, passing below busy avenues and adjacent to Santiago's old Cathedral and other important historic building. For this endeavor, which would be decisive for the future of mined construction in Santiago, Metro S.A. requested local assigned consultant Cade-Idepe to get support from foreign tunneling experts. For this, Geoconsult of Austria was called in to help with the design of running mined tunnels.

A comprehensive and robust tunnel design was developed by Geoconsult/Cade Idepe with basis on the principles of the NATM (New Austrian Tunneling Method). Soil conditions were the typical Ripio de Santiago, with presence of local ground water infiltration. Tunnel cover was typical with round surface about 10–11 m above the crown. In view of the lack of previous relevant experience, the noviceship of contractors and the sensitivity of the surrounding buildings and structures, running tunnels were intentionally designed as conventional NATM for soft ground conditions.

The tunnel transversal section was ovoidal with an area of about 65 $\mathrm{m^2}$. Tunnel support comprised of a primary shotcrete lining of 200–250 mm, installed immediately after each round, followed by a secondary in situ reinforced watertight concrete lining, with a thickness of 40–45 cm, cast to the invert and arches in a later stage. Excavation was carried out in 0.8–1.4 m rounds with the closed invert no more than 7 rounds behind the top heading. In some sections, micro-piles curtains were installed next to relevant buildings to control deformations.

Stations were constructed as open cuts, but incorporated for the first time the use of ground anchors to

support the piles and soil nailing, avoiding the need for the disturbing internal bracing. Even so, very large ground settlements and adjacent building damage was registered within the area of influence of these excavations.

Tunnel construction was carried out from 1997 to 2000 with the incorporation of systematic monitoring of deformations and stresses in tunnel and surrounding ground. Results from this monitoring program showed that ground behavior was very favorable with low convergences and ground surface deformations, mostly in the range of 4–8 mm.

2.4 *Mined tunnels get established – The first mined stations*

In view of the favorable results obtained in the line 5 and the practically inexistent impact on the urban surface and structures, Metro S.A. decided to apply extensive mined tunneling methods on the following subways expansions.

Therefore, for the new Line 2 and 5 extensions, with a total length of more than 6 km, mined methods were applied not only for the running tunnels but also for station tunnels. Construction was carried out from 2001 to 2003. Design and site supervision work was carried out by 3 different JVs of local with international consultants, namely Cade-Idepe with Geoconsult Austria, Ingendesa-ARA with Dr Sauer Co. from USA and Arcadis-Geotecnica with Bureau de projetos from Brazil.

These new extensions marked the return of the use of shotcrete for both primary and secondary tunnel linings. The tunnel lining concept was based on the consideration of a double and monolithic tunnel lining, where both linings would work together to provide the long term tunnel support and service conditions. This was possible basically due to the favorable ground conditions of the Ripio de Santiago, the inexistence of significant ground water and application of state-of-the-art shotcrete technology, including low dosages of alkali-free accelerators, additives, meticulous shotcrete installation, curing and use of steel fibers to increase quality of the secondary lining.

For the running tunnel sections, horse-shoe tunnels (without invert) were extensively applied and the thickness of the primary lining was reduced to only 15 cm. Tunnels with structural ring closure were applied only at singular sections, such as intersections or heavily loaded sectors.

Stations were typically constituted by one or two lateral shafts, located in a place as to not interfere in public roadways and require extensive utilities relocation, and associated access tunnels, placed mainly in a direction transversal to the main line alignment so that it crosses in a perpendicular way with the main station tunnel.

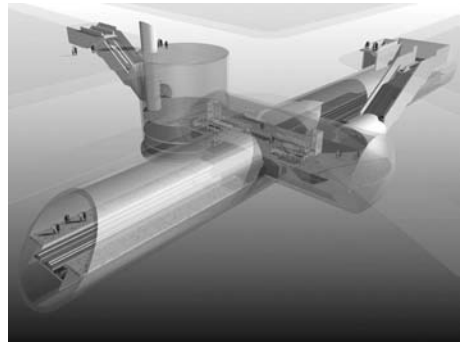


Figure 4. View of a mined station tunnels.



Figure 5. Excavation of access tunnel under pipe roof.

Station tunnel cross sections varied from 100 m^2 at intermediate stations to up to 180 m^2 at terminal or multi-modal stations. With rail levels at a depth of 17–18 m, the crown of cross sections up to 17 m wide were only 6–7 m below the ground surface.

Access tunnels were constructed under the protection of a pipe roof umbrella, as to control ground deformations and allow full-face exaction of the top heading section, which was completely excavated and supported, including a temporary invert, before carrying out the excavation of the bench and invert headings.

After the access tunnel excavation was finished, the break-out for the excavation of the main station tunnel was done. The station tunnel was constructed subdividing the section in 3 or 2 separated headings with the provision of temporary lateral walls, demolished as the excavation stages advanced. No pipe roof or forepoling was installed for these sections. Significant lessons regarding design and construction aspects were drawn from the construction of these two extensions. The most relevant are listed below:

– ground conditions response to the excavation of large dimension tunnels were favorable and safe (max. settlements were in the order of 2 cm);



Figure 6. View of access station tunnel end wall.



Figure 7. View of a mined station tunnel excavation.

- stresses on the linings were below those foreseen in the design, allowing the further optimization of tunnel support;
- The control of shotcrete technology and installation was proven critic to ensure the required lining quality;
- Efforts should be made to reduce the amount of reinforcement in shotcrete linings, as there was a clear limit to get rebars fully embedded and obtain good quality linings, avoiding the need to carry out extensive repair works by post-injection;
- It was not possible to obtain watertight linings with the use of shotcrete (the installation of a sprayable waterproofing membrane between the two linings was proposed in the design but not applied during construction);
- The provision of a qualified and expert engineering team (Site Supervision) on site is of most relevance for tunneling works, providing vital control and solutions to guarantee safety, construction schedule and the specified quality.

2.5 *Tunneling under tunnels and old bridges*

Another line 2 extension's landmark was the construction of a tunnel section below the bottom slab of the six-lane cut & cover highway tunnel "Costanera Norte" and of a large subway mined tunnel section directly under the abutment foundation of an old bridge for vehicular traffic across the Mapocho River, in the centre of the city (Gomes, A., Boefer, M. & Cruz, J.H. 2004).



Figure 8. Interior view of a finished mined station in shotcrete.

Whereas the passage below the cut & cover tunnel constituted no major challenge, the crossing below the bridge abutment required special construction methods and additional auxiliary measures to allow tunnel construction and prevent damages to the bridge. These included the underpinning of the bridge abutment, the installation of an active jacking system, the use of a subdivided excavation face and the implementation of a comprehensive and continuous monitoring system of loads and deformations, designed specifically for this project.

2.6 *New grounds and wet shotcrete*

With the new line 4, constructed from 2003 to 2005, Metro S.A, started one of its more impressive investments in the subway network. The new line encompassed app. 32–33 km, with 12 km of mined tunnels, 14 km at grade and 7 km of elevated rail.

Since its construction overlapped with the construction of the Line 2 and 5 extensions, there was a market peak, which generated a certain overstrain in the local construction industry. Nevertheless, this also helped to create the right scenario for major improvements in technology and a doorway for new local and foreign contractors and companies.

Metro S.A. used the line 4 to foster the use of more advanced techniques for tunnel construction. Therefore, the JV Geoconsult-Cade Idepe was hired to carry out a comprehensive feasibility study on the use of mechanized tunneling (TBM). By using the typical NATM design as a baseline, a comparative study was carried out for different TBM alternatives. This study



Figure 9. Tunneling below the Fray Andresito bridge.

concluded that the NATM approach was the most appropriated approach for the line 4 underground works, as it was less expensive, generated more benefits to the local industry and posed fewer risks for the project schedule.

Another important decision taken by Metro S.A. at the new line 4 was the specification of state-of-the art wet shotcrete for tunnel support, allowing the further development of this technology in Santiago.

The construction of the line 4 also marked the first tunnel excavation in soft ground and the harshest handling of ground water at the Station Puente Alto (Gomes, A. & Boefer, M. 2005). Actually, a large part of the alignment crossed sediments deposited by erosive streams from the Andean Cordillera, consisting mainly of clay and silt with low to moderate plasticity and sand lenses with different thickness. In Puente Alto, even tough the ground was the typical and favorable Ripio de Santiago, the presence of water inflow (up to 15 l/s) from water bearing layers, associated with the contractor inexperience caused important construction problems and program delay. Problems of ground water were also found in other sections of the line 4, without causing many difficulties.

Design concepts were kept basically similar to those used for previous lines. However, some new construction methods were applied, such as the design of the Plaza Egaña station with the use of a composite geometry with double cell and a central pillar, as to reduce excavation area, avoid sinking of rail level and limit deformations to acceptable values. Besides, some sectors presented local instability problems required the establishment of a comprehensive and monitored excavation procedure to control local ground collapse and reduce the risk of global cave-ins. This was managed by the provision of geologists at the face, under the supervision of the site Engineer and in close work with the contractor. Another change was the consideration of an in situ inner concrete lining for the Station Puente Alto due to the presence of ground water.



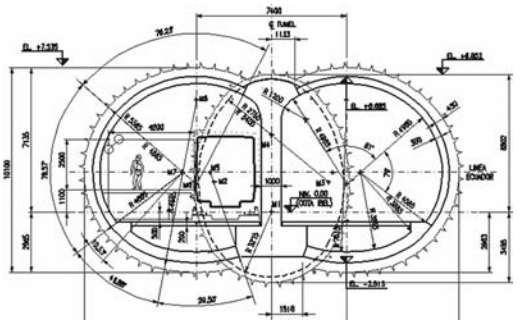


Figure 10. View of station tunnel with central pillar solution.

2.7 *More soft grounds and further expansion*

In the 13 km new line 2 extension to the North, constructed in 2004–2005, aside from typical Ripio de Santiago conditions, tunnels were also excavated in soft alluvial ground (clay, silt and sand layers, intercalated with sand lenses and gravels). Similarly to the experienced in the line 4, local instability problems required the establishment of a comprehensive and monitored excavation procedure.

For this extension, a significant optimization of the lining design was achieved, reducing both thickness and amount of reinforcement in station tunnel crossings.

2.8 *The latest expansions*

With construction start planned for the beginning of 2007, the new extensions of Line 1 to the East and Line 5 to Maipu (West): 17.5 km, will also shown some novelties and new challenges to designers and contractors. At the line 1, ground conditions are the typical Ripio de Santiago. Aside for some tunnel crossing and other singular situations, no significant novelty is expected. However, at the Line 5 to Maipu, tunnels will cross not only the typical fluvial deposits of gravel but also other ground conditions where there is no previous tunneling experience.

The most challenging will be the sectors with raveling gravel, which may require special pretreatment of the excavated surfaces, prior to installation of the shotcrete lining. There will also be sectors running through fine silt-sands deposits of volcanic origin with low cementation, the sol-called "Pumicita", and mixed soft ground conditions with the presence of clay, silt, sand and gravel layers. Additionally, a tunnel sector may experience relevant ground water inflow, requiring proper water control. At the time of preparing this paper, the design was still being carried out. However, even tough not all particularities are defined yet, it can be anticipated that the design of these new structures will incorporate many lessons learned in the past, providing even more optimized solutions, such as the flexibilization of invert installation to account for the different ground conditions.

3 PROCUREMENT AND FINANCING

3.1 *Procurement*

The typical approach to design and construction is based on the development of basic and detail designs by consultants hired by Metro S.A. and bid and build contracts. Bidders are pre-qualified contractors and contracts are awarded to the lowest technically complying bid. Contracts are administrated by Metro S.A. managers, together with a dedicated site Inspection, also provided by local consultants. Additionally, the site engineering supervision, which oversees the overall tunnel construction, is granted to consultants together and as an extension of the detail design works carry out for each contract.

3.2 *Financing*

Since 1990 Metro S.A. is an independent government-owned institutions that own, operate and maintain the subway system. In general, costs of civil works are borne by the National budget through funds granted by the Ministry of Finance. M&E and rolling stock costs are generally financed directly by Metro S.A. itself by means of loans lent by the international banking system. Regarding operation costs, those are totally covered by Metro S.A. own revenues.

4 COSTRUCTION COSTS, PRODUCTIVITY

During this decade of development, construction costs have decrease and productivity increased significantly for the Metro de Santiago underground works. During the first years of tunneling, average advance rate of running tunnel excavation was inferior to or maximum 1.0 m daily. Nowadays, average advance rate reaches up to 2.5 m daily.

Costs have also decreased substantially. Initial ruining tunnel costs per lineal meter were in the range of U$15.000–20.000. Currently, these costs lay typically in the range of U$7.000–8.000. Another important cost reduction aspect was the continuous optimization of the monitoring program, as more knowledge of the ground behavior became available. This effort allowed a reduction from the initial cost of U$1million/km to the current figures, which are lower than U$250.000/km.

5 CONCLUSIONS

On the basis of a successive array of investments in new subway projects and a strong compromise to pursue low disturbance, cost-effective and pragmatic technical solutions, Metro S.A. has managed to develop in a short period of time a remarkable, safe and efficient subway network, which shall still continue to expand in the future.

In this quest, Metro S.A. has also helped to forge a new tunneling industry with qualified and competent tunneling contractors, consultants, suppliers and workers, able to respond to Metro S.A. needs to further develop its subway network, which constitutes the backbone of the integrated Urban Transportation Plan of Santiago (UTPS).

REFERENCES

Gomes, A. & Boefer, M. 2002. Aspectos de diseno y construccion de las obras de tuneleado del metro de Santiago; proceedings of the 12nd COBRAMSEG / 1st CLBG / 3rd SBMR, ABMS; São Paulo 2002.

Gomes, A. & Boefer, M. 2004. Metro de Santiago: Tunnelling under the Fray Andresito bridge; proceedings of the 30th ITA-AITES World Tunnel Congress "Underground Space for Sustainable Urban Development; Singapore 22–27 May 2004.

Gomes, A. & Boefer, M. 2005. Proyecto y Construccion de las Obras de Tuneleado de la estacion Puente Alto, linea 4 – Metro de Santiago; proceedings of the 1st International Symposium of Engineering Geology , Geotechnics, Geomechanics and Environment. CIP APIG; Lima 17–20 August 2005.

Mercado, C., Chamorro, G. & Egger, K. 2004. Santiago's Metro Expands. Proceedings of the North American Tunneling (NAT 2004) Conference, Atlanta, GA, May 2004.

Wallis, S. 2003a. "Evolving NATM for Santiago's Metro": Focus on South America. In T&T International, pp. 16–20, March 2003.

Wallis, S. 2003b. "Metro's Evolution": Focus on South America. In T&T International, pp. 34–37, In T&T International, April 2003.

Underground Space – the 4th Dimension of Metropolises – Barták, Hrdina, Romancov & Zlámal (eds)
© 2007 Taylor & Francis Group, London, ISBN 978-0-415-40807-3

The Slivenec Tunnel on the Prague City Ring Road

O. Hasik & K. Závora
METROPROJEKT Praha, Prague, The Czech Republic

ABSTRACT: A motorway-type ring road is being developed to reduce traffic in Prague. The southern section is currently under construction. The route in this section traverses the Vltava and Berounka valley, to which it descends from a quite steeply rising hilly country along both river banks. In addition, there is a protected landscape area there. For this reason, the authors of the design have proposed underground sections for this locality (construction lots no. 513 Lahovice-Vestec and no. 514 Lahovice-Slivenec). These sections consist of uni-directional tunnels, with two lanes in descending sections and three lanes in ascending ones. In addition, given the steep 4% gradient, the ascending sections are provided with a slow lane for trucks. The tunnel safety equipment is on the top worldwide level. In order to verify the geological conditions thoroughly, an exploration gallery has been designed to pass through the entire three-lane tunnel section. The position and shape of this gallery have been selected in such a way that the gallery will substitute the initial tunnel excavation sequence, the top heading. The gallery bottom will be identical with the floor of the tunnel top heading. The exploration gallery situated in this way will not only serve its primary exploration purpose. The site facility built for the works will even be utilised for the future tunnel excavation. The concept and the technical design of the tunnel sections meet the latest EU safety regulations. The Slivenec tunnel is 1,610 m long in total.

1 THE ABSENCE OF A RING ROAD AROUND PRAGUE AND ITS CONSEQUENCES

The number of vehicles significantly grew in recent years in the Czech Republic. The high traffic volume, unusual in the past, is obvious everywhere. If you look at a road map of the Czech Republic, you will see the apparent centralism in the layout of main roads and motorways; the majority is heading to Prague.

Today's Prague, however, has changed for many drivers from a target city to a transit city. This fact can be related to the political change of the formerly closed socialist state to a state with a democratic system, which is open for the whole Europe. The current large proportion of international transit is one of the effects. International transit routes cross the Czech Republic from Germany in the southwest or northwest to Poland and Slovakia in the east, from Austria in the southeast to Germany in the northwest, etc. The vehicles only passing through Prague put an unnecessary burden on Prague streets and municipal roads. In rush hours, this situation is often unbearable. A ring road around Prague is being badly missed.

The main task of the ring road will be to reduce the traffic volume within the network of Prague streets and local roads, and interconnect all motorways and fast highways before entering Prague, thus to allow the transit transportation to switch fluently between all long-distance radial routes leading from Prague. Considering the location of our republic in the centre of Europe and with respect to the planned cancellation of borders (incorporation of the Czech Republic into the union of Schengen countries), and owing to the actual process of completing the basic network of our motorways, a considerable volume of transit through our territory can be expected in the years to come. The increase in the proportion of truck transit which was recorded after the accession of the Czech Republic to the EU in May 2004 has confirmed the anticipation that all of this traffic will prefer the PRAGUE CITY RING ROAD to the problematic and slow passage through the centre of Prague.

This fact has become clear to members of parliament, mayors, directors of big companies, investors, designers, contractors and all other people who would like to promote the development of the ring road. They have founded the Prague City Ring Road Development Association, which has been creating space for dialogue and, lately, has been helping to accelerate the work on the design and construction of the ring road.

2 THE PRAGUE CITY RING ROAD HISTORY

The first ideas of the Prague ring road project are dated the 1920s. This period even saw first efforts for development of a general plan of the traffic solution for Prague.

Other proposals for the development of a ring road around Prague emerged before World War II. They were based on a contention that "the city of this magnitude cannot cope without a project like this". The ring road, as a basic principle of diverting transit transportation to bypass the centre of the city and to interconnect city centres found in the outskirts was the subject of numerous studies carried out in Prague.

However, the construction of the ring road was approved as late as 1963, and the implementation of the PRAGUE CITY RING ROAD started in the 1980s. The decision that the ring road will be only of the fast highway type instead of the motorway type was made in 1987. This decision also meant the end of discussions about the number this motorway was to be assigned (the D1 motorway had already existed then).

3 THE DESIGN OF THE HORIZONTAL ALIGNMENT AND CONSTRUCTION OF THE SOUTHWESTERN PART OF THE PRAGUE CITY RING ROAD

The process of designing the alignment of each of the segments of the Prague ring road has always risen lots of questions and problems, which were solved and analysed in studies and designs carried out in the particular period. The pressing character of the task to solve the problem became fully obvious only in the 1990s, in the context of the social changes after 1989 and the enormous increase in the vehicular traffic volume associated with this process. Today, there are two parts of the PRAGUE CITY RING ROAD in operation, namely the Slivenec – Ruzyně section (construction lots No. 515, 516 and 517) on the west edge of the capital, and the Satalice – Běchovice section (construction lot No. 510) on the eastern edge.

The most pressing traffic situation is currently on the Barrandov Bridge, where traffic jams even last over 12 hours in a day. The entire length of the Southern Connection Road, which is part of the inner City Circle Road, is filled with standing vehicles. Each driver can experience there the passage through a big city lacking a road loop. The traffic volume on this road, which is today one of the roads most loaded by traffic, should be reduced by the south-western part of the ring road consisting of the construction lots No. 513, 514 and 516, which together form a road link between the D1 motorway for Brno and the D5 motorway for Plzeň. The alignment of the southern part of the Prague City Ring Road crosses the valley formed jointly by the Vltava and Berounka Rivers. It falls to the valley from a relatively steeply rising hilly area lining the river banks. For this reason, and also because of the fact that it passes through protected areas, the alignment of the sections of the construction lot No. 513, Lahovice – Vestec, and construction lot No. 514, Lahovice – Slivenec, is designed to pass through tunnels. The right-hand tunnel tubes are offset from the centre line of the route by means of radii slightly differing from the radii of the route so that an optimum distance between the tubes is achieved.

4 VERTICAL ALIGNMENT AND DIFFERENCES IN THE CONFIGURATION OF TRAFFIC LANES

The revised norm currently valid for road tunnels recommends gradients up to 3.0%; tunnels with steeper gradients need an assessment to be performed whether additional safety measures are necessary. The 4% gradient at the lengths over 1.5 km means, in our specific case, that an additional a traffic lane for slow moving vehicles and trucks is necessary.

Traffic engineering measurements showed that freight traffic makes up a 40% proportion of the total traffic volume, while a 15% proportion had been assumed before the measurements. From this viewpoint, the addition of one traffic lane at an uphill section is obviously necessary even for a smaller gradient. For this reason, three-lane tunnels are designed for the tubes carrying the traffic ascending from the confluence of the rivers up the plateaus. The solution of the question whether the capacity of the 4% uphill gradient three-lane roads is sufficient will remain to be answered in the future. The descending tunnel tubes have two traffic lanes.

The width of the right traffic lanes of 3.75 m, which is increased compared with the standard width of 3.50 m, was designed with respect to the significant proportion of truck traffic. The widths of the roadway were binding for the designer.

5 ARCHITECTURAL DESIGN OF THE PORTALS

Tunnel portals are nearly always difficult items of any tunnel construction. Even the choice of their location depends on many factors, mainly on the terrain configuration, the horizontal and vertical alignment of the route, geological conditions in the particular location, proper incorporation of the structure into the landscape and other factors. All of the above circumstances also apply to the portals of the tunnels built on the Prague ring road. The Lochkov portal of the construction lot No. 514 belongs among the most difficult. It is located on a steep slope above Radotín, where the nappe (gravelly soils) is over 10 m thick. In this case, the portal of the mined tunnel is properly shifted as deep to the rock massif as possible, to a point where at least the bottom part of the tunnel will be excavated in rock conditions. When you walk in this area you can see nothing exceptional. The terrain above the future tunnel, a meadow with naturally seeded trees and brushes, looks

subdued. Unfortunately, there is a biological protected zone located just in the place most suitable for the portal. It means that the initial section of the tunnel must be shifted to a place where, simply put, the conditions for tunnelling are the most difficult. The design of the construction trenches for the portals of the mined tunnels comprises mighty vertical piles keyed in the bedrock, with the steep slopes stabilized by shotcrete, anchors and needles. The trenches will be used for the construction of both the cut-and-cover tunnel sections and the architectural concrete portals. The C25/30 reinforced concrete lining of the cut-and-cover tunnels is 600 mm thick at the vault. The waterproofing system applied to the cut-and-cover tunnels consists of a membrane installed on the outer surface, which is protected on both sides by non-woven geotextile. The cut-and-cover tunnels are founded on strip footings; the invert will be built at the portal.

All portals are designed as cast-in-situ reinforced concrete structures. The elliptic front ends of the portals of the construction lot No. 514 are provided with "ribbed canopies", which improve the architectural impression of the portals and help to incorporate them into the landscape.

This architectural design is used for tunnels designed in our country for the first time and, as you can judge by yourselves, it certainly will make the passage along this section of the route brighter. The finish of the terrain around the portals will be created by the backfill of the adjacent cut-and-cover tunnels, and by a part of portals inclined approximately at 1:1.75. The side slopes of the portals are terminated by retaining walls and service buildings, which are incorporated into the walls.

The chimney of the ventilation structure is also designed as an architectural feature.

6 MINED TUNNELS, CROSS SECTIONS THROUGH TUNNEL TUBES AND CROSS PASSAGES

Mined structures (tunnels, cross passages etc.) form a substantial proportion of the construction lots No. 513 and 514 of the road ring. In terms of the structure, all of the tunnel structures are similar, consisting of reinforced C 20/25 sprayed concrete primary lining, cast-in-situ C 25/30 concrete final lining and intermediate waterproofing layer. The vaults of both liners are circular. All of the tunnels will be driven using the New Austrian Tunnelling Method with a horizontal excavation sequence. The excavated cross-section areas of the double-lane tunnel and three-lane tunnel will be 95 m^2 and 130 m^2 respectively. The internal profiles of the tunnel tubes are vaulted, uniform along the entire lengths, irrespective of the construction technique.

Walkways 1.0 m wide are provided on both sides of the roadway. The height clearance is 4.80 m; higher vehicles could pass through the tunnel exceptionally if they ride under the middle of the vault.

7 SAFETY IN TUNNELS – TUNNEL EQUIPMENT

The scope of safety equipment of road tunnels is wider than that of railway tunnels because of the fact that much more subjects (vehicles) move in a road tunnel, the freedom of their movement is much higher, thus the chance that a dangerous situation will occur during the operation is much greater.

The safety equipment meets the ČSN 73 7507 norm and is designed in compliance with the Directive of the European Parliament and of the Council on minimum

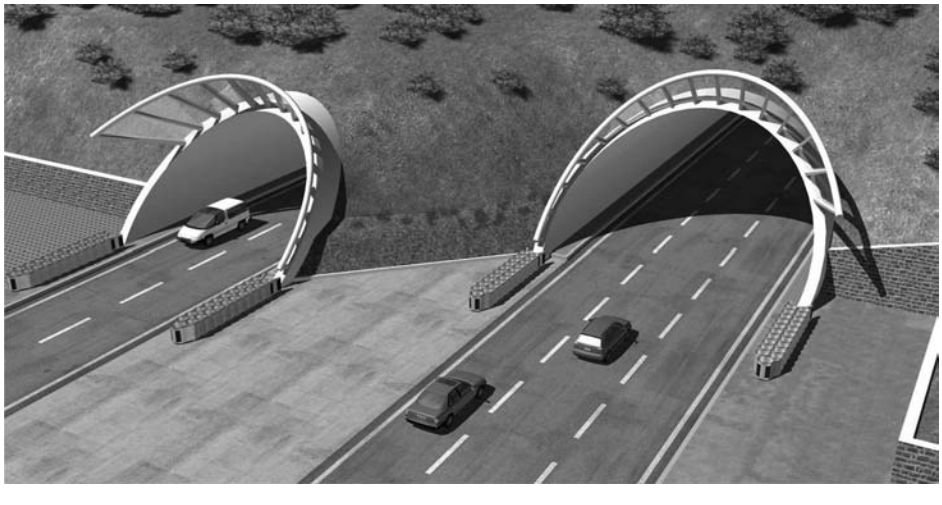


Figure 1. Architectural image of the portals.

safety requirements for tunnels in the Trans – European road network.

The recent conflagrations in European tunnels have shown us that the possibility of escaping from the tunnel is the most important factor of safety in a tunnel. This possibility is provided by construction of the above-mentioned cross passages, which are always equipped with fire resisting doors and separate ventilation systems. In addition, there is an emergency lay-by in each double-lane tunnel to be used for stopping and parking immobile vehicles; the lay-bys also facilitate contingent exiting of trucks from the cross passages passable for vehicles to the double-lane tunnels.

SOS boxes are installed every 150 m. They contain telephones, fire extinguishers and other equipment. A fire main with big hydrants, which is intended for the use only by firemen, is installed in each tunnel.

Of course, tunnel illumination with threshold and transition zones at portals, where the gradual reduction/increase in the lighting intensity provides gradual darkening/lightening and driver eyes can accommodate at the tunnel entry/exit, are a design standard. Stand-by lighting to be used in the case of an accident or fire is also installed in each tunnel.

The traffic control will be possible by variable traffic signs installed both inside the tunnels and on the open road before the tunnels. The tunnel control system is connected to the Traffic Information System and the data is transferred to control centres in Rudná and Prague, where the traffic data collected from the route is assessed. The processes in the tunnel will be observed by video cameras.

The tunnels are ventilated by jet fans installed under the tunnel crown at intervals about 200 m. In the basic regime, they are operated in the direction of traffic movement. The position and output of the fans is designed with respect to a fire emergency. The ventilation will be started during a fire after roughly 6 minutes to 8 minutes, when the cooling of smoke under the tunnel arch causes destratification of the smoke, which starts to threaten the passengers. The hot smoke keeps under the arch till that time and the escape of passengers is possible. The fans in the neighbouring smoke-free tunnel tube will be started in the same direction as those in the tunnel with the fire so that the smoke and other pollutants are not sucked to the clean tunnel via the portals. A ventilation plant for an exhaust ventilation system is designed, which will provide the required dispersion of pollutants in the right-hand (ascending) tunnel tube and partially at the beginning of the left tube.

The power consumption of all of the above-mentioned facilities is very high.

A transformer station and distribution substations are installed in single-storey buildings located in front of the portals; points where the electrical installations in the tunnels can be disconnected are available every 400 m. The power supply is backed up in case of a power failure.

Even the roadway drainage is designed with safety taken into consideration. Inverted siphons preventing a fire caused by an accident from spreading interrupt the drainage ducts installed along the curbs every 50 metres.

8 GEOLOGICAL CONDITIONS

The tunnels of the construction lot No. 514 will be driven through Ordovician and Silurian rocks, which are tectonically faulted and have pervasive faults and folds. Heavy fracturing of the rock occurs along the

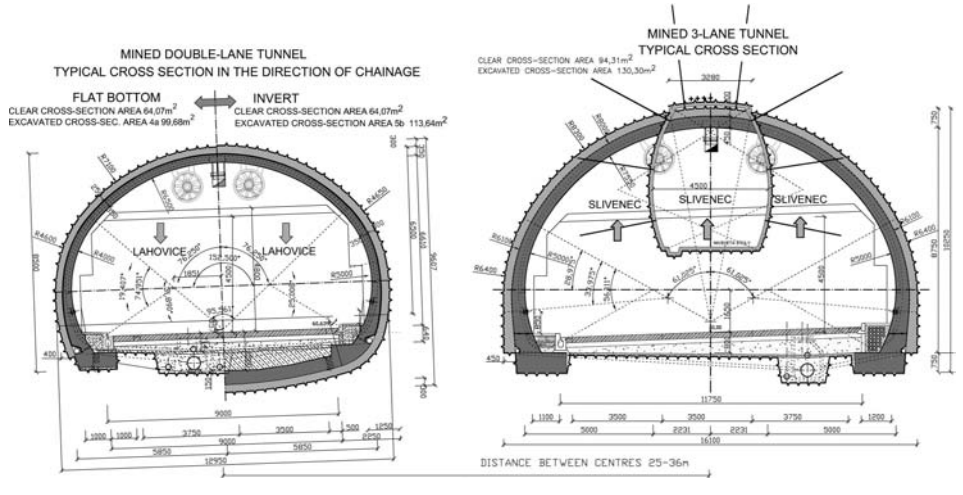


Figure 2. Cross sections.

faults. The shales, which are crushed by remoulding, are slickensided. Fissures are frequently open or partially filled with crushed rock and water. The numerous faults vary in their trends; the NE – SW trend dipping 45° to 60° to northwest can be considered prevailing. However, even transverse down-faults sub-parallel with the route are frequent. The filling of the down-faults consists of breccias of a character of shale fragments or clay. The information about quantity and quality of the faults was refined by an exploration gallery, which was driven along the central line of the top heading of the three-lane tunnel tube.

The hydrogeological conditions are relatively favourable for the excavation despite the fact that nearly the entire length of the mined tunnels passes under the water table lowered by the drainage effect of the exploration gallery. The aquifer existing in the area of the mined tunnels is bound to a fissure-type collector in the weathered zones of the bedrock. The water table copies to a certain extent the ground surface. The yield of the inflows at the excavation face may reach tenths of litres per second, in the case of quartzite or diabase it may grow to roughly 1 l/s, and in the case of water bearing faults up to 3 l/s.

9 THE EXPLORATION GALLERY – A PRE-CONSTRUCTION ELEMENT IN THE AREA

Geological conditions anticipated according to a geological survey can be verified during the planning phase of larger projects by excavation of an exploration gallery.

The exploration gallery, however, is always a matter of discussion in terms of the tunnel excavation; pros and cons of exploration drifts are relatively well known.

Today we would like to draw attention to a little bit different aspect. In addition to the exploration of the geology proper, the exploration gallery will test, on a smaller scale, even other relationships, and will "teach" the inhabitants and the entire region how to coexist with the future construction activities. In practice, it means that the condition survey of the affected buildings must be carried out and the blasting permit must be obtained; truck traffic to the construction site will start, thus the haul routes will be tested. Some utility networks will have to be relocated, the land for the site facility will have to be obtained, selected areas paved, power, water and sewerage services built etc. The inhabitants will feel all of these activities similarly as they will feel them during the future tunnel construction, only to a smaller extent. This process will help to forecast their future attitudes and requirements.

The results obtained by the exploration will be available to the designer and the contractor, who will use them in the process of optimisation of the construction procedures and selection of adequate tunnelling equipment.

10 TECHNICALLY SUITABLE SETTING OF THE EXPLORATION GALLERY

Till now, small cross-section exploration galleries have usually been designed with the aim of minimising the cost. Geological conditions have lately ceased to be the main factor in the design of the alignment passing through a more densely populated area. The final alignment is the result of strenuous searching for a "practicable" corridor.

The extent of tunnel projects, their exactingness and cost demands, the requirement for quick and economic excavation using up-to-date high-performance equipment, require broad knowledge of geology as well as knowledge of the rock response to excavation by heavy equipment. For this reason, "hand excavation" of minimum cross-section galleries with imperfect temporary support is today unsuitable.

The utilisation of heavy equipment requires the exploration gallery cross section to be enlarged; the enlargement requires the setting of the gallery to be selected which is optimal with respect to the subsequent tunnelling work so that the in advance excavated exploration gallery interferes with the excavation of the future tunnel as little as possible, and, on the other hand, contributes to facilitation and acceleration of the work.

The issue of the size and setting of the exploration gallery has been step by step solved for tunnels on the Prague City Ring Road.

The first gallery was designed as a traditional small horseshoe shaped profile gallery with the cross section of 13.8 m^2, set in the centre of the top heading of a three-lane tunnel. The aim of this design probably was to prevent the rock disturbance effects from reaching the surface of the future tunnel excavation. Such the setting will influence the further progress of the excavation of the tunnel tubes in a minimum extent, although, it can contribute to the facilitation of the future tunnel excavation also in a minimum extent if we consider the fact that the floor of the gallery is at least 1 m above the expected bottom of the top heading.

Metroprojekt Praha a.s. negotiated with the client a change in the cross section and setting of the exploration gallery when the work on the final design for the tunnels of the construction lots 513 and 514 was commencing. They incorporated a new setting and an enlarged cross section of 25.6 m^2 into the design; the floor of the gallery was designed at the level of the future tunnel. The height of the gallery is an optimum for utilization of high-performance equipment and for its radius of handling at the excavation face. The



Figure 3. A passing bay in the exploration gallery.

passing bays even represent complete top headings of the tunnel.

The setting and shape of the exploration gallery were selected so that the crown of the primary lining of the gallery extended into the primary lining of the future tunnel and became its part; later, because of the lapse of time between the gallery construction and the tunnel excavation, the gallery arch lining was shifted above the tunnel lining. Owing to this setting, the exploration gallery will create the first partial excavation (sequence) of the top heading of the three-lane tunnel. The primary lining of the gallery will act as a mighty anchor during the course of the top heading excavation. At the same time, it will significantly reduce the excavation face, which will become stable even without any additional measure. This gallery will not deteriorate the conditions for the excavation of the three-lane tunnel proper; just opposite, it will significantly contribute to the tunnel excavation safety.

Apart from its exploratory purpose, the completed exploration gallery, in its new setting, will become an important ventilation adit, escape route and access adit for rescue services in case of an emergency, even an optional supply route. It will allow gravitational drainage of the excavation during the downhill excavation of the large tunnels. The ideal opportunity of installing anchors in the crown of the vault in advance of the tunnel excavation and implementing in advance extraordinary or required measures in locations of weakness zones or other extraordinary conditions identified by the exploration gallery must not remain unmentioned. As a last resort in case of unfavourable rock conditions, a segment of the primary lining of the tunnel can be cast in the crown of the gallery (at a width equal to the width of the gallery) reinforced sufficiently to be capable of acting as a stiff longitudinal beam significantly reducing deformations in the rock mass and surface settlement during the work on the enlargement of the top heading and installation of the excavation support.

11 CONCLUSION

Today, the excavation of the exploration galleries for the 514 and 513 tunnels and the refining the information on geological conditions have been completed. The information and experience gained from the excavation of the exploration galleries have been incorporated into the detailed designs for both tunnels. The excavation of the tunnel 514 has commenced.

Underground Space – the 4th Dimension of Metropolises – Barták, Hrdina & Romancov (eds)
© 2007 Taylor & Francis Group, London, ISBN 978-0-415-40807-3

Portals – The architecture visible in cities and landscape

O. Hasik
METROPROJEKT Praha, Prague, The Czech Republic

P. Sourek
SATRA, Prague, The Czech Republic

ABSTRACT: Tunnels are civil engineering works where emphasis is mostly laid on their technical and economic design. The public usually view them as very important, even though unsightly rather than nice; as a structure that only serves its purpose and is no aesthetic complement or enhancement of the landscape in which it is located. In the past, tunnel portals were integrated with the ambience without affecting the ambience significantly, in a somewhat uniform style and often intentionally overshadowed by other structures. With the new upswing of the tunnelling industry in the Czech Republic over the last ten years, even tunnel designers dared involve capable architects, whose task was to complete this technical work so that it not only serves its purpose but its appearance also completes the architecture of the territory, and thus underlines the clear meaning of this large investment. The new approach has even made some of the current portals landmarks of the respective territories. The paper illustrates and describes the architectural concept of the tunnel portals being currently under construction or in the preparations phase, and brings back to mind the most important historic portals in Prague.

1 INTRODUCTION

The focus of this paper is on picturing tunnel portals. Photographs of structures built in the past or visualisation of projects being prepared are provided with brief descriptions.



Figure 1. Rudolph's Gallery, the year 1593.

2 SMALL TUNNELS

2.1 *Rudolph's gallery*

It is an underground gallery leading between the embankment of the river Vltava and Kralovska Obora (Royal Deer Park), which is the oldest tunnel in Prague. This historic monument was built in the years 1581–1593 to supply water to a pond in the deer park. The about 1000 m long gallery was excavated simultaneously from both ends and additional five shafts. The dimensions of the cross section are approximately 3.5 m × 2.2 m. The shafts and the gallery were supported only with round timber, which was replaced by masonry during the 18th century. This remarkable piece of technical work has been preserved up to the present time.

2.2 *The tunnel under the Prasny Bridge embankment*

A possibility of interconnecting both parts of Jeleni Prikop (Deer Moat) divided by a road embankment was under consideration from 1990. The tunnel has opened the access to another part of Prague Castle. The shape of the new tunnel and portals as well as the whole construction were sensitively designed by



Figure 2. The tunnel under the Prasny Bridge, 1990.

an architect. The route of the passage is identical with a former Theresian gallery allowing Brusnice stream to pass through the embankment.

The new egg-shaped tunnel is 84 m long. Three basic materials were used for the construction: concrete, hard-burnt brick cladding and, for pavements and the stream channel, natural stone.

3 ROAD TUNNELS

3.1 *The tunnel under Vysehrad*

The 34 m long × 9 m wide tunnel was opened to traffic on 11th December 1904.

The tunnel was considered necessary for vehicular and pedestrian traffic, which was a condition for further development of Prague districts of Podoli, Branik and Hodkovicky (villages on the outskirts then). The ambience around Vysehrad, which is a significant, nearly mythical historic monument, has always a romantic air. This was probably why the authors used crenelation and turrets for the portal decoration, which enhances this romantic character.

3.2 *The Letna tunnel*

The first real road tunnel was the Letna tunnel built in 1949–1953. It is 426 m long × 10.3 m wide × 6.5 m high. The gradient of the S-shaped alignment is uniform at 5.4%.

The tunnel links the area of Letna with the centre of Prague. It was excavated using the Modified Austrian Tunnelling Method.

3.3 *The Strahov tunnel*

The Strahov tunnel route connects the areas of Brevnov and Dejvice with the area of Smichov. The history of this connection can be followed in proposals developed

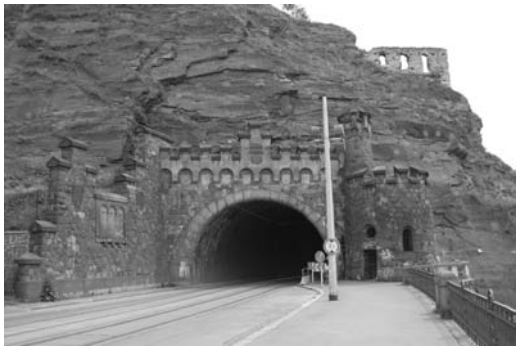


Figure 3. The tunnel under Vysehrad decorated with crenelation; 1904.



Figure 4. The Letna tunnel, 1953.



Figure 5. The Strahov tunnel, 1990.

as long ago as 1847 and 1937. The Strahov tunnel was inaugurated in 1997 as a part of the inner circle road.

The tunnel was driven using the side-drift method, which was probably a little bit archaic at that time.

3.4 *The Mrazovka tunnel*

The Mrazovka tunnel on the City Circle Road in Prague was built recently. The portals have been



Figure 6. The Mrazovka tunnel, 2004.



Figure 7. South-East Portal of The Mrazovka tunnel, 2004.

properly incorporated into the surroundings, from both architectural and town planning viewpoints.

The construction of the Mrazovka tunnel started in the autumn of 1998. It was opened to traffic in August 2004. The tunnel is 1300 m long; three traffic lanes are provided in the major part of its length. The excavated cross-section areas in the three-lane section and in bifurcation chambers were 165 m^2 and up to 340 m^2 respectively. The excavation of the tunnel passing under the relatively densely developed area was carried out by the New Austrian Tunnelling Method.

The northern portal is nearly directly connected to the southern portal of the Strahov tunnel. A cascade of greenery troughs suspended above the portal ends in a park on the top of Mrazovka Hill. The southeastern portal is provided with a staircase leading to a lookout located on the hillside.

3.5 *The Blanka tunnel*

The further development of the City Circle Road in Prague will comprise the Czech Republic's longest road tunnel at a total length of 5.5 km. The construction is planned to begin in 2007.



Figure 8. Troja axonometry – visualisation.



Figure 9. Portals of the Prague City Ring Road – visualisation.

The Blanka tunnel starts at the Malovanka grade-separated intersection, at the northern portal of the Strahov tunnel. In strict sense, the only real portal is the Troja portal.

3.6 *A portal and ventilation shaft of a tunnel on the Prague City Ring Road*

The construction lot 514 of the Prague City (outer) Ring Road project comprises tunnel tubes with "ribbed canopies" skirting the elliptic crowns of the portal ends. This architectural design will certainly relieve the dullness of the passage along this section of the route.

3.7 *The Pisarky tunnel in Brno*

The Pisarky tunnel is the first motorway tunnel completed in the Czech Republic and the first tunnel excavated using the observational method. The variant consisting of a tunnel with relatively long cut-and-cover sections was chosen as the most considerate towards the surroundings.



Figure 10. The Pisarky tunnel, 1998.

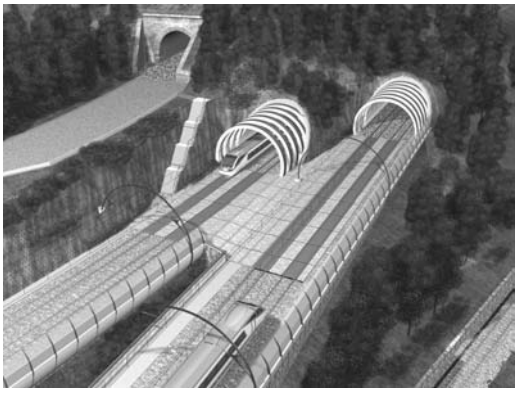


Figure 11. The new connection – visualization of the portal built in the centre of the city.

The tunnel is connected to a bridge over Certik stream on one side and to a bridge over the river Svratka on the other side.

4 RAILWAY TUNNELS

4.1 *The new connection in Prague*

Based on the EIA developed in 1996, it was decided that the railway lines from the Prague Libeň station and Prague Hlavni Nadrazi station and from Prague to Turnov would be led under Vitkov Hill, through a pair of double-rail tunnels. The reason for this solution was the effort to minimise the impact of railway traffic on inhabitants. Both 2400 m long double-rail tunnels were driven using the NATM.



Figure 12. The Vinohrady railway tunnels, 1944.

4.2 *The Vinohrady tunnels*

The year 1866 saw the commencement of the construction of the Franz Joseph's single-track railway line. As a part of this construction, the Vinohrady I single-rail tunnel construction started. The tunnel was later reconstructed and converted to a double-rail tunnel. The growth in the transportation outputs after the foundation of Czechoslovakia and the poor structural condition of the Vinohrady I tunnel resulted in the decision that a second double-rail tunnel (Vinohrady II) be built in 1940.

The recent reconstruction of the Prague railway junction which was carried out around the year 1985 required the addition of the Vinohrady III tunnel. It was driven using the ring method.

The Hlavni Nadrazi portal is located directly in the contact with the historic centre of Prague. We can say that it has become part of the unmistakable local colour of this area.

Underground Space – the 4th Dimension of Metropolises – Barták, Hrdina & Romancov (eds)
© 2007 Taylor & Francis Group, London, ISBN 978-0-415-40807-3

Study of the ship lift structure at the Slapy Dam

M. Jakoubek & J. Kuňák
Metroprojekt Praha, Prague, The Czech Republic

P. Uher
Pöyry, Prague, The Czech Republic

ABSTRACT: The paper deals with the design of the driven structures of the ship lift at the Slapy Dam, which is some 35 km upstream from Prague on the River Vltava. The dam profile is the main reason why the water route from Prague to České Budějovice is not navigable for ships of tonnage up to 300 tons. At present studies deal with several variants of the ship lift structure. Despite the fact that none of the variants has been chosen for further stages of the project preparation, the text describes in detail only one of the planned variants – the lock with high lift, which is the most interesting one from the point of view of tunnelling. This design of the ship lift uses to the maximum extent the newly built underground structures and at the same time it requires minimum work on the right bank. The excavation of the shaft and the driving will take place in the nearest surroundings of the dam and the hydraulic power plant which will require that extra safety and anti-vibration measures should be taken.

1 INTRODUCTION

The Vltava water route from Prague upstream ends at present below the Slapy Dam. The Slapy Dam is the only structure of the Vltava Cascade where the structure of the ship locking system is not finished. In 1955 the hydraulic structure was put into operation without the locking system and this situation still lasts.



Figure 1. View of the dam downstream side. In the left-hand bottom corner you can see the diversion tunnel outlet.

When the Slapy hydraulic structure was under development, its first studies already planned that the locking system should be constructed. This goal was not met due to the lack of time, high building costs and technological difficulties in connection with the filling of the reservoir. Only the building part of the navigation lock on the right bank in the upstream pool was built.

The original project planned the ship lift structure for ships of tonnage up to 300 tons. A vertical ship lift in a reinforced-concrete tower structure on the right bank below the dam was planned, situated out-side the dam body. The structure should have been connected to the diversion tunnel, which was used during the construction activities for the purpose of diverting water from the dam construction site.

2 STRUCTURE HISTORY

2.1 *Dam*

The decision to build the Slapy Dam was made as early as 1933. The gorge in the place once called Midsummer Streams (Svatojánské proudy) was chosen as the most suitable one for the dam. The structure was approved in 1949. In the same year the work on the diversion tunnel and auxiliary structures was commenced. It was the first big structure of the Vltava Cascade after the World War II. The dam was built

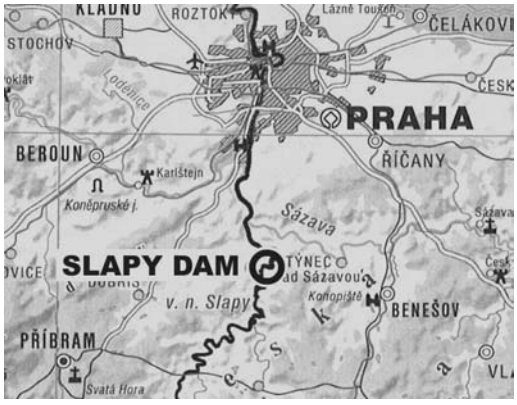


Figure 2. Map plotting.

in a dry pit, protected by fill dams on the upstream and downstream sides of the dam foundation surface. The dam was completed in 1955. The dam crest is 65 m above the bottom; the level difference is 54.6 m. The hydraulic power plant is situated in the concrete dam body. Water runs through four spillways with crest gates built above the hydraulic power plant.

2.2 *Diversion tunnel*

The diversion tunnel 10.0×12.0 m was built to allow rafts and vessels to navigate through while the construction activities were under way and most of all to divert water away from the construction site. The tunnel, 321 m long, was driven in a sound rock on the right bank and it is provided with concrete walling only in short sections by portals. The tunnel longitudinal slope is 0.15%. The diversion tunnel was closed shortly before the dam crest concreting. A concrete plug was constructed at the tunnel upstream end. It rested on cone-shaped pockets created in the wall and grouted with vertical holes, at the length of 30 m. Then, in April 1954, the filling of the reservoir was commenced. In July 1954 a vast flood came (a fifty-year one with the flow of 2200 $m^3.s^{-1}$), however the dam under construction withstood it. A positive result in favour of the capital of Prague downstream was the considerable transformation of the flood wave filling the empty reservoir.

At present the unsupported length of the tunnel is 291 m. The tunnel is accessible from the downstream water level (Fig. 3). The disposition of the tunnel and especially its length on the downstream side of the dam were designed from the beginning so that it could later be used as a navigation canal by the entrance to the locking system. The condition of the diversion tunnel was checked in detail some 20 years ago within trial blasting in connection with the shaft of the locking system. At that time the tunnel condition was quite good, only in a few places the rock under the vault toe.

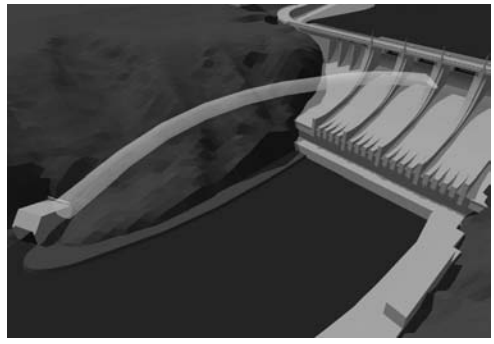


Figure 3. Existing diversion tunnel.

3 GEOLOGIC SITUATION

3.1 *Geologic conditions*

The Slapy hydraulic structure is situated in an area with monotonous occurrence of amphibolites of the argillaceous zone. The amphibolites are of the character of a fine-grained, solid, dark grey-green rock with high unconfined compression strength of up to 300 MPa. Occasionally in complete sections of amphibolites there is the so-called cushion lava forming longitudinally oval-shaped compressed schistose bodies, approx. 1.0×0.8 m. Amphibolites are very tough and resistant to chemical weathering, their faults are caused by slope movements of rock blocks and tectonic movements resulting from intensive compression of the argillaceous zone which is evident in schistose formations.

3.2 *Hydrogeologic conditions*

Groundwater absorbed in the rock base does not form a continuous horizon, its yield is small and the groundwater circulates in fissures without any relations. Apart from the surface sections, the fissures are close, frequently healed with calcite and almost water impermeable. The rock ambience permeability had been tested within research, before work on the dam was started, in holes by means of water-pressure tests and grouting tests. The value of the specific water loss was from 0.001 to 0.014 $l.s^{-1}.m^{-1}$ at the water pressure from 0.4 to 1.0 MPa. The dam profile was sealed with a grouted curtain during the construction activities. Since the dam was completed, the effect of the fissure systems pressure after afflux in the reservoir has not been tested.

4 SHIP LIFT CONCEPTION

4.1 *Original designs*

The heated discussions among experts in the Czech Republic, focused on the locking system structure at

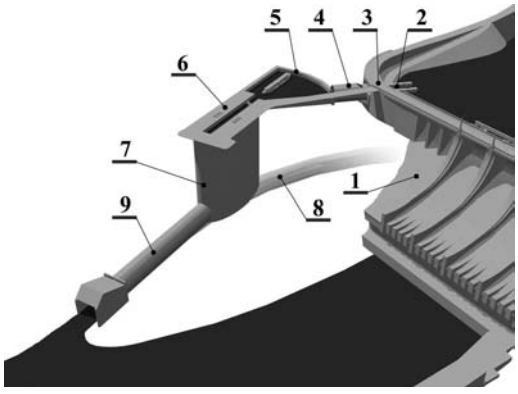


Figure 4. Design diagram. 1. Slapy dam, 2. Existing navigation lock, 3. Existing bridging, 4. New tunnel on the upstream water, 5. Passing bay, 6. Navigation lock platform, 7. Lock with high lift, 8. Closed part of the existing diversion tunnel, 9. Lower navigation tunnel, straightening the existing diversion tunnel.

Slapy, have lasted for more than 50 years. Up to the present several technological conceptions have been prepared (a lock with a high lift, a vertical ship lift in a shaft and a sloping ship lift). There were considered also alternatives of a navigation lock with s reversible pumps, a navigation lock with spare basins, a navigation lock with an ejection effect or a vertical ship lift with a complete balancing. Another proposal was an innovative design of a revolving ship lift when the ship channel moves along one carrying rail the shape of a helix Záruba (1960). Another original solution protected with a patent is a ship lift with pushed chains Záruba (1987).

4.2 *The existing state of project preparation*

The solution is designed in accordance with currently valid parameters of Water Routes European Classification Class I as regards ships of tonnage up to 300 tons. The ship lift must be able to lock a ship of effective dimensions 45.0×6.0 m. The navigation lock construction brings about a number of problems both hydraulic, nautical and static.

The last expert study (Uher and team 2006) contained three variants of the ship lift design: a shaft ship lift with a complete balancing, a lock with high lift with spare basins and a sloping ship lift.

The first and second variants have in essence the same layout, which is also used in all the previous designs. It uses as much as possible the existing navigation lock in the upstream water and part of the existing diversion tunnel for ships arriving to the lift on the downstream water.

The next part of the paper describes the most interesting variant from the point of view of tunnelling – the lock with high lift (Fig. 4). One of the problems of this design is the arrangement of structures with respect to ensuring optimum entry and exit conditions from upstream and downstream pools. In order that a ship enters and leaves on the downstream water it is necessary that this manoeuvre on a straight line. For this reason it is necessary to straighten the existing diversion tunnel in the point of the connection of the vertical shaft. The sudden change of the course of a ship which is necessary with respect to the above specified disposition will take place when the ship stops in the passing bay on the upstream water.

5 LOCKING SYSTEM STRUCTURAL DESIGN

5.1 *Upper navigation canal*

An upper navigation canal will be driven from the existing navigation lock, running partly through an open cut and partly through a short navigation tunnel. The new profile will be driven by means of NRTM (New Austrian Tunnelling Method) with a primary support of the excavation with a sprayed concrete layer and a system anchorage. Final walling will be of cast-in-situ reinforced concrete. On both sides of the tunnel will be (escape) footbridges, their vertical parts will be, within the fluctuation of water level of 1.50 m, used as guard rails.

The navigation tunnel will end in the passing bay tank of trapezoidal layout. The passing bay will be situated in an excavated pit, slopes of the cuttings will be supported with permanent anchors and protected with a sprayed concrete layer. The passing bay tank structure will be made of cast-in-situ reinforced concrete for water structures. The foundation surface of the passing bay bearing structure will be permanently drained with a drain system connected to the downstream water because of the pressure effects on the structure. The passing bay will have two mobile binding systems. With the systems it will be possible to turn the ships if they avoid each other in the passing bay.

In the downstream direction the passing bay tank is connected to the lock with high lift.

5.2 *Lock with high lift*

The navigation lock will be situated in a shaft of an elliptic layout 60.0×25.0 m, cross-section area is approx. 1300 m^2 and depth 60.0 m. The clearance of the lock is 45.0×6.0 m, the intermediate space will be used for spare basins (Fig. 6).

The shaft will be excavated gradually from the surface, it will be secured with primary walling of sprayed concrete with a system anchorage. To prevent the effect of shocks on the structures of the dam and the operated hydraulic power plant, before the excavation is commenced a secured perimeter nick will be

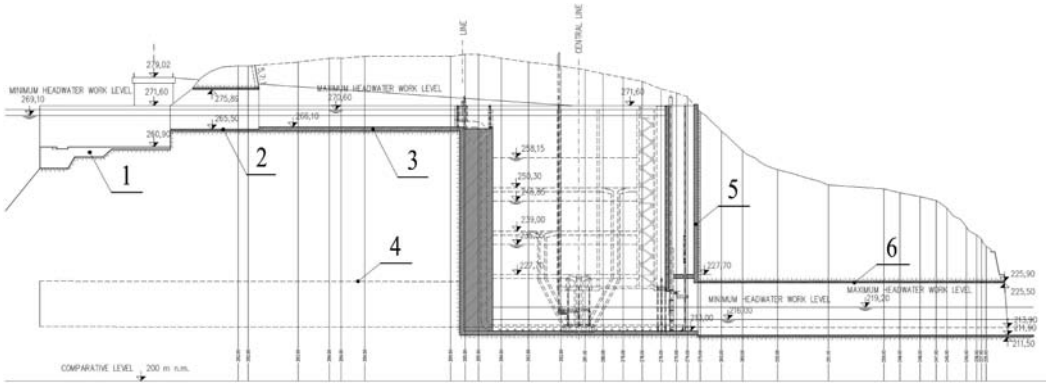


Figure 5. Longitudinal profile. 1. Existing navigation lock, 2. New tunnel on upstream water, 3. Passing bay, 4. Closed part of the existing diversion tunnel, 5. Lock with high lift, 6. Lower navigation tunnel, straightening the existing diversion tunnel.

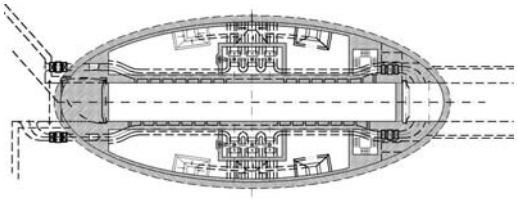


Figure 6. Plane section of lock with high lift.

made by means of a hydro cutter along the height of the shaft. The trench, 0.6 m wide, will be filled with bentonite mud. The final (secondary) walling will be of cast-in-situ reinforced concrete. Waterproofing with a permanent drain system connected to the downstream water will be inserted between the primary and secondary walling. This will eliminate effects of possible hydrostatic pressure from fissure systems on the final shaft structures. The inner clearance of the shaft enclosure will be approx. 60.0×25.0 m.

The shaft inner structures that will be used as spare basins are designed to transfer different hydrostatic pressures during regular water level fluctuation while the navigation lock is being filled and discharged. The lock will be filled and discharged by means of long bypasses closed with check gates. Bypass inlets on the upstream water will be on side walls between the tank and the lock. Check gates will be controlled with hydraulic face jacks. Shafts of bypass closures will be up to the level of the lock platform. In the downstream head the hydraulic face jacks of check gates of bypasses will be situated above the level of maximum downstream water. The navigation lock platform will be at 271.60 meters above sea level and the minimum water depth in the lock will be 3.0 m, the bottom at 213.00 meters above sea level. On the walls of the navigation lock will be installed floating binding elements for big and small ships and ladders. The lock platform will be lit.

The lock will have three twos of spare basins, interconnected with filling and discharging channels in the middle of the lock length with long bypasses. Particular channels will be closed with check gates controlled by hydraulic face jacks installed in the dry shaft integrated into the layout of spare basins. For the purposes of installing technology and its operation the shaft will be accessible from the lock platform. In the section of the channels between the check gates and the lock will be slots of box dam and the space will be filled with air. Particular levels of the spare basins will be connected to the atmosphere through the aeration pipe.

The head gate will be of boards with a vertical axis of rotation controlled by a hydraulic face jack. The gate sill with surface at 266.10 meters above sea level will be of minimum length, thus a ship hull will be prevented from sinking to the bottom when the water level drops while the lock is being emptied. In front of the gate will be the slot of the box dam for filled tube stop logs.

The tail gate situated outside the navigation lock layout will consist of a lift gate controlled by a hydraulic face jack installed in the dry shaft. The shaft floor will be at 227.70 meters above sea level, a box dam board will be permanently installed in the slots against downstream water. Access allowing technology installation and its operation will be possible from the lock platform top. The gate sill will be at 213.00 meters above sea level. The long bypasses will be emptied into the downstream water in the profile between the tail gate and the box dam.

For the purposes of operation and maintenance of the navigation lock and the spare basins there will be two dry access shafts with a staircase and a central

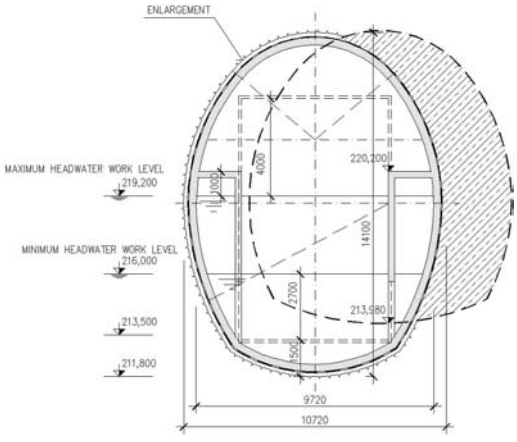


Figure 7. Cross-section of the lower navigation tunnel. Extension of the existing profile of excavation in the place of connection to the shaft.

space for material and equipment transport. Particular landings of the staircase will allow access to the floor of the machine room of tail gate closures, the machine rooms of closures of filling and discharging channels of spare basins and pressure covers provide access to particular spare basins. A small passenger lift will be designed to transport people.

5.3 *Lower navigation canal*

The lower navigation canal will consist of a tunnel running right in the direction of the longitudinal axis of the lock with high lift, connected to the straight end section of the diversion tunnel. The existing tunnel will have to be profiled anew (while using principles of NRTM with the primary support of the excavation with a sprayed concrete layer and a system anchorage). Final walling will be of cast-in-situ reinforced concrete (Fig. 7).

The remaining part of the diversion tunnel, approx. 130 m long, will be used for the fill of muck which will be subsequently grouted and the tunnel profile will be closed. When the operating level in the channel is at 216.00 meters above sea level, the minimum water depth will be 2.70 m (2.20 ship draught and 0.50 m margin). The tunnel bottom at the depth of 2.70 m will be min. 213.30 meters above sea level. Maximum level will be at 219.20 meters above sea level. On both sides of the tunnel will be (escape) footbridges with the top at 220.20 meters above sea level, their vertical parts will be, within the fluctuation of water level of 3.20 m, used as guard rails. The tunnel will be lit.

While the lower navigation tunnel is being driven and equipped, a pit will be excavated outside the tunnel portal in the River Vltava bed.

6 SAFETY ISSUES

6.1 *Safety measures taken during construction activities*

According to the task the work on the construction should be carried out while the hydraulic power plant works full out and the water level in the reservoir must not get lower.

The vertical shaft, some 60 m deep and some 1300 m^2 of excavated area, is a mining work of extraordinary dimensions. Excavation and driving will take place in relatively complicated hydrogeologic conditions (extremely hard amphibolites with compression strength of 300 MPa, broken into blocks with fissure groundwater under the pressure of up to 50 m of water column). Work will be carried out in the nearest surroundings of the dam and the hydraulic power plant, in the nearest place the shaft is 100 m away from the dam body. The establishment of the perimeter nick along the entire height of the shaft before the excavation is commenced is an extensive anti-shock measure taken for the purpose of separating the blasting operations from the outdoor environment. The said designs will be worked out in detail in the following stages of the project documentation.

6.2 *Safety measures during the ship lift operation*

As similar structure is found neither in the Czech Republic nor even abroad, the proposal of safety measures will be based on structures of a similar character, that means navigation locks with a big gradient.

If an accident of a ship in the lock occurs, the advantage of this variant is that it is possible to fill or discharge the lock as an emergency and thus the ship can be relatively quickly moved to one of utmost positions. For purposes of inspections and access of rescue teams there will be a section with ladders along the entire height of the navigation lock.

It is possible to anticipate that despite all the safety measures there will be a group of people that will refuse this way of transporting. In this instance these tourists will be transported by minibuses.

7 INCORPORATING THE WORK IN THE LANDSCAPE

7.1 *Effects on the environment*

The variant of the lock with high lift is to the maximum possible extent situated in the underground so that its adverse effect on the landscape is minimal (Fig. 8). In comparison with the other variants this one offers the slightest impact on the surroundings.

The lock with high lift construction is designed to meet the strictest ecological requirements as it is

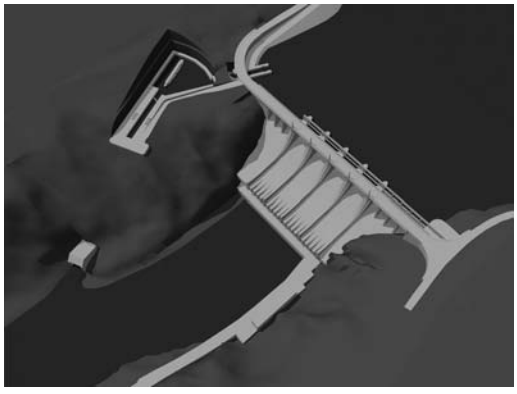


Figure 8. Perspective – bird's eye view.

situated in a beautiful landscape of the River Vltava valley, used as a holiday area by inhabitants of the capital which is some 35 km away.

7.2 *Ship lift as a draw for tourist*

It is expected that the entire ship lift system will be accessible tot the public. The variant of the lock with high lift is probably the least attractive from among the assessed variants if compared with the sloping ship lift when the ship is on the ground level all the time and thus the passengers can watch the valley. In order that the peace of mind of passengers is preserved the navigation lock and the lower navigation tunnel will be lit on walls. Within the reach of the work will be founded a centre to be visited by both ship passengers and the people who will only come to see the work. It is anticipated that the public will be interested in the work as it will be, owing to its extraordinary parameters and its design, a popular destination of tourists. This is also taken into account when the return on the investment is considered.

8 CONCLUSION

It is possible to say that the presented design prepared as a study is feasible on the basis of current conditions.

Safety risks in connection with the construction and operation of the locking system do not exceed common risks associated with the use of water routes and therefore they do not represent any obstacles to the construction.

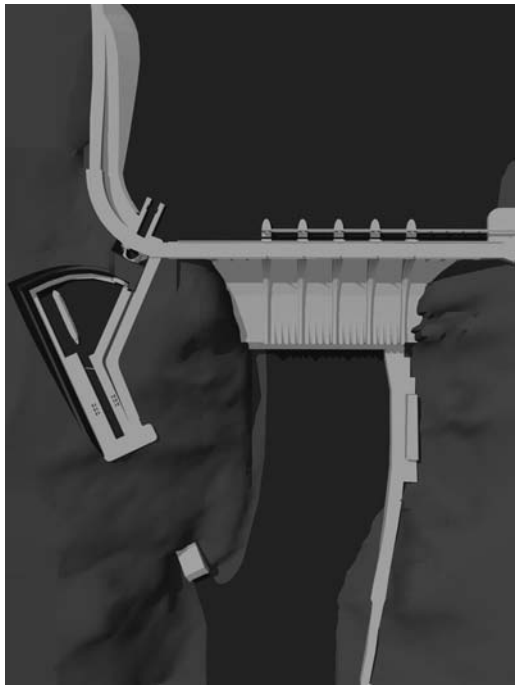


Figure 9. Incorporating the work in the landscape.

REFERENCES

Broža, V. & kol. 2005. Dams in Bohemia, Moravia and Silesia. Liberec: Knihy 555

Uher, P., Trnka, M., Suchý, J., Veselý, R., Jakoubek, M. & Kuňák, J. 2006. Expert Technical and Economic Study on Ship Lift Structure at the Slapy Dam

Záruba, L. & kol. 1953. The Slapy Hydraulic Structure. Ship Lift Design

Záruba, L., Gabriel, P. & Němec, M. 2002. Completion of Locking Systems at the Slapy and Orlík Dams. Water Routes

Záruba, Q. & kol. 1967. Geology of Dams on the Vltava River. Prague.

Underground Space – the 4th Dimension of Metropolises – Barták, Hrdina & Romancov (eds)
© 2007 Taylor & Francis Group, London, ISBN 978-0-415-40807-3

Design of the District Heating Tunnel in Copenhagen

T. Kasper, C. Edvardsen & M. Faurschou
COWI A/S, Kongens Lyngby, Denmark

ABSTRACT: The 3.9 km long District Heating Tunnel in Copenhagen is intended to supply the inner city of Copenhagen with district heating. Starting from a 37 m deep access shaft at the power plant on the island Amager, the tunnel is bored by an EPB shield machine and passes under the city to a 44 m deep shaft at Adelgade and a 30 m deep end shaft at Fredensgade. The tunnel has an internal diameter of 4.2 m and will carry 2 steam pipes, 2 hot water pipes and 2 condensation pipes. Under operation with 12 hours ventilation per day, the inside of the tunnel will heat up to a temperature of approx. 50 degrees. With its axis between 25 and 38 m below the ground surface, the tunnel is located at its full length within the Copenhagen limestone. The lining for this tunnel is designed with steel fibre reinforced concrete (SFRC) segments without conventional steel bar reinforcement based on the German SFRC design guideline. Apart from a general overview on the project, this paper is concerned with the methods and calculations applied in the structural design of the tunnel lining including the special aspect of the heating of the tunnel. Further attention is paid to the durability design, laboratory tests and experiences during construction.

1 INTRODUCTION

To upgrade the production and supply of district heating in Copenhagen it has been decided to move the current production from the two older plants Svanemølleværket and HC Ørestedsværket to the completely renovated block 1 at the Amager Power Plant (Amagerværket). In order to minimise the disturbance at the surface in the Copenhagen city it was decided to place the pipelines in a tunnel (Figure 1). The tunnel starts with a straight 2.4 km long stretch between the access shaft at the Amager Power Plant and the shaft at Adelgade, turns about 56° northwards and continues in a straight 1.5 km long stretch to the end shaft at

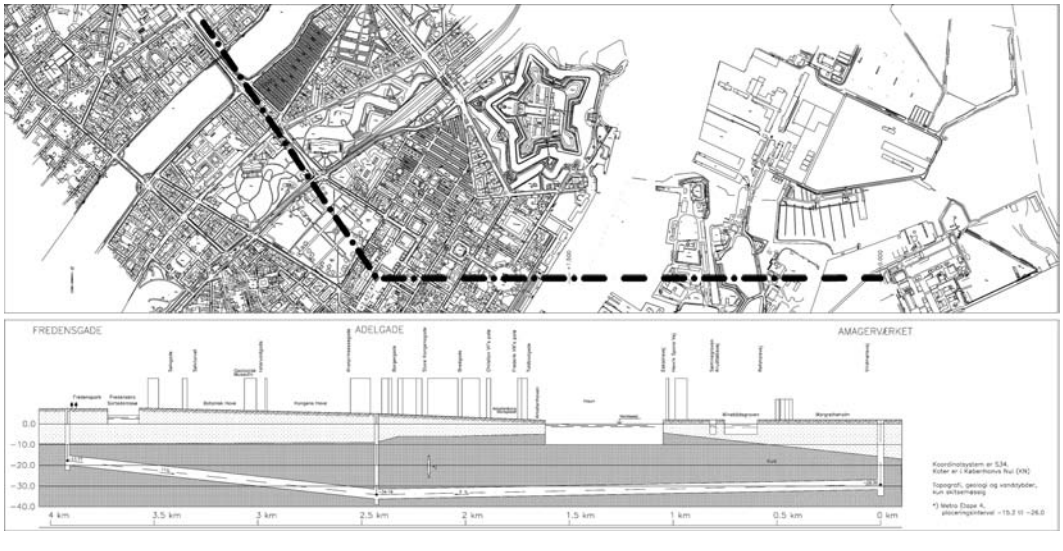


Figure 1. Layout of the District Heating Tunnel in Copenhagen.

Fredensgade. The tunnel is located at a depth between 25 and 38 m. The alignment is governed partly by the wish to excavate the tunnel primarily in the middle Copenhagen limestone and partly by minimum inclinations needed to deal with condensates in the steam pipes during operation. The heating tunnel passes below the future metro tunnel on the first stretch to the shaft at Adelgade. The geology along the alignment is characterized by quarternary layers of fill, clay and sand tills and melt water units down to depths between 14 and 18 m below the surface and Copenhagen limestone underneath (Knudsen et al. 1995, Hansen & Foged 2002, Jackson et al. 2004).

The shafts for the tunnel are constructed with secant pile walls in the upper part and are temporarily lined with shotcrete in the lower part. Permanent concrete linings with membranes at the outer faces will be constructed after the tunnel works are finished. The shaft at the Amager plant is the largest one. It has an oval cross-section with final internal diameters of 25/15 m and an excavation depth of 37 m.

The tunnel is excavated with an EPB shield machine. This type of TBM was also successfully applied in the Copenhagen metro project (Nymann & Taylor 2003). For the installation, launch, turning and arrival of the TBM, NATM caverns with temporary shotcrete linings are excavated from the three shafts. As the shafts, these caverns will also be lined with permanent concrete linings.

Although passing under densely built inner city areas with historical buildings and sensitive infrastructure, no surface settlement problems need to be investigated compared to shallow tunnels in soft soils (Kasper & Meschke 2006a, b) due to the deep location of the tunnel in the intact limestone rock mass. This conclusion is further supported by a comprehensive investigation of settlements experienced during construction of the Copenhagen metro phase 1 + 2A.

The District Heating Tunnel is lined with steel fibre reinforced concrete (SFRC) segments without conventional steel bar reinforcement (Figure 2). Although the properties, design and possible application of SFRC have been a topic of research for a longer period (see e.g. Maidl 1995) only relatively few applications for precast segmental tunnel linings have been reported so far. To the authors' knowledge, the first large-scale test application of SFRC segmental linings without steel bar reinforcement was in 140 m of a pressurized water tunnel in the Lesotho Highlands Water Project in South Africa (Wallis 1995). Further application examples are the baggage handling tunnel at London Heathrow Airport (Moyson 1995) and, on a large scale, about 20 km twin-tube sections of the Channel Tunnel Rail Link (Davis et al. 2006). Design guidelines for SFRC have been worked out in various countries. However, no standards are available yet. The lining design for the

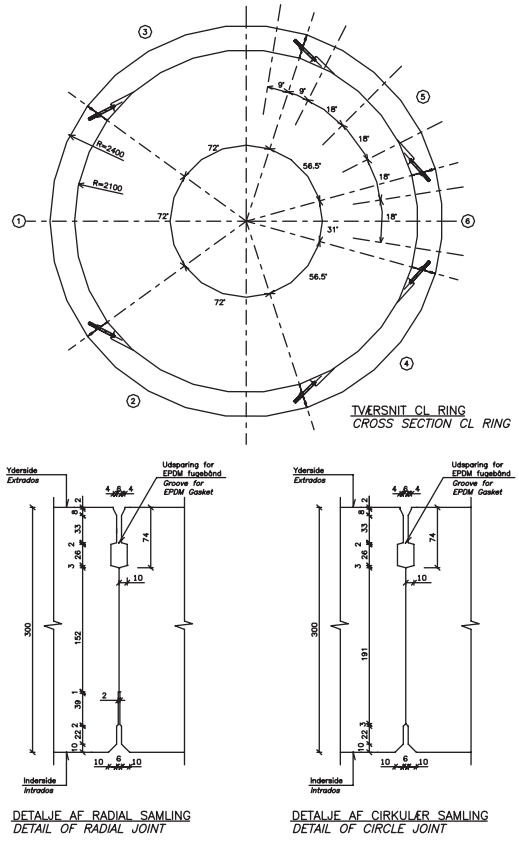


Figure 2. Layout of the segmental lining.

District Heating Tunnel is based on the German SFRC design guideline (DBBV 2001).

The annular gap around the lining is injected with a two-component grout (cement, bentonite, water and stabilizer as component A, water glass and water as component B), which is characterised by short gelling and setting time. This ensures a quick stabilization of the tunnel lining, avoids uplift of the rings and shear displacements between the segments.

The operation of the heating system has been optimized (Matlock et al. 2005). The tunnel is assumed ventilated 12 hours each day during night time leading to a predicted uniform temperature elevation along the circumference to max 54°C on the inside of the lining and to max 50°C on the outside of the lining.

The design and construction of the tunnel is performed based on a partnering model (late partnering) between the involved parties. The design work started in October 2004, the excavation works for the shafts started in September 2005 and the tunnel is due for operation of the pipelines end of March 2009. The total costs of the project are estimated to be DKK

750 million incl. the piping works tendered for in late 2006. The use of steel fibres was included as an option in the tender documents. Apart from direct commercial benefits to the contractor, it is anticipated that the client will gain from the use of SFRC by reduced operation and maintenance costs during the life time of the tunnel.

2 STRUCTURAL DESIGN OF THE SEGMENTAL TUNNEL LINING

The lining has a thickness of 30 cm (Figure 2). The concrete is C50/60 and contains 35 kg/m^3 fibres of type DUOLOC 47/0.80. According to its bending strength characteristics (cp. Figure 5), the SFRC is classified as fibre class 1.4/0.6. The lining has flat concrete-to-concrete radial joints and flat longitudinal joints with 0.9 mm thick bituminous packers. It is equipped with EPDM gaskets. The segments are designed to form tapered rings with a width of 1.50 m and a taper of 2 cm consisting of 3 standard segments, 2 counter key segments and 1 key segment. The final loading situation of the circular tunnel lining in the limestone rock mass is characterised by predominant compression with only small bending moments. Steel fibres in the concrete lining improve the resistance against spalling of corners and edges, introduce a ductile post-cracking behaviour, eliminate corrosion problems and therefore increase the durability. However, special care is required during segment production, transport and construction in the tunnel, as SFRC segments cannot compete with the bending capacity of conventionally reinforced segments. The segments are erected with a vacuum pad erector in combination with a shear key of 110 mm diameter in the centre of the segments. The segments are bolted together with straight bolts in bolt pockets. The bolts are removed after construction.

The sectional forces in the lining for the loading situation without heating of the tunnel have been determined by two-dimensional numerical models using the finite difference code FLAC (Figure 3). The model considers the different soil layers and the grout by continuum elements and the tunnel lining by beam elements. A fine grid is used in the vicinity of the tunnel. The lining is modelled in a simplified way as a continuous ring without consideration of the radial joints. This is a conservative approach leading to the largest possible bending moments while the normal forces in the ring are not affected by this assumption. Table 1 contains the material parameters applied in the analyses. Both an upper and a lower bound estimate of the limestone stiffness are investigated.

The calculated sectional forces contain a circle shape tolerance of the ring of 25 mm and lipping of 15 mm. The load bearing capacity of the lining is verified based on the stress-strain relationship shown in

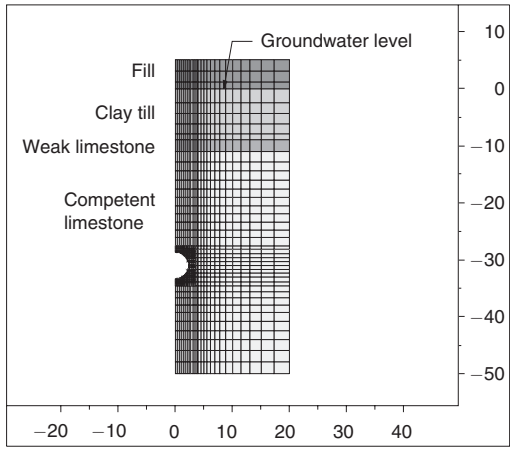


Figure 3. Numerical model for the determination of sectional forces without heating of the tunnel, shown for the deepest section.

Table 1. Geotechnical parameters of the different soil layers.

Material	γ (kN/m^3)	E (MPa)	ν –	ϕ' (°)	c' (kPa)	K_0 –
Fill	22	10	0.3	30	0	0.5
Clay till	23	150	0.3	34	10	0.44
Limestone crushed zone	22	1000	0.25	45	50	0.29
Competent limestone	22	1500 (min) 10000 (max)	0.25	45	100	0.29

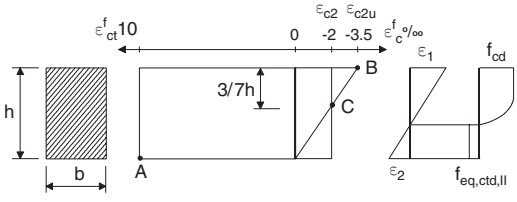


Figure 4. Rectangular SFRC cross-section: Definition of admissible strain ranges and assumed, simplified stress-strain relationship for the verification of the bearing capacity.

Figure 4. A parabolic-rectangular compressive stress block is assumed for the concrete and a simplified (conservative) rectangular tensile stress block is assumed for the cracked concrete. The actual tensile stress-strain relationship of the SFRC determined from bending tests is shown schematically in Figure 5. The resulting failure envelope in the M-N interaction diagram is shown in Figure 6 and Figure 7 together with the calculated sectional forces for the two limit cases

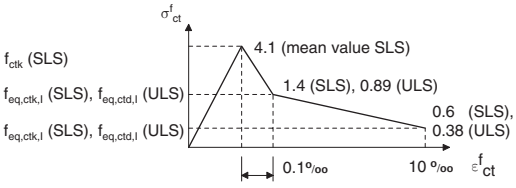


Figure 5. Tensile stress-strain relationship of the SFRC according to laboratory 4-point bending tests.

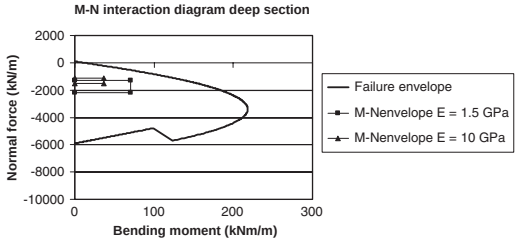


Figure 6. Failure envelope and envelope of the sectional forces for the deepest tunnel section without heating, for the upper and lower bound estimate of the limestone stiffness.

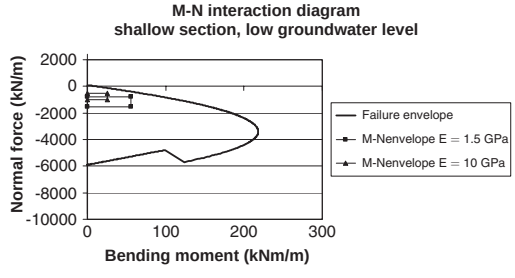


Figure 7. Failure envelope and envelope of the sectional forces for the shallowest tunnel section with low groundwater level, without heating, for the upper and lower bound estimate of the limestone stiffness.

of the deepest and the shallowest section of the tunnel. The ranges of the sectional forces are shown as rectangles, bounded by the lines min N, max N, min M = 0 and max M. The discontinuity of the failure envelope is due to the required higher safety factor of 1.8 for failure of uncracked cross-sections compared to the normal safety factor of 1.5 for failure of cracked cross-sections. It can be observed that without heating of the tunnel the smallest safety margin for the bearing capacity is obtained for the shallowest section with low groundwater level.

The heating of the tunnel leads to an axisymmetric temperature and, consequently, thermally induced strain and stress distribution and has therefore been analysed with an axisymmetric thermo-mechanical numerical model. The model contains the lining, the

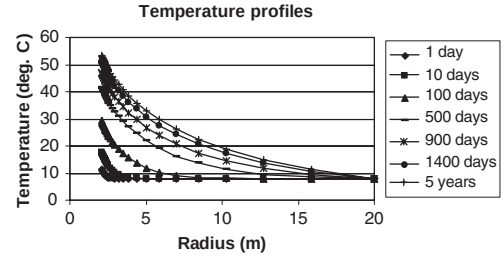


Figure 8. Computed axisymmetric temperature profiles in the lining, grout and limestone at different points in time. The steady state is reached after approximately 5 years.

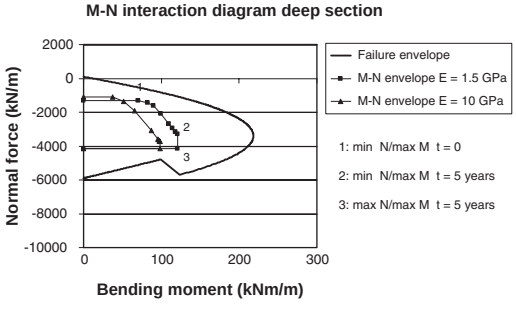


Figure 9. Failure envelope and envelope of the sectional forces for the deepest tunnel section including heating, for the upper and lower bound estimate of the limestone stiffness.

grout and the limestone and considers a constant heat flux on the inside of the lining of 19.7 W/m^2 in the SLS (totally 261 W/m, cp. Matlok et al. 2005). The initial temperature is assumed to be 8 °C in all materials and is assumed to remain unchanged at a distance of 20 m. For the mechanical plane-strain analysis, the displacements are fixed at a distance of 20 m. Figure 8 shows the evolution of the temperatures due to heating of the tunnel. The steady state is reached after approximately 5 years with a temperature of 53.3 °C on the inside of the lining and 49.4 °C on the outside of the lining. For the verification of the bearing capacity of the lining (ULS), a heat flux of $1.35 \times 19.7 = 26.6$ W/m^2 is applied resulting in steady-state temperatures of 66.1°C on the inside and 60.8°C on the outside of the lining.

The temperature induced sectional forces in the lining are obtained by integration of the computed tangential stresses and are added to the sectional forces without heating of the tunnel. The result is shown for the deepest section of the tunnel in Figure 9. The temperature increase causes a considerable increase of the normal force in the lining ring. Due to the temperature gradient over the lining thickness and the lipping tolerance the bending moment increases as well. Only the deepest section is shown as it is obvious that this gives the most critical sectional forces after heating.

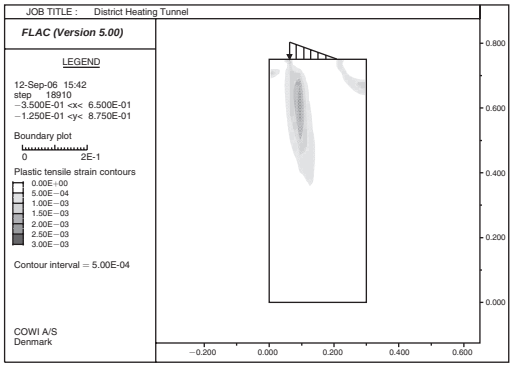


Figure 10. Computed plastic tensile strains (cracking) at the radial joints based on $f_{eq,ctd,I} = 0.89$ MPa (ULS).

The concentrated transfer of the sectional forces at the radial joints through the 152 mm wide contact area (cp. Figure 2) leads to bursting stresses in the vicinity of the joints. The most onerous sectional forces (M = 121 kNm/m and N = 4141 kN/m (ULS) and M = 90 kNm/m and N = 3074 kN/m (SLS)) have been transformed into an equivalent triangular contact pressure distribution and have been applied in a 2D-plane strain numerical model as shown in Figure 10.

Although the formation of a larger crack is observed in the ULS the predicted strain level in the crack of about 2 ‰ is small (cp. Figure 5). It is concluded that the cracks do not represent a critical failure state and that the integrity of the structure can be maintained by the steel fibres. In an SLS computation, no cracking is predicted as the bursting stresses remain below the mean characteristic tensile strength of 4.1 MPa.

3 DURABILITY DESIGN OF THE SEGMENTAL TUNNEL LINING

The client has required that the tunnel shall be designed to satisfy a service life of 100 years, where the structure should not require major maintenance and repair. The elevated temperature in combination with the aggressiveness of the environmental exposure requires special attention. The tunnel is located in salty water, mainly close to the harbour with chloride contents of 1–1.5%. Due to this, the most critical deterioration process in case of traditionally reinforced segments would be chloride induced reinforcement corrosion which, for structures in marine environment, would require special measures to guarantee a service life of 100 years (end of service life is usually defined by the start of reinforcement corrosion). In the present case, the situation is even more serious due to the increased temperature, as the temperature level is decisive for the rate of transporting aggressive substances such as chlorides into and within the concrete. All chemical and electro-chemical reactions are accelerated by an increase in temperature. According to a simple rule of thumb an increase in temperature by 10°C causes a doubling of the rate of reaction. In the present case the temperature is approx. 40°C higher than in usual, bored tunnels with approx. 10°C, which will lead to a $4 \times 2 = 8$ times faster ingress of chlorides in the heating tunnel compared to the ingress rate in normal, bored tunnels. In addition, the corrosion process may be accelerated due to the risk of accumulation of chlorides on the internal tunnel surfaces due to evaporative effects. These factors would make it very difficult to design the heating tunnel for a 100 years corrosion free service life when trusting alone on the traditional durability measures such as sufficiently large and sufficiently dense concrete layers. In the present case, the traditional design would require covers of approx. 70-80 mm. These covers would induce a high risk of spalling during handling and installation of the segments (ram thrust forces etc.).

Several research investigations (Raupach et al. 2004, Weydert et al. 1998) have shown a favourable behaviour of steel fibre reinforced concrete with respect to durability. This is due to the fact that the critical chloride content of steel fibre reinforced concrete (so-called threshold value) is much higher than that of normal steel reinforcement, although identical steel compositions are used. Further, the corrosion activity of steel fibre reinforced concrete is limited to surface rusting of some protruding single fibres. Although rust spots near the surface are expected to occur, corrosion will not penetrate deeply as a result of the following reasons in case of uncracked concrete:

- Continuous corrosion between individual fibres is not possible because each fibre is individually embedded in and thus protected by the concrete. Therefore, no electrical conduction occurs which would result in a continuous process (no macrocell corrosion possible).
- Corrosion of fibres will not cause the concrete to spall. The stresses caused by the expansion of the fibre diameter are negligible and do not lead to more damage.

In summary, steel fibre reinforcement instead of steel bar reinforcement has been found to be the best solution to ensure the required durability of the District Heating Tunnel.

4 LABORATORY TESTS AND EXPERIENCES DURING CONSTRUCTION

The following material tests are made:

- Petrography analyses on plan-sections of extracted cores to investigate the distribution of the fibres in

the hardened concrete. In the beginning, the distribution of the fibres was not always as homogenous as desirable with some higher amounts of fibres in the lower part of the cores. This concrete test has proven to be very useful and almost indispensable, at least during the pre-testing and starting phase of the production.
- Wash-out tests of fresh concrete to determine the amount of fibres. The intention was to find a simple test method which gives a second control of the actual fibre amount in addition to the automatic weighing determination at the mixing plant.
- 4-point bending tests to ensure the required strength properties.
- Splitting tests (Brazilian tests) as additional tensile strength tests.
- Unconfined compressive strength tests to ensure the specified C50/60 concrete class.

About 300 rings have been built so far. The design, the segment production and the construction works appear to be satisfactory as segment damages are limited to 15 visible cracks with wet spots and some irrelevant spalled edges at the bolt pockets and erector cone recesses. Most of the cracks have occurred at the corners of key segments. Only a small number of further minor water leakages have been detected.

5 CONCLUSIONS

The construction works for the District Heating Tunnel in Copenhagen comprise the excavation of three deep shafts, short NATM caverns and 3.9 km of TBM tunnelling in the Copenhagen limestone. Following previous applications in some tunnel projects, the lining for the bored tunnel is made of SFRC segments without conventional steel bar reinforcement. This eliminates the problem of corrosion, ensures the required durability and helps to achieve a cost-efficient segment production as well as an efficient construction with low segment damage rates.

ACKNOWLEDGEMENTS

The authors gratefully acknowledge the permission of Copenhagen Energy to publish this paper.

REFERENCES

Davis, H., Woods, E. & Shuttleworth, P. 2006. Focusing on fibres: CTRL experience. *Tunnels & Tunnelling International* 20(3): 29–32.

Deutscher Beton- und Bautechnik-Verein (DBBV) 2001. *Guideline "Stahlfaserbeton"*.

Hansen, H.K. & Foged, N. 2002. Kalkens bjergmekaniske egenskaber. In J.K. Frederiksen et al. (eds), *Ingeniørgeologiske forhold i København*. dgf-Bulletin No. 19: 31–34, Danish Geotechnical Society.

Jackson, P.G., Steenfelt, J.S., Foged, N. & Hartlén, J. 2004. Evaluation of Bryozoan limestone properties based on in-situ and laboratory element tests. In *Proceedings of the 2nd International Conference on Geotechnical Site Characterization, 19–22 September, Porto*, Vol. 2: 1813–1820.

Kasper, T. & Meschke, G. 2006a. On the influence of face pressure, grouting pressure and TBM design in soft ground tunnelling. *Tunnelling and Underground Space Technology* 21(2): 160–171.

Kasper, T. & Meschke, G. 2006b. A numerical study of the effect of soil and grout material properties in shield tunnelling. *Computers and Geotechnics* 33: 234–247.

Knudsen, C., Andersen, C., Foged, N., Jakobsen, P.R. & Larsen, B. 1995. Stratigraphy and engineering geology of København Limestone. In *Proceedings of XI ECSMFE Copenhagen*. dgf-Bulletin No. 11, Vol. 5: 117–126, Danish Geotechnical Society.

Maidl, B. 1995. *Steel Fibre Reinforced Concrete*. Ernst & Sohn.

Matlok, S., Hansen, B. & Frederiksen, M. 2005. Cooling of concrete lining in a district heating tunnel. In *Proceedings of the International Conference on Tunnel Design and Systems Engineering, 12–13 September, Basel*, 155–164. Kempston: Independent Technical Conferences Ltd.

Moyson, D. 1995. The construction of a steel fibre reinforced concrete segmental lining in London. In STUVA (ed.), *Weltneuheiten im Tunnelbau. Proceedings of the World Tunnel Congress / STUVA-Tagung '95 Stuttgart*, 274–278.

Nymann, J. & Taylor, S.D. 2003. Construction of the Copenhagen Metro. In J. Saveur (ed.), *(Re)Claiming the Underground Space*, Vol. 2, 607–612. Lisse: Balkema.

Raupach, M. & Dauberschmidt, C. 2004. Corrosion Behaviour of Steel Fibres in Concrete Containing Chlorides. In *Long Term Prediction and Modelling of Corrosion. Proceedings of the EUROCORR 2004, European Corrosion Conference, 12–16 September, Nice.*

Wallis, S. 1995. Steel fibre developments in South Africa. *Tunnels & Tunnelling International* 27(3): 22–24.

Weydert, R. & Schiessl, P. 1998. Corrosion of steel fibres in cracked and uncracked steel fibre reinforced concrete. In *Research report No. 516*, University of Aachen (ibac), Germany.

Underground Space – the 4th Dimension of Metropolises – Barták, Hrdina, Romancov & Zlámal (eds)
© 2007 Taylor & Francis Group, London, ISBN 978-0-415-40807-3

Excavation connecting the underground ventilation station and the underground expressway tunnels

Yoshihito Konishi & Isao Kamegaya
Metropolitan Expressway Company Limited, Tokyo, Japan

Akio Ueda & Yasutaka Imanaka
Obayashi Corporation, Tokyo, Japan

ABSTRACT: Construction of the Nakaochiai Ventilation Station requires the underground connection of the shaft structure and the tunnels. Due to schedule constraints, the entire 50 m-section is to be opened up at the same time, so several countermeasures, such as heavy soldier piles, wedge concrete and soil struts, are adopted for construction. The construction sequence is thoroughly examined and instrumentation of the structures is planned. This paper introduces one successful example of underground ventilation station construction, focusing particularly on the connection between the ventilation station and the tunnels.

1 INTRODUCTION

In recent years, traffic congestion in urban areas has become a major problem as the Japanese population becomes more and more concentrated in large cities. To alleviate traffic congestion, expressways have been constructed in the large cities. The construction of the expressway system in the Tokyo metropolitan area began in the 1960s, but the construction of circular expressways lags far behind the construction of radial expressways, as shown in Fig. 1. When expressway construction started in the 1960s, elevated expressways over the public right-of-way were built to expedite the construction schedule and to minimize the construction cost. However, due to environmental problems and overcrowded ground-level space, plans were made to construct the first underground expressway in Tokyo.

The Central Circular Shinjuku Route is an 11 km-long western section of the Central Circular Route and the first underground expressway in Tokyo, as shown in Fig. 2. The Shinjuku Route is designed as a tunnel structure under the Ring Road No.6, which has an average daily traffic of 18,000 vehicles. One of the problems of underground expressways is the ventilation of exhaust gas. Ventilation stations are being constructed at approximately every 1,500 m. Most of the tunnel sections are built using the shield method, but the ventilation stations are built using a cut-and-cover method above the tunnels. Therefore, connections are made underground between ventilation stations and expressway tunnels, and new techniques will be developed to accommodate underground construction of expressways, such as underground tunnel enlargement and diversion.

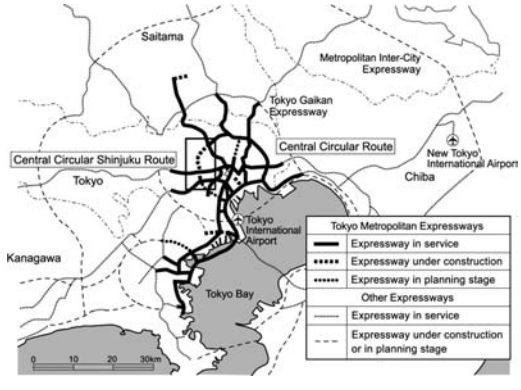


Figure 1. Greater Tokyo Expressway network.

2 DESIGN AND DETAILS OF THE NAKAOCHIAI VENTILATION STATION

The Nakaochiai Ventilation Station is 230 m long, 35 m wide and 22 m deep. The expressway road was built under the ventilation station using the shield method, so the excavation for connecting the ventilation station and the expressway roads reaches a depth of 36 m. Our contract concerns the southern 130 m of

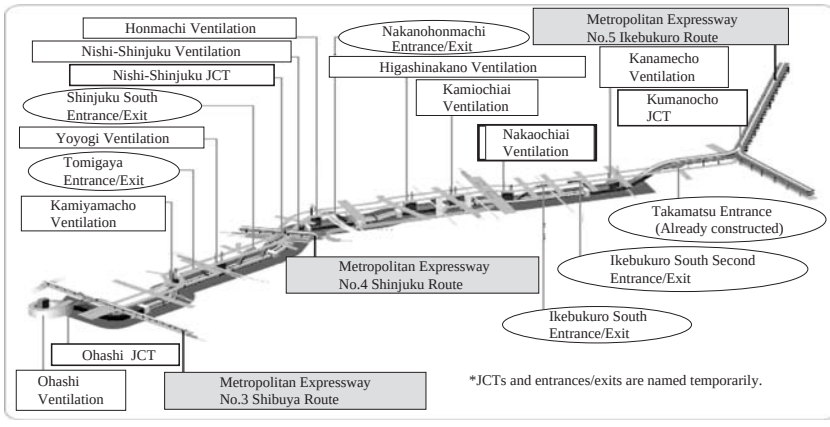


Figure 2. Over view of the Central Circular shinjuku.

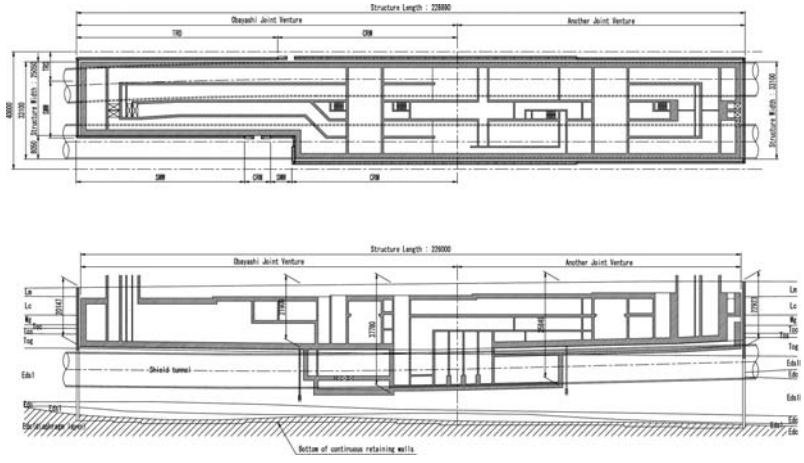


Figure 3. Plan view and longitudinal view of the ventilation station.

the station structure construction. The shaft, which will provide a connection to the tunnels, is 8.1 m wide, 50 m long and between 35 m to 37 m below the ground.

The ventilation station is built in stable diluvial strata. There is a layer of Kanto loam and clay from the surface to a depth of 10 m, followed by a layer of Musashino gravel and Tokyo gravel to a depth of 22 m. The ground underneath the Tokyo gravel layer is the 1st Edogawa sand layer, which is stable diluvial sand, and its N value is more than 100. The 1st Edogawa clay layer lies under the 1st Edogawa sand layer.

The underground water level is about 10m from the surface, which is approximately at the top of the Musashino gravel layer. The Tokyo gravel layer and the 1st Edogawa sand layer both have artesian ground water. When an earth retaining system was designed for the Nakaochiai Ventilation Station, a continuous retaining wall was adopted to prevent adverse effects on the surrounding area by dewatering. Therefore, the retaining wall extends to the 1st Edogawa clay layer, which is about 46 m below the surface.

The wall in the standard section consists of H-488×300 steel piles at 600 mm spacing. In the section where excavation is 36 m deep for connection to the tunnels, H-900×300 steel piles were used at 450 mm spacing, because no ground resistance was expected where the section between the two tunnels was excavated. The plan view and the longitudinal view of the ventilation station are shown in Fig. 3. The cross-sections are shown in Figs. 4 and 5. The Continuous Walls Using Recycled Mud (CRM) method, a kind of slurry wall method in which a horizontal multi-axis

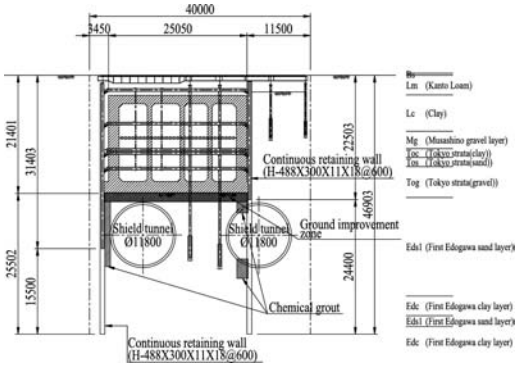


Figure 4. Cross-section of the standard section.

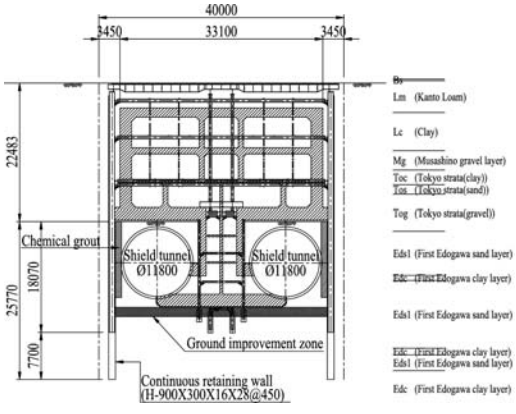


Figure 5. Cross-section of the connection to the tunnels.

Table 1. Quantities of the major work items.

Work items	Unit	Amount
Cotinuous retaining wall (SMW)	m^2	3,930
Cotinuous retaining wall (CRM)	m^2	5,590
Cotinuous retaining wall (TRD)	m^2	3,560
Intermediate piles	本	104
Metal decking	m^2	4,800
Earthwork	m^3	89,000
Trench timbering	t	1,890
Chemical grout	k?	1,120
Ground-improvement	m^3	4,900
Filling	m^3	3,600
Concrete	m^3	31,350
Reinforcement	t	2,760

cutting wheel excavator is used, was adopted for a slurry wall where H-900 × 300 steel piles were used. The size of the element, which is 1,100 mm wide and 3,200 mm long, is the same as for a conventional slurry wall. The quantities of the major work items are shown in Table 1.

3 FORESEEABLE DIFFICULTIES AND CONSTRUCTION SEQUENCE OF THE VENTILATION STATION

3.1 *Foreseeable problems with the ventilation station construction*

Due to schedule constraints, the entire ventilation station structure could not be completed before the shields came through, so the ventilation shaft and the connection work could begin only after the shields passed through the station area. The completion of the expressway has long been awaited and the opening date for the public has been set. Accordingly, every effort to expedite the construction schedule had to be implemented. The construction sequence was planned in order to minimize the work remaining after the shields passed through, and all necessary preparation work was planned as well as possible before the shields came through. Only excavation and concrete placement of the shaft and the connection area were planned after the shields passed through, and the ventilation station structure, shaft construction, and connection had to be conducted concurrently. Connection is usually performed by dividing the entire area into several sections and completing the excavation and concreting of each section before moving on to the next section. However, due to the schedule constraints, the entire length of the connection section between the shaft and the tunnels had to be excavated at the same time.

3.2 *Planned construction sequence*

The following measures were planned to expedite the completion of the entire project.

(1) The slurry wall was extended to the impermeable clay layer so that all shaft and connection work could be done in dry conditions.
(2) Heavy H piles (H900 × 300 × 16/28@450 mm) were used for soldier piles so that the retaining wall was strong enough to be supported between the base slab of the ventilation station structure and the ground underneath the tunnels. These heavy soldier piles were adopted so that no passive earth pressure inside the soldier piles between the base slab of the station structure and the ground under the tunnels was measured.
(3) The ground underneath the tunnels had to be consolidated by jet grouting to form soil struts.
(4) When the shaft was excavated to the top of the tunnels, the upper arches of the tunnels were secured at the top to prevent lateral movement of the tunnels and to secure the ground between tunnels and the base slab of the ventilation station structure.
(5) The shaft structure was concreted before excavation between the shaft and tunnels began.

(6) Though the segmental rings at the ventilation openings were cut, the main beams were not cut as long as possible. The connection of the segments and the shaft structure was designed as a pin connection. Stiffeners and gusset plates were welded to the main beams where they come into contact with the concrete to secure the bearing capacity, and the axial loads of the segmental rings were transferred to the shaft structure. The details of the connection are shown in Fig. 6.

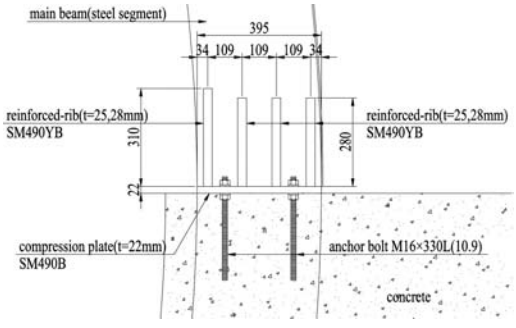


Figure 6. Details of the connection of the segment.

3.3 *The construction sequence*

The construction sequence is shown in Fig. 7.

Step 1: The struts for reinforcement of the tunnel linings were installed in the tunnels by tunnel contractors. The shaft was excavated approximately to the spring line of the tunnels and the pipe roofing was put into place. Steel pipes 87.6 mm and 114.3 mm in diameter were used for the pipe roofing. Then, the ground between

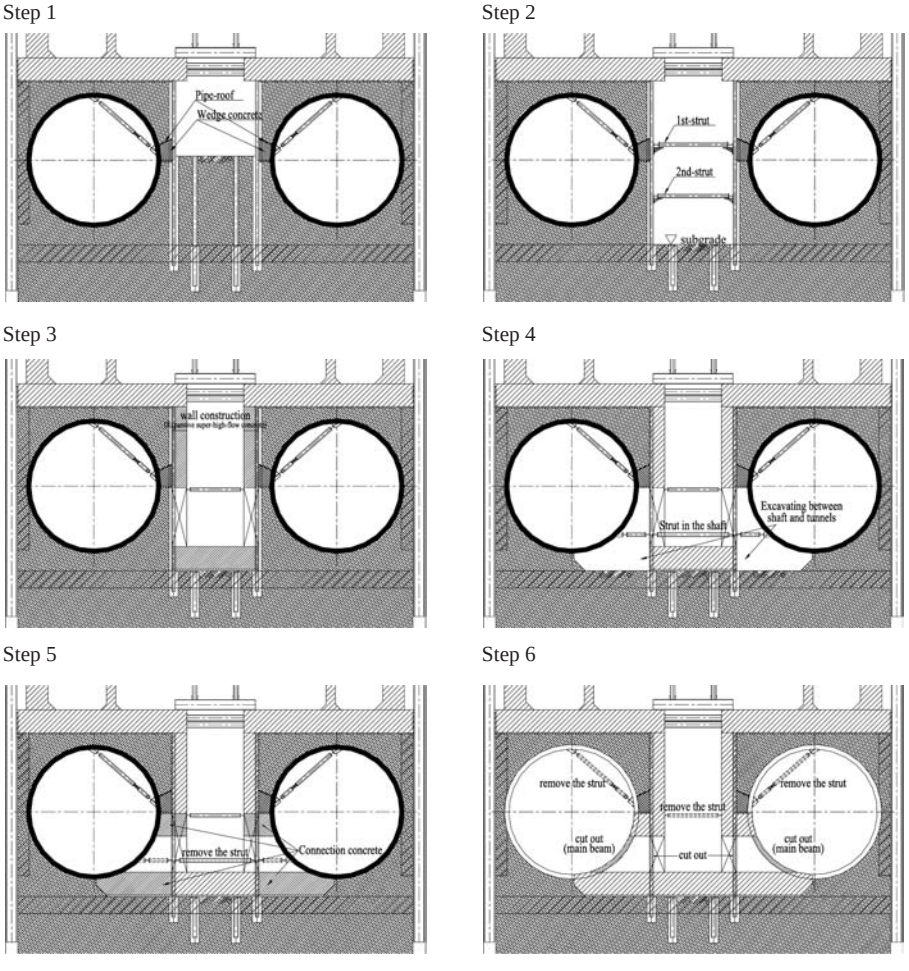


Figure 7. Construction sequence.

the shaft and the tunnels was excavated and the opening was filled with structural concrete, which prevented the lateral movement of the tunnels and secured the ground between the base slab of the station structure and the tunnels.

Step 2: The shaft was excavated to the bottom. Deformation of the soldier piles in the outside retaining wall was monitored by inclinometers, and the load cells were installed on the struts in the shaft excavation to monitor the axial loads.

Step 3: To secure the rigidity of the shaft structure, the concrete of the shaft structure was placed before the ground between the shaft and the tunnels was excavated.

Step 4: The ground between the shaft and the tunnels was excavated, while deformation and displacement of the tunnels and loads on the struts in the shaft was carefully monitored.

Step 5: When excavation was complete and the tunnels were exposed, the skin of the segments was cut out. The ribs and main beams were kept intact until the connection concrete was complete. The base slab of the connection was poured and then rest of the connection structure was completed. Bearing plates and gusset plates were welded to the main beams of the segments and embedded into the concrete.

Step 6: The main beams of the segments were cut out and struts inside the tunnels and the shaft were removed.

Since a wide area was open at the same time on both tunnels, deformation of the tunnels and stress of the shaft concrete and struts were measured. The following measurements were taken while the shaft and connection work was being conducted.

(1) Measurements of the tunnel's inner diameter
(2) Movement of the segmental lining
(3) Strain on the segmental lining
(4) Stress on the reinforcing bars of the connection structure
(5) Load on the struts inside the shaft

4 CONSTRUCTION RESULTS

4.1 *Installation of the pipe roof and placing the support concrete (wedge concrete)*

The pipe roof had to be put into place via the shaft, which was only 8 m wide, and excavation to the tunnels had to be performed by hand because of limited space.



Photo 1. Construction of wedge concrete.

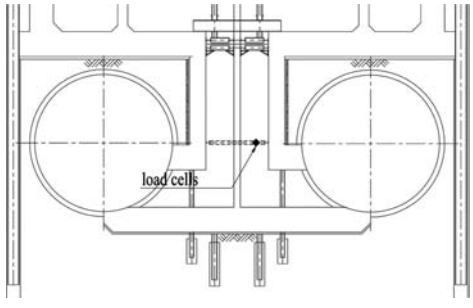


Figure 8. Location of the load cells on the struts.

The ground was hard, so the work was very time consuming and tough, as shown in Photo 1. However, this wedge concrete contributed significantly to the stability of the ground between the base slab of the station and the tunnels and to the stability of the segmental linings against lateral displacement. No detrimental movement was detected during the shaft construction, even though the entire 50 m-section was opened at the same time.

4.2 *Measurement of the load on the struts in the shaft*

After the shaft concrete was placed, the struts for the shaft excavation were replaced with new ones in the shaft structure and the axial load was monitored by load cells. The locations of the load cells are shown in Fig.8. Judging from the measurement results, which are shown in Fig.9, little change in the axial load on the struts was detected until the upper slab of the connection section was poured. It is believed that the expansion pressure of the non-shrink concrete, which was used on the upper slab due to its workability, may have caused the increase in axial load. The axial load far exceeds the design value, but it is still less than the maximum capacity of the concrete, and no major cracks were detected in the concrete either.

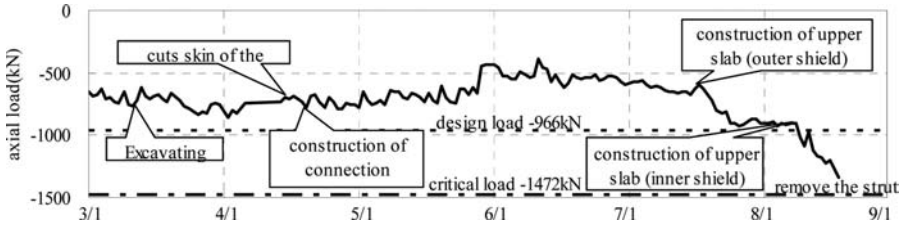
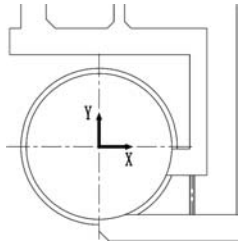
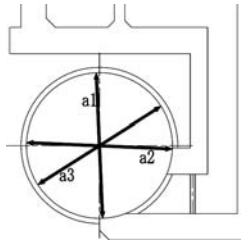


Figure 9. Measurement records of the load cells on the struts.



a) Measurement of displacement

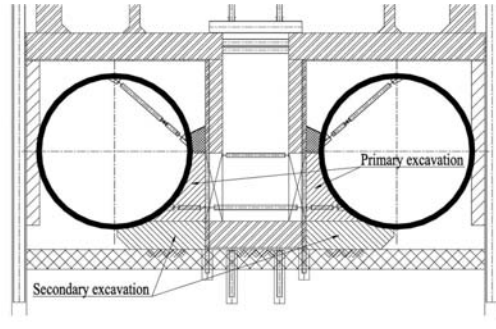


b) Measurement of deformation

Figure 10. Displacement and deformation measuring.

Table 2. Maximum displacement and deformation of the segmental linings.

Construction step	X (mm)	Y (mm)	a1 (mm)	a2 (mm)	a3 (mm)
Primary excavating	7	−3	−14	18	5
Secondary excavating	7	−13	−20	9	5



4.3 *Displacement and deformation of the segmental lining*

Once a day during excavation and once a week when concrete work was being conducted, the movement of the segments was measured using an automatic theodolite, while the deformation of the segmental lining was measured by an inner diameter-measuring device that uses lasers. The measurement locations are shown in Fig.10. The maximum deformation values in each stage are tabularized in Table 2. When the first stage of the excavation was completed, lateral movement was shown to have occurred, but the vertical movement was small because the bottom area of the segments had not been excavated. At the second stage of the excavation, the ground under the segments was excavated and 13 mm of settlement was recorded.



Photo 2. Excavation at the base slab of connection by a small backhoe.



Photo 3. Hand excavation under the segment.



Photo 4. Cutting out the skin of the segment.

As for the inside diameter of the segmental linings, the vertical diameter became smaller and the horizontal diameter grew larger as the excavation between the shaft and the tunnels proceeded. This tendency and the magnitude were within the expected range and no ill-effects were observed on the permanent structures.

Photos 2, 3 and 4 show the connection construction.

5 CONCLUSION

Due to the great challenge posed by the tight schedule, additional measures, such as installation of the wedge concrete and soil struts, were implemented. This was the first attempt to construct the entire 50 m section of the connection between the shields and the shaft at the same time. The field work was conducted carefully while measurements of the instrumentation were evaluated to ensure that the construction process proceeded as designed. Because the working area was relatively confined, work had to be performed by hand in many places, which could have resulted in schedule delays if it had not been planned in advance. The entire work of the shaft and the connection construction was completed as scheduled and without any major problems.

Construction plans vary according local geology and conditions, so foreseeable problems need to be investigated as much as possible in advance and necessary countermeasures must be prepared before construction starts.

Since underground connection work will become increasingly required in the future, this paper may help to assist in the planning of such work.

This page intentionally left blank

Underground Space – the 4th Dimension of Metropolises – Barták, Hrdina & Romancov (eds)
© 2007 Taylor & Francis Group, London, ISBN 978-0-415-40807-3

Prague – Beroun, new railway connection

D. Krása, J. Růžička & O. Hasík
METROPROJEKT Praha, Prague, The Czech Republic

ABSTRACT: A large investment, the modernisation of railway corridors, has been under way in the Czech Republic for approximately 10 years. The preparation of the modernisation of the Third Railway Corridor, leading from Prague through Plzen and Cheb to Germany, has progressed to an advanced stage. This corridor also includes the Prague – Beroun section. The existing route, which is 39 km long, currently leads through the valley of river Berounka. The design documentation for the reconstruction of this route following the existing route was prepared first. However, given the parameters required to be met by a design for a modernised railway corridor, the horizontal alignment of this route is very problematic in terms of the track speed, the direct interference with the Protected Landscape Area of Ceský Kras, and the problems stemming from the route passage through a densely populated area. This route modernisation would require large investment without achieving the expected improvement of the track parameters. This gave rise to the idea of a qualitatively different option of delineation of the route from Prague to Beroun. A new Prague – Beroun railway connection will be built to meet the high-speed track parameters, with the speed up to 300 km/h. Given the character of the landscape, the new route, with the total length of 28 km, mostly leads through a tunnel, approximately 24,7 km long, with the longitudinal gradients about 5‰.

1 THE EXISTING CONDITION

The route of the western part of the Transit Corridor III from Prague to Beroun, which is the route heading toward Plzeň and the border with Germany, leads along the densely developed Berounka River valley, and directly touches the Protected Landscape Area of Český Kras (Bohemian Karst).

The horizontal alignment contains sections with maximum design speed of 80 km/h. It was proven during the work on the draft design for the optimisation of this section that modification of the existing alignment was virtually unfeasible and, in addition, the investment would not result in the expected improvement of the parameters of the track. For those reasons the decision was made to seek a new solution that would follow parameters required for a high-speed railway track.

2 THE NEW DESIGN

A new solution to the western part of the Railway Transit Corridor III, the section Prague – Plzeň – state border, was approved by the Government in July 2005. This section is considered as a priority for it is part of the Corridor IV of the European network of main railway lines (AG-TC – C40), (AGTC – E40) Lvov – Čierná nad Tisou – Žilina – Ostrava – Olomouc – Prague – Plzeň – Frankfurt – Paris.

Given the terrain configuration, the newly designed route is 28 km-long, with a major part of its length (approximately 24.7 km) passing through a tunnel to be driven on a minimum longitudinal gradient of 5‰, under an overburden higher than 100 m. Obviously, given the anticipated length of the tunnels, the choice of dimensions of the tunnel clearance will also play an important role.

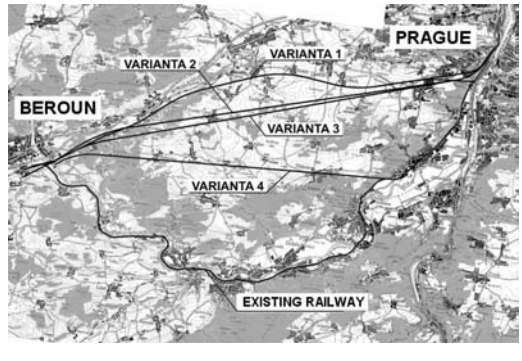


Figure 1. Variants of the route.

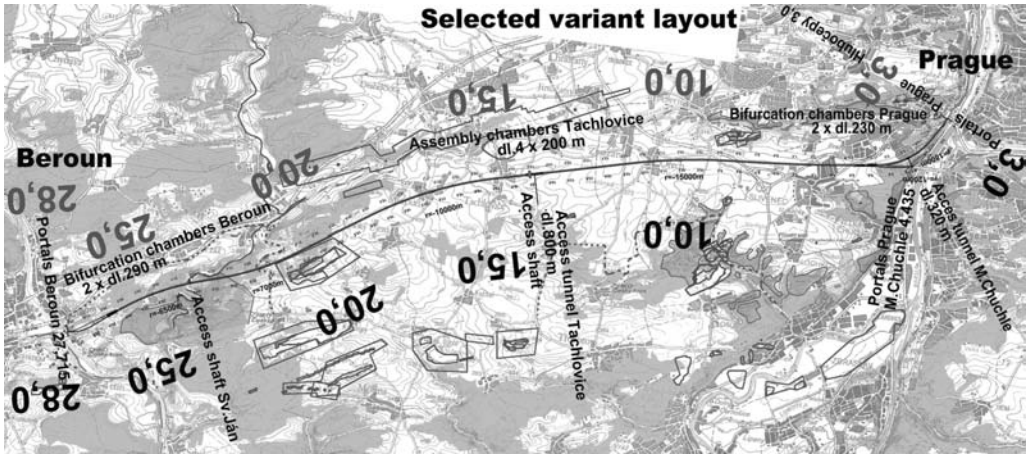


Figure 2. Selected variant layout.

The existing route, leading through the Berounka River valley, will remain without modernisation, only subjected to common maintenance, to serve the dense commuter traffic and as a by-pass route.

The studies which were submitted were assessed on the basis of a risk analysis. The most suitable solution was used as a basis for preparation of the design documentation for issuance of the zoning and planning decision, which is currently underway.

3 THE RISK ANALYSIS AND THE DOCUMENTED SELECTION OF VARIANTS

The risk analysis was carried out in the initial phase of the designing process. Naturally, it did not bring surprising results because the hazards defined at the beginning of the analysed progressions of segments of sources and concurrences are easily foreseeable even without any analysis. However, the risk analysis provides a consistent image of the entire design, not only of isolated parts. The particular risks, including their assessment, were processed in a tabular form.

The result of the risk analysis is a source of recommendations for the owner, designer and others, which are aimed at minimising the design risks. The recommendations cover the risk management, insurance, bank guarantees, dispute prevention and contract procurement.

As required by the order, the designer developed several variants of the possible design approach to the new railway link to be assessed. They consisted primarily of various variants of the alignment and variants of cross sections with various sizes and configurations. The route started at the Prague-Smíchov railway station, and ended in the Berounka River valley, on the edge of Beroun. The variants of the alignment differed in the end section found on the edge of Prague, in the location of the Prague portals, and in the vertical arrangement.

The alignment and configuration of the cross section which were selected on the basis of the risk analysis should meet the highest of all the requirements for basic design parameters, feasibility, safety and overall economy.

The most differing variants of the alignment are shown in Fig. 1; the selected variant is marked with No. 1. The following aspects were taken into consideration in the process of selection: the location of tunnel portals in relation to residential areas; conflicts of interest; passage through conservation areas; outlets to the surface in conservation areas; the possibility of achieving the design speed of 300 km/h; separation of the new high-speed railway line from the existing track; a necessity for modification of the existing track; a possibility for gradeseparated crossings of the two opposing traffic directions in the case of branching off; geotechnical conditions along the route in relation to the construction technique; problems associated with alteration of rock types; occurrence of karst phenomena and caverns during the course of the excavation; passage through a deposit area or its reservation; existing buildings above the tunnel; requirements for ventilation during the excavation and operation; feasibility of establishing site facilities; feasibility of the construction in terms of time; possibility of rail haulage of spoil; road haulage; spoil disposal; the tunnel length-cost relationship.

4 THE MAIN DESIGN PRINCIPLES

Apart from the basic order to connect Prague with Beroun by a double-rail line, the following main principles were sat out to be met:

4.1 *Feasibility*

The railway line will run through a pair of single-track tunnels, each 24.7 km long, according to the map No. 2 enclosed. The alignment must allow the travel at the speed of 300 km/h in the future.

The track will carry freight traffic and passenger traffic. For that reason the track must be split into two directions in Prague: passenger traffic to lead to the Smíchov station and freight traffic to the Krč station.

On the Beroun side, the possibility for the high-speed line to continue past the city as well as to branch off to the station in the city must be maintained. However, only the tunnels to the Beroun station will be built.

The horizontal alignment conditions do not allow branching off in the open-air track, the only branching possible is that in the tunnel.

The longitudinal gradient of the tunnel is 5‰ uphill from the portals to the mid point of the tunnel. The gradient changes at the grade-separated intersections.

The open-air route adjacent to the portals has not been designed to pass through residential areas so that the process of construction approval is not threatened by negotiations with the public, and a possibility of a conflict of interest with owners of existing properties is minimised. The areas for temporary site facilities were designed with the same attitude. The access to the tunnel is at chainages km 4.5 and 14.5 via two access adits and at chainages km 14.5 and 24.0 via two shafts.

The originally designed short at-grade section of the track near the village of Sv. Jan pod Skalou, which is also found in a conservation area, was also located underground as a result of forewarning of problems with the negotiation.

The tunnel will be driven by a TBM, with the sections between the portal and the branching off points excavated using traditional tunnelling methods. The profile of the tunnels is enlarged at the branching off locations and at the access adits connection points.

4.2 *Safety aspects*

The pair of single-track tunnels with separate portals is the basis of the safety concept. The tunnels are interconnected by cross passages every 400 m. This is how safe escape of persons from any point of the tunnel is ensured.

Dangerous contra-flow travels at the branching-off points have been eliminated by designing grade-separated intersections.

Access to the technical services centres are possible from the surface, therefore closing of the line in the tunnel to traffic is not necessary.

The ventilation system has been designed with respect to the needs for maintenance, contingent emergencies and a fire.

State-of-the-art equipment, which provides safety at the world's highest level, has been designed for the tunnels.

4.3 *Service life*

The structure has been designed for a minimum service life of 100 years. It will be solved so that optimum conditions for a long service life of the tunnel and equipment is secured in the way of which we have experience from Prague Metro. The tunnels and equipment rooms will be dry, ventilated and with relatively constant temperature.

4.4 *Environmental aspects*

The in the past completed tunnel structures have persuaded us that a continuous aquifer exists even in the relatively impervious Ordovician shales of the Prague Basin, up to the level of the tunnel at a depth of 100 m. Similarly, it was determined by measurements that the water table returned back nearly to the original level when the construction of a perfectly watertight tunnel had been finished. For that reason a waterproof lining around the entire circumference, the so-called 'submarine' type, has been designed for the tunnels on the new railway link between Prague and Beroun. This design, which does not require removal of groundwater by underground drains, eliminates permanent decline of water table and origination of dead wells or dry woods. It is very environmentally friendly a solution, which guarantees that the natural water regime will be restored.

5 ECONOMIC TUNNEL CROSS-SECTION AND SINGLE-TRACK TUNNELS THROUGHOUT THE ROUTE

The completed studies took into consideration variants with variously differing cross section sizes. The difference between the economic cross-section area and the large area which is assumed in German Railways' regulations amounts to 25%, which means a difference of about 6.5 billion CZK in terms of the cost.

The opposing traffic flows have been thoroughly segregated owing to the grade-separated design of crossings with the branching off tracks. The unfavourable effect of the pressure wave on passengers in common trains travelling in opposing directions will not, therefore, be experienced. The internal space of high-speed trains is sealed so that passengers are protected against these unfavourable effects.

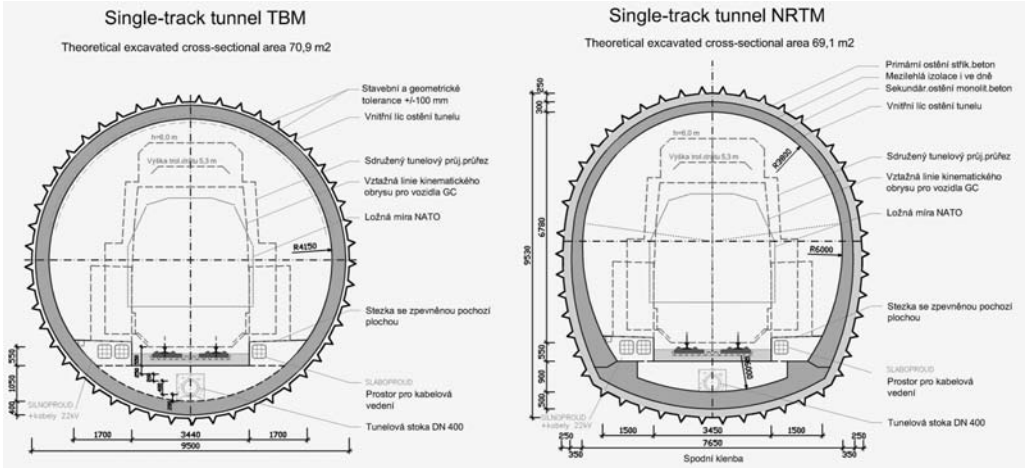


Figure 3. The typical driven tunnel cross-sections.

The above-mentioned measure allowed the owner to choose the economic cross-section. At the same time, the owner decided that the two tunnel tubes would be constructed simultaneously. The fact that a complete double-track railway line will be operated from the very beginning is a great benefit for quality and safety of the traffic. Regarding the environmental impact, the construction site surroundings will be inconvenienced for as short time as possible. Naturally, the total project cost is lowest when the construction programme is not divided into stages.

6 GEOLOGICAL CONDITIONS

Geological conditions are one of the main factors in terms of selection of the alignment. The tunnel route keeps clear of areas with mineral deposits and undermined areas.

The railway line passes through the Early Palaeozoic area forming the central part of the Barrandiene Member. The Palaeozoic rock layers rest unconformably on the basement formed by Proterozoic rock, which was folded during the Cadomian orogeny. The overall knowledge of this area is high, but, for example, a state-of-the-art survey of the tectonic pattern is missing and information from great depths is scarce.

The core of the Barrandiene Basin in Prague consists of a sequence of strata of Ordovician and Devonian sediments and volcanites. The rocks were folded during the Varisan orogeny and disturbed by transverse and longitudinal fault tectonics.

The western part of the tunnel passes through Ordovician rock, i.e. silty shale, siltstone and through quartzite of the Kosov Member, and Silurian rock types. The Silurian rock types are represented by graptolitic shale and marl slate. Shale and claystone prevail and frequent diabase intercalations occur in the lower part of the Silurian strata. The Upper Silurian rock mass contains larger proportion of limestone. It is characterised by a high degree of facies variability, frequent alternation of shale, various types of limestone and volcanic products disturbed by thrust faults.

The carbonate evolution following from the Silurian basement prevails in the Devonian strata in the eastern part of the tunnel. The Lochkov Member contains the Radotín and Kotýz limestone facies. A limestone sequence (Loděnice, Slivenec, Řeporyje, Koněprusy) can be distinguished in the Prague Member. The Zlíchov Member consists of grey, bedded limestone with hornstone. Significant karstification must be expected in the Devonian limestone. The current degree of knowledge obtained by surveys allows us to determine the border of possible karstification in the map with an accuracy of about 100 m. This border runs from the southern edge of Prague-Radlice through Ořech, past the southern edge of Tachlovice to Sv. Jan pod Skalou. According to the results of an information search based on long-term karstological surveys of the Bohemian Karst, it is impossible to determine the depth of a zone which would be beyond the karstification reach. Conversely, manifestations of karstification are expectable throughout the depth of the limestone bodies, which are affected by folding to the depth of about 100 m. It has been ascertained that the occurrence of karst phenomena, tapping of karst cavities, water irruptions etc. are a source of serious risks and threats for mechanical excavation using TBMs.

North of this border, the possibility of occurrence of karst cavities can be completely excluded. The Dalejské Valley Shale is characterised by prevalence of greenish, in higher levels even reddish colour. The Srbsko Member consists of siltstone and shale. The thickness may exceed 250 m in synclines.

7 THE EXCAVATION METHOD

7.1 *TBM drives*

A major part of the tunnel, from the bifurcation chambers in Prague to Beroun, will be driven by a large-profile TBM. Most long tunnels in the world have been driven by TBMs. It is so for the following reasons:

Faster advance rate compared to traditional methods. The shorter construction time means less uncertainties for the owner and the tunnel is cheaper.

The equipment is ever more perfect after the numbers of tunnels driven mechanically in the world. They are capable of coping with mixed geological conditions.

Mechanical excavation is safer; workers do not get into contact with rock and cannot be injured by collapsing rock mass.

Mechanical excavation allows accurate control over the excavated volume; at the same time, it does not disturb the surroundings of the excavation by blasting operations, thus overexcavation is avoided, cavities do not originate behind the lining and settlement of the surface is minimised. This is advantageous when residential areas are being passed under.

The circular profile of the tunnel is the most advantageous in terms of structural analysis, thus the safest at an adequate cost.

With respect to the anticipation that stretches with relatively low hardness of the rock mass will be passed through, the TBM type which has been chosen is not equipped with grippers. This means that the TBM-driven tunnel will have a single-shell segmental lining consisting of reinforced concrete segments, which will provide support to the thrust cylinders propelling the TBM. The lining segments will be made of water retaining concrete; they will be provided with sealing gaskets on all sides, thus the lining will be waterproof.

7.2 *Traditional NATM excavation*

The NATM will be utilised for the excavation of the single-track tunnels which starting at the Prague portals in Hlubočepy and Malá Chuchle and continue up to the bifurcation chambers, for the bifurcation chambers at Prague and Beroun, the access adits and shafts, assembly chambers, cross passages and equipment rooms. There are the following explicit reasons for this decision:

Frequent changes in the shape of the cross section (each of the above-mentioned openings has a different shape).

The NATM-excavated parts are enabling works for preparation of the TBM sets and access adits and shafts.

The majority of karst phenomena which will be encountered in the Prague area are much easier for the NATM to overcome. The access adit in Malá Chuchle or other works may even be utilised for geological exploration purposes.

The NATM excavated works, e.g. the access adits and assembly chambers, can be carried out in advance of the TBM excavation or concurrently with it; it will result in reduction of the construction time.

The NATM-excavated tunnel lining structure will consist of a sprayed concrete primary liner, intermediate waterproofing and cast-in-situ concrete secondary liner. The waterproofing will be of the 'submarine' closed type, covering the entire circumference including the bottom. The secondary lining will have an invert structure throughout the NATM-excavated tunnel length to resist the hydrostatic pressure.

8 THE CONSTRUCTION PROCEDURE AND LOGISTICS

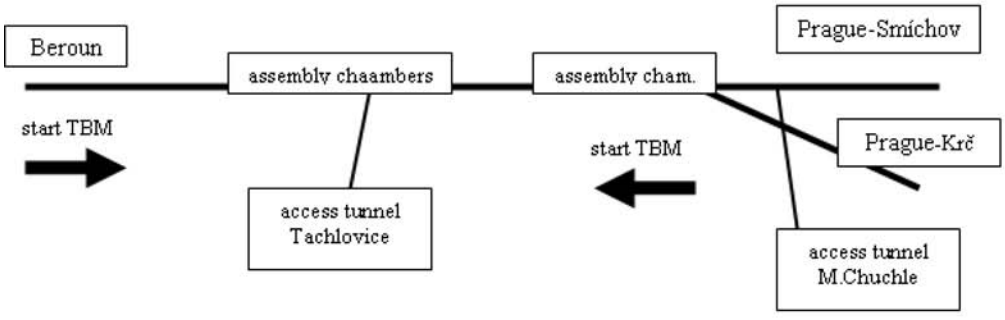
A single TBM would need approximately seven years to drive the about 22 km-long tunnel. This is a too distant horizon. Tunnel cost analyses have shown that over a half of the total cost consists of components dependent on time. The total construction time is therefore a deciding factor. For that reason, two TBMs must work concurrently on the drive of one single-track tunnel tube.

Problems may be encountered during the course of the simultaneous excavation by two TBMs when geological weakness zones are being passed through, which may result in suspension of the drive so that measures improving the rock mass can be implemented. In such a case, the work is much simpler and faster if an auxiliary adit can be driven from one tunnel to the other and the operation be carried out from this adit. Such the situation has already taken place in the world and examples of solutions are known. This is the reason why simultaneous drives of both single-track tunnels must be recommended. This recommendation is supported by the results of the risk analysis.

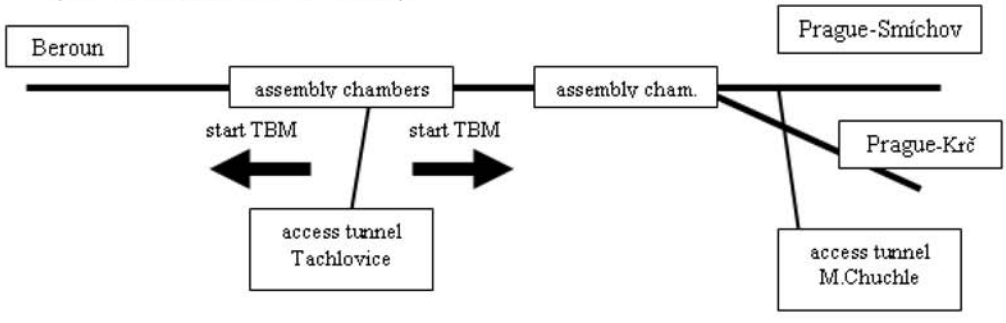
The excavation procedures possible are presented in the following chart. The duration of the tunnel drives is, according to the programme, about 4 years, the total construction time is 6.5 years.

In the case of volumes of material transfer during excavation of tunnels of so great length there

1. **heading from both portals simultaneously** (logistics cannot be provided on the Prague side)



2. **heading to both sides from the access adit connecting in the middle of the tunnel** (one construction site for TBMs)



3. **heading from the portal and from the access adit in the middle of the tunnel**, in the identical direction

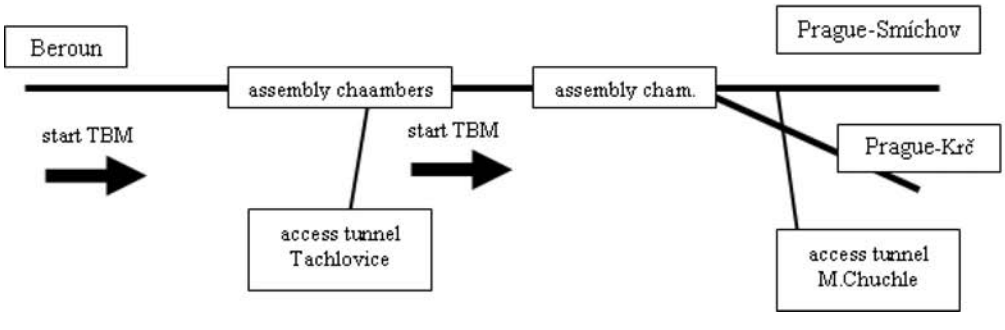


Figure 4. TBM excavation procedures.

is a significant problem associated with logistics, prefabrication and transport of the lining segments, and, primarily, haulage of muck. The design of the areas in front of the access adits and tunnel portals which are necessary for intermediate stockpiles of muck and intermediate storage of the segments allows for the needs; it has been proven that the project is feasible.

Underground Space – the 4th Dimension of Metropolises – Barták, Hrdina, Romancov & Zlámal (eds)
© 2007 Taylor & Francis Group, London, ISBN 978-0-415-40807-3

Underground high-speed railway – The phenomenon of urbanistic development in Prague

E. Kyllar
METROPROJEKT Praha, Prague, The Czech Republic

ABSTRACT: The Prague subway clearly demonstrates how important the utilization of the underground is for city life. A survey of the development of views about how to organize the basic pillar of the public transportation system. Realization of individual lines and subway stations in the historic section of Prague, in the central city, in the surrounding quarters and in the new suburbs. The transformation of conceptions concerning urban planning from the dominance of automobile traffic to the preference of walk-only zones in city centres. The subway in Prague is one of the crucial factors of urban life and development.

1 INTRODUCTION

After more than thirty years of operation of subway in Prague, we can consider as proven that the underground high-speed railway has besides the basic transport effect also urbanistic significance – city-making. I am going to prove this thesis on an example of several subway stations. Prague has unique specifications in the terrain configuration, geological conditions, but mainly in cultural and historical value of its historical centre, whose total area is almost 900 ha. It has been declared by UNESCO organization as the world cultural heritage for its thousand year's continuity, exceptional well-preservance and integrity and quality of monument sets. This heritage binds for systematic caution and modesty when executing any construction activity and therefore its makers have to deal not only with technical problems.

2 DEVELOPMENT OF OPINIONS ON THE CONCEPTION OF HIGH-SPEED RAILWAY

At the end of 19th century requirements on the transport were increasing with the development of housing. An extensive clearance of the Old Town and Josefov – the Jewish town was carried out, as well as the construction of infrastructure, embankment streets and walls regulating the flow of the Vltava River. Omnipresent construction activity inspired in 1898 Ladislav Rott to propose to use the wide trenches and demolitions for the construction of underground railway (Fig. 1).

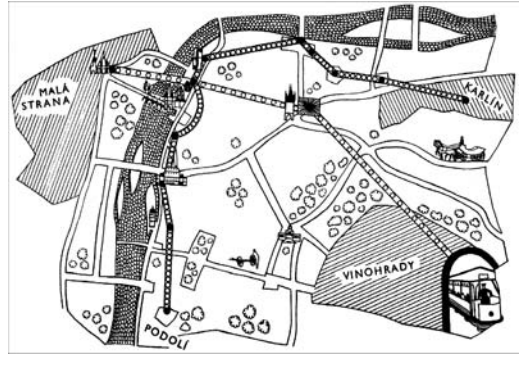


Figure 1. The scheme of Ladislav Rott proposal from 1898.

City technical officer Bohuslav Vondráček proposed in 1912 underground tram railway between Jindřišská str. to the Wenceslas square to Kaprova street. The number of citizens was close to 700 000 after the creation of Czechoslovakia in 1918 and Big Prague in 1922. Jiří Hruša published a proposal in July 1926 to solve the underground high-speed railway by placing it to deeply based tunnels with 3 diametrical lines through the city centre (Fig. 2).

First technically elaborated and complex proposal for the subway system in Prague was a study proposed by *Vladimír List* and *Bohumil Belada* from December 1926, which counted with 4 underground lines (Fig. 3).

A *competition* was announced for the solution of transport in the Big Prague in the year 1930. Results of this competition proved the necessity to introduce

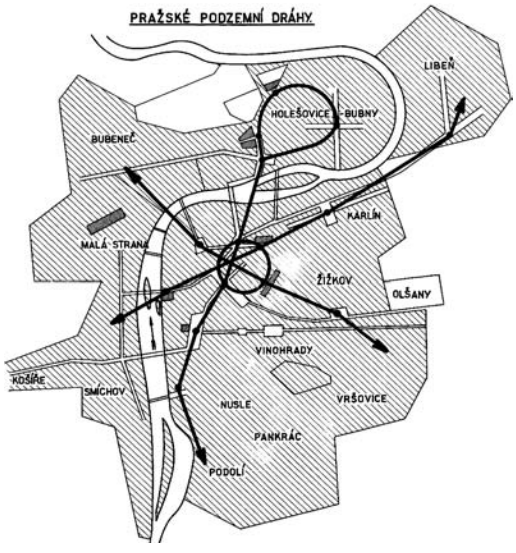


Figure 2. The proposal of Jiří Hruša from 1925.



Figure 3. The proposal of Vladimír List and Bohumil Belada from 1926.

a bearing element into the public transport into the underground.

The study department of municipal Electric companies elaborated in 1938 so called *Project D*, according to which the lines of dominant transport directions through the city centre were supposed to be carried out by cut-and-covered tunnels (Fig. 4).

Project D was rejected and *Konsorcium* of all considered partners for the construction was created. They proposed in 1941 the *Project M* of a classical subway underground railway. They supposed a system with 3 underground lines carried mainly shallowly under the ground with an exception of overcoming the Vltava River. Stations were supposed to be also cut-and-covered with lateral or insular platforms, underground halls and underpasses (Fig. 5).

It was even supposed after the Liberation in years 1946–1947 that it would be possible to begin with the

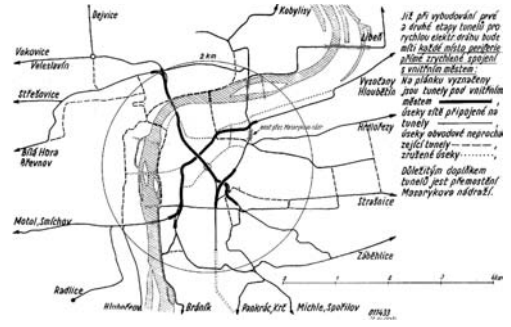


Figure 4. Project "D" from 1939.



Figure 5. Project "M" from 1941.

subway construction in Prague according to the Project M, but it was not possible.

In 50's when the number of inhabitants exceeded 1 million, were elaborated several proposals of territorial plans and also several studies on the solution of subway situation, but they have not succeeded to pass the *Directional master plan* until 1964, whose part was also the solution of public transport with a system of 3 underground lines in the city centre. The system called *Underground tram* (*PPT*). It required extensive groundwork in confined conditions of medieval streets, demolition of historical monument buildings, which evoked big conflicts with city infrastructure. The construction of PPT begun in January 1967 in Opletalova Street, close to the Central Railway Station (Fig. 6).

International expertise rejected project PPT in 1967 and the government then decided that a *classical subway* is going to be constructed in Prague. Projects were reelaborated and the construction was without interruption reoriented from the cut-and- covered tunnels to the bigger proportion of driven works.

3 CURRENT SITUATION IN THE SUBWAY NETWORK IN PRAGUE

There is a majority of railway tunnels between the stations with single or twin-track with stations in the

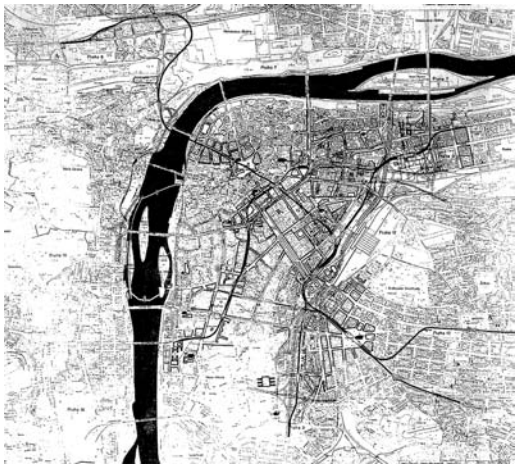


Figure 6. Project of the underground tram from 1964.

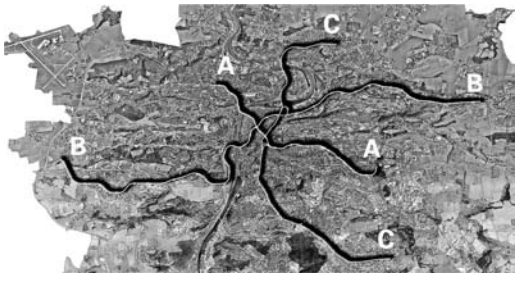


Figure 7. Current situation of Prague subway network.

historical centre and inner town driven and in the outer town cut-and-covered from the surface. All stations except for one are cut-and-covered or surface on the line C (Fig. 7).

An overview of Prague subway network.

Line	Construction length	Stations			
		Driven	c. and c.	Surface	Total
A	10,79	9	3	1	13
B	26,399	13	8	3	24
C	18,77	1	15	1	17
Total	55,959*	23	26	5	54
%		45,6	48,1	9,3	

*from which: 41,5 km driven tunnels = 74%,
13,5 km cut-and-covered tunnels = 24,1%,
1,6 km surface track = 1,9%.

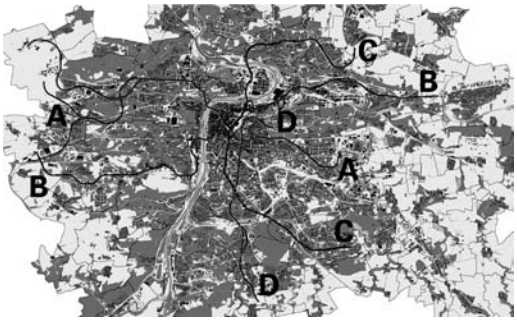


Figure 8. Prague subway network with development intentions.

4 DEVELOPMENT OF SUBWAY NETWORK IN PRAGUE

Subway in Prague is considered as a priority in solving the complete transport problems, because it currently realizes up to 40 % of all transport requirements for the public transport. This proportion is going to even increase by broadening the network. Strengthening the performance of subway is for Prague one of the most effective weapons against clogging of the city areas by car transport and against restricting pedestrian transport mainly in the city centre.

On the *northern end of C line* begun construction of 3 new stations, which are going to be opened in 2008. The construction of *a new 4th line D* is being prepared, from the Central Railway Station through Vršovice, Nusle, Pankrác to Krč, Lhotka and Písnice with the change to all three lines and with extension to the west to Žižkov.

The *extension of line A* westwards should be another extension to the subway network from Dejvice through Veleslavín, Petřiny to the hospital in Motol, to Bílá hora and from here to the airport Ruzyne and with a branch to Řepy and Zličín.

There is prepared turning of the branch on the East from the station Strašnická to Zahradní město and Hostivař and a branch from the station Skalka further on to the industrial area can be executed also (Fig. 8).

The system of Prague subway is fully opened and it allows anywhere and anytime to connect to the current system and to increase the quality of transport service in the city.

5 PRAGUE SUBWAY IN THE HISTORICAL CENTRE

The centre of Prague had a determining influence on the arrangement of subway network and its space solution. Saving majority of railway, stational and escalator parts of tunnels to the underground enables to limit

the intervention to the medieval city only to entrance halls and underpasses. In the area of historical centre is altogether 10 stations, 8 of which are driven and 2 cut-and-covered and 14 shallowly based halls.

Both shallowly based stations on C line, Hlavní nádraží and Muzeum were built in 1974 including their halls on unfinished buildings according to the PPT project.

Hlavní nádraží station – integral part of underground foreground of central railway station, initialized its reconstruction and its finishing to its current appearance (Fig. 9).

A component of the station *Muzeum* on C and A lines is a wide underpass, which provides not only the entrance to both the crossroad station on C and A lines, but also an important connection for the city between Wenceslas square and the area of Vinohrady with the National Museum (Fig. 10).



Figure 9. The central railway station with subway station under the hall in the park.

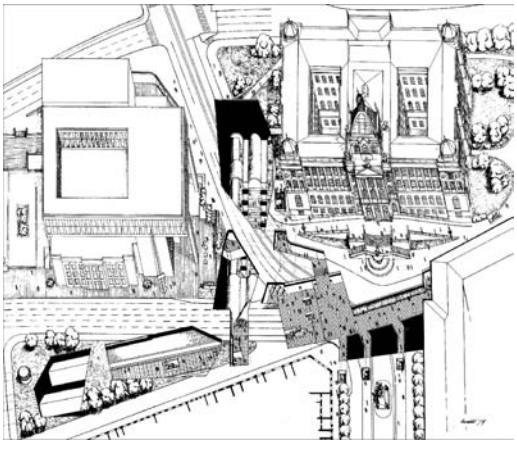


Figure 10. Axonometry of the change point by National Museum.

Malostranská station on A line is the foreground of unique area of Malá Strana with beautiful palaces, gardens and town houses in the area under the Prague Castle. Space solution with deeply based platform limited negative intervention to the valuable organism of the city on several temporary constructions. A surface entrance pavilion and atrium with a garden are a substitute for them. Their surroundings cultivated and brought new quality by enriching the historical heritage (Fig. 11).

Realization of the two stations *Můstek* with changes to line A and B was one of the most demanding in the network of Prague subway (Fig. 12). Station on line A was finished in 1978 and its part is also the underpass to Můstek. Nowadays it is a certain anachronism, but was adequate to the requirements of the times, during

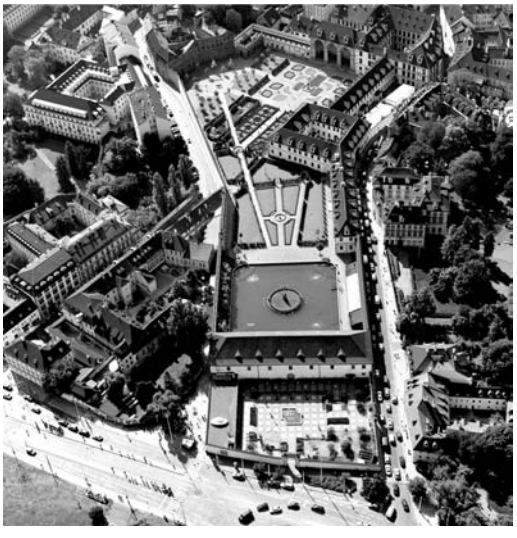


Figure 11. Malostranská station is a part of historical construction.



Figure 12. The diagram of the change point arrangement on Můstek station.

which it was constructed. A huge underground hall and the exit with the underpass to Jungmannovo square was also constructed together with finishing the station on B line in 1985. Shortly before its opening was decided that tram transport here is going to be cancelled and that car traffic is going to be significantly limited and that there is going to be a pedestrian zone. Both underpass areas are used as commercial zones (Fig. 13).

The construction of *Náměstí Republiky* station with deeply based platforms and two escalator tunnels was in the area concentrated on the western hall with the underpass under own square and to eastern hall with underpass to the Masarykovo railway station Free areas were used for their construction without demanding demolitions. Modifications of the parter on the square and foreground of the station were executed together with the construction.

Releasing once unsightly street V Celnici originated conditions for construction of new important hotels and multifunctional buildings in their surrounding, which created new urban cultural area. There is currently a construction of a big multifunctional complex Palladium in the area of former barracks and underpass will become the entrance area to the commercial area (Fig. 14).



Figure 13. Pedestrian zone under the underpass on Můstek station from 1989.



Figure 14. The area over the western hall of Náměstí Republiky station.

6 PRAGUE SUBWAY IN THE INNER CITY

Line C goes from the historical city centre to Pankrác terrace in the tunnel of the Nuselský bridge. On its southern foreground originated unique station Vyšehrad. The bridge was constructed together with the subway construction in 70's of the last century and became a connection of new city areas to the Pankrác plain with the central area. Thanks to this station once deserted place started to change its surroundings to new spacious city dominant with huge composition of Congress centre, hotels, office buildings and houses (Fig. 15).

A new centre grew by the station *Budějovická*. Projects on its construction originated simultaneously with subway projects and became mutually coordinated. The station was originally located on the free area, but a department store and sale gallery were established already during the subway construction. They were able to maintain fixed urbanistic conception for the creation of the centre of Budějovické square up to now and the square with the surrounding sets of offices, commercial buildings and houses is almost complete. This example of usefulness of good planning and coordination deserves to be followed (Fig. 16).

From many localities, where the subway initiated the reconstruction and development of the area, can be presented on the first place the new urban centre Smíchov and surroundings of *Anděl* station. There was still in eighties of the last century a big and old factory in the middle of Smíchov. Unattractive, mixed housing site remained in its surroundings. They managed to substitute in 1985 part of this housing site by surface pavilion of the northern hall together with realization of the subway station. The base of the new centre Smíchov became the Palác Zlatý Anděl, which was creating the new square along the Nádražní Street and originated



Figure 15. The bridgehead of Nuselský bridge with Vyšehrad station.



Figure 16. The Budějovické square with the subway station in the underground.



Figure 17. Centrum Smíchov over the subway station Anděl.

over the reconstructed northern hall (Fig. 17). The Southern hall of the station is placed in the area, around which is being prepared a new construction of urban sets on the currently problematically used areas. In the surroundings of Zlatý anděl gradually originated the centre of commerce, culture, accommodation, alimentation, housing, offices, garages and clubs even in more distant surroundings. Smíchov was really transformed into a modern city and the subway plays a major role.



Figure 18. A commerce centre grew over the subway station Chodov.



Figure 19. A new centre is growing by the hall of Roztyly station.

7 PRAGUE SUBWAY IN THE OUTER CITY

There were two stations on the II. part of C line – realized in almost free area. Both these stations evoked in the end of nineties a huge construction works in the surroundings of business, services, culture, sports and accommodation centres, administration and housing. A huge international technological park and commercial centre Centrum Chodov originated by the Chodov station, which is supposed to be the biggest in the Czech Republic (Fig. 18).

Station *Roztyly*, which was formerly called as the station for rabbits from surrounding forests, is nowadays important terminal for suburban and long-distance bus transport lines, a T-mobile centre was also created here and a big department store. A construction of the centre of a big travel agency, hotel and other buildings is prepared (Fig. 19).

Stations *Stodůlky*, *Luka*, *Lužiny*, *Hůrka* and *Nové Butovice* originated as natural local centres of housing sets on the South-western part of Prague. The preparation of the construction of this outer city began in the area, when it was already decided about the realization of subway in Prague. Authors could therefore create a conception of real *high-speed railway city*, which

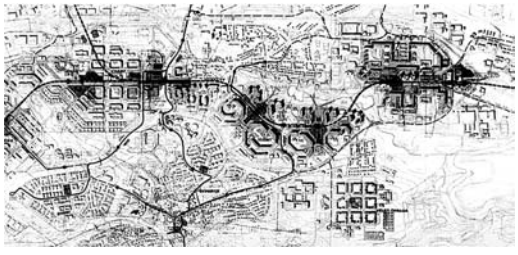


Figure 20. The plan of South-western City with a subway station.

does not have many parallels in the world (Fig. 20). They were successful to coordinate projects of the new residence area with projects for the preparation of subway construction so that a symbiosis of both buildings was created here. The construction of *South-western City* was quicker than the realization of the subway, but areas and corridors in determined localities were prepared for further construction of subway stations and track tunnels. Around stations in all localities were created natural centres for the life of inhabitants of housing complexes. The whole territory of South-western city is thanks to its transport availability in the interest of different, often multinational developers, so that 13. Prague district is the area, where many building of all kinds, importance and size, are constructed. A valuable and attractive city part was created from originally stark block of flats. Subway helped this development to a great extent (Fig. 21).

Rajská zahrada station and its original architectonic solution is inspiration for future. It is not exceptional in terms of traffic, but it is a modern investment to the values, according to which Prague is regarded as a beautiful city (Fig. 22).



Figure 21. South-western City from the East in 2003.



Figure 22. Station Rajská zahrada is an innovation in solution of stations.

Subway in an old town, such as Prague, represents a phenomenon, which helps the city in creation of the environment for its inhabitants, in the development of city's equipment, in using the historical centre and in its protection and preservation and broadening cultural heritage.

Source: Kyllar E., 2004. *Praha a metro*. For Inženýring dopravních staveb, a. s., published Gallery, Prague

This page intentionally left blank

Underground Space – the 4th Dimension of Metropolises – Barták, Hrdina, Romancov & Zlámal (eds)
© 2007 Taylor & Francis Group, London, ISBN 978-0-415-40807-3

Railway line Prague centre – Ruzyně airport

J. Martinec & P. Zobal
METROPROJEKT Praha a.s., Prague, The Czech Republic

ABSTRACT: Prague, the capital of the Czech Republic, still does not have sufficient railway transport capacity serving the city centre and Ruzyně, the international airport in Prague. This should be changed by some 20 km of a new railway line which considerably uses the existing single-track line from Prague to the city of Kladno. In addition to the quick and reliable rail connection between the airport and the capital centre the modernised line will be accompanied with development of architectural and urban centres and important interchanges in the territory. The project comprises several tunnels which cover some 10% of the total length of the line.

1 BASIC IMPORTANCE OF THE RAIL CONNECTION

At present there is not quick, comfortable and especially reliable connection of sufficient capacity between the capital centre and Ruzyně, the international airport in Prague, provided by public transport. The existing bus transport is insufficient and with respect to the expected rise in the air transport volume (at present it is some 11 million passengers a year) it will be inefficient in the future.

From the point of view of a systemic nature it is definitely more suitable for the traffic channels of the airport if the railway transport is used as it removes the disadvantages of the bus transport with its limited capacity and poor travelling standard in general. Major airports in Europe and other countries all over the world are served by railway transport.

It is an advantage that it is possible to use the existing Prague – Kladno railway line, running through stations in Praha Dejvice and Praha Ruzyně. By modernising this line, its current substandard condition will be improved, incl. negative effects elimination such as noise, vibrations and the barrier effect (tunnels and elevated sections, grade-separated intersections). Despite the widening of the line (especially for the reason of doubling of the track) no acquisition of land of greater extent will take place. The new development of the line from Ruzyně station to the end station of Ruzyně Airport runs mostly in the existing traffic corridor (along the Prague ring road).

With respect to the prospective volume of transport when it is possible to expect that as at 2015 some 20,000 passengers will be transported in 24 hours in one direction (METROPROJEKT Praha a.s. 2002–2006), the railway transport is the optimum system as regards capacity.

At the same time the railway system provides a higher travelling standard, preferring seating room, luggage hold, allowing seat booking, etc. – in general it gets closer to the air transport standard. In addition to this the connection between the airport and the capital centre will be quick, regular and reliable.

The modernised railway line will also improve the standard of traffic channels of the biggest city of Central Bohemia and its region. This will be a through train connection without any need to change and therefore it will be competitive in comparison with individual car transport.

2 COMPLEX TRANSPORT RELATIONS, IMPACTS ON THE TERRITORY

The railway transport connection to Praha Ruzyně Airport creates conditions for its natural integration into the PID system and is fully in harmony with the policy of development of the traffic channels of the capital of Prague. The railway connection to the airport is of a radial and central character, the railway line ends right in the city centre, its historical core, Praha Masaryk Station. A possible connection of the airport to the long-distance transport can be dealt with in the future through further development of railway lines in the area of the airport.

The route runs through a highly urbanised area providing good conditions for being directly served and conditions for establishing relations with transports of other types. Nine railway stations and stops will be major traffic junctions and the most important

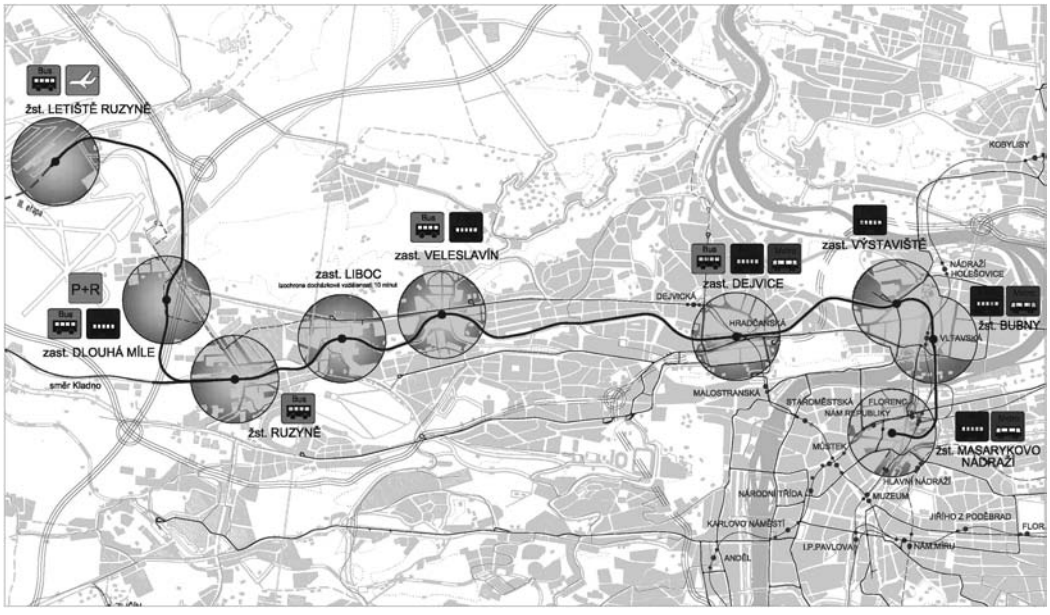


Figure 1. General layout of railway line.

ones – Masaryk Station, Bubny – Vltavská, Dejvice – Hradčanská and Dlouhá Míle – will also be natural architectural and urban centres of the particular locality. This transport connection will also provide an attractive change of all routes of Prague Metro (route A – Hradčanská station, route B – Náměstí Republiky station, route C – Vltavská station). Modernisation of the line will also eliminate all level crossings with the existing road network and thus improve the provision of transport services in the area in general.

3 PARTICULAR STATIONS AND STOPS

The starting point of the route, Praha Masaryk railway station, is situated in the very capital centre, allowing the possibility of changing to the metro route B and tram lines. The station is directly linked to the adjoining area which is important especially as regards accessibility of services and job opportunities (shopping and office centres, major accommodation capacities, etc.). The development of the line and its terminus in the premises of Masaryk station will also considerably contribute to the improvement of the devastated northern part of the station where extensive conversions are planned in connection with the introduction of the line.

The newly planned Bubny – Vltavská station is part of the development area of Holešovice – Zátory and is of an important potential as an interchange point and a destination of trips in relation to the newly planned urbanisation of this area. It is expected that the adjoining area will meet residential and servicing purposes. A new northern hall of the route C Vltavská metro station will be built there and a tram stop will be near.

The new overhead Výstaviště stop will be of its greatest importance especially as regards access to the premises of Výstaviště (Exhibition Ground) and the Stromovka Park (especially as regards services, leisure time activities, culture and sports). At the same time the particular area should be improved from architectural and urban point of view. There will be a direct connection to the tram transportation.

Dejvice – Hradčanská underground stop will provide a short connection to Hradčanská station of the metro route A. At the same time a construction of the metro station western hall is planned. It will also be possible to change to trams and busses. Next future intensive urban development of the area between Hradčanská metro station, the existing Praha Dejvice railway station and Prašný most (Powder Bridge). The station will thus be important as regards availability of services and residential zones. The fact that the station will be underground will improve availability of Prague 6 to pedestrians and in general it will allow its urbanisation.

The partly underground Veleslavín stop moved to the north will be close to Evropská avenue and will make changing to trams or busses possible. Close to the station should be built a new multipurpose building. The station will thus serve also the adjoining area.

The new Liboc stop will both serve the adjoining area (especially residential areas) and allow indirect pedestrian connections to Evropská avenue and the holiday areas of Divoká Šárka and Džbán.

Ruzyně station, moved in the western direction, will be in a space contact with the new grade-separated intersection with Drnovská street, where a bus stop could be established. The station could be important also as regards accessibility of adjoining storage premises. It also creates conditions for urbanisation of the surroundings and allows its direct servicing. Behind the station the line branches off, one branch runs to the airport and one to Kladno, passengers coming from Kladno can change for the airport (until the development of the direct line from Kladno to the airport).

The new Dlouhá Míle stop is an important terminal in the north-western part of the capital where all bus services coming from this direction should end. At the terminal it will be possible to change to the public busses as well as to the trams whose stop will be built in the future. Part of the part of the junction will also be a capacity car part of the P + R system for the purposes of the individual car transport, close to the ring road. Dlouhá Míle terminal is thus the basic junction in this part of the capital owing to which it is possible to reduce the non-railway transport (BUS, individual car transport) in the territory of Prague 6.

The new Ruzyně Airport end station, in the premises of the international airport of Prague, is directly connected to the existing and new terminal and other structures within the airport halls. At the same time it is possible to change to busses here and it is also the required element of integration of the air transport with the PID capital transport system of a corresponding functional and quality standard.

4 BASIC DATA

- Length: 20.3 km, with 5.6 km newly built section Praha Ruzyně railway station – Praha Ruzyně Airport railway station.
- Total number of stations (stops) 9; it is completely a double-line railway.
- Design speed: 80 km/hour.
- Min. curve radius R = 325 m, max. gradient 25‰.
- Traffic completely as electric traction (direct-current, 3000 V).
- Regular shuttle service of the airport and Kladno trains, the interval corresponding to the demand and the chosen transport standard. The peak interval for airport: 10min., for Kladno: 20min.
- Journey time from Praha Ruzyně airport to Masaryk station: 26.5min (stopping train).
- Journey time from Kladno – Masaryk station 40min (stopping train).

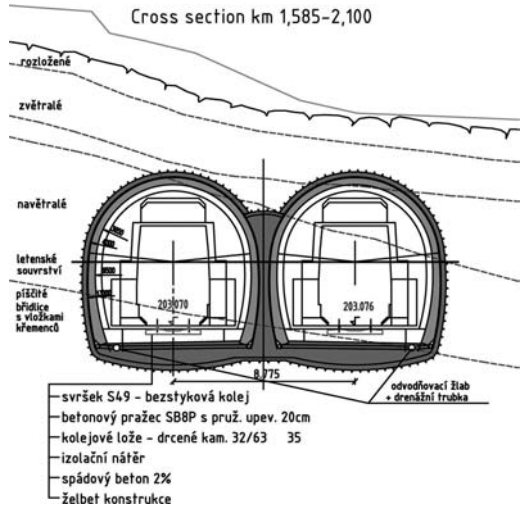


Figure 2. Cross section km 1,585–2,100.

5 UNDERGROUND STRUCTURES ON THE ROUTE

It is not possible to build a structure of this extent within the capital without underground sections of which there will be a great number.

5.1 *Tunnels in the area of Stromovka Park*

If proceeding in the direction from the capital centre, the first tunnels are designed in the Stromovka Park in length of 800 m. They are designed here to minimise negative effects of the new route on the environment. Stromovka is listed as a cultural monument and it is a nature park. The section of tunnels starts with a portal right outside the vaulted overbridge adjoining Kamenická street. The portal is situated next to the overbridge so that the overbridge will be preserved. Tunnels of the double-track line pass partly under the park and partly under the development adjoining the park and are designed on principle as single-track tunnels with a common supporting pillar. This solution with a minimum axial distance of rails allows minimisation of the impact on the outside environment, whether it covers the width of the influenced zone as regards the development area and valuable park area or also overlying rock drifts and surface drops.

Another section is the subway under the existing bridge in Korunovační street. In this place one tunnel tube runs under the existing line and under the right pier of the bridge. If full operation of the bridge is to be maintained, it will be necessary to underpin both its piers of the bridge and secure its right support for the driven subway. Both the tunnel tubes will be gradually

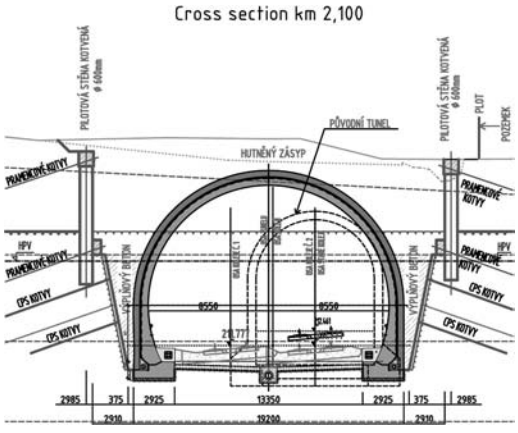


Figure 3. Cross Section km 2,100 – another variant.

inserted, along the bridge subway, under the railway cut so that 1.5 to 2.0 m of rock remain above the top section. In this section the driving of the left tunnel tube will be combined with the development of the right tunnel tube under the protection of the concrete ceiling which will be supported, in the area of the common intermediate pillar, with a number of root piles, which will become part of the common intermediate pillar of the primary lining of both tunnel tubes.

Tunnels will be driven in layers of shale of Letná. The tunnelling and the primary supporting of the tunnel tubes or the intermediate adit is to be performed in accordance with the principles of the New Austrian Tunnelling Method.

Another discussed variant of this passage through Stromovka is a mere doubling of the track of the existing line and its partial covering. This solution requires the necessity of reconstructing the existing single-track Dejvice tunnel, approx. 100 m long, which is a listed structure (the oldest railway tunnel in the Czech Republic). This tunnel had been built in a cut and then covered. The new tunnel of the required arched shape would have to be built also cut-and-cover with pile walls shoring of the building pit. On the basis of experience of similar structures the vaulted, arch structure of an excavated tunnel is built by means of formwork formed from inside with a formwork vehicle and from outside with a system formwork or with auxiliary primary lining.

This variant also requires a complete reconstruction of the bridge in Korunovační street with necessary stoppage of traffic on the bridge.

5.2 *Cut-and-cover section in Letná*

This section is adjoined by a 640 m-long section of a cut-and-cover double-track tunnel in Letná, situated right under the surface. It runs as far as the underground Praha Dejvice-Hradčanská station. It is a cast-in-situ reinforced concrete one-nave frame in an open cut. This solution allows a grade-separated intersection with several cross streets outside the station. The tunnel structure is close to the structure of the exit ramp of the tunnels of the City Ring Road (Ramp 1 – Letná City Ring Road) and the progress of both the building activities will have to be coordinated with respect to the course of time of both the structures.

5.3 *Praha Dejvice – Hradčanská station*

The new Praha Dejvice – Hradčanská underground station will be situated between Milady Horákové avenue, Dejvická street, the existing ČD Praha Dejvice station and Bubenečská street in direct relation to the existing hall of the metro station. The space around Hradčanská metro station and the new station is one of the most complex places on the route. The development of the new underground cut-and-cover station is in close contact with the planned development of road tunnels of the City Ring Road.

It will be connected to the metro station on the level of the existing subway of the metro station from which it will be possible to get into the middle of the railway platform. From the north-western end of the platform of the new station it will be possible to change to metro or leave for Dejvice through the newly planned western metro vestibule. The perimeter walls of the station are diaphragm walls, which will also shore the foundation pit. They are strutted with the foundation plate of the station, on the upper level partly with concrete floor structure, partly anchored with permanent anchors and partly strutted within the final glazed steel structure of the ceiling above the platform.

5.4 *Cut-and-cover tunnels behind Praha Ruzyně station*

In the section between Praha Ruzyně station and Praha Ruzyně Airport end station there are planned several sections of cut-and-cover tunnels where it is not possible to run the route on the surface for the reason of crossing the road beds and protecting airport systems (impact of electric traction on the radio beacon, protection of the route under the planned runway) on this edge of the city. There are altogether five sections of the total length of 1250 m.

Tunnels are designed as cast-in-situ reinforced concrete frame which is not closed in the lower part, longitudinal strip foundations are interconnected transversely only with ribs of max. distance of 8 m. Inside dimensions were determined on the basis of the maximum moving dimensions and requirements for drainage of roadbed. They will be built in an open pit either sloped or shored by Stent Walls.

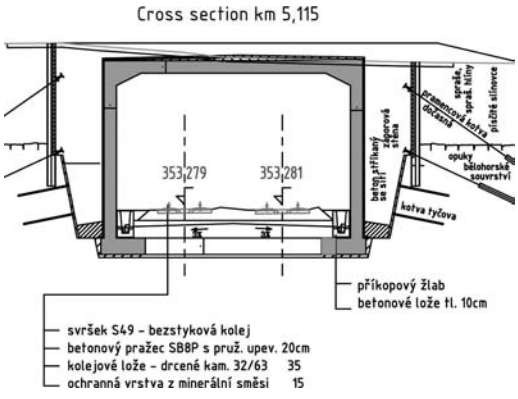


Figure 4. Cross Section km 5,115.

5.5 *Praha Ruzyně Airport station*

This end station with an intermediate platform is situated in the area between air terminals along the elevated roads. The station is the underground one, the bearing structure is a closed cast-in-situ reinforced concrete frame. The station area will be, in addition to the direct exit leading to the surface, also interconnected with the airport buildings with two underground connecting corridors – the eastern one connecting the station with the original terminal and the western one connecting the station with Sever 2, the recently completed new terminal. For the purposes of this corridor, in connection with the construction of the new terminal there was built an underground advanced structure which will allow completion of the corridor without any impact on the surface.

The station will be built in a cut-and-cover system. It will be necessary to anchor gradually the piers of the parallel elevated road. The elevated road was founded so that it would be possible to excavate the pit for the station structure.

6 CONCLUSION

At present the project documentation is being discussed at the stage for planning proceedings and number of additional studies are being completed.

REFERENCE

METROPROJEKT Praha a.s. 2002–2006. Studie obsluhy hlavního města Prahy a jeho okolí hromadnou dopravou osob, fáze C, Praha (Study of public transport services of the capital of Prague and its environs, phase C, Prague)

This page intentionally left blank

Underground Space – the 4th Dimension of Metropolises – Barták, Hrdina & Romancov (eds)
© 2007 Taylor & Francis Group, London, ISBN 978-0-415-40807-3

The Trans Hudson Express (THE) Tunnel

Nasri Munfah
Parsons Brinckerhoff, New York, NY, USA

Arthur D. Silber
NJ TRANSIT, Newark, NJ, USA

ABSTRACT: Meeting New York Metropolitan area mobility needs is critical to keep pace with growing demand, to achieve the forecasted economic growth, and to maintain midtown Manhattan as a centre of regional, national and global importance. The possibility of insufficient access to midtown Manhattan was recognized as a significant problem, leading to this project major goal of doubling trans-Hudson rail capacity. With a budget of over six billions dollars (2005) and a completion plan by 2016, the Trans Hudson Express (THE) Tunnel project will fulfil these needs. The project faces many technical, environmental, and regulatory challenges including tunnelling under the Hudson River in soft silts and with limited cover; tunnelling through mixed ground in the New Jersey shore; crossing under existing historic bulkhead; tunnelling under high rise buildings in one of the most congested region; constructing a six-track cavern station under 34th Street, one of Manhattan's busiest cross-town thoroughfare; underpinning and supporting existing facilities; maintaining NJ Transit, Amtrak, Long Island Rail Road and New York City Transit operations during construction; and developing the design concepts to meet environmental requirements and regulatory constraints. This paper presents the planning process of the project, the environmental and engineering challenges, and measures taken to address them.

1 GENERAL

The New York/New Jersey metropolitan area is one of the most densely developed areas in the United States. Within the trans-Hudson Midtown corridor, almost 300,000 people commute into Manhattan each weekday on various modes from counties west of the Hudson River. This demand has grown to exceed available capacity on the trans-Hudson transportation network which includes roadways, buses, ferries, PATH trains, and commuter rail to Penn Station New York (PSNY), the existing trans-Hudson rail tunnels, and within PSNY itself. The consequence is that NJ TRANSIT's (NJT) options to provide additional rail service into midtown Manhattan during peak hours have been exhausted without major new infrastructure. Compounding the situation is that demand for additional public transportation solutions are certain to increase, as population and employment across the region grow. Recent projections for commercial development in Manhattan estimate more than 200,000 additional office-sector jobs will be created over the next two decades. Furthermore, maintaining a safe and secure rail system is the highest priority of rail operators. The post 9/11 attack security environment demands rail redundancy across the trans-Hudson Midtown corridor, where one incident can quickly impact hundreds of thousands of commuters, to be critical.

Presently, NJT operates 23 trains per hour during the morning and evening peak periods to and from Penn Station carrying about 42,000 passengers each way during the peak period and about 140,000 passengers per day each way. By 2025, ridership is expected to increase by about 70% to more than 200,000 passengers per day. The Trans Hudson Express (THE) Tunnel project, formerly known as the Access to the Region's Core (ARC) project is vital to accommodate the increased ridership. THE Tunnel will support the New York/New Jersey metropolitan area's future economic well-being by improving trans-Hudson mobility, maintaining a safe and secure transit system, maintaining and enhancing the economic viability of the region, improving the quality of life for transit passengers, and preserving and protecting the environment.

2 PROJECT DESCRIPTION

The project consists of providing additional tracks in New Jersey along the North East Corridor (NEC), new tunnels across the Palisades and the Hudson River,

new tunnels in Manhattan, and a new cavern station under 34th Street. See Figure 1. In New Jersey the project consist of the construction of loop tracks connecting the Main/Bergen/Pascack Valley lines to the NEC near the Secaucus Junction Station, to provide a one-seat ride to and from midtown Manhattan from northern New Jersey, and from Orange and Rockland Counties in New York; a new rail yard in Kearny to accommodate 45 to 50 train sets; and improvements along the NEC to increase its capacity. New tunnels under the Palisades in New Jersey and the Hudson River will connect to a new 34th Street Station in New York and the existing PSNY. The new station will be connected to the existing PSNY, and the Sixth, Seventh, and Eighth avenues, and Broadway Subway lines. With a budget of $6.1 billion (2005) and anticipated completion date of 2016 the project will provide infrastructures, facilities, and rolling stocks to accommodate a total of 48 trains per hour to New York carrying more than 86,000 riders each way during the morning peak period. In addition, NJT is implementing, independently from this project, improvements in PSNY to accommodate the increase in capacity and ridership. These improvements include platform extensions, vertical circulation elements, track modifications and additional storage capacity.



Figure 1. Alignment in New Jersey.



Figure 2. Alignment in New York.

2.1 *Project alignment*

The project extends from just east of the Hackensack River on the NEC to West 34th Street and Sixth Avenue in New York City and includes a new rail yard in Kearny. The alignment includes new loop tracks (Secaucus Loop) from the outer tracks of the existing Main Line on the lower level that connect with the upper level NEC tracks west of Secaucus Junction Station. The new loop tracks will utilize the former Boonton Line right-of-way, and allow Main-Bergen/Pascack Valley Line trains to continue to PSNY or the proposed 34th Street Station through either the existing North River tunnels or the new tunnels. This arrangement will create a direct, one-seat ride for passengers from Northern New Jersey to New York City.

East of the Hackensack River, the alignment includes a new bypass track that would split off to the northern side of the NEC, creating four tracks along the NEC from the Hackensack River to the new tunnel portals. This would allow express service along the NEC in either direction. Two tracks would connect to the existing North River tunnels, and two tracks would connect to the new proposed tunnels, descending and turning southward under the Palisades through Union City and Hoboken. Interlocking configurations along the NEC are developed to provide full flexibility between the existing tunnels and the new tunnels to facilitate emergency operations or periodic closures of the tunnels for maintenance. See figure 1.

Near the Hudson River in Hoboken, the new tunnels will turn eastward to cross the river. At the eastern shore of the river in New York, the alignment will begin to ascend in grade, and turn in a northeast direction, passing under the Hudson River bulkhead. Connections to PSNY will split from the main tracks after passing the bulkhead. The PSNY connector tracks will continue to ascend, before turning east to tie into existing PSNY tracks. Beyond the point where the PSNY connector tracks will split off, the main tracks leading to a new 34th Street Station will descend, and split to four trackways, arranged two-over-two. At West 34th Street, the alignment will turn eastward to match the street grid. Each tunnel level will split into four platform tracks serving two island platforms in a two-cavern station. See figure 2.

3 PROJECT GEOLOGY

The New Jersey portion of the project area is located within the Piedmont physiographic province broad

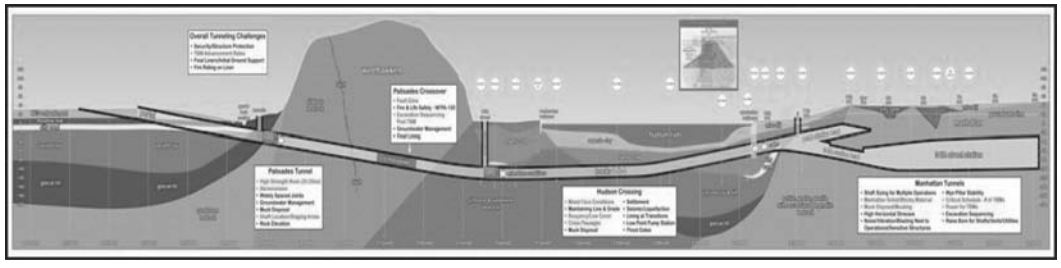


Figure 3. Geological profile.

lowland interrupted by long, northeast-trending ridges and uplands. The most prominent physiographic feature in the eastern part of the province is the Palisades, a striking north-south topographic ridge near the Hudson River that rises above the surrounding lowlands of the Meadowlands. Most of the project area in New Jersey is underlain by rocks of the Newark Basin, a northeast-trending late Triassic – early Jurassic rift basin filled with a thick sequence of sedimentary rocks and intrusive and extrusive igneous rocks. The topography of the bedrock surface shows two narrow, deep, glacially scoured troughs, one on either side of the NJ Meadowlands. Metamorphic rocks in the project area occur only along the Hudson River waterfront in Hoboken and Jersey City. The Hartland Formation consists of gray, interbedded schist, granulite, and amphibolite.

Thickness of surficial materials in the project area in NJ varies from one meter to greater than 75 m (250 feet) at a glacially eroded bedrock trough in the vicinity of the New Jersey Turnpike east of Kearny. Surficial materials consist of deposits of glacial, eolian, alluvial, and marsh/estuarine origin. The Rahway till is a surficial unit directly overlying bedrock. It is a nonstratified, compact deposit with pebbles, cobbles, and boulders in a reddish-brown matrix of sand, silt, and clay. Its thickness is generally less than 10 m (30 ft). Overlying the till are glacial deposits along the west flank of the Palisades ridge, at scattered locations near the Hudson River, and near the Passaic River. The unit includes both deltaic deposits of sand, sand and gravel, and silty sand and lake-bottom deposits of fine sand, silt, and clay. Thickness ranges from about 8 m (25 feet) to over 30 m (100 feet) in the Meadowlands east of Kearny. Passaic terrace deposits, consisting of moderately sorted sand and gravel, are present along the Passaic River in the vicinity of Newark and Harrison. Light brown eolian deposits of very fine to medium sand occur locally near Laurel Hill and just west of Penhorn Creek. A large percentage of soils in the project area have been altered by excavation or filling. Earth and manmade materials that have been placed as fill include gravel, sand, silt, clay, trash, cinders, ash, and construction debris. In the cut and cover section in New Jersey the soil stratigraphy from the ground surface consists of 2.5 to 3 m (8 to 10 ft) of marsh deposits, underlain by about 1.5 m (5 ft) of alluvial sand, underlain by about 6 to 12 m (20 to 40 ft) of hard blue clay deposits of glacial Lake Hackensack, which are in turn underlain by 15 to 24 m (50 to 80 ft) of hard red to brown clay deposits of glacial Lake Bayonne. In the centre of the trough, bedrock is overlain by a glacial deposit of till or hard sand and clay about 15 m (50 ft) thick.

The Hudson River portion of the project area is located between the Piedmont physiographic province on the west and the Manhattan Prong of the New England Upland physiographic province on the east. The topography of bedrock surface underlying the Hudson River shows a narrow, deep, glacially scoured trough that extends to more than 100 m (300 ft) below sea level. Depth to rock is about 40 m (125 ft) below mean low water at the New York bulkhead line and about 55 m (180 ft) below mean low water at the New Jersey bulkhead line in Hoboken. The maximum total thickness of surficial materials overlying bedrock of the Hudson River in the project area is about 100 m (300 ft), with a complex stratigraphy of glacial, fluvial, lacustrine, and estuarine deposits. It is anticipated that the soil materials through which the Hudson River tunnel would be constructed would be primarily estuarine deposits of organic clayey silt and fine sand, with sand or glacial till possible near the New Jersey waterfront and sand or organic clay near the New York waterfront. Gas pockets due to natural methane have been reported in the estuarine silts, mostly at shallow depths. It is also anticipated that hidden offshore obstructions within soil materials, such as boulders, piles, wrecks, or miscellaneous fill exist on both sides of the Hudson River.

The New York portion of the project area is located within the Manhattan Prong of the New England Upland physiographic province. Within the Hartland Formation, granitic intrusions are present near the Hudson River. A large granitic sill has been mapped between Ninth and Twelfth Avenues, and between West 34th Street and West 40th Street. Serpentinite associated with the Hartland Formation has been reported

between Tenth and Eleventh Avenues, at the northern part of the project area, and at scattered locations as far south as West 26th Street. Thickness of surficial materials is variable and they generally have been altered by excavation, filling, or paving for various developments. The entire length of the Hudson River waterfront in the project area is reclaimed beyond the original mid-19th Century shoreline. Filled for urban development, these areas are typically former bays or tidal marshes with organic deposits beneath the fill. Most of the Manhattan tunnels east of Eleventh Avenue, are expected to be excavated primarily in schist of the Hartland Formation, including some granite or pegmatite and possibly serpentinite. Rock along the proposed alignment in this section is likely to be moderately weathered and of fair to good quality within the first 1.5 m (5 ft). Below this zone, weathering is likely to be slight, with good to excellent rock quality. The schist is typically of intermediate strength, with unconfined compressive strength generally ranging from about 28 to 100 MPa (4,000 to 15,000 psi). It may contain significant percentages of abrasive accessory minerals such as garnet or sillimanite, as well as thin veins of quartz. The granite or pegmatite is likely to be of high strength, with unconfined compressive strength from about 100 MPa (15,000 psi) to greater than 170 MPa (25,000 psi) and it is likely to contain a very high percentage of abrasive minerals, mostly quartz. Groundwater levels are within the overburden about 3 m (10 ft) of the ground surface and generally parallel to the bedrock surface. Rock mass permeability is relatively low but with higher permeability and greater water inflow along weathered joints or fault zones.

4 34TH STREET STATION CAVERN

The proposed station concept incorporates a potential four-over-four track configuration in two caverns with two tracks and an island platform over two tracks and an island platform in each. Initially six tracks with three island platforms will be provided. A mid-level mezzanine would be provided in each cavern to provide for circulation and pedestrian distribution. The two caverns will be connected to each other with cross passages and will be connected to PSNY through the 33rd Street LIRR concourse. See figure 4. Street entrances along 34th Street between Eighth and Sixth Avenues will be provided.

The conceptual design incorporates belowground connections to the Broadway, Sixth, Seventh, and Eighth avenues subway lines. The station caverns will be approximately 20 m (60 ft) wide by 23 m (70 ft) high and would be placed about 35 m (110 ft) below street surface at the mid-level mezzanine elevation. The southerly cavern will be located under 34th Street, and

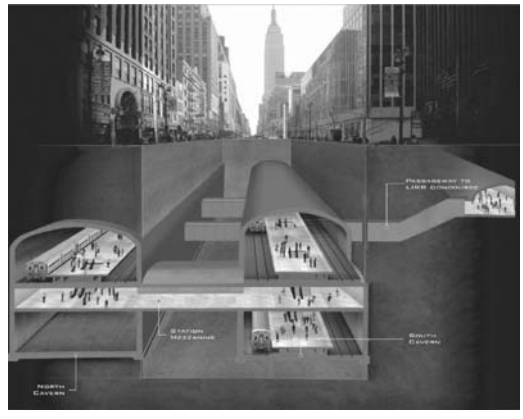


Figure 4. 34th Street station concept.

the northerly cavern will be located under properties along the northern side of 34th Street. The caverns crown will be located approximately 17 m (50 ft) below the top of rock to provide suitable rock cover.

5 TUNNELING CHALLENGES

Building the Trans Hudson Express project will involve construction of a number of tunnels using a variety of construction methods. Selection of an appropriate tunnelling method for each section of the alignment will have a major impact on the successful completion of the project. The project faces many technical challenges:

- Selecting an alignment to meet the transportation needs and minimize environmental issues, while meeting tunnelling method technical challenges.
- Developing a versatile, yet economical and constructible tunnel cross section capable of meeting present and future equipment, and accommodating the required utilities and ventilation.
- Developing track vertical alignments that meet the required design grade to provide connectivity to the existing PSNY and to provide sufficient cover over the tunnel under the Hudson River.
- Utilizing suitable construction techniques in soft silts of the Hudson River with a limited cover.
- Constructing a new cavern station in New York City with access to the existing PSNY, and the existing transportation systems in New York, while minimizing impact on the surface, businesses, and the public.
- Identifying locations for construction staging especially in Manhattan and meeting the needs of other projects in the area.
- Identifying provision for emergency egress and ventilation with minimal impact on land use.

- Minimizing impact on the Hudson River, the Hudson River Park, future developments and existing and future facilities along the alignment.
- Tunnelling in mixed face conditions under the Hudson River.

5.1 *Tunnelling methods*

The construction of the alignment in New Jersey along the NEC would mostly be constructed using the existing or an enlarged embankment, viaduct structures, retained fill, and cut-and-cover tunnels. As the alignment diverges from the NEC and dives under the embankment the construction would be done either by cut and cover, tunnel jacking, or by using sequential excavation or NATM. Cut and cover method will be used to construct other underground segments of the New Jersey alignment to the tunnel shaft west of the Palisades. The cut and cover construction will use slurry walls for support of excavation and water cut off. Staging, rerouting, and decking will be provided to maintain traffic across the excavation. The Palisades tunnels will be constructed using rock TBM starting in a shaft located near Route 1&9. The shaft will be used for access, material delivery, and mucking. Upon completion of the construction it will be converted to a ventilation shaft where a ventilation facility will be located. The tunnels are located about 120 m (350 ft) below surface in the Palisades diabase, with argillite and hornfels of the Lockatong formation for short lengths on either side of the diabase. A cross-over will be constructed between the two tunnels using controlled drill and blast method utilizing the previously excavated tunnels. Crossing the Hudson would be done by a pressurized face soft ground TBM using either Earth Pressure Balance (EPB) TBM or slurry TBM. The TBM will be lowered in a shaft in North Hoboken and would mine the tunnels toward Manhattan under the Hudson River. The tunnels will be lined using one pass gasketed and bolted precast segmental liner. As the alignment approach Manhattan, the cover over the tunnels is limited and special measures would be needed as discussed later. The TBM will be retrieved via a cofferdam constructed in the river at the edge of the bulkhead. Cross passages would be required under the Hudson River that will be constructed using NATM with localized ground freezing. Crossing the river bulkhead, the Hudson River Park, and 12th Avenue in Manhattan would be done using either the cut and cover method with decking and staging to maintain vehicular and pedestrian traffic or alternatively soft ground NATM can be used to construct the crossing with jet grouting and/or ground freezing for ground improvement. The Hudson River TBM can then continue through the previously constructed NATM tunnels and retrieved on land.

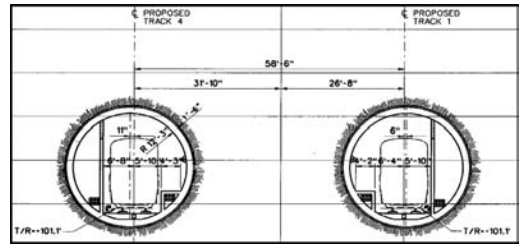


Figure 5. Tunnel cross section.

Tunnelling in Manhattan is challenging in term of access and staging. It is planned that most of the tunnelling in Manhattan would be done from a staging site at 11th Avenue. Two rock TBMs would be used to excavate four tunnels along the alignment through the station caverns. After the initial two runs, the TBMs will be retracted through the tunnels to the 10th Avenue interlocking caverns where they will be re-launched again to excavate the second pairs of tunnels. Subsequently the caverns will be excavated by sequential excavation using controlled drill and blast method from the mined tunnels to create the complex underground track configurations as the tunnels split to serve potential eight-track station. Access and mucking will be through the previously excavated tunnels. The initial liner in the rock tunnels will consist of rock bolts, lattice girders and shotcrete and the final liner will be cast in place concrete liner over a drained waterproofing system.

5.2 *Tunnel cross section*

The tunnel size was established to allow all available vehicles through the tunnel. Its size was based on the Amtrak Super-liner locomotive, with a 4.928 m (16′-2″) vehicle height. The inside tunnel diameter was established to be 7.47 m (24′-6″) to accommodate in addition to the largest equipment, the catenary power requirements, a suitable emergency walkway, and the required systems and utilities. See figure 5. This size tunnel allows the use of the available space for a ventilation plenum created within the bored tunnels to meet NFPA 130. The plenum would be equipped on the top side with motor operated dampers at certain intervals to be used to exhaust smoke in case of fire. In the event of an incident, the dampers in the immediate vicinity would be opened to extract the smoke and hot gases from the trainway. The tunnels will be spaced 17.8 m (58′-6″) on centre to allow sufficient pillar between them especially in the soft silts under the Hudson River.

5.3 *Limited cover over the Hudson Tunnel*

There are several challenges that constrained the design of the connection to existing PSNY. The

engineering alignment underwent many alternative designs to address these challenges. The connection to PSNY was only possible south of the existing North River Tunnel due to the LIRR yard access tracks north of the tunnels and NJT's use of the southern half of PSNY. The operational analysis indicated that 2.0% is the maximum allowable effective grade for locomotive-hauled trains; however with such grade the cover over the tunnels under the Hudson River is inadequate. In an attempt to address this issue two possible solutions were evaluated: an increase in the grade to 3% for approximately 600 m (1800 ft) or artificially increasing the effective cover over tunnel by providing suitable ground improvement. A maximum grade of 3% may be permitted on the PSNY connection if equipment is limited to EMU train sets with multiple-powered coaches. However this will limit the operational flexibility of the railroad. On the other hand, intervention in the Hudson River would trigger environmental and permitting issues. For an effective grade of 2.5% the cover over the tunnel will be about 5 m (15 ft). In this case grouting a canopy over the tunnel from within the TBM can be provided to stabilize the ground and to protect the tunnel face against stability and buoyancy. The TBM would then advance under the protection of the grouted canopy without impact on the Hudson River.

5.4 *Crossing the Hudson River bulkhead*

The Hudson River Bulkhead is constructed of sheet pile walls with stone façade and timber relieving platform and supported by timber piles 18 to 30 m (50 to 90 ft) deep spaced about 1 m (3 ft) apart. The bulkhead is part of the Hudson River Park and is considered a historical structure. Therefore, it is important to preserve and protect it to the maximum extent possible. The piles will intercept the tunnel profile and are expected to be at variable spacing at the tunnel level. Three different methods have been conceptually evaluated for intercepting the Hudson River bulkhead and for constructing the tunnels in the Hudson River Park: continuation of the Hudson River Tunnel Boring Machine through the timber piles with special measures if needed, extraction of the piles, cut-and-cover construction, or excavation using the NATM method with ground improvement.

5.5 *Connection to existing Penn Station*

In order to connect to existing tracks in Penn Station, the track alignment in Manhattan at 12th Avenue diverge to four tracks. The inner tracks descend toward the new station at 34th Street while the outer tracks ascend to meet the existing tracks at the approaches to Penn Station. The track connections to PSNY pass under the Long Island Rail Road (LIRR) storage yard and the LIRR maintenance shop at 10th Avenue in close proximity to their foundations. These tunnels will be constructed using the cut and cover method or NATM. Special measures will be used to minimize the impact on the yard and the shop operations. The yard tracks and the shop will be underpinned prior to the excavation of the tunnels. Underpinning and pre-treatment of the ground will be done at night and on weekends to minimize impact. Conventional tunnelling will be done beneath the yard and the shop with extensive monitoring.

6 CONSTRUCTION COST AND SCHEDULE

At a budget of $6.1B (2005) construction is expected to begin in 2009 and to be completed with revenue operation by late 2016. The peak construction is expected to be in 2011. In order to establish a reliable construction schedule and cost estimate an initial construction packaging plan was established. The plan identified sixteen different contracts ranging in sizes and durations. The packaging plan took into consideration the type of construction, size of the contracts, and their durations and dependency on each other. The Manhattan segment with the TBM tunnels, the 34th Street Station caverns, and subsequently the railroad system work and the station finishes are on the project critical path.

7 CONCLUSION

The Trans Hudson Express (THE) Project is the largest transportation project ever undertaken by NJ TRANSIT. It will improve the overall New York metropolitan area transportation system, will stimulate economic growth, and will maintain midtown Manhattan as a centre of regional, national and global importance. The project has been planned using state-of-the-art design concepts, latest construction techniques and approaches, and with careful attention to environmental issues and concerns.

REFERENCES

NJ Transit "Access to the Region's Core DEIS – Engineering Report" June 2005

NJ Transit "Access to the Region's Core – Draft Environmental Impact Statement" September 2005

Underground Space – the 4th Dimension of Metropolises – Barták, Hrdina & Romancov (eds)
© 2007 Taylor & Francis Group, London, ISBN 978-0-415-40807-3

CTA Block 37 Tunnel Connection in downtown Chicago

V. Nasri & P. Razgha
STV Incorporated, NY

ABSTRACT: Block 37 Station Tunnel Connection project will include construction of two short tunnels to connect the existing subway tunnels (Red and Blue lines) in the northern loop area of downtown Chicago through a new station. The Southeast Tunnel will connect the Red Line to the new station below the intersection of State and Washington Streets and the Northwest Tunnel will connect the Blue Line to the new station below the intersection of Dearborn and Randolph Streets. The connection tunnels are located in a very dense urban area of downtown Chicago and under several important historical buildings. Both tunnels are curved at the intersections and located at a depth of about 7.5 m below ground surface in saturated soft clay with an average undrained shear strength of approximately 25 kPa. The design calls for minimizing surface disruption and ground displacement while maintaining normal operation of the existing subways during the construction of the connections tunnels.

1 INTRODUCTION

To create an express train service linking O'Hare International and Midway Airports, the Chicago Transit Authority (CTA) decided to build two short tunnels to connect the Blue and Red transit lines in Chicago. The connection will be at Block 37, located between State and Dearborn Streets, and will link the two subways through a new station (Figure 1). The new Block 37 station structure will be constructed as part of the Block 37 development project using slurry wall construction and a top down technique. The new connection tunnels will be constructed using mining methods. Mining operations will originate from access shafts to be built within Block 37. The project will also include modifications to the continuous platforms at the existing State Street and Dearborn Street subway tunnels to accommodate the new connections. This project will be accomplished under a complex and tight schedule and must be completed with minimal disruptions to the non-stop subway service. The anticipated subsurface conditions and the stringent project settlement criteria create difficult conditions for the design and construction of the tunnels.

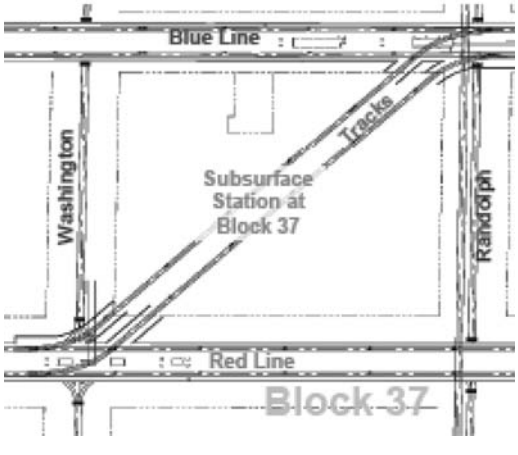


Figure 1. Plan view of project site.

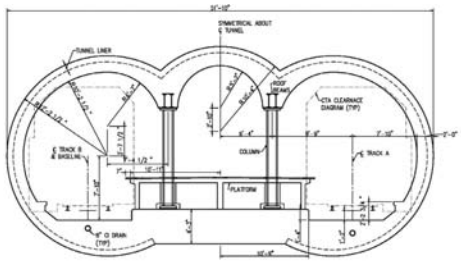
The soft deposits at the project site with their low shear strength can experience large deformations during tunneling. Application of a pre-support interlocking pipe arch method and fiberglass face reinforcement technique ahead of the advancing tunnel face are proposed to limit the ground deformation.

Continuous and swift excavation and support installation combined with an appropriate staging and support system is necessary to minimize short and long-term deformations. The tunnels will be constructed using fiber reinforced shotcrete and lattice girders as an initial support lining. The final lining will be installed using a composite system of steel fiber reinforced shotcrete and lattice girders.

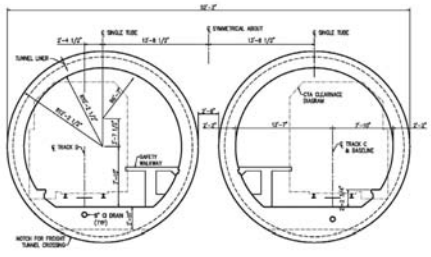
For the connection of the new short tunnels to the existing subway tunnels, a new larger span tunnel will be constructed using the interlocking pipe arch

technique which will be parallel to the existing Tunnel. The new expanded tunnels will transfer the imposed loads to the column line of the existing tunnels. To facilitate the construction of the new expanded tunnels, two cross adits will be constructed perpendicular to the existing tunnels. These cross adits will originate from within Block 37 and extend below State and Dearborn Streets and above the existing Track B and Track C. This construction approach allows all tunneling work, including excavation, temporary and final lining work, to take place outside of the existing tunnel envelopes. Revenue operation can continue practically uninterrupted until the final breakthrough of the existing tunnels is required.

Structural modification and reinforcement of the existing tunnels must take place prior to the excavation of the new tunnels. These structural modifications and reinforcement consist of platform demolitions, erection of new tunnel roof structural support systems and installation of permanent tie down anchors. Removal of some of the existing columns and longitudinal beams will take place after construction of the new tunnels and breakthrough of the sidewall of the existing tunnels. Most of these construction activities will be performed using enclosures separating the work areas from the revenue operations.



a) Station cross section (triple arch)



b) Tunnel cross section (circular arch)



c) Existing subway station (triple arch)

Figure 2. Existing tunnels.

2 EXISTING SUBWAY TUNNELS

The initial subway system of Chicago included two routes, State Street Route and Dearborn Street Route. The tunnel portion consisted of 7.7 miles of double tube and station sections. All the tunnels were entirely constructed in Chicago clay. The bottom of the tunnels is located at a depth of about 15 m below the street surface.

For constructing the tunnels two different methods were used: the liner plate method and the shield method. In the liner plate method the pressure which acts on the roof of the tunnel is carried by steel ribs which transfer the load onto the footings. In order to use this method the clay located beneath the bottom of the tunnel must be stiff enough to withstand the downward pressure exerted by the footings. This condition was satisfied north of the river, where liner plate method was used. On the other hand, the clay at the south of the river was too soft to support the heavily loaded footings. Inadequate support of the footings of the arch ribs in a liner plate tunnel could cause not only tunnel roof failure but also adjacent buildings collapse. Therefore, in the loop district, shield method was employed in spite of the higher construction cost. Figure 2 shows cross sections of the existing station and tunnels built in 1940's. The outside diameter of the individual tubes is about 7.5 m and the minimum horizontal distance between them at the mid-height of the tunnels is about 2′–8″ (Figure 2).

3 SUBSURFACE INVESTIGATION

The subsurface investigation for this project consisted of performing geotechnical borings with standard penetration tests and cone penetration tests with shear wave velocity measurements. Laboratory tests were also conducted on representative and undisturbed

samples of soils which consisted of index tests, unconsolidated-undrained triaxial tests, consolidated-undrained compression and extension triaxial tests in conjunction with laboratory shear wave velocity measurements.

The subsurface soils consist of an upper layer of miscellaneous sandy fill underlain by layers of glacial deposits above the limestone bedrock. The glacial deposits are Blodgett, Deerfield, Park Ridge, Tinely and Valparaiso. The three layers of Blodgett, Deerfield, and Park Ridge are predominantly clay ranging in strength from soft to stiff. The top of the clay is located at a depth of about 4.5 m below the street surface, approximately at the level of the Lake Michigan. The existing tunnels and the proposed construction are predominantly in Blodgett layer.

Blodgett stratum is characterized as very soft to soft silty clay with trace of fine sand and gravel and shale and mostly shows a variable distribution of water content. Red and Blue line subways were constructed in this layer and the proposed connection at Block 37 is expected to be constructed entirely in this stratum. The upper part of the Blodgett layer to a depth of about 1.5 m is desiccated clay crust and much stiffer than the underlying soft clay. However, the clay crust is very variable in thickness and strength and therefore, the entire stratum was considered as Blodgett layer with softer clay characteristics. The groundwater table is approximately at the top of the Blodgett stratum.

4 DESIGN CONSIDERATIONS

Minimum surface settlement, minimum disturbance to the street traffic and minimum impact on the operation of the existing tracks were the main requirements for the design. The critical design criteria consisted of strict limitation of surface subsidence due to tunneling at the location of existing building foundations. Based on these criteria the angular distortion at these locations can not exceed 1/1000, and no surface point shall subside more than 12 mm below its pre-construction location. Presence of important high rise historical buildings supported on shallow spread footings in the zone of mining influence dictated such strict settlement criteria.

The state of the art geotechnical testing and interpretation program has been carried out by Northwestern University to define the behavior of different Chicago clays at the project site. The type of ground in which the tunnels will be mined is classified as soft clay with very low strength characteristics. Different ground improvement techniques and various pre-support methods were considered in initial phases of design. Ground improvement approaches such as jet grouting and ground freezing were excluded due to their unsatisfactory performance in similar geological settings and also their incompatibility with the densely distributed utilities and other site constraints.

Use of forepoling and interlocking pipe arch techniques as pre-support methods were studied in detail. The interlocking pipe arch concept was selected for the final design to achieve the above described surface settlement criteria. An interlocking pipe installation technology was recommended to minimize installation induced soil disturbance, excess pore water pressure and surface settlement. This technique combines drilling with continuous controlled jacking and auguring.

To limit the face extrusion and its resulting ground deformation and to increase the excavation stand up time, fiberglass face reinforcement bars were designed as an element of the pre-support system. The reinforced core in the excavation face reduces ground deformations including extrusion, convergence and pre-convergence components. The design provides either interlocking pipe support or fiberglass reinforcement in all the exposed excavation surfaces including crown, sidewalls, invert and face of all excavations.

The sequential excavation method has been selected as a means of progressively excavating and supporting the ground. The longitudinal tunnels and cross adits are to be excavated with two headings in accordance with the specified sequences designed to stabilize the ground in limited excavation rounds. The excavation sequences of specified round lengths consist of application of steel fiber-reinforced flashcrete to newly exposed surfaces, installation of lattice girders at predetermined intervals, and application of fiber reinforced shotcrete support with variable thicknesses depending upon final opening dimensions.

Due to its particular geometry, the State Street tunnel BD is to be excavated full face. The proposed steel fiber reinforced shotcrete of initial and final liners are combined and the lattice girder is not used as a support element. For shorter connections in State and Dearborn streets a horizontal secant concrete cylinders concept is used as pre-support system. The design of State Street tunnel BD and the longitudinal tunnel were adapted to accommodate the presence of the paid transfer tunnel and the abandoned freight tunnel. The design of the longitudinal tunnel at Dearborn Street was modified to account for the presence of the active and abandoned freight tunnels in Randolph Street.

The final tunnel lining will be designed to carry the combination of full overburden and hydrostatic groundwater loads as well as surcharge loads. Due to the varying tunnel shapes and short tunnel lengths, it is proposed to use high quality shotcrete for the permanent tunnel support lining.

Because of very low assumed permeability of the ground and small expected water head, combination of relatively thick shotcrete initial and final liner with

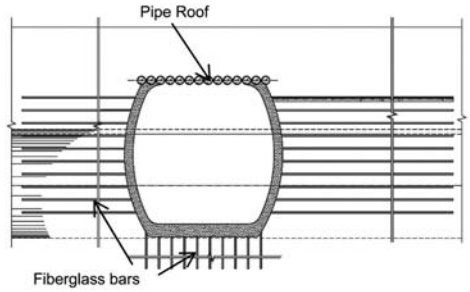
appropriate mix design is considered sufficient to provide acceptable watertightness for the new tunnels. Fuko grouting hoses at construction joints and intersections can be used for repairing the possible leaks.

Monitoring of surface movements will be conducted with series of surface settlement points installed in a series of arrays perpendicular to tunnel centerline across the expected settlement trough. In addition, inclinometers, extensometers and piezometers will be installed to detect horizontal and vertical subsurface movements and ground water level. Total station technology will be used to determine buildings deformation in the zone of influence of tunneling operation. Monitoring points and tiltmeters will be installed to observe any building movement. In-tunnel monitoring will primarily comprise convergence monitoring of the new and existing tunnels and deformation and stress measurement of liner using strain gauges and concrete and soil pressure cells.

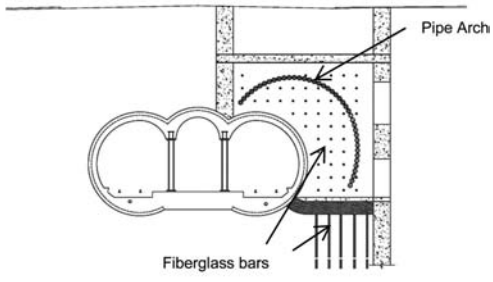
5 CONSTRUCTION ELEMENTS

The construction elements and the corresponding sequences are as follows:

- Building a stairway tunnel under the center arch of the existing tunnel (Figure 4),
- Reinforcement of existing tunnels by erecting new columns, beams and temporary columns (shoring) and installing tie down anchors for both existing Red and Blue line tunnels,
- Installation of 0.6 m diameter interlocked steel pipe roof system and filling them with cement grout (Figure 3),
- Construction of two cross adits under State and Dearborn Streets based on prescribed excavation sequence and support of face, side walls and invert by steel fiber reinforced shotcrete and fiberglass bars (Figure 3),
- Construction of the new expanded tunnel based on prescribed excavation sequence and installation of initial steel fiber reinforced shotcrete and lattice girder support (Figure 4),
- Completing final support system consisting of a combination of cast in place reinforced concrete framing and steel fiber reinforced shotcrete and lattice girder allowing for opening arches at breakthrough points,
- Construction of Tunnel BD at State Street side using interlocking steel pipe arch and fiberglass face reinforcement techniques based on prescribed excavation sequence together with steel fiber reinforced shotcrete as the final liner,
- Connection of track BD at Dearborn Street to the new expanded tunnel at the cross adit location using a short reinforced concrete box structure,

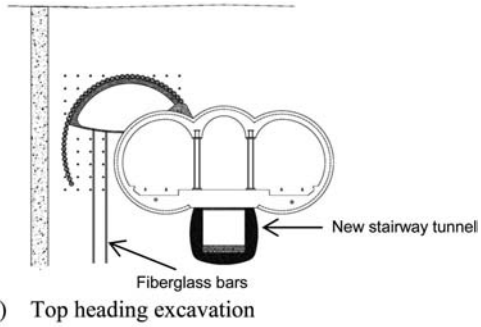


a) Longitudinal section

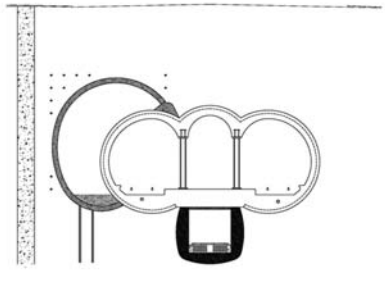


b) Transverse section.

Figure 3. Cross adit sections.

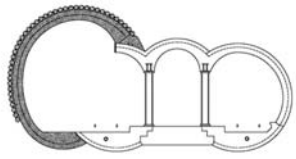


a) Top heading excavation

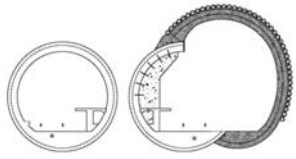


b) Completed initial liner

Figure 4. New expanded tunnel (during construction).



a) Cross section at triple-arch tunnel



b) Cross section at circular-arch tunnel

Figure 5. New expanded tunnel (after construction).

- Connection of Track AC at State Street and Dearborn street with two new expanded tunnels at intersection points using horizontal secant concrete cylinders pre-support system and steel fiber reinforced shotcrete and lattice girder as the final liner,
- Backfilling both cross adits based on prescribed backfilling schedule,
- Breakthrough sidewalls of existing tunnel (Figure 5),
- Transferring the loads of removed beams and columns of existing tunnels to new framing systems by means of jacking.

The excavation of both expanded new tunnels will be performed in two stages of top heading and bench. Maximum distance between faces of top heading and bench will be 9 m. The more desirable full face excavation cannot be applied due to constructability constraints which would require hand mining or the use of a movable platform for mechanical excavation. The Tunnel BD at State Street side will be excavated full face in one stage.

6 NUMERICAL ANALYSES AND MODELLING

The three layers of Blodgett, Deerfield, and Park Ridge along with the miscellaneous fill were modeled in the finite element analysis. The Hardening Soil (H-S) model (Schanz, 1999) was used for modeling Blodgett, Deerfield and Park Ridge strata. H-S model is an advanced model with stress-dependant soil stiffness using the following three different input stiffnesses: the triaxial loading stiffness (E_{50}), the triaxial unloading stiffness (E_{ur}) and the oedometer loading stiffness (E_{oed}). The limiting states of stress are defined by the friction angle (ϕ), cohesion (c) and dilatancy angle (Ψ). The relatively simple Mohr-Coulomb model tends to overestimate soil dilatancy. For miscellaneous fill, Mohr-Coulomb soil model was used in the analysis. Material properties used for analysis of Block 37 tunnel connections were obtained from Geotechnical Baseline Report (Patrick Engineering, Inc., 2005) and hardening soil parameters developed for this project at Northwestern University (Finno, 2005).

The excavation and support of various elements of the project such as the extended stairway tunnel, cross adits, expanded tunnels and tunnel BD have been modeled according to the construction stages of the existing and new tunnels using PLAXIS software (Brinkgreve, 2002). As an example, the stages used to model the construction of expanded tunnels are as follows:

1. Initialization of stresses. In this stage the soil layers and ground water table are defined and vertical and horizontal stresses are generated before the construction of existing tunnel.
2. Construction of existing tunnels (initial liner). Construction of existing tunnels, which took place in 1940's, was modeled by creating their geometry as closely as possible and then modeling the excavation using undrained analysis. The initial liner consisting of a steel segmental liner was installed in this stage. This liner was modeled using a structural beam element. The beam element section properties were obtained from the existing drawings. To model the effect of compressed air used during the construction of these tunnels, the groundwater pressure inside the excavated tunnel was kept active, since the pressure of air was originally designed to compensate the existing groundwater pressure during the excavation of these tunnels. Moreover since the concrete final liner was installed at a considerable distance from the face of excavation, 100% of excavation induced stresses are released at this stage. A uniform surcharge of 12.5 kPa was applied at ground surface at this stage representing traffic live load. This surcharge was kept active during the following stages.
3. Construction of existing tunnels (final liner). In this stage, the concrete final liner for the existing tunnels was installed and the groundwater pressure inside the tunnels was deactivated to model the removal of compressed air.
4. Consolidation for 65 years. This stage was added to create the existing state of stress in soil layers, as closely as possible, before the new construction for Block 37.
5. Pre-construction support. Prior to new construction, the existing tunnels were supported by installation of tie-down rock anchors. The displacements

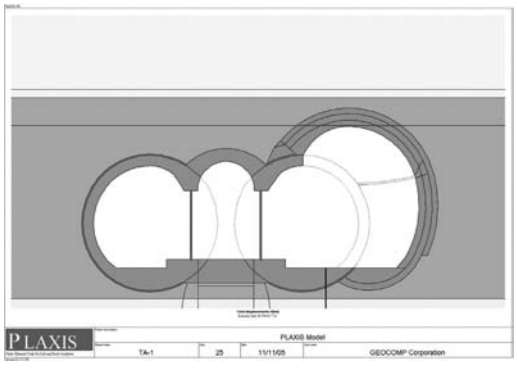


Figure 6. PLAXIS model used in the analysis.

from previous stage were set to zero at this stage, which marks the start of Block 37 construction. Undrained analysis was used for this stage.

6. Construction of new arch (top heading-1). In this stage the top heading of the expanded tunnel was excavated after activating the longitudinal pipes of the pipe arch. It is assumed that 50% of the excavation induced initial stresses are released in this stage. Undrained analysis was used for this stage.
7. Construction of new arch (top heading-2). In this phase, top heading initial liner was activated (shotcrete and vertical fiberglass bars in invert) and 100% of the initial stresses at the excavation boundary were released. Undrained analysis was used for this stage.
8. Construction of new arch (bench-1). The bench of the expanded tunnel was excavated and 50% of the initial stresses were released. Undrained analysis was used for this stage.
9. Construction of new arch (bench-2). In this phase, bench initial liner was activated and 100% of the initial stresses at the excavation boundary were released. Undrained analysis was used for this stage.
10. Cutting the existing tunnel liner. At this stage final liner was installed and part of the existing tunnel liner was cut.
11. Consolidation for 100 years. A 100-year consolidation was performed to calculate long-term ground movements and stresses in surrounding soil and liner.

The tensile stresses in the existing tunnel liner were checked against the rupture modulus of concrete after applying the appropriate load and resistance factors. The analysis indicates that the surface settlement and angular distortion were within the acceptable limits (Figure 6).

7 CONCLUSIONS

A brief history of tunnel construction in Chicago area in the past century including the complexities and challenges involved was presented followed by an overview of construction activities for development of Block 37 in downtown Chicago. A comprehensive geotechnical investigation has been carried out to identify soil parameters required for the design of the connection tunnels at Block 37.

The methodology applied for selection of optimum construction techniques and their complexities were discussed. The construction method included application of fiberglass bars for face reinforcement and interlocking pipe roof technique to minimize the surface settlement induced by tunneling work.

To verify the efficiency of the applied construction technique, series of finite element analyses were performed to investigate: (a) the initial state of stress in soil due to construction of the existing tunnels, (b) the soil-structure interaction during various stages of construction, and (c) the structural response of the existing tunnels.

REFERENCES

Brinkgreve, R.B.J. 2002. PLAXIS 2D Version 8 Manual. Balkema Publishers, the Netherlands.

Finno, R.J., 2005. Hardening Soil Parameters for Block 37 Tunnel Project. Internal Report.

Patrick Engineering Inc., 2005. Geotechnical Baseline Report 100% Submittal to the Chicago Transit Authority, Engineering Department, Capital Improvement Program Management, Block 37 Tunnel Connections.

Peck, R.B., and Reed, W.C., 1954. Engineering Properties of Chicago Subsoils. Engineering Experiment Station, University of Illinois, Vol. 47, No. 423, 63p.

Schanz, T., Vermeer, P.A., and Bonnier, P.G., 1999. The hardening soil model-formulation and verification. Proc. Plaxis Symposium Beyond 2000 in Computational Geotechnics, Belkema, Amsterdam, The Netherlands, pp. 281–296.

Terzaghi, K., 1942. Shield Tunnels of the Chicago Subway. Journal of the Boston Society of Civil Engineers, Vol. 29, No. 3, pp. 163–210.

Underground Space – the 4th Dimension of Metropolises – Barták, Hrdina & Romancov (eds)
© 2007 Taylor & Francis Group, London, ISBN 978-0-415-40807-3

Construction of a large underground station under a station in operation

T. Niibori, Y. Seki, T. Sato & T. Yamada
East Japan Railway Company Tokyo Construction Office, Tokyo, Japan

T. Fujiwara
East Japan Railway Company Construction Engineering Center, Tokyo, Japan

ABSTRACT: A four- and five-tier box-shaped underground station, measuring 25 m in width and 420 m in length, was constructed by East Japan Railway Company at a depth of about 25 m immediately under Yokohama Station through which about 2.3 million passengers pass each day, to link the Minatomirai Line with the Tokyu Toyoko Line. The construction work faced various challenges, including excavation through special geology, the high level of groundwater, tunneling for a railroad immediately under a large terminal station, and severe restrictions on construction due to live flows of passengers. These obstacles were overcome by meticulous engineering studies and technical development, as a result of which the underground station was finally completed two months ahead of schedule.

1 OUTLINE OF THE PROJECT

Operated by the Yokohama Minatomirai Railway Company and initiated under the Minatomirai 21 Plan, one of Yokohama City's urban plans, the Minatomirai Line is a new 4.1-km line connecting Yokohama Station with Motomachi-Chukagai Station. The Minatomirai Line directly connects with the 2-km line between Higashi-hakuraku Station on the Tokyu Toyoko Line and Yokohama Station, which was also recently built underground. This Project has reduced the time taken to travel from Shibuya Station, Tokyo, to Motomachi-Chukagai Station to a minimum of 37 minutes. East Japan Railway Company (JR) constructed an underground station immediately under the present Yokohama Station under a contract with the operator (Fig. 1).

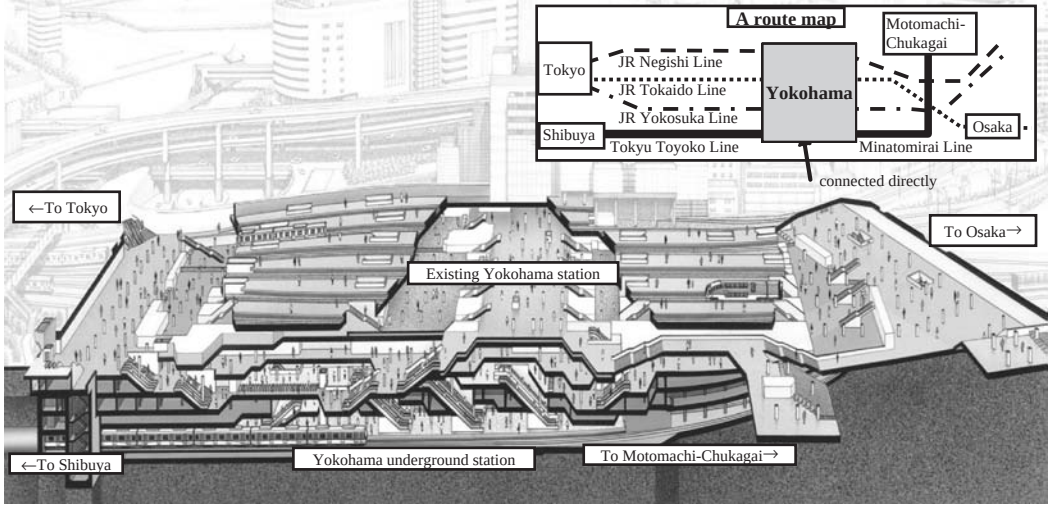


Figure 1. As-built of Yokohama underground station and a route map.

Yokohama Station is used by about 2.3 million passengers every day, serving JR's Negishi Line, Tokaido Line, and Yokosuka Line, the Tokyu Toyoko Line, the Keihin Kyuko Line, the Sotetsu Line and the Yokohama municipal subway through various structures, viaducts and underground tunnels. Yokohama Station is surrounded by station buildings to the east and west, as well as the Aratama River and Katabira River that run north to south.

With no vacant space available above ground, the connecting point of the Minatomirai Line and the Tokyu Toyoko Line was set at about 25 m under the JR Yokosuka Line and the Tokyu Toyoko Line, and a four- to five-tier box-shaped underground station measuring 25 m in width and 418 m in length including the crossing part was constructed.

This paper reports mainly the challenges in terms of geological conditions, working space, available working hours and many other restrictions that were met while constructing this large underground station under a busy, large terminal railway station.

2 AREA SURROUNDING YOKOHAMA UNDERGROUND STATION

2.1 *Geology and underground conditions*

The geology of the ground is very different between the Tokyo side of Yokohama Station and the Kobe side in terms of the depth of bearing stratum, status of geological stratification, and other geological parameters. The Tokyo side ground has good geological conditions, with the Kazusa Group lying between a depth of about 15 m and the ground surface and having an N-value of over 50, whereas the Kobe side ground has a cohesive geological condition down to a depth of greater than 40 m from the ground surface, with an N-value of less than 2. It was a major design and engineering challenge to construct the underground station in such complicated ground.

In addition, a high level of groundwater and the presence of confined groundwater over the entire construction site posed further difficulties for the construction work, including the potential lifting of the underground station structure. Therefore, meticulous design and engineering studies had to be conducted (Fig. 2).

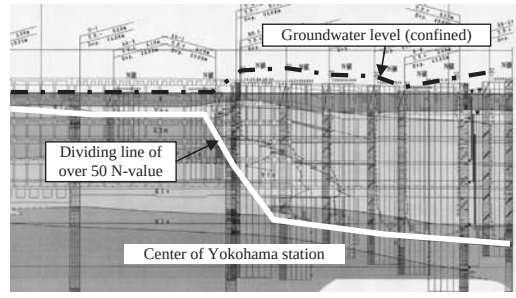


Figure 2. Schematic diagram of Yokohama underground station, geology and groundwater.

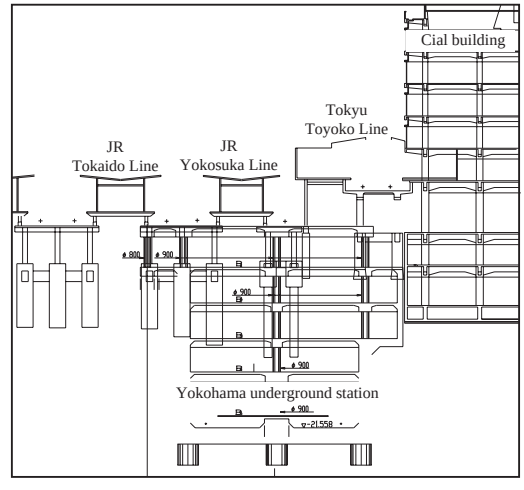


Figure 3. Main body of station – standard section.

2.2 *Structural outline of the underground station*

The Yokohama underground station for the Minatomirai Line and the Tokyu Toyoko Line is a box-shaped structure measuring about 418 m in length, 25 m in maximum width, and 25 m in height. The dimensional details include 24 m for a vertical shaft, 209 m for the structural shell of the station, and 185 m for the crossing under the JR tracks. The structural shell of the station is located immediately under the track of the Yokosuka Line and the viaduct of the Tokyu Toyoko Line. The underground station is thus composed of five layers: one aboveground level that is integrated with the existing JR Line viaduct and four underground levels, as well as two spans (Fig. 3).

In view of the fact that a building is planned to be constructed on the ground above the underground station, specifically a 85-m section from the starting point of the station shell, the steel reinforced concrete construction is adopted for the 85-m section to ensure architectural consistency with the specifications of the future building. The remaining 124-m section was constructed using two different types of construction to reduce the construction period of the underground station although the original plan was to use reinforced concrete construction only. To be specific, steel construction was adopted for the beams and columns of the aboveground part (B0F) and part of the underground level (B1F and B2F), while reinforced concrete construction was used for levels from B3F to B5F.

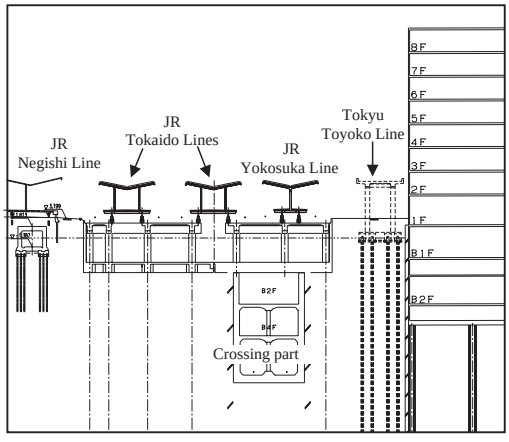


Figure 4. Crossing part – standard section.

The crossing section, which is near the end of the underground station, is a 185-m tunnel that crosses sideways immediately under the existing eight JR lines and connects the main body of the station to the shield-excavated tunnel near Motomachi-Chukagai station.

The structural shell of the crossing section is a reinforced concrete box rigid-frame tunnel, measuring about 14 to 18 m in total width and about 18 to 20 m in height, and with the number of levels and spans varying from 4 and 2 for the station proper to 3 and 1 for the shield-excavated tunnel (Fig. 4).

2.3 *Construction of the underground station*

2.3.1 *Restrictions on work*

Yokohama Station is a large terminal station with some 2.3 million passengers daily, and also operates cargo trains running on a tight schedule. Construction of the underground station faced various restrictions, including that no trains of the existing lines should be forced to reduce speed during excavation. A subway station is generally constructed perpendicular to the direction of the existing track to minimize the influence on the track, but the Yokohama underground station had to be built parallel with the existing tracks since the station buildings and their basements already stand along the existing tracks. Therefore, temporary girders to support train loads had to be built for about 2.4 km in total (283 spans in total). Further restrictions included very short night-time working hours of 3 hours minimum and about 4 hours on average between the last train and the first train.

2.3.2 *Construction procedure*

The Yokohama underground station was constructed as follows, as illustrated in Figure 5.

The existing Yokohama Station, before commencement of the underground station work, had train tracks both on viaducts and embankments. Before excavating

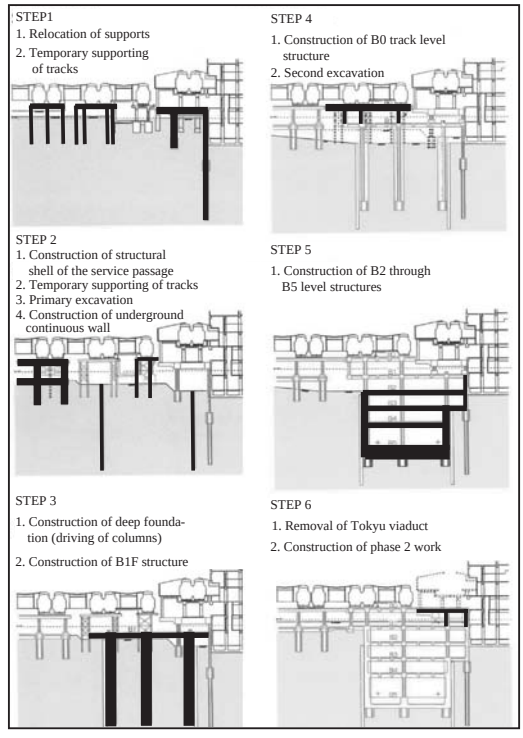


Figure 5. Construction procedure of Yokohama underground station.

the ground, the JR line tracks and the Tokyu Toyoko Line tracks had to be temporarily supported to ensure their structural stability.

[Step 1]
A tentative viaduct was constructed by JR East Japan to support the JR line tracks, while the Toyoko line tracks were temporarily supported by the underpinning method by Tokyu Railroad Company.

[Step 2]
The ground was excavated down to the B1F level of the underground station to create a working space immediately under the existing railroad tracks. Then, the cast-in-situ diaphragm walls were constructed as earth retaining walls to allow further excavation down to the B5F level.

[Step 3]
The ground was excavated down from the B1F level to the B5F level by means of the deep foundation method, and steel pipe columns were constructed from down to up. Then, the structural shell of the B1F was constructed.

[Step 4]
The viaduct to support the JR line tracks was constructed and replaced the temporary viaduct, which was then demolished and removed.

[Step 5]
During construction of the viaduct for the JR line tracks and demolition of the temporary viaduct, the process of excavation and construction of structural shells was repeated to construct the underground station, using the inverted lining method as the main construction method.

The underground station was opened on January 31, 2004, which was the timing when Step 5 was completed.

[Step 6]
From February, the Tokyu Toyoko Line was relocated to a newly constructed tunnel under Yokohama Station, and the former viaduct was demolished. Ongoing construction of the ground level structure of the underground station is the last step, completion of which will mean the completion of the Yokohama underground station.

3 NEWLY INTRODUCED OR DEVELOPED TECHNOLOGIES

The staff repeatedly studied various ways to complete the project within the schedule, and a number of technologies were improved and newly developed to meet the challenge and cope with various restrictions posed by the surrounding conditions and associated engineering difficulties.

3.1 *Development of screwed rotational jack steel piles*

Temporary piles for work girders had to be driven to a depth of about 30 m because of the soft ground and the deep bearing stratum, but as there was only a 2.5-m clearance due to the feeder lines, 17 parts had to be connected to form a single pile. In addition, each pile had to be constructed during just a two- to three-hour period at night when the trains were not running. The screwed steel joint technique was therefore developed and used, as shown in Figure 6. This technique successfully increased the amount of work done each night and reduced the pile construction time. In detail, the conventional method requires 90 minutes to construct a welded joint pile, whereas the screwed steel joint technique can accomplish a single pile in 20 minutes. With the conventional welding joint technique, it would have taken 5 or 6 years to complete all the piles, while the new technique could finish it in almost half the time, or about 3 years.

3.2 *Development of attachable pile cap joint*

Steel pile caps needed to be quickly, neatly and precisely treated to construct lateral girders of temporary viaducts. With the conventional welding connection,

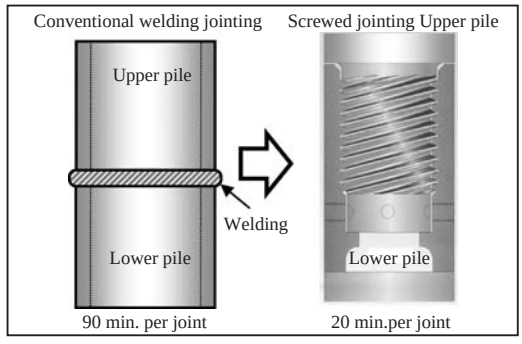


Figure 6. Schematic diagram of screwed steel pipe joint technique.

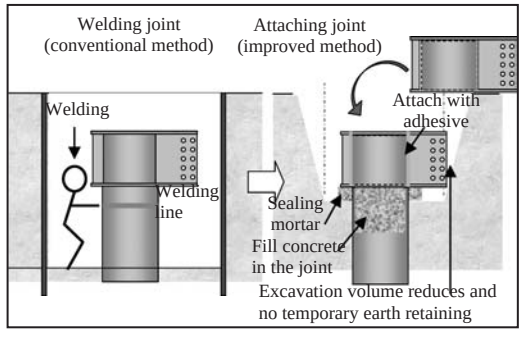


Figure 7. Schematic diagram of attachable pile cap joint technique.

not all the procedures for pile cap treatment could have been completed in just three hours at night. With the screwed technique, however, sufficient precision in the connecting joint was not possible, so a new technique, as shown in Figure 7, was developed. In the new technique, a connecting joint is put over a steel pile head like a cap, the cap-like joint is connected to the steel pile with acrylic resin adhesive filled into the space between the joint and the pile top, and concrete is filled inside the joint to ensure integration. This technique reduced the work load and the volume of excavation, eventually finishing the pile cap treatment work in a single night, down from two nights.

3.3 *Development of the mechanical deep foundation construction technique*

It was necessary to construct main posts for the underground station (2.6 m in diameter and about 30.0 m in length) under limited working conditions with a short overhead space immediately below the existing railroad tracks, and so a deep foundation had to be constructed. However, the conventional approach could not have completed the necessary work safely and smoothly because of the poor working conditions

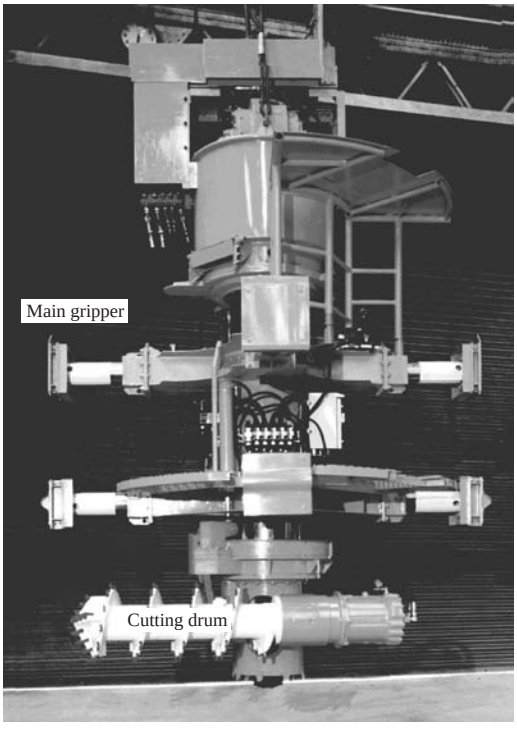


Figure 8. Deep foundation construction machine.

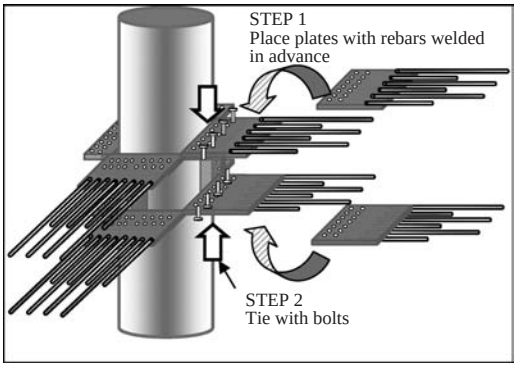


Figure 9. Illustration of connection.

and small number of experienced workers. Therefore, an automatic machine designed to excavate and install liner plates was developed, as shown in Figure 8. This machine successfully allowed safe and smooth construction of a deep foundation in small working spaces.

3.4 *Development of a new technique to connect steel pipes and RC beams*

Steel pipe columns were used for the main columns of the underground station to shorten the construtionperiod, while reinforced concrete beams were used for those connecting the columns to improve economic efficiency. Since there were about 400 places where steel pipes had to be connected to RC beams, a simple connecting technique was needed. A new technique was developed involving an integrated structure in which diaphragm plates at the connection of the steel pipe columns are tied by bolts to plates with mechanical joint rebars welded in advance. The application of this type of precasting technique to the connections of steel pipes and RC beams successfully reduced the field working hours and greatly shortened the total working period (Fig. 9). Before being put to practice, this new technique was proven to be effective by conducting a scale-model experiment and three-dimensional FEM analysis.

3.5 *Development of the steel element continuous wall*

For excavation for the external part of the western side continuous wall (referred to as "extended part") of the main part of the station, and construction of the structural shell, the original plan was to first construct the main body of the station under B2F, without which no extended part could be constructed in terms of structural stability. However, we were requested by the client to bring the start-up timing forward by two months, so we had to shorten the construction period. We drove angular steel pipes called JES (jointed element structure) vertically while manually excavating the ground, and filled the inside of the pipes with concrete. This work eliminated the need to construct the main structure of the station and allowed construction of the main walls that also serve as temporary earth retaining walls without affecting the structural stability of the underground station. Eventually, this technique shortened the original schedule by three months, and it was applied over an area of some 500 m^2. JES are generally applied horizontally in the construction of a tunnel crossing under a railroad track, but for this project they were used vertically (Fig. 10).

4 CONCLUSION

The Tokyu Toyoko Line tracks were relocated to the underground tracks on January 31, 2004, which allowed use of the Yokohama underground station. Then, the Minatomirai Line was opened on February 1, 2004. The work faced a number of challenges, including various restrictions posed by operation of train services, fluctuating loads of station users and special geological conditions immediately under the existing large terminal station. Strenuous efforts were made to study the conditions and develop new engineering ideas, and the project was successfully completed

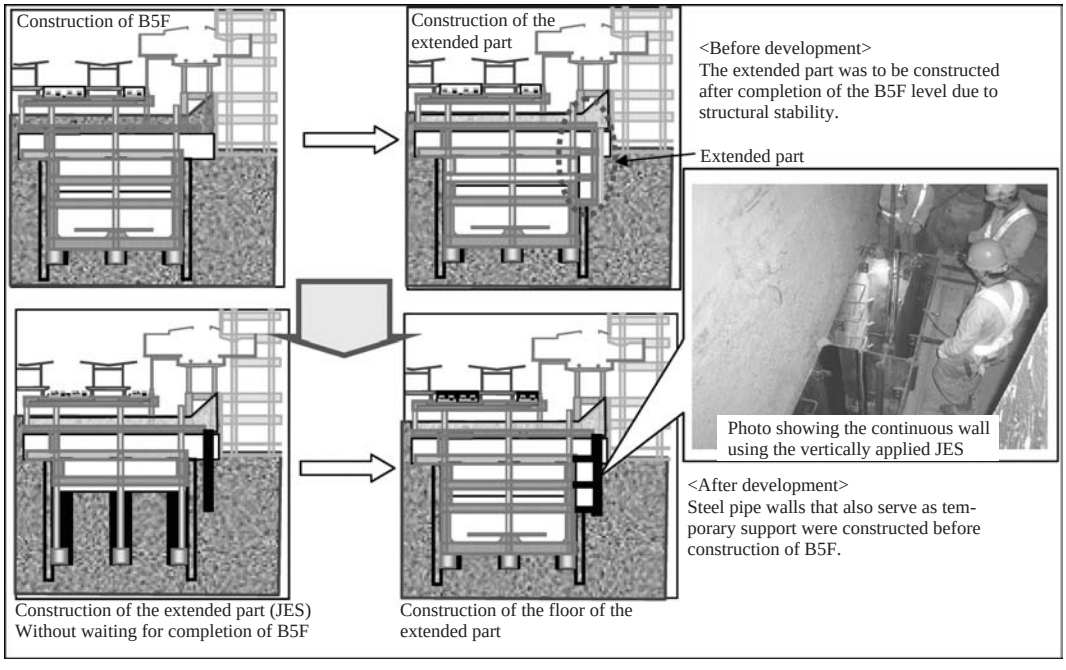


Figure 10. Schedule reduction by construction of continuous diaphragm walls.

about two months earlier than originally planned (March 2004).

The Minatomirai Line has started operation, but some work remains to be done, including deconstruction of the former Tokyu Toyoko Line viaduct and associated construction of the second phase of the underground station. The authors hope that this report may be of help to similar projects in future. Finally, the authors would like to thank all the people involved in this project.

REFERENCES

Fujiwara, T. & Niibori, T. 2004. Construction of a Large-scale underground Railroad Station-The Yokohama Underground Station for the Minatomirai Line and Tokyu Toyoko Line, *Concrete Engineering, No.42, No.2*: 48–53. Tokyo: Japan Concrete Institute.

Sunaga, K. & Morimoto, T. 1999. Construction of the Minatomirai 21 Line Yokohama Underground Station, *Tunnnel and Underground, Vol.30, No.2*: 7–16. Tokyo: Doboku Kogakusha.

Underground Space – the 4th Dimension of Metropolises – Barták, Hrdina & Romancov (eds)
© 2007 Taylor & Francis Group, London, ISBN 978-0-415-40807-3

The next step: The Very Long Tunnel (VLT)

Dr. Havard Ostlid
Norwegian Public Roads Administration

Walter C. Grantz, P.E. & Ir. Jan Saveur
Immersed Tunnel Consultant

Dr.ing. Bernt Jakobsen
COWI AS

ABSTRACT: This paper attempts to see into the future of subaqueous tunneling and look at some exciting technologies that are beginning to come together to make possible the efficient underwater transportation of people and cargo over heretofore unheard of distances. Further this paper identifies some of the unique environmental benefits of the Submerged Floating Tunnel concept when combined with underground and commercial and municipal facilities. stations, shops and any other suitable activity needing space.

1 INTRODUCTION

At the beginning of the 20th century the only known ways to construct a tunnel under a waterway were by simple digging, sometimes under air pressure and by a new "high tech" method, just emerging initially referred to as "Sunken Tube Tunnel". During the 20th century over 150 tunnels were constructed by this Immersed Tunneling(IT) method. These tunnels were used for many purposes including rail and highway transport, material transport, and the subaqueous crossing for various utilities such as water, sewer, petroleum etc. The Immersed Tunnels are prefabricated in sections 100–200 m. long, sealed by bulkheads at the ends, floated to the tunnel site and lowered into a trench whereby they are joined hydraulically and later backfilled.

Another idea for underwater tunnels had been around for nearly 150 years but was never seriously considered until recently. The idea of a tunnel with a vertical alignment above the bottom of the waterway and either floating with some form of stabilizing support, or simply supported on underwater piers in the form of an underwater bridge. This is what is termed the Submerged Floating Tunnel (SFT). This idea was originally proposed in 1865 for an underwater bridge crossing the English Channel, by a British Naval Engineer, Sir Edward James Reed.

In the 1980's and 90's several crossings of this kind were seriously considered and preliminary designs were developed, notably in Norway (Hogsfjord), Sicily (Strait of Messina), Italy (Lake Lugano) and others in Japan.

As a result of the increasing use of the immersed tunnels for underwater crossings all over the world and the new found interest in the SFT Concept, in 1987 at the World Congress in Manchester, UK, ITA established Working Group 11 "Immersed and Floating Tunnels" to foster these tunneling technologies internationally.

Since then WG 11 has presented many technical papers and has also published two editions and most recently an on-line version of the "Immersed and Floating Tunnels State of the Art Report".

This paper is now intended to take these existing technologies for underwater tunnels and suggest means by which they can be extended perhaps by a factor of 100 or more to serve the developments in long distance transportation in MAGLEV.

We name these extended tunnels "VLT", (Very Long Tunnels)

An extension of VLT is very briefly mentioned at the end of this paper, the Trans Ocean Tunnel (TOT) The combination of land based tunnels and submerged floating tunnels facilitate the use of underground space for a long list of purposes, such as underground parking, service stations, shops and any other suitable activity needing space.

2 EXISTING TECHNOLGY

2.1 *The immersed tunnel*

The immersed tunnel method is a well developed technology of great versatility. None of the existing tunnels

are alike. Each is designed to serve a set of specific requirements for interior space, type of throughput, environmental conditions, construction constraints, ventilation, structural strength, seismic loads, accidental loads, etc. Because of this, there exists a wide range of available design and construction experience on which to draw in moving to the development of the as yet untried SFT.

There are, for example, a few basic structural configurations used in immersed tunnels. The most prevalent, particularly for vehicular traffic, is the rectangular concrete box section. This has been widely used in Europe and other parts of the world. In the United States where the technology started however, various forms of single and double steel shell structurally composite sections largely became the norm. In these sections, the steel shell both acts as a structural composite medium with an interior concrete load carrying lining and as a waterproof enclosure..

The construction of these tunnels is a shipyard operation with steel shell elements being assembled from prefabricated modules into long single or double tubes. Bulkheads are fitted to the ends and the element can either be end or side launched or it can be floated out if assembled in a drydock. The interior concrete structure is then largely constructed while the element floats at a jetty. The foregoing methodology is particularly well suited to the development of the SFT.

2.2 *The Submerged Floating Tunnel*

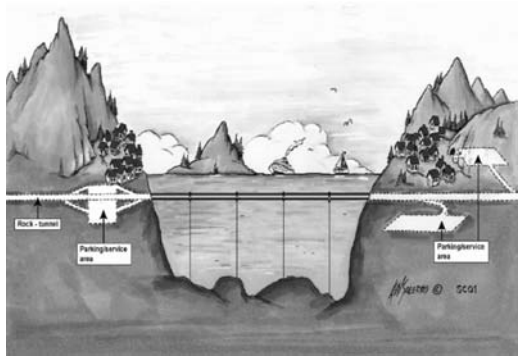
It is now time to describe the SFT as this is the bridge between the immersed tunnel and the Very Long Tunnel (VLT) the subject of this paper. The SFT takes the immersed tunnel and raises it out of the mud, so to speak. The immersed tunnel has an important advantage over the excavated tunnel in that its depth need only be a few meters below the bottom of the waterway. A shield driven tunnel, for example, must be at least a diameter below the stable bottom putting it perhaps ten meters deeper or more. For a rail tunnel with flat gradients of say 0.015 this will increase the total length of the tunnel by $(10/.015)2 = 1{,}333$ m.

Take the example of a crossing under a fjord where the depth might be 500 m. Given the same navigation depth requirements as for the previous example, the SFT would only be as long as the immersed tunnel, but in this case the immersed tunnel would be outside of the range of feasibility for IT's and a bored tunnel would be say $(530/.015)2 = 71$ km longer!

At such a depth to cross, it could be anchored directly by steel tethers attached to bottom anchors spaced along the tunnel alignment.

2.3 *Design of the SFT*

As for the IT, almost any configuration can be adapted for the SFT. The structure can be solely concrete, solely steel, or a steel/concrete composite. It can be multilane or multi-track. It can be rectangular or it can be circular. Whatever the configuration, as the depth is made greater the structure increasingly favors a circular cross section for efficient design. Tethered SFTs must float with sufficient positive buoyancy to maintain stable tension in the tethers under all loading conditions. At greater depths, the concrete becomes too much of a dead load so that steel alone may be used. Exterior flotation material may be used to augment positive buoyancy.



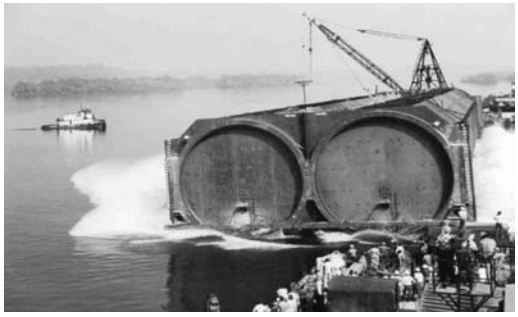
Dynamic loads caused by waves, swell, wave drift forces, vortex shedding or varying currents can cause trouble if these forces are not well understood and properly accounted for. Often physical modelling can be helpful directly or can be used to calibrate and verify software for appropriate modelling of such phenomena. Such model testing and evaluation of the test results with particular emphasis on the slowly-varying motions have been done in the Høgsjord project. Based on the present state of the art, circular cross-sections are favoured also from a hydrodynamic point of view.

The terminal ends of the SFT where the tunnel enters the rock or the ground will require special design to limit the motion without focusing load, especially if seismic forces must be taken. Potential lateral, vertical, and longitudinal motions must be taken into account.

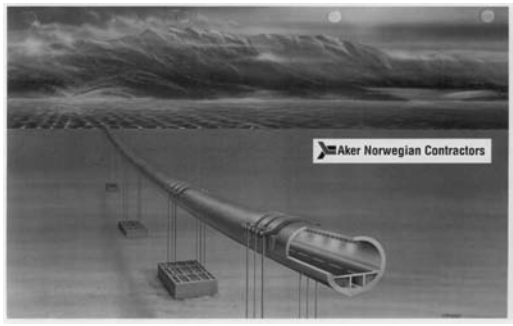
2.4 *Construction of the "unsinkable" SFT*

As this discussion will eventually lead us to the next step, the VLT, let us say that we are going to build a tethered, steel shell SFT to cross a 2000 m wide waterway 400 m deep at the center. This SFT will carry three tracks for electric trains. The signal system will be operated so that no more than one train can be in the tunnel on two of the tracks at any one time. Further the tunnel will be designed so that it will not sink and self-destruct if it is breached and filled with water.

The bottom of the water channel is soft and has a low bearing capacity so it must be improved by piling or simply gravel replacement of the soft strata. Large gravity anchors will be used. The elements will be



Example of immersed tunnel of steel.



An approved alternative for SFT and possible anchoring system for (VLT).

200 m long and the anchors and double tethers (on each side) will have a longitudinal spacing of 50 m or four sets per element located so that they miss the joint areas.

Each of the ten elements is constructed on side launching shipways and all are straight as drainage will all be toward one end. A 2 meter thick layer of syntactic foam (made of glass microballoons that will not crush or deteriorate in water pressure) covers the circumference of the tunnel except at the joint areas providing reserve flotation capable of supporting the tunnel if the interior floods. For the SFT to be unsinkable it must have sufficient flotation capacity to allow the entire running tunnel tubes to flooded while maintaining a nominal tension in the tethers.

The joints are designed and the elements are connected very much using the well-proven method used for immersed tunnels. in that an initial seal is first made to seal the joint area so that the water pressure can be released and the full hydrostatic force at the other end of the element being placed can compress the gasket (GINA) and permit a full structural connection to be made.

2.5 *Tethers and anchorages, offshore Technology*

Over the last few decades offshore platforms have been constructed and operated in deep waters, such as in the Gulf of Mexico, the North Sea and off Brasil.

Vast experience has been gained regarding forces exerted on offshore structures by waves and current, the motions induced by these forces and on the hydroelastic interaction between the forces and the motions. Better understanding of phenomena and sources for slow-varying motions has been acquired. This understanding is of vital importance for the safe design and configuration of an SFT with its anchorages.

The Tension Leg Platform (TLP) with its tethered connections to the sea bottom has in particular paved the way for the use of this technology also for structures like the SFT. This applies both to the design and installation of the tethers and their anchoring elements on the sea floor.

For relatively shallow SFT's with depths in the order of 100 m. cable or pipe tethers may be suitable but as the depth gets deeper, the tethers themselves must be more sophisticated. The offshore oil industry has led the way in this respect in the design of tethers for their Tension Leg Platforms (TLP's). Special pile anchorages and floating hollow tethers have been used offshore. This technology is well developed and should be adaptable and suitable for use for SFT's and VLT's.

2.6 *Tunnel saddles*

The method used to connect and fine tune the tethers to the tunnel structure is an area that still requires a great deal of study. The configuration of the tethers themselves and how they attach to the tunnel and transfer huge loads requires special attention in the structural design of the tunnel itself.

A limitation on the use of the SFT is the depth of water. At some point the tethers become too long and laterally flexible allowing unacceptable deflections. It is doubtful that a completely stable SFT can be built in more that 1000 m. of water depth. Unless measures as described to provide enough flotation in the SFT to prevent its destruction in the event of accidental flooding, such a tunnel would be high insurance risk.

For Høgsfjord it was found that, where the tunnel would arch between the abutments, it would be too vulnerable to slowly-varying wave/current forces, and concluded that tethers with sufficient high lateral stiffness was preferable.

2.7 *Stability of tethers:*

The tethers can be unstable due to varying tether forces (so-called Mathieu-instability) also for relatively short tether lengths. The key thing here is to configure a tether system with high enough stiffness both vertically and horizontally. A combination of inclined and

vertical tethers every second pair of tethers might be one interesting possibility.

3 THE VLT

3.1 *The very long SFT + MAGLEV + Vacuum = the VLT*

Say you want to cross the Irish Sea between England and Ireland. It is some 100 km wide and less than 200 m deep. How would one do this. Vehicles are out, but trains maybe. . .

One concept that has been given some attention recently, is the building of a long tunnel and keeping it at a full or partial vacuum. By using frictionless MAGLEV propulsion, theoretically, trains could travel a very high speeds of say 1000 km/hr or faster in such a vacuum and make the 100 km crossing in ten minutes or less allowing some time for acceleration and deceleration.

MAGLEV or Magnetic Levitation of course is the technology now being used to propel trains at great speed by magnetically raising them above what in effect is the stator part of an alternating current motor. By so doing there is only air resistance to overcome. By removing most or all of the air, the train can operate at very high speeds with little energy usage. Most of the energy used is due to resistance losses in the MAGLEV "rails".

So if we take the SFT example we developed above, build the special termini with airlocks and vacuum pumping stations, provided MAGLEV trains equipped with self-contained breathable air/oxygen and assured a very stable precisely aligned leak-proof tunnel, a new international travel system will have been created.

3.2 *Things to consider*

Of course it is not quite as simple as it sounds. For these tunnels to operate safely and comfortably, their alignment must be maintained to precise tolerances. This is not easy to do in open ocean conditions with storms, waves, currents, varying water densities and the weight of the trains themselves acting to displace the tunnel. This favors the idea of going deeper to stay away from the turbulent surface conditions that may prevail. But going deeper requires more structural strength and more weight. Leakage is not an option as any water entering the tunnel will flash into vapor in the tunnel and provide a local pressure that might buffet the train besides that salt would be deposited everywhere and salt is an enemy of electrical equipment.

A long list of problems will have to be solved, among these the amount of electrical power needed, how to produce it and transport it.

The construction and maintenance of the MAGLEV system, the vacuum system, the air-locked train stations and switching yards would be costly and complicated but certainly doable.

For intermediate access and exit to and from the VLT one can imagine intermediate (tethered) submerged stations provided with shafts to a platform above the wavezone. Very much like the existing Tension Leg Platforms. These stations can initially serve for the construction of the tunnel, later for maintenance and for emergency evacuation.

3.3 *Construction time and cost*

Continuing with our 100 km crossing example what will the components of the system be and how long will it take to construct them? At 200 m. per element, there would be 500 elements to construct.

These units would likely be built in shipyards or specially equipped fabrication sites. For easy installation and hookup, most of the electrical mechanical "guts" of each element would be in place when connected into the tunnel so that only the work in the joint would be required.

It is likely then that the fastest any element could be constructed would be 3–6 months. Based on the present day industrial practice for steel tunnels at shipyards, we assume a learning curve for each shipyard so that the average production speed would be 4 months per element, 500 elements would require 2000 shipyard months. To complete the production in say 10 years would take $2000/120 = 17$ shipyards working continuously.

The cost of such a structure would be high compared with the cost of present day tunnels, however these tunnels may be a possibility to help solving future transport problems.

3.4 *Safety*

3.4.1 *Collision from vessel*

While the chances of such a collision should be very low since the SFT and the VLT are essentially exposed to the danger of a ship sinking or a submarine collision, it may not be possible to design a tunnel to absorb such an impact. However small ships would not be a problem given the mass and strength of the tunnel. It is noted that the current practice in designing immersed tunnels provide for accidental loads by sunken ships that could easily be carried by the VLT. Especially if constructed to be unsinkable. Furthermore, it is entirely possible to replace a damaged or destroyed section of tunnel underwater given that the design has provided for a stable flooded tunnel.

If an SFT/VLT is not capable of floating in a flooded condition it will of course then be lost by collapsing to the ocean floor.

3.4.2 *Terrorism*

For bored or immersed tunnels the danger of terrorism is from the inside. For SFT or VLT the outside is also

exposed. The danger of terrorist is always present, any underwater tunnel could be a target with the larger, longer tunnel being a bigger "statement" . As the case of airlines, security will be the first countermeasure. However the use of interior foam for flotation can also be designed to absorb explosive energy so that even though a car and train be destroyed, there may be a way to design and prevent the breaching of a SFT or VLT tunnel.

4 ADVANTAGES OF THE SFT/VLT

The SFT can be environmentally attractive as they put roads or railroads out of sight. This is especially beneficial in areas of natural beauty where congested roads or noisy railroads along lake shorelines can be a real blight.

In certain cases, since the roads entering shoreline towns are entirely hidden underground, they might be connected to parking garages and shopping malls also underground and hidden.

These tunnels save fuel/energy by keeping tunnel alignments flat. Steep grades in conventional tunnels require heavy fuel consumption, especially for cargo trucks.

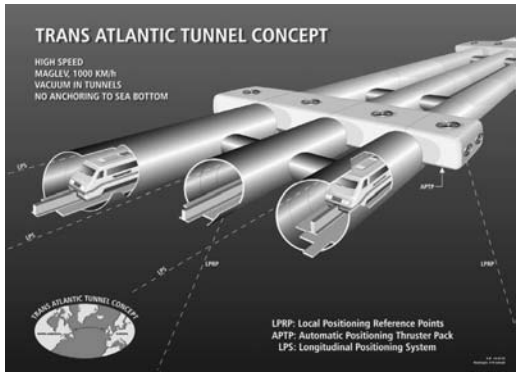
Of course, the proposed combining fast transport with very long tunnels has many potential benefits. While these benefits and technical breakthroughs are very attractive, in the end their costs must be justified by the traffic they will carry.

4.1 *Preliminary conclusion for Submerged Floating Tunnel*

The SFT is a viable environmentally friendly alternative method for underwater transport both vehicular and rail as well as other pipeline, conveyor, or services that might be desired. It is an extension of the immersed tunnel technology with new aspects and engineering problems to solve. No SFT has yet been constructed. This may be because all the SFT's put forward so far are vulnerable to collapse if flooded, but as indicated above, SFT may be made unsinkable. SFT's are more costly on a unit basis of cost per kilometer than tunnels that are excavated but may make up for that by shortening the tunnel significantly.

4.2 *Preliminary conclusion for Very Long Tunnels*

The VLT is an extension to the SFT. The idea of a high speed MAGLEV railroad within a vacuum tunnel seems very novel and interesting. It would only seem to justify itself for significant distances of say more than 50km. Such a tunnel would seem to take many years to amortize its cost and the energy involved in its construction. However with the industrial base in place to produce such tunnels and efforts to standardize components, it might well turn into a wave of the future



A futuristic example of a Trans Ocean Tunnel

with longer and longer subsea tunnels eventually transitioning from VLT's to Trans ocean -Tunnels (TOT's)

40 years ago when containerized cargo began to appear in ports, who could have visualized the huge ships carrying 10–15,000 standardized containers of present day?

4.3 *Some thoughts on Trans Ocean Tunnels (TOT)*

Connection between continents may be called for in future for reducing the use of energy in transport of people and goods.

Combination of all kinds of tunnels and tunneling technology would be required, soil and rock tunnels, immersed and submerged floating tunnels and completely new technologies and solutions.

This would be one of the big challenges of the future in the tunneling industry and preliminary investigations and research should start now.

5 HISTORY AND BACKGROUND

5.1 *Brief history*

In 1865, Sir Edward James Reed, MP for Cardiff put forward the idea of crossing the English Channel in a tunnel suspended on top of caissons. The concept did not win much support, as members of Parliament feared this to be a possible route for invasion of the British Isles.

Recently , a number of studies have been carried in Italy, Japan and Norway. One of these studies, for the Høgsfjord Project in Norway was taken as far as being approved for final engineering design by the Public Roads Administration. This project brought forward four separate concepts, three as concrete tunnels and one alternative in steel as the main construction material. The anchoring methods were by pontoons on the surface or as tethers to caissons on the sea bed.

5.2 *Publications and Conferences*

The following is a summary of recent SFT publications, project studies and conferences , this list is by no means complete, but will illustrate the interest this special structure has received .In addition to this list a large number of presentations have taken place in conferences and seminars over the last 20 years or so.

1973 Vallavik-Bu, Norwegian Public Roads Administration (NPRA), reports
1984 Messina Strait
1989 AIOM Congress , Napoli, Italy
1990 Wegen naar de toekomst (Roads to the future) Robbert and Rudolf Daas, publ.Tirion, Baarn, NL
1996 First International Conference on SFT, under the auspices of the NPRA
1996 FEHRL Report on Analysis of SFT concept
1997 ITA, Working Group no.11, State of The Art Report
1999 Strait Crossings Working Group, ITA, NPRA
2000 Seminar Varenna, Italy, Ponte di Archimede, NPRA
2002 First US workshop on SFT, AUCA
2003 The elevated immersed tunnel James Felch, WCT, Amsterdam, 2003
2004 Discovery Channel, Extreme Engineering, Program: “Trans-Atlantic Tunnel”

Some examples of Project studies known to the authors, there are likely other studies not recorded below:

Vallavik-Bu, NPRA, Norway
Høgsfjord Project, NPRA, Norway
Strait of Messina, Italy
Lake Lugano, Switzerland
Funka Bay, Hokkaido, Japan
Lake Mjøsa Crossing, NPRA, Norway
The Storfjorden Crossing, NPRA, Norway
Lake Washington, Washington State , USA
Lago di Como and Magiore, Italy

6 OVERALL CONCLUSIONS

SFT, VLT and possibly TOT will be challenging future opportunities for cooperation within the whole tunneling industry. ITA may be the most important forum for these exciting possibilities.

Underground Space – the 4th Dimension of Metropolises – Barták, Hrdina & Romancov (eds)
© 2007 Taylor & Francis Group, London, ISBN 978-0-415-40807-3

Planning and construction of major infrastructure works in Croatia

J. Radic
Faculty of Civil Engineering, University of Zagreb, Zagreb, Croatia

P. Djukan
Civil Engineering Institute of Croatia, Zagreb, Croatia

Z. Zderic
Konstruktor-inzenjering, Split, Croatia

ABSTRACT: The paper presents recent accomplishments in tunnel construction in Croatia, which was part of a much bigger undertaking – development of national motorway network. Over the last decades Croatia made large investments in order to construct the planned 1500-km of motorways. The total length of motorways and semi-motorways currently operated in Croatia amounts to 1020 km, half of which were constructed over the past 5 years. Further works comprise extension of motorway network, as well as rehabilitation of older sections. Development of highway network required construction of a large number of motorway structures. Overall 55 tunnels will in the end provide for little over 86 km of Croatian motorways, including two longest tunnel structures in Croatia: Sveti Rok tunnel (5670 m) and Mala Kapela tunnel (5780 m) completed in 2003 and 2005, respectively.

1 INTRODUCTION

The last decade is marked by extreme growth of construction in Croatia, mainly in terms of intensive development of motorway network. Numerous structures were build to carry motorways across wide rivers, large valleys or deep gorges, cut through mountains, or simply provide facilities for safe and comfortable transport.

Motorway network construction is currently the most important development project in the country. After gaining its independence in 1991, Croatia was faced with insufficiently developed road network.

The strategic significance of the construction of motorways for the Republic of Croatia was soon recognized (Radic et al. 1999) with the long-term development programme of the Croatian road network outlined in Road Network Development Strategy (Banjad et al. 1996) adopted by Croatian Government in 1996 and Croatian Parliament in 1999 (Fig. 1).

Subsequently the construction gained speed and currently the total length of motorways operated in Croatia amounts to 1020 km (www.huka.hr), half of which have been constructed over the past five years. It is planned to construct the total of 1501 km of motorways, and the works are advancing as scheduled (www.hac.hr). Figure 2 indicates the current stage of completion of Croatian motorway network.

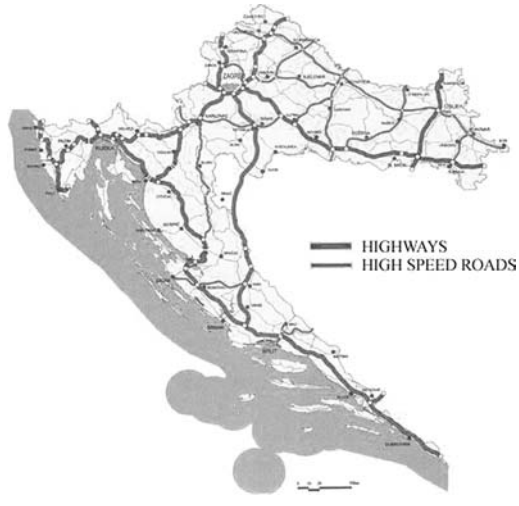


Figure 1. Road network development strategy.

The Croatian motorway network may not seem long, but it is worth mentioning that Croatia already has more kilometres of motorways per 100 000 citizens than UK, Ireland, Greece or Italy.

Development of motorway network required construction of a large number of motorway structures

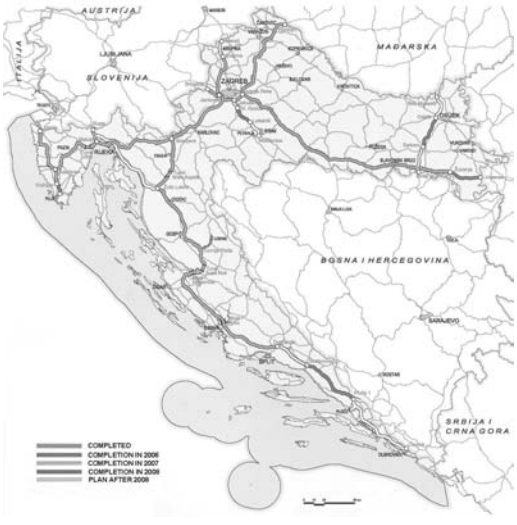


Figure 2. Motorway network in croatia (2005).

Table 1. Number and length of tunnels on Croatian motorways (Mlinaric et al. 2005).

Motorway	No. (pcs)	Length (km)
A1: Zagreb-Bosiljevo-Split-Dubrovnik	22	42.28
A2: Macelj-Zagreb	6	5.31
A4: Goričan-Zagreb	2	2.18
A6: Bosiljevo-Rijeka	12	10.03
A7: Rupa-Rijeka-Zuta Lokva	12	21.21
A8: Kanfanar-Matulji	1	5.06
Total	*55*	*86.08*

(Radic et al. 2006): tunnels, bridges, viaducts, overpasses, underpasses, wildlife crossings etc. For instance, 292 motorway structures account for 19% of the 380-km long Zagreb to Split motorway route. Large-span bridges and long tunnels are the most complex and most expensive part of the network.

2 TUNNELS

2.1 *General*

Overall 55 tunnels (refer to Table 1) will in the end provide for little over 86 km of a total of 1501 km long Croatian motorway network. Two structures stand out – Sveti Rok Tunnel, with total length of 5670 m and Mala Kapela Tunnel with total length of 5780 m, which is the longest tunnel in Croatia, and these shall be described in more detail.



Figure 3. Bisko tunnel.

2.2 *Current works*

Currently, work is in progress on several tunnel structures on Zagreb to Rijeka motorway, Zagreb-Macelj motorway, as well as on motorway sections in the most southern parts of Croatia, which provide for the motorway extension from Split to Dubrovnik.

Most of the structures are constructed as twin-tube tunnels, except on the Rijeka to Zagreb motorway where the current works comprise addition of the second tube to already existing two-way traffic single tubes.

We shall mention only two tunnels among many structures currently under construction: Bisko Tunnel and Strazina Tunnel.

Bisko Tunnel shown in Figure 3 is a twin-tube tunnel with the total length of the left-hand side tunnel tube of 493.5 m and the right hand side tunnel tube of 500.9 m.

Tunnel tubes are spaced at a minimum distance of 35.0 m. The eastern tunnel portal is located at 392.3 m above the sea level, and the western tunnel portal is at 400.2 m above the sea level, resulting in difference of 7.9 m.

Grade in the longitudinal direction is approximately 1.5%. Each of the four portal structures is 12 m long.

Tunnel tube accommodates two-lane roadway (3.75 m + 3.60 m) with the overall width of 7.35 m. Transversal slope of the roadway varies from 2.5% to 3.5%.

Clear cross-sectional area of the tunnel is 56.17 m^2, but the excavation area is in the range of 71.86 m^2 to 86.26 m.

Overburden is approximately 50 m. Total of 76 400 m^3 of material was excavated.

The minimum thickness of the concrete lining is 30 cm. It is constructed of C 25/30 concrete class and total of 9 432 m^3 of concrete was used.

Construction of the tunnel has started in August 2004.



Figure 4. Strazina tunnel.

The entire section between Dugopolje and Bisko of Zagreb-Split-Dubrovnik motorway is scheduled for opening to traffic in 2007.

Strazina Tunnel shown in Figure 4 is another twin-tunnel tube further to the south along the same motorway route. It is somewhat longer than the Bisko Tunnel, with 565.4 m long left-hand side tube and 587.2 m long right-hand side tunnel tube.

Construction of the tunnel started in June 2005 with the opening to traffic scheduled in 2007.

Tunnel tubes are spaced at a minimum distance of 25.0 m. Averaged overburden amounts to 50 m. Eastern and western tunnel portals are located at 282.5 m and 278.7 m above the sea level, respectively. The longitudinal grade in the tunnel is 0.6%.

The roadway in the tunnel is 7.70 m wide, providing for two traffic lanes of 3.85 m. Transversal slope of the roadway is 2.5%.

Cross-sectional area of the tunnel is the same as that of the Bisko tunnel (56.17 m^2), while the excavation are between 70.60 m^2 and 84.05 m^2. Total of 85 800 m^3 material was excavated for this tunnel, and the amount of concrete needed for the construction amounts to 11 800 m^3.

Each of the four portal structures is 12.0 m long, and there is a cut & cover section in the left-hand side tunnel tube in the length of 24.0 m. Secondary tunnel lining is made of concrete class C 25/30, and is 30 cm thick.

2.3 *Sv. Rok Tunnel*

At the time of its construction the Sv. Rok Tunnel was the longest tunnel ever to be constructed in Croatia. It cuts through the Velebit Mountain (Fig. 5), in a total length of 5680 m.

Prior to the completion of the Sv. Rok Tunnel, the longest tunnel in Croatia was Ucka Tunnel near Rijeka, with a total length of 5062 m, which was opened to service back in 1981 (Fig. 6). But, while the Ucka Tunnel is a single-tube tunnel, two separate tunnel tubes were excavated for the Sv. Rok Tunnel.



Figure 5. Sv. Rok tunnel through Velebit mountain.



Figure 6. Ucka tunnel dating back to 1981.

Sv. Rok Tunnel is located on Zagreb to Split motorway, on section between Sv. Rok Interchange and Maslenica.

The preparation work for the construction including clearing the site of landmines started back in 1996, but the excavation itself began in 1997 and was completed in 1999. The tunnel was opened to traffic in 2003.

Two tunnel tubes are spaced at a distance of approximately 35 m.

At the northern entrance located at 561 m above the sea level the slope of the grade line is 0.40%, and at the southern portal located at 511 m above the sea level the slope is 1.5%.

The clear cross-sectional area of a single tube of the Sv. Rok Tunnel is 58.90 m^2. The area of excavation ranges from 70.90 m^2 to 82.30 m^2.



Figure 7. Inside of the Sv. Rok Tunnel.

Table 2. General data on Sv. Rok tunnel.

	Unit	Value
Northern portal	(m above MSL)	561
Southern portal	(m above MSL)	511
Upward slope beginning of tunnel	(%)	1.5
Downward slope end of tunnel	(%)	0.4
Cross-sectional area	(m^2)	58/tube

The roadway in the tunnel is 7.7 m wide (2×3.85 m; refer to Figure 7) with a slope in transverse direction varying from 1.5% to 2.5%.

Tunnel tubes were excavated using New Austrian Tunnelling Method (NATM), which is the only excavation technique that can be used in the region where tunnel passes through all types of soil.

The excavation of twin-tube tunnel was carried out in two stages.

The first stage included excavation of the entire right-hand side tube and 2700 m of the left-hand side tube (almost 50% of its length).

The lining of the right tube is already executed when the second stage of excavation on the remaining portion of the left tube of the Sv. Rok Tunnel takes place. Blasting induces energy in a form of movement and impact on surrounding soil. The distance between two tubes is not large enough to ignore the effect of blasting.

Thus, the design of the concrete lining of the right-hand side tube had to take into account an additional loading due to blasting in the adjacent tunnel tube (Tkalcic et al. 2002).

Finite element analysis was used for this purpose. Data on velocity of the impact were obtained by on-site testing. Movement of the rock mass was measured in the right-hand side tube were the lining had not yet been constructed. The results provided relation between rock movement speed and time.



Figure 8. Twin-tube Mala Kapela tunnel; currently only one tube is opened for two-way traffic.

The main objective of this investigation was to determine excavation step length at which the existing lining in the right-hand tube can remain without reinforcement. It was concluded that from the economical point of view this goal cannot be achieved.

It would be neccesary to make blasting steps so small that it would be more reasonable economicaly to put some reinforcement in the lining.

The second intention was to keep lining reinforcement at the minimum level which would comply with the requirements of Croatian standards.

Since more than 3000 m of the left-hand tube were not excavated at the first stage, placing reinforcement in the existing lining at that length represents a substantial increase in tunnel cost.

This was the main reason that reinforcement in existing tunnel lining was to be kept at the minimum level.

Only the right-hand side tube of the Sv. Rok Tunnel is opened to traffic, while the other one serves as a service tunnel and escape route, refer to Figure 8.

Completion and opening to traffic of the second tube is anticipated when the traffic intensity requires it.

This tunnel tube contains 4 turning points, 12 stopping lay-bys and 14 cross-passages for pedestrian use.

2.4 *Mala Kapela Tunnel*

Mala Kapela Tunnel is located on Zagreb to Split motorway, on section III between Bosiljevo interchange and Sv. Rok.

The tunnel runs through both Mala Kapela and Velika Kapela massif.

It was opened to traffic in June 2005, together with the final 33 km long motorway section between Vrpolje and Pirovac, thus completing motorway connection between the two largest Croatian cities.

Table 3. General data on Mala Kapela Tunnel.

	Unit	Value
Northern portal	(m above MSL)	562
Southern portal	(m above MSL)	573
Upward slope beginning of tunnel	(%)	1.5
Downward slope end of tunnel	(%)	1.2
Cross-sectional area	(m^2)	56/tube

The initial design of the Mala Kapela Tunnel envisaged right-hand side tunnel tube of 5680 m in length, and left-hand side tunnel tube of 5683.2 m in length.

According to these, Mala Kapela Tunnel would have surpassed Sv. Rok Tunnel as then the longest tunnel structure in Croatia by approximately 10 m.

The length of the tunnel was later changed to facilitate the construction of the adjacent Jezerane viaduct. Thus, the completed structure consists of the 5760-m long right tube, and the 5761.7-m long left tube.

Two-tube tunnel was designed, with one-way traffic in both tubes. From the point of view of safety, a twin-tube system with two separate tunnels has a clear advantage over a single tube tunnel. In a case of fire or some other accident, the other tube serves as an escape route.

Longitudinal ventilation of the tunnel also contributes to fire safety in the tunnel as in the case of fire smoke is driven in the direction of travel.

Additionally, one-way traffic in tube provides for traffic safety, as frontal vehicle collisions are excluded.

The clear cross-sectional area of a Mala Kapela Tunnel tube is 56.17 m^2, thus fulfilling all the requirements of both Croatian and Austrian safety standards.

Austrian regulations and recommendations concerning safety in road tunnels were used to supplement the Croatian standards, which date back to 1973. This was only natural, as the tunnel was excavated using New Austrian Tunnelling Method (NATM).

The tunnel is designed for the speed of 100 km/h. Two parallel tubes of the Mala Kapela Tunnel are spaced at a distance of 25 m.

Tunnel grade at the northern entrance (Josipdol) is 0.82%, and at the southern portal (Jezerane) is 1.466%.

The northern portal is located at 562 m above the sea level, while the south tunnel portal is located at 573 m above the sea level, resulting in the difference of 11 meters. The highest point of the tunnel is located at 604 m above the sea level.

The roadway in the tunnel is 7.7 m wide consisting of two 3.5-m wide traffic lanes with 0.35 m wide edge strips on both sides. 90 cm wide sidewalks are elevated 15 cm, and accommodate utility ducts.



Figure 9. Twin-tube Mala Kapela tunnel; currently only one tube is opened for two-way traffic.



Figure 10. Inside of the Mala Kapela Tunnel.

The slope of the roadway in transverse direction is 2.5% directed towards the outer side of the tunnel tube.

Closed drainage system collects the water from the roadway and transfers it to a separate treatment facility.

Construction works started in 2002, and were successfully completed with excavation of both tunnel tubes.

The excavation rate depended naturally on the geology, but on occasions it reached 50 m a day i.e. 200 m a week.

Both tunnel tubes were excavated simultaneously, but at the moment only the right-hand side tunnel tube is opened to two-way traffic, as shown in Figures 9-10, while the other one serves as a service tunnel and escape route.

Completion and opening to traffic of the second tube is anticipated when the traffic intensity requires it. Tunnel tube serving the traffic has 12 emergency and stopping lay-bys.

Additionally, 6 turning points for traffic redirection (spaced at 840 m) were constructed and equipped with sliding fireproof doors providing cross-passage to the



Figure 11. Portal structure on the southern entrance to the Mala Kapela Tunnel.

second tube. There are a total of 14 inches provided in between these cross-passages, spaced at 280 m.

The tunnel is equipped with highly sophisticated traffic surveillance systems which provide 24-hour-a-day surveillance by experts at road maintenance and traffic control centres.

The minimum thickness of the concrete lining is 30 cm. It is constructed of C 25/30 concrete class.

Generally, there is no reinforcement in the concrete lining, except at the location of inches and cross-passages, sections where the large ventilations fans are installed, as well as in the first and last tunnel sections.

Waterproofing layer is installed between the primary and secondary lining.

The primary lining of each tunnel tube contains 19 000 m^3 of shotcrete, while the tunnel tube itself comprises approximately 55 000 m^3 of concrete.

Figure 12 illustrates the construction of the Mala Kapela Tunnel.

3 CONCLUSIONS

Over the last 15 years Croatia made large effort and investments in order to construct motorway network which would integrate the most distant parts of the country and provide for quick, easy and comfortable transportation of people, goods and services.

Several sections of new motorways cut through mountainous regions, thus construction workers were challenged to excavate a substantial number of tunnels, under very tight deadlines and unusually dangerous circumstances posed by landmines left over from the recent War for independence.

Many extraordinary structures have been constructed using the most modern technologies, and the record of the longest tunnel ever built in Croatia was surpassed on two tunnels.



Figure 12. Construction of the Mala Kapela Tunnel.

Most of the tunnels on new Croatian motorways are built as twin-tube structures. The vast majority of those tunnels which were initially constructed as a single-tube structure, are currently being added a second one. Two longest tunnels in Croatia – the Mala Kapela and Sv. Rok tunnels have both been constructed as twin-tube tunnels, but for the time being only one tube is serving two-way traffic as the present traffic volume does not justify the huge cost of equipping the second tube.

In addition to structural safety, much attention and resources were assigned to ensuring traffic and fire safety in tunnel structures. This was confirmed by European Tunnel Assessment Programme which put one of Croatian tunnels – Plasina tunnel on Zagreb to Split motorway – on very high second place while testing tunnels all across Europe with respect to tunnel system, lighting and power supply, communication, escape and rescue routes, fire protection, ventilation and emergency management.

REFERENCES

Banjad, I.; Djukan, P. & Radic, J. 1996. Road Network Development Strategy, in Veselin Simovic (ed), *Building in Reconstruction and Development of the Republic of Croatia; Proceedings of the Congress of Croatian Builders 1996, Cavtat, 7–9 November 1996:* 41–56, Zagreb: Croatian Society of Civil Engineers. (in Croatian).

Mlinaric, D. et al. 2005. *Motorways in Croatia.* Goran Puz (ed.), Zagreb: Croatian Motorways Ltd. Company for Operation, Construction and Maintenance of Motorways. (in Croatian).

Radic, J.; Bleiziffer, J.; Zderic, Z.; Savor, Z. & Tkalcic, D. 2006. *Concrete Structures in Croatia: 2002–2006 Croatian National Report for the 2nd fib Congress Naples, 5–8 June 2006.* Zagreb: *fib* Croatian Member Group & Croatian Society of Structural Engineers.

Radic, J.; Djukan, P. & Banjad, I. European road corridors in Croatia. *Oesterreichische Ingenieur und Architekten Zeitschrift* (144) 1999 (3): 117–123.

Tkalcic D., Hranilovic, M. & Krecak, A. Construction and Exploitation Problems at Sveti Rok Tunnel in Croatia. In *Proceedings of the 1st fib Congress 2002:* 29–34, Osaka: Japan Prestressing Association.

www.huka.hr – Croatian Association of Toll Motorways Concessionaires official website

www.hac.hr – Croatian Motorways Ltd. official website

Underground Space – the 4th Dimension of Metropolises – Barták, Hrdina & Romancov (eds)
© 2007 Taylor & Francis Group, London, ISBN 978-0-415-40807-3

The Dulles Corridor Metrorail Project – Tunneling aspects of the Metrorail extension to Washington, DC Dulles International Airport Phase I and Phase II

J. Rudolf
Bechtel Infrastructure Corporation, Vienna, Virginia, USA

V. Gall & K. Zeidler
Gall Zeidler Consultants, LLC, Ashburn, Virginia, USA

ABSTRACT: The Virginia Department of Rail and Public Transportation (DRPT) is currently undertaking the extension of Washington Metropolitan Area Transit Authority's Metrorail service to Washington Dulles International Airport. The 37 kilometers long Metrorail alignment is scheduled for completion in 2015. The project features two single-track, 700 meter long NATM tunnels at shallow depths in soft ground. At Dulles Airport two 3.3 kilometer long, single-track tunnels will be bored by TBM in siltstone rock. A 25-meter deep station will be constructed using NATM techniques. The total cost of the Metrorail project is estimated to be approximately US $4.0 billion (2006 dollars). Upon completion of preliminary engineering in early 2007 the design build contractor, a joint venture of Bechtel and Washington Group International and referred to as Dulles Transit Partners (DTP) will submit a negotiated, firm, fixed price to DRPT and the project will be implemented under a public private partnership agreement.

1 INTRODUCTION

The Dulles Metrorail project will extend WMATA's rail services from the Metrorail Orange Line in Fairfax County, Virginia to Route 772 near Ashburn in eastern Loudoun County, Virginia. This corridor encompasses several activity centers including Tysons Corner, Reston, Herndon, and International Airport Dulles (IAD) as well as emerging activity centers in eastern Loudoun County. The project alignment within the Dulles Corridor is displayed in Figure 1.

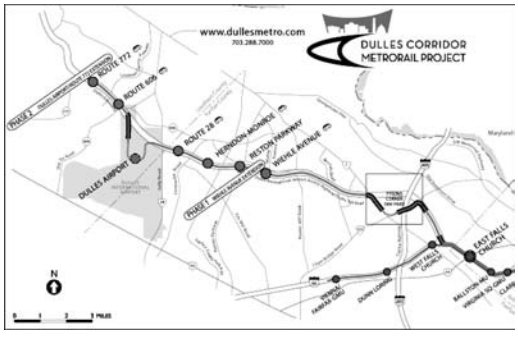


Figure 1. Dulles Corridor Metrorail project.

Rapid Transit for the Dulles Corridor was initially explored in the 1950's as part of the planning process for Dulles Airport. At that time it was decided to reserve the median of the Dulles Airport Access Highway for future transit access to the airport. Preservation of this median allows the alignment to be at grade for most of its length within the corridor. Since the initial planning the need for transit in the Dulles Corridor had been studied and although rail transit in the corridor was not part of WMATA's originally adopted rapid transit system, rapid transit service for the corridor remained a local and regional goal (Schrag, 2006).

The strong growth of the activity centers within the corridor in particular during the1990's and recent 2000's that continues today has led to inception of Metrorail in the Dulles Corridor. Current and projected, future regional growth data exemplify the need for rapid transit and its timely implementation (Dulles Transit Partners, 2006):

- Tysons Corner is the largest employment center in Virginia with 115,000 jobs and close to 4 million square meters of commercial space.
- Reston/Herndon is home of 70,000 jobs and 2.7 million square meters of commercial space.
- In Fairfax County employment is expected to increase 63 percent in the next 20 years.

– Loudoun County grew by 49 percent in the last 5 years and is currently the fastest growing county in the US.
– In the last nine years traffic on the Toll Road in Loudoun County has increased from 50,000 to 90,000 cars per day.
– Dulles International Airport employs more than 18,000 people and serves 23 million passengers per year and presently is being expanded and modernized. Modernization includes a new underground automated people mover system with multiple stations at main and mid terminals.

Regional growth and progress result however in urban and social challenges:

– Washington, DC region has the 3rd worst congestion in the US.
– The annual delay amounts to 69 hours per traveler resulting in a "congestion cost" of US $2.5 billion per year.
– 5 of 8 main roads in the corridor will be gridlocked by 2010.

The much-needed implementation of the project began with Preliminary Engineering in 2004 under a public private partnership agreement between DRPT and DTP. Other funding partners in financing the preliminary engineering effort are the Federal Transit Administration (FTA), the Metropolitan Washington Airports Authority (MWAA), WMATA, County of Fairfax, Loudoun County, and the towns of Reston and Herndon.

This extension to be known as the Silverline once completed will significantly extend the existing Metrorail system. The original system as conceptualized in the 1960's included 103 miles (166 kilometers) and was designed and built between 1969 and 2001. Additions including the Largo Line were accomplished between 2001 and 2004 extending the total system length to about 171 kilometers. The planned extension to the Airport will therefore constitute an addition of some 23% in length.

2 WMATA METRORAIL SYSTEM – COMPONENTS AND TUNNELING EXPERIENCE

A summary of the existing WMATA Metrorail system components is provided in Table 1 followed by a summary of WMATA's tunneling experience of the three decades between the early 1970's through late 1990's.

WMATA's over 80 Kilometers of subway construction provides many examples of tunneling methods and types of tunnel construction and displays a continuous development of tunnel design and construction methodology spanning some 30 years.

Table 1. Current Metrorail system.

Systemwide	Double track length (Km)	Stations (Number)
Subway Includes cut-and-cover construction	80.55	47
Surface	70.41	32
Aerial	14.84	7
Metro System (Total in 2001) Without Largo segment	**165.79**	84
By Jurisdiction		
District of Columbia	61.64	40
Maryland	61.55	24
Virginia	47.43	20
Total Metro System With Largo segment added in 2004	**170.62**	86

In the 1970's WMATA had employed tunneling methods nowadays considered an "old-standard." In soft ground methods involved mandatory dewatering for tunneling with open face digger shields, breasting and temporary support by steel ribs and lagging. These soft ground tunnels were designed for loading conditions assuming a load equivalent to full overburden. Consequently, the final tunnel lining was a rigid, heavily reinforced cast-in-place concrete structure with PVC waterstops in contraction joints as the only means of positive waterproofing. Such construction was used on the Inner City A-Redline, D-Orangeline, and Outer G-Blueline. During that time there are examples of utilizing cast iron bolted segmental lining with lead waterproofed joints between the liner segments. Cast iron linings were used for the Potomac River tunnel crossing on the Orangeline and the Waterfront Tunnel on the F-Greenline. Immersed ("sunken") tube construction was used across the Washington Channel (L-Yellowline).

For tunneling in rock drill-and-blast methods were used for excavation with steel ribs and cribbing as temporary support followed by cast-in-place reinforced concrete for final tunnel support. During this period WMATA already used a modern, gripper-type rock TBM when good bedrock conditions were present, with cast-in-place reinforced concrete lining as final tunnel support. An example is a section on the A-Redline. For the construction of large, approximately 20 meters wide mined station vaults pilot tunnels followed by multiple drift mining were employed. These openings were supported by heavy rock bolting and massive steel ribs embedded in shotcrete for both temporary and permanent support. The final structure was established as an independent architectural precast concrete structure within the mined vault. For the design of the permanent support in rock some arching

effect was considered. Tunnel construction on the A-Redline under Connecticut and Wisconsin Avenues is an example for such rock tunneling.

In the 1980's soft ground tunneling was accomplished using sophisticated Earth Pressure Balance Machines (EPBM) and a single pass segmental, pre-cast concrete lining with gaskets fabricated with tight tolerances. The tunneling was performed under the Anacostia River in adverse ground conditions with 3 bar hydrostatic pressure. It resulted in a very successful waterproofing largely as a result of well-designed and tight tolerances that were required for segment construction and gasket fabrication. This EPBM tunneling was used on two different sections under M Street namely Sections F3a and F3c on the Greenline. Successful installation of bolted segments depended on contact grouting within the time specified. On other sections an open face TBM was utilized. On a section with a low hydrostatic pressure compressed air was employed to control ground water. On another section with an open face TBM systematic dewatering was performed. Both open face TBM drives utilized a one-pass segmental, gasketed, pre-cast concrete lining which was successfully installed.

Also, in the 1980's WMATA allowed new, at that time progressive tunneling and waterproofing approaches. Consequently, in 1984 WMATA accepted the use of NATM rock tunneling proposed by the contractor. This was the first application of a dual lining NATM with PVC waterproofing in the US. It was utilized for running tunnel and station construction on the B-Redline to Wheaton, MD. The design considered arching of the surrounding ground and interaction between ground and the initial lining. Un-reinforced, thin, cast-in-place concrete lining was used for final support. Tunnel and station waterproofing was by an "umbrella type" PVC membrane with fully immersed sidewall drains on both sides of the vault. This resulted in completely dry tunnels in contrast to the A-Redline tunnels experiencing persistent leaks. At the end of the 1980's and at the beginning of the 1990's NATM tunneling was used again, but this time in soft ground for running tunnels and complicated, split station vault construction. The station was built using five different drifts. The first center drift was excavated for installation of a column line located in the middle of the station platform. Both, station and running tunnels were fully encased by a PVC membrane (Fort-Totten Station on the E-Greenline).

In the mid 1990's the NATM was used again for soft ground tunneling by employing dewatering from inside the tunnel and a grouted pipe arch as a crown pre-support to control surface settlement. The grouted pipes were installed by "directional drilling" methods under the Rock Creek Cemetery from a shaft at New Hampshire Avenue. This section was part of the Mid-City E-Greenline.

Also in the 1990's WMATA adopted a "two-pass" lining system for the circular soft ground tunnels excavated by the open face digger shield method (Outer E-Greenline tunnels; Sections E6e and E8a). Besides the need for dewatering this method also required the use of ground modification techniques such as chemical grouting systematically applied from the surface prior to tunneling (Mid-City E-Greenline tunnels; the Under/Over tunnels at Park Road & 14th Street Tunnels). The two-pass tunnel in soft ground with an initial pre-cast concrete liner usually considered as "throw-away" temporary lining was accounted for in the design of the final lining support system. The premise for this assumption was that solid, closed concrete rings were used for the initial support by not allowing any wooden wedges between segments. Rather, the pre-cast lining was required to be fully stabilized before the final concrete lining was cast. The combined liners for final support were designed considering flexibility of the initial lining and soil-structure interaction for "Short Term Loading" and all WMATA loading combinations including full hydrostatic pressure acting on the final lining for "Long Term Loading." Using these assumptions the initial pre-cast and the final cast-in-place linings share the loading combination. This allowed the use of an un-reinforced, cast-in-place final concrete lining. For the initial liner segments installed as expanded rings, success depended upon chemical pre-grouting, dewatering, immediate expansion by jacking the segments against the ground.

Depending on the nature of the soils, ground water level and difficulty in dewatering, such as from aquifers of artesian nature, it was necessary to use EPBM technology again but with the initial liners of non-expansion type but bolted segments similar to those in single-pass installations but with temporary gaskets. This installation was followed by an un-reinforced cast-in-place concrete lining and referred to as "Modified Two-Pass" with a PVC waterproofing membrane between initial and final linings. Such systems were used on the Outer F-Greenline, Sections F6a and F6c, Suitland Parkway to Branch Avenue. Here, the two-pass lining system was used for the first time with the EPBM tunneling method on the WMATA system. In this application the usual rings of four (4) reinforced concrete segments with added key segment forming rings are lightly bolted in the longitudinal joints. The gaskets in joints and the initial liner are designed for temporary hydrostatic pressure as the final waterproofing is achieved by the PVC membrane installed around the entire lining circumference. This system obviously is more costly, but it was necessary to overcome the most adverse ground and water condition where dewatering was not allowed due to environmental concerns. For the initial liner the segments were installed as bolted rings, and success depended upon water control, proper erection scheme and

accomplishing contact grouting immediately behind a sealed tail of the TBM shield (Rudolf, 1997).

3 DULLES CORRIDOR METRORAIL PROJECT DESCRIPTION

The project description concentrates on the tunneling aspects of the work at Tysons Corner (Phase I) and at Dulles Airport (Phase II). The preliminary engineering of Phase I essentially followed the general plans of the Locally Preferred Alternative (LPA) selected by WMATA out of many alternate alignments studied including a tunnel at Tysons Corner. The LPA as portrayed in the approved Final Environmental Impact Statement (FEIS) is designed mainly as an aerial guideway with short tunnels through Tysons Corner.

Late in the preliminary engineering of Phase I WMATA in conjunction with a Spanish contractor and an Austrian design group strongly supported by a local developer proposed an all-underground option for the roughly 6.0 kilometers long segment at Tysons Corner. The envisioned tunnel would have been a large bore, 12 m-diameter TBM driven tunnel to accommodate two over/under tracks and stacked station platforms. It was based on a deep tunneling experience gained at the Barcelona Light Rail system recently constructed (Della Valle, 2002 and 2005). Despite strong support of an underground option by all parties involved, its realization was found to cost from US $250 to $800 million more, based on various estimates, than the mostly elevated and partially at-grade alignment. Furthermore the tunnel option would have significantly deviated from the NEPA selected and approved alignment as portrayed in the preliminary engineering documents. This new tunnel concept would have involved another environmental approval process, and additional geotechnical studies to be followed by a new preliminary engineering. This in turn would have resulted in a project delay of some 2 1/2 to 3 years. The additional projected cost for the tunnel alternative would have practically led to the loss of funding by the Federal Transit Administration (FTA). Due to these factors and the fact that delaying the relief of every-day traffic congestion in Tysons Corner by another up to 3 years, the option was found unacceptable and therefore not pursued further.

3.1 *Phase I tunneling*

The mined tunnel segment includes twin single track NATM tunnels at a length of 700 meters each and an emergency cross-passage. Short cut-and-cover sections will be utilized at the portals. These tunnels will be constructed in soft ground and will be located adjacent to existing structures and utilities that are sensitive to ground movements.

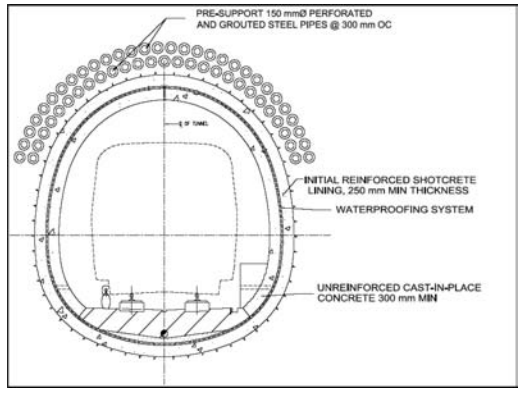


Figure 2. NATM tunnel with pipe arch pre-support.

The soils include mainly residual soils and soil like, completely decomposed rock. The residual soils encountered along the alignment are the result of in-place weathering of the underlying bedrock and are typically fine sandy silts and clays, and silty fine sands. Ground water at portal locations is generally at invert elevation, in mid-point of the tunnel alignment it rises up to the tunnel spring line.

Prominent building and infrastructure elements located in the tunnel's vicinity include an underground parking garage at a distance of some 8 meters from the outbound tunnel wall and bridge piers of the Route 123/Route 7 overpass, at a clear distance of approximately 15 meters from the inbound tunnel, as well as International Drive, a six-lane divided highway located about 4.5 meters above the future tunnel crowns. Deepest overburden cover exists at about mid-point of the alignment with nearly 12 meters. At the west portal and in the center of Route 7 the overburden cover is just 4 meters.

Because of the shallow depth, the prevailing soft ground conditions, the relatively short tunnel length, and the need to control settlements the NATM has been chosen as the preferred tunneling method. To enhance stand-up time of the soils and minimize settlements a single row of a grouted pipe arch umbrella will be utilized for the entire length of the tunnels. This will be sufficient for pre-support where the overburden is greater and surface structures are less sensitive. An additional row of pipe arch umbrellas, using closely spaced 150 mm diameter sleeved steel pipes (tube-a-manchette) will be used on the first 100 m length at the portals where tunneling is shallow with less overburden under International Drive. Figure 2 displays the double row pipe arch umbrella above a typical single track NATM tunnel with shotcrete initial lining, closed PVC membrane waterproofing system and a cast-in-place concrete final lining.

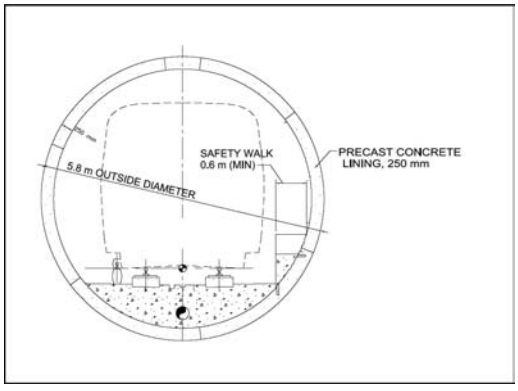


Figure 3. Typical TBM tunnel section.

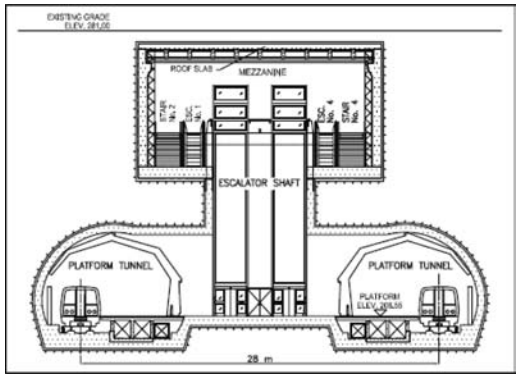


Figure 4. Station typical structural cross section.

3.2 *Phase II tunneling*

The underground segment of Phase II lies within Dulles International Airport property with the metro station referred to as Dulles Airport Station in front of the main terminal. The main terminal has considerable traffic and existing infrastructure with much of the project area having a high concentration of existing utilities. The underground structures include twin single-track TBM tunnels, emergency cross passages, shafts and mined caverns for the Dulles Airport underground station. These structures will be constructed in bedrock and will be located below existing structures and utilities that are sensitive to ground movements. The host geologic formation for tunneling will be generally competent siltstone bedrock whereas the over burden includes fill, residual soils, and decomposed rock.

The TBM tunnels have an approximately 6 meter outside diameter and are about 3.31 kilometers long each. The tunnels will be constructed by either a shielded rock TBM using a single pass, pre-cast concrete, gasketed lining or a rock gripper type TBM with an initial rock support followed by installation of a PVC membrane waterproofing and a final cast-in-place concrete lining. Figure 3 displays a typical, single pass lining cross section for the TBM tunneling.

The mined portions of Dulles Airport Station will be constructed using NATM techniques in sedimentary, typically siltstone bedrock. Excavation will be by road headers. Initial support will consist of rock reinforcement and shotcrete lining. All mined station and associated structures will be waterproofed using an open, "umbrella type" waterproofing system with sidewall drain pipes. Figure 4 displays a typical station tunnel configuration at the central cross passage with 5.2 meters wide platforms. The station platform is about 25 meters below the ground surface.



Figure 5. Station tunnel rendering (by diDo menico + Partners, Architectural Design Consultant).

To allow for a twin station tunnel configuration, where there are two parallel station vaults, the centerline track-to-track distance is 28 meters. Both station platform tunnels are 183 meters (600 feet) long and unobstructed by vertical circulation. The station platforms are connected with cross-passages between the station tunnels. Access to the platforms is provided by a central access structure located between the two station vaults. Architectural rendering for the station tunnel configuration is shown in Figure 5.

All station construction will be mined except for the mezzanine and ancillary rooms, which will be constructed using cut-and-cover techniques. Mined station construction has been selected to minimize disruption to airport activities. Surface disruptions will therefore generally be limited to Mezzanine and ancillary room construction using cut-and-cover excavation while maintaining airport pedestrian circulation above, except for the time period when the mezzanine box will be connected to an existing pedestrian tunnel "Node" that will provide Metrorail Station access.

4 IMPLEMENTATION

4.1 *Public Private Partnership (PPP)*

The project is being implemented in a Public-Private-Partnership under the Public Private Transportation Act (PPTA) an innovative project delivery framework as established by the Virginia Department of Transportation (VDOT) in 1995. Its implementation is in accordance with the guidelines as amended by the General Assembly in 2005 (The Commonwealth of Virginia, 2005). The essential goals of the PPTA are to encourage investment in the Commonwealth by creating a more stable investment climate and increasing transparency and public involvement in the procurement process. According to the guidelines the private entity charged with project implementation is required to provide certain commitments or guarantees and enters into a mandatory risk sharing.

4.2 *Design and construction*

The project is being realized under a design-build contract. The design-builder, Dulles Transit Partners (DTP) is required to initially develop preliminary engineering for the rail project. The cost for the preliminary engineering is shared between the design-builder and the project partners, DRPT, FTA, MWAA and the counties of Fairfax and Loudoun. The preliminary engineering then forms the basis to develop a fixed firm price by the design-builder. To maintain previously established budget limits this results in design challenges and the need to optimize design and construction methods to build to budget. Consequently, many design iterations are required during preliminary engineering. The design and construction team constantly weighs the benefits of underground space to keep everyday routines undisrupted versus its increased cost when compared to at grade and above ground construction.

Value Planning (VP) and Value Engineering (VE) exercises are a central activity of the design development in pursuit of the most economical approach with least impact on the surroundings. In Phase I these exercises led to a series of transformations of the underground segment at Tysons Corner. This alignment was initially envisioned as deep, 1.6-kilometer long twin TBM tunnels and a roughly 24 meter deep underground station constructed by cut-and-cover methods within Route 7, a busy traffic artery. Analysis of construction cost however favored the implementation of the short NATM tunnels with a quasi at-grade station within the median of Route 7 at a cost saving of roughly US $200 million. In Phase II the VP exercises led to selection of a deep TBM tunneling and NATM station construction in rock instead of a cut-and-cover excavation for station and running tunnel construction originally depicted in the FEIS. Since the rock formation at the Airport is close to the surface this selection resulted in considerable cost and schedule savings. This construction will also considerably reduce impacts on the Airport operation. VE exercises, which are to follow, will search for further cost reductions; if successful these will become the basis for construction.

REFERENCES

Capital Transit Consultants. (2002). Engineering Design Report, Dulles Corridor Rapid Transit Project. *Virginia Department of Rail and Public Tansportation and Washington Metropolitan Area Transit Authority*.

Della Valle, N. (2002). Barcelona's New Backbone Runs Deep. *Tunnels and Tunnelling International.* March 2002.

Della Valle, N. (2005). The Barcelona TBMs' Learning Curves. *Tunnels and Tunnelling International*. February 2005.

Dulles Transit Partners. (2006). Project Update Presentation. March 2006.

Rudolf, J. (1997) Waterproofing and Its Effects on the Design and Construction of WMATA Subway Tunnels. *Proceedings, 1997 APTA Rapid Transit Conference.* Washington, DC.

Schrag, Z.M. (2006) The Great Society Subway: A History of the Washington Metro. *The Johns Hopkins University Press.* Baltimore, MD.

The Commonwealth of Virginia (2005). The Public-Private Transportation Act of 1995, (as Amended, Implementation Guidelines, Revised October 31, 2005).

Underground Space – the 4th Dimension of Metropolises – Barták, Hrdina & Romancov (eds)
© 2007 Taylor & Francis Group, London, ISBN 978-0-415-40807-3

Experience from architectural design and build of the underground space

P. Šafránek
Architektonický a Projekční Ateliér, Prague, The Czech Republic

ABSTRACT: The paper presents meditations, examples and visual prompts of architectural design concerning some Prague metro stations and their incorporation into the city organism and road tunnels of the Prague road ring. There are mentioned also portals of tunnels and their connection with neighbouring bridge – two engineering works, which are applied in close co-operation of architects.

1 GENERAL THOUGHTS ABOUT ARCHITECTURAL DESIGN OF TUNNELS AND UNDERGROUND SPACES

The architectural solution of underground spaces and tunnel interiors is a special discipline, where the arguments of the static and construction needs seem to have the priority. The cooperation of statics and tunnel engineers with architects is sometimes on the edge of common interest, but still needed and contributional. Underestimating of architectonic and aesthetic qualities of such a work can be dangerous. Even a useful and well-functioning technical work can be devaluated in eyes of public this way.

As an introduction, let us spend a while with several ideas of our big theoretist of aesthetic, arts and architecture, professor Mukarovsky:

While thinking of architecture, we come to a need to define an aesthetic norm; By professor Mukarovsky has an aesthetic norm the characteristic of a rule, which is but not fixed, static, but which is changable in time. Rule with dynamic validity. For example, Fechner's so-called experimental aesthetic was based on experimentally detected and further appointed basic aesthetic

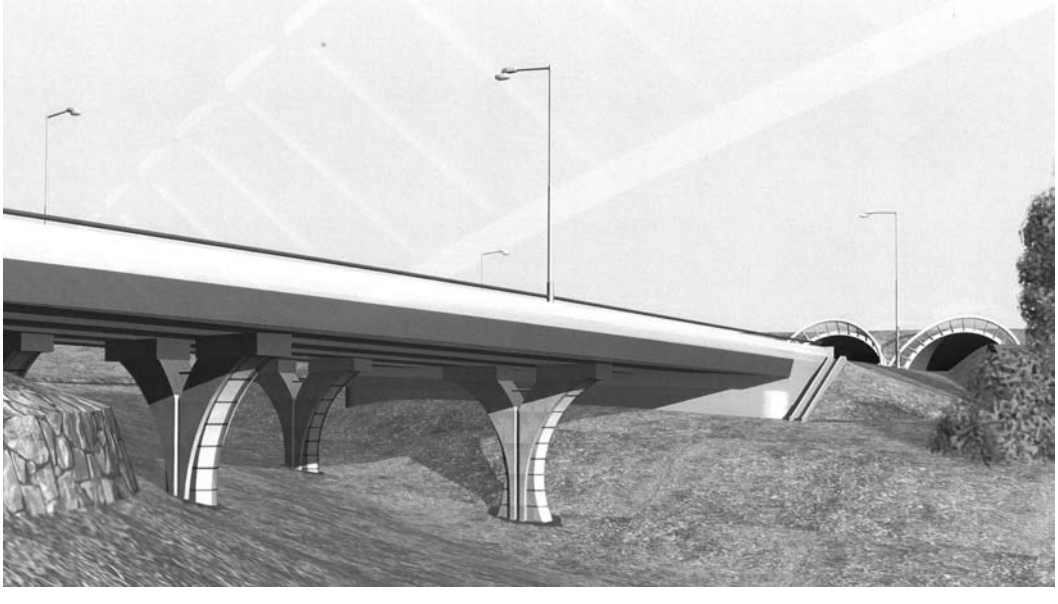


Figure 1. The cooperation of statics and tunnel engineers with architects.

norms. But their further simple applications failed to represent the ideal aesthetic sample.

My personal conviction in a best way represents Mukarovsky's quotation:

If we look at the history of art and architecture from the position of the aesthetic norm, then we see the history of revolts against rulling norms.

This introduction has an ambition to show, that rating and judging the architecture as an art discipline can be problematic and we should keep in mind, that our judgements and objections are rather of subjective and relative character.

The statement about the changebility und unpredictability of the aesthetic norms we should not forget. Therefore more than trying to appoint flatly fitting criterions, we should learn how to be tolerant and pluralist. Because tolerance and pluralism lead to richness, variability and spectacularity of the creative works around us. This means freedom of choice and so plurality as a feedback returns from our society.

Upon the positive influence of aesthetic function in arcitecture on the society agree a big amount of philosophers and theoretists from the times of Aristotel to our days. Professor Mukarovsky comments it: With the means of aesthetic value appeals the art work directly on the man's thinking process and behavior. In comparison, the science or the philosophy needs to pass through the man's willing and thinking process to be able to touch him and influence.

Therefore the aesthetic function means much more than only "the spume on the surface".

At the underground works, tunnels and engineer works, the function, safety, constructive and technical demands are widely pointed out, while the architectonic solution and aesthetic function can be considered to be "the spume on the surface". This attitude is often to be seen as an argument for the financial-costs cut. This attitude represents the narrow minded opinion, that on something, which is not quite important, such as an architecture, the expenses can be radically lowered. These pressures can be very dangerous. Because the simplyfied thinking is tempting.

This article above all refers to some underground stations, highway tunnels and their portals.

2 THE ARCHITECTONIC CONCEPTIONS AND ALTERNATIVES TO THE SOLUTION OF UNDERGROUND STATIONS

Interesting is how the architectural concept of subway stations is approached in different cities:

For example, in Stockholm's subway, the sweedish architects created so-called Cave architecture by using



Figure 2. Design of interior is binded with circle construction of the tunnel.

a local 2 miliards years old granit in a station's interior. In Marseille the mayor at the time, monsieur Gaston Defferce, enforced the idea of specifying each underground station with the local symbols. In the station Sainte-Marguerite was placed a composition reminding the watter-mills on the river Huveanne, which belonged to this fertile land in history.

In Buffalo, USA was organized exhibition, where the public voted for the most favorite art works and conceptions to be used for local subway's design.

Interesting principle was used in Vienna's: At the striked underground stations especially, the dominating idea lies in the division of platform space and railway space. By the highlighting the middle arc's edge, where it penetrates the side arc and placing the light-source on this edge, where the platform is ending, is clearly shown, which space is dedicated to the public and is ment to be pleasant and bright and which space serves as a tunnel-route for the train. That one is left in a rough condition and is rather dark. This difference factor functions as a warning: here the safety of platform is ending. The artistic principle of this extreme contrast further creates a particular tension – dynamism and let the interior talk itself. On the other side stands the conception of the Prague's metro, where even the wall behind the railway is worked out with the surface materials and is intensivelly delighted.

However contradictory these two attitudes are, both seem to have certain reason and bring the contribution to the interior design.

Mr. Liebaerse, president of the comittee for art for the Brusel's metro says:

"The people don't travel by metro for their pleasure, they have to face the stressful atmosphere, closed in a train moving through the dark tunnel. Therefore we try to lead our artists to create bright interiors, which will humanize this oppressive clima."

The fact, that these architectural works are fully under the ground and there are no fascades, which a man can perceive and overview, can be deprivating for a human beeing. This kind of architecture doesn't have an outter volume and can't join the common environment and that can be frustrating.

On the other side in the underground stations is extremelly visible the original characteristic, which differentiates architecture from the other visual-arts such as painting, sculpturing: the possibility to visit and perceive it from inside.

In any case the underground architecture works function as a vital spring for the city organism. The presence of underground traffic net improves the city functions, urbanistic development and architectural design of the buildings in a close neighbourhood.

Such architectural works bring advantages to many people, more than most of other public buildings and that's where lies their strength, competency and reliability.

3 LIGHT AND COLOUR

Very important part of architectural design is colour and ilumination of the surfaces. The undeground spaces, above all the artificial delighted ones, seem to tolerate brighter and richer colours, than the surfaces reflecting the day-light.

Rich encouraging colorcode and sufficient amount of light can ballance the oppressive atmosphere under the ground.

Using the colours in highway tunnels can provide better orientation and safety of moving traffic: In the Radotin tunnel on the Prague road ring are used two tones of blue as a basic colour together with the light gray colour of concrete. As we are approaching the emergency zones, the blue is alternated first by dark and as we come closer , by light yellow colour. This change of colour signs the existence of emergency exits or the end of the tunnel. In front of each portal, the light yellow changes instantlly in a light gray tone of concrete. Therefore the leaving the tunnel is decent.



Figure 3. Expressive colourfulness in the underground of the Hloubetin station.

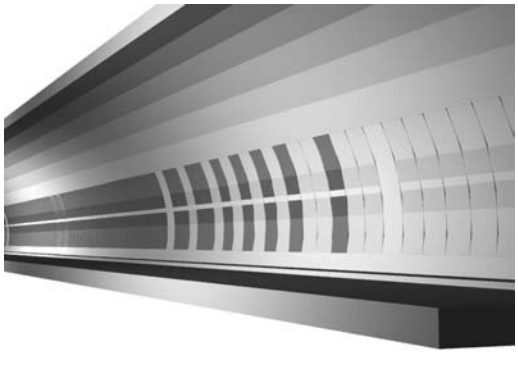


Figure 4. Coloured solution of the road tunnels Radotin.



Figure 5. Tunnel portal Radotín – authoritative element.

The light yellow, already delighted surfacecould feel agressive in contrast with the outter green.

This basic colourcode is symptomatic for the whole Radotin segment of the Prague road ring, where the functions of the colours are: informative, architectonic and safety.

4 TUNNEL PORTALS

The tunnel portals sign the beginning and the end of the underground route and at the same time mark the hidden underground part and therefore should have the representative character.

The function of the portals is not to radically disturb the environment, respect the landscape and show to the approaching in advance, that they are entering the undeground route.

The tunnel portals on the Prague road ring have the appearance of a fan bowing over the cutted arch-segment of the tunnel profile. This shape is a result of an effort to create a shield protecting the entry against falling rocks and the authoritative element serving as an important orientation point for the higway travellers.

At the portal of the railway tunnel in Brezno, the main motto was to connect the surrounding rough terrain with the entry by the natural materials. Therefore the system of supporting walls made of gabions was used to shape the portal.

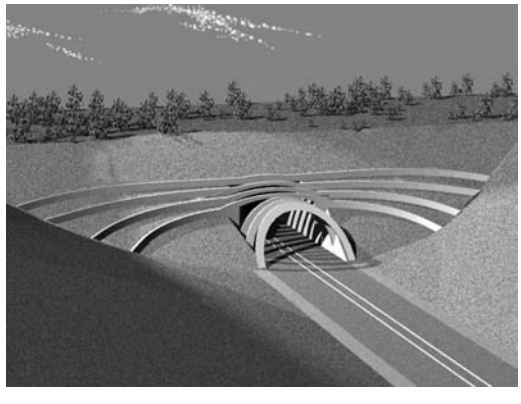


Figure 6. Railway tunnel portal Brezno.

5 THE MUTUAL INSPIRATION OF CONSTRUCTION AND ARCHITECTURAL DESIGN

The construction of tunnel works can expressivelly influence its interior appearance and also engineer works in its neighbourhood.

The west portals of the higway tunnel on the Prague road ring at Lochkov are in the close neighbourhood of the bridge over the Nightingale valley. This locality touches the protected area of natural reservation, therefore the designing process of the both works was



Figure 7. Tunnel portal Slivenec – authoritative element.

accompanished with increased attention and sensibility. For the both objects the common base idea was used and the mutual influence on each other's design is visible: The specific architecture of the fan-portals appeared also on the bridge's soft arch-shaped piers.

6 JUDGING THE ARCHITECTURAL AND ARTISTIC DESIGN OF UNDERGROUND SPACES

While we pass a judgement on the aesthetics of underground spaces (but also other architectural works), we have to admit, that all instructions how to set our rates are very problematic and relative.

Although we should stay watchful and resistant against the absolute judgements, still we can learn: Especially the cooperation of an architect and static – tunnel engineer is contributional, because the contradictory professions can enrich each other and in this cooperation the next impulse and inspiration for the creative work can be founded and cause, that the new aesthetic (or the common) norms are born. And their validity grows upon the norms which are passing over.

This page intentionally left blank

Underground Space – the 4th Dimension of Metropolises – Barták, Hrdina & Romancov (eds)
© 2007 Taylor & Francis Group, London, ISBN 978-0-415-40807-3

Study on underground space planning of Shanghai Expo 2010

H.H. Zhu, P. Li, X. Wang, F.L. Peng & Y.S. Li
Research Center for Underground Space of Tongji University, Shanghai, China

ABSTRACT: The World Expo 2010 will be held in Shanghai, which theme is "BETTER CITY BETTER LIFE". According to the program, large-scale underground space constructions will be built in the Expo Park. For their features that huge investments and non-disassembly, it needs more complex study and planning to satisfy various demand both during and after the Expo. This paper mainly focus on the following aspects: The logical scope of underground space constructions in Expo Park; the Expo Park's underground planning; Re-use of the underground infrastructure facilities by post expo. In conclusion it will be shown that: put the ecological infrastructure facilities underground can not only form a positive cycle of energy utilization, but also a effective way to make the Park ecology, compact and sustainable development. The World Expo underground urban complexes will be connected together to form regional public transit transferring hub and commercial center by post Expo.

1 INTRODUCTION

The World Exposition 2010 will be held in Shanghai in year 2010. Its theme is so called "BETTER CITY, BETTER LIFE". For the first time in the history using *city* as the theme, expresses the desire of all mankind seeking a better life in the future. The philosophies of building up a World Expo are such concepts as constructing a greenwood city, ecological city, digital city, gardening city, co-existing living city, information city and intelligent city. Meanwhile through comprehensive exchange among different points of views and among inter-acting sciences, the new concept and new knowledge as well as new technology of urban development will be enriched, and the urban function will be upgraded, the urban space enhanced. As a result, Shanghai's urbanization will be promoted.

From the figure 1 it can be seen that the Park site was confirmed in the city center, composed of Puxi and Pudong two sections, include the Huangpu River which is the Mother River of Shanghai as a part and the total length of 8.3 km alongside the River. The Park's fencing area (the area with ticket entrance) occupies an area of 3.1 km^2 , parking area is 0.6 km^2, World Expo Village 0.3 km^2, backup land as well as municipal engineering and other facility land plus land reserved land for city resident's use totally consumes 1.4 km^2. The total area of the World Expo Park within the programmed limit is 5.7 km^2 (excluding Huangpu River area), among which there are 1.44 km^2 for Puxi area (West Shanghai) and 4.26 km^2 for Pudong Area (East Shanghai).

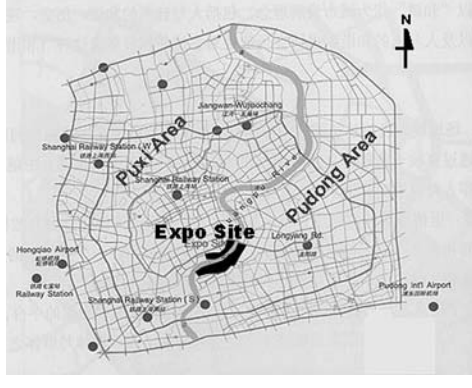


Figure 1. The location of the World Expo Park.

2 THE NECESSITY OF DEVELOPING AND CONSTRUCTING THE UNDERGROUND SPACE IN THE WORLD EXPO PARK

For the purpose of enabling the World Expo Park's construction to fully manifest the main theme of the World Expo and the city life's concept in the 21st century, it is necessary to, based on the features of the World Expo Park is located in the center of the city, make full use of the land development and utilization potential so as to meet the following demands.

2.1 *Demand for fully utilizing the land resources*

Since programmed World Expo Park's halls and pavilions are located in Shanghai city center area, the

control on index of land occupied rate is rather strict, thus it is necessary to study carefully on land resources utilization value and, on this basis reasonable planning and layout of ground and underground space, through the development and utilization of underground space to meet the requirements land occupied rate.

2.2 *Demand for building up ecological and sustainable development World Expo Park*

In the course of the constructing the World Expo Park, enlarging Park's greenwood area and open area are vital to energy saving, environmental protection, Expo Park's climate enhancement as well as improving ability of handling emergency accident, etc. With a view to constructing an ecological and sustainable development World Expo Park, it is a must to develop and utilize the underground space resources, some areas such as man-less space, space where mankind activity consumes little time and Park's municipal engineering infrastructures will be built down to underground area so as to enlarge Park's greenwood area to the most extent to construct ecological gardening World Expo Park, to reveal the theme of "BETTER CITY BETTER LIFE" and reveal urban development trend in the 21st century.

2.3 *Demand for Building up urban traffic system with high efficiency, speedy convenience and safety*

As a comprehensive exposition, the World Expo Park during the expo will receive 70∼80 million person-time visitors from the nation and the world, with averagely 400,000 per day and 800,000 per day in ultimate peak time, thus will create a World Expo record. As a result, huge pressure will be imposed to traffic status.

Therefore it is necessary to build up an underground traffic system with multi-layer both underground and on the surface ground, with multi functions and with information technology. This said underground space will integrate all patterns of traffic facilities and provide reasonable layout so as to form a closely interacted and functionally supplemented tangible space and bring entire effect of the facilities into full play. Meanwhile, it will also reasonably arrange and distribute all types of traffic movement based on resources of space and time. It imposes balance and coordination for the traffic direction layout and time and space layout under the principle of highly effective network operation, and though information technology it reasonably allocates the occupation of tangible space by all types of traffic pattern. Generally speaking, it is an organic combination for all types traffic facilities to play scale effect into full play.

2.4 *Demand for building up modern municipal engineering facility system for the Park*

The municipal engineering facilities are the basis and safeguards that a city relies on for survival and development, they are the nerve and blood vessel to enable the city to normally play its function and enable the people to enjoy peaceful and comfortable life.

For the World Expo Park's being put to show it is need Large quantity of municipal pipelines which will consume tremendous amount of land resources. Thus it is necessary to fully use underground space for those pipelines' planning and construction, so that the valuable land resources can be saved.

2.5 *To establish basis for the Park's post Expo use*

Since the construction of the World Expo Park will definitely impose important impact on city's structure and pattern, and according to the World Expo's features, the roads inside the World Expo Park play different roles between the period during the Expo and post Expo in terms of the road's function. Therefore the utilization of the World Expo Park shall consider the post Expo use. For this purpose, the World Expo Park needs to be included into comprehensive consideration of Shanghai city's organic system. To utilize underground space resources to reduce, to an utmost extent, the negative impact on city of Shanghai due to World Expo Park's construction, and to enable the Park's pattern and structure to meet requirements by post Expo use.

3 PLANNING OF THE UNDERGROUND SPACE

The World Expo Park's underground space development mainly focus on buildings' underground space, the underground commercial facility, the underground walk space, the underground opening space and so on to construct by stages. In Pudong area, the Park's underground space utilization will bring the comprehensive construction of permanent buildings (shown in figure 2, points A, B, C and D denote four permanent buildings respectively), Metro stations, transport hubs into consideration. While in Puxi area of the Park, as the region with the tunnels and Metro lines installed more intensive, and there is a larger surface area of the historical buildings, the remainder underground space is limited. And it can not be connected to form an overall economic even if the limited space is used. Therefore, no more underground space will be developed in Puxi area of the Park.

3.1 *Underground transport facilities*

The Park's underground transport facilities mainly including the Metro lines, cross river tunnels, underground walking space and underground parking lots.

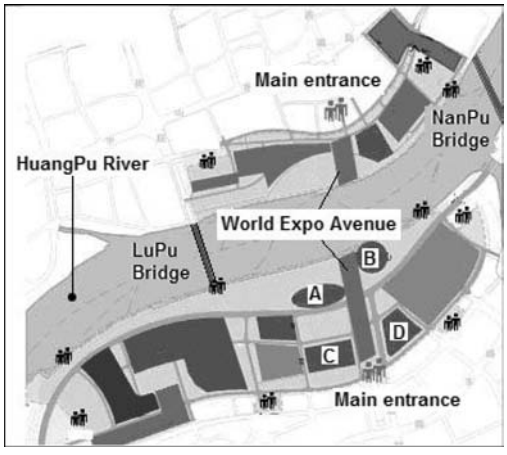


Figure 2. General ground layout in The World Expo Park.

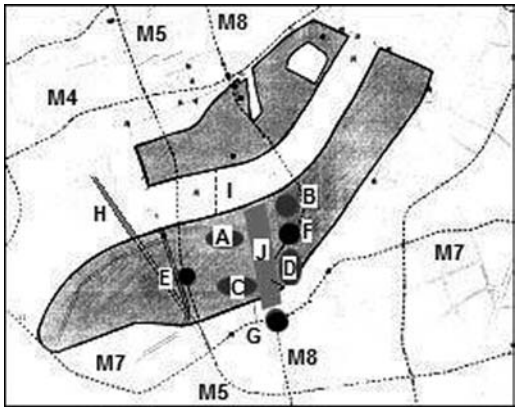


Figure 3. Main underground facilities around The World Expo Park.

3.1.1 *Metro*

In figure 3 it can be seen that there are four Metro lines going through the World Expo Park, namely, M5 and M8 penetrate center of World Expo Park in S-N direction, while M4 and M7 respectively come from Pudong and Puxi going through periphery of World Expo Park in E-W direction. M5 and M8 have set up Metro stations in the World Expo Park's Pudong area (shown in figure 3, point E denote M5's station, Point F denote M8's station). But in considering the convenience for transport organization and ticket – checking, this two stations will be closed during the Expo and re-opened after the Expo.

3.1.2 *Cross river tunnel*

In consideration for cross river transport between Pudong and Puxi Park area, a new cross river tunnel (shown in figure 3, broken line I) will be constructed in the core area of the World Expo Park under Huangpu River. This new tunnel, together with a existed tunnel (shown in figure 3, line H), will be a part of the ring road for public bus.

3.1.3 *Underground walking space*

Between two main entrances of the World Expo Park, a aerial Plaza (called "World Expo Avenue", shown in figure 2) will be built in S-N direction. The World Expo Avenue's width is 80 m and the elevation is +10 m. It is the most important landscape axis of the World Expo Park, is the main place for celebration activities.

A parking lot on the ground is built beneath the World Expo Avenue (shown in figure 4). And a underground walking system (called "World Expo Underground Street" in this paper. shown in figure 3, rectangle J) whose width is equal to that of the World Expo Avenue will be built beneath the parking lot. The World Expo Underground Street extend from the transit transferring station (shown in figure 3, point G) of M7 & M8 to the bank of the Huangpu River in Pudong side in S-N direction. It will be connected with the basements of the permanent buildings that around it (shown in figure 3, points A, B, C and D denote the basements of permanent buildings).

During Expo, the World Expo Underground Street will play the role of the underground walking hub, and the corresponding commercial, leisure facilities will be set in it. Tourist can chose the visit route on the ground or underground.

3.1.4 *Underground parking lots*

In the Park, a certain scale of underground parking lots will be set up under the permanent buildings, and connect them with motorway underground. These underground parking lots are for the use of public bus, tourism passenger bus, VIP vehicles, logistic lorries and fire engine during the Expo, while they will be for the use of cars serving for the Park's internal business or leisure and entertainment by post Expo.

3.2 *Underground municipal engineering facilities*

The World Expo Park may accommodate approx 170 exhibition spaces, large quantity of facilities of electricity, telecommunication, gas, water and dewater are requested to ensure all sorts of requirement during the Expo.

3.2.1 *"Point" layout pattern*

What facilities included in the "point" municipal engineering layout pattern are water treatment plan, pressure pump station, pump station for rain and drainage, gas pressure station, Pressure regulating station, high voltage substation, switch station, rubbish collection

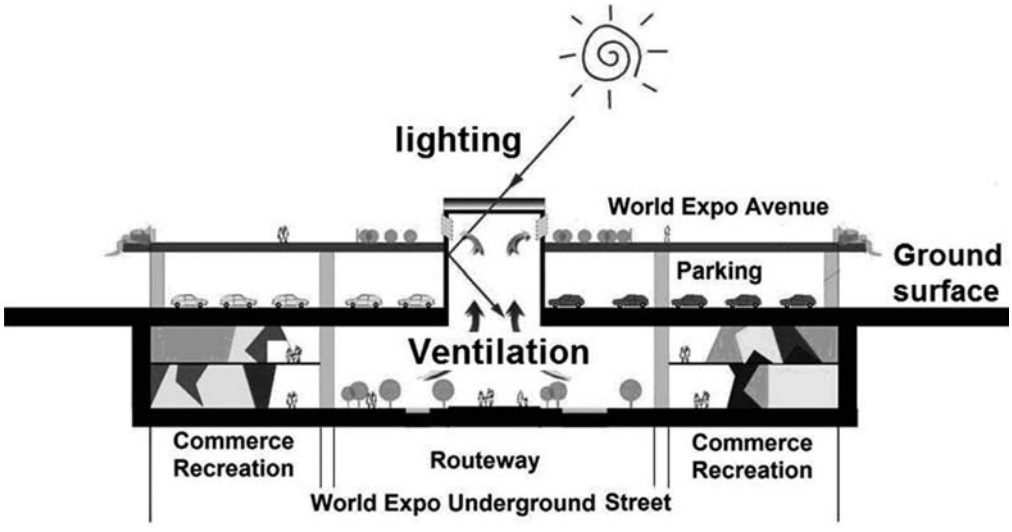


Figure 4. Cross-sectional view of the World Expo Avenue.

station and regional energy station, etc. These facilities have the feature of consuming large area above the ground and causing contradiction to ambient environment, meanwhile bring about negative impact to the development and utilization of the surrounding areas.

With a view to the said features, the layout pattern of these municipal engineering facilities will be set up alongside the areas around the World Expo Park. While in terms of the structure, it shall be best to construct them underground or semi underground.

3.2.2 *"Linear" layout pattern*

The municipal engineering facilities of the "Linear" layout pattern includes running water pipelines, waste water pipelines, rain water pipelines, gas pipelines, concentration heating or cooling pipelines, rubbish collecting pipelines, electricity pipelines and telecommunication pipelines, etc. These municipal engineering pipelines could be laid put based on need underneath trunk road or less important roads with an advantage of lowering cost and being convenient to lay out. But this could also cause repeat cutting and covering the road due to pipelines burying or maintenance. Plus, the pipelines' life time will be shortened by corrosion because of touching the soil and underground water, and this is not good for re-construction or expansion in the future.

Therefore, to pave the main road in & around the Park with so called protection shell, under which the main line comprehensive pipelines tunnel containing all sorts of municipal engineering supply pipelines will be installed.

3.3 *Underground urban complex*

The underground passenger volume during the World Expo will be intensively huge. There will be wide range of service items and concentrated peak time. The traffic volume's peak time coverage during a day will be very distinct according to different ticket-pricing system. Normally the time when evening peak hour comes before closing the Park is the time when the day's most extreme peak time is seen. Therefore the planning of the underground urban complex of the World Expo Park shall play the function to mitigate and disperse the crowded stream of people.

In the Park, large scale compound underground urban complexes will be constructed at the underground railway hub and comprehensively developed and constructed in connection to metro interchange and underground public utility. The World Expo Underground Street will be the main body of the underground urban complexes. These underground urban complexes will play the function to mitigate and disperse the crowded stream of people during Expo, while, the function to mitigate underground traffic congestion will be somewhat weaken and the commercial function of the underground urban complexes will be strengthen by post Expo.

From figure 4 it can be seen that, in the underground urban complexes, light & ventilation wells will be created in order to lead nature light and air into, thereby saving energy sources maximized.

Meanwhile, such landscapes as plant, water, sculpture and so on are settled in the underground urban complexes (shown in figure 5) to create the environment similar to the feeling that on the ground in order



Figure 5. Conceptual scheme of the World Expo Park's underground complex.

to provide a safe and comfortable walking, leisure and shopping space for tourist.

4 RE-USE OF THE UNDERGROUND INFRASTRUCTURE FACILITIES BY POST-EXPO

According to the overall urban planning of Shanghai, the waterfront of two sides across Huangpu River will be the landscape axis, the important ecological corridor, and urban public gathering areas of the city in the future. The World Expo Park's construction will be integrated with the magnificent overall development projects alongside the two banks of Huangpu River by fully utilizing river side's features and the location advantages to build a batch of large service facilities for cultural activity, conference, exhibition, residence, leisure and entertainment as well as commercial service. Therefore in the post Expo stage, the World Expo Park's development positioning is to become important cultural exhibition center, luxury business district and featured river side residence area in Shanghai.

Under this background, those underground traffic and municipal facilities built for the World Expo need to extend further to satisfies the local development demand. The World Expo underground street will be with peripheral underground urban complex, the basement of buildings and Metro stations to become regional public transit transferring hub. Meanwhile, as an important component of the regional commercial network, the underground complex unites the decentralized shops together as an organic body to form regional commercial center. Fat commercial profit will attract the investment to develop underground space to compensate deficient income of the underground transport facilities. This function will also provide convenient and comfortable shopping, F & B, rest and entertainment services to the passengers who use the underground walking system and underground railway hub.

5 CONCLUSION

It is necessary to implement underground space project in order to better manifest the BETTER CITY BETTER LIFE theme of the World Expo 2010. The Park's construction shall consider underground space resources, and try best effort to include the expressway and municipal public facilities down to underground to leave more greenwood space on the ground so as to let Shanghai become ecological city. Meanwhile, put the garbage disposal system, as well as the green energy system and so on the ecological infrastructure underground can not only form a positive cycle of energy utilization, but also a effective way to make the Expo Park ecology, compact and sustainable development. Moreover, in the underground space, constructing the ecology & humanities landscape and carrying on the reasonable layout to them, can promote the quality of the Expo Park, make the underground constructions attractive.

From the context mentioned above it can be seen that large-scale underground space constructions will be constructed in the World Expo Park. For their features that huge investments and non-disassembly, it need to accord with the long-term urban planning to

satisfy various demand both during and after the Expo. Having the largest scale among all underground facilities that would be constructed in the World Expo Park, the underground urban complex will become regional public transit transferring hub. Its principal function is transportation, meanwhile, commercial, cultural, entertainment and other services will be provided in it to both enjoy the local residents & tourists and gradually reclaim the construction costs of underground space, thereby achieving sustainable economic development.

REFERENCES

Parriaux, A., Tacher, L. & Joliquin, P. 2004. The hidden side of cities – towards three-dimensional land planning. *Energy and Buildings* 36: 335–341.

Sellberg, B. 1996. Environmental benefits: a key to increased underground space use in urban planning. *Tunnelling and Underground Space Technology* 11(4): 369–371.

Roberts, D.V. 1996. Sustainable development and the use of underground space. *Tunnelling and Underground Space Technology* 11(4): 383–390.

He, J.J. & Liu, Y. 2003. Investigation on Ecological Urban Construction and Development and Utilization of Underground Space. *Chinese Journal of Underground Space* 3: 83–86.

Pasqual, J. & Riera, P. 2005. Underground land values. *Land Use Policy* 22: 322–330.

Durmisevic, S. 1999. The future of the underground space. *Cities* 16(4): 233–245.

Section 2
Geotechnical survey and improvement of ground mass

This page intentionally left blank

Part 2.1
Geotechnical survey

This page intentionally left blank

Underground Space – the 4th Dimension of Metropolises – Barták, Hrdina, Romancov & Zlámal (eds)
© 2007 Taylor & Francis Group, London, ISBN 978-0-415-40807-3

The impact of puncturing support on the expansion of seismic effects during blasting activities in tunnels

Hrvoje Antičević
Croatian road authorities, Širolina, Zagreb, Croatia

Zvonimir Ester & Mario Dobrilović
Department of Mining and Geotehnical Engineering, Faculty of Mining, Geology and Petroleum Engineering

ABSTRACT: This paper outlines the research of the impact of puncturing support during blasting activities in tunnels. The puncturing support, whose main purpose is to bypass unexcavated section in poorer ground categories that is to prevent the material fall from the tunnel calotte after the completion of excavation, has additional functions aimed at decreasing negative impacts caused by blasting. By drilling and placement of puncturing support the rock will get perforated and thus by means of the shielded zone the rock mass will get separated from the excavation area which will prevent excessive loosening of the rock mass and diminish the expansion of seismic effects.

1 INTRODUCTION

As a part of the future motorway Bregana – Zagreb – Dubrovnik, section Žuta Lokva – Ličko Lešće there is a tunnel Brezik with approximate length of 400 m (Figure 1). Tunnel is located in western suburban area of the town Otočac, at an altitude of 450 m. Maximum overburden was 38 m. Tunnel excavation has been performed in full profile, with 2 driving lanes, one for each driving direction. Excavation works began at south portal in midst of April 2003, and both tunnel pipes have been broken through at the beginning of year 2004. Average advance rate was 1.5 m per day for each pipe. Average excavated cross section varied from 74.3 to 85.6 m^2, which depended on rock mass category.



Figure 1. Portal of tunnel Brezik.

Tunnel construction has been performed by N.A.T.M., by drilling and blasting. In better rock mass category, excavation has been performed entirely by drilling and blasting operations; while in worse rock mass category there was a combination of drilling and blasting with excavator operation. Solely excavator method was applied in critical areas.

2 GEOLOGICAL ROCK MASS STRUCTURES

Rock mass through which tunnel is passing is built from carbonate rocks of Jurassic, cretaceous and Paleocene time. Paleocene and Jurassic limestone make up a karsted and broken stratum, upon which limestone Jelar breccias left sediments. These Jelar breccias and breccias conglomerates occupy rather a large area. As in other areas with Jelar type layers it is also obvious here that the contact zone with ground rocks is characterized by significant tectonically disturbances (Figure 2).

Predominant part of Jelar is characterized by fine grains (very rarely bigger than 1 cm, occasionally there are some grains with diameter of few cm). Size of upper Jurassic grains became significantly enlarged from ground rocks.

Generally the boundary between layers in the lower bed is karsted, very uneven, and very often

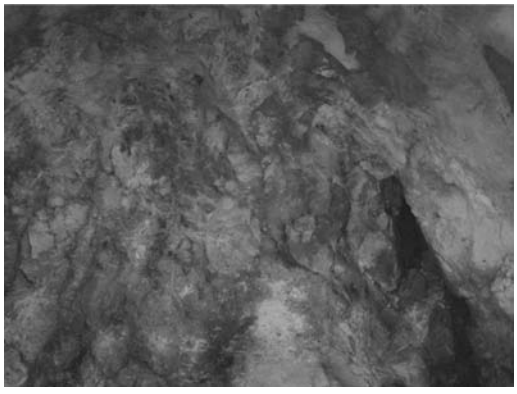


Figure 2. Geological structure – excavation face.

Table 1. Rock mass geotechnical parameters.

	σ_c (MPa)	ρ (kg/dm^3)	E (GPa)
Limestone	70–100	2.64–2.65	35–50
Limestone Jelar breccias	60–110	2.57–2.69	31–60

exceptionally karsted, cavernous dolomitized and recrystallized.

According to hydro geological characteristics rock mass is classified mostly as watertight sediments. Today, flow dynamics of underground water depends on rock fabric, tectonic and level of karst modification on rock. Significant impact on flow dynamics has top cover made from clay sediments.

Condition of surface and underground waters in above mentioned area is partly connected to hydro geological relations in wider area of river Gacka basin. Seepage waters in the tunnel excavation area with regard to small basin area and small overburden are of limited range. Table 1 show Rock mass geotechnical parameters.

3 IMPACT OF DETONATION ON THE ROCK MASS

By the initiation of explosive charge in a blast hole, high-speed chemical reaction occurs whereby large amount of energy and detonation products are being released. Released energy causes occurrence of shock waves in the explosive, which are further transmitted to surrounding rock. Released energy is transmitted in to surrounding rock mass in the form of shock wave and expanded gasses.

Shock wave energy causes primary rock brakeage, meaning rock destruction. The strength of shock wave depends on density of explosive charge and detonation velocity. Further progress of shock wave in the area, where destruction stops, causes generation of radial cracks.

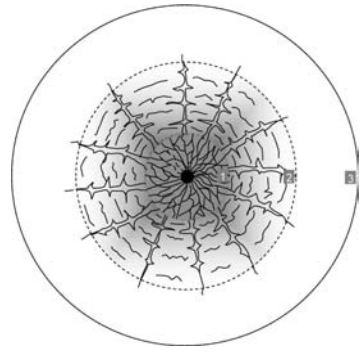


Figure 3. Zone of detonation activity in the rock.

Expansion gasses energy or thrust energy under the impact of expansion gasses with high pressure and high temperature continues process of widening of radial cracks generated by shock wave.

Quantity portion of shock energy is smaller but more far-reaching then gas energy rate, because rock breaking and widening of radial cracks causes release of space around blast hole and fast decrease of pressure.

By increasing the distance from center of explosion, stresses caused by shock wave decrease until they are smaller then tension strength of rock and generating of radial cracks is stopped. Shock wave is continuously spreading as an elastic wave and causes ground oscillations (Figure 3).

Elastic wave could cause undesirable effects on wider surrounding during its traveling route. There are three determinate zones in rock: 1. Zone of plastic deformations (crushing), 2. Zone of generated radial cracks, 3. Zone of elastic deformations (ground particle oscillation).

4 CRITERIA FOR CRITICAL VELOCITY OF DETONATION

Amount of explosive charge which does not cause damage of the rock and supporting system is estimated upon:

- predicted oscillation intensity as a function of the amount of explosive charge per level of ignition,
- Distance between blasting field and supporting system,
- Attenuation of seismic waves as a consequence of geological characteristics of a rock,
- Maximum allowed level of ground oscillation.

Connection between maximum oscillation velocity at a measuring point, amount of explosive charge per level of ignition and a distance from a blasting point

to a measuring point is given by empiric formula after M. A. Sadovski (Krsnik 1989)

$$v = k\left(\frac{\sqrt[3]{Q}}{R}\right)^{n} \text{ (cm/s)} \quad (1)$$

where
v ground oscillation velocity (cm/s), Q amount of explosive charge used for detonation (kg), R distance between measuring point and blasting field (m), k and n constants depend on the geological characteristics of a rock.

Based on the results of measuring of the oscillation velocities and consequential damages of rock mass in surroundings of the blast hole, a ground oscillation velocity was estimated for Swedish gneiss and granite which causes increase in rock deformations (Holmberg 1979). Damage was noticed up to 32 m away from the blasting point by velocity $v = 700$ mm/s.

Langefors and Kihlström suggested the level of $v = 300$ mm/s for unsupported tunnels constructed in rocks like granite.

I.D. Isaac suggested level of $v = 450$ mm/s based on measurements taken by construction of underground engine room of the power plant Dinorwic (Isaac et al. 1981).

T.R. Yu and S. Vongpaisal suggested the criterion for estimation of allowed ground oscillation velocity for underground constructions (Yu et al. 1998) given by blast damage index:

$$\text{BDI} = \frac{vdC}{K_t T} \quad (2)$$

where BDI (Blast Damage Index), v ground oscillation velocity (m/s), d rock density (g/cm^3), C compressive pulse velocity in a rock (km/s), K_1 constant of rock quality, T dynamic compressive consistency of rock (MPa). Value of BDI index varies between 0.125, with no damage occurring, and 2 when great damage occurs related to ground oscillation velocity $v = 85$ mm/s (no damage) and $v = 1750$ mm/s (rock collapse).

A.K. Chakraborty had applied the suggested criterion by construction of underground chambers in basalt rock and found out that the level of possible damages $v = 85$ mm/s is far too low (Chakraborty et al. 1998).

For the orientation about possible support structure damage, standard DIN 4150 is applied.

Table 2; subsection 1, under DIN 4150-3-1999-02, gives values of oscillation velocity for support structures, like armour-concret columns, massive foundations and other.

4.1 *Hopkinson's effect theory*

Based on the observation data we conclude that the ground oscillation velocities reached, at least at one detonation level, values above allowed velocities according to standards for industrial objects. Possible deformations increase in the rock on which measuring was done, can be defined upon analysis of cores before and after blasting or by seismic tomography.

Table 2. DIN 4150-3 1999-02, part 3.

	Maximum oscillation velocity V_{max} (mm/s)			
Frequency (Hz)	1–10	10–50	50–100	over 100
Support structures	40	40–80	80–100	min. 100

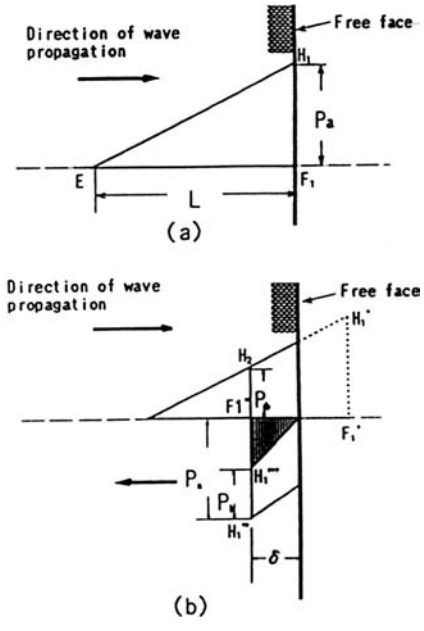


Figure 4. Theory of Hopkinson's effect.

Nearly each blast triggered exfoliation of rock along the lower left side of the right tunnel pipe. This phenomenon, known as Hopkinson's effect, was noticed by Johansson et al. (1970) as an effect of cylindrical explosive charge on metal plate 15 cm thick.

Later on, influence of Hopkinson's effect on rock samples was tested in a laboratory (McCarter et al. 1993, Katsuyama et al. 1993).

Figure 4 explains the simplified influence of Hopkinson's effect which appears as a consequence of interference of pressure shock pulse H1 F1 (triggered by detonation) and a reflected compressive strain pulse of free surface H1" F1". The amount of strain is a sum of strains (Pa-Pb) of a compressive pulse and a reflected compressive pulse, and δ is a thickness of blasted rock.

In case of sufficient kinetic energy exfoliation of rock occurs on a free surface. It is assumed that

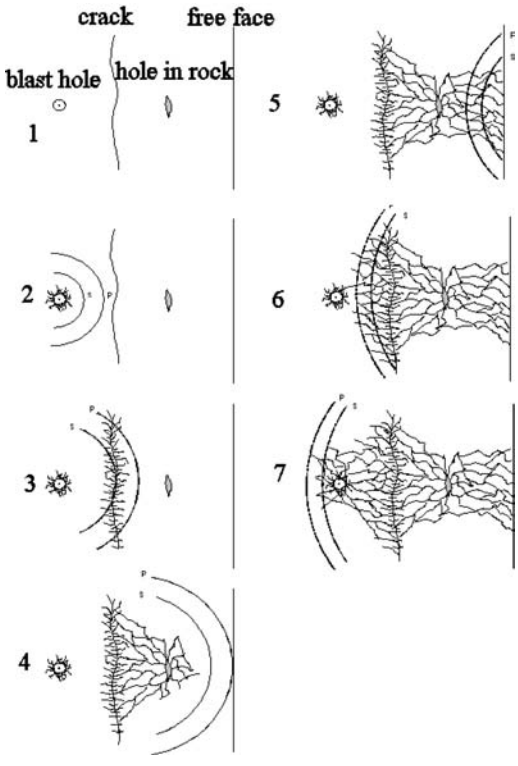


Figure 5. Schematic view of theory of core or shock wave.

velocity of free surface movement above 8.0 cm/s causes exfoliation of rock on the tunnel side.

4.2 *Theory of core or shock wave/cracks*

This theory is based on tests developed in materials, which characterize geological conditions in the rock mass.

Authors of this theory started with examinations on homogeneous materials and from these results they have derived basic assumptions and certain regularities that were later proven on samples as a defined geological structure of rock mass (Figure 5). Other authors continued further investigations on this theory, whereby tests have been performed in actual surrounding, i.e. with respect to rock mass.

Passing of P and S waves through material containing cracks and voids generates new system of cracks around old ones, in the larger scope than in the area without voids. Reason is that they represent area of rock weakening through which waves are spreading. (1–4). When a P wave reaches a free surface it is reflected backwards in form of a shear wave, it collides with a S wave and interference occurs. This interference causes further spreading of existing and generating of new cracks. (5 and 6). After reflection from free surface or crack, new wave system occurs (PP, PS, SP, SS, PP, and S, PS, and S) that causes additional spreading and generating of new cracks.

5 IMPACT VALUES ON BLASTING RESULT

There is a chain of values that have influence on final blasting results and they could be divided in 2 groups.

The first group contains values to which we do not have any influence and they define blasting environment. Those values are: tectonics, mineralogical-petrologic composition, physical and mechanical characteristics, crack system, type of fill, primary condition of stress, subsurface water level, climate conditions (seepage waters) etc.

At inhomogeneous anisotropy rocks with very complex structure, special attention should be paid to cracks system and its fill, that have crucial impact on blasting results.

The second group contains values to which we do have influence, and they are divided into 3 subgroups: drilling, loading and blasting with accompanying elements. These elements should be adjusted to geologic structure of blasting location in a way to perform test blastings and define characteristics of environment in order to perform corrections on existing blasting design.

6 MEASURING AND INSPECTIONS

Excavation area was $P = 80\,m^2$. Drilling depth was from 1,2 to 3,0 m, and total number of holes was from 103 to 132 holes (Picture 4-1 and 4-3) with explosive consumption of 174 to 329 kg explosive per round. For creation of a new free face, a double V cut was applied with drilling patterns shown on Picture 5-3. Daily progress on 2 faces amounts to 3 to 4.5 m. A reason for such poor progress was poor rock category (IV and V), which determines a short “step” per blasting cycle.

Measurements were performed with three-compound seismographs White Digital Seismograph Mini-Seis II and INSTATEL Blast Mate III.

These instruments have the possibility to measure frequency, displacement, acceleration and ground particle velocity. Value of particle velocity is a standardized value for evaluation of possible damages and it is incorporated in the majority of international standards (DIN 4150, OSMRE, B.S. 7385, G.F.E.E.). None of these standards defines limit value for ground particle velocity for tunnels and roads.

6.1 *Blasting without puncturing support*

In total, tree measurements have been performed, whereby each measuring was performed in different conditions. Each measurement was carried out on 2

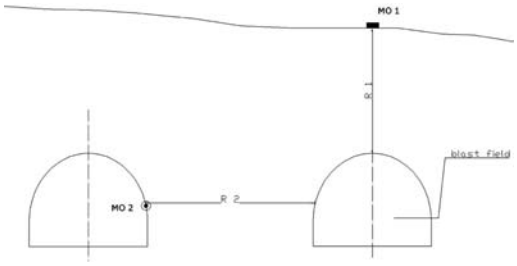


Figure 6. Measurement points positions.



Figure 7. Measurement point no. 2.

monitoring points whereas the first monitoring point was vertical to the terrain, above the blasting point in the tunnel and the second monitoring point was on the concrete lining of the second tunnel tube as it is shown in Figure 6.

The first measurement was performed in the condition without puncturing support (deformed reinforcing steel bars), (Figure 7). The total of 107 holes have been drilled. The depth of holes was from 1.2 to 1.5 m with explosive consumption of 174 kg. Maximum quantity of explosive per delay was 18.30 kg. In measurement point No.1, 28 m away from the blasting location (R 1), ppv reading was 62 mm/s, whereas on the primary support of the adjacent tunnel tube, in measurement point No. 2 (Figure 7), 19 m away from blasting location, ppv reading was maximum 85 mm/s.

6.2 *Blasting under the puncturing support*

Different from above at this measurement a puncturing support (reinforcing steel bars) was drilled and installed before blasting above last lattice girder next to the face. Design of puncturing support, i.e. of deformed reinforcing steel bars contains rebar (RA 400/500–2), diameter 25 mm, length 4 m installed in to calotte with spacing of 0.30 m as it is shown in the Figures 8 and 9.



Figure 8. Tunnel face with blasting field and the puncturing support.

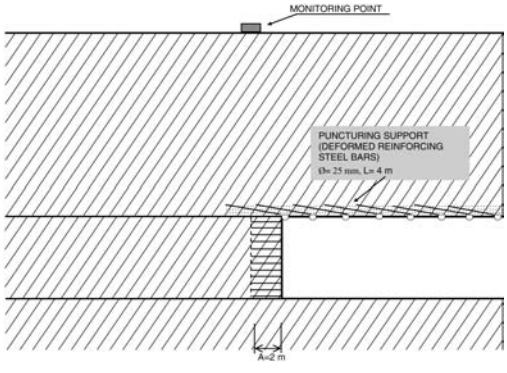


Figure 9. Schematic view of puncturing support.

Although this support system element is considered a beam, which will stop falling of unconsolidated strata in poor categories of rock from calotte after blasting, the significance of puncturing support is ambiguous.

Apart from the above stated, the perforation of rock in calotte along the excavation line will be achieved by drilling and installing of deformed reinforcing steel bars. In that manner excessive squander of surrounding rock mass and lowering of bearing capacity of rock will be avoided. Rock is considered a main support element and it is presumption that ground oscillation above blasting location will be lowered.

In the first measurement below puncturing support drilling the depth was increased to 2.5 m. In total 132 holes were drilled and 275 kg of explosive was spent. Maximum quantity of explosive per delay amounted to 22.6 kg. Distance from the first monitoring point to blasting location was 26 m, and recorded maximum ppv was 71.5 mm/s. The second monitoring point on primary support of adjacent tunnel tube was 26 m away, and ppv was double as high, i.e. 142.7 mm/s.

Table 3. Results of measurements.

No.	Drilling lenght (m)	Hole no. (Pcs.)	Total explosive quantity (kg)	Max. explosive quantity per delay (kg)
1.	1.2–1.5	107	174	18.3
2.	2.5	132	275	22.6
3.	2.0	119	202	18.6
No.	factor (kg/m^3)	Puncturing support	PPV-M.P.1 (distance) mm/s (m)	PPV-M.P.2 (distance) mm/s (m)
1.	1.61	–	62 (28)	85(19)
2.	1.8	yes	71.5 (26)	142.7 (26)
3.	1.26	yes	35 (15)	168 (26)

The second measurement was performed at the drilling depth of 2 m (119 holes) with total explosive consumption of 202 kg. In the first monitoring point (M.P.1) ppv up to 35.5 mm/s at 15 m distance from the blasting location were recorded. Ppv in the second tunnel pipe (M.P.2) amounted to 168.1 mm/s at the distance of 26 m.

7 ANALYSIS OF TEST RESULTS

In Table 3 are the results of measurement with blasting patterns with and without puncturing support. The first test was performed without puncturing support and it serves as a stub, i.e. as a standard for the remaining two measurements. From the other 2 measurements it is obvious that from the monitoring point MO1 above the tunnel calotte, particle velocities are lower than when applying the puncturing support system opposite to the measurement without it.

During testing the quality of tunnel contour has been monitored and recorded. In the places without puncturing support there was an over break along the whole contour of the tunnel. During the excavation below puncturing support the contour quality depended on 3 group of parameters; blasting method, installation of puncturing support and geological excavation structure. In order to achieve proper installation of puncturing support (deformed reinforcing steel bars), the ratio between loading concentration of contour hole and spacing between holes and deformed reinforcing steel bars must be determined. Collar of deformed reinforcing steel bar must have contact and should be covered with shortcrete. Beside that, the diameter of deformed reinforcing steel bar (25 mm) is not strong enough and should be at least 32 mm large; used on the semi motorway project Karlovac-Rijeka, and it was proved very efficient. Proper installation of puncturing support is shown on Figure 10. Improper installation of puncturing support is shown on Figure 11.

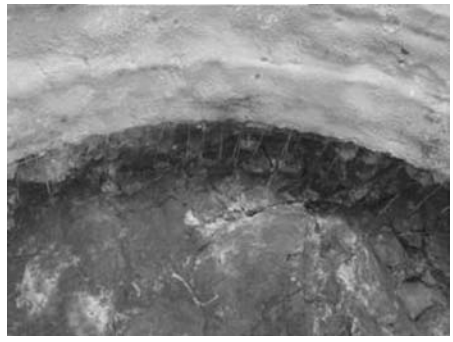


Figure 10. Proper installation of puncturing support.



Figure 11. Improper installation of puncturing support.

8 CONCLUSION

Based on the principle of New Austrian Tunneling Method, stating that the rock is primary a support element, it is necessary to preserve primary strength of rock during the excavation as much as possible. In rock mass next to the tunnel opening there occurs squander of ring-like support structures, which range of disturbance zone depends on the quality of applied blasting method. Implementation of puncturing support has larger significance than beam supporting of calotte material itself. During drilling of puncturing support (4 m) by monitoring of drilling fluid it could be defined what type of material can be expected, and with this knowledge blasting method could be adjusted to forthcoming conditions. Drilling and installing of rebar Ø 25 mm on each 30 cm in tunnel calotte generates broken perimeter arch (shielded zone) that attenuates ground vibrations along the monitoring point and in such a manner prevents unwanted squander of rock mass. Puncturing support (4 m) was installed on each 2 m of excavation, which meant that the overlap was each 2 m, so even two attenuating zone existed. Concluding from all the above stated facts, the puncturing

support has proven to be a useful and multi-valued support element, which only deficiency is a diameter that should be at least Ø 32 mm, because on former projects this diameter has been proven more appropriate.

REFERENCES

Chakraborty, A.K., Raina, A.K., Ramulu, M., Jethwa, J.L., Gupta, R.N. 1998. *Lake Tap at Koyna.* World Tunneling, November, pp. 456–460.

Ester, Z., Antičević, H. 1997. *Determination of a particular regime of blasting in a tunnel with thin overburden*, Proceedings of the International Conference Tunnelling Under Difficult Conditions, ITC, Basel, pp. 145–151.

Ester, Z., Vrkljan, D., Dobrilović, M. (2002). *The effects of blasting on rock support in tunnel*, Proceedings of Conference Blasting Tecniques, Stara Lesna, Slovak Republic, pp. 71–79.

This page intentionally left blank

Underground Space – the 4th Dimension of Metropolises – Barták, Hrdina, Romancov & Zlámal (eds)
© 2007 Taylor & Francis Group, London, ISBN 978-0-415-40807-3

Two different concepts of geotechnical survey and monitoring in exploration galleries for tunnels in Prague – Lahovská exploration gallery and Blanka exploration gallery

R. Chmelař & B. Březina
PUDIS a.s, Prague, The Czech Republic

ABSTRACT: In the article, two different concepts of geotechnical survey adopted in newly realized exploration galleries in Prague are discussed. The first of them is the Blanka exploration gallery with cross section 10 m^2, in which the geological and geotechnical conditions have been verified especially by means of a series of pressuremetric tests and large scaled in-situ tests performed on rock blocks. Rather different concept was adopted in the Lahovská gallery, where both in-situ geotechnical measurements (pressuremetric tests) and measurements of geotechnical monitoring (especially convergence and extensometric measuring) were concentrated into turnout areas, which were driven with cross section 64 m^2, corresponding to that of top heading of the proposed three lane tunnel.

1 INTRODUCTION

At present, two important underground constructions on different road circuits are performed in Prague, the capital of the Czech Republic. Together with radial connecting roads, these two circuits – the inner City Circle Road (CCR) and the outer Prague City Ring Road (CRR) – are expected to create an up-to-date global traffic system in Prague.

In order to verify the geological and geotechnical circumstances, two exploration galleries have been carried out beforehand for two already finished tunnels – the Strahov Tunnel (built during 1985–1997) and the Mrázovka Tunnel (1998–2004), both forming a part of the CCR.

Currently, the above mentioned exploration galleries are followed by third one, namely the Blanka gallery (2002–2005), performed in the route of the next part of the CCR between Špejchar and Pelc Tyrolka.

At the CRR, two parallel driven tunnels are proposed to become a part of the construction lot No. 514 from Slivenec to Lahovice. Before starting their construction at the end of 2006, the Lahovská exploration gallery has been performed (2004).

As to their general concepts, both above mentioned galleries are reasonably different. In the following text, the differences of the conception of geotechnical survey and monitoring in both exploration galleries are discussed.

2 THE BLANKA GALLERY

2.1 *Purpose of exploration gallery*

Geotechnical survey during tunnelling the gallery was aimed to verification of geotechnical conditions along the difficult parts of the tunnels proposed, especially below the Vltava River and in the area of the Stromovka Natural Park, where the tunnels will be driven immediately below highly water-bearing terrace sediments.

For this purpose, both the total length (1950 m in the left tunnel tube) and the section area (10,5 m^2, or 18,7 m^2 at turnouts) have been adapted. The gallery was driven from its entrance shaft located in Troja (city quarter on the right Vltava bank), and shot firing together with track transport were applied for its driving.

2.2 *Geological conditions*

In the total length of the gallery, its driving was performed in the rock massif consisting of Lower Palaeozoic Ordovician sediments covered with highly water-bearing terrace fluvial sediments.

Along the gallery, the geotechnical character of Ordovician sediments varies extremely, from the softest clay shales (Libeň strata group) and sandy shales (Dobrotiv) with medium strength up to very hard

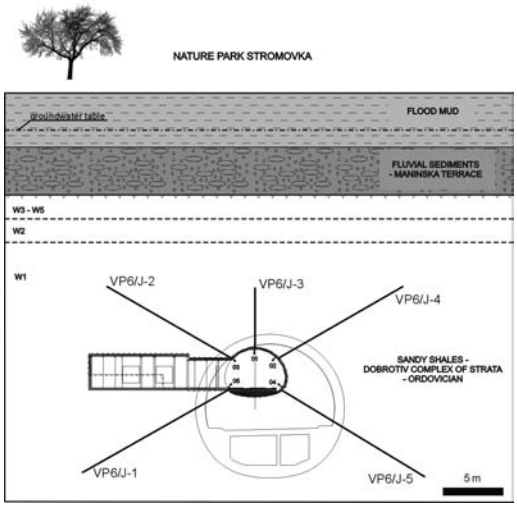


Figure 1. Cross section in turnout of the BLANKA exploration gallery with lateral testing drift for in-situ geotechnical tests.
Legend:
VP6/J-1 pressuremetric bore J-1 in VP-6 bore flapper
01 convergence measuring point
W1 degree of weathering by ČSN 72 1001 standard.

quartzites (Řevnice and Skalka substrata). All these rocks were formed within Varisan orogeny and locally they display tectonic failures of various degree.

Geotechnical survey has been aimed not only to geological documentation of particular geological types, but also to the verification of their geotechnical properties. As well, great importance was put on hydrogeological conditions of the rock massif and waterflows into the body of the gallery.

As well, the level of underground water in terrace sediments has been monitored, especially in the Stromovka natural park area.

2.3 *Geotechnical tests*

Geotechnical properties of rocks have been determined both by means of laboratory tests (especially strength of the rock mass itself) and in-situ tests. The latter were represented by two main types – pressuremetric tests, performed in 14 bore flappers, each consisted 4–5 radially oriented bores, and large scale strength and deformation tests of rock blocks, situated in two short testing drifts of the gallery. A scheme of the pressuremetric flapper and the testing drift is shown on Figure 1.

In two testing shafts, the following types of large-scaled in-situ tests have been performed: uniaxial and triaxial strength tests on the rock blocks of 50×50 cm cross section and 100 cm height (Fig. 2), shear strength

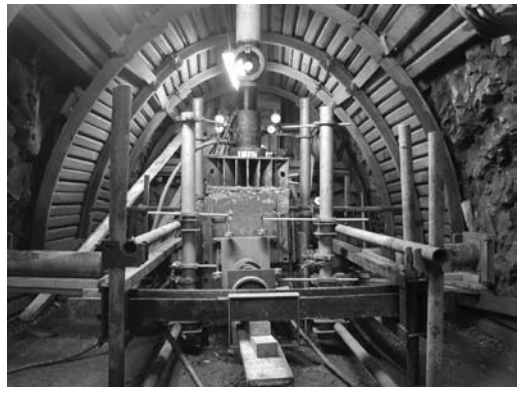


Figure 2. Assembly of large scale in-situ triaxial strength test.



Figure 3. Assembly of in-situ shear strength test with predetermined plane of disturbance.

test with pre-determined plane of disturbance (located along stratification, along fissuration or into tectonic zones, respectively – Fig. 3) and plate load tests (both in horizontal and vertical direction). Thus it was possible both to observe and measure the properties of the rock massif (including the discontinuities) on the rock blocks in the testing drifts and to verify the deformation parameters around the exploration gallery by means of pressuremetric tests performed in bore flappers. As the result, the laboratory and in-situ tests performed gave the opportunity to collect reasonable quantity of geotechnical information not only along the exploration gallery, but also in the environs (and especially the overburden) of the tunnel proposed.

Development of intact rock strength and of pressuremetric modulus along the Blanka gallery and the diagram of shear strength as derived from the results on large-scale rock blocks in the testing drift are shown on Figures 4–5.

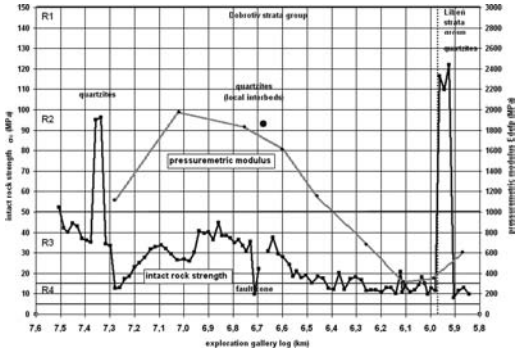


Figure 4. Development of intact rock strength and pressuremetric modulus of deformation in along the Blanka gallery.

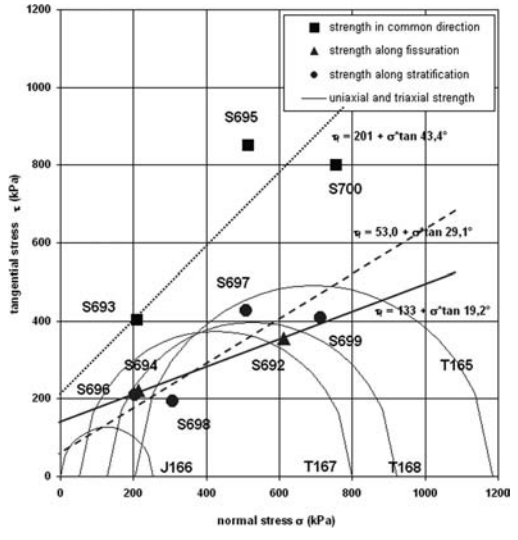


Figure 5. Diagram of shear strength as derived from the results on large-scale rock blocks in a testing drift.

2.4 *Geotechnical monitoring*

As the components of the geotechnical monitoring, especially the convergence measurements, the ground surface deformation measurements and the primary lining pressure measurements have been performed. In the critical tunnel sections with minimum rock overburden, also the extensometric measurements were carried out, with a rod extensometer located above longitudinal axis of the tunnel. All measurements gave the information on the deformation behaviour of the primary lining and the rock massif (and in some case also on the development of a depression basin) invoked from advancing the 10.5 m^2 cross section gallery (18,7 m^2 in turnouts). Even if very valuable, the data of the deformation response obtained during the tunnelling of the gallery should not be overestimated when applied for future tunnels with the cross section over 100 m^2, and some additional prediction method (e.g. pregnant parametric study by means of the mathematical modelling) is definitely needed. Anyway, driving the large cross section tunnels in complicated geological circumstances (as e.g. nearby the end of the Blanka gallery, with only 3 m of rock overburden and under highly waterbearing terrace sediments of the Vltava River) remains always less or more risky and unsafe, and thus most demanding for maximum engineering experience as well as safety precautions applied.

3 THE LAHOVSKÁ GALLERY

3.1 *Purpose of exploration gallery*

Geotechnical survey in the Lahovská exploration gallery was aimed to the verification of geological and geotechnical conditions in route of the tunnels proposed, the driving of which is planned with a minimum delay after finishing the gallery. Therefore, the gallery has been driven from two opposite ends of the future tunnels, i.e. from the Radotín and from the Lochkov portals. The gallery with total length 1313 m has been adapted for wheel traffic and thus its cross section was reasonably larger than in the Blanka gallery (24.5 m^2 against 10,5 m^2). Moreover, all turnouts have been driven in full profile of the tunnel top heading, thus reaching almost 64 m^2 (18.7 m^2 in Blanka). The gallery has been driven by means of shot firing.

3.2 *Geological conditions*

Within its total length, the gallery has been driven in rock massif, consisting of Lower Palaeozoic Silurian and Ordovician sediments, with Quarternary deluvial sediments in overburden. The rock massif was formed during Varisan orogeny, with local tectonic failures of various degree.

In the following text, the dip-advanced half of the gallery (performed from the Lochkov portal) is introduced as an example. In this part, the gallery has been driven exclusively in the Silurian rocks, nevertheless highly heterogeneous. Generally, both strata groups occurred (i.e. the Motol and Kopaniny strata) consist of clay shales with interbedded limestones. Besides Palaeozoic rocks, some basaltic effusive rocks (diabases and basaltic tuffes) also occurred here and there.

3.3 *Geotechnical tests*

Geotechnical survey within tunnelling the gallery included the routine measurements and activities, i.e. geotechnical observation and documentation of

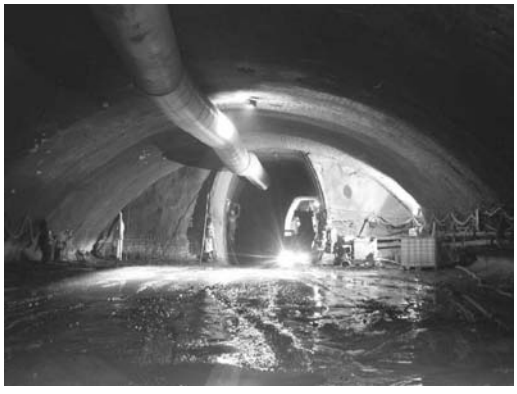


Figure 6. View into the monitored turnout extended into full size of the top heading of a three-lane tunnel in Lahovská exploration gallery.

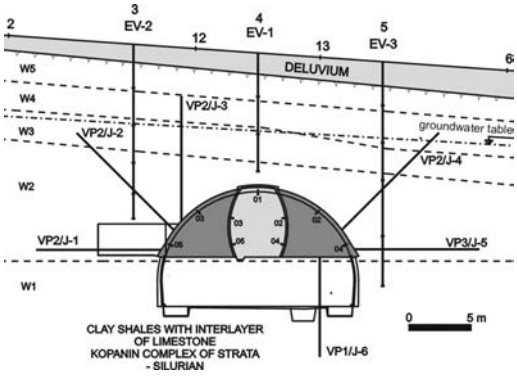


Figure 7. Complex solution of geotechnical survey and monitoring in associated profile situated at the turnout extended into full size of the top heading of a three-lane tunnel in Lahovská exploration gallery.
Legend:

VP-2/J-1	pressuremetric bore J-1 in VP-2 bore flapper
EV – 2	rod extensometer
01	convergence measuring point
2	geodetic point on terrain
W1	degree of weathering by ČSN 72 1001 standard

gallery faces, laboratory tests on rock samples (including abrasivity and disintegration tests) as well as geotechnical in-situ tests.

In the original concept of the field tests, two testing drifts for in-situ tests on large-scale rock blocks were proposed. However, with regard to the rapid advance of the tunnelling and the decision of extending the section area in all turnouts, the scheme of in-situ tests has been revised – the original concept of testing drifts has been abandoned and replaced by a series of pressuremetric measurings with the particular tests located in bore flappers consisting of 4–5 radially oriented boreholes, i.e. similarly as in the Blanka gallery. The bore flappers were located into all extended turnouts (top headings) and one of them also nearby the future Lochkov portal.

In first turnout, a series of pressuremetric tests have been executed also in the extensometric bores from the ground surface, in order to determine the deformation properties of the rock massif when under primary stress conditions, i.e. not influenced by the driving. Later, the results collected have could be compared with those from the underground bore flapper situated in the same cross section.

3.4 *Geotechnical monitoring*

After extending the gallery turnouts into full section of the top heading of the three-lane tunnel (Fig. 6), it has been possible to monitor a real response of the rock massif, which is already comparable with that of the driving of the tunnel itself. An example of the associated measuring profile for geotechnical survey and monitoring in the extended first gallery turnout near the Lochkov portal is shown on Figure 7. From such a measuring profile, a great volume of the most important information for designing the future tunnels can be obtained.

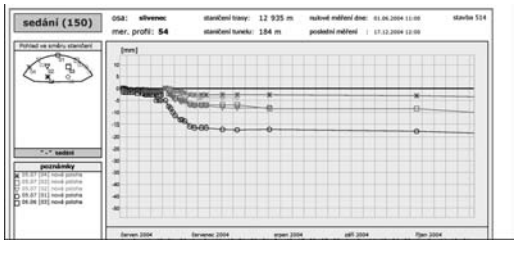


Figure 8. Results of convergence measuring from the monitored turnout displaying vertical deformations of lining – gradually from driving the gallery and then from driving the top heading of a three-lane tunnel.

Unlike the two further turnouts, the first turnout (including the above mentioned associated profile) has been driven gradually. At first, the exploration gallery has been tunnelled in this section, which has been successively extended into full width of the top heading, and geotechnical monitoring has been designed in such a way that could enable the observation of deformations evolved both from driving the gallery itself and from the extended tunnel top heading.

Similar development of vertical deformations from driving the gallery and, successively, the top heading, is evident both from the results of the convergence measurements of the primary lining (Fig. 8) and from a three-stage rod extensometer, situated above the longitudinal axis of the tunnel.

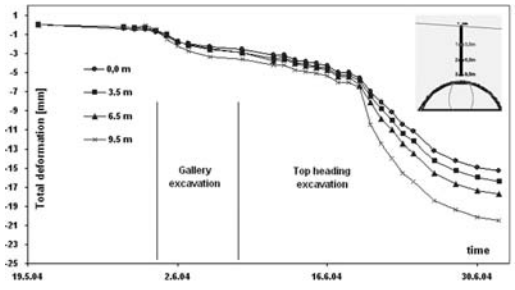


Figure 9. Extensometric measuring – development of vertical deformations of the rock massif in overburden from tunnelling the gallery and successively from extended top heading.

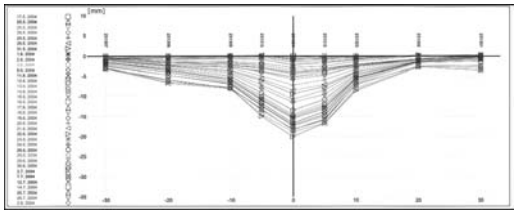


Figure 10. Development of a terrain depression basin from tunnelling the gallery and successively from extended top heading.

From the results of this extensometer, if has been confirmed that a decreased stress zone around the tunnel stope remains relatively narrow – it has been indicated only at the last (lowest) measuring level of extensometers. As well, it has been repeatedly proved that the extensometres are more suitable to be installed from the ground surface, thus obtaining the possibility of measuring the vertical deformations even before the gallery/tunnel face reaches the profile of measuring.

The influence of driving the gallery (and then the top heading) on the development of vertical deformations in the tunnel overburden as detected by the extensometric assembly is shown at Figure 9. Such values are already directly applicable for the design of the tunnel.

Besides the overburden and the lining deformations, also the development of the transverse depression of the ground surface can be observed when the gallery is being extended into the full tunnel top heading. As the result, the limits of the depression basin during the driving of the tunnel itself can be predicted much more precisely. The development of the depression basin above the top heading-sized turnout nearby the Lochkov portal is shown at Figure 10.

4 COMPARISON OF BOTH CONCEPTIONS

Both conceptions of the geotechnical survey the monitoring, as applied in the Blanka and Lahovská exploration galleries, are well-founded. For the sake of the tunnel design, the latter concept seems to be evidently more advantageous and sophisticated, for several reasons: wheel traffic has been applied similarly as for the future tunnels, the turnouts have been extended into the full width of the tunnel top heading, which enabled to monitor the impact of tunnelling on the tunnel overburden and the ground surface intensively, as well as to determine the deformations of the primary lining in the top heading area. Thus, with the geotechnical parameters of the rock massif collected from the in-situ tests carried out, a complex set of information on the properties of the rock massif and its behaviour during driving the top heading of three-line tunnels can be obtained. However, the possibility of application of the above characterized modern survey conception may sometimes be limited, since the exploration gallery with its turnouts extended into full top heading can be proposed only for the tunnels with their horizontal and vertical position finally fixed; otherwise it can hardly be applied. On the other hand, the galleries with smaller cross section area (as e.g. the Blanka gallery) can be used even if the final location of future tunnels is not yet exactly determined, and greater accent is put on the survey activities here. For example, besides pressuremetric in-situ tests, also large-scale tests on rock blocks can be executed under such conditions, in order to compensate the fact that the results of geotechnical monitoring in the smaller-sized galleries are much less comparable with those of the tunnel itself. In similar circumstances, some supporting prediction method, e.g. a parametric study with the application of mathematical modelling is definitely needed.

5 CONCLUSION

Generally, especially the concept of geotechnical survey and monitoring as applied in the Lahovská exploration gallery is evidently perspective. Besides the positives on the field of geotechnical survey, its most important aspect consists in application of the same type of excavation technology and transport as for the tunnels proposed. Moreover, the gallery turnouts extended into the full profile of the tunnel top heading becomes a full-value and in-advance-finished part of the tunnel, thus having an undisputable technological and economical importance for the successive driving of the tunnel itself.

REFERENCES

Březina, B., Chmelař, R. & Butovič, A. 2006: Construction lot No. 0079 Špejchar-Pelc-Tyrolka. Final report on the geotechnical survey. Satra s.r.o. & PUDIS a.s., Praha.

Hudek, J. & Chmelař, R. 2001: Geotechnical conditions of the west Mrázovka tunnel. Tunel 10 (1): 2–7.

Chmelař, R. & Hudek, J. 2006: The role of fault zones in Prague shallow Mrázovka tunnels. *Felsbau* 24 (5): 76–81.
Chmelař, R., Březina, B. & Síla, L. 2005: Prague City Ring Road, construction lot No. 514 Slivenec-Lahovice. Lahovská tunnels, exploration gallery, part I. Final report on geotechnical survey and monitoring. PUDIS a.s., Praha.
Chmelař, R. 2006: Lahovská exploratory gallery – new conception of geological survey and monitoring adopted for tunnel constructions of the construction lot No. 514 Slivenec – Lahovice. *Proc. Intern. Conference Underground Constructions, Bojnice, 1–3 October 2006*: 12–17.
Vorel, J., Chmelař, R. & Březina, B. 2003: Geotechnical survey for driven tunnels of the construction lot No. 514 Slivenec-Lahovice. *Proc. Intern. Conference Underground Constructions, Prague, 18–20 November 2003*: 50–56.

Underground Space – the 4th Dimension of Metropolises – Barták, Hrdina, Romancov & Zlámal (eds)
© 2007 Taylor & Francis Group, London, ISBN 978-0-415-40807-3

Inverse analysis on measurements realized during a tunnel excavation

S. Eclaircy-Caudron, D. Dias & R. Kastner
URGC Géotechnique, INSA de Lyon, Villeurbanne, France

ABSTRACT: One of the major difficulties for geotechnical engineers during project phase is to estimate in a reliable way the mechanical parameters values of the adopted constitutive model. In project phase, they can be evaluated by laboratory and in situ tests. But, these tests lead to uncertainties due to the soil reworking and to local character of the test which is not representative of the soil mass. Moreover for in situ tests interpretation difficulties exist due to the non homogeneous character of the strain and stress fields applied to the soil mass. In order to reduce these uncertainties, geotechnical engineers can use inverse analysis processes during construction. This article shows the application of two of these processes on convergence leveling measurements realized during the excavation of the Bois de Peu tunnel (France).Two inverse analysis method have been tested (an optimization method and an evolutionary algorithm), coupled with the finite element software CESAR-LCPC to identify soil parameters.

1 INTRODUCTION

The purpose of inverse analysis processes is the identification of parameters using tests results or/and experimental measurement carried out during works. Various methods exist. Hicher (2002) distinguishes three kinds: analytical methods, correlation and optimization methods. Optimization methods are applied when model parameters are not appropriate to be used in a direct approach by graphic construction or in an analytical approach. By this method, the inverse problem is solved using an algorithm which minimizes a function depending on all parameters. This function is generally called "cost function" and corresponds to the difference between numerical and experimental measurements. The experimental results can come from various origins: laboratory tests, in situ tests or work measurement data. Two types of optimization methods are distinguished: deterministic and probabilistic methods. The deterministic methods include gradient, Newton, Gauss-Newton or Levenberg Marquardt optimization algorithms. Several researches aiming at parameter identifications based on deterministic methods were carried out in the last years. Zentar (2001) tried to identify some mechanical parameters of the Saint-Herblain clay using the results of pressuremeter tests and the optimization software SiDoLo. He considered an elastoplastic model with or without hardening. In spite of the identification methods development, a few of them were applied to real cases like tunnels or deep excavations (Finno et al. 2005).

The deterministic methods present some advantages. The iteration number required to achieve the optimization process is relatively low. But, if the cost function presents several local minima, the deterministic methods can converge towards the first found minimum. This major drawback explains why these methods are seldom used for complex problems. For such problems probabilistic methods are preferred. Probabilistic methods include evolutionary algorithms such as genetic algorithms and evolution strategies. Evolutionary algorithms reproduce the natural evolution of the species in biological systems and they can be used as a robust global optimization tool. The major principles of genetic algorithms were developed by Goldberg (1991). Evolution strategies (Schwefel, 1985) start searching from an initial population (a set of points) and transition rules between generations are deterministic. The search of new points is based on mutation and recombination operators. Recent researches applying genetic algorithms to soil parameters identification for a constitutive model have been undertaken in geotechnics (Levasseur et al. 2005). Evolution strategies were also recently applied to problems in many domains (Costa et al. 2001).

First, this paper presents briefly the used optimization software, SiDoLo and the used evolutionary algorithm. Then the numerical modelling of the tunnel and the followed approach are detailed. Finally, results obtained by the two processes are compared.

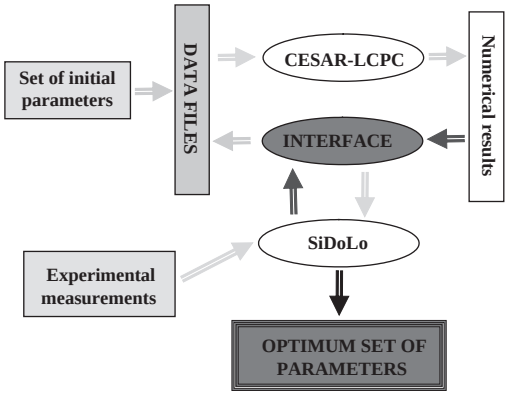


Figure 1. Principle of the coupling.

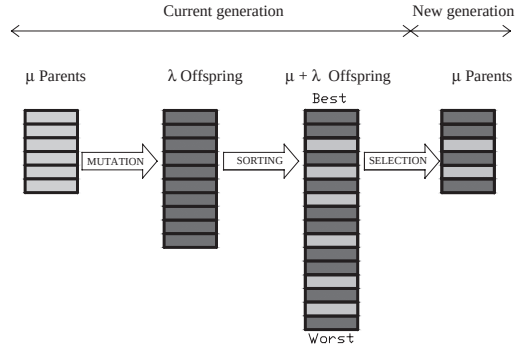


Figure 2. Principle of the $(\mu/\rho+\lambda)$ evolution strategies (Costa et al. 2001).

2 PRESENTATION OF THE OPTIMIZATION METHODS USED

2.1 *The optimization software, SiDoLo*

SiDoLo is coupled with the finite elements code CESAR-LCPC. The coupling principle is illustrated in figure 1.

Though this coupling, SiDoLo compares numerical results with experimental measurements, in order to calculate the cost function. When the cost function is lower than a fixed value, then the optimization process stops. The cost function L(A) is expressed by the following finite sum:

$$L(A) = \sum_{n=1}^{N} \frac{1}{M_n} \sum_{i=1}^{M_n} {}^{T}[Z_s(A,t_i) - Z_s^*(t_i)].D_n.[Z_s(A,t_i) - Z_s^*(t_i)]$$

where A are the model parameters, N is the number of experimental measurements; $[Z_s(A,t_i) - Z_s^*(t_i)]$ is the difference between numerical and experimental results evaluated only at M_n steps of observation t_i and D_n is the weighting matrix of the nth test. Measurements accuracy is taken into account by weighting coefficients.

SiDoLo uses a hybrid optimization algorithm, which combines two typical minimization methods: the gradient method and a variant of the Lavenberg-Marquardt method to accelerate the convergence when the solution is close. More details on the SiDoLo approach can be found in Eclaircy-Caudron et al. (2006).

2.2 *The algorithm based on evolution strategies*

The algorithm used was developed by Costa (Costa and al. 2001). This algorithm was adapted to the problem studied in this paper, and as for SiDoLo, requires to create an interface with Cesar-LCPC. The population individuals are vectors of real coded decision variables that are potential optimal solutions. An initial population is generated and then each following generation, λ offspring are generated from μ progenitors by mutation and recombination. Then the best individuals are selected for next generation among the $\mu+\lambda$ members according to their cost function value. Finally, the μ best of all the $\mu+\lambda$ members become the parents of the next generations. Important features of evolution strategies are the self adaptation of step sizes for mutation during the search and the recombination of individuals that is performed between ρ individuals. This algorithm, named generally $(\mu/\rho+\lambda)$ algorithm, is illustrated in figure 2.

The algorithm stops when one of the following conditions is verified:

- The maximum number of generations is reached
- The difference between the two extremes values of the cost functions is lower than 10^{-5}
- This difference divided by the average of the cost functions values is lower then 10^{-5}

3 THE FOLLOWED APPROACH

3.1 *Presentation of the tunnel*

The Bois de Peu tunnel is situated near Besançon in France. It is composed of two tubes. The excavation length is about 520 meters per tube for a cover height which varies between 8 meters and 140 meters. Four kinds of supports were foreseen in the project phase for the four types of materials: limestones, marls, interbeding of marls and limestones and clays. The studied section is located near one of the two tunnel portals where interbeding of marls and limestones were expected. A face levelling of this section is showed in figure 3. The lining support set up in this area is composed of a mixed support of the tunnel walls by shotcrete with a thickness of 0.2 m and steel ribs. The tunnel is dug with a constant step of 1.5 m. The height

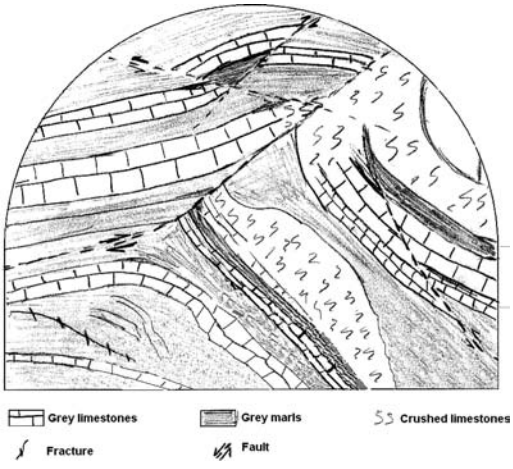


Figure 3. Face levelling.

Table 1. Design characteristics.

Parameters	γ (kN/m^3)	E (MPa)	C (MPa)	ϕ (°)	ν –
Probable	24.8	1600	0.70	40	0.3
Exceptional	24.0	750	0.21	36	0.3

of cover is equal to twenty six meters. At the end of site investigations, two kinds of design characteristics were defined: probable and exceptional. They are resumed in table 1.

3.2 *Numerical model*

Due to time consuming of three dimensional calculations, tunnel excavations are often taken into account by two dimensional modelling. We adopted a transverse plane strain model, taking into account the real geometry, the excavation and tunnel support being modelled by an unconfinement coefficient (Panet, 1995). Only a half section is represented because a symmetrical deformation of the section is assumed. The grid dimensions are 75 m (= 6D) in the two directions in order to avoid the influence of the boundaries. The grid (figure 4) contains around 3900 nodes and 1850 elements with quadratic interpolation (Six nodes triangles and 8 nodes quadrangles). The initial stress field is anisotropic. An earth pressure ratio of 0.7 is adopted. This value was obtained by means of in situ tests. Steel ribs and sprayed concrete are simulated by a homogeneous support with equivalent characteristics. This support is assumed to have a linear elastic behaviour. A linear elastic perfectly plastic model with a Mohr Coulomb failure criterion and non associate flow rule is considered to represent the soil mass.

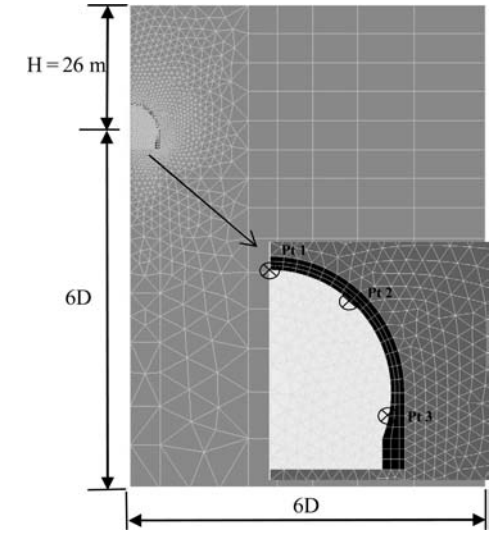


Figure 4. The grid and its dimensions.

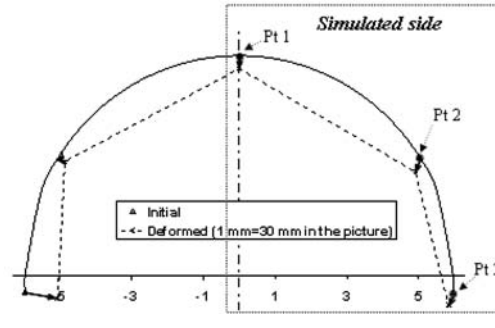


Figure 5. The observations points and deformed section.

Three computing phases are defined. First the initial stress field is applied. After, the tunnel is excavated. In this phase the unconfinement ratio at the time of the support installation is applied. Finally the homogeneous support with a 0.238 m width is activated. A total unconfinement is applied.

3.3 *Experimental results*

Figures 4 and 5 locate the three experimental measurements points used for optimization. Five measurements are observed for these three points: leveling for these three points and horizontal displacements for the points 2 and 3. They correspond to convergence and leveling measurements of the tunnel wall in a given cross section (point 1 to 3 in figures 4 and 5). The convergence and levelling measurements of this section are reported in figures 6 and 7. These measurements permit to deduce the horizontal and

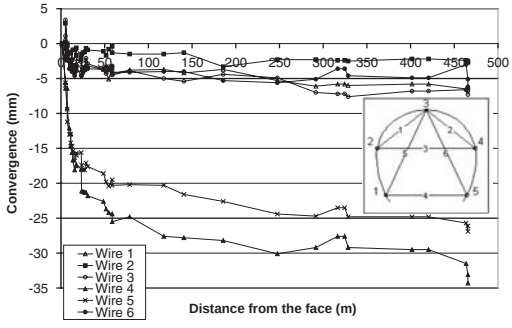


Figure 6. Convergence measurements.

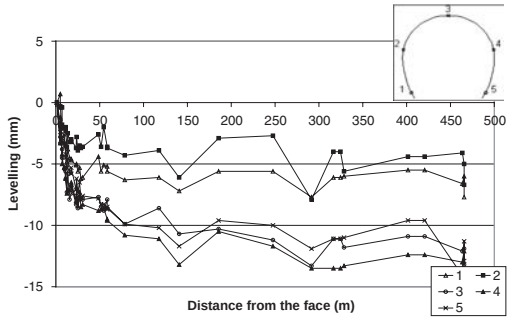


Figure 7. Leveling measurements.

vertical displacements of each point. The convergence is maximal for wires 4 and 5. It reaches 30 mm for wire 4. Moreover levelling is more important for targets 3, 4 and 5 than for the others. It reaches 13 mm. So, these measurements showed a dissymmetrical deformation of the section. In optimization process average displacements measured at equilibrium are used. The dissymmetry is confirmed by the section deformation presented in figure 5 where the crown displacement is assumed purely vertical. The experimental results considered in the optimization process correspond to the average displacements observed at the two sides.

3.4 *Unknown parameters*

In the frame of plane strain calculation, the introduced unconfinement ratio λ at the time of support installation might be calculated by the convergence-confinement method (Panet, 1995) if the constitutive model parameters were well known. But in this study, it is considered as an additional parameter to identify. Before using inverse analysis, a sensibility study was performed. The Poisson ratio and the dilatancy angle are parameters which have low influence on the observed variables. So, these parameters could not be identified with these measurements. Only parameters λ, C, E and ϕ, might be evaluated.

Validation studies (Eclaircy-Caudron et al. 2006) were performed with SiDoLo on this numerical model in order to define which parameters might be identified according to the available experimental measurements. These studies showed that with convergence and levelling measurements no more than two parameters could be identified. But SiDoLo always succeeded to identify ϕ and λ even if they were unknown with other parameters because they have more influence on the convergence and levelling measurements than the others. In order to verify the provided solution an evolution strategies algorithm is used in complement of the software SiDoLo.

4 RESULTS

Several identification attempts were performed with SiDoLo, confirming that SiDoLo provides approximately the same values of ϕ and λ in all cases.. They also showed that the friction angle was lower than the project value (between 10 and 20°).

Two examples of identification are presented here, where three vertical and two horizontal displacements are used in the optimization process. For each identification several initial values (referred as a, b and c) of unknown parameters are tested in order to show the influence of the initial value.

In the first example, the four parameters E, C, λ and ϕ are identified. Table 2 gives the obtained values and the enabled respective ranges in SiDoLo. Several solutions are found by the optimization process according to the introduced initial values but provided values of ϕ and λ are similar. ϕ varies between 12.2 and 15.6° and λ between 0.7 and 0.75. Figure 8 compares the displacements obtained with the optimized values provided by first identifications to the measurements. Displacements computed with the design characteristics (probables or exceptionals) are also reported in this figure. They are very low compared to the measurements. The displacements computed after optimization for points 2 and 3 are close to the measured displacements. The vertical displacements computed at point 1 are lower than the one measured. The iteration number required to achieve the optimization process varies between 16 and 52 according to the initial value. These results highlight the fact that the optimization problem has not a single solution when more than two parameters are unknown. The major drawback of the probabilistic optimization methods is that they can converge to local minima.

In the second identification only the Young modulus E and the cohesion C are identified. λ and ϕ are fixed respectively to the average of values provided by the first identification. A friction angle of 14° and an unconfinement ratio of 0.717 are adopted. The enabled ranges in SiDoLo are the same. Table 3 gives the obtained values. Several solutions are also found by

Table 2. The first identifications results realized with SiDoLo.

Set	E (MPa)	C (MPa)	ϕ (°)	λ –
a	202.3	0.12	15.6	0.7
b	102.3	0.19	13.4	0.7
c	100.3	0.20	12.2	0.7
Range	100–2000	0.10–1	10–30	0.7–0.8

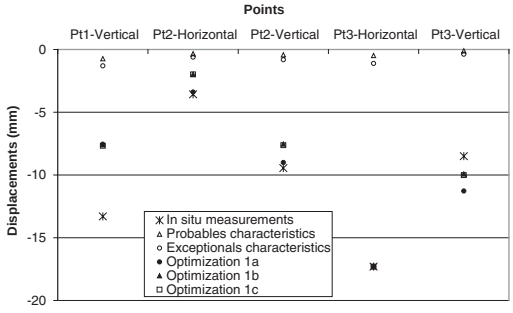


Figure 8. Comparisons between the measured and computed displacements after optimization by SiDoLo (tests 1).

Table 3. The second identifications results realized with SiDoLo.

Set	E (MPa)	C (MPa)
a	217	0.13
b	100	0.19
c	102	0.19

the optimization process according to the introduced initial values. SiDoLo does not succeed to find the best couple. It provides local minima. Displacements computed after identifications 2 are similar to those obtained after identifications 1. The vertical displacement measured at the tunnel crown appears difficult to reproduce in the numerical model. Although the face levelling showed in figure 3 highlights a disturbed geology with folds and faults a homogeneous medium is considered in the model. A more complex model seems to be required to simulate the real behaviour of the tunnel crown.

In order to avoid local minima, the evolution strategies algorithm is used. The same identifications than those previously presented are realized. These identifications allow to verify the solutions found by SiDoLo. The same ranges are enabled for parameters. The number of generations is limited to 50 in order to keep acceptable computation times. The parent population size is 10 and the offspring population size is 20. For two identifications the evolution strategies algorithm

Table 4. Design characteristics and optimized values.

Parameters	E (MPa)	C (MPa)	ϕ (°)	λ –
Probable	1600	0.7	40	–
Exceptional	750	0.21	36	–
SiDoLo (test 1)	102–202	0.12–0.2	12–16	0.7–0.75
SiDoLo (test 2)	100–217	0.13–0.19	14*	0.717*
ES (test 1)	288.5	0.1	19.4	0.7
ES (test 2)	242.7	0.12	14*	0.717*

* Fixed values

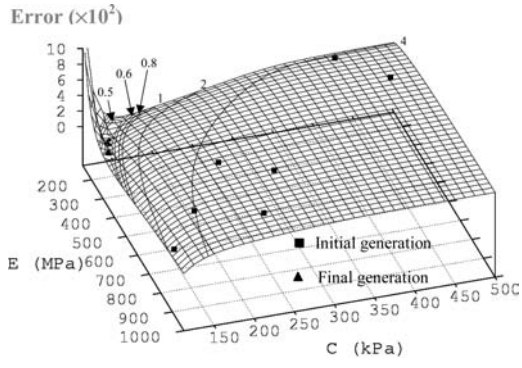


Figure 9. Evolution of the cost function for tests 2. Representation of initial and final generation's parents.

stopped when the maximum number of generations is reached, the cost function being still relatively important and the stop criteria on this function cannot be reached. So the problem seems to be badly formulated. The design characteristics, the best member provided by the Evolution Strategies algorithm (ES) and solutions provided by SiDoLo are resumed in table 4.

For the first identification where four parameters are unknown the evolution strategies algorithm provided a solution different from those provided by SiDoLo. This solution corresponds to a global minimum.

Figure 9 presents the evolution of the cost function in the case of two unknown parameters E and C while λ and ϕ are introduced as input parameters (identifications 2). The cost function is not convex and shows a valley. A decrease of parameter E is counterbalanced by an increase of C in a small variation domain. So it is difficult to identify these two parameters with only convergence and levelling measurements. Moreover the value of the cost function is important, confirming that the numerical model should be improved. Figure 9 shows also the parents at initial and final generations. At initial generation parents are dispersed in all research space. At later generation they are located in the valley and are close to each other. Figure 10 locates the three couples found by SiDoLo and the best

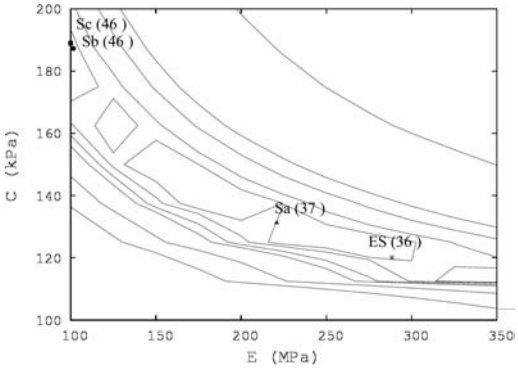


Figure 10. Location of the solution found by SiDoLo (Sa, Sb and Sc) and the best member found by the evolution strategies algorithm (ES) during tests 2.

member found by the evolution strategies algorithm after identifications 2. The error function value is also reported. Solutions found by SiDoLo are situated in the valley and correspond to local minima. The evolution strategies algorithm provides a global minimum.

5 CONCLUSIONS

The use of inverse analysis on in situ measurements carried out during the construction of a real work is rare. This might be due to the difficulty met to apply inverse analysis on real work. In a tunnel case the numerical model required many simplifications in order to obtain acceptable computation times. Moreover, boundaries conditions should be representative. The adopted constitutive model should not be too sophisticated with many parameters but should properly simulate the soil behaviour.

The use of a deterministic method in two steps permits to obtain local minima. The probabilistic method based on evolution strategies makes it possible to find the global minimum. But this method required more important computation time: more than 2 days for the 50 generations against 1h30 for SiDoLo per identification and for the three initial values. Here with two unknown parameters the cost function is not convex and presents a valley. Moreover the error values are important. Thus the problem is more difficult to solve.

In this study a linear elastic perfectly plastic model with a Mohr Coulomb failure criterion is considered to represent the soil mass. In order to improve results a non linear elasticity and a Young modulus which varies with depth could be introduced. Maybe the evaluation of the earth pressure ratio by means of in situ tests needs to be more investigated. This ratio might be considered as a supplementary parameter to identify. Moreover uncertainties exist on the lining stiffness. Due to the face levelling showed in figure 3 and to the section deformed in figure 8 the studied section is not homogeneous. So it could be interesting to realize two optimizations by considering each side. Optimizations could be realized by considering only points 1 and 2 where dissymmetry is less visible.

In order to improve the results provided by the two optimization methods tested in this paper other measurements have to be used like stress measurements in steel ribs or displacements measured along extensometers. Moreover, two numerical models could be coupled in the optimization process. So the optimization could be realized at the same time on displacements measured during the exploration gallery excavation in a zone near the studied section and on convergence measured in tunnel.

REFERENCES

Costa, L. & Oliveira, P. 2001. Evolutionary algorithms approach to the solution of mixed integer non linear programming problems. *Computers and Chemical Engineering* 25: 257–266.

Eclaircy-Caudron, S., Dias, D., Kastner, R. & Chantron, L. 2006. Identification des paramètres du sol rencontré lors du creusement d'un tunnel par analyse inverse. *Proc. JNGG 2006*. Lyon, France.

Finno, R.J. & Calvello, M. 2005. Supported Excavations: the Observational Method and Inverse Modeling. *Journal of Geotechnical and Geoenvironmental Engineering* 131(7): 826–836.

Goldberg, D. 1991. *Algorithmes génétiques : exploration, optimisation et apprentissage automatique.* Adisson-Wesley Edition.

Hicher, P.Y. & Shao, J.F. 2002. *Modèles de comportement des sols et des roches 2: lois incrémentales, viscoplasticité, endommagement*. Hermès Science Publications.

Levasseur, S., Malecot, Y., Boulon, M. & Flavigny, E. 2005. Analyse inverse par algorithme génétique en géotechnique: application à un problème d'excavation. *17th Congrés Français de Mécanique*. Troyes, France.

Panet, M. 1995. *Le calcul des tunnels par la méthode convergence-confinement*. Presse de l'école nationale des Ponts et Chaussées.

Schwefel, H.-P. 1985. *Evolution and optimal seeking*. John Wiley and Sons.

Zentar, R. 1999. Analyse inverse des essais pressiométriques : Application à l'argile de Saint-Herblain. *Ph. D. thesis*. Ecole Centrale. Nantes, France.

Underground Space – the 4th Dimension of Metropolises – Barták, Hrdina, Romancov & Zlámal (eds)
© 2007 Taylor & Francis Group, London, ISBN 978-0-415-40807-3

Prediction of the ground conditions ahead the TBM face in the tunnels of Guadarrama (Spain), using geophysical methods and in situ testing

José Miguel Galera
Geocontrol S.A. Universidad Politécnica de Madrid

Salvador Pescador, Ángel Rodríguez & Manuel Torres
In Situ Testing S.L.

ABSTRACT: The tunnels of Guadarrama are new twin tunneles crossing the Central Range between Madrid and Segovia, as part of the new High Speed Railway Line to the NW of Spain. Their length is 28,3 km with a maximum overburden of 900 m. The geology consists mainly of crystalline rocks, gneiss and granites, with a main graven in the Lozoya valley where poor quality sedimentary rocks from the Cretaceous are crossed. Nevertheless several faults have also been detected with mylonites and water. The tunnels have been done using four double-shield TBMs, all of them with an excavation diameter of 9,5 m. In order to predict in detail the ground conditions ahead the TBM face, a review of the geological features has been done. This has consisted in detailed geological mapping with a precise photogeological study and systematic Electrical Resistivity Tomography (ERT) profiles along the axis of both tunnels. Also several geophysical investigation methods have been applied, in order to allow a good knowledge of the rock mass. In situ geotechnical tests have been also carried out, yielding ground geomechanical parameters. They can divide as follows:- Surface tests, carried out from the South Portal, previous to the TBM – Surface tests, carried out from the North Portal, previous to the TBM – La Umbría Fault, where various methods have been applied at the surface, in borehole, surface to borehole or borehole to borehole. This paper describes the field campaigns and shows the most significant results of the geophysical investigation in Guadarrama tunnel. In the main faults inclined boreholes were drilled in order to perform dilatometer and permeability in situ test. With all these data it was decided in advance if the double-shield was going to work in a single or double mode. A type of expert system have being used to interpret the data coming from TBM after crossing the expected faults, so allowing a feedback to the entire process.

1 INTRODUCTION

The Tunnels of Guadarrama are new twin tunnels crossing the "Sistema Central" (Central Range) of the Iberian Peninsula, between Madrid and Segovia, for the new High Speed Railway Link Madrid-Valladolid, to the NW of Spain.

Figure 1 shows the location of these tunnels.

The length of each tunnel is 28,3 km with a maximum overburden of 900 m.

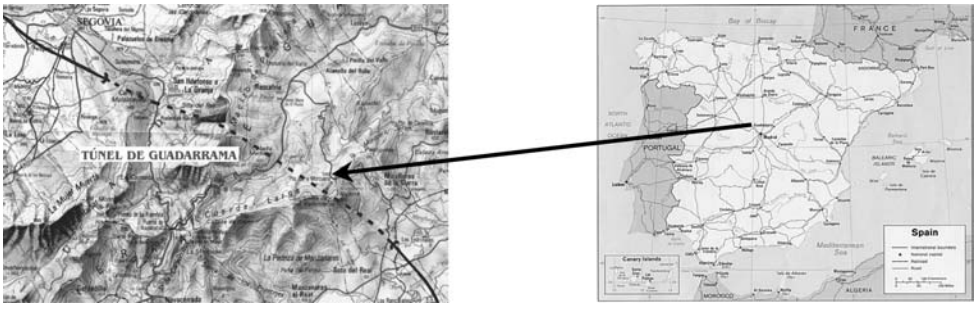


Figure 1. Location of Guadarrama's tunnels.

The tunnels have been excavated using four double-shield TBMs; all of them with an excavation diameter of 9,5 m.

2 MAIN GEOLOGICAL FEATURES

The geological conditions consist of crystalline rocks, gneiss and granites crossed by several types of dykes. A main graben in the Lozoya valley where poor quality sedimentary rocks from the Cretaceous, including loose sands under water table, were crossed is the most problematic section of both tunnels. Nevertheless several faults and dykes have also been detected in the site characterization jobs, inside the crystalline bodies with different mylonites and water conditions.

In the Figure 2 a longitudinal geological section of the tunnel is shown. It can be appreciated, the two main faults encountered that have been intensively investigated in advance using geophysical methods.

There two faults corresponds to Valparaiso and to La Umbría fault areas.

3 METHODOLOGY USED FOR THE PREDITION OF GROUND CONDITIONS AHEAD THE TBM FACE

Since the beginning of the excavation, the major importance of having a prediction of the ground conditions ahead the TBM face has been demonstrated, in order to take the decision to advance in a single or in a double-shield way or if it is necessary to make a ground improvement ahead the face of the tunnel.

For this purspuse a review of the main geological features has been done.

This review has consisted of a detailed (1:1000 scaled) geological mapping with a precise photogeological study.

Following this geological mapping an intensive geophysical survey of both tunnels was done. This survey has consists in the following works:

- Geophysical methods applied from surface.
- Geophysical methods applied between boreholes or between borehole and surface.

In Figure 3 it is shown a block-diagram showing the relationships between the different technologies used (Capote, 2005).

As a prediction tool a systematic Electrical Resistivity Tomography (ERT) profiling along the axis of both tunnels has been carried out.

In the main faults and accidents further inclined boreholes were drilled in order to perform dilatometer and permeability in situ tests, as well as to make some geophysical logging.

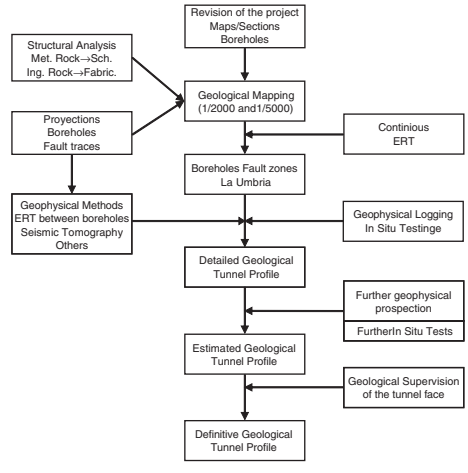


Figure 3. Methodology used for the prediction of the ground conditions ahead the TBM face (modified from Capote, 2005).

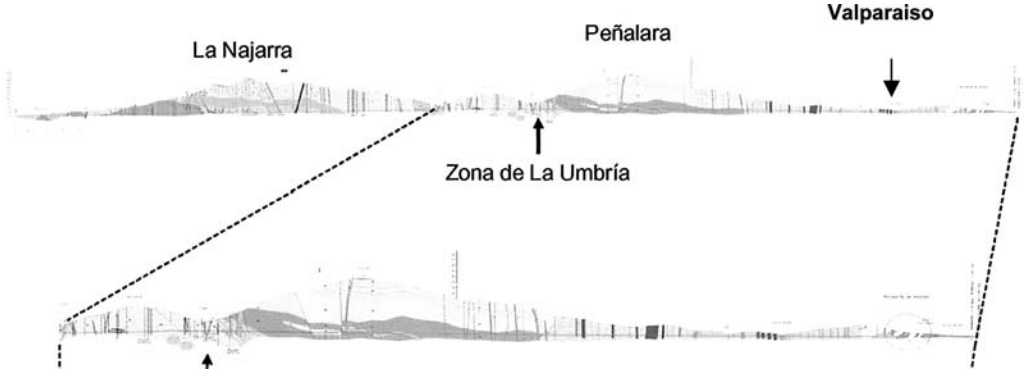


Figure 2. Geological profile of the tunnels of Guadarrama.

This methodology has proven to be effective and very precise down to an overburden around 150 m.

A special remark was done in relation with La Umbría Fault were several geophysical methods have been applied.

In this area most of the geophysical and in situ tests methodologies were used, to precise the structural position of the creataceous loose sands, as well as the position of the main gouge faults zones. It was encountered that the tectonized zones were located in the northern part of the valley.

3.1 *Electrical resistivity tomography (ERT)*

The use of Electrical Resistivity Tomography (ERT) for the detection of faults has already been used since faults usually give low values of resistivity because of the presence of day minerals and high water contents.

The method is based in the measurement of the potential drop between two electrodes (MN), obtaining the resistance of the ground to a current flow (AB).

The multi-electrods mode used has been an axial dipole-dipole, as this is the best mode for the detection of vertical resistivity anomalies.

After several trials a unit electrode spacing of 10,0 m has been used for low overburden, obtaining a constant depth of investigation of about 60 m.

Two parallel profiles along both axis of the tunnels have been done. With this geometry, a good correlation is assured in the strike and dip of the resistivity anomalies.

For the definition of the characteristic of the faults, a very detailed interpretation process has been used.

It has the following steps:

- The apparent resistivity pseudosection is measured.
- Secondly the resistivity is calculated from the resistance value.
- Thirdly, an iterative inversion process is done, minimizing the error between the measurement and the calculated values of resistivity. This accordance is given by the value of RMS error expressed as a percentage.

Finally, as is shown in the Figure 4, the model is corrected to allow for the real topography.

For the final interpretation it is very significative to analyze the chargeability section. This analysis has provided data for the prediction of water inflow into the tunnel.

Since the beginning of the excavation from the North Portal of the tunnels, more than 1.1980 ml of ERT profiles have been done, while the excavated length is 13.500 m for each tunnel (Tunnels 3 and 4).

The prediction system has proven to give satisfactory results. Figure 5 shows the correlation between the geological and the resistivity sections in one of the main faults encountered.

3.2 *3D interpretation of ERT*

In La Umbría fault 4.600 m of ERT profiles from surfaces were done, as well as 5 electrical tomography

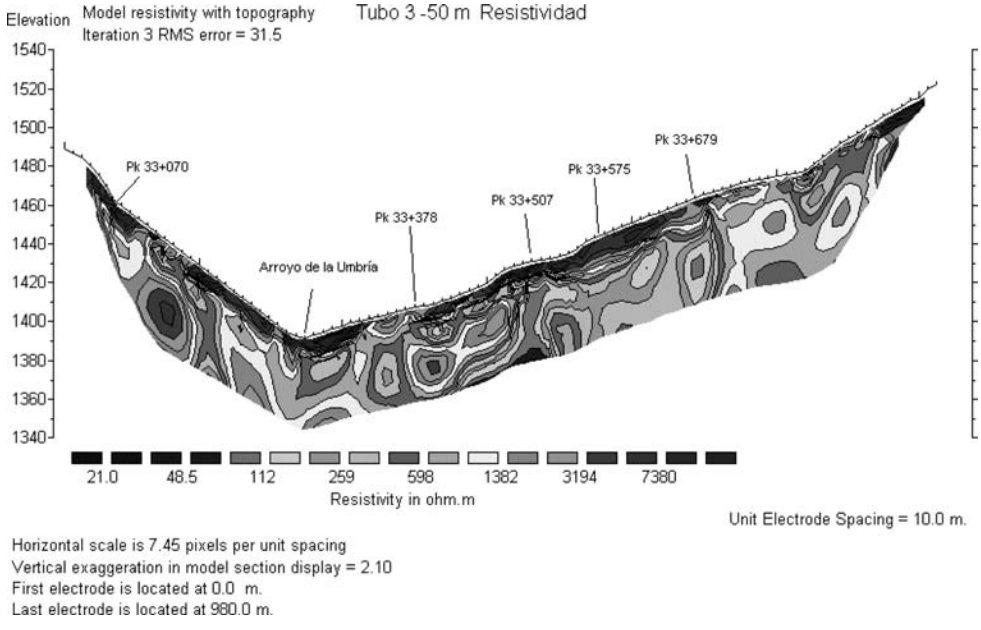


Figure 4. Final section with real topography.

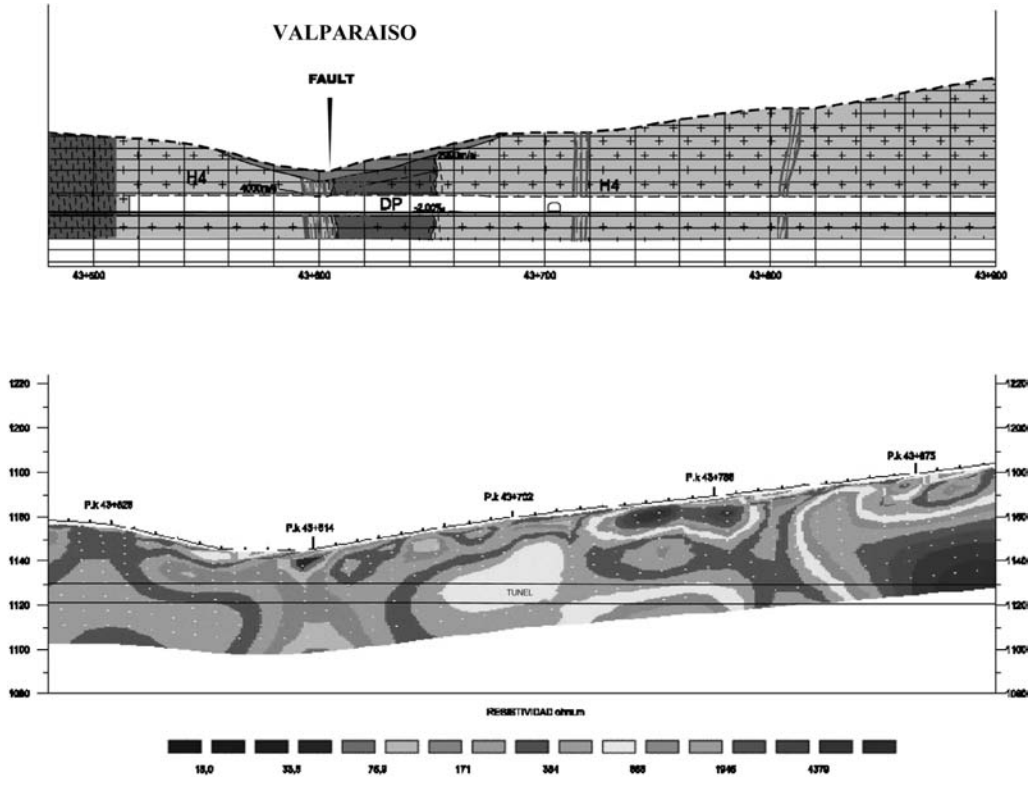


Figure 5. Example of the correlation between the resistivity and the geological profiles. (Valparaiso Fault).

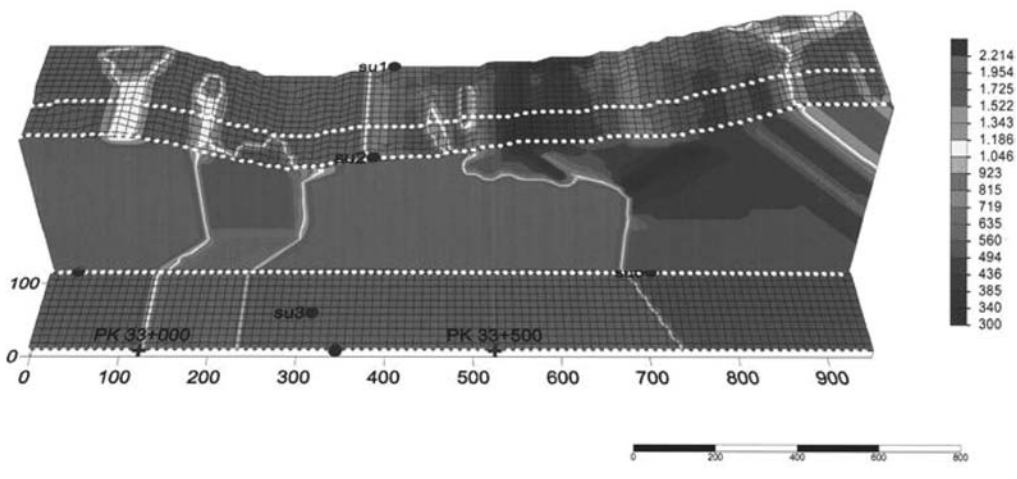


Figure 6. Resistivity 3D model of La Umbria Fault zone. (In the horizontal plane, both tunnel axis have been marked).

borehole-borehole and 6 ERT borehole-surface. This has allow to make a complicate 3D interpretation of the fault.

Figure 6 shows a tridimensional section of Tunnel 3, in which the two low resistivity main faults can be appreciated.

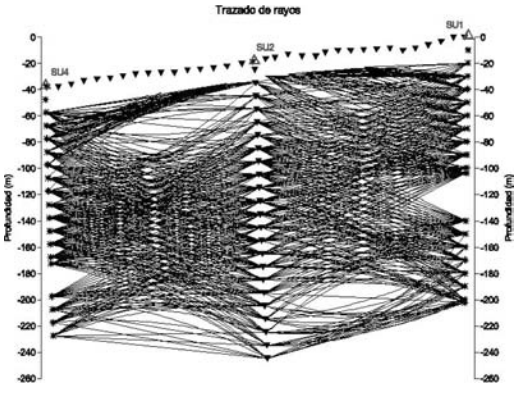


Figure 7. The raypaths of one of the sections measured with seismic tomography in La Umbria Fault zone.

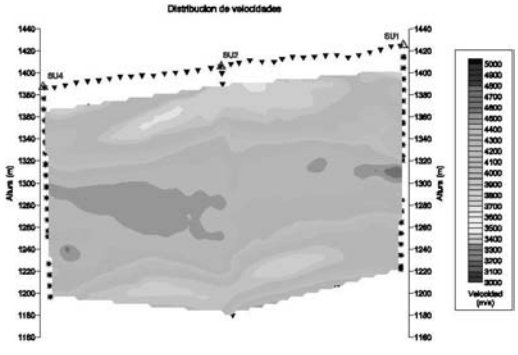


Figure 8. Results of the interpretation, of seismic tomography in La Umbria Fault zone.

As it has been said, these two zones are located in the northern part of the valley.

3.3 Seismic crosshole tomography

The seismic tomography is based on the elastic waves propagation to obtain a spacial distribution of the velocities inside a volume of rock mass.

Once the data acquisition is done, it is calculated the velocities between all the nots of the mesh.

In La Umbria Fault it was done a seismic survey between boreholes.

Considering:

- The distance between boreholes: As bigger this distance is lesser is the accuracy.
- The distance between geophones an shot points.
- The accuracy in the knowledge of the position of emissor and receptors.

Figure 7 shows the raypath, of one of the sections measured. While Figure 8 show the results of the interpretation carried out.

Table 1. Geophysical logging used in boreholes.

Equipment	Log
SCHLUMBERGER	HALS-PEX-Laterolog-Plataform Express Logs HNGS – Espectometría Gamma Nuclear FMI-Fullbore Fm. Microimager DSI-Dipolo Shear Imager GR-Gamma Ray
MOUNT SOPRIS	Caliper Acoustic Televiewer Full wave sonic Temperature Gamma Ray Conductivity Resistivity SP

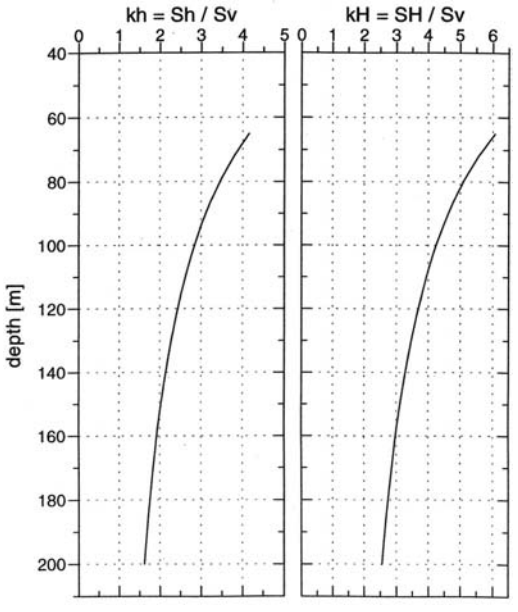


Figure 9. Result of the Hidrofract tests carried out in one borehole, showing high horizontal stresses.

3.4 *In situ testing*

The following techniques have been used:

- Geophysical logging (see Table 1).
- Hidrofract tests (see Figure 9).
- Dilatometer Tests.

These tests have been very useful for geotechnical site characterisation of La Umbria fault, as well as for other tectonical features.

The geophysical logging and in situ test carried out inside the drilled boreholes, have provided a very valuable information concerning:

- structural data.
- natural stress field (with a high ratio k_0, between horizontal and vertical stresses).
- rock mass deformability, specially in the sedimentary rocks of the Cretaceous, including loose sands.

4 DISCUSSION AND CONCLUSIONS

The geophysical surveys and in situ tests carried out, have contribute to define the geological and geomechanical profile of Guadarrama tunnels.

This methodology has allow to predict in advance, the constructive difficulties of the rock mass to be excavated by the 4 TBMs.

The figures of these measurements are the following:

- 3.501 ml seismic profiles.
- 24.870 ml surface ERT.
- 3.860 ml of VLF.
- 11.019 ml of geophysical logging.
- 5 ut. ERT borehole-borehole.
- 6 ut. ERT borehole surface.
- 18 ut. Seismic Tomography borehole-borehole.
- 25 ut. Dilatometric tests.

The ERT has proven to be an efficient system for the prediction of faults and dykes ahead the TBM face in the gneiss and granites of Guadarrama Tunnels.

The use of the chargeability profiles is very interesting for the prediction of water inflow conditions.

The interpretation is very difficult when the strike of the resistivity anomaly is parallel to the axis of the tunnel.

Using the resistivity profile it has been decided in advance, if the TBM has to work in a single or in a double shield way.

For an overburden higher than 250 m, Najarra and Peñalara massifs, no geophysical survey has been used, as all the tests done didn't give enough reliability and accuracy in the interpretation.

For the Umbria Fault, the electrical and seismic tomographies, have contribute to define the position of cretaceous loose sands.

The in situ tests have contributed, in conjuction with the geotechnical logging of the drilled boreholes and the last test to the mechanical characterization of the rock mass.

BIBLIOGRAPHY

Capote, R (2005). La geología del proyecto del túnel de Guadarrama. In: Túnel de Guadarrama. ADIF. Ed. Entorno Gráfico: 67–93.

Galera, J.M.; Peral F.; y Rodríguez, A (2004). Prediction of the ground conditions ahead the TBM face in the tunnels of Guadarrama (Spain), using Electrical Resistivity Tomography (ERT). In Proc. 2nd Int. Conf. on Site Characterization. Ed. Millpress: 1443–1447.

Galera, J.M.; Pescador, S; Rodriguez, A y Torres, M. (2005). Empleo de las técnicas geofísicas y de los ensayos in situ en los túneles de Guadarrama. In: Túnel de Guadarrama. ADIF. Ed. Entorno Gráfico: 97–115.

Loke, M. H. & Barker, R. D. 1996. Practical techniques for 3D resistivity surveys and data inversion. *Geophysical Prospecting, 44, 1996:* 499–523.

López, F. (2005). Perfil geológico del túnel de Guadarrama. Estudios de caracterización de fallas: La Umbría: In: Túnel de Guadarrama. ADIF. Ed. Entorno Gráfico: 149–187.

Oteo, C (2005). Geotecnia, auscultación y modelos geomecánicos en los túneles ferroviarios de Guadarrama: In: Túnel de Guadarrama. ADIF. Ed. Entorno Gráfico: 191–220.

Sasaki, Y. 1994. 3-D resistivity inversion using the finite element method. *Geophysics, vol. 59, no. 11, December 1994:* 1839–1848.

Underground Space – the 4th Dimension of Metropolises – Barták, Hrdina, Romancov & Zlámal (eds)
© 2007 Taylor & Francis Group, London, ISBN 978-0-415-40807-3

Risk analysis of soil transition in tunnel works

Q.F. Hu
Shanghai Institute of Disaster Prevention and Relief, Tongji University, Shanghai, China

H.W. Huang
Department of Geotechnical Engineering, Tongji University, Shanghai, China

ABSTRACT: Recent years the demands for systematic risk analysis of soil transition for tunnel works are more and more increasing to minimize the construction accidents. The probabilistic geologic prediction model based on Markov process is being established to characterize the probabilistic form of ground uncertainty. This paper studied how to modify 1D (one dimension) Markov process, and then improved to establish a new method of the conditional Markov Process, which can uses all available ground class information. For analyzing the spatial soil transition, the 2D (two dimension) conditional Markov process is also proposed and discussed. The modified 2D conditional Markov process can predict the soil transition and get the probabilistic risk index by Monte Carlo simulation. Finally a case study of Shanghai Yangtze River Tunnel, the biggest diameter and longer shield tunnel now in the world, showed that the predicted data using the proposed method has very good agreements with the real borehole data.

1 INTRODUCTION

Before the construction of tunnels and underground works is started, engineers should make the site investigation based on the character of the soil, and analyze the random distribution of soil combined with geological borehole samples to create the geological soil transition along the tunnel profile. Due to the information of limited number of boreholes are not enough, which are just discrete point information of the deterministic area around the borehole locations, the soil transition process between the boreholes is a big random uncertainty. The conventional methods of boreholes driven for a tunnel construction are linear interpolation and engineering experience, which can not reflect the soil random distribution. Therefore it has become a critical problem and a challenging task for the tunnel and underground working engineers that how to reduce the random uncertainty between boreholes, and to establish a precise soil transition along the tunnel profile.

At present, the internationally geological researchers (Einstein H.H. 1984; Whitman, R.V. 1984, Isaaks, E.H. 1989) are using the random field theory to study the soil random transition, and therefore analyze the characters of soil random distribution in tunnel and underground works. They use stochastic technology to establish some models to obtain the tunnel profile, which are quantitative, dimension-extendable and faithful to the known borehole information, and establish spatial distribution of soil random field for forecasting the soil character in the tunnel site. Based on Markov Random Field Model (MRFM), and combined with the engineering geological borehole data, the paper studied how to modify the 1D Markov process, and to establish a new method of the conditional Markov Process. This method can use all available ground class information. Then the 2D conditional Markov process is also purposed and discussed for analyzing the spatial soil transition. The modified 2D conditional Markov process can predict the soil transition and get the probabilistic risk index by Monte Carlo simulation. And finally a case stubby about the Yangtze River Tunnel is shown in the end.

2 RISK ANALYSIS OF SOIL TRANSITION BASED ON MARKOV MODEL

In tunnel works, the vertical boreholes only show the soil types that are available in the borehole location. The soil profiles between different boreholes are uncertain. It could be analyzed and defined as an obscure Markov Chain by adopting the model of Markov Process. Currently, many scholars (Likhitruangsilp, 2003; Ioannou, 2003) make use of the method of the Markov chain to study the soil transition and establish the soil profile at engineering site. But they only focused on studying the soil order of the

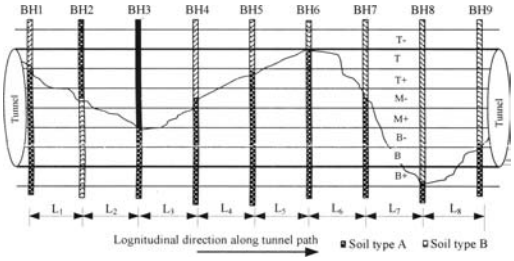


Figure 1. The longitudinal soil profile and transition along tunnel.

perpendicular direction. So their methods could not be used for analyzing the soil transition at two deferment direction like horizontal and vertical direction, and their result was physically poor for reflect the obscure soil random fields. In order to improve the current methods, a 2D modified conditional Markov Process was established to predict the soil transition between the boreholes along the tunnel alignment base on the geological statistics methods (Hou jinyu, 1998; Liu Zhenfeng, 2004).

2.1 *Model hypothesis*

One-demission Markov Model could be mainly used to study the geologic strata deposition and obtain the soil type form at vertical direction. The character of soil deposition sequence is actually hidden in the ground (see Figure 1). And great deals of site investigation data were proved the soil sequence distribution (Ruwanpura A., 2004) and the soil statistic relation in a historical way (Schwarzacher, 1984). So the character and condition of soil transition could be described by the model of Markov Process on the supposition that:

(1) Each soil layer types appear randomly inside the construction site. And all different soil types are district and random distribution, their spread distance is also discrete;
(2) The different boreholes are absolute, and each borehole can only provide the local soil random information around borehole location of construction site;
(3) The condition of soil transition is a homogeneous and smooth Markov Process

Based on the above model hypothesis, Markov Random Field Model (MRFM) was established to study the soil transition and to quantify the risk of soil uncertainty.

It is well known, the key parameters of MRFM are soil tally matrix or soil probability matrix which reflects the soil transition condition (see Figure 2). It is established through dividing the soil sequence

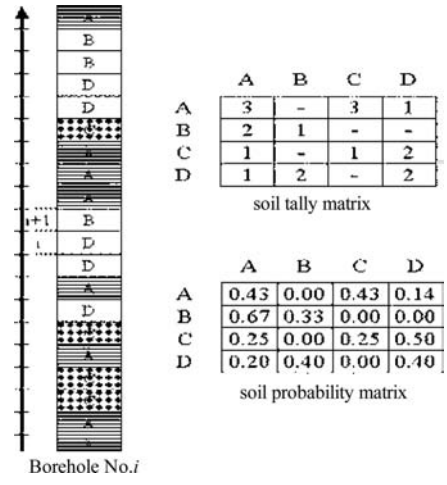


Figure 2. Soil tally matrix or soil probability matrix of borehole data.

of borehole into different soil interval length. Then the soil tally matrix is easily obtained from the borehole data. Generally, the soil interval length is difficult to determine than the soil type through borehole data, so the probability of soil transition is also difficult to calculate. There are two kinds of methods which can establish the soil tally matrix as follows.

(1) Divide the borehole length by the fixed distance. That is the same distance which is equal to the minimal thickness of soil in borehole.
(2) Divide the borehole length by different soil types. That is the same soil type whose thickness is equal to the soil distance.

Different dividing methods have different advantage. The second method is suitable for studying the soil type of borehole, and is non-useful for predict the soil transition condition. Comparatively, the first method is suitable for studying the soil distribution and get soil thickness. In order to get the soil transition for predicting soil profile along tunnel alignment, the first method is used here and the probability of soil transition is calculated by the fixed distance along the borehole.

2.2 *The model of 2D Markov process*

2D Markov model could be established on 1D Markov model. If the method of fixed distance in borehole is used, the probability of soil transition condition of two different directions can be calculated (see Figure 3). It is assumed that the soil transition of up-side and left-side are known, the space of soil transition condition is $S\{s_k \in S, k = 1, 2, \cdots, n\}$, and the probability $P^{(h)}, P^{(v)}$

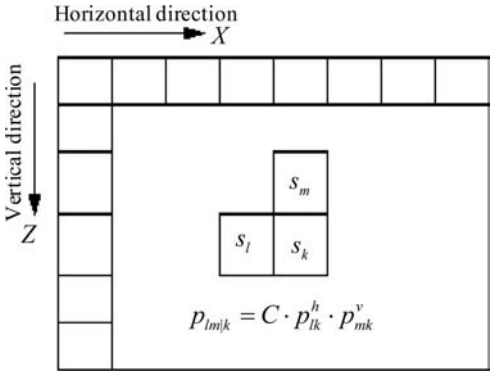


Figure 3. 2D model of Markov Process.

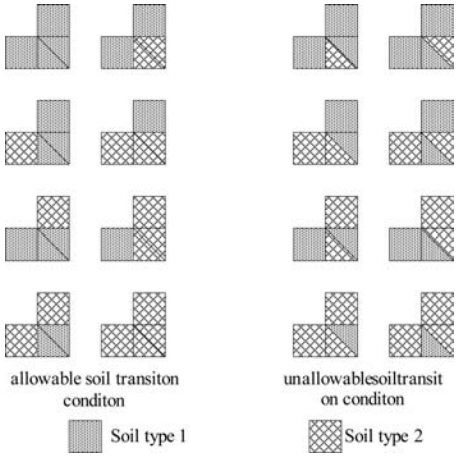


Figure 4. Soil transition condition of two different soil types.

of horizontal and vertical direction, then the probability of certain location, which is soil type k in the space, is defined as:

$$\begin{aligned} p_{lm|k} &= P_r\{X_{i+1} = s_k, Z_{j+1} = s_k \mid X_i = s_l, Z_j = s_m\} \\ &= C \cdot P_r\{X_{i+1} = s_k \mid X_i = s_l\} \cdot P_r\{Z_{j+1} = s_k \mid Z_j = s_m\} \\ &= C \cdot p^h_{lk} \cdot p^v_{mk} \end{aligned} \quad (1)$$

$$C = (\sum_f p^x_{lf} \cdot p^z_{mf})^{-1}, f = 1, 2, \cdots, n \quad (2)$$

Where, C is a unitary parameter, which is defined as Figure 4.

Based on the theory of 2D Markov Process, the soil condition which is two type of soil in the same location by the method of fixed distance does not exist there (see Figure 4). Therefore, the unitary parameter of C is defined as formula (2).



Figure 5. Conditional 1D Markov Process.

Similarly, considering the 3D of soil transition in tunnel construction site, the space of soil transition condition is $S\{s_k \in S, k = 1, 2, \cdots, n\}$, the probability of certain location with soil type k in the space is defined based on the 3D model of Markov Process:

$$\begin{aligned} p_{lmq|k} &= P_r\{X_{i+1} = s_k, Y_{j+1} = s_k, Z_{r+1} \\ &= s_k \mid X_i = s_l, Y_j = s_m, Z_r = s_q\} \\ &= C \cdot P_r\{X_{i+1} = s_k \mid X_i = s_l\} \cdot P_r\{Y_{j+1} \\ &= s_k \mid Y_j = s_m\} \cdot P_r\{Z_{r+1} = s_k \mid Z_r = s_q\} \\ &= C \cdot p^x_{lk} \cdot p^y_{mk} \cdot p^z_{qk} \end{aligned} \quad (3)$$

$$C = (\sum_f p^x_{lf} \cdot p^y_{mf} \cdot p^y_{qf})^{-1}, f = 1, 2, \cdots, n \quad (4)$$

Therefore, if the soil boundary and borehole data are available by site investigation, the soil transition condition can be calculated by modified the 1D Markov Process into Multi-dimension Markov Process, and the uncertainty between different borehole is reduced to build the soil profile along tunnel alignment.

2.3 *The model of 1D conditional Markov Process*

It is known that the soil boreholes only provide the soil transition condition in vertical direction. It is difficult to get the information of soil transition in horizontal direction between two neighborhood boreholes. In order to solve the problem and improve the prediction veracity of soil transition, the 1D model of Markov Process is modified into conditional Markov Process.

Assuming the modified 1D model of Markov Model like Figure 5, the space of soil transition is $S_k, k = 1, 2, 3, \cdots N$, the white fields of soil transition means that the soil type in the certain location is clear, and grey fields are unknown to be determinated by the Markov Model. Therefore, the probability in grey location of soil type S_i is calculated as follows:

$$P_r(X_i = S_i \mid X_{i-1} = S_{i-1}, X_N = S_N) \quad (5)$$

$$\begin{aligned} &P_r(X_i = S_i \mid X_{i-1} = S_{i-1}, X_N = S_N) \\ &= \frac{P_r(X_{i-1} = S_{i-1}, X_i = S_i, X_N = S_N)}{P_r(X_{i-1} = S_{i-1}, X_N = S_N)} \end{aligned} \quad (6)$$

The formula (6) can be changed as through the theory of C-K equation in Markov Process.

$$\begin{aligned} &P_r(X_i = S_i \mid X_{i-1} = S_{i-1}, X_N = S_N) \\ &= \frac{P_r(X_N = S_N \mid X_i = S_i, X_{i-1} = S_{i-1}) \cdot P_r(X_{i-1} = S_{i-1}, X_i = S}{P_r(X_{i-1} = S_{i-1}, X_N = S_N)} \end{aligned} \quad (7)$$

Because the Markov Process is without aftereffect, then the formula (7) was changed to:

$$P_r(X_i = S_i \mid X_{i-1} = S_{i-1}, X_N = S_N) = \frac{P_r(X_N = S_N \mid X_i = S_i) \cdot P_r(X_{i-1} = S_{i-1}, X_i = S_i)}{P_r(X_{i-1} = S_{i-1}, X_N = S_N)} \quad (8)$$

Similarly, based on the theory of C-K equation and the character without aftereffect, the formula (8) can be simplified as:

$$P_r(X_i = S_i \mid X_{i-1} = S_{i-1}, X_N = S_N) = \frac{P_r(X_N = S_N \mid X_i = S_i) \cdot P_r(X_i = S_i \mid X_{i-1} = S_{i-1}) \cdot P_r(X_{i-1} = S_{i-1})}{P_r(X_N = S_N \mid X_{i-1} = S_{i-1}) \cdot P_r(X_{i-1} = S_{i-1})} \quad (9)$$

By the same way, the end calculation formula is got:

$$P_r(X_i = S_i \mid X_{i-1} = S_{i-1}, X_N = S_N) = \frac{p_{i,N}^{(N-i)} \cdot p_{(i-1),i}}{p_{(i-1),N}^{(N-i+1)}} \quad (10)$$

In the end, the probability of soil transition condition is calculated as:

$$p_{i-1,i|N} = \frac{p_{i,N}^{(N-i)} \cdot p_{(i-1),i}}{p_{(i-1),N}^{(N-i+1)}} \quad (11)$$

2.4 *The model of 2D conditional Markov model*

The vertical information of soil transition was explored by many borehole data of site investigation. The soil type of ground surface is also known through some geological survey. Therefore, the soil boundary condition in local field of construction site is clear. A new modeling algorithm to predict the soil transition between the boreholes along tunnel alignment can be established based on the above 2D model and 1D conditional model of Markov Process.

Assuming that the soil transition condition is 2D Markov Process, and the left-side, right-side and surface-side soil information is known after site investigation (see Figure 6), the space of soil transition is $S, \{s_k \in S, k = 1, 2, \cdots, n\}$, then the probability of soil type s_k in a certain location (i, j) between the boreholes can be calculated as follows:

$$\begin{aligned} p_{l,m\to k|q} &= P_r\{Z_{i,j} = s_k \mid Z_{i-1,j} = s_l, Z_{i,j-1} \\ &= s_m, Z_{N_x,j} = s_q\} = C' \cdot P_r\{Z_{i,j} = s_k \mid Z_{i-1,j} = s_l, Z_{N_x,j} = s_q\} \cdot \\ P_r\{Z_{i,j} &= s_k \mid Z_{i,j-1} = s_m\} = C' \cdot p_{lk|q}^x \cdot p_{mk}^z \end{aligned} \quad (12)$$

Where, C' is a unitary parameter, which is defined as:

$$C' = [\sum_f (p_{lf|q}^x \cdot p_{mf}^z)]^{-1}, f = 1, 2, \cdots, n \quad (13)$$

By using of the model of 1D conditional Markov process Model, the formula (14) can be established after the formula (10) is inputted in the formula (12).

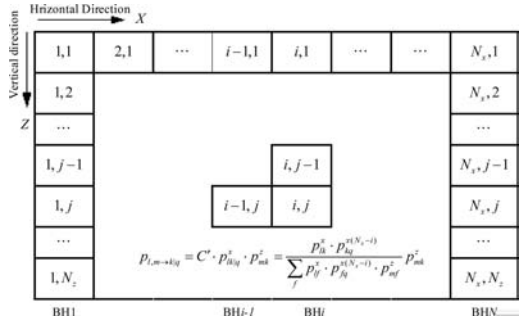


Figure 6. 2D conditional model of Markov Process.

$$p_{lk|q}^x = p_{i-1,i|N_x}^x = \frac{p_{kq}^{x(N_x-i)} \cdot p_{lk}^x}{p_{lq}^{x(N_x-i+1)}} \quad (14)$$

Therefore, the formula (15) is obtained based on the formula (13) and (14).

$$p_{l,m\to k|q} = C' \cdot p_{lk|q}^x \cdot p_{mk}^z = \frac{p_{lk}^x \cdot p_{kq}^{x(N_x-i)}}{\sum_f p_{lf}^x \cdot p_{fq}^{x(N_x-i)} \cdot p_{mf}^z} p_{mk}^z \quad (15)$$

$f = 1, 2, \cdots, n; k = 1, 2, \cdots, n$

In the end 2D conditional model of Markov Process is established to predict soil transition. It shows that the proposed new model can make use of all available borehole data and improve the precise of soil distribution prediction by adding more borehole data.

Three key probability matrixes, vertical soil transition matrix, horizontal soil transition matrix and surface soil transition matrix, are supported in the prediction of soil transition condition by using 2D conditional model of Markov Process. These three soil matrixes could be established by borehole data from site investigation (Qunfang Hu, 2006).

2.5 *The prediction and risk analysis of soil transition*

The 2D conditional model of Markov Process for predicting the soil type in tunneling is carried out by computer. The modeling algorithms were based on the method of Monte-Carlo (Huang Kezhong, Mao Shanpei, 1987).

Assuming that there were three different soil types in the site field, like soil type 1, soil type 2 and soil type 3. Firstly the key three soil transition matrixes is calculated, and the probabilities p_1, p_2, p_3 of those three different soil types in a certain location could

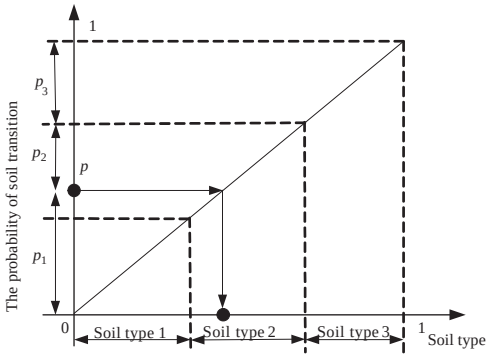


Figure 7. The simulation method based on the method of Monte-Carlo.

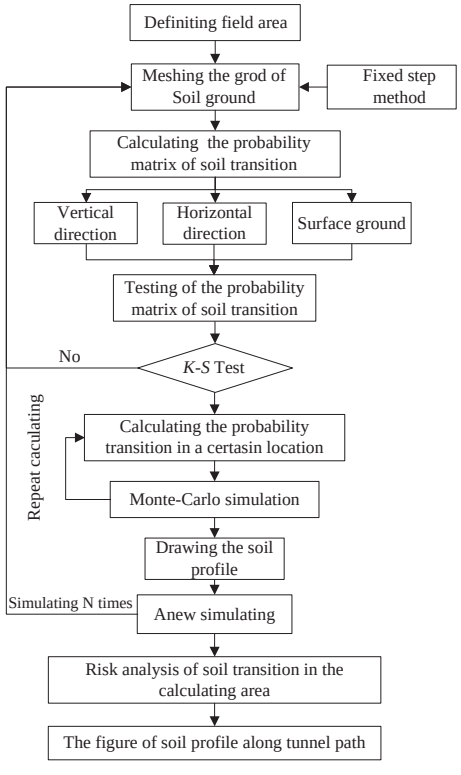


Figure 8. The simulation flow and calculation method for predicting soil transition condition.

be obtained by the 2D conditional model of Markov Process. Then three uniform numbers are produced by the method of Monte-Carlo. It can be seen that those different uniform numbers are represented by different soil type. Therefore the soil type in the certain location is decided (see Figure 7).

Up to now, the simulation method and calculation flow can be given as follows based on the 2D conditional model of Markov Process and the method of Monte-Carlo (see Figure 8).

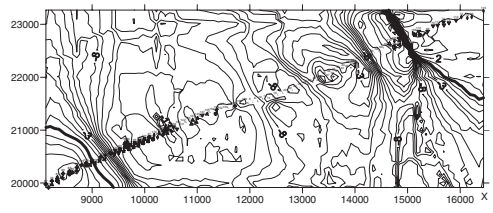


Figure 9. Borehole feature of Shanghai Yangtze River tunnel.

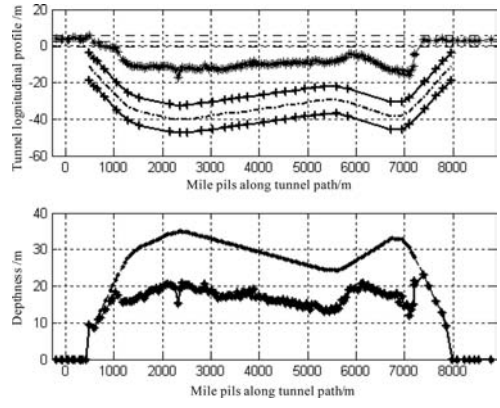


Figure 10. The depth and overburden thickness of Shanghai Yangtze River tunnel.

The simulation method was programmed by the software Matlab2006a (Yin Zheming, 2002). By using the 2D conditional model of Markov Process, the soil transition condition could be clear for drawing the soil profile along the tunnel alignment. The uncertainty between different boreholes is reduced for tunneling. Furthermore, if there are more new borehole data, the prediction precision can be easily increased by adding the new borehole information. So the new prediction model of soil transition is a good way for risk analysis the soil transition.

3 CASE STUDY

Yangtze River tunnel is the south crossing way from Pudong to Changxing island in Shanghai. This tunnel has a 7.5 km in length and 15 m in outside diameter. At present there are 164 geological drilling holes. The specific information of each hole along the axis is shown in Figure 9.

Based on the geological investigation information of Yangtze River tunnel and its longitudinal axis design, the vertical layout of the entire tunnel is shown in Figure 10. The up figure is the depth layout

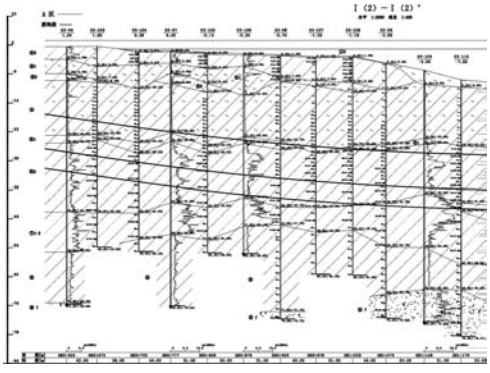


Figure 11. XK0 + 633∼XK1+179 soil layers probabilistic distribution by the method of linear interpolation and experience.

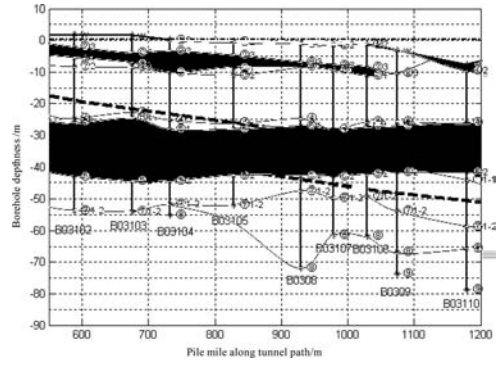


Figure 12. XK0+585∼XK1+180 soil layers probabilistic distribution by the 2D conditional Markov Model.

and the below one is the overburden thickness of tunnel.

Because the Yangtze River tunnel is very long, it is hard to have a one-time simulation. Here, we focus on the critical area using the conclusion of regional soil transition process analysis.

According to geological survey data, the authors draw the stratigraphic profile using linear interpolation in Figure 11. From this figure, we know the shield tunnel transverse ④, ⑤$_1$ and ⑤$_2$ layers in the local area and the soil types are complex comparatively. Especially in the XK0 + 800∼XK1+180 segments, the shield construction will transverse some composite soil layers. The ⑤$_1$ layer is grey clay with thin powder and a little shell chipping and has high compressibility, so the shield construction gesture control is difficult. As the shield launching, the cover soil layer is very thin and the least thickness is only about 8.69 m. Therefore, the construction risk is severely.

After adopting the 2D conditional Markov chain model process, the soil layers distribution from the numerical modeling is shown in Figure 12. Comparing Figure 11 with Figure 12, the soil layers distribution using model predicting is the same with that from the linear interpolation basically except the interlayer ⑤$_1$. However, the soil layer probabilistic distribution token by the stratigraphic profile is more in series and reliable than the general method.

4 CONCLUSIONS

Tunneling works are characterized by high degree of uncertainty. The geologic uncertain factor, here means soil transition condition, may have greater impaction on tunneling. Furthermore, because the boreholes driven for a tunnel construction project only can provide a handful of deterministic information at discrete locations either in the tunnel alignment itself or adjacent to the tunnel, it is necessary to establish a new method to improve the soil predication for tunnel engineering. Some conclusions were drawn in the paper.

(1) It is very essential to consider the uncertainty of soil transition condition which could lead to risk in tunneling work.
(2) The 2D conditional model of Markov Process is established based on the geostatistic theory and Markov Process, and this model can predict the soil transition.
(3) The case study shows the proposed prediction method of soil transition can reflect the adverse soil conditions for risk analysis.

ACKNOWLEDGEMENTS

This study was funded by the Program for New Century Excellent Talents in University under Education Ministry of China and Shanghai Municipal Science and Technology Commission (No.04dz12021), here great thanks should be given to them.

REFERENCES

Einstein H.H., (Vick SG 1984), Geological model for a tunnel cost model [J], Proceedings Rapid Excavation and Tunneling Conf, 2nd:1701–1720.

Isaaks, E.H., and Srivastava, R.M. 1989. Applied geostatistic. Oxford University Press [M], New York, N.Y.

Jingru, Hou & Zhennan, Yin., etc.1998. Practical Geostatistic (Spatial information statistics). Beijing: Geological Publishing House.

Kezhong, Huang & Shanpei, Mao. 1987. The theory of Probabilistic Method and Fuzzy Mathematics and its application. Shanghai: Tongji University Press.

Likhitruangsilp, V. & Ioannou, P.G. 2003. Stochastic evaluation of tunneling performance using discrete-event simulation. Contruction Research Congress, Winds of Change: Integration and Innovation in Construction, Proceedings of the Congress, 933–940.

Qunfang, Hu. 2006. Risk Analysis and Its Application for Tunnel Works based Research of Stratum and Soil Spatial Variability [D]. Dissertation of tongji university.

Ruwanpura, J.Y., AbouRizk, S.M., & Allouche, M. 2004. Analytical methods to reduce uncertainty in tunnel construction projects. Canadian Journal of Civil Engineering, 31(2), 345–360.

W.Schwarzacher. 1984. Sedimentation Models and Quantitative Stratigraphy. Beijing: Geological Publishing House.

Whitman, R.V. Evaluating calculated risk in Geotechnical engineering. Journal of Geotechnical Engineering, ASCE, 1984. 110(2): 145–188. Zhenfeng, Liu. 2004. The Use of MRF Model in Stochastic Reservoir Attribute Modelin [D]. Institute of Ggeology and Geophysics Chinese Academy of Sciences.

Zeming, Yin & Chunli, Ding. etc. 2002. Mastery the Software of MATLAB 6.Beijing: Tsinghua University Press.

This page intentionally left blank

Underground Space – the 4th Dimension of Metropolises – Barták, Hrdina, Romancov & Zlámal (eds)
© 2007 Taylor & Francis Group, London, ISBN 978-0-415-40807-3

Feasible Boulder treatment methods for soft ground shielded TBM

Warren Wangryul Jee & Sang-Gui Ha
Daehan Consultant, Co. Ltd., Seoul, South Korea

ABSTRACT: Boulder detection methods, treatments and its compensations are discussed with the geotechnical consideration of the boulder conditions in soft ground tunneling by shielded TBM. The prior objective of this topic is to overcome the existing problems to excavate the boulder rich deposits by the EPB shield, or slurry shield in downtown areas. There are three phases of this research work including the boulder detection technology during the design and construction stages of the tunneling projects, secondly developing the appropriate boulder treatment methods at the tunnel site depending on the geological and hydro geological conditions including with dimension issues, and compensation for boulder obstruction removal or weight is not practical for most tunneling situation, but compensation by crew time, is probably for the optimal design modification of the existing EPB shield, and slurry shield TBM to minimize the boulder cutting problems in soft ground. If boulders are anticipated on tunnel project at the design stage, boulder removal plan must be considered with proper equipment selection to handle it easy way.

1 INTRODUCTION

As the number of urban tunneling projects are increased within a soft ground, more and more of difficulties lies to overcome the boulder treatments during the tunnel excavation. This paper covers the major considerations to detect the boulders and existing treatment methods that influence the design and construction of soft ground tunnels which could be excavated by mechanized tunneling machine like EPB shielded TBM or slurry shielded TBM. The objective of this paper is to establish an knowledge of boulders and study the boulder detection technologies and its optimal treatment methods to suggest the developing requirements of the strong shielded TBM to excavate the tunnels in the complex geological conditions.

There are three phases of this research work including the boulder detection technology during the design and construction stages of the tunneling projects, secondly developing the appropriate boulder treatment methods at the tunnel site depending on the geological and hydro geological conditions including with dimension issues, and compensation for boulder obstruction removal or weight is not practical for most tunneling situation, but compensation by crew time, is probably for the optimal design modification of the existing EPB shield, and slurry shield TBM to minimize the boulder cutting problems in soft ground. If boulders are anticipated on tunnel project at the design stage, boulder removal plan must be considered with proper equipment selection to handle it easy way.

Boulders are justified as big dimensional rocks compared with the cobbles, and the gravels, but its real scales are much smaller than the bed rocks which are developed at the construction sites. Therefore, it is not easy to find them along the given alignment of roadway, and railroads during the design and construction stages through the direct boulder detection. However, if the designers find some information related to the possible existence of boulders in a certain geological layers, then, they could better to perform the geophysical exploration and doing the face mapping focusing on the boulder detection during the tunneling works.

2 BOULDER DETECTION TECHNOLOGY

2.1 *Origins of boulders*

In general, boulders are defined as solid objects larger than 300 mm (one foot), which is defined significantly stronger than the surrounding ground. Boulders are typically a part of rock blocks of various origins and sometimes carried to the site by stream works, or natural falls from the mountain sides, or frequently transported by glaciers, and often they including the man-made solid materials, too.

Boulders are commonly found in river beds, glacial tills, and at the bottom of slopes. Another source of boulders is the bedrock itself as a core stones. For example, Doublin boulder clay is a glacial till which overlies the bedrocks.



Figure 1. Boulders collected during the geotechnical investigations.



Figure 2. Full face shielded TBM.

In practice, the hard boulder would neither break up nor pass through spoil holes on either side of the discs, which forced loose boulders to slip sideways off the edge of the head where they encouraged over-break and made the machine difficult to maneuver. Removing calibration bars from across the spoil holes eased the problem. In addition, plans are being considered to grout from the surface and further bouldered areas along the route to hold the boulders firm so that improved cutters can break them down.

2.2 *Geotechnical investigations of boulder detections*

Normally, the aim of geological and geotechnical investigations is to characterize the natural environment in which an underground structure is intended to be built. The results of such studies form the basis for decisions concerning the general construction method, the specific design of the underground structure as well as for numerical analysis. By means of borehole drilling, the excavation of test pits, geophysical probing and other field methods to geological situation in the project area is classified.

All characteristics which will be encountered during tunnel construction have to be identified, including their spatial relation and the extent of geological boundaries. Furthermore, field or laboratory tests have to be applied to determine the geotechnical properties of the rock or soils. For tunneling projects the following parameters are needed (Table. 1).

Where the soft ground tunnels in urban area will be excavated with a shielded TBM , then, the mineral content and the abrasively of the penetrated soil and rock

Table 1. Required geotechnical parameters for the tunneling project.

Materials	Geotechnical parameters
Rock & Soil	Specific weight Poisson number Permeability Stiffness parameters (Deformation modulus, elasticity) Strength parameters (Friction angle, Cohesion)
Rocks	Mineral content Abrasivity Hardness
Soils	Grain size distribution Water content Plasticity Density
Ground water	Chemistry Flow direction & Velocity

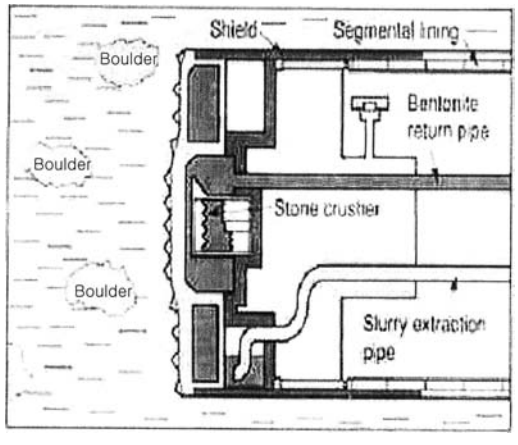


Figure 3. Problems of boulders at the tunnel face.

layers are very important. General site geotechnical investigations are:

– Core drilling (Sampling)
– Geophysics
– General geological pictures
– Geophone (Sonar or seismic systems)

The Geological character of boulder deposits and probability of encountering boulders should be assessed. Hunter and Angulo, 1999 suggested six boulder occurrence characteristics that should be investigated by a subsurface investigation.

– Frequency
– Distribution
– Sizes
– Shapes
– Rock composition
– Matrix soil composition

2.3 *Problems of existing geotechnical investigations*

Due to the small drilling diameter (NX: 76 mm) and the flushing method it is impossible to define the exact composition of boulder, gravel, and cobble layers. The problems are in particular with respect to the choice and operation of the shielded TBM should be considered. Also the other question, whether the jet grouting technique is applicable largely depends on the exact composition of sand / gravel / cobble / boulder layers for the effective pre-reinforcement to increase the face stability. Every soft ground tunnel projects have a crucial question which is whether boulders have to be expected during tunnel excavation or not. When the boulders spread in sedimentary layers, however, are difficult detect by drilling. Due to its implications on shielded TBM design and operation the position is of special interest.

Seismic tomography and seismic sounding from the surface are definitely good method to trace the bedrock boundary, in particular since there seems to be a distinct physical contrast between the sound bedrock and its cover.

2.4 *Boulder detection at the design stages*

For soft ground tunnels, key investigations are focused on the boulder distributions and the groundwater conditions along the designed alignment.

If the boulders are presented in the soft soils, and rocks,

1. Boulders can be the resistive target around the electrically conductive conditions.
2. Elastically, boulders can be the locally high velocity anomaly in the low velocity zones.
3. Response to the radar waves, boulders have a different electromagnetic property like as electric conductivity, magnetic susceptibility, dielectric constant, etc., with the surrounding materials, and boulders have a unique reflection to the radar waves.



Figure 4. Geologger-3 is a multi-purpose field data logger.

It is supposed to be able to use the electrical resistant exploration, the seismic exploration, and the ground penetration radar (GPR) methods to detect the boulders. Some of the possible methods are suggested the electric resistivity tomography (ERT), surface seismic reflection survey, and GPR methods in practice.

But, the depth of exploration target is deeper, the ERT and seismic survey have a difficult by the shortage of analysis limits, and the GPR has a low detect ability by way of reduction of penetration energy.

Therefore, ERT and seismic surveys are available in the target depth range between 20 and 30 m. However, GPR method has accuracy from 5 to 10 m range of the target depth.

Normally, ERT and seismic refraction methods along the alignment are carried out to detect the boulders in the massive hard rocks, after they get the results of analysis to classify the geological layers like soils/ soft rocks, then they can do the more accurate survey at the suspicious area by the 3-D exploration, geotomography, or core drill works. Geotomography can be achieved by the seismic wave, electrical resistance, and Geo-radar.

2.5 *Boulder detection at the construction stages*

2.5.1 *Seismic reflection methods in tunnels*

Seismic reflection method in tunnel TRT method by NSA in Colorado, HSP, and TSP method by Amberg in Switzerland are famous commercial code for this survey ways in underground space during tunneling to take the source by the small blasting or noise generated by rock breaker through the tunnel excavation. Through the source which is generated by the tunnel excavation, and collect the reflect signals from the

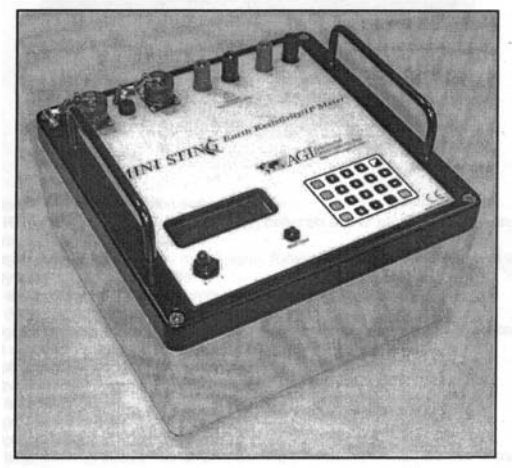


Figure 5. New geophysical electrical resistivity instrument.

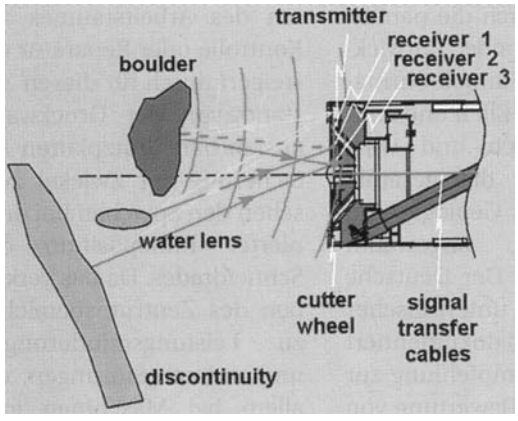


Figure 6. Boulder detection by sonic system.

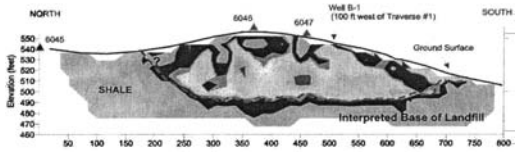


Figure 7. The results of geophysical resistivity and its images.

front face discontinuities like faults, fracture zones, cavity, and boulders, to detect the position of those through the analysis of the reflected data. However, the accuracy of this method is measured very low, because of the data receiving system in the underground conditions, because of the shortage coverage of the cross-hole tomography.

Especially, boulders have a very small scaled anomaly compared with its wave length, which acts the very small reflection signals, therefore, this method only have a possibility to find the boulders in the 5 m distance from the working faces.

2.5.2 *GPR survey*

In general, GPR survey has a limited survey range in soil layers less 5 m distance, but this method is very simple and cheap method, they can use it every tunneling working face to guess the frontal geological conditions at the working face. However, it can not cover the above area of the working face, only possible to discover the just parallel front area from the working site, sometimes, with this survey system mistake to search the boulders above the working faces cause the fatal dangers.

2.5.3 *Pilot core drilling method*

This is the reasonable method to check the existence of boulders by the parallel core drill works in the expected boulder reserved area.

2.5.4 *Special geophysical probe system*

The variation of soil materials will be much easier to predict with a forward looking geophysical technique. A possible method is seismic prospection in soft ground which is currently used in EPB and slurry shield machines. The description of a system, which has been used with success, is presented below:

The sonic soft ground probing system continuously monitors the soil formation ahead of the tunnel face. It is permanently installed in the cutter wheel of the shield machine. This device serves to perform the following.

- To classify soft ground in terms of strength, homogeneity and other physical characteristics.
- To localize and define planar discontinuities ahead of the cutting wheel. Planar discontinuities can be distinct changes between geological formations, for instance from soil to rock, or fault zones.
- To detect and localize irregular bodies and obstacles within a range of about 50 m ahead of the tunnel face.

This sonic system provides the results immediately after the measurement, such that appropriate tunnel construction measures can be adopted before zones of potential problems are excavated.

3 BOULDER TREATMENT METHODS

3.1 *Possible removal methods*

Boulders might be handled during tunneling by one or more of the following methods.

- Removal boulders from the outside of shielded TBM

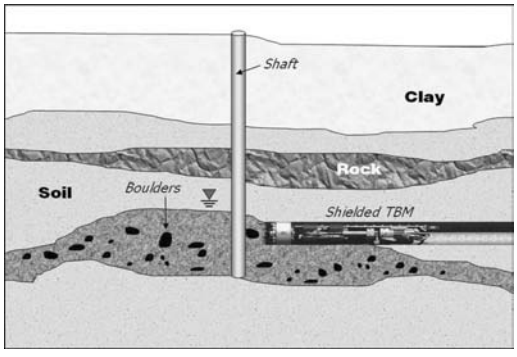


Figure 8. TBM pushing the boulder into a temporary access shaft.

– Piece removal boulders through shielded TBM after fracturing
– Intact removal through shielded TBM
– Pushing aside by shielded TBM

3.2 *Removal boulders from outside shielded TBM*

When a boulder obstruction is encountered with a microtunnelling TBM that is not equipped with rock cutters and boulder is too large for crushers, the obstruction has to be removed from outside of the TBM. The following options might be considered.

– Removal from a temporary access shaft or cross passage tunnel
– Pushing into a drilled hole
– Drilling & Blast

If the boulder is within a granular aquifer, dewatering or grouting will likely be required to maintain stability. After boulder removal, tunneling can resume without trouble.

3.3 *Piece removal boulders through shielded TBM after fracturing*

Boulders can be fractured and ingested by one of three methods.

– Crushing within the plenum
– Cutter fracturing at the heading
– Mechanical splitting through openings

3.4 *Intact removal through shielded TBM*

Boulders can be ingested intact or mostly intact when the openings at the heading are large enough for boulders to pass through. The boulder size that may pass through the heading openings depends on the size and shape of both the boulder and openings. Smooth, spherical boulders will generally pass through cutting wheel openings more readily than oblong and angular boulders. Oblong and angular boulders are more likely to become stuck in an opening or roll around in front of the heading until fractured. Most rotary cutting wheel TBMs are able to ingest boulders with sizes smaller than 15 to 30 percent of the excavated diameter.

3.5 *Pushing aside by shielded TBM*

Boulder might be pushed aside before being fractured or ingested. To be pushed aside, requires mining with a partially closed face TBM through soil that is sufficiently soft or loose to allow boulder penetration into the soil in response to the forces being applied to the heading. Boulders encountered within weak or loose soil that are not pushed aside and are too big to be ingested are likely to roll around in front of the cutters or to become lodged in a cutting wheel door.

4 COMPENSATION METHODS FOR BOULDER OBSTRUCTION

4.1 *Compensation by boulder number encountered*

A simple method of boulder obstruction compensation is payment at a unit rate per obstruction that is bid. This method would provide the same payment for removal of small boulder obstructions that might be split with one blast taking 15 minutes of time as a big boulder obstruction requiring several blasts and over an hour of time. It would also pay the same whether or not the boulder is within a wet sand matrix that must be dewatered or grouted for stability as within a stable cemented granular soil or stiff cohesive soil. Uncertainties such as these will likely lead to contingencies in the bid price.

4.2 *Compensation by boulder size*

Payment based on boulder size may be a more equitable method but requires size measurement. Size measurement is often difficult as previously discussed. The measurement method should be carefully defined to avoid disputes.

One use of payment by size is to avoid payment for boulders anticipated to be small enough to pass through the cutting wheel doors and mucking system. This size might be defined as 20 percent of the excavated tunnel diameter or smaller.

Another option is categorize boulders into two or three size ranges and to pay at bid rates for quantities of each size encountered. This approach may be more equitable and reduce contingencies needed to cover the potential cost of removing very large boulders.

4.3 *Compensation by boulder volume*

The volume method of compensation is not considered viable with most tunneling methods, particularly those where boulders are fractured with cutters or split through cutting wheel doors. It may be a viable method when tunneling with a shield or digger shield where

whole boulders or fragments may be readily removed from the tunnel and sorted for measurement. However, determining boulder volume accurately is not easy. Boulders have irregular shapes that allow only an approximate boulder volume to be calculated based on dimensions. Perhaps the only accurate method of measurement would be to suspend boulders into a tank of water and computed their volume base on increased height of the water.

4.4 *Compensation by boulder weight*

Boulder obstruction removal compensation by weight of boulders removed has been used on some projects and should be easier to measure than volume. The payment item could be limited to boulders greater than a selected weight or size. Bids could also be taken for ranges of weights to allow contractors to bid more for removal of large boulders.

With this method, the contractor must segregate and stockpile boulders and qualifying boulder fragments. However, separating, stockpiling and weighing qualifying boulders is additional work that may not be practical for many projects, particularly where most boulders will be fractured rather than excavated whole or in large pieces.

4.5 *Compensation by crew time to remove boulders*

Payment for boulder obstruction removal by TBM crew hours should be an equitable method of compensation, provided that an obstruction event and qualifying removal work are clearly defined. Mason, Berry & Hatem, 1999 provide a thorough discussion of issues associated with payment for obstruction removal by crew hours. Key aspects of the method include:

- The contract should indicate the various anticipated potential obstructions and anticipated obstruction locations.
- Obstructions to tunneling progress might be defined with a time limit.
- The contractor should be required to provide immediate notification to the resident engineer when an obstruction event has occurred.
- The means and methods of boulder removal not be specified, but left to the contractor.
- Crew hours for obstruction removal should be estimated, baselined and included as a bid item quantity.
- The contract should indicate that crew time unit prices will apply to quantities within a range such as ± 25 percent.
- Mason, Berry & Hatem, 1999 recommend not allowing obstruction removal time to impact the schedule unless the time exceeds 125 percent of the baselined removal time.

5 CONCLUSIONS

1. The GPR method is not possible to be equipped with TBM, and pilot boring system requires to install the special equipment to work on the TBM at the site. Seismic reflection method inside the tunnel will not disturb the TBM operation, but it will take long times to the installation of the measuring system at the site, and also requires to ask the expensive analysis cost with the involvement of specialist.
2. With the present status of arts, there are no confidential survey methods for the boulder detection with reasonable cost, and it is hard to guess that the reasonable boulder detection could not be able to be developed in a near future.
3. The modified pilot boring system like LIM system will be more attractive to develop the boulder detection systems during the tunnel excavation for the tunnel contractor to increase the better operation rate of TBM machines.
4. Compensation for boulder obstruction removal by crew time is probably the most equitable method of those considered.
5. When boulders are spread at the tunnel face, tunnel advance should be halt, and creating very expensive delays, and result in the construction claims. Cutters need to break the boulders too large to fit into the machine mucking system. It is necessary that tunnel engineer try to find the general boulder cutters extremely effective to treat boulder cut.

REFERENCES

W. Jee, Technical Report of Seoul Metro Line Number 9, Construction Lot 9-9, April, 2001, Seoul, Korea

W. Jee, Design of the Slurry Type Shielded TBM to Excavate the Alluvial Strata in Downtown Area, 2001 International Symposium on Application of Geosystem Engineering, October, 18–19, 2002, Seoul, Korea

Tunnelbautechnischer Bericht (Technical report of tunneling, railway tunnel in Berlin)

Unterirdisches Bauen in Deutschland (Underground Construction in Germany) 2000

Mano Walis, Suitability of Mechanized Tunneling in Various Ground Conditions, Proceedings of Symposium on the Mechanized Tunneling Techniques, Sep 2001, Korea Tunneling Association

M. Goss, Finite Element Modeling of Boulder Excavation in Soft Ground Tunneling by Earth Pressure Balance and Slurry Machines Using Disc Roller Cutters. Ph. D Thesis, CSM, 2000

S. W. Hong, Engineering Geology in Geotechnical Failure. Proceeding of 2002 ISRM Regional Symposium July, 2002, Seoul, Korea

Warren Jee & Sang-Gui Ha, Boulder Detection Methods and its Compensation for Obstruction in Soft Ground Tunnels by Shielded TBM, Journal of the Korean Society for Railway, No.1, Vol.9, pp.110–117, March, 2006, Seoul, Korea

Underground Space – the 4th Dimension of Metropolises – Barták, Hrdina, Romancov & Zlámal (eds)
© 2007 Taylor & Francis Group, London, ISBN 978-0-415-40807-3

Reasons of swelling of Miocene clays near Třebovice in Bohemia

F. Kresta
Stavební geologie – Geotechnika a.s., branch Ostrava

ABSTRACT: Track section Třebovice – Rudoltice on the border between Bohemia and Moravia and European watershed is one of the most complicated sections in Czech republic. Main difficulties in that area result from expansive clays with high plasticity. Swelling of these clays caused destruction of the Třebovice tunnel built in 1842–1845. This tunnel was restored after great difficulties in 1932. Reasons of swelling were not completely known just at the beginning of construction works on the re-alignment in 2004. Detailed mineralogical analysis has confirmed a hypothesis that swelling of Miocene is caused mainly by the dispersed coal matter content. Organic matter initialises the swelling.

1 INTRODUCTION

Track section Třebovice – Rudoltice on the border between Bohemia and Moravia and European watershed is one of the most complicated sections in Czech republic. Main difficulties in that area result from expansive clays with high plasticity. Swelling of these clays caused destruction of the Třebovice tunnel built in 1842–1845.

The Třebovice tunnel was built in 1842–1845. Constructors in that time had no experiences with tunnelling in expansive plastic clays. Therefore Negrelli, main designer of railways in Austria, proposed to build open cut instead of a tunnel or to build cut-and-cover tunnel. Austrian railways did not accept these proposals and the first tunnel in Bohemia was built by German coring method. Tunnel was finished in 1845 after great difficulties resulting from expansive clays with high plasticity and water coming from saturated sand lenses inside the clay mass and saturated sand layers above clays. Expected costs (188000 guldens) increased more than six times over 1 mil. guldens. Swelling of these clays caused destruction of the lining and in 1866 tunnel was closed.

In 1866 a new track was built that followed the surface, however, with worse track gradient (9.5‰). That was the reason for reconstruction of the closed tunnel. Tunnel was restored after great difficulties in 1932 (advance in digging per round was only 5–30 mm). New lining from granite blocks was placed to the old one from sandstone. Restored tunnel has been operated since that time till 6.4.2005 when the last train came through it.

Modernisation of railway track in that area was solved by re-alignment of existing tracks. Crossing through the soils with the worst mechanical properties (highly plastic expansive clays) was designed as double-track tunnel built by diaphragm walls with invert. However, contractor in tender proposal suggested to build an open cut and proclaimed significant reduction of costs (approx. 10 MEUR). This solution was accepted and constructed. One-track operation started in 2.8.2005, track No. 2 was opened in 18.10.2005.

2 GEOLOGICAL SITUATION, LITHOLOGY AND LITHOFACIES OF MIOCENE SEDIMENTS

The area is located in the Miocene fill of the Ústí – Česká Třebová trench near the elevation of the Třebovice walls and the Hřebeč edge where it is crosses with the transversal trench Třebovice – Damníkov that communicated with the Lanškroun trench (existing watershed). Miocene sediments in the Ústí – Česká Třebová trench near Třebovice are formed by the Lower Baden clays that are overlapped on the Lower Turonian marls, Ca-spiculites and sandstones. The Upper Cretaceous rocks formed the Třebovice walls and the Hřebeč edge.

Thickness of the Miocene fill reaches up to 170 m. A part of Miocene sediments was eroded (approx. 100+/−30 m). Miocene sediments are formed by marine clays (highly plastic clays stiff to very stiff). In the Eastern part of the area they contain intercalations of sands with terrigenous clasts and re-deposited wooden material. This indicates communication with the Lanškroun trench with fresh and brackish sedimentation with typical coarse-grained sediments. The right stratigraphic position of the Miocene sediments within the Lower Baden complex is not known due to

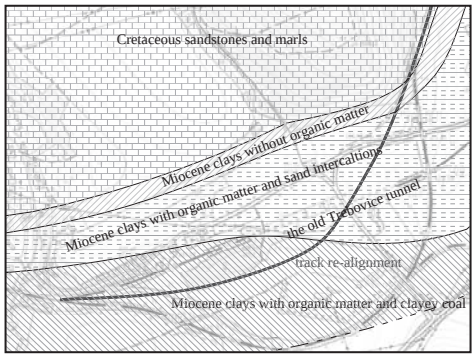


Figure 1. Lithofacies of the Miocene sediments above the level of 420 m above the sea level.

a lack of detailed paleontological data. Lithofacies of the Miocene sediments above the level of 420 m above the sea level are presented in figure 1.

From the geotechnical point of view the most important area contains clays with organic matter. The second factor influencing mechanical properties of clays is the Quaternary weathering crust (a zone of the hypergenous alteration). The depth of the alteration depends on the paleorelief, the erosion history and profile lithology. It however reflects in rock composition (removing off calcite), susceptibility to swelling, etc.

2.1 *Petrography and mineralogy of Miocene clays*

Clays are grey-green, highly plastic, in dry conditions lightly green-grey, very stiff just with conchoidal fracture and contract cracks. They contain variable amount of sand and organic matter. Matrix is clayey (illit-kaolinitic, with variable amount of authigenous montmorillonite). Clasts are formed by sandy grains under 1 mm.

Allochtonous, detritic coal matter represents also a clay component Presence of lens shape clayey sands in clay complex allow us to define this sedimentary milieu as distal proto deltas sediments (in sense Einsele 1992).

2.2 *Clay matter in clays and sands*

Flaky clay particles forming the matrix have not got stable mineralogical composition. A core of primary detritic mica flake is formed by very argillised mica (1.0 nm), continually it is originated a cover from authigenous illite (1 nm), eventually illite-Ca-montmorillonite. Terrigenous clay mineral is represented by kaolinite.

Clay matter in fraction 0.063–0.005 mm as it is presented in grain size tests and in electron microscope snaps (see fig. 2) is formed by agglomerates of particles bounded by cement and authigenous clay

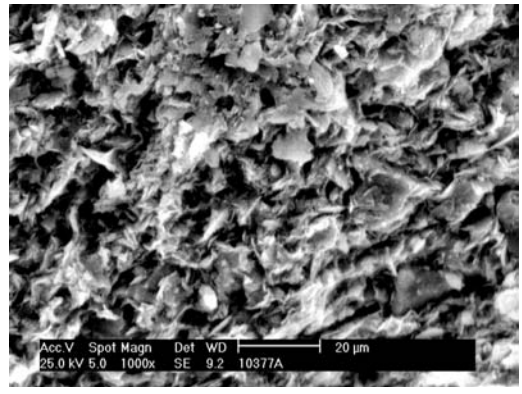


Figure 2. Light grey-greenish clay (illitic type) (borehole VI-1, depth of 11.8–12.0 m). Chaotic flakes of clay matter (illite predominates) and very small angular clasts compose clay matrix. SCAN, metal coated, enlargement on scale (20 µm).

matter and soft clasts. They represent 20–30% of total volume. The rest is formed by clay matter with particles under 0.005 mm.

Dominant mineralogical associations in clays are as follows:

- a clast part is formed by quartz, feldspar and clast muscovite
- cement is formed by authigenous carbonate – calcite. A carbonate content increases with depth under the erosion boundary Quaternary – Miocene
- clay matter is represented by association: (**illite + mica 1.0 nm $\gg$ kaolinite $>$chlorite $\pm$ Ca- smectite (montmorillonite or chlorite 1.38 nm)**, in temperature of 550°C :**(illite + mica) − chlorite − smectite (?).**)

2.3 *Organic matter and humic material in clays*

Coal matter is re-deposited and detritic, washed especially to the foreland of the distal fan of terrigenous floating sediments to the trench formed by clays and sands. Coal matter is formed by unsorted wooden and plant detrite with carbonisation corresponding to lignite. Although coal matter sedimented in marine water milieu it contains high share of extracted humic materials that in interaction and through authigenous clay matter influence local clay properties.

It is not allochtonous sediment (i.e. peat bog), however allochtonous coal matter that was more or less transformed by transport (oxidation, sorption) and more carbonised to the lignite stage in place of sedimentation. Humic materials were not changed. Their partial oxidation is not possible exclude. A transformation of coal matter during the transport was supported either by infrared spectra, either by the presence of oxidized resin of the amber type – valchovite in coal.

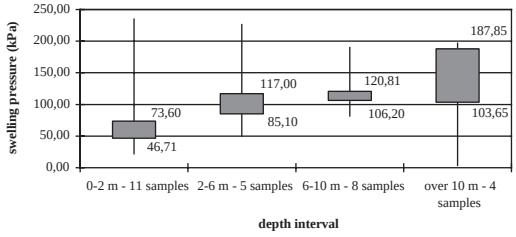


Figure 3. Robust analysis – dependence of swelling pressure on the depth of samples (distance from Quaternary – Miocene boundary).

Ca-humite complexes originated on the contact of the clay and organic matters.

3 GEOTECHNICAL PROPERTIES OF MIOCENE CLAYS

Miocene clays with high plasticity (CV, CE) represent the most important geotechnical hazard. Expansive clays caused great difficulties during construction of existing tunnel in 19th century and they complicated its reconstruction in 20th century too.

Miocene clays were tested by the wide set of laboratory tests (Kresta – Sekyra 2002), Kresta 2003a, Kresta 2003b).

Swelling of Miocene clays was solved individually. Statistical analysis used also results of previous laboratory tests (Pavlík 1998, Tomášek et al. 1998, Dudík 2001).

Detail observation of swelling process showed that start of volume changes begins firstly on the contact of clay matter and cola matter accumulation, i.e. in places with Ca-complexes of humic matter.

Linear swelling of Miocene clays achieve values up to 25% (median from 45 samples was 5%); the maximum value of swelling pressure was 276 kPa (median from 28 samples was 111 kPa.). Robust statistic analysis was used to identify any dependence of linear swelling and swelling pressures on the depth of sampling. The depth was taken as the distance of sample from the boundary between Quaternary and Miocene soils. Results are presented in figure 3 by box-and-whiskers diagrams.

In case of linear swelling no significant dependence of the distance of samples from the Quaternary – Miocene boundary was proven. Values of swelling pressure increase with distance from boundary of Quaternary sediments and Miocene clays. Correlation coefficient of linear regression is 0.57.

Swelling of clays is a long-term process as it is evident from laboratory tests of volume changes in time. Shape of all curves is similar and resembles de-consolidation curve, however stabilisation of deformations is very slow (see fig. 4).

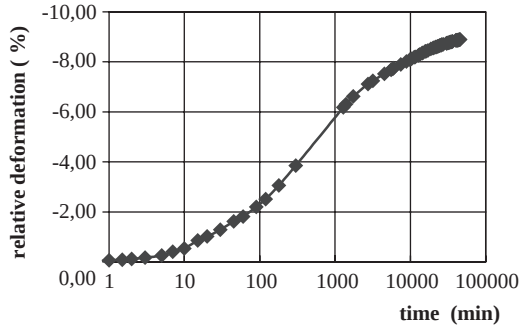


Figure 4. Relative deformations of Miocene clays depending on time (J207, depth 11.7–11.9 m).

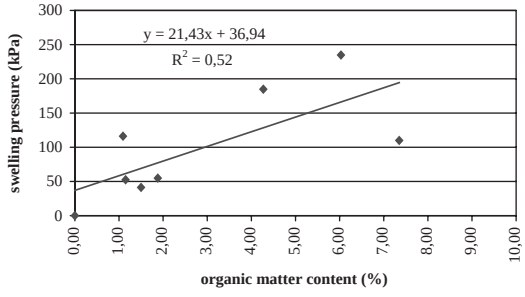


Figure 5. Dependence of values of swelling pressure on the content of organic matter.

It is mainly organic matter dispersed inside the clay matrix that causes swelling of them. The organic matter content is 4–7%, maximally 12%. Values of swelling pressure increase with increasing content of organic matter (see fig. 5) although the correlation coefficient is only 0.52.

4 CONCLUSIONS

The old Třebovice tunnel damaged by swelling of Miocene clays was in 6.4.2005 closed. In the area of its crossing with the track re-alignment it was filled by the fly-ash-cement mixture. The rest of the tunnel will be filled by soils excavated from the construction place. Unique construction documenting the fight between man and nature that was after many problems successful finished its existence.

A track re-alignment leads in deep cuts and short cut-and-cover tunnel. Cut and tunnel walls were protected by diaphragm walls with invert.

During construction of the track re-alignment great size monitoring were carried out. Fortunately, no deformations caused by volume changes of Miocene clays under the bottom of tunnel and in lower parts of cuts were observed (Kresta – Sloboda 2005).

The presence of humic matter bounded as Ca-humic complexes of organic matter is a principal reason of Miocene clays swelling.

Construction of track re-alignment coming through the area with complicated geotechnical conditions was finished in 18.10.2005. I hope that its destiny will not be so dramatic as in case of the old and now liquidated Třebovice tunnel.

REFERENCES

Borovský, K. 1994. The Třebovice tunnel in track Olomouc – Prague. *Tunne*l, vol. 25, No. 1, 25–27 pp. (in Czech).

Dudík, F. 2001. Modernisation of the track section Krasíkov – Česká Třebová. New Třebovice tunnel, detailed geotechnical survey. *MS GeoTec GS Prague* (in Czech).

Jefferson, I., Murray, E.J., Faragher, E., Fleming, P.R. 2001. Problematic soils. – Thomas Telford Publishing London.

Kresta, F. & Sekyra, Z. 2002. Modernisation of track section Krasíkov – Česká Třebová, Analysis of geotechnical hazards during construction of cut in km 7.330–8.210. *MS Stavební geologie – Geotechnika a.s.* (in Czech).

Kresta, F. 2003a. Re-alignment of railway track Třebovice – Rudoltice (Czech republic), tunnel or open cut, analysis of geotechnical hazards. *Railway Engineering 2003*, London.

Kresta F. 2003b. Modernisation of track section Krasíkov – Česká Třebová, additional geotechnical survey of re-alignment in km 7.330–8.210. *MS Stavební geologie – Geotechnika a.s.* (in Czech).

Kresta, F. 2004. Expansive clays in track subgrade in deep cut (section Třebovice – Rudoltice, Czech republic). *Railway Engineering 2004*, London.

Kresta, F. 2005. Geotechnical hazards of the deep cut and tunnel construction in re-alignment of the Třebovice – Rudoltice track. *Proceedings of the conference Railway bridges and tunnels*, Prague (in Czech).

Kresta, F. & Sloboda, J. 2005. Modernisation of the track section Krasíkov – Česká Třebová. Realignment of track between Třebovice – Rudoltice. Final report of monitoring. *MS Stavební geologie – Geotechnika a.s.* (in Czech).

Martinec, P. et al. 2003. Mineralogical, petrographical and chemical study of desensibiliation of clays from Třebovice. *MS Geonics Institute of Czech Academy* (in Czech).

Martinec, P. et al. 2005. Mineralogical analysis of Miocene clays with high organic matter content in cut of railway track in the Třebovice – Rudoltice area. *MS Geonics Institute of Czech Academy* (in Czech).

Lambe, W. T. & Whitman, R. V. 1976. Soil Mechanics. *Wiley Eastern*, New Delhi.

Pavlík, J. 1998. Geotechnical and construction survey of the Třebovice tunnel. *MS Geotest Brno* (in Czech).

Tomášek, J. et al. 1996. Modernisation of the track section Krasíkov – Česká Třebová., final report of geological survey of the track. *MS SGS Prague* (in Czech).

Underground Space – the 4th Dimension of Metropolises – Barták, Hrdina, Romancov & Zlámal (eds)
© 2007 Taylor & Francis Group, London, ISBN 978-0-415-40807-3

Geophysics method used to recognize the boundary between different deposits

R. Kuszyk & M. Superczyńska
Warsaw Uniwersity of Technology, Warsaw, Poland

ABSTRACT: The Warsaw underground line is situated in glacial and pliocen deposits which have quite different geotechnical parameters. Additionally some of those deposits were extrenally distributed during quaternary glaciations. In spite of underground tunnel construction, deep dewatering and possible surface displacements it is very important to clearly specify how proceed the boundary between two different kinds of soil. In some cases the geophysical research is very helpful to recognize this blurred boundary in Warsaw. The authors would like to present one of the example of such research and present also general soil parameters used to design tunnel construction in Warsaw.

1 INTRODUCTION

Geophysics method was used on north part of first Warsaw underground line to localize the boundary between two different kinds of deposits – tertiary clay formation and quaternary sandy river valley. The target was to localize the slope of pliocen clay elevation which strongly subside in the direction of local, deep interglacial period sandy valley full of underground water. It was important because of decision where should finish diaphragm wall tunnel and start shield tunnel. The geophysical research also discovered potencial areas of soil pads in pliocene clay characterize by different geotechnical parameters.

2 GEOLOGY AND GEOTECHNICS

2.1 *Tertiary clay*

In central Poland, in region of Warsaw and its surrounding the Poznań Formation has developed as a clay – soil strongly overconsolidated in a result of complicated geological history. These clay often appears as a soil foundation for high buildings and underground construction. Soil shows the anisotropy features resulting of anisotropy of structure or anisotropy of state tension features. It is the effect of sedimentation as well as geotechnical processes, which soil was subjected in its geological history.

The sedimentation of clay began 13 millions years ago, in central Miocene, and it lasted 9 millions years. The processes of soil erosion connected with forming the river net as well as glacitectonic effects on this region appeared afterwards. It led to coming into existence folding and dislocations in mass of clay. The decompression, erosion and weathering processes followed.

Warsaw area clays lie under Quaternary deposits. The thickness of Pliocen Formation in Warsaw is in range for several metres to 150, however its original thickness is 100–140 m.

Piocen formation include compact clay and sandy clay with fine sand and dusty sand formed lenses inside clay.

In many places in Warsaw the clay formation exists on the surface of the tarraine. This situation take place in the edge of the Vistula valley slope on the left side of the river or under thin cover of quaternary deposit.

There are numerous depressions and elevation on NNW-SSE direction in tertiary clay formation (after glacitectonics and erosion processes). The average thickness of tertiary deposits is 50 meters, and its differences reach 100 m. The biggest and the highest is downtown elevation of altitude about 100–113 m over see level. In elevation the roof of pliocen deposits is secondarly uplifted by glacitectonic process. Original, sedimented surface of the pliocen roof reached the altitude 60–80 m over see level. Present roof surface of the pliocen formation was formed by glacitectonic process during three glaciations and next cut by rivers during three interglacial periods. Major dislocations are connected with Warta glaciation.

Particularly important for clays is the history of loads. The glaciers covered the terrain of Poland three times. The maximum thickness of ice during the earliest glaciation was about 800–1000 meters. Poznań Formation clay is expansive kind of soil, strongly swell. In spite of its geological history there are a lot of

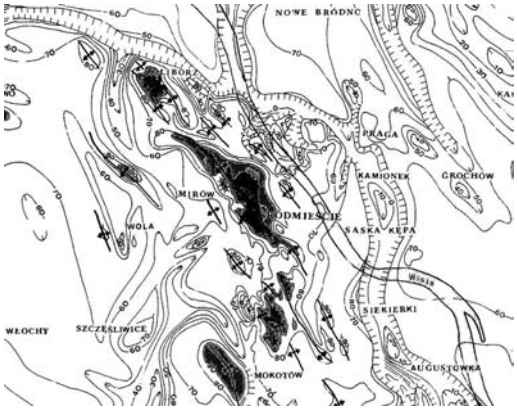


Figure 1. Downtown elevation of tertiary clay and site of geophysical tests.

cracks, dissections, interbeddings and also sand lenses including water under high pressure. Because of it this is important to precisely recognize the roof of those deposits.

Figure 1 presents all the downtown elevations of tertiary clay deposits and their directions and also site of geophysics test. Figure 2 presents those elements in focuse.

2.2 *Geology of the site*

Geology of the investigated site was presented on the cross-section on figure 3. In the base there are the following series of soil:

- Tertiary deposits
  Pliocen Clay – clay and sandy clay, Sandy lenses in Pliocen Clay – medium and thick sand, gravel;
- Quaternary deposits
  Glacial Till – bouldary clay, silty clay, sandy silt, River Sand – interglacial period deposits – medium and thick sand, gravel;
- Contemporary deposits
  Embankment – mixed soil and foundations fragments (mainly war remainders).

2.3 *Geotechnical parameters*

Soil recognition on the site was made by series in situ test verificated by laboratory test.

During in situ test there were done many exploratory drilling, CPT tests made by Borros equipment with Memocone end and Marchetti dilatomiter tests.

On the base of the in situ tests there were determined geotechnical parameters. All the basic parameters are shown in the table 1 and additional parametres in table 2 below.

As it is shown on geological cross-section of this region on figure 3, there are two main formations – clay and sand which have quite different history of sedimentation and geotechnical parameters. In spite of this it is important to have a good knowledge how proceed the border to design economically and safety new construction.

Table 1.

Soil	γ [kN/m^2]	ϕ' [^{0}]	c′ [kPa]	E [MPa]
Embankment	–	–	–	–
River sand	19.0	40.0	0.0	70.0
Glacial till	22.5	23.0	30.0	42.0
Pliocen clay	20.5	15.0	20.0	11.5

Table 2.

Soil	OCR [–]	Ko [–]	I_L [–]	I_D [–]
Embankment	–	–	–	–
River sand	NC	0.40	–	0.80
Glacial till	1.3	0.70	0.10	–
Pliocen clay	2.0	0.80	0.05	–

3 GEOPHYSICAL TESTS

The target of geophysical tests was to define morfology of tertiary deposits roof – pliocen clay in the region of planed underground line. Between Wloscianska street and Armii Krajowej street were designed three section measurement – two along underground line and one perpendicular to it.

The principal difficulty during tests was developed technical infrastructure of terrain. On the ground – marketplaces and subterranean – electro-power industry lines, collectors, canals and deep foundation of bridge pillars.

Geophysical tests were carry throught by ARS-200 equipment – electro-resistance probing method SGE, electro-resistance tomography method in Wenner-Schlumberger configuration. Length of measurement spacing took out 220 m on A-A and B-B profile. Those spacing gave about 30 m of the penetration depth. On the C-C profile length of measurement spacing took out about 130 m what gave less than 25 m of the penetration depth. Spacing between measurement electrodes took out 5 m.

Figure 4 presents one of the geophysical cross-sections in B-B profile.

For the Warsaw soil conditions there are characteristic range of the specific resistance given below:

dry sand – over dozens Ω m,
sand with water – over 20 Ω m,
bouldary clay – over 20 Ω m,
clay – 0–18 Ω m.

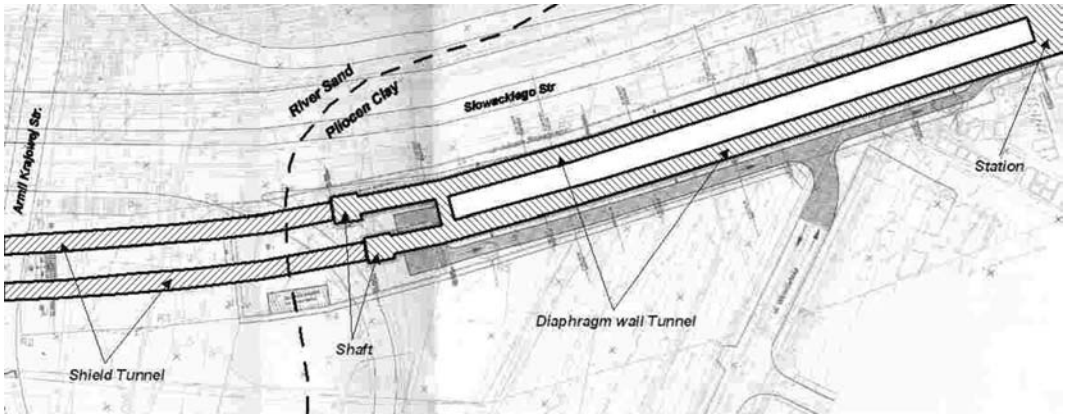


Figure 2. Site of tests.

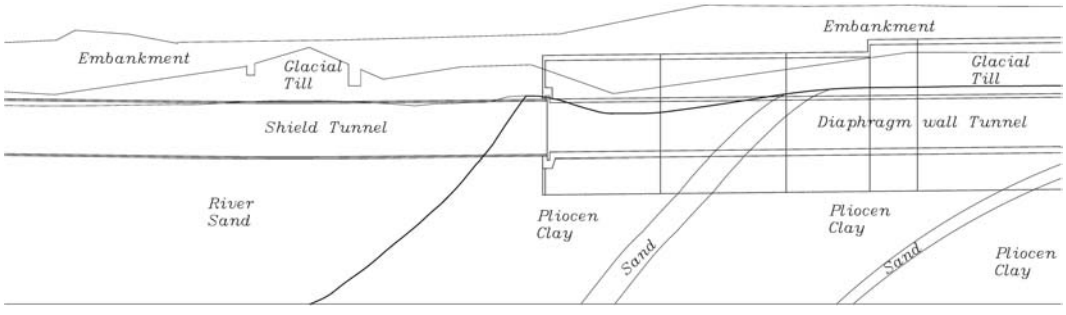


Figure 3. Geological cross-section.

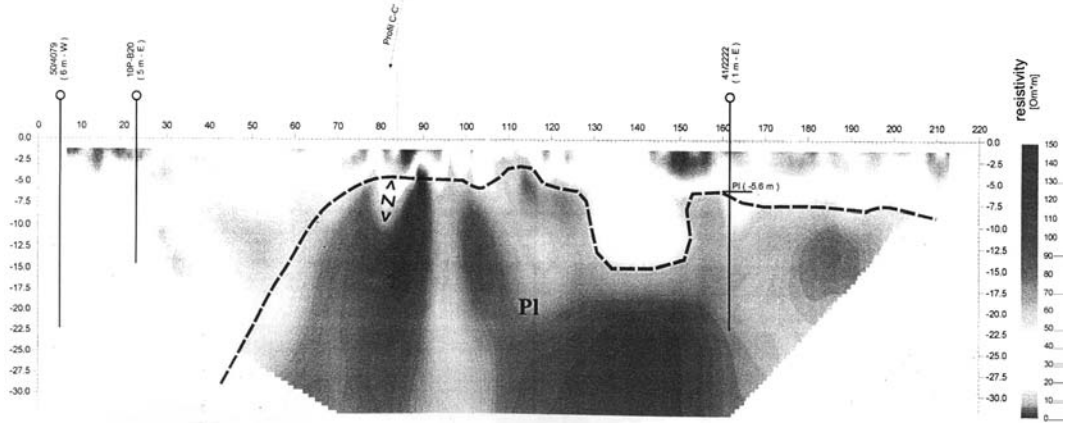


Figure 4. Geophysical cross-section B-B.

On the geophysical cross-sections there is visible high-resistance zone just below surface of the terrain. This zone reach several meters deep and is connected with embankment layer and developed technical infrastructure of subterranean.

Generally low resistance indicates pliocen clay layers but high-resistance zones within the precincts of the clay are connected with sandy dissections in its roof. Generally the roof of pliocen formation sharply subside to the north direction where is the border between river sand and pliocen clay.

4 CONCLUSIONS

In spite of the underground tunnel construction, deep dewatering and possible surface displacements it is very important to clearly specify how proceed the boundary between two different soil formation. In some cases the geophysical research is very helpful to recognize this blurred boundary in Warsaw.

In presented example important element is that pliocen roof fall in very steeply and it is hard to specify its course only by the exploratory drilling. Well known course of the border between this two formation is required because of different designe parameters and especially of pliocen clay expanding property. In spite of this it is important to decide which method of tunnel construction will be apply. Finally the section of the tunnel located in pliocen clay formation was designed as diaphragm wall tunnel and the section located in river sand was designed as shield tunnel.

REFERENCES

Kaczyński, Ryszard. 2000. Lithogenesis, microstructures and geological-engineering properties of Pliocene clays from Warsaw region (in polish). Project KBN nr 9T12B00516. Warsaw.

Kuszyk, Rafal. 2002. Geological-ingineering subsoil evaluation along 1st Metro line in Warsaw – Bankowy Square to Wilson Square section (in polish) . Warsaw. UW.

Sarnacka, Zdzislawa. 1992. Stratigraphy of Quaternary sediments of Warsaw and its vicinity (in polish). Prace Państw. Inst. 138 pages. Warsaw.

B.P. Metroprojekt. 2003. Geological-ingineering dokumentation for A19-B21 section. 1st Metro line in Warsaw (in polish). Warsaw.

ITB. 2003. In situ tests and labolatory tests for geological-ingineering dokumentation of 1st Metro line – section A19 to A23 (in polish). Warsaw.

PBG. 2003. Technical report from geophysical tests made by SGE method on the 1st Metro line in Warsaw between Wloscianska street and Armii Krajowej street (in polish). Warsaw.

Underground Space – the 4th Dimension of Metropolises – Barták, Hrdina, Romancov & Zlámal (eds)
© 2007 Taylor & Francis Group, London, ISBN 978-0-415-40807-3

Geotechnical exploration for the Dobrovského tunnel in Brno

J. Pavlík, D. Rupp & L.Klímek
GEOtest Brno, a.s., The Czech republic

ABSTRACT: Object of the exploration – Tunnel Dobrovského, as part of the constructed Large City Ring Road in Brno, consists of two route tubes which essential length fall on the mined part. Commission for the exploration estimated the excavation of three exploratory galleries with approximately triangular cross section in the area of tunnel tubes at the bases of their vaults, which will be used during the future construction of the tunnel structure. Design of the exploratory works consisted of extensive complex of works, mostly focused on analysis of the behavior of tertiary clays, within which predominant part of the future tunnel tubes will be excavated. Main parts of the exploration are geological observation and documentation during the construction, open-trench works at the surface, laboratory analysis of rock mechanics and chemical tests of waters, geophysical measurement, hydrogeological measurement, field geotechnical tests and measurements in test galleries – loading and shear tests, measurement of massif stress. Article evaluates results of the complex geotechnical exploration works in relation to the future tunnel construction what to be started this year. Exploratory and monitoring activity proved the possibility of realization of the designed tunnel structure and set the conditions for the design intent to be accomplished.

1 INTRODUCTION

Constantly unacceptable high density of traffic in Brno urgently requires relief in terms of large traffic structures. As part of the constructed Large City Ring Road in Brno, the cut-and cover Husovický tunnel and mined Pisárecký tunnel on the highway feeder Prague Radial Road already been constructed. Preparation of the third structure – Dobrovského tunnel has markedly advanced.

Thanks to the support of investment bodies represented by the Brno municipality and the Directorate of roads and motorways in the CR, the process of the investment and preparation was launched in form of exploratory galleries, which represent underground exploratory works constructed using the mining method that cost 300 mil. CZK. A consortium of company Štoly Dobrovského was delegated to be the general contractor of the geotechnical exploration. It consisted of GEOtest Brno, a.s. – leader of the consortium guarantee ling the exploration results, and three construction companies Metrostav, a.s., Subterra, a.s. and ŽS Brno a.s. responsible for excavation of the galleries and connected engineering works.

Three exploratory galleries were completed in August 2003, whose purpose was to find an optimal technology of excavation as well as total design solution of the construction. General designer Amberg Engineering Brno, a.s. considers realization of the tunnel structure using the technique of vertically and horizontally segmented excavation. Shape and location of the exploratory galleries, which will become permanent part of the full tunnel profiles, have been conformed to this technology.

The purpose of realization of the exploratory galleries and connected exploratory works was to:

- Analyze engineering-geological and hydrogeological conditions in the tunnel area;
- Verify the proposed excavation technology and remove potential problems during excavation;
- Determine the maximum range of impact of excavation on the urban area;
- Excavate app. 20% of the total tunnel volume.

2 OBJECT AND CONCEPT OF THE EXPLORATION

Object of the exploration was the tunnel route of two tubes in lengths of 1237 m (northern – designated as tunnel I) and 1258 (southern – designated as tunnel II), from which 1019 m and 1060 m fall on the mined part. Commission for the exploratory galleries with approximately triangular section in the area of tubes at the bases of their vault, which will be used during the future construction of the tunnel structure. Total length of the exploratory galleries reaches something over 2 km (IIA 831 m, IIB 831 m and IB 365 m). Due to technological reasons the galleries did not pursue the entire length of the designed tunnel tubes (Fig. 1).

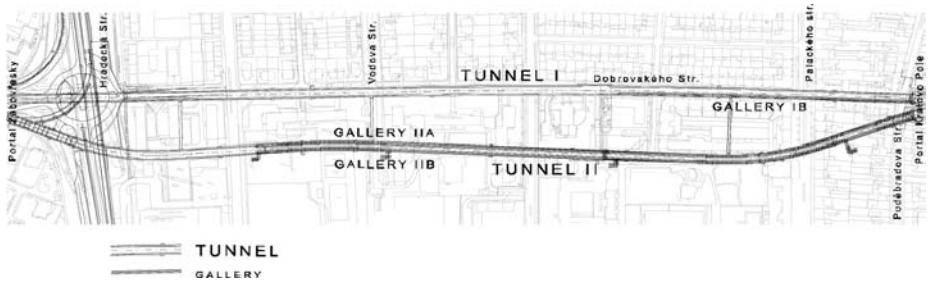


Figure 1. Exposure of galleries and designed tunnels in urban area of Brno.

Proposal of the exploratory works respected requirements laid forth by general designer of the work. It consisted of extensive complex of works, mostly focused on analysis of the behavior of tertiary clays, within which predominant part of the future tunnel tubes will be excavated:

- Factual evaluation of the Brno clays.
- Geological observation and documentation during the construction – constant geological monitoring, documentation of the faces, collection of soil samples, measurement of structure.
- Open-trench works at the surface – engineering-geological core-bores, structure bores, monitoring hydrogeological, geotechnical bores and penetration probes.
- Laboratory tests of rock mechanics, mineralogical and x-ray analyses, chemical analyses of waters.
- Geophysical measurements – vertical electric probing and shallow refraction seismic survey, seismic documentation in the galleries for determination of the massif anisotropy, determination of the Poisson's ratio from measurements of velocity of axial and lateral waves, seismic radiation between the bore and surface and between the galleries using seismic tomography, measurement of corrosiveness and stray currents.
- Passportization of water resources and regime hydro geological measurement – regular complex observation of excavation on water resources as well as their quality and quantity.
- Field geotechnical tests and measurements in test galleries – loading tests for determination of deformation statistics, shear tests with predestined area of faulting, measurement of massif tension using convergence method in a circular cross section during the excavation of test galleries, measurement of clay contraction and in situ permeability.
- Geotechnical tests and measurements in the boreholes – measurement of deformation attributes and trial stress measurements.
- Geotechnical monitoring realized both at the surface and inside the exploratory galleries – it is presented in the special article in the section 4.

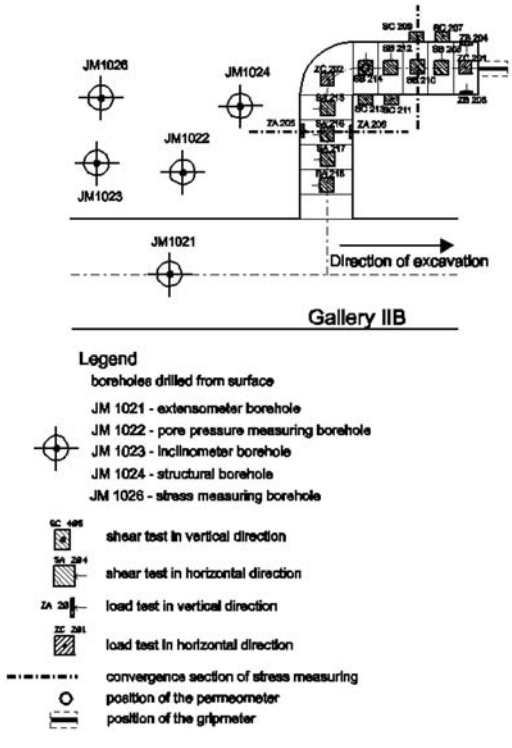


Figure 2. Layout of geotechnical works in places of concentrated investigation.

- Physical modeling using equivalent materials, determination of deformations after gallery excavation and also during the sectional excavation of tunnel for separate phases of the excavation.

For this purpose, 4 bent tests galleries of circular cross section Ø 1900 mm were designed for location of the special field tests. Their floor was bend in ground plan elevated by 0,5 m against level of floor of axial corridor of the IIB gallery, from whose left-side wall the tests galleries were started The tests galleries were part of the so-called places of concentrated exploration, which brought together all main exploratory

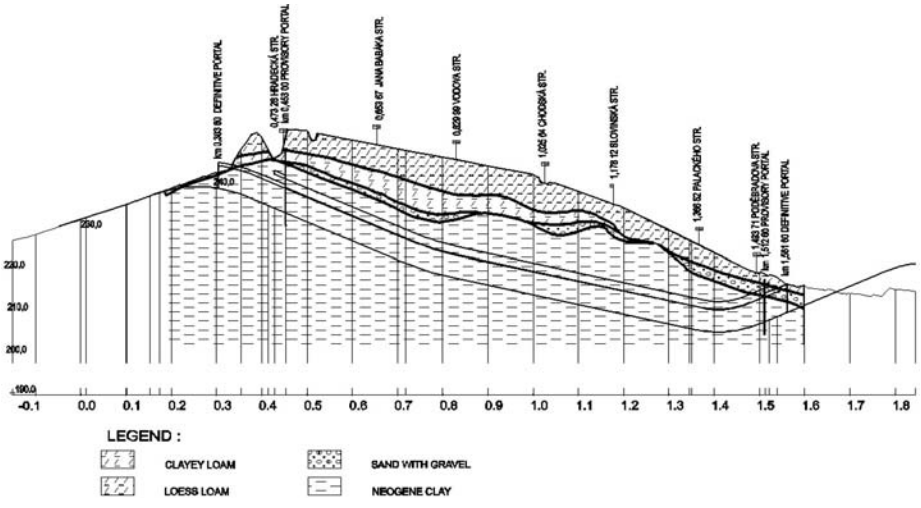


Figure 3. Geological longitudinal section through the axis of the tunnel.

and testing methods of geotechnical exploration as well as monitoring. These places further contained a total of 5 bores, carried out from the surface (see Fig. 2).

The concept of engineering-geological exploration was selected so that exploratory works realized from the surface would be coordinated with the activities underground. A total of 22 core bores was bored in the line of these designed tunnels. Bore depths ranged between 8 and 20 meters. These bores were designed to reliably uncover cross-section of the tunnel overburden and at the same time not interfere with free area of the future tunnels. Selected bores were equipped for observation of groundwater level oscillation. The mentioned places of concentrated exploration consisted of four 60 m deep bores for determination of the geological profile in the estimated zone of impact of the tunnel structure on state of stress in the massif.

3 THE PROCESS OF EXCAVATION

First, the provisory portal Královo Pole was realized by framework with fixed 18 m deep diaphragm wall, into which, following uncovering of the front section, openings were cut using special diamond devices in the shape of consequently excavated galleries with width of the floor 4,75 m and max. height of the niche 4,03 m Prior to the own excavation, which proceed from Královo Pole towards Žabovřesky, 16 m long classic micropile umbrellas were created around the gallery periphery. Lining of the galleries consisted of bearing frames from rolled mining reinforcement K24 with spacing and 10 cm thick B20 shotcrete reinforced with KARI net.

Immediately after the excavation started, the most complicated geological conditions of the track with occurrence of Quaternary watered gravels were encountered in first 60 m. Unfavorable geology in the initial gallery section was further complicated by extensive groundwater inflows, by low overburden and recent reconstruction of the multi-storey houses. Special technical measures had to be adopted in order to provide for stability of the gallery excavation as well as urban area in the overburden of this initial section. These were represented by realization of five rows of 12 m long micropile fans with a four-meter cover, bored from the underground along periphery of all three exploratory galleries. Although it was supposed to be complicated and excavation-retarding measure, it proves effective.

4 ENGINEERING-GEOLOGICAL AND HYDROGEOLOGICAL CONDITION IN THE LOCALITY

The area of the designed tunnel Dobrovského belongs to the expanded pelagic Neogene of Carpathian foretrough, which in this case reaches several hundred meters deep. Sediments lay directly on rock of the Brno massif.

Significant area of the target for exploration is urbanized; predominant part of free areas is covered with fills, or eventually with road structure layers. Terrain surface, which is slightly aligned in uniform gradient in the entire overburden of the exploratory galleries, is in the western part formed by mostly road-type structures, namely cloverleaf crossroad.

Natural cover of the terrain surface is represented by loess loams, sedimented by eolic activity during

Pleistocene. This layer experiences several decimeters thick dark-brown layers representing fossil horizons. Bases of the Quarternary cover is represented by gravel sediments, very often full of loam and clay. Their occurrence is not continuous. The largest thickness of the gravel strata was documented below the municipal bathing pool. In this place, the tunnel overburden will have only 1,5–2,5 m of Neogene clays, yet the gravel layer should not be encountered.

Prequarternary underlay is in the entire given area formed by rock of Neogene (Miocene) lower Badenian age. From the engineering-geological point of view it is limely, largely silty clay. Considering the risk of deformation there is the most vital presence of expanding clayey minerals due to their ability to swell and contract. Newer rock has a greenish-gray color, near the surface it is colored yellow to reddish-brown. Exploratory works revealed that the clays are heavily tectonically faulted, locally in zones up to several tens of meters thick. More significant tectonics areas are rubbed, grooved in the direction of movement and highly undulated.

Groundwater in the given area is mostly bound to the occurrence of Quarternary fluvial sediments in the form of gravel to sand-gravel sediments, which create very good conditions for the origin, transport and accumulation of groundwater. Neverthless, the water collectors are not continuous, and therefore the groundwater is of mostly static resource character.

5 GEOTECHNICAL ATTRIBUTES OF ROCK AND ROCK MASSIF

Attributes of the rock massif, in which tubes of the Dobrovského tunnel are designed, as well as attributes of soils that form this massif were determined based on evaluation of results of several laboratory tests of samples, collected from bores and underground openings, and field tests, realized mainly underground, in lower scale also at the surface in bores. Analysis of the geotechnical attributes proceeded in the mentioned four locations of concentrated explorations that characterized corresponded quasi-homogenous units. Attributes of the covering formations were further explored outside these locations of concentrated exploration using samples collected from bores located along the entire length of both tunnel tubes.

Laboratory tests analyzed the attributes of materials formed the rock massif, among those common index attributes on disturbed samples, on undisturbed samples volume weight in the original condition and after drying-out also permeability, density of the solid particles, total and effective parameters of shear strength, constrained modules, swelling, swelling pressures and contractibility. With regards to the fact, that each location of the concentrated exploration included one 60 m deep bore, it vas possible to observe the process of

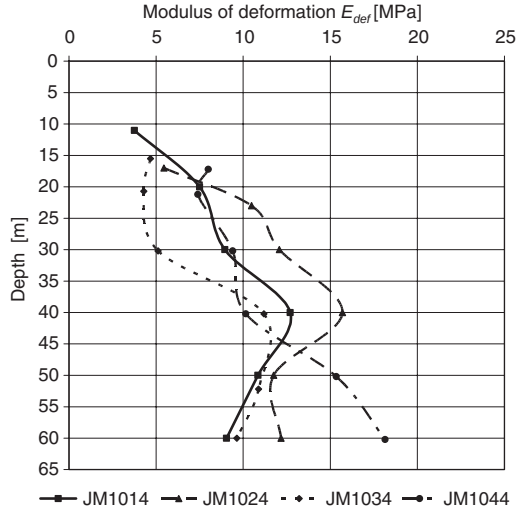


Figure 4. Relation of the modules of deformation into depth.

modification of attributes in the clay massif not only along the gallery length, but also in vertical direction. Figure 4 graphically illustrates the influence of depth on the modules of deformation of clays evaluated from the measured constrained modules.

Field tests were focused on analysis of the Neogene clay massive. Based on their purpose, they were divided into five groups: tests of massif deformability, strength tests, tests of the massif stress, tests of massif permeability and technological tests. Moreover, results and evaluation of the penetration probes were assorted with field determination of geotechnical attributes.

The first group includes mostly loading tests, which were located into test galleries in locations of the concentrated exploration. Determination of a total 6 deformation modules was realized in each test gallery, always in all mutually perpendicular directions. The tests were realized using tough 0,5 m square loading plates, gradually loaded up to the maximum average contact load 0,5 MPa and subsequently relieved to zero in two phases.

Measurement of deformability also proceeded in bores that were carried out from surface using pressiometer up to depth of 40 m below surface. These measurements were realized by employees of SG-Geotechnika Praha. Based on these results of this activity, pressiometric modules and their course of the depth were determined.

The second group is represented by shear tests with predetermined area of faulting under influence of tangential (shear) force in similar directions as for the loading tests – parallel with axis of the IIB gallery, in perpendicular horizontal and vertical direction. The tests were performed on $50 \times 50 \times 30$ cm block, which

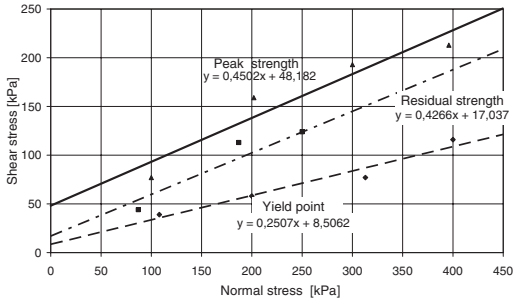


Figure 5. Strength lines of Neogene clays in vertical plane measured in the test gallery 2.

had been prepared pressing steel frames into tested environment and by gradual removal of the surrounding material. Four block formed one set, in which each block was loaded with a different combination of normal and tangential load up to disconnection of the block by shearing of its basis. From measured deformations during loading of the blocks were evaluated lines of the yield point, peak and residual strength of clay massif (see Mohr's diagram in Fig. 5). Altogether, 34 tests were performed.

Measurement of the massif stress (third group) represents the most complicated and least mastered part of rock mechanics, especially in the conditions of underground openings. Magnitudes and direction of principal stresses that occur in the massif of Neogene clays were measured by three methods, none of which had been applied in similar rock environment. Therefore, the stress measurement had a rather experimental nature. For this purpose were used three methods: the Hydrofrac, which measures horizontal stress by a probe inside of a bore that is expanded into its faulted walls by pressure of a liquid medium, the method of stress determination based on measurement of convergence of the circular opening during its excavation and finally the stress measurement by probe inside of bores that observed contracting effect of plastic clays (called method of Svěrometr).

The Hydrofrac method was developed for stress measurement of massif with solid rock, in this locality was used for the first time in a clay massif. This measurement was applied by Institute of Geonics by ČAV Ostrava in three bores. This method, however, proved unsuitable for use in a clay massif.

On the contrary, very good results were achieved by stress measurement using convergence method, although this is an indirect method that determines magnitudes and direction main stresses by calculation from measured values of other factor – deformations of the circular opening during its excavation. This method was used in all tests galleries in their both parts – in parts perpendicular to a axis of the IIB gallery and those curved, which had been excavated

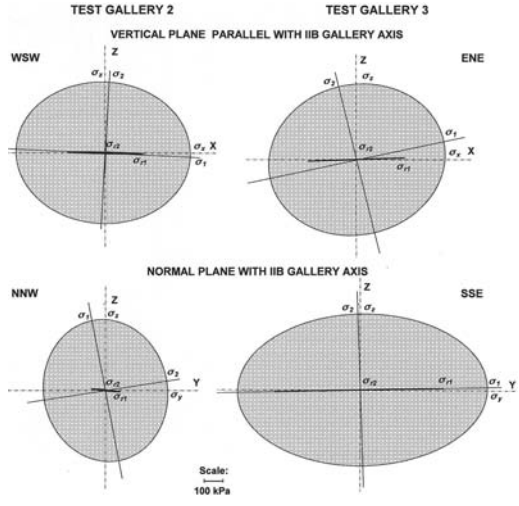


Figure 6. Ellipses of stress of rock massif in the central part of tunnel evaluated of the convergence measurement in the test galleries 2 and 3.

in parallel direction with this axes. This measurement submitted the magnitudes of normal and shear stresses in vertical and horizontal direction in planes perpendicular to axes of the cut, from its were calculated magnitudes and direction main stresses actuates in this plane and finally the residual stresses existing in the massif before excavation of the underground openings obtained by subtraction of the stresses evoked by weight of the overburden. The measurement showed that there is a horizontal residual stress, which is, in perpendicular direction to the tunnel axis, almost constant at 80 kPa with the exception of one short section below Vodova Street, where an enormous five-fold increase of value of this stress was discovered. In the axial direction, the residual stress in end section was measured with slightly reduced values (60 kPa), which increased three-fold in the middle sections. Existence of the residual stress can be attributed to preconsolidation of clays by originally high, now denudated overburden (reaching up to 80 m above the current surface); its elevation in the middle section probably to an existence of faulting line. For magnitudes of stresses measured in middle section of the explored area see ellipses of stress on Figure 6.

The method of stress measurement using contractionmeter probe is a direct method, which uses geological attributes of clays that become expressed in contraction of bored holes. It is a generally simple test, yet a very demanding one, and therefore due to time reasons the measurement could be realized only on two test galleries. The measuring device was developed for measurement in this locality, and therefore had an experimental nature. Nevertheless, achieved results

proved that use of this method of stress measurement can be considered as successful. This method can determine stress in planes perpendicular to axis of trial bore as well as magnitudes and directions of residual stresses in the same way as with convergence method. Moreover, this method enables measurements in different levels based on length of trial bores.

Four group of the field tests measurement included measurement of permeability of the rock massif by infiltration method using the Horn permeability-meter, which proceeded in all test galleries, into whose permeability-meter located. The method uses principle of measurement according to Maag, the Horn's device removes disadvantages of using the original method by its application in low permeable soils. The measurements proceeded for a long period of time, which also allowed contemplating possibilities of modification of the clay massif permeability based on the duration of the open excavation in the floor. These measurements showed permeability higher by two orders than laboratory results and slight reduction in permeability based on the time of excavation opening.

Fifth group – technological tests include only pulling tests of anchors, which had been realized in two trial fields in the trench near IB gallery portal.

The aim of these tests was to analyze effectiveness and attributes of rod anchors in the environment of Neogene clays. The task was solved in two phases – The supplier of anchoring CarboTech Bohemia installed a total 12 anchors in the first phase (4 anchors of SN type, 2 glass-fibre and 4 self-boring anchors TITAN. In the second phase following completion of the pulling tests, GEOtest Brno, a.s. installed 2 anchors of SN type and 2 anchors TITAN. After testing of the second phase anchors it was possible evaluate the self-boring anchors TITAN as the most suitable for subsequent construction of the underground work.

Penetration probes analyzed attributes of overburden of the never realized gallery IA in lower part of Veleslavínova Street – near the provisory portal of the tunnel tube I. They were carried out as dynamic enabling determination of the value of deformation module as well as parameters of the shear strength from the number of hits of the ram needed for driving the measuring pike in given depth interval and from toque at the string of rods. They were focused on exploration of the Quaternary rock and surface zone of Neogene clay massif.

6 CONCLUSIONS

As results of the realized exploratory activity showed, the tunnel structure will be realized in an environment of over-consolidated Neogene clays with specific attributes that need to be respected during the design of its dimensions as well as during the technology of realization. This environment is marked by relatively low strength, high contraction, slow creep and volume modifications due to changing water amount.

There is a very positive factor for the excavation in very low permeability of the clay massif, and therefore running groundwater will be unfavorably affecting the excavation only in section to the exit portal, where the cut penetrates into Quaternary rocks.

Exploration proved that there are relatively high horizontal residual stresses in the clay massif. As for excavation of the tunnel tubes by which horizontal directions outweigh the vertical ones, occurrence of higher horizontal stress will be an advantage.

Geotechnical conditions thus require for the excavation to be realized in shortest time possible and immediately equipped with non-permeable lining the entire periphery. Moreover, organization of works will have to be adjusted to these geotechnical conditions – it will be necessary to select such technological procedures that would only minimally interrupt otherwise continuous excavation.

Finally, along with the excavation, it will be necessary to monitor behavior of the rock massif, lining of the excavation and deformations of surface and especially the impact of underground works in urban area in the settlement trough in order to immediately evaluate the acquired data for potential guidance of realization of the tunnel structure.

REFERENCES

Pavlík, J. & Klímek, L. & Rupp, D. 2004. Geotechnický průzkum pro nejvýznačnější stavbu na Velkém městském okruhu v Brně – tunel Dobrovského. Geotechnical Exploration for the Dobrovského Tunnel, the Most Significant Structure on the Large City Ring Road in Brno. *Tunel. Magazine of the Czech Tunneling committee and Slovak Tunneling Association ITA/AITES, Vol.13 No.2/2004: 2 – 12* Praha.

Underground Space – the 4th Dimension of Metropolises – Barták, Hrdina, Romancov & Zlámal (eds)
© 2007 Taylor & Francis Group, London, ISBN 978-0-415-40807-3

Design and construction of a large underground cavern in Atlanta, Georgia, USA

T.W. Pennington, R.F. Cook & D.P. Richards
Parsons Brinckerhoff, Portland, Oregon, USA

G. Barnes
City of Atlanta, Department of Watershed Management, Atlanta, Georgia, USA

ABSTRACT: The Southern Piedmont Geologic Province in the state of Georgia (USA) consists primarily of moderate to high-grade metamorphic rock that lends itself well to underground development, particularly within the Atlanta metro area. The Custer Avenue Storage Facility was designed and constructed within this massive, high quality metamorphic rock of the Piedmont. Design of the ground support originally consisted of three types of patterned rock bolts with shotcrete and incorporated a combination of widely accepted empirical design methods for underground excavations in rock. During construction, contract requirements directed the contractor to excavate a 20-feet (6.1 meters) wide pilot drift at the top heading of the cavern excavation to confirm rock mass conditions along the length of the cavern and to serve as the initial drift of the cavern excavation. Where zones of weakness or less favorable conditions were identified in the pilot drift, the ground support was modified based on the in-situ rock Q-values. Ultimately, the pilot drift provided valuable data on the geologic conditions encountered prior to enlargement of the cavern and allowed flexibility in the design of the ground support for the final cavern.

1 BACKGROUND

Under federal mandate by the federal Environmental Protection Agency (EPA), the City of Atlanta was required to implement long-term planning and combined sewer overflow (CSO) controls throughout the city's combined sewer areas. Originally, a 1-mile (1.6 kilometer) storage and transport tunnel was considered to provide CSO control for the East Area Combined Sewer Basin. Following a value engineering study, the tunnel was replaced with an above ground CSO storage tank with an estimated cost savings of $150 million ($US). During preliminary design, a review of operational hydraulics; available property; protection of the mature, stately trees in the area; impacts of construction and future operation to the area residents; and cost, led to the consideration of options to provide the required additional CSO storage in an underground configuration. The selected option was a 60-feet (18.3 meters) wide, 600-feet (183 meters) long underground cavern with a storage capacity of 10 million gallons (3.8 million liters) excavated into the massive granite bedrock. Favorable bedrock conditions were subsequently confirmed at the site following a detailed site investigation. Ultimately, the cavern proposal reduced cost and only came to the surface at the mining shaft, minimizing the impact to the neighboring community. Furthermore, the Custer Avenue Storage Facility only required the acquisition of one property.

2 GEOLOGIC SETTING

2.1 *Southern Piedmont*

The Custer Avenue site is located within the Midland Georgia Subsection of the Southern Piedmont Physiographic Region of Georgia. The Piedmont is a region of moderate to high-grade Precambrian and Paleozoic metamorphic rocks such as schist, quartzite, amphibolite and gneiss, as well as various igneous rocks. Peak metamorphism occurred 365 million years ago in the Devonian Period with igneous intrusions dating to the late Paleozoic Period. The Piedmont Province has undergone several periods of intense deformation resulting in a great deal of folding, faulting and thrusting.

The deformation and recrystallization of the Piedmont metamorphic rocks produced parallel planar structures, schistosity and banding with a general structure that has a northeasterly strike and an accompanying southeasterly dip. The structure is reflected in rock foliation, fold axes and orientation of major thrust faults, as well as joints that developed in the

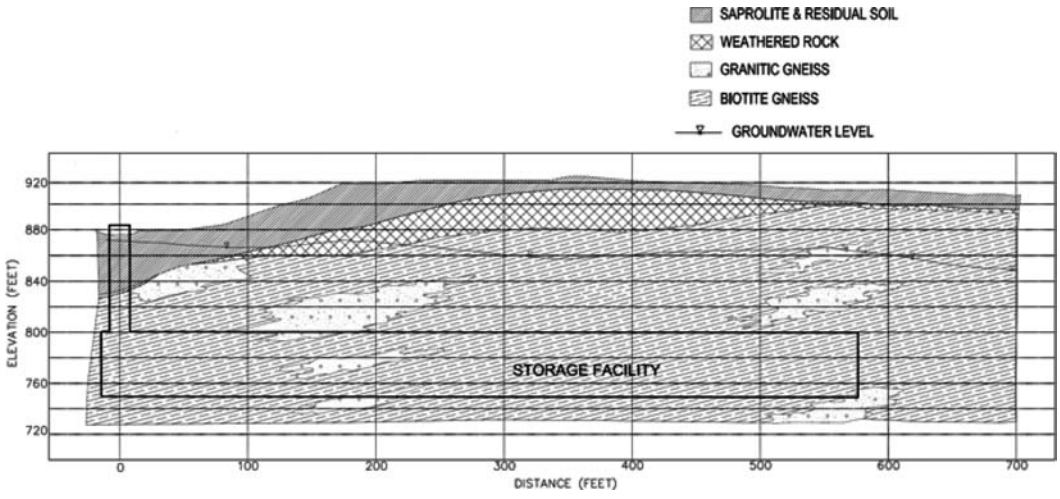


Figure 1. Storage facility geologic profile.

rock due to volume changes caused by slow cooling of the rock mass. Joints in the metamorphic rocks can assume many orientations but it is common to have one orientation parallel to the rock foliation strike and another that is perpendicular to the strike direction.

2.2 *Geologic units*

Along the Storage Facility alignment, the bedrock consisted primarily of biotite gneiss with lesser amounts of granitic gneiss (Figure 1). Local geologic mapping indicated that the project area was underlain by granitic gneiss, but borings drilled during geotechnical site investigation penetrated predominantly biotite gneiss. Quartz veins (up to four feet thick) were encountered in nearby borings drilled for the adjacent Intrenchment Creek Tunnel at the northern terminus of the proposed facility alignment.

2.3 *Weathering profile*

Following uplift and erosion of the Piedmont, the exposed bedrock was subject to deep chemical weathering that has resulted in a weathering profile that is irregular, with gradational contacts between weathering zones. The boundary between soil and rock is a transition zone, grading with increasing depth from residual soil to fresh unweathered rock. Since weathering is facilitated by fractures, joints and the presence of less weathered material, the weathering profile was expected to be highly variable and the contact with the underlying fresh rock irregular and erratic. For the Storage Facility, the following criteria were established for characterization of the weathering profile:

A. Residual zone (residual soil and saprolite with N-values < 100 blows/foot)
B. Partly weathered zone (weathered rock with N-values > 100 blows/foot)
C. Bedrock Zone (Unaltered, unweathered, or slightly weathered rock)

The boundaries between weathering zones in the Piedmont are generally not horizontal. Weathering is often deeper and more advanced adjacent to fractures that transmit water and in mineral bands that are more susceptible to decomposition (as found in foliated gneiss). Vertical foliation in the bedrock also enhances weathering resulting in deep saprolite deposits. Weathering in the highly foliated rock proceeds inward from joints through less resistant rock producing deep soft seams alternating with seams of hard, relatively unweathered rock.

2.4 *Structural geology*

The sub-parallel foliation within the rock mass was identified as the primary joint set (and potential plane of weakness during cavern excavation). Infrequent high angled joints and shear zones up to five feet thick were also identified in three of the borings drilled along the alignment as follows.

2.4.1 *Foliation and schistosity*

The biotite gneiss encountered during subsurface explorations contained abundant biotite mica that produces a strong foliation. The granitic gneiss contained less mica and thus shows less foliation. Since the majority of the cavern would be located within biotite gneiss, foliation orientation would influence the overbreak and stability of the resulting excavation. Foliation within the biotite gneiss and granitic gneiss consisted of thin laminations of contrasting mineralogy; however, large-scale foliation would be present.

Laminations generally dipped from 0° to 60° from horizontal, but the average dip of the majority of the foliation was less than 30° from horizontal.

2.4.2 *Jointing*

Bedding planes, foliation, and jointing were confirmed within cores obtained from subsurface explorations. A minimum of three joint sets were assumed along the proposed Storage Facility. Based on the history of metamorphasism in the Piedmont, joint frequency was expected to decrease with depth below top of rock. Average fracture frequencies for individual core runs varied from about one to 20 fractures per 10 feet (3.0 meters). Measured dip angles (measured from the horizontal) on the vertical drill core were estimated to vary from 0 to 45 degrees. In the deeper portions of the Storage Facility, joints were expected to become tight and in most cases to have no apertures or openings. Occasional localized joints containing small amounts of clayey gouge material (indicating minor shear or altered zones) were expected at depth.

2.4.3 *Groundwater*

In the Atlanta area, the main source of groundwater is infiltration from the ground surface into the overlying soil zone. The soil zone acts as a reservoir consistently recharged by the substantial precipitation in Georgia. The saprolite and weathered rock have significant storage capacity within abundant open fractures and small voids and act as a conduit for groundwater transmitted into the underlying bedrock. Groundwater in the underlying bedrock is present in irregularly distributed, highly localized, discontinuous water-bearing zones. Groundwater is typically conveyed along foliation planes, fractures, joints, boundaries between different rock types, veins, and other geologic features that have been enhanced by differential weathering. Within the bedrock units themselves, permeability is largely controlled by secondary porosity, i.e. open joints, fractures and shear zones, rather than through the porosity of the crystalline rock material.

2.4.4 *In-situ stresses*

In-situ horizontal stress in the Atlanta area has been reported to vary from 800 to 2,500 psi (5.6 to 17.1 MPa) (Lindner and Halpern, 1978), with maximum principal stress direction approximately perpendicular to the fold axes in the area. At the planned depth of the Storage Facility, these stress levels were not expected to introduce any stress related modes of instability. However, stress levels ere considered high enough to either hold in or force out blocks depending upon the geometric details of the block with respect to the excavation, and depending upon the shear strength properties of the controlling discontinuity surfaces.

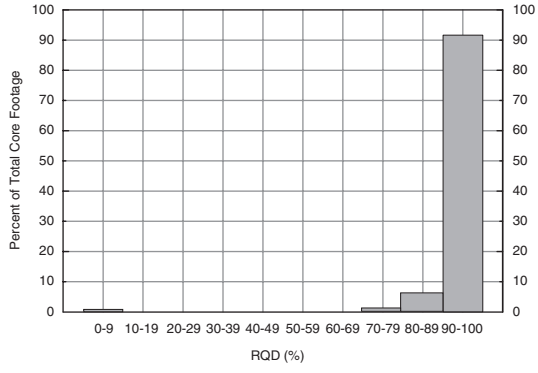


Figure 2. Distribution of RQD.

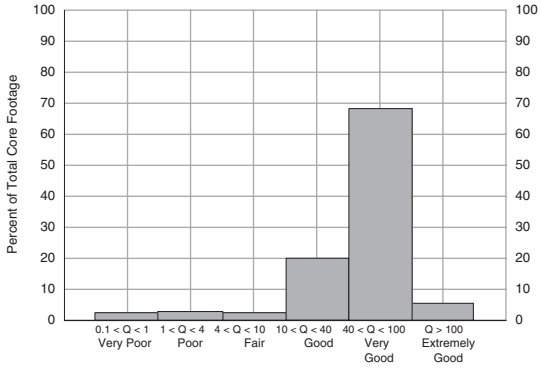


Figure 3. Distribution of Q-values.

3 ROCK MASS PROPERTIES

3.1 *Rock quality*

The rock mass within the Storage Facility excavation was relatively unweathered (moderately weathered to fresh) except for localized weathered zones and a few potential shear zones. Rock Quality Designation (RQD) values in the granitic gneiss and biotite gneiss ranged from six to 100 percent, with a median value of 95 percent. Distribution of RQD values are provided in Figure 2.

The Norwegian Geotechnical Institute (NGI) Q system (Barton, 1988) was used to characterize the rock mass and to assist in establishing and sizing the permanent ground support. Q-values were estimated along the Storage Facility alignment at the approximate depth of excavation by interpretation of rock discontinuity data for core runs within the Storage Facility envelope (defined as 30 feet, (9.1 meters) above the Storage Facility crown and 30 feet below the invert). Distribution of Q-values is provided in Figure 3. NGI parameters assumed along the Storage Facility are summarized in Table 1. Q-values were anticipated to

Table 1. NGI parameters selected for Q-values.

NGI parameter	Selected value
J_n – Joint Set	3.0
J_r – Joint Roughness	1.0 to 3
J_a – Joint Alteration	0.75 to 8
J_w – Joint Water Reduction Factor	1.0
SRF – Stress Reduction Factor	1.0 to 5.0

Table 2. Summary of point load test strength and UCS.

	$I_{S(50)}$	UCS (psi)
Axial point load test	0.66–1.82	15,840–43,680
Diametrical point load test	0.38–1.14	9,120–27,360
UCS	–	6,700–12,270

span a range of support categories from very poor ($Q < 1$) to extremely good ($Q > 100$).

3.2 *Rock strength*

Unconfined Compressive Strength (UCS) tests and Point Load Strength Index tests were performed on representative core samples. UCS values obtained during laboratory testing ranged from 6,700 to 12,270 psi (46 to 85 MPa). Review of the photos of failed test specimens indicated that many of the samples appeared to have failed prematurely as they did not exhibit a traditional shear failure. These results were assumed to underestimate the intact rock compressive strength.

Point load tests were used augment rock strength data and to estimate rock strength anisotropy (due to foliation and variation in crystal structure) present in the rock mass. Test results were correlated to UCS using compressive strengths estimated from the Point Load Index values, $I_{S(50)}$. As shown in Table 2, compressive strength from the axial and diametrical Point Load Strength Index tests indicated that strength along the foliation was approximately 60% of strength perpendicular to foliation.

3.3 *Anticipated ground behavior*

Results of the Point Load Strength Index and UCS tests, as well as foliation observed in core samples obtained during the subsurface investigation program, suggested foliation would influence excavation of the cavern, particularly when excavated by drill and blast techniques. Influence of foliation would be more pronounced where excavating through the strongly foliated biotite gneiss. Excavation in the crown would break along foliation planes and discontinuities, resulting in localized areas of overbreak and a corbelled surface across the crown. Additional rock breaking across the roof to remove protrusions was also anticipated.

Excavation of the sidewalls would also result in breakage along foliation planes, as well as joint sets subparallel to the walls, again requiring removal of protrusions and resulting in excessive overbreak. It was anticipated the breakage pattern across the crown and sidewalls would not be fully controlled by means of smooth-wall blasting. The excessive overbreak over the crown of the excavation would require application of shotcrete to provide a final lining over the crown to meet the final lining shape.

Where zones of blocky rock were anticipated, blocks formed by intersecting joint surfaces would be prone to fallout when they are oriented adversely relative to the excavation orientation, open, or contain mineral coatings or gouge material. The probability for fallout was judged to be high where closely to moderately spaced persistent joints, especially in fractured zones, would be encountered. Unless promptly supported during excavation, the blocks would tend to fall out of the crown and sidewalls due to the interaction between foliation, potential shear zones and joints oriented across foliation.

The main types of block fallouts from the crown, sidewalls and the face of the excavation are as follows:

Wedge-shaped fallout – characterized by blocks bounded by three or more intersecting joints. In general, these would occur due to the presence of steeply dipping joints intersecting the cavern excavation combined with shallow dipping foliation joints. Such instabilities would occur both during pilot drift excavation and cavern excavation.

Slab fallout – occurring at intersections of discontinuity planes, such as altered, shear, or weathered zones. Slab fallout would also occur due to the presence of a combination of closely spaced shallow foliation joints or shear zones and one or more moderately to widely spaced steeply dipping joints.

4 GROUND SUPPORT

Three ground support types were specified for construction based on expected rock mass conditions, as well as Q-values and RQD values along the cavern alignment. Typical details of each support type are provided in Figure 4. Ground support for Type I and Type II consisted of patterned rock bolts ranging from 10 to 20 feet (3.0 to 6.1 meters) in length, with alternating offset patterns ranging from four to 8 feet (1.2 to 2.4 meters). This support category corresponded to “good” to “extremely good” rock conditions in accordance with the NGI classification. Ground support for Type III consisted of lattice girders spaced at 4 feet (1.2 meter) with 20 feet (6.1 meter) long rock bolts spaced at 8 feet (2.4 meters) to support the crown. Sidewall support was provided by 10 and 20 feet (3.0 to 6.1 meter) rock bolts. This support category corresponded to “poor” to

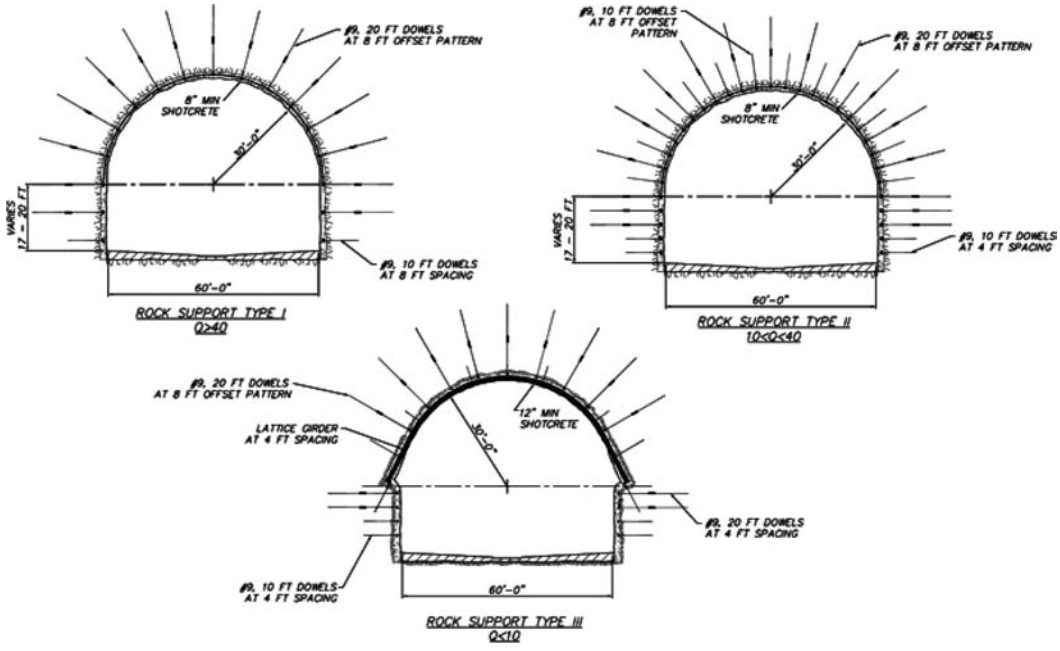


Figure 4. Ground support details.

Table 3. Ground support criteria.

Type	Q-Values	RQD (%)	Cavern Length (%)
I	>40	>95	60
II	10–40	75–95	35
III	<10	<75	5

"fair" rock in accordance with NGI classification and was intended for zones within the cavern where weathering or alteration of the massive rock was expected.

All ground support types also required a minimum of 8 to 12 inches (20 to 30 cm) of shotcrete following installation. The distribution of each ground support type along the cavern alignment is shown in Table 3.

4.1 *Pilot drift excavation*

Excavation of the pilot drift extended along the length of the cavern alignment prior to enlargement of the cavern. Approximate dimensions of the excavated drift were 25 feet (7.6 meters) wide by 20 feet (6.1 meters) high. Advance rates ranged from nine to 20 feet (2.7 to 6.1 meters) per day. Geologic mapping provided along the pilot drift indicated better than anticipated rock mass conditions than assumed during design. Based on the ground support criteria defined during the design stage (Table 3), 80% of pilot drift length, or 480 feet (146 meters) required Type I ground support, with calculated Q-values greater than 50 and frequently exceeding 100. Approximately 20% of the pilot drift length, or 120 feet (37 meters) required Type II ground support, with Q-values ranging from 17 to 36.

Discontinuities encountered along the pilot drift consisted of wide to very widely spaced healed shears and pegmatite veins with near vertical orientation, as well as wide to very widely spaced steeply dipping joints (>70 degrees). Few shear zones and joints oriented parallel to the sub-horizontal foliation were encountered. The shear zones observed ranged in thickness from 0.25 to 10 inches (0.6 to 25 cm) in thickness, with occasional clay coating. Where these discontinuities intersected the near vertical joints, potential rock wedges were identified and supplemental rock bolts were installed. No extensive zones of weakness or significantly altered zones requiring Type III ground support were observed along the length of the pilot drift excavation.

The pilot drift was primarily dry during excavation. Localized groundwater inflows were encountered primarily from the sub-parallel shear zones and foliation joints and maximum seepage rates were less than 25 gallon per minute (75 liters per minute).

4.2 *Cavern excavation*

Enlargement of the cavern excavation encountered conditions similar to those encountered during the pilot drift excavation. Rock mass conditions and rock quality were comparable to those mapped in the



Figure 5. View of fully excavated cavern.

pilot drift and similar ground support types were utilitized. Overbreak along foliation was encountered and required localized milling and shotcrete infilling to provide a relatively smooth excavated surface.

Potential rock wedges were evaluated as the cavern was enlarged and supplement rock support in the form of spot and patterned rock bolts were provided. No slab-type fallouts were encountered due to wide to very wide spacing of discontinuities.

Similar to the pilot drift excavation, minimal groundwater control was required during enlargement of the cavern excavation.

5 CONCLUSIONS

The Custer Avenue Storage Facility successfully utilized the massive, high quality metamorphic rock to provide a cost effective underground solution to providing CSO control for the City of Atlanta. Project designers were able to rely on excellent rock quality, as well as documented local construction experience, to develop a successful and cost effective solution for the project owner. At 60 feet (18.3 meters) in width, the Custer Avenue Storage Facility is among the largest underground spans in the Atlanta area.

Characterization of the rock mass using the NGI Q-value system, combined with comparison of local construction experience, was imperative to the successful design and construction of the Custer Avenue CSO Storage Facility. Construction of the pilot drift prior to enlargement of the cavern to the design dimensions allowed identification and mapping of potential zones of weakness, as well as development of supplemental ground support.

ACKNOWLEDGEMENTS

The authors of this paper gratefully acknowledge the cooperation of the City of Atlanta, Department of Watershed Management for their kind permission to publish this paper. Thanks are also extended to Bill Gray, Vice President of Parsons Brinckerhoff for his contributions and support in preparing this paper.

REFERENCES

Barton, N.R., R. Lien and J. Lunde. 1974. Engineering Classification of Rock Masses for the Design of Tunnel Support, *Rock Mechanics,* Vol. 6, No. 4.

Barton, N.R. 1988. Rock Mass Classification and Tunnel Reinforcement Selection Using the Q-System. *Rock Classification Systems for Engineering Purposes, ASTM STP 984,* Philadelphia: 59–88.

Cressler, C.W., C.J. Thurmond and W.G. Hester. 1983. *Groundwater in the Greater Atlanta Region*. Information Circular 63, Georgia Geologic Survey.

Deere, D.U., R.B. Peck, J.E. Monsees and B. Schmidt. 1969. *Design of Tunnel Liners and Support Systems.* Report for the U.S. Department of Transportation, OHSGT Contract 3-0152, No. PB 183 799, Springfield, Virginia.

Kuesel, T. R. and E. H. King. 1979. "MARTA's Peachtree Station," Proceedings, *Rapid Excavation and Tunneling Conference*, (RETC).

Lindner, E.N. and J.A. Halpern. 1978. In-situ Stresses in North America – A Compilation. *International Journal of Rock Mechanics and Mining Science and Geomechanical Abstracts,* Vol. 15, pp. 183–203, London: Pergamon Press Ltd.

Lyman, Tracy J. 1978. *Selection of Permanent Tunnel Support for the Intrenchment Creek Tunnel*. Three Rivers Water Quality Management Program, City of Atlanta, Georgia.

Underground Space – the 4th Dimension of Metropolises – Barták, Hrdina, Romancov & Zlámal (eds)
© 2007 Taylor & Francis Group, London, ISBN 978-0-415-40807-3

Development of in-situ tunnesl-ahead detection system using electromagnetic wave

H.H. Ryu, G.C. Cho & Y.J. Sim
Korea Advanced Institute of Science and Technology, Daejeon, Korea

G.H. Lee
POSCO Engineering & Construction Co. Ltd., Seoul, Korea

J.K. Lee
Dept. of Tunneling, Dodam E&C Co. Ltd., Anyang, Korea

ABSTRACT: During tunnel construction, ground failures are often reported due to occurrence of weak zones such as faults, joints, and cavities. By using conventional geophysical characterization methods, it is hard to detect detailed weak rock and fault zone which can lead underground structure to fail after excavation and before supporting. In this study, an enhanced detection system of predicting weak zones ahead of tunnel face is developed for making up the problems of the conventional characterization methods. Using the developed system, case studies are performed for detection of a spherical shaped weak zone and an oriented fault. The experimental results show that the presence of weak zones and their sizes, location, and states can be accurately predicted from electrical resistance measurements through a proper inversion process.

1 INSTRUCTION

Rapid urbanization has necessitated the creation of underground spaces such as tunnels and underground structures. Unfortunately, a considerable number of accidents have occurred in such sites, including tunnel collapses. Accidents of this nature mostly occur in areas under construction and around tunnel faces. During tunnel construction, the unexpected occurrence of anomalies ahead of tunnel face, such as weak zones, fault zones, and cavities, may cause mechanical failures and ultimately result in casualties. So, various methods to predict geotechnical ground conditions in advance have been studied while conventional geophysical characterization methods have been relied upon. However, the application of conventional geophysical characterization methods is quite limited because of their failure to yield reliable prediction, especially for weak zones near the tunnel face. For this reason, it is necessary to develop an enhanced geophysical characterization method which allows predicting ground-condition ahead of tunnel face during construction.

The Tunnel Seismic Profiling (TSP) method has been generally used for that purpose. This is suitable for detection of weak zones for hard rock mass in 100 m∼200 m ahead of tunnel face. However, the TSP is not applicable to detection in a near range such as 10 m∼20 m ahead of tunnel face (Sattel et al., 1992; Lee, 2001; Lee et al., 2002). Therefore this study will present an enhanced electrical resistivity prospecting system. This method overcomes shortcoming of elastic wave and performs more precise analysis than other conventional resistivity-based geophysical characterization methods.

2 ELECTRIC FIELD ANALYSIS IN ROCK MASS

2.1 *Homogeneous intact rock*

The electric field analysis in intact rock can be done in a semi-infinite medium that is homogeneous and ideal. Let us consider that two spherical electrodes are placed at a certain distance in an ideal infinite medium. An electric field at any point can be expressed using Coulomb and Gauss' laws, so that intact rock resistance (ρ_{IR}) can be expressed as follows:

$$R_{IR} = \rho_{IR} \frac{1}{\pi a} \tag{1}$$

where ρ_{IR} ($=1/\sigma_{IR}$) is the electrical resistivity of intact rock, σ_{IR} is the conductivity of intact rock, and a is the electrode radius.

2.2 *Jointed rock mass*

In electric field analysis, joints in a rock mass are assumed to be saturated with water (e.q., most underground sites are below the groundwater table). Figure 1 shows a configuration of two electrodes (radius = a) on the face of the rock mass (x-y plane) having joint sets in x, y, and z directions. The origin for the rectangular coordinate system is at the center of the left electrode. The direction of excavation is on the z-axis. The width of each joint is 't' and the distance between joints is 'd'. The electric field at the joint surfaces (E_J) and intact rock (E_{IR}) can be expressed as follows:

$$E_J = \frac{Q}{2\pi\varepsilon_J}\frac{L/2}{\left[(L/2)^2 + y^2 + z^2\right]^{3/2}}\cdot\hat{r} \tag{2}$$

$$E_{IR} = \frac{Q}{2\pi\varepsilon_{IR}}\frac{L/2}{\left[(L/2)^2 + y^2 + z^2\right]^{3/2}}\cdot\hat{r} \tag{3}$$

where ε_J and ε_{IR} are the dielectric permittivity in joint and intact rock, respectively. The electric current of the rock mass along the y-z plane (I_{RM}) can be expressed by the summation of the electric current of joints parallel to x-z plane (I_{xz}), the electric current of joints parallel to x-y plane (I_{xy}) and the electric current of intact rock (I_{IR}) as follows:

$$I_{RM} = I_{xz} + I_{xy} + I_{IR} \tag{4}$$

where

$$I_{xz} = \frac{1}{2}\sum_{k=-\infty}^{\infty}\int_{-\infty}^{\infty}\int_{k(d_y+t_y)-t_y/2}^{k(d_y+t_y)+t_y/2}\sigma_J E_J dy dz = \frac{\sigma_J Q}{\pi\varepsilon_J}\cdot\alpha_{xz} \tag{5}$$

$$I_{xy} = \frac{1}{2}\sum_{l=-\infty}^{\infty}\int_{l(d_z+t_z)-t_z/2}^{l(d_z+t_z)+t_z/2}\int_{-\infty}^{\infty}\sigma_J E_J dy dz = \frac{\sigma_J Q}{\pi\varepsilon_J}\cdot\alpha_{xy} \tag{6}$$

$$I_{IR} = \frac{1}{2}\sum_{l=-\infty}^{\infty}\sum_{k=-\infty}^{\infty}\int_{l(d_z+t_z)-t_z/2}^{l(d_z+t_z)+t_z/2+d_z}\int_{k(d_y+t_y)-t_y/2}^{k(d_y+t_y)+t_y/2+d_y}\sigma_{IR}E_{IR}dy dz = \frac{\sigma_{IR}Q}{2\pi\varepsilon_{IR}}\cdot\beta \tag{7}$$

$$\alpha_{xz} = \sum_{k=-\infty}^{\infty}\left[\sin\left(\tan^{-1}\left(2k\left(\frac{d_y}{L}+\frac{t_y}{L}\right)+\frac{t_y}{L}\right)\right) - \sin\left(\tan^{-1}\left(2k\left(\frac{d_y}{L}+\frac{t_y}{L}\right)-\frac{t_y}{L}\right)\right)\right] \tag{8}$$

$$\alpha_{xy} = \sum_{l=-\infty}^{\infty}\left[\sin\left(\tan^{-1}\left(2l\left(\frac{d_z}{L}+\frac{t_z}{L}\right)+\frac{t_z}{L}\right)\right) - \sin\left(\tan^{-1}\left(2l\left(\frac{d_z}{L}+\frac{t_z}{L}\right)-\frac{t_z}{L}\right)\right)\right] \tag{9}$$

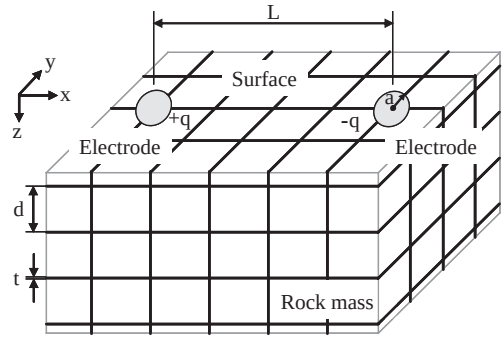


Figure 1. Rock mass with joint set.

$$\beta = \sum_{l=-\infty}^{\infty}\sum_{k=-\infty}^{\infty}\int_{l(d_z+t_z)+t_z/2}^{l(d_z+t_z)+t_z/2+d_z}\frac{2/L}{1+4(z/L)^2}\left[\sin\left(\tan^{-1}\left(\frac{2k\left(\frac{d_y}{L}+\frac{t_y}{L}\right)+\frac{t_y}{L}}{\sqrt{1+(z/L)^2}}\right)\right) - \sin\left(\tan^{-1}\left(\frac{2k\left(\frac{d_y}{L}+\frac{t_y}{L}\right)-\frac{t_y}{L}}{\sqrt{1+(z/L)^2}}\right)\right)\right]dz \tag{10}$$

where σ_J is the electric conductivity of a joint, d_y and d_z are the distance between joints along the y- and z-axis, respectively, t_y and t_z are the joint thickness along the y- and z-axis, respectively, k and l are integers and L is the distance between electrodes. If $d_y = d_z$ and $t_y = t_z$, which is a specific case, $I_{xz} = I_{xy}$.

Finally, using Eq. (4) through Eq. (7), electrical resistance (R_{RM}) and resistivity in rock mass (ρ_{RM}) where joints are included can be written as follows:

$$R_{RM} = \frac{1}{a}\cdot\frac{1}{\left[2\sigma_J\left[\alpha_{xz}+\alpha_{xy}\right]+\sigma_{IR}\beta\right]} \tag{11}$$

$$\rho_{RM} = \frac{\pi}{\left[2\sigma_J\left[\alpha_{xz}+\alpha_{xy}\right]+\sigma_{IR}\beta\right]} \tag{12}$$

3 ELECTRIC FIELD ANALYSIS IN ROCK MASS WITH A SPHERICAL WEAK ZONE

Consider that a weak zone is ahead of tunnel face. The shape of the weak zone is assumed to be a spherical shape.

Figure 2 shows electric field variation in spherical. The electric field of a weak zone (E_w) can be expressed

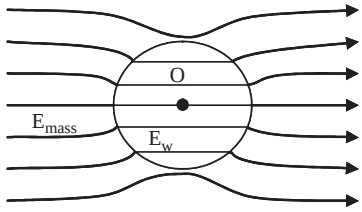


Figure 2. Electric field variation in spherical.

in terms of relative permittivity (K) and the electric field of rock mass (E_{mass}) (Reitz et al., 1993):

$$E_w = \frac{3}{K+2} E_{mass} \tag{13}$$

where K = the ratio of the permittivity of rock mass to the permittivity of weak rock mass ($=\varepsilon_w/\varepsilon_{mass}$).

Using the configuration shown in Figure 3, the current of rock mass with a spherical weak zone can be calculated as follows:

$$I = \int_0^{l-r} \sigma_{mass} \overline{E}_{mass} \cdot \pi l dl + \int_{l-r}^{l+r} \sigma_w \overline{E}_w \cdot \alpha l dl + \int_{l-r}^{l+r} \sigma_{mass} \overline{E}_{mass} \cdot (\pi - \alpha) l dl + \int_{l+r}^{\infty} \sigma_{mass} \overline{E}_{mass} \cdot \pi l dl \tag{14}$$

where $\alpha = \sin^{-1}(r/l)$, r = the radius of weak zone, l = the distance between the center of electrode and that of weak zone, σ_w = the conductivity of weak zone and σ_{mass} = the conductivity of rock mass. After substituting Eq. (13) for Eq. (14), the resistance of total rock mass with a weak zone is

$$R = \frac{1}{\left[\pi \sigma_{mass} A + \left[\frac{3\sin^{-1}(r/l)\cdot\sigma_w}{K+2} + \left[\pi - \sin^{-1}(r/l)\right]\sigma_{mass}\right] \cdot B\right] \cdot \frac{a}{2}} \tag{15}$$

where

$$A = 2 + \cos\left(\tan^{-1}\frac{l+r}{x}\right) + \cos\left(\tan^{-1}\frac{l+r}{L-x}\right) - \cos\left(\tan^{-1}\frac{l-r}{x}\right) - \cos\left(\tan^{-1}\frac{l-r}{L-x}\right) \tag{16}$$

$$B = \cos\left(\tan^{-1}\frac{l-r}{x}\right) + \cos\left(\tan^{-1}\frac{l-r}{L-x}\right) - \cos\left(\tan^{-1}\frac{l+r}{x}\right) - \cos\left(\tan^{-1}\frac{l+r}{L-x}\right) \tag{17}$$

where x = the distance from electrode $+q$ to the point, meeting perpendicularly the line passing the center of spherical weak rock mass with the line passing the center of two electrodes simultaneously, and L = the distance between two electrodes.

In practice, multiple sensors are installed on the tunnel face. Although the electric current (or resistance) can be measured only between two sensors at a time, each resistance measured is dependent upon each

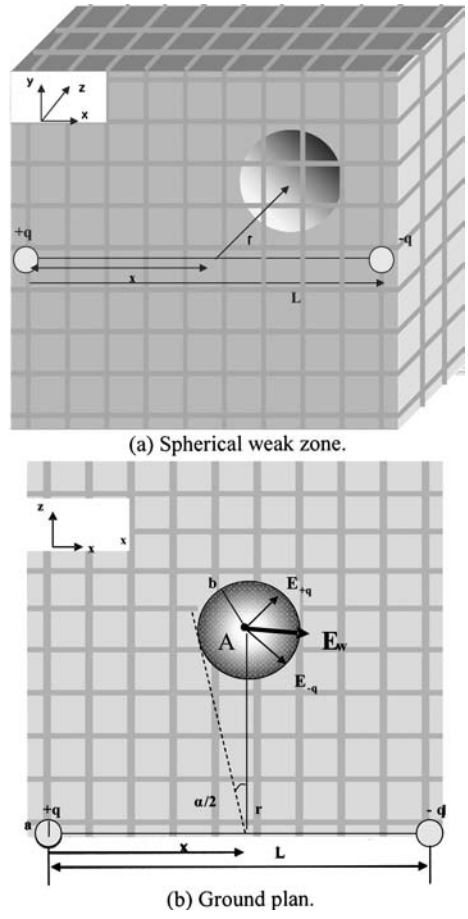


Figure 3. Electric field analysis of weak zone in a semi-infinite medium.

sensor configuration. For changing three-dimension to two-dimension, the parameters L, l, x must be changed. Figure 4 shows a spherical weak zone in three-dimension. ⓐ coordinate is ($x1$,$y1$,0), while ⓑ coordinate is ($x2$,$y2$,0). Each parameter is obtained as follows:

$$L = \sqrt{(x2-x1)^2 + (y2-y1)^2} \tag{18}$$

$$l = \sqrt{g^2 + e^2} = \sqrt{\left(\frac{\left|x3(y2-y1) - y3(x2-x1) - x1(y2-y1) + y1(x2-x1)\right|}{\sqrt{(y2-y1)^2 + (x2-x1)^2}}\right)^2 + z^2} \tag{19}$$

$$x = \sqrt{(x3-x1)^2 + (y3-y1)^2 + z^2 - l^2} \tag{20}$$

Substituting Eq. (18) through Eq. (20) for Eq. (15), it is possible to obtain a resistance for any arbitrary sensor configuration.

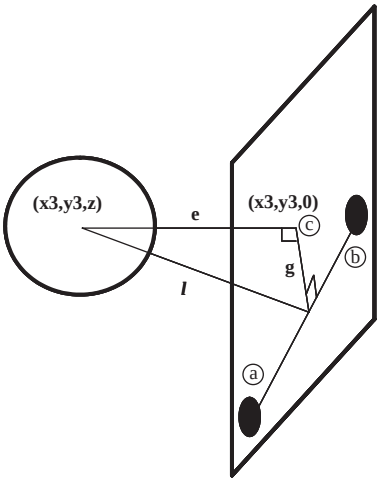


Figure 4. Spherical weak zone in three-dimension.

4 ELECTRIC FIELD ANALYSIS IN ROCK MASS WITH A FAULT ZONE

Consider that a fault zone is ahead of tunnel face. The shape of the fault zone is assumed to be a rectangular shape. If no a fault zone exists ahead of tunnel face, the equation is as follows:

$$I = \iiint \sigma_{mass} E \cdot dxdydz \tag{21}$$

A fault zone is considered as a plane (Figure 5). If a fault zone exists ahead of tunnel face, the equation is as follows:

$$I = \iiint \sigma_{mass} E \cdot dxdydz + \iint\int_{Z}^{Z'} (\sigma_f - \sigma_{mass}) E \cdot dzdxdy \tag{22}$$

$$Z = \frac{-AX - BY + D}{C} \tag{23}$$

$$AX + BY + C(Z' - t) = D \tag{24}$$

$$Z' = \frac{-AX - BY + Ct + D}{C} \tag{25}$$

where Z is the equation of the fault zone front, Z' is the equation of the fault zone back (i.e., the equation that Z plane moves toward z-axis by an extent of the fault zone's thickness, t), σ_f is the conductivity of the fault zone and A, B, C, D are constant values.

As shown in Figure 6, the electric field can be expressed as follows:

$$E = \frac{Q}{4\pi\varepsilon_0}\left(\left(\frac{1}{k^2}\times\cos\theta 1\right)+\left(\frac{1}{q^2}\times\cos\theta 2\right)\right)i$$
$$= \frac{Q}{4\pi\varepsilon_0}\left(\left(\frac{1}{k^2}\times\frac{\sqrt{k^2-l^2}}{k}\right)+\left(\frac{1}{q^2}\times\frac{\sqrt{q^2-l^2}}{q}\right)\right) \tag{26}$$

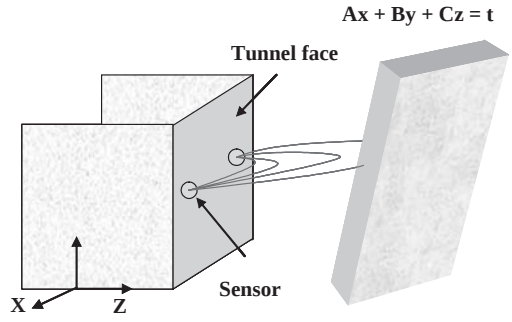


Figure 5. Fault zone.

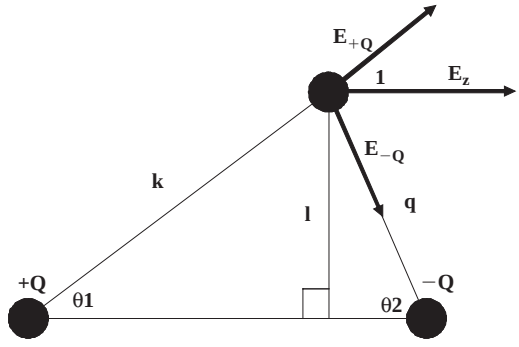


Figure 6. Electric field, E

$$k = \sqrt{(x-x1)^2 + (y-y1)^2 + z^2}$$
$$q = \sqrt{(x-x2)^2 + (y-y2)^2 + z^2} \tag{27}$$

where $x1$, $y2$, $x2$, $y2$ are coordinates of sensors. L is expressed in Eq. (19). So using Eq. (21) through Eq. (25), the current can be expressed as follows:

$$I = \int_{\infty}\int_{\infty}\int_{\infty} \frac{dV\sigma_{mass}}{2}\left(\frac{\sqrt{k^2-l^2}}{k^3}+\frac{\sqrt{q^2-l^2}}{q^3}\right)dzdxdy$$
$$+\int_{\infty}\int_{\infty}\int_{\frac{AX-BY+D}{C}}^{\frac{-AX-BY+D}{C}} \frac{dV(\sigma_f-\sigma_{mass})}{2K}\left(\frac{\sqrt{k^2-l^2}}{k^3}+\frac{\sqrt{q^2-l^2}}{q^3}\right)dzdxdy \tag{28}$$

where V is the voltage. As a result, if a fault zone exists ahead of tunnel face, the resistance can be obtained as follows:

$$R = 1/\left(\int_{\infty}\int_{\infty}\int_{\infty} \frac{d\sigma_{mass}}{2}\left(\frac{\sqrt{k^2-l^2}}{k^3}+\frac{\sqrt{q^2-l^2}}{q^3}\right)dzdxdy + \right.$$
$$\left.\int_{\infty}\int_{\infty}\int_{\frac{AX-BY+D}{C}}^{\frac{-AX-BY+D}{C}} \frac{d(\sigma_f-\sigma_{mass})}{2K}\left(\frac{\sqrt{k^2-l^2}}{k^3}+\frac{\sqrt{q^2-l^2}}{q^3}\right)dzdxdy\right) \tag{29}$$



Figure 7. Model test setup.



Figure 8. Sensor configuration on a tunnel face.

5 DEVELOPMENT OF PROGRAMS

Using the derived equations, an inversion method is developed for predicting weak zones and fault zones ahead of tunnel face from in-situ resistance measurements. Inversion methods are composed of loop forms. Comparing the measured resistances with the calculated resistances through loop forms, the unknown parameters can be determined at the smallest error.

An integrated program with the inversion process is developed, composed of two other programs. One is a program which can be utilized when a fault zone exists ahead of tunnel face. The other is a program which can be utilized when a weak zone exists ahead of tunnel face. Given that resistances measured for each sensor configuration, the location of sensors and the conductivity of the rock mass, the unknown parameters such as the size of the anomaly, the conductivity of the anomaly and the location of the anomaly can be obtained using the developed program.

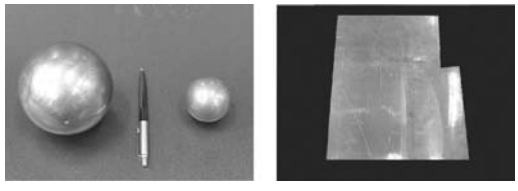


Figure 9. Materials used for simulation of weak zones and fault zones.

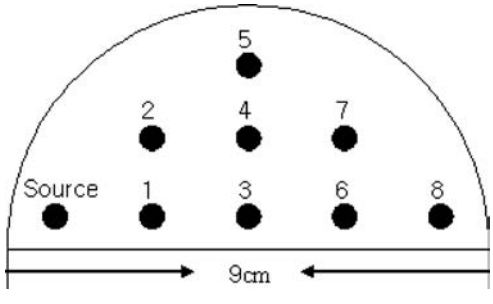


Figure 10. The location of sensors.

6 EXPERIMENTAL TESTS

Laboratory experimental tests are performed to verify the derived equations, inversion methods and developed programs. Figure 7 shows a model test setup that simulates a tunnel under the ground, Figure 8 shows sensor configurations on a tunnel face, Figure 9 shows the materials simulating weak zones and fault zones, and Figure 10 shows the location of sensors. Table 1 shows the measured resistances for different sensor locations when weak zones and faults zones exist ahead of tunnel face. Table 2 shows the comparison of the real values such as the location, size, and conductivity of a weak zone and the predicted values for the case of a weak zone. Table 3 shows the comparison of the real values such as an equation of plane, the thickness, and conductivity of a fault zone and the predicted values for the case of a fault zone. The results show that the predicted values are in good agreement with the real values. Thus, the detection system developed in this study can be used for predicting a weak zone and a fault zone ahead of tunnel face effectively.

7 CONCLUSIONS

This study presents an enhanced electrical resistivity-based detection system for predicting a weak zone and a fault zone ahead of tunnel face. The electric field analyses are based on Coulomb's law and Gauss' law considering electrical characteristics of rock mass properties. The equations for resistance are derived for the presence of a weak zone and a fault zone ahead of

Table 1. Measured resistances.

Sensor #	A weak zone (Ω)	A fault zone (Ω)
1	11456	11627
2	11299	11320
3	11069	11251
4	11002	11076
5	10753	11031
6	10747	10549
7	10653	10636
8	10408	10166

Table 2. Real values and predicted values (a weak zone).

Characteristics	Real values	Predicted values
x coordinate(m)	0.02	0.02
y coordinate(m)	0.03	0.04
z coordinate(m)	0.26	0.26
Radius(m)	0.05	0.04
Conductivity($\Omega^{-1}m^{-1}$)	1.1	1

Table 3. Real values and predicted values (a fault zone).

Characteristics $Ax+By+Cz=D$	Real values	Predicted values
A	5	5
B	−4.3	−4.5
C	5.3	5.5
D	136	135
Thickness (m)	0.01	0.0089
Conductivity ($\Omega^{-1}m^{-1}$)	20	19

tunnel face. The developed algorithms and programs are verified through laboratory experimental tests. The experimental results suggest that the presence of weak zones and their sizes, location and states can be effectively predicted from electrical resistance measurements through a proper inversion process. This method would benefit from verification using more elaborate field measurements.

ACKNOWLEDGMENTS

This paper was supported by the Korea Institute of Construction and Transportation Technology Evaluation and Planning under the Ministry of Construction and Transportation in Korea (Grant No. 04-C01) and Brain Korea 21 Project in 2006.

REFERENCES

Archie, G. E. 1942. The electrical resistivity log as an aid in determining some reservoir characteristic. *Trans, AIME*, Vol. 146, pp. 54–62.

Bittar, M.S., Rodney, P.F., Mack, S.G.. and Bartel. R. P. 1993 A multiple-depth-of-investigation 7. Electromagnetic Wave Resisivity Sensor. *Theory, Experiment, and Field Test Results, SPE Formation Evaluation*, pp. 171–176.

Blaricom, R. V. 1992. Practical geophysics 2 -for the exploration geologist. *Northwest Mining Association, Spokane*, pp. 39–139.

Chinh, P.D. 2000. Electrical properties of sedimentary rocks having interconnected water-saturated pore spaces. *Geophysics*, Vol. 65, pp. 1093–1097.

Cho, Y., Lim, J. S., Jeong, Y. Y., and Choi, S. Y. 1999. A case study on the ground reinforcement method and effect of the failed tunnel. *KTS Spring Conference*, pp. 293–300.

Hasegawa, M., Usui, M., and Gotoh, K. 1993. Geological prognosis ahead of a tunnel face. *Engineering Geology*, Vol. 35, pp. 229–235.

Herrick, C. D., and Kenndy, W. D. 1994. Electrical Efficiency – A Pore Geometric Theory for Interpreting the Electrical Properties of Reservoir Rocks. *Geophysics*, Vol. 59, No. 6, pp. 918–927.

Jackson, J. D. 1999. Classical Electrodynamics. *John Wiley& Son*, U.S.A, pp. 24–134.

Karwatowski, J., and Habberjam, G.. M. 1981. A tunnel resolution investigation using automated resistivtiy tank analog. *Geophysics Prospecting*, Vol. 29, pp. 891–905.

Kim, N. Y., Kim, S. H., and Joeng, H. S. 2000. Analysis of collapse shape and cause in the highway tunnel (in Korea). *Korea Tunnel Association*, Vol. 2, pp. 13–23.

Lee, I. M., Choi, S. S., Kim, S. T., Kim, C. K., and Jun, J. S. 2002. 3D analysis of fracture zones ahead of tunnel face using seismic reflection (in Korea). *Tunneling Technology*, Vol. 4, pp. 301–317.

Lee, S. W. 2001. Investigation skill of TBM tunnel ahead of tunnel face (in Korea). *Construction Skill Information*, pp. 25–27.

Militzer, H., Rösler, R., and Lösch, W. 1977. Theoretical and experimental investigations for cavity research with geoelectrical resistivity Methods. *Geophysics Prospecting*, Vol. 25, pp. 640–652.

Olivar A. L. de Lima, 1995. Water saturation and permeability from electrical resistivity, dielectric, and porosity log. *Geophysics*, Vol. 60, pp.1756–1764.

Reitz, J. R., Milfore, F. J., and Christy, R. W. 1993. Foundations to Electromagnetic Theory. *Addison Wesley*, U.S.A., pp. 26–126.

Sattel, G., Frey, P., and Amberg, R. 1992. Prediction ahead of the tunnel face by seismic methods. *Pilot project in Centovalli Tunnel*, Locarno, Switzerland. First Break, Vol.10, pp.19–25.

Sen, P. N., Scala, C., and Cohen, M. H. 1981. A self-similar model for sedimentation rocks with application to the dielectric constant of fused glass beads. *Geophysics*, Vol. 46, pp. 718–795.

Suzuki, K., Nakata, E., Minami, M., Hibino, E., Tani, T., Sakakibara, J., and Yamada, N. 2004. Estimation of the Zone of Excavation Distribution around Tunnels, using Resistivity and Acoustic Tomography. *Geophysics Prospecting* Vol. 33, pp. 62–69.

Underground Space – the 4th Dimension of Metropolises – Barták, Hrdina, Romancov & Zlámal (eds)
© 2007 Taylor & Francis Group, London, ISBN 978-0-415-40807-3

A modified design of a large section tunnel as an auxiliary spillway along large faults

Y.W. Shin, I.K. Lee, T.S. Park, H.S. Choi & S.C. Park
Tunnel & Geotech. Div., Hakyong Eng. Co., Korea

J.K. Kim, M.S. Lee, K.H. Shin & B.H. Han
Division of Civil Works, Samsung Corporation, Korea

ABSTRACT: An auxiliary spillway tunnel of 18 ~ 15 m height and 24 ~ 15 m width is planed for increasing flood control capacity of the Soyang river dam in South Korea. It is composed of two parallel tunnels, T1 and T2. Some faults unexpected in design stages are revealed in transition section of entrance. Two times of roof falls are caused by those faults. Additional vertical borings at ground surface and horizontal borings at tunnel side wall are executed. Some alternative reinforcement methods based on additional borings are carefully investigated. Roof falls were occurred in entrance section of T1 and T2 tunnel. Steel pipes are inserted and cement mortar is filled temporarily. The results of additional geological investigation indicate that T1 tunnel are planned parallel to faults of maximum width 20 m. Four faults are intersected with T2 tunnel. Extremely poor mica gneiss is widely distributed and stability of tunnel face is not guaranteed. It is concluded that original support system is deficient and alternative support system is needed. Several alternative methods such as cut and cover tunnel, double support system and steel pipe insertion method are profoundly investigated considering ground and construction conditions. Double support system is selected as the most suitable alternative. Numerical analyses considering field ground condition and dimension of tunnel cross section manifest the tunnel stability.

1 INTRODUCTION

A localized heavy rain is often caused by a worldwide unusual change of weather. The magnitude of flood disaster is gradually increased. Therefore, an auxiliary spillway has been constructed in order to improve the safety of existing dams in Korea. For the purpose of this, a large section spillway tunnel of the Soyang river dam is constructing of 25 m width and 18 m height. And this spillway tunnel is the first case in Korea. It is composed of two parallel tunnels, T1 and T2. Some faults unexpected in design stages are revealed in transition section of upper entrance tunnel through additional ground investigation. Two times of roof falls are caused by those faults. In addition, the spillway tunnel should be obliged to construct through a large fault of 20 m width. Therefore, an alternative method for excavation and reinforcement is needed to guarantee the stability of the spillway tunnel. Double support system is selected as the most suitable alternative in very poor ground with large faults.

2 PROJECT OUTLINE

2.1 *Design status*

This spillway tunnel for increasing of flood control capacity is composed of two parallel tunnels of T1 and T2 and two domains of upper and lower. Tunnel length is about 1,300 m respectively. The large inlet part of 155 m length with horseshoe-shaped section in upper domain is transition section for smooth inflow of overflow water. From that point, tunnel section narrow more and more, and become most safe circular section by hydraulics in lower domain Incline of upper tunnel section is steep slope of 14.036°. The whole status of auxiliary spillway tunnel is shown in Figure 1.

2.2 *Construction status*

Upper tunnel was excavated upward toward inlet. Roof fall of T1 tunnel was caused directly after 47 m advance during upper section excavation. Mucks were accumulated and reinforcement was executed in the

rear of roof fall area. Roof fall of T2 tunnel was caused immediately after 130 m advance of pilot tunnel and excavation of left and right parts of upper section. Mucks were stacked up and face shotcrete was shot in the roof fall area of T2 tunnel. Also, cement mortar was filled up in the roof cavity. The status of construction and roof fall are shown in Figure 2.

2.3 *Geological conditions*

On the excavation of the spillway tunnel, the unexpected large faults were appeared and an additional geological investigation on the ground will be excavated was needed. Borings and an outcrop investigation were preferred than physical investigation such as electrical resistivity survey. Geological characteristics were reevaluated by additional investigation. Results of additional geological investigation are shown in Figure 3. C1∼C7 are horizontal boring and C8∼C10, C12 are vertical boring.

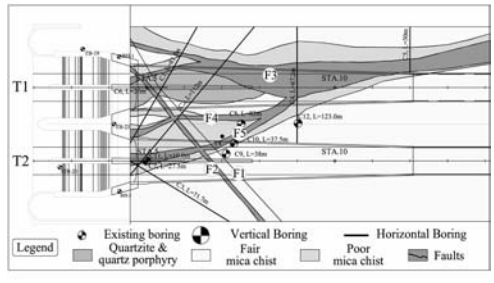
5 faults of F1∼F5 in the construction area were investigated by additional borings. Considering the fault width and distribution range, an original support is not insufficient. It was estimated that roof falls during excavation were caused by many faults. Geological condition of the roof falling section and transition section are shown in Figure 4. Analyzing roof falling status and results of an additional detailed geological investigation, probable reinforcement methods were examined.



(a) The Soyang river dam and the auxiliary spillway tunnel

(b) Auxiliary spillway tunnel

Figure 1. The auxiliary spillway tunnel of the Soyang river dam.



Faults	Width	Characteristic
F1	~ 1.0m	clay filling
F2	2.4m	groundwater
F3	4.0 ~ 20.0 m	faults superposition
F4	2.2 ~ 6.0m	disturbance structure
F5	2.5 ~ 5.4m	large scale shear zone

Figure 3. Results of additional borings.

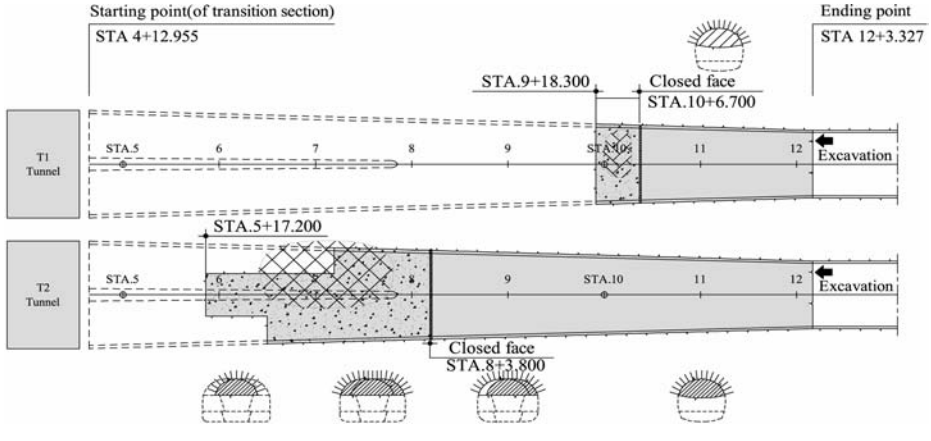


Figure 2. Construction status.

3 ALTERNATIVE EXAMINATION

For successful construction of the auxiliary spillway tunnel, possible alternatives were investigated considering construction status and new-revealed geological condition. First of all, the design and construction cases of large tunnel like the inlet cross section of spillway tunnel and those of constructed in very poor ground condition were investigated. Geological survey technology, reinforcement method and numerical analysis method were investigated. Probable alternatives to solve this problem were NATM, cur and cover tunnel, and pipe insertion method. The first alternative of NATM is more economic than the others and continuous with section constructed in former times. However, various support patterns are needed due to uncertainty of ground condition.

The second alternative, cut and cover tunnel can eliminate the possibility of roof fall at faults area and reduce uncertainty of ground condition. But application to whole section is impossible and uneconomic in comparison with NATM because of large excavation and temporary retaining wall.

The third alternative is the pipe insertion method of inserting a large diameter pipe into the ground prior to excavation. The benefit of this method is the increasing of tunnel stability and foresight of fore ground condition. However, construction cost is very expensive and its application cases are scarce.

Results of giving careful consideration to geological condition and stratum show that NATM with additional reinforcement is more suitable method than the others from a economical point of view and considering the construction convenience. Cut and cover tunnel method is applicable to the entrance section of 30∼50 m length, but the impossibility of temporary heaping of blasted rocks and a widespread damage of mountains and forests. Finally, NATM is chosen as the most suitable alternative considering the results of construction, construction cost and construction period.

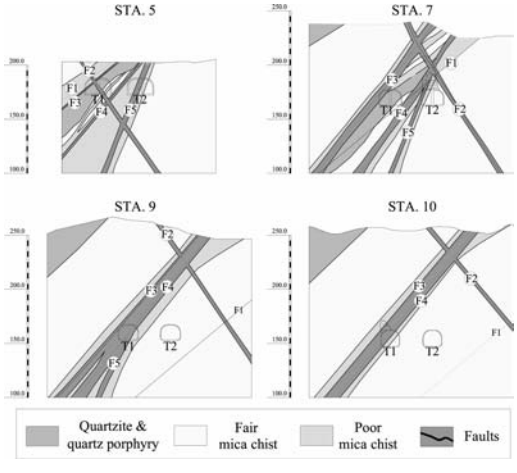


Figure 4. Faults condition.

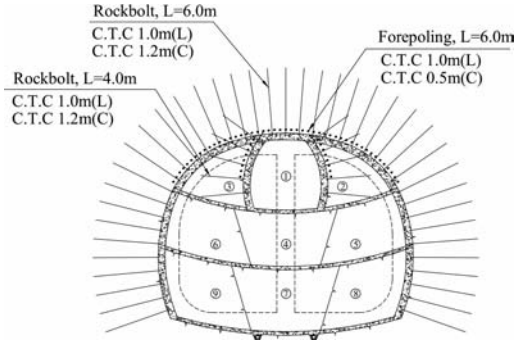


Figure 5. NATM.

4 MODIFIED DESIGN

Detailed excavation and reinforcement method of NATM concluded as the most suitable alternative were investigated.

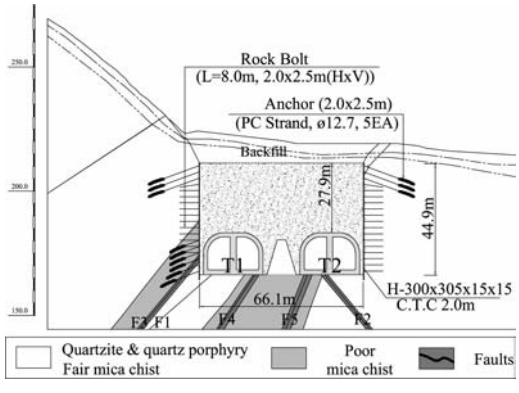


Figure 6. Cut and cover tunnel.

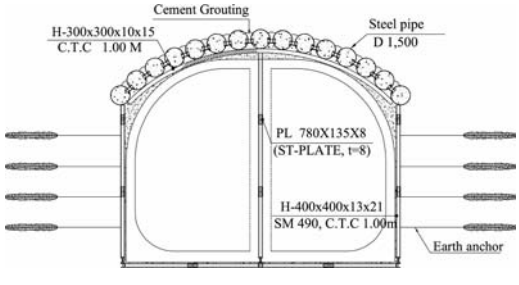


Figure 7. Pipe insertion method.

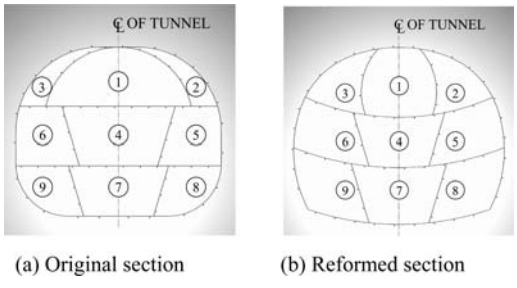


Figure 8. Improvement of cross section.

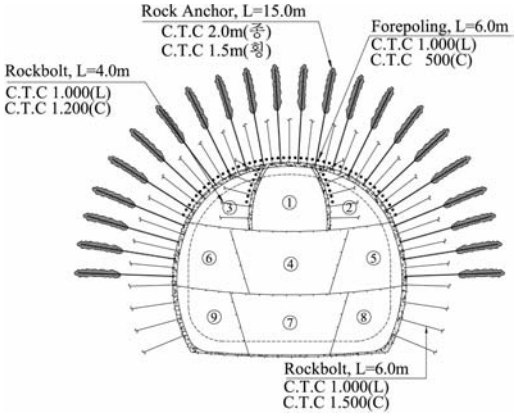


Figure 9. Anchor system.

4.1 *Improvement of tunnel cross section*

Cross section of an original design is unfavorable to support rock loads because crown and side wall of cross section are flat. Obtaining the supporting capacity by arching effects is probably difficult in the section of poor ground condition. Therefore, the shape of excavation cross section is converted into arch shape although excavation area is more or less increased.

4.2 *Supporting pattern*

Section of roof fall is located in very poor ground condition. Reinforcement of supporting system is needed because the maximum width of fault is about 20 m and overburden of 100 m height is very excessive. First of all, numerical analysis for original supporting system is carried out in the changed ground condition. Countermeasure reducing or supporting ground stress is needed because engineering properties of faults are very poor and ground stress induced by overburden is very excessive. Accordingly, anchor system that can reduce the ground stress and double support system that can uphold rock loads are evaluated as suitable countermeasure for the mechanical stability and construction convenience.

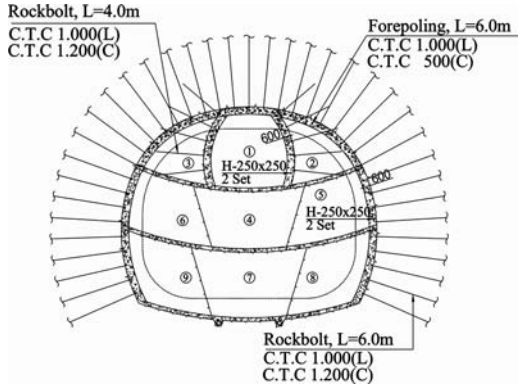


Figure 10. Double support system (Double steel-rib support).

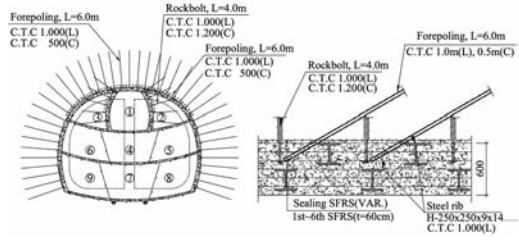


Figure 11. Outline of double support system.

Investigation results show that both two systems guarantee the tunnel stability. Double support system is chosen as an alternative method for faulted ground because it is more preferable than anchor system considering construction convenience, economical efficiency and construction period. The first steel rib of the double support system make ground permit some deformation for extremely rock loads and swelling pressure. Behind the first support release the rock loads, the second steel rib is installed to secure the stability of general support system. Some successful application cases has been reported in Japan that overall ground condition is poor. Tunnel cross section and construction sequence of double support system chosen as an alternative are shown in figure 11 and figure 12.

4.3 *An auxiliary reinforcement method*

An auxiliary reinforcement method is needed because self-supporting time of the face is insufficient even if the face is excavated into 8 m width separately. Therefore, forepoling, face bolt, face shotcrete, temporary invert, and umbrella arch method are chosen as an auxiliary reinforcement method to insure the stability of tunnel crown and face.

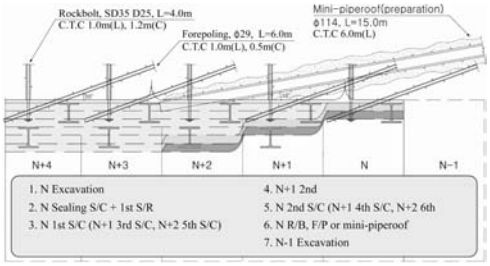


Figure 12. Construction sequence of double support system.

4.4 *Excavation direction*

Considering a longitudinal steep inclination with 14° and very poor ground condition, an original upward excavation is profitable to drain of itself. However, when the upper, middle and lower part of tunnel section is excavated separately, construction is very difficult because the maximum longitudinal inclination of mount road is 14°. On the contrary, when tunnel is excavated downward, a pumping drainage is needed because groundwater is collected at the face. When the upper, middle and lower part of tunnel section is excavated separately, the longitudinal inclination of mount road is less than 14°. Accordingly, the downward excavation is very profitable because the upper, middle and lower part of tunnel section can be excavated simultaneously. In addition, downward excavation is more profitable than upward excavation, because the reinforcement effect of mini-piperoof of excavating downward is more preferable than the other. In conclusion, the downward excavation is selected for the face stability.

4.5 *Numerical analysis*

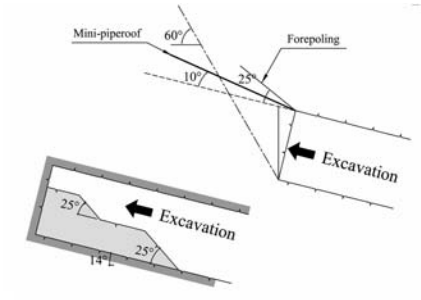
Numerical analysis is performed to investigate the stability of double support system using FLAC of Itasca consulting group. In Korea, the support capacity of steel rib is not considered conservatively in numerical analysis because steel rib is regarded as temporary support till shotcrete hardening.

A role of steel rib is great in very poor ground with fault. For that reason, the supporting capacity of steel ribs of double support system is reflected to analyze the tunnel stability.

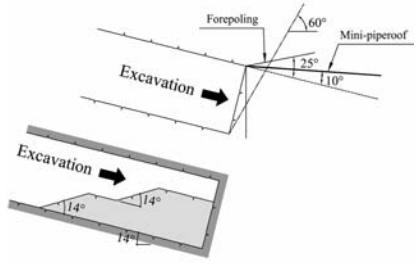
Equivalent elastic modulus(E_0) and equivalent moment of inertia(I_0) are Eq. (1) and Eq.(2). Bending moment is only supported by steel ribs.

$$E_o = \frac{E_c A_c + E_s A_s}{A_c + A_s} \quad (1)$$

$$I_o = \frac{I_s E_s}{E_o} \quad (2)$$



(a) Upward excavation



(b) Downward excavation

Figure 13. Excavation direction.

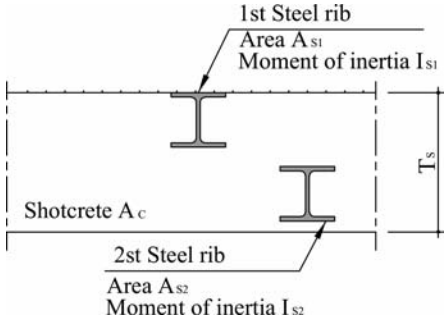


Figure 14. Structural properties of shotcrete and steel ribs.

where, Ec : elastic modulus of shotcrete, Es : elastic modulus of steel rib

Numerical analysis shows that the maximum crown settlement is 124.0 mm and the maximum convergence is 43.19 mm. The maximum compression stress of shotcrete is 4.59 MPa and that of steel rib is 269.43 MPa. All are lower than allowable criterion.

5 CONCLUSIONS

A large section spillway tunnel of large dam is constructing of 25 m width and 18 m height. It is composed of two parallel tunnels, T1 and T2. Some faults

unexpected in design stages are revealed in transition section of the inlet of upper tunnel. Two times of roof falls are caused by those faults. The countermeasure based on an additional geological survey was investigated as follows.

NATM, cut and cover tunnel, and pipe insertion method are investigated considering the ground condition and construction status for the purpose of choosing an countermeasure. NATM is chosen as the most suitable alternative considering the results of construction, construction cost and construction period.

Double support system is chosen as an alternative method for faulted ground because it is more preferable than anchor system considering construction convenience, economical efficiency and construction period.

REFERENCES

Hoek, E. 2001. 3, Design of large underground caverns-A case history based on the Mintan Pumped Storage Project in Taiwan, Discussion paper #2

Hoek, E. 2004. 2, Anchored crane beams in hydroelectric caverns, Discussion paper #1

Hoek, E. 2002, Rock Engineering, pp.232∼249

Kitagawa Syusan, 2003. 2, Double support system is an effective countermeasure on swelling ground, Tunnels and Underground, Vol.34, No.2, pp.55∼65

Korea Water Resources Corporation, 2004. 4, Detailed design report on the spillway construction of the Soyang river dam

Samsung Corporation, 2005. 6, Report on an Additional Site Investigation for the spillway construction of the Soyang river dam

Underground Space – the 4th Dimension of Metropolises – Barták, Hrdina, Romancov & Zlámal (eds)
© 2007 Taylor & Francis Group, London, ISBN 978-0-415-40807-3

Geotechnical control during the excavation of the tunnel of Guadarrama

Isidoro Tardáguila, Benjamín Celada & José Miguel Galera
Geocontrol S.A.

ABSTRACT: The tunnels of Guadarrama are new twin tunnels crossing the Central Range between Madrid and Segovia, as part of the new High Speed Railway Line to the NW of Spain. Their length is 28.3 km with a maximum overburden of 900 m. The geology consists mainly of crystalline rocks, gneiss and granites, with a main graven in the Lozoya valley where poor quality sedimentary rocks from the Cretaceous are crossed. Nevertheless several faults have also been detected with mylonites and water. The tunnels have been done using four double-shield TBMs, all of them with an excavation diameter of 9.5 m. The information that can be accessed from the face during its excavation with a Double-Shield TBM is generally limited. Nevertheless during Guadarrama tunnels excavation a close control of the excavated ground has been carried out, in order to allow the prediction of ground conditions ahead the TBMs. The applied methodology consists in: – geotechnical face characterization – inspection of the excavated chips – analysis of TBM drilling parameters. In relation with face characterization, conventional mapping of the face has been done as well as short boreholes (<1 m) through the lining segments. These cores have provided samples for laboratory conventional tests (UCS, PLT, Vp,…). The inspection of the waste chips has consisted not only in the weight in the belt but also in the size and shape of the waste. Finally, the drilling parameters controlled were: – rate of advance – time of excavation – weight of material in the belt – thrust – rotation speed – torque. These basic drilling parametes have been used to obtain the drilling specific energy, that has shown to be a very powerful index to predict ground conditions in the face. By means of this analysis the prediction of ground conditions ahead the TBM face was successfully done, specifying discontinuities spacing and condition.

1 INTRODUCTION

The construction of a tunnel using a TBM requires an accurate knowledge of the rock mass as the face is almost inaccessible and therefore the information that can be obtained from it is limited. Also because the TBMs are very sensible to the rock mass characteristics and its possibilities to adaptation to other conditions not foreseen is quite difficult.

In Guadarrama tunnels one of the tunnels (In the North Portal, the eastern one) goes always ahead the other. This circumstance makes very interesting to make a precise supervision in the first one, in order to:

- Foreseen the ground behaviour in relation with the TBM performance.
- Extrapolate the TBM behaviour from one tunnel to the parallel one.

The methodology set up includes the following activities:

- Geological and geomechanical prediction.
- Information collected from the tunnels excavation.
- Data storage and exploitation.

2 GEOLOGICAL AND GEOMECHANICAL PREDICTION

The main objective of this activity is to have a prediction of the ground conditions ahead the TBM face.

In Galera *et al.* (2006) it has been explained the importance of geological mapping as well as geophysical prospecting and in situ testing, for this purpose.

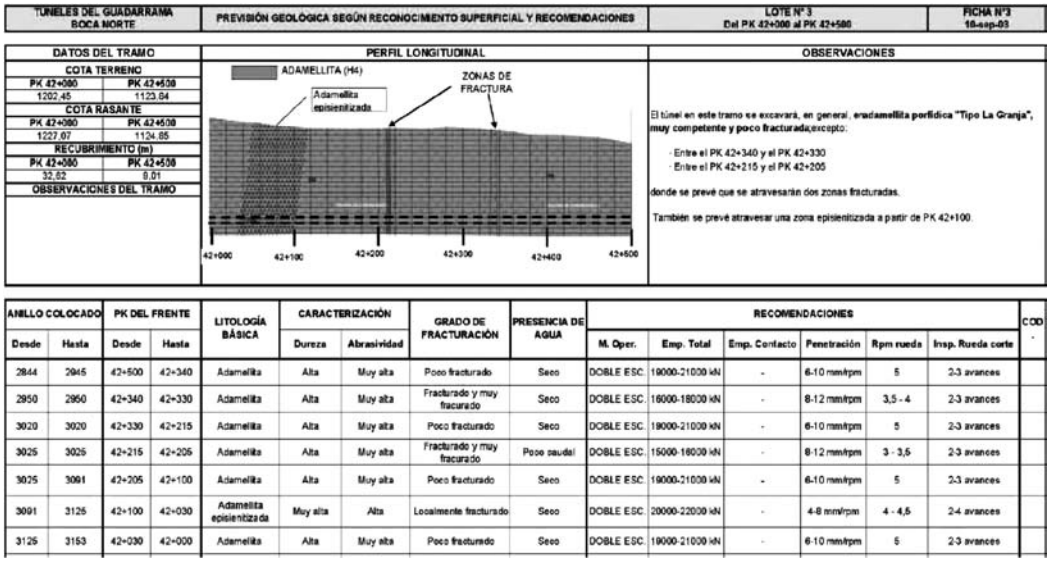
Following that methodology for the each 500 m of tunnel that roughly correspond to a month of advance a prediction sheet was done. Figure 1 shows an example of this prediction sheet.

It can be observed that this prediction sheet includes the following information:

- Geological profile and description.
- Lithology.
- Discontinuity spacing.
- Hardness and abrasivity.
- Water presence.

Also in the right hand side it includes the recommendations for the TBM, as follows:

- Working mode (Double or Single Shield TBM).



ANILLO COLOCADO		PK DEL FRENTE		LITOLOGÍA BÁSICA	CARACTERIZACIÓN		GRADO DE FRACTURACIÓN	PRESENCIA DE AGUA	RECOMENDACIONES						COD.
Desde	Hasta	Desde	Hasta		Dureza	Abrasividad			M. Oper.	Emp. Total	Emp. Contacto	Penetración	Rpm rueda	Insp. Rueda corte	
2844	2945	42+500	42+340	Adamellita	Alta	Muy alta	Poco fracturado	Seco	DOBLE ESC.	19000-21000 kN	-	6-10 mm/rpm	5	2-3 avances	
2950	2950	42+340	42+330	Adamellita	Alta	Muy alta	Fracturado y muy fracurado	Seco	DOBLE ESC.	16000-18000 kN	-	8-12 mm/rpm	3,5 - 4	2-3 avances	
3020	3020	42+330	42+215	Adamellita	Alta	Muy alta	Poco fracturado	Seco	DOBLE ESC.	19000-21000 kN	-	6-10 mm/rpm	5	2-3 avances	
3025	3025	42+215	42+205	Adamellita	Alta	Muy alta	Fracturado y muy fracurado	Poco saudal	DOBLE ESC.	15000-16000 kN	-	8-12 mm/rpm	3 - 3,5	2-3 avances	
3025	3091	42+205	42+100	Adamellita	Alta	Muy alta	Poco fracturado	Seco	DOBLE ESC.	19000-21000 kN	-	6-10 mm/rpm	5	2-3 avances	
3091	3125	42+100	42+030	Adamellita episienitizada	Muy alta	Alta	Localmente fracturado	Seco	DOBLE ESC.	20000-22000 kN	-	4-8 mm/rpm	4 - 4,5	2-4 avances	
3125	3153	42+030	42+000	Adamellita	Alta	Muy alta	Poco fracturado	Seco	DOBLE ESC.	19000-21000 kN	-	6-10 mm/rpm	5	2-3 avances	

Figure 1. Example of a prediction sheet for the ground conditions ahead the TBM face.

– Thrust (kN).
– Penetration (mm/rpm).
– Rotation speed (rpm).
– Time for inspection of the cutter wheels (TBM head).

3 INFORMATION COLLECTED FROM THE TUNNEL EXCAVATION

3.1 *Tunnel face*

The access to the tunnel face in a Double-Shield TBM is very restricted. Nevertheless in some maintenance gaps,…, it is possible to access to it. Usually this access is done through the windows included in the TBM head (cutter-wheels, bucklets or man windows).

The information collected from the face is shown in the sheet included in Figure 2, that contains the following:

– Face scheme, mapping lithologies and geological structures.
– UCS estimation, using point load tests (I_{S50}).
– RMR determination (Bieniawski, 2003).
– Discontinuities (strike, dip, spacing, roughness, filling).
– Photos.

Figures 3, 4 and 5 include photos taken on the tunnel face.

These photos have been systematically taken from the three different available windows at the TBM head.

Exceptionally it has been possible to visit the face of the tunnel while some maintenance stops. Figure 6 shows the aspect of the face in one of these occasions.

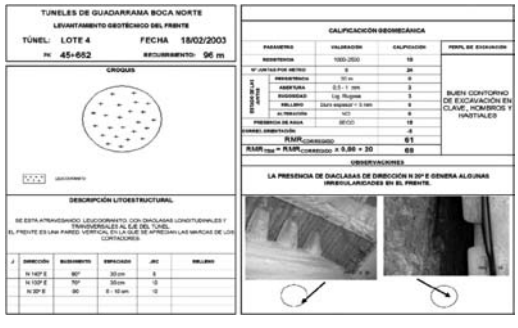


Figure 2. Example of the geotechnical information obtained from the mapping of the face.

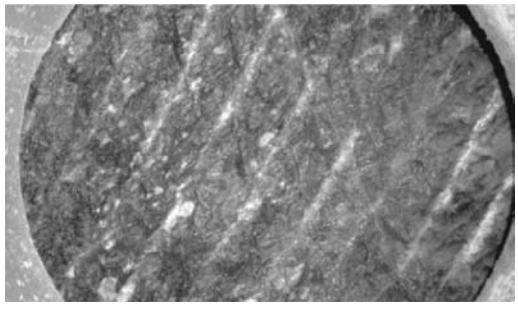


Figure 3. Face view taken through the man window in the TBM head.

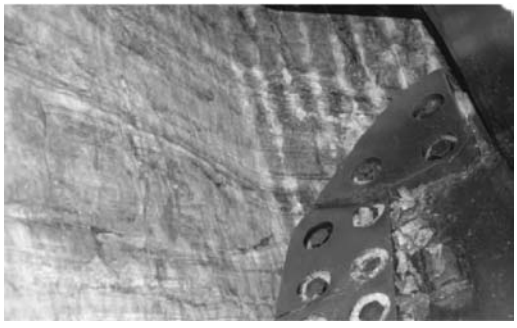


Figure 4. Face view taken though the bucklet window in the TBM head.



Figure 5. Face view taken through the cutter-wheel window in the TBM head.



Figure 6. Face of the tunnel taken during one maintenance stop.

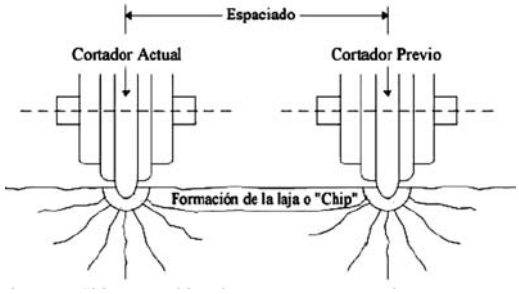


Figure 7. Chip created in a homogeneous ground.

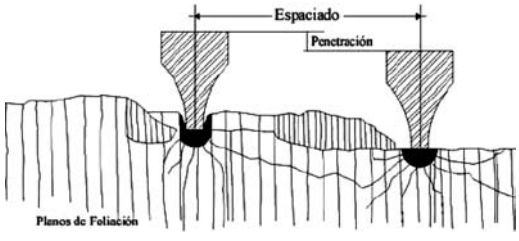


Figure 8. Chip created in a ground foliated longitudinally.

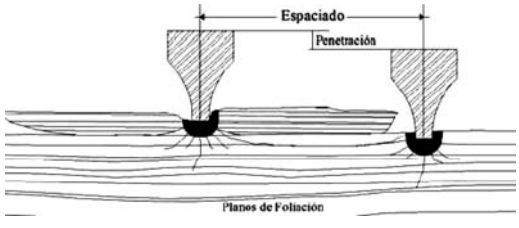


Figure 9. Chip created in a ground foliated perpendicularly.

3.2 *Chip inspection*

The most usual way to analyse the ground condition in a tunnel excavated using a TBM, is following the chips coming from the TBM head.

Figures 7, 8 and 9 shows the way in which the cutter wheel creates different types of chips, depending on the kind of ground.

Figures 10, 11 and 12 include photos showing the type of chips coming from a homogeneous face, fractured face and faulted-gouge.

3.3 *TBM drilling parameters*

The following TBM drilling parameters have been systematically recorded:

- Advance rate (ARA)
- Time of excavation
- Weigh of the debris in the belt
- Thrust (total/contact) (F)

– Rotation speed (N)
– Torque (T)

Two different interpretations can be done:

– Qualitative
– Quantitative

In the first type the following circumstances have been noticed:

– A significant increase in the rate of advance with an decrease in the geomechanical ground quality.



Figure 10. Chips coming from a homogeneous ground.



Figure 11. Chips coming from a fractured face.



Figure 12. Chips coming from a faulted face.

– An increase in the debris weight with a face instability.
– Instantaneous torque increase with a face instability.
– The difference between the applied and the contact thrust is equivalent to the TBM friction. If this value increase the TBM can get stucked.

In relation with a quantitative interpretation, the following values have been considered:

– Penetration rate (p)

$$p\,(mm/r) = \frac{V\,(mm/m)}{N\,(rpm)} \tag{1}$$

that gives the ground resistance to be excavated.

– Penetration index (I_p)

$$I_p = \frac{F_c\,(kN)}{p} \tag{2}$$

that proportionates the thrust per cutter to penetrate 1 mm per revolution.

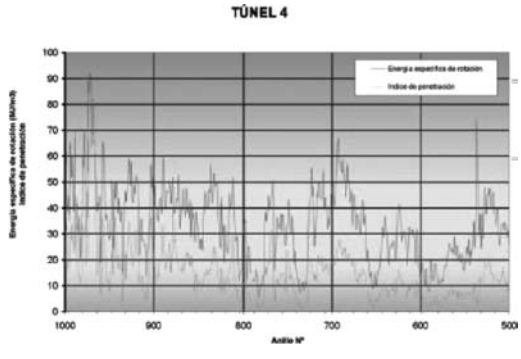


Figure 13. Relationship between I_p and E_{sr} for 500 segments rings.

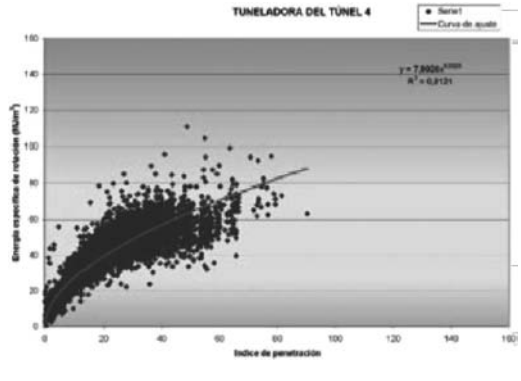


Figure 14. Correlation between E_{sr} and I_p ($E_{sr} = 8 \cdot I_p^{0.52}$).

– Specific energy of excavation (E_s)

$$E_s\ (kJ/m_3) = \frac{F}{A} + \frac{2\pi \cdot N \cdot T}{A \cdot ARA}\ \text{(Teale, 1965)} \qquad (3)$$

where E_s = specific energy of excavation (kJ/m^3), F = total cutterhead thrust (kN), A = excavated face area (m^2), N = cutterhead rotation speed (rps), T = applied torque (kN·m) and ARA = average rate of advance (m/s).

As it can be observed there are two addends, the first one corresponds to the thrust energy (E_{st}) while the second one corresponds to the rotation energy (E_{sr}).

– Correlation between I_p *vs.* E_{sr}.

Figures 13 and 14 shows the existing relation between the penetration index and the specific rotation energy of excavation.

In the first one it can be observed the direct relation between both parameters considering 500 segment units. From this relation it can be concluded that the specific energy depends on the geomechanical quality of the rock mass as the penetration index does.

Table 1. Rock mass classification, considering discontinuities spacing (NTNU, 1994).

Rock mass classification	Discontinuities spacing (cm)
0	Massive
0–I	160
I	80
I–II	40
II	20
III	10
IV	5

Table 2. Criteria to establish the rock mass spacing discontinuities at the excavation face, considering different criteria.

Rock mass type	Spacing (cm)	Joints/m	I_p	E_{sr} (kJ/m^3)	Debris
I	>40	4	20–30	40–60	chips
II	20	4–8	10–15	20–30	chips and occasional blocks
III	10	8–15	4–7	10–15	cm and dm blocks
IV	5	15–30	1	5	heterometrical blocks (dm, cm, fines)
V	<5	>30	>0	<5	sand and fines

3.4 *Discontinuities at the excavation face*

The Norges Lekmsk-naturritenskapllige Universitet (NTNU, 1994) made a classification (see Table 1).

In the Guadarrama tunnels the discontinuities spacing has been determined:

– Directly from the mapping of the face.
– Indirectly from the debri type at the belt.
– Indirectly from the TBM drilling parameters.

In Table 2 it is shown the relation between them.

3.5 *Rock sampling*

The aim of this activity was to obtain information about basic rock mechanics properties of the excavated rock mass.

Each 125 m of tunnels a small borehole (70 cm aprox.) was drilled, obtaining samples to carry out the following tests: density, sonic velocity, UCS, brazilian, point load test, petrographical analysis, DRI and Cerchar abrasivity.

In Table 3 it is shown the average parameter obtained for the different lithologies excavated in the tunnels of Guadarrama.

Table 3. Geomechanical properties of the Guadarrama lithologies.

Lithology	Density (gr/cm^3)	UCS (N/mm^2)	Is50	σ_t (N/mm^2)	V_p (m/s)	Qz (%)	Quartz equivalent (%)	DRI	CLI	Cerchar
Ortogneiss	2.703	89.6	8.30	9.5	5100	33	53	46	13.0	3.4
Adamellite	2.625	85.9	7.50	7.6	5095	33	55	55	11.7	3.1
Leucocratic Granite	2.591	95.1	7.71	9.0	4737	33	57	42	9.7	3.2
Episienite	2.582	75.6	4.50	5.6	4686	3	34	55	18.6	2.4
Granitic Porphyr	2.598	125.0	9.18	13.0	5530	22	47	37	12.3	3.0
Diorite	2.723	152.1	10.34	–	5577	1	32	38	27.7	2.5
Paragneiss	2.759	–	9.00	10.1	–	–	–	–	–	–
Marble	2.711	–	5.30	7.3	–	0	9	71	64	1.4
Skarn	2.726	–	8.10	9.9	–	3	20	–	–	–
Pegmatite	2.756	110.3	–	9.7	–	47	–	–	–	–
Quartz	2.657	76.0	6.84	–	5805	99	99	47	5.3	3.1

4 CONCLUSIONS

The methodology followed during the excavation of the tunnel of Guadarrama for its geotechnical control, has consisted on:

- Mapping of the tunnel face.
- Chips inspection.
- TBM drilling parameters record.
- Discontinuities spacing at the excavation face.
- Rock sampling.

This methodology has proved to be efficient for the geological and geomechanical prediction of the rock mass to be excavated.

BIBLIOGRAPHY

Galera, J.M. *et al.* (2006). "Prediction of the ground conditions ahead the TBM face in the Tunnels of Guadarrama (Spain), using geophysical methods and in situ testing". ITA World Congress 2007 Proceedings.

Tardáguila, I., Suarez, J.L. (2005). "Metodología para el seguimiento y control del terreno en el interior de los túneles de Guadarrama". In: Túnel de Guadarrama. Ed. Entorno Gráfico, pp. 479–501.

Teale, R. (1965). "The concept of specific energy in rock drilling". Int. J. Rock Mech. and Min. Sci., vol. 2, pp. 57.73.

NTNU (1994). "Hard Rock Tunnel Boring". The Norwegian Institute of Technology.

Bieniawski, Z.T. (2003). "New tendencies in Rock Mass Characterization". Cedex. Madrid. 27 p.

Underground Space – the 4th Dimension of Metropolises – Barták, Hrdina, Romancov & Zlámal (eds)
© 2007 Taylor & Francis Group, London, ISBN 978-0-415-40807-3

Assessment of rock mass properties using machine performance data from roadheaders

K. Tsukamoto, H. Hamada & S. Ebisu
Okumura Corporation Technical Research Institute, Tsukuba, Japan

ABSTRACT: The authors have developed and continue to refine a rock mass assessment system, which is based on machine performance data from roadheaders. This assessment system utilizes measured data on thrust force by the roadheader, electrical energy consumed, machine vibration and excavation rate and it evaluates in-situ rock mass conditions objectively and quantitatively. It is shown that the estimated rock strength and elastic wave velocity of rock mass are in accordance with data from rock mass investigations, Point Load tests, and elastic wave exploration and it is effective in assessing rock mass conditions and rock strength at the tunnel face on real time basis.

1 INTRODUCTION

It is important to determine economic considerations as well as appropriate support systems on the basis of accurate assessment of rock mass properties during the construction of mountain tunnels. The tunnel face evaluation method is widely used in Japan for quantitative evaluation of stability by experienced engineers. However, the conclusions derived from evaluation of rock mass conditions and stability, using this method, differ from person to person even though the engineers are all very experienced. Therefore, these evaluations are somewhat subjective and require some improvements. The Japan Highway Public Corporation (JH) introduced a new tunnel face evaluation method. The JH system is a rock mass rating system, which relies primarily upon the following four general observation data related to rock mass strength: "compressive strength", "weathering", "spacing of joints" and "condition of joints" (Akagi et al., 2002). In this method, simple in-situ tests are performed on the rock obtained from the tunnel face to get a better grasp of the mechanical characteristics of the rock. A typical in-situ test may include one or more intrusive examinations, such as the Point Load test, Rock Schmidt Hammer test, etc. The compressive strength of the rock is estimated based upon historical data. Moreover, seismic explorations and core borings might be performed at the tunnel face, if deemed necessary. However, these tests may require interrupting tunneling work, while the tests are performed. Generally, the testing can be limited to small scale test instruments, in which case this process can be accomplished comparatively quickly. But, these tests cannot be performed when the rock mass at the tunnel face is fractured, due to the danger of falling rocks or collapse of the tunnel face. If the evaluation method used to determine rock properties is based upon real time data taken from roadheader operations, objective and quantitative rock mass conditions can be determined without interruption of the tunneling work. In view of this, the authors have developed a rock mass assessment system, which is based on machine performance data taken from roadheaders (Tsukamoto et al., 2002).

Excavation experiments were performed on mortar material to investigate the effects of machine performance data. In addition, the assessment system, which relies upon machine performance data from roadheaders, was applied to two tunnel sites. In this paper, the practicable effectiveness of this system is presented.

2 LABORATORY EXCAVATION EXPERIMENTS

2.1 *Overview of excavation experiments*

To clarify the relationship between machine performance data from roadheaders and rock mass strength, experiments were performed on mortar specimens with different compressive strengths. A roadheader with a milling cutting head with an electrical power rating of 65 kW and total weight of 22 tons was used for the experiment.

2.2 *Mortar specimens*

The size of the mortar specimens were 2 m (width), 2 m (height), and 1 m (depth). Table 1 shows the properties

Table 1. Properties of the mortar specimens.

Specimen no	Mass density (t/m^3)	Unconfined compressive strength (MPa)	Elastic modulus (GPa)
1	2.0	12.8	12.9
2	2.1	38.5	20.4
3	2.3	63.3	27.6
4*	2.3	63.3	27.6

*Contains 9 slits, which are 9 mm (thickness), 1.2 m (width), 0.8 m (depth).

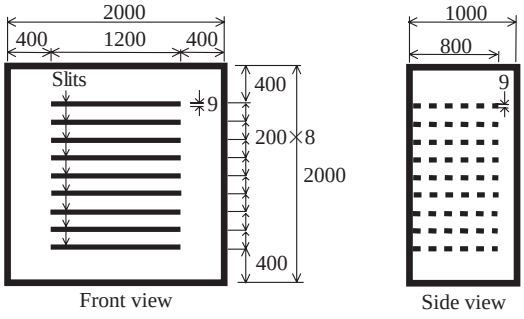


Figure 1. Overview of specimen No. 4 (Unit: mm).

of the mortar specimens. Specimen No.4 had the same unconfined compressive strength (63.3 MPa) as specimen No.3, but to simulate the effects of joint in the rock mass, nine slits were cut into the face of this specimen (see Figure 1).

2.3 *Procedure of the experiments*

The specimens were fastened to the reaction wall and floor by steel H-beams and steel rods (see Figure 2). Because the boom extension was limited to only 0.4 m, the experiments had to be performed in two steps. In the first step, the cutter performed its cutting operation until the boom was fully extended, whereupon the boom was retracted and the roadheader was advanced and the cutting operation continued to completion.

Measurements were taken for the cutter head motor current, penetration, thrust force and cutter boom acceleration. An accelerometer was attached to the boom casing and was used to monitor accelerations transmitted from the cutter head to the boom. The Root-Mean-Square (RMS) value was calculated by using boom acceleration data from the sampling frequency of 1 kHz.

2.4 *The results of the experiments*

The mean values, such as thrust force, electrical power consumption for cutting, boom vibration and

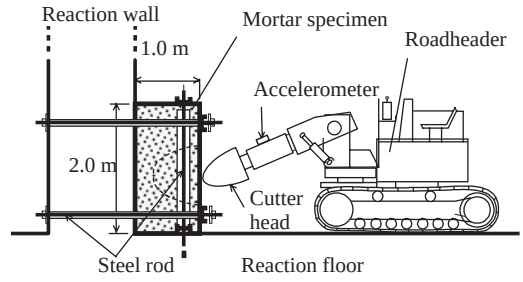


Figure 2. Overall view of excavation experiments.

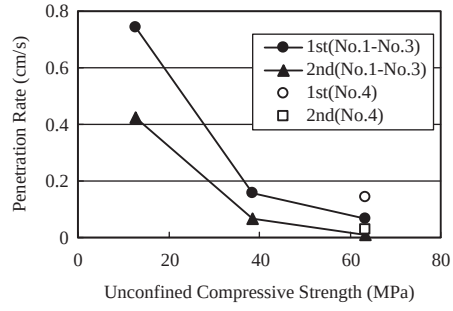


Figure 3. Relationship between penetration rate and unconfined compressive strength.

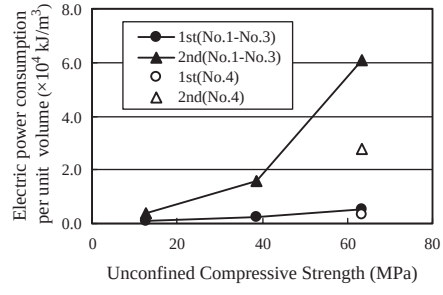


Figure 4. Relationship between electric power consumption and unconfined compressive strength.

penetration rate were calculated from measured data from the roadheader during cutting operations.

Figure 3 shows that there is an inverse relationship between penetration rate and unconfined compressive strength. Penetration rate decreases rapidly when compressive strength increases, because cutting time, per unit volume, is lengthened.

Figure 4 shows the relation between electrical power consumption for cutting, per unit volume, and unconfined compressive strength. Similarly, electrical power consumption tends to increase rapidly, when compressive strength is increased. Perhaps, specimen No.3, which had the highest compressive strength of the

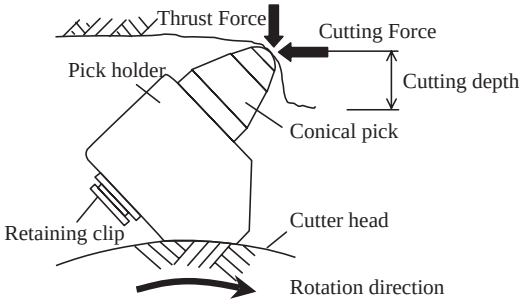


Figure 5. Bit of a cutter head cutting a specimen.

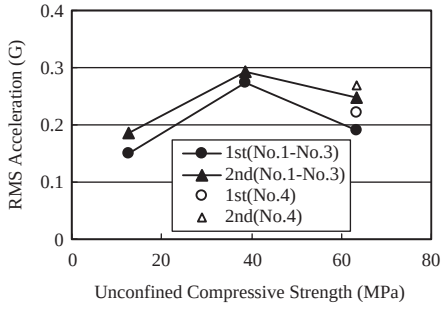


Figure 6. Relationship between RMS acceleration and unconfined compressive strength.

specimens, may have been at the strength limit for the roadheader's cutting ability.

Figure 5 shows the bit of a cutter head cutting a specimen. During normal cutting, the penetration rate is proportional to the cutting depth of the bit. And, it is a given that the cutting depth is related to thrust force and cutting force (Hurt et al., 1979). Cutting depth is inversely proportional to the compressive strength of the specimens, so that the cutting bit depth is deeper for lower compressive strength specimens (No.1 and No.2) and more shallow for higher compressive strength specimens (No.3 and No.4). In the latter case, since the output of the cutting motor was not consumed in cutting, the current decreased. However, the electrical power consumption per unit was increased, because the overall cutting time was lengthened, with very little cutting progress accomplished.

Figure 6 shows the relationship between the measured RMS acceleration of the boom vibration during cutting and the unconfined compressive strength of the specimens. From the results of cutting specimens No.1 and No.2, it is evident that RMS acceleration during cutting is proportional to increased compressive strength. However, RMS acceleration is inversely proportional to compressive strength for specimens No.3 and No.4, with higher strengths.

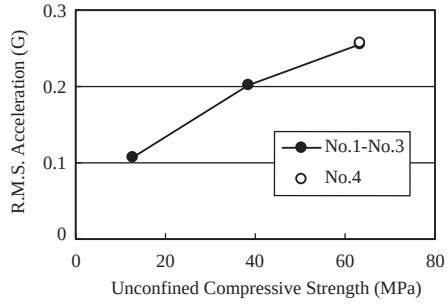


Figure 7. Relationship between RMS Acceleration and Unconfined Compressive Strength for a Penetration Depth of 10 cm.

Figure 7 shows that RMS acceleration is proportional to unconfined compressive strength given a constant cutting depth of 10 cm. It seems evident that it is not practical to continue excavation under conditions which result in shallow cutting depths. It is anticipated that RMS acceleration would be further increased for specimens No.3 and No.4 than for specimen No.2, where a very large thrust force was applied by the roadheader. The RMS acceleration and penetration rate for specimen No.4 was only slightly higher than for specimen No.3, even though slits in its face were present.

From the above results, it is evident that there is a correlation between RMS acceleration of the boom, penetration rate, and electrical power consumption per unit volume and unconfined compressive strength.

3 ASSESSMENT SYSTEM OF ROADHEADERS

The assessment system consists of the following three subsystems (See Figure 8).

1. A "Measurement subsystem" that automatically measures machine performance data with a measurement device installed on the roadheader. Various sensors that measure the current of the cutting head, thrust force, boom acceleration, etc., are installed on the roadheader. Control sequence devices are programmed to take measurements in the range of 1 kHz (for boom acceleration) to 10 Hz (for other items to be measured). The device can transmit the averaged measurement data at intervals of one second, wirelessly. At the same time, the data is saved to hard disk on a notebook computer. It automatically starts saving data, when the current value on the cutting motor exceeds a threshold level and continues to record data until the current falls below the threshold level for a fixed period of time (e.g., 20 minutes).
2. A "Face observation subsystem" that inputs the results of geological data, face observations and in-situ tests. Face rating values, which are determined

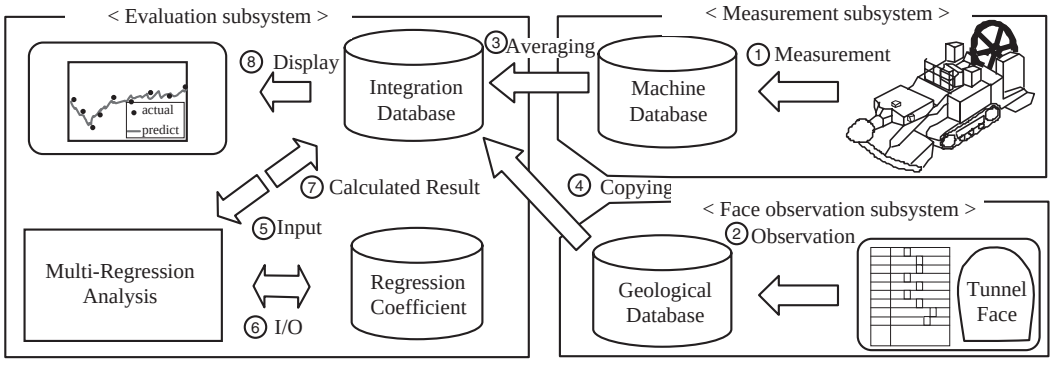


Figure 8. Assessment system of for a roadheader.

by tunnel engineers in the field, unconfined compressive strength estimated from Point Load tests or Rock Schmidt Hammer tests, after excavation, are inputted into the computer and stored in a geological database.

3. An "Evaluation subsystem" that evaluates geological conditions. The mean of the machine performance data from roadheaders, for each excavation cycle, is calculated for each item to be measured. The face rating and unconfined compressive strength are predicted by substituting the above noted mean value in the regression equation obtained through multiple regression analysis in advance. The regression coefficients, are adjusted to correspond to the amount of data accumulated in an early stage of the application. The face rating, unconfined compressive strength and elastic wave velocity of rock are calculated using the following equation.

$$y = a \times X_1 + b \times X_2 + c \times X_3 + d \times X_4 + e \qquad (1)$$

Where, y = face rating, unconfined compressive strength, elastic wave velocity; a, b, c, d, & e = regression coefficients, X_1 = electric power consumption to excavate a unit volume of rock; X_2 = thrust force of the cutter head; X_3 = RMS acceleration of the boom; and X_4 = excavation rate (cutting volume per hour).

Table 2. The contribution rate by multiple regression analysis.

Number of independent variables	Independent variables				Contribution rate	
	X_1	X_2	X_3	X_4	Takahara tunnel	Yanbe tunnel
4	○	○	○	○	0.71	0.59
3	○	○	○	—	0.69	0.58
3	—	○	○	○	0.71	0.56
3	○	—	○	○	0.70	0.58
2	○	○	—	—	0.33	0.22
2	—	○	○	—	0.69	0.56
2	—	—	○	○	0.70	0.56
2	○	—	○	—	0.69	0.57
2	○	—	—	○	0.15	0.21
2	—	○	—	○	0.32	0.20
1	○	—	—	—	0.08	0.20
1	—	○	—	—	0.31	0.01
1	—	—	○	—	0.68	0.56
1	—	—	—	○	0.01	0.19

○ Used — Not used

4 SYSTEM PERFORMANCE EVALUATION

4.1 *Overview of application tunnels*

The JH system, which utilizes the measured data from roadheaders, was applied to the Takahara tunnel and the Yanbe tunnel, where the new face observation method had been adopted. The rock units of this site consisted mainly of rhyolitic tuff and rhyolite of Neogene Miocene epoch. Due to hydrothermal alteration and weathering, the tuff was in a softened condition. A boom-type roadheader with a cutting head power rating of 240 kW and total weight of 54 tons was brought to these sites. Moreover, the Point Load tests were examined by using the rock taken from the tunnel face, where deemed appropriate.

4.2 *Selection of independent variables*

Cutting electric power consumption, excavation rate, boom acceleration and thrust force were selected as independent variables, based on the results of excavation experiments. All possible regression methods were applied, and the case where the contribution rate, of the combination of the four independent variables was maximum, was calculated. The results of the contribution rate calculations for the Takahara tunnel and the Yanbe tunnel are shown in Table 2.

Because the contribution rate is maximum, when all the independent variables are used, the expression

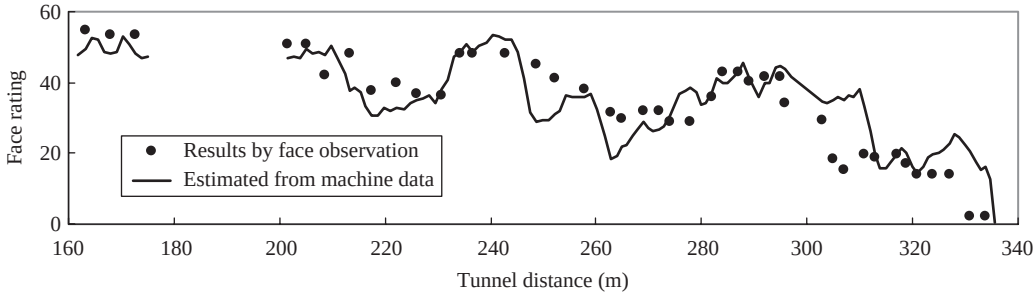


Figure 9. Comparison with face rating by face observation and estimated from machine data.

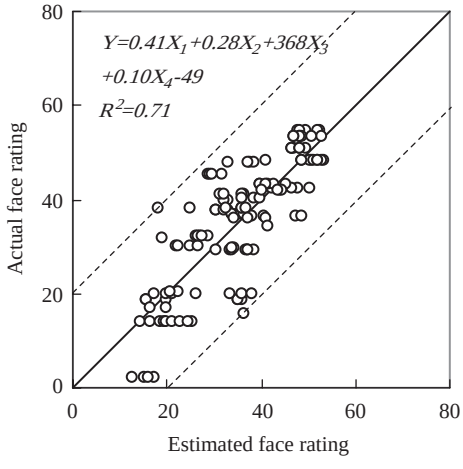


Figure 10. Estimated face rating from machine data and face rating by face observation.

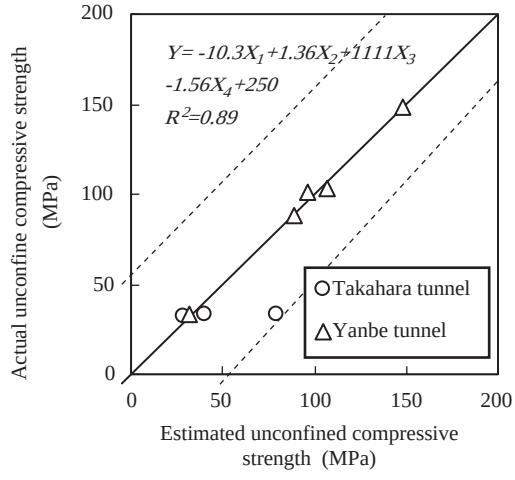


Figure 11. Estimated unconfined compressive strength from machine data and unconfined compressive strength by Point Load test.

shown in equation (1) is used for the regression analysis.

4.3 *Predictive performance of face rating calculated from roadheader machine performance data*

Figure 9 shows that estimated values from methods using machine data and from face observations were both in the upper 40's for the 165 to 175 m, 202 to 247 m, 286 to 289 m, and 293 to 296 m ranges. In addition, both methods showed a minimum value at about 335 m, indicating that these methods were in good agreement. Also, note that a higher face rating indicates a more competent rock mass.

Figure 10 shows the correlation between face rating values evaluated by the JH system and estimated face rating values calculated from roadheader machine data taken from the Takahara tunnel. We can see that contribution rate of regression is high (0.71) and the estimated face ratings are within the error range 2.5 Standard Error. This indicates that the predictive performance of the assessment system developed is reliable and practical.

4.4 *Predictive performance of unconfined compressive strength and elastic wave velocity*

Although there were relatively few samples, the assessment system may be verified by using the results of in-situ tests. More specifically, a multiple regression analysis can be performed, with unconfined compressive strength and elastic wave velocity as dependant variables, and the four machine data values in equation (1) as independent variables.

At the locations selected on the Takahara and the Yanbe tunnels, Point Load tests were performed on rock obtained from the face and the unconfined compressive strength was estimated using the failure load of the rock. Since, the contribution of regression was large (0.89), it was determined that it reliably predicted unconfined compressive strength based upon machine data from roadheaders (Figure 11).

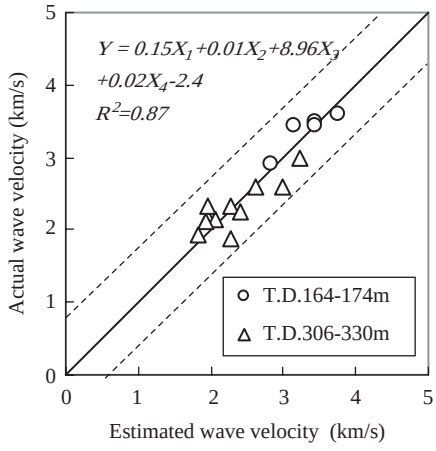


Figure 12. Estimated wave velocity from machine data and wave velocity by seismic exploration.

Seismic explorations were performed at two locations in the Takahara tunnel, primarily due to the presence of hard tuff, from 164 m to 174 m, as well as the presence of weathered, very soft tuff from 306 m to 330 m. The elastic wave velocity of hard tuff is 1.8 km/s to 3.0 km/s and that of very soft tuff is 2.8 km/s to 3.8 km/s. A multiple regression analysis was done based upon machine data measured at the same locations as the seismic explorations. The contribution of regression was high (0.87) and its estimation reliability was found to be in good agreement with the elastic wave velocity (See Figure 12). The contribution rate of unconfined compressive strength and elastic wave velocity are higher than the contribution rate of face rating. And, the data shown in Figures No.11 and No.12 show less scattering than those in Fig. 10. This indicates that the results of unconfined compressive strength and elastic wave velocity provide an objective assessment of the properties of the in-situ rock. In contrast, face ratings, which involve error by face observers, are a less reliable means of assessment. Therefore, the use of objective information obtained from roadheader machine data is more effective for the reliable evaluation of tunnel face ground conditions.

5 CONCLUSIONS

This rock mass assessment system, was developed to analyze real time data from roadheaders, which are commonly used in tunnel excavation, to accurately predict rock mass conditions at the tunnel face, without interrupting the progress of work during construction. It was confirmed that this system has sufficient accuracy to be effectively and reliably used to evaluate in-situ conditions during construction. Furthermore, this system may be further developed to be used for the assessment of rock mass properties. The following conclusions can be drawn from the results obtained in this study:

1. Boom acceleration is increased with increased compressive strength of rock at tunnel face. However, when the cutting performance of the roadheader is inadequate, boom acceleration is reduced.
2. It was confirmed that this assessment system can reliably predict rock mass properties at tunnel face from the results of multiple linear regression analysis using four independent variables for machine data taken during one excavation cycle of tunneling work.
3. It was demonstrated that the predictive reliability of this assessment system, which uses unconfined compressive strength from Point Load tests and the elastic wave velocity from seismic explorations, exceed the reliability of other assessment systems, which rely upon determining face ratings from evaluation of observations of the tunnel face.
4. It was also demonstrated that the application of this assessment system, based upon objective machine data was effective and reliable as compared to a face rating assessment system, which is subject to personal and estimation errors by tunnel engineers.
5. The operation of the system begins by determining a correlation coefficient for the roadheader from historical data collected at an earlier stage of tunnel construction. However, the same correlation coefficient cannot be applied to different types of roadheaders. Subsequently, it is necessary to assess the correlation coefficient and confirm the presumption accuracy.

REFERENCES

Akagi, W., Ito, T., Shiroma, H., Kunimura, S., Shinji, M. & Nakagawa K. 2002. Study about relationship between estimation of rock mass by JH system and applicability to tunnel excavation control by field measurements. *AITES-ITA Downunder 2002 World Tunnel Congress.*

Hurt, K.G. & Laidlaw, D.D. 1979. Laboratory comparison of three rock cutting tools. Tunnels & Tunneling 11(5):13–16.

Tsukamoto, K., Ebisu, S., Kurimoto, M., Kurita, T., Ishihara, M. & Nakagawa K. 2002. Study on the rock mass evaluation system using the mechanical data of a boom-type roadheader (in Japanese). *The 11th Japan National Symposium for Rock Mechanics.* CD-ROM H02.

Underground Space – the 4th Dimension of Metropolises – Barták, Hrdina, Romancov & Zlámal (eds)
© 2007 Taylor & Francis Group, London, ISBN 978-0-415-40807-3

Deep tunnelling in hardrock with large diameter TBM: What's up? An experience from the Gotthard Base Tunnel

I. Vicenzi, S. Pedrazzini, A. Ferrari & G. Gubler
Lombardi Consulting Engineers Ltd., Minusio, Switzerland

O. Böckli
Implenia Ltd., Aarau, Switzerland

ABSTRACT: In the driving of underground openings, two main factors are to be borne in mind. First, the existence of failed rock and second, the control of displacements. The general problem devolves into questions of excavation geometry, sequence and support specification while adverse performance of the rock mass in the post-excavation stress field may be caused by either failure of the medium or slip on the weakness planes. During the excavation of the southern section of the Gotthard Base Tunnel, the rock mass response to TBM tunneling activities described unusual magnitudes of displacements in so far as the thrust of the machine couldn't overcome the shield's frictional forces. A smooth-blasting technique was implemented so that pressures on it went back to a sustainable magnitude. This paper describes how appropriate design and contractual approach are critical in assuring both efficient geomechanical and economic performance of hardrock tunnelling by large diameter TBM.

1 INTRODUCTION

1.1 *The new Gotthard Base Tunnel Project*

By constructing the New Rail Link through the Alps, Switzerland is integrating itself into the growing European high-speed network. AlpTransit Gotthard Ltd. – a completely state owned subsidiary of Swiss Federal Railways charged with the overall planning and supervision of the construction works of the New Rail Link on the Gotthard axis – is creating a flat rail link for future travel through the Alps.

At the heart of the new transalpine rail route is the world's longest tunnel – the 57 km Gotthard Base Tunnel – whose highest elevation at 550 meters above sea level is much lower than the highest point of the existing route through the mountains at 1,150 meters, so that gradients will be no steeper accordingly to those of a modern high performance rail link making freight transportation more productive, while passenger traffic benefits from massively shorter journey times.

In 1995, after intensive political, financial and technical studies of several options the Swiss Federal Council approved the plan for the Gotthard Base Tunnel and spoke in favor of a tunnel system with two single-track tunnels. The two rail tunnels are about 40 meters apart and joined approximately every 3,125 meters by connecting galleries. Two double crossovers allow trains to change from one tunnel to the other – which may be necessary to allow maintenance work if an accident occurs. Trains can switch tunnels in the multifunction stations which also house ventilation and technical equipment, safety and signaling systems, as well as two emergency stop stations which are directly linked by separate access tunnels.

Other then the two portals, intermediate headings provide additional accesses to the tunnel from above (shafts) and from the sides (adits), shortening also the construction time and dividing the tunnel into five sections: this paper focuses on the southern section of Bodio.

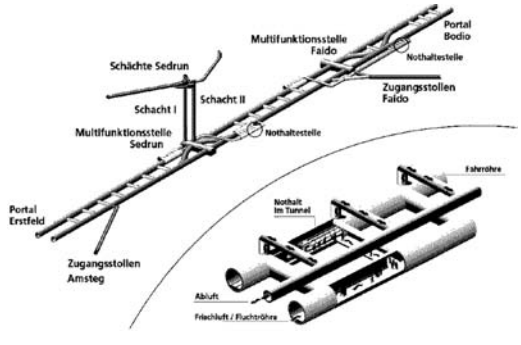


Figure 1. Gotthard Base Tunnel. Tunnel systems with shafts and adits.

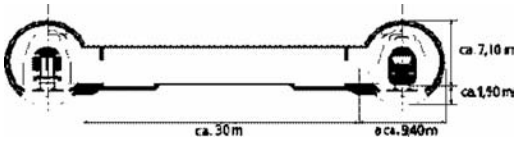


Figure 2. Typical cross section of the two twin tube tunnel in the section of Bodio.

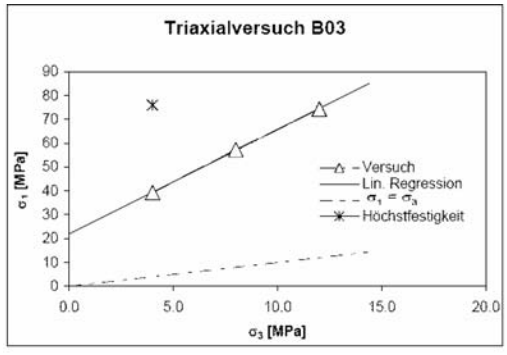
1.2 *Site description*

The section of Bodio is located in Southern Switzerland (Ticino) at the southern portal of the tunnel. This section is the longest one of the Gotthard Base Tunnel. To allow faster construction of the underground assembly caverns for the TBM, a bypass tunnel was driven out round the site of the portal. From the assembly caverns, two 400 m long – complete driving unit with backup train – open gripper TBMs with a diameter of 8.9 m started driving north towards the next section of Faido in 2003: the length of the TBM driven tunnels reaches 13.4 km in the eastern tube respectively 14.1 km in the western tube, the headings facing steadily an uphill gradient of 7‰. The Breakthrough is expected in the "multifunction station" 16 km from portal.

1.3 *The event at chainage 13,692 EST W*

The sensitivity of large diameter TBM to adverse rock mass conditions has been a major issue since the very beginning of the design and tendering stages of the Gotthard Base Project; in view of the crossing of zones allocated to the poorest excavation classes accordingly to the contract specifications, the owner commissioned TBMs with reaming equipment by pull-out cutters fitting the driven diameter up to 30 cm over the standard one. The sensitivity of the TBMs was particularly well highlighted by the event occurred in the western tube at ch. 13,692 (2006, March 3rd), where unusual large displacements brought – even without evidence of major failure of the surrounding rock mass – one of the two TBM – the so called West TBM – to be overcome by the frictional forces acting on the short front shield while the second one could pass throughout the same ground unit without getting blocked as well.

This paper presents an attempt to quantify and understand both the records and the limitations in poor ground related to the response of the managing TBM's operator – as well as the importance of reaming opportunities – by driving through low quality rock masses on the basis of the experience of the above-mentioned event; moreover, the importance of both appropriate design and contractual approach for achieving efficiency in geomechanical and economic performance by TBM tunnelling is showed by the same case study.



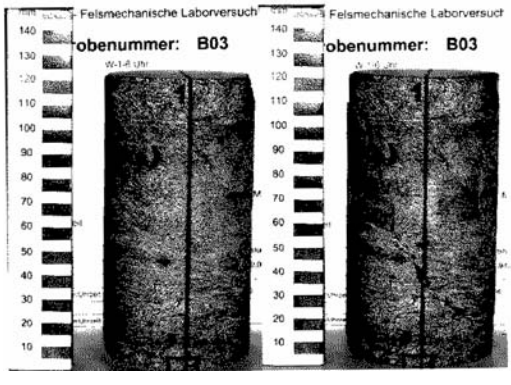


Figure 3. Core sample recovered in the near field of the jammed West TBM before (left) and after (right) lab test.

2 GEOLOGY AND POTENTIAL MODES OF OPENING BOUNDARY FAILURE

2.1 *General geological and geomechanical data*

The section of Bodio lies in the hard rock formations of the Penninique gneiss, which are typical of southern Switzerland. The geological longitudinal section shows at the location mentioned in 1.3 a biotite rich gneiss with prominent sub-horizontal weakness planes with relatively low shear strength compared to that of the intact rock; the overburden at the same location slightly exceeds the km mark.

Average geotechnical parameters of intact rock were determined by a large series of triaxial compressive tests carried out by the lab of the Federal Institute of Technology in Zurich on core samples recovered in the near field of the jammed West TBM: Young's modulus ranging around 10 GPa, uniaxial strength ranging from 5 MPa to 35 MPa. The mechanical properties of the weakness planes of the intact rock were also assumed on the basis of the same lab tests, i.e. cohesion $C' = 1{,}200$ kN/m^2 and friction angle $\phi' = 32°$.

Volumen [m³]	<0.001
Höhe [m]	<0.5
Gewicht [to]	
KS	225-057 /0-85
K I+ II	150(320) /89
K IV	045-070 /80-85
K III + V	220-230(050) /80-85

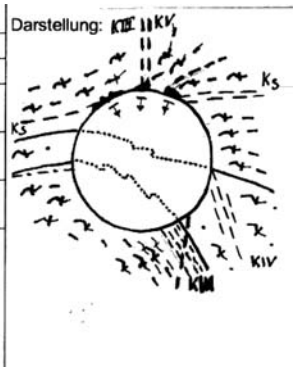


Figure 4. Tunnel mapping and potential modes of boundary failure reported for the western tube from ch. 13,569 to ch. 13,743.

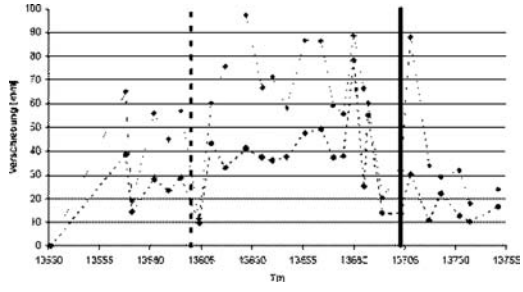


Figure 5. Total measured convergences of the opening between ch. 13,530 and ch. 13,755. Zero measure was taken 4 m from the heading. Rock support already set. The figure shows largest (max. 10 cm) and medium (max. 8 cm) displacements lines, i.e. from 5 points.

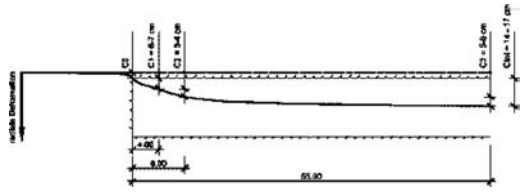


Figure 6. Schematic representation of the progression and extension of the roof displacements between ca. ch. 13,600 and ca. ch. 13,700: ca. 7 cm (40% of the whole displacement) at 4 m from heading, ca. 10 cm (60%) at 8 m from heading and finally ca. 17 cm at 55 m from heading.

2.2 *Potential modes of rock mass failure*

Following the two main factors mentioned in the abstract for designing the rock supports, particular attention has been given to ensure that large, uncontrolled displacements of excavation peripheral rock couldn't occur in order to satisfy the tunnel duty requirements, such as minimum dimensions required both for excavating equipment as well as for the minimum clearance of the mined section. The first main factor – major boundary failure – could be neglected due to the fact, that around chainage 13,692 no one was reported; nevertheless, the effect of any major discontinuities which will transgress the excavation has been examined by consideration of both the general effect of the structural features on boundary stresses and local stability problems in the vicinity of the discontinuity/ boundary intersection. These considerations educed support design adjustments to achieve simultaneous satisfaction of local and general stability conditions for the excavated perimeter near chainage 13,692.

The potential mode of boundary failure is depicted in Figure 4, where the banding (i.e. K_s) running with sub-horizontal banding is showed. Local phenomena of minor parting or slabbing couldn't be excluded if two or more families of joints (i.e. K_I to K_V) come to intersect each other.

The mapping of the tunnel sets forth the bent of that geological unit to large displacements; this feature has been then confirmed by monitoring the behavior of the rock mass surrounding the tunnel; in fact, the largest displacements were measured between chainage 13,595 and chainage 13,695 (Figures 5 and 6, western tube).

It is important to note that, the possibility to comfort the opening with rock support is not given before the end of the short TBM shield, i.e. at 4 m from the heading, where over 40% of the total displacement has already took place. In other words, the pre-mining stress field came to be disturbed in a quite large extent before any opportunity to control it by rock support were given.

2.3 *Rock support*

The adverse performance of the opening boundaries in the post-excavation stress field illustrated in the previous chapter were mainly caused by slipping on the pervasive weakness planes while a few sloughing due to induced tensile stress exceeding the strength of the rock occurred.

The opening reinforcement was defined in the attempt to reach as soon as possible a stable equilibrium between the rock mass and rock supports by placing the reinforcement close to the TBM short shield soon after excavation. Heavy rock support consisting of blocked steel sets (TH 29 each meter, all around) combined with a wire mesh and two layers of shotcrete (first layer of 9 cm, second layer of 5 cm, both sprayed on 260°) were installed for a maximum stiffness of the reinforcement.

Although heavy rock supports were installed, evidence of suffering from the disadvantage of a poor stiffness by the blocking points of the steel arches, where overlapping of two neighboring elements often

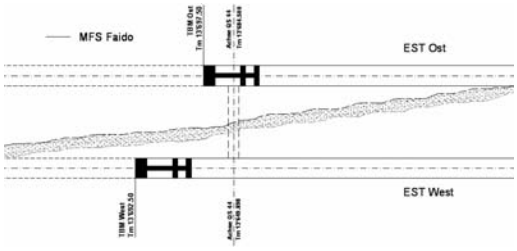


Figure 7. Layout of the heading progress of both TBMs on 2006, March 3rd.

happened, as well as from failure by sideways buckling were reported.

3 TBM JAM AT CHAINAGE 13,692, WESTERN TUBE

3.1 *TBMs working progress*

On 2006, March 3rd the western TBM reached chainage 13,692 before getting blocked by the rock mass pressure acting on the short TBM shield; in fact, the machine was no more able to overcome the frictional forces solely with its own thrust. By that time the eastern TBM was progressing at chainage 13,698. The actual distance between the advance headings came to 40 meters (ch. 0 milestones slightly differ each other, of exactly 34,612 m); nevertheless, no mechanical interaction between the openings could be evidenced confirming thus the general rule saying that the zone of influence of one opening lies outside one another's when the distance between their centers is $D_{I,II} \geq 6r$ where r is the opening's radius (ideal case, hydrostatic stress field).

A fault striking the tunnels with an acute angle and dipping almost vertical was intercepted coming from east and going straight westwards was feared to influence the behavior of the tunnel system in addition, of course, to those to the single tubes. The fault, consisting of a strong weathered, loose material with a thickness of in the m range, hit the two tubes in a distance of about 300 m.

Accordingly to a back analysis carried out by a 2D-model using both a FLAC code and the characteristic curve method, the influence of that fault would have significantly affected the pre-mining stresses field around the western tube so far as the fault location reached the centerline between the two tubes. One can take also reference to Figure 5 again, where the left vertical line points out the chainage – respectively the displacements – by which the fault was located at 3 m away from the tunnel sidewall while the right one do the same for the fault location in the middle

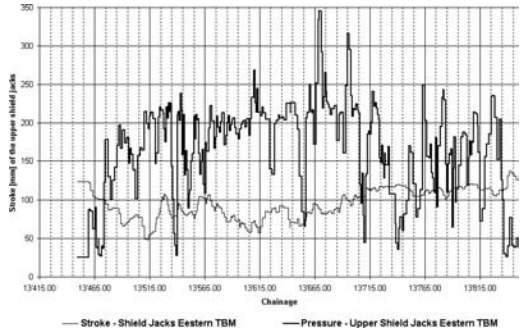


Figure 8a. Stroke vs. pressure in the upper shield jacks of the eastern TBM.

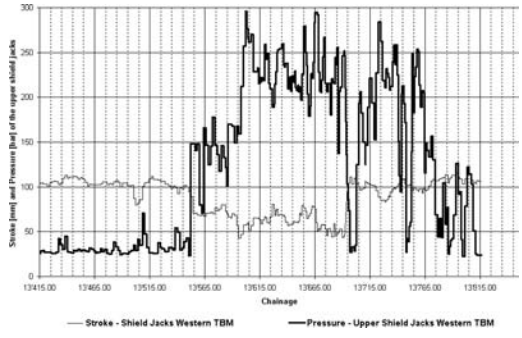


Figure 8b. Stroke vs. pressure in the upper shield jacks of the western TBM.

distance between the tubes: from this location on, the displacements clearly decrease due to the fact, that the influence of the fault is vanishing.

3.2 *TBMs crossing of the zone with large displacements*

Both TBMs are equipped with automatic data log instrumentation recording a wide range of operating parameters, mostly of which are directly related to the steering system of the TBM: of particular interest are then the data of the thrust cylinders and that of the shield jacks which supply informations about the advance of the TBM as well as the encountered rock mass pressures. Such data are recorded online by the contractor and delivered to the site engineer in real time.

The site engineer disposes of a code named SISO, which first selects the useful ones and in a second stage processes them; as a result, the whole operation's track is stored in a data bank and ready for the rendering as graphs or in tables.

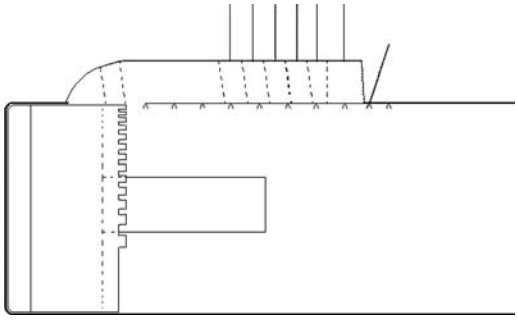


Figure 9. TBM recovery.

By comparing several data coming from the TBM, the stroke's progression of the jacks moving the upper part of the TBM shield in function of the time delivered the most feasible explanation for the jamming occurred only to the western TBM at chainage 13,692 while the eastern one could successfully manage the similar bad conditions, this with although reported damages of the jacks of the shield ant of the shield itself.

The TBM guidance on the vertical and horizontal planes basically results from the control of two sets of elements: the grippers and the shield. By adjusting them the operator can drive the TBM accordingly to the given alignment as well as reacts in case of troubles, that's for instance when the ground collapses underneath the gripper or soft rock formations let the cutting head to depart from the horizontal plane.

Seemingly, the western machine entered the difficult zone, characterized by unusual large displacements, with the strokes of the shield jacks being more or less just half way extended (ca. 70 mm out of 150 mm of the total stroke). By the sudden increase of the rock mass pressure – topping 300 bar on the shield jack gauge – the only way let to the operator in order to shift away from such a zone is to lower the upper part of the shield and release then the frictional forces on it. This procedure is usual successful in the short period but not if the extent of the zone is important; in fact, the stop line of the jack is quickly reached. From this point on – if a natural release of the rock mass pressure does not take place – one has to overcome then by other methods.

3.3 *Western TBM recovery*

Contractor, designer and the site engineer agreed to recover the jammed TBM by taking back the rock pressure to a sustainable magnitude. The implemented technique was based on firing shotholes in short sequences in the upper part of the TBM (smooth blasting). The recovery lasted about 10 days.

4 DISCUSSION

4.1 *The importance of the contract*

The contract governing the project is a fixed price one, ruled also accordingly to Swiss construction standards such SIA 118 and 198.

The contractor accepted with its tender the risks for stipulated sum or rates nominated in its bid. However, provisions for adjustments have been included; in particular, the risk of a diverting, unexpected geology and delays caused by the owner are compensated to the contractor.

Provisional items, which also are a part of the contract, allow to cover works for which complete details were not known at the time of tendering without creating new ones. Time related costs are covered by separated items offered by the contractor with its bid, so that unexpected variations of order could easily, upon agreement, be integrated in the contract.

That's to say, the unexpected additional works caused by the recovery of the TBM could be well managed by the existing contract in case of agreement on the liabilities.

4.2 *The importance of the TBM data logs*

More attention should be paid to the interpretation of the TBM parameters in real time. This should be true at any level of the operation's management and should be achieved by a more intensive education of the involved technicians.

Contractor and site engineer should take more advantage of the possible fine tuning of the TBM operations, especially in adverse conditions, accordingly to the long learning curve which long lasting, well monitored projects allow.

4.3 *What about reaming?*

Reaming has been a major issue from the very beginning of this project; in fact, the contract specifications included the opportunity to shift the cutting head of the TBM for 15 cm in radius – on short sections going through the mapped faults for some 200 m in accordance to the contract – for overcoming adverse rock mass conditions requiring a thicker reinforcement and enough comfort for controlled displacements. Accordingly to the literature, no successfully reaming hasn't yet been carried out in crystalline hard rock.

Actually, any attempt to reaming up to 30 cm in diameter on the section of Bodio failed since the beginning of the operations because of technical problems. Those problems were considered to be insuperable from both the technical and the contractual point of view. As a result, the contractual parties agreed to close any dispute: the owner abandoned the request accepting an equitable technical proposal for replacing

reaming – shift of 10 cm in diameter – along with a fair price adjustment.

5 CONCLUSION

The accident occurred to the western TBM driving the longest section of the Gotthard Base Tunnel would cause delay and extra costs due to the compulsory stop of the operations.

It is not the goal of the authors to argue hereby on the liabilities of the contractual parties.

The goal of the paper is to incentive the discussion on the way to improve TBM operations in deep, long tunnels taking benefits from the experiences learned on the Bodio site and, last but not least, to generally question the ones involved in full face, mechanized tunnelling: still reaming a challenging issue for hardrock TBM manufacturers or is just a designer's chimera?

ACKNOWLEDGMENT

The authors cordially thank Mr. Stefan Flury, head of the AlpTransit Gotthard Ltd. for the section of Bodio, for his appreciated cooperation and review of the paper as well as AlpTransit Gotthard Ltd. in Lucerne for giving us the permission to publish it.

REFERENCES

AlpTransit Gotthard Ltd. 2004. The New Gotthard Rail Link

Swiss Federal Institute of Technlogy, 2006. Felsmechanische Laborversuche, Bericht Nr. 1, ATG, Teilabschnitt Bodio.

Brady, B.G.H., Brown, E.T. 1985. Rock Mechanics for Underground Mining. New York: Chapmann & Hall

SISO, Site Information SOftware, www.sisonet.ch

Underground Space – the 4th Dimension of Metropolises – Barták, Hrdina, Romancov & Zlámal (eds)
© 2007 Taylor & Francis Group, London, ISBN 978-0-415-40807-3

Laboratory tests for EPB tunnelling soil conditioning

R. Vinai, D. Peila, C. Oggeri & S. Pelizza
Tunnelling and Underground Space Center – Dept. of Land, Environment and Geotechnology, Politecnico di Torino. Italy

ABSTRACT: The screw conveyor system plays a fundamental role during the EPB tunnelling operations for the tunnel face pressure control. On the other hand, the use of additives such chemical foams is even more applied in order to extend the EPB technology to the cohesionless soils. Despite the extensive use of the EPB technique in urban environment, little knowledge exists in the understanding of the behavior of such conditioned soil during the excavation operations. At the Turin University of Technology the Tunnelling and Underground Space Centre, in the mainframe of a wider research on soil conditioning, has developed an experimental apparatus that simulates the extraction phase with screw conveyor from a pressurized tank. In this paper the apparatus is presented and the results of a first series of tests carried out on sand are discussed.

1 INTRODUCTION

EPB tunnelling in the last years has experienced a great increase in the number of applications and it can be considered the most used technology of mechanized tunnelling in urban area, challenging the primate of slurry shield both for size and field of applicability. This has been possible from one side thanks to the mechanical development that brings even more power on the TBM, from the other thanks to the more effective use of additives (foams, polymers, bentonite, fillers) injected in the soil and in the bulk chamber, following the practise that is currently named "soil conditioning".

Since the application of such conditioning agents is relatively recent, a little experience on the use of them is achieved, particularly from the research point of view. In fact there have been a few studies concerning on this issue: Peron & Marcheselli (1994) report the first case of foam injection in Europe with the Milan Passante Ferroviario project in Italy; Maidl (1995) in Germany and Quebaud (1996) in France exploit this subject giving the first quantification of the effect of the foam when mixed with soil. Other interesting contributions can be found in Bezuijen et al. (1999), Herrenknecht & Maidl (1995), Jancsecz et al. (1999). Milligan (2000) gives the mainframe in which all the researches on the soil conditioning are organized and reports the state of the art. EFNARC (2005) also provides some guidelines for the use of conditioning products and their characterization. More recently, Mair et al. (2003) carried out studies on the effect of foam and polymers on the London Clay using a special experimental apparatus that simulates the extraction of material from a pressurized tank by means of a screw conveyor. An apparatus with the same features has been used by Peña (2003) at the Oxford University for the assessment of foam effects on fine and medium sand.

In this frame a research on the effects of conditioning on soils, developing a screw conveyor experimental apparatus able to apply relatively high pressure in the chamber, to better simulate the effects which are present ahead of a EPB machine was developed (Vinai, 2006; Gallina, 2006; Vinai et al., 2006). The description of the built up device and the used test procedures are described to explain their vantages and disadvantages and the results obtained from tests carried out on a medium sized sand are analyzed and discussed in the following sections to focus the applicability of the proposed test procedure for the choice of the optimum conditioning when EPB tunneling in cohesion-less soil.

2 DESCRIPTION OF THE EXPERIMENTAL DEVICE

2.1 *Screw conveyor system description*

Starting from the experimental system and procedure developed in Oxford as well as in Cambridge (Mair et al., 2003; Peña, 2003) it is clear that only a test able to simulate the complex EPB operation that involves both the conditioning of the soil but also the interaction with

Table 1. Transducer description.

Number	Description	Type	Range
1	Displacement wire transducer	Potentometric	0–1000 mm
2, 3	Pressure cell	De-aired liquid pressure	0–500 kPa
4, 5, 6	Pressure cell	Load cell	0–500 kPa
7	Torque meter	Slip ring contacts	0–500 Nm
8	Scale	load cell	0–50 kg

machine-member for the extraction operation would be really significant for the mix (soil + conditioning agents) behavior understanding.

It has also been observed that, in order to extend the tests on gravely soils and to try to obtain a relationship between the test results and real size excavation data, it would have been necessary to construct a large-sized system, follow the real geometry of the screw position and measure the same data recorded on a real scale EPB.

The apparatus has been designed and constructed to fulfill these goals: it consists of a iron tank 800 mm height with an outer diameter of 600 mm, on which an aluminum plate 40 mm thick fits. The plate is then connected to a hydraulic cylinder, with a stroke of 500 mm, driven by a hydraulic pump with a maximum pressure capacity of 400 bars.

The 1500 mm long screw conveyor is coupled with the tank with an inclination of 30° on the horizontal line. The inner diameter of the screw case is 162 mm, the flights have a pitch of 100 mm, and the screw shaft is 60 mm diameter. Following safety considerations, in order to avoid the possibility for the operator to be injured by accidental plate movement while working around the charging point of the tank, a metal grid has been placed around the tank, which interrupts via a micro-switch the power supply of the hydraulic pump is the hydraulic cylinder is started before rising it up to protect the connection between the plate and the tank. The screw is equipped with a three-phase motor with an installed power of 1.1 kW, coupled with a mechanical gear that gives screw rotation speeds between 6 and 15 rpm.

2.2 *Data acquisition system description*

In order to monitor the test parameter the sensors described on Table 1 were installed on the device while figure 1 shows the complete system and the sensor positions.

The transducers are connected with a pc-driven data logger. Signal conditioning, real time visualization, sampling and data memorization steps are executed through a specific software, supplied by the data logger constructor.

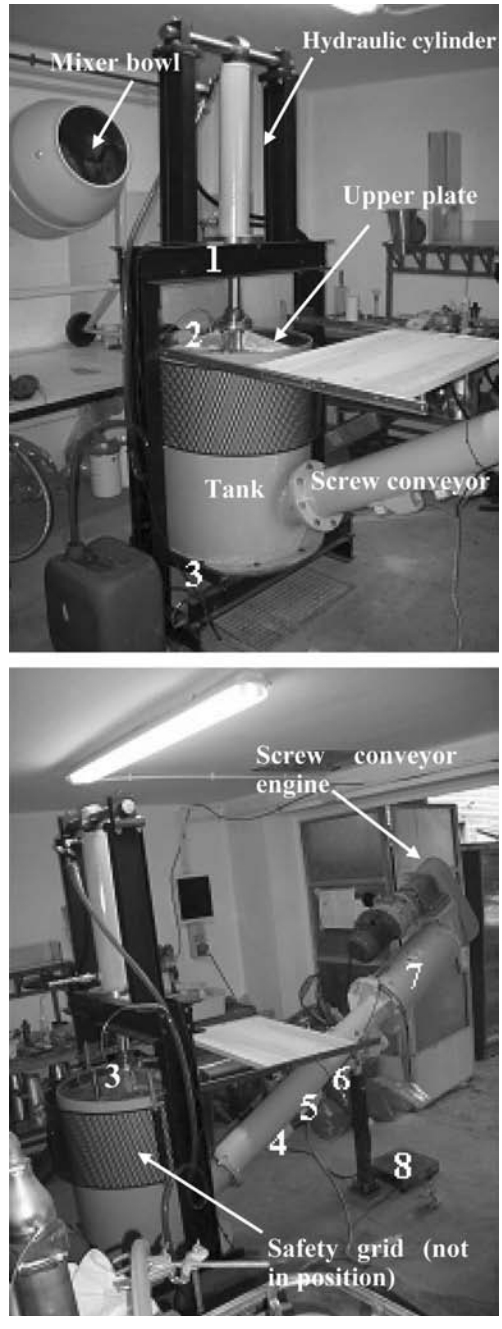


Figure 1. Experimental apparatus views where the numbers refer to the installed transducers.

2.3 *Foam generator system description*

The foam is obtained from an industrial generator redesigned for lab purposes. The generation unit

allows the control of the liquid flow (maximum flow 15 l/min) and air flow (maximum air flow 150 n.l/min), as well as the electronic control of the foaming agent concentration. The required expansion ratio can be achieved by the regulation of both fluid flows. The system is completed with an air compressor and a collector tank (Figure 2).

3 CARRIED OUT TESTS AND RESULTS

3.1 *Procedure description*

The tests are carried out following this procedure: a certain quantity of sand (approx. 25 kg), with defined moisture, is placed into a concrete mixer and the required amount of foam is added into the mixer bowl. As soon as the mix is ready (according to the operator check) it is poured into the tank and this operation is repeated until the tank is full (about 330 kg of sand required for each test). Subsequently the plate is positioned and pushed down by the hydraulic cylinder until the test pressure in the tank is reached. The screw conveyor is then started and the material is collected at the discharging point of the screw where it is weighted. The test is stopped when the hydraulic cylinder reaches its maximum stroke. Slump tests on the material coming out from the screw as well as on soil sampled in the tank at the end of the test are carried out in order to check the final plasticity of the material. The duration of each test, saving the loading phase, is about 15–20 min.

3.2 *Test operative conditions*

In order to assess the effects of foam on a medium graded sand with the grain size distribution shown in Figure 3, several tests have been carried out with different values of moisture, Foam Injection Ratio (FIR – as defined for example in Milligan, 2000) and pressure applied in the tank. The used conditioning agent was a commercial foam agent.

Here the results coming from six tests, respectively three on saturated sand without additives and three on conditioned sand, are presented and discussed. The conditioning parameters were defined after a specific study carried out by means of slump tests and mixing tests, varying systematically the water content (w) and the FIR. This test campaign allowed defining the optimum conditioning settings. Therefore the tests with the screw conveyor apparatus were carried out to compare the best conditioning with nil to focus the advantages of the additivation.

The following parameters were used in this set of tests: $FIR = 40\%$, $w = 10\%$ while the screw conveyor was set for a rotation speed of 6 rpm which is close to the one normally used in the EPB machines.

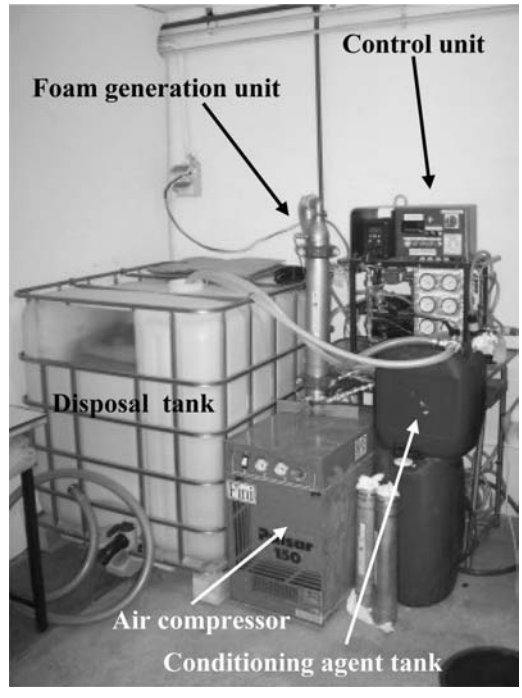


Figure 2. Foam generator equipment.

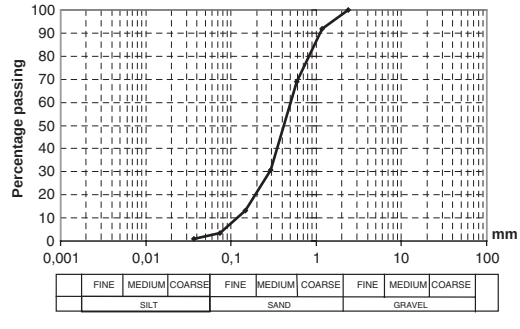


Figure 3. Grain size distribution of the sand used for the tests.

3.3 *Results and comments*

The efficiency of the conditioning can be verified through the analysis of several monitored parameters in the screw conveyor apparatus:

- the pressure distribution into the tank,
- the required torque,
- the displacement gradient,
- the discharged weight gradient
- the trend of the pressure along the screw conveyor.

The obtained results are summarized in Table 2.

The analysis of the pressure transmission in the tank indicates that in case of conditioned soil the material

Table 2. Summary of the results obtained from the tests on saturated and conditioned sand.

Test #	Theoretical pressure [kPa]		Measured pressure [kPa]		Torque [Nm]	∂disp. [mm/s]	∂weight [kg/s]	Cell 1 [kPa]	Cell 2 [kPa]	Cell 3 [kPa]
	Top	Bottom	Top	Bottom						
S1 saturated	60	75	N.A.	N.A.	35–45	0,299	0,159	6–8	4–6	2–4
S2 satuarated	90	105	150–230	110–120	30–40	0,327	0,137	4–8	4–6	2–4
S3 saturated	90	105	90–150	75–85	35–40	0,283	0,145	4–6	7–9	2–4
C1 conditioned	30	45	35–40	45–50	6–8	0,517	0,215	15–20	12–15	4–6
C2 conditioned	90	105	80–95	90–100	6–10	0,546	0,183	20–23	12–14	4–6
C3 conditioned	90	105	60–80	60–80	8–10	N.A. (0,431)	0,193	23–28	12–17	4–7

Key: Theoretical pressure = pressure in the tank derived from the pressure in the cylinder. Top and Bottom cells should differ, for the weight of the material acting on the bottom one, by about 15 kPa; Measured pressure = pressure measured by the cells located respectively on the top and on the bottom of the tank; Torque = torque acting on the shaft of the screw conveyor; ∂disp. = gradient of displacement of the plate; ∂weight = gradient of the weight recorded by the scale; Cell X = pressure cell on the screw case (cells numeration goes from the closest to the most far from the tank).

is far more homogeneous and plastic, whereas in case of saturated sand the material is too stiff and is not able to transmit properly the stresses in the tank (Figure 4).

In the latter case the top pressure is higher than the bottom one, and it is even higher than the maximum theoretical one.

This might be due to the partial reduction of the contact area between plate and sand from the theoretical section, because the material doesn't flow homogeneously under the plate and the sensor encounters a stiffer area. The torque is dramatically reduced in case of conditioning. The value in stationary conditions falls between one fourth to one fifth of the value recorded for the saturated sand. It is also to be pointed out that the diagram becomes smoother for the conditioned sand, whereas for the saturated sand periodic peaks, related to the screw rotation speed, are visible (Figure 5). The displacement gradient shows a higher speed for the downward movement of the plate in the case of conditioned sand: this means that the screw conveyor increases its efficiency, since more material is extracted during the same time interval.

This aspect is less evident analyzing the extracted material weight gradient, because the saturated sand is heavier than the conditioned sand, therefore less quantity of material gives similar weight.

Finally, the analysis of the pressures along the screw case shows clearly that the conditioned material is more able to transmit pressure, as well as that the screw is completely filled with material: the value recorded by the cell closest to the tank is of the same magnitude of the pressure in the tank and it is clearly visible the pressure fall along the screw (Figure 6). The same is not observable for the saturated sand case, where the pressures are low and similar along the entire case and periodic peaks, due to the effect of the screw flights on the cells, are evident.

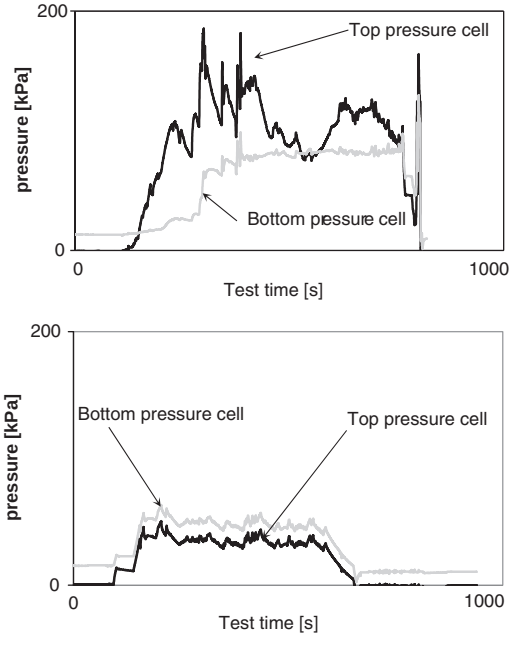


Figure 4. Pressures measured in the tank. Upper diagram: saturated sand. Lower diagram: conditioned sand.

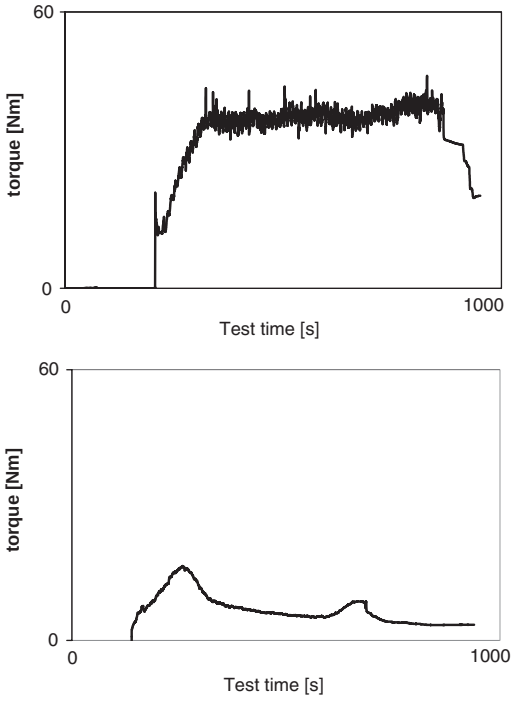


Figure 5. Torque required for the screw conveyor. Upper diagram: saturated sand. Lower diagram: conditioned sand.

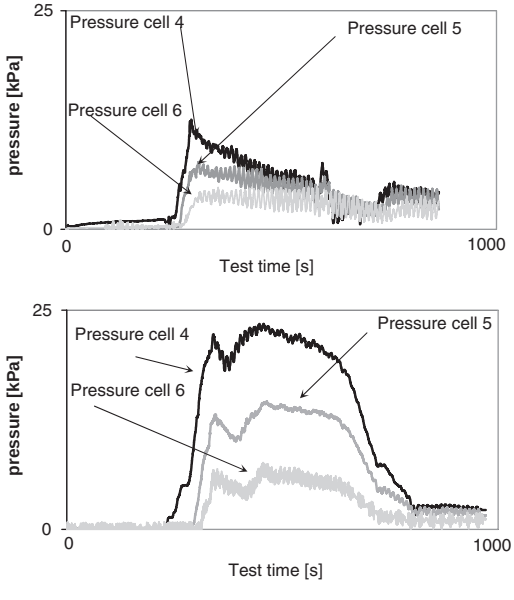


Figure 6. Pressures measured along the screw case. Upper diagram: saturated sand. Lower diagram: conditioned sand.

4 CONCLUSIONS

The soil conditioning is nowadays a crucial task for EPB tunneling application, because of the huge diffusion of this method even soils previously thought not suitable are now excavated using EPB machines with a systematic soil conditioning with foam and polymers. It is therefore very important to define some feasible and reliable laboratory test procedures able to improve the understanding in the design stage of the conditioned soil behavior rather than slump test only, which is one of the most used test.

A reliable test procedure, that might be used for this goal, foresees the extraction of conditioned soil from a pressure chamber with a screw driver thus allowing the measurements of many parameters which are very close to the real behavior of an EPB machine.

A device with a screw conveyor device that simulates the extraction phase from a pressurized chamber has been designed and constructed to study the effect of conditioning on cohesion-less soil. The obtained results, from a tests campaign carried out on a medium sized sand, show that this device is efficient to study the effects of foam conditioning of the soil. Particularly some monitored parameters, like the pressure distribution into the tank, the required torque, the displacement gradient, the discharged weight gradient and the trend of the pressure along the screw conveyor, are good markers for the definition of the conditioning quality, since differences are evident between conditioned and non-conditioned sand tests.

ACKNOWLEDGMENTS

The authors want to thank MAPEI S.p.A. for the technical and financial support to this research . A special thank is to be given to Eng. D. Gallina for the help which he gave to this study during the development of his MSc thesis work.

REFERENCES

Bezuijen A., Schaminee P.E.L. & Kleinjan J.A. 1999. Additive testing for earth pressure balance shields, In *Proc. of 12th Eur. conf. on Soil Mech. and Geotech. Engng.*: 1991–1996. Amsterdam, June 1999, Rotterdam: Balkema.

EFNARC 2005. Specification and Guidelines for the use of specialist products for Mechanised Tunnelling (TBM), *Soft Ground and Hard Rock*, EFNARC web page.

Gallina D. 2005. Scavo di gallerie con EPB. Studio del condizionamento del terreno, *Tesi di laurea di II livello in Ingegneria per l'Ambiente e il Territorio*, Politecnico di Torino, Italy, unpublished, (in Italian).

Herrenknecht M. & Maidl U. 1995. Applying foam for an EPB shield drive in Valencia, *Tunnel 95 (5)*: 10–19.

Jancsecz S., Krause R. & Langmaack L. 1999. Advantages of soil conditioning in shield tunnelling: experiences of LRTS Izmir, Challenges for the 21st Century, Alten et al. (eds), 1999, Balkema-Rotterdam, pp. 865–875.

Maidl U. 1995. Erweiterung der Einsatzbereiche der Erddruckschilde durch Bodenkonditionierung mit Schaum. Dissertation Ruhr-Universität Bochum, Germany (in German).

Mair R., Merritt A., Borghi X., Yamazaki H. & Minami T. 2003. Soil conditioning for Clay Soils, *Tunnels & Tunnelling International*: 29–33, April.

Milligan G. 2000. Lubrication and soil conditioning in tunnelling, pipe jacking and microtunnelling state of the art review, *Geotechnical consulting group* – London.

Peña M. 2003. Soil conditioning for sands, *Tunnels & Tunnelling international* July: 40–42.

Peron J.Y. & Marcheselli P. 1994. Construction of the "Passante Ferroviario" link in Milan, Italy, lots 3P, 5P, and 6P: excavation by large EPBS with chemical foam injection. In *Tunnelling '94: 679–707*, IMM, London: Chapman & Hall.

Quebaud S. 1996. Contribution à l'étude du percement de galeries par boucliers à pression de terre: amélioration du creusement par l'utilisation des produits moussants, PhD thesis, Université des Sciences et Technologies de Lille, France.

Vinai R. 2006. A contribution to the study of soil conditioning techniques for EPB TBM applications in cohesionless soils, PhD thesis, Politecnico di Torino, Italy.

Vinai R., Oggeri C., Peila D., Pelizza S. 2006. Condizionamento con schiuma dei terreni per applicazioni EPB: sperimentazione mediante un nuovo apparato di laboratorio, *Gallerie e grandi opere sotterranee*, 78: 39–47.

Underground Space – the 4th Dimension of Metropolises – Barták, Hrdina, Romancov & Zlámal (eds)
© 2007 Taylor & Francis Group, London, ISBN 978-0-415-40807-3

3D geo-modeling for spillway tunnel construction in the complex fault region

W.S. Yoon & U. Jeong
NEXGEO Inc., Seoul, Korea

B.H. Han, K.H. Shin, S.S. Lee & Y.K. Kim
Samsung Corporration, Sungnam-Si, Korea

ABSTRACT: Existence of main fault zone is one of main hazardous factors of tunnel construction. In this case, a part of fault zone was exposed on the spillway tunnel face. The fault zone with graphite triggered some failures of the tunnel. According to the result of face mapping to an adjacent slope, the fault zone estimated a complex thick fault system consisted with sub-parallel faults in meta-sedimentary rocks. Detail geological survey including concentrated vertical and horizontal drillings was carried out in order to evaluate geometry and engineering properties of the fault system. We could construct a 3D Geo-Model of the unexcavated tunnel ground using the results of detail geological survey. The 3D Geo-model consisted with 3 rock units (quartz-schist, fair mica-schist and poor mica-schist) and fault zone unit. Individual units were characterized by core condition with RMR values and lab/field test properties. This 3D Geo-Model provided useful information about spatial and engineering relationship between the complex fault system and the tunnel to re-design excavation and supporting method for the unexcavated tunnel ground.

1 INTRODUCTION

Engineering Geological Model is a representation of the geology for engineering practice in a particular location. The form of the model can vary widely and include written descriptions, section or plans, block diagram, or be slated towards some particular aspect such as groundwater or geomorphological process, rock structure and so on (Fookes, 1997). Classification and reconstruction of geological units are very important in order to engineering geological modeling. Figure 1 shows elements of engineering geological modeling.

This process of engineering geological is just ground investigation and characterization. We classify geo-materials and define their engineering properties and distribution under surface. Figure 2 shows relationship between ground investigation and geological modeling. Engineering geological model is upgraded and detailed during the process (Dearman, 1991).

This case is an engineering geological modeling for construction stage of a spillway tunnel in Korea. The Geological maps and sections of the design stage were used to pre-construct engineering geological model of this tunnel site. In the maps and sections of design stage, some fault zones developed across the spillway tunnel. These fault zones were sub parallel with the tunnel. Some borehole logging sheets showed that graphite materials are in the fault zones.

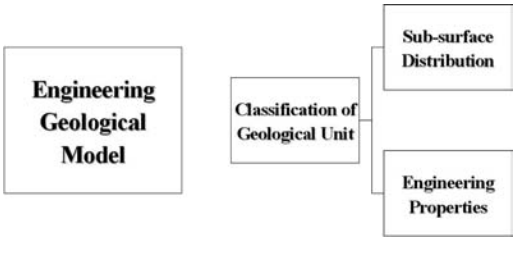


Figure 1. Elements of engineering geological modeling.

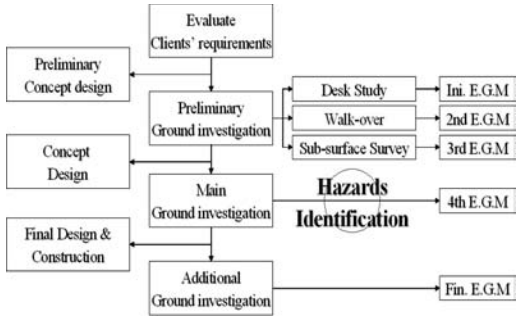


Figure 2. Process of engineering geological modeling.

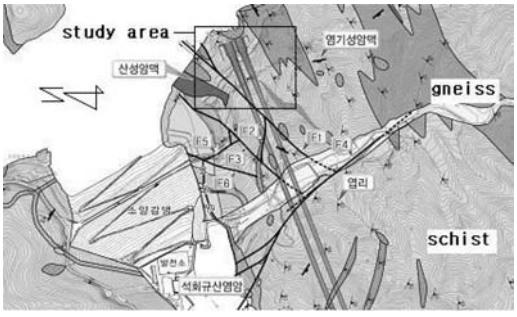


Figure 3. Geological map drown in design stage.

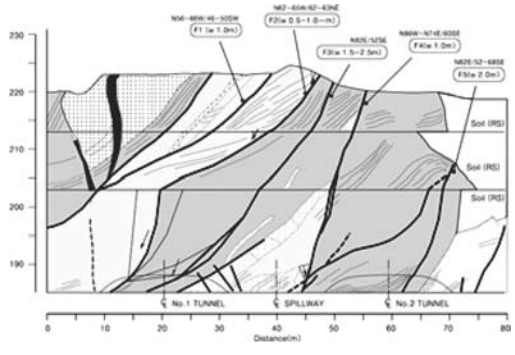


Figure 4. Geological map of tunnel slope.

A part of fault zone was exposed on the spillway tunnel face. The fault zone with graphite triggered some failures of the tunnel. Tunnel excavation was stopped and additional geological survey was planed in order to detailed engineering geological modeling for safety of tunneling. LYNX S/W (Geosystems, 2004) was used for 3D computational modeling.

2 GROUND INVESTIGATION

2.1 *General geology*

Pre-Cambrian metamorphic rocks are in the tunnel site. Schist group is consisted with mica-schist, quartz-schist and calc-silicate rocks. Some main faults cross the tunnel sun parallel or normally (Figure 3).

Some failures occurred in the study area of figure 3. Fault material like graphite was estimated main factor of these failures.

2.2 *Slope and tunnel face mapping*

Detailed geological mapping was carried at tunnel slope and faces. Figure 4 was a geological map of tunnel slope.

Figure 4 shows five faults with 1∼5 m thickness in slope face. Five faults have complex shape and various fault materials. Some faults have thick graphite zone and sub parallel direction against tunnel axis. These faults were occupied at tunnel face around failures. Distance between slope and tunnel faces is about 50 m. Table 1 shows characteristics of faults in the slope face.

Table 1. Characteristics of faults in the slope face.

Fault	Orientation		Matrial type	Fault zone thickness
	Strike	Dip		
F1	N60W	50SW	clay	∼1.0 m
F2	N60W	60NE	clay	∼1.0 m
F3	N80E	50SE	graphite	∼3.0 m
F4	EW	60SE	graphite	∼2.0 m
F5	N80E	60SE	graphite	∼2.0 m

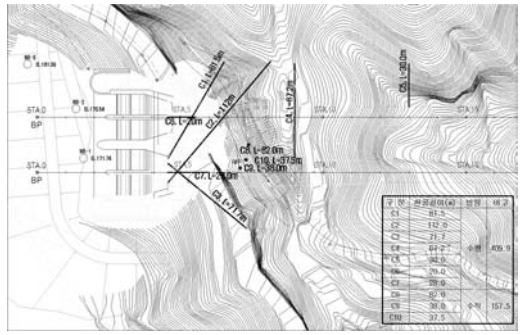


Figure 5. Location of boreholes in the under tunneling region.

2.3 *Drilling and logging*

In order to characterize geological condition including faults, drilling survey is planned in the region under tunnel excavation. Seven horizontal and inclined boreholes and five vertical boreholes were drilled. Figure 5 indicates location of boreholes.

Detailed geological logging of all cores was carried out. Engineering geological parameters based on ISRM standards (ISRM, 1981a,b) were decrypted and RMR (Beiniawski, 1989), Q value (Barton, 1974) and GSI (Hoek, 1995) were rated.

3 3D GEOLOGICAL MODELLING

3.1 *Classification of engineering geological units*

Engineering geological condition were classified five geological units of quarts-schist (QS), fair mica-schist (FMS), poor mica-schist (PMS) and fault zone (FZ) based on above mentioned geological survey. Individual units have characteristics in Table 2.

Table 2. Characteristics of faults in the slope face.

Units	QS	FMS	PMS	FZ
Class	Good	Fair	Poor	Very Poor
RMR	38–74	30–47	16–39	8–21
Q	15.813	2.156	0.869	0.027
GSI	32–88	30–57	22–49	11–34
Em (Gpa)	15,000	6,000	2,500	400
C (Mpa)	1.95	0.69	0.24	0.05
Friction A.	42	38	35	25

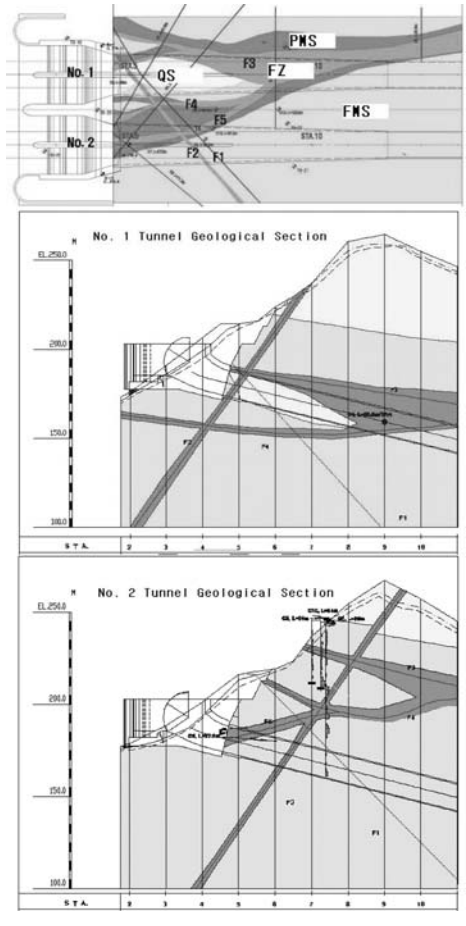


Figure 6. Geological map and section of No. 1&2 tunnels.

Engineering properties of units were evaluated through field and Lab. tests. These results were summarized in Table 2.

3.2 *Construction of plan and sections*

Geological plan and longitudinal geological sections of No. 1 and 2 tunnels were drawn (Figure 6).



Figure 7. Representaion of geological survey results.

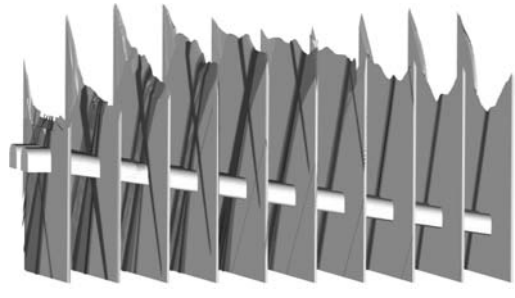


Figure 8. Geological cross sections using 3D geo-model.

Fault Zone (FZ) and Poor Mica Schst (PMS) units have very complex shape. Occupied failures located at fault zone across No. 1 and 2 tunnels in longitudinal sections.

3.3 *Reconstruction of 3D geo model*

In the site, tunnel is inclied and geological structures are complex shapes and spatial relationships. In order to fully understanding relationship between tunnel and geological structures, 3D geological model was constructed.

Figure 7 summaries all geological survey results, i.e. tunnel face mapping and core logging and etc.

3.4 *Use of 3D geo model*

Reconstructed 3D geological model can provide useful information for understanding geological condition and making concept of engineering practice.

Figure 8 shows geological cross sections using the geo-model. If 3D computational geological model is constructed, engineers can get any geological section with any direction and shape.

Additionally, engineers can easily recognize the relationship between structure and geological units.

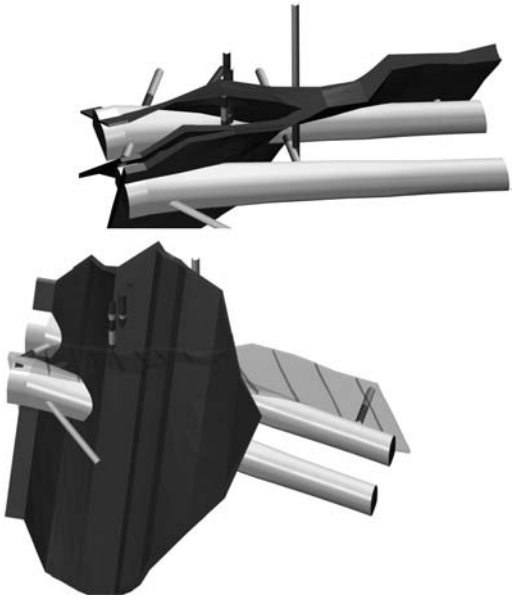


Figure 9. Spatial relationship between tunnels and zone.

Figure 9 shows spatial relationship between No. 1, 2 tunnels and fault zone.

In this work, No. 1 and 2 tunnels under excavation were successfully redesigned using 3D geo-model

4 CONCLUSION

3D Geo-Model of the unexcavated tunnel was constructed using the results of detail geological survey. Redesign of tunnels was carried out based on the 3D Geo-model with four engineering geological units, quartz-schist, fair mica-schist, poor mica-schist and fault zone unit. This 3D Geo-Model provided useful information about spatial and engineering relationship between the complex fault system and the tunnel to re-design excavation and supporting method for the unexcavated tunnel ground.

ACKNOWLEDGMENT

This study was supported by CTRM research project (project no. C105A1020001-05A0502-00419) of MOCT.

REFERENCES

Barton, N., Lien, R. & Lunde, J. 1974. *Engineering classification of rock masses for the design of tunnel support*, Rock Mrch. Rock Eng. 6(4), 189–236

Bieniawski, Z.T. 1989. *Engineering rock mass classification*. New york, John Wiley & Sons

Dearman, W.R. 1991. *Engineering geological mapping*. London, Butterworth-Heinemann Ltd

Fookes, P.G. 1997. Geology for engineers: the geological model, prediction and performance. The Quarterly Journal of Engineering Geology 30(4): 293–408

Hoek, E. 1995. Strength of rock and rock masses, ISRM News Journal 2 (2)

ISRM. 1981a. Rock and soil description and for geological mapping report. IAEG Bull. (24) 235–274

ISRM, 1981b. Suggested method for the quantitative description of discontinuities in rock mass, ISRM Suggested Methods, Pergamon Press, 3–52

Underground Space – the 4th Dimension of Metropolises – Barták, Hrdina, Romancov & Zlámal (eds)
© 2007 Taylor & Francis Group, London, ISBN 978-0-415-40807-3

Dilatometer tests in deep boreholes in investigation for Brenner base tunnel

M. Zalesky & Ch. Bühler
Solexperts AG, Mönchaltorf, Switzerland

U. Burger
BBT SE, Innsbruck/Bolzano, Austria/Italy

M. John
John Tunnel Consultant, Innsbruck, Austria

ABSTRACT: Results from more than one-year of in-situ deep borehole dilatometer testing and data evaluation for the Brenner base tunnel geotechnical investigation project are presented. The principle of dilatometer measurements is explained. Dilatometer measurements describe deformation properties of rock massif. Deformation modulus and modulus of elasticity are determined in relationship to applied pressure. Equipment for testing in deep boreholes with diameters ranging from 96 to 158 mm is described. Information needed prior to measurements, testing procedures as well as evaluation of recorded data are discussed. Examples of in-situ dilatometer measurements are presented. Range of use of gained results is discussed and conclusions are drawn.

1 INTRODUCTION

The Brenner base tunnel will be a significant part of European railway axis Berlin – Napoli – Palermo. The 55.6 km long tunnel route will be built from Austrian Innsbruck to Italian Franzensfeste (Fortezza). Numerous deep boreholes up to 1351 m depth were simultaneously drilled during the second phase of geological exploration in 2004–2005. Depth of the boreholes required drilling in several sections with decreasing diameter. Other reason for various borehole diameters was that six different drilling companies participated in the project. To comply with the proposed procedure of "drilling – logging – measuring", Solexperts AG was obliged to perform tests in boreholes with diameters ranging from 96 mm to 158 mm.

Several types of borehole measurements were performed: geophysical logging, packer tests, stress measurements using hydraulic fracturing and dilatometer measurements. In this paper we focus on in-situ determination of deformation properties of rock massif using Solexperts dilatometer.

2 SOLEXPERTS DILATOMETER SYSTEM

The dilatometer probe developed by Solexperts AG has been successfully used for more than 30 years (Thut 1977). Determination of the mechanical properties of the rock mass is based on real-time measurement of the applied pressure and the resulting deformation – the change of the borehole diameter.

The dilatometer probe consists of a metal core, which holds three potentiometeric displacement transducers placed in the centre of the core, Figure 1. The axes of the transducers are oriented 120° to each other and vertical distance between the transducers is 75 mm. The borehole wall is loaded by means of a reinforced packer sleeve fixed to the core of the probe at its both ends. The packer can be expanded by compressed nitrogen or air via a high-pressure hose connected to either nitrogen bottles or a compressor. The dilatation of the borehole wall is directly measured by the transducers, which contact the borehole wall through steel pins with spherical heads. The applied pressure is measured at the surface using a pressure sensor. The electronic signals of the displacement transducers are transmitted to the dilatometer logger through a coaxial cable within the high pressure-hose. The probe can be additionally equipped with a compass for oriented strain measurement or with two pressure sensors: one measuring the formation pressure underneath the probe and the other measuring the pressure inside the packer. To simplify installation and minimize risk of damage when retrieving the probe from the borehole a steel cone is attached to the lower end

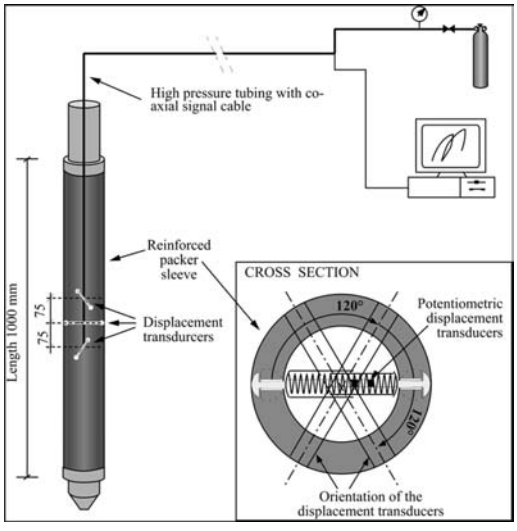


Figure 1. Scheme of the Solexperts dilatometer.

Table 1. Diameters of Solexperts dilatometer.

Diameter		
Unexpanded probe mm	Borehole – minimum mm	Sign
92	96	HQ
95	101	
118	122	PQ
142	146	
148	152	

of the probe and an open type bailer, called sedimentation tube, to its upper end in order to prevent blocking the probe by loose material falling down the drill hole.

The maximum measurement range of the displacement transducers is 25 mm, also due to their high accuracy of 0.001 mm. The packer is designed for this range of strain too. To perform tests in boreholes with diameters ranging from 96 mm to 158 mm there had to be either a single probe for each diameter or one type of probe, where the packer element and transducer extension pins could be easily changed. Solexperts has developed a dilatometer probe body (core), which can be equipped by packer elements of different diameters. A set of corresponding sedimentation tubes and calibration tubes have also been provided, Table 1. The probe is installed with so called hydro-frac tubing of 1″ using a drilling rig.

The high-pressure hose containing signal cable is wound on a winch on the surface. The hose/cable was manufactured in sections of 200 m with the appropriate connectors. Connecting multiple sections, made it possible to perform measurements up to 1400 m in depth. One or more 200 m sections of the hose/cable can be replaced, if needed.

The inflation pressure is manually regulated and automatically measured at the control panel with a pressure sensor. Additionally it can be observed together with the pressure in the system and the rest pressure in the nitrogen bottle (or compressor) with mechanical pressure gauge in the control panel. For special long-term dilatometer experiments a fully automated monitoring system (the Solexperts GeoMonitor II) can be used. In this case however, the dilatometer system is pressurized with silicon oil.

The pressure sensor and the signal cable from the probe are connected to special dilatometer data acquisition system, which is controlled by a computer via the software program DilatoII developed by Solexperts. This program provides data acquisition, testing control, graphical and numerical real-time data presentations, as well as test analysis and reporting.

3 DILATOMETER TESTS

3.1 *Planning and preliminary information*

To comply with a “drilling – logging – measuring” procedure requires a significant planning, decision making and preparation is necessary prior to execution of each series of tests.

In-situ testing i.e. dilatometer measurements or hydraulic tests using a double packer system can be done during the drilling phase or after the entire length of the borehole has been drilled. Performing measurements according to the state of drilling progress may be difficult to manage especially when several boreholes are being drilled simultaneously, as it was for the Brenner exploration project.

In most cases however, measurement campaigns are carried out after the drilling has been successfully finished. The geologist in charge usually overviews the entire borehole and specifies the borehole sections of interest. Results of tests might be affected by “borehole history effect” (especially affecting the hydraulic tests results). Another problem to be considered for testing after drilling is the stability of the borehole. Especially, investigation of faults and shear zones is of interest for the design of planned excavation. In cases of poor borehole stability only the “measurement-while-drilling” approach can be applied.

The approach chosen for the geotechnical and hydrogeological investigation for the Brenner base tunnel was a compromise of the presented possibilities: a series of test measurements was done after a first section of the borehole with one diameter was drilled.

Borehole logging and geophysical measurements were carried out at the beginning of a testing campaign.

The logs were used to decide about the subsequent testing strategy and number of tests. For the dilatometer tests the most important information was:

- nominal borehole diameter,
- test depths,
- type of rock / inspection of borehole cores,
- dipping of shistosity,
- calliper log for actual borehole diameter or
- borehole scan for geologic structure and
- ground water table / hydrostatic pressure at each test depth.

The calliper log and/or the borehole scan provided information about the true borehole diameter as well as the possible existence of caverns, discontinuities, large cracks and fractures of the massif. Uneven borehole walls result in higher risk of packer damage and, in the extreme case, the possible blockage of the borehole by an irretrievable probe. Additionally, to high artesian water pressure (determined by the hydrogeological tests) can cause difficulties during the tests.

3.2 *Test procedure*

The dilatometer probe must be calibrated prior to testing. The calibration is done by inflating the probe inside a steel tube of known diameter. The DilatoII software then records the data from each displacement transducer and calculates offsets so that a "zero reading" corresponds to the known inner diameter of the tube. The actual borehole diameter can then be precisely determined. It is needed for control of the probe expansion state during the test and for test analysis.

The test sequence usually begins at the lowest test position in the borehole. During installation into deep boreholes the probe must be partially inflated in order to counterbalance the acting hydrostatic pressure. After lowering the probe to the depth given by the geologist, the dilatometer measurement can start. The actual borehole diameter can be determined with the dilatometer probe in cases where the calliper log shows significant variations in borehole diameter along the borehole section selected to be the test position, or the borehole cores showed discontinuities, but especially if no core could be retrieved. The actual diameter can be determined by inflating the probe just enough to overcome the hydrostatic pressure and the stiffness of the packer. Then the packer is in contact with the borehole wall. Under low inflation pressure there is no danger for the probe even if a cavern or fracture exists at this borehole section. The risk of damaging the equipment can be minimized by selecting a test position with an appropriate diameter after measuring the borehole diameter at several locations along the test zone using the described procedure.

The dilatometer tests for Brenner base tunnel project were performed with four loading cycles. At first, the probe was inflated to a base pressure, which was about 0.5 MPa higher than the hydrostatic pressure at the test position in order to establish a good contact between the packer and the borehole wall. The first cycle consisted of initial loading and subsequent unloading to the base pressure. The following cycles consisted of reloading up to the maximum pressure of the previous load cycle, initial loading to a higher level and then unloading to the base pressure level.

The maximum level of loading pressure has to be chosen with respect to the rock type, its assumed compressibility and the aim of the test. In case of measurements for a future base tunnel, the applied pressure should reach the same order as the horizontal pressure at rest in the mountain massif. One of the aims of a good dilatometer test is to describe the ratio of plastic and elastic deformations together with general behaviour of the rock, which can be also mostly elastic or plastic. The range of applied pressures should be chosen so, that the maximum of elastic deformation phase of the rock is used, but causing massive plastification or fracture of the rock is to be avoided if possible.

After the test is finished, the probe is unloaded under the level of acting hydrostatic pressure and raised to the next higher measurement zone.

3.3 *Evaluation of dilatometer test*

The moduli are calculated based on Lamé's equation for a tube with infinite wall thickness (1):

$$E = \frac{\Delta p * d * (1 + \nu)}{\Delta d} \tag{1}$$

where Δp = pressure difference; d = borehole diameter; Δd = change of borehole diameter; ν = Poisson's ratio. In case where no results of laboratory tests are available for the tested rock formation, we assume the Poisson's ratio of 0.33 with respect to rock quality.

The deformation modulus (V) is calculated based on data of initial loading from each load cycle. The modulus is computed using a linear regression along the corresponding section of the curve. The deformation modulus from reloading phase of each cycle is calculated in a similar manner.

The modulus of elasticity (E_1) is calculated from the slope of a secant connecting the first and the last point of the unloading phase, which corresponds to the initial loading range for each cycle. However in cases of very step slopes which correspond to very small elastic deformation of the borehole wall and thus to very high moduli, it appears to be more appropriate to calculate E_2 (Fig. 2) from the entire unloading curve for each load cycle.

The averaged displacement measurements of the all three transducers are mainly used for the calculation

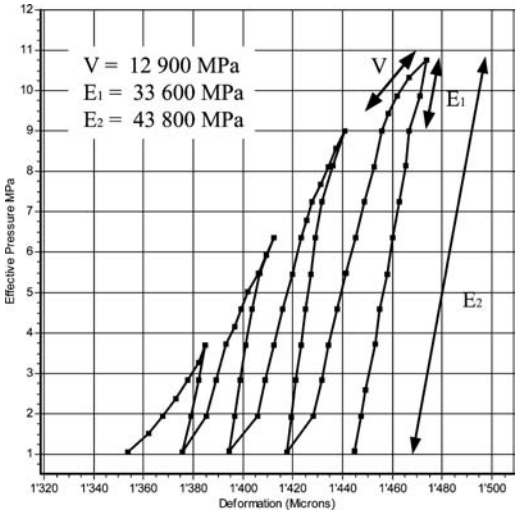


Figure 2. Dilatometer test in borehole Va-B-03/04s, 986.5 m depth, chlorite schists. Graphical representation from the DilatoII software program: average from deformation measurements of all three extensometers.

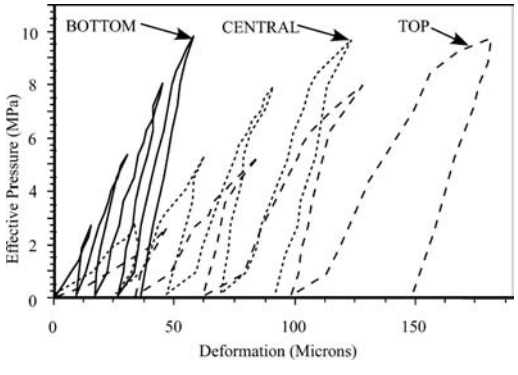


Figure 3. Dilatometer test in borehole Va-B-03/04s, depth 986.5 m. Comparison of pressure/deformation graphs for three extensometers.

of the moduli. Based on comparison of all three pressure / deformation graphs, conclusions on elastic or plastic behaviour of the rock massif can be drawn and estimates of anisotropy can be made. Figures 2 and 3 show a dilatometer test in chlorite schists at 986.5 m depth. The borehole Va-B-03/04s is inclined 30° from vertical.

The method of analysis described above allows assessing one dilatometer test at a time. The stiffness of the examined rock can be classified according to the values of deformation and elasticity modulus from the last loading cycle. For this purpose we use the classification based on E-modulus values, which was proposed by AFTES (1993).

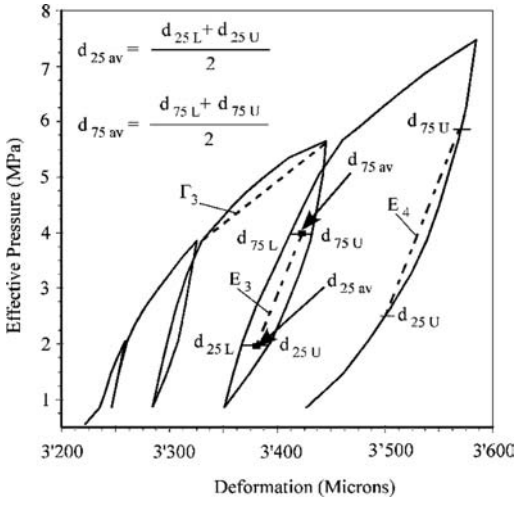


Figure 4. Schema for computation of E and Γ for Schneider's criterion. Graph: Test in borehole Pf-B-03/05, depth 39 m, quartzphyllite. Average from deformation measurements of all three extensometers.

Another approach, Schneider's criterion (1967), also uses the Lamé's equation, but allows interpretation and comparison of series of dilatometer tests from a wide range of rocks. Development of the deformation properties can be evaluated with respect to acting pressure. Measurements with four loading cycles are required for the Schneider's criterion, which describes the relationship of a factor of permanent deformation C_p (2) to a ratio of elasticity modulus E to deformation modulus Γ (3):

$$C_p = \frac{d_p}{p_{max}} \quad (2)$$

$$\frac{E}{\Gamma} \quad (3)$$

where d_p = permanent deformation after a complete loading cycle; and p_{max} = maximum loading pressure applied with this cycle. The factor of permanent deformation is calculated for each loading cycle.

The modulus of elasticity E is defined as a slope of a straight line, which connects points $d_{25\ av}$ and $d_{75\ av}$. These points represent average deformation from unloading ($d_{25\ U}$, $d_{75\ U}$) and reloading ($d_{25\ L}$, $d_{75\ L}$) phase of the corresponding load cycle (see Fig. 4). Values of d_{25} and d_{75} are determined at pressure levels of 25% and 75% from the maximum pressure applied in the loading cycle. The E moduli are calculated for the first to the third load cycle. The calculation of E-modulus from the last (fourth) cycle is based on data from the unloading phase only. These calculations

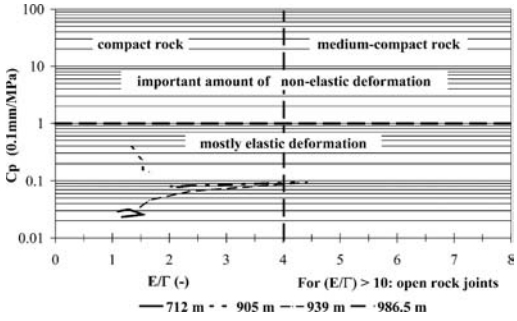


Figure 5. Schneider's criterion, after Schneider (1967). Graph: dilatometer tests in shales, borehole Va-B-03/04s.

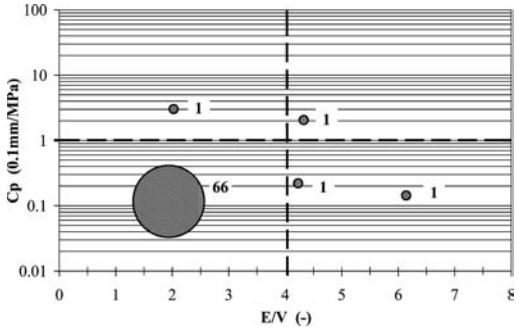


Figure 6. Modified Schneider's criterion. Distribution of 70 test results. The position of the points corresponds with average of E/V and C_p for each presented rock class. The size of points relatively depicts the number of tests.

can be done by interpolation between the data points recorded during the measurement (see Figure 2) or estimated in the chart. The analysis data presented in this article were interpolated. The deformation modulus Γ is determined as the slope of a secant, which connects the first and last point of an initial loading phase of a load cycle, Figure 4.

The resulting data is plotted in a semi-logarithmic graph, which is also used for rock classification, after Schneider (1967), Figure 5. All four data sets presented in this example indicate compact rocks with mainly elastic deformation behaviour.

Data analysis for Schneider's criterion is not integrated into the analysis part of DilatoII program. Therefore the analysis was made with a spreadsheet program, which is rather time consuming. Further, presentation of a large number of tests in a diagram according to Schneider can become confusing. For these reasons we propose a modified version of Schneider's criterion based on the values from the last (fourth) loading cycle only. The results of a complete dilatometer test are reduced to only one point in the Schneider's graph, instead of a polygon line in the original Schneider's criterion. This method allows a quick comparison of rock properties in a large set of dilatometer tests. This procedure does not depict the development of the moduli and the amount of plastic deformation with respect to pressure changes during the test but makes evaluation of the distribution of measured moduli much easier.

We use the data of V (deformation modulus calculated as regression) and E (elasticity modulus) computed by the DilatoII program in the modified Schneider's analysis. The E_2 modulus calculated from the entire unloading phase of the fourth loading cycle was chosen, because it is closer to the original Schneider's criterion than the E_1 value determined from the upper part of the corresponding unloading phase only, Figure 2. This simplifies determination of coefficient E/V (instead of original E/Γ), whereas the coefficient C_p remains unchanged. All results are then displayed in Schneider's graph. To get a better overview of the distribution of test results, the average is calculated for each rock class. Seventy dilatometer tests executed during the exploration campaign for Brenner base tunnel project are shown in Figure 6.

The proposed analysis and graphic presentation gives an overview of the deformation properties along the whole project. Based on the modified Schneider's criterion, it is obvious, that that about 95% of the tests indicate a compact rock, of mainly elastic behaviour in the range of applied pressures. Only four tests (roughly 5%) represent rock with partly plastic deformation behaviour. In the next step, these tests should be reviewed in detail and further investigation might be considered if these results appear to be critical for the project.

This approach might be helpful for decision making in the early stages of geological and geotechnical survey. The knowledge gained from the modified Schneider's criterion may be used:

- as another point of view for preliminary characteristics the rock mass,
- to find areas, where further investigation may be required,
- to obtain an overview of the deformation properties of the rock mass and
- to estimate suitable tunnelling techniques and the type of primary tunnelling supports.

4 APPLICATION OF RESULTS

For the determination of the stiffness parameters of the rock mass at the Brenner base tunnel various formulas given in the literature such as Hoek et al 2002 have been used. Results obtained revealed a considerable scatter. The results of the dilatometer tests have been used to verify calculated results. Due to the fact

that dilatometer tests represent the deformability of sections of rock mass of less than 1 m, whereas during excavation stress redistributions affect sections of up to 10 m results of dilatometer tests have been regarded as an upper limit taking into consideration the scale effect.

5 CONCLUSIONS

Results of dilatometer in-situ measurements describe deformation properties of rock mass. A large number of tests were performed during the second phase of geological exploration for the Brenner base tunnel in 2004–2005. The borehole diameters were ranging from 96 to 158 mm and the boreholes were reaching to depths of more than 1300 m. The results from the provided dilatometer tests were used to verify calculated stiffness parameters of the rock mass at the Brenner base tunnel. Based on our experience with test analysis and interpretation, a modification of Schneider's analysis of dilatometer tests has been created in order to allow quick overview and comparison of numerous dilatometer tests. The most important modifications are: moduli calculated only from the last loading cycle are directly used. Each dilatometer test is then represented by only a single point in the Schneider's graphical classification. Even large series of tests covering the whole explored area of interest can be assessed. Evaluation of the distribution of points in the resulting graph allows characterization of the major type of rock mass deformability. The rock classes where few tests occur can indicate areas to be reviewed or further investigated.

ACKNOWLEDGEMENTS

The authors would like to thank BBT SE for the permission to publish results from the 2004/2005 exploration campaign.

REFERENCES

AFTES, Groupe de travaille No. 1, Géologie – Géotechnique. Texte des recommandations pour une description des massifs rocheux utile à l'étude de la stabilité des ouvrages souterrains. *Tunnels et ouvrages souterrains, supplément au No117, Mai 1993, pages 12–21, Annexe 1.*

Hoek, B., Carranza-Torres, C., Corkum, B. 2002. *Hoek-Brown Failure Criterion – Edition 2002*. Vancouver.

Schneider, B. 1967. Moyens nouveaux de reconnaissance des massifs rocheux. In Nouredine Dinia et al, *Méthodologie des essais au dilatomètre: application à quatre grands barrages Marocains; Proc. intern. Symp. Essais en place volume 2, Paris 1983.*

Solexperts 2005. *Brenner Basistunnel Erkundungsbohrungen 2004 B0008-Wipptal Bohrung Va-B-03/04s Dilatometerversuche*. Final report. Mönchaltorf: Solexperts.

Solexperts 2005. *Brenner Basistunnel Erkundungsbohrungen 2004 B0008-Wipptal Bohrung Pf-B-03/05 Dilatometerversuche*. Final report. Mönchaltorf: Solexperts.

Thut, A. 1977. Deformationsmoduln der Mergelschiefer der Flyscherie und des verlehmten Gehängeschuttes Vergleiche zwischen Dilatometer- Lastplatten- und Druckversuchen. *Mitteilungen der Schweizerischen Gesellschaft für Boden- und Felsmechanik No. 96, Frühjahrstagung, Luzern, 13. Mai 1977.*

Zalesky, M., unpubl. 2006. Comparison of all results of dilatometer test form Brenner base tunnel (2nd phase of exploration) and modification of the Schneider's criterion.

Part 2.2
Improvement of ground mass

This page intentionally left blank

Underground Space – the 4th Dimension of Metropolises – Barták, Hrdina, Romancov & Zlámal (eds)
© 2007 Taylor & Francis Group, London, ISBN 978-0-415-40807-3

The dimensioning of tunnel face reinforcement

G. Anagnostou & K. Serafeimidis
ETH Zurich, Switzerland

ABSTRACT: Ground reinforcement using fiberglass or steel bolts is a very efficient measure for stabilizing the face in conventional tunneling. The reinforcement needs a careful design in order to optimize the construction process. This paper presents a computational method which is based upon limit equilibrium considerations and which can be applied to heterogeneous, layered ground as well as to arbitrary reinforcement layouts in terms of the spacing, length, longitudinal overlapping and installation sequence of the bolts. Additionally, design nomograms are presented for the assessment of tunnel face stability in the special case of a homogeneous ground with uniform reinforcement.

1 INTRODUCTION

The most serious risks in tunneling through weak ground are associated with a collapse of the tunnel heading. In shallow tunnels the instability may propagate towards the surface, thereby creating a crater on the ground surface. In mechanized tunneling through soft ground, closed shields are applied for stabilizing the face. In conventional tunneling, ground reinforcement using face bolts is a very efficient measure besides partial excavation or ground improvement through grouting or artificial freezing.

The face reinforcement needs a careful design because it slows down construction progress considerably as it is carried out ahead of the face intermittently with the excavation. Besides experience and engineering judgment, calculations are indispensable. Basic considerations for the stabilizing action of face reinforcement may be found elsewhere (Anagnostou 1999). In the following pages, a dimensioning method as well as design nomograms will be presented.

2 COMPUTATIONAL METHOD

2.1 *Failure mechanism*

As in past contributions (Horn 1961, Anagnostou & Kovári 1994), the computational method is based upon the limit equilibrium of a failure mechanism that consists of a wedge and the overlying prism (Fig. 1). Mohr-Coulomb failure condition will be assumed for the ground. Cohesion c and angle of internal friction ϕ may vary over the face (layered ground). Both the inclination ω of the slip plane and the elevation z_f of the wedge foot are in general unknown at the start. Their

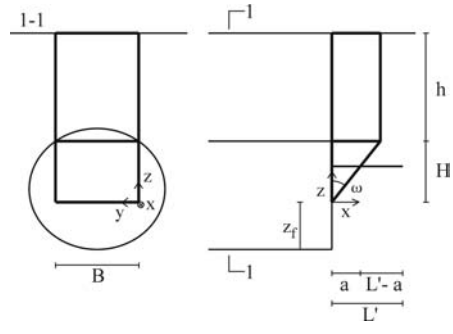


Figure 1. Failure mechanism.

critical values, i.e. the values that maximize support requirements, depend on the shear strength and on the stratigraphy of the ground and they will be determined iteratively.

2.2 *Effect of reinforcement*

During ongoing excavation (without anchorage plates), the supporting effect of the face bolts relies solely on the strength of the bond between grout and soil. The support force of one bolt depends thus on its tensile strength F_z, on the diameter d of the grouted borehole, on the shear strength τ_m of the soil – grout interface, on the bond length a inside the wedge as well as on the bond length $(L' - a)$ in the ground ahead of the inclined slip surface, where L' denotes the actual bolt length (Fig. 1).

If anchorage plates are present (e.g. during an excavation standstill) and the bond length a inside the wedge is insufficient, the bolt force will be transmitted to the ground through the plates being thus limited by

the bearing capacity F_p of the anchorage system at the face (bolt plates and soil).

In general, the support pressure s offered by the face reinforcement is given by

$$s = n \cdot min[F_z, max(\pi d \tau_m a, F_p), \pi d \tau_m (L'-a)], \quad (1)$$

where n denotes the reinforcement density, i.e. the number of bolts per sqm.

Note that the bond lengths a and $(L' - a)$ vary over the height of the wedge and, moreover, they depend also on the specific mechanism considered, i.e. on the angle ω and on the elevation of the wedge foot z_f. Consequently, the support force offered by the reinforcement will not be uniformly distributed even in the case of constant bolt spacing (Fig. 2a).

Depending on the initial lengths of the bolts and on the longitudinal overlapping of the successive installation stages, bolts of different lengths may be present at the same time. It is interesting to note that the same total quantity of bolts (linear meters bolts installed per linear meters tunnel) may lead to different support pressures, depending on the installation sequence (Fig. 2b and 2c).

2.3 *Equilibrium assessment*

The wedge is loaded by the overlying prism. The bearing capacity of the wedge depends on the shear resistance of the ground and on the support force offered by the bolts.

The shear resistance of the two lateral, vertical slip surfaces of the wedge contributes to stability considerably. The frictional part of the shear stress depends, however, on the respective normal stress (i.e. on the horizontal stress σ_x), which cannot be derived from the equilibrium conditions. Following Anagnostou & Kovári (1994), the horizontal stresses will be derived here by assuming that their ratio to the vertical stresses σ_z is constant and equal to $\lambda = 0.8$. The vertical stress σ_z will be obtained by considering the equilibrium of a horizontal, infinitesimal slice of the wedge (Fig. 3). Walz and Prager (1978) first proposed such an approach for the stability assessment of slurry walls (so called "method of slices"). It is very similar to the one of silo theory, eliminating the need for an *a priori* assumption of the distribution of the vertical stress σ_z and offering the possibility of analyzing a layered ground with an arbitrary distribution of reinforcement.

The infinitesimal slice is acted upon the following forces (Fig. 3): its weight dG; the "supporting" force $V(z)$ exerted by the underlying ground; the "loading" force $V(z) + dV$ exerted by the overlying ground; the forces dN and dT at the inclined slip surface; the shear force dT_s at the vertical slip surfaces; and the supporting force dS of the reinforcement (i.e. $s(z) \cdot B \cdot dz$, where B is the width of the wedge and dz the thickness of the slice).

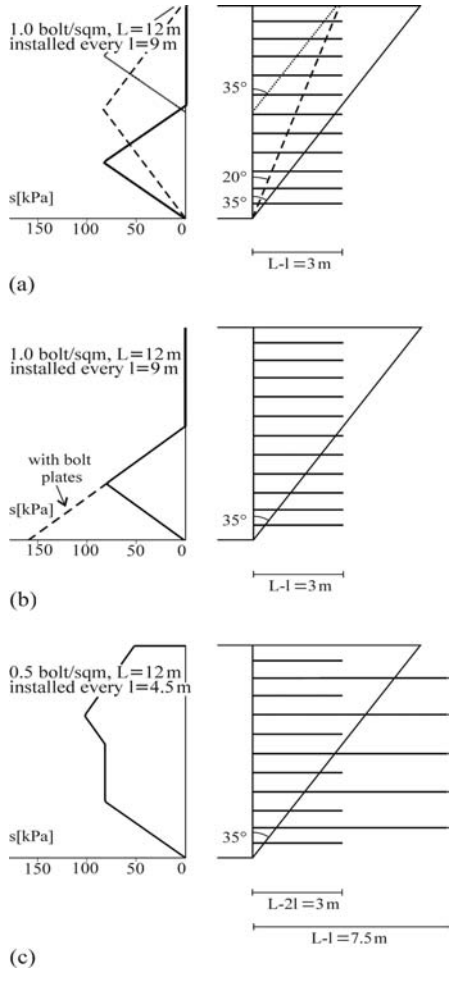


Figure 2. Support pressure distribution for different reinforcement densities and installation sequences.

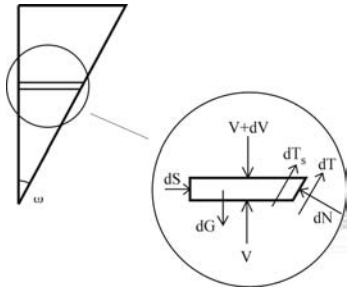


Figure 3. Forces acting upon infinitesimal slice.

The equilibrium conditions parallel and perpendicular to the sliding direction, i.e.

$$dT_s + dT + S \sin\omega = (dV + dG) \cos\omega \quad (2)$$

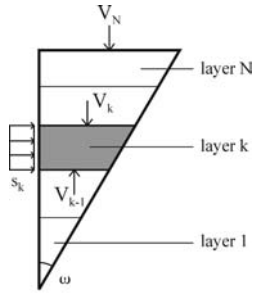


Figure 4. Division of wedge in layers.

and

$$dN = (dV + dG)\sin\omega + dS\cos\omega \quad , \tag{3}$$

lead to the following differential equation for the vertical force $V(z)$:

$$dV/dz - A(z)\,V = \Gamma(z)\,z + \Delta(z) \, , \tag{4}$$

where the coefficients $A(z)$, $\Gamma(z)$ and $\Delta(z)$ depend on the shear strength constants $c(z)$ and $\phi(z)$, on the soil unit weight $\gamma(z)$, on the ratio λ of horizontal to vertical stress, on the wedge width B, on the support pressure $s(z)$ and on the angle ω.

For the solution of Eq. (4), the wedge is divided into an arbitrary number N of finite thickness layers (Fig. 4). Each layer k is homogeneous (constants c_k, ϕ_k and γ_k) and is supported by a uniform pressure s_k, i.e. the irregularly distributed support pressure $s(z)$ (Fig. 2) is approximated by a piecewise constant pressure. The support pressure s_k of each layer is calculated based upon its reinforcement density n_k and by taking into account the average bond length (at mid-height of the layer). Under these conditions the coefficients A, Γ and Δ are constant within each layer and Eq. (4) can easily be integrated layer-wise.

As a result one obtains the following equation for the k.th layer:

$$V_k = C_{sk}\,s_k + C_{Vk}\,V_{k-1} + C_{ck}\,c_k - C_{\gamma k}\,\gamma_k \, , \tag{5}$$

where

$$C_{vk} = e^{A_\kappa\cdot(z_\kappa - z_{\kappa-1})} \, , \tag{6}$$

$$C_{sk} = \frac{(C_{v\kappa}-1)\cdot B\cdot\tan(\omega+\varphi_\kappa)}{A_\kappa} \, , \tag{7}$$

$$C_{ck} = \frac{(C_{v\kappa}-1)\cdot B\cdot A_\kappa + 2\cdot F_\kappa\cdot\sin\omega}{A_\kappa^2\cdot\cos^2\omega\cdot(1-\tan\omega\cdot\tan\varphi_\kappa)} \, , \tag{8}$$

$$C_{\gamma k} = \frac{F_\kappa\cdot\tan\omega\cdot B}{A_\kappa^2} \, , \tag{9}$$

$$A_k = \frac{2\cdot\lambda\cdot\tan\varphi_\kappa}{B\cdot\cos\omega\cdot(1-\tan\omega\cdot\tan\varphi_\kappa)} \, , \tag{10}$$

$$F_k = C_{v\kappa}\cdot\left(1+A_\kappa\cdot z_{\kappa-1}\right) - 1 - A_\kappa\cdot z_\kappa \, , \tag{11}$$

and z_k denotes the elevation of the upper layer boundary. Eq. (5) expresses the "loading" force V_k acting at the upper boundary of the k.th layer as a function of the "supporting" force V_{k-1} acting on its bottom boundary (Fig. 4). The forces V_k are calculated by applying Eq. (5) successively from down to top starting with $V_0 = 0$.V_k represents the force that can be sustained by a wedge consisting of the layers 1, 2, . . . k. A negative value of V_k (tensile force) means that the wedge must be hanged in order to remain stable, thus indicating a collapse of the face up to layer k. So the following constraint has to be fulfilled by the chosen reinforcement:

$$V_k \geq 0 \;(k = 1, 2, 3, \ldots N). \tag{12}$$

V_N represents the bearing capacity of the entire wedge up to the overlying prism: In order that the face remains stable, V_N must be higher than the load V_S exerted by the prism. The latter is calculated based upon silo theory. At limit equilibrium,

$$V_N = V_S \tag{13}$$

applies. The iterative solution of this equation together with the constraints according to Eq. (12) yields the required reinforcement densities for the specific mechanism considered (i.e. for a given inclination ω and wedge foot elevation z_f). The critical mechanism, i.e. the one necessitating the maximum support quantities, is found by repetitive application of the procedure outlined above. In general, a multi-parametric optimization problem has to be solved because any layer may have another bolt density. A unique solution can be obtained, however, by specifying the bolt distribution (e.g., uniform distribution).

2.4 *Homogeneous ground, uniform reinforcement*

In this special case, one can readily verify, by inspecting Eqs. (5) and (1), that the required bolt density n depends linearly on the ground cohesion c, and can, therefore, be expressed in the following way:

$$n = n_o\,(1\text{-}c/c_{crit}) \, , \tag{14}$$

where n_o is the necessary reinforcement density in the case of cohesionless ground ($c = 0$) and c_{crit} denotes the minimum cohesion required in order that the face remains stable without support ($n = 0$). A dimensional analysis shows, furthermore, that the following dimensionless dependencies exist:

$$\bar{c}_{crit} = c_{crit}/\gamma H = f(\phi,\, B/H,\, h/H,\, \lambda) \, , \tag{15}$$

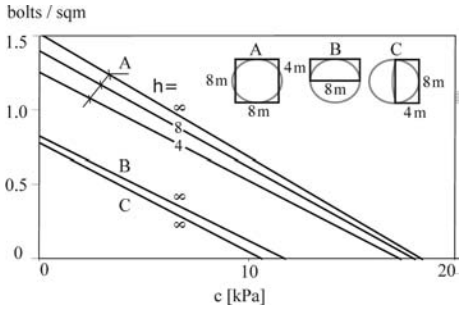


Figure 5. Numerical example on the influence of shape and of depth of cover h ($L = 12$ m long bolts installed every $l = 9$ m).

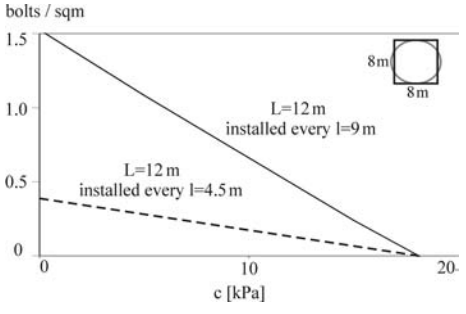


Figure 6. Numerical example on the influence of installation sequence.

$$\bar{n}_0 = n_o\, d\tau_m/\gamma = f(\phi,\ B/H,\ (L\text{-}l)/H,\ l/L,\ h/H,\ \lambda)\ , \quad (16)$$

where L denotes the initial bolt length (at installation), l the distance between the successive installation stages and L-l the longitudinal overlapping of the bolts (see Fig. 7).

Eq. (16) does not take into account the tensile strength of the bolts and the bearing capacity of the plates. This is a reasonable simplification as experience shows that shear failure at the grout-soil interface is the most critical mechanism, at least for soft ground.

The effect of depth of cover (h/H) is negligible as can be seen from the computational results of Figure 5 (lines A). The shape of the wedge (expressed by the width-height ratio B/H) is, however, an important parameter (see Fig. 5, lines for $h = \infty$). The smaller the width, the more pronounced becomes the stabilizing effect of the shear resistance at the vertical slip surfaces of the wedge. So, for example, case C of Figure 5 needs about the same bolt quantity as case B, in spite of the greater height of the wedge.

The reinforcement installation sequence (expressed by the parameters l and L) is also important. In the example of Figure 6, up to 1.5 bolts/sqm are needed if installed every 9 m (upper line). In the case of frequent installation (every 4.5 m, see lower line), only

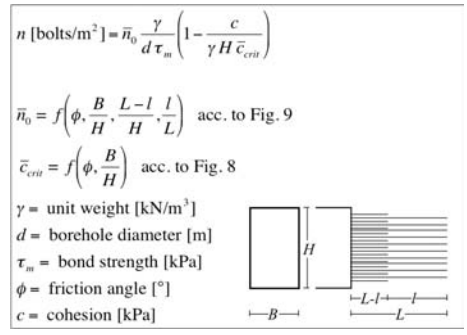


Figure 7. Synopis of equations for using the nomograms.

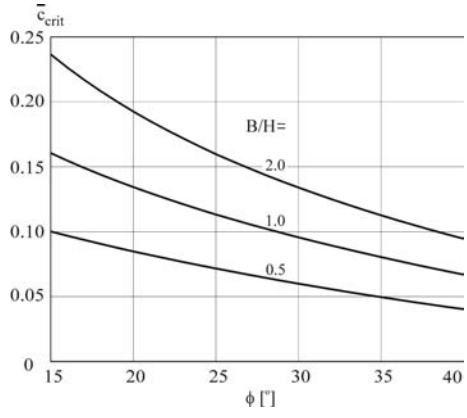


Figure 8. Dimensionless critical cohesion $\bar{c}_{crit}$ as a function of friction angle ϕ and of shape factor B/H.

0.4 bolts/sqm must be installed. The total quantity of bolts (meter bolts installed per linear meter tunnel) is given by $n{\cdot}B{\cdot}H{\cdot}L/l$ and amounts up to 130 m/m in the first case, and up to 65 m/m in the case of frequent installation. This considerable saving is due to the more favorable pressure distribution (cf. Fig. 2a and 2b). A frequent installation of bolts interferes, nevertheless, with the excavation works and may therefore be advantageous only if the reinforcement quantities are large.

2.5 *Design nomograms*

Based upon these considerations, design nomograms have been prepared. Figures 8 and 9 show the dimensionless critical cohesion $c_{crit}/\gamma H$ and the dimensionless reinforcement density $n_o d\tau_m/\gamma$, respectively, as a function of the friction angle ϕ for cross section shapes $B/H = 0.5$ to 2, $h/H = \infty$ and $\lambda = 0.8$ (cf. Eqs. 15 and 16). The solid lines in the nomograms of Figure 9 concern the common case of short overlapping lengths (L-$l < L/2$). The dashed lines apply to the case

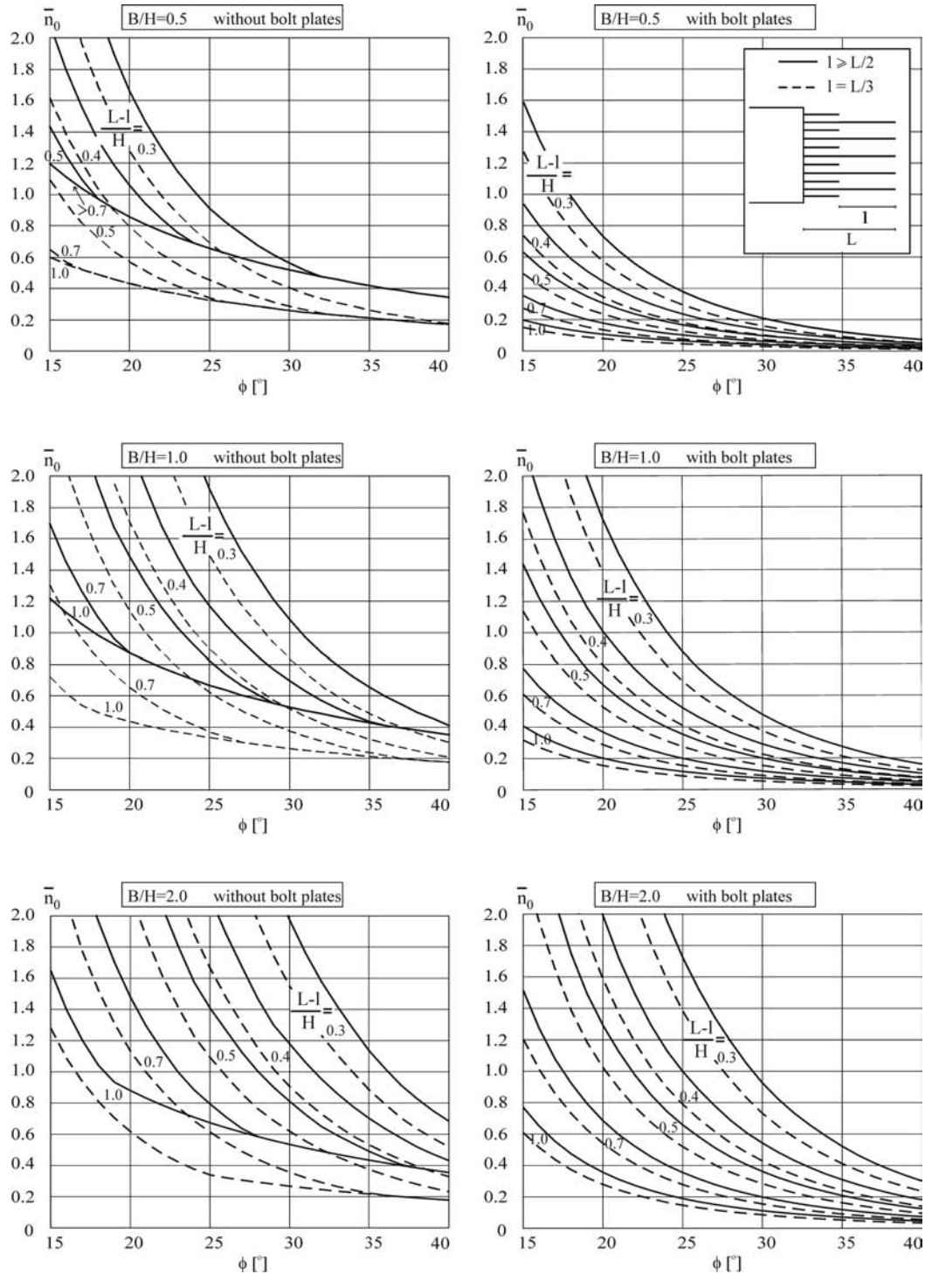


Figure 9. Dimensionless reinforcement density $\bar{n}_0$ as a function of friction angle ϕ.

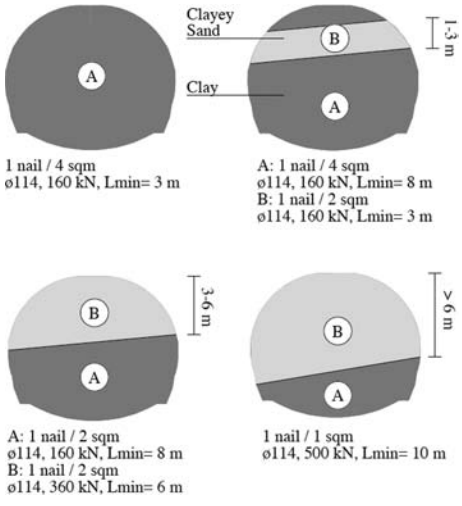


Figure 10. Example of face stabilization according to stratigraphy (after Anagnostou 2001).

$l = L/3$, i.e. to frequent reinforcement installations. All diagrams have been calculated for a safety factor of 1.0. A safety factor ν can easily be taken into account through an appropriate reduction in the shear strength parameters (c/ν, $tan\phi/\nu$ and τ_m/ν).

3 CLOSING REMARKS

The presented nomograms cover a wide range of conditions and represent a very useful design aid for conventional tunneling through soft ground. One should, nevertheless, keep in mind the underlying assumptions and their limitations. Besides a global instability of the tunnel heading, local failures may also occur and endanger safety on the work site. For example, the nomograms suggest that a cohesionless ground can be stabilized by bolts. Without a minimum cohesion, however, the ground will fail between the bolts particularly in the presence of water. On the other hand, according to Figure 8 the face should remain stable without any measures if the cohesion is higher than a threshold value of about $0.2\gamma H$, i.e. 40–50 kPa for common cross-sections of traffic tunnels. This conclusion oversimplifies reality, because failures such as detachment of wedges along wet slickenslides, may occur even in a stiff clay. Heterogeneous ground is particularly demanding (Fig. 10). Design calculations in that case provide only rough guidelines for decision-making during construction.

REFERENCES

Anagnostou, G. & Kovári, K. 1994. The face stability of slurry-shield driven tunnels. *Tunnelling and Underground Space Technology*, 9 (2), 165–174.

Anagnostou, G. 1999. Standsicherheit im Ortsbrustbereich beim Vortrieb von oberflächennahen Tunneln. *Symp. "Städtischer Tunnelbau – Bautechnik und funktionelle Ausschreibung"*, Zürich, 85–95 (in German).

Anagnostou, G. 2001. Two shallow tunnels in soft ground. *AITES-ITA 2001 World Tunnel Congr. "Progress in Tunnelling after 2000,"* Milano, 21–28.

Horn, M. 1961. Alagutak homlokbiztositására ható vizszintes földnyomásvizsgálat néhány eredménye. *Az országos mélyépitóipari konferencia elóadásai*, Közlekedési Dokumentációs Vállalat, Budapest (in Hungarian).

Walz, B. & Prager, J. 1978. Der Nachweis der äusseren Standsicherheit suspensionsgestützter Erdwände nach der Elementscheibentheorie. *Veröff. des Grundbauinstitutes der TU Berlin*, **4** (in German).

Underground Space – the 4th Dimension of Metropolises – Barták, Hrdina, Romancov & Zlámal (eds)
© 2007 Taylor & Francis Group, London, ISBN 978-0-415-40807-3

Cost-effective pre-injection with rapid hardening microcement and colloidal silica for water ingress reduction and stabilisation of adverse conditions in a headrace tunnel

A.K. Bahadur
Uttaranchal Water and Power Department, Dehradoun, India

K.G. Holter
BASF UGC Europe, Zürich, Switzerland

A. Pengelly
BASF Construction Chemicals, Delhi, India

ABSTRACT: During the drill-and-blast excavation of the headrace tunnel, difficult rock conditions were encountered in a zone caused by a regional fault. Tunnelling through the zone was initially done without pre-treatment of the ground, resulting in severe difficulties and a lengthy delay. Therefore it was decided to excavate a bypass tunnel utilizing pre-excavation grouting from the tunnel face. A two-stage pre-injection scheme was laid out in order to achieve the desired penetration of grout into the ground. First stage grouting was done with rapid hardening microcement, in which a limited grout take was achieved. The second stage of grouting was done with liquid colloidal silica, thus achieving penetration into the finest discontinuities. The result was an acceptably fast advance, excellent ground stability and virtually dry ground conditions. This enabled the safe installation of rock support with steel sets combined with sprayed concrete.

1 BACKGROUND

1.1 *The project*

During the drill-and-blast excavation of the 16 km long headrace tunnel of 4×76 MW Maneri Bhali Hydro Electric Project, difficult ground conditions were encountered in the stretch passing below a stream. The ground cover mostly consists of river born material (RBM).

Tunneling through this section was initially done without any pre-treatment of the ground, resulting in the puncturing of the small rock cover over the tunnel crown, causing severe leakages from the water saturated RBM zone and chimney formations. The difficulties caused lengthy delays, so much so that a 56 m long problem zone in the tunnel took nine months to excavate.

Moreover, due to problems faced in negotiating this sitaution, the tunnel could not be excavated to full required cross section. As a result the designers of the tunnel lining advised the reduction of the tunnel section and the installation of steel lining.

The work on the project was stopped in early nineties. When it was resumed in 2002, the project management did not feel comfortable with the idea of having a reduced tunnel section with steel lining in this portion due to the of extra time required for the steel lining, as well as the increased friction losses associated with this arrangement.

1.2 *Geological conditions*

The challenge in this situation was to 'again' cross this fault zone in the bypass tunnel, without ground collapse and in dry conditions, thereby allowing lining construction in dry and stable conditions. The rock mass consisted of heavily jointed quartzites and metabasics on each side of a regional fault zone.

A river valley at surface followed the fault zone alignment with subsequent thick deposits of river born materials over lying the quartzite and metabasics. The fault zone exhibited highly crushed material with associated high water seepages that resulted in significantly reduced stability of the excavated rock-mass. Joint fillings consisted of fine grained quartzite material of clay and silt fractions.

1.3 *The problem*

During the initial phase of the project, the tunnel was excavated through this zone without any pre-treatment

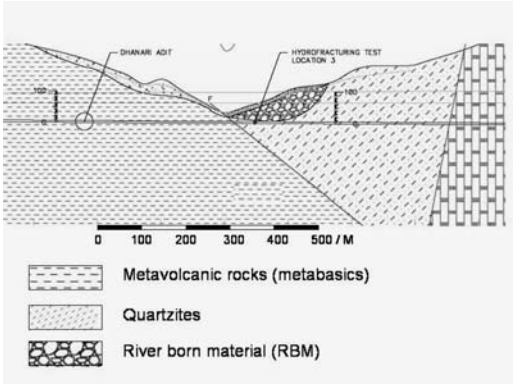


Figure 1. Longitudinal geological section with the tunnel alignment passing under the weak zone. Note that the rock overburden is indicated as uncertain. The vertical lines indicate exploratory holes.

of rock mass. Large water ingress and cave-ins were experienced. A very irregular tunnel contour with less than required excavation diameter was the result. The tunnel was supported with steel sets and bakfill concrete. The tunnel has suffered from major seepages in this section since the excavation in the eighties.

After the work was restarted in 2002, it was decided to reconsider the design of the tunnel lining in this section, with a intent of reducing the lining construction time and friction losses. The first option was to re-excavate this part of tunnel to the fully required cross section. This was not implemented since this would have caused stoppage of all excavation/lining activities further downstream.

Moreover, with the rate of water seepage being observed it was considered uncertain if a structurally sufficient support of the tunnel could be achieved in the already excavated tunnel. For these reasons, it was decided to excavate a by-pass tunnel around the problem area. Pre-treatment ahead of the excavation was decided in order to improve the properties of the ground as well reduce water ingress to a minimum.

The by-pass tunnel was located at approximately 25 meters distance running parallel to old Head Race Tunnel alignment. Limited relief in the form of already happening seepage in the original Head Race Tunnel alignment was anticipated, though it could not be considered adequate to create desirable dry excavation conditions.

When excavating through the zones, the exploratory holes drilled ahead of the tunnel phase always showed a significant amount of water seepage. Hence, a pre-injection scheme was considered necessary, to consolidate the ground and reduce the seepage to a minimum.

2 PRE-INJECTION SCHEME

2.1 *Required results of the pre-injections*

The main goal of the pre-injection works was to achieve penetration of the ground with a grout with a significant mechanical strength. The extent of the penetration had to be sufficient in order to reduce the water seepage to a virtually dry rock mass.

The densely fractured competent quartzitic schist which was the rock mass to be encountered, would require an improvement of the joint characteristics in order to achieve a general improvement of the rock mass. General weathering of the rock mass or voids in the rock were not encountered. Hence, the pre-injection scheme was a pure issue of achieving good penetration into fine joints with fillings of in-situ crushed rock material.

2.2 *Pre-injection strategy*

The first attempts with pre-injections with ordinary Portland cement (OPC) were not convincing. Penetration of the ground was not achieved. In most cases, one only achieved filling of the drill holes with the grout. It was therefore obvious that one had to employ a more sophisticated injection system, including a well laid out method in order to achieve the desired result.
The strategy for the injection works consisted of the following main elements:

a) Injection with pressure up to 60 bars to achieve sufficient penetration
b) Injection rounds up to 15 m ahead of the tunnel face, covering the full tunnel circumference
c) A method for the establishment of drill holes to desired length in the fractured rock
d) Injection materials which would penetrate into the rock mass to the necessary extent to provide the desired improvement result
e) A second stage of injections (if necessary) with low viscous grout
f) A simple method to verify the achieved result of the injections, and hence, decide further advance of the tunnel face

2.3 *Method considerations*

After the initial attempts with injection with OPC as well as microcements, it was obvious that a two-stage injection scheme would be required. Basically this consisted of a first stage injection with microcements with a limit to the injection pressure.

Following the first stage of microcement injections, one drilled a few holes ahead of the tunnel face to verify the achieved water seepage reduction and improved properties of the rock mass (by drillability). In the case the result were unsatisfactory, one would decide the second stage injection.

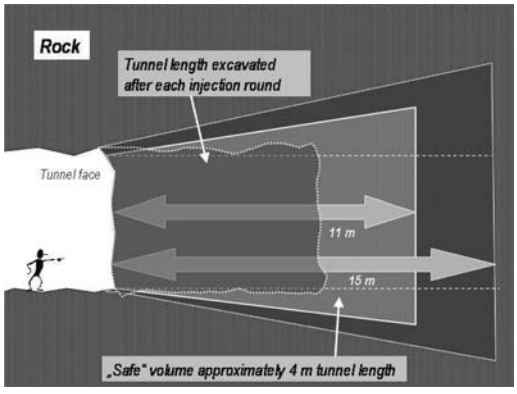


Figure 2. Principal sketch showing coverage of the two injection stages ahead of the tunnel face. The dark area indicates the coverage of the first stage with microcement injections. The lighter area shows the second stage with colloidal silica injections.

The second stage of injections was designed as an inner injection fan which was entirely covered by the rock mass volume treated under the first stage of injections. Figure 2 shows the layout of the two stages of injections.

With this method it was possible to advance the tunnel face approximately 7–8 m before a new injection cycle had to be undertaken. This provided a 'safe' volume of treated ground of minimum 3–4 m ahead of the tunnel face which had been injected during both injection stages.

The jointing of the rock mass imposed a limit to the feasible drilling length with normal percussive drilling. In untreated rock the holes would partially collapse and create difficulties with the retracting of the drilling rods. It was also difficult to achieve good and tight placements of the injection packers in open drill holes under such high extent of jointing and unstable rock.

For this reason it was decided to establish the drillholes through grouted steel pipes. Furthermore, the drilling and injection through the steel pipes was done in advancing steps with lengths of approximately 3 m. Hence, one would re-drill and inject through the same steel pipe several times, advancing longer for each time. In this way one would be re-drilling through a stabilized length and hence, one could drill further into un-treated rock. This method allows making long holes but limiting the drilling length in untreated ground to sections of 2–5 m.

This particular method was applied for injections in adverse ground with rapid hardening microcements during the construction of the Bjoröy subsea road tunnel in Norway in 1994. A controlled improvement of the ground was achieved and safe drill-and-blast excavation through the zone could be realized. (Holter et al. 1995, Holter et al. 1996)

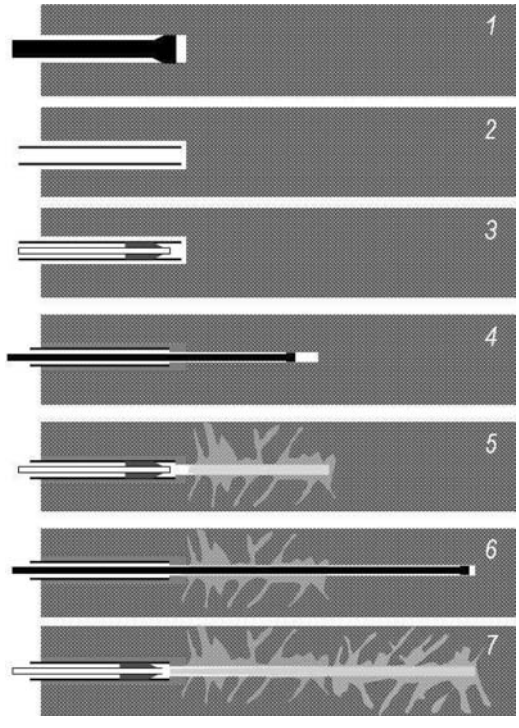


Figure 3. Sketch showing the main steps in the method of establishing drillholes through steel pipes for injection in difficult rock. Repeated drilling and stepwise advance through grouted steel pipes.

The method of stepwise advancing repeated drilling and injection through grouted steel pipes was one of the key issues to achieve any success with pre-injections under these ground conditions. This method is therefore explained in detail below. Figure 3 below illustrates the method graphically.

- *Step 1:* Drilling of 65–70 mm diameter hole to 3 m length
- *Step 2:* Installation of a steel pipe with internal diameter 50 mm (or diameter to fit the expandable packers)
- *Step 3:* Placement of packer (diameter 48 mm) at the very end of the steel pipe and injection of a stiff (very viscous) cement based grout which fills the annular space between the rock and the steel pipe. Hardening for approximately 12 hours
- *Step 4:* When the grout is hardened, drilling through the steel pipe to feasible length (approximately 3 m beyond the steel pipe)
- *Step 5:* Placement of packer and pressure injection with microcement grout for penetration into the rock mass in the drilled length of the hole.

Termination criteria for the injection set to 60 bars injection pressure, or 300 kg injected cement per meter drillhole

- *Step 6:* After hardening of the injected grout, re-drilling through the pipe and injected area to approximately 3 m beyond last drilled length
- *Step 7:* Placement of the packer in the pipe and inject (repetition of step 5)

The length of the drilling steps was adjusted to the encountered rock conditions.

Normally it was possible to advance the drilling to a depth 4–5 m beyond the preceding injection depth. The same method was used when injecting the liquid colloidal silica. However, drilling lengths were normally 5–6 m in untreated rock due to the improvement effect in the rock of the preceding microcement injections.

2.4 *Injection materials*

Bearing in mind the relatively low rock cover and the poor ground, it was necessary to inject with moderate pressures. In order to achieve penetration of the different joint features with moderate injection pressures, one recognized the need for two different grouts. One grout was designed to penetrate into the largest fissures and the other grout type to penetrate into the fine joint features which were partially filled with the in-situ crushed rock material (silt and clay fractions).

2.4.1 *Microcement grout*

In order to achieve the best possible penetration in the first stage of injection, a microcement with particularly good penetrability properties was chosen. Furthermore the chosen microcement had rapid hardening properties. Initial set of the grout mix took place after approximately one hour with water/cement ratio 1:1 at 20°C (typical temperature in the tunnel). The grain size characteristics of the microcement was a d_{95} of 16 μm.

The standard utilized mix design of the microcement grout had a water/cement ratio 1:1 with the dosage of a special dispersing agent. This gave an exceptionally good stability combined with low viscosity of the grout (Marsh cone time 32 sec) which was considered essential for the penetrability properties. The rapid hardening properties of the microcement grout enabled the continuous work without any delay between the different steps in the injection operation. For the microcement a maximum injection pressure of 60 bars was experimentally established, based on when hydrofracturing with a grout would with water/cement ratio 1:1 would occur. Furthermore, at 60 bars injection pressure with this mix a relatively limited grout take was experienced. Hence, a risk of a significant pressure build-up in the ground fed by an injected volume of grout could be neglected.

2.4.2 *Colloidal silica grout*

For the second stage injection an injection gel based on liquid colloid silica was chosen. The reason for this was the penetrability properties that this gel offered. The chosen gel had a viscosity of 5 mPas in liquid state (during injection) and a particle size of 0.016 μm. This allowed for extremely good penetration under difficult ground conditions.

The workability properties of this grout were exceptionally favourable under these conditions. One could easily utilize the same injection equipment for the microcement and the colloidal silica grout, a cement injection plant with a high pressure single component plunger pump.

The open time of the colloidal silica grout could be easily and precisely controlled from approximately 10 minutes up to 2 ½ hours.

Colloidal silica is a pure mineral grout. The gelling process takes place by a physical reaction between particles of silica (SiO_2). The accelerator for this grout is a solution of sodium chloride. Hence, this grout is very user and environmentally friendly, imposing no health risks due to chemical reactivity or toxicity during the injection works.

Furthermore, colloidal silica offers long term chemical stability and durability (resistance to washout or leaching). For this reason colloidal silica was preferred to silicate (waterglass) based gels.

3 ACHIEVED RESULTS

During injection it was necessary to limit the maximum injection pressure to approximately 60 bars. The reasons for this were occurrence of backflow of grout into the tunnel and sliding of the packers in the steel pipes.

The first stage injections with rapid hardening microcement showed a relatively limited grout take of only 100–150 kg per m drillhole when the termination pressure of 60 bars was reached. Bearing in mind the seepage which was encountered in the drillholes one would expect a higher grout take.

The reason for the relatively low grout take was joint fillings which consisted of the silt and clay particles, which in turn limited the penetration of the grout created by filtration.

The first stage injection fan with microcement was always completed in the full circumference of the tunnel before the secondary fan was attempted. The reason for this was that the first stage injection provided penetration of grout into the joints with the largest apertures. Hence, the second injection stage with an extremely low viscous grout could be targeted for the finer joints and the joints which were partially filled with clay and silt.



Figure 4. A typical situation during ongoing injection works. The steel pipes for injection are seen along the perimeter of the tunnel face.



Figure 5. Tunnel under excavation through successfully treated ground in the weakness zone. Litterally dry and stable conditions at the tunnel face, as well as a favorable shape of the tunnel contour have been achieved.

The secondary fan was drilled and injected with liquid colloidal silica with a termination pressure of 25 bars, or approximately 100 kg per m drillhole length.

Injection beyond a pressure of 25 bars usually showed signs of hydrofracturing. The control of the achieved result was done in two ways. Firstly, the water seepage situation after the injection of the two stages was controlled in drillholes. Secondly, the result was observed in the tunnel contour after the excavation of the first round starting from the injection location. In this way the detailed criteria for termination of the injection were fine tuned and continuously adjusted.

The result was a literally dry and stable tunnel contour. No excessive breakouts of rock or cave-ins occurred during excavation through the weakness zone. (Figure 5).

4 CONCLUDING REMARKS

This proactive approach to pre-grouting fault zones ahead of the excavation face resulted in the tunnel being excavated without a single incidence of collapse and with virtually dry conditions. The effects could be directly compared to the poor conditions and heavy water flows observed in the adjacent tunnel where pre-injections were not used. A direct comparison of the effectiveness of microfine cements and colloidal silica gels versus OPC was also clearly evident.

This exercise also showed that a proactive approach to drilling and grouting with a clearly defined method statement and utilizing materials with the proper penetration, viscosity and rapid hardening characteristics can significantly reduce the construction time through such highly faulted and unstable zones (6 months in by-pass tunnel versus 18 months in original tunnel). The low cost of pre-injection in comparison with post-injection techniques can also be clearly seen. The cost for materials on this project came to a material cost of approximately Euro 1,200/m versus a similar condition in another tunnel in India where polyurethane post-injections were utilized at a cost of approximately Euro 12,000/m and currently almost 2 years behind schedule.

The post-injection then cost about 10 times more just in materials. Considering that materials are mostly less than 10% of the total cost, post-injection as a method may easily cost 20 to 30 times more than pre-excavation injection. (Stenstad, 1998)

REFERENCES

Stenstad, O. 1998. Execution of injection works. (in Norwegian), *Proceedings of Post Graduate Training Course sponsored by the Norwegian Chartered Engineer Association and the Norwegian Rock Mechanics Group* 1998. Fagernes. Norway

Holter, K.G., Johansen, E.D. & Hægrenæs, A. 1996. Tunnelling through a Sandzone. Experiences with Ground Improvement from the Bjoröy Subsea. *North American Tunnelling, World Tunnelling Conference, Washington D.C 1996*. Rotterdam. Balkema

Holter, K.G., Aagaard, B. & Johansen, E.D. 1995. Geomechanical Considerations and Methods for Ground Improvement during Tunnelling through a Sandzone. The Bjoröy Subsea Road Tunnel. (in Norwegian) *Norwegian rock Mechanics Conference 1995 (Norwegian)* Oslo. Tapir

This page intentionally left blank

Underground Space – the 4th Dimension of Metropolises – Barták, Hrdina, Romancov & Zlámal (eds)
© 2007 Taylor & Francis Group, London, ISBN 978-0-415-40807-3

Experimental investigation on backfill grouting deformation characteristics of shield tunnel in sand

Yue-wang Han[1], Wei Zhu[1,2], Xiao-chun Zhong[1] & Rui Jia[1]
[1]*Geotechnical Research Institute, Hohai University, Nanjing, China*
[2]*College of Environmental Science and Engineering, Hohai University, Nanjing, China*

ABSTRACT: Backfill grouting is an important technique to decrease stratum deformation in shield tunnel construction. After backfill grouting completed, grout gradually convert from liquid to solid due to the grout draining and consolidating. Grout volume shrinkage has an important influence on stresses and deformation of soil around tunnel. An element model apparatus was used to test grout deformation under various grout pressures and groundwater pressures. In sand soil, grout deformation time is short; high grout pressure can accelerate drainage and consolidation; high groundwater can slower the grout deformation rate, and minimize the final grout deformation.

1 INTRODUCTION

With the fast development of economy in China, there is a huge demand for the development of underground space in large and medium cities (Qian Qihu 1998). Nowadays shield tunneling technology has widely applied to the construction projects of subway and cross-river tunnels, such as Nanjing subway and the South-to-North Water Transfers Middle Route Cross Yellow River Tunnel. The stratum disturbance would be induced more or less in process of shield tunneling, then cause ground settlement. So predicting ground settlement and decrease the settlement caused by tunnel excavation is a major engineering challenge (Qu et al., 1995 & Bernat et al., 1998). The stratum displacement can be mostly induced by two aspects: the supporting pressures in chamber cannot balance the earth pressure and groundwater pressure ahead of working face, and induce the working face instability; the tail void closure and backfill grout shrinkage induce periphery soil deformation. It is shown in Figure 1 that mostly ground settlement occurs in excavation stage and tail void grouting stage (Hwang et al., 1995 & Kuwahara et al., 1997).

Apart from control working face stability strictly during shield tunnel excavation, the tail void backfilled by grout is an active measure to reduce stress release of soil and soil deformation. After backfill grouting completed, grout convert from liquid to solid under grout pressure during the action with soil and liner (Bezuijen et al., 2004, Hashimoto et al., 2004 & Zhou Xiaowen et al., 2001). So the grout mechanical properties and grout volume shrinkage vary with time is relevant to

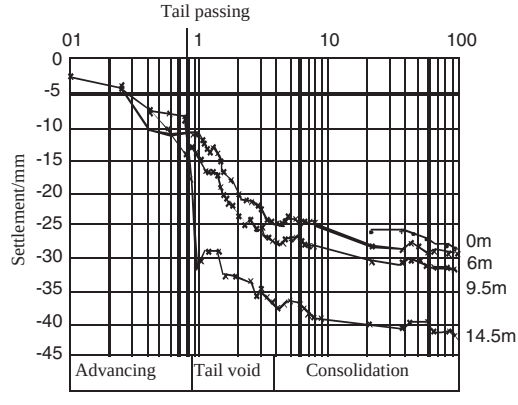


Figure 1. Settlement of shield tunnel construction in Taibei.

grout pressures, surround soil parameters, groundwater level and grout material properties(Snuparek et al., 2000).

With the proceeding of backfill grouting, tail void gradually backfilled, the water content drained slowly from grout to soil under grout pressure. Then grout volume shrunk, grout pressure dissipated, grout become hardened. Many numerical calculation methods have taken into the function of backfill grouting. The hardening of the grout materials with the process of shield excavation were simulated by varying parameters such as the stiffness, the internal friction angle and cohesion at different construction stages (Bernat et al., 1999). But the parameters of grout are defined based on presupposition, especially at the stage of state

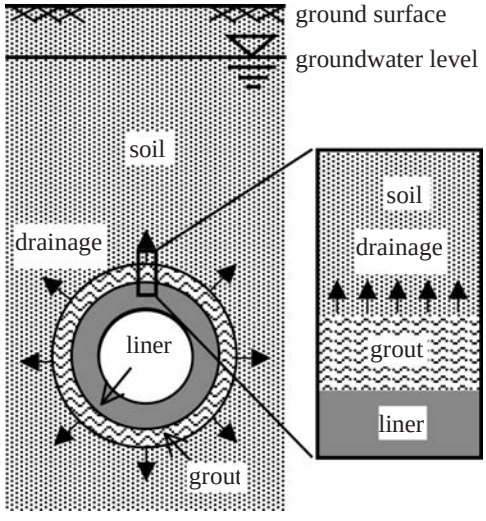


Figure 2. Sketh of consolidating grout around tunnel liner.

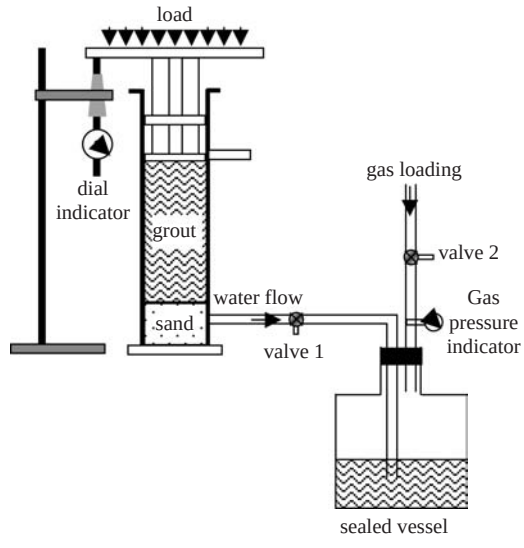


Figure 3. Experimental setup of grout volume shrinkage.

conversion from liquid to solid. So the changes of the grout parameters are very important to predict the ground settlement.

2 TEST SCHEME

2.1 *Test introduction*

After backfill grouting completing, grout formed an annular layer between liner and surrounding soil. The sketch is shown in Figure 2. An element is taken out from tunnel crown. The element model includes soil, grout and liner. Liner is considered impervious. Water content penetrates through soil from grout under grout pressure. Based on the element model, experimental setup was designed, see Figure 3.

Test sample is chosen from the medium and fine sand stratum of South-to-North Water Transfers Cross-Yellow River Tunnel. Sand particle size distribution curve see Figure 4. Sand mechanical parameters see Table 1. Grout is hard grout, and mixture ratios see Table 2.

2.2 *Test procedure*

Sand must be saturated by air extraction before test. Close valve 1, the sealed vessel must be inflated up to preset gas pressure to simulate groundwater pressure, then inject the grout and load weights up to plunger to preset grout pressure. Open the valve 1, the data of dial indicator be recorded simultaneously.

Complete trial scheme adopted, grout pressures are 150 kPa, 200 kPa, 250 kPa, 300 kPa respectively, groundwater pressures are 0 kPa, 50 kPa, 100 kPa respectively.

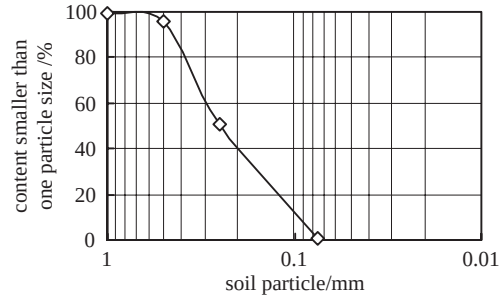


Figure 4. Particle size distribution curve of sand.

Table 1. Mechanical parameters of sand.

	γ/kN/m^3	c/kPa	ϕ/^{o}	E/MPa	ν	K/cm/s
sand	17.21	10	38	34	0.3	1.16E−3

3 TEST RESULTS AND ANALYSES

1. Figure 5 to Figure 7 present comparisons of grout deformation vary with time between different grout pressures (Pg) under same groundwater pressure (Pw). With the increase of grout pressure, the grout volume shrinkage rate is accelerated, the final deformation is large, and the deformation stabilization time is short. It is obvious that high grout pressure accelerates the rate of permeation of grout-water to soil, then promotes the grout harden rate. It is advantageous to tunnel early stage stability.

Table 2. Mixture ratio of backfill grouting material.

material	cement	Flyash	bentonite	sand	water	water reducing agent
percentage ratio	1.0	1.67	0.21	4.10	2.0	0.02
content /kg/m^3	195	325	40	800	390	4.5

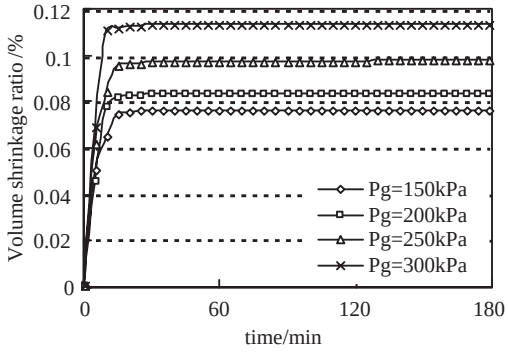


Figure 5. Shrinkage ratio curves versus time under different grout pressure Pg and groundwater pressure Pw = 0 kPa.

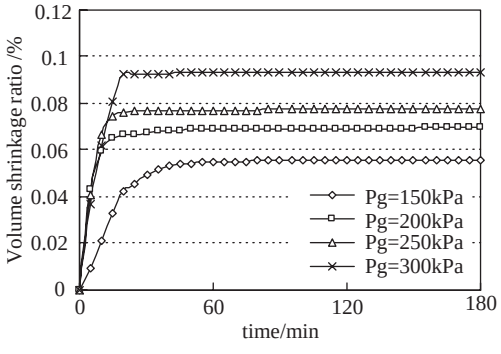


Figure 6. Shrinkage ratio curves versus time under different grout pressure Pg and groundwater pressure Pw = 50 kPa.

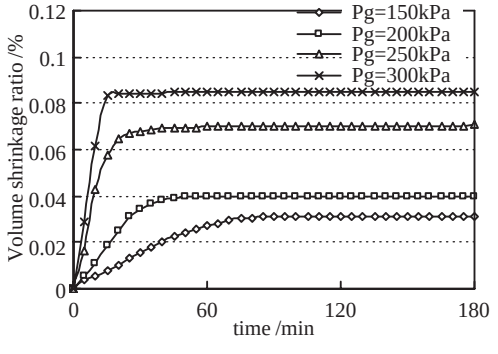


Figure 7. Shrinkage ratio curves versus time under different grout pressure Pg and groundwater pressure Pw = 100 kPa.

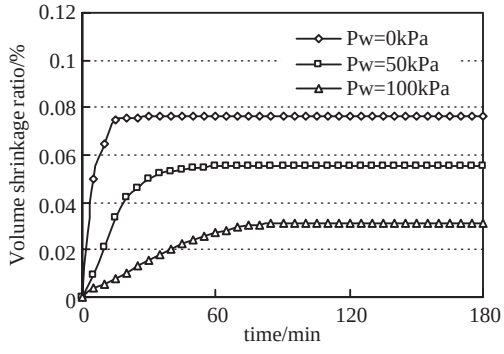


Figure 8. Shrinkage ratio curves versus time under different groundwater pressure Pw and grout pressure Pg = 150 kPa.

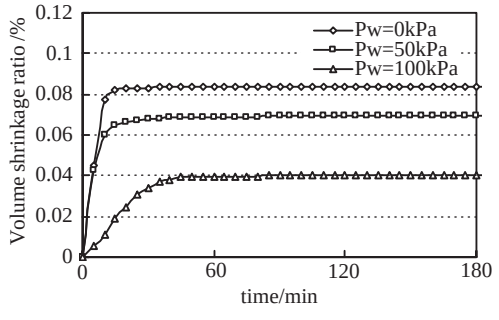


Figure 9. Shrinkage ratio curves versus time under different groundwater pressure Pw and grout pressure Pg = 200 kPa.

2. Figure 8 to Figure 11 present comparisons of grout deformation vary with time between different groundwater pressures (Pw) under same grout pressure (Pg). With the increase of groundwater pressure, the grout volume shrinkage rate is slower, the final deformation is small, and grout deformation stabilization time is longer. It is obvious that the main function of groundwater is to slow down the rate of permeation of grout-water, then influence on the grout harden rate.
3. Figure 5 to Figure 11 show the major change of deformation complete within about 1 hour, and the final deformation is not exceed 12%. The grout pressure compare with groundwater pressure is higher, the curves of deformation is more steeply. The groundwater pressure has big effect on grout

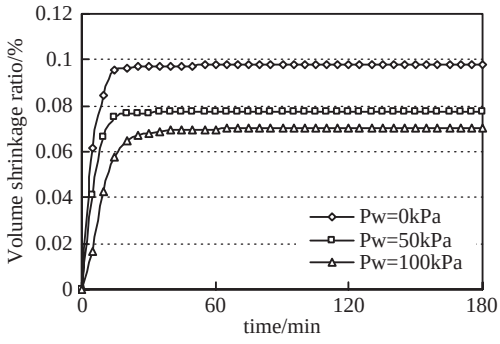


Figure 10. Shrinkage ratio curves versus time under different groundwater pressure Pw and grout pressure Pg = 250 kPa.

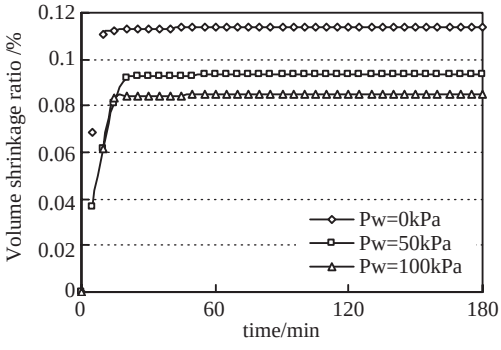


Figure 11. Shrinkage ratio curves versus time under different groundwater pressure Pw and grout pressure Pg = 300kPa.

deformation rate under relatively minor grout pressure. Grout volume shrinkage occurs during the stage of grout drainage and consolidation due to the big permeability of sand.

4 CONCLUSIONS

The grout is injected in a fluid state with a high value for the water content. As the tunnel is located under the water table, the grout mechanical properties variation is a very complicated process. The grout deformation characteristic has studied by element model apparatus. The following conclusions can be drawn:

1. High grout pressure is advantageous to accelerate the permeation of grout-water, then short the time of grout deformation time.
2. The main function of groundwater pressure is slow down the rate of grout-water drainage, and reduces the final grout deformation.
3. Due to the high permeation rate of sand, grout consolidated drained time is short, grout deformation rate is fast.

REFERENCES

Qian Qihu. 1998. Welcome the high tide of development of underground space in china. Chinese Journal of Geotechnical Engineering 20(1): 112–113.

Ou, C.Y. & Cherng, J.C. 1995. Effect of tail void closure on ground movement during shield tunneling in sandy soil. Geotechnical Engineering 26(1)17–32.

Bernat, S. & Cambou, B. 1998. Soil-structure interaction in shield tunneling in soft soil. Computers and Geotechnics 22(3): 221–242.

Hwang, R.N. & Fan, C.B. 1995. Consolidation settlements due to tunneling. Proceedings of South East Asian Symposium on Tunnelling and Underground Space Development, Bangkok. 76–86.

Kuwahara, H. & Yamazaki, T. 1997. Ground deformation mechanism of shield tunneling due to tail void formation in soft clay. Proc., 14th Int. Conf. on Soil Mech. and Found. Engrg. The Netherlands 2: 1457–1460.

Bezuijen, A. & Talmon, A.M. 2004. Grout pressures around a tunnel lining, influence of grout consolidation and loading on lining. Proceeding of the 30th ITA-AITES World Tunnel Congress, Singapore. F01: 1–8.

Hashimoto, T. & Brinkman, J. 2004. Simultaneous backfill grouting, pressure Development in Construction Phase and in the Long-Term. the 30th ITA-AITES World Tunnel Congress, Singapore. F04: 1–8.

Zhou Xiaowen & Pu Jiaju, 2001. Effect of shield tail void closure on lining earth pressure. Proceedings of 15th Int. Cont. on Soil Mech. and Geotech. Engrg. San Francisco: 1441–1444.

Snuparek, R. & Soucek, K. 2000. Laboratory testing of chemical grouts. Tunneling and Underground Space Technology 15(2): 175–185.

Bernat, S. & Cambou, B. 1999. Assessing a soft soil tunneling numerical model using field data. Geotechnique 49(4): 427–452.

Underground Space – the 4th Dimension of Metropolises – Barták, Hrdina, Romancov & Zlámal (eds)
© 2007 Taylor & Francis Group, London, ISBN 978-0-415-40807-3

Advances in synthetic injection technology, do they improve tunnel construction productivity?

Willie Kay
Managing Director – WAK Consultants Pte Ltd/WAK Trading Pte Ltd/MC Bauchemie Muller GmbH & Co

Thomas Yang
General Manager – Hydroseal Enterprise Co Ltd

ABSTRACT: As tunnelling in urban areas continues to expand problems of sink holes and traffic disruption become less acceptable. Delays in the construction process become costly and can lead to subsequent claims from follow on contracts such as track laying, lighting and others. Build Own Operate companies want the tunnel in use on the time and with minimum maintenance. Chemical injection resins have been available in crude forms for many years. The available materials in the 1970 to 1985 were often highly toxic and carcinogenic and could injure the operatives as well as pollute the ground. Polyurethane technology was normally single component water reactive often with brittle open cell foams. Problems of running sands, silts and high water pressure need a variety of solutions. Material set times and pot life has to adjust from seconds to minutes and often need some structural strength. Modified and new equipment coupled with advance chemical resins have provided solutions to solve some of these problems. Case histories will outline how contractors were able to speed up tunnel excavation and solve unstable soil conditions. The new generation resins have their long properties listed opening up new possibilities for solving problems. Costs are examined showing often the overall saving in the contract by spending relatively small amounts of money in critical areas.

1 INTRODUCTION

Injection techniques using cements, modified cements and resins as means of solving problems in the tunnelling industry have been available for many years. Materials technology has advanced rapidly over the last two decades and due to this some manufacturers no longer use the historic generic names as they are no longer specific enough to describe their actual use and application. As more and more structures move underground and often nearer to other underground structures new methods of injection have been developed. Today methodology is the key word, that is not just material but also equipment, trained experienced applicators and technique.

1.1 *Materials*

The early injection resins consisted of cements, later these were modified with supplementary materials such as bentonite, fly ash and other pozzolans. Often there was a need for acceleration of the set time and this was achieved by the use of silicate and similar materials. These materials are still in use today and are cost effective and a practical solution to many ground and water ingress problems.

Marotta & Peach. 2006. High Pressure …
Bossard & Mattar.2005. How the Zimmerbert…

In the early seventies water based chemical grouts appeared in the market. Compared to epoxy and polyurethane resins in 1970–1975 they had much lower viscosity were flexible and apparently easier to use. However many of them were carcogenic and not environmentally acceptable. However the ability to adjust set times from seconds to minutes plus ultra low viscosity opened up new methods of sealing structures against water ingress.

Developments in epoxy and polyurethane resins continued and by the late 80s and into 1990 had became less viscous and capable of exhibiting properties from flexible to rigid depending on the formulation. Micro cement technology was improving allowing penetrations into soils and other substrates that was previously impossible.

The twenty-first century has seen even more accelerated progress and Tables I. Highlight some areas of application needed in injection materials. Table II. Look at specific injection properties.

1.2 *Equipment*

With the constant advancement of materials in both viscosity and gel time change in the pump and packer technology was inevitable.

To use injection resins with set times from 10 seconds to 3 minutes require the use of twin line pumps where the resin is mixed at the point of application in a specially designed mix head. Twin line pump technology is not new and in epoxy injection was used in the mid 1970 for epoxy crack injection. What has changed is the understanding of the methods of mixing resins in the mix head.

Early mix heads had brushes or inserts of a fixed length so no change in mixing shear could be introduced. This could lead to resins of different viscosity or chemistry not being mixed properly and thus not developing full performance. We have developed mix head technology that varies the shear energy in the mix head thus ensuring all mechanical properties of the resin we achieved.

Other developments in equipment include very high volume pumps up to 60 litres per minute. Diagram A illustrates a modern twin line pump and correct mix head technology.

To place injection resins in the right place requires a packer. Standard packer is available from many sources but in out experience custom designed packers are often needed. Diagram B illustrates a specific packer developed for a tunnel injection.

Diagram A

	2 component High Pressure Piston Pump		
MC I 200	Mixing Ratio		1 : 1
	Max Pressure		200 bar
	Max Volume		8.5 lit/min
MC 2 Comp Mix Head Static Mixer	For a homogeneous mixing of the injection resins in the mix head	Standard 2 grid mixer	Resin A
		4 additional grid mixers (6 in total)	Resin B
		12 additional grid mixers (18 in total)	Resin C







Diagram A

Table I. MC Injection rigid/flex types – filing materials/ areas of application.

			Water bearing	
Situation	Dry	Damp	No pressure	No pressure
Product	EP C PUR	(EP) C PUR AY	 C PUR AY	 (C) PUR AY

1.3 *Case histories – Singapore MRT circle line*

A suburban MRT Station was being built underground where the ground conditions were variable. The construction method was to build a secant pile diaphragm wall and then excavate and strut. As in most situations some leakage at the pile joints is inevitable. In good clay or rock this is never an issue but in sandy soils it can have disastrous consequences.

In this particular project and advance plan was made to counteract this situation should it arise. The first line of defence was sandbags on the site near the area of excavation. The second line of defence was to keep on site specialised twin line pumps and quantities of hydro-structure resin. This meant in emergency mobilisation would be fast and effective.

Table II. Injection resin properties.

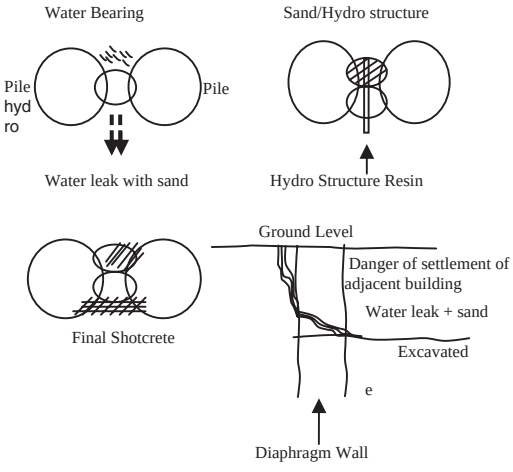
	Viscosity CPS	Set time	Strength N/mm^2	Resistant to water pressure wash out	Relative cost index
Epoxy (EP)	250	10–60 min	40–90	Limited	3–5
Mineral suspension/ Micro cement (C)	25–100	60–180 mins	10–35	Limited	1–2.5
Polyurethane (PUR)	95–250	5–200 secs	1–90	Good/Excellent	1.5–3.0
Acrylic Gel (AY)	10–40	5–300 secs	1–5 (in sand)	Good	1.5–4.0

Table III.

	Cement Grout	Hydro Structure Resin
Placed cost	60 m^3 @400 = 24,000	½ m^3 = 20,000
Time to mobilise	2–3 days	Max 6 hours
Cost of site downtime S$	15,000/day	15,000/day
Time to grout	1–3 days	1–4 hours

The hydro-structure resin has ultra low viscosity and an ability to vary the gel time between 8 seconds to three minutes. The twin line pump has a mix head near the point of injection and built in water flush.

This technique of injection was used on a number of occasions and proved totally successful. The sketches below show the sequence of work.



1.3.1 *Cost benefit*

Cost savings are difficult to quantify due to a large number of variables however Table III shows a cost estimate. The cement grout is disrupted by the water flow and this is why the grouting time is longer.

The water pressure and flow are not having the same effect on the resin injections as compared to cement grout. If the volume flow is too high then the cement grout will always be washed out and will not be able to seal the leaks. The skill and experience of the specialist applicator is critical in ensuring the resin injection is cost effective.

1.4 *SMART tunnel Malaysia*

One of the largest tunnels in Asia is being constructed using slurry shield Tunnel Boring Machines. When cutter heads need to be replaced or other essential maintenance is required it is critical to be able to stabilise the air pressure.

Table IV. Case benefits – KMRT C01 LUO04 shield machine arrival.

Item	Injection water Glass-cement grout	Injection MC-Injekt GL 93/95 Acrylic Gel
Volume	26 m^3 × NT$25,000/$m^3$ = NT $650,000	105,690 kg × NT$280/kg = NT $2,959,320
Length Progress	2.4 (Not finished)	7.2 (Arrival End)
Time	60 days	7 days
Time Cost	Shield Machine Operations Cost 60 days × NT $100,000 = NT $6,000,000	Shield Machine Operations Cost 7 days × NT $100,000 = NT $700,000
Time Delay	55 days	Normal
Problem	Not solvent	Solvent
Payment cost	NT $6,650,000	NT $3,659,320

Hydro structure resins have been adopted as a means of ensuring this pressure can be maintained.

This is not a new technique – it was used in Singapore on Contract T05 for the Deep Tunnel Sewage System and in Holland on the Westerschladen Tunnel.

We have however due to experience and better resin technology been able to substantially reduce costs. Hydro structure resins can be both retarded and accelerated to ensure the optimum reaction time.

This means that we can pump less resin as the setting time to some degree dictates the flow pattern. Packer spacing can then be optimised which again saves time and costs. Typically at the SMART project we are using some 60%–70% less material than on other projects with a downtime of hours rather than days.

1.5 *Taiwan MRT*

The breakthrough of a TBM into the station box can be difficult or easy depending on ground conditions. Where a high water table sandy soils and moving water is expected hydro structure resins can be an economic solutions.

The choice of using Portland cement injections or resin injection is often made on the basis of comparative cost of a litre of material. However in areas of high water flow it is often impossible to prevent cement grout wash out.

The accelerators used in cement grouts are often stiffness or gelling agent not true set admixtures and depending on flow/pressure of the water they do not have the physical properties to stop the water.

In Table IV we summarise the actual costs involved in a tunnel break through with a high water table and sandy substrate.

2 CONCLUSION

In every part of our lives technology changes are forever increasing. In construction this is also true and it is difficult to keep up with all these changes. We are not suggesting that all traditional materials be abandoned but rather that there is an awareness of the new technologies. To be able to create resins with strengths greater than 60 N/mm^2 in 12 seconds creates problem solving system which previously were non existent. New applications are being discovered and the technology changes continue. Cost comparisons are important and if traditional materials are the correct technical answer then it would be foolish to use alternatives. However it is important that a total evaluation including down time, project delay costs and other parameters are included.

REFERENCES

A DA Via/Marotta & G Peach. 2006. High Pressure Jet Grouting for a Collapsed Tunnel , International Conference and Exhibition on Tunnelling and Trenchless Technology 7–9 March 2006.

M Bossard & J Mattar. 2005. How the Zimmerberg Base Tunnel is being built in the city of Zurich, Tunnels & Underground Structures, Singapore November 2006.

Underground Space – the 4th Dimension of Metropolises – Barták, Hrdina, Romancov & Zlámal (eds)
© 2007 Taylor & Francis Group, London, ISBN 978-0-415-40807-3

Injection techniques used at the old workings and karst voids abandonment under the built-up residential areas in the Urals

A.B. Kondratov
State Specialized Research & Production Operations "Geoinjection", Perm State Technical University, Russia

ABSTRACT: Results of a special injection technique development and application for the old underground workings and karst voids abandonment under the built-up residential areas are examined. Field and analytical studies data and specific examples of the technique practical application to provide for surface structures and facilities safety are presented.

1 INTRODUCTION

Many cities, medium-size and small towns in the Urals (Perm, N. Taghyl, Kungur, etc.) are located in karst terrain as well as in the areas undermined in the 17–18th centuries. To date no surveying records are retained. These underground openings of hundreds to thousands cubic meters volume are located at a depth of a few tens of meters from the surface presenting a real hazard to the surface structures, facilities and services.

Ensured protection of the municipal structures in the areas specified is provided for by the injection techniques developed in the Specialized Research & Production Operations "Geoinjection". These techniques are based on:

- geophysical methods of voids detection (seismic survey, electrical prospecting, ultrasonic location, teleinspection, etc.) with further verification through core drilling and core recovery;
- geomechanical analysis of surface movement through parameters before and after abandonment works;
- design of injection technique parameters and procedures in terms of the preliminary studies and geomechanical analysis;
- monitoring of rock mass injection treatment quality by means of submersible TV and ultrasonic equipment;
- geodetic monitoring of protected surface structures carried out by conventional means as well as GPS satellite geodetic control.

2 FIELD SURVEYING OF STRUCTURES

One of the typical structures located in the area of karsting is a brick 87 apartment house in Kungur, a small town in Perm Province. The building was constructed over pile foundation of 9 m depth. Geologic section of the foundation is presented by filled soil (0–3 m), loam with peat partings (3–6 m), loamy sand (6–10 m), loam (10–17.5 m), gravel and sand (17.5–22 m), limestone debris (22–28.5 m). It is underlain by thick hypsoanhydrite formation.

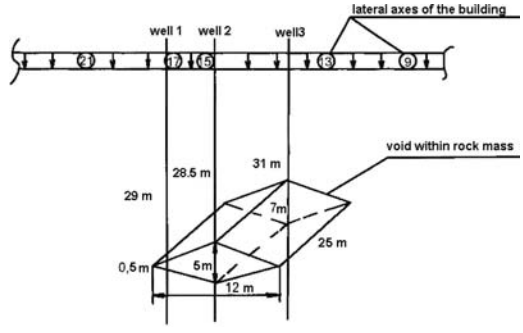


Figure 1. Configuration of the karst void in the formation under the building.

Deformations of the building have occurred right away on construction completion. In order to find the cause of this phenomenon the earth foundation study has been carried out by means of low-depth seismic survey of high resolution, core drilling and core recovery, ultrasonic echo-location and bore teleinspection. The building settling geodetic monitoring station has been deployed.

Studies enabled to establish that an extensive channel like solution cavity of volume about 900 m^3 is located under central part of the building at a depth of 28.5 m–33.5 m, 31 m and 38 m in the formation of hypsoanhydrite. The cavity is oriented perpendicular to longitudinal axis of the building. Configuration of the cavity of interest is illustrated in Figure 1.

Table 1. Filling material size distribution.

Sieve diameter, mm								
>10	10–5	5–2	2–1	1–0.5	0.5–0.25	0.25–0.10	<0.10	Total, %
Percentage								
25.01	22.89	14.60	9.55	8.96	11.47	5.87	1.65	100

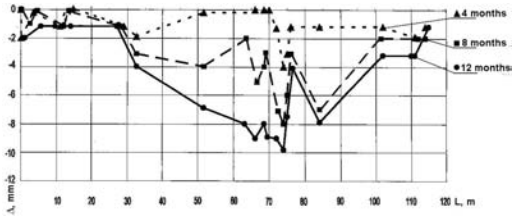


Figure 2. The building annual settling dynamics.

Underground void is filled with water and aggregate composed of chippings, gravel and sand. Aggregate grain size distribution is presented in Table 1.

Dynamics of the building annual settling is illustrated in Figure 2.

Comparing Figures 1 & 2 we may see that maximal settling of the building is observed directly over the solution cavity. In order to choose the measures preventing the building from further settling respective geomechanical analysis has been made.

3 GEOMECHANICAL ANALYSIS

A concept of safe mining depth can be found in various regulations on buildings and facilities protection against underground workings adverse effect on them. According to [1] safe mining depth may be calculated from the formulae:

$$H_s = \sqrt{Rk \cdot m} \quad \text{or} \quad H_s = 25K_l\sqrt{\frac{D \cdot m}{\varepsilon}} \tag{1}$$

where
R – the minimum allowable design radius of curvature, km;
k – proportionality factor;
m – height of a mine goaf;
K_l – a factor related to an angle of a seam dip;
D – the minimum size of a goaf, m;
ε – the maximum allowable relative lateral strain, mm/m.

The formula enabling to calculate the minimum depth of mining that manifests itself in surface

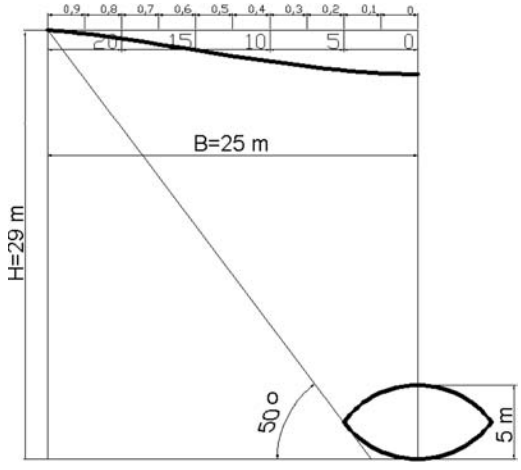


Figure 3. Counting circuit to estimate the surface subsidences and strains.

subsidence is given in the document [2]:

$$H_s = \frac{D}{0.15} \tag{2}$$

where

$$D = \sqrt{L_1 \cdot L_2}$$

L_1 and L_2 – dimensions of a goaf in two normal directions.

Taking the values of K, ε, k, k_α as it is recommended in the document [3], we have found the values of H_s from the formulae presented above. Respective values are 121 m, 220 m and 67 m, i.e. these three values exceed the goaf location depth therefore rock movement process will manifest itself in surface subsidence.

Proceeding from stated above we made analysis to find expected and design values of surface subsidences and strains for service life of the structure located in Commune Str., 45 with the goaf features being accounted for. Structural model is given in Figure 3.

The following assumptions have been made: $H = 29$ m, $B = 25$ m, $L_1 = 10$ m, $L_2 = 10$ m, $m = 5$ m.

Maximum expected subsidences as of the end of ground movement process are estimated by the formula:

$$\eta_0 = 0.9 \cdot f_0 \cdot m \cdot \omega \tag{3}$$

where:
f_0 – a factor accounting for effect of goaf and mining depth on maximum subsidence value is a function of

$$\chi = \frac{D}{H} = \frac{\sqrt{L_1} \cdot L_2}{H}, \tag{4}$$

$$\chi = \frac{\sqrt{10 \cdot 10}}{29} = 0.345 < 1.4 \qquad \text{therefore}$$

Table 2. Expected surface subsidences and strains per life of a building located over packed goaf.

Points of trough principal sections	Expected surface subsidences and strains per life of a building located over a packed goaf				
	Subsidences, m	Inclination, $i_0 \times 10^{-3}$	Curvature, $k_0 \times 10^{-4}$, l/m	Lateral strains, $\alpha_0 \times 10^{-3}$	Radius of curvature, R_0, km
0	0.130	0	0	0	∞
0.1	0.122	2.60	−6.35	−1.52	−1.575
0.2	0.108	4.88	−5.67	−1.36	−1.763
0.3	0.085	6.50	0	0	∞
0.4	0.059	5.69	3.81	0.91	2.626
0.5	0.039	4.06	4.65	1.12	2.148
0.6	0.026	2.76	2.37	0.57	4.220
0.7	0.016	1.95	1.69	0.41	5.908
0.8	0.009	1.46	1.27	0.31	7.877
0.9	0.004	0.98	0.85	0.20	11.815
1.0	0	0	0	0	∞

$f_0 = \beta\left[\beta_1\left(\beta_0\chi^{\alpha_0} - 1\right) - \chi\right]$ where β, β_1 β_0 and α_0 – variables of approximation, $\beta = 0.5953$ $\beta_1 = 3.7678$ $\beta_0 = 1.6708$, $\alpha_0 = 0.25$;

$f_0 = 0.5953[3.7678 \cdot (1.6708 \cdot 0.345^{0.25} - 1) - 0.345] = 0.422$

$\eta_0 = 0.9 \cdot 0.422 \cdot 5 \cdot 1 = 1.9$ m.

Predicted maximum subsidence value for residual service life of the structure (50 years) is calculated by the formula:

$$\eta_m = k_t \cdot \eta_0 \tag{5}$$

where η_m – time factor specifying $\frac{\eta_m}{\eta_0}$ ratio variation with time:

$$k_t = \beta_z \cdot \eta_t^{\alpha_z},\ \eta_t = \frac{t}{100} = \frac{50}{100} = 0.5,\ \beta_z = 0.385,$$

$$\alpha_z = 0.807, \eta_m = k_t \cdot \eta_0 = 0.385 \cdot 0.5^{0.807} \cdot 1.9 = 0.418\,m$$

Length of the ground movement trough margin in view of small size of the goaf is calculated by the formula:

$$L = H \cdot ctg\delta_0 = 29ctg50 = 24.33 \tag{6}$$

Expected values of surface subsidences and strains in the points of the trough principal sections within time in question are calculated by the formulae:

Subsidence $$\eta(z_i)_t = \eta_m S(z)_i \tag{7}$$

Inclination $$i(z_i)_t = \frac{\eta_m S'(z)_i \cdot q_i}{L} \tag{8}$$

Curvature $$K(z_i)_t = \frac{\eta_m S''(z)_i \cdot q_k}{L^2} \tag{9}$$

Curvature radius $$R(z_i)_t = \frac{1}{K(z_i)} \tag{10}$$

Rock strains $$\varepsilon(z_i)_t = m_e \cdot K(z_i)_t \cdot L,\ mm/m \tag{11}$$

where z_i – dimensionless coordinate of a point in the ground movement trough margin;

$S(z_i)$, $S'(z_i)$, $S''(z_i)$ – dimensionless functions of distribution in subsidence, inclination and curvature.

In view of the subsidence trough margin low length the following values have been adopted: $q_i = 0.5$, $q_k = 0.7$;

m_e – curvature – lateral strains transfer factor;

$$m_e = \beta_e \times \beta_k \tag{12}$$

where $\beta_e = 0.05, \beta_k = 1.0$ at $\lambda_{ok} = \frac{\eta_m \cdot S''(z_i)}{1 \cdot 10^{-4} \cdot L^2} < 1$

Let's make similar analysis for a case of a packed goaf with the filling factor making A = 0.8. Maximum subsidence as of the end of ground movement process can be found by the formula:

$$\eta_0 = 0.9 \cdot f_0 \cdot m \cdot \omega \cdot (1 - A(1 - B)) \tag{13}$$

$B = 0.18;\ \eta_0 = 0.9 \cdot 0.422 \cdot 5 \cdot 1 \cdot 0.34 = 0.646m$

At a filling factor A = 0.9 maximum subsidence as of the end of ground movement process will make

$\eta_0 = 0.9 \cdot 0.422 \cdot 5 \cdot 1 \cdot 0.242 = 0.130$

To estimate the undermining-induced loads at designing of a structure to be located on the undermined area design strains have to be calculated through multiplication of expected strain values by respective overload factors, o [4]: $o_l = 1.1$; $o = 1.2$; $o_k = 1.4$; $o_e = 1.2$.

The estimates are presented in Tables 2 & 3.

Table 3. Design surface subsidences and strains per life of a building located over packed goaf.

Points of trough principal sections	Design surface subsidences and strains per life of a building located over a packed goaf				
	Subsidences, m	Inclination, $i_0 \times 10^{-3}$	Curvature, $k_0 \times 10^{-4}$, l/m	Lateral strains, $\alpha_0 \times 10^{-3}$	Radius of curvature, R_0, km
0	0.143	0	0	0	∞
0.1	0.134	3.12	−8.89	−1.83	−1.125
0.2	0.119	5.85	−7.94	−1.63	−1.260
0.3	0.093	7.80	0	0	∞
0.4	0.064	6.83	5.33	1.10	1.875
0.5	0.043	4.88	6.52	1.34	1.534
0.6	0.029	3.32	3.32	0.68	3.014
0.7	0.017	2.34	2.37	0.49	4.220
0.8	0.010	1.76	1.78	0.37	5.626
0.9	0.004	1.17	1.18	0.24	8.440
1.0	0	0	0	0	∞

The estimates enabled to come to the following conclusions and make the following recommendations:

- solution cavities are located at a depth that is less than its safe value, therefore in case of their caving the process of ground movement will actively manifest itself in surface subsidence and strains with the latter many times exceeding allowable values ($i_g \leq 3.0 \times 10^{-3}$; $R_g \geq 20$ km; $\varepsilon_g < 1.0 \times 10^{-3}$); in particular, maximal surface subsidence will make 1.9 m and failure of the building will be catastrophic;
- in case of a cavity being filled with sand grout 90% full strain values in some points of the ground movement trough principal sections will also exceed allowable values, therefore the solution cavities have to be filled 100% full with further pressure testing to be carried out by polymer mortar injection.

4 PRACTICAL DESIGN IMPLEMENTATION

In terms of studies and analysis made the building foundation soil stabilizing has been carried out by injection technique. The activities included cementation and resin injection stabilizing of weak loose ground underlying the pile foundation base as well as abandonment of the solution cavity located in rock mass under the building. For this purpose cement-water slurries, urea resins and sand grouts have been used. Sulfate-resisting Portland cement amount made up 320 t, KF-MT urea resin amount made up 68 t. At present works on the solution cavity abandonment are still in progress.

The situation now is under control. The taken measures resulted in stabilization of the building settlement and deformation. All works have been carried out without evacuation of the tenants.

The next objective is to furnish the "problem" building and similar structures (only in Kungur their number exceeds 40) with a GPS satellite geodetic control station equipped with "Trimble" complex. Our experience of work in cooperation with the Institute of Mining of the Ural Branch of the Russian Academy of Science, Ekaterinburg, has shown that proposed technique provides for sufficient accuracy of measurements (1–2 mm), their continuity and gives an opportunity of simultaneous data transmission to personal computers of various services to rectify a situation in due time.

REFERENCES

1 Petukhov, I.A. 1968. On safe mining depth estimation. In the book "Rock pressure, rock movement and VNIMI mine survey transactions".

2 Directions for mine flood and surface structures protection from underground goafs adverse effect under conditions of the Upper Kama Basin potash deposit. 2004. St.-Petersburg.

3 Regulations on the procedure of the mineral deposit area construction authorization. 1999. Approved by the State Mines Inspectorate of Russia. # 64, Mining Code 07-309-99.

4 Territorial Building Code 22-301-98 of Perm region. Buildings in the undermined areas of the Upper Kama Basin potash deposit. Specification of the building protection measures.1998. Perm.

Underground Space – the 4th Dimension of Metropolises – Barták, Hrdina, Romancov & Zlámal (eds)
© 2007 Taylor & Francis Group, London, ISBN 978-0-415-40807-3

Instabilities at the Messochora tunnel, Greece: ground improvement and safety evaluation based on observational data

V. Kontogianni
Geodesy Lab., Dept of Civil Engineering, Patras University, Greece

Y. Thanopoulos
Public Power Corporation, Messochora Hydroelectric project, Messochora, Greece

ABSTRACT: The Messochora road tunnel, central Greece, 1100 m long and 10 m diameter, aims to serve transportation after flooding of the nearby Messochora reservoir. The tunnel opened through medium to poor flysch was excavated at the heading level with no significant deformations but during the bench excavation, high distortion of the steel sets and fractures along the shotcrete shell were observed at a 36 m long 'failure zone'. To stabilize strains and avoid a generalized failure, the bench was re-filled and additional support was installed at the affected zone. During these works systematic monitoring, based on geodetic techniques and rock extensometers was performed to confirm effectiveness of ground improvement and evaluate tunnel safety. Detailed analysis of recorded deformation revealed strains at the '*failure zone*' and other nearby stable locations immediately after the failure, generated from stresses re-distribution within the rock. Furthermore, careful analysis of the monitoring data indicated that post-failure strains correspond to a clearly time-dependent effect, with strains in the '*failure zone*' and adjacent sections accumulating for several days, until reinforcement works were fully completed. Strains stabilization permitted the bench re-excavation a few months later; minor displacements recorded during this last stage of construction suggest that the restoration works carried out indeed improved the rock mass and reinstated stability of the tunnel.

1 INTRODUCTION

Seventy years ago, Karl Terzaghi first methodized continuous recording of ground surface and tunnel walls displacements to evaluate the Chicago Subway excavation procedure and maintain safety and stability during construction (Terzaghi 1942). This innovative technique, i.e. to judge about the effectiveness of the excavation technique and support measures and need for construction modifications in tunnelling based on the detailed recording of ground-support interaction, revolutionized a new methodological approach for underground excavation, later named the '*observational method*' (Peck 1969). The '*observational method*', widely spread to all kind of underground projects, remains till today the most essential tool for construction of safe and low-cost underground structures.

In the last years, though, the evolution of electronics made possible to obtain, store and process great amounts of observational data even in real time and opened up new possibilities to tunnelling works optimization by providing early detection of potential failures in unstable ground conditions, a study particularly important for project economy and critical for overall safety of construction. In modern tunnels both geodetic techniques and geotechnical instrumentation are utilized: (i) to record the ground response to excavation-induced stresses, by extensometers, load cells etc. and (ii) to describe the subsequent reduction of the excavated opening, by surveying the support shell distortion (Kontogianni & Stiros 2003; Kavvadas 2005). These records, planned to control tunnel behaviour at various ground conditions, are particularly valuable in failure cases, where special supporting and modifications in construction are crucial for future stability.

In this study, the planning of restoration of the Messochora tunnel, immediately after instabilities affected a 36 m long part of the tunnel in Aug. 2005, based on geodetic techniques and extensometers data, are presented. Aim of the study is to describe the post-failure kinematics of the ground-support system based on the collected measurements at the 'failure zone' and at its neighboring locations during and after the ground improvement works.

2 THE MESSOCHORA PROJECT

Messochora hydroelectric project, a part of the Acheloos River diversion project owned by the Public Power Corporation of Greece, is planned to provide hydroelectric power to the national grid, with a 2×80 MW installed capacity (Fig. 1). The formation of an artificial lake upstream of Messochora Dam for water storage will cause inundation of the existing road network. A new road, aiming to serve local traffic across the lake is currently under construction, as part of the Trikala – Arta main road, including the 1099 m long Messochora tunnel.

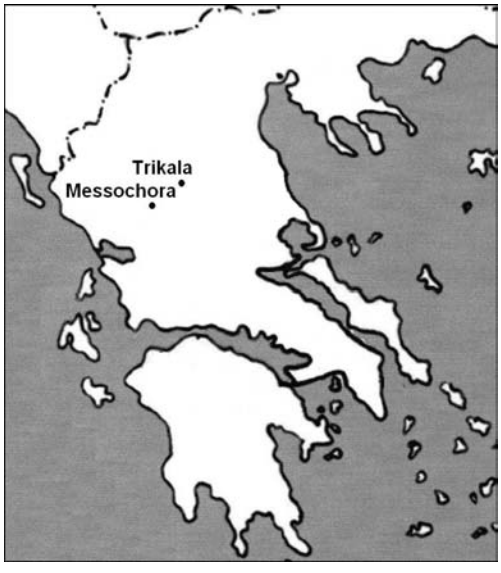


Figure 1. Location map.

3 THE MESSOCHORA ROAD TUNNEL

The Messochora tunnel, 10 m in diameter, is excavated through a flysch complex, widespread in the Pindos Mt. range, at a maximum overburden height of ~150 m. The tunnel cuts through ~500 m of cretaceous limestone before entering a claystone formation, of medium to poor quality, representing a 'transitional zone' to the neighboring flysch formation. This zone is composed of limestone mixed with claystone and clay materials at increasing ratio near the surface. At the NE portal, shear zones, substantially deteriorate geotechnical conditions of the ground. A geological section of the tunnel with 'transitional zone' divided in two different zones representing material with different mechanical characteristics is shown in Figure 2.

The tunnel was constructed at the framework of two different contracts. The first, 1997–1998, involved the excavation of 48 m at the NE portal of the tunnel, which proved extremely difficult due to low strength rock masses met and high risk of triggering a landslide. The second, 2004–2006, involves the excavation of the rest 1051 m, at the limestone and the transitional zones, with severe damages and high convergence along a 36 m zone of the tunnel, and restoration and safe completion of the tunnel.

3.1 *Tunnel excavation and failure*

3.1.1 *Excavation from the NE tunnel portal – ch.1 + 495 m to ch.1 + 447 m*

Excavation of the N-E portal of the tunnel from 1997 to 1998 at highly weathered rock proceeded in full

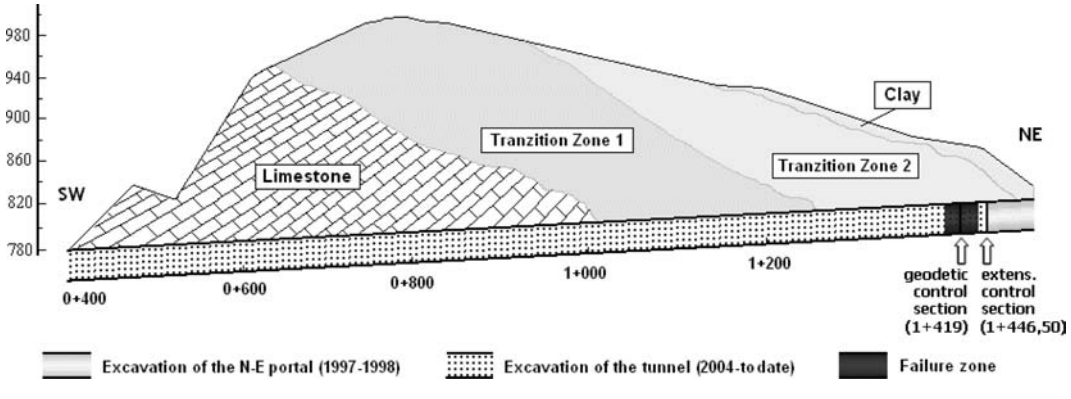


Figure 2. Geologic cross section of the Messochora tunnel. The tunnel cuts through Limestone and a 'Transiotional Zone' divided in two separate sections: 'Transition Zone 1' with medium and 'Transition Zone 2' with poor geomechanical characteristics. Segments of the tunnel excavated at the first and the second contract are shown. The 'failure zone' and the two control sections (at ch.1 + 419 m and ch.1 + 446.50 m) where displacements associated with stress and strain re-distribution in the ground were recorded are also indicated.

face in steps of ∼1.0 to 2.0 m. A basic requirement of construction was the immediate installation of stiff support measures (steel ribs HEB140 and 180 and shotcrete) with full closure at steps of 1.0–1.5 m, to prevent ground displacements that might induce instability of the slope. In addition, 12 m long Forepoling tubes were installed, to minimize ground movements until ring closure, following closely the tunnel front (1.0 to 2.0 m). Displacements, measured with geodetic techniques and rock extensometers, did not exceed safety levels and proved that the excavation technique adopted was successful (Thanopoulos et al. 1998).

3.1.2 *Excavation from the SW portal – ch.0 + 395 m to ch.1 + 447 m*

Messochora tunnel was excavated from the SW portal from 2004 to 2006 in two phases including: *first*, excavation of the heading with installation of steel sets (IPB 120), rock bolts at the lining footings and 15 cm of shotcrete and *second*, bench excavation with rock bolts and shotcrete. The excavation, however, did not follow the predefined steps given at the technical specifications for Rock Class IV, i.e. face advance 1.0 to 2.0 m and ring closure maximum at 12 m, for rock mass properties were overestimated during excavation. The whole tunnel was excavated at the heading level with no stability problems. However, a few weeks after the bench excavation a failure suddenly occurred at the weathered 'transition zone'. At ch.1 + 401 m to ch.1 + 437 m, high distortion of the steel sets and fractures along the shotcrete were observed, on August 29th, 2005, indicating extremely 'weak' rock conditions at the 36 m long tunnel segment ('failure zone'; Fig. 2).

3.2 *Tunnel restoration*

A restoration program was developed after the failure. Its purpose was to maintain tunnel stability both immediately after the failure and in the long-term permitting installation of the final lining. Tunnel restoration involved two phases:

(1) Immediate measures. They aimed to prevent further instabilities and stop all movements in the tunnel and involved re-filling of the bench area and additional self-drilling, injection boring bolts; 9 m long bolts were installed at the crown and 12 m at the tunnel springline (Fig. 3).
(2) Full section restoration. After all movements were stabilized a few months later, the bench was re-excavated following small steps (1–1.5 m). A new lining, including 2 rows of 6 m-long self-drilling, injection boring bolts at each of the bench sidewalls and a layer of 30 cm shotcrete, was installed at each excavation cycle. Removal of the bench filling was definitely the most difficult part of restoration since the already yielded rock at the 'failure zone' would be loaded again.

To evaluate stability during the above stages of restoration, a monitoring system including a geodetic and an extensometer control section was established (see Fig. 2). Geodetic data permitted the estimation of the absolute displacements of the support shell while the extensometer records permitted to assess rock reaction at the vicinity of the 'failure zone' during restoration. Yet, these data offered the possibility:

(i) to control post-failure ground movements at the 'failure zone' and neighbor sections, confirm effectiveness of the immediate measures and plan full restoration when all strains are stabilized and
(ii) to evaluate stability at the 'failure zone' and neighbor sections during the full section restoration.

Collected monitoring data and post-failure tunnel behavior are analyzed below.

3.3 *Monitoring data and analysis*

Seven geodetic control sections were initially installed along the tunnel between ch.0 + 480 m and



Figure 3. Left: Injection boring bolts installation for immediate support of the Messochora tunnel. Right: A photo from the Messochora tunnel taken on August 30th, 2005, shortly after re-filling of the bench area. A several meters long and a few cm wide crack of the lining are visible in this photo.

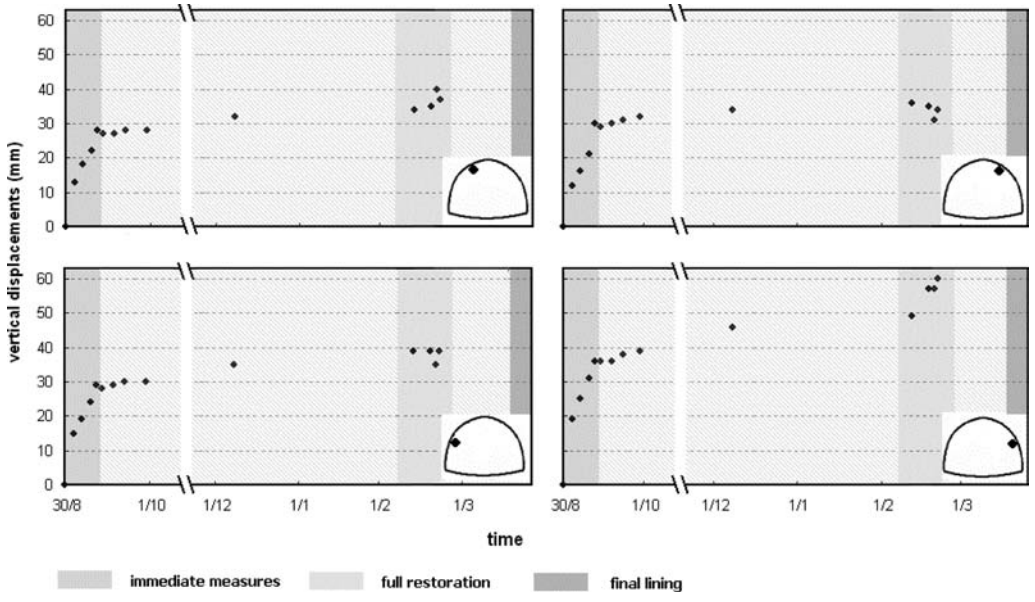


Figure 4. Time-history of vertical displacements geodetically measured at ch.1 + 419 m, immediately after the failure. It is evident that movements accumulated till Sept. 10th, when ground improvement and re-filling of the bench was completed. Afterwards, all movements tended to stabilize. On Feb. 2006 when bench was re-excavated minor displacements were detected.

ch.1 + 319 m shortly after heading excavation. Recordings at six of these revealed minor displacements and only at ch.0 + 979 m, at maximum overburden, displacements reached 60 mm but did not affect tunnel stability. However, instabilities at the 36 m long 'failure zone' on August 29th, led to the installation of an eighth control section in the middle of the 'failure zone' (ch.1 + 419 m) on August 30th. Continuous measurements for over a month revealed post-failure displacements accumulating till Sept. 10th when immediate reinforcement works, i.e. refilling of the bench area and ground improvement at the 'failure zone', were completed. After Sept. 10th only slow-rate creep strains were recorded for several months testifying to ground stresses were fully compensated. Recordings of all four targets of control section at ch.1 + 419 m are shown in Figure 4.

Additionally, two sets of 3 extensometers (Fig. 5a) were initially installed at ch.0 + 949 m and ch.1 + 051 m and one set of 4 extensometers (Fig. 5b) was installed at ch.1 + 446.50 m close to the breakthrough point of the tunnel (ch. 1 + 447 m). Records at ch.0 + 949 m and ch.1 + 051 m did not exceed ±6 mm at any of the extensometers sensors, indicating minor stress distribution and subsequent deformation within ground volume. At ch.1 + 446.50 m, only 9.5 m far from the 'weak' zone (distance <D), minor displacements were recorded after installation of the instruments on August 1st, but on August 29th, the day failure appeared at the 'failure zone', records at two

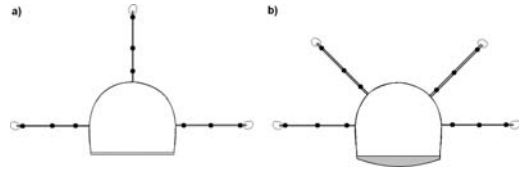


Figure 5. Positions of rock extensometers installed at the Messochora tunnel: (a) at ch.0 + 949 m and ch.1 + 051 m and (b) at ch.1 + 449.50 m, which recorded later strains after the nearby failure.

of the extensometers revealed movements within the rock (Fig. 6). Displacements continued to accumulate for several days and stabilized on Sept. 10th. Afterwards, only slow creep deformations were recorded for several months.

4 DISCUSSION

Messochora tunnel sections excavated from the SW portal at the heading level were stabilized a few weeks after excavation, with geostatic stresses on the lining fully compensated. However, on Aug. 29th, 2005, a few weeks after the bench excavation, an entirely sudden, episodic failure, characterized by high closures and failure of the lining, affected a 36 m long segment of the tunnel. Failure and disablement of the lining to accommodate additional loadings led to post-failure

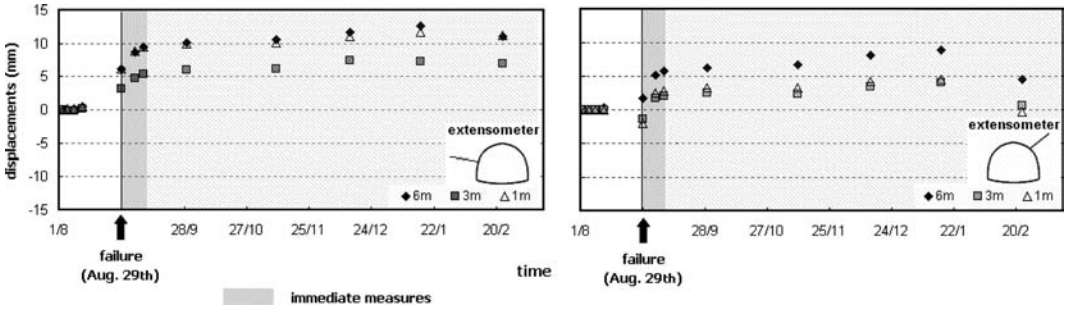


Figure 6. Time-history of displacements of all sensors (at 1 m, 3 m and 6 m from the tunnel wall) of two extensometers installed at ch.1 + 446.50 m. Extensometers were installed at the heading excavation on Aug. 1st, 2005 and practically no movements were recorded. Suddenly on Aug. 29th, the day failure appeared at the 'failure zone', rock displacements were detected and accumulated till Sept. 10th when movements at the 'failure zone' were also stabilized. Afterwards, only slow creep movements were recorded.

deformations at the 'failure zone' which continued accumulating for several days after, till installation of the immediate measures was completed (Sept. 10th). However, these measurements, did not alarm site engineers for strain rates were kept at low levels (they did not exceed 8 mm/day) and strain curves had a clear tendency to stabilization (Fig. 4).

Though, a similar time history of displacements was observed at the ch.1 + 446.50 m extensometers control section showing additional unforeseen ground displacements of up to 8 mm (as shown in diagrams of Figure 6). The fact that this new phase of deformation started on the day failure initiated at the 'failure zone' and stabilized with strain stabilization at the latter is far from coincidental and suggests that strains, originated from 'failure zone' induced further deformation at stable sections at short distances (∼1-2D) outside it, as is schematically shown in Figure 7.

This conclusion clearly suggests that failure actually affected a wider area with strains from the 'failure zone' transferred at distance >D from the edge of the 'failure zone' – an effect related to stresses distribution at the vicinity of the tunnel sections, analogous to the face advance effect – though with no apparent signs, as lining cracking or high deformation. Furthermore, analysis of monitoring data proved this strain transfer to be a clearly time-dependent effect; deformation at the 'weak' zone and the adjacent sections continued for 12 days since initial damage (Aug. 29th to Sept. 10th) and both stabilized only when ground improvement was fully completed at the 'weak' zone.

Stabilization of the 'failure zone' and adjacent areas for several months after allowed the full restoration of the 'failure zone' sections on February 2006. Displacements were recorded at the geodetic control section (ch.1 + 419 m) during the bench re-excavation, carried out on Feb. 7th to Feb. 27st, 2006. Records indicated only minor displacements at the heading area (Fig. 4) and permitted installation of the final

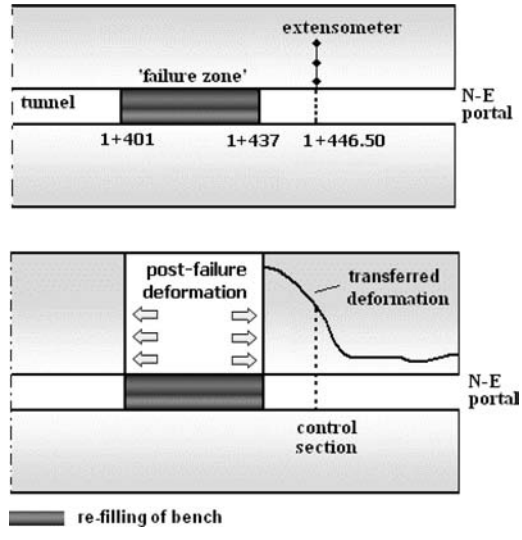


Figure 7. An ideal sketch showing the transfer of ground deformation from the 'failure zone' to adjacent stable areas of the Messochora tunnel due to stresses re-distribution at the vicinity of the 'failure zone'.

lining one month later (Mar. 2006). Interestingly, no movements were detected at the extensometers control section during that period, which revealed that the ground-support system at the failure zone was adequately strong to accommodate all the stresses generated after bench re-excavation. This effect suggests that despite the extremely weak rock conditions and rock yielding, ground improvement carried out contributed to the development of the physical bearing capacity of the rock around the excavation; a process characterizing response of ground around successful tunnels (i.e. 'arch effect'; Lunardi, 2000).

5 CONCLUSIONS

A detailed monitoring system established to evaluate stability during restoration of the Messochora tunnel, recorded post-failure strains at the 'failure zone' and other sections at short distances (∼1D) apparently testifying to stresses and strains transfer along the tunnel. Such transfer of strains could possibly trigger high closures or even more generalized failures propagated even at distant areas; an effect detected in many other tunnels in the past leading to costly failures and great project delays (Kontogianni & Stiros 2006). However, immediate development of ground improvement and section reinforcement obviously interrupted a possible uncontrolled propagation of strains along the tunnel.

Besides, this study made clear that appropriate ground improvement and support installation, planned on the basis of systematic ground monitoring, may help even yielded rock masses around failed tunnel sections to recover their bearing capacity and eventually maintain tunnel stability.

ACKNOWLEDGMENTS

We are deeply indebted to Mr A. Dimitriou (Hydropower Corporation of Greece) and Mr. K. Skourlis (Michaniki S.A.) for data and discussions.

REFERENCES

Peck, R.B. 1969. Advantages and limitations of the observational method in applied soil mechanics. *Geotechnique*, 19(2): 171–187.

Terzaghi, K. 1942. Shield tunnels of the Chicago Subway. *Journal of the Boston Society of Civil Engineers*, 29(3): 163–210.

Thanopoulos, Y., Sofianos, A., Karinas, A., Katsaris, D. 1998. Initial support of the mixed ground eastern portal of the Messochora highway tunnel. Proc. of the 2nd International Symposium on Hard Soils Soft Rocks. October 12–14, Napoli.

Kavvadas, M.J. 2005. Monitoring ground deformation in *tunnelling: Current practice in transportation tunnels. Engineering Geology*, 79 (1–2): 93–113.

Kontogianni, V. & Stiros, S. 2003. Tunnel Monitoring during the Excavation Phase: 3-D Kinematic Analysis based on Geodetic Data. *Proc. of the 11th FIG Symposium on Deformation Measurements*, Santorini, Greece, 397–402.

Kontogianni, V. & Stiros, S. 2006. Convergence in weak rock tunnels. *Tunnels and Tunnelling International,* February issue, 36–39.

Lunardi, P. 2000. Design and constructing tunnels – ADECO-RS approach. *Tunnels & Tunnelling International special supplement.* Internet ref: www.rocksoil.com.

Underground Space – the 4th Dimension of Metropolises – Barták, Hrdina, Romancov & Zlámal (eds)
© 2007 Taylor & Francis Group, London, ISBN 978-0-415-40807-3

Rock bolt integrity evaluation in tunnelling using ultrasonic NDT techniques

J.S. Lee, H.J. Kim, I.M. Lee
Dept. of Civil Engrg., Korea University, Seoul, Korea

S.I. Han
Dept. of Civil Engrg., Korea University, Seoyeong Engrg. Co., Ltd., Seoul, Korea

Y.J. Lee
POSCO E&C Co., Ltd., Seoul, Korea

ABSTRACT: Rock bolts play a crucial role in the reinforcement of Single-shell tunnels and rock slopes as rock bolts become a main support system. Numerical and experimental studies are performed to evaluate the integrity of rock bolts encapsulated by grouting paste using a transmission method of ultrasonic guided waves. Numerical simulation shows that the optimal frequency range is 20∼70 kHz in the first longitudinal L(1) mode for the rock bolt NDT system. Analytical and experimental results represent the velocities of the ultrasonic guided wave increase with increase in the defect ratio. This study demonstrates that the transmission method of ultrasonic guided waves may be a valuable tool for the evaluation of the rock bolt integrity.

1 INTRODUCTION

For the construction of tunnels by using a conventional method, NATM, rock bolts with shotcrete are widely used as a subsidiary tunnel support system. Furthermore, rock bolts play a crucial role in a Single-shell tunnelling method and rock slope reinforcement as rock bolts become a main support system.

Generally, to install the rock bolt on the rock mass, a 38 mm diameter grouting hole is drilled, cement-mortar grouting is pumped into the hole, and a 25.4 mm diameter steel bar is inserted. After the grouting is cured, the steel bar and rock work as a composite material. Rock bolts are commonly installed in a whole section of the tunnel: from sidewall to crown. When rock bolts are installed on the crown, the cement-mortar grouting is easily running out due to the gravity. Thus, the grouting may be poorly or partially plugged in the tip of rock bolt. This phenomenon is a typical example of defects in rock bolt systems. The defect of rock bolts on the ceiling may result in falling of rock mass during and/or after tunnel construction. Therefore, the evaluation of rock bolt quality is essential to the safety and reliability of tunnels.

The traditional methods of inspecting rock bolt integrity are the destructive pull-out tests or the over-coring methods. As these methods are generally expensive and time-consuming, a new method is required. Therefore, nondestructive evaluation may be an alternative.

A number of nondestructive evaluation techniques have been conducted for the inspection of the slenderness material including rock bolts surrounded by rock mass, steel bars in a concrete block, steel tendons in a bridge deck, and even concrete piles in soil and rock mass. The techniques included numerical, analytical, and experimental methods. The experimental methods covered the reflection (impact-echo) and transmission of waves. The waves used for the integrity evaluation of the slenderness material were ultrasonic guided waves including flexural, longitudinal, and lamb waves.

Thurner (1988) introduced the non-destructive testing using the reflection method "Boltometer", which compares the amplitude of the reflected ultrasonic guided waves. However, it should be noted that the amplitude of the reflected guided waves is dependent on not only rock bolt conditions but also the length of the rock bolt, rock condition and even coupling conditions of the transducers.

The delamination of the steel bar from concrete mass using ultrasonic guided waves was investigated by Na et al. (2002). They used flexural, longitudinal, and lamb waves. Furthermore, the dispersion curve, which shows the relationship between the phase velocity and the frequency, was used. Hassan & Nagy (1999) measured the change of the velocity of copper

wire (1.0 mm in diameter and 500 mm in length) with frequency in fluid. The intensive analysis of the dispersion curve shows that the velocity of ultrasonic guided waves changes with frequency in the slenderness material due to the different modes (Beard et al. 2003). Beard et al. (2003) also did experimental studies by using reflected ultrasonic guided waves in the longitudinal mode.

Madgena et al. (2006) investigated the effect of the curing time and testing frequency on the ultrasonic guided wave velocity. Zhang et al. (2006) showed the numeral simulation solution and experimental data. The velocity and amplitude were compared with frequency.

The purpose of this paper is to extend the application of ultrasonic waves to evaluate the integrity of rock bolts encapsulated by grouting paste. A transmission method rather than the reflection method is adopted for simplicity in analysis. This paper includes numerical studies for the dispersion analyses of ultrasonic guided waves in rock bolt systems, experimental studies for both embedded in the concrete block and non-embedded conditions, and simple analytical solutions.

2 DISPERSION OF GUIDED WAVES IN ROCK BOLT SYSTEM

2.1 *Guided wave and dispersion*

Equation of motion in an elastic medium is:

$$\rho \frac{\partial^2 \mathbf{u}}{\partial t^2} = (\lambda + \mu)\nabla(\nabla \cdot \mathbf{u}) + \mu \nabla^2 \mathbf{u} \tag{1}$$

where body forces such as gravity are absent, ρ is a mass density of an elastic medium, **u** is the displacement vector in a specified direction with a Cartesian coordinate system, λ and μ are Lame's constants, and t is time.

Using Helmholtz decomposition, the displacement field **u** can be expressed with a scalar potential ϕ and a vector potential **H** (Kolsky 1963, Graff 1975):

$$\mathbf{u} = \nabla\phi + \nabla \times \mathbf{H}. \tag{2}$$

Hence, substituting Equation 2 into Equation 1 yields:

$$c_1^2 \nabla^2 \phi = \partial^2 \phi / \partial t^2 \tag{3}$$

$$c_2^2 \nabla^2 \mathbf{H} = \partial^2 \mathbf{H} / \partial t^2 \tag{4}$$

where c_1 and c_2 can be represented as follows,

$$c_1 = \left[(\lambda + 2\mu)/\rho\right]^{0.5} \tag{5}$$

$$c_2 = \left[\mu/\rho\right]^{0.5}. \tag{6}$$

Table 1. The material properties used for the analysis.

Layers	Steel	Grouting	Rock
Young's modulus [GPa]	206	10	20
Poisson' ratio	0.30	0.27	0.25
Density [g/cm^3]	7.90	2.10	2.40
Thickness [mm]	12.5	6.50	infinite
Remarks	D25	cement mortar	

If a wave propagates in cylindrical elastic system, which is axially symmetric and infinitely long, the constants c_1 and c_2 are real valued, and equal to the longitudinal and shear bulk wave velocities respectively. In a cylindrically embedded rock bolt system composed of arbitrary several layers, the characteristic equation for wave propagation may be described, which satisfies the boundary conditions of stresses and displacements for each interface.

The solution of the characteristic equation can be expressed by several types of graphs, what are called "dispersion curves", which are series of roots of the equation, for example, frequency versus phase velocity and/or group velocity etc. In other words, characteristic properties including dispersion, changes of wave modes and attenuation can be determined through the dispersion curves.

2.2 *Analysis of dispersion*

The selection of the nondestructive test equipment can be acquired by the inspection of wave propagation. When ultrasonic guided waves propagate through the steel bar in the rock bolt system, the energy leakage occurs from the steel bar into surrounding layers including grouting paste and rock mass. Note the energy leakage includes geometrical spreading, material losses, and apparent attenuation due to partial transmission and scattering. Apparent attenuation and geometrical spreading are the main sources on the decay of the wave amplitude in the rock bolt system. Furthermore, as the frequency increases, the change of velocities such as phase and group velocities is accompanied during ultrasonic guided wave propagation.

For the purpose of finding dispersion in the rock bolt system, the numerical code "DISPERSE", developed in Imperial College, UK, has been used (Beard et al. 2003, Pavlakovic & Lowe 2003). The material properties taken in this study are listed in Table 1, and a schematic diagram, which models the embedded rock bolt system, is shown in Figure 1. Figure 1 describes the system consisting of a steel bar, cement-mortar grouting materials and surrounding rock mass.

The predicted energy velocities are plotted versus frequency for the non-embedded, free end rock bolts and the embedded rock bolts in Figures 2 and 3. The

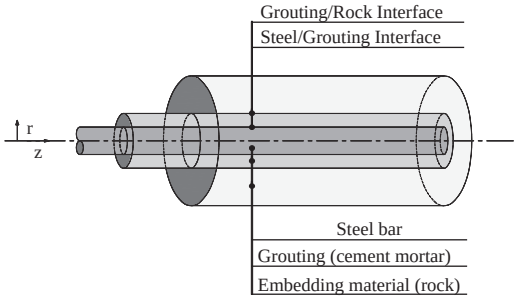


Figure 1. Schematic diagram of the rock bolt system.

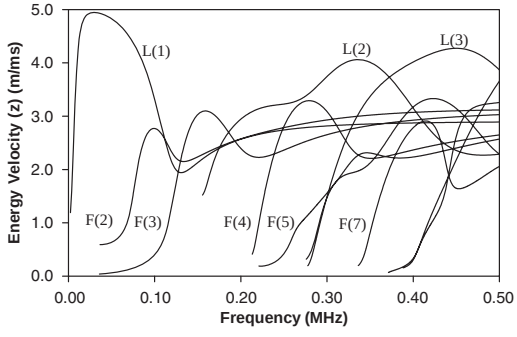


Figure 2. Energy velocity dispersion curves in the non-embedded, free end rock bolt. L and F mean longitudinal and flexural modes respectively. Number in parentheses is a mode number counted with increasing frequency.

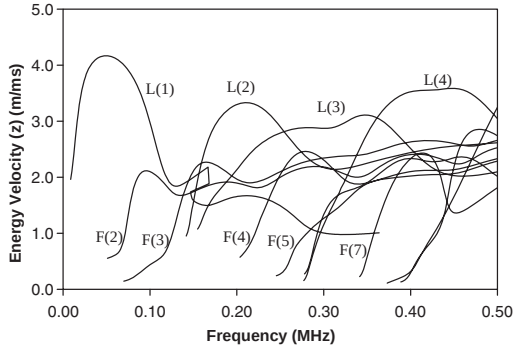


Figure 3. Energy velocity dispersion curves in the embedded rock bolt. L and F mean longitudinal and flexural modes respectively. Number in parentheses is a mode number counted with increasing frequency.

velocity range is 0∼5000 m/sec and the frequency range is 0∼0.5 MHz.

The dispersion curves represent that the maximum energy velocities appear at the first longitudinal mode L(1) with the frequency range 20∼70 kHz for the non-embedded, free end bolt and the embedded rock bolt. Note L(2) and L(3) show the second and/or third maximum energy velocity. However their frequency depends on the embedded condition. In addition, the flexural mode shows the lower energy velocity with the higher attenuation. Therefore, the L(1) mode is used for the attenuation analyses.

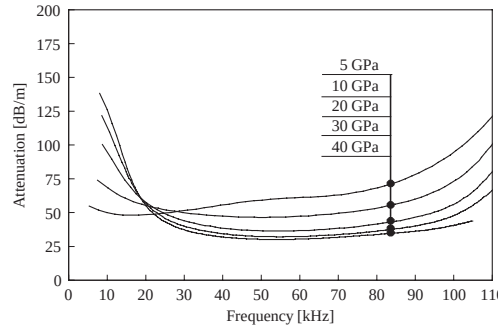


Figure 4. The effects of the Young's modulus of rock mass on attenuation for L(1) mode in the embedded condition. Number in figure denotes the Young's modulus.

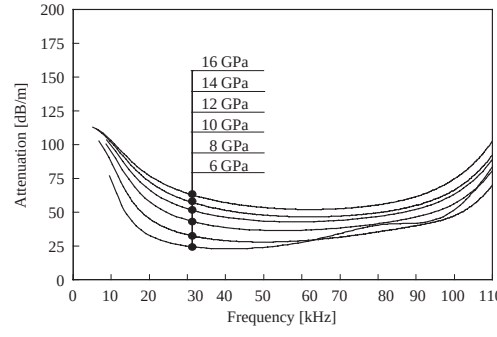


Figure 5. The effects of the Young's modulus of grouting materials on attenuation for L(1) mode in the embedded condition. Number in figure denotes the Young's modulus.

The effects of the modulus of rock mass, which surrounds grouting and a steel bar, is shown in Figure 4 in terms of attenuation for the L(1) mode. The attenuation of the L(1) mode is not affected by the rock modulus at about 20 kHz. The attenuation of the L(1) mode increases with decrease in rock modulus if the frequency is ranged about 30∼110 kHz. Figure 4 shows that the optimal frequency is about 20∼70 kHz for the L(1) mode.

The modulus of the grouting material between a steel bar and rock mass is easily affected by the ground water condition and the water-cement ratio. The effect of the modulus of the grouting material is plotted in Figure 5. Figure 5 shows the attenuation increase with increasing grouting modulus. The attenuation is about 25∼70 dB/m at 30∼100 kHz in frequency.

3 EXPERIMENTAL STUDIES

The numerical studies by using "DISPERSE" suggest that the appropriate frequency range is about 20∼100 kHz in the L(1) mode for the integrity test in the rock bolt system. Therefore, the system for experimental study is prepared in accordance with the numerical study. For the simplicity, the transmission method is used in this study.

3.1 *Specimen preparation*

Experimental studies are carried out by using 3.1 m in length and 25.4 mm in diameter steel bars encapsulated with grouting paste. The grouting material is mixed with cement, fine grain sand and water in a weight ratio of 1:1:0.4. The external diameter of grouting, which encapsulates the steel bar, is fixed at about 38 mm. However, the length of grouting L_G changes from zero meter to the full length of the steel bar L_S in accordance with the intended defect ratio DR (see Figure 6):

$$DR(\%) = \left(\frac{L_S - L_G}{L_S}\right) \times 100 . \tag{7}$$

The specimen with 0% in DR is prepared for the non-embedded, free end rock bolt condition. After nondestructive test is carried out by using the non-defect specimen (0% in DR), the grouting of this specimen is gradually taken out to increase the defect ratio. The increment of the defect ratio is about 10%. For the application of the same technique in the embedded rock bolt, five specimens with different defect ratio are prepared in the non-embedded, free end rock bolt condition: 0, 25, 50, 75, 100% in DR. Five specimens are carefully installed in the concrete block as shown in Figure 7. Note the non-grouted area is maintained in the concrete block. The dimension of the concrete block is 3.0 m in length, 0.8 m in height and 0.9 m in width.

3.2 *Experimental device*

The piezo ceramic elements (PZT elements) are used for the generation of ultrasonic waves (see Figure 7).

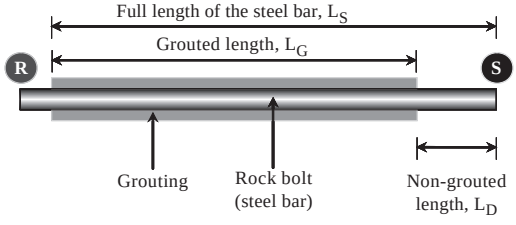


Figure 6. Schematic diagram of the rock bolt partially encapsulated with grouting. Non-embedded, free end condition. S: PZT element (source). R: AE transducer (receiver).

The piezo ceramic element is attached by using the epoxy resin at the end of the rock bolt (see Figure 6). The dimension of element is 14mm in ceramic diameter, 20 mm in element diameter and 0.45 mm in thickness.

The single square signal was delivered from the signal generator (Agilient A3441) to the element. The ultrasonic guided waves, which is emitted from the source elements and traveled through the rock bolt system, was captured and transformed into the electrical signal in the receiver. The receiver used in this study is an acoustic emission sensor (Physical Acoustics A3). Note a typical accelerometer is not applicable due to the operating frequency range. The electrical signal was fed through a pre-amplifier and post-amplifier. The amplified signal was digitized through oscilloscope. Note the 500∼1000 signals were averaged to remove the high frequency uncorrelated noise.

3.3 *Experimental results*

Measured signals in non-embedded, free end condition are plotted in Figure 8. Figure 8 shows that the amplitude of the signal increases and first arrival time decreases with defect ratio.

The calculation of the velocity of ultrasonic guided waves is based on the steel bar length and travel time. The evolution of the ultrasonic wave velocity is plotted versus the defect ratio in Figure 9. Figure 9 shows the wave velocity increases with increase in the defect ratio. When the ultrasonic waves propagate through the mixture composed of the steel bar and grouting, the mixture condition affects the travel time. In other words, the velocity reflects the property of the composite material. The equivalent velocity of the composite material may be simply expressed as follows.

$$V_{eq} = \sqrt{\frac{E_{eq}}{\rho_{eq}}} = \sqrt{\frac{A_s \rho_s V_s^2 + A_c \rho_c V_c^2}{A_s \rho_s + A_c \rho_c}} \tag{8}$$

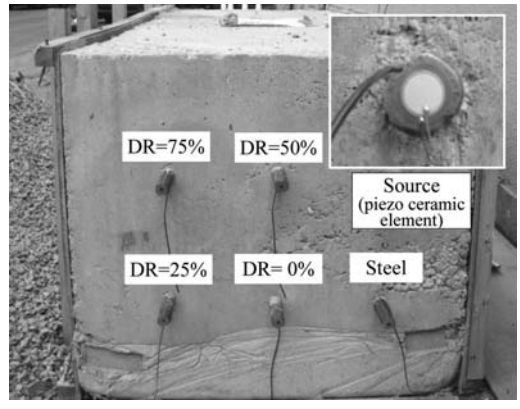


Figure 7. Picture of the concrete block with rock bolt specimens for the embedded condition.

where E is elastic modulus, A is cross-sectional area, ρ is a mass density, and subscripts eq, s, c are equivalent, steel bar and cement-mortar, respectively.

The calculated velocity by equation 8 is plotted versus the defect ratio in Figure 9. Figure 9 shows the relatively good agreement between the simple analytical solution and experimental results in non-embedded, free end condition. Thus, the defect ratio can be evaluated by measuring the ultrasonic wave velocity of installed rock bolts.

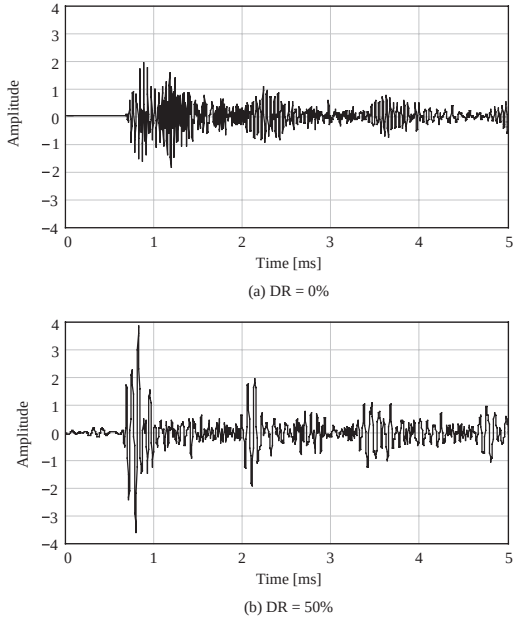


Figure 8. Ultrasonic wave velocity versus defect ratio (DR) in non-embedded, free end condition.

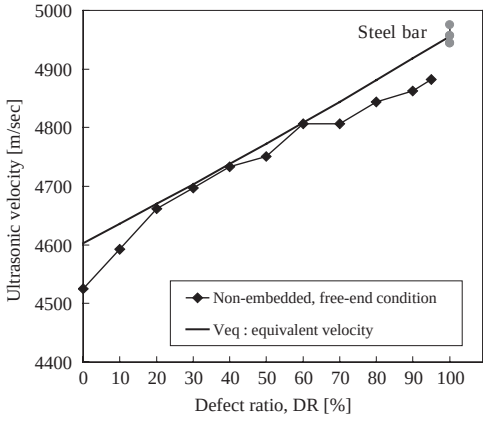


Figure 9. Ultrasonic wave velocity versus defect ratio (DR) in non-embedded, free end condition.

Responses of the embedded rock bolt into the concrete block are plotted in Figure 10. Figure 10 shows that the amplitude of the signal increases and first arrival time decreases with defect ratio. The calculated velocities are plotted in Figure 11.

The test result shows that the velocities increase with increase in the defect ratio in both embedded and non-embedded conditions. However, the velocities are slower in the embedded rock bolt than in

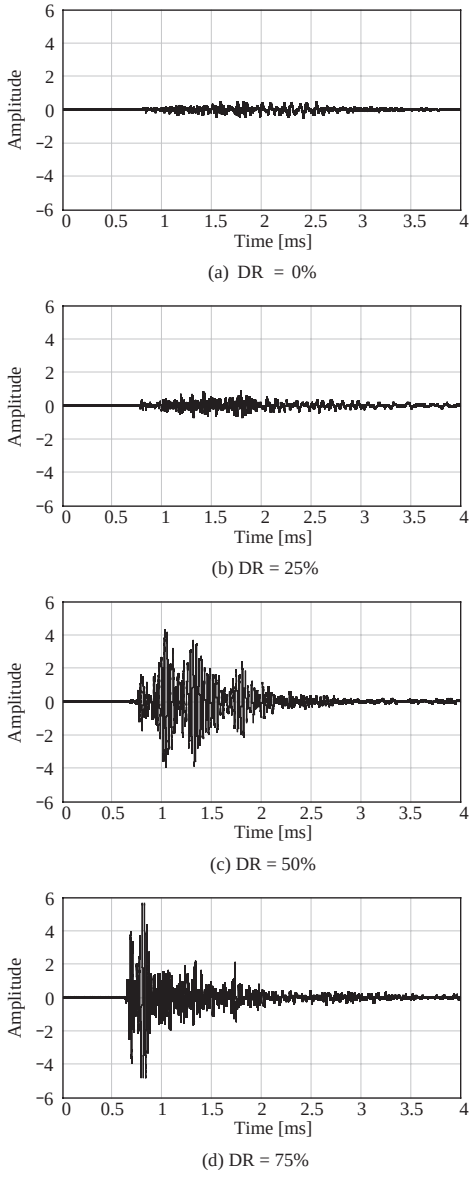


Figure 10. Responses of AE sensor for the embedded rock bolt with 3.1m long in the concrete block specimen.

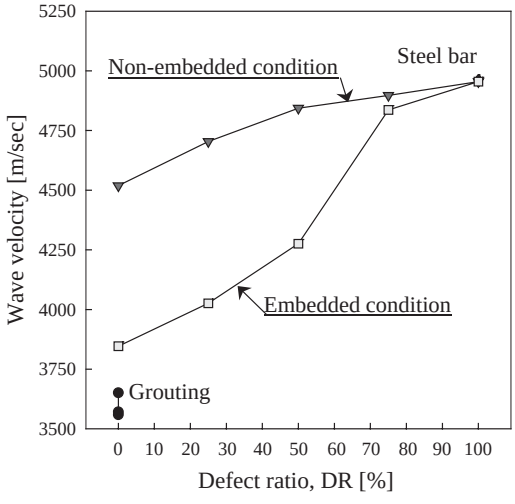


Figure 11. Ultrasonic wave velocity versus defect ratio(DR) in non-embedded condition.

the non-embedded rock bolt. The slower velocity in the embedded rock bolt results from the increase of the affected zone, where the guided wave travels (see Figure 11).

4 CONCLUSION

Numerical and experimental methods using ultrasonic guided waves have been implemented to evaluate the integrity of rock bolts encapsulated by the cement-mortar grouting in both embedded and non-embedded condition. The numerical code "DISPERSE" is used to identify the dispersion characteristics in ultrasonic guided waves in the cylindrical geometry. The numerical code shows that the maximum energy velocity is expected at the frequency range 20∼70 kHz on the first longitudinal mode L(1) for the grouted rock bolt system.

Experimental studies were carried out with different defect ratios in both of the non-embedded and embedded conditions. The measured ultrasonic wave velocities increase with increase in the defect ratio for the embedded condition as well as the non-embedded condition. The simple analytical solution, which is based on the volume fraction, shows a good agreement with measured velocities in the non-embedded rock bolt. Note velocities of the embedded rock bolt are lower than those of the non-embedded rock bolt at the lower defect ratio due to the increased affected zone.

The numerical simulations, experimental studies, and the analytical solution suggest that the integrity of rock bolts can be easily evaluated by the transmission method of ultrasonic guided waves.

REFERENCES

Beard, M.D., Lowe, M.J.S. & Cawley, P. 2003. Ultrasonic guided waves for inspection of grouted tendon and bolts. *Journal of materials in civil engineering, ASCE*, 15(3): 212–218.

Beard, M.D. & Lowe, M.J.S. 2003. Non-destructive testing of rock bolts using guided ultrasonic guided waves. *International journal of rock mechanics and mining sciences*, 40: 527–536.

Graff, K.F. 1975. *Wave motion in elastic solids.* London: Oxford university press.

Hassan, W. & Nagy, P.C. 1999. Experimental verification of the opposite effect of fluid loading on the velocity of dilatational waves in thin plates and rods. *Journal of the acoustical society of America*, 105(6): 3026–3034.

Kolsky, H. 1963. *Stress wave in solids.* New York: Dover publications Inc.

Madenga, V., Zou, D.H. & Zhang, C. 2006. Effects of curing time and frequency on ultrasonic wave velocity in grouted rock bolts. *Journal of applied geophysics*, 59(1): 79–87.

Na, W.B., Kundu, T. & Ehsani, M.R. 2002. Ultrasonic guided waves for steel bar concrete interface testing. *Materials evaluation*, 60: 437–444.

Pavlakovic, B. & Lowe, M. 2003. *DISPERSE user's manual(ver. 2.0).* London: Imperial college.

Thurner, H.F. 1988. Boltometer-instrument for non-destructive testing of grouted rock bolts. *2nd international symposium on field measurements in geomechanics. Sakurai(ed.)*: 135–143. Rotterdam: Balkema.

Zhang, C.S., Zou, D. H. & Madenga, V. 2006. Numerical simulation of wave propagation in grouted rock bolts and the effects of mesh density and wave frequency. *International journal of rock mechanics and mining sciences*, 43(4): 634–639.

Underground Space – the 4th Dimension of Metropolises – Barták, Hrdina, Romancov & Zlámal (eds)
© 2007 Taylor & Francis Group, London, ISBN 978-0-415-40807-3

Jet-grouting in underground construction

A.G. Malinin & P.A. Malinin
EPC close corporation, Perm, Russia

ABSTRACT: Recently jet-grouting technology becomes more popular at solution of different tasks of underground construction in Russia. Developed calculation method of deformation mode of one- and two-row cofferdams from jet-grouting columns is realized in the application software, which allows to get jet-grouting cofferdam parameters.

The main point of the jet-grouting technology is using of high-pressure grout jet for destruction and simultaneous mixing of soil with cement grout. As a result columns from new material – soil-concrete are formed in the ground. The new material has high strength and antifiltering characteristics. Depending on the technology the diameter of pile is 600–2000 mm.

The most significant application of jet-grouting is soft ground consolidation. There is no doubt that in this case the jet-grouting technology has advantages over historically preceding, simpler, but practically uncontrolled technology of injection ground strengthening, where cement grouts or mixtures on the basis of liquid glass or artificial resins are used.

For example, at the construction of highway tunnel in Ufa, plastic clays in walls and roof of one of the technological adits were reinforced using jet-grouting technology. The works were made from the ground surface at a depth of 30 m.

Another interesting task is stabilization of clays at subway tunnel crossing with one of the auxiliary underground course. In order to do this work a small drill rig was installed in the course, so 9 m long protective circular shield was made towards forthcoming TBM 5.6 m in diameter.

On the territory of one of the metallurgical plants two 20 m deep technological pits were constructed in watered sandy ground using jet-grouting technology. So with the help of intersecting piles vertical cofferdam and horizontal curtain grouting were made.

Meanwhile the jet-grouting technology allows also to solve the other, in our opinion, more complicated problems of underground construction.

Among them first of all there is a construction of deep foundation pits in difficult geological conditions. Importance of such problem has increased recently because of appeared and annually rising demand for the underground multilevel parking construction, located under the dwelling houses. It is well-demonstrated in such megalopolis as Moscow, where at the construction of practically each building in center underground parking is planned. That makes such project very attractive for investors.

Application of jet-grouting technology in this case has the following advantages:

- absence of negative influence on the nearby buildings foundations in the process of cofferdam making from jet-grouting piles;
- providing of cofferdam water impermeability from intersecting piles;
- possibility of safe horizontal waterproofing membrane performance in the foundation pit bottom, artificial aquifuge layer.

Reinforcement of jet-grouting piles is usually made using centrally located pipes 89–219 mm in diameter or single reinforcement bar. For such schemes of reinforcement authors got formulas which allow to calculate limit moment of pile section.

When natural aquifuge layer occurs at a big depth, jet-grouting technology allows to form in watered ground massif horizontal waterproofing membrane – layer of artificial aquifuge from intersecting jet-grouting piles.

1 STRENGTH ANALYSIS OF JET-GROUTING COFFERDAMS

Strength analysis of jet-grouting cofferdam and reliability assessment of construction is the main stage of design and decision-making. In this process the most important cofferdam characteristics are taken, such as – diameter, positional relationship and depth of columns, type and parameters of columns reinforcement.

Strength analysis of jet-grouting cofferdam is made by determination of maximum bending moment. Analysis of longitudinal bending stresses is made taking into consideration soil-concrete deterioration in terms of stretching longitudinal strains and comparing obtained maximum stresses values in soil-concrete and reinforcement with allowed values.

In this paper a method of jet-grouting cofferdams strength analysis is presented. This method can be used for different types of cofferdams: one-row, two-row.

2 PROBLEM DEFINITION FOR ONE-ROW JET-GROUTING COLUMN COFFERDAM

In problem of cofferdam mode of deformation the following suggestions are made:

- in cofferdam mode of deformation and strength analysis we consider longitudinal component of stress tensor only;
- soil-concrete doesn't resist stretching;
- hypothesis of plane sections in design section of jet-grouting cofferdam.

Strength analysis of jet-grouting cofferdam is made in section with maximum value of bending moment. Stresses in section are obtained from equilibrium equations for external forces.

Among the external forces are:

- normal and tangent forces, which act on the column from the soil side, R = resultant of forces of normal pressure; S = resultant of tangent force;
- gravity force, G = resultant force;
- reaction, acting from the side of jet-grouting column, which is situated below the design section, p = distribution of normal forces for section, T = resultant of intersecting forces.

To make equilibrium equations the external forces are given in the point O – figure 1. At parallel translation of R and S forces in the point O we add a couple of force with moment $M_o(R+S)$, equal to bending moment in section from soil pressure on the cofferdam. Reaction of the lower jet-grouting column part in design section is resulted in two components of main vector T and $N(p)$ and main moment $M_o(p)$. Neglecting the bending column deformation, the gravity force G is transferred along the line of action to the point O, reduced forces are shown on the figure 1, forces R and S are marked as R' and S'.

For the reduced forces we will write two statistical equilibrium equations:

$$N(p)-G-S=0 \tag{1}$$

$$M_o(p)+M_o(R+S)=0 \tag{2}$$

where distribution of normal forces p is unknown.

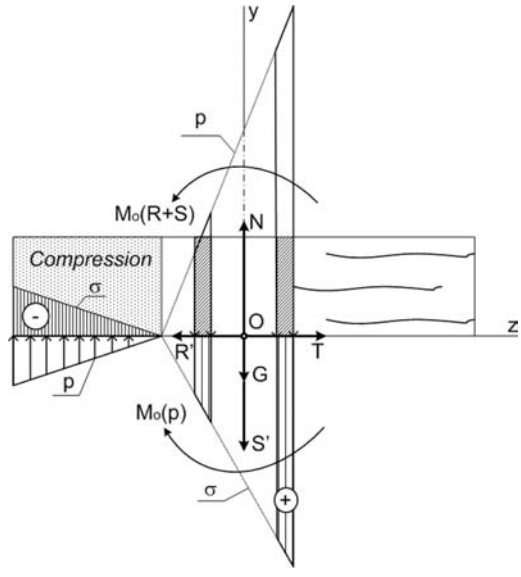


Figure 1. System of balanced forces.

In order to make a closed set of equations we will use the following:

- Koshi correlations, according to which $p_y = -\sigma_y$, where p_y = projection of force p on the axis oy; σ_y = longitudinal component of stress tensor;
- hypothesis of plane sections. Its application gives the following formula for the bending deformation:

$$\varepsilon(z)=\frac{\delta+z}{\rho} \tag{3}$$

- Hooke's law, which connects longitudinal bending deformation with longitudinal stresses.

For reinforcement material:

$$\sigma(z)=E_s\varepsilon(z) \tag{4}$$

For jet-grouting column:

$$\varepsilon(z)<0 \Rightarrow \sigma(z)=E_b\varepsilon(z),\quad \varepsilon(z)\geq 0 \Rightarrow \sigma(z)=0 \tag{5}$$

where ρ = curvature radius of neutral line in the design section, δ = distance from column axis to neutral line in the design section.

Let's consider the variant of intersecting jet-grouting columns. Calculation of separate columns is a particular case of intersecting columns calculation.

There are two variants of neutral line position:

1. Neutral line is out of the columns crossing area. For this case the area of compression and tension in soil-concrete is shown on the figure 2.

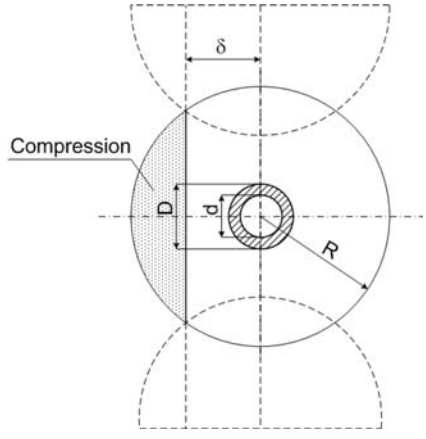


Figure 2. Neutral line is out of the intersecting columns crossing area.

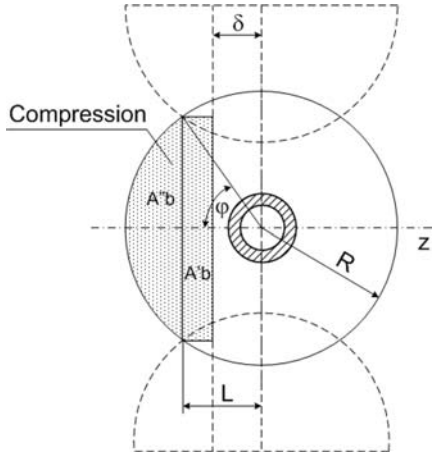


Figure 3. Neutral line goes through the crossing area of intersecting columns.

2. Neutral line goes through the crossing area of columns sections – figure 3.

For the second case $\delta \le L$ we will calculate integrals of the main vector and main moment from forces *p*.

$$N(p)=-\int_{A_b}\sigma_y dA_b-\int_{A_s}\sigma_y dA_s=$$
$$=-\int_{A_b'}E_b\frac{\delta+z}{\rho}dA_b'-\int_{A_b''}E_b\frac{\delta+z}{\rho}dA_b''-\int_{A_s}E_s\frac{\delta+z}{\rho}dA_s \quad (6)$$

$$\int_{A_b'}E_b\frac{\delta+z}{\rho}dA_b'=\frac{bE_b}{\rho}\left(-\frac{1}{2}\delta^2+L\delta-\frac{1}{2}L^2\right) \quad (7)$$

$$\int_{A_b''}E_b\frac{\delta+z}{\rho}dA_b''=\delta\frac{E_bA_b''}{\rho}-\frac{b^3E_b}{12\rho},$$
$$A_b''=\frac{1}{2}R^2(2\varphi-\sin 2\varphi),\quad b=2R\sin\varphi \quad (8)$$

$$\int_{A_s}E_s\frac{\delta+z}{\rho}dA_s=E_s\frac{\delta}{\rho}A_s=E_s\frac{\delta}{\rho}\frac{\pi}{4}(D^2-d^2) \quad (9)$$

$$M_o(p)=-\int_{A_b}\sigma_y zdA_b-\int_{A_s}\sigma_y zdA_s=$$
$$=-\int_{A_b'}E_b\frac{\delta+z}{\rho}zdA_b'-\int_{A_b''}E_b\frac{\delta+z}{\rho}zdA_b''-\int_{A_s}E_s\frac{\delta+z}{\rho}zdA_s \quad (10)$$

$$\int_{A_b'}E_b\frac{\delta+z}{\rho}zdA_b'=\frac{bE_b}{\rho}\left[\frac{(L^3-\delta^3)}{3}-\frac{\delta(L^2-\delta^2)}{2}\right] \quad (11)$$

$$\int_{A_b''}E_b\frac{\delta+z}{\rho}zdA_b''=-\frac{\delta b^3E_b}{12\rho}+$$
$$+\frac{E_b}{4\rho}\left[R^4\left(\varphi+\frac{\sin 2\varphi}{2}\right)-2L^4tg\varphi\right] \quad (12)$$

$$\int_{A_s}E_s\frac{\delta+z}{\rho}zdA_s=\frac{\pi E_s}{64\rho}\left(D^4-d^4\right) \quad (13)$$

Substitution of integrals (6)–(13) in the equilibrium equations (1) and (2) results in set of two nonlinear algebraic equations relative to δ and ρ.

3 PROBLEM DEFINITION FOR TWO-ROW COLUMNS COFFERDAM

Calculation of mode of deformation is made for cofferdam part, width *b*, situated above the design section (Fig. 4).

Let's consider the case when $-\delta < L$.

$$N(p)=-\int_{A_b}\sigma_y dA_b-\int_{A_s}\sigma_y dA_s=$$
$$=-\int_{A_b'}E_b\frac{\delta+z}{\rho}dA_b'-\int_{A_b''}E_b\frac{\delta+z}{\rho}dA_b''-$$
$$-\int_{A_{s1}}E_s\frac{\delta+z}{\rho}dA_{s1}-\int_{A_{s2}}E_s\frac{\delta+z}{\rho}dA_{s2} \quad (14)$$

$$M_o(p)=-\int_{A_b}\sigma_y zdA_b-\int_{A_s}\sigma_y zdA_s=$$
$$=-\int_{A_b'}E_b\frac{\delta+z}{\rho}zdA_b'-\int_{A_b''}E_b\frac{\delta+z}{\rho}zdA_b''-$$
$$-\int_{A_{s1}}E_s\frac{\delta+z}{\rho}zdA_{s1}-\int_{A_{s2}}E_s\frac{\delta+z}{\rho}zdA_{s2} \quad (15)$$

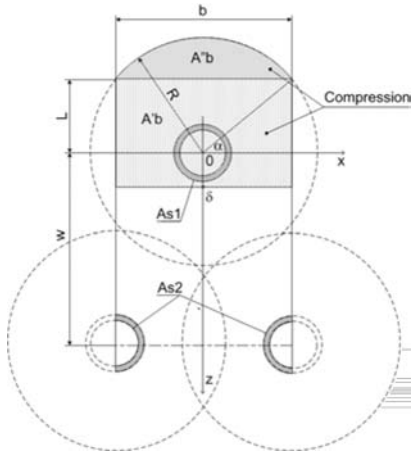


Figure 4. Design section for two-row columns cofferdam.

In case $-\delta \geq L$ there are no integrals in area A_b' in forms (14) and (15).

Substitution of integrals (14), (15) in the equilibrium equations (1) and (2) results in set of two nonlinear equations relative to ρ and α parameters.

We summarize suggested method of calculation in case of reinforcement over one or two columns. For example, in case of each second column reinforcement, the main vector and main moment of longitudinal forces for reinforcement is multiplied by reinforcement ratio equal to 0.5.

4 STRENGTH ANALYSIS OF JET-GROUTING COFFERDAMS

Solution of nonlinear equations set (1), (2) relative to ρ and α parameters, or ρ and δ, is made using Newton-Rafson method. In the process of parameters value iteration a set of equations was selected depending on neutral line position.

Developed calculation method of deformation mode of one- and two-row jet-grouting columns cofferdams was realized in the application software. The following example will show its work.

One-row cofferdam is made from columns 900 mm in diameter, located with interval $b = 900$ mm and reinforced with steel pipe 159×9 mm. Stress-strain properties of soil-concrete: deformation module $E_b = 1000$ MPa, compressive strength $R_b = 5$ MPa. Stress-strain properties of steel: modulus of elasticity $E_s = 20,000$ MPa, tensile strength $R_b = 250$ MPa. Bending moment from external forces $M_o(R+S) = 166$ kN/rm, specific weight of soil-concrete is 20 kN/m^3.

So the task solution relative to desired quantities is found: $\delta = 47$ mm, $\rho = 104,708$ mm. The maximum stresses in jet-grouting columns are $\sigma_b = 3.85$ MPa, maximum reinforcement stress is $\sigma_b = -242.1$ MPa.

5 SUMMARY

The choice of cofferdams construction from jet-grouting columns is based exclusively on the calculation results of cofferdams strength and reliability. Lack of developed methods of jet-grouting cofferdams strength analysis, development of new designing approaches and its practical application is still an actual problem.

In this paper the calculation method of one- and two-row cofferdams from jet-grouting columns, based on the numerical solution of bending beam equilibrium equations with longitudinal compression is suggested. This method is realized in the application software, which allows to get jet-grouting cofferdam parameters.

Underground Space – the 4th Dimension of Metropolises – Barták, Hrdina, Romancov & Zlámal (eds)
© 2007 Taylor & Francis Group, London, ISBN 978-0-415-40807-3

Modelling of ground freezing in tunnelling

E. Pimentel, A. Sres & G. Anagnostou
ETH Zurich, Switzerland

ABSTRACT: Depending on the prevailing soil, the project location and the environmental requirements, the artificial ground freezing may be advantageous or even the only technically feasible method for strengthening, stiffening and sealing the ground. The potential problems of this method are associated with high groundwater seepage velocities (which hinder the development of a frozen body) and surface heaves (due to the expansion of the frozen soil) or settlements (due to the consolidation in the thawing phase). To avoid such problems careful analysis and design of the freezing operation is necessary. A new numerical model has been developed and implemented in order to simulate the time-dependent, three-dimensional growth of the ice body, taking into account the complex thermal and seepage flow interactions. For the verification of the numerical model a large scale laboratory model was conceived and constructed. The tests performed show the high quality of the laboratory measurements. The respective simulations with the numerical model agree very well with the measurements.

1 INTRODUCTION

Due to the ever increasing extent of underground space utilization, urban construction projects are realized ever more frequently in very difficult conditions. Construction methods in shallow soft ground tunneling beneath the water table must ensure control of the ground at the tunnel heading and, additionally, prevent seepage flow towards the working face. For these reasons, tunnel construction in saturated soils is being carried out ever more frequently with closed shields, which provide support to the tunnel face continuously during excavation. Slurry and EPB-shield tunneling has been successfully applied worldwide in recent years. Under extremely unfavorable geological conditions, however, face instabilities may occur. Furthermore, stability of the tunnel face must also be ensured during maintenance works on the cutter head or other activities at the face (e.g. removal of large blocks, tree trunks etc.). Finally, for special underground works (crossovers, caverns, adits etc.) only conventional tunneling methods can be applied. In all these cases, auxiliary ground improvement measures are still indispensable for maintaining face stability and preventing groundwater drainage.

The ground can be strengthened and sealed either by grouting or by artificial freezing. Grouting is in most cases the first choice due to economic and technological considerations. Its applicability may be limited, however, by the grain size distribution of the soil as well as by environmental constraints. In such cases artificial ground freezing is an alternative. The potential problems of this method are associated with surface heaves (due to the expansion of the frozen soil) or settlements (due to the consolidation in the thawing phase). Furthermore, high groundwater seepage velocities may prevent the closure of the freezing body. Systematic experimental investigations hardly exist for these topics. Jessberger (1996) outlines for the development of the freezing body a critical velocity for seepage flow of more than 2 m/d. Based on Darcy's law and thermodynamic considerations, Sanger & Sayles (1979) developed an equation for the critical seepage flow, which is useful for preliminary design.

In order to evaluate the above-mentioned problems from case to case and to plan appropriate measures, the temperature distribution of flowing groundwater as well as the deformations of the ground over time have to be known. With the aim of being able to plan this construction method for the threshold cases more safely and thus more economically, numerical 3D models that can simulate thermal and hydraulic (TH model) processes as well as the mechanical ones coupled to them (THM model) on the basis of the FE-method were implemented. In the present contribution the TH model and its experimental verification is described. With this model it is possible to simulate the distribution of the temperature in the frozen body, the required freezing-time and the energy demand. The creep behaviour of frozen soil is not part of our research, since other authors are investigating this (Cudmani 2006, Orth 1986).

2 MATHEMATICAL MODEL

The time-dependent temperature distribution of the soil in flowing groundwater during the application of the ground freezing method may be prognosticated realistically only by means of thermo-hydraulic models (TH-model). An overview of the state of the art of numerical models for the ground freezing method taking into account seepage flow and frost heaves is shown in Sres et al. (2006). At the present the known models have been developed for simulations in 2D only and are, thus, not suitable for the modeling of complex geometries and soil stratification. Thus, when planning this construction method for the threshold cases, the uncertainties associated with not having an adequate model have to be compensated by costly over-dimensioning of the freezing operation (refrigeration capacity, number of the freezing pipes) as well as by additional auxiliary measures such as grouting or ground densification.

In a first stage of the ongoing research project a TH-model in 3D was formulated. Here, a temperature field T and a piezometric height H were coupled. This is defined as:

$$H = \frac{p}{\rho^w g} + z \tag{1}$$

where p is the pore water pressure, p^w the water density, g the gravity acceleration and z the geodetic height. The field temperature is governed by the equation of heat transport:

$$C^s \dot{T} - \partial_k(\lambda \partial_k T) + C^w v_k \partial_k T = 0 \tag{2}$$

where λ is the thermal conductivity, C^w the volumetric heat capacity of the water and C^s the so-called effective heat capacity of the saturated soil. C^s includes the latent heat that occurs during phase change. Darcy's law gives the velocity v^k

$$v_k = -k \cdot \partial_k H \tag{3}$$

where k denotes the hydraulic conductivity. The velocity field fulfils the equation of continuity, which for a quasi steady-state seepage process is reduced to

$$\partial_k v_k = 0 \tag{4}$$

The equation 4 of continuity and the equation 2 of heat transport are coupled by the Darcy velocity v_k and the temperature dependency of the hydraulic conductivity k.

The equations 1 and 2 are solved numerically by the FE-method in a given 3D domain. With the increasing size of the model, 3D calculations rapidly consume more memory and computing time. Therefore for the numerical implementation special attention was paid to simple and efficient algorithms. The spatial discretization is accomplished by means of the Garlekin method. Integration over time is managed by a single-step, non-iterative backward Euler scheme (Reddy & Gartling 2001). In order to save computer memory space, the fields H and T are calculated one after another in each time-step, namely each with the actual value of the other. Furthermore and in order to increase computational efficiency isoparametric hexahedral elements with biquadratic shape functions were chosen. Since all elements have the same shape but different dimensions, the Jacobi matrix and its determinant become very simple, depending thus only on the side length of a cube.

3 EXPERIMENTAL TESTS

The verification of the numerical model was carried out in a multi-stage approach on the basis of laboratory tests results. In the literature, there is a lack of well-documented tests with seepage flow. Only the experiments of Beggren (1979) are well documented and allow some verification calculations.

In the first stage, the Beggren-tests have been numerically modeled. The TH-model shows a good agreement with the measurements (Sres et al. 2006). Nevertheless, the apparatus of Beggren showed some restrictions on comprehensive verification, e.g. small dimensions ($H \times L \times W = 0.5 \times 0.5 \times 1.3\,m^3$), low hydraulic gradients ($i < 0.1$ m/m) and seepage velocities ($v < 1$ m/d). A new testing program was therefore developed, consisting of an element test without seepage flow and a large-scale laboratory test with seepage flow. The element test is composed of a cooling system, a barrel with a diameter of 0.5 m and thermal isolation. The test and the verification results are described in Pimentel et al. (2006). The calculations showed a very good agreement with the measurements. Later, the large-scale laboratory test with seepage flow will be described.

The laboratory model includes a watertight box with effective dimensions $H \times L \times W = 1.2 \times 1.3 \times 1.0\ m^3$ (Figure 1), assembled from 2 cm thick PVC plates. The dimensions and components of the model have been designed so as to achieve a large degree of flexibility in defining the test conditions and for obtaining comprehensive information on soil behavior. Depending on the boundary conditions, the position and alignment of a row with three frozen pipes can be varied. For the verification of the TH-model a vertical alignment of the pipes has been chosen. In the next stage of the laboratory test program, i.e. tests for the verification of the THM-model, a horizontal alignment of the pipes is intended in order to simulate the formation of ice lenses and the associated soil deformations.

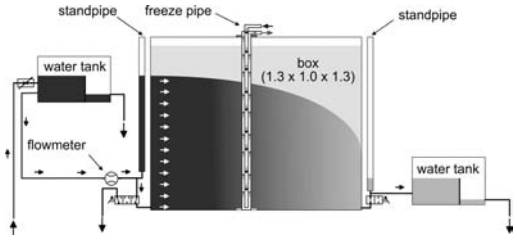


Figure 1. Plan of the large-scale laboratory model.

The freezing pipes consist a PVC down pipe with an inner diameter of 21 mm and a copper pipe with an outer diameter of 41 mm. The head and foot of the frozen pipe is made from PVC. The brine hoses were insulated with neoprene.

The box has an all-around thermal insulation of at least 18 cm of foam. The box was placed on a layer pallet and a layer of wood beams with a total thickness of 36 cm. All the spaces in the pallets and beams were filled with foam. The tests are performed in an air-conditioned room with a constant temperature. Using the insulation described above, it was possible to achieve controlled thermal boundary conditions.

In order to simulate ground freezing with seepage flow the box has a water inlet and outlet at the bottom of the two frontal faces. They were connected to water tanks with spill (Figure 1). Standpipes control the hydraulic gradient. The amount of water, which inflows the model is being recorded over time with a flow meter.

The cooling system consists of an electronically controlled cooling machine with an electrical power of 1.6 kW. The cooling machine and the other components were designed for a temperature range down to $-30°C$. The cooling liquid used is brine (water: glycol 1:1). The temperature at the inlet and outlet of the machine is being electronically registered as well as the amount of cooling liquid pumped through the system.

The monitoring of the tests includes sensors distributed in the model for measurement of temperature and pore water pressure, i.e. 40 temperature sensors PT100 and 8 miniature tensiometers (Figure 2 and 3). The data logging was done with a conventional PC (Figure 4).

Several tests with different seepage flow velocities were performed. The average flow velocity measured at the location of the frozen pipe was varied between $v = 0$ and $v = 3$ m/d. By each test the water tanks were positioned at a given level. After having achieved stationary conditions all over, i.e. no changes over time of the water table and temperature in the model, the cooling phase was started. The cooling phase was stopped either when the frozen body closed (no seepage flow) or when approximately steady state conditions were achieved (no drop of temperature in the model). The experimental results are presented later in Section 5, together with the results of the respective computer simulations.



Figure 2. Top view of empty box with freeze pipes and sensors.



Figure 3. Top view of half-full box with freeze pipes and temperature sensors along the measuring line 1 (parallel to tape measure) and line 2 (between freeze pipes).

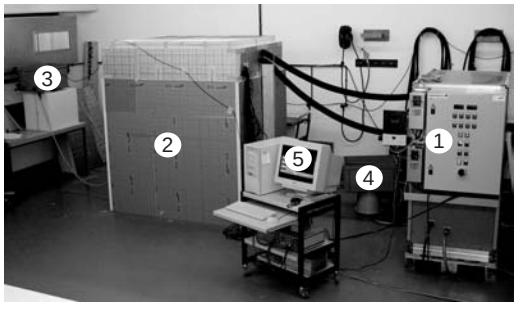


Figure 4. General view of the laboratory model (1 cooling machine, 2 box with thermal insulation, 3 and 4 water tanks and 5 data logging system).

Table 1. Geotechnical parameters.

γ_s [kN/m^3]	$\gamma = \gamma_d$ [kN/m^3]	n [%]	e [−]	k* [m/s]	k/ρ^{w*} [m^{2}s/Pa]
26.13	15.52	40.60	0.683	10^{-4}	2.45×10^{-8}

* for T = 15°C.

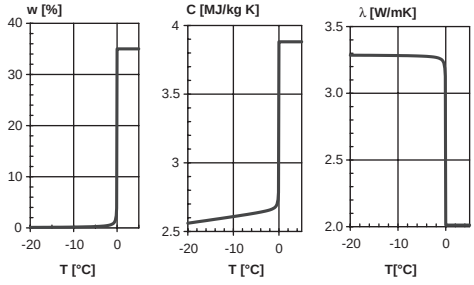


Figure 5. Thermodynamic parameters against temperature. From left to right: water content, heat capacity and heat conductivity.

4 MATERIAL PARAMETERS

For the laboratory tests a medium sand with maximum grain size of $D_{max} = 1$ mm was used. The hydraulic conductivity was determined with a big permeameter and the specific weight with a pyknometer. The box was filled with dry sand in layers of 10 cm. The filled material was weighted continuously and each layer was compacted locally by hand, so that the density of the sand in the box could be calculated. In Table 1 the geotechnical parameters were listed.

The thermodynamic parameters were also determined experimentally. The specific heat of the sand was determined calorimetrically. For the other parameters in addition to temperature sensors, a Time-Domain-Reflectometer (TDR) system for measuring the water content, a Non-Steady-State-Probe sensor for measuring the heat conductivity and an environmental chamber were used. The chamber has effective dimensions of $H \times L \times W = 0.25 \times 0.25 \times 1.0\,m^3$. The temperature is controlled by a thermostat down to −30°C. Dry sand was filled in a watertight PVC cylinder with a diameter of 150 mm and a height of 450 mm. After positioning the above-mentioned sensors in the sample this was saturated and placed in the chamber. The temperature in the chamber was dropped gradually until the whole pore water was frozen. In Figure 5 the temperature dependence of the thermodynamic parameters is shown. The heat conductivity was calculated using the equation of Johansen & Frivik (1980).

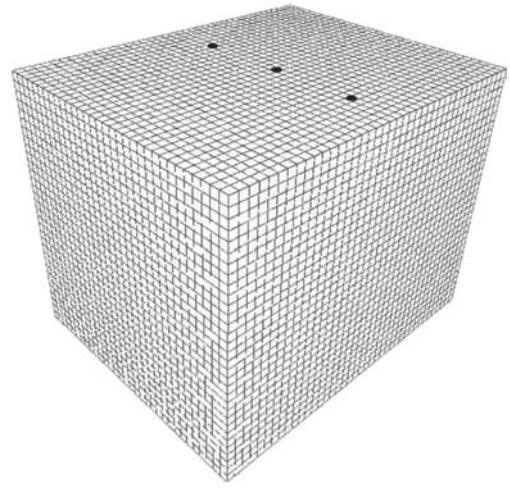


Figure 6. Perspective view of the FE mesh. The three dark elements in the center represent the freeze pipes.

Table 2. Closing time of the frozen body.

Test	v [m/d]	t_c_{bottom} [h]	t_c_{middle} [h]	t_c_{top} [h]
v0	0	11.50	12.54	15.08
v1	1	39.92	44.27	73.02
v2	2	–	–	–

5 NUMERICAL SIMULATIONS

Figure 6 shows the 3D mesh. As mentioned above isoparametric hexahedral elements were used. The laboratory test was modeled with $H \times L \times W = 32 \times 40 \times 32 = 40{,}960$ elements.

Three selected laboratory tests were calculated, namely for the conditions without water flow (v = 0), with high flow velocity but with a closed frozen body (v = 1 m/d) and with excessively high flow velocity, i.e. no closed frozen body (v = 2 m/d). The closing times of the frozen body at the bottom, middle and top of the water table are listed in Table 2.

The measurements (points) and their respective calculations (lines) along two lines located on a horizontal plane at half of the height of the model are shown in the Figures 8 to 13. Line 1 runs from the center of the frontal plate (inlet) to the center of the back plate (outlet) and line 2 runs perpendicular to this from the freeze pipe in the middle to the center of the side plate on the right (Figure 7 and 3).

The measurements of the test v0 shows, as expected, a symmetrical temperature distribution along line 1 and between the freeze pipes in line 2. This symmetrical distribution could also be observed during the tests

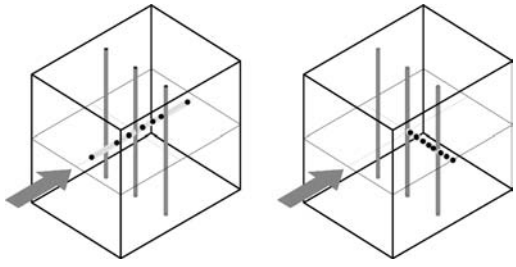


Figure 7. Line 1 (left) and 2 (right) of measurements.

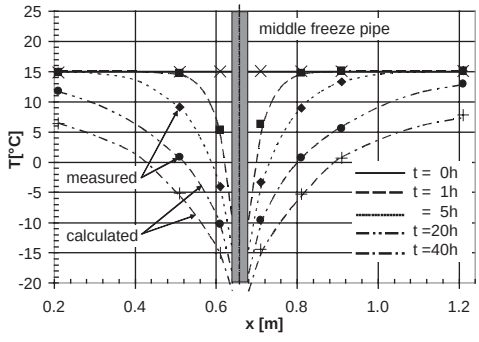


Figure 8. Measurements and calculations. Test v0 – line 1.

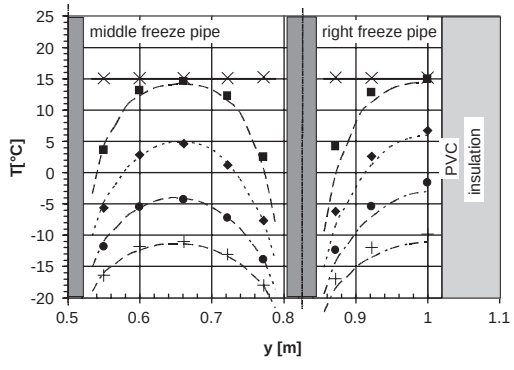


Figure 9. Measurements and calculations. Test v0 – line 2.

with seepage flow along line 2. The distribution along line 1 for these cases is plausible, since the water in the inlet is warmer than in the outlet due to the cooling work of the pipe. These measurements provide evidence of the high quality of the laboratory tests. Their results are therefore appropriate for verification purposes.

The calculated values show a very good agreement with the measurements all over, including the cases with high seepage flow velocities.

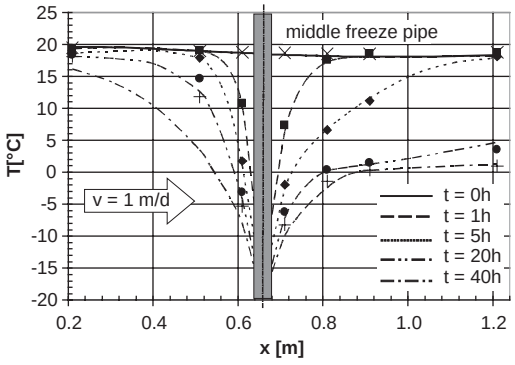


Figure 10. Measurements and calculations. Test v1 – line 1.

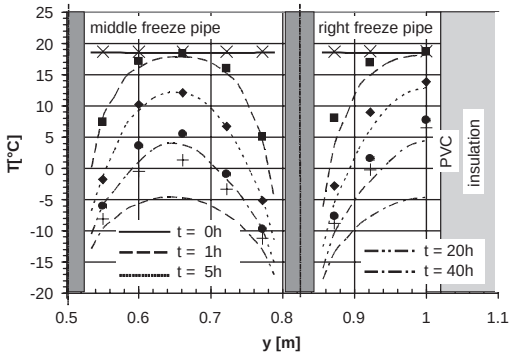


Figure 11. Measurements and calculations. Test v1 – line 2.

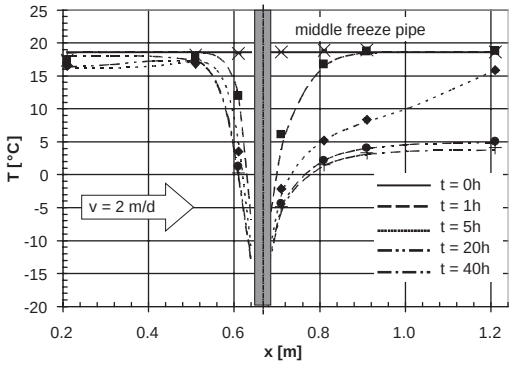


Figure 12. Measurements and calculations. Test v2 – line 1.

6 CONCLUSIONS

A new TH-model in 3D with optimized algorithm has been successfully implemented. The verification of the model on the basis of external tests published in the literature and particularly on the basis of our own large scale tests covering a wide range of seepage

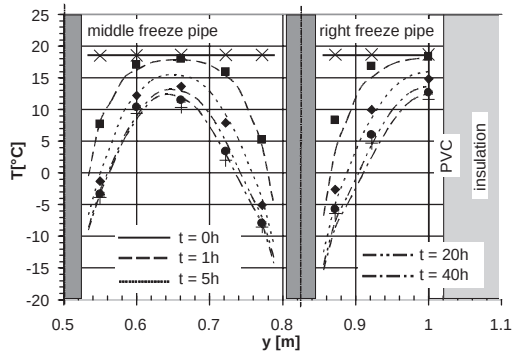


Figure 13. Measurements and calculations. Test v2 – line 2.

flow conditions shows a very good agreement with the measurements. The large-scale laboratory model conceived and constructed has shown itself to be adequate for the purposes of verifying tests involving complex boundary conditions.

Our research work includes the following additional tasks:

- analysis and variation of relevant design parameters for the ground freezing method with seepage flow
- enhancement of the model with a coupled mechanical component (THM-model) in order to simulate the formation of ice lenses
- element tests with ice lense formation
- numerical simulation of the element tests
- large scale test with ice lense formation
- numerical simulation of the large scale test
- analysis and variation of relevant design parameters for the ground freezing method in grounds susceptible to ice lense formation

REFERENCES

Berggren, A. 1979. Artificial Freezing of Seepage Flow (B.Sc. thesis in Norwegian). *Division of Refrigeration Engineering NTH.* Trondheim

Cudmani, R. 2006. An elastic-viscoplastic model for frozen soils.*Proc. Numerical Modelling of Construction Processes in Geotechnical Engineering for Urban Environment, 177–184.*

Jessberger, H.L. 1996. *Grundbau Taschenbuch.* Berlin: Ernst & Sohn, Verlag für Architektur und techn. Wiss.

Johansen, O. & Frivik, P. E. 1980. Thermal Properties of Soils and Rock Materials. *Proc. 2nd International Symposium on Ground Freezing. NTH*. Trondheim

Korvink, J.G. 1993. An implementation of the adaptive finite element method for semiconductor sensor simulation (PhD Thesis). *Institute of Structural Engineering ETH.* Zurich.

Orth, W. 1986. Gefrorener Sand als Werkstoff (PhD Thesis). Karlsruhe: Veröffentlichungen des Institutes für Bodenmechanik und Felsmechanik der Universität Fridericiana in Karlsruhe.

Pimentel, E., Sres, A. & Anagnostou, G. 2006. Numerische FE Simulation in 3D der Frostkörperbildung und Frosthebung beim Gefrierverfahren und der Vergleich zu experimentellen Labormessungen. *Proc. 29. Baugrundtagung Bremen.* Essen: Verlag Glückauf.

Reddy, J.N. & Gartling, D.K. 2001. The Finite Element method. *In Heat Transfer and Fluid Dynamics, second Edition.* Boca Raton (USA): CRC Press LLC.

Sanger, F. J. & Sayles F. H. 1979. Thermal and rheological computations for artificially frozen ground construction. *Ground Freezing developments in geotechnical engineering, Eng. Geol. 13, vol. 26*, Amsterdam: Elsevier.

Sres, A., Pimentel, E. & Anagnostou, G. 2006. Numerical and physical modeling of artificial ground freezing. *Proc. Numerical Modelling of Construction Processes in Geotechnical Engineering for Urban Environment, 185–191.*

Underground Space – the 4th Dimension of Metropolises – Barták, Hrdina, Romancov & Zlámal (eds)
© 2007 Taylor & Francis Group, London, ISBN 978-0-415-40807-3

Performance evaluation of ground improvement by electrical resistivity tomography

T. Shimizu, K. Narumoto & S. Ebisu
Okumura Corporation, Technical Research Institute, Tsukuba City, Ibaraki Prefecture, Japan

ABSTRACT: Electrical resistivity tomography was carried out in order to identify the chemical grouting range in ground improvement. Experiments were conducted on imitated ground and imitated improved ground prepared using sand and mortar, respectively. The results confirmed that it was possible to accurately grasp the range for imitated improved ground by designing the appropriate electrode array.

1 INTRODUCTION

The procedures for initial excavation in general shield tunneling are as follows: 1: Seepage control work and ground reinforcement around the starting shaft, as shown in Figure 1, are carried out using ground improvement methods such as chemical grouting; 2: Improved ground of the excavation part is exposed; and 3: Shield propulsion starts.

Moreover, an impervious zone is constructed at the face in cases where diluvium soil below groundwater level is excavated by mountain tunneling method without lowering the groundwater level. Similar seepage control work and ground reinforcement methods are used when constructing a tunnel in soft ground in urban areas. However, in actual practice, the thickness of the improved ground layer is designed on the safe side, since the technique for accurately predicting and evaluating improvement performance is not yet sufficiently established. Therefore, it is expected that the technique will enable accurate evaluation of the impervious performance of improved ground for enhanced reliability and cost reduction in tunnel construction.

We applied multiple geophysical exploration such as electrical resistivity tomography, acoustic tomography, and ground temperature distribution measurement for the purpose of accurately visualizing the imitated improved ground and detecting artificially generated water leakage for wall-like imitated improved ground prepared in the imitated ground. This paper reports the results of examining the applicability of electrical resistivity tomography applied in order to specify the shape of the improvement range.

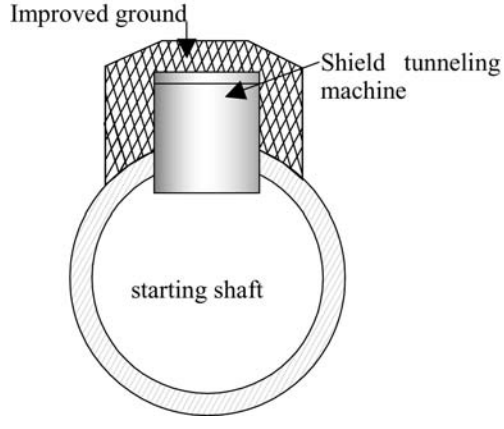


Figure 1. Ground improvement around the starting shaft in shield tunneling method.

2 OUTLINE OF THE EXPERIMENT

2.1 *Specifications for the imitated improved ground*

The imitated improved ground used in the experiments was composed of 20 cm-thick mortar and was constructed so as to bisect the excavation in the east-west direction. First, a 9.5 m area around the excavation was dug to a 2.5 m depth as shown in Figure 2. An impervious rubber sheet was laid between the peripheral ground and imitated ground in order to cut off any effects from the peripheral ground and to easily control the groundwater level in the imitated ground. River sand was used to fill the area on both sides of

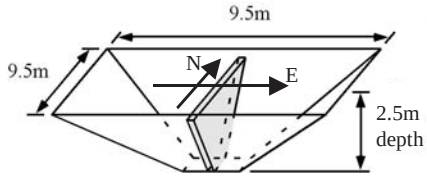


Figure 2. Schema of imitated ground and imitated improved ground.

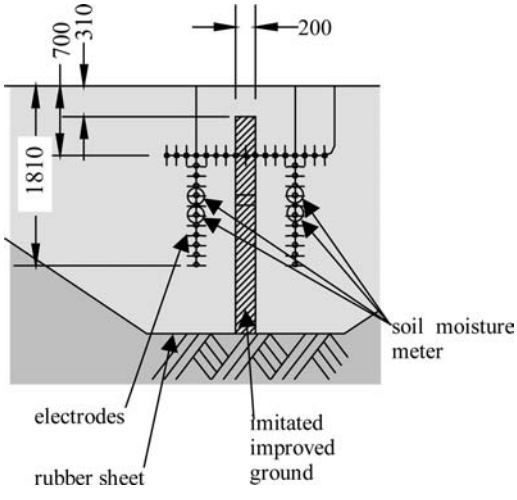


Figure 3. Position of electrodes and surrounding conditions.

the imitated improved ground, and with equal pressure. The resistivity of the mortar was 26.2 Ωm and that of the river sand in a saturation state was about 70 Ωm. For the groundwater conditions, multiple cases were created. For example, the water level of both sides was changed, and water leakage was intentionally generated by drilling the imitated improved ground.

2.2 *Measurement*

The electrodes used for measuring resistivity were placed at 10 cm intervals, forming a 'π' in left-right symmetry, around the imitated improved ground, as shown in Figure 3. Sensitivity seemed to improve by placing electrodes at all four corners of the rectangle as the exploration object within the three boundaries of the π. However, considering that such an arrangement would be difficult in practical use, the above-mentioned arrangement was used. Since contact resistance is lowered, a copper disk with 10 cm outer diameter and 3.2 cm inner diameter was used for the electrode. Each electrode was connected by polyvinyl chloride pipe.

It was difficult to establish an infinite electrode because it was measured in a closed region electrically isolated by the impervious sheet for the peripheral ground. Therefore, the four-electrode method was used in the measurement.

3 COMPARISON OF THE ELECTRODE ARRAY PATTERN

3.1 *Electrode array*

The two-dimensional electrical resistivity method, which is nearly established, seems to obtain inversion analysis results for resolution corresponding to the quantity of data, if the data has been acquired in the correct manner. However, it is important to accurately grasp the position of the boundary in the improved and unimproved area in order to estimate the improvement range from the resistivity distribution. Therefore, resolution beyond the conventional electrical resistivity method is necessary. Since the resolution is closely related to the stability of the inversion analysis solution, it is important to examine the boundary-value problem described next in order to stabilize the solution of the inversion analysis (Wang 2003).

i. Stability and uniqueness of the inversion analysis solution are improved if the survey point is placed within the boundary surrounding the region to be investigated, if possible, even if not all data space is proven.
ii. The best possible estimation is given for a boundary where data is lacking, using all known information, when above survey point placing cannot be achieved.
iii. Useless estimated calculation is not carried out for subspace of the model, which cannot be controlled in known data.

In this study, the arrangement of the survey point described in i was observed; that is, the selection of the electrode array was examined, and efforts were made to enhance the estimation accuracy of the improvement range. The basic pattern (a, b, c, d, e) of the electrode array applied in this study is shown in Figure 4.

Pattern-a was created by combining a Wenner electrode array with a dipole-dipole array. Pattern-b was devised by predicting that a clear image of the improved ground would be obtained by putting the imitated improved ground between two current electrodes. Pattern-c was thinned out from all available combinations except for Pattern-a and Pattern-b. Pattern-d and -e were made similar to a two-electrode array by fixing the positions of one current electrode and potential electrode as shown in Figure 4, and applying the other current electrode and potential electrode to all combinations considered.

3.2 *Quantitative evaluation of the tomogram*

Quantitative evaluation was performed on the tomogram obtained from measured data using the inverse

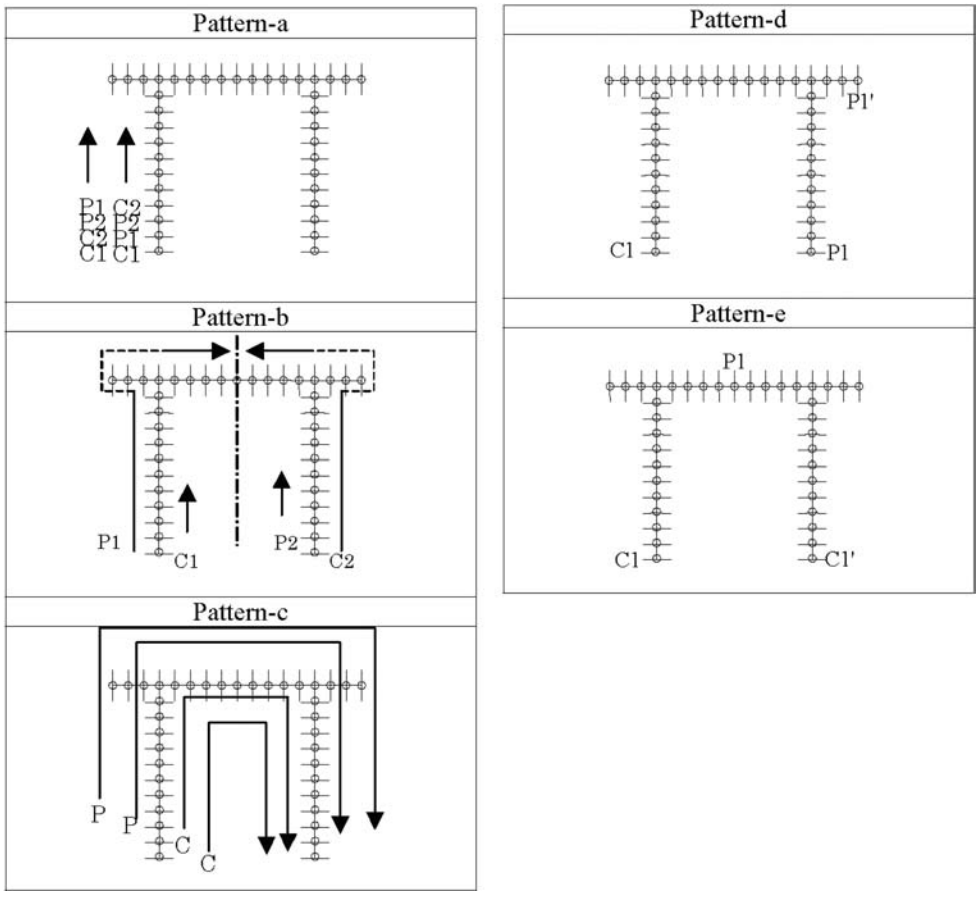


Figure 4. Basic pattern of the electrode array. C1, C2: Current electrode. P1, P2: Potential electrode. Pattern-a: Combining Wenner electrode array with dipole-dipole array. Pattern-b: C1 and P1 were selected from only the left side, and C2 and P2 were selected from only the right side. Pattern-c: Electrode array thinned out from all available combinations except for Pattern-a and -b. Pattern-d: C1 and P1 (or P1') were fixed at electrodes shown in the figure. C2 and P2 were selected from the remainder. Pattern-e: C1 (or C1') and P1 were fixed at electrodes shown in the figure. C2 and P2 were selected from the remainder.

analysis method. In this study, resistivity distribution based on known information is assumed for the true model, because the position of the boundary and the resistivity of sand and mortar are known. Then, the degree of difference between the true model and the tomogram was used as an index for the evaluation. That is, the least mean squared error (*LMS*) was calculated using the following equations. The objective range is one surrounded by three measurement lines of electrodes.

$$LMS = \sum_i \varepsilon_i^2 \tag{1}$$

$$\varepsilon_i = y - y' \tag{2}$$

$$y = \frac{Y - Y_{ave}}{\sigma_Y} \tag{3}$$

$$y' = \frac{Y' - Y'_{ave}}{\sigma_{Y'}} \tag{4}$$

where Y = resistivity of true model; Y_{ave} = average of Y; σ_Y = standard deviation of Y; Y' = resistivity calculated by inversion; Y'_{ave} = average of Y'; $\sigma_{Y'}$ = standard deviation of Y'.

The effect of the exception value (noise) was strongly received, as the *LMS* increased linearly in the inversion analysis results separate from the true model. On the other hand, the *LMS* can catch sharply even slight signal in the inversion analysis results obtained from data with low noise. Then, it is considered that the

Table 1. Combinations of basic study patterns.

Pattern No.	Basic pattern a	b	c	d	e
A	o	–	–	–	–
B	–	o	–	–	–
C	–	–	o	–	–
D	–	–	–	o	–
E	–	–	–	–	o
F	–	–	–	o	o
G	o	o	–	–	–
H	o	–	o	–	–
I	o	–	–	o	–
J	o	–	–	–	o
K	o	–	–	o	o
L	–	o	o	–	–
M	–	o	–	o	–
N	–	o	–	–	o
O	–	o	–	o	o
P	–	–	o	o	–
Q	–	–	o	–	o
R	–	–	o	o	o
S	o	o	–	o	–
T	o	o	–	–	o
U	o	o	–	o	o

o: use, –: not use.

electrode layout pattern with smaller *LMS* has better performance to specify the shape of the improvement range in this study.

Still, the observed resistivity of sand and mortar for the true model was 73 Ωm and 26.2 Ωm, respectively. The finite element method was utilized in forward analysis, and the constrained least squares method was used in inversion analysis. In the inversion analysis, the convolution in which a minimum residual is reached in 20 times iterations was adopted. Because it was predicted that 20 times iterations were sufficient to reach minimum residual empirically.

3.3 *Patterns to compare the perfomance of electrode array pattern*

In measuring the resistivity, 21 composite electrode array patterns, as shown in Table 1, which combined the above-mentioned 5 basic patterns, were used to examine the estimation accuracy. And, considering its potential importance as a parameter affecting the performance evaluation of the electrode array, the constraint of inversion analysis was also parametrically examined. Examination was conducted on the 9 patterns of constraint shown at Table 2, making a sum total of 189 cases. These are all combinations able to examine within limitation of the computer soft for inversion calculation.

Still, this paper reports the results of examination at a groundwater level of 40 cm beneath the surface on both sides of the imitated improved ground.

Table 2. Constraint of inversion analysis.

No.	Constraint	Horizontal continuity*
1	A	–
2	B	0.0
3	B	0.5
4	C	0.0
5	C	0.5
6	D	0.0
7	D	0.5
8	E	0.0
9	E	0.5

* Degree of continuity in horizontal direction.
A : Initial model is not significantly different.
B : Minimize the difference between resistivity of neighboring elements.
C : Minimize the curvature of resistivity distribution.
D : Minimize the difference between resistivity modification of neighboring elements.
E : Minimize the curvature of distribution of resistivity modification.

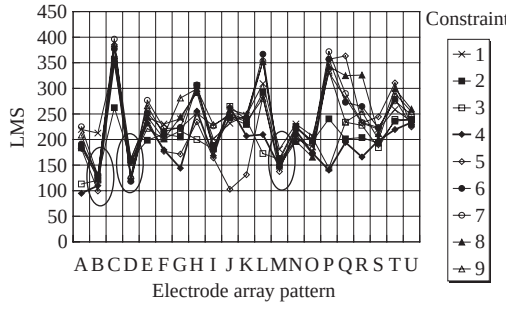


Figure 5. Value of *LMS* in each case.

3.4 *Results of the examination*

The *LMS* of each case is shown in Figure 5. The *LMS* seems to be more dependent on the electrode array than on the constraint, because all plot lines in each constraint gather together. The value is small for the *LMS* of pattern B, D, and M (= B + D) in most constraints. The *LMS* of pattern A is also small only in the case of constraint 4 and 5. Tomograms of case B5, in which the *LMS* is small, and of case E4, in which the *LMS* is medium, are shown in Figures 6 & 7 as examples. Two length lines in the center of the figure show the width of the imitated improved ground. The form of π shows the line of electrodes. The *LMS* of cases B5 and E4 are 99 and 232, respectively. The shape of the imitated improved ground is clearly recognized in Figure 6, but not in Figure 7. From these results, it was proven that the *LMS* could be used as an index for the accuracy of the tomogram, because the shape of the

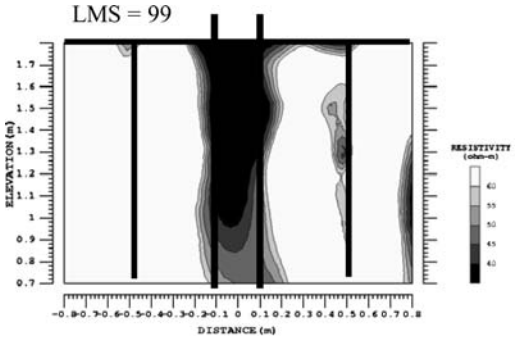


Figure 6. Tomogram for case B5.

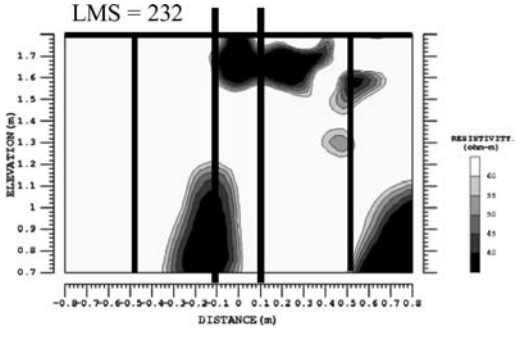


Figure 7. Tomogram for case E4.

imitated improved ground was accurately recognized, as the *LMS* is smaller.

Pattern B, in which the *LMS* is averagely small, is distinguished by the many arrangements for the position where current electrodes and potential electrodes respectively hold the imitated improved ground. Moreover, it is also a characteristic of pattern B that there are many measurement frequencies compared to the other pattern in the lower half of the π form in which the measurement density is low. The cause-and-effect relationship has not yet been clarified. The accuracy should have improved with the increase of information. However, the results were not good for the combined patterns used in this study.

On the other hand, Wenner Method or Dipole-Dipole Method, which are contained in Pattern-a, are usually used in four-electrode resistivity tomography as standard method. But the *LMS* of them takes not only small value but also medium value, though the LMS of Pattern-b mostly takes small value.

4 APPLICABILITY IN DIFFERENT MEASUREMENT CONDITIONS

The examination described in the previous chapter revealed which electrode array pattern should be selected to accurately visualize the imitated improved ground in the disposition of measurement line in this study. This chapter presents the results of inversion analysis based on data measured adopting the electrode array pattern of case B5 and changing the measurement conditions to ground water conditions.

Table 3. Measurement conditions.

	Imitated water-leaking holes	Ground water conditions
Stage 1	not exist	Saturated on both sides
Stage 2	not exist	E*: saturated; W*: unsaturated
Stage 3	exist	E*: saturated; W*: unsaturated

* E: east side W: west side.

Table 3 shows the measurement conditions. At first, the ground on both sides was saturated up to the ground surface by injecting water (Stage 1). This stage is the same as in the examination of electrode array patterns. After that, the water level on the west side (left side on paper) was lowered to the level at the lower end of the imitated ground by pumping up ground water. In other words, the ground on the east side was saturated, and that on the west side unsaturated (Stage 2). The imitated improved ground was sound up to this point.

Next, holes forming a horizontal line were made in the imitated improved ground at 250 mm intervals and at half its depth. This imitated the condition of water leakage. The same ground water conditions as in Stage 2 were created by pumping up ground water on the west side (Stage 3). The difference in water head between the two sides caused a steady water leak in Stage 3, which was maintained by pumping the water leaking from the west side and returning it to the east side.

The ground water conditions and the tomogram of the electrical resistivity at each stage are shown in Figures. 8–10. The form that is taller than broad in the figure for the ground water conditions shows the imitated improved ground, and the π form shows the line of electrodes. The tomogram is enlarged to show the resistivity distribution in and around it

The tomogram of the electrical resistivity at every stage shows the shape of the imitated improved ground clearly. The change in ground water conditions is also reflected to a certain degree. That is to say, while the resistivity of the ground on both sides ranges from 60 to 100 Ωm in Stage 1, the resistivity on the west side ranges from 140 to 290 Ωm for the most part in Stage 2. This reflects the increase in resistivity due to the decrease in water content by volume after pumping up the ground water on the west side.

In this experiment, soil moisture meters were buried at the locations shown in Figure 3 in order to grasp the water content by volume, automatically taking measurements once every hour. According to the results,

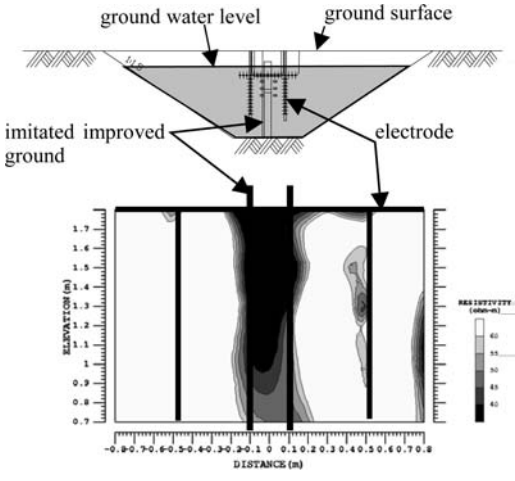


Figure 8. Ground water conditions and tomogram of electrical resistivity in Stage 1.

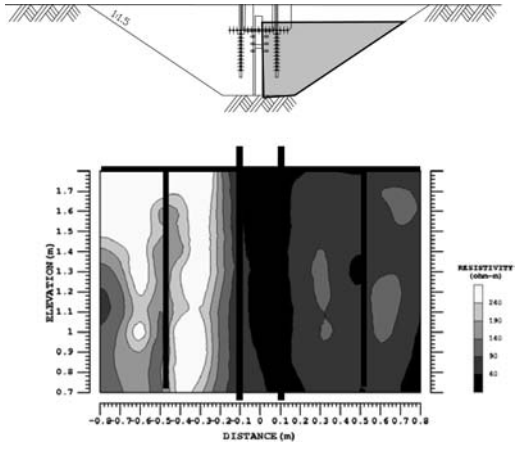


Figure 9. Ground water conditions and tomogram of electrical resistivity in Stage 2.

the change in water content by volume on both sides ranged from 46 to 50% in Stage 1. In Stage 2, the change ranged from 13 to 15% on the west side, and from 47 to 50% on the east side.

On the other hand, the relationship between the water content by volume and the resistivity was examined for the sand used for the imitated ground by a laboratory test. Figure 11 shows the relationship between the water content by volume and the electrical conductivity, which is a reciprocal of the electrical resistivity. Correlate coefficient between them was 0.998. So they were related with hard linear relationship.

Figure 12 shows the relationship between the water content by volume and the resistivity. When the resistivity shown in the above-mentioned tomogram and

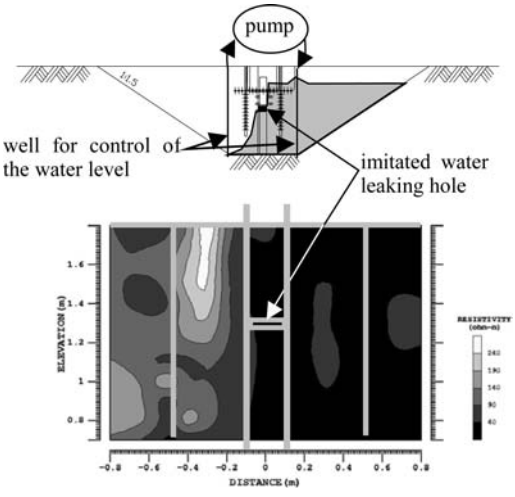


Figure 10. Ground water conditions and tomogram of electrical resistivity in Stage 3.

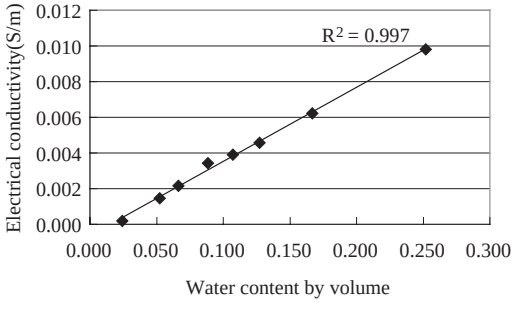


Figure 11. The relation between the water content by volume and the electrical conductivity.

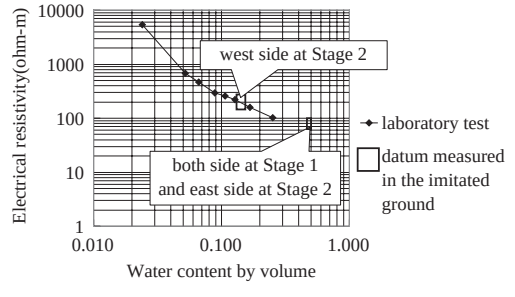


Figure 12. Relationship between water content by volume and resistivity.

the water content by volume measured by the moisture meter are plotted in the figure, the plotted points agree with the relationship or its extrapolation. Therefore, the validity of the absolute value is ascertained.

The resistivity in the lower half area on the west side is somewhat lower in Stage 3 compared to Stage 2. It seems that the condition of water leaking from the imitated holes wet the lower area, reflected by the water leakage caused in Stage 3.

5 CONCLUSIONS

The following conclusions were obtained in this experiment:

i. Pattern-b, the electrode array pattern that emphasized the low, center area where the measurement density is thin, enabled to visualize the shape of the imitated improved ground clearly, and the ground water distribution to a certain degree.
ii. Although the measurement conditions changed using Pattern-b, the imitated improved ground and the change of water table were visualized regardless of the difference in measurement conditions.
iii. From the above, it is considered that an estimate of the range of improved ground by electrical resistivity tomography can be sufficiently practical by Pattern-b.

After this, we would examine reproductiveness of this result besides improvement of accuracy. Moreover, we hope to examine the required technique for detecting water leakage in addition to this method, and suggest a system to detect water leakage for improved ground using a combination of techniques.

REFERENCE

Wang, Z. 2002. On the 3-D Data Interpretation in Resistivity Method Using Numerical Coordinate Transformation. *Thesis for a degree at Waseda University*, Tokyo, Waseda University.

This page intentionally left blank

Underground Space – the 4th Dimension of Metropolises – Barták, Hrdina, Romancov & Zlámal (eds)
© 2007 Taylor & Francis Group, London, ISBN 978-0-415-40807-3

Reinforcing effects around tunnel face by crown & face reinforced

J.H. Shin
Dept of Civil Eng., Konkuk University, Seoul, Korea

S.H. Choi & S.B. Woo
Daewon Soil co., Ltd, Karacbon-dong, Songpa-gu, Seoul, Korea

Y.K. Choi
WIN Consulting, Karacbon-dong, Songpa-gu, Seoul, Korea

ABSTRACT: One of the most popular pre-reinforcement methods of tunnel heading in cohesionless soil would be the fore-polling of grouted pipes. This technique allows safe excavation even in poor ground condition by creating longitudinal arch parallel to the tunnel axis as the tunnel advances. Some previous studies on the reinforcing effects have been performed using numerical methods and/or laboratory-based small scale model tests. The complexity of boundary conditions imposes difficulties in representing the tunneling procedure in laboratory tests and theoretical approaches Full-scale study to identify reinforcing mechanism of the tunnel heading has rarely been carried out. In this study, a large scale model testing for a tunnel in granular soils was performed. Reinforcing patterns considered are non-reinforced, crown-reinforced, and crown & face-reinforced. The behavior of ground and pipes were fully measured as the tunnel advanced. The influence of reinforcing pattern, pipe length, and face reinforcement were investigated in terms of stress and and displacement, It is revealed that the pipe reinforcement of heading increases longitudinal arching sufficiently along the tunnel axis, consequently decrease settlement sufficiently at the heading, and improves the face stability significantly.

1 INTRODUCTION

Generally tunneling in granular soils is performed with the protection of a shield providing to support the excavated perimeter and to, when necessary, support the tunnel face until the initial/final supporting system can be erected. One common and economical alternative for the case would be the pre-reinforcement of tunnel heading. One of the most popular pre-reinforcement methods id the fore-polling of grouted pipes above the tunnel crown. This technique allows safe excavation even in poor ground conditions by developing longitudinal arching parallel to the tunnel axis as the tunnel advances. Lunardi(2000) identified the advantages of heading reinforcement based on field instrumentation. It is clear that the pre-reinforcement reduces plastic strains in the tunnel heading, decreases in lining loads, increases face stability and prevents damages from structures nearby.

The method is initially developed in 1970s(Barisone, 1982; Pelia, 1994) and has been used increasingly with the improvement of grouting equipments. Figure 1 shows arching effect at the tunnel face (Gnilsen, 1989) and design factors. Although some previous studies on the reinforcing effects have been performed, the complexity of boundary conditions imposed difficulties in representing the procedure in laboratories and theory. Therefore, full scale research to identify reinforcing mechanism quantitatively has rarely been carried out. In this study a large scale model testing was performed to evaluate and improve the design method of the heading reinforcement

2 LABORATORY TESTS PREPARATION AND PROCEDURE

The tunnel was excavation in a test tank of which length is 3.6 m long, width is 4.0 m and depth is 3.3 m as shown in Fig 1. Steel structures were used for the frame of the soil tank. The floor and lateral sides and a back-end of the tank were built of reinforced concrete of which thickness is 30 cm. The floor and lateral sides and a back-end of the tank were built of reinforced concrete of which thickness is 30 cm The front wall was made of steel plate with the thickness of 10 mm. Inner sides of the concrete and steel wall were covered with thin clay layer to reduce friction between the soil and the wall. The tunnel was 1.1 m in diameter and 1.0 m in cover depth.

To identify full effect of reinforcement, it would be appropriate to consider all design factors.

Total 8 cases of tests were considered. To explore the effect of reinforcement, firstly an unsupported model was considered, two different pipe lengths were considered to investigate the effect of pipe length and finally the effect of face-reinforcement was examined by modeling face reinforcement with different length of pipes. All Test cases considered are summarized in Table 1.

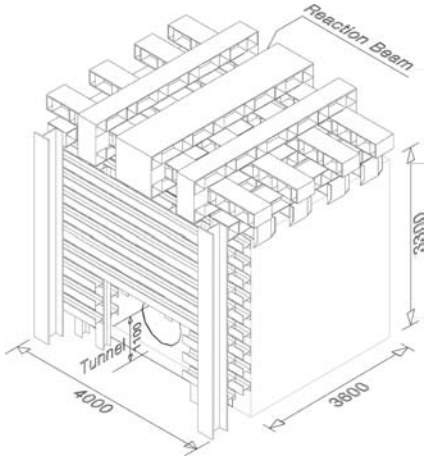


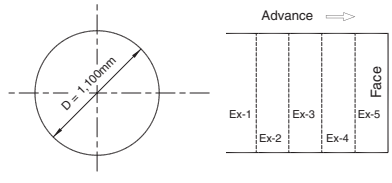
Figure 1. Layout of the model.

2.1 *Model ground*

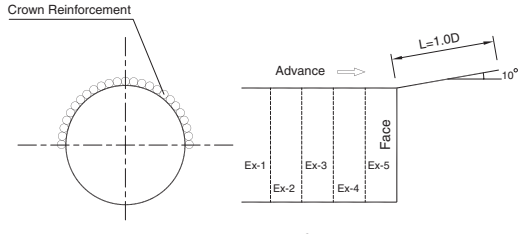
Model ground was prepared by falling sand from a certain height of the tank and compacting it in every 30 cm layer with constant energy. The soil properties are summarized in Table 2.

2.2 *Install pipe and grouting*

Grout pipe with external diameter of 25 mm and thickness of 3 mm were used. Grouting was performed to



(a) Non reinforced (NR)



(b) Crown reinforced (c1.0)

Figure 2. Schematic diagram of the reinforced type (continues).

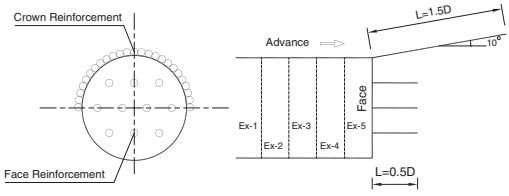
Table 1. List of the model tests.

Reinforced Type	Test Notation	Reinforcement					
		Crown Zone	Face Line	Angle		Length	
				Crown	Face	Crown	Face
Non	NR	–	–	–	–	–	–
Crown	C1.0	180	–	10	–	1.0D	–
	C1.5	180	–	10	–	1.5D	–
Crown	C1.5F0.5	180	3(ea)	10	0	1.5D	0.5D
+	C1.5F1.0	180	3(ea)	10	0	1.5D	1.0D
Face	C1.5F1.5	180	3(ea)	10	0	1.5D	1.5D
Face	F1.0	–	3(ea)	–	0	–	1.0D
	F1.5	–	3(ea)	–	0	–	1.5D

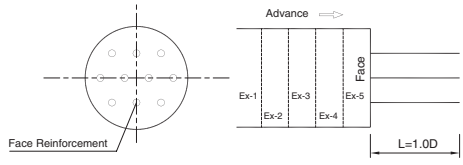
Table 2. Physical properties of testing material.

Unit weight (kN/m^3)	Relative density (%)	Specific gravity	Friction angle (°)	Cohesion (kN/m^2)	Soil classification (USCS)
16.47	56	2.64	38	5.9	SP

determine appropriate grouting pressure and the diameter of the grout. Cement mortar of 200% W/C ratio was used as grout material. At the far-end of pipes, the required diameter of grout was 90 mm which was obtained under the pressure of 1.2 kgf/cm^2. The lining was made of steel plates of which shape is circular shape. Each lining segment has 30 cm in width and is assembled with epoxy resin.



(c) Crown-force reinforced (c1.5F0.5)



(d) Face reinforced (F1.5)

Figure 3. Schematic diagram of the reinforced type.



Figure 4. Strain gage install process.

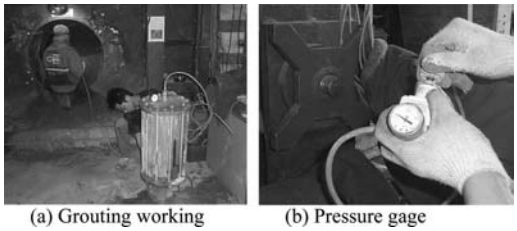


Figure 5. Grouting using pressure apparatus in the FRP pipe.

2.3 *Tunnel excavation*

Model testing was performed sequentially as shown. The lining was made of steel plates of which shape is circular shape. Each lining segment has 30 cm in width and is assembled with epoxy resin as shown in Fig 6.

2.4 *Surcharging*

After completion of excavation to the desired location, surcharge is given to induce sufficient displacement and stress, and failure behavior of tunnel heading is investigated. Surcharge was applied to a stress-controlled boundary at the top of the model ground surface. Surcharge is loaded in six steps;

2.5 *Instrumentation*

To monitor the ground behavior, settlement gages earth pressure cells were pre-installed. Behavior of pipes was also instrumented by measuring axial forces and bending moments in the pipes using strain gages. The

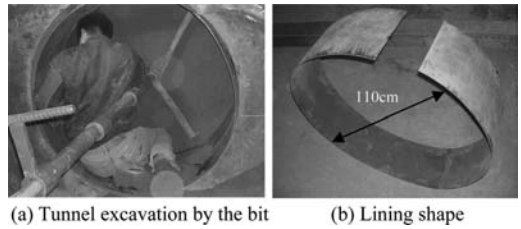


Figure 6. Inserting a steel ring after excavation.



Figure 7. Strain gage attached on the steel bar.

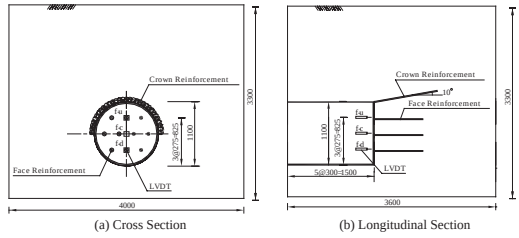


Figure 8. Horizontal displacement instrumentation(LVDT).

horizontal movements of face were measured at three point; crown (f-u), center (f-c) and invert (f-d).

2.6 *Summary of testing procedures*

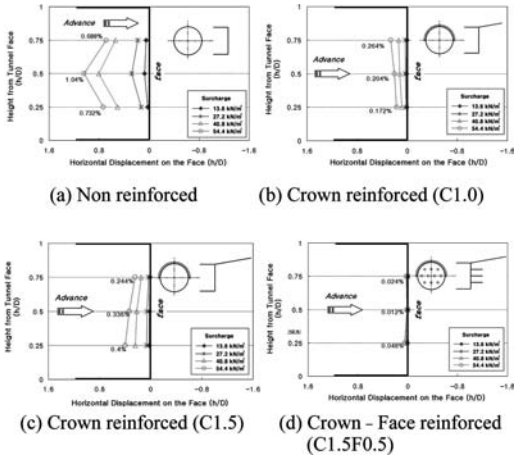
The testing procedures mainly consists of three steps: firstly boreholes are drilled at the tunnel face, then FRP pipes are inserted and finally grouts are injected. The testing procedure is as following:

a) Test ground are prepared by falling sand from the soil tank and relative density of 56%.



(a) Crown reinforced (b) Face reinforced

Figure 9. The umbrella shapes of field model tests.



(a) Non reinforced (b) Crown reinforced (C1.0)

(c) Crown reinforced (C1.5) (d) Crown – Face reinforced (C1.5F0.5)

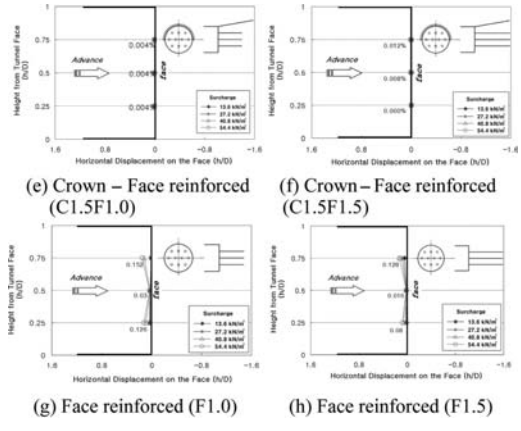
Figure 10. Face displacement due to surcharge (Continue).

b) While preparing model ground, measuring devices are installed at the predetermined locations and connected them to data loggers, and the PVC pipes of 32 mm diameter were pre-installed at the desired locations of FRP pipes.
c) Remove steel plate-tunnel face at the front and excavate a tunnel with a specially devised mechanical excavator.
d) For every excavation of 30 cm, steel plate lining is installed. The excavation process is repeated until the desired location has been reached.
e) After completing excavation, extract the PVC pipes and insert FRP pipes. Grout the pipes with cement milk under the pressure of 1.2 kgf/cm^2.
f) Surcharge is loaded on the surface of model ground.

3 TEST RESULTS

3.1 *Grouted shape of pipes*

Figure 9 presents the grouted pipe arch exposed after testing. The success tests were carried out by the continuous grout formation.



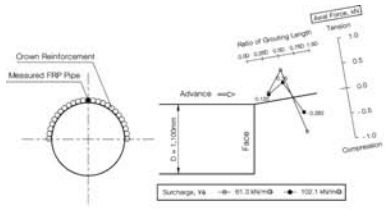
(e) Crown – Face reinforced (C1.5F1.0) (f) Crown – Face reinforced (C1.5F1.5)

(g) Face reinforced (F1.0) (h) Face reinforced (F1.5)

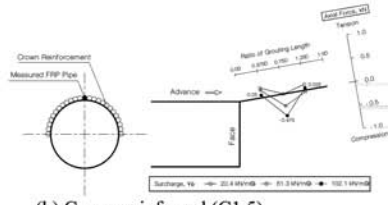
Figure 11. Face displacement due to surcharge.

Table 3. Average horizontal displacement ratio on the face compared to the non-reinforced changing the length of crown reinforcement. (surcharge = 54.52 kN/m^2).

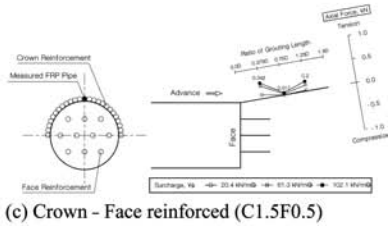
Reinforced type	Test notation	Height from tunnel face (h/D)			Average horizontal displacement ration(%)
		0.75	0.5	0.25	
Crown	C1.0	0.264	0.204	0.172	0.213
	C1.0	0.244	0.336	0.400	0.327
Crown + Face	C1.5F0.5	0.024	0.012	0.048	0.028
	C1.5F1.0	0.040	0.040	0.040	0.040
	C1.5F1.5	0.012	0.012	0.000	0.010
Face	F1.0	0.030	0.030	0.126	0.193
	F1.5	0.128	0.016	0.080	0.075



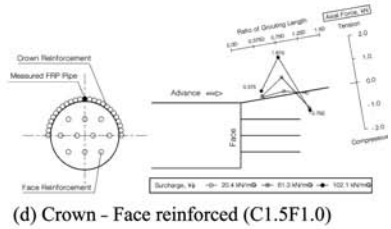
(a) Crown reinforced (C1.0)



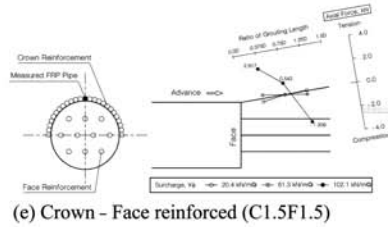
(b) Crown reinforced (C1.5)



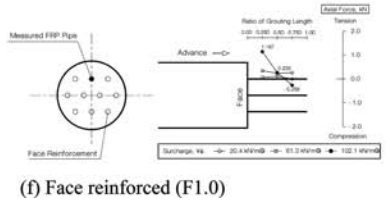
(c) Crown - Face reinforced (C1.5F0.5)



(d) Crown - Face reinforced (C1.5F1.0)

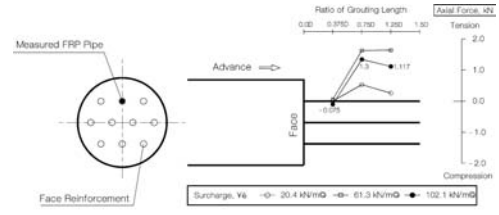


(e) Crown - Face reinforced (C1.5F1.5)



(f) Face reinforced (F1.0)

Figure 12. Comparison of increments of axial force in the FRP pipe due to the surcharge (continues).



(g) Face reinforced (F1.5)

Figure 13. Comparison of increments of axial force in the FRP pipe due to the surcharge.

3.2 *Horizontal displacement shape of the face*

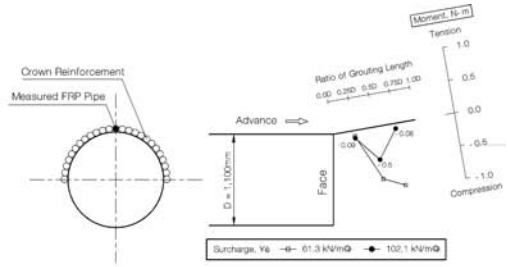
Surcharging after completion of excavation is also useful in investigating the failure mechanism of the face. The influence of face reinforcement on stability can also be investigated by comparing test in Figure 10. The horizontal movement is negligibly small for the test of face reinforcement. The Average Horizontal displacement ratio at tunnel face has decreased from 0.01 to 0.327. Increase in pipe length reduced displacement slightly at the tunnel crown from 0.264 to 0.244(Table 3). It is shown that the face reinforcement, particularly combined with crown reinforcement is considerably beneficial in securing face stability.

3.3 *Behavior of grouted pipes*

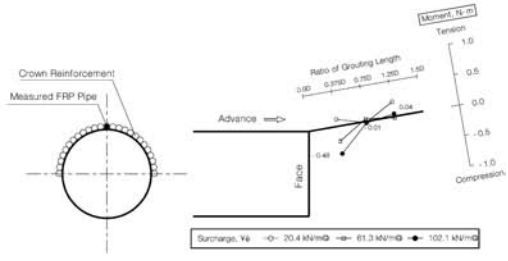
Figures 11 & 12 presents axial forces and bending moments in the grouted-pipes for the tests result. High tension load and bending moments were obtained in the pipes installed at the tunnel crown. The behavior indicates that the deformed shapes for the pipes are downward concave. At initial stage maximum axial loads and bending moments were observed at the middle of pipes. However, the location of maximum loads and bending moments moved towards tunnel face with an increase of sur-charge. Measured results indicate that the grouted-pipes resist effectively against face collapse mechanism which is being developed close to tunnel face. Pipes installed at the face showed less axial forces and moments in comparison with those in the pipes at the crown.

4 CONCLUSIONS

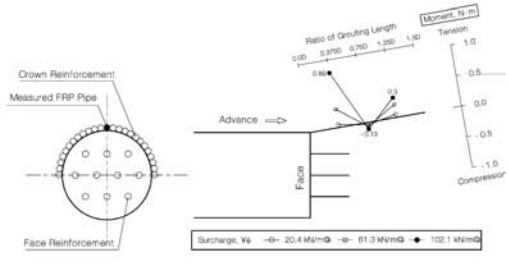
A series of large scale model test were carried out to investigate the behaviour of tunnel heading in granular soils reinforced by pipe grouting. It is revealed that the pipe grouting of heading is an efficient measure in reducing settlement, consequently preventing damages from surface structures



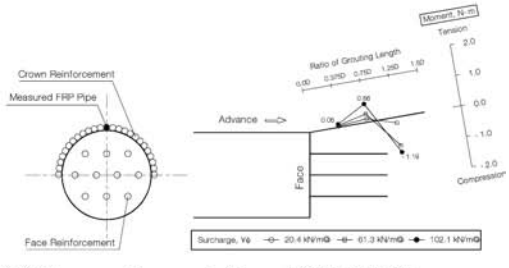
(a) Crown reinforced (C1.0)



(b) Crown reinforced (C1.5)

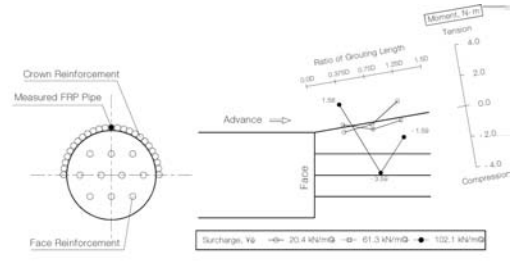


(c) Crown - Face reinforced (C1.5F0.5)

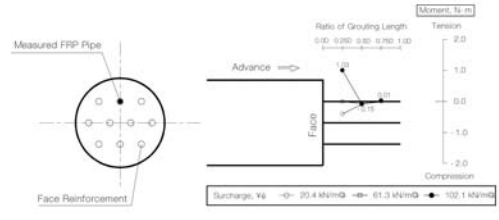


(d) Crown - Face reinforced (C1.5F1.0)

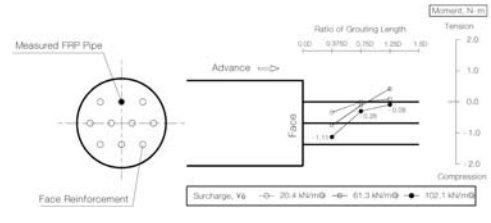
Figure 14. Comparison of bending moment in the FRP pipe due to the surcharge (continues).



(e) Crown - Face reinforced (C1.5F1.5)



(f) Face reinforced (F1.0)



(g) Face reinforced (F1.5)

Figure 15. Comparison of bending moment in the FRP pipe due to the surcharge.

and increasing face stability. Results are summarized below.

(a) surcharge increduce may not be significantly reduced before failure because the straining of pipes is counteracted after considerable sur-charge.

(b) Face reinforcement combined with crown reinforcement improves face stability significantly during excavation. Shorter pipes length can be employed at the face than at the crown.

(c) The grouted-pipes resist effectively against face collapse mechanism.

REFERENCES

Anderson, J. M.(1996), Reducing Risk and Improving Safety with Particular Reference to NATM, *Proc. North American Tunnelling '96*, Balkema, pp. 453–458.

Chambon, P. and Corte, J. F.(1994), Shallow Tunnels in Cohesionless Soil: Stability of Tunnel Face, *Journal of Geotechnical Engineering*, ASCE, Vol. 120, No. 7, pp. 1148–1165.

Gnilsen, R.(1989), Numerical Analysis, *Underground Structures Design and Instrumentation*, Elsevier, Developments in Geotechnical Engineering, 59A, pp. 84–128.

HSE(1996), *Safety of New Austrian Tunnelling Methods (NATM) Tunnels* – A review of sprayed concrete lined tunnels with particular reference to London Clay, Health and Safety Executive, UK, HSE Books, pp. 87.

Leca, E. and Dormieux, L.(1990), Upper and Lower Bound Solutions for the Face Stability of Shallow Circular Tunnels in Frictional Material, *Geotechnique*, Vol. 40, No. 4, pp. 581–606.

Peila, D.(1994), A Theoretical Study of Rein-forcement Influence on the Stability of a Tunnel Face, *Geotechnical and Geological Engineering*, Vol. 12, No. 3, pp. 145–168.

Peila, D., Oreste, P. P. and Pellizza, S.(1996), Study of the Influence of Sub-horizontal Fiber-glass Pipes on the Stability of a Tunnel Face, *Proceedings of International Conference on North American Tunneling 96*, Vol. 1, pp. 425–431.

Terzaghi, K.(1943), *Theoretical Soil Mechanics*, John Wiley & Sons, Inc. New York, pp. 66–77.

Vlasov, S. N., Makovsky, L. V. and Merkin, V. E.(2001), *Accidents in Transportation and Subway Tunnels*, Elex-KM Publ. Moscow.

Walter W.(1990), *Rock Mechanics: Theory and Applications with Case Histories*, Springer-Verlag, pp. 444–471.

This page intentionally left blank

Underground Space – the 4th Dimension of Metropolises – Barták, Hrdina, Romancov & Zlámal (eds)
© 2007 Taylor & Francis Group, London, ISBN 978-0-415-40807-3

Laboratory testing of chemical grouting effects in rocks

K. Souček, L. Staš & R. Šňupárek
Institute of Geonics, ASCR, Studentska Ostrava-Poruba, The Czech Republic

I. Kroutilová
Institute of Macromolecular Chemistry, ASCR, Heyrovskeho nam. Prague, The Czech Republic

ABSTRACT: This paper deals with investigation and testing of targeted properties on the basis of laboratory research of geo-composites, which are prepared form rocks and chemical grouts including their rheological and chemo-rheological study (particularly epoxy material, which is not in common use in domestic grouting practice). The paper presents some testing methods and procedures for research of both clean grouting media and composites with the grouted discontinuity, which enables to optimize a choice of grouting media for affecting the properties of rock mass.

1 INTRODUCTIONS

Discontinuities affect significantly stress and deformation phenomena in rock mass. Moreover, they affect its cohesion and therefore, they affect negatively the stability and the construction of underground structures and reduce occupational safety at construction works. The worsened stability occur primarily at shallow depths and in rock mass with de-stressed areas where structurally controlled failures may be the prime concern in the underground constructions and excavation design (Brady 1993).

In the cases when discontinuities of rock mass complicate the construction, it is possible to improve its quality with targeted geo-technical steps in rock mass. One of the options of application of such geo-technical procedures is the grouting technology with utilization of progressive chemical grouts. With application of chemical grouts into discontinuities, it is possible to affect properties of rock mass.

With application of chemical grouts, primarily on the basis of polymers, new geo-composite materials come into existence in the grouting process. The important factors, which affect a choice of grouting media and at the same time, the effectiveness of grouting technology, are resulting properties of geo-composites. Generally geo-composites are materials that are produced in the process of pressure grouting on the basis of rocks as a skeleton and grouts s as a binding agent. With stabilizing grouting of petrean types of rocks, the grouts are grouted into the void of discontinuities in rock mass. A new composite material comes into existence consisting of the system of rock-cured grouts-rock, the so called "geo-composites with the grouted discontinuity".

In present grouting practice, epoxy resins are not currently used despite their high target strength and adhesion parameters. Therefore, we have examined the possibilities of available epoxy materials utilizable in grouting practice, primarily in the field of rehabilitation of fissures in petrean rocks.

The presented material deals with the knowledge in the field of targeted treatment of properties of rock mass for geotechnical purposes gained from laboratory research. At the same time, there are described some general procedures for the research and assessment of properties of pure chemical grouts in the liquid and cured condition relating both to grouting process and to properties of geo-composites with the grouted discontinuity.

The achieved results and procedures described in this paper are based on the results from the completed Grant Project GA AVČR No.B3086907 and project aimed research carried out by the Academy of Sciences of the Czech Republic No. S3086351.

2 MATERIALS USED

Polymer systems based on epoxy resins cured with aliphatic amines have been used for the purpose of rehabilitation of discontinuities. There are three epoxy-amine systems identified as Epoxy A, Epoxy B and Epoxy C cured with the usual hardener T used in dry conditions, and/or hardened with the hardener T1 for application in humid conditions. All the epoxy

Table 1. Basic properties of epoxy resins.

	Epoxy A	Epoxy B	Epoxy C
Properties of non-cured resins			
Viscosity (23°C) (Pa.s)	0,1–0,2	1,2	1–3
Epoxy index (mol/1 kg)	3.5–4	4,9–5,1	Min 0,5
Properties of cured resins			
Tensile strength (MPa)	> 25	> 50	> 50
Compressive strength (MPa)	> 45	> 120	–
Bending strength (MPa)	> 40	> 85	> 90

systems have been chosen also with respect to the application at lower temperatures than is, for example, the temperature of the Carboniferous massif, i.e. at least 8°C. Originally, these epoxy systems have been intended for preparation of the putties with mineral fillers, polymer-mortar and polymer-concrete composites. The following table shows some general properties of these epoxy systems taken over from material sheets of the company Spolchemie (Table 1).

For comparison, the three types of chemical grouting resins, that are currently used today, have been used in the laboratory research; there are grouting polyurethane materials Bevedan – Bevedol S and WF (BBS and BBWF) and the organic-mineral material Bevedan – Bevedol OM.

The drill cores with the diameter of 48 mm, of prevailingly light grey medium-grain carboniferous sandstone, with a slight content of mica, non-calcareous, well sorted out, with uniform grain size with massive texture – fresh rock have been used for preparation of geo-composites.

3 USED CHEMICAL GROUTS PROPERTIES

Several experimental methodologies have been used for the comparison and assessment of the applicability of chemical grouting polymer systems in the liquid and/or hardened condition on the basis of the following criteria:

- Viscosity of reactive mixture – affecting directly the flow itself (velocity, pressure gradient in the grouts, etc.) of grouting media in rock environment; the higher viscosity of grouting mixture requires higher pressures under the comparable conditions;
- Velocity of hardening reaction (the period of gel formation) determining the workability of reactive mixture, the time of grouting process and the reach of grouting process;
- Mechanical properties of hardened grouting material – modulus of elasticity (at room temperature, and/or at increased temperature in rubber-like condition), strength, ductility, etc;
- Thermal stability of permanency of form (temperature of glass transition T_g);

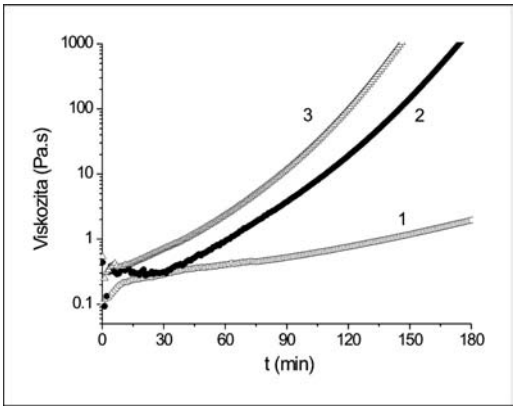


Figure 1. Growth of viscosity in the course of hardening of epoxy systems at temperature of 30°C, 1 Epoxy A-T, 2 Epoxy B-T, 3 Epoxy C-T.

- Thermo-oxidation stability against degradation and combustion resistance.

3.1 *Dynamic-mechanical analysis (DMA)*

3.1.1 *Chemorheology*

Chemo-rheology as part of DMA is the methodology determining rheological changes of reactive mixture in the course of curing, i.e. the growth of viscosity and modulus of elasticity. This methodology is used for determination of initial viscosity of reactive system, the course of hardening at the given temperature, gelation and/or system vitrification. A very important parameter is primarily the dynamic viscosity and the time of workability of the mixture, which depends on the speed of curing process. This period can be determined as reactive time in which the reacting system reaches a certain defined value of dynamic viscosity. The point of gelation corresponds with the utmost limit of workability of reactive mixture. However, the mixture viscosity considered as workable depends on the technological method of preparation of mixture, grouting method and on the physical condition of discontinuities in rock environment.

The Epoxy A-T (see Figure 1) shows the lowest initial viscosity of polymer mixture (i.e. 100 mPa.s). The speed of formation of a net was characterized by determination of the times of gelation t_g (at 20°C) that are outlined in the following table (see Table 2). From this table and the following figure (see Figure 1) it results that the fastest growth of polymer structure occurs in the case of the Epoxy C-T. It can be stated, from the development of viscosity values in the graph in this table that the more favorable rheological properties, from the viewpoint of grouting process (the lower values of viscosity, i.e. better grouting through the less opened fissures, the lower grouting pressure and higher reach of grouting medium) have the Epoxy A

Table 2. Gelation time, thermo-mechanical and strength characteristics of epoxy systems cure at temperature of 20°C.

	t_g (min)	η (Pa.s)	T_g (°C)	$G'_{120°C}$ (MPa)	$G'_{25°C}$ (MPa)
Epoxy A-T	540/2160*	0,1	30/20*	5,0/0,8*	600/100*
Epoxy B-T	250/1200*	0,3	51/29*	8,0/0,9*	880/200*
Epoxy C-T	190/900*	0,3	87/40*	8,8/3,0*	920/760*

	σ_b (MPa)	σ_k (MPa)	ε_b (%)	ε_k (%)
Epoxy A-T	31 ± 2	36 ± 2	$5{,}8 \pm 2$	4 ± 1
Epoxy B-T		49 ± 7		$1{,}8 \pm 0{,}5$
Epoxy C-T		62 ± 3		$2{,}8 \pm 1{,}5$

T_g – Temperature of glass transition; η- initial viscosity; $G'_{25°C}$, $G'_{120°C}$ – Dynamic conservative shear modulus at temperature of 25°C and 120°C; σ_b, ε_b – stress and/or relative, longitudinal deformation at breakage; σ_k, ε_k – stress and/or relative longitudinal deformation at tensile strength; * – values of parameters stated for reaction temperature 8°C.

and B roughly in the first 30 minutes of reaction. It was found out that hardening of reactive mixtures of Epoxy B and C was significantly faster in comparison with Epoxy A. In the case of Epoxy B and C, the systems gelate in the period of approx. 3–4 hours, while the system based on Epoxy A gelates in approx. 9 hours.

3.1.2 *Temperature dependence of dynamic module (DMA)*

DMA gives the information about the modulus of elasticity in the glass-like and rubber-like condition and at the temperature of glass transition T_g, characterizing the thermal stability of material permanency of shape (See Table 2).

3.2 *Strength characteristics*

The determination of strength characteristics (strength, ductility, toughness) by means of a tensile or pressure test is one of general criteria of material quality (see Table 1, 2). In the case of foaming grouting systems, it is appropriate and desirable to determine their mechanical properties according to their degree of foaming (Snuparek 2000).

3.3 *Thermo-gravimetric analysis – (TGA), thermo-oxidation stability and combustion resistance*

The TGA analysis informs about thermal stability of material and resistance against oxidation degradation and combustion. The methodology gives the information about the loss of material mass when the temperature rises. Samples have been heated in air atmosphere with velocity of 10°C/min. The values $T_{5\%}$ a $T_{50\%}$ have been chosen for characterization

Table 3. Thermo-oxidation stability of epoxy, PUR and OMR materials.

	$T_{5\%}$ (°C)	$T_{50\%}$ (°C)	Char (at 700°C) (%)
Epoxy A-T	234	381	0
Epoxy B-T	331	385	0
Epoxy C-T	304	360	0
BBOM	91	409	27
BBS	311	452	0
BBWF	314	422	1

of hardened materials corresponding to temperatures when a 5% and 50%, respectively, of mass loss occurs. While the parameter $T_{5\%}$ characterizes the thermo-oxidation stability, $T_{50\%}$ can be considered for a degree of resistance of material against the general degradation and combustion. An important parameter is also non-burnt residual mass (Char) at very high temperatures, which characterizes the resistance of material against combustion as well as (see Table 3).

4 SOME KNOWLEDGE CONCERNING THE USED EPOXY RESINS

It can be stated, on the basis of the carried out investigations by means of the above-mentioned experimental procedures, that due to vitrification of the system, the course of hardening depends very much on the reaction temperature. At the low temperature, the reactive mixture vitrifies early at lower conversion, which affects the next course of reaction, its resulting mechanical properties and thermal stability of permanency of shape characterized by the value of glass transition T_g. Therefore, we have observed the effect of reactive temperature and compared the course of reaction and properties of the systems hardened at the temperature of $T = 8°C$ and $T = 20°C$ (see Table 2). If the temperature of hardened mixture approaches the value T_g, the grouting material will be capable of more deformable behavior, for instance, during the tensile tests – the occurrence of residual strength behind the tensile strength (see Epoxy A in Table 2 – temperature of tests of approx. 24°C). The quantity (volume) of reactive mixture affects also the mechanical properties. For example, in the case of Epoxy A, the thermo-mechanical behavior is almost independent on the quantity of reactive mixture. In this case the reaction is slow, the originating reactive heat is efficiently dissipated and the reactive mixture is not heated even in a thick layer. On the contrary, in the case of the fast reacting Epoxy C, there was an apparent rise of T_g at reaction in a thick layer almost by 50°C; $T_g(\text{weak}) = 48°C$, $T_g(\text{thick}) = 87°C$. It is apparent that with Eoxy C-T, the exothermic reaction heats up the

sample in the event of the sufficiently great quantity of reactive mixture. Due to the increased reactive temperature, the system vitrifies, characterized by the condition of $T_g = T_{react}$ and the reaction takes place in a higher conversion. Therefore, this sample shows a higher T_g and the modulus of elasticity G′. The effect of the quantity of the reactive mixture Epoxide on resulting properties of the hardened system is important, because it shows that the material hardened in a narrow gap will show the worsened properties in comparison with the epoxy system, which has reacted in a thick layer (Kroutilová 2006).

Polyurethane materials show significantly a greater resistance against the total thermal degradation of material and combustion in comparison with epoxy materials. The relatively small resistance against degradation (characterized by the parameter $T_{50\%}$) has been observed in Epoxy A-T and the high resistance has been observed in Epoxy B-T and C-T, which relates apparently to a greater net thickness of these systems. The hybrid organic-inorganic mixture is resistant against flammability due to a high content of non-combustible inorganic component (char). However, it contains a considerable quantity of thermo-oxidation instable low-molecular components and a quite significant loss of material occurs early at the temperature below 100°C.

5 STRENGTH PARAMETERS OF GEO-COMPOSITES WITH THE GROUTED DISCONTINUITY

The adhesion of chemical grouts to rock surface is of a crucial importance on strength parameters of geo-composites with the grouted discontinuity. A limiting factor for assessment of the quality of geo-composite system "rock – cured grouts – rock" is its capability to resist tensile and shear stress. Principles and procedures of tests of geo-composites with the grouted discontinuity have been similar as for tests of rocks; however, with the difference that, in the preparation phase of test bodies, the discontinuity has been formed on the tested samples and afterwards this discontinuity was glued with the tested grouts, so as its orientation corresponded to the tested type of loading (tension, shear). Tests with geo-composites with the grouted discontinuity based on the selected grouts have been carried out in dependency on quality of their surfaces (natural – by breaking or artificially created – by cutting) and humidity of surfaces of discontinuities (i.e. the rocks glued in dry or wet conditions after they have been taken out from a water bath; the time of submersion in water bath for approx. 24 hours).

5.1 *The used testing methods*

The types of tests have been chosen with regard to the desired requirements for curing grouts in practice. This

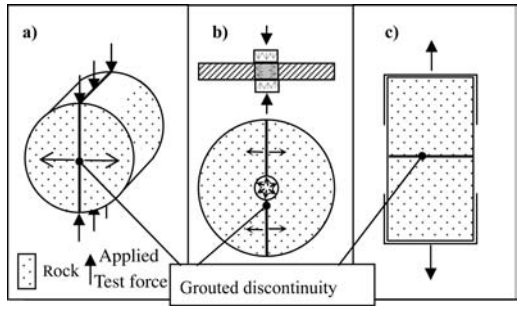


Figure 2. Scheme of used tensile tests a) Brazilian test and, b) tensile strength test by coaxial punches in axiator, c) direct tensile test

is the mobilization of capabilities of discontinuities to transfer tensile stress (which is almost zero or very low before the grouting process itself), the improved capability to transfer shear (shearing) loads on fissures, especially at zero or very low normal stress. To assess the quality of bonding the rocks with selected grouts, the three types of tests have been used. There are tensile, shear c and pressure tests (the so called "bond strength test" (ref.). In the first type of test, the adhesion of tested grouting resins to rocks is tested; in the second type of tests, the shear strength of the grouted discontinuity is measured. As in the tensile tests of geo-composites with the grouted discontinuity the strength parameters are ascertained, which are directly affected by adhesive bonds of tested grouted medium to the surface of rocks, the bonds are identified as "tensile adhesive strength (TAS)".

5.1.1 *Tensile tests*

Originally, the three types of tensile tests have been used for testing of capability of bonded discontinuities to transfer the tensile stress. One test was a direct test and two types of tests were indirect tests:

- Simple tensile test
- Transversal tensile test (Brazil test)
- Tensile strength test with the coaxial punches in the axiator.

Figure no. 2 shows schematically the used types of tests. With respect to the description of results achieved from tests, the method of disintegration of test bodies and demanding character of their preparation, the direct tensile test was mainly used in the research, because this test describes better the values of adhesive tensile strength of geo-composites with the grouted discontinuity in comparison with the indirect tests that are more appropriate only for comparison of the quality of reinforcement of rock mass by means of various types of grouting resins.

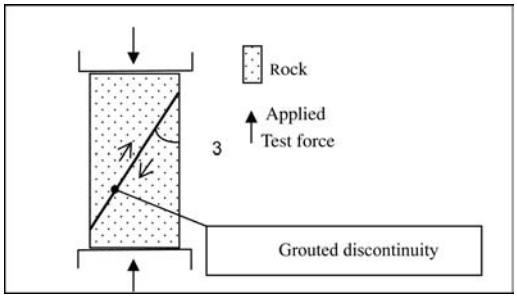


Figure 3. Scheme of Bond strength test

5.1.2 *Bond strength test*

In principle, the bond strength test is a pressure test. Originally, this test was carried out on cylindrical concrete test bodies with the slenderness ratio 2 (diameter of test body 76 mm) with the glued discontinuity inclined at 30 degrees from the longitudinal axis of the sample (see Figure 3). This type of test is used to assess and compare the capability of different types of the bonding agents to glue the surfaces of discontinuities. In our case, the test bodies consisted of sandstone with medium grain size and with the diameter of 48 mm and with the slenderness ratio 2. The result of this test is expressed in a percentage share of uniaxial compression strength of specimen with the bonded discontinuity pressure to the compression strength of undisturbed cylindrical body without discontinuity (PPG). In this test, the area of failure is not pre-determined with the design of testing equipment as in the case of shear cut tests, but with the total state of stress in the specimen. Therefore, in this test, we can differentiate three general types of failures in test bodies.

5.2 *Discussion of the achieved results*

5.2.1 *Tensile adhesion strength (TAS)*

In the majority of cases, the simple tensile test was used for the measurement of values of TAS. From the reason of non-homogeneity and generally low simple tensile strength of rocks, good adhesion of resins to the used rocks, the TAS was not always measured, but often the tensile strength on unconventional test bodies was measured.

With test bodies of geo-composites based on the tested epoxy systems with a dry discontinuity formed with a cut, the values of TAS exceeded the tensile strength of sandstone used, i.e. c. 6 MPa. With test bodies with discontinuities glued in humid conditions, the situation was different.

On all the test bodies, the failure occurred in the glued discontinuity, so the TAS of the observed epoxy systems was measured. The lowest values of tensile adhesion strengths have been recorded in the system Epoxy A-T1 (c. 1,3 MPa); the highest values have been recorded in the system Epoxy C-T1 (c. 3 MPa). In the case of the system Epoxy B-T1, the values of TAS were measured slightly lower than in the system Epoxy C-T1 (c. 2.7 MPa).

TAS decrease significantly with the increased humidity of grouted discontinuities and vary below the limit of 1 MPa for all the three compared and commonly used grouting systems (BBS, BBWF and BBOM). In all cases in these tests, the failure was in area of the glued fissure too.

The quality of grouted discontinuities surfaces affects the values of TAS. The majority of tests carried out on the samples with discontinuity caused by a fracture (a higher roughness of the fissure surface) show higher values of such adhesion strengths in comparison with the samples with a fissure created by cutting. In these tests it is not possible to define a precise value of TAS due to the failure of PUR and OMR geo-composites outside the glued discontinuity; however, it can be certainly stated that these values of adhesion were greater than 3 MPa.

From comparison of TAS in the case of polyurethane resins in simple tension it is apparent that the samples grouted with resin with a smaller capability to create foam in dry environment show slightly higher values of adhesion i.e. BBWF. In the conditions with a dry discontinuity formed by cutting, the values of tensile adhesion strength showed in this resin approx. 2,8 MPa (in the conditions with wet discontinuity of c. 0,4 MPa) in comparison with the values measured with the grouting system BBS, i.e. c. 2,5 and 0,3 MPa, respectively. Under the same conditions, with the grouts BBOM the TAS were approx. 4 MPa and 0,2 MPa, respectively. In the wet condition of discontinuity surfaces, the values of such TAS are very low and approximately on the same level.

5.2.2 *Bond strength test*

As it has been already mentioned, one of potential assessments of this test is the expression of a share of uniaxial compression strength (UCS) of geo-composite with the glued discontinuity and original rock material expressed in percentage (PPG). The results of individual tests for the particular systems are shown in the following table (see Table 4). The average value UCS of the used rock in was 43 ± 5 MPa. The PUR and OMR systems show prevailingly a smaller capability to bond the rock used (discontinuity in the dry condition) in comparison with epoxy systems (see Table 4).

The test bodies of geo-composites based on the grouting system BBOM with the discontinuity bonded both in the dry and wet condition have shown approx. $2 \times$ higher pressure strengths in comparison with geo-composites based on BBS and BBWF. From the comparison of results of compression strengths on geo-composites with the glued discontinuity by means of epoxy systems it is apparent that Epoxy A is less

Table 4. Strength parameters - "Bond Strength Test"

Chemical grouts	Dry condition		Wet condition	
	UCS (MPa)	PPG (%)	UCS (MPa)	PPG (%)
BBS	9 ± 2	21	4 ± 2	9
BBWF	7 ± 3	16	6 ± 2	14
BBOM	23 ± 4	53	10 ± 5	23
Epoxy A-T(T1)	31 ± 5	72	7 ± 1	16
Epoxy B-T(T1)	47 ± 4	109	44 ± 8	102
Epoxy C-T(T1)	43 ± 2	100	43 ± 7	100

capable to bond the used rock both in the dry and wet condition (see Table 3). The compression strength of test bodies of geo-composites with Epoxy B and C vary on the limit of strength of the used rock, and/or they exceed it slightly, which is caused by non-homogeneity of the used rock, higher adhesion bonds and strength parameters of Epoxy B and C in the hardened condition (see Table 1,2).

In these tests, the three types of failure of test bodies have been diagnosed. The first type presents a fragile failure in diagonal bonded discontinuity with the immediate drop of pressure force. This group includes the BBOM based geo-composite (the discontinuity glued in the wet and dry condition) and Epoxy A-T1 (the discontinuity glued in the dry condition). The second type of failure represents also a failure in the glued discontinuity, but there does not occur a fragile disintegration of a test body. The slippage occurs only in the diagonal discontinuity and on the deformation graph, there is apparent a significant residual strength beyond the ultimate strength in uniaxial compression. This category includes the geo-composite based on BBWF and BBS (the discontinuity glued in the wet and dry condition) and Epoxy A-T1 (the discontinuity glued in wet condition). In the group of geo-composites with the glued discontinuity based on the epoxy resin Epoxy B and C, the situation is different from the viewpoint of the manner of failure of test bodies. With these geo-composites with the glued discontinuity (in the dry and wet condition), the test bodies were disturbed primarily outside the glued discontinuity and disintegrated into more parts outside the glued discontinuity. The character and manner of failure of test bodies of these geo-composites was characteristics for failure of compact rock test bodies in uniaxial compression. At failure of test bodies of geo-composites based on these two epoxy systems, the compression strength of the used rock was a constraining factor.

6 CONCLUSIONS

From the results of research of the properties of geo-composites with the grouted discontinuity it can be stated that by means of tested chemical grouting systems it is possible to reinforce the rock mass significantly. The degree of reinforcement will depend both on used grout and on the roughness of rehabilitated discontinuities surface and their humidity.

A higher level of reinforcement can be achieved by means of epoxy systems, eventually, with organic-mineral system in comparison with the polyurethane grouts. The epoxy resins Epoxy B and C have shown the most favorable results even under the conditions of wet discontinuities. TAS achieved c. 3 MPa in comparison with polyurethane, and/or organic-mineral grouts, where these TAS did not exceed the limit of 1 MPa. Tensile and compression strength was a constraining factor at test bodies failure of geo-composites based on Epoxy B and C in the both discussed tests (the discontinuity was glued in the dry condition and formed by a cut).

Cohesion of test bodies beyond the ultimate strength was found out at the certain kinds of geo-composites. This behavior was observed primarily with geo-composites based on BBS and BBWF, which is probably caused by different deformation properties of grouting systems. BBS and BBWF show foaming during chemical reaction on the contrary with the BBOM, which behaves more fragile. In the case of the Epoxy A, this behavior can be affected by a low temperature of its glass transition (c. 30°C) and low temperature difference (i.e. c. 5°C) during geo-composites testing.

The described general methodologies and procedures enable to optimize a choice of grouting medium for affecting the properties of rock mass and to gain the necessary information on the degree, quality of reinforcement and rehabilitation of discontinuities in rock mass.

From the results of research into chemo-rheological behavior of epoxy systems in the course of reaction it is apparent that the tested resins will be probably more applicable in rock mass with a higher temperature. There is potential problem with vitrification of epoxy systems in the course of reaction at low temperature. Tests of thermo-mechanical properties have shown that the Epoxy B and C are more favorable in the conditions with higher temperature too. They show higher temperature of glass transition.

REFERENCES

Brady, B. H. G., Brown E. T. 1993. *Rock Mechanics for Underground mining*, second edition, Kluwer Academic Publisher, Dordrecht

Šňupárek R., Souček K. 2000 Laboratory testing of chemical grouts, *Tunneling and Underground Space Technology*, volume 15, No. 2, p. 175–186

Kroutilová I., Matějka L. Sikora A., Souček K., Staš L. 2006. Curing of epoxy systems at sub-glass transition temperature, *Journal of Applied Polymer Science*, p. 3669–3676

Section 3
Research, development and design of underground constructions in built-up areas

This page intentionally left blank

Underground Space – the 4th Dimension of Metropolises – Barták, Hrdina, Romancov & Zlámal (eds)
© 2007 Taylor & Francis Group, London, ISBN 978-0-415-40807-3

Deformation computation based on numerical modelling for urban NATM tunnelling

M. Zaki Abd Elrehim
Civil Engineering Department, Minia University, Minia, Egypt

ABSTRACT: In this paper, numerical studies in the context of plane-strain Finite Element analyses are presented, comparing the effect of different parameters on deformations' values. Height of overburden, stiffness of the ground, underground water level and size of a tunnel among others are influential factors in the developed deformations. A special cell mesh generation is presented to reduce the effort and calculation time needed for repeated calculations and parametric studies. Based on the calculated results it would become necessary to modify or change the used construction method even during the planning and design stages. On the basis of the numerical results, a definition for the critical deformation related to a certain tunnel project can be defined. Hence, the original design/construction method can be modified and the optimal method of soil reinforcement can be determined. It is the aim of this paper to help the geotechnical engineer to decide which deformation limits can be allowed to achieve a safe and economical tunnel design that meets all construction and operational requirements.

1 INTRODUCTION

NATM (the New Austrian Tunnelling Method) has become one of the main tunnelling concepts. It has originally been developed for rock conditions in the Alps. As a matter of fact, soft ground tunnelling with NATM has a shorter history than NATM tunnelling through rock. Currently, an increasing number of tunnels in urban areas is excavated according to the principles of NATM. During construction, the main aim is to preserve and improve the potential of the ground to support itself as far as possible by making use of an arching effect in the ground around the tunnel. Too large deformations should be avoided otherwise loosening in the ground will take place which significantly reduces the potential of the ground to support itself. This results in an increase of load on the tunnel lining which may cause critical situations for tunnelling safety.

An essential part when planning urban tunnels is to indicate the expected deformations. Surface deformation is important to ensure the stability and safety of surface structures and utilities (Sozio 1998, Mair 1998, Netzel & Kaalberg 2000) whereas deformation within the tunnel is important to ensure the safety of tunnelling procedure and construction technique. The task of the geotechnical engineer is to decide which deformations can be allowed to achieve a safe and economical design that meets all operational requirements. Efficient numerical methods could provide the geotechnical engineer with an additional tool for getting better insight into the behaviour of the ground. Consequently, a numerical model for predicting possible deformation behaviour of the ground could support the engineer and avoid dangerous situations during tunnelling.

In order to achieve more efficient control for the ground deformation, the load-carrying capacity of soil surrounding the tunnel may be improved by means of many techniques. Grouting techniques, soil freezing, pipe-roofing, jet-grout arch, micro-piles, grouted-fiber glass or re-bar nails…etc are examples of soil reinforcement techniques (Guatteri et al. 1994, Fitl 1997, Liebsch and Haberland 1998, Gioda and Locatelli 1999, Tan and Ranjith 2003). The engineer needs a helpful tool to select the optimum technique that will reduce the deformation to the required levels. So, there is an increasing demand to firstly know the deformation limits of the natural soils in the planning stage and hence deciding the optimum reinforcement technique.

Compared with shield tunnelling methods, there is currently no NATM design method that has been established for urban areas (Ishibashi et al. 2004), and there are some reports of ground settlement being greater than expected and cost and time overruns occurring because of the use of various reinforcement methods.

2 MODELLING OF URBAN NATM TUNNELS

The urban NATM tunnelling is usually characterized by the sub-division of the tunnel cross section in multiple stages. The subdivision can be on the form of a top heading, bench and invert sequence, the side-wall drifting procedure or the use of advance pilot tunnels. All these sequences are based on the principle that ground deformations are practically proportional to the size of the tunnel cross section.

Finite Element Method (FEM) in usual soft-ground tunnelling design practice is one of the main tools to simulate complicated three-dimensional stress distribution in the tunnel vicinity in both cases of using three or two dimensional calculations. It is very important to carefully simulate the construction sequences to analyse the expected loading conditions. Despite the merits of three dimensional analyses in realistic modelling of tunnel face, 92% of the published tunnel analyses are still performed in two dimensions, using plane strain models and mostly elastic-perfectly plastic ground behaviour (Farias et al. 2004).

As a result of FEM calculation there is a stress and strain distribution related to each loading condition. The most important two cases that characterize the final deformational behaviour of the ground are:

1. Deformations due to stress relieve (after considering the initial stress condition) which take place just before excavation in every cross section.
2. Deformations after excavation and after developing final strength of the initial shotcrete lining.

In the present analyses, a 2D plane strain elastoplastic soil model based on Mohr-Coulomb failure criterion has been used. The excavation of each part of the tunnel is simulated in two steps according to the stiffness reduction method (Swoboda 1990). In the first step (called loosening), the stiffness of the soil inside the tunnel part is reduced to the value corresponding to the z-location along the tunnel axis where temporary support is installed. In the second step (support), the excavated soil is removed and its primary stresses are eliminated simultaneously with the installation of the secondary shotcrete lining with its fresh state. The lining helps in controlling further deformation of the soil. In multi-stage excavation, the above two steps are repeated for each excavation stage. This simulation can achieve the three-dimensional effect near the tunnel face. Figure 1 illustrates the basic investigated load conditions for top heading and bench excavation sequence. With respect to deformation consideration, these loading cases correspond not only with the three dimensional modelling requirement, but also with the practical feasibility of measurement possibilities at the face.

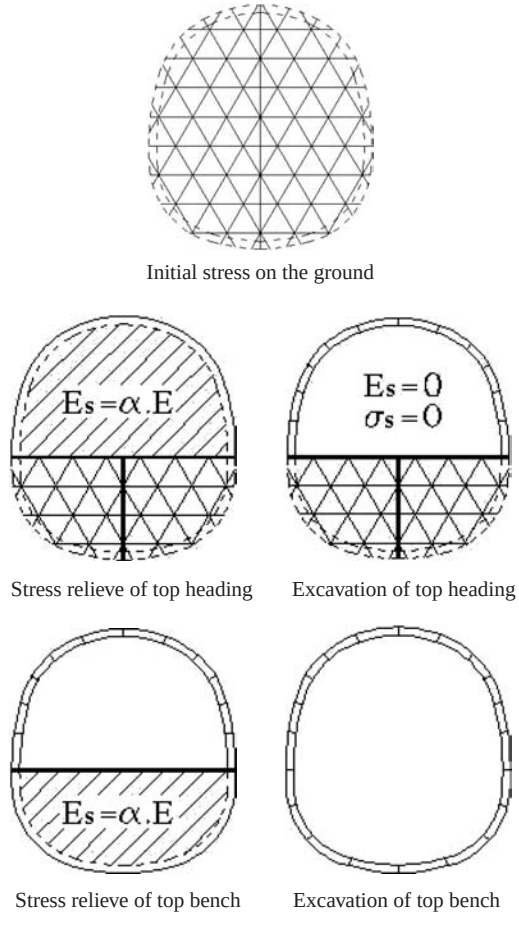


Figure 1. Loading conditions related to construction sequences.

Modern geomechanical measurements methods have been developed to measure very accurately deformations caused by stress relieve (loosening) as well as by excavated and initially lined tunnels. Comparing both types of measurements leads to better values for the stiffness reduction factor.

It is important to check, whether the calculated deformations correspond with the associated measured deformations or not especially before the installation of the final lining. Therefore, the calculated stress relieve deformation has to be compared with the measured one to check whether the analysis corresponds satisfactorily with the construction or not. Numerical models are continually updated by back analyses of the observed behaviour (Sakurai et al. 2003) to update the most critical ground parameters used in the model.

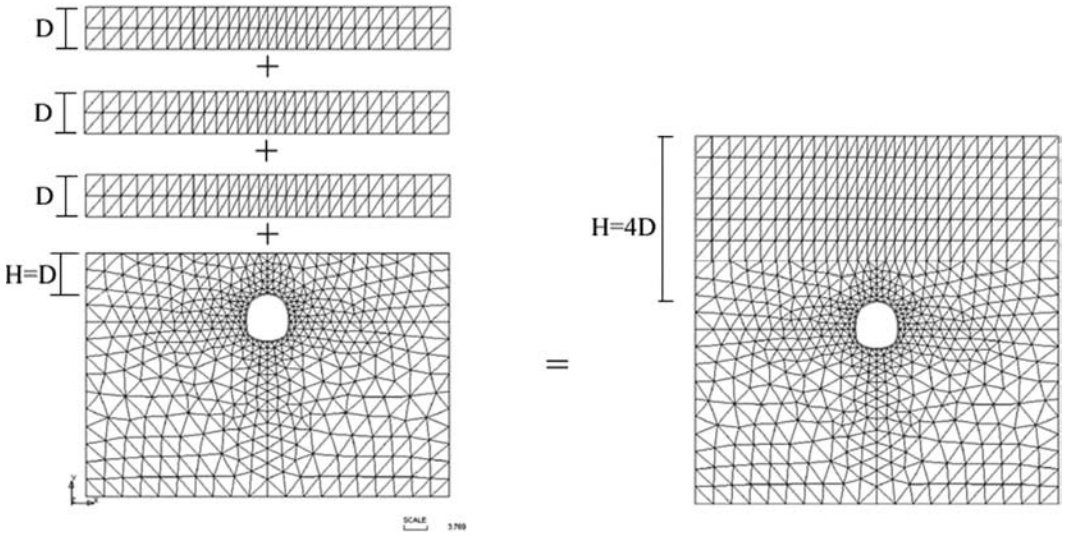


Figure 2. Mesh-generation cell technique.

3 CRITICAL SECTIONS AND CRITICAL DEFORMATIONS

The determination of the most critical sections along a tunnel route is mainly based on, among other factors, the following parameters:

1. The depth of the tunnel.
2. The mechanical parameters of the soil layers.
3. The ground water pressure exerted on lining.
4. The surface loading.

For large tunnel projects with several kilometers of excavation and various cross sections, it is impractical to analyse all sections along the tunnel route. It will be more helpful to have a round figure about the deformation limits along the route and then to determine the most critical sections for detailed analysis. The deformation limits can be used to define the critical deformations along the tunnel route. If these critical deformations are acceptable, the design process continues to the next detailed step otherwise modifications for the construction sequence and/or tunnel alignment, especially for the depth factor, are to be considered.

At this preliminary stage, the first parameter for the tunnel depth can be considered more effective especially if the variation in ground condition is not too much. Many calculations are to be made according to the variations on tunnel depth to have a more clear idea about the deformations. With the help of numerical techniques a lot of work for meshing and deformation calculation within the context of FEM can be saved.

It should be noted that each tunnelling project must be treated on its own characteristics, the issues discussed in this paper should be given due consideration for the proper modelling and analysis of the construction sequences.

3.1 *Mesh-generation cell technique*

Relating the studied varied height of overburden above tunnel cross section with the maximum diameter (D) of the tunnel, leads to very tidy mesh layout in the zone beyond the tunnel and near the ground surface. In order to save the time needed to generate many repeated larger meshes, a mesh-generation cell technique was developed. Using this technique a mesh for a regular cell representing the required varied height is first generated. The basic mesh containing the tunnel is generated in the usual way. Then, the entire mesh is generated with the required number of cells using a cell mesh-generation program. The process is performed numerically and without regeneration of the mesh again every time we change the height of overburden (D). Figure 2 shows three cells of height equals (D) each and the whole FE mesh with a total overburden of ($4D$) above the tunnel.

Finite element meshes for models with regularly varied height are generated by a mesh generation cell method. These meshes are composed of Linearly Strain Triangular (LST) elements. To meet the requirement of accuracy of the calculation, the meshes of triangular elements near the tunnel axis should be suitably dense.

The calculation and results of deformation development presented in this paper are performed using general FE package, FINAL package (Swoboda 2001).

The mesh generation-cell technique is coded, linked and used with the main FINAL package.

The procedure of mesh-generation cell can be described as follows:

- Define the cell geometry. This includes the depth (D) and the width (W).
- Generate a mesh for the defined cell.
- Transform the mesh to FINAL input file.
- Generate an original mesh for the tunnel with the minimum depth.
- Transform the original mesh to FINAL input file.
- Use the cell program to merge both generated files with any number of repeated cells and check for nodes/support compatibility and connectivity.
- Run FINAL to get the required results for deformations, stresses...etc for the larger meshes.

The procedure was firstly checked for small examples and then generalized for tunnels meshes. The method is found to be useful and time saving for repeated calculations and parametric studies. The precondition to be carefully noted during the application of the method is that cells must be regular in rows and ranks. With the increasing of total mesh height, attention should be paid to total mesh width (aspect ratio) to have reasonable far field and support conditions at the mesh boundary.

4 ANALYSIS OF A TYPICAL EXAMPLE

A typical cross section of a shallow single-track railroad tunnel has been modeled. The geotechnical soil parameters are excluded from the investigation report of Cairo Metro line III phase II (NAT documents 2003). The soil at this phase is characterized by the existence of uniform sand and clay layers without ground water within the tunnelling zone which more encouraging the use of NATM technique. Thus, it is expected that the most important factors for deformation calculation along the tunnel route is the height of overburden and the construction technique.

The initial overburden over the tunnel crown was chosen to be roughly equal to the tunnel diameter. The analysed domain has horizontal fixations at both sides of the mesh whereas the bottom nodes of the mesh are vertically fixed. The used FE mesh is illustrated in Figure 2 for the basic mesh and the extended ones for the overburden variations. The loading conditions related to the chosen method of construction are illustrated in Figure 1 for a top heading excavation followed by a bench excavation.

Results regarding deformations and critical deformations as will be made here are strictly related to shallow tunnels under soft ground or mixed face conditions. It is assumed that whatever construction concept will be used the ring closer time is short and is about one diameter from the face. This precaution will minimize the effect of face stability on the developed deformation in two dimensional analyses.

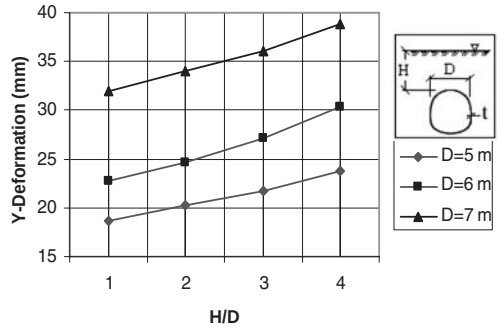


Figure 3. Surface settlement (t = D/30).

A series of FE calculations is performed for different tunnel diameters each having different height of overburden and for different lining thicknesses. The height of overburden and the lining thicknesses are chosen as a function of tunnel diameter (D) and within the practical engineering values.

Based on structural calculations, the relation between lining thickness and tunnel diameter is in the range of (1/30). Two other values (1/15 and 1/40) can be considered as the upper and lower limits of lining thickness of shallow tunnels under soft ground conditions. However, it is possible to interpolate any other different relation between lining thickness and tunnel diameter between these two limits.

A lot of curves and relations may be resulted from the FE calculations. As an example, the effect of NATM tunnelling on surface settlement for different tunnel's diameter and different values of overburden is illustrated in Figure 3 for a lining thickness of ($D/30$). The thickness is thus ranging between 15 cm and 25 cm which agree well with the engineering experience.

Figure 3 dictates that surface settlement is directly proportional to the height of overburden. The variations in settlement values are nearly within *25%* for the indicated range of H/D for each diameter. It can also be noticed that the settlement increases with the increase of tunnel diameter for the same H/D value.

The settlement values at the tunnel crown for different H/D values and for different tunnels diameters are shown in Figure 4. The same trends noticed in Figure 3 can also be noticed here but with more effect for the height of overburden. The settlement values nearly doubled for the indicated range of H/D for each tunnel diameter.

Both Figures 3 and 4 can be used to investigate the optimal diameter for the specified construction method. Studying the intervals between the curves of different diameters shows a larger interval beyond

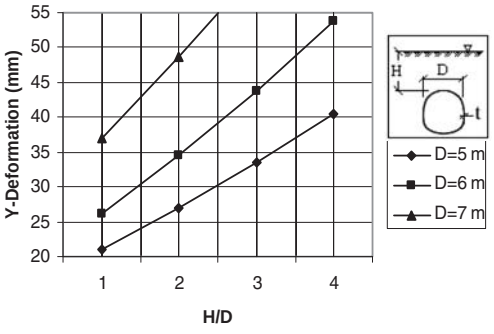


Figure 4. Crown settlement (t = D/30).

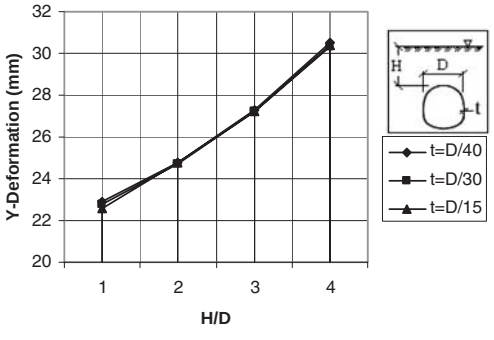


Figure 5. Effect of lining thickness on surface settlement (D = 6 m).

a diameter of 6 m. This indicates that the optimal acceptable limit for a top heading bench sequence of construction in the specified soil is up to 6 m. For a diameter of 7 m, a modification in the construction sequence by more tunnel section subdivision or by introducing a soil reinforcement technique is recommended if a reasonable level of deformation is required.

The effect of lining thickness on reducing surface settlements for NATM tunnels in the specified conditions of the considered example is not significant, Figure 5.

Many FE calculations was performed and used to define the critical deformation in a simple and usable way, Figure 6. The recommended value of critical deformation can be found by using the data of the tunnel diameter, the height of overburden and simple interpolation between the indicated curves. The curves help to define the critical deformation in the early design stage to decide if the construction method is appropriate or some modifications should be considered for the tunnelling process, tunnel

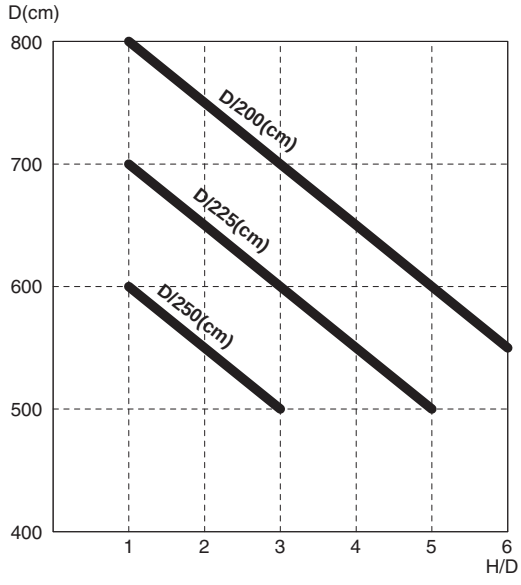


Figure 6. Critical surface deformation of the considered typical example.

alignment (especially tunnel depth) and/or soil reinforcement. The principle ideas in the curves of Figure 6 can be extended systematically and developed in design tables and charts easy to use by engineers for the studying of the deformational behaviour of different soil/structure interaction problems.

5 CONCLUSION

An essential part when planning urban NATM tunnels is to indicate the expected deformations. The ideas presented in the paper help the geotechnical engineer to decide which deformations can be allowed to achieve a safe and economical design that meets all operational requirements. A criterion for defining the critical sections along the tunnel route was pointed out. A mesh-generation cell technique was developed, coded and linked to a FEM package to facilitate and save the time needed for repeated calculations and parametric studies. A typical cross section of a shallow single-track railroad tunnel has been analysed and used to clarify the main ideas of deformation analysis. A set of characteristic curves for deformation was given and from which a simple definition for the critical deformation is indicated. The principle ideas as presented in the curves can be extended systematically and developed in simple design tables and charts easy to use by engineers. Although the tunnel engineers understand that each NATM case must be treated on its

own characteristics, the issues discussed in this paper should be given due consideration for the studying of deformational behaviour in the early design stage.

REFERENCES

Farias, M.M., Moraes, A.H. and Assis, A.P. 2004. Displacement control in tunnels excavated by the NATM: 3-D numerical simulations. *Tunnelling and Underground Space Technology*, 19:282–293.

Fitl, D. 1997. Der Tunnel Frankfurter Kreuz [The Frankfurter Kreuz tunnel]. *Felsbau* (*Rock and Soil Engineering*); 15(5):347–350 (in German).

Gioda, G. and Locatelli, L. 1999. Back analysis of the measurements performed during the excavation of a shallow tunnel in sand. *International Journal for Numerical and Analytical Methods in Geomechanics*; 23:1407–1425.

Guatteri, G., Mosiici, P., Koshima, A., Doro-Altan, V. 1994. Application of jet grouting to tunnel portals and top headings in NATM tunnelling: Brazilian experience. In Bell AL (ed.). *Grouting in the Ground*. Thomas Telford: 455–471, London, England.

Ishibashi, T., Setoguchi, Y., Aoki, T. and Izumi, T. 2004. Consideration of the limitations of NATM methodology in urban area tunnelling. *Proc. of the 16th International Conference on Engineering Mechanics*, ASCE, Seattle, USA.

Liebsch, H. and Haberland, C. 1998. Soft ground tunnelling in urban areas by NATM. *Felsbau–Rock and Soil Engineering*, 16(2):78–90.

Mair, R.J. 1998. Geotechnical aspects of design criteria for bored tunnelling in soft ground. *Proc. World tunnel congress 98 on Tunnels and Metropolises*: 183–199, Sap Paolo, Brazil, Balkema.

NAT, National Authority for Tunnels, 2003. Greater Cairo Metro Line III, *Geotechnical investigation report*. Cairo, Egypt.

Netzel, H. and Kaalberg, F.J. 2000. Numerical damage risk assessment studies on masonry structures due to TBM tunnelling in Amsterdam. *Geotechnical Aspects of Underground Construction in Soft Ground*: 235–244, O.Kusakabe et al, (editors), Balkema.

Sakurai, S., Akutagawa, S., Takeuchi, K., Shinji, M. and Shimitu, N. 2003. Back-analysis for tunnel engineering as a modern observational method. *Tunnelling and Underground Space Technology*, 18:185–196.

Sozio, L.E. 1998. Urban constraints on underground works. General report. *Proc. World tunnel congress 98 on Tunnels and Metropolises*:425–430, Sap Paolo, Brazil, Balkema.

Swoboda, G. 1990. Numerical Modelling of Tunnels, in C.S. Desai and G. Gioda: *Numerical Methods and Constitutive Modelling in Geomechanics, Courses and Lectures*, Springer-Verlag, Wien, No. 311:277–318.

Swoboda, G. 2001. Programmsystem FINAL, *Finite Elemente Analysis linearer und nichtlinearer Strukturen*, in German, Version 7.1, Druck Universität Innsbruck, Austria.

Tan, W.L. and Ranjith, P.G. 2003. Numerical analysis of pipe roof reinforcement in soft ground tunnelling. *Proc. of the 16th International Conference on Engineering Mechanics*, (in CDRom) ASCE, Seattle, USA.

Underground Space – the 4th Dimension of Metropolises – Barták, Hrdina, Romancov & Zlámal (eds)
© 2007 Taylor & Francis Group, London, ISBN 978-0-415-40807-3

Numerical analysis of TBM road tunnels under Suez Canal at Port Said

Ashraf Abu-Krisha
National Authority for Tunnels (NAT), Cairo, Egypt

ABSTRACT: Due to the construction of the international littoral road, the road tunnels at Port Said under the Suez Canal are required and studied. This road consists of two identical tunnels (twin tunnels) with inner diameter 10.8 m that run parallel to each other with length of about 2.30 km. The two tunnels will be constructed by Tunnel Boring Machine (TBM). These tunnels are analyzed using a two-dimensional (2D) numerical simulation by FEM, with allowance for three-dimensional (3D) effects. Several 2D numerical models, based on the finite element technique, were generated in plane strain analysis at different depths to simulate TBM process and to investigate the effect of ground movements due to tunneling. The soil mass were modeled as a non-linear perfect elastic-plastic, based on the proper constitutive laws according to the soil layers type. The long-term ground response is contributed to simulating the second tunnel.

This paper presents the results of the numerical studies performed to investigate the effect of different conditions on the predicted ground behavior and tunnel lining. Also, the results of these analyses are compared with the laboratory scale model.

1 INTRODUCTION

Egypt has a rapidly expanding economy, which consequently requires the construction of the necessary transport infrastructure. As part of this infrastructure it is proposed to construct twin road tunnels to form a permanent and durable road link between Port Said city in the west and Sinai Peninsula in the east. This project will link the international coastal express highway from the North Africa to Asia via Sallume – Alexandria – Port Said and going to Sinai Peninsula – Ghaza under the Suez Canal. The tunnels are to be located at Kp 19.15 of the Suez Canal south of Port Said while the Mubark Al-Salam Bridge is far from south of Port Said by 48.5 Km. So, the project will save approximately 100 Km from the international coastal express highway.

The road tunnel shall have two tunnels, each one have two lanes in each direction with minimum clear lane width of 3.75 m and clear height of 5.5 m minimum vertical clearance. Figure 1 shows the cross section of the proposed road tunnel. Each tunnel has four ventilation shafts, two at the sides of the canal bank by distance 100 m, the others at the entrance and exit of the TBM. The total length of each tunnel is approximately 2300 m. The tunnel will be protected by a fire barrier system.

The present Suez Canal is 214 m width at level – 11.0 m and 22.5 m depth at the location of the project. The project will take into account the forecast of the Suez Canal for the depth and the width. The future depth is 27.0 m and the future width is 270 m at level – 11.0 of the Suez Canal. Figure 2 shows the proposed longitudinal section of the project.

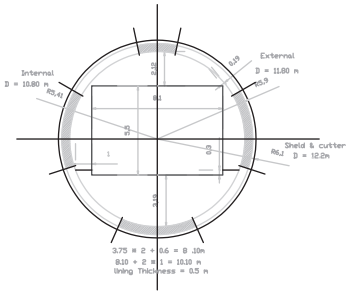


Figure 1. The proposed cross section of road tunnels under Suez Canal.

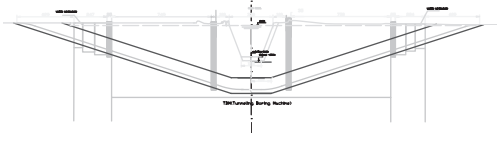


Figure 2. The proposed longitudinal section of road tunnels under Suez Canal.

Numerical simulation of the interaction between ground and structure using the Finite Element Method (FEM) as implemented with Plaxis software (2002) is performed. The behavior of soft soils is complicated

Table 1. Layers and geotechnical parameters.

Soil layer	Depth (m)	γ	E MPa	ν	ϕ	C
Fill	0–2	17.0	20	0.2	24	0
Silty clay	−2–35	16.0	10–45	0.40	22	5
Sand (1)	−35–45	18.5	70	0.35	36	0
Sand (2)	−45–70	20.0	100	0.3	38	0

and hardly accurately modeled, even with the most elaborate constitutive models; moreover, parameters such as soil deformation modulus, which are essential to output of numerical analysis, can hardly be estimated with sufficient accuracy with exist testing techniques. The more recent advances related to FE techniques were further analyzed by Mair and Taylor (1997), Leca and Mestat (1999) and Abu-Krisha (2002). FE modeling can be considered as a powerful means of analysis, because it allows the main parameters involved in the tunneling process and construction sequence.

2 GEOLOGY AND GEOHYDROLOGY

The geological knowledge of the site collected from the extensive studies on the basis of deep drillings, surface surveys and analysis of geostructural surveys. The subsoil consists mainly of, medium dense to dense sandy gravel, covered with a top layer of silty clay and fill. During soil surveys a 34 to 36 m thick layer of stiff to very stiff silty clay was encountered. The lab results from the oedometer tests show a large bandwidth of stiffness, which is an important design parameter for bored tunnel. The sand layers which were encountered at depths below 46 m displayed refusal N values in field STP tests, indicating very dense conditions.

According to the geotechnical reports by NAT 2004 the recommended design parameters for the four main soil deposits are given in Table 1. The ground water depth stabilized inside the open boreholes at 1.5 m to 2.0 m. The ground water level will be taken −2.00 m from the ground level as a critical case in the FE analysis. The results of the chemical tests indicate to high concentrations of chlorides, sulphates and total dissolved salts (TDS).

3 MODELS SIMULATION STUDIES

3.1 *Structural properties*

Two identical 10.8 m diameter TBM tunnels will be used for installing a concrete lining as it advances. The diameter of the cutter head of TBM is 12.2 m. One tunnel is constructed with two way and then- in future- it will be with one-way direction. The second tunnel will be construed in future with one-way direction.

Table 2. Material properties of the tunnel lining (beam).

Parameter	Name	value	Value in long term	Unit
Type of behavior	*Material type*	Elastic	Elastic	
Normal stiffness	*EA*	0.75E7	0.5E7	KN/m
Flexural rigidity	*EI*	1.5E5	1.0E5	KNm2/m
Thickness	*t*	0.5	0.5	m
Weight	*w*	12.5	12.5	KN/m/m
Poisson's ratio	*v*	0.2	0.2	

Each tunnel having four ventilation shafts, two at the sides of the canal bank by distance 100 m, the others at the entrance and exit of the TBM. The lining thickness is 0.5 m and the gap between the soil and liner associated with the over cutting is 0.2 m. The material properties suggested for the tunnel lining are listed in table 2.

3.2 *Analysis model*

In the present analysis, the straining actions acting on the tunnel lining resulting from the soil and groundwater pressure is evaluated along the TBM route. The 2D finite element method code Plaxis was adopted in this numerical study. Full-face excavations in two stages of the Twin bored tunnel with lining is supporting the tunnels immediately after the excavation were modeled to allow of 3D effects. Three particular and representative sections are chosen for the analysis in order to get a realistic range of values of the deformations, the stresses and the internal forces in the lining that could be developed under tunneling process. These sections are a plane strain non-linear elastic plastic model that resembles the soil by 4th order 15-node isotropic Strain Triangular elements. The lining is modeled with the help of beam element as a linear. This beam element with interface was used to perform realistic analysis of geotechnical structure. The volume loss is simulated by applying a contraction to the tunnel lining. The range of contraction values are 1.5% – 2% according to the depths. Three sections were chosen for analyses:

- Section 1(lowest one): case of the maximum normal force and located just at the canal axis where tunnels are included into sands. The maximum water pressure is 40 m. the minimum soil cover is 13 m (13 m after 3 m dredging).
- Section 2 (middle): case of the maximum bending moment. The maximum soil cover is, 33 m corresponding water pressure 31 m.
- Section 3 (shallow): The soil cover is, 11 m corresponding water pressure 9 m.

The analysis cases are included the long-term effects of the construction of the second tunnel. Also, the horizontal distance between the two tunnels was

Table 3. Internal Forces and Displacement for three sections.

Tunnel No.	Forces/Disp.	Sec.1	Sec.2	Sec.3
No. 1	B. M. KN m/m	57.4	110.8	46.8
	S. F. KN/m	19.4	52.1	17.9
	N. F. KN/m	2700	2420	1110
	Displacement.mm	33	42.5	68.7
No. 1	B. M. KN m/m	58.75	116.4	49.5
Long-term	S. F. KN/m	20.7	58.5	19.1
	N. F. KN/m	2740	2500	1170
	Displacement. mm	35.5	45	71.7
No. 2	B. M. KN m/m	62.1	120	57.0
	S. F. KN/m	21.2	59.0	24.5
	N. F. KN/m	2710	2450	1140
	Displacement. mm	35.5	45	72.8

performed for investigation. The results of these FE analyses are compared with the results of tests to investigate the techniques that should be applied to obtain reliable solution to this type of project. Also, the water uplift stability is studied in the present analysis.

4 RESULTS AND DISCUSSION

The analysis results of the internal forces that developed in the tunnel lining for the three sections according to the construction stages and the conditions of every section are compared in table 3. The tunnel lining displacement obtained from the analysis included the tunnels movements due to soil deformation beside the lining distortion are shown in table 3. Table 3 showed the results of internal forces and displacement for the first tunnel in long term. The excavation of the second tunnel beside the first one lead to significant increase in bending moment in the lining of the first tunnel according to the volume loss.

Figure 3 shows the plastic zones distributed around the tunnels obtained from the analysis of section 2. The thickness of the plastic zones sideward from the tunnel lining was limited. These plastic zones lead to increase the internal forces in lining of the second tunnel compared to the first one.

The contours of the total deformation of the mesh for the section 1 are illustrated in figure 4 for the soil mass. The surface settlement for the section 3 is illustrated in Figure 5. The contours of the vertical effective stress at the final loading step for the two tunnels at sections 2&3 are shown in Figure 6. The stresses obtained at the region between the two tunnels were out the limits of ultimate strength of that soil layers.

5 RESULTS COMPARISON WITH PHYSICAL MODEL TESTS

The results presented here are limited to the comparison between the results of test PS3 given by Kim (1996,

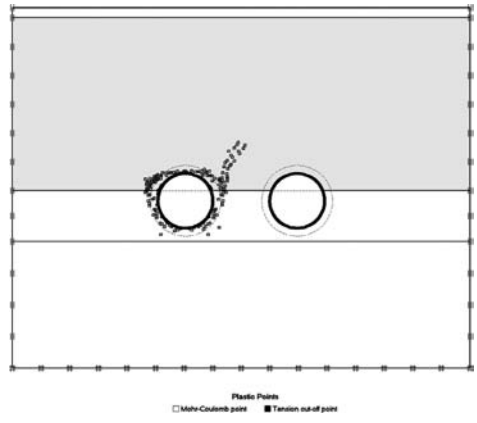


Figure 3. Plastic zones distributed around the tunnels obtained from the analysis of section 2.

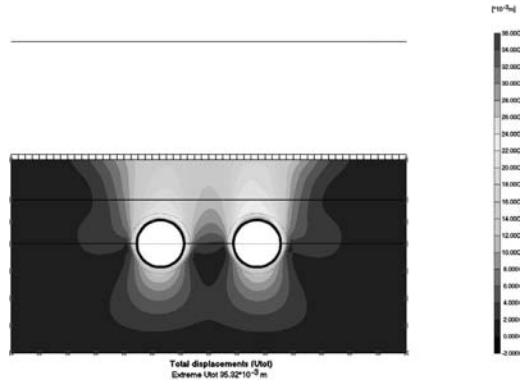


Figure 4. The total deformation of the mesh for the section 1.

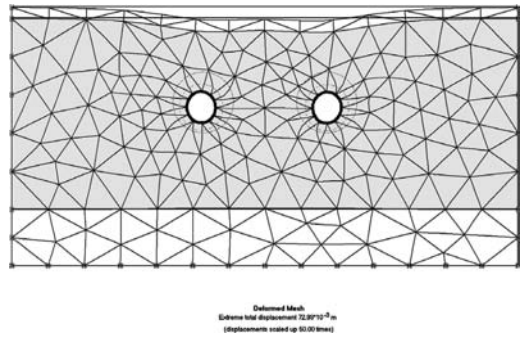


Figure 5. The surface settlement of the mesh for the section 3.

2004) and the corresponding FE analysis of section 3 where the tunnel is located in silty clay layer. The diameter changes of the first tunnel immediately after the

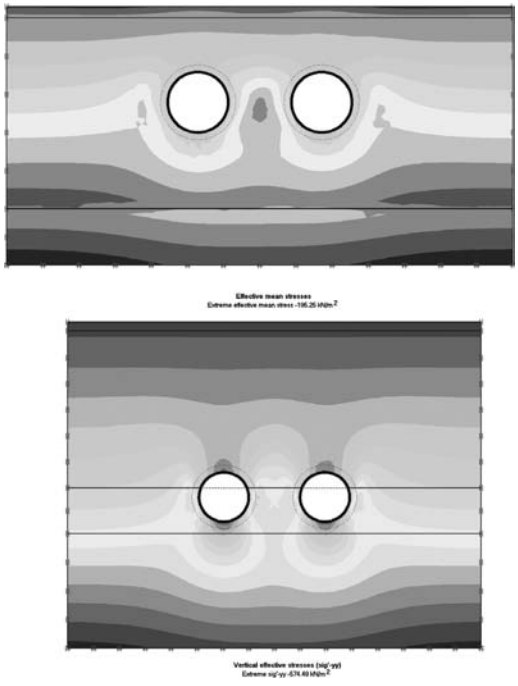


Figure 6. The effective stresses at final loading for sections 2 & 3.

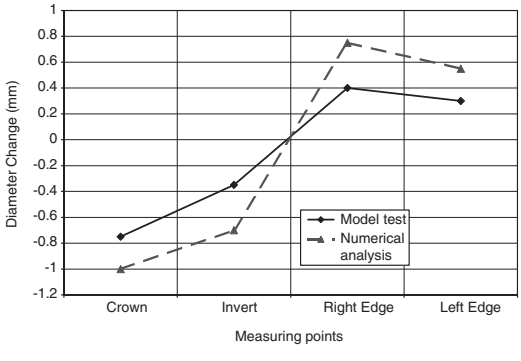


Figure 7. Diameter change at 4 points against tunnel test PS3.

construction of the second one. Figure 7 indicates good agreement between the physical and numerical results of the deformation for the four main points. Figure 8 shows the incremental Bending moments induced in the instrumented lining due to the installation of the second tunnel. These results indicate that the numerical and the model test data are well agreed. Figure 9 shows typical results of total displacements of the lining.

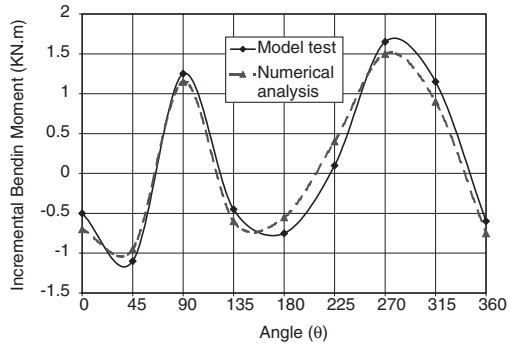


Figure 8. Incremental Bending Moments against tunnel test PS3.

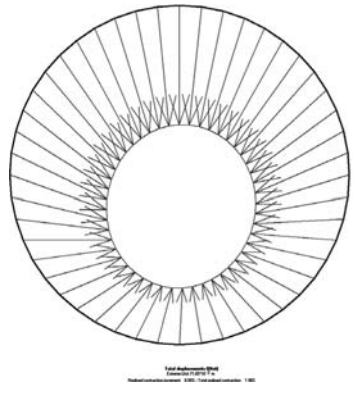


Figure 9. Total displacements in lining of section 3.

6 OVERALL STABILITY OF THE TUNNELS

One of the important aspects of the water uplift stability is developed in the present analysis. The water level in the area of construction is too high and the weight of the structure shall overcome the water uplift forces. The stability is ensured for the critical section located under Suez Canal where the soil cover is minimum 13 m after dredging. Any resisting forces due to soil friction are neglecting.

7 CONCLUSIONS

One of the major advantages of the numerical studies is to allow the very complex soil structure interactions involved in the tunneling process to be accurately investigated. The technique has been developed to include 3D effect in 2D analysis was succeed.

The straining actions acting on the tunnel liner resulting from the soil and groundwater pressure is evaluated along the TBM Tunnel route through the three sections considering in the analysis.

Based on the results of the analysis providing to the stresses and the plastic zones, it can be shown that the interaction between two tunnels is unlikely to be significant unless the spacing between them centers is more than about two tunnel diameters.

The non-linear FE analysis with a hydrostatic procedure gives results that appear to be in good agreement with the results of the physical model tests for the internal forces and deformations.

The stability is ensured for the tunnels against the uplift pressure with safety factor of 1.5. The soil cover that must remain on the tunnels should be at least about 6 m.

The results obtained from this study are believed to be useful for design of the project and to facilitate the interpretation of the monitoring results. Also, it is benefit for the back analysis that can be achieved privilege during the construction of project.

REFERENCES

Brinkgreve, R.B.J., 2002. *PLAXIS, Finite Element Code for soil and Rock analysis*, Version 7.2, A.A. Balkema, Rotterdam, Netherlands.

Mair R.J. and Taylor R.N., 1997. Bored tunneling in the urban environment. Theme Lecture, Plenary session 4, 14th *Inter. Conference on Soil Mechanics and Foundation Engineering*, Hamburg, 6–12 September.

Leca, E. and Mestat Ph., 1999. Modelisation des ouvrages souterrains. Chapter 5, *AFPC, Emploi des elements finis en genie civil: ouvrages en interaction, Ph. Mestat & M. Prat Eds*., pp. 305–389.

Abu-Krisha, A., 2002. New 2D simulation of TBM tunneling and application on EL-AZHAR road tunnels. 28th *ITA-AITES world tunnel congress*, Sydney, Australia.

National Authority for tunnels (NAT). 2004. *Project Documents, Soil repots.*

Sang-Hwan Kim, 2004. Interaction behaviors between parallel tunnels in soft ground. 30th *ITA-AITES world tunnel congress, Underground space for sustainable urban development*. Singapore, pp. 899–904.

Sang-Hwan Kim, 1996. Model testing and analysis of interactions between tunnels in clay. *D. Phil. Thesis*, Oxford University, UK.

This page intentionally left blank

Underground Space – the 4th Dimension of Metropolises – Barták, Hrdina, Romancov & Zlámal (eds)
© 2007 Taylor & Francis Group, London, ISBN 978-0-415-40807-3

Numerical modeling of face stability for TBM tunneling

Ashraf ABU-KRISHA
National Authority for Tunnels (NAT), Cairo, Egypt

ABSTRACT: Several approaches have been developed to analyze the face stability for TBM tunneling in soft ground. The face stability for TBM is a three-dimensional (3D) problem. As a consequence of the TBM procedure, 3D analyses are the most realistic, especially the modeling of the face stability. In the present numerical examples, the effects of face supports at the front of the shield have been considered in the analyses. Incremental stage-by-stage analysis simulating excavation scheme is used.

In this study, the face stability in underwater tunnels was evaluated by simultaneously considering the effective stress acting on tunnel face and the seepage force. The effect of permeability anisotropy on the seepage force acting on the tunnel face was also assessed by conducting a coupled analysis. This presented model is namely a four-dimensional (4D) numerical model. The support pressures calculated by the analytical methods taking seepage forces into account were compared with the results of the coupled finite element analysis.

Keywords: Numerical Analysis, TBM Tunnelling, Face stability, four-dimensional.

1 INTRODUCTION

Advances in computer systems have allowed complex conditions to be accurately modeled by means of numerical methods, thus providing new approaches for characterizing the face stability of TBM tunnels constructed in soft soils. Front stability is usually maintained by bentonite slurry or pressure balance shields. Recently, several studies are developed to deal with the face stability of the TBM tunnels. Many approaches can be applied to tunnel subject to seepage forces during tunnel construction which are located under the ground water level. The upper bound solution by modifying the failure mechanism was provided by Leca and Dormieux (1990). The wedge stability model that taking full account of the three-dimensional geometry at the tunnel face, was proposed by Anagnostou and Kovari (1996–1997), using limit equilibrium principles. This model is not valid when different soils are present within the tunnel face, and those soils have different angles of internal friction and cohesion. Also, there is no straightforward way to approximate or average the soil properties to obtain the correct support pressure. Two slice methods are proposed according to the shape of sliding surface, In-Mo Lee and Seok-Woo Nam (2004). The first sliding surface is employed to be a logarithmic spiral while the second sliding surface is assumed to be a straight line. The critical support pressure at the tunnel face can be determined by iteratively altering the inclination angle between the sliding surface and the horizontal. Figure 1 shows the critical surfaces for the methods of the analysis of tunnel face in longitudinal section.

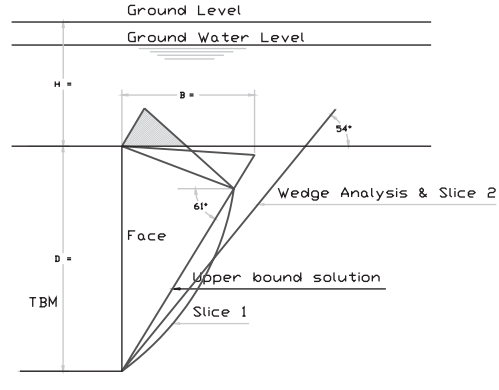


Figure 1. Critical surface of the analysis of TBM tunnel face.

In the TBM tunneling, the penetration of the support medium into the soft soils simultaneously with the removal of soils at the face is taken into account. This infiltration may in turn leads to excess pore pressures in the front of the TBM as well as a reduction of the effective support force. The penetration distance is governed not only by the filtration velocity but also by the advance rate. Thus, the support pressure is then transported onto the soil skeleton over this infiltration length. Consequently, there are three cases of the slurry infiltration; formation of filter cake only,

pure penetration without filtration, and combination of filtration and penetration.

In a soil problem with the consideration of water flow, there are two methods to analyze the forces that acting on an element. One is to use boundary water forces along with the total weights and the other is to use seepage forces along with the submerged weights. The two methods give approximately the same results exactly. The support pressure that is calculated by latter one in wedged analysis is used in this study. In this paper, 3D FEM model that include face pressure is performed describing time-dependent in longitudinal section deformations. These types of model are known as a four-dimensional (4D) model analysis.

The 4D face stability model was derived from the twin tunnel of El-Azhar road tunnels, Cairo, Egypt. Each tunnel is 2.7 km long and has inside diameter of 8.35 m with 0.4 m lining thickness. Construction used a TBM with bentonite slurry shield. A system of monitoring was installed for the project. This system at considering north tunnel section consists of surface settlement points, deep extensometer with 4 points, inclinometer and contraction section. Face pressure transducers have been inserted in ring 171 of the northern tunnel beneath the monitoring section. This instrumented ring was monitored during excavation and construction and after lining installation, NAT Monitoring Documents (1999).

2 DATA ANALYSIS AROUND MONITORING SECTION

The monitoring results around ring 171 of north tunnel have been analyzed in details. Surface settlement versus time was plotted as settlement versus TBM position, NAT Monitoring Documents (1999). For a uniform tunnel boring posses these plots should show the influence of face stability pressure and TBM volume loss. Surface settlement at ring number can be compared with face pressure at ring number x-10 in figure 2. Also, the ground displacements are given as a function of time from the deep extensometer and inclinometer. The extensometer is located at the tunnel centerline by 6.6 m near the ring 171. Heave was mainly found during boring of TBM for ring numbers 150 through 200. This heave is limited to the zone directly above the tunnel. Figure 3 shows the monitoring results of the face stability pressure and vertical settlement at the considering section versus the time. From the above mentioned, it is evident that tunnel boring from rings 130 to 210 has not been constant.

3 GEOLOGY AND GEOTECHNICS

The geological formations along El-Azhar road tunnels project are typical Cairo Nile Alluvial deposits.

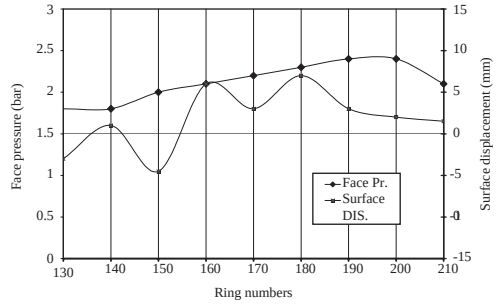


Figure 2. Face stability pressure at crown and surface settlement versus ring numbers.

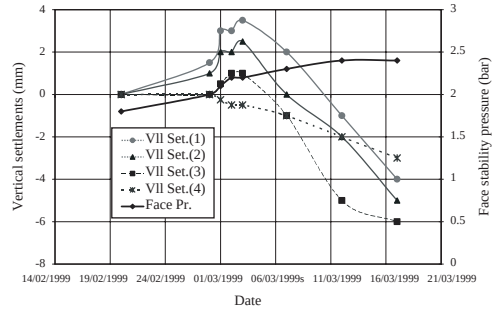


Figure 3. Vertical displacement extensometer at 4 points and face pressure as a function of time.

Table 1. Layers and geotechnical parameters.

Soil Layer	Depth (m)	γ KN/m^3	E Mpa	v	K_0	ϕ	C Kpa
Fill	0–6	18.0	10	0.4	1.0	26	15
Sand (1)	−6–9	20.0	40	0.35	0.37	37	0
Clay (1)	−9–12	18.5	13	0.4	1.0	0	90
Sand (2)	−12–15	20.0	50	0.3	0.4	38	0
Clay (2)	−15–25	18.5	14	0.4	1.0	0	100
Sand (2)	−25–60	20.0	50	0.3	0.45	39	0

The tunnels are mostly bored in slightly silty sand. Soil parameters were derived from in situ and laboratory tests. Geotechnical parameters that used for the analysis are given in Table 1. Water table is −8 m from the ground level, NAT soil report (1998).

4 NUMERICAL MODEL

Half north tunnel is modeled with standard boundary conditions for soil and lining using FINAL code (1998) for coupled analysis, as shown in figure 3. In coupled

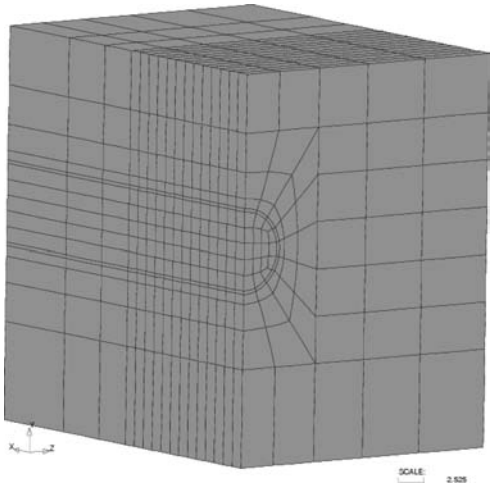


Figure 4. 3D finite element model.

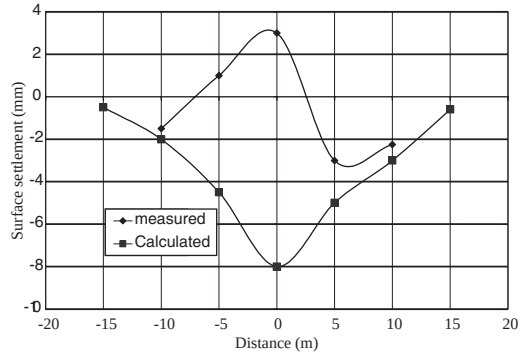


Figure 5. The comparison between the calculated and measured transverse surface settlement.

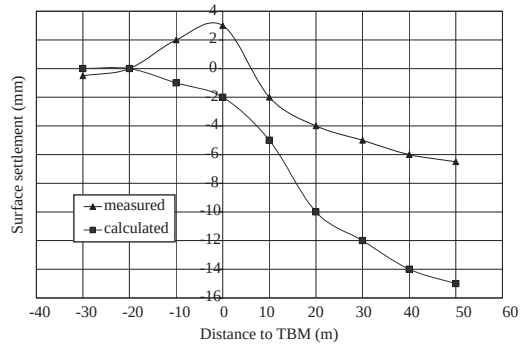


Figure 6. The comparison between the calculated and measured longitudinal surface settlement.

analysis, the hydraulic boundary conditions must be defined. These conditions are identical to those that used in seepage analysis. The model is divided in longitudinal direction according to the one tunnel ring that is 1.5 m to simulate the phase's construction. The number of stages will cover a constant bending moment at some distance from both TBM and model boundaries. The total length and width of the model are 120 m and 40 m respectively. The upper part section of the tunnel is in sand and the remaining lower section is in plastic to very plastic clay. The tunnel axis is 8 m below the water table level. The coefficient of horizontal permeability to the coefficient of vertical permeability (K_h/K_v) is 10 time.

The soil has been modeled using the hardening soil model. This model implements soil behavior under the unloading-reloading conditions governing the tunnel construction. The TBM and Tunnel lining are modeled by shell elements. TBM face pressure is modeled by applying slurry pressure at the crown and the pressure gradient of 20 KN/m^2/m. This face support pressure is modeled as external forces and not linked to the TBM. The tunnel boring process has been modeled by incremental stage-by-stage analysis construction calculation; where there is approximately 30 stages, one ring per stage is bored.

The summation value of the slurry pressure at the face of TBM (slurry confining pressure) consists of the hydrostatic pressure, over-burden pressure and factor of safety pressure. At any section the hydrostatic pressure and over-burden pressure are constant while the factor of safety pressure will be changed according to the allowable settlement and soil parameters.

5 RESULTS OF 4D FEM ANALYSIS

The results of the analyses have been compared with monitoring soil deformations. Some of the calculations have been conducted in order to determine the model's sensitivity to the face stability pressure.

The results show that the maximum of the calculated final surface settlement is about 8 mm. Figures 5 & 6 show the comparison between the calculation under the effect of measured face slurry pressure and measured surface settlement in the transverse and longitudinal direction respectively. The final deformation at surface level measured at the monitoring section is varied between approximately 6 mm heave and 5 mm settlement. Hence the 4D model with best estimate parameters calculates the maximum of measured settlements. The calculated transverse through is symmetric, while the measured one is not. The deformations measured by inclinometer and the calculated horizontal displacements are plotted in figure 7. The calculated curve is closely matches these measured. It is found that magnitude of horizontal components of the displacement vectors is much larger than that of

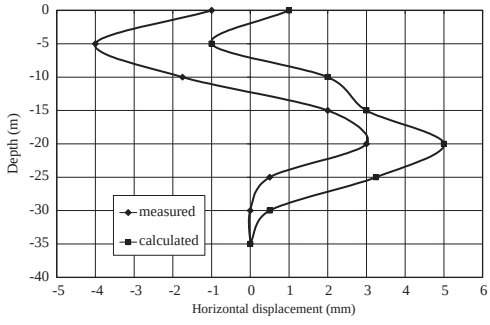


Figure 7. The comparison between the calculated and measured horizontal displacement.

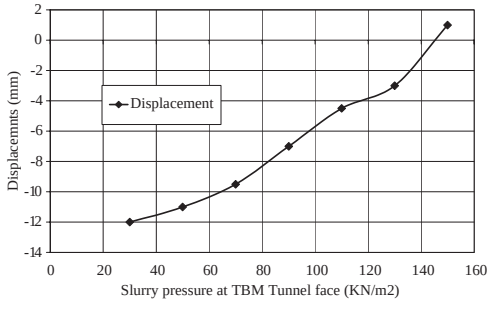


Figure 8. Slurry pressure versus horizontal displacement at tunnel face.

vertical components with small slurry face pressure and depends on the seepage flow vectors.

The horizontal displacements at center node of the tunnel face are plotted against the slurry pressures as shown in figure 8. The support pressure estimated was compatible with the wedge stability method using limit equilibrium principles.

The effects of permeability anisotropy on support pressure for face stability are illustrated in figure 9. It can be noted from this figure that the higher horizontal permeability compared with the vertical one (k_h/k_v) has a favorable effect on the TBM face stability. This result was the same trend as that obtained by Buhan et al. (1999). The critical failure surface might vary due to the permeability anisotropy of the soil. So, the critical failure surface can be determined by iteratively changing of the slurry face stability pressures in the coupled analysis until matching with one of suggested calculation method.

6 CONCLUSIONS

The face stability of TBM tunnel was studied in this paper and the methods of calculate the slurry pressures required for the face stability were reviewed. The coupled numerical analysis was performed for the slurry

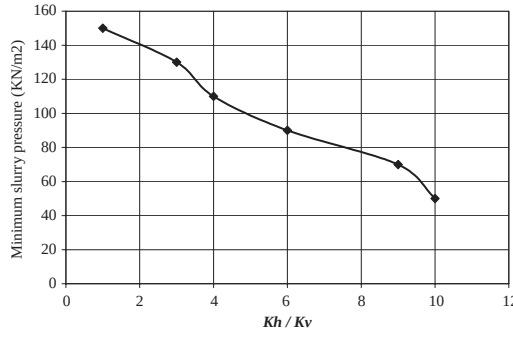


Figure 9. Slurry pressure as a function of permeability anisotropy.

pressure of face stability and checked with estimation methods.

The presented results show that the FEM for face stability combined with the practical experience currently available it is feasible to model TBM with 4D approach. The monitoring data show that the boring process has not been constant at the section used for the history match with the FE model.

The stability model that deals with layered soils, especially at the tunnel face, is clearly needed. The existence of ground water may seriously affect the face stability.

REFERENCES

Anagnostou, G.and Kovari, K., 1996. "Face Stability in Slurry and EPB shield Tunneling." *Tunneling and Underground Space Technology,* Vol. 9, No. 2, pp. 165–174.

Anagnostou, G.and Kovari, K., 1997. "The Face Stability of Slurry-shield-driven Tunnel." *Proceeding Int. Symposium Geotechnical Aspects of Underground Construction in soft Ground,* London, pp. 453–458.

Leca, E. and Dormieux, L., 1990. "Upper and Lower Bound Solutions for the Face Stability of Shallow Circular Tunnels in Frictional Material." *Geotechnique,* Vol. 40, No. 4, pp. 581–606.

In-Mo Lee, Jae-Sung Lee and Seok-Woo Nam, 2004. "Effect of seepage on tunnel face stability reinforced with multi-step pipe grouting." *Tunneling and Underground Space Technology,* Vol. 19, No. 6, pp. 551–565.

Swoboda G., 1998. Program System FINAL, Finite Element Analysis Program for Linear and Nonlinear Structures, *Version 7.1, University of Innsbruck,* Austria.

National Authority for Tunnels (NAT), 1999. El-Azhar Road Tunnels Project, *Monitoring Documents*.

National Authority for Tunnels (NAT), 1998. El-Azhar Road Tunnels Project, *Geology and Geotechnical Investigation Documents, Soil Design parameters.*

Buhan, P.D., Culvillier, L. Dormieux, L. and Maghous, S. 1999. "Face Stability of shallow circular tunnels driven under the water table: a numerical analysis". *Int. journal for Numerical and Analytical Methods in Geomechanics* 23(1), pp. 79–95.

Underground Space – the 4th Dimension of Metropolises – Barták, Hrdina, Romancov & Zlámal (eds)
© 2007 Taylor & Francis Group, London, ISBN 978-0-415-40807-3

Impact of the face anchoring on the stability of underground working

J.Aldorf, E. Hrubesova & L. Duris
VSB –Technical University Ostrava, Ostrava-Poruba, The Czech Republic

ABSTRACT: Underground working stability depends on many objective and subjective factors. One of the important condition participant in the underground working stability is the face stabilization. These condition resulted from the fact, that after excavation the primary state of plane -deformation on working face and ahead of it changes into complex spatial (3-D) stress–deformational characteristics. The area ahead of face get deformed in the transverse plane as well as in longitudinal axis of the working. Without the adoption of appropriate stabilisation measures at the face (e.g. anchoring) , this qualitative change of stress-strain state can lead to loss of face stability and, eventually, may lead to the loss of stability of the whole section of the underground working. The paper is concerned with the mechanism of the face stability, with the stabilization effect of face anchoring, including the possibilities for the determination of optimum anchoring parameters.

1 FACTORS DETERMINING FACE STABILITY OF UNDERGROUND WORKING

Leaving aside the factors like shape and dimension of the tunnel, depth, characteristics of rock mass (deformational, strength, structural) and hydro-geological conditions of the rock environment in which the tunnel is being realized, among the basic factors, which determine the face stability and loading of the support, belong the technological factor of tunnelling and supporting of the tunnel, particularly the system of division of the face of the excavation and the length of the unsupported part behind the face. From this point of view, it is necessary to evaluate the time factor of supporting of the tunnel from two viewpoints, one is with regard to the influence on face stability and the other is with regard to its influence on loading of the support. Increased time lag between the stoppage of excavation and it's supporting may indicate increase in stability problems in transverse as well as in longitudinal direction. On the contrary, however, from the view point of loading of the support, the optimum time lag in supporting may contribute to the reduction of loading of rock mass on the support. Effective utilisation of co-acting of system "rock-support", for attaining minimum loading of the support while maintaining the stability and allowable deformation of rock mass (in transverse as well as in longitudinal direction), assumes, among others, objective determination of manifestation of deformation in the rock mass, not only in the part behind the face but also ahead of it, with the objective to determine that part of the total deformation which is not brought on the support. Stress–deformational manifestations of the rock mass are, however, influenced as well by the stabilisation measures at the face. For the purpose of stabilisation, it is possible to use different types of anchors and bolts, whose purpose is not only to anchor the potential unstable area around the face, but also to increase parameters of deformational and strength properties in the anchored part ahead of the face.

2 MODELLING OF FACE STABILITY AND IT'S INFLUENCE ON THE LOADING OF THE SUPPORT

Problem of face stability and the problem of determination of loading of the support are, therefore, mutually closely interconnected. Different types of physical models (Broms and Bennermark, 1967, Chambon and Corté, 1994) and simplified models based on evaluation of working–deformational characteristics of rocks and supports (Lombardi and Amberg, 1979) have contributed towards the understanding of the mechanism of stress-deformational behaviours around the face and towards the quantification of stability conditions at the face. These models, however, due to their simplification cannot take into account the influence of all the determining factors mentioned

earlier. Numerical methods of spatial (3D) modelling have wider possibilities for more reliable and objective solution of stability in tunnel and in determining the loading of the support.

A tunnel lying at a depth of 30 m below the surface has been modelled by using the program system 3D Tunnel, which works on the basis of finite elements method, developed by the Dutch company Plaxis. Dimensions of the model are $60 \times 60 \times 100$ m. The tunnel has arched transverse cross-section. Height of the tunnel is 5,5 m and the width, as measured along the floor, is 7 m. In this model case, the drivage has been considered as undivided face, the concrete support (E = 20000 MPa) of thickness 25 cm has been initiated in the model at a distance of 1 m behind the face. The spatial (3D) model works with homogeneous, isotropic environment. Behaviour of this environment has been described on the one hand by means of an elastic model and on the other hand by an elastic – plastic Mohr – Coulomb material model. The rock environment is characterised by the following parameters: Weight per unit volume $\gamma = 22$ kN/m^{3,} modulus of elasticity Ed = 50 MPa, cohesiveness c = 100 kPa, angle of internal friction $\varphi = 17°$.

Simulation of face stabilisation has been conducted within the framework of the model by means of fibreglass anchors (length 5 m and diameter of rod 25 mm) located in the direction of the longitudinal axis of the model. The influence of the anchor density has been investigated on the following variants: density 1 m × 1 m/anchor (representing 27 anchors at the face); density 1 m × 1,5 m/anchor (representing 14 anchors at the face);density 1.5 m × 1.5 m/anchor (represents 14 anchors at the face). Influence of anchoring of the face on the change of deformational and strength parameters of rock environment in the surrounding of the face has been considered in the model by modifying the value of modulus of elasticity and cohesiveness. Simplified assumption has been adopted that the increased values of deformational and strength properties, which are, among others, functions of number of anchors at the face, are constant in the whole anchored part ahead of the face. Percentage increase of modulus of elasticity stems from the parametric studies conducted by using finite elements method. Value of increased cohesiveness "c" comes from the relationship.

$$c' = \frac{1+\sin\varphi}{2\cdot\cos\varphi}\cdot\frac{P}{F} \qquad (1)$$

where P is the load – bearing capacity of the anchor, F is the area of transverse cross-section of the face coming under one anchor.

The following increased values of the mentioned parameters have been considered (table 1).

Table 1. Increasing parameters depending on anchor density.

	Increase of parameters	
Anchor density	Modulus E %	Cohesion c %
27	30	197
22	25	98
14	20	32

3 RESULTS OF MATHEMATICAL MODELLING

Parametric computations have been conducted for the stated variants of anchor density utilising the mentioned program 3D – Tunnel and the stress – deformation and stability state in the rock environment around the tunnel (inclusive of the face) has been determined as well as the internal forces and deformation in supports of the tunnel and fibreglass anchors have been evaluated. Some of the results of 3 D – modelling have been presented in figures 1 to 7. Evaluation of the results of parametric computations is possible to summarise as follows:

- final maximum value of the vertical displacement of the roof of the excavation (15 mm) has been achieved at a distance of approximately 50 m behind the face (approximately seven times the width of the excavation as measured along the floor), this remains valid not only in the case of an elastic model but also in the case of an elasto-plastic model and is not dependant on the anchor density at the face
- the influence of stress release in the rock mass, as a consequence of realisation of the tunnel, has been observed at a distance of 50 m ahead of the face and has been manifested by vertical displacement of the roof (0,3 mm to 0,5 mm) in connection with the chosen constitutive relationship and the density of anchoring of the face
- the character of the graphs of vertical displacement at the face and in the immediate surroundings differs in relation with the chosen type of behaviour of the rock environment. Realized computations have shown substantial quantitative and qualitative differences between the results of computation of displacement on the assumption of elastic behaviour of the rock environment and on the assumption of elastic – plastic behaviour of the medium (figure 1 and 2).
- in case of elastic model, approximately 36% of final vertical deformation of the roof has occurred ahead of the face in case of unanchored face, while in the case of anchored face the final vertical deformation of the roof has been reported to be only 30% (influence of anchor density has not been almost

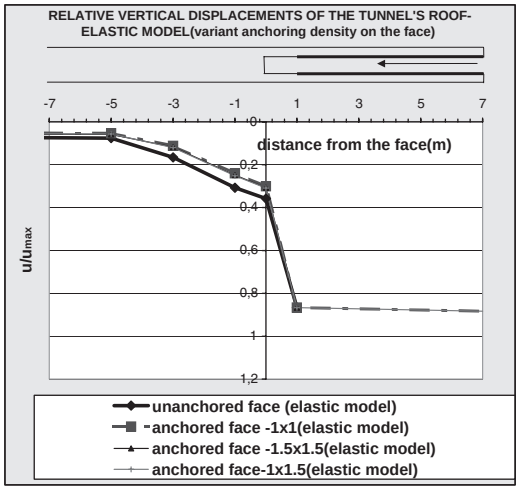


Figure 1. Vertical displacements in the roof (elastic model).

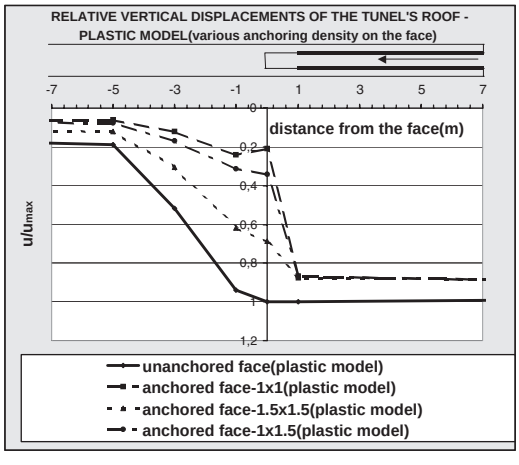


Figure 2. Vertical displacements in the roof (elasto-plastic model).

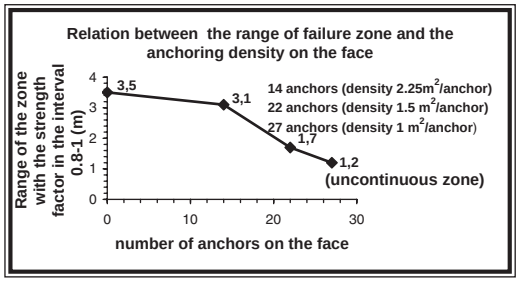


Figure 3. Relationship of the range of the zone of failure on the number of anchors at the face.

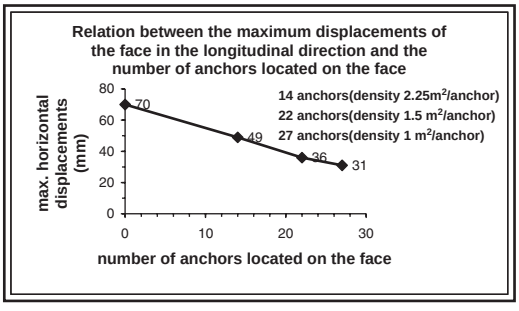


Figure 4. Relationship of the maximal longitudinal displacements on the number of anchors at the face.

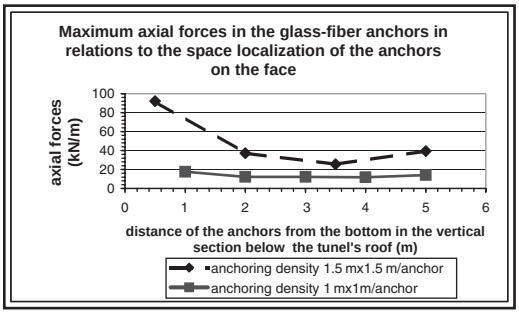


Figure 5. Relationship of the maximal axial forces in the fibreglass.

manifested in that model). In case of unanchored face, 100% of the vertical deformation of the roof has occurred ahead of the face on the assumption of plastic behaviour of the rock environment, which implies probably from the effects resulting forming the longitudinal arches. With the increase of anchor density, this share of vertical roof displacements which have already occurred ahead of the face gradually decreases within the boundary of 69% to 21% of the total vertical displacements. The share of total displacements changes proportionally (directly proportional) to the degree of face stabilisation, which corresponds to the unsupported metres behind the face (66% for maximum considered anchor density, 19% for minimum considered anchor density). The influence of anchor density at the face on the value of vertical displacements of the roof, which is brought on to the tunell support does not demonstrate practically.

– in case of the elastic model with the unsupported face, the results of computation show higher percentage of the total vertical displacements of the roof, which is brought on the support in comparison with the elasto-plastic model. In case of anchored face, the loading of the support increases as a result of stabilisation, subject to the the assumption of elasto-plastic deformation. The used numerical

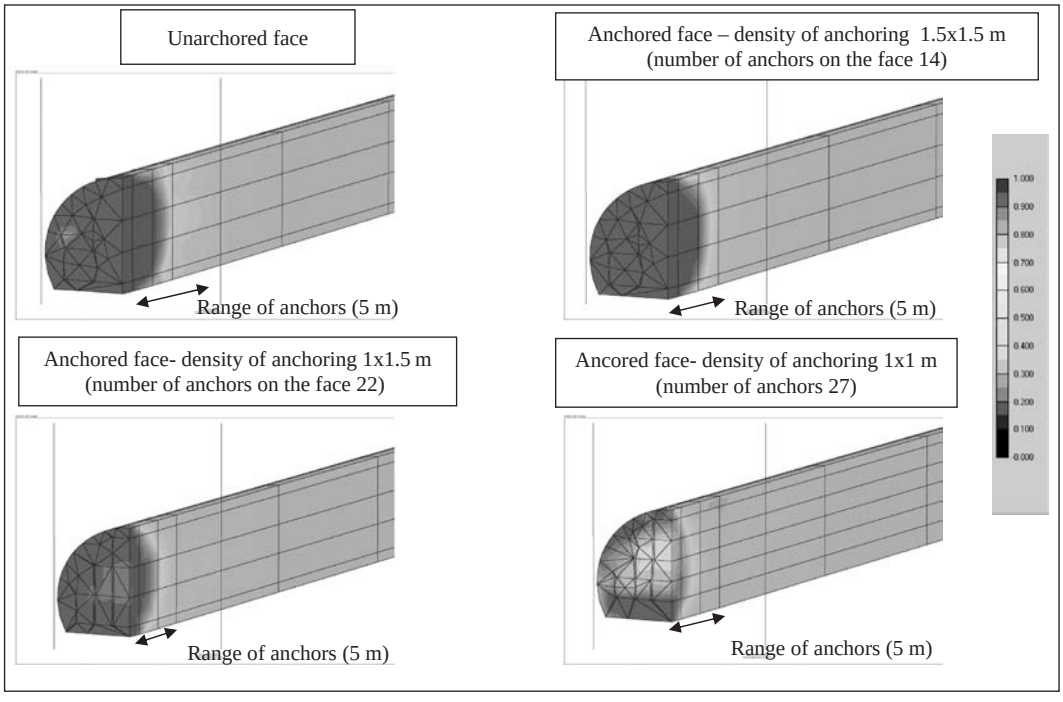


Figure 6. Strength factor on the face and it‘s forefield.

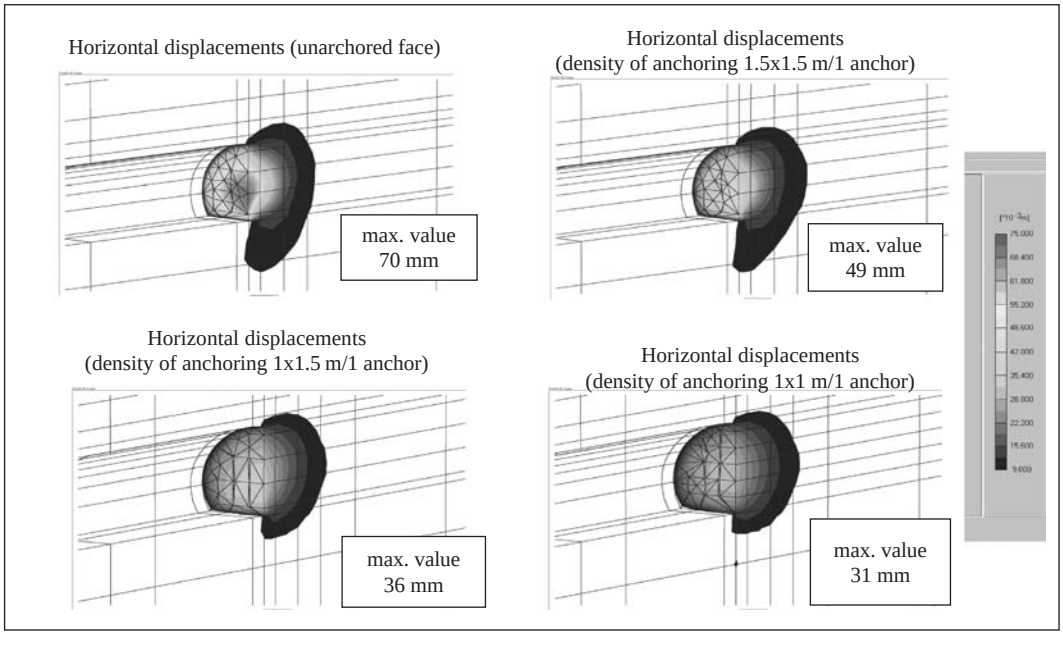


Figure 7. Horizontal displacements in the longitudinal direction.

model, however, in this case did not prove the influence of anchor density on the magnitude of that part of the support loading, which implies from the shifting of vertical displacements to the supports.
– graphs in figure 3 and fig. 6 illustrate increase in drawing of strength with the reduction of anchor density at the face and further show the indirectly proportional relationship of the range of the zone of fracturing on the number of anchors at the face. Extent of the area of fracturing, corresponding to drawing of strength in the range of 0,8–1 varies in the interval of 3,5 m (unanchored face) to 1,2 m (anchor density 1 m^2/anchor). Face stability is increased with the increase of anchor density.
– horizontal displacements in the direction of longitudinal axis of the excavation are inversely proportional to the anchor density at the face. It varies in the range of 70 mm (unanchored face) to 31 mm in the case of anchor density of 1 m^2/anchor (graph in fig 4 and fig 7).
– from the evaluation of axial forces in the anchors, whose heads are localised in the vertical section passing through the centre of the transverse cross - section of the excavation, it appears that in case of lowest considered anchor-density (2,25 m^2/anchor), the highest axial forces are located closest to the floor (92 kN/m). The axial forces are lowest (25 kN/m) in the middle part of the transverse section of the face. Axial forces in anchors are gradually decreased with the increase of anchor density at the face and their values then practically do not depend on the distance of the anchor from the floor (graph in fig. 5).

4 RECOMMENDATIONS IMPLIED FROM THE RESULTS OF THE MODEL

– from the viewpoint of the evaluated extent of fracturing ahead of the face, the minimum length of the bolts should be 0,5 times the width of the excavation.
– anchor density with area higher than 2 m^2/anchor do not any further markedly influence the stability state. Therefore, the recommended anchor density at the face is 1,5 m^2/anchor.
– due to the determined not very high values of the axial forces in the anchors (maximum 92 kN/m), the requirements regarding the load bearing characteristics of the anchors are quite little.

5 CONCLUSION

Results of the parametric computations show, except others, mutual close relationship between face stabilisation and loading of the support, particularly in the case of elasto-plastic model of behaviour of the rock environment. Optimisation of this mutual state is not possible to carry out in an objective and reliable manner without the realisation of the respective spatial (3 D) mathematical model which enables to take into account the complicated spatial (3D) character of the stress – deformation state ahead of the face. The paper also points towards the quantitative and qualitative differences of results of modelling in relation to the accepted model of behaviour of the rock environment (elastic model, elasto – plastic model). This reality has, in case of low strength rocks where it is possible to assume the creation of zone of plastic deformation, great consequence not only for the effective stabilisation of face but also for more objective determination of loading of the support.

REFERENCES

Zaman, M. & Gioda, G. & Booker, *J. Modelling in Geomechanics*, J. Wiley, 2000. ISBN 0-471-49218-3.
Manual of the Programme System 3D Tunnel, Balkema, 2001. ISBN 90-265-18196.

This page intentionally left blank

Underground Space – the 4th Dimension of Metropolises – Barták, Hrdina, Romancov & Zlámal (eds)
© 2007 Taylor & Francis Group, London, ISBN 978-0-415-40807-3

Bentonite and grout flow around a TBM

A. Bezuijen
GeoDelft, Delft, The Netherlands

ABSTRACT: The flow of grout and bentonite around a slurry shield TBM is investigated, using a 1-dimensional calculation model. The results show that the shield of the TBM is only partly in contact with the surrounding soil and that for a large extent it is in contact with the liquid grout and, depending on the amount of over cutting, also in contact with the bentonite that is injected at the tunnel face. These liquids also determine the forces on the TBM shield. The calculation model presents the pressure distribution on the shield and shows the influence of the soil properties, the overcutting and the properties of the grout and the bentonite.

1 INTRODUCTION

The cutting wheel of a TBM is in most cases a bit larger than the TBM itself. There is only a small difference (a few centimeters on a TBM with a diameter of 10 meters or more), but this difference is significant. It means that for a slurry shield bentonite can flow from the tunnel face back to the grout used to fill up the tail void. However, it is also possible that grout can flow from the tail void to the tunnel face. It is important to quantify the flow of both the bentonite and the grout because these flows determine the quality of the tail void grouting and in non-cohesive soils these flows have to be controlled to avoid erosion of the soil around the TBM. Furthermore these flows determine the pressure distribution on the TBM shield that is important in both the design of the TBM and to calculate the soil settlement that is caused by the TBM tunnelling. Lack of knowledge on the pressure distribution on the TBM led to deformations of the TBM during tunnelling (Barends, 2005).

A 1-dimensional model is developed to get information on the order of magnitudes of the flow of the grout and the betonite, the pressure distribution and the soil deformation around the TBM shield. The model assumes a given pressure distribution at the tunnel face (the face pressure) and at the tail of the TBM (the grout pressure) and incorporates the yield strength of both the grout and the bentonite. It takes into account the over cutting of the cutting wheel and the conical construction of the TBM (with a bit smaller diameter at the tail compared to the front). Linear elastic soil behaviour is assumed. This last assumption is justified to a certain extent by the observation that only small deformations will occur during TBM tunnelling under normal operation.

Finite element calculations (Hoefsloot & Verweij, 2005; Kasper & Meschke, 2006) have shown that the calculated settlement trough is too deep when it is assumed that the TBM shield is in contact with the soil all over the TBM. The model described in this paper presents a framework that quantifies the amount of contact between the soil and the TBM and indicates what volume loss can be expected depending on the face pressure and the grout pressure.

2 GEOMETRY OF A TBM

A TBM shield seems to be a tube with a constant diameter, sketched in a way as in Figure 1.

However, looking more in detail the shield is part of a cone. The diameter at the front is larger than at the tail. The difference is only small, normally around 0.4% of the diameter of the TBM. For a TBM shield

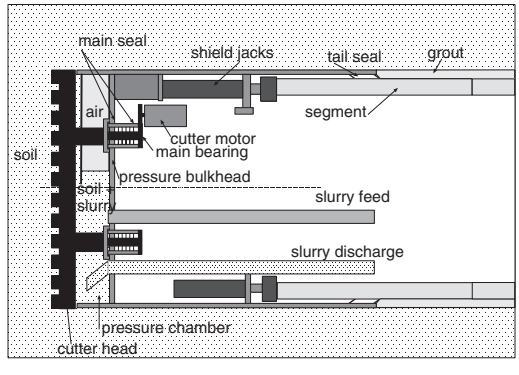


Figure 1. Sketch of a slurry shield TBM.

with a diameter of 10 m, this means that the diameter of the shield is 4 cm smaller at the tail compared with the diameter just after the cutter head. This small difference in diameter allows the TBM to maneuver in the soil.

3 GROUT FLOW AROUND A TBM

3.1 *Theory*

Assume a TBM with a small change in diameter (a diameter decrease from front to back). The TBM is boring in soil that is assumed linear elastic with a shear modulus G.

Assume that the soil flows around the shield and the soil is in contact with the shield. This leads to a decrease in stresses in the soil around the TBM going from the tunnel face to the tail. A simple approach is to neglect the influence of gravity and assume a tunnel that is positioned perfectly symmetric in the bore hole. In such a situation the relation between deformation and stress reduction can be written as:

$$\Delta\sigma = 2\frac{\Delta r}{r}G \tag{1}$$

Where $\Delta\sigma$ is the change in pressure, Δr the change in radius, r the radius of the tunnel and the grout and G the shear modulus of the soil around the tunnel. The interaction between soil and grout was also described with this formula in Bezuijen & Talmon. (2003) and proved to be useful in that research.

Calculating the pressure from front to tail of the TBM, without the influence of grout, will lead to an ongoing pressure reduction. However, grout is injected at the tail of the TBM. If this is injected with a pressure higher than the pressure calculated with Equation (1) the soil will be pushed from the TBM and the situation sketched in Figure 2 will occur. The grout will flow in the joint between the soil and the TBM. Flowing into this joint will lead to a pressure drop in the grout. The pressure is the highest in the tail and decreases going to the tunnel face of the TBM. This pressure drop is determined by the yield stress in the grout and the width of the joint. Assuming that most flow induced friction will develop between the soil and the grout, the pressure drop can be written as:

$$\Delta P = \frac{\Delta x}{s}\tau_\gamma \tag{2}$$

Where ΔP is the change in pressure due to the flow, Δx a length increment along the TBM, s the joint width between the tunnel and the soil and τ_γ the shear stress of the grout around the TBM. In this formula we neglect viscous forces. This is allowed due to the low flow velocities that can be expected. With these equations and the known shape of the tunnel it is possible to calculate what joint width can be expected and for how far the grout in the tunnel flows over the TBM shield.

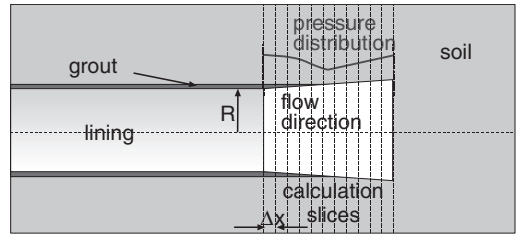


Figure 2. Idealized sketch of a TBM and lining in grout (picture not to scale).

Table 1. Parameters used in calculation.

Length TBM	5	m
Diameter	10	m
diameter reduction	0.2	%
1 or 2 side (1 with non-symm. TBM)	1 or 2	
Grain stress	200	kPa
Grout pressure drilling	500	kPa
Pore pressure	200	kPa
Shear modulus (G)	90	Mpa
Yield stress grout with soil	0.8	kPa

The following calculation procedure is used. The soil around the tunnel is assumed to behave as independent slices with a thickness Δx, see Figure 2. Knowing the geometry of the tunnel, the grouting pressure, the soil pressure and the elastic properties of the soil, the joint width at the tail of the TBM can be calculated using Equation (1). That joint width can be used to calculate the pressure drop due to the flow of the grout to the front of the TBM over the distance Δx with Equation (2). The resulting pressure (the original grouting pressure minus the pressure drop) is used to calculate the deformation and joint width of the next slice and so on. For each calculation it is checked if the calculated joint width is still positive. If this is not the case then the soil is in contact with the TBM and the pressure is calculated from Equation (1) using the actual diameter of the TBM for that slice.

3.2 *Calculation*

The diameter of the TBM at the front face is 10 m, the diameter at the tail is 20 mm less. All values used in this calculation are mentioned in Table 1 are used. 1 or 2 side is mentioned in this table. “2 side” assumes a symmetric situation as shown in Figure 2. “1 side” indicates the asymmetric situation in which the tunnel is on one side in close contact with the soil and as a result the joint on the other side is wider.

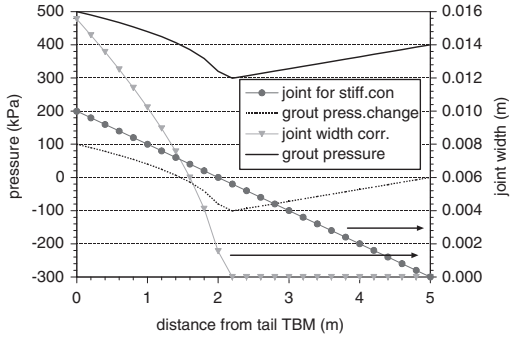


Figure 3. Calculated pressures at the tail of a TBM and the resulting joint width. Symmetric situation (lines with markers refer to the right vertical axis, the others to the left), see also text.

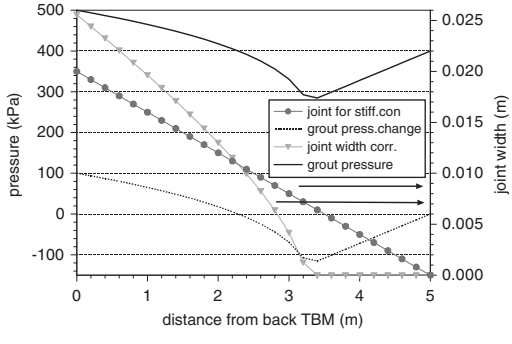


Figure 4. Calculated pressures at the tail of a TBM and the resulting joint width. Asymmetric situation (lines with markers refer to the right vertical axis, the other to the left), see also text.

The calculation shows that there is a considerable amount of the shield, which is not supported by soil but is in the grout (2.2 m from the back of the TBM is in the grout).

In these figures the line with the round dots represents the joint width that would occur if the tunnel is boring trough a completely rigid soil. In that situation the diameter of the hole in the soil would be constant and the diameter of the TBM shield decreases (going from the tunnel face to the tail. This line is simply the difference between these 2 values. The line with the triangles is the correction due to elastic deformation in the soil caused by the diameter differences in the TBM and the grout pressures. The solid line presents the grout pressures along the TBM, and the broken line the grout pressure minus the static soil pressure.

In this first example it was assumed that the TBM was perfectly symmetric in the soil. However, it is likely that this is not true. The tail of the TBM weights less than its front and if this tail is embedded into the grout, it is likely that buoyancy forces lift the tail. The lifting will be counteracted by the yield stress of the grout. Therefore the second calculation is made for the situation that the TBM is as asymmetric as possible. One side of the TBM is in contact with the soil over the full length the other side has a joint that is twice the joint in the symmetric situation. The symmetry was used to calculate the soil deformation and therefore this solution is strictly spoken not valid. However, this solution can be used to get an indication on the possible pressure distribution.

In both cases the grout pressure at the end of the TBM is higher than the soil pressure. As a result the soil is pushed away from the TBM. The corrected width of the joint between the tail of the TBM (the line with the triangles) and the soil is therefore bigger at the end of the TBM than it would be by the cutting of the TBM only (the line with the round dots). The difference is small, only 6 mm, but significant compared with the original joint width of 10 or 20 mm. Going from the back of the TBM along the shield to the front, the joint width decreases and the corrected joint width becomes smaller than the original. At 2 respectively 3.5 m from the back of the TBM the corrected width of the joint between the soil and the TBM becomes zero. The soil pressure is at that location 100 kPa less than the original value. Going further to the front of the TBM the soil pressure increases because the diameter of the TBM increases.

4 INFLUENCE OF BENTONITE FROM THE TUNNEL FACE

The calculations presented in the section above have some simplifications. The over cutting that occurs at the tunnel face by the cutting wheel was not taken into account neither the influence of the bentonite that is present at the tunnel face at a certain pressure (the face pressure). In this section these two effects are incorporated.

In normal operation a TBM has an over cutting of 10 to 30 mm (depending on the state of the teeth at the cutting wheel) with respect to the TBM itself. This will result in a larger joint between the TBM and the soil. The joint at the tunnel face is not zero as was assumed in the section above, but the value imposed by the over cutting. Bentonite will now flow to the tail of the TBM and grout will flow to the face. Somewhere in the middle around the TBM these flows will meet. Calculating the pressure distribution is now complicated by the fact that the direction of the flow is of importance. Both grout and bentonite are usually described as Bingham liquids. This means that a certain pressure gradient is needed to start a flow. Therefore there are 3 possible flow situations, see also Figure 5.

1 Grout flows from the tail to the tunnel face and bentonite flows from the tunnel face to the tail this

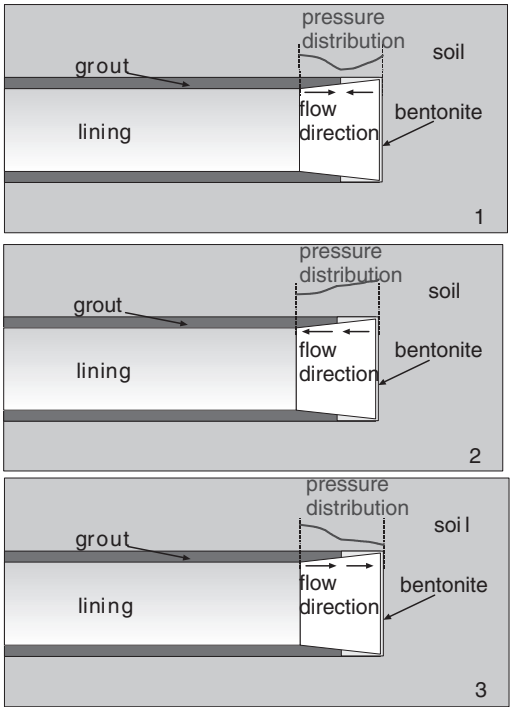


Figure 5. Possible flow directions and sketched pressure distributions along the TBM. The 3rd situation is worked out quantitatively, see Figure 6.

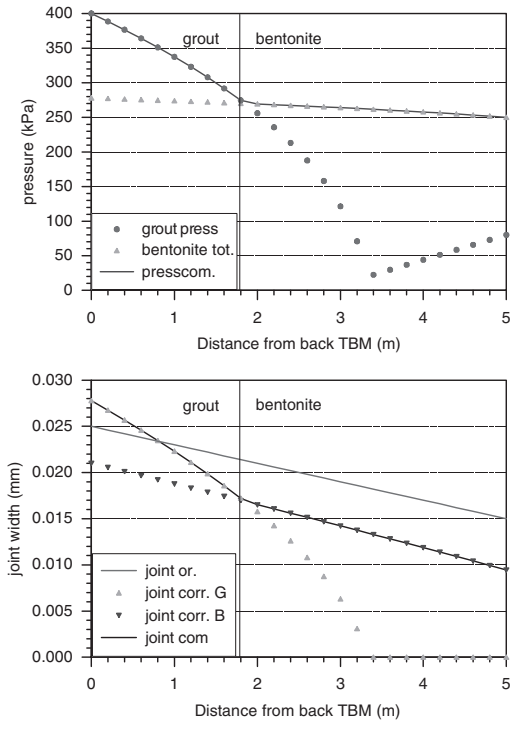


Figure 6. Pressures and joint width along a TBM. Grout pressures and bentonite pressures. Parameters see Table 2. Plots show pressures and joint width for the bentonite and grout pressure separately and the combined result.

situation can only occur when there is some volume loss in the joint between the TBM and the soil for example due to bleeding of the grout or penetration of the bentonite into the soil. For this situation the lowest pressure will be present there where the bentonite and the grout meet.

2 Bentonite is flowing backwards to the tail and pushing the grout out of the joint between the TBM and the soil. The pressure will be the highest at the tunnel face and will decrease when going to the tail. This cannot be a continuous situation, but can occur temporally.

3 Grout is flowing to the tunnel face and pushes the bentonite to the tunnel face. The pressure is highest at the tail close to the injection points of the grout and will decrease going to tunnel face.

The model developed can in principle cope with all these 3 options. However, for simplicity in this paper we will only deal with the 3rd option because this is the most realistic situation for most of the drilling process. Starting with a certain grout pressure at the tail void, this pressure will decrease due to the flow from the grout into the joint between the TBM and the soil. This pressure decrease will depend on the viscosity of the grout and the joint width. The joint width depends on the pressure at that location as is explained in Section 3. This grout flow is completely comparable to the calculation of that section. The pressure at the tunnel face will be the bentonite pressure. Since the bentonite is pushed forward from the tail to the tunnel face, the bentonite pressure will be highest at the tail and lower at the face. It is assumed that there is no mixing from the bentonite with the grout. In such a situation the grout pressure and the bentonite pressure can be calculated. When the grout pressure is higher than the bentonite pressure, there will be grout in the void and if the bentonite pressure is higher there will be bentonite. The result of such a calculation is shown in Figure 6.

The upper plot of this figure shows the pressures and joint widths that would occur if there were only grout (G) or only bentonite (B) in dots and in lines the combined joint width and pressure. In this calculation the grout penetrates between the shield and the soil up to 1.3 m from the tail. The remaining part of the joint between the TBM and the soil is filled with bentonite. The amount of penetration varies with the pressures and shear strength that are chosen. The parameters used in this calculation are shown in Table 3. Although there is an open connection between the face and tail of

Table 2. Input parameters used in calculation with bentonite and over cutting.

Length TBM shield	5	m
Diameter	10	m
Diameter reduction	0.2	%
over cutting	0.015	m
Asymmetric (1) or symmetric (2)	2	
Grain stress	150	kPa
soil pressure	400	kPa
pore pressure	200	kPa
Pressure on tunnel face	250	kPa
Shear modulus (G)	90	MPa
Shear strength grout, 1 sided friction assumed	1.6	kPa
Shear strength bentonite 2 sided friction assumed	0.08	kPa

Table 3. Input parameters used in calculation joint pressures and joint width.

Length TBM shield	8	m
Diameter	6.5	m
Diameter reduction	0.4	%
over cutting	0.015	m
asymmetric (1) or symmetric (2)	2	
Grain stress	100	kPa
Soil pressure	350	kPa
pore pressure	150	kPa
Pressure on tunnel face	200	kPa
Shear modulus (G)	1.7	MPa
Shear strength grout, 1 sided friction assumed	1.6	kPa
Shear strength bentonite 2 sided friction assumed	0.08	kPa

the TBM (See the lower plot of Figure 6, the joint width of the combined calculation is never zero), there is still a stable boundary between the grout en the bentonite. Since both liquids behave as a Bingham liquid there can be some decrease in the grout pressure and still the position of the grout-bentonite front will be the same.

According to the results, the tail of the TBM is never in contact with the soil. In reality there can be some contact due to forces not taken into account in this calculation (vertical loading from the lining, moments induced by the hydraulic jacks). However, it is clear that tapering of the shield does not necessarily lead to a certain volume loss, as is suggested by Kaspar & Meske (2006). The calculation results presented here are also in line with the TBM data, which normally show that more grout have to be pumped into the tail void than the original tail void. The grout that flows into the joint between the soil and the TBM is not an extra volume, because it is a constant volume during tunnelling, but the grout volume increases because the grout pressure makes a wider joint.

5 EXAMPLE CALCULATIONS

The calculation method can now be used to test the influence of various parameters. In a set of example calculations the length of the TBM has been changed (the length used up to now is with 5 m a bit short compared to the usual TBMs) and/or the grout pressure or the soil properties. In all example calculations Table 2 is used as a reference and the parameter changed is mentioned.

Assuming the same amount of tapering but a longer tunnel leads to a comparable distance over which grout flowed over the tail of the TBM (approximately 2 m). Most of the shield is in that situation covered with bentonite, increasing the face pressure to 370 kPa results in a joint completely filled with bentonite. But then the assumptions of the 3rd picture in Figure 5 are not valid

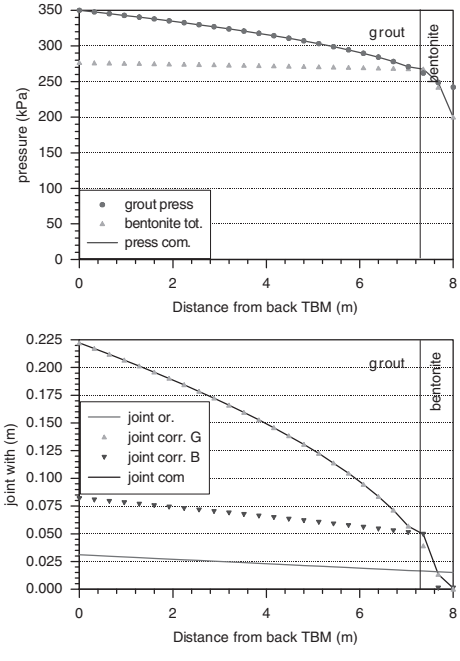


Figure 7. Pressures and joint width along a TBM for a TBM drilling in clay. Grout pressures and bentonite pressures. Parameters see Table 3. Plots show pressures and joint width for the bentonite and grout pressure and the combined result.

anymore, because there it was assumed that the grout pushed the bentonite in the direction of the face during drilling. This is obvious not the case when no grout is present at all anymore in the joint. In this situation (thus with a shield of 10 m length and the other parameters taken from Table 2) the grout pressure can be increased until 750 kPa before the bentonite flows through the joint between the TBM and the soil into the pressure chamber. Assuming that the minimum grout pressure

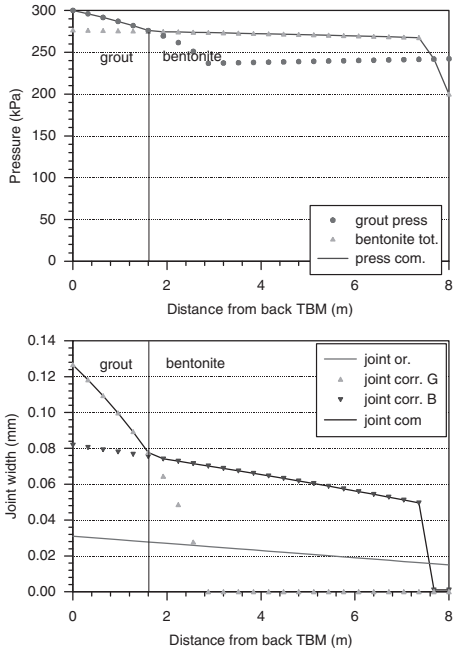


Figure 8. Pressures and joint width along a TBM for a TBM drilling in clay. Grout pressures and bentonite pressures. Parameters see Table 3 but grout pressure lowered until 300 kPa. Plots show pressures and joint width for the bentonite and grout pressure and the combined result.

is somewhat higher than the total stress (350 kPa in this situation), this result indicates that quite a variation in grout injection pressure is possible before the grout really reaches the pressure chamber.

Interesting is to investigate the influence when the TBM drilled through holocende clay layers as will be the case in the Netherlands for the RandstadRail project, (Pachen et al. 2005) and also possibly in future projects. Clay has a much lower shear modulus. Pachen et al. (2005) assumed an average value of 1.7 Mpa at the centre of the tunnel. A first calculation was run with the parameters of Table 3. In this calculation the assumed geometrical parameters for the RandstadRail tunnel are used, the (face and grout) pressures are set on a level that is usual for boring a tunnel in sand, but the shear modulus of the clay is used (1.7 MPa).

The results of such a calculation are shown in Figure 7. The results show that the applied grout pressure will lead to a considerable joint width above the shield of 0.225 m. This means that this joint width is wider than the original designed tail void, which will be 0.15 m and this would also have enormous consequences for the amount of grout used, which will more than double. This problem can be overcome by reducing the grout pressure. In a second calculation the grout pressure was reduced to 300 kPa and for this situation the joint width reduces until approximately 0.125 m (Figure 7). Still considerable but only halve the value of the original calculation. This model therefore shows that when drilling in soft clay the grouting process is even more critical than during drilling in sand. Considerable changes in joint width above the TBM shield and therefore also considerable changes in volume loss (or gain) can be achieved by only limited changes in the grout pressure.

6 CONCLUSIONS

1-dimensional calculations showed that it is very likely that the tail of the TBM is to a large extent supported with bentonite and grout and not with soil. Therefore there is no direct relation between the tapering of the TBM and the volume loss, as is sometimes suggested. There is, however, in this model a direct relation between the grouting pressure and the volume loss. 4-D FEM calculations performed for COB in The Netherlands (Hoefsloot et al., 2005) are in agreement with these results.

The model shows that a good pressure control is essential when tunneling in soft soil (holocene clay).

ACKNOWLEDGEMENT

The author wants to thank Dr. K.J. Bakker from Plaxis B.V. and Dr. Ulrich Rehm from Herrenknecht for stimulating discussion.

REFERENCES

Barends F.B.J. (2005), Associating with advancing insight. Terzaghi oration, proc. 16ICSMGE, Osaka.

Bezuijen A., Talmon A.M. 2003, Grout the foundation of a bored tunnel, 2003, *Proc ICOF 2003 Dundee.*

Bezuijen A., Talmon A.M., Kaalberg F.J. and Plugge R. (2004), Field measurements of grout pressures during tunneling of the Sophia Rail tunnel. *Soils and Foundations vol, 44, No 1, 41–50, February.*

Hoefsloot F.J.M, & Verweij A., 2005, 4D Grouting pressure model PLAXIS Proc. 5th. Int. symposium on Geotch. Aspects of Underground Construction in Soft Ground, Amsterdam, pp. 529–534.

Kasper T. & Meschke G. (2006), On the influence of face pressure, grouting pressure and TBM design in soft ground tunnelling. *Tunnelling and Underground Space Technology 21, 160–171.*

Pachen H.M.A., Brassinga H.E., Bezuijen A. (2005), Geotechnical centrifuge tests to verify the long-term behaviour of a bored tunnel. *Proc. 5th. Int. symposium on Geotch. Aspects of Underground Construction in Soft Ground, Amsterdam.*

Underground Space – the 4th Dimension of Metropolises – Barták, Hrdina, Romancov & Zlámal (eds)
© 2007 Taylor & Francis Group, London, ISBN 978-0-415-40807-3

Volume changes in grout used to fill up the tail void

A. Bezuijen & W.H. van der Zon
GeoDelft, Delft, The Netherlands

ABSTRACT: Volume changes in grout to be applied in the tail void of a tunnel were measured in the laboratory. Two different mechanisms that lead to volume changes have been distinguished: Bleeding of the grout, which is the dominant mechanism when a tunnel is constructed in a permeable soil; and volume changes during the hardening process. The last volume changes are the only volume changes that occur when a tunnel is constructed in an impermeable soil. Two test set-ups have been developed to test these two different causes of volume changes. It appeared that the volume changes caused by bleeding varied between 3 and 8%. Volume changes during the hardening process were less than 3% for a two component grout that was tested. A 2-component grout mixture with air appeared to have a certain elasticity also after hardening of the grout. As a result small volume changes did not result in large pressure changes, which will lead to smaller loading on the lining compared with grout without air.

1 INTRODUCTION

The tail void between the lining and the soil in a tunnel is filled with grout during the construction of a tunnel. This tail void grouting appears to be an important process in tunnelling. This process appears to have an important influence on the resulting settlement trough and on the loading on the lining. Volume changes in the grout after its application in the tail void will lead to surface settlements above the tunnel and/or will change the loading on the lining. Two different mechanisms can lead to volume changes:

1. Bleeding of the grout. The water in the grout is expelled to the surrounding soil when applied in a permeable soil. The amount of bleeding depends on the permeability of the grout, the consolidation properties and the hardening properties.
2. The hardening of the grout. Even when there is no bleeding, as will be the case when the tunnel is bored in nearly impermeable soil as rock or clay, volume changes can occur during the hardening of the grout.

Two test set-ups have been developed to measure the volume changes during bleeding and hardening of grout.

This paper presents detailed information on the set-ups and the results of various tests. Results will be compared with small scale tests on samples with a thickness of 0.02 m. Consequences for tunnelling will be discussed.

2 SET-UP OF TESTS

2.1 *Types of tests*

Two different set-ups were used to test the volume change caused by the two mechanisms mentioned above for four different types of grout.

The first setup was a consolidation cell with a diameter of 0.3 m in which a grout layer of 0.2 m thickness was tested. The 0.2 m is comparable with the thickness of a grout layer around a tunnel. This is important because the ratio between hardening time and consolidation time determines the bleeding. When the hardening time is much less than the consolidation time (for a layer of grout of a certain thickness) the bleeding loss will be small. During a test the pressure was kept constant and volume change was measured continuously.

The second set-up was again a cell with a diameter of 0.3 m and 0.2 m thickness. However, in this cell there was no bleeding of the grout. The set-up was designed to measure volume changes accurately. The set-up was developed to see how a grout behaves that is injected between the lining and the soil in the case the surrounding soil is impermeable.

2.2 *Bleeding tests*

Tests have been performed to investigate the hardening and bleeding of conventional grout, see Figure 1 and Figure 2. In this test a grout layer of 0.2 m is

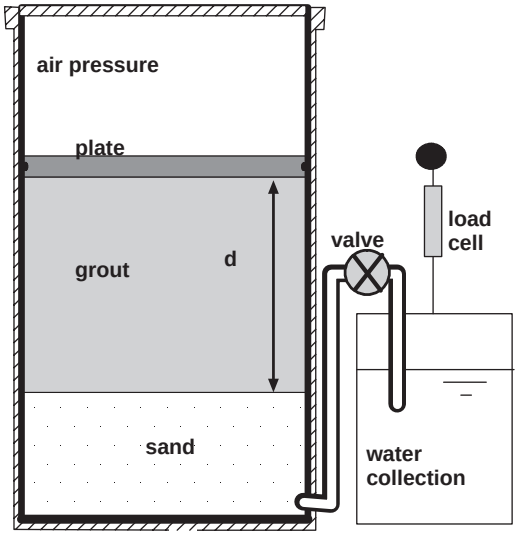


Figure 1. Measurement principle.

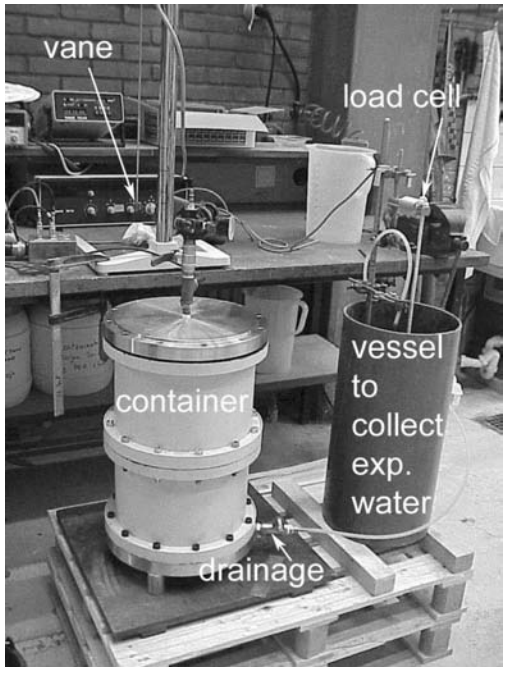


Figure 2. Experimental setup.

loaded mechanically with a constant load of 1–3 bar. The expelled water is a measure of the consolidation of the grout. After several minutes of consolidation the sample was unloaded and the shear strength of the grout was measured at different locations in the grout. An example of results of such a test is shown

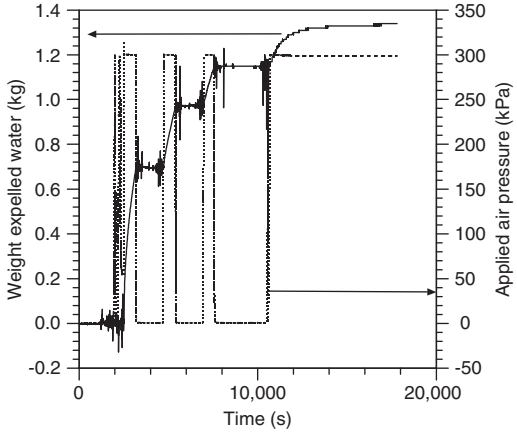


Figure 3. Test result expelled water as a function of time and applied pressure.

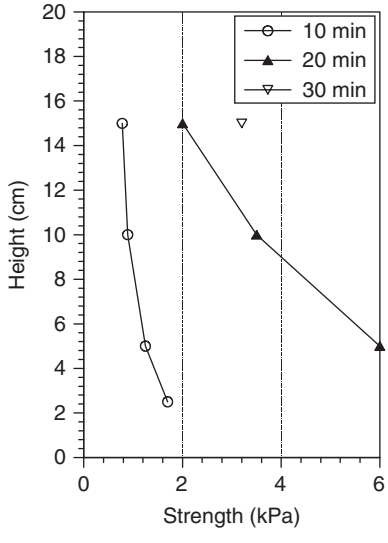


Figure 4. Strength development as measured with a vane.

in Figure 3 and Figure 4. Figure 4 shows the amount of expelled pore water as a function of time and the applied pressure. In this test a pressure of 300 kPa was applied. Pressure was relieved several times to be able to take the vane tests. Figure 4 shows the measured shear strength after various times that pressure was applied. In this test it was focused on the lower values of the shear strength. Therefore only shear strengths up to 6 kPa were measured and presented in the plot.

The type of grout tested here was tested before at atmospheric pressure (Bezuijen *et. al. 2002*). In that test it appeared that the measured shear strength remained more or less constant until 5.5 hours and after that time the hardening of the grout started.

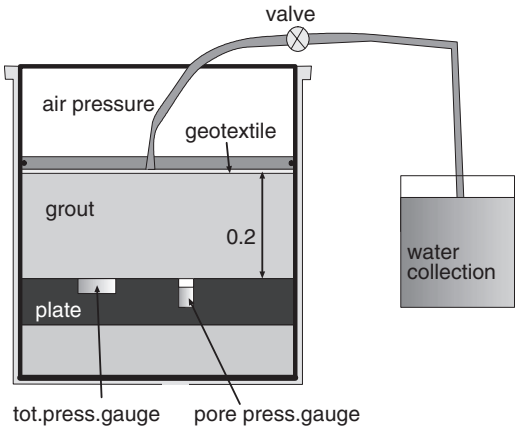


Figure 5. Modified test set-up to measure the bleeding of grout.

Comparing the result from the test at atmospheric pressure with the results of the tests at 1–3 bar over pressure it became clear that the increase in strength in the over pressure case is caused by consolidation of the grout and not by the hardening of the grout. To understand the grout properties just after injection in the tail void it is therefore necessary to understand consolidation. If the grout layer is consolidated it will have certain strength to act as a foundation for the tunnel lining, even before hardening of the grout commences. If it is not consolidated, it is possible that the shear strength is too low to counterbalance the buoyancy forces of the tunnel. Another important consequence of consolidation is an increase of flow resistance, which directly affects the pressure distribution behind the TBM when drilling.

The vane test as shown in this Figure 4 was only possible in case a grout was used with a relatively long hardening and consolidation time. For tests performed with two-component grout or grout without cement, the strength development was not measured. For later tests the set-up was changed, to avoid the preparation of the sand sample and to be able to measure the pore pressure and total pressure in the grout. The set-up for these later tests is shown in Figure 5. The principle is the same, but the drainage is in a different direction to the top of the grout sample.

The test where evaluated using the theory developed by Bolton & Mckinley (1997). There formulation written in porosity changes in stead of void ratio (as in the original paper) reads:

$$x = \sqrt{2k \frac{1-n_i}{n_i - n_e} \Delta\phi \, t} \qquad (1)$$

Where x is the thickness of the consolidated layer, n_i the initial porosity, n_e the porosity after consolidation, k the permeability of the consolidated layer, $\Delta\phi$ the difference in piezometric head over the column and t the time.

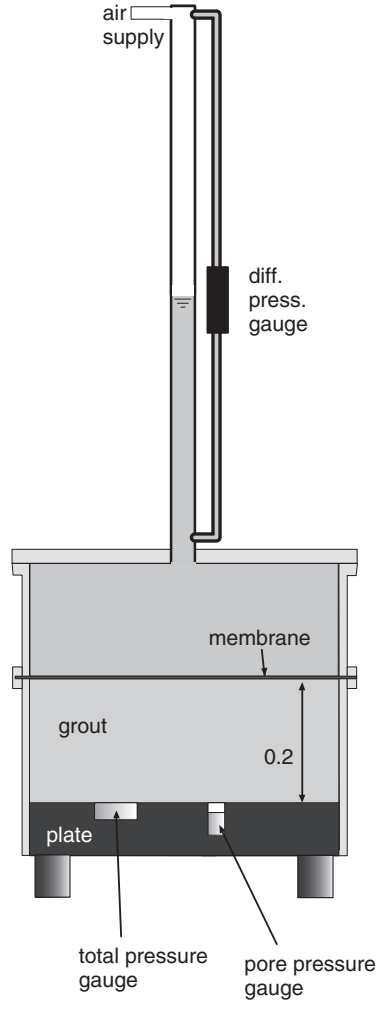


Figure 6. Sketch test set-up, grout tests for rock applications.

2.3 *Measuring the volume changes in the grout without bleeding*

The test set-up for these tests is sketched in Figure 6. The test set-up was designed to be able to exert a constant pressure on the grout and to measure volume changes accurately during hardening of the grout. The pressure was kept constant by applying a constant pressure at the air supply on top of the set-up. An excess pressure of 1 bar was used during the tests. Volume changes were measured by measuring volume changes in the water cylinder on top of the container.

Table 1. Properties of the grout samples used.

Parameter	CG	2CG	NCG	Dim.
Density	2109	1225	1840	Kg/m^3
water content.	16	225	36.3	%
D_{15}	–	–	0.0043	mm
D_{50}	–	–	0.017	mm
D_{85}	–	–	0.095	mm
Conf. pressure	300	100	100	kPa
Volume loss	8	3.5	4.5	%
Permeability cake	4.10^{-8}	$1.3.10^{-8}$	$1.6.10^{-7}$	m/s

A differential pressure gauge is attached to this cylinder and a change in water level leads to a change in differential pressure. Changes in the water level also lead to pressure variations in the grout, but these variations will be relatively small compared with the applied excess pressure of 1 bar. The container with the grout has an inside diameter of 0.284 m, the cylinder on top a diameter of 0.03 m. The height of the tube was 1 m.

3 TESTS PERFORMED

3.1 *Bleeding tests*

Three different types of grout were tested. A 'traditional' cement based grout (CG), a 2-component grout (2CG) and a grout mixture without cement (NCG) that gets the desired properties by choosing the right grain size distribution of the granular material in the grout. The properties of the grouts selected and the volume strains that were found in the consolidation tests are summarized in Table 1. It should be noted that the volume strain of the CG grout is higher than of the other 2 but that this was also measured with a higher confining stress. For the same confining stress the difference will be smaller.

As examples the results of the bleeding tests for 2CG and NCG are shown in Figure 7 and Figure 8. These materials were tested with the set-up of Figure 5. The pressures are measured with the pressure transducers in the plate below the grout. The vane tests were not performed in these tests.

Although the 2 component grout has a certain strength within a very short time (seconds) the volume decrease due to bleeding continues until 5 hours after the beginning of the test. In the hardening process that starts after approximately 5 hours the pore pressure decreases sharply until −100 kPa because the water is bounded by the chemical reaction that leads to hardening.

With the pressure applied (100 kPa) the bleeding of the NCG grout is only present for a period of approximately 0.5 hour. Since there is no chemical hardening reaction with the water the pore pressure decreases until 0 kPa, but negative pressures are not found. The

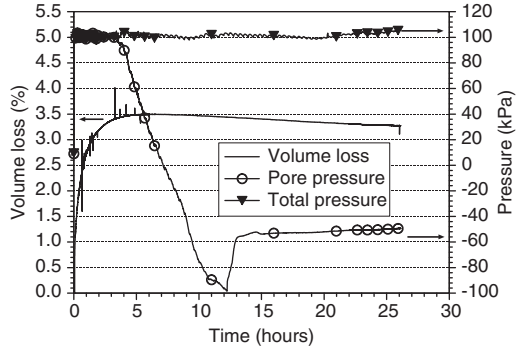


Figure 7. Result Bleeding test for the grout 2CG.

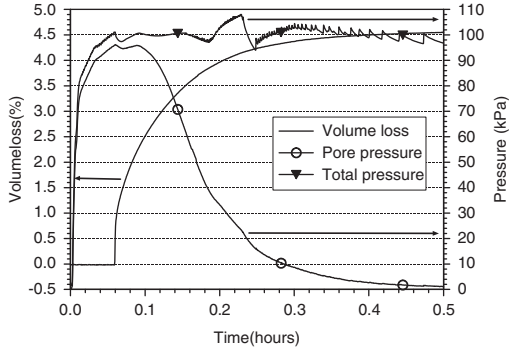


Figure 8. Result Bleeding test for the grout NCG.

measured pore pressure is not in agreement with the theory of Bolton & McKinley (1997). According to that theory the pore pressure should remain constant at 100 kPa until all material is consolidated. During the test it appears that the pore pressure at the bottom of the sample already starts to decrease before the end of consolidation, showing that the theory is only an approximation of the real process.

The 2-component grout was also tested on bleeding properties using a standard oedometer test with a sample height of 0.02 m. In such a test the consolidation times are theoretically 100 times shorter than in a sample with a thickness of 0.2 m. Therefore the influence of the hardening of the sample on the result will be less. This resulted in a much larger volume loss of around 30%. This result shows that for grouts where the hardening component is significant, the bleeding has to be tested using a layer with a comparable thickness as is expected in the application, thus for tail void grouts this has to be the actual thickness of the tail void.

3.2 *Results tests without bleeding*

The tests without bleeding, with the set-up shown in Figure 6, were only performed on grout type 2CG. One

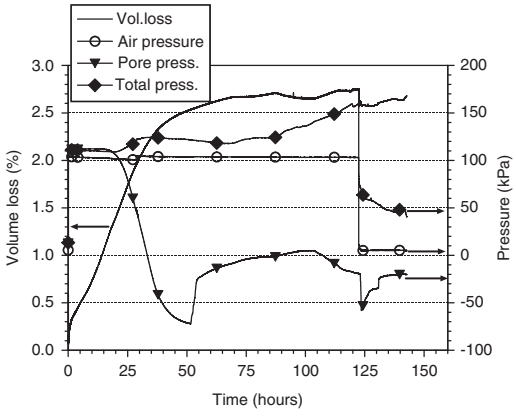


Figure 9. Test volume change during hardening. 2CG without air.

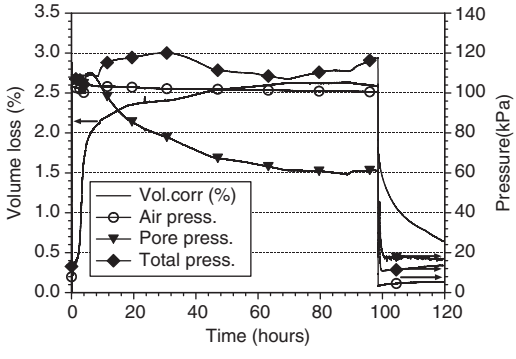


Figure 10. Test volume change during hardening. 2CG with air.

sample with only 2CG and one sample where air was mixed into the grout. Results are shown in Figure 10 and Figure 9.

Figure 9 shows the result without air. There is a constant rate of volume loss until approximately 50 hours. After 50 hours the rate of volume loss decreases, but even after 125 hours of testing the volume is still not constant. The volume loss is then around 2.8%. The experiment is stopped after 125 hours and the pressure is released. This leads to a small decrease in the volume loss. The results from the pore pressure gauge showed again that during hardening of the grout all water is used, leading to a very low pore water pressure.

The result with air, as shown in Figure 10, is different. Now the pore water pressure remains positive. It is likely that this is caused by the elastic storage that is brought into the sample by the air. It appears that even after 100 hours the grout has still some elasticity, as can be seen when after nearly 100 hours of testing the pressure is released resulting in a decrease of the volume loss from 2.6 to 0.6%.

4 DISCUSSION ON THE RESULTS

The grout mixtures tested all appeared to have some volume loss. This is caused by bleeding of the grout, but also in the case bleeding is not possible during the test there is a few percent of volume loss. The volume loss will lead to a decrease in the pressure loading on the lining in case the lining is placed in sand (Bezuijen & Talmon, 2003). This means that the original stress distribution in the sand is of no importance any more when the tunnel is made, because this stress distribution changes during the tunnel process itself (Bezuijen, 2006) and during the grouting process. Calculation methods that use the original stress distribution will over predict the loading on the tunnel, as was proven by Hashimoto et al. (2002).

The 2CG was tested for the situation without bleeding. This is the situation that can occur when the grout is used in a rock tunnel or for a tunnel made in soft clay. The 2.7 % volume loss will have not significant influence on the pressure distribution of the soil around the tunnel when this is soft clay, but may lead to considerable pressure changes in case the tunnel is made in rock, because both lining and surrounding (the rock) will react very stiff. A situation where there is some elasticity in the grout itself, as was the case for the second test where the grout had 17% air, seems to be advantageous. However, this will depend heavily on the quality of the mixture, which is more difficult to control when air is applied. Another advantage from the air is that the density of the grout decreases, which lead to a reduction in the buoyancy forces on the lining (Bezuijen et al. 2005).

5 CONCLUSIONS

Bleeding characteristics of different grout mixtures have been tested. Pressurizing these mixtures with a constant pressure of 100 to 300 kPa led to a volume loss of 3 to 8%. It was shown that these bleeding characteristics can only be tested accurately in a setup where the thickness of the grout layer is comparable to the thickness of the layer that will be applied during tunneling. Although in literature (see for example, Bolton and McKinley, 1997) the bleeding process is described as a kind of consolidation process only, it is a consolidation process that is influenced by the hardening of the grout. The time scale for consolidation is proportional with the square of the thickness, but the hardening time is independent from the dimensions.

The hardening leads to a large decrease in the pore pressure in the grout. This can result in negative pressures (relative to the atmospheric pressure).

In the tests without bleeding the presence of air appears to have a remarkable influence on the results. The grout mixture tested appeared to have an elastic

behaviour even after 120 hours when the hardening of the material is finished.

REFERENCES

Bezuijen A., Talmon A.M, Kaalberg F.J., R.Plugge, 2002, Field measurements on grout pressures during tunnelling, *4th Int. Symp. on Geotechnical Aspects of Underground Construction in Soft. Ground – IS Toulouse, 23–25 October.*

Bezuijen A., Talmon A.M, 2003, Grout the foundation of a bored tunnel, 2003, *Proc ICOF 2003 Dundee.*

Bezuijen A., Zon W.H. van der, Talmon A.M., 2005, Laboratory testing of grout properties and their influence on back fill grouting, Proc. ITA 2005 Istanbul.

Bezuijen A., 2006, Bentonite and grout flow around a TBM. Sub. to Proc. ITA2007, Prague.

Bolton M.D. & McKinley J.D., 1997, Geotechnical properties of fresh cement grout – pressure filtration and consolidation tests, *Géotechnique 47, No 2, 347–352.*

Hashimoto T, Nagaya J, Konda T, Tamura T, 2002, Observation of lining pressure due to shield tunnelling, *3rd Int Symp. on Geotechnical Aspects of Underground Construction in Soft Ground, IS-Toulouse.*

Underground Space – the 4th Dimension of Metropolises – Barták, Hrdina, Romancov & Zlámal (eds)
© 2007 Taylor & Francis Group, London, ISBN 978-0-415-40807-3

Laboratory tests on compensation grouting, the influence of grout bleeding

A. Bezuijen
GeoDelft, and Delft University of Technology, Delft, The Netherlands

M.P.M. Sanders
Delft University of Technology, Delft, The Netherlands

D. den Hamer
GeoDelft

A.F. van Tol
GeoDelft and Delft University of Technology, Delft, The Netherlands

ABSTRACT: The process of compensation grouting has been investigated by a series of laboratory tests. In previous test series all tests resulted in an injection body of grout that had an irregular shape relatively close to the injection point. Shape of the fractures and necessary injection pressure indicate that the process was more comparable to compaction grouting than to fracture grouting. It was assumed that this was caused by bleeding of the grout mortar. Therefore a new test series was performed with larger variations in permeabilities and amounts of solid material between the injection fluids of different tests. Here it appeared that the injected 'grout' sometimes created fractures. Calculation models are described to calculate the interaction between soil and the injection fluid and a conceptual model what parameters determine the shape of the injected volume.

1 INTRODUCTION

Compensation grouting or fracture grouting has been successfully applied in several projects to compensate for surface settlements induced by for example tunnelling. Fracture grouting is planned to compensate possible settlements of buildings in Amsterdam during the construction of the tunnels for the North/South Metro Line.

Fracture grouting uses hydraulic fracturing to get a heave that can compensate the settlement. Hydraulic fracturing of competent material has been studied extensively in the oil industry where it is used successfully to enhance the capacity of oil wells. Hydraulic fracturing can also be an unwanted phenomenon in tunnelling or horizontal drilling when high pressures can cause a blow-out that starts with a hydraulic fracture (Bezuijen & Brassinga 2001).

The area where heave can be expected is determined by the shape of the fracture. Some pictures taken near Antwerp Station and a theoretical model by Te Grotenhuis (2004) showed thin fractures propagating over a large distance. However, experiments on fracture grouting in sand performed by Gafar & Soga (2006) and experiments reported by Kleinlugtenbelt (Kleinlugtenbelt 2005 and Kleinlugtenbelt et al. 2006) showed no fractures but a shape that looks as a perfect ball or an irregular ball with something that looked like the beginning of a fracture, see Figure 1.



Figure 1. Grout body formed in sand during a compensation grouting test.

That sand can be fractured was proven by experiments with different fracture materials (Khodaverdian & McElfresh 2000, Pater & Bohloli, 2003 and Bezuijen, 2003iii).

This paper starts with a conceptual idea how fracturing of sand can occur. This idea shows what parameters are of importance to determine the shape of the fracture. It describes briefly the set-up and the results of the model tests on fracturing that has been performed and the tests to characterize the injection material and will end up with conclusions.

2 CONCEPTUAL MODEL

2.1 *Fracturing*

When a grout is injected into an opening of sand, as is done by compensation grouting, there will be an elastic deformation of the opening, the opening will increase. Assuming the injection fluid (the grout) forms a plastering layer we can describe this first deformation with cavity expansion theory. The radial stress will increase and the tangential stress will decrease. This will go on until, according to the Mohr-Coulomb criterion for cohesionless soil, the stress ratio (σ_r/σ_θ) in the sand at the boundary of the injection hole fulfils the relation:

$$\frac{\sigma_r}{\sigma_\theta} = \frac{1+\sin\phi}{1-\sin\phi} \qquad (1)$$

Where ϕ is the friction angle of the sand. For sand with a friction angle of for example 35 degrees this ratio is 3.7. If the radial stress increases further, the stress ratio will remain constant and plastic deformation will occur.

Classical cavity expansion theory assumes that there will be a radial expansion, which is uniform in all directions. However, in reality the sand is never perfectly homogeneous. Looking at the scale of the grains at the boundary of the opening there will be some grains that are in closer contact and some between which there is some space, see Figure 2.

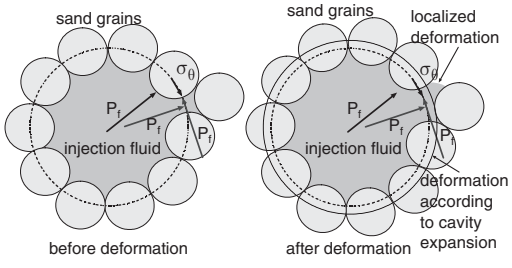


Figure 2. Sketch with possible deformation modes of the injection hole.

If the radial pressure is exerted by the injection fluid, the pressure in the fluid will be the same in all directions. As a result the pressure working on two grains on the boundary of the opening, which are not in direct contact will lead to a tangential stress that wants to remove the grains form each other and that is higher than the opposing tangential stress from the soil. As a result the grains will be pushed apart. A micro mechanical calculation has shown that this situation, in which 2 grains are pushed apart, is stable in case the soil has a plastering function and most forces work on the grains at the boundary of the opening. From hereon this process can go further and more grains can be pushed apart by the injection fluid until a full fracture occurs.

The model as described above, explains why the injection pressure is difficult to predict. There is no clear boundary where a fracture starts. The injection pressure must be high enough to create plastic deformation in the sand, but it is always possible that some plastic deformation occurs before a fracture starts. Literature presents the injection pressure in most cases as a ratio of the vertical stress on the soil sample (Bezuijen et al. (2003i). It appears from our tests and literature that this ratio can vary between 3 and 20. However, the highest values do not produce real fractures. The reason for that is, that there will always be cavity expansion in case pressures are high enough. Fracturing is an additional failure mechanism that can only occur at a lower injection pressure than cavity expansion.

The conceptual model described above also explains why the properties of the injection fluid are of importance. The injection pressure has to work close to the boundary. When there is too much plastering than the injection pressure is not applied on the sand, but on the plaster, see Figure 3. In that case the tangential force that is exerted on the grains at the boundary of the opening is much less and depends on the mechanical properties of the plastered material.

The mechanism described here for injecting in loose granular material is different for cohesive soils and

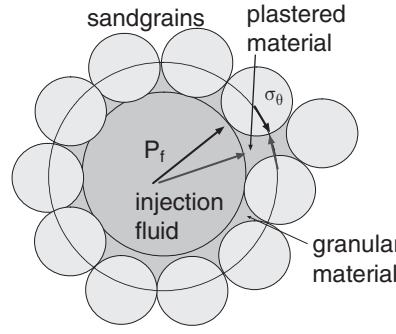


Figure 3. Influence of plastering.

rock where tension cracks can occur. In sand there will never be tension, because there is no cohesion in the material and therefore plastic deformation will occur in the material before tension stresses develop.

2.2 *Injection fluid*

The injection fluid used in compensation grouting is a mixture of water, bentonite and cement. Plastering can occur by 2 different mechanisms:

1. Bleeding of the injection fluid, as described by Bolton and McKinley (1997). The amount of bleeding depends on the injection pressure, the duration and the permeability of the plastered material.
2. Leak-off of the injection fluid. This phenomenon occurred when most of the particles in the fluid are very small. In that case the injection fluid will penetrate into the sand. In the situation that there are also larger particles, these will not penetrate, but will end up at the boundary between the fluid and the soil, see Figure 4.

The injection fluid for compensation grouting has 3 different components. Looking at the particle size only, the cement particles will not penetrate into the sand, but the very small bentonite particles will. However, from literature (Mitchell, 1976) it is known that these particles cannot be dealt with separately. The calcium in the cement leads to flocculation of the bentonite, which results effectively in larger particles and therefore in a larger permeability of the cake. Due to this the bleeding will increase but the leak-off will decrease.

3 MODEL EXPERIMENTS

3.1 *Test set-up*

A circular container with a diameter of 0.9 m was used for the tests (see Figure 1). This container was filled with saturated sand up to 0.84 m height. A PVC plate was placed on top of the sand sample. There was an air tight connection between the plate and the container by means of a rubber ring. It was therefore possible to pressurize the sand sample, using air pressure, simulating sand at a larger depth. The injection nozzle is comparable to the system developed for compensation grouting. A pipe with a rubber sleeve has been used (see Figure 2). The sleeve will only allow outflow of the grout when the grout pressure is higher than the soil pressure. The injection nozzle was located 0.37 m above the bottom of the tank.

Tests were performed with Baskarp sand ($d_{50} = 130\,\mu m$). The sand was wet pluviated into water in the container. The loose sand was densified by dropping the whole container over a few centimetres several times depending on to the required density. The sand was 'pre-stressed' by applying a high vertical pressure before the test to achieve a higher K_0. This pre-stressing was only partly successful. The K_0 achieved with this procedure was around 1. During grout injection K_0 rises rapidly to values well above 1 and even to 4.5 in the case of dense sand. Pore pressure transducers and total stress transducers were installed at various locations in the container, see Figure 7.

Special attention was paid to the measurement of the volumes. The increase in volume of the sample due to the injection and the drainage of pore water was measured continuously during the tests, more details

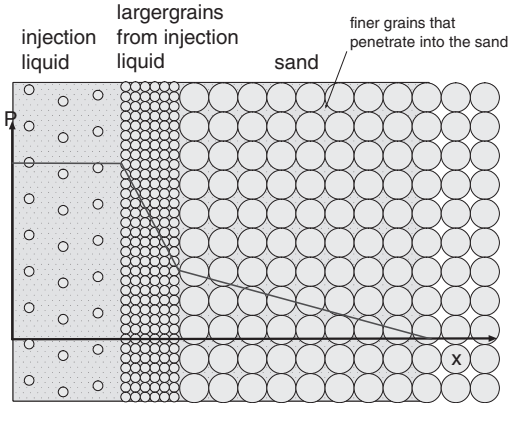


Figure 4. Plastering that can occur during leak off due to larger grains in the liquid that cannot penetrate into the sand and sketch of the pressure distribution over the injection liquid.

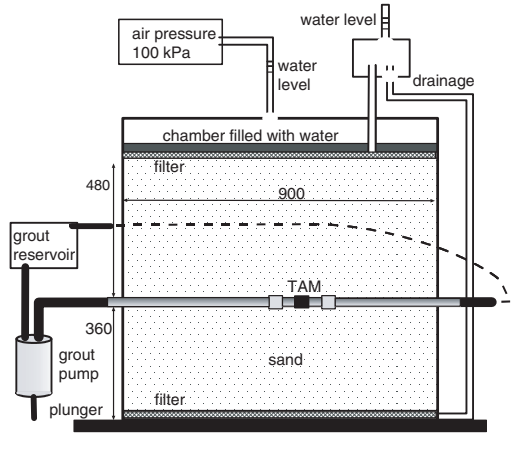


Figure 5. Set-up of the experiments. Note that changes in pore volume and sand volume can be measured as changes in the water levels.

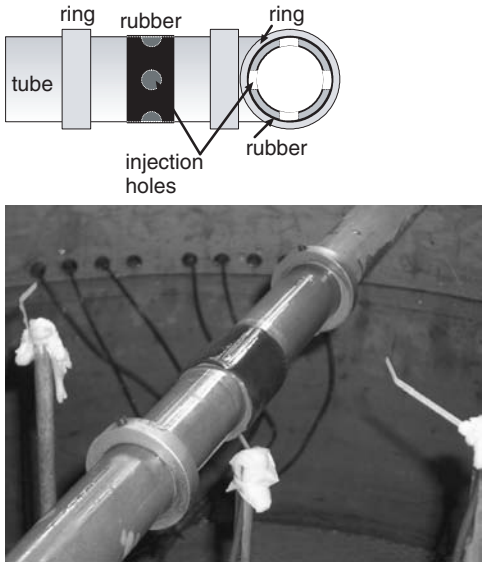


Figure 6. Injection system with rubber sleeve. The steel rings were placed on the tube to prevent grout flow along the tube.

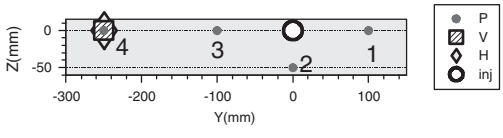


Figure 7. Position of the instruments with respect to the injection tube (inj). P are the pore pressure gauges, V measures the vertical pressure and H the horizontal.

on the measurements of the volume can be found in (Kleinlugtenbelt, 2005).

Grout was injected by means of a plunger pump. This pump pumped water and by means of a bladder the grout was pumped into the system (the sketch in Figure 5 does not show the bladder). The bladder system was installed to avoid damage to the pump by the granular particles in the grout. The maximum injection pressure of the injection pump was 25 bars.

The grout was allowed to harden for one day after the test before the sand was washed away and the shape of the injected grout became visible. There was no hardening of the grout in the test without cement. After these tests the capillary forces in the sand were used to see the shape of the fracture.

3.2 *Classification experiments*

The properties of the injection fluids were determined for each test. Viscosity and yield point were determined using a Fann V.G. viscometer that was operated at 300 and 600 rpm. Leak-off and bleeding

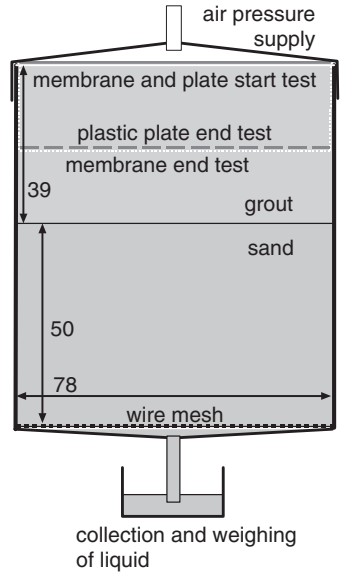


Figure 8. Sketch of the apparatus used for the bleeding tests, see also text (dimensions in mm).

were determined using a modified consolidation test, see Figure 8.

A cylindrical pressure vessel with an inward diameter of 78 mm and a height of 89 mm can be pressurized on one side and has drainage capabilities on the other side. A fine wire mesh allows water to flow through, but prevents sand particles to pass. In an experiment 50 mm of medium fine sand (d_{50} = 130 μm) is applied on the wire mesh and densified until the maximum density. 39 mm of injection fluid was applied and the pressure vessel was sealed off with a rubber membrane and a plastic plate. The latter is to achieve an even settlement of the grout. An air pressure of 4 bar is applied on top of the membrane and the amount of liquid expelled is continuously measured with a balance. The membrane and plastic plate will settle as is indicated in the figure during the experiment. The experiment is continued until the amount of expelled water remains constant.

The result of the test depends on the type of injection fluid. For a grout without any leak- off the amount of expelled water is proportional with the square root of time, as in agreement with the findings of Bolton and McKinley (1997) and can be described with the formula:

$$x = \sqrt{2k\frac{n_i - n_e}{1 - n_i}\Delta\phi\, t} \qquad (2)$$

Where x is the thickness of the consolidated layer, n_i the initial porosity, n_e the porosity after consolidation,

Table 1. Parameters of tests performed.

No	Yield stress (Pa)	Visc (Pas)	σ_v peak (kPa)	σ_h peak (kPa)	Perm. $\times 10^{-12}$ (m/s)	Peak press. (kPa)	Frac.
1	39	7.5	145	250	211	1600	No
2	35	17	150	270	17	1200	No
3-1	98	11	195	300	35	1200	No
3-2	39	7.5	210	400	470	1060	No
4	n.d.	n.d.	160	225	5.6	750	Yes
5	8	9	150	170	6	1200	Yes
6	51	21	170	200	50	1700	Yes

Notes: Yield stress = the yield stress of the grout, Visc = the viscosity of the grout, σ_v = the vertical total stress, σ_h = the horizontal total stress, Perm = the permeability of the grout filter cake, peak pressure = the maximum pressure measured and Frac = the fracturing of the sand. n.d = not determined.

Table 2. Additives injection fluid.

No	Bentonite (%)	Cement (%)	Silica flower (%)	Fly ash (%)	Retarder (%)
1	7	-	-	33.3	5.3
2	7	-	33.3	-	5.3
3-1	12	-	0.5	33.3	5.5
3-2	7	-	0.5	33.3	5.3
4	-	-	0.5	-	-
5	6.2		0.5	-	-
6	6.2	0.5	-	-	-
7	6.2	5	-		-

Note: All values are related to the real water content of the grout mortar.

k the permeability of the consolidated layer, $\Delta\phi$ the difference in piezometric head over the column and t the time. The formula was used to describe bleeding tests on tail void grout and appeared to describe the bleeding process quite well (Bezuijen & Talmon, 2003ii).

In case there is leak-off, there is a quick discharge in the first few seconds when leak-off is dominant, after that the curve follows again the curve that is expected from the bleeding.

3.3 *Tests results*

The typical conditions of the tests performed with the set-up of Figure 5 are listed in Table 1. The idea for this test series was that the grout properties are determining the result of the test, more than variations in other parameters (changing the sand into silt of clay will also have an influence, but the aim was to create compensation grouting in sand). For that reason most parameters were kept constant but a wide variety of

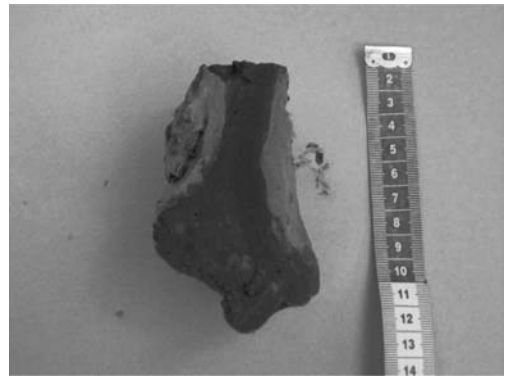


Figure 9. Injection results test 3.

'grout mixtures' was used in the tests as an injection fluid. To compare with other results, injection fluids without cement were used and in one case we used X-linked gel, a fracture fluid that is used in the oil industry to create fractures.

The injection rate in all tests was 167 ml/s. All tests were run with a relative density of the sand sample of around 65%. The confining stress on the sand was 100 kPa on all tests and the pore pressure in the sand was only a few kPa.

The first two tests resulted from the conclusions of the test series described before (Kleinlugtenbelt et al. 2006). A very impermeable grout mortar was used, but this did not lead to fractures, probably due to the relative high percentage of solids in the injection fluids. Even with a limited amount of leak-off this leads already to a plastering layer that prevents fractures, see also the discussion section.

Two injections were performed with the sand model of test 3. It appeared that the second injection was capable to fracture the grout body that was formed by the first injection, but was not able to fracture the sand any further, see Figure 9.

The fourth test was performed with X-linked gel. This test was performed to test the model set-up. X-linked gel produces fractures in a comparable model set-up (De Pater & Bohloli, 2003). We also found fractures in our test set-up for this injection fluid, see Figure 10.

The last two tests also resulted in fractures, but only to a limited extent, because in both cases there was a considerable leak-off, see Figure 11.

4 DISCUSSION

The results of these tests, together with the results of Kleinlugtenbelt et al. (2006) and De Pater & Bohloli (2003) show that it is not easy to get long hydraulic fractures in sand. Fractures as predicted by the model

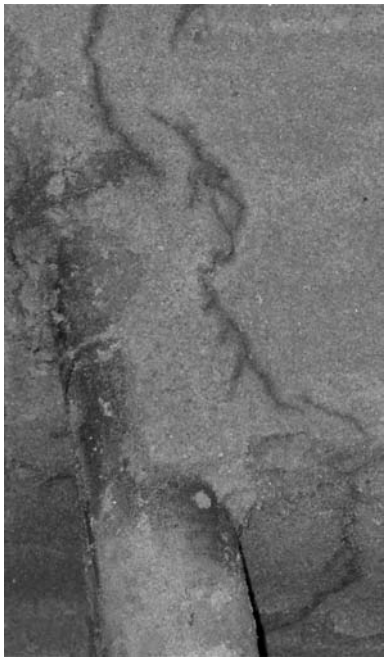


Figure 10. Fractures obtained using X-linked gel.

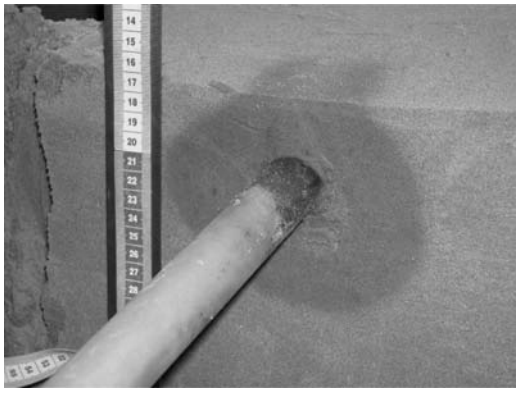


Figure 11. Results test 6 with some fractures and a considerable leak-off.

of Grotenhuis (2004) could not be produced in the tests using mixtures of bentonite slurry and cement or silica flour.

The reason is that the traditional grout mixtures (5% bentonite and a WCR of 3 or less) are too permeable, when pressurized the consolidated material will form a cake, which will prevent a fracture as described in Section 2. This can be shown by using Equation (2) that is plotted in Figure 12. Calculations were run for

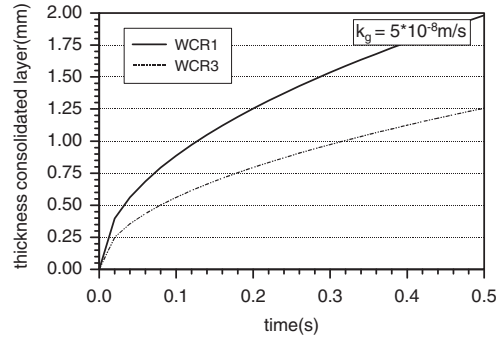


Figure 12. Plot of equation (1) for relevant permeabilities and injection times. Results show that with WCR 3 a filter cake of several tenths of mm is formed with one second.

0.5 s, approximately the time necessary to pressurize the injection hole. It can be seen that in this period the consolidated layer is already significant compared with the grain size diameter (d_{50} = 130 μm).

The mixture in test 1 and 2 did not fracture because of the leak-off. This leak-off causes the fly ash and the silica flour to gather at the interface between the injection fluid and the sand. The leak-off after the test was approximately 10 mm. The ratio (with respect to the weight) between water and fly ash or silica flour was 3. Neglecting the weight of the bentonite (only 7%) the ratio in volume for silica flour is 3*2650/1000 = 7.95 (the correction for the difference in density), for fly ash this is 3*2900/1000 = 8.70. Assuming that the porosity of the silica flour after sedimentation is roughly comparable to the porosity of the sand this means that a leak-off of 10 mm into the soil will result in a layer of silica flour of 1.3 mm, which is again much more than the grain size of the sand. Leak-off itself does not hamper fractures, as long as no filter cake is formed, but leads to less fluid that can contribute to the fractures. This is shown from the results from Test 5 and 6.

The results show that fracture grouting in clean sand will be more an exception than the normal result of a compensation grouting process. Projects where, according to the contractor, settlement in sand is corrected by fracture grouting will in most cases be examples of compaction grouting, unless there is cohesion in the soil or the soil is much more impermeable than the soil tested here (with a permeability of 10^{-4} m/s). Since compensation grouting projects are executed deep under the soil surface it is seldom known what is created, only in few cases where there was the opportunity to investigate the fracture afterwards because some soil has to be removed. Some projects report high injection pressures, which indicate that there is a kind of compaction due to cavity expansion.

How compensation is achieved, is of importance for the field situation, because it indicates how localized the compensation will be. Fracture grouting will result in heave over a wider area than compaction grouting.

5 CONCLUSIONS

From the tests performed we came to the following conclusions:

1. The grout as used in practice formed a dehydrated cake between the injection fluid and the sand where through a fracture could not propagate.
2. More cement in the grout mortar results in a thicker and more permeable filter cake.
3. Tests implemented with a low amount of particles and impermeable filter cake gave small fractures. From this we concluded that the dry mass entity of the hydraulic fracture fluid also has a major influence on the mechanism of fracturing.
4. Too much leak-off decreases the amount of injection fluid that can really contribute to the fracturing, where through the fracture stays small. (Cement can counteract the leak-off through the acting reactions of calcium.)

REFERENCES

Bezuijen, A. & Brassinga, H.E. 2001. Blow-out pressures measured in a centrifuge and in the field Proc. *XIII ECSMGE* 2001, Istanbul.

Bezuijen, A., Pruiksma, J.P. & Pater, C.J. 2003i. Maximum pressures in tunnelling limited by hydraulic fractures, (Re)claiming the underground Space, *Proc ITA* 2003, Saveur, Amsterdam: 1007–1008.

Bezuijen, A. & Talmon, A.M. 2003ii. Grout the foundation of a bored tunnel. *Proc ICOF*. Dundee: Thomas Telford.

Bezuijen A. 2003iii, *Hydraulic fracturing experiments ant low stresses in sand.* rep. Delft University of Technology TA/TG/02-03.

Bolton M.D. & McKinley J.D., 1997, Geotechnical properties of fresh cement grout – pressure filtration and consolidation tests, *Géotechnique 47, No 2, 347–352.*

Gafar K. & Soga K. 2006. Fundamental Investigation of soil-grout interaction in sandy soils, Un. of Cambridge report, August.

Grotenhuis te, R. 2004. *Fracture grouting in theory*, MSc thesis, Delft University of Technology.

Khodaverdian M. & McElfresh P. 2000. Hydraulic fracturing simulation in poorly consolidated sand: Mechanism and consequences, *Proc. Conf. Soc. of Petroleum Engineers*, Dallas no. 63233.

Kleinlugtenbelt, R. 2005. *Compensation grouting, laboratory experiments in sand*. MSc thesis, Delft Un. of Technology.

Kleinlugtenbelt, R., Bezuijen, A. & Tol A.F. van. 2006. Model tests on compensation grouting. Proc. ITA 2006, Seoul.

Mitchell, J.K. 1976. Fundamentals of soil Behavior, University of California, Berkely ISBN 0-471-61168-9.

Pater de, H.J. & Bohloli, B. 2003. *Fracturing unconsolidated rock*, rep. Delft University of Technology TA/TG/02-03.

This page intentionally left blank

Underground Space – the 4th Dimension of Metropolises – Barták, Hrdina, Romancov & Zlámal (eds)
© 2007 Taylor & Francis Group, London, ISBN 978-0-415-40807-3

Software solutions for sensitivity studies in design of tunnels

E. Bieth
Centre d'Etudes des tunnels, Lyon, France

L. Chantron
BG Bonnard & Gardel Ingénieurs-conseils, Lyon, France

P. Roure
Itech, Paris, France

ABSTRACT: The design of a tunnel is characterized by certain degrees of uncertainty, particularly in regard to the characteristics of the rock mass. As a result, in the design of tunnels a certain level of risk is not completely avoidable and therefore, sensitivity studies are highly recommended. The design and sizing studies of tunnels require different calculation methods providing connected information. Many cases require a finite element method analysis. Yet, during the initial study phases for ordinary tunnel designs, the geometry of the excavation and structures stems from a systemization of standard profiles commonly employed. A complete software (C-Tunnel) dedicated to tunnel design has been developed by CETU (The "Centre d'Etudes des Tunnels" is the French tunneling study Center which is part of the French transports Ministry) and the producer of computation software ITECH. This software includes a finite elements tool (Plane strain Module), a convergence-confinement tool and many other state of the art tools dedicated to design. It allows to create automatically a calculation note and offers the possibility of a fast sensitivity study of the involved parameters.

1 DEALING WITH UNCERTAINTY

Dealing with uncertainty, caused by material parameters varying in a wide range or simply by a lack of knowledge, is one of the important issues in geotechnical analyses. In underground construction, it often leads to design and construction conservatism and hence to inflated costs. Nevertheless, different ways to take uncertainty into account exist. On the one hand, there are deterministic methods associated with sensitivity studies, and on the other hand there are probabilistic ones.

1.1 *Probabilistic modelling*

The mathematical representation of uncertainty has started with the concept of probability theory. Re-cent developments made in computational modelling have established various probabilistic related methods such as stochastic finite element analysis or random set finite element method. Despite the fact that they can give a more formal consideration of uncertainties, the use of such method is not common practice. The most difficult task is to characterize input parameters with density distribution function in view of having insufficient data available for a particular project, especially in the very preliminary design steps.

1.2 *Deterministic modelling with sensitivity studies*

This is the classic engineering analysis. One runs deterministic sensitivity analyses which means varying each variable at a time while keeping all others constant. The range of variation is usually either the range between the extremes or the standard deviation.

Since using probabilistic analyses is more complex than doing deterministic ones, it is advisable to only include parameters (variables) in the probabilistic analysis which have a major effect on the out-come. For this purpose, those two approaches are complementary.

The software solution presented in this article was developed with that concern: giving a user friendly tool dedicated to tunneling design and able to assist and facilitate such sensitivity studies.

2 TUNNELING DESIGN METHODS

2.1 *Most commonly used tunneling design methods*

Calculation – or rather the justification – of underground works is a relatively recent science. It is the know-how of the engineer which prevails because

designing tunnel support was for many years considered too complex for strict engineering analysis and remained an empirical art repeating techniques that had proven satisfactory under similar conditions in the past. This similarity approach is principally based on various geotechnical classification systems (Bieniawski's RMR, Barton's Q system,. . .).

In addition to that approach, the design and sizing studies of tunnels require different calculation methods providing connected information. We can first quote the convergence-confinement method. Recent advances made in computational modelling have extended the use of numerical methods. Because of the huge of time required by a full three dimensional analysis, the most commonly used numerical methods in current design are the followings:

– plane strain analysis
– axisymmetric

2.2 *Provide connected information*

As it was said, there is not only one method to compute a tunnel support, and even less only one solution. According to the geological and geotechnical configuration, as well as the geometry and the environment of the work, a technique will be more suitable than another to provide the wanted result. And very often, the only choice of the kind of result conditions the choice of the method !

As illustration, let us take the case of a not-circular tunnel, dug at strong depth in a homogene-ous and isotropic ground. The particular geometry of the excavation section makes one choose a plane strain finite-element computation. To determine the confinement-loss value at the installation of support, required for the phased-computation, it will be nec-essary to use the convergence-confinement method principles or better, to carry out an axisymmetric computation with an « equivalent » circular tunnel. A data-processing tool making it possible to handle all these methods at the same time, while passing from the one to the other and preserving the under-ground « state of the art », thus constitutes a price-less saving of time.

3 SOFTWARE SOLUTION

3.1 *Purpose*

The reports established in the preceding paragraphs underline the complexity and the complementarity of calculations for tunnel design. The main characteristic is the permanent interaction ground-structure.

The studies carried out by CETU (The "Centre d'Etudes des Tunnels" is the French tunneling study Center which is part of the French transports Ministry) and a professional of FEM calculations and producer of computation software ITECH deal with the design of support and lining structures for tunnels and the subsequent development of a complete software (C-Tunnel) which makes it possible to lead huge sensitivity studies starting from the most elaborate methods of calculation.

It was also developed to responds to two main issues:

– the pre-design of tunnels may require the analysis of a great number of alternative scenarios
– the large majority of preliminary studies can be performed on a restricted number of standard geometries

3.2 *Many tools dedicated to design*

The functionalities proposed are based on the state that most of tunnel calculation reports mainly use simultaneously the three methods described just before. Furthermore, a pre-design study also requires the practitioners to estimate some of the parameters and in the previous steps of a project, engineers do not spend lot of time on various calculations. Therefore, they need help to build the numerical model and practical tools to analyze the results.

In order to respond to these demands, the software would be articulated around three methods of calculation:

– The analytical convergence-confinement method analysis
– FEM analysis: plane strain FEM analysis and axisymmetric FEM analysis (axisymmetric analysis is not available yet)

The other main characteristic is that the model would be only defined by project parameters (geometry, soil properties) and the results automatically extracted on pre-selected sections and summered in an automatic report.

In fact, most of the steps of the model generation process can be automated, from the definition of the tunnel geometry to the publishing of the report. The usual modelling steps specific to the finite element method such as meshing, definition of the boundary conditions and application of the loads are here fully automated according to finite element best-practice.

Finally, the software works as it is presented in figure 1.

The different tools are presented in detail just bellow.

3.2.1 *Analytical convergence-confinement tool*

This tool allows to carry out studies for pre-design of tunnels according to the convergence-confinement method.

Several configurations are proposed:

1 The convergence curve of soil is defined selecting one of the four following material behaviors:
– Mohr-Coulomb,
– Mohr-Coulomb with softening,

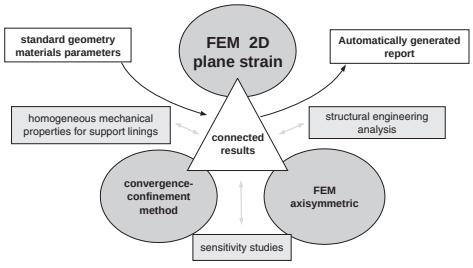


Figure 1. Software architecture.

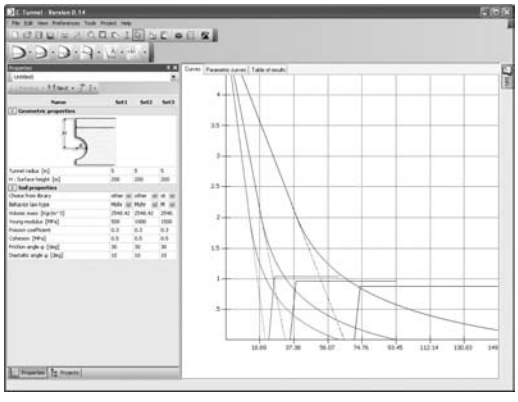


Figure 2. Parametric study with the convergence-confinement tool.

– Hoek and Brown,
– Hoek and Brown with softening.

2 The displacement curve at lining setup is defined from one of the two following methods:
– Elastic method (AFTES)
– Similarity principle

Using an input in grids, the convergence-confinement tool enables to vary very simply parameters in order to test their sensitivity (Fig. 2).

It displays simultaneously the results of all the studies, allowing a graphic visualization of the influence of a parameter.

The user can also visualize curves of variation of a result according to a parameter.

An automatic report will synthesize the results.

3.2.2 *FEM tool*

C-tunnel implements the finite element method for two-dimensional calculations in plane strain. It uses for these calculations solver CESAR-LCPC designed by the LCPC (Laboratoire Central des Ponts et Chaussées, France). The steps of the user are as follows:

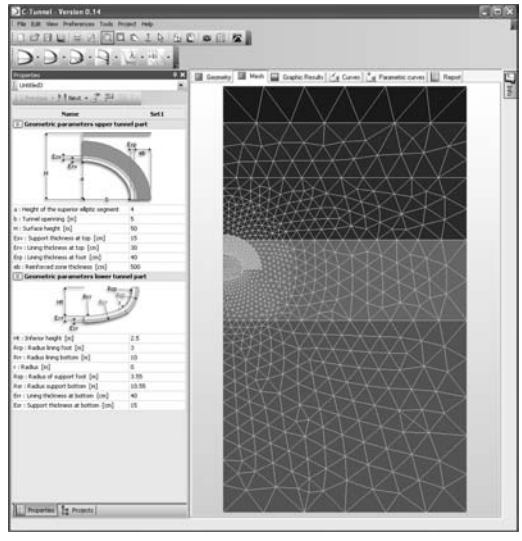


Figure 3. FEM tool: automatic creation of the mesh from geometrical parameters.

– Description of typical section (from many current sections)

  Model is defined from geometrical parameters; Finite Element mesh used by solver CESAR is automatically generated. Yet, during the initial study phases for ordinary tunnel designs, the geometry of the excavation and structures stems from a systemization of standard profiles commonly employed.
– Input of material properties: Soil layers, reinforced soil, lining, support, lateral pressure coefficient, long-term effects coefficient, ground water level,. . .
– Input of confinement loss coefficient: (Manual definition or use of convergence-confinement tool)
– Choice of the method of tunnel excavation: excavation in full section or half-section, that determines the phases of calculation.

All the steps dedicated to finite elements modelization are automatically managed by the software: creation of the mesh, definition of the boundary conditions. . . That enables to be freed from the modelization errors and gives once again the possibility of testing the influence of parameters.

The results are graphically exploited and synthesized via a report generator, selecting, phase per phase, required results for design.

The choice is offered to simulate full face or half section excavation.

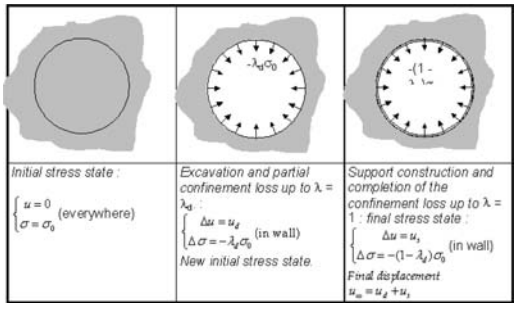


Figure 4. Modelling steps for full face advance.

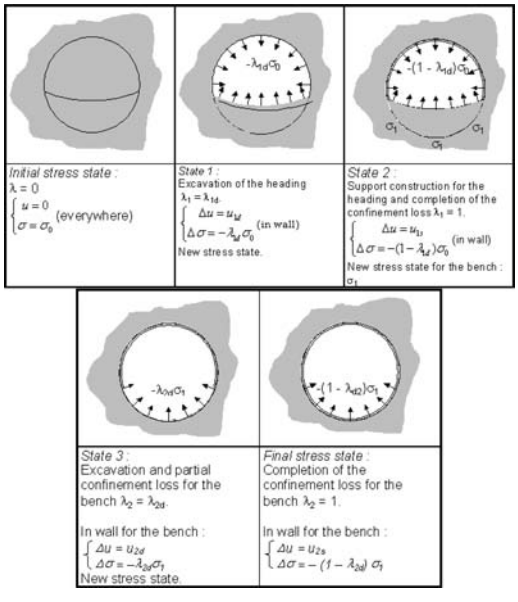


Figure 5. Modelling steps for top heading and bench excavation.

– For full face excavation, the tunnel advance is simulated by a single confinement loss (Fig. 4).
– For top heading and bench excavation, two confinement loss are needed (Fig. 5).

3.2.3 *The additional wizard*

Using the direct characteristics of projects, the wizards bring their technical "appreciation" around the software C-Tunnel.

The wizard for Bolting: It allows, starting from the mechanical characteristics of the bolts, to deter-mine the increase of the cohesion in the reinforcement area.

The wizard for mixed Supports: it makes it possible to calculate, starting from the properties of the concrete and of the steel arches, the homogeneous characteristics of the supports. It also enables

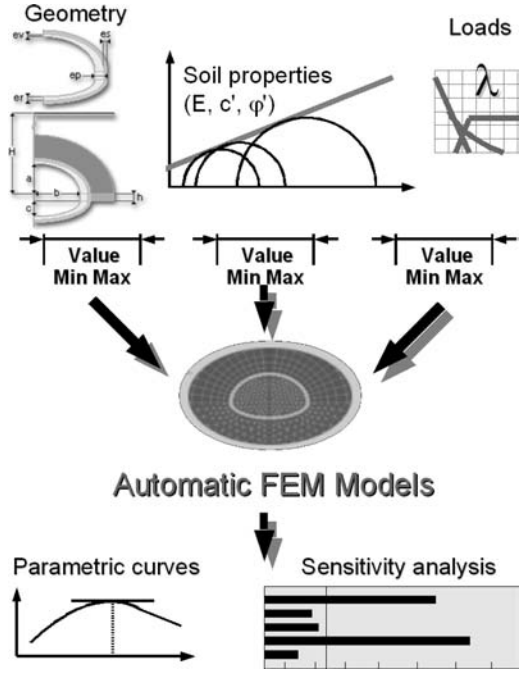


Figure 6. Sensitivity studies principles.

to calculate the distribution of the efforts within the concrete and the arches.

In addition, each module of calculation or wizard uses material libraries which are managed like true data bases by the user.

3.3 *Leading sensitivity studies easily*

In tunneling design, the advantages of numerical modelling have been appreciated by practitioners. Therefore, it seems to be logical to combine numerical modeling with concepts for sensitivity studies.

Then, each tool is developed to encourage those studies. The user only have to choose one or more project parameter and define min and max values. The software will automatically compute models and propose parametric curves for the selected parameters (Fig. 6).

4 CONCLUSIONS

Tunneling design studies are hard work especially for an engineering structure due to uncertainty in geotechnical properties. Therefore, sensitivity studies are highly recommended for the pre-design studies. In order to encourage taking that uncertainty into account, a new software has been developed, based on the FEM code CESAR LCPC. It allows the use of various connected calculation methods and structural

tools and offers help to make fast and easy sensitivity studies.

It is thus beneficial to make use of "trade"-specific tools, as a complement to the geotechnical computation codes for more specialized interfaces; such tools apply this systematization by automatically conducting both a numerical model and the standardized interpretation of results.

REFERENCES

AFTES (Association française des travaux en souterrain), 1993. Considerations on the usual methods of tunnel lining design. *TOS (n°*117*)*.

AFTES (Association française des travaux en souterrain), 2002. Recommendations on the convergence-confinement method *TOS (n°*170*)*.

CETU, 1998, Dossier pilote des tunnels – Génie civil, France.

Favre, J-L., 2004. Sécurité des ouvrages. Modélisation de l'incertain, fiabilité, analyse des risques. Paris: Ellipses.

LCPC - Logiciel CESAR-LCPC, 1992. Modélisation des phases de construction d'un tunnel, *Bibliothèque d'exemples*. France.

Mestat, P., 1997. Maillages d'éléments finis pour les ouvrages de géotechnique - Conseils et recommandations. *Bulletin des laboratoires des Ponts et Chaussées (212)*: 39–64.

Saïtta, A., Bieth, E. & Roure, P., 2004. Des outils "métiers" pour le dimensionnement courant des tunnels, *Geoquebec 2004; Proc. intern. symp., Quebec, 24–27 October 2004*, Canada.

Saïtta, A. & Bieth, E., 2005. Outils-métiers d'aide à la conception des soutènements et revêtements des tunnels, *TOS (n°*188*)*.

Saïtta, A., Bieth, E., Martin, F. & Roure, P., 2005. PFD-Tunnels: une plateforme informatique pour l'aide à la conception et au dimensionnement des tunnels, *AFTES 2005; Chambery*, France.

This page intentionally left blank

Underground Space – the 4th Dimension of Metropolises – Barták, Hrdina, Romancov & Zlámal (eds)
© 2007 Taylor & Francis Group, London, ISBN 978-0-415-40807-3

Safety problems of underground structures in the design

N. Bulychev & N. Fotieva
Tula State University, Tula, Russia

A. Levchenko
Department of City-Planning Policy Development and Reconstruction of Moscow, Russia

ABSTRACT: A high degree of safety of underground structures such as lining and support in the design is provided by a strength computation. Design methods of underground structures are very difficult in comparison with other structure types because of the interaction between the structures and the surrounding rock mass. That is why the first problem of the safety provision of the underground structures consists in choosing the design method is that which faithfully valid physical essence of the lining – rock mass interaction.

The second problem lies in the authentic input data securing for computation or modeling the underground structures. Obligatory input data are the following: characteristics of the intact rock mass stress state (magnitudes and directions of principal stresses) as well as deformation characteristics of rock mass in the position taking into account the scale effect. The fact is that the concrete lining is loaded at the same time when the shuttering demoulds.

1 INTRODUCTION

1.1 *Fundamentals*

Safety of underground structures contacted with the rock mass such as a lining or support is provided in the design by strength computation. The basic principle in modern theory of underground structures design is that of joint contact interaction of the rock mass and the lining. In accordance with that principle the lining and the rock mass are elements of a united deformable "rock-support" system subjected to external loads and actions (Bulychev 1994, Bulychev & Fotieva 1999, 2001). According to the theory it has been established that the rock pressure or, more precisely, contact stresses on the interface between rock mass and support, is not fixed but depends from both technology and support stiffness. Due to that peculiarity underground structures methods have been recognised as not having analogies among other engineering structures in respect to the design.

That is why the first problem of the high degree of safety of underground structures during the process of the structures design resides in proper choosing the design method for them.

The next problems depend from the chosen design method and lay in determination of input data for the design method.

Obligatory input data are the following:

- characteristics of the intact rock mass stress state (magnitudes and directions of principal stresses),
- deformation characteristics (modulus and Poisson ratio) of rock mass in the position taking into account the scale effect,
- strength and deformation characteristics of tunnel lining materials,
- characteristics of tunnel (shaft) lining erection technology especially lining lag behind tunnel face advancing.

2 BRIEF REVIEW OF TUNNEL LINING DESIGN METHOD

2.1 *Methods of fixed loading*

The first attack the problem of the tunnel lining design was application of the ordinary design methods considering underground structure as ordinary one. The design method was discussed as consisting of two steps: design (calculation, as such) and loads (rock pressure) determination. It was proposed that the rock pressure is conditioned only by rock mass properties.

The next step of the underground structures design evolution was a model of ring beam on elastic

(Winkler) base (rock mass). It should be pointed out that the design scheme of bedded ring beam and the corresponding widely spread method of tunnel lining design was developed by Russian engineers-designers when the Moscow Underground construction has been started (Bodrov & Matery 1936).

The rock mass model (the elastic Winkler foundation) is not loaded in relation to lining because of that the bedded ring beam method involves fixed "active loads" taking into account a "passive loads" due to the reaction of the elastic base.

At the present time the traditional calculation methods of both fixed and fixed active loads as well as a century-long efforts to understanding the rock pressure independently of the tunnel lining characteristics are not correct in general. That is proved today. In spite of that those methods are discussed and practically currently recommended for use (IBSM 1995, Japan Society 1996, ISSMGE ERTC 9 1997, ITA 2000).

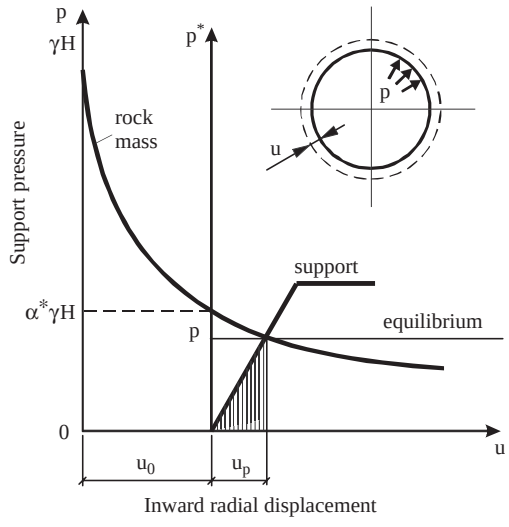


Figure 1. Scheme of interaction between rock mass and tunnel lining (u_0 is initial displacement before the lining is installed, u_p is joint displacement of rock mass and lining as result of their interaction).

2.2 *Methods of interactions between lining and rock mass*

Notions about tunnel lining function were sufficiently changed by Fenner (1938) and Ruppeneyt (1954). They have given us insight into the mechanism of the rock mass and lining (support) interaction. The curve in Figure 1 illustrates response of lining to tunnel walls displacements resulting in establishment of equilibrium. Owing to them a great step has been made towards the theory.

Thanks to that investigations it has been found the principal peculiarity of underground structure, namely, the interaction between a structure and surrounding rock mass. It has been established that the rock pressure or, more precisely, contact stresses on the interface between the rock mass and support, is not fixed but depends from both technology (u_0) and support stiffness (u_p). Due to that peculiarity underground structures methods have been recognised as not having analogies among other engineering structures in respect to the design.

One may distinguish three directions of the following development of the underground structure design methods taking into account the principle of rock-support interactions:

- New Austrian Tunnelling Method (NATM)
- physical equivalent material (sand and plaster) modeling
- numerical modeling (FEM)
- analytical design method.

The NATM is the first that found a practical implementation of Fenner-Ruppeneyt investigation. It is well known that generally recognised NATM is based on the philosophy of following relations represented at the Figure 1 (Rabcewicz 1973, Muller 1990). The concept of the NATM is to construct a tunnel on the basis of scientifically established principles and ideas which have been proved in practice, the main idea being that by mobilising the bearing capacity of the rock mass. The NATM philosophy is the use of instrumentation to monitor the deformation of the excavation and the build-up of load in the support or reinforcing elements. In this manner the NATM is not design method. It is empirical method of underground support constructing.

The analytical methods of underground structures design are developed according to the modern theory "Underground Structures Mechanics". The theory consists in applying rigorous analytical solutions of the elasticity theory contact problems simulating interaction between rock mass and different types of supports and linings when the rock-support system is subjected to all kinds of loads and actions including a seismic effects.

The mathematical elasticity theory developed in the classical works by Muskhelishvily, Sherman, Lekhnitsky and others may be used to solve the problems of underground structures design. The analytical methods allow to obtain both direct and inverse solutions (back analysis) and optimal solution too. The analytical methods of underground structures design are developed by Savin (1947), Muir Wood (1975) as well as Fotieva, Bulychev and others.

As to numerical methods such as FEM we would like to note that numerical methods are modeling ones (not design) and they are approximate. Because of that they need to be checked for accuracy. Analytical

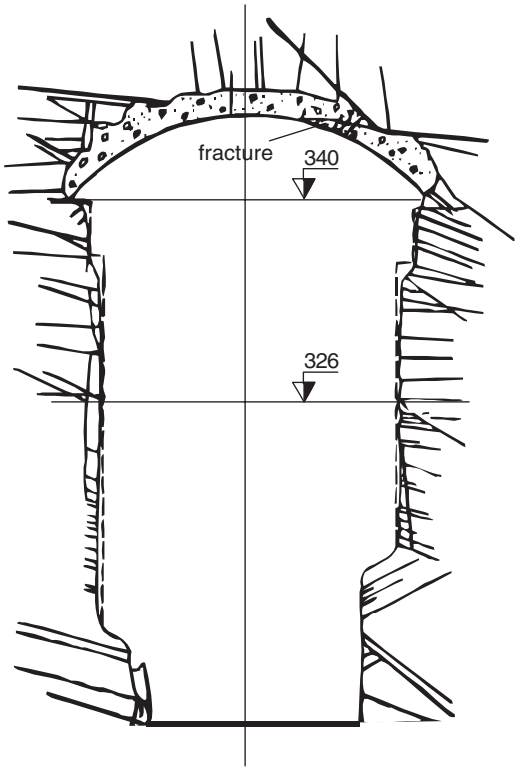


Figure 2. Scheme of fracture in the vault of Kolymskaya. Power station chamber. After Mostkov.

solutions are the only to check for accuracy numerical methods. By the way comparing results of analytical underground structures design with numerical (FEM) and physical (equivalent materials) modeling we discovered to our surprise that the result obtained by physical modeling most closely corresponds.

2.3 *Case history*

Case history is a failure of the reinforced concrete vault of Kolymskaya Power House in Siberia (Fig. 2) during the process of construction at a depth of 60–70 m (Mostkov et al 1993). The powerhouse was constructed in jointed and fractured granite with fractures filled by ice. Span of the arch was 24.7 m. According to field measurements horizontal stresses in the intact rock mass were 3.3–4.9 MPa consequently the lateral pressure coefficient represented about 2.5.

These rock mass intact stress state characteristics were ignored and the vault was worked out the design for a prescribed vertical pressure. But vault facture was caused by convergence of the chamber walls. A fracture appeared in the arch. Somewhere along the fracture the concrete was spalled and reinforcing bars were uncovered. As the chamber was constructed that fracture extended along the arch of the chamber up to 84 m length. Then the new spalling of the concrete protective layer appeared and reinforcing bars experienced buckling. The fracture in reinforced vault has the aspect of shear. In specific places the fracture is through.

According to further field measurements the convergence of the arch skewbacks comprises from 20 up to 70 mm within 7 years. The rate of the convergence at the beginning period ranges up to 7.6 mm per month.

It cannot be doubted that the reason of the vault fracture is not expected compressive stress due to convergence of the chamber walls as the powerhouse was constructed. Consequently the design methods not correlate with physical essence of the vault and rock mass interaction.

3 ROCK MASS CHARACTERISTICS

3.1 *Intact rock mass stress state*

The very important problem of the high degree safety provision of underground structures in the design consists in plausible input data securing. Among the obligatory input data are characteristics of the intact rock mass stress state.

In gravitational stress field that take place in sedimentary rocks the main characteristic of the intact stress state is only the lateral pressure coefficient. But different matter is in magnetic or metamorphic rocks especially in tectonic and seismic areas. In these cases the intact rock mass stress state characteristics represent magnitudes and directions of three principal stresses in a region of underground construction. It allows presenting those characteristics in statistic form.

The design intact rock mass stress state may be not only natural but also man-made due to technology of underground construction. These situations take place when applied frozen technique of construction (Bulychev 2005).

Let us consider the following instance preparing a shaft sinking. Rock mass – mergel at depth of 300 m, the deformation modulus is 4000 MPa, the Poisson's ratio is 0.3, the moisture transformed into ice is 6%. Natural intact horizontal stress in the rock mass is 3.2 MPa. Additional horizontal stress produced by the action of freezing is in the range of 5.9 MPa. Influence of rock freezing is obvious.

Similar situation take place when press concrete tunnel lining method is applied (Bulychev at al 2003). Pressing the stiff concrete behind a sliding shutter using the shield jacks under pressure 1–2 MPa carries out the concreting of the tunnel lining. The concrete sets and hardens under that pressure. One has to consider this pressure as a design initial soil stress state especially for shallow tunnels.

A sewer tunnel of 4 m diameter has been constructed in the center of Moscow with use the press concrete technology. Engineering geological condition was complicated: weak water bearing ground at depth up to 30 m. Operating pressure on concrete mix was 1.3–1.5 MPa what was about two times as great than vertical stress in the ground mass. According to surveying of a subsidence of buildings positioned over the tunnel the subsidence along the whole alignment of the tunnel was effectively zero.

3.2 *Deformation characteristics of rock mass*

Tunnel lining stress-strain state sufficiently depends on deformation characteristics of the rock mass namely on deformation modulus and Poisson's ratio.

At the present time there are mistakes in determination of these characteristics especially the deformation modulus. For instance real deformation modulus of clay obtained as a result of geotechnical monitoring in the course of underground tunnel construction in Saint Petersburg (Kulagin et al 2004) appears to be more than 10 times in comparison with official input data.

Similar case takes place when drainage adit in Tomsk City was driving. In this instance the difference comprises almost 100 times.

The fallacies in these instances are that the ground mass characteristics were obtained as results of specimens laboratory test. To eliminate the trouble it needs to execute of ground mass testing in the immediate occurrence of a place of tunnel driving.

4 CHARACTERISTICS OF LINING MATERIAL

4.1 *Characteristics of monolithic concrete*

Cast-in situ concrete is erected behind shuttering. The concrete mix is compressed between shuttering and rock walls due to the rock walls displacements and is hardening sometimes. Then according to the sequence diagram of the work organization the shuttering is ripped from the concrete lining.

The concrete is remoulding and because of that radial stresses that have been before at the inner surface of concrete lining are reliefed and the lining is loaded. So the lining is loaded in early age of the concrete mix hardening. Under these conditions monolithic concrete lining is subjected to twice simultaneously acting factors: hardening concrete in early age and the lining loading due to rock mass deformation.

The first accidents and concrete shaft lining failure were established on Tashtagol iron ore deposit in Siberia at the depth more than 400 m in jointed and faulted sienites and carbonate-chlorite shales. According to results of investigations the distinguished feature of the rock mass is a tectonic intact stress state: sub horizontal normal stresses are 2–3 times as much as vertical ones.

The reason of the accidents was deficient the shaft lining bearing capacity because loading in early age of concrete hardening together with increased horizontal stresses in rock mass.

Because of that the following characteristics of concrete are necessary for the tunnel (shaft) lining design taking into account the early age hardening of it: deformation modulus and compressive strength for the moment of the concrete demould. The concrete lining is to be designed for the above moment and the second design has to be executed for operating period.

4.2 *Case history*

Combined shaft sinking method is characterized that cast-in situ concrete is erected immediately above the shaft face. After rock blasting the shaft face advance and the concrete mix is compressed behind shuttering. After taking away the crushed rock the shuttering is ripped from the concrete lining and lowered to the face.

According to shaft sinking experience (Mindely et al 1970) the period of the concrete mix hardening time may range between 10 and 20 hours. In the process of rapid shaft sinking technique the hardening time may be reduced up to 3–4 hours.

It happened in 1984 at chromite ores deposit in Kazakhstan. In the Central Mine, a 8.8 m diameter cage shaft, 766 m deep, was been sinking. Inner diameter is 8 m. Rock mass consists of jointed and faulted serpentinits with cracks filled by talc. Compressive strength of the rock mass as whole is 15–20 MPa, the angle of the internal friction is 18–20° (due to talc). In addition to that intact stress state of the rock mass is characterized as tectonically with heightened normal horizontal stresses. The lateral pressure coefficient is from 1.0 up to 1.5. Because of that the rock mass may be estimated as instability. In the process of the shaft sinking unsupported rocks in shaft walls were crushed and failure.

The situation on the eve accident is the following. The face of the shaft was at the depth 765 m. Holes were drilled and blasted; the shuttering was put down on crushed rock. At that time rock failure occurs behind shuttering and part of before installed lining was fractured. To prevent further failure of rock and lining 117 rock bolts were installed and 50 m^3 of concrete mix was placed against shuttering. In spite of that cracks occur above in the lining in the range of depth 737–743 m. Work in the shaft was stopped but next day increasing fracture of shaft lining started. A total of near 200 m of the shaft lining above the face including three shaft insets was crushed.

Cause of the accident is deficient the shaft lining bearing capacity because loading in early age of concrete hardening. We emphasize that deficient the lining bearing capacity took place on 200 m part of the shaft during near two month.

It needs to be noted that the above-mentioned press concrete lining was loaded in early age of concrete hardening but the tunnel was constructed with increased requirements to the concrete quality and lining technique were made

- average length of advance of the press concrete operation was 0.33 m
- concrete mix pressing cycle took 2.5 hours
- the class of concrete strength was B60
- the strength of high-early-strength concrete mix after 5 hours was 5.0 MPa and after 7.5 hours was 11 MPa
- the brand of watertight was W16.

5 CONCLUSIONS

A high degree of safety of lining in the design is provided by a strength computation.

The first problem consists in proper choosing the design method correlate with physical essence of the lining-rock mass interaction. The next problems lay in obtaining obligatory reliable input data for the design method.

ACKNOWLEDGEMENT

The work is supported by grant of President of Russian Federation on Leading Scientific Schools 1013.2003.5.

REFERENCES

Bodrov, B.P. & Matery, B.F. 1936. *The ring in elastic medium (methods and examples of calculation)*. Bulletin No 24, Part 2. Moscow: Metroproyekt.

Bulychev, N.S. 1994. *Mechanics of underground structures.* Moscow: Nedra.

Bulychev, N.S. 2005. About shaft lining design in sinking by rock frozen method. *Izvestiya of Tula State University. Series Geomechanics. Underground Structures Mechanics.* 3: 42–46.

Bulychev, N.S., Amusin, B.Z., Olovjanny, A.G. 1974. *Design of main mining working support.* Moscow: Nedra.

Bulychev, N.S. & Fotieva, N.N. 1999. Once more about the modern theory of underground structures design. challenges for the 21st Century. *Vol. 1. Proc. of the World Tunnel Congress'99, Oslo. In Alten et al (eds.)*: 1:327–333. Rotterdam: Balkema.

Bulychev, N.S. & Fotieva, N.N. 2001. Theory and practice of tunnel linuing design. *Proc. of the Int. Symp. on Modern Tunnelling Science and Technology. In Adachi et al. (eds.), Kyoto, Japan, Tokyo*: 445–450. Rotterdam: Balkema.

Bulychev, N., Abramov, A., Gilstein,S., Semenov, A. 2003. Design method of monolithic press concrete tunnel lining. *Underground Construction 2003. International Conference & Exhibition.* London Docklands: 491–495. Brintex.

Bulychev, N.S., Fotieva, N.N., Sammal, A.S., Savin, I.I. 2000. Theoretical aspects of monitoring and back analysis in tunnels. In T.R.Sacey et al. (eds). *AITES-ITA 2000 World Tunnel Congress. Symp. Series S*24: 73–78. The South African Inst. of Mining and Metallurgy.

Fenner, R. 1938. Untersuchungen zur Erkenntnis des Gebirgsdruckes. *Gluckauf* : 32:681–695, 33:705–715.

Fotieva, N.N. 1974. *Design of Non-Circular Cross-Section Tunnel Linings*. Moscow: Stroyizdat.

Fotieva, N.N. 1980. *Design of support of underground structures in seismically active regions*. Moscow: Nedra.

Fotieva, N.N. & N.S. Bulychev 1997. Design of undersea and under-river tunnel linings. *Proc. of the 1st Asian Rock Mech. Symp.: ARMS' 97- Seoul, Korea. In Hi-Keun Lee et al. (eds.):* 211–216. Rotterdam: Balkema.

Fotieva, N.N. & A.S. Sammal 1993. Design of linings of large cross-section tunnels undergoing construction in rock. *Proc. ISRM Int. Symp. Eurock'93*: 545–549. Rotterdam: Balkema.

ITA. Working Group 2. 2000. Guidelines for the design of shield tunnel lining. *Tunnelling and Underground Space Technology.* 15 (3): 303–331.

Japan Society of Civil Engineers, 1996. Japanese standard for shield Tunnelling. Tokyo: Japan Society of Civil Engineers.

Kulagin, N.I., Bezrodnyi, K.P., Krjukovsky, Ju.A. 2004. Results of geotechnical monitoring accompaning construction of Saint Petersburg underground tunnels in zone "Razmyv". *Metro & Tunnels*: 17–18.

Levchenko, A.N. 2001. Crack resistance design of lining of sewer tunnel main line. *Mining Inform. Analytic. Bulletin*: (10): 88–90. Moscow State Mining University.

Mindely, E.O., Tjurkjan, R.A. et al. 1970. *Technique and technology vertical shaft sinking.* Moscow: Nedra.

Mostkov, V., Dmitriev, N. Rachmaninov, Ju. 1993. *Design and construction of underground structures of large cross-section.* Moscow: Nedra.

Muir Wood, A. M. 1975. The circular tunnel in elastic ground. *Geotechnique* 25(1): 115–127.

Muller, L. 1990. Removing misconceptions on the New Austrian Tunnelling Method. *Tunnel & Tunnelling, Special Issue*: 15–18.

Protodyakonov, M.M. 1930. *Rock pressure and mining support. Part one. Rock pressure.* Moscow: Gostechizdat.

Rabcewicz, l.V. & Gosler, I. 1973. Principles of dimensioning the support system for the New Austrian Tunnelling Method. *Water Power.* Vol 25. No 3: 88–93.

Ruppeneyt, K.V. 1954. *Some problems of rock mechanics*. Moscow: Ugletechizdat.

Savin G.N. Impact of support on stress distribution near narrow mining working. 1947. *Notes of Mining Mechanics Institute of the UkrSSR Academy Sci.* No 5.

Terzaghi, K. 1943. *Theoretical soil mechanics.* New York: John Willey.

This page intentionally left blank

Underground Space – the 4th Dimension of Metropolises – Barták, Hrdina, Romancov & Zlámal (eds)
© 2007 Taylor & Francis Group, London, ISBN 978-0-415-40807-3

Stability and deformations in large-scale underground constructions

A. Butovic
Satra spol. s r.o.

ABSTRACT: As the tunnel construction under the town develops, also technical demands of their implementation increase. The underground location of factories, hydropower stations, road networks etc. lead to a demand for construction of large-scale underground works. Modern technology allows for the development of incredible feats of engineering, which could not be even dreamt of by our predecessors. But, of course, even today there are certain limits. The article analyses the stress and deformation response to the excavation process. Possible solutions of constructing in such loose rock have been calculated from mathematical modeling using the final element method (FEM). The choice face are sequencing and influence of anchoring from the point of view of the stress and deformations influence on the rock. Examples are shown on completed constructions in different geotechnical conditions in the Czech Republic. The article compares and provides quantity assessment of the influence of individual measures and sets possible limits for some particular cases.

1 LARGE-SCALE UNDERGROUND CONSTRUCTIONS IN THE CZECH REPUBLIC

1.1 *Introduction*

Geomorphology of the terrain in the Czech Republic does not call for the construction of a high number of the tunnels. In most cases it is beneficial to find cheaper, non-tunnel solutions for the direction of the road and railway routes. In spite of this, many interesting underground constructions have been built over the last century. As a reference we can show almost 60 km of the Prague's metro underground network plus the new Mrazovka tunnel.

A significant chapter of the Czech underground architecture is the construction of the large – scale underground structures. Except for the military construction it is possible to mention at least:

- Pumped storage "Dlouhe strane"
- Excavated tunnel forks of the Mrazovka tunnel
- The Kobylisy excavated one-vault metro station
- The "Blanka tunnel" ventilation machinery room

Basic information about the above examples is adduced in the following paragraphs.

1.2 *Pumped storage "Dlouhe strane"*

The construction of the pumped storage "Dlouhe strane" is one of the most technically unique constructions in the Czech Republic. It is located in the Northeast part of the Czech Republic in Jeseniky Mountains. It was built in a period from 04.1978 to 12.1996 and in the time of its construction it was one of the world's top structures. The extended time of a construction was due to different non-technical reasons, which are not pertinent from underground construction point of view.

Main construction parameters :

Storage cavern	$87 \times 25.5 \times 50$ m (l, w, h)
Transformer station cavern	$115 \times 16 \times 21.7$ m
Declivity	534.3 m
Supply tunnels	d. 3.6 m, l. 1547 m (1499 m)
Waste tunnels	d. 5.2 m, l. 354 m (390 m)
Volume of the excavated space	290.000 m^3

All construction was built into the stable rock, which represent gneiss.

The excavation site of the caverns was reinforced by steel rock bolts and by a primary lining from the shot crete. A final lining was constructed from reinforced concrete and the supply tunnels were lined with steel.

A point of interest: Two Francis turbines were installed with a total performance 2×325 MW. During electricity production there are 68 m^3/s traversing there, by reverse it pumps up to the height 534.3 m 55 m^3/s.



Figure 1. "Dlouhe strane" cavern.



Figure 2. East tunnel fork excavation.



Figure 3. East tunnel fork – current state.

1.3 *Excavated tunnel forks of the Mrazovka tunnel*

The Mrazovka tunnel is about 1.1 km long tunnel, which is a part of Prague city ring, and its construction was completed in 2004. Complicated motoring solution requested implementation of two excavated tunnel forks. This concerned those parts of the tunnel where three-lane tunnels, with the area of excavation of 165 m^2, gradually broaden and are divided into independent two-lane (122 m^2) and one-lane (85 m^2) tunnels. Vertical sequencing was chosen for excavating by experience from previous excavated parts and math modelling by final element method (FEM).

Main construction parameters:

Total length	53.7 m	(21.1 m)
Excavated cross section	322.0 m^2	(335.1 m^2)
Excavation clearance	16.0 m	(16.6 m)
Excavating width	23.8 m	(24.2 m)
Volume of the excavated space	13.090 m^3	(12.790 m^3)

The excavation proceeded in bad clay-dust shales (E_{def} = 100–200.000 Mpa, ν = 0,31–0,29, φ = 31–35°, c = 35–60 kPa) with the total overburden depth of 19–24 m (20–35 m). There were many houses and engineer networks in the area. The performed excavation was protected by hydraulic rock bolts 6–8 m in length and by primary lining from shot-crete with the width up to 700 mm reinforced by steel frames and meshes.

1.4 *The Kobylisy excavated one-vault metro station*

The Kobylisy Station of the Prague metro route 4.C is the first station, which was constructed as one-vault. It was installed in rock of Ordovician age, which represents clay-dust shales (E_{def} = 100–350.000 Mpa, ν = 0,3–0,27, φ = 30–34°, c = 40–100 kPa) and crushingly roughed quartzites. There were blocked sandstones in overburden. There were many houses and engineer networks on the surface of this area corresponding with Mrazovka tunnel fork.

Main construction parameters:

Total length	148 m
Excavated cross section	220 m^2
Excavation clearance	13.8 m
Excavating width	21.2 m
Volume of the excavated space	32.560 m^3
Sequencing	combined



Figure 4. The Kobylisy metro station excavation.



Figure 5. The Kobylisy metro station – current state.

A combination of the vertical and horizontal sequencing was chosen for excavation. The excavation site was reinforced by hydraulic rock bolts 6 m in length and by shot-crete, reinforced by steel frames and meshes.

Maximal surface settlement did not exceed 75 mm, the deformation of the primary lining reached in maximum 60 mm.

1.5 *The "Blanka" tunnel ventilation machinery room*

Currently next large scale underground construction is being prepared. It will be the construction of the excavated ventilation room designed as a part of the continuation Prague city ring.

Main construction parameters:

Total length	123.3 m
Excavated cross section	298.8 m^2
Excavation clearance	18.3 m
Excavating width	20.2 m
Volume of the excavated space	36.850 m^3
Sequencing	vertical

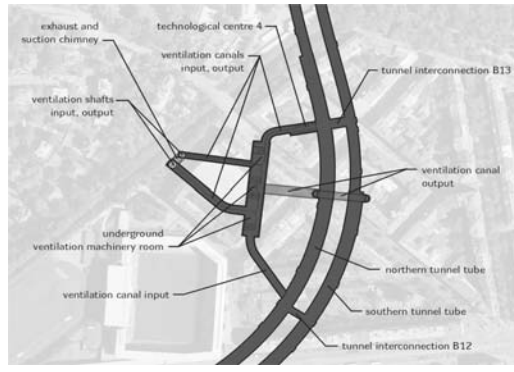


Figure 6. The ventilation machinery room – situation.

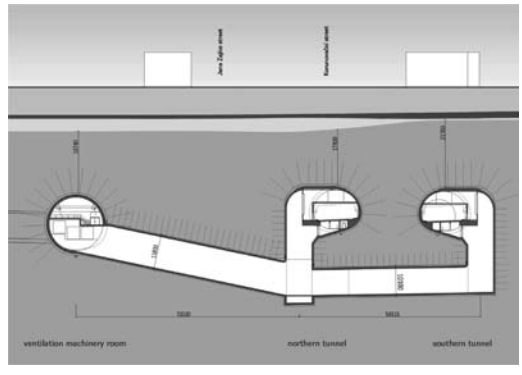


Figure 7. The ventilation machinery room – cross section.

It will be constructed in good sandy shales ($E_{def} = 200–600.000$ Mpa, $\nu = 0{,}27–0{,}24$, $\varphi = 34–37°$, $c = 45–150$ kPa) with total overburden depth 32–33 m. There are many buildings on the surface.

The ventilation machinery room excavation is not main problem, there are five another big tunnel profiles (about 120 square meters), which cross it.

This tunnel will be under construction at the end of year 2007.

2 DEFORMATIONAL – TENSENSESS ANALYSIS

The above constructions have one thing in common; the size of the excavation complicates their performance from two main reasons:

1. Technological – available mechanical mechanization is not able to work in a heights transcend 7 m (except TBM)
2. Deformational-tenseness – depending on quality of the rock condition, overburden height etc. it is necessary to choose suitable performing procedure and

completion of unsupported excavation. Except for cases when the underground construction is carried out in carefully chosen conditions it is the deformaltensensess that plays the most important role.

Different variants of the excavation approach were solved based on the example of the East Mrazovka tunnel fork by mathematical modeling by Final element method (FEM):

1. Full profile excavation without rock bolting
2. Horizontal sequencing (top heading and invert) without rock bolting
3. Vertical sequencing without rock bolting
4. Full profile excavation with 8 m long hydraulic rock bolts
5. Horizontal sequencing (top heading and invert) with 8 m long rock bolts
6. Vertical sequencing with 8 m long rock bolts
7. Full profile excavation with 12 m long hydraulic rock bolts
8. Horizontal sequencing (top heading and invert) with 12 m long rock bolts
9. Vertical sequencing with 12 m long rock bolts

Number 6 variant has been used for tunnel fork excavation.

Annotation: The calculations of the full profile excavations without rock bolting have not been finished.

Program that was used is Tunnel by RIB Stavební software Company, version no.12. The rock condition has been modelled as homogeneous isotropic material considering Mohr – Coulomb material law, with an assumption of strain plain.

The influence of the rock bolting was implemented into the model as a change of material characteristics of the rock bolted area elements by (5).

The calculations have been executed just for one particular example of the rock condition.

Variant number 6 was chosen as a base for percentage results comparing; it represents the real excavation of the Mrazovka tunnel forks.

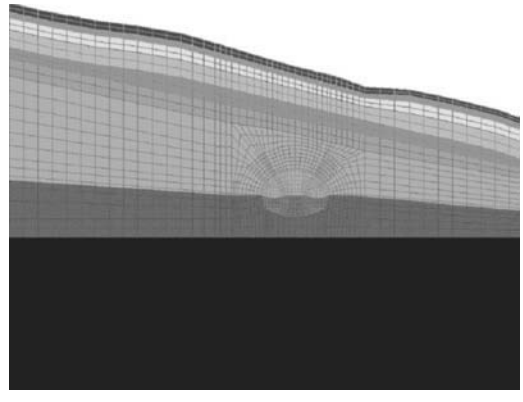


Figure 8. Model geometry.

Table 1. The results of the modelling.

		Full profile			Horizontal sequencing			Vertical sequencing		
Quantity	Units	Without	8 m	12 m	Without	8 m	12 m	Without	8 m	12 m
Lining deformation	mm	–	265	234	186	136	134	59	57	55
Settlement	mm	–	194	163	127	82	80	50	46	46
N	kN	–	−3387	−3273	−3290	−3112	−2999	−3295	−3013	−2951
M	kNm	–	597.2	592	431.6	415.8	412.3	126.5	124	115.1
Stress	MPa	–	−3.991	−3.908	−3.089	−3.091	−2.993	−2.654	−2.631	−2.631

Table 2. Results of the modelling (%).

		Full profile			Horizontal sequencing			Vertical sequencing		
Quantity	Units	Without	8 m	12 m	Without	8 m	12 m	Without	8 m	12 m
Lining deformation	%	–	464.9	410.5	326.3	238.6	235.1	103.5	100	96.5
Settlement	%	–	421.7	354.3	276.1	178.3	173.9	108.7	100	100
N	%	–	112.4	108.6	109.2	103.3	99.5	109.4	100	97.9
M	%	–	481.6	477.4	348.1	335.3	332.5	102	100	92.8
Stress	%	–	151.7	148.5	117.4	117.5	113.8	100.9	100	100

Where: Lining deformation – vertical element of the lining displacement in an arch crown; Surface settlement – vertical element of surface settlement above tunnel geometrical axis; N – Axial force in a lining in an arch crown; M – Bending moment in a lining in an arch crown; Stress – main stress in rock conditions on left side of the excavation.

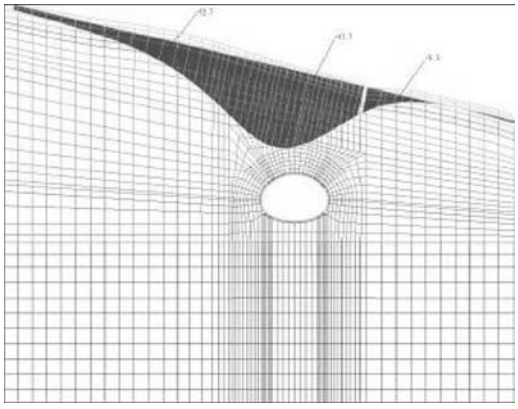


Figure 9. Model results – settlement of the surface.

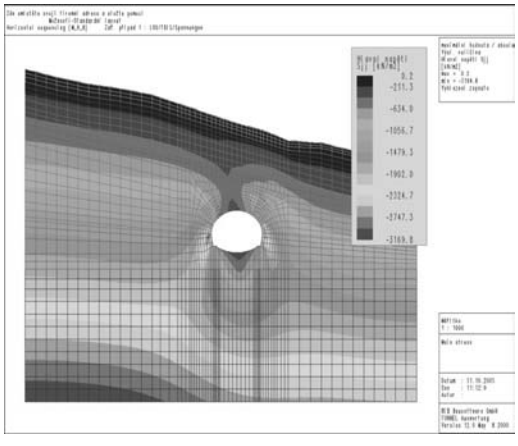


Figure 10. Vertical stresses – horizontal sequencing.

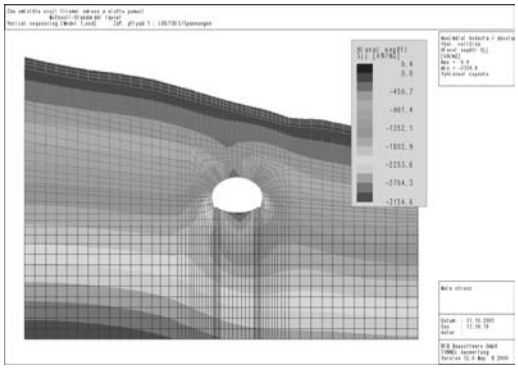


Figure 11. Vertical stresses – vertical sequencing.

3 CONCLUSION

1. The calculation simulating the tunnel fork full profile excavation without influence of rock bolting was not successfully finished. The results considering the influence of the rock bolting show unreal values. The above mentioned indicates that full profile tunnel fork excavation is according to the deformal – tensensess analysis unreal.
2. The choice of the sequencing has fundamental influence on the values of the displacements of the primary lining, rock conditions and surface settlement. In this case the displacements of the primary lining with horizontal sequencing are about 140% higher than at vertical sequencing. The similar result was registered at surface settlement where calculated difference is 70%.
3. The values of the axial forces in the primary lining are similar in both cases; the type of sequencing has no influence on it.
4. Large influence has been registered at bending moment (top of the arch), which in the case of the horizontal sequencing increased about 230%. This result is real and is related to a different history of rock massif loading and different span of the arch (the influence of the side wall tunnels).
5. The vertical sequencing is distinctively more "careful" to the rock massif, which can be seen from the side rock massif stress comparing, see pict.10, 11.
6. The rock bolting influence is certainly in all cases positive, particularly in the case of the horizontal sequencing. I expect its influence to be larger, calculated values probably relate with the implementation of the rock bolts to the mathematical model.

REFERENCES

Butovic, A., Nemecek, J., 2001. "Mrazovka tunnel forks", documentation for excavation

Bucek, R., Kolesa, K., Rozsypal, A., Vrba, O., 2003. "Comprehensive application of geotechnical methods to the excavation of the Kobylisy one-vault metro station", *"Tunel"* journal, no. 3/2003

Kunes, V., 1992. "Transformation of rock massif in caver surroundings of the THS at "Dlouhe strane", *"Tunel"* journal, no. 2/1992

Nemecek, J., Butovic, A., 2001. "Excavation of the Mrazovka tunnel in the capital of the Czech Republic", *WTC 2001-Milano*, Proceedings

Zapletal, A., 1999. "The calculation of the rock bolted rock conditions parameters", reference manual

Zelenka, M., 2003. "Excavation of the first one-vault station on the IVC1 line of the Prague metro", *"Tunel"* journal, no. 3/2003

The monitoring results during the Mrazovka tunnel excavation

Promote brochure of the pump storage "Dlouhe strane"

This page intentionally left blank

Underground Space – the 4th Dimension of Metropolises – Barták, Hrdina, Romancov & Zlámal (eds)
© 2007 Taylor & Francis Group, London, ISBN 978-0-415-40807-3

Particular design for nuclear long term interim storage

N. Dias & J. Triclot
Scetauroute DTTS, Pringy, France

H. Lagrave & E. Breton
CEA, Valrho, France

ABSTRACT: The third research topic of the 1991 French nuclear waste management act covers long-term interim storage. Two options are being investigated for waste packages: surface and subsurface storage. The object of this article is to describe the particular designs of the subsurface storage, which are based on a network of shafts and tunnels. In this study, we propose the organisation methodology of civil engineering construction for two kinds of waste: high-level waste and intermediate-level waste.

1 INTRODUCTION

The French Atomic Energy Commission (CEA) has carried out a major R&D programme on underground interim storage for spent fuel and nuclear waste (CEA., 2005). The programme concerns the design of storage facilities, durability and functional performance demonstrations.

The R&D aspect conducted by the CEA includes the demonstration of the long-term performance of concrete structures subjected to thermal and mechanical stresses.

The CEA asked SCETAUTOUTE DTTS to carry out the civil engineering construction design and the associated organisation methodology. It should be emphasised that many earlier studies were carried out in order to finalise these particular designs.

In this study, the organisation methodology of Civil Engineering construction is described for two kinds of long-term interim storage:

1 High-Level long-lived Waste Storage (this entire process will be referred to as "HLWS" as follows) and spent fuel storage.
2 Intermediate-Level long-lived Waste Storage. (referred to as "ILWS").

The storage design of these two wastes is different due to their thermal and mechanical characteristics: the high-level wastes are exothermic. The required design conditions are that, the subsurface facilities must have a target 300 years life, where the first 100 years should be without major repairs.

After a description of each kind of subsurface storage design, this article focuses on excavation processes for underground works, different logistic ways to link with milestones, and construction costs for the options considered are presented.

2 PROJECT DESCRIPTION

2.1 *Location*

The subsurface storage for the two facilities is located between 50 m and 100 m below ground level on the hillside, above the water table. This geometrical situation allows water to drain by gravity.

2.2 *Geological and geotechnical conditions*

At present, the real construction site has not been identified, so this research is based on a "generic" site represented by limestone rock with enhanced geotechnical parameters. The rock mass fracturation is considered to be moderate. (Fig. 1)

The main 150 m thick geological layer of is composed of good quality limestone called F1. Layer F1 is situated between two geological layers called F2 and F3 represented by marling limestone. The site is

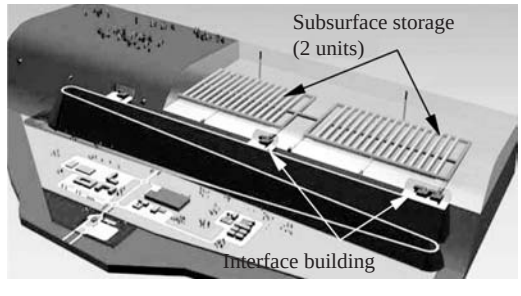


Figure 1. Geological location of subsurface facilities.

Table 1. Geotechnical parameters.

Characteristics	F1a	F1b	F2/F3
Rock compressive strength (R_c) [MPa]	60	40	30
Rock mass tensile strength (R_t) [MPa]	5	2	1
Young's modulus (E)[GPa]	40	20	10
Poisson's ratio (ν)	0.25	0.25	0.25
Density (ρ) [kg.m^{-3}]	2700	2700	2600

Table 2. Geotechnical parameters according to Bieniawski rock mass classification.

		F1a	F1b	F2/F3	ZF1	ZF2
Rc [MPa]	Value	60	30	40	–	–
	Note	7	7	4	0	0
RQD	Value	90	85	90	40	30
	Note	17	17	17	8	8
Spacing of	Value	0.4	0.25	0.4	0.1	0.1
Discontinuities	Note	20	10	20	10	10
Condition of discontinuities		12	12	12	0	0
Groundwater		7	7	10	7	7
RMR		63	60	56	25	25

intersected by two major geological faults (ZF1 and ZF2). (AFTES GT1).

The geotechnical parameters are represented in table 1. (AFTES GT7).

According to the rock mass classification published by Bieniawski (Barton & al. 1974b), (Bienawski, 1984), the RMR value for each layer is as shown in table 2.

2.3 *High level waste storage (HLWS)*

The design of the HLWS is composed of several units, for instance, the spent fuel is made up of six units.

Each unit is composed of 6 parallel galleries divided into two levels, and linked to each other by vertical shafts. In these shafts the waste packages are stocked. The dimensions of each underground unit are approximately 800 m long by 160 m wide. The number of shafts depends on the kind of waste, varying between 600 and 720 per unit (100 or 120 per gallery). The access for each unit is provided by a single interface building, situated in the hillside. Figure 2 presents the scheme of one unit.

Seven types of gallery are distinguished. As an example, table 3 describes different gallery types for spent fuel.

The distance between the upper ventilation galleries is 26 m. The distance between vertical storage shafts is 3.70 m.

Two packages of HLWS waste are set down in each vertical shaft. The package loading is carried out by a special handling vehicle, which accesses through the upper ventilation gallery (Fig. 3).

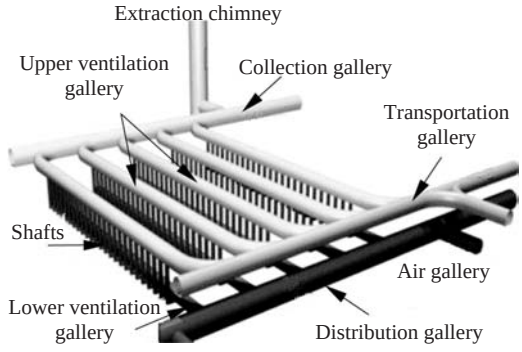


Figure 2. Scheme of one unit (HLWS).

Table 3. Gallery characteristics in terms of length and section.

Gallery name	Length m	Excavated section m^2 (Profile N2)
Transportation and handling gallery	182	108
Upper ventilation gallery	4620	60
Lower ventilation gallery	3782	46
Storage shaft (720 per unit)	12384	13
Distribution gallery	156	97
Collection gallery	156	108
Chimney	65	89

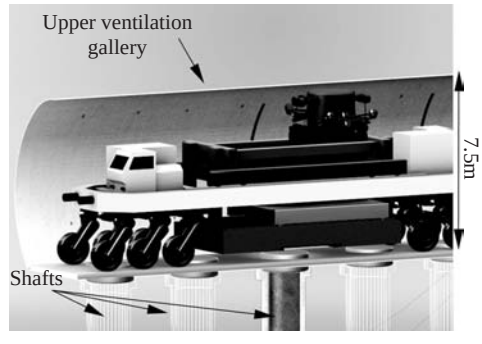


Figure 3. Handling in the upper ventilation gallery.

The HLWS design takes into account the waste temperature effects in the underground structure (with a maximum temperature of about 80° C). (Lagrave & al. 2006).

The ventilation concept plays an important role in the storage of exothermic HLWS waste packages.

The cooling air arrives by the distribution gallery from outside in order to supply the lower ventilation gallery. As a result, the packages are cooled by natural

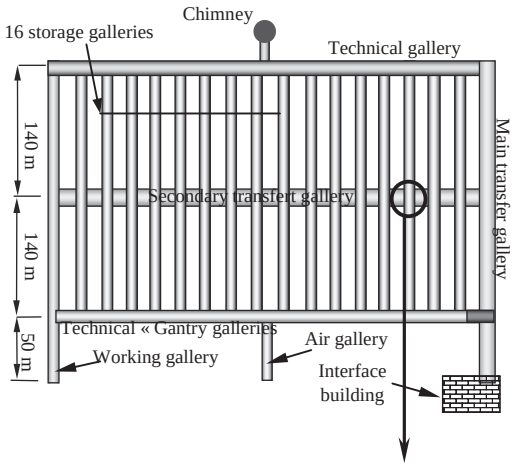


Figure 4. Scheme of ILWS unit.

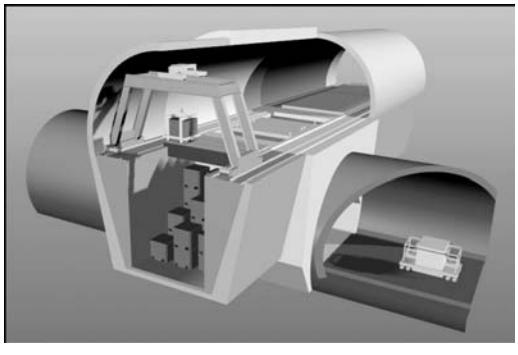


Figure 5. Crossing between the secondary transfer gallery and the storage gallery.

ventilation due to the temperature difference between outside and inside which draws air into the collection gallery and then towards the extraction chimney. (Lagrave & al. 2005).

2.4 *Intermediate-level waste storage (ILWS)*

The conception of intermediate-level waste storage (ILWS) is different due to the absence of waste exothermic effects. Consequently the design contains only one level. Three units compose the ILWS storage. Each unit comprises sixteen parallel galleries (15 storage galleries + 1 empty gallery). Finally, the complete facility consists of 48 galleries (45 storage galleries + 3 empty galleries). The access to each unit is ensured by an interface building. The storage gallery is 280 m wide by 520 m long (Figs 4–5).

Every unit comprises 9 types of gallery (Table 4).

The crossing between 16 storage galleries and the secondary transfer gallery is perpendicular and

Table 4. Gallery characteristics in term of length and section.

Name of gallery	Length m	Excavated section m^2 (Profile N°2)
Working gallery	340	64
Air entrance/exit gallery	50	20
Chimney	50	23
Technical gallery ≪gantry≫	460	99
Technical gallery	525	72
Assembly gallery	61	81
Main transfer gallery	345	108
Secondary transfer gallery	465	108
Storage gallery (16 per unit)	4480	147

halfway up the level. This configuration ensures complete insulation of the storage galleries from a ventilation point of view as well as providing protection against radiation.

The principle of waste storage is as follows: the handling vehicle takes the main transfer gallery, then the secondary transfer gallery, and stores the waste packages at each storage gallery.

The travelling gantry crane is situated in the upper part of the technical "gantry" gallery and plays an important role in the waste package handling. The gantry crane accesses every storage gallery via the technical "gantry" gallery and moves the packages along from the crossing to each storage gallery.

The functions of the gantry crane are as follows: handling the waste packages from secondary transfer gallery to the storage gallery by means of the hatch.

Even if the waste of the ILWS is not exothermic, the ventilation is important to evacuate the hydrogen, which is given off by some packages, the humidity in galleries and to reduce the impact of water streaming.

3 CHOICE OF EXCAVATION METHOD

The choice of tunnel excavation method must be adapted to the rock masses encountered, to the cross-sections and it has to be effective, speedy and safe (AFTES GT29).

Taking into account non-circular gallery sections, short lengths and differing cross sections, the excavation by means of TBM is not suitable.

In this study phase, the excavation by roadheader cannot be adopted because of its operational limit, which is related to ground geotechnical features, particularly the compressive strength Rc and the rock mass abrasivety.

The most adapted excavation method for this complex network of shafts and tunnels seems to be the conventional method known as the "drill and blast method". This method permits the excavation of the

rock mass under very difficult and variable geological conditions.

The shafts for the HLWS facility will be excavated by the "raise drill" method.

4 TUNNELING SUPPORTS

In this design stage, three kinds of tunnel support have been chosen. The lighter support is for very good bearing rock mass quality and the heavy support is for poor bearing rock mass quality. (AFTES GT29).

Profile N°1: very good quality limestone (RMR > 80).

- Occasional rock bolts in crown : 1 bolt/4 m^2, Ø25, L = 2.5 to 4 m;
- Shotcrete 0.05 m in crown.

Profile N°2: good quality rock (60 < RMR < 80).

- Systematic rock bolts: 1 bolt/4 m^2, Ø25, L = 2.5 to 4 m;
- shotcrete 0.1 m.

Profile N° 3: poor quality rock and fault zones ZF1 et ZF2 (20 < RMR < 30).

- Colliery arches 0.18 m H sections at 1 m centres;
- Shotcrete, concrete fill, concrete facing;
- Concrete strip footings reinforced with four 0.25 m diameter high tensile bars;
- Self-drilling bolts if necessary 1 bolt /2 m^2.

5 TUNNEL EQUIPMENT

Another major condition for design of this kind of facility is the reduced maintenance due to the 300 year design life objective of the waste storage where there should be no major repairs for the first 100 year. Consequently, a strict minimum of mechanical and electrical equipment will be used in the galleries.

6 ORGANISATION OF UNDERGROUND WORK

6.1 *HLWS*

6.1.1 *Access and in-situ installation*

In the scheduled programme of underground work for high-level waste storage, we considered two principal attacks per level, which represent four principal attacks with four construction installations (Figure 6).

Upper level:

1 Attack N°1 corresponds to an uphill drive and comprises the main underground site in the transport gallery entrance. The access building will be situated at the end of the underground works.

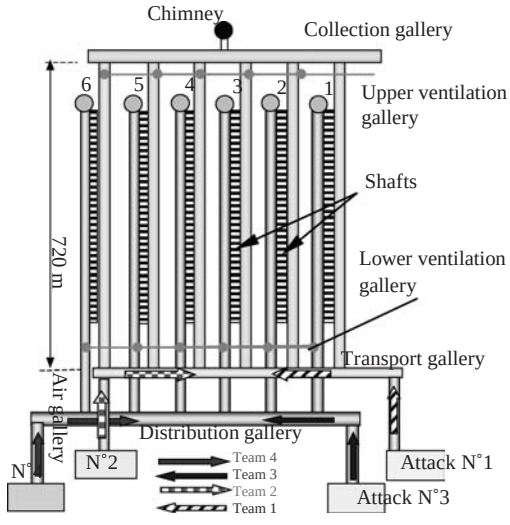


Figure 6. Scheme of on-site installation and excavation phase.

2 Attack N°2 corresponds to a second uphill drive and is situated along the temporary work gallery, which will be closed afterwards.

Lower level:

The lower level is located about 10 to 17 m lower than the upper level. The two attacks are separate. They are linked to each other by a site access haul road.

3 Attack N°3 is located at the front of the air gallery.
4 Attack N°4 is at the face of the second air gallery.

6.1.2 *Excavation phases*

6.1.2.1 Phase 1

For the workers' security, during the whole underground excavation it is vital to ensure ventilation at all times (CRAM). The drilled air chimney will allow natural ventilation in the upper level. Additionally, six temporary ventilation shafts will be drilled between the two levels in order to ensure natural site ventilation.

The first excavation phase starts with four main parallel attacks. The whole face is excavated by the "drill and blast" method:

- Attacks N°1 and N°2 (upper level) correspond to excavation of the transport gallery from two galleries, which are perpendicular to the transport gallery.
- Attacks N°3 and N°4 (lower level) correspond to the excavation of the distribution gallery from two air entrance galleries.

6.1.2.2 Phase 2 – Excavation phases of ventilation galleries.

Upper level:

Two attacks (N°1 and N°2) are used to excavate the first upper ventilation gallery. After finishing the excavation of the upper ventilation gallery, construction team N°1 continues to excavate the collection gallery as far as the air chimney. Once the extraction chimney is accessible, the boring of the pilot hole can begin (0.3 m). After boring the first hole, the raise-drill reams a hole of 3 to 4 meters in diameter. The final diameter (about 12 m) of this chimney is obtained by the "drill and blast" method.

Attack N°2 excavates the upper ventilation galleries N°2, N°4 and N°6. Attack N°1 excavates galleries N°1, N°3 and N°5.

Lower level:

The lower level excavation is carried out by construction teams N°3 and N°4. The underground work for the lower level is carried out after the upper level, thus avoiding a stress concentration in the rock mass.

Attack N°3 drills the upper ventilation galleries N°1, 3 and 5. Attack N°4 excavates the upper ventilation galleries N° 2, 4 and 6 (Fig. 6).

The drilling of the access to the storage shafts requires particular attention for many reasons (Fig. 3). On the one hand, the excavation must not penalise the deadline of the gallery excavation. On the other hand, the cost (per meter) of their accesses is about twice that of the gallery.

6.1.2.3 Phase N°3 – Shaft drilling

The storage shafts (600 or 720 per unit) will be drilled by the "raise-drill" method with specific boring machines adapted for industrial drilling.

This drilling phase will be carried out by four construction teams after the tunnel lining phase in the upper ventilation galleries.

6.1.3 *Tunnel lining phase*

All the underground galleries, except the transport gallery and the air entrance gallery, will be lined but not waterproofed.

The lining operation is carried out with non-reinforced in-situ concrete of 0.35 to 0.5 m thickness, depending on the profile. The reinforced concrete will probably be applied in the gallery where the concrete is subjected to high temperatures (80°C), notably in the upper ventilation gallery. The 3D numerical modelling carried out by CEA, shows that a weak section is situated at the crossing between the bottom and the side wall of the upper gallery.

6.1.4 *Scheduling aspects*

The expected average rate of advance by "drill and bast" used in this study is presented in table 5. The work assumptions take into account 24 hour working five days per week.

Table 5. Expected average rates.

Tunnel support	Rates
Profile N°1	5 m/day
Profile N°2	4 m/day
Profile N°3	1.5 m/day
Lining	
All 3 Profiles	10 m/day

The construction period for one HLWS unit was estimated at 5 years and 4 months. Consequently, for six units of spent fuel, the total construction period is 32 years and 4 months.

6.1.5 *Cost of the HLSW unit*

Here we present the cost for the reference profile, N°2. The construction cost (for year 2005) of one unit of spent fuel is estimated at 132 M€ exc. tax, so for 6 units the total costs is 792 M€ exc. tax.

6.2 *ILWS*

6.2.1 *Access and in-situ installation*

In the operating phase of the ILWS unit, two principal in situ installations are provided (Attacks N°1 and N°3) as well as one secondary in-situ installation (attack N°2).

Attack N°3 is situated along the working gallery. In the operating phase, this working gallery will be used for access, but afterwards, in the maintenance phase, it will be closed.

6.2.2 *Excavation phases*

6.2.2.1 Phase 1 – Ventilation during the construction phase.

As noted previously, ventilation of the underground space is necessary during construction for the workers' security. (CRAM). Consequently, the first excavation phase will start on the perimeter unit in order to drill the air chimney to ensure natural air ventilation. An additional air supply is also used during excavation.

Excavation starts with two main parallel attacks, N°1 and N°3. The first attack drills the main transfer gallery, half of technical gallery and after the access to the air chimney. Attack N°3 excavates the working gallery and half of technical gallery (Fig. 7).

The drilling of the air chimney is carried out by the "raise-drill" method.

After the perimeter excavation, both construction teams will be used for boring attack N°3, first the air entrance gallery and after the upper part of "Gantry" gallery. The lower part of the "Gantry" gallery will be excavated later.

6.2.2.2 Excavation of 16 storage galleries

In order to optimise the deadline, a third construction team is used, altogether representing 3 parallel attacks.

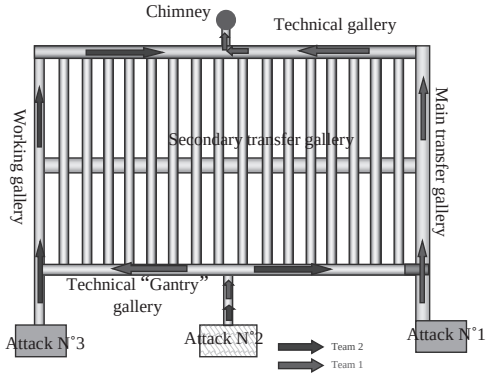


Figure 7. Scheme of excavation phases.

The storage gallery excavation will be carried out in two successive stages:

1 Upper part of the gallery (handling zone).
2 Lower part of the gallery (storage zone).

6.2.2.3 Excavation phase of secondary transfer gallery

After finishing the upper part of the storage galleries, construction team N°1 starts the excavation of the secondary transfer gallery. These two galleries have different levels, the secondary transfer gallery being lower (Figure 5). Their connection points are very delicate, there are 16 per unit.

At the same time, attacks N°2 and N°3 will excavate the lower part of the storage galleries by vertical boring.

6.2.2.4 Excavation of the lower part of the storage gallery

When the excavation of the secondary transfer gallery is finished, the phase "Blast and muck removal" of the lower part of storage gallery commences. It was decided to first excavate the secondary transfer gallery in order to use this gallery as an optimal means to evacuate the muck for all lower parts.

6.3 *Scheduling aspects*

The assumptions are the same as for HLWS (§6.1.4). The construction period for one ILWS unit is 4 years and 9 months, thus the total construction period for 3 units is estimated at 14 years and 7 months.

The construction of one access building will take over 5 years.

6.4 *Cost of ILSW unit*

The construction cost for the ILWS unit for profile N°2 is estimated at 141 M€ exc. tax, so for 3 units the costs is 423 M€ exc. tax.

7 CONCLUSIONS

In this paper we have described two particular designs for two kinds of waste storage (HLWS and ILWS) and we have proposed the organisation methodology for each facility. This network composed of shafts and tunnels is non-typical and complex to design and to manage. We have then givensome of the main considerations.

According to the scheduling aspects, the maximum total construction period for the HLWS waste storage (spent fuel) is 32 years and 4 months. For the ILWS it is 14 years and 7 months. It is necessary to note that this construction schedule is not penalised by the storage waste process, which lasts 50 years.

In terms of muck removal, the excavation volume mass for one HLWS unit is estimated at 960 000 m^3, so the maximum total volume of spent fuel is 5 760 000 m^3. For one ILWS unit, the excavation volume mass is estimated at 1 116 000 m^3, so the total volume for 3 units is 3 348 000 m^3.

It is important to emphasise that, in today's economical context with sustainable development it is necessary to identify how to enhance the value of this enormous volume of excavated rock mass.

REFERENCES

AFTES. GT1. 1982. Characterisation of rock masses useful for the design and the construction of underground structures.

AFTES. GT7 – Choice of geotechnical parameters and tests for tunnel design.

AFTES. GT29. Utilisation des règles et normes de conception pour les revêtements en béton.

CRAM. R 352. Recommandation de la ventilation des ouvrages souterrains en phase travaux.

Barton, N. & al. 1974b. Engineering classification of Rock Mass for the design of tunnel support, *Rock Mechanics*, vol. 6, n°4: 189–236.

Bienawski, Z.T. 1984. Rock mechanics design in mining and tunnelling. Rotterdam : Balkema.

CEA. 2005. Les déchets radioactifs à haute activité et à vie longue, loi du 30 décembre 1991. Dossier final sur le conditionnement et l'entreposage de longue durée; Décembre 2005.

Lagrave, H & al. 2005. Thermo-aerailics of high level waste storage facilities. *European Nuclear Conference*. Versailles: France.

Lagrave. H. & al. 2006. Durability design of heated concrete structures. Methodology and application to long-term storage. *Corrosion and long term performance of reinforced concrete in nuclear power plants and waste facilities. Proc. intern. Symp, NUCPERF 2006.* Cadarache: France.

Underground Space – the 4th Dimension of Metropolises – Barták, Hrdina, Romancov & Zlámal (eds)
© 2007 Taylor & Francis Group, London, ISBN 978-0-415-40807-3

Design and construction of a tunnel using the technology for controlling muck flow in the cutting chamber of an earth pressure balance shield of large cross section

H. Dobashi & M. Matsuda
Metropolitan Expressway Co., Ltd.

K. Matsubara & A. Kitayama
Obayashi Corporation

ABSTRACT: Of the Metropolitan Expressway Central Circular Shinjuku Route, which is being constructed by the Metropolitan Expressway Public Corporation, tunnels of the SJ51 to SJ53 Sections were decided to be excavated using a world-largest earth pressure balanced shield, which has an outer diameter of 12.02 m. In the conventional earth pressure balanced shield method, plastic flow of excavated soil within the cutter chamber, which is indispensable for stable excavation, has never been analyzed, and the method has been little used to excavate tunnels of over 10 m in diameters. In this project, a system for visualizing the flow of soil inside the chamber was decided to be developed and introduced. This paper describes an overview of the system and results of its application.

1 INTRODUCTION

Metropolitan Expressway Company Limited is now constructing the Central Circular Route of the Metropolitan Expressway with a total length of approximately 47 km outside the Inner Circular Route, approximately 8 km in radius from the city center. The goal is to alleviate traffic congestion by diverting or dispersing traffic passing through the city center and thereby form a well-balanced circular traffic network. Sections of approximately 26 km, about 60%, of the Central Circular Route have been completed and are currently in service. The remaining 20-km sections consist of the Shinjuku Route on the west side and the Shinagawa Route on the south side. In the Shinjuku Route with a length of approximately 11 km, construction is being carried out rapidly mainly with the shield tunneling method to perform construction work smoothly under heavily congested roads and minimize adverse effects of construction on residents in surrounding areas. Shields of large cross section with a diameter of more than 10 m are used in all of the eight sections where shield tunneling takes place. Figure 1 provides an outline of the project.

As shields of large cross section with a diameter of more than 10 m, slurry shields have frequently been employed because they facilitated the stabilization of the face. In this project (work sections SJ51 to SJ53 (clockwise route) of a highway tunnel), an earth pressure balance shield of cross section with an outer diameter of 12.02 m, largest in the world at the time of receipt of the order, was adopted because the construction base was narrow, so no space could be secured for installing equipment required for a slurry shield and because effects of leaking slurry on the ground surface or surrounding structures in sections with shallow depth of overburden during the operation of a slurry shield was of concern. Figure 2 gives a geological profile at the construction site.

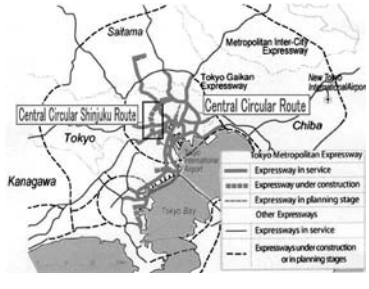


Figure 1. Project outline.

In the earth pressure balance shield, establishment of plastic flow of excavated material in the cutting chamber is important to the stabilization of the face and smooth removal of excavated material through the screw conveyor. In the earth pressure balance shield of large cross section, it has been unknown whether

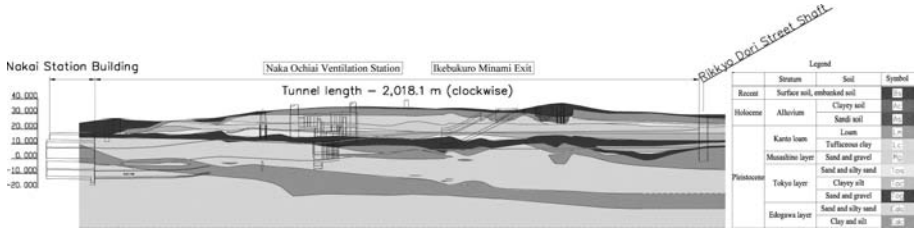


Figure 2. Geological profile.

appropriate agitation is possible to ensure the plastic flow of slurry or not, which has been preventing the earth pressure balance shield from being applied to tunnels of large cross section. The problem has yet to be solved because no method has been established for quantitatively grasping the establishment of plastic flow.

In this project, technology for controlling muck flow in the cutting chamber of an earth pressure balance shield was developed and applied to maintain face stability and ensure safe excavation solving problems involved in the use of an earth pressure balance shield of large cross section. The technology enabled the contractor to quantitatively grasp the plastic flow of excavated material in the cutting chamber and to carry out the following work.

(i) Quantitative excavation control by evaluating the plastic flow of the muck in the chamber
(ii) Appropriate system design for agitation and muck removal in the chamber

This paper outlines the technology developed, describes the results of its application to actual construction and presents case studies of design of an agitation and muck removal system.

2 OUTLINE OF MUCK FLOW CONTROL TECHNOLOGY

"Plastic flow" is essential to the stabilization of the face and smooth removal of excavated material through the screw conveyor. Where there exits plastic flow, excavated material starts flowing at a deformation rate (shear strain occurs) when the shear stress in the material exceeds a certain yield value (Figure 3). In the case where the plastic flow of the excavated material in the cutting chamber is in a good condition, the rotation of the cutter face causes the excavated material to flow and be mixed with additives for excavation and agitated. As a result, the excavated material flows at a deformation rate. When the chamber is clogged, the velocity of the material is high and deformation rate is low (Figure 4). Where the excavated material is blowing from the screw conveyor, velocity is low and deformation rate is high.

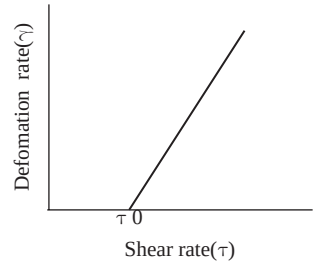


Figure 3. Plastic flow of excavated material.

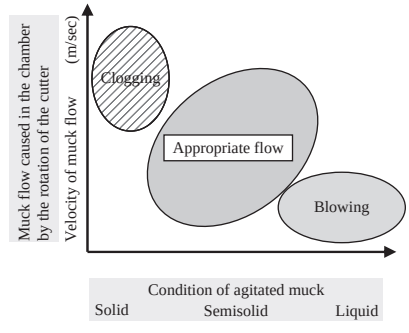


Figure 4. Muck flow velocity and deformation rate.

The technology we have developed involves the making of a three-dimensional model of the inside of the cutting chamber in the shield for analyzing muck flow, calculation of velocity and deformation rate in the chamber and evaluation of plastic flow. To reflect the actual condition in the chamber in analysis, a flapper (Photograph 1) was developed and four flappers were installed on the bulkhead in the chamber (Figure 5). Flaps were rotated with electric motors during excavation to measure the variations of torque due to muck flow. The flapper was also modeled for analysis. In the case where analysis results were in good agreement with measurements, it was determined that the calculated velocity and deformation rate were actually found in the chamber. The muck flow control technology enables visual display of velocity and deformation rate in the chamber based on analysis results. Then, quantitative control of



Photo 1. Flapper.

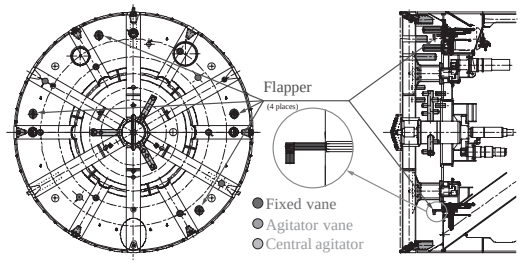
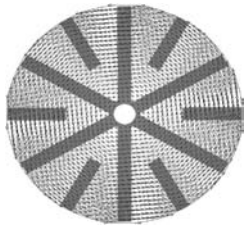
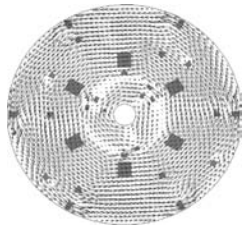
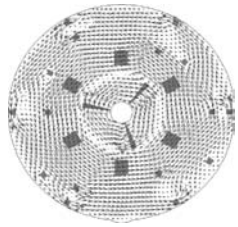
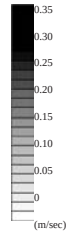
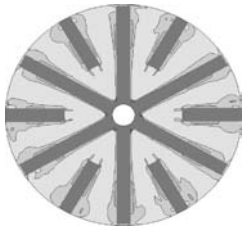
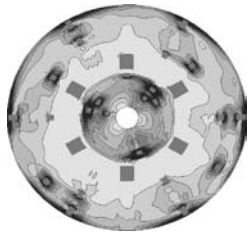
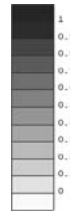


Figure 5. Positions of flappers.

Table 1. Inside the chamber during smooth excavation.

	Near the cutter face	At the middle of the chamber	Near the bulkhead	Legend
Velocity (m/sec)				
Deformation rate (1/sec)				

injection of additives for excavation becomes possible. For example, additives are injected exclusively at points where no appropriate plastic flow seems to have been established.The condition in the chamber can also be grasped real-time by controlling the variation of torque of the flapper during excavation. Thus, actions can be taken promptly in response to changes in property of the muck in the chamber. The technology therefore contributes to safe excavation. The technology also enables quantitative design of an agitation system beneficial to the establishment of plastic flow based on the results of analysis using an arbitrary model of the agitation system in the chamber.

3 APPLICATION IN ACTUAL CONSTRUCTION PROJECTS

3.1 *Condition in the chamber during smooth excavation*

In the actual construction project, muck was removed smoothly through the screw conveyor without any blowing throughout the tunnel alignment along which shield tunneling took place. It was then assumed that there was plastic flow of the muck in the chamber and that the face remained stable.

Results of analysis of plastic flow in the chamber are listed in Table 1.

Table 1 shows distributions of velocities and deformation rates in the chamber in three cross sections: near the cutter face ($z = 1.7$ m, where z represents the distance from the bulkhead), at the middle of chamber ($z = 0.9$ m) and near the bulkhead ($z = 0.45$ m) (Figure 6). Velocity is a vector quantity. The directions and lengths of arrows indicate the directions and levels of velocities.

Deformation rate, a scalar quantity, is expressed by brightness. Analysis results show that distributions of velocities and deformation rates are not uniform transversely but are different in the cutter peripheral area, cutter support area and agitator area. In the longitudinal direction, distributions of velocities and deformation rates are different in the three cross sections between the cutter face to the bulkhead.

Figure 7 shows logarithms of velocities (m/sec) plotted along the vertical axis and logarithms of deformation rate (l/sec) along the horizontal axis in the areas shown in Figure 6. The plotted points move toward the center of the graph in the agitator and cutter peripheral areas as the cross section move from the cutter face to the bulkhead. Plastic flow of the muck is therefore assumed in these areas. In the cutter support area on the other hand, the movement toward the center of the graph is not so outstanding. Velocity is available owing to the rotation of cutter supports, but no mixing and agitation takes place. Plastic flow is therefore unlikely to be established. In the project, excavation could be carried out while maintaining face stability. As a result of analysis, however, plastic flow was found unlikely to start at some points. Then, additives for excavation were injected also at such points shown in Figure 8.

3.2 *Condition in the chamber during muck blowing from the screw conveyor*

At the time of blowing, excavated material pressurized in the chamber moves through the screw conveyor remaining in the form of a liquid and the pressure is not reduced to air pressure at the outlet, and the volume of muck can no longer be controlled by adjusting the speed of rotation of the screw conveyor. When muck is being removed smoothly, the pressure of the muck pressurized in the chamber is reduced to air pressure owing to resistance in the screw conveyor by the time the muck reaches the outlet, and the volume of muck can be controlled by adjusting the speed of rotation of the screw conveyor.

In this project, excavation was carried out smoothly while maintaining face stability owing to smooth muck removal throughout the tunnel alignment along which the shield tunneling method was adopted. The condition in the chamber at the time of blowing of the muck from the screw conveyor was therefore not measured. The muck flow control technology was used to calculate the pressure in the chamber through the outlet of the screw conveyor in analysis. Figure 9 shows the pressure in the screw conveyor during smooth excavation and at the time of muck blowing. The pressure acting on the muck in the chamber was reduced in the screw conveyor and no longer acted at the outlet of the screw conveyor during smooth excavation. At the time of blowing of the muck, pressure was not reduced at the outlet.

Table 2 shows the condition in the chamber when an analysis was made at the time of muck blowing (Figure 9). Figure 10 presents mean velocities and deformation rates during smooth excavation and at the time of muck blowing for comparison.

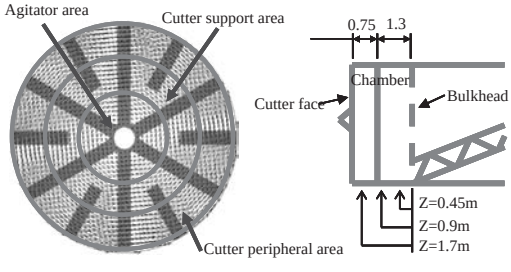


Figure 6. Points of evaluation.

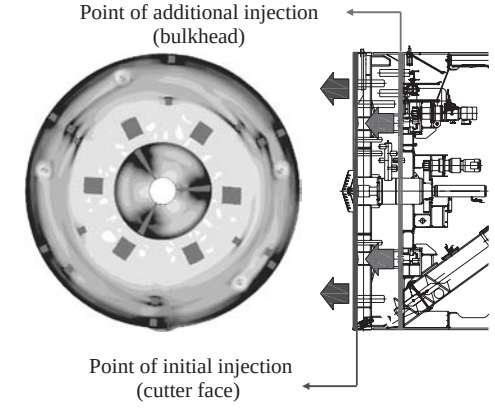


Figure 8. Points of additive injection.

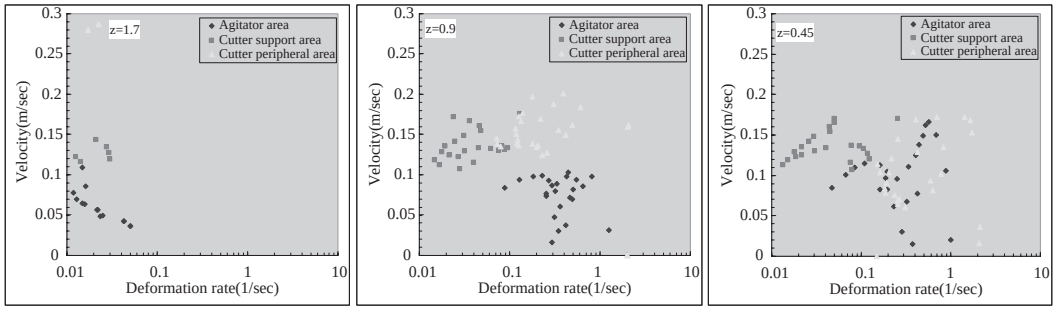


Figure 7. Velocity and deformation rate in each cross section.

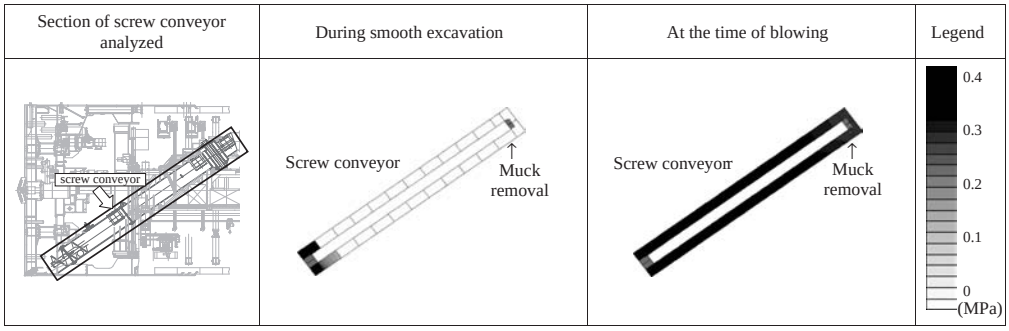
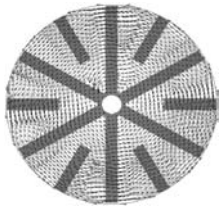
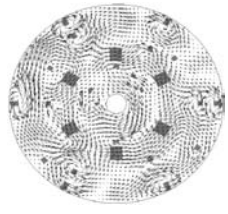
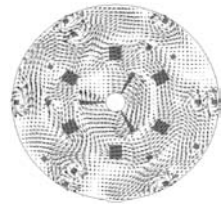
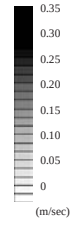
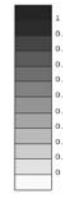


Figure 9. Pressure in the screw conveyor.

Table 2. Condition in the chamber at the time of muck blowing.

	Near the cutter face	At the middle of the chamber	Near the bulkhead	Legend
Velocity (m/sec)				
Deformation rate (1/sec)				

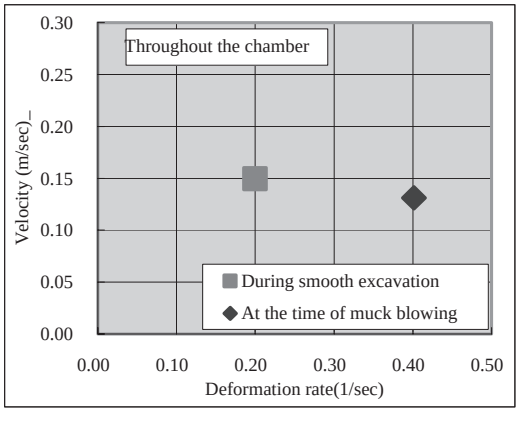


Figure 10. Velocity and deformation rate during smooth excavation and at the time of much blowing.

Velocity at the time of muck blowing was similar to that during smooth excavation. Deformation rate was higher at the time of muck blowing. Deformation rate was in the area of muck blowing shown in Figure 4. In the case where the condition shown in Table 2 is found during tunnel construction similar to this project, measures should be taken promptly such as those for modifying the property of the muck.

3.3 *Excavation control based on the variation of flapper torque*

To establish plastic flow of excavated materials in the chamber, the property of the muck removed through the screw conveyor has conventionally been evaluated by visual inspection or slump tests. Where and how much additives for excavation should be injected were adjusted based on the evaluation results. In this project,

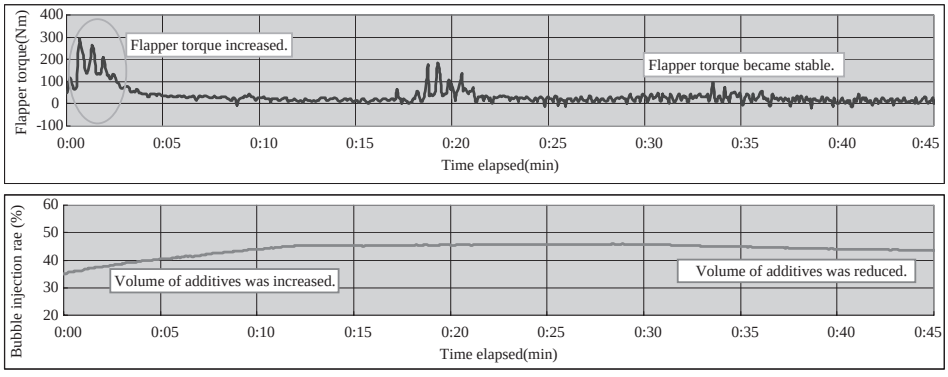
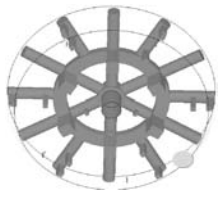


Figure 11. Excavation control using flappers.

Table 3. Model of agitation system designed.

CASE 1 Cutter	CASE 2 Cutter and agitation vane	CASE 3 Cutter, agitation vane and fixed vane	CASE 4 Cutter, agitation vane, fixed vane and agitator
			

injection of additives was controlled also using the muck flow control technology.

Additives for excavation were injected not only on the front face of the cutter but also at points where plastic flow was found unlikely to be established based on the distributions of velocities and deformation rates identified in analysis. The volume of additives was adjusted according to the variations of flapper torque. Figure 11 shows an example of control of additive injection in the project.

In the excavation work shown in Figure 11, the torque of the flapper increased rapidly, so more additives were injected. When the flapper torque became stable, the volume of additives was reduced. Flapper torque changes earlier than the change in property of the excavated material that is removed through the screw conveyor. Actions therefore can be taken quickly in response to the change in plastic flow in the chamber by controlling the volume of additives according to the flapper torque. Thus, safe excavation can be carried out.

In this project, the tunnel was excavated over a length of 2020 m and the geology varied from cohesive soil to grave layers. The muck flow control technology helped complete excavation smoothly without any adverse effects on the ground surface or on adjacent structures including railway tracks and land bridge foundations.

4 OPTIMAL DESIGN OF AGITATION AND MIXING SYSTEM IN THE CHAMBER

The muck flow control technology involves the modeling of the system of agitation and mixing in the chamber for controlling muck flow. Making an arbitrary model of agitation and mixing system and making analysis under one and the same conditions enable optimal design of an agitation and mixing system beneficial to the establishment of plastic flow of excavated material based on the results of comparison in calculated velocity and deformation rate. In this study, agitation and mixing systems were designed in four cases for analysis (Table 3). Figure 12 shows mean velocities and deformation rates in the chamber in respective cases.

As a result of analysis, it was found that velocities were more or less the same in all cases. Deformation

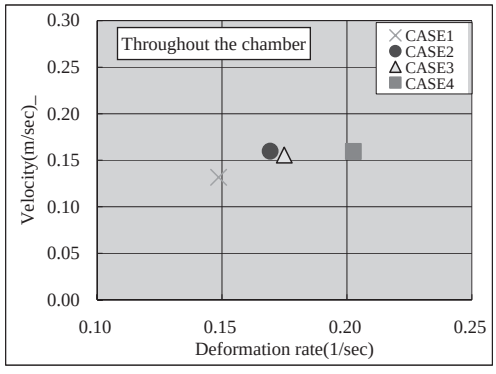


Figure 12. Velocity and deformation rate.

rate in the chamber was highest in case 4. This was considered the optimal agitation system that is capable of establishing the plastic flow of the muck.

As discussed above, it has been confirmed that the muck flow control technology provided for the evaluation of the effects of agitation and mixing systems quantitatively for the first time. Thus, the technology enables smooth mixing of muck with additives in the chamber and the design of an agitation system effective for establishing plastic flow of the muck.

5 CLOSING REMARK

The “technology for controlling muck flow in the cutting chamber of an earth pressure balance shield” enables tunnel excavation based on the results of evaluation of the plastic flow of the muck in the chamber. Thus, greater face stability can be ensured.

The shield tunneling method has been playing a leading role in urban tunnel construction and is expected to play a greater role. In big cities in particular, tunnel construction is expected to be more demanding for such reasons as the shortage of construction sites, need of construction adjacent to important structures, construction at great depths and requirements for cost reduction. Earth pressure balance shields need to play a greater role to solve these problems. The “technology for controlling muck flow in the cutting chamber of an earth pressure balance shield of large cross section” will help increase the cross section of an earth pressure balance shield and apply earth pressure shields in an increasing number of projects.

This page intentionally left blank

Underground Space – the 4th Dimension of Metropolises – Barták, Hrdina, Romancov & Zlámal (eds)
© 2007 Taylor & Francis Group, London, ISBN 978-0-415-40807-3

Estimation of front-end stability using field displacement

R.M. Faure
Centre d'études des Tunnels, France

J.F. Thimus, F. Desmoulin & S. Delvaux
Université catholique de Louvain, Génie civil et environnemental, Belgium

ABSTRACT: The stability of a front-end of a bored tunnel is for safer works a crucial estimation. It depends of soil reinforcement or slurry pressure following the means of boring. Based on a 3D analysis, we propose in this paper a new approach of safety estimation that can be summarized through the following steps. Determination of 3D failure surfaces by an automatic process and estimation of stresses on these surfaces. This estimation is based on Mohr circle analysis. Determination of 3D fields displacement, in a parametric approach, at each vertices of a spatial net, which allows 3D interpolation. Determination of behaviour laws (stress – displacement laws) for any soils and inclusions. Using homothetic fields of displacement we can so compute the equilibrium and define a kind of distance to failure, that is an estimation of safety. It is very easy to change any parameters like soil nails and so, to optimize the design.

1 INTRODUCTION

Lot of methods try to assess the front face stability using failure schemas and soil failure equations. Among these methods we can notice the Terzaghi method, taking into account some vault effects for determining the vertical load. The resistance is the integration of shear stress along chosen failure surfaces. Except DEM, no method is able to take into account the displacement of blocks of soils moving relatively to each others.

With the possibilities of computer it is now possible to check 3D failure surfaces and obtain a more realistic result.

If safety is not checked, the two main way for reinforcing the stability is the slurry pressure in case of TBM or nailing in case of traditional boring.

This paper presents a new method that can determine the efficiency of the two reinforcement systems already mentioned. This method can be summarized in three steps.

2 SOLVED PROBLEM

As to define the given problem, we use the name of the different data screens we can find using the computer code available on the net.

2.1 *Tunnel geometry*

The tunnel section is circular and the axe of the tunnel is horizontal. The ground is defined by two layers, and the interface of the two layers is parallel to the tunnel axe, but can be inclined in the transverse direction. (Figure 1)

2.2 *Failure surface*

The failure surface is determined using parametric curves defined by only two points, one at the vertical of the front face, the second at a given distance from the front face, on a horizontal line at the top of the front face. (Figure 2)

2.3 *Reinforcement system*

2.3.1 *Pressure*

If boring is done by a TBM a pressure transmitted by air or slurry can be applied to the front face. In the equilibrium of the instable soil mass, the pressure is

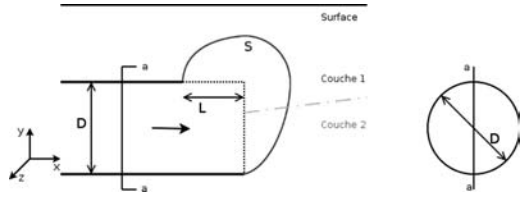


Figure 1. Tunnel geometry.

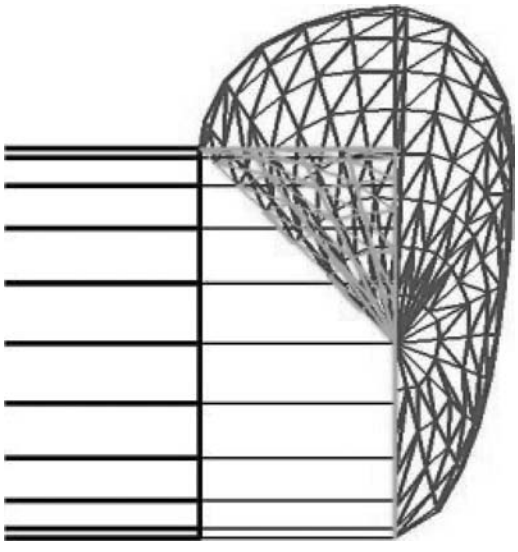


Figure 2. Example of 3D surface failure (see annex 1).

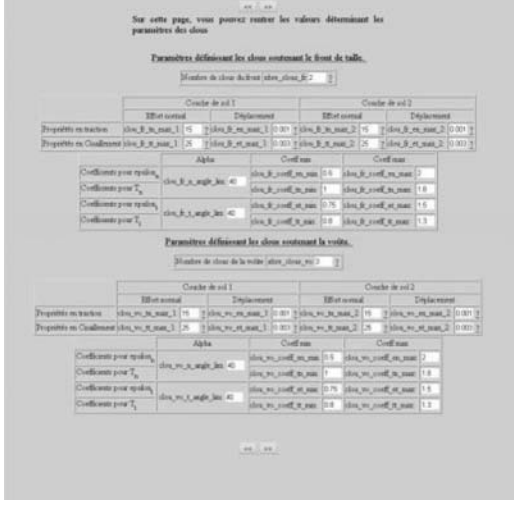


Figure 3. Data for nails definition.

equivalent to a non uniform force on the front face depending the altitude of each facet.

2.3.2 *Nails*

The definition of nails takes lot of values. So, usual nails are stored as tables. Figure 3 is an example of nail data sheet.

Data are numerous because the behavior of the nail is given in terms of displacements. This model was obtained after numerous giant shear box tests with nails inside.

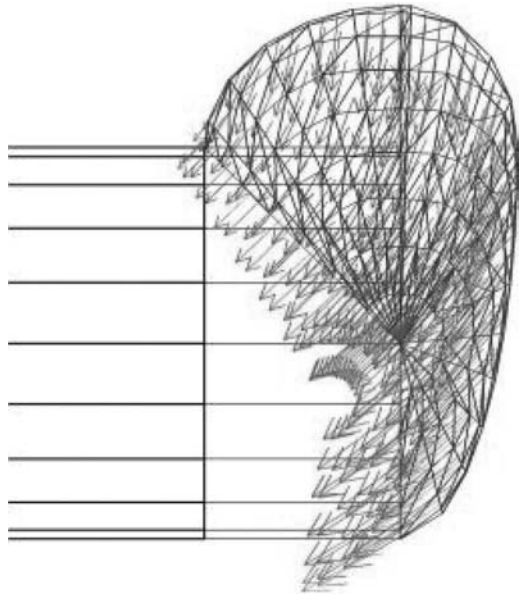


Figure 4. Example of displacement field.

2.4 *Given displacements*

A displacement field is compulsory for the calculation. This field that represents the maximum of displacement on the failure surface will be divided into ten steps and equilibrium is computed at each step. With this approach it is possible to have an approximation of the displacement leading to stabilization when the balance of forces is satisfied. The field is a combination of translational and rotational movements, as shown on figure 4.

2.5 *Water table*

Taking into account the water table is important and the water table is defined by a level.

3 CALCULUS

3.1 *Stresses determination*

3.1.1 *Static : the perturbation method*

Before taking into account displacements a static calculus is done using the perturbation method. This method was developed for 3D slope stability evaluation.(Faure et al, 1998) The main advantage of the perturbation method is in the realistic determination of stresses on the surface failure. The analysis is done using the Mohr circle criterion, respecting the failure criteria of the soil. Starting with this accurate value of stresses on the failure surface, extensions with nails or displacement are easier because all used values are limited and stay in range.

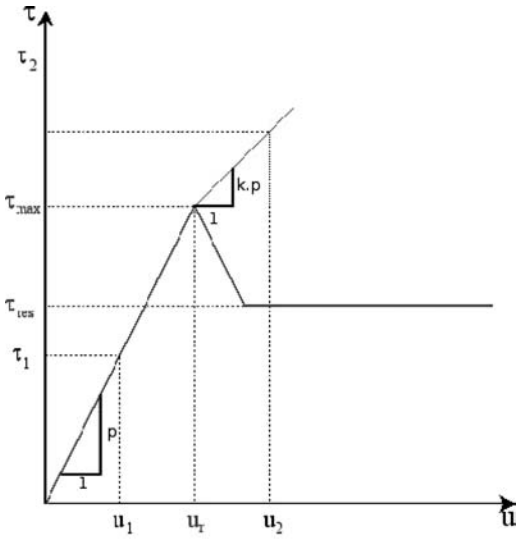


Figure 5. Behavior of soils.

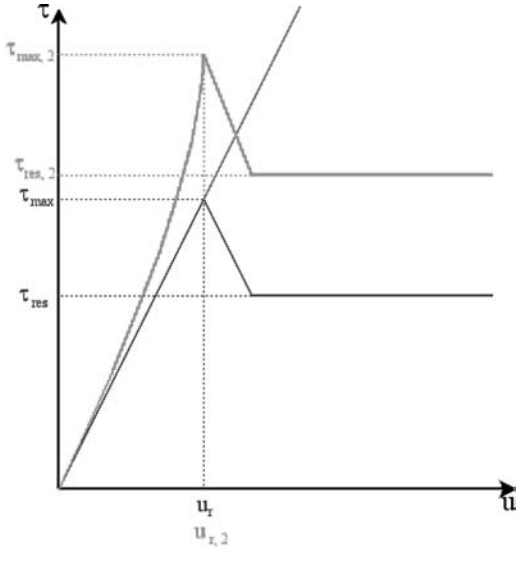


Figure 6. Modified soil behavior when pressure.

3.2 *With displacement*

The two displacement models are the soil model and the nail model.

In the soil the parameters c, ϕ, ε_r, R_f defined the curve on figure 5 and in case of external pressure this curve is modified following figure 6.

In this model, τ_{max} is computed by the Coulomb law using the realistic value of σ given by the perturbation method. u_r (or ε_r) is a given value in correspondence

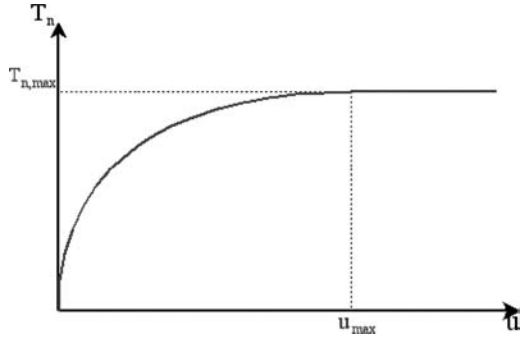


Figure 7. Axial effort in the nail.

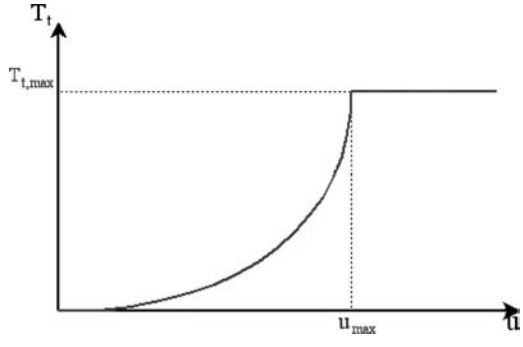


Figure 8. Transverse effort in the nail.

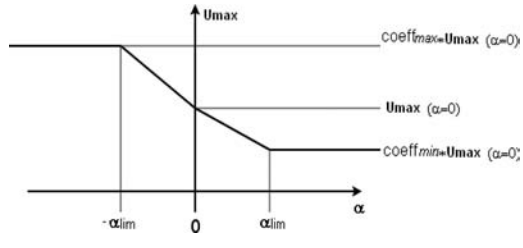


Figure 9. Influence of α.

with the maximum displacement of the field displacement, and R_f define τ_{res} following $\tau_{res} = R_f * \tau_{max}$.

With nails it is more complex; the displacement model is obtained following giant shear box trials with nails included in the shear box. One of the important parameter is the inclination of the nail on the failure surface. For all the nails given as a family this inclination is computed, and allows the determination of ratios that modify the value of nail strength when they are perpendicular to the shear surface. Figures 7 and 8 show the variation of axial and tangential forces in the nail following the shear displacement on the failure surface.

Figure 9 gives the ratio function depending of inclination of the nail on the failure surface. All the

parameters describing these curves are defined on the data sheet corresponding to each kind of nail.

4 RESULTS

With the use of displacements we can't have a unique safety factor because at each point on the failure surface, the displacement is not the same (the sliding mass is not a block and have deformations) and we have to define new parameters that can represent the safety level of the front face with its reinforcements for a given displacement.

So we define that we call "safety margin" that is an expression infinite when no displacement and going to 1 when the large displacement put all element on residual failure. At each point the difference between failure shear stress and shear stress evaluated using the displacement is computed. Integration of all these stress reserve gives, when normalized, the 'safety margin'.

In another approach, we can define the "global safety factor" that is an integral of local safety factors, that is zero when no displacement and going to a limit value when large displacements occur.

These two ratios give a good idea of front face stability. But this approach is more efficient when we compare two solutions of reinforcement, because we can make a choice between the two (or more) solutions in terms of displacement, that very important at the front face.

5 CONCLUSION

This method seems complex because lot of concepts must be used together. But it is simple because all concepts are easy to understand, and the computer manages all of them. This code is now available on the web site of Solem or UCL supporting the DIDACTU learning system. We hope that with this code any student can understand the challenge of front face reinforcement for minimizing front face displacement.

BIBLIOGRAPHY

Faure R.M., Pham M., Robinson J., Jolly P., 1996, Three dimensional Slope stability by the perturbation method. ISL 96, Trondheim, pp 1207–1212.

Esfehani M.,1999, Etude de la stabilité et du tassement engender lors du creusement d'un tunnel sans pressurisation. Phd thesis, INSA Lyon, France.

Leca E., 1989, Analysis of NATM and shield tunneling in soft ground. PhD thesis VPI, USA

ANNEX 1 **Parametric data for failure surface.**

In Leca, 1989 and Esfehani, 1999, lot of failures and experimental failures are described that can be approached with only few parameters using ellipsoid curves. Figure 10 shows this kind of surface and figure 11 shows the input of this description.

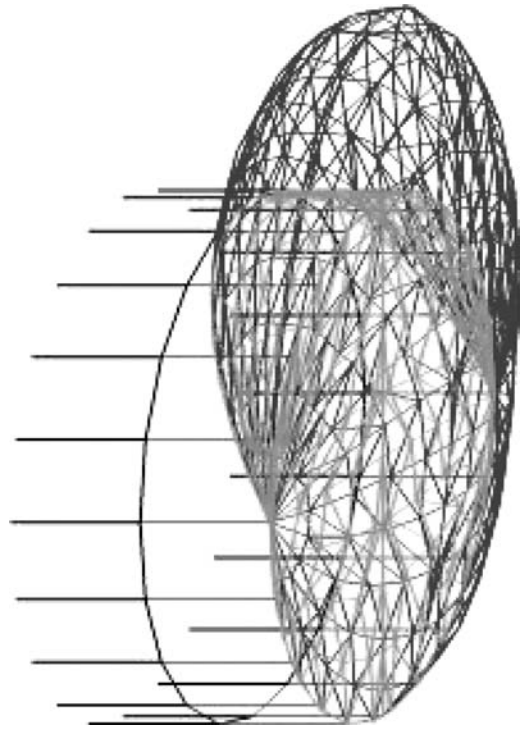


Figure 10. 3D view of a failure surface.

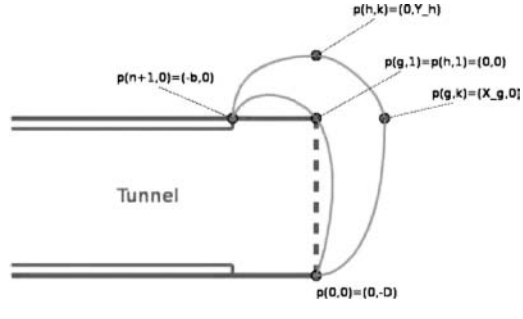


Figure 11. Points for surface description.

Underground Space – the 4th Dimension of Metropolises – Barták, Hrdina, Romancov & Zlámal (eds)
© 2007 Taylor & Francis Group, London, ISBN 978-0-415-40807-3

Influence of soil grouting on the shallow tunnel linings stress state in urban areas

N. Fotieva, N. Bulychev, S. Antziferov, A. Sammal & P. Deev
Tula State University, Tula, Russia

ABSTRACT: An analytical method for determining the stress state of multiple shallow circular tunnel linings constructed with the application of grouting in build up areas is proposed based on consideration of interaction of underground structures and the surrounding soil mass as elements of a united deformable system and on the new analytical solutions of corresponding plane problems of elasticity theory with approximate taking the 3-D character of surface loads into account.

1 INTRODUCTION

In tunnels being constructed in complicated hydrogeological conditions special techniques such as grouting (cementation) the surrounding soil mass are applied. Strengthening by grouting allows anisotropy of soils around a tunnel to be reduced and their deformation modulus to be raised. In this case a soil zone around the opening the mechanical properties of which are different from those of the rest massif is being created. This circumstance resulting in a redistribution of the "lining – soil mass" system stress state, may exert a substantial influence on the lining bearing capacity and it is necessary to be taken that influence into account in the lining design.

At present there are methods by Fotieva & Sammal (1986) and by Fotieva, Bulychev & Sammal (1993) for the design of deep tunnel linings of an arbitrary cross-section shape under the actions of the soil's own weight and external water pressure taking the influence of grouted zone into account, based on analytical solutions of the corresponding plane problems for a single double-layer non-circular ring in a linearly deformable medium. Similar methods for the design of shallow non-circular tunnel linings constructed with the application of grouting are described in the paper by Fotieva, Bulychev & Deev (2006).

There is also a method for designing multiple shallow circular tunnel linings in grouted soils developed by Fotieva, Bulychev & Antziferov (2003) allowing the linings stress state under the actions of the soil own weight and the weight of a building or structure both existing before the tunnels driving and erected nearly to the already constructed tunnels to be determined. Some improvements giving the possibility of this method application for the design of tunnels constructed in built-up areas are described in the paper presented.

2 THE DESIGN METHOD

The method proposed is based on analytical solutions of the corresponding plane problems of elasticity theory for a weighty linearly deformable semi-infinite medium simulating the soil or rock mass, weakened by a finite number of arbitrarily located circular openings of different radii supported by double-layer rings (the internal layers simulate the tunnel linings, the external ones simulate the soil zones around openings strengthened by grouting). The general design scheme is given in Figure 1.

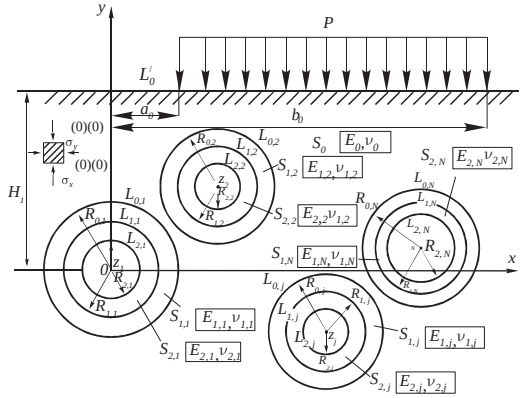


Figure 1. The design scheme.

Here a heavy semi-infinite linearly deformable medium S_0 the mechanical properties of which are characterized by the deformation modulus E_0 and the Poisson's ratio ν_0, simulates the soil or rock mass. The layers of double-layer rings $S_{m,j}$ ($m = 1, 2$; $j = 1, \ldots, N$) from materials possessing the deformation characteristics $E_{m,j}$, $\nu_{m,j}$ ($m = 1, 2$; $j = 1, \ldots, N$) simulate correspondingly soil zones strengthened by grouting ($m = 1$) and tunnel linings ($m = 2$), located on depths H_j ($j = 1, \ldots, N$), counted off from centers having complex coordinates $z_j = x_j + iy_j$ ($j = 1, \ldots, N$).

The medium S_0 and layers of rings $S_{m,j}$ ($m = 1,2$; $j = 1, \ldots, N$) undergo deformation together i.e. conditions of continuity of vectors of displacements and complete stresses are satisfied on the contact lines $L_{m,j}$ ($m = 0,1$; $j = 1, \ldots, N$). The internal outlines $L_{2,j}$ ($j = 1, \ldots, N$) of the rings are free from loads.

The action of the soil own weight is simulated by a presence of initial stresses in the medium S_0 and layers $S_{1,j}$ ($j = 1, \ldots, N$) determined by formulae:

$$\sigma_y^{(m)(0)} = -\gamma(H_1 - y),\ \sigma_x^{(m)(0)} = -\lambda\gamma(H_1 - y), \qquad (1)$$

where γ = soil unit weight, λ = lateral pressure coefficient in an intact soil mass.

The weight of a building or structure on the surface is simulated by a vertical load of the P intensity uniformly distributed along the part $a_0 \le x \le b_0$ of the straight boundary L'_0 of the semi-plane.

There are two cases under consideration – when a new building is erected near the already existing tunnels and when the building was erected before the tunnels driving. In the latter case the ground displacements appearing before the tunnels construction are excluded from the boundary conditions connected the displacements.

The described problems have been solved with the application of the complex variable analytic functions theory (Muskhelishvili 1966), analytical continuation of complex potentials regular in the lover semi-plane out of the openings into the upper semi-plane (Aramanovich 1955) and the method of solving problems for an infinite medium weakened by a finite number of supported circular openings (Fotieva & Kozlov 1992). Such an approach allowed to reduce the problems considered to the iteration process (Fotieva, Bulychev & Sammal 1996) in every approximation of which the solution of the problem for a single double-layer ring supporting an opening in a whole plane is applied at the boundary conditions including some additional items reflecting the influence of the straight boundary of the semi-plane and the other openings. These items are represented in the form of the Laurent series the unknown coefficients of which assumed to be equal to zero in the first approximation then are specified on each step of iterations.

For approximate account of the influence of the distances $l_j (j = 1, \ldots, N)$ between the lining constructed in every tunnel and the tunnel face the correcting coefficients are introduced into the results of the lining design under the action of the soil own weight and weight of buildings existing before the tunnel driving. These coefficients are determined by empirical formulae obtained on the basis of 3-D numerical modeling (Bulychev 2002):

$$\alpha_j^* = 0.6\exp(-1.38\ l_j / R_{1,j}) \quad (j = 1,..., N). \qquad (2)$$

The sequence of the tunnels construction may be taken into account in the same way as described in the work by Fotieva & Kozlov (1992) by means of consequent consideration of all stages of the tunnel complex construction applying the above correcting coefficients.

For approximate taking the limited size of the surface load in the direction along the tunnel axis into account in the work by Fotieva, Bulychev & Antziferov (2003) the correcting multiplier k was introduced in to the results of calculations obtained as the relation between maximal vertical stress appearing in a solid semi-plane on the level of the tunnel arch due to the action of the load of a limited width and due to an infinite load corresponding to the conditions of the plane strain. However formula for determining this coefficient needed to be improved because it did not take the length b of the load into account and gave no possibility to take into account a presence of several buildings located on some distances to one another along the tunnel axis. This is why an improved technique is offered for an approximate account of the 3-D character of problems caused by limited sizes of buildings in the direction along the tunnel axis and by their 3-D locations with respect to the tunnel.

The technique is based on a hypothesis that the relation k between stresses in the ring simulating the tunnel lining obtained from the solution of a 3-D problem, to the ones given by a 2-D problem, is approximately the same as a similar relation between vertical stresses appearing in the point of a solid half-space (without tunnel) corresponding to the center of the tunnel cross-section considered. The coefficient k may be determined in way described in publication by V.B, Shvetz et al. (1987).

The above hypothesis has been confirmed to a certain degree by comparison of results obtained in this way for a single tunnel, with the data from physical modelling on the equivalent materials published in the paper by Fotieva et al. (2005) and from 3-D linear and non-linear numerical modeling carried out by J. Aldorf, E. Hrubesova & K. Voitasik in the framework of joint project supported by the INTAS grant No01-0647. Some examples of compared results are given below.

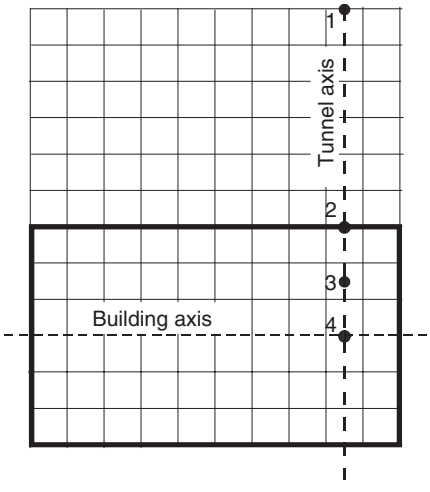


Figure 2. Plan of the building location.

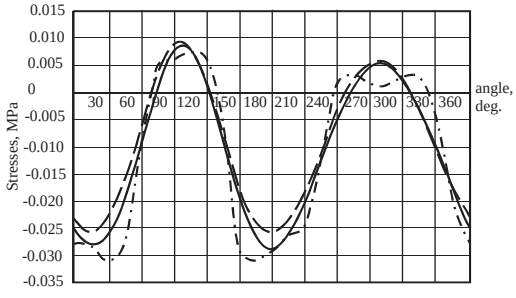


Figure 3. Comparative diagrams of stresses along the internal outline of the lining cross-sections 1.

A circular tunnel located on the depth $H = 18$ m in the rock mass with the deformation characteristics $E_0 = 5000$ MPa, $\nu_0 = 0.3$ has been considered. The lining of radii $R_0 = 3.0$ m, $R_1 = 2.7$ m is produced from concrete with characteristics $E_1 = 23000$ MPa, $\nu_1 = 0.2$. The load $P = 0{,}075$ MPa simulates the weight of the building of sizes $b = 10$ m, $l = 6$ m, erected nearly to the already existing tunnel. The plan of the building location with respect to the tunnel axis is shown in Figure 2 (one grid side corresponds to 1×1 m). Non-linear 3-D numerical modelling has been carried out taking the plastic deformations of rocks with $C = 5$ KPa and $\varphi = 30^\circ$ into account. The stresses have been determined in the lining cross-sections 1, 2, 3, 4.

Diagrams (in involute) of circumferential stresses $\sigma_\theta^{(in)}$, MPa along the internal lining outline obtained with the aim of the approximate technique proposed, are shown in Figures 3–6 by solid lines. The same stresses determined from 3-D linear and non-linear

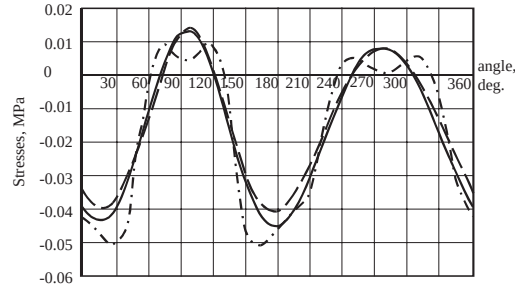


Figure 4. Comparative diagrams of stresses along the internal outline of the lining cross-sections 2.

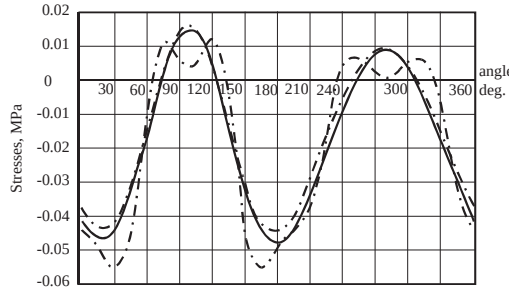


Figure 5. Comparative diagrams of stresses along the internal outline of the lining cross-sections 2.

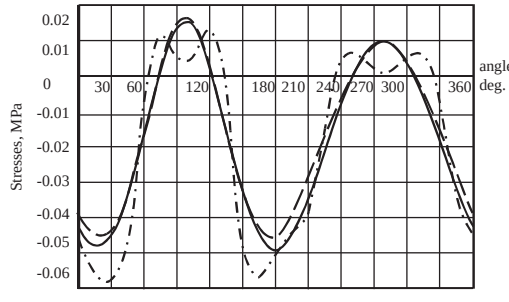


Figure 6. Comparative diagrams of stresses along the internal outline of the lining cross-sections 4.

numerical modeling are given for comparison by dotted and dot-and-dash lines correspondingly.

One can see from Figures 3–6 that the compared results of approximate analytical approach and 3-D linear modelling are in wholly satisfactory agreement. A similar conclusion has been drawn from physical modeling on equivalent materials described in papers by Fotieva, Sammal et al. (2004) and by Fotieva, Bulychev et al. (2005).

There are some differences with the data from non-linear 3-D modeling showing the increase of maximal compressive stresses and the decrease of maximal tensile stresses in the lining up to 18–20% due to the

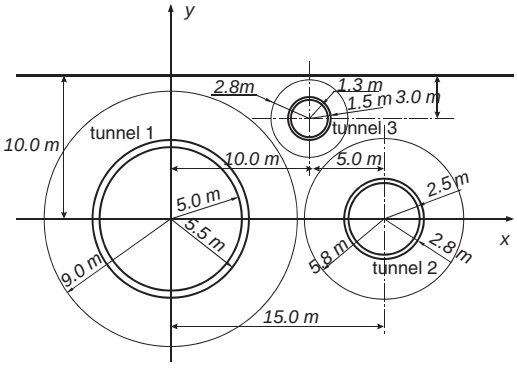


Figure 7. Tunnels cross-section.

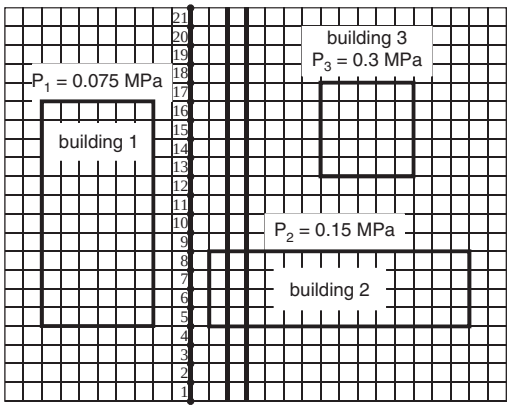


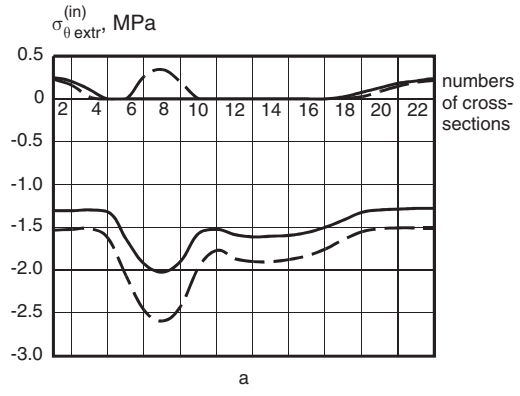
Figure 8. Plan of buildings locations.

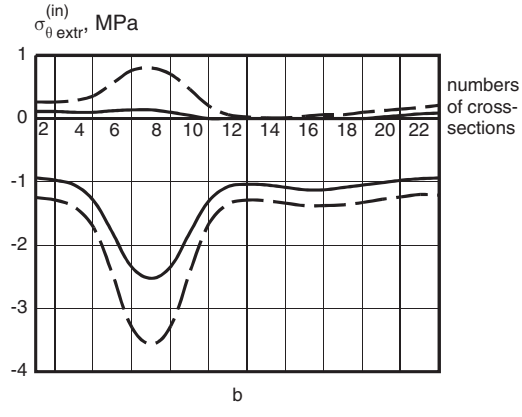
influence of plastic soil deformations. Since the tensile stresses are substantially more dangerous for the lining than the compressive ones, it is save to say that applying the linear model of soils lays only some additional margin of the lining safety.

3 EXAMPLES OF THE DESIGN

The example of the design of concrete linings of three parallel tunnels is given below. The input data are the following: $E_0 = 300$ MPa, $\nu_0 = 0.35$, $E_{1,1} = E_{1,2} = E_{1,3} = 900$ MPa, $\nu_{1,1} = \nu_{1,2} = \nu_{1,3} = 0.35$, $E_{2,1} = E_{2,2} = E_{2,3} = 30000$ MPa, $\nu_{2,1} = \nu_{2,2} = \nu_{2,3} = 0.2$, $\gamma = 0.022\,MN/m^3$, $\lambda = 0.54$, $l_1 = l_2 = l_3 = 1$ m. A cross-section of the tunnels is given in Figure 7.

Tunnel linings are subjected to the actions of soil own weight and the weight of three buildings erected close to already existing tunnels. The plan of the buildings locations is given in Figure 8.





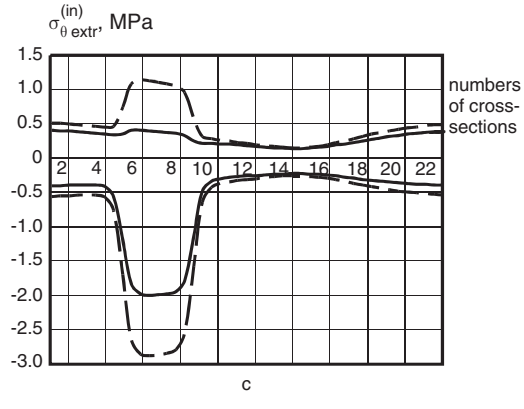


Figure 9. Distributions of maximal tensile and compressive stresses along the tunnel axes: a – tunnel 1; b – tunnel 2; c – tunnel 3.

One mesh on the plan has corresponds actual size 5 m × 5 m.

Distributions of maximal tensile (positive) and compressive (negative) stresses along the tunnel axes

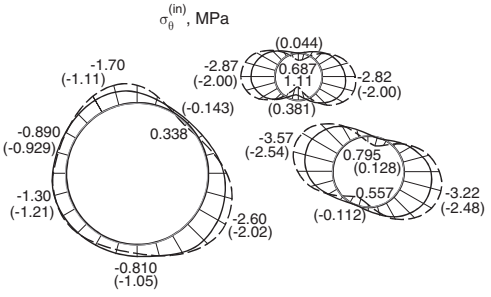


Figure 10. Circumferential stresses along the internal linings outlines in the cross-section 7.

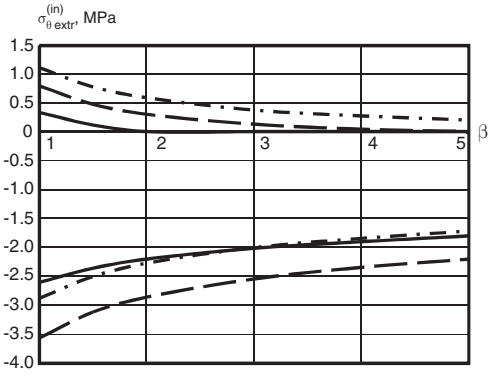


Figure 11. Dependencies of extreme stresses in the linings on the degree of strengthening.

are shown in Figures 9a, b, c by solid lines. Dotted lines correspond to the case when the tunnels are constructed without grouting.

One can see from figures 9 a, b, c that section 7 is the most dangerous for tunnels 1 and 2 and section 6 is the most dangerous for tunnel 3.

Diagrams of circumferential stresses along the internal linings outlines in the cross-section 7 are represented in Figure 10.

From Figure 10 one can see that the applying of grouting significantly reduce total stresses in tunnel linings. For example, maximal compressive stresses in tunnel linings fall by 22. . .30%, maximal tensile stresses disappear in the lining of tunnel 1 and drop by 38% and 84% in the linings of tunnels 2 and 3 correspondingly.

Dependencies of extreme (maximal compressive and maximal tensile) circumferential stresses $\sigma_{\theta\,extr}^{(in)}$ on the degree of strengthening $\beta = E_1/E_0$ are shown in Figure 11. Solid, dotted, dash-and-dot lines corresponds to stresses in the linings of tunnels 1, 2, 3.

On can see from Fig. 11 that the rise of the degree of strengthening leads to the decrease of extreme stresses in all three tunnels.

4 CONCLUSIONS

A new analytical method and the corresponding software for the design of multiple shallow circular tunnel linings including the ones constructed with the application of soil grouting in build-up areas has been developed. The method allows the influence of the distance between the lining been installed in every tunnel and the tunnel face and the sequence of tunnel complex construction as well as the 3D character of problems connected with surface loads caused by the weight of nearly located buildings to be approximately taken into account. This give a practical possibility to evaluate the linings stress state and their bearing capacity depending of thickness of zones strengthened by grouting and on the degree of strengthening by multi-variant calculations of a high accuracy requiting a few time.

REFERENCES

Aramanovich, I.G. 1955. Distribution of stresses in an elastic semi-plane weakened by a supported circular opening. *Reports of AN USSR, Vol. 104, No 3*: 17–23. Kiev: *AN USSR.*

Bulychev, N.S. 2002. On tunnel linings design in very soft soils. *Problems of Underground Construction in XXI Century; Proc. of the International Conference*: 35–37. Tula: TGU.

Fotieva, N.N. & Kozlov, A.N. 1992. *Design of the parallel openings support in seismic areas.* Moscow: Nedra.

Fotieva, N.N. & Sammal, A.S. 1986. Design of the closed monolithic lining with the rock strengthening taken into account. *Mining Systems Adjusted to High Rock Pressure Conditions; Proc. of the 9th Plenary Scientific Session of the International Bureau of Strata Mechanics, Varna 18–21 June 1985.* Rotterdam: Balkema.

Fotieva, N.N., Bulychev, N.S., Antziferov S.V. 2003. Designing multiple shallow tunnel linings constructed with the application of grouting. *Geotechnical Problems with Man-made and Man Influenced Grounds; Proc. of the XIIIthEuropean Conference on Soil Mechanics and Geotechnical Engineering, Prague, Czech Republic, 25–28th August 2003, Vol. 2*: 259–264.

Fotieva, N.N., Bulychev, N.S., Deev, P.V. 2006. Design of shallow tunnel linings constructed with the application of soil grouting. *Active Geotechnical Design in Infrastructure Development; Proc. of 13th Danube-European Conf. on Geotechnical Engineering. 29–31.04 2006. Ljubljana, Slovenia. – Vol.2: papers*: 893–897.

Fotieva, N.N., Bulychev, N.S., Sammal, A.S. 1993. Design of tunnel linings, constructed in weak water bearing rocks improved by cement grouting *Geotecnical Engineering of Hard Soils – Soft Rocks; Proc.of Int. Symp. 20–23 September 1993. Greece.* Rotterdam: Balkema.

Fotieva, N.N., Bulychev, N.S., Sammal, A.S. 1996. Design of shallow tunnel linings. *Proc. of the ISRM International Symposium Eurock'96, Torino, Italy, 2–5 September 1996*: 677–680. Rotterdam: Balkema.

Fotieva, N.N., Bulychev, N.S., Sammal, A.S., Golitsynskiy, D.M., Frolov, Yu.S., Fowell, R.J. 2005. Some aspects of shallow tunnel lining design in urban areas. *Underground Construction – 2005. Conference & Exhibition 26th–27th October, Olympia 2, London, UK, presented at the Conference (full text on CD-ROM).*

Fotieva, N.N., Bulychev, N.S., Sammal, A.S., Hrubesova, E., Aldorf, J., Voitasik, K., Fowell, R.J. 2005. Evaluation of a sewer tunnel linings durability in urban areas. Underground Space and Rock Mechanics. *Underground Space: Economy and Environment; Proc. of the 10th ACUUS Int. Conf. January 24–28, 2005*: 79–84. TA Engineering.

Fotieva, N.N., Sammal, A.S., Bulychev, N.S, Golitsynskiy, D.M., Frolov, Yu.S., Kavkazskiy V.I., Hrubesova, E., Aldorf, J., Voitasik, K., Malik, I., Fowell, R.J. 2004. Stress state of tunnel linings constructed in urban areas. *Ukrainsko-Polskie Forum Gornicze, Jalta, Krym, 13–19 Wrzesnia. 2004, Materialy Forumu*: 140–147.

Muskhelishvili, N.I. 1966. *Some basic problems of mathematical theory of elasticity.* Moscow: Nauka.

Shvetz, V.B., Ginzburg L.K., Goldstein, V.M., Kapustin, V.K., Feklin, V.I., Shvetz, N.S. 1987. *Guide on Soils Mechanics and Dynamics*. Kiev: Budivelnik.

Underground Space – the 4th Dimension of Metropolises – Barták, Hrdina, Romancov & Zlámal (eds)
© 2007 Taylor & Francis Group, London, ISBN 978-0-415-40807-3

Analyses of underground structures crossing an active fault in Coronado, California

T. Gregor & B. Garrod
Hatch Mott MacDonald, Mississauga, Ontario, Canada

D. Young
Hatch Mott MacDonald, Pleasanton, California, USA

ABSTRACT: The City of Coronado, California, has initiated the design for the State Route 75/282 Transportation Corridor Project. This project includes the design of approximately 5700 feet (1740 m) long twin road tunnels. The shallow, 32′–6″(9.9 m) finished diameter, tunnels will be crossing the seismically active Coronado Fault. A cut-and-cover box structure or twin bored tunnels lined with precast segmental concrete linings, have been considered as options in the area of the fault crossing. Assessment of the structural behaviour of these options during fault rupture consisted of the development of finite difference (bored tunnels) and finite element (cut-and-cover boxes) analytical models. Both types of models reflected non-linear stress-strain ground behaviour. The results of the design analyses have shown that it is possible to assess the structural behaviour of underground structures under severe ground displacement conditions using numerical analysis and to develop structural solutions.

1 INTRODUCTION

The City of Coronado has initiated the State Route 75/282 Transportation Corridor Project to improve traffic flow between the San Diego-Coronado Bay Bridge and the Naval Air Station North Island, a distance of approximately 1.4 miles (Figure 1). The project is in the Project Report / Environmental Document (PR/ED) phase. Several alternative alignments and associated construction methods are under consideration, including both cut-and-cover and twin bored tunnel options.

The tunnel length is approximately 5700 feet (1740 m). For the twin bored tunnels alternative, pressurized face tunnel boring machines (TBMs) will be used to install a single-pass lining system consisting of gasketed, precast concrete segmental rings concurrent with TBM advance. These rings are referred to as a Precast Concrete Tunnel Lining (PCTL) system. PCTL systems have been extensively used in seismically active locations in the United States and around the world (Dean, et. al. 2006).

In order to complete the PR/ED phase of the project, preliminary designs are required as a basis for estimating, and feasibility of designing fault crossings must be confirmed.



Figure 1. Project area.

2 GEOTECHNCIAL AND SEISMIC CONDITIONS

The excavations will be in soils, consisting of interbedded clays and sands of the Quaternary-age Bay Point Formation overlain by younger deposits of dune sand and fill. Bed thickness in the Bay Point Formation typically varies from a few inches to tens of feet. The natural water contents for these materials are

Table 1. Design ground motion levels.

Designation	FEE	SEE
Return period	150 years	Not applicable
PGA	0.17 g	0.57 g
PPV	7.8–8.3 inches/second	26.3 inches/second
Free field shear strain	0.04%	0.28%

Notes: PGA: Peak Ground Acceleration, PPV: Peak Particle Velocity, 1 inch = 25.4 mm

typically at or near the plastic limit, and the over consolidation ratio of these materials is typically in the range of 2.5 to 2.9.

The Bay Point Formation sands are medium dense to very dense, with an effective friction angle typcally ranging from 33 to 38 degrees.

Groundwater exists 10 to 15 feet (3.0 to 4.5 m) below ground surface, and depth to invert varies from 40 feet (12 m) for the cut-and-cover option to 100 feet (30 m) for the bored tunnel option.

Site seismicity and geologic hazards were assessed by Kleinfelder (2006). Three faults, the Coronado, Silver Strand, and Spanish Bight Faults, have been identified in and around the project area but only the Coronado fault crosses the proposed tunnel structures, as shown on Figure 1.

The project is being designed for a Functional Evaluation Earthquake (FEE) event and a Safety Evaluation Earthquake (SEE) event. As the anticipated lifetime of the project is on the order of 100 years, the FEE will conform to the 150-year return period event. The SEE event is similar to the maximum credible earthquake. The maximum moment magnitude for the SEE is 7.0. A summary of proposed design seismic ground motion levels for the SR75/282 Project is provided on Table 1. Return period and peak ground acceleration (PGA) values are provided in the table as well as peak particle velocity (PPV) and free field shear strains that consider near source effects.

3 CORONADO FAULT

The fault is only expected to rupture in the SEE event. It will rupture through the soil to the ground surface in an oblique sense of movement, with displacement spread over a fault zone thickness of 2 feet (600 mm). Displacement values for design are described in terms of vector components along strike and down dip.

The primary fault rupture occurs along the 2 foot (600 mm) wide zone that can occur anywhere within a 70 foot (20 m) wide zone along the alignment. In addition to primary rupture, secondary fault rupture would occur within a zone 50 feet (15 m) in each direction outside of the primary zone.

Table 2. Maximum fault rupture design parameters in the main zone.

Scenario	Lateral (Along Strike) Displacement (1 inch = 25.4 mm)	Sub-vertical (Along Dip) displacement
Right lateral	22 inches	11.75 inches
Left lateral	14 inches	11.75 inches

Table 3. Maximum displacements in secondary zone – footwall (hanging wall similar).

Scenario	Lateral (Along Strike) displacement	Sub-vertical (Along Dip) displacement
Right lateral	11 inches	5.9 inches
Left lateral	7 inches	5.9 inches

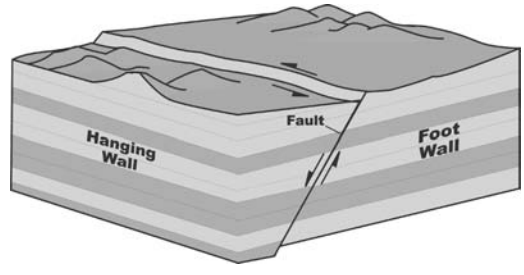


Figure 2. Hanging wall and Foot wall.

The lateral design offsets were estimated by deterministic methods. The two fault rupture lateral and vertical displacements for the SEE are outlined on Table 2 below for the main zone and in Table 3 for the secondary zones. A graphic depicting a hanging wall and foot wall is shown on Figure 2.

Lateral displacements occur in the same direction as the strike of the fault which intersects the tunnel at an angle of 78 degrees. The dip of the Coronado Fault was observed to be 70 degrees. (Kleinfelder, 2006).

4 BORED TUNNELS

4.1 *Tunnel structure properties and geometry*

Geometry of the planned tunnels and assumptions that were built into the analytical models were as follows:

- External tunnel diameter: 36.5 feet (11.12 m)
- Lining thickness: 1.5 feet (457 mm)
- Ring length 5 feet (1.52 m)
- Number of segments in a ring: 6 + a key
- Spacing between the twin tunnels 62.5 feet (19.05 m) center-to-center
- Lining modulus of elasticity 4354 ksi (30000 MPa) (uncracked concrete)

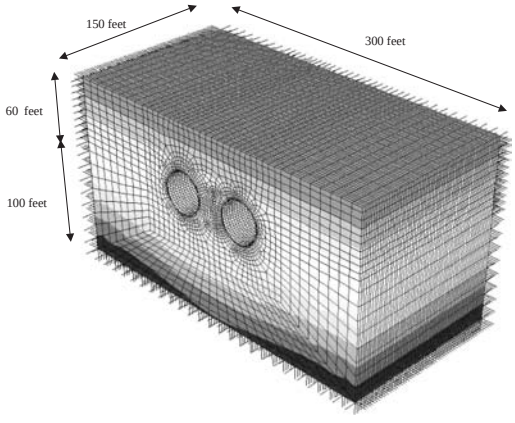


Figure 3. FLAC^{3D} model.

- Closure of the convergence gap between the extrados of the lining and the soil was assumed to be 0.25″ (6 mm) before grouting.
- The friction angle between the extrados of the lining and soil/grout was assumed to be 15°, reflecting the smooth surface of the extrados and presence of the tail seal grease from the TBM.

4.2 *FLAC^{3D} model size*

The block of ground represented in the models is 300 feet (91.4 m) wide 150 feet (45.7 m) long and 160 feet (48.8 m) deep with the tunnels located with their horizontal axis 60 feet (18.3 m) below the ground surface. See Figure 3.

Only the primary slip zone displacements were modeled for the bored tunnels, since the gradient of displacement is much more severe in the primary rupture zone in comparison to the secondary zone and it seems to be reasonable to assume that if the structure can withstand the primary zone displacement it can withstand the secondary zone displacements at the same time.

4.3 *Lining ring stiffness*

The precast lining is a segmental lining therefore its flexural stiffness in the hoop direction will be less than that of a solid tube. Muir Wood (1975) proposed that the stiffness of the segmental lining can be approximated by:

$$I_e = I_j + \left(\frac{4}{n}\right)^2 I \qquad (1)$$

With $I_e \leq I, n > 4$

Where I_e is equivalent moment of inertia, I_j is the moment of inertia of the joint (assumed 0 in this case) and n is the number of radial joints and I is the moment of inertia of the solid section of the lining. The formula has been derived under the assumption that the radial joints are uniformly distributed along the ring circumference. Typically, with the key segment being much smaller than the rest of the segments the radial joints adjacent to the key are much closely spaced than the rest of the radial joints and thus the two joints adjacent to the key were conservatively considered as one joint.

In order to preserve the true axial load stiffness of the lining the following calculations had to be performed where t_m is the lining thickness in the model, t is the actual thickness of the lining, E_m is the modulus of elasticity of the lining in the model, E is the actual modulus elasticity of the lining and A is the actual lining area per unit length:

$$I_e = \frac{t^3}{12}\left(\frac{4}{6}\right)^2, A = t, I_j = 0, n = 6 \qquad (2)$$

$$t_m = \left(\frac{12 I_e}{A}\right)^2 \text{ and } E_m = \frac{EA}{t_m} \qquad (3)$$

4.4 *Lining ring connectivity*

Precast rings are connected along the circumferential joints by bolts or dowels. In addition, the thrust of the TBM on the lining during the tunnel construction results in locked in compression along the circumferential joint interface between adjacent rings. Therefore, the relative displacement (slip) between adjacent rings is difficult to estimate. To capture the limits of behaviour we have assumed three extreme cases:

Case 1. Adjacent rings cannot slip relatively to each other along the circumferential joints but the joint can open and only compression force can be transmitted across the joint.

Case 2. Adjacent rings behave independently of each other, where no force (axial or shear) is transferred from ring to ring across the circumferential joint.

Case 3. Adjacent rings are fully connected to each other, the tunnel is a continuous structure. This would approximate a structure with special provisions to prevent joint opening and transfer forces across the joint.

4.5 *Modeling process*

- In-situ stresses including pore pressures from the water table were generated in the soil block.
- Soil in the tunnel void was removed and a stress free linear elastic lining, was installed. A 0.25″ (6 mm) gap (corresponding to the 0.23% volume loss) was left between the lining and the soil.
- The gap was pressurized to the level of the water table head.

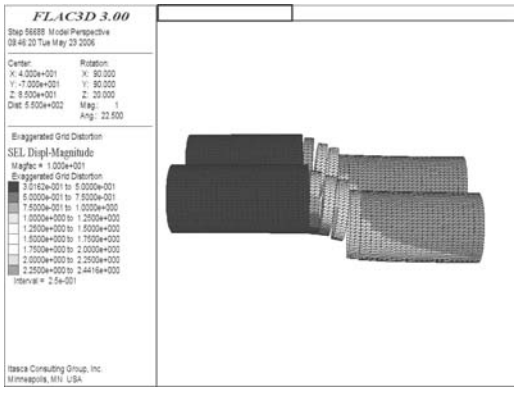


Figure 4. Case 2 tunnel ring displacements (x10).

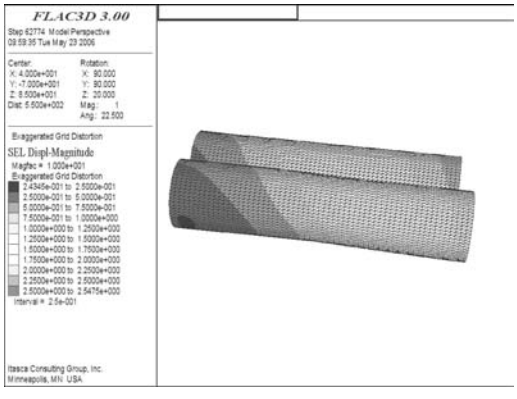


Figure 5. Case 3 tunnel ring displacements (x10).

- The system was brought to equilibrium, while the gap was allowed to close.
- In the next phase, the fault offset displacement pressures have been gradually applied to the boundaries of the model while concurrent solving of the model towards equilibrium was performed. Once the prescribed displacements at the model boundaries were reached the model was brought into the final equilibrium.
- A similar gradual loading process was applied to model the SEE shaking. A free field strain of 0.34% was applied gradually along the boundaries of the model, perpendicularly to the tunnel direction thus imposing ovaling deformations.
- Non-linear material simulation of the concrete lining was performed.

4.6 *Observations from the analyses*

Figure 4 shows that for ***Case 2*** the tunnel displacements follow the ground displacements. Figure 5 shows that for ***Case 3***, however, the tunnel

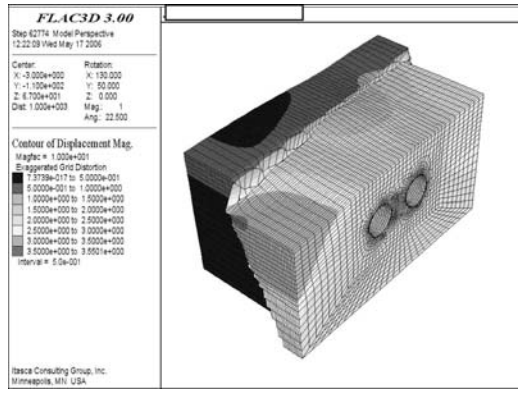


Figure 6. Case 3 soil block displacements (x10).

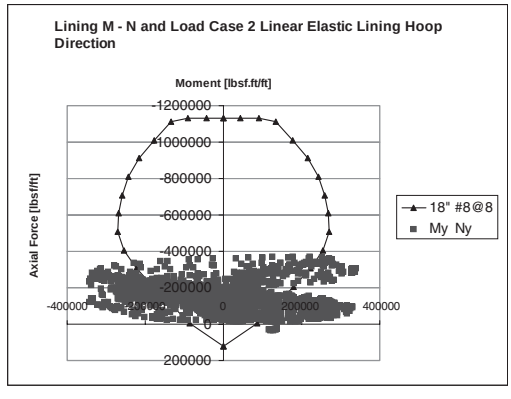


Figure 7. Capacity and loads, linear elastic lining hoop direction, case 2.

displacement is gradual, extending beyond the model limits and smoothes out the abrupt ground displacement. ***Case 1*** results were intermediate between these two extremes.

4.6.1 *Post processing*

A moment-axial force interaction curve was developed for the precast lining assuming the reinforcement of about 1% in each direction. Values of axial loads and corresponding moments were read from all elements representing the tunnel lining in the model and plotted against the capacity curves.

4.6.2 *Lining as linear elastic material*

As the first step in the evaluation, the lining rings were conservatively assumed to be a linear elastic material. This would correspond to uncracked lining. Figure 7 shows the critical curve for ***Case 2*** connectivity assumption.

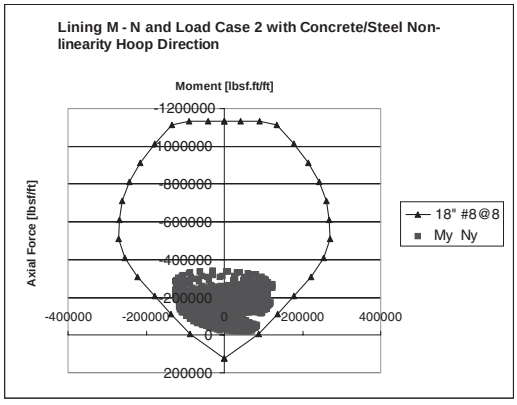


Figure 8. Capacity and loads, non-linear lining hoop direction case 2.

As it can be seen, the lining capacity appears to be insufficient in the hoop flexure for ***Case 2*** when the lining is considered to be linear elastic material.

4.6.3 *Lining as non-linear material*

The loading on the lining rings has been applied by prescribed ground displacements rather than by applied forces, which would remain constant throughout the loading process. If the flexibility of the structure increases (say by cracking) the forces in the lining will decrease. The key is to ensure that there is a sufficient ductility in the lining ring structure and that with additional small displacements the internal forces in the structure decrease.

The reinforced concrete material has been simulated using a HMM developed FISH function (FLAC^{3D} internal programming language). The method takes each lining model element and divides it into 10 layers. Strain in each layer is evaluated. Based on a parabolic and no-tension stress-strain relationship for concrete and elasto-plastic relationship for rebars, stresses in each layer are calculated. Stresses are summed into sectional forces and added into the equilibrium equations which are rebalanced in the solving process.

Figure 8 shows the lining capacity curves for the same case and direction as in Figure 7 but with the lining as non-linear material. Strains in the rebars in no case exceed 6%, the typical rebar rupture limit. The results clearly show that the lining strength is sufficient once the non-linearity of the lining is considered. This was true for all configuration cases.

5 CUT AND COVER BOXES

5.1 *Boxes properties and geometry*

A 3-D model of the cut-and-cover box was built using StaadPro software. The model represented a 294 feet (89.6 m) long section of the concrete box. The box geometry is outlined in Figure 9. The box is assembled from rectangular linear elastic plate elements.

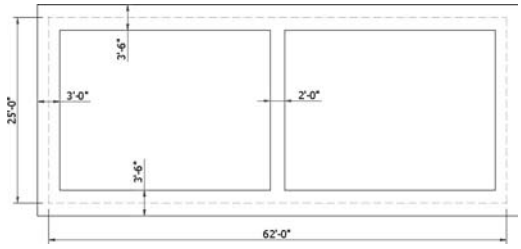


Figure 9. Box geometry.

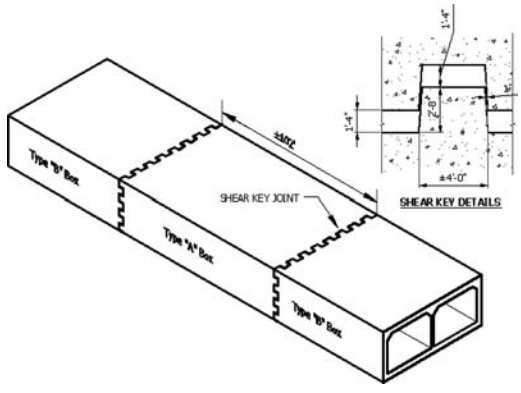


Figure 10. Box layout.

The soil was represented by compression-only springs that were placed at every exposed model node of the structure. The springs act perpendicularly to the corresponding face of the box and are capable of transmitting axial compression only. These springs have variable stiffness and are defined by multi-linear curves.

In order to simulate the long tunnel, elastic springs were assumed at both ends of the box. In trial runs we found that a seamless continuous box would produce very high compressive and tensile forces along the box length that required heavy reinforcing. For that reason shear key joints were introduced in the structure so that axial stresses are relieved during fault rupture event. A conceptual sketch of shear key joint is presented in Figure 10. Box A is the box crossing the main rupture zone, boxes type B are adjacent boxes. In the model these joints are simple hinges that are only capable of carrying in-plane shear forces only along the joint edges. The two shear key joints were placed 102 feet (31.1 m) apart so that fault rupture plane is at equal distance from each joint.

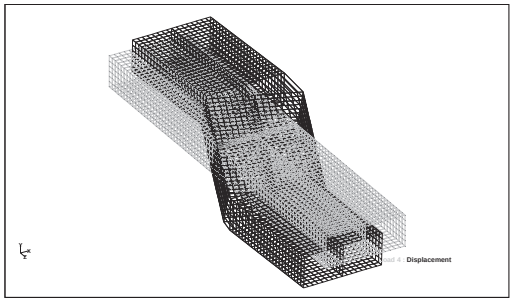


Figure 11. Box displacements.

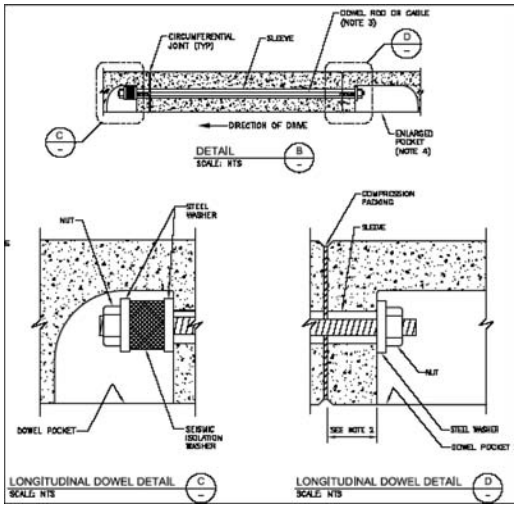


Figure 12. Circumferential joint opening control.

5.2 *Modeling sequence in StaadPro*

A two stage modeling sequence was used to circumvent some of the StaadPro loading modeling limitations.

Soil shear strains causes by ground shaking were applied as an additional, racking, displacement derived from the calculated soil shear strain and the ratio of the ground and structure stiffness.

Consideration has been given to using compressible material around the box structure to reduce the forces on the structure due to ground movements.

5.3 *Analyses results*

Figure 11 shows the resulting box displacement. The results also showed that with providing the special joints the effect of the fault rupture was actually secondary to the effects of the ground shaking.

6 CONCLUSIONS

From application of numerical analyses tools to assess the effects of a rupture of the Coronado fault on underground structures crossing the fault it can be concluded that:

- It is feasible to design a structure crossing the fault that would withstand the SEE and rupture event without a structural collapse.
- Both bored tunnels and cut-and-cover boxes can be used for this purpose.
- Both structures would show some degree of post-rupture damage (concrete cracks, large deformations).
- Bored tunnels constructed using segmental lining are more prone to inundation by water and soil during and after the fault rupture event. However, providing longitudinal ties connecting the rings and/or soil treatment around the tunnels over the tunnel length affected by the fault rupture could mitigate this issue. Some type of circumferential joint opening control is required, an example of which is shown in Figure 12.

REFERENCES

Dean, A., Young D.J., and Kramer G.E. 2006. The Use and Performance of Precast Concrete Tunnel Linings in Seismic Areas. *Proceedings of the 10th IAEG Congress, Nottingham, United Kingdom:* Paper No 679, Geological Society Publishing House

Kleinfelder, Inc., 2006. Final Preliminary Engineering Geotechnical Investigation, Volume I&II, State Route 75 and 282 Transportation Corridor Project Report, Coronado, California.

Muir Wood, A M. 1975. The circular tunnel in elastic ground. *Geotechnique 25* No 1:115–127.

USGS 2000, The web site of the U.S. Geological Survey, http://www.usgs.gov/

Underground Space – the 4th Dimension of Metropolises – Barták, Hrdina, Romancov & Zlámal (eds)
© 2007 Taylor & Francis Group, London, ISBN 978-0-415-40807-3

Numerical modeling of tunnel excavation and lining under high initial stresses and high underground water pressures at Jinping Mountain

Wei Chen & Huai-Ning Ruan
Institute of Geotechnical Engineering, Hohai University, Jiangsu Province, China

ABSTRACT: The Jinping underground hydroelectric power plant is one of major hydropower projects in China. Four high-pressure tunnels at about 2000 m depth below JinPing Mountain surface act as waterway towards the power plant. The phreatic water table is located at about 900 m above the tunnels. This paper presents the tunnel excavation and lining procedures under high initial stresses and high underground water pressures at Jinping Mountain. Coupled hydro-mechanical (HM) behavior of fractured rock during tunnel excavation is analyzed. A three-dimensional stochastic continuum model that accounts for the heterogeneity of the permeability has been developed to simulate the excavation and lining processes. The random permeability field is generated using sequential indicator simulations, which is then mapped into the finite element mesh. The concrete lining is modeled by shell elements and assumed impervious. Truss elements embedded in a set of three dimensional solid elements are used to model anchors with the embedded element technique. Some simulation results are discussed in details in this paper.

1 INTRODUCTION

The Jinping hydroelectric power generation plant with a maximum generating capacity of 4400 MW is one of the major hydropower projects in China. The pressure tunnels, which act as waterway towards the power plant, have an excavated span of 12 m and are approximately located at 2000 m depth below the Jinping Mountain surface. The water table is at about 900 m above tunnels. An understanding of the mechanical behavior of the support system and the hydro-mechanical (HM) processes of fractured rock are major challenges when assessing the performance of pressure tunnels under high initial stresses and high water pressures.

Natural spatial variability in hydraulic and mechanical variability can play an important role in the hydro-mechanical processes in fractured rock (Hudson et al, 2001). In this paper a three-dimensional stochastic continuum model that accounts for the heterogeneity of the hydraulic properties of fractured rock has been developed by using a non-parameter geostatistical technique. The results are then imported into a finite element model that resolves the HM behavior in detail. The tunnels are excavated in full-section and supported with rock anchors and concrete lining after excavation. The compliant joint model (CJM) (Chen, 1991) has been employed to perform mechanical calculations; both drained and undrained conditions are discussed in our numerical model. Coupled HM simulations were implemented with the commercial code ABAQUS 6.6 (ABAQUS, 2005).

2 MATHEMATICAL FRAMEWORK

2.1 *Fluid mass balance equations*

The final form of mass balance equation of flow in a deformable porous medium is expressed as:

$$\phi\frac{\partial(S_w\rho_w)}{\partial t}+S_w\rho_w\left[\frac{\partial\varepsilon_v}{\partial t}+\frac{(1-\phi)}{\rho_s}\frac{\partial\rho_s}{\partial t}\right]=-\nabla\cdot(\mathbf{q_w}) \quad (1)$$

where ϕ is the porosity, S_w is the saturation, ρ_s and ρ_w are the density of the solid and the fluid respectively, ε_v is the skeleton volume strain, and $\mathbf{q_w}$ is the mass flux. The rate of change of fluid mass is caused by changes in saturation, fluid density, volume strain of solid skeleton and grain volume (Lewis, 1987).

The mass flux, $\mathbf{q_w}$, can be written as

$$\mathbf{q}_w=-\rho_w\frac{\mathbf{k}}{\gamma_w}(\nabla P_w-\rho_w\mathbf{g}\nabla z) \quad (2)$$

where $\mathbf{k}$ is the hydraulic conductivity, P_w is the pore pressure. The permeability is assumed constant and heterogeneous in our numerical model.

2.2 *Mechanical constitutive relations*

The compliant joint model is used for modeling the mechanical behaviour. The CJM provides a simple, continuum model for materials containing a high density of parallel joint surfaces in different orientations. It can model joint opening/closing and the plastic behaviour of a joints system, which is defined as:

$$f_a = \tau_a - P_a \tan \beta_a - d_a \tag{3}$$

where f_a is the failure surface, τ_a is the magnitude of the shear stress resolved onto the joint surface, P_a is the normal pressure stress acting across the joint, β_a is the friction angle for the joint system a, and d_a is the cohesion for system a.

3 GENERATION OF THE HETEROGENEOUS PERMEABILITY FIELDS

The hydraulic conductivity of the rock matrix is ignored because the matrix permeability is several orders of magnitude lower than the fracture permeability. The dimensions of the domain are $700 \times 1000 \times 1100$ m in the x, y, z directions, respectively. The domain is discretized into $5 \times 10 \times 5$-m grids for a total of 3,080,000 elements. The random field generation was performed with the sequential indicator simulation routine SISIM (version 2.9) of the geostatistical library GSLIB (Deutsch and Journel, 1992). The sequential indicator simulation allows users to assign different isotropic or anisotropic correlation scales to different segments of the probability density function. The permeability data used for the creation of the random fields are mainly based on pumping test in Jinping Mountain and the fracture surveys in the drift tunnel. A spherical correlation structure with an isotropic correlation length of 5 m is adopted for permeability values less than $10^{-13.5}$ m. A correlation length of 90 m in the x-direction and the z-direction, and a correlation length of 10 m in the x-direction, both using a spherical correlation structure, are given to permeability values larger than $10^{-13.5}$ m. Figure 1 shows a generation of the permeability field.

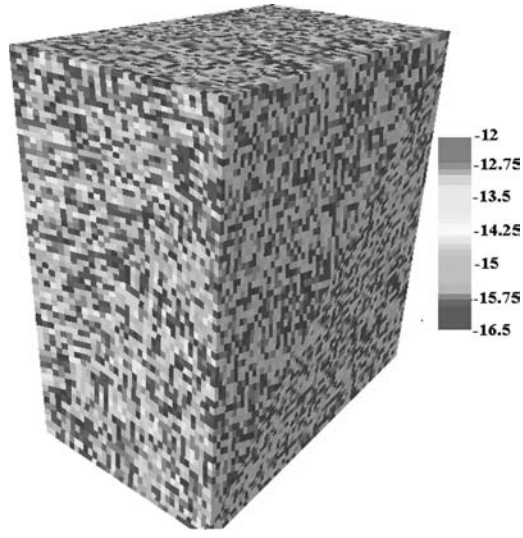


Figure 1. Permeability distribution generated by GSLIB (the legend indicates log10 permeability in m^2.

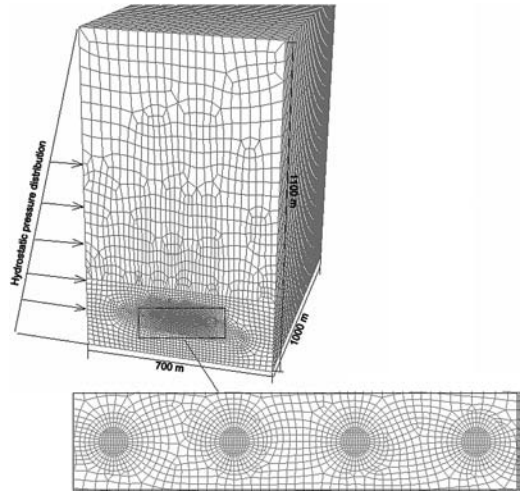


Figure 2. The finite element model (the mesh near tunnels are enlarged).

4 MODELLING OF EXCAVATION AND LINING

4.1 *Model domain geometry and boundary conditions*

It is impractical to model the whole mountain for the coupling calculations. Therefore a 'local model' was developed in our study. The 3D domain chosen for the simulation is 700 m wide (x-direction), 1000 m deep (y-direction) and 1100 m high (z-direction). In order to limit the computational load, a relatively coarse mesh with high resolution grids near the tunnels is used. The finite element mesh is shown in Figure 2. The heterogeneous permeability distribution is interpolated from the previous high-resolution onto this finite element mesh.

The vertical boundaries have a constant hydrostatic pressure, and the top and bottom boundaries have a no flow condition. The initial stress was obtained from the calibrated data based on a regression analysis.

Table 1. Material parameters for coupling analysis.

Material type	Properties		value
Fluid	γ_w, specific weight		10 kN/m^3
	E, Young's modulus		2.5e + 07 kPa
	γ_s, specific weight		27 kN/m^3
	ν, Possion's ratio		0.3
	n, porosity		0.007
Fractured rock	φ, Friction angle	Parameters	35°
	ψ, dilation angle	for joints	15°
	C, cohesion		40 kPa
	φ, friction angle	Druker-Prager	45°
	ψ, dilation angle	parameters for	35°
	C, cohesion	bulk material	1350 kPa
Concrete lining	E, Young's modulus		3.0e + 07 kPa
	ν, Possion's ratio		0.2
	d, thickness		0.5 m
Steel anchors	E, Young's modulus		2.1e + 08 kPa
	ν, Possion's ratio		0.3
	L, length		6 m

4.2 *Numerical analysis steps*

The tunnels are excavated in full-section and are supported by steel anchors and concrete lining after excavation. Steel anchors are modeled by truss elements which are embedded in solid elements. Shell elements are used to represent concrete lining. The details of analysis steps are as follows:

(1) Initial stresses were imported, and lining and anchor elements were deactivated. Geostatic equilibrium was established during this step.
(2) Excavated rock elements were deactivated and nodal forces and fluxes were ramped down to zero in the excavation stage.
(3) Anchor and lining elements were activated. Both drained and undrained conditions during tunnel excavation are included in our model. The properties of rock and fluid are summarized in table 1. The physical deterioration of the components of rocks due to pore water was not considered.

5 RESULTS

5.1 *Displacements*

Figure 3 illustrates the radial displacement of a tunnel section after excavation under undained conditions. The calculated results have indicated inward, non-uniform convergence of the tunnel. The maximum value of radial displacement is 2.2 cm, which occurs at the side walls of the tunnel.

Figure 4 shows the radial displacement of the section under drained condition. It is found that the inward

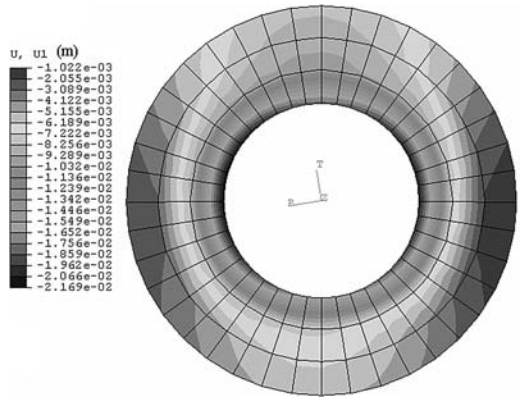


Figure 3. Radial displacement of a tunnel control section under undrained conditions.

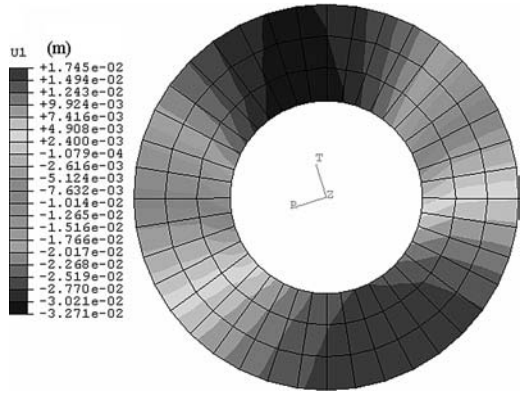


Figure 4. Radial displacement of a tunnel control section under drained conditions.

deformation of the crown is relatively large. The bottom of the tunnel section has an outward deformation. This is caused by drainage-induced consolidation of rock in the vicinity of the tunnel. The pore pressure is much reduced after drainage, which will induce a new non-uniform deformation of the opening.

5.2 *Stresses and moments*

The tangential stresses of rock around the tunnel under drained and undrained conditions are illustrated in Figure 5 and Figure 6, respectively. When the tunnel is assumed undrained, tensile stresses occur in rock, which are not found in the calculated results when assuming full-drainage conditions. A comparison between the two results indicates that drainage conditions have significant effects on mechanical response of rock.

Figure 7 and Figure 8 show the stresses in the steel anchors. It is found that the tensile stresses in anchors under non-drainage conditions are larger than

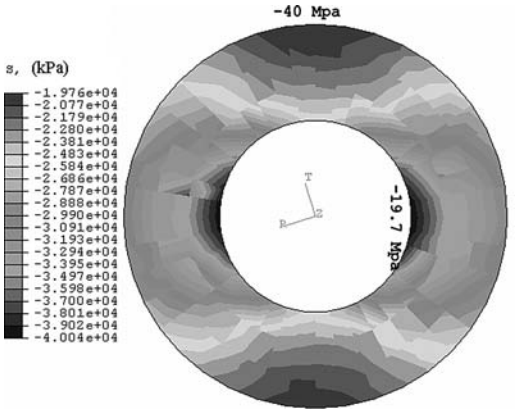


Figure 5. Tangential stresses of a tunnel control section under drained conditions.

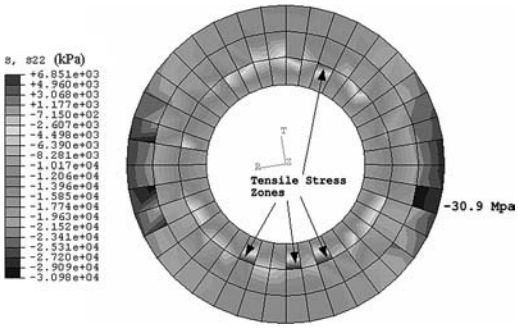


Figure 6. Tangential stresses of a tunnel control section under undrained conditions.

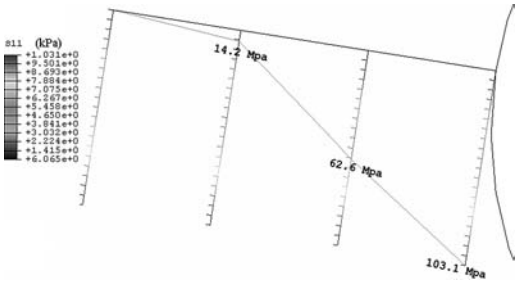


Figure 7. Axis tensile stresses of an anchor under drained conditions.

that under full-drainage conditions. The maximum value of tensile stresses under undrained conditions is 236.4 MPa.

However, the stresses in the concrete lining are not affected by the drainage conditions, which is also presented by Bobet using analytical solutions (2003). The calculated moments in the lining are shown in Figure 9.

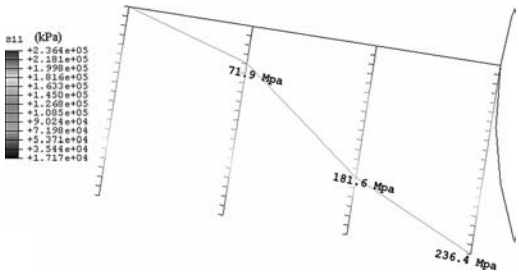


Figure 8. Axis tensile stresses of an anchor under undrained conditions.

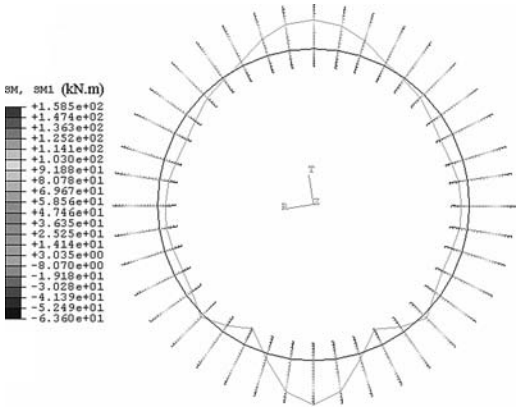


Figure 9. Moments in the lining.

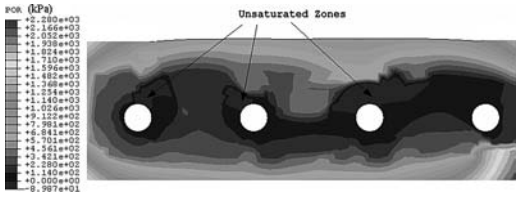


Figure 10. Pore pressure contours at a slice under full-drainage conditions.

The maximum moment occurs in the bottom of the lining, with the value 158.5 kN.m.

5.3 *Pore pressure*

Figure 10 presents the pore pressure results at the slice 400 m from the tunnel access. Negative pore pressures have been predicted near the tunnel after drainage using the heterogeneous permeability field as shown in the contours, which indicates the development of an unsaturated zone. This is the result of highly permeable fractures in the tunnel vicinity. The contours indicate a non-uniform pore pressure distribution, which reflect the heterogeneity of the model area.

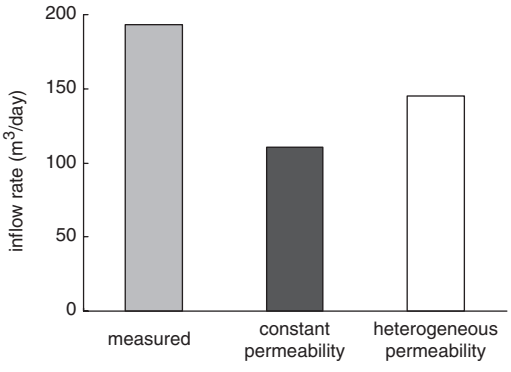


Figure 11. Inflow rates to the tunnel.

5.4 *Inflow rates to the tunnel*

The calculated inflow rates are compared to the measured data in Figure 11. The maximum water inflow rate to the tunnel, in calculations with heterogeneous permeability, is about 145 m^3/day, which is close to the measured value (194 m^3/day). Assuming constant permeability, the result is much smaller (110 m^3/day).

Both simulated results of maximum inflow rate were below the actual measurements, which may be caused by the ignorance of the underground water recharge in our study.

6 CONCLUSIONS

A 3D finite element model with heterogeneous permeability has been developed for simulating coupled hydro-mechanical behavior during tunnel excavation. The calculated results of hydraulic and mechanical response have been discussed in detail.

The results have indicated that the presence of groundwater in rock has a negative effect on the stability during tunnelling as a result of strength reduction due to the reduction of effective confining stress caused by high pore water pressures. Tensile stresses, which are found under non-drainage conditions, are eliminated when assuming full-drainage conditions. The stresses in steel anchors also change significantly from drainage to non-drainage conditions. It can be concluded that with the application of the drainage and removal of pore water and water pressure from fractured rock, tensile forces will be eliminated and rock masses can be strengthened.

The heterogeneous model gives a better prediction of inflow rates compared to the homogeneous model. Due to highly permeable features in the heterogeneous model, unsaturated zones are predicted. The heterogeneity of permeability has a significant effect on the hydraulic behavior of fractured rock during tunnel excavation.

ACKNOWLEDGEMENTS

The authors are grateful to Wouter Karreman at Delft University of Technology, the Netherlands for a careful review of the manuscript and his critical comments.

REFERENCES

ABAQUS 6.6. 2005. *Finite Element Program*, from Hibbit, Karlson, Sorensen, Inc. 1080 Main Street, Pawtucket, RI, USA.

Bobet, A. 2003. Effect of pore water pressure on tunnel support during static and seismic loading. *Tunnelling and Underground Space Technology. 18: 377–393.*

Chen, E.P. 1991. A constitutive model for jointed rock mass with two intersecting sets of joints. *SAND89-0592.* Albuquerque, New Mexico: Sandia National Labs.

Deutsch, C.V. & Journel, A.G. 1992. *GSLIB—Geostatistical Software Library and User's Guide*. Oxford University, Press, New York.

Hudson, J.A., Stephansson, O., Andersson, J., Tsang, C.-F. & Jing, L. 2001. Coupled T-H-M issues relating to radioactive waste repository design and performance. *International Journal of Rock Mechanics & Mining Sciences 38: 143–161.*

Lewis, R.W. & Schrefler, B.A. 1987. *The finite element method in the deformation and consolidation of porous media.* John Wiley, New York.

This page intentionally left blank

Underground Space – the 4th Dimension of Metropolises – Barták, Hrdina, Romancov & Zlámal (eds)
© 2007 Taylor & Francis Group, London, ISBN 978-0-415-40807-3

Simulation of failure around a circular tunnel using a bonded particle model

Dae-Sung Cheon & Chan Park
Korea Institute of Geoscience & Mineral Resources, Korea

Seokwon Jeon
Seoul National University, Korea

Young-Sik Jeong
Sambo Eng. Co. Ltd., Korea

ABSTRACT: To evaluate brittle failure around deep tunnels, true triaxial compression tests were performed, using cement mortar with a circular tunnel. In order to simulate the observed failure zone around the tunnel, the particle flow code (PFC) was applied. The PFC is a distinct element geomechanical modeling program in which rock is represented by an assembly of thousands of round particles bonded together at each contact point. The modeling program reproduced complex macroscopic behavior such as strain softening and dilation by simulating micro-mechanisms without resorting to complex constitutive laws. To determine the micro-mechanical parameters needed in the calibration process of the simulation, laboratory uniaxial tests were performed. Compared to the continuum models with traditional failure criteria, PFC^{3D} simulated the localization behavior of the brittle materials, and the numerical model reproduced the failure zone observed in the physical model test.

1 INTRODUCTION

At low in-situ stress magnitudes, the continuity and distribution of natural fractures in a rock mass control failure processes. However, at highly stressed levels, the failure process is affected and eventually dominated by stress-induced fractures growing preferentially parallel to the excavation boundary. And in these geological environments, brittle failure is the dominant failure mode. Brittle failure results from the growth and accumulation of tensile cracks around tunnels. This failure is usually described as "spalling" or "slabbing," and the shape of the failure zone is commonly called the "breakout" or "V-shaped notch."

To model the observed spalling, numerical simulations were carried out using the Mohr-Coulomb or Hoek-Brown criterion (Read & Martin, 1996). However, none of the suggested modeling simulations predicted a V-shaped failure zone. This is because conventional continuum modeling approaches overlook a fundamental observation of brittle failure, which is that the formation of tensile crack is the first step in the failure process.

In this study to simulate an observed failure zone around a tunnel, the particle flow model (PFC^{3D}), which does not need specific failure criteria, was applied. To determine the micro-mechanical parameters needed in the calibration process of the simulation, laboratory uniaxial tests were performed. And to investigate the effect of particle size on macro-properties, the resolution test was carried out.

The results of PFC^{3D} modeling were verified with the physical model tests, which were performed under true triaxial stress conditions using a cement mortar block with a circular tunnel. Also, the results of the modeling were compared to the continuum modeling.

2 BONDED PARTICLE MODEL

2.1 *Theory*

The particle flow code (PFC) is a discontinuum code that represents a rock mass as an assemblage of balls confined by planar walls. The distinct element method is used to model the forces and motions of the particles within an assembly. This method is similar to that used in explicit finite difference analyses and allows information to propagate dynamically through the system.

The particles move independently of one another and interact only at contact points. They are assumed to be rigid (non-deformable), but overlap can occur at the contacts. Contacts are assumed to exist only at a point and not over some finite surface area as would be the case with fully deformable particles. The particles

can be bonded together to simulate a competent rock. The contact bonds can be envisaged as a pair of elastic springs with constant normal stiffness and shear stiffness acting at a point. The values assigned to these stiffnesses influence the macro deformation properties of the rock sample. The contact bonds also have a specified shear and tensile strength. The values assigned to these strengths influence the macro-strength of the sample and the nature of cracking and failure that occurs during loading.

After a bond breaks in PFC, stress is redistributed, and this may then cause more cracks to form nearby. If the rock model is suitably stressed, then these bond breakages will localize into an inclined macro-fracture. Eventually, the macro-fracture will cause sample failure. In this way, deformation and fracture of rocks is modeled directly by allowing micromechanical damage to evolve, instead of indirectly by using constitutive equations, as is the case in most continuum models (Itasca Consulting Group Inc., 1999; Hazzard & Young, 2000).

2.2 *Bonding type*

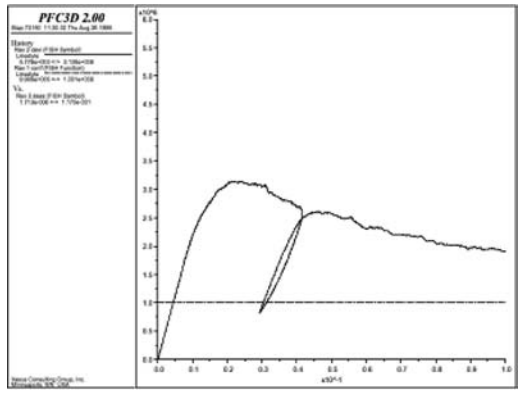
PFC^{3D} allows particles to be bonded together at contact points. Two bonding models are supported: a contact bond model and a parallel bond model. Both bonds can be envisioned as a kind of glue joining the two particles. The contact-bond glue is of a vanishingly small size that acts only at the contact point, while the parallel-bond glue is of a finite size that acts over a circular cross-section lying between the particles. The contact bond can transmit only a force, while the parallel bond can transmit both a force and a moment.

Both types of bonds may be active at the same time: however, the presence of a contact bond inactivates the slip model. Once a bond is formed at a contact between two particles, that contact continues to exist until the bond is broken. Only particles may be bonded to one another; a particle may not be bonded to a wall.

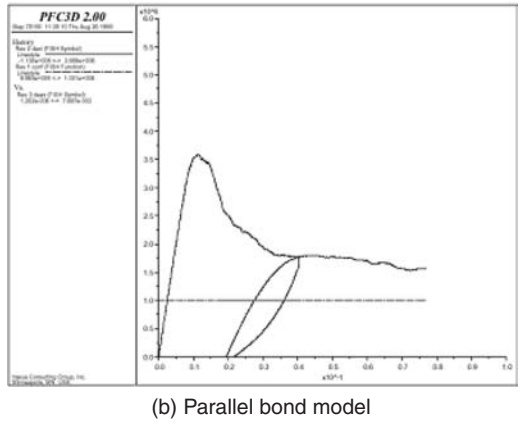
Two simulations are performed with a contact bond and a parallel bond (Fig. 1). In the unload/reload cycle during the test with the contact bond, there is only minor degradation in the elastic modulus. This reflects the nature of contact bonds, which represent only the drop in the load-carrying ability of a contact, not the change in stiffness. The parallel bond, on the other hand, also models stiffness reduction during failure. A parallel bond is more suitable to materials such as rock. Thus, in this study, parallel bonds are adopted for the simulation.

2.3 *Effect of resolution on macro-properties*

If the PFC is used to predict damage formation surrounding an excavation, then the absolute size of the potential damage region is fixed, and successively finer resolution models can be produced by decreasing



(a) Contact bond model



(b) Parallel bond model

Figure 1. Axial deviatoric stress and confining stress vs. axial strain.

particle size. It is expected that as the resolution continues to increase, the coefficients of variation will converge to specific values. These values should be a true measure of the effect of both packing and strength heterogeneities in the model materials, because the number of particles across the specimen has become large enough to obtain a representative sampling of the material response. A high resolution must be present for the model to resolve and reproduce the failure mechanisms that influence the strength properties.

To evaluate the effect of resolution on macro-properties, six PFC^{3D} materials were produced using the same micro-properties with different values of resolution. In this study, the resolution is defined as the number of particles within the model width. Table 1 shows the tested resolution and run time.

The Young's modulus and peak strength, etc. except for Poisson's ratio, exhibits a dependence on the resolution (Fig. 2). The characterization of the elastic grain-cement micro-properties in terms of the ball-ball contact modulus, parallel bond modulus, ball stiffness

Table 1. Mean radius of particle at each resolution.

Resolution	Mean radius (mm)	Run time (min.)	No. particle
5	5.2	1	298
10	2.6	11	2837
15	1.73	36	8103
20	1.3	94	19098
25	1.04	222	37301
30	0.87	517	63719

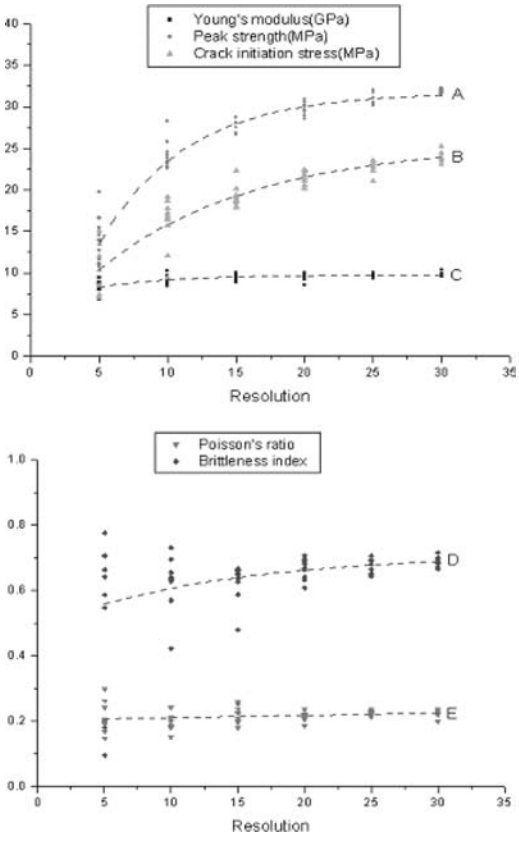


Figure 2. Result of resolution test.

ratio, and parallel bond stiffness ratio provides a size-independent means of specifying the Poisson's ratio of the material, but the Young's modulus exhibits a minor size effect (Potyondy & Cundall, 2004).

PFC^{3D} modeling in high resolution needs a much more efficient computer CPU and run time than PFC^{2D}. And some times the modeling does not run. Thus, in this study a 25 resolution was used to predict failure.

Table 2. Micro-parameters used in modeling.

Parameter	Description	Value
ρ	ball density [kg/m^3]	2,020
Ec	ball-ball contact modulus[GPa]	9.7
k_n/k_s	ball stiffness ratio	2.1
$\overline{\lambda}$	parallel bond radius multiplier	1.0
$\overline{E_c}$	parallel bond modulus	9.7
$\overline{k_n/k_s}$	parallel bond stiffness ratio	2.1
μ	ball friction coefficient	1.5
(mean)	parallel bond normal strength (mean)	35
$\overline{\sigma}_c$ (std.dev)	parallel bond normal strength (std.dev)	15
(mean)	parallel bond shear strength (mean)	37
$\overline{\tau}_c$ (std.dev)	parallel bond shear strength (std.dev)	15

2.4 *Determination of micro-parameter*

In order to determine the micro-parameter necessary for bonded particle modeling, preliminary analyses with varying micro-parameters were carried out.

The model width for determining the micro-parameter was set to 50 mm as the average diameter of the test samples used in the uniaxial compressive tests. The model height was set to 100 mm in order to satisfy the height/diameter ratio of 2:1. The measurement circles were located in the top, bottom, and middle of a test sample, and in each time step, the stress and stain of a model were calculated by averaging the stress and strain of particles within a measurement circle. The determined micro-parameters are listed in Table 2.

3 PHYSICAL MODEL TESTS

Physical model tests under true triaxial stress conditions were carried out, in order to evaluate brittle failure around deep tunnels.

3.1 *Specimen and test procedure*

The specimen used as substitute rock was cement mortar. This mortar was formed by mixing cement, fine sand, and water in the proportion of 3:6:2 by weight and air curing more 28 days. The size of the specimen was 290 mm × 290 mm × 290 mm. It had a half-excavated circular tunnel of 60 mm in diameter. The specimen width was five times the tunnel diameter to eliminate edge effects.

The physical model tests were carried out using a true triaxial testing system (Cheon et al., 2006). The testing system consists of two main parts: the biaxial loading apparatus and the polyaxial pressure chamber. The test procedure was conducted as follows.

To avoid intrusion of fluid into the specimen during tests, the surfaces of the specimen were coated with a thin film. Also, the entrance of the tunnel was isolated by a tunnel plug to prevent fluid from entering the tunnel.

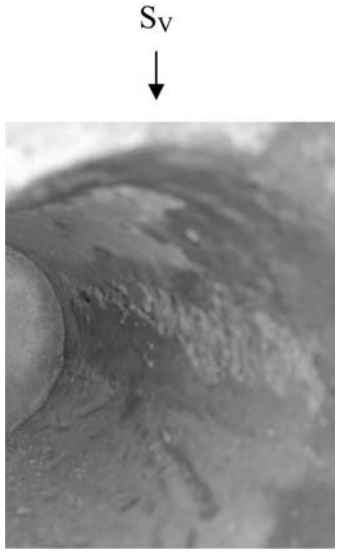


Figure 3. Failure around the tunnel in the physical model test.

The prepared specimens were carefully transferred into the polyaxial chamber. Using a hoist and an electric lift, the chamber was settled into the Interlaken rock testing machine. Next, the two independent stresses (S_V and S_{H2}: perpendicular to the tunnel axis) were applied initially in small amounts (about 1 MPa). And then S_{H1}, which was parallel to the axis of the tunnel axis, was increased to a constant value. After reaching the predetermined level of S_{H1} and S_{H2}, S_V was increased monotonically to a constant level ($S_V > S_{H2} > S_{H1}$). During the tests, acoustic emissions and source locations were detected to determine the S_V level. The tests were performed for 5 to 10 minutes using load control.

3.2 *Test results*

The failure around the tunnel observed in the physical model tests is depicted in Figures 3 and 4. As Figure 3 reveals, spalling occurred parallel to the S_V, and it was V-shaped, as in previous research studies (Martin et al., 1999; Kaiser et al., 2000). Little damage occurred around the tunnel face due to the 3D arching effects. As the distance from the tunnel face increased, the failure zone became wider and deeper.

4 NUMERICAL SIMULATION

The numerical investigation was performed using the PFC^{3D}, and this was compared to the result of physical model test and FLAC^{3D} simulation using the Mohr-Coulomb criterion. In order to simulate the physical model test as reliably as possible, the axial stress (S_v) was monotonically increased until it reached the tested stress level.

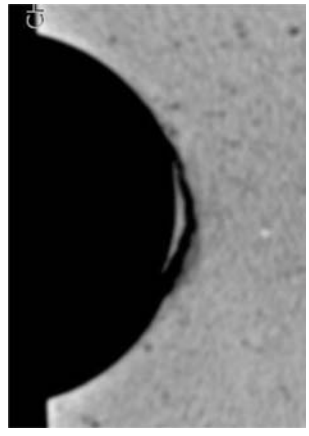


Figure 4. V-shaped notch in CT image.

4.1 *Comparison of PFC^{3D} and FLAC^{3D}*

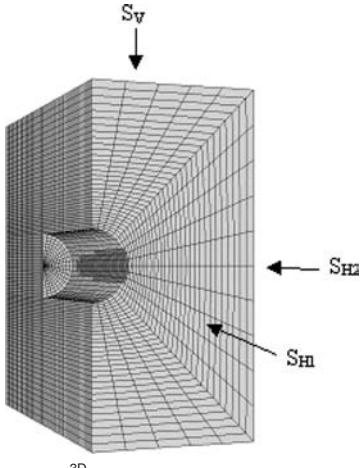
Figure 5 shows the results of PFC^{3D} simulation and FLAC^{3D} simulation. As shown in Figure 5, FLAC^{3D} using the Mohr-Coulomb criterion did not show a V-shaped notch as observed in the physical model test. The continuum modeling using the Mohr-Coulomb criterion seems to be inappropriate for brittle materials, because this criteria ignores material weakening in its constitutive equation, whereas the PFC^{3D} modeling could be simulate the V-shaped notch. However, in 3D simulation it is sometimes difficult to detect the notch formation compared to 2D simulation (Bae, 2005). If the continuum model does not use a specific constitutive equation for brittle material, it would be better to use the particle flow code to simulate brittle failure.

4.2 *Failure characteristic with stress conditions*

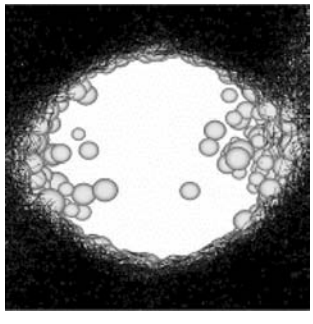
Based on the physical model tests, crack initiation stress was considered to be the brittle failure initiation stress level. In this study, crack initiation stress is equal to the stress when the 10% cracks of total cracks were occurred. As the S_{H1} and S_{H2} increased, crack initiation stress also increased (Figure 6). From the multi-variable regression on stress conditions and failure initiation stress, $f(S_v, S_{H1}, S_{H2})$ was proposed as below.

$$f(S_v, S_{H1}, S_{H2}) = -\frac{S_V}{\sigma_c} + 1.700\frac{S_{H1}}{\sigma_c} + 0.930\frac{S_{H2}}{\sigma_c} + 0.452 = 0 \qquad (1)$$

PFC^{3D} can describe spalling as a splitting of particles. Figure 7 shows the failure pattern and displacement



(a) FLAC^{3D} simulation using Mohr-Coulomb model



(b) PFC^{3D} simulation

Figure 5. Comparison of failure shape between PFC^{3D} and FLAC^{3D}.

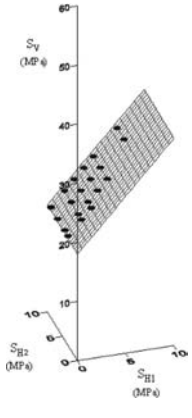
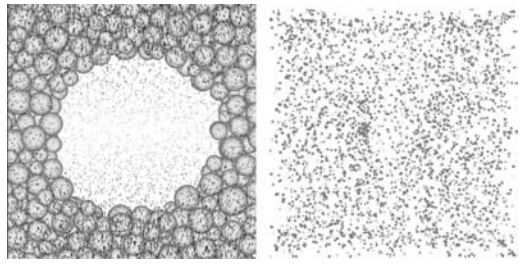
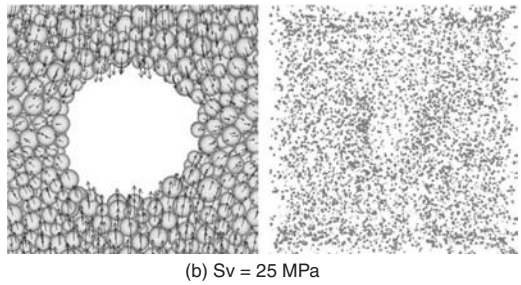


Figure 6. Crack initiation stress from PFC^{3D} modeling with different stress conditions.

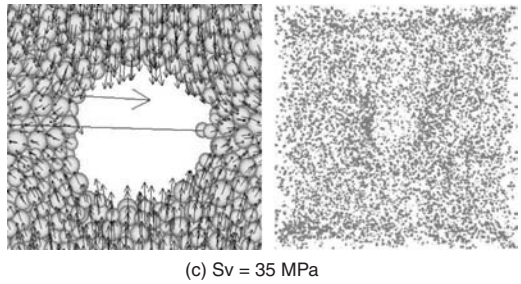
vector around a tunnel with S_V stress conditions (S_v: parallel to the tunnel axis). Figure 7 (a) is the state when S_v is at 20 MPa. There were no significant changes,



(a) Sv = 20 MPa



(b) Sv = 25 MPa



(c) Sv = 35 MPa

Figure 7. Particle displacement, crack distribution with different Sv level.

but as S_v increased, the displacement vector greatly increased and cracks were concentrated at the side-wall parallel to S_v. In particular, when S_v reached 35 MPa, particle splitting was clearly detected with visual observation.

5 CONCLUSIONS

To evaluate brittle failure around a deep tunnel, numerical simulations using PFC code were performed, and the results were compared with the physical model test and the simulation using FLAC. From this study, the following results were obtained:

– The Young's modulus and peak strength and etc. except for Poisson's ratio exhibits a dependence on resolution in PFC simulation. As the resolution continues to increase, the coefficients of variation will converge to specific values.

– The particle flow code (PFC) could simulate a V-shaped notch and describe spalling as a splitting of particles.
– Based on the physical model test, crack initiation stress was considered to be a brittle failure initiation stress. As the applied polyaxial stress increased, crack initiation stress also increased.

REFERENCES

Bae, S.H. 2005, Characteristics of initial rock stress state in Korean tectonic provinces by hydraulic fracturing stress measurement, *Ph. D Dissertation*, Seoul National University, Korea.

Cheon, D.S., Jeon, S., Park, C. & Ryu, C. 2006. An experimental study on the brittle failure under true triaxial conditions, *Tunnelling and Underground Space Technology*, No 44.

Hazzard, J.F. & Young, R.P. 2000. Simulating acoustic emissions in bonded-particle models of rock, *Int. J. Rock Mech. & Mining Sciences*, 37: 867–872.

Jeong, Y.S., Jeon, S. & Cheon, D.S., 2005, Numerical study for mechanical behavior of cement mortar using 3D particle flow code, *Proc. Autumn Korea Society of Rock Mechanics*, 157–162.

Kaiser, P.K., Diederichs, M.S., Martin, C.D. & Steiner, W., 2000, Underground works in hard rock tunnelling and mining, *Proceedings of GeoEng2000*: 841–926, Melbourne.

Martin, C.D., Kaiser, P.K. & McCreath 1999. Hoek-Brown parameters for predicting the depth of brittle failure around tunnels, *Can. Geotech. J.* 36: 136–151.

Potyondy, D.O. & Cundall, P.A. 2004. A bonded-particle model for rock, *Int. J. Rock Mech. & Mining Sciences*, 41: 1329–1364.

Read, R.S. & Martin, C.D. 1996, Technical summary of AECL's Mine-by experiment phase 1: Excavation response, *AECL Report AECL-11311*.

Underground Space – the 4th Dimension of Metropolises – Barták, Hrdina, Romancov & Zlámal (eds)
© 2007 Taylor & Francis Group, London, ISBN 978-0-415-40807-3

Deformation prediction for tunnels at PiccEx junction in London heathrow – An engineering approach

J.Jäger & A.Stärk
Beton-und Monierbau Ges.m.b.H, Innsbruck, Austria

ABSTRACT: The capability of three relatively simple soil models to predict movements in stiff clay are investigated in this study. Calibration of material parameters and theoretical justification for selecting these models are discussed. Finally the predictions are compared with the actually measured deformations and the overall performance of the models discussed.

1 INTRODUCTION

To connect the newly constructed Piccadilly Line Extension tunnels that go to Terminal 5 at London Heathrow with the existing Piccadilly Line tunnels a structure called PiccEx Junction has been built. The structure encloses two turnouts connecting the eastbound and westbound Piccadilly Line Extension to the existing Piccadilly Line tunnels. The two turnouts are enclosed in a combination of sprayed concrete lined (SCL) tunnels and a cut and cover box. Construction and Monitoring of PiccEx Junction is explained in a companion paper (Stärk & Jäger 2007).

This paper deals in particular with the prediction of movement of existing Piccadilly Line tunnels as a result of close by tunnelling operation for the new Piccadilly Line Extension tunnels. The smallest distance between the old segmentally lined tunnels and the new sprayed concrete lined tunnels is only 40 cm.

For carrying out the movement assessment a full 3D finite element model has been chosen. All major construction steps like construction of diaphragm wall of the cut and cover box, plugging of the existing tunnels to control movements, excavation of SCL tunnels using full face excavation according to Laser Shell™ method of construction (Eddie & Neumann 2004) and removal of plug in existing tunnels. As several calculation runs with varying input parameters are required to learn about the sensitivity of the results on modelling assumptions, a numerically efficient model is important for an efficient design process.

Generally soil models taking into account small strain stiffness nonlinearity are recommended for stiff clay. For every days design work a robust model with sound theoretical basis is vital. The mathematical formulation should be such that efficient and robust numerical algorithms can be used. In addition a small number of material parameters should facilitate the model calibration. A further requirement is that the assessment of material parameters should be possible with available test data.

A simple model for predicting short term deformation is considered to be a modified von Mises plasticity model, formulated in total stress space. In order to improve the model performance a nonlinear isotropic and a kinematic hardening law has been added to account for the prefailure nonlinearity.

2 GROUND CONDITIONS

The soil at Heathrow is typical for the greater London area. There is a several meter thick layer of earth and gravel on the surface, which is followed by around 50 m of London Clay and 20 m Lambeth Group. The tunnels at PiccEx Junction are well embedded in London Clay so that there is about a tunnel diameter thick clay cover between the tunnels and the clay/gravel interface. The low permeability of around 10^{-10} m/s and the homogeneity of London Clay make sure that dry conditions prevail during tunnelling.

2.1 K_0-*value*

The heavy overconsolidation of London Clay gives rise to high horizontal effective stresses. In the upper 10 m of the London Clay K_0 varies between 2 and 2.5 and this value tends to decrease with increasing depth, falling to 1.5 at about 30 m depth.

Therefore a typical horizontal in-situ stress at tunnel level is around 1.5 times the vertical stress.

Table 1. Parameters for small strain stiffness model

ε_a	E_u/C_u
$\leq 0.003\%$	5000
0.01%	2800
0.1%	750
1%	150

2.2 *Strength*

The undrained shear strength C_u (in kPa) is depth dependent. The origin of the depth coordinate z (in m) is at the clay/gravel interface.

$$C_u = 37.5 + 6 \cdot z \quad (1)$$

2.3 *Stiffness*

It is well known, that the stress-strain behaviour of soil is highly non-linear and soil stiffness may decay with strain by orders of magnitude.

The mathematical formulation used originally for strain dependent (secant) undrained stiffness Eu is given below (Jardine 1986)

$$\frac{E_u}{C_u} = A + B\cos\left\{\alpha\left[\log_{10}\left(\frac{\varepsilon_a}{C}\right)\right]^{\beta}\right\} \quad (2)$$

In (2) C_u denote undrained shear strength and ε_a is the axial strain of an undrained cylindrical sample. All the other constants A, B, C, α, β are material parameters and must be assessed from tests using curve fitting techniques. Rather than carrying out the curve fitting exercise the strain levels and corresponding stiffness values are given in Table 1.

3 CONSTRUCTION PHASES

The construction phases can be outlined as follows:

- Building diaphragm wall box structure with short ending D-Walls above existing Piccadilly line Tunnels
- Filling foam concrete plug (over a length of 8 m) into existing tunnels to provide sufficient stability and to limit movements of existing tunnels during construction of adjacent tunnels
- Create opening in D-Wall for new Eastbound tunnel and start mining Eastbound Tunnel
- Remove plug from existing Eastbound Tunnel
- Fill plug in existing Westbound Tunnel
- Create opening in D-Wall for new Westbound Tunnel and start mining Westbound Tunnel
- Remove foam concrete plug from existing old tunnels

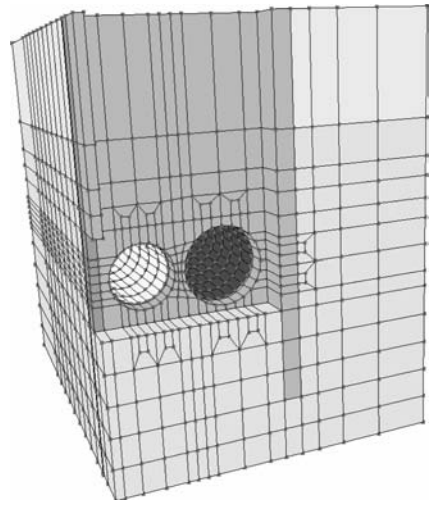


Figure 1. Full 3D model – view from within the box.

4 NUMERICAL MODEL

To take into account the beneficial effect of foam concrete plug and the increasing width of ground pillar with increasing distance from the diaphragm wall a full threedimensional finite element model has been chosen. The finite element program ZSoil v 6.2 (Z_SOIL.PC 2003) has been used. Ground materials (gravel and clay) have been modelled with continuum elements and diaphragm wall and tunnel linings haven been modelled with shell elements. The elastoplastic von Mises material is part of the material library being available in ZSoil. The isotropic hardening and the kinematic hardening model extensions have been added using the interface provided by ZSoil to ad user defined materials.

4.1 *Spatial model*

The model is shown in Figure 1. For greater numerical efficiency symmetry along a vertical plane in the middle between the existing Eastbound and Westbound Tunnels has been taken.

4.2 *Total stress vs effective stress*

As one purpose of this study is to investigate how much sophistication in material modelling is actually required to get a reliable deformation prediction the pros and cons of a total and effective stress analysis shall be discussed. It is well accepted that stress-strain behaviour of soil is correctly described in terms of effective stresses. For some problems involving the deformation of clay, the soil may be idealised as undrained, and for these problems a total stress analysis may be used – provided the following conditions

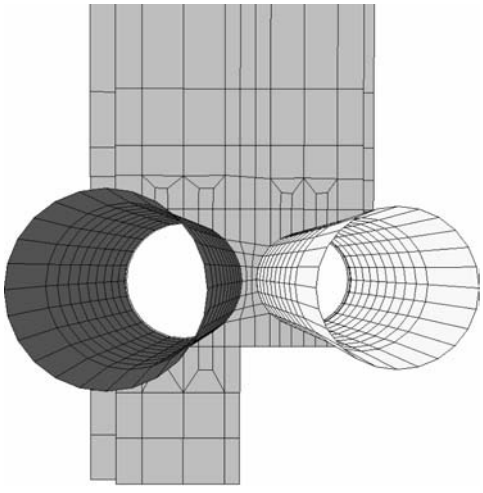


Figure 2. Shell elements for D-Wall, SCL-tunnel (left) and existing segmentally lined tunnel (right) – view from outside the box.

apply. A total stress analysis is only valid in the short term while there is no significant dissipation of the negative pore water pressures induced on clay around the excavation.

4.3 *Material models*

The analysis has been carried out using relatively simple elastoplastic material models adopting total stress approach. The first step was to run the analysis with a simple elastoplastic material selecting an elastic modulus and a corresponding K-value such that they compensate the obvious shortcomings of the existing model. In the next two steps analyses have been run with isotropic and kinematic hardening. A common feature of all three models is that they are based on linearised theory of elastoplasticiy. The linearised strain tensor ε may be decomposed into an elastic part ε^e and a plastic part $\boldsymbol{\varepsilon}^p$

$$\boldsymbol{\varepsilon} = \boldsymbol{\varepsilon}^e + \boldsymbol{\varepsilon}^p \tag{3}$$

The stress is defined by an isotropic tensor function of the elastic part of the strain tensor following Hooke's law expressed. The elastic parameters are the shear modulus G and the Poisson ratio v.

$$\boldsymbol{\sigma} = 2G\left[\boldsymbol{\varepsilon}^e + \frac{\nu}{1-2\nu} tr\left(\boldsymbol{\varepsilon}^e\right)\mathbf{1}\right] \tag{4}$$

The plastic strain rate is calculated from an associated flow rule.

$$\dot{\boldsymbol{\varepsilon}}^p = \gamma \frac{\partial f}{\partial \boldsymbol{\sigma}} \tag{5}$$

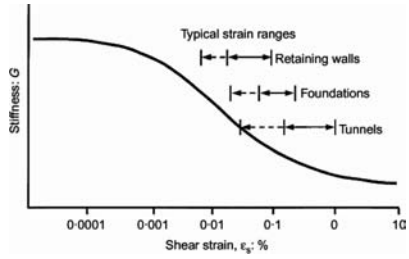


Figure 3. Characteristic stiffness-strain behaviour of soil with typical ranges for laboratory tests and structures (after Mair 1993).

Only stress states inside the yield surface are allowed. This can be the case for purely elastic loading or for strains beyond the elastic limit. The consistency parameter γ ensure that there is no stress state outside the yield surface. Those rules can be expressed mathematically be the Kuhn Tucker complementary conditions. (Simo & Hughues 1998)

$$\gamma \geq 0,\ f \leq 0,\ \gamma \cdot f = 0 \tag{6}$$

4.3.1 *Elastoplastic Model and Parameter Selection*

To compensate for the obvious inability of the elastoplastic model without hardening to simulate small strain stiffness nonlinearity parameters like the elastic modulus and the K-value must be modified.

One possibility to deal with small strain stiffness in a practical way is to take into account the expected strain amplitude in selecting the moduli used. Typical strain ranges for geotechnical structures are those proposed by Mair (Mair 1993).

The proposed strain ranges in Figure 3 are based on stiffness which gave reasonable designs for structures in stiff, overconsolidated clay. A typical characteristic strain in London Clay due to tunnelling has been found to be 0.1%. According to Table 1 this strain corresponds to an undrained stiffness of Eu = 750× Cu.

The von Mises yield surface can be expressed mathematically in the following way

$$f(\boldsymbol{\sigma}) = \|\mathbf{s}\| - \hat{C}_u \tag{7}$$

where **s** is the deviatoric stress tensor and $\hat{C}_u$ is related to the undrained cohesion C_u as shown in (8).

$$\hat{C}_u = 2\sqrt{\frac{2}{3}} C_u \tag{8}$$

It should be mentioned that C_u is depth dependent as defined in (1).

The high K-values near the ground surface are typical for heavily overconsolidated clays. When modelling those initial stress conditions together with low

elastic stiffness material unrealistic movements can be observed. To be able to come up with meaningful analysis results a modified K-value must be introduced. For London Clay it has been found that figures ranging between 0.6 and 1.0 may lead to realistic results. Based on this information the analysis has been carried out with K-value of 1.

4.3.2 *Isotropic hardening model and parameter selection*

The yield surface of the isotropic hardening model is similar to (7)

$$f(\boldsymbol{\sigma}, p) = \|\mathbf{s}\| - \left[\hat{C}_y + \hat{K}(p)\right] \tag{9}$$

The yield limit is expressed by $\hat{C}_y$. To account for nonlinear isotropic hardening with a saturation term an exponential formulation has been chosen, similar to Voce (Voce 1955). The saturation term ensures that there is no stress state beyond undrained shear strength possible. The isotropic hardening modulus is a function of the plastic strain *p*.

$$\hat{K}(p) = \hat{K}_\infty \left(1 - e^{-\delta \cdot p}\right) \tag{10}$$

The rate of plastic strain *p* is defined as

$$\dot{p} = \left\|\dot{\boldsymbol{\varepsilon}}^p\right\| = \gamma \tag{11}$$

Similar to (8) the following relations hold:

$$\hat{C}_y = 2\sqrt{\frac{2}{3}} C_y \,,\; \hat{K}_\infty = 2\sqrt{\frac{2}{3}} K_\infty \tag{12}$$

As the yield limit is given through the yield strain of 0.003% (see Table 1) the yield limit C_y can be calculated from elasticity theory. From undrained shear strength C_u and with C_y the second parameter K_∞ can be computed.

$$C_u = K_\infty + C_y \tag{13}$$

The third parameter δ can be found by curve fitting. For the isotropic hardening model a K-value of 1.5 has been selected for the analysis which is the actually assessed earth pressure coefficient at the elevation of the tunnel axes.

4.3.3 *Kinematic hardening model and parameter selection*

The elastic domain is defined by a von Mises yield function *f* in the stress space

$$f(\boldsymbol{\sigma}, \boldsymbol{\alpha}) = \|\mathbf{s} - \boldsymbol{\alpha}\| - \hat{C}_y \tag{14}$$

where $\hat{C}_y$ again represents the yielding parameter. The evolution equation for the stress type kinematic hardening tensor α is the Armstrong-Frederick evolution equation of the back stress (Armstrong & Frederick 1966).

$$\dot{\boldsymbol{\alpha}} = A \cdot \dot{\boldsymbol{\varepsilon}}^p - B \cdot \dot{p} \cdot \boldsymbol{\alpha} \tag{15}$$

A and B are material parameters and can be assessed considering ultimate state condition. At ultimate state the rate of the back stress is zero and equation (15) can be rewritten.

$$A \cdot \dot{\boldsymbol{\varepsilon}}^p = B \cdot \dot{p} \cdot \boldsymbol{\alpha} \tag{16}$$

Using the definitions for plastic strain rate tensor and plastic strain rate as well as the yield conditions finally leads to the following equation.

$$A \cdot (\mathbf{s} - \boldsymbol{\alpha}) = B \cdot C_y \cdot \boldsymbol{\alpha} \tag{17}$$

From (17) it is evident that the deviatoric stress tensor and the backstress tensor have got the same direction in ultimate state and therefore the ultimate shear strength can be expressed in the following way.

$$\hat{C}_u = \hat{C}_y + \frac{A}{B} \tag{18}$$

From (18) we see that the ratio of A over B determine the undrained shear strength of the model and the absolute values of A and B govern the stiffness between yield initiation and ultimate state. Like for the isotropic hardening model a K-value of 1.5 has been chosen.

4.3.4 *Comparison of models in simple strain path*

To investigate the performance of the three models with regard to their ability to reproduce the required small strain stiffness non-linearity a single element has been subject to a monotonically increasing strain path ranging from 0.001% to 1%. The results thereof are shown in Figure (4).

From Figure 4 it can be seen that for axial strains ε_a greater than 0.1% all three models are close to the required small strain stiffness nonlinearity. For axial strains smaller than 0.1% the deficiencies of elasto-plastic von Mises material become evident. Only the two hardening plasticity models are capable of reproducing the varying secant stiffness at small strains.

5 ANALYSIS RESULTS

Figures 5 to 7 show analysis results and compare predicted horizontal movements along the tunnel alignment (starting at the headwall and ending in 20 m distance from headwall) with actually measured

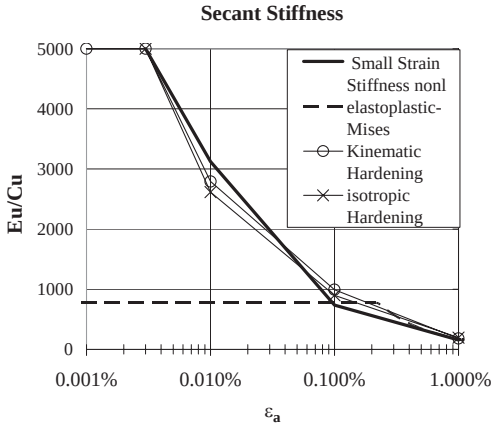


Figure 4. Secant stiffness computed from axisymmetric single element test.

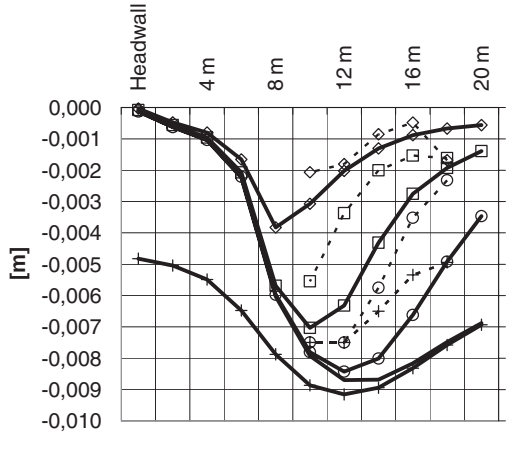


Figure 5. Measured and predicted movements – elastoplastic model.

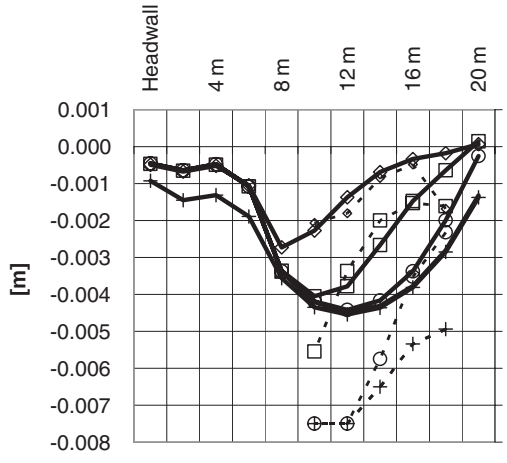


Figure 6. Measured and predicted movements – isotropic hardening model.

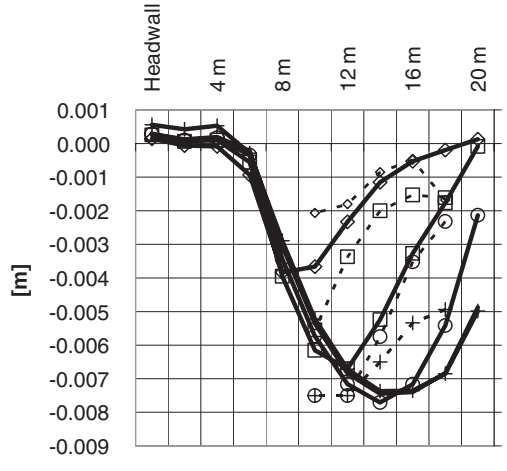


Figure 7. Measured and predicted movements – kinematic hardening model.

movements. The results of five construction stages are shown on the diagrams. For each construction stage there is a separate line for predicted as well as for measured movements. The continuous lines indicate predicted movements and the dotted lines indicate measured movements. The legend in Figure 8 should help to identify each construction stage.

The results shown in Figure 5 suggest that the simple elastoplastic model provides a reasonably conservative prediction of a maximum of 9 mm lateral movement. The maximum measured lateral deformation however is 7.5 mm only. In general there is a more pronounced peak of deformation to be observed in the measured data than in the predicted data. A significant difference between measured data and predicted data is the resilience of the predicted data after removal of the plug. There has been observed no additional movement at all after removing the plug.

The isotropic hardening model in Figure 6 significantly underestimates the lateral deformation predicting a maximum deformation of 4.5 mm only. The resilience after removal of the plug is much smaller than in the elastoplastic model. Looking at the stiffness calculated from monotonic strain path as shown in Figure 4 a better fit with measured data could have been expected. However it seems that the stress reversals taking place in the ground because of the advancing face and the lining installation have got a significant impact on the deformations.

The total deformation predicted by the kinematic hardening model (see Figure 7) is close to 7.5 mm

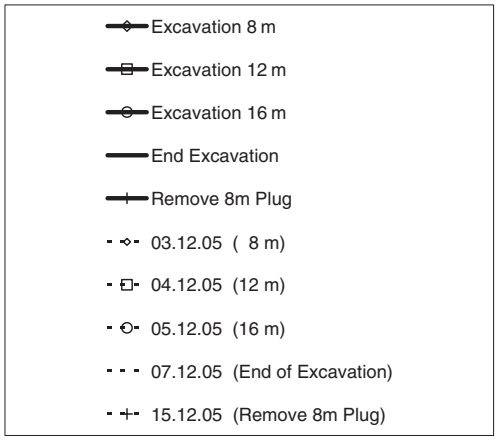


Figure 8. Legend for figures 5 to 7.

which have been measured on site. In general however the locations of peaks of predicted and measured deformation are around 2 m offset. The resilience after plug removal is small, which compares well with actual movements. The strain dependent stiffness in the monotonic strain path is similar for isotropic and kinematic hardening models, however the analysis results from the 3D model with complex loading path show quite significant different performance.

6 CONCLUSIONS

The simple elastoplastic model was relatively successful in predicting the maximum deformations. However it must be noted that some significant assumptions (K-value and stiffness according to 0.1% strain) have been made to end up with realistic results. Those assumptions came from previous experience from tunnelling in London Clay which may not be available elsewhere.

The isotropic and kinematic hardening models on the one hand do not rely on those assumptions, on the other hand however the results are not really better.

To exploit the capability of isotropic and kinematic hardening models more fine tuning of the models based on more complex stress path is necessary. Calibration of models based on monotonic strain path as shown in Figure 4 is probably not sufficient to justify use of more complex models.

Finally it should be mentioned that apart from soil modelling there are some more parameters not addressed in this study (lining stiffness, advance length, actual excavation sequence etc.) which may cause discrepancies between predicted and measured movements.

REFERENCES

Armstrong,P.J., Frederick,C.O., 1966, A Mathematical Representation of the Multiaxial Bauschinger Effect.*Technical Report RD/B/N731*, General Electric Generating Board.

Eddie, C & Neumann, C 2004. Development of LaserShell™Method of Tunneling. Proc. *North American Tunneling Conference 2004*, Atlanta. Rotterdam: Balkema.

Jardine, R. J., Potts, D. M., Fourie, A. B. & Burland, J. B. (1986). Studies of the influence of non-linear strain characteristics in soil-structure interaction. *Geotechnique 36, No. 3, 377–396*.

Mair, R.J (1993) Unwin Memorial Lecture 1992 Developments in geotechnical engineering research: application to tunnels and deep excavation. *Proc. Instn Civ. Engng, 1993, 93, Feb. 27–41*.

Simo, J.C., Hughes, T.J.R (1998) *Computational Inelasticity*, Springer Verlag 1998 New York.

Stärk, A. & Jäger, J., (2007). London Heathrow Terminal 5 - Construction and monitoring of Piccadilly Line Extension Junction, *AITES World Tunnel Congress 2007, Prague, 5–10 May 2007*. Rotterdam: Balkema.

Voce, E., 1955, *Metallurgica 51*,219

Z_SOIL.PC, 2003-Zace Services Ltd, see http://www.zace.com.

Underground Space – the 4th Dimension of Metropolises – Barták, Hrdina, Romancov & Zlámal (eds)
© 2007 Taylor & Francis Group, London, ISBN 978-0-415-40807-3

Improved design method for 2-arch tunnel

Wan Gi Jeon, Kyeong-Han Jeong & Ju Hyoung Lee
Dodam Engineering & Construction CO., LTD, Korea

Hyun-Ho Ahn & Seok-Won Lee
Dept. of Civil and Environmental System Engineering, Konkuk University, Seoul, Korea A.T.

ABSTRACT: Most conventional 2-arch tunnels have been constructed with pilot excavation of center tunnel-utilized 3-step excavation. However, such method has low constructability due to the confined space of the center tunnel and is exposed to various issues, including leakage from the required complex waterproofing-drainage system. Accordingly, this research studied designing an improved 2-stage 2-arch tunnel excavation method in which the proceeding tunnel is constructed after establishing structural stability of preceding tunnel through reinforcement shotcrete or concrete. First, a scaled model test using plaster was conducted to validate the improved 2-arch tunnel construction method. Based on the experimental test results, various parametric studies were conducted through numerical analysis. Findings from those studies yielded a standard cross section with the central support thickness at 40 to 60 cm. The suitable amount of support and a standard supporting pattern were then suggested through converted breadth estimation. Bench cut and/or CD cut excavation sequences were suggested for excavation of the proceeding tunnel.

1 INTRODUCTION

As the number of tunnels with considerably close separation distance increases in consideration for inferior ground conditions, civil complaints, minimization of environmental impact, etc., application of the 2-arch tunnel has recently been on the rise. Most of current 2-arch tunnels are a 2 arch-1 pilot that utilizes supporting function of the central wall. 2 arch-1 pilot tunnels are, however, complex in constructing the central tunnel and inherent with issues such as waterproofing-drainage. To this end, this research aims to present an improved 2-arch tunnel design method capable of attaining safety, constructability, and economic efficiency.

2 2-ARCH TUNNEL CONSTRUCTION METHOD

2.1 *Issues with conventional 2-arch tunnels*

While conventional tunnels are constructed in two mining phases of left and right main tunnels, the standard construction sequence of 2-arch tunnels, as shown in Figure 1, take place in three-phases of central tunnel mining, central pillar, and main tunnel mining. Consequently, the cycle time in 2-arch tunnel construction is longer in comparison to conventional tunnels,



Figure 1. Panoramic view of a conventional 2-arch tunnel construction.

resulting in lowered constructability and economic efficiency.

On the construction front, the narrow central tunnel width makes equipment use difficult and main tunnel blasting and shotcreting causes damage of waterproofing system (Figure 2). Furthermore, protective facilities need to be installed to the central wall unit during blasting.

Maintenance wise, water can leak from the upper sections of the central wall unit and the upper lining joint of the main tunnels to cause road surface freezing. Furthermore, icicles could form on the ceiling to impede vehicle safety and cause additional erosion of the surrounding concrete. These aforementioned

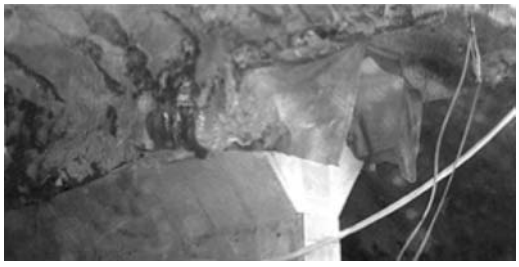


Figure 2. Waterproof sheet damage.

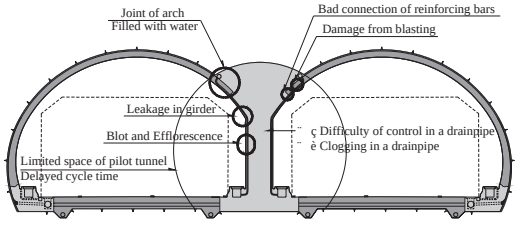


Figure 3. Issues with conventional 2-arch tunnels.

issues with the conventional 2-arch tunnel construction method are summarized in Figure 3.

2.2 *Improved 2-arch tunnel design method*

Improved 2-arch tunnel design method eliminates the preceding excavation of the central tunnel found in the conventional 2-arch tunnel construction method and, like adjacent tunnel construction, excavates the preceding tunnel first and then installs reinforcement shotcrete to gain structural safety first before excavating the proceeding tunnel. The matter of improvement here is that reinforcement shotcrete or concrete are added as substitutes to the central wall unit in preventing stress concentration on the central section between the expected preceding and proceeding tunnels. This effectively controls the displacement and stress generated as per excavation of the proceeding tunnel.

Consequently, previously raised issues of constructability, economic efficiency and waterproofing-drainage issues can be resolved at the source through this improvement.

3 VERIFICATION THROUGH SCALED MODEL TESTS

3.1 *Model material and dimension analysis*

The material used in the scaled model tests must be able to sufficiently reflect the physical properties of the base rock from the research subject site. In this respect, a mixture of sand, plaster, and water was used. The strength of the model required in this research was

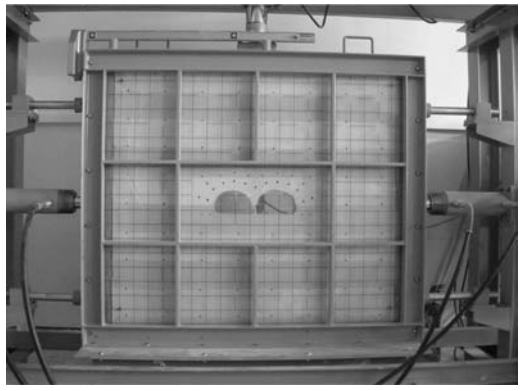


Figure 4. Scaled model testing device.

3 kgf/cm^2. Various mixture ratios were experimented with, and it was found that a ratio of 2.8:1.0:1.9 that has been cured over fifteen days yielded the desired strength.

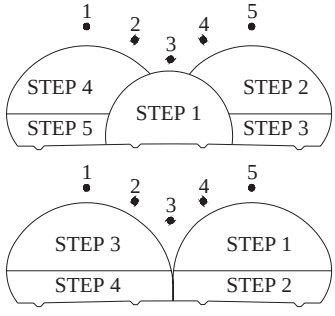
Dimension analysis (Everling, 1964; Hobbs, 1968) between the construction site condition and the reduced model must be conducted so that the site conditions can be sufficiently recreated in the reduced model test. Where the three fundamental dimensions are Length [L], Mass [M], and Time [T], the reduction ratio of the length is calculated first and then the length reduction ratio is used to derive time, density, mass, stress, and strength reduction ratios in that sequence.

The length reduction ratio was set to 1/89.8 after determining the model tunnel width to be 30 cm in consideration for the model's dimensions ($1000 \times 1000 \times 100$ mm) and the onsite tunnel's width of 2,694 cm. The time reduction ratio then became 1/9.48. With the mixture density being 1.75 g/cm^2 and with the in-situ density being 2.141.75 g/cm^2, the density [ML^{-3}] reduction ratio became 1/1.22. Where the length reduction ratio has been set at 1/89.8, the mass reduction ratio became $1/(8.83 \times 10^5)$. Subsequently, the stress, elastic modulus, and strength [ML^{-1}T^{-2}] reduction ratios became 1/109.4.

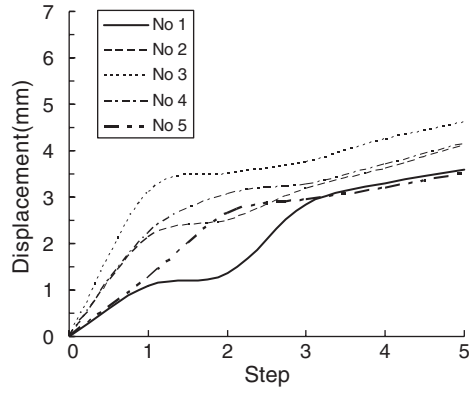
3.2 *Testing method and analysis program*

A model testing device with dimensions of $2290 \times 1930 \times 710$ mm (L × H × W), was fabricated for this research as shown in Figure 4. The lower section is secured with a steel plate, and the front and rear sides are made of acrylic boards. In addition, three pressure devices, one on the top, one on the right side, and one on the left side, were installed.

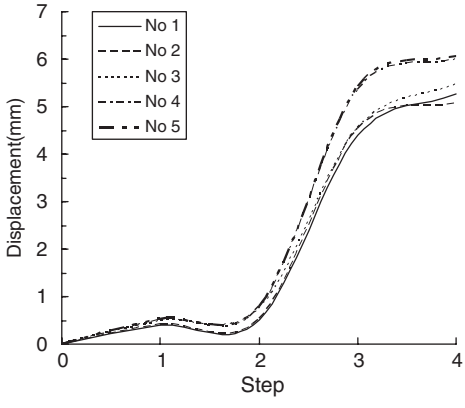
First, the model was prepared according to the mixture and then cured over fifteen days. Dots were then drawn in specific distances to be used in measuring displacements using PhotoModeler Pro 5. Once the model was prepared, the load was pressurized.



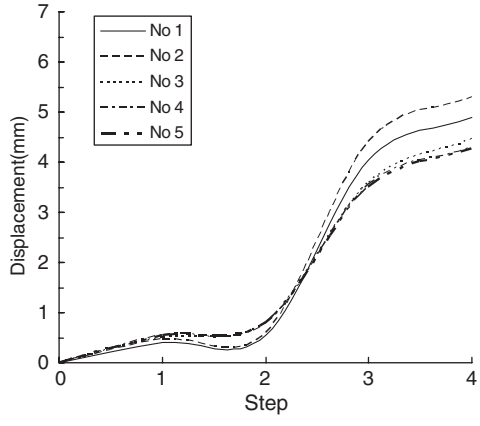
(a) Construction step for 2-arch tunnel.



(b) Result based on the conventional method.



(c) Result based on the improved method without central rein-forcement.



(d) Result based on the improved method with central rein-forcement.

Figure 5. Experimental test results.

Digital pictures were taken at each stage of the load increase and the displacement was analyzed using PhotoModeler.

3.3 *Model testing results*

Figure 5 shows the results from the three model tests conducted in this research. Figure 5(b) is the results based on the conventional 2-arch tunnel construction method. Figure 5(c) is the results based on the improved 2-arch tunnel construction method, but without the reinforcement shotcrete installed to the central section. Figure 5(d), on the other hand, is the results based on the improved 2-arch tunnel construction with reinforcement shotcrete.

As shown in Figure 5(b), the conventional 2-arch tunnel construction produces significant displacement during central tunnel excavation(step 1). In the case of left and right main tunnel excavations, however due to the installation of central pillars, the ratio of increment of displacement showed somewhat of a decrease. Figure 5(c) reveals that the improved 2-arch tunnel construction method without central reinforcement resulted in greatest displacements at the preceding tunnel's crown (No. 5) and the sidewalls (No. 4) and in significant displacement at the proceeding tunnel's crown (No. 1). In the case of the improved 2-arch construction method with central reinforcement shown in Figure 5(d), however, displacements at the preceding tunnel's crown (No. 5) and the sidewalls (No. 4) were significantly reduced, and the greatest displacement took place at the proceeding tunnel's sidewalls (No. 2).

Considering that the tests did not replicate the rockbolt, shotcrete, and other supports, although comparison of the conventional 2-arch tunnel construction technique to the improved version shows similar displacement results from the tests, it is clear that installation of supports such as rockbolt and shotcrete

in actual constructions does support the validity of the improved 2-arch construction method. This validity will be described in following numerical analysis results.

4 IMPROVED 2-ARCH TUNNEL DESIGN THROUGH NUMERICAL ANALYSIS

Through the aforementioned model testing, the improved 2-arch tunnel construction method has been proven to be capable of attaining constructability and economic efficiency through use of suitable supports. Consequently, in this section, the various numerical analyses were conducted to determine the central reinforcement shotcrete thickness, suitable amount of supports and the excavation sequence for the proceeding tunnel. Finally, improved design method for 2-arch tunnel was suggested.

4.1 *Tunnel cross section design*

The improved 2-arch tunnel, as mentioned before, is free of the central tunnel excavation phase. Therefore, it does not require installation of the central wall unit but produces stress concentration at the central section between the preceding and proceeding tunnels. Consequently, reinforcement shotcrete or concrete has to be installed additionally as a substitute to the central wall unit in supporting the stress concentration in order to control the displacement and stress resulting from excavation of the proceeding tunnel. A numerical analysis was conducted to derive the suitable shotcrete thickness as shown in Figure 6. Included in Table 1, Figure 7 and Figure 8 are input properties applied to the analysis, 3D modeling and analysis results, respectively.

As shown in Figure 8, 2D finite difference analysis (FLAC) and 3D finite element analysis (Pentagon-3D) with central reinforcement shotcrete thickness as the parameter showed that the central section's bending compressive stress was stabilized to within the permissible range when the thickness is over 60 cm in the 2D analysis and when over 40 cm in the 3D analysis.

With the results from the analysis of the improved 2-arch tunnel's behavioral characteristics as per the shotcrete thickness as the basis, a standard cross section of 40 cm or thicker central reinforcement thickness as shown in Figure 9 is suggested in this study.

Case Categorization by Support Thickness

- 2D : 40 cm, 50 cm, 60 cm, 70 cm, 80 cm
- 3D : 20 cm, 40 cm, 60 cm, 80 cm

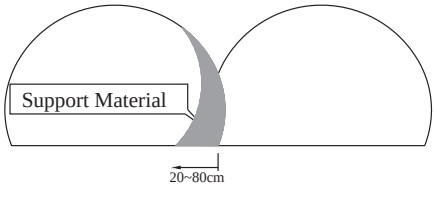


Figure 6. Central reinforcement and analysis case.

Table 1. Base rock and central reinforcement shotcrete properties.

Category	γ_t	E	v	c	ϕ	K_0
Base rock class	2.3	180,000	0.28	60	33	1.0
Shotcrete	1.8	1500,000	0.2	50	40	1.0

4.2 *Calculation of a suitable amount of supports*

The entire 2-arch tunnel breadth is similar to a four-lane tunnel. However, because the central section is supported by central supports and the stress can

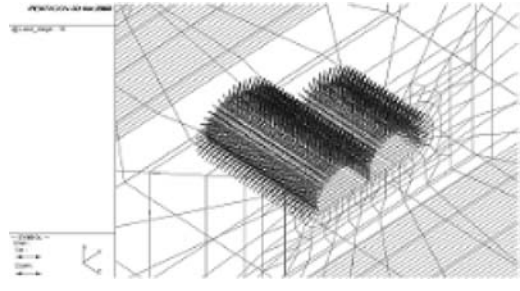


Figure 7. Modeling of 3-D element analysis.

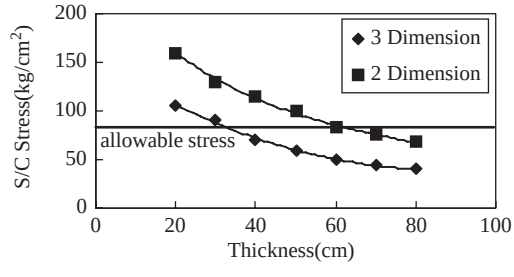


Figure 8. Bending compressive stress of central section.

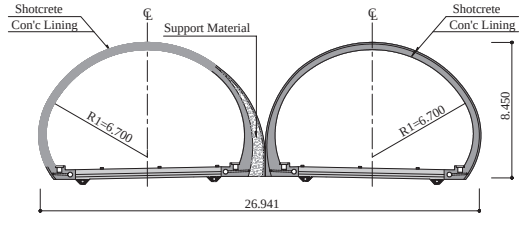


Figure 9. Suggested cross section of the improved 2-arch tunnel.

be reduced through arching effect during main tunnel excavation, designing the 2-arch tunnel with the four-lane breadth can result in an excessive design. Therefore, in reviewing the amount of supports in the improved 2-arch tunnel, 2-, 3-, and 4-land tunnel cross sections and the 2-arch tunnel's displacement were numerically compared and analyzed to determine the converted tunnel width. This width was then applied as the maximum width in calculating the suitable amount of supports.

As shown in Figure 10, the analysis resulted in a 2-arch tunnel's displacement at crown and convergence similar to those of a 2-lane or a 3-lane tunnel, with maximum displacement distributed between 2-lane and 3-lane tunnel values. Consequently, the 3-lane tunnel breadth was applied in determining the support pattern for the improved 2-arch tunnel and then Q-system and RMR were used to derive the suitable amount of supports as shown in Table 2.

4.3 *Excavation sequence of proceeding tunnel*

Excavating the proceeding tunnel after excavating the preceding tunnel and reinforcing the central section results in transference of the preceding tunnel's load over to the proceeding tunnel and greater stress concentration on the proceeding tunnel than the preceding tunnel. To this end, a proceeding tunnel excavation method capable of providing tunnel stability was sought after.

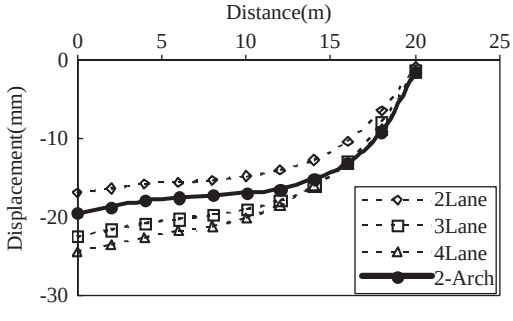


Figure 10. Displacement at crown by excavation distance.

Bench cut and CD cut excavation techniques were selected as four proceeding tunnel excavation cases and then numerically analyzed. After which preceding tunnel, proceeding tunnel, and central support stabilities were reviewed.

Figures 11 and 12 show the analysis cases and modeling, respectively, for which the following analysis criteria were applied :

- Analysis Criteria
  - Program: MIDAS GTS
  - Foundation: Base Rock Class – IV (Table 2)
  - Support Strength: fck = 210 kg/cm^2
  - Support Thickness: 60 cm (Figure 6)

Based on the analysis results, the displacements of preceding and proceeding tunnel were stable to within

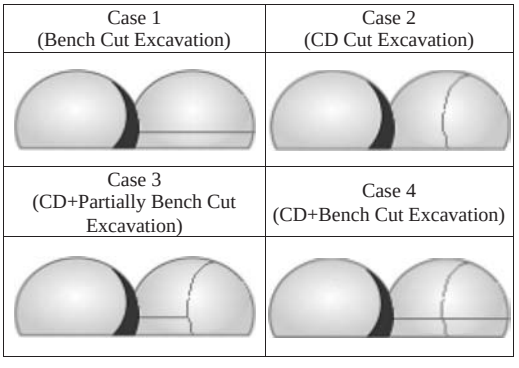


Figure 11. Analysis cases.

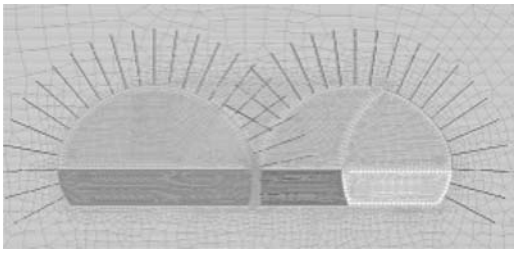


Figure 12. Finite element analysis modeling (GTS).

Table 2. Calculation of a suitable amount of supports.

Support Class		1	2	3	4	5
Base rock category	Q	Over 40	40 ~ 10	10 ~ 1	1 ~ 0.1	Under 0.1
	RMR	Over 81	80 ~ 61	60 ~ 41	40 ~ 21	Under 20
Shotcrete (cm)		80	80	100	180	200
Rock Bolt	Length (m)	4.0	4.0	4.0	5.0	5.0
	Vertical Distance (m)	3.0	3.0	2.0	1.2	1.0
	Horizontal Distance (m)	3.0	1.5	1.5	1.2	1.0

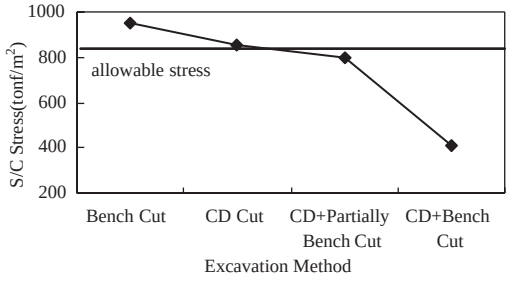


Figure 13. Bending compressive stress of shotcrete by excavation method.

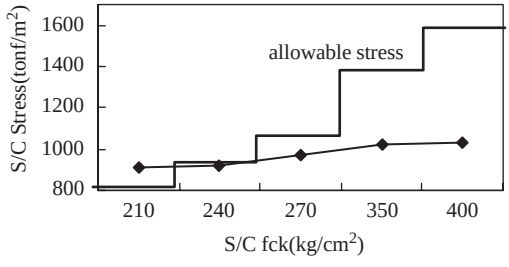


Figure 14. Bending compressive stress of shotcrete by support strength.

11 mm in all cases and, as shown in Figure 13, bending compressive stress of shotcrete satisfied the permitted value in Case 2 (CD cut excavation).

However, because proceeding tunnel's CD cut excavation, which is the only case to satisfy the allowed value, is a constructability lowering cause, the range of possible bench cut excavation with enhanced central support system strength was reviewed. The support strength applied to this was $f_{ck} = 210$, 240, 270, 350, 400 kg/cm^2, and all other input data remained the same. Figure 14 shows stability review results by support strength.

According to the analysis results, bench cut excavation is possible on a foundation of base rock class IV (Table 2) or higher when support strength is $f_{ck} = 240$ kg/cm^2 or greater. For soft ground conditions of base rock class V or lower, portals, and fault zone, it is recommended that application of CD cut excavation or CD + bench cut excavation is safe.

5 CONCLUSIONS

Conventional 2-arch tunnels carry clear areas of improvement, such as construction of a central tunnel and waterproofing/leakage issues, and are not economically efficient due to the need to increased cycle times from installation of a central tunnel and a central wall unit. To this end, this research has presented an improved 2-arch tunnel construction method that eliminates the central tunnel and that involves excavating the preceding tunnel first and then reinforcement shotcreting to gain structural safety first before excavating the proceeding tunnel. Conclusions from the research are:

(1) As the result of reviewing the improved 2-arch tunnel construction method's validity through scaled model tests, it has been found that there is no problem when a suitable support system is installed.
(2) As the result of support system stress review through 2D and 3D numerical analysis, the suitable central shotcrete thickness is found to be 60 cm under 2D analysis and 40 cm under 3D analysis. This is a difference as per the existence of longitudinal arching effect and load distribution rate. Finally, the improved 2-arch tunnel's cross section that has been applied with a 40 to 60 cm reinforcement shotcrete was suggested.
(3) As the result of calculating the converted breadth for calculation of the amount of supports for the improved 2-arch tunnel, the displacement of 2-arch tunnel was found to be similar to that of a 3-land tunnel. Therefore, the amount of supports as per a 3-lane tunnel was calculated and suggested.
(4) As the result of reviewing the excavation sequence of proceeding tunnel, bench cut excavation for foundations of rock base class IV or higher and CD cut excavation for foundations of rock base class V or lower were suggested. It was also found that here the central support system's strength needs to be $f_{ck} = 240$ kg/cm^2 or higher.

ACKNOWLEDGEMENTS

This paper was funded by the Korea Institute of Construction and Transportation Technology Evaluation and Planning under the Ministry of Construction and Transportation in Korea (Grant No. 04-C01).

REFERENCES

Everling, G. 1964. Model study of rock-joint deformation. *Int. J. Rock. Mech. Min. Sci & Geomech. Abstr.* 1: pp. 319–326.

Hobbs, D.W. 1968. Scaled model study of strata movement around mine roadways. The dependence of roadway closure upon rock strength. *Int. J. Rock. Mech. Min. Sci & Geomech. Abstr.* 5: pp. 219–235.

Underground Space – the 4th Dimension of Metropolises – Barták, Hrdina, Romancov & Zlámal (eds)
© 2007 Taylor & Francis Group, London, ISBN 978-0-415-40807-3

Evaluation of strength parameters for the single shell tunnel in Korea

Kim, Hak Joon
Daejeon University, Dept. of Geological Engineering

Lee, Seong Ho, Shin, Hyu Seong & Bae, Gyu Jin
Korea Institute of Construction Technology

ABSTRACT: Shotcrete is used as a permanent lining in single shell tunnels even though shotcrete has been used as a temporary lining in NATM tunnels. Therefore, the accurate evaluation of strength parameters is very crucial because the reliable estimation of loads acting on the shotcretes is necessary to maintain the stability of tunnels. The evaluation of strength parameters of the ground for the single shell tunnels should be investigated to adapt the method in Korea because the geological condition of Korea is different from those of other countries. Rock classification and strength parameters obtained from 25 tunnel sites were investigated for this study. Support types for the different rock classes are suggested for the single shell tunnels in Korea based on the NMT. The support types in terms of both Q and RMR values are given based on the correlation of Q and RMR values obtained from the case studies.

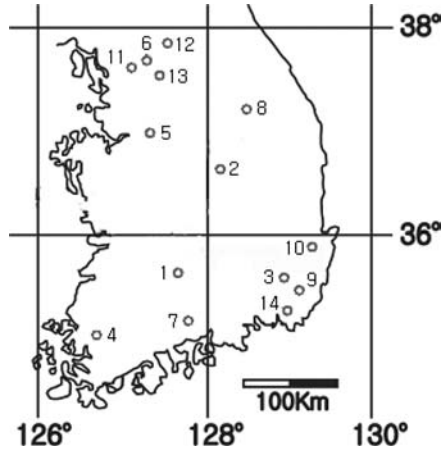
1 INTRODUCTION

Shotcrete and rockbolts are used as a permanent lining in the single shell tunnel. The method has been widely used in several countries such as Norway, Sweden, and Finland. However, the method was not used in Korea even for very good rock mass conditions because the research for the single shell tunnel was not actively conducted in Korea.

Rock classification and strength parameters obtained from 25 tunnel sites were investigated for the application of single shell tunnels in Korea. The characteristics of rock masses and the values of strength parameters for each rock mass class were obtained from the case studies. Support types for the single shell tunnels were suggested considering the characteristics of rock mass conditions in Korea and support patterns used in the other countries. The support types in terms of both Q and RMR values are given based on the correlation of Q and RMR values obtained from the case studies.

2 CASE HISTORIES OF ROCK MASS CLASSIFICATION IN KOREA

Rock classification system, the RMR system and the Q system, and strength parameters obtained from 25 tunnel sites were investigated for the application of single shell tunnels in Korea. The location of 25 tunnel sites is shown in Figure 1. The following results were obtained from the case studies.



Tunnel Name
1. Jeom-gok
2. Ma-gu, Ho-buk, Geon-cheon
3. Neung-dong
4. Cheong-ho, Nam-ak
5. Geum-gang No.3
6. Wol-mun, Do-gok, Pal-dang
7. Jin-sang, Ok-gok Nos.1 & 2
8. Song-hak
9. Beop-ki
10. Yang-buk
11. Yong-ma
12. Dae-seong No.1~No.4, Cheong-pyeong, Keun-bong
13. Dae-ssang
14. Su-jeong-san

Figure 1. Location of case histories used for this study.

2.1 *Correlations between the Q and the RMR*

The correlation between the Q-index and the RMR were given by several authors (e.g. Bieniawski, 1974;

Rutledge & Preston, 1978; Goel et al., 1995). The correlation is not so good because the two systems use different parameters and different weightings to similar parameters. However, the correlation between the two systems is pretty good according to the current study as shown in Figure 2 and the following relationship is applicable:

$$RMR = 7.40 Ln(Q) + 39.5 \quad (r^2 = 0.81) \qquad (1)$$

The correlation between the Q and the RMR systems shown in Equation 1 is very close to the correlation given by Geol et al. (1995).

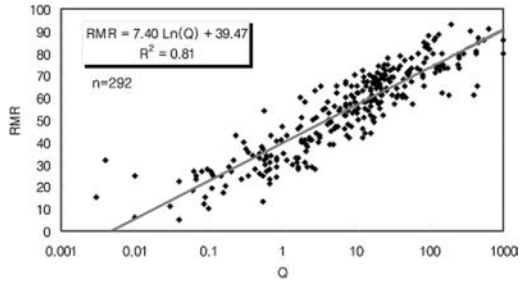


Figure 2. Correlation between RMR and Q in the study area.

2.2 *Values of strength parameters for each rock mass class*

The values of strength parameters used in 25 tunnelling sites were investigated with respect to rock mass classes of the RMR as shown in Figure 3 and summarized in Table 1. The deformation modulus and the cohesion show wide range of values even for the same rock mass class, whereas the friction angle, Poisson's ratio, and unit weights have small range of values within the same rock mass class.

The obtained values of cohesion are generally higher than those given by Bieniawski (1989) but lower than those given by Trueman (1988). The values of friction angles are comparable with those suggested by Bieniawski (1989) except for Classes IV and V, which show higher values than Bieniawski's. Poisson's ratio and unit weight values are generally agreed with those reported in Korea (e.g. Shin et al., 2000).

The strength parameters given in Table 1 are expected to use in the preliminary tunnel design in Korea.

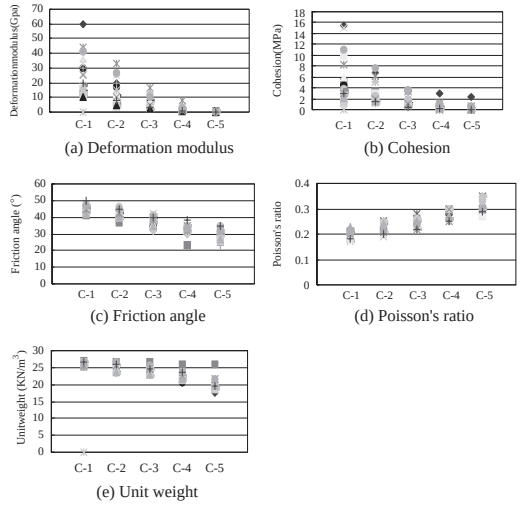


Figure 3. Values of strength parameters with respect to rock mass classes (C).

Table 1. Average values of strength parameters for rock mass classes.

Rock mass class	Deformation modulus (MPa)	Cohesion (MPa)	Friction angle (°)	Poisson's ratio	Unit weight (kN/m^3)
I (Very good rock) RMR: 81–100	23.34	5.32	43	0.20	26.1
II (Good rock) RMR: 61–80	12.16	2.88	42	0.22	25.0
III (Fair rock) MR: 41–60	5.49	1.47	38	0.24	23.9
IV (Poor rock) RMR: 21–40	1.71	0.60	33	0.28	22.3
V (Very poor rock) RMR: < 20	0.36	0.26	30	0.30	20.0

3 ROCK MASS CLASSIFICATIONS FOR SINGLE SHELL TUNNELS

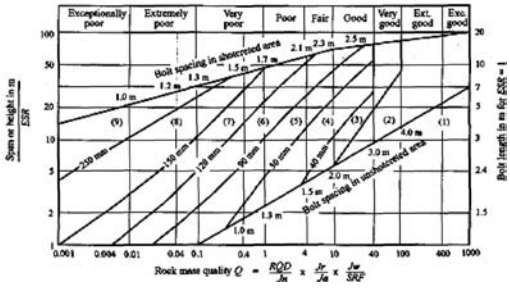
3.1 *Rock mass classifications for single shell tunnels in other countries*

Barton et al. (1974) proposed a Q-system on the basis of a large number of case histories of underground excavations. The proposed support system is based on the rock bolts and shotcretes or the rock bolts and wire mesh reinforced shotcretes. Barton et al. (1992) presented the methods, philosophy, and materials of Norwegian Method of Tunnelling (NMT). In essence, NMT combined the use of Q-system characterization, Q-system permanent support design, and the rock bolts and steel fibre reinforced shotcretes.

Grimstad & Barton (1993) updated the original chart of support categories suggested by Barton et al. (1974) to reflect the increasing use of steel fibre reinforced shotcrete in underground excavation as shown in Figure 4.

Geofront (2000) suggested rock mass classifications for the single shell tunnel in Japan. According to Geofront (2000), the NMT cannot be applied directly for the single shell tunnel in Japan because the geological condition of Japan is very much different from that of European countries.

Geofront (2000) considers the rock mass as a soft rock if the uniaxial compressive strength of a rock specimen is lower than 30 MN/m^2 or absorption index of a rock specimen is greater than 5%. Additional support materials for resisting the bending moments or the concrete lining in the invert of a tunnel are recommended to use because the safety of the single shell tunnel cannot be guaranteed for such ground conditions. The contents of steel fibres are determined to be 30 kg/m^3 and 40 kg/m^3 for the amount of water inflow of less than and greater than 50 *l*/min/km, respectively. However, the contents of steel fibres can be increased up to 50 kg/m^3, depending on the site conditions.



1) Unsupported
2) Spot bolting
3) Systematic bolting
4) Systematic bolting with 40-100mm unreinforced shotcrete
5) Fibre reinforced shotcrete, 50-90mm, and bolting
6) Fibre reinforced shotcrete, 90-120mm, and bolting
7) Fibre reinforced shotcrete, 120-150mm, and bolting
8) Fibre reinforced shotcrete, >150mm, with reinforced ribs of shotcrete and bolting
9) Cast concrete lining

Figure 4. Estimated support categories based on Q for NMT. (After Grimstad & Barton, 1993)

The support categories for the single shell tunnels in Japan are based on Figure 4 with some modifications. The thickness of inner layers in single shell tunnels are the same as the thickness of shotcretes in NATM tunnels, whereas the thickness of outer layers in single shell tunnels is determined using the equivalent thickness of the concrete lining in NATM tunnels, considering the high strength of shotcretes in single shell tunnels.

3.2 *Rock mass classifications for single shell tunnels in korea*

Even though new rock mass classification system is proposed for the single shell tunnel in Korea, the verification of the system is difficult due to the lack of case histories of the single shell tunnel in Korea. Therefore, rock mass classification based on the Q-system will be appropriate, considering the wide use of the Q-system in Korea and similarities of rock mass conditions between Korea and Norway.

The Q-system has several advantages over other methods because the system was verified from a large number of case histories. However, the outcrop which is necessary to investigate the rock mass conditions in Korea for the determination of support categories may not be enough compared to that of Scandinavia. Therefore, the credibility of the investigation for the parameters determined in the tunnel face can be questioned. The RMR system, which is widely used in Korea due to its simplicity, is suggested to use in this study with the Q-system for the determination of the support categories of the single shell tunnels in Korea.

It is necessary to limit the application of the single shell tunnels to the good ground conditions because the single shell tunnelling method is very new in Korea. However, various rock mass classes generally occur even in the same tunnel site. The rock mass classes distributed in the 11 tunnel sites are summarized in Table 2. The rock mass classes between I and III from the RMR-system are distributed along the 87% of the tunnel section, whereas the rock mass classes of IV and V are also distributed 13% of the tunnel section. Therefore, the poor ground conditions should be also considered for the application of the single shell method in Korea.

The application of the single shell method for the road and railway tunnels in Korea is recommended to use for the Jw value greater than 0.66 and the Q value greater than 1. The limitation of Jw value is due to the difficulties of the groundwater handling in the single shell tunnel. The limitation of the method to

Table 2. Distribution of rock mass classes along the tunnel section.

Tunnel name	Class (Units: %) I	II	III	IV	V	Total
Jeom-gok	29.1	25.2	24.3	10.9	10.4	100
Ma-gu, Ho-buk, Geon-cheon	13.1	21.2	45.2	17.3	3.2	100
Neung-dong	39.4	42.1	10.9	1.4	6.4	100
Cheong-ho, Nam-ak	34.4	54.0	6.9	3.4	1.4	100
Geum-Gang No.3	21.0	36.5	29.4	9.6	3.5	100
Wol-mun, Do-gok, Pal-dang	50.7	27.6	10.9	9.8	1.0	100
Average	31	35	21	9	4	100

Table 3. Percent distribution of Jw and Q suitable for the application of the single shell method.

Tunnel	(Units:%) (Jw ≥ 0.66)	(Q ≥ 1)	Jw ≥ 0.66 &Q ≥ 1
Jeom-gok	100	83.3	83.3
Ma-gu, Ho-buk, Geon-cheon	57.1	61.9	33.3
Neung-dong	66.7	66.7	41.7
Cheong-ho, Nam-ak	100	100	100
Geum-Gang No.3	68.8	75	68.8
Wol-mun, Do-gok, Pal-dang	100	48	48
Average	82	73	63

Table 4. Rock mass conditions for tunnels without support requirement.

Rock mass classifications	Rock mass classes
RMR	RMR(No Support) = 22 ln(Equivalent dimension) + 25, Kaiser et al. (1986) ex) For a 12 m wide tunnel RMR ≥ 80 Class I(RMR ≥ 81) : No support required except for occasional spot bolting
Q system	Maximum unsupported span = 2 ESR $Q^{0.4}$ ex) Equivalent dimension 10 m tunnel, Q > 60, Barton et al. (1974) Unsupported span = 2 $Q^{0.66}$, Barton et al. (1980)

the Q value above 1 is related to the lack of experiences making the high strength shotcrete in excess of 360 kN/m^2 and corrosion protected rock bolts. However, support categories should be considered for the Q values lower than 1 because various rock mass classes generally occur together as shown in Table 2. What percentage of the tunnel length along the entire tunnel length should satisfy the above requirements of Jw and Q for the application of the single shell method needs to be determined considering the construction cost. If the construction of the single shell tunnel continues with the accumulation of field measurements, the single shell method can be extended for the more challenging rock mass conditions.

3.3 *Suggested support requirements for the single shell tunnel in korea*

The application of the single shell method for the road and railway tunnels in Korea was recommended to use for the Q value greater than 1 and the Jw value greater than 0.66 as mentioned in the previous section. Table 3 shows the investigated results of 11 case histories for the Q value greater than 1 and/or the Jw value greater than 0.66. Average values of 82% and 73% of the total tunnel length have a Jw value greater than 0.66 and the Q value greater than 1, respectively. An average value of 63% satisfies both Jw and Q requirements at the same time.

Table 4 shows rock mass conditions without support requirements for the construction of a tunnel. Generally no support is required for this kind of rock mass conditions except spot bolting.

The selection of support for the single shell tunnel in Korea is proposed based on Figure 4, Table 4, and the study of Geofront(2000) as shown in Table 5. Table 5 is for a 12m wide tunnel and Figure 4 may be used for the other size tunnel.

Support for the single shell tunnel is given in accordance with the RMR values as well as the Q values using the correlation of the RMR and the Q in order to improve its usability. The correlation between the RMR and the Q for Table 5 is obtained based on the studies of Bieniawski (1974), Rutledge & Preston (1978), and Equation 1 because they have good correlation ratios compared to other suggestions. Conservative RMR values are chosen among the correlative values as shown in Table 6.

Field measurements are necessary to verify the suggested support for the single shell tunnel in Korea even though field monitoring is less used in NMT compared to NATM. More reliable support requirements for different ground conditions can be proposed if field measurements are collected from various case histories.

4 CONCLUSIONS

Rock classification and strength parameters obtained from 25 tunnel sites were investigated for the application of single shell tunnels in Korea. The values of strength parameters for each rock mass class were presented from the case studies.

Table 5. Guidelines for the support of 12 m wide single shell tunnels in Korea. (Modified after Geofront, 2000)

		NATM support	Shotcrets for single shell tunnels			
Q	RMR	Total thickness of lining (cm)	Inner layer (cm)	Inter-mediate layer (cm)	Outer layer (cm)	Total thickness of lining (cm)
>60	>81	30	5		5 (30)	10
>10	65–80	30–35	5	5	5 (30)	15
3–10	55–65	35	5	10	5 (30)	20
1–3	45–55	40	10 (30)	10 (30)	5 (30)	25
0.1–1	30–45	40	10 (30)	10 (30)	5 (30)	25
0.01–0.1	15–30	45	15 (40)	10 (40)	5 (30)	30
<0.01	<15	50	25 (50)	10 (50)	5 (30)	40
(Tunnel portal)		55	25 (50)	10 (50)	10 (30)	45

* Note: ( ) is contents of steel fibers in shotcrets in kg/m^3.

Table 6. Correlation between Q and RMR used for the support requirements of single shell tunnels.

Q	RMR (Bieniawski, 1974)	RMR (Rutledge & Preston, 1978)	RMR (Current Study)	RMR (Chosen)
10	65	57	57	65
3	54	49	48	55
1	44	43	40	45
0.3	33	36	31	35
0.1	23	29	22	30
0.01	3	16	5	15

Support types for the different rock mass conditions are suggested for the single shell tunnels in Korea based on the NMT. Support for the single shell tunnel is given in accordance with the RMR values as well as the Q values using the correlation of the RMR and the Q in order to improve its usability.

The application of the single shell methods for the road and railway tunnels in Korea is recommended to use for the Q value greater than 1 and the Jw value greater than 0.66 because the single shell tunneling method is very new in Korea. However, support categories should be considered for the Q values lower than 1 because various rock mass classes generally occur together at the same tunnel site in Korea. What percentage of the tunnel length along the entire tunnel length should satisfy both the Q and Jw requirements for the application of the single shell method needs to be determined considering the construction cost.

Even though support requirements for the single shell tunnel are suggested conservatively, the validation of the proposed support categories cannot be evaluated due to the lack of case histories. More reliable support requirements for the various and challenging rock mass conditions can be proposed if the construction of the single shell tunnel continues with the accumulation of field measurements. The single shell tunnelling method is expected to contribute to the economical construction of tunnels in Korea.

ACKNOWLEDGEMENTS

The authors wish to acknowledge the support provided by the Korea Institute of Construction and Transportation Technology Evaluation and Planning under the Ministry of Construction and Transportation in Korea (Grant No: 03-A01-06).

REFERENCES

Barton, N., Lien, R. & Lunde, J. 1974. Engineering classification of rock masses for the design of tunnel support. *Rock Mech* 6: 183–236.

Barton, N., Loset, f., Lien, R. & Lunde, J. 1980. Application of Q-system in design decisions, Subsurface Space, *ed. M. Bergman, Pergamon, New York*: 553–561.

Barton, N., Grimstad, E., Aas, G., Opsahl, O. A., Bakken, A., Pedersen, L., & Johansen, E. D. 1992. Norwegian method of tunnelling, *WT Focus on Norway, World Tunnelling.*

Bieniawski, Z. T. 1974. Estimating the strength of rock materials, *J. S. Afr. Inst. Min. Metall* 8(74): 312–320.

Bieniawski, Z. T. 1989. Engineering rock mass classifications, *New York, Wiley* : 251.

Geofront, 2000. Report on the design of single shell tunnel using shotcrets, Japanese Single Shell Study Division, Committee on the Shotcrete Design.

Goel, R. K., Jethwa, J. L., & Paithankar, A. G. 1995. Indian experiences with Q and RMR systems, *Tunnelling and underground space technology* 1(10): 97–109.

Grimstad, E. & Barton, N. 1993. Updating of the Q-System for NMT, *On sprayed concrete -modern use of wet mix sprayed concrete for underground support; Proceedings of the International Symposium*, Fagernes: 46–66.

Kaiser, P. K., Mackay, C., & Gale, A. D. 1986. Evaluation of rock classifications at B. C. Rail Tumbles Ridge Tunnels, *Rock Mech. Rock Eng* 19: 205–234.

Rutledge, J. C. & Preston, R. L. 1978. Experience with engineering classifications of rock, *Proc. International Tunnelling Symposium*, Tokyo: A 3.1–A 3.7.

Shin, H. S., Sunwoo, C., & Lee D. H. 2000. Geological investigation and rock mass classification, *Goomibook, (In Korean)*: 491.

Trueman, R. 1988. An evaluation of strata support techniques in dual life gateroad. Univ. of Wales, Ph. D. Thesis.

Underground Space – the 4th Dimension of Metropolises – Barták, Hrdina, Romancov & Zlámal (eds)
© 2007 Taylor & Francis Group, London, ISBN 978-0-415-40807-3

Measurements and seismic effects of vibrations caused by urban tunneling

Z. Kaláb
Institute of Geonics of the Academy of Sciences of the CR, Ostrava – Poruba; also at VŠB – Technical University of Ostrava, Faculty of Civil Engineering, Ostrava – Poruba, The Czech Republic

J. Knejzlík
Institute of Geonics of the Academy of Sciences of the CR, Ostrava – Poruba, The Czech Republic

ABSTRACT: This paper presents description of experimental seismic measurements that were performed during construction of underground spaces. Numerous site and source factors influence seismic effects on the surface. Therefore, individual measurements have to be completed by geological and geotechnical parameters. Seismic apparatuses GCR-16, GeoSIG Ltd. were used for our measurements. Their amplitude range is 1, 10 or 100 mm.s-1; recording bandwidth is up to 315 Hz using the sampling rate 1 kHz. Experimental instrumentation of PCM3-EPC type was also used. Generally, the most intensive seismic effects are generated in cases when blasts were used as a part of the technological process. It is usually used timing of blast, therefore wave patterns are short, and they have sharp inputs and very often documented vibrations on high frequencies.

1 INTRODUCTION

Urban tunneling induces not only changes in rock massif (e.g. Rozsypal 2001), but buildings and inhabitants in the nearest surroundings above the tunnel or a mine working can be affected too. Vibrations are one of the most significant effects, especially when blasting operations are used as part of technological process. Seismic load on buildings and constructions can be evaluated with use of maximum velocity amplitude V and prevailing frequencies f in records. There is an effort to compile a universal relation for prediction of the maximum amplitude V. So-called Langerfor's relation (Bongiovani 1991) is often used:

$$V = K.Q^{m}.R^{-a}. \quad (1)$$

There, Q is the total charge or charge fired in one stage, R is distance, K is a coefficient representing physical properties of medium where the waves spread, m and a are empirical constants. Properties of medium (local geological pattern) influence attenuation, refraction and reflection of seismic waves and their modification into different types on boundary; therefore they have significant influence on resulting wave field, e.g. Isaac (1991). Similar empirical relations, which optimally satisfy local geological conditions and conditions for blasts performing, are presented in many other publications. All relations are based on empirical constants that represent studied locality and that can be obtained by parametric measurements. Analyses of wave patterns can be performed for either a whole record or parts of a records representing blast of charge in individual stages (e.g. Pandula & Leššo 2005).

Blasting operations generate seismic waves with a wide spectrum of frequencies. This process depends on type of broken-up rocks, properties of charges and technology of blasting. With increasing distances the components of higher frequencies are absorbed faster in the rock massif than components of lower frequencies. It is documented in publications that frequency spectrum of seismic signals generated by near blasting operation in rock massif can contain frequencies up to 250 Hz. It is also known that shear waves can evoke vibration in soil or rock on defined frequencies (Isaac 1991). Graph of general dependence of frequency content of seismic signal on distance from the point of shot is presented on Figure 1.

2 CONDITIONS DURING URBAN TUNNELING

When studying urban tunneling, distances exceeding 10 m must be taken into account; it means frequency ranges up to several hundred Hz. From the metrology viewpoint, it is a very complicated task, because the wave field of high frequencies of seismic signal is significantly interfered on the surface and an important part of this field is also response of buildings' constructional elements. As an example: if wavelength $\lambda = 10$ m and frequency 200 Hz determine vibration

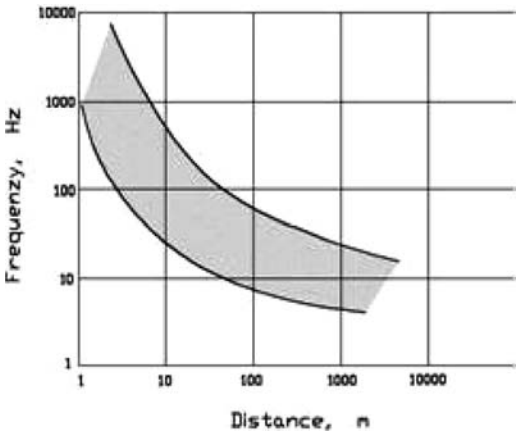


Figure 1. Graph of general dependence of frequency content of seismic signal on distance from the point of shot (according to Rock Blasting Technique).

velocity $v = 2\,\mathrm{km \cdot s^{-1}}$, mechanic constructional elements with n*λ/4 must be to taken into account. Therefore, selection of point for mounting of detecting sensors is very significant in order to obtain measured velocity value, which is fully representative for wide surroundings. Boundary between mediums (rocks) with differential acoustic impedances can generate transform waves; this fact complicates studied wave field even more. Searched predictor dependence of maximum velocity value V on charge Q and distance R can be determined using statistic method only, while it is necessary to check existing values of maximum velocity by an experimental measurement. This conclusion is consequence of influences mentioned above.

Local geological setting, especially shallow sedimentary layers, level of underground water and other factors have significant influence on value of maximum velocity on surface, as described above. Therefore, seismic load on farther construction can be smaller.

3 CONDITIONS FOR PERMANENT MONITORING OF SEISMIC LOADING

Temporary or permanent monitoring system of seismic vibration is suitable for construction in case when seismic loading is expected to last for a long period and/or vibration sensitive apparatuses are installed inside affected objects. Generally, it is necessary to account local conditions and to perform detailed parametric measurement in order to derive basic information about:

- Behavior of seismic noise in a particular region
- Maximum amplitudes and frequency spectra of vibrations
- Type of movement (particle motion)
- Validity of measured values for surroundings.

Detailed parametric measurement must be performed using seismic digital instrument. Obtained data have to provide:

- Analyses in time and frequency domain, especially to determine frequency of wave with maximum amplitude of space vibration component
- Polarization analysis to determine types of recorded parts of wave pattern (e.g., occurring of Rayleigh and Love surface waves and subsequently to define influence of geological pattern)
- Evaluation of character, sources and seismic noise on surface.

Basic parameters from technical point of view are amplitude and frequency range of seismic channel. Usually, the amplitude and frequency ranges of seismic records for monitoring structures on surface are determined in local regulations; frequency range 2–200 Hz is often used. This range was determined from amount of experimental measurements. The frequency range of signals and prevailing frequencies form demands for parameters of sensors and their mounting (concrete pillar, grounding …), needed sampling frequency for digital data and needed storage volume. It is necessary to point on exacting installation of sensors for first quality data with the highest frequencies (e.g. Ground Vibration 2001).

Following significant parameter for preparation of monitoring system is behavior and level of vibration noise in given area. Noise generated by automobile and rail transports and operation of technological instruments can be detected very often in cities. Amount of vibrations induced during mining of underground tunnel and level of common seismic noise on surface establishes the type of recording and preprocessing of measured data.

(a) Level of vibrations induced during mining of underground tunnel significantly exceeds common seismic noise. Apparatuses with triggering regime, which means exceeding of defined vibration level, can be used in such conditions. Generally, short time history that runs over fulfillment of triggering conditions is recorded. Advantage of this type of recording is a small volume of recorded data and, therefore, easy transportation of recorded data to interpretation centre. During preprocessing the technical staff detaches useful signals for further interpretation.

(b) The level of vibrations induced during mining of underground tunnel is practically the same as the level of seismic noise. In this case it is not possible to use monitoring system based on triggering and it is necessary to realize continuous record of situation. Recorded data volume is

very large and therefore telemetric transport (e.g. by modem) from field station without Internet is complicated from both technical and financial viewpoint. For example, three-component record from 16-bit seismic instrument and using sampling frequency of 500 Hz is about 260 MB per day. These data have to be stored on high-volume media and interpretation is then realized off-line. A specialist or a professional technical staff performs preprocessing of these records.

4 EXAMPLE FROM EXPERIMENTAL MEASUREMENT

Presented parametrical measurement was realized in Prague in January 2006. Blast operation was performed as a part of mining technology in terms of preparations for new plumbing. Total charge was 5.95 kg in 17 holes, timing in 10 steps. Mining works were made about 10 m below the surface; working face was contained by slates with mica.

Three seismic apparatuses GCR-16, GeoSIG Ltd. were used for our measurements. Their amplitude range was 1 or 10 mm·s^{-1}; recording bandwidth was up to 315 Hz using the sampling rate 1 kHz. Experimental instrumentation of PCM3-EPC type (Knejzlík & Kaláb 2002) was also used (Figure 2). This apparatus enables semi-continuous records of industrial seismic noise generated by common working activities. Basic problem for seismic measurement in these conditions is good anchorage of sensors as it is not possible to construct special seismic pillars (usually we do not have a place well connected with soil that is needed).

Permanent buildings do not exist in surroundings of preparation of plumbing. Therefore, solid plane areas were utilized for sensor installing (sensors were flatted by rock). Furthest station (instrumented by PCM3-EPC2) was installed about 250 m from source of vibration (station 1). Evaluation of seismic effect in this distance was main reason for this position. By contrast, the nearest station was about 25 m far from source of vibration (station 2). Here two apparatuses GCR-16 with different sampling frequency of digital signal (500 Hz and 1 kHz) were installed. Evaluation of wave patters recorded in the immediate vicinity of source and check of influence of sampling frequency on shapes of records. Last position was about 190 m from source (station 3); see Figure 3.

Duration of seismic effect on station 1 is almost 3 s, maximum recorded velocity amplitude is 0.078 mm·s^{-1} (vertical component), space component is 0.098 mm·s^{-1}($\sqrt{(Z^2+(N-S)^2+(E-W)^2)}$). Wave patterns do not contain sharp inputs except first one because significant damping of inputs generated by subsequent shots, occurring of secondary wave groups and their interferences. Spectral analysis documents frequency range 10–40 Hz.

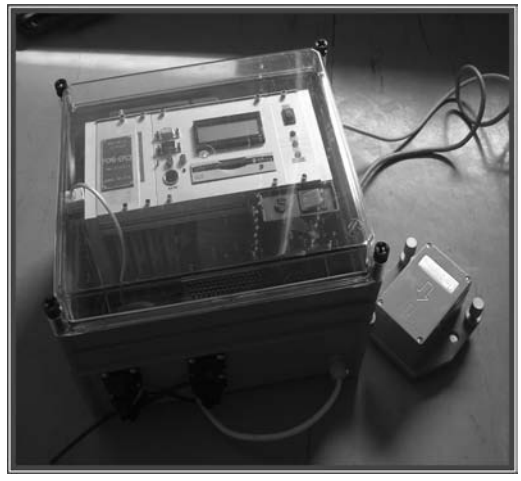


Figure 2. Photo of experimental instrumentation of PCM3-EPC type (developed in Institute of Geonics).



Figure 3. Sketch of position of source of vibrations (star) and seismic stations (St. 1 – St. 3) at experimental measurement.

Records on station 2 are shorter (about 2 to 2.4 s). Maximum recorded velocity amplitude is 1.12 mm·s^{-1} (vertical component); space component is 1.33 mm·s^{-1}. Wave patterns contain clearly recognizable sharp inputs that correspond to individual shots of holes and quick damping of individual seismic wave groups that have character of harmonic wave with different damping. The FFT of records show prevailing frequency range 40–55 Hz.

Records on station 3 represent transient type of records. Their durations are approximately 2.5 s, maximum recorded velocity amplitude do not exceed 0.3 mm·s^{-1}. Prevailing frequency range is up to 40 Hz.

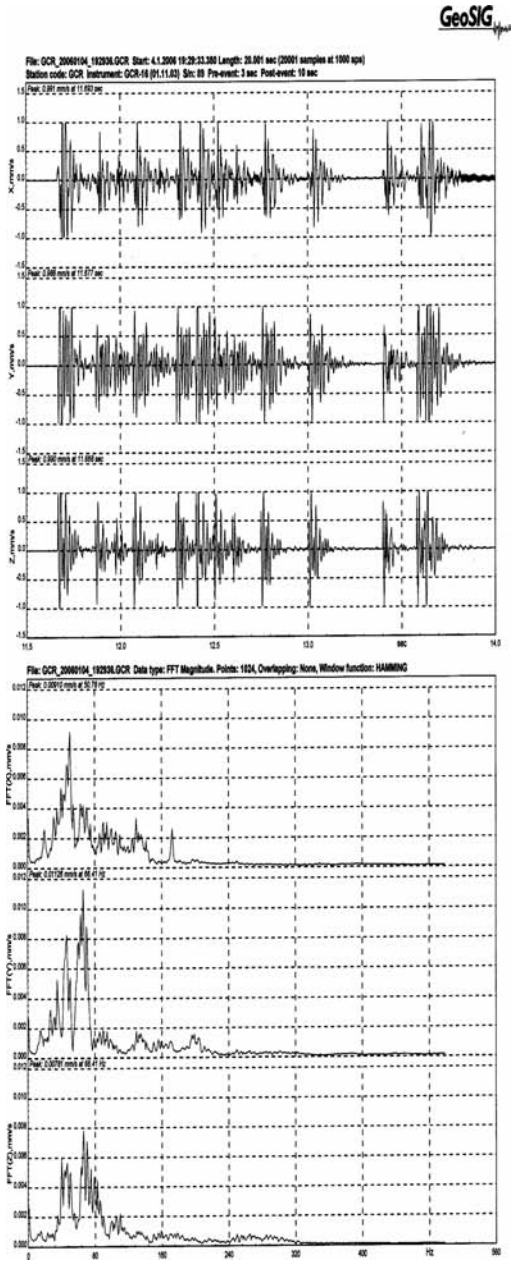


Figure 4. Example of wave pattern of blast, sampling frequency 1 kHz, distance to source about 25 meters.

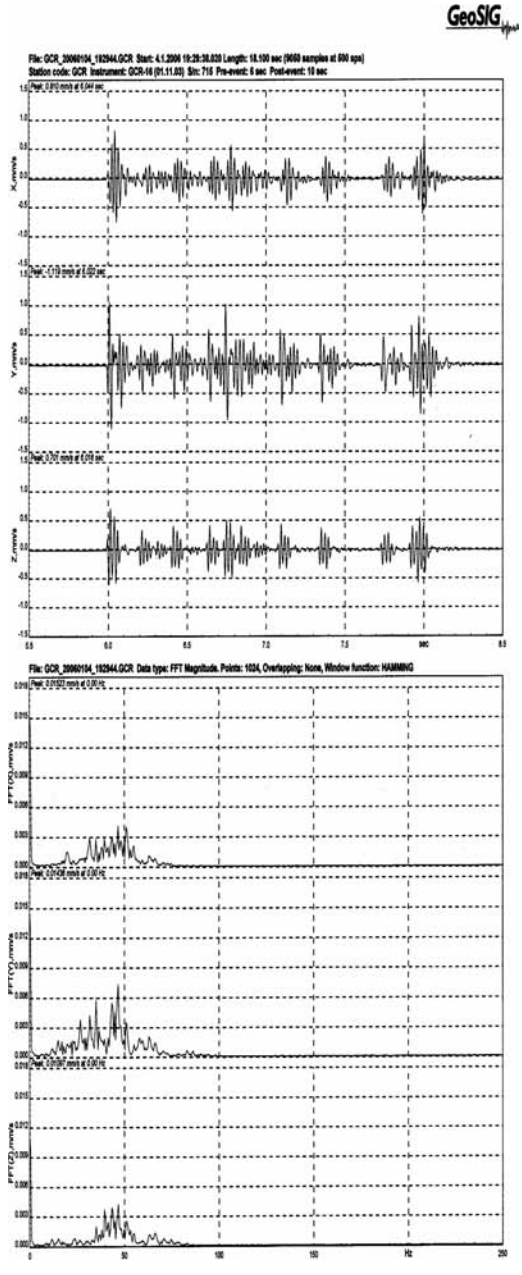


Figure 5. Example of wave pattern of blast, sampling frequency 500 Hz, distance to source about 25 meters.

Figures 4–5 document the changes of shape of recorded wave patterns due different sampling frequency. First figure presents wave pattern (top-down horizontal radial component, horizontal normal component and vertical component) and their spectra (Fast Fourier Transform) using sampling frequency 1 kHz, the second figure presents the same situation but with sampling frequency 500 Hz.

Values of maximum amplitudes of both records are almost the same (differences up to 15%). However,

frequency capacity of recorded signals is different; the 1 kHz record has wider frequency range, especially in higher values.

5 REMARKS RESULTED FROM MEASUREMENT

Obtained knowledge from experimental measurement is possible to summarize as follows:

- In short distances from source of vibration, it is necessary to provide high dynamic range of recorded apparatuses.
- Frequency range of seismic channel (i.e. both sensors and apparatus) should be as wide as possible, especially for higher frequencies.
- To record data of first quality, it is necessary to use high value of sampling frequency of digital signal, optimally 1 kHz or at least 500 Hz.
- Very good contact between sensor and basement is necessary to realize; to best solution is anchor sensors to basement using bolts or suitable additional load (it must not vibrate).
- All demands are possible to reduce adequately if seismic station is located in larger distance.

Behavior of signals, especially sharp inputs of first wave group, gives good conditions for possibility to use apparatuses with trigger regime of data recording. It is true that common seismic noise (other technical seismicity) do not often exceed preset trigger level. This fact is very important in case when medium-term or long-term monitoring is necessary to use.

Generally, the most intensive seismic effects are generated in cases when blasts were used as a part of the technological process. It is usually used timing of blast. Therefore, wave patterns are short, and they have sharp inputs and very often documented vibrations on high frequencies, mainly in short distances between source of vibration and sensor.

6 CONCLUSION

Evaluation of technical seismicity induced during urban tunneling on buildings and structures on surface results from experimental measurements usually. Realization of temporary seismic stations that will operate in suitable buildings during whole period of seismic loading (generally weeks or first months) is supposed. As was mentioned above, vibrations can be produced by different sources. Amount of measurements illustrates that the highest values are induced by blasts of explosives. Damage of buildings within the meaning of limitation on usability is not expected when referential values specified in standards, e.g. Czech Standard CSN 73 0040 or German Standard DIN 4150, are not exceeded (Kiehl & Werfling 2003).

At present, permanent seismic monitoring with automatic data acquisition and primary interpretation of basic parameters is favored in urban regions when significant vibrations are generated. Obtained results are at disposal to civil engineers, firefighters and also to custodians and occupants of influenced buildings. Usually, web application is used with different access authority. This web continuously presents basic parameters and results of seismic monitoring (and other information). Limit and critical values of vibrations for appropriate damages of buildings are determined for evaluated area. These values, of course, depend on technical wear of building and local geological conditions.

ACKNOWLEDGEMENT

This research was partially supported by the Grant of Czech Mining Bureau (Project No. 38/05) and the Czech Grant Agency (Project No. 105/05/2712).

REFERENCES

Bongiovanni, G. 1991. Experimental Studies of Vibrations Caused by Blasting for Tunnel Excavations. *In: Earthquake, Blast and Impacts: Measurements and Effects of Vibration*, Elsevier Applied Science: 201–210.

Ground Vibration Monitoring for Construction Blasting in Urban Areas. *F-00-OR-10, Final Report, State of California*, Department of Transportation, USA, 2001, unpublished.

Isaac, I.D. 1991. Effects of Constructional Vibrations upon an Urban Environment. *In: Earthquake, Blast and Impacts: Measurements and Effects of Vibration*, Elsevier Applied Science: 442–462.

Kiehl, J.R. & Werfling, J. 2003. Measurements and Analyses of Blasting Vibrations. *ISRM 2003 – Technology Roadmap for Rock Mechanics.* South African Institute of Mining and Metallurgy: 635–640.

Knejzlík, J. & Kaláb, Z. 2002. Seismic Recording Apparatus PCM3-EPC. *Publs. Inst. Geophys. Pol. Acad. Sc.*, No. M-24(340): 187–194.

Pandula, B. & Leššo, I. 2005. Spectral Analysis of a Coyote – hole Blast. *Transactions (Proceeding of VŠB – Technical University of Ostrava, Civil Engineering Series)*, Vol. V, No. 2/2005: 105–112 /in Slovakian/.

Rock Blasting Technique. Blasting with Restriction. *Project Report 14A-98*. NTNV, Department of Building Construction, Norway, unpublished.

Rozsypal, A. 2001. Inspectional Observations and Hazards in Geotechnics. *Jaga group – Publishing*, Bratislava, Slovak Republic /in Czech/.

This page intentionally left blank

Underground Space – the 4th Dimension of Metropolises – Barták, Hrdina, Romancov & Zlámal (eds)
© 2007 Taylor & Francis Group, London, ISBN 978-0-415-40807-3

Design method considering construction loads during shield tunneling using a three-dimensional FEM analysis model

Kiyoshi Kasuga, Naruhiko Kawada & Akira Shiratori
Metropolitan Expressway Co., Ltd., Japan

Naomitsu Fukai & Masayuki Saitou
Nippon Civic Consulting Engineers Co., Ltd., Japan

ABSTRACT: With recent technological advancements, secondary linings have been eliminated, segmental linings have become thinner and lining rings have become wider to reduce the cost of constructing shield tunnels of large cross section. There have, however, been concerns about the functional deterioration of linings due to the effects of loads during construction, which are difficult to handle in conventional design processes.

In the Shinjuku Route of the Central Circular Route of the Metropolitan Expressway, the effects of loads on tunnels during construction have been analyzed using the data on the control of construction with shields and the measurements of the behavior of segmental linings. No measurements were, however, available to identify the effects of loads during construction, and no detailed studies could be made.

In this study, construction control data and measurements were collected in the Kamiyamacho-Yoyogi shield work section of the Shinjuku Route based on a measurement plan aimed at analyzing the loads during construction. Three-dimensional FEM analysis was made using the measurements. A method for analytically checking the effects of loads on tunnel linings during construction was examined. The concept of the method and problems involved in its future application are described in this paper.

1 INTRODUCTION

A growing number of shield tunnel projects have been implemented for constructing road tunnels with an outer diameter of as large as 11 to 13 m and without any secondary lining. With recent technological advancements, segmental linings have become thinner and lining rings have become wider to reduce construction costs. Then, safety margin against loads during construction, which were difficult to handle quantitatively in conventional design processes, has been reduced and lining damage is more likely to be caused.

Segmental linings of a shield tunnel are subjected to jack thrust, tail seal pressure and backfilling pressure during construction. The surrounding ground is not expected to provide support right after the assembly of segmental linings, so the deformation of segmental linings, joint opening and joint unevenness are likely to occur. Records on past construction show that such effects of loads during construction are found outstanding in curved sections where segmental linings deviates from the direction of shield advance. In the design of a shield tunnel, loads such as jack thrust, tail seal pressure and backfilling pressure are generally examined separately, but they probably combine with one another and damage segmental linings. The authors, with the view to reproducing the behavior of segmental linings, have conducted field measurement of their behavior during construction, and analyzed the behavior of the shield machine and made three-dimensional FEM analysis.

This paper presents the results of evaluation of the effects of construction loads on segmental linings based on the results of measurements of segment linings that were taken in the field.

In this study, the behavior of segmental linings was analyzed using a three-dimensional FEM model of shield tunnel in order to identify the effects of construction loads on segmental linings based on the results of measurement of the behavior of segment linings conducted in the field and on the data on construction with shield machines. The analysis results were compared with field measurements to verify the validity of behavior analysis. Based on the above results, a segmental lining design method was examined that took the effects of construction loads into consideration.

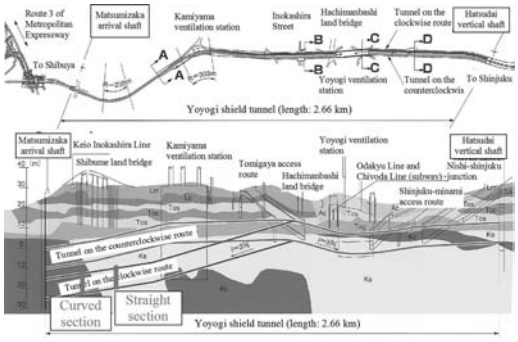


Figure 1. Measurement sections (Kamiyamacho-Yoyogi shield work section).

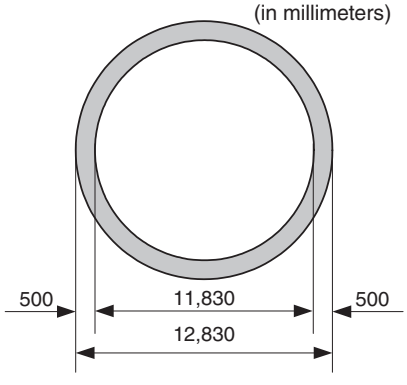


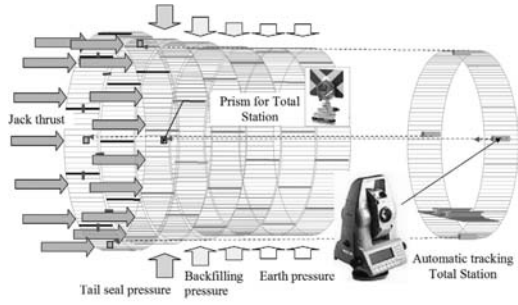
Figure 2. Tunnel cross section (on the clockwise route).

2 FIELD MEASUREMENTS OF LOADS DURING CONSTRUCTION

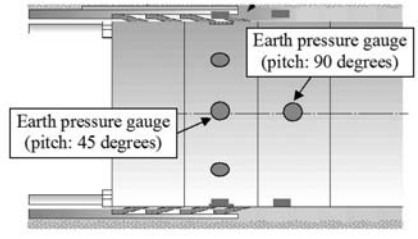
2.1 *Outline of the site*

Field measurements were taken of the loads during construction in straight and curved (radius: 238 m) sections of varying cross section of the Kamiyamacho-Yoyogi shield tunnel on the Shinjuku Route of the Metropolitan Expressway to evaluate the effects of loads in different types of alignment (Figure 1).

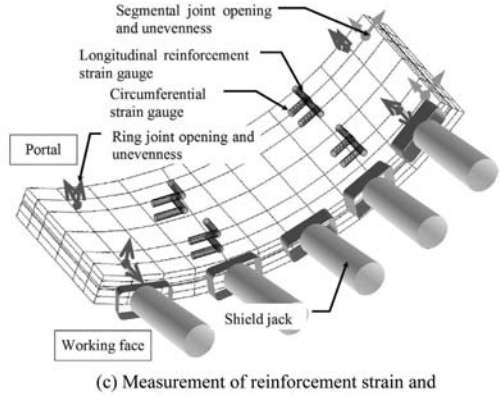
The Kamiyamacho-Yoyogi shield tunnel is constructed using slurry shields over a length of 2,660 m between Hatsudai icchome, Shibuya ward to Aobadai yonchome, Meguro ward under Central Circular Route 6 (Yamatedori Avenue). The tunnel passes through consolidated ground mainly composed of Kazusa formation. The tunnel on the clockwise route has a diameter of 12.83 m and is 3.5 to 9 m away from the other of twin tunnels. The two horizontally parallel tunnels change into vertical parallel ones. Reinforced concrete segmental linings with a thickness of 500 mm are used in the sections where measurements were taken. Segmental rings are divided into nine segments.



(a) Measurement of displacement



(b) Measurement of earth pressure



(c) Measurement of reinforcement strain and joint opening and unevenness

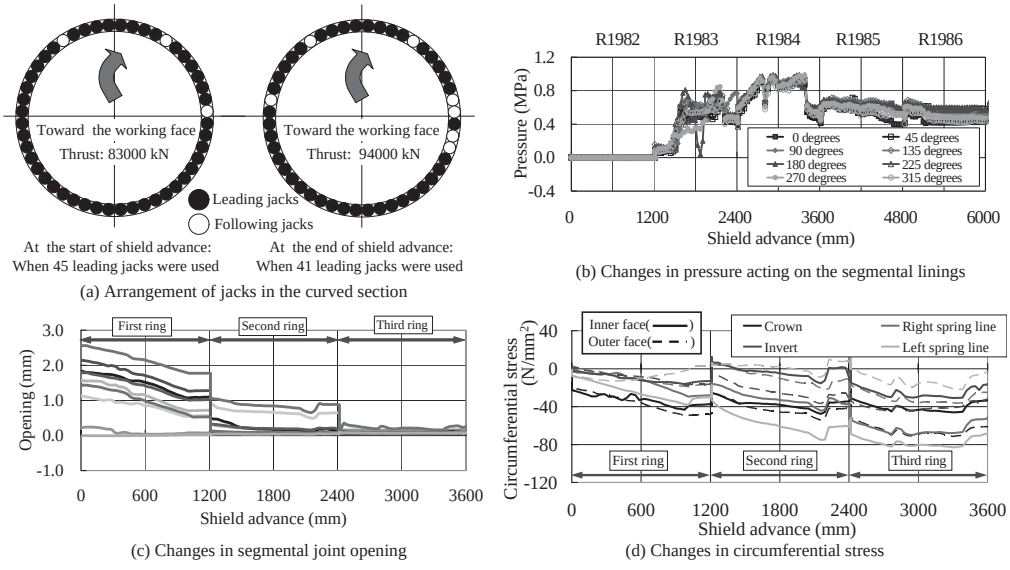
Figure 3. Measurement instruments.

2.2 *Details of measurement*

In the field measurement of loads during construction, displacement, earth pressure, strain of reinforcement, and joint opening and unevenness were measured. In the straight section, only displacement and joint opening were measured (Figure 3).

For displacement measurement, Total Stations were installed at a pitch of 90 degrees to identify the three-dimensional behavior of the tunnel.

Earth pressure gauges were installed in two rings, main and sub rings, to grasp tail seal pressure and backfilling pressure acting on the segmental linings during excavation.



(a) Arrangement of jacks in the curved section

(b) Changes in pressure acting on the segmental linings

(c) Changes in segmental joint opening

(d) Changes in circumferential stress

Figure 4. Results of measurement (in curved section).

Reinforcement strain gauges were used to obtain changes in strain in segmental linings right after assembly and during construction. Gauges were installed at 36 positions in a ring, or at four positions per segment, to measure circumferential and longitudinal strains.

Gauges for measuring joint opening and unevenness were installed at segmental and ring joints at the four corners of a segment. They were used to monitor how the initial joint opening and unevenness right after assembly would vary with shield advance.

2.3 *Results of measurement*

Results of measurement were shown in terms of the arrangement of jacks, and changes in earth pressure with shield advance, in segmental joint opening and in circumferential stress (Figure 4).

The number of jacks was gradually reduced to enable the shield to follow the tunnel alignment in the curved section. Jacks on the concave face of the curve were reduced earlier. The jack thrust was greater at the end of shield advance than at the start. Thrust per jack increased by 24%.

The pressure acting on the circumference of the segmental lining is represented based on the reading of the earth pressure gauge and the stroke of the jack. The segmental ring did not reach the tail seal while the shield was used to assemble the first ring following the ring for measurement. Then, no pressure from areas around the tunnel was acting. While the shield was used to assemble the second ring, the segmental ring was subjected to tail seal pressure and rapid variation of earth pressure was found. The segmental ring was subjected to the highest pressure due to the effect of backfilling pressure while the shield was assembling the third ring because the segmental ring passed the tail of the shield. Little variation of pressure was observed in the fourth and subsequent rings.

Segmental joint opening was approximately 2 mm at the maximum near the key segment right after assembly, but decreased with the advance of the shield. All the joints had an opening of less than 0.2 mm after the excavation in the second ring.

Circumferential stress gradually increased after the start of shield advance, similar to the circumferential pressure and segmental joint opening.

Conventional three-dimensional FEM analysis [4], [5], [6] considered jack thrust (arrangement of jacks) and changes in circumferential pressure acting on the tunnel. In the analysis model adopted in this study, segmental joint opening was also considered. The results of analysis were verified by comparing the stress and deformation with measurements.

3 THREE-DIMENSIONAL FEM ANALYSIS

3.1 *Analysis model*

A three-dimensional FEM analysis model was adopted for analyzing loads during construction (Figure 5). Segments were modeled using solid elements and connected to one another via spring elements. The first three rings were analyzed because variations of circumferential pressure were confirmed in these rings based on the measurements. The tunnel was compressed by jack thrust along the tunnel axis during excavation. To reproduce the behavior, values of springs at the boundary were specified as boundary

conditions for the analysis model based on the relationship between the absolute value of shield tunnel displacement and the jack thrust obtained in field measurement (Figure 6).

Physical property values of segment are listed in Table 1. Concrete was regarded as a perfectly elastic body when the model was made.

Values of springs of segmental and ring joints were specified around the tunnel circumference, along the tunnel radius and along the tunnel axis based on the results of element tests (Figure 7).

In this study, the curve representing the joint spring passing the origin was shifted based on the changes in segmental joint opening with time shown in Figure 4 to make a model similar to the ring in actual construction.

3.2 *Loading conditions*

For analysis, jack thrust that varied according to the arrangement of jacks and varying pressures acting on the circumference of the tunnel (Figure 4) were adopted as the loads during construction. Circumferential pressure was measured at a pitch of 45 degrees, so it was interpolated linearly around the tunnel circumference for input.

3.3 *Analysis cases*

Analysis was made in a curved section subjected to outstanding effects of loads during construction in four cases (Table 2). The timing of measurement, at the start or end of shield advance where different numbers of jacks were used, and whether there was a segmental joint opening or not were used as parameters.

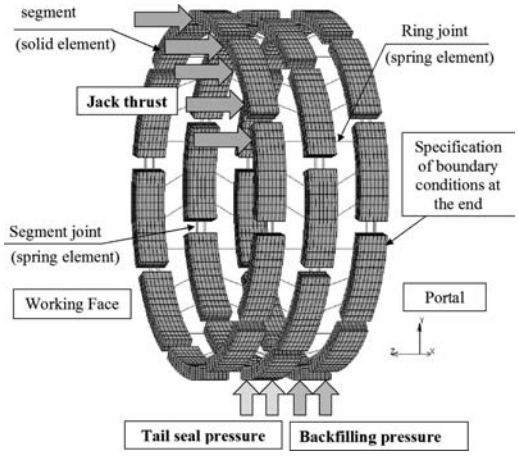
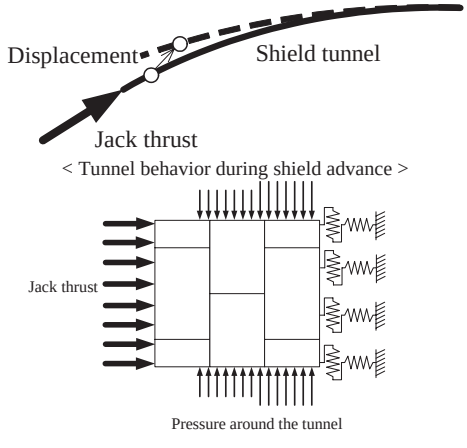


Figure 5. Analysis model.



Type of spring		Characteristics
Longitudinal		Tension (joint spring)/ compression (specified based on measurement)
Transverse		Shear (joint spring)

Figure 6. Specification of boundary conditions.

Table 1. Physical property values of segment [1], [2].

σck (N/mm^2)	E (kN/m^2)	ν	σca (N/mm^2)	ftk (N/mm^2)
48	3.9×10^7	0.17	$18 \times 1.5 = 27$	3

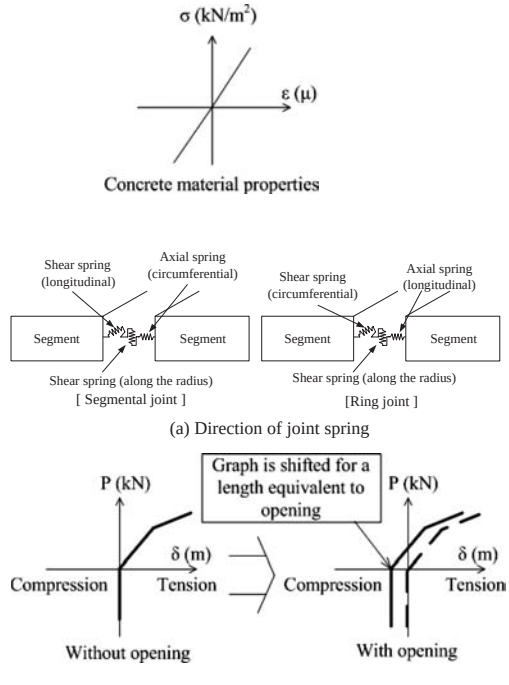


Figure 7. Characteristics of joint spring.

3.4 *Results of analysis*

3.4.1 *Distribution of acting stresses*

Measurements and analysis results for stress are represented by points and solid lines in Figure 8. Analysis results are given only for cases 2 and 4 at the end of shield advance without and with segmental joint opening, respectively.

Where joint opening was considered, circumferential stress varied at segmental joints although the variation was small. In both cases 2 and 4, analysis results were in good agreement with measurements in terms of stress level. No local variance in stress on the outer and inner faces are reproduced in the figure. Local stress varied greatly at different measurement positions. This may have been caused by the rotation of segmental joints (variance in mode of contact between segments), which was not considered in analysis.

It was confirmed based on the longitudinal stress that little axial compression occurred on the inner face of the segmental lining in the second and subsequent rings as shown by the results of measurement where joint opening was considered.

Table 2. Analysis cases.

Measurement section	Case	Construction condition	Segmental joint opening
Curved section	1	At the start of shield advance	Without opening
	2	At the end of shield advance	
	3	At the start of shield advance	With opening
	4	At the end of shield advance	

3.4.2 *Deformation*

Tunnel deformation is shown in Figure 9. Black circles indicate measurements and solid lines indicate analysis results. Analysis results are given only for cases 2 and 4 at the end of shield advance without and with segmental joint opening, respectively as for stresses.

Transverse deformation shows that tunnel cross section was reduced with shield advance when joint opening was taken into consideration as reflected in the measurements.

Longitudinal deformation is more or less the same in cases 2 and 4, and is nearly in agreement with measurements. The boundary conditions of the analysis model specified based on measurements are therefore determined to be appropriate. Longitudinal deformation was partially different in a cross section probably because boundary conditions were specified

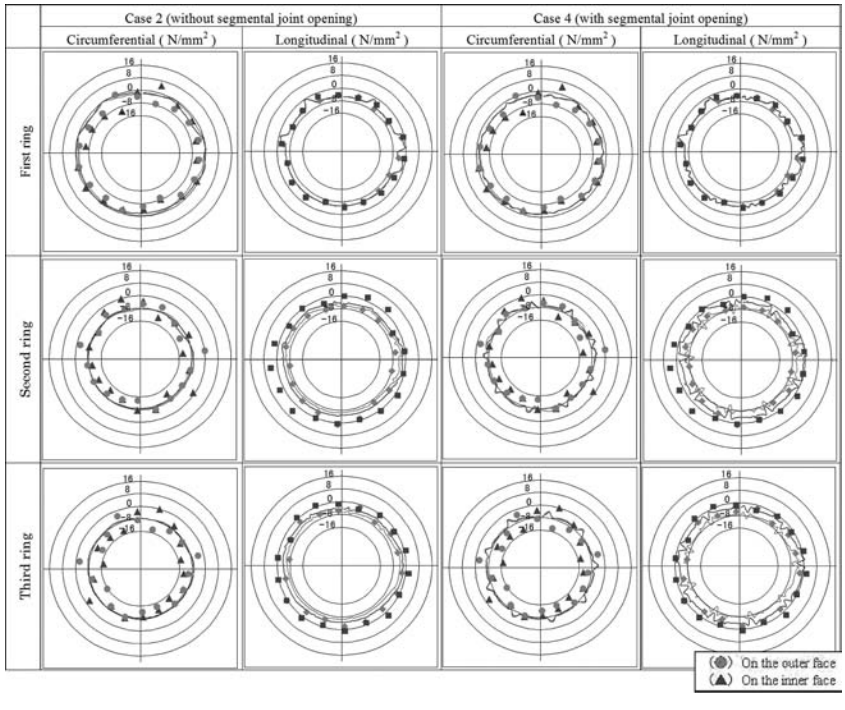


Figure 8. Stress (in N/mm^2).

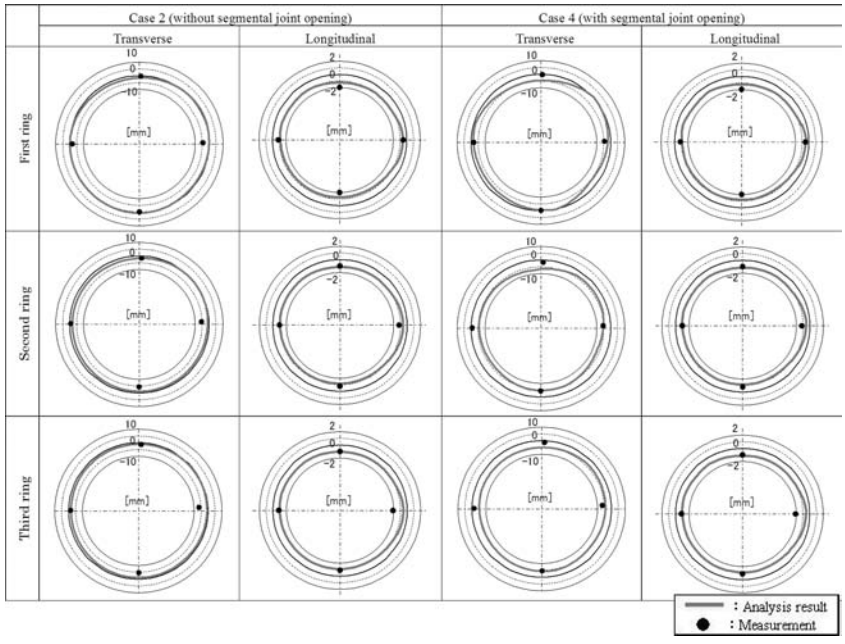


Figure 9. Tunnel deformation.

uniformly in a cross section. More detailed specification of boundary conditions is expected to increase the accuracy of analysis.

4 CONCLUSIONS

In this study, evaluation was made of a method for examining the effects of construction loads on the tunnel based on the field measurements of the behavior of segmental linings during shield advance and using three-dimensional FEM analysis. The results of evaluation and future tasks involved in the application of the method are described below.

It was confirmed that a three-dimensional FEM analysis model could reproduce nearly satisfactorily the behavior of segmental linings that was identified in field measurement if segmental joint opening was considered in addition to jack thrust, pressure along the circumference of segmental linings and boundary conditions obtained based on the absolute displacement of the tunnel.

In the future, variations of stress occurring locally along the circumference will be verified analytically.

Loading conditions and the accuracy of shield assembly are now defined based on measurements. In order to establish a design method, a method should be developed for specifying these parameters quantitatively.

In this study, verification was made in highly consolidated ground with an N-value of more than 50. For application in weak soils, further verifications will be required.

The analysis model proposed in this study is highly complicated, so making analysis frequently with the model in daily design process is difficult. Design methods using two-dimensional models are now being examined based on the knowledge obtained in this study. Simpler design methods will be proposed in the future.

REFERENCES

Metropolitan Expressway Public Corporation: Tunnel structures design procedures, Metropolitan Expressway Public Corporation, pp. 61–66, 2003.

Japan Society of Civil Engineers: Standard Specifications for Design and Construction of Concrete Structures – Structural Performance Check –, Japan Society of Civil Engineers, pp. 21–24, 2002.

M. Kishida, H. Tajima, A. Dan and M. Saito: Analysis of behavior of shields of large cross section based on the field construction data, Proceedings of Tunnel Engineering, JSCE Vol. 14, pp. 345–351, November 2004.

H. Tajima, M. Kishida, N. Fukai and M. Saito: Study on construction loads during shield tunneling using a three-dimensional FEM model, Proceedings of Tunnel Engineering, JSCE Vol. 14, pp. 353–360, November 2004.

H. Tajima, K. Kasuga, N. Fukai, A. Dan and M. Saito: Study of construction loads in shield tunnels of large cross section based on the measurement of the behavior of segmental linings, Proceedings of Tunnel Engineering, JSCE Vol. 15, pp. 293–300, December 2005.

Underground Space – the 4th Dimension of Metropolises – Barták, Hrdina, Romancov & Zlámal (eds)
© 2007 Taylor & Francis Group, London, ISBN 978-0-415-40807-3

Development of a new center-cut method: SAV-cut (Stage Advance V-cut)

Donghyun Kim, Seunghwan Noh & Sangpil Lee
GS Engineering & Construction Corp., Seoul, Korea

Byungki Park & Seokwon Jeon
Seoul National University, Seoul, Korea

ABSTRACT: In most tunnels in South Korea, blasting has been widely used as an excavation method. The key of blasting method in tunnel is the center-cut, which creates first free surface. This paper introduces new center-cut method named SAV-cut (Stage Advance V-cut) developed on the concept of V-cut. An important factor of SAV-cut is center holes drilled and partly charged for maximizing tensile failure effect and satisfying optimum charge density. Field tests and numerical analysis were carried out to analyze the mechanical behavior and blasting vibration. In the numerical analysis, PFC 2D (Particle Flow Code 2D) was used and two field tests were performed to verify the high performance of SAV-cut. From the results, the newly developed SAV-cut was proved as an effective center-cut method for both increasing blasting efficiency and decreasing blasting vibration.

1 INTRODUCTION

In South Korea, the ground is mainly composed of hard rock such as granite and gneiss, but the complex geology generally limits blasting method as a main tunnel excavation method rather than mechanical excavation using TBM or shield method. In tunnel blasting, the center-cut inducing first free surface is very important for enhancing excavation efficiency and reducing vibration caused by exploding.

In general, V-cut and cylinder-cut are commonly used for center-cut. V-cut is a representative type of angle-cut having inclined holes that nearly meet at the bottom. Charging at the bottoms of the holes play a role to pull out the rock mass by the shape of V. Cylinder-cut is a type of parallel cut having 2-4 large empty holes (generally over 102 mm in diameter) drilled at middle of the center-cut. This method is most commonly used for long advance over 2 m.

But there are some problems in applying these methods as center-cut because there may be considerable difficulties in accurate drilling of inclined holes for V-cut and the narrow width (0.2-0.4 cm) of parallel holes makes drilling work difficult for cylinder-cut. Also, due to the regulations in South Korea, cartridge explosives are generally used rather than bulk type explosives. Therefore, tight loading at the bottom of the holes, yielding center-cut blasting, is not always successful.

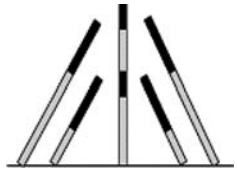
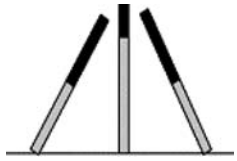
In this study, a new center-cut method named SAV-cut (Stage Advance V-cut) was developed to overcome these problems on the concept of V-cut. In order to verify the performance of the SAV-cut, field tests and numerical analysis were carried out.

2 CONCEPT OF SAV-CUT

The principle of V-cut is to create the first free surface by wedge failure. For the success of V-cut blasting, accurate drilling and sufficient failure at the bottom of inclined holes are important. The concept of SAV-cut is focused on these two factors. The center hole that is the significant feature of SAV-cut makes the rock mass around bottoms of inclined holes weakened by being ignited at first. As the rock mass constant is diminished, it can be enabled to decrease the amount of charging in the inclined holes. Also, the adverse effect of inaccurate drilling is to be reduced because the bottom spacing between two inclined holes can be more widened due to the center hole.

In the SAV-cut, the angle of inclined holes could be extended to 70 degrees and the spacing between two holes could be increased due to the added center holes. Therefore, SAV-cut is more effective for long hole blasting than V-cut in consideration of drilling work. Cross section and main features of SAV-cut were described in Table 1. Figure 1

Table 1. Cross sections and the main features of SAV-cut.

Classification	Cross section	Features	Application
Pattern for long hole blasting		– Center hole – Baby cut hole – Deck charge of center hole – Ignition sequence: center hole(1) → baby cut hole → center hole(2) → main cut hole	– Advance of 2.0 m or more
Pattern for short hole blasting		– Center hole – Ignition sequence: center hole → main cut hole	– Advance of 2.0 m or less

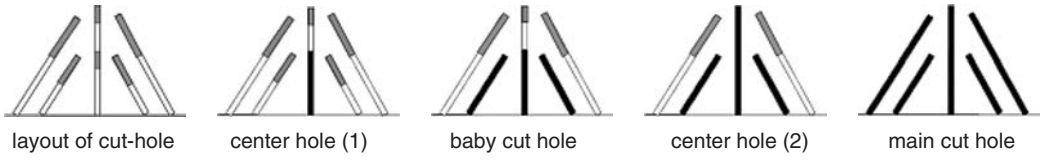


Figure 1. Ignition sequence of SAV-cut (long hole blasting).

shows the ignition sequence of SAV-cut for long hole blasting.

3 NUMERICAL MODELING WITH PARTICLE FLOW CODE

3.1 *Input parameters for numerical modeling*

In PFC2D, particles interact with other particles and walls, through the forces that develop at their contacts. Each contact model may be divided by three models: (1) a contact-stiffness model, (2) a slip and separation model and (3) a bonding model (Itasca, 1999a).

In this study, a linear model as a contact-stiffness model and a contact-bond model as a bonding model was used. Micro-mechanical parameters, which define the contact-bonded material, include ball density, ball-ball contact modulus, ball stiffness ratio, ball friction coefficient, contact-bond normal strength and contact-bond shear strength.

The parameter analysis was carried out to determine the input parameters, i.e., micro-mechanical parameters of the particle assembled model which has similar mechanical behavior of the rock mass based on the macro-mechanical parameters of the rock mass shown in Table 2. In Table 2, the deformation modulus of rock mass E_m and the rock mass strength σ_{cm} were estimated from the uniaxial compressive strength of intact rock σ_{ci} and the geological strength index (GSI) from Equations (1) and (2) (Hoek et al., 2002).

$$E_m(GPa) = \left(1 - \frac{D}{2}\right)\sqrt{\frac{\sigma_{ci}}{100}} \cdot 10^{\frac{GSI-10}{40}} \quad (1)$$

$$\sigma_{cm} = \sigma_{ci} \cdot \frac{\left[m_b + 4s - a\left(m_b - 8s\right)\right]\left(m_b/4 + s\right)^{a-1}}{2\left(1+a\right)\left(2+a\right)} \quad (2)$$

where, D is factor to allow for the effects of blast damage and stress relaxation ($0 \le D \le 1$).

$$m_b = m_i \exp\left(\frac{GSI-100}{28-14D}\right), \quad s = \exp\left(\frac{GSI-100}{9-3D}\right)$$

$$a = \frac{1}{2} + \frac{1}{6}\left(e^{-GSI/15} - e^{-20/3}\right)$$

The micro-mechanical parameters determined by the trial-and-error method through many numerical simulations were summarized in Table 3.

3.2 *Blasting pressure-time history curve*

Sudden release of energy and reaction products at high pressure by rapid chemical reaction in explosive charged in a blast hole gives rise to compression waves

Table 2. Micro-mechanical parameters of the model.

Parameter	Rock mass class I	Rock mass class IV
Modulus of deformation of rock mass	75 GPa	24 GPa
Poisson's ratio	0.20	0.22
Rock mass density	2,700 kg/m^3	2,600 kg/m^3
Rock mass strength	92 MPa	41 MPa

Table 3. Micro-mechanical parameter values used in the PFC2D simulation.

Parameter	Rock mass class I	Rock mass class IV
Ball density	2,700 kg/m^3	2,300 kg/m^3
Ball-ball contact modulus	156.13 GPa	5.60 GPa
Ball stiffness ratio	4.50	25.00
Ball friction coefficient	0.50	0.50
Contact-bond normal strength, mean	69.00	5.73
Contact-bond normal strength, SD*	6.90	0.57
Contact-bond shear strength, mean	91.94	3.82
Contact-bond shear strength, SD*	9.19	0.38

* SD: Standard deviation.

in the explosive and surrounding rock material. The detonation waves play an important role in the function of the explosive and fragmentation of rock mass (Persson et al, 1994).

Detonation is the first step of fragmentation process. After detonation, components of explosives are immediately converted into high-pressure and high-temperature gases. In general, it is impossible to measure the detonation pressure directly. Many researchers, however, such as Atlas Powder Company (1987) and Liu and Tidman (1995) have proposed equations to calculate the detonation pressure employing the chemical equilibrium equation of explosives and the empirical factor obtained from field tests. In this study, Equation (3) suggested by National Highway Institute (1991) was applied to estimate the detonation pressure.

$$P_D = \frac{4.18\times10^{-7}\times\gamma_e\times D_e^2}{1+0.8\gamma_e} \tag{3}$$

where, P_D is detonation pressure (kbar), γ_e is explosive density (g/cm^3), and D_e is detonation velocity (ft/s).

Time history of dynamic pressure was considered in order to simulate its effect of rock blasting accurately

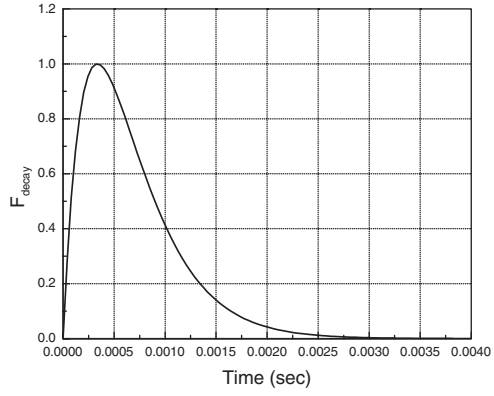


Figure 2. Time history curve for the dynamic pressure acting on the wall of blast hole.

because dynamic pressure acting on the wall of blast hole varies with time. The time history of dynamic pressure can be obtained by using window function proposed by Starfield and Pugliese (1968) as shown in Equation (4).

$$P_D(t) = 4P_B\left[\exp\left(\frac{-Bt}{\sqrt{2}}\right)-\exp\left(-\sqrt{2}Bt\right)\right] \tag{4}$$

where, P_D is detonation pressure, P_B is decoupled detonation pressure, B is loading constant (=16,338 in this study), and t is time.

Also, the decay function, Equation (5), was used to consider the extent of attenuation with time. However, it is difficult to determine the time when the pressure arrives its maximum value.

$$F_{decay} = \exp\left(1-\frac{t}{t_0}\right)\times\frac{t}{t_0} \tag{5}$$

where, F_{decay} is decoupled detonation pressure.

The detonation pressure calculated by Equations (4) and (5) is for the fully coupled holes. In order to take into account the decoupling effect, the borehole pressure is calculated by Equation (6).

$$P_B = P_D\times\left(\frac{d_c}{d_h}\right)^3 \tag{6}$$

where, P_B is decoupled detonation pressure, P_D is detonation pressure, d_c is charge diameter, and d_h is borehole diameter.

The borehole pressure was simulated to consider the characteristics of decay function using Equation (5) and detonation pressure using Equations (4) and (6). Figure 2 shows the time history curve for dynamic pressure acting on the wall of blast hole.

This study was carried out under following assumptions. (1) The viscous damping effect was neglected in the numerical simulation because its influence on the response of high-velocity explosives was insignificant. (2) The cracks in the numerical simulation were formed as a result of contact-bond breakage between balls. (3) The damage to the rock mass due to the penetration/explosion of the explosive gas into the existing fracture was not considered.

However, numerical results obtained by the past researches suggested that the damage of modeling induced solely by stress wave propagation could give reasonable prediction of rock mass response to blasting load (Hao et al, 2002).

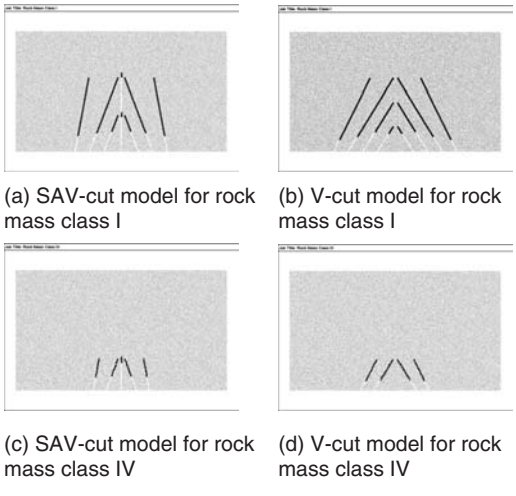
3.3 *Modeling*

The domain of model is 6 m long and 10 m wide and the radius of particle used in the simulation is 0.04 m. A total of 4 cases including two rock mass classes (class I and IV) and two blasting patterns (V-cut and SAV-cut) were considered as shown in figure 3.

3.4 *Results of numerical modeling*

3.4.1 *Blast efficiency in the bottom area of cut holes*

Blast efficiency of each cut blasting pattern was measured by the number of crack generated in the bottom area of cut holes. The boundary of bottom area was defined as 1.0 m ahead from the end of blast hole in rock mass class I, 0.5 m ahead in rock mass class IV. Table 4 shows cut volume, drill length, charge, the number of tensile crack and shear crack in four cases, respectively.



(a) SAV-cut model for rock mass class I

(b) V-cut model for rock mass class I

(c) SAV-cut model for rock mass class IV

(d) V-cut model for rock mass class IV

Figure 3. PFC 2D model for efficiency comparison.

In the case of rock mass class I, total number of tensile cracks and shear cracks by SAV-cut was increased by 41% and 128%, respectively than that of V-cut. In case of class IV, total number of tensile cracks by SAV-cut was increased by 108%, while the number of shear cracks was decreased 19%. The simulation showed that SAV-cut generated more cracks than V-cut in rock mass class I and IV.

The propagation pattern of cracks of each ignition step is shown in Table 5. The rock mass around cut holes is broken by step-by-step blasting within 0.2 sec. In spite of more cracks, the broken rock mass area of SAV-cut was expressed smaller than that of V-cut on the simulation results because the displacement of rock mass occurred by failure was transferred to the center hole in case of SAV-cut by the limitation of 2D numerical analysis.

3.4.2 *Blast vibration attenuation*

In order to measure peak particle velocity, the particle velocity in the x- and y-direction at specific points was measured and peak vector sum was calculated with particle velocities. There are three measuring points located in the vicinity of left boundary as indicated in Figure 4. On the assumption that the center of model domain is the origin, coordinates of each measuring point (A,B,C) are shown in Table 6.

Table 4. Blast efficiency comparison of SAV-cut and V-cut in the bottom of cut holes (PFC 2D).

	Class I		Class IV	
Factors	V-cut	SAV-cut	V-cut	SAV-cut
cut Volume (m^2)	15.22	13.72	4.00	3.8
Drill Length (m)	25.48	24.94	7.2	8.9
Charging (kg)	16.8	13.2	4.00	3.25
Tensile failure crack (Ea)	332	469	136	283
Shear failure crack (Ea)	25	57	422	341

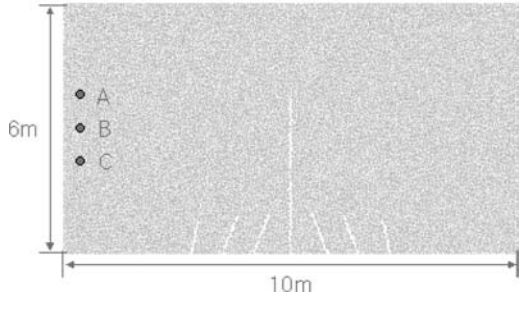


Figure 4. The location of measuring points to monitor peak particle velocity.

The peak particle velocity of SAV-cut was compared to that of V-cut by numerical analysis using PFC 2D as detailed in Table 7. In comparison with V-cut, the peak particle velocity of SAV-cut was reduced by 24∼39% in rock mass class I and 16∼51% in rock mass class IV.

Table 8 shows the peak particle velocity of each ignition step measured at point B.

Table 9 shows the time history of particle velocity in the x-direction, y-direction and vector sum of V-cut and SAV-cut. In case of rock mass class I, the peak particle velocity was occurred at 0.12 sec in SAV-cut and 0.06 sec in V-cut respectively. In case of rock mass class IV, the peak particle velocity was occurred at 0.065 sec in SAV-cut and 0.025 sec in V-cut.

The peak particle velocity of SAV-cut was occurred 0.06 sec later than that of V-cut because the delay time of main inclined holes after center hole ignition was designed to be 40 ms for preventing cementation effect. Due to the delayed time and smaller amount of charging, blast vibration of SAV-cut was lower than that of V-cut.

Table 6. Coordinates of measuring points (A,B,C).

location	A	B	C
x coordinate	−4.7	−4.7	−4.7
y coordinate	0.75	0	−0.75

Table 7. Peak particle velocity(m/sec) of SAV-cut and V-cut.

		Position		
Class		A	B	C
Class I	SAV-cut	2.33	2.43	2.64
	V-cut	3.07	3.97	3.92
	Vibration attenuation	24.1% ↓	38.8% ↓	32.7% ↓
Class IV	SAV-cut	1.14	1.16	1.26
	V-cut	2.36	1.39	1.69
	Vibration attenuation	51.7% ↓	16.6% ↓	25.4% ↓

Table 5. Normal bondage failure.

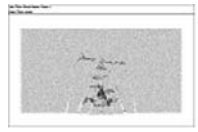
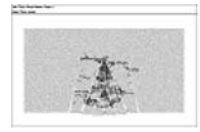
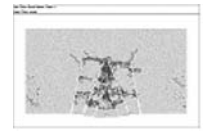
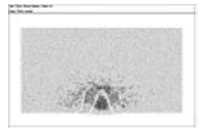
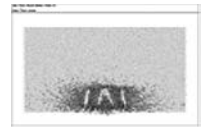
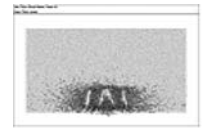
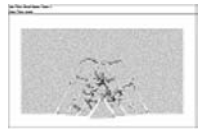
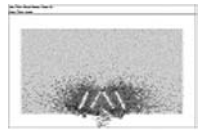
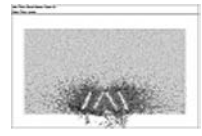
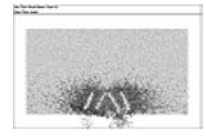
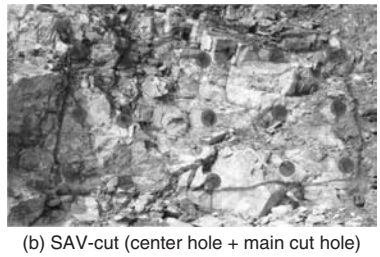
Center-cut	Rock mass class	Crack pattern			
SAV-cut	I				
		0.0 sec	0.06 sec	0.12 sec	0.20 sec
	IV				
		0.0 sec	0.04 sec	0.08 sec	0.20 sec
V-cut	I				
		0.0 sec	0.04 sec	0.08 sec	0.20 sec
	IV				
		0.0 sec	0.04 sec	0.08 sec	0.20 sec

Table 8. Peak particle velocity (m/sec) of each ignition step.

	Class I		Class IV	
	Step	PPV (m/sec)	Step	PPV (m/sec)
SAV-cut	1st Center hole	0.328	center hole	0.597
	baby cut	0.038	1st main cut	0.150
	2nd Center hole	0.049	2nd main cut	1.16
	1st main cut	0.135	–	–
	2nd main cut	2.43	–	–
V-cut	1st baby cut	0.324	1st main cut	0.863
	2nd baby cut	0.048	2nd main cut	1.35
	1st main cut	0.219	–	–
	2nd main cut	3.76	–	–



(a) V-cut (inclined hole)



(b) SAV-cut (center hole + main cut hole)

Figure 5. cut-hole layouts of V-cut and SAV-cut.

Table 9. Particle velocity of SAV-cut and V-cut.

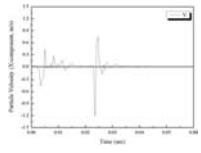
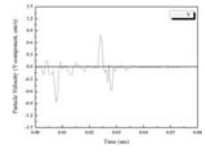
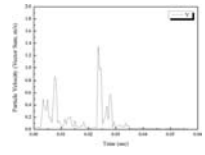
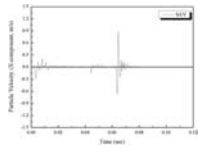
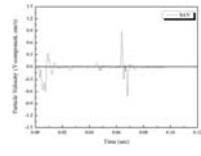
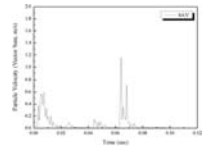
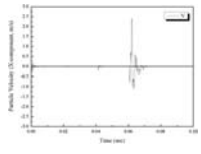
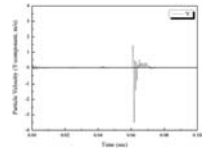
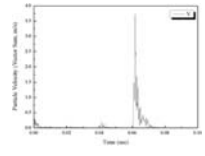
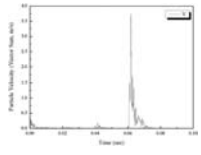
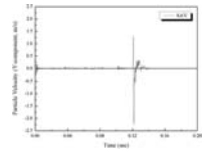
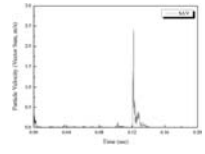
		Particle velocity		
Rock mass class	Center-cut	X	Y	Vector sum
Class IV	V-cut			
	SAV-cut			
	V-cut			
Class I	SAV-cut			

Table 10. Performance of SAV-cut and V-cut from field tests.

Tunnel center-cut	Sapaesan		Chungho	
	V-cut	SAV-cut	V-cut	SAV-cut
Rock type (Drill length)	IV (1.3 m)	IV (1.3 m)	I (3.8 m)	I (3.8 m)
Total charging weight (kg)	79.825	78.70	275.17	268.425
Blasting efficiency (%)	84.6	93.8%	82.9	92.1
PPV (cm/sec)	0.164	0.143	0.179	0.170
Distance (m)	75	75	260	260

4 FIELD TEST RESULTS

The performance of SAV-cut and V-cut was compared by two field tests. Figure 5 shows the cut-hole location of V-cut and SAV-cut marked on the tunnel excavation face.

From test results, the blasting efficiency of SAV-cut was 10 % higher than that of V-cut. Also, the peak particle velocity was decreased as shown in table 10.

5 CONCLUSION

This paper introduced SAV-cut (Stage Advance V-cut) developed to overcome the disadvantage of V-cut and Cylinder-cut. Field tests and numerical analysis were carried out to analyze the mechanical behavior and blasting vibration. The results of studies are summarized as follows.

(1) In numerical analysis, a total of 4 cases including two rock mass classes (class I and IV) and two blasting patterns (V-cut and SAV-cut) were compared using PFC 2D.
(2) In case of rock mass class I, tensile cracks and shear cracks induced by SAV-cut were increased by 41% and 128%, respectively. In case of class IV, tensile cracks of SAV-cut was increased by 108%, while the number of shear cracks was decreased 19%. The simulation showed that SAV-cut generated more cracks than V-cut in both rock mass class I and IV.
(3) The peak particle velocity of SAV-cut was compared to that of V-cut by numerical analysis. In comparison with V-cut, the peak particle velocity of SAV-cut was reduced by 24∼39% in rock mass class I and 16∼51% in rock mass class IV.
(4) The performance of SAV-cut and V-cut was compared by two field tests. The blasting efficiency of SAV-cut was 10 % higher than that of V-cut. Also, the peak particle velocity was decreased.

REFERENCES

Atlas Power Company. 1987. Explosives and rock blasting: 662.

Cundall, P.A. & Strack O.D.L. 1979. A discrete numerical model for granular assemblies, *Geotechnique* Vol. 29 : 47–65.

Hao, Ho., Wu, C. & Zhou, Y. 2002. Numerical analysis of blast-induced stress waves in a rock mass with anisotropic continuum damage models – Part I: Equivalent material property approach, *Rock Mechanics and Rock Engineering* Vol. 35 : 79–94.

Hoek, E., Carranza-Torres, C. & Corkum, B. 2002. Hoek-Brown failure criterion – 2002 Edition, *Rocscience, Inc.*

Itasca. 1999a. PFC2D-Particle Flow Code in 2 Dimensions, *Itasca Consulting Group, Inc.*

Itasca. 1999b. PFC3D-Particle Flow Code in 3 Dimensions, *Itasca Consulting Group, Inc.*

Jong, Y.H., Lee, C.I., Jeon, S., Cho, Y.D. & Shim, D.S. 2005. Numerical modeling of the circular-cut using particle flow code, *31st Annual Conference of Explosives and Blasting Technique, Orlando, CO, USA* : CD-ROM.

Kim, J.-H. 2000. The circular center cut with large empty hole and pre-splitting in tunnel, *Master's thesis of Kangwon National University, Korea.*

Liu, Q. & Tidman, P. 1995. Estimation of the dynamic pressure around a fully loaded blasthole, *Technical Report MRL 95–014, CANMET/MRL* : 15.

Starfield, A.M. & Pugliese, J.M. 1968. Compression waves generated in rock by cylindrical explosive charges: A comparison between a computer model and filed measurements, *International Journal of Rock Mechanics and Mining Science & Geomechanics Abstracts,* Vol. 5 : 65–77.

Persson, P.A., Holmberg, P. & Lee, J. 1994. Rock blasting and explosives engineering, *CRC press* : 540.

This page intentionally left blank

Underground Space – the 4th Dimension of Metropolises – Barták, Hrdina, Romancov & Zlámal (eds)
© 2007 Taylor & Francis Group, London, ISBN 978-0-415-40807-3

A study of the invert tunnel's behavior in a weathered-rock using laboratory model test and numerical analysis

K.J. Kim & S.Y. Koh & S.Y. Choo
DANWOO Engineering co. LTD, Seoul, Korea

C.S. Hong & D.J. Hwang
SAMSUNG Engineering & construction, Seoul, Korea

ABSTRACT: Invert is a kind of the tunnel structure which is applied to weathered rock or poor ground condition. In this study we grasped the efficiency of the plate and invert section by the laboratory model test and numerical analysis for the korea high speed railway's tunnel section and verified that invert is more superior than plate section for the load resistance ability. We analysed tha failure mode of the tunnel peripheral ground for the each test case using the critical shear strain rate among the indicated parameters of the failure mechanism. To control ground deformation in a weathered rock, the invert section is more effective than the plate section. But the invert's shotcrete section force exceeded the allowable limit and this was checked using a numerical analysis. When the invert section is applied, it should be installed permitting a maximum ground deformation in order to prevent failure of supporting system.

1 INSTRUCTIONS

The invert which is installed on the base of the tunnel floor is applied to the tunnels outer wall to resist external pressure from weathered rock or poor ground condition. The invert is stabile solution in soft ground but it is often omitted in fine ground because of economical reasons.

In bad ground conditions, it is more effective to install the invert as soon as possible, but if the invert is installed too early (before settling) supporting capacity can not effectively be controlled, so it should be installed after permitting sufficient rock deformation.

Pre-estimating of the failure mechanism using a model test with different mathmatical modeling and numerical analysis to determine tunnel failure behavior is important process. A laboratory model and centrifuged model test represent the bearing and failure behavior which can be observed with the naked eye. To analyze the ground failure use the numerical analysis on a computer for quicker and more effective conclusions.

In this study the invert section's resistance from external pressure is estimated quantitatively through the 2- axis compression test and numerical analysis. This is for the Korean express train tunnel which has a height of 15.3 m and a width of 11.0 m.

A failure state around the tunnel is estimated from different test results with the critical shear strain and this also provides basic information to set up an effective installation analysis through the invert and plate section's behavior with consideration to the ground conditions.

2 STUDY OF THE TUNNEL MODEL TEST AND NUMERICAL ANALYSIS

2.1 *Equipment of the model test*

When using a downsized scale model test of real site conditions deformation behavior of the tunnels stability can be verified using a reduction rate calculation. The down-scaled model tester using hydraulics has a bearing of 25 ton, $48 \times 48 \times 20$ cm (width $\times$ height $\times$ length) The down sized scale model test is a 2-dimensional space test, the upper side of the tunnel model is fixed with a displacement control bar. A digital camera (type EF 28$\sim$105 mm, 6.5mega pixels) is installed at a distance of 2 m from the down-scaled model. A displacement (error range $\pm$0.1 mm) of the model test is measured by comparing pictures taken at regular intervals with pre-marked measuring points.

2.2 *The down-scaled model test*

The purpose of this study is quantity estimation of resistance capacity against external pressure through



Figure 1. The down-scaled model tester.

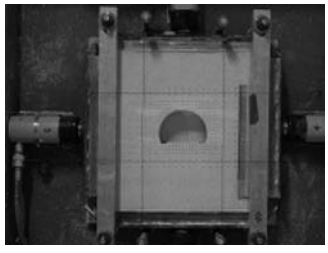


Figure 2. The measuring points are marked.

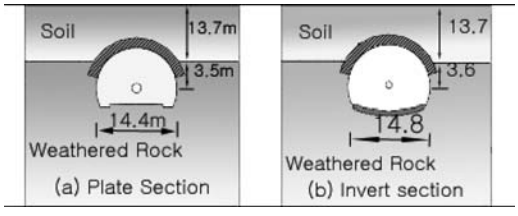


Figure 3. Down-scaled model test section.

a 2-axis compression test and the use of numerical analysis, using a section of the Korea express train tunnel. The area of excavation is about 140 m^2 (width 15.3 m, height 11.0 m).

The model test is performed at tunnel depth G.L −11.0 m, the reinforced space in the crown has a range of approx. 150° of the umbrella roof reinforcement. The materials used in this model test are the same as in real site's engineering properties and test material used in sand, gypsum(or lime), and water.

To get an exact test result, a dimensional analysis is performed. The three physical factors, that is length [L], time [T], and mass [M], are used to assist in the result of the reduction rate. The reduction rate is then applied to the model test as the result of a dimensional analysis. The displacement measured in the invert section and plate section is constantly updated and has a variable pressure, which is measured in hydrostatic pressure (Ko = 1).

Table 1. Material properties.

Classification	Soil	Weathered rock	Hard rock
rt (tf/m^3)	1.9	2.1	2.7
E (tf/m^2)	8×10^3	9×10^4	4×10^6
υ	0.35	0.31	0.2
Cohesion(tf/m^2)	2	10	1,000
Φ	31	35	48
qa (tf/m^2)	25	180	15,000

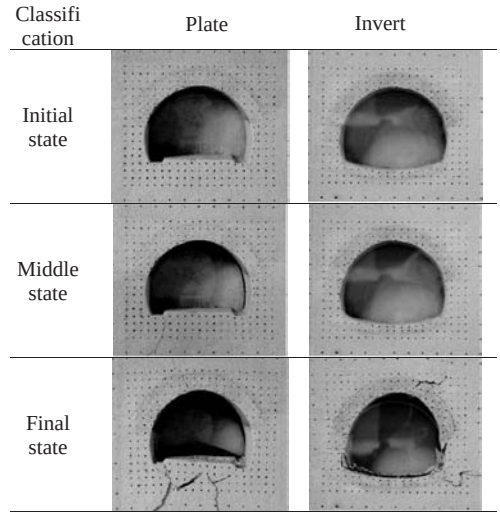


Figure 4. Result of plate & invert section test.

2.3 *The result of down-scaled test*

When 2.2 kgf/cm^2 pressure is applied to the plate section as seen in fig. 4, a crack developed from the left corner of the tunnel and additional failure occurred along the tunnel floor. A big displacement has formed on the tunnel floor and a crack has occurred on the crown of the tunnel in its final stage.

On the other hand, when 2.7 kgf/cm^2 pressure is applied to the invert section in fig. 4, a crack has developed from the upper soil layer and left corner of the tunnel. The right side crown of the tunnel and the bottom side of the tunnel experienced failure in the final stage, but the tunnel has no floor heaving.

2.4 *Numerical analysis – Investigate numerical analysis*

FLAC 2D,2-dimensional finite element Method, is used to analyze more details of the tunnel failure behavior after the model test. The numerical analysis modeling uses the same soil properties and scale as the model test. Load is increased step by step at model boundary.

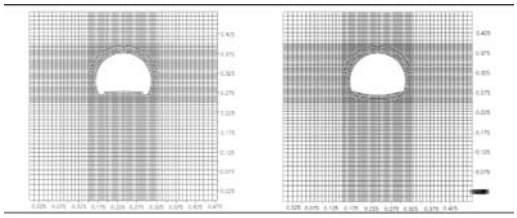


Figure 5. Numerical analysis modeling.

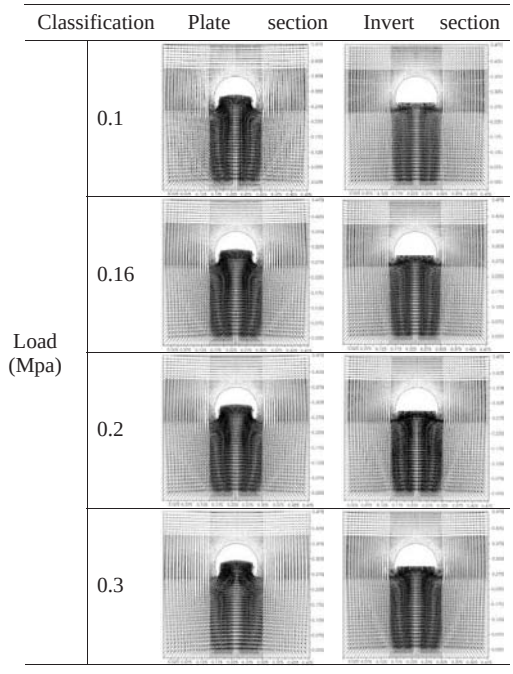


Figure 6. The strain vector depend on load pressure.

In the plate section each analysis section's displacement vector is displayed with fig. 6., the tunnel displacement is increased fundamentally when the load pressure exceeds 1.6 kgf/cm^2 and floor heaving occurs on the tunnel floor when the load pressure exceeds 2.0 kgf/cm^2. But in the invert section, displacement has gradually increased but floor heaving has not occurred when the load pressure is over 3.0 kgf/cm^2. Plasticity area has extended from the bottom edge of the tunnel according to the increase in load pressure, and most of the bottom of the tunnel has failed(fig. 7), this represents for the distribution shape of the plasticity area on loading pressure, but the invert section has smaller plasticity areas compared with the plate section these have no failure on the bottom of the tunnel at 3.0 kgf/cm^2 load pressure. The results are very similar with the model test.

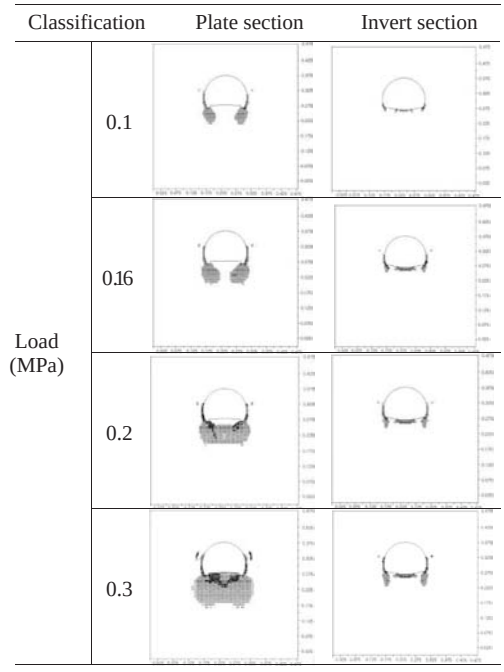


Figure 7. Distribution form of plasticity area depend on loading pressure.

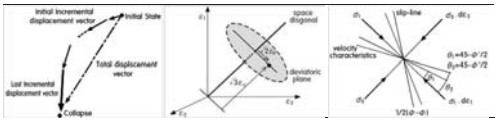
3 ESTIMATES OF EFFECTIVENESS OF INVERT ON ANALYZING OF THE FAILURE MODE

3.1 *Characteristics of failure mechanism around tunnel*

If the plate section permits displacement without support in the weathered rock or bed ground condition, the bottom of the tunnel will have failure by floor heaving. The invert section has fixed condition effect, so that support's stress increase with ground deformation, and support's failure precedes ground failure. To analyze tunnel failure mode by numerical analysis, it is important to consider choice of parameters and how to use these parameters. A pre-estimate of failure mechanism is possible from increment strain vector, shear strain rate, velocity properties but failure mode must be decided by supplemental investigation of new parameters in Shin et al; (2001)

(a) Incremental strain vector
(b) Deviatoric Strain Space
(c) Relation between Velocity Characteristics and Slip Line

Shear deformation, which is one of the indicated parameters, is defined as an exact failure surface when shearing deformation has a narrow and conspicuous direction(Shin et al; 2001). Failure behavior in the



(a) Increment strain vector | (b) Deviatoric Strain Space | (c) Relation Between Velocity Characteristics and Slip Line

Figure 8. A failure mechanism of indicator parameter (Shin et al; 2001).

invert section and plate section is estimated by Mohr-Coulomb, which can be compared to critical shear strain rate. If the area around the tunnel ground adapts a standard failure by Mohr-Coulomb, a formula will be applied to deviator stress.

$$\sigma_1 - \sigma_3 = (\sigma_1 + \sigma_3) \cdot \sin\Phi + 2 \cdot c\cos\Phi \text{ ----------(1)}$$

And deviator strain will be expressed by Hook method as below.

$$\varepsilon_1 - \varepsilon_3 = \frac{1+\upsilon}{E} \cdot (\sigma_1 - \sigma_3) \text{ ---------- (2)}$$

A indicated parameter of the failure ε_1, ε_3 is Max, Min deformation rate, E is elastic modules, and υ is poison rate. The critical shear stress strain will be defined by combination of the two above formulas as below

$$\gamma_c = \varepsilon_1 - \varepsilon_3 = \frac{1+\upsilon}{E} \cdot (\sigma_1 - \sigma_3)\sin\Phi + 2 \cdot \frac{1+\upsilon}{E} c\cos\Phi$$

$$\approx \frac{1+\upsilon}{E} P_o \sin\Phi + \frac{1+\upsilon}{E} c\cos\Phi \text{----------(3)}$$

3.2 *Failure mode analysis of tunnel model test*

Figure 9. shows the tunnel's failure behavior depends on the load condition by shear strain of model tests. In the plate section, ground failure caused the concentration of shear strain rate on both sides of the tunnel bottom when loading pressure exceeded over 1.0 kgf/cm^2, and shearing deformation has extended at the tunnel bottom. But the invert section shows a very stable state compared with the plate section with the same load conditions.

3.3 *The invert section is behavior characteristics in weathered rock*

Maximum Shearing deformation, under weathered rock condition, is about 15,000 kgf/cm^2 based on many test carried out in Korea fig. 10. the purpose of this study is to estimate the invert section's effectiveness and tunnel failure behavior using weathered rock deformation such as 500, 1,000,

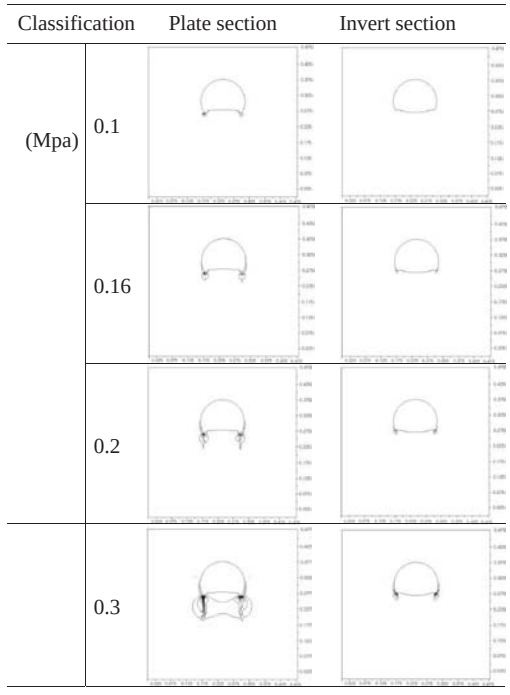


Figure 9. A increasing chart of shearing deformation according to loading pressure.

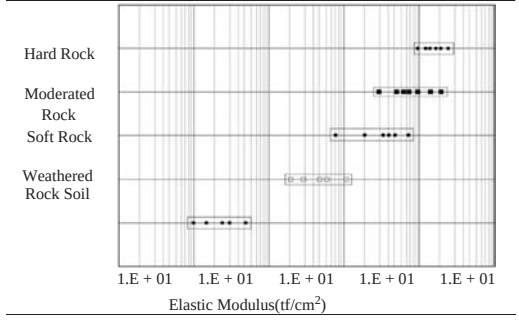


Figure 10. Range of deformation according to ground condition(in Korea).

5,000, 10,000 kgf/cm^2, which correspond with Mohr-Coulomb criteria.

The Korean express train tunnel section is applied to estimate the invert section's effectiveness, in the modeling range was included 1D for depth and over 3D for the left and right side in numerical modeling. A portion of 20% loading was applied before installing supports and 80% after. A result of critical shear strain rate and displacement, is shown in table 2 at formula 3, these are applied to properties in numerical modeling.

Table 2. Critical shear strain (rate) each case.

Classification	Case1	Case2	Case3	Case4
E (tf/m^3)	5,000	10,000	50,000	100,000
C (tf/m^3)	2	4	8	10
Φ ( )	25	28	30	35
Critical shear strain rate	0.0107	0.0061	0.0013	0.0007
Critical shear strain (mm)	161.3	92.7	20.4	11.7

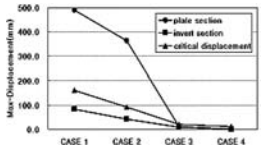


Figure 11. Critical shear strain according to case analysis.

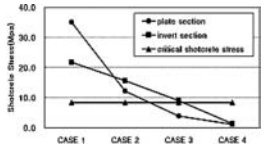


Figure 12. Stress at supporting to case analysis.

In plate section displacement over the critical shear strain in case 1, 2 but in the invert section, a displacement was under a critical shear strain in all cases (fig 11).

In the invert section bending-compressed stress of shotcrete was over the limit bending-compressed stress in case1, 2, 3, but in the plate section bending-compressed stress of shotcrete over the limit bending-compressed stress in case 1, 2 (fig 12).

The plate section is installed under weathered rock condition and soft ground, ground failure started from the bottom of the tunnel when tunnel displacement is in a unconfined condition. But the invert section's support stress is larger than the plate section's support stress, that means invert section's stress is increased because of the fixed condition effectiveness. Therefore, the plate section have more advantages in good ground conditions because displacement of tunnel bottom is smaller than the critical shear strain in good ground conditions. But the invert section have more advantages in bad ground condition because ground will be failed by deformation of tunnel when deformation of tunnel is over the critical stress strain. When the invert section is needed, the invert section should be installed as soon as possible but if it is installed too soon, the inverts supporting stress will be over the allowable stressed. So when the invert section is

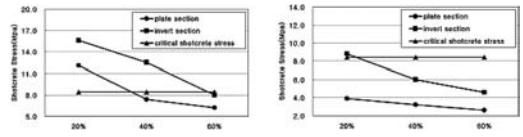


Figure 13. Supporting stress according to allowed displacement.

applied, the invert section should be installed after permitting a maximum of ground deformation within critical shear strain. To verify this, displacement is increased by a portion of load distribution which is applied 20%, 40%, 60% before installing the invert. Figure 13. shows a result of section force in support.

When a distributed loading pressure of 20% is applied, the shotcrete's stress is over the allowable limit as in case 2, 3 but the shotcrete's stress is under the allowable limit when 60% distributed loading pressure as in case 2 and over 40% distributed loading pressure as in case 3, and the support such as shotcrete is installed in inferior ground, it is more effective to install an support after displacement has occurred. That means when the invert section is installed after until the critical shear strain has occurred, it can be prevented from ground failure and an anchor failure.

4 CONCLUSION

The invert section is a very effective structure to control failure influence around the tunnel in a under weathered rock condition. Tunnel down-sized test and numerical analysis is executed for the Korean express tunnel section and the invert section is quantitatively estimated compared with the plate section in a weathered rock condition.

1) These results shows that the invert section is more effective against external pressure compared with the plate section.
   (a) From the result of a laboratory model test, cracks in the plate section started approximately at 20% pressure higher than the plate section.
   (b) Floor heaving and plasticity area is noticeable reduced when the invert section is applied to the tunnel compared with the plate section.
   (c) In the invert section, small floor heaving and plasticity area, which has shown noticeable reduction in the failure area around the tunnel. When the shearing deformation and the critical shear stress strain are used, which is a standard from Mohr-Coulomb.
   (d) Using the indicator parameter of failure mechanism which are incremental strain vector, shear strain rate and velocity property, these are tested individually in the laboratory model test.

2) To analyze the behavior of the invert section in a weathered rock condition, parameter study is carried out to analysis of invert section's behavior properties. Smaller displacement has occurred in the invert section compared with the plate section, but the supporting system showed stress in excess of the allowable stress. That means invert sections of the shotcrete show stress has increased due to ground deformation because of confined conditions. To prevent ground failure and the supporting system concrete failure, the invert section should be installed after ground deformation in the critical shear strain range.

REFERENCES

Atkinson, J.H. and Potts, D.M. (1977). "Subsidence above shallow tunnels in soft ground", J. Geotech. Eng. Div. ASCE, Vol.103, GT4, pp.307∼325.

Chambon, P and Corte, J.F. (1994). "Shallow tunnels in cohesionless soil: stability of tunnel face", J, of Geotech. Eng. Div. ASCE, Vol.120. GT7, pp.1149∼1165.

Davis, E.H., Gunn, M.J., Mair, R.J. and Seneviratne, H.N. (1980). "The Stability of Shallow tunnels and underground opening in cohesive material", Geotechnique, Vol.30, No.4, pp.397∼416.

Eisenstein, Z. and Samarasekera, L. (1992). "Stability of unsupported tunnel in clay", Can. Geotech. J. Vol.29, pp.609∼613.

Kim, Y.M. (2001). "Analysis for Effects of Slope Failure Behavior by Finite Element Method", Journal of the *Korea Geotechnical Society*, Vol.00, No.0, pp.000∼000.

Hong, C.S. et al (2006) "An Assessment of Safety Zone for Mountain Tunnel Portal Using Strength Reduction Technique", Korea Geotechnical Society Spring Conference, pp.000∼000.

Kim, Y.M. (2001). "A Study on Comparision of Numerical Simulation with Model Test of Shallow Tunnel Failure", Journal of the Korea Society of Civil Engineering, Vol.21, No.2-C, pp.91∼98.

Leca, E., and Dormieux, L. (1990). "Upper and lower bound solutions of the face stability of shallow circular tunnels in frictional material", Geotechnique, Vol.40, No.4 pp.581∼606.

Shin, J.H. and Lee, I.K. (2001). "A Study on the Failure Mechanism of the Mixed-face Tunnels in Decomposed Granite", Journal of the *Korea Geotechnical Society*, Vol.14, No.4, pp.317∼329.

Shin, J.H. and Potts, D.M. (2001). "Constitutive Models for Decomposed Granite Soil and Their Application to Tunnelling Problem", Journal of the *Korea Geotechnical Society*, Vol.17, No.1, pp.131∼139.

Underground Space – the 4th Dimension of Metropolises – Barták, Hrdina, Romancov & Zlámal (eds)
© 2007 Taylor & Francis Group, London, ISBN 978-0-415-40807-3

Design and installation waterproofing system for access shafts of service tunnels on Palm Jumeirah Island

M.K. Kundu
General Manager, Al Naboodah Engineering Services (L.L.C.), Dubai, UAE

M.E. Ryjevski
Technical Manager, Al Naboodah Engineering Services (L.L.C.), Dubai, UAE

D.G. Solter
Deputy Project Manager, Al Naboodah Engineering Services (L.L.C.), Dubai, UAE

ABSTRACT: The man-made island, created in Dubai, UAE in the shape of a palm tree is known as the 8th Wonder of the World. To the Island it was given a name of Palm Jumeirah Island. The Palm Jumeirah will measure approximately 5 km in length and 5 km in width. The crescent Island surrounding the Palm will measure approximately 11 km in length. Infrastructure construction for this island has comprised amongst others, the construction of several bridges, waste water collection and maintenance systems, storm water drainage system, irrigation and domestic water supply network, pipe-gas system, telecommunications, electrical system, tunnels, marinas facilities and landscaping. Among numerous tasks the service tunnels supplying electricity from the Palm Island to the Crescent is one the most difficult and expensive. This paper describes the design and construction issues for tunnel and shafts sophisticated waterproofing system, which will warranty dry condition during the life time of all underground structures.

1 INTRODUCTION

The man-made island, created in Dubai, UAE in the shape of a palm tree is known as the 8th Wonder of the World.

The complex of the islands that is called "The Palm Jumeirah" was artificially reclaimed of sand in the Arabian Gulf approximately 30 km away from the center of Dubai (Fig. 1).

About 100 million cubic meters of sand have been used to create this island. The height of "The Palm" (i.e. the length of the island) is about 5 km, the distance between the tips of the biggest branches – the Fronds (i.e. the width of the island) is about 5.5 km.

"The Palm" is framed by another man-made island named "The Crescent", which is approximately 1.5 km away from the top branches – the Spine of "The Palm" and was designed in order to protect the coastline from possible storms (like breakwaters).

The project suggests the construction of about 60 high-class fashionable hotels, more than 5000 villas and over 100 residential buildings. Numerous entertaining and cultural leisure centers such as parks, yacht and golf clubs, a delphinarium, restaurants, shopping malls, cinemas and many more will be built.

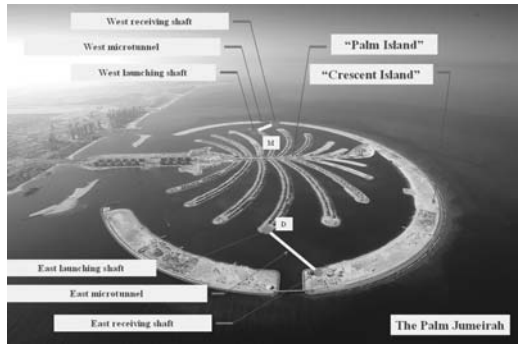


Figure 1. The Palm Jumeirah Island and service shafts location plan view.

"The Crescent" and "The Palm" are linked to each other by a road tunnel and a monorail, the services and communication means will be supplied thanks to 2 microtunnels and 12 Horizontal Directional Drilled (HDD) pipes with the diameter of 0.5 m.

The Eastern and the Western microtunnels are meant to be the energy supply to "The Crescent". Each

of them about 700 m long and has the internal diameter of 2.4 m, they approximately go as deep as to 25 m below the sea level.

One of the largest and well-known Construction Companies of Dubai "Al Naboodah Engineering Services LLC" (ANES) was entitled to an authority to design and construct the service tunnels and HDD on "The Palm".

The construction of the tunnels was carried out thanks to the modern microtunneling method which suggests the usage of the TBM AVN3 manufactured by well-known company "Herrenknecht" and specially designed concrete jacking pipes. The tunnels construction using the afore-named method required the design and the excavation of two launching and two receiving shafts which were supposed to be used afterwards, while functioning, in order to have an access to the tunnel and to accommodate the electric cables and the required electric equipment.

The TBM complex AVN3 was installed one by one on the Fronds "D" and "M" in launching shafts and the feeding of the concrete jacking pipes which were subsequently jacked and served as a tunnel liner. The launching shafts are about 12 m in diameter and with the depth of around 28 m. (Fig. 2).

The receiving shafts located on "The Crescent" are about 9 m in diameter and around 20 m deep.

The main difficulty while designing and constructing all four shafts was the necessity to excavate them in totally unstable and saturated drudged sand, which actually reacted as "quicksand". Only going as deep as to 17 m the reclaimed sand underlined by natural sandstone which was classified as a weak and heavy fractured rock formation.

Existing subsurface geological conditions made it necessary to excavate the shaft using shoring system made of from secant piles.

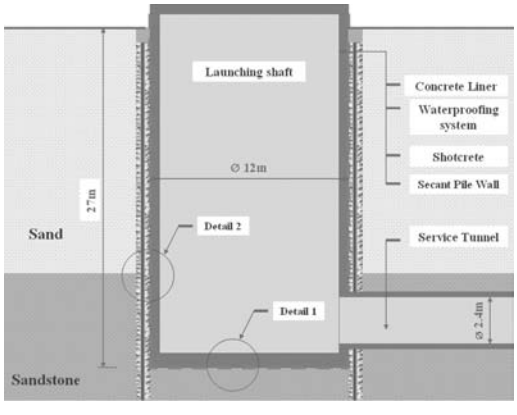


Figure 2. Launching shafts at Frond "M" & "D".

Thus, in general the shafts construction scheme can be described as below:

1) The construction of shafts shoring system made of from secant piles with the diameter of 1.0 m and 30 m deep, the suggested distance between the piles' axes was about 0.85 m;
2) The soil excavation to the project level of approximately −28 m fixing several levels of bracing beams made of pre-cast reinforced concrete;
3) The shafts' walls surface preparation for the installation of a waterproofing system by applying shotcrete around 10 cm thickness;
4) The waterproofing system installation around of 5000 m^2 using PVC membrane;
5) The reinforcement installation at the bottom of the shafts and base slab casting with thickness of 1.0 m;
6) Shafts walls casting with thickness of 0.45 m;
7) The roof pre-cast slabs (the weight of slabs around 90 tons) installation.

Taking into consideration the sever geological conditions, the high level of underground water and the high level of aggression of the seawater towards shafts concrete, the high level demands to the water tightness of the shaft liner while functioning, the major concern was as follows: to develop a waterproofing system that would meet the demands and provide reliability during all shaft operation period as per project specification and international standards has to be not less than 120 years.

2 THE DESIGN SOLUTIONS OF THE SHAFTS WATERPROOFING SYSTEM

The long-term experience in tunneling and in general underground constructions shows that to reach the above-mentioned requirements require quite considerable investments, but make sense from economical point of view as investing once in the future they allow to use the equipment without wasting huge sums to struggle with water-suppression and grand construction overhauls.

To fulfill the mentioned above task considering the accepted construction scheme, the analysis of the building elements' mutual relocations, the climatic conditions, the surrounding environmental factors etc., there has been made a comparative analysis. It analyses the characteristics of various types of membranes which are well known in underground construction, such as highly elastic polyethylene (VFPE), high density pressure polyethylene (HDPE), a polyvinylchloride (PVC) and other alternatives, after which the final decision was made. The PVC membrane has been selected as a basic material of the waterproofing system.

PVC membranes of various manufactured companies, such as "Sika" (Switzerland), "Flag" (Italy), "Alkor Draka Ltd." (UK) and the other companies offering analogous product in the UAE market have been thoroughly and carefully studied paying heed to the comparative characteristics of the materials, suggested technological schemes of the system installation, "the know-how", the technical assistance possibility, the supply terms, the cost and some other factors. Considering all the afore-named factors, the choice has finally been made in favor of the company "Flag-Degussa".

In the process of the collaboration of the experts between the companies "ANES" and "Flag - Degussa" there was developed a basic concept of the shafts waterproofing system installation that is as follows:

The PVC membrane stacking up on a blinding concrete layer of a base slab and a shotcrete layer which evens the secant piles surface. Before fixing the membrane the base surface should be in corresponding conditions: smooth to the utmost extent, with no contain of off and other uneven substances, capable to break the PVC membrane layer subject to the influence of the water's negative effect and reinforced construction weights, the surface. Generally, the admissible radius of unevenness with more than 200 mm or their width relation towards the height more than 5/1 is acceptable. In spite of the fact that the membrane underlying layer course is not directly relevant to the waterproofing system, it importance in terms of it preparation quality shouldn't be neglected.

The layer of Geotextile Drefon S with specific gravity not less than 500 g/m^2 is applied on the prepared base. This layer prevents the PVC-membrane from possible damages under the loading influence from shafts concrete slab and it is a drainage layer as well, in order to direct the water from the walls into the gravel drainage layer installed under the base slab;

The main element of waterproofing system is PVC membrane Flagon BSL (3 mm) for a base slab and Flagon BSL (2 mm) for the walls, which is defined further to the liquid pressure water volume and the conditions of interactivity between the constructions of the base slab and the shoring in the process of functioning;

The additional – Flagon PZ with the thickness of 1.5 mm, which is also used to insure the safety, is fixed onto the main layer of the PVC membrane. Almost all the manufactured companies of PVC and HDPE membranes around the world apply a similar technical solution, which is called Fail-Safe System (the destruction preventing system). This layer does not fulfill the main waterproofing function, but along with the injection tubes it allows the leakage observation and to carry out the repairing structure injection between the two layers of the membranes when needed;

The waterproofing system surface was divided by waterproofing tape Waterstop W4 into compartments not more than 200 m^2, in order to have a precise control over the possible leakage areas, and to save the repairing contents injection as well. The installation site of the waterproofing tape was figured out in a way so that the center of Waterstop would coincide with the center of a concrete construction joint that was also an additional safety element to prevent the shafts from water access.

A protective layer of the Drefon S Geotextile with specific gravity not less than 200 g/m^2 was applied over the PVC membrane in order to protect the main membrane from accidental punctures in the process of the subsequent constructional works including reinforcement installation, the casing and concreting. There was an additional protective layer of a cement screed applied over the Geotextile coating for the base slab.

The design of "shear key" between a base slab and secant piles with expectable water pressure up to 3Bar and the utmost maximum displacement of the structural components was a matter of a major concern. The displacement of the structural elements had a potential danger in terms of the membrane's possible destruction; the concrete finishing construction joints have been paid a certain attention too, as they were critical for the water filtration into the structure. The shear key Waterstop W4 along with the multiple use injection system Masterflex 900 has also been fixed in all similar construction joints, allowing to prevent leaking applying the repairing structure.

Summarizing the aforesaid, there has been developed and later on used a waterproofing system unique for this project. A system, which not only prevents the shafts from water infiltration (PVC membrane) but also repeatedly protects the construction from interior water filtration which may occur due to poor quality welding of a membrane, its unforeseen infringements in the process of work, etc., and making it possible to have a simple repairing of the membrane across the total construction area having the control and the water display elimination throughout the whole period of its usage.

3 THE WATERPROOFING SYSTEM INSTALLATION PROCEDURE

Due to the construction constrains and not-so-beneficial construction of "working scaffolds" from a base slab (−28,00 m) up to the top point of the shafts (+1,00 m) the project management decided to carry out the work on a step-by-step basis capturing the height from 4.0 m up to 8.0 m in accordance with the height of a concrete area.

It is important to mention that this working scheme can be favorable for the general work organization but not for a waterproofing system, i.e. actually while

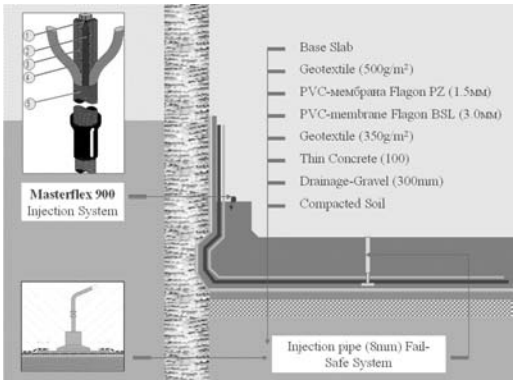


Figure 3. Waterproofing Details at the Base Slab level.

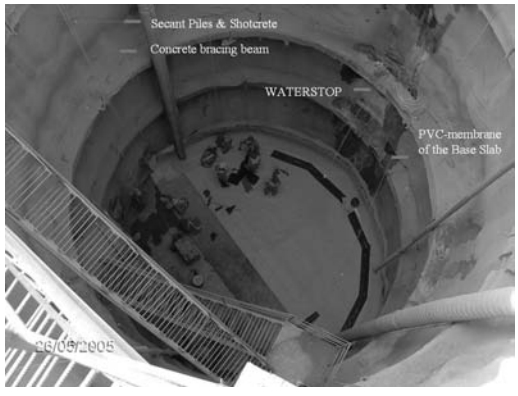


Figure 4. Waterproofing membrane installation.



Figure 5. Waterproofing membrane seam testing.

installing the 20 m high PVC-membrane we are limited to 4 (8) m that has a great impact on membrane installation speed, therefore the cost of the installation works and the most important factor- its quality as there may appear between 3 to 5 additional welded joints overall the shaft perimeter, repeatedly increasing the leakage risk through possible poor quality connections.

Thus the general work scheme can be described as below:

3.1 *Stage 1*

The drainage layer installation and concrete preparation of the shaft base slab with drainage pit for water accumulation and evacuation using the pumps during working time (fig. 3).

3.2 *Stage 2*

The base slab waterproofing system installation stacking the first layer of Drefon Geotextile, the main layer of waterproofing membrane Flagon BSL, fixing the separating element WATERSTOP, a safety layer of Flagon PZ membrane, a protective layer of Drefon S Geotextile (350 g/m^2) and a protective screed of blinding concrete (fig. 4). All the works are listed in a technological order.

A drainage pipe Ø160 mm which had a joint point with a waterproofing membrane due to a special element of waterproofing system Flagon Pipe Collar has been fixed in a pre-cast pit.

The injection tubes Ø18 mm that would allow the application a repairing structure in case of the membrane damage were fixed between the two layers of the PVC membrane Flagon.

Due to the fact that the most critical design loads that effect the PVC membrane thanks to the mutual displacement of the structural components are located in a zone of a base slab joining with the mine non-load-bearing construction the additional injection tubes were installed across the bottom perimeter of a base slab (4 pieces) and in a zone where a base slab is joint with the secant piles (4 pieces).

Works on automatic welding joints of the membrane were implemented using the equipment Leister Twinny S with a nozzle, allowing to carry out the quality test of the membrane welded joint by air pressure through the special test channel with a pressure of 2 Bars. The welded joint is considered to be accepted in case of the pressure drop not more than 20% within 10 minutes (fig. 5).

Manual welding was done applying the equipment Leister Triac S with a 100% quality control by means of a non-destructive method.

During the works on the sites of all the waterproofing system installation works were controlled starting with the quality tests of the supplied materials and their correspondence to the confirmed specification, their storage conditions up to the technological order and quality of the installation works (the membrane welded joints control). All the examination results were daily reported in a special journal that is dedicated to the waterproofing system installation works.

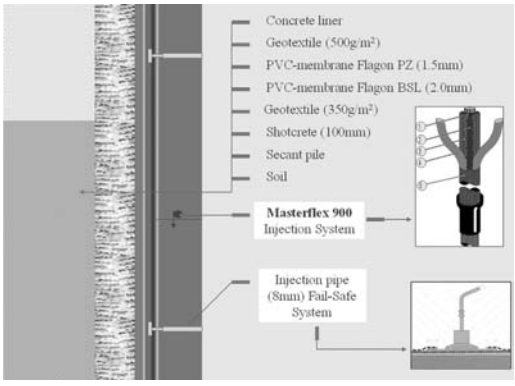


Figure 6. Waterproofing Details on the Walls.

3.3 *Stage 3*

The additional reinforcement and concreting of a base slab.

3.4 *Stage 4*

While installation of the working scaffolds step-by-step, the evening of the secant piles surface by shotcrete, the installation of the two layers of the PVC membrane according to the technology described in a stage 2 and concreting of shafts in-situ concrete liner (fig. 6).

A separating element Waterstop W4 was fixed in each construction joint of the reinforced walls of the shaft and 4 injection tubes were mounted in areas between the construction joints. Every zone of the suggested repairing works did not go beyond 200 m^2.

In addition, each concreting industrial joint was equipped with a multiple use injection system of Masterflex 900 divided along the length into areas 9.0–11.0 meters that became necessary by simplifying of the installation works system and in the future carrying out repair works if required, lessening the injection contents volume.

3.5 *Stage 5*

The separating element Waterstop W4 installation into the reinforced wall of the mine while carrying out the reinforcement works at the level of a return soil coating and the subsequent concreting. The last layer of the waterproofing PVC membrane was welded after dismantling the casing on Waterstop.

3.6 *Stage 6*

The drainage pit elimination, the ability to stop the pumps work and the waterproofing system work reliability control.

There were several local leakage spots defined at this stage both through the injection tubes and in concreting construction joints, that became possible either as a result of the poor-quality welding of a joint or by a membrane puncture during reinforcement installation. However the presence of the two additional protective systems against the leakages allowed their elimination within a short period achieving a 100% result.

4 THE PROSPECTS

Along with the waterproofing system installation for the project “Service Tunnels” the company ANES got orders and has started the works on designing and installation of the analogous systems for the other underground project on the palm islands. In total the capacity of the prospective installation works for the year 2006 has increased from 5000 m^2 in 2005 up to 60,000 m^2 in 2006.

Each new project has its specific features, both in technological solutions and in the companies – the manufacturers of waterproofing membranes, but what they have in common is their unique tendency to switch of from the second safety layer of the membrane as the experience in the construction of this project shows:

1) The cost of the required materials increases 1.5 times;
2) The industrial input therefore the cost of the installation works increases more than twice;
3) The time required for the waterproofing membrane installation almost doubles and this has a negative effect on the object’s work conditions in general;

Considering that the concrete quality and all the works relevant to concrete respond the high standards in the UAE, and selecting the concrete of the right grade in terms of its water tightness and competent calculation of the reinforced concrete structure, we can be confident declaring that one layer of a waterproofing membrane is sufficient making it necessary to use the additional elements related only to the touching areas, joints and similar constructive units.

To make the final decision on this matter it is necessary to have the additional observations over the completed construction done, to analyze all the results as aspiring to create and put into practice the effective waterproofing system that would satisfy the Customer in all respects, it is important to keep in mind the profitability and the terms of construction and all the other way around.

5 CONCLUSION

Despite the fact that the waterproofing of the underground constructions on “The Palm, Jumeirah” using

the PVC materials was the first experience both for the whole island and the company "Al Naboodah Engineering Services LLC" in particular, we can confirm it is a success.

Upon the results of the carried out works the Client received the structure which was completely free from leakages and the possibility of their total control in the future while it's functioning. The repairing works of the PVC membrane can be done at any times if required, without significant labour and material expenses, without creating an obstacle to the operation of the structure.

The correct technical solutions, well trained personnel, a strict fulfillment of all technological processes and the continuous control both internal and from the Client's side made it possible to perform to the utmost extent, the least expenses and within the demanded period.

While designing the shafts not many people were assured in the effectiveness and expediency of waterproofing membranes of this kind, but the successfully gained experience was a proof to all that despite the relatively higher cost of the materials compared to the traditional methods, this direction of underground construction waterproofing is one of the most effective and should be given a priority.

REFERENCE

Al Naboodah Engineering Services LLC, 2004. Project specifications for Constructions of Service Tunnels (JAP 006 – C113), The Palm Jumeirah, Dubai, UAI.

Underground Space – the 4th Dimension of Metropolises – Barták, Hrdina, Romancov & Zlámal (eds)
© 2007 Taylor & Francis Group, London, ISBN 978-0-415-40807-3

Seismic behavior of Tubular Roof & Trench method (T.R.&T) by numerical analysis

Kwak, Chang-won
Civil Engineering Task Force, Korea District Heating Engineering Co. Ltd, S. Korea

Park, Inn-joon
Dept. of Civil Engineering, Hanseo University, S. Korea

Kim, Sang-hwan
Dept. of Civil Engineering, Hoseo University, S. Korea

Kim, Jeong-yoon
KNTS. Co. Ltd, S. Korea

ABSTRACT: T.R.&T (Tubular Roof & Trench) method has been invented for safety and effectiveness on underground construction, then, applied to some projects recently. In this research, the practical site where T.R.&T method was applied is selected and dynamic response was analyzed by 2-dimensional numerical analyses. The behavior of T.R.&T under seismic excitement is important because it is constructed near ground surface normally and composed of various sizes of steel pipes which means enormous differences of stiffness. It may cause tremendous ground amplification and stress concentration at the connection part of steel pipes. Therefore, it is necessary to examine the general behavior and seismic performance of T.R.&T structure under troublesome ground conditions such as fault zone and highway underpass. Stress concentration and displacement occurrence trends are investigated thoroughly in those two cases Consequently, case study on practical sites showed the weak part of T.R.&T structure under dynamic loading and characteristics of seismic behaviors.

1 INSTRUCTIONS

1.1 *T.R.&T (Tubular Roof & Trench) method*

A new excavation method, T.R.&T, has been invented for safety and effectiveness on underground construction, especially for the excavation under the existing road or railway with shallow cover. Several steel pipes have large section($D = 2{,}000$ mm) are injected to the ground for restraining surface settlement and excavated inside the pipes. Smaller pipes connect main pipes transversely to build up stable steel structure. The area between pipes is grouted to prevent water leakage. Concrete slabs and walls are placed after cutting the inner section of whole structure. These procedures offer stability of ground during excavation. That is why this method is broadly applied to the excavation under existing roads, railways, boxes, etc. Figure 1 shows the typical T.R.&T section.

T.R.&T method has advantage on water leakage, erosion and stability during construction. In addition, it is tremendously economical because construction period reduction under the difficult conditions (for example, adjacent excavation or urban tunneling with shallow depth, large sectional tunneling, etc.).

Otherwise, T.R.&T tunnel is normally constructed near the ground surface, earthquake load may cause stability problem. Connecting pipes can be the weak part of the structure, therefore, seismic behavior of T.R.&T structure should be examined.

In this study, 2-dimensional dynamic numerical analysis has been performed in two practical sections, respectively. Stresses and displacement occurrence trends are investigated thoroughly to investigate the behavior of T.R.&T structure.

1.2 *Analysis procedures and conditions*

First of all, static analysis has been performed to simulate in-situ condition of the structure and ground. The input load is applied as artificially composed acceleration time history which has 10 second of duration and 0.154 g of peak acceleration. Peak acceleration and other guidelines for dynamic analysis are determined by the seismic design code of civil structure in S. Korea.

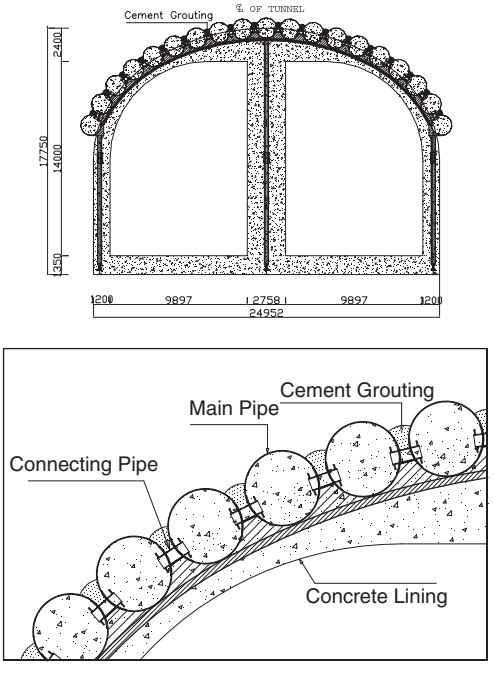


Figure 1. Typical T.R.&T section (arch type).

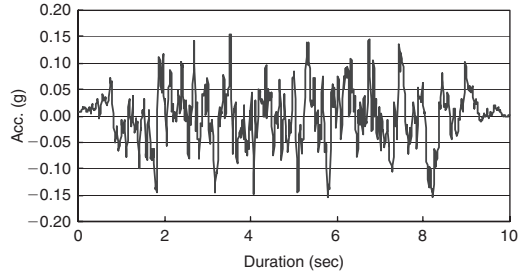


Figure 2. Artificial wave time history.

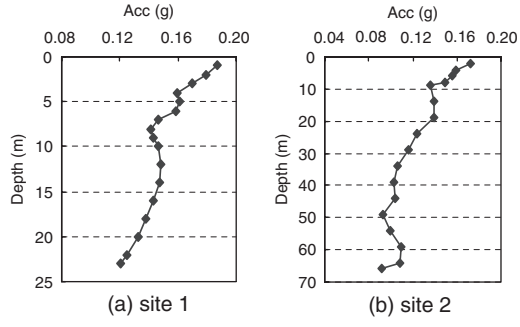


Figure 3. Ground response analysis results.

To find the input motion of wave, one dimensional linear ground response analysis has been performed. As the result of ground response analysis, raw values of artificial acceleration are changed into the base rock motion by deconvolution, then, applied to the base rock. 2-dimensional finite difference method is used to calculated dynamic response of the model.

2 GROUND RESPONSE ANALYSIS

2.1 *Overview*

The mechanism of epicenter, wave propagation through multi-layered soils and other intricate parameters are required to perform ideal ground response analysis. Practically the fracture mechanism of faults and energy propagation are too difficult to obtain precise solution. Therefore, ground response analysis has been performed based on empirical and simplified theory such as 1-dimensional equivalent linear method. SHAKE91, 1-D equivalent linear analysis program has been employed, hereafter.

In the first section, soil layers are composed of weathered soil (thickness = 8 m) and weathered rock from the surface. SPT-N value varies from 6 to 28 in weathered soil. Load of road on the surface are applied on the surface, which may cause the large displacement of surface and large sectional excavation may trigger settlement of the slab and wall.

In the second section, soil layers are composed of weathered soil (thickness = 9 m), weathered rock and soft rock from the surface. SPT-N value varies from 13 to 50 in weathered soil. Large sectional arched tunneling (width = 25 m, height = 18 m) may trigger settlement of the crown and surface ground. Figure 2 shows artificial wave history and Figure 3 shows the results of ground response analysis.

Based on the results, base rock motions have been acquired and displayed in Figure 4.

As the result of ground response analysis, accelerations have been amplified about 55 and 87 per cent in each site. Peak accelerations in the base rock motion are estimated as 0.113 g and 0.092 g at the site 1 and 2, respectively. In both cases, the amplification near the ground surface shows rapid increase, which means the typical tendency of ground excitement.

Time history above will be applied at the lower boundary of FDM mesh as the input loading of dynamic numerical analysis.

3 DYNAMIC ANALYSIS

3.1 *General*

Several methods to estimate the behaviour of civil structures under the dynamic loads have been invented and developed. In order to arrive at rational and correct result, geological investigation of the site and

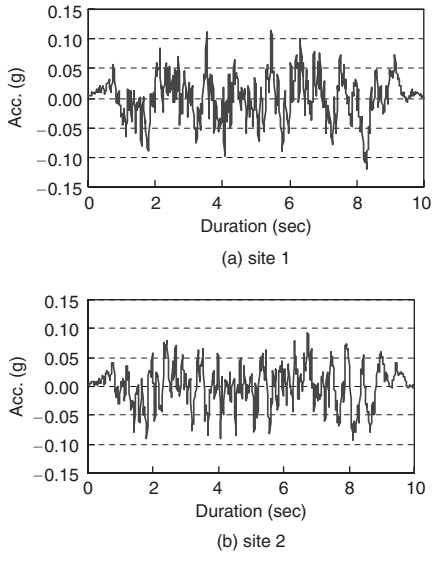


Figure 4. Base rock motion.

appropriate analysis procedures are inevitable. Additionally, elaborate insight into the dynamic analysis method and sufficient understanding of computational tools are also required. In this study, dynamic numerical analysis using the finite different method has been performed to minimize the inaccuracy of other approximate method.

FLAC^{2D}, universal code of numerical analysis using FDM, has been chosen to estimate dynamic response of the structures. It has been utilized in many practical projects in Korea and also verified in previous study. Finite difference method (Explicit method) has several advantages, then, most importantly, no iteration process is necessary when computing stresses from strains in an element. In an implicit method which is normally used in FEM program, several cycles of iteration are necessary before compatibility and equilibrium are obtained.

3.2 *Case-1: Dynamic analysis on the box type*

T.R.&T method is applied to the large sectional underground box structure which has 17 m of width and 7 m of height. Road is passing on the surface. Site section is demonstrated in Figure 5.

Based on the practical site profile, 2-dimensional FDM mesh is built. Static analysis is performed first, then free-field boundary condition and base rock motion are applied to the model. Steel pipes are modeled as consecutive beam element in elastic model and ground as Mohr-Coulomb model. Mesh and vertical stress distribution results are shown in Figures 6 and 7, respectively.

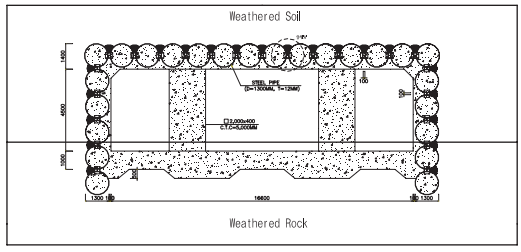


Figure 5. Section (Case-1).

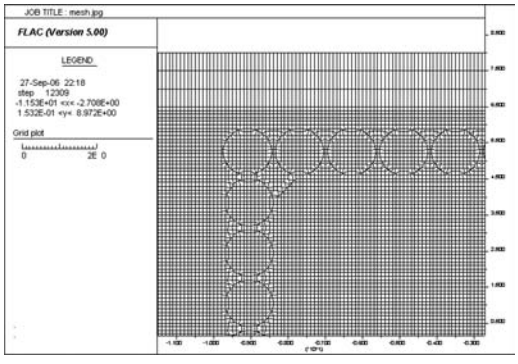


Figure 6. Mesh for 2D analysis (left edge).

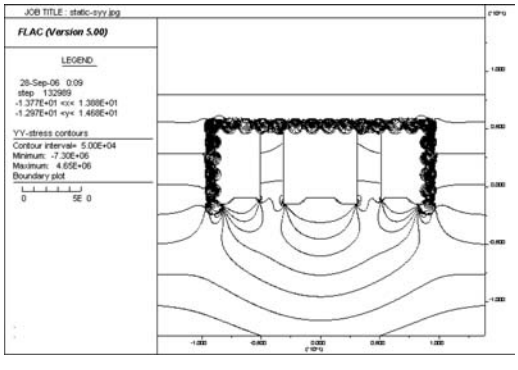


Figure 7. Vertical stress distribution (static analysis).

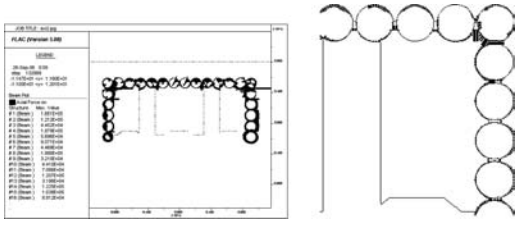
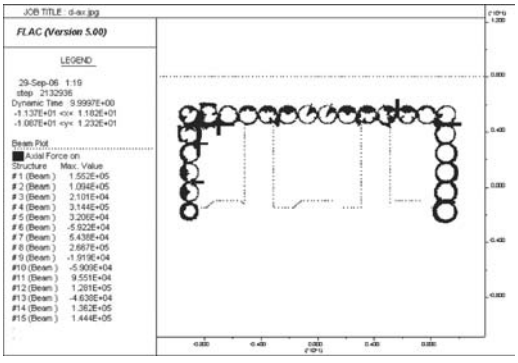
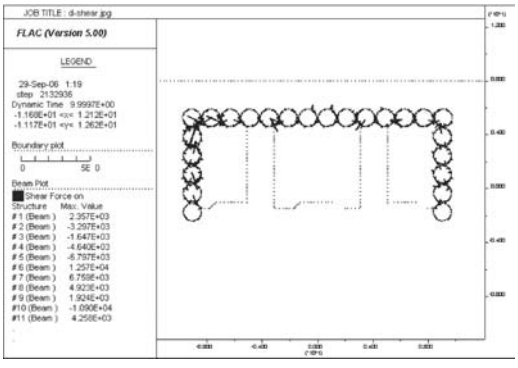


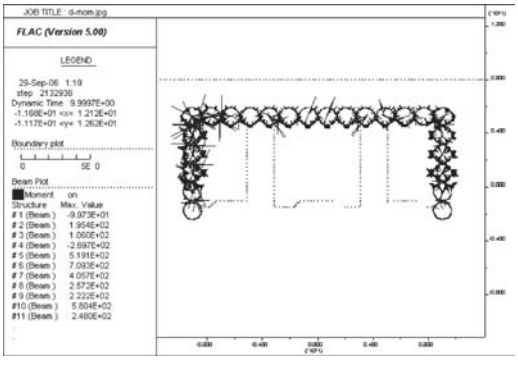
Figure 8. Axial forces of steel pipe elements.



(a) axial forces



(b) shear forces



(c) bending moments

Figure 9. Structural forces (Case-1).

Target values are axial stress, velocity and displacement of steel pipes and displacement, velocity and acceleration of the upper slab.

Maximum axial stress in all steel pipes are estimated 93.17 MPa and presented 45.3% of yield stress in static analysis.

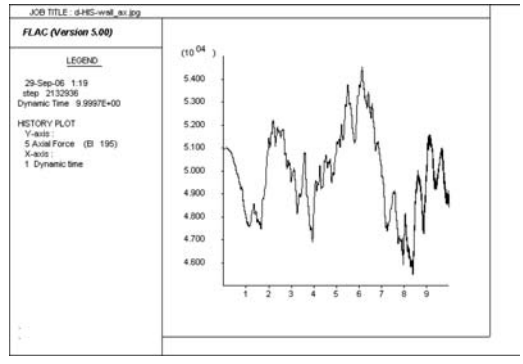


Figure 10. Axial force history at side wall.

Dynamic analysis is performed in addition to the result of static analysis. Free-field boundary condition is applied to side edge and base rock motion history is loaded at the base of mesh. Acceleration in y-direction is set to 0 to preventing rocking along base. Target positions are upper slab between columns and side wall. Maximum axial stress of pipes is 123.44 MPa which occurred at the upper slab edge. Displacement shows quite small value, 8.85 mm at the Figure 9 displayed structural forces and moment.

Figure 9 designates the critical position of T.R.&T box structure can be the edges between wall and upper slab, especially connecting points under the dynamic loading. Force and moment are concentrates at that position of structure, however, shows quite small values. Moment and shear forces display relatively large values at the side walls due to lateral seismic load.

Figure 10 shows axial force history at the side wall on the inner position. Axial forces are tensional and vary from 54.54 kN (t = 6.14 s) to 46.50 kN (t = 8.39 s).

3.3 *Case-2: Dynamic analysis on the arch type*

T.R.&T method is applied to the large sectional tunnel which has 25 m of width and 18 m of height. Site section is demonstrated in Figure 11.

Procedures are same as Case-1. Mesh and vertical stress distribution results are shown in Figures 12 and 13, respectively.

The smallest length of mesh is only 0.12 m to avoid being distorted. Mesh and vertical stress of the model are demonstrated in Figure 13.

Maximum axial stress in all steel pipes are estimated 133.84 MPa and presented 65% of yield stress. Figure 14 shows axial forces of steel pipe elements.

Dynamic analysis is performed in addition to the result of static analysis. Target positions are crown and shoulders of the tunnel. Results are

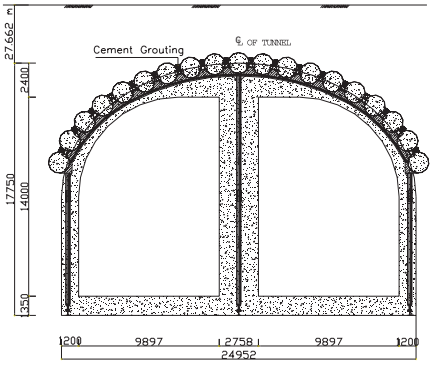


Figure 11. Section (Case-2).

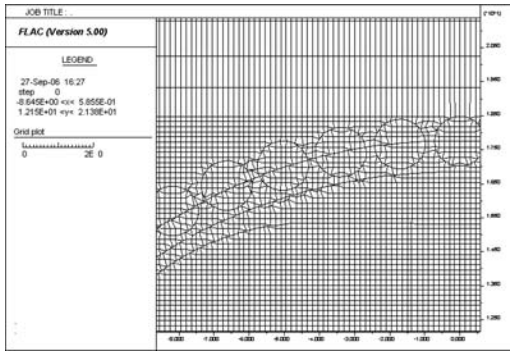


Figure 12. Mesh for 2D analysis.

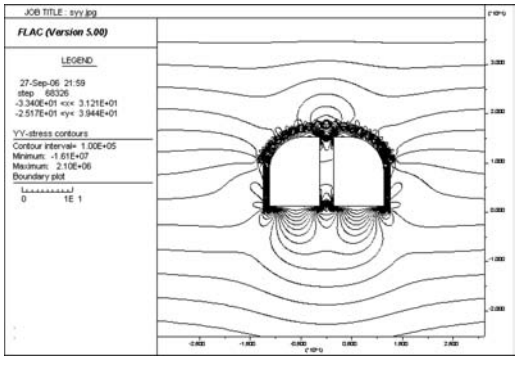


Figure 13. Vertical stress distribution (static analysis).

also obtained in time history. Maximum axial stress of pipes is 134.12 MPa which occurred in the shoulders. Figure 15 displayed structural forces and moment.

Figure 15 designates the critical position of T.R.&T tunnel (arch type) which penetrates in weathered rock can be shoulder, especially connecting points under the dynamic loading.

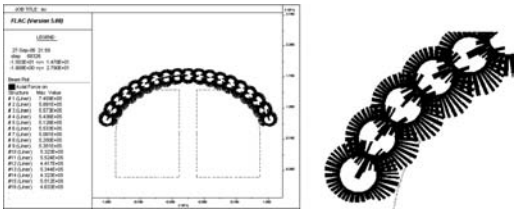
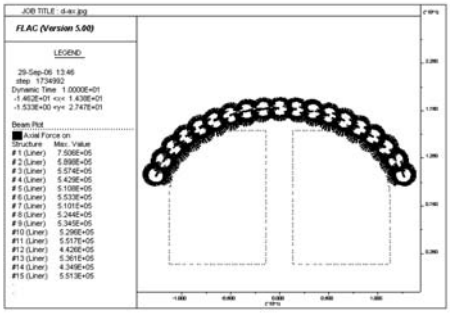
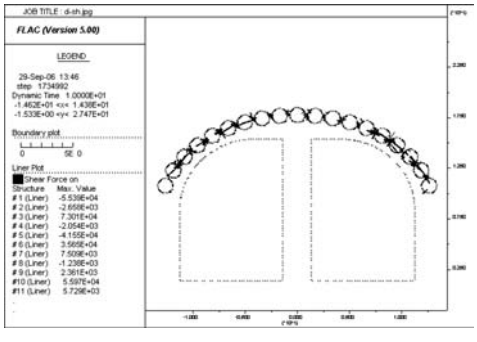


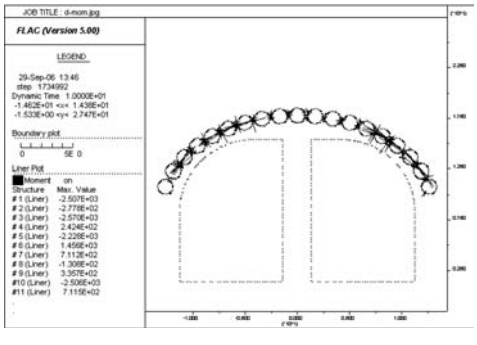
Figure 14. Axial forces of steel pipe elements.



(a) axial forces



(b) shear forces



(c) bending moments

Figure 15. Structural forces (Case-2).

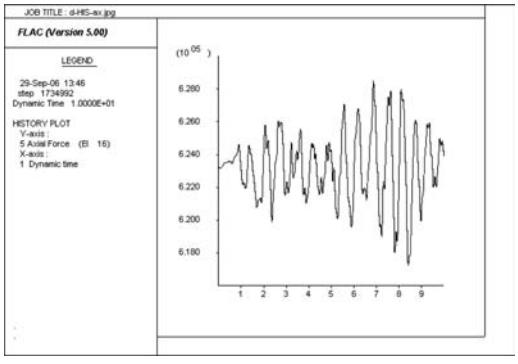


Figure 16. Axial force history at shoulder.

Figure 16 shows axial force history at the side wall on the inner position. Axial forces are compressions and vary from 628 kN (t = 6.86 s) to 617 kN (t = 8.43 s). The range of fluctuation shows large extent comparing to Case-1 due to the depth of structure, however, difference of peak values between static an dynamic is quite small which means the effect of seismic load is not so significant to tunnel.

4 CONCLUSIONS

2-dimensional dynamic numerical analysis has been performed in this study. Some reviews are as follow according to the analysis results.

1. The maximum axial stresses of pipes are increased to 32.5% (93.17 to 123.44 MPa) in Case-1 (box type) and only 0.2% (133.84 to 134.12 MPa) in Case-2 (arch type). Enormous difference is shown between two cases due to the depth from the surface. Ground amplification in deep position is relatively small, therefore, the depth of T.R.&T structure has the key role under dynamic load.
2. The stability of T.R.&T structure is governed by joining position of transversely connecting pipe and main pipes. The stress of structural elements at wall or shoulder displayed larger value than at upper slab or crown. In box type(Case-1), stresses are concentrated to the edge between wall and upper slab. In arch type(Case-2), stresses are concentrated to the shoulders, normally.
3. Axial force history fluctuates according to time. In box type (Case-1), the difference between initial value, i.e the result of static analysis and peak value of axial force is 5.35 kN (11.75%). In arch type (Case-2), the difference between initial value and peak value is 6.00 kN (1%). This result also prove that seismic load amplification is more severe near the ground surface than near the base rock.

ACKNOWLEDGEMENT

This study has been funded by the Korea Institute of Construction and Transportation Technology Evaluation and Planning under the Ministry of Construction and Transportation in Korea (Grant No. 04-C01).

REFERENCES

Cundall, P.A. 1976. Explicit Finite Difference Methods in Geomechanics. *Proceedings of the EF Conference on Numerical Mehtods in Geomechanics*. Blacksburg. Virginia. June. Vol. 1. pp. 132–150.

Idriss, I.M. & J.I.Sun. 1992. *User's Manual for SHAKE91*. Berkeley: Univ. of California, Davis, Dept. of Civil & Environmental Engineering, California Center for Geotechnical Modeling.

Kim, Jeongyoon, Park, Innjoon, and Kim, kyunggon 2003. The development of underground structure using new tubular roof method. *Journal of the Korean Tunneling Association.* Vol. 5, No. 4.

Kim, Jeongyoon 2003. The method of building underground structure using the space in the steel pipes injected to the ground. Application of new technology authorization, *Ministry of Construction and Transportation*, Seoul, Korea.

Park, Innjoon, Kim. Jeongyoon, Yu, Kwangho, Kwak, Changwon, Kim, K. G. 2005. The underground drainage system using New Tubular Roof method. *ITA-AITES 2005*.

Shin, Jongho, Potts, D. M., and Addenbrooke, T. I. 2002b. "Three-dimensional modelling of NATM tunnelling in decomposed granite soil." *Géotechnique*, 52(3), pp. 187–200.

Wolf, J.P. 1985. *Dynamic Soil-Structure Interaction.* New Jersey. Prentice-Hall.

Underground Space – the 4th Dimension of Metropolises – Barták, Hrdina, Romancov & Zlámal (eds)
© 2007 Taylor & Francis Group, London, ISBN 978-0-415-40807-3

A laboratory test for determination of the optimum installation number of face bolts

K.W. Seo & S.W. Lee
Korea Institute of Construction Technology, Republic of Korea

T.Domon & K. Nishimura
Tokyo Metropolitan University, Japan

ABSTRACT: This study dealt with the analysis of behavior of ground and face bolts in a tunnel supported by face bolts by means of laboratory experiments and it mainly focused on the installation number. The followings are conclusions of this study. The support effect increases up to 8 bolts in one section ($N_p = 8$) and the effect of the more face bolts does not increase. Also, the axial force decreases more with the more installation number. The axial force on a face bolt decreases with more installation number and therefore, the number should be determined for 1 face bolt to display maximal axial force.

1 INTRODUCTION

Among various supplementary support methods, the face bolt installation is one of the frequently used methods due to simplicity of work, economical reason and effective control of axial displacement. Its use increases dramatically by introduction of new materials and development of the method in Japan. In more than 70 working site per year, face bolt method is employed in Japan. Active researches are being conducted for investigating the support effect of face bolts and site investigation.

As the study of installation number of face bolts, D.Pelia et al (1996) studied the relationship between the number of face bolts and axial displacement of the face. They reported that more than about 100 bolts in numerical analysis and more than 80 bolts in the site measurement do not have any effect against the face displacement. Yoo (2003) found that support effect by face bolts in his numerical analysis would not increase any more if the installation density is more than 1.1 bolts/m^2. According to the investigation of 33 tunnels in Japan by Ohtsuka (2006), the numbers of bolts have been predominantly determined by experience and the calculation method which uses the axial force of the face, proposed by Murayama (1966).

However, the effect of face bolts depend chiefly on the axial force and, therefore, its support effect is very dependant on the specification of the bolt. Also, every working site has different ground conditions and then it is fairly hard to determine the installation number.

Fig. 1 shows the elastic modulus, one of ground properties, based on the real data from 11 tunnel sites measured by the writers. There seems to have no relationship between the elastic modulus and the installation number of face bolts as shown in the figure. Because most of tunnels where the face bolt method is employed require strong control for the surface subsidence, more than two support methods are used together. Therefore, unless the support effect of the other method or methods employed is determined, the exclusively direct relationship between the modulus and the number cannot be found easily.

The relationship between tunnel depth and installation number of face bolts and Reinforced Protective Umbrella (RPUM) steel pipes is represented in Fig. 2. Both methods are applied in the ground deeper than 40 m often. Despite this, their relation with tunnel depth is vague.

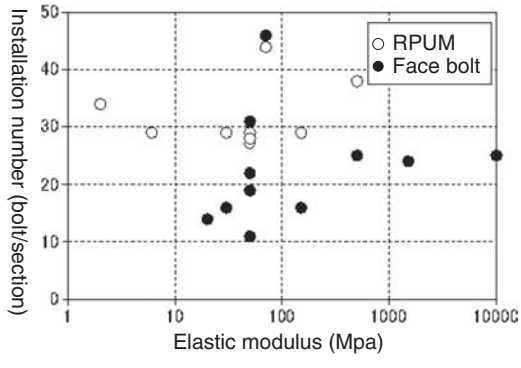


Figure 1. Elastic modulus of ground and the installation number of face bolts and steel pipe.

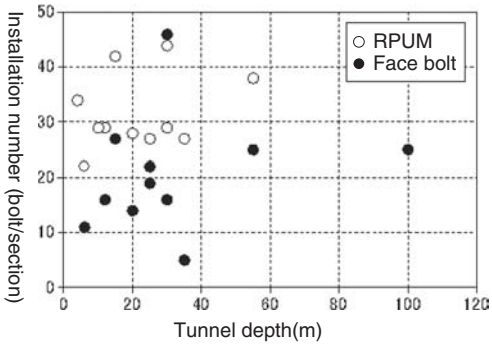


Figure 2. Tunnel depth and the installation number of face bolts and steel pipes.

This is, as mentioned, because the other support methods are employed in many cases and hence the installation number does not increase even under very bad ground condition. Also, the number of RPUM steel pipes is almost fixed but that of face bolts is rather dependent on the working site. RPUM has abundant cumulated data due to frequent use and, in many cases, is designed systematically with installing it in 120° or 180° on the basis of the tunnel axis. Contrarily, face bolt is employed together with the other support method and consequently there is no established design scheme. Thus, the installation number of face bolts has no verified interrelationship with ground properties.

The installation number of face bolts depends on the sites there is no design pattern for it.

In this study, a laboratory test will be conducted to obtain the relationship between the installation number of face bolts and their displacement prevention, and a method to determine the installation number will be introduced.

2 LABORATORY TEST

2.1 *Test procedure*

Ground behavior around and behind the face due to the alternatively repetition of face bolt installation and excavation (cutting) are examined, which is similar as the real installation and excavation process. To model this working process, the laboratory test is planned.

2.1.1 *Material of the ground*

The artificial soil used here is the mixture of copper bead, Vaseline and zincous oxide in the weight ratio of 200:1:0.3 respectively. Although copper bead is not light enough to handle easily and required to be kept in the stable temperature, it could provide some adhesive power, and could be preserved for a long time. The soil is filled 6 times up to totally 30 cm of its thickness and

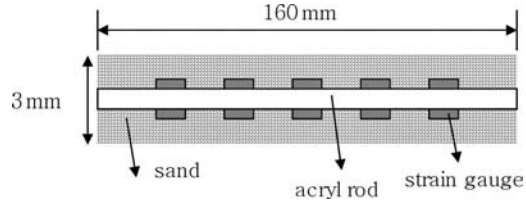


Figure 3. Diagram of a face bolt.

the compaction with 23 gf/cm^2 is done at every time the soil is filled.

The density of copper bead, main material, is 5.4 g/cm^3, and the effective size (D_{10}), uniformity coefficient (U_c) and coefficient of curvature (D_{60}) for the ground are 0.88 mm, 2.18 and 1.92 mm, respectively.

2.1.2 *Test box*

The test box used in this study is an aluminum box of which the width is 0.88 m, the length is 1.08 m and the height is 0.6 m. A removable plate is located on the lower side for the entrance of the model tunnel (see Fig. 5).

2.1.3 *Face bolt*

The face bolt used in this test, of which the section is a 2 mm wide square, is a 1D (160 mm) long acryl rod. On its surface, sand is attached with epoxy and it is 8 pairs of strain gauges are placed on a pipe. And this is installed in the center of the face to measure the axial force (Fig. 3). The bolts are installed by pushing into the face during excavation with hand, and every 20 mm of each pipe is cut at the each step of excavation.

2.1.4 *Excavation method*

The model tunnel is advanced 2 cm(1step) sequentially to 2.8D (44 cm) by hand. This excavation method was successfully carried out by Ishimura (1998).

Fig. 4 shows the complete setup of test box with artificial soil and gauges, and Fig. 6 represents the surface settlement after completion of excavation to 2.8D (44 cm) with $N_p = 3$.

2.2 *Test case*

Test cases are represented in Table 1. The longitudinal pipes are placed 6 times, until the tunnel reaches 2.8D (44 cm) with 0.5D (8 cm) of the overlap length. Because the tunnel model is excavated sequentially and, therefore, its face displacement cannot be measured. Fig. 7 illustrated the laboratory test's case.

3 TEST RESULT AND DISCUSSION

In this study, the axial displacement of the tunnel face could not be measured directly due to the sequential

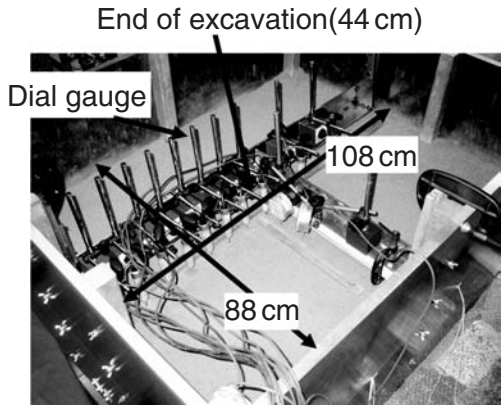


Figure 4. Complete setup of test box.

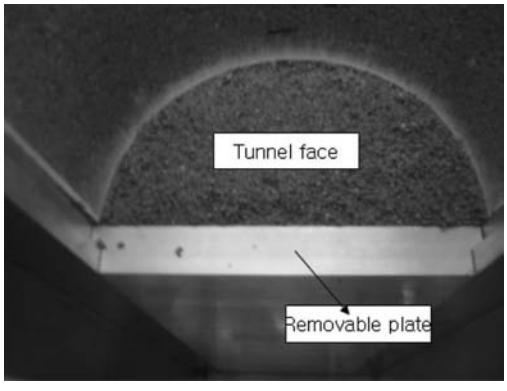


Figure 5. Lower part of the model tunnel (removable plate).

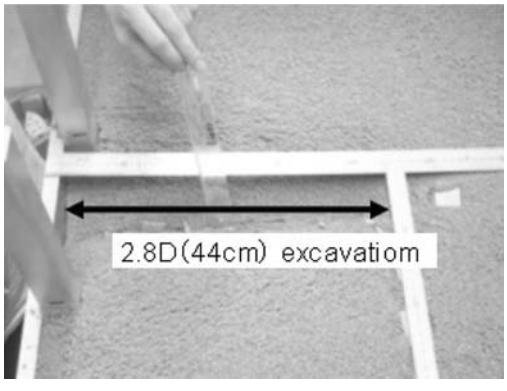


Figure 6. Surface settlement after completion of excavation (2.8D (44 cm) with $N_p = 3$).

excavation. Therefore, only the surface settlement is analyzed.

The surface settlement of axial direction according to the installation number after 2.0D (32 cm) excavation is represented in Fig. 8. It can be found in the figure that the settlement is reduced by the face bolt installation. As the installation number increases up to 8 bolts, the settlement decreases.

The surface settlement at the final excavation position 2.8D (44 cm) is shown in Fig. 9 (see Fig. 4 for the measurement position). The settlement decreases as the installation number increases same as above cases. Comparing $N_p = 6$ and $N_p = 11$, the difference of N_p is almost twice, but the support effect increases only 31% at the face and 32% at 1.9D position. In other words, the growth of the support effect by increasing the installation number has limitation.

Fig. 10 shows the surface settlement in transverse direction of the tunnel after 2.8D (44 cm) excavation

Table 1. Test case.

Test case		Layout of face bolts
	Model	Characteristics of layout
1	$N_p = 0$	No bolt
2	$N_p = 3$	Installed on 1 outer round line
3	$N_p = 6$	Installed on 2 round lines
4	$N_p = 8$	Installed on 2 round lines
5	$N_p = 11$	Installed on 2 round lines

- Tunnel depth (D): 1.4D (22 cm)
- Overlap of bolts: 0.5D (8 cm)
- Total installation shift: 6
- Total excavation length: 2.8D(44 cm)
- Excavation method: hand excavation
- 1 excavation distance: 2 cm (1step)

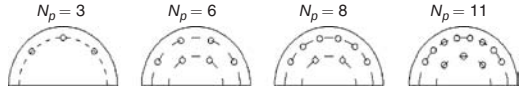


Figure 7. Layout of face bolts.

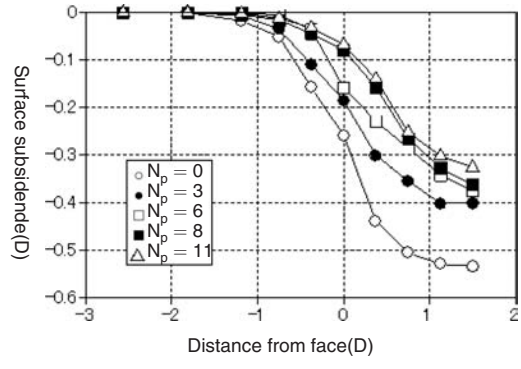


Figure 8. The surface settlement after 2.0D (32 cm) excavation – axial direction.

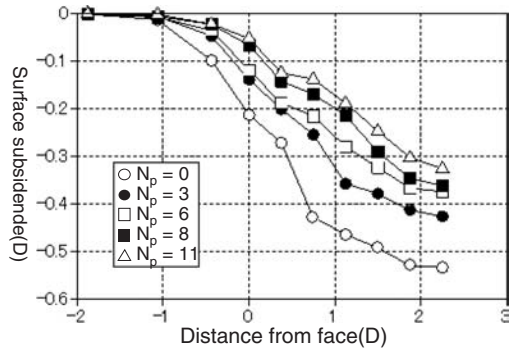


Figure 9. The surface settlement after 2.8D (44 cm) excavation – axial direction.

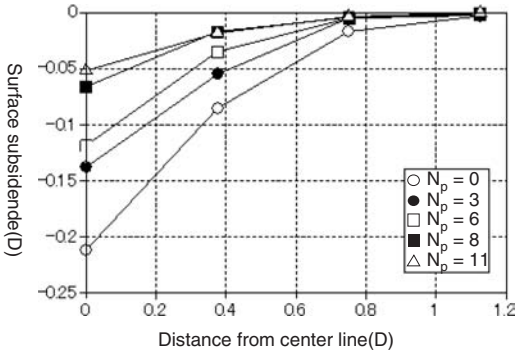


Figure 10. The surface settlement after 2.8D (44 cm) excavation – transverse direction.

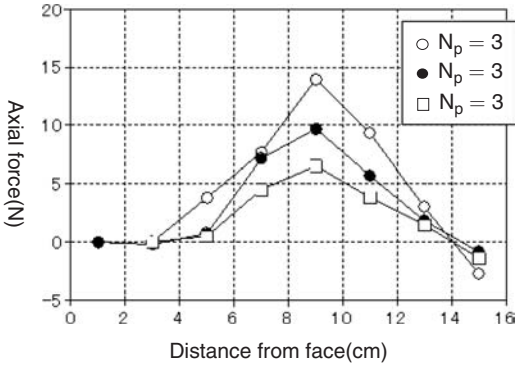


Figure 11. This is a comparison of excavation steps showing the maximal value.

(see Fig. 4 for measuring position). The surface length of settlement part from the tunnel center (x = 0) is about 0.8D without a face bolt ($N_p = 0$). Comparing cases of $N_p = 8$ and $N_p = 11$, the support effect of $N_p = 11$ has only 6% more than that of $N_p = 8$. Therefore, it is thought that $N_p = 8$ is the maximal installation number of face bolts under the conditions of this paper.

The axial force according to the installation number is shown in Fig. 11. The bolt used for measurement is the one in the face center in Fig. 7. Strictly, the actual positions of the bolts for measurement are somewhat different. The forces when $N_p = 3$, 8 and 11 are 14 N, 10 N and 6 N, respectively. That is, the axial force is smaller with more face bolts. Because the axial force of a bolt is a function of relative displacement of a bolt and ground, the force is smaller with smaller displacement.

4 CONCLUSION

In this paper, a basic laboratory test is carried out to introduce a method for determination of the optimum installation of face bolts. From the test, the following conclusions are obtained.

(1) The maximal optimum installation under the condition in this test is 8 ($N_p = 8$). Increase of support effect by more than 8 bolts is too small.
(2) The axial force on a face bolt decreases with more installation number and therefore, the number should be determined for 1 face bolt to display maximal axial force.

The result of this laboratory test has been reported, and the determination method will be introduced by the study using the real data.

REFERENCES

Chungsik Yoo, hyun-kang Shin. 2003. Deformation behaviour of tunnel face reinforced with longitudinal pipes-laboratory and numerical investigation, Tunnelling and Underground Space technology, 18, pp.303–319

D. Peila, P.P. Oreste & S. Pelizza. 1996. Study of the influence of sub-horizontal fiber glass pipes on the stability of a tunnel, North American Tunnelling 96, pp.425–432

Isamu Ohtsuka, Tomoyuki Aoki, Tadashi Okabe, Shingo Morito. 2006. Study on performance and application range of long face bolts, Proceedings of the 35th Symposium on Rock Mechanics, JSCE, pp.41–46

Toshiaki Ishimura, Hideto Mashimo, HidetoMayumi, Kunino Hujii. 1998. A 3-dimensional excavation model test about the effect of a tunnel pre-lining for the restraint of the ground deformation, proceeding of tunnel engineering, JSCE, Vol.8, pp.199–204

Underground Space – the 4th Dimension of Metropolises – Barták, Hrdina, Romancov & Zlámal (eds)
© 2007 Taylor & Francis Group, London, ISBN 978-0-415-40807-3

Development of tunnel drainage system using drain board

G.P. Lee, H.S. Shin, G.J. Bae & S.W. Lee
Geotechnical Engineering Research Dept., Korea Institute of Construction Technology, Republic of Korea

ABSTRACT: The objective of this study is development of economical drainage system by omission of construction step such as trench, paving stone in trench and set up of drain pipes etc, at the existing drainage system. Pavement is generally make up with sub base, base and pavement and the drain board is constructed at the top of sub base with concrete. The concrete layer is used base and cavity is formed at the lower part of base act as drain line. For this study, numerical analysis and laboratory tests are performed to investigate fatigue behavior by dynamic load and to make pillar shape of drain board. At the result of hydrological model test, drain capacity of rectangular with half circle at both side pillar shape is more superior than the capacity of rectangular and circle pillar shape and distance of pillars for inflow direction affects the drain capacity. And at the result of numerical analysis and investigation of fatigue behavior, structural safety of the concrete layer which is constructed to make drain line for the dynamic load by vehicle is verified.

1 GENERAL INSTRUCTIONS

A drainage system is required in all tunnels to remove water that could accumulate from rainfall, tunnel washing operations, tunnel seepage, vehicle dripping, fire-fighting operations, or any combination of these sources. Drainage of a tunnel can be accomplished either by a gravity flow system or a pumped system. A gravity flow system will suffice for tunnels with continuous grades, provided that the collected water can be properly disposed of at the lower end of the tunnel. It may be necessary to have a pumped system to dispose of collected water when a low point occurs within the tunnel.

The objective of this study is development of economical drainage system by omission of construction step such as trench, paving stone in trench and set up of drain pipes etc, at the existing drainage system. Pavement is generally make up with sub base, base and pavement and the drain board is constructed at the top of sub base with concrete. The concrete layer is used base and cavity is formed at the lower part of base act as drain line. For this study, laboratory tests are performed to investigate to make pillar shape of drain board.

2 TUNNEL DRAINAGE SYSTEM

2.1 *Existing tunnel drainage system*

Existing tunnel drainage system in South Korea is divided in two types such as partially or fully separation system between ground water and contaminated water. Gravity flow system is generally common used in South Korea, standard drainage system is composed longitudinal perforated drain and gravity drain line such as side drain pipe, transverse drain pipe and spiral seam duct(or T.H.P.) etc,.

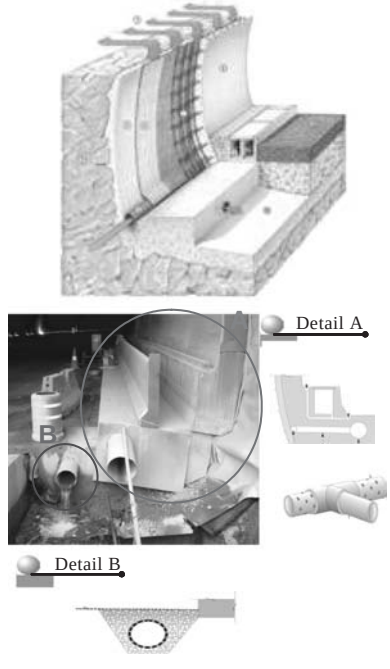


Figure 1. Drainage system using perforated pipe.



(a) upper part



(b) lower part

Figure 2. Drain board sample.

2.2 *Tunnel drainage system using drain board*

As illustrated figure 2∼3, a channel within concrete slab which is constructed by concrete and then aging on drain board installed at invert is formed. Therefore side drain pipe, transverse drain pipe and perforated pipe etc, are omitted in tunnel drainage system using drain board. The slab is used to base in road tunnel and to sub-roadbed in railway tunnel.

3 CORRELATION INVESTIGATION OF DRAIN BOARD PILLAR SHAPE VS. DRAINAGE CAPACITY

Drainage capacity of drain board is affected by pillar shape. But circle or rectangular pillar shape is generally common used without examination of correlation between the shape and drainage capacity to improve the drainage capacity.

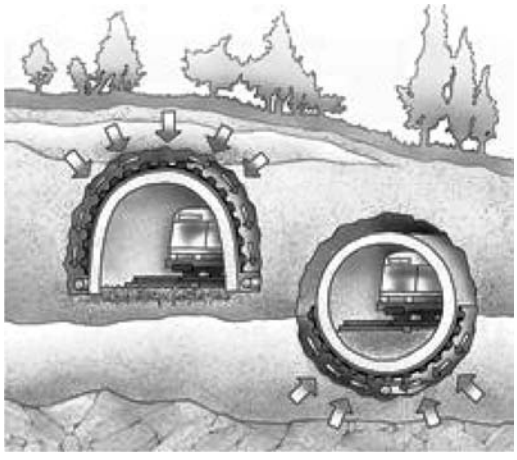


Figure 3. A concept of tunnel drainage system by using drain board.

Table 1. Resistance coefficient of flow in river for bridge pillar shape.

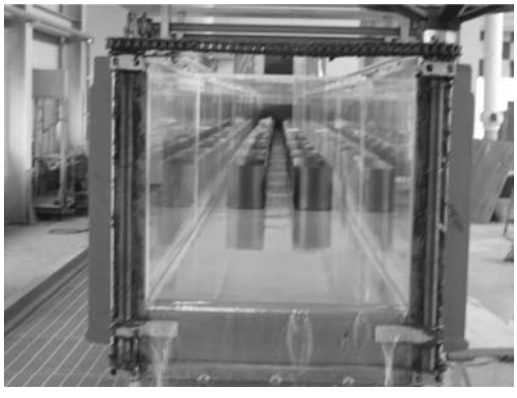
Shape	Resistance coefficient
(Rectangular)	0.07
(Circle)	0.04
(Rectangular with half circle at both side)	0.04

As illustrated table 1, resistance coefficient of flow which is determined by pillar shape in case of rectangular pillar shape is 1.75 times higher than circular or rectangular with half-circle at both side pillar shape(standard of bridge design, South Korea, 2003). Therefore, rectangular pillar shape more obstruct water flow than circle or rectangular with half-circle at both side pillar shape. But, different condition between drain board and bridge such as pillars group is not considered in the standard.

To improve the drainage capacity, hydrological model test was performed with conditions of pillar shape(rectangular, circle, rectangular with half-circle at both side) and width for flow direction between pillars.



(a) a general view of channel



(b) cross section of channel

Figure 4. A general view of channel used to hydrological model test.

4 HYDROLOGICAL MODEL TEST

To improve the drainage capacity by determine pillar shape and disposition, analyzed the resistance of flow by water level measurement in hydrological model test for each pillar shape and width for flow direction between pillars.

4.1 *A summary of hydrological model test*

Dimension of the channel used in hydrological model test is 12,000 mm × 400 mm × 400 mm (total length × width × height). To minimize effect of Froude resemblance law, rectangular specimens (width × length = 114 mm × 114 m), circle specimens (ø114 mm) and rectangular with half circle at both side specimens(width × length = 114 mm × 500 mm) which are reproduced from drain board pillar are prepared (figure 4∼5). The channel gradient affecting on flow at open channel is fixed on 0.25%.

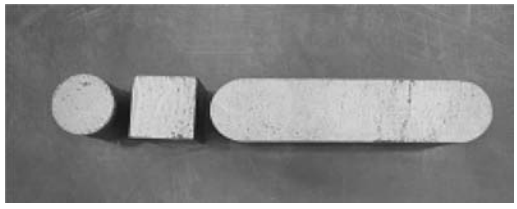


Figure 5. A specimens used to hydrological model test.

Table 2. Amount of flowing water conditions.

	Amount of flowing water
1	0.0045 m^3/sec/m
2	0.0103 m^3/sec/m
3	0.0170 m^3/sec/m

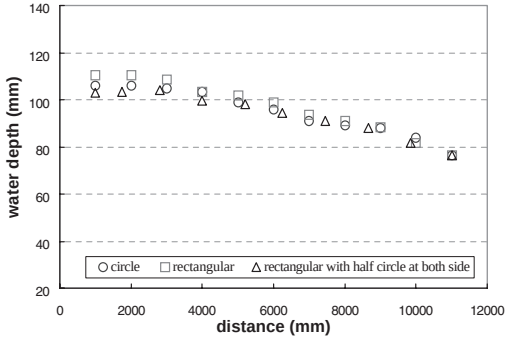


Figure 6. Drainage water level with specimen shape.

The specimens is lined up in a double file, distance between specimens for flow direction is 86 mm to rectangular and circle shape specimens and the distance is 86 mm, 61 mm, 36 mm and 0 mm to rectangular with half circle at both side specimens. The amount of flowing water conditions are follow as table 2.

4.2 *Test results*

The depth of water according to the variation of specimens shape from upper stream to down stream in the channel is plotted at figure 6(at q = 0.0170 m^3/sec/m). The highest water depth is in case of rectangular specimen and water depth is decreased in circle specimen shape, half circle at both side specimen shape sequence.

As a result of measure the depth of water at varied condition of the distance decreased in 86 mm, 61 mm, 36 mm and 0 mm sequence, the highest water depth decreases with decreasing the distance. There is difference of drainage water level between 86 mm, 61 mm and 36 mm, 0 mm(figure 7).

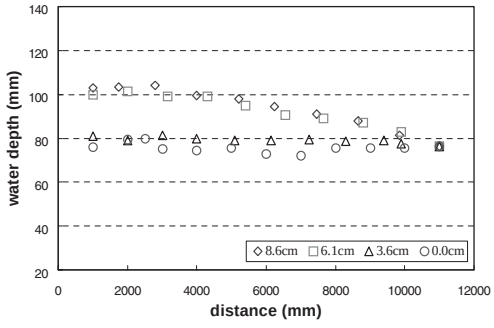


Figure 7. Drainage water level with the distance.

5 CONCLUSIONS

The hydrological model test have been examined, to improve drainage capacity of drain board in tunnel drain system.

From the hydrological model, drainage capacity of rectangular with half circle at both side shape is more effect than the drainage capacity of rectangular or circle shape. And it is of utmost importance to the distance between specimen for flow direction.

There is a correlation between drainage capacity of drain board and the distance, the highest water depth decreases with decreasing the distance. And there is difference of drainage water level between 86 mm, 61 mm and 36 mm, 0 mm according to decrease head loss.

REFERENCES

John O. Bickel, Thomas R. Kuesel, Elwyn H. King, (1996) Tunnel Engineering Handbook, pp. 467–484.

Crowe C. T., Elger D. F. and Roberson J. A., (2001) Engineering Fluid Mechanics, pp. 531–538.

Ding Y., Jia Y. and Wang S.S.-Y., (2004) Identification of manning's roughness coefficients in shallow water flows, ASCE, Journal of Hydraulic Engineering , Vol. 130(6).

Underground Space – the 4th Dimension of Metropolises – Barták, Hrdina, Romancov & Zlámal (eds)
© 2007 Taylor & Francis Group, London, ISBN 978-0-415-40807-3

The effects of tunnelling on an adjacent single pile

C.J. Lee, S.H. Jun & N.J. Yoo
Department of Civil Engineering, Kangwon National University, Korea

G.W. Kim
Department of Geology, Kyungpook National University, Korea

ABSTRACT: Three-dimensional numerical analyses have been conducted to study the effects of tunnelling on an adjacent single pile constructed in weathered soil and rock. The study includes ground settlement trough, pile settlement and shear transfer mechanism at the pile-soil interface. In particular, the change of apparent pile capacity associated with the tunnel advancement has been analysed. The computed results show that the ground settlement trough might not be represented by the well-known Gaussian distribution curve. Due to the reductions in vertical soil stress underneath the pile base and settlement of the surrounding ground, pile settlement was induced, thereby changing shear stress distribution along the pile. Some insights into the pile behaviour under the influence of tunnelling obtained from the numerical analyses will be reported and discussed.

1 INTRODUCTION

In recent years, there have been a number of tunnel construction projects in urban areas where the performance of nearby piled foundations might have been affected by the tunnelling activities (Fig. 1, Pang 2006). This might have resulted in increasing pile settlement and changes in the shear stress distribution in the piles. There have recently been several studies on the influence of tunnelling on the behaviour of piles located near a tunnel (Vermeer & Bonnier 1991; Bezuijen & Schrier 1994; Mroueh & Shahrour 2002; Jacobsz 2002; Lee 2005; Selamates et al. 2005; Pang 2006 and others). These were based on field observations, numerical simulations and experimental studies. These studies considered the effects of tunnelling on piles constructed mainly in clayey or sandy ground. Compared to the overseas studies, however, research on this issue is rather limited in Korea (Lee et al. 2006). Moreover, geological condition in Korea is completely different from above-mentioned ground types. Typically the ground in Korea consists mainly of weathered soils, weathered rock and soft rock. These materials might have resulted in different tunnel-pile interaction compared to the overseas studies. Furthermore, the behaviour of piles affected by tunnelling has attracted less attention among engineers.

In this study, three-dimensional (3D) numerical analyses have been performed to study the influence of tunnelling on an adjacent single pile. The analyses have concentrated on the ground settlement trough, pile head settlement, change of apparent pile capacity and shear stress transfer to the pile. It is expected that the current analysis can be used to understand the fundamental mechanism of pile-tunnel interaction caused by tunnelling.

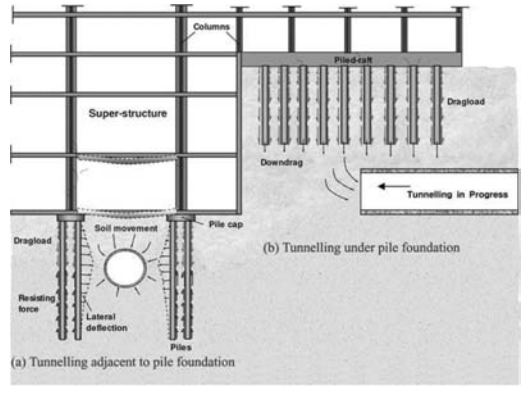


Figure 1. An illustration of pile response caused by tunnelling (Pang 2006).

2 NUMERICAL MODELLING

In the current study, the finite difference analysis package Flac 3D was used in the numerical analyses to study the effects of tunnelling on a single pile located above a tunnel. Totally there numerical analyses have been conducted (i.e., Analysis 1 : pile loading test,

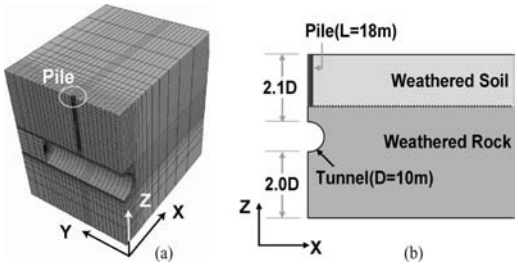


Figure 2. (a) A 3D finite difference grid, (b) Location of pile and tunnel.

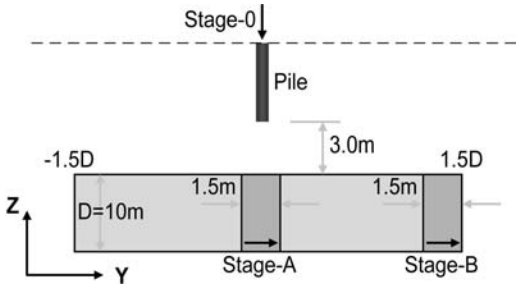


Figure 3. Numerical modelling procedure (not to scale).

Table 1. Material parameters assumed in the numerical analysis.

Analysis	E (MPa)	γ_t (kN/m^3)	ν	c' (kPa)	ϕ' (°)	K_0
Weathered soil	50	20	0.3	20	30	0.5
Weathered rock	100	20	0.3	50	35	0.5
Soft shotcrete	5000	20	0.2	–	–	–
Hard shotcrete	15,000	20	0.2	–	–	–
Pile	20,000	24	0.2	–	–	–

Note: E = Elastic modulus, γ_t = Unit weight, ν = Poisson's ratio, c' = Cohesion, ϕ' = Internal friction angle, K_0 = Earth pressure coefficient.

Analysis 2 : tunnel-pile interaction, Analysis 3 : tunnelling in the green field condition). In analysis 1 pile-soil interaction was studied, while in analyses 2 and 3 tunnelling in the green field condition and pile behaviour under an axial loading excluding tunnelling were simulated respectively. Figs. 2a∼2b show a 3D finite different grid used in the numerical analysis (Analysis 1). A single square concrete pile above the tunnel crown is shown. The pile was 18 m in length L and 0.5 m in size. The pile base was assumed to rest at an elevation of 3 m above the tunnel crown as shown in Fig. 2b. The tunnel diameter is 10 m and the tunnel centreline was located at a depth of 26 m below the surface. Considering the plane of symmetry, only a half of the whole grid was used in Fig. 1a. The ground was divided into two layers, i.e. weathered residual soil above the tunnel and weathered rock below the weathered residual soil. The bottom of the grid was pinned and its lateral boundaries were supported by rollers.

Table 1 summarises the material parameters assumed in the numerical analyses, which are typical design values widely used in Korea. An isotropic elastic model was used for the pile and the shotcrete. A Mohr-Coulomb failure criterion was used for the ground. All the analyses were based on drained analyses, assuming a hydrostatic pore pressure distribution in the ground with the water table located at the surface. In the numerical simulation, interface modelling at the pile-soil interface was not included since the relative displacement between the pile and the soil was expected to be insignificant.

The numerical modelling consisted of three stages, i.e., initial geostatic equilibrium, application of axial pile load under the service condition, followed by tunnel excavation. The analysis stages referred to in the current research are shown in Fig. 3 (Stage 0 : application of axial load, Stage A : tunnel excavation below the pile, Stage B : end of tunnel excavation). Following the initial geostatic stage, an axial load of 1000 kN was applied to the pile head to simulate a service load prior to the tunnel excavation. The axial load was decided based on computed load-settlement relation from analysis 1. The tunnel excavation was then simulated in several stages. In each advancement, the tunnel was excavated in increment of 1.5 m. The simulation of tunnel excavation was performed by using the "Null Element" provided by the Flac 3D programme. At the same time, a shotcrete of 200 mm in thickness was applied on the excavated soil face by specifying material parameters corresponding to soft shotcrete. The elastic modulus of the soft shotcrete was then changed to that of the hard shotcrete (E = 15,000 MPa) during the tunnel excavation in the next excavation stage. The tunnel excavation was simulated from −1.5D to 1.5D in the longitudinal direction (Y direction) as shown in Fig. 3.

Upon completion of the numerical calculation, the axial force on the pile, P_a, was calculated using $[P_a = (\sigma_{zz})_{avg} \times A_p]$, where $(\sigma_{zz})_{avg}$ is the averaged vertical stress component in the pile zones at a certain elevation, A_p is the sectional area of the pile. In addition, the shear stress τ acting on the pile shaft was calculated by using $[\tau = (P_{i+1} - P_i)/A_c \times dz]$, where i and i + 1 are the reference points, A_c is the circumferential area of the pile, dz is the distance between i and i + 1. Finally the volume loss V_l was calculated based on [V_l = amount of ground lost in the region near the tunnel per unit length/sectional area of the tunnel per unit length)].

3 PILE-TUNNEL INTERACTION COMPUTED FROM NUMERICAL ANALYSIS

3.1 *Load-settlement characteristic (Analysis 1)*

Fig. 4 shows load-settlement characteristic of the pile under an axial loading (Analysis 3). It is demonstrated that when the axial loading is more than 2000 kN, a sudden increase in the pile settlement occurred, indicating development of yielding at the pile-soil interface. Similarly when applied the Davisson's method (1972) widely used in Korea to determine pile capacity, the ultimate pile capacity of about 2100 kN can be obtained as shown in the figure. Hence in the current study the pile capacity was assumed to be 2000 kN (Pile head settlement: 7.38 mm) and applying the factor of safety of 2.0 the design pile capacity was 1000 kN. At the design load the pile head settlement was 2.84 mm. The load-settlement curve in Fig. 4 was used to analyse the change of pile behaviour under the influence of adjacent tunnelling. In particular, the change of apparent pile capacity during the tunnelling was studied.

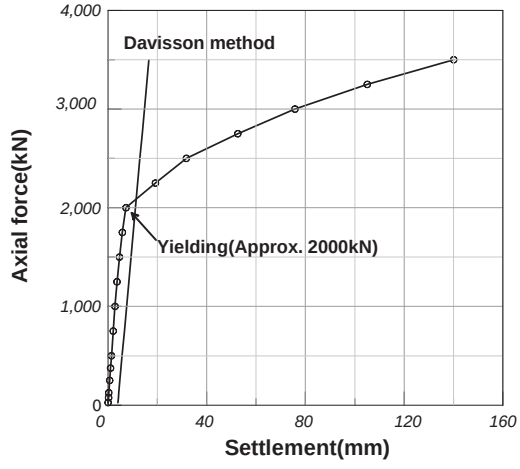


Figure 4. Load-settlement relation (Analysis 1).

3.2 *Pile head settlement (Analyses 1∼2)*

Fig. 5 shows changes in the pile settlement during tunnel excavation. The pile head settlement δ is normalised by the pile head settlement δ_i at analysis stage 0 (prior to the tunnelling). Fig. 5 shows how the pile head settlement increased as the tunnel excavation proceeded. As expected, it is clear that the longer the distance from the tunnel, the smaller the effect of tunnelling on the pile settlement would be. It is noted that the rate of pile settlement increase is at a maximum when the tunnel was excavated underneath the pile (during the analysis stage A). At stages A and B, δ/δ_i of 1.99 and 3.04 was computed, respectively. Upon completion of tunnel excavation, maximum pile settlement of 8.63 mm was computed. This is substantially larger than that computed from analysis 1 (2.84 mm). Hence, when using load-settlement relation in Fig. 4 apparent axial load of about 2100 kN can be deduced. Therefore the apparent pile capacity perhaps reduced substantially with a reduced factor of safety of about 0.95. Similarly, Lee & Ng (2005) reported a reduction in the apparent pile capacity due to tunnelling. This probably affects the serviceability of piled foundation.

The computed results showed that tunnelling might have resulted in a substantial increase in the pile settlement. On the contrary, it was found that pile movements in the lateral and longitudinal direction were insignificant, suggesting that bending moment in the pile might be insignificant. In the current study the majority of deformation developed in the vertical direction. However, when a pile locates near the tunnel horizontally from a tunnel, a significant lateral deflection might be induced in the pile (Lee & Ng 2005).

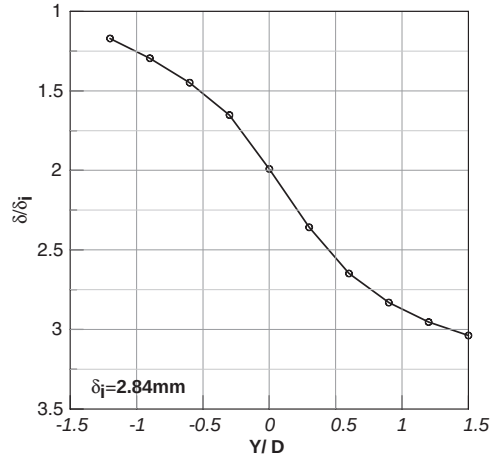


Figure 5. Distribution of pile settlement with tunnel advancement (Analyses 1∼2).

The computed results showed that tunnelling might have resulted in a substantial increase in the pile settlement. On the contrary, it was found that pile movements in the lateral and longitudinal direction were insignificant, suggesting that bending moment in the pile might be insignificant. In the current study the majority of deformation developed in the vertical direction. However, when a pile locates near the tunnel horizontally from a tunnel, a significant lateral deflection might be induced in the pile (Lee & Ng 2005).

3.3 *Distribution of settlement trough (Analyses 2∼3)*

Figs. 6a∼6b show the distribution of the settlement trough in the lateral direction (X direction in Fig. 1)

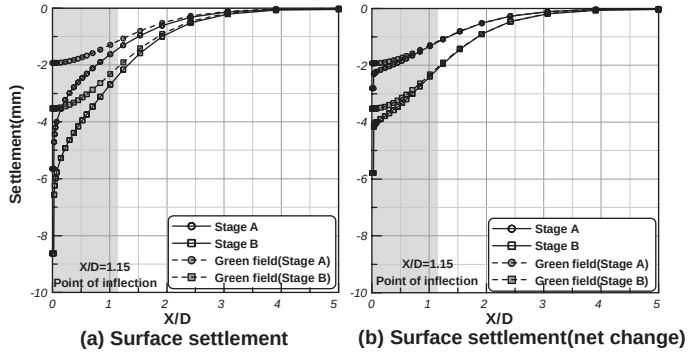


Figure 6. Distribution of surface settlement (Analyses 2∼3).

at the location of the pile for analysis stages A and B. In Fig. 6b, only net changes in the ground settlement purely associated with the tunnel construction are considered. Hence, the ground settlement developed at stage 0 (i.e., axial loading) is not included.

The ground settlement profile for the green field condition in the lateral direction is similar to the well-known Gaussian distribution curve based on $[s_m \times \exp(-0.5(X/i)^2]$, where s_m is the maximum ground settlement at the tunnel centreline, X is the lateral distance from the tunnel centreline, i is the point of deflection in the settlement distribution curve. The computed ground settlement distribution was compared with the Gaussian settlement curve. The point of deflection (i) was about 11.5 (X/D = 1.15) and the trough width parameter, K, was calculated to be about 0.45 ($K = i/Z_C$), where, Z_C, is the vertical distance between the ground surface and the tunnel centre. Mair & Taylor (1997) has reported that K values for clay and sand/gravel ground are 0.5 and 0.25 respectively. The computed K value of about 0.45 was somewhat larger than the typical value for sand/gravel (0.25).

When there is a pile in the ground, settlement trough is not following the Gaussian distribution curve (Analysis 2). In addition, the point of deflection was unable to be decided in the settlement trough. This is perhaps related to the stress concentration of the ground near the pile, thereby leading to large ground settlement near the pile. Hence to express settlement trough other settlement distribution pattern other than the Gaussian curve may probably required. In this case the maximum ground settlement is about 65% larger than that computed in the green field condition [Maximum surface settlement: analysis 2 (5.79 mm), analysis 3 (3.50 mm)]. Hence pile settlement estimation using the green field condition may result in underestimation of pile settlement leading to unsafe design.

Prior to tunnel excavation volume loss of 0.03% was computed at stage 0 due to pile loading. The volume loss deduced from the computed ground settlement trough in the green field condition was 0.07% and 0.13% at stages A and B, respectively. This is substantially smaller than those observed in the tunnelling excavation in London clay (1.0∼2.0%) (Mair & Talyor 1997). This is perhaps related to higher stiffness of weathered soil and rock. When there is a pile in the ground volume loss of 0.08% and 0.14% was calculated at stages A and B (net change only related to tunnelling). This is larger than those in the green field condition perhaps due to an increase in the pile settlement near the tunnel as shown in Fig. 6b.

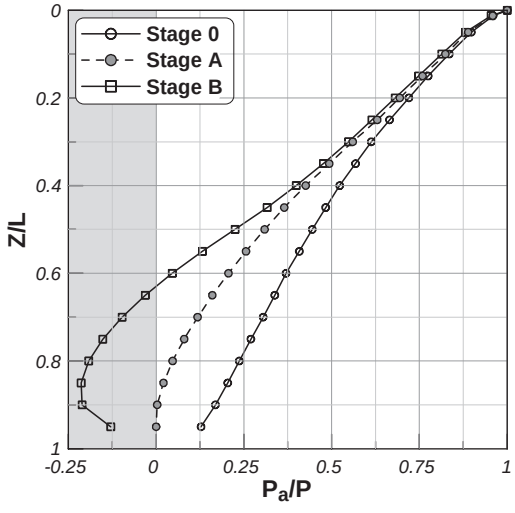


Figure 7. Distribution of axial forces in the pile (Analysis 2).

3.4 *Axial force distribution in the pile (Analysis 2)*

Fig. 7 shows changes of the normalised axial forces on the pile with the normalised pile depth, Z/L. The axial

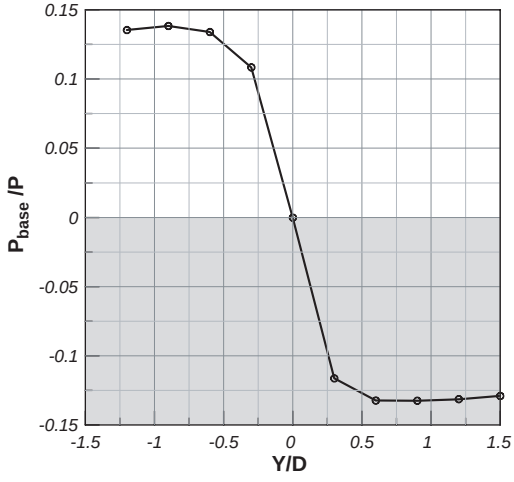


Figure 8. Changes of pile force at the base (Analysis 2).

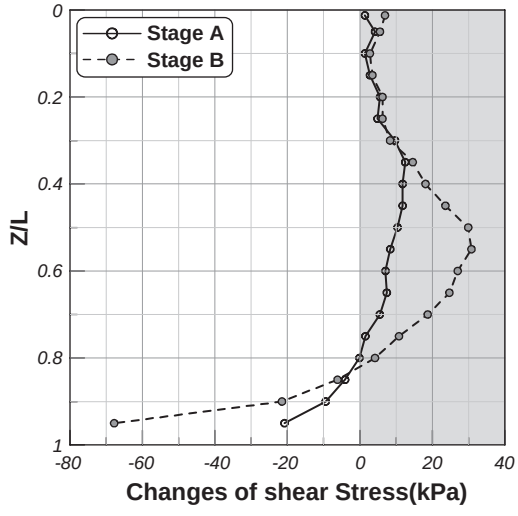


Figure 9. Changes of shear stress along pile (Analysis 2).

force on the pile, P, is normalised by the axial load, P_a, applied on the pile head at stage 0 prior to the tunnel excavation (i.e., Stage 0), most of the axial force is carried by skin friction, implying the pile behaviour is similar to that of a friction pile. Only about 15% of the pile load reached the pile base. This is probably due to insufficient pile head settlement (2.84 mm) to fully mobilise end bearing capacity. It is shown that the axial forces reduced as the tunnel excavation proceeded. Hence, a portion of the axial load carried by the pile base prior to the tunnel excavation was now supported by skin friction as reported by Jacobsz (2002). In particular, the axial force actually reduced to below zero, implying the development of tension near the pile base. A maximum tensile force of 217 kN was calculated, which equals about 11% of the tensile capacity of pile (2000 kN) assuming a tensile concrete strength of 8 MPa. Hence, the probability of a tensile crack developing in the pile therefore appears low.

Fig. 8 shows changes of the tensile forces at the pile base, P_{base}, normalised with the axial force, P, during tunnelling. Prior to the tunnel excavation a compressive force of about 0.135P developed, but as tunnelling proceeded the compressive force decreased gradually. At the end of tunnelling a tensile force of 0.132P developed. It is noted that when tunnelling near or underneath the pile ($Y/D = -0.3 \sim 0.3$) the compressive force reduced rapidly and turned to tensile force indicating the major influence zone maybe about 0.3D (Y direction) measured from the tunnel centre.

3.5 *Shear stress distribution along the pile (Analysis 2)*

Fig. 9 shows distribution of net changes in the shear stress purely due to the tunnel excavation with the normalised pile depth, Z/L, excluding the effect of the axial loading on the pile at stage 0. The shear stresses are deduced from the axial force distribution in the piles. It is shown that the shear stresses at the most part of the pile (from $Z/L = 0.0$ to $0.85 \sim 0.90$) increased at stages A and B, while those near the pile base decreased in a similar pattern. The negative shear stresses near the pile base were large up to 68 kPa, perhaps indicating that the substantial relative displacement between the pile and the surrounding ground might have taken place. This illustrates that the development of the tensile force near the pile base as mentioned previously was related to the downward shear stress component (Pang 2006). The reason for this observation is probably attributed to the soil around the pile base settling less than the soil around the upper parts of the pile shaft due to tunnelling. Depending on the amount of volume loss, this might even result in negative friction on the upper sections of the pile (Jacobsz 2002).

3.6 *Development of plastic yielding in the soil (Analysis 2)*

Changes of stress state of the soil next to the pile prior to tunnel excavation and during the tunnel excavation was studied. At stage 0, the zone of plastic yielding in the soil prior to tunnelling only extended to $Z/L = 0.25$ from the surface. This is probably due to the large relative shear displacement developed at the pile-soil interface near the surface. The extent of plastic yielding during tunnelling increased at stages A and B. The range of plastic yielding increased to $Z/L = 0.45$ at stage A and $Z/L = 0.60$ at stage B. In addition, a plastic zone developed near the pile base ($Z/L = 0.95 \sim 1.0$)

at stage B due to the large shear displacement which developed there. Generally pile behaviour under the service condition can be explained based on the elastic model. However, the computed results indicate that substantial plastic yielding can be developed in the soil near the pile which will in turn affect the performance of the pile significantly.

4 CONCLUSIONS

Parametric numerical analyses have been conducted to study the influence of tunnelling on an adjacent single pile. The following conclusions can be drawn from the present study.

1. Due to tunnelling pile settlement increased and shear stress distribution along the pile changed.
2. The pile settlement increased as the tunnelling proceeded. The computed pile settlement was larger than that computed from the green field condition. Moreover, the ground settlement distribution was severely deviated from the Gaussian settlement distribution. Hence, a relation that can include this phenomenon is perhaps necessary to estimate ground settlement trough. The apparent pile capacity deduced from load-settlement of the pile during tunnelling was reduced. At the end of the tunnel excavation, the apparent pile capacity was reduced to about 50%. Therefore, a significant reduction in the pile capacity is expected affecting serviceability of the piled foundation.
3. Due to development of the relative shear displacement at the pile-soil interface the shear stress distributions along the pile changes, and so is the distribution of axial force of the pile. The analysis showed that axial forces near the pile base reduced while those at the upper part of the pile increased, implying an increase in the shaft resistance of the pile. In addition, tensile forces developed near the pile base up to 13% of the axial load.
4. The extent of plastic soil yielding next to the pile expanded as the tunnelling proceeded and hence when large ground settlement is expected, soil slip at the pile-soil interface very likely to be developed.
5. It may be necessary to study the effects of ground reinforcement on the pile performance where tunnel excavation is to be conducted near the piled foundation to minimise damages of superstructures.

ACKNOWLEDGEMENTS

This study was supported by 2006 Research Grant from Kangwon National University.

REFERENCES

Bezuijen, a., & Schrier, J.V.D. (1994). The influence of a bored tunnel on pile foundations, *Centrifuge 94*, (Edited by Lee & Tan), Balkema, Rottterdam, 681–686.

Davisson, M.T. (1972). High capacity piles, *Proceedings and Lecture Series in Innovations in Foundation Construction*, ASCE, Illinois Section, 82–112.

Jacobsz, S.W. (2002). The effects of tunnelling on piled foundations, PhD thesis, University of Cambridge.

Lee, C.J., Lee, J.Y., Yoon, S.H., & Kim, J.S. (2006). The design and construction of the Dae Gu subway near Geum Ho river: A case history, ITA 2006, CD

Lee, G.T.K., & Ng, C.W.W. (2005). The effects of advancing open face tunneling on an existing loaded pile, *Journal of Geotechnical and Geoenvironmental Engineering*, ASCE,131(2), 193–201.

Lee, Y.J. (2004). Tunnelling adjacent to a row of loaded piles. PhD Thesis, University College London, University of London.

Mair, R.J., & Taylor, R.N. (1997). Theme lecture: bored tunnels in the urban environment, *Proc. 14th International Conference on Soil Mechanics and Foundation Engineering*, Hamburg, Balkema, 2353–2385.

Mroueh, H., & Shahrour, I. (2002). Three-dimensional finite element analysis of the interaction between tunnelling and pile foundation *Int. J. Numer. Anal. Meth. Geomech.*, 26, 217–230.

Pang, C.H. (2006). The effects of tunnel construction on nearby pile foundation, PhD thesis, The National University of Singapore.

Selemetas, D., Standing, J.R., & Mair, R.J. (2005). The response of full-scale piles to tunnelling, *5th Int'l Symposium Geotechnical Aspects of Underground Construction in Soft Ground*, Balkema

Vermeer, P.A., & Bonnier, P.G. (1991). Pile settlements due to tunneling. *Proc 10th European Conference on Soil Mechanics and Foundation Engineering*, Florence, Balkema, 2, 869–872.

Underground Space – the 4th Dimension of Metropolises – Barták, Hrdina, Romancov & Zlámal (eds)
© 2007 Taylor & Francis Group, London, ISBN 978-0-415-40807-3

Loads on the center pillar of two-arch tunnel under the influence of discontinuity planes in the ground

Sang Duk Lee
Prof. Dr-Ing. Dept. of Civil & Transportation Eng., Ajou University, Suwon, Korea

Gwang Wook Byun, Bum Jin Oh & Il Woo Lee
Grad. Student Dept. of Civil & Transportation Eng., Ajou University, Suwon, Korea

ABSTRACT: Load on the center pillar of two-arch tunnel and behavior of the ground around it under the influence of discontinuity planes were studied. Large scale model tests in the scale of 1/10 were performed in the biaxial loading test apparatus. Tests ground with various angle of discontinuity in 0, 30, 60, and 90 degrees were built, which was 3.3 m in width, 3 m in height, 0.45 m in length. During the construction sequences were pillar loads, deformation of the ground around the two-arch tunnel, liner stress, and the distortion of tunnel measured. Tests results show that pillar load and ground deformation are distinctly depended on the angles of discontinuity. The construction sequences should be considered in the construction of two-arch tunnel in the ground including discontinuity planes.

1 INTRODUCTION

Recently two-arch tunnel has been commonly constructed because it has many advantages such as the minimization of tunnel section, less loading on the environment and easy connection to adjacent roads. But the behavior of two-arch tunnel and ground around it have not been fully clarified because of its complex construction sequences and relaxation history. Effects of the existing discontinuities in the ground and the construction sequences on the behavior of two-arch tunnel, especially loads on the center pillar, are not well known yet.

This research was focused on the analysis of pillar load, liner stress, and deformation of the ground around two-arch tunnel depending on the lateral stress coefficient, the construction sequences, and the inclination of discontinuities.

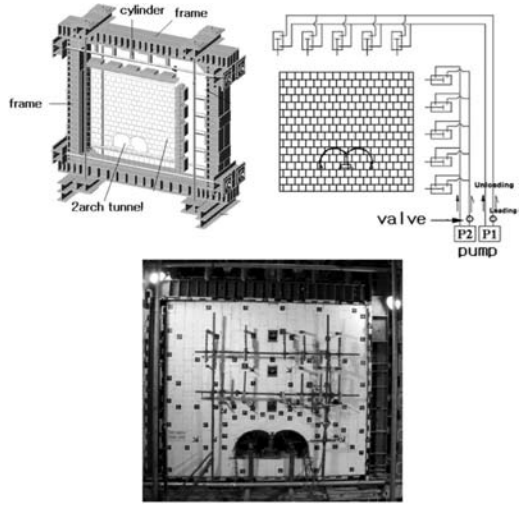


Figure 1. Test equipment and model ground.

2 LARGE SCALE MODEL TEST

2.1 *Development of model test*

Large scale model tests in 1:10 scale were accomplished in the biaxial load test facility which was 5 in width, 5 m in height and 0.8 m in length. Load capacity was 2.50 MN in both vertical and horizontal directions (Fig. 1).

Figure 2 shows a model test ground including various discontinuities, which is 3.3 m in width, 3.0 m in height, and 0.45 m in length. The ground, whose RMR value was about 67, was constructed by using the hexahedral concrete blocks which are 0.2 m in width, 0.15 m in height, and 0.45 m in length. And the discontinuity inclination test ground was in 0, 30, 60, and 90 degrees. The model tunnel in 1:10 scale was 1.2 m in width, 0.6 m in height and 0.45 m in length. The steel liner in 0.4 mm thickness was designed according to the similitude law by Duddeck and Erdmann (1985), to have the same moment of inertia as the standard

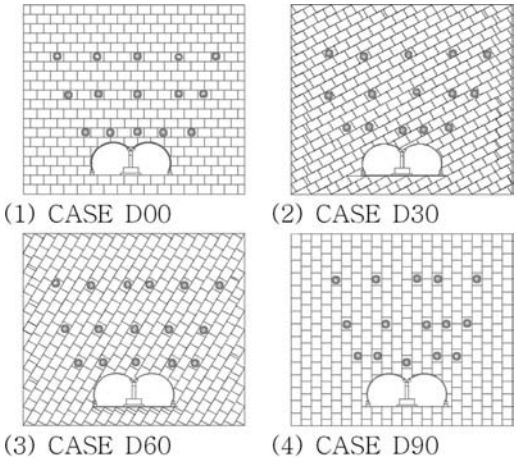


Figure 2. Test ground including discontinuities and displacement measuring points.

supporting type III. Friction at the boundary of test ground was minimized by installing rollers. The center pillar load, ground deformation and tunnel distortion were measured during the construction sequences.

2.2 *Test procedure*

Before tunnel excavation, the test ground was loaded not only vertically but also laterally. Lateral stress coefficient was kept constant as 0.4.

Model tunnel was excavated in the sequence of pilot tunnel, upper right face, upper left face, lower right face, and lower left face. After tunnel construction, horizontal stress was increased to change the lateral stress coefficient in 0.3, 0.325, 0.35, 0.375, 0.5, 1.0, 1.4, 2.0.

3 TEST RESULTS

3.1 *Ground deformation*

Ground deformation around tunnel was measured by using LVDT(Linear Variable Displacement Transformer), and was shown in contours. And maximum displacement was illustrated in construction stages. Results showed that most part of displacements was occurred during the excavation of upper face. Ground deformation was distinctly dependant on the inclination of discontinuity planes.

3.1.1 *CASE D00*

When a two-arch tunnel was excavated in the ground, which had horizontal discontinuity planes, ground deformed symmetrically to the center pillar. Maximum displacement was measured at the ground above pillar.

Displacement history at the location of the maximum displacement during excavation procedure is

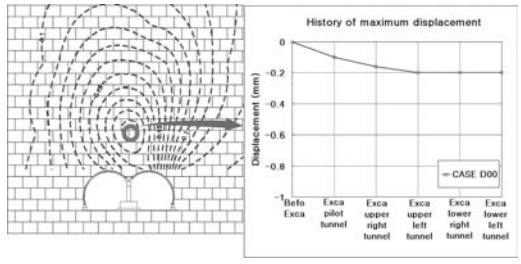


Figure 3. Displacements contour and the history of the maximum displacement in CASE D00.

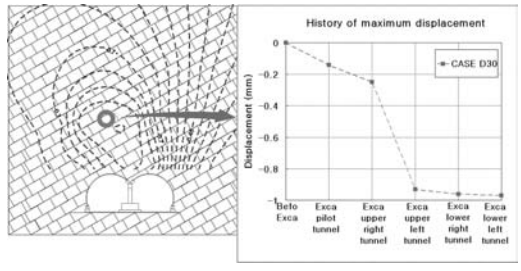


Figure 4. Displacements contour and the history of the maximum displacement in CASE D30.

illustrated in figure 3. Most part of the displacement was measured during the excavation of pilot tunnel and upper face of main tunnel. But almost no displacement was measured during the excavation of lower face of main tunnel.

3.1.2 *CASE D30*

In case of D30, when discontinuity was inclined 30 degrees, most part of the displacement was occurred during the excavation of the upper face of left main tunnel. And maximum displacement was occurred at the ground above the crown of left tunnel.

Maximum displacement due to the excavation of upper left face in CASE D30 was 20 times larger than that in CASE D00. And that due to the excavation of pilot tunnel and upper face of right tunnel in the CASE D30 was 1.5 times larger than that in the CASE D00. Ground was deflected perpendicular to the discontinuity planes and directed to tunnel.

3.1.3 *CASE D60*

In CASE D60, when discontinuity inclined 60 degrees, ground deformed in the very wide area above the crown of left tunnel during the tunnel excavation. But maximum displacement was occurred in the ground direct above the crown of right tunnel.

Displacement due to the excavation of upper face of right tunnel was 3 times larger than that, which happened due to the excavation of any other faces. The angle of discontinuity planes and the lateral stress

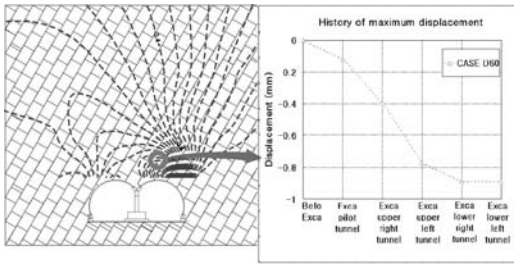


Figure 5. Displacements contour and the history of the maximum displacement in CASE D60.

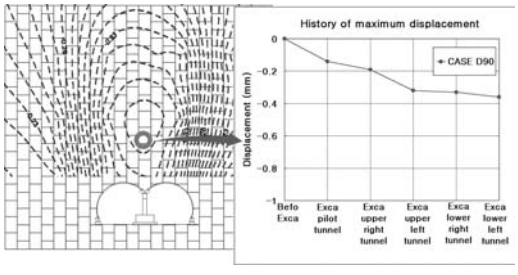


Figure 6. Displacements contour and the history of the maximum displacement in CASE D90.

coefficient were the most important factors for the ground deformation. Displacement due to the excavation of upper face of left tunnel in CASE D60 was greater than that in CASE D00 and D90.

3.1.4 *CASE D90*

In CASE D90, when discontinuity planes were vertical, ground deformed almost symmetrically to the center pillar. Displacement contours showed that ground deformation was concentrated on the upper part of center pillar. The ground above center pillar deformed as if it was sliding into the tunnel (fig. 6).

Displacement at every tunnel excavation stages was almost same amount at every tunnel excavation stages. Maximum displacement in CASE D90 was slightly larger than that in CASE D00.

3.2 *Pillar load*

In the tests, initial stress condition was produced by applying both vertical and horizontal loads at the horizontal and vertical boundary. Lateral stress coefficient was kept constant (K = 0.4).

Firstly, pilot tunnel was excavated and then center pillar was installed. Excavation of main tunnel began with upper face and right tunnel.

During the main tunnel excavation, load on the center pillar at each construction procedure is normalized thru rock mass load by Terzaghi and shown at

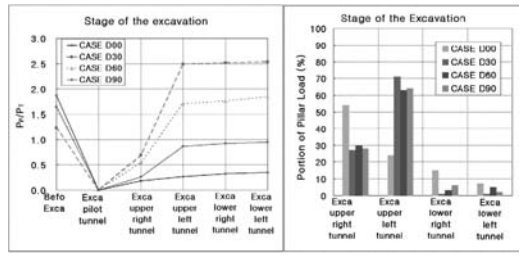


Figure 7. Pillar loads during construction sequences.

Table 1. Pillar loads during construction, P_P/P_T*.

Joint dip	Right upper	Left upper	Right lower	Left lower
0°	0.19	0.27	0.33	0.35
30°	0.70	2.52	2.55	2.57
60°	0.55	1.73	1.78	1.87
90°	0.26	0.87	0.94	0.96

*P_P : Pillar load after lower left tunnel was excavated,
P_T : Rock mass load by Terzaghi

Table 2. Ratio of pillar load to Matsuda and Lee equation.

Joint dip	P_P/P_M	P_P/P_L
0°	0.62	0.77
30°	4.53	5.67
60°	3.3	4.13
90°	1.69	2.11

table 1 and figure 9. It shows that pillar load increases depending on the excavation sequences.

Measured pillar loads were compared with the calculated loads by Matsuda(1997) and Lee(2004), which are for continuous ground. Lee took into consideration the liner stiffness for the calculation of pillar loads.

The calculated loads did not coincide with the measured value. Calculated pillar load was larger than the measured value in case of horizontal discontinuity planes (D00), but much smaller in other cases (D30, D60, D90).

Especially, in CASE D30, measured pillar load P_P was 4.53 times (P_M by Matsuda) and 5.67 times (P_L by Lee) larger than the calculated values.

3.2.1 *CASE D00*

Measured pillar load was smaller than the calculated by Matsuda's equation.

About 53% of the total pillar load was developed during the excavation of upper face of right tunnel, and 25% during upper face of left tunnel. That means about 80% of total pillar load was developed during the upper face excavation.

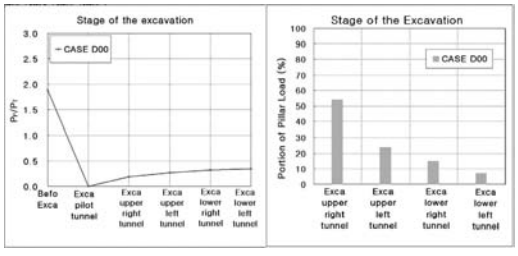


Figure 8. Pillar loads in CASE D00.

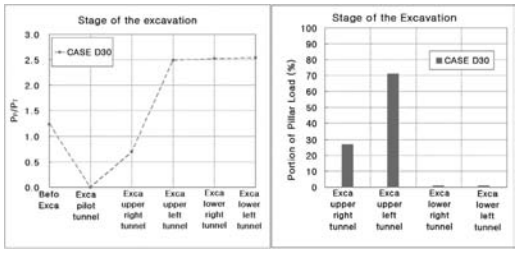


Figure 9. Pillar loads in CASE D30.

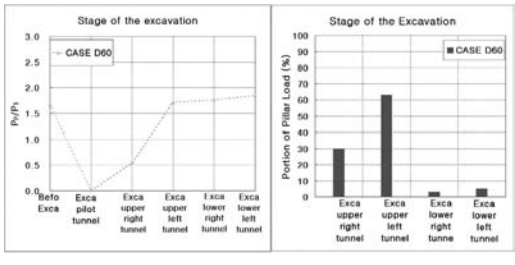


Figure 10. Pillar loads CASE D60.

3.2.2 *CASE D30*

Measured pillar load was 4.53 times larger than P_M.

Measured pillar load at the time of complete excavation in CASE D30 was 7 times larger than that of in CASE D00. But pillar loads due to the excavation of upper right face and upper left face in CASE D30 were 3.75 times and 21.8 times larger than that of D00.

3.2.3 *CASE D60*

After complete excavation in D60, the measured pillar load was 3.3 times larger than that of calculated by Matsuda.

Pillar load due to the excavation sequences showed almost the same trends but was slightly lower value than that in CASE D30. Largest pillar load was measured at the excavation of upper face of left tunnel, and its increment was largest when excavation line was parallel to discontinuities.

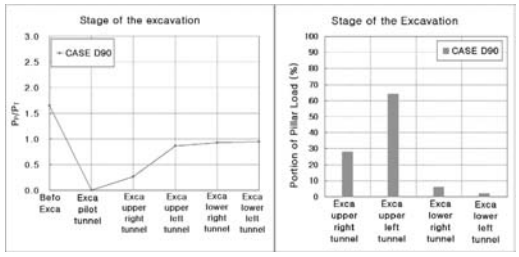


Figure 11. Pillar loads and its development during the excavation stages in CASE D90.

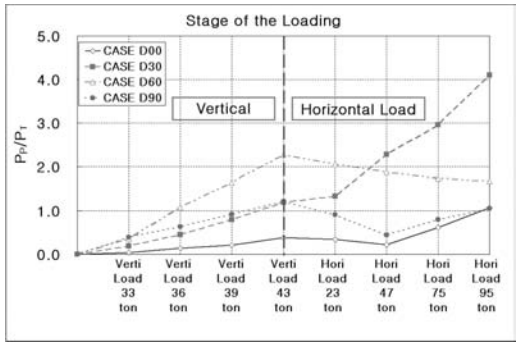


Figure 12. Pillar loads under vertical and horizontal loading.

3.2.4 *CASE D90*

When two-arch tunnel was completely excavated, pillar load in CASE D90 was 2.72 times larger than that in CASE D00. When upper left tunnel was excavated, almost 60% of total pillar load was developed.

3.3 *Vertical and horizontal loading*

Loads at the vertical and horizontal boundary were increased, in order to see the behavior of two-arch tunnel and the ground around it due to the changed loading condition.

Vertical load was increased gradually from initial value 300 kN to 330, 360, 390, 430 kN to change the lateral stress coefficients from 0.4 to 0.375, 0.35, 0.325, and 0.3, respectively. And horizontal load was increased from initial value 140 kN to 230, 470, 650, and 950 kN to change the lateral stress coefficient 0.5, 1.0, 1.4 and 2.0 respectively.

During these loading stages, the pillar load, liner stress, and the deformation of tunnel and ground around the two-arch tunnel was measured.

3.3.1 *Pillar load*

Pillar load due to extra boundary load is shown in figure 12. Pillar load at the time of completion of construction was the largest in CASE D30. Due to the

vertical load, the largest pillar load was developed in CASE D60, and it was more than 4 times larger than that of CASE D00.

On the other hand, due to the horizontal load, pillar load was developed depending on the inclination of discontinuities and the lateral stress coefficient.

In CASE D00 and D90, pillar load was decreased due to horizontal load if lateral stress coefficient was smaller than 1.0 ($K<1.0$). But it was increased in case lateral stress coefficient larger than 1.0 ($K>1.0$).

In CASE D60, due to the horizontal load, pillar load was decreased proportionally to lateral pressure, but in CASE D30, it was increased continuously.

4 CONCLUSION

Conclusion of large scale model tests for two-arch tunnel could be drawn as follows;

1 Largest pillar load due to the excavation of main tunnel was developed in horizontal discontinuity (D00) and then in the order of 0°, 90°, 60° and 30°.
2 Measured pillar load in the ground with horizontal discontinuity was smaller than the calculated values by Matsuda equation (1997) and Lee (2004) for continuous ground. But much larger pillar load was measured in the ground with inclined discontinuity than the calculated for continuous ground.
3 Most part of the pillar load was developed during the excavation of upper face of right tunnel in the ground with horizontal discontinuity(D00), but it was developed during the excavation of upper face of left tunnel in the ground with inclined discontinuity (D30, D60, D90).
4 Due to vertical load, the pillar load was eventually increased irrelevant to the load, pillar load was developed depending on the inclination of discontinuity and the lateral stress coefficient.

REFERENCES

Duddeck, H. & Erdmann, J., 1985. On structural design models for tunnels in soft soil. Underground Space, Vol. 9. Pergamon Press, pp. 246–259

Lee, S.D., et al., 2002. Influence of the discontinuity planes on the Shallow Tunnel. 28th *ITA General Assembly and World Tunnel Congress, ITA*, pp. 217–225

Lee, S.D. & Jun, E.S., 2003. A Behavior of Two-Arch Tunnel at Sandy Ground. *A Journal of Korean Tunneling Association*, Vol. 6, No.2. pp. 171–182

Lee, S.D., et al., 2004. A Behavior of Pillar in 2 Arch Tunnel according to Stiffness of shotcrete liner. *Conference of Korean Society of Civil Engineering*, Vol. 4H

Kouthabeloulis, N.C. & Griffiths, D.V., 1989. Numerical modeling of the trap door problem, *Conf. Soil Mech. Found. Engng., Cambridge*, Vol. 39. No.1

Matsuda, T. (1997) A study on design methods for twin tunnel constructed by the single drift and central pier method, *Proceeding of studies on tunnel engineering*, Vol. 7

Matsuda, T. (1998) Ground behavior and Settlement control of twin tunnels in soil ground, *Tunnels and Metropolises* pp. 1193–1198

Terzaghi, K., 1936. Stress distribution in dry and in saturated sand above a yielding trap-door, *Proc. 1st int. Conf. Soil Mech. Found. Engng., Cambridge*, Vol. 1

Vardoulakis, I., et al., 1981. Trap-door problem with Dry Sand: A Statical Approach based upon Model test Kinematics, *Int. J. Num. Analy. Meth. Geomech.*, Vol. 5

This page intentionally left blank

Underground Space – the 4th Dimension of Metropolises – Barták, Hrdina, Romancov & Zlámal (eds)
© 2007 Taylor & Francis Group, London, ISBN 978-0-415-40807-3

A case study of tunnel excavation adjacent to a steep slope

Shen-Chung Lee & Lin-Bin Chiou
Taiwan Area National Expressway Engineering Bureau, Taipei, Taiwan

Gwo-Fong Lin
National Taiwan University, Taipei, Taiwan

ABSTRACT: The Hsintien No.1 tunnel located in the northern section of National Expressway No.3 in Taiwan passes through the toe of a steep slope in parallel manner, due to the unfavorable topographical and geological conditions as well as the onslaughts of torrential rains during the construction, the project was on the brink of total collapse. Assessing the monitoring data and evaluating the failure mode, the engineering layout was changed so that the slope could stop cutting downward; the stability of the slope was enhanced by massive backfilling and heavier tunnel supports. After a series of remedial measures, the stability of the slope and tunnel was reached. Current construction of expressways in Taiwan has expanded to the mountainous terrains; thus a big portion of tunneling works is expected. It is hoped that this case study will shed some light on the future projects of similar nature.

1 INTRODUCTION

The National Expressway No.3 connects both the northern and southern ends of Taiwan. The feasibility study of this expressway commenced in 1983, followed by the planning, design and construction, and was completed for operation in January 2004. The total length of this expressway (Fig. 1), including the main route and branches, is 518 km (TANEEB, 2004). There are 14 tunnels with a total length of 13.6 km in Expressway No.3 of which 12 of them are located in the northern section, thus a tunnel group is formed. Most of these twin-tube three lanes tunnels passing through unfavorable topography and adverse geology; therefore, the tunneling works were always critical during the construction.

The Hsintien No.1 Tunnel is one of the tunnels in the tunnel group that runs through the hilly area at the rim of Taipei Basin. This tunnel cuts through the toe of an 80 m steep slope. There are high-voltage electric towers on the top of the slope and a community with hundreds of residential buildings near the toe, thus the topographical condition around the site is complicated. The rock formations are loosely cemented and low in strength, as well as affected by the thrust fault nearby the site, the geological conditions are unfavorable for constructions. To aggravate the matter, three consecutive torrential typhoon rains invaded the site during the construction and resulted the sliding of the slope. There was tremendous deformation in the tunnel excavated simultaneously with the slope cut.

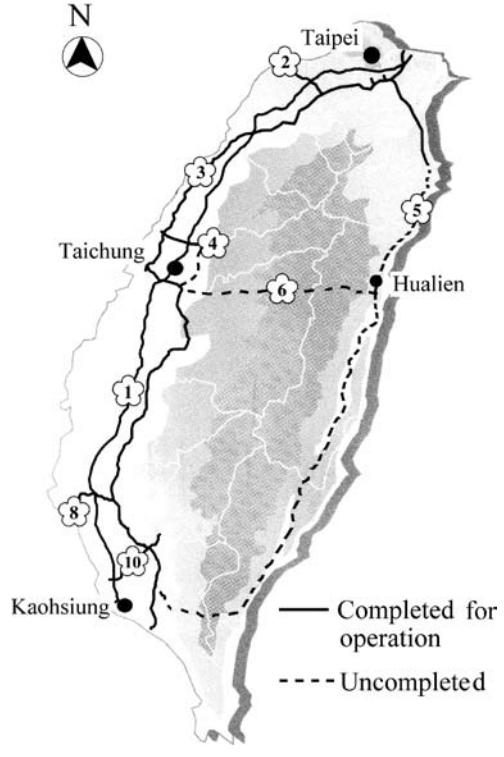


Figure 1. Taiwan National Expressway Network.

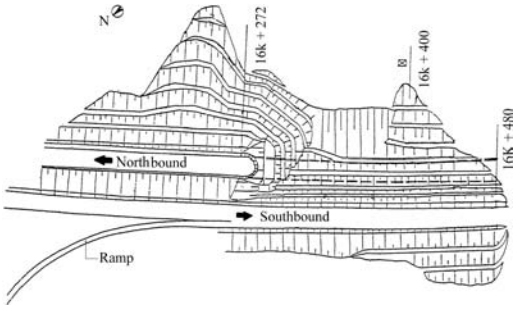


Figure 2. Original plane view of Hsintien No.1 Tunnel.

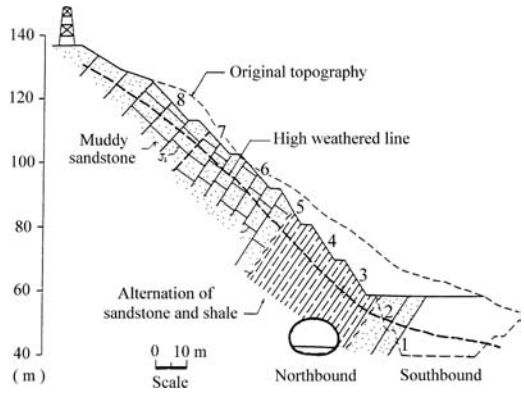


Figure 3. Geological section of Hsintien No.1 Tunnel.

This paper first gives a general description of the project, followed by the construction procedures, the interactive factors that affected the stability of the project, and the remedial measures adopted. Finally, the causes of construction delay were summarized and presented.

2 GENERAL DESCRIPTION OF THE PROJECT

2.1 *Original design*

Due to the topographic restriction, Hsintien Tunnel was constructed by four separated tunnels, namely Hsintien No.1 to Hsintien No.4 Tunnels. These four separated tunnels were connected in the concrete lining installation stage. According to the original design, the northbound of Hsintien No.1 Tunnel was cut through the bottom of the slope by tunneling, while the southbound was designed by open cut in the original design owing to the interchange ramp merge into the main route. The original plane view is shown in Figure 2.

The slope is steep with a height of 80 m in the original design. The slope was designed to cut by 8 benches; each bench is 10 m high with a 3 m berm. The primary supports of the slope are shotcrete, rock bolts and stressed rock anchors.

2.2 *Topography and geology*

The Hsintien No.1 Tunnel is located at the rim of Taipei Basin where the topographic surface is rugged. It runs in parallel manner to the slope, an unbalanced earth pressure thus occurred on the tunneling work. It passes through the Nankang Formation where its geological age is middle Miocene. It is a marine sedimentary sequence. The formation is divided into two parts according to lithological differences: the upper part is mainly composed of thick-bedded muddy sandstone, while the lower part is mainly composed of thin alternation of sandstone and shale. As a result of squeezing effects from the thrust fault nearby the site, shale beds in the sandstone and shale alteration are transformed into clay seams. The bedding planes are often open with smooth surfaces, thus its shear strength is low. The beds are smooth with attitude of N44° E / 55°S. The strike of the beds intersects the tunnel axis and the excavated slopes at a small angle or the two are extending in parallel. They incline into the hill, thus a scarp slope was formed (Cheng et al. 1997). A representative cross-section showing the geologic units is shown in Figure 3.

3 CONSTRUCTION PROCESSES AND REMEDIAL MEASURES

3.1 *Initial remedial measures*

The slope was excavated from June 1992 and when the slope was cut to the fifth bench, the excavation of northbound tunnel at the bottom of the slope was commenced from the south portal (Sta.16 k + 480). When the tunnel was excavated to 16 k + 342 (138 m far from the south portal), the cut slope reached the third bench. During this time, the shotcrete on the slope began to crack and propagated upward toward the top of the slope, the slope toe showed signs of bulging, and a few tendons of rock anchor were broken. After reviewing the monitoring data and evaluating the failure mode, the slope was belief to be in the state of creeping. The northbound tunnel also showed increased convergent displacement; the shotcrete had the phenomena of cracking and stripping, and the steel ribs seriously buckled. If the project were to proceed according to the original design, more slope slides might occurred and the stability of tunnel would than be affected. Based on the long term stability analysis, initial remedial measures were proposed and adopted for the construction:

1. Installation of rock bolts and rock anchors on the completed slope to enhance stability.

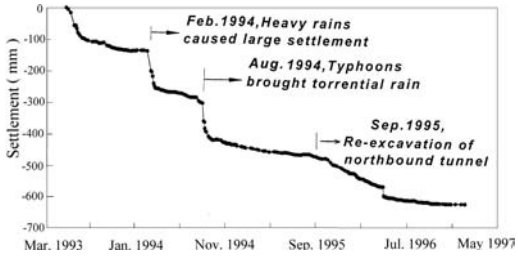


Figure 4. Time-settlement plot measured on the top of the slope.

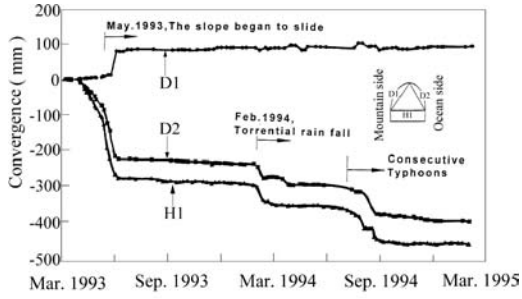


Figure 5. Time-convergence plot measured at sta. 16k + 391 of northbound tube.

2. Construction of 1.0 m diameter by 25 m long bored piles on the slope between Sta. 16 k + 375 to 16 k + 445. The piles are tied back by 50 m long anchors.
3. For the sake of reducing the cut slope area, the north portal of northbound tunnel was extended 40 m, i.e. the station of north portal was moved from 16 k + 272 to 16 k + 232.

After the completion of all the initial remedial measures, the slope resumed excavation downward from the third bench in June 1994. In the mean time, the excavation of the northbound tunnel was stopped to avoid interactive effects between the tunnel and the slope. During the resuming of slope excavation, there were onslaught of three consecutive typhoons which brought heavy rain falls, the remedied slope cracked and deformed again as the rock mass strength was weakened by the water. In that time, the inclinometer on the fifth bench measured a maximum movement of 60 cm; the disc load cell on the fourth bench indicated the tendons had reached 77 tons (design stress was 60 tons), the accumulated settlement of electric tower on the top of the slope was 40 cm (Fig. 4), and the convergence of northbound tunnel at station 16 k + 391 reached 35 cm (Fig. 5). The cracking of the shotcrete and buckling of the steel ribs in the tunnel became worsen. It was obvious that the tunnel suffered tremendous deformation due to the formidable slope sliding. Thus, the entire project was stopped again for the further remedial measures.

3.2 *Subsequent remedial measures*

After reviewing the monitoring data and evaluating the failure mode it was revealed that the slope and the tunnel were at critical state. Further excavations of the slope and the tunnel might trigger a total collapse that would damage the residential buildings at the toe and the electric towers on the top of the slope. The following construction should be performed in such a way that the tunnel must be completed safely without having to perform any more downward excavation on the slope. After a through evaluation and considering

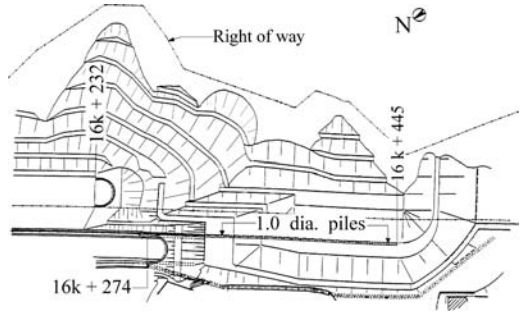


Figure 6. Plane view of the subsequent remedial measures.

the workability, the following remedial measures were adapted (TANEEB, 1998):

1. Installation of more rock anchors on the slope to counter the slope slide.
2. To extend the north end of bored piles from station 16 k+375 to 16 k+270, thus the length of the bored piles was increased to 175 m.
3. Performed massive backfilling at the toe of the slope, in two benches to a height of 20 m with a total volume of 60,000 m^3, to ensure long term slope stability.
4. The southbound was changed from open cut to tunnel excavation. In addition, the southbound tunnel was excavated by both side galleries method.
5. Heavier tunnel supports were adopted in the northbound tunnel thus the rigidity of supports was increased.

The plane and cross-section views for the subsequent remedial measures are shown in Figures 6, 7. After the completion of the subsequent remedial measures, the displacement rates of slope and tunnel work were significantly reduced. Moreover, the contractor and engineers had sufficient understanding of the geological conditions and the failure mechanisms, more effective measures were adopted in the subsequent construction stages.

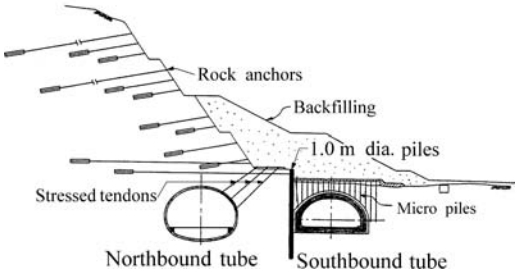


Figure 7. Cross-section view of the subsequent remedial measures.

4 TUNNEL CONSTRUCTION

4.1 *Northbound tunnel*

The northbound tube of Hsintien No.1 Tunnel is a three-lane, one traffic direction tunnel. The original designed station, from 16 k + 272 (north portal) to 16 k + 480 (south portal), was 208 m in length, with a horse-shoe shape cross-section and an excavation area of 157 m^2. The excavation sequence was top-heading first, followed by the bench and invert excavations. In order to avoid vibration caused by explosion to the local inhabitants, the tunnel was excavated by mechanical means such as road-headers or breakers. The rock mass rating (RMR) was the major engineering rock mass classifications used for this tunnel. It was divided into six grades, namely class I to class VI. The tunnel was excavated and supported in rock mass class VI. The thickness of shotcrete is 25 cm, rock bolts diameter (φ) was 29 mm with lengths varied between 6 to 9 m long. After the primary support, the tunnel was lined with 40 cm thickness concrete.

In order to reduce the cutting area of the slope and to avoid the accidents caused by rock falling during operation, the north portal was extended 40 m in the initial remedial measures, thus the length of northbound tunnel was increased to 248 m. In the subsequent remedial measures, the thickness of the shotcrete was increased from 25 cm to 35 cm to restrict the increased convergent displacement. Some additional 40 tons-stressed anchors were installed inside the tunnel. It is noteworthy that the fixed end of some rock anchors installed from the slope surface were exposed during the tunnel excavation, in this situation the exposed tendons were stressed again toward opposite direction from the excavated tunnel, thus both-end-stressed tendons were formed and the rock pillar was reinforced (Fig. 7).

In addition to increase the strength of primary supports, a more rigid concrete lining was also adopted. The thickness of concrete lining was increased from 40 cm to 50 cm; the compressive strength of concrete was also increased from 210 kgf/cm^2 to 350 kgf/cm^2; the reinforcing bars inside the concrete also added.

The monitoring data showed that the rapidest deformation of the tunnel occurred at station 16 k + 420; for the sake of diminishing the deformation by the rigid concrete lining, steel form was transported to the vicinity of station 16 k + 420 and placed the concrete lining by priority herein. It was different from the ordinary operation that the concrete lining was placed consecutively from the portal. Though the "jumping lining" required more construction time, it reduced the tunnel deformation significantly and provided a great help to the tunnel stability.

4.2 Southbound tunnel

In order to prevent further slope movement when the slope was cutting down to the third bench, the proposal of changing the southbound from open road to tunnel excavation had been adopted in the subsequent remedial measures. The southbound tunnel is 206 m long, from 16 k + 274 to 16 k + 480. Owing to the ramp of Hsintien Interchange merge into the main route at the north portal section, there is a 49 m long section near the north portal with 4 traffic lanes with cross-section excavation area of 230 m^2—the biggest cross-section road tunnel in Taiwan. The following 48 m long is the transition section from 4 lanes to 3 lanes, and the other 109 m near the south portal is 3 traffic lanes.

When the southbound was changed from open road to tunnel excavation, the slope had been cut down to the third bench; therefore, the overburden above the tunnel was only 8∼10 m thick. In such situation of big cross-section, shallow overburden and unbalanced earth pressure, the construction encountered extreme perplexities. After investigation, the following measures were adapted for the southbound tunnel:

1. The overburden above the tunnel was reinforced by micro piles: Before the backfilling at the toe of the slope, the shallow overburden was reinforced by vertical micro piles. The construction methods for these micro piles were to drill 4″φ bored holes until the tunnel crown at 1.5 m × 1.5 m c/c. The bored holes were filled with 1:1 cement-sand grouting, and then the piles which composed of four 25 mm φ reinforcing bars with spacer were installed into the bored holes. Finally, all of the top ends of micro piles were placed with a 50 cm thick concrete, similar to the cap slab of foundation piles. After the completion of micro piles, backfilling at the toe of the slope was performed on the cap slab, as shown in Figure 7.
2. Installation of pipe roofing at the portal section: Pipe roofing often used as auxiliary support for the treatment of tunnel disasters such as cave-in, collapse, etc. The portals of Hsintien No.1 Tunnel were sensitive to the disturbance; in case of tunnel collapse, it would cause great damages to the slope and the inhabitants. Therefore, the 4″φ by 25 m long

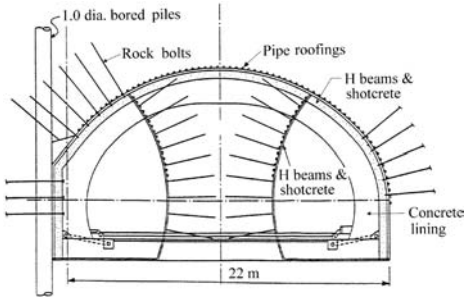


Figure 8. Cross-section view of southbound tunnel.

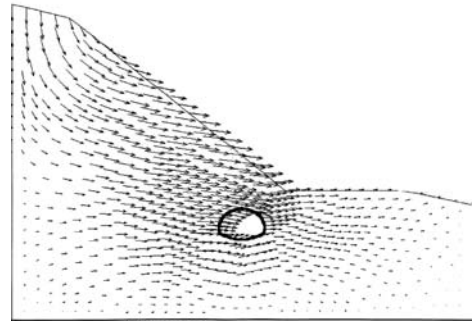


Figure 9. Displacement field after the excavation of slope and northbound tunnel.

pipes were installed adjacent to each other before the portal excavation.

3. Side gallery excavation: Owing to the adverse geology and topography as well as the shallow overburden, the southbound tunnel was designed and constructed by both side galleries method. The construction sequences are (Fig. 8): (i) side galleries excavation (round length 8∼12 m) ,(ii) placing the foundation concrete of side galleries, (iii) excavation of central pillar (round length 8∼12), (iv) placing the foundation concrete of central pillar, (v) erection of steel form, (vi) installation of waterproofing membrane and reinforcing bars, (vii) placing of concrete lining (8 m long), and (viii) curing of concrete lining for 3 days. The thickness of the shotcrete in the primary support is 50 cm, and the inner concrete lining is between 1.2 ∼ 2.0 m thick; therefore, the rigidity of tunnel support was significantly increased. During the construction, the deformation of this tunnel was generally found to be less than 2 cm.
4. Flexibility principle: The tunnel cross-section varies from 4 to 3 traffic lanes at the north portal section. During the installation of concrete lining, the width of steel form has to be modified according the dimensions of the tunnel cross-section. To do this, the contractor separated the original 3-lane steel form, and inserted a transition steel panel at the center part; thus a changeable-dimension steel form was formed and adapted for the variable tunnel cross-sections. Moreover, as the thickness of concrete lining is over 1.2 m, the space was enough for workers to use this steel form as the working truss for the erection of waterproofing membrane and reinforcing bars, it was not only convenient for the construction but also cost and time effective. The both side galleries method resulted a very small deformation during the construction, thus the contractor could changed the construction sequences and support systems with ease, this was also the main reason that the construction time of southbound tunnel could be reduced significantly.

As the contractor was getting familiar with the side galleries excavation, the cycle time (round length was 8 m) could be reduced from 45 days to 23 days. The southbound tunnel was excavated simultaneously from both portals; it was completed in 11 months, 3 months earlier than the anticipate time. After the completion of concrete lining for both tubes and the earth backfilling between the portals of Hsintien No.1 and No.2 tunnels, the entire project of Hsintien Tunnel is in a stable condition, no more disasters happened again.

5 CAUSES OF DELAY

Hsintien No.1 Tunnel was only a short tunnel in the tunnel group, but it took 7 years and 3 months to complete, twice the contract construction time of 3 years and 6 months. Except the Hsuehshan Tunnel (composed of two main tunnels and one pilot tunnel, each is 12.93 km in length) of National Expressway No.5, which was just completed for operation in June 2006, the Hsintien No.1 Tunnel is one of the most formidable construction among all expressway tunnels in Taiwan. The causes of such delay are:

1. Complicated and unfavorable topographic conditions: Expressway No.3 had been planned to pass through Taipei metropolitan area. To avoid large scale demolition of residential buildings and to minimize the environmental impact to schools along the alignment, it was decided to align the expressway along the hilly areas around the Taipei Basin. In terms of topography of Hsintien No.1 Tunnel, the slope is high and steep, and the tunnel runs through and parallel to the toe of the slope. The project was in an unbalance pressure situation, and the displacement was toward to the ocean side, as shown in Figure 9. This situation also can be verified from the convergence measurement. In Figure 5, the diagonal measurements D2 was

convergence, while the D1 was divergence, it is different to the normal situation.

2. Adverse geological condition: The rock formations around the site are mostly of tertiary sedimentary sequences, their lithology, thickness and geologic structure are often vary within even for a short distance, this became the main cause of many design changes and the progress of the project was delayed considerably.
3. Rock mass strength was weakened by water: It was learned from the monitoring data that many rapid displacements occurred after torrential rains; it showed that the failures of the slope and the tunnel were related to the water. The study of rock strength performed by Lin & Hung (1982) shows that: (a) the uniaxial compressive strength of sandstone reduced 50% if moisture content was increased from dry to 75%; (b) the uniaxial compressive strength for shale reduced 56% and the elasticity modulus reduced 25% if the moisture content increased from dry to 75%. Moreover, according to Jeng et al. (1996), the strength of submerged soft sandstone weakened obviously if the soft sandstone was submerged in water for 120 minutes. Its peak uniaxial compressive strength reduced 60%, the shear deformed modulus reduced 60%, and the bulk modulus reduced 70%. From the above studies, if the soft rock submerges in the water or situated in a high moisture content surroundings, its strength will be weakened and deformed significantly.
4. Unfavorable engineering layout: Due to the restriction of route alignment, the northbound tunnel passes through the bottom of the slope by tunnel excavation, while the southbound runs at the toe of the slope by open cut in the original design; thus the interactive effects between the excavation of the slope and the tunnel were sensitive. At the beginning of the slope cut, the slope was stable because the tunnel was not excavated yet. When the slope was cutting down to the third bench, the northbound tunnel was also excavated to the section with the most unbalanced pressure (in the vicinity of station 16 k + 400). During this time, the slide of the slope became serious, and the deformation of tunnel became rapid. After the engineering layout was changed, i.e. the southbound was changed from open road to tunnel excavation, and backfilling was performed at the toe of the slope, the stability of the whole project was fulfilled.

6 CONCLUSIONS

From this case study, the following conclusions can be made:

1. The route selection should be prudent. If the tunnel is designed to excavate through the bottom of a slope in parallel manner, then detailed geological investigations and stability analyses are necessary.
2. The stability issues of scarp slope can not be neglected, especially in the steep slope with adverse geological condition. In the present case, the slope is a scarp slope, but the joints are loosened due to construction operations, topping failure could be easily induced.
3. The strength of rock mass is easily weakened by water. Slope protection measures and drainages facilities can not be overlooked during the design and construction stages.
4. Prevention is always better than remedial measures. Disasters of tunnel and slope are not generated abruptly. By evaluating the monitoring data carefully, many disasters can be prevented in time. A well-planned monitoring system is important for tunneling project.
5. The present project was on the brink of collapse several times during the construction, it was prevented because of the effective remedial measures especially the stoppage of downward excavation of slope and the earth backfilling at the toe contributed the stability greatly on this project.
6. Flexibility is important in tunneling project. Owing to the flexible design and construction of tunneling works, the present project could be completed safely in time.

REFERENCES

Cheng, W.L., Hu, C.J., Wang, S.K. 1997. Stability issues of tunnel excavation on slopes: A case study based on Hsintien No.1 Tunnel. *Proceedings of the symposium on arduous tunneling works of Northern Second Freeway*: 45–67.

Jeng, F.S., Lin, M.L., Huang, T.H. 1996. Investigations on natural obstacles of weak rock tunnel in the northern area of Taiwan. *Proceedings of conference on the construction of rock tunneling*. Taipei.

Lin, M.L., Hung, J.J. 1982. The influence of moisture contents on the mechanical property of sedimentary rock in Taiwan. *Proceedings, 7th Southeast Asian Geotechnical Conference*. Taipei.

Taiwan Area National Expressway Engineering Bureau (TANEEB) 1998. *The final report of Northern Second Freeway*. Taipei: Taiwan Area National Expressway Engineering Bureau.

Taiwan Area National Expressway Engineering Bureau (TANEEB) 2004. *Planning volume of the construction of National Expressway No.3*. Taipei: Taiwan Area National Expressway Engineering Bureau.

Underground Space – the 4th Dimension of Metropolises – Barták, Hrdina, Romancov & Zlámal (eds)
© 2007 Taylor & Francis Group, London, ISBN 978-0-415-40807-3

Subsurface settlement profiles above shallow and deep model tunnels at large ground loss

Yong-Joo Lee
Senior Researcher, Soil-Structure Interaction Group, Steel Structure Research Laboratory, Research Institute of Industrial Science & Technology (RIST), South Korea

Chung-Sik Yoo
Professor, Department of Civil & Environmental Engineering, Sungkyunkwan University, South Korea

ABSTRACT: A major concern in the construction of any tunnel in urban areas is the ground movements that inevitably take place. Geotechnical engineers are responsible for assessing these ground movements in association with tunnel design and have to demonstrate that neighbouring structures will not be subject to excessive differential settlements. The study presented in this paper focuses on the subsurface settlement profiles above shallow and deep tunnels in granular material simulated by aluminium rods. In order to provide theoretical deformation patterns during two-dimensional volume loss, CRISP is used for the finite element analysis. Comparison is then made with idealised laboratory tunnel model tests using close range photogrammetry to measure displacement pattern in a multi sized rod mixture. FEA based on the test results is shown to be in good agreement with the physical model data.

1 INTRODUCTION

The construction of any tunnel will give rise to ground movements in the form shown in Figure 1. Geotechnical engineers are responsible for assessing these ground movements related to the tunnel design and an assessed construction quality, usually expressed as a volume loss (V_L, %). They should demonstrate that neighbouring structures will not be subject to excessive differential settlements.

The pattern and magnitude of ground movements depends on the soil type, the stress history of soil through which tunnel is constructed, the tunnelling methods (open face tunnelling – NATM and closed face tunnelling – slurry shield and EPB) adopted, the geological setting, ground water level, speed of construction and workmanship.

Numerous studies on the tunnelling-induced ground movements in clay soils have been carried out, but few studies have focused on the behaviours of granular soils to date. In particular, there is spare data on the subsurface deformations at the large ground loss.

The study presented in this paper focuses on the subsurface settlement profiles above shallow and deep tunnels in a granular mass. In order to provide theoretical deformation patterns, the CRISP code is used for the finite element analysis. In addition, the close range photogrammetric technique is adopted to generate displacement data from the laboratory two-dimensional tunnel model tests using the multi-sized aluminium rods.

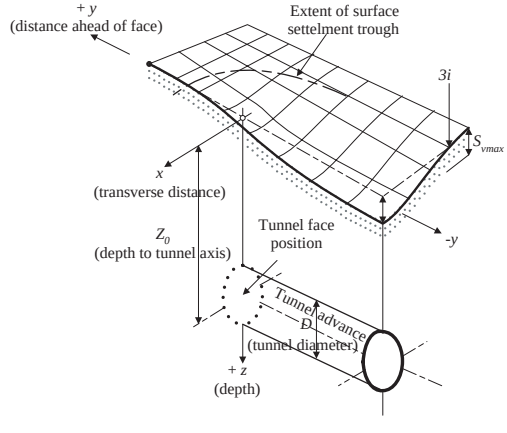


Figure 1. Three dimensional shape of surface settlement above advancing tunnel (Attewell et al., 1986).

Digital image processing has allowed overall deformation patterns of ground movements to be obtained from the analysis of digital images. Detailed patterns of ground movements can be obtained which give a clear insight into deep and shallow tunnelling events and are particularly valuable for validation of numerical analyses.

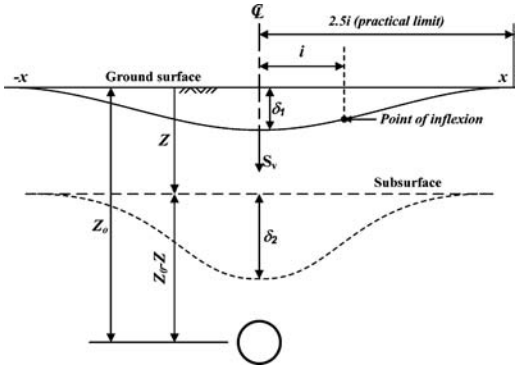


Figure 2. Form of surface and surface settlement profiles (after Mair et al., 1993).

2 SUBSURFACE SETTLEMENT PROFILES

In contrast to the collections of surface settlement measurements, there are relatively few field measurements of subsurface profiles available. It is common to assume that the shapes of subsurface settlement profiles developed during tunnel construction also approximate to a Gaussian distribution, as shown in Fig. 2. However, field and model measurements of subsurface settlements in clay soils indicate that the parameter K does not remain constant but increases with depth, giving proportionally wider settlement profiles closer to the tunnel crown (Mair et al., 1993). For the above subsurface settlement profiles, Mair et al. (1993) proposed a relation between K and the dimensionless subsurface below ground level (Z/Z_0):

$$K = \frac{0.175 + 0.325(1 - Z/Z_0)}{1 - Z/Z_0} \quad (1)$$

where K = trough width parameter; Z = depth of subsurface settlement trough below ground surface; and Z_0 = depth of tunnel axis below ground surface.

3 2D MODEL TEST

3.1 *Deep and shallow tunnel model tests*

Three tunnel model tests were conducted with respect to three tunnel embedment depths, viz. Z_0 = 270 mm; Z_0 = 420 mm; and Z_0 = 470 mm. No surcharge was applied to the surface as all stresses being provided by self-weight of the aluminium rod material.

The tunnel model tests did not precisely reproduce real tunnel construction replicating the method of excavation and support but carefully reduced tunnel diameter to simulate increasing 2D volume loss. The authors investigated the resulting deformation patterns as the tunnel cavity diameter was reduced in a displacement-controlled manner rather than by reducing the support pressure. This method approximates to the condition within a tunnel during excavation where the controlled physical support is provided and limited (i.e. deformation is the aim). The boundary conditions associated with plane-strain conditions are shown in Fig. 3.

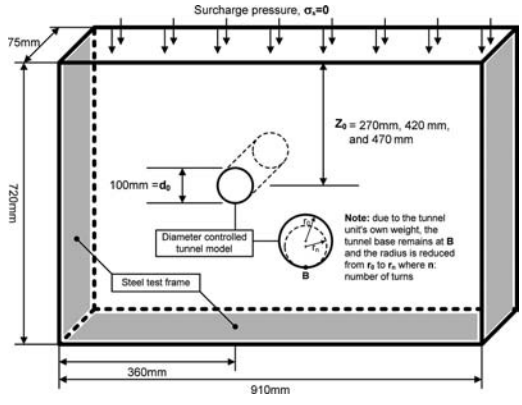


Figure 3. Boundary conditions for two-dimensional tunnel model test (non-scale).

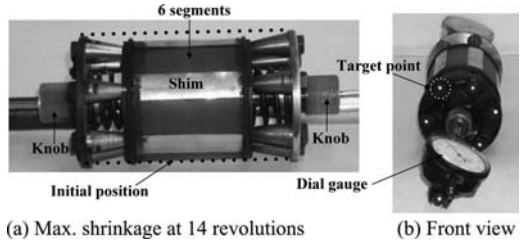


Figure 4. Two-dimensional tunnel device (diameter reduction system).

3.2 *Test equipments*

The model tunnel consists of 6 segments, the two ends of a segment being carved on the tapered cones. Each segment will move inward as the tapers are withdrawn, simulating the two-dimensional volume loss during tunnelling operations. The tunnel diameter is reduced by rotating the two knobs as shown in Fig. 4. The outer diameter of the tunnel is initially 100 mm. The reduction of the tunnel diameter gives directly a 2D volume loss (V_L). This 2D volume loss per revolution is determined from the calibration result (Lee, 2004). The model tunnel itself is a stiff element in the soil but is not fixed in space, so it can move freely during the development of the volume loss.

The aluminium rod mixture consists of six different diameters (viz. 2 mm, 3 mm, 6 mm, 9 mm, 12 mm and 20 mm), which have the same length of 75 mm.

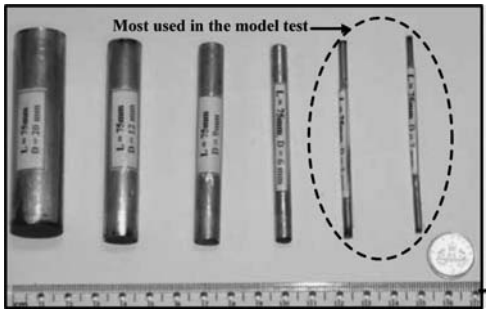


Figure 5. Multi-sized aluminium rod material.

It represents a well graded, idealised two-dimensional granular material, as shown in Fig. 5. The smallest rods (2 mm and 3 mm diameters) were mainly used in the specific area of the model test. However, the biggest rods were only used at boundaries which could not affect the stress-strain behaviour around the tunnel model.

The main features of the modelling of the ground by aluminium rods are as follows: (a) rigid motions such as movement and micro-rotation are visually observed; (b) aluminium rods satisfy plane-strain conditions; (c) as aluminium rods are self-sustaining, there are no side walls. Thus, the aluminium rod models are free from lateral wall friction; (d) the specific gravity of aluminium is comparable to that of sand and gravel. However, the irregular roughness of the shape of soil particles which would normally prevent the rotation of particles is neglected.

The testing time is much quicker than any conventional test using sand or clay. In addition, detailed observation of the side section is easily carried out enabling details of deformation patterns, which are associated with strain fields rather than stress fields, to be determined.

3.3 *Calibration of tunnel model and test procedures*

The tunnel model provided a surface of negligible bending stiffness adjacent to the rod material. The two-dimensional volume loss was determined from the calibration test result, as shown in Fig. 6. The relationship between 2D volume loss and number of revolutions based on the dial gauge was polynomial.

The test procedures are as follows: (a) Preparation of the rod model; (b) Preparation of the test equipment (e.g. model tunnel); (c) Stacking the rod model with the silver reflective markers and insertion of the tunnel at the correct level in the steel test frame; (d) Recording 10 digital images for the initial stage of the photogrammetric measurement; (e) Reduction of the tunnel diameter by the controlled rotation of the knobs at the front and back of the tunnel unit. The following were normally recorded: - 1 revolution

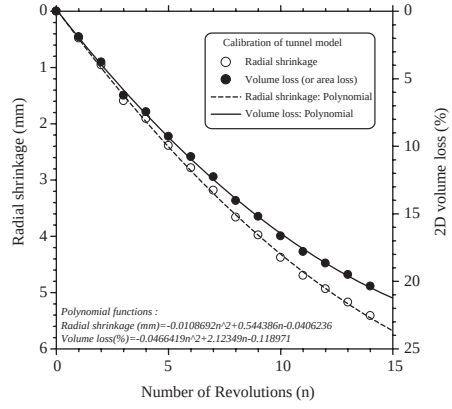


Figure 6. Calibration result of 2D tunnel model.

(V_L = 1.96%), 3 revolutions (V_L = 5.83%), 6 revolutions (V_L = 10.94%), and 9 revolutions (V_L = 15.21%); and; (f) Recording 10 digital images for each chosen stage of (e) above.

The physical position of the tunnel model was not restrained. Care was taken that adjustments made never disturbed the rod material, great care being taken not to apply load or to distort or to twist the unit. The resulting physical location of the tunnel centre during the model test was investigated by using the reflective nodes immediately adjacent to the model tunnel and this actual location was inserted into the finite element analysis (FEA) to mimic the actual physical conditions. The triangular mesh of reflective silver markers used in the Z_0 = 270 mm tunnel model test is shown in Fig. 7. The mesh is comparable with the FE meshes. They are generated by the EngVis program. The horizontal and vertical location of every reflective point is calculated for each 2D volume loss. The incremental displacements and the associated strains within triangular elements were calculated on completion of the whole imaging process.

Specific details of the digital imaging process and strain generation were introduced by Lee and Bassett (2006).

4 NUMERICAL ANALYSIS

4.1 *Numerical simulation*

In order to simulate the "floating" model tunnels in the CRISP FE code, the actual centre point movements of the physical model tunnel were investigated for each of the tunnel depths (Lee and Yoo, 2006). The vertical movements appeared to increase almost in proportion to the volume loss, as shown in Fig. 8. The centre point of the model tunnels moved vertically down while the invert remained at very nearly the same level, which is what would often be the situation in real life, the

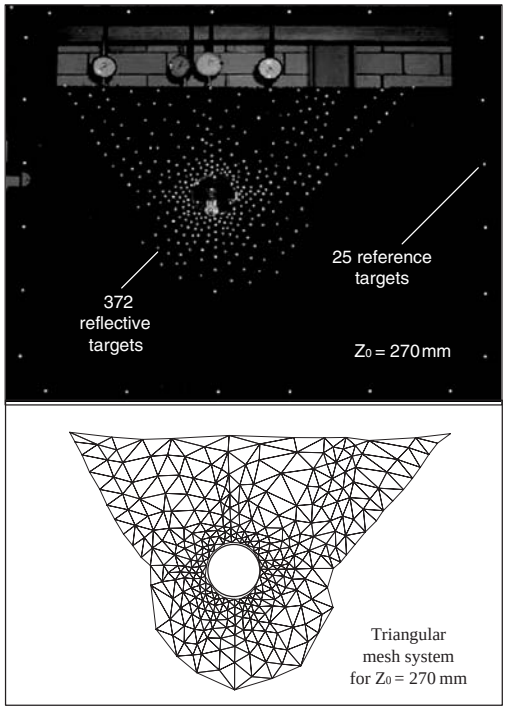


Figure 7. $Z_0 = 270$ tunnel model test and corresponding triangular mesh.

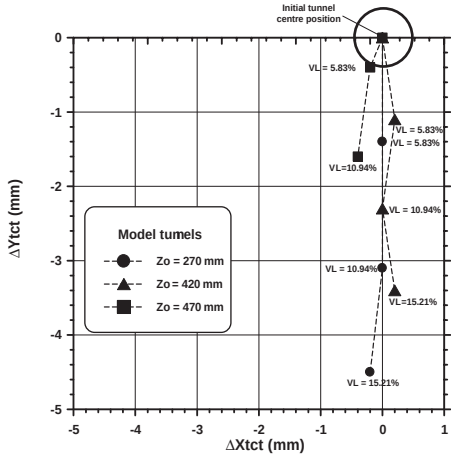


Figure 8. Horizontal and vertical movements (ΔX_{tct}, ΔY_{tct}) of a centre point of a "floating" tunnel model.

level of the invert being the key control. The horizontal movements of the tunnel centre point were assumed to be zero throughout the tests.

The correspondent 2D finite element mesh for the $Z_0 = 270$ mm is shown in Figure 9. It should be noted

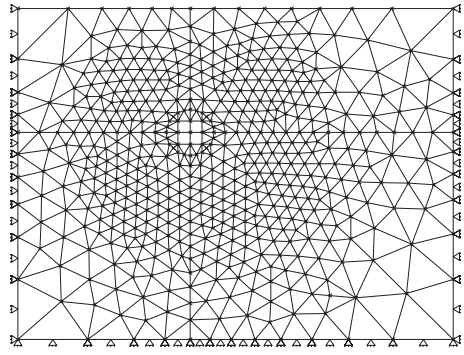


Figure 9. Finite element mesh for $Z_0 = 270$ mm.

Table 1. Soil parameters used in the FEA.

Reference level, Y_0*(m)	0.72
Young's modulus at Y_0, E_0*(kPa)	1600
Gradient of Young's modulus, m_E**(kPa/m)	10,000
Poisson's ratio, ν	0.35
Unit weight of soil, γ (kN/m^3)	24
Effective cohesion, c′ (kPa)	0.1
Effective angle of friction, ϕ' (degrees)	23
Angle of dilation, ψ (degrees)	15

Note: * at ground surface; ** varying with depth.

that for the finite element mesh shown the FE tunnel centre was not located at the middle line of the mesh. This was because in the physical model the tunnel model was not at the centre of the test equipment. This fact was dictated by a later study of pile-soil-tunnel interaction.

4.2 *Constitutive model and model parameters*

Soil behaviour was assumed to be governed by an elastic-perfectly-plastic constitutive model based on the Mohr-Coulomb failure criterion with a non-associated flow rule. The effective angle of friction (ϕ') and the angle of dilation (ψ) were determined to 23° and 15° for granular material, respectively (based on a best FEA fit of load-settlement relationship for the wall model loading tests, Lee, 2004). The effective cohesion (c′) was assumed to be 0.1 kPa. The variation of E (Young's modulus) was assumed to increase linearly with depth. The soil parameters are summarised in Table 1.

The tunnel support is modelled as two-noded bar element and linear elastic material respectively. The Young's modulus and Poisson's ratio for the tunnel support are assumed to be 15.5 GPa and 0.2. The cross section area of the tunnel support ring is 0.003 m^2.

Numerical FNR (full Newton-Raphson) iterative solution scheme was used with a tolerance of 0.05 and a maximum iteration number of 100. K_0 was applied to the initial in-situ stress conditions and a double

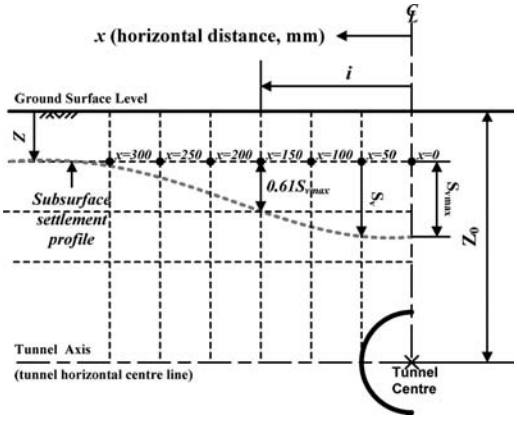


Figure 10. Typical subsurface settlement profile for this study.

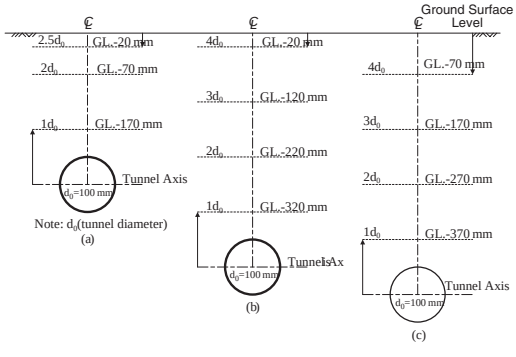


Figure 11. Subsurface levels for three model tunnels: (a) $Z_0 = 270$ mm; (b) $Z_0 = 420$ mm; (c) $Z_0 = 470$ mm.

convergence check applied. A total of 250 increments were used.

5 RESULTS

The authors investigated the vertical displacement (S_v) for a half width for the following 2D volume losses, viz. $V_L = 5.83\%$, 10.94% and 15.21% and at the various subsurface levels, as shown in Figs. 10 and 11. The ground deformation data S_v was extracted from the vertical displacement contours provided by the FE runs and by the photo imaging process for the 2D tunnel model tests. For comparative purposes between the numerical and physical models, the authors concentrated the settlement data close to the ground surface (GL.-20 mm) and on a level $1d_0$ above the tunnel axis. It should be noted that the "surface line" of reference markers in the physical models was actually located at GL.-20 mm.

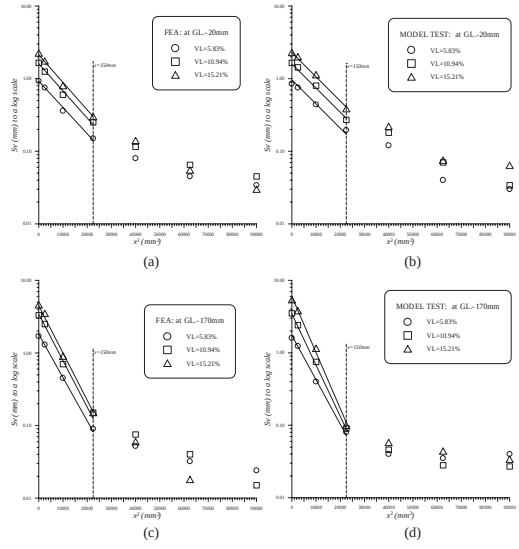


Figure 12. S_v (log scale) – x^2 ($Z_0 = 270$ mm): (a) FE data at *GL.-20 mm*; (b) model data at *GL.-20 mm*; (c) FE data at *GL.-170 mm*; (d) model data at *GL.-170 mm.*

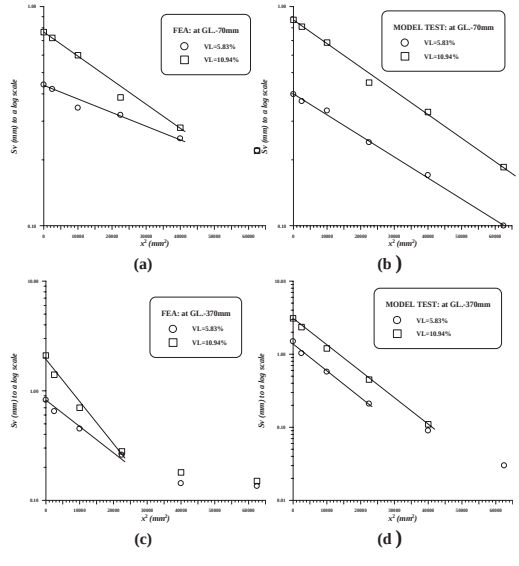


Figure 13. S_v (log scale) – x^2 ($Z_0 = 470$ mm): (a) FE data at *GL.-70 mm*; (b) model data at *GL.-70 mm*; (c) FE data at *GL.-370 mm*; (d) model data at *GL.-370 mm.*

5.1 *Investigation of i values*

In order to investigate whether an inverted Gaussian is an acceptable approximation to both the numerical and the experimental subsurface settlement profiles, all $S_v - x$ data was re-plotted in the form of log scaled settlement to x^2 (Figs. 12 and 13). A true

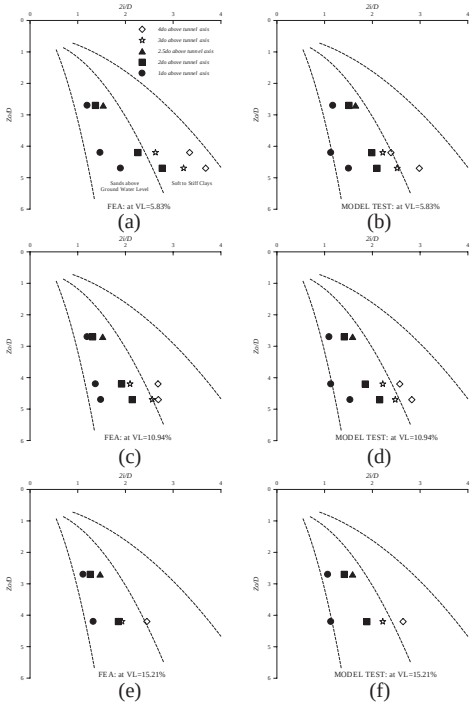


Figure 14. Subsurface settlement profile with tunnel depths: (a) FE ($V_L = 5.83\%$); (b) model ($V_L = 5.83\%$); (c) FE ($V_L = 10.94\%$); (d) model ($V_L = 10.94\%$); (e) FE ($V_L = 15.21\%$); (f) model ($V_L = 15.21\%$).

Gaussian function will provide a straight line on the S_v to a log scale against x^2 plot. The magnitude of i being found at $\underline{S}_v = 0.61 S_{\text{vmax}}$ for which $x^2 = i^2$. The assumed Gaussian error function associated with i values appear to fit both the surface and the subsurface settlement data up to a horizontal distance of 1.5 to 2i in both the FEA and the laboratory model tunnel test (Fig. 12). Beyond that horizontal location, the data does not appear to comply with the same Gaussian function at all. For the deepest case (Z_0 = 470 mm) the model data shown in Fig. 13 the FE analysis shows a similar break at GL.-370 mm but the model data shows subsurface settlement profiles that appear to fit a single Gaussian curve. In the FE case, where the fit does not occur, the authors believe that this is due to the roller boundary conditions applied at the mesh side boundaries which were not remote enough. A fictitious frictional boundary would have been a better assumption or the use of an element to represent the effect of a remote extent of material.

5.2 *The variation of i with depth*

These i values were determined from the data within 200 mm either side of the centre line (i.e. $x^2 < 40{,}000$)

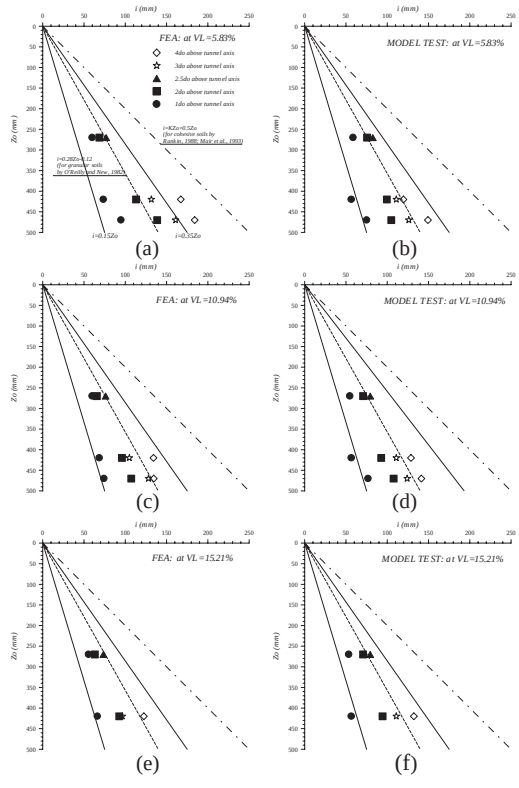


Figure 15. Trough width parameter (i) with tunnel depths: (a) FE ($V_L = 5.83\%$); (b) model ($V_L = 5.83\%$); (c) FE ($V_L = 10.94\%$); (d) model ($V_L = 10.94\%$); (e) FE ($V_L = 15.21\%$); (f) model ($V_L = 15.21\%$).

as discussed above. In Fig. 14, $2i/D$ has been plotted against Z_0/D (D is a tunnel diameter, d_0). As expected, the rods are a dry granular material, the authors' model data all falls in Peck's zone "sand above the water table" (Peck, 1967). The FE data agrees except for the data at small volume loss (Fig. 14 (a)). The physical model values change slightly with increasing 2D volume loss. The FEA values appear to vary quite considerably at high Z_0/D values and different 2D volume loss values. In FEA the zone of influence of a tunnel does not appear to remain consistent throughout its construction. Simple constant spread angle from the centre point or the centre of the invert are not a good representation of the situation throughout the soil depth.

The FE and model data are replotted as i against Z_0 in Fig. 15 and as Z/Z_0 against K in Fig. 16. The settlement trough width parameter (i) for both the FEA and the model tunnel test lie close to O'Reilly and New (1982) for levels 2.5d_0 above the tunnel, but fall to values close to or less than $i = 0.2Z_0$ for levels close to the tunnel crown (i.e. 1d_0 to 2d_0 above the tunnel axis).

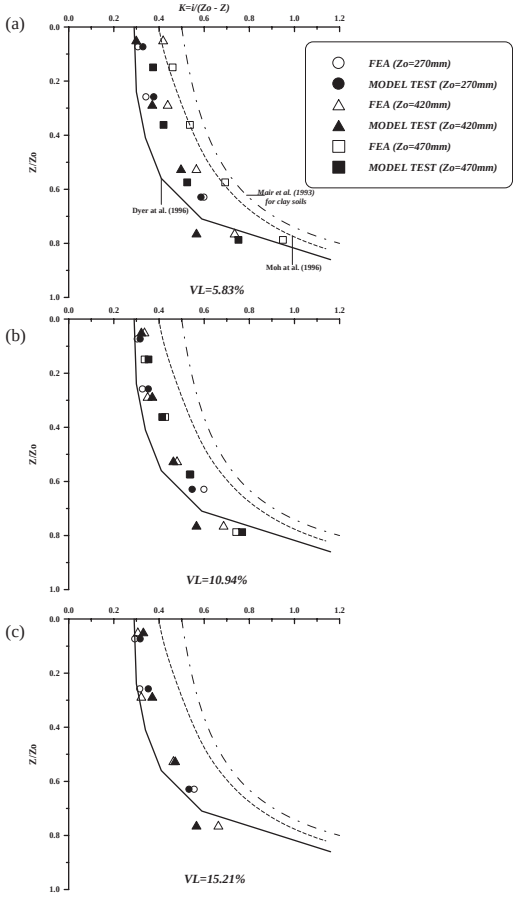


Figure 16. K with tunnel depths for subsurface settlement profiles above FE and model tunnels: (a) $V_L = 5.83\%$; (b) $V_L = 10.94\%$; (c) $V_L = 15.21\%$.

The values of K from both the FEA and the model test lie in a band according to Dyer et al's (1996) field observation as 2D volume loss increased.

6 CONCLUSIONS

In order to provide theoretical deformation patterns associated with shallow and deep tunnels in granular material with increasing 2D volume loss, the CRISP code was used for the finite element analysis and comparisons were made with an idealised laboratory model. Throughout the above comparison the authors reached the following conclusions:

(a) Attention was drawn to a single Gaussian curve, which did not fit well for both the FE and physical model data (Fig. 12), except for the model data for the case of a deep tunnel (Fig. 13).
(b) The i values agreed well with Peck's zone of real field values (Fig. 14) and K values range between 0.15 and 0.35 for dry granular materials (Fig. 15).
(c) The values of K agree very closely with Dyer et al's (1996) field observation data (Fig. 16).

REFERENCES

Attewell, P. B., Yeates, J. and Selby, A. R., 1986. *Soil movements induced by tunnelling and their effects on pipelines and structures*. Glasgow: Blackie.

Dyer, M. R., Hutchinson, M. T. and Evans, N. 1996. Sudden valley sewer: a case history. In Mair, R. J. and Taylor, R. N. (eds), *International Symposium on Geotechnical Aspects of Underground Construction in Soft Ground*: 671–676. London: Balkema.

Lee, Y. J. 2004. *Tunnelling adjacent to a row of loaded piles.* PhD Thesis, Department of Civil and Environmental Engineering, University College London, University of London.

Lee, Y. J. and Bassett, R. H. 2006. Application of a photogrammetric technique to a model tunnel. *Tunnelling and Underground Space Technology,* 21(1): 79–96.

Lee, Y. J. and Yoo, C. S. 2006. Behaviour of a bored tunnel adjacent to a line of loaded piles. *Tunnelling and Underground Space Technology,* 21(3–4): 370.

Mair, R. J., Taylor, R. N. & Bracegirdle, A. (1993). Subsurface settlement profiles above tunnels in clays. *Gétechnique* 43(2): 315–320.

O'Reilly, M. P. & New, B. M. (1982). Settlements above tunnels in the United Kingdom – their magnitude and prediction. *Tunnelling '82*: 173–181. London: IMM.

Peck, R. B., 1969. Deep excavations and tunnelling in soft ground. *Proceedings of 7th International Conference on Soil Mechanics and Foundation Engineering*: 225–290. Mexico: State of the Art Volume.

This page intentionally left blank

Underground Space – the 4th Dimension of Metropolises – Barták, Hrdina, Romancov & Zlámal (eds)
© 2007 Taylor & Francis Group, London, ISBN 978-0-415-40807-3

Application of digital image processing in tunnel excavation

Leng Biao*, Qiu Wen-ge, Liu Yang & Wei Hong-chun
School of Civil Engineering, Southwest Jiaotong University, Chengdu,Sichuan, China

ABSTRACT: With the development of civil traffic, more and more roads and railways have been built. Correspondingly, the number of tunnels becomes larger. During tunnel excavation, geological logging and rock mass classification are two major tasks to be concerned, so tunnel face image analysis is essential. Traditional analysis is time-consuming, costly and the effect is different because of different operators. While conventional approaches are limited, graph and image processing and 3D modeling technology are adopted for tunnel face imaging. Tunnel Face Geology Image System (TFGIS) is designed to manipulate tunnel faces. After processing a series of face images which are snapped by tracking tunnel logging, rock edges and rock characteristic information can be acquired, by which rock masses are classified. According to rock corresponding relation between adjacent face images, 3D tunnel model is built up, which can be regarded as reference information on tunneling.

FOREWORD

Traffic–the basis of national economic development– is the prerequisite to social production currency consumption distribution, and it is also very important to ensure national economic persistent healthy development and accelerate national modernization construction.

With the enhancement of national basis construction, roadway net construction will be one of investment emphasis. In many places, tunnel length took up a big proportion of the whole roadway length. In some sections, the proportion came to more than 40–50%. Therefore, tunnel logging and geology detection are very important to totally roadway construction. During tunnel logging, tunnel excavation volume (includes overbreak and underbreak) reckoning geology prediction and tunnel mechanics structure transformation research are often encountered. If those questions can not be well processed, disasters including tunnel collapse and underground water flooding may take place when tunnels are excavated. Traditional observations are manual record face description and photography, which are diverse with different operators. As a result, the data obtained are inconsistent and incomparable. Photos gained from photography have to be rinsed, which can not be digitized and processed in time. The effects of manual analysis are very limited. If the experience and knowledge of analyzers are different, the analysis outcome will be distinct. There is something that can not be touched by manual analysis. For example, in order to know the geology construction of tunnel logged part, tunnel 3D model need to be built, which nearly can not be manually achieved. However, 3D modeling with computer is easier. In 1990's, researchers in Japan applied imaging technology to tunnel faces so as to extract parameters about surrounding rock classification, predict geology structure in front of tunnel faces, observing lining cracks. In 1993 year, QingShui civil construction company developed tunnel face imaging system[1]. In China, software and hardware of under-well drilling vidicon had been systemic designed, which can not only display deep geology structure and play it, but also determine structural plane attitude and joint width[2]. In document [3], the digital photogrammetry was applied into rock mass joint measurement to overcome traditional methods' disadvantage. An interpretation scheme for images of rock mass joints based on digital photogrammetry is put forward. In document [4], the author had studied on rock mass joint measurement based on digital photogrammetry.

Above all, most of study work is still not systemic. However, photogrammetry always includes job site measurement and image interpretation. In this paper, the author systemic analyzes image interpretation. Graph & image processing technology and OpenGL 3D modeling technology are adopted to deal with tunnel face images gained from job site. Rock mass edges are automatically acquired, and manual interference is

* The connection way of the first author Leng Biao
Tel: 86-28-86465636 Fax: 86-28-87602793
E-mail: bleng@126.com, biaoleng@163.com
Address: 301#, School of Civil Engineering, Southwest Jiaotong University, Chengdu,Sichuan, 610031, China

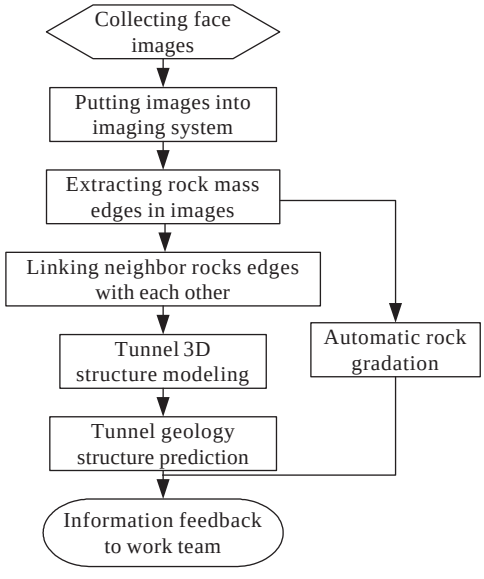


Figure 1. Tunnel face processing flow.

taken as assist step. At last, all rock mass edge information in face images is obtained, then tunnel 3D model is built. According the 3D model tunnel forward geology structure can be predicted.

1 BASIC THINKING

During tunnel logging, tunnel face images are gained by photogrammetry. These face images snapped along with construction schedule are input into imaging system. Every image is processed by digital imaging technology[4]. All rock mass edge information is extracted. After being analyzed by characteristics extraction, rock mass area character parameters are acquired so that rock masses can be classified. At the same time, these corresponding relationships are established between neighboring digital images according rock mass edge information. When all rock mass corresponding relations of all neighboring face images are established, tunnel 3D model then can be set up according edge information. Through this 3D model, tunnel interior geology structure can be observed from all directions. Relevantly, tunnel forward part is predicted from the 3D model. The information is very useful to tunnel construction safety, construction quality and so on. Fig. 1 is the whole flow sheet from photogrammetry to imaging system operation[5].

In the whole procedure, digital image and graph processing pattern recognition and OpenGL 3D modeling technology are needed. Digital image intensification image restoration image segmentation characteristics extraction and so on, which can extract rock mass edges from tunnel face images. Graph processing includes line curve movement distortion and so on, which can edit rock edges. Pattern recognition includes neural network genetic arithmetic vector machine, which can be used to automatically classify surrounding rocks. OpenGL is a 3D graph and model library, which can finish tunnel 3D modeling.

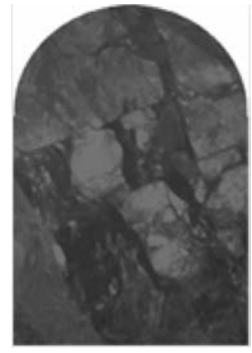


Figure 2. Source image.

2 DIGITAL IMAGE PROCESSING TECHNOLOGY

Digital image[6] and graph processing technology is the base of the whole system. They are complementary to each other. It uses imaging technology to extract rock mass edges of tunnel faces in images. These edges are not always automatically achieved. Therefore, graphing technology is introduced to edit and modify rock mass edges.

Ordinarily, according to processing way, digital image processing includes image preprocessing image segmentation and characteristics extraction.

2.1 *Image preprocessing*

At first, tunnel face images are imported to the imaging system, then these images sorted by shooting time. These images' brightness are often dim. In order that images can be better observed and analyzed, image preprocessing arithmetic is needed. Color equalization processing arithmetic can balance colors distributing among these images, which have a good effect on intensify images. Fig.2 is the source image, and Fig.3 is the result by color equalization processing.

It can be seen from the processing result that the whole brightness and contrast ratio are obviously improved.

2.2 *Image Segmentation*

After preprocessing, the system considers two ways to process images. One way is that edge detection



Figure 3. Color equalization processing result.

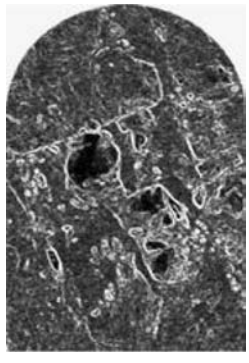


Figure 4. Face image edge detection result.

operators are used to detect image edges. After that, rock mass edges in these images will be more conspicuous. Then these result images are processed to extract edge information. The other preprocessing way is target rock masses segmented directly. From the result, the rock mass edges can also be extracted.

2.2.1 *Edge detection*

The aim of edge detection is that rock mass edges are displayed more clearly. Fig.4 is tunnel face image edge detection result. It can be seen that the edges of rock masses can be well marked using while lines while the none-edge area is darker. The next step is to study how to extract rock edges, then automatic link none-continuous edges.

In practical face images, rock edges and rock mass interior color varies from large range. After being processed binary images, white edges is not always continuous. The result of edge detection is that all edges are detected. Then how to determine which edges are real rock mass edges, and how to link none-continuous edges is difficult. Therefore, it should be considered manual interfere way to link rock edges so that all rock mass edges of rock can be intacted.



Figure 5. Image segmentation result.

2.2.2 *Target segmentation*[7]

Specific arithmetic is used to segment images, and target rocks' internal will become foreground color blocks. Meanwhile, target rocks' external will become background color block. If rocks' internal color block is gained by segmentation, it can be easy to extract these block edges. This can be seen from Fig. 5.

In Fig. 5, white blocks are target rock blocks. From the result of image segmentation, target rock blocks can be well segmented. It will be of great benefit to edge extraction of target rock masses.

Compared to edge detection, target segmentation is more difficult which have to determine whether each area in images belongs to some rock mass target. If target segmentation problem is determined, then it will be easy to find out the boundary of rock target.

2.2.3 *Boundary extraction*

After edge detection and target segmentation, it needs extracting the boundary of rock target blocks in images. From these blocks, rock size can be determined and rock block character parameters can be achieved. According to rock mass block boundary, 3D tunnel model can be rebuilt.

Edge detection is much more difficult than target segmentation when rock mass boundary is extracted automatically. In TFGIS, after rock boundary being extracted from rock mass blocks, the boundary is processed by polygon simulation arithmetic. In Fig. 6, the gray boundary marks are the processing outcome of Fig. 5.

2.3 *Character extraction and pattern recognition*

After rock mass targets are determined, some character parameters can be farther gained from those targets. The purpose of characteristics extraction is that surrounding rock mass level is classified according to character parameters extracted from rock mass. The classification information can be referred to tunnel construction, so that units in charge of construction



Figure 6. Object rocks boundary extraction result.

clearly understand rock level in tunnels and cut down the incidence of emergency accidents.

Characteristics extraction directly analyzes rock mass targets. According to pixel gray level in rock mass target areas, nth moment estimation and texture statistical characters can be acquired. Based on area shape, target long axis short axis round degree and rectangular degree can be acquired. 1D characteristic vector is established with these characters. In some given rule, this vector is compared with all kind of standard rock mass characteristic vectors. If the vector is closer to a standard vector than others, then the rock mass is classified to the standard one. Target rock mass characteristic parameter extracted from some rock mass targets can be seen from Table 1, in which slice number marks different face images, target number names diverse objects in the same face image, gradation is pixels' gray average value in object rocks when separating image color into 256 gray scale, centering coordinate x and y means object's x-axis and y-axis respectively when both face images' length and width are 1 unit.

In general, if the section is different, the geological condition always differs from each other. It is impossible to obtain all standard rock characteristic vector data, so if compared with all standard rock character vector in databases, the actual rock mass characteristic vector data is very different, the actual rock mass image and vector data will be saved in databases so as to provide references for analyzing this kind of rock masses next time.

3 TUNNEL 3D REBUILDING AND 3D PREDICTION

In order to know geology structure of tunnels, it's necessary to rebuild tunnel 3D model. Tunnel geology structures are observed in all directions from the tunnel 3D model.

OpenGL 3D modeling technology was adopted in 3D rebuilding. OpenGL's full name is Open Graphics Library, which is a 3D graph and model library, and it is a new 3D graph industry criterion. OpenGL is not only a graph library, but also an Application Programming Interface.

Table 1. Object rocks character parameter.

Slice No.	Object No.	Gradation average	Center coordinate x	Center coordinate y
1	1	199.179	0.368	0.361
1	2	190.603	0.078	0.687
1	3	192.111	0.839	0.331
1	4	198.727	0.370	0.361

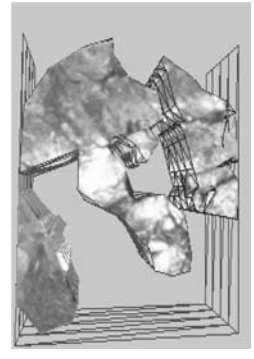


Figure 7. Tunnel 3D model.

3.1 *Tunnel 3D rebuilding*

During tunnel 3D rebuilding, the most important thing is how to link the same rock mass edges in all neighboring face images. Only if the corresponding connections are formed correctly, the 3D model can be exactly restituted. In TFGIS, neighboring image rock mass edges were linked through pattern recognition arithmetic. After that, all face image sequence corresponding relations were constituted. Considering some special construction conditions, rock mass edges can not be linked through pattern recognition arithmetic. Especially when rock dislocation takes place, manual interfere needs to be introduced to modify real corresponding relations between neighboring rock masses. Tunnel 3D model was shown in Fig.7 which was established according to face sequence.

In Fig.7, the outer outline is tunnel profile. The 3D model can be observed in all directions.

3.2 *Tunnel 3D prediction*

According to the 3D model, however, only logged part geology structure can be observed, which is not very useful. The unit in charge of construction always hopes to learn about the geological structure around the

tunnel. This function is offered in TFGIS, by which the structure around the tunnel can be automatically predicted and displayed. Thus the system affords more information, which will be great helpful to tunnel logging and construction units will make much more feasible measures. As a result, construction process will be safer.

4 THE END

Tunnel face image processing and tunnel 3D modeling have been studied for a moment. Yet there is low correlative information that can be found overseas.

(1)There is lots of image processing arithmetic applied in the system, and some new arithmetic is included on the base of real instances. When using this system, operators can process tunnel face with different image processing arithmetic according to different actualities.

(2)When 3D model was built, neighboring face rock corresponding relations were established through pattern recognition arithmetic. Tunnel 3D model was set up according to corresponding relations.

(3)In this system, it is necessary to study much more arithmetic about tunnel overbreak area and excavation volume computing, and it can predict tunnel unlogging geology structure 3D model.

REFERENCES

[1] Guan Baoshu. The application of digital camera and image processing methods in the geological interpretation[A]. *Key Point Anthology for Tunnel Engineering[C]*. Beijing: China Communications Press, 2003. 25–32.(in Chinese)

[2] Wang Chuanying, Ge Xiurun, Bai Shiwei. Study on the digital panoramic borehole camera system[J]. *Chinese Journal of Rock Mechanics and Engineering*, 2002, 21(3): 398–403.(in Chinese)

[3] Wu Zhiyong. The application of digital image interpretation in the statistics of rock joints in field[J]. *Journal of Chengdu University of Technology*,2001, 28(Supp.): 157–161.(in Chinese)

[4] Liu-ming, LI Ning. STUDY ON ROCK MASS JOINT MEASUREMENT BASED ON DIGITAL PHOTOGRAMMETRY FAN [J].*Chinese Journal of Rock Mechanics and Engineering*, 2005, 24(5): 792–797.(in Chinese)

[5] Soe-Sen Leu, Shiu-Lin Chang. Digital image processing based approach for tunnel excavation faces [J]. *Automation In Construction*, 2005, 14:750–765

[6] Castleman K R. Digital Image Processing[M]. *Translated by Zhu Zhigang.* Beijing: Publishing House of Electronics Industry, 2002. 375–394.(in Chinese)

[7] TIAN Chun Xiou-xing. Computer Image Processing. *Science Publication*, 2004,6

This page intentionally left blank

Underground Space – the 4th Dimension of Metropolises – Barták, Hrdina, Romancov & Zlámal (eds)
© 2007 Taylor & Francis Group, London, ISBN 978-0-415-40807-3

Recent development of tunneling techniques in Taiwan

H.S. Liu, P.C. Hou & C.T. Chang
Sinotech Engineering Consultants, Ltd. Taiwan, ROC

ABSTRACT: Located along the tectonic boundary of the Eurasian Continental Plate and the Philippine Sea Plate, Taiwan is a mountainous island with complicated geological environment. The unfavorable ground conditions pose a severe challenge to tunneling works. Many national development projects such as water transmission lines, railway and highway projects, and hydropower development projects, involve lots of tunneling works. Both of the size and the scale of these tunneling works have been increased significantly from time to time. And the construction techniques have also been improved substantially from project to project. In this paper, the geological environments, which are closely related to tunneling works, are outlined. Then, some technical developments such as support systems etc. are presented. Finally, handling of difficult ground is illustrated. It is hoped that the development of the tunneling techniques can help upgrade the competition capability of Taiwan in international tunneling industries.

1 PREFACE

The current Taiwan tunneling works, including mainly the tunnels of highways, railway, mass rapid transits systems (MRT) and hydropower development projects, are positively pushed forward. However, the future main tunneling works are focusing on the tunnels of urban pipe lines, the extended MRT systems, the island wide highways and railway systems, the hydraulic and hydropower development projects and so forth. It is therefore estimated that approximately 150 tunnels are to be built in the future with total length of more than 400 km.

With the application of the new concepts, new techniques, new construction equipment and new materials as well as the accumulated experiences, Taiwan tunneling works, no matter in quality or quantity, have been achieved with a great development in the current decades. In order to consolidate the results gathered from the previous tunneling experiences in planning, designing and tunneling techniques and to provide as the guidance for the future tunneling works, this paper addresses major subjects of Taiwan tunneling techniques, beginning with a brief description on geological background and geotechnical investigation techniques, following by an overview on the current development of Taiwan tunneling techniques, and a discussion on the concepts and practices to overcome the extremely difficult ground when tunneling. It is hoped that a common consensus among the tunneling industry can be manifested and Taiwan tunneling techniques can be led into a new frontier.

2 GEOLOGICAL BACKGROUND AND EXPLORATION

The island of Taiwan can be geologically divided into four distinct provinces, namely, the Western Coastal Plain, the Western Foothills, the Central Ranges and the Eastern Coast Range, each having different engineering geological characters. The Central Range with precipitous cliff is mainly formed by argillite, slate, meta-sandstone in the Hsuehshan Range and schist, marble, amphibolites and some ultra basic rock in the eastern slope of Central Range. Due to multiphase metamorphism and orogenic process, the rocks in the Central Range are highly contorted and are structurally complicated. Separated by the longitudinal fault with the Central Range, the Coastal Range is formed of a core of Miocene andesite covered with thick andesitic agglomerate, tuffaceous and pyroclastic deposits. Outcropped in the southern section of the Coastal Range is the mélange chaotic with serpentine inclusions. The mélange material in this area is tectonically related with the collision between the Eurasian Plate and Philippine Sea Plate. The Western Foothill Province is formed by Tertiary sedimentary rocks that were folded and faulted during orogenic processes. This imbricate folded and faulted belt system represents

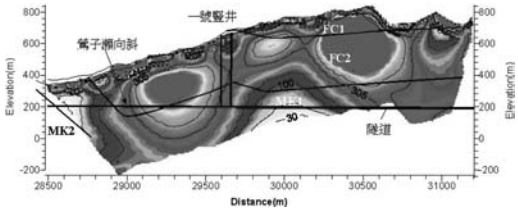


Figure 1. Rip profile showing groundwater distribution along tunnel alignment.

a west-verging deformation front. The Chichi earthquake of 1999 with magnitude of 7.3 can be considered as the outcome of the on-going orogenic process. West of the Foothill area is the Western Coastal Plain mainly composed of unconsolidated material including lateritic gravel tableland, piedmont deposits and recent alluvial deposits.

In the early days the geological investigation was mainly performed by surface mapping supplemented by local subsurface drillings but the drilling depth was highly limited due to technique constrain. In recent years investigation approaches are versatile and more important is that the concept of investigation during construction being part of the overall exploration program is widely accepted in the tunneling industry. The techniques used in explorations include surface mapping, aero-photo or remote sensing interpretation, drilling, geophysical exploration and trench excavation, etc. Among the above-mentioned items, geophysical explorations are widely adopted such as resistivity study, seismic refraction study, tunnel seismic profiling, True Reflective Tomography (TRT). Figure 1 is the results of the resistivity imaging profiling performed along a part of Hsuehshan tunnel of 12.9 km long. For some important project such as at Hsuehshan tunnel project, pilot tunnel parallel to the main tunnels is sometimes adopted for geological exploration purpose. As for the coring technique, drill holes with length more than several hundred meters are very common. Furthermore, horizontal directional drilling technique as shown in Figure 2 was also applied in the undersea exploration for the Circulating Water Discharging System of the Forth Nuclear Power Plant Project in northern Taiwan. The versatile exploration techniques make engineers have a deeper insight into the subsurface geological conditions.

3 RECENT DEVELOPMENT OF TAIWAN TUNNELING TECHNIQUES

3.1 *Portal excavation and slope protection*

Tunnel portal is the critical construction item of the whole tunneling works. In the recent years, due to high rising of environmental protection consciousness, the extent of portal excavation is required as little as

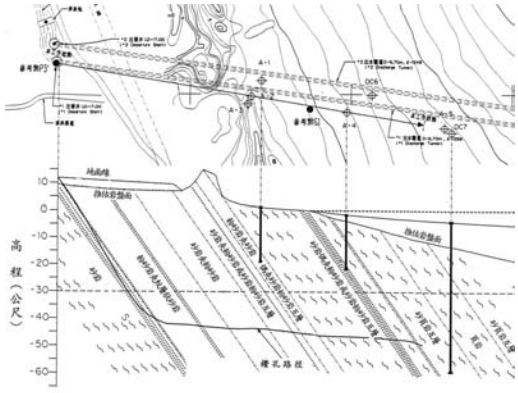


Figure 2. Geological exploration of undersea tunnel project using directional drilling technique.

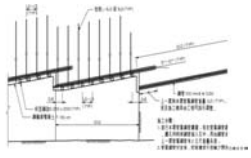


Figure 3. The layout figure of pipe roofing application.

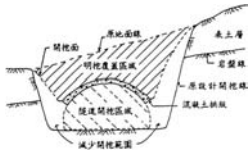


Figure 4. Schematic sketch showing the pre-arch cover method.

possible. In order to comply with such a tendency, most of the tunnel portals are now excavated by the adopting the pipe roofing method to reinforce the stability of portal section. Pipe roofing method is one of the many common methods used in Taiwan for the poor ground sections. The method is carried out by drilling horizontal boreholes on the crown area before inserting steel pipes and then injecting the bonding grout for the ground consolidation, which could build up at the arch of tunnel to form a reinforced umbrella protection ring. Steel pipes used for pipe roofing combined with the rock bolts, steel supports, and the (steel fiber reinforced) shotcrete can create a lattice support system with high support stiffness both in the longitudinal profile and in transversal profile, as Figure 3 indicated. Recent examples in Taiwan are the Lantan Tunnel of Second Freeway, and the Hsinkuanyin Tunnel of North Link Railway, etc.

Alternatively, the false portal section can also be constructed by means of pre-arch cover method as Figure 4 indicated. (Liu et al. 1999) By Pre-arch Cover

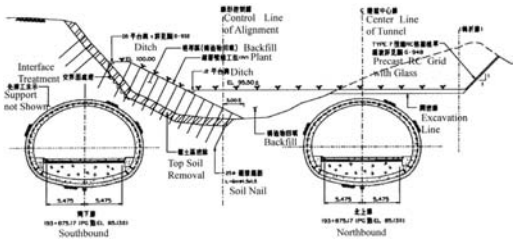


Figure 5. The layout figure of shallow coverage thickened section of Lantan Tunnel.

Method, the portal slope is slightly excavated and cast with the RC cover on the crown before mining in. Depending on ground condition, the feet of the Prearch Cover sometimes need to be pre-reinforced with micro-piles or grouting. The major advantages of the above mentioned methods are to minimize the extent of excavation and the environment impacts. Recent cases in Taiwan are the Lantan Tunnel, the Hsichi Tunnel of Second Freeway Group, etc.

The slope stability of the portal must be assured before mining. Normally, the slope of portal is covered with slope wash or weathered rock. Adequate slope protections are required to avoid slope failure when excavating the portal slope. Factors need to be considered during portal excavation include ground condition, incident angle into the slope, etc. Slope stability analysis should be made with the incorporation of the tunnel portal excavation method. The analysis then can be used as a basis to select an appropriate stabilizing measure, which is constructably, economically, safely and landscape wisely justified. Case examples of measures with ecological approach are the prestressed tendons coordinated with precasted or cast-in-place rebar reinforced concrete grid with plantation for the slope protection or the thickening of the lateral tunnel cover reinforced with grouted rebar, etc. as shown in Figure 5.

3.2 *Support design*

Due to the complexity of ground and the difficulty in the direct application of theoretical mathematic analysis, the design of semi-rigid tunnel support is proceeded in accordance with the experiences of previous design based on the rock mass classification. It must be then examined and verified by means of numerical analysis based upon the estimated parameters of geological investigation and the data of laboratory tests. At the design stage, the ground at the tunneling level must be, in advance, classified into different grades to which adequate support patterns are designed in accordance with the estimated ground conditions. During construction, adequate support system is selected according to the exposed rock conditions. Based on the monitoring data and feedback analyses, it will then be decided whether the support system need to be enhanced or not.

The RMR System of South Africa and Q System of Norway for the rock mass classifications are most popularly used in Taiwan tunneling works today. However, due to the unique geological and geomorphologic characters of Taiwan such as young geological age, drastic change of rock conditions, high cover, on-going orogenic belt, etc., the application of the foreign rock classifications are still not satisfactory based on the monitoring data. In addition, the existing rock classifications are not applicable to the unconsolidated material in western foothill area and western coastal plain of Taiwan. To deal with the young and drastic geological change, the Public Construction Commission of Taiwan establish Taiwan Rock Classification System (PCCR-System) and the tunnel support system which could be more suitable to be used in the local geological conditions and make the design of tunnel support more realistic. The recommended support system for A Rock Mass (uniaxial compressive strength greater than 25 MPa) and B Rock Mass (uniaxial compressive strength between 5–25 MPa) are as Table 1 indicated. (Chang et al. 2004)

3.3 *The excavation methods and construction equipments*

Traditional drill and blast (D&B) method and mechanized tunneling method are widely used in tunneling in Taiwan. In the recent years the drilling machine used in D&B has been advanced to multiple arms Jumbo. As for the explosives, the standard bar type with diameter of 32 mm of 60% to 80% nitroglycerin gelatine dynamite or ammonium nitrate (AN) gelatine dynamite or emulsion gelatine dynamite have been adopted. For the perimeter holes on the excavation face, the detonating cord of containing dynamic at 10 g/m and multiple dynamite bar of half in size collaborated with bamboo spacing filled with the explosive agent or slender bar with external diameter 18 mm contained with 45% to 60% gelatine dynamite is constantly adopted in the recent years as shown in Figure 6. In addition, MS or DS electric delay detonator or nonelectric delay detonator are commonly used in blasting to secure the blasting safety and to improve the construction quality and advance rate.

In addition to the traditional D&B excavation method, mechanized excavation methods such as shield machine, roadheader and TBM are also common in many recent tunneling cases. The shield machine is mostly used in the soft and the weak ground while the roadheader is used in the medium strength rock tunnel. The TBM is merited with average faster speed, less man power required, economic support systems as well as less environmental impact, and

Table 1. The standard tunnel support of types A&B rock mass in Taiwan district.

Type A rock mass	Type B rock mass	Rock mass class.	Excavation method	Shotcrete (cm)	Steel support		Rock bolt(m)		
					Size	Space(m)	length	Lon. space	Cir. space
10 m ≤ Tunnel spans ≤ 16 m Max. overburden ≤ 400 m									
RMR ≥ 81		I Very good	Top heading	5∼10	–	–	4	–	–
RMR 80∼61	RMR ≥ 81	II Good	and bench				(if req.)		
RMR 60∼41	RMR 80∼61	III Fair	Top heading and bench	15	H100 × 100 (if req.)	–	4∼6	1.5∼2.0	1.5∼2.0
RMR 40∼21	RMR 60∼41	IV Poor	Top heading and bench	15∼20	H125 × 125	1.2∼1.5	4∼6	1.2∼1.5	1.5∼2.0
RMR 20∼11	RMR 40∼21	V Very poor	Top heading and bench or side gallery	25	H125 × 125	1.0∼1.5	6∼9	1.0∼1.5	1.5∼2.0
RMR ≤ 10	RMR ≤ 20	VI Ext. poor	Top heading and bench or side gallery	25	≥ H150 × 150	0.8∼1.2	6∼9	0.8∼1.2	1.0∼1.5
Tunnel spans < 10 m, Max. overburden ≤ 400 m									
RMR ≥ 81		I Very good	Full face or top	5	–	–	4	–	–
RMR 80∼61	RMR ≥ 81	II Good	heading and bench				(if req.)		
RMR 60∼41	RMR 80∼61	III Fair	Full face or top heading and bench	10	H100 × 100 (if req.)	–	4	1.5∼2.0	1.5∼2.0
RMR 40∼21	RMR 60∼41	IV Poor	Top heading and bench	15	H125 × 125	1.5∼2.0	4∼6	1.5∼2.0	1.5∼2.0
RMR 20∼11	RMR 40∼21	V Very poor	Top heading	20∼25	≥	1.0∼1.5	4∼6	1.0∼1.5	1.2∼2.0
RMR ≤ 10	RMR ≤ 20	VI Ext. poor	and bench		H150 × 150				

Remark: The shotcrete and the steel support, in the table, all must be based upon the result of individual assessment and to see if it can be replaced by the steel fiber reinforced shotcrete or the lattice girder.



Figure 6. The standard bar type dynamite and the slender type Nitroglycerin gelatine dynamite.

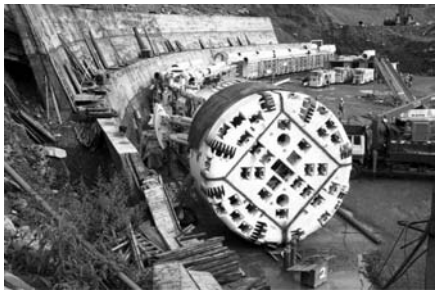


Figure 7. Open type TBM assembled at the outside of portal of Newwuchieh Diversion Tunnel Project.

therefore will be expected to be a major construction method in Taiwan in the future.

The first introduction of rock TBM into Taiwan commenced in the year of 1992 in Hsuehshan tunnel. The performance of the TBM is not as expected mainly due to extremely poor geological condition with large water inflow of the eastern section of the tunnel and lack experience of mechanized construction method. However, many valuable experiences have been accumulated and have been applied to the headrace tunnel of Shihlin Power Project, the diversion tunnel of Newwucheih Project, the circulating water discharging tunnel of Nuclear Power Project No.4, etc. Especially, the Newwuchieh Diversion Tunnel, for instance, had created the fastest monthly advancement record of 659.3 m, as shown in Figure 7.

3.4 *The support materials and the inner lining steel form*

To stabilize the surrounding rock, inner support (permanent support) and outer support (primary support) system are normally required. Since the concept of NATM was introduced into Taiwan, shotcrete, rock bolt, steel support, auxiliary measurement and reinforced concrete lining, etc. have been playing a key role for tunneling support system. The function and the development of main support materials and the inner lining steel form are briefly described as follows:

3.4.1 *Shotcrete*

The main functions of the shotcrete are to seal and fill the rugged surfaces, preventing the ground from stress concentration, and slaking. It will form a thin shell and can contact tightly with the excavated surface. Although the conventional dry-mixed shotcreting are proved to have good capability of compressive resistance, yet the tensile strength, the flexural strength and the ductility performance concerned are relatively poor. However, the mentioned deficiencies can be improved if appropriate amount of steel fiber, superplasticizer, silica fume, etc. can be added into the shotcrete mix. By doing so the advantages include reducing dry shrinkage, preventing the support material from cracking, enhancing the strength of durability, increasing the abrasion resistantability, minimizing the damage caused by collision, increasing the ductility and strengthening the shock resistance. For the application on the design and construction, steel fiber can substitute the wire mesh to save the time of installation for the wire mesh and the thickness of shotcrete. Should the wet-mix shotcrete be used together with robot spray device, not only the rebound ratio but the dust volume can be significantly reduced. With these advantages, the steel fiber reinforced shotcrete can be seen as one of the safe, fast and economic supporting element. The typical steel fiber reinforced shotcrete mix proportion of Lantan Tunnel is as shown in Table 2 (Chang et al. 1998). Similar cases in Taiwan are the Mingtan Pump Storage Power Caverns, the Lantan Tunnel of Second Freeway, etc.

3.4.2 *Rock bolt*

The rock bolts installed in the surrounding rock are designed to assist the surrounding rock to form the rock arch and provide with shearing resistance for potential shear failure in jointed rock. In the early days, the resin rock bolt had been widely used and proved that it can provide with the support function within a short period of time and also provide with anchoring effect when encountered with water seepage. However it needs second corrosion proof grouting, and the resin mix quality can not be easily controlled. With this reasons, the resin rock bolts is currently seldom used in Taiwan. For the moment, the full section grouting type anchor bolt (such as SN anchor bolt) are much widely used. As the system is made of high tensile strength rebar, cement mortar and the fast set accelerator, it is much cheaper than those of other type rock bolts as far as the cost is concerned. Along with drastic progress of the material science, many new type rock bolts have been developed, such as the Swellex bolt, the Hardi bolt, the self drilling rock bolt, the expansion end rock bolt, the glass fiber rock bolt

Table 2. The steel fiber shotcrete mix proportion of Lantan Tunnel. (kg/m^3)

Cement	water	Fine agg.	Coarse agg.	Steel fiber	Silica fume	Accerator	S. p.	Slump
440	207	1,031	566	55	40	8.8	6.6	22 cm

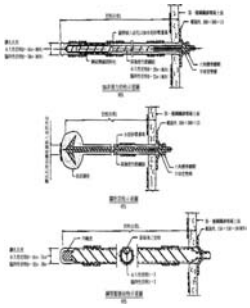


Figure 8. The typical rock bolts.

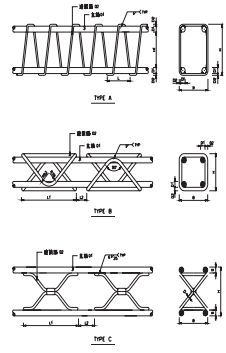


Figure 9. The typical lattice girders.



Figure 10. The needle beam steel form.

and etc., the typical rock bolts as shown in Figure 8. The Swellex bolt, among them, has the advantages of easy installation, quick support effect, suitability to various geological conditions, less environmental contamination, and to meet the requirements of TBM fast advancement. Cases in Taiwan where Swellex rock bolts are used include the tunnel group of Newtenlun Power Project, the tunnel section by TBM of Shihlin Power Project, etc.

3.4.3 *Steel support*

The steel support is designed to share most of rock stress in early age when shotcrete strength is still low and can function as reinforced material for the shotcrete. Furthermore, it can prevent the loose rock from falling down when used with wire mesh. In addition, it can be applied as the template for the subsequent excavation outline. The conventional H beam steel support used in poor ground condition is designed to make use of its wider extensive wing boards which can undertake bigger rock loads. However, the extensive wing boards sometimes hinder the shotcrete from closely contacted with the cut face, which weaking the support performance. To solve the above-mentioned problem, the lattice girder is usually applied to most current projects. The lattice girder usually used was assembled with either 3 or 4 main rebars and spiral hoop rebars (or connection rebars) after the welding. As the space is large enough for the shotcrete to penetrate through, the shotcrete can tightly contact with the rock, and to create with the lattice girder strong rebar reinforced shotcrete structure. The typical lattice girders are shown in Figure 9. The cases where lattice girder were used include the Lantan Tunnel of Second Freeway, most of tunnels of Taiwan High Speed Rail Tunnel Group, etc.

3.4.4 *Inner lining steel form*

To speed up the construction schedule, enhance the construction quality and reduce construction cost, the traditional steel form, with length 8–12 m each are popularly adopted for the most of tunnel inner linings. Nevertheless, it is still limited by the time for the form assembly, the form positioning, the form sealing, the concrete placement, the form maintenance, the form dismantling, the form moving, the form reassembling, etc. , which must be carried out step by step accordingly. Therefore, it causes that the rate of monthly advancement is only about 120 m. In order to overcome the mentioned obstructions, the needle beam steel form and the telescopic steel form, which are provided as the inner lining forms. Normally, all the length of needle beam steel form is not extended over 15 m, as Figure 10 indicated. The telescope steel form

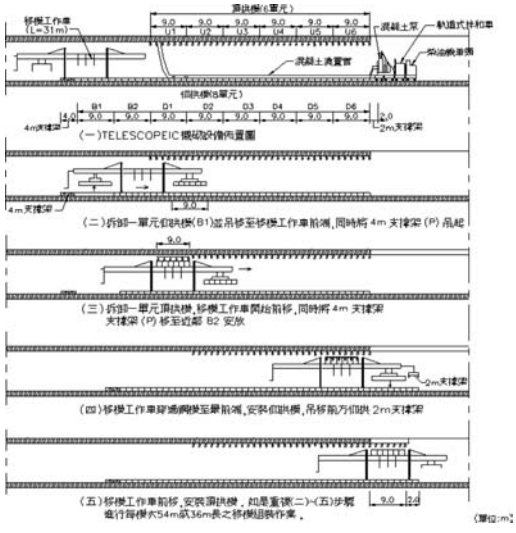


Figure 11. The form moving sequences of telescopic steel form adopted in the headrace tunnel of shihlin power project.

which is used to complete the lining work can be contacted and taken apart, then it must be moved to pass through the steel form at the movement of maintenance and moved to the next work face standing by. Also the steel form must be re-assembled and positioned for the afterward operation of lining works. Thus the steps must be preceded repeatedly until it reaches at the expected terminal position of lining work, so that the telescope steel form can be used for the continuous concrete lining placement. Sequences of telescope steel form moving, as figure 11 indicated (Sinotech 2002). Owing to that the support manner of telescopic steel form is by means of external support with systematic support studs, installed on the outside of steel form and stretched on the excavated rock face (or shotcrete) to against the gravity forces, the buoyant and the lateral forces reacted on the steel form when placing concrete lining. Meantime, owing to that the length of allowable tolerance for support stud adjustment is limited, thus the telescopic steel form is suitably to be used to excavate the tunnel surface which is relatively smooth such as tunnel section by the TBM. The whole set of telescopic steel form is assembled with several sub-forms, generally, with total length of 30–60 m. For the telescopic steel form to carry out its utmost performances, the non-rebar (utmost with re-bar of single layer), the steel fiber of high performance concrete which must be adopted as inner lining materials, thus the form head sealing and the vibration compaction can be eliminated. Meanwhile, the concrete placement can be continuously proceeding. The Headrace Tunnel of Shih Lin Power Project, for instance, the needle beam steel form with the length of 12 m and the monthly average advancement rate 179 m was adopted in the D&B section of upstream while as the telescopic steel form, with length of $9\,\text{m} \times 6$ ones $= 54$ m, and the monthly average advancement rate about 345 m, was adopted in the TBM section of downstream.

4 NEW TECHNIQUES FOR THE DIFFICULT GROUND

The geological structure of Taiwan is very complicated, meantime, the fault zones and the shear zones always cause the tunnel squeezed phenomenon after the tunnel is excavated. Moreover, as Taiwan is located in the subtropical zone with the abundant rainfall, the water inflow is frequently encountered during underground excavation. Obviously, the long and large tunneling works would be faced with big challenges : such as the Hsuehshan Tunnel of Chiangweishui Freeway with total length of 12.9 km (opened to the traffic on June 16, 2006) and etc. In addition to the mentioned fault squeezed zone and the water inflow problem, the high rock pressure, the geo-thermal, the toxic gases, the ventilation, the maintenance, etc. are the major problems need to be solved one by one accordingly. In addition, the tunnel to be cut through the Western Foothills soft and weak sandy clay layers or the gravel strata is really to be faced with big challenge. To overcome such difficult geologies, based upon the present development conditions of domestic and foreign new tunneling techniques, the typical Taiwan Tunneling Methods are developed.

5 CONCLUSION

Tunneling work in Taiwan before 1950 had been carried out by human labors using simple and crude techniques for the excavation of short and small tunnels. However, the conventional long tunnel engineering techniques have been evolved and gradually replaced by machineries today. It fully reflects that Taiwan tunneling techniques has been achieved with a great development. For the coming future, when faced with extremely soft ground and high ground water level in the densely populated metropolitan area, and extremely hard rock and lithological change area in high mountainous area, stringent difficulties could not be avoided. However, the experience gained through previous projects such as Second Freeway Project and Chiangweishui Freeway Project provide us with more confidence to undertake future underground works involved, for example, in cross island freeway systems and many more. In technological improvement, sharing of experience is a very important factor. Taiwan has unique geological conditions for tunneling, and the

local engineers will be glad to share the Taiwan experience with our foreign counterparts. Undoubtedly, international cooperation will contribute to the further upgrading of the technique level of our tunneling industry.

REFERENCES

Liu, H. S. & Chang, C. T. 1999. Tunnel portal chapter 4. *Tunneling design and cases manual*. Taipei: Scientific & technical publishing co., ltd. (in Chinese)

Chang, C. T., Hou, P. C., Lee, M. C., Lee, I. T. & Chang, P. H. 2004. Extension of RMR and Q-System in Taiwan. *Sino-geotechnics.* (99): 15–22. (in Chinese)

Chang, C. T & Liu, H. S. 1998. The current and prospective applications of steel fiber reinforced concrete/shotcrete in Taiwan. *Civil and hydraulic engineering.* 25(3):25–39. (in Chinese)

Sinotech engineering consultants ltd. 2002. The construction completion report of Liyutang Reservoir Shulin Hydropower Project. Liyutang Project Office of Taipower Co. (in Chinese)

Underground Space – the 4th Dimension of Metropolises – Barták, Hrdina, Romancov & Zlámal (eds)
© 2007 Taylor & Francis Group, London, ISBN 978-0-415-40807-3

Construction method of connecting tunnel in a shield-driven tunnel

J. Liu
Beijing Municipal Engineering Research Institute, Beijing, China

F. Zhang & H. Kong
Beijing Municipal Engineering Company, Beijing, China

ABSTRACT: According to the design, there should be a connecting tunneling between two shield driven tunnels, the connecting tunnel is often built by NATM in China. In a real project, the geological condition of the ground is typically complex consisting of clayey soil, saturated fine sand, and saturated gravel soil. The soil cover above the crown of connecting tunneling is about 8.0 m, and there are three existing utility pipes passing above the tunnel. Heavy traffic road is directly above the tunnel and there are many old buildings in the same directions as the tunnel center line. Therefore, the construction of this connecting tunnel may take a high risk; moreover, two segments of existing shield-driven tunnels should be removed before this tunnel is dug. Because the location of this connecting tunnel is very sensitive to the surrounding environment, how to construct is a challenge to us, especially, how to remove the two segments is very important in this difficult ground condition. This similar engineering accident has ever appeared in Shanghai. According to the results of numerical simulation, the detailed construction method was constituted to affect the pipelines less and to avoid the large disturbance above the ground, including the remove order of two segments. Besides these, a series of in-situ measurement were carried out during the whole period of construction. After the project was finished, the maximal ground settlement was only 4.1 mm, the whole project was successfully completed without any accident and the surrounding environment was protected very well. At last, the results of numerical simulation were compared with the in-situ measurement, the result indicated that numerical simulation can predict the ground settlement well. It can be said that the experience on this project is valuable to solve similar problems in connecting tunnel between two shield driven tunnels.

1 INTRODUCTION

According to the design, there should be a connecting tunneling between two shield driven tunnels, the connecting tunnel is often built by NATM in China, and the location to be excavated has been designed as two rings of steel segment. The connecting tunnel is located at Dongsi Hutong. Dongsi Hutong is a street, which often has heavy traffic. The soil cover above the crown of connecting tunneling is about 8.0 m, and there are many old buildings directly above this tunnel, especially, there are three existing utility pipes passing above the tunnel: (1) waste pipe, which cross the tunnel, the crown of it is about 2.0 m, the diameter is about 0.5 m; (2) telecom pipe, which is in the same direction of the tunnel, the crown of it is about 1 m; (3) tap water pipe, which is also in the same direction of the tunnel, the crown of it is about 1 m.

According to the report of engineering geologic investigation, the condition of the ground is typically alluvium, consisting of backfill, silty clay, silty-fine sand, medium-coarse sand and gravelly sand, and the groundwater level is about 4 m below the surface. Because of the soft ground and abundant groundwater, the old buildings, utility pipes and road surface are very sensitive to the excavation of the connecting tunnel. Therefore, the construction of this connecting tunnel may take a high risk; moreover, two segments of existing shield-driven tunnels should be removed before this tunnel is dug. It can be seen how to construct is a challenge to us, especially, how to remove the two segments is very important in this difficult ground condition. This similar engineering accident has ever appeared in Shanghai.

In order to solve these problems, numerical simulation was used to study the ground settlement when excavating the tunnel, including the remove order of two segments. Besides these, a series of in-situ measurement were carried out during the whole period of construction. It is well known that the ground settlement may directly affect the surrounding environment, so the most important task is to control the ground settlement.

2 NUMERICAL SIMULATION AND ANALYSIS

2.1 *The calculating model*

The FLAC^{3D} program is performed in this calculation. The calculating model can be found in Figure 1, and the connecting tunnel between two shield-driven tunnels can be found in Figure 2.

The calculating parameters are listed in Table 1.

In this table, material 1 represents segment, material 2 the grouted ground, material 3 the primary support, and material 4 the secondary lining; γ is density, E is elastic modulus, μ poisson's ratio, c cohesion, and ϕ angle of internal friction.

In this calculation, elastoplastic model and Mohr-Coulomb yield criterion are used.

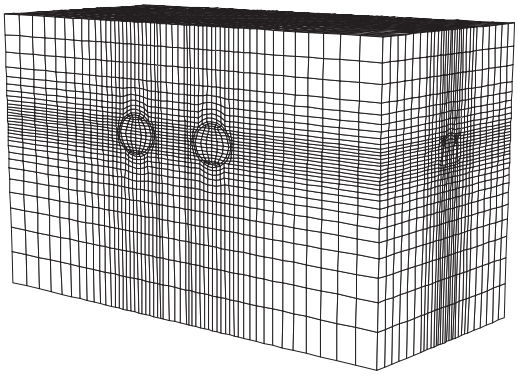


Figure 1. The calculating model.

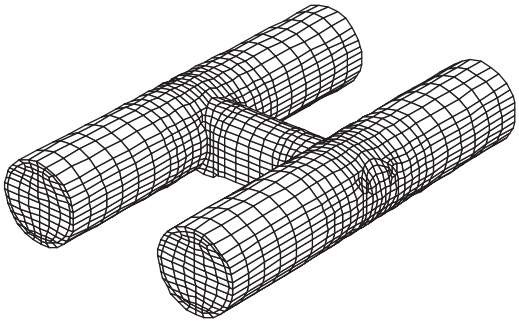


Figure 2. The connecting tunnel model.

Table 1. The calculating parameters used in calculation.

Material	γ (kN/m^3)	E (MPa)	μ	c (kPa)	ϕ (°)
1		34500	0.17		
2	22	30	0.25	75	40
3	25	18	0.2		
4	24	30	0.2		

2.2 *The calculating results*

Through the calculation, the following results are obtained.

(1) The maximal deformation of the crown of the remaining segments is about 9 mm, when the segment is removed and the connecting tunnel is finished (Figure 3).
(2) The convergence of the remaining segments is about 3 mm (Figure 4).
(3) After the segments are removed and the connecting tunnel is finished, the major principal stress of other segments near the excavation face is changed greatly, from compressive stress to tension stress, the value is about 2.77 MPa, but it remains the same opposite the excavation face.
(4) After the two shield-driven tunnels are finished, the maximal settlement of surface is about 15 mm. After the connecting tunnel is finished, the total settlement of surface is about 28 mm, therefore the ground settlement is about 13 mm when excavating the connecting tunnel (Figure 5).

On the basis of theory analysis, the remaining segment will be deformed after the connecting tunnel is

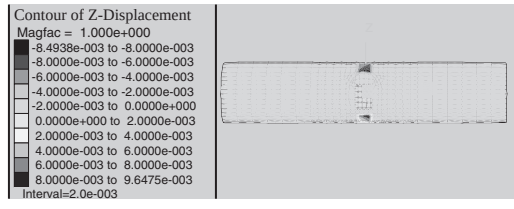


Figure 3. The maximal deformation of the crown of segment.

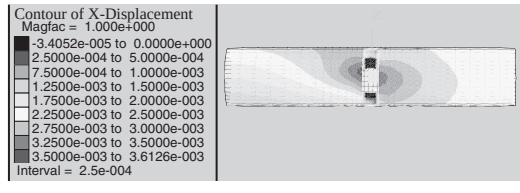


Figure 4. The convergence of the remaining segments.

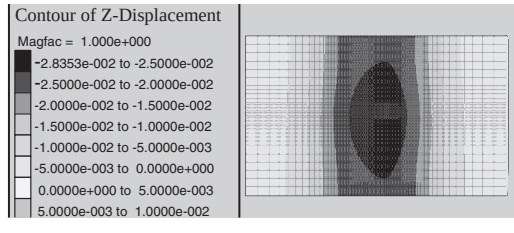


Figure 5. The ground settlement after the connecting tunnel finished.

excavated, and the surface above the connecting tunnel will subside. In order to protect the surrounding environment well, some construction measures should be taken.

3 CONSTRUCTION METHOD

Because of the difficulty ground, the surface above the tunnel may collapse induced by quicksand when removing the segments and excavating the tunnel. Therefore, the ground must be reinforced using cement and soluble glass. The area to be grouted is about 3 m around the tunnel (Figure 6). When grouting, two steps are carried out, that is, the small hole of soil is injected, then the grouted soil is crushed and injected using higher pressure in second step.

Before remove the steel segments in the shield driven tunnel, the remaining segments should be braced temporarily using I-shape steel (Figure 7).

After grouting and bracing, the steel segments of shield-driven tunnel should be removed, and the construction method of connecting tunnel can follow 6 steps as below till the connecting tunnel is finished.

(1) dewater: the remnant groundwater should be drained using small pipe;

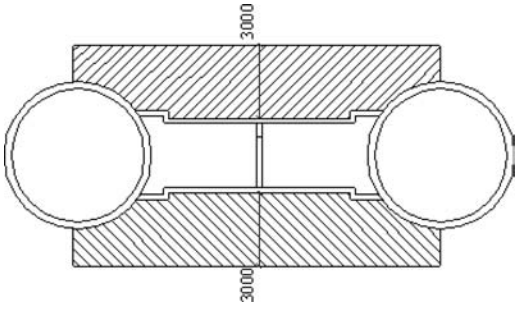


Figure 6. The area to be grouted.

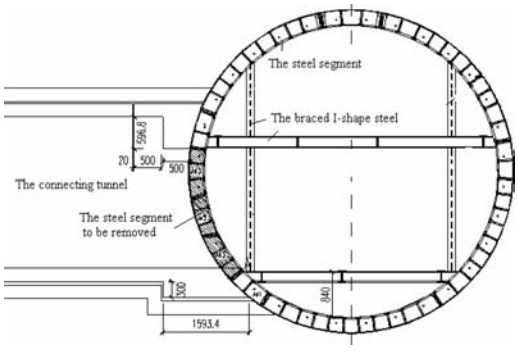


Figure 7. The temporary braced I-shape steel.

(2) removing steel segments: the steel segments should be removed from top to bottom;
(3) excavating: the whole section was divided two steps, and using benching tunneling method. After the upside step was finished, concrete should be sprayed immediately;
(4) install steel frame: three steel frames should be fixed in time;
(5) spray concrete: after steel frame was finished, concrete should be sprayed again;
(6) secondary lining: the primary support could be completed through the steps mentioned above. When the primary support of the whole connecting tunnel was finished, and the deformation of it became stable, the secondary lining should be constructed.

4 IN-SITU MEASUREMENT

In order to ensure the ground settlement and the deformation of segment within the prescribed limit, a series of in-situ measurement were taken out during the period of excavation. For example, the crown settlement of remaining segments, the convergence of remaining segments, the stress of remaining segments, the ground settlement, and the others (Figure 8).

The ground settlement observation points are set along the axis above the connecting tunnel.

As regards the crown settlement of remaining segments, the maximal value occurred (about 6 mm) when the steel segment was removed and upside step of the connecting tunnel excavated into 3 m (Figure 9).

The convergence of remaining segments was about 2.9 mm.

The major principal stress of the segments near the excavation face was about 2.8 MPa, which was tension stress, and opposite the excavation face, the stress was 0.6 MPa, which was compressive stress.

As regards the ground settlement, the maximal value was about 4.1 mm.

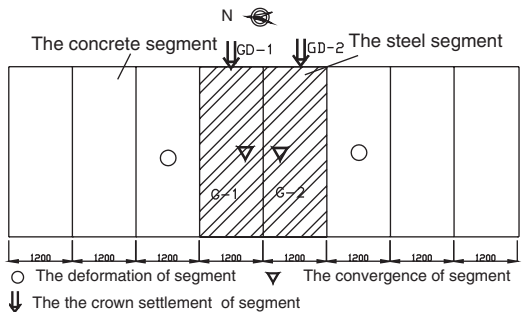


Figure 8. The map of observation points in shield-driven tunnel.

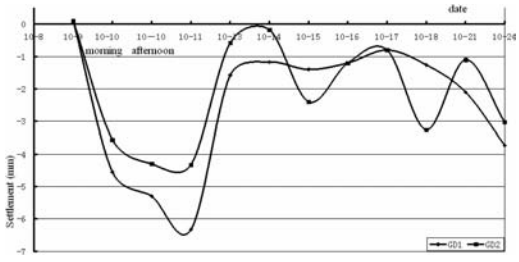


Figure 9. The crown settlement of remaining segment.

5 CONCLUSIONS

Because of the difficult ground and complex surrounding environment, the construction of the connecting tunnel between two shield-driven tunnels may take a high risk, the construction method has been studied in detail. Firstly, the mechanical behavior of the connecting tunnel is simulated using FLAC^{3D}. Then the construction method has been presented, and some measures have been taken, such as grouting the soft soil, using the braced I-shape steel, fixing three steel frame in time, and dewatering in the shield-driven tunnel. The results of in-situ measurements were smaller than that of theory analysis, which indicated that the construction method was suitable for this project, and all values were within the prescribed limit. The pipes and old buildings were protected very well. It is can be said that the experience on this project is valuable for solving similar problems in difficult ground and complicated surrounding environments in urban areas.

REFERENCES

Liu, J. & Li. P. Z. 2005. A study on construction technology for traverse channel of connecting tunnels based on shield-driven tunnel. *3rd Japan-China Technological Exchange of tional shield-driven tunneling*. Tokyo, Japan, 352–356

Liu, W. N. & Luo. F. 2000. A new construction method for a metro station in Beijing. *Tunneling and Underground Space Technology.*15(4): 409–413

Liu, J. & Li. P. Z. 2005. Numerical simulation for construction steps of single connecting tunnel between two shield-driven tunnels. *Proceedings of the fourteenth national conference on structural engineering (No.1)*. Qingdao, China, 330–333

Liu, J. & Li. Z. K. Stability analysis of a deep cut slope using the DDA method. *The 6th international conference on analysis of discontinuous deformation*. Orkanger, Norway, 334–337

Underground Space – the 4th Dimension of Metropolises – Barták, Hrdina, Romancov & Zlámal (eds)
© 2007 Taylor & Francis Group, London, ISBN 978-0-415-40807-3

Closely constructing influence forecast of hydraulic tunnel under-cross existing railway tunnel

Gong Lun*, Qiu Wen-ge & Wang Fei
School of Civil Engineering, Southwest Jiaotong University, Chengdu, Sichuan, China

ABSTRACT: This paper gives an analysis of the influence which under-cross hydraulic tunnel construction imposed on the existing railway tunnel and discusses the security countermeasure of existing railway tunnel's structure, Using three-dimensional numerical modeling methods associated with the practical situation of Shoupayan Tunnel in the Neijiang - Kunming railway which was under-crossed by Baishuijiang 3-level electric station hydraulic tunnel in Yanjin country of Yunnan province. The results indicate: the hydraulic tunnel construction circle which affects the existing railway tunnel has relation with driving direction. The circle is 2*D* (*D* means the hydraulic tunnel excavation diameter) when adjacence to the existing railway tunnel, while it is 4.5*D* away from; the inflection area of the existing tunnel is 6.5*D* in longitudinal direction and 3*D* in transversal direction. When closely constructing the hydraulic tunnel, the railway tunnel will be occurred deformation such as twist rotation. Monitoring of railway tunnel baseboard settlement, lining distortion, lining transversal/vertical force and vertical vibration velocity at the two tunnels' crossover point in the influence circle of existing railway tunnel must be carried out. In additional, the rail should be reinforced by clasp in order to insure the existing tunnel structure and the train traffic safety.

FOREWORD

With the development of national economy, the building needs were increased constantly for foundation projects in our country[1], the using of underground space was gained developments unparalleled, there were many of closed construction projects which new building structure adjacency existing construction.

At present, there has a certain extent individual research towards appearance underground engineering closed construction in home and overseas: the classification, partition and adjacent degree of underground engineering closed construction; the vibrancy influence of up-down across tunnels[2]; the vibrancy influence of closed blasting towards existing tunnels[3]; the influence of exploiting coal bed to the above highway tunnels[4]; discussing adjacent influence from different position and distance[5]; closed construction influence to each other of overlap and interlace subway interval tunnel when in different distance[6]; the stress redistribution which caused by the new building tunnel driving to the two parallel closed tunnels[7]; the deforming of vertical crossing tunnel in shield construction[8]; surrounding rock stability of the overpass place in up and down run tunnel[9] and so on. in this paper, through the analysis of water tunnel down through railway tunnel in the Yanjin country of Yunnan province, the forecasting and countermeasure research were carried out towards railway tunnel by the construction influence of under-cross water tunnel.

* The connection way of the first author Gong Lun. Tel: 028-86465636. E-mail: gonglun33@126.com. Communication address: 2-16 of number 4 of Shuying street number 12 of Ying menkou Jinniu zone of Chengdu of Sichuan province. Postal-code: 610031.

1 ENGINEERING GENERAL

The angle between water tunnel and rail track plane is 82 degree, water tunnel down through railway tunnel, which foundation height mark of plane intersect position is 465.55 m, the water tunnel's top contour is 452.49 m, the clear distance between two tunnels is 13.06 m.

The construction delimitation of Shoubayan tunnel was tunnel limited-2A, macadam track bed, it has cross-section size: clear height 6.55 m, clear width 4.9 m, C20 concrete lining with 40 cm thickness (III degree), grate layer with 20 cm thickness; Water tunnel cross-over the stratum layer of limestone, marlstone rock, sandstone and so on, the circle cross-section with inner diameter 7.0 m, outer diameter 8.1 m, C20 concrete lining with 55 cm thickness.

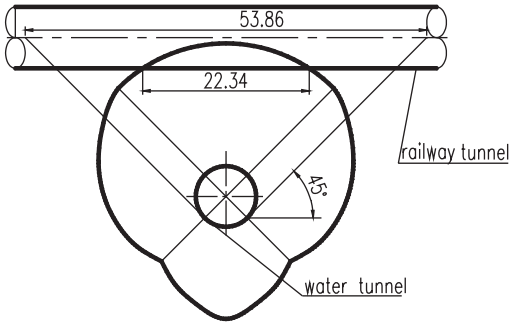


Figure 1. Influence range of railway tunnel by the closed construction of water tunnel (Unit: m).

2 INCIDENCE BY THEORETICAL CALCULATION

For the influence problems of up-down cross closed tunnel construction, longitudinal effect was mainly considered. The existing tunnel which in the weak influence area of new building tunnel was needed to consider longitudinal effect partly; while in the strong influence area was needed to not only consider longitudinal effect but also consider transverse effect partly.

In order to ensure the influence range for which railway tunnel by the closed construction of water tunnel, based on the K. Terzaghi theory, leading-out 45° oblique line as potential break gliding plane, intersect with railway tunnel axial line in order to ensure the longitudinal influence range of railway tunnel, while transverse influence range was determined based on the closed influence partition standard between the two crossing tunnels (Figure 1).

From figure 1: the longitudinal influence range of railway tunnel was 53.86 m (about 6.5D, D was excavation diameter of water tunnel, same as below), transverse influence range was 22.34 m (about 3D).

3 THE INCIDENCE OF NUMERICAL CALCULATION

When using 3D FEM numerical calculation, it could simulate the time and space effect, the mechanics effect of stratum layer and supporting structure during construction, the effect of railway tunnel by the closed construction of water tunnel could be understood generally.

3.1 *Calculation model*

The range of calculation model was consulted to the theoretical calculation result: the left, right and bottom boundary were all adopted 50 m away from the edge of water tunnel, the top boundary has a distance 30 m higher than the existing railway tunnel, the length was adopted 120 m; model constraint: there has horizon constraint of for and after, right and left direction, vertical constraint of bottom plane, top surface was free face; the calculation model was divided to 37008 elements and 38711 nodes totally; using elastic shell element to simulate the linings of railway tunnel and water tunnel, using elastic-plastic entity element to simulate surrounding rock, using Drucker-Prager elastic-plastic nonlinear constitutive model as the constitutive equations of rock and soil[10], calculation model such as figure 2.

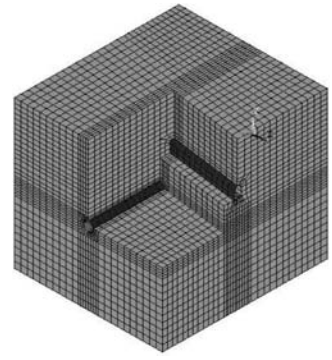


Figure 2. FEM model.

Table 1. Physics mechanics parameter.

Stratum and material	Young's modulus E/GPa	Poisson ratio μ	Bulk density γ/kN/m^3	Cohesion force c/MPa	Internal friction angle f/°
III level wall rock	10.0	0.25	23.0	0.7	39
Lining concrete	28.0	0.18	23.0	—	—

3.2 *Calculation physics mechanics parameter*

The physics mechanics parameter of surrounding rock and lining such as table .1[11]

3.3 *Calculation load and construction process*

The stratum layer's deadweight stress and gravity of concrete lining was mainly considered as calculation load, vertical stress was applied based on the practice depth of burial of tunnel top surface.

Using element kill and alive function which supplied by ANSYS calculation software to implement rock mass's excavation and lining's application during construction, so that it could complete dynamic

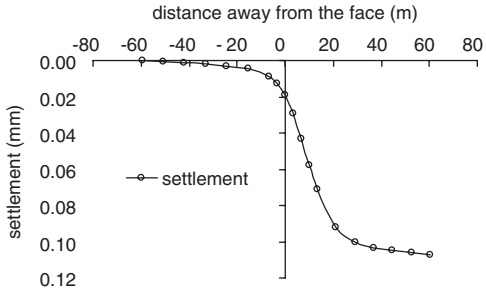


Figure 3. Relationship curves of cross point settlement and distance away from the face.

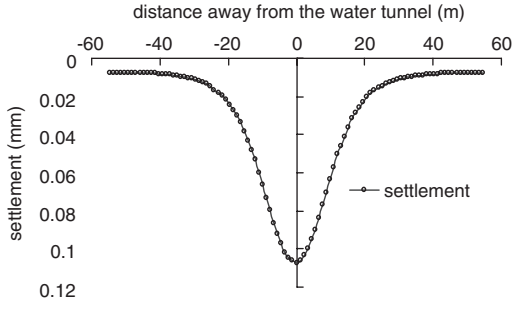


Figure 4. Longitudinal settlement canal of railway tunnel.

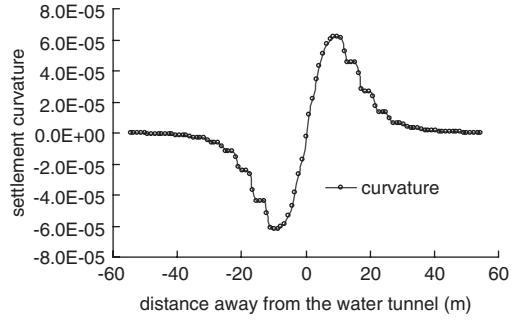


Figure 5. Longitudinal settlement curvature of railway tunnel.

simulation of total construction process. The concrete construction process in calculation were: original ground stress field-tunnel excavating and lining applying-the first step excavating and lining applying of water tunnel-· · · · · ·-the last step excavating and lining applying of water tunnel.

3.4 *Calculation result and analysis*

3.4.1 *Water tunnel's construction range which has impact on the railway tunnel*

The relationship curves between settlement which at the cross point of railway tunnel and water tunnel and the horizon distance away from the face of water tunnel as the following figure 3.

The settlement value was 0.005 mm when the face has 15 m distance away from railway tunnel; when the face just at the lower side of railway tunnel, settlement value was not at the most, when the face depart 37 m away from the railway, settlement value at the most (that was 0.102 mm). When the construction of water tunnel in this area, it needed to carry out monitoring for railway tunnel; when out of this area, the settlement impact by the construction of water tunnel to railway tunnel could be ignored.

From the analysis we could know, the construction range of water tunnel which has impact on the railway tunnel was related to the tunneling direction, the distance was 2D when near the railway tunnel, while 4.5D when far away from the railway tunnel.

3.4.2 *The influence that railway tunnel by water tunnel*

1) Deformation analysis

(1) Longitudinal influence range of railway tunnel

The longitudinal settlement canal and its settlement curvature at right side wall basement of railway tunnel such as figure 4 and 5.

A The settlement value was 0.015 mm when the distance was 25.11 m away from the two tunnels' axis cross point left side of the railway tunnel, curvature was $-1.18 \times 10-5$; While at the right side the settlement value was 0.014 mm and the curvature was $1.31 \times 10-5$; The finally settlement value at the cross point was 0.107 mm, so this range was get to the influenced area (length about 50.22 m).

B The Max curvature about longitudinal settlement of railway tunnel was $6.20 \times 10-5$, that was less than the limited value of rail vertical curve $1.0 \times 10-4$, considered the influence of train getting through and blasting vibration in railway tunnel, it needed to make pinch rail for the influenced rail, and make settlement monitor for the ground floor during construction.

C The longitudinal settlement deformation of railway tunnel was similar to the free beam, it needed to carry out checking about longitudinal bend moment and axis force of concrete lining of the tunnel.

(2) The transverse deformation of railway tunnel

The deflection condition of railway tunnel cross section which intersect with the horizon cast shadow of water tunnel at different position of face such as figure 6.

During the whole process of water tunnel down through the railway tunnel, the differential settlement would yield on the cross section.

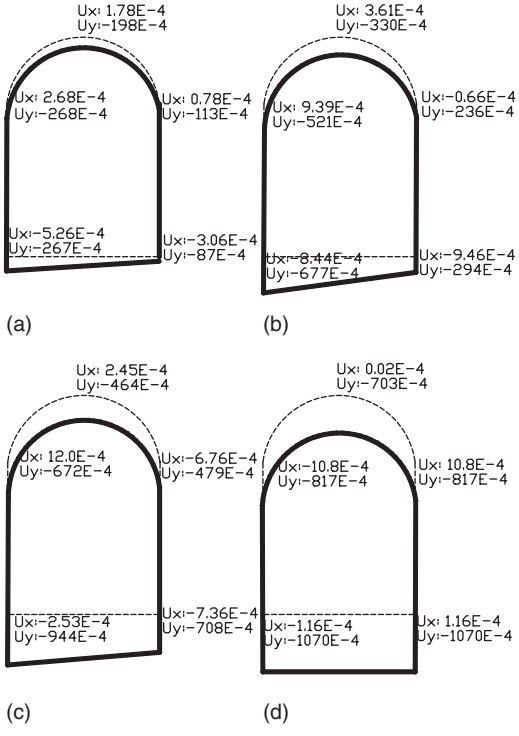


Figure 6. (a) The distance between the face and railway tunnel was 10 m; (b) The face just at the lower position of railway tunnel; (c) The face down through railway tunnel over 10 m; (d) The face over through the influenced area. The cross section displacement of railway tunnel.
Note: Ux: horizon settlement; Uy: vertical settlement.

The face was not at the position of railway, cross section would incline to the face direction, such as figure 6(a); when the face at the just lower position of railway tunnel, the slant value of cross section was reach the Max, such as figure 6(b); since with the driving of the face, the slant value of cross section would release gradually, such as figure 6(c); when the face out of the influenced area, cross section would not incline, getting back standing state, but brook away the original position, there were vertical settlement at each observed points and the horizon settlement with the character of symmetry, such as figure 6(d).

From the deflection process of cross section we could know, the twist rotation deformation would be yielded of railway tunnel by the construction influence of water tunnel. When discussing the structure security of railway tunnel, it needed to carry out inner force examination of bend moment and axis-force about the transverse section of concrete lining.

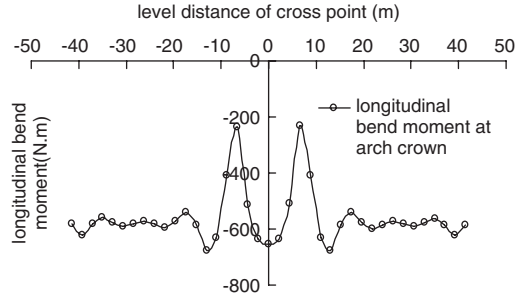


Figure 7. Longitudinal bend moment at the arch crown of railway tunnel.

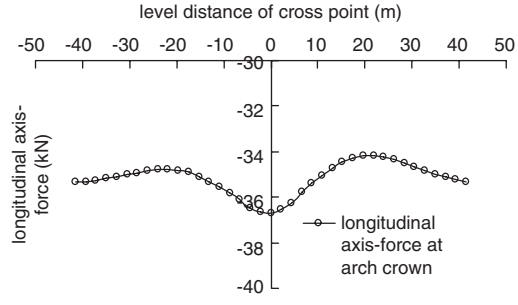


Figure 8. The longitudinal axis-force at arch crown of railway tunnel.

In theory, when symmetry construction was adopted for water tunnel at the both sides of railway tunnel, because the symmetrical characteristic, it could avoid creating twist distortion for the railway tunnel.

2) Stress analysis

(1) Longitudinal stress

The longitudinal bend moment and axis-force at the arch crown of railway tunnel after the water tunnel down through such as figure 7 & 8.

The longitudinal bend moment (678.58 N.m) reach the Max at the cross point $\pm$ 13.10 m away from the railway tunnel; while reach the Min (232.52 N.m) at the point $\pm$ 6.55 m. The longitudinal axis-force at the Max bend moment point was -34735 N. Based on the bending press structure the inner force checking was carried out to the Max bend moment section, the Max longitudinal press stress of concrete lining was $4.39 \times 10 - 3$ MPa, the value was less than the concrete tolerance press stress 11.0 MPa.

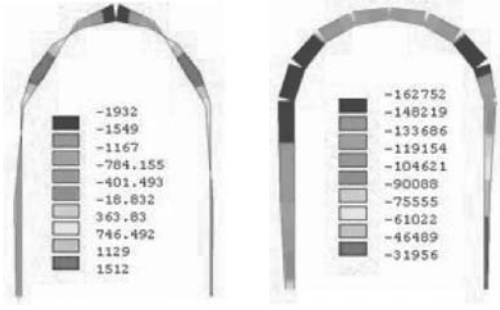
(2) Transverse stress

The bend moment and axis-force of cross section such as figure 9.

Known from the longitudinal and transverse direction stress checking of lining concrete of

Table 2. The stress checking table of lining structure.

Check computation part	Concrete grade	M/N.m	N/N	Linear eccentricity e_0/m	Resist compression safe coefficient	Resist extension safe coefficient
Vault	C20	1932	104621	0.018	59.5(>2)	–
Hance	C20	1512	162752	0.009	38.4(>2)	–



(a) bend moment (unit: N · m) (b) axis force (unit: N)

Figure 9. The bend moment and axis force of cross section.

railway tunnel, the lining of railway tunnel could satisfy the safety requirement, it needn't to carry out special reinforcement for lining concrete. Considering the influence of blasting by mining method construction and train getting through in the tunnel, it needed to carry out monitor for longitudinal and transverse direction lining concrete of railway tunnel.

4 INFLUENCE FORECASTING AND COUNTERMEASURE

Based on the calculation analysis above, the countermeasure of railway tunnel by the construction influence of water tunnel and the construction forecasting area of water tunnel which has influenced on the railway tunnel such as below:

(1) The construction area of water tunnel which has influenced on the railway tunnel was related to the driving direction, while the distance was 2D when near the railway tunnel and 4.5D when away from the railway tunnel. When adopting the blasting construction method of water tunnel in this area, it needed to carry out vertical vibration monitor for the cross point of two tunnels in the railway tunnel.
(2) The longitudinal influenced area of railway tunnel was 6.5D, while transverse influenced area was 3D. It needed to carry out buckle rail method for the rail which in the influenced area of railway tunnel, and to carry out monitor for the ground floor of railway tunnel.
(3) By the influence of tunnel construction of down through water tunnel, twist rotation deformation would be occurred of railway tunnel. If using the method of symmetry construction at both sides of railway tunnel for the water tunnel, such deformation would be avoided; If using one-way construction method, it needed to decide deformation value strictly, and to carry out lining deformation monitor of railway tunnel during construction.
(4) The lining concrete could satisfy safety requirement of railway tunnel, it needn't to carry out special reinforcement for lining concrete. Considering the influence of blasting by mining method construction and train getting through in the tunnel, it needed to carry out monitor for longitudinal and transverse direction lining concrete of railway tunnel.

The implement of each influence countermeasure above, the main purpose was to ensure the safety of railway tunnel structure and train operation.

5 THE END

During the construction water tunnel of Baishuijiang three degree hydroelectric station down through Shoubayan tunnel of Neijiang-Kunming railway in Yanjin country Yunnan province, this influenced forecasting result was applied sufficiency. During construction process, the monitoring was carried out for the ground floor settlement, lining deformation and stress and vibration speed when in blasting, and buckle rail method for the rail. At present, the water tunnel was getting through the closed influenced area of two cross tunnels successfully, so it showed the correctable and feasible of this influenced forecasting result.

REFERENCES

[1] Qiu wenge. The closed construction mechanics principal and countermeasure research of underground engineering. *Sichuan Chengdu: The Doctor academic*

thesis of southwest jiaotong university, 2003. 3.1–3:188–192.

[2] Gong lun, Qiu wenge. The research of closed construction vibration influence about up-down and crossing tunnel[A]. *The academic thesis of China traffic civil engineering [C]*. Sichuan Chengdu: The publishing company of southwest jiaotong university, 2006. 654–661.

[3] Peng daofu, Li zhongxian, Yang nianhua. The vibration influence of closed distance blasting towards existing tunnel[J]. *China railway Science*. 2005, 26 (4):73–76.

[4] Gaoyang, Qiu wenge, Zhengyuchao. The excavation influence forecasting and countermeasure research of highway tunnel by underside coal bed[J]. *Modern tunnel technical*, 2003, 42(2): 15–24.

[5] Qiu wenge, Zhang zhiqiang. Numerical simulation analysis of overlapped tunnel by closed construction influenced in Shenzhen metro[J]. *Railway standard design*, 2000, 20(6∼7):41–42.

[6] Liao huisheng, Ye wenqian, Chen junrong. The closed construction influence evaluation and analysis of hidden shield tunnel[J]. *The rock mechanics and engineering transaction*, 2004, 23:4876–4881.

[7] Pan xiaoma, Zhang chengman, Wen xiangdong and so on. The safety influence numerical analysis of new building railway tunnel to closed existing tunnel[J]. *Railway construction technique*, 2002(1):29–31.

[8] Li qiang, Zeng deshun. 3D FEM numerical analysis about the deformation of vertical cross tunnel in shield construction[J].*Rock and soil mechanics*, 2001, 22(3):334–338.

[9] Zhang yujun, Liu yipping. FEM numerical calculation about surrounding rock stabilization at the cross position of up and down run tunnel[J]. *Rock and soil mechanics*, 2002, 23(7):511–515.

[10] Pan changshi. *Tunnel mechanics numerical method[M]*. Beijing: China railway publishing company, 1995.

[11] (TB 10003–2005). *Railway tunnel design criterion[S]*.

Underground Space – the 4th Dimension of Metropolises – Barták, Hrdina, Romancov & Zlámal (eds)
© 2007 Taylor & Francis Group, London, ISBN 978-0-415-40807-3

Monitoring of the state of pipes in sewage networks as an element of adapting such networks to the technical demands of modern, urban subterranean infrastructure

C. Madryas & B. Przybyła
Wrocław University of Technology

ABSTRACT: A strategy for adapting sewer networks to the demands of modern cities is becoming more and more vital. Intensification of the usage of underground space has brought about the need for new research on the operation, modernization and renovation of sewer networks. Leaving this issue unsolved would make the sustainable development of cities impossible. As an element of such a strategy, the monitoring of technical conditions in sewers concentrates on: (1) determining short-term actions leading to an improvement in the operational reliability of a sewage network, (2) predicting the technical condition of a network, in order to optimally plan the financial resources allocated to renovation and improve long-term reliability, (3) optimising, given the existing constraints: the technology used for renovation, the materials used, the range and form of renovation and the modernization of a network (including integrated systems i.e. utility tunnels). This will enable the adaptation of a network to modern methods of utilizing underground space. This paper presents the current issues, guidelines and principles for the monitoring of sewers, together with a discussion on practical aspects.

1 INTRODUCTION

The elements in a sewage network were built in different eras, from various materials with greatly differing properties (stone, brick, concrete, polymer concrete, stone, cast iron, PEHD, PCV, GRP), which leads to problems in maintaining the condition of such systems. Damaged elements in the network cause many negative effects on the surrounding environment.

The location of sewage networks under roads (from 2 to 10 m) and, in particular of gravitational pipes, cause serious problems and sometimes even prevent changing the location of these pipes, in order to build other subterranean installations. These traits are fundamental constraints on the construction of e.g. pedestrian subways or shallow tunnels for road traffic. However, they have become an important incentive for the dynamic development of non-invasive techniques and technologies for renovating and monitoring the technical state of pipes.

A strategy for adapting sewage networks to the needs of cities of the future are particularly necessary. In order to adapt cities to an increased density of subterranean installations, it is above all necessary to undertake research into perfecting the processes of exploiting, modernizing and restructuring sewage networks. The balanced development of urban agglomerations will not be possible without such work. Monitoring the elements in a sewage network is an element of such operations aimed at obtaining the necessary information to assess their technical state and choose the appropriate means of renovation and improving the reliability of the network.

2 MONITORING DURING THE PROCESS OF NETWORK RENOVATION

2.1 *Monitoring as an element of the renovation process*

The process of renovation is conducted for a specific time referred to as the renovation time. This is the length of time from assessing a pipe to be unsuitable until its return to active service and is the sum of the following times:

- monitoring time, determining the location of damage – t_K,
- diagnosis time, determining the cause and scale of the damage – t_D,
- repair time (sum of the following times: for carrying out formal procedures, preparing projects, transporting the required materials and carrying out construction work – t_N,
- for testing after repair – t'_K.

Figure 1 illustrates these elements of the renovation time along the time axis

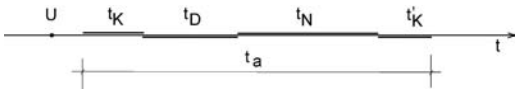


Figure 1. Components of renovation process: U – demage, t_K – monitoring, t_D – diagnosis, t_N – renovation, t'_K – testing after repair.

As can be seen from figure 1, the time at which the damage occurs us not the time at which the renovation of the pipe starts (the time at which the pipe is monitored). This is due to the fact that damage in sewage networks is often not immediately observable and the damage caused depends, to a large extent, on the length of time that passes between inspections. Hence, it is necessary to choose the frequency at which inspections are made, such that the costs caused by undetected faults are less than the costs of inspection.

A fundamental question is the optimization of the renovation time, particularly in cases when a so called by-pass is necessary or (even worse) when invasive renovation, which disturbs the normal functioning of the city, is required. In such cases, the social costs caused by extended renovation times may well be extremely high. Ignoring the renovation time t_N, the most important determinants of the renovation time are the monitoring and diagnosis times. Assuming that diagnosis is in the form of a in-depth inspection of the technical state of a pipe, the sum of the monitoring and diagnosis times to a large extent determines the efficiency of the renovation process. The inspection techniques used, competency of the inspectors and the skill of the diagnosticians play a fundamental role in minimising these times. These and other factors imply the need to continuously search for optimal renovation and diagnostic techniques, as well as inspection timetables and improving formal procedures.

The fundamental task of monitoring and diagnostics is to discover damage and determine the cause, respectively. An inspection may result from the observation or evidence of damage to the network. Such inspection is unplanned and occurs at an unknown rate. Diagnosis and repair of appropriate elements in the network is required. An inspection may also be carried out as part of a monitoring strategy.

In practice, the time required to localise the damage may sometimes exceed the repair time. The inspection/localisation of damage may be carried out by workers either directly observing the pipe or with the aid of remote monitoring devices. In organisational terms, an inspection may by facultative, logical or logical-facultative. It should be noted that sewage pipes (in contrast to the majority of technical installations) may well be able to carry out their function even when damage has been caused to several elements (e.g. leakage at junctions), although from a technical point of view the state of such elements would be deemed to be non-operational. This means that diagnosis must cover the entire section of the network in which a fault may have occurred and must be continued, even when a fault has been found.

If an element is found to be faulty and the fault localised, then the next step is diagnosis. The goal of diagnosis is to determine the cause of a fault and seriousness as quickly as possible. Additional inspections are sometimes needed within the framework of diagnosis. This requires the appropriate procedures and equipment. Such inspections should be carried out by a technical specialist and sometimes require laboratory tests in addition to in situ tests, particularly in order to define the parameters of the construction materials and the degree of the degradation caused by chemical and biological corrosion. It should be stressed that sometimes inspections are commissioned to incompetent individuals or firms, which may result in mistakes and unsuccessful renovation.

The testing time t'_k depends on the type of work carried out, the equipment used and the skill of the inspectors. Standard testing after repair is based on observing the renovated channel using CCTV or by direct inspection from inside large pipes. Due to the complexity and high costs of some repair techniques, there are cases in which testing after renovation requires laboratory testing of the parameters of the construction materials used to renovate a channel. In this case the testing time may be long.

2.2 *Monitoring as an element of a strategy for renovating a network*

Companies involved with the running of a sewage system carry out a planned or quasi-facultative monitoring strategy, which may be classified into the groups described below. These are presently treated as conventional strategies for the technical renovation of a sewage network.

The "Fire Service" Strategy. Such a strategy calls for inspections only in the case when an element has failed (analogous to a fire service which simply puts out fires). Due to the "hidden" nature of subterranean infrastructure (unforeseen faults suddenly appear), such a strategy is very commonly used. However, analysis of previous faults can lead to significant improvements. Sections of networks which have been particularly prone to faults may be systematically monitored. In this way, without carrying out expensive inspection, statistical analysis may be used to attain a higher level of reliability. It should, however, be stated that most unexpected failures have to be repaired using invasive strategies, which create large "social costs" in the functioning of a city. This means that the "fire service" strategy should be replaced by other strategies, which remove negative changes in the network before

they cause a failure, even though the costs of such monitoring schemes are higher.

Strategy of "relieving". Such a strategy does not call for the renovation of old elements in the network, but is based on the building of new elements in order to e.g. relieve the burden placed on older elements. Strictly speaking, this is not a renovation strategy, but rather a system for increasing the reliability of the system. Since they are less burdened, older elements in the system are less often subject to failure, which increases the reliability of the system. This strategy is often used in transport industries, transporting water and gas and less often for sewage networks and supplying heat. It should be stressed that such strategies are associated with costs for predicting the future demand of a good and does not solve the problem of old elements which are subject to gradual decline. Thus, this cannot be treated as the only option for water supply companies.

Strategy of regular replacement (prevention). Elements of the system are replaced by new elements at regular intervals, regardless of whether they are in a poor state or not. Of course, an element is replaced if it fails (hence we can distinguish between profilactic and forced changes). Such a strategy is normally used in systems, whose elements have short operative lives whose variance is small. It is possible to mathematically estimate the optimal time at which an element should be replaced (such a strategy is called a preventative strategy with the optimal replacement time T_{opt}). In practice, due to the multiplicity of factors affecting the operative life of pipes (such elements are designed to have a long operative life, at least 50 years independently of the material used), this strategy is not used in sewage networks, but only for minor elements in the system eg. manhole covers, safety valves, locks.

Strategy of renewal based on monitoring. While the previous systems do not require a system of monitoring a network, in this case renovation comes as a result of inspection and assessment of the state of elements in the system. If, as a result of an inspection, an element is assessed to require repair (its state is in some defined critical set), it is renovated. Such an approach requires the definition of indicators of the state of an elements and the states requiring renovation, based on the level of wear/damage of the element. The methods used for monitoring (inspection) must be specified, i.e. observation of these indicators, time between inspections, the methods for storing and analyzing the results of inspections. The costs involved depend on the strategy adopted and the reliability of the system.

In the case where the results of an inspection are used only to determine which elements should be renovated, the scope of a firm's medium-term planning and records are constrained. In order to eliminate this problem, the results of inspections may be stored and then analyzed in order to obtain prognoses regarding the behaviour of the system in the future. This leads to the final strategy to be considered here:

Strategy of renewal based on monitoring and prediction. A prognosis for the evolution of the wear/aging of elements in a sewage network using long-term monitoring of a system, taking into account all possible constraints, together will the boundary conditions of the functioning and characteristics of the materials used, is the basis of such a strategy.The dates of future inspections and renevations are planned with reference to this prognosis. The prognoses made basically regard the physical process of wear on the elements. Another question is the determination of the so called "moral" level of wear of an element, which is an important factor when a firm plans its budget.

It is easy to see that a strategy of renewal based simply on monitoring can be developed into such a strategy when enough material has been collected to carry out the appropriate statistical analysis.

3 SYSTEMS OF MONITORING

The systematic monitoring of sewage network is carried out in order to observe the state of its elements and the level of corrosion. This is part of a firm's maintenance programme. Moreover, monitoring the network includes inspection of the elements of the network which lie above the surface and detection of collapses along the channels.

The implementation of a strategy of prevention with the optimal replacement time T_{opt} requires information regarding the reliability of the system. Since water companies do not normally have such information, it seems reasonable to start by using a renovation strategy based on monitoring and gradually switching to a renovation strategy based on monitoring and prediction when enough information has been obtained. This is the standard approach to the monitoring of elements in most modern, well-managed firms.

A monitoring system, which is a key element in a renovation strategy, can be defined as an multilevelled inspection system carried out at constant or variable intervals based on criteria indicating the order in which inspections should be made in the various parts of the network. In organisational terms we may distinguish the following types of inspection: routine, detailed and specialist. This classification is based on the exactitude and frequency of inspections. Routine inspections (with the lowest degree of exactitude q_1) are carried out with the most frequency and at regular intervals, Δt, detailed inspections (with a higher degree of exactitude q_2) are carried out at intervals which are multiples of Δt. Specialist controls are only carried out when the results of a routine or detailed inspection are unsatisfactory. Hence, such inspections appear at random intervals and do not have to be

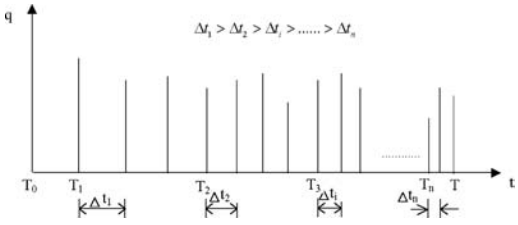


Figure 2. System of sewer inspection (Madryas, 1993) T_i – general overhauls, Δt_i – mean time between inspections, q – coefficient of the exactitude of an inspection.

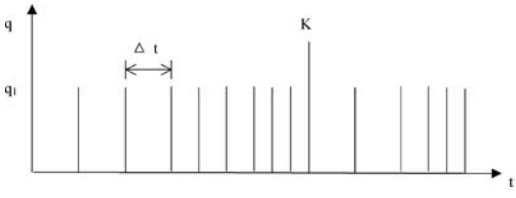


Figure 3. Generalised system for monitoring a sewage network Δt_i – mean time between inspections, which is constant or variable depending on the state of the pipe or the prognosed age/level of wear. q – coefficient of the exactitude of an inspection. K – coefficient of the exactitude of a detailed inspection carried out when planning the renovation of an element or testing after carrying out emergency repair resulting from a fault.

included in the calculations for optimising the costs of routine and detailed inspections.

In order to limit the losses associated with an undetected fault, it is necessary to minimise the length of time between the ocurrence of the fault and the moment of its discovery. Hence, it is necessary to inspect pipes which are more subject to faults than other pipes. Figure 2 illustrates a system which on observing a worsening of the state of a pipe, increases the frequency of inspection, together with an appropriate change in the exactitude of inspection q (Madryas 1993).

The majority of pipes in a sewage network are of large enough diameter to allow inspections by workers from inside the pipe. Hence, it is relatively straightforward to adopt the appropriate exactitude of inspection. In this case, the appropriate recording instruments should be used to analize the state of the system, which is used to determine the time and the exactitude (or at least a bounded interval for the exactitude) of future inspections. However, in the case of smaller pipes a significant increase in the exactitude of inspection requires direct, specialist observation and this requires exposure of the element under observation (invasive work) and normally the element should be isolated from the rest of the network. At the same time, similar methods may be used in pipes of larger diameter. Hence, a generalised system may be proposed for monitoring a sewage network (see figure 3). Such a scheme is adapted to each specific case, according to the goals of each individual inspection, the goals of the whole system of monitoring, as well as the skills and technology available in a given water supply company. In the simplest form of such a system, one may assume that inspections carried out using video cameras are of exactitude q_1, whereas an inspection of exactitude $K > q_1$ enables detailed planning of any repair work to be done.

4 SELECTIVE AND EXHAUSTIVE INSPECTIONS, THE PRIORITY OF INSPECTIONS

4.1 *Exhaustive inspections*

Taking into account the size of an urban sewage network and the constrained funds of water supply companies, the choice of the length of time between inspections should depend on the classifaction of an element, together with the possible consequences of a fault. It is necessary to choose:

– the elements which are to be inspected first,
– a policy for adapting the monitoring strategy according to the results of inspections.

At present two basic approaches are used. These are called exhaustive inspections and selective inspections. The first approach involves inspection and assessment of all of the elements in a given area. The order of the inspections does not have to be fixed. Monitoring is carried out in chosen areas, e.g. A district of a city. Due to the number of elements involved, such inspections tend to take a very long time. Thus, inspections are more often carried out according to a specified plan, which defines the order in which the inspections are made (elements whose failure would lead to the largest costs). A possible scheme for choosing the order in which inspections are made is shown in figure 4.

This scheme chooses the order of inspections according to the seriouness of the consequences associated with leaks in channels. However, it should be stressed that this should not be the only criterion. An analysis of the consequences of a fault in an element may result in improved criteria for choosing the ordering. The scheme illustrated above is thus an illustration of a scheme that can be practically implemented. Such a scheme should be adapted to the characteristics of the local sewage network.

Good results can be obtained by highlighting critical channels and treating such channels as the core of the system. These channels should have priority treatment, with respect to both inspections and planning renovation work. A method for choosing these critical channels was proposed by WRC (1990).

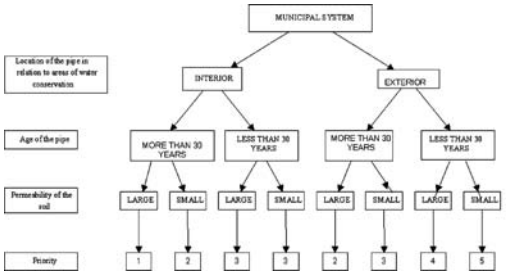


Figure 4. Determining the order for assessing the state of pipes (Schaaf, 1997).

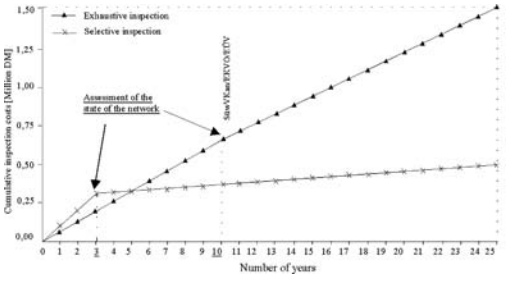


Figure 5. A comparison of the costs of selective inspection and exhaustive inspection for a 100 km network (Hertwig & Krug, 1999).

Ascribing priority to certain channels obviously does not undermine the assumptions of exhaustive control that over a given period of time all the pipes from a given class will be inspected and only then will the appropriate conclusions regarding the state of the network be taken (in order to specify the future course of inspections).

4.2 *Selective inspection*

Selective inspection is an alternative to exhaustive inspection. Information regarding the state of the network as a whole is obtained by generalising the assessments of a sample of elements chosen from each class using appropriate statistical techniques. According to the EN 752-5:1997 norm, both methods are equally acceptable.

Figure 5 presents a comparison of the costs of using selective selection for the first and following inspections and the analogical costs when exhaustive inspection covering the same fraction of the network at each stage is used (Hertwig & Krug, 1999). To begin with the costs of selective control are higher than the costs of exhaustive inspection. After carrying out a general appraisal of the state of the network (this can be done at an earlier stage if selective inspection is used), the costs of using selective inspection are decidly lower.

In Poland, when assessing the state of a network there is often an additional problem associated with an incomplete inventory of its elements. Hence, inspections are used as an element in creating a full inventory. Adopting selective control seems particularly appropriate in this case, since costs can be significantly lowered. In order to make accurate general conclusions regarding the state of a network, it is necessary to inspect about 20% of the elements.

The selective control of pipes embraces the following stages:

– a classification of the elements in the network, elements in a class have similar characteristics (e.g. age),
– selection of a random sample from each each class that is to be inspected,
– inspection and assessment of these random samples,
– statistical analysis of these assessments and then generalising, firstly for each class and then at the level of the network as a whole.

One may define various criteria to be used in defining classes. Among other things, these may be:

– the load carried by a pipe,
– the type of material the pipe is made from,
– the diameter and the cross-section type,
– the sewage system to which a pipe belongs,
– the corrosiveness of waste waters carried,
– other…

In situations where there are a large number of categories of varying importance, such a procedure may lead to an excessive number of classes. This is a result of the number of criteria (which directly depends on the classification used) and the characteristics of a given network. It seems useful in this case to resign from the use of certain criteria and group similar classes together. In cases where such a classification is still too rich, classes which contain too few elements to carry out the appropriate statistical analysis (there should be at least 30 elements in a class) should be subject to exhaustive inspection.

Another question regards the choice of the number of pipes (a random sample) to be inspected in a given class. Muller and Krug 2001 argued that at least 12–15 pipes in a class should be inspected. Also, in order for the random sample to be representative of a given class, a random sample should contain at least 10–20% of the elements in the class.

According to the results of an inspection, the pipes from these random samples are graded with respect to their state. Various aspects of changes in pipes may be used to grade the state of a pipe (e.g. the technical state of the pipe, aspects regarding possible ecological consequences resulting from a fault, the social costs resulting from renovating a pipe). If one has observed

the distribution of the states of the pipes in the random samples from each class, one may generalise these results to each class and then to the network as a whole. The mean grade of pipes in a given class can be characterised by a confidence interval, which gives bounds which are very likely to contain the mean grade of the pipes in the whole of a class given the grades of the pipes in the random sample from that class.

A fundamental question when using selective inspection is the verification of the results obtained. The random samples taken may give a false picture of the network as a whole due to: inappropriate choice of classes, small size of random samples, poor quality of assessments, differences between assessments carried out at different times, lack of consistency in the assessments (despite using the same assessment scheme) and inappropriate statistical analysis.

In order to verify the results of inspections, according to standard practice a water supply company commissions additional inspections. The results obtained in these inspections are compared with the results of the original inspections.

5 SUMMARY

- Monitoring is crucial in ensuring a reliable sewage network and protect areas surrounding the network (road surfaces, buildings and other urban infrastructure).
- The need to optimise the process of renovating sewage networks implies the need to constantly find improved monitoring systems, methods of diagnosis and formal procedures. Considering the techniques available at present, renovation strategies based on prognosing the future state of the network seem to be the most appropriate strategies.
- Due to the size of sewage networks and associated costs of inspection, exhaustive inspections in a short period of time are impractical.
- Due to the size of sewage networks and associated costs of inspection, selective inspections are a more practical solution, especially when carrying out an inventory of the system.
- Inspection of the system is a fundamental element of its reliability and is necessary in order to adapt a sewage network to the needs of a modern city.

REFERENCES

Madryas, C. 1993. Odnowa przewodów kanalizacyjnych. *Prace Naukowe Instytutu Inżynierii Lądowej Politechniki Wrocławskiej*. Seria Monografie 42/16: Wrocław.

Schaaf, O. 1997. Neue Landesbauordnung fordert Kontrolle der Grundstückentwasserungsleitungen. *Kommunalwirtschaft*. 9: 468–474.

WAA/WRC. 1990. Sewerage Rehabilitation Manual. Second Edition.

Hertwig, E. & Krug, R. 1999. Selektive Inspektionsstrategie und statistisch/prognostische Sanierungsmodelle. *Korrespondenz Abwasser*. 11: 1703–1708.

Müller, K. & Krug, R. 2001. Selektive Erstinspektion von Kanalisationen. *wwt awt*. 1: 30–33.

Underground Space – the 4th Dimension of Metropolises – Barták, Hrdina, Romancov & Zlámal (eds)
© 2007 Taylor & Francis Group, London, ISBN 978-0-415-40807-3

Investigation behavior of vertical shaft under loadings of intake tower at first filling of Doosti Dam

Daliri-Massoud
TOOSSAB Consulting Engineers Co, Dams & Hydropower Department

ABSTRACT: Intake Tower of Doosti Dam is constructed on the left bank of Dam body with 54 m height. Regarding to the concept of Intake Tower's Load conditions and Mechanical Parameters of rock foundation (soft Rock), Evaluation of Foundation and effects on Behavior of Shaft's Lining under Tower are important. In this Studies considering to Monitoring of foundation with extensometers' and Modeling with Numerical Method, effect of Static Loads at duration of construction and first filling on Shaft's behavior are investigated and compared Results with Monitoring Data. Finally Intake Tower's Foundation with Shaft under Static Loads conditions is evaluated.

1 INTRODUCTION

Doosti Dam is located at 260 km from the north-East of Mashhad city on the border of Iran and Turkmenistan. This dam is constructed by two countries at 2004 on Harirrud River and supplied agricultural water of two countries and drinkable water of Mashhad city. Doosti Earth fill Dam has 78 m height and 700 m crest length. water intake system of dam has 50 m^3/s capacities and is included Intake Tower with 54 m height, Vertical Shaft with 24 m depth and transmission galleries. Doosti Dam and Intake Tower are shown in figure 1. [1].

Intake Tower is constructed on the left bank of dam body on the Argillite bed rock that it is one of the soft rocks type and Shaft as part of transmission section was constructed under Intake Tower.

Vertical Shaft under Tower is affected by Tower loadings and acts as a part of tower foundation, Therefore investigation behavior of shaft and safety control of Tower foundation is important. For monitoring of tower and foundation, some extensometers after finishing of tower were installed on tower foundation. After installation of instruments, left side of dam body extended on tower foundation and 26 m of tower height were buried by embankment. Then reservoir elevation increased after finishing of dam construction. During stage construction of dam body and first filling, instruments were monitored. In this study, regarding to form of loading, shaft and tower rock foundation with numerical method, are modeled and analyzed. Then results checked and comparing with instruments data. In figure 2 section of Tower, Shaft and Dam body are shown.



Figure 1. View of Doosti Dam and Intake tower from upstream.

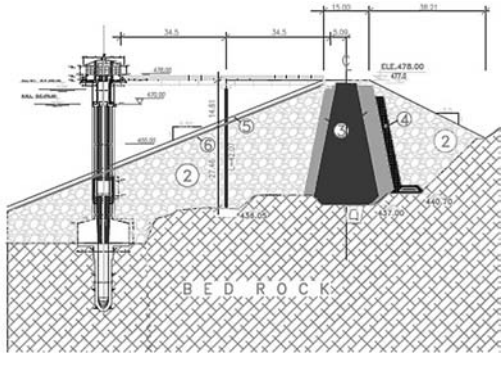


Figure 2. Section of dam body, Intake tower and Shaft.

Table 1. Geomechanical parameters of foundation rock.

Geomechanical parameter	
Module of elasticity (Gpa)	2.6
Module of deformation (Gpa)	1.1∼1.9
Friction angle ϕ (Deg)	27°
Cohesion C (Mpa)	0.1
Poisson's ratio υ	0.3
Density (ton/m^3)	2.32

2 GEOTECHNICAL CHARACTERCTIC

According to the results of explorations program at Feasibility study stage, foundation rock of Intake Tower and Shaft located in the "Koape_Dagh" formation, that consisted of argillite with small spacing and are slightly jointed filled with clay and gypsum. Rock at surface is very weathered and degree of weathering to the depth decreases and apparent strength of intak rock are weak. Regarding to the type of rock, after excavation of Shaft, some field and laboratory tests were performed and properties of rock measured. For determination module of deformation were used Dilatometery test method. In this method expanding of borehole diameter derived of cell pressure are measured directly. This test is reasonable for some weak rock like Argillite. In this stage six vertical boreholes and two horizontal borehole of the Shaft wall were tested. Summery Result of in-situ and laboratory tests of rock's periphery of the shaft is shown in table 1.[1].

Considering to the physical and mechanical parameters of rock, especially in the vicinity of water, consolidation grouting of foundation were performed. Furthermore, according to result of analysis for stability of Intake Tower in extreme load conditions numbers of 32 bar anchors were installed on the foundation of Tower. Length of anchor in the rock is 16m that 6 m end of them are restraint with grout and then prestressed up to 80 kpa, next fully grouted. These conditions are affected on the mechanical parameters of foundation rock that is considered on modeling with back Analysis, which is explained later.

3 MONITORING

One of the important methods for monitoring of rock for controlling of safety is regular measurement of deflection and displacements. With this method regarding to the rate of variations, behavior of system are predicted. On the Intake Tower of Doosti Dam besides some surveying points on tower body, numbers of 4 Extensometers on the foundations were installed. Every extensometer has four fixed points, that it monitored four level of rock around the Shaft. Length of

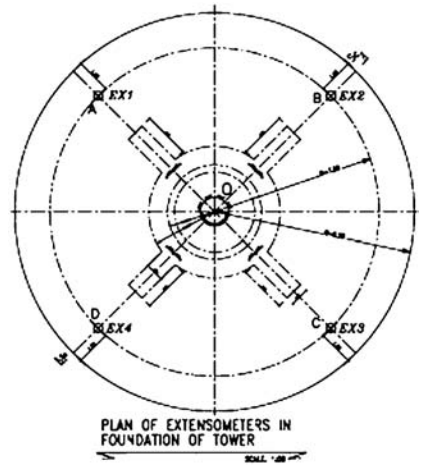


Figure 3. Position of extensometers on foundation of tower.

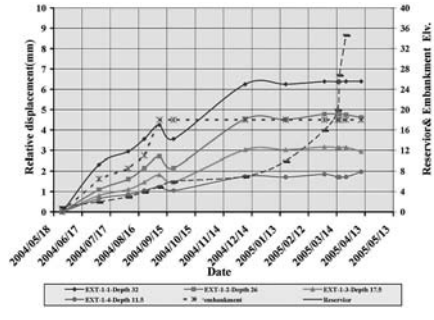


Figure 4. Variation of foundation relative displacement No. 1 with embankment and water level from March 2004 to 2005.

restraint of extensometer is performed in 11.5, 20, 28 and 32 m from top of tower foundation. Thickness of tower foundation is 8 m. Positions of extensometeres in figure 3 are shown.

Extensometers were installed after completion main part of Tower, foundation treatment with consolidation grouting and anchors bars installation. Therefore effect of dead load of tower and prestressed force of anchor bars weren't considered. But effects of stage construction of embankment were monitored by extensometers. In figure 4 variation of deflection on the tower foundation at the duration of dam body construction and the impounding of reservoir from 2004 to 2005 are shown. [2]. Horizontal axis is date and vertical axis at left side is relative displacement of extensometer No. 1 in millimeter. Furthermore, variation of embankment on foundation and depth of reservoir water are shown at right side of graph in meter from Bed River.

Like it is shown in figure 4, large proportion of displacement is related to the effect of loading's embankment and trend of increasing on graphs is

similar. But effect of water rising in reservoir on deflection of extensometer is low that the main reason is unloading due to buoyancy effects on weight of tower and embankment's materials. In this graph sensible short term effects of water on physical and mechanical parameters of rock not observed too.

4 MODELING AND ANALYSIS

Modeling of Shaft-Rock and Tower system was made using with Flac3D software. This software is an explicit finite difference program to study numerically the behavior of a continuous three dimensional medium as it reaches equilibrium or steady plastic flow. [3]. Modeling in this software are performed by making of 3D meshed model with brick elements that they behave according to the mechanical properties and model of materials under external or internal loading and boundary conditions and are developed to the yield state. In this software regarding to method of analysis and solution of equations (Explicit Lagrangian method), calculation time and solution problems is less than other FEM soft wares.

In the first stage of modeling, limitation of model is recognized and rock in dimension of 100 m by 100 m and 50 m depth were modeled. Then shaft are excavated and lined. In the Next, Intake Tower on the shaft is constructed. According to the stage of construction, modeling was performed in program. In the modeling procedure, has been made an attempt real conditions of model was considered. In figure 5 models of Rock, Shaft and Tower is shown.

4.1 *Material model*

In the second stage regarding to material properties, behavior of materials are determined. For rock foundation materials around the shaft Mohr-Coulomb plasticity model was used. This model is one of the most applicable for Geoengineering studies. Mohr-Coulomb model is used for materials that yield when subjected to shear loading, but the yield stress depends on the major and minor principal stresses only. Main Parameters for model is cohesion and friction angle that the initial amounts of them in table 1 are available. Final parameters for rock after back analysis were determined and are used for calibrated model. Material model for the Shaft lining and Intake Tower are considered elastic. These materials are assumed homogeneous, isotropic and continuous that exhibit linear stress – strain behavior.

4.2 *Boundary conditions*

In the next stage boundary conditions of model should be recognize. The boundary conditions in a numerical model consist of the value of the field variables that are prescribed at boundary of the numerical grid. Boundary can be either real or artificial. The model boundary must be far enough away from the region of study so that response is not adversely affected, that appropriate distance depends on the purpose of analysis. Generally boundary should be 3 to 5 time the size of the cavern. In this model distance of boundaries in x and y directions 50 m are considered that enough for this type of analysis. Roller Displacement boundary has been applied on all five sides that causes the stress and displacement to be underestimated. This fact has to be considered while interpreting the result.[4].

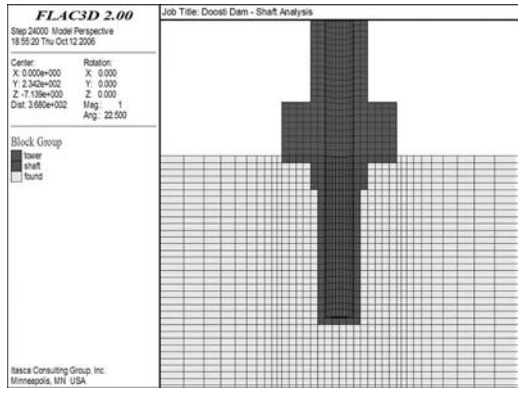


Figure 5. Modeling of Rock-Shaft-Tower in Flac3D.

4.3 *Stage analysis*

As it explained at the last parts, three stages for analyzing of model before loading are considered. At the First stage, model before excavation was analyzed to equilibrium of model that initial stresses in model generated. Displacements at end of this stage reset to zero. Second, shaft is excavated and lined with Thickness and geometry In the real state, consolidation grouting in the shaft's rock was performed in this stage and effect of them as increasing module of deformation in the back analysis are considered. Third, in this stage Intake Tower was modeled. Weight of tower is about 7800 tons that is considerable for determination of initial stresses in the shaft rock before instrumentation. The number of anchor bars is 32 with post tension forces about 80 kpa per anchors, that loading as uniform load on model was considered. At end of this stage, reset displacement to zero. In the last three stages, for material parameters of rock and concrete in model, initial parameters of the field and laboratory test of the studies stage are used. In the next stage, considering to the installation of instruments, model were calibrated after back analysis and determination of final parameters. Result of stress analysis of model and relative displacements before installation of extensometers in figure 6 are shown.

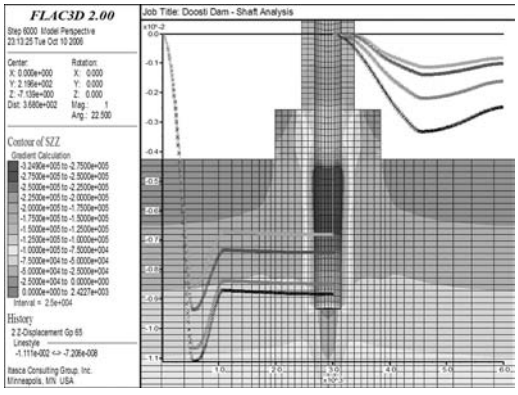


Figure 6. Results of stresses and relative displacements before installation of instruments.

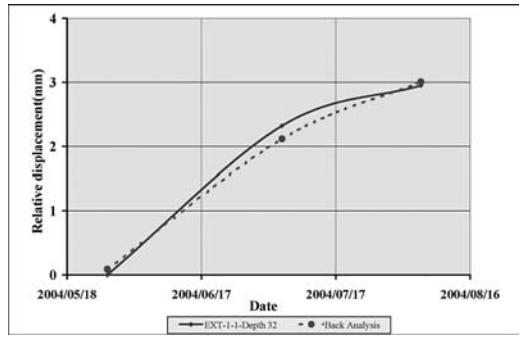


Figure 7. Compare displacement of extensometer and analyzing with final parameters.

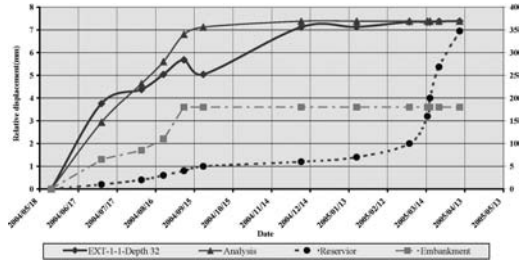


Figure 8. Displacements variation during of loading.

4.4 *Back analysis*

Considering to the variation of mechanical rock parameters at during of construction of Shaft and Tower and effect of foundation treatments, it is necessary that the main parameters of rock are determined. In this stage regarding to data of extensometers, Back Analysis was carried out. Before back analysis, for determination of main parameters, sensitive analysis on friction angle, cohesion and module of deformation are done and module of deformation according to the effect on displacements of model was defined for back analysis. Initial amounts of friction angle and cohesion regarding to the range of variation and effect on results are selected. For module of deformation, Back Analysis with direct method was performed [5]. In this method with minimizing of deference's square of displacement for extensometers and displacement of analyzed model, as equation (1), reasonable amount for module of deformation are determined.

$$\sum (U_m - U_p)^2 = Min \qquad (1)$$

In this equation U_m is amount of measured displacement from extensometers and U_p is predicting displacements of model after analyzing. This equation is used for 16 points that extensometers have had data. Regarding to the range of modules 1.1 Gpa to 2.6 Gpa from reports and site investigations, during 18 analysis minimum of error for 1.5 Gp is determined. As it explained, the first stage of embankment's loads for back analysis was applied, because in this stage, loading are uniform. In figure 7 Data's extensometer compared with displacement of analyzed model using final parameter of back Analysis.

After determination parameters of analyze, model are calibrated for applying loads with final parameters. In this stage, loading are included effects of embankment and reservoir elevation that were applied gradually. Maximum elevation of embankment on the shaft's rock is 26 m with density 2.0 ton/m^3. Loading of embankment was applied to model as uniform load that increased to 26 m in three stages.

Effect of water as pressure was applied to the model. Because this load acts after embankment, sequence of loading was considered. In this stage weight of intake Tower and embankment's materials reduced caused effect of buoyancy and Reservoir elevation rose up to the normal water level. In this study, notwithstanding, reservoir elevation haven't rose to this elevation yet, but for control safety of Tower and Shaft, up to normal water level in reservoir, model was analyzed and stresses and deflections were checked. Variation of displacements during the whole of loading is shown if figure 8. As it is shown, parting of loads stages in excavation of shaft, construction of shaft lining, Tower and embankment are cleared and coincidence of results with instrument's data is acceptable.

Stresses in Shaft are shown in figure 9. As it has shown, increasing of vertical stresses in Shaft lining regarding to the weak parameters of around rock is important. Structural function of shaft's lining in distribution of loads effect on the rock is reasonable.

Regarding to the maximum deflection of foundation and stresses in the shaft lining (8.6 Mpa), Intake Tower and shaft under maximum static loads in normal condition of loadings is safe.

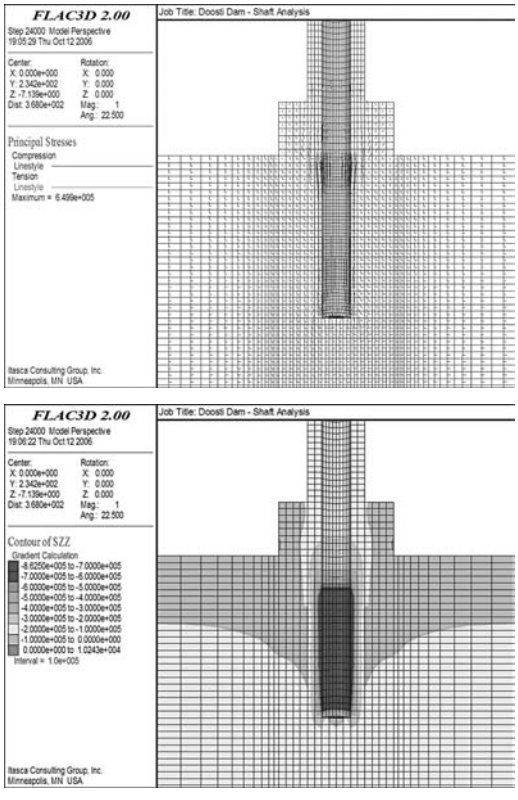


Figure 9. Distribution vertical and horizontal stress in shaft and rock.

5 CONCLUSIONS

1. contrary to the result of some laboratory tests, effect of water on physical and mechanical quality of shaft's rock in the short term is low.
2. considering to the weak rock around the shaft, effect of geometry and structural parameters of lining for reasonable distribution of tower loads on rock is more important.
3. comparing results of dilatometery tests after excavation of shaft and final parameters of back analysis indicate positive effect of foundation treatments.
4. regarding to the analysis results, condition of Shaft and Intake Tower at end of first filling is acceptable.

REFERENCES

[1] Technical Reports of feasibility studies for Doosti Dam, Toossab Consulting Engineers Co., 2000
[2] Monitoring Report of Doosti dam 2004 to 2005, Toossab Consulting Engineers Co., 2006
[3] Itasca Consulting Group Inc., FLAC, User manual version 2.0, 2000
[4] "Engineering and design tunnels and Shafts in Rock", Engineering manual 1110-2-2901, USACE, 1997
[5] Goida. G., "Some Remarks on Back Analysis and characterization problems in geomechanics", 5th Int. Conf. Numer. Meth. In Geom. – Nagaya, Japan, 1985

This page intentionally left blank

Underground Space – the 4th Dimension of Metropolises – Barták, Hrdina, Romancov & Zlámal (eds)
© 2007 Taylor & Francis Group, London, ISBN 978-0-415-40807-3

Membrane waterproofing – Activation of the grouting system and its re-sealing ability

R. Matzner
Matteo spol. s r.o., České Budějovice, The Czech Republic

M. Grossmann
Minova Bohemia s.r.o., Ostrava, The Czech Republic

ABSTRACT: For new tunnel structures and underground line structures, then in existing practice the lining of these constructions is designed for waterproof class 0. However, the lining of these structures contain many activities where human factor plays an important role. This presents many risks to the waterproof layer which is the most problematic and the worst repaired element of the lining – in fact after production of the secondary lining, this layer is not accessible, i.e. it cannot be repaired in a standard manner. Therefore, in the case of tunnel structures it is purposeful to apply a safety system for the waterproof insulation which enables effective action in the case of problems with the waterproof insulation. If such a system is correctly designed, performed and used, it is possible, if necessary, to be used again and this system will maintain its functionality in the long term.

1 INTRODUCTION

Waterproof insulation of the lining of tunnel structures is currently made of special waterproof foils. This mostly concerns a sophisticated system of products which, in addition to the waterproof foil, contains sealing strips for the expansion joints, various shaped units and anchoring elements, protection geotextiles and special glues. Foil insulation systems function very reliably but their 100% functionality is characterized by several aspects. First of all they are very demanding for the quality of the base, for maintaining the placement technology and, in particular, for the exact performing of all joints and other details. Protection of the placed insulation is also important in order to prevent damage during subsequent work starting from the placement of the reinforcement through to the placement of the form of boarding up to the concreting of the secondary lining. Within such a complicated construction process influenced by many inputs it is very difficult to prevent errors which can have a negative influence on the efficiency of the waterproof insulation. It is necessary to take these problems into consideration in advance and to prepare conditions for fast and effective action. Therefore, it is recommended to complete the injection protection system in the design phase where it can be easily activated if necessary, i.e. in the case of the occurrence of leakages and to remove these leakages. This is mainly valid in the case of intermediate foil insulations performed along the whole perimeter of the structure (the so-called "submarine" type) where the underground structure is submerged into the underground water and no its drainage effect is reflected.

Such an injection protection system was used in 2004 for prolongation of northern line C of the Prague Metro in the operating system indicated IV.C1 and in the same year it was also used in the Mrázovka road tunnel which is the part of the Prague inner city ring road.

2 UNDERGROUND IV.C1

2.1 *Tunnel design*

The tunnel was excavated using the NRTM method in the areas of rock with the rock clay and sand stone types. The work was reinforced depending on the stability of the rock by hydraulically expandable beams of the BOLTEX type and by boring R type anchor bars in combination with injection by cement suspension. The primary lining is from sprayed concrete and the secondary lining is made of cast concrete. The intermediate insulation is made of strips from Sikaplan V Tunnel transparent TR 30 softened PVC with a thickness of 3 mm, joined by welding by hot drift or hot air. In the cross-lateral and longitudinal working and expansion joints there are Sika Fugenband joint sealing strips to which the Sikaplan foil is connected.

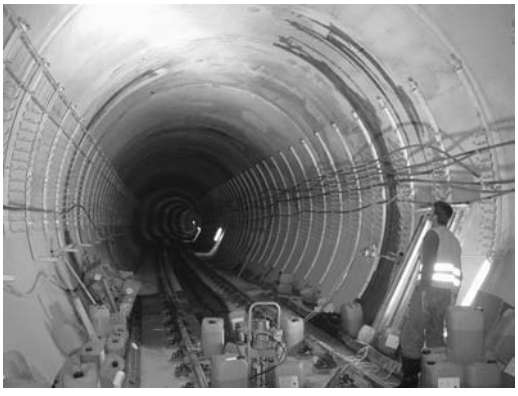


Figure 1. Metro IV.C1 – grouting in the single-track running tunnel.

Waterproof insulation is completed with the injection protection system consisting of two parts. In the expansion and working gaps are injection hoses and in individual sectors throughout the whole area there are injection and aeration hoses fixed to the foil insulation which terminates in the boxes of the central outlet in the secondary lining. The length of the individual sectors is 10 m for the two-rail tunnel and 7.0 m or 7.5 m for single-rail tunnels according to the type of the boarding. The length of the construction joint on the perimeter of the tunnel tube is 29 m. The area of one sector is about 290 m^2. The division of the tunnels into sectors enables to rehabilitate only those sectors which were damaged and had leakages. In Kobyliská station the protection injection system is designed as a floor type with two collection boxes on each side of the section.

2.2 *Defects*

The underground line in the section between Holešovice railway station and the new Kobylisy station has a height difference of 112 m and runs through a territory containing complicated hydro-geological conditions. The Kobylisy station is very unique by its design and it is the largest single-aisle bored station to ever have been constructed in the Prague Metro. In the final stage of the final (secondary) lining, leakages were reflected. The most frequent symptoms were:

- leakages in construction and expansion joints,
- leakages in the area of sectors which were reflected by leaks from the lining,
- local leakages, in particular in the places of the control points of the concreting in the top points of the arc (working name “spy”),
- escapes in complicated construction areas (e.g. connection of the station to escalator tunnels and the contact of the cable shaft with the railway tunnels).



Figure 2. Metro IV.C1 – grout injection into a joint in the vault of the Kobylisy station.

These leakages were removed with the use of the injection protection system, but because there was no experience with the activation in such a scope in the Czech Republic, it was necessary to look for the optimal solution. In particular, it was necessary to find suitable injection material which would fulfil the stated criteria. The common requirement of the general designer, the general supplier and the supplier of the waterproof foil system was to perform the rehabilitation of penetration through such injection material which would fulfil the following requirements – high flexibility, excellent sealing properties, ability to permanently ensure the sealing function, resistance to aggressive influences and, at the same time without any damage to the intermediate waterproof foil by any chemical composition.

2.3 *Activation of the backup grouting system*

The company CarboTech – Bohemia s.r.o. (now Minova Bohemia s.r.o.) was requested to prepare a technical proposal for the rehabilitation of individual types of defects with the aim to prevent penetration into the tunnel tube. For injection work both protection systems were used – injection hoses and local injection. Penetration on construction joints with inserted injection hoses was proposed to be stopped by



Figure 3. Metro IV.C1 – grouting in the double-track running tunnel.



Figure 4. The Mrázovka tunnel – testing of the passableness and continuity of the grouting system.

using CarboCryl T methacrylate gel, developed specially for this case. For stopping the penetration in the area of individual sectors it was proposed, due to the impossibility of precisely localising the defect in such large area, the complete filling by CarboCryl Hv, or CarboCryl Wv methacrylate gel. Prior to this step each section was "separated" by injection into joint strips. Injection work was performed by low-pressure injection with the use of a WIWA pneumatic pump followed by the Booster 10A pump which has a higher output. The consumption of injection material in individual sections was different depending on the scope and the manner of the defect of the intermediate insulation. On the basis of knowledge achieved during the activation of the protection system, on regular control days the further procedure was stated. Immediately after termination of injection, the filling hoses of the injection system were cleaned in order to endure their throughput for the next injection in the case of an occurrence of penetration.

Stronger local escapes in the top points of the arch were pre-sealed by high-pressure injection with Bevedan – Bevedol WF and Bevedan – Bevedol WFA polyurethane resin (currently the delivered modified CarboPur WF and CarboPur WFA types). The injection was performed through packets mounted into the holes in the concrete secondary lining. A DV 97 electric pump was used to do the work. Consumption in these cases did not exceed the volume of 10 litres per one sealing area.

In the Kobylisy station the situation was more complicated. After commissioning, the access to the face of the inside walling was disabled due to the additional mounted lower ceiling tiling from enamelled metal sheet. Therefore, it was decided to perform a whole surface injection of the station. Moreover, it is not possible to design the insulation of the arch as a sector due to technical reasons. Using the whole surface injection a similar effect was achieved with lower financial costs. Local penetration and leakages were removed and in fact, the waterproof insulation was doubled. The average consumption of the CarboCryl Hv injection gel during the whole surface injection did not exceed 5 litres/m^2 of the sealed area.

Costs for activation of the injection system did not exceed the values of similar constructions which were confirmed by expert opinions.

The injection work was performed by MATTEO s.r.o., and CarboTech – Bohemia s.r.o. delivered the injection materials and performed the technical consultancy, in particular during the preparation of the technical proposal for rehabilitation and during the commencement of the injection work.

After commissioning of a new underground section, one additional sealing of five newly created escapes was performed. In none of these places had any sealing injections been performed by that time. These additionally created defects were evidently caused by additional firming of the upper layers or an increase in the level of underground water. These latest activities were performed during night closures between 01:00 and 03:00 in the morning during the common operation of the Metro. During this time-restricted work the accessibility and functionality of the injection system was positively evaluated. When using another system than the used injection system, during the 45–60 minutes reserved for the injection, it would not be practical to perform the sealing within the necessary scope. Last but not least, the success of these actions was supported by the experience and the organisation of the work of the injection teams. Consumption of material during this action varied by only approximately 200 kg gel per penetration.

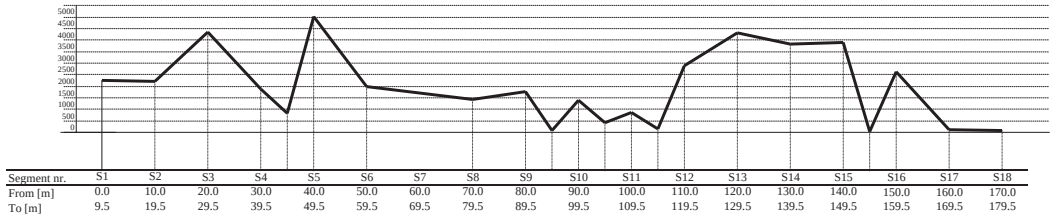


Diagram 1. Metro IV.C1 the Kobylisy station – the time story of the injection gel consumption (lt.).

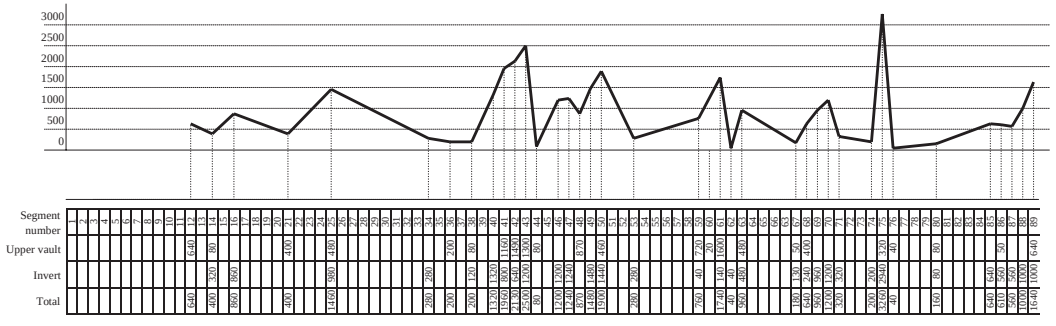


Diagram 2. The Mrázovka tunnel – the western tunnel tube – the time story of the injection gel consumption (lt.).

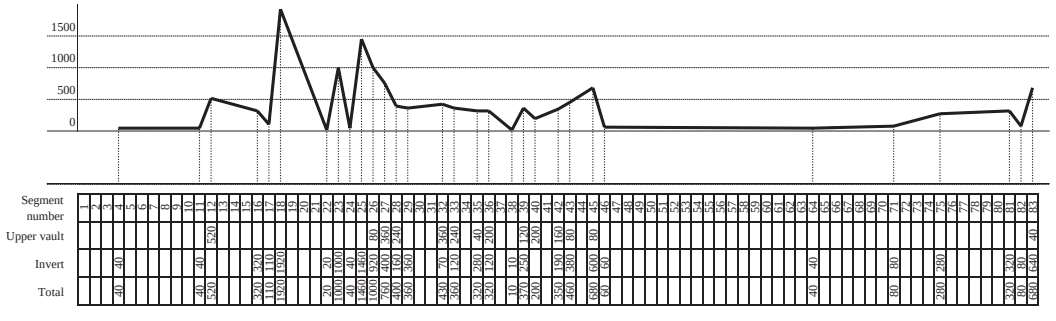


Diagram 3. The Mrázovka tunnel – the eastern tunnel tube – the time story of the injection gel consumption (lt.).

3 MRÁZOVKA

The second completed tunnel for which part of the waterproof system was the protection system of injection hoses was the Mrázovka road tunnel.

3.1 *Tunnel design*

The tunnel was excavated by the NRTM method in the rock environment of slate with the occurrence of quartz rock. In the case of the Mrázovka tunnel in the mentioned locality there are very complicated hydro-geologic conditions which led to a similar proposal of waterproof insulation as in the case of the Metro tunnel – whole surface closed foil insulation located between the primary and secondary lining. For the Mrázovka tunnel, a SARNAFIL MP 915-30 B2 polyethylene waterproof foil was used with a thickness of 3.2 mm with a signal layer. Geotextile NETEX 800 B2 was used as the protective layer. In the place of the working joints between the construction of a calotte, bridge deck and supports located in parallel to the longitudinal axis of the tunnel tube, the waterproof insulation is equipped with a reinforcing strip of insulation with a width of 500 mm. In the whole area of the lower arch is a waterproof layer which is protected against damage by N8-25 protective foil with a thickness of 2.5 mm. Welding of the foil was performed by semi-automated welding machines on the principle of hot drift, details were performed manually by hot-air electric welding devices.

The insulation system is based on the creation of individual cross-lateral sectors which are mutually separated by Fugenband AFI 600/35 MP joint strips located in the cross-lateral joints. In addition to the cross-lateral joints the same joint strips are used for horizontal construction joints between the lower and upper arch. In both cases the strips are welded on their perimeter to the insulation foil. This construction divides the whole tunnel tube into segments with average lengths of 7.5 m. The mutual connection of horizontal and vertical strips was performed by manual welding. As cross joints were not permitted, the lower strips are continuous and the cross-lateral strips are shifted at the upper and lower arch by approximately half of the segment.

The protection system consists of two separate circles. The first circle is represented by injection hoses located in the upper arch of the secondary lining. These are used for filling of the wall cavity and holes which may originate in the top part of the upper arch during the concreting of secondary lining. In these cases, cement plaster is used for injection.

The second circle of the protection system is used for additional sealing injection in the case of the occurrence of defects in the waterproof layer. The principle of the solution is similar to that used in the Metro IV.C1 tunnel. In segments specified by horizontal and vertical joint strips, injection and aerating hoses are spread out which are fixed to the insulation foil and directed to the central outlet in boxes. These are mounted at about 10 m in the support of the tunnel. In the place of the joint strips it is not necessary to mount injection hoses because the joint strips contain channels which fulfil the same function as the injection hoses. It was only necessary to perform the connection of the filling hoses to the channels and perform their termination in the boxes on the central outlet.

3.2 *Activation of the backup grouting system*

In the case of the activation of the protection system in the Mrázovka tunnel, the situation was significantly simplified by the acquired experience from the Metro IV.C1 tunnel. Due to the fact that the system for both tunnels was very similar, it was possible to perform the sealing injection in a similar manner with the use of the same substances – CarboCryl Hv and CarboCryl T methacrylate gels. This work was performed by MATTEO s.r.o. in cooperation with CarboTech - Bohemia s.r.o. as the supplier of injection substances.

Very small resistance of the protection injection system and channels in joint strips against outside pressure was a big problem. This caused blocking of the system during the filling injection by cement and low tightness and leakage during the activation of the protective injection system by gels.

Additional sealing of newly originated escapes ascertained during revision inspections after the commissioning of the tunnel was performed during three regular closures of the tunnel. This concerned very minor escapes or penetration into the collection boxes and in most cases it concerned areas in which the activation of the protection inspection system was not performed. Similarly as in the case of the metro tunnel there was effecting by underground water increased to the stable level.

4 CONCLUSION

It is possible to demonstrate with the examples of the prolongation of the Metro in section IV.C1 and the Mrázovka road tunnel that the completion of waterproof insulation systems of constructions by injection protection systems has its importance mainly for intermediate foil insulations performed along the whole perimeter of the underground structure (“submarine” type). It uniquely contributes to the achievement of the full functionality of the insulation which, due to the scope of the described structures, the complicated hydro-geological conditions and other limited requirements would mean in the case of a standard manner of performing injection work a significantly higher time and price demand. The important aspect for selection of the technical solution submitted by CarboTech – Bohemia s.r.o. was the fulfilment of the requirement to keep the throughput of the protection system after the performed injection. This requirement could be fulfilled due to the application of CarboCryl methycrylate gels and the experience of MATTEO s.r.o.

The main idea of the combination of waterproof insulation and a protection injection system is not only the simplification of the injection work in the time of the completion of the construction of the work and before commissioning. If such a solution is applied which keeps the functionality of the protection system in the future, it is possible to use this system at anytime. It is possible to rehabilitate leakages which can be reflected later and are adapted to the final completion of the work, change of outside conditions, etc.

This page intentionally left blank

Underground Space – the 4th Dimension of Metropolises – Barták, Hrdina, Romancov & Zlámal (eds)
© 2007 Taylor & Francis Group, London, ISBN 978-0-415-40807-3

Geomechanical studies for a road tunnel in volcanic formations

A.T. Menezes, F.M. Varela & L. Ribeiro e Sousa
University of Porto, Porto, Portugal

F. Moura
University of Minho, Guimarães, Portugal

ABSTRACT: The extremely mountainous and the heterogeneous volcanic rock formations of the Madeira Island led to the construction of an important road network where the tunnels are dominants, representing about 14% of the total network. In this paper the analysis of a road tunnel between Caniço and Camacha is presented, along with the description of the construction and of the geotechnical information. The evaluation of the geomechanical rock mass properties using empiric systems and 2D and 3D numerical analysis of sections of a tunnel are presented. Finally an empirical system that was developed for tunnels in volcanic rocks common at Madeira Island is also presented.

1 ROAD TUNNELS AT MADEIRA ISLAND

The road tunnels of new transport system of Madeira Island were strongly affected by the heterogeneous and complex volcanic formations, by the topography and by the land occupation. All these factors originate the design of a large spectrum of innovative structural solutions that permit to achieve economic solutions more adequate to the topographic and geological conditions.

The new road transport network, with high radii curves and more reduced longitudinal inclinations permitted easy and comfortable accesses to the whole island. The regional road system length is about 546 km, with about 78 km in tunnels. In the new highways the relation is about 43% in tunnels, in total of 173 km. More important works are still planned, mainly in the Northern part of the island, also with an important of these being tunnels (Moura and Sousa 2006).

The geology of Madeira Island comprise five volcanic complexes (Figure 1): $\beta 1$ – mio-pliocenic volcanic complex of Curral das Freiras, Serra de Água, Vale de São Vicente and Vale da Boaventura, in west part of the island and Ruivo e Areeiro mountains, São Roque, Porto da Cruz, Machico and Ponta de São Lourenço; $\beta 2$ – pos-miocenic volcanic complex at Ribeira da Janela, Porto Moniz, Ponta do Pargo, Ribeira Brava and Câmara de Lobos, in the west part, and Funchal, Camacha, Santa Cruz and Santana, including tuffs at Arco de São Jorge; $\beta 3$ – pos-miocenic volcanic complex of Paúl da Serra, Achada da Pinta and Lombada das Vacas, at west part, and Lombada do Meio, Cabeços de Fajã dos Vinháticos and Terreiro da Luta, in the east part of the island; $\beta 4$ – Superior basaltic complex of Paúl da Serra, Chão dos Balcões, Poiso and Achada do Teixeira; $\beta 5$ – Modern basaltic lava of Porto Moniz and the valleys of São Vicente and Seixal.

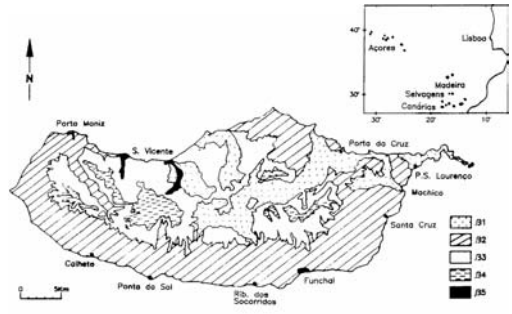


Figure 1. Identification of the geological-geotechnical formations at Madeira Island.

The transversal section of the road tunnels at Madeira Island Region have a horse-shoe (semi-circulat arch) cross section with a span of 9.0 m, for tunnels with one directional of traffic and 9.6 m for tunnels with two directions of traffic. Both types of tunnels consist of two lanes with a width of 3.5 m. In some older tunnels a semi-elliptic arch was adopted (João Gomes and Jardim Botânico tunnels). Some tunnels may have up to three (Pestana Júnior tunnel) or

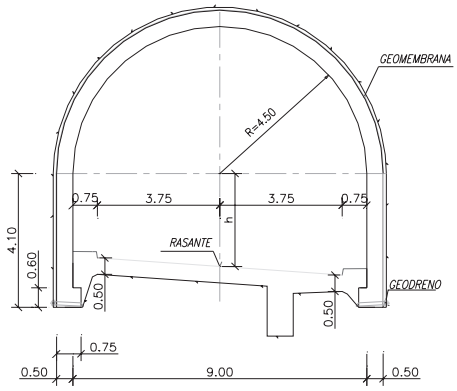


Figure 2. One traffic directional tunnel with two lanes.

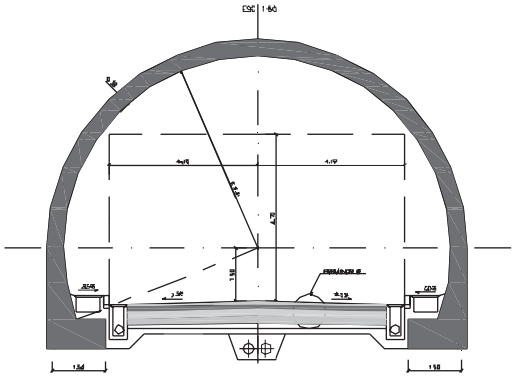


Figure 3. One traffic directional tunnel with two lanes.

four lanes (Santa Cruz West and East tunnels). Here the width is 18.5 m, in order to allow 2 lanes in each direction, separated by a central separator.

Figures 2 to 4 presents examples of geometric characteristics of road tunnels constructed at Madeira Island.

2 CANIÇO-CAMACHA TUNNELS

In order to establish a road liaison between Cancela and Nogueira located in the towns of Caniço and Camacha, respectively, important viaducts and tunnels were constructed in a mountainous region of Madeira in an extension of about 3.9 km. Of these an extension of 2.44 km (63% of the total) consisted of four tunnels. They have two directional of traffic with a lane in each direction (until km 0+725 including Tunnel 1) and with two lanes in the North direction (since km 0+725) for heavy traffic (trucks).

This paper is focus in Tunnel 2. Two sections are being considered, A (km 1+167) and B (km 1+256). Section A crosses a zone of disaggregated to moderate

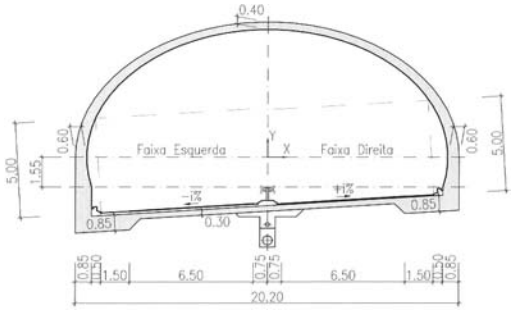


Figure 4. Two traffic directions tunnel with four lanes.

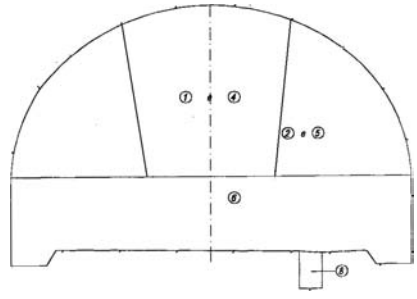


Figure 5. Construction sequence for section A.

compacted breccias. Section B corresponds to a zone of disaggregated and compact breccias, and compact basalts.

The design of supports adopted for the different types of rock formations were based on empirical methodologies (Viés 2001). In this tunnel supports used on both sections A and B were the following: bolts – length of 4 m, 20 mm in diameter and a capacity of 177 kN, 1.5 m spacing in the ceiling and 2.0 m in the walls for section A and 1.0 m for section B; shotcrete −10 cm in thickness for section A and 5 cm for section B; steel linings – only for section A, a profile HEB 160 spacing of 0.8 in upper part of the section. As usually done at Madeira Island a final concrete support was adopted with a thickness of 30 cm was adopted.

The construction process adopted is the Sequential Excavation Method (SEM). Due to the strong heterogeneity of the volcanic formations the construction was versatile in order to consider the adaptability to the different geotechnical conditions. Section A of Tunnel 2 has an overburden of about 3.9 m, composed by rock material of weak geomechanical quality. The construction sequence is illustrated in Figure 5. Section B has an overburden of 26 m composed of basalt of good geomechanical. The construction sequence is presented in Figure 6.

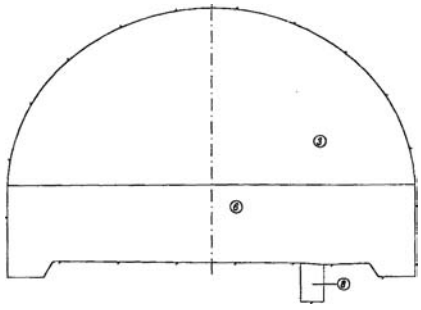


Figure 6. Construction sequence for section B.

Table 1. Results of uniaxial tests.

Samples		E	σ_c
Borehole	Depth(m)	(GPa)	(MPa)
S2	19.8–20.25	–	117.5
S5	8.55–8.85	–	1.55
S12	12.6–12.97	14.7	63.8
S13	31.4–31.7	–	316.0
S14	9.2–9.55	37.0	63.3
S38	20.3–20.95	–	2.2

3 EVALUATION OF THE GEOMECHANICAL PARAMETERS

Tunnel 2 is located in the volcanic complex β^2, that is composed by basalts and by piroclastic materials with variable dimensions like tuffs, breccias and scoria. The geotechnical survey of the tunnel consisted of boreholes and laboratory tests. The deformability and strength properties were estimated based on laboratory tests results. Table 1 shows some results of the Young modulus (E) and uniaxial strength (σ_c). The results from the survey show highly complex heterogeneous formations from complex β^2 with different types of formations apart the surface soil formations with about 3 m thickness:

Compact basalt – predominant lithology with a weathering degree between W3 to W1-2; RQD between 60–100; E = [17–46]GPa and σ_c = [35–100]MPa.

Volcanic breccias – with the basalts is also an important lithology with a matrix highly variable, being more or less compact. The weathering degree varies between W4 to W3; RQD is in average 50, being null in the disaggregated breccias; E = [0.1–33]GPa and σ_c = [1–35]MPa.

Volcanic tuffs – the less important lithology appearing in the upper part of the rock mass. The weathering degree varies between W4-5 to W3; RQD is in average 60, with a wide spectrum; E = [0.1–5]GPa and σ_c = [0.9–18]MPa.

Table 2. Geomechanical parameters.

Parameter	Disaggregated breccia	Moderate compact breccia	
Section A			
γ(kN/m^3)	25	25	
E (GPa)	1.5	3.6	
σ_c (MPa)	10.3	10.3	
m_b (HB crit.)	0.154	0.682	
s (HB crit.)	5.44×10^{-6}	0.0002	
Parameter	Disaggregated breccia	Compact breccia	Compact basalt
Section B			
γ(kN/m^3)	25	25	29
E (GPa)	1.6	5.6	19.5
σ_c (MPa)	10.3	10.3	170
m_b (HB crit.)	0.154	0.605	1.572
s (HB crit.)	5.44×10^{-6}	0.0002	0.0023

The geomechanical parameters were determined through the RMR empirical system. Relevant average geomechanical parameter values are presented in Table 2. Probabilistic approaches and a software developed for underground construction designated GEOPAT were used to obtain a probabilistic distribution and average values (Costa et al. 2002; Miranda et al. 2005).

4 STRUCTURAL BEHAVIOR OF CANIÇO-CAMACHA TUNNEL

The structural analysis of Tunnel 2 was performed using the software Phases2 from Rockscience for 2D analysis and FLAC 3D from Itasca, for the 3D analysis. The two referred sections A (portal section) and B.(inside the rock mass) were considered. The in situ state of stress adopted considered a ratio of 0.8 between in situ state horizontal and vertical. Section A analysis required a 3D model using 93527 nodal points and 2464 shell elements (Figures 7 and 8). For section A and using 2D approaches Figures 9 and 10 reveals the initial and final meshes.

The maximum settlement at the tunnel crown was about 5.8 mm and maximum convergences measured were equal to 10,0 mm. Settlements at surface were also evaluated in order to assess any possible damage on the buildings. The yielded zones were evaluated. They are mainly located at the disaggregated breccia that exhibited low strength.

Some results of the 2D analysis of section A are presented in Figures 11 and 12.

As a result two situations for the reinforcement of the crown tunnel were analyzed. One considered the

use of forepoling and other the use of bolts. The use of forepoling led clearly to the reducing of the yielded zones of the rock mass.

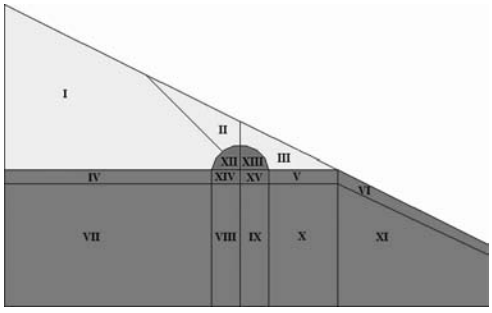


Figure 7. Detail of the 3D mesh near the tunnel.

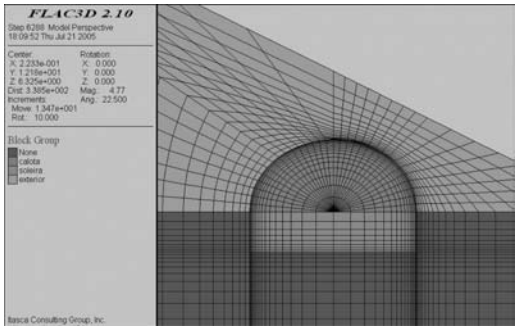


Figure 8. Detail of the 3D mesh near the tunnel.

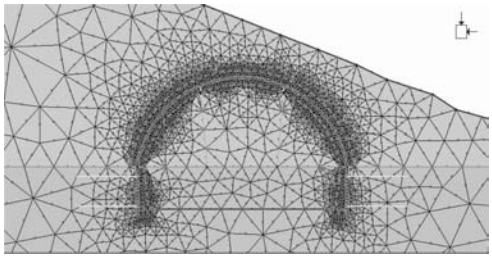


Figure 9. Initial 2D mesh for section A.

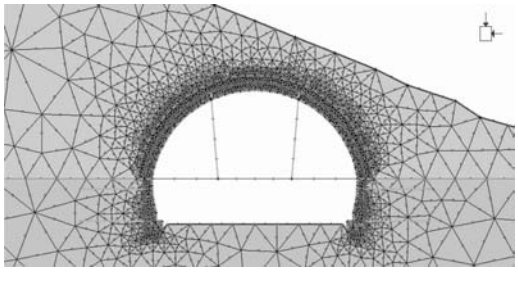


Figure 10. Final 2D mesh for section A.

In the portal 3D analysis were performed considering a 5 step excavation sequence following as proxy as possible the construction procedure. Table 3 indicates the geomechanical properties adopted at FLAC 3D.

Figures 13 to 15 present some obtained results at the last excavation stage. A comparison with 2D results shows that the displacements obtained with the 3D

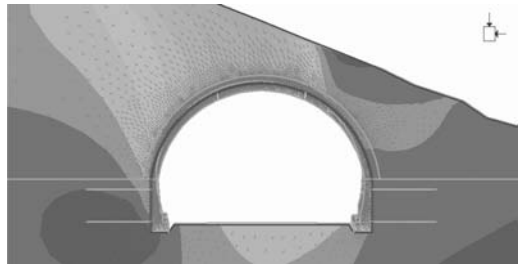


Figure 11. Displacements in the last stage.

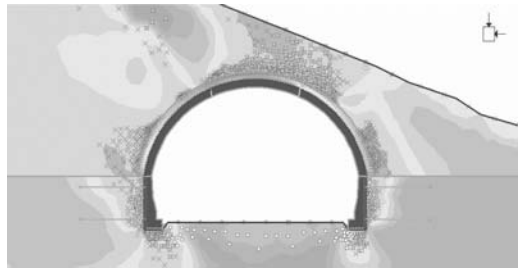


Figure 12. Yielded points at last stage.

Table 3. Geomechanical properties for FLAC 3D model.

Formation	K (Pa)	G (Pa)	c' (Pa)	ϕ (°)	σ_c (Pa)
Disaggregated breccia	1.03 E+09	6.15 E+08	9720	36.6	10.25 E+06
Median compact breccia	2.39 E+09	1.43 E+09	7880 0	36.8	10.25 E+06

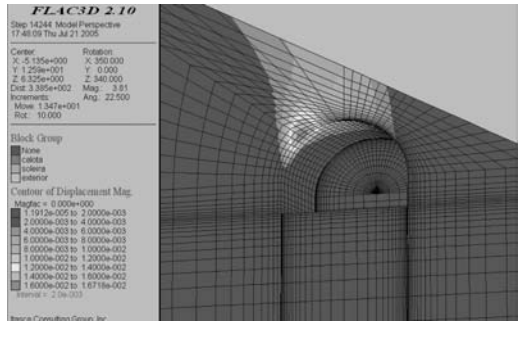


Figure 13. Vertical displacements in the last stage.

model were higher. The maximum displacement is in this case of about 1.7 cm, in the left side of the crown. The maximum stresses are registered in the vicinity of the excavation e mainly in the walls.

5 EMPRICAL SYSTEM FOR VOLCANIC ROCK FORMATIONS

An empiric system was developed specifically for volcanic rock formations. It was adapted by the RMR system and by a classification developed at IPT, São Paulo, for the design of several tunnels in basaltic formations (Ojima 1981).

The geomechanical characterization developed at Tunnel 2 revealed that the volcanic formations were mainly composed by breccias and basalts from the volcanic complex β^2 existing regions with a high level of weathering and crashed.

The following parameters were considered for this empirical system:

- Uniaxial compression strength
- Rock characteristics

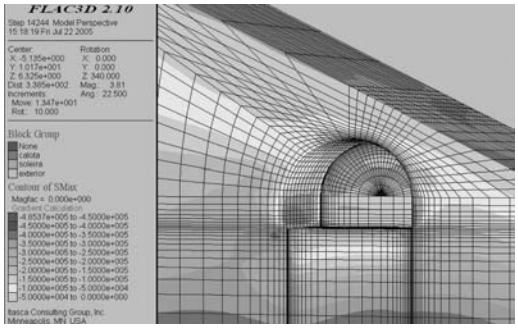


Figure 14. Principal stresses at final stage

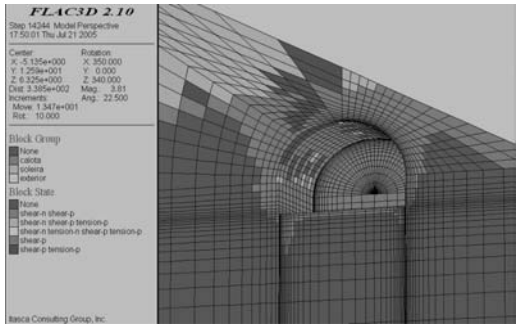


Figure 15. Yielded elements in the last stage

Table 4. Application of the proposed classification for volcanic rocks.

Parameters	Rock Mass classification and weights				
P_1	Uniaxial strength	R_1	R_2	R_3	R_4	R_5
		>120 MPa	60–120 MPa	30–60 MPa	15–30 MPa	<15 MPa
	Weight	15	9	6	3	1
P_2	Rock weathering	A_1		A_2		A_3
	Weight	20		12		4
P_3	Joint frequency	F_1	F_2	F_3	F_4	F_5
	Weight	25	20	15	10	5
P_4	Joint surface conditions	B_1	B_2	B_3	B_4	B_5
	Weight	30	25	17	10	0
P_5	Presence of water	C_1	C_2	C_3		C_4
	Weight	10	7	4		0
P_6	Block position	Very favorable	Reasonable	Acceptable		Not favorable
	Weight	0	−2	−5		−10

Classification of the rock mass

Final indexes	Rock mass class	Description of the class
100–91	I	Excellent
90–76	II	Good
75–61	III	Reasonable
60–41	IV	Regular
40–21	V	Poor
20–0	VI	Very poor

Table 5. Parameters for rock weathering.

Parameter	Description
A1	Sound or practically sound
A2	Median weathered
A3	Highly or very highly weathered

Table 6. Parameters for joint frequency.

Parameter	Description
F1	Joint spacing >1 m
F2	Joint spacing 0.25–1 m
F3	Joint spacing 0.1–0.25 m
F4	Joint spacing 0.06–0.1 m
F5	Joint spacing <0.06 m

Table 7. Parameters for joint surface conditions.

Parameter	Description
B1	Rough joints without continuity, closed and hard walls
B2	Slight rough joints with an aperture <1 mm and hard walls
B3	Slight rough joints with and aperture >1 mm and soft walls
B4	Joints with soft walls with filling material and aperture <5 mm
B5	Joints with filling material, continuous and aperture >5 mm

– Intensity of jointing
– Discontinuity conditions
– Presence of water
– Disposition of blocks.

In the proposed empirical system different weights were attributed for the different conditions of each parameter. Table 4 represents the used methodology and the classification proposed. The meaning of the different parameters is referred in Tables 5 to 8. The new system was applied to the several volcanic formations with the results shown at Table 9.

A rock mass formation designated by VI has a behavior conditioned by the rock characteristics in terms of deformability and strength; while a formation designated by class I behave in accordance with the characteristics of discontinuities. In relation to the remaining classes their behavior is determined by the conjugation of both types of characteristics.

Other parameters were not taken into consideration in the proposed classification as is the case of discontinuity orientation and the operational parameters. The evaluation of the discontinuity orientation is a complex process since the identification of discontinuity

Table 8. Parameters for presence of water.

Parameter	Description
C1	Dry
C2	Wet
C3	Dripping
C4	Flowing

Table 9. Application of the new empirical system to the different formations of Tunnel 2.

Formation	Weight		Classification	
	Min.	Max.	Min.	Max.
Disaggregated breccia	20	53	VI	IV
Median compact breccia	43	63	IV	III
Compact breccia	48	58	IV	IV
Compact basalt	62	93	III	I

sets in volcanic rocks is extremely difficult. The attitude of a discontinuity set is not only conditioning the block falls since to create instability it is necessary the occurrence of the discontinuity intersection. Thus it was judged more important to consider as a criterion the disposal of rock blocks.

This classification has the disadvantage of being basically based in the survey of the rock masses. Due to this fact certain parameters can not be evaluated directly. It is necessary, therefore, to perform visits to the works in order to have a detailed knowledge of the properties of the rock masses.

6 CONCLUSIONS

A reference is made for the important highway network at Madeira Island recently built. The percentage of tunnel length is perhaps unique.

A behavior analysis was performed of a road tunnel recently constructed in Madeira Island. It is part of the connection Caniço-Camacha and it was constructed in volcanic formations.

In this work special emphasis is made to an empirical system developed for volcanic formations. The system needs to be calibrated and correlated with other systems mainly developed for other formations. A study is initialized using Data Mining techniques or the so-called pattern recognition in order to the check the system and the parameters used for the evaluation, as well as the evaluation of deformability and strength parameters.

Finally the importance of the numerical studies is emphasized for two sections following 2D and 3D approaches. It was not possible to compare the obtained numerical results with the observed ones,

since only convergences were measured in a certain distance of the front of excavation.

ACKNOWLEDGEMENTS

The authors are greatly indebted to Road Regional Direction of the Autonomic Region of Madeira for authorizing the publication of this paper. They also wish to thank Mr Tiago Miranda from the University of Minho for his help in the 3D modeling.

REFERENCES

Costa, P.; Monteiro, A.; Oliveira, R.; Gaião, R.; Baião, C.; Sousa, L.R. 2002. Geotechnical analysis of the Caniçal tunnel, Madeira Island. *ISRM Symposium EUROCK 2002 on Rock Engineering for Mountainous Regions, Funchal, Ed. D. Gama and R. Sousa, pp. 579–588.*

Miranda, T.; Correia, A.; Sousa, L.R.; Lima, C. 2004. Numerical modeling of a large underground powerhouse using geomechanical parameters obtained by artificial intelligence techniques. *ISRM Int. Symposium on Contribution of Rock Mechanics to the New Century, Kyoto, Ed. Y. Ohnishi & K. Aoki, pp. 579–584.*

Moura, F., Sousa, L.R. 2006. The road tunnels in Madeira. Methodologies of construction and safety. *University of Minho, Individual Project, Guimaraes, 14p.*

Ojima, L.M. 1981. Methodology of rock mass classification applicable to tunnels (in Portuguese). *LNEC thesis, Lisbon.*

Viés 2001. Geological-geotechnical study – Road highway Caniço-Camacha (Madeira). *Viés, Consultoria, Estudos e Projectos de Engenharia, Lda.*

This page intentionally left blank

Underground Space – the 4th Dimension of Metropolises – Barták, Hrdina, Romancov & Zlámal (eds)
© 2007 Taylor & Francis Group, London, ISBN 978-0-415-40807-3

Large-scale model tests for the verification of Braced Rib Arch Method for shallow overburden tunnel

S.M. Na, S.H. Moon, S.P. Lee & S.H. Cho
Technical Division, GS E&C Corp., Seoul, Korea

S.D. Lee
Professor, Ajou University, Suwon, Korea

ABSTRACT: The large-scale model tests are conducted to verify BRAM (Braced Rib Arch Method). The BRAM is developed to excavate the shallow overburden tunnel. This method uses the rib arch structure that consists of H-beams and braced walls. The rib arch structure takes a role to distribute the load to the ground. To verify mechanical behavior of the proposed rib arch structure, the large-scale model tests were performed to reduce the scale effect. The large-scale model tests are carried out backfill process and tunnel excavation process. To simulate displacement of the ground with tunnel excavation process, the fulcrums are able to move downward manually. Some experimental results of the behavior of the rib arch structure and the backfill ground are introduced. The reaction force of fulcrums, grid reinforced effects, displacements of surface and in-ground and earth pressure are monitored to investigate the stability of the method. From the results, it can be concluded that the effect of the displacement with tunnel excavation is not serious to the stability of the rib arch structure. And verified using grid is an effective method to lesson the load when the ground has not sufficient bearing capacity.

1 INTRODUCTION

1.1 *BRAM*

In concept of NATM, tunnel stability is based on the ground arching effect. Shallow overburden tunnel is the weakest section of the tunnel construction because of the arching effect is hardly showed up in this section. Therefore several assistance methods are applied for the stability of the shallow overburden tunnel. These methods are generally expensive and take a long time.

So the BRAM is developed to excavate shallow overburden tunnel. This method is a kind of the arch slab method. Conventional arch slab methods have concrete arch slab. However it is not easy to make arch shape surface for pouring concrete. And concrete arch slab is a weak structure in vibration of blasting. So we replace the concrete arch slab with the rib arch structure that consist of H-beams and braced walls. This structure is not requiring arch shape surface and it is easy to assemble. Fig. 1 shows the rib arch structure.

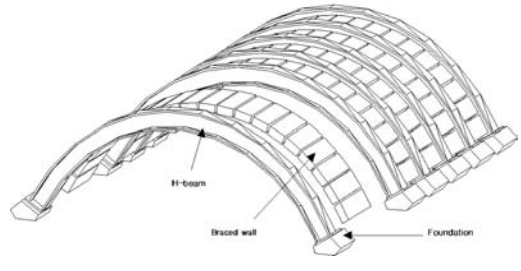


Figure 1. Diagram of the rib arch structure.

1.2 *Construction sequence of the BRAM*

The construction sequences of the suggested method are as follows:

(i) Excavating from surface to tunnel arch (Fig. 2(a)),
(ii) Installing the rib arch structure (Fig. 2(b)),

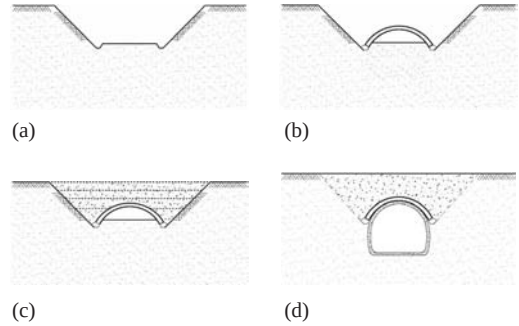


Figure 2. Construction sequences of the BRAM.

Table 1. The properties of the model ground.

Property	Value
Max. unit weight (kN/m^3)	16.86
Min. unit weight (kN/m^3)	13.82
Dryness unit weight (kN/m^3)	15.57
Relative density (%)	62
Specific gravity	2.63
Water content (%)	7∼7.59
Internal friction angle (°)	38
Cohesion (kN/m^2)	11

(iii) Backfilling with hardening (Fig. 2(c)),
(iv) Excavating tunnel section with conventional tunneling method, drilling and blasting or mechanical method (Fig. 2(d)).

The rib arch structure that is used in the suggested method consists of H-beams, braced walls and foundations (Fig. 2). The H-beams are installed at intervals of 1∼2 m longitudinally depend on the ground condition. The braced walls are installed between H-beams. The foundations take a role of load transfer to the ground. The type of foundation can be varied with ground.

2 LARGE-SCALE MODEL TESTS

2.1 *Preparing the tests*

Soil chamber, 4 m (width) × 3.3 m (height) × 3 m (length), is prepared for large-scale model tests. The front and rear walls are attached 10 mm steel plate with double anointment, bentonite and grease, for the minimum friction between soil and walls. The both slope sides are attached steel mesh to simulate real ground friction.

The model ground is tested particle distribution test, KS F2301, specific gravity test, KS F2343, and max./min. dryness unit weight test, KS F2345 for physical properties and direct shear test, KS F2348, for mechanical properties. The particle distribution of model ground is SP according to the unified soil classification system. The properties of model ground are summarized in Table 1.

For the rib arch structure, five H-beams, H-100×100×6×8, are prepare in bending. The wood is used as braced wall for convenience. Its size is 5 cm (width) × 3.5 cm (height) × 95 cm (length).

The fulcrums are hinge condition and horizontal and vertical forces are measured with load cells (Fig. 3).

2.2 *Measuring instruments*

Total five H-beams are used. To measure the stresses on the H-beams, 64 strain gages are used (Fig. 4). To measure the displacement of the H-beams and braced walls, 18 LVDTs are installed (Fig. 5).

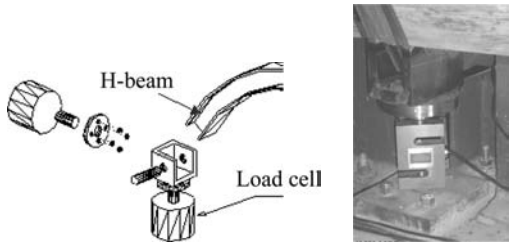


Figure 3. Diagram and picture of the fulcrum.

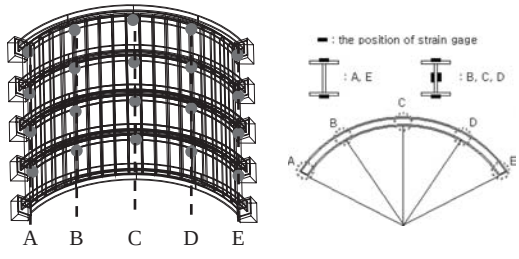


Figure 4. Diagram of the positions of strain gages.

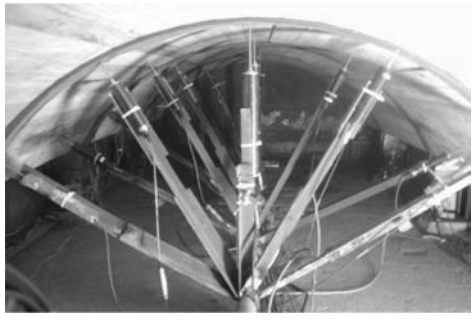


Figure 5. Picture of installed LVDTs.

To measure the reaction forces of fulcrums, 20 load cells are installed. Figure 3 shows vertical load cell.

To measure the ground pressure, the pressure meters are installed in ground. The whole measurements of surface and in-ground displacement and ground pressure are designed to get the 3-dimensional effects of the fulcrum subsidence. Figure 6 shows 3-D diagram of measurement points of the surface and in-ground displacement and ground pressure.

2.3 *Cases of the model tests*

The large-scale model tests have two main objects. First, verifying the ground load on the arch structure with backfill process. Second, investigating the amount of load transfer in neighboring fulcrum with tunnel excavation process. In the tests, two slope angles are used; the slope angel of 60° for general ground condition and 90° for special site condition such as

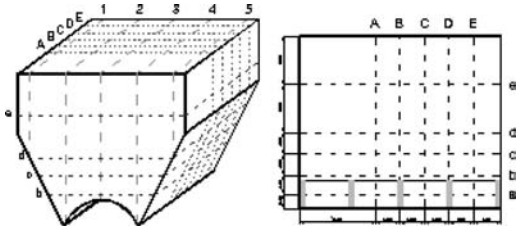
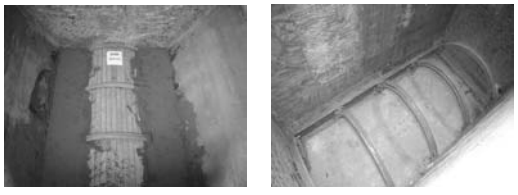


Figure 6. Diagram of the positions of LVDTs and pressure meters.



(a) 60° (b) 90°

Figure 7. Pictures of 60° and 90° slope angle cases.

existing adjacency building. Figure 7 shows the 60° and 90° slope angel models.

The tests have two sequences, backfill and fulcrum displacement process. Backfill process has several stages. To investigate the effect of the unequal backfill, left and right sides are backfilled take turns. Figure 8 shows the sequences of the backfill process up to the top of the rib arch structure.

The fulcrum displacement process is simulating the tunnel excavation process. The circumference ground moves with the tunnel face advancing. Therefore this is simulated fulcrum displacement in the large-scale model test. The third fulcrums of both sides are able to move vertical downward maximum 10 mm (Fig. 9).

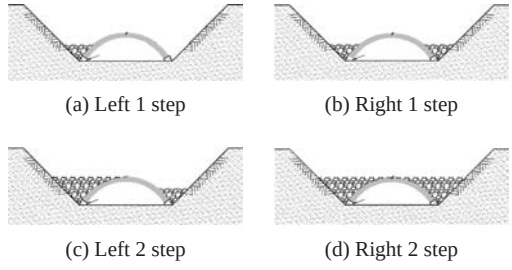
If the ground bearing capacity is low, there are necessary to reduce the load on the rib arch structure. Therefore the grid is tested to reduce that load. The total test cases are summarized in Table 2.

2.4 *Test results*

The large-scale model tests are carried out in two stages. In this paper, the results of the fulcrum displacement process are showed only.

2.4.1 *Reaction force*

The load on the rib arch structure is concentrate on the fulcrums. During the fulcrum displacement process, the loads on the third fulcrums are decreased. These loads transfer to the neighbor fulcrums or side slopes. Figure 10 shows the loads transfer to the neighbor fulcrums. The amount of the loads transfer is increasing according to the slope angle is steeper. However the absolute amount of that is not serious on the stability of the rib arch structure.



(a) Left 1 step (b) Right 1 step

(c) Left 2 step (d) Right 2 step

Figure 8. Backfilling sequences.

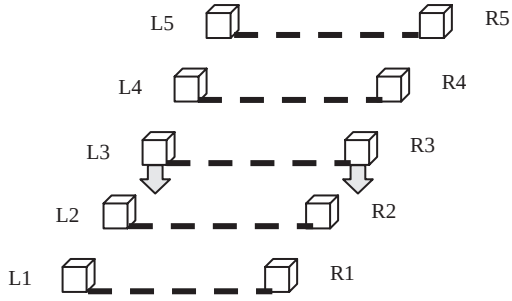


Figure 9. The displacement condition of fulcrums.

Table 2. The cases of the model test.

Case	Slope angle	Backfill height	Reinforcement
Case 1	60°	1.5D∗	No
Case 2	60°	0.5D	No
Case 3	60°	1.5D	Grid
Case 4	90°	1.5D	No

∗ Tunnel diameter.

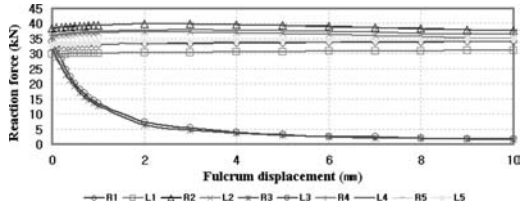


Figure 10. Graph of the load change with fulcrum displacement.

2.4.2 *Earth pressure*

The earth pressure is changed with fulcrum displacement process. Figure 11 shows vertical pressure in section B.

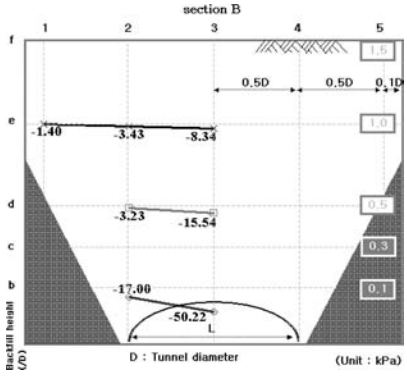


Figure 11. The variation of vertical earth pressure in section B.

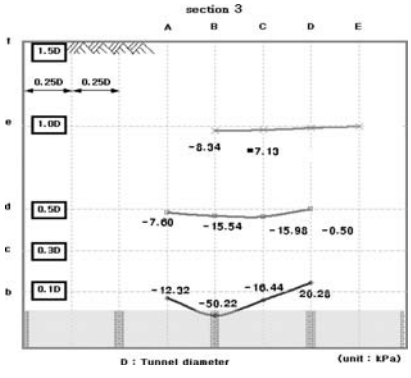


Figure 12. The variation of vertical earth pressure in section 3.

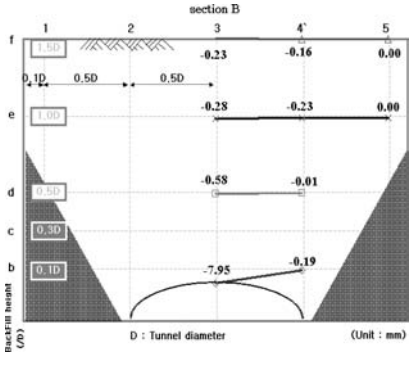


Figure 13. Surface and in-ground displacement at transversal section.

The variation of vertical earth pressure above the top arch is pretty much. And the absolute amount is decreased very rapidly with backfill height. The effect of fulcrum displacement on the earth pressure is decreasing with go away from the center. The variation

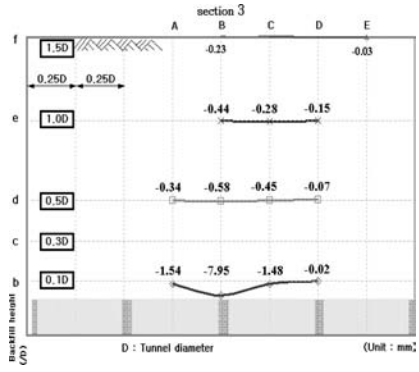


Figure 14. Surface and in-ground displacements at longitudinal section.

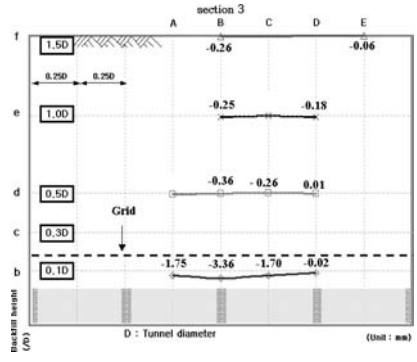


Figure 15. Surface and in-ground displacements at longitudinal section in Case 3.

of vertical earth pressure in longitudinal section is shown in figure 12. It can be seen that longitudinal arching effect is appeared with fulcrum displacement.

2.5 *Surface and in-ground displacement*

The maximum in-ground displacement is 7.95 mm at 3b (Fig. 13) above the top arch. However the in-ground displacement at Ab and Cb (Fig. 14) (in longitudinal section, the distance between 3b and Ab or Cb is 0.25D) is occurred only 20% compare with that of 3b. Also the in-ground displacement at 4b (Fig. 13) (in transversal section, the distance between 3b and 4b is 0.5D) is very small.

Therefore it is explained that the small form of soil above the top arch is subsided by the effect of fulcrum displacement. The surface settlement is started at 6mm fulcrum displacement. The maximum surface settlement is 0.23 mm at 3f (Fig. 13).

2.6 *Reinforcement effect of the grid*

The position of the grid is 0.2D from the top arch. In the reinforced case, the displacement at Bb is decreased

about 58% compare with the Case 1 (Fig. 15). The displacements at Bd and Be are also decreased about 40%. However it does not appear that reducing effect of the load on the fulcrum in backfill process with grid reinforcement.

3 CONCLUSION

The developed method, BRAM, is a kind of the arch slab method. It improves the construction efficiency and vibration resistance compare with conventional arch slab methods. It was carried out the large-scale model test because of it reduces the scale effect of the model test. And another object of this test is to find any problem to apply the BRAM to the construction site. Hence, we obtained some practical results to apply this method. The following conclusions can be drawn from this study.

- The load on specified fulcrum is transferring to the neighborhood fulcrums with displacement of that. However the amount of load transfer with fulcrum displacement is not serious effect to the stability of the rib arch structure.
- The arching effect of ground is appeared with fulcrum displacement. This phenomenon advantages to the stability of the rib arch structure.
- The grid reinforcement method is not effective to reduce the load on fulcrum in backfill process. However it is effective to reduce the in-ground displacement during the fulcrum displacement process.

REFERENCES

Na, S.M., Lee, S.J., Kim, S.H. & Lee, S.D. 2005. An experimental study on the half cut-and-cover method for shallow overburden tunnel, *Korea Tunneling Association 2005 symp., Seoul, 9 November*.

Sauer, G. 1992. The Schurzegerg tunnel, Oberrieden, *Proceedings of the 1st Int. symp. on tunnel construction and underground structures*, Chap. 2; 151–165.

This page intentionally left blank

Underground Space – the 4th Dimension of Metropolises – Barták, Hrdina, Romancov & Zlámal (eds)
© 2007 Taylor & Francis Group, London, ISBN 978-0-415-40807-3

An investigation into the effects of Shiraz metro tunnels on the stability of Ghadir bridge

I. Namazi, R. Rahmannejad & M.A. Ebrahimi Farsangi
Mining Engineering Department, Shahid Bahonar University of Kerman, Kerman, Iran

H. Jamshidi
Industrial advisor, Shiraz Metro, Shiraz, Iran

ABSTRACT: Tunneling in the shallow area, through the soft ground and under the water level is a difficult job. In such an environment, the associated effects of tunnel driving on the surface structures is one of the main concerns. Generally, the appropriate selection of tunneling method as well as the type of support prevent surface settlements and having less effect on the surface structures.

In the constructing plan of Shiraz metro, two parallel tunnels, in an alluvial, clay and siltstone environment with a diameter of 6.88 m and length of 14 Km are excavating. These two tunnels pass under heavy structures, such as Ghadir bridge for which EPB machines are being used. In this paper, by a three-dimensional analysis, using Plaxis 3D, the effects of excavating such tunnels on the stability of Ghadir bridge and the effects of the bridge piles on the pressure at the tunnel faces are investigated. Furthermore, a settlement profile prediction was carried out, considering the effects of piles.

1 INTRODUCTION

In the Shiraz metro, which is under construction, in some part twin tunnels with a diameter of 6.88 m, length of 14 Km and an axial distance of 10.88 m are driving. These tunnels are located at the depth of 16 m for which the water level is 5 m from the surface.

For tunneling in such a ground two EPB machines were designed by WirthNFM company. Supporting is being carried out using concrete segments with a thickness of 30 cm and external diameter of 6.6 m. The gap of 14 cm between the segments and the soil is filled by grouting.

These two tunnels are driving under heavy structures such as Ghadir bridge. The loads accounted in the numerical modeling including dead and traffic transfer through the side and middle pillars to the foundations with a length of 16.4 m, width of 6 m and a thickness of 1.5 m. The middle pillars have a pattern of two rows and 8 pillars in each row. The foundations are supported by 40 friction piles with a length of 24 m and a diameter of 1.2 m. As it can be seen in Figure 1, the twin tunnels are driven through the middle piles with a distance of 4 m and 3.4 m to the piles in the left and right sides respectively.

In the present paper, using Plaxis 3D software, the load-bearing of friction piles as well as the effects of tunnel driving on the load-bearing were studied.

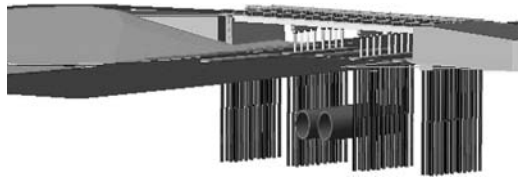


Figure 1. A schematic view of Ghadir bridge and associated twin tunnels (Bamrah, 2005).

Furthermore, the effects of loaded friction piles on the tunnel face pressure as well as possible settlement were investigated.

2 THREE-DIMENSIONAL MODELLING

In the three-dimensional modeling carried out, all process involved in mechanized excavation were considered. The model with a length of 80 m, a height of 40 m and width of 40 m including 26 segments were taken into account. Due to long distance between the side piles and the tunnels, the effects of such piles were ignored and only the middle piles were considered.

The amount of total loading, 300 tones on each pillar, was determined based on the bridge weight and

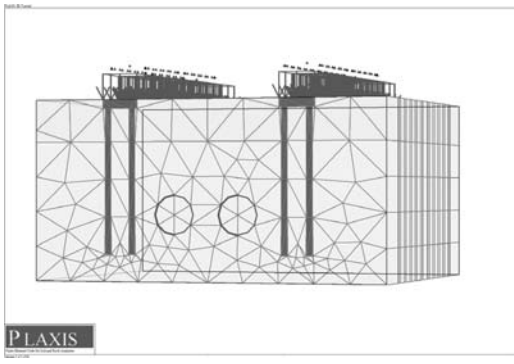


Figure 2. The three-dimensional numerical model of Ghadir bridge.

traffic loads, which is transferred to foundations in a distributed form (Figure 2) (Shiraz metro, 2002).

The Mohr-Columb and linear elastic models were considered for soil and piles respectively. The modeling of contact zone between the tunnels supports and soil, and also, piles and soil was carried out using contact interfaces. In this case, the amount of internal friction angle and cohesion are 0.6 of the nearby soil (Shiraz metro, 2002). Boundary conditions with fixed nodes were applied on the model.

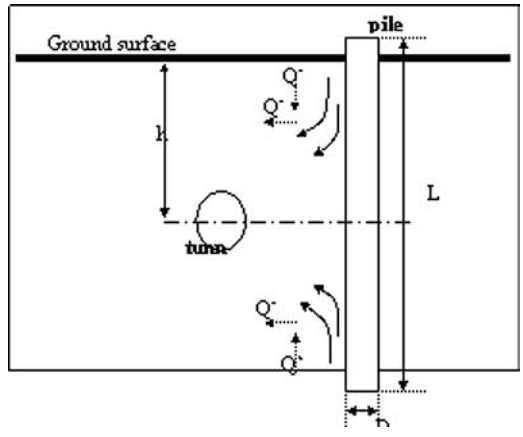
3 THE MECHANISM OF THE EFFECT OF TUNNELING ON THE LOAD-BEARING OF PILES

In practice, in construction engineering, if the hard rock formation is located in deep ground, the piles construction carries out without reaching hard rock. The stability of such piles can be achieved by the friction between the soil and pile. If the pile is constructed in the soil-claystone formation, load-bearing of such a pile extremely depends upon the cohesion between the pile and the clay. In the case of Ghadir bridge, having the top layers of clay and the hard rock formation is located in deep ground, the friction piles were used. In clays, the load-bearing of such piles can be determined using Equation 1 (Tahooni, 2001):

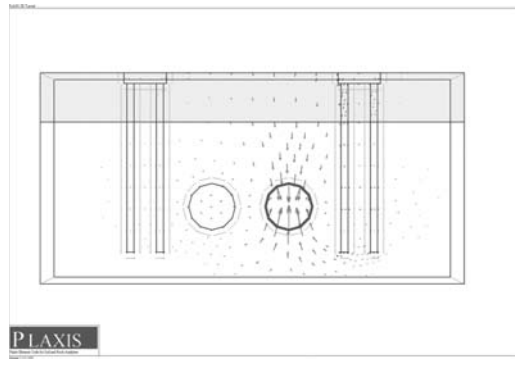
$$Q=Qp+Qs \quad (1)$$

Where Q = the permitted load-bearing of pile (N); Qp = the permitted load-bearing of the top part of pile (N); and Qs = the permitted load-bearing of the body of pile (N).

In the first step of modeling, prior to tunnel driving, the displacement of soil-mass due to the weight of the bridge as well as traffic loads was calculated. The results revealed that piles settled 20 mm, which is accounted as zero at the next step of modeling.



(a)



(b)

Figure 3. The mechanism of effects of tunnel excavation on a: the load-bearing of piles (Ghazavi, 2001); b: soil-mass displacement.

While the tunneling is carried out close to the piles, the soil near to the piles is dislocated causing changing in the load-bearing of piles, which depends on the soil type, the distance between piles and tunnel, the tunnel geometry, pile geometry and the amount of load on the pile (Ghazavi, 2001).

The soil displacement close to the piles has two horizontal and vertical components. Horizontal displacement around piles and toward tunnels causing weakness at the intersection between soil and piles, which results in reducing load-bearing capacity of friction piles. Furthermore, vertical movement of soil in the crown area of tunnel also decreases the load-bearing capacity (Q^-).

With an upward movement of soil, located below the horizontal symmetry axis of tunnel, the friction force at the intersection between soil and pile will be increased resulting in increasing load-bearing capacity of piles (Q^+) (Figure 3) (Ghazavi, 2001).

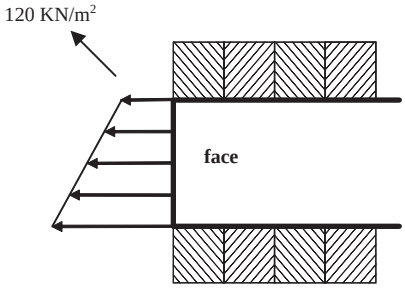


Figure 4. Applied pressure on the tunnel face (Namazi 2006).

4 EARTH PRESSURE BALANCE MODELING

Usually Earth Pressure Balance (EPB) TBM uses in the soft ground tunneling in the urban area to minimize the ground deformation during and post-tunneling. Also, in presence of water, it is used to prevent water flow toward tunnel.

The amount of real face pressure depends on: soil properties, water level, method of tunneling, tunnel geometry, overburden and surface loads (Broere 2001). Finding the optimum pressure at the tunnel face while using EPB machine was carried out by many researchers based on the mechanism of failure (Broere 2001). In these models, the effects of piles on the face pressure were not taken into account. In this research, such an effect is investigated using Plaxis 3D software.

In the first step, neglecting piles effects, using wedge method, the face pressure at the level of tunnel crown was calculated (120 KN/m^2) (Namazi 2006), which is increased with a gradient of 12 KN/m^2 downward from the tunnel crown. In the next step, using Plaxis 3D software, applying the above mentioned pressure, the operation of driving for a round and installation of supporting system was modeled.

But, by applying such a condition, while tunneling under the Ghadir bridge, the soil in the tunnel face centre was displaced 45 mm and failure occurred at the face. With a try and error base, the pressure at the face was increased, reaching to a pressure for which no failure at the tunnel occurred. The final amount of pressure obtained at the face on the crown part is 120 KN/m^2 with a gradient of 16 KN/m^2 downward (Figure 4).

5 THE EFFECTS OF PILES ON THE SUBSIDENCE PROFILE

Usually, prediction and control of subsidence due to underground excavation in the urban area is an active field of research (Peck 1969). In the excavation by

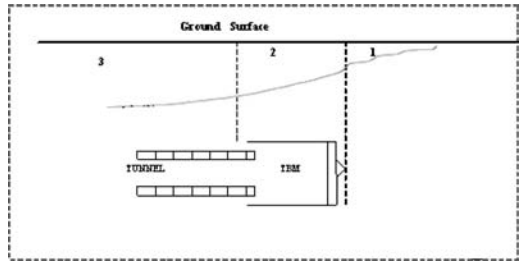


Figure 5. Different stages associated with subsidence due to EPB tunneling (Cording 1975).

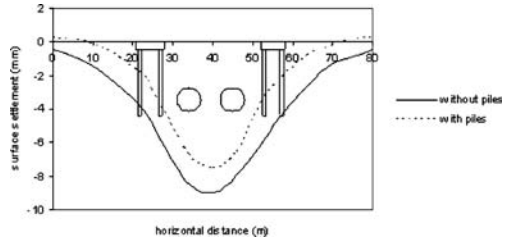


Figure 6. The profile of subsidence.

EPB machine, subsidence occurs in different stages as follows (Figure 5) (Cording et al 1975):

Stage 1: Front zone,
Stage 2: On the shield,
Stage 3: After excavation and grouting.

In stage 1, the amount of subsidence is depended upon the EPB pressure on the face-wall, which sometimes in the case of unbalancing reaches to 50 m front of machine (Mari et al 1997). While the pressure is balanced, the amount of subsidence goes to zero.

In stage 2, as shown in Figure 5 the shield is in contact with soil-mass for which a little amount of subsidence is observed.

In stage 3, due to gap between segments and soil-mass or grouting material, more subsidence is expected.

In the case of Ghadir project, also, the effects of existing friction piles on the subsidence is investigated for which two models were taken into account.

In the first model, it was assumed that there is no pile present. In the second model, the effects of piles were considered. In this case, the presence of axial force (weight) on the piles causing increasing in the stresses around the piles for which more stresses on the top and the base of piles were observed (Broere 2001). Since the tunnels are located in the lower part of piles, such stresses causing upward movement which in return results in less subsidence on the ground surface. Figure 6 shows the subsidence profile in two cases, without piles and with piles using numerical analysis.

Considering the effects of piles, the subsidence profile is squeezed causing reducing in maximum subsidence and the width of surface subsidence profile.

6 CONCLUSIONS

Studies reveal that the interaction between piles and tunnels is depended upon: the distance between piles and tunnel, geometry of piles and the amount of load on piles.

An investigation into the interaction of system of pile-soil-mass and tunnel showed that the presence of piles affects the face pressure during excavation, which results in increasing of this pressure. Also, it causes decreasing of maximum settlement and the width of settlement curve.

REFERENCES

Bamrah Co., 2005. Three-dimensional maps of Ghadir bridge. Technical report. Shiraz.

Broere, W. 2001. Tunnel face stability and new CPT applications. PhD thesis. Delft: Delft University press.

Cording, E.J. and Hansmire, W.H. 1975. Displacements around soft ground tunnels. The 5th panamericam conference on soil mechanics and foundation engineering. General report. session IV. Buenos Aires: 571–632.

Ghazavi, M. (2001). Influence of tunneling in soft soils on axial response of piles, the 5th Iranian tunneling conference: 1–2.

Mair R.J. and Taylor R.N. 1997. Bored tunneling in the urban environment. 14th international conference on soil mechanics and foundation engineering. Hamburge.

Namazi I. 2006. An investigation into the effects of Shiraz metro tunnels excavation on the stability of Ghadir bridge. MSc Thesis. Mining Engineering Department. Shahid Bahonar University of Kerman.

Peck, R.B. 1969. Deep excavations and tunneling in soft ground. The 7th ISSME Conference. Mexico.

Shiraz metro. 2002. Geotechnical engineering of Shiraz metro report. Shiraz.

Tahooni, Sh. 2001. Fundamental of geotechnical engineering. Vol. 2. Tehran: Pars Aien.

Underground Space – the 4th Dimension of Metropolises – Barták, Hrdina, Romancov & Zlámal (eds)
© 2007 Taylor & Francis Group, London, ISBN 978-0-415-40807-3

Extension of the Underground space Information Management System: Road tunnel maintenance

Y. Ohnishi & P.A. Bruines*
Kyoto University, Department of Urban and Environmental Engineering, Kyoto, Japan
**Currently: Obayashi Corporation, Tokyo, Japan*

T. Nakai & M. Ryu
Earthtech-Toyo, Kyoto, Japan

T. Katou
Ministry of Land, Infrastructure and Transport, Kinki Regional Development Bureau, Japan

K. Tsujimori
Road Management Technology Center, Kinki Branch, Japan

ABSTRACT: This paper presents the use of an Underground Space Information Management System (USIMS) for road tunnel maintenance. The USIMS is a three-dimensional representation of an underground structure and the surrounding rockmass, coupled to a database which holds all data gathered during planning, construction, inspections and repairs. Data can be accessed interactively and some of it directly visualized in the three-dimensional virtual underground structure. A number of applications are presented in this paper including a USIMS model developed for road tunnel maintenance. Instant access to all data, the ability to investigate three-dimensional relations as well as the ability to track development of specific locations over time are important advantages for optimizing planning, executing and controlling maintenance and inspections.

1 INTRODUCTION

Economic, political and societal changes in Japan have forced the construction industry to shift the focus from building new, to maintaining existing infrastructure. Good maintenance can extend the life of an engineering structure considerably. Overlooked defects can have devastating results. This is especially true for tunnels and other underground structures. However, to reach the goal of extending the life time of a tunnel while maintaining safety, a well carried out maintenance program needs to be implemented.

For this purpose we have developed new extensions to our Underground Space Information Management System or USIMS (Ohnishi et al., 2006; Bruines et al., 2006). USIMS is a system that can improve the way data is managed by providing a system that:

- Allows for examining 3-D relationships between data
- Stores data in a systematical way, and
- Is easily extendible to include additional data and data sets.

This is achieved by sorting data by location and making the data available in a 3-D virtual representation of the underground structures. The user can navigate through this virtual version of an underground structure and access all available data at each particular location. By using one data management system for all datasets, the user can access all data even after many years, which means that no datasets are lost or forgotten.

In the following chapter we will discuss the USIMS in more detail. We will tell why we have adopted the USIMS, explain the advantages and illustrate some of the concepts by presenting some of the previous USIMS models we have developed. In the next chapter the road maintenance USIMS is presented. We will conclude this paper with a discussion of the results and the next steps of our research.

2 THE UNDERGROUND SPACE INFORMATION MANAGEMENT SYSTEM

In this chapter we will first explain why we have developed an Underground Space Information Management

System. In the following section some of the advantages of the USIMS will be presented. The last section will present our previously developed USIMS models.

2.1 *Why an Underground Space Information Management System?*

Underground engineering structures need to be evaluated in the context of the geology surrounding the underground space. This geology is three-dimensional and by its nature largely unknown.

The geology is usually revealed only during construction. It is therefore important to collect geologic and construction related data and store it for future use. After the completion and commissioning of the underground space, inspections have to be carried out, and repairs made if defects are found. At each of these steps large amounts of data are gathered that have to be stored and retrieved at a later stage.

At first sight the data collected seems to be only relevant for its particular phase or for the first steps of the next phase. However, for a number of tasks a complete database can be of great help. Some examples are:

- Performance evaluations of different methods, materials and crews,
- Support for past and future decisions,
- Research of deterioration mechanisms, or
- For the purpose of asset management.

Nowadays most information can be made available in an electronic format. For instance, construction drawings are made using a Computer Aided Design program; during construction digital photographs will be taken of each excavation stage; inspection reports are written using a word-processing program; repairs might be documented using a spreadsheet program on a handheld device.

For regulatory, administrative or contractual reasons most of these data have to be stored. Very often this means that the data is printed out as a hard copy and archived as such. Although there are some efforts on the way to store information digitally, more often electronic data tends to disappear over time.

Data in general will be stored with different people and organizations, and datasets are organized by type of data. The construction drawings might be at the planning department of the general constructor, the rock mechanical analysis with an external consulting firm, the construction records with a subcontractor and inspection records with the regulatory agency.

The way in which the data is collected is usually different from one project to the other, even if the same file format is used.

With the USIMS we have developed we hope to address most of the before mentioned problems.

2.2 *Advantages of adopting a USIMS*

We are of the opinion that using a USIMS has a number of advantages. The USIMS is a three dimensional virtual representation of the underground structure that can be used both for navigation and display of information, where all data at a location is available by the click of the mouse, and data in the database is sorted by location. The USIMS is also a platform for storing data generated at every stage of the underground structure, from conception to decommissioning, preferably for the entire lifetime of the structure. It is readily extendable and very flexible with regards to the data types that can be included. Data is readily accessible, and the individual databases can be easily updated or imported, yet, if required, different levels of access can be created. Adopting a USIMS will standardize the data gathering effort. It can be extended with modules for analyzing data, exporting findings and generating checklists and forms.

The current version of the USIMS is developed using freely available software that allows the system to be accessible to everybody with a web browser, a VRML plug-in and standard office software.

2.3 *Examples of previous USIMS models*

The USIMS can be seen as being built up of three main components which will be discussed in the following sections. The components are:

- The three-dimensional virtual representation
- The data exploration
- The database

2.3.1 *Three-dimensional virtual representation*

The main feature that distinguishes the USIMS from a regular database system is the ability to explore data in a three-dimensional virtual representation.

Almost any level of detail can be included. In Figure 1 for instance all installed bolts have been included. For the walls a color code has been used to identify the different construction steps.

In Figure 2 additional ground class measurements are visualized. This approach allow for a very quick visual evaluation of the ground classes of a tunnel.

Photographic material can be incorporated into the model. It can be projected onto the wall or on a movable screen as shown in Figure 3. At regular intervals during the construction of the tunnel the excavation face has been photographed and described in detail. The image of the excavation face can be pushed backward or pulled forward. At each location the correct photograph is displayed. Comparing the excavation face at different stages in three-dimensions can yield additional information.

There is no limit to the amount of detail that can be incorporated. Photogrammetry data have been used to visualize details of 3-D rock surfaces. By taking

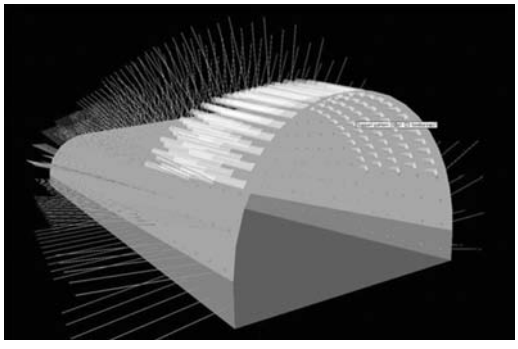


Figure 1. Three-dimensional virtual representation of the entrance section of a tunnel showing the different support patterns used. The tunnel is constructed in two steps by using a bench. The second excavation step is indicated by a different color.



Figure 2. Gradual coloring is used to visualize a dataset of ground class measurements. The view is into the tunnel with generally higher quality rockmass values towards the deeper end of the tunnel.

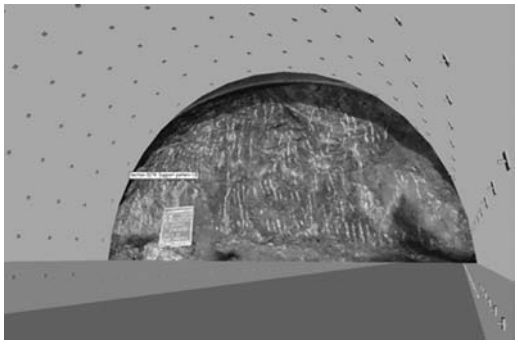


Figure 3. The three-dimensional model of a tunnel located in Kyoto prefecture, Japan. Digital photographs of the excavation face at each stage are included.

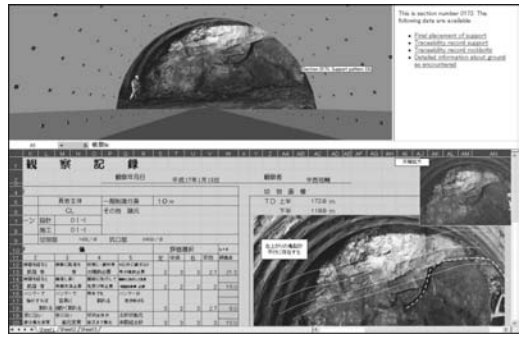


Figure 4. By incorporating the virtual representation in a set of frames additional data can be accessed. Concise data of each tunnel section is available using the mouse over event. A mouse click event will open links to all data available at the particular location in the upper right frame. When a link is clicked the data opens in the lower frame. In this case the detailed engineering geological description is displayed.

photographs from different perspectives of the same surface, the three-dimensional coordinates can be reconstructed. The photographs can than be projected on the three-dimensional frame work. In a tunnel environment this could be used for key block analysis.

2.3.2 *Data exploration*

The different locations in the model can include links to the data. To enhance the navigation of the data, the 3-D model is integrated in a set of frames. A summary of the data can be included in a small pop-up that moves with the mouse. When clicking the mouse, a file is opened in an adjacent frame that shows links to all available information at that particular location. Activating one of these links will open the detailed data in a separate frame. This could be a detailed investigation of the excavation face at that location (Fig. 4) or data of the location, time of installation and description of materials used (Fig. 5).

2.3.3 *Database management*

To generate the three-dimensional model, and all the links, a small program has been made using a scripting language that goes through all the directories and files in the database and automatically generates the entire USIMS. This does mean that the database needs to be structured. However once the computer program has been made and the user strictly respects the database structure, the USIMS can be updated on-the-fly when new data becomes available.

It will be beneficial in the long run to invest time to agree on a good database structure, because the data of an underground construction project in a USIMS should be preferably stored and updated until decommissioning.

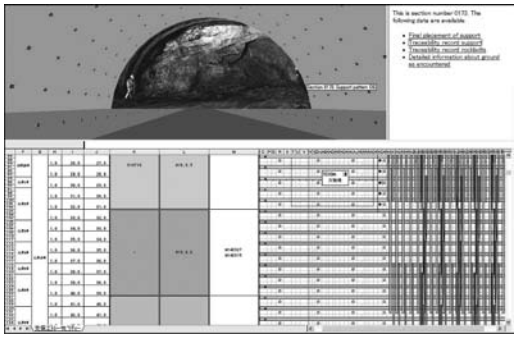


Figure 5. In this data frame the traceability record of installed support is opened. It shows the exact location of each rockbolt, the date of installation as well as a reference to the batch of materials used.

3 ROAD TUNNEL MAINTENANCE INFORMATION MANAGEMENT SYSTEM

If during an inspection a problem is encountered it will be at a location within a tunnel. For the analysis of the observed defect the inspector is not interested in the entire inspection report of last year, but only in the information from last year's inspection at that particular location. However, it would be more helpful if all relevant data of that location would be available: all the previous inspection findings at that particular location as well as a complete repair history. If the inspection and repair data indicates that deterioration is particularly fast additional data would be useful to perform a more detailed analysis. "What was the ground-class classification?"; "Was there excessive groundwater inflow recorded?"; "Has the correct support been installed?" are just a few of the questions that might come up. If a likely scenario for accelerated deterioration is formulated, locations with similar conditions could be identified by the Information Management System for more detailed inspection or for preventive maintenance measures.

In the next part we would like to show the development of a USIMS for an actual tunnel located in Kinki district.

The data available are:

- location maps, construction drawings and other general information about the tunnel,
- sketches of the tunnel lining from inspection,
- database with a detailed description of each observed defect, and
- photographs of defects.

All available information has been incorporated into the USIMS. A three-dimensional representation of the tunnel has been modeled. Since the entire lining of the tunnel has been mapped, the sketches with the observed defects are projected on the walls and floor of the tunnel. Clicking on each of the sections opens links to all available data of that section. This additional data can than be investigated by a click of the mouse.

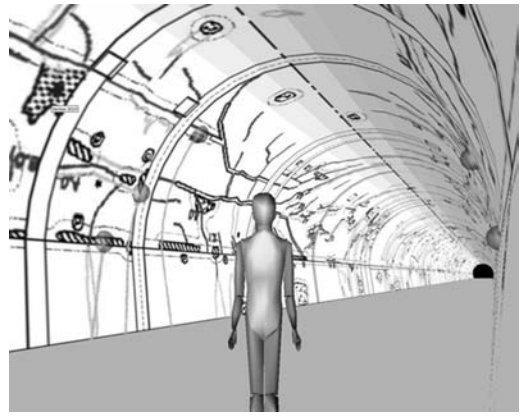


Figure 6. Sketches made during an inspection are projected on the walls. Blue spheres link to additional information about individual trouble spots.

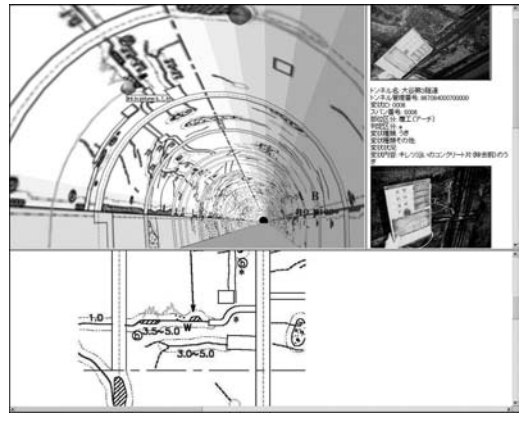


Figure 7. Clicking on the wall or one of the blue spheres opens a frame with a short summary of available data on the right. Photos, sketches and data can be closer examined in the data frame on the bottom.

Apart from the tunnel section, detailed descriptions of each of the observed defects are available. They are marked in the three-dimensional representation with a blue sphere so that the information is available from the inside and from outside the tunnel. Clicking the sphere will open a small picture together with a description of the defect. The small picture can be clicked to investigate the problem area in detail. The generation of the HTML code necessary to visualize all the data is automatically extracted from the database using a scripting language.

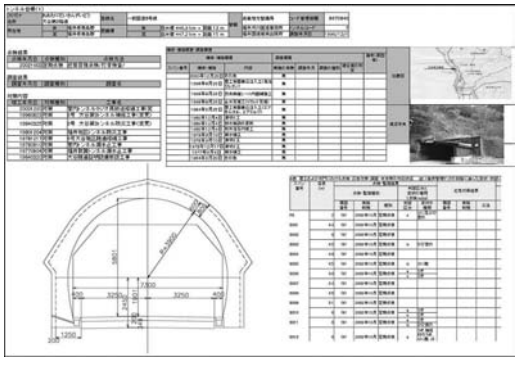


Figure 8. A small selection of non-location specific data available in the USIMS.

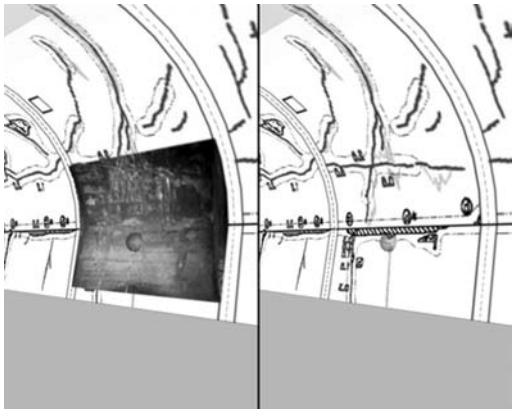


Figure 9. The user can switch between different projections at any time. In this case a projection of the sketches only or of a projection with integrated photographic information.

Data that is not directly related to a particular location can be accessed at anytime. A navigation menu will be available at all times in the lower right corner of the USIMS. The navigation menu links to files on the construction history, the technical details, the location, a cross-section of the tunnel as well as information on the history and the costs of inspection and maintenance.

The pictures taken of the defects have been added as an overlay to the sketches. The user can switch between the sketches with and without pictures at any moment using the navigation menu.

A few other applications which fit in the frame work of inspection and maintenance have been developed. Especially in the early stages after construction of the tunnel the geology has to readjust which can lead to convergence. Although a slight movement can help to stabilize the tunnel, excessive movements can lead to disaster. It is for that reason movements of control



Figure 10. Reflective targets in a tunnel. Reflective targets are ideal reference points to be used for three-dimensional photogrammetric measurements.

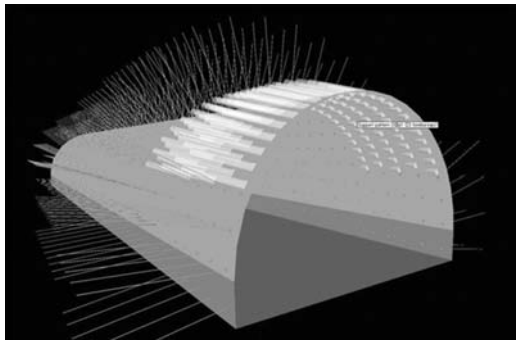


Figure 11. Visualization of the displacements from photogrammetric measurements.

points have to be measured. Nakai et al., (2002) have developed a new method that can calculate these movements using digital photography. When many photographs are taken of the same object from different angles the 3-D position of this object can be determined. The methodology developed is unique because it doesn't have any constraints on the location and direction of photographs taken. It gives the photographer the maximum freedom to take pictures. This means that pictures can be taken faster, outside of dangerous areas and of unreachable locations. Figure 10 shows a picture of the inside of tunnel where reflective targets are used.

By comparing the 3-D measurements over time the movements can be determined. The precision of the method used is less than 1.0mm. The USIMS is an ideal platform to visualize these results.

Further development of this method is ongoing, which might lead to other applications that can be incorporated in the USIMS, such as for instance 3-D analysis of excavation faces for real time key block analysis.

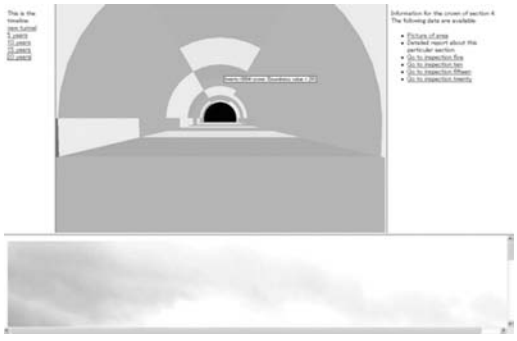


Figure 12. In this example for maintenance purposes an additional timeline frame is included that lets the user investigate the condition of the tunnel at different times. This shows the same three-dimensional model after 20 years. Different colors indicate that certain parts of the tunnel have deteriorated. Different colors relate to suggested actions to be taken such as e.g. “special attention during next inspection”, “preventive maintenance suggested”, “immediate repair required”.

In another application a visualization of the results from deterioration analysis has been developed. Using a questionnaire a soundness rating can be assigned to different sections of a tunnel . The analysis is performed at different times and using a deterioration model, predictions for the future are made. Figure 12 shows a USIMS that includes an additional frame for the time line, which lets the user jump between the different soundness values over time. It shows the soundness value of the tunnel lining as determined after 20 years of operation. Different colors correspond to different suggested responses.

4 DISCUSSION

The models presented in this paper have to be regarded as preliminary explorations of the possibilities of what could offer a fully developed USIMS. The USIMS models that have been developed nevertheless are fully functional.

We have not yet encountered data that can not incorporated. The size of the database has proven to be not a big issue. As long as some care is taken to the design of the database, building the USIMS can be easily automated.

The system is very flexible as to what can be displayed. Three-dimensional shapes, textures, colors indicating values, pictures of the geology during excavation, pictures of observed defects, location of boreholes, borehole scan pictures, three-dimensional rock surfaces for the interpretation of discontinuities are just some of the features that have already been implemented.

A number of ideas are currently being worked out. These include the development of an inspection system. Before the inspector goes to a tunnel for an inspection a questionnaire is generated. This module is downloaded to a tablet computer or handheld device. In the tunnel the inspector is guided by the questionnaire that has been generated from the previous inspection results. His questionnaire would attend the inspector to recent repairs, or to locations that during a previous inspection was a border case. If the inspector has identified a certain problem the questionnaire opens a special set of detailed questions that are relevant for this type of problems. When the inspector comes back from the inspection the results are uploaded to the USIMS that automatically updates the database, perform a number of analyses and updates the three-dimensional model.

Another idea is to incorporate modules into the USIMS to make it an asset management tool. Some research has already been carried out to come up with the best strategies for scheduling inspections and maintenance. A full-fledged USIMS with a complete set of data would have the possibility to do many more analyses. It could be a tool to compare the efficiency of different contractors, materials, construction methods or maintenance schedules.

REFERENCES

Ohnishi, Y., Bruines, P., Hanaoka, S. & Kimura, K. 2006. Development of an Underground Space Information Management System. In Proceedings of the 11th Underground Space Symposium of the Japan Society of Civil Engineers, Tokyo, Japan.

Bruines, P., Ohnishi, Y. and Nakai, T. 2006. Extension of the Underground Space Information Management System: maintenance and 3-D structures. In The proceedings of the 35th Rock Mechanics Symposium of the Japan Society of Civil Engineers, Tokyo, Japan.

Nakai, T., Ohnishi, Y., Ohtsu, H., Nishiyama, S., Ryu, M. 2002. Monitoring and Analysis of Tunnel in Discontinuous rock Masses by using Digital Photogrammetry and Key Block Theory at Houou Tunnel, In The proceedings of the EIT-Kyoto University-AIT Joint Work-shop on Development of Rock Mechanics and Engineering, Bangkok, Thailand.

Underground Space – the 4th Dimension of Metropolises – Barták, Hrdina, Romancov & Zlámal (eds)
© 2007 Taylor & Francis Group, London, ISBN 978-0-415-40807-3

Performance of pile due to tunneling-induced soil movements

C.W. Ong, C.F. Leung, K.Y. Yong & Y.K. Chow
Centre for Soft Ground Engineering, Department of Civil Engineering, National University of Singapore

ABSTRACT: Tunneling would inevitably induce vertical and lateral soil movements on piles supporting adjacent buildings. In the present study, centrifuge model tests were conducted to evaluate the free-field soil movements due to tunneling and the effects of soil movements on a free-head single pile located nearby. Three-dimensional finite element analysis was also performed to back-analyze the centrifuge test data. The measured and predicted pile responses due to tunneling show fair agreement in both short-term (immediately after tunnel excavation) and long-term.

1 INTRODUCTION

In many large heavily populated cities, tunnel excavations very close to adjacent buildings. In view of this, an assessment on the performance of piles due to tunneling is important to ensure that the structural integrity of the piles can be maintained. In the present study, centrifuge model studies were carried out at the National University of Singapore (NUS) to examine the pile behavior due to tunneling-induced soil movement.

As tunnelling is an unloading process, it will cause stress relief and redistribution in the ground and induce soil movement. In such scenario, piles will be subjected to simultaneous vertical and lateral soil movements. Different modes of tunnelling deformations in centrifuge were evaluated by a good number of early researchers (Feng, 2003; Ghahremannejad et al. 2006; Grant and Taylor, 2000; Jacobsz et al. 2005; Lee et al.2006; Loganathan et al. 2000; Ran, 2004; Sharma et al. 2001).

In the present study, inward tunnel deformation at the tunnel springline is simulated using both centrifuge and finite element models. Free-field soil movements and tunneling-induced pile lateral and axial responses in both short-term (immediately after tunnel excavation) and long-term are evaluated. The study is limited to a single free head pile only.

2 CENTRIFUGE MODEL SETUP

Two centrifuge tests were conducted at an acceleration field of 100 g on the NUS centrifuge. Unless otherwise stated, the test configuration and results are presented in this paper. The first test was conducted without the presence of pile to solely study the free-field soil movements due to tunneling. During this test, high resolution photographs were taken at regular intervals and the soil displacement trajectory was derived using particle image velocimetry (White et al. (2003), an advanced image processing technique. The second test was conducted to study the tunneling-induced responses of a pile located at 6 m away from the tunnel axis. Figure 1 shows a photograph of the centrifuge model setup in the present study.

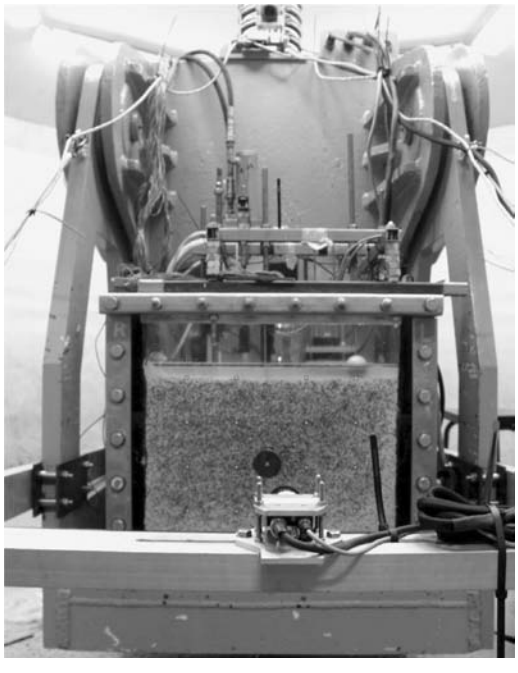


Figure 1. Centrifuge model setup.

Table 1. Test parameters (prototype scale).

Parameter	Value
Volume loss	6.6%
Tunnel diameter (D)	6 m
Tunnel depth (Z)	15 m
Tunnel cover (C)	12 m
Pile cross-section	1.26 m × 1.26 m
Pile length	23.5 m
Pile bending rigidity	3.97×10^6 kNm^2
Pile axial rigidity	3.64×10^7 kN
Pile distance from tunnel axis	6 m

The strong box soil container used is made of stainless steel alloy and has internal model dimensions of 525 mm × 200 mm × 490 mm (length × width × height). One sidewall of the container is made of transparent Perspex plate and all sides of the container were heavily greased to minimize the soil/container side friction.

In both tests, the elevation of the crown of the 6 m diameter tunnel was at 12 m beneath the ground surface. In the second test, a long free head single pile with its tip beneath the tunnel was investigated. In this test, two instrumented piles (one for measuring axial pile responses and the other for lateral responses) were placed at equidistance from the tunnel. The test parameters are given in table 1.

The model piles were fabricated using square aluminium tubes. Ten pairs of strain gauges were attached along the pile shafts to measure the bending moment along one pile (termed 'bending' pile) and axial forces along the other pile (termed 'axial pile'), as shown in Figure 2. The strain gauges were protected by a thin layer of epoxy resin for waterproofing. The 'bending' and 'axial' piles were connected to the strain meter (placed on the centrifuge arm) with half-bridge mode and full-bridge mode, respectively. The prototype pile configurations are also listed in table 1.

Figure 3(a) shows the cross-section of the model tunnel. The tunnel was made of stainless steel of 6 m diameter. A technique has been developed to simulate the inward tunnel deformation at the tunnel springline by dissolving the over-shaped high density polystyrene foam placed outside a model tunnel lining using an organic solvent, acetone, while the centrifuge was in-flight at 100 g. A discharge outlet has been made to allow the drainage of acetone into the tunnel cavity. This technique was initiated by Sharma et al. (2001). In this paper, the gap parameter GAP as proposed by Lee et al. (1992) has been adopted to quantify the degree of over-cut of tunnel. The simulated tunnel opening for this model has a GAP of 200 mm in prototype scale with an equivalent imposed volume loss of 6.6%.

The model ground was prepared from slurry of kaolin clay at a water content of 120% preconsolidated under a pressure of 20 kPa before accelerated to

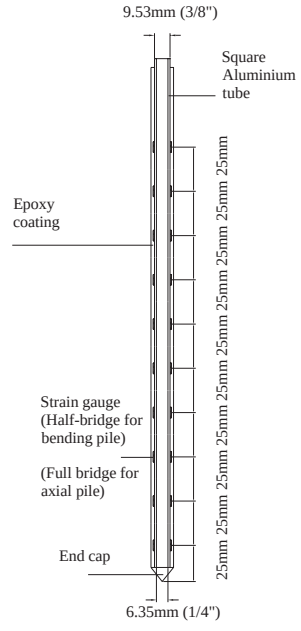


Figure 2. Instrumented model pile.

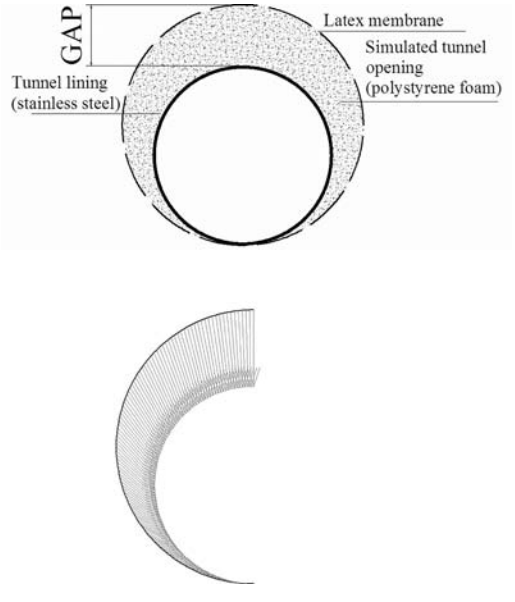


Figure 3. (a) Cross-section of model tunnel in centrifuge. (b) Simulation of tunnel over-cut in numerical analysis.

100 g. After the ground settlement and pore water pressure readings stabilized, the centrifuge was stopped and the front and back walls of the container was removed to install the model tunnel, transducers and to place marker beads onto the soil behind the perspex front wall.

The model piles were then installed and two non-contact laser displacement transducers were used to measure the lateral deflection and rotation of the pile head. The pile settlement was measured by one transducer resting on the pile head. The model setup was then subject to reconsolidation at 100 g until the pore water pressure reached a steady state. The test began by draining Acetone to dissolve the high density polystyrene foam. All instruments were monitored regularly throughout the test. In order to study the post-excavation effects, the centrifuge would be kept at 100 g for 2.3 years (i.e. 2 hours in model scale) after the completion of tunnel excavation.

3 NUMERICAL ANALYSIS

The 3-dimensional numerical back analysis was performed using the PLAXIS 3D Tunnel program (version 2). Similar to the centrifuge model tests, the tunnel excavation was simulated under plane strain condition. The Hardening Soil model, which is a general second-order and an elasto-plastic type hyperbolic model, was adopted for the clay. In contrast to an elastic perfectly-plastic soil model, the yield surface of a hardening plasticity model is not fixed in the principal stress space and can expand due to plastic straining.

Due to symmetry, only one-half of the centrifuge setup was modeled. Simulation of tunnel over-cut in numerical analysis is shown in Figure 3(b). The finite element mesh shown in Figure 4 has an overall dimension similar to the centrifuge container size, i.e. width = 26 m, depth = 28 m and width = 20 m. It is assumed that no horizontal or vertical displacement takes places at the bottom boundary as it is beyond the influence of tunnel excavation. The mesh sides were restrained from moving laterally but free to settle. The right-hand boundary was the line of symmetry. The ground water level was at the ground surface.

The same geometry and pile parameters given in table 1 were adopted in the numerical simulation. The model tunnel lining was modeled such that it was rigid having nil deformation. The soil parameters are given in table 2.

Undrained analysis was performed to evaluate the short-term pile behavior whereas drained analysis was conducted to examine the pile responses at 720 days after tunnel excavation.

4 TUNNELING-INDUCED SOIL MOVEMENT

In the present study, a centrifuge model test has been conducted without the presence of pile to study the green-field soil movements due to tunneling. The measured soil movements are computed by comparing the bead locations from high resolution photographs

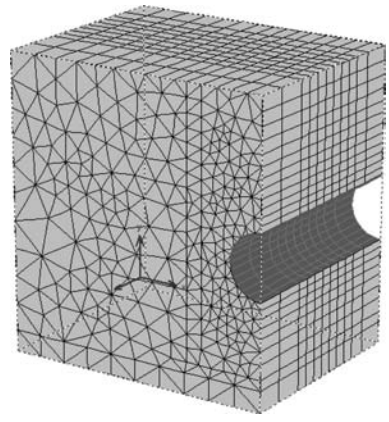


Figure 4. Finite element mesh.

Table 2. Soil properties (After Goh, 2003).

Parameter	Value
Saturated unit weight, γ_w	16.39 kN/m^3
Permeability k_x	2.0×10^{-8} m/s
Permeability, k_y	6.0×10^{-8} m/s
Angle of friction, Φ	23°
Angle of dilation, Ψ	0°
Cohesion, c	0.001
E_{oed}^{ref}	1520 kPa
E_{ur}^{ref}	8500 kPa
E_{50}^{ref}	1900 kPa

before and after tunnel excavation using particle image velocimetry (PIV) (White et al. 2003).

It is observed that the soil movement wedge above the tunnel crown behaves as an active zone and it moves towards the tunnel lining to fill the gap above the tunnel crown created by tunneling. The soil beyond the wedge acts like a passive zone, with the soil in the wedge gradually deforms by arching.

Figure 5 shows the comparison of the tunneling induced surface settlement troughs between the centrifuge test results and the numerical calculations. The volume loss immediately after tunneling (short-term) was 6.6% with a maximum ground surface settlement of 91.5 mm. This corresponds to the imposed volume loss with simulated tunnel opening of GAP = 200 mm. The measured value of the surface trough is similar to the volume loss imposed at the tunnel depth; hence confirming the modeling method is appropriate.

The horizontal distance from the tunnel axis to the point of inflection, i, of the settlement trough is determined to be 7.50 m. This value is close to the prediction of 7.5 m by Peck (1969), in which the trough width parameter k is 0.5 for tunnels in clay, as suggested by Mair et al. (1993). Thus it can be established that the

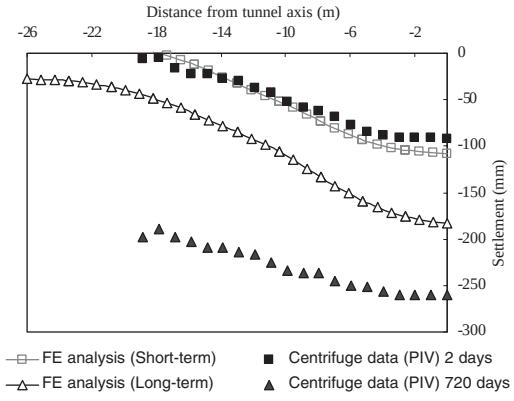


Figure 5. Comparison of surface settlement troughs.

observed settlement trough in the short-term can be reasonably predicted by the finite element analysis.

It is noted that in the long-term, the observed ground settlement continued to increase with time, as shown in Figure 5. This can be attributed to the reconsolidation of the clay, with the dissipation of pore water pressure caused by tunneling. As a result, the settlement trough becomes wider with time after tunnel excavation. Shirlaw (1993) presented examples of long-term settlements and reported that the ground settlement due to tunneling and the extent of settlement trough can increase significantly in the long term in some cases. Figure 5 also shows that the calculated ground settlements also increase with time after tunnel excavation, but the magnitude of increase is smaller than that observed in the centrifuge test.

5 TUNNELING-INDUCED PILE RESPONSES

Piles adjacent to tunneling are subjected to simultaneous vertical and lateral soil movements, which in turn induce axial (pile axial force and settlement) and lateral responses (pile bending moment and deflection) on the piles. It should be noted that the induced bending moment and axial load are additional loads over and above the design working moment/load of the pile.

This additional loading caused by soil movement must be taken into account in order to avoid excessive pile settlement or exceeding pile structural capacity.

5.1 *Induced pile axial force*

In general, the soil settlement due to tunneling would induce negative skin friction along the shaft of an adjacent shaft. This response is evident from the observation shown in Figure 6. Owing to large soil settlement above the tunnel springline, the settling soil drags the pile down. In addition, the magnitude of negative skin friction increases significantly with time. The neutral plane, below which positive shaft friction occurs,

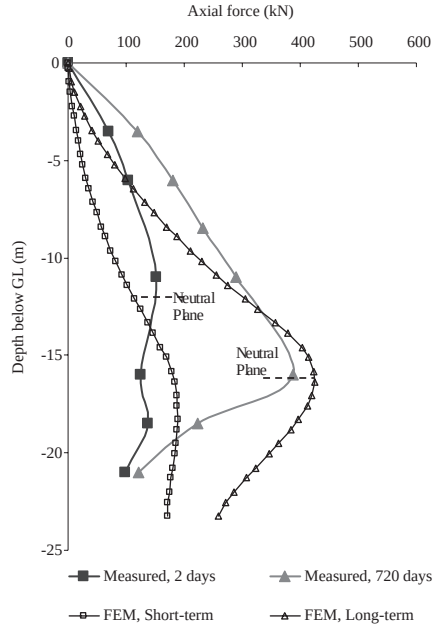


Figure 6. Induced pile axial force (Test 2).

moves downward with time with the final neutral plane located around the tunnel springline elevation.

Figure 6 reveals that the observed short and long-term pile axial force profile can be reasonably predicted by the finite element analysis. As an example, the magnitude of observed negative skin friction increase from 151 kN at the end of excavation (short term) to 387 kN at 720 days after excavation (long term), an increment of 156%. For the numerical calculations, the negative skin friction increases from 188 kN in the short term to 424 kN in the long term. Although the FE analysis over predicts the peak axial force, but the difference is relatively small.

Considering the ultimate axial force capacity of the model pile of 1800 kN, the negative skin friction induced by tunneling reveal that the factor of safety of the pile against pile material failure has been considerably reduced.

5.2 *Induced pile settlement*

Figure 7 shows the observed short and long term green field vertical soil movement profile at the pile location and the corresponding pile settlement. It is evident that the pile has suffered large settlement which increased significantly over time. The high axial stiffness of the pile is evident as the pile body compression is very small.

By comparing the pile settlement with the free field soil movement, the elevation of the neutral plane, where there is no relative movement between the soil

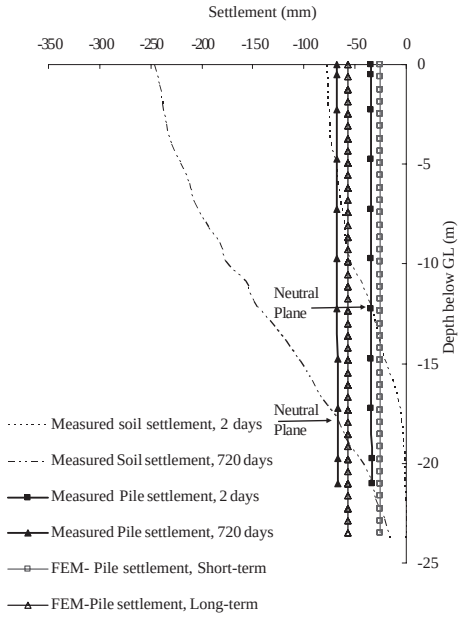


Figure 7. Induced pile settlement (Test 2).

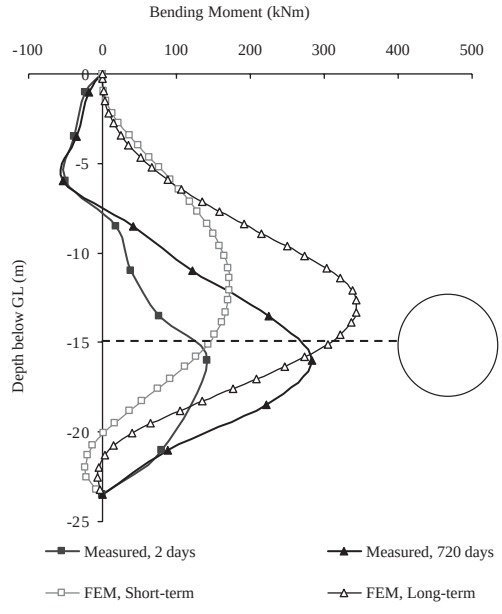


Figure 8. Induced pile bending moment (Test 2).

and pile, can be obtained. The elevation of the neutral plane is consistent with that observed in Figure 6.

5.3 *Induced pile bending moment*

Tunneling-induced soil movement would impose additional bending moment on adjacent piles. As the tunneling process is modeled as plane strain, the bending moment in the transverse direction is much higher than that in the longitudinal direction. Pang (2006) reported that during a tunnel excavation in, Singapore, it was observed that the bending moment in the longitudinal direction was consistently either equal to or smaller (up to 5 times) than the bending moment in the transverse direction. Hence, the modeling technique adopted in the present study is justified.

Figure 8 shows the tunneling-induced pile bending moment profiles at different times. The induced bending moment profile has a double curvature with the moment increasing with depth and time. The bending moment at the pile head and tip is zero because the pile head is free while the pile tip behaves as a hinge. The shape of bending moment profile remains fairly constant over time with the maximum induced bending moment occurs approximately at the tunnel springline. Owing to tunnel over-cut, the soil moves towards the tunnel spring elevation due to volume loss and therefore pushes the pile towards the tunnel.

The induced pile bending moment obtained from the centrifuge test and numerical analysis has a similar profile but the maximum bending moment back analyzed by numerical analysis is located at a higher elevation. This is because the largest negative horizontal soil movement occurs at the tunnel crown elevation, rather than at the tunnel spring line elevation.

In the present study, the ultimate bending moment capacity of the model pile used in centrifuge is estimated to be 3000 kNm. In the short-term, soil movements due to tunneling cause the soil to flow past the pile and induce a maximum bending moment of 141 kNm on the pile and increases to 283 kNm after 720 days. In the numerical analysis, the maximum induced pile bending moment is 172 kNm in short-term and increases by about 100% to 343 kNm in long-term. The percentage of increment of pile bending movement in both centrifuge test and numerical analysis are the same in long-term although the finite element analysis slightly over predict the peak bending moment.

5.4 *Induced pile horizontal displacement*

The horizontal displacement of the pile is related to the free-field horizontal soil movements, pile bending stiffness and the horizontal pile-soil interaction. A comparison of pile and free-field horizontal displacements is shown in Figure 9.

The free-field horizontal soil displacements are obtained in test 1 where as the pile horizontal displacement profile is obtained by integrating the spline function for the bending moment profiles twice with two specified boundary conditions in the double integration, i.e. the measured pile head displacement and assume no pile toe rotation.

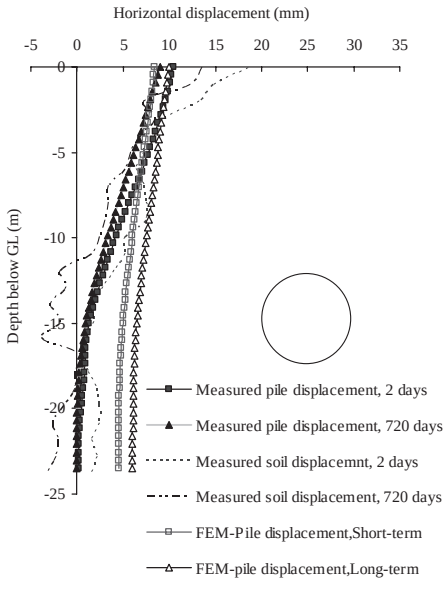


Figure 9. Induced pile lateral deflection (Test 2).

Generally, the pile and soil are moving in the same direction, i.e. toward the tunnel. In this case, the pile head moves laterally more than pile tip because the upper portion of the model tunnel has a higher magnitude of over-cut than that of the lower portion. Both results from centrifuge and numerical analysis exhibit a similar profile. However, the pile horizontal displacement profile obtained from the numerical analysis shows a stiffer pile behavior in which it has a larger toe movement compared with the negligible displacement of pile toe in centrifuge test.

6 CONCLUSIONS

Two plane strain centrifuge model tests have been conducted at NUS to study the tunnel-pile interaction in clay. A technique has been developed to simulate the inward tunnel deformation at the tunnel springline in centrifuge model tests. Besides, 3D numerical analysis has been performed to back analyze the centrifuge test results.

The results reveal that the observed and calculated surface settlement trough in clay generally agreed well in the short-term. The trough extends much wider in the long-term. Tunneling induces both vertical and horizontal soil movements simultaneously and hence affects the axial and lateral behavior of adjacent piles. Back analysis of centrifuges studies has demonstrated the ability of the 3D finite element analysis in predicting the soil movement and pile responses, although the numerical method predicts somewhat slightly over-estimated the pile responses.

ACKNOWLEDGEMENTS

The authors wish to express their gratitude to Mr Eddie Hu and the laboratory officers in the NUS Geotechnical Centrifuge Laboratory for their assistance in carrying out the centrifuge model experiments.

REFERENCES

Feng, S.H. 2003. Centrifuge modeling of tunnel-pile interaction. M Eng thesis, National University of Singapore.

Ghahremannejad, B., Surjadinate, J., Poon, B. & Carter, J.P. 2006. Effects of tunnelling on model pile foundations. *Physical Modelling in Geotechnics-6th ICPMG'06-Ng,Zhang & Wang (eds)*, 1157–1162.

Goh, T.L. 2003. Stabilization of an excavation by an embedded improved soil layer. PhD thesis, National University of Singapore.

Grant, R. J. & Taylor, R. N. 2000. Tunneling-induced ground movements in clay. *Geotechnical Engineering, Proc. Institutions of Civil Engineers*, Vol. 143, No. 1, 43–55.

Jacobsz, S.W., Bowers, K.H. & Moss, N.A. & Zanardo, G. 2005. The influence of tunnelling on piled foundations. *Proc. 16th International Conference on Soil Mechanics and Geotechnical Engineering*, 1611–1614, Osaka.

Katoh, Y., Miyake, M. & Wada, M. 1998. Ground deformation around shield tunnel. *Proceeding of Centrifuge 98*, 1998, Rotterdam. 733–738.

Lee, C.J., Chen, P.S., Chiang, K.H., Chen, H.T. & Lin, W.L. 2006. Evolution of arching effect during the tunnelling in sandy soil. *Physical Modelling in Geotechnics-6th ICPMG'06-Ng,Zhang & Wang (eds)*, 1171–1176.

Lee, K.M., Rowe, R.K. & Lo, K.Y. 1992. Subsidence due to tunnelling: Part I – Estimating the gap parameter. *Canadian Geotechnical Journal*, Vol. 29, No. 5, 929–940.

Loganathan, N., Poulos, H.G. & Stewart, D.P. 2000. Centrifuge model testing of tunneling induced ground and pile deformations. *Geotechnique*, Vol. 50, No. 3, 283–294.

Mair, R.J., Taylor, R.N. & Bracegirdle, A. 1993. Subsurface settlement profiles above tunnels in clay. *Geotechnique*, Vol. 43, No. 2, 315–320.

Pang, C.H. 2006. The effects of tunnel construction on nearby pile foundation. PhD thesis, National University of Singapore.

Peck, R.B. 1969. Deep excavations and tunneling in soft ground. *Proc. 7th International Conference Soil Mechanics and Foundation Engineering, Mexico City, State of the Art* Volume, 225–290.

Ran, X. 2004. Tunnel pile interaction in clay. M Eng thesis, National University of Singapore.

Shirlaw, J.N. 1993. Pore pressure around tunnels in clay: Discussion.*Canadian Geotechnical Journal*, Vol. 30, 1044–1046.

Sharma, J.S., Bolton, M.D. & Boyle. R.E. 2001. A new technique for simulation of tunnel excavation in a centrifuge. *Geotechnical Testing Journal*, Vol. 24, No. 4, 343–349.

White, D.J., Take, W.A. & Bolton, M.D. 2003.Soil deformation measurement using particle image velocimetry (PIV) and photogrammetry. *Geotechnique*, Vol.53, No.7, 619–631.

Underground Space – the 4th Dimension of Metropolises – Barták, Hrdina, Romancov & Zlámal (eds)
© 2007 Taylor & Francis Group, London, ISBN 978-0-415-40807-3

The continual load development measurement of the central concrete pillar in the Valík tunnels

J. Pacovský, J. Svoboda & R. Vašíček
Centre of Experimental Geotechnics, Faculty of Civil Engineering, Czech Technical University in Prague, The Czech Republic

ABSTRACT: The safe and cost-effective construction of tunnels employing modern technologies requires that systematic geo-monitoring be carried out. It is often necessary to supplement basic monitoring with further measurements and observations. In the case of complicated geological conditions or in the case of the use of complicated, atypical construction methods, stress measurements are required. The continual measurement of stress on the contact between the rock and the primary tunnel lining and between the rock and the central concrete supporting pillar was carried out during the construction of the Valík tunnels. The measurement results provided information on the development of loading by rock pressure over the course of time.

1 INTRODUCTION

The present-day construction of underground structures requires constant geo-monitoring. The amount of monitoring needed is open to debate and, despite professional advice, it is often the case that underground structures are either subjected to unnecessary and costly over-monitoring or, at the opposite end of the spectrum, insufficient monitoring. The cost of geo-monitoring can make up a considerable portion of the overall construction budget, therefore the investor would be well advised, in cooperation with the designer, to approach the issue in a responsible manner and to take full advantage of the professional advice on offer.

Continual stress measurements are not usually considered an integral part of geo-monitoring and are only utilised when tunnels are constructed in areas with complicated geological conditions, or at sites where non-traditional tunnelling technologies are employed. Stress measuring, as well as being costly, requires a high level of professional knowledge. It is advisable therefore to employ specialised, experienced companies with a proven track record in the taking of such measurements. Only a limited number of geo-monitoring companies are able to provide such services and the employment of unskilled companies in the past who have provided unsatisfactory stress measurement data has led to a general lack of trust in the field.

2 PRINCIPLE OF CONTINUAL STRESS MEASUREMENT

The principal advantage of stress measurement at the contact of the rock mass with the tunnel lining is that it may provide information on changes in the load acting on the lining before such changes cause any real damage. Since measuring is carried out on a continual basis, a decision can be made, based on load change development in the risk area, to increase the frequency of basic deformation measurements thus preventing, well in advance, any dangerous deformation of the lining.

Since these measurements are fully automated, any measurement interval can be selected allowing practically any number of gauges to be connected to the datalogger.

Contact stress measurement is performed by means of hydraulic pressure cells (Fig. 1) and the continual recording of measurement results is provided by an ADSYS-ASOFT datalogger which is tough enough to withstand the demanding environment of an underground site (Fig. 2).

3 VALÍK TUNNELS

3.1 *Basic information*

The Valík Tunnels are located on the D5 highway, which runs from Prague to Rozvadov (on the German

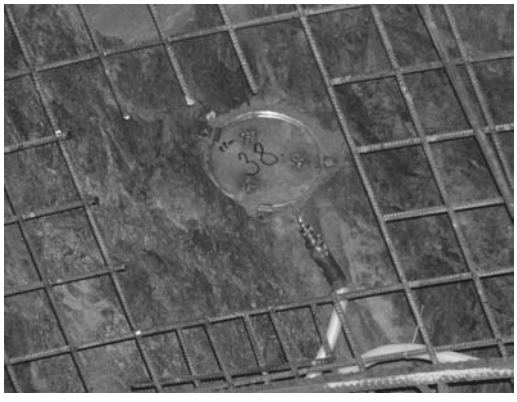


Figure 1. Hydraulic pressure cell (HPC).



Figure 2. Data transport from the ADSYS – ASOFT datalogger.

border). The construction investor is Ředitelství silnic a dálnic ČR Praha, i.e. Road and Highway Management for the Czech Republic, Prague, and the construction contractor Metrostav a.s., SG-Geotechnika a.s., responsible for comprehensive geotechnical monitoring during the construction of the tunnel. The driven tunnel section is 330 m in length and is made up of two separate tunnel tubes, 12 m wide and 8.2 m high. Two traffic lanes each with a width of 3.75 m were designed in each direction plus one emergency lane with a width of 3.25 m. There is no rock pillar between the tunnel tubes, the tubes being separated by a central reinforced concrete pillar built in advance. The construction of the driven tunnel sections is of the double-jacket design with intermediate insulation.

3.2 *Geological conditions*

The geological conditions along the whole length of the highway tunnel were verified in 2002 using a driven prospecting drift. Both the tunnel construction

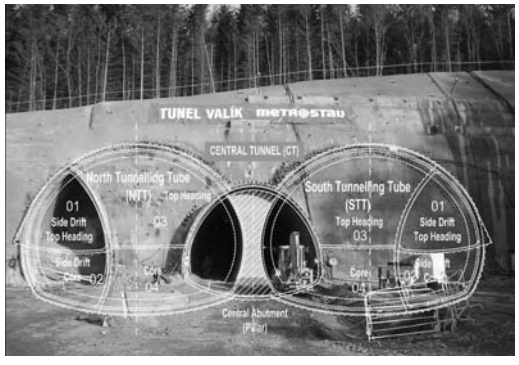


Figure 3. Tunnel cross section – excavation sequence.

technology and the level of geotechnical monitoring were subsequently designed according to the exploration results.

The tunnels were driven into weathered, tectonically highly affected Proterozoic shales. In terms of hydrogeology, the prevailing rock mass was dry.

3.3 *Tunnel technology and construction procedure*

The basic partial excavation procedure can be seen in Figure 3. Combined zoning (vertical and horizontal) was chosen because of the complex geological conditions, the minimum roof thickness above the tunnels and the considerable width and height of the breakings.

The primary lining consists of shotcrete, truss arches (BTX), a lattice grid and anchoring elements. The final lining is designed to be of in-situ reinforced concrete cast in 10 m lengths in monolithic form.

In terms of technology and structural design, the most complicated problem was the construction of the central reinforced concrete pillar which bears a considerable part of the rock load above the tunnels. The pillar was built in advance in the central tunnel.

Excavations, performed to 70% without blasting, commenced in March 2004 with the excavation of the central tunnel, which was completed one month ahead of schedule at the end of July 2004. In September 2004, the concreting of the central pillar commenced so that the excavation of the main tunnels could be in full swing by the beginning of October. The concreting of the central pillar was completed in January 2005; the excavation of the main tunnels was completed in May 2005. The tunnel was put into operation in early October 2006 (Bernard, 2004).

3.4 *Geotechnical monitoring system*

Geotechnical monitoring (GTM) is a component part of the New Austrian Tunnelling Method (NATM), used in the construction of the majority of tunnels in the Czech Republic.

Basic geo-monitoring in this case included: the geological observation of the faces, the measurement of settlement on the surface of the area observed, extenzometric measurements in vertical drills from the surface of the terrain, the measurement of horizontal deformations in the surrounding massif using inclinometers, the measurement of primary lining deformations (measurement of convergence), stress measurement in the primary lining as well as on the rock - lining contact (Bernard, 2004).

4 CONTINUAL CONTACT STRESS MEASUREMENT

Based on the results of geological prospecting, 3 driving sections along the tunnel length were selected in which geo-monitoring was extended to include automated continual contact stress measurements carried out in the vicinity of the central concrete pillar at the rock-lining – lining-pillar contact. Such measurements performed hourly provided immediate information on the on-going redistribution of stresses in the surrounding rock continuum and in the central concrete pillar itself. Stress redistribution in a complex rock continuum is a long-term process (Pacovský, 2002). The measurement results allowed predictions to be made concerning future changes in lining deformation due to changes in loading (stress-state).

In these 3 difficult driving sections, 3 joint measurement profiles were instrumented. In all, 36 hydraulic pressure cells (HPC) were installed at various stages of the excavation work. As the result of long-term experience, continual temperature measurements at the stress measurement points were carried out simultaneously. The measurement of temperature is relatively both simple and cheap and is able to provide some very useful information.

Gauges were installed in stages with respect to the stope subdivision. The mounting process was designed to keep as many gauges in operable condition as excavation progressed.

4.1 *Installations and measurements in the central tunnel*

The driving process of both Valík tunnels commenced by driving the central tunnel in which a central supporting pillar for both tunnel tubes was concreted (Fig. 3). Since the main task of continual stress measurement was to monitor the development of the load acting on the central concrete pillar, installation of the HPC gauges was concentrated in the area immediately above and below the future concrete pillar. The gauges were first mounted in the upper vault area and, subsequently, below the lower vault, at the contact point with the rock or at the contact point of the pillar with the primary lining of the central tunnel. Due to the long distances between the measuring profiles, 3 collecting dataloggers were installed along the tunnel.

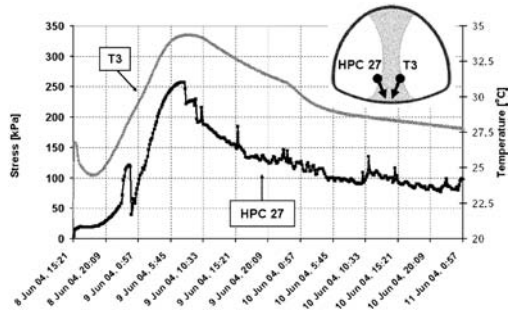


Figure 4. Stress-temperature time distribution at rock – primary lining contact – joint profile 2.

Each stress measuring gauge (HPC) installed on the surface of the stope was covered with a layer of shotcrete during the spraying of the primary lining. During the shotcrete hydration process, there is an increase in temperature and hydration pressure, which loads the stope surface. When the concrete cools, the falling hydration pressure can, for a certain time, locally load the contact with the rock with tensile stress and, eventually, the lining starts to take over the load from the rock continuum.

In cases where shotcrete is not applied into the formwork in the shotcrete lining, hydration pressure values are relatively low (max. x*100 kPa) while, conversely, in the lining which is concreted into the formwork, values increase to several MPa. The difference in the hydration stresses is the result of permitting or eliminating volume changes in the concrete during hydration. A typical example of a hydration phase time pattern is shown in Figure 4.

In 2002, as part of the prospecting stage, an exploration gallery was driven along the whole length of the future tunnel. The gallery subsequently caved in as work commenced on driving the central tunnel in 2004. During driving operations on the central tunnel this gallery was reopened which increased the amount of natural ventilation, which in turn led to a slight temperature drop in the central tunnel. Subsequently, a slight temperature drop was observed at the primary lining-rock contact which caused a change in the load acting on the lining (Fig. 5). Although the change in loading was insignificant, it proved the usefulness of the monitoring of temperature together with the development of stress.

4.2 *Installation and measurement during concreting of the central concrete pillar*

An important part of the continual measurement process was the monitoring of temperature development

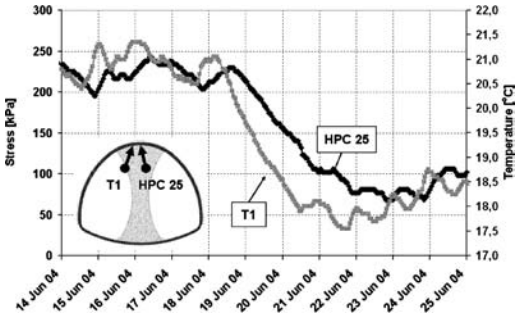


Figure 5. The effect of temperature change in the tunnel on the change in the load on the lining – joint profile 1.

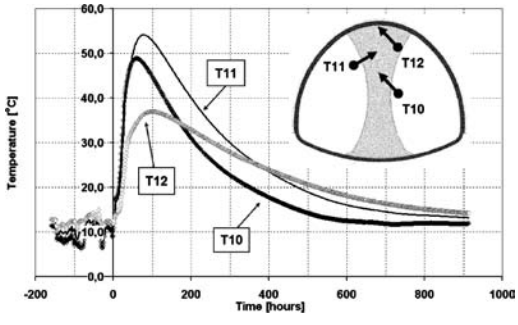


Figure 6. Time pattern of concrete hydration in the central pillar – joint profile 1.

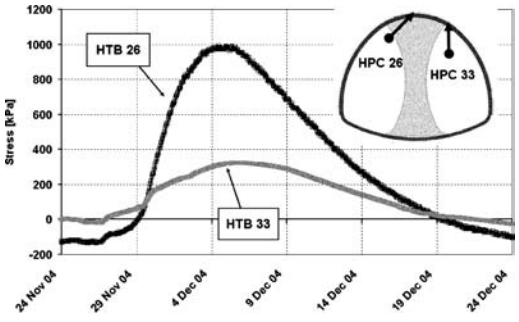


Figure 7. The effect of the concrete hydration of the central pillar on increased load at the rock-primary lining contact in the central tunnel – joint profile 2.

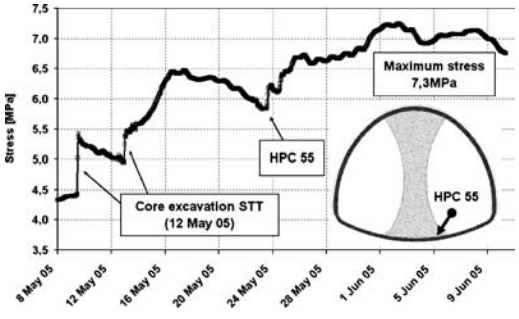


Figure 8. Load changes on the pillar footing bottom – joint profile 3.

during the hydration of the concrete of the central supporting pillar. Exceeding the maximum temperature could have resulted in a reduction in the quality of the concrete thus reducing the load-bearing capacity of the pillar (Fig. 6).

Hydration stress developed along with temperature. The development of hydration stress in the concrete of the pillar was initiated by the time-limited increase in the load at the rock-primary lining contact of the central tunnel. At the end of the hydration process, contact stresses (load) in some places above the pillar became tensile stresses which in turn, due to rock stress state redistribution, became compressive stresses (Fig. 7). More significant changes in the pillar load, however, occurred only with the approaching partial stopes of the south and north tunnel tubes as construction progressed.

4.3 *Measurement of the development of pillar loading due to the advance in partial driving*

The main reason for extending the range of geomonitoring to include continual stress measurement was the need to verify that the load on the central concrete pillar would not exceed the values determined in the dimensioning stage, in any of the various construction phases.

After the pillar in the central tunnel (CT) was concreted, the primary lining assumed practically all the load exerted by the rock massif. The pillar started to assume the load as partial driving operations in the north and south tunnel tubes (NTT and STT) approached. In some places, the load change was very fast. Figure 8 shows the rapid increase in the load on the footing bottom due to the excavation of the STT core. These rapid changes in loading justified the automated reading of measured data at 1 hour intervals.

A gradual increase in the load on the pillar was recorded at all the measuring profiles. The discontinuous, non-homogenous rock continuum exerted a considerable influence on non-uniform pillar loading. Stress concentration values locally reached 11 MPa (Fig. 9). During partial driving operations on the STT and NTT load acting on the pillar increased many times over several days (Fig. 10).

Approximately one month after the driving operations came to an end, the load on the pillar stabilised within a range of 4–8 MPa.

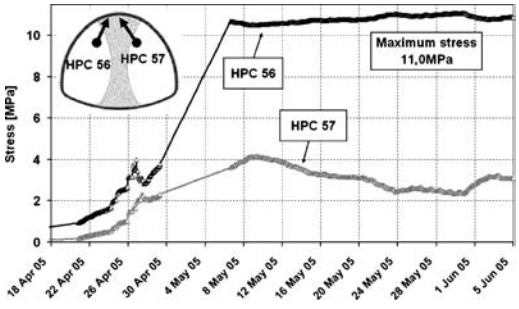


Figure 9. Maximum load on the central pillar – joint profile 3.

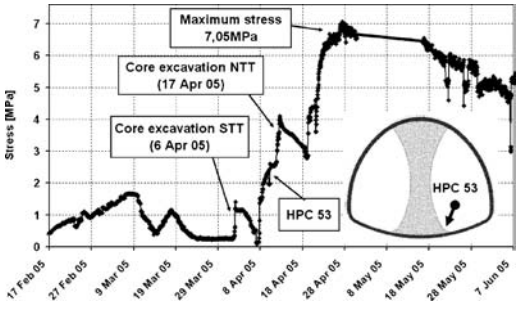


Figure 10. The effect of partial driving operations on load on the central pillar.

5 CONCLUSION

The measurement of changes in stress is one of the most difficult geotechnical measurements to perform. The continual measurement of contact stress is a method whose results depend upon the quality of each step of the installation and monitoring process. The greater the non-homogeneity and discontinuity of the rock continuum, the more difficult such measurement becomes. Any slight imperfection in the mounting of the gauges can drastically affect the usefulness of the results. It is, therefore, essential that the company chosen to do this work is able to prove its suitability for the task in terms both of qualifications and previous experience. A common underestimation of the complexity of such measurements has tended to drive commercial clients to distrust the results and to question the usefulness and relevance of this method.

The information obtained through continual stress measurement during the construction of the Valík tunnels has contributed to the safety and cost-effectiveness of the project. It is clear that the use of this method, in combination with other geo-monitoring methods, has an important part to play in the driving of tunnels in complicated geological conditions and/or where non-traditional tunnelling technology is employed.

ACKNOWLEDGEMENTS

The research team gratefully acknowledges support provided by the Grant Agency of the Czech Republic, project No.103/05/2231.

REFERENCES

Bernard, R. 2004. Project of Geotechnical Monitoring of Valík Tunnel. *Technical report*, Prague: Stavební geologie – Geotechnika. a.s.

Pacovský, J. 2002. Possibilities and Limits of Stress Measurements Performed on Geotechnical Constructions with the Use of Hydraulic Pressure Cells. *Proc. 30th Conf. Foundations*, Czech Republic, Brno: CERM

This page intentionally left blank

Underground Space – the 4th Dimension of Metropolises – Barták, Hrdina, Romancov & Zlámal (eds)
© 2007 Taylor & Francis Group, London, ISBN 978-0-415-40807-3

The Josef underground educational facility project

J. Pacovský, J. Svoboda & R. Vašíček
Centre of Experimental Geotechnics, Faculty of Civil Engineering, Czech Technical University in Prague, The Czech Republic

ABSTRACT: The Faculty of Civil Engineering, CTU in Prague, is in the process of establishing a new, modern experimental facility to be used for both educational and research purposes – the Josef Underground Educational Facility (UEF). The reason for the establishment of this underground workplace arose from the need for a facility which would contribute towards providing an increased amount of practical education for students in the fields of underground structures, rock mechanics, material testing, engineering-geological surveying, geodesy and mapping, blasting, ventilation and safety training. It is envisaged that this facility will contribute towards closer collaboration between universities and outside institutions, allow the performance of national and foreign experimental projects and will be available for use as a training facility for experts in the practical application of new technologies etc.

1 INTRODUCTION

The reasons for establishing a new, modern underground educational facility as part of the Faculty of Civil Engineering, CTU in Prague, resulted from the following:

- the need for further development of experimental research at universities, particularly with regard to material engineering, environmental geotechnics, geology and hydrogeology in a natural, "in-situ" environment
- the present lack of facilities (at a convenient distance from Prague) for the practical training of students in the fields of engineering-geological and geotechnical investigation and mapping in underground spaces
- the establishment of this workplace will contribute towards closer collaboration between universities and outside institutions
- there are a number of closed, unexploited minor underground workings currently available in the Czech Republic the utilization of which for such purposes is self-explanatory.

2 LOCATION SELECTION

The basic requirements for the selection of a suitable underground site were defined as follows:

- financial feasibility (purchase price, operating and closure costs)
- varied geological conditions (occurrence of non-monotonous geological formations)
- the site's potential for future expansion (short insets for individual experiments)
- distance of up to 60 km from Prague.

Selection of a suitable location was based on the precondition that the facility should be sited in a horizontal gallery, rather than a vertical pit the operation of which would be considerably more expensive.

Economic considerations dictated that the most favorable of the various alternatives was clearly the purchase of an unexploited underground gallery. From the very beginning of the selection process it was evident that the most suitable of all the locations which fulfilled the basic site requirements and had a good local infrastructure and the potential for future expansion (reconstruction of the existing structure) was the Josef Gallery situated in the Mokrsko-Čelina area.

3 BASIC DESCRIPTION OF THE JOSEF GALLERY

The Mokrsko-Čelina area in which the Josef Gallery is located belongs to the Jílové gold bearing zone (Morávek, 1996). The Josef exploration gallery was excavated as part of renewed prospecting activities which commenced in 1981 (Fig.1). It was decided, however, that mining operations would be discontinued since ore extraction and dressing would result in the devastation of an area of natural and recreational potential and consequently, in 1991,



Figure 1. Josef exploration gallery construction yard in 1981.

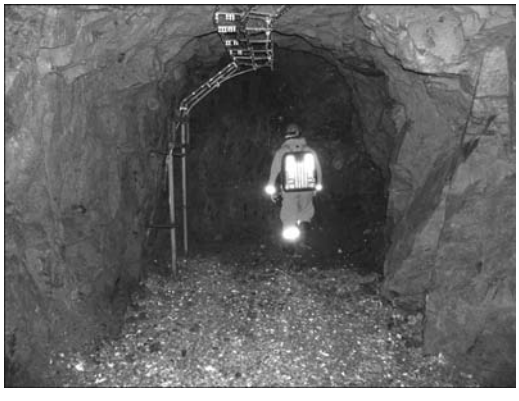


Figure 2. Typical prospecting drift profile.

prospecting activity in the Josef Gallery finally came to an end. In 2000, the entrance portals were plugged with concrete to prevent access to the underground areas.

The Josef exploration gallery is cut into the Mokrsko Hill rock massif. The total length of the main drift is 1700 m, with a cross-section of 14–16 m^2. The overlying rock thickness is 90–110 m.

The main exploration gallery is connected to various other exploration workings by numerous insets (total length of 8.6 km) which follow ore formations and provide access to two further levels. Approximately 90% of the breakings are not fitted with linings (Fig. 2).

The end of the main gallery is connected to the ground surface by means of an unsupported 90 m vent.

The geological continuum is made up of Jílové zone volcanic (basalts, andesites, rhyolites) and sedimentary (hornfels) rock types and their combinations (tuffs, tuffites) characterized by younger intrusive rock types (granodiorites, albitic granites).

4 THE PLAN TO EXPLOIT THE JOSEF UNDERGROUND GALLERY

The idea of exploiting the Josef underground gallery originated as early as 2003. Following extensive discussions and consideration of the information available, the management of the Czech Technical University in Prague gave its support to the Faculty of Civil Engineering's scheme to establish the Josef Underground Educational Facility (UEF) as a CTU multidisciplinary workplace. Unlike a number of foreign underground laboratories, the CTU workplace will not be single topic-oriented; the size of the Josef underground gallery and its geological diversity allow the participation of a wide spectrum of those interested in experimental research.

Since Josef is to be a university workplace, its primary mission is the education of young scientists – specialists in their respective branches; it is envisaged that the Josef facility will significantly improve the level of practical instruction provided by the Faculty of Civil Engineering.

One of the facility's most important areas of activity will be collaboration with outside institutions in solving topical problems concerning construction engineering, ecological engineering, verification of new building technologies and materials etc. The underground educational facility will provide space for specialized instruction and training of staff of building companies (shotcrete technology, bolt lining and anchorage, operation of modern building machinery and devices, health and safety training etc.).

A further use for Josef will be in providing facilities for domestic and international single- as well as multi-disciplinary research projects (grants); the Josef underground exploration gallery allows the performance of extensive experiments.

The organizers of the project have gained extensive experience in the exploitation of underground workplaces as part of their research participation in a number of international projects assigned by the European Union. Such experience has shown that performing experimental projects in underground facilities sets high financial demands and that without EU grant support such projects would not be practically feasible in the Czech context. It is envisaged that the Josef Facility will allow a wide range of interested parties to work on their research projects in ideal underground conditions and, moreover, that good value for money will attract academic institutions from other EU member states.

5 PROJECT IMPLEMENTATION

In 2004, the Faculty of Civil Engineering, CTU in Prague, signed a contract of cooperation with the company Metrostav a.s. in which both parties agreed to build a joint workplace, UEF Josef. At the same time,



Figure 3. Survey of the newly opened Josef underground gallery.



Figure 4. UEF Josef 's commissioning kick off.

Metrostav a.s. undertook to put the Josef gallery into operation at its own expense.

In March 2005, a loan agreement, the subject of which was the Josef underground exploration gallery, was concluded between the Faculty of Civil Engineering, CTU in Prague, and the owner of the Josef gallery, the Ministry of the Environment of the Czech Republic (MŽP). In August 2005, Metrostav a.s. removed the concrete plug blocking the entrance to the main gallery.

In September 2005, the Prague Mining Rescue Service carried out a detailed survey of the Josef complex concluding that: "The condition of the Josef underground complex allows its use as an underground educational facility" (Fig. 3).

In February 2006, the Faculty of Civil Engineering, CTU in Prague, concluded a lease contract with the owners (Lesy ČR s.p.) of the land concerned (15,000 m^2). At the same time, negotiations on their purchase were started. Based on the results of the above-mentioned survey, Metrostav a.s. ordered a project concerning the commissioning of the underground facility.

In April 2006, the Faculty of Civil Engineering won a grant from European Structural Funds JPD3, which will cover the funding of the first two years of trial instruction of students specialized in geotechnics and geodesy.

The building permit for the start of work was granted on 21st July 2006, and the commissioning of the underground was begun by Metrostav a.s. – Division 5 on 21st August 2006 (Figs 4, 5).

Discussions with the designer of the underground part of UEF Josef, IKP Consulting Engineers s.r.o., and the experts from Metrostav a.s. resulted in a decision to cater for the needs of student instruction in the first phase of the Josef Underground Facility commissioning (total length of 8.6 km of drifts) by putting into operation a section of the main gallery and the west part of the Èelina zone (Fig. 6).



Figure 5. Removal of concrete portal plugs.

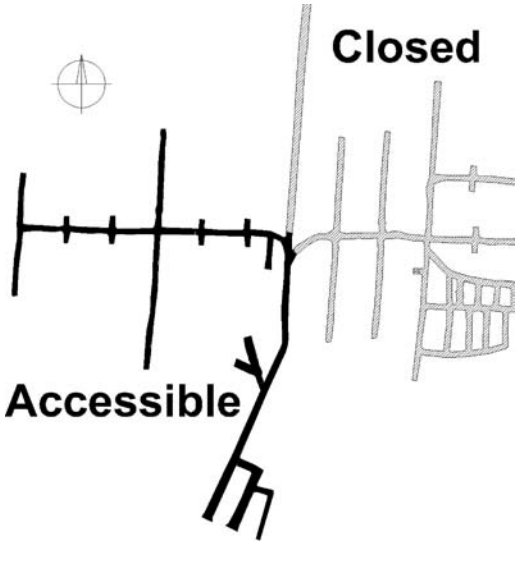


Figure 6. The size of underground spaces put into operation.



Figure 7. Current condition of Josef underground work.

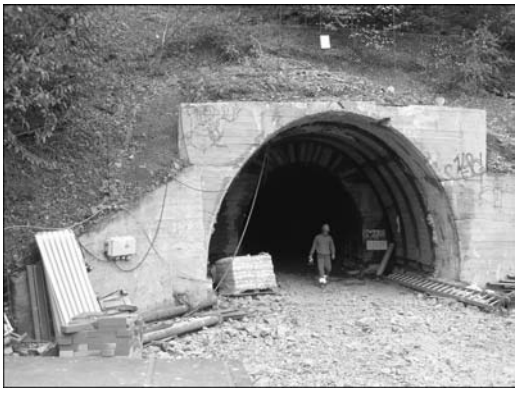


Figure 8. Adaptations of Josef gallery.

Although the Josef underground work was found in very good condition (Fig. 7), in accordance with the IKP project Metrostav a.s. started works necessary for ensuring the safety of the underground facility for student instruction (Fig. 8).

All activity within the commissioning of the underground will be completed by the end of 2006 when, following the approval of construction, Metrostav a.s. will hand the underground work over to the Faculty of Civil Engineering, CTU for further use. The following process is set by the time schedule of the JPD3 project. January 2007 is the start of the implementation of a pilot (trial) project of instruction, June 2007 is the month of presumed festive opening of UEF Josef, and from September 2007 the underground part put into operation will be used for regular instruction following newly designed study plans of the Faculty of Civil Engineering, CTU. It is envisaged that over 300 students will use the Josef facility in the first year of teaching, mainly in teaching blocks covering several days (Pacovský, 2006).

6 CONCLUSION

The exploitation of a part of the unused underground work Josef for practical educational purposes will be the first step towards the use of the total volume of the underground spaces available. Step by step, the galleries are presumed to be used for research on domestic and international experimental projects, for specialized training and instruction of staff members of building companies, and for the presentation of modern building technologies and products by both Czech and foreign construction companies.

The disused two-storey building at the Josef site, which was donated to the Faculty of Civil Engineering by its owner (MŽP) in 2005, will be converted into surface premises to serve the underground educational facility. If the underground area is to be exploited to its full extent, good quality surface premises will be required for use as offices, laboratories, accommodation, storerooms, workshops etc.; therefore plans have been made for the building's complete reconstruction.

The UEF Josef complex is situated in a beautiful natural locality. Based on an agreement with Chotilsko Municipality, UEF Josef will become part of an existing instructive foot trail with public access to the exploited part of the underground.

ACKNOWLEDGEMENT

This project would not be feasible without funding obtained from European Structural Funds – project CZ.04.3.07/3.1.01.3/3148, and financial and professional support provided by the joint-stock company Metrostav. We would also like to thank the Ministry of the Environment of the Czech Republic and Chotilsko Municipality.

REFERENCES

Morávek, P. 1996. The Mokrsko Gold Deposit. *Gold Deposits in Bohemia,* Czech Geological Survey, Prague: 31–56.

Pacovský, J. 2006. The Josef Underground Educational Facility Project. *Proc. 9th International Conference on Engineering Education*, Puorto Rico, San Juan. pn 3079.

Underground Space – the 4th Dimension of Metropolises – Barták, Hrdina, Romancov & Zlámal (eds)
© 2007 Taylor & Francis Group, London, ISBN 978-0-415-40807-3

Displacements estimate due twin tunnel excavation under low overburden

E.A. Palma Filho, A.C. Zingano, J.C. Koppe & J.F.C.L. Costa
Federal University of Rio Grande do Sul, Porto Alegre, Brazil

ABSTRACT: The study of the stresses and strains caused by an underground excavation can currently be modeled with better precision and much faster than a few years ago. However, the tools which allow numerical analysis in two or three dimensions, for any geometry of excavation, need data for input into the system. In the Reversion tunnel project, the contractor measured a series of displacements of the walls of the tunnels. This was done in conjunction with the mechanical characterization of the rock and the geomechanical classification of the tunnel workmanship. Using these three parameters, it was possible in this study to calculate the stress in the rock mass, by means of backward-analysis, and the ratio between the horizontal stress and vertical stress, K_0. This was accomplished using finite element software. With parameterized geomechanical data, it was possible to calculate the stresses acting on the support system for each phase of excavation.

1 INTRODUCTION

1.1 *General view*

The opening of an underground excavation, for civil, military or mining use, is an activity that has for thousands of years followed the development of civilization. Beside the diversification of use, over the years excavation techniques have developed the stage that today involves the modern technology in all the stage of an underground excavation.

1.2 *Objectives*

In this work the objective was to estimate by means of numerical simulation the displacements resulting from the excavation of twin road tunnels constructed in an area of low overburden (depth varying from 0.5 to 4 tunnel diameter), and of in the side of a hillside. For this, the software Plaxis® Tunnel 3D (Brinkgreve & Broere, 2004), that allows the three-dimensional simulation of the excavation process using the Finite Element Method, was used.

1.3 *Methodology*

The necessary data for input into the Plaxis® software (Deformability Modulus – E, Cohesion – c, Friction Angle – Ø, Stress ratio – K_0) was obtained from three sets of information: (i) the instrumentation of the tunnel; (ii) geomechanical classification carried out during the excavation; (iii) laboratory assays for characterization of the rock. Whit this information, Roclab software (Rocscience, 2006) was used to estimate the parameters, as show in Figure 1.

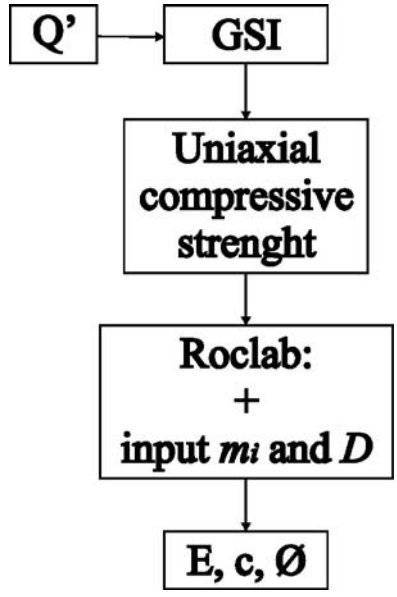


Figure 1. Sequence to estimation of the parameters.

From the information of deformability modulus, cohesion and friction angle obtained from the Roclab software, and with the displacements of the walls of the tunnels already known from the instrumentation, a

backward-analysis with the Plaxis® software was carried out, in order to get estimates of the stress ratio K_0.

2 CASE STUDY

A case study involving the stress distribution was carried out during the construction of twin road tunnels in the RS-486 road, the "Route of the Sun", that is located in Rio Grande do Sul State, in the southern region of Brazil. The double tunnels of Km 10, the so called "Reversion Tunnels", are being executed with the New Austrian Tunneling Method (NATM), along with technique of drilling and blasting. They possess an arched passage way, with 7% inclination and they are being excavated with a partialized section (Figures 2 and 3).

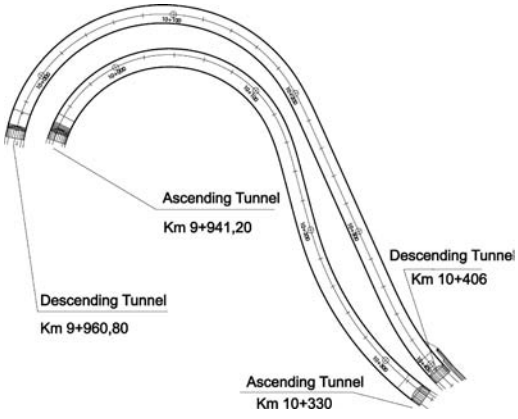


Figure 2. Road tunnel way.

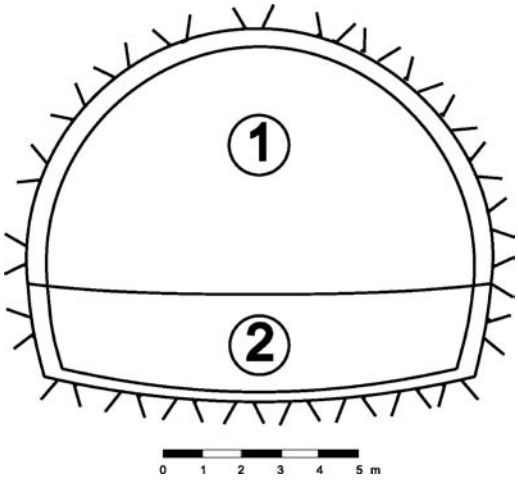


Figure 3. Typical section of the tunnels, with excavation sequence.

2.1 *Local geology*

The "Três Forquilhas" river valley cuts through a sequence of acid and basic volcanic rocks (lava flows) of the Serra Geral Formation (Cretceous period). In the base of this sequence, occurs lenses of sandstones of the Botucatu Formation. In the lowest areas of the valley Quaternary fluvial sediments of the Três Forquilhas river basin are found and, above these, sediments of the Coastal Plain (Nummer, 2003).

2.2 *Backward-analysis*

From the information of the instrumentation of the tunnel, where the measures of displacement carried out by the contractor of the project gave a divergence between the walls of the order of 3 mm, a parameterized backward-analysis was made, in order to estimate the stress ratio K_0. The parameterized values used in the analysis are described in Table 1, and lead to a stress ratio of the order of $K_0 \approx 0.2$.

2.3 *Geomechanical classification*

Since the beginning of the execution of the tunnel a geologic-geotechnical classification of the rock mass was made, by means of the Q System. Three maps were generated with this information: (i) description of the rock mass; (ii) commercial classification; and (iii) geomechanical classification.

This work classification gave values of Q between section $10+075$ and $10+149$, in the ascending tunnel, and between $10+110$ and $10+180$, in the descending tunnel. The summarized information is presented in Table 2.

Table 1. Geomechanical data for backward-analysis.

N° of simulation	Defomability modulus (GPa)	Coesion (MPa)	Friction angle (°)
1	14.60	1.011	64.04
2	14.60	1.011	64.04
3	8.51	0.565	63.02
4	3.25	0.466	60.59
5	2.40	0.467	60.37
6	2.56	0.510	60.51

Table 2. Q′ value, in the section $10+075$ to $10+149$ (ascending), and $10+110$ to $10+180$ (descending).

Information	Value
Number of data	120
Minimum value	0.10
Maximum value	35
Standard deviation	8.02
Mean	8.64

2.4 *Laboratory assays*

Concerning the quality of the rock, values from laboratory assays are summarized in Table 3.

From the value of known resistance of uniaxial compression, and the value of Q′ obtained from the classification, RocLab software was used in order to estimate the Mohr-Coulomb parameters to input into the software. Table 4 shows the average values obtained using the RocLab software. The Disturbance Factor *D* used was 0.5.

2.5 *Numerical simulation*

With the geometry known; the geomechanical parameters estimated; and with the excavation sequence also already known, a numerical simulation of the excavation was made. The resulting mesh was as shown in Figure 4.

Table 3. Rock quality, from laboratory assays.

Litology	Riolite
Rock parameter	mean – standard deviation – number of samples
UCS (MPa)	79.91 – 14.91–11
Point load (MPa)	101.87 – 33.45–9
c (MPa)	19.80
Ø (°)	47°
E (GPa)	67.11 – 17.71–9

Table 4. Mechanical parameters of the rock mass – average.

TUNELL	Q	Q′	σ_{ci} (MPa)	GSI	E_m (GPa)*	Ø′ (°)*	c′ (MPa)*
Ascending	2.54	2.54	79.91	47.63	6.82	59.37	0.45
Descending	14.75	14.75	79.91	67.14	18.60	64.18	0.99

* estimated in accordance with Hoek *et al.* 2002.

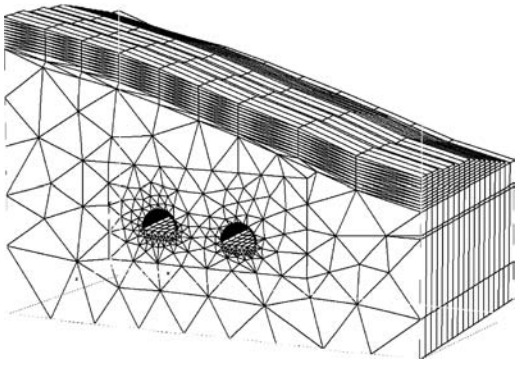


Figure 4. Mesh for the numerical simulation.

For the simulation in the Plaxis®, the sequence of the work was:

- the general configurations had been defined (file name, model declivity, dimensions of the work area, grid spacement, and units);
- extension and geometry mesh was defined;
- in the tunnel designer auxiliar command was draw the geometry of twin tunnels;
- the restrictions of the mesh had been defined; the properties of the material, and the K_0 ratio had been input;
- was defined the support system (shotcrete and bolts);
- the Finite Element mash was generated;
- the eighteen slices of four meters each had been inserted (three-dimensional);
- the excavation sequence was defined.

3 RESULTS

A 72 meters section of excavation was simulated three-dimensionally, split into 4 meters slices, for the section between stations $10 + 075$ and $10 + 146$ of the ascending tunnel. In the excavation, in this stretch, there are sections of instrumentation at stations $10 + 075$, $10 + 110$ and $10 + 146$, from where the data for the comparison with the simulation was obtained. The results of the estimated displacements between the walls of the tunnels are given in Tables 5 and 6, as a function of each stage of excavation.

Other information was also obtained by means of the numerical simulation software an the forces acting

Table 5. Estimated displacements, for half section.

Section	Horizontal displacements, ascending tunnel, in mm	Horizontal displacements, descending tunnel, in mm
01	2.35	2.60
02	2.05	2.10
03	1.90	1.60

Table 6. Estimated displacements, for full section.

Section	Horizontal displacements, ascending tunnel, in mm	Horizontal displacements, descending tunnel, in mm
01	1.84	2.00
02	1.56	1.50
03	1.24	1.10

Table 7. Forces acting on the support system.

Full section excavation – maximum value	
Axial force	1.80×10^3 kN/m
Shear force	62.38 kN/m
Bending moment	19.15 kNm · m

on the support system of the excavation, as presented in Table 7.

4 CONCLUSIONS

It was possible to carry out, by means of numerical methods, the three-dimensional simulation of the excavation of double twin tunnels.

The value estimated from parameterized backward-analysis for the stress ratio K_0 was of the order of 0.2 and is consistant with the topographical situation of the project, having little overburden and in the side of a hillside.

The estimated values of total displacements of the excavation for the full section stage are slightly lower than the displacements estimated for the half section stage of excavation.

REFERENCES

Geoprojetos. 2004. Reversão Tunnel Project – RS-486. Geoprojetos.

Hoek, E.; Carranza-Torres, C.; Corkum, B. 2002. Hoek-Brown failure criterion – 2002 edition. In: <http://www.rocscience.com/ library/pdf/RL_1.pdf>, in 20 abr. 2006.

Nummer, A. V. 2003. Parâmetros Geológico-Geotécnicos controladores dos movimentos de massa na Rota do Sol/RS 486 – Itati, RS. Porto Alegre. 241 p. Tese de Doutorado. PPGEC/UFRGS. *In Portuguese*.

Rocscience. 2006. Software RocLab versão 1.021. In: <http://www.rocscience.com>.

Underground Space – the 4th Dimension of Metropolises – Barták, Hrdina, Romancov & Zlámal (eds)
© 2007 Taylor & Francis Group, London, ISBN 978-0-415-40807-3

Parametric study of displacements on sequential and full-face tunnel excavation

S. Papakonstantinou & W. Schubert
Institut of Rock Mechanics and Tunnelling, Graz, Styria, Austria

ABSTRACT: When constructing tunnels with low overburden in built-up areas face stability and in the unsupported span, as well as displacements of ground and subsidence are major issues. Presently two different concepts to deal with such tunnels can be observed. One concept is to subdivide the face into several excavation steps, like top heading bench and invert excavation with a certain distance between the single steps. The other concept is a full-face excavation with a quick ring closure and heavy support of the face to account for the face stability problem. The different concepts have been compared in a parametric study, using the code FLAC3D.

1 INTRODUCTION

According to the Austrian Guideline for Geomechanical Design of Underground Structures, the system behaviour is defined as the behaviour of the compound system resulting from rock mass and selected construction measures (excavation and support method, auxiliary measures). In tunnels with low overburden, the stress redistribution, combined with poor quality of the ground can lead to instability of the face and the crown. Shear failures can develop progressively without significant sign (Schubert & Vavrovsky 1994). This can lead to serious overbreak of the crown or even to a chimney type failure in case of poor ground and low confining stress (Feder 1981). Therefore, deformations should be carefully controlled to minimize the risk and scale of collapses, as well as surface settlements.

The advocates of the full face method claim that the increase of the rigidity of the core ahead of the face is the main medium of controlling pre-convergence and convergence in the cavity (Lunardi 2000). In cases of low face stability extensive face reinforcement is applied, ranging from a number of 50–60 anchors in shallow tunnels, up to 200 in tunnels with higher overburden (100–200 m) or even 400 in extremely poor ground.

Quick final ring closure was also demanded by some protagonists of the NATM (Müller 1978). Over the decades in poor ground, sequential excavation with the installation of a temporary invert in the top heading however has become common practice. In very weak ground, the face usually is supported by shotcrete and a small and adequate amount of anchors.

An unbiased evaluation of the advantages and disadvantages of the different construction methods so far has not been attempted. To allow an objective comparison of the two approaches, a parametric study has been conducted. The emphasis in this work was put on the evaluation of displacements of the tunnel, the ground ahead of the face, and the surface settlement.

2 3D NUMERICAL MODEL

The Flac3D code was used for the simulation of the tunnel excavation.

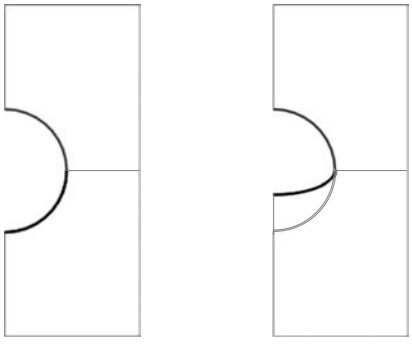
2.1 *Model geometry*

The length of the model was chosen with 150 m and the width with 60 m and 80 m respectively for the weaker ground. The tunnel diameter was chosen with 10 m, while the overburden was 20 m. For the sequential excavation, the top heading height in the model is 5 m with a depth of the temporary invert of 2 m. The thickness of the slices in longitudinal direction was chosen with 2 m. The two construction methods simulated are shown in Figure 1a, b.

2.2 *Material parameters*

The Mohr-Coulomb failure criterion was used for the soil, while the shotcrete was modelled elastically. The parametric study included variations of cohesion, friction and K_0 (Table 1).

The shotcrete was modelled with elastic behaviour, considering the effects of time dependent hardening,



(a) Full-face excavation method.

(b) Sequential excavation method (top heading stage)

Figure 1. Excavation methods.

Table 1. Ground parameters used in the study

Model	Cohesion (kPa)	Friction angle (degrees)	E (MPa)	ν (–)	k_0 (–)
1	10–100	25	40	0.3	1.0
2	20	15–25	40	0.3	1.0
3	30	25	40	0.3	0.5–1.0

Table 2. Development of effective Young's modulus of shotcrete.

Input parameter Ec,eff	1 (MPa)	2 (MPa)	3 (MPa)
	500	1000	2000

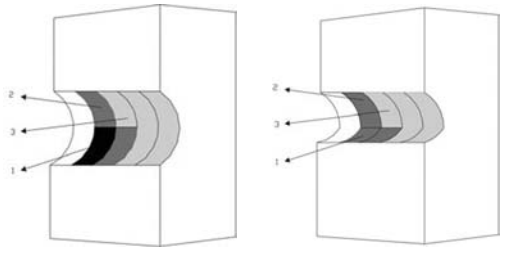
shrink and creep by using an effective Young's modulus with a maximum value of 2000 MPa (Wittke et al. 2003, Schubert 2001, Leitner 2005). Three stages of hardening were considered (see Table 2).

For all simulations a shotcrete thickness of 20 cm was chosen.

2.3 *Sequence of excavation and support installation*

Excavation of 80 m in the longitudinal direction was simulated step by step with round lengths of 2 m. The installation of the support is done 2 m behind the face. The process of installing the support in both construction methods is illustrated in Figure 2a, b. Numbers 1, 2, and 3 in the diagrams correspond to the table 2 values above.

For the top heading – bench excavation sequence it showed, that due to the invert in the top heading and the immediate invert closure after bench and invert excavation only negligible displacements occurred. Hence,



(b) Installation of support for full-face excavation.

(b) Installation of support for top heading excavation.

Figure 2. Installation of support behind the face for both methods.

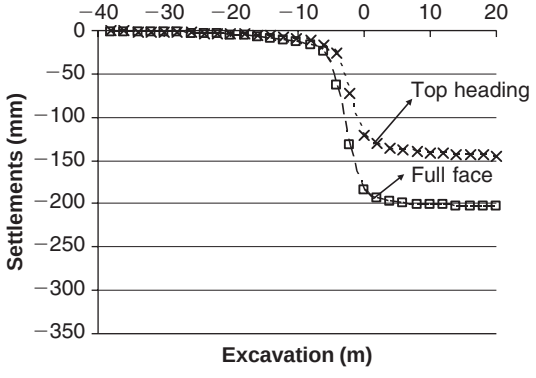


Figure 3. History plot of crown settlements for station 40, $\varphi = 25°$, $K_0 = 1.0$, $c = 10$ kPa.

the results of the bench excavation are not shown in this paper.

2.4 *Face support*

The face support was simulated with a uniformly distributed pressure on the face. The influence of the face pressure on the displacements was studied for both excavation methods. The support was simulated in cases, which would not stabilize without it. To evaluate the equivalent number of face bolts, the average load taken by each bolt was chosen at 100 kN. Some authors use the ultimate load of bolts (Peila 1994) to evaluate the equivalent face support pressure. Other studies show, that the load taken by a bolt is in the range of maximally 100 kN, regardless of its strength (Dias 1999, Trompille 2003, Leitner 2005).

3 RESULTS

3.1 *Terminology*

In this study, pre-settlement refers to the settlement, which takes place ahead of the face.

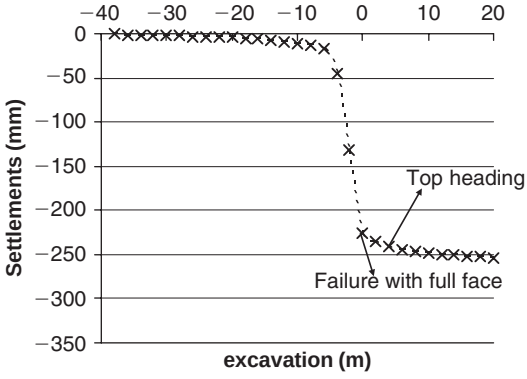


Figure 4. History plot of crown settlements for station 40, $\varphi = 25°$, $K_0 = 1.0$, for c = 15 kPa.

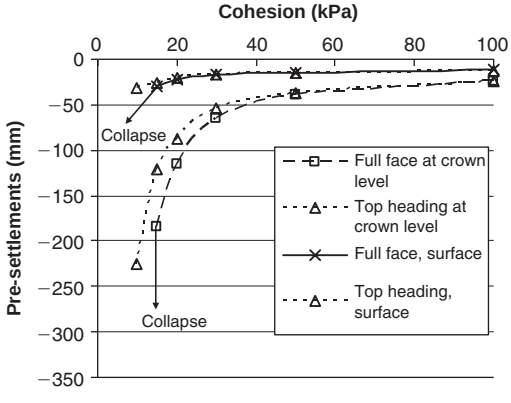


Figure 5. Pre-settlements at crown level and surface, $\varphi = 25°$, $K_0 = 1.0$, cohesion varied.

3.2 *Influence of cohesion*

For a cohesion below 50 kPa, pre-settlements (at the crown as well as at the surface level) caused by sequential excavation are smaller than those with full -face excavation, even if they both increase with decrease of cohesion (See Fig. 5). Disturbance of ground ahead of the face increases with full-face excavation. This soon leads to larger final crown settlements as well as slightly larger surface settlements (Fig. 6). The main difference is that with the full-face excavation the pre-displacements are considerably higher. Face displacements in the case of full-face excavation are much larger (Fig. 7) than those with sequential excavation. Higher displacements of the face increase the hazard for the labour force and lead to the requirement of face support.

A critical cohesion of 30 kPa was detected for which final crown settlements with staged construction are lower than the ones with full-face (Fig. 6).

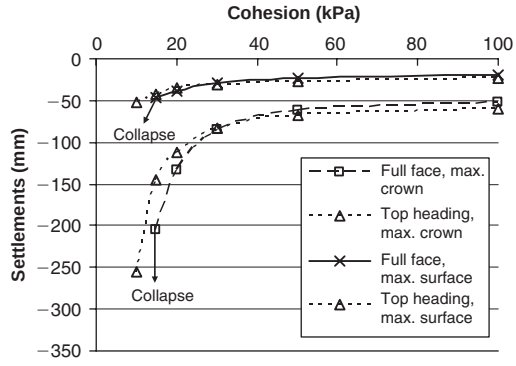


Figure 6. Settlements at crown level and surface, $\varphi = 25°$, $K_0 = 1.0$, cohesion varied.

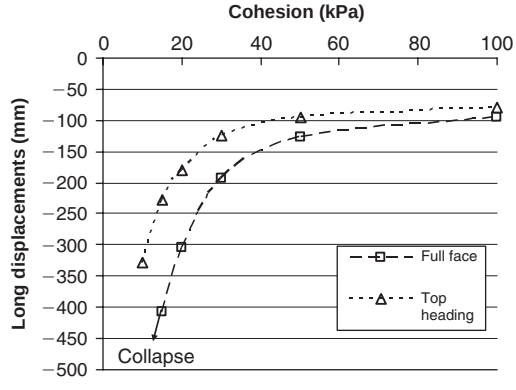


Figure 7. Face displacements, $\varphi = 25°$, $K_0 = 1.0$, cohesion varied.

With a further decrease of cohesion below 20 kPa the final crown settlements increase with the full-face excavation more than those with the staged excavation.

When the cohesion is reduced to 10 kPa the tunnel excavated full face collapses while the top heading remains stable.

3.3 *Influence of coefficient of stresses* K_0

A variation of the coefficient of stresses was investigated for cohesion of 30 kPa. It showed that this parameter had a minimal influence on the development of displacements with different construction methods.

3.4 *Influence of friction angle*

A high sensitivity of displacements to this strength parameter was revealed even with small changes of its value, keeping the cohesion at 20 kPa and K_0 at 1.0. Crown and surface settlements increase significantly

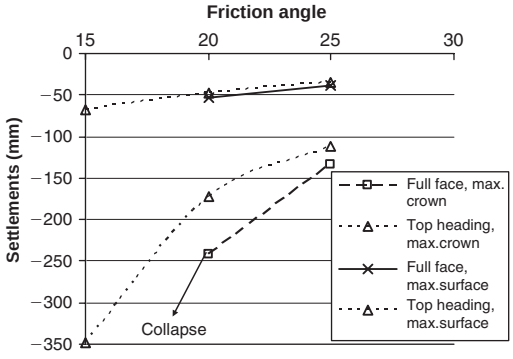


Figure 8. Crown and surface maximal settlements, $c = 20$ kPa, $K_0 = 1.0$, friction varied.

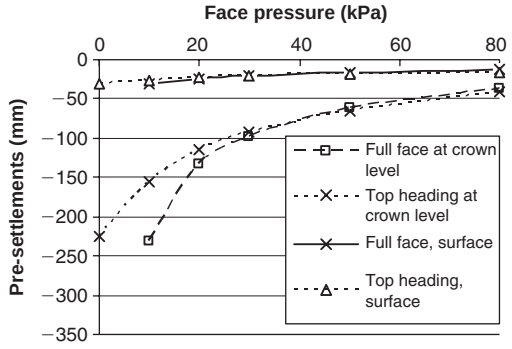


Figure 9. Pre-settlements at crown level and surface, $\varphi = 25°$, $K_0 = 1.0$, $c = 10$ kPa, face pressure varied.

for a lowering of 5 degrees in the friction angle, from 25° to 20° (see Fig. 8).

When the friction angle is reduced to 15°, the tunnel excavated full-face collapses.

In case of a pronounced variation of the friction of the ground, tunnelling with full-face excavation appears to be risky, because displacements escalate rather fast and can not easily be controlled on site.

3.5 *Variation of face pressure*

In cases, where the full-face excavation would lead to failure (in this case $c = 10$ kPa) a pressure was applied on the face at each excavation step. A parametric study for top heading stage was also made to find with what pressure same level of crown settlement, surface settlement or facial displacement occurs. As pointed out before, only a small amount of the face bolts' strength in shallow tunnels is activated, approximately 100 kN. This still is an optimistic estimation, as the activated force in each anchor depends on the position and overlapping length (Leitner 2005). Assuming such a load mobilised in each anchor, we found that full-face excavation demands 24 face bolts and top heading excavation 12 face bolts to achieve nearly the same crown and surface settlements. If the design criterion is only face displacement the full face excavation would require 16 bolts more than the face of the top heading.

Additionally, one can observe that an increase of the bolt density beyond a critical value decreases the displacements only in an insignificant way. Such an effect has been already proved, but only for deep tunnels. A critical bolt density of 0.5 b/m^2 and 0.2 b/m^2, up to which there is a significant influence of the bolts on the displacements was found for full face excavation by Cosciotti (2001). In our study, an optimum face pressure of 30 kPa for both methods and for each examined displacement was found (see Figs. 9–10), meaning 0.3 b/m^2 for top heading stage and 0.6 b/m^2

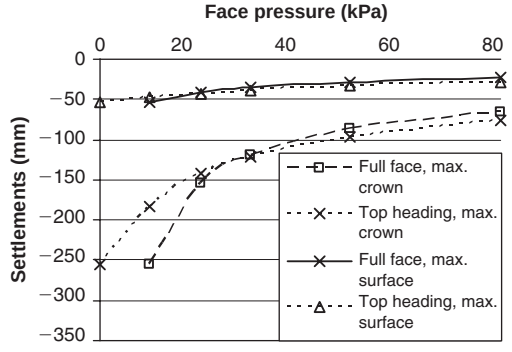


Figure 10. Settlements at crown level and surface, $\varphi = 25°$, $K_0 = 1.0$, $c = 10$ kPa, face pressure varied.

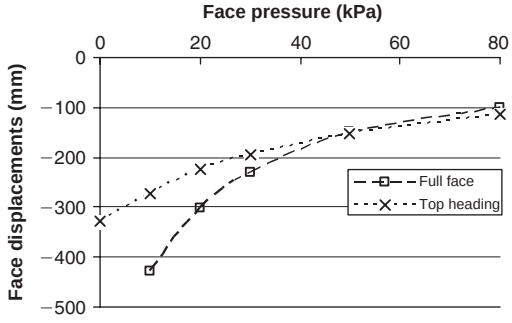


Figure 11. Face displacements, $\varphi = 25°$, $K_0 = 1.0$, $c = 10$ kPa, face pressure varied.

for full face excavation, which is close to the findings of Cosciotti (2001). Face pressure more than 50 kPa makes full-face excavation slightly better than the staged excavation with respect to roof settlements (Fig. 9). However, in such a case the number of bolts is large (40 bolts).

4 CONCLUSIONS

The results of this parametric study demonstrated that for a crucial value of cohesion, the sequential excavation leads to smaller pre-displacements and total displacements than with the full-face approach. The portion of predisplacements dominantly controls the rate and final value of crown and surface settlements.

Collapse occurred at a cohesion value equal to 10 kPa with full face driving, while the top heading remained stable. Full-face tunnel excavation also led to collapse for a soil with cohesion of 20 kPa and friction angle of 15°. This means that for very poor ground the most safe tunnel construction method is sequential excavation. The friction angle proved to be more influential parameter on evolution of displacements than the cohesion. Consequently, in a geological environment with low or frequently changing of friction angle, staged construction of a tunnel reduces the risk of abrupt and uncontrollable propagation of displacements as well as a collapse.

As recent research has shown, forces mobilized in the face bolts are rather low. When using the bolt strength for the estimation of the equivalent face pressure, the effect of the bolts is overestimated.

The study also showed that with the sequential excavation a considerably lower amount of face support is required than with the full-face method to achieve the same deformation magnitudes. It has shown, that with sequential excavation support of the bench face is not required, providing a sufficient distance between top heading and bench excavation is maintained.

The effectiveness of face bolting progressively decreases beyond a density of 0.3 bolts/m^2 and 0.6 bolts/m^2 for the top heading and full-face excavation respectively.

The study shows, that in very poor ground sequential excavation is preferable in terms of crown, face, and surface displacements and risk of collapse of the face. To achieve an equivalent level of safety, the full-face excavation would require a considerable number of face bolts.

The final decision on which construction method is preferable for specific soil conditions has to be based on an analysis of time, costs, and risk associated with each method.

REFERENCES

Cosciotti, L., Lembo, F., Boldini, D. & Graziani, A. 2001. Simplified behaviour models of tunnel faces supported by shotcrete and bolts. International Symposium of Modern Tunneling Science and Technology, Kyoto.

Dias, D. 1999. Renforcement du front de taille des tunnels par boulonnage. Etude numérique et application à un cas réel en site urbain. Doctorat, Institut National des Sciences Appliquées de Lyon.

Feder, G. 1981. Firstniederbrüche im Tunnelbau. Forschung und Praxis 27: 52–63

Leitner, R. 2005. Numerical Investigation on Failure Mechanisms and Function of Tunnel Support systems. Diploma Thesis, Institut of Rockmechanics and Tunneling, Graz University of Technology.

Lunardi, P. 2000. Design and constructing tunnels: A.DE.CO.- RS approach. Tunnels and Tunneling International, May 2000.

Müller-Salzburg, L. 1978. Grundgedanken und Grundsätze der "Neuen Österreichischen Tunnelbauweise". Felsmechanik Kolloquium Karlsruhe 1978: 247–262. Trans Tech Publications.

Österreichische Gesellschaft für Geomechanik. 2001. Richtlinie für die Geomechanische Planung von Untertagebauarbeiten mit zyklischem Vortrieb.

Peila, D. 1994. A theoretical study of reinforcement influence on the stability of a tunnel face. Geotechincal and Geological Engineering 12: 145–168.

Schubert, P. & Vavrovsky, G-M. 1994. Interpretation of Monitoring Results. World Tunneling, November 1994: 351–356.

Schubert, W. & 3G- Gruppe Geotechnik Graz. 2001. Remarks on input for shotcrete properties for numerical models, Eastern Highway Tunnel Project Section Suao-Hoping, Tunnels 6 & 7.

Trompille, V. 1998. Mouvements d'extrusion du front de taille d'un tunnel renforcé par des boulons en fibre de verre: comparaison entre des measures in situ et un modèle analytique dévéloppé à l'ENTPE. DEA. ENTPE, Lyon, France.

Wittke, W., Tegelkamp, M., Wittke-Gattermann, P. & Wittke, M. 2003. Tunnelling under Stuttgart airport runway. World Tunnelling 16(8): 317–321.

This page intentionally left blank

Underground Space – the 4th Dimension of Metropolises – Barták, Hrdina, Romancov & Zlámal (eds)
© 2007 Taylor & Francis Group, London, ISBN 978-0-415-40807-3

Characteristics of the ice-ring with phase change of water to ice for LNG underground storage

C. Park, D.S. Cheon & S.K.Chung
Korea Institute of Geoscience & Mineral Resources, Korea

H.D. Lim
Chungnam National University, Korea

Y.J. Park
University of Suwon, Korea

S.D. Lee
Korea Highway Corporation, Korea

ABSTRACT: Recently, interest has increased in the underground storage of cryogenic materials such as LNG. When designing and constructing underground storage for LNG, it is very important to evaluate the characteristics of the rock mass under cryogenic conditions. The formation mechanism and extent of the ice-ring, which is a key factor in the new concept for storing LNG and is the frozen zone including ice in several joints within the rock mass, should be studied especially when considering the stability of underground storage for LNG. However, little research exists on ice-ring formation and the thermo-mechanical behavior of rocks exposed to cryogenic conditions. In this study, in order to investigate the characteristics of the ice-ring caused by cooling, we measured the swelling pressure within the joints caused by the phase change of water to ice. We also performed the cryo-suction test to investigate the flow characteristic after ice formation. The results of tests show that the swelling pressure was approximately 2.43 MPa at the phase change temperature, 0°C, and the swelling pressure increased about 11.66 MPa/°C as cooling took place. In the cryo-suction test, the growth rate of the ice in the joints was 1.0 mm/day to 1.1 mm/day and varied minimally in joint apertures.

1 INTRODUCTION

The demand for liquefied petroleum gas (LPG) and liquefied natural gas (LNG) is increasing rapidly, and there are plans to build new liquefied gas storage facilities in Korea. To construct underground storage for cryogenic temperature materials such as LNG, the thermal effects on structural stability underground should be considered.

A number of unsuccessful attempts to store LNG in unlined rock caverns have been tried (Kim, Amantini & Chanfreau, 2003). Those failures were mainly caused by the opening and generation of cracks by a cryogenic thermal load (−162°C) on the cavern wall. In order to overcome this problem, a new concept for storing LNG in a lined rock cavern (LRC) has since been developed and tested for several years (KIGAM, 2004). In this concept, a containment system with a gas-tight steel liner and insulation protect the host rock against the extremely low temperature. In addition, a new groundwater control system was introduced to create an ice-ring (ice barrier) around the LRC cavern to protect it from groundwater intrusion into the containment system. The ice-ring is supposed to play an important part as a secondary barrier against leakage of the stored material. In the case of groundwater intrusion into the containment system, the integrity of the containment system can be destroyed because of the volume expansion of the groundwater during the freezing process. Therefore, the location and thickness of the ice-ring and the characteristics of the ice-ring are important factors for the stable storage of LNG in a lined rock cavern.

To validate this new concept of storing LNG in a lined rock cavern, a pilot plant has been constructed and operated in an existing research cavern in KIGAM since 2003 by storing LN_2 (−196°C) instead of LNG for safety and practical reasons.

In this research, in order to investigate the characteristics of the ice-ring caused by cooling, we measured

the swelling pressure within the joints caused by the phase change of water to ice. And we performed the cryo-suction test to investigate the flow characteristic after ice formation. We also measured the propagation of the ice-ring with joint apertures.

2 ICE-RING FORMATION IN PILOT CAVERN

The schematic construction sequences are outlined in Figure 1. In this new concept of LNG storage, groundwater near the cavern must be drained in order to avoid the freezing of groundwater that causes instability of the rock cavern and the concrete lining. After completing the drainage around the cavern, the cavern was filled with LN_2. Then a heat transfer occurred from the cavern to the rock mass due to the temperature gradient. After checking the spread of an 0°C isotherm location by temperature monitoring, the drainage system stopped, and the groundwater table returned to the original state. Consequently, an ice-ring formed around the 0°C isotherm.

The pilot underground cavern is located at Daejeon, Korea, and the depth from the surface to the cavern roof is about 20 m. Detailed information about this cavern has been described in KIGAM research reports (KIGAM, 2004). A comprehensive geotechnical monitoring system was applied to measure the temperature and the thermo-mechanical responses of the rock mass and concrete during the construction and operation of the LNG storage. Temperature and displacement were monitored from 6 borehole extensometers, which have 6 measuring points, respectively. After several commissioning tests, operation began on 10 January 2004 with a 2.6 m level of LN_2; the drainage rate was reduced gradually from 10 June 2004 to 8 July 2004. Filling of LN_2 was completely stopped on 5 July 2004. The cavern was completely emptied on 12 August 2004. In addition, through groundwater level monitoring, it was found that the groundwater level rose to the roof of the cavern on 1 July 2004.

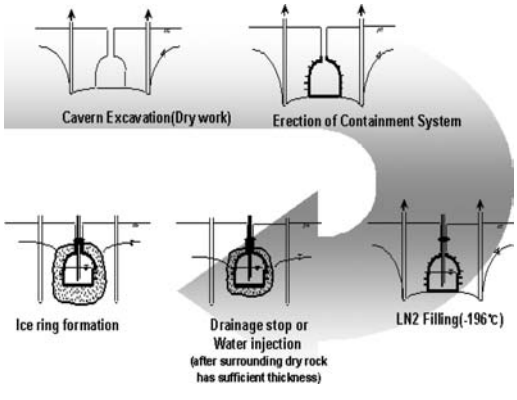


Figure 1. Schematic construction of the Daejeon pilot LNG cavern.

The cavern and containment system were dismantled after the completion of the scheduled operations in order to judge the validity and safety of the proposed concept. The decision criterion was based on the occurrence of thermal cracks in the rock mass and concrete lining. No remarkable thermal cracks were detected in the rock mass and concrete lining; thus, the experiment was considered a success.

3 ROCK SPECIMENS

The rock specimens used in the experiment were biotitic granite, which were sampled by the LNG pilot plant. The basic properties of the tested rocks are as follows.

3.1 *Mechanical properties*

The mechanical properties of the tested rocks are summarized in Table 1.

3.2 *Thermal properties*

The thermal properties of the granite were measured by Korea Research Institute of Standard and Science. Thermal conductivity, specific heat, and the linear thermal expansion coefficient are listed in Table 2.

Table 1. Mechanical properties of the tested rocks.

Properties	Values
Bulk specific gravity	2.66
Absorption ratio (%)	0.32
P-wave velocity (m/s)	3,740
S-wave velocity (m/s)	2,010
UCS (MPa)	129
Young's modulus (GPa)	43.2
Poisson's ratio	0.22

Table 2. Thermal properties of the tested rocks.

Properties	Values
Specific heat (J/g °C)	0.7282
Thermal conductivity (W/mK)	2.382
Linear thermal expansion coefficient ($\times 10^{-6}$/°C)	7.411

These properties vary with temperature. Table 2 shows the numerical value at room temperature.

4 LABORATORY TESTS

4.1 *Swelling pressure test by phase change*

To measure the swelling pressure during the phase change of water to ice, a new testing system was manufactured as shown in Figure 2. The vessel is made with 10 mm thick circular steel to prevent deformation with phase change. The environmental chamber (Fig. 3) supplied by the Interlaken rock testing system was used to obtain a cold environment. The swelling pressure was measured using a PG-1TH (Kyowa) pressure transducer, which has a capacity of 100 MPa and thermal correction to −10°C. As shown in Figure 2, the inner space was filled with water and silicon oil. The swelling pressure by the phase change was transmitted to the pressure transducer through the silicon oil.

The tests were performed from room temperature to −3°C, from −3°C to −6°C and again −6°C to −8°C. The temperature was lowered at the rate of 1°C/min to minimize the thermal stress buildup during refrigeration. The test sampling rate was 0.1 Hz for consideration of test time.

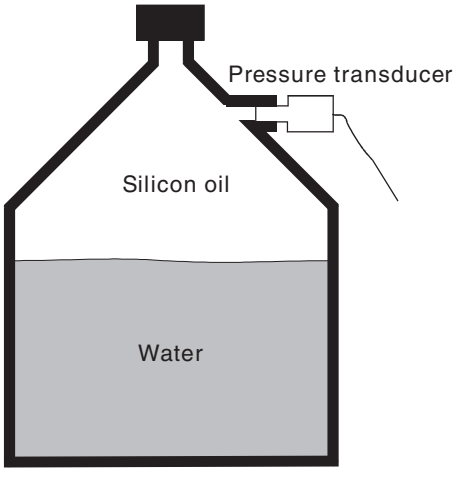


Figure 2. Schematic diagram of test equipment.

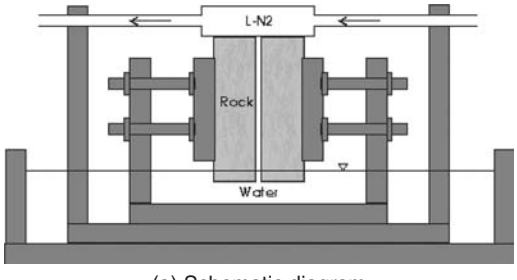


Figure 3. A view of environmental chamber for cryogenic test.

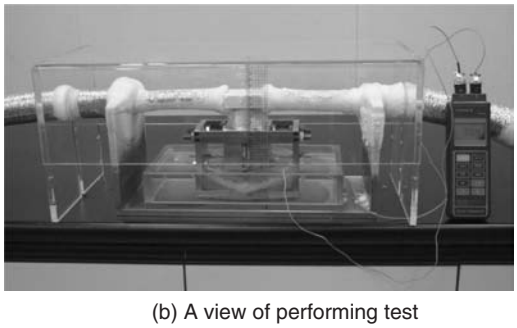
4.2 *Cryo-suction test*

For the cryo-suction test, new test apparatus also was manufactured (Fig. 4). The purpose of this cryo-suction test was to identify the possibility of progressive ice-ring movement to the LNG cavern. For this test, we measured the progress length of ice within the joints. To reproduce the joints, a rock specimen with a 150-mm height was separated into two parts. The tested apertures between the two rock specimens were 1.5 mm and 3.0 mm.

As shown in Figure 4(a), cryogen was conducted to the specimens through the LN_2 pipe located at the upper end of the specimens. The lower end of the specimens was under water. After the water within the joint changed to ice, the progress length of the ice was measured with visual observation for 12 hours. From these measurements, the growth rate was calculated.



(a) Schematic diagram



(b) A view of performing test

Figure 4. Cryo-suction test.

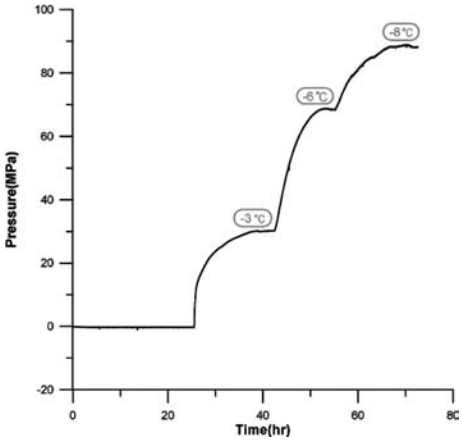


Figure 5. Results of swelling pressure test.

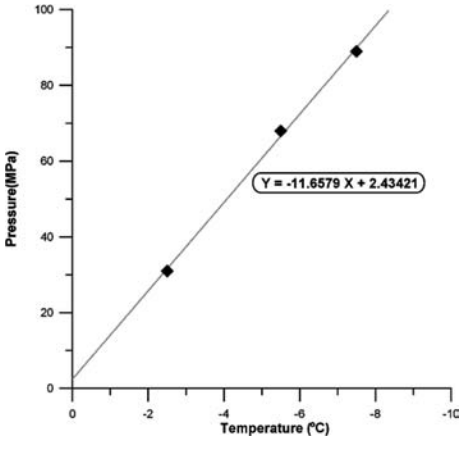


Figure 6. Swelling pressure as a function of temperature.

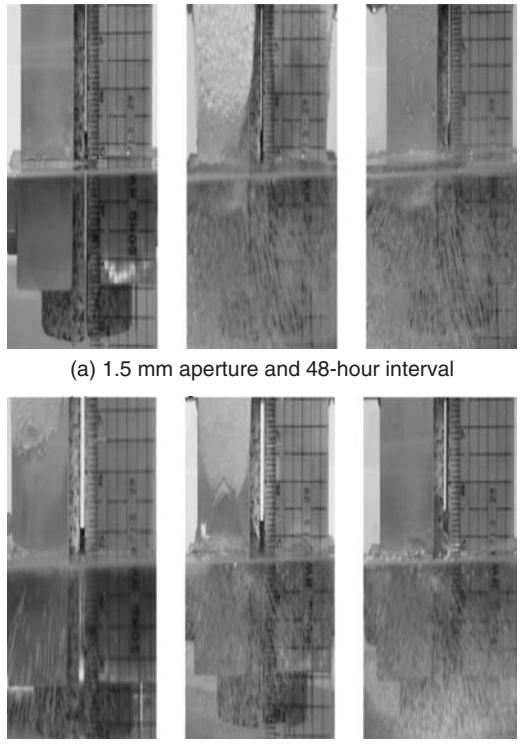
5 TEST RESULTS

5.1 *Swelling pressure test*

The test results show that swelling pressure by the phase change of water to ice was about 31 MPa when the temperature was lowered from room temperature to −3°C. The swelling pressures were 68 MPa from −3°C to −6°C and 89 MPa from −6°C to −8°C (Fig. 5).

From the linear regression on the temperature, swelling pressure was 2.43 MPa at 0°C and increased at a rate of 11.66 MPa°C (Fig. 6).

According to previous research, the swelling pressure occurring within the pore or joint was about 14 MPa (Blyth et al., 1984), and when the water was completely confined, the swelling pressure was 25 MPa (Andersland et al., 1978). Compared to the previous research, the different swelling pressure observed in our study was due to the effect of the state of the water confinement and test temperatures.



(a) 1.5 mm aperture and 48-hour interval

(b) 3.0 mm aperture and 48-hour interval

Figure 7. A view of cryo-suction test.

Table 3. Results of cryo-suction test.

Elapsed time (day)	Cryo-suction (mm)	
	1.5 mm aperture	3.0 mm aperture
0.5	0	0
1.0	0.5	0.5
1.5	0.5	1.0
2.0	0.5	1.5
2.5	1.0	2.0
3.0	1.5	2.5
3.5	2.0	3.0
4.0	2.0	3.5
4.5	2.5	4.5
5.0	3.5	5.0
5.5	4.0	6.0
6.0	4.5	6.0

5.2 *Cryo-suction test*

From the observation of the progress length of ice, ice growth rates were measured. Figure 7 shows the test

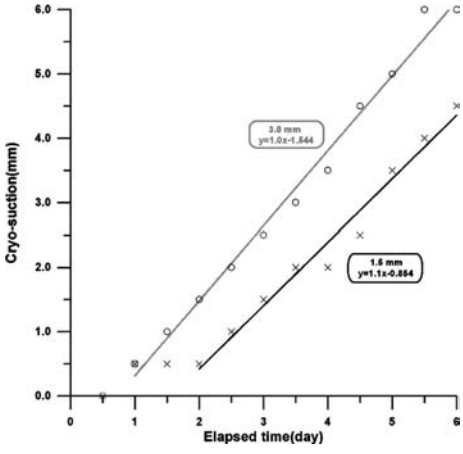


Figure 8. Cryo-suction with elapsed time.

results at the 1.5 mm aperture and 3.0 mm aperture. The numerical values with reading visual observation are listed in Table 3.

As shown in Figure 8, the ice growth rate was 1.0 mm/day at the 1.5 mm aperture, and the ice growth rate was 1.1 mm/day at the 3.0 mm aperture. There is no significant difference with variation of apertures.

6 CONCLUSION

To investigate the characteristics of the ice-ring caused by cooling, we manufactured new test apparatus and measured the swelling pressure and growth rate of ice within joints caused by the phase change of water to ice. From this study, the following results were obtained:

- The Swelling pressure by the phase change of water to ice was about 31 MPa, 68 MPa, and 89 MPa when the temperature was lowered from room temperature to −3°C, from −3°C to −6°C and from −6°C to −8°C, respectively.
- From linear regression on temperature, the swelling pressure was approximately 2.43 MPa at the phase change temperature, 0°C. The swelling pressure increased about 11.66 MPa/°C.
- The growth rate of ice within the joint was 1.0 mm/day to 1.1 mm/day and varied minimally in the joint apertures.

REFERENCES

Andersland, O.B. & Anderson, D.M. 1978. *Geotechnical engineering for cold regions*, New York: McGraw-Hill.

Blyth, F.H. & de Freitas, M.H. 1984. *A geology for engineers*, London: Edward Arnold.

KIGAM. 2004 Development of base technology for underground LNG storage and the analysis on the operation results of pilot plant, *KIGAM report*.

Kim, H.Y. Amantini, E. & Chanfreau, E. 2003. Pilot project: lined cavern LNG storage. *The Korean Society for Geosystem Engineering* 40: 140–145.

This page intentionally left blank

Underground Space – the 4th Dimension of Metropolises – Barták, Hrdina, Romancov & Zlámal (eds)
© 2007 Taylor & Francis Group, London, ISBN 978-0-415-40807-3

Underground exploitation of a granite mine by large voids: stability aspects

D. Peila, S. Pelizza, & C. Guardini
Tunnelling and Underground Space Center Dept. of Land, Environment and Geoengineering, Politenconco di Torino, Torino, Italy

ABSTRACT: This paper describes the geomechanical and stability aspects of an underground granite mine located in Canal San Bovo (Trento district, North – East Italy). The exploitation of the granite, which is used in the ceramic industry, is carried out the by room and diaphragm method. The rooms are 12 m wide and they cross the main discontinuity set of the rock mass in the perpendicular direction. This work presents the analyses that were performed to verify the local and global underground void stability.

1 INTRODUCTION

Industrial mineral exploitations are usually carried out in open pit mines, since they are characterized by lower production costs than the underground exploitation of the same ore. The underground option is however unavoidable when environmental preservation is necessary and when the topography of the area does not allow the creation of an open pit mine.

An interesting example of these conditions is the underground granite mine in Canal San Bovo (Trento District, Italy) (Fig. 1), which is exploited to obtain feldspar for the ceramic industry. The exploitation method consists of the excavation of long rooms separated by diaphragms, which are excavated starting from a main tunnel sub-parallel to the mountain slope. The choice of the exploitation method was influenced by the geomechanical parameters of the good quality rock mass, which therefore, allows the rooms to be excavated with an annual production of about 30000 m^3 of granite. It is important to point out that the chosen geometry is very interesting since it does not require large infrastructural works, can be selective and allows a large flexibility in terms of production quantities (if necessary, more rooms can be exploited simultaneously).

2 GEOLOGICAL AND GEOMECHANICAL ENVIRONMENT

2.1 *Geological conditions*

The exploitable granite rock mass is located on the left side of Vanoi stream valley, between Canal San Bovo and Caoria (Trento District), and enters inside the Col Tondo mountain for about 500 m. It is a coarse

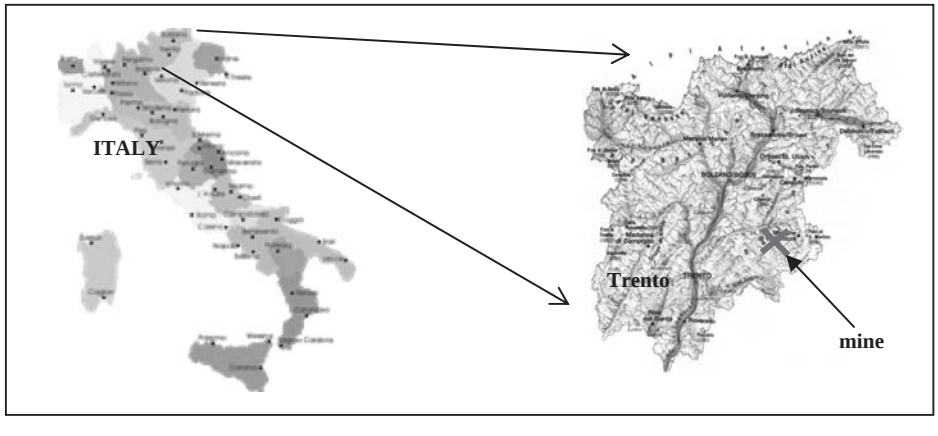


Figure 1. The position of the mine inside the Trento district.

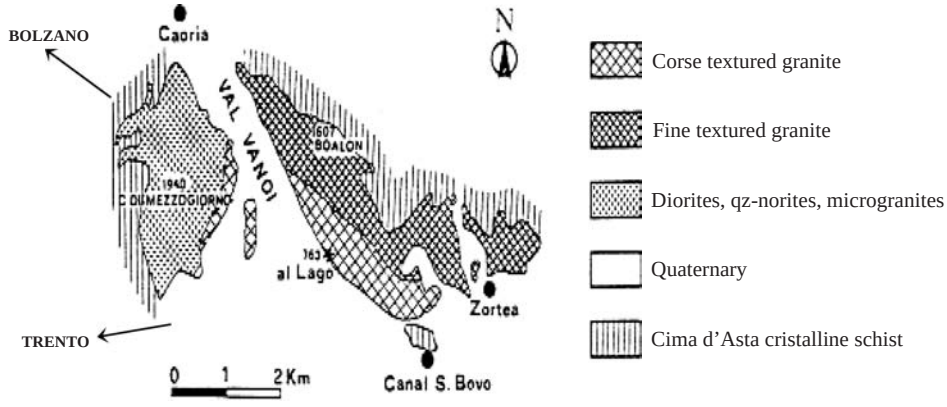


Figure 2. Simplified geological map of the area where the mine is located (Siena, 1977).

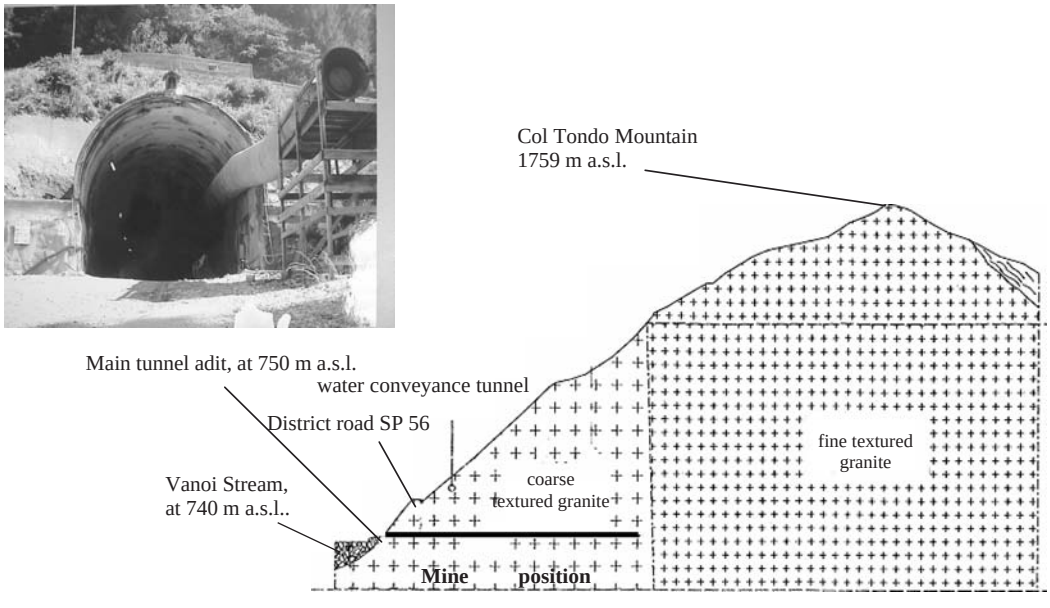


Figure 3. Rock mass geological section.

textured granite, with medium grains size (ranging between 1 mm and 3 mm), mainly composed of quartz, k-feldspar, plagioclase, biotite and muscovite.

The excavated ore is subject to a crushing treatment in order to separate the biotite from the other minerals, which are the useful products for the ceramic industry.

2.2 *Geomechanical investigations*

Detailed investigations, both in the laboratory and in situ, with a geotechnical survey in the first exploration tunnel, were carried out to provide reliable geotechnical data for the stability analyses of the mine voids. The results of the in situ survey were processed using the Dips code (Ver. 5.2, Rocscience) (Figs. 4–5). Four main discontinuity sets are present in the rock mass (Tab. 1), the most important is the A set, which has a 233° dip direction and a dip of 77°, and is therefore sub-parallel to the mountain slope. The discontinuity set indicated as C is also noticeable since it has a high persistence and if coupled to the previous one may cause block collapses in the rooms. The B and D sub-horizontal and the sub-vertical discontinuity sets are less important since they are less persistent than the A and C ones (Fig. 6). Globally speaking, the geomechanical conditions of the rock mass are generally good and, according to the Bieniawski rock mass classification, the calculated RMR

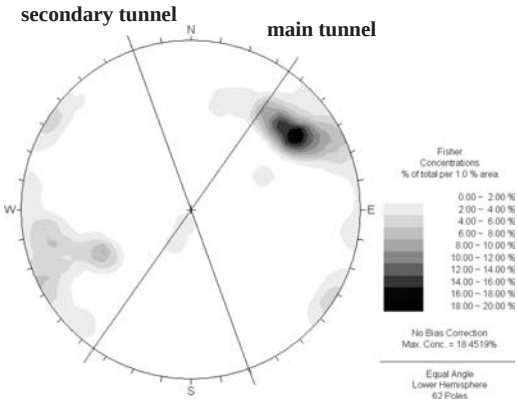


Figure 4. Stereoplot of joint poles.

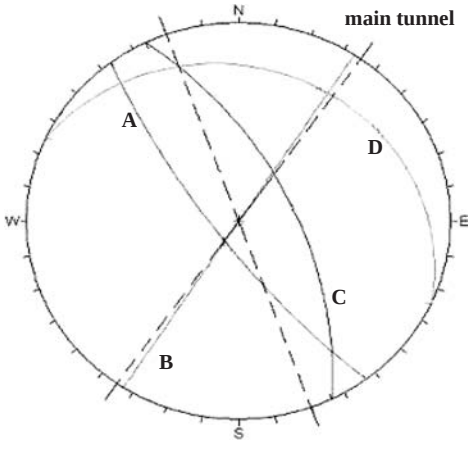


Figure 5. Representation of the main discontinuity sets.

Table 1. Orientation of the discontinuity sets.

Discontinuity sets	Dip	Dip direction
A	77°	233°
B	90°	123°
C	61°	64°
D	15°	25°

values are between 59 and 74 (class II) (Bieniawski, 1989; Hoek et al., 2002). The most important geomechanical parameters of the intact rock, evaluated by laboratory tests, are summarized in Table 2.

3 LAYOUT OF THE MINE

The mine consists of sub-parallel rooms separated by rock diaphragms, as shown in Figure 7. The slopes

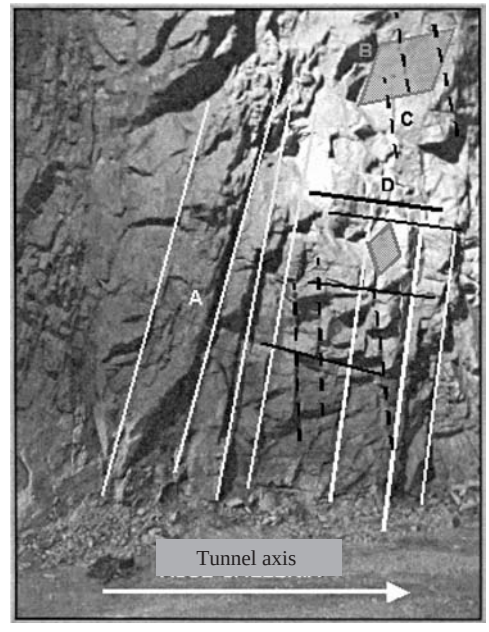


Figure 6. Photograph of the main tunnel wall and indication of the main discontinuity sets.

Table 2. Geomechanical parameters of the rock mass.

Rock mass Young's modulus	$E_M = 2RMR - 10$ [GPa]	40
Rock mass Poisson's ratio	ν	0.3
Uniaxial compressive strength of the intact rock	σ_c [MPa]	170
Rock mass m (peak) and s (peak)	m_p, s_p	8.595–0.0205
Rock mass m (residual) and s (residual)	m_r, s_r	1.000–0.0100

overhanging the adit are very steep and they have therefore made it necessary to place the mine adit at 750 m a.s.l. and pass under the local SP 56 road with forepoling (Fig. 3). The main tunnel axis orientation is N35°E, with a section of about 53 m^2. A secondary tunnel was driven from the main tunnel and the exploitation rooms are excavated from this secondary tunnel. The rooms are 12 m wide and 18.5 m high and their axis is almost parallel to the main entrance and is perpendicular to the main discontinuity set (A), in this way it was possible to obtain more favorable stability conditions.

The sequence of operations used to exploit each room is as follows:

– driving the top gate from the secondary tunnel to the end of the room;
– exploitation of the room by blasting with a bench height of 10 m.

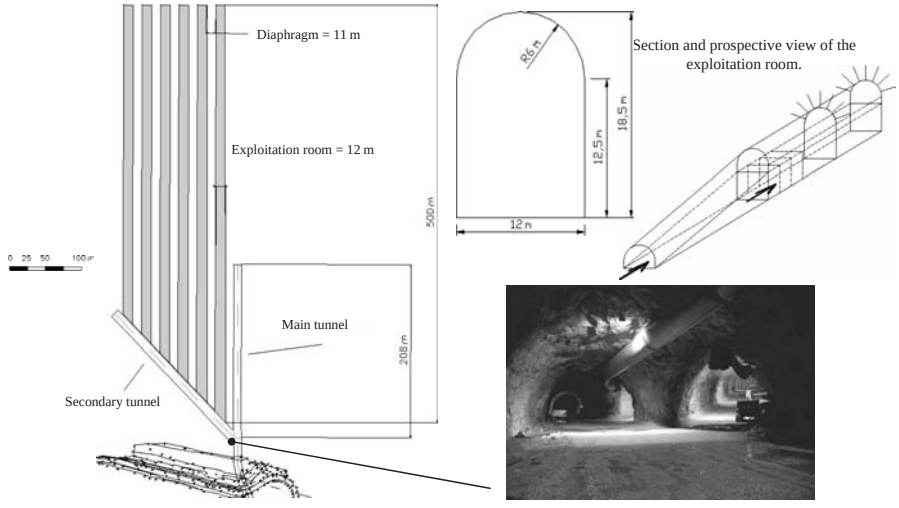


Figure 7. Plan of the mine, prospective view and transversal section of an exploitation room.

Table 3. Results of the Unwedge calculation . In order to improve the quality of the results, three different orientations were assumed for joint set A, corresponding to medium and extreme values of the distribution (A (medium): dip = 77°, dip dir = 233°; A1: dip = 71°, dip dir = 211°; A2: dip = 77°, dip dir = 248°). SF = safety factor.

Analysis number	Joint sets	Cohesion of the joints [kg/cm^2]	Total number of expected wedges	% of wedges with SF < 1.5	% of wedges with SF < 1
1	A (medium), B, C, D	0.1	18	11.1%	5.5%
2	A1, B, C, D	0.1	19	15.8%	5.3%
3	A2, B, C, D	0.1	17	5.9%	5.9%
4	A (medium), B, C, D	0.05	18	27.8%	11.1%
5	A1, B, C, D	0.05	19	21.1%	10.5%
6	A2, B, C, D	0.05	17	29.4%	11.8%

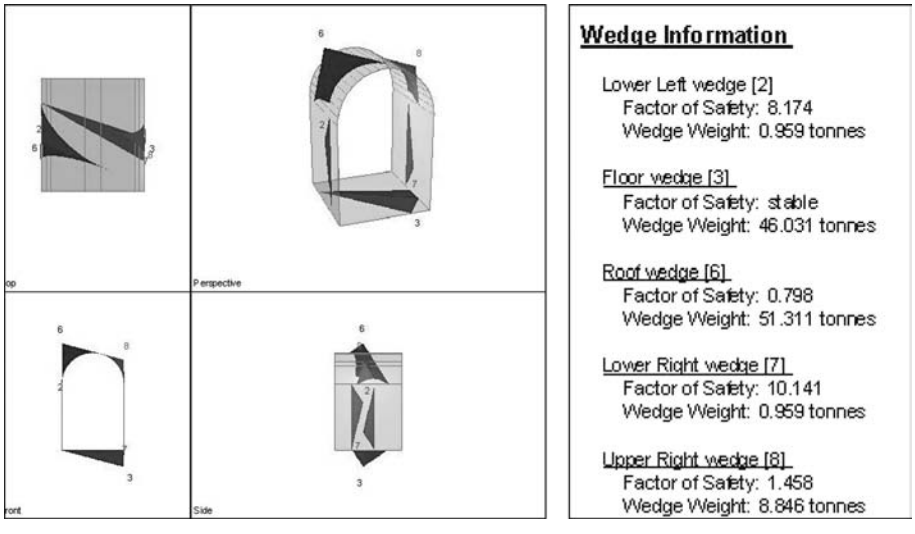


Figure 8. Graphical and analytical results of analysis n.1 using the Unwedge code.

Spot bolting is foreseen for the areas where the geo-structural survey and jobsite observations have detected unstable rock wedges. Systematic rock bolting, wire mesh and shotcreting is also used when crossing fault zones.

4 NUMERICAL MODELS

The study of the stability conditions of the exploitation rooms was carried out using two numerical analyses. The first one was carried out to evaluate the possible presence of unstable rock wedges, due to discontinuities, using the Unwedge code (ver. 3.0, Rocscience) (Guardini, 2005). The second one had the aim of analyzing the global stress and deformation conditions of the rock mass during the exploitation, which depend on the height of the overburden, in a transversal section of the mine. These numerical models were developed using the FEM Phase^2 code (ver. 6.0, Rocscience).

4.1 *Wedges stability analysis*

The used code allows the maximum wedges, which are present on the room walls and roof, to be simulated, and their volume and the safety factor (defined by the ratio between the stabilizing and destabilizing forces acting on the wedge) to be calculated, based on the geometry of the joint sets and the geomechanical properties.

The results of the calculation are summarized in Table 3 and an example of calculation output is shown in Figure 8.

The study of the stability of the wedges was carried out focusing on the cohesion of the joints and the influence of the persistence on the safety factor value. In the first set of analyses, the joint persistence was assumed equal to 100% in order to highlight only the cohesion effect. The results showed that the most critical area in the room is the roof, where local wedge falls could occur. However, it is possible to observe that a reduced increase of the cohesion ensures the stability of all the computed rock wedges. The second set of analyses was carried out to analyse the influence of the joint persistence on the safety factor values. The comparison between the obtained results showed that a small decrease in joint persistence leads to a large increase in the value of the safety factors (Fig. 9). This analysis was repeated for all the possible values of joint persistence and the final results are summarized in the graphics shown in Figure 10. From the study of the results of analysis 1, 2 and 3 (assumed cohesion value = 0.1 kg/cm^2), with 100% joint persistence, 11% of all the possible wedges have a SF < 1.5; this value increases to 26% when analyses 4,

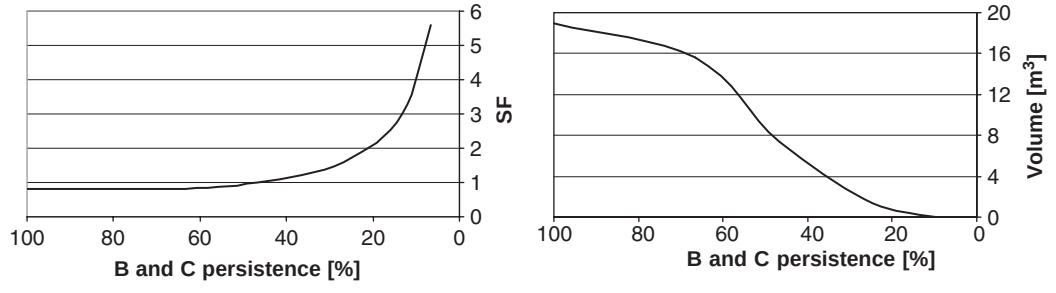


Figure 9. Examples of parametrical analysis of the persistence of the discontinuities. In the left graph it is possible to observe that with a decrease in the persistence value to 30%, SF shows a higher value than 1,5. The decrease in the wedges volume is shown in the right graph in function of the decrease in discontinuity persistence.

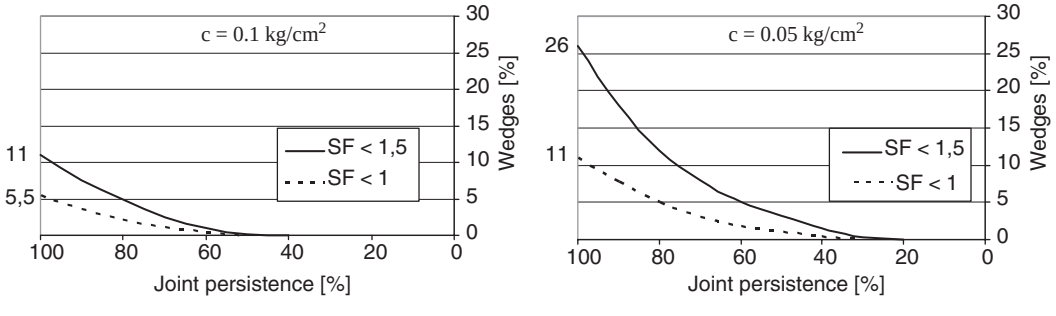


Figure 10. Discontinuity persistence effect on the safety factor of the wedges.

5, and 6 (assumed cohesion value = 0.05 kg/cm^2) are considered. The reduction in joint persistence to 50% leads to the reduction in the wedges with a SF < 1.5 at about 0%, with c = 0.1 kg/cm^2, and at 3%, with c = 0.05 kg/cm^2. The discussed results highlight that the presence of some rock bridges along the discontinuities could ensure a consistent increase in the safety factor of the wedges and therefore it is possible to state that the technical choice of spot rock bolting would guarantee roof stability for most of the possible joint geometries.

4.2 *Rock mass stress condition analysis*

The study of stress and deformation around the mine rooms was carried out by applying both the two-dimensional Phase^2 FEM code (ver. 6.0, Rocscience) and the tributary area analytical method. The use of a two-dimensional model is suitable for the analysis of this problem because the exploited rooms are developed mainly in the longitudinal direction and it is therefore possible to disregard the three-dimensional effect due to the excavation face when the rooms have been excavated. The developed numerical models, which simulate the excavation of six rooms at different depths, allowed the rock diaphragm stability to be verified. The model is 607 m wide and its height ranges between 318.5 m and 718.5 m, in function of the overburden (Tab. 4 and Fig. 10); two different K_0 (σ_o/σ_v) were considered: $K_0 = 0.5$ and 1.

Table 4. Main parameters assumed in the Phase^2 numerical analysis.

		Overburden height [m]	Exploitation room advancement [m]	k
Analysis 1	1a	100	50	1
	1b	200	180	
	1c	300	300	
	1d	400	450	
Analysis 2	2a	100	50	0.5
	2b	200	180	
	2c	300	300	
	2d	400	450	

The following stages were considered in the model:

1. application of the original stress field;
2. simulation of the excavation of the upper part of the first room;
3. simulation of the room exploitation with 10m vertical benching;
4. repetition of stages two and three till the end of the mine exploitation (i.e. excavation of 6 rooms).

The stresses (Figs 12 and 13), the horizontal and vertical displacements after the exploitation of each room (Fig. 14) and the plastic zones (Fig. 15) were analysed from each simulation.

From these calculations, it was possible to evaluate the underground stability conditions during and at the end of the mine exploitation: the vertical stress inside the diaphragms never overcame 24 MPa and the displacement maximum value was 6 mm (Fig. 13).

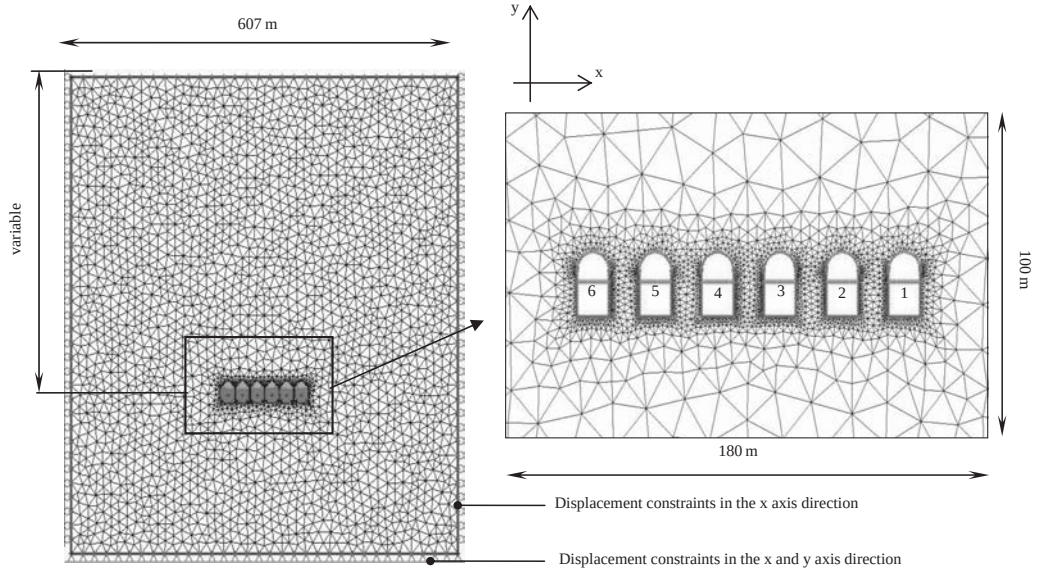


Figure 11. Numerical model section and zoom of the excavation boundaries.

The plastic zones around the room walls had a maximum thickness of 2 m, where the overburden height is 400 m, however this plastic zones do not compromise the global underground stability, though they could cause the local detachment of rock wedges from the room walls, therefore a particular attention is required during the vertical benches exploitation.

Yielding phenomena on the crowns of the rooms is almost absent.

The results obtained from the numerical models were verified by applying the tributary area method. The analytical equations used for the calculation of the vertical stress acting on the diaphragms are defined in technical literature (Brady & Bown, 1985) and allow the safety factor to be defined by comparing the computed stress value to the rock mass uniaxial compressive strength (σ_{cRM}), which in this case was assumed equal to 60 MPa. The results of the tributary area calculations are summarized in Table 5, while Figures 16 and 17 report the stresses acting on the diaphragms and the computed safety factors.

From the results of the analytical and numerical calculations it is possible to point out that average vertical stress values, calculated according to the analytic method, are usually very close to the maximum value obtained with the numerical model, while the safety factor, evaluated according to the analytic method, usually shows higher values than the ones obtained with the numerical model.

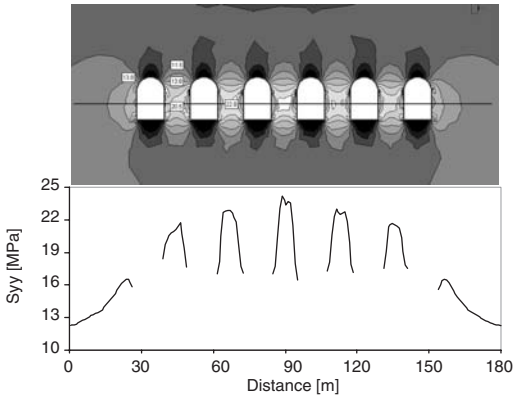


Figure 12. Vertical stress (σ_{yy}) distribution in the numerical analysis n. 2d (overburden height = 400 m, k = 0.5). The σ_{yy} value along the horizontal section in the middle of the diaphragms is shown. The maximum σ_{yy} value is 24 MPa in the central diaphragm (stress values increase from black to white).

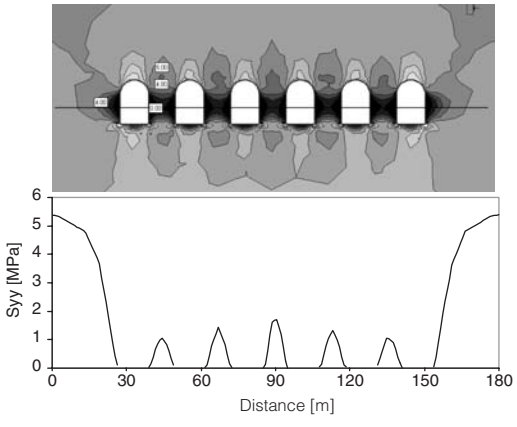


Figure 13. Horizontal stress (σ_{yy}) distribution in the numerical analysis n. 2d (overburden height = 400 m, k = 0.5). The σ_{xx} value along the horizontal section in the middle of the diaphragms is shown. The maximum σ_{xx} value is 1.7 MPa (stress values increase from black to white).

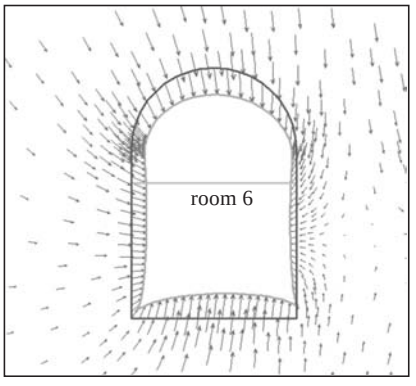


Figure 14. Displacements of the walls of room 6 obtained from the analysis n. 2d, the maximum displacement value is 5.5 mm (scale factor = 500).

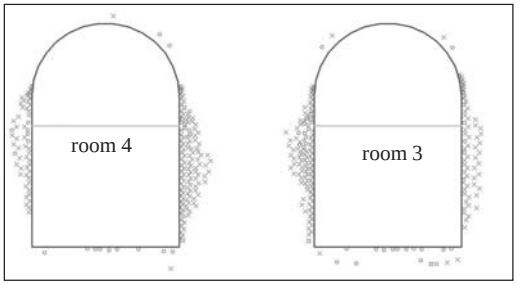


Figure 15. Plastic zones (maximum value = 2 m) in the central diaphragm, obtained from the analysis n. 2d, at the end of mine exploitation.

Table 5. Vertical stress and safety factor values of the diaphragms obtained using the tributary area method.

Overburden height [m]	100	200	300	400
σ_p [MPa]	5.6	11.3	16.9	22.6
SF	10.6	5.3	3.5	2.7

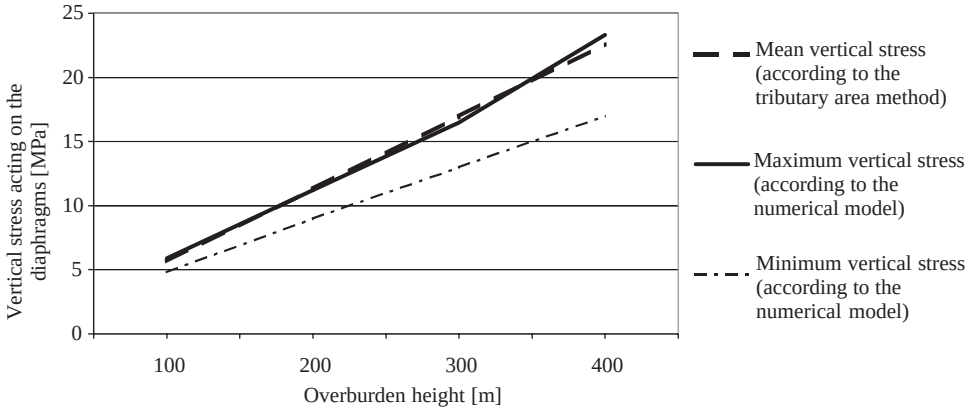


Figure 16. Vertical stress acting on the diaphragms for increasing overburden heights computed with the analytical and numerical approaches.

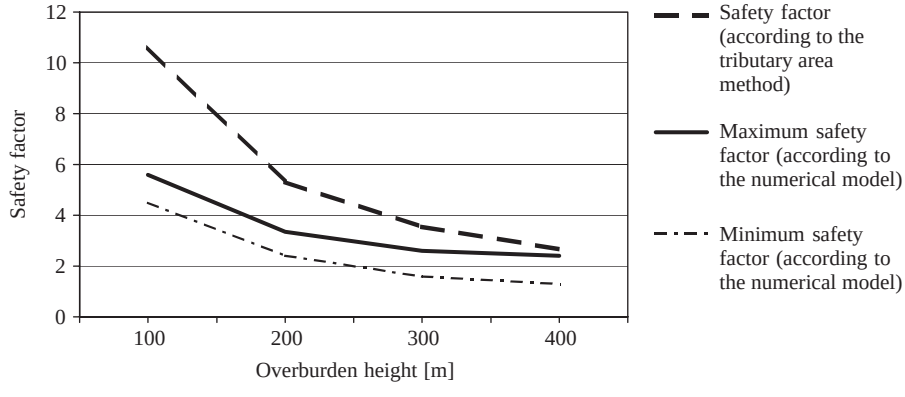


Figure 17. Safety factor of the diaphragms computed with the numerical and analytical approaches. Analytical safety factor values correspond to the ratio between rock mass uniaxial compressive strength and mean vertical stress acting on the diaphragm: while, for the numerical model, the safety factor is defined by $SF = [\sigma_3 + \sqrt{m\sigma_c\sigma_3 + s\sigma_c^2}]/\sigma_1$.

In the last part of the analysis, the tributary area method was applied again, in order to verify the stress condition which would be induced in the diaphragms if the plasticized zones detached from the room, thus reducing the width of the diaphragm itself. The results make it possible to affirm that, also in this case, global stability of the diaphragms would not be compromised because the safety factor never has a value lower than 1.5.

5 CONCLUSIONS

In order to verify the "near field" and the "far from field" (Brady & Brown, 1985) stability condition of an underground room and pillar mine, it is necessary to carry out computations that are able to check both the rock wedge stability, which can form around the rooms, and the stress redistribution around the room and in the pillars. The computation carried out for the study of an underground granite exploitation, in Canal San Bovo (Trento district, Italy), is a good example of how this analysis should be carried out. In this specific case, it can be pointed out that the underground exploitation of a good geomechanical quality granite rock mass to obtain feldspar to be used in the ceramic industry, is an interesting application of how surface constraints can prevent exploitation from being carried out in a open pit mine.

REFERENCES

Bieniawski Z. T. (1989). *Engineering Rock Mass Classification.* J. Willey, New York.

Brady B. H. G. & Brown E. T. (1985) *Roch Mechanics or Underground Mining.* George Allen & Unwin, London.

Cravero M., Iabichino G., Mancini R., Pelizza S. & Stragiotti L. (1987). *The potential of underground mining small dept in the light of environmental, economical and rock stability considerations.* 13th World Mining Congress, Stockholm.

Del Greco O., Ferrero A.M., Oggeri C. & Peila D. (1993). *Analysis of exploitation mine room instability in weak rocks.* Int. Symp. "Assessment and prevention of failure phenomena in rock engineering", Istanbul. 441–447.

Guardini C. (2005). Studio geomeccanico e della ventilazione di una coltivazione mineraria per camere e diaframmi. Tesi di Laurea, Politecnico di Torino (Unpublished).

Hoek, E., Carranza-Torres, C. & Corkum, B. (2002). Hoek-Brown criterion, 2002 edition. Proc. NARMS-TAC Conference, Toronto.

Pelizza S., Oreste P.P., Peila D. & Oggeri C. (2000). Stability of a large cavern for quarrying exploitation of a pink marble in Italy. Tunnelling and Underground Space Technology, 15, n. 4, Pergamon Press. 421–435.

This page intentionally left blank

Underground Space – the 4th Dimension of Metropolises – Barták, Hrdina, Romancov & Zlámal (eds)
© 2007 Taylor & Francis Group, London, ISBN 978-0-415-40807-3

Analysis of input parameters of the rock mass

J. Pruška
CTU in Prague, Faculty of Civil Engineering, Prague, The Czech Republic

ABSTRACT: The main goal of the paper is focused on the effect of the input parameters to the suitable mathematical models of the underground structures. Within the introduction of the paper the inaccuracy in the geotechnical tasks modelling is performed. In the following part the Fuzzy techniques are summarized and the Fuzzy arithmetic using on the Index Q rock mass classification is mentioned. The next part of the paper is focused on the stochastic simulation – Monte Carlo Simulation is shortly described while Latin Hypercubes method is described in detailed. At the end the application of the statistical analysis of the input parameters on the numerical modelling of Prague tunnels Mrázovka and Špejchar – Pelc Tyrolka is shown.

1 INTRODUCTION

The inherent variability of rock mass is difficult to take into account and for this reason engineers very often solve the question "What value should be used in analyses?". The answer on such question requires a probabilistic approach in the evaluating the uncertainty in the input parameters in geologic media. In the recent time specialists encounter problems of the input parameters in using uncertainty modelling based on the Fuzzy set theory, Monte Carlo Simulation, Latin Hypercube Sampling etc.

To illustrate this concept, the variability in the strength R and stress S (given by their probability density functions) is shown in Figure 1. The overlap between the strength and stress distributions indicates the zone that contributes to the probability of failure P_f. The probability of failure can vary from a very low value to nearly unity (depending of the degree of overlay).

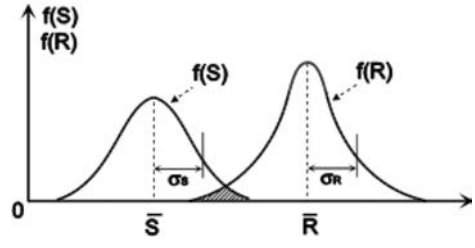


Figure 1. Probability of failure (Pauli 1991).

2 FUZZY METHODS

In underground structures design is very difficult to take into account inherent variability of rock mass using the current rock mass classification. One of the main methods in improving rock mass classification is by accounting for variations in the individual parameters using fuzzy mathematics (Hudson 1998).

The fuzzy set was first introduced in 1965 by Lofti A. Zadeh (Zadeh 1965) as a mathematical way to represent linguistic vagueness. In a classical set, an element belongs to or does not to a set. The concepts and definitions of the fuzzy set theory are mentioned in many publications. Dubois and Pride (Dubois & Pride 2000) provide the following definition: "Fuzzy set is a generalization of ordinary or classical set theory it consists of mathematical tools developed to model and process incomplete and/or gradual information, ranging from interval – valued numerical data to symbolic and linguistic expressions".

Contrary to crisp (or ordinary) set, fuzzy set have no sharp or precise boundaries. In crisp set, element x belongs to or does not to a set A and membership function (or degree of membership) $\mu_A(x)$ is a unique. Fuzzy set assigns membership function $\mu_A(x)$ for each element x to range over the interval (0,1). This type of membership function is characteristic by smooth transition from "belong to a set" (1) to "not belong to a set" (0) and gives fuzzy sets flexibility in modeling used linguistic expressions of engineering practice (such as "Fairly rough surface"). Membership functions can be represented by analytical method too.

Two types of variables are used in the fuzzy model: fuzzy variables and fuzzy numbers. Fuzzy variables are defined directly as fuzzy sets on the set of reference

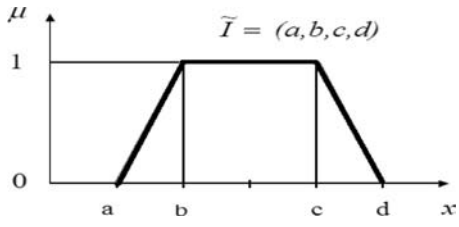


Figure 2. Trapezoidal fuzzy number.

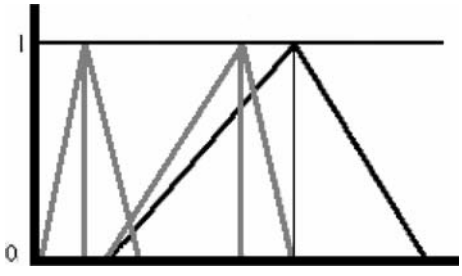


Figure 3. Fuzzy addition.

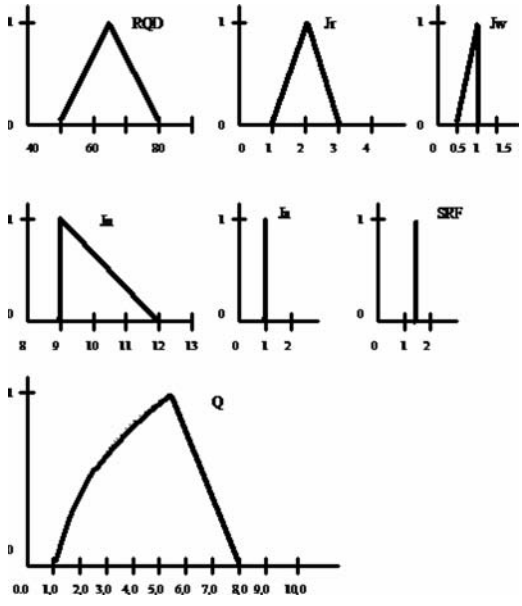


Figure 4. Applying fuzzy arithmetic to the Q-system (Hudson 1998).

linguistic terms. Generally, a fuzzy variable x_j can acquire any value expressing various shades between the reference terms. For the linguistic terms the fuzzy variables are fuzzy singletons. Fuzzy variables need not to be associated with any numerical universe. This can be because their values are qualitative in nature, or are respected as qualitative for the sake of convenience. Fuzzy numbers are defined over a continuous domain – triangular or trapezoidal membership functions (or numbers). Trapezoidal number is defined by the height and four distinct elements of the fuzzy set interval – Figure 2. Taking $b = c$ reduce the trapezoidal number to those of triangular.

Fuzzy Logic provides a number of functions for performing fuzzy arithmetic. The fuzzy arithmetic functions are a little different than the rest of Fuzzy Logic's functions in that they operate on lists of above mentioned fuzzy numbers. In the Figure 3 is fuzzy addition of two triangular fuzzy numbers.

The application of fuzzy arithmetic in the rock mass classification is direct and generate a fuzzy number representing the classification value. Fuzzy mathematics even introduce the uncertainty in the evaluating of parameters to the rock mass classification. Let us have for example Index Q rock mass classification. This classification was established in 1974 in Norway (by Barton, Lien, Lunde and Loset) and is based on six parameters (Bieniawski 1989):

$$Q = \frac{RQD}{J_n} \cdot \frac{J_r}{J_a} \cdot \frac{J_w}{SRF} \qquad (1)$$

where $RQD =$ rock quality designation, $J_n =$ joint set number, $J_a =$ joint alteration number, $J_w =$ joint water reduction number, $SRF =$ stress reduction factor.

By applying the fuzzy logic to the equations for Index Q (Equation 1) we obtain results in the fuzzy classification value (Figure 4) with non-linear distributions. The convex nature of the flanks has the effect of increasing the possibility that the conditions will be worse than a single computed index Q.

3 MONTE CARLO SIMULATION

Monte Carlo simulation is a well-known toll that is used to analyze random phenomena. In Monte Carlo simulation is the random problem transformed into several deterministic problems that are much easier to solve – sample inputs are used to generate sample outputs with statistical or probabilistic information about random output quantity. Monte Carlo simulation is simple to use and therefore has found much favor in geomechanics, particularly in stability analysis of rock slopes (McMahon 1971).

The simplest sampling scheme of a Monte Carlo simulation approach is to use a pseudorandom number generator to select random numbers between 0 and 1 and swap them with randomly generate values for each variable which will be input to the calculation. However, this simple (and best-known) random sampling scheme required for good accuracy and repeatability

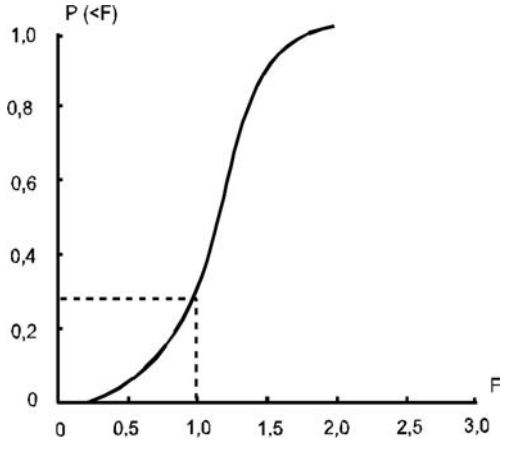


Figure 5. Cumulative distribution of Monte Carlo results (Mahtab 1992).

many samples – in practice for generating a probability distribution of the safety factor of rock slopes is the minimum number of selection between 200 up to 2000 (depending on the desired accuracy).

The simulation output (random variable which depends upon random input variables, fields and processes) may be in several approaches. One way is to define the probability that safety factor F is less than a prescribed value Fp:

$$P\left(F < F_0\right) = \frac{n}{N} \tag{2}$$

where $n =$ number of trials in which $F < F_n, N =$ number of selections.

Another approach (Mahtab 1992) is to plot a cumulative distribution of random F, which can be used to define the probability of F being less than a given value (Figure 5).

4 LATIN HYPERCUBES

To reduce the number of samples required for good accuracy in Monte Carlo simulation have been developed other sampling methods. One of the best is Latin hypercube sampling (Bažant 1987). Latin hypercube sampling preserves marginal probability distributions for each simulated variables. To fulfilled this aim, Latin hypercube sampling constructs a highly depend joint probability density function for the random variables in the problem, which allows good accuracy in the response parameter using only a small number of samples.

In Latin hypercube sampling is the bounded interval $<0, 1>$ uniformly divided into N non-overlaying intervals (with the same probability of accuracy). Than is one value per interval generated. This can be performed by initially generating N random numbers within range $<0, 1>$. These values are linearly transformed to the random numbers in the non-overlaying intervals for each random variable:

$$u_i = \frac{u}{N} + \frac{(i-1)}{N} \tag{3}$$

where $i = 1,2\ldots.n$ (n number of values), $u =$ a random number ($u \in <0,1>$), $u_i =$ random numbers in the ith interval, $N =$ number of the non-overlaying intervals.

From the above equation follows that we generated only one value for each random variable (this value is randomly selected within each of N intervals):

$$\frac{(i-1)}{N} < u_i < \frac{1}{N} \tag{4}$$

where $i = 1, 2 \ldots .n$ (n number of values), $u_i = a$ random numbers in the ith interval, $N =$ number of the non-overlaying.

The n values obtained fir the first random variable x_1 are paired in a random manner with the values of the second random variable. These n pairs of (x_1, x_2) are combined in a random manner with n values of the third random variable. This combination results in the n triads (x_1, x_2, x_3) which are combined in a with n values of the 4th random variable and so on until (K-2) triads are formed (K is a number of random variables). Thus we can assembled N^*K matrix. It can be seen that a certain statistical correlations among columns of the matrix may have a significant influence on the results of simulation (Spolehlivost 2001).

5 APPLICATION OF LATIN HYPERCUBE SAMPLING

The north-western sector of the City Circular Road in Prague contains three major road tunnels of large cross section area. While the Strahov and Mrázovka tunnels are already open for traffic, the Špejchar – Pelc Tyrolka tunnel is still in the planning phase. The very difficult Prague Ordovician geological conditions make it necessary to apply NATM. Stabilization of the deformations was always achieved only after closure of the whole primary lining, but the following supporting technical measures were performed: anchoring, widening of the top heading legs, micropile support under the top heading legs, reinforcing grouting performed in advance from the exploratory gallery (Fig. 6), and closing the top heading by a temporary invert. Due to increased deformations occurring at the excavation with a horizontally divided face, a vertical pattern of the sequence was used in the further course of excavating the Mrázovka tunnel.

The outputs of two tunnel Mrázovka models were verified by Latin Hypercubes method (Barták at al. 2002). The numerical analysis was carried out by means of the PLAXIS program system. 3D behaviour of the excavation face area, and correct description of the influence on the deformations and the state of the massif were simulated by means of the frequently used procedure of loading the excavation and lining using the so-called β-method. The modelled area of the profile covers an area of about 200 m wide and 110 m high and was divided into eight basic sub-areas according to the types of rock encountered. The rock mass behaviour was approximated by means of the Mohr-Coulomb model. The intervals of input parameters of the rock mass (E_{def}, ν, c, φ, γ) were determined on the basis of the engineering-geological investigation results (Hudek 1999). The modulus of deformation of the tectonic zone was determined according to the results of plate bearing tests. A comparison of theoretically determined deformations with the values obtained by monitoring (Kolečkář 2000) was used verifying the applicability of the mathematical model.

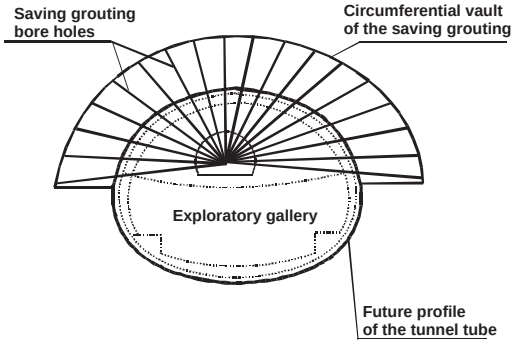


Figure 6. Scheme of the execution of the saving grouting.

The results of statistical study of West Tunnel Tube (WTT) in profile km 5.160 are shown in Table 1. They show that final settlements will be with probability 95% between values 71 mm and 213 mm. The interval of settlement without deformations caused by excavation of pilot adit is from 65 mm to 198 mm. The recognised range was in coincidence with measured value 194 mm (value does not include effect of pilot adit).

The construction package Špejchar – Pelc-Tyrolka is 4,320 m long – the length of the tunnelled section amounts to 3,438 m. The construction package also contains underground garages in Letná, four underground Technology Centres and the Trója Bridge. According to the design, the excavation will be carried out using the New Austrian Tunnelling Method (NATM). Due to the given conditions, a vertical excavation sequence will be applied to the three-lane tunnel excavation. Regarding the two-lane tunnels, a horizontal sequence is expected.

The position of the exploratory drift is selected with respect to complicated sections so that the vertical sequence can be applied to the top heading, or the vertical sequence can be used for the entire cross section. Mechanical rock breaking is expected, or also in combination with the drill-and-blast when passing through the Quartzites. A transition zone between the Quartzites exists at the foot of the slope falling from the Letná Plain. Due to the gradient parameters, the tunnels run at a close vicinity of fully saturated Quaternary sediments. A multicriteria analysis resulted into selection of the variant of pre-excavation grouting (Dvořák at al. 2004).

The outputs of the exploratory drift near the transition zone (km 5,900 ETT) were verified by Latin Hypercubes method with coperation with design and consulting company SATRA (Louženský 2006). The 2D and 3D numerical analysis was carried out by means of the CESAR – LCPC program system. The

Table 1. Results for WTT km 5,160.

	Total settlement (mm)		Pilot adit settlement (mm)		Settlement without the pilot adit effect (mm)	
Calculation	Surface	Tunnel	Surface	Adit	Surface	Tunnel
1	79	107	15	8	64	99
2	153	197	29	14	124	183
3	92	125	18	10	74	115
4	85	111	15	8	70	103
5	134	171	25	12	109	159
$\overline{X}$(average)	108.60	142.20	20.40	10.40	88.20	131.80
s (standard deviation)	29.41	35.61	5.64	2.33	23.80	33.31
$\overline{X}+2s$ (p=95.45%)	167.42	213.42	31.69	15.06	135.81	198.43
$\overline{X}-2s$ (p=95.45%)	49.78	70.98	9.11	5.74	40.59	65.17
$\overline{X}+s$ (p=68.27%)	138.01	177.81	26.04	12.73	112.00	165.11
$\overline{X}-s$ (p=68.27%)	79.19	106.59	14.76	8.07	64.40	98.49
VAR X (variance)	5.69	6.22	2.65	1.75	5.15	6.02

Table 2. Results for STT km 5,900.

Calculation	Total settlement (mm)		Pilot adit settlement (mm)		Pilot adit settlement (mm)	
	Surface	Tunnel	Surface	Tunnel	Surface	Tunnel
1	13,6	22,6	2,2	4,1	6,5	10,2
2	17,5	26,9	2,5	4,7	4,9	11,1
3	13,1	21,6	3,4	6,2	5,9	13
4	12,1	18,4	1,68	3,4	6,9	13
5	25,5	35,8	2,4	6,6	6,6	13,8
$\overline{X}$(average)	16,4	25,1	2,4	5,0	6,2	12,2
$\overline{X} + 2s$ (p = 95.45%)	26,2	37,1	0,6	1,2	0,7	1,3
$\overline{X} - 2s$ (p = 95.45%)	6,6	13,1	0,4	1,9	0,8	2,3

rock mass behaviour was approximated by means of the Mohr-Coulomb model. The intervals of input parameters of the rock mass were determined on the basis of the engineering-geological investigation results (Butovič 2004). The results of statistical study of South Tunnel Tube (SWTT) in profile km 5,900 is shown in Table 2. They show that final settlements of the tunnel lining will be with probability 95% between values 13 mm and 347 mm. The interval of surface settlement above excavated tunnels is from 7 mm to 26 mm.

6 CONCLUSION

The results of analysis show the effect of variation of input parameters of rock mass behaviour on results of FEM. It can be seen, how different can be this influence. Difference of outputs is given by disparity of geological layout. However it can be clearly seen, how important is at least basic study of input parameters variation for determination of final structure behaviour. Latin Hypercubes method is advantageous procedure for qualified statistical evaluation of FE calculation. These methods make possible radical time saving in regards to common statistical methods (Monte Carlo method, estimations of probability moments etc.). Latin Hypercubes method is also not bonded with concrete rock mass classification with respect to fuzzy technique.

ACKNOWLEDGEMENT

The authors wish to express their gratitude to Ministry of Education of the Czech Republic for research project *MSM 6840770003* "Developments of the Algorithms of Computational Mechanics and their Application in Engineering" for allowing to develop this article. Thanks also to Ing. A. Butovič of the SATRA company for their supporting in the analysis of the Spejchar – Pelc Tyrolka tunnel.

REFERENCES

Barták, J., Hilar, M., Pruška, J. 2002. Statistical Analysis of Input Parameters Influence to the Tunnel Deformations Modelling *In: Fourth International Conference on Computational Stochastic Mechanics [CD-ROM]*. Houston: Rice University, 280–292.

Bažant, Z.P., Křístek, V. 1987. The effect of shear lag on creep deformation. *Journal of Structural Engineering, ASCE*, Vol. 113, No. 3, 557–569.

Bieniawski, Z.T. 1989. Enngineering Rock Mass Classification. *John Wiley and Sons, New York*, ISBN 0-47160172-1.

Butovič, A. 2004. Exploratory drift for the Blanka twin tube (Průzkumná štola pro tunely Blanka) *Tunel, 2004/1*, CTuK Praha, 13–18.

Dubois, D. & Prade, H., (Eds.) 2000 Fundamentals of Fuzzy Sets, *Kluwer*, Norwell, MA.,647)

Dvořák, J. et al., 2004 Špejchar – Pelc-Tyrolka construction lot of the city circle road in Prague and underground engineering techniques *Tunel, 2004/1*, CTuK Praha, 2–12.

Hudek, J. 1999. The Mrazovka tunnels – measurement and monitoring at construction of the WTT – presiometric checking on the success of saving grouting – profiles 003 to 009. *PÚDIS* Praha.

Hudson, J.A. 1998. Rock Engineering Systems : Theory and Practice. *Ellis Horwood, Chichester*, ASIN: 0137826249.

Kolečkář, M.- Zemánek I. 2000. *Monitoring of the Mrazovka tunnel*. In: "Volume of papers of the Int. Conf. Underground Construction 2000", Praha, ITA/AITES, pp. 427–433.

Louženský, T. 2006 Mathematical modeling of primary lining influence on rock mass stress, CTU in Prague, FCe, Prague, *Diploma Thesis* (in Czech).

Mahtab, M.A., Grasso, O. 1992. Geomechanics Principles in the Design of Tunnels and Caverns in Rock. *Elsevier*, ISBN 0-4440883088.

McMahon, B.K. 1971. A Statistical method for the design of rock slopes. *Proceedings, 1st Australia – New Zealand Conference on Geomechanics*, Melbourne, Australia, Vol. 1, 314–321.

Pauli, J. 1991. Rock Mechanics. *ČVUT Praha*, (in Czech)

Spolehlivost konstrukcí 2003. Téma Cesta k pravděpodobnostnímu posudku bezpečnosti, provozuschopnosti a trvanlivosti konstrukcí. *Ostrava. Dům techniky*, ISBN80-02-01410-3 (in Czech).

Zadeh, L.A. 1965. Fuzy Sets, *Inform Control*, 8,338–53.

This page intentionally left blank

Underground Space – the 4th Dimension of Metropolises – Barták, Hrdina, Romancov & Zlámal (eds)
© 2007 Taylor & Francis Group, London, ISBN 978-0-415-40807-3

Study on neighboring construction of three parallel shield tunnels in soft ground by centrifugal model test

Wenge Qiu, Yuchao Zheng*, Shufeng Li, Ruiguo Wu & Hongbo Guo
School of Civil Engineering, Southwest Jiaotong University, Chengdu, Sichuan, China

ABSTRACT: Based on the prototype of three-tube parallel shield tunnel of R413 bid segment of the ninth route in Shanghai track traffic, stratum loss of shield tunnel was simulated by the control of injecting and releasing water quantitative of pockets around tunnel model, centrifugal model test study was carried out on ground face settlement of three-tube parallel shield tunnel. There were two group of centrifugal model test in all, one group with stratum reinforcement and another not, and the construction of three-tube tunnel was divided into two stages. The comparison was carried out between the result in site and in model test. The result shows that this method, injecting and releasing water quantitative of pockets around tunnel model, could simulate stratum loss effectively. The settler would create superposition with the construction of tunnel one by one, ground face settlement could be controlled effectively through the method of stratum reinforcement, the Max ground face settlement value would not ultralimit in each stages of construction, but the Max accumulated settlement would ultralimit, so it needed the cooperation of railway department and could deal with combining the railway maintenance.

1 INTRODUCTION

In the prevision of surface settlement induced by shield driving for the time being, the routine methods are empirical formula, numerical simulation and model test. With help of centrifugal machine in high speed, centrifugal model test can impose more than n times centrifugal force, and compensate weight loss caused by 1/n shrinkage rule. Which also can maintain the same stress, strain, fracture mechanism and similar deformation between the proto and model. So studying geotechnics problem on which the most important load is gravity by the way of centrifugal model test is a perfect way[1]. However, because it difficult to simulate drilling of shield machine in earth. Model test faces large difficulty in studying shield tunneling. Some scholar like Zhou has made a lot of model test in tunnel engineering of South-to-North Water TransferProject by control of injecting and releasing air quantitative of pockets around tunnel model, and studied the relationship between support stress and stratum displacement, influence of construction space, and mechanism about the stability and destruction[2][3]. Wu, Liu and other scholars simulated drilling tunneling by the way of melting paraffin with coupling between stress field and filtration[4][5].

A large number of study and engineering experience have indicated that in shield tunneling surface, settlement is in relation to stratum loss. A lot of empirical formulas for forecasting surface settlement are in relation to stratum loss, for example, Peck advanced Gaussian distribution curve in 1969[6], Loganathan and Poulos advanced an empirical formula[7]. Demestic TongJI University advanced correction Peck formula considering cross settlement value based on construction space and consolidation[8], Academician Liu advanced correction Peck formula for forecasting portrait settlement[9]. Author got an idea from it, considering that the centrifugal test equipment of author's work station can't compressed air and water, author decided to simulate the stratum loss of shield tunneling driving by injecting and release water. So the model test of three-tube parallel shield tunnel can be implemented.

2 ENGINEERING GENERAL SITUATION

Based on the prototype of three-tube parallel shield tunnel of R413 bid segment of the ninth route in Shanghai track traffic, the tunnel segment between east and west slip road DK20 + 664 (= L2DKO + 220) across under NanXin circle railway (railway mileage DK31 + 820). NanXin circle railway is double-track

* Communication of Yuchao Zheng:
Tel: 86-28-86465636 Fax: 86-28-87602793
E-mail: jddx@home.swjtu.edu.cn
ADD: 301#, School of Civil Engineering, Southwest Jiaotong University, Chengdu,Sichuan, 610031,China

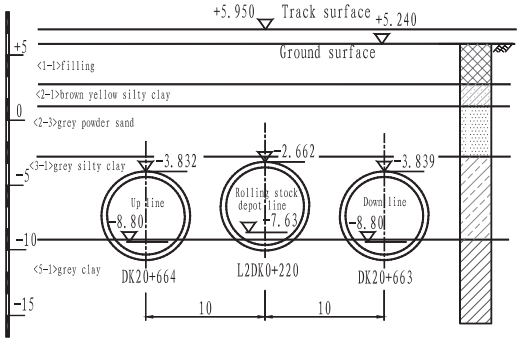


Figure 1. Cross section of three-tube parallel shield tunnel underthrough railway.

main way(the width of subgrade is 13 m), it lay over the tunnel, it is orthogonal to the tunnel (the angle of intersection is 88), the cross segment is in the north of HuSong highway, the distance from eastside to westside of slip-road delve is 60 m.

There are three parallel line, that is up-line, down-line and east rolling stock depot line, are all straight line, the distance between rolling stock depot line and down-line is 20 m, and east rolling stock depot line is in the middle of up-line and down-line. The clear distance between the three line is only 3.8 m, the longitudinal gradients from east to west of cross segment are as following: the degree of slop of up-line is 16.427‰ falling gradient, the degree of slop of down-line is 16.263‰ ascending gradient and the degree of slop of east rolling stock depot line is 3‰ ascending gradient. The depth of embedment of up-line and down-line is 9.1 m, the depth of embedment of rolling stock depot line is 7.8 m.

According to the detailed engineering geology survey report of ninth track traffic between JiuTing station and QiBao station, the stratum situation of parallel and overpass segment is as following: filling, brown yellow silty clay, grey powder sand, grey silty clay, grey clay and so on.

Most of study and construction are based on the driving of one-tube tunnel, there are less study on surface settlement cased by three-tube parallel tunnel driving. Considering that the tunnel goes under crowed railway main line, safety is quite important, so forecasting the surface settlement and regular cased by three-tube shield tunnel driving by centrifugal modest test is useful.

3 TEST WAY AND TEST MODEL

3.1 *Test equipment*

Test was made on centrifugal machine of Southwest Jiaotong University. The major parameter of the equipment are as following: (1) 100 g·t; (2)effective radius: 2.7 m; (3)effective size of model is 0.8 m × 0.8 m × l m, 06 m × 0.6 m × 0.8 m; (4)working range of centrifugal machine is 10∼200 g; (5)the longest working time is 12; (6)survey pattern: sensor + amplifier + intellectual survey macheng + data digitization parallel transmination(computer); (7)monitoring and recording test procedure by camera system.

Table 1. Trial field value.

Sort	Crosswise scope (m)	Longitudinal scope (m)	Vertical scope (m)
Prototype	80	60	50
model	0.8	0.6	0.5

Table 2. Parameter ratio of similitude.

Physical quantity	Ratio	Physical quantity	Ratio
Geometry ratio/C_l	100	Acceleration ratio/C_g	1:100
stress ratio/C_s	1	Yong's modulus ratio/C_E	1
cohesion ratio/C_C	1	Friction angle/C_f	1
strain ratio/C_e	1	Displacement ratio/C_u	100
Density ratio/C_e	1	Time ratio/C_t	10000

3.2 *Model test field and similarity rate*

06 m × 0.6 m × 0.8 m model case is used, considering the size and space position of the three tunnel, influence of boundary effect and size of model case, we used 100 as the similarity rate in this test, geometry size of test field is shown as Table 1. Double-skin plastic film is used in boundary to remove boundary constraint effect, according to basic principle of centrifugal model test and π theoren of Buckingham, the similarity rate of physical quantity is shown as Table 2.

3.3 *Test material*

Substratum soil is allocated by people in testing laboratory, matching rate is controlling nonconfined compressive strength, the we tamped the soil field stratal soil is adopted as padding of the rest strate. Because most of stratum is made of soft clay. It is remolded according to the moisture content offered by geologic examination report, and it is consolidated on centrifugal machine, the index c and ϕ is controlled by shear test[10]. For lining structure of shield tunnel, if we use material index as prototype, structure will be too thin as concrete, it can't meet the need, so we choose steady LYZ aluminium product as similar material, which has similar density and Poisson ratio with concrete, we can get the aluminium product of similarity criterion can be got from documentation[3].

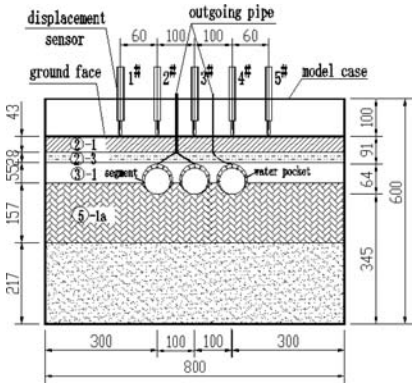


Figure 2. Layout figure of tunnel, stratum and sense organ.

3.4 *Stratum loss and model way*

Stratum loss of shield tunnel by the control of inject and releasing water quantitive of pockets around tunnel model, the pocket is made of rubber, the single width is 1 mm, the external is 64 mm, the inner diameter is 62 mm, the length of one sector is 60 mm, long conduct pipe of 1000 is located on one sector, a value is located in the outside. According to document[11], the stratum loss rate of Shanghai subway shield construction is 0.3%∼0.6% generally, considering the fact situation, we choose 0.5%, we can get the value of stratum loss per mater 0.158 m^3 from the diameter of shield machine, we can get the water discharge value 0.95 ml, we choose the value 1ml,according to equation of state of ideal gas, if compression force increases to 100 times, air will be compressed to 1%, so injecting water to fill the pocket will be nice, and the influence of air compression can be ignored, put the pocket full of water on the outside of tunnel lining model, injecting and releasing can be realized by injector.

3.5 *Displacement test original production and layout of measuring point*

Displacement sensors used in test are MDA-5 series line displacement sensor. Survey rod is controlled by spring, the measuring range is 10 mm, the measurement accuracy is 0.1%F · S, the current source ±12VDC, the output rate 0∼5VDC. Other cross-section lays in center, five sensors are located in it, the locating point is shown as Picture 2.

3.6 *Experiment process*

There were two groups of test in all, one group with stratum reinforcement and another not. The reinforcement scope was a cuboid with one time diameter apart from the tunnel. The Portland cement with grade 425 was adopted to mix with the ground, and the content of the cement was 10%. The various soils and the tunnel with 3 holes was enclosed into the model box following the Figure 3, the enclosing height of each layer soil should be strictly controlled and be symmetrically tamped. The wire and water pocket pipe were put out of the model box.

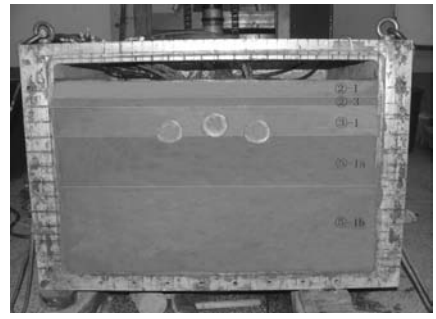


Figure 3. Model obverse figure.

The basic construction sequence of the three tunnels is following: firstly the tunnel(the first tunnel in the experiment) on the down line and the tunnel(the third tunnel in the experiment) on the up line were excavated face to face at the same time, the tunnel on the down line advanced from east to west (from inside to outside in the experiment), the tunnel on the up line advanced from west to east (from outside to inside in the experiment), finally the tunnel on the rolling stock depot line advanced from east to rolling stock depot (from inside to outside in the experiment). The water pockets were gradually released one by one (or by twos), in order to simulate the gradual advance of stratum loss. The idiographic process of the experiment simulation is as follows:

(1) Clean up the scene, close the centrifugal room armor door, then start to carry out the experiment. Gradually increases the centrifuge rotational speed to cause the acceleration to 100 g, and continue revolving for 1 hour (to be equal to 417 days in the prototype), in order to simulate the solidifying of the soil layer, observe the reading of each sensor for displacement measurement, if the reading is out of the measuring range, readjust the position of the sensor for displacement measurement after the engine is off.
(2) Slow down until stop, open the armor door, extract 1 milliliter of water in the first and second water pocket of the third tunnel and in the ninth water pocket of the first tunnel through the conductor pipe and the injector, after cleaning up the scene, close the armor door, gradually speed up to cause the acceleration up to 100 g and continue revolving for 10 seconds (to be equal to 27.8 h in the prototype), and gather displacement data dynamically, the sampling frequency is set to 0.03 k.

(3)∼(6) The operating procedure is similar to that of the step (2), Slow down until stop, open the armor door, gradually extract 1 milliliter of water in the other water pockets through the conductor pipe and the injector, after cleaning up the scene, close the armor door, gradually speed up to cause the acceleration up to 100 g and continue revolving for 10 seconds, and gather displacement data dynamically.

(7) Slow down until stop, open the armor door, extract 1 milliliter of water in the ninth water pocket of the third tunnel and in the first and second water pocket of the first tunnel through the conductor pipe and the injector, after cleaning up the scene, close the armor door, gradually speed up to cause the acceleration up to 100 g and record the reading and continue revolving for 10 minutes (to be equal to 69 days in the prototype), finally complete the simulation of the stratum loss in the third and first tunnel.

(8)∼(12) The step (8)∼(12) are similar to that of the step (2)∼(6), gradually complete the simulation of the stratum loss in the second tunnel and gather data.

(13) Slow down until stop, open the armor door, extract 1 milliliter of water in the first and second water pocket of the second tunnel and through the conductor pipe and the injector, after cleaning up the scene, close the armor door, gradually speed up to cause the acceleration up to 100 g and continue revolving for 1 hour (to be equal to 417 days in the prototype), gather displacement data dynamically.

4 THE ANALYSIS OF THE EXPERIMENTAL RESULT ABOUT SRUFACE DISPLACEMENT

According to the obtained data, the writer draws ground surface settlement curve of cross section under different construction simulation steps, as well as ground surface settlement curve of various measuring points along with the position of the water pocket (stratum loss driving distance). See Figures 4 to 7. In the chart, the frontal 0 to 60 of the position of releasing water pocket (prototype: m model: cm) is the driving distances of the first and the third tunnel, and 60∼120 (prototype: m model: cm) is the driving distances of the second tunnel.

As a result of the insufficient measuring points, the experiment does not obtain the entire settler scope, but

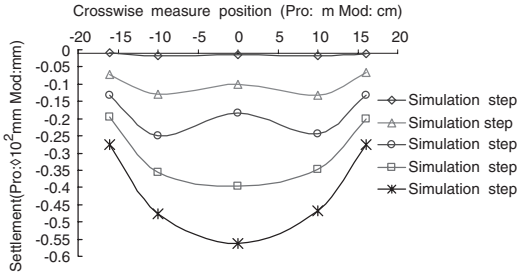


Figure 4. Settlement curve of each stage with non reinforcement of ground.

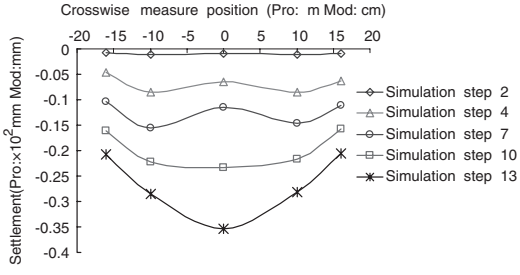


Figure 5. Settlement curve of each stage with reinforcement of ground.

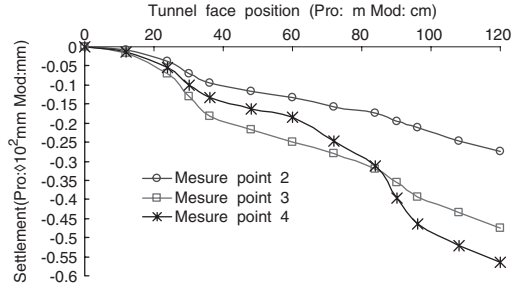


Figure 6. Relationship of measuring point settlement with position of releasing water pocket with non reinforcement of ground.

it is still seen from chart 4 to 7 that the surface displacement has the following characteristics (the following analyzing values are all prototype values):

(1) When the first and third tunnel are tunneling, the settlement value of the measuring point 2 (above the first tunnel) and the measuring point 4 (above the third tunnel) is bigger than that of the measuring point 3 (above the second tunnel), after the construction of the first and third tunnel is finished, the surface settler assumes shape of W, which is crosswise settlers' superposition of

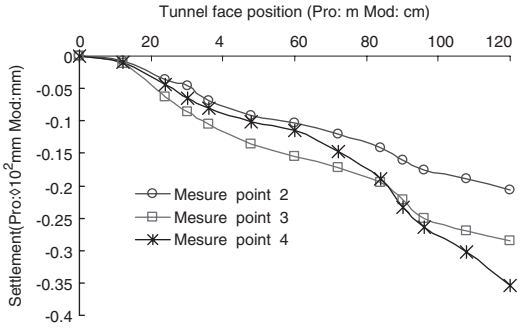


Figure 7. Relationship of measuring point settlement with position of releasing water pocket with reinforcement of ground.

the first and third tunnel. After the second tunnel's construction, the measuring point 4 subsides quicker, and the settlement value of the measuring point 4 surpasses that of the measuring point 3 and the measuring point 5, then forms a settler of U shape.

(2) When the stratum is not reinforced, the biggest surface settlement value is 25.0 mm the latter 69 days after the first and third tunnel are completed, and the accumulative biggest surface settlement value is 56.4 mm (prototype) the latter 417 days after the three tunnels are completed; when the stratum is reinforced, the biggest surface settlement value is 19.5 mm the latter 69 days after the first and third tunnel are completed, and the accumulative biggest surface settlement value is 39.4 mm (prototype) the latter 417 days after the three tunnels are completed. The accumulative biggest surface settlement value with reinforcement of ground is 30% less than without reinforcement of ground, so it indicates that the stratum reinforcement may effectively reduce the surface settlement.

(3) If dividing the construction of the first and third tunnel and the construction of the second tunnel into two stages, thus the biggest settlement value without reinforcement of ground which is caused in the first stage is 25 mm and 19.5 mm with reinforcement of ground, and the corresponding value is respectively 38 mm and 23 mm, the settlement value in the second stage is remarkably bigger than in the first stage, so it indicates that the later period consolidation settlement of shield driving is bigger in the clay stratum.

The permitted settlement value which is proposed by the railway department is 10∼30 mm, so looking from the single stage, the surface settlement overruns the permission without reinforcement of ground, while the surface settlement satisfies the requirement with

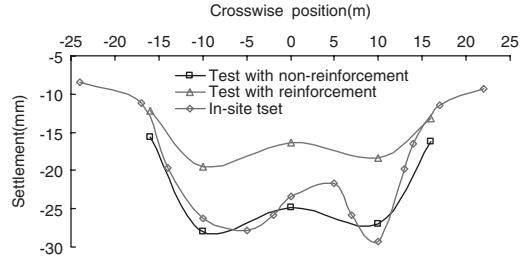


Figure 8. Model test and actual measurement settlement curve after up and down line tunnel completed.

reinforcement of ground, but looking from the accumulative biggest surface settlement after three tunnels' construction, the both experiment values overrun the permission, especially considering that the stratum needs experience a long-term consolidation and secondary consolidation process in the clay, hence besides requiring strictly control the construction measure and strengthening monitor in the construction as well as the forward monitor, and it is needed that we cooperate with the railroad department closely, if necessary, we would unite maintaining job of the railway to adjust plane and vertical parameter of the line through track lifting.

5 THE COMPARISON BETWEEN THE MEASURED VALUE IN THE FIELD AND THE EXPERIMENTAL VALUE

Before the construction of shield passing the railroad, the stratum among 6m scope around the tunnels is reinforced through compaction grouting. At present, the shields in the up and down lines have passed through the railroad smoothly, thereamong, the down line passed ahead, after 20 days, the up line also passed successfully. Thus we have obtained ground surface settlement curve after 2 months when the down line passed, and the article draws ground surface settlement curve during around 2 months after the up and down line passed from the experiment, see Figure 8. From Figure 8, it can be seen that measured ground surface settlement curve with reinforcement of ground is consistent with experimental settlement curve without reinforcement of ground, and it is obviously bigger than experimental settlement curve with reinforcement of ground, through analyzing reason preliminary, it is thought that the effect of adopting compaction grouting in the soft clay is difficultly to meet the design requirement, while the experiment adopts mixing method which is similar to churning up, thus the effect is better. The measured ground surface settlement curve assumes the remarkable asymmetry; it has something to do with the two

tunnels' asynchronous construction and the soft clay's obvious upper settlement.

6 CONCLUSIONS

(1) Stratum loss of shield tunneling was effectively simulated through the method of injecting and releasing water by water pockets, sequentially the ground surface settlement in the shield construction would be researched.
(2) Crosswise settler which is aroused by near various tunnels' construction would create superposition, and the ground surface settlement is effectively controlled by stratum reinforcement.
(3) Looking from the single stage, ground surface settlement without reinforcement of ground overruns the permission, and ground surface settlement with reinforcement of ground meets the requirement, but looking from the accumulative biggest surface settlement after the construction of three tunnels, the both experiment values overrun the permission, hence, besides requiring to strictly control the construction measure and strengthen monitor, and it is needed that we cooperate with the railroad department closely, if necessary, we would unite maintaining job of the railway to adjust plane and vertical parameter of the line through track lifting.
(4) The comparison between the measured ground surface settlement in the field and the experimental settlement shows that the effect is better to adopt mixing method in the soft clay.

REFERENCES

[1] Bao C G, Rao X B. Principle of the Geotechnical Centrifuge Model Test[J]. *Journal of Yangtze River scientific Research Institute.* 1998,15(2): 2∼5.

[2] Zhou X W, Pu J L, Bao C G.A Study of the Movement and Failure Characteristics of Sand Mass Above the Crown of a Tunnel[J]. *Rock and Soil Mechanics.* 1999,20(2):32∼36.

[3] Zhou X W, Pu J L. Centrifuge model test Study of the earth Pressure and deformation of tunnel lining[J]. *J Tsinghua Unlv.* 2001,41(8): 110∼113.

[4] Ma L, Gao BO. Centrifugal model test of ground surface sedimentation control in construction of tunnels[J]. *Construction technology*,2005,34(6): 6–8.

[5] Wu Bo, Liu WeiNing, Gao Bo. Study of construction technique of Shenzhen metro running tunnel on watery strata non-precipitaion[J]. *China Civil Engineering Journal.* 2004,37(4): 93∼98.

[6] Peck R B. Deep excavations and tunneling in soft ground[A]. *Proceedings Of the 7th International Conference on soil Mechanics and Foundation Engineering[C]*. Mexico City: State of the Art Volume, 1969: 225–290.

[7] Fang Jiang H, Liu H Y, Jiang Y S. Identification on surface subsidence effect by shield tunneling[J].

[8] Hou Xue-yun, Liao Shao-ming. Settlement Predicted in Shield Tunnel [J]. *Underground Engineering and Tunnel*.

[9] Liu Jian-hang, Hou Xue-yuan. *Shielding tunnel[M]*. Beijing: China Railway Press.1991.

[10] Yang L C, Zhou shun-hua, Yao M Y. Ground Surface Settlement during Excavation of variety span tunnel[J]. *Journal of Tongji University.* 2003, 31(4), 408–412.

[11] Shen Pei-liang, Zhang Hai-Bo,Yin Zhong-ze.Ground settlement due to shield construction in Shanghai metro tunnel project[J]. *Journal of Hehai University.* 2003, 31(5): 556–559.

Underground Space – the 4th Dimension of Metropolises – Barták, Hrdina, Romancov & Zlámal (eds)
© 2007 Taylor & Francis Group, London, ISBN 978-0-415-40807-3

The effect of advance rate on shield loading in squeezing ground

M. Ramoni & G. Anagnostou
ETH Zurich, Switzerland

ABSTRACT: Squeezing ground may slow down or even obstruct TBM operation and, if occurring over frequent tunnel intervals or persisting over longer portions of a tunnel, may be decisive for the economic viability and the feasibility of a TBM drive. Among other problems, a low strength or high deformability ground may cause jamming of the shield. From tunnelling practice, it is well known that squeezing is a time-dependent process, which may take place over a period of days, weeks or months. The risk of shield jamming therefore essentially depends on the TBM advance rate. This paper investigates the complex problem of the interaction between the advancing machine and the creeping or consolidating ground. Numerical analyses highlight the effect of advance rate, ground permeability, shield length and installed thrust.

1 INTRODUCTION

Squeezing refers to the phenomenon of large time-dependent deformations during tunnel excavation. It occurs mostly in weak rocks with a high deformability and a low strength, often in combination with a high overburden (Kovári 1998). It is also known that a high pore water pressure promotes the development of squeezing. If suitable preventive measures are not implemented, squeezing may even lead to complete closure of the tunnel cross section. In the presence of a lining, the ground exerts a gradually increasing pressure which can lead to it becoming damaged or even completely destroyed.

Squeezing ground may slow down or even obstruct TBM advance and – if occurring over frequent tunnel intervals or persisting over longer portions of a tunnel – may be decisive for the economic viability and the feasibility of a TBM drive (Lombardi & Panciera 1997). An overview of the specific problems of mechanized tunnelling in squeezing ground can be found elsewhere (Ramoni & Anagnostou 2006). Depending on the TBM type (thrusting system, type of support, existence or not of a shield etc.) a series of potential hazards must be considered concerning the machine (sticking of the cutter head, jamming of the shield) or the back-up area (inadmissible convergences of the bored profile, damage to the support).

The present paper deals with the risk of shield jamming, with particular emphasis placed on the time-dependency of squeezing, on understanding the mechanisms governing the ground response to tunnelling operations and on some of the practical questions of mechanized tunnelling through water bearing squeezing ground.

2 TIME-DEPENDENCY OF DEFORMATIONS

2.1 *Observations*

Experience shows that squeezing may take place over a period of days, weeks or months. Usually it is a slow process, although there have also been cases of intense and rapid development of ground deformations close to the working face.

As an example, the "Strada"–section of the headrace tunnel Tavanasa-Ilanz in Switzerland may be mentioned. This tunnel crosses a phyllitic verrucano and was bored in the period 1985–1988 by a gripper TBM ($Ø = 5.20$ m). During the drive in an overthrust zone, measurements revealed that within just a half day the convergence was greater than 25 cm, i.e. 5% of the diameter (Marty 1989).

Another interesting example is the water tunnel Evinos-Mornos in Greece. This tunnel crosses mainly Flysch and it was constructed in the years 1993–1994 by two gripper TBMs ($Ø = 4.20$ m) and two double shielded TBMs ($Ø = 4.04$ m). During the gripper TBM drives through some thrust zones, the ground squeezed so rapidly that the radial displacements amounted 3–5 cm right at the cutter head and 5–8 cm at the location of support installation (Vigl & Jäger 1997). The double shielded TBMs encountered squeezing conditions in an overthrust zone more than 650 m long. Within less than one hour after the excavation, at a distance of only 2 m from the working face, the convergences reached 15 cm, i.e. 4% of the diameter (Grandori & Antonini 1994, Grandori et al. 1995).

The New Viola water tunnel (Italy) was constructed in the years 1999–2004 by a double shielded TBM ($Ø = 3.60$ m). The machine was trapped first during

excavation in a phyllitic rock. The ground deformation was fast enough to close the gap (8 cm) between the double shield (L = 9 m) and the rock mass within a time period of six to ten hours (Höfle 2001). The same machine was later stopped again because of squeezing ground, although this was after a one 1-week holiday stop.

2.2 *Mechanisms*

The gradual increase of the ground deformation or pressure is first of all a consequence of the *spatial stress redistribution* associated with progressive excavation (Lombardi 1973). The stress redistribution is completed within a relatively short distance from the face (about two tunnel diameters), and cannot therefore explain long-term phenomena but is, nevertheless, essential for the convergence close to the working face and, consequently, for the loads acting upon the shield.

Long-term deformations can be traced back to the *creep* and *consolidation* processes taking place in the ground surrounding the tunnel (Gioda & Cividini 1996). In the vicinity of the working face, creep and consolidation are in general superimposed on the spatial stress redistribution associated with the advancing excavation. Consolidation comes into play when tunnelling through a water-bearing, low-permeability ground. Creeping depends on the rheological properties of the ground and becomes evident especially when the ground is highly stressed as the state of failure is approached. It is therefore of great importance in the case of squeezing ground (Fritz 1981). In order to reduce complexity, creeping will not be considered further in this paper. Instead, attention will be paid to the consolidation processes around the advancing face.

2.3 *Pore water pressure generation and dissipation*

Squeezing is in general accompanied by a volume increase of the ground. In theory one speaks of "plastic dilatancy", in tunnelling practice of "loosening". The water content of a saturated ground increases during squeezing. This occurs more or less rapidly depending on the permeability of the ground. In a low-permeability ground, the water content remains constant in the short term. Since the pore water hinders dilatancy, excess pore water pressures develop, which dissipate over the course of time. Tunnel excavation in a saturated squeezing ground thus triggers a transient seepage flow process. Seepage flow and ground deformation are coupled to each other. The pore water pressures and the effective stresses change with time, the latter leading to additional deformations or, in the presence of a lining, to increasing loading (Anagnostou & Kovári 2005).

Two important limiting states of the transient process are: the state at time $t = 0^+$ ("short-term behavior") and the state at $t = \infty$ ("long-term behavior"). The first is characterized by the condition of a constant water content (so-called "undrained conditions"), while the second is governed by the steady state pore water pressure distribution (so-called "drained conditions"). According to theoretical and experimental investigations (Vogelhuber 2006), the negative excess pore pressures developing under undrained conditions strengthen the ground (so-called "dilatancy hardening"). The short-term behavior is therefore more favorable than the long-term behavior.

During tunnel excavation, consolidation takes place in general simultaneously with the stress redistribution caused by the advancing tunnel heading. In the case of rapid excavation through a low-permeability ground, the favourable "undrained conditions" prevail in the vicinity of the advancing face. If the excavation proceeds slowly or the permeability of the ground is high, the unfavourable "drained conditions" prevail practically right from the start. A simple dimensional analysis shows that the time development of deformations is governed by the ratio of advance rate v to permeability k.

Subsequently, the role of pore water pressure dissipation will be illustrated by means of numerical results concerning a 500 m deep, Ø 10 m tunnel which crosses weak ground at a depth of 100 m beneath the water table. Information on the modelling assumptions and numerical procedures can be found in the Appendix. For simplicity, the hypothetical case of an unsupported tunnel will be considered first.

Figure 1 shows, for different v/k-ratios, the contour lines of pore water pressure, the distribution of volumetric strain ε_v (in the radial direction and along the tunnel axis ahead of the face) as well as the radial displacement u of the tunnel wall (after subtracting the deformations taking place ahead of the face). With increasing permeability (or an equivalent decreasing advance rate), dissipation of the excess pore water pressures accelerates, i.e. it takes place more and more closely to the tunnel heading. The higher the permeability of the ground (or, in equivalent terms, the slower the tunnel excavation), the quicker the consolidation process develops and the larger are the deformations occurring at a fixed distance from the face.

3 THRUST FORCE

When tunnelling with a shielded TBM, some limited convergence may occur because the gap which exists between the shield and the rock provides space for deformations. In the case of intense and rapid squeezing, the ground closes the gap at a short distance from the tunnel face and starts to develop a pressure upon the shield. Figure 2 shows, for the example discussed before, the distribution of the ground pressure p alongside the tunnel assuming a normal gap

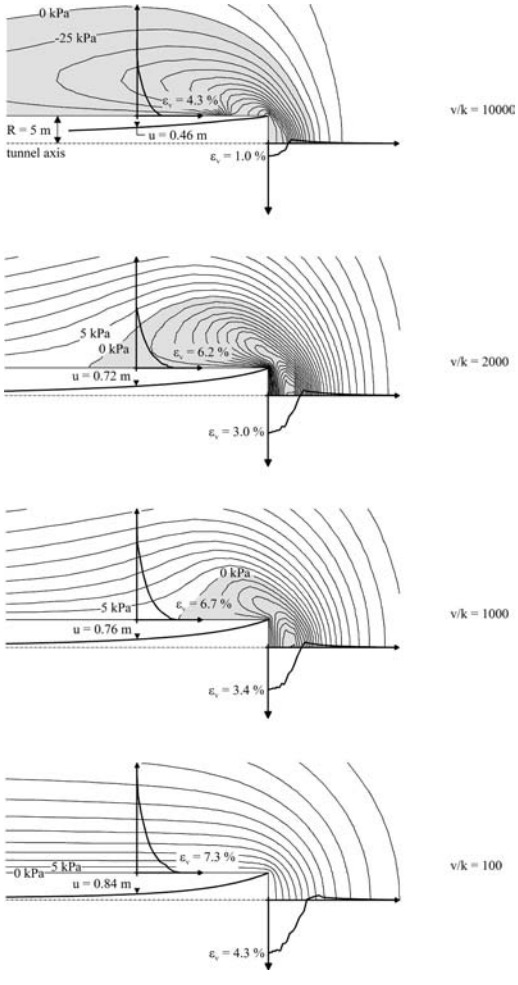


Figure 1. Contour lines of the pore water pressure, convergence of tunnel wall u and distribution of volumetric strain ε_v for different values of the ratio of advance rate v to permeability k (other parameters: see Table 1).

ΔR of 5 cm. Again, the ratio of advance rate v to ground permeability k governs the pressure development. If the permeability is low and the advance rate high ($v/k \geq 10^6$), the gap remains open for the first 6 m. Consequently, the pressure acting upon, e.g., a 10 m long shield would be very low, while a gripper TBM with a short canopy ($L \leq 3$ m) would not experience any squeezing pressure at all. In the case of high permeability, a low advance rate or a standstill ($v/k \leq 10^2$), however, the ground will close the gap in a distance of 2 m from the face and exert a considerable pressure on the shield, possibly endangering its structural stability and also posing the question of the thrust force needed to keep the TBM advancing.

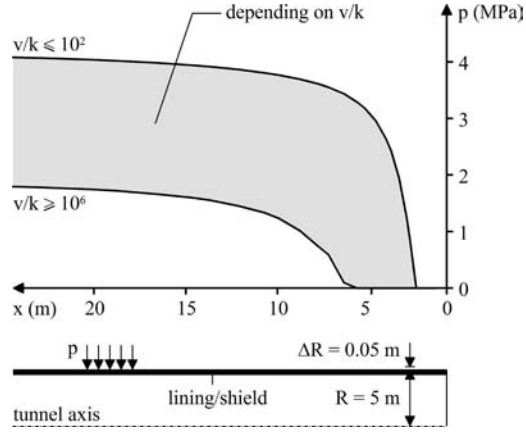


Figure 2. Radial pressure p acting upon the shield or lining for different values of the ratio of advance rate v to permeability k (gap between shield and ground $\Delta R = 0.05$ m; other parameters: see Table 1).

Figure 3 shows the thrust needed to overcome the friction of a 10 m long shield as a function of the advance rate v in a low permeability ground ($k = 10^{-9}$ m/s). The curves have been calculated by integrating the ground pressure p (Fig. 2) over the shield length L and taking into account additionally the thrust needed for the boring process (15 MN). The skin friction coefficient was taken equal to $\mu = 0.25$. In the case of a normal gap ($\Delta R = 5$ cm, upper curve), a continuous excavation rate of $v = 10$ m/cd in combination with a high but still feasible thrust of 90 MN would be necessary to overcome squeezing. The lower curve applies to a gap of $\Delta R = 15$ cm. Accordingly, the thrust requirements can be reduced considerably by overboring – this comes, however, at the cost of possible steering difficulties and reduced production rates.

The permeability of the ground governs the rate of the consolidation process and thus the intensity of the deformations close to the advancing face. Figure 4 shows the effect of permeability k on the thrust needed to overcome friction. The curves apply to different advance rates v and gap sizes ΔR. The lowest curve is rather theoretical as it presupposes a high advance rate inspire of the extreme overboring. Figure 4 shows that for feasible production rates the consolidation process is practically irrelevant if the permeability is higher than about $10^{-7}-10^{-8}$ m/s. The unfavorable steady state conditions apply immediately after excavation, i.e. in the vicinity of the tunnel face. High ground pressures and, consequently, also high thrust forces characterize the steady state. The thrust requirements reach, in the present example, the limits of feasibility. On the other hand, for a practically impermeable ground ($k < 10^{-10}-10^{-11}$ m/s) and even moderate advance rates ($v = 1-10$ m/cd),

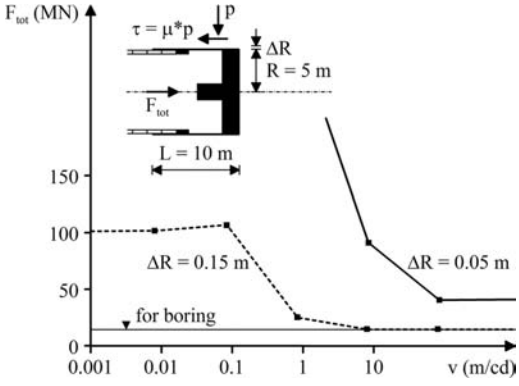


Figure 3. Needed total thrust force F_{tot} as a function of the advance rate v (permeability $k = 10^{-9}$ m/s, gap between shield and ground $\Delta R = 0.05$ or 0.15 m, shield length L = 10 m, skin friction coefficient $\mu = 0.25$; other parameters: see Table 1).

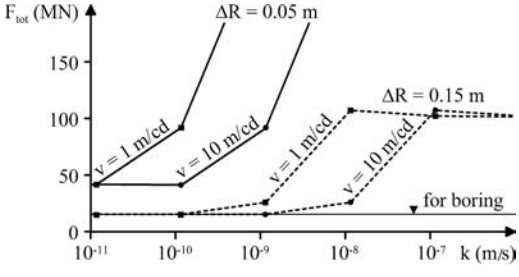


Figure 4. Needed total thrust force F_{tot} as a function of the permeability k (advance rate $v = 1$ or 10 m/cd, gap between shield and ground $\Delta R = 0.05$ or 0.15 m, shield length L = 10 m, skin friction coefficient $\mu = 0.25$; other parameters: see Table 1).

the favorable undrained conditions prevail. The thrust needed to overcome friction is considerably lower.

In the permeability range of $k = 10^{-10} - 10^{-8}$ m/s, a large sensitivity of the results can be observed. This permeability range is thoroughly relevant in practice. For example, the extensive laboratory testing program carried out for investigating the kakiritic rocks of the Gotthard Base Tunnel (Lot Sedrun) revealed permeabilities between 1.1×10^{-10} and 1.5×10^{-9} m/s (Vogelhuber 2006). The large sensitivity in the results indicates a major source of prediction uncertainty, as permeability cannot be estimated reliably. This is particular true for heterogeneous ground (Anagnostou & Kovári 2005).

4 CLOSING REMARKS

The thrust force *needed* to overcome shield friction in given ground conditions depends on the length of the shield, the amount of overboring, the skin friction coefficient and the advance rate. A reduction in the advance rate leads as a rule to an increase in the ground pressure, and thus to further deceleration or even standstill of the machine.

The *available* thrust force depends on the installed thrust and on the capacity of the thrusting system. In a single shielded TBM, for example, the possible thrust force is limited by the bearing capacity of the segmental lining and depends, therefore, on the structural design of the segments and on the quality of the annulus grouting. A quick, proper installation and backfilling of the segmental lining may be impeded by poor ground conditions or water inflows. These difficulties lead to a reduction of the advance rate with the result that the ground pressure acting upon the shield, the required thrust force and the force to be introduced into the lining all increase. Similar feedback effects exist also for gripper TBMs. The time needed for support installation in a poor quality ground reduces machine utilization and may lead to a higher ground pressure on the cutter head shield, to a higher thrust force in order to avoid jamming and therefore to problems with the bracing of the grippers.

In conclusion, on the one hand, the ground-machine–support interaction is decisive for the advance rate, but on the other hand the advance rate influences this interaction too. Besides adverse ground conditions, undesirable events such as electric power stoppages, mechanical breakdowns of the TBM or problems in the back-up system may slow-down excavation progress unpredictably. Maintaining a high production rate is of course a main goal of any TBM drive. For tunnelling through squeezing ground, it may also help avoiding trapping of the machine. Nevertheless, a high advance rate cannot be seen as a panacea for coping with squeezing, as several uncertainties exist with respect both to ground and the machine.

APPENDIX. COMPUTATIONAL MODEL

The numerical investigations are based on an axial symmetric model. The ground is modelled as a saturated porous medium according to the principle of effective stresses. Seepage flow is taken into account using Darcy's law. The mechanical behaviour is modelled as an isotropic, linear elastic, perfectly plastic material obeying the Mohr-Coulomb yield criterion and a non-associated flow rule. The material constants (Table 1) are typical for kakiritic rocks from the Gotthard Base Tunnel (Vogelhuber 2006). For simplicity, both the lining and the shield are assumed to be rigid and only the simplified case of a constant gap size ΔR is considered.

At the far-field boundary the radial stress is kept constant and equal to the initial value σ_0. The respective hydraulic potential Φ is fixed to 78 m. This value is slightly lower than the initial value of $\Phi_o = 100$ m. It

Table 1. Parameter Values.

Tunnel radius R	5 m
Radial gap size ΔR	0.05 or 0.15 m
Advance rate v	variable
Initial stress σ_0	12.5 MPa
Initial hydraulic head Φ_0	100 m
Young's Modulus E	1000 MPa
Poisson's ratio ν	0.25
Angle of internal friction φ	25°
Cohesion c	500 kPa
Dilatancy angle ψ	5°
Permeability coefficient k	variable

takes into account the deviation from axial symmetry and it was estimated based upon a preliminary two-dimensional seepage flow analysis. At the excavation boundary the initial stress is reduced to zero. In order to avoid water inflow from the excavation boundary, a mixed seepage flow boundary condition is prescribed (no flow condition in the case of negative pore water pressures, atmospheric boundary pressure in the case of positive pore water pressures).

The pore water pressure dissipation takes place in general simultaneously with the spatial stress redistribution in the vicinity of the advancing face. Consequently the analysis of an advancing tunnel heading is inherently a time-dependent, three-dimensional problem with a moving boundary. Usually, the tunnel excavation is simulated by a step-by-step excavation and support installation procedure. Since high deformation- and pore water pressure- gradients prevail in the vicinity of the tunnel face and the latter moves during the step-by-step simulation, the finite element mesh has to be fine everywhere. Such an analysis is, therefore, extremely time-consuming even in the case of linear material behavior. The calculations of this paper are based upon a new numerical solution method, which solves the advancing tunnel heading problem in just one single computational step (Anagnostou 2007). This is possible (i) by re-formulating and solving the underlying transient equations in a reference frame which is fixed to the moving face (Anagnostou 1995), and (ii) by applying a special stress-point algorithm to the integration of the incremental, elasto-plastic stress-strain equations which takes into account appropriately the stress path dependency of the material's behavior. The numerical solution was accomplished with the finite element program HYDMEC (Anagnostou 1992).

REFERENCES

Anagnostou, G. 1992. Untersuchungen zur Statik des Tunnelbaus in quellfähigem Gebirge. Veröffentlichungen des *Instituts für Geotechnik (IGT) der ETH Zürich* Band 201. Zürich: vdf Verlag der Fachvereine an den schweizerischen Hochschulen und Techniken AG.

Anagnostou, G. 1995. The influence of tunnel excavation on the hydraulic head. *International Journal for Numerical and Analytical Methods in Geomechanics* 19: 725–746. Chichester: John Wiley & Sons Ltd.

Anagnostou, G. & Kovári, K. 2005. Tunnelling through geological fault zones. Proceedings of *International symposium on design, construction and operation of long tunnels* (Taipei) Volume 1: 509–520. Taipei: Chinese Taipei Tunnelling Association.

Anagnostou, G. 2007 (in preparation). Continuous tunnel excavation in a poro-elastoplastic medium. Proceedings of *NUMOG X Tenth International Symposium on Numerical Models in Geomechanics* (Rhodes).

Fritz, P. 1981. Numerische Erfassung rheologischer Probleme in der Felsmechanik. *Institut für Strassen-, Eisenbahn- und Felsbau der ETH Zürich* Mitteilung Nr. 47. ETH Zürich.

Gioda, G. & Cividini, A. 1996. Numerical methods for the analysis of tunnel performance in squeezing rocks. *Rock Mechanics and Rock Engineering* (1996) 29 (4): 171–196. Wien New York: Springer-Verlag.

Grandori, R. & Antonini, F. 1994. Double shield TBM excavation technique – Recent experiences and future development. *Felsbau* 12 (1994) Nr. 6: 490–494. Essen: Verlag Glückauf GmbH.

Grandori, R., Jäger, M., Antonini, F. & Vigl, L. 1995. Evinos-Mornos Tunnel – Greece / Construction of a 30 km long hydraulic tunnel in less than three years under the most adverse geological conditions. Proceedings of *Rapid excavation and tunnelling conference* (San Francisco): 747–767. Littleton: SME Inc.

Höfle, H. 2001. Wasserstollen bei Bormio – Einsatzerfahrungen mit einer Teleskopschildmaschine. Proceedings of *6. Internationales Symposium Tunnelbau bauma 2001* (München): 169–174. Essen: Verlag Glückauf GmbH.

Kovári, K. 1998. Tunnelling in squeezing rock. *Tunnel* 5/98: 12–31. Gütersloh: Bertelsmann Fachzeitschriften GmbH.

Lombardi, G. 1973. Dimensioning of tunnel linings with regard to constructional procedure. *Tunnels and Tunnelling* 5 No. 4 – July-August 1973: 340–351. London: Morgan-Grampian Ltd.

Lombardi, G. & Panciera, A. 1997. Problems with TBM & linings in squeezing ground. *Tunnels & Tunnelling International* 29 No. 6 – June 1997: 54–56. London: Miller Freeman plc.

Marty, T. 1989. Tunnelboring in difficult rock conditions with a fullface machine as part of the Ilanz Power Station Project. *World Tunnelling and Subsurface Excavation* 2 Special edition – April 1989: 14–20. London: The Mining Journal Ltd.

Ramoni, M. & Anagnostou, G. 2006. On the feasibility of TBM drives in squeezing ground. *Tunnelling and Underground Space Technology* 21 (2006) No. 3–4: 262. Oxford: Elsevier Ltd.

Vigl, L. & Jäger, M. 1997. Double shield TBM and open TBM in squeezing rock – A comparison. Proceedings of *ITA World tunnel congress '97 Tunnels for people* (Vienna) Volume 2: 639–643. Rotterdam Brookfield: A.A.Balkema.

Vogelhuber, M. 2006. Der Einfluss des Porenwasserdrucks auf das mechanische Verhalten kakiritisierter Gesteine. *PhD Thesis*. ETH Zurich.

This page intentionally left blank

Underground Space – the 4th Dimension of Metropolises – Barták, Hrdina, Romancov & Zlámal (eds)
© 2007 Taylor & Francis Group, London, ISBN 978-0-415-40807-3

Benefits and life-cycle costs of underground projects

John Reilly
John Reilly Associates International, Framingham, Massachusetts, USA

Harvey Parker
President, International Tunneling Association; Harvey Parker & Associates, Bellevue, WA USA

ABSTRACT: Prior to 2002, ITA's Working Group (WG) 13 addressed the "Direct and Indirect Benefits of Underground Structures. In 2002 WG20 continued this theme with the topic "Urban Problems – Underground Solutions" (the principal author was an Animateur of both groups). Much progress has been made in understanding the issues, however in many parts of the world it is very difficult to obtain funding and approval for underground projects, even if the benefits are positive, because the higher initial capital cost of underground projects means that a cheaper elevated or above ground project is frequently chosen. However, selection of an alternative only on the basis of initial capital cost is misleading and in many cases precludes the realization of very substantial long-term benefits. Underground projects have long-term (life cycle) benefits that are, in many cases, much greater than those for above ground projects. These and other benefits mean that the tunnel alternative can return more benefits if long range benefits and costs are considered.

1 INTRODUCTION

There are many complex political and technical issues and decisions in the planning and financing of any infrastructure project. Perceived high cost is an assumption that prematurely eliminates consideration of tunnels in many cases. These premature decisions are usually made only on the basis of initial capital cost since there is a general misconception that tunnels cost too much and therefore need not be considered at all. In fact the true long-term cost of a tunnel may or may not be more expensive than surface or elevated schemes. When evaluated from the standpoint of Life Cycle Cost and Benefits there are examples of tunnels having benefits that outweigh their higher initial capital cost and many examples of tunnels being "in the competitive range".

Therefore, the true cost of a tunnel should be evaluated, not in terms of initial capital cost which is often the only factor considered, but in terms of life cycle costs and benefits considering the generally much longer useful service life of tunnels and their contribution to the environment and sustainability.

The underground industry has been remiss in not developing methodologies and databases that can allow evaluation of projects using life cycle costs and benefits. In 2001, in Seattle, USA the authors organized an American Underground Association Regional conference which discussed these issues (see also, Hess 2001). It is noted that life cycle cost methodology is used routinely for selection of highway pavement alternatives and by private businesses but is seldom used for a complete evaluation of major infrastructure projects.

Fortunately, new tools have been developed to better identify cost, risk and value (*Reilly, 2003 et. seq.*). These tools can include life-cycle costs and benefits as well as funding and revenue projections. An outline of this is presented later in this paper.

1.1 *Overview – The decision to build underground*

More cities are deciding to construct urban transportation projects underground for several reasons.

- They are often the shortest route between two points.
- Tunnels are a way to maintain mobility, using space that is not in conflict with surface functions.
- Tunnels allow multiple use of real estate, essentially doubling the potential use of any parcel of land.
- They provide significant environmental benefits (reduction of noise and visual impacts) and social opportunities (better public use for the surface space).
- They allow movement of people, goods and services, without having to change modes of conveyance.
- Tunnels operate in, and can provide shelter from, adverse weather conditions – safety is improved by the absence of glare, distractions, rain and snow.

- They allow movement under or through obstacles (preserving the obstacles if necessary).
- They conserve energy and are inherently energy efficient.
- They are ideal for preservation of the environment and sustainability.

Examples of international cities building transportation tunnels include: Amsterdam, Hamburg, Stuttgart, Melbourne, Moscow, Oslo, Paris, Shanghai, Stockholm, Sydney and Tokyo. In these cities, there is a relationship between sustainable development and tunnel demand. These tunnels have environmental and social benefits that are recognized by decision makers and voters.

Population, and urban concentration are major factors to consider. In Japan, the lack of available land for infrastructure is driving demand for tunnel construction, and the country builds more tunnels than any country with over 1200 km of tunnels. Switzerland builds mostly through mountains in rock tunnels. Sweden has a policy to first consider underground solutions. All of these factors are relevant, many quantified specifically for a particular city, region or country – however, we need a process to allow this quantification to be more reliable in the determination and political environment of the jurisdiction.

2 COST OF UNDERGROUND PROJECTS & LIFE-CYCLE BENEFITS/COSTS

It is generally true that the initial capital cost of underground construction is significantly greater than elevated or surface facilities. This was documented in the ITA WG 13 Report "Underground or Aboveground", Making the Choice for Urban Mass Transit Systems. (ITA, 2004). The cost factors for underground were reported, in general, to be around 4.5 times that of surface and 2.25 times elevated. These are very significant cost factors in the choice of an underground facility.

Significant conclusions of the WG13 report follow (only some of the findings are given):

1. The decision on whether to place an urban mass transit system underground or aboveground is a complex planning, engineering, construction, urban design, economic and political decision.
2. In many cases – for example in the center areas of older cities – there is no alternative to the choice of an underground alignment for new mass transit systems because of for functional, social, historic environmental and economic reasons.
3. In newer cities, cities without extensive historical districts, and cities with wide streets, elevated alignments can offer full grade separation typically at substantially lower initial construction cost than underground alignments, with certain exceptions usually related to right-of-way costs.
4. The initial capital cost is only a part of the total long-term financial commitment. Costs include capital (including financing), operations, maintenance, security and rehabilitation. A rational and quantified consideration of all costs and benefits (direct and indirect) is necessary.
5. Many aspects of the long-term cost-benefit relationships are hard to quantify. Reference analyses and reports with the experience of other cities are very useful – particularly in the early stages of planning and design – however such quantification must be considered.

2.1 *Long-range cost-benefit analysis*

Cost-benefit analysis should include capital, operating and maintenance costs, road user time savings, public transport user time savings, travel time variability, pedestrian time savings, vehicle operating cost savings, accident reduction, etc. The benefits accrued to underground projects should include the time value of the use of the surface over the tunnel (a value can be assigned even if it is a park), right of way advantages, increased property values and employment in the general vicinity, and overall energy savings that might result from shorter travel times, flatter grades, etc. Moreover, an equivalent accrued value should applied for the less tangible environmental and sustainability benefits such as noise impacts, air quality impacts, and greenhouse gases which are significant over the life cycle (Parker, 2004, Hess, 2001). The following examples include many of these elements and this issue is developed further later in this paper.

2.2 *Maintenance and operating costs – underground vs. above-ground*

Increased maintenance and operational costs for underground facilities may or may not be greater than surface or elevated facilities. Operating costs for light, ventilation, communications and safety systems will cost more for a tunnel. Maintenance costs however may be the same or could be less than for an elevated structure. For example a study for the Newfoundland and Labrador Fixed-Link project, 18 km long, which compared the estimated capital, maintenance and operating costs for several alternatives including bridges compared to immersed tube, drill and blast and TBM tunnels, found significantly lower maintenance and operational costs for the tunnel configurations in the order of $CA16.9 million/year for the bridge and between $CA 6.8 and $CA7.6 million for the tunnel (Newfoundland and Labrador Fixed-Link project).

In Sydney (see following) the projected Net Present Value (NPV) of operating and maintenance costs

Table 1. Estimated Long-Term Savings, Sydney.

Element	Estimated benefit ($A m)
Time savings – road	738.15
Time savings, public	83.48
Time savings, pedestrian	67.15
Vehicle cost savings	211.27
Accident reduction	10.17
Reduction in noise	10.94
Reduction in pollution	0.13
Greenhouse gases	50.58
Increased property	3.41
Total	1,175.28

were projected at about 8% of the cost of construction. These costs were included in the cost-benefit analysis which showed a positive investment return. Hess (2001) reported a similar very comprehensive life-cycle evaluation of the Prague Metro in which he concluded that over the life cycle, a subway project brings a profit to public budgets in spite of increased operational costs compared with the surface transport.

3 EXAMPLES – BENEFITS OF URBAN UNDERGROUND TRANSPORTATION PROJECTS

The following examples outline major transportation projects in dense urban environments where an underground solution has been chosen or preferred over a surface or elevated solution. These are road projects, but the same considerations would apply to rail or transit projects. In a few cases the cost-benefit of the underground solution has been quantified and is reported here.

3.1 *Cross-City Tunnel, Sydney, Australia*

Sydney, Australia examined the costs and benefits of the construction of the Cross-City Tunnel which occupies a critical location in relation to the flow of traffic in the inner metropolitan area. It is the crossing point for major road and public transport flows in both north–south and east–west directions. The economic assessment of the Cross-City Tunnel (NSW Roads and Traffic Authority Working Paper 2000) found a very positive benefit for the underground facility. The project had an estimated a capital cost of $A330 m and a delivered capital cost of $A680 m (see other papers for cost growth of major infrastructure projects e.g. Reilly, 2005a) but was estimated to deliver total benefits of some $A1,175 m as shown following. The net present value of the benefits was $A448 m.

3.2 *Rheinufertunnel (Rhine embankment tunnel), Düsseldorf, Germany*

As in many old cities, which are situated along rivers, the road along the embankment of the Rhine in Düsseldorf was frequented by 55,000 cars per day until the early 90s. This road separated Düsseldorf's "Altstadt", the famous historic part of the town, which is also frequented by many tourists, from the river Rhine, preventing the public from enjoying the special urban quality of living next to a river. In 1993 a 4-lane road tunnel under the previous embankment road was opened, also opening the chance for an immense improvement of the urban quality in this part of Düsseldorf. The tunnel partly is under the water line of the Rhine and therefore was built using compressed air under a lid with the help of diaphragm walls. The area today has proved to be one of the most beautiful parts of the city and its recreational value, esp. on weekends, is inviting thousands of citizens. The case history is being evaluated by ITA Working Group 20, Urban Problems, Underground Solutions.

The tunnel provided the following benefits:

- Valuable surface space made available again
- Additional traffic capacities provided for individual transport
- Relief from traffic congestion achieved
- Time savings in transport achieved
- Noise levels brought to acceptable levels
- Pollution (especially air pollution) reduced
- Architectural quality of urban environment improved
- Service quality of the urban environment improved
- Safety and security in urban environment improved
- The project was completed on time and within the original 300 million Euro budget.

3.3 *Alaska Way Viaduct and Seawall Replacement, Seattle, USA*

The Washington State Department of Transportation (WSDOT), the City of Seattle and the U.S. Federal Highway Administration are working to replace the old Alaskan Way Viaduct and Seawall, considering two basic alternatives – a tunnel along the waterfront or an elevated highway structure. These two alternatives were carried forward in 2004, following three years of environmental and engineering review, 76 initial concepts, over 200 community meetings and over 4,500 public comments.

The viaduct plays a major role in sustaining the regional and city economy and maintaining mobility throughout Seattle. One quarter of all north-south traffic through Seattle (103,000 vehicles) use the viaduct every day. When the project was closed temporarily after the 2001 Nisqually Earthquake there was extreme congestion on adjacent freeways and the downtown

city grid. The earthquake also damaged the seawall and subsequent investigations revealed that the seawall also needs to be replaced. Options considered for the Alaska Way Viaduct replacement were:

- Boulevard Along Alaskan Way (Multi-Modal Transportation)
- Elevated Roadway Along Alaskan Way
- Cut & Cover Tunnel Along Alaskan Way
- Deep Bored Tunnels
  - Along Alaskan Way
  - Along 1st & 2nd Aves.
  - Along 5th Avenue
  - Under Interstate – 5
- Sunken Tube Under Elliott Bay
- Deep Bored Tunnel Under Elliott Bay
- Submerged Floating Tube Under Elliott Bay
- Elliot Bay Signature Bridge

As of this writing, the City of Seattle believes the Cut & Cover Tunnel along Alaskan Way using the outboard wall of the tunnel to replace the seawall is the preferred project and the State is working with the City to find funding for the extra capital cost of this alternative. The additional funding is not yet assured.

4 BENEFITS OF UNDERGROUND FACILITIES – WITH REFERENCE TO SEATTLE

One of the primary findings from the Seattle review is that relevant tunnels and underground structures last a significantly longer time than the equivalent above-ground structures. Tunnels constructed over one hundred years ago in the U.S. and elsewhere are still in useful service today.

For example, the Seattle Alaskan Way (elevated) Viaduct is 52 years old but needs to be urgently replaced. The West Side Highway in New York City was taken out of service after 42 years. The Embarcadero Freeway in San Francisco was demolished after approximately 30 years.

A review of transportation corridors shows that underground structures last much longer, often over a century and more. The Burlington Northern (BN) Rail Tunnel beneath Seattle is over 100 years old – it was opened in November 1904 and is now on its second century of low-maintenance service. The Seattle Battery Street Tunnel, now 53 years old, will continue to take traffic well into the future.

A significantly longer service life means that the present value (worth) of that structure (the tunnel) can be less than a shorter-life structure (elevated viaduct) although the initial capital cost of the elevated structure is usually less than that of the tunnel.

Table 2. Benefits associated with the tunnel option, seattle.

Element	Benefit
Increased values associated with the waterfront:	\$0.7–\$1 billion over 25 years
New visitor spending:	\$1 billion for each 1% increase in visitors
Increased property values:	\$280–\$960 million.

5 ECONOMIC STUDIES

An economic case for the tunnel was outlined recently to the Downtown Seattle Association (Pascall, 2006). This study reported that, by funding the tunnel option (at an additional cost of over \$1 billion more than the elevated viaduct replacement), property values could increase by \$450 million, as much as \$2 billion in additional property development could occur and \$325 million a year could be generated by tourism.

A previous (but limited) had review indicated that the following potential benefits for the tunnel might be realized in addition to the environmental improvements:

In total these numbers indicate that the present worth value of the tunnel could exceed the extra initial capital cost by a factor of between 1 and 3. However, because it is hard to quantify these numbers sufficiently or accurately in the context of current practice this is an area for further study and development by ITA.

6 NEW TOOLS TO QUANTIFY COSTS AND BENEFITS

There are new tools that can better address cost, probable cost, risk identification, risk management, value engineering, life-cycle costs and benefits and probable funding. An example of one of these is the U.S. Washington State Department of Transportation's Cost Estimate Validation Process CEVP® which is a process to identify ranges of probable costs by identifying and combining "base costs" and risks plus opportunities to produce a "range of probable cost and schedule" for the explicit and implicit conditions of the evaluation. The process has been described previously (Reilly, 2005a, 2004b & c, 2003c).

Current thought is to extend this process to include life-cycle and value-engineering components. An outline has been drafted for the value engineering process and one could be readily developed for life-cycle costs. This Life Cycle Cost Estimation Process (LCCEP) would allow us to tie together cost validation, ranges of probable costs and benefits and value-added returns in order to better assist determination of alternatives considering long-range costs and benefits.

7 CONCLUSIONS

1. There is rising skepticism toward the underground design and construction industry, particularly for large expensive projects in cities. This is due to many major cost over-runs and sometimes mismanagement – which need to be addressed. We also need to improve design standards for safety, security, environmental soundness and user friendly tunnels and to and communicate this effectively to the public and political decision makers.
2. We cannot do this unless we develop reliable methodologies to systematically estimate and manage costs and risk, and to use those methodologies to reduce the out-turn costs of tunnels and underground space. Adding value engineering and life-cycle costs and benefits will enable better total cost comparisons for alternatives if the environmental and political decision processes are also aligned.
3. The concepts outlined in this paper, including the proposed Life Cycle Cost Estimation Process (LCCEP) if developed and applied, would allow, practical and more reliable comparisons on the basis of cost and benefits to select a preferred project alternative from significantly different alternatives such as elevated, surface, cut-and-cover, various bored tunnel and other underground schemes and alignments.
4. This can be done because of the comprehensive nature of the proposed process, which could fully take into account relevant factors and could provide the equivalent monetary value of all the environmental benefits the proposed project provides. It is anticipated that underground projects would become more economically attractive as a result.
5. The referenced CEVP process (Reilly, 2005) has improved our ability to predict a project's probable cost and schedule in ways that incorporate the effects of risks, technical and non-technical. The same concepts and attitudes necessary to be successful with CEVP are also those that are needed to quantify for life cycle costs and benefits.
6. When fully developed, LCCEP will allow engineers, planners, decision makers, politicians, the general public, and the media to better understand the compromises and tradeoff choices that are made in planning a given infrastructure project.
7. When this methodology becomes mature, the authors believe that tunnels and underground space will be found to be more competitive with other alternatives and many decisions regarding alternates can be made on the basis of issues such as the environment and quality of life. It is likely that the underground alternative will be selected more often – provided funding can be found.
8. The concept of life cycle costs is not new as it has been applied to pavement replacement for decades. The approach regards cost as an investment to be managed prudently. The same is true for major transportation projects, but the methodology has not been applied similarly and, as a result, engineers and planners do not commonly apply it to major infrastructure projects.
9. The underground industry should have already developed this acutely needed methodology. We must be proactive to develop these concepts and to get them to be understood and accepted by the decision makers. We must continue to explain that tunnels and underground facilities are "investments and not costs".
10. Much needs to be done to develop and simplify practical methodology to accomplish the goals of a complete Life Cycle Cost Process. If this initiative is successful, the result will be benefits to urban communities in the form of more value and improved environmental quality and sustainability. And, there will be more underground facilities designed and constructed.

8 SUMMARY

To make a more equitable case for appropriate selection of underground alternatives, the following actions must be considered:

1. Planning and public policies must consider long-term life-cycle costs and benefits
2. The long-term life-cycle costs and benefits need to be quantified through an accepted methodology
3. Benefits must be communicated to the public and political decision-makers
4. The political process must recognize that this is an appropriate planning and selection process
5. A funding mechanism that will support the higher initial capital cost must be found
6. Revenue to support the funding mechanism needs to be collected
7. The credibility of this process must be demonstrated.

REFERENCES

Hess, 2001, Presentation to AUA conference on Life-Cycle Costs, Seattle, USA, March 2001

ITA 2004, Working Group 13, "Underground or Aboveground", Making the Choice for Urban Mass Transit Systems, *Tunneling and Underground Space Technology*, Vol. 19, No. 1, pp 3–28

ITA 1995, "General Considerations in Assessing the Advantages of Using Underground Space" WG13 report, *Tunneling and Underground Space Technology*, Vol. 10, No. 3, pp 287–297

Newfoundland and Labrador Fixed-Link project http://www.gov.nf.ca/publicat/fixedlink/pdf/completereport.pdf).

NSW Roads and Traffic Authority Working Paper, 2000: "*Economic and Financial Assessment of the Cross-City Tunnel*", Spiller Gibbins Swan Pty Ltd, April

Pascall, G, 2006, study presented to the Downtown Seattle Association, August

Parker, H.W 2004 "Underground Space: Good for Sustainable Development, and Vice Versa," *Proceedings, World Tunnelling Conference*, International Tunnelling Association, Singapore, May 2004

Reilly, J.J 2005a "Cost Estimating and Risk Management for Underground Projects", *Proc. International Tunneling Association Conference*, Istanbul, May, Balkema

Reilly, J.J 2004b w. Brown, J "Management and Control of Cost and Risk for Tunneling and Infrastructure Projects" *Proceedings, World Tunneling Conference*, International Tunneling Association, Singapore, May 2004

Reilly, J.J 2004c w. McBride, M, Sangrey, D, MacDonald, D & Brown, J. "The development OF CEVP®, WSDOT's Cost-Risk Estimating Process" *Proceedings, Boston Society of Civil Engineers*, Fall/Winter 2004

Reilly, J.J 2003c "The Relationship of Risk Mitigation to Management and Probable Cost", *Proc International Tunneling Association*, World Tunnelling Congress, Geldermalsen, Netherlands, April

Underground Space – the 4th Dimension of Metropolises – Barták, Hrdina, Romancov & Zlámal (eds)
© 2007 Taylor & Francis Group, London, ISBN 978-0-415-40807-3

New York Second Avenue Subway – Initial support design of shallow rock caverns

K. Rossler & C. Stone
DMJM Harris, New York, USA.

ABSTRACT: New York Metropolitan Transportation Authority Capital Construction (MTACC) has authorized the DMJM+HARRIS•Arup Joint Venture team with preliminary engineering of the $16 billion 2nd Avenue Subway project consisting of 14 km of twin tunnels and sixteen underground stations. The project will include large, shallow caverns for stations and crossovers mined in rock, which will be featured in this paper. Clear span openings up to 30 m, low rock cover ranging from 6 m to 12 m, and non-circular shapes below groundwater level presented many design challenges and dictated unique design considerations to assure prudent solutions. Confronting the caverns' design intricacies, a robust design procedure was developed to increase the design safety margin and to assure economic feasibility. The core of the design procedure was the adoption of ground behavior rules identifying support types, and verification by a simultaneous deployment of the best-known tunnel design methods.

1 INTRODUCTION

The Second Avenue Subway (SAS) project alignment (Fig. 1) is planned for the east side of Manhattan Island in New York City. The project includes six underground mined station caverns and five mined crossover caverns.

2 GEOLOGY

Manhattan Schist along the alignment typically has three joint sets with scattered shear zones. Joint spacing ranges from moderate to close within the top 9 m of bedrock. Top of rock elevation is variable, and typical soil overburden is about 6 m.

The design intact rock parameters are shown in Table 1. With respect to the compressive strength, the intact rock cores measured higher tensile strength (Brazilian test), and lower Young's modulus (uniaxial compression test) likely influenced by the mica schist content.

The direct shear test results revealed an elasto-plastic behavior of joints with zero displacement weakening, and peak friction angle equal to residual friction. The joint parameters are provided in Tables 2–3.

Base friction angle of Set 2 in conditions I, II, and III was increased to account for effect of joint waviness by 5 deg. Cohesion was zero.

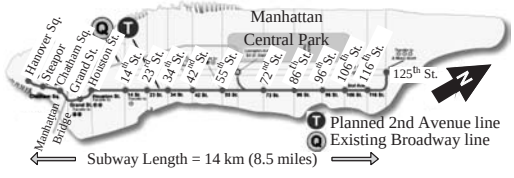


Figure 1. Plan of second avenue subway.

3 DESIGN METHODOLOGY

The design methodology relied on three design concepts:

1. Initial support design chart structured by ground behavior rules.
2. Four verification methods with fundamentally different design approaches.
3. Rock load as a parameter of ground behavior.

Table 1. Design intact rock parameters.

Unit weight (kN/m^3)	27.5
Secant modulus (GPa)	20.7
Poisson's ratio	0.15
Compressive strength (MPa)	48
Tensile strength (MPa)	14

Table 2. Measured rock joint shear strength parameters (Snee & Rocha 2005).

	Joint sets∗			
	Set 1, and Set 3,		Set 2,	
Base friction, and dilation angles	ϕ_b deg	ϕ_d deg	ϕ_b deg	ϕ_d deg
I Fresh to slightly weathered with iron-oxide staining	30–40	5–10	42	5–10
II As condition I with heavy iron-oxide staining	30	5–10	35	5–10
III Slightly to moderately weathered with mineralization, chlorite, kaolinite, sericite	20–35	2–10	40	5–10
IV As condition III with heavy iron-oxide staining and clay coating	20–30	0–5	20–36	5
V Condition I–III with slickensides	25	3	25	3

∗ Set 1 = Foliation; Set 2 = Cross-foliation; Set 3 = Conjugate to foliation.

Table 3. Design rock joint parameters.

Shear displacement for zero dilation (mm)	4
Joint normal stiffness (kN/m^3)	1.6E+07
Joint shear stiffness (kN/m^3)	6.0E+06

3.1 *Initial support design chart*

The design chart in Table 4 includes:

- Five support types (Types I thru V), and their support quantities.
- Ground behavior rules defining design ranges of the five support types.

The five ground support types have been developed to cope with anticipated changes in ground conditions. The ground behavior rules, which recognize the impacts of both rock quality and excavation geometry, were used to arrange the five support types in hierarchy from bolt-reinforced rock to structural shotcrete arch in recognition of a boundary between "good" and "bad" ground behavior.

3.2 *Methods with fundamentally different design approaches*

Four methods with fundamentally different design approaches were utilized in verification and optimization of initial support quantities to comply with design criteria, and performance requirements for given geotechnical parameters:

1. Empirical methods (Q, RMR).
2. Stress-strain method of discontinuum (UDEC).
3. Stress-strain method of continuum (STAAD).
4. Force-equilibrium method (UNWEDGE, Closed-form).

The four methods allow accounting for a broad range of the tunnel design aspects to assure safe and economic construction. The methodology recognized the strengths of each method, and maintained a premise of the methods equal importance for the design. Neither method was considered an inferior or superior analytical tool in making design decisions. The key, however, was to distinguish the method's range of applicability. An engineer with tunnel design experience and familiar with the methods would make design decisions based on understanding the features that impact the design and which methods include the features.

Table 5 describes the methods, their strengths and weaknesses, and their range of applicability. Table 6 provides selection guidelines of verification methods appropriate for given ground conditions.

3.3 *Rock load parameter*

Rock load is required input for structural design of the final concrete lining, and the initial shotcrete structural arch. In the design chart, rock load was also recognized as a parameter to measure ground behavior, and to identify the support types because it accounts for all the impacts including the rock quality and the excavation geometry, and is directly proportional to the amount of support required.

4 FUNDAMENTAL CAVERN DESIGN CONSIDERATIONS

Loading considerations and dimensional elements relating to the transit station and crossover cavern design were discussed and agreed upon with the client, MTACC, early in the design phase. These included the following:

- Station and crossover geometries,
- Two-pass lining system, in which initial lining does not contribute to the final support.

4.1 *Performance requirements*

The mined cavern linings were designed to ensure stability of the rock mass and to protect the existing structures. The design was required to comply with the following requirements:

- Maximum permissible vertical movement in crown, and at street level = 0.020 m.
- Maximum permissible differential settlement for a historic structure near cavern = 1/1000.
- Maximum permissible differential settlement for a modern structure near cavern = 1/750.

Table 4. Initial support design chart.

Good ground behavior. Reinforced rock arch. ⟷ Bad ground behavior. Structural arch required

		TYPE I				TYPE II				TYPE III				TYPE IV				TYPE V			
		Excavation span (m)				Excavation span (m)				Excavation span (m)				Excavation span (m)				Excavation span (m)			
Initial support design chart		6–8	8–15	15–23	23–30	6–8	8–15	15–23	23–30	6–8	8–15	15–23	23–30	6–8	8–15	15–23	23–30	6–8	8–15	15–23	23–30
Ground rules																					
Rock tunneling quality index > Q, and		>6	>13	>21	>35	>0.5	>1.4	>2.5	>4	>0.04	>0.14	>0.25	>0.4	>0.0028	>0.017	>0.05	>0.1	<0.0028	<0.017	<0.05	<0.1
Rock Mass Rating > RMR, and	RMR	>80	>80	>80	>80	>60	>60	>60	>60	>40	>40	>40	>40	>20	>20	>20	>20	<20	<20	<20	<20
Rock Mass Class < / = C_{RM}, and*	1	1	1	1	1	1	1	1	1	1	1	1	2	2	2	2	3	3	3	3	
Rock Cover(m) > RC	RC	>3	>5	>8	>10	>3	>5	>8	>10	>3	>5	>8	>10	>2	>4	>6	>8	<2	<4	<6	<8
Design rock load (m)**	RL_1	3	5	8	9	3	5	8	9	3	5	8	9	5	8	12	15	5	9	14	18
Design rock load (if rock cover < RL_1)	RL_2	–	–	–	–	–	–	–	–	–	–	–	–	80%	80%	80%	80%	100%	100%	100%	100%
Support																					
Support description		Unsupported – Spot bolting				Systematic bolting				Syst. bolting, thin shotcrete				Structural arch, syst. bolt.				Structural arch, syst.bolt.			
Bold diameter (mm)		25	28	32	32	25	28	32	32	25	28	32	32	25	28	35	35	25	28	35	35
Bolt length (m)		2.5	4	5	6	2.5	4	5	6	2.5	4	5	6	2.5	4	5	6	2.5	4	5	6
Bolt spacing (m)		spot	3	3	3	1.5	3	3	3	1.2	1.5	1.5	1.5	1.2	1.2	1.2	1.2	1.2	1.2	1.2	1.2
Shotcrete thickness (m)		–	–	–	–	–	–	–	–	<0.10	<0.10	<0.10	<0.10	0.15	0.15	0.20	0.30	>0.15	>0.15	>0.20	>0.30
Shotcrete fiber reinforcement (J)		–	–	–	–	–	–	–	–	700	700	700	700	700	700	700	700	1000	1000	1000	1000
Lattice girder type		–	–	–	–	–	–	–	–	–	–	–	–	3/70	3/70	3/115	4/220	3/70	3/70	3/115	4/220
Lattice girder spacing/weight (m)/(kg)		–	–	–	–	–	–	–	–	–	–	–	–	1.2/10	1.2/10	1.2/12	1.2/15	To be determined.			
Excavation sequences***		F	C or M	C or M	C or M	F	C or M	C or M	C or M	F	C or M	C or M	C or M	HB	C or M	C or M	C or M	HB	M	M	M
Excavation advance (m)		2	2	2	2	2	2	2	2	2	2	2	2	1.2	1.2	1.2	1.2	1.2	1.2	1.2	1.2

* Cording 1984.
** RL_1 = Rock load as equivalent rock column. RL_2 = Rock load as percentage of full overburden including soil (rock unit weight = 27.5 kN/m^3; soil unit weight = 19 kN/m^3).
*** F = Full face excavation; C = Center cut w side slash; M = Multiple side drift; HB = Heading and benching.

Table 5. Description of the method's applicability, strengths, and weaknesses.

	Empirical Q, RMR CLASSIFICATION	Stress-strain discontinuum UDEC	Stress-strain continuum STAAD	Force equilibrium UNWEDGE, CLOSED FORM
Strength:	Incorporates construction experience, incl. 3D geometry, material variability, etc.	Verification of displacements, and rock loads. Rock-structure interaction.	Structural arch verification for design loads.	3-D wedge stability supported bolts and shotcrete. Pillar stability (closed-form).
Caution:	Limited use for shalow, sequential, or non-circular excavations. Thin rock pillars	2-D models tend to be conservative	Springs and final loads have to be known beforhand.	Structural arch can be represented only by its shear strength.
Not applicable:	Verification of displacements.	Modeling of heavily broken rock may be impractical.	Rock reinforcement. Rock stability. Rock-structure interaction.	Shallow exc. External loads. Displacements or rock-structure interaction.

Table 6. Guide to application of design verification methods.

Support types	Excavation geometry		Verification methods		
	Span	Excavation	1	2	3
I, II, III	<8 m	Full face	Empirical	UNWEDGE	–
I, II, III	8–30 m	Sequential	Empirical	UNWEDGE	UDEC
IV, V	6–30 m	Full, Seqntl	Empirical	UDEC	STAAD

4.2 *Design criteria*

Initial support was designed as a temporary structure over the time period prior to installation of the final liner; this involved:

1. Non-factored loads.
2. Strength reduction factors applied in structural verifications of shotcrete arch and steel sets.
3. Safety factors applied in bolt design and wedge stability.

Design criteria were summarized in Table 7.

5 DESIGN ISSUES

This paper focuses on issues that have generated controversial points of view. The adopted solutions shall not be taken as definitive statements, rather as project-specific design approaches that are offered for discussion.

5.1 *Rock load magnitudes*

The rock load ranges of the design chart were defined by the minimum rock load of 3 m of NYCT design guidelines (NYCT 2003), and by empirical data from previously constructed mined station caverns in Washington, D.C. and New York, which were correlated with geological data and cavern geometry using the Q value and scaled crown span (Fig. 2).

The rock loads are generally in compliance with the U.S. Army Corps of Engineers guidelines, and were confirmed by UDEC analyses (Fig. 3).

Rock loads of shallow caverns are limited by the low rock cover, however due to proximity of the top of rock, the loads may approach full overburden loads by adding the pressures of soil overburden, as shown in Figure 3.

Force equilibrium methods (Closed form solutions or UNWEDGE) cannot fully account for the impact of low rock cover, and were utilized to verify wedge loads for Types I thru III.

5.2 *Low rock cover*

Various design methods define shallow tunnels differently. The Q tunneling index considers the impact of low rock cover when it is less than the excavation span. Low cover of soil tunnels is defined by three excavation spans by considering the impact of gravity gradient on ground load distribution.

In the design of the SAS caverns, the adverse impact of low rock cover was defined by the rule of minimum rock cover thickness equal to 1/3 and 1/4 of

Table 7. Design criteria of initial support.

Bolts			
Max bolt force (kN)	Min ultimate strength × 0.6		
Max yield strain	4%		
Shotcrete plain, with wire mesh, fiber, or lattice girder			
Unit weight, γ (kN/m^3)	23.6		
Compressive strength, f'_c (MPa)	41.4		
Young's modulus, E (GPa)*	19.8		
Poisson's ratio, ν	0.17		
Adhesion to rock, c_a (kPa)	517 (Clements 2003)		
Shear strength, f_v (MPa)	0.05 f′c (Cording 1984)		
Structural shotcrete arch**	Plain, wire mesh	Fibers	Lattice girder
Tensile strength, f_t (MPa)	0.1 f'_c	0.1 f'_c	***
Res. tensile strength, f_{tr} (MPa)	0	0.1 f'_t	0.1 f'_t

* Elastic modulus reduced by 35% to account for plastic deformation, and microcracking.
** Structural shotcrete arch defined as a curved structural member with thickness >15 cm, which relies on rock support along the walls and under the footings to generate axial thrust, enhancing the arch flexural strength. Fiber content of 0.6, 0.9, 1.2% (by volume) may account for 20, 35, and 40% shear strength increases, respectively, (ACI 544.4R-88).
*** The design tensile strength of shotcrete arch enhanced by lattice girder shall be determined from moment-thrust diagram in correspondence to the steel bar reinforcement per foot. The compressive strength of shotcrete shall be considered without contribution of lattice girder.

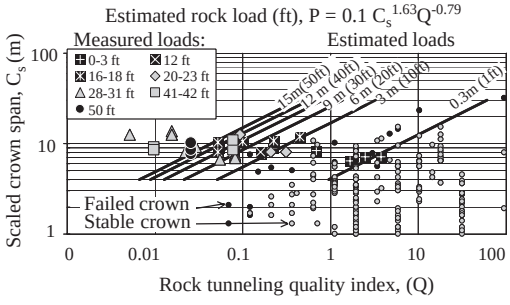


Figure 2. Estimation of rock loads for shallow caverns via the scaled crown span.

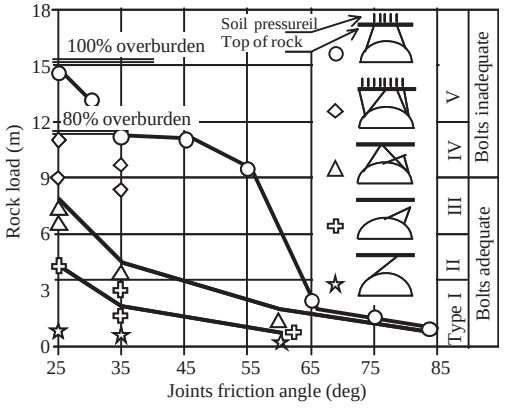


Figure 3. UDEC rock loads on 30.5 m wide cavern liner, under 5 m of soil, 12 m of rock cover with various joint dips.

excavation span in support Types IV, and V, respectively. It was assumed that a rock mass reinforced by bolts would be capable of supporting the excavation in compliance with the definition of good ground behavior with rock cover more than the defined minimum. Bad ground behavior or excavation with rock cover thickness less than the minimum would require support via a structural shotcrete arch.

The minimum rock cover thickness is less restrictive than the Q or the soft ground tunnel rules, and therefore it was verified by the numerical method UDEC, (Fig. 3), including the adverse impacts of low rock cover, as follows:

1. Overstressing and limited rock arching in the roof.
2. Tensile stresses and joint opening due to bending of the roof under the soil overburden.
3. Failure mechanism defined by steep discontinuities and by the top of rock surface.
4. Limited roof thickness for productive drill and blast operation.
5. Limited rock thickness for proper bolting lengths.

5.3 *Verification of structural shotcrete arch*

Design aspects of the shotcrete arch for support of Types IV, and V are described in the following sections.

5.3.1 *Rock load distribution diagrams*

The uniform rock load distribution (Fig. 4), and unbalanced rock load distribution (Fig. 5) were utilized in STAAD analyses to obtain shotcrete design forces.



Figure 4. Uniform rock load diagrams; RL = rock load magnitude in Table 4.

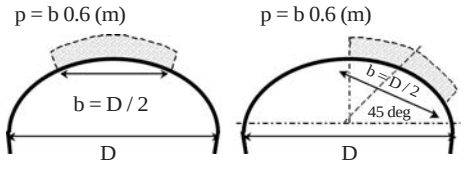


Figure 5. Unbalanced rock load diagrams.

Table 8. Rock mass modulus and spring stiffness magnitudes.

Rock quality classification	Q ≥ 4, or RMR ≥ 60	Q < 4, or RMR < 60
Rock mass modulus, E_m (GPa)	16.5	4.1
Radial spring stiffness, k_r(kN/m^3)	9.4E+05	3.1E+05
Vertical spring stiffness under footings, k_v (kN/m^3)	9.4E+06	3.1E+06
Horizontal spring reaction under footings, k_h (kN)*	<N_u tan(15 deg)	

* N_u = vertical thrust force exerted by the footing.

5.3.2 *Springs*

Rock mass modulus estimated from correlations of RQD (Bieniawski 1984), and Q (Barton 2002) with derived spring stiffness are shown in Table 8.

Convergence of UDEC and STAAD results was utilized in the calculation of spring stiffness, which represented passive resistance of the rock mass. Figure 6 shows agreement between axial thrust, moments, and shear forces calculated by UDEC, and STAAD in the shotcrete arch, which confirmed similar boundary conditions in both models, and yielded the spring stiffness equivalent to the rock mass behavior.

5.3.3 *Comparison to Q*

The Q support chart (Grimstad 2002) defines structural arch support by shotcrete ribs reinforced with steel bars, while the SAS design chart recommended a structural arch of uniformly thick shotcrete liner reinforced by lattice girders. For comparison purposes, Figure 7 converted the Q reinforced shotcrete ribs into equivalent support of the uniform shotcrete liner reinforced by lattice girders. The comparison showed, that the SAS subway design chart prescribed smaller shotcrete thickness, and less reinforcement than the Q design, which demonstrated the effect of support optimization of the robust design methodology. Note that the SAS shotcrete lining is to be followed by a concrete final lining.

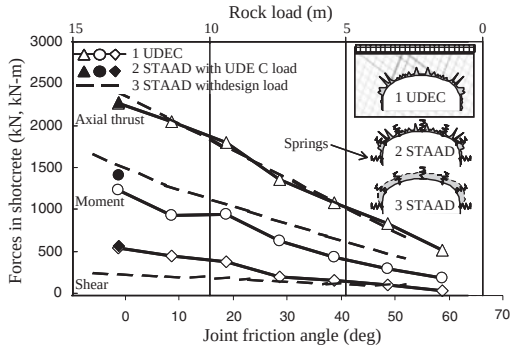


Figure 6. Forces in shotcrete arch (30.5 m wide cavern, under 6 m of soil, 10 m of rock cover, joint dips +50 × −50 deg.)

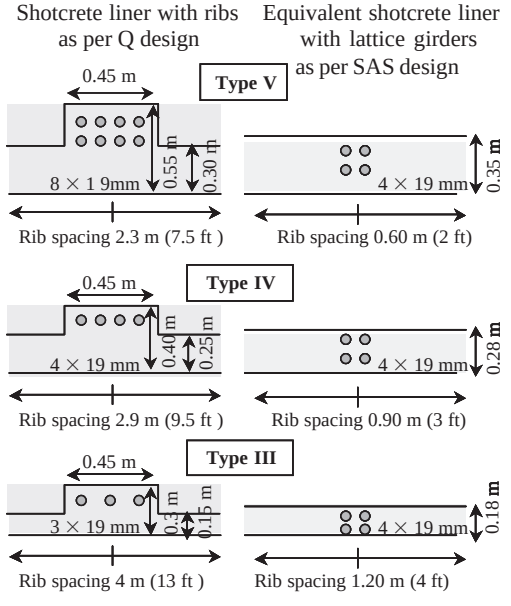


Figure 7. Shotcrete liners reinforced by lattice girders equivalent to the Q design requirements.

5.4 *In situ stress and Ko*

With respect to the low stress environment of shallow caverns, overstressing of intact rock blocks is unlikely, and the planes of weakness of joints, faults, and shear zones will control the excavation stability.

In preliminary engineering, the design of shallow caverns adopted a design value of Ko = 0.75, with lithostatic vertical stress equal to the weight of overburden. However, later in the project, the hydrofracture field tests measured high in situ stresses in the range of 1724 to 2758 kPa within the depths of 18 m, which would lead to Ko values of more than 10.

UDEC analysis demonstrated that before any excavation, the rock joints with the known design strengths would not support the high in situ stresses and failed, which led to a hypothesis that the measured stresses, would not transfer across the joints. The in situ measurements are to be re-examined.

5.5 *Groundwater*

Monitored groundwater levels indicated that the cavern construction would take place below the ground water table. Nevertheless the initial support design assumed zero groundwater pressures. In faulted areas the pressures are expected to be zero due to the recharge being less than the joints conductivity, while in tight rock mass areas the excavation is expected to be dry.

5.6 *Size of drill and blast drift*

The initial support design supported the excavation throughout all stages of excavation sequencing. General limitations that apply to drift size, round length, installation of support, and cut sequences were specified.

For cost estimating purposes, the SAS project adopted a round length of 2 m, which complied with the limited mucking capacity at the shafts, although, rock mechanics issues would allow larger round lengths of up to 6 m.

Applying the round length of 2 m, and considering vibration impacts on the surface structures yielded maximum drift size of 37 m^2. Drift height and span ranged from 4.5 to 8 m to accommodate mining equipment.

5.7 *Initial lining contribution*

Complying with the client's request and considering liability issues, the initial support, rock bolts and shotcrete liner were considered temporary support and would not contribute to the support capacity of the final lining during the 100-year design life. As a permanent support, the initial support would have to comply with strict quality assurance procedures, including inspection of lining thickness, shotcrete quality, steel cover, and corrosion protection.

Considering the shotcrete separation from the final liner by a waterproofing membrane, the analyses showed that the contribution of the 0.15 m thick shotcrete arch to the permanent support of a 0.9 m final liner would be only 15%.

ACKNOWLEDGEMENTS

The authors wish to thank Jeff Fosbrook, Project Manager of DMJM Harris•Arup Joint Venture, and Anil Parikh, Program Manager, of MTACC for permission to publish the project information. Our thanks also extend to Stanley Niemiec of Jenny Engineering for his mentoring, Sakir Selcuk, and Nils Pettersson of DMJM Harris who performed design analyses.

Views and/or opinions expressed in this paper do not necessarily express the views and opinions of the MTA and/or the Agencies.

REFERENCES

ACI 544.4R-88. 1999. Design considerations for steel fiber reinforced concrete. American Concrete Institute.

Barton, N. 2002. Some new Q-value correlations to assist in site characterization and tunnel design. *Int. J. Rock Mech. Min. Sci*. 39 (2): 185–216.

Bieniawski, Z.T. 1984. *Rock mechanics design in mining tunneling*. Rotterdam: Balkema.

Clements, M. 2003. Shotcreting in Australian Underground Mines: A Decade of Rapid Improvement. *Shotcrete* (Spring): 6–9.

Cording, E., Van Sint Jan, M., Rodriguez, C., Mahar J. & Fenrnadez, G. 1984. Ground and lining behavior of station chambers in rock for the Washington, D.C. metro. *U.S. DOT Federal Highway Administration*, 10/1983–07/1984.

Desai, D. & Naik, M. & Rossler, K. & Stone, C. 2005. New York Subway Caverns and Crossovers – A Tale of Trials and Tribulations, *RETC 2005, Seattle.* Colorado: SME.

Geotechnical Interpretative Report. 2004. Tunnels 92nd Street to 62nd Street. Internal doc of 2nd Ave Subway project.

Grimstad, 2002. Rock mass classification. *Norwegian Tunnelling Society*. (14): 25–27.

NYCT 2003. Structural Design Guidelines. Subway and Underground Structures, Issue No. 0, July 2003. New York.

Snee, Ch. & Rocha, S. 2005. Rock joint shear strength parameters. Internal doc of 2nd Ave Subway project, May 2, 2005.

STAAD.Pro. 2005. Structural analysis and design. Research Engineers International, A division of netGuru, Inc.

UDEC 3.1. 2003. Universal distinct element code. Itasca Consulting Group, Inc. Minneapolis, Minnesota.

UNWEDGE 3.0. 2006. Rockscience Inc. Toronto, Ontario.

U.S. Army Corps of Engineers. 1997. Tunnels and shafts in rock, *Engineer Manual*, EM 1110-2-2901, 30 May 1997.

This page intentionally left blank

Underground Space – the 4th Dimension of Metropolises – Barták, Hrdina, Romancov & Zlámal (eds)
© 2007 Taylor & Francis Group, London, ISBN 978-0-415-40807-3

Laboratory and numerical investigation of tunnel reinforced with face bolts

K.W. Seo, T. Domon & K. Nishimura
Tokyo Metropolitan University, Japan

ABSTRACT: During the excavation of tunnel, to prevent the collapse of tunnel face and settlement of ground the face bolts have been being frequently used in the soft ground. In this study, the face bolts were installed near to excavation line upwardly and radially on purpose and their supporting effects according to the installation angles were examined. Based upon the results of the laboratory and numerical investigation, the following conclusions were obtained. The axial displacement of the tunnel face depends on the installation angel under the same construction condition. The upward installation of the face bolts is fairly effective on controlling the vertical settlement. Inclined installation of face bolts depending on the purpose of support may be required for effective control of axial displacement of the face and/or the vertical settlement of surface.

1 INSTRUCTION

Construction of a NATM tunnel in soft ground usually calls for a supplementary method or methods to secure the stability of its working face and minimize its effect on the structures on surface. Especially face bolts prevent collapse of the face and settlement of ground during excavation. Therefore, they are frequently used in soft ground. (Geofronte research Association, 2002). As the main characteristic, the face bolts are installed in the excavation area and cut off during excavation process. (Geofronte research Association, 2002). Geofronte research Association (2002) reported that the face bolts has been used with other supplementary methods in 84% tunnel construction sites out of 29 tunnels where the bolts are employed. The reason of this is thought that the vertical settlement, such as surface settlement, as well as the axial displacement of the face is needed to be controlled.

Although the current construction standard prescribes that boring for bolts should be done horizontally as possible, it often deviates from the designed boring line due to geological condition, working condition, etc. (Seo, 2006). In this study, we give the angle, upward and radial, to the face bolt being installed near to the excavation line and examine its support effect against the vertical settlement of surface.

2 LABORATORY TEST AND NUMERICAL ANALYSIS

2.1 *Laboratory test*

Face bolts, as described above, are cut during the excavation. To model this, the following test method is used employed.

2.1.1 *Material of the ground*

The artificial material used as soil here is the mixture of copper bead, Vaseline and zincous oxide in the weight ratio of 200:1:0.3 respectively. Although copper bead is not light enough to handle easily and required to be kept in the stable temperature because of using Vaseline, it could provide some adhesive power, and the properties are stable due to not using water and could be preserved for a long time.

2.1.2 *Test box*

The test box used in this study is a aluminum box of which the width is 0.88 m, the length is 1.08 m and the height is 0.6 m.

2.1.3 *Face bolt*

The face bolts used in this test, of which the section is a 2 mm wide square, is a 1D (160 mm) long acryl rod. On its surface, sand is attached with epoxy.

2.1.4 *Excavation method*

The model tunnel is advanced 2 cm sequentially to 2.8D (44 cm) by hand. This excavation method was successfully carried out by Ishimura (1998). Picture 1 shows the test box set with artificial ground and gauges.

2.2 *Numerical analysis*

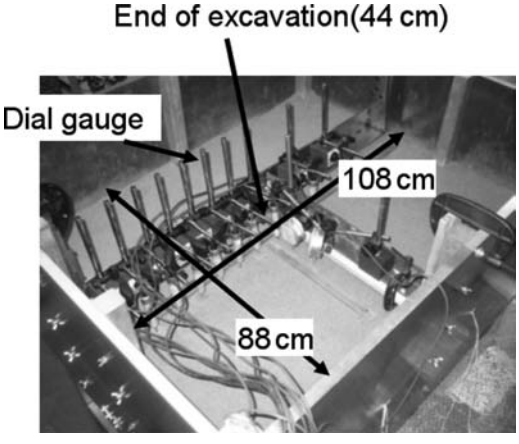
The axial displacement is not easy to measure directly on the face. Therefore, it is analyzed by numerical analysis. The ground material is presumed as elasto-plastic material of Mohr-Coulomb.

Figure 1 represents the numerical model and its input properties are listed in Table 1.

2.3 *Test case*

To compare face bolts with angles to horizontally installed bolts, the test cases shown in Table 2 are analyzed. Figure 2 shows the layout of the <0°> model.

Here, <none> represents a model without a face bolt, and <0°> does that with horizontally installed bolts. <0°> model is compared with 4 models of which face bolts on line 1 in Figure 2 are installed with radially upward angles of 15° and 30° and the upward 15° and 30° in parallel to the tunnel axis. The bolts on line 2 are horizontally installed. Both the laboratory test



Picture 1. Test box set up with artificial ground and dial gauges.

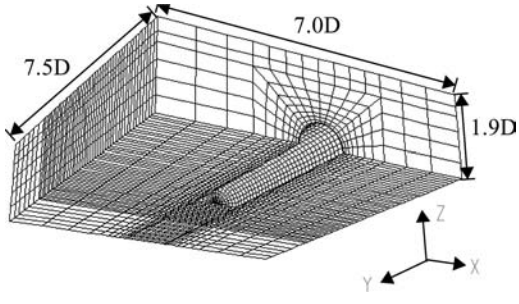


Figure 1. Numerical model.

Table 1. Input properties.

Ground	Material	Artificial material of copper bead
	Density	5.4 g/cm^3
	Elastic modulus	2900(KPa)
	Poisson ratio	0.45
	Frictional angle	35(°)
	Cohesion	7.3(KPa)
Face bolt	Material	Sand adhered Acryl
	Elastic modulus	4.5E5(MPa)
	Area	7.0E-2(cm^2)
	Overlap	8 cm(0.5D)
	Length	16 cm(1D)
Adhesive Characteristic between bolt and ground	Shear stiffness	7.3(KN/m/m)
	Shear strength	0.35(KN/m)

Table 2. Test case.

Model	Pipe		Number of installation	Analysis
	Line 1	Line 2		
<none>	none			Lab test, numerical analysis
<0°>	0°	0°	6 bolts/ section	Lab test, numerical analysis
<R15°>	Radial 15°	0°	6 bolts/ section	Numerical analysis
<R30°>	Radial 30°	0°	6 bolts/ section	Lab test, numerical analysis
<U15°>	Upward 15°	0°	6 bolts/ section	Numerical analysis
<U30°>	Upward 30°	0°	6 bolts/ section	Lab test, numerical analysis

- overlap: 0.5D 8 cm
- excavation distance 2.8D 44 cm
- the number of excavation: 6 times



Figure 2. Layout of model <0°>.

and numerical analysis are conducted on <R30°> and <U30°> models and only the numerical analysis is carried out on <R15°> and <U15°>. The overlap length is 0.5D (8 cm) and the tunnel is excavated six times to 2.8D (44 cm).

Radially and upwardly installed face bolts are remained in ground after excavation although horizontally installed bolts are removed by excavation. Upward installed face bolts on Line 1 reach the outside of the tunnel face. The more angle the face bolts have, the bolts reach further, that is, in the order of <U15°>, <R15°>, <U30°>, <R30°>, the bolts are installed further out of the tunnel. As the tunnel progresses, horizontally installed face bolts on Line 2 are cut off and those installed upwardly and radially on Line 1 are remained in the ground.

3 TEST RESULT AND CONSIDERATION

Figure 3 shows the maximum axial displacement according to the installation angle by numerical analysis. As shown in the figure, the axial displacement with the face bolts of 0° installation angle is minimal and it is greater with greater installation angle. The displacement of <U15°> and that of <R30°> are 27% and 45% greater than that of <0°>, respectively. The reason that the displacement of <U30°> and that of <R30°> are so big is thought that the installation angle of bolts on Line 2 is 0° and only those on Line 1 have the angle. It is believed that this is because horizontally installed face bolts mainly have the effect on axial displacement prevention.

This explains that the face bolts should be installed horizontally as possible to prevent axial displacement.

The axial force after horizontal installation of face bolts on Line 2 (See Figure 2) is represented in Figure 4. In every step of excavation, ground behind the face has the maximal axial force and it is the maximum after 2 step excavation. Further behind location with the maximal axial force, the force decreases. This phenomenon matches to the real measurement data (Nishizaki, 2002; Shimizu, 2003) and, therefore, it can be said that the laboratory test is successfully done.

The axis-direction vertical settlement after 2.0D excavation is shown in Figure 5. The settlement with radial installation is bigger than that with horizontal one. The reason is thought that the face bolts are stretches out of the face area and, therefore, the displacement on the face is large. Also, the bolts left in the ground may not affect much on supporting. Figure 6 represents the vertical settlement in axial direction after 2.8D (44 cm) excavation. Comparing the effects of horizontal installation and upward installation of face bolts, the vertical settlement with upward installation is about 10% less than that with horizontal installation and 17% less than that at 1.9D of the

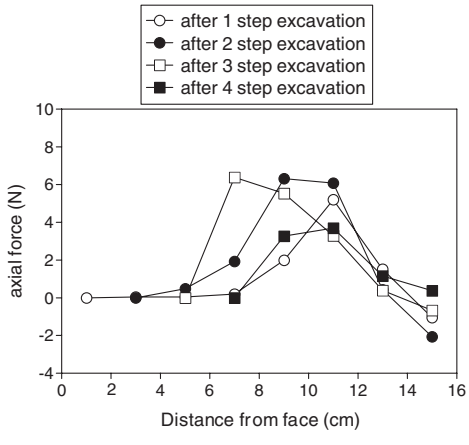


Figure 4. Axial force distribution on horizontally installed face bolts <0°> according to the excavation.

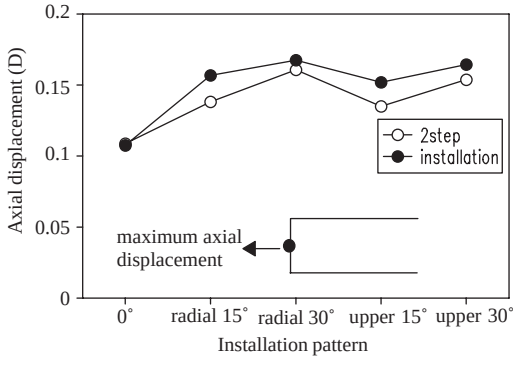


Figure 3. Maximum axial displacement according to the installation angle – numerical analysis.

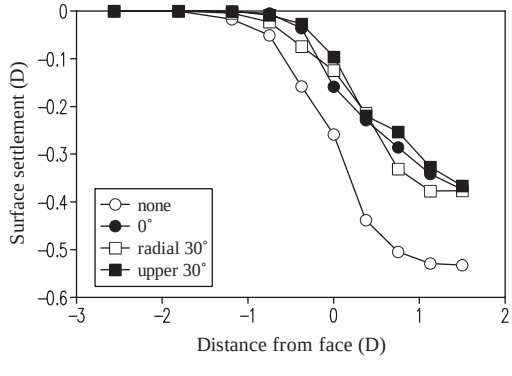


Figure 5. The vertical settlement according to the installation angle (after 2.0D excavation).

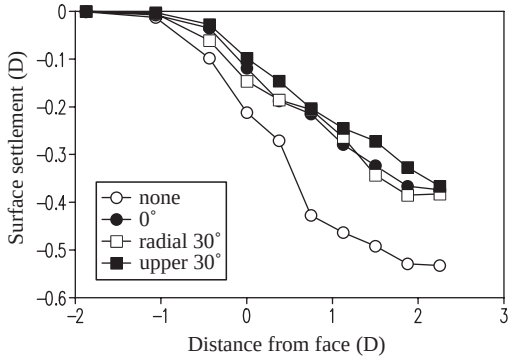


Figure 6. The vertical settlement according to the installation angle (after 2.8D excavation).

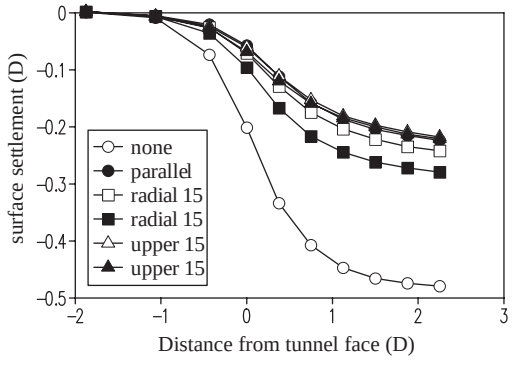


Figure 7. The vertical settlement according to the installation angle (after 2.0D excavation).

tunnel. The reason why the axial displacement with upward angle installation in Figure 3 is bigger and the vertical settlement is smaller than those with horizontal installation is believed that the bolts are installed in the opposite direction of surface settlements.

Figure 7 is the vertical settlement after 2.8D excavation calculated with numerical model. The settlement with radial installation is obviously larger than that with horizontal installation and that with upward installation is almost same as it. This may represent that the bolts left in ground become disjoined from the ground and then they don't affect on supporting.

According to the results shown above the following can be said: horizontal installation is effective on controlling the axial displacement of the tunnel face and the larger installation angle leads to the larger axial displacement. Also, the upward, not radial, is effective on controlling vertical settlement. Therefore, the installation design for face bolts proper to the support purpose may be required.

4 CONCLUSION

During the excavation of tunnel, to prevent the collapse of tunnel face and settlement of ground the face bolts have been being frequently used in the soft ground. Also, in the current construction standard for working the bolts prescribe that boring must be as horizontal as possible (in some cases, a slight inclination is given for the convenience of boring) , but in the field boring often deviates from the original boring line due to geological condition, working condition, etc. In this study, the face bolts were installed near to excavation line upwardly and radially on purpose and their supporting effects according to the installation angles were examined.

Based upon the results of the laboratory and numerical investigation, the following conclusions were obtained.

(1) The axial displacement of the tunnel face depends on the installation angel under the same construction condition.
(2) The upward installation of the face bolts is fairly effective on controlling the vertical settlement.
(3) Inclined installation of face bolts depending on the purpose of support may be required for effective control of axial displacement of the face and/or the vertical settlement of surface.

REFERENCES

GeoFronte Research Association Tunneling New Technology. 2000. Application trend and analyses of longitudinal facebolts-Part pp. 15–229

Kyoungwon Seo. et. Al. 2006. Behaviour of a tunnel face reinforced by bolts: Influence of an inclination installation, ITA-AITES World tunnel congress & 32nd ITA Generel assembly, 2006. 04

Toshiaki Ishimura, Hideto Mashimo, HidetoMayumi, Kunino Hujii. 1998. A 3-dimensional excavation model test about the effect of a tunnel pre-lining for the restraint of the ground deformation, *Proceeding of tunnel engineering*, JSCE Vol.8 pp.199–204

Shoushi Nishizaki, Tohru Haba, Tadashi Okabe. 2002. Application tend of long length facebolting and analytical study of its behaviour characteristics *Proceeding of tunnel engineering*, JSCE Vol.12 pp.131–136

Shimizu et al. 2003. Behaviour of the ground ahead of the face reinforced with long GFRP face forepiling, *Proceeding of tunnel engineering*, JSCE Vol.13 pp.225–230

Underground Space – the 4th Dimension of Metropolises – Barták, Hrdina, Romancov & Zlámal (eds)
© 2007 Taylor & Francis Group, London, ISBN 978-0-415-40807-3

Non-linear FE analysis of a grouted pipe-roofing reinforcement applied to a tunnel portal area

H.S. Shin, G.J. Bae, D.G. Kim & S.W. Lee
Geotech. Eng. Res. Dept., Korea Institute of Construction Technology (KICT), Gyunggi-Do, South Korea

ABSTRACT: This paper deals with a grouted pipe-roofing reinforcement method (GPRRM) which is used in construction of tunnels on weak grounds. This reinforcement method has proven to be very efficient in reducing amount of tunnel convergence and water inflow taking place in tunneling on weak grounds. However, due to the geometrical and mechanical complexity of the reinforcement, existing finite element frameworks are very difficult to simulate the kind of reinforcements for tunneling. Therefore, a mathematical framework for modeling a grouted pipe-roofing reinforced ground (GPRRG) by introducing a homogenization technique and its implementation into a 3-D finite element program are presented. The constitutive model developed allows considering the main design parameters of the problem and only requires geometrical and mechanical properties of the constituents. Additionally, the use of a homogenization approach implies that the generation of the finite element mesh can be easily produced and that re-meshing is not required as basic geometrical parameters such as the orientation of the pipes are changed. The model developed is used to simulate tunneling with the UARS. From the analyses, the effects of the main design parameters on the elastic and the elastoplastic analyses are considered.

1 INTRODUCTION

The GPRRM for ground reinforcement has been commonly applied in tunnelling under difficult ground conditions, with satisfactory results. Previous experience on the use of the technique has shown effective reductions on potentially large tunnel convergence, ground settlement and water inflow (KICT, 1986; Societa Italiana Gallerie, 1991; Pelizza and Pelia, 1993; Pelia, 1994; Bae et al., 1997). However, due to the geometrical and mechanical complexity of the problem, there have been very few attempts to analyse this problem and no adequate method for determining the design parameters of the reinforcement system has been developed.

In this study, a mathematical framework based on a homogenization technique similar to the one used by Lee et al. (2000), but with a different geometrical definition of the reinforced ground is adopted to derive an anisotropic composite material representing the elastoplastic macroscopic behaviour of GPRRM. A new algorithm for nonlinear stress integration is also proposed. The constitutive model developed is then incorporated into a FE program, capable of considering stage construction, to produce a tool that allows considering the effect of the main design parameters of GPRRM.

2 HOMOGENISATION TECHNIQUE FOR GPRRM

The general idealised geometry of the system to simulate is shown in Figure 1. As shown, two sets of axes are defined, a global axis X-Y-Z associated with the geometry of the tunnel and a local axis x-y-z associated with the geometry of the reinforcement system. The latter coincides with the axis of orthotropy of the reinforcement system, z being parallel to the pipe and y perpendicular to the arch formed by the set of pipes. As shown in Figure 1, it is assumed that the injected grout produces a continuum in the x direction but a finite

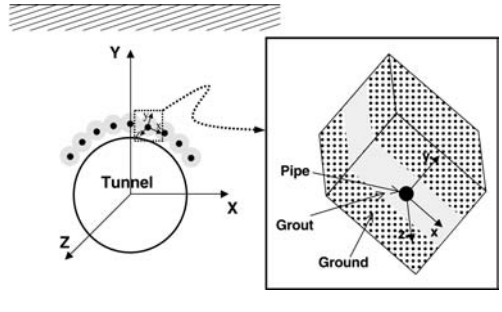


Figure 1. Geometrical description of GPRRM model.

depth band in the y direction. The use of the local axes allows defining the properties of the reinforced ground in its axis of orthotropy regardless of the orientation of the pipes with relation to the tunnel. The orientation of the reinforcement system at each location is included in the model by converting the properties of the reinforced ground into the global axes. For this, transformation matrices are composed by introducing angles θ and β, shown in Figure 2. This procedure allows defining the FE mesh independently from the orientation of each constituent of the GPRRM.

Then, a two-stage homogenisation procedure as shown in Figure 3 is employed to define the composite GPRRM, which contains three basic isotropic constituents, i.e. ground, pipes and grout (see Figure 1). The mathematical formation of the procedure in details can be found in a reference (Bae et al., 2003). The basic mathematical framework is similar to that given by Pietruszczak and Niu (1992) for the simulation of structural masonry. In the local axes of the GPRRM, the properties of the homogenised material at the end of each step, depends only on the volume fraction of each constituent and its constitutive law. The stress-strain relationship for each constituent can be described as shown in Equation (1), where [D] indicates either an isotropic elastic or an elastoplastic constitutive matrix. The same equation can be used to describe the constitutive behaviour of the stage 1 and stage 2 homogenised equivalent composite materials. In the first stage, the ground (constituent 1) and the pipes (constituent 2) are homogenised, leading to a homogenised material (composite I). In the second stage, composite I is homogenised with the grout (constituent 3) to obtain the final equivalent composite material (composite eq).

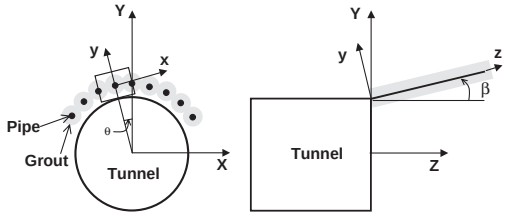


Figure 2. Typical arrangement of pipes.

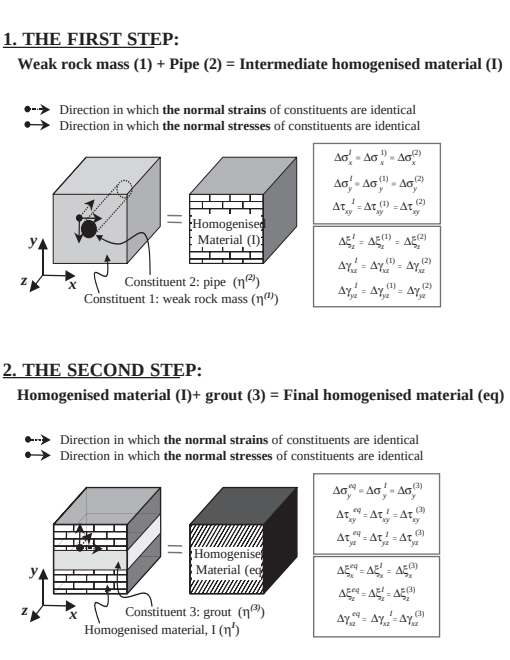


Figure 3. Schematic diagram of dual homogenisation procedure.

3 ELASTOPLASTIC SIMULATION IN HOMOGENISATION FRAMEWORK

The nonlinear behaviour of the GPRRG material is considered at a constituent level. As constituents undertake elastoplastic straining, their constitutive matrices [D] are modified according to the classic elastoplastic theory (Zienkiewicz and Taylor, 2000). A detail of the nonlinear stress integration algorithm developed can be found in a reference (Bae et al, 2003). At the end of each convergence iteration, within each load increment iteration, the basic homogenisation procedure described in the previous section is repeated, using the constituent elastoplastic matrix for the constituents that have yielded. From this procedure, the matrix for the homogenised material and the elastic or elastoplastic structural matrices for the constituents are obtained. The structural matrices and the stiffness matrix for the homogenised material used for the ith iteration are shown as follows.

$$\begin{aligned}\left[S_{k,ep}^{i-1}\right] &= S_{k,ep}^{i-1}\left(\nu_1,\nu_2,\nu_3,\left[D_{1,ep}^{i-1}\right],\left[D_{2,ep}^{i-1}\right],\left[D_{3,ep}^{i-1}\right]\right)\\ \left[D_{h,ep}^{i-1}\right] &= D_{h,ep}^{i-1}\left(\nu_1,\nu_2,\nu_3,\left[D_{1,ep}^{i-1}\right],\left[D_{2,ep}^{i-1}\right],\left[D_{3,ep}^{i-1}\right]\right)\end{aligned} \quad .(1)$$

At each iteration, the updated elastoplastic structural matrices are used to obtain the strain increment in each constituent from the increment in strain in the homogenised material (Equation (2)). Following the classic elastoplastic algorithm, the admissible stress increment in each constituent is computed. The admissible stress increment in the homogenised material is then obtained using the averaging rule and added to the stress state at the end of the previous iteration (Equation (3)). Following standard elastoplastic theory, the equivalent nodal forces are computed from

the stresses in the equivalent homogenised material and compared with applied load increment to check convergence.

$$\Delta\varepsilon_k^i = \left[S_{k,ep}^{i-1} \right] \cdot \Delta\varepsilon_h^i \tag{2}$$

$$\sigma_h^i = \sigma_h^{i-1} + \sum_{k=1}^{3} v_k \Delta\sigma_k^i \tag{3}$$

In the current version of the code, each constituent can be considered using either Mohr-Coulomb, Drucker-Prager, Tresca or Tension cut-off as a yield criterion, combined with either a linear or an exponential softening/hardening rule (Zienkiewicz and Taylor, 2000). The use of the elastoplastic structural matrices instead of the elastic ones ensures that the kinematic and equilibrium conditions of the homogenisation formulation are satisfied incrementally and therefore at all stages. As shown in Equation (3), the averaging rule is applied incrementally instead of being applied in total stresses due to the conditions of the construction procedure. Nevertheless, a certain approximation is introduced, since the elastoplastic structural matrices employed correspond to the previous iteration and, therefore, do not consider the changes in the [D] matrices of the constituents that will take place in the current iteration. This approximation induces an accumulation of error in the results. However, if the load increments considered are sufficiently small the errors accumulated are not significant. In order to avoid this accumulation of errors, the stresses and strains of constituents and homogenised material could be adjusted to satisfy fully the homogenisation conditions. However, this adjustment would be arbitrary and would not provide any benefit to the formulation.

A method of stress adjustment was used by Lee et al. (2000). In that approach, instead of updating the structural matrices and equivalent constitutive matrix, the stresses were adjusted. Although this approach had a much lower computational cost, the accuracy of the results was severely affected on the areas where yielding took place.

3.1 *Implementation in staged construction*

For simulating the staged construction, nodal forces are calculated at all the nodes on the excavated surfaces at every excavation stage, from the initial stresses around the tunnel. These initial stresses have been generated by considering the depth of the points under the ground surface and the ground specific weight. Similarly, as the GPRRG is applied, a series of elements within the FE model change from ground elements into homogenised GPRRG elements. In order to maintain global equilibrium within the model, the stress state in the ground element is transferred into the homogenised material. Internally, all the stress is transferred into the ground constituent (Equation (4)).

$$\begin{aligned} \sigma_h &= \sigma_{ground} \\ \sigma_{ground\ constituent} &= \sigma_{ground} \\ \sigma_{pipe\ constituent} &= 0 \\ \sigma_{grout\ constituent} &= 0 \end{aligned} \tag{4}$$

Stress is only absorbed by the grout and the pipes as more loads are introduced in system. As a result of this, however, the kinematic constraints and equilibrium conditions to be satisfied are only valid incrementally. Similarly, the averaging rule is also only valid incrementally.

4 STUDY ON THE REINFORCING EFFECT OF GPRRG

4.1 *Orthotropic elastic characteristics of GPRRG*

In this section, a series of parametric studies on the effects of the main design variables of the problem on the orthotropic elastic properties are presented. The isotropic elastic material properties and volume contributions of the constituents assumed in these studies are given in Table 1.

When considering the effects of modifying the volume fractions, the volume of the constituent considered is modified while the volume of the other two constituents is left unchanged. Since this results in a change on the total volume, the volume fractions of all constituents change. The volumes of the constituents not modified are shown on in Table 1.

Figure 4(a), (b) and (c) show the effects of changes in the volume of ground, pipe and grout, respectively, on the nine orthotropic elastic constants of GPRRG. The results have been normalised by the properties of plain ground material. Figure 4(a) represents the effect of increasing the zone affected by the reinforcement, while maintaining the level of reinforcement introduced. As expected, the Young's and shear moduli decrease as the volume of ground material increases, due to the lower stiffness of the ground material. The

Table 1. Elastic material properties of constituents of GPRRG.

Constituents	Young's modulus (MPa)	Poisson's ratio	Volume contribution (m^3)
Ground material	500	0.33	89.6
Grout material	5,000	0.17	10.0
Pipe	200,000	0.25	0.4

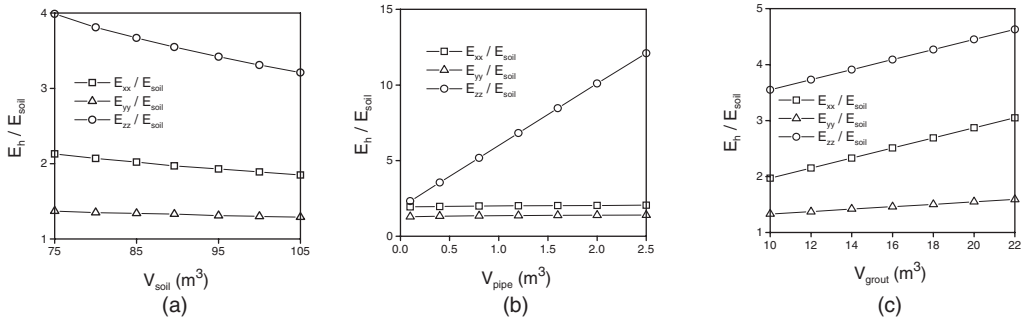


Figure 4. Evolution of orthotropic elastic constants.

effects are most significant in the z direction, i.e. parallel to the pipe, as a result of the kinematic conditions imposed. The effects of varying the degree of reinforcement are shown on Figure 4(b). The results show a very significant effect on all the properties, but particularly in the z direction. This suggests that the elastic characteristics of GPRRG are mainly governed by the contribution of pipes. Figure 4(c) illustrates the effect of modifying the extent of grouting on the properties of GPRRG. As a result of the geometric arrangement, i.e. grout is injected through the set of pipes, and the modelling assumptions, i.e. the grout is assumed to form a continuum in between the pipes, the most affected properties are the Young's moduli in x and z directions. Conversely, the Young's modulus in y direction is only slightly affected. This result is in disagreement with the prediction by Lee et al. (2000), as a result of the different geometrical hypotheses. The results obtained suggest that grouting enhances the arching effect in the circumferential direction but provides a small reinforcing effect on the ground stiffness in the radial direction.

4.2 *Direct tension test with elastoplastic medium of GPRRM*

In order to verify the results of the elastoplastic model proposed, a simple arrangement was first considered. The arrangement consists of a single GPRRG under direct tension at an angle with the reinforcement varying between 0 and 90˚ , as shown in Figure 5. The results are also compared with the case of plain ground material. In this model, the constituents have the material properties given in Table 2, a Mohr-Coulomb yield criterion with associated flow rule and perfect plasticity. The volume fractions considered are 63, 2 and 35% for the soil, pipe and grout, respectively.

As expected, the stiffness and yielding stress increase as the direction of loading becomes more parallel to the direction of the pipes. For the case of $\theta = 90°$, an elastic response of obtained due to the very high stiffness of the pipes in their axial direction.

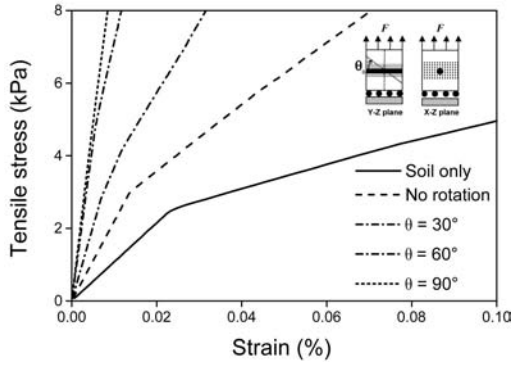


Figure 5. Elastoplastic response of GPRRG.

5 APPLICATIONS TO A TUNNEL PORTAL AREA

5.1 *Brief description of the site*

The tunnel site is OO twin road tunnels constructed at mountain area in Korea which are in 500 m long and 11.7 m width each. One of the tunnel gates is in quite weak ground condition which, therefore, requires a special auxiliary reinforcement system to be installed such as GPRRM. The analysis technique proposed in this study is used for determining the optimum major design variables of the reinforcement. The portal site of concern is described in Figure 6.

5.2 *Model set-up*

A FE model is set up for 3D FE analysis incorporating the GPRRM model developed in this study. The analysis is to determine a set of optimum values for three major design parameters which are overlapped length (4 m, 6 m, 8 m), angular range of reinforcements in tunnel section (120°, 150°, 180°) and CTC (centre to centre) of pipes (50 cm, 75 cm, 100 cm) chosen from other possible design variables. Three cases for

Table 2. Material properties of constituents of GPRRG used in FE analyses.

Material		Young's modulus (MPa)	Poisson's ratio	Volume fraction (%)	Cohesion (kPa)	Internal friction angle (°)
Soil		200	0.33	–	100	35
GPRR	Soil	200	0.33	89.6	100	35
G I	Pipe	200,000	0.25	0.4	–	–
	Grout	4,900	0.17	10	1500	30
GPRR	Soil	200	0.33	89.2	100	35
G II	Pipe	200,000	0.25	0.8	–	–
	Grout	4,900	0.17	10	1500	35

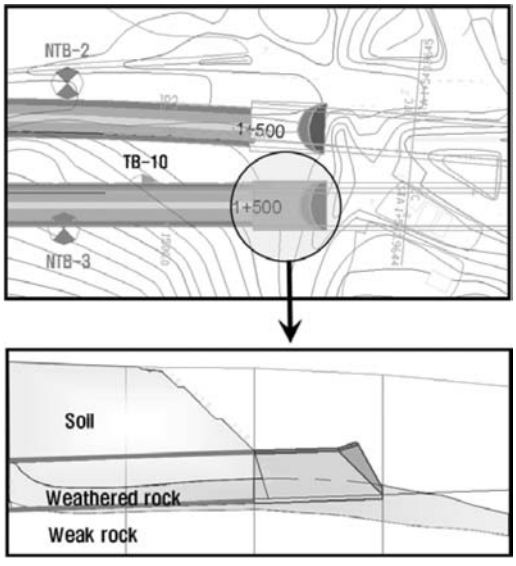


Figure 6. Description of the considered tunnel portal site.

each design parameters under consideration are set up. Therefore, total number of sets to be simulated is 27 sets. The optimum set chosen could confirm the safety as well as economical efficiency in construction.

Figure 7 shows the FE mesh and dimension of the model used. The mesh is generated by importing the exact geometry of the tunnel and ground levels. The colors in Figure 8 denote the ground conditions and different material properties.

Material properties of the grounds and reinforcements are given in Table 3. The properties have been determined by laboratory tests with the specimens from a number of borehole tests at NTB-2 & NTB-3 in Figure 8. It is noted that each material properties of pipe and grout material is given individually which are the same as in Table 2.

Young's modulus (Poisson's ratio) of shotcrete are 5 GPa (0.17), and 15 GPa (0.17) in soft and harden

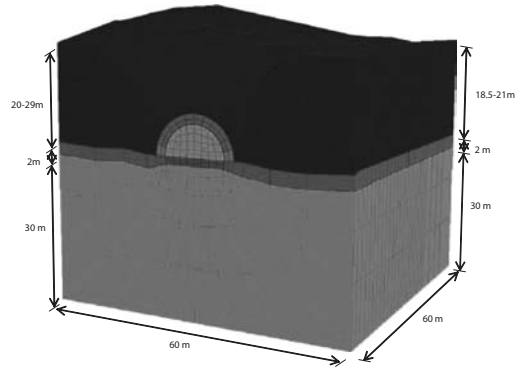


Figure 7. A FE mesh and dimensions.

condition, respectively. Elastic constants of rock bolt with section area of 5 cm^2 are the same as ones of the pipe in Table 2. In analysis, it is possible to involve one to three set(s) of pipes to be overlapped. The overlapped layers are simulated by changing the volume fractions of constituents which would be subjected by the volume of pipes occupied on unit volume of GPRRG. Excavation and installation stages of reinforcements are taken into account in the simulation.

5.3 *Results*

The orthotropic Young's modulus of GPRRG automatically calculated during the analysis are given in Table 4. In fact, twenty-one orthotropic elastic constants are calculated but only three Young's modulli (Ex, Ey, Ez) are given for comparison because of a lack of space.

As mentioned in Section 4.2, Young's module in longitudinal direction of pipe is sensitively increasing depending on the volume fraction of pipes while the one in horizontal direction changes insensitively. The Figure 9 shows total displacement distribution resulting from the analysis case without application of GPRRM, in which tunnel collapse with a localized large deformation at tunnel crown can be seen.

Table 3. Material properties used for FE analysis.

Material	Young's modulus (MPa)	Poisson's ratio	Cohesion (kPa)	Internal friction angle (°)	Unit Weight (kN/m^3)
Weathered soil	23	0.35	20	28	19.2
Weathered rock	500	0.33	70	29	23
Weak rock	5,000	0.25	1,320	38.3	25.1

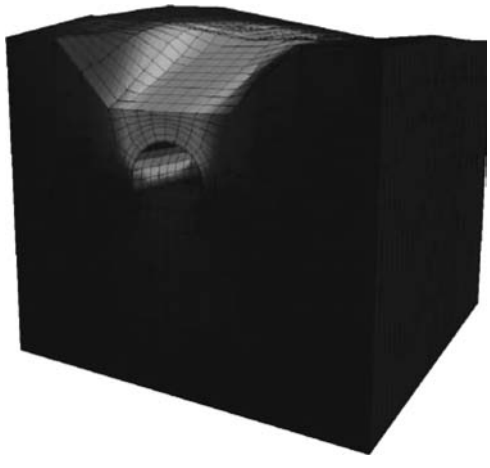


Figure 8. Displacement distribution on the analysis case without application of GPPRM (collapsed zone in green).

Table 4. Orthotropic Young's modulli of GPRRG with overlapped pipes.

Number of overlapping	Ex (MPa)	Ey (MPa)	Ez (MPa)	Volume fraction of pipes (%)	Volume fraction of grout (%)
1	889.9	363.4	1230.2	0.168	13.564
2	1089.5	392.7	1775.4	0.336	17.503
3	1191.1	408.0	2224.1	0.504	19.523

Then, an optimum set of design parameters has been determined from the case that contains no plastic strains at any elements and has minimum displacement at crown and side wall. Based on this, the final design parameters have been decided as the set of angular range of 180, CTC of 50 cm, overlapped length of 6 m. The case shows no plastic zone and maximum displacement of about 8 mm at crown. The details of the results from all the cases considered are omitted because of lack of space.

6 CONCLUSIONS

In this study, a new mathematical framework for modelling the ground reinforcement system known as GPRRM has been proposed using a homogenisation technique. This tunnelling method has been previously applied successfully in the construction of tunnels in weak ground conditions.

The framework developed provides the 12 independent orthotropic elastic constants of the reinforced ground material and the structural matrices that allow deriving the stresses/strains in each constituent from the stresses/strains in the homogenised ground material. The constitutive matrix of the equivalent material and the structural matrices are obtained as functions of the mechanical properties, volume contribution and internal geometrical arrangement of the three constituents of the reinforcement system, i.e. ground, steel pipes and grout.

This homogenisation framework is capable of considering the effect of the main parameters of the problem, i.e. amount of reinforcement and grout, the geometry of the pipe installation, the length of pipes, the extent of the grouted area, the length of excavation prior to the installation of additional reinforcement and the length of pipe overlapping. Additionally, the use of a homogenisation approach implies that the generation of the Finite Element mesh for the complex geometry of the problem can be simulated easily and that re-meshing is not required as basic geometrical parameters such as the orientation of the pipes are changed.

The use of a homogenisation approach also allows considering the elastoplastic behaviour of the composite material at a constituent level, using well-known constitutive models. This approach, therefore, only requires constituent parameters, instead of composite parameters, which would be very difficult to define and obtain. In order to satisfy the kinematic and the equilibrium constraints of the two stages of the homogenisation procedure during the non-linear computations, the homogenisation is applied incrementally. Then, the homogenisation procedure proposed has been implemented in a Finite Element model capable of considering stage construction situations.

The tool developed allows the effective simulation of tunnelling operations using the GPRRM and flexibility in the design stages.

The mathematical formulation proposed has been used to determine optimum design parameters in a tunnel portal area on a quite weak ground condition. Since this work was able to be undertaken in reasonable computing time by using the model proposed, it enables us to achieve optimum design of the GPRRM. It lead to achievement of economical efficiency with confirmation of the safety against tunnel collapses.

However, experimental data are required to fully validate the model proposed. A number of investigations are currently being undertaken in the authors' research groups to further understand the validity, range of applications and effectiveness of this homogenisation technique for tunnelling. Results of these studies will be reported shortly. The model proposed has also been used to undertake the elastoplastic analysis of a tunnelling operation. The results indicate that, in the example considered, the nonlinear effects have a limited effect on the results. It is expected, however, that the nonlinear effects will have a greater influence in weaker grounds.

REFERENCES

Bae, G.J., Kim, C.Y., Moon, H.D. & Hong, S.W., 1997, A study on the ground movement around tunnel reinforced by Umbrella Arch Method, Tunnel & Underground-Journal of Korean Society for Rock Mechanics, Vol. 7, pp. 299–309.

Bae, G.J., Shin, H. S., Sicilia C., Choi, Y. G., 2003, Study on Anisotropic Reinforcing Mechanism of Umbrella Arch Reinforcement Method in Tunnelling, Journal of The Korean Geotechnical Society, (submitted).

KICT (1986), A study on Design and Construction of Auxiliary Techniques of Underground Excavation, KICT-86-GE-2, p. 308.

Lee, J. S., Bang, C. S., Choi, I. Y. & Um, J. H., 2000, A study on the design approach of the pipe roofing reinforcement, Journal of the Korean Society of Civil Engineers, Vol. 20, No. 3-C, pp. 305–314.

Societa Italiana Gallerie (1991), Tunnelling in Italy: 1990, Tunnelling and Underground Space Technology, Vol. 6, No. 3, pp. 299–316.

Pelia, D., 1994, A theoretical study of reinforcement influence on the stability of tunnel face, Geotechnical and Geological Engineering, Vol. 12, No. 3, pp. 145–168.

Pelizza, S. & Peila, D., 1993, Soil and rock reinforcements in tunnelling, Tunnelling & Underground Space Technology, Vol. 8, pp. 357–372.

Pietruszczak, S. and Niu, X., 1992, A mathematical description of macroscopic behaviour of brick masonry, Int. J. Solids Structures, Vol. 29, No. 5, pp. 531–546.

Zienkiewicz, O. C. and Taylor, R. L., 2000, Finite element method, fifth edition, Volume 1–3, London, McGraw-Hill Book Company.

This page intentionally left blank

Underground Space – the 4th Dimension of Metropolises – Barták, Hrdina, Romancov & Zlámal (eds)
© 2007 Taylor & Francis Group, London, ISBN 978-0-415-40807-3

An enhanced pre & post processing techniques for three dimensional tunnel analysis: Tunnel Modelling Wizard

J.H. Shin
Dept of Civil Eng., Konkuk University, Seoul, Korea

J.H. Moon & D.S., Shin
MIDAS Information Technology Co., Ltd., Seongnam, Korea

ABSTRACT: An enhancement to pre & post processing techniques, which is encapsulated in 'Tunnel Modelling Wizard (TMW)' for three dimensional tunnel analysis, is developed and described in this paper. The techniques include geometry modelling, mesh generation, virtual transformation, flying view and utilization and interpretation of analysis results. The TMW automatically generates full analysis data including mesh, loads, boundary conditions and construction stages from the user-defined parameters. The TMW also provides its own file I/O service to help users expedite modelling tasks for similar models and build their own tunnel templates. Implementation of the TMW into a FE Program is described, and applications of the TMW to practical tunnel problems will be demonstrated.

1 INTRODUCTION

Tunnel construction entails complex three dimensional operations. Consequently, any numerical modelling methods should, in principle, attempt to closely represent such characteristics. It has been a common practice, however, that two dimensional modelling methods have been used for convenience to perform parametric studies for the optimization of tunnel design and construction. The main limitation of such two dimensional modelling methods is that they do not provide any information on the behaviour of tunnel headings. A recent investigation on NATM tunnel collapses revealed that most failures occurred during or soon after excavation of tunnels before completing linings, which suggests that intermediate stages of construction are becoming more critical. A conclusion can be drawn that three dimensional analyses are required for the cases of tunnel headings.

Three dimensional analyses are becoming more and more practical with high performance computer systems. Engineering costs are nevertheless still remaining high as the preparation of input data and the interpretation of results require a significant amount of time.

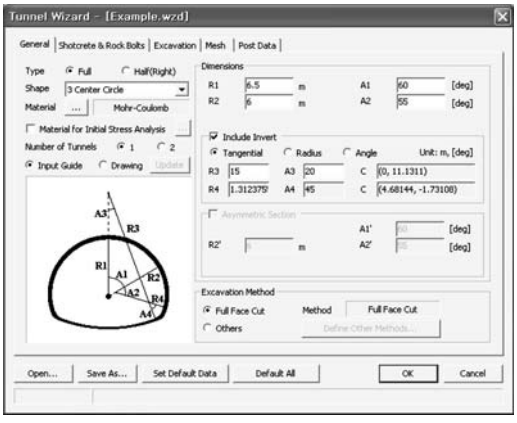
In order to overcome these difficulties of three dimensional tunnelling analyses, an enhancement to pre & post processing techniques, which is called 'Tunnel Modelling Wizard (TMW)', is developed. TMW automates almost all time-consuming operations of three dimensional modelling and produces reports of output data for swift interpretation of analysis results. With respect to the enhancement to pre-processing, it provides various tunnel templates, NATM tunnelling method, advanced surface modelling tool for terrain and strata, and automatic hexahedral mesh generation. In addition, results of construction stage data are generated in an MS-Excel file, which is a most widely used data solution. This paper describes the implementation of the TMW into a FE Program, and applications of the TMW to practical tunnel problems are demonstrated.

2 TUNNEL MODELLING WIZARD

2.1 *Modelling procedures*

The general modelling procedure for TMW consists of 5 major steps; (a) configuration of a tunnel cross section and excavation type; (b) specification of shotcrete and rock bolts; (c) definition of excavation and construction stages; (d) configuration of mesh data with terrain and strata; and (e) preparation for reports with output data.

In the first step, TMW provides a template for various tunnel cross sections and excavation types. Most common tunnel cross sections can be chosen from TMW such as circular, 3-center circle and 5-center circle including their inverts. A tunnel cross section does not necessarily have to be symmetrical; unsymmetrical sections can be defined. Figure 1 (b) shows all the excavation types available in TMW.



Step 1: definition of tunnel cross section

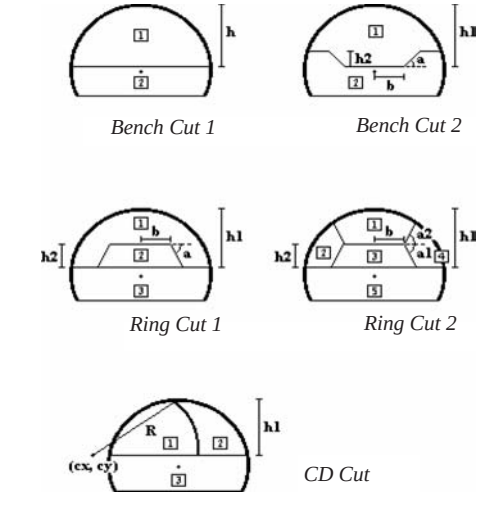


Figure 1. Templates of tunnel cross sections and excavation types.

The ground material is also specified in this step. TMW provides 4 material models; an elastic model and three most popular non-linear material models used in geotechnical engineering, which are Mohr-Coulomb, Hoek-Brown and Drucker-Prager.

In the second step, the parameters for shotcrete and rock bolts, which are considered as general reinforcements in a NATM tunnel, are defined. If shotcrete is installed, it is configured for material, thickness and hardening property for the transition from the initial soft shotcrete. Similarly, rock bolt's material, section property and a position arrangement can be established herein. With the defined parameters, TGM models shotcrete with shell elements and rock bolts with embedded truss elements, which can retain element stiffness regardless of mesh connectivity (Figure 2(a)).

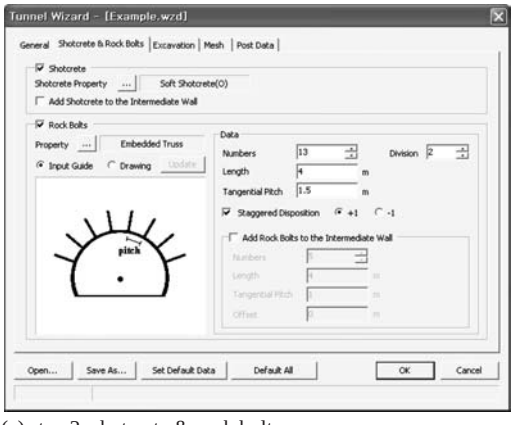
The third stage involves excavation sequence and construction stage definition. Advancing length, rock bolt locations and pattern, and the duration of shotcrete and rock bolt installation after excavation can be specified. Construction stages are arranged in a tabular format, and discrete options such as Load Distribution Factor can be defined for each stage (Figure 2(b)).

The fourth stage of TMW is used to define the location of tunnel(s), the boundaries of subsurface and pillar width in case of two tunnels. If the location of the tunnel is relatively close to the ground, it is crucial to consider the impact of the ground weight difference in the analysis. Consequently, TMW provides advanced surface modelling tools, which can generate an analysis model with actual terrain and strata. Having defined all the geometric parameters, information for mesh generation should be provided. The geometrical algorithms for terrain and strata surface modelling and the method of three dimensional mesh generation are explained in Section *2.2 Surface and mesh generation.*

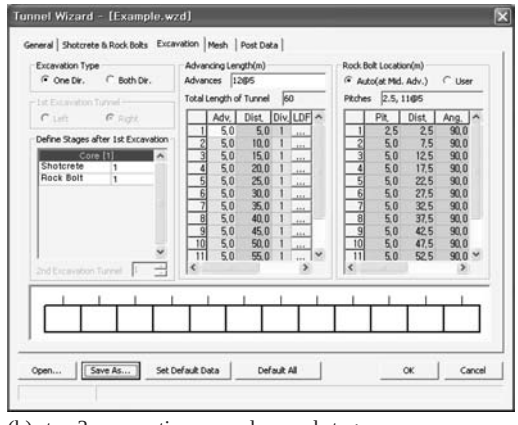
Since not every project readily has the required elevation information for its terrain surface, TMW provides 'Terrain Geometry Maker (TGM)', which is a module of TMW. This module can automatically obtain the elevation data from a digital map. In order to create a terrain surface from a digital map, TMW goes through the following algorithm. As shown in Figure 4(a), the modelling area is first defined on a digital map, and contours that are included in or crosses through the region are uniformly divided for sampling. After performing Delaunay triangulation in the xy plane, they are mapped into three dimensional facets Figure 4(b). Then, it determines to which facet a sampling point belongs. Using the area coordinate system shown in Figure 4(c), it interpolates the elevation at each sampling point. Figure 4(d) shows an example of a terrain surface, which has been generated using a digital map.

Once it completes the construction stage analysis of an assembled NATM tunnel model, TMW autogenerates post processing data for the purpose of preparing reports and provides the related functions to arrange and generate graphs. The last step defines the range of post-processing and construction stages for desired output, which are automatically produced in MS-Excel files. The data file contains the displacements of crown, wall and invert, stresses of shotcrete and axial forces of rock bolts.

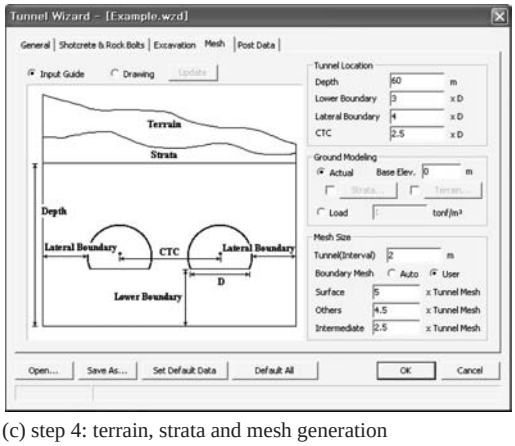
Upon completion of Steps 1 through 5, TMW automatically performs mesh generation, while applying loads and boundary conditions and generating construction stages. Subsequently, it performs a construction stage analysis based on stress-displacement using the finite element method. TMW generates MS-Excel files for the interpretation of output results, which are specified in Step 5.



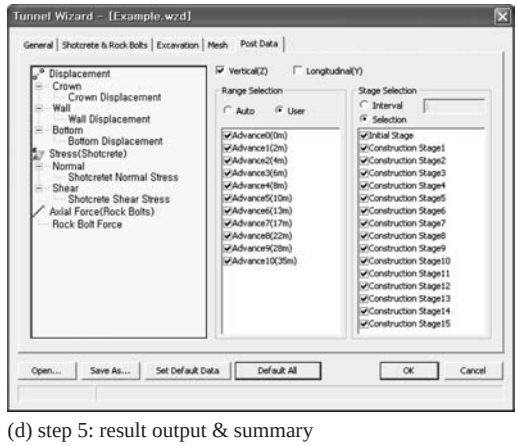
(a) step 2: shotcrete & rock bolts



(b) step 3: excavation procedure and stages

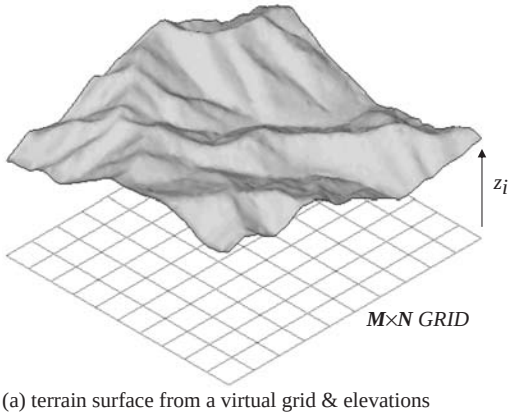


(c) step 4: terrain, strata and mesh generation

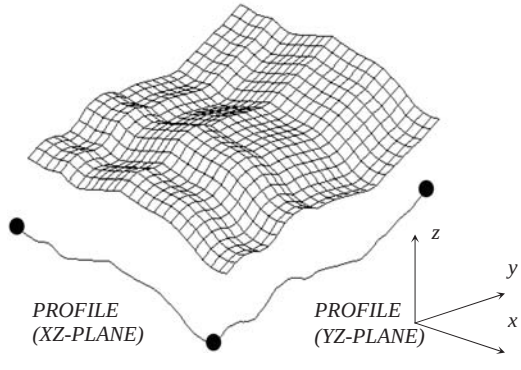


(d) step 5: result output & summary

Figure 2. Modelling procedures Steps 2∼5.

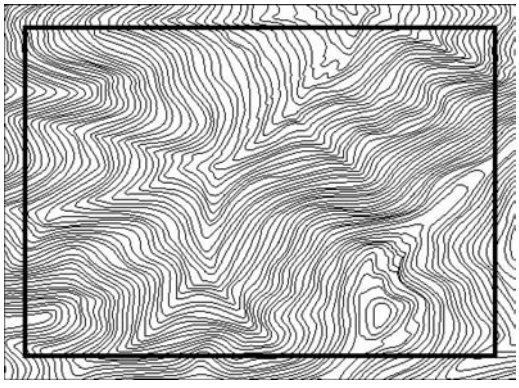


(a) terrain surface from a virtual grid & elevations

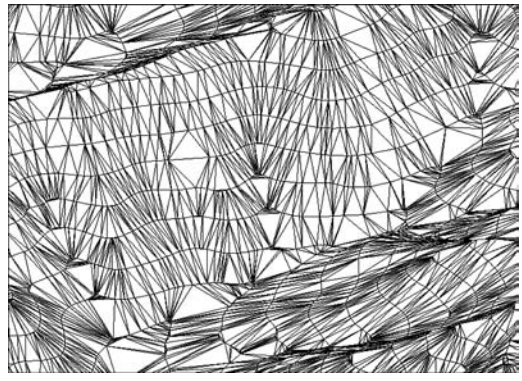


(b) stratum surface from profiles

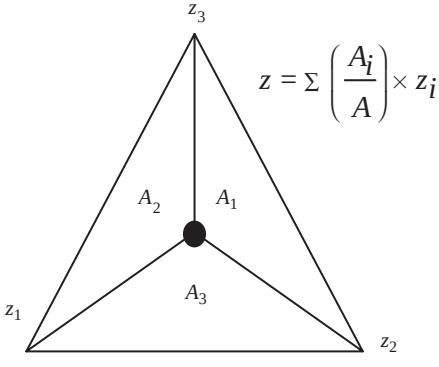
Figure 3. Definition of terrain and stratum surface.



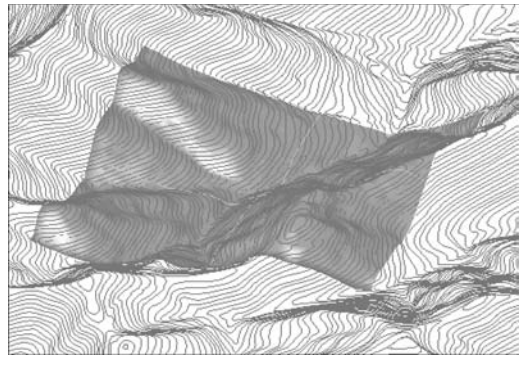
(a) digital map (top view)



(b) triangulation & facets



(c) area coordinate system



d) generated terrain surface

Figure 4. Terrain surface generation from a digital map.

Using its own file I/O service, the user can generate similar models by simply updating the parameters. This enables the user to undertake comprehensive parametric studies of multiple analysis models without significant efforts.

2.2 *Surface and mesh generation*

TMW internally creates surfaces from the input data for terrain and stratum generation. As shown in Figure 3(a), the terrain surface is a B-spline surface, which is generated using the elevations at each grid points of a virtual rectangular grid. The stratum surface, as shown in Figure 3(b), is created by Coons Patch, which is a bi-linear interpolation surface with defined coordinates and offsets of profiles in the x-z and y-z planes. All input data for the terrain and stratum are entered in a table. TMW can create up to five strata in a single model.

In order to obtain accurate analysis results, TMW generates an analysis model using a hexahedral mesh. First, a two dimensional quadrilateral mesh is created within the defined rectangular analysis area including the tunnel cross section by the looping mesh generation algorithm as shown in Figure 5(a).

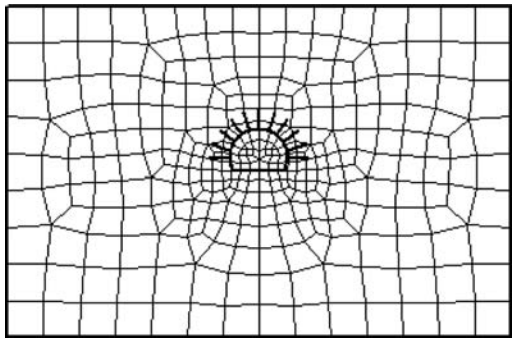
The quadrilateral mesh is then extruded based on the excavation stages to generate a box-shape hexahedral mesh for each stage Figure 5(b). After the extrusion, the top faces of the hexahedral meshes are projected onto the stratum and terrain respectively. This completes the final mesh, which appears in Figure 5(c).

TMW is exclusively implemented in the commercially available geotechnical analysis software, MIDAS/GTS, in the form of the NATM tunnel wizard.

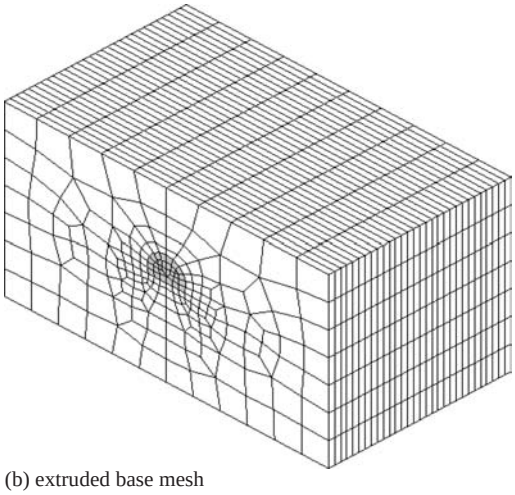
3 EXAMPLES

3.1 *Mountain tunnels*

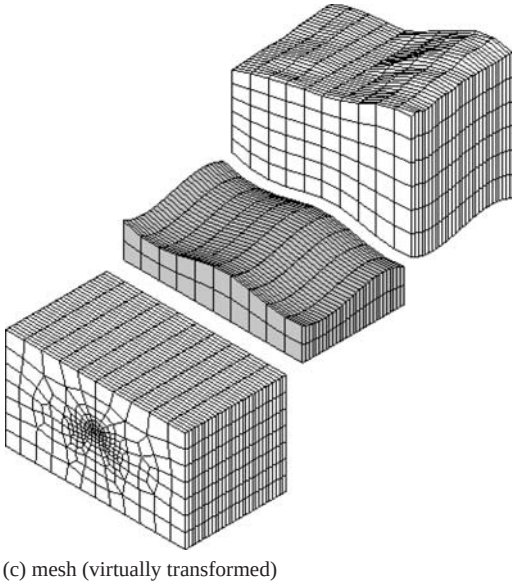
This example pertains to an analysis model of parallel mountain tunnels, which is generated by TMW in MIDAS/GTS. The overview of the analysis model is shown in Figure 6(a). It contains a single stratum above



(a) two dimensional mesh

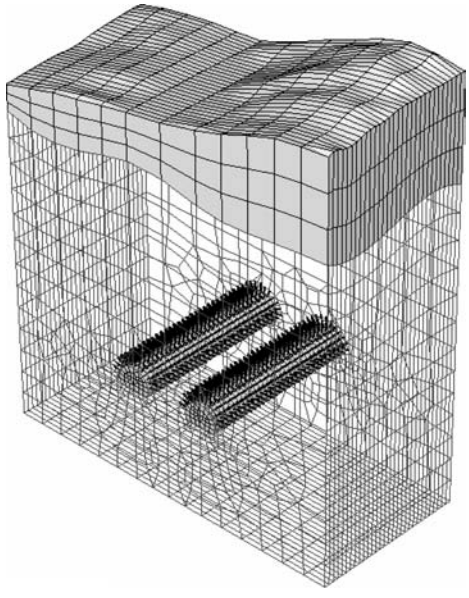


(b) extruded base mesh

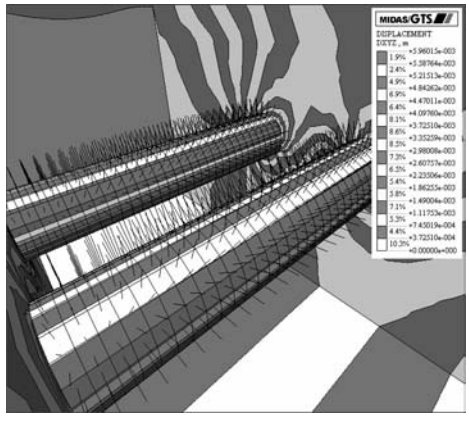


(c) mesh (virtually transformed)

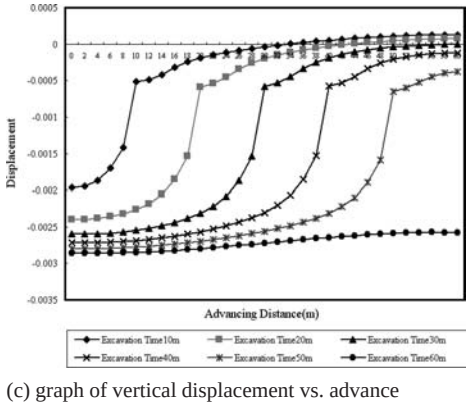
Figure 5. Three dimensional mesh generation.



(a) analysis model

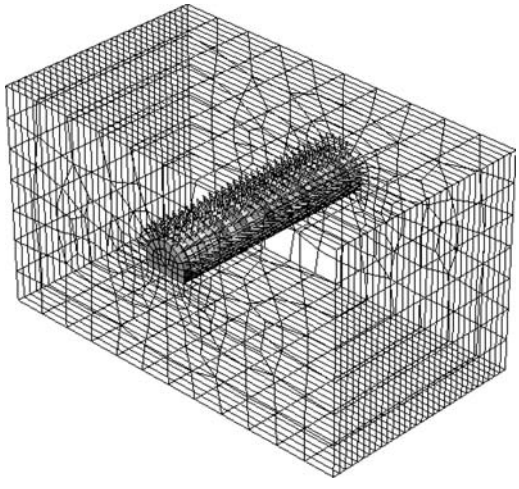


(b) analysis results (flying view)

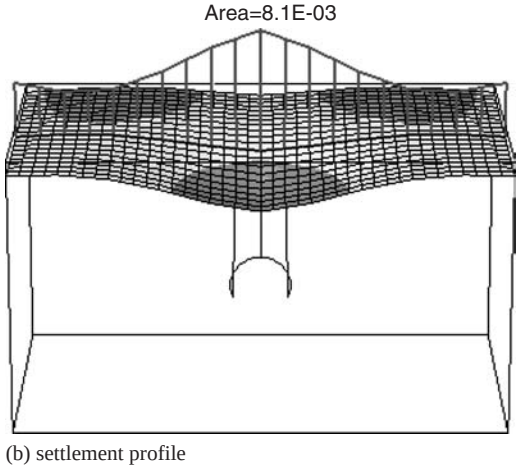


(c) graph of vertical displacement vs. advance

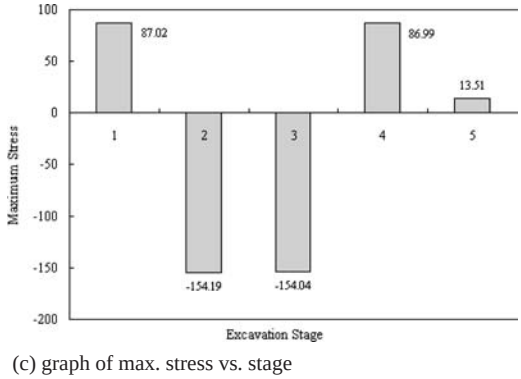
Figure 6. Example of mountain tunnels.



(a) analysis model



(b) settlement profile



(c) graph of max. stress vs. stage

Figure 7. Example of subway tunnel.

the tunnels. Figure 6(b) represents the displacement contour after the analysis, and its interior results are checked using the 'Flying View' function. Figure 6(c) shows a graph of vertical displacements at the crown relative to advancing distances, which is captured from the automatically generated MS-Excel result file.

3.2 *Subway tunnels*

The second example of TMW, as shown in Figure 7(a), is the analysis model of a subway tunnel. The deformation and settlement of the ground surface are checked in Figure 7(b) using 'Settlement Profile', which is one of the post processing functions in MIDAS/GTS. Figure 7(c) displays a graph of maximum stresses of shotcrete for each excavation stage prepared by TMW.

4 CONCLUSIONS

This paper describes the implementation of TMW, which provides an automated pre & post-processing procedure for three dimensional NATM tunnel analyses. The templates provided in TMW enables the user to model various tunnel types and specify different excavation methods. TMW permits the user to simply enter necessary parametric variables in a simple five-step definition process in order to readily create a complex three dimensional model. Moreover, TMW provides advanced surface modelling and hexahedral mesh generation functions, which are ideal for modelling complex strata and terrains encountered in practice. Not only does TMW provide the capabilities of modelling complex geo-structures, but it also enables the user to readily interpret the analysis results to reflect in design by the automatic summary arrangement and graphic processing of the analysis results. For a reasonably complex tunnel problem, TMW enables the user to complete the overall tasks of pre & post processing and analysis within about two hours. Such dramatic reduction in engineering time provides the user much more time to undertake numerous preliminary analyses, carry out parametric studies for various patterns, and investigate for potential problems during construction.

TMW is intended to be further developed to support automatic repetitive analyses for self parametric studies and more complex geometric configurations such as tunnel intersections.

ACKNOWLEDGEMENTS

The work presented in this paper was sponsored by Ministry of Construction and Transportation of Korean Government (No.C105A108001). Its support is gratefully acknowledged.

REFERENCES

John O. Bickel, Thomas R. Kuesel, and Elwin H. King, 1996, *Tunnel Engineering Handbook*, 2nd edition, Chapman & Hall.

Gerald E. Farin, 1996, *Curves and surfaces for computer aided geometric design: a practical guide*, 4th edition, Academic Press.

Joseph O'Rourke, 1998, *Computational geometry in C*, Cambridge University Press.

Jeffrey A. Talbert, and Alan R. Parkinson, 1990, Development of an automatic two-dimensional finite element mesh generator using quadrilateral elements and Bezier curve boundary definition, *International Journal for Numerical Methods in Engineering*, Vol. 29, pp. 1551–1567.

MIDAS IT Co., Ltd., 2005, *MIDAS/GTS Manual*, MIDAS IT Co., Ltd. (http://eng.midasit.com/gts).

This page intentionally left blank

Underground Space – the 4th Dimension of Metropolises – Barták, Hrdina, Romancov & Zlámal (eds)
© 2007 Taylor & Francis Group, London, ISBN 978-0-415-40807-3

Design parameter determination for modeling of pre-reinforced zones in a tunnel

K.I. Song, G.C. Cho & S.R. Lee
Dept. of Civil and Environ. Eng., Korea Advanced Institute of Science and Technology, Daejeon, Korea

J.H. Lee
Civil Projects Department, Daelim Ind. Co. Ltd., Seoul, Korea

ABSTRACT: This paper suggests that a simple micro-scale approach combined with a macro-scale approach to determine equivalent design parameters provides effective numerical modeling of pre-reinforced zones in a tunnel. This new technique enables the determination of the equivalent stiffness of pre-reinforced zones with a series or parallel combination of ground, grout bulb, and steel pipe stiffness. For verification, the authors compared the 3D numerical results from the suggested approach with the results of a precisely-simulated model. The comparison suggests that two cases achieve the best approximation to the solution: one case is related to the series-parallel stiffness system (SPSS) in which a bulb and steel are coupled in parallel and then connected to the ground in series; the other case is related to the series stiffness system (SSS) in which only a bulb and steel are coupled in series. The SPSS suggested in this paper effectively represents the behavior mechanism of pre-reinforced zones when compared to a precisely-simulated model.

1 INTRODUCTION

The construction of a large underground space has many risk factors such as difficulties with predicting arching effects and determination of various uncertain underground properties. Researchers have suggested various techniques for auxiliary support systems such as the reinforced protective umbrella method (RPUM), which has the advantage of combining a modern fore-poling system with the grouting injection method (Barisone *et al*., 1982). This method is used for pre-reinforcement design before the underground excavation: not only for small section tunneling within weathered and crashed zones, but also for large underground spaces. In addition, to decrease the risk of a collapse or failure in large excavation caverns, researchers developed various techniques and construction methods: the tunneling method using an advanced reinforcing system, where a double steel pipe is used for water-proofing and a urethane injection is used for reinforcement; the Trevi jet method which involves constructing an arch-shell structure around a tunnel crown with cement grout; and steel pipe reinforced multistep grouting where a beam arch is constructed around the tunnel crown with large diameter steel pipes, and a multilayer cement grouting injection.

However, the design and analysis of pre-reinforcement techniques require design assumptions that are problematic at best resulting in the increase of uncertainty in tunnel design. The pre-reinforcement effect is typically modeled by simulating the construction sequence of setting the reinforced zone and then increasing the stiffness, thereby obviating the need for complex modeling of each bulb and steel pipe. However, this approach has been found unsuitable when the center-to-center between pipes is larger than the expansion of the grout bulb. This approach assumes that the stiffness of the pre-reinforced zone is the same as the stiffness of the grout bulb, which may be either completely hardened or arbitrary and that the pre-reinforced zone become two to four times stronger than before reinforcement. Therefore, this study presents a new technique of determining a reasonable equivalent parameter of a pre-reinforced zone.

2 PROPOSED APPROACH

The RPUM design procedure is based on a combination of theoretical and numerical methods: the micro-scale approach which uses equivalent design parameters; and the macro-scale approach which uses a mathematical model.

2.1 *The macro-scale approach*

A mathematical model of reinforced media is defined in terms of the geometrical and mechanical characteristics of the ground and each reinforcing

component. Using derived constitutive equations, various researchers have numerically modeled struc-tural response of tunnels. Zienkiewicz and Pande (1977) used a multilaminate model to derive a constitutive relation of the composite material. The multilaminate model subsequently became the foundation of the homogenization constitutive relation used by Bernaud *et al*. (1995) to derive mathematical models of rock-bolted ground. The mathematical model could simulate anisotropic elastic behavior of a grouted zone. In addition, Bae *et al*. (2005) used the homogenization technique to develop constitutive relations for elasto-plastic FEM codes. The macro-scale approach differs from realistic conditions where the relation between the ground, the steel pipes and the grouted zone needs to be assumed.

2.2 *The micro-scale approach*

The micro-scale approach uses predefined structural element with a commercial program to individually model each component of a reinforcing system. In recent years, this approach has been supported by the evolution of computers and the development of various finite element method (FEM) programs specific for underground applications. The modeling method for RPUM design assessment has been developed for many years. For example, Kotake *et al*. (1994) considered a reinforced zone as a shell element. Later, beam elements were used to simulate inserted pipes with shell elements to model the reinforced zone around the pipes. In addition, steel pipes were modeled as beam elements with a weighted Young's modulus, which is the series summation of Young's modulus of pipes weighted by an area ratio. The micro-scale approach, however, can be controlled and affected by the intuition and experience of a designer and the analytical results are sensitive to the size and shape of finite elements and boundary conditions. Moreover, the pre- and post-processing of the micro-scale approach are significantly more time-consuming than those of the macro-scale approach.

2.3 *A micro-scale approach based on a macro-scale approach*

The pre-reinforced zone can be considered as a composite of pipe, grout and in-situ formation material. For the proposed micro-scale approach of a pre-reinforced zone, orthotropic material properties such as the elastic modulus, Poisson's ratio and the shear modulus should be considered as the equivalence composite parameters of reinforced soil and/or rock obtained on the basis of mean field theory and strain energy theory. However, this approach is hard to apply for a field design. We therefore present a micro-scale approach which is based on a macro-scale concept that can be applied effectively in commercial FEM programs. The new

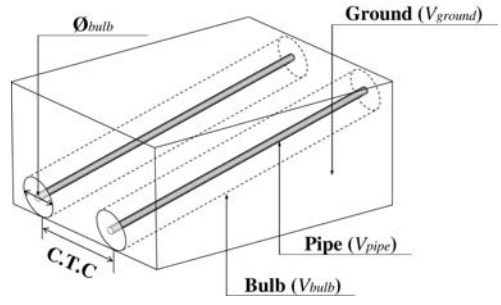


Figure 1. Diagram of simplified pre-reinforced zone.

approach determines the equivalent system composite stiffness of pre-reinforced zones developed by combining ground, grout bulbs and steel pipes in series or in parallel formation. For verification of our approach, we compared the results of a 3D numerical analysis using this system composite with the results of a precisely-simulated model. In precisely-simulated model, all components such as ground, grout bulb and steel pipe were modeled in realistic condition. This model therefore has the best exactness. We now discuss a proposed approach and comparative assessment for analysis of pre-reinforced zone.

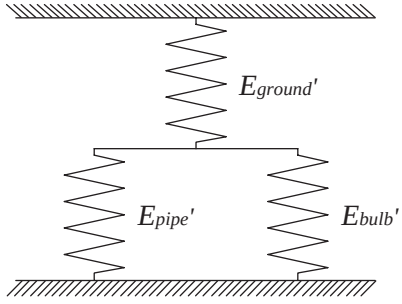
3 DETERMINATION OF EQUIVALENT DESIGN PARAMETER FOR PRE-REINFORCED ZONE

A pre-reinforced zone consists of ground, grout bulbs and steel pipes. It may be simplified, as shown in Fig. 1, to a condition of when the space between the pipes is wider than the grout expansion range. In weathered rock, the injected grout along the bore holes permeates into the gaps and joints; it also binds jointed rocks together and increases the stiffness of rock around the bore holes. In sandy soil and weathered soil, the bulb may be cylindrical. We assessed five cases of conditions to model the pre-reinforced zone.

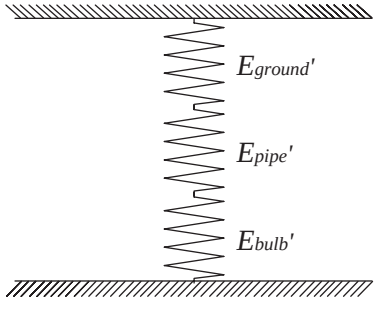
3.1 *Case 1: grout bulbs and steel pipes only*

The equivalent design parameters that we obtained from a SSS(series stiffness system) of a bulb and steel pipes are based on the micro-macro scale approach. As shown in the following equation (1), the equivalent design parameters are the sum of the parameters of the pipe weighted by the volume ratio and the parameters of the grout bulb weighted by the volume ratio in series:

$$E_{eq} = \frac{V_{pipe}}{V_{bulb} + V_{pipe}} E_{pipe} + \frac{V_{bulb}}{V_{bulb} + V_{pipe}} E_{bulb} \qquad (1)$$



(a) Series-parallel stiffness system (SPSS)



(b) Series stiffness system (SSS)

Figure 2. Series and/or parallel stiffness system of pre-reinforced zone.

3.2 *Case 2: a series-parallel stiffness system for the ground, grout bulbs and steel pipes*

The fan-shaped pre-reinforced zone is comprised of the ground, grout bulbs and steel pipes. We obtained the equivalent parameters from a SPSS(series-parallel stiffness system) in which the stiffness of gout bulbs and steel pipes was coupled in parallel and then connected to the stiffness of the ground in series as shown in Fig. 2(a). Each stiffness value of the constitutive components was weighted with a volume fraction as follows:

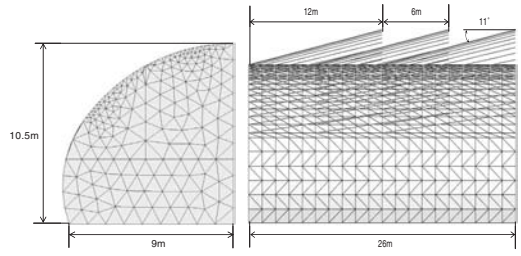
$$E_{eq} = E_{ground}' + \frac{E_{pipe}' \cdot E_{bulb}'}{E_{pipe}' + E_{bulb}'} \tag{2-1}$$

$$\text{where,} \quad E_i' = \frac{V_i}{\sum V} E_i \tag{2-2}$$

3.3 *Case 3: the ground and gout bulbs only*

Equivalent design parameters, which were weighted by a volume fraction, are based on a SSS of grout bulbs and the ground.

$$E_{eq} = \frac{V_{bulb}}{V_{bulb} + V_{ground}} E_{bulb} + \frac{V_{ground}}{V_{bulb} + V_{ground}} E_{ground} \tag{3}$$



(a) Transversal section (b) Longitudinal section

Figure 3. Profile of four-lane tunnel and condition of pre-reinforcement.

3.4 *Case 4: a series stiffness system for the ground, grout bulbs and steel pipes*

As with Case 2, the pre-reinforced zone in Case 4 is comprised of the ground, grout bulbs and steel pipes.

The equivalent design parameters were calculated by a SSS in which the stiffness of the ground, grout bulbs and the steel pipes were connected in series as shown in Fig. 2(b).

$$E_{eq} = E_{bulb}' + E_{pipe}' + E_{ground}' \tag{4}$$

3.5 *Case 5: supposition of a pre-reinforced zone with a high level of stiffness*

Case 5 is the most general method for modeling the pre-reinforcement. In this case, the properties of the fan-shaped pre-reinforced domain are replaced by a level of stiffness that is twofold to tenfold the original level of stiffness. When a grout bulb is not connected to neighboring bulbs, this method does not represent the practical and real behavior of a pre-reinforced zone and causes wrong and biased results. The equivalent parameters are expressed as follows:

$$E_{eq} = E_{bulb} \tag{5}$$

4 NUMERICAL MODELLING

4.1 *Analytical model: a four-lane tunnel*

For a more practical and realistic simulation of the tunneling process for each case, we used the 3D FEM program MIDAS-GTS (MIDAS-IT, 2005), which enabled us to consider and model the construction sequences and boundary conditions in detail. We selected a four-lane tunnel to make our comparison. Fig. 3(a) show our simulated four-lane tunnel, constructed 50 m under the surface of the ground, a radius of 9 m, and a height of 10.5 m. This simulated tunnel is an actual section of a four-lane tunnel that was designed and constructed in weathered rock in Korea. We modeled four subsectional excavations with a length of 1.2 m per stage.

Table 1. Mohr-Coulomb material properties of ground and structure.

Properties	E (MPa)	C (kPa)	υ	γ (kN/m^3)	φ (°)	σ_t (kPa)
Weathered soil						
Ground	49.04	58.84	0.35	18.63	30	98.07
Grout bulb	490.35	588.42				
Weathered rock						
Ground	490.35	245.18	0.30	20.59	35	490.35
Grout bulb	2451.75	1225.9				
Double steel pipe	205947	78456	–	–	–	–

Where, E: Elastic modulus, C: Cohesion, υ: Poisson's ratio, γ: Unit weight, φ: Friction angle, σ_t: Tensile strength.

Table 2. Equivalent design properties used for numerical modeling.

Ground Type	Weathered Soil		Weathered Rock	
Equivalent design properties	E_{eq} (MPa)	C_{eq} (kPa)	E_{eq} (MPa)	C_{eq} (kPa)
Case 1	1748.21	1065.04	3697.61	1698.57
Case 2	107.35	91.21	569.3	260.87
Case 3	117.81	141.22	796.02	398.16
Case 4	315.22	216.73	992.78	472.7
Case 5	490.35	588.42	2451.75	1225.88

Fig. 3(b) shows the case of a double steel pipe being modeled as a beam element: a 12 m steel pipe is installed at an inclination of 11° with a 6 m overlap; there is a 0.7 m interval between the steel pipes that are installed along the tunnel crown 60° from the center; and the grout expansion range is 0.5 m.

Table 1 lists the material properties used in this analysis. For the strengthening of the grout bulb reinforcement, we followed the method of Kikuchi *et al*. (1995). The grout injection consequently produced a tenfold increase in the stiffness of the weathered soil and a fivefold increase in the stiffness of the weathered rock. Table 2 shows the equivalent design parameters for the various compositions.

5 COMPARATIVE ANALYSIS OF NUMERICAL RESULTS

We analyzed numerical models for the weathered rock and the weathered soil. First, we examined the effect of precisely-simulated models that were modeled with different sized finite elements. On the basis of these results, we constructed five equivalent models of the pre-reinforced zone and compared these models to the precisely-simulated model results in terms of the vertical displacement of the tunnel crown and the horizontal displacement of the springline.

5.1 *Effect of finite element size*

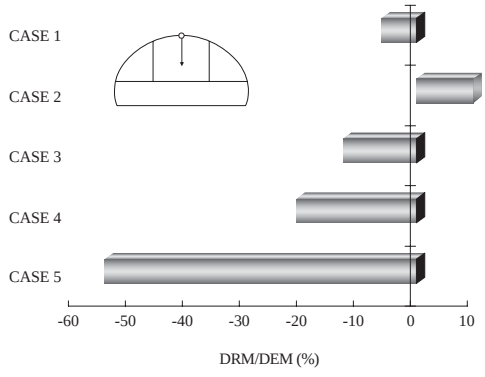
To deduce a reasonable reference for a comparison of a precisely-simulated model and an equivalent model, we completed a 3D FEM parametric analysis of a precisely-simulated model with respect to the size of the finite elements. As the number of elements of model increases, the displacement converges. Rather than the model that used the biggest finite elements, the model that used the smallest finite element shows a 4% to 5% increase in both the vertical displacement at the tunnel crown and the horizontal displacement at the springline, as well as a 13.4% increase in the ground surface settlement. The outcomes can be changed with respect to the size and shape of the finite element, which are inherent characteristics of FE analysis. Hence, to support a rational comparison between a precisely-simulated model and equivalent models, we used the small finite elements for the comparison models.

5.2 *Comparative analysis of equivalent models: vertical displacement at the tunnel crown*

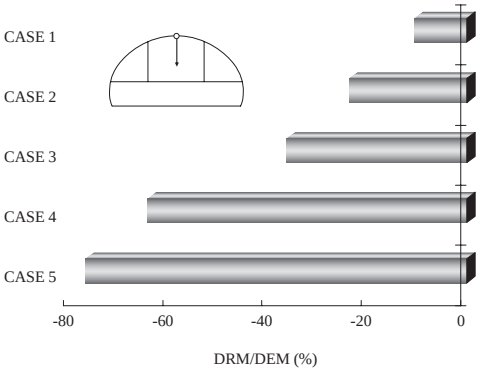
Fig. 4 shows the vertical displacement at the tunnel crown. To obtain this value, we averaged the five nodes located at the center and left areas of the tunnel crown at a depth of 4.5 m from the portal. The DRM/DEM parameter, as shown in the following equation (6), is the fraction of the displacement of the referential model (DRM) to the displacement of the equivalent model (DEM). A precisely-simulated model is represented by a value of 0%.

$$DRM / DEM = \left(\frac{Disp_{case}}{Disp_{real}} - 1 \right) \times 100(\%) \quad (6)$$

Case 1 gives the closest result to the precisely-simulated model in weathered rock and weathered

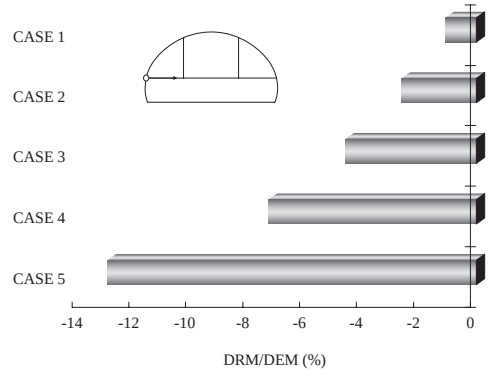


(a) Weathered soil

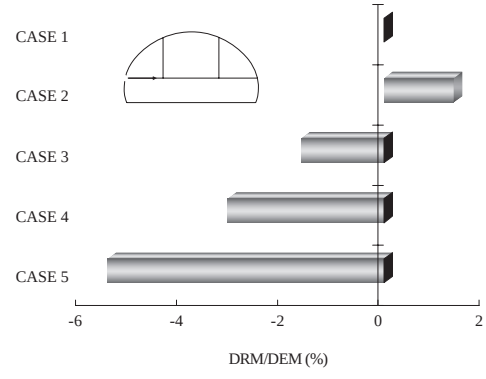


(b) Weathered rock

Figure 4. Comparison of the vertical displacement at tunnel crown.



(a) Weathered soil



(b) Weathered rock

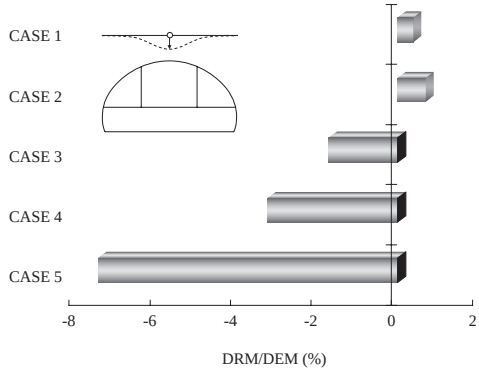
Figure 5. Comparison of the horizontal displacement at springline.

soil because of the similarity in the geometry and the finite element mesh of the equivalent model and the precisely-simulated model. Case 2 predicts an increase of around 10% for the DRM/DEM in weathered rock, though it provides a close prediction for the vertical displacement at the tunnel crown in the precisely-simulated model and ensures a safe design. As the equivalent elastic modulus and the equivalent cohesion increase, the vertical displacement at the crown decreases. In the general method (Case 5), the DRM/DEM value is 76% for the weathered soil and 54% for the weathered rock, indicating that general methods tend to overestimate the effect of pre-reinforcement. Moreover, the DRM/DEM decreases so significantly in soft ground that, in modeling the pre-reinforcement, we must simulate cylindrical bulbs rather than equivalent pre-reinforced zones.

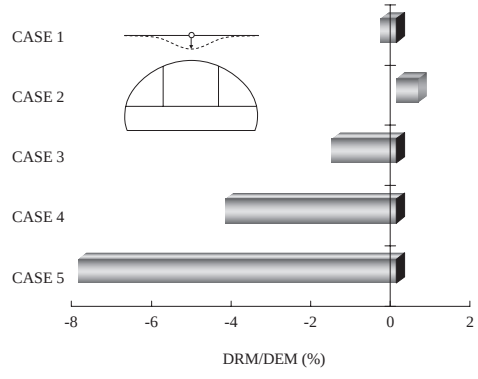
5.3 *Comparative analysis of equivalent models: horizontal displacement at the springline*

To determine the horizontal displacement at the springline, we averaged the four nodes around the springline at a depth of 4.5 m from the portal. The results of each case are plotted in Fig. 5. From Fig. 4 and Fig. 5, we can see that for each ground condition the phase behavior of the horizontal displacement is very similar to the horizontal displacement at the tunnel crown. The DRM/DEM value of the horizontal displacement at the springline is smaller than that of the vertical displacement at the crown. Thus, depending on the location of the four-lane tunnel, the geometrical effect induces a displacement difference in the internal direction.

The DRM/DEM value increases as the ground properties change from weathered rock to weathered soil. For all weathered soil cases, the horizontal displacement of the equivalent model was smaller than that of the precisely-simulated model. On the other hand, the DRM/DEM value increased by 1.3% in Case 2 for weathered rock. Although there is only a slight difference between Case 2 and Case 3, Case 2 predicts a similar horizontal displacement at the springline for the precisely-simulated model and the design is rather safe.



(a) Weathered soil



(b) Weathered rock

Figure 6. Comparison of the ground surface settlement.

5.4 *Comparative analysis of equivalent models: ground surface settlement*

To determine the ground surface settlement, we averaged the two middle nodes of the four nodes at the top of the model immediately above the tunnel crown. Fig. 6 shows that the surface settlement characteristics were not greatly affected by the material properties of the ground. The ratio between the precisely-simulated model and the equivalent model in weathered rock and weathered soil is analogous even though the scale of the induced displacements differs in each case. The DRM/DEM value ranges from 0.55% to 0.7% in Case 1 and Case 2. Thus, the equivalent model offers a satisfactory prediction of the ground surface settlement.

5.5 *The Apprehension of behavior of a pipe-grout pre-reinforced zone*

Case 1 exemplifies a proper equivalent modeling technique for simulating the pre-reinforcing mechanism in sandy ground. Case 2, which is a SPSS in which the stiffness of the bulb and steel pipes are coupled in parallel and then connected to the stiffness of the ground in series, exemplifies a simple equivalent modeling technique that predicts the vertical displacement at the tunnel crown, the horizontal displacement at the springline, and the ground surface settlement.

When the ground, grout bulbs and the steel pipes are regarded as an individual support system, the pre-reinforced zone is not a series or parallel stiffness system but a series-parallel compound stiffness system. Thus, a small degree of stiffness support receives the biggest stress; moreover, the linear combination of big stiffness supports resists ground displacement. The SPSS explains the failure mechanism of the pre-reinforced zone: namely, the rupture of the steel pipes and the grout bulb follows the yielding of the ground. The SPSS should be used in various studies related to the analysis of pre-reinforced tunnels.

6 CONCLUSION

We conducted a comparative analysis in order to suggest a technique of determining the equivalent design parameters for effective numerical modeling of pre-reinforced zones in tunnels. We deduced the following conclusion after verifying the technique of determining the equivalent design parameters. The general method (Case 5) leads to an unconservative design for predicting vertical displacement at the tunnel crown. In contrast to other cases, Case 2, the SPSS model, predicts that the vertical displacement at the tunnel crown is likely to conservatively resemble the vertical displacement of a precisely-simulated model. In addition, we can use the SPSS a degree of horizontal displacement that is approximately the same as that of a precisely-simulated model. The DRM/DEM value of the horizontal displacement at the springline increases as the ground property changes from weathered rock to weathered soil. However, for each ground condition, the displacements behave similarly to the vertical displacement at the tunnel crown. In addition, the material property of the ground does not affect the DRM/DEM value of the surface settlement. Moreover, Case 1 and Case 2 produce similar results for predicting ground surface settlement in close agreement with the precisely-simulated model.

The pre-reinforced zone before the excavation tunnel can be simplified as a composite system of the ground, grout bulbs and steel pipes. The Case 1 of SSS, which relies on the stiffness of steel pipes and a grout bulb, is a reasonable simulation method for analysis under specific conditions. However, to model cylindrical grout bulbs, we need considerable time and manual labor to establish and run the model. We therefore recommend that another technique be used for determining the equivalent parameters with the SPSS; namely, by coupling the stiffness of grout bulbs and

the steel pipes in parallel and then connecting them to the stiffness of the ground in series. This alternative approach is simple and effective relation for numerical analysis of a pre-reinforcement with the RPUM. The failure mechanism of pre-reinforced zone can be explained by SPSS, where the yielding of the ground occurs before the failure of the steel pipes and the grout bulbs.

7 ACKNOWLEDGEMENTS

This paper was funded by the Korea Institute of Construction and Transportation Technology Evaluation and Planning under the Ministry of Construction and Transportation in Korea (Grant No. 04-C01) and Brain Korea 21 Project in 2006.

REFERENCES

Bae, G.J., Shin, H.S., Sicilia, C., Choi, Y.G. & Lim, J.J. 2005. Homogenization framework for three-dimensional elasto-plastic finite element analysis of a grouted pipe-roofing reinforcement method for tunneling. *Int. J. Numer. Anal. Methods Geomech*., 29, 1–24.

Bernaud, D. 1995. Numerical simulation of the convergence of a bolt-supported tunnel through a homogenization method. *Int. J. Numer. Anal. Methods Geomech*., 19, 267–288.

Kikuchi, K., Mito, Y. & Adachi, T. 1995. Case study on the Mechanical Improvement of Rock Masses by Grouting. *Rock Foundation*, Balkema, 393–398.

Kotake, N., Yamamoto, Y. & Oka, K. 1994. Design for Umbrella Method based on Numerical Analysis and Field Measurements. *Proc. Tunnelling and Ground Conditions*, Ed. M. Abdel Salam, 501–508.

MIDAS-GTS. 2005. Geotechnical & Tunnel Analysis System, MIDAS Information Technology Co., Ltd.

Zienkiewicz, O.C. & Pande, G.N. 1997. Time-dependent multilaminate model of rocks-a numerical study of deformation and failure of rock masses. *Int. J. Numer. Anal. Methods Geomech.*, 1, 219–247.

This page intentionally left blank

Underground Space – the 4th Dimension of Metropolises – Barták, Hrdina, Romancov & Zlámal (eds)
© 2007 Taylor & Francis Group, London, ISBN 978-0-415-40807-3

Computer aided hierarchical ground characterization for underground structures

A. Steiner & W. Schubert
Graz University of Technology, Institute for Rock Mechanics and Tunneling, Austria

ABSTRACT: The characterization of the ground comprises an integral part in the design of an underground structure. For this reason several classification systems have been developed in the past. They were derived from specific project conditions. The Austrian "Guideline for the Geomechanical Design of Underground Structures with Conventional Excavation" describes a consistent procedure for the characterization of the ground and determination of excavation and support. The software GEOCLASS has been developed in order to accelerate the calculation process following this guideline. GEOCLASS allows dealing with Ground Types, failure mechanisms, and ground behavior. The result of the calculation is a classification of identified ground behaviors into Ground Behavior Types. It allows the application of deterministic and probabilistic methods due to the automatic processing of the data. The results are used to determine excavation and support, as well as costs, time and risks of the construction works.

1 INTRODUCTION

The development of a tunnel project contains several investigations and design phases. Those start with a preliminary site assessment and typically end with a final design. The particular investigation and design steps are usually executed by various companies and/or working groups. Results from these subsequent steps lead to continuous increase of knowledge on the tunnel project and finally end with the final design.

The Austrian "Guideline for the Geomechanical Design of Underground Structures with Conventional Excavation" (ÖGG 2001) illustrates a coherent procedure for both the design- as well as the construction stage of a tunnel. The procedure for the design phase includes the following intermediate stages: definition of Ground Types (GT), assessment of ground behavior and classification into Ground Behavior Types (BT), evaluation of System Behavior (SB), and determination of excavation and support methods.

Reliable results require sufficient and representative data sets for input, which have to be processed by using predefined rules and definitions. Due to the large amount of data obtained from investigation campaigns, this analysis calls for an efficient, automated processing, accelerating the entire process. For this reason, the program GEOCLASS was created following the procedure illustrated in the previously mentioned Austrian Guideline. In this paper, the computer aided data processing is presented up to the determination of the Ground Behavior Types comprising the basic result of the ground characterization.

2 GUIDELINE FOR THE GEOMECHANICAL DESIGN OF UNDERGROUND STRUCTURES WITH CONVENTIONAL EXCAVATION

The guideline considers two main phases, the design phase the construction phase. The procedures described in the design phase lead to a coherent determination and characterization of support and excavation methods related to the expected ground conditions. The expected ground, excavation and support interaction is assessed (System Behavior) (ÖGG 2001, Goricki 2003). Additionally during the design process, the natural spread of the input parameters is considered.

During the construction phase, the observed System Behavior can be compared to the behavior that was determined for the associated Ground Type during the design phase. When all concepts, considerations, and decisions are documented during both phases, the systematic procedure described in the guideline allows a review of the decision making process, whenever new findings from the site are gained.

The design phase consists of five general steps: determination of Ground Types, assessment of ground behavior and classification into Ground Behavior Types, evaluation of System Behavior, Baseline Construction Plan, and determination of excavation classes

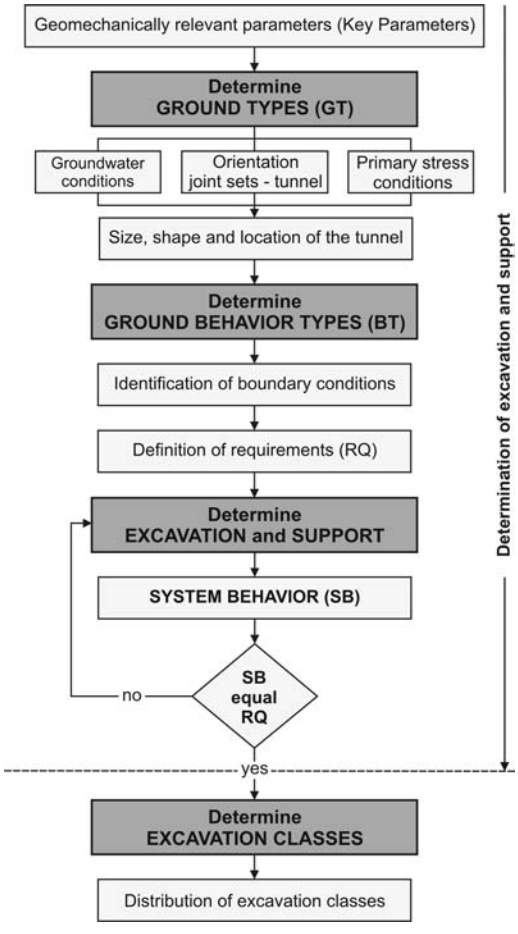


Figure 1. Fundamental design procedure based on ground characterization and classification according to the Austrian society for Geomechanics (ÖGG 2001, Goricki 2003) modified by Steiner (2005).

(Figure 1). In order to account for the variability of the input parameters they should be described with statistical values to enable the evaluation with probabilistic procedures later on.

The basis for the determination of the Ground Types is the geological model for the project area. The information about the geological architecture allows correlating geological units with geomechanically relevant parameters (key parameters). The key parameters describe the relevant properties of the ground within a geological unit. Ground Types are defined by similar material and properties. The number of necessary Ground Types for one geological unit is dominated by the variation of the key parameter values.

The ground behavior is the response of the ground to the excavation a tunnel without consideration of excavation and support methods as well as auxiliary measures. It considers the specific local influencing factors (primary stress situation, ground water conditions, discontinuity orientation relative to the excavation direction, etc.). These analyses evaluate only involved failure mechanisms. The observed mechanisms characterize the behavior caused by the excavation. Similar behavior is subsequently grouped into the Ground Behavior Types. The basic Ground Behavior Types, mentioned in the Guideline, are presented in Table 1.

Table 1. Eleven general Ground Behavior Types (ÖGG 2001), for a detail description (Goricki 2003).

Number	Ground behavior types
1	Stable
2	Discontinuity controlled block failure
3	Shallow stress induced failure
4	Deep seated stress induced failure
5	Rock burst
6	Buckling failure
7	Shear failure under low confining pressure
8	Raveling ground
9	Flowing ground
10	Swelling
11	Frequently changing behavior

The evaluated ground behaviors form the basis for the determination of excavation and support methods as well as auxiliary measures (Schubert et al. 2000). Several combinations of excavation and support methods may result in a stable excavation fulfilling all project requirements but only one regarding to economical and safety issues has to be chosen. Based on this result the Baseline Construction Plan is developed. The Baseline Construction Plan defines the excavation and support measures for each tunnel section.

The final step in the design phase includes the preparation of the tender documents as well as costs and construction times estimated for the entire project consistent with the determined amount of excavation and support measures.

Since the input parameters have a natural spread, the influence of varying key parameters on the ground and System Behavior has to be assessed for a realistic risk assessment in the design, the use of probabilistic methods is recommended and described in this paper.

3 COMPUTER AIDED DESIGN PROCEDURE

The Austrian guideline describes a consecutive approach for the design of an underground structure. Due to the consideration of the natural spread in the input parameters via statistical and probabilistic approaches, calculation and time efforts increase for the design process. To optimize these time consuming processes the program GEOCLASS was developed

for the evaluation of the first two steps in the design procedure.

The core of GEOCLASS is the determination of the response of the ground using empirical and closed-form solutions for 2D failure mechanisms under current boundary conditions.

3.1 *Basic procedure in GEOCLASS*

GEOCLASS requires for computation the definition of several input parameters, which are related to the implemented approaches, and the assignment of boundary conditions. The parameter values are simultaneously processed with all models resulting in specific output values for each model. Typical output categories are depth of the failure zone, rock burst potential, or displacement magnitudes. Each of the output categories is characteristic for a particular ground behavior. The output values of each category are used to classify the ground into a particular Ground Behavior Type. Due to the use of several calculation models, it is possible that for a particular ground several Ground Behavior Types apply. Therefore, it is necessary to assign the dominating Ground Behavior Type with a hierarchical sequence.

3.1.1 *Input*

At the beginning, the mechanical ground properties are assigned to the predefined Ground Types. Typical properties used in the program are uniaxial compressive strength, Hoek's constant, Young's modulus, Poisson's ratio, etc. These parameters describe the properties of the intact ground. They are usually determined by laboratory tests, and additionally by field tests, index tests, or from literature.

The influence of the ground structure has to be considered, in order to enable the determination of ground properties from the intact rock values. Presently the GSI model (Hoek et al. 1998, Marinos & Hoek 2001) is implemented in the software to account for fracturing, block interlocking, weathering, etc. of the ground. Appropriate GSI values are assigned for each Ground Type.

When the Ground Types have been determined, the project related geometry and other influencing factors have to be defined. The project geometry includes the geometry of the excavation (size, shape, and length), the corresponding overburden, and the assignment of the Ground Types along the tunnel axis according to the geological model. For the calculation, it is necessary to assign the Ground Types to discrete locations, so called calculation segments. One characteristic parameter set is assigned for each calculation segment. The length of the calculation segments is project specific and depends on the complexity of the geological architecture. Typical length values range between 10–50 m. Singular structures such as faults can be individually discredited. Other project dependent influencing factors are also assigned directly to the calculation segments, such as ground water conditions, the lateral confining coefficient, discontinuity orientation relative to the tunnel direction, etc.

In order to enable the software to classify automatically different Ground Behavior Types the input of delimiting criteria are necessary. The delimiting criteria are compared with the output parameters of the calculation models. Delimiting criteria are given, for instance, for rock burst potential, depth of the failure zone, overbreak, etc. Reasonable delimiting criteria should be based on a geotechnical model and take into account practical relevance.

Finally, a hierarchy of Ground Behavior Types has to be defined because the analysis can result in several Ground Behavior Types for each calculation segment. However, the following automated processing only considers one Ground Behavior Type per calculation segment. For this reason, the dominating Ground Behavior Type has to be defined for each particular calculation segment, though secondarily defined Ground Behavior Types have an impact on later steps of the design procedure (e.g. swelling).

3.1.2 *Data processing*

In the first step, the defined intact ground properties of the Ground Types are processed into ground properties. Presently GEOCLASS uses for the upscaling process of intact properties to ground properties the GSI system (Hoek et al. 2002).

Using the ground properties and the boundary conditions assigned to each calculation segment the response of the ground to the excavation is determined based on the analytical models implemented in the software. For example, GEOCLASS includes two models for the determination of the failure zone depth and the displacements (Carranza-Torres 2003, Feder & Arwanitakis 1976), one model for rock burst potential (Wang & Park 2001), as well as one model for determining dome and chimney type failures (Feder 1980). The models are simultaneously applied for each calculation segment.

The results of the analysis are compared to the defined delimiting criteria. For a particular parameter, whose magnitude complies with the range of the delimiting criteria, the corresponding Ground Behavior Type is assigned to the calculation segment. Several Ground Behavior Types can be assigned due to the simultaneous use of different calculation models. The relevant BT is determined according to the previously defined BT hierarchy (Figure 2).

3.1.3 *Results*

In order to judge the results of the ground characterization, several tables and visualizations can be created. The obtained BT for all calculation segments can be

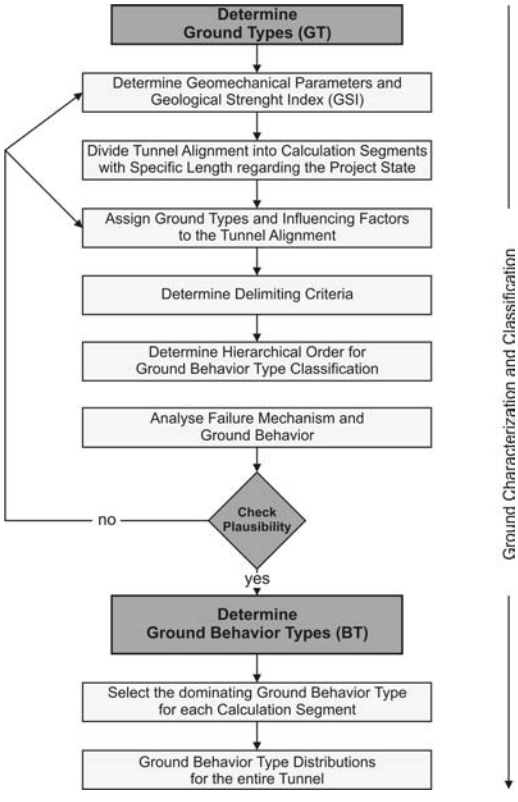


Figure 2. Deterministic procedure for the ground characterization and classification implemented in GEOCLASS.

visualized in a longitudinal tunnel section. This way of illustrating the results descriptively shows the different BT location, as well as their variation along the tunnel, and geotechnical units can be derived. Based on these units the conceptual layout of the excavation and support is established.

Diagrams, showing the displacement magnitudes and depth of failure zone can also be created. All diagrams are generated relative to the geometric project layout (Figure 3). All these visualizations allow the engineer a fast and clear judgment of the analysis and provide valuable input for the subsequent design of excavation and support.

3.2 *Exemplary calculation for Ground Behavior Type 7*

Practically input parameters are determined by laboratory tests and measurements during the geological investigations. In GEOCLASS the parameters UCS_{intact} and Hoek's constant (m_i) describe the intact ground and the GSI value is used to consider the discontinuity condition. These input parameters result in

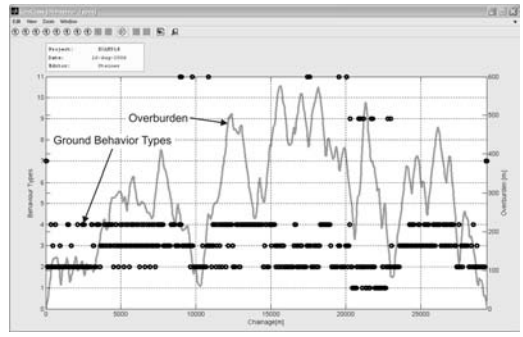


Figure 3. Distribution of the Ground Behavior Types in the longitudinal direction of a project; with the associated overburden.

the parameters describing the homogenized ground (UCS_{rm}, E_{rm}, c_{rm} and φ_{rm}).

These parameters can be used to classify the Ground Behavior Type 7. The analysis of the BT 7 (Formula 1-3) considers a failure criterion delimiting a chimney type failure from stable conditions (Feder 1980).

$$T_{shear} = \frac{h_{overburden}^{2} * \gamma_{rm}}{2} * K_0 * \tan(\varphi_{rm}) \quad (1)$$

$$G_{block} = h_{overburden} * \gamma_{rm} * D_{tunnel} \quad (2)$$

$$2 * T_{shear} \leq G_{block} \quad (3)$$

where T_{shear} = shear force in the sliding plane; $h_{overburden}$ = overburden; γ_{rm} = specific weight of the ground; K_0 = lateral confining coefficient; φ_{rm} = friction angle of the ground; G_{block} = weight of the block over the excavation; D_{tunnel} = excavation diameter.

3.3 *Exemplary calculation for Ground Behavior Type 1/3/4*

For the classification between Ground Behavior Type 1, 3, and 4, the UCS_{rm} is used in the calculation model from both Feder & Arwanetakis (1976) as well as Carranza-Torres (2003). The second one is limited to hydrostatic stress situations.

The result of this calculation is the size and shape of the failure zone (secondary stress condition > UCS_{rm}). The delimiting criterion between BT 3 and 4 is determined depending on project conditions and practical issues. In GEOCLASS an empirical formula (4), which is primarily based on the size of the excavation, is used for the classification (Figure 4).

$$DBZ_{\lim it} = 2.5 * \sqrt{R_{equivalent}} \quad (4)$$

where $DBZ_{\lim it}$ = delimiting depth of failure zone; $R_{equivalent}$ = equivalent radius of excavation.

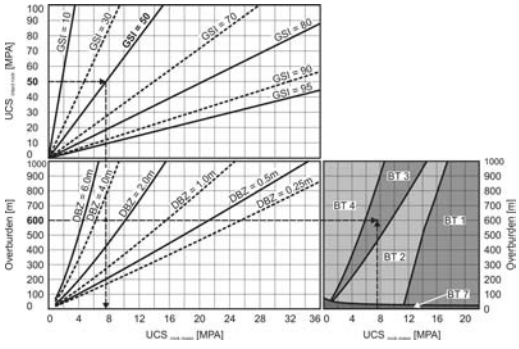


Figure 4. Nomogram for the Ground Behavior Types classification based on uniaxial compressive strength (intact rock), geological strength index, and overburden including different delimiting criteria; excavation diameter = 10 m; Hoek's constant = 10.

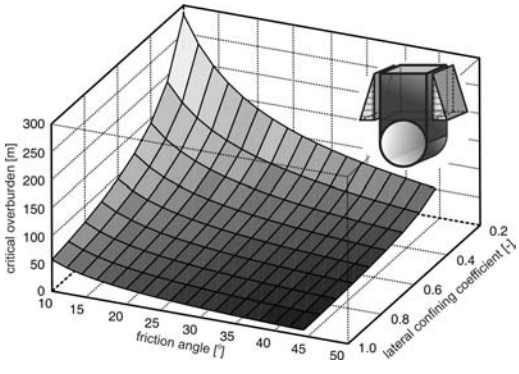


Figure 5. Delimiting criteria to determine the critical overburden depending on the friction angle and the lateral confining coefficient.

4 PROBABILISTIC APPROACH

In contrast to the deterministic calculation that proceeds with one representative parameter set during the entire calculation, the probabilistic approach uses a number of such calculations with varying input parameter sets. Those input parameter sets are determined by the natural spread of the values for each GT. The probabilistic approach results in a statistical distribution for the calculation results, hence also for the Ground Behavior Types after a sufficient high number of calculations (Figure 6).

At the ideal case, a number of laboratory results for each geotechnical unit can be used for the determination of the statistic distribution type and its characteristic values. If there is a lack of laboratory results, the determined input parameters can be used as average values. In this case, expert knowledge can

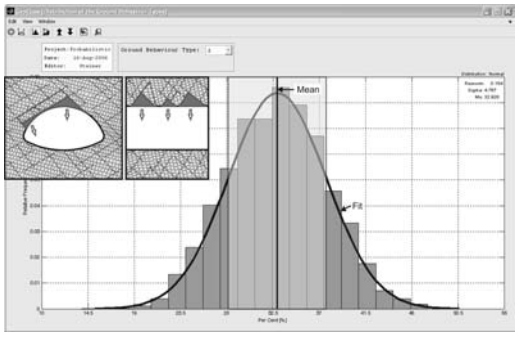


Figure 6. Histogram of the Ground Behavior Type 2 with a sketch of the appropriate failure mechanism.

be used to assume a realistic distribution. Now the random input values can be determined. In GEOCLASS this determination is done by using the Monte Carlo Simulation (Haldar & Mahadevan 2000).

The previously described deterministic calculation is executed with each of these random parameter sets, which represent the natural spread of the ground properties. The evaluation of the probabilistically determined results offers relevant conclusions (e.g. risk assessment, etc.).

During the following steps in the design procedure, each Ground Behavior Type is assigned with specific excavation and support measures. Those measures result in costs and time. The distribution, showing the expected length of each Ground Behavior Type, is later used for the determination of the costs and their possible spread.

Even when the natural spread of the input parameters is used for the calculation, some calculation segments can clearly be assigned to one expected Ground Behavior Type. Others may possibly be assigned to several Ground behavior types. In early stages of a project, these may indicate a lack of information about the ground conditions possibly resulting in further ground investigations. During final design these results represent the natural spread inherent in the explored data sets.

5 CONCLUSION

The estimation of costs and time requires rules for the determination of excavation and support during design stage. Both depend on the ground behavior. For this reason characterization systems were developed (GSI, RMR, RMi, RSR, Q-System, etc.). These systems are mostly based on measurable and/or observable values, which are used to classify the ground quality. The determined ground quality is then used to associate support methods without considering the ground behavior (Edelbro 2004, Goricki 2003).

The complexity of projects effort a lot of calculation works, so a program (GEOCLASS) was developed to accelerate the design procedure following the rules of the Austrian Guideline for the Geomechanical Design of Underground Structures with Conventional Excavation (ÖGG 2001). In the program, different approaches can be used to analyze the ground behavior. The simple illustrations of the results allow a continuous engineering judgment of the results during the first steps of the design process. Normally only deterministic procedures are used to analyze project conditions. The implementation of the Monte Carlo Simulation in GEOCLASS additionally provides the use of probabilistic procedures for the entire procedure.

The results of the probabilistic approach contain the natural spread and/or variability of the ground. When this statistic results are used for the determination of excavation and support, the variability of expected costs, and time can also be determined.

By the consideration of the natural spread inherent in the input parameters, the results for the design process are more significant in each project stage.

REFERENCES

Carranza-Torres, C. 2003. Elasto-Plastic Solution of Tunnel Problems Using the Generalized Form of the Hoek-Brown Failure Criterion. *In Hudson, J., Xia-Ting, F. (eds.), Rock Characterization, Modelling and Engineering Design Methods; Proceedings of the ISRM SINOROCK 2004 Symposium, Spec. Iss. Int. J. Rock Mech. Min. Sci., 41(3), Paper No. 2B 28, Elsevier*

Edelbro, C. 2004. Evaluation of Rock Mass Strength Criteria. *Licentiate Thesis, Department of Civil Environmental Engineering, Division of Rock Mechanics*, Lulea University of Technology

Feder, G. & Arwanitakis, M. 1976. Zur Gebirgsmechanik ausbruchsnaher Bereiche tiefliegender Hohlraumbauten. *Berg- und Hüttenmännische Monatshefte 4*, Springer Verlag, Wien, 103–117

Feder, G. 1980. Firstniederbrüche im Tunnelbau. *Berg- und Hüttenmännische Monatshefte 4*, Springer Verlag, Wien, 52–63

Goricki, A. 2003. Classification of Rock Mass Behavior based on a Hierarchical Rock Mass Characterization for the Design of Underground Structure. *Doctoral Thesis, Institute for Rock Mechanics and Tunneling*, Graz University of Technology

Haldar, A., Mahadevan, S. 2000. Probability, Reliability and Statistical Methods in Engineering Design. *JohnWiley & Sons Inc*, New York

Hoek, E., Marinos, P., Benissi, M. 1998. Applicability of the Geological Strength Index (GSI) Classification for very Weak and Sheared Rock Masses, the Case of the Athens Schist Formation. *Bulletin of Engineering Geology and Environment 57*, 151–160

Hoek, E., Carranza-Torres, C.,Corkum, B. 2002. Hoek-Brown Failure Criterion – 2002 Edition. *Mining Innovation and Technology*, University of Toronto, 267–273

Marinos, P., Hoek, E. 2001. Estimation the Geotechnical Properties of Heterogeneous Rock Masses such as Flysch. *Bulletin of Engineering Geology and Environment 60*, (85–92)

Schubert, W., Moritz, B., Sellner, P. 2000. Tunneling Methods for Squeezing Ground. *GeoEng 2000*, Melbourne

Steiner, A. 2005. Criteria for the Determination of Ground Behavior Types. *Diploma Thesis, Institute for Rock Mechanics and Tunneling*, Graz University of Technology

ÖGG Österreichische Gesellschaft für Geomechanik. 2001. Richtlinie für die Geomechanische Planung von Untertagebauarbeiten mit zyklischen Vortrieb. Salzburg, Austria

Wang, J.-A., Park, H.D. 2001. Comprehensive Prediction of Rock Burst based on Analysis of Strain Energy in Rocks. *Tunneling and Underground Space Technology 16*, 49–57

Underground Space – the 4th Dimension of Metropolises – Barták, Hrdina, Romancov & Zlámal (eds)
© 2007 Taylor & Francis Group, London, ISBN 978-0-415-40807-3

Developments of structural performance assessment for sewer liners

C. Madryas & A. Szot
Wrocław University of Technology, Poland

ABSTRACT: Wide application of strengthening and sealing CIPP and FFP liners in sewage sewers imposes taking into detailed consideration their structural performance. Some research has been conducted to capture and describe rules that govern their behaviour. The specificity and complexity of those constructions, as well as still insufficient long term experience in this subject has not allowed to work out fully relevant principles of structural design. Instead some approximate solutions based on different classic pipe approaches have been used. The behaviour of liners indicates significant degree of non-linearity, both geometrical and physical along with the unsteady boundary conditions, which is an outcome of the contact between liner and host-pipe. The results of latest research for verifying previous approaches and establishing relevant algorithm for structural design of liners have been presented in the paper.

1 INTRODUCTION

Renewal of gravity flow sewer pipeline with the use of continuous polymer liners is one of the most efficient methods for restoration of its former technical and functional condition. In general, the method consists in inserting and forming a polymer liner to make it close-fit to the pipeline. The purpose of the liner installing is to seal and strengthen the pipeline with minimum reduction of the pipeline cross-section. Among materials used for liner productions the most popular is so-called "prepreg" made of thermosetting polyester, epoxy or vinyl ester resins as well as HDPE or PVC. Liners may be inserted in loose form (prior to installation – resin prepreg; CIPP technology) or with the use of thermo-mechanical deformation (HDPE, PVC; FFP technology). In the manufacturers' specifications such constructions are commonly called "liner" or "sleeve".

Although liners have already been in use for over 30 years it seems that many theoretical aspects of this technology related to structural design and long-term liner exploitation under chemical load have not been thoroughly examined and identified. The chief questions refer to load pattern and its magnitude which hinge upon installation conditions, failure modes and relevant criteria of bearing capacity of liners.

The structural performance of sewage pipeline liners is known to be affected by the following factors:

- geometry of the ideal circular model – thickness and diameter
- geometrical imperfections – deviations of the ideal model that occur in the real model
- material physical properties of the liner with consideration of rheology
- structural condition of the host-pipe – the degree of deterioration, which might govern the loading pattern to which liner is subject
- loading pattern – mainly ground water pressure, sporadically soil pressure passed by the host-pipe
- altering boundary conditions – depending on the contact between liner and host-pipe

Vitally important in the case of liners is defining a relevant model for the structural design. There are two potential sources of failure, namely instability and exceeding material yield point. According to some research concerning that matter (Bakeer et al. 1996, Boot 1998, El Savy et al. 1998, Falter 1997), liners in sound but leaking host-pipe are reported to collapse mainly due to acting of ground water pressure and the failure usually takes form of one-lobe snap-through buckling.

Since there is no reliable bond between polymer liners and host-pipes after installation it is usually assumed that there is no obstructions for ground water to penetrate the gap and the pressure is acting along the circumference. The liner installed in a host-pipe is known to be subject to ground water pressure in most real-life cases, which is the main cause of failure. Although, in practice, the load pattern is non-uniform along the circumference of the liner the uniform distribution is accepted in publications presented to date (Bakeer et al. 1996, Boot 1998, El Savy et al. 1998, Falter 1997). In this research project, the non-uniform pressure is incorporated into FEM analysis as accurate

enough at this stage of problem examination. Moreover, there may be certain circumstances where liner is also subject to ground and overburden load. This occurs where the host-pipe is severely structurally deteriorated which results in transferring some part of loading on the liner by the local contact interaction. For liners installed in cracked host-pipes the failure mode is exceeding yield point.

2 GENERAL STABILITY FOR 2D MODEL

Performance of the shell subject to uniformly distributed ground water pressure is described in publications by several approaches. The analytical model by Glock (Glock 1977) apparently predominates and, in its evaluation by means of FEM, it was proven to comply very good with the results of laboratory tests of liners with no initial imperfections (Boot 1998, Szot 2002).

Glock's model embraces stability problem of thin, circular ring confined in rigid boundary, which corresponds with ideal conditions of liners application. The ring is subject to uniformly distributed pressure on its circumference. Since this approach is based on the potential energy balance calculation, the post-buckling form was assumed. The formula for critical water pressure resulting in instability, dependent on geometrical parameter and modulus of elasticity, takes the following form:

$$P_{cr} = \frac{2 \cdot E_L}{1 - \nu^2} \cdot \left(\frac{t}{2 \cdot R} \right)^{2.2} \tag{1}$$

where: R = liner radius (mean value of the inner and outer diameter), t = wall thickness of the liner, E_L = long-term modulus of elasticity as an equivalent of creep modulus, ν = Poisson ratio.

The formula is currently considered to be the base for further development of the load-bearing capacity assessment. Although it is relevant for ideal conditions that assume perfect circular geometry, the formula can be used as a point of reference for introduction of initial geometrical imperfections influence as a simplification of the real, highly complex model. The important topic is to combine all the kinds of imperfections into the design algorithm.

The simulations of liner performance in the natural-like conditions were performed with the use of Finite Element Method. Taking non-uniform distribution of ground water pressure into consideration, which exist in practice and may be an another relevant factor for large diameter liners. A wide range of calculations have been performed by the authors of this paper to describe dependencies between important geometrical or load factors and, relevant for structural design, critical pressure. The aim of this calculations was to identify the importance, compare and confirm the influence of initial geometrical imperfections and some other factors like buoyancy (non-uniform pressure distribution), interaction between the liner and the host-pipe and dead loads.

Results of the current analysis pertain only to the cases, where the host-pipe fully maintains ability of bearing loads, so the assumption of no traffic and ground dead loads passed to the liner was established. Such assumption covers most of the real cases of the liners' installations. Also no exact rheological behaviour was introduced into calculation. Instead, simple reduction of the modulus of elasticity as an equivalent of the creep modulus was set.

3 STABILITY AND DETERMINED GEOMETRICAL IMPERFECTIONS

The aim of the analysis was to establish the quantitative influence of imperfections combined in the model on the critical groundwater pressure. Some previous results have been used both as a point of reference and intermediate values, namely individual imperfection reduction charts. Formulae for individual reduction factors have been incorporated into a combined model, which was then calibrated with the use of FEM and regression analysis.

Three types of imperfections have been taken into account to examine the influence they produce on the critical pressure value. Geometrical imperfections have been set as follows:

- gap between the liner and the host-pipe,
- local imperfection (wave form).

Circumferential gap is a general measure of liner geometrical mismatch to the internal host-pipe surface caused by design errors, liner shrinkage and installation procedure quality. Local intrusion is a departure from the ideal circular liner cross-section resulting from installation inaccuracy, presence of bottom solidified sediment or local host-pipe surface irregularity. Local intrusions take forms of an inward bulge. Furthermore, ovalisation is often indicated to be another form of initial imperfection but in the author's opinion this form refers rather to the case of a liner installed in deteriorated host-pipe, which is a separate problem. The normalised size of a gap is often expressed as a percentage fraction as nominal gap to liner radius ratio Δ_g/R. The form of intrusion used by the author is adapted from displacement description presented in Glock's analytical solution and expressed by intrusion wave amplitude in relation to liner radius Δ_{wi}/R.

The impact of combined imperfections on the structural performance of sewer liners is of vital importance in the process of its structural design. Detailed study into this problem may allow the thickness of the liner

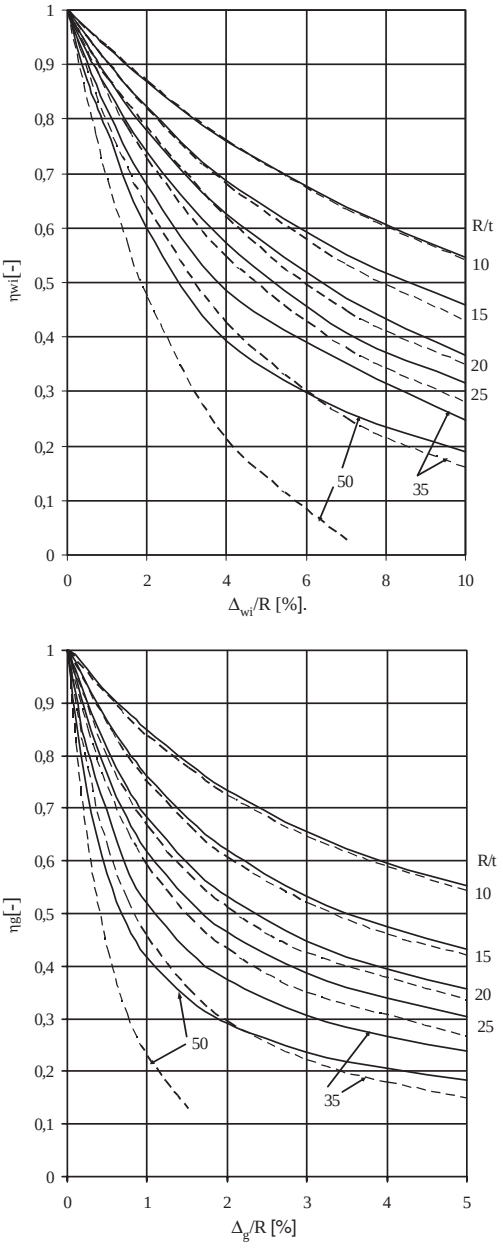


Figure 1. Diagrams of critical pressure reduction factors due to local imperfection and gap for uniform pressure distribution (solid line) and non-uniform (dashed line).

wall to be reduced, which when considering the economy of the technology, is highly desirable. Apart from rheological variation of the liner material, this issue is the main point of current discussion concerning liner performance.

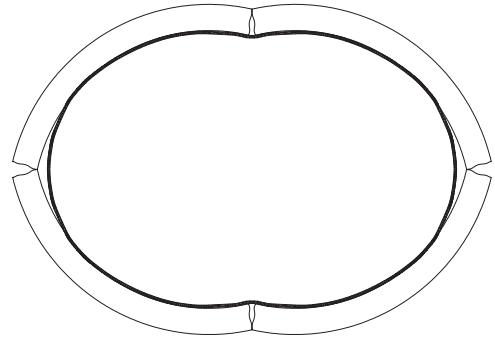


Figure 2. Mechanically deteriorated sewer and typical liner geometry.

As an intermediate parameter of the analysis there has been assumed the height of ground water pressure, being the cause of the liner instability. The parameters resulting from the analysis include reduction factors (Fig. 1), which express the ratio of pressure load in the model with imperfections to that of the corresponding, perfectly circular model. They express the influence produced by a simple-type geometrical imperfection. In the scope of the analysis combined imperfections were studied.

4 BEARING CAPACITY OF LINER IN CRACKED HOST-PIPE

The aim of the research subproject was the quantification of maximum stress in liner walls as well as the deflection of pipe-and-liner system for continuous polymer liners installed in sanitary sewers. Determination of functions of key parameters in relation to installation conditions was carried out with the use of finite element method, theory of similarity and dimensional analysis. The performed analysis enabled to work out universal formulae describing the wanted mechanical parameters for a variety of geometrical and soil conditions.

Results of the conducted analysis help assessing maximum stress and deformation of liners of all size with satisfactory accuracy. Range of geometrical and physical properties taken into account covered most practically existing cases.

Derived formulae (2) do (3) can completely describe limit states of bearing capacity and deformation. Following conclusions were drawn from the analysis:

– there are two limits of the liner stiffness envelope – upper limit depending on maximum stress and lower limit depending on maximum deformation,

– contrary the intuitive prediction setting higher stiffness does not lead to a safe solution. This effect leads to exceeding stress threshold due to increase of load on the liner,
– too low liner stiffness results in large deformation, which is unfavorable due to decreasing hydraulic performance.

In conclusion, it is recommended to use in structural design optimum magnitude of liner stiffness located within the limit envelope.

Analysis carried out with the use of finite element method and multivariable non-linear regression models led to formulae describing maximum stress and maximum deformation (ovalisation):

$$y_1 = 8{,}966 + 0{,}064 \cdot x_1 - 0{,}370 \cdot x_2 + 0{,}006 \cdot x_2^{\,2} - 0{,}002 \cdot x_1 \cdot x_2 \tag{2}$$

$$y_2 = 0{,}323 \cdot x_1^{\,1{,}017} \cdot x_2^{\,0{,}332} \approx \frac{1}{3} \cdot x_1 \cdot x_2^{\frac{1}{3}} \tag{3}$$

$$y_1 = \frac{\sigma_{\max}}{E_L} \cdot 10^3 \tag{4}$$

$$y_2 = \left(\frac{\Delta D}{D}\right) \cdot 10^3 \tag{5}$$

$$x_1 = \frac{\gamma_g \cdot h + p_k}{E_{gr}} \tag{6}$$

$$x_2 = \frac{R}{t} \tag{7}$$

where: $\sigma_{\max}$ = maximum existing stress in liner wall, D = liner diameter, γ_{gr} = ground density, E_{gr} = ground modulus of deformation, p_k = overburden pressure, h = host-pipe ground cover height.

5 STABILITY OF 3D LINER MODEL

Numerical analysis of the stability of sewer liner model was performed in the research project. The aim of the analysis was to compare results generated by plane and spatial solutions concerning stability of shell in rigid boundary subject to non-uniform circumferential pressure. Significant raise of the critical circumferential pressure was observed for the spatial model in comparison with the plane one. A linear multiplying factor for the critical pressure was determined and incorporated as a modification of the analytical plane model solution. The modification makes the analytical solution approach the laboratory test results and significantly improve accuracy of the entire solution.

The direct result of the performer simulation was water table height resulting in snap-trough instability. Only first level of critical pressure was taken into account, which complies with general stability consideration in structural design algorithms.

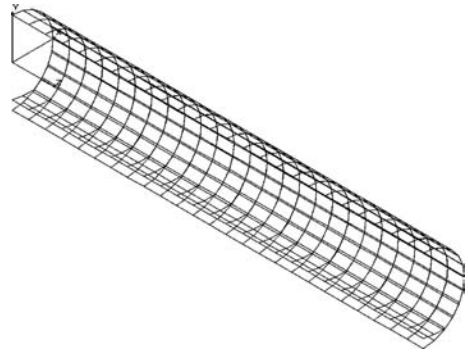


Figure 3. Typical post-critical snap-trough configuration according to FEM simulation for spatial model.

Observer results of FEM simulations for spatial liner model showed that deformations tend to be uniform along the liner axis (Fig. 3). This phenomenon does not comply with the laboratory test results (Aggarwal et al. 1984, Wagner 1992). In fact, these discrepancies can be attributed to specificity of laboratory models geometry, which were rather short. Also, boundary conditions applied in laboratory tests affects strongly the critical pressure and post-critical configuration.

Numerical critical pressure results showed that there is linear relation between spatial and plain strain model. As expected, results for spatial model showed higher magnitudes of critical pressure, which means that plain strain model is conservative and safe. This also complies with results of laboratory test, where generally linearly higher magnitudes of critical water pressure comparing to analytical ones can be observed.

Approximation of numerical results was carried out to derive modification to formula (1) in order to include spatial stability performance for liners. After linear modification the general formula for critical groundwater pressure took the following form:

$$p_{cr} = 1{,}255 \cdot \frac{E_L}{1-\nu^2} \cdot \left(\frac{t}{2R}\right)^{2{,}2} \tag{8}$$

Taking spatial performance into account leads to critical pressure higher by about 25% comparing to the 2D model. This means that current structural design algorithms are far conservative. Laboratory test results (Aggarwal et al. 1984, Wagner 1992) and the authors' solution showed good compatibility. However, in the range of low liner stiffness convergence slightly lower was observed. This could be attributed to local of liner to host-pipe adherence occurring in laboratory model, which affected boundary conditions.

6 CONCLUSIONS

Some basic results of bearing capacity analysis for continuous polymer liners used for sewer renewal have been presented in this paper. Identified valid structure load parameters and expected failure modes were shown. Circumferential ground water pressure was pointed out to be the dominant liner load. One-lobe snap-through instability localised at the liner bottom turned out to be both the predicted and observed failure mode. The model which appeared to comply best with FEM results was that proposed by Glock (Glock 1977). The assumptions and procedure proposed therein were used to work out the author's own improved approach which takes into account non-uniform water pressure. Further on, based on FEM simulations the influence of initial geometrical imperfections (circumferential gap and local intrusion) on critical pressure was analysed with taking into consideration uniform and non-uniform pressure distribution.

The impact of combined imperfections on the structural performance of sewer liners is of vital importance in the process of its structural design. A detailed study into this problem may allow the thickness of the liner wall to be reduced, which when considering the economy of the technology, is highly desirable. Apart from rheological variation of the liner material, this issue is the main point of current discussion concerning liner performance.

The problem of stability of the polymer non-circular sewer liner subject to the action of ground water pressure has been studied. In comparison with computational results the first approximate analytical solution by Glock turned out to be fairly accurate and useful for practical purposes. The magnitudes of the snap-through pressure calculated in this way were in good agreement with those obtained from FEM analysis.

Analysis of the liner installed in cracked host-pipe was performed. Formulae describing liner performance were determined with the use of FEM. General solution presented herein may be universally used for various geometries and installation conditions.

Numerical analysis of the stability of spatial model of sewer liner model was conducted. Significant raise of the critical circumferential pressure was observed for the spatial model in comparison with the plane one. A linear multiplying factor for the critical pressure was determined and incorporated as a modification of the analytical plane model solution. The modification made the analytical solution approach the laboratory test results and significantly improve accuracy of the entire solution.

All the examinations performed led to improving the general liner performance assessment.

ACKNOWLEDGEMENTS

The study presented in the paper was supported by The Polish Ministry of Science and Education within the project No. 4 T07E 023 27 and Fundation for Polish Science within the Professorial Grant.

REFERENCES

Aggarwal S.C. & Cooper M.J. 1984. External pressure testing of Insituform lining. Internal report. Coventry Polytechnic. Coventry.

Bakeer R.M., Barber M.E. & Chunduru S. 1996. Buckling behaviour of polyethylene liner system. *Journal of Materials in Civil Engineering*. 8(4): 201–206.

Boot J.C. 1998. Elastic buckling of cylindrical pipe linings with small imperfections subject to external pressure. *Trenchless Technology Research*. 12(1–2): 3–15.

El Sawy K. & Moore I.D. 1998. Stability of loosely fitted liners used to rehabilitate rigid pipes. *Journal of Structural Engineering*. 124(11).

Falter B. 1997. Structural analysis of sewer linings. *Trenchless Technology Research*. 11(2): 27–41.

Glock D. 1977. Überkritisches Verhalten eines starr ummantelten Kreisrohres bei Wasserdruck von außen und Temperaturdehnung. *Der Stahlbau*. 7: 212–217

Guice L. & Li J.Y. 1995. Buckling of encased elliptic thin ring. *Journal of Engineering Mechanics*. 121(12): 1325–1329.

Shaw W.J., Sun C. & Vinogradov A.M. 1995. One-way buckling of circular rings confined within a rigid boundary. *Transactions of the ASME – Journal of Pressure Vessel Technology*. 117: 162–169.

Szot A. 2002. Nośność rurociągów kanalizacyjnych wzmacnianych polimerowymi wykładzinami ciągłymi. Dissertation. Wrocław University of Technology.

Wagner V. 1992. *Beulnachweis bei der Sanierung von nichtbegehbaren. undichten Abwasserkanälen mit dem Schlauchverfahren*. Dissertation. Technical University Berlin.

This page intentionally left blank

Underground Space – the 4th Dimension of Metropolises – Barták, Hrdina, Romancov & Zlámal (eds)
© 2007 Taylor & Francis Group, London, ISBN 978-0-415-40807-3

Experimental verification of final tunnel lining performance

P. Šourek
SATRA, Prague, The Czech Republic

J.L. Vítek
METROSTAV, Prague, The Czech Republic

ABSTRACT: Design of final tunnel lining is influenced by many factors – rock/soil performance, concrete and geometry of the lining, technology of construction, etc. The input data for the analysis have usually a large statistical scatter. The design used to be conservative, in order to guarantee the safety of the tunnel. This paper deals with the experimental work carried out with the aim of monitoring the actual performance of the tunnel lining in selected tunnels. The measured values are recorded for a period 1 to 4 years.

1 INTRODUCTION

The progressive development of transport infrastructures in the Czech Republic resulted in design of many tunnels. The new trends of design and construction of underground structures came mostly from abroad. Tunnels represent very important parts of roads and railways, no limitations of traffic should be allowed, and therefore the tunnels must be safe, economical and they must serve the users without any restrictions during their entire service life. The experiences concerning the long term tunnel performance are sufficiently different in many countries, so that it was considered useful to verify the tunnel lining performance in the Czech conditions. The objective of this paper is to provide information on measurements carried out in selected tunnels, which should provide a basis for tunnel assessment and, later, for possible modification of the design methods.

2 CONSTRUCTION OF TUNNELS IN THE CZECH REPUBLIC

Geological conditions, tunnel alignment and but above all, the equipment of contractors resulted in the fact, that most of the new tunnels are built using the New Austrian Tunnelling Method (NATM). The principle of the NATM is based on the interaction of the rock massive with primary lining in the first phase. The temporary primary lining is made of sprayed concrete, reinforced by steel mats supplemented by rock nails and temporary anchors. In this phase, the deformations become stabilized and the stress in the rock massive is redistributed.

In the second phase, the definitive secondary lining is cast into the free space supported by primary lining. It forms a final structure, which should carry all the permanent loads during the entire service life of the tunnel. The secondary lining is usually made of reinforced concrete composed of the heading, side foundation blocks and, in some cases, also by an invert.

The reinforcement used to be assembled from mats at each surface which are supplemented by individual bars. The final lining made only of plain concrete was applied in very few tunnels. The individual sections of the lining are cast in sequence, the invert using a classical system formwork, and the top using a hydraulically operated formwork. The length of individual casting segments varies in dependence on the size of the tunnel cross-section; tunnel alignment and length of the formwork from 5 to 15 m. Individual segments are statically independent.

3 DESIGN ASSUMPTIONS OF THE FINAL LINING

The application of advanced numerical methods has become standard over recent years. Internal forces and deformations in the tunnel lining are analyzed using a method of finite elements. The complete rock/soil massive, including a secondary lining, is modelled together with its time development and important construction stages like installation of individual linings.

The structural analysis is focused on the most complex cross-sections regarding many loading stages and

their combinations. The most important loadings are as follows:

– self-weight of the lining,
– geostatic load of the rock/soil massive,
– hydrostatic pressure of underground water (if the waterproofing is applied),
– shrinkage of concrete,
– changes of the ambient temperature, etc.

The loading of classical structures, such as buildings and bridges can be relatively precisely defined. Above the ground structures may be also built with a high degree of accuracy and their deviations from the designed shape and dimensions are minor. The material parameters are given with an acceptable statistical scatter.

To the contrary, the underground driven tunnel forms a system which includes the tunnel lining and the rock/soil massive. Both parts interact and the response of the lining is highly dependent on the rock/soil massive performance. The determination of actual parameters of the system composed of a rock/soil massive and a tunnel lining is a rather complex task. Therefore, during the tunnel design, it is necessary to accept many simplifying assumptions. In addition, the safety reserves are subject to the code requirements as well as to the subjective considerations of the designer. This results in the design of the tunnel lining being significantly dependent on the experience of the designer and on the availability of the data describing the performance of the rock/soil massive. It can be expected that in this situation, the designs will be rather conservative. The non-existing unified methodology of the design in terms of loading stages consideration and the interaction of the rock/soil massive with the secondary lining including their deformation and strength characteristics variable in time contributes to the complexity of the design.

4 EXPERIMENTAL MEASUREMENTS

The uncertainties described above led to a decision to observe the actual tunnel performance, and to compare the measured values with those obtained from the design calculations. Within the research project of the Grant agency of the Czech Republic, the strain gauges were embedded into the secondary or primary linings of selected tunnels. The vibrating wire strain gauges produced by the Gauge Technique Company were used since they are rather robust and reliable, and the research team had had a long term experience with their application.

The vibrating wire strain gauges were installed in the final lining of some road tunnels, for example:

– Tunnel Valik, motorway D5, 4 measured sections
– Tunnel Panenska, motorway D8, 2 measured sections

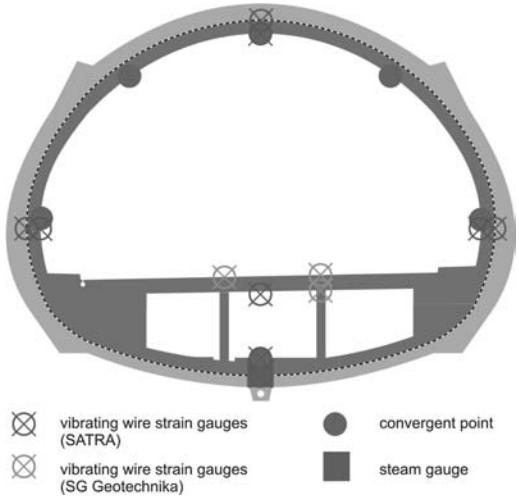


Figure 1. Cross-section of the tunnel Mrazovka including the position of vibrating wire strain gauges.

– Tunnel Libouchec, motorway D8, 2 measured sections.

Besides these tunnels, the results of the measurements that had begun earlier were used. Similar strain gauges were embedded in the secondary lining of the tunnel Mrazovka in Prague, where about 6 sections have been measured and in the surveying gallery of the tunnel Blanka, where the two sections are monitored.

Using the vibrating wire strain gauges, the strain and temperature developments in the secondary lining are recorded at regular time intervals. This method of measurement has been verified over the past 20 years when the same types of gauges were installed in different structures, and the strains are within many projects successfully recorded until now.

The changes in stress and strain in the secondary linings are assumed to be rather slow; therefore, the readings are taken only several times a year. The cross-sections, where the gauges are embedded, are supposed to be subjected to a significant loading. The locations deep in the rock/soil massive or the locations with a high hydrostatic pressure of underground water were given preference. The position of gauges within the cross-section was chosen according to the bending moment distributions. The locations in the top of the vault or above the abutments are typical for appearance of the large bending moments. The symmetry of the cross-section is used as an independent check of the recorded strains. It is assumed that if the loading is symmetrical, the recorded strains should also satisfy the condition of the symmetry. Figure 1 shows the positions of the vibration wire strain gauges in one of the sections of the tunnel Mrazovka. The section is not typical; therefore the strain gauges are also located in

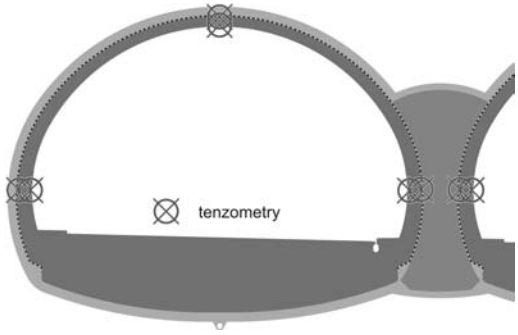


Figure 2. Cross-section of the tunnel Valik including the position of vibrating wire strain gauges.

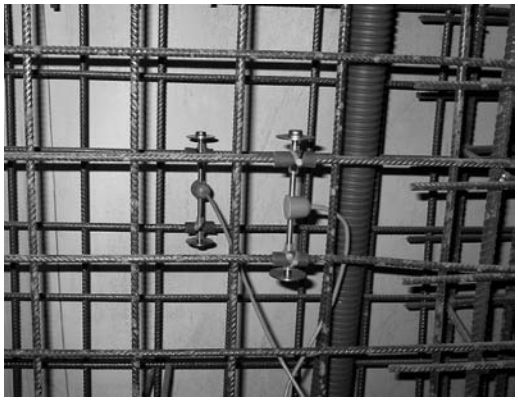


Figure 3. Vibrating wire strain gauges attached to the reinforcing bars prior to pouring of concrete.

a slab under the pavement (called bridge deck). This slab also works as a tie which stiffens the complete cross-section of the tunnel. In this tunnel two independent measurements are carried out by the SATRA and by the SG Geotechnika companies. The results are shared and the evaluation is based on the results of both measurements. Additionally, the deformations of the lining measured by surveying and measurements of the underground water pressure are taken into account as part of the evaluation of all the measured values.

The vibrating wire strain gauges are attached to the reinforcing bars (Fig. 3). The leads from the gauges are connected into the box which is installed at the surface of the tunnel lining. The boxes are also accessible during the operation of the tunnel, which allows for recording of the strains after the opening of the tunnel to the traffic as well. No calibration is necessary before taking the new readings, which is one of the advantages of this strain gauge. The electric impulse sent by the reading device starts the string in the gauge to vibrate and immediately its frequency is measured. The frequency varies with the strain, which is then calculated. The measuring length of the used gauges is 140 mm, which is suitable for measurements in heterogenic materials like concrete. The initial reading is taken just after the pouring of concrete and further readings are taken approximately 4 times a year. Fig. 2 shows the positions of the gauges in the tunnel Valik.

5 MEASURED VALUES

The measured strains are compared with the strains measured in other similar tunnels or with the strain values obtained from the structural analysis of the secondary lining. The measured strain is a result of many effects, including an elastic strain due to the applied stress, creep and shrinkage of concrete, temperature effects, and sometimes, increased strain due to cracking. Within the evaluation, it is necessary to measure the concrete properties in order to estimate the stress values in the instrumented locations. The bond between steel and concrete is assumed to be perfect since the stresses are rather low. It is necessary to note that the stress in steel reinforcement is also influenced by internal stresses induced by shrinkage and temperature changes of concrete. The smaller the reinforcement ratio, the higher the internal stress in steel.

The secondary lining of the tunnels Valik, Libouchec and Panenska was built mostly in 2005. The strains measured in these tunnels are therefore rather low. The stress in steel is in the order of the tens of MPa and the stress in concrete does not exceed 2 MPa. The strain development in time at the tunnel Valik is plotted in Fig. 4. The secondary lining (in this case without the closed waterproofing), is loaded by the self weight of concrete, shrinkage, and by temperature changes. The effect of the self-weight is not in the reading involved since the first reading was taken after demoulding. The load induced by the rock/soil pressure will be active later, at present it is transferred still by the primary lining. After its degradation, the secondary lining will be slowly loaded. The degradation of primary loading will be dependent on the design parameters and on the aggressiveness of the rock/soil environment.

The secondary lining of the tunnel Mrazovka was finished in 2003. The tunnel was open to traffic in 2004. The tunnel is completely protected by waterproofing which is located between the primary and the secondary lining. The measured strains also in this tunnel do not show that the secondary lining would be loaded up to the expected design level. The maximum measured stress in the reinforcing steel has reached about 12 MPa, while the compression on concrete does not exceed 1 MPa. The time development of strains proved the growth of the stress due to the growing pressure of underground water after the pumping

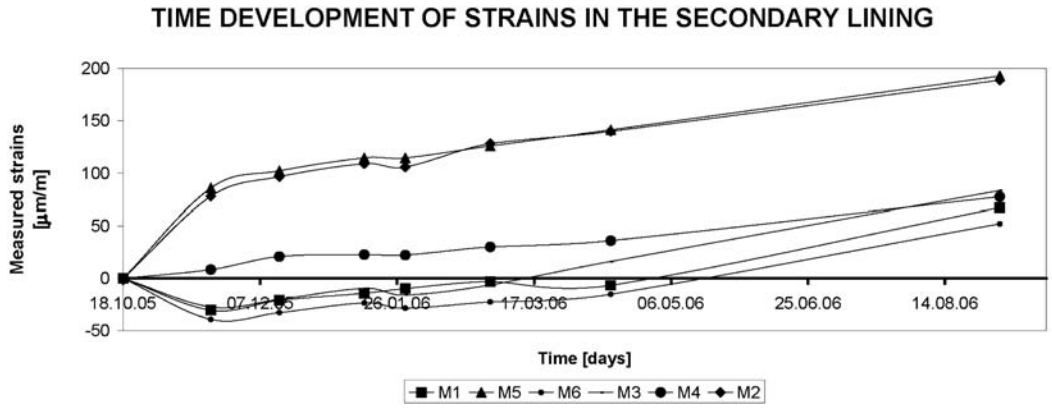


Figure 4. Time development of strains in the secondary lining – Valik tunnel.

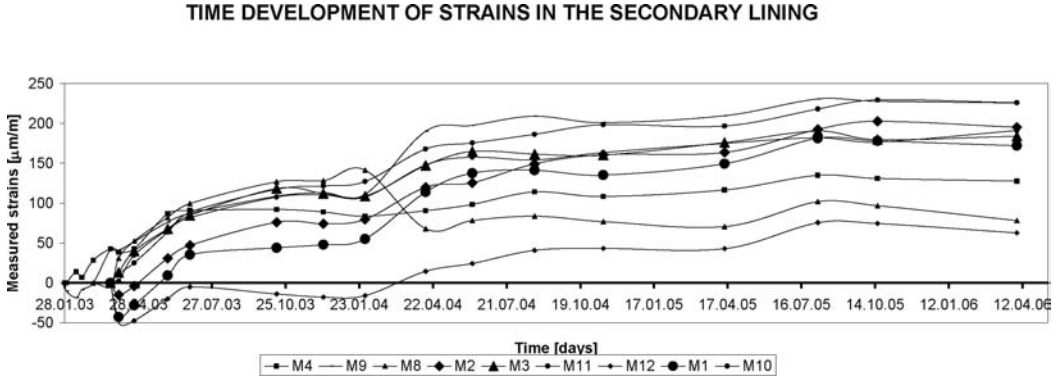


Figure 5. Time development of strains in the secondary lining – Mrazovka tunnel.

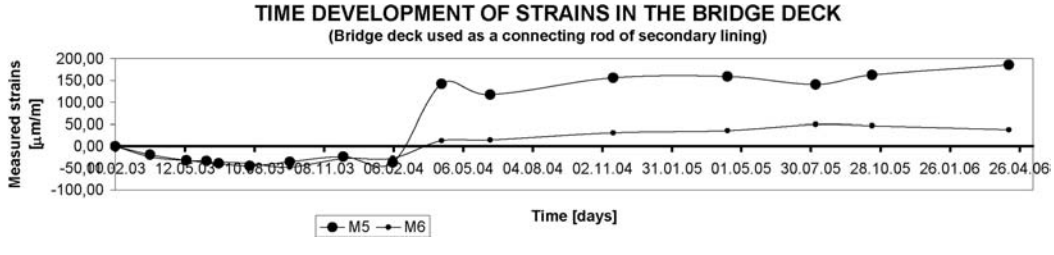


Figure 6. Time development of strains in the bridge deck – Mrazovka tunnel.

shafts had been closed. The water pressure stabilized after some period (see Fig. 5 and 6). The measured values also prove the functionality of the designed system, where the road slab works like a tie and stiffens the whole cross-section of the tunnel. The slab transfers the tensile force and the measured strain values correspond to the stress in the steel about 70 MPa (the effects of traffic excluded).

6 CONCLUSION

The primary lining initially carries the complete loading at all the instrumented tunnels, since they were built by the new Austrian tunnelling method (NATM). In the later stages, the secondary lining is cast. It is usually separated from the primary lining by a waterproofing. A structural analysis assumes that the

primary lining will disintegrate in time and the total loading will be carried by the secondary lining. If it happens, to what extent and when, is still rather uncertain. The measurement carried out under the mentioned research project should help to explain how the transfer of load will influence the measured strains. The instrumented tunnels are rather new, and the actual load of the secondary lining is small, which is in accordance with the design philosophy of the NATM. Even the shrinkage alone exhibits smaller strain than that measured on the small concrete specimens. It can be assumed that the actual shrinkage of the tunnel lining is rather small. The reason may be (a) the environment in tunnels is rather wet, the drying of concrete is slow, (b) the concrete lining is thicker than the usual dimensions of the standard laboratory specimens and (c) the surface of the lining is exposed to the environment only from one side.

The significance of the proposed measurements consists of long term observation of the actual performance of tunnel linings. The strains will be recorded for many years, and it is expected that there will be a possibility to register changes in strains, which could indicate the degree of loading carried by the secondary lining (it would also provide information about the degradation of the primary lining). When the secondary lining is exposed to the pressure of underground water, it is possible to trace this loading from the measured strains. This was evidenced in the case of the measured strains in the Mrazovka tunnel. One can assume that the measured strains in instrumented segments of selected tunnels will bring information on the behaviour of the system primary and secondary lining in the future. Such knowledge will hopefully be of interest in the design of the new tunnels, along with the evaluation, and possibly for modification, of the currently used design procedures.

ACKNOWLEDGEMENT

The research team gratefully appreciates the support of the Grant Agency of the Czech Republic, Project No.103/2005/2231.

REFERENCE

Pacovský, J., Šourek, P., Vítek, J.L.: Experimental verification of tunnel construction. Proc. of the 2nd CCC Congress, Hradec Kralové , Czech Concrete Society, Prague 2006, 485–490.

This page intentionally left blank

Underground Space – the 4th Dimension of Metropolises – Barták, Hrdina, Romancov & Zlámal (eds)
© 2007 Taylor & Francis Group, London, ISBN 978-0-415-40807-3

Stability analysis and excavation schemes of large-span highway tunnel under complex geological conditions

J.S. Tang, S.Y. Liu & L.Y. Tong
Transportation College, Southeast University, Nanjing, jiangsu, P.R. China

C.H. Shen
Transportation College, Hohai University, Nanjing, jiangsu, P.R. China

ABSTRACT: More and more practice problems arise during the construction of the big-span highway tunnels due to the complexity of the geological conditions, such as geological disasters, failure of the shot and lining concrete, etc. Tunneling excavation is actually the process of stress redistribution and rock deformation, which are much influenced by different construction methods and sequences. A case study of the east Mao Mountain tunnel on the Ning-Chang highway, China, is carried out in this paper. The three dimensional numerical simulation is conducted on different excavation schemes in the condition of pre-designing support system using the FLAC^{3D} software. The displacement behavior and stress characteristics are analyzed to propose the reasonable tunneling scheme. Accordingly, the stability of selected scheme is predicted. Moreover, the simulation results are compared with field monitoring data. The pre-designing support parameters of the large-span highway tunnel are evaluated. The results of this study are expected to be useful for the successive design and construction control.

1 INTRODUCTION

The stress and deformation of the surrounding rock are influenced by different tunneling methods and sequences. Especially, for partial excavation methods, different construction sequences have different stress paths, which affect final stress and displacement fields of surrounding rock as well as support structures. Accordingly, tunneling methods and construction sequences are of importance for tunneling safety and are also key concerns for the engineers.

Numerical simulation is mostly applied to validate rationality of pre-designing schemes by theory and engineering analogy. However, most papers on simulation of construction schemes are two-dimensional and three-dimension analysis are rather few. Moreover, the single tunnel model based on symmetry theory is mostly used. The change of surrounding rock is not revealed using two-dimensional model, which doesn't consider space effect during tunneling process. The interaction of two separate tunnels isn't also considered by single tunnel model. So, it is more reasonable for two separate tunnels analysis using three-dimensional model.

In this paper, the three-dimensional model of east Mao Mountain tunnel, on the Ning-Chang highway, China, is founded. The construction schemes and sequences under Class III surrounding rock is simulated using FLAC^{3D} software. The reasonable construction scheme for large-span highway tunnel is recommended and the corresponding stability of the surrounding rock is evaluated.

2 BACKGROUND OF EAST MAO MOUNTAIN TUNNEL PROJECT

The east Mao Mountain tunnel is a typical large span tunnel under complex geological conditions. It locates the highway from Nanjing to Changzhou, China. The total length of the double-direction tunnel is 513 m. It has a shape of ellipse with the maximum values of 17.33 m in width and 11.89 m in height. Moreover, the shallow overburden mostly varies from a few meters up to approximately 45 m.

The excavation scheme of east Mao Mountain tunnel is designed based on NATM theory. It adopts compound lining structure. The initial support consists of rock bolts, steel arch girder, wire mesh and shotcrete. The grouted rock bolt has diameter of 25 mm and length of 3.5 m. The distribution of rock bolt is 1 m × 1 m. The type of steel arch girder is I20a and the space is 1 m in each round. The wire mesh has diameter of 8 mm and space of 20 cm. The shotcrete is

C25 polypropylene fibre concrete, which has thickness of 23 cm. The inner lining is C30 waterproof-self reinforced concrete, which has thickness of 45 cm. The EVA waterproofing membrance are in the gap between the initial support and the inner lining.

For rock mass of Class III, the CRD tunneling method is proposed in pre-designing based on engineering analogy method. However, the bench cut method is suggested on the basis of real surrounding rock conditions during construction. It needs to be verified whether the bench cut method is more feasible compared with the CRD method.

3 GENERAL GEOLOGICAL SITUATIONS

3.1 *Stratum and lithology*

There are complex stratums in region where the east Mao Mountain tunnel passes through from west portal to east exit. The surrounding rock consists of conglomerate of Pu-kou group, cretaceous and andesite of Long-wang-shan group, Jurassic. Especially, the species of andesite are rather complex, which include andesite, tuff and cracked gravel tuff. Granitic porphyry makes inroads into andesite at some sections. The uni-axial compressive strength of conglomerate is from 33.5 MPa to 82.6 Mpa. The andesite species has mostly disintegrated structure and the uni-axial compressive strength varies from 7.6 MPa to 37.3 Mpa.

3.2 *Geological structural features*

The tunnel locates in the active Mao Mountain fault zone. However, there are few major faults crossing the tunnel alignment. But many small faults are revealed during excavation.

3.3 *Hydrological geological conditions*

The groundwater is mainly porous phreatic water and bedrock fissure-water. The quantity of groundwater is small and controlled by rainfall mainly. However, in view of the characteristics of shallow overburden, particular area with weak structural plane combination is deserved to consider.

3.4 *Rock mass classification*

According to rock mass structure, rock mass integrality, RQD index and other influencing factors, the appropriate classification of the rock mass is proposed on the basis of Code for Design of Road Tunnel (JTG D70-2004, China).The percentage of Class III is 67.3% in uplink and 88.8% in downlink. It is obvious that the surrounding rock is weak and the stability is deserved to consider during excavation.

Table 1. Physic-mechanical parameters of rock mass.

Material name	Young's modulus (GPa)	Poisson ratio	Density ($kg \cdot m^{-3}$)	Cohesion (MPa)	Frictional angle (°)
Rock mass	0.5	0.35	2300	0.1	38

4 SIMULATION AND ANALYSIS OF CONSTRUCTION SCHEMES

4.1 *Calculation model of east Mao Mountain tunnel*

As theory analysis indicates, for circular cavern in infinity homogeneous elastic media, the change of stress and displacement is less than 1% outside 5 times of excavation diameter and less than 5% outside 3 times of excavation diameter on account of load release. The error may satisfy the needs of practical engineering. Considering calculation reliability and reasonable computing time, the range of the three-dimensional model is proposed as following: The transverse computing range, that is, the central line to the side boundary, is 3 times of the tunnel span, which is actually 60 m. The vertical range is 57 m from the tunnel bottom to the model bottom. The space between uplink and downlink is 50 m according to the central line. Taking into account the shallow overburden, the upper boundary of the model reaches to the ground plane surface and the depth from the top of the tunnel to the ground surface is approximately 17 m. Considering the space effect of construction process, the longitudinal length of the model is 60 m.

The boundary conditions of the model are described as: the side-face boundaries are respectively restricted by horizontal displacement of x-axial and z-axial direction. The bottom boundary is restricted by vertical displacement of y-axial direction. The ground surface is free boundary.

The surrounding rock is modeled using zone element. The shotcrete is simulated using shell structural element. The equivalent principle is introduced to simulate the effect of supporting system, which consists of small grouting pipe, steel arch girder and rock bolts.

4.2 *Determination of computational parameters*

The surrounding rock of class III is assumed as simplex homogeneous continuous media in this study. The physic-mechanical parameters of surrounding rock are obtained from the engineering geological exploration (showed in Table 1). The parameters of C25 and C30 concrete are showed in Table 2.

The pre-supporting effect of small grouting pipe, which is treated as assistant construction measurement, is simulated by increasing physic-mechanical parameters of rock mass. The reinforced effect of rock bolts is also treated with equivalent principle, that is, by increasing Young's modulus, cohesion and inner friction angle of surrounding rock. Here, the improvement of inner friction angle is less and doesn't take into account. The Young's modulus and cohesion of reinforced surrounding rock are respectively proposed by equation 1 and 2 as following:

$$E = E_0(1 + \frac{f}{e \cdot i}) \tag{1}$$

$$C = C_0 + \frac{f}{e \cdot i}\tau_b \tag{2}$$

where $E =$ Young's modulus of reinforced rock mass by rock bolts; $C =$ cohesion of reinforced rock mass by rock bolts; $E_0 =$ Young's modulus of rock mass not reinforced by rock bolts; $C_0 =$ cohesion of rock mass not reinforced by rock bolts; $\tau_b =$ maximal shearing strength; $f =$ area of cross section of rock-bolt; $e =$ longitudinal spacing of rock bolts; $i =$ transverse spacing of rock bolts.

The effect of steel arch girder is also simulated by increasing the Young's modulus of shotcrete (Wu B. et al. 2005). The calculation method is as following:

$$E = E_0 + S_g E_g / S_c \tag{3}$$

where $E =$ Young's modulus of reinforced shotcrete considering steel arch girder; $E_0 =$ Young's modulus of shotcrete; $E_g =$ Young's modulus of steel arch girder; $S_g =$ cross section area of steel arch support; $S_c =$ cross section area of shotcrete.

Owing to shallow depth of the east Mao Mountain tunnel, the initial stress field of the model is the self-gravitational stress field. The ideal elastic-plastic model is adopted for the constitute model of rock mass, which is submitted to Mohr-Coulomb yield rule. The initial support is simulated as ideal elastic material.

Table 2. Physic-mechanical parameters of support structure.

Material name	Grade	Young's modulus (GPa)	Poisson ratio	Density (kg · m^{-3})	Thickness (cm)
Shotcrete	C25	26*	0.25	2200	23
Reinforced concrete	C30	31	0.2	2500	45

* Young's modulus of C25 shotcrete in the Table is the Young's modulus considering the equivalent effect of steel arch girder in initial support.

4.3 *Simulation of construction schemes*

According to pre-designing scheme and practical geological conditions, the bench cut and CRD method are respectively simulated. Figure 1 is the sketch map of construction sequence of them.

The excavation sequences of bench cut method can be simplified as following: step 1, top-heading excavation; step 2: top-heading initial support; step 3: bench and invert excavation; step 4: bench and invert initial support.

The excavation sequences of CRD method can be simplified as following: step 1: top-heading1 excavation; step 2: top-heading1 initial support and temporary support (including diaphragm wall and temporary invert arch); step 3: top-heading2 excavation; step 4: top-heading2 initial support and temporary support; step 5: bench and invert 3 excavation; step 6: bench and invert 3 initial support and temporary support; step 7: bench and invert 4 excavation; step 8: bench and invert 4 initial support.

Because of time limit for tunnel project, the uplink and downlink tunnel are usually excavated in turn in the same direction. In this study, each length of tunneling step is 3 m. The interval of each cutting face in one tunnel is 12 m. Moreover, left tunnel is excavated at first and the least interval of the advancing excavation face between left and right tunnel is 21 m. The excavation sequences with the same or reverse direction synchronously aren't simulated.

Considering the complexity of the problem, the step of removing temporary support in this study isn't simulated with CRD construction method. The inner lining is calculated by load-structure method according to the Code for Design of Road Tunnel (JTG D70-2004) and isn't simulated in this study.

4.4 *Analysis of calculation results and excavation scheme*

Considering influence of boundary conditions and space effect, the typical cross section of z = 21 m along tunnel alignment is selected. The analysis consist of stress distribution, displacement change, plastic area of surrounding rock and stress state of initial support structure. The final displacement and stress of the selected section are listed in Table 3 after excavation completed. The vertical displacement distribution of two schemes is showed as Figure 2. The minimal principle stress distribution of surrounding rock is showed



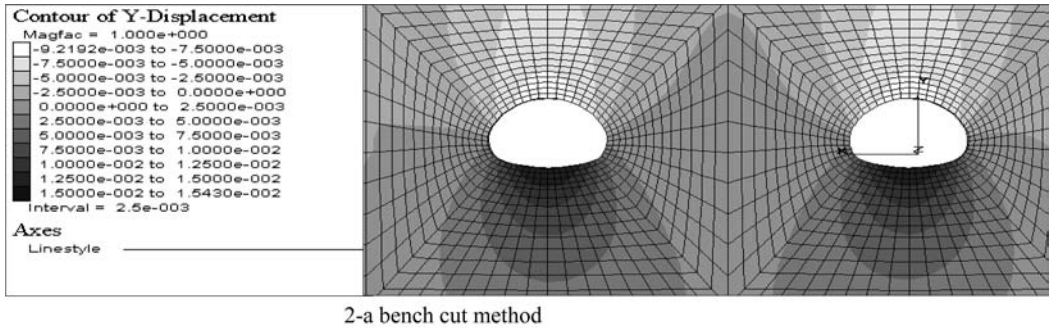
(a) bench cut method (b) CRD method

Figure 1. The sketch map of construction sequence.

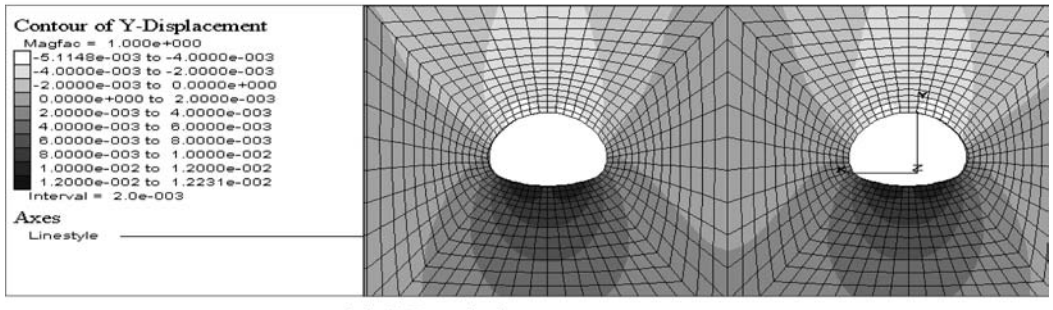
Table 3. The calculation results of two tunneling schemes.

Tunneling method	The maximal settlement of arch crown (mm)	The maximal rise of invert (mm)	Principal stress of surrounding rock*		Principal stress of initial support*	
			(σ_1/MPa)	(σ_3/MPa)	(σ_1/MPa)	(σ_3/MPa)
Bench cut method	9.22	15.43	0.11	−1.26	2.42	−6.57
CRD method	5.11	12.23	0.06	−1.14	7.94	−14.75

* The rule of stress sign is that '+' denotes tensional stress and '−' denotes compressive stress.



2-a bench cut method



2-b CRD method

Figure 2. The vertical displacement sketch of surrounding rock.

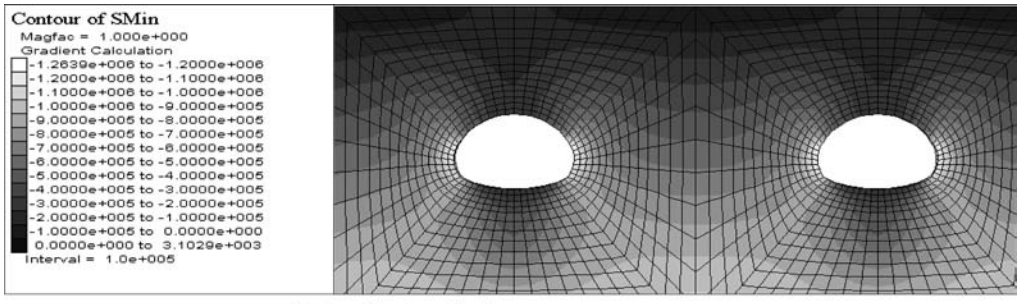
as Figure 3. The minimal principle stress distribution of initial support structure is showed as Figure 4.

The vertical displacement of surrounding rock in Figure 2 shows that the maximal settlement of arch crown using CRD method is 55% of that using bench cut method. The maximal rise of invert arch using CRD method is 80% of that using bench cut method. It is obvious that CRD tunneling method may effectively lessen disturbance to surrounding rock and temporary support can control displacement of surrounding rock better.

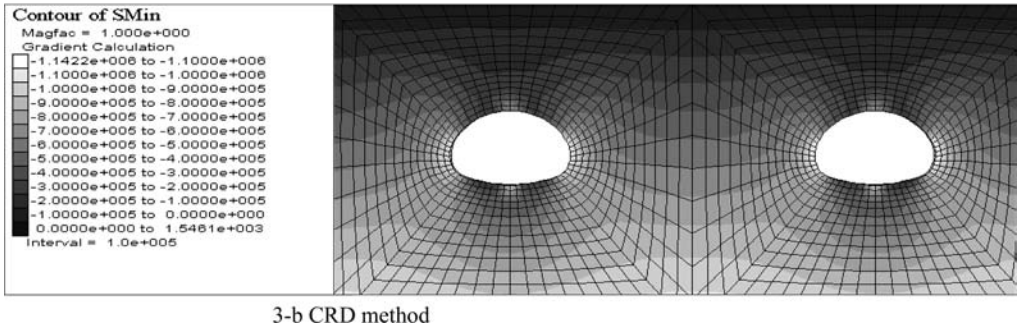
This is very important for subway construction in urban region. According to the safety of adjacent structures and residing living, the maximal subsidence of ground surface should be controlled to within 30 mm. So, the release of displacement of surrounding rock must be effectively restricted. The results of numerical simulation indicate that CRD method can do it well. But for mountain tunnel, the subsidence of ground surface isn't the primary controlling target. It is allowable that deformation of surrounding rock is tended to stability and doesn't exceed allowable deformation synchronously.

Figure 2 also indicates that the maximal settlement of arch crown using bench cut method occurs at the center of arch crown. However, the maximal settlement of arch crown using CRD method takes place at two side spandrels. This is because of the restriction of temporary support and the maximal settlement of arch crown transfers from the center of arch crown to two sides.

Shown as Figure 3, the minimal principal stress is mainly compressive stress, which is concentrated in the sidewall within 1m range. So, the surrounding rock on the sidewall should be reinforced especially to ensure safety in the process of construction.

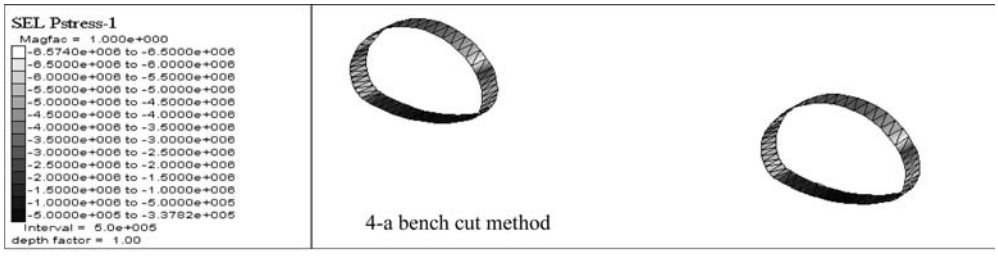


3-a bench cut method

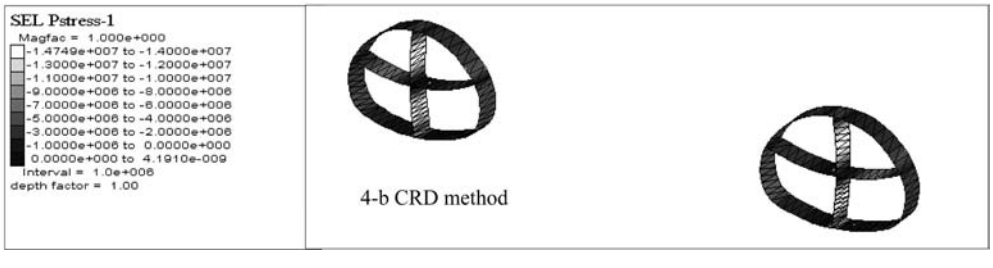


3-b CRD method

Figure 3. The minimal principal stress sketch of surrounding rock.



4-a bench cut method



4-b CRD method

Figure 4. The sketch for the minimal principal stress of initial support.

The minimal principal stress of bench cut method is greater 10% than that of CRD method. It is shown that the surrounding rock is lesser disturbed using CRD method because the excavating face of each round is smaller, which reduces stress concentration on both sidewall. However, the minimal principal stress of bench cut method is only 1.26 MPa, which can be endured by surrounding rock.

Figure 4 shows that the minimal principal stress of initial support structure is also compressive stress. The stress value using bench cut method isn't larger than 5.5 MPa except several parts, where the value reaches

6.57 MPa. The stress value using CRD method indicates that temporary support, especially diaphragm wall, endured biggish compressive stress, which reached 14.75 MPa. This is a baptism to initial support. However, the minimal principal stress of shotcrete doesn't exceed 5 MPa using CRD method. So we can say that displacement of surrounding rock is effectively controlled, which is obtained at the cost of biggish compression bearing by temporary support. Reinforced temporary support, especially diaphragm wall, is the primary task to ensure safety and stability.

All the analysis above indicate that the stability of surrounding rock itself is the primarily concern for bench cut method. The displacement of surrounding rock is biggish. But the stress of initial support structure is lesser. So, the initial support system can be properly decreased and cost can be saved. Comparatively, the stress of surrounding rock can't effectively be released using CRD method because initial support is in the wake of excavation and closed to ring at each stage. Although displacement of surrounding rock is lesser, biggish compression is acted on initial support. So cost of reinforcing initial support must be increased and it isn't economical for mountain tunnel.

Considering construction convenience and economic rationality, bench cut method is better appropriate construction method for big-span highway tunnel under Class III surrounding rock conditions, which can exert self-bearing capacity of surrounding rock. However, CRD method, which may effectively control surface subsidence, is more reasonable for city subway.

4.5 *Evaluation of selected excavation scheme*

According to the analysis mentioned above, the bench cut method is selected as the excavation scheme for east Mao Mountain tunnel. Moreover, the displacement, the maximal principal stress and plastic zone of surrounding rock are simulated as well as the former analysis.

The stress distribution and deformation characteristics of typical cross section can be summarized as following:

- The vertical displacement of surrounding rock using bench cut method for big-span tunnel primarily occurs at crown and invert area. The horizontal displacement on sidewall is very small.
- The maximal principal stress of surrounding rock is mainly compressive stress. The tension stress occurs at arch crown, invert area and near ground surface. But tension stress is small except near ground surface, where tension stress reaches 0.11 MPa.
- The plastic failure of surrounding rock is shear failure and no tension failure. Biggish plastic zone takes place at the intersection between invert and sidewall, sidewall and arch crown. The maximal depth of plastic zone is approximately 2.5 m. The length of rock bolts is 3.5 m for initial support. The plastic zone doesn't exceed the reinforced range of rock bolts, so the initial support design scheme is reasonable.

Above analysis indicate that surrounding rock is stable and the bench cut excavation is reasonable construction scheme for the east Mao mountain tunnel.

5 CONSTRUCTION TEST OF EXCAVATION SCHEME

During the process of excavation and support workings, the continuous field stress and deformation monitoring are conducted. The measurement data show that the maximal settlement of arch crown is approximately 5 mm, which is less than the simulation value. That is because of the installation of monitoring points was slightly delayed. Generally speaking, the monitoring data accord with the results of theoretical calculation. It indicates that the surrounding rock of east Mao Mountain tunnel is stable and the selected construction scheme is reasonable.

6 CONCLUSIONS

The three-dimensional numerical simulation shows that different excavation schemes have significant impact on tunnel stability and deformation. So the optimal construction scheme should be selected before construction, especially for poor rock conditions.

In the case studied for the east Mao Mountain tunnel, the bench cut method is a better scheme than CRD method, as the former takes a much shorter time to complete the opening and the initial support may be properly decreased. The numerical results also accord well with the field results. It is hoped that this case study will provide a good reference for the design and construction of similar tunnel engineering projects.

REFERENCES

Hu X.B. & Qiao Y.Y. 2005. Numerical analysis of construction method for partial press double-arch tunnel [J]. Chinese Journal of Underground Space and Engineering. 1(3) 374–378

Jiang S.P. & Hu X.B. 2004. The numerical analysis of constructional mechanical responses of Yangzong tunnel [J]. Chinese Journal of Geotechnical Engineering. 26(2) 178–182

Wang Y.F. et al. 2005. Study on the mechanical properties of four-lanes tunnel during the construction [J]. Journal of Highway and Transportation Research and Development, 22(6) 134–137

Wu B. et al. 2005. Mechanical simulation and analysis of construction behavior of urban metro tunneling with small interval [J]. China Journal of Highway and Transport. 18(3) 84–89

Underground Space – the 4th Dimension of Metropolises – Barták, Hrdina, Romancov & Zlámal (eds)
© 2007 Taylor & Francis Group, London, ISBN 978-0-415-40807-3

Introductory tunnel design – Lining types and selection: A case history of large span soft ground tunnel design

B.F. Townsend
Hatch Mott MacDonald, LLC

C.R. Speers
Arcus Gbb

ABSTRACT: This paper presents a general design methodology for linings. *Inter alia* it discusses typical lining types and functions and factors governing the selection of a lining, geometrical considerations, ground and groundwater considerations, loadings acting on linings, lining-ground strength-stiffness interaction, allowable working stresses, factors of safety, load factors, etc, and presents strength design and serviceability design approaches. A case study is presented in the form of the design of a final lining for a large diameter railway tunnels, excavated in extremely saturated weak ground using sequential excavation and support methods.

1 INTRODUCTION

This is the second in a series of papers addressing practical tunnel lining design. The format for this and future papers is to present a particular topic and support the presentation of the guidelines by the practical application of a case history. The primary intent is to provide guidelines for the geotechnical and structural design of tunnels where the tunnel size and/or ground conditions dictates that systematic support of the excavation is required following each increment of excavation. This method of tunneling is commonly referred to as Sequential Excavation and Support (SES) and is also commonly termed the New Austrian Tunneling Method (NATM).

The authors developed the design guidelines from experience gained over the past two decades during the design and construction of several major railway, highway and water-transfer tunnel projects in Africa and Asia. During this time it has been possible to compare the performance of the as-constructed structures to the predicted performance as given by the design process. Excavation was typically carried out in widely varying ground conditions (weak-bedded rock, jointed hard rock, and soil-like poorly cemented rock with groundwater). It is therefore intended that the design guidelines could be applied, in general terms at least, to any tunnel excavated in any ground mass condition with any ground material type (hard rock, soft rock, bedded rock, soft ground, and soil) with or without ground water.

This paper is a continuation of the introductory paper that defines the scope and a brief outline of the design issues that are required for lining selection and may be presented in detail in later papers.

A tunnel is a relatively long horizontal or near horizontal opening located below ground surface (underground), typically for the purpose of transportation of one form or another, for example, of water, sewerage, utilities, road or rail traffic. The construction of a tunnel is in most cases carried out by underground excavation that commences at one or more tunnel entrances termed portals. This type of tunnel is often referred to as a "mined tunnel". In some cases, normally in low cover areas such as less than 15 meters, and as an example close to the portals, the tunnel is constructed in open cut and then backfilled to restore the original ground line as close as possible. This type of tunnel is called a "cut-and-cover tunnel". The content of this paper is focused on mined tunnels and lining requirements.

2 GENERAL

The mining of an underground opening introduces a new stress boundary condition in the ground in that the ground stresses are significantly changed along and adjacent to the boundary of the opening. The normal and shear stresses on the boundary reduce from their original pre-construction *in-situ* values to zero. In the ground immediately inside from the excavation

boundary the stress at right angles to the excavation boundary is also reduced to zero but the stress tangential to excavation boundary increases considerably to a value that typically depends on the ratio of the original vertical and horizontal stresses at that point in the ground. For example, if the original vertical and horizontal stresses were equal, the induced tangential stress in the ground will be twice the original stress. However, if the original horizontal stress was twice that of the vertical stress (for example, in over-consolidated sediments), the induced tangential stress will be five times that of the original vertical stress. These stresses are given by equations originally derived by Kirsch (1858) and are based on the assumption that the ground material is perfectly homogeneous, isotropic, linearly elastic with an infinite strength in both compression and tension.

In most cases the ground material will not act in this manner due to the following two factors:

(1) the ground is not homogenous, isotropic and elastic but rather contains incipient planes of potential weakness, in the form of bedding planes and geologically-induced fractures caused by cooling of rock, shrinkage of soil, etc (normally called "joints"), fault zones, shear zones, etc; and
(2) the intact material itself (that is the material between the joints) has a limited strength.

Depending on the original stresses in the ground relative to the respective strengths of the intact material and joints, two typical types of failure of the ground can be expected:

(3) shear or tensile failure of the intact material; and
(4) shear or tensile failure on the joints.

The combined action of the intact material and the joints determines the ground mass behavior, which is typically non-linear, resulting in an inward displacement, commonly termed "convergence", of the tunnel boundary that will continue with time until a collapse of part or all of the ground around the opening will occur.

In order to prevent such potential failure the opening boundary requires that it be supported. The support, which can vary greatly, depending on the ground or rock mass strength relative to the induced ground stresses and other loads, from light support comprising for example nominal "spot" or "random" widely spaced ground bolts, to a medium lining comprising reinforced shotcrete, to heavy support comprising for example heavily reinforced concrete, prestressed concrete or steel. The applied support may be termed as "tunnel lining" or simply "lining". Notwithstanding its support function, a lining can often be used for non-structural reasons, for example for hydraulic reasons, etc.

3 LINING TYPES FUNCTION AND SELECTION

Tunnel linings may be classified in a number of ways, for example as follows:

- In terms of the lining function
- In terms of permanency (temporary or permanent)
- In terms of timing of their application in relation to excavation phase
- In terms of the lining material
- In terms of load bearing capacity
- In terms of durability

No matter how the lining is termed, each of all conditions must be evaluated in relation to not only each above mentioned requirement but in terms of cost, schedule and constructability.

Tunnel lining types usually considered are typically constructed from the following:

- Cast-in-Place Unreinforced Concrete
- Cast-in-Place Reinforced Concrete
- Spayed Shotcrete (w/ or w/o Steel Fibres)
- Precast Reinforced Concrete Segments
- Steel Liner Plate
- Spheroidal Graphite Iron Segments

Combinations of these types of linins are possible and sometimes required based on project design and in-situ conditions.

3.1 *Lining function*

The type of tunnel to be designed and constructed often defines the requirements. Generally there are five (5) types of tunnels and each category generally has its' own specific requirements for functionality. The most common types of civil works tunnels are:

- Road Tunnels
- Railway Tunnels (Mass Transit, Commuter, Freight, High Speed)
- Hydraulic Tunnels (Water, Wastewater, Storm Water, Head/Tail Race)
- Utility Tunnels
- Pedestrian Tunnels

Each of the above tunnels generally require a clear statement of performance requirements regarding but not limited to the following:

- Tunnel cross-section(s) (twin bores versus single bores)
- Tunnel Orientation
- Alignment (horizontal and vertical)
- Portal Locations
- Structure gauge/size
- Water Tightness / Leakage
- Ventilation/Purging
- Drainage

- Design Life
- Durability
- Lighting
- Power
- Aerodynamics
- Noise
- Vibration

As described above, a lining is normally required to provide support to the surrounding ground, i.e. it must carry the ground loadings and provide sufficient pressure to the ground to prevent ongoing convergence ultimately leading to rupture of the ground and fall of ground into the opening.

However, in many cases, the lining may be primarily required for reasons other than that of support of ground. For example, in water transfer tunnels, a final concrete lining is often specified for hydraulic reasons to reduce friction losses, for durability reasons (loss of the ground through the ongoing action of the water), or to prevent water leakage into the surrounding ground.

A careful definition of a lining's function/functions is required before a selection of the lining type is made.

3.2 *Geometry requirements*

Once the "User" defined requirements identified, there are always select issues which need to be accounted for in the design which will adequately allow sufficient space to construct the final tunnel structure following the excavation and support phase for SES/NATM type of tunnels.

There are several major design decisions which must be identified and resolved prior to the excavation phases such as:

- Pressure Design Requirements (if not environmentally required)
- Allowance for Outer lining Installation and Deformations
- User Requirements such as:
  - Ventilation Requirements
  - Alignment Constraints
  - Water Tightness Criteria
  - Emergency Egress & Niches/Laybys
- Constructability Requirements for Excavation and Lining Installation

It is extremely important that there is a complete and full understanding of how these issues relate to the determination of the tunnel excavation opening size. Once a tunnel excavation is underway, it is very difficult and costly to have to increase the size of the existing opening as a result of a design errors or omissions.

3.3 *Lining permanency*

A lining can be temporary or permanent depending on a number of factors such as the excavation method, lining type and timing of installation in relation to the excavation phase, costs, etc. For example, in a rock tunnel excavation using drill and blast or in soft ground tunnel excavation using sequential excavation-support methods, the largest cost of the completed tunnel is that of the excavation phase. In order to minimize this cost it is important that the tunneling advance rate be as fast as possible subject to proper effective stabilization of the tunnel being implemented. For this reason relatively rapidly applied lining methods that provide minimum initial support are used. These would vary from light bolting in strong rocks with widely spaced joints or highly cemented hard to stiff ground, to medium bolting with shotcrete in weaker rocks/round mass, to lattice girders or steel arches covered with thick mesh-reinforced shotcrete and closely spaced dowels in soft ground open face tunneling without a shield. Following completion of the excavation and installation of the initial support, which is often referred to as the "outer lining", typically a second lining is added for reasons of permanency in terms of durability, seepage, etc. In this case the outer lining is often designed using a lower factor of safety, subject to the correct use of monitoring to confirm ground stabilization and ensure tunnel safety and then the final lining is designed according to standard norms of structural practice. This method of tunnel lining construction is often referred to as a "two pass" lining system.

It is also possible to provide a permanent lining immediately following excavation, i.e. a "single pass" lining system is used, if a tunnel-boring machine ("TBM") is used or selection of precast elements are to be used for typical SES/NATM methods.

For a TBM excavated drive, this construction method consists of erecting rings of reinforced pre-cast concrete segments from within a double shield type machine. Provided the segments are properly backfilled with grout or pea gravel at a suitable distance behind the shield and provided with gaskets, if waterproofing is a design issue. The installed rings can serve the dual function of initial stabilization of the ground and final permanent lining.

The choice of this type of lining is dictated by the choice of the tunnel excavation method using a TBM, which in turn is often dictated by other factors. For example, the use a tunnel boring machines in relatively large size and short tunnels in good ground is not economical, but in relatively small and long tunnels in the same ground or in saturated soft ground, it could be a viable method of tunnel construction. Another example might be in urban tunneling where drill-blast may not be permitted or where the groundwater table may not be lowered. In these cases, a tunnel-boring machine may be the most desirable method of construction the tunnel. This is the extent of discussion on TBM driven tunnels as this is considered a separate topic.

However, precast segmental liners are not only used with TBM driven tunnels. These liners often constructed from Spheroidal Graphite Iron (SGI), steel liner plate or precast concrete segments may be used in smaller drives or complex arrangements where special openings or alignment curvatures are required.

3.4 *Lining application timing*

A lining applied at or close to the excavation face has been referred to in a number of ways, for example "initial support", "primary support", "outer lining", etc. The term "initial support" is the preferred terminology; as it leaves no uncertainty about its main role, initial stabilization of the opening. Depending on how effective this initial support proves in meeting its main requirement, there is an opportunity to add additional support further behind the excavation face. The term "primary support" is not recommended as it could be construed to mean that it is the most important part of the final completed tunnel lining and that may not be the case depending on the requirements of the tunnel and the permanency of the initial lining.

In two-pass linings systems the second lining is often referred to as a "secondary" lining, as it is placed as a second lining, or as an "inner lining", as it is placed inside the initial lining. If the initial lining is discarded as part of completed tunnel lining, the second lining is often referred to as a "final lining". Terminology is often project related, but it is important to understand the primary roles of each lining type and the following is recommended:

- The "initial lining" must stabilize the opening (limit all ground movements) and provide safety and security, which must be confirmed by ongoing tunnel convergence monitoring. Depending on the design of the initial lining with respect to stresses, deflections and durability, the initial lining may or may not form part of the completed tunnel final lining system.
- The "final lining", whether it incorporates the initial lining or not must provide the permanent support of the tunnel against all applied loads.

It is typically permitted to assume that the outer lining, unless located in an aggressive water environment, could support part of the ground load, depending on the relative stiffness. In the event that the initial lining is used as part of the final lining the following rule is a good starting point for the determination of load bearing capacity allocated to each lining type.

Shear interaction should not be considered unless special provisions have been made for shear transfer from the outer lining to the inner lining. However, generally the benefits of ground support from the outer lining are ignored in designs due to the small contribution to overall lining stiffness. The following is a recommended distribution of stiffness between the inner and outer linings if the outer lining is to be used to support part of the total ground load.

$$EI_{\text{shotcrete lining}} + EI_{\text{inner lining}} = EI_{\text{total}}$$

$$P_{\text{ground}} \times \left(EI_{\text{shotcrete lining}} / EI_{\text{total}}\right) = P_{\text{shotcrete lining}}$$

$$P_{\text{ground}} \times \left(EI_{\text{inner lining}} / EI_{\text{total}}\right) = P_{\text{inner lining}}$$

where:

- $EI_{\text{shotcrete lining}}$ is flexure stiffness of shotcrete lining
- $EI_{\text{inner lining}}$ is flexure stiffness of inner lining
- EI_{total} is flexure stiffness of shotcrete lining + inner lining
- P_{ground} is the total ground load
- $P_{\text{shotcrete lining}}$ is part of the ground load acting on the shotcrete lining
- $P_{\text{inner lining}}$ is part of the ground load acting on the inner lining.

3.5 *Lining materials*

Typically, when a two-pass lining system is used, initial linings comprise various combinations of support elements that can be installed rapidly, such as shotcrete, rock bolts, ground dowels, etc, so that the cycle time can be minimized and thus the tunneling advance rate maximized. In this case, final linings would be cast-in-place concrete, with or without steel reinforcement, depending on whether tensile strains are induced by the applied loads; post-stressed concrete; or steel linings.

Typically, when a one-pass lining system is used, the lining would comprise bolted pre-cast segmental linings placed within a shield near the tunnel face followed by grouting of the annulus at a short distance behind the erection area.

4 SELECTION OF FINAL PERMANENT TUNNEL LININGS

4.1 *Geometric considerations*

In terms of lining design and tunnel stability the best shape for a lining is circular as it is the best shape structurally and minimum, if any, bending moments and thus shear forces would be induced by the applied loads. However, in many tunnel cases, the final lining is not fully circular, often for reasons relating to the excavation phase and economy. For example in traditional drill-blast excavation of a rock tunnel or sequential-support excavation of a soft ground tunnel, the tunnel invert is often made flat or near flat to facilitate rapid mucking out of the excavated material and thus maximize the tunneling advance rate.

In these cases the final lining would be non-circular over the invert section of the lining and often, depending on the applied loads, steel reinforcement may be required in the cast-in-place concrete for strength.

For high loads the geometry may be used to limit bending moments in the liner and to increase axial thrust which would be considered beneficial to the liner design.

4.2 *Ground and groundwater considerations*

Fundamentally, as described earlier, the main reason for a lining is to provide long-term stabilization to the excavated perimeter. Thus, the weaker the ground relative to the stresses induced by the excavation, the higher the ground loadings acting on the lining will be. Conversely, in competent ground the structural demand on the installed lining would be lower than in weaker ground.

In cases where there is a high groundwater table, the final lining can be required to perform in one of two possible ways; firstly as an undrained tunnel whereby the lining must be able to resist the maximum possible groundwater that could act on the back face of the lining; and secondly as a drained tunnel whereby pressure relief is provided such that no adverse groundwater pressures can develop on the lining back face. The latter implies that a residual pressure may act on the tunnel lining even when designed as a drained tunnel.

The development of groundwater pressure with time is dependent on factors such as the rate of recharge of the ground and the permeability of the ground. For example, in poorly consolidated sand-like sediments such as in the western coastal plain of Taiwan, the void ratio of the sediments is typically 0.5 and thus the permeability of the ground is relatively high. With sequential-support excavations the driving of the tunnel typically requires that the groundwater table be lowered ahead of the tunnel face. After completion of the tunnel drive and final lining installation, the groundwater would tend to recover to its original elevation in the case of a fully undrained tunnel. On the other hand in highly consolidated hard mudstone in the Karoo Sequence in Southern Africa the ground permeability is so low that the tunneling may not materially affect the groundwater table. Nevertheless, with time after completion of the tunnel final lining, groundwater pressure may develop on the back face of the lining.

5 CONCLUSION

Further issues regarding individual lining types will be presented in later papers. However this paper is provided to present the basic issues and option related to tunnel lining selection and design. The are many issues regarding ground loading and groundwater drainage requirements that will influence how the liner is required to perform. Among issues to be discussed in future papers is the selection of appropriate load factors to e used in ultimate strength design of reinforced concrete liners as well as the liner stiffness and the development of tunnel liner load.

However, this paper has presented in introduction to liner selection and the factors and use of terminology that need to be considered in the tunnel design process.

This page intentionally left blank

Underground Space – the 4th Dimension of Metropolises – Barták, Hrdina, Romancov & Zlámal (eds)
© 2007 Taylor & Francis Group, London, ISBN 978-0-415-40807-3

Effectiveness of zonal ground mass pre-stressing round an opening at grouting

K. Vojtasik & J. Aldorf
VŠB–Technical University of Ostrava, Ostrava, The Czech Republic

ABSTRACT: The ground changes due grouting find out their impact not only on the area touched just by grouting material but go beyond penetrated area. The explanation of the outside impacts resides in the volumetric expansion getting on penetrated ground. Non penetrated ground is subdued to compaction and state strain-stress is altered too (pre-stressing). The article reports knowledge regarding the quantitative and qualitative state strain-stress changes beyond penetrated area and what next circumstances of grouting technology are working essentially upon these changes. The findings are benefited finally to boost ground stability round an opening.

1 INTRODUCTION

The modification of ground became a routine practice to pass over the unfavourable circumstances have been met in geotechnical constructions such as insufficient strength-strain properties of ground, permeability and so on.

The grouting of ground is classified as one of the major method that has branched out to many mutations to cope with the operative objectives and nature of the ground conditions.

The fundamental idea of grouting is in favour of ground which is mostly faulted and split in particles with free voids (pores, fissures) in the between of them. The voids are not just cause of ground weakens but a likely track of grouting medium to flow through. In this manner a grouting medium simply penetrates the ground, fills voids in. After mediums hardening ground gets for new qualities. A cohesionless soil aggregates and becomes cohesive, a low strength-strain properties of weak rock intensifies and a faulted rock mass turns up to a continuous unit. The water permeability of ground decreases in proportion to the degree of void saturation with grouting medium. The ground is penetrated with a grouting medium in first hand and this area and their changes in it noted above are usually taken into account as a tangible result we wish to achieve.

The grouting of the ground is very much complex process featured of a few phenomena such as flow progression of grouting medium through ground voids. The velocity, pressure, operating period, pumped volume of grouting medium as well as material transformation change from liquid to solid state of grouting material are significant constituents not being involved satisfyingly into account. They strike not only the penetrated area but they are essential on changes of condition round penetrated area.

The article pursues the grouting volume increase effect occurring in penetrated area on the adjoined non penetrated ground. There are also envisaged the ways to put to use the detected findings within the field of underground constructions.

2 PROBLEM ANALYSIS

2.1 *Fundamentals*

The pre-stressing of the ground by means of the grouting is executable only in grounds being apt to absorb uniformly grouting medium around a source of the grouting medium (grouting borehole). As representatives of these may be shown cohesionless porous soil, backfill, crushed hard rock. The component unit of these grounds may be found in softened state. The forces and stress-strains on boundary points and planes between the units of ground are relaxed. A ground in such state is prone to collapse as it comes on when circumstances are fit to. This unfavourable state of ground its low shear-strength and strain parameters are changeable. They all can be raised up and preserved in the end embodying measurements which are capable to bring about change in stress-strain state of the boundary points and planes between the units of ground. The ground units lock tightly in and compact those in also.

The grouting technology seems to be a tool to achieve the wanted change of a softened ground in its stress-strain state and compaction.

The pre-stressing of ground is based on grouting technology. It supposed to run grouting in several steps and on different grouting regimes.

The first grouting step has to set up the area of a regular circular shape penetrated by a grouting medium filling up voids around a grouting borehole. The units of ground should be glued partly within this area. After the first step there is made a new structure body in the ground. This body is bounded and detached sharply by the boundary line from the rest of ground. It differs from those part of ground non touched by grouting material in the manner it will act in the second grouting step.

The second grouting step is intended to star up increasing volume of grouted area. The pressure of grouting material fed in this step dilates cracks and the partly glued ground units shift in the flow direction of grouting medium.

The pre-stressing shift impulse comes into being on the boundary line and it goes from here over to the non penetrated units of ground. The ground units behind the boundary line close to this one are compacted. The ground units lying far-away the boundary line are only press together (pre-stressed) more intensively than they were before. The same effect of pre-stressing is in progress also in the compacted zone. The enhancement of stress-strain parameters of ground is due the compaction and the value increment of the normal stress on the contacts between the ground units. The pre-stressing is more significant than the compaction for being throughout the ground around penetrated area and spreading more deeply the ground than the compaction.

2.2 *Ground pre-stressing analysis*

A ground behavior under circumstances of pre-stressing has been neither investigate in detail yet nor sufficiently clarified and also it fails any quantitative findings at all.

The pre-stressing of ground is a complex process conditioned by many factors. Generally the factors split in two substantial groups regarding the possibilities to handle them.

The first group encompasses the conditions met in ground. They have to be identified and next evaluated reliably. Any lapse made in this group brings about the unavoidable failing in operation. The learned facts have to be taken into account and a it can't then change subjectively in any significant manner.

The second group takes the wide spectrum of grouting technology aspects in. Each of them can be modified to get the best outputs.

The following topics have a decisive signification for pre-stressing of ground.

– Grouting medium. Two various grouting mediums in each step of pre-stressing grouting operation are supposed to be used. In the first step the grouting medium has to penetrate uniformly the ground and fill all its voids in. A regular cylindrical or conic solid body should be made in ground. The volume of grouted area doesn't grow in this step. The second grouting step has to start before the first step grouting medium solidifies and cements a ground units together firmly. It has to cause a volume expansion and to hold grouting pressure till it hardens. It effects only the penetrated area at first step.
– Parameters of grouting procedure. Alike the grouting mediums there are two different regimes to put grouting medium to ground considering the medium's qualities and the performance they have to do. The grouting pressure for both grouting steps is governed by hydraulic features of ground and mediums. In the second step grouting pressure takes extra into the account the desired value of pre-stressing.
– Design of grouted area and attained value of pre-stressing. The design of pre-stressing compounds the above discussed factors within the context of looking for an accord between them with respect to intensify a ground quality. There are several issues to be thought out as the size of ground penetrated area the impact radius of efficacious pre-stressing in ground and the value of attained change at ground. Beaten track to start surveying such issues is mathematical modeling. The following paper section shows a few outputs detailing the last reported issues.

3 MATHEMATICAL MODEL

A survey on some essential pre-stressing phenomena was carried out by 2D FEM model (PHASE2D) see figure 1. The situation contains the basic objects taking part in pre-stressing. They are borehole, grouted area, plain ground, forked cracks put in the grouted area. Other necessary conditions are chosen the simplest. The zero primary strain state, isotropic elastic material represents both the ground and penetrated ground, values of elastic modulus are related by multiplier. The start value of ground elastic modulus equals 100 MPa. The pressure of grouting medium with inside the cracks is in keeping with real grouting pressure values and it equals 10 MPa. The grouted area extends from borehole to distance of 0.3 m deep into ground. The model calculates only the second step referring to the pre-stressing volume expansion.

4 MODEL CALCULATION RESULTS

The diagrams presented in figures below summarize results of the parametric calculation aimed to

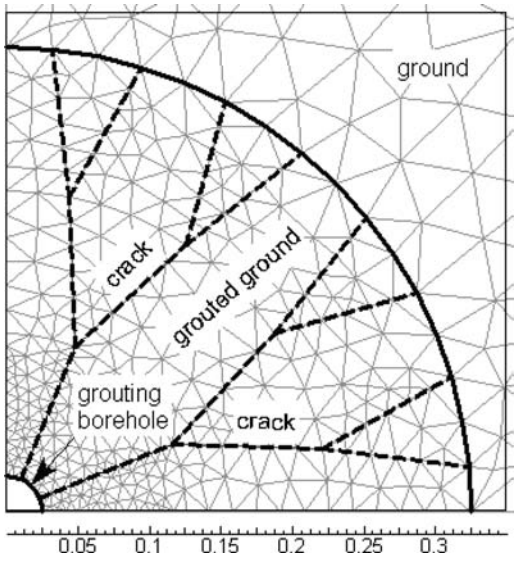


Figure 1. The analysis model – detail showing the concept of a mathematical simulation of a volume change at the grouted area.

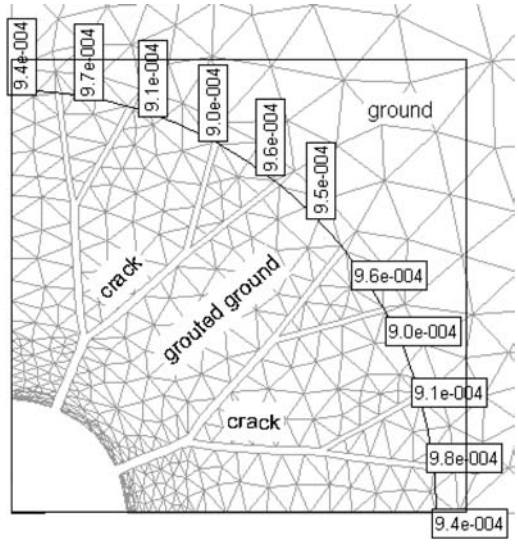


Figure 2. The displacements on boundary line between the grouted ground area and non grouted ground [m].

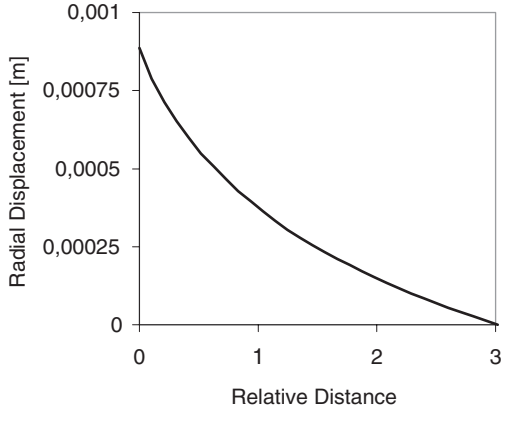


Figure 3. Radial displacement in non penetrated area. (Note: Relative Distance = Real Distance/Thickness of penetrated ground area; Thickness of penetrated ground area equals 0,3 m).

investigate the development of impacts of ground pre-stressing. Especially an accent is put on the ground movements at grouted area boundary line and on the dependence of ground movement off penetrated area. Analogously to ground movement attention is paid to ground stress changes on the identical areas. The insight into both dependencies is significant to pre-stressing feasibility evaluation.

The figure 2 displays the values of displacements on boundary line between the grouted ground area and non grouted ground.

Graph at figure 3 tracks development of displacement in non penetrated ground in radial direction starting at boundary line.

Development of radial and circumferential stresses on the identical line as previous dependency is brought in figure 4.

5 IMPLEMENTATION

The employment of ground pre-stressing in underground construction practice illustrates figure 5. The ground surrounding the underground opening is usually grouted continually to form a shall stabilizing the hanging wall. Implementation of the pre-stressing doesn't necessitate a continually grouted area to achieve the stabilizing effect. The ground is grouted in discrete areas and the space between them is pre-stressed. The stabilizing effect intensifies if the penetrated area is deeply fixed by the bolts or cables. The conical shape of penetrated area seems to be better than cylindrical as the pre-stressing effects are heading into the hanging wall opposite the destabilizing forces. The effects of cylindrical shape follow the tangential direction to the opening line.

6 CONCLUSION

The achieved appealing results allow to draw some principal conclusions.

– the softened ground seems to be capable to be pre-stressed by means of grouting technology

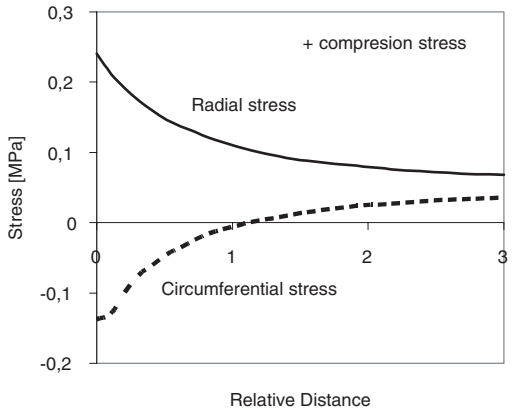


Figure 4. Radial and Circumferential stresses in non penetrated area.

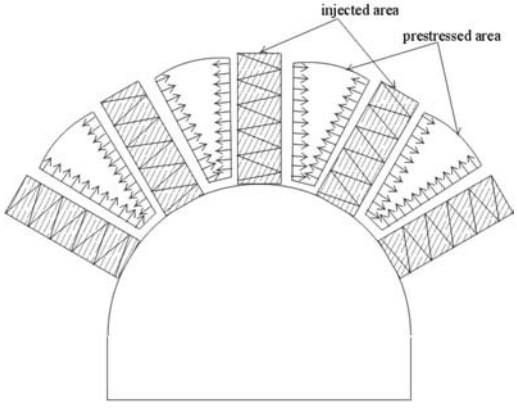


Figure 5. The implementation of ground pre-stressing to stabilizing the hanging wall of an excavation.

- the fundamental cause for pre-stressing of ground by means of grouting technology is volume expansion at grouted area.
- in non penetrated ground area the ground units may be compacted at section in which the circumferential stress causes tension (fig. 4).
- all over the non penetrated ground area the increment of radial stress causes the pre-stressing. Intensity of pre-stressing wanes gradually in dependency of distance form boundary line of penetrated ground (fig. 3).
- an intensity of ground pre-stressing depends on the value of the grouting pressure.
- an intensity of ground pre-stressing depends as well upon the ratio of elasticity modulus ($E_{grouted\ ground}/E_{ground}$). The higher it is this ratio the more intensive it is the pre-stressing of ground. The value of this ratio doesn't extend significantly the intensively pre-stressed area.
- an extend of intensively pre-stressed area is proportional just only to a value of thickness of penetrated ground area.
- an extend of intensively pre-stressed area intensifies due to conjunction effect when the pre-stressed areas overlap. There are three lay-outs to place the grouted areas each other in. A triangle, square and hexagon lay-out.
- tracking the curves on figures 3 and 4 showing the development of displacement a stresses it can be established the value of effective distance between the two neighboring grouted areas. The distance seems to be the double of the thickness of penetrated ground area. This distance guarantees the pre-stressing efficiency in the ground.
- a quantitative evaluation of ground pre-stressing isn't possible to achieve only on model calculation now owing to problem complexity.
- the ground pre-stressing is applicable in geotechnical practice. Its effects is necessary to assess first of all following the monitored values on real situation and subsequently to use them in model calculation as inputs data (back analysis).
- the pre-stressing was applied to stabilizing a mining drift traversing heavily faulted shift area.

ACKNOWLEDGEMENTS

This paper is part of a research program provided by Czech Grant Agency under No. GACR 105/05/2712 "Construction of shallow galleries in territories affected by mining activities". The authors greatly appreciated this support.

REFERENCES

Vojtasik, K. 2000. Research on the methods of partial prestressed strengthening of a solid rock in the surroundings of underground works as means of optimizing the support loading. *The final report of the grant project No. 103/99/1495 of the Czech Grant Agency, Ostrava, December 2000.*

Vojtasik, K., Aldorf, J., Hrubesova, E., Lahuta, H. & Durove, J. 2000. A method of partial rock mass pre-stressing in the surrounding of the underground excavations as the means of its stability improvement. *International conference "Underground construction 2000"; Proc. intern. conf., Cracow, 25–27 September 2000: 624–631.* Krakow Wydavnictwa AGH.

Underground Space – the 4th Dimension of Metropolises – Barták, Hrdina, Romancov & Zlámal (eds)
© 2007 Taylor & Francis Group, London, ISBN 978-0-415-40807-3

Geotechnical model for pipe roof supports in tunneling

G.M. Volkmann
ALWAG Tunnelausbau GesmbH, Austria

W. Schubert
Graz University of Technology, Institute for Rock Mechanics and Tunneling, Austria

ABSTRACT: Pipe Roof Support systems have increasingly been used in weak ground tunneling although the design is often based solely on experience. The results of an intensive measurement campaign, including settlement measurements ahead of the face, were used to determine a geotechnical model for this pre-support system. The measured ground-support interaction was reproduced utilizing three-dimensional numerical calculations with FLAC-3D. This study confirmed the model created by the in situ data and clarified the influence of the design parameters on both the support effect and the ability to control displacements. This enables a more informed decision in the design stage on whether a Pipe Roof System or more cost- and time-consuming support systems must be used to guarantee the project requirements during construction.

1 INTRODUCTION

The increasing population in metropolitan areas requires a concomitant upgrade of the infrastructure. The majority of the infrastructure is subterranean, especially in congested urban areas. Due to the pre-existing structures on the surface, the construction of new projects is subject to specific restrictions such as subsidence and/or noise limitations during construction. In urban areas, the ground generally consists of sedimentary soil and/or highly weathered rock mass. Both types of ground are prone to major displacements during tunneling. These settlements control the entire design process due to the project limitations, as compliance with the design requirements may demand additional support systems including ground freezing, jet grouted columns or pipe jacking, which are time and cost intensive.

An alternative support system is the "Pipe Roof Umbrella" System, which is also referred to in literature as "Steel Pipe Umbrella" (Oreste & Peila 1998), "Umbrella Arch Method" (Kim et al. 1996), "Pipe Fore-Pole Umbrella" (Hoek, 2003), "Long-Span Steel Pipe Fore-Piling" (Miura, 2003) or "Steel Pipe Canopy" (Gibbs et al. 2002). Compared to this system the previously mentioned pre-support systems are stiffer but pipe roof systems are less time and cost intensive. These facts have led to an increase in the use of the pipe roof method without an accompanying increase in the knowledge about the ground support interaction associated with this system.

Inclinometer chains, installed parallel to the pipe roof support, were used to perform in situ measurements in order to obtain a better understanding of this support system. The measurements of the inclinometer chain were linked to the geodetical displacement measurements taken inside the tunnel and on the surface. These measurements observe the longitudinal distribution as well as the magnitudes of settlements in the crown level of the tunnel (Volkmann et al. 2003). The outcome was a geotechnical model for pipe roof systems.

Additional laboratory investigations were performed on the ground and the pipes in order to obtain their strength- and stiffness parameters. Both the geotechnical model and the parameters, describing the behavior of the applied materials, were used for the numerical investigations.

2 TYPES AND DEFINITIONS

The pipe umbrella system is one among the group of pre-support systems. The terminology for pre-support systems is not clearly defined and in order to avoid confusion with other systems a brief description is given below.

The aforementioned terms are simply descriptions of the system itself. Steel pipes, and sometimes fiberglass pipes, are installed from the actual tunnel face to the front (fore-poling system) in an umbrella or canopy shape around the area to be excavated (Figure 1).



Figure 1. West portal of the Birgl tunnel (AUSTRIA) supported by a pipe roof.

The diameter of the steel pipes is usually between 60 mm and 200 mm with a wall thickness of 4 mm to 8 mm. The length of one umbrella is generally 12 m or 15 m. The excavated length underneath (length of a pipe roof field) ranges from 6 m to 12 m. When the end of a pipe roof field is reached, there is still a part of the pipe remaining in the ground ahead of the face. This length is called the "overlapping length" of the pipe roof system.

3 SYSTEM BEHAVIOR

The observation and the interpretation of movements caused by tunneling is one of the principles when using the New Austrian Tunneling Method (NATM) (Rabcewicz 1944, Rabcewicz 1975). The observations and their interpretation are used to control the ground support interaction. Specific evaluation techniques allow the prediction of changes in the ground conditions in front of the face (Steindorfer & Schubert 1997). The support system is continuously adapted to the actual ground conditions encountered during tunneling, leading to economical construction progress. This is possible as the measurements represent the ground-support interaction and not the ground or the support reaction separately. The observed interaction is commonly referred to as System Behavior (Goricki 2003, ÖGG 2001).

The main issue with developing the geotechnical model for pre-support systems is that the geodetical survey only measures the system behavior in the already supported section of a tunnel, while the pre-support systems primarily influences the system behavior ahead of the supported tunnel. The observation of the system behavior, influenced by a pipe roof system, was enabled by performing measurements

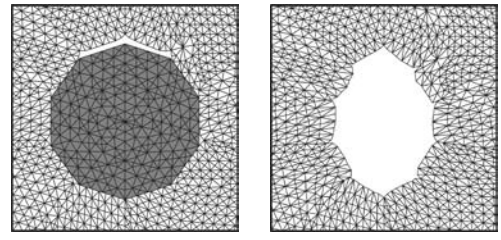


Figure 2. Result of a numerical study in UDEC on the deformation characteristic of the cased drilling system (left) and the pre-drilling system (right) (Volkmann & Schubert 2006).

with horizontal inclinometer chains, installed in the tunnel crown.

4 MEASURED BEHAVIOR

4.1 *Installation*

Conventional drill jumbos or special machines can be used to install the pipes. From the geotechnical point of view, there are two different methods for the installation: the pre-drilling system and the cased-drilling system. The significant difference is, when using the cased-drilling system the pipe follows directly behind the drilling bit providing immediate support for the installation hole. When using a pre-drilling system, the hole for the installation is drilled first and in a second step, the pipe is installed in the unsupported hole. In weak ground a pre-drilling system carries a higher risk for settlements than a cased-drilling system (Figure 2) (Volkmann 2004).

In weaker ground the stress transfer related to the drilling of the installation holes may cause the closure of the annular gap between the ground and the pipes before the excavation under the pipe roof starts. However, this closure does not result in any significant pre-stressing and hence the internal forces of the pipes are still practically zero. The initial loadings are not influenced by the flushing method (water or air) used to remove drill cuttings. However, one must consider that the use of water may result in a decrease in the engineering performance of the ground. Additionally, the fan of pipes operates as a drainage system until the pipes are grouted (Sellner 2005).

4.2 *The first meters*

The space that is needed for the installation of the next pipe roof fan requires a constant widening of the profile during the excavation of a pipe roof field. The new installation generates a ring of shotcrete at the end and/or the beginning of every pipe roof field. During the excavation of the first 1 to 3 rounds after the installation, the inclinometer measurements presented lower

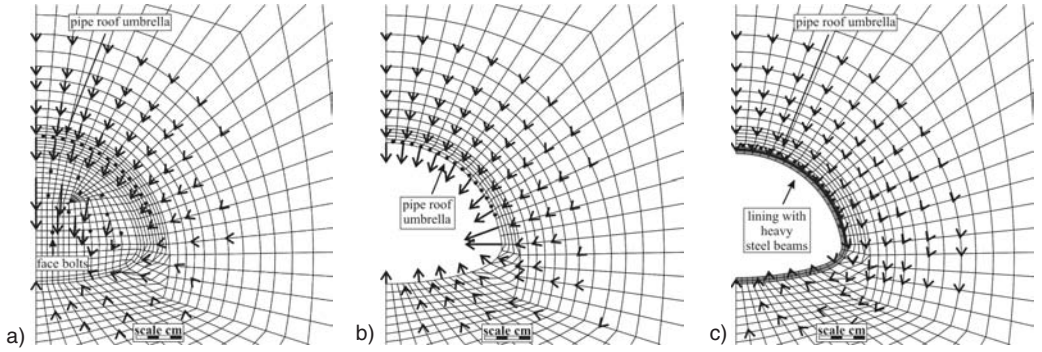


Figure 3. Three cross sections showing the displacement vectors normal to the tunnel axis; (a) 2 m ahead of the face, (b) in the unsupported span, (c) 2 m backwards in the supported section (one excavation round only).

settlement magnitudes. This observation is explained by the stiff shotcrete arch that creates a foundation for the longitudinal arching effect during stress transfer processes.

4.3 *Normal excavation rounds*

The foundation effect of the stiffer shotcrete ring decreases with distance. The data from two case studies show the following rounds of excavation induce a uniform settlement characteristic. This characteristic contains the magnitudes and positions of the measured settlement values relative to the face and the three-dimensional behavior in the already supported sections (Figure 4 for example). It depends on the strength- and stiffness contrasts between the ground and the installed support.

4.4 *Last meters*

Depending on the ground quality and the height of the tunnel, the effectiveness of the pipe roof foundation ahead of the face decreases with decreasing length. This decrease in effectiveness is associated with an increase of the settlements ahead of the face. Therefore, when the pipe roof support system is used to minimize displacements caused by the excavation a new pipe roof should be installed before the foundation effectiveness decreases. When the pipe roof system is only applied to increase the stability of the unsupported span, further rounds may be excavated as long as the stability of the face is guaranteed.

5 BASIC GROUND DISPLACEMENT

The numerical results shown in the Figures 3a, 3b, 3c, and 4 are calculated with the program "Fast Lagrangian Analysis of Continua in three dimensions" (FLAC-3D). Although the Trojane tunnel (Slovenia) was constructed in a slight hillside situation with a few buildings on the surface, the numerical model was created using the assumption that the tunnel was constructed in a topographically flat area. The selected section, with a crown cover of 15 m, was supported by a pipe roof system to help minimize surface displacements within a major fault zone (UCS $\ll$ 1.0 MPa) where distress to surface structures had been observed. The input parameters were determined by laboratory tests (ground, pipes), as well as taken from literature (ground, shotcrete) (Zlender 2003, Aldrian 1991, Müller 2001). Further information on these calculations can be found in Volkmann et al. 2006. The displacements presented in the Figures 3a, 3b, 3c, and 4 result from excavating only one 1.0 m long excavation round.

5.1 *Radial displacements*

The shown cross sections are 2 m ahead of the face (Figure 3a), in the middle of the unsupported span (Figure 3b), and 2 m backwards in the supported section (Figure 3c). All three figures demonstrate that the orientation of the incremental displacement is almost perpendicular to the shape of the tunnel in the area where the pipe roof is installed.

The maximum displacement vector in Figure 3a is about 3.0 cm but is situated in the area to be excavated later. The maximum displacement in the zone where the pipes are installed is 2.1 cm.

The displacement vectors in the unsupported span (Figure 3b) have nearly the same magnitude (2.0 cm) and are practically uniform around the upper section of the tunnel perimeter. The displacements only increase to 3.3 cm in the region below the installed pipes (lower sidewall).

Due to the very stiff support system in the supported section behind the face, the displacements decrease to 0.5 cm only 2.0 m behind the unsupported span (Figure 3c).

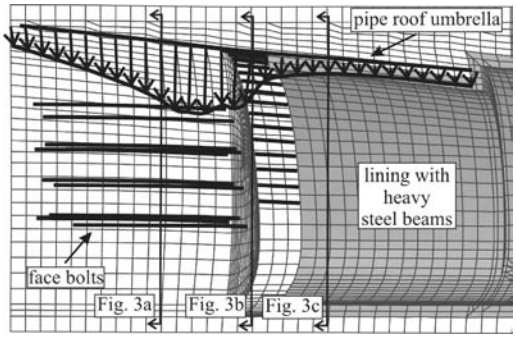


Figure 4. This longitudinal section shows the vertical and longitudinal displacement in the crown (one excavation round only).

5.2 *Distribution of displacements in the longitudinal direction*

Elastic numerical calculations normally result in 30% of the total displacements ahead of the face (Steindorfer 1998). When the stress level is higher than the strength of the ground near the tunnel the displacement distribution changes considerably, resulting in significantly higher displacements ahead of the tunnel face. The strength weakening characteristics of the material associated with the post peak behavior control these changes. This condition agrees with the measured data from the Trojane tunnel where up to 80% of the total displacements occurred ahead of the supported section in the tunnel.

Figure 4 exemplifies a calculated displacement distribution in the longitudinal section. The calculated values increase to 2.5 cm approximately 1.0 m ahead of the face while the displacement vectors in the supported section are lower than 0.5 cm. In the other direction, the settlement values start decreasing with distance.

This example shows that the displacements are orientated against the excavation direction in the sections ahead of the face, except the last 2.0 m ahead of the face. This area moves vertically or slightly in the excavation direction. In the unsupported span and in the first supported meter the displacements are orientated towards the face. The previously supported region again displaces against the excavation.

6 GEOTECHNICAL BEHAVIOR

The internal forces of the pipes are almost zero after the installation, comparable other passive support measures (rock bolts). The stress transfer, due to the previous excavation steps, has an influence on the ground and on the already installed support. The newly installed pipes are not affected by previous activities, whereas every construction process after the installation, that causes a stress transfer, starts to activate the support effect of the pipes. The displacements mainly caused by the excavation process during tunneling so the three-dimensional displacement characteristic control the activation of the support effect after the installation of the pipe roof.

Each pipe is founded in the ground (ahead of the face) as well as on the lining (behind the face) in the longitudinal- and radial direction. The strength and stiffness of the pipe roof therefore depend on both the ground properties as well as on the time dependent strength and stiffness properties of the lining (shotcrete, steel beams).

6.1 *Radial support effect*

Figure 5 presents the calculated result of the ground pipe interaction after every second excavation step. The pipes bend primarily at two positions with ongoing excavation steps under the pipe roof as long as the pipe foundation effectiveness does not decrease ahead of the face. One position in this example is 3 m ahead of the face. The second one is 1 m behind the face. These sections indicate the positions where the pipes operate as support and where the pipes transfer the loads to the ground and the lining. The supported section is between chainage 47 and 50 (for bottom line) while on both ends of this area the loads are transferred to the foundation regions. The position ahead of the face corresponds to the orientation change of the displacements shown in Figure 4. The loads are only transferred in the longitudinal direction and the pipe roof support does not create any arching perpendicular to the tunnel axis. It is therefore necessary to model each pipe individually in the numerical simulation; because in numerical calculations both a stiffer homogenized region as well as the use of shell elements would additionally cause an arch effect perpendicular to the tunnel axis. Both simplifications could lead to an underestimation of the displacements and/or to an overestimation of the stability conditions.

This pipe roof support effect is affected by the bending of the pipes so the second moment of the area defines the activation speed of the support effect by bending. Pipes with a larger diameter activate a more powerful support effect at similar displacements compared to smaller diameters. The pipe wall thickness, on the other hand, defines the critical moment and/or the maximum bending.

This example demonstrates that a pipe roof system supports the face region, the unsupported span, and sometimes a short zone at the beginning of the lining (fast excavation). The support effect decreases in these critical sections the risk against possible local or global failures associated with the tunnel face.

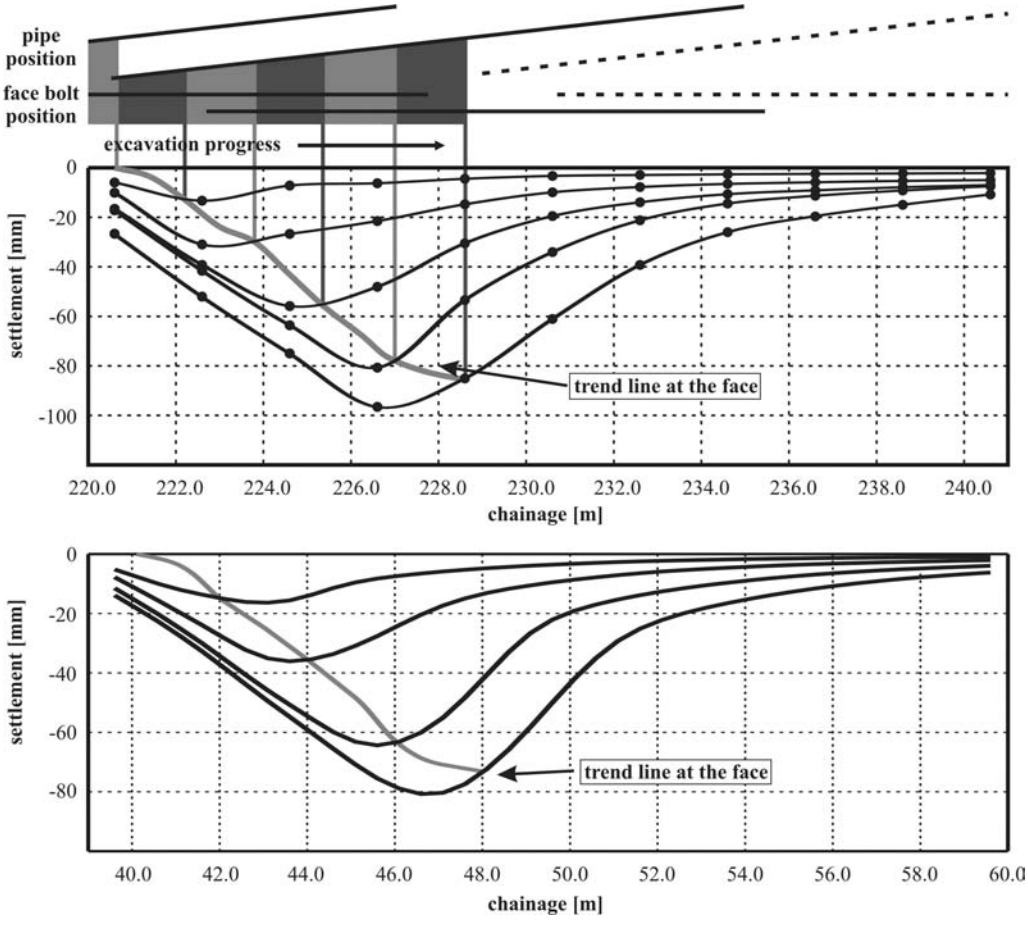


Figure 5. This deflection curve diagrams demonstrates measured settlement values from the Trojane tunnel (upper diagram) and results of a three-dimensional numerical calculation (lower diagram) after every second excavation round.

6.2 *Longitudinal support effect*

The stiffness of a steel pipe is much higher compared to the stiffness of ground that needs additional support by a pipe roof system during tunneling. The relative movements in the longitudinal direction therefore create a second support effect of pipe roof systems during excavation. The pipes are subjected to longitudinal compression. This influences the stress distribution ahead of the face positively so the displacements in the ground decrease ahead of the face.

This support effect is controlled by the area that can be used for the transfer of interaction forces so the outer pipe diameter defines the activation of this support effect.

6.3 *Pipe gap in the unsupported span*

Both previously mentioned support effects are also influenced by the number of pipes. This design parameter and the diameter of the pipes define the remaining gap in between the pipe roof pipes. A local arching effect in between the pipes (Stöckl 2002) increases the stability in the unsupported span and decreases the overbreak volume as long as this local arch can be formed.

A comparison of calculated results can be found in Volkmann & Schubert 2006. Those results explain both the effect of larger pipe diameters and different numbers of pipes on the displacement characteristic.

6.4 *Validation of numerical results*

Complex three-dimensional numerical calculations are influenced by all input parameters. These include geometric conditions, material properties, installed support systems, and time dependent changes of strength- and stiffness properties.

The comparison of the measured and calculated displacements (Figure 5) for this case study shows good

agreement ahead of the face, in unsupported-, and supported sections. This fact provides evidence that the relevant mechanisms, which occurred during the excavation of the Trojane tunnel, could be reproduced in the numerical calculations.

7 CONCLUSION

The advantages of being cheap and less time consuming during the installation, increased the use of Pipe Roof Support systems over the last few decades even though, neither formulas nor clear rules for the design of this pre-support system were determined. An intensive monitoring campaign, including settlement measurements ahead of the face at the tunnel level, enabled the determination of the geotechnical model for this support system. Using this knowledge design parameters of the Pipe Roof System were investigated in numerical calculations.

The results of the numerical investigations demonstrate that the pipe roof system supports the critical section around the heading by transferring the radial loads to both the ground in the front as well as the lining in the supported section. This support effect increases the safety because the risk, that local or global failures occur in the working area, decreases.

Compared to the stiffness of the ground, the high stiffness of the steel pipes positively influences the stress distribution ahead of the supported section. This effect and the radial support around the heading decrease the settlement amounts.

Numerical calculations enable an adaptation of the pipe roof support system by a knowledge-based change of the design parameters: overlapping length, pipe dimensions, and number of pipes. So the calculated system behavior can be optimized with respect to the project requirements.

REFERENCES

Aldrian, W. 1991. Beitrag zum Materialverhalten von früh belasteten Spritzbeton. *Ph.D. Thesis, Leoben: Montan Uni Leoben 1991*.

Gibbs, P.W., Lowrie, J. Keiffer, S. & McQueen, L. 2002. M5 East – Design of a Shallow Soft Ground Shotcrete Motorway Tunnel. *In Proc. of the 28th ITA-AITES World Tunneling Congress, Sydney, Australia, March 2002*.

Goricki, A. 2003. Classification of Rock Mass Behaviour based on a Hierarchical Rock Mass Characterization for the Design of Underground Structures. *Doctoral Thesis, Graz University of Technology, Institute for Rock Mechanics and Tunneling.*

Hoek, E. 2003. Numerical Modeling for Shallow Tunnels in Weak Rock. *PDF available at www.rocscience.com/library/rocnews/Spring2003/ShallowTunnels.pdf.*

Oreste, P.P. & Peila, D. 1998. A New Theory for Steel Pipe Umbrella Design in Tunneling. *World Tunnel Congress '98, Sao Paulo, Brasilien, 25.-30.04.1998* ISBN 90 5410936X, p 1033–1039.

ÖGG 2001. Richtlinie für die Geomechanische Planung von Untertagebauarbeiten mit zyklischem Vortrieb. *ÖGG-Österreichische Gesellschaft für Geomechanik, Salzburg, Austria*.

Miura, K. 2003. Design and Construction of Mountain Tunnels in Japan. *Tunneling and Underground Space Technology, 18 (2003): 115–126.*

Müller, M. 2001. Kriechversuche an jungem Spritzbeton zur Ermittlung der Parameter für Materialgesetze. *Master Thesis, Leoben: Montan Uni Leoben 2001*.

Kim, C.Y., Koo, H.B. & Bae, G.J. 1996. A Study on the Three Dimensional Finite Element Analysis and Field Measurements of the Tunnel Reinforced by Umbrella Arch Method., *Proc. of the Korea-Japan Joint Symposium on Rock Engineering.* ISBN 89-950028-0-8, pp. 395–402.

Rabcewicz, L.v. 1944. Gebirgsdruck und Tunnelbau. *Wien: Springer Verlag.*

Rabcewicz, L.v. 1975. Die Bedeutung der Messung im Hohlraumbau III. *Der Bauingenieur 50 (1975) Nr. 10, 369–379.*

Sellner, P.J. 2005. Tunnel Paierdorf – Drainage of the Ground. *Presentation at the Symposium Koralmtunnel 2005, November 24th–25th. Graz University of Technology, Geotechnical Group Graz*

Steindorfer, A. 1998. Short Term Prediction of Rock Mass Behaviour in Tunnelling by Advanced Analysis of Displacement Monitoring Data. *Doctoral Thesis, Graz University of Technology, Geotchnical Group Graz, Institute for Rock Mechnaics and Tunneling, Heft 1, ISBN 3-900 484 171*.

Steindorfer, A. & Schubert, W. 1997. Application of new Methods of Monitoring Data Analysis for Short Term Prediction in Tunneling. *In Proc. of the 23rd General Assembly of the International Tunneling Association, Vienna. Balkema, Rotterdam, 65–69*.

Stöckl, Ch. 2002. Numerische Berechnung der Tragwirkung von Rohrschirmen mit PFC-2d. *Diplomarbeit, Graz University of Technology, Institute for Rock Mechanics and Tunneling.*

Volkmann, G.M., Button, E. & Schubert, W. 2003. Influence of the Zero Reading Time and Position on Geodetical Measurements. *In Proc. of the International Symposium on GeoTechnical Measurements and Modeling, Tucson, 7 – 12 January 2001, eds. O. Natau, E. Fecker, E. Pimentel, 101–104.* Karlsruhe: A.A. Balkema.

Volkmann, G.M. 2004. A Contribution to the Effect and Behavior of Pipe Roof Supports. *In Proc. of the 53rd Geomechanics Colloquy and EUROCK 2004, Copyright VGE, October 2004, Salzburg, Austria.*

Volkmann, G.M. & Schubert, W. 2006. Optimization of Excavation and Support in Pipe Roof Supported Tunnel Sections. *In Proc. of the 32nd ITA-AITES World Tunneling Congress, Seoul, 2006.*

Volkmann, G.M. & Schubert, W. 2006. Contribution to the Design of Tunnels with Pipe Roof Support. *In Proc. of the 4th Asian Rock Mechanics Symposium, Nov. 8th–10th, in print*.

Zlender, B. 2003. Triaxial Tests of Carboniferous Slates with Static and Dynamic Loading. *In Proc. of the 10th ISRM 2003 – Technology roadmap for Rock Mechanics, South Africa, 2003, eds. M. Handley, D. Stacey*, 1391–1394. Johannesburg: Camera Press.

Underground Space – the 4th Dimension of Metropolises – Barták, Hrdina, Romancov & Zlámal (eds)
© 2007 Taylor & Francis Group, London, ISBN 978-0-415-40807-3

Model analysis of pre-lining methods used in tunnel construction

V. Vrba
Bachy Soletanche Ltd., Burscough, Lancashire, United Kingdom

J. Barták
Dpt. of Geotechnics, Faculty of Civil Engineering, Czech Technical University, Prague, The Czech Republic

ABSTRACT: A series of centrifuge model tests has been conducted to investigate ground movements around tunnel heading reinforced by so called pre-lining structure. The outcomes have been evaluated by direct comparison with the numerical model analysis. The results show that a pre-lining structure influences the progress of ground deformations above the tunnel heading. The research work undertaken also highlighted the complexity of the problem and its potential for future research development.

1 INTRODUCTION

1.1 *Background*

In an urban environment the need for construction of tunnels for transportation or utility systems is always present. For practical reasons such as accessibility, serviceability and economy these tunnels are constructed at shallow depths. Since the ground near the surface consists very often from soils or weak rocks, the shallow tunnels are usually constructed using either tunnel boring machines or tunnelling methods based on NATM (New Austrian Tunnelling Method) principles often combined with certain type of soil or rock improvement and reinforcement. These techniques are used to modify stresses within the layers of soil adjacent to underground works and/or to modify geotechnical parameters of the soil. So-called pre-lining methods form one important group of available improvement processes.

As an alternative to field measurements of deformations associated with the underground excavation modelling of in situ prototype situations can be employed. Generally, tests may be performed on physical models where geotechnical centrifuge can become useful tool. To validate the physical models numerical analysis can be used.

Tunnel construction operating with the pre-lining structure is in general composed of two phases. During the first one the protecting arch made from concrete (pre-cutting), from jet-grouting columns or from steel pipes is created into the ground ahead of the tunnel face around its upper circumference. Due to technology of overlapping of each new arch with the previous one their resulting shape is of a truncated cone. The excavation of the new space under the protection of this structure is the second part of the process - see Figure 1.

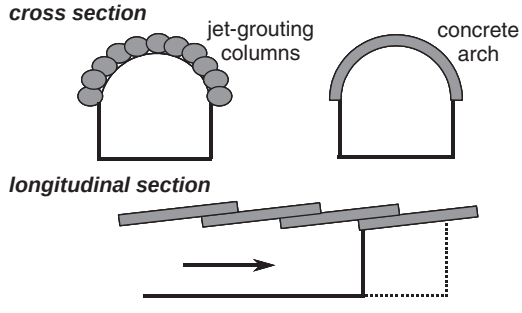


Figure 1. Principle of pre-lining methods used in tunnelling.

1.2 *Methodology*

Geotechnical centrifuge model testing was the method of investigation on physical models. Within the Czech Republic there is no geotechnical centrifuge laboratory in operation. The research work presented in this paper has been undertaken during the author's stay at City University in London (UK) under kind supervision of Professor R N Taylor.

Centrifuge testing allows the simulation of full scale prototype stress distributions with depth. This is due to the nature of centrifuge imposed loading – increase in radial acceleration imposed by the rotation of the centrifuge. With this technique, self-weight stresses and gravity-dependent processes are correctly reproduced and observations from small-scale models can be related to the full-scale prototype situation.

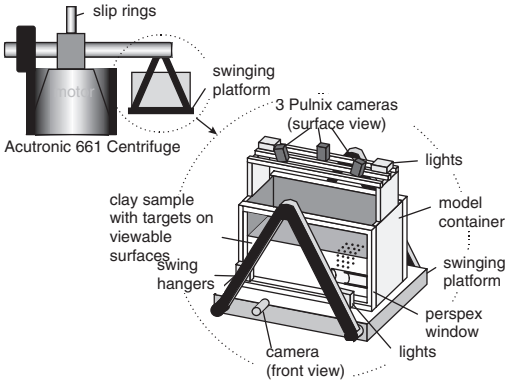


Figure 2. Diagram of the centrifuge and arrangement of the model (after Calvello & Taylor 1999).

Centrifuge models were conducted under 3D conditions. The tunnel was cut into overconsolidated kaolin clay material. Part of the tunnel was supported by a stiff lining while the heading was supported by the model of pre-lining structure together with air pressure within a rubber lining. Movements were generated by reducing the pressure in the tunnel so that tunnel heading started to collapse. A schematic diagram of typical centrifuge model used for this study is presented in Figure 2.

Finite element analyses were carried out using version 4.3a of SAGE CRISP finite element program and models were conducted as two dimensional under plain strain conditions and certain assumptions were made to approximately represent the three dimensional situation. All analyses were conducted at centrifuge model scale. Finite element analyses were evaluated by direct comparison with centrifuge model test results.

2 GEOTECHNICAL CENTRIFUGE – PHYSICAL MODELLING

2.1 *Tests undertaken*

A total of three tunnel heading tests were conducted. The aim of the test series was to observe and evaluate the effect of so called pre-lining structure installed ahead of tunnel face in reducing the risk of collapse of a tunnel excavation and also its influence on movements of ground above the tunnel. The diagram of the typical model set up is shown in Figure 3. All the tests were conducted with the same stress histories. They were pre-consolidated to 175 kPa (clay sample in consolidation press). Pore pressure equilibrium conditions were achieved at full acceleration on the centrifuge before the pressure reduction in the tunnel was carried out.

The model of a pre-lining structure is shown in Figure 4. The semicircular profile of a brass tube was used to model the stiff tunnel lining which occupied

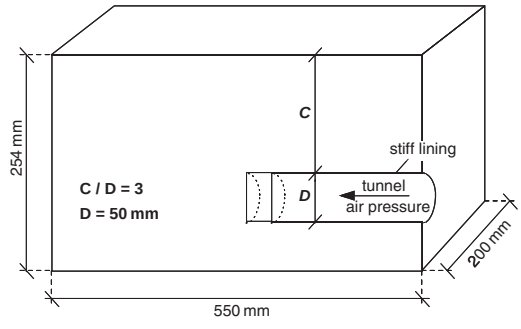


Figure 3. Diagram of typical model set up.

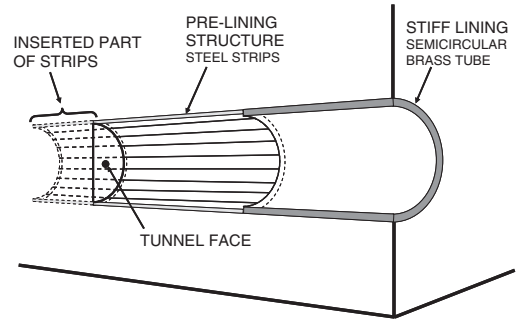


Figure 4. Pre-lining structure model.

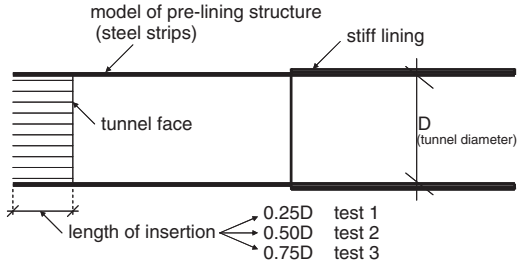


Figure 5. Geometry of the tunnel arrangement.

only approximately half of the tunnel length. The pre-lining structure was modelled by thin steel strips 6 mm wide and approximately 1.25 mm thick. They were pushed one next to another into the ground ahead of the tunnel face around the circumference of the face in order to create a protective shell around the ground to be excavated.

The rear part of these strips was supported by the stiff lining of the tunnel. The length of insertion of the strips ahead of the face was the difference between the tests (the ratio between the length of insertion and the tunnel diameter was 0.25 or 0.5 or 0.75 – see Figure 5).

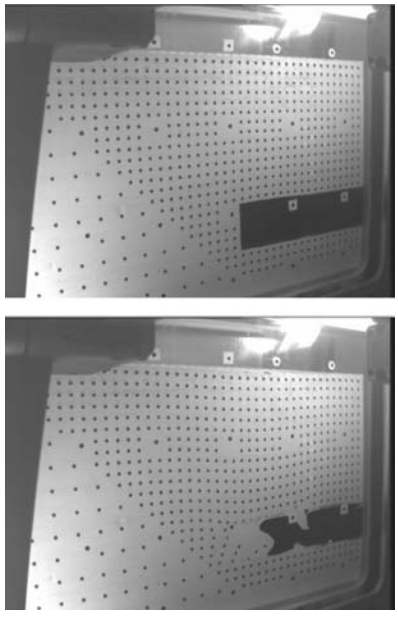


Figure 6. Digital images of Test 1 (before reducing the tunnel pressure & tunnel collapse in progress).

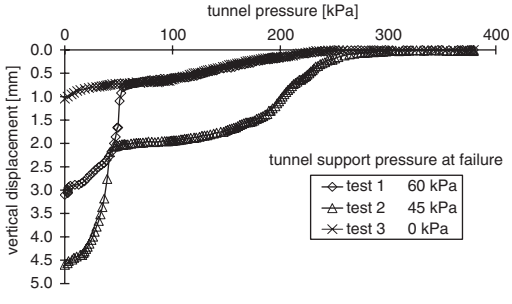


Figure 7. Tunnel support pressure at failure.

2.2 *Test results*

Digital images from the centrifuge mounted cameras were taken during the test and stored in the computer for later processing. In images presented in Figure 6 the pattern of black targets pushed into the front surface of the model can be seen. Special software was used to capture the black target positions from these images and calculate their coordinates and also changes in these coordinates during the course of the test.

In Figure 7 the vertical displacement near the ground surface directly above the centre of the unsupported length of the steel plates was plotted against the support air pressure. After decreasing the tunnel pressure to the value of about 200 kPa, the settlement process was initiated and stabilized at a value of 1 mm; then the collapse of the tunnel heading followed.

This shows that the pre-lining type of tunnel heading stabilization could prolong the period between the occurrence of the first significant deformations above the unsupported tunnel heading and final collapse of the tunnel. In another words, the pre-lining structure contributes with its structural capacity to the stability of tunnel crown. Other question is how this "structural" capacity is defined. In this case, the model was made of steel strips placed around the tunnel circumference and the collapse most probably occurred in the moment when these strips started to bend. The proper arching effect cannot be taken into account here, because the strips were not interconnected with each other.

As it is obvious from Figure 7, the curve for test 2 has almost entirely moved down by about 1.5 mm, which was caused by a mistake in the model preparation. During the test, all the targets on the front face of the model moved down. Despite of this event, the development of deformations near the surface and the collapse pressure can be read from this curve.

According to these observations, it was possible to say that the length of the part of a pre-lining structure, which remains inside the ground ahead of the tunnel face, plays a certain role at the tunnel heading stability. The longer the insertion into the ground is the stable the tunnel face and entire tunnel heading area.

Figure 8 shows the overall patterns of subsurface movements in the vertical plane passing through the longitudinal axis of the tunnel. The crosses indicate the initial coordinates of the targets, whereas the lines show their displacements vectors from the beginning of the tests (tunnel pressure 380 kPa) to failure (tunnel pressure 60, 45 and 0 kPa for tests 1, 2 and 3 respectively). In the figures, the vectors are magnified 4 times with respect to the grid scale. Displacement patterns do not vary significantly throughout all three tests. The biggest deformations of the ground above the tunnel occur approximately in the middle of the unsupported length of the steel strips. This is obviously dependant on the material the pre-lining structure model is made of. Using stiffer and more brittle material would definitely bring different results.

3 NUMERICAL MODELLING

3.1 *SAGE CRISP software*

The numerical analyses presented in this section were conducted using a non-linear elasto-plastic soil model (modified Cam-clay) and the finite element method. The focus was to model the soil sample stress history as accurate and closely as possible. Linear strain triangular elements were used together with coupled consolidation (Biot) facility in CRISP software. CRISP is an incremental finite element program which was developed at Cambridge University during the 1970's

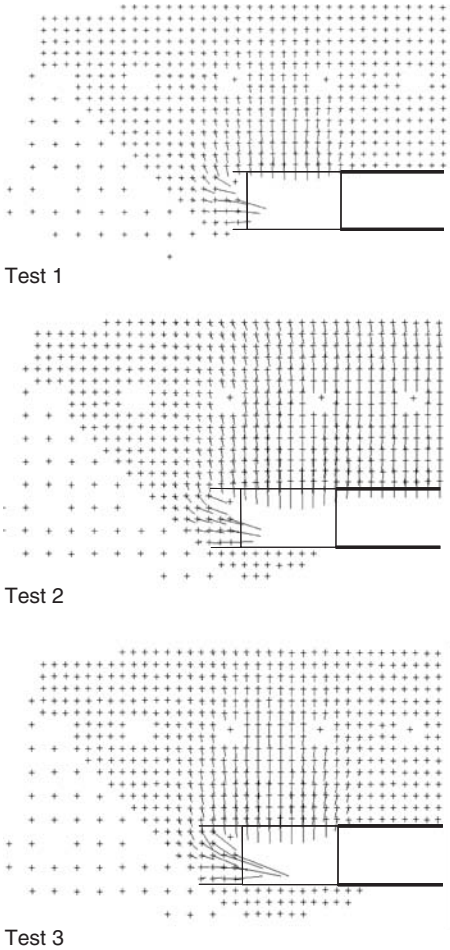


Figure 8. Displacement vectors from beginning of tests to failure.

specifically to carry out geotechnical analyses using Critical State framework to describe soil behaviour.

3.2 *Numerical models*

To model the three-dimensional problem by means of plane strain models needed to think through what potential pitfalls such simplification can bring. Three-dimensional centrifuge model was designed to reflect the overall acting of a tunnel heading while it is being excavated, which is truly three-dimensional.

The numerical analysis was planned as follows. Firstly, two cross-sectional models were conducted – see top of Figure 9. The first one (A) had completely same dimensions as the cross-section of the centrifuge model through the open tunnel. In the second one (B) the "tunnel" excavation was modelled as cut much

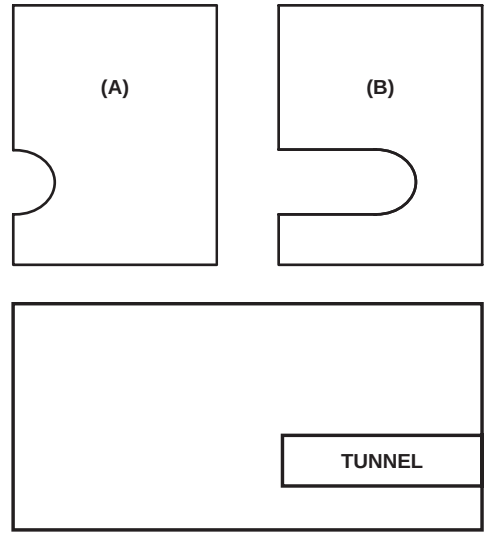


Figure 9. Cross-sectional representations for initial analyses (top) and longitudinal section, the main model for ground movement observation.

deeper inside the soil mass; the only reason being the intention to eliminate the contribution of the arching effect to the tunnel stability. The third model was the one of longitudinal section – see bottom of Figure 9. For all three models the sample stress history was the same, the dimensions of the models were as per the centrifuge models and the way of modelling the tunnel excavation remained the same (i.e. by reduction of supporting pressure inside the tunnel).

The reason for the two different cross-sectional models was to try to evaluate the difference between the progress of deformations during the collapse of the tunnel for these two. Next step was to try to apply this difference (in the form of some coefficient) to the results from the longitudinal section model because the three-dimensional acting of the tunnel heading is not reflected there. It was not necessary to model any tunnel lining here because the purpose of those models was only to asses the influence of different tunnel geometries on the movements of the ground above the tunnel.

The vertical movements at the ground level for both models (A) and (B) were compared, which is shown in Figure 10. As can be observed there is a significant difference between the failure progress in model (A) and (B). This is no surprise because in model (B) there is no physical support of the far left side of the tunnel cavity (tunnel arch far away) and so the vertical ground movements begin to progress straight after the tunnel support pressure reduction is initiated. The failure comes very soon in model (B), at around 330 kPa of tunnel support pressure, which is roughly 100 kPa

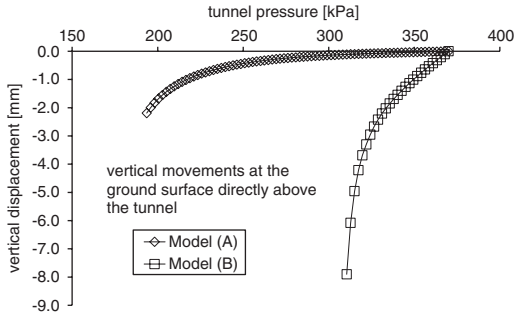


Figure 10. Comparison of the vertical movements at the ground level above the tunnel for models (A) and (B).

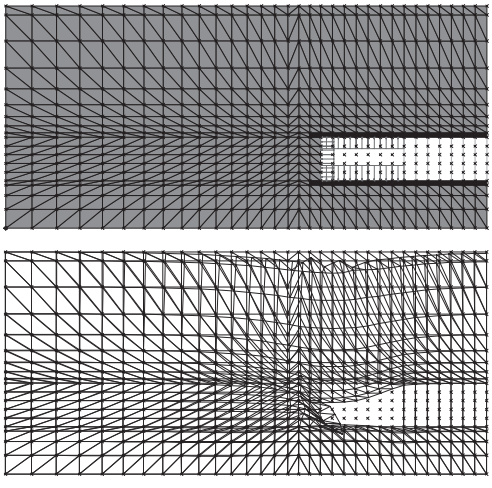


Figure 11. Longitudinal section, Test 1 model – original and deformed finite element mesh.

earlier than in model (A). Another feature which can be assessed is the gradient of the two settlement curves before the tunnel collapse. Vertical movements at the ground surface for model (A) increase with approximate gradient of 1mm per 420 kPa of tunnel pressure reduction whereas for model (B) the gradient is 1 mm per 19 kPa pressure reduction. This means the deformations in model (B) progress approximately 22 times faster than in model (A) during the tunnel support pressure reduction.

In the final stage of numerical modelling the longitudinal section finite element mesh was assembled and three model tests were conducted based on the centrifugal tests. Figure 11 shows the original finite element mesh for the longitudinal section model. The elements representing the stiff lining and pre-lining structure are distinguished by darker colour from the elements representing the soil. Shown here is Test 1

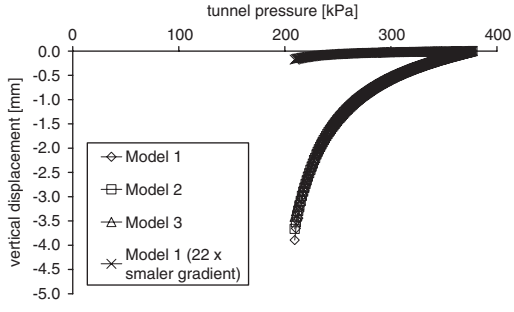


Figure 12. Near surface vertical movements directly above pre-lining structure – numerical analysis (compare with Figure 7).

with 0.25 D insertion length of the pre-lining structure ahead of the tunnel face. The second diagram represents deformed finite element mesh of longitudinal Test 1. The movements are presented at the time of tunnel failure and are magnified 4 times to emphasize their patterns.

4 COMPARISON OF RESULTS

The stress history, centrifugal loading and boundary conditions have been numerically modelled with great accuracy to the physical model tested on geotechnical centrifuge. The pre-lining structure has been modelled by simply swapping the soil elements around the tunnel cavity for linear strain isotropic elastic elements normally interconnected with the surrounding soil elements. This proved not to be an ideal solution. However, certain outcomes from both analyses can be compared and analysed here.

In Figure 12 vertical movements near ground surface directly above the middle of pre-lining structure from numerical models are plotted to be compared with the same situation from centrifuge models shown in Figure 7. At the first glance, it seems difficult to find any similarities between the two ground movement illustrations. Describing the centrifuge testing, it has been distinguished between different collapse pressures for the three model tests. Looking at them again, they are not too distant and all appear to be around 50 kPa (models 1 and 2). Model 3 carried on until the supporting pressure was zero without showing any signs of more rapid increase in vertical movements. Apart from being moved down (model 2 settlement curve) by approximately 1 mm, the shapes of model 1 and 2 curves are very similar. This was definitely the case of numerical models where all three model tests performed nearly identical pattern of ground movements above the pre-lining structure. This similarity in ground movements even for various lengths of pre-lining structure insertion into the

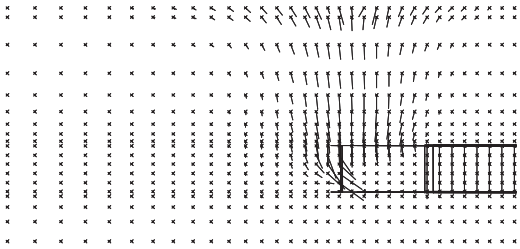


Figure 13. Model 1 – numerical test. Displacement vectors, magnified by factor 4, from beginning of tests to failure.

ground would suggest that it is not of such importance for tunnel heading stability how far the pre-lining will be inserted. However, these tests have been conducted with only one soil material type (consolidated kaolin clay sample with rather plastic behaviour) and it should be expected that for other types of soil or soft rock material this phenomenon would still play major role in overall tunnel heading stability.

The normalised vertical movement curve (22 times smaller gradient) in Figure 12 could be extrapolated further towards lower pressure values. Setting the collapse pressure value somewhere around 130 to 110 kPa would bring it closer to the centrifugal analysis values. The collapse pressures in this type of analysis depend to great degree on the material used to model the pre-lining structure. Since it is fairly difficult to find a numerical model which would closely describe such physical prototype as steel strips inserted into clay soil with elasto-plastic behaviour, the difference between 50 kPa (collapse pressure for centrifuge models) and 120 kPa (numerical models – extrapolated normalised curve) does not seem so unjustifiable.

In Figure 13 the overall patterns of subsurface movements are shown for Model 1 from numerical analysis (compare with centrifugal test data in Figure 8). The crosses in centrifugal model grid represent the positions of black plastic targets inserted into model front surface, whereas the crosses in numerical analysis represent the node positions.

5 CONCLUSIONS

The work that has been presented was conducted to investigate ground movements around a tunnel heading reinforced by so called pre-lining structure. The overall patterns of subsurface movements in vertical plane passing through the tunnel axis were modelled numerically with great degree of conformity with centrifugal tests. Both models show the "sagging" behaviour of the pre-lining structure supported on one side by the stiff tunnel lining and on the other by the soil which it protects. Both numerical and physical models showed very small or even negligible differentiating between different collapse pressures for the three model tests. This would suggest that the structural behaviour of pre-lining structure is more significant to tunnel heading stability than its length of insertion into the ground ahead of tunnel face. The main drawback is that the model experiments were limited to "green-field" site conditions and the findings have not been assessed against any field observations.

REFERENCES

Atkinson, J.H. 1993. *An Introduction to the Mechanics of Soils and Foundations.* Maidenhead: McGraw-Hill Book Company.

Barták, J. & Bucek, M. 1989. *Podzemní stavby.* Praha: ČVUT.

Calvello, M. & Taylor, R.N. 1999. Centrifuge modelling of a spile-reinforced tunnel heading. *Proc. 2nd International Symposium on Geotechnical Aspects of Underground Construction in Soft Ground.* Tokyo.

Grant, R.J. 1998. *Movements Around a Tunnel in Two-layer Ground.* PhD. Thesis. London: City University.

Longelin, R., Le Goer, Y. & Van Walsum, E. 1992. Mechanical pre-cutting as a tunnelling technique. SIPREMEC company report, France.

Lunardi, P. 1997. Pretunnel advance system. *Tunnels & Tunnelling International* October 1997: 35–38.

Mair, R.J. 1979. *Centrifugal Modelling of Tunnelling Construction in Soft Clay.* PhD. Thesis. Cambridge: University of Cambridge.

Papež, P. & Jánský, J. 1999. Kolektor příkopy. *Tunel – Časopis Českého tunelářského komitétu a Slovenského tunelářského komitétu ITA/AITES* 3/99: 18–22.

Peila, D., Poma, A. 1995. Study of tunnel face reinforcement with longitudinal elements. *Gallerie e grandi opere sotterranee* vol. 45: 39–49.

Peila, D., Oreste, P.P., Rabajoli, G. & Trabucco, E. 1995. The pretunnel method, a new italian technology for full-face tunnel excavation: a numerical approach to design. *Tunnelling and underground space technology* vol. 10. No. 3: 367–374.

Rozsypal, A. 2000. From the New Austrian Method to the peripheral slot Pre-cutting Method. *Tunel – Časopis Českého tunelářského komitétu a Slovenského tunelářského komitétu ITA/AITES.* 1/2000: 6-15.

Spyropoulos, I. 2001. Effects of the 3rd dimension in tunnelling. *Proc. of the XIV European Young Geotechnical Engineer's Conference, Monastery "Sts. Cyricus and Julitta". Bulgaria:* 319–328.

Stallebrass, S.E. & Taylor, R.N. 1997. The development and evaluation of a constitutive model for the prediction of ground movements in overconsolidated clay, *Gèotechnique* 47 No. 2: 235-253.

Taylor, R.N. 1995. *Geotechnical Centrifuge Technology.* Glasgow: Blackie Academic &. Professional.

Vrba, V. 1998. *Tunel Březno.* Diplomová práce. Praha: ČVUT.

Wheeler, S.J. 1999. Critical state soil mechanics. *MSc. lectures.* Glasgow: University of Glasgow.

CRISP Consortium Limited 2001. SAGE CRISP Technical reference manual and examples. Version 4.

Underground Space – the 4th Dimension of Metropolises – Barták, Hrdina, Romancov & Zlámal (eds)
© 2007 Taylor & Francis Group, London, ISBN 978-0-415-40807-3

L-SurF – Large scale underground research facility for safety and security

Volker Wetzig
VSH – Hagerbach Test Gallery Ltd., Sargans, Switzerland

ABSTRACT: Security and stability rank among the most important aspirations in everybody's life. Mobility of people and reliable transport of goods are key issues in our society. Both economic growth and societal development rely heavily upon safe and secure infrastructure, in which road, rail and metro tunnels and other enclosed spaces of infrastructures are important elements. To date, the increasing awareness of safety and security caused by severe heavy accidents with partly enormous damage on health and goods and terrorist attacks in underground infrastructures, leads to the necessity of R&D projects that work on safety and security and make an improvement of both existing and projected infrastructure in enclosed spaces possible. This also finds its expression in the description of the 7th framework programme of the EC where safety and security is explicitly addressed as an individual topic for R&D activities. The European Community supports actively the design of new RTD infrastructure on a European level with the aim to both structure the European Research Area and to support the design and the construction or further development of research infrastructure which justify not only a national but a European wide support. The necessity for large scale test and R&D on safety and security in enclosed spaces – and correspondingly for adequate R&D facilities – was identified during the programmes of the 5th EU framework programme. The L-surF project is running with the 6th EU framework programme and will propose a solution to define a European wide R&D approach and real scale research facility which cover safety and security aspects in enclosed spaces.

1 THE IMPORTANCE OF SAFETY & SECURITY – THE EUROPEAN APPROACH

Security and stability rank among the most important aspirations in everybody's life. Mobility of people and reliable transport of goods are key issues in our society. Both economic growth and societal development rely heavily upon safe and secure infrastructure, in which road, rail and metro tunnels and other enclosed spaces of infrastructures are important elements.

To date, the increasing awareness of safety and security caused by severe heavy accidents with partly enormous damage on health and goods and terrorist attacks in underground infrastructures, leads to the necessity of R&D projects that work on safety and security and make an improvement of both existing and projected infrastructure in enclosed spaces possible. This also finds its expression in the description of the 7th framework programme of the EC where safety and security is explicitly addressed as an individual topic for R&D activities or in the fact that a first "European Conference on Security Research" was held in February 2006.

1.1 *EC supports the Design of New R&D Infrastructure*

The European Community supports actively the design of new RTD infrastructure on a European level with the aim to both structure the European Research Area and to support the design and the construction or further development of research infrastructure which justify not only a national but a European wide support.

Within the frame of the Sixth Framework Programme of the European Community, the L-surF project is run as a Specific Support Action (SSA) under the specific programme "Structuring the European Research Area", the project in other words responds exactly to the aims of the EC.

1.2 *The L-surF project*

L-surF, acronym of the project and abbreviation of Large Scale Underground Research Facility on Safety and Security, is a feasibility study. It is carried out through the cooperation of some of Europe's leading institutions on safety and security, started in March

2005 and will finish after 36 months, say in the spring of 2008. The five partners of the consortium are:

- VSH Hagerbach Test Gallery Ltd., Switzerland (Coordination)
- SP Fire Technology, Swedish National Testing and Research Institute, Sweden
- STUVA, Studiengesellschaft für unterirdische Verkehrsanlagen e.V. , Germany
- TNO, Netherlands Organisation for Applied Scientific Research, The Netherlands
- INERIS, Institut National de l'environnement industriel et des risques, France

The budget for the feasibility study is approximately 3.3 Mio €.

2 WHY L-SURF

2.1 *Various EC programmes*

A couple of EC funded RTD programmes on safety in underground infrastructures within the 5th Framework Programme, for example FIT (Fire In Tunnels), DARTS (Durable And Reliable Tunnel Structures), Virtualfires, Uptun (cost-effective, sustainable and innovative upgrading methods for fire safety in existing tunnels), SafeT etc, have been dealing with the improvement of safety in tunnels. The fact that all these programmes have been carried out, shows that the EC identified clearly the need for such efforts on safety and security in enclosed spaces.

The necessity for large scale test and R&D on safety and security in enclosed spaces – and correspondingly for adequate R&D facilities – was identified during these programmes and expressed at the First International Symposium on safe and reliable tunnels, held in Prague in February 2004. The projects of the 5th framework programme also showed a highly fragmented and a mostly unstructured research industry for safety and security in enclosed spaces with many national or even local "players" – a fact which must be addressed if a higher quality level of the R&D work and larger R&D infrastructures are considered being necessary. Also other issues are currently not taken care of sufficiently within the existing industry: Matters like education and training are entirely left to national or regional efforts, there are no harmonized test and R&D procedures available which makes it very difficult to compare R&D work carried out in various sites under various and often quite differing conditions etc.

2.2 *Large scale problems*

If one thing has become apparent from the EU co-financed projects such as mentioned above, it is that accurately assessing the safety level of complex systems such as tunnels on the basis of laboratory test on sub-systems and single elements, even in combination with advanced modelling techniques (CFD, FEA), is hardly possible. This is due to:



Figure 1. Preparation for water mist tests at VSH-Hagerbach test gallery.



Figure 2. Beginning of water mist tests at Hagerbach test gallery.

- scale effects
- unexpected (adverse or positive) interaction between (mitigating) measures
- limited (read: costly) options to validate models to realistic scale events
- a lack of understanding or even unknown physical phenomena regarding fire development (spread of fire to other vehicles or rolling stock)

As long as there is no correspondingly versatile test and R&D facility available that allows working under realistic conditions these problems can't be addressed properly. However such a facility is only possible to be set up on a European approach.

2.3 *Content of the design study*

In order to answer these questions and to overcome the identified shortcomings a basic analysis of all relevant aspects was needed.

A design – study seemed to be the most appropriate tool to do so.

Table 1. Responsibilities and objectives to achieve.

Task n°	Descriptive title	Leading participant	Short description and specific objectives of the task
WP 0	Project management	VSH	Steering and coordinating the project Implementing the business plan and setting-up of a legal entity for L-surF
WP 1	Integration	INERIS	Survey on existing or project development facilities, integrative activities to integrate existing and under development European research facilities and organisations, development of potential L-surF scenarios for integration within the ERA (European Research Area).
WP 2	Research needs	TNO	Identifying and prioritising of scientific and technological research necessities on safety and security in enclosed underground spaces, finding future users and clients of L-surF.
WP 3	Lay-out	VSH	Defining of civil-works, auxiliaries, installations of L-surF, evaluation of measures to minimise environmental impact, development of technical specifications for converting the geometry and the lay-out of the L-surF research facility.
WP 4	Equipment/ Measuring technique	SP	Defining of ultra-modern test methods and the corresponding use of measuring installations, development of technical specifications for innovative 2- and 3-dimensional data acquisition sensors.
WP 5	Activities	STUVA	Defining all the activities of L-surF (R&D, training and educations, external-services, maintaining and operating) in accordance with the existing national organisations and thus reshaping the European R&D – environment.
WP 6	Funding/ business plan	VSH	Fund raising for the realisation of L-surF, establishing a business plan for L-surF based on public private partnership (PPP) and evaluation of legal forms.

Aim of the project is to respond to all aspects mentioned and the main objectives of the design study are thus:

- to describe the constructional lay-out of the facility, based – if the concept is feasible – on a entirely new concept for easily creating any contours, shapes and sizes of enclosed spaces needed, but also all other aspects like installations, environmental impacts etc. The concept will allow novel approaches to R&D work, e.g.
- to describe innovative measuring sensors, based on the latest technologies (e.g. nanotechnology) available
- to evaluate the research needs and to outline the R&D – activities
- to develop an integration process for the existing and projected national facilities with their competences and researchers, thus restructuring and improving the relevant EU competence while simultaneously showing ways for using R&D funds more economically
- to show ways and means to raise the necessary funds for the different stages in the setting up of the facility
- to include a business plan for a new legal entity dedicated to the establishing of L-SURF

2.4 *The work-packages*

To reach this aim all tasks are grouped within six work packages (WP) within the implementation plan and briefly described including responsibilities and objectives to achieve.

2.5 *Short report of the actual state of the project*

One of the general decisions was the making of our choice of the bottom-up approach through a design study to the purpose. From our current point of view it was a good decision because it allows to carefully working out the relevant issues. However, the actual state calls for corresponding top-down activities. Safety and security have to stay main requests within the European Community's 7th Framework Programme. The European Strategy Forum on Research Infrastructure (ESFRI) for example has the role to support a coherent approach to policy-making on research infrastructures in Europe, and to act as an incubator for international negotiations about concrete initiatives. In particular, ESFRI is preparing a European Roadmap for new research infrastructures of pan-European interest. To find entrance into this roadmap is one of our targets of the next months.

3 THE L-SURF LEGAL ENTITY

Within the Design Study for L-SURF all relevant aspects for such a facility will be elaborated to a level that the facility could be established at least as a legal entity with the necessary structures and activities and that preliminary concepts and plans for the physical construction are laid out.

3.1 *Possibilities*

The legal form will first of all highly depend on what kind of organisations, public administrations and private companies will participate and in which way in the establishment of the legal entity and secondly on the business plan developed within the frame of the design study. For working out the legal form of the coming legal entity for the L-surF legal advice will be necessary and accordingly subcontracted. As a result the proposal for a legal form of the L-surF that finds approval of the consortium will be put into reality.

3.2 *Site of the new legal entity*

The choice of the site for the erection of the large scale research facility may also be a criterion in addition to the above mentioned criteria for the legal form, but moreover it will either open or eliminate possibilities for testing and training in connection with fire and smoke as far as environmental impact is concerned, which is a problem not to be sneezed. The analyses of both financial and economical aspects will probably strongest influence the decision where to establish L-surF.

4 CONCLUSION

Safety and Security are among the most urgent challenges of the European Community in the coming years. The EC answers to these challenges with its strategic initiative on safety and security, also in underground and enclosed spaces. The L-surF concept which is both about safety but also about security, because there are similarities in the effect and the need for large scale R&D, testing, training and education is certainly one part of these answers.

Underground Space – the 4th Dimension of Metropolises – Barták, Hrdina, Romancov & Zlámal (eds)
© 2007 Taylor & Francis Group, London, ISBN 978-0-415-40807-3

New high-speed railway lines Stuttgart 21 and Wendlingen-Ulm-Approximately 100 km of tunnels

W. Wittke
WBI – Prof. Dr.-Ing. W. Wittke Consulting Engineers for Tunneling and Geotechnical Engineering Ltd., Aachen/Stuttgart, Germany

ABSTRACT: For the large scale projects new high-speed railway line (NBS) Wendlingen-Ulm and Stuttgart 21, a total of approx. 100 km long single- and to a small extent also double-track tunnel tubes are foreseen.

In the course of the NBS Wendlingen-Ulm, among other structures, the 8.7 km long Boßlertunnel and the 4.7 km long Steinbühltunnel are planned. The Boßlertunnel is located in Brown Jurassic. Locally, squeezing rock is to be expected. The Steinbühltunnel is located in White Jurassic, which is locally strongly karstified. For both tunnels, it was investigated whether an advancing test section and through-going exploratory adits respectively would lead to a safer design with regard to construction costs and time.

A total of approx. 52 km single- and double-track tunnel tubes is foreseen for the project Stuttgart 21. The paper exemplary illustrates the Fildertunnel. With regard to tunneling, the tunnel sections in swelling unleached Gypsum Keuper are of major importance. The principle of resisting support is planned to be carried out.

1 INTRODUCTION

Approximately 100 km of tunnels are foreseen for the construction of the new high-speed railway lines Wendlingen-Ulm and Stuttgart 21. Tunneling in squeezing rock as well as in karstified rock is decisive with regard to construction time and costs of the tunnels for the new high-speed railway line from Wendlingen to Ulm (Wittke W. 2004b). The design and construction of tunnels in swelling rock is a major challenge in connection with the project Stuttgart 21.

2 NEW HIGH-SPEED RAILWAY LINE WENDLINGEN – ULM

2.1 *Tunnels*

The new high-speed railway line Wendlingen – Ulm is planned to go from Wendlingen, passing Aichelberg and Merklingen, to Ulm (Fig. 1). Four comparatively large tunnels are foreseen. The Albvorlandtunnel near Wendlingen is planned with a length of 7.9 km. The ascent to the Swabian Alb from Aichelberg to Merklingen with a length of approx. 13.5 km is also planned to go below ground. In this section, the line is crossing the Filstal. This valley needs to be spanned by a bridge. Therefore two separated tunnels, the Boßlertunnel with a length of 8.7 km and the Steinbühltunnel with a length of 4.7 km, are required. The fourth tunnel is the 5.9 km long Albabstiegstunnel near the city of Ulm (Fig. 1).

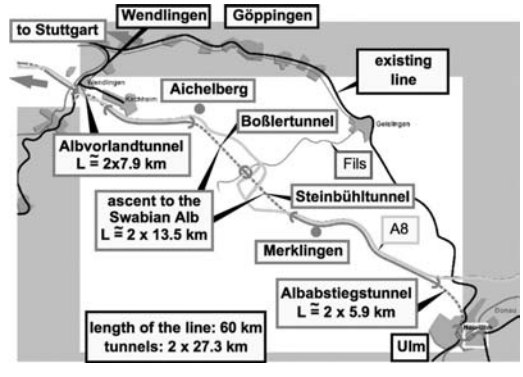


Figure 1. New high-speed railway line from Wendlingen to Ulm.

All tunnels are to be constructed as single-track tubes with cross-cuts at distances of $\leq$1000 m. The total length of all single-track tunnel tubes results to approx. 55 km.

2.2 *Boßlertunnel – Tunneling in squeezing rock*

For the ascent to the Swabian Alb to the west of the Filstal, the Boßlertunnel is planned with a length of 8.7 km (Fig. 2).

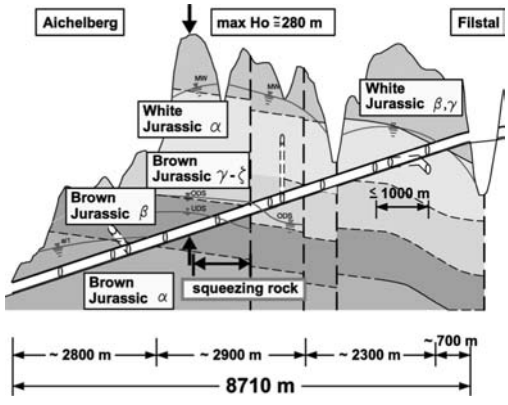


Figure 2. Geological longitudinal section, Boßlertunnel.

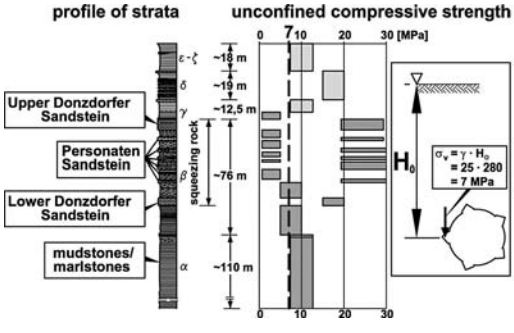


Figure 3. Layers of the Brown Jurassic.

Over a length of approx. 6 km, the tunnel tubes are crossing the layers of the Brown Jurassic (Figs 2 and 3). The Brown Jurassic α, which is also known as Opalinuston, consists of a sequence of mudstones and marlstones. The thickness of the Brown Jurassic β amounts to approx. 75 m. In the lower and upper part two sandstone layers, the Lower and Upper "Donzdorfer Sandstone", are located. The middle part is formed by an alternating sequence of mudstones and sandstones, the so-called "Personatensandsteinzone". Above the Brown Jurassic β, mudstones and marlstones, in which layers of limestone are embedded, are located. The permeability of the mudstones and marlstones is very low. The sandstone and the limestone are aquifers.

Above the Brown Jurassic the layers of the White Jurassic α to γ are located (Fig. 2). The White Jurassic α consists of an approx. 90 m thick sequence of marlstones. In the lower part of it mudstones are embedded and in the upper part limestones. The White Jurassic β and γ, which consists of limestones with deposits of marlstone and are partly karstified, are located above the White Jurassic α.

According to the results of explorations carried out up to now, several ground-water reservoirs exist in the Brown and White Jurassic, which are separated by mudstone and marlstone deposits with very low permeability. At the moment, the water pressures at the level of the tunnel tubes are estimated to be $\leq$9 bar for the White Jurassic.



Figure 4. Tunnel Yacambu (Venezuela), squeezing rock.

The unconfined compressive strength of the mudstones of the Brown Jurassic β, δ and ε to δ is comparatively low (Fig. 3). For the Brown Jurassic β, values of 0.5 and 5.0 MPa were evaluated. In the section in which the tunnel is located in the Brown Jurassic, the overburden amounts to 280 m. It cannot be excluded that in these layers the low strength of the mudstones will be exceeded during excavation of the tunnel tubes and squeezing rock conditions occur.

The effect of squeezing rock is illustrated in Figure 4. The Yacambu tunnel in Venezuela could not be completed for a long time, because the shotcrete support could not withstand the high rock pressure.

The excavation of the Boßlertunnel in the Brown Jurassic β with an overburden of some 280 m, therefore, is one of the challenges of the new high-speed railway line Wendlingen – Ulm. Using the shotcrete method, a yielding support could be taken into consideration (Rückel & Wittke 1991, Zimmer & Wittke 1996, Fig. 5). With regard to a possible TBM heading, it is presently planned to excavate an advancing test section in the Brown Jurassic β for additional exploration. If this full scale exploration leads to the conclusion that a TBM heading in the layers of the Brown Jurassic β, which are difficult with respect to tunneling, is associated with a too high risk, the tunnel section in the Brown Jurassic β would have to be excavated using the shotcrete method. In the remaining tunnel section of approx. 10 km, however, TBM headings could be carried out.



Figure 5. Shotcrete method in squeezing rock, deformable lining.

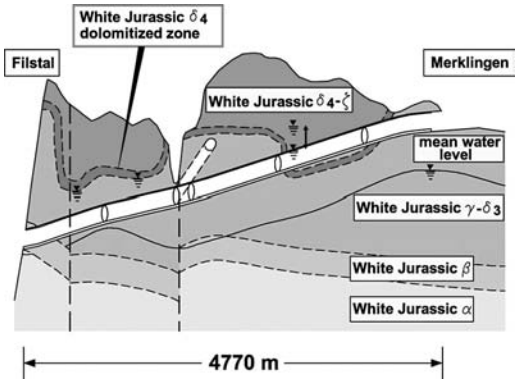


Figure 6. Geological longitudinal section, Steinbühltunnel.

2.3 *Steinbühltunnel – Tunneling in karstified rock*

Figure 6 shows a geological longitudinal section of the Steinbühltunnel, which is located to the south of the Filsbachtal. The length of this tunnel amounts to approx. 4.8 km.

The tunnel tubes are located in the layers of the White Jurassic β to δ_4 above the average water level. The alignment and the gradient were chosen correspondingly. The water level of the karst aquifer varies. During rainfalls, it is rising by several 10 m. Thus, also for this tunnel the water pressure is expected to be within 3 to 5 bars and the tunnel tubes need to be sealed along the whole circumference by a watertight lining which is dimensioned against water pressure.

The layers of the White Jurassic are karstified. In the Swabian Alb, many karst phenomena and cavities are known. Examples are the "Mordloch" (Fig. 7) and the "Falkensteiner Höhle", a 5 km long cave in the White Jurassic δ. Furthermore, karstified master joints occur in the layers of the White Jurassic β to δ (Fig. 8).

In Figure 9, the main types of karstification in the layers of the White Jurassic are illustrated.



Figure 7. Mordloch, karst channel in the White Jurassic β (Binder 1989).



Figure 8. Karstified master joints in the White Jurassic γ.

Figure 10 shows a vertical section through the cave "Laichinger Tiefenhöhle", in which the contour of one tunnel tube of the new high-speed railway line is plotted.

Since it cannot be excluded that karst phenomena of importance for tunneling are encountered during the excavation of the Steinbühltunnel, corresponding support measures are foreseen in the tunnel design. Figure 11 exemplary shows the support of a tunnel tube in case of a karst cavity located above the tunnel's roof. For stability reasons a concrete body is to be constructed between the tunnel and the karst cavity. Thus, the karst cavity as the main flow path will be maintained so that groundwater conditions remain unchanged during tunneling. Figure 12 exemplary shows the support in case of a karst cavity located underneath the invert of the tunnel.

Also for the Steinbühltunnel it was investigated whether the excavation of advancing exploratory adits in karstified rock is of use. This investigation led to the recommendation to drive two advancing exploratory adits located within the cross-sections of the tunnel tubes over the full length of the Steinbühltunnel (Fig. 13). From these adits, karst cavities adjacent to both tunnel tubes can be explored by seismic methods and supplementary drillings and also stabilized if required. If these measures are carried out prior to

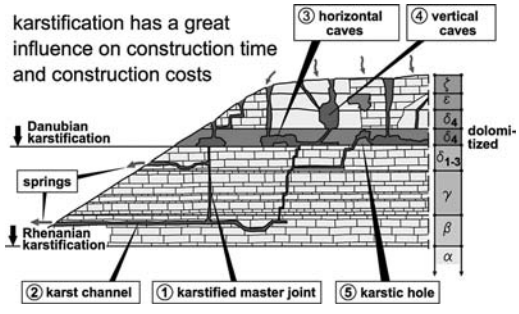


Figure 9. Main types of karstification in the White Jurassic.

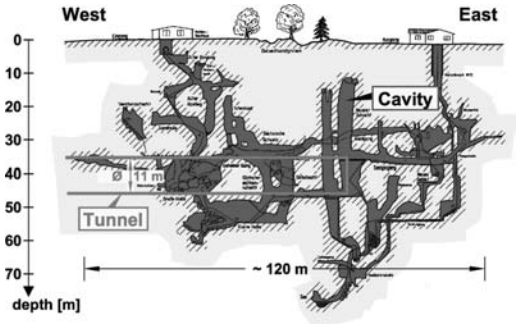


Figure 10. Possible cavities in the cross-section of the tunnel.

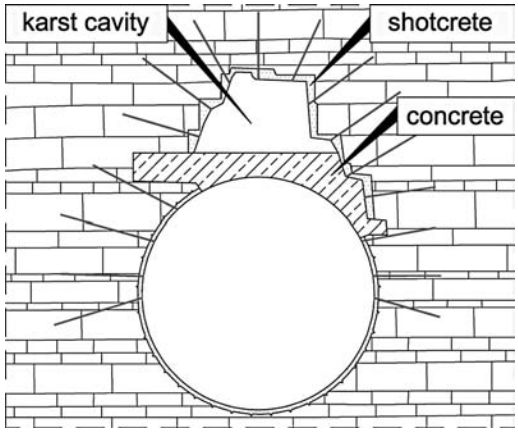


Figure 11. Support of tunnel in karstified White Jurassic, karst cavity above the roof.

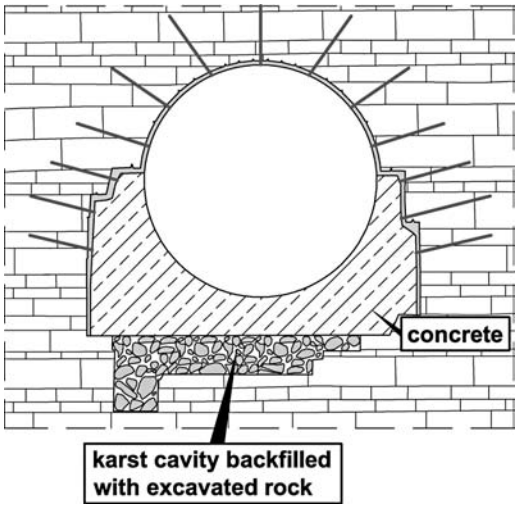


Figure 12. Support of tunnel in karstified White Jurassic, karst cavity underneath the invert.

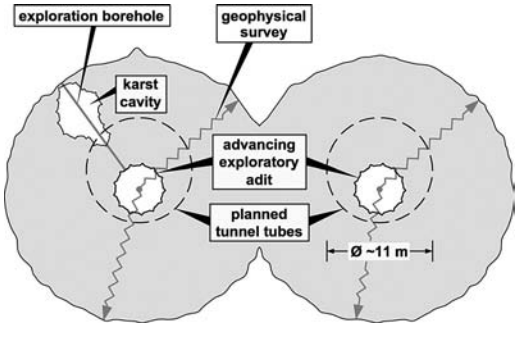


Figure 13. Exploratory adit in karstified rock, Steinbühltunnel.

the excavation of the tunnel tunnel tubes, the risk for TBM-tunneling is considerably reduced.

3 STUTTGART 21

3.1 *Tunnels*

In the city of Stuttgart, five tunnels are planned (Fig. 14). The tunnel Feuerbach with a length of approx. 3.2 km is connecting the high-speed railway line Mannheim-Stuttgart with the new main station. The Fildertunnel with a length of approx. 9.5 km shall provide the main connection from the new main station to the Stuttgart airport and further to the new high-speed railway line Wendlingen-Ulm. As further essential tunnel structures, the tunnel Bad Cannstatt with a length of approx. 3.8 km and the tunnels to Ober- and Untertürkheim are to be constructed. The tunnel Obertürkheim undercrosses the Neckar river in a comparatively low depth. The total length of this tunnel is approx. 6 km.

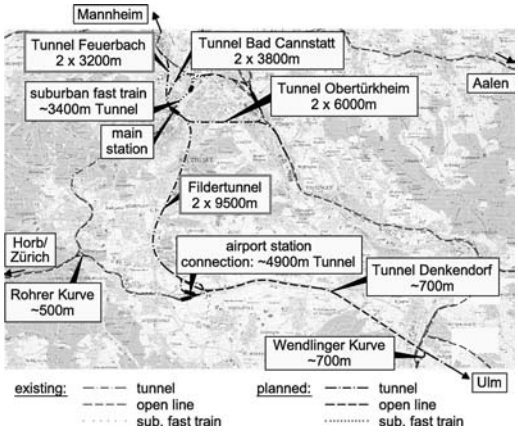


Figure 14. Stuttgart 21, overview.

To remove traffic from the ground surface and to improve the suburban fast train connections, additional tunnels with a length of approx. 3.4 km are planned. For the connection to the airport, further tunnels with a length of approx. 4.9 km are foreseen. In addition several comparatively short tunnels like the Rohrer Kurve, the Wendlinger Kurve and the tunnel Denkendorf are planned.

The total length of all single-track and double-track tunnel tubes for the project Stuttgart 21 is approx. 52 km. In the following, the Fildertunnel with its special features with respect to tunneling will exemplary be presented.

3.2 *Fildertunnel – Tunneling in swelling rock*

The Fildertunnel, which leads from the new Stuttgart main station to the Filder Plain, has a length of approx. 9.5 km (Fig. 15).

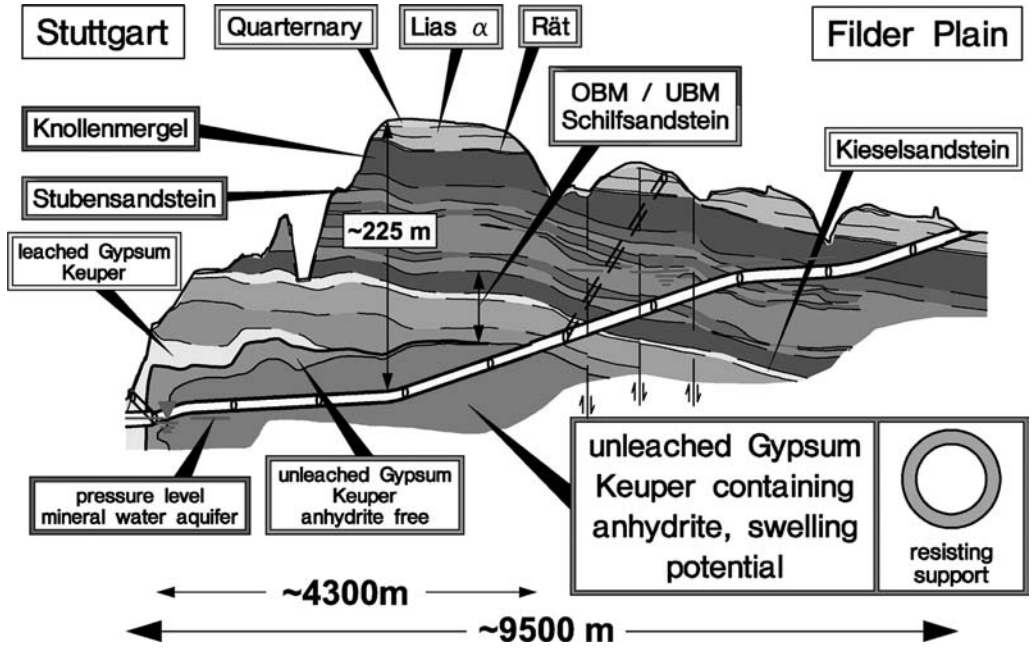


Figure 15. Geological longitudinal section, Fildertunnel.

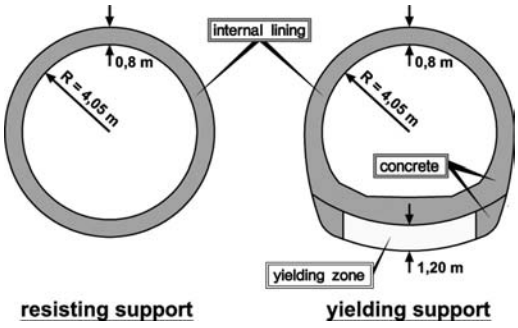


Figure 16. Design principles for tunnels in swelling rock.

The tunnel crosses all layers forming the valley of Stuttgart, which are located above the "Lettenkeuper". At the beginning of the tunnel, the cross-section is located in the leached Gypsum Keuper over a length of 200 to 300 m. In the following, it passes sulfate rock containing gypsum and anhydrite over a length of approx. 4.3 km. Here, the leaching front is located 30 to 45 m above the roof of the tunnel. Underneath the anhydrite level, which is located 20 to 30 m above the tunnel's roof, the sulfate rock consists mainly of anhydrite. The tunnel is located in the "Schilfsandstein", the "Kieselsandstein" as well as the "Unteren Bunten Mergel" and "Oberen Bunten Mergel" over a length of approx. 750 m. The sandstones and siltstones of the "Stubensandstein" are crossed by the tunnel over a length of some 2.5 km. The remaining tunnel sections are located in the "Knollenmergel" and the silty mudstones and sandy limestones of the Black Jurassic (Lias α).

The unleached Gypsum Keuper is a major challenge for design and construction of the Fildertunnel. It consists of a horizontal alternating sequence of sulfate-containing clay- and siltstones and pure sulfate rock. The sulfate is found in two different modifications, as gypsum and as anhydrite. Both modifications can be found at the same time, if the rock is dry. If water gains access to the rock, however, anhydrite transforms into gypsum. This chemical process results in an increase of the solid volume by approx. 60%. This volume increase is denoted as swelling.

The swelling behavior of the unleached Gypsum Keuper is also influenced by the water uptake of clay minerals.

The volume increase due to swelling causes major swelling deformations. If these are confined, great swelling pressures occur, which have led to severe damages of tunnel linings in many cases in the past.

The maximum overburden of the Fildertunnel amounts to 225 m. The design concept for the Fildertunnel is based on the principle of resisting support (Fig. 16). Thus, the lining is designed to resist the developing swelling pressure.

In a greater distance to the leaching front the unleached Gypsum Keuper has a very low permeability according to experience. Because of the comparatively great distance of the tunnel gradient to the leaching front, it is to be expected that the rock mass remains dry and thus no swelling occurs, if no water gains access to the rock during the stages of construction. This was an important criterion for determination of the gradient. Another criterion was to have the tunnel passing the leaching front in an area in which the overlaying rocks are almost dry. Furthermore, due to the chosen deep location of the gradient, a tunnel lining subjected to swelling pressure underneath the invert can be supported by a sufficiently thick rock layer consisting of hard rock. Thus, significant heavings of the tunnel tubes due to swelling are not to be expected.

The principles of resisting support and yielding support respectively are presently used for the design of tunnels in anhydritic, swelling rock (Fig. 16). In both cases, it is assumed that water to initiate the maximum swelling load and full swelling respectively is available in sufficient quantities. Consequently, the designed measures have to be carried out over the full length of the tunnel in swelling rock.

Based on observations, the hypothesis was made that, in the area of the transition from water bearing to anhydritic rock, self-sealing due to swelling occurs around the tunnel, if the resisting principle is applied. As a consequence of this self-sealing effect, seepage through the rock along the tunnel, and thus also swelling, is interrupted at a certain distance from the water bearing formation (Wittke M. 2003, 2004).

In a research project carried out by WBI, a rock mechanical and hydraulical model and a corresponding 3D-FEM-code have been developed, which describe the corresponding phenomena. It is expected that the results of this work will lead to remarkable cost savings along with the design of tunnels in swelling rock.

3.3 *Tunnel Feuerbach*

The tunnel tubes to Feuerbach run through both, the unleached Gypsum Keuper containing anhydrite and the leached Gypsum Keuper (Fig. 17). Within the approx. 150 m long tunnel section located near Feuerbach, which crosses the zone containing anhydrite the principle of yielding support is foreseen. Within the approx. 420 m long anhydrite containing tunnel section located near the planned main station as well as in the following more than 1 km long section containing anhydrite the principle of resisting support is ought to be carried out. Here, according to the results of exploration seepage water is to be expected only to a very limited degree. If during excavation unexpectedly heavings due to swelling occur a changeover to the more expensive principle of yielding support is planned.

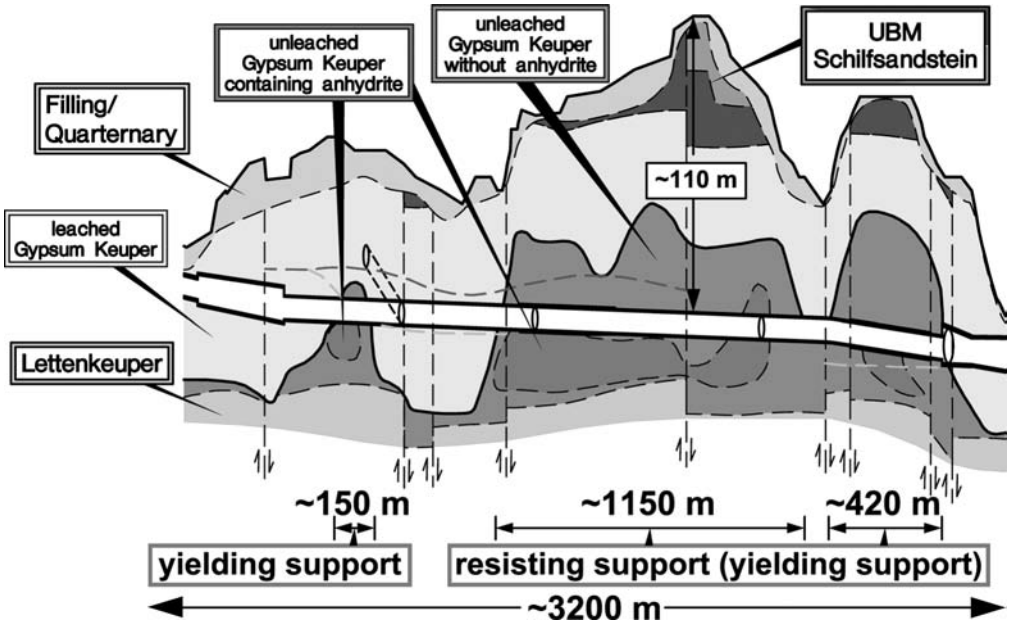


Figure 17. Geological longitudinal section, Tunnel Feuerbach.

REFERENCES

Baur, R. 2002. *Tunnelbau im Projekt Stuttgart 21. Geotechnik* 25 (3): 153–156.

Baur, R. & Erichsen, C. 2000. *Challenges in tunneling according to 40 km tunnels for the DB Projekt Stuttgart 21. Proc. of the EUROCK 2000 symp., Aachen 2000*. Essen: Verlag Glückauf.

Beiche, H. 1991. *Bemessung und Bau eines Tunnels in anhydrithaltigem Gebirge. Proc. 9. Nat. Felsmechanik Symposium, Aachen 1990*. Essen: Verlag Glückauf.

Bernhardt, K. & Rock, D. 1995. *Der Engelbergbasistunnel: Bau und Finanzierungskonzept eines Autobahntunnels mit außergewöhnlichen Querschnittsabmessungen in schwierigen Gebirgsverhältnissen. Forschung + Praxis 36, Proc. World Tunnel Congress, Köln 1995.*

Binder, H. 1989. *Höhlenführer Schwäbische Alb.* Konrad Theis Verlag.

Grob, H. 1972. *Schwelldruck am Beispiel des Belchentunnels. Proc. Int. Symposium für Untertagbau.* Luzern: 99–119.

Grüter, R. & Liening, B. 1976. *S-Bahn Stuttgart, Planung und Bau der Haltestelle Schwabstraße (Baulos 11) und der unterirdischen Wendeanlage (Baulos 12), Teil I. Proc. Baugrundtagung, Nürnberg 1976.*

Jäckle, P. 2002. *Die Tunnel der Neubaustrecke Wendlingen – Ulm. Geotechnik* 25 (3): 157–161.

Kiehl, J. R. 1990. *Ein dreidimensionales Quellgesetz und seine Anwendung auf den Felshohlraumbau. Proc. 9. Nat. Felsmechanik Symposium, Aachen 1990*. Essen: Verlag Glückauf.

Kirschke, D., Kuhnhenn, K. & Prommersberger, G. 1991. *Der Freudensteintunnel: Eine Herausforderung für den planenden Ingenieur.* Ibw 7: 5–39.

Klonsdorf, G. & Schaser, F. 1991. *Baudurchführung des Freudensteintunnels, Bergmännische und offene Bauweise.* Ibw 7: 118–172.

Marquart, P. 2004. *Die Geologie weist ihren Weg – Tunnelbau in den Gebirgsformationen rund um Stuttgart und auf der Schwäbischen Alb. Geotechnik* 27 (2): 99–103.

Paul, A. & Wichter, L. 1992. *Das Langzeitverhalten von Tunnelbauwerken im quellenden Gebirge – Neuere Meßergebnisse vom Stuttgarter Wagenburgtunnel. Proc. 10. Nat. Felsmechanik Symposium, Aachen 1992.* Essen: Verlag Glückauf.

Rückel, M. & Wittke, W. 1991. *Abschluß von Einlagerungskammern in druckhaftem Gebirge, Konzept und in situ Nachweis. Proc. 9. Nat. Felsmechanik Symposium, Aachen 1990.* Essen: Verlag Glückauf.

Wittke, M. 2003. *Begrenzung der Quelldrücke durch Selbstabdichtung beim Tunnelbau im anhydritführenden Gebirge. Geotechnik in Forschung und Praxis, WBI-PRINT 13.* Essen: Verlag Glückauf.

Wittke, M. 2004. *Bemessung von Tunnels im quellfähigen Gebirge unter Berücksichtigung der Selbstabdichtung. Geotechnik* 27 (2): 136–141.

Wittke, W. 2004a. *Planung, Bau und Überwachung von Tunneln in quellfähigem Gipskeuper. Geotechnik* 27 (2): 104–111.

Wittke, W. 2004b. *Ursachen und Vermeidung von Termin- und Kostenüberschreitungen bei Tunnelbauten der Infrastruktur,* unpubl.

Wittke, W. & Rißler, P. 1976. *S-Bahn Stuttgart, Planung und Bau der Haltestelle Schwabstraße (Baulos 11) und der unterirdischen Wendeanlage (Baulos 12), Teil II. Proc. Baugrundtagung, Nürnberg 1976.*

Wittke, W., Wittke, M. & Wahlen, R. 2004. *Zum Quellgesetz für anhydritführenden, unausgelaugten Gipskeuper. Geotechnik* 27 (2): 136–141

Wittke-Gattermann, P. 1998. *Verfahren zur Berechnung von Tunnels in quellfähigem Gebirge und Kalibrierung an einem Versuchsbauwerk. Geotechnik in Forschung und Praxis, WBI-PRINT 1*. Essen: Verlag Glückauf.

Zimmer, M. & Wittke, W. 1996. *Entwurf und Ausführung eines verformbaren Ausbaus in stark durckhaftem Gebirge. Proc. 11. Nat. Felsmechanik Symposium, Aachen 1994*. Essen: Verlag Glückauf.

Underground Space – the 4th Dimension of Metropolises – Barták, Hrdina, Romancov & Zlámal (eds)
© 2007 Taylor & Francis Group, London, ISBN 978-0-415-40807-3

Estimation of multi-well dewatering induced pile foundation settlement in phreatic zones

Y. Xiang, S. Chen & C. Yu
School of Civil Engineering, Beijing Jiaotong University, Beijing, China

ABSTRACT: Dewatering induced soil consolidation may cause additional settlement of nearby pile foundations. A simplified procedure is adopted to estimate pile foundation settlement induced by multi-well dewatering in phreatic zone, and sensitivities to various parameters can be analytically calculated. A synthesized case analysis indicates: (1) when the drawdown surface is above the pile tips, the dewatering-induced pile foundation settlement is influenced by the drawdown, consolidation of soil surrounding the pile shafts and strength of pile-soil interaction; (2) when the phreatic surface is lowered deeper than the pile tips, the additional pile foundation settlement due to the consolidation of the underlain soils should be accounted for; and (3) due to the additional negative skin friction exerted on the pile shafts above the initial phreatic surface as well as the additional compaction of the soil beneath the pile tips, dewatering induced pile foundation settlement could be larger than the settlement of nearby soils.

1 INTRODUCTION

1.1 *Background*

In urban areas there often exist tall buildings and overpasses that are mostly supported on pile foundations. Restrained by spatial and/or other environmental conditions, some geotechnical and underground excavations have to be carried out in the vicinity of existing piles. When the excavations are below the water table, artificial dewatering is needed in order to provide the undertaking a relatively dry condition. Dewatering of the ground may cause increases in the effective stress and the compression of the soil, and consequently the settlements of the nearby piles.

1.2 *Present work*

In order to estimate the pile foundation settlement induced by artificial dewatering, the drawdown of each dewatering well and its effect on each pile are estimated, then for multiple wells, neglecting inter-well and inter-pile interactions, linear superposition of the effects of the wells amounts to the total dewatering-induced action on the pile foundation, which then can be employed to calculate the corresponding pile foundation settlement. The sensitivities of the pile foundation settlement thus obtained with respect to the related parameters, including the total pile length, the pile length below the initial phreatic surface, the Poisson's ratio and the modulus of compression of the soil, the drawdown at pile location, the distance between pile tip and the depressed phreatic surface, and the pumping rate, can be analytically calculated. A synthesized case analysis of a near-pile dewatering situation for the construction of a metro tunnel in Beijing is presented.

2 CALCULATION OF PUMPING-INDUCED PILE FOUNDATION SETTLEMENT

2.1 *General procedure*

Dewatering induces soil settlement, as a result of soil compression due to the increase in the effective stress caused by groundwater drawdown, and such soil settlement exerts negative skin friction on nearby pile shafts and thus causes additional pile foundation settlement. The following procedure (Chen & Xiang 2006) is employed to estimate the dewatering induced pile settlement: (1) calculation of pumping induced groundwater drawdown, (2) calculation of the corresponding effective stress and compressive strain increments, (3) calculation of the corresponding negative skin friction on pile shaft, (4) calculation of the dewatering induced pile foundation settlement.

2.2 *Calculation steps*

2.2.1 *Calculation of drawdown*

For a partially or fully penetrated well in phreatic zone, pumping induced groundwater drawdown can be

calculated by using the theory developed by Neuman (1972, 1973, 1974):

$$w(r,z,t)=\frac{Q}{4\pi T}\int_0^\infty 4yJ_0(y\beta^{1/2})[u_0(y)+\sum_{n=1}^{\infty}u_n(y)]dy \tag{1}$$

where Q denotes pumping rate; T initial transmissivity, a product of horizontal radial hydraulic conductivity, K_r, and thickness of the phreatic zone, H; J_0 zero-order Bessel function of the first kind; $\beta = K_z r^2/K_r H^2$, with K_z being the vertical hydraulic conductivity, and r the horizontal radial distance; z the vertical location; u_0 and u_n denote known functions with parameters involving the storage coefficient, the hydraulic conductivity, time of pumping duration, initial phreatic zone thickness, position of the pumping screen, specific yield of the ground, and coordinates of the point of interest.

When multiple wells are involved, the linear relationship between the drawdown and the pumping rate allows superposition for calculation of the total drawdown.

2.2.2 *Calculation of effective stress and compressive strain increments*

As shown in Figure 1, the depressed piezometric surface at the pile may be above or below the pile tip. With the objective being to evaluate the total effective stress increment, it is convenient and rational to average the effective stress and the corresponding compressive strain over the vertical range of drawdown (assuming instantaneous consolidation and vertical 1-D compression):

$$\bar{\varepsilon}=\frac{\overline{\Delta\sigma}}{\overline{E_s}} \tag{2}$$

where with the bar symbolizing averaging, $\Delta\sigma$ denotes the effective stress increment in the soil around the pile, E_s the modulus of compression (with soil settlement as the subject of concern, harmonic averaging can be employed for layered soils), and ε the compressive strain.

For case (a) as shown in Figure 1(a), the averaged effective stress at the pile can be expressed as:

$$\overline{\Delta\sigma}=\gamma_w\cdot w_c/2 \tag{3a}$$

and for case (b) as shown in Figure 1(b):

$$\overline{\Delta\sigma}=\gamma_w\cdot l_p/2 \tag{3b}$$

where w_c represents the drawdown at the pile center location, and l_p the pile length in the phreatic zone.

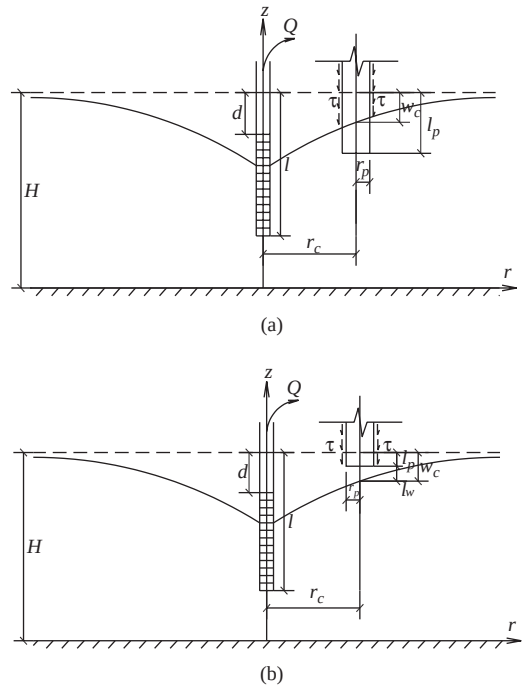


Figure 1. Effects of dewatering on a nearby pile: (a) $w_c \le l_p$, (b) $w_c > l_p$ (τ denotes the dewatering induced negative skin friction on pile shaft, w_c drawdown at pile center, l_p the pile length below the initial phreatic surface, and l_w the distance between the pile base and the depressed piezometric surface below).

2.2.3 *Calculation of negative skin friction on pile shaft*

According to Randolph & Wroth (1978), the relationship between the soil settlement, s, and the induced skin friction, τ, can be assumed as:

$$\tau=\frac{G_s}{r_p\ln(r_m/r_p)}\cdot s \tag{4}$$

where G_s denotes the averaged shear modulus of the soil around pile shaft, r_p the pile radius, r_m the effective radius of influence, $r_m = 2.5L\rho(1-\nu)$ with L, ν and ρ being the effective pile length influenced by the dewatering-induced negative skin friction, the Poisson's ratio and the ratio of the shear modulus at the pile mid-depth to that at the tip, respectively.

The pumping induced soil settlement can be estimated as, for case (a):

$$s=\bar{\varepsilon}w_c \tag{5a}$$

and for case (b):

$$s=\bar{\varepsilon}l_p \tag{5b}$$

2.2.4 *Calculation of pile foundation settlement*

Denoting the surcharge load that the negative skin friction amounts to as F, using a semi-theoretical method recommended in the Chinese code (China Ministry of Construction 2002), the total pile settlement can be calculated as:

$$\delta = \psi \sum_{j=1}^{m} \delta_j = \psi \sum_{j=1}^{m} \frac{F}{abE_{sj}} (z_j \alpha_j - z_{j-1} \alpha_{j-1}) \tag{6}$$

where a and b denote the length and width of the pile foundation base, respectively, E_{sj} stands for the modulus of compression of the jth layer of soil below the pile tip, z_j the distance of the bottom of the jth soil layer below the pile tip, α_j a coefficient for the averaged incremental stress over the range of z_j, Ψ an empirical coefficient, and m the number of soil layers adequate for calculation of pile settlement. Both α_j and Ψ can be obtained via empirical tables, and m is related to the depth of calculation, z_m, which must satisfy:

$$\Delta\delta_m \le 0.025 \sum_{j=1}^{m} \delta_j \tag{7}$$

where $\Delta\delta_m$ stands for the settlement of the soil zone Δz distant above z_m, and Δz is an empirical number dependent on the pile diameter.

Substituting all the interim relationships into equation (6) yields the following expressions:

$$\delta = \psi \sum_{j=1}^{m} \frac{\pi l_m \gamma_w w_c^2 (2\nu - 1)}{2(\nu\text{-}1) abE_{sj} \ln 20} (z_j \alpha_j - z_{j-1} \alpha_{j-1}) \tag{8a}$$

$$\delta = \psi \sum_{j=1}^{m} \frac{\pi l \gamma_w l_p^2 (2\nu - 1)}{2(\nu - 1) abE_{sj} \ln 20} (z_j \alpha_j - z_{j-1} \alpha_{j-1}) + \frac{\gamma_w (l_p + w_c)}{2\overline{E_s}} l_w \tag{8b}$$

for case (a) and (b), respectively.

3 EXAMPLE

3.1 *Sensitivity calculation*

Shown in Table 1 are the relevant parameters of a typical soil profile for the construction of a metro line in Beijing, where excavations often have to be conducted in the vicinity of municipal overpasses supported on pile foundations. Consider a phreatic zone with the water table located 10 m below the ground surface, a pumping well with a flow rate of 2.4 m^3/h and a pile of a length 10.5 m and a diameter of 1 m located 10 m away from the well. Treat the well as a line sink along its perforated portion (neglecting well storage and presence of seepage face), and the phreatic zone with a thickness of 14.3 m is assumed to be homogeneous and isotropic with an averaged hydraulic conductivity of 0.0928 m/h, a storage coefficient of 2.4×10^{-3} and a specific yield of 0.24. Referring to Code for Design of Building Foundation (China Ministry of Construction 2002), Ψ is assumed to be 0.2.

Table 1. Physical-mechanical parameters of soils.

Soil layer	Thickness/m	E_s/MPa	v	G_s/MPa
sand & gravel	13.4	19.8	0.27	6.3
silt	0.8	11.4	0.30	3.3
sand & gravel	3.8	43.9	0.26	14.2
pebble	6.3	87.8	0.2	32.9
clay	4.8	10.2	0.3	2.91

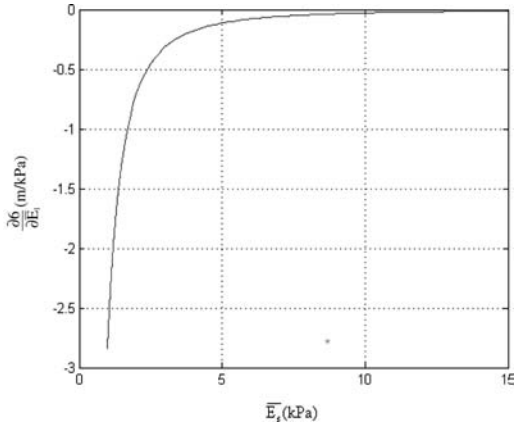


Figure 2. Sensitivity of the pile settlement in case (b) with respect to the averaged modulus of compression of soil.

The sensitivities of the pile foundation settlement with respect to the relevant parameters can be easily calculated by using the expressions in equations (8a) and (8b). For example, the pile settlement in case (a) is not explicitly related with the averaged modulus of compression of the soil around the pile shaft, whereas at steady state, the depressed phreatic surface is below the pile tip, corresponding to case (b), the sensitivity of the pile settlement with respect to the averaged modulus of compression of the soil around pile shaft can be calculated as shown in Figure 2.

3.2 *A synthesized case analysis*

Dewatering is needed for the construction of a metro tunnel in Beijing, with the same soil condition as in Table 1, and a total of 13 wells, each with a pumping rate of 2 m^3/h, are employed. As shown in Figure 3 and Figure 4, two pile foundations of a municipal overpass are located at the left and the right hand sides of the tunnel, respectively; the 1# foundation consists of

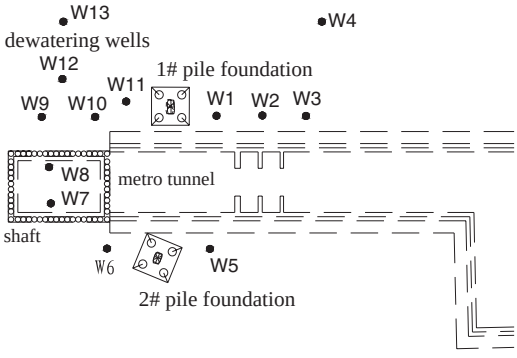


Figure 3. Layout of dewatering wells and pile foundations.

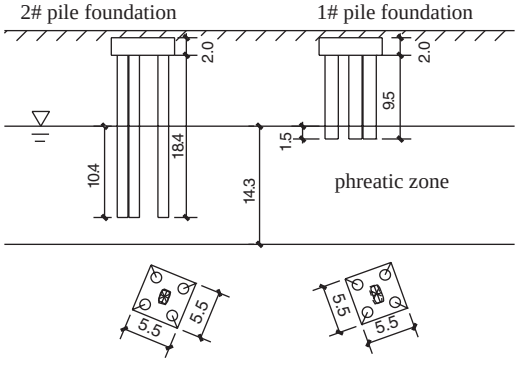


Figure 4. Profile of phreatic zone and pile foundations (m).

four piles of a diameter 1.5 m, and the 2# foundation four piles of a diameter 1.2 m. The relative distances between the wells and the pile foundations are shown in Table 2.

Shown in Table 3 are the dewatering induced drawdown, negative skin friction, additional force and pile foundation settlements, from which the following observations may be obtained:

(i) For the 1# foundation (with shorter piles), during the earlier stage of pumping, when the depressed phreatic surface is above the pile tips, the additional forces on the piles and the foundation settlement increase quadratically with the drawdown, and when the depressed phreatic surface goes below the pile tips, the compression of the soil below the pile tips due to consolidation results in further foundation settlement until steady state is reached, even though there is no increase in the additional forces on the piles.

(ii) The 2 # foundation consists of longer piles, thus the depressed phreatic surface in the entire dewatering operation is always above the pile tips, and the additional force and settlement increase with pumping duration and the final values at steady state are larger than those for the 1# foundation.

(iii) Because of the combined effect of the negative skin friction on the portion of pile shafts that is above the depressed phreatic surface and the consolidation settlement of the soil below the pile tips, the dewatering induced pile foundation settlement could exceed the consolidation settlement of the surrounding soil.

Table 2. Horizontal distances between wells and pile foundations (m).

Well	w1	w2	w3	w4	w5	w6	w7	w8	w9	w10	w11	w12	w13
1 F.	6.8	13.4	19.7	21.9	21.3	22.5	22.4	19.8	18.9	11.1	6.6	16.3	19.9
2 F.	22.2	25.6	29.8	43.5	7.7	7.5	17.4	20.5	26.5	22.3	23.1	29.3	36.8

Table 3. Dewatering induced additional force on and settlement of 1# and 2# pile foundations.

Time/h		w/m	τ/kPa	F/kN	δ/mm		w/m	τ/kPa	F/kN	δ/mm
t = 1	1#	0.037	9.17E−04	0.139	0.00	2#	0.023	3.27E−04	0.040	0.00
t = 5	F.	0.189	0.024	3.631	0.03	F.	0.121	0.009	1.146	0.00
t = 10		0.334	0.073	11.531	0.10		0.222	0.032	3.939	0.03
t = 50		0.805	0.426	70.738	0.62		0.621	0.248	32.213	0.23
t = 100		1.025	0.691	117.523	1.03		0.830	0.442	58.873	0.41
t = 500		1.543	1.481	265.188	2.35		1.339	1.150	161.999	1.14
t = 1000		1.763	1.481	265.188	2.53		1.560	1.562	225.185	1.59
t = 5000		2.211	1.481	265.188	2.97		2.030	2.645	400.017	2.82
t = 10000		2.343	1.481	265.188	3.12		2.209	3.133	482.266	3.39
t = ∞		2.403	1.481	265.188	3.19		2.393	3.676	576.095	4.05

4 SUMMARY

The main influencing factors for dewatering induced pile foundation settlement in phreatic zone include: drawdown, seepage and deformation characteristics of soil, and the interaction between soil and pile. A theoretical model for multi-well pumping in phreatic zone, an averaged effective stress approach and a linear elastic interaction model are adopted to estimate the dewatering induced pile foundation settlement. Illustrative examples, including sensitivity calculation and a synthesized case analysis, are presented.

Two situations may be distinguished: (1) when the depressed phreatic surface is above the pile tip, the pile settlement are mainly influenced by drawdown, consolidation compression of the soil around the pile shaft and the degree of interaction between soil and pile, the additional force and the pile settlement increase with the drawdown squared; (2) when the phreatic surface is depressed to below the pile tip, the consolidation of the soil below the pile tip needs to be included. The dewatering induced pile foundation settlement could exceed the settlement of the surrounding soil as a result of the combined effect of the negative skin friction on the portion of pile shafts that is above the depressed phreatic surface and the consolidation settlement of the soil below the pile tips.

REFERENCES

Chen, S. & Xiang, Y. 2006. A procedure for theoretical estimation of dewatering-induced pile settlement. *Computers and Geotechnics* 33(4–5): 278–282.

China Ministry of Construction 2002. *Code for Design of Building Foundation* (GB50007-2002) (in Chinese).

Neuman, S.P. 1972. Theory of flow in unconfined aquifers considering delayed response of the water table. *Water Resources Research* 8(4): 1031–1045.

Neuman, S.P. 1973. Supplementary comments on 'Theory of Flow in Unconfined Aquifers Considering Delayed Response of the Water Table'. *Water Resources Research* 9(4): 1102–1103.

Neuman, S.P. 1974. Effect of partial penetration on flow in unconfined aquifers considering delayed gravity response. *Water Resources Research* 10(2): 303–312.

Randolph, M.F. & Wroth, C.P. 1978. Analysis of deformation of vertically loaded piles. *Journal of Geotechnical Division* 104(GT12): 1465–1488.

This page intentionally left blank

Underground Space – the 4th Dimension of Metropolises – Barták, Hrdina, Romancov & Zlámal (eds)
© 2007 Taylor & Francis Group, London, ISBN 978-0-415-40807-3

Estimation of rock load for the design of 2-arch tunnel lining

Kwangho You
University of Suwon, Hwasung-Si, Kyeonggi-Do, Korea

Myung Sagong, Jun S. Lee
Korea Railroad Research Institute, Uiwang-Si, Kyeonggi-Do, Korea

ABSTRACT: In this study, the existing methods proposed to estimate relaxed rock load due to a tunnel excavation are compared and analyzed. Also a new approach, by which the stress relaxed zone around an excavated tunnel periphery can be systematically estimated, was suggested for the design of 2 – arch tunnel lining. To this end, local factors of safety are calculated from the redistributed stresses after the excavation of a tunnel. The height of the relaxed rock load is inferred based on the assumption that the stress relaxed zone might coincide with the region corresponding to the local safety factor of 2.0 or 3.0. The new approach proposed in this study has the advantage of estimating the height of rock load regardless of the shape of a tunnel and the ground conditions. Since the height of the relaxed rock load is estimated from the local factor of safety, which is a relatively clear criterion, the designer's subjectivity involved in the design of concrete tunnel lining might be reduced.

1 INTRODUCTION

The estimation of rock load is very important for the design of tunnel lining. Terzaghi's rock load method, Bierbäumer's equation, empirical methods based on RMR and Q system, and numerical approaches have been mainly used for the estimation of rock load.

To estimate rock load of a tunnel excavated in rock mass, Terzaghi's rock load classification table, RMR index, or Q value can be used but these methods are merely empirical. The Terzaghi's and Bierbäumer's proposed equations are also applied. However, these equations were derived based on the limit equilibrium theory with the assumption that the rock mass was continuous. In numerical approaches, on the other hand, rock load is inferred from the stresses behind shotcrete or plastic zones occurred due to tunnel excavation during the stability analysis of tunnels. Nevertheless, these approaches are so ad hoc that the estimated rock load may be different designer by designer.

In this study, therefore, the existing methods are compared and analyzed, and a new systematic way is demonstrated to estimate the stress relaxed zone of a tunnel due to excavation. Also, the proposed method is applied for the design of 2-arch tunnel lining.

2 THE ESTIMATION OF TUNNEL ROCK LOAD

2.1 *Terzaghi's equation*

Terzaghi(1946) applied the failure mechanism shown in Figure 1 to calculate rock load which a tunnel lining should support when the tunnel was excavated in cohesionless dry coarse soil. Vertical rock load (P_{roof}) was suggested by Equation (1) for shallow tunnels.

$$P_{roof} = \frac{\gamma B}{2K\tan\phi}(1 - e^{K\tan\phi\frac{2H}{B}}) \quad (1)$$

where B is the relaxed range ($= 2[\, b/2 + m\,tan(45 - \phi/2)]$), v is the unit weight of rock mass, K is coefficient of lateral earth pressure, ϕ is friction angle, b, m, and H are the width, height, and depth of a tunnel respectively.

For deep tunnels, the vertical rock load was also suggested as follows;

$$P_{roof} = \frac{\gamma B}{2K\tan\phi}(const.) \quad (2)$$

2.2 *Bierbäumer's equation*

Bierbäumer (1913) assumed that the shape of stress relaxed zone occurred due to tunnel excavation might

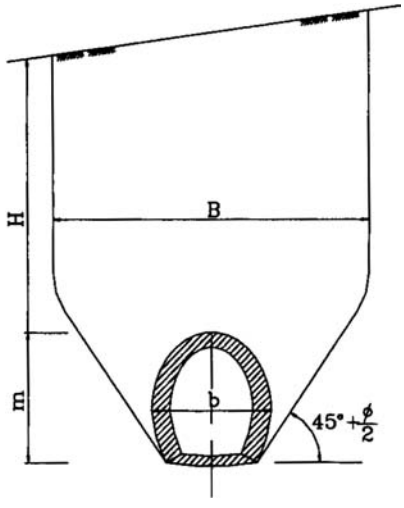


Figure 1. The assumed failure mechanism for Terzaghi's rock load.

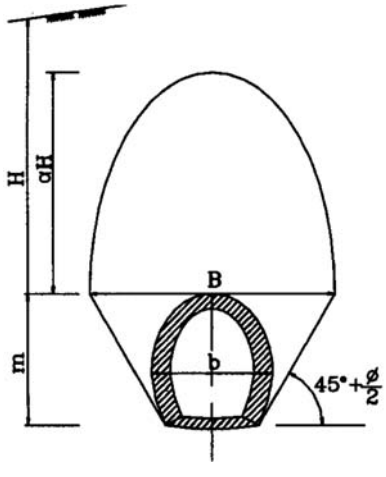


Figure 2. The assumed relaxed zone of Bierbäumer.

be a parabola as shown in Figure 2 (Part, 2003). In Figure 2, b is the internal friction angle of rock mass, m is the tunnel height, and B is the width of the relaxed zone.

As can be seen in Figure 2, the upper relaxed zone acts on the tunnel along $45+\phi/2$ inclined plane as a vertical load. The height of the relaxed zone (h) is assumed to be proportional to the depth of the tunnel (H); $h=\alpha H$ (α is reduction factor). At tunnel crown, the vertical relaxed load (P_{roof}) can be given as follows;

$$P_{roof} = \alpha H \nu \tag{3}$$

where, ν is the unit weight of rock mass. And the reduction factor can be obtained as follows;

- when H is very small;

$$\alpha = 1 \tag{4}$$

- when $H \leq 5B$;

$$\alpha = 1 - \frac{\tan\phi \tan^2(45-\phi/2)\, H}{b + 2m\tan(45-\phi/2)} \tag{5}$$

- when $H \geq 5B$;

$$\alpha = \tan^4(45-\phi/2) \tag{6}$$

2.3 *Empirical approaches*

2.3.1 *Terzaghi's rock load classification*

Terzaghi (1946) proposed rock load classification for steel rib support and then Rose modified it as shown in Table 1 in 1982. In the system, rock load conditions are divided into 9 categories. However it is very subjective and can be applicable only for the horseshoe shaped tunnels.

2.3.2 *Approach based on the RMR classification system*

Unal(1983) proposed the following empirical equation for the estimation of vertical rock load (P_{roof}) based upon RMR values which a tunnel should be supported:

$$P_{roof} = \nu b\left(\frac{100-RMR}{100}\right) \tag{7}$$

where ν is the unit weight of rock mass and b is tunnel width.

2.3.3 *Approach based on the Q system*

Barton et al. (1974) proposed an empirical equation for the estimation of vertical rock load (P_{roof}) based on Q values as follows;

if the number of joint sets ≥ 3;

$$P_{roof} = 2\,Q^{-1/3} J_r^{-1} \quad (kg/cm^2) \tag{8}$$

if the number of joint sets <3 ;

$$P_{roof} = \frac{2}{3}\sqrt{J_n}\,Q^{-1/3} J_r^{-1} \quad (kg/cm^2) \tag{9}$$

where Q is Q value, J_n is the number of joint sets, and J_r is the joint roughness coefficient.

Also, horizontal rock load (P_{wall}) can be calculated from the same equations applied for P_{roof} with the transformed Q value (Q′) according to Table 2.

2.4 *Numerical approach*

Chun and Shin (2001) investigated a methodology to estimate rock load numerically for the design of concrete lining of a tunnel. They assumed that concrete

Table 1. Terzaghi's rock load classification (Rose, 1982).

Rock condition	RQD	Rock load height, H_p(m)	Remarks
1. Hard and intact	95 ~ 100	0	Light limiting required only if spalling or popping occurs.
2. Hard stratified or schistose	90 ~ 99	0 ~ 0.5b	Light support, mainly for protection against spalling. Load may change erratically from point to point.
3. Massive, moderately jointed	85 ~ 95	0 ~ 0.25b	
4. Moderately blocky and seamy	75 ~ 85	0.25b ~ 0.20 (b + m)	Types 4, 5 and 6 reduced by about 50% from Terzaghi values because water table has little effect on rock load. (Terzaghi, 1946; Brekke, 1968)
5. Very blocky and seamy	30 ~ 75	(0.20 ~ 0.60) (b + m)	
6. Completely crushed but chemically intact	3 ~ 30	0.60 ~ 1.10 (b + m)	
6a. Sand and gravel	0 ~ 3	1.10 ~ 1.40 (b + m)	
7. Squeezing rock, moderate depth	NA	(1.10 ~ 2.10) (b + m)	Heavy side pressure, invert struts required. Circular ribs are recommended.
8. Squeezing rock, great depth	NA	(2.10 ~ 4.50) (b + m)	–
9. Swelling rock	NA	Up to 250ft irrespective of value of (b + m)	Circular ribs required. In extreme cases, use yielding support.

Note: b: tunnel width, m: tunnel height.

Table 2. Transformed Q value.

Range of Q value	Q′
$10 < Q$	5Q
$0.1 \leq Q \leq 10$	2.5Q
$Q < 0.1$	Q

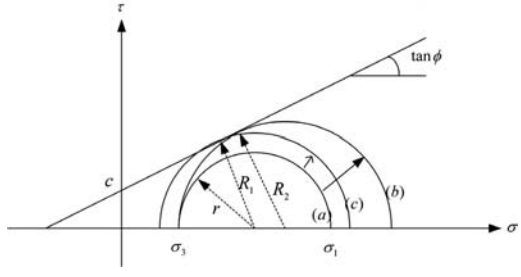


Figure 3. Local factor of safety.

lining must support the whole load when the shotcrete lost its support capability after long period time.

They compared two ways of calculating rock load which the lining supports. One way is that rock load can be proportional to the size of the plastic zone occurred around tunnel excavation periphery. The other way is that rock load can be a function of radial stresses occurred behind shotcrete.

As the results, it was concluded that the radial stresses behind shotcrete might not be properly used as rock load because it became much greater around lower corner than around crown and its magnitude was very small. Also when the rock load is estimated to be proportional to the size of plastic zone, it can be very sensitive to the ground properties such as cohesion and the coefficient of lateral earth pressure etc. Therefore, they recommend that great care must be given in estimating ground parameters for the design of tunnel lining.

3 LOCAL SAFETY FACTOR OF A TUNNEL

In numerical analysis, state of stresses can presented at each elements in terms of principal stresses (σ_1 and σ_3) as shown in Figure 3. This stress state is, in general, depicted by a Mohr's circle (*a*) with a radius *r* in

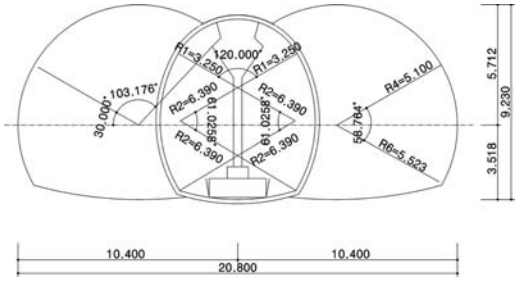


Figure 4. Tunnel section of interest.

the σ-τ plane. Failure is assumed to occur when the circle touches the failure envelope. If failure occurs at a certain stress state, σ_1 should increase keeping σ_3 unchanged until the circle touches the failure envelope like circle (*b*). (Itasca Consulting Group, 1999). Also, failure can be reached by increasing the radius of the circle keeping the center of a circle fixed like circle (*c*). The ratio of two circles' radii (R_1/r, or R_2/r) is a kind of strength/stress ratio in a given state of stresses and is often called as 'local factor of safety (FS)'.

In this study, local factor of safety is obtained with the assumption that failure occurs by increasing σ_1 and keeping σ_3 unchanged. The maximum principal stress at the moment of failure (σ_{1f}) can be written as follows;

$$\sigma_{1f} = (\frac{1+\sin\phi}{1-\sin\phi})\sigma_3 - 2c\sqrt{\frac{1+\sin\phi}{1-\sin\phi}} \quad (10)$$

This approach can be very effective in explaining how close the failure is at each element. In addition, it is very useful in searching potential weak zones from tunnel excavation and the zone where supports are required (You, et al., 2000).

$$FS = \frac{R_2}{r} = \frac{\sigma_3 - \sigma_{1f}}{\sigma_3 - \sigma_1} \quad (11)$$

Therefore, it is expected that the size of relaxed zone occurred by tunnel excavation could be found by finding the contour of local safety factor of 2.0 or 3.0.

4 NUMERICAL ANALYSIS

In this study, a numerical analysis was performed to estimate rock load height for the design of 2-arch tunnel lining. The 2-arch tunnel has a cross section of 20.8 m wide and 9.23 m high as shown in Figure 4. In numerical modeling, the construction sequence are simplified into 3 stages; excavation of center tunnel (stage I), excavation of left arch tunnel (stage II), and excavation of right arch tunnel (stage III).

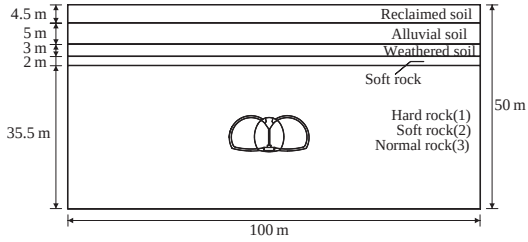
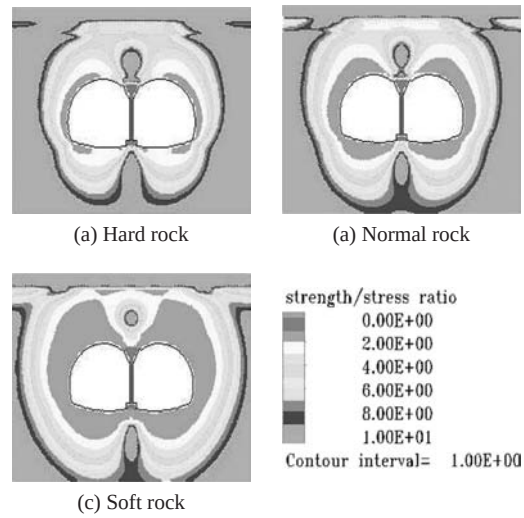


Figure 5. Configuration of numerical analysis.

Table 3. Properties for layers.

Layer	Unit weight (tf/m^3)	Cohesion (tf/m^2)	Friction angle (°)	Deformation modulus (tf/m^2)	Poisson's ratio
Reclaimed soil	1.8	1.0	27	800	0.35
Alluvial soil	1.8	0.5	28	900	0.40
Weathered soil	2.0	1.0	30	3,000	0.30
Soft rock	2.3	10.0	33	260,000	0.27
Normal rock	2.6	20.0	34	300,000	0.25
Hard rock	2.7	30.0	38	550,000	0.22



(a) Hard rock (a) Normal rock

(c) Soft rock

Figure 6. Contours of local safety factors at final construction stage for 3 different rock conditions.

As can be seen in Figure 5, reclaimed soil layer, alluvial soil layer, and weathered soil layer are located at the top of the tunnel. Three different layers; hard, soft, and normal rock layer at which the tunnel is located was modeled respectively to get an idea how ground conditions influence the rock load height. The properties of each layer used for the numerical analysis are listed at Table 3.

Table 4. Estimated thickness of relaxed zone.

Layer	Excav. stage	Elevation of local safety factor (m)		Thickness of relaxed zone (m)		Elevation of tunnel crown (m)
		FS = 2.0	FS = 3.0	FS = 2.0	FS = 3.0	
Hard	I	9.44	10.0	0.59	1.15	8.85
rock	II	10.0	11.6	0.7	2.3	9.3
	III	10.3	12.25	1.0	2.95	9.3
Normal	I	10.07	10.75	1.22	1.9	8.85
rock	II	11.4	13.25	2.1	3.95	9.3
	III	11.95	13.9	2.65	4.6	9.3
Soft	I	11.4	12.45	2.55	3.15	8.85
rock	II	14.6	17.1	5.3	7.8	9.3
	III	15.75	17.15	6.45	7.85	9.3

FLAC version 3.4 was used for the numerical analysis. At each element, the local safety factor was calculated and its contour was obtained at 3 different construction stages. Figure 6 shows the contour of local safety factors at construction stage III which is the final stage of the construction. The thickness of relaxed zone which can be considered to be rock load height was obtained by subtracting the elevation of tunnel crown from the elevation of local safety factor contour and the results are arranged in Table 4.

From Table 4 and Figure 6, it can be known that as rock conditions become weaker and construction advances, the relaxed zone expands and its thickness increases. Especially, it can be concluded that local safety factor of 2.0 or 3.0 can give a realistic rock load height for the design of concrete lining. In addition, this approach can be effectively used as a systematic way of estimating rock load height for concrete lining design.

5 CONCLUSIONS

In this study, the existing methods of estimating rock relaxed load were compared. A systematic way was proposed to estimate the relaxed zone around a tunnel periphery due to the excavation for the design of 2-arch tunnel lining. In this approach, first of all, local safety factor is calculated from the redistributed stresses due to the tunnel excavation. Then rock load height is estimated based on the assumption that the region corresponding to the local safety factor of 2.0 or 3.0 might be the relaxed zone.

The proposed approach in this study is independent of the shape of a tunnel and ground conditions since rock load height is estimated from a fairly clear and well established criterion of local safety factor. Additionally, it is expected that a tunnel designer' subjectivity might be avoided in the design of concrete lining.

ACKNOWLEDGEMENTS

This study was partly funded by the Korea Institute of Construction and Transportation Technology Evaluation and Planning under Korean Ministry of Construction and Transportation in Korea (Grant No.: 05-D01, Development of Water Control Technology in Undersea Structures). The authors deeply appreciate the authorities concerned.

REFERENCES

Barton, N., Lien, R. and Lunde, J. (1974), "Engineering Classification of Rock Masses for the Design of Tunnel Support", *Rock Mechanics*, Vol. 6, No. 4, pp. 189–236.

Bierbäumer, A. (1913), *Die Dimensionnierung des Tunnelmanerwerks*.

Itasca Consulting Group, Inc. (1999), FLAC, Fast Lagrangian Analysis of Continua, Version 3.4, Itasca Consulting Group, Minneapolis, Minnesota, USA.

Rose, D. (1982), "Revising Terzaghi's Tunnel Rock Load Coefficient", *Proc. 23rd U.S. Symposium on Rock Mechanics*, AIME, New York, pp. 953–960.

Terzaghi, K. (1946), "Rock Defects and Loads on Tunnel Support", *Rock Tunneling with Steel Supports*, eds. R. V. Proctor and T. White, Commercial Shearing Co., Youngstown, Ohio, USA, pp. 15–99.

Unal, E. (1983), Design Guideline and Roof Control Standards for Coal Mine Roofs, Ph.D. Thesis, The Pennsylvania State University, 355p.

Park, Si-Hyun (2003), "A study on the review of Terzaghi's tunnel load theory", *Tunnelling Technology*, Vol. 5, No. 3, pp. 261–268.

You, Kwang-Ho, Yeon-Jun Park, Gyu-Jin Bae (2000), "An assessment of safety factor for tunnels excavated in a weak rock layer", *J. of Korean Tunnelling Association*, Vol. 2, No. 3, pp. 47–57.

Chun, Byung-Sik, Young-Wan Shin (2001), "A study on the design loads of NATM tunnel concrete lining", *J. of Korean Society for Rock Mech.*, Vol. 11, No. 2, pp. 96–108.

This page intentionally left blank

Underground Space – the 4th Dimension of Metropolises – Barták, Hrdina, Romancov & Zlámal (eds)
© 2007 Taylor & Francis Group, London, ISBN 978-0-415-40807-3

An analytical solution of shield tunnel based on force method

Xiaomin You, Zixin Zhang, Yongsheng Li
Department of Geotechnical Engineering, Tongji University, Shanghai, P.R.China

ABSTRACT: Based on the released assumption of the given distribution of soil resistance pressure, the 'force method' is used to determine the internal forces, displacements and the distribution range of soil resistance of shallow shield tunnel lining. This paper considers those factors which would affect the distribution range in detail, such as tunnel geometry, stiffness, soil resistance coefficient, etc. The comparison is also made between the numerical results and the analytical solution under the same condition. And the analytical solution makes a good agreement with the numerical results.

1 INTRODUCTION

With the rapid development in modern city, people's demands for convenience in commuting and living are expanding, while the city space is limited. Recent advancements in tunnelling construction technology help to mitigate the problem, for its virtue to minimize the influence to superstructures and so people's daily life.

Nowadays, shield tunnels in urban area have two points in common, i.e. large section and shallow embedded depth. The outer diameter of shield tunnels constructed in Shanghai in recent years has increased from 6.2 m to 15 m while the ratio of thickness versus diameter correspondingly decreased from 0.060 to 0.043. To reduce the influence to the surrounding environment, the embedded depth of shield tunnel should be 1–1.5 times of its diameter (Zhang et al. 2004). However, shield tunnels are usually embedded at the depth less than its diameter, especially when they are advanced away or close to shafts. Shanghai Yangtse River Tunnel with diameter of 15 m is embedded 6.9 m when near the shafts.

On the other hand, different design models (Morgan 1961, Muir Wood 1975, I.T.A. 2000) are presented with the advancements in theoretical analysis. Models (Lee et al. 2001, Koyama 2003) based on Force-method are still widely used even in today, for the reason of clear mechanics concepts and simple and effect calculation. However, in most common models, soil resistant pressure is assumed to be distributed in the range of 45°∼145°. Considering the special characteristic of large section, relative thinner thickness and shallow embedded depth for current tunnels, whether the distribution of soil resistant pressure will change and how the effect this kind of change will bring to behavior of tunnel lining should be carefully studied.

The purpose of this paper is to develop an analytical solution for shield tunnel to study the change of distribution of soil resistant pressure. The proposed solution is then compared with conventional model solution and numerical simulation results.

2 DEDUCTION BASED ON FORCE-METHOD

The proposed solution focuses on the change of the distribution of soil resistant pressure around tunnel lining, so the existence of joints is not under consideration in this paper. Tunnel lining is assumed to be a continuous circle ring, and the load pattern is shown in Figure 1. The loads $p_1 \sim p_6$ on the tunnel lining have been defined

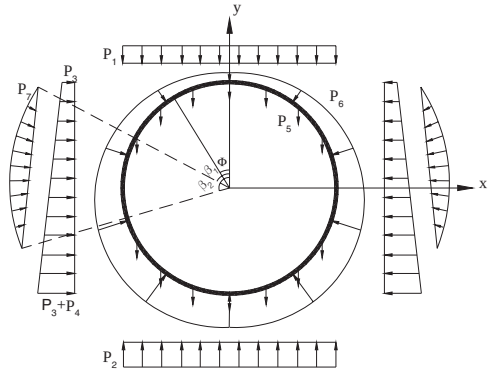


Figure 1. Load Condition of Tunnel Lining.

by Liu & Hou 1991, where p_1 is the vertical earth pressure at crown of lining; p_2 is the reaction pressure at bottom of lining; p_3 is the horizontal earth pressure at the crown level of tunnel lining; p_4 is the additional horizontal earth pressure at the bottom level of tunnel lining; p_5 is the self-weight of tunnel lining; and p_6 is the hydrostatic pressure. In the proposed solution, the distribution of soil resistant pressure p_7 ranges from β_1 to β_2. The soil resistant pressure, p_7, is defined as:

$$P_7 = -K\delta \cdot \cos(A\varphi + B\pi) \tag{1}$$

where δ is the largest radial displacement of tunnel lining, which is assumed to be at the middle of β_1 and β_2, $A = \pi/\Delta\beta$, $B = (\beta_2 - 3\beta_1)/\Delta\beta$, $\Delta\beta = \beta_2 - \beta_1$. β_1 is the first angle where the radial displacement is zero, measured from the vertical direction; β_2 is the second angle where the radial displacement is zero, also measured from the vertical direction. K is the soil resistance coefficient. The typical values of K are shown in Table 1.

For the convenience of describing the deduction, the sign conventions in this paper are: the bending moment is positive when the inside surface of tunnel lining is subject to tension; the axial force is positive when the tunnel lining is subject to compression; the shear force is positive when it tends to make the lining rotate counterclockwise.

For the symmetry of tunnel structure and load pattern, the model for calculation can be simplified as Figure 2, and the Force-method equation can be given as follows:

$$\begin{cases} \delta_{11}x_1 + \Delta_{1p} = 0 \\ \delta_{22}x_2 + \Delta_{2p} = 0 \end{cases} \tag{2}$$

where x_1 and x_2 are, respectively, the bending moment and the axial force at the elastic centre; δ_{ii} is the displacement at the location of x_i on the direction of x_i due to the unit force $x_i = 1, i = 1, 2$; Δ_{ip} is the displacement at the location of x_i on the direction of x_i due to the loads around the tunnel lining.

Solve the Equation (2), and then x_1 and x_1 are given as follows:

$$\begin{cases} x_1 = -\dfrac{\Delta_{1p}}{\delta_{11}} \\ x_2 = -\dfrac{\Delta_{2p}}{\delta_{22}} \end{cases} \tag{3}$$

Let $x_1 = 1, x_2 = 0$, and $x_1 = 0, x_2 = 1$, respectively, then the internal forces, $\overline{M}_1$, $\overline{N}_1$, $\overline{Q}_1$ and $\overline{M}_2$, $\overline{N}_2$, $\overline{Q}_2$ are:

$$\begin{cases} \overline{M}_1 = 1 \\ \overline{N}_1 = 0 \\ \overline{Q}_1 = 0 \end{cases} \text{ and } \begin{cases} \overline{M}_2 = -R \cdot \cos\varphi \\ \overline{N}_2 = \cos\varphi \\ \overline{Q}_2 = -\sin\varphi \end{cases} \tag{4}$$

According to the virtual work principle, δ_{11} and δ_{22} can be determined by

$$\begin{cases} \delta_{11} = \int_0^{\pi} \dfrac{\overline{M}_1^{\,2}}{EI} ds = \dfrac{R\pi}{EI} \\ \delta_{22} = \int_0^{\pi} \dfrac{\overline{M}_2^{\,2}}{EI} ds = \dfrac{R^3\pi}{EI} \end{cases} \tag{5}$$

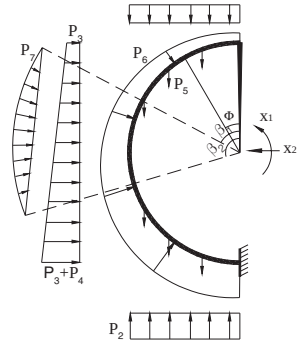


Figure 2. Simplified model for calculation.

Table 1. Typical values of soil resistance coefficient for clay (Zhang et al. 2004).

Ground Condition	Clay					Sand		
	Silt	Soft	Medium	Stiff	Very stiff	Loose	Dense	Very dense
$K(10^3\text{kN/m}^3)$	0	0∼5	5∼10	10∼30	30∼50	0∼10	10∼30	30∼50
SPT N-value	0∼2	2∼4	4∼8	8∼25	>25	<15	15∼30	>30

The internal forces, M_p, N_p, Q_p, caused by surrounding loads, is the accumulation of seven loading cases as shown in Figure 1:

$$\begin{cases} M_p = \sum_{j=1}^{7} M_{pj} \\ N_p = \sum_{j=1}^{7} N_{pj} \\ Q_p = \sum_{j=1}^{7} Q_{pj} \end{cases} \tag{6}$$

where M_{pj}, N_{pj}, Q_{pj} are bending moment, axial force, and shear force due to the loading case j, respectively.

For loading case 1–6, the solution is as usual one. However, the solution for case7 is as follows:

$$M_{p7} = \begin{cases} 0 & 0 \le \varphi < \beta_1 \\ \dfrac{\Delta\beta K\delta R^2}{\Delta\beta^2 - \pi^2}\left[\Delta\beta\cos(A\varphi + B\pi) + \pi\sin(\varphi - \beta_1)\right] & \beta_1 \le \varphi < \beta_2 \\ \dfrac{\pi\Delta\beta K\delta R^2}{\Delta\beta^2 - \pi^2}\left[\sin(\varphi - \beta_1) + \sin(\varphi - \beta_2)\right] & \beta_2 \le \varphi \le \pi \end{cases} \tag{7}$$

$$N_{p7} = \begin{cases} 0 & 0 \le \varphi < \beta_1 \\ \dfrac{-K\delta R}{\Delta\beta^2 - \pi^2}\left[\Delta\beta^2\cos(A\varphi + B\pi) + \pi\cdot\Delta\beta\sin(\varphi - \beta_1)\right] & \beta_1 \le \varphi < \beta_2 \\ \dfrac{\pi\Delta\beta K\delta R}{\Delta\beta^2 - \pi^2}\left[\sin(\beta_1 - \varphi) + \sin(\beta_2 - \varphi)\right] & \beta_2 \le \varphi \le \pi \end{cases} \tag{8}$$

$$Q_{p7} = \begin{cases} 0 & 0 \le \varphi < \beta_1 \\ K\delta\cdot R\dfrac{\pi\cdot\Delta\beta\left[\sin(A\varphi + B\pi) - \cos(\varphi - \beta_1)\right]}{\Delta\beta^2 - \pi^2} & \beta_1 \le \varphi < \beta_2 \\ -K\delta\cdot R\dfrac{\pi\cdot\Delta\beta\cdot\left[\cos(\varphi - \beta_1) + \cos(\varphi - \beta_2)\right]}{\Delta\beta^2 - \pi^2} & \beta_2 \le \varphi \le \pi \end{cases} \tag{9}$$

Based on aforementioned equations, Δ_{1p} and Δ_{2p} can be written as:

$$\begin{cases} \Delta_{1p} = \sum_{j=1}^{7} \Delta_{1pj} \\ \Delta_{2p} = \sum_{j=1}^{7} \Delta_{2pj} \end{cases} \tag{10}$$

Where Δ_{1pj} and Δ_{2pj} are for the loading case j ($j = 1, \ldots, 7$), and can be written based on virtual work principle.

For loading case 1–6, the solutions for Δ_{1pj} and Δ_{2pj} are also as usual ones. However, for case7,

$$\begin{aligned} \Delta_{1p7} &= \int_0^{\beta_1} \frac{\overline{M}_1 M_{p7}}{EI} ds + \int_{\beta_1}^{\beta_2} \frac{\overline{M}_1 M_{p7}}{EI} ds + \int_{\beta_2}^{\pi} \frac{\overline{M}_1 M_{p7}}{EI} ds \\ &= \frac{K\delta\cdot R^3\Delta\beta}{EI\left(\Delta\beta^2 - \pi^2\right)}\left[-\frac{2\Delta\beta^2}{\pi} + \pi\left(\cos\beta_1 + \cos\beta_2 + 2\right)\right] \end{aligned} \tag{11}$$

$$\begin{aligned} \Delta_{2p7} &= \int_0^{\beta_1} \frac{\overline{M}_2 M_{p7}}{EI} ds + \int_{\beta_1}^{\beta_2} \frac{\overline{M}_2 M_{p7}}{EI} ds + \int_{\beta_2}^{\pi} \frac{\overline{M}_2 M_{p7}}{EI} ds \\ &= \frac{K\delta\cdot R^4\Delta\beta}{2EI\left(\Delta\beta^2 - \pi^2\right)}\left\{-\frac{2\Delta\beta^2\pi\left(\cos\beta_1 + \cos\beta_2\right)}{\Delta\beta^2 - \pi^2}\right. \\ &\quad + \pi\left[(\pi - \beta_1)\sin\beta_1\right. \\ &\quad \left.\left. + (\pi - \beta_2)\sin\beta_2\right]\right\} \end{aligned} \tag{12}$$

Based on the previous equations, the values of δ_{11}, δ_{22}, Δ_{1p}, Δ_{2p} are obtained, so the redundant forces, x_1 and x_2, can be expressed by Equation (3), and then the total internal forces can be given by the following equation:

$$\begin{cases} M = \overline{M}_1\cdot x_1 + \overline{M}_2\cdot x_2 + M_p \\ N = \overline{N}_1\cdot x_1 + \overline{N}_2\cdot x_2 + N_p \\ Q = \overline{Q}_1\cdot x_1 + \overline{Q}_2\cdot x_2 + Q_p \end{cases} \tag{13}$$

The following is to determine the radial displacement of tunnel lining and the distribution range of soil resistant pressure. In the simplified calculation model, the center of tunnel lining would have a settlement. Here, we assume the settlement at the lining center has the same value as the tangential displacement at the lining where $\varphi = \pi/2$. Then the final radial displacement, u, can be expressed as:

$$u = \sum_{j=1}^{7} u_{pj} + u_x + v_o\cdot\cos\varphi \tag{14}$$

where u_{pj} is the radial displacement due to the loading case j; u_x is the radial displacement due to the reluctant forces; v_o is the tangential displacement in the simplified model. Based on virtual work principle, u_{pj} can be given as:

$$u_{pj} = \int_{\varphi}^{\pi} \frac{\overline{M}_u M_{pj}}{EI} R d\alpha = \int_{\varphi}^{\pi} \frac{R\sin(\alpha - \varphi)\cdot M_{pj}}{EI} R d\alpha \qquad j = 1, \ldots, 7 \tag{15}$$

where $\overline{M}_u$ is the bending moment at α due to the virtual unit force acting on the tunnel lining along the direction of radius at φ.

For the redundant forces x_1 and x_2:

$$u_{px} = \int_{\varphi}^{\pi} \frac{\overline{M}_u M_x}{EI} Rd\alpha = \int_{\varphi}^{\pi} \frac{R\sin(\alpha-\varphi)\cdot\left(\overline{M}_1 x_1 + \overline{M}_2 x_2\right)}{EI} Rd\alpha = \frac{x_1 R^2}{EI}(\cos\varphi+1) + \frac{x_2 R^3}{2EI}\sin\varphi(\pi-\varphi) \quad (16)$$

v_o, the tangential displacement where $\varphi = \pi/2$, is consist of two parts, one for seven loading cases and the other for the redundant forces, given as follows:

$$v_o = \sum_{j=1}^{7} v_{opj} + v_{ox} \qquad j = 1,\ldots,7 \quad (17)$$

where v_{oj} is the tangential displacement where $\varphi = \pi/2$ due to the jth loading case,

$$v_{opj} = \int_{\frac{\pi}{2}}^{\pi} \frac{\overline{M}_{vo} M_{pj}}{EI} ds = \int_{\frac{\pi}{2}}^{\pi} \frac{R(1-\sin\varphi)\cdot M_{pj}}{EI} ds \quad (18)$$

where $\overline{M}_{vo}$ is the bending moment due to the virtual unit force acting on the tunnel lining along the tangential direction at φ.

For the redundant forces x_1 and x_2,

$$v_{ox} = \int_{\frac{\pi}{2}}^{\pi} \frac{\overline{M}_{v0} M_x}{EI} ds = \int_{\frac{\pi}{2}}^{\pi} \frac{R(1-\sin\varphi)\cdot\left(\overline{M}_1 x_1 + \overline{M}_2 x_2\right)}{EI} ds = \frac{x_1 R^2}{EI}\left(\frac{\pi}{2}-1\right) + \frac{x_2 R^3}{2EI} \quad (19)$$

3 COMPARISON

3.1 *Analysis of the parameters*

Soil resistant pressure in the new analytical solution is not known initially, so radial displacement has to be calculated by iterations until the value and the distribution range are in accordance with soil resistant.

Here two cases are chosen, one in sand layer and the other in clay layer to do the analysis. As shown in Table 2, all the natural parameters of the soil are from the actual project constructing in China.

3.1.1 *Effect of horizontal soil pressure coefficient*

The effects of horizontal soil pressure coefficient are examined by comparing the results of the case in clay layer embedded 0.7D with different horizontal soil pressure coefficient. For the convenience to describe, β is defined as $\beta = (\beta_1 + \beta_2)/2$ which describes the general location and $\Delta\beta$ describes the distribution range of soil resistant pressure.

The result of distribution of soil resistant pressure is shown in Figure 3. In Figure 3, two curves of $\Delta\beta$ do not show clear trends with the increase of K_0 until K_0 reaches 0.65, while both of the two β curves have the same trend. The values of β decrease obviously with the increase of K_0. It decreases more quickly at higher value of K_0. As shown in the figure, when t/D = 0.043, β decreases 2.5 degrees when K_0 increases from 0.35 to 0.65, while β decreases 2.25 degrees when K_0 increases from 0.65 to 0.70. On the other hand, the thickness of tunnel lining is also another factor to influence the results. For the case of t/D = 0.060, β totally decreases 2.5 degrees while β decreases 5.75 degrees in the case of t/D = 0.043.

The aforementioned observations have shown the effect of horizontal soil pressure coefficient. The increasing horizontal soil pressure coefficient will intensify the inhomogeneity of horizontal earth pressure, which means that additional horizontal earth pressure at the bottom level of tunnel lining,p_4, will take great weight to determine the internal forces in the tunnel lining, if the embedded depth is smaller comparing with the tunnel diameter.

Table 2. Detailed information about cases adopted in analysis.

	R	h_w	γ	γ_w	K	
Cases	m	m	kN/m^3	kN/m^3	kN/m^3	K_0
Clay layer	5	0	16.9	10	5000	055
Sand layer	5	0	19.8	10	10000	0.25

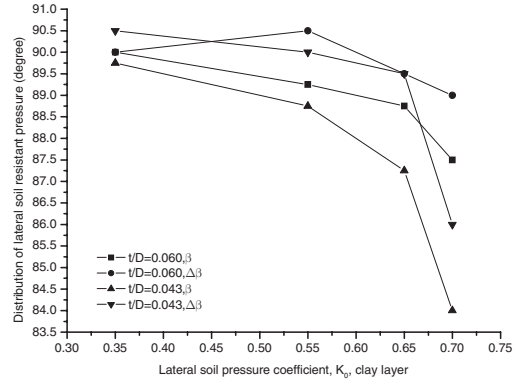


Figure 3. Distribution range of soil resistant pressure Vs. K_0.

3.1.2 *Effect of soil resistance coefficient*

The effects of soil resistance coefficient are examined by comparing the results of the case in sand layer embedded 0.7D with different soil resistance coefficient. The result of distribution of soil resistant pressure is shown in Figure 4.

In Figure 4, both of the two curves of β have some decrease with the increase of soil resistance coefficient K, and the one with thinner tunnel lining (i.e. $t/D = 0.043$) decreases a little more than that with thicker tunnel lining (i.e. $t/D = 0.060$).Both of the two curves of $\Delta\beta$ in Figure 4 have shown relatively obvious increasing trend with the increase of K. The increasing $\Delta\beta$ describes the extended range of soil resistant pressure, and the one with thinner tunnel lining (i.e. $t/D = 0.043$) increases much more than that with thicker tunnel lining (i.e. $t/D = 0.060$). As shown in the figure, $\Delta\beta$ increases 6 degrees in the case of $t/D = 0.043$, while $\Delta\beta$ only increases 2.5 degrees in the case of $t/D = 0.060$ when K increases from 0 to 50000 kN/m^3.

The effect of soil resistant pressure is obtained from the aforementioned observations. The soil resistance coefficient, K, as the significant factor to determine the value of the soil resistant pressure and the displacement of tunnel lining, directly describes the interaction between soil and tunnel lining.

3.2 *Comparison with different solutions*

To verify the proposed analytical solution, different solutions are used to analyze the same case with characteristic parameters of soil from the real project (Sha 2005, shown in Table 3). The results of conventional model and FEM are compared with those from the new analytical solution. The numerical simulation adopts the professional finite element software, PLAXIS-2D.

Figure 5 shows the numerical model, in which soil is decomposed into solid elements and tunnel lining is simulated with beam elements. Figure 6 shows the meshwork of tunnel lining.

With the proposed analytical solution, two significant parameters controlling the distribution of soil resistant pressure, β and $\Delta\beta$, are 89° and 93°, respectively, which means the acting range of the soil resistant pressure has moved and extended along the tunnel lining. Comparisons of internal forces calculated by the proposed analytical solution, conventional model solution and FEM are shown in Figure 7, Figure 8 and Figure 9, respectively.

In Figure 7, both the results from the proposed analytical solution and the conventional model solution

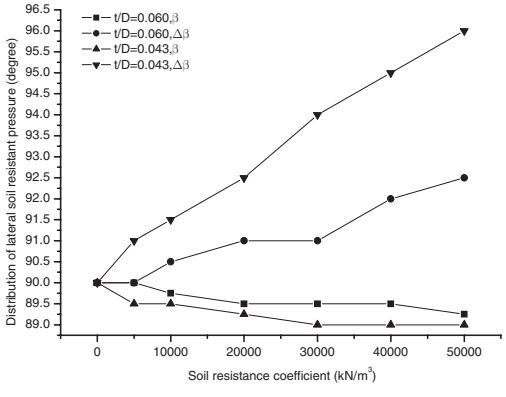


Figure 4. Distribution range of soil resistant pressure Vs. K.

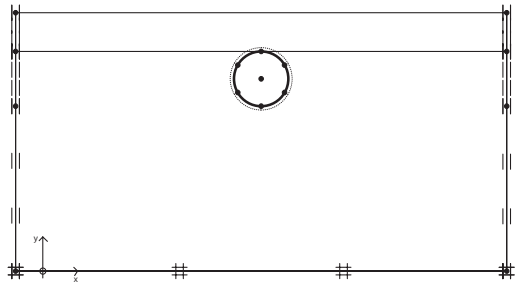


Figure 5. Numerical model of shield tunnel.

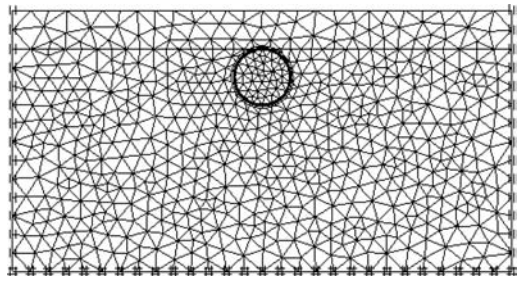


Figure 6. Meshwork of shield tunnel and soil.

Table 3. Parameters of the shield tunnel.

R m	h_w m	H* m	t m	γ kN/m^3	γ_w kN/m^3	C kPa	φ °	SPT N-value	K_0	K kN/m^3	E_c* kN/m^3
5	0	7	0.43	19.8	10	1	38	18.7	0.33	20000	22000

* H is the embedded depth and E_c is compression modulus.

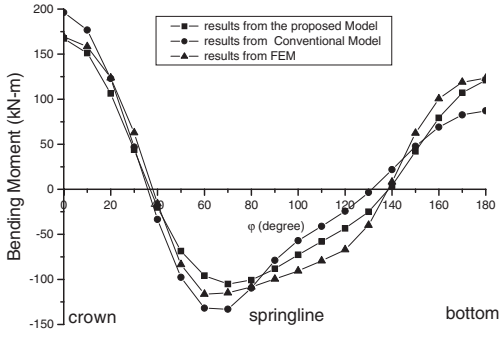


Figure 7. Comparison of bending moment.

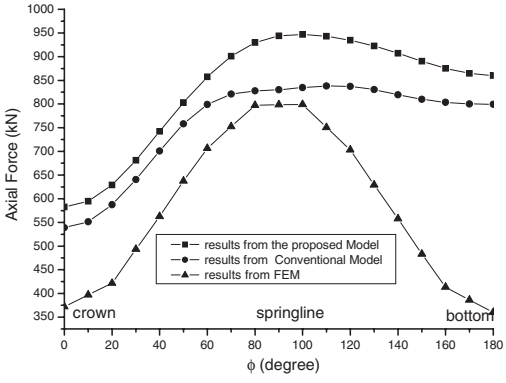


Figure 8. Comparison of axial force.

are generally accordant with those of numerical simulation, while the former results agree with those from FEM better than the latter. Before φ reaches 70°, all the results of the three curves reasonably agree with each other and after 70°, the curve of proposed analytical solution is closer to the curve of FEM than that of conventional model solution both in shape and value. The difference between the curves of proposed model and FEM is about 10%∼30% and the difference between the curves of conventional model and FEM is about 20%∼60%.

Figure 8 shows the comparison of axial force calculated by different solutions. As shown in the figure, neither the curve from proposed analytical solution nor the curve from conventional model solution is close to the curve from FEM. The reason should be relevant with the truth that FEM adopts the continuum mechanics model, in which the surrounding soil layer and the tunnel structure is treated as a whole, so the soil layer can also bear some loads, while in the other two solutions, the soil layer is only considered as loads.

The comparison of shear force from different solutions is shown in Figure 9, where the curve for the

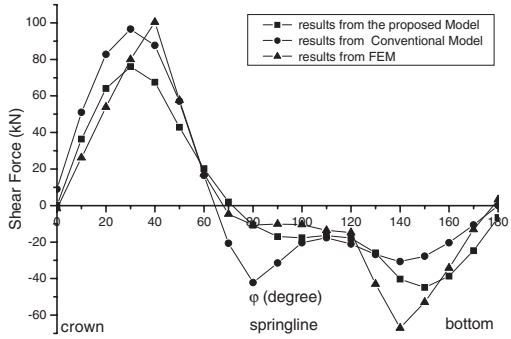


Figure 9. Comparison of shear force.

proposed analytical solution agrees with the results of FEM better than that for the conventional model solution, which is also consistent with the comparison of bending moment in Figure 7.

Based on the previous comparison of internal forces, the proposed analytical solution is relatively more suitable to analyze the shallow tunnel than conventional model, considering the change of distribution of soil resistant pressure.

4 CONCLUSION

Based on the Force-method, this paper develops an analytical solution for shield tunnel to study the change of distribution of soil resistant pressure, the effect of horizontal soil pressure coefficient and soil resistance coefficient, with consideration of different ratio of lining thickness versus diameter. The proposed solution is compared with conventional model solution and numerical simulation results. On the basis of the calculated results, the following conclusions can be drawn:

(a) For a given soil resistance coefficient and a shallow embedded depth, the distribution of soil resistant pressure is significantly effected by the value of horizontal soil pressure coefficient, K_0, and also the ratio of thickness versus diameter is a influencing factor. In the typical range of 0.35∼0.70 for K_0, the soil resistant pressure moves up along the tunnel lining. The magnitude of change in large highway tunnels (t/D = 0.043) is 2.5 times of that in subway tunnels (t/D = 0.060).

(b) For a given horizontal soil pressure coefficient and a shallow embedded depth, the distribution of soil resistant pressure is significantly effected by the value of soil resistance coefficient, K, and also the ratio of thickness versus diameter is a influencing factor. In the range of 0∼50000 kN/m^3 for K, the distribution range of soil resistant pressure

extends along the tunnel lining. The magnitude of extension in large highway tunnels (t/D = 0.043) is 2.4 times of that in subway tunnels (t/D = 0.060).

(c) The results predicted by the proposed analytical solution are compared with those of numerical simulation and the conventional model solution. The comparison indicates that the proposed solution agrees more reasonably, and it provides a new approach to better predict and make the preliminary design of shield tunnel lining.

REFERENCES

I.T.A. Working group No.2 (ITA). 2000. Guidelines for the design of shield tunnel lining. *Tunnelling and Underground Space Technology* 15(3): 303–331.

Koyama, Y. 2003. Present status and technology of shield tunneling method in Japan. *Tunnelling and Underground Space Technology* 18(2–3): 145–159.

Lee, K.M., Hou, X.Y., Ge, X.W., Tang, Y. 2001. An analytical solution for a jointed shield-driven tunnel lining. *International journal for numerical and analytical methods in Geomechanics* 25: 365–390.

Liu, J.H., Hou, X.Y. 1991. *Shield-driven tunnels*. Beijing: China Railways Press.

Morgan, H.D. 1961. A contribution to the analysis of stress in a circular tunnel. *Geotechnique*, 11(3): 37–46.

Muir Wood, A.M. 1975. The circular tunnel in elastic ground. *Geotechnique* 25(1): 115–127.

Sha, M.Y. 2005. Shield machine type selection in Nanjing Yangtse River Tunnel.*Proceedings of 2005 Shanghai International Forum on Tunnelling*: 41–48.

Zhang, F.X., Zhu, H.H., Fu, M.D. 2004. *Shield Tunnelling Method*. Beijing: China Communications Press.

This page intentionally left blank

Underground Space – the 4th Dimension of Metropolises – Barták, Hrdina, Romancov & Zlámal (eds)
© 2007 Taylor & Francis Group, London, ISBN 978-0-415-40807-3

Expert system for D&B tunnel construction

C.W. Yu & J.C. Chern
Sinotech Engineering Consultants, Inc., Taipei, Taiwan

ABSTRACT: To improve the technology for drill and blast tunnel construction in Taiwan, an expert system consisted of data bank, tool bank and decision making auxiliary system has been developed. Various tools can be used efficiently in carrying out data collection, processing, analysis and evaluation work required in the tunneling process. Using the successful tunnel case histories data learned from the past experiences, the system can provide multi-expertise assistance on the decision of support system and excavation procedures to be adopted in the construction site. The system can also provide rational estimation on the tunnel deformation under the selected support system and construction procedure with the aid of an artificial neural network approach. Application of the system to actual tunnel construction is given for demonstrating the capability of the system.

1 INTRODUCTION

The engineering practice for drilling and blasting (D&B) tunnel construction in Taiwan adopts similar approach used in the western countries. In the design stage, support requirements and construction procedures were pre-determined by using empirical rock classification method, mainly based on limited geological information and rock mass conditions obtained from the preliminary investigations.

During construction, actual rock mass rating was obtained at the tunnel face, and appropriate support system and construction procedures were selected and implemented. Monitoring instruments were installed for observing the performance of rock masses surrounding the tunnel. Revision and remediation were made on the support system or construction procedures, if necessary, to achieve a safe and economic tunnel construction.

However, due to the poor rock condition often encountered in Taiwan, excavation large span tunnel through poor quality rock mass has resulted in numerous engineering difficulties in the past two decades. These difficulties included uncontrolled excessive tunnel deformation, serious damage to the support system and even tunnel cave-in.

Figure 1 shows an example of driving a large span tunnel through a fault zone in northern Taiwan by using the traditional rock classification method. It required systematic pre-stressed tendons and re-mining and re-supporting the tunnel to overcome the uncontrolled excessive deformation. Controversies over the adequacy of tunnel support design and construction procedures based on experiences of different geological environments have become issues for the local tunneling community. This also calls for the development of a more rational system to deal with the processes in D&B tunnel construction. This paper presents the system and its application in a tunnel construction project.



Figure 1. Systematic pre-stressed tendons, re-mining and re-supporting had to be used to control large deformation of tunnel through a dry fault zone in the construction of the Second Freeway in northern Taiwan.

2 EXPERT SYSTEM FOR TUNNEL CONSTRUCTION

The tunnel expert system compiles expert knowledge and tools for facilitating the data collection and processing, data analysis and evaluation, and decision

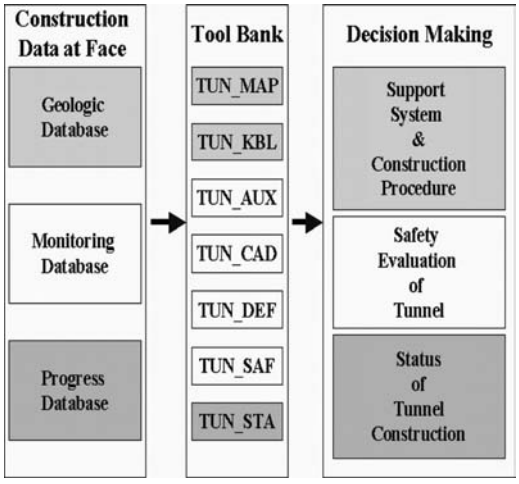


Figure 2. Working processes of the expert system developed.

Table 1. Tool bank of the expert system.

Tools	Main functions
TUN_MAP	Geological Information Collecting and Processing
TUN_KBL	Key Block Analysis
TUN_AUX	Construction Decision-making Assistance
TUN_DEF	Deformation Prediction
TUN_CAD	Construction Simulating
TUN_SAF	Tunnel Safety Evaluation
TUN_STA	Construction Status Demonstrating

making in the tunnel construction processes. Figure 2 shows the working processes of the system.

The working processes contain 3 major blocks, i.e., (1) construction data collection at the site, (2) tool bank for various data processing, analysis, simulation and evaluation, and (3) decision making for support design and construction procedures recommendation, safety evaluation and construction status demonstration.

The functions of each module in the tool bank are outlined in Table 1. The working process will be described further in the following sections.

3 TOOL BANK

The tool bank of the expert system comprises of 7 subsystems as shown in Table 1, and the main functions of the subsystems are:

(1) Geological Information Collecting and Processing System (TUN_MAP) utilizes digital image taken on the tunnel face to retrieve the geological information for statistical analysis of joint systems and production of developed geological map of tunnel surface.
(2) Key Block Analysis System (TUN_KBL) can be used to perform key block analysis from the actual recorded joint information or statistically generated joint information.
(3) Construction Decision Making Auxiliary System (TUN_AUX) is a case history based artificial intelligence system for making multi-expertise recommendations on tunnel support system and construction procedures.
(4) Tunnel Deformation Prediction System (TUN_DEF) is an numerical analysis data based artificial neural network system for providing a rational estimation on the tunnel deformation under various geological and construction conditions.
(5) Tunnel Construction Simulation System (TUN_CAD) provides numerical analysis programs for carrying out back analysis of monitoring data and forward prediction analysis of tunnel performance by simulating the construction processes in the field.
(6) Tunnel Safety Evaluation System (TUN_SAF) utilizes the monitoring tunnel deformation for evaluating the safety of tunnel construction by using a case history based empirical tunnel safety criterion.
(7) Construction Status Demonstration System (TUN_STA) uses the records collected during tunnel excavation, including geological information, monitoring data and construction progress records, for demonstrating the status of tunnel construction.

The application for some of the systems will be demonstrated by the results of case study presented.

4 DECISION-MAKING MODULES

Decision-making modules include the recommendation of optimum tunnel support requirement and construction procedures, tunnel deformation estimation and safety evaluation during tunnel construction stages. It also provides the status of tunnel construction for better control of construction progress and tunneling conditions by the tunnel engineer.

4.1 *Optimum support requirement*

A Decision Making Auxiliary System (TUN_AUX) is a case-based artificial intelligence system together with the traditional empirical rock classification system. The working processes of system TUN_AUX are shown in Figure 3.

In the field, the parameters, including the tunnel span, strength of rock material, rock mass classification and overburden depth, collected are used for the

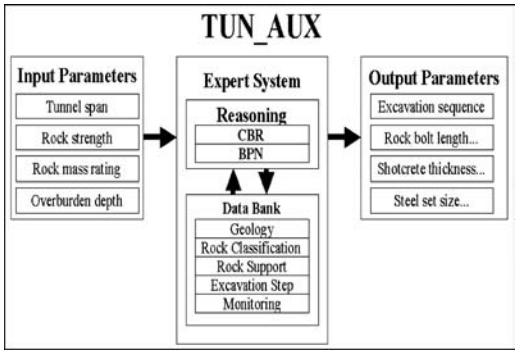


Figure 3. Flow chart of application of rock support decision-making auxiliary system.

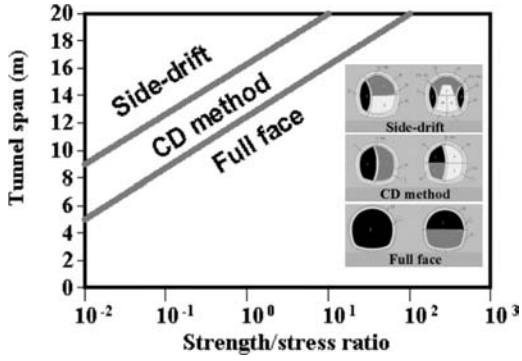


Figure 4. Optimized chart for selecting a suitable excavation procedure according to tunnel span and the strength stress ratio.

expert system. TUN_AUX can give a multi-expertise recommendations on the major support elements such as the length and spacing of rock bolts, thickness of shotcrete, size and spacing of steel sets, etc.

4.2 *Optimum construction procedures*

The Decision Making Auxiliary System (TUN_AUX) also provides a function for the recommendation of optimum construction procedure. The excavation procedures suitable for various tunnel spans and ground conditions were categorized into full face, central diaphragm (CD) and side drift. Based on the expert knowledge collected from experienced tunnel engineers and the results of construction simulation under various tunneling conditions, the optimum construction procedure is suggested by the tunnel span and strength/stress ratio at the construction site. The chart for selecting a suitable construction procedure is shown in Figure 4. Figure 5 shows the construction of a four-lane freeway tunnel under poor ground and very shallow rock cover by using dual side-drift method. Severe unstable condition was developed in a 3-lane adjacent tunnel with top heading and benching procedure.

4.3 *Tunnel deformation estimation*

Tunnel Deformation Prediction System (TUN_DEF) provides an estimation on the magnitude of tunnel deformation expected under various geological and construction conditions. The system was developed based on large amount of 3-D numerical simulations of the tunnel construction under various geological conditions, excavation sequences and support measures. Tunnel deformations, including roof settlement, horizontal convergency, as well as plastic zone thickness were given by a back propagation artificial neural network from the data base. It is intended to provide a rough estimate on the order of magnitude of tunnel deformation expected as guidance for tunnel engineer.



Figure 5. Four-lane freeway tunnel driven by dual side-drift excavation method adjacent to a shallow slope.

4.4 *Tunnel safety evaluation*

Empirical tunnel safety criterion based on case histories in Taiwan (Chern, et al. 1998) is used in the safety evaluation of tunnel. In the criterion, the information of the tunnel inward movement (δ), tunnel radius (R), rock mass strength (UCS) and actual performance of tunnel case histories were used to establish 3 warning levels of tunnel safety and the necessary measures to be taken.

Below warning level I, tunnel is considered to be in stable condition, and no special measure is required. Between warning levels II and III, tunnel is susceptible to instability, and review of support system and construction procedures adopted should be made. Above warning level III, tunnel is in unstable condition, and remedial measures should be taken to stabilize the tunnel.

Figure 6 shows the flow chart of tunnel safety evaluation using TUN_DEF and TUN_SAF systems.

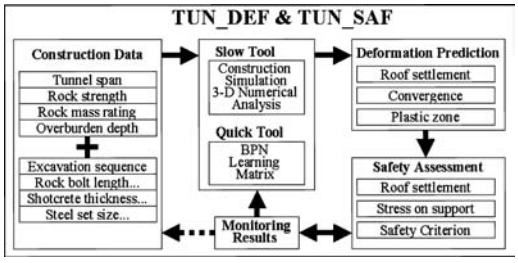


Figure 6. Flow chart of tunnel deformation prediction and safety evaluation.

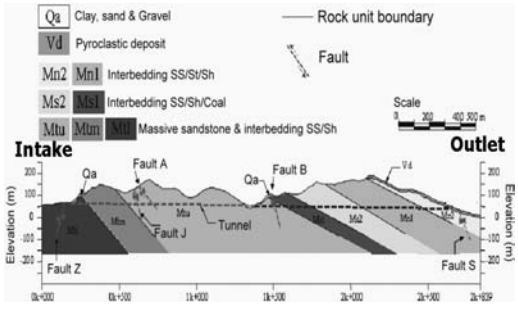


Figure 7. Geological profile of the flood diversion tunnel.

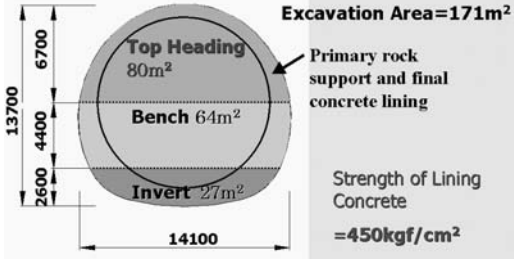


Figure 8. Tunnel section showing the excavation span and excavation steps.

5 CASE STUDY

To illustrate the application of the system developed, a case study on a flood diversion tunnel in northern Taiwan is presented.

The diversion tunnel is 2,835 m long driving through sedimentary rock formation of Miocene Age. The geological profile is shown in Figure 7. The maximum excavation span is 14.1 m and was excavated in 3 stages as shown in Figure 8. The major difficulties encountered in tunneling are associated with the fault zones and the disturbed zones adjacent to a volcanic intrusion.

The rock support system was designed according to the traditional RMR rock classification method.

Table 2. Suggested support elements predicted by the system.

Support type	Advance per round	Rockbolt length	Shotcrete thickness	Steel-rib size
Design Type III	1.0–1.4 m	4 m	20 cm	G220*
Design Type IV	0.8–1.2 m	6 m	25 cm	G220*
Suggested Type III	1.5–2.0 m	6–8 m	20–25 cm	H125†
Suggested Type IV	1.0–1.5 m	8–10 m	20–25 cm	H150†

* Use lattice girdle. †Use H-beam.



Figure 9. The highly disturbed rock exposed at 2k+008.

Five support types were proportioned according to the RMR rating. The rock support requirements were also examined by using the expert system TUN_AUX during construction. The results for type III and type IV rock are shown in Table 2 along with the original design of support system.

Most of the tunnel sections belong to the good quality rock with type II and type III support systems. The type III support adopted worked quite well. However, in a disturbed zone adjacent to the volcanic intrusion near station 2k+008, the poor quality rock mass (Figure 9) with RMR values in the range of 28 to 34 showed squeezing behavior under 140 m overburden stress. The monitoring results during tunnel excavation are shown in Figure 10.

The monitoring data for top heading excavation showed potential unstable condition according to the tunnel safety evaluating system TUN_SAF as shown in Figure 11. This proved to be true by the tunnel convergence occurred during subsequent benching.

Reviewing the support requirement and excavation procedure, it was found that the expert system would suggest a more conservative support system and excavation procedure. These can be shown by the longer bolt length as suggested in Table 2, and excavation by CD or side drift method recommended as shown in Figure 12.

Before benching, various remedial measures were further studies by using 3-D numerical simulations.

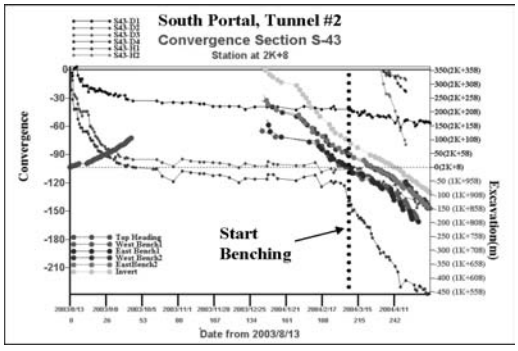


Figure 10. Monitoring results during tunnel excavation in disturbed zone near 2k+008.

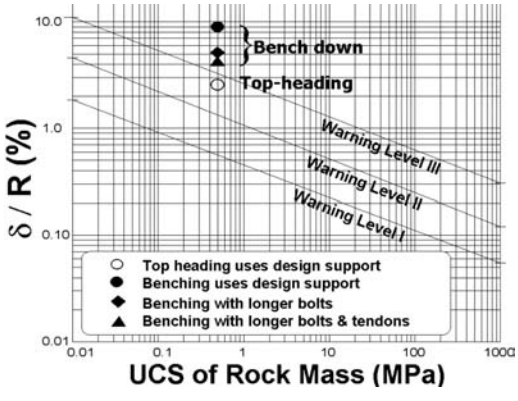


Figure 11. Potential unstable condition according to TUN_SAF evaluation.

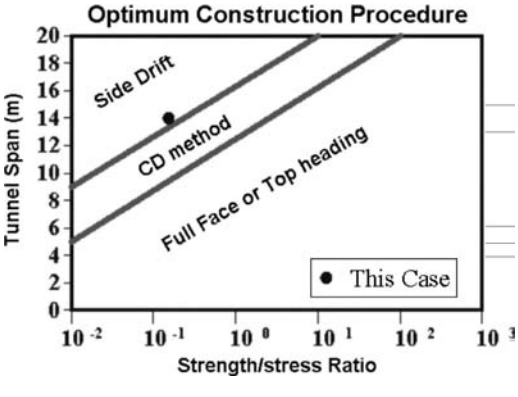


Figure 12. Excavation by CD or side drift method as recommended.

The predicted tunnel deformations after benching down are shown in Figure 11. Due to limited option available at the construction site, only additional 9-meter long systematic bolts were installed to enhance the tunnel stability. The tunnel did not suffer from severe unstable condition during benching, but rather large tunnel convergence occurred with accompanying cracks of shotcrete in the tunnel crown area. This is also predicted by the tunnel safety evaluation system as shown in Figure 11.

6 CONCLUSIONS

An expert system consisted of tools and expert knowledge for performing construction data collection and processing, data evaluation and analysis, and decision making assistance in the working process of D&B tunneling was developed. The results of preliminary application of the system in the construction of a flood diversion tunnel showed the system can provide efficient tools for carrying out various data collection, analysis and evaluation work in the tunneling process. Rational suggestions on support requirement, construction procedure and safety evaluation can also assist the field engineer in the decision making process.

However, In a practical application sense, the system developed is considered to be a prototype due to the lack of precedence and case histories with sufficient accuracy covering wide range of tunnel conditions. For further improvement of the system, trial application and collection of additional case information are still needed.

REFERENCES

Hoek, E. and Brown, E.T. 1980, *Underground excavations in rock*, London: Institution of Mining and Metallurgy.

Dershowitz, W.S. and Einstein, H.H. 1984, Application of Artificial Intelligence to Problems of Rock Mechanics, *25th W. S. Symp. Rock Mechanics*, pp.483–494.

Zhang, Q., Mo, Y. and Tian, S. 1988, An Expert System for Classification of Rock Masses, *Proc. 29th U.S. Symp. Rock Mech*., pp.283–288.

Butler, A.G. and Franklin, J. A. 1990, Classex: Expert System for Rock Mass Classification, *Proc. ISRM Int. Symp. Rock Mech*., Mbabane, Swaziland, pp.73–80.

Zhang, Q., Nie, X.Y. and Tian, W.T. 1995, A Case-Based Reasoning for Tunnel Support, *Proc. 8th Int. Cong. Rock Mech.*, Tokyo, pp.907–909.

Chern, J.C., Shiao, F.Y. and Yu, C.W. 1998, An empirical safety criterion for tunnel construction. *Proc., Reg. Symp. Sedimentary Rock Engineering*, Taipei, 325–330.

Palassi, M. and Franklin, J.A. 1998, *Tunnex: An Expert System for Tunnelling through Rock.* Tunnelling Association of Canada (TAC) News, Vol. 16, No. 1, pp.12–18.

Hoek, E. 2001. Big tunnel in bad rock. *Journal of Geotechnical & Geoenvironment Engineering*, Vol.127, 726–740.

Liu, J.M. 2005. River Yuanshantzu flood-diversion project. *Proc., Int. Symp. Design, Construction and Operation of Long Tunnel*, Taipei: 923–933.

This page intentionally left blank

Underground Space – the 4th Dimension of Metropolises – Barták, Hrdina, Romancov & Zlámal (eds)
© 2007 Taylor & Francis Group, London, ISBN 978-0-415-40807-3

Progress of drill and blast tunnelling efficiency with relation to excavation time and costs

S. Zare & A. Bruland
Department of Civil and Transport Engineering, Norwegian University of Science and Technology (NTNU), Trondheim, Norway

ABSTRACT: The productivity and efficiency of the drill and blast method have been investigated by means of NTNU prediction models for excavation time and costs since 1975, when the first time and cost models were published. The technological developments have improved the productivity in terms of increased advance rate and reduced excavation costs. For a typical 60 m^2 road tunnel assuming 100 working hours per week, the normal advance rate without rock support installation is increased from 50 m/week to 80 m/week, i.e. 60% improvement and the excavation costs are reduced from 16000 NOK/m to 10200 NOK/m, indicating a 36% reduction from 1975 to 2005.

1 INTRODUCTION

The drill and blast method has for long time been used for excavation of underground spaces in rock for various applications. The method may be applied in tunnels, rock caverns and mines. The major part of underground excavation in Norway is drill and blast (Norwegian Tunnelling Society 2004).

The Department of Civil and Transport Engineering at NTNU has recently published updated models for blast design and excavation time and costs (NTNU 2006a,b,c). The models are developed based on field studies and technological progress of different elements involved in the tunnel excavation process. The models can be used through all phases of tunnel projects for:

- Economic dimensioning
- Choice of alternative
- Time planning
- Cost analysis, tender, budget and cost control
- Choice of excavation method and equipment

The first version of the models was published in 1975 and has later been updated and revised five times. From the first publication, substantial development has been achieved in drilling jumbos, drilling tools, explosives efficiency, loading and hauling equipment as well as HES regulations.

The paper reviews the latest versions of the NTNU prediction models for excavation time and costs, as well as technological developments. Then development of the productivity and cost efficiency of the method by means of empirical prediction models for excavation time and costs has been investigated since 1975.

2 TIME AND COST MODELS

2.1 *Time model*

The complete time or advance rate model is published in NTNU 2006b. The model is based on the round cycle time consumption. The round cycle is divided into four major operations:

I Drilling and charging
II Ventilation
III Loading and hauling
IV Scaling and rock support

The operations I and III are divided into three different categories of time, i.e. fixed lost time (rig time), proportional operational time and incidental lost time. The time consumption for each operation is given in NTNU 2006b for various tunnel cross sections.

By applying the model for 3 km tunnel length, 5 m drillhole length, 48 mm drillhole diameter, parallel hole cut, medium rock drillability and blastability and 100 working hours per week, the weekly advance rate without rock support installation varies from 100 m/week for 10 m^2 tunnel to 54 m/week for 120 m^2 tunnel, depending on equipment combination and number of drilling hammers (Zare & Bruland 2006b).

2.2 *Cost model*

The cost model is based on detailed cost calculation for excavation operations, i.e. drilling, charging,

scaling, loading, hauling, additional work, niches and labour. The complete cost model is published in NTNU 2006c. Equipment and material prices, labour wages and expected life time for equipment are main input for detailed cost calculation. Depreciation, interest, wages, repairs and power consumption are included in the costs of each operation. Linear or degressive depreciation method is assumed, depending on equipment type and repair costs over life time.

In addition, 10% extra for unforeseen costs and uncertain assumptions is added in the end to the excavation costs. As in the time model, rock support cost is not included in the excavation costs, in order to provide the basis to compare the costs for different tunnel cross sections. The amount of rock support much depends to the rock conditions and tunnel application.

The equipment combinations are chosen according to the tunnel cross section and excavation method, i.e. track tunnelling for cross sections up to 16 m^2 and trackless tunnelling for cross sections between 16 m^2 and 120 m^2.

For rough estimation, the excavation costs for a tunnel with the same assumptions in the time model, varies from 6500 NOK/m for 10 m^2 tunnel to 17500 NOK/m for 120 m^2 tunnel, depending on equipment combination and number of drilling hammers. The costs input are based on June 2005 price level.

3 TECHNOLOGICAL DEVELOPMENT

3.1 *Drilling*

Currently, computerised hydraulic drilling jumbos with different level of automation are widely used in drill and blast tunnelling (Atlas Copco 2004, Sandvik Tamrock Corp. 1999). The current generation of drilling jumbos is designed for high productivity, quality drilling, and comfortable working conditions for operators.

The drill plan is stored in the drilling jumbo computer and therefore the face does not need to be marked up; the navigation is done by laser alignment and is very precise in deciding the position of the drilling jumbo. The excavated tunnel profiles can be scanned by electronic instruments, whereby over-break and under-break can be recorded to be used for the optimisation of the drilling process in the coming rounds (Nord 2003).

3.1.1 *Rock drills*

Obviously, invention of the hydraulic rock drills in the 1970s was a great progress in drilling speed, economy and improvement of the operator's working conditions. Figure 1 supports the fact and shows general development of rock drills and jumbos.

As an example, one may look at the Cop 3038. The latest rock drill from Atlas Copco is designed to increase the penetration rate in hard rock tunnelling. According to Atlas Copco; the Cop 3038 is 50% faster than its predecessor Cop 1838 ME, the time saved with Cop 3038 compared to Cop1838 ME on 3-boom jumbos in a 90 m^2 tunnel could be about 40 minutes per round. The high penetration rate may be utilized in limited space to replace 3-boom to 2-boom jumbos (Mining & Construction 2004).

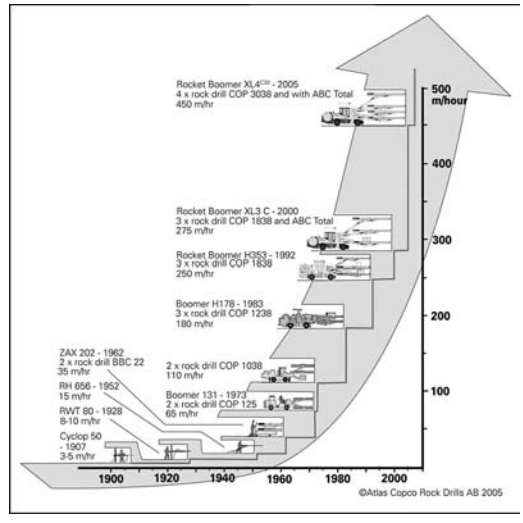


Figure 1. Drilling development 1905–2005, drilled metres per hour and operator (Atlas Copco 2006).

Table 1. Development of Atlas Copco hydraulic rock drills for face drilling (Mining & Construction 2004).

Type	Year	Impact power	Impact rate
COP 1038HD	1973	12 kW	42–60 Hz
COP 1238ME	1983	12 kW	40–60 Hz
COP 1440	1986	21 kW	70 Hz
COP 1838ME	1990	18 kW	60 Hz
COP 1838HF	2000	22 kW	73 Hz
COP 3038	2004	30 kW	102 Hz

The Cop 3038 delivers the same energy per percussive blow as the Cop 1838 ME, but the frequency has been increased from 60 to 102 Hz.

In the Table 1 the development of Atlas Copco hydraulic rock drills for face drilling is presented.

3.1.2 *Drill steel*

Drill bits, drill rods and shank adapters may be referred to as the drill steel, which has been concurrently developed with introduction of more powerful hydraulic rock drills. New conical thread system, Magnum SR35, is devised to cope the weakness of the old threads. The advantages of the new thread

system are intended to solve rod breakage at the bit end, less tendency for deviation when collaring, straighter holes, and longer service life (Atlas Copco 2004).

The rod length has also increased, even though the 18 feet rods are common in civil tunnelling and gives around 5 m drilled length, the tendency towards longer round is increased (Nieminen 2003) and some tunnels have been excavated with 6 m round length (Tunnelling and Trenchless Construction 2005).

3.2 *Charging and explosives*

Emulsion explosives combined with non electrical initiation system like NONEL have increased the safety of the charging and blasting operations and become more efficient.

The pumpable emulsion explosives, SSE (Site Sensitised Explosives) are not explosives until pumped in the hole, which means safety in transportation and handling (Johansen & Mathiesen 2000, Atlas Copco 2006).

The modern emulsion explosives are oxygen-balanced, producing a minimum of noxious fumes and far less smoke (Olofsson 2002), provides better working conditions and less ventilation requirements.

The emulsion explosives are water resistant and can be used when water is a problem and ANFO can not be used efficiently.

In addition, the pumpable emulsion explosives can be pumped into the blastholes by a computer controlled system and the amount of explosives in each hole and total explosives consumption can be measured, which can be used to control the amount of explosives in different holes in the face, especially in the contour and row nearest the contour where less explosives is needed for smooth blasting (NTNU 2006a, Zare & Bruland 2006a). The measuring system may also help to control the uncharged length of blastholes for optimum blasting results.

Recently, after a feasibility study, a prototype machine for automatic charging of emulsion explosives was completed and tested in Norway (Hermann & Elvoy 2004). The project is meant to reduce the time consumption for drilling and charging by 20% with improved work safety. The charging system is mounted on the drilling jumbo as a separate boom and charging is accomplished automatic during drilling without human interface at the face, in compliance with the regulations that prohibits simultaneous manual charging and drilling at the face.

3.3 *Ventilation*

The harmful gases and dust particles above the certain level of acceptance must be removed by the ventilation system.

For the cost efficiency and improvement of the work environment, the intelligent ventilation system is developed and tested in two tunnels (Lima & Blindheim 2004). The project includes development of new duct materials and duct support system as well as recording of air quality and automatic control of the ventilation fans.

3.4 *Loading and hauling*

The loading and hauling capacity is dependent on the tunnel cross section size and excavation method. Using adequate size equipment as the cross section increases is an efficient way to increase loading capacity. By NTNU field studies in large cross sections (NTNU 2006b), a capacity up to 500 lm^3/h is attainable when using wheel loader and dump truck combination and the loader is fully utilised, i.e. the loader is not waiting for a hauling unit.

Crusher, conveyor belt and mucking trains are also employed in drill and blast tunnels. The average capacity is 300 m^3/h (understood as loos cubic metre). 500 m^3/h should be achievable by the method in the future (Girmscheid & Schexnayder 2002). The crusher and conveyor belt is used as part of "high performance drill and blast excavation concept" which uses a suspended platform system for higher performance. Even though, the crusher capacity is the limiting factor, by other benefits of the method, the total cycle performance has been increased by 30% (Girmscheid & Schexnayder 2002).

3.5 *Rock support*

Rock bolts and sprayed concrete (shotcrete) are two common types of rock support, both developed towards more durable; high strength, and quick installation by means of mechanised and automated equipment.

CT-bolt, the newest bolt type in the market can first be used as an ordinary end-anchored bolt for temporary support and later on be grouted to a permanent bolt (Norwegian Tunnelling Society 2004).

During the past two decades the sprayed concrete has faced a significant improvement; today fibre-reinforced sprayed concrete by wet mix method is widely applied.

Sprayed concrete robot is one of the modern equipment for applying sprayed concrete. The capacity by manual spraying is less than 5 to 8 m^3/h, while using robot it reaches up to 20 m^3/h (Girmscheid & Moser 2001). The robot has better safety and quality control.

By the NTNU models it possible to estimate excavation time and cost including rock support, but since the rock support much depend on the rock mass conditions, the time and costs which are presented in the paper do not include the rock support.

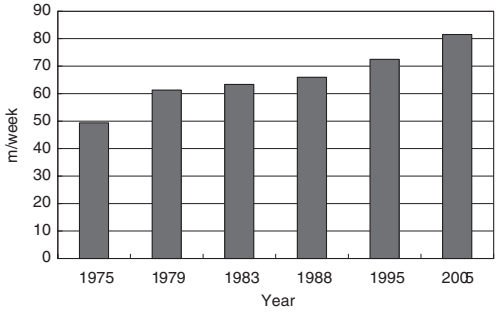


Figure 2. Development of weekly advance rate for a 60 m^2 tunnel.

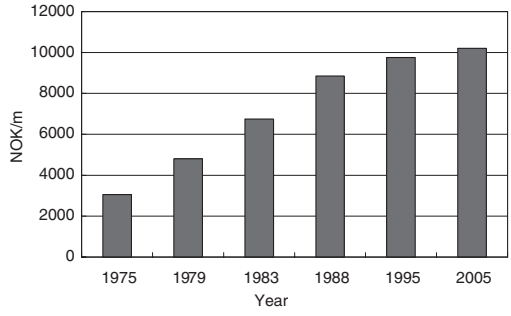


Figure 3. Development of uncorrected excavation cost for a 60 m^2 tunnel.

4 TIME AND COST TRENDS

To investigate time and cost trends or productivity and efficiency of the method, a 60 m^2 tunnel with 3 km length is chosen as a typical two-way road tunnel. Medium rock blastability and rock drillability is assumed.

The advance rate per week and unit costs per tunnel metre without rock support installation are estimated from 1975 to 2005 by the NTNU models. The NTNU model was first time published in 1975 and has been revised five times; in 1979, 1983, 1988, 1995 and 2005.

Weekly advance rate is shown in Figure 2. The weekly advance rate is normalised based on 100 hours working time per week. The advance rate is increased from some 50 m/week to 81 m/week during the past 30 years, indicating a 60% increase in production rate. The excavation method itself does not change significantly, development in the equipment capacity and efficiency, tools and materials leads to that the current tunnel will be excavated faster and the excavation time is shortened.

For example in 1975 the maximum penetration rate for medium drillability was 140 cm/min whilst in the recent model of 2005, it reaches to some 300 cm/min and the maximum loading capacity for same size cross sections is increased from 160 sm^3/h to 280 sm^3/h.

The uncorrected excavation costs are shown in Figure 3, the unit cost is presented in Norwegian Kroner per metre of tunnel. The cost in Figure 3 is not corrected for price level; only representing the unit excavation costs in each year. To find the comparable figures, the cost must be corrected for price level.

The Department of Civil and Transport Engineering at NTNU has published a cost index for construction equipment (NTNU 2006d). The corrected excavation costs are shown in Figure 4. The trend of excavation cost is not consistent such as the time trend (Fig. 2). One reason is different working hours per week; which is 112 hours in 1975, 75 hours in 1979 and 1983

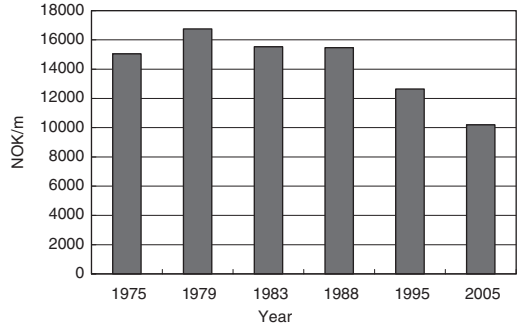


Figure 4. Development of excavation costs for a 60 m^2 tunnel, price level June 2005.

models, and 100 hours for the rest. Based on 100 working hours the costs for 1975 model should be higher and for the 1979 and 1983 models, lower than the presented values.

In spite of this minor deviation the excavation cost is decreased from some 16000 NOK/m to 10200 NOK/m, indicating a 36% reduction. The technological development is the main reason of decreasing cost trend. Changes in the investment tax and interest rate are included in the price level correction.

5 CONCLUSIONS

In line with development in tunnelling, the productivity and efficiency of the drill and blast method has increased. Drilling is now using computerised drilling jumbos with various levels of automation, faster rock drills and more durable drill steel. Charging is accomplished safer and more efficient by using NONEL detonators and emulsion explosives which causes less pollution and is not considered as an explosive until placed in the holes. Ventilation may utilise intelligent ventilation system. The loading and hauling capacities

are increased and advanced rock support equipment with higher performance is employed.

By means of the NTNU prediction models, the investigation shows substantial increase in the productivity and reduction in the costs. For a 60 m^2 road tunnel, the productivity has increased 60% and the cost has been reduced by 36% from 1975 to 2005.

Furthermore, the time and cost trends confirm the importance of updated models for time and cost prediction. The NTNU models are unique and should be revised based on technological development in the excavation methods and equipment.

ACKNOWLEDGEMENTS

The paper is prepared as part of the first author's PhD research project financed by the Ministry of Science, Research and Technology of Iran.

REFERENCES

Atlas Copco. 2006. Available from <*www.atlascopco.com*>.

Atlas Copco. 2004. *Face Drilling* third edition. Orebro: Atlas Copco Rock Drills AB.

Girmscheid, G. & Moser, S. 2001. Fully automated shotcrete robot for rock support. in *Computer-Aided Civil and Infrastructure Engineering 16*: 200–215. Blackwell: Malden.

Girmscheid, G. & Schexnayder, C. 2002. Drill and blast practices. *Practice periodical on construction design and construction* 7(3): 125–133.

Hermann, R. & Elvoy, J. 2004. Automatic charging of emulsion explosives to increase safety, productivity and quality. In *Health and safety in Norwegian Tunnelling*. Publication No 13. Oslo: Norwegian Tunnelling Society.

Johansen, J. & Mathiesen, C.F. 2000. *Modern trends in tunneling and blast design*. Rotterdam: Balkema.

Lima, J. & Blindheim, O.T. 2004. Development in ventilation methods. In *Health and safety in Norwegian Tunnelling.* Publication No 13. Oslo: Norwegian Tunnelling Society.

Mining & Construction. 2004. The development of the COP 3038. *Mining & Construction No.3*: 26–27.

Neiminen, P. 2003. Blasting into the 21st century. *Tunnels & Tunnelling International* 35(7): 43–44.

Nord, G. 2003. Use and misuse of the logging system. *Tunnels & Tunnelling International* 35(7): 46–47.

Norwegian Tunnelling Society. 2004. *Norwegian Tunnelling*. Publication No 14. Oslo.

NTNU. 2006a. *Report 2A-05 Drill and Blast Tunnelling; Blast Design*. Trondheim: NTNU, Department of Civil and Transport Engineering, to be printed in 2007.

NTNU. 2006b. *Report 2B-05 Drill and Blast Tunnelling; Advance Rate*. Trondheim: NTNU, Department of Civil and Transport Engineering, to be printed in 2007.

NTNU. 2006c. *Report 2C-05 Drill and Blast Tunnelling; Costs*. Trondheim: NTNU, Department of Civil and Transport Engineering, to be prined in 2007.

NTNU. 2006d. *Cost index of construction machinery*, published monthly since 1978. Trondheim: NTNU, Department of Civil and Transport Engineering.

Olofsson, S.O. 2002. *Applied explosives technology for construction and mining.* Arla: Applex AB.

Sandvik Tamrock Corp. 1999. *Rock excavation handbook for civil engineering*.

Tunnelling and Trenchless Construction. 2005. TTC Nordic Focus. *Tunnelling and Trenchless Construction.* November 2005:16–20.

Zare, S. & Bruland, A. 2006a. Comparison of tunnel blast design models. *Journal of Tunnelling and Underground Space Technology* 21(5): 533–541.

Zare, S. & Bruland, A. 2006b. Estimation model for advance rate in drill and blast tunnelling. *Intern. symp. on utilization of underground space in urban areas, 6–7 November 2006*. Sharm El-Sheikh, Egypt.

This page intentionally left blank

Underground Space – the 4th Dimension of Metropolises – Barták, Hrdina, Romancov & Zlámal (eds)
© 2007 Taylor & Francis Group, London, ISBN 978-0-415-40807-3

Analysis of the ultimate states of the underground tunnel lining

Ing. Jaromír Zlámal
POHL cz, a.s., Prague, The Czech Republic

ABSTRACT: Evaluation of the load-bearing capacity of underground tunnel linings under emergency conditions (as with structural cracks and deformations), must be conducted rapidly, and in a way that static analysis will immediately reveal points of fault, stress and excess loading, as well as areas of spare capacity. Coefficient *s* of bearing capacities, calculated according to measures of internal forces and within technical parameters, can give an immediate indication of the state of a tunnel lining. Analysis, by mathematical modelling of such extreme states, can reveal points in the lining structure which are close to capacity limits, and points where spare capacity is very small. Use of this method for two different cases of lining deformations in the Prague Underground demonstrate its simplicity, speed and reliability.

1 INTRODUCTION

During construction and use of underground rail tunnels made from reinforced concrete segments, the lining is only rarely in a state nearing the limit of its bearing capacity, and only very rarely in a state which is actually at that limit. (For such extreme conditions, the term 'ultimate state' of the structure will be used.)

However, once the structure reaches the ultimate state, there is typically very little time to decide what measures to take in order to stabilize the structure. Suggested mitigations are usually based on detailed static analysis of the tunnel lining.

For this type of analysis, a static model of the structure is created and extreme conditions are simulated in numerous runs, such that deformations in the model are maximally close to the real situation of the tunnel.

The goal of this study is to evaluate the load bearing capacities and reserves, of concrete circular tunnel linings with inside diameters of 5,1m, as used in the Prague Underground.

The tunnels were installed beneath apartment buildings and stress on the structures (cracks and deformations), were evident with only visual examination. However, the design of the tunnels and their geometry allows for their use with minimal mitigation when actual deformations are not considered extreme.

2 METHOD OF ANALYSIS OF THE ULTIMATE STATE

The design of each structure has to satisfy two basic but often contrasting conditions – the structure has to be economical and safe. Underground structures are continuously loaded by stress and deformation, which can be expressed mathematically on the basis of structural mechanics. The durability of the structure is defined by three factors:

- *support structure*
- *load applied on the structure*
- *natural environment surrounding the structure*

Static computation reveals the bearing-capacity of the lining at the rock mass, considering rock-support interaction. To apply the computation that is closest to our real circumstances, we will use static parameters M_i, N_i, T_i to establish the ultimate state of the structure. Based on this analysis, it is then possible to decide what measures would be necessary to stabilize the tunnel lining structure if its ultimate state is reached. Let $p_{Umax}(t)$be the limiting bearing-capacity of the tunnel lining, $p_{Lmax}(t)$ the limiting loading capacity of the tunnel lining (Fig. 1), and p_i, p_j the loading in points i, j for the calculated static values M_i, N_i, T_i and M_j, N_j, T_j then

$$p_{i(t)} = f\,(M_i, N_i, T_i);\; p_{j(t)} = f\,(M_j, N_j, T_j) \qquad (1)$$

The limiting bearing-capacity of the tunnel lining corresponds to static values of M_U, N_U, T_U, so we can simply write

$$p_{Umax(t)} = f\,(A_b, A_s, R_b, R_s) = f\,(M_U, N_U, T_U) \qquad (2)$$

where A_b is the effective area of concrete, R_b is the strength of concrete, A_s is the effective area of steel

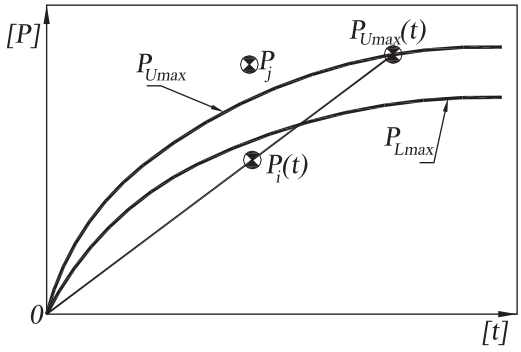


Figure 1. The limiting bearing-capacity and the limiting loading of the tunnel lining.

reinforcement, R_s is the strength of steel reinforcement. If we compare values of the loading $p_i(t)$ a $p_j(t)$ and the bearing-capacity $p_{Umax}(t)$we can then evaluate the bearing-capacity of the tunnel lining in points *i* and *j*. If loading $p_j(t)$ is less than $p_{Umax}(t)$then

$$p_i(t) < p_{Umax}(t) \tag{3}$$

governs inequality. We can say that the tunnel lining satisfies the limiting conditions of the bearing-capacity.If loading $p_j(t)$ is greater than $p_{Umax}(t)$ then

$$p_j(t) > p_{Umax}(t) \tag{4}$$

governs inequality. Here we can say that the strength limit is overrun and the bearing-capacity of the construction is unsatisfactory. The coefficient of the bearing-capacity of the lining *s* is defined as the ratio of $p_{Umax}(t)$ and $p_j(t)$

$$\frac{P_{U\max(t)}}{P_{i(t)}} = s \tag{5}$$

the bearing-capacity of the tunnel lining is then specified by the coefficient s_i on the whole perimeter of the tunnel lining. Where the value s_i {5} is smaller than 1,

$$s \leq 1$$

the construction's total strength is unsatisfactory. The limiting bearing-capacity of the lining is usually reached at one point only, and other static calculations of the lining are usually necessary to evaluate the lining for limiting state usability (deformation) and the limiting state of cracks.

3 UNDERGROUND TUNNEL LINING

We will conduct analysis of the ultimate state of the tunnel lining using bearing capacity coefficient *s* on

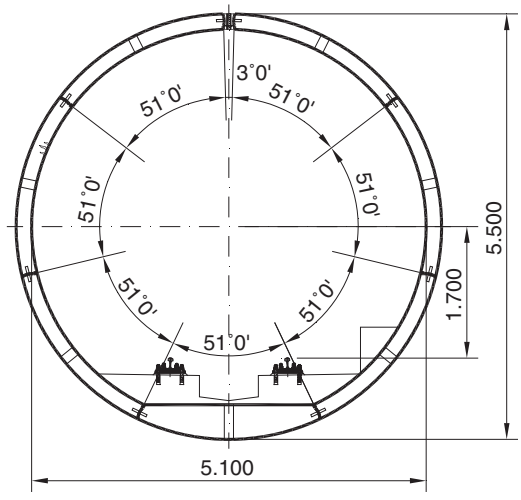


Figure 2. The tunnel lining of the Prague Underground.

two samples of reinforced concrete lining in track tunnels of the Prague Underground. In one of the cases, there was only one visible horizontal crack in the lower part of lining, and in the other case, there were two horizontal cracks visible in the upper part of lining. Linings were at the limit of bearing capacity, so after the static analysis was conducted, measures towards stabilizing the lining were taken. The inside diameter of the lining is 5,1 m, width is 0,2 m, and the base is 0,62 m wide. Concrete B400 was used in horizontal reinforcement of concrete tubing 4×Ø12 mm and vertical reinforcement Ø8 mm, steel 10 425. Separate tubings (segments) are connected by hinges, and each tubing has openings for grouting. Rings are 1m wide and they are not connected with each other. Levels between tubing are prepared to be filled with waterproof mortar. The shape of the concrete segments lining is on Figure 2.

4 POLYGONAL COMPUTATION METHOD

This computation method (used for analysis) is universal and able to affect any shape of construction and allows ease of change to the input parameters for calculation (loading, construction and geotechnical parameters). However, the calculation informs us about deformation and internal forces in lining only and says nothing about the state of stress in the rock mass. The exact shape of the tunnel lining is replaced by a polygon. Radial rods imitate rock mass with hinge connections at the corner points of the polygon.

Action of the rock mass on lining is imitated by the outside active loading applied in the corner of the polygon, and the passive resistance of rock is imitated

by Winkler's springs. The calculation runs in iterative cycles and in the first iterative cycle all radial rock imitative rods are in function, and the calculation runs until all tensile rods are removed and all pressed radial rods are in function only.

The characterization of the elastic rods can be written in the form

$$\overline{K}_i = K_{(\sigma)} \frac{l_i + l_{i+1}}{2} b \tag{6}$$

where $K_{(\sigma)}$, the coefficient of elastic resistance of rock, depends not only on geotechnical parameters of the rock, but also on the shape of the construction and is usually determined according to B.G. Galerkin.

$$K_{(\sigma)} = \frac{E}{R(1+\nu)} \tag{7}$$

where l_i is the length of the member of the polygon and b is the width of the ring, which is usually 1,0 m. Let us assign the deformation and the movement of i joint U_i, V_i, θ_i and internal forces of i joint X_i, Y_i, M_i and outside loading $\underline{X}_i, \underline{Y}_i$.

We then download the columnar matrix $\{P_i\}$ for the internal calculation parameter, and columnar matrix $\{P_i\}$ for outside loading, where

$$\{P_i\} = \begin{Bmatrix} U_i \\ V_i \\ \theta_i \\ X_i \\ Y_i \\ M_i \end{Bmatrix}; \qquad \{P_i\} = \begin{Bmatrix} 0 \\ 0 \\ 0 \\ \underline{X}_i \\ \underline{Y}_i \\ 0 \end{Bmatrix}; \tag{8}$$

So we take the reaction of the supports as the internal forces for i joint, inclusive of the deformation of elastic supports, leading to the changed coefficient $[K_i]$ which affects computation parameters. In general, case loading can be applied to any joint (joints have unique numbering, with the label j).

The matrix notation of the equation for calculating parameters for the joint n, including known perimeter conditions, has the form

$$\{P_n\} = \prod_{i=n+1}^{1} [K_i]\{P_o\} + \sum_{j=1}^{n} \prod_{i=n+1}^{j+1} [K_i]\{\underline{P}_i\} \tag{9}$$

where $\{P_o\}$ is a columnar matrix of initial calculation parameters.

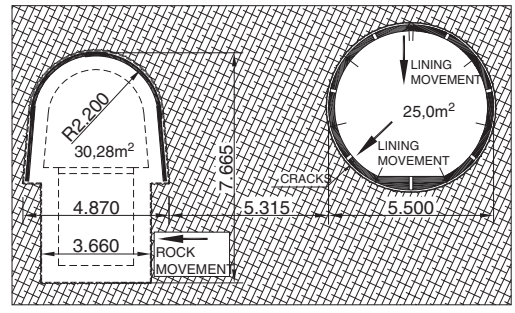


Figure 3. Ultimate state of tunnel lining as a result of drilling the gallery and base sump 38 m long.

5 ANALYSIS OF ULTIMATE STATES

5.1 *Tunnel with a lack of resistance on the side of lining*

The rock mass had lost resistance on the side of the track tunnel lining during drilling of both the gallery and the base sump. At the time of drilling the space for the base sump, tectonically irregular rock mass shifted into the sump space causing the tunnel lining to become deformed. Cracks and crushed zones appeared on the bottom segment of tunnel lining that joins the gallery Figure 3.

In this case, the tunnel lining needs to be restored, as deformations were in the range of centimetres. The primary gallery lining was 4.87 m wide and 7.66 m high, and the tunnel lining outside diameter was 5.5 m. The gallery was drilled after the drilling of the metro tunnel, at 10.5 m axis spacing and 38 m length. The gallery and base sump drilling surface was 30.28 m^2, tunnel drilling surface was 25.0 m^2, spacing of drilling was 5.3 m. The gallery was drilled into Ordovician rocks, in Bohdalecke layers with cover 38.5 m.

After visual observation of cracks in the lining, a detailed analysis of the state of the lining was conducted using bearing capacity coefficient s, results are shown in Figure 4, which illustrates the bearing capacity of the metro structure. At the point of deformation and its immediate surroundings, the value of bearing-capacity coefficient is close to 1. This means, that the bearing capacity of the lining is spent at these locations and it is necessary to take mitigating action to ensure lining stability. The analysis showed two locations on the tunnel lining that are close to capacity limits, although visually the cracks were observed only in one location. The second point close to bearing capacity limits had cracks that were facing the rock wall. The values of the bearing-capacity coefficient higher than 1 represents places with spare capacity. Figure 4 clearly shows points where reconstruction of crushed areas are necessary.

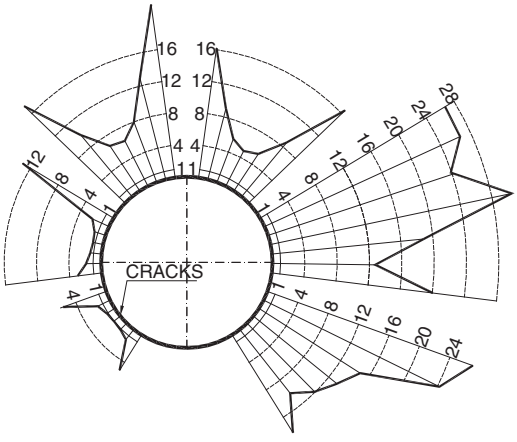


Figure 4. Graph of bearing capacity coefficient of tunnel lining with a lack of side resistance as result rock shift behind metro tunnel lining.

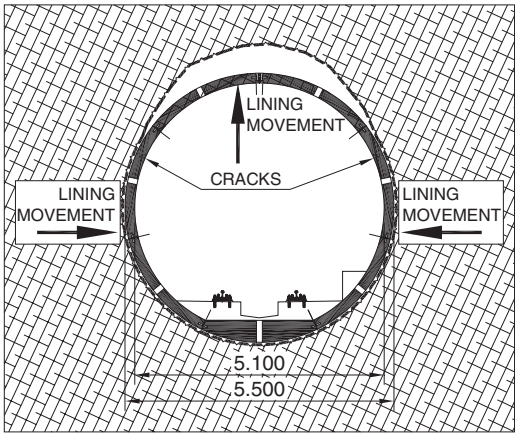


Figure 5. Ultimate state of metro tunnel lining as a result of empty space above the arch at least 8 m long.

5.2 *Lack of resistance in arch of lining*

The same mass concrete lining also reached another ultimate state. After a longer time of use horizontal cracks 8 m long appeared in the concrete tubings (segments) in the upper part of tunnel lining. Crushed places appeared and joint fillings started to fall out. The first signs of damage appeared already in 1990, and the problem was monitored during regular nightly checks of the metro. In 1991, the damage got worse, with the number cracks growing and underground water was starting to seep into the structure. At these points, the metro tunnels go through folding rocks of earlier Paleozoicum, belonging to Ordovicum.

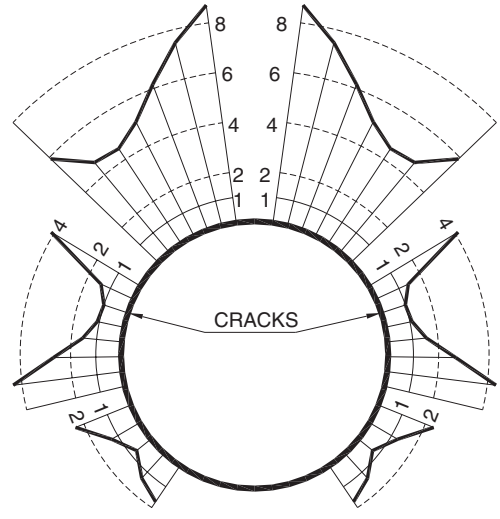


Figure 6. Graph of bearing capacity coefficient with lack of resistance in the upper part as result of an empty space at least 8 m long over the arch. Bottom is bearing capacity overrun also, but cracks are on the outside of the lining and could not be seen.

The largest part of cracks in the tubings appeared in points of contact between Bohdalecke and Vinicke layers, where the horizontal tectonic line is, according to geological research. The cover over the arch of the tunnel lining at this point was 42 m. By modelling different ultimate states of the tunnel lining, we discovered that this kind of deformation is possible only if there is an empty space above the arch of the tunnel.

After this analysis the lining in the arch was drilled through and results of the static analysis was confirmed. There was an empty space above the arch of the lining along the length of cracks. Analysis showed, that on the left and right side of tunnel lining there are two places at the limit of bearing-capacity, although there were cracks only on one place. The second spot at the limit of bearing capacity had rock facing cracks Figure 6.The bearing-capacity reserves shows values of coefficient *s* higher than 1. There were no cracks observed in these places. Reconstruction of crushed areas is necessary at the points where bearing capacity coefficient *s* is close to 1.

6 CONCLUSION

The coefficient of the bearing capacity of the lining *s* describes reserves in the bearing capacity of the lining, and also shows the point where ultimate state will be reached first.

The location of the critical point of the lining depends upon the loading, resistance of the rock and material parameters of the lining.

After evaluation of analysis results we concluded that for simple projects, the static analysis results calculated by the polygonal method are safest, on the condition that this calculation method is supplemented by another analysis, e.g. calculations reviewing the overburden, the pillar of rock or the settlement.

For simple analysis of a tunnel lining, the polygonal calculation method is fully sufficient. Results of detailed analysis of bearing-capacity coefficient *s* of the tunnel lining were presented in a form of graph and they were confirmed by deformations visually observed. Further detailed analysis showed that there are other points of ultimate state of the lining. At these points, cracks are on the outside of the lining and could not be seen from inside the tunnel. Analysis of the ultimate state of the structure can locate points that are very near to the bearing-capacity limit, and direct preventive measures to these points, as well as points where the reserve capacity is very small. Use of this method for two different cases of lining deformations of the Prague Underground demonstrates its simplicity, speed and reliability.

REFERENCES

Aldorf, J., Exner, K. & Škrabiš, A. 1979. *Stability and reinforcing of long mining works*, Prague: SNTL (in Czech).

Aldorf, J. 1992. *The influence of time-dependant deformation properties of concrete on load and loading capacity of support of underground working, Proceedings of Geomechanics 91*- Hradec n. Moravicí, Rotterdam (in English).

Bulychev, N.S. 1982. *Mechanics of underground constructions*, Moscow: Nedra (in Russian).

Dausvili A.P. 1972. *Rascet tonnelnych obdelok v matricnoj forme*, Moscow: Transport, (in Russian).

Muschelisvili N.I. 1966. *Nekotorye osnovnye zadaci matemaiceskoj teorii uprugosti*, Moscow: Nauka, (in Russian).

Pokorný, J. et al. 1990. *II B – 2nd Operational Section Of B Line; Florenc – Českomoravská*, Prague: MON Praha (in Czech).

Srpa, J. et al. 1991. *III B – 3rd Operational Section; Dukelská – Smíchovské nádraží*, Prague: DP Metroprojekt (in Czech).

Széchy, K. 1966. *The Art Of Tunnelling*, Budapest: Akadémiai kiadó (in English).

Závora, K. 1979. *Metro-Driven Tunnel Linings; Textbook Of The Profiles And Segments*, Prague: DP IDS (in Czech).

Závora, K. 1979. *Metro-Driven Tunnels – Design Guidelines*, Prague: DP IDS (in Czech).

This page intentionally left blank

Section 4
Urban tunnelling and its monitoring: conventional and mechanized tunnelling

This page intentionally left blank

Part 4.1
Monitoring

This page intentionally left blank

Underground Space – the 4th Dimension of Metropolises – Barták, Hrdina, Romancov & Zlámal (eds)
© 2007 Taylor & Francis Group, London, ISBN 978-0-415-40807-3

Redesign and monitoring of a portal structure in built-up area

E. Akis, Z. Etkesen, T. Solak & R. Mucukgil
General Directorate of Highways, Ankara, Turkey

E. Durukan
Distinct Directorate of Highways, Trabzon, Turkey

M. Unver
ARGEM Drill. Geotech. Eng. Res. Consult. and Trade Co. Ltd., Ankara, Turkey

ABSTRACT: In this work, the redesign studies and the construction of the ground anchorages of the portal structure of a shallow urban tunnel, which is located on the main transportation artery of Black Sea Coast Road, are given. This tunnel has been constructed near an old existing tunnel under heavy traffic conditions and surrounded by residential area. During the research studies of the design stage, restricted number of boreholes was opened because of the expropriation problem. In view of the site observations and information obtained from these boreholes, it was observed that the rock encountered at the portal sites is a weathered and weak volcanic rock composed of medium to fine-grained pyroclastic material. Due to this reason, a portal structure that consists of bored piles, ground anchorages and cut and cover was designed. The original project of the tunnel was approved by General Directorate of Highways in December 2000. The construction of the tunnel was started at June 2003. After completion of the first test anchorage, it was observed that it could be pulled out only one third of the design load. After solving the expropriation problem, additional boreholes could be opened and the existing project was redesigned using the new data. During the construction of anchorages, special care was given and the monitoring of the portal structure was performed using load cells, extensometers and inclinometers. This study contains two main parts: Firstly, the redesign of the pre-stressed anchorages and construction techniques of them for improving the capacity will be given and then the evaluation of the monitoring data during construction of portal structure will be explained.

1 INTRODUCTION

Kalepark Tunnel, which is the scope of this study, is located on the main transportation artery of Black Sea Coast Road, city crossing of Trabzon. It is a shallow urban tunnel that is surrounded by residential area and located under a historical reputational area and military zone. This tunnel has been constructed near an old tunnel under heavy traffic conditions and surrounded by residential area (Photograph 1). The length of new tunnel was 144 m including 15.5 m and 28.5 m cut and cover sections at entrance and exit sections respectively. The horizontal distance between the old and new tunnel at the entrance and exit portals are 11 m and 20 m, respectively. The overburden of the new tunnel is varied between 2.5–3.5 m at portal areas and the maximum overburden through the tunnel is 11.5 m.

In the entrance zone there was a permanent excavation from 6.5 to 13.5 m depth. In 1997, during the research studies of the design stage, restricted numbers of boreholes were opened because of expropriation problem. Only four boreholes were drilled during the tunnel research studies at that time. As it was shown in Figure 1, ESK-1 borehole, quite far from deep permanent excavation, was representative for the portal structure. In view of the site observations and information obtained from these boreholes, it was observed that the rock encountered at the portal sites is a volcanic rock composed of medium to fine-grained pyroclastic material. Due to this reason, a portal structure that consists of bored piles, ground anchorages and cut and cover were designed. Besides, at the design stage it is advised that the confirmation of the geotechnical values and the assumptions of the project should be checked. The original project of the tunnel was approved by General Directorate of Highways in December, 2000.

During the design stage, the geotechnical model for the right section of the entrance portal, which is the scope of this study, was described as weathered tuff and



Photograph 1. A view from entrance portal of Kalepark Tunnel.

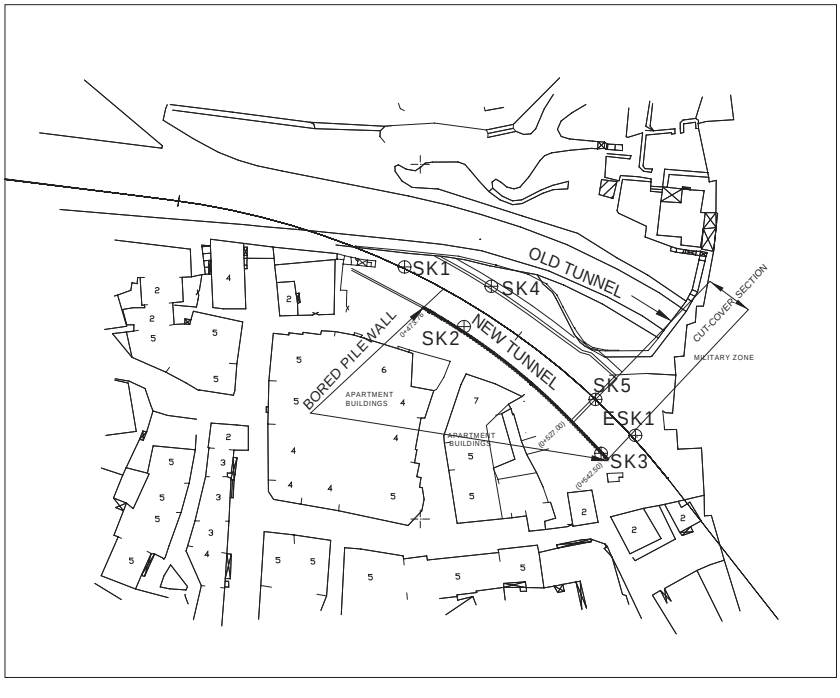
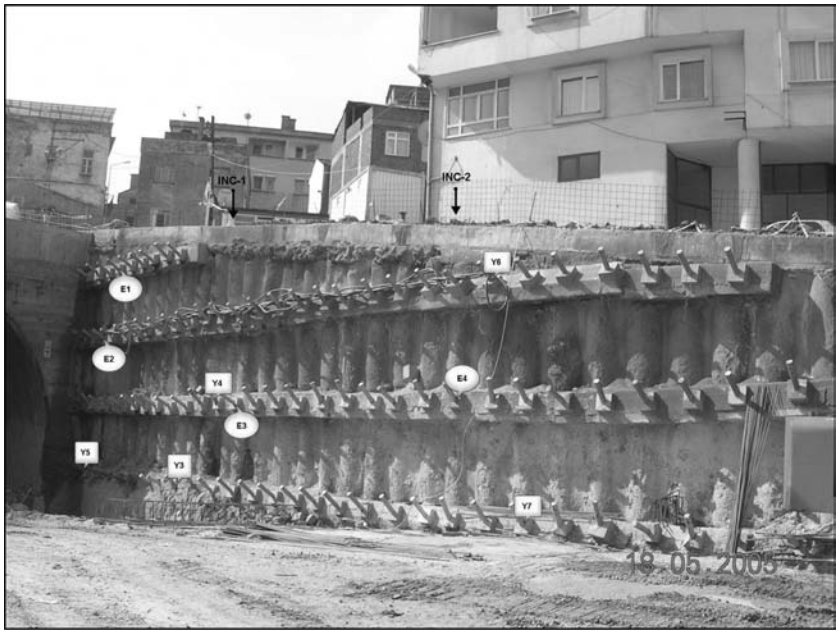


Figure 1. Plan view of Kalepark Tunnel entrance portal and the location of boreholes.



Photograph 2. Monitoring system and retaining structure of Kalepark Tunnel.

agglomerate that contains clay layers. The retaining structure of the entrance portal at the design stage was determined as bored pile wall with pre-stressed ground anchorages (Photograph 2 and Figure 1).

The construction of the tunnel was started at June, 2003. Construction and research studies for comparison were performed simultaneously. After solving the expropriation problem, additional boreholes were drilled. Bored piles were constructed. Three pre-stressed anchorages at the first row were constructed and anchor tests were performed. During the drilling process of anchorages, it was seen that soil around the anchor bond length was containing water. The test results were not in consistent with the project values as it was expected. During anchor tests, some of the anchorages could be pulled out only one third of the design load. In view of the evaluation of the new borehole data, the results of anchor tests and the observations made during the pile drilling, it was concluded that the foreseen geotechnical evaluation was different from the actual site. Due to this fact, the existing project was redesigned using the new data.

2 GEOTECHNICAL EVALUATION

2.1 *Geotechnical evaluation at the first design stage*

The site was described as weathered, weak and water susceptible tuff and agglomerates containing thin clay layers. The rock quality designation (RQD) values are zero and the core recovery ratio (TCR) values were differing from 5–43%. The water level was approximately 10 m below the ground surface. The strength parameters for the weathered tuff and agglomerate and clay layers were decided as $c = 100$ kPa, $\Ø = 25°$ and $c = 0.5$ kPa, $\Ø = 9–10°$, respectively. Using these parameters, intermittant bored piles (Ø80) with 15 cm clear space and pre-stressed ground anchorages were designed.

2.2 *Geotechnical evaluation at the construction stage and new project studies*

At the entrance portal four additional boreholes were drilled. Two of these boreholes (SK2 and 3) could be representative for the right section of the portal. Pressuremeter tests were performed in these boreholes.

Unfortunately, no additional boreholes that could give information about the fixed anchor zone were drilled because of residential buildings surrounding the site. In order to overcome this problem, results of anchor tests were evaluated. From this investigation, it was seen that, approximately the first 4 m of the geotechnical profile was formed of road fill. Then, highly weathered and water susceptible clayey tuff was encountered up to approximately 10th meter. After this layer, weathered tuff with 0–60% RQD value and 30–80% TCR value is laid down. The water level was 2.70–5.45 m below the ground surface. The water level was different from the former boreholes, the main

Table 1. Soil parameters used in the redesign stage.

Layer	c′ (kPa)	Ø′ (°)	E (kPa)	ν
Fill	0.5	27	7500	0.33
Tuff 1	2.0	27	15000	0.30
Tuff 2	10.0	28	25000	0.30

reason for that was thought as the percolation of the surface runoffs and the percolation of water due to surrounding buildings.

The pressuremeter test results were used in determining the elasticity modulus and friction angle of the layers. Menard and Calhoon Methods were used and it was seen that friction angle values obtained from Calhoon method gives more conservative values than Menard Method. As it was a permanent excavation, without any boreholes drilled at the anchor fixed zones and since it was a residential area, lower values were chosen as design friction values. Moreover, lower cohesion values were chosen as shown in Table 1 due to reasons mentioned above.

From the results of the evaluation of new borehole data, the results of anchorage tests and the observation made during the pile drillings, the parameters used in the redesigned project was given in Table 1.

3 PROJECT DESCRIPTION

3.1 *New design project details*

The safety of permanent retaining structures in such residential areas is very important. In the entrance portal structure, the depth of the excavation was varied between 6.5 m to 13.5 m. As expected, horizontal and vertical displacements are normally occurred in every deep excavations. But it is important to keep these deformations in permissible limits in this project due to surrounding built-up area.

At the redesign stage, the construction of the intermittant bored piles (Ø80) with 15 cm clear space was constructed. Firstly, the existing bored pile wall was taken into consideration and redesign was performed by considering new parameters obtained from new investigations. The location of pre-stressed ground anchorages is another important factor since the construction was located in a residential area. All the buildings near the portal structure were reevaluated and the anchorage patterns and inclination of anchorages were decided.

On the other hand, the pre-stressed anchorages and pile wall of the system were modeled by finite element program PLAXIS. In this program all the construction stages can be modeled with any loading conditions. Forces acting on the ground anchorages and pile wall can be evaluated for all stages of the construction.

The design of retaining wall was made based on six typical types of solution depending on the depth of excavation and surrounding buildings near to the excavation. The working loads of the anchorages were calculated from the program. Additional analyses were performed in order to see the displacements occurred at prescribed locking loads. By evaluating the results of the analyses, locking loads for the ground anchorages were adjusted. As a result of these analyses, it was seen that the anchorage working loads (service load) were varied between 20–30 tons.

Horizontal and vertical displacements just near and around the retaining walls were restricted between 5–15 mm depending on the neighboring conditions. As a result, no any visible cracks were observed around the permanent excavations.

The moment and shear capacities of the piles were high. Depending on that fact, pre-stressed ground anchorages were designed as they located at every space between piles in the new design project. As a result of this pattern, the dimensions of breasting beam would be smaller and the construction rate would be fast. The anchorage pattern in the design project was determined as 0.95 m × 2.5 m (horizontal × vertical). Because of the adjacent buildings, the inclination of the anchorages was 20°, 25° and 35° from the horizontal. These inclinations were applied variably ±2 degrees in horizontal direction of the breasting beams, in order to prevent the fixed anchor zone interactions. After the construction of anchorages, the anchorage tests were made and it was observed that the working loads can be carried by these anchorages.

3.2 *Practical aspects in ground anchorage constructions*

Drilling and grouting methods are the main practical aspects that influence the anchorage capacities. Suitable diameters of augers (minimum 15 cm) were used in drilling operation in this project. After drilling without using any water, hole was filled with grouting material immediately in order to prevent the collapsing of the hole-walls. The ground anchorage assembly then was located through the grouted hole before setting time of grout. Some grout material was come back from the hole and some of it was percolated to the surrounding soil as was expected. Therefore, a post grouting process was found necessary to get desired capacities. Special packers were designed just between the free and fixed parts of the ground anchorages. A grout pipe entering into this packer was used to give grouting material. Thus a barrier was formed between free and fixed zones. After 1 to 3 hours, a post grouting was performed under 2 to 4 bars through another grout pipe. Thus, the final fixed zone of the anchorage does not contain any voids that may be produced after primary grouting which was performed by tremie method. The diameter of the fixed zone is also greater

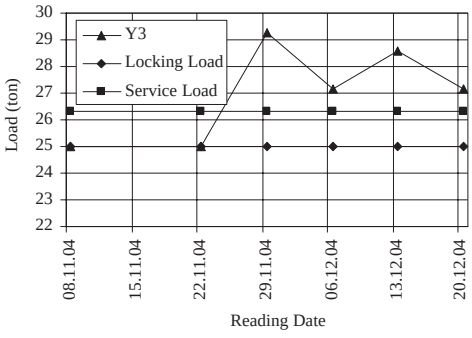


Figure 2. Data measured from load cell Y3.

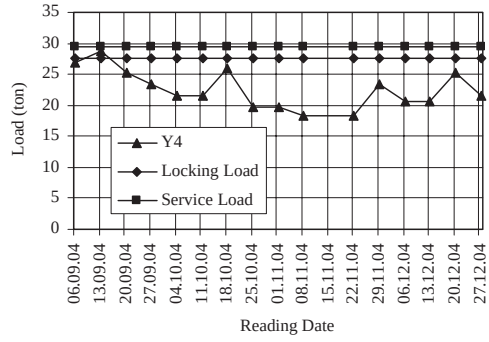


Figure 3. Data measured from load cell Y4.

after this post grouting process. All of these increase the capacity of the ground anchorages.

4 ANCHORAGE TESTS, MONITORING AND EVALUATION

Anchor tests were done during construction according to SIA 191 Standard. The anchor tests were performed in order to check the design assumptions.

4.1 *Anchor tests*

The working loads of the ground anchorages were about 60 tons in the original project. These capacities were found quite high after testing first anchorages. Additional site investigations confirmed these results. The working loads of the anchorages were decreased in the redesigned project. The results of anchor tests were satisfactory in the redesigned project. Thus, the permanent excavations were finished based on new site investigation and design studies with special measures in ground anchorage constructions as mentioned above.

4.2 *Load cell readings at anchorages*

Five load cells were located at the anchorages in order to monitor the load distribution (Photograph 2). The load variation during the construction process was followed with periodical readings.

As it can be seen from the Figures 2,3,4,5,6 during the intermediate construction stages, some data measured from Y3, Y5, Y7 load cells are 3, 4, 3 tons higher than service loads respectively. But it was observed that, the final readings taken after completion of the retaining wall showed that, the loads acting on the anchorages were all lower than the service loads.

4.3 *Extensometer results constructed on pile wall*

Four extensometers were located at the pile wall in order to monitor the deformations during construction. (Photograph 2). The values measured were followed

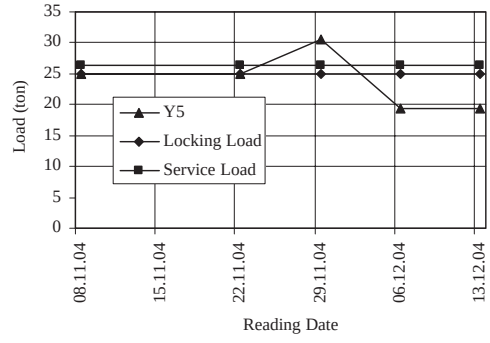


Figure 4. Data measured from load cell Y5.

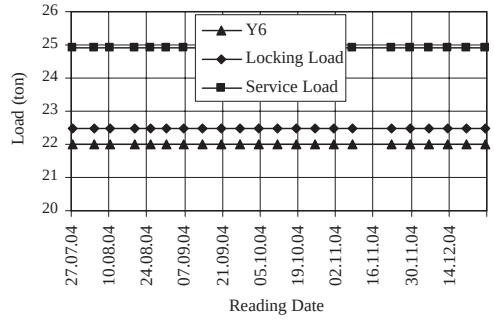


Figure 5. Data measured from load cell Y6.

with periodical readings and is given in Figure 7. The results were showed that, maximum measured deformations were about 80% of the calculated ones.

4.4 *Inclinometer measurements constructed on behind the pile wall*

Two inclinometers were located in order to control the displacements during the construction of the portal structure (Photograph 2). If the measurements taken

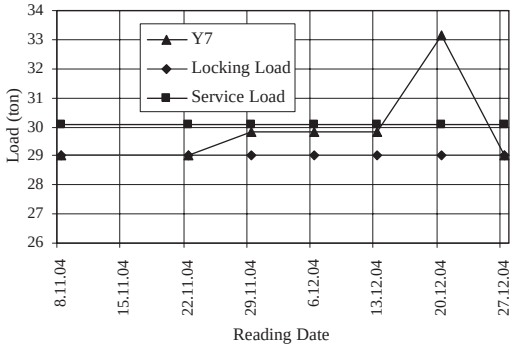


Figure 6. Data measured from load cell Y7.

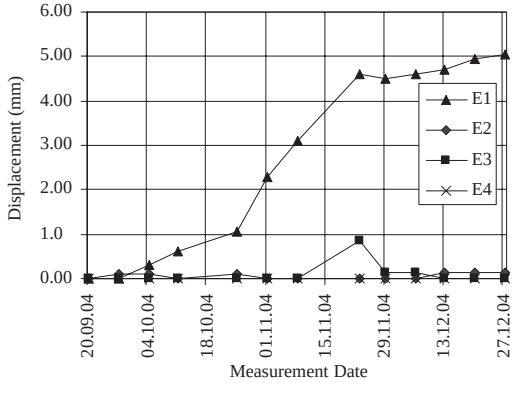


Figure 7. Data obtained from extensometer E1, E2, E3, E4.

from inclinometers and the extensometer data (E3 and E4) are compared, it is seen that the maximum displacement values are in 5–8 mm and convenient with each other.

5 CONCLUSION

In this case study, the importance of the confirmation of the assumptions at the project stage due to compulsory incomplete research studies was seen. Loads measured from the load cells at intermediate stages may show higher values than assumed ones in project due to improper construction sequence. Excavation, breasting beam and anchor construction activities should be adjusted carefully so that no any horizontal and vertical excavations are to be performed without locking the neighboring ground anchors. But on the other hand, by cross checking the inclinometer and extensometer readings it was concluded that no additional support was needed. As a result, detailed research studies, anchor tests and confirmation of project assumptions and also monitoring have vital importance on the safety of retaining structures especially in built up areas.

REFERENCES

Geological, Geotechnical Project Report, Yüksel Domaniç Co. Ltd., 1997.
Geological, Geotechnical Project Report, Yüksel Domaniç Co. Ltd., 2000.
Support Project for the Entrance of Kalepark Tunnel, MNG Zemtaş, 2004.
Ground Anchors, SIA 191, 1977.

Underground Space – the 4th Dimension of Metropolises – Barták, Hrdina, Romancov & Zlámal (eds)
© 2007 Taylor & Francis Group, London, ISBN 978-0-415-40807-3

The influence of vibrations and noise on the housing development on the cover of the Mrazovka tunnel in Prague during tunnel driving and its putting into service

L. Bartos & L. Bartos jun.
Bartos- Engineering, Brno, The Czech Republic

ABSTRACT: This paper sums up the knowledge acquired from measuring the seismic and acoustic impacts on the housing development on the cover during the tunnel driving of the Mrázovka tunnels and after putting the tunnels into full service. The inhabitants complained mainly about the noise propagating through basement rocks into the building construction and housing premises, i.e. vibrations within the audible frequency spectrum during the night. During day-time the complaints were scarce due to the raised level of noise from the nearby roads. The results of measurements of vibration and acoustic effects caused by blasting as well as machinery used in the underground during the working process are compared with the limits permissible according to the valid regulations and standards. After putting the tunnels into service, vibration and noise measurements were carried out that proved that even with low cover thickness (12 m) the vibrations and noise propagating into the buildings are below the human perception threshold. The motor-traffic in the tunnels can by no means exert negative influence on the comfort of living in the respective housing development.

1 INTRODUCTION

This paper deals with the summary and assessment of the data obtained from seismic impact measurements affecting the housing development on the cover during the tunnel driving of the Mrázovka tunnels and after putting the tunnels into full service.

The complexity of geological conditions represented by the Letná shales of both monotone and flysch-type evolution, Libeň shales and Řevnice quartzites did not allow a unified technique of rock fragmentation to be specified for the sequential excavation of the tunnels. For fragmentation of hard or very hard rocks (over 60 Mpa) i.e. namely Letná shales of flysch-type evolution and quartzites blasting was therefore used. Otherwise mechanical technologies of driving were used.

The vibration effects sources were:

a) blasting, applied in sequential tunnel driving using NATM driving (New Austrian Tunnelling Method)
b) machinery used in construction technology
c) current motor- traffic on nearby roads

After finishing the construction of the tunnel, vibration effects in the tunnel, caused by motor- traffic and propagating through the rocks into building constructions in the cover, were investigated.

2 PERMISSIBLE VIBRATION LIMITS

Depending on the character and duration of the vibrations, the permissible limits for building constructions in the stage of failure O (no harm) according to the technical standard (ISO) were set:

a) for blasting maximum vibration velocity (v_{max})
b) for long-term impact load by virtual value of vibration speed
c) for steady periodical load by effective value of vibration speed (v_{ef})

2.1 *Blasting*

The permissible limits of dynamic excess load for building constructions that were found in the field of operations (with frequency characteristic of seismic impacts over 50 Hz) were set for reference points

(the lowest construction spot, bottom construction) in the following range:

Assessed structure – characteristics	Resistance class	V_{max} (mm/s)
Dilapidated buildings, nonconforming to building rules, historic building	A	6 až 15
Common masonry buildings up to 3 levels	B	15 až 30
Big masonry buildings (brickwork or blockwork), well reinforced panel and prefabricated buildings from concrete elements	C	20 až 40

The blasting limits were represented by the lowest values in the given range. Thus the variety in the construction and technical state of buildings, their age, and way of foundation reflected. Engineering communications and service pipelines that find themselves under the surface in shallow depths have a markedly higher dynamic resistance (40 to 100 mm/s) and therefore represented no limit to blasting.

2.2 *Technical bumps from machinery*

Dynamic reponse caused by long-term impact load or stabilized periodic vibrations is given by virtual value of vibration velocity $v^{ef(1)}$ in mm/s:

Resistance class	Vibration velocity $v^{ef(1)}$ mm/s			
	Construction class according to Czech standard ČSN 730031			
	U	I	II	III
A	0.2	0.4	0.7	1.1
B	0.4	0.6	1.0	1.8
C	0.7	1.5	2.0	2.8
D	0.9	2.0	2.5	3.5

Construction class II : civic and residential constructions

The given values are valid for the so called reference point.

2.3 *Vibrations in protected parts of the constructions*

Vibrations in the protected indoor parts of the constructions are judged from the Hygienic regulations about "health protection from unfavourable effects of noise and vibrations". For the protected indoor parts, the decisive role will be played by low-frequency wake-up elements (app. 10 to 80 Hz).

The highest permissible virtual values of vibration acceleration a_{etp}(interrupted and continuous vibrations) for dwelling rooms, time of the day (06–22) and time of the night (22–06) for the given 1/3 octave medium frequency range are presented in the table:

Frequency range 1/3 octave (Hz)	a_{ez} (m/s^2)	a_{etp} (m/s^2) 06–22 o'clock	a_{etp} (m/s^2) 22–06 o'clock	a_{etp} (m/s^2) 06–22 o'clock	a_{etp} (m/s^2) 22–06 o'clock
		Interrupted and continuous vibrations		Repetitive bumps (1 to 3 × daily)	
2	0.0036	0.0072	0.0051	0.0576	0.005
5	0.0045	0.009	0.0063	0.072	0.0063
8	0.005	0.01	0.0071	0.08	0.007
20	0.0125	0.025	0.0176	0.2	0.018
40	0.025	0.05	0.0352	0.4	0.035
80	0.05	0.1	0.0705	0.8	0.07

a_{ez} – basic vibration acceleration value (no corrections).

The highest permissible weighted frequency acceleration level L_{awp} of building constructions in protected indoor parts depend on the type of the room, daytime and vibration influence on man, or vibration acceleration virtual value a_{ewp}, respectively.

	L_{awp} (dB)		a_{ewp} ($m.s^{-2}$)	
Room type	day	night	day	night
Dwelling rooms	77	74	0.0072	0.005

The highest permissible bump acceleration weighted values in constructions (max. 1 to 3 occurences a day):

	L_{awp} (dB)		a_{ewp} ($m.s^{-2}$)	
Room type	day	night	day	night
Dwelling rooms	95	74	0,056	0,005

3 PERMISSIBLE NOISE VALUES

The limit site work noise values from hygienic regulations:

7 to 21 o'clock ……. 65 dB(A)
6 to 7, 21 to 22 o'clock. ….. 55 dB(A)
22 to 06 o'clock……..……. 45 dB(A)

4 VIBRATION MEASUREMENT RESULTS

4.1 *Blasting*

From the set of bumps measured on 47 houses, caused by shooting and blasting while driving the tunnels (western and eastern), maximum bump values were assessed, including other technical parameters:

Constr.	Length (m)	m_{evn} (kg)	$m_{celk.}$ (kg)	L (m)	Cover (m)	$v_{max.}$ (mm/s)
Western tunnel	325	2.4–3.2	60–110	2	42–50	5
Western tunnel	148	0.4–0.8	10–15	1	15–18	14.5
Machine room	105	2.4–5.3	75–132	2	50–65	5.2
Branch A	180	2.4–6,0	60–223	2	38–40	2.2
Eastern tunnel	235	0.6–2.4	30–93	1–2	30–32	9.8
Eastern tunnel	135	0.4	6–10	1	15–20	14.5
Branch B	100	0.6–1.6	15–45	1	20–22	11.1

Table legend:
m_{evn} – equivalent charge
$m_{celk.}$ – total charge for the blasting event
L – pull.

The set dynamic stress permissible limits of the monitored constructions were kept in all cases.

4.2 *Machinery*

The results of vibration effects measurements concerning the machinery used underground, such as rigs, winding machines, pneumatic drill units, which were transported into groundfloor rooms of dwellings, exceeded the hygienic limits for night with cover thicknesses 12 to 16 m (max. 58.5 dB or $a = 0.1$ m/s^2, resp.). For the cover thicknesses from 18 to 20 m the hygienic limits were already kept, thanks to increased vibration loss in the cover (below 55 dB, or 0.07 m/s^2 resp.). On higher floors permissible limit values were registered, thanks to the vibration loss in the construction.

In order to compare the effects of different vibration sources, measurements of vibration caused by motor-traffic were carried out with buildings on the main roads, to assess the "the backgroung vibration". The maximum vibration values measured, depending on the distance of the passing vehicles (3 to 6 m), ranged $v_{ef} = 0.2$ to 0.6 mm/s.

4.3 *Motor-traffic in tunnels*

After putting the tunnels in service, measurements were carried out on the groundfloor level of the houses above the tunnels, to find out the maximum

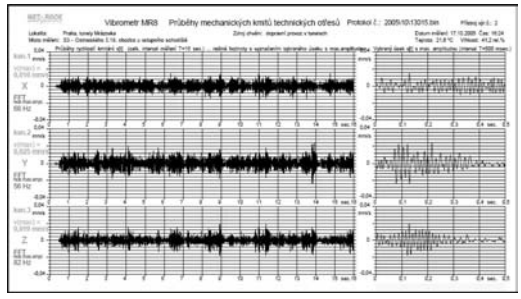


Figure 1.

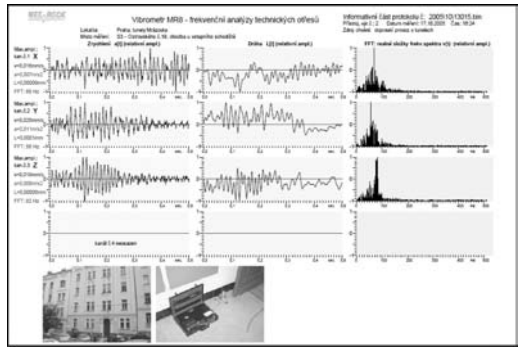


Figure 2.

vibration and noise values propagating into the buildings. The measurements proved that even with low cover thickness (app. 12 m), both vibration and noise values transmitted are below the threshold of human perception, i.e. $L_{awp} = 59$ to 65 dB, or vibration acceleration value $a_{awp} = 0.001$ to 002 m/s^2, respectively.

The motor-traffic in the Mrázovka tunnels can by no means exert negative influence on the comfort of living in the housing development.

Mechanical vibrations record diagram of technical bumps (vibration velocity) caused by motor – traffic in the tunnel, as registered on the groundfloor of 19 Ostrovská St. house (12 m above the tunnel vault) – figure 1.

Interpretation of path deviation, acceleration and frequency analysis from vibration velocity record – figure 2.

Motor – traffic vibration measurement record in the tunnel with interpretation according to a hygienic regulation – figure 3.

5 RESULTS OF NOISE MEASUREMENTS

5.1 *Blasting*

The noise measurements from blasting, propagating through the rock, proved no excess to the maximum

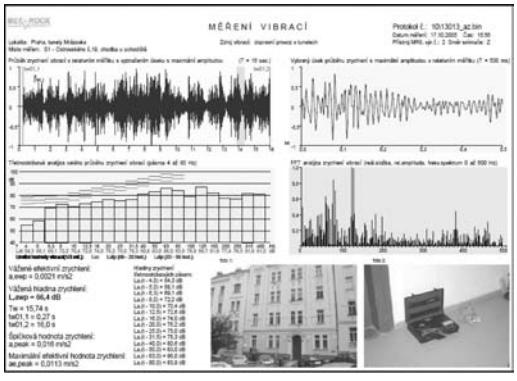


Figure 3.

acoustic pressure equivalent level for daytime (40 dB), with maximum values in parts of housing development with low cover reaching 35 to 38,5 dB. From 21 to 07 o'clock there was no blasting going on.

5.2 *Machinery*

Maximum acoustic pressure equivalent levels in inhabitated places caused by construction works, i.e. drilling, driving, rock fragmentation, lining demolition etc. were within permissible range (below 55 dB) for cover thickness of 18 to 20 m during daytime, with maximum vibration level of 53.5 dB. With lower cover thickness (12 to 16 m) the maximum vibration level was 61.5 dB. Fot nightime the only technology applicable was machine drilling with acoustic level below 30 dB.

5.3 *Motor-traffic in the tunnel*

The motor-traffic noise in the tunnels was also considerably below the human threshold of perception.

6 SOLUTION OF COMPLAINTS

When driving tunnels in the vicinity of housing development there were complaints about vibration and acoustic effects of blasting. Because these two elements combine and work concurrently, they are percieved as physiologically unpleasant bumps with vibration velocity of 3 mm/s.

Therefore people attribute to them common cracks in painting, plaster and masonry which, in fact, have a totally different cause.

There were frequent complaints from nearby surroundings even about vibration and acoustic effects of driving or drilling, which propagated through the cover into the houses and caused disturbances especially during the night.

All the complaints were dealt with by the developer, were discussed by the monitoring board and investigation into their justification was commanded. Through systematic checking of blasting bumps and through blasting charges adjustment the permissible limits of dynamic excess load were kept in all houses. In critical parts, blasting was reduced to the minimum applicable values and the process was segmented.

There were several complaints from the distance of 100 and more meters, claiming serious disturbances to construction elements (fallen stone bridge, fallen retaining wall, disturbance of newly constructed villa and some old houses). After inspections being carried out it was concluded that these claims are unsubstantiated and had different causes.

The unjustified claims of these damages were proved by a variety of measurements, the very nature of the disturbances and the statement of their real causes.

REFERENCES

Bartos, L. & Bartos, L. 2003. Evaluation of the influence and noise on the surrounding development during excavation of the Mrazovka tunnels, *Proc. international conference Uderground construction, Praha 18–20 nov.2003*

Bartos, L. & Bartos, L. 2002. The impact of vibrations and noise on the surrounding development and environment during excavation of the Mrazovka tunnels, with respect to application of blasting, *Tunel 2/2002.*

Underground Space – the 4th Dimension of Metropolises – Barták, Hrdina, Romancov & Zlámal (eds)
© 2007 Taylor & Francis Group, London, ISBN 978-0-415-40807-3

Advanced online monitoring for urban tunnelling projects

N. Benecke, P. Althaus & U. Kalz
Deutsche Montan Technologie GmbH, Essen, Germany

ABSTRACT: Tunnelling in urban environments causes several impacts to existing buildings and infrastructures as well as to the urban population. In particular surface movements, sound and vibrations from tunnelling work (e.g. tunnelling machines, blasting or rams) may have negative impacts on people up to damages on existing buildings and infrastructures. Therefore a monitoring system is urgently needed to know as early as possible about any surface movements and vibrations to take measures to avoid damages. More and more calls for proposals for urban tunnelling projects require monitoring systems for these purposes. An advanced online monitoring system with alert function is presented in this paper. The system includes different components for continuous monitoring of surface movements (e.g. DGPS, TPS and radarinterferometry) and vibrations (seismic event registration) with high accuracy and reliability. Also remote data-transmission and real-time alert functions are included. Especially some examples from practise will demonstrate the effectiveness of the system.

1 INTRODUCTION

Wherever tunnel projects are being developed in urban environments, the knowledge about geodynamic and environmental conditions plays a crucial role in the management and reduction of risks. Important data required are three-dimensional surface movements and vibrations, both for the whole area as well as for individual objects, which are exceptionally sensitive to deformations and/or vibrations, e.g. houses or infrastructures. For a long time DMT is measuring surface movements and vibrations as a service contractor for mining and tunnelling industries as well as for governmental agencies in Germany and worldwide. With regard to the increasing demand for information and cost effectiveness, DMT is in a continuing process to integrate advanced surveying, remote sensing and geophysical techniques.

This contribution deals with:

- Deformation monitoring using online GPS and TPS techniques as well as differential SAR interferometry, and
- Vibration monitoring.

Depending on the conditions of each single project the monitoring conception, possibly containing traditional survey as well as online-methods, radarinterferometry or vibration monitoring, has to fit the specific demands on site. Typically early-warning features and automatic reporting and documentation features are realized.

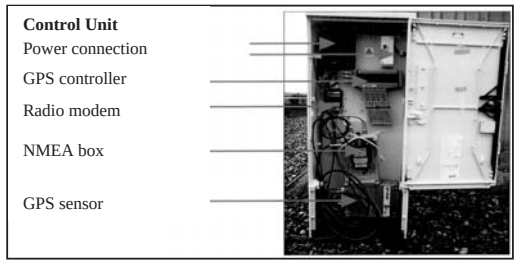


Figure 1. Control unit for GPS real time station.

2 DEFORMATION MONITORING

2.1 *GPS-Real-Time-Monitoring*

For a period of 17 months three public buildings in a city in Western Germany have been monitored by GPS real time measurements during underground mining operations. Therefore on each building a GPS station has been mounted inaccessible for the public (see Figures 1 and 2). Additionally a reference station has been operated over the whole monitoring period.

All stations have been linked. All captured data have been transmitted to a central processor unit, where an direct data evaluation has been realized (Figure 3). The data have been captured with a frequency of 180 seconds. This frequency has been proven and tested in several projects, but also other frequencies up to 1 second are possible.

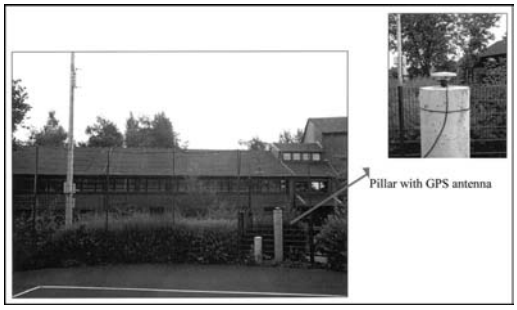


Figure 2. Secured pillar with GPS antenna.

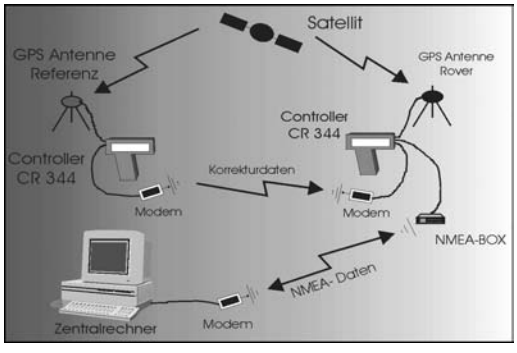


Figure 3. System components and cross linking.

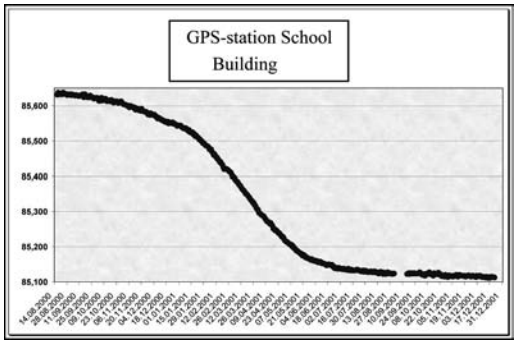


Figure 4. Measured vertical movements.

Meanwhile similar measurement designs have been used successful in several mining and tunnelling projects. If reasonable defined thresholds for horizontal and vertical movements can be set up. In case of overstepping these thresholds an alert will be send immediately to a computer or mobile phone.

In Figure 4 the effect of a mining induced subsidence is shown. These data are compared to subsidence modelling data to find abnormous behaviour. Subsidence modelling at DMT covers all kind of effects from tunnelling, mining in 3D and time dependent.



Figures 5 and 6. Monitoring system with totalstation and pillar with prism.

GPS-Real-Time-Monitoring is especially applicable for monitoring single objects, e.g. public or historical buildings, sensitive industrial plants and infrastructures, which have to be monitored for longer periods (several months up to years) with high accuracy. Reasons therefore will be specific sensitivity against movements, expected large damages or public interest.

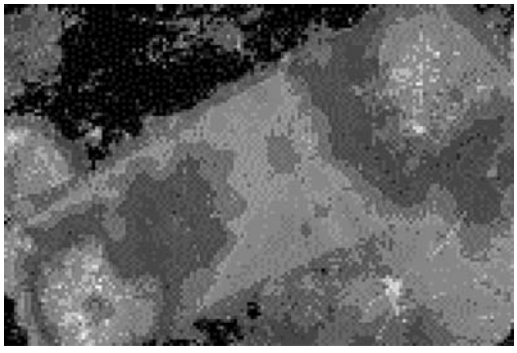
In comparison of different measurement methods, GPS-Real-Time-Monitoring start with high basic costs, but with very low running costs. In opposite traditional repeating measurements have linear increasing costs with each repetition. Therefore it is necessary to calculate for each project the individual break-even-point from which the real-time monitoring system is cheaper than traditional measurements (Benecke et. al. 2001).

2.2 *Totalstation monitoring*

A shaft, closely located to residential buildings, has been reconstructed over a period of 10 months. During the construction movements with damages to the residential buildings have been feared. For monitoring the movements a continuous monitoring with a Totalstation and 10 monitoring points (pillars with prism) have been installed (Figures 5 and 6).

The totalstation has been erected on a nearby building and has been connected with a central processor unit by radio control to drive automatically to each of the prisms for measurements each 20 minutes. The measured data have been transferred directly to the processor unit for evaluation. Additionally an alert system has been integrated, which send an alert SMS to the mobile phones of the site manager and the responsible surveyor in case of movements bigger than 1 cm.

The use of totalstation monitoring is especially reasonable if several points on a small object or area have to be monitored over a long period. Every measurement point needs only a prism. Therefore a large number of points can be measured very cost effective. As a pre-condition a stable position for the totalstation is needed. Alternatively the movements of the



Figures 7. Surface movements detected by radarinterferometry in an oilfield.

totalstation can be measured simultaneous by real-time GPS (Korittke et. al. 2004).

2.3 *Radarinterferometry*

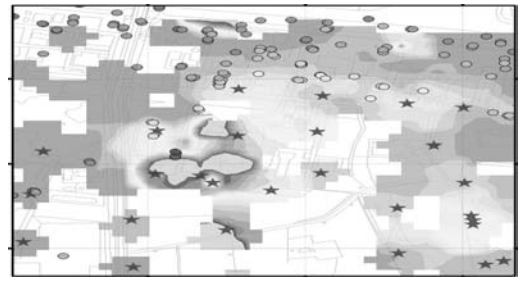
A dense monitoring of large area surface movements of with traditional methods as mentioned above is time consuming and expensive. Instead radarinterferometry is coming up as an innovative and at least very economically methods for this purpose. In addition only radarinterferometry can look into the past for several years by processing older scenes. DMT and partners have developed an integrated conception for monitoring surface movement in large areas with influences from underground mining, oil and gas exploitation and groundwater measures.

Using data of current satellites ERS, ENVISAT or ALOS as well as archives data of ERS since 1992, it is possible to detect small movement rates of few millimeters per year with good spatial coverage and point density, especially in urban or less vegetated areas. Figures 7 and 8 point out typical results (Wegmuller et. al. in prep.).

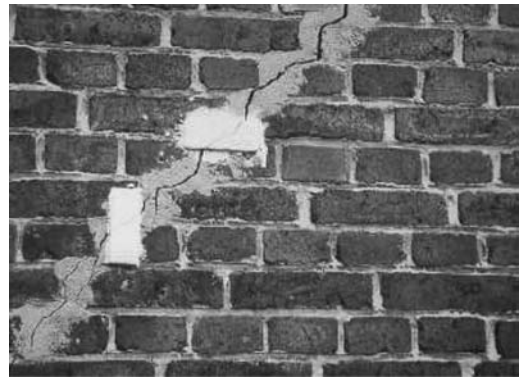
2.4 *Vibration monitoring*

Tunnel construction activities often cause serious vibrations, e.g. from blasting, drilling or machine driving. If the tunnel construction work is located close to buildings or infrastructures, the vibrations are potentially able to induce damages to these objects (Figure 9) or strongly affect people living in the neighborhood.

The following example deals with blasting during tunnel excavation. Depending on the specific blasting scheme drill holes have to be executed at the rock face to contain the blasting agent. The allocation of blasting time levels and the time lapses are driven by the blasting scheme. Of course, the tunnelling is running through different geological strata, therefore the used



Figures 8. Surface movements detected by radarinterferometry in a salt caverns field.



Figures 9. Damage from vibrations.

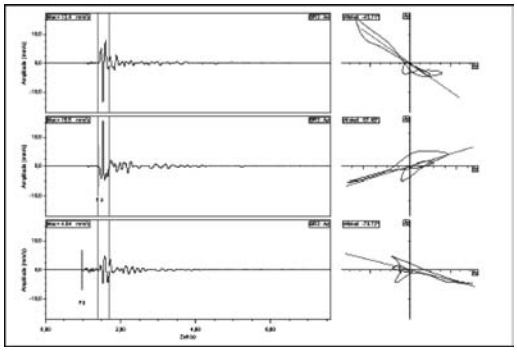
blasting schemes are varying in dependency on rock strength, tectonics and other geological features.

Outside the source vibration waves occur due to the elastic behaviour of the rock. There are different mechanisms of wave propagation, which lead to different types of waves. In practise the wave propagation is affected by additional factors, e.g. damping, reflection, refraction or conversion.

The registered vibration at the place of imission is a superposition of all relevant wave types. How vibrations caused by blasting affect a building can be registered by basement measurements in 3 rectangular directions and can be visualised in a hodogram (Figure 10).

Different wave types can be identified in the hodogram by their typical signatures. Of course, the registration of the vibrations has to be done with calibrated instruments (Figure 11) and have to meet the valid standards, e.g. in Germany DIN 45669. The registration can be performed as one-day measurement, but typically long-term measurement with online registration, database, and early- warning and alert system. Often additional sound measurements are made.

The evaluation of imissions caused by vibrations is important for the permission of any blasting activity as well as for liabilities in case of damages.



Figures 10. Hodogram.



Figures 11. DMT vibration monitoring instrument SuMo.

In case of changing operational parameters a prediction of the expected vibrations can be provided as well as an optimization of the blasting to minimize the vibrations can be proposed (Althaus et al. 2002).

All the techniques mentioned above can be combined together in an environmental impact documentation system including:

- GIS based topographic maps
- Subsidence monitoring with GPS, TPS and radarinterferometric satellite scene processing
- Sound and vibration database
- Model calculation
- Blast optimisation
- Document database for quality control
- Automatic reporting and documentation
- Early warning and alert systems

3 CONCLUSIONS AND OUTLOOK

Surface movements and vibrations are important impacts of mining and tunneling activities. The monitoring of these impacts is necessary for different reasons, e.g. permit procedure, preservation of evidence and documentation of damages or better prevention against damages.

The examples have shown innovative, but operational conceptions to monitor surface movements and vibrations, especially with advanced online monitoring techniques.

REFERENCES

Althaus, P. & Hellman, J. 2002. Vibrations in blasting. *In: Erzmetall 55 (2002) No. 2, 105–117*.

Benecke, N., Korittke, N. & Raekers, E. 2001. 3D-determination of subsidence using differential-GPS-and radarinterferometric techniques as well as GIS supported analyses. *3rd workshop on geodynamic and environmental safety in the development, storage and transport of gas. St. Petersburg, 27–29 June 2001*.

Korittke, N., Benecke, N. Lüttmann, A. & Petrat, L. 2004. Innovative strategies for monitoring movements caused by mining. *41st scientific congress of German Society of Mine Surveyors, Bochum 15–18 September 2004*.

Wegmuller, U. & Benecke, N. in prep. Land Motion services for the Mining sector. *Final report for an Earth Observation Market Development Project of the European Space Agency (ESA).*

Underground Space – the 4th Dimension of Metropolises – Barták, Hrdina, Romancov & Zlámal (eds)
© 2007 Taylor & Francis Group, London, ISBN 978-0-415-40807-3

Geotechnical monitoring of the Valik tunnel construction near Pilsen

Radek Bernard, SG-Geotechnika a.s. Praha
Geologická, Praha

ABSTRACT: This paper describes geo-monitoring of the Valík tunnel construction near Pilsen. General description of geology uncovered during the tunnel drive and an overview of construction works is given. Geo-monitoring, carried out during the tunnel construction, its main objectives and measurement techniques are presented in detail. Data acquired as part of geo-monitoring was collected, presented and archived using the Barab© online database system, developed by SG-Geotechnika. In conclusion, assessment of geo-monitoring benefits, including financial savings, are presented.

1 INSTRUCTIONS

Tunnel drive of the Valík tunnel under the Valík hill between municipalities Černice and Utušice is a part of the construction of the 510/1B highway D5 from Prague to Rozvadov and the highway by-pass of the city of Pilsen. Full-scale geo-monitoring of the tunnel drive is carried by our company, SG-Geotechnika, for the client, ŘSD ČR, Praha.

These highway tunnels are 390 m, or 380 m long respectively, (the bore portion of 330 m) and are formed by two independent tunnel tubes less than 12 m wide and 8.2 m high (definitive lining). The maximum longitudinal grade is 4% descending to the West. Both tunnel tubes are in close proximity without a rock pillar. They are separated by a central reinforced concrete pillar constructed in advance, leading to significantly lesser extent of surface land take in the area affected by the construction (discussed in detail later). Construction of bored tunnel sections is designed as double skin with intermediate insulation. For stability and static reasons, it was necessary to construct countervaults in both primary and secondary casings along full bore lengths. Tunnel bore was done according to the guidelines of the New Austrian Tunneling Method (NATM).

1.1 *Geology encountered during tunnel bore*

The bore encountered Proterozoic sediments, slightly metamorphosed rocks of the Blovice-Teplice series. These Proterozoic slates, mostly greyish-brown in color, in the central bore portion higher in silica, are complemented by greyish-black graphitic slates of varying thickness. Slates are weathered to strongly weathered and limonitized near cracks. Strong tectonic effects are prominent as slates are fissured, in places intensively.

Several dyke structures, ranging from decimeters to tenths of meters, appear in the massif. Weathered to strongly weathered grey-beige porphyry and grey-greenish metabasalt (spilite), weathered to a varying degree are common. Tunnel excavation took place in predominantly dry conditions with local and insignificant groundwater water leaks in the lower vault of the tunnel sections. Neither tectonic fissures nor dyke structures were considered to be the source of groundwater.

Results of detailed geological engineering survey lead to the assignment of one basic technological grade of rocks for the tunnel bore according to the NATM. The grade is 5a, further subdivided into grades 5aI, 5aII and 5aIII, where 5aIII was used in the most favorable geological conditions and 5aI in the most unfavorable ones. Complete geotechnical monitoring was proposed for these technological grades and forms the main topic of this paper.

1.2 *Description of construction works*

Field work commenced in November of 2003 and the western, Rozvadov portal was excavated. The Prague portal was excavated at the same time as the bore of the central section of the tunnel (May–August of 2004). The tunnels' bore was initiated by the drive of the central tunnel from the mentioned Rozvadov portal. Concrete work on the mid-pillar began in September, 2004, and the bore of the main tunnels could begin in early October. Concrete work on the mid-pillar was completed in late January 2005 and satisfied project requirements for further tunnel excavations.

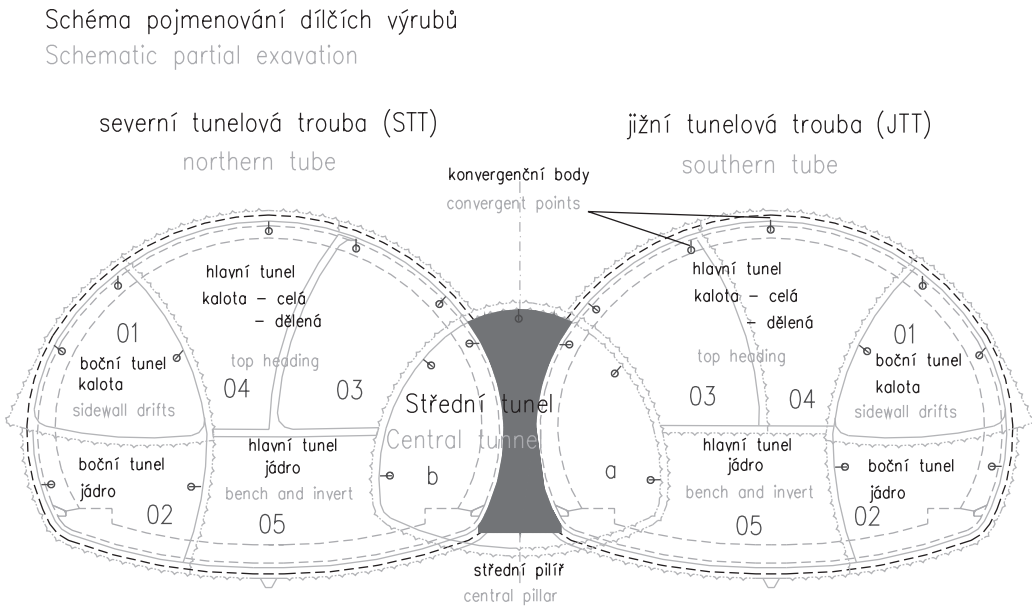


Figure 1. Progression of partial tunnel bores.

Figure 1 shows the progression of bores, divided by a combined method into sections using predominantly a less common, and more time consuming vertical division. This method was used due to complex geology encountered during the bore of an exploration gallery in 2002 and minimal overburden thickness above the tunnels ranging from 5 to 15 m along the tunnel length. Tunnel height is 16 m and width 12 m (primary lining).

The front portion of all divided stopes passed under an 18 m long micropilot umbrella, drilled in two rows from the Rozvadov portal. Similar measures were used to prevent the end-points of bores from breaking through in the Prague portal. Subsequent to the passage of the central tunnel bore (approx. 50 m^2) under the above mentioned security micropilots, the contractor proceeded with a two-part bore using calottes with a slight lead in the left portion (in the bore direction). Evaluation of all available measurements acquired during the initial bore (in approx. 30 tunnel meters, or TM), the IG documentation and recommendations of the GTM office formed the basis of the decision of RAMO members to proceed with the bore using calottes in full profile. This decision turned out to be favourable as the remaining section of the central tunnel was bored the same way leading to considerable time savings. The bottom, or lower vault of the mid-tunnel was closed every BTX 6–7 steel frames while leaving 2–3 m of bench at the forefield.

Generally positive conditions during the bore of the central tunnel resulted in the overall favourable assignment of technological NATM grade which turned out as more beneficial to the developer than the original project assumption. Minimal overbreaks were documented during the bore of the central tunnel, for the most part described as fortuitous as they were caused by tectonic disturbance or intensive cleavage of the rock massif. This was not expected as during the bore of the exploration gallery, high rates of overbreaks from bored profile were reported (approx. 15 m^2). As it turned out, this exploration gallery, placed in the profile of the mid-tunnel, had a positive impact on the tunnel drive acting as an anchor ensuring the stability of the forefield. Minimal rate of overbreaks in this tunnel section was due to the use of tunnel dredger in medium hard rocks in approx. $^2/_3$ length of the mid-tunnel. The use of non-explosive methods of rock excavation did not cause substantial disintegration of the surrounding rock mass. Permanent rainfall deficit, recorded since 2003, leading to gradual subsidence of groundwater levels by 3–4 m was another positive factor in tunnel excavation. The bore of main tunnel tubes commenced in September–October 2004 and was completed during May of 2005. Only first two NATM grades were used during the excavation of the two main tunnels. Owing to these facts it is obvious, that geological conditions during these tunnel drives were quite diverse as relatively favourable conditions during the bore of the central tunnel were not matched during bores of the surrounding main tunnels.

The overall geological conditions of tunnel drives were relatively simple lithological environment but

very complex tectonic framework. Several orogenic phases affected Proterozoic rocks and subdivided them into separate blocks. These blocks were unevenly moved and turned which is obvious from measured foliation. In addition, repeated tectonic movements occurred on some fault planes.

2 GEOMONITORING

2.1 *Geotechnical monitoring (GTM) of the Valík tunnel construction*

Geotechnical monitoring is an integral part of the New Austrian Tunneling Method (NATM) which is used during construction of most tunnels in the Czech Republic. The purpose of geo-monitoring is to provide sufficient information about the response of the rock massif to the bore of the tunnel. An important objective is continuous cross-referencing of project's assumptions with the reality and obtaining information for the assignment of NATM grades to stopes. Geomonitoring during the Valík tunnel construction included the following measurements and observations:

- forefield monitoring by means of geological engineering
- measurements of slope deformations in excavated sections of portals
- convergent measurements in tunnels
- surface terrain subsidence measurements (transverse subsided basin and longitudinal wave)
- extensometric and inclinometric measurements in wells from the surface
- tension measurements using tensometers on the contact between rock and primary lining and in secondary lining
- tension measurements using pressure cells in primary lining of the mid-tunnel and in the central pillar
- seismic control measurements of the effects of blasting operations on the surroundings
- measurements of the actual shape of stopes and the primary and secondary linings
- control measurements of concrete strength using Schmidt's hammer
- control measurements of forces in bolts and ties
- complex monitoring of the cottage settlement Amerika (pasportisation)

Complex evaluation of interaction between the rock massif and the tunnel lining required measurements in 3 aggregate profiles. Convergent, extensometric and inclinometric measurements were carried out in these profiles as well as measurements of tension in primary lining, tension measurements on the contact between primary lining and the rock massif and measurements of surface terrain deformations. Complex analysis and evaluation of geotechnical measurement results in relation to all completed measurements and actually observed geotechnical conditions, particularly in aggregate profiles. All measurements described above were regularly placed on the Barab© internet online server at the GTM office with access provided to all qualified construction participants, including invited experts. Evaluation of all types of measured data, – in relation to determined warning situations constituted a very important activity of the GTM office. Criteria for determination of warning situations were set prior to construction by the project engineer from static computations based on measurements done during the bore of the exploration gallery. These criteria were regularly refined during construction from periodic evaluations of measurement results (Monitoring Committee) – depending on the new information on the behavior of the underground construction.. In addition, static calculations were updated during the course of tunnel bore taking into account new observations. Thus, warning situation parameters were adequately refined. In relation to the evaluation of GTM results and warning situations, measures concerning the following issues were taken:

- measurements and evaluation of geomonitoring (rate of measurements, measurement type modifications, speed and method of evaluation)
- emergency regime (direction and speed of information flow and decision making process)

modifications of bore technology and lining reinforcement (according to RDS), work safety and its organization (according to the construction accident plan)

2.2 *Evaluation of geotechnical measurements from the bore of the mid-tunnel*

As described above, bore of the mid-tunnel was done predominantly according to a horizontal division (calotte and lower vault). The entire profile of the mid-tunnel occupied an area of approximately 71 m^2 (calotte of 50 m^2 and lower vault approx. 21 m^2). During convergent measurement in the front part of the tunnel, individual five-point profiles were designed in 10 m spacing and from 30 TM station every 20 m. Due to the occurrence of a thick disturbance spanning over more than half of the bored profile, RAMO members decided to add an inserted KVG profile in this section. The threshold value of warning situation was different for individual points due to the location of each point on the lining. Generally, the lowermost warning threshold of all points was 13 mm in the vertical and 11 m in the horizontal direction. These values fall into the 3rd warning stage on a five stage scale – *the state of cutoff acceptance*. Maximum deformation measured in the mid-tunnel was 11 mm in the vertical and 10.5 mm in the transverse direction. We can conclude that measured deformation values of KVG points on primary

lining of the mid-tunnel fell at most into the IInd warning stage and therefore it was not necessary to adopt any special measures during the tunnel drive.

Similar evaluation of deformation measurements on surface including extensometric and inclinometric surveys was carried out. Maximum deformation measured from extensometric wells was found on the lowest tie No. 4 within the 3. aggregate profile at station 30 TM. The value of 12.6 mm was measured on extensometer 24.22 which is situated slightly left (in the direction of bore stations) from the longitudinal axis of the tunnel. Measurements on the same extensometer yielded a maximum deformation of 10.4 mm at its head (the warning situation at the surface is set to 40 mm). It is obvious, that deformation of the deepest tie of the extensometer is almost identical as the deformation of its head at the surface. This is caused by the presence of a minimum overburden at station 30 TM of approx. 6 m which does not allow for the formation of a natural rock vault in surrounding rocks above the bored tunnel. Largest absolute deformations were measured on profile No. 3 which is clearly caused by lesser overburden above the tunnel and highly problematic geological conditions at the initial portion of the construction. Deformations on subsequent transverse profiles (190 a 290 TM), measured at individual extensometric ties, reached values of around 5 mm. Interestingly, maximum deformations on all transverse profiles, recorded during the bore, were not observed at extensometers along the axis above the tunnel, but rather, always at accessory extensometers (see scheme on Figure 3) located on the right hand side in the bore direction. Encountered foliation and dip angles of about 80° were a contributing factor as maximum deformation did not evolve along a vertical but followed the dip of the foliation. Maximum measured surface deformation (13 mm) along a longitudinal axis



Figure 2. Division of bores inside the tunnel during the drive of the south tunnel tube.

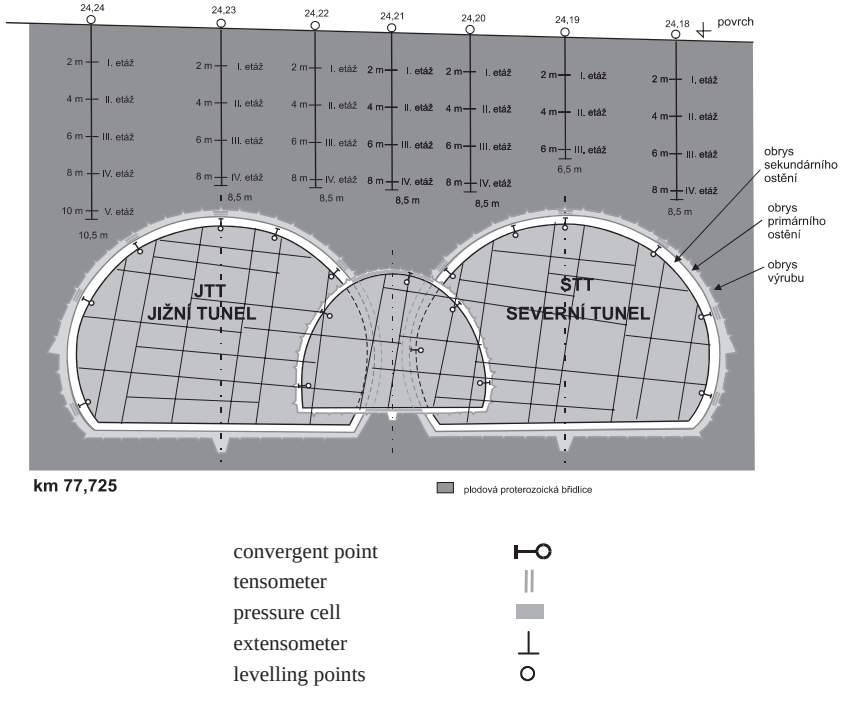


Figure 3. Scheme of measuring elements in the 3. aggregate profile (30 TM).

above the mid-tunnel, measured within the longitudinal subsidence wave, was recorded at point No. 22 at the tunnel station 310 TM.

Lesser horizontal deformations of 4–7 mm were recorded in the surrounding rock massif in six inclinometric wells during the bore of the mid-tunnel. The deformation propagated always in the direction from the inclinometers towards the tunnel. Minimal deformations at this stage of the construction were affected by the fact, that individual inclinometers was approx. 8 m from both sides.

Continuous control GTM measurements of encountered overbreaks using a profile machine turned out to be an independent and useful method during the construction of the Valík tunnel during the bore of the mid- and main tunnels. The client delegated the responsibility for these measurements to the geomonitoring office and therefore was responsible for random measurements done by the contractor. Individual documents on stope profiles were given to construction technical supervisors by means of weekly protocols always prior to RAMO meetings in order to secure possible approvals for overbreaks by the client.

2.3 *Description of work flow and brief evaluation of GTM during the bore of main tunnels*

Main tunnel drives (North and South Tunnel Tubes) commenced during the end of September and beginning of October, 2004. Bores with vertical division of individual parts began from the Rozvadov portal gradually through individual side tunnels (gothic galleries). Following-up approx. 30 meters of the side tunnel bore, the main calottes of the main tunnels were bored. Under close supervision, they were bored in one take (not divided, as proposed in the project), see Figure 2. After boring of a section of the main calotte, (approx. 50 m), the core of the tunnel was mucked and the bottom closed along the full length of the lower tunnel vault. After closing of the bottom, the partition between the side gallery and the middle part of the tunnel was dismantled and the full profile of the primary tunnel lining was formed. Maximum transverse deformation of 12 mm in the South Tunnel Tube was recorded at the inserted profile No. 20 (due to intersected rock disturbance) at station 59 TM. Deformations, measured in the North tunnel reached slightly higher values. This was caused by a less favourable geological situation encountered during the bore of the South tunnel as the rocks were weathered to a higher degree, particularly at the initial third of the bores. Maximum vertical deformation was recorded on profiles No. 6 (90 TM) and 7 (110 TM). Both measured values of 19 mm came close to the set levels for warning situation. These values were recorded during additional excavation works and construction of a stall near both profiles. Maximum transverse deformation of 13 mm was measured on profile No. 2 (20 TM) (the value of warning situation).

Maximum deformation at the terrain surface of 31 mm within the 3. aggregate profile at station 30 TM. In contrast, extensometric measurements in the rock massif yielded a maximum deformation of 47.5 mm at the lowermost tie of the extensometer 24.05, located above the vault of the South Tunnel Tube, in the 2nd aggregate profile at the station 190 TM. The mentioned additive vertical deformation is affected by the passage of the bores of the mid-tunnel and all partial components of large tunnels.

Due to gradual drop in groundwater levels to the lower tunnel vault level in 2002 to 2005, hydrogeological observations of tunnel bores indicate isolated minimal inflows of groundwater only at the tunnel bottom. Long-term GTM observations and monitoring in surrounding water wells confirmed no effects and subsidence of groundwater levels due to the construction of the Valík tunnel.

2.4 *Contributions of geomonitoring to the construction thus far*

Results of measurement evaluations and recommendations of the GTM office formed the basis of the decision not to use division of the calotte stope of the mid-tunnel according to the project. After approx. 10 meters of drive behind the micropilot umbrella (18 m long), the entire upper part (calotte) was bored as one profile, of an approx. diameter of 50 m^2 under constant supervision of the GTM office. As per measurement results, anchoring in the lower vault in the most favourable grade 5aIII was not carried out. Adopting of these decisions (approved by RAMO), savings of more than a month of planned bore works in the mid-tunnel were made in addition to saved financial resources for unused BTX truss rip, spared anchors and air-placed concrete.

Similar situation occurred during the bore of main tunnels (10/2004 to 05/2005) as the GTM recommended to RAMO to simplify the design of the division of both tunnels. Thus main calottes of both tunnels were bored as one stope. At the same time, in accordance with the recommendation of the GTM office, securing of micropilots BODEX above the tunnel vaults was not completed. The original project called for drilling of these from chapels built above the upper tunnel vault. The simple reason was not to endow the overburden massif by technological water from drilling which would likely make the forefield situation considerably worse, under the circumstances. Due to the above mentioned measures the time frame for tunnel boring was shortened by more than 4 months and considerable financial resources were saved.

3 CONCLUSION

Albeit documented very difficult geological conditions of the Valik tunnel and close scrutiny of the public in the affected region, it was possible to deal with these difficulties very successfully. This was possible due to the contractor's discipline, project engineer's experience and a well functioning geo-monitoring expert team. Even prior to the tunnel trial operation in October, 2006, it was concluded, that the more costly but unique solution with the reinforced pillar will provide considerable financial savings due to reduced surface land take – as opposed to similar large highway construction projects.

CITED LITERATURE

Geotechnical monitoring project of the Valík tunnel on highway D5 – st. 0510/IB in km 77,405–77,785 (R. Bernard – 01/2004)

RDS – Tunnel Valík, 600.06 Bored portion – primary lining (J. Svoboda – 03/2004)

Congress paper, WTC 2006 in Seoul – "Geomonitoring applied during the construction of the Valík tunnel. (R. Bernard, J. Pacovský, I. Zemánek – 04/2006)

Underground Space – the 4th Dimension of Metropolises – Barták, Hrdina, Romancov & Zlámal (eds)
© 2007 Taylor & Francis Group, London, ISBN 978-0-415-40807-3

The use of guide lines in tunnelling

G. Cassani & L. Mancinelli
Rocksoil SpA, Milan, Italy

ABSTRACT: In several conditions, design of tunnel is based on a limited number of data, deduced from geological and geotechnical investigations, laboratory and in-situ tests, bibliography information and experience. This kind of approach obliges the designer to make strong hypotheses that have heavy influence on his product. Guide lines allow to

– define different possibilities of application of a same section type, modulating the quantity and the quality of the reinforcements on the basis of the real ground or rock conditions in conventional tunnelling;
– calibrate working parameters as a function of the front conditions in mechanized tunnelling.

Real-time monitoring activity, geological observation and analysis of working data are the instruments that drive every choice, proceeding by fitting real needs and reducing risk.

In works, like tunnelling, where costs are high, the introduction of variability can optimize a design, making all process cheaper and safer.

1 INTRODUCTION

Guide lines represent a modern approach to design that are used increasingly by engineers and are now present in numerous official national and international regulations. In general terms they are a set of criteria that allow variability in the application of a design and constitute an integral part of it.

This approach is particularly useful when predictive work leaves too much open to chance, a situation which may be due to many different factors.

From a geotechnical viewpoint, and more particularly from that of the construction of tunnels whether excavated using tradition methods of mechanised means, the use of guide lines appears to be of fundamental importance.

Survey data is in fact often limited and insufficient at the design stage to justify fully deterministic approaches such as statistical approaches. In the past, this limit was not overcome until the operational stage when the real conditions became clear, giving rise to quite a number of problems in terms of safety, operations and, in the final analysis, contracts.

The idea of defining guide lines for construction operations is designed to solve all these not inconsiderable problems before work starts, by acting while still at the design stage and therefore in terms of general organisation.

From a practical point of view, guide lines for tunnel construction allow a series of quantitative and qualitative possibilities in the application of a design. The engineer defines different activities or action on the basis of the studies carried out that can be proposed according to the conditions encountered. For underground tunnels this concerns initial ground support, ground improvement work and the placing of the finally lining.

For mechanised excavation, performed using a tunnel boring machine (TBM), the variability relates entirely to the manner in which the machine advances and is operated.

2 TRADITIONAL EXCAVATION

The construction of underground tunnels has always required excavation and support operations to be adapted to the actual in situ conditions encountered. In design terms this translates into defining different tunnel section types to be employed as a function of requirements. A certain type of initial ground support, ground improvement, drainage and lastly final lining is specified for each tunnel section type. All these items, except for the final lining, can be easily defined in terms of ranges of variability within which they can be applied. Final linings on the other hand possess very rigid geometries for a given tunnel section type which is determined by the area excavated and the inner profile which must be complied with.

The criteria for selecting when to apply these variable items constitute a fundamental working instrument for the approach discussed here. It is monitoring

Table 1. Variability in traditional excavation.

Item	Modifiable quantity
Shotcrete	Rate of reinforcement, strength class and frequency of implementation
Steel ribs	Interval
Radial roof bolts	Number, length and frequency with which placed
Ground improvement at the face	Number, length and geometry
Ground improvement around the tunnel	Number, length and geometry
Ground improvement at base of ribs	Number, length and geometry
Drains	Number, length, frequency with which placed and geometry
Tunnel advances	Length
Stage at which final lining is cast	Distance from face

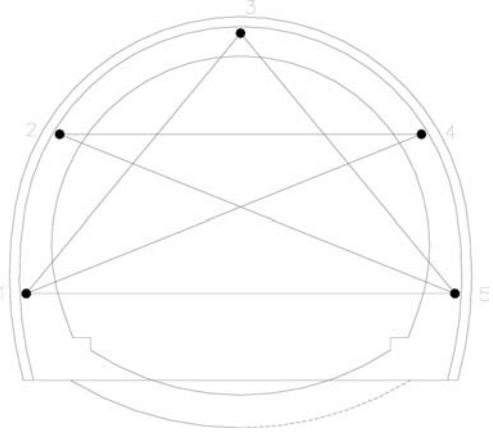


Figure 1. Section type for tunnel monitoring – Convergences.

operations which furnish the necessary information in terms of extrusion at the face and cavity convergence, when tunnelling underground.

A list is given below of the main items typically subject to variability, which are then briefly mentioned and described.

It is important to always keep in mind that the guide lines must contain an indispensable consistency between the different items subject to variability; many of these are *de facto* intrinsically interrelated one with the other.

2.1 *Shotcrete*

Shotcrete, together with steel ribs or radial roof bolts, constitutes the primary lining of an underground tunnel. Its thickness is generally limited by the area excavated and the geometry of the final lining. It can be reinforced to a greater or lesser degree using different types of steel wire or mesh, or different percentages of fibre and even the type of mix used can be easily modified. It can be placed on each tunnel advance or after a number of advances depending on the behaviour of the excavation.

2.2 *Steel ribs*

Steel ribs have the same fixed geometry within a given section type. In the case of cylindrical section types, the interval at which they are placed can be easily varied. They are usually placed on each tunnel advance. When variable section types are used (truncated cones) if the intervals at which the ribs are placed changes then so does the geometry; they are in fact different from each other within the range of the tunnel advance. In this case it is advisable to develop a new section type.

2.3 *Radial roof bolts*

Roof bolts are mechanical elements for supporting the roof arch. They can be placed with a large variety of geometries (different types of grid) according to need. The number can also be easily changed in real time. They can be placed on each tunnel advance or after a number of advances depending on the behaviour of the excavation.

2.4 *Ground improvement at the face or around the tunnel*

Ground improvement at the face or around the tunnel, consisting of cemented tubes, injected tubes or jet-grouting, for example, constitute very important advance support elements for the progress of operations. They can be adjusted very easily in terms of the number and length, factors which will also be related to the length of tunnel advance decided. It is often only the number of elements which is varied because of supply and operational considerations. Finally the reciprocal positioning of the elements can be optimised and modified.

2.5 *Ground improvement at base of ribs*

Ground improvement at the foot of ribs, also consisting of cemented tubes, injected tubes or jet-grouting, for example, constitute elements of protection against potential local instability. As with the ground improvement techniques already described, these too can be easily varied in terms of number, length and geometry.

2.6 *Drains*

When water is present, section types are often fitted with appropriate drainage structures consisting basically of PVC tubes with valves. In terms of design, these are always allowed for as possibilities and can

therefore be varied in terms of presence/absence, number, length and geometry to optimise drainage capacity.

2.7 *Tunnel advances*

A tunnel advance is the length of tunnel excavated which is performed before proceeding to place primary linings. It can be easily varied according to the context. This quantity obviously affects many of the items already described.

2.8 *Stage at which final lining is cast*

The casting of the final lining is performed as a function of the response of the cavity to excavation. If convergence or extrusion values are high, it may be advisable to cast linings closer to the face, either just for the tunnel inverts or even for the roof arches. These activities must be defined during construction, considering work on the construction site and real operations *in situ.*

In addition to the items specified, the following can be considered as particular intervention covered by guide lines: ground freezing, placing of special ribs or of steel struts in the tunnel invert, etc.

3 TUNNEL EXCAVATION WITH TBM

When excavation is mechanised, many aspects of the application of the design are necessarily decided before work starts in such a way that they cannot be changed. These include the dimensions of the machine, the type of machine, the geometry and the characteristics of the final lining. These factors must in fact be decided before proceeding with the works. There is one single cross section for tunnel advance and there is no concrete possibility of changing it.

The guide lines intervene in terms of excavation operations. A list of the main items typically subject to variation is given below.

Here too, it is monitoring that furnishes information on which decisions on construction operations are based. Activity involves both observations of movements at the surface and analysis of machine operating parameters. At present the latter items can be varied continuously and, by exploiting the latest technology for data transmission, this can even be done remotely. Combined study of all items allows works to proceed with minimum side effects on the surface and with guarantees of greater safety margins.

The technical objective is basically that of keeping the value for volume lost (the space invaded within the cavity by the excavated material before support structures take effect) to a minimum and consequently minimising surface subsidence responsible for damage to structures or infrastructures that may be present.

Table 2. Items for TBM.

Modifiable quantity
Torque
Advance velocity – Quantity of material extracted
Containment pressure at the face
Conditioning of the material treated in the excavation chamber

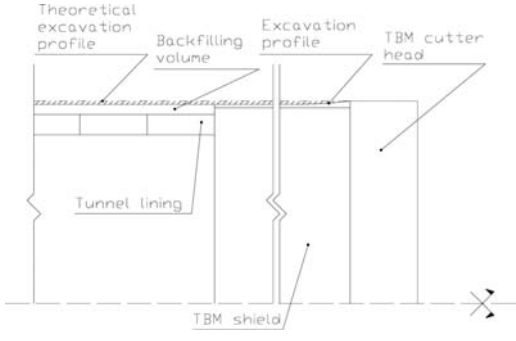


Figure 2. TBM Work diagram.

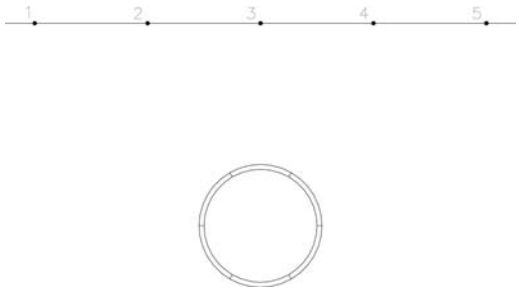


Figure 3. Section type for surface monitoring.

3.1 *Torque*

Torque is the stress exerted by the action of the shield at the front of the TBM. It can be selected as a function of the consistency of the material excavated. Its value is closely correlated with the pressure in the excavation chamber for machines designed for this type of excavation.

3.2 *Advance velocity – Quantity of material extracted*

The advance velocity is closely correlated with the quantity of material extracted. A proper balance between these two items leads to good performance in the execution of the works, without causing dangerous over excavation (too much material extracted) or unadvisable TBM advance (too high a value for the torque).

3.3 *Containment pressure at the face*

Various machines allow the face to be supported by applying pressure to it. This pressure makes it possible to counter thrusts and water, if present, coming from the ground. Proper application of pressure allows tunnel advance to be optimised and surface subsidence to be kept to a minimum.

3.4 *Conditioning of the material in the excavation chamber*

The material loosened by the TBM and present in the excavation chamber is usually conditioned before it is extracted. The treatment in question consists of adding appropriate material to produce a mixture that can be easily conveyed away.

4 CONCLUSIONS

The definition of underground designs and, more specifically, of tunnel designs contains a series of intrinsically unknown factors. This aspect is in itself, however, well known as a result of experience above all. As we have seen Guide lines constitute an excellent instrument for managing these random elements, a set of criteria which define how a design can be implemented in practice. As is happening increasingly more often, they are starting to form part of the designs themselves, basically constituting a fundamental element of the application.

The guide lines must therefore be thought of as a set of rules which make the design dynamic. Design therefore loses its character as a precise definition of activities and becomes a more complex entity which responds more appropriately to real requirements.

BIBLIOGRAPHY

Anagnostou, G. & Kovari, K. 1996. Face stability condition with Earth-Pressure-Balance Shields. In *Tunnels and Underground space Technology, Vol. 11, No. 2, pp. 165–173.*

Cassani, G. & Mancinelli, L. 2005. Monitoring surface subsidence for low overburden TBM tunnel excavation: computational aids for driving tunnels. *Proc. 11th International Conference of IACMAG Symposium, Turin 2005 – Vol. 2 – pp. 631–638.*

Lunardi, P. 2000. Design and tunnel construction – ADECO-RS approach. *Tunnels & Tunnelling International special supplement.*

O'Really, M.P. & New, B.M. 1982. Settlements above tunnels in the United Kingdom, their magnitude and prediction.

Peck, R.B. 1969. Deep Excavation and Tunnelling in soft ground. In *State of the Art Report International Conference on S.M.F.E. Mexico.*

Russo, G. 2003. Una riflessione sui criteri di valutazione della pressione di stabilizzazione del fronte nello scavo con EPBS. In *Gallerie e grandi opere sotterranee No. 71.*

Underground Space – the 4th Dimension of Metropolises – Barták, Hrdina, Romancov & Zlámal (eds)
© 2007 Taylor & Francis Group, London, ISBN 978-0-415-40807-3

Rio de Janeiro subway – Challenges of the access tunnel to the Cantagalo station

Aluisio de Abreu Coutinho Jr.
Odebrecht Engenharia e Construção

Marco Antonio de Lima Rocha
Rio Trilhos

Luis Eduardo Sozio
Promon Engenharia

Werner Bilfinger
Vecttor Projetos Ltda

ABSTRACT: The Rio de Janeiro Metro Line 2 was expanded recently in 1230 m, including the new Cantagalo Station. In this stretch, the tunnel and station were excavated mainly in sound gneiss. To connect the station to the highly populated Copacabana area, a 95 m long, main access tunnel connecting the station to the entrance area at Praça Eugênio Jardim, had to be built. This 9.1 m wide and 11.6 m high tunnel had to cross sharp and irregular transitions between the sound gneiss and a silty residual soil, underlying a sedimentary sand, below groundwater.

The access tunnel, additionally, crosses under a specially settlement sensitive building. The 11 story high, approx. 60 years old building, is founded on shallow footings. Few of the footings are bearing on rock and the remaining on sedimentary sand, which, is characterized by a loose to medium dense condition.

Sand compaction resulting from vibrations due to drill and blast excavation technique induced less than 15 mm additional settlements in the footings on sand, but lead to important structural damages.

To avoid further deterioration of the already critical structural condition, this building was underpinned with 84 root piles and 1.50 m thick reinforced concrete slab.

The main difficulties encountered during tunnel excavation under this building, the mitigating construction method adjustments, and building performance are detailed in the paper.

1 INTRODUCTION

Rio de Janeiro has a population of approx. 10 million inhabitants and is continuously growing. As so many other big cities, traffic is one of the main problems and, therefore, Line 2 of Rio de Janeiro Metro was recently expanded in another 1230 m, adding the new Cantagalo station. Excavation works are finished and delivery to operation is due in 11/2006.

The south area of Rio de Janeiro is densely populated and, especially in Copacabana, where Cantagalo station is located, buildings are concentrated in a relatively narrow strip between the shoreline and steep mountains. These particular conditions oriented main design guidelines, which located the main subway line inside the rock massif, beneath mountains. Only access tunnels and relatively short crossings are constructed beneath buildings and roads.

During the construction of the access tunnel, significant damage to a specific building was detected. To avoid further deterioration, the building was underpinned with 84 root piles and a 1.5 m thick concrete slab.

After completion of underpinning, excavation continued without further problems.

2 PROJECT DESCRIPTION

The recently built Metro stretch is 1230 m long, including approx. 1 km of a twin lane tunnel and a 180 m long cavern, where Cantagalo station is located. 3 short access and ventilation tunnels where also constructed. Figure 1 presents typical cross sections of the tunnels.

The main line tunnel and the station were excavated mainly in sound gneiss, occasionally crossing faults and weathered zones.

To access the station, 2 relatively short tunnels, approximately perpendicular to the main line, were build, crossing from the sound gneiss, through weathered gneiss and sedimentary sands, beneath several relatively old, more than 10 story high buildings, founded on direct footings.

Figure 2 presents a schematic view of the lay-out of the project:

The access tunnel connects a cut & cover entrance structure, where the main public will enter the Metro, to the station. This excavation was built using 80 cm thick and 25 m deep diaphragm walls.

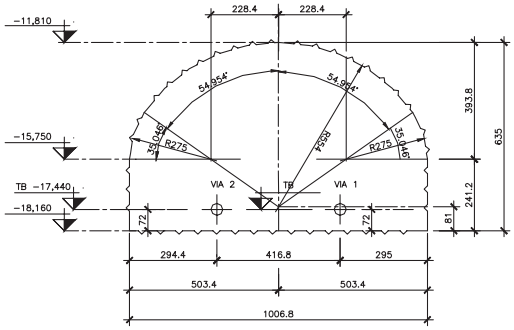
The emergency tunnel is connected to a 10 m diameter and 20 m deep circular shaft.

Excavation method in rock was conventional Drill & Blast, using a 3 boomer Jumbo.

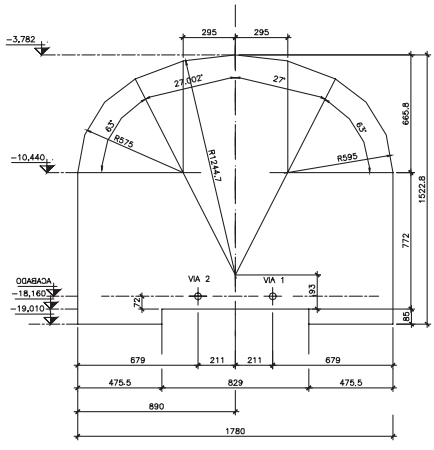
Along the access tunnels, drill & blast method was used, where applicable, and conventional excavation with hydraulic excavators, front-loaders and hammers.

Along critical stretches, like fault zones, 62.5 mm tubular metallic forepolling was used, together with cement grout injections.

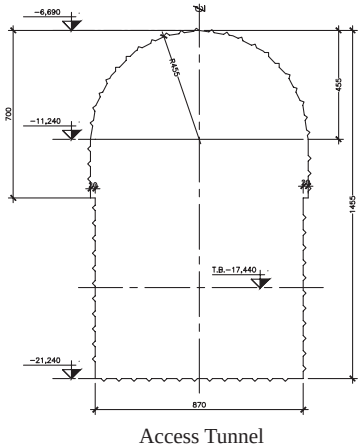
The access and emergency tunnel excavation was protected by horizontal and vertical Jet-Grouting, used together with 62.5 mm tubular metallic for pollings.



Line Tunnel



Station Tunnel



Access Tunnel

Figure 1. Typical tunnel cross sections.

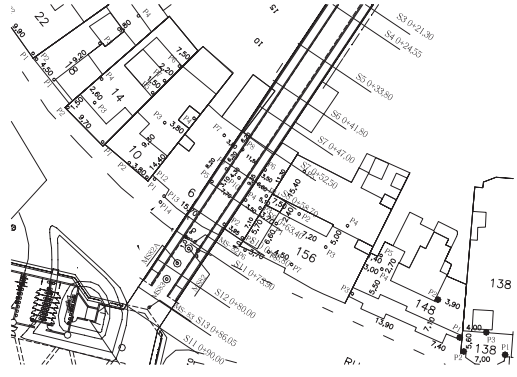


Figure 2. Plan view of the access tunnel. In the lower left corner, the cut & cover section.



Aerial View of buildings above access tunnel.

An extensive monitoring program was foreseen, mainly monitoring surface settlements of buildings and instrumented cross sections, as well as water level. Inside the tunnels, convergence and settlements were also measured. Additionally, periodic visual inspections of buildings located in the vicinities of excavations, to detect cracks and other signs of differential movements.

3 GEOLOGICAL BACKGROUND

The typical geological cross section along the line tunnel and station tunnel is a relatively thin silty residual soil cover, occasionally covered by colluvial soils, and its transitions to the sound gneiss.

Local gneisses are Kinzigitic, generally with three sets of discontinuities, one of then associated to the southward dipping xistosity. Rock quality index Q is in general between 15 and 35, and as low as 3 to 4 at faulted zones.

Along the 2 access tunnels (access tunnel and emergency tunnel) a transition from the conditions above, close to the station, to a cross section with the crown of the tunnels in saturated sedimentary sands, and side walls in residual soils and its transitions to the sound gneiss, occurs. The transition is sharp and irregular. Similar conditions where encountered in previous sections of Rio de Janeiro Metro (Nieble et al, 1998; Mello et al, 1998; Mello et al, 2001, Bilfinger et al, 2001).

Figure 3 below presents a typical longitudinal section along the access tunnel.

The sedimentary sands are loose to medium dense, with and NSPT blow count between 5 and 20. Natural groundwater level is some 8m above tunnel crown.

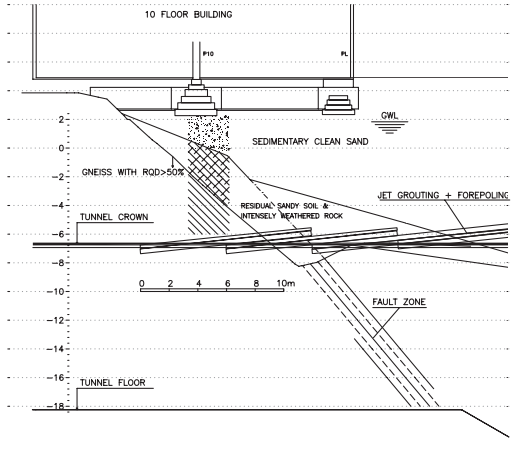


Figure 3. Geological cross section.

4 STRUCTURAL PROBLEMS – DESCRIPTION AND INTEPRETATION

Settlements, as mentioned, previously, were continuously monitored, including building no.6 of "Praça Eugênio Jardim". Settlements of some of the monitored columns started to increase with excavation still 15 m behind the buildings. Other columns showed no movements and, in some cases, slight heave. After visual inspections, severe cracking of walls and structural elements was detected (Photo 1). Calculated differential settlements were still only 1:480. Construction methodology was changed, reducing advance rates, but the settlements continued, with some columns not settling. Figure 4 presents the layout of the settlement gauges and Figure 5 the recorded settlements of these gauges.

Analysis of available data showed that the direct footings beneath some of the building rear columns



Photo 1. Cracks inside the building.



Figure 4. Plan view of building and settlement gauges location.

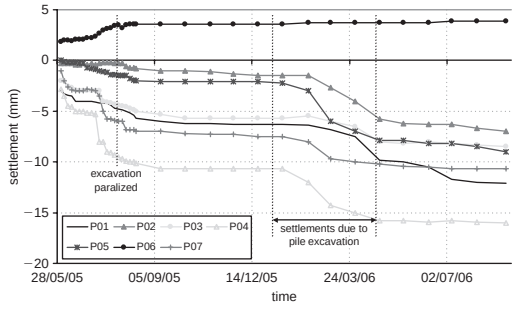


Figure 5. Building settlements.

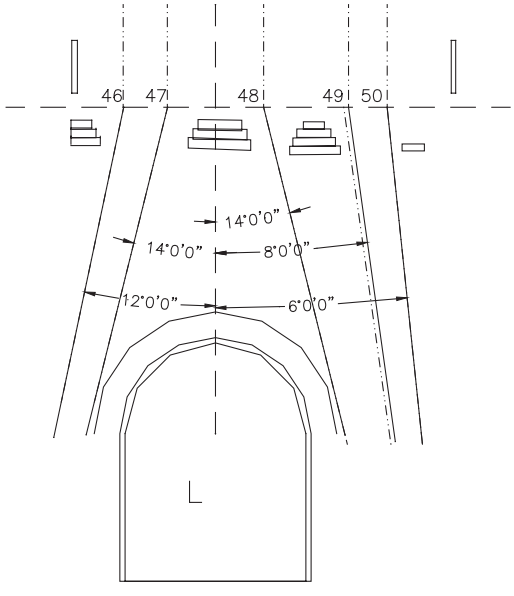


Figure 6. Schematic cross section of the access tunnel and the root piles.

were founded on residual soil or rock, the remaining footings being founded on the typical Copacabana sand.

Analysis of the structure showed that average bearing pressures applied by the footings on the subsoil was around 350 KPa. And in opposition to a standard foundation design, there were no structural cantilever beams to balance the eccentric load at the peripheral footings.

Structural damage seemed to be excessive, when compared to differential settlements; however, probably, the building settled, during construction and 60 years of use, suffering considerable distortions and, when the settlements increased slightly due to tunnel construction, the effects were significant.

Interpretation of cause of the settlements was that the vibrations due to the blasting caused compaction of the loose to medium sand and the footings resting on it. On the other side, the foundations on rock/residual soil, did not settle; instead, some of the footings showed slight heave, interpreted as being associated to high horizontal/sub horizontal in situ stress relief due to the excavation. Similar results (heave) where observed on other stretches along the line.

Evaluations by the designer and an independent consultant showed that the risk of severe structural damage due to additional settlements was high and should be avoided. Considering that the excavation was still not beneath the building itself, the only solution that could be considered safe was underpinning, with the use of root piles. Figure 6 shows a schematic cross section of the tunnel, the building and the root piles.

5 SOLUTION

The solution conceived consisted of 84 root piles and a 1.5 m thick concrete slab. The root piles were concentrated in the region were the original footings were founded on the sedimentary sands.

The root piles were founded in the sound rock, avoiding direct loading of tunnel crown. Additionally to the underpinning, horizontal jet grounting and forepoling with 63.5 mm dia. steel tubes were used to guarantee treatment of the interface between the rock, residual soils and sedimentary sands.

The existing footings were incorporated to the slab using pre-stressed Dywidag bars. Adequate concrete adherence was ensured along the 1.5 m length where piles crossed the slab.

This enabled creation of a monolithic behavior that was confirmed by checking differential settlements between slab and columns, during subsequential tunnel excavation.

6 PERFORMANCE

The building settled less than 1mm after the completion of the underpinning system and of tunnel conclusion.

During tunnel excavation it was noted that although the horizontal jet grouting system resulted in a moderately improved soil strength, it was not watertight, and therefore a risk of a progressive piping failure was high. Deep wells previously drilled from the building basement, and horizontal vacuum drains were activated in order to control groundwater pressure and mitigate this risk. Some minor settlement associated with groundwater lowering was induced to the neighbor buildings, however with no structural damage.

7 CONCLUDING REMARKS

The behaviour of the more than 60 year old building, suffering severe cracking with only limited settlements showed that the routine type of induced settlement analysis, where distortions are evaluated and compared to predetermined limit values, should be revisited. Previous settlements, not measured and technically documented, can reduce normally considered safety margins.

The underpinning solution showed adequate performance; after its construction, no additional significant settlements were measured and adverse behaviour detected.

Jet grouting soil treatment was not capable of creating an impervious barrier or reduction permeability significantly; this behaviour probably associated to the extremely variable rock-soil interface.

ACKNOWLEDGMENT

The authors want to thank the Owner, Rio Trilhos, the Contractor, Odebrecht Engenharia e Construção and the Designer, Promon Engenharia, for the opportunity of publishing and supporting this paper.

REFERENCES

Nieble, C.N., Mello, L.G., Melo, J.T.L.P., Camara, G.J. & Primo, C.N.P. 1998. Experiences in the excavation of tunnels and underground station in rock in Botafogo-Copacabana stretch of the subway in Rio de Janeiro, Brazil. In Negro Jr. & Ferreira (eds.), *Tunnels and Metropolises*; *Proc. WTC, São Paulo, 25–30 April 1998*. Rotterdam: Balkema.

Mello, L.G., Bilfinger, W., Fialho, M.S.M., Rideg, P., Primo, C.N.P. & Rocha, M.A.L. 1998. Access tunnel to the Arcoverde Station of the Rio de Janeiro Subway: Design and Construction. In Negro Jr. & Ferreira (eds.), *Tunnels and Metropolises*; *Proc. WTC, São Paulo, 25–30 April 1998*. Rotterdam: Balkema.

Mello, L.G., Bilfinger, W., Primo, C.N.P., Carvalho, F.C. & Cortes, M. J. 2001. Rio de Janeiro Subway System: Jet-Grouting Treatment Design and Control. In Teuschser P. & Colombo, A.(eds.), *Progress In Tunneling after 2000*; *Proc. WTC., Milan, 10–13 June 2001*. Bologna: Patrone.

Bilfinger, W., Mello, L.G., Primo, C.N.P., Carvalho, F.C. & Cortes, M.J. 2001. Rio de Janeiro Subway System: Settlements due to Horizontal Jet Grouting and their Control. In Teuschser P. & Colombo, A.(eds.), *Progress In Tunneling after 2000*; *Proc. WTC., Milan, 10–13 June 2001*. Bologna: Patrone.

This page intentionally left blank

Underground Space – the 4th Dimension of Metropolises – Barták, Hrdina, Romancov & Zlámal (eds)
© 2007 Taylor & Francis Group, London, ISBN 978-0-415-40807-3

Prediction of subsidence during tunnel construction

K. Grossauer & R. Leitner
Institute for Rock Mechanics and Tunnelling Graz University of Technology, Austria

W. Schubert & P. Sellner
3G Gruppe Geotechnik Graz ZT Gmbh Graz, Austria

ABSTRACT: Stress redistribution, ground loss and change of groundwater table in the course of tunnel excavation cause surface settlements. These surface movements may cause damage to structures above and beside the tunnel. Experience shows that the timely and spatial influence of underground excavations on the surface settlements varies in a wide range. The domain of influence mainly depends on the ground structure and properties, the quality and quantity of the tunnel support as well as on tunnel dimension and the construction method. In some cases the surface movements are limited to some meters ahead and aside of the tunnel and stabilisation is reached within a few days after excavation. In other cases an extended surface area is influenced for a long period and the stabilisation process is slow. Accurate predictions of surface movements are difficult in the design phase. To enable a timely adjustment of the construction method an extensive observation program in the tunnel and on the surface is established in many cases, and warning and alarm criteria defined to ensure safety and serviceability. These levels and criteria of the observed properties should consider not only fixed values – such as maximum settlements – but account for the evolution of these parameters (i.e. settlement path or history). It is indispensable to consider the timely development of surface movements in all three dimensions over the time and as a function of the tunnels progress. Efficient and easy to use procedures to predict and check the surface movements are required to ensure a safe and economical construction. Numerical methods require a more or less time consuming input, calculation time and interpretation work, limiting their applicability for the day-to-day use.

An efficient way to predict displacements caused by tunnel excavation is to use analytical functions that describe the movements as a function of time and the face advance. A procedure based on analytical functions has been developed to support the prediction of the tunnel performance and surface movements. The tool can also be used to study the influence of variations of the tunnel progress and support on the surface movements. In this way the construction planning can be optimized in a way to minimize damage to surface structures. Two case histories from shallow tunnels in Austria are used in this paper to illustrate the application of the prediction tool.

1 INTRODUCTION

To prevent surface structures from (excessive) damage due to surface movements (subsidence) an extensive observation program in the tunnel and on the surface is established in many cases. The measurements describe the actual state of the system consisting of ground and support. The monitored values can be compared to values from the design allowing judging whether the system behaviour is in a "normal range" or in an "abnormal one" (see the design procedure described in ÖGG, 2001). Considering the time depending evolution of displacements and to ensure an adequate reaction time usually warning levels and alarm levels or criteria are defined, dependent on local requirements. Those levels are determined at a rather cautious level at the beginning of construction work and are updated with increasing knowledge of the system behaviour. Additionally, the observation of trends may be used as a criterion for "normal" or "abnormal" behaviour.

To ensure safe and economic tunnel projects a detailed description of the system behaviour and its "normal" range is indispensable and has to be defined during the design phase. For the judgment of the systems state and to check the efficiency of different measures routine predictions are required during the construction which describe the expected reactions of the ground to the excavation and support. These predictions are compared to the observed behaviour on a daily basis. Any deviation between prediction and observation must be related to either a wrong estimation of the geological model in combination with wrong or inaccurate material parameters and/or an inadequate prediction to the construction's response to the stress redistribution. In both cases measures have to be established in time to ensure safety and economy.

The definition, the prediction and the comparison of the system behaviour requires a calculation method which considers various inputs as ground properties, support properties and construction methods. This calculation method should also allow estimating the efficiency of additional measures or mitigation measures in time.

2 STATE OF THE ART & METHODS REQUIRED

During design the expected normal system behaviour is determined and various alarm levels and alarm criteria defined and continuously updated during construction, if required. The use of displacement monitoring data is quite effective for describing, predicting and controlling the system behaviour. Additionally other parameters like pore water pressures, lining stresses, ground stresses and so on can be monitored.

Practice has shown that sometimes the projects success is hampered by shortcomings in the definition, the prediction and the observation of the system's behaviour. A few points which have to be considered when dealing with surface settlements in tunnelling are listed below:

- Sometimes certain values are compared to a predefined fixed threshold instead of accounting for the evolution of the displacement. Especially when differential settlements of the surface areas (subsidence troughs across as well as along the tunnel axis) may damage or reduce the serviceability of an object, it is indispensable to consider the timely development of surface movements in all three dimensions over the time and as a function of the tunnels progress.
- During the construction the tools or techniques used for the prediction are time consuming and therefore costly. This may or will lead to a low frequency in the update of the prediction and consequently to a late identification of unacceptable displacement trends. Efficient and easy to use procedures to predict and check the surface movements are required to ensure a safe and economic construction.
- Current prediction techniques such as analytical solutions (see Park 2005, Chou & Bobet 2002) are limited in their prediction accuracy due to simplifications. Although an extended surface area is influenced for a long period and the stabilisation process is slow (Burland 2001), common analytical methods can only be used for estimating the maximum settlement trough perpendicular to the tunnel axis. In addition such methods do not consider relevant influencing factors, such as excavation rates and methods, different support types and ground conditions leading to inaccurate predictions. Certain counter measures (as additional bolting, installation of temporary top heading invert, etc.) can not be judged with regard to their efficiency. To be on the safe side the tunnel engineer has to overdesign the support accepting cost increase. Thus the prediction tools should account for the ground properties, the supports, and the excavation rate and method.
- The commonly pure empirical assessment of the system behaviour may lead to problems in the case of change of personnel on site. Former experience is difficult to communicate if no consistent rules are established. Thus such rules have to be developed, which describe the timely and spatial local development of certain values and allow predicting the system's state.

In the design phase mostly numerical simulations are used to predict subsidence. These time consuming simulations may consider influencing parameters as size of the structure, overburden, ground structure and quality, ground water conditions, excavation method, supports and progress rate. However, the knowledge of the parameters of the ground, the ground-support interaction, quality of construction, the influence of ground water disturbance etc. is limited during the design phase. In addition, numerical models contain simplifications and constraints regarding the material parameters and the difficult choice of an appropriate material law (see Kofler 2002, Potts & Zdravkovis 2001), which further decrease the accuracy of the prediction. Due to computational limitations surface and subsurface structures are rarely integrated in the numerical model and consequently the ground model needs to be updated during construction and the real behaviour controlled by monitoring. These drawbacks, as well as the effort required make numerical simulations unsuitable for a day-to-day updating of the geological-geotechnical model and its alarm levels. Quick, flexible and easy to use tools are required to continuously predict and control the system behaviour.

3 PROPOSED METHOD

An efficient way to predict the system behaviour of underground excavations is to use analytical functions, which describe the displacements as a function of time and the face advance (tunnel progress). The displacement behaviour of the rock mass and support basically is represented by function parameters. These parameters can be back-calculated from data of case histories. Using those function parameters the development of displacements of the tunnel wall and the ground surface can be predicted. Artificial intelligence methods (expert systems) interlink the function parameters and appropriate ground and support features. Special visualization techniques of the results allow an easy recognition of critical conditions. The tool can also be used to study the influence of variations of the tunnel

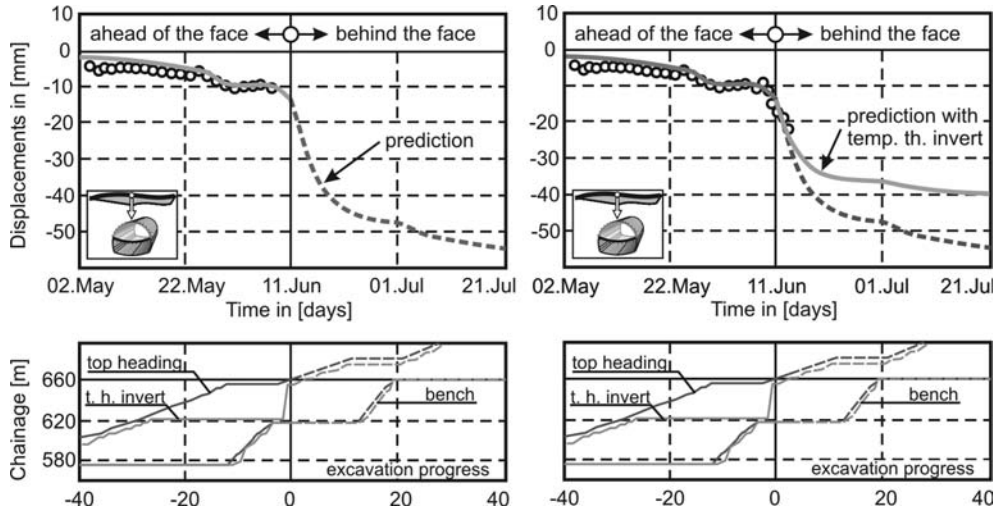


Figure 1. Time – displacement history plot for the surface point. Measured and predicted displacement history some days before (left side) and after (right side) the face passes the monitoring section 661.

progress rate and support type on the surface movements. In this way the construction planning can be optimized in a way to minimize damage to surface structures. The proposed method (GeoFit©) provides the following major advantages (Sellner, 2000):

- it predicts and simulates the evolution of displacements over time depending on the tunnel progress,
- it is an efficient, quick and easy to use procedure using graphical user interfaces and calculation takes a few seconds only,
- it considers relevant inputs, such as supports, excavation sequence and ground conditions,
- it allows to establish certain "rules" predicting critical system states in advance by considering both, the evolution of the function parameters and displacements over time or tunnel advance, and
- a continuous comparison of the monitoring results to warning levels is possible.

4 PRACTICAL APPLICATION

4.1 *Prediction technique and how to set counter measures*

The first example illustrates the technique for the subsidence prediction of points above a shallow tunnel which underpasses a freeway. The tunnel is situated in a tectonic melange and is excavated according to the NATM. The prediction technique proposed is demonstrated on the monitoring section 661.

Figure 1 shows the time – displacement history plot for the considered surface point in the upper axis system and the construction advance in the lower diagram. The zero reading was done approximately 110 m before the tunnel face passed the monitoring section on 11th of June. The circles in the displacement plots represent the monitored subsidence, which are used to back calculate the four function parameters X, T, C and m. The solid grey line shows the back calculation ("fitting") and the dashed line represents the predicted displacements according to the back calculated function parameters and a progress rate, which was extrapolated for the next few days.

In this case, the subsidence prediction for this monitoring section is done three days before the tunnel face reaches this section (see left side of Figure 1). It can be seen, that the settlements will reach a maximum value of about 60 mm. The accuracy and reliability of the prediction can be checked by looking on the development of the function parameters along the alignment.

Figure 2 (left side) shows the back calculated function parameters for the system behaviour which should show a reasonably "smooth" trend as they are correlated to certain geological-geotechnical properties of the ground (Grossauer, Schubert & Kim, 2002; Schubert, Button, Sellner & Solak, 2003). Abrupt changes in magnitude are most unlikely except there are abrupt changes of ground conditions. In this case the back calculated function parameters follow a rather consistent trend which increases the prediction's accuracy and reliability. If changing rock mass conditions are expected, the parameters can be modified accordingly. Methods for short term prediction of rock mass conditions are described by Steindorfer (1998) and Sellner & Steindorfer (2000).

If expected displacements exceed the acceptable range additional measures can be set in time. The

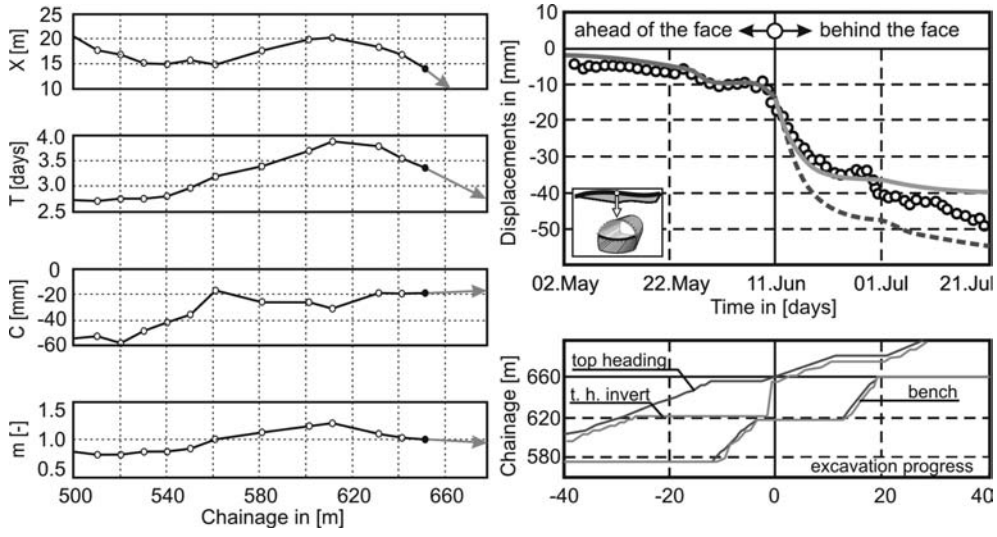


Figure 2. Trend of the function parameters X, T, C and m along the tunnel axis (left side) and the comparison of predicted and observed subsidence (right side) for monitoring section 661.

efficiency of such counter measures is shown in figure 1 (right side). The grey solid line shows the expected settlements considering that a temporary top heading invert is installed. The final displacement on the surface will be reduced by approximately 20 mm.

The right side of figure 2 shows a comparison of the finally observed and the predicted surface settlements due to top heading excavation. The prediction fits the monitoring with a high degree of accuracy until the 28th of June. On this day the bench excavation reaches the monitoring section resulting in additional displacements. For this excavation step an analogous prediction can be performed but is not shown here.

4.2 *Early detection of problem areas*

The next example shall demonstrate the potential of detecting critical situations in time and check the effectiveness of mitigation measures. The example is derived from a tunnel at shallow depth in very poor ground conditions. An intense observation program was conducted. The left part of figure 3 shows the observed subsidence (circles) and predicted (solid line) subsidence of a single observation point on the surface. The right part of figure 3 shows the outline of surface structures and the tunnel alignment. The dark dots represent the monitoring points on the surface. When the tunnel face has reached chainage 785 m a displacement prediction is performed (shown here as contour plot) which represents the surface settlements when the face will be located at chainage 825 m. The dark area ahead of the tunnel indicates settlements exceeding the defined alarm level.

To meet displacement restrictions, countermeasures have to be taken. In this case a temporary top heading invert is installed and the bolt density increased. The efficiency of these measures is predicted and shown in figure 4. The left part shows the settlement of the surface point in case of installing the temporary top heading invert and intensifying bolting (solid line). For comparison the settlements without additional measures are shown too (dashed line). Due to the installation of the top heading invert and the denser bolting pattern the settlements are significantly reduced and the defined alarm level will not be exceeded.

The prediction of subsidence can be performed for any time or chainage and visualized with movies, contributing to detect critical areas in advance. A better understanding of the timely and spatial influence of the construction on the subsidence can be archived.

The visualisation as plan view or three dimensional surface plots is of significant importance when dealing with surface inclinations. A two dimensional evaluation of observations along a monitoring sections will not show the total inclination but the projection of the inclination which is of lower quantity.

5 CONCLUSION

Considering subsidence, two main features can be found. Firstly, they can be measured and observed long before the tunnel passes the domain of interest. Secondly, they may cause damage on surface structures due to a variety of settlements, movements,

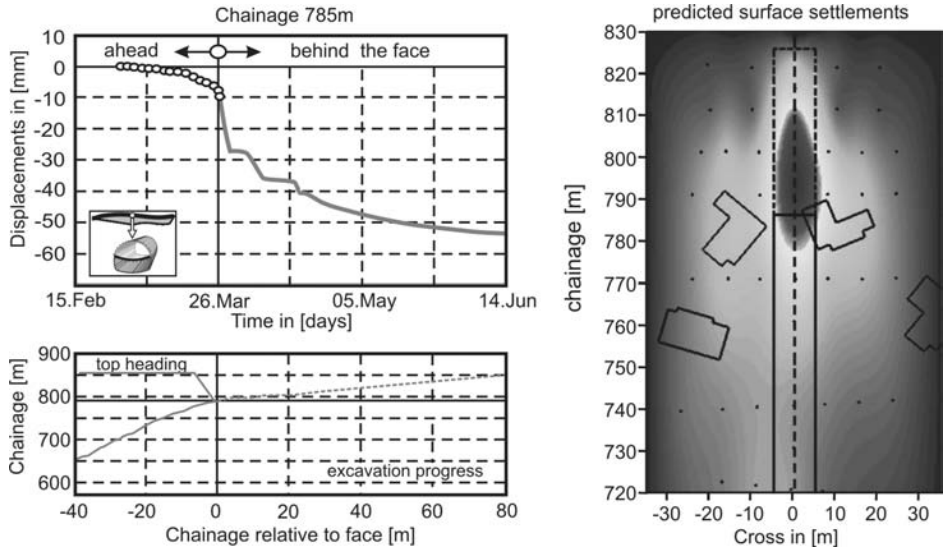


Figure 3. Left side: Settlement prediction for a single point on the surface; right side: outline of surface structures, tunnel alignment and contour plots of predicted subsidence without additional measures.

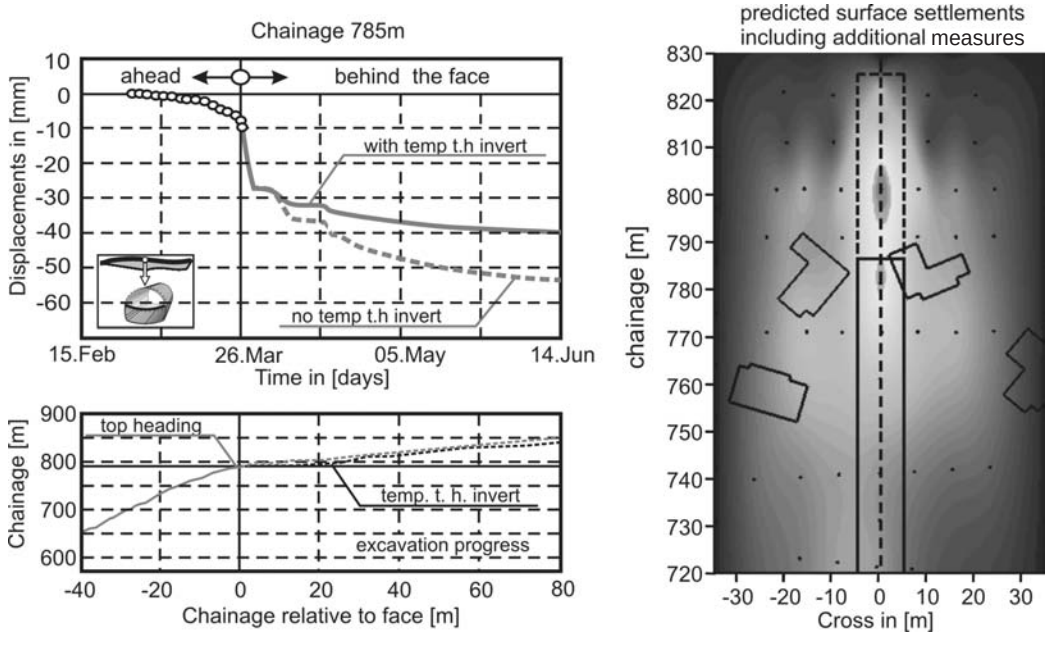


Figure 4. Left side: Settlement prediction for a single point on the surface; right side: outline of surface structures, tunnel alignment and contour plots of predicted subsidence considering additional measures.

rotations, and deflections. This requires that the engineers permanently control the settlement trough above an advancing tunnel and its compatibility to surface structures. The degree of damage is reduced by predicting displacements and establishing measures to reduce or compensate them. As a matter of fact, pre-displacements can be observed and used to back calculate the displacement behaviour of the ground in an early stage resulting in a better understanding of the ground's reaction to tunnelling and thus in a better

quality of the subsidence prediction for any stage of the tunnel project.

The proposed method provides tools for back calculation and prediction of subsidence and supports the tunnel engineer in his daily work. A permanent comparison of predicted "normal behaviour" and observed "real behaviour" allows to detect critical domains in time and to set counter measures. The efficiency of the planned counter measures can be checked "virtually" before implementation.

The decision making process regarding support and construction method can be supported with this method. The basis of the predictions – the function parameters and the resulting definition of the system behaviour – is stored and thus reproducible. This storage of decisions represents a specific knowledge, a correlation of geological, geotechnical and construction parameters, which can be used for further sections and projects.

REFERENCES

Burland, J.B. 2001. Assessment methods used in design. In Burland, J.B. Standing, J.R. & Jardine, F.M. (eds.), Building Response to Tunnelling, Case studies from the Jubilee Line Extension, London: 23–43. London: Thomas Telford.

Chou, Wei-I & Bobet, A. 2002. Predictions of ground deformations in shallow tunnels in clay. Tunnelling and Underground Space Technology 17 (2002). 3–19. Elsevier.

Grossauer, K., Schubert, W. & Kim, C.Y. 2003. Tunnelling in heterogeneous ground – stresses and displacements. In Technology Roadmap for Rock Mechanics; Proc. of the 10th Congress of the ISRM, Johannesburg, South Africa, 8–12 September 2003: 437–440. Johannesburg: The South African Institute of Mining and Metallurgy.

Kofler, M. 2000. Praxisorientiertes Stoffgesetz für Böden unter Berücksichtigung hoher Anfangssteifigkeiten. In G. Riedmüller, W. Schubert, S. Semprich (eds.). Schriftenreihe der Gruppe Geotechnik Graz, Heft 6. Graz.

ÖGG – Austrian Society for Geomechanics, 2001. Guideline for the Geomechanical Design of Underground Structures with Conventional Excavation. Austria.

Park, Kyung-Ho 2005. Analytical solution for tunnelling-induced ground movement in clays. Tunnelling and Underground Space Technology 20 (2005). 249–261. Elsevier.

Potts, D.M. & Zdravkovic 2001. Finite Element Analysis in Geotechnical Engineering: Volume two – Application. London: Thomas Telford.

Schubert, W., Button, E., Sellner, P.J. & Solak, T. 2003. Analysis of Time Dependent Displacements of Tunnels. Felsbau 21 (2003), Vol. 5: 96–103. Essen: VGE.

Sellner, P.J. 2000. Prediction of Displacements in Tunnelling. Ph.D. thesis, Graz University of Technology, Austria. In G. Riedmüller, W. Schubert, S. Semprich (eds.). Schriftenreihe der Gruppe Geotechnik Graz, Heft 9. Graz.

Sellner, P.J. & Steindorfer, A.F. 2003. Prediction of Displacements in Tunnelling. In Felsbau 18 (2000), Vol. 2: 22–26. Essen: VGE

Steindorfer, A.F. 1998: Short term Prediction of Rock Mass Behaviour in Tunnelling by advanced Analysis of Displacement Monitoring Data. PhD thesis, Graz University of Technology, Austria. In G. Riedmüller, W. Schubert, S. Semprich (eds.). Schriftenreihe der Gruppe Geotechnik Graz, Heft 1. Graz.

Underground Space – the 4th Dimension of Metropolises – Barták, Hrdina, Romancov & Zlámal (eds)
© 2007 Taylor & Francis Group, London, ISBN 978-0-415-40807-3

Monitoring of ground massif using TR-GEO georadars while drifting tunnels

S.V. Izyumov
Geological Prospecting Co., Ltd, Moscow, Russia

I.I. Goltsman
MosInzStroi, Moscow, Russia

ABSTRACT: Geological Prospecting Co., Ltd has gained for nearly a decade a lot of experience in practical application of TR-GEO georadars on construction sites in Moscow. TR-GEO georadars are designed for remote sounding of grounds and other structures with low and moderate absorption of electromagnetic waves: hard rocks, wet sandy grounds and sandy loams as well as low wet clay loams. Various areas of practical application of TR-GEO georadars as well as results of monitoring are discussed in this paper.

1 INTRODUCTION

Geological Prospecting Co., Ltd has been involved with development and application of TR-GEO georadars for nearly a decade. This article gives examples of practical applications of TR-GEO georadars as well as short description of their design and software used.

2 SHORT DESCRIPTION OF TR-GEO GEORADARS

2.1 *Principle of operation and field of application*

TR-GEO georadars are designed for remote sounding of grounds and other structures with low and moderate absorption of electromagnetic waves: hard rocks, wet sandy grounds and sandy loams as well as low wet clay loams. They are able to detect local irregularities (metallic and dielectric ones) as well as boundaries of ground layers differing from each other in electrical parameters. The performance of georadars is based on radiation of video pulse having wide spectrum and recording of video pulses being reflected from irregularities. The results of processing of those signals make it possible to make an image of reflecting boundaries of irregularities of structure under sounding presented as three-dimensional one or as vertical cross-sections. The georadars in use differ in range of operating frequencies, dimensions of antennas, resolution and depth of sounding. Performance data for TR-GEO georadars are given in Table 1.

TR-GEO-01 and TR-GEO-02 georadars are designed for imaging of geological cross-sections, for detection of karst cavities, decompaction zones in ground, boundaries of lenses, floating earth, alluvial sediments, local objects – metallic or dielectric ones (big boulders) of no less than 0.3–0.5 m in size as well as for location of cables and pipes.

Table 1. Essential characteristic of TR-GEO georadars.

Georadar	Dimensions of antenna (cm)	Average frequency (MHz)	Maximum depth* (m)
TR-GEO-D	$100 \times 90 \times 20$	20–30	30
TR-GEO-D	$55 \times 55 \times 13$	120–150	15–20
TR-GEO-01	$40 \times 40 \times 7$ $41 \times 33 \times 5$	150–200	10
TR-GEO-02	$25 \times 25 \times 5$ $30 \times 20 \times 5$	150–250	5–7
TR-GEO-03	$12 \times 12 \times 3$ $8 \times 8 \times 3$	~1000 ~1500	1

*The depth of sounding is given for sandy ground with moderate moisture content.

Figure 1 shows the most recent model of TR-GEO-01 georadar. TR-GEO-03 georadar is designed for detecting faults in building constructions, voids, cables, pipes, local objects of no less than 0.05 cm in size as well as for measuring the depth of pavement layers.

The signals are recorded by antenna unit moving over surface under sounding. A small gap (1–5 cm) between antennas and surface is allowable during moving. The best results are achieved with close contact between antennas and ground and with even surface



Figure 1. TR-GEO-01 georadar.

of ground. The antenna unit moves usually along several parallel profiles. When counting the coordinates one can use distometer. The distance between adjacent profiles depends on how close the supposed object under sounding is placed and makes up to 0.2–1 m. To achieve the more accurate locating of object the range of moving area of antenna unit over surface should be approximately twice as large as the depth of object under sounding.

TR-GEO georadars are equipped with slot antennas. This provides for a large "front to back" ratio, i.e. low level of parasitic reflections from objects placed in air half-space. This feature is of special value when foreign objects are available, when operating radar in close vicinity to walls of buildings as well as in conditions of strong electromagnetic interference. If necessary the antennas are additionally screened by blocks of resistive material.

2.2 *Methods of processing of signals*

Radar Program is used for recording and processing of signals. Signal processing consists of preliminary processing, deconvolution algorithms, three algorithms of three-dimensional focusing and algorithms of three-dimensional visualization.

The preliminary processing includes detection of directly between the antennas passing signal and deduction of that signal from all recorded signals. The preliminary processing includes also subtraction of low-frequency component which remains as a result of non-complete deduction of slowly attenuating exponential of directly passing signal. If required also "noise" which as a rule originates from multiple signal reflections becomes subject to zonal filtration. Such a "noise" appears in particular when sounding over surface of reinforced concrete constructions. The elimination of occasional thermal noise as well as of electromagnetic interference is achieved through accumulation and multiple averaging of signals. The numerical value of accumulation of measured data in each point of time base is given as a function which is in increase towards the end of time base and which ensures the required "signal – noise" ratio over all radar time base. This function takes into account exponential attenuation of reflected signals in ground. The averaging of signals is also effected as the georadar slowly moves along the profile within short distances defined by distometer.

The result of preliminary processing represents the sum of signals reflected from objects. Every signal of this type reflected from local object or from dividing line appears as attenuating oscillating signal consisting of several (3–5) half-periods. The algorithms of deconvolution make the transformation of those reflected signals into signals which consist of one half-period, or those algorithms specify moments of appearance and amplitude of reflected signals. Radar Program uses following deconvolution methods: method of inverse filtration, method of least squares with regularization method developed by A.N. Tikhonov. Also correlation and autocorrelation methods were investigated. The autocorrelation method provides for searching for similar reflected signals in adjacent positions of the antenna unit.

3 RESULTS OF MONITORING OF GROUND MASSIF USING TR-GEO GEORADARS

Geological Prospecting Co., Ltd has gained for nearly a decade a lot of experience in practical application of TR-GEO georadars on construction sites in Moscow. We consider various areas of practical application of georadars as well as results obtained using TR-GEO georadars. Following are results of preliminary processing presented as vertical wave profiles.

3.1 *Monitoring of ground mass when drifting tunnels*

The sounding ahead of tunneling machine is necessary due to risk of hitting and destroying underground utilities which were mismarked or unmarked on geological cross-sections. Furthermore available geological cross-sections of ground do not often correspond with actual geological mass. This is due to impossibility of drilling appraisal wells in conditions of dense urban building. Lenses, buried channels and alluvial cuttings can be smaller in size than the distance between wells.

Monitoring of ground ahead of face of collectors under construction allowed for timely detection of several objects including five metallic water mains pipes, two gas mains pipes, one ceramic collector, one high-voltage cable, five buried appraisal wells, two large water-filled karst cavities with volume of 150 m^3 as

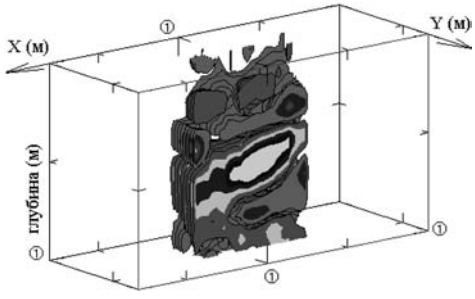


Figure 2. Results of sounding of five shells of 152 mm caliber in clayer ground.

well as of a great number of large in size boulders. Twenty nine shells of 152 mm caliber with length of about 50 cm, which have been remained in ground since World War Two, were detected. Figure 2 shows results of sounding on the spot of mass burial of those shells. Five shells were placed closely to each other at distance of about 0.5 m from tunnel face.

3.2 *Sounding from surface to check geological cross-sections*

This type of sounding is necessary when drifting tunnels and other shallow utilities in particular when using micro-tunnelling method. The results of georadar sounding are used in combination with data on well prospecting in order to image or check geological cross-sections between geological appraisal wells.

3.3 *Sounding of rocky ground*

The sounding in galleries and transport tunnels being under construction in rocky grounds seeks detection of fractures and faults in rocky mass. Figure 3 shows the process of sounding in engineering gallery of transport tunnel while Figure 4 shows one of sounding results. As a result of sounding fractures at distances of up to 3–4 m were revealed (shown by arrows).

3.4 *Sounding of urban underground utilities*

When laying new pipes or cables or proceeding with repair works of old mains it is necessary to know the exact disposition of all underground utilities and their expansions which are available at particular place. It often occurs that old underground utilities are unmarked on geological maps. It can lead to failures or breakdowns of tools when laying new mains.

3.5 *Sounding on construction sites*

In this case the sounding seeks surveying of geological subbasis as well as search for karst cavities and buried cellars on future construction sites. Let us give



Figure 3. Sounding of engineering gallery of transport tunnel using TR-GEO-02 georadar.

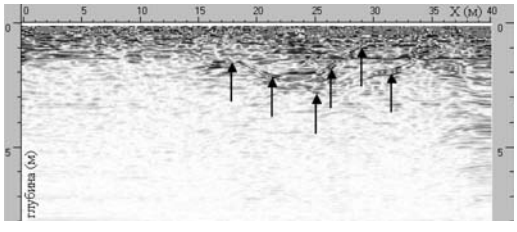


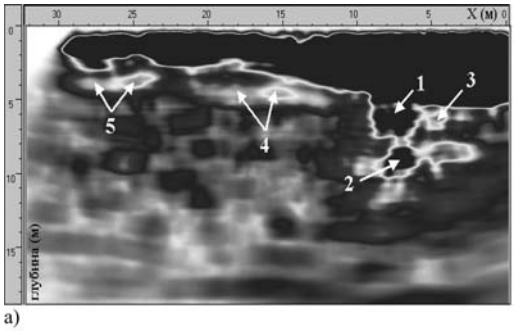
Figure 4. Results of sounding of fractures in rocky ground using TR-GEO-02 georadar.

an example of sounding which resulted in detecting of buried cellar on the spot of intended foundation pit. Figure 5a shows results of sounding after making focusing. Figure 5b shows photo depicting the wall of excavated foundation pit on site under sounding. The irregularities in the resultant picture correspond with dug-up reinforced concrete constructions. Always use the Figure caption style tag (10 points size on 11 points line space). Place the caption underneath the figure (see Section 5). Type as follows: 'Figure 1. Caption.' Leave about two lines of space between the figure caption and the text of the paper.

3.6 *Application of georadars when laying underground utilities using micro-tunnelling method or further trenchless technologies*

This type of sounding seeks searching for industrial and natural inclusions (large boulders) as well as checking of location of underground utilities. The detection of those objects allows for correct engineering of a run and for avoiding failures when proceeding with micro-tunnelling.

Ground surveying is necessary to be carried out upon completion of construction works because when drifting using micro-tunnelling machine voids and decompaction zones in ground are sometimes formed. Sounding of one of collectors using TR-GEO radars which carried out by Geological Prospecting Co., Ltd upon construction completion has revealed those decompaction zones what was verified by following checking.



a)



b)

Figure 5. Results of sounding after making focusing (a) and wall of foundation pit which has been dug out on the spot of sounding (b).

3.7 *Sounding of mine tunnel walls when proceeding with monolith pressed concrete lining*

The sounding using high-frequency radars (with average frequency of 1 (GHz) makes it possible to detect potential faults in lining as well as to control the thickness of concrete walls of tunnels. The sounding using radars with lower average frequency seeks detection of karst cavities and wet zones in the immediate vicinity to mine tunnel. The sounding using radars with lower average frequency seeks detection of karst cavities and wet zones in the immediate vicinity to mine tunnel.

4 CONCLUSIONS

The results of practical activities carried out by Geological Prospecting Co., Ltd demonstrated that it is strongly necessary for ground condition to be controlled using TR-GEO georadars and that TR-GEO georadars are appropriate to successfully solve this task.

Underground Space – the 4th Dimension of Metropolises – Barták, Hrdina, Romancov & Zlámal (eds)
© 2007 Taylor & Francis Group, London, ISBN 978-0-415-40807-3

Application of tunnel information system for construction supported by international cooperation

C.Y. Kim, K.Y. Kim, Y.Z. Lee, S.W. Hong, S.H. Baek, & K.W. Seo
Geotechnical Engineering Research Dept., Korea Institute of Construction Technology, Korea

Wulf Schubert
Institute of Rock Mechanics and Tunnelling, Graz University of Technology, Austria

Y.S. Seo
Department of Earth and Environmental Science, Chungbuk National University, Korea

ABSTRACT: The system (ITIS, Intelligent Tunnel Information System) which can manage and analyze the tunnel information in design and construction stage has been developed through several years' research. This system is being modified and improved for the international sharing of tunnel construction information. Since each country has each management system for tunnel construction information, the new system should allow the different forms of information. In this research, Austrian system (DEST, Data Evaluation System for Tunneling) is adopted for the international cooperation with Korea. The system under development (ITCISS, International Tunnel Construction Information Sharing System) is operated in web-based environment. Therefore, it is possible that the tunnel construction information can be shared and cross-reviewed internationally by use of ITCISS.

1 INTRODUCTION

Recently, tunnels with length over 10 km are constructed increasingly all over the world including Europe and Asia. In Korea, various tunnels are planned to be constructed for express way, subway, railway and utility. However, tunneling cost in Korea is relatively higher than in Europe, thus current problems of tunnel construction in Korea should be investigated. Sufficient investigation and analysis of European tunnel construction information is also required for the precise comparison. Tunnel construction information (monitoring, face mapping, construction history etc.) and its practical use on site should be examined carefully for the establishment of the sharing system because the philosophy of tunnel design and construction could be different between countries.

In this research, core components of tunnel construction information are determined by analyzing various management systems of tunnel construction information and the standard relational database model is established for international tunnel construction information sharing system (ITCISS). Also, internet-based ITCISS is developed to share tunnel information during construction between Austria and Korea for the initial development. In addition, ITCISS is designed in consideration for extension of this system and connection with other countries.

2 TUNNEL INFORMATION SYSTEM

2.1 *Requirements of database system*

The data stored in the system would be provided from many construction sites of different countries, which have not only conventional and compatible type of information but also their unique type of information characterized by their own construction method, construction condition, geological environment and so on.

The requirements of database system for the storage and manipulation are:

- That the data would be stored in a commercially and practically acceptable database standard, enabling future access and migration.
- That the data could be protected against unauthorized access, and was secure during use from accidental or deliberate corruption.
- That the data could be accessed as soon as it becomes available at any location.
- That manipulation and display of the data would need no special knowledge and should be intuitive for the user.
- That creation of data by the contractor should be simple and consistent, using commonly available software and transmission techniques.

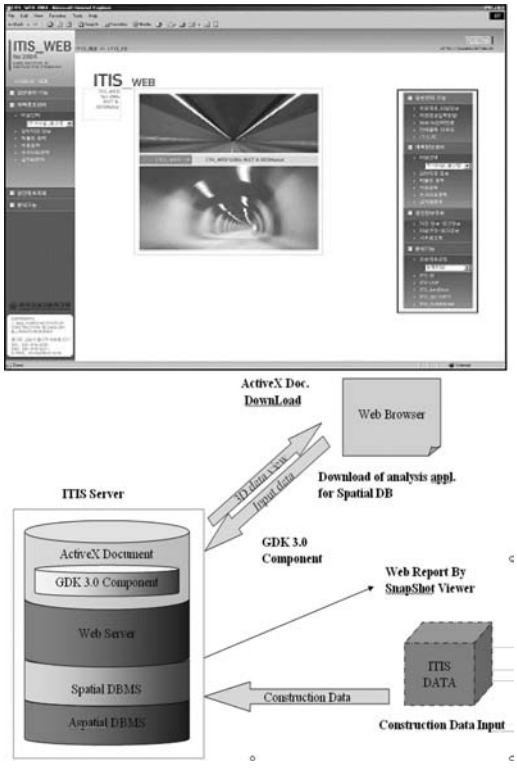


Figure 1. ITIS GUI feature.

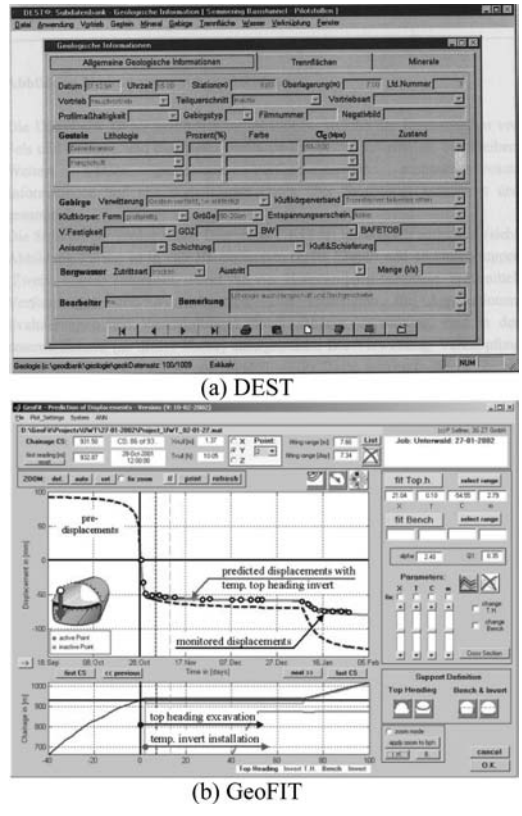


Figure 2. DEST & GeoFIT GUI feature.

2.2 *Existing system*

ITIS (Intelligent Tunnel Information System) had been developed by Korean Institute of Construction Technology (KICT) for the purpose of integrated D/B management, analysis and visualization system for geotechnical projects especially tunnel construction in Korea (Hong et al. 2002, see figure 1) ITIS is being modified to make up integrated tunnel construction information system both in domestic and foreign countries.

For tunnel information system shared between different countries, several important constraints such as database structure, system architecture, environment and infrastructure of operation should be considered. The first counterpart country is decided to be Austria because New Austrian Tunnelling Method (NATM) is applied commonly in Korea.

DEST (Data Evaluation System for Tunnelling) is an in-house database system developed by Institute for Engineering Geology and Applied Mineralogy of Graz University of Technology. Geofit is an in-house software developed by Institute for Rock Mechanics and Tunnelling of Graz University of Technology for the interpretation of geodetic monitoring data (see figure 2).

3 INTELLIGENT TUNNEL INFORMATION SYSTEM (ITIS)

3.1 *System outline*

Arriving at the correct design for the information system before embarking on its development is very important. Site investigation, tunnel design and construction data are generally existed in forms of manually completed documents, project reports, regional geotechnical maps and geotechnical relational database, etc. And the analysis of these data that located against some form of map or plan is generally two dimensions. ITIS is an integrated D/B management, analysis and visualization system for geotechnical projects especially in tunneling. It is a true client-web server database system. The client-web server model for distributed computing allows multiple client PCs to request data from a single server PC on which resides a database and the software for servicing client requests. The structure of ITIS is shown in figure 3.

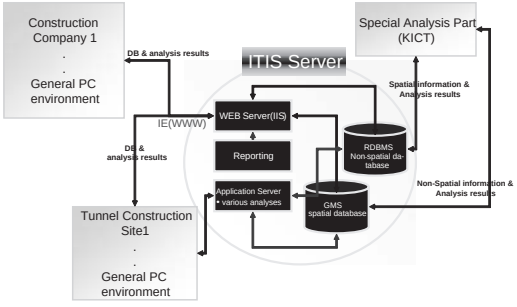


Figure 3. System structure of ITIS.

3.2 *Visualization of the information*

In ITIS system, the techniques of 3-D visualization and VR are used to visualize a complicated geotechnical structures in the 3-D space and many kinds of analysis and investigated data in tunneling. Because tunnel construction is performed under 3-D space with complex discontinuities such as fault, joint and bedding, 2-D drawing design is difficult to figure out, so 3-D graphic technique is necessary to utilize and give out information rapidly and efficiently. Besides, VR technique can make users control all the movements and actions not by programmers but by his willing. That is, users can enter into VR space, experience the defined world, and interact each other by their eyes, ears and hands. Thus, it is one of the substitutive recommendations to apply VR technique to visualization of geotechnical information in order to make users comprehend it easily. All useful information acquired from 3-D graphic technique and site investigation can be used to simulate many possible and critical circumstances that may be faced or experienced during construction. In addition, VR is helpful to choose the appropriate construction procedures(see figure 4).

4 ITCISS (INTERNATIONAL TUNNEL CONSTRUCTION INFORMATION SHARING SYSTEM)

In this research, two different systems (ITIS (Korea) & DEST (Austria)) are to be integrated for sharing system of tunnel construction information. Numerous experience and construction information are stored in each system, so that ITCISS can be a very meaningful tool in the light of combining them with powerful analysis modules in one system. For this purpose, all the data should be produced under consistent quality control and the various types of data (figures, pictures or qualitative description) should be digitized and managed in an appropriate system.

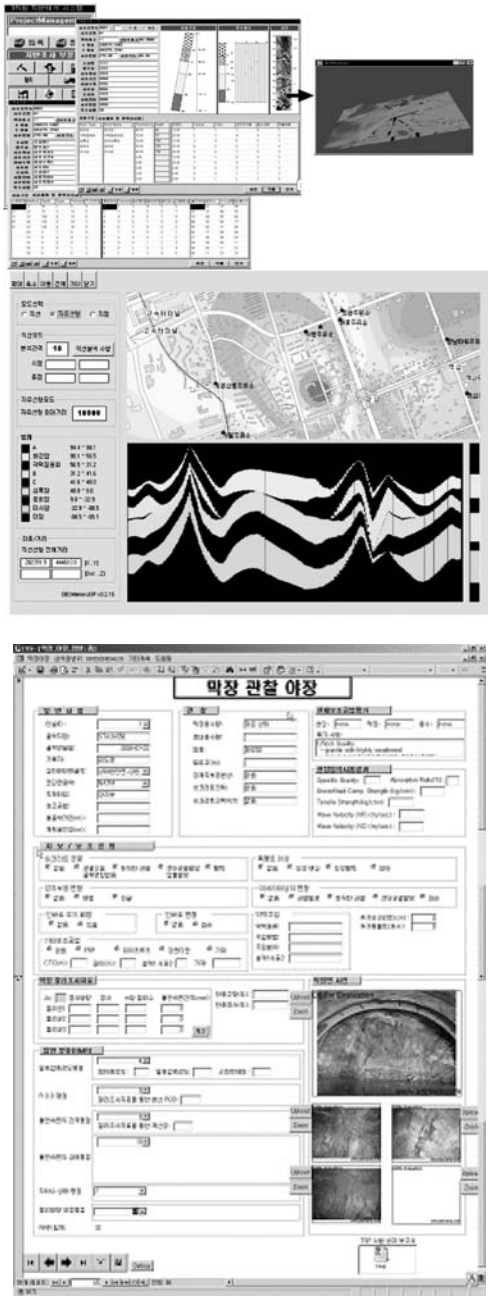


Figure 4. Visualization of the information in ITIS.

Table 1 shows the differences of ITIS and DEST. To combine the database systems and access in each country, linkage between ITIS and DEST was developed as shown in figure 5.

Table 1. Comparison of ITIS and DEST.

Item	ITIS	DEST
System architecture	On-line Networking RDBMS	Stand-alone General DBMS (non relational)
Principal functions	GIS-application (Visualization/Various stability analysis modules included)	Powerful analysis for monitoring (with GeoFIT module)
DB items	Non changeable DB schema (Unified database)	Changeable DB schema by user (Site-specific database)

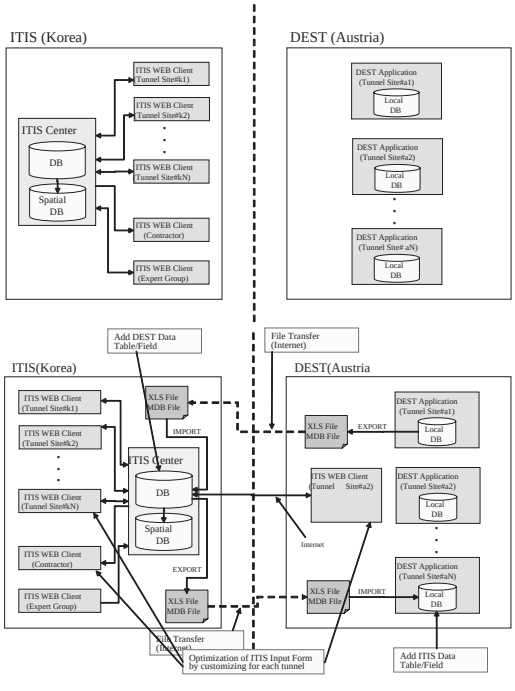


Figure 5. Linkage between ITIS and DEST in ITCISS.

5 CONCLUSIONS

This paper introduced improved way of utilizing tunnel construction information as a model system sharing international tunnel construction information. Advanced system to share tunnel construction information between countries can be meaningful not only in accumulation of various experience and data but also in cooperation of on-line support for decision making on site.

Several topics are being researched, related with database system. For instance, the database system of construction information will be used for the research of the expert system for tunneling, prediction of tunnel displacement or risk Assessment of excavation. The application of this database system will be enhanced more and more in the future and the cooperation with related countries will produce a fruitful result.

REFERENCES

Hong, S.W., Bae, G.J., Seo, Y.S., Kim, C.Y., Lee, S.W. & Lee, K.H. 2001a. The development of geotechnical interpretation system for tunnelling. AITES-ITA 2001. 715–721.

Hong, S.W., Bae, G.J., Seo, Y.S., Kim, C.Y., Lee, S.W. & Lee, K.H. 2001b. 3-D simulation analysis for visualizing geotechnical site investigation. Proc. 15th Int. Conf. Soil Mech. and Geotech. Engng. Istanbul. 27–31. Aug. 2001.

Kim, C.Y., Bae, G.J., Hong, S.W., Park, C.H., Moon, H.K. & Shin, H.S. 2001a. Neural network based prediction of ground surface settlements due to tunneling. Computers and Geotechnics. 28. 517–547.

Kim, C.Y., Park, C.H., Bae, G.J., Hong, S.W. & Oh, M.Y. 2001b. Countermeasure Expert System for Tunnelling Failure. AITES-ITA 2001. 409–416.

Underground Space – the 4th Dimension of Metropolises – Barták, Hrdina, Romancov & Zlámal (eds)
© 2007 Taylor & Francis Group, London, ISBN 978-0-415-40807-3

Influence of water back rise on tunnels and surface

M. Kolečkář
VIS, a.s., Prague, The Czech Republic

J. Němeček
SATRA, s.r.o., Prague, The Czech Republic

I. Zemánek
SG-Geotechnika, a.s., Prague, The Czech Republic

ABSTRACT: The aim of this paper is to present information about results of measurement of the influence of underground water level back rise on secondary lining of large tunnels and on the surface development. Measurement results and related conclusions provide investors with sufficient information in order to enable them decide about the timing of repairs of the surface development damaged by tunnelling.

1 INTRODUCTION

The results concern two tunnel structures in Prague which were commissioned in 2004. These were: Mrázovka road tunnel with the cross-section of 165 square meters and Kobylisy one bay driven underground station on line IV-C with the cross-section of 220 square meters.

As both structures are located in densely built-up municipal areas, extensive surveying took place both under ground and on the surface and it continued even after commissioning of both structures. This was not usual with other structures.

Both tunnels were constructed using similar technology – New Austrian Tunnelling Method and their complete perimeter was provided with pressure insulation. After the construction is completed, the underground water level rises back to its original level, loads the tunnel structure, and influences also the surface.

As both tunnel structures are located in different geological conditions, results of measurement of their impact on the surface differ considerably.

First measurement results on Mrázovka tunnel were published during the 28th ITA International Congress in Sydney in 2002. Other measurements Since 2002, when insulations and secondary tunnel lining were completed, and after the commissioning of the tunnels, additional measurements were carried out. These measurement have given some interesting and surprising results.

Due to the scope of this paper, we are only able to provide elementary information relating to the topic hereof. List of literature at the end of this paper provides more details about publications containing details about the monitoring and construction issues.

2 MRÁZOVKA TUNNEL

2.1 *Basic data*

Mrázovka road tunnel consists of two three-lane tubes which further fork into two-lane and single-lane tubes in driven tunnel forking. The tunnel is one kilometer long.

The most difficult part of tunnel construction was the passage under Ostrovského street where five-storey apartment houses are located (Figure 1).

The bedrock in this area consists of silty-clayey shales. The total thickness of overlaying formations above the tunnel vault was 9.0 meters. From that, 3.5 meters consisting of weathered shales and 5.5 meters consisting of partly weathered shales. The eastern tunnel tube also intersected with quartzites. Surface layers consist of made-up ground and deluvial gravel and sand deposits. The total overburden height is 16.0 meters. Distance between the tunnel profile vault and the foundations of the buildings was as short as 12.0 meters. Remedial grouting was carried out from the exploratory tunnel with the aim of improving the overburden quality. Compensation grouting was carried out under three buildings during the western tunnel tube construction.

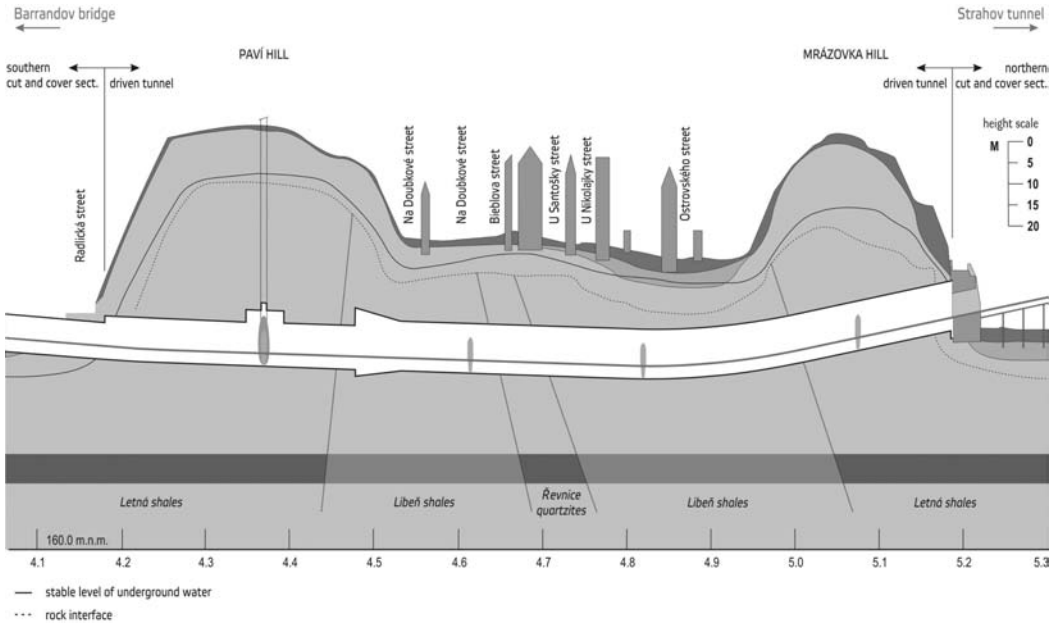


Figure 1. Longitudinal section of Mrázovka tunnel.

2.2 *Consequences of the underground water rise in Ostrovského street*

Significant oscillation of the underground water level both in the capping mass and in the bedrock occurred during tunnels construction. The soil mechanics theory and subsidence calculations show that surplus loading and resulting compression occur in emerged soils (strata in which the underground water level drops). These deformations subsequently propagate to the surface and various effects causing terrain deformations and subsidence of buildings on the surface thus sum up (tunnel driving, underground water level decrease, sealing and compensation grouting).

- exploratory tunnel construction in the western tunnel tube (Figure 2) .....20 mm (from that the calculated effect of the underground water decrease by 14 meters stands for 10 mm)
- gradual driving of the western and eastern tunnel tubes.....45 through to 51 mm (causing additional decrease of the underground water level by 8 meters with unidentified contribution to the overall deformation. Expert estimates indicate between 5 and 10 mm).

The total deformations on the surface ranged between 65 and 71 mm (Figure 3).

It is therefore possible to state that the impact of the underground water level decrease after the overall underground water level decrease by 22 meters, construction of the tunnels, and after completion of primary lining in both tunnels represented the terrain subsidence by approximately 15–20 mm. After the full insulation of both tunnel tubes was completed and after the secondary lining was constructed, the underground water rose back to the original level which was registered before commencement with tunnel construction. Monitoring has indicated terrain rise by 5 mm and rise of the buildings by 8–12 mm. Reasons for this can be seen firstly in relieving the ground layers re-saturated with water and secondly in the great static lift force of approximately 1.6 MN per meter of each tunnel tube (Archimedes' principle).

Theoretical analysis would be a speculation because the soil does not behave as an elastic material and changes of the deformation modulus depend on stress condition of the ground. Undoubtedly, there have also been at least partial degradation of the ground environment in the tunnel overburden.

Reverse deformations of the buildings in Ostrovského street represented approximately 50% of the values caused by the underground water level decrease.

Such a great rise of 8–12 mm was not expected and some previously reconstructed structured had to be repaired again. Owners of the buildings insisted on immediate repairs right after completion of tunnels driving while the reverse deformations occurred some 18 months later due to the time required for construction of complicated secondary lining in the tunnels.

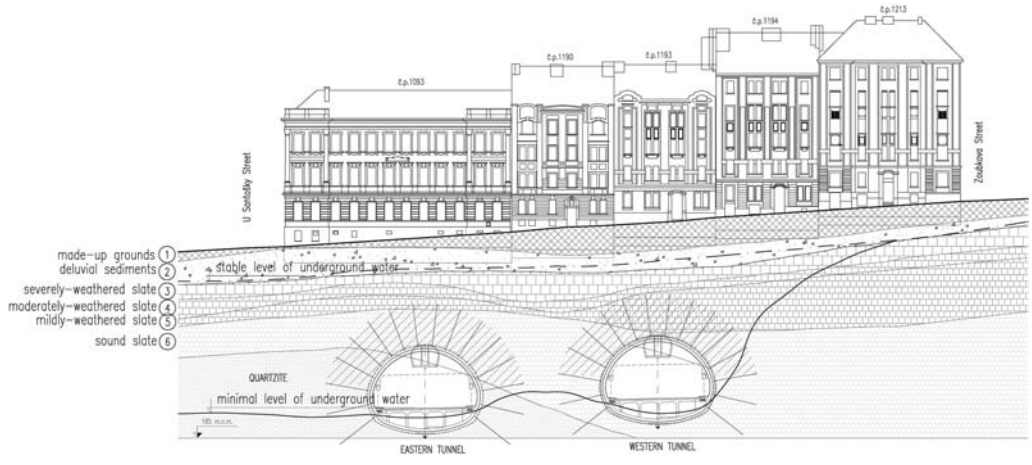


Figure 2. Cross-section in Ostrovského street.

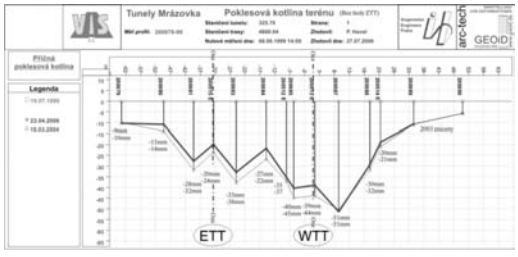


Figure 3. Subsidence though in Ostrovského street.

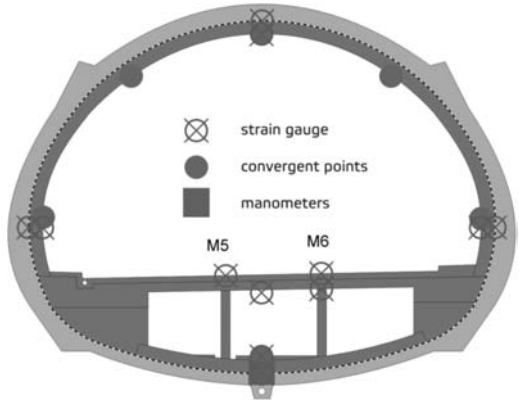


Figure 4. Measuring points placement in the tunnel.

2.3 *Impact of underground water rise to the tunnel structure*

The impact of the underground water level back rise has been documented firstly by the movement of the metering points installed on the secondary lining of the tunnels (Figures 4, 6), and secondly by changes of stress in the deck, which forms part of the secondary lining structure (Figure 5).

From the time perspective, the following essential terms have to be mentioned:

- completion of driving and primary lining execution (underground water decrease by 22 meters) in 06. 2002
- secondary lining construction in both tunnels in 06. 2003
- packing of the tunnels and closing of pumping pits, underground water level rise in 06. 2004
- commissioning of the tunnels 26.8. 2004
- back rise of the underground water level to the original level recorded before commencement with construction in 04. 2005.

2.4 *Stress in the deck*

When designing the cross-section of the three-lane Mrázovka tunnels, a non-standard solution of the lower parts of the secondary lining has been adopted. The deck structure supporting the road is used as a strutting bar in the lining structure (Figure 4). This eliminated the necessity of strengthening the bottom of the tunnel and increasing its profile.

The structural design of the deck has respected the requirement on observing the maximum crack width in order to ensure the corrosion protection of the reinforcement.

Stress of the deck reinforcement was measured during the monitoring and results of this measurement are documented on Figure 5 .

During the first phase (June, 2003–November, 2003) when the underground water level was low, the

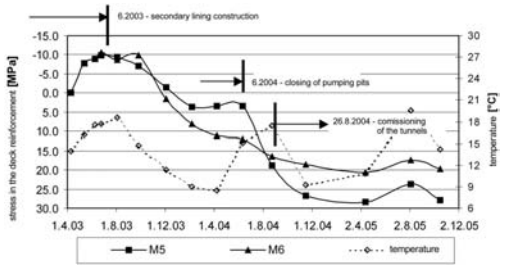


Figure 5. Stress in the deck reinforcement.



Figure 6. Secondary lining deformations.

deck acted as a compression brace. Once the insulation was closed and the underground water level rose, the compressive stress changed into tensile stress during December, 2003 and since then the deck acted as a tendon with reinforcement tension values between 20 and 28 MPa. The increase of the values which took place before April, 2005, corresponds to the underground water rise back to the original level.

2.5 *Secondary lining deformations*

Hydrostatic pressure represents dominant part of the overall loading of the secondary lining. Movement of six points in a number of diameters along the tunnel length and stress inside the lining were measured within the framework of the monitoring (this is described in a separate article).

Resulting movement of metering points in the secondary lining in the three-lane tunnel under Ostrovského street are documented in Figure 6 (vector scheme). Individual frames indicate dates and absolute values of measured vertical deformations at each particular point.

The diagram shows that the hydrostatic pressure affecting the bottom of the tunnel is so considerable that it lifted the tunnel tubes by 4–11 mm until April, 2005 despite of the overburden resistance. Other loading factors also occur and there is no doubt that after many years, when the primary lining degrades, the ground pressure will rise considerably. This upward movement of the tunnel tubes has contributed to lifting the terrain and surface development in Ostrovského street as indicated in the previous section of the paper.

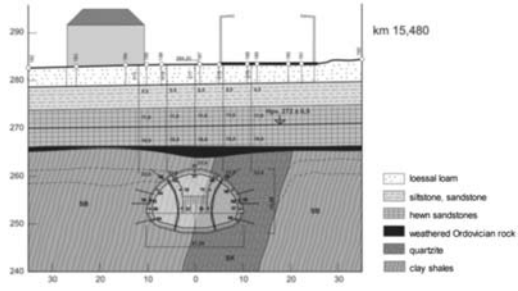


Figure 7. Cross section.

3 KOBYLISY ONE BAY DRIVEN STATION

3.1 *Basic description*

Kobylisy single-aisle underground station is located in the densely built-up center of Kobylisy. The large cavern is 148 meters long and the theoretic stope area was 220 square meters (which is approximately 30% more than in the case of Mrázovka tunnels). The excavation width is 21,2 m.

The rock environment, in which the tunnel was driven, consists of Ordovician skalecké shales and skalecké quartzites. This geologic environment is characterized by extraordinary inhomogeneity of the rock environment and by a great heterogeneity of geotechnical properties as for example strength, deformation properties, shear strength on discontinuities, stability, saturation, and permeability. As regards the mechanical and physical properties, this rock environment is similar to that in which Mrázovka tunnels were constructed. However, both locations differ in the geology of the overlying strata. The overburden of the stope consists of thick sub-horizontal formation of hewn sandstones which establish a bearing element above the cavern stope. This bearing slab has favorably influenced the development of deformations in the vicinity of the stope and on the terrain surface. The total overburden thickness is 22 meters.

3.2 *Monitoring results*

Geotechnical monitoring established in advance before commencement with the construction works has focused on monitoring the deformation behavior of the tunnel lining, stope overburden, terrain surface, and buildings on the surface.

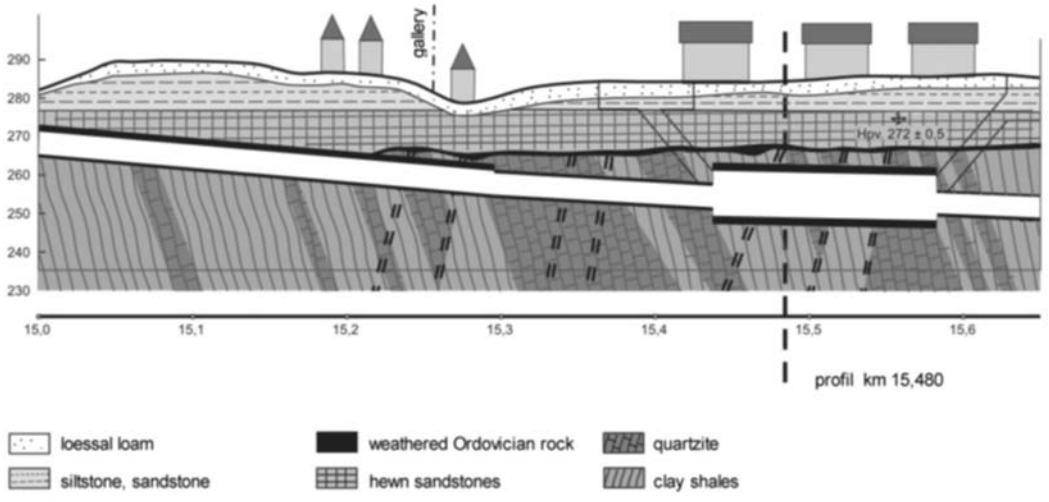


Figure 8. Longitudinal profile.

Another important part of the geomonitoring was the underground water level monitoring in the overlaying strata (in the rock of horizon). These surveys have been carried out in 21 wells and in four observation boreholes.

The measurement results have shown that construction of the cavern and line tunnels caused decrease of the underground water level by 1–2 meters only. Wells with the depth over 11 meters did not dry out at all. This documents the productiveness of the cenomanský aquifer.

For the purpose of monitoring the effects of underground water level rise after insulation and secondary lining completion, we have selected a characteristic levelling profile on the terrain surface located at chainage 15.480 km. Underground water level monitoring was carried out during the entire construction duration, as well as after its completion. The results have indicated that the saturation with water and the underground water stabilization to the original level took approximately one year.

The levelling profile on the terrain surface located at chainage 15.480 km was subject to systematic geodesic surveying during the entire term of driving works, i.e., until the half of 2003 when the deformations stabilized at approximately 45 mm.

Outside the scope of the monitoring project, we executed leveling surveying of points in profile June 17, 2004 and June 1, 2004 after the final lining was completed and after the underground water stabilized back at its original level. The results are illustrated in the Figure 9. The results shown below indicate that, unlike at Mrázovka, the effect of lift force on the terrain surface denivelation has not occurred here. It is

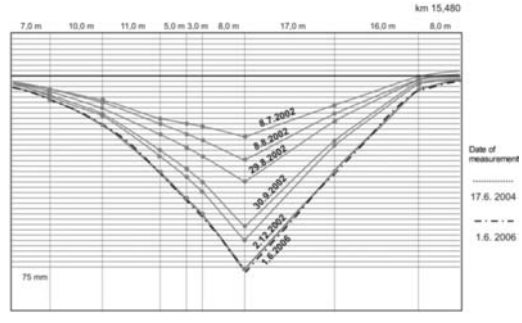


Figure 9. Levelling measurement in KM 15.480 profile.

obvious that despite of the considerably greater volume of the cavern (and therefore also greater lift force), the overburden thickness and its stability given by the Ordovician formation and the sandstones are the decisive factors for the balanced state of the underground structure.

4 CONCLUSIONS

1. The paper informs about results of monitoring two large tunnel structures in Prague from the perspective of underground water effects and its back rise after commissioning of the structures in 2004. Two structures with different geological conditions were compared.
2. As regards Mrázovka tunnels where significant decrease and subsequent rise of underground water

level was encountered, the monitoring and calculations identified deformation effects of underground water decrease between 15 and 20 mm in the area of Ostrovského street (from total deformations between 65 and 71 mm).

3. Back rise of the water caused lifting of surface structures by 8–12 mm, i.e., approximately 50% of the value caused by the underground water level decrease. This lifting occurred approximately one year after the secondary tunnel lining completion and after the end of water pumping from the pits under the tunnels.
4. In similar cases of tunnels with full insulation and in the hydrogeological conditions with soil overburden, it is necessary to carry out final repairs of surface buildings only after full underground water level rise and after stabilization of the buildings confirmed by leveling measurements.
5. Monitoring of Mrázovka tunnel still continues (subject to approval of the operator) and its continuity can be beneficial for design of other large tunnel structures.

REFERENCES

Havrda, A., Dvořák, J., Kolečkář, M., Němeček, J.2002, Monitoring of Mrázovka tunnel in Prague, *World tunnelling congress ITA-AITES,* Sydney

Kolečkář, M. 2003, Main problems encountered during construction Mrázovka tunnel and monitoring, settlements above the big cross section tunnels, *International conference:Underground construction,* Prague

Kolečkář, M. & Zemánek, I., 2000, Monitoring of Mrázovka tunnel, *International conference :Underground construction,* Prague

Růžička, J. 2004, Final lining of Kobylisy one bay driven station, *Tunnel magazine 04*

Růžička, J., Němeček, J 2006, Specifications of tunnelling in conditions of Prague, *World tunnelling congress ITA-AITES,*Sydney

A great number of authors, 2004, *Tunnel Mrázovka,* Prague SATRA

Underground Space – the 4th Dimension of Metropolises – Barták, Hrdina, Romancov & Zlámal (eds)
© 2007 Taylor & Francis Group, London, ISBN 978-0-415-40807-3

Geotechnical support of construction and operation of the Underground and transport tunnels

N. I. Kulagin, Sc. D. & K. P. Bezrodny, Sc. D.
NIPII Lenmetrogiprotrans OJSC, St. Petersburg, Russia

ABSTRACT: Geotechnical monitoring applied by the Institute in the design, construction, and operation of the Underground of St. Petersburg and transport tunnels is presented. Its structure and survey methods used are discussed. The results are presented in brief. In 1993, the Lenmetrogiprotrans Institute, in addition to its design and survey functions, became also a research facility. It has established a special division comprising three laboratories for geotechnical, geophysical, and environmental research. Development and implementation of geotechnical monitoring in the design, construction, and operation of the Underground and transport tunnels has recently become one of its major priorities.

1 ST. PETERSBURG UNDERGROUND

As St. Petersburg is Russia's second city in terms of its population (5 million), the problems of development of up-to-date passenger transport are very acute, all the more so because the city is located on over 40 islands in the Neva's estuary, while the existing bridges are heavily overloaded with ground transport.

Currently, St. Petersburg has 4 operating underground lines about 130 km long (face-to-face length) with 59 stations. The Underground daily carries over 3.0 million passengers, and its proportion in the total passenger traffic is constantly growing. A feature of its construction engineering geology is that under the mass of labile aqueous soils of quaternary strata (peat, sands, sandy loams, ribbon clays, and boulder rocks) there is a quite thick stratum of dense dry Proterozoic clays, which are a convenient environment for both construction and operation of underground facilities. Therefore, the city's underground space at these depths is mostly allocated for the Underground construction. An advantage of great depths (40…80 m from the ground surface) in these conditions is that construction in dense clays has a very slight effect on the city's life and on preservation of historically valuable monuments and compact city housing, especially in the historic center, and offers high roadheading rates.

As examples of station facilities where geotechnical monitoring has been used in the construction and operation, we will review three stations.

Sportivnaya Station (Fig. 1) is a two-storey single-vaulted interchange station for two Underground lines at once. Prior to designing, a large set of research efforts by physical and mathematical simulation methods was carried out. On the basis of these results, a design was developed for the station that for the first time ever, in such geological conditions, enabled construction of such a colossal underground facility with a sectional area of abt. 430 m^2. During the construction, field geotechnical monitoring with the use of various instrumentation was provided, which has been carried out also in operation for 9 years up to this day, and which enabled updating of the design parameters of tunnel structures.

Krestovsky Ostrov Station: Tri-vaulted, of a tower type, for one Underground line. For the first time in St. Petersburg's conditions, it was built entirely of reinforced concrete, without shaped cast iron components, with the three tunnels' lining extruded into the rock, and with the tower installation's girders prestressed between themselves. During the construction, geotechnical monitoring was applied with various sensors mounted in structures, which also continues during operation.

Admiralteyskaya Station: Tri-vaulted, of a tower type, for one Underground line. It is located under the city's historic part at a considerable depth.

Prior to designing, research by physical and mathematical simulation methods was carried out. Its results enabled solutions in the design documents for the station's facilities and its erection technology that ensure minimum surface sagging.

The middle hall was driven with a forepoling temporary arched concrete support installed in a slot made with a specially designed bar (Fig. 2).

During the construction, geotechnical monitoring of the station's facilities and ground surface was set up, which still continues during the line operation. Prior to the station tunnels driving, a system of compensating injection into the rock was built on the surface,

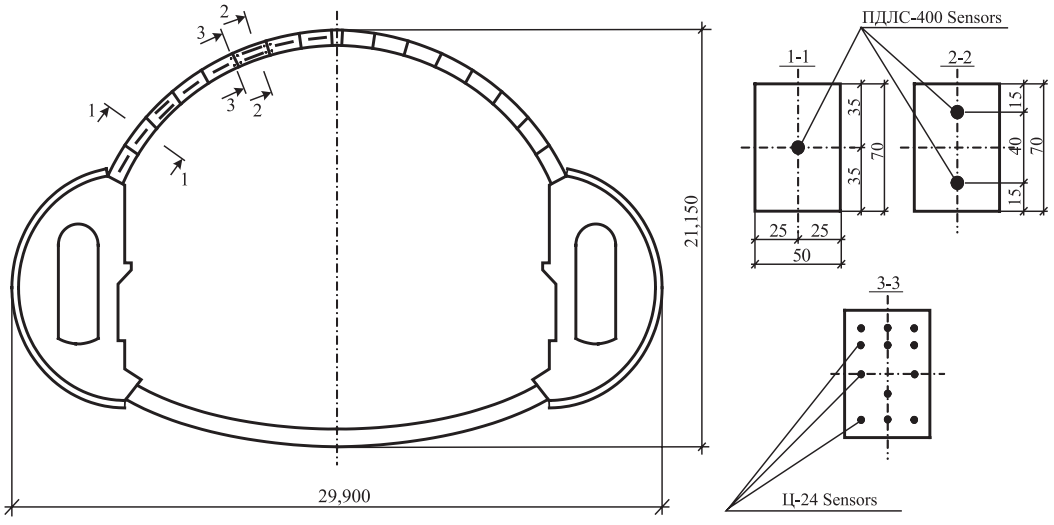


Figure 1. Sportivnaya Station: Arrangement of sensors in the top vault.

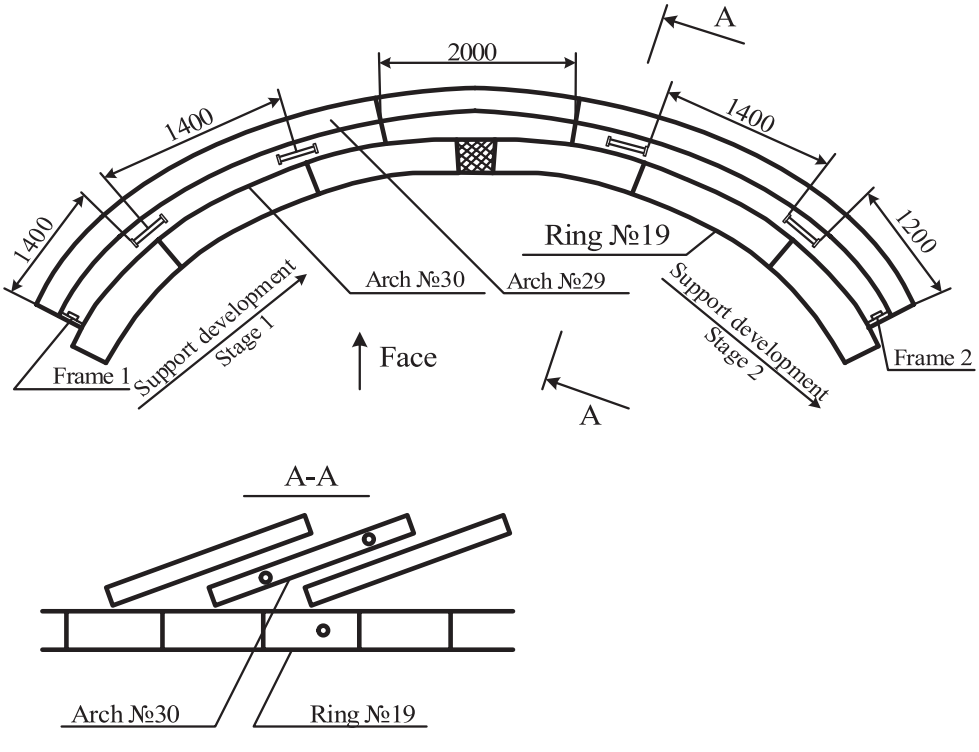


Figure 2. Arrangement of sensors in Arch No. 30 of the forepoling support.

with a grid of deep-seated reference points. During the tunneling, the system allowed to greatly reduce buildings' setting, to prevent their deformation by injecting solidifying spacer fluids into the strata movement zone under buildings (Fig. 3), and to preserve historic buildings without any distortions.

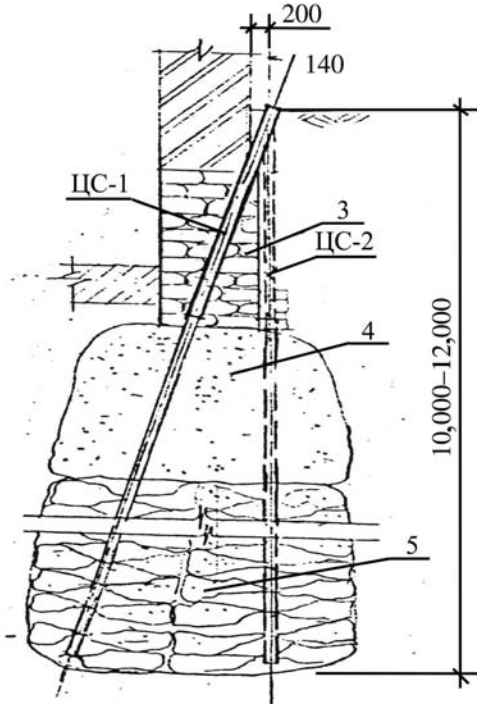


Figure 3. Compensatory injection soil fixing: LIC-1,2 – injection holes; 3 – building foundation; 4 – fixed soil under the foundation; 5 – compensating injection zone.

Geotechnical monitoring enabled to get full information on strain-stress states of the "station structures-soil block" system in every phase of construction and operation.

We should dwell in more detail on geotechnical monitoring in the design, construction, and operation phases of the new route of St. Petersburg Underground tunnels between Lesnaya Station and Ploschad Muzhestva Station, in quaternary aqueous soils at hydrostatic pressures of up to 0.5 MPa.

The tunnels were driven by a tunnel-boring machine with face surcharging at the depth of 50 m to 55 m, 1573 m long in single-track terms (Fig. 4).

To survey the soil block, 162 vertical survey holes 60 to 120 m deep were drilled at various design stages. Static sounding was made in 16 holes. 48 holes were drilled to install strain sensors in them. At 137 points, subsurface geological radar was applied from the surface to a depth of up to 90 m by ultra-broadband (UBB) sounding. Gravity prospecting was performed at 396 points, seismic survey, at 953 points, temperature survey, at 319 points, resistivity sounding, at 700 points, and caliper logging, at 115 points; cleanup pumping was performed in 19 holes; 696 soil samples were taken.

Extremely difficult geological engineering and hydrogeological conditions along the tunnel route, the one-side tunneling technology and lining design solutions that were novel for those conditions, and several questions posed by research organizations required development and implementation geotechnical monitoring of construction safety and subsequent safe operation of tunnels.

Monitoring comprised the following tasks:

– observation of lining strain-stress states in the plane perpendicular to the tunnel axis and along the tunnel axis

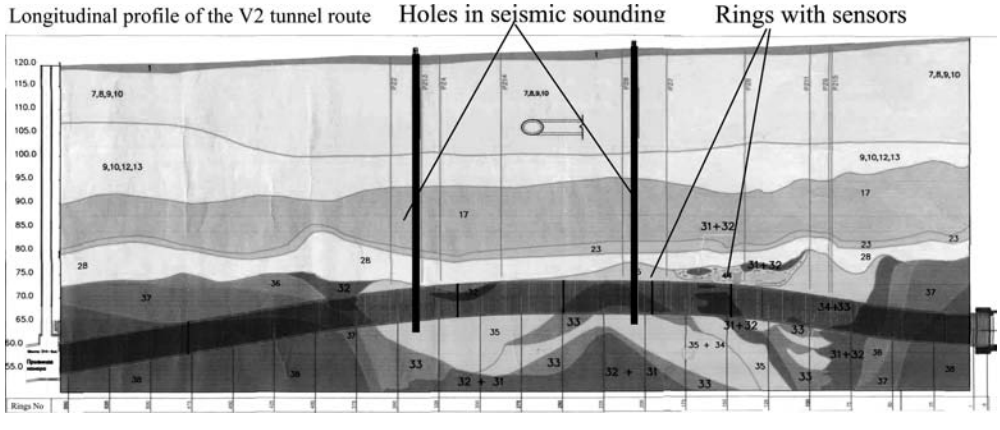


Figure 4. Longitudinal profile of the V2 tunnel route.

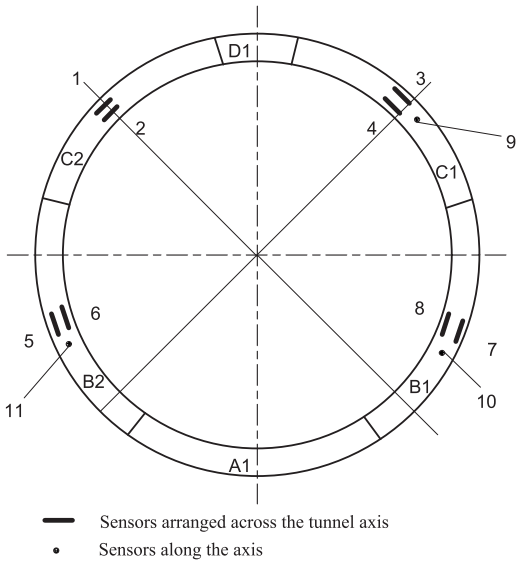


Figure 5. Arrangement of sensors in a lining ring.

– observation of linear and angular shifts of annular and radial lining joints
– observation of hydrostatic and pore pressure variations in the block
– monitoring of variations of geological engineering and hydrogeological conditions
– observation of surface shifts and structures during tunneling
– observation of inner geological processes
– detection of cavities not filled with fluid behind the tunnel lining
– acoustic sounding of the soil block.

The tunnel lining, 710 cm in outside diameter, was assembled from wedge-shaped rings to ensure the tunnel lateral and profile turning. The average width of a ring is 1.4 m. The ring consists of six reinforced concrete blocks 35 cm thick.

20 rings (Fig. 5) of the lining, with 220 sensors mounted thereon, were installed in both tunnels during their boring.

The sensor measurements showed that the normal tangential stresses were far below the concrete ultimate strength, all stresses are far below the ultimate compression, and their distribution along the lining perimeter is close to uniform.

The compression values between and within the rings are retained along the tunnel, following the temperature changes inside it. The dynamic stresses from trains passing make 1…3% of the static values.

The observations of the lining block joints with an error of 0.01 mm showed their practical invariability.

The pore pressure in the block was changing with the tunnel-boring machine approaching; after the tunneling, it stabilized and slightly varied with atmospheric pressure variations.

The method of UBB radar ranging from the ground surface along the tunnels' route was used to monitor expectable changes in the geological engineering and hydrogeological conditions before, during, and after the tunneling. These results showed their invariability.

The geodetic measurements of the ground surface, and buildings thereon, showed that the overall sagging from the two tunnels driving did not exceed 20 mm.

The ultrasonic detection showed that the stand-off between the soil boundary and the lining was filled with solidifying fluid of the preset thickness in every part.

Acoustic sounding of the soil block was performed before and after the tunneling and during operation. The tunneling actually did not affect the condition of soils near the tunnels.

Subsequent operation of the tunnels did not cause any vibratory liquefaction of soils. Moreover, the S-wave speed rates are far from the threshold criterion when such an effect is possible.

Prior to the tunnels' startup, an attitude position monitoring system was assembled in the first track tunnel. The system operates automatically and enables monitoring of the X-coordinate (length of the monitored tunnel sector between Planes 1–9), Y-coordinate (horizontal coordinate of the plane perpendicular to the tunnel axis), and Z-coordinate (vertical coordinate of the plane perpendicular to the tunnel axis) (Fig. 6).

During the observations, the variation of the length of the monitored tunnel part (624.8 m) was oscillatory. The maximum span of oscillations throughout the period of observations was about $\pm$ 6 mm relative to the average measurement error value.

The variation of the maximum shift of the monitored tunnel part in its center was within $\pm$ 5 mm both horizontally and vertically.

This information indicates sufficient stability of the monitored object throughout the period of operation of the tunnel attitude position monitoring system.

Elongation/contraction of the tunnel is related to seasonal temperature variations therein, and its vertical changes, to loads from trains in the morning, afternoon, and evening, and no-load in the night time.

2 TRANSPORT TUNNELS

The Institute has developed a system of geotechnical monitoring starting from the design stage and through the construction and operation support stages.

Monitoring purposes:

– safety during construction
– safe operation
– information about the strain-stress states of the "block-support-lining" system, geological

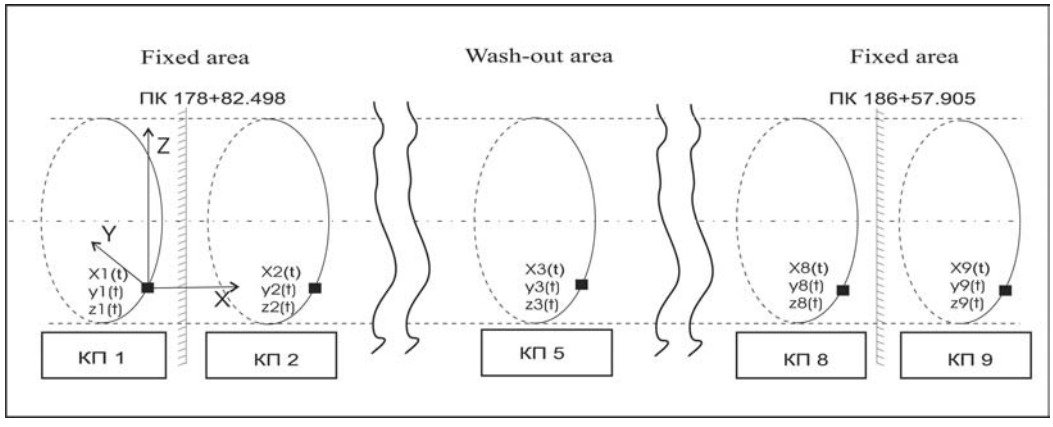


Figure 6. Attitude position monitoring system of Tunnel No. 1 by 9 monitored planes.

engineering and hydrogeological conditions ahead of the tunnel face, and actual physical/mechanical properties of soils, to take timely action to prevent development of negative processes
– generation of a data bank for assessment of construction risks and feasibility of analog design.

It should be noted that surveys conducted at various stages of designing do not provide sufficiently detailed data on the geological engineering and hydrogeological conditions along tunnel routes, especially for subvertical structures.

Geotechnical monitoring comprises the following stages:

– updating of geological engineering and hydrogeological conditions ahead of the tunnel face by the ultra-broadband (UBB) radar method at distances of up to 100 m
– analysis of the strain-stress states of the soil block and the "block-support" system in the working area by the electromagnetic emission re-cording method
– analysis of the strain-stress states of the "block-support" system using string transducers, or by the excavation pattern shift
– determination of actual stress-strain and strength properties of the soil block in the bored part of the tunnel by seismic profile shooting and by measured stresses in the structures
– on the basis of the results obtained, updating of design documentation as regards modifications in the tunneling processes and support design, and application of special techniques
– assessment of hydrostatic pressures and water production, and updating of drainage system designs
– observation of movements of the ground surface and structures thereon, and where necessary, actions to keep buildings and structures in their proper status
– geotechnical monitoring system switchover to the tunnel operation mode
– generation of a data bank for the tunnel.

Such geotechnical monitoring is provided actually in all transport tunnels under construction.

On the basis of completed geotechnical monitoring and surveys of tunnels, we develop experimental and theoretical methods of analysis of the strain-stress states of the "block-support-lining" system, and study the effect of operating loads on the system interaction variations. We analyze the degree of peripheral soil degradation and its influence on operation of the entire system. On the basis of a new-generated and updated geotechnical monitoring results data bank, we assess construction risks and feasibility of analog design.

As of this day, the following field observation methods have been invented/developed by the Institute:

– seismic methods
– ultrasonic methods
– electrical survey
– electromagnetic emission recording
– ultra-broadband (UBB) geological radar sounding
– analysis of hydrostatic and intrastratal pressures using string transducers
– stress testing in operated structures: by partial relieving, in concrete structures, and by magnetostriction, in steel/ironwork
– analysis of strain-stress states of supports/lining using string transducers, or by the excavation pattern shift.

The use of geotechnical monitoring in the construction of underground railways and transport tunnels in cities enables getting complete information about processes going on in the soil block, and timely engineering action for preservation of buildings and structures on the day surface.

This page intentionally left blank

Underground Space – the 4th Dimension of Metropolises – Barták, Hrdina, Romancov & Zlámal (eds)
© 2007 Taylor & Francis Group, London, ISBN 978-0-415-40807-3

Influence of the primary support stiffness on the surface subsidence during tunnel construction

J. Likar & M. Venta
University of Ljubljana, Faculty of Natural Sciences and Engineering, Slovenia

ABSTRACT: The usage of underground structures is increasing which is the reason that in many cases construction takes place in heavy and difficult geological geotechnical conditions. The main goal to reduce surface settlement on the minimum is connected with stiffness of the primary lining and effective protection excavation face against deformation process realized in rock pillar ahead the excavation. The construction process was modelled with *PLAXIS 3D tunnel program*. Input parameters were determined by 3D back analyses with Soft-Soil-Creep (SSC) constitutive material model, which takes into account rheological phenomena. 3D development of stress-strain fields during the tunnel excavation was performed to show major stress-strain changes in the surrounding rocks and support elements. The calculations showed that during excavation of the top heading substantial deformations are developed ahead of the top heading. Influence of the support stiffness has strong connection with amount of surface movements above the tunnel.

1 INTRODUCTION

The influences of tunnelling on surface in areas of low overburden are sometimes still difficult to predict, despite contemporary computer techniques. The cause for that could be in quite changeable physical and mechanical properties of the surrounding rocks mass and soils and also in selected construction method related with stiffness of primary support, which is installed after the excavation.

In technical literature at this area we could find some numerical models, which deals with relations between stresses and strains in the support system and surrounding rock mass for different distances between closed primary support and the face of excavation also for the particular stiffness of the support system.

In fact this is the effect of the support stiffness in function with surrounding rock mass in which the stiff support system has the biggest contribution. Stiff support system is usually combination of steel support together with shotcrete, rock bolts or anchors and also with additional support systems like steel pipe roof, micro piles, temporary invert with elephant foot, etc. In rocks with low bearing capacity, the arrangement of stresses and the amount of deformations which occurred, could be a serious problem regarding to the acceptable surface subsidence. In reality deformations in tunnel shell usually make no problems with stability and excavation process. The technological procedures are schematic shown in the Figure 1.

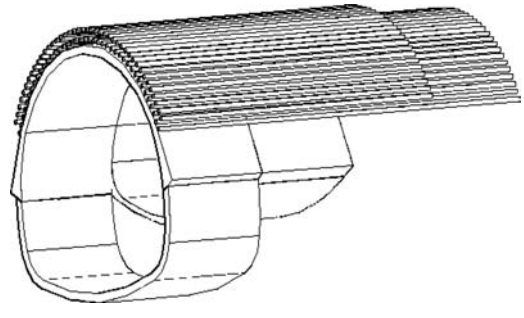


Figure 1. Technological sequences during the tunnel tube excavation.

Regarding to that, this demands detailed analysis of stiff support effect taking in to account development of deformation fields with excavation progress and installation of primary support.

2 SOME NUMERICAL MODELS WHICH DEALS WITH STIFFNESS OF PRIMARY SUPPORT SYSTEM

The question, which is related with the share of primary state in rock mass, which the support system has to take over, is in professional literature treated in different ways by many authors (Whittaker and Frith,

1990; Kim and Eisenstein, 1998; etc.). But in latest past, the usage of complicated models were less desired, because it took a lot of knowledge and time for engineers to obtain some results in practice and on the other hand the input parameters were complicated and difficult to define with standard laboratories tests. This causes some problems at planning and execution of detailed laboratories tests, which also could had limited practicability at wider area of the surrounding rock. This fact is quite related with inhomogeneous and anisotropic behaviour and anomalies, which often occur in surrounding rock mass. Reduction factors, which were used by some authors, show us, that they were fully aware of the complexity of rock mass structures.

Experiences that we have with usage of that numerical models indicated, that they are useful for tunnels or others underground objects with low overburden, which are construct in compact rock mass with high cohesion. In cases, where the rock mass has low cohesion, the results are questionable and not so reliable. Kim in Eisenstein 2006 suggested, that calculation method developed by Schwartz in Einstein 1980, could be used, when the quotient came to $L'_d/R < 1$. In this equation the $L'_d = 0.7\,m$ is the distance between the excavation face and the centre of gravity of the latest closed segment of primary lining and $R = 5.5\,m$, which is the equivalent radius of excavation.

In our case is $\lambda_d = 0.7 - 0.57(L'_d/R) = 0.63$, which corresponds their recommendation.

3 TECHNICAL PARTICULARITY OF CONSTRUCTION OF THE TROJANE TUNNEL AT THE SECTION OF SHALLOW COVER CLASS

The construction of the tunnel at the section of shallow cover class was adjusted to unfavourable conditions. The following working phases were performed:

(a) An excavation of top heading was carried out in 5 phases with simultaneous protection of working face by wire mesh Q189, 15 cm thick shotcrete. 35 pieces of 15 m long IBO rock bolts with bearing capacity 250 kN and over covering at 5 to 7 m were also installed. The amount of excavation step was 0,8 m.
(b) After excavation of the 3rd phase, the steel support was installed, which included 2 steel segments IPE 180 and 2 steel micro piles at every side of top heading, with length 6 m and 64 mm in diameter.
(c) After excavation of the 4th and 5th phase, temporary invert was installed with the thickness of 25 cm and one layer of wire mesh Q283. Also the second layer of wire mesh Q283 and shot concrete was installed, so that final thickness of primary support came to 35 cm.

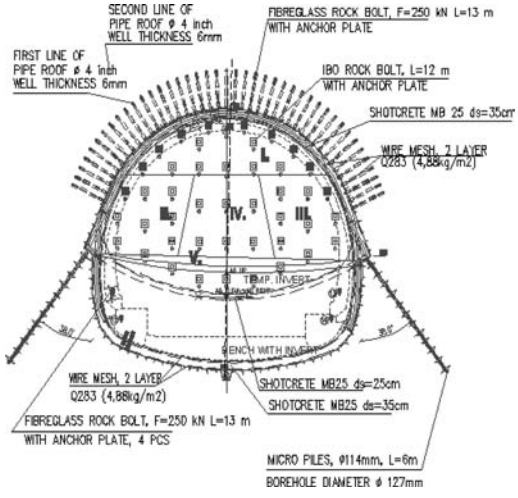


Figure 2. Cross section of tunnel tube with supported measures.

(d) An installation of pipe roof contained 42 pieces of pipes with 114 mm in diameter and over covering of 5 to 8 m.
(e) An excavation at top heading was followed by excavation and installation of primary support at bench and invert. Distance after working face of top heading was 10 to 20 m with excavation step 0,8 m.

Figure 2 presents the cross section of the tunnel tube with the supported measures.

4 CHANGES OF STRESS STRAIN RELATIONS IN ROCK-SUPPORT SYSTEM AROUND THE TUNNEL'S WORKING FACE

Excavation in low bearing and tectonic damaged rocks like tectonic clays, clay grain and gravel stone, which are present at the section of Trojane was connected with large amount of stress strain changes in front of the working face and wider area around the tunnel. In mostly clayey and relatively soft rocks, the influence was 3D or even 4D in front of the working face, where D stands for the diameter of the tunnel tube. This phenomenon was extremely unfavourable because of influence to the time dependent subsidence at the wider area. From the so far completed analysis and engineering interpretations, it could be estimated that large amounts of clayey components essentially influence the time dependent deformations. That was significant for the right judgment of possible deformations in a long time period.

Very heterogeneous geological structure and primary damaged rocks were often indicated in the differential subsidence of tunnel sidewalls. That also

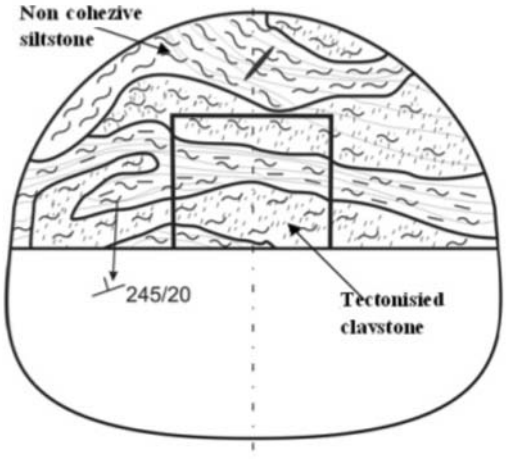


Figure 3. Typical geological cross section of the tunnel tube Trojane (East left tube).

unfavourably affected the governing of the amount of deformations in the tunnel roof and on the influential section at surface.

5 BACK STATIC ANALYSIS OF STRESS STRAIN FIELDS

Modern computer techniques based on numerical methods make quick and qualitative assessment of the changes, which are the result of excavation and installation of the support system. Anyhow, input parameters, which we obtain from standard laboratory and in situ tests, are not always quite realistic, comparing results from analysis obtained with those parameters to actual influences that developed between excavation and support measures. These statements were confirmed during construction of the Trojane tunnel, especially on the sections with clayey material.

Absolute values of the deformations calculated with analysis for estimation were quite smaller than those that actually occurred during the construction and later on. It is interesting that values of the differential deformations were more in accordance with the measured values.

The reasons for increased deformations are:

- The fact that in two-dimensional analysis the three-dimensional effect is not considered which is essential for this kind of rocks.
- The fact that input parameters, especially deformational, which we obtain from standard laboratory and in situ tests are not always quite realistic.

The application of the two-dimensional static analysis for realistic assessment of deformational fields demands much lover values of the input parameters.

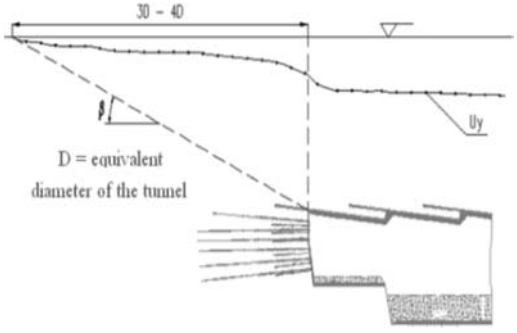


Figure 4. Angle of influence and deformations on the surface due to tunnel excavation.

This contradicts the correct scientific and engineering work. Figure 4 presents in schematic form the influence of excavation on the surface above the tunnel.

5.1 *Influence of support system stiffness and rock pillar in front of the working face*

Influence of the supporting system stiffness on amount and time depended behaviour of deformations is essential for an adequate planning of construction. Increased stiffness of supporting system could be achieved in several ways:

- By installing the supporting system, which ensures a quick undertaking of additional loads, which are the consequence of the excavation;
- By excavating and supporting its sections, e.g. excavation with side gallery, where balance is reached in smaller cross sections;
- By installing the auxiliary support elements with low deformability for increasing stiffness of rock pillar in front of the working face;
- By combining it all.

The question of the intensity of increasing the stiffness of rock pillar in front of the working face by installing the auxiliary supporting elements, which allow normal evolution of the technological process of excavation and support, remains. This understanding is essential for normal operation with fewer interruptions and more continuous construction work.

So far it hasn't been determined, how increasing stiffness of rock pillar in front of the working face by installation of auxiliary support elements effects on technology of excavation and supporting. This understanding is essential for normal operation with fewer interruptions or more continuous construction work.

5.2 *Results of back geotechnical analysis*

3D analysis of stress strain relations were made with software PLAXIS Tunnel 3D, Version 2.0.

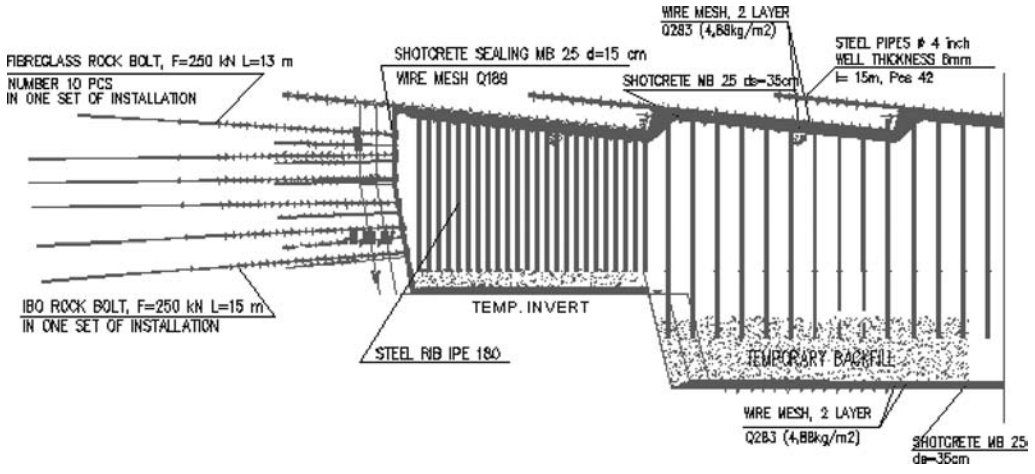


Figure 5. Installation of support system, which ensures quick undertaking of additional loads due to excavation.

Table 1. Input parameters for calculation with SSC model.

Model parameters	Clay schist and mudstone
Unit weight γ [kN/m^3]	24
Cohesion c [kN/m^2]	28
Angle of the internal friction φ [°]	26
Modified swelling index $\kappa^\bullet$ [/]	0,035
Modified compression index $\lambda^\bullet$ [/]	0,04
Modified creep index $\mu^\bullet$ [/]	0,0003

Table 2. Strength support with different stiffness.

Support type	EA [Kn/m]	EI [Knm^2/m]
PIPE ROOF 2X	10.480.000,00	406.134,55
PIPE ROOF 1X	4.520.000,00	31.704,91
SHELL + IPE180 (ES.C. = 3000 MPa)	3.097.500,00	17.648,75
SHELL + IPE180 ES.C. = 7000 MPa)	4.497.500,00	31.940,42
SHELL + IPE180 (ES.C. = 15000 MPa)	7.297.500,00	60.523,75
SHELL + TH 21 (ES.C. = 3000 MPa)	1.541.400,00	11.430,65
SHELL + TH 21 (ES.C. = 7000 MPa)	2.941.400,00	25.722,32
SHELL + TH 21 (ES.C. = 15000 MPa)	5.741.400,00	54.305,65

Geotechnical input parameters for calculation of stresses and strains in supporting system and surrounding rock were partially determent in previous investigations. The values are presented in Table 1.

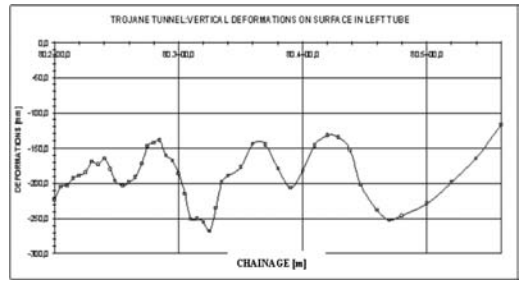


Figure 6. Measured subsidence on the surface along the longitudinal axe of the tunnel tube.

The simulation of excavation and primary supporting were carried out in such manner that first, the excavation and supporting in top heading in the length of 10 m were performed.

This was followed by the excavation and installation of supporting elements at bench, invert and top heading for 10 m more. Excavation and supporting step was 0,8 m. Deformations were in amount of 200–250 mm in the tunnel and 150–200 mm on the surface. These values are similar to those measured at many points. A part of these measurements is presented in Figure 6, where we could see irregular subsidence, which is a consequence of the extremely unfavourable geologic and geotechnical conditions on this section.

The way of excavating and supporting was the same at this section, but over covering of the pipe roof in the sections of bigger deformations was greater, even in the range of 8 m. This caused the stiffness to increase in the roof section of top heading together with primary support, which contained 2 steel segments IPE 180, 2 micro piles, wire mesh and shotcrete of final thickness of 35 cm.

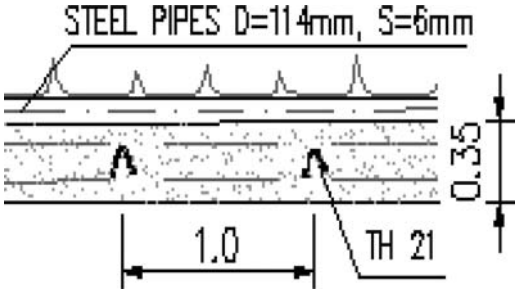


Figure 7a. Standard support elements with steel pipes, steel rib, wire mesh and shotcrete.

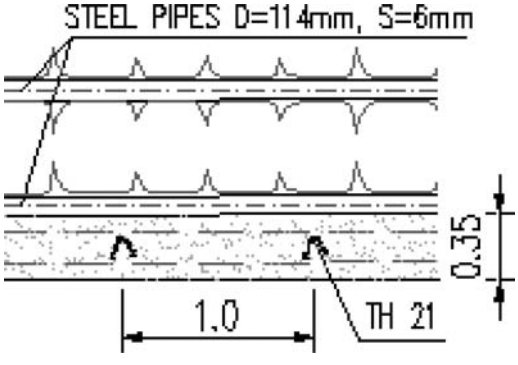


Figure 7b. Support elements with double steel pipes, TH21 steel rib, wire meshes and shotcrete.

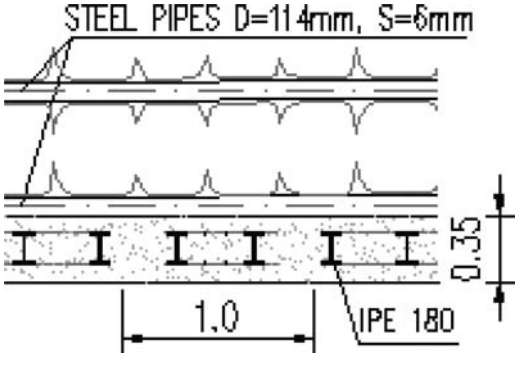


Figure 7c. Support elements with double steel pipes, double IPE180 steel rib, wire meshes and shotcrete.

The results of calculation are presented in figure 9 in form of deformation field. In calculation was also included passive resistance of rock bolts and shot concrete lining in working face in amount of 250 kN/m^2.

Comparison between deformation fields obtained with consideration of single pipe roof and over covered

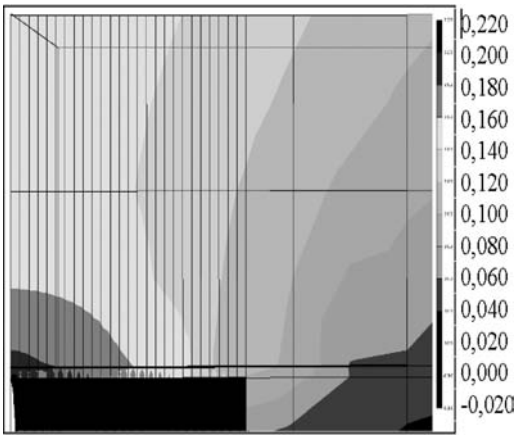


Figure 8a. Deformation fields for normally over covered pipe roof.

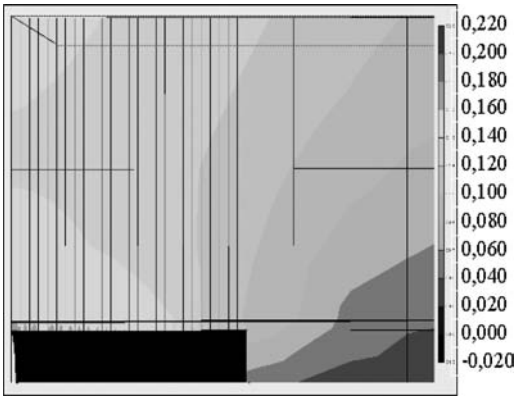


Figure 8b. Deformation fields for fully over covered pipe roof.

pipe roof shows us that influence of increasing stiffness in soft ground is important. Deformations on surface are 20–30% smaller when double pipe roof is used. This was also established during the construction, where in sections with over covered pipe roof deformations were smaller.

Figure 8a and Figure 8b shows differences in deformation fields for normal over covered and fully over covered pipe roof.

5.3 *Time dependent processes*

Development of deformations at the time of excavation and primary supporting of the tunnel is distinct in carbonic rock, since evolution of deformations is completed only in time period of 180 days or more.

This was also established in analysis with finite element method, where soft soil creep model was used.

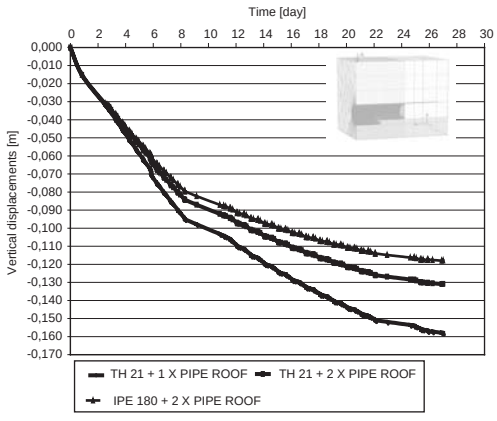


Figure 9. Time dependent surface displacements calculated for different stiffness of the primary lining.

In calculation the hardening of shotcrete was simulated, which gives us increased stiffness of support. During the construction, the support stiffness was also increased with installation of stiff steel segments (2 IPE 180 on section of excavation 0,8 m). The weakness of this combined steel and shotcrete system is that quality of filling in the empty spaces around the steel segments is not easily achieved.

6 CONCLUSIONS

- Tunnel construction in specific conditions such as in low bearing time dependant rocks under habited area depends of the technological procedure and primary support lining, which were used.
- The area of the surface displacements caused by tunnel excavation is closed to geological and geotechnical conditions and type of surface relief with dipping of the natural slopes and local stabilities.
- The results of presented numerical analyses of the surface displacement caused by tunnel construction were usable. Time dependant displacements which were presented help us to make danger volume assessment of objects on the surface.
- Comparison between calculated and measured displacement show us, that this method can be used in similar geological and geotechnical circumstances.

REFERENCES

Brinkgreve R. & Vermeer P. 2004. Plaxis 3D Tunnel-Version 2. Set of manuals. Plaxis bv Delft, Netherlands.

Karakus M. 2006. Appraising the methods accounting for 3D tunnelling effects in 2D plain strain FE analysis, Tunnelling and Underground Space Technology, Article in press, Elsevier, pp.10.

Kim, H.J., Eisenstein, Z. 1998. Prediction of lining loads from case histories. World Tunnel Congress'98, Sao Paolo, Brazil, pp. 299–304.

Whittaker, B.N., Frith, R.C., 1990. Tunnelling-Design, Stability and Construction. The Institution of Mining and Metallurgy, London.

Wittke W. 2000. Stability Analysis for Tunnels. Fundamentals. Verlag Glückauf GmbH. Essen.

Wittke W. 2002. Statik und Konstruktion der Spritzbetonbauweise. Verlag Glückauf GmbH. Essen.

Underground Space – the 4th Dimension of Metropolises – Barták, Hrdina, Romancov & Zlámal (eds)
© 2007 Taylor & Francis Group, London, ISBN 978-0-415-40807-3

Deformation behavior of west Mao Mountain highway tunnel in gravel deposits layers during excavation

L.Y. Tong, S. Y. Liu, C.H. Shen & L.M Liu
Transportation College, Southeast University, Nanjing, Jiangsu, P.R. China

ABSTRACT: Construction of the large-span tunnel and other underground space in urban areas is of particularly challenge because it has impact on the adjacent existing buildings, public transportation and resident living. Accordingly, stability and deformation behaviors of the surrounding rock and soil are the major concerns for the tunneling construction control. The experiences and techniques of large-span tunnel construction are mostly accumulated from rock and soil tunnel construction. However, relatively rare experiences have been reported on gravel tunneling. A case study of west Mao Mountain tunnel on the Ning-Chang highway, China, is carried out in this paper. Systematic monitoring on the displacements of ground surface and surrounding rock is undertaken for evaluation the deformation behavior of gravel tunnel during excavated. Moreover, with the measurement data, displacement-based back analysis is introduced to get the Young·s modulus of gravel deposits. The findings are useful for design optimum and construction control for this project or other projects with similar conditions.

Keywords: Large-span, gravel deposits, west Mao Mountain Tunnel, deformation, back analysis.

1 INTRODUCTION

A number of urban tunneling and other underground space construction take place as the social demand for public transportation and communication increases, such as large-span highway tunnel, subway, underground supermarket and parking lots, civil defence projects, etc. Accordingly, the adjacent structures, ground surface transportation and even resident living are subject to the surrounding rock and soil movements and potential damages due to tunneling. In general, the tunnel and underground space projects are constructed in rock or soil stratum. However, gravel deposits, which kept properties between rock and soil, are often encountered at such locations as floodplain, valley, piedmont and seacoast. The typical projects involved the Paghuashan tunnel for Taiwan High Speed Rail project, the tunnels traversing Yangtse Rive in Nanjing or Wuhan, China. Valuable knowledge and experiences for rock or soil tunnels have been already accumulated. However, the experiences for the design and construction of the gravel tunnel are still lacking.

The west Mao Mountain tunnel in the Ning-Chang Expressway is selected as an example in this study. With the displacement measurement data that carried from gravel excavation, deformation behavior of the surrounding rock is discussed in detail. Then, based on the vault settlement data, back analysis is undertaken to get the Young·s modulus of gravel deposits using the SHUGUANG FEM software designed by Tongji University of China.

2 BACKGROUND OF WEST MAO MOUNTAIN TUNNEL PROJECT

The Ning-chang expressway travels across the hills of south of Jiang-su province, China, of which the most critical project is the Mao mountain tunnel with mining over 1.5 km. The tunnel consists of a major twin-track tunnel with typical oblate cross-sections of 170 m^2 excavated faces and one emergency interpenetration tunnel between the uplink and downlink lines. Among the two subsections, the west Mao Mountain locates at the hillside of the Tao-hill with maximum span of 17.21 m and maximum height 12.04 m, the uplink and downlink of which contain three driveways respectively. The space between the tunnel axial lines of the two tracks is 51 m maximum and 34.35 m minimum. The total length of the west Mao Mountain is 1034 m.

According to the investigations and tunnel excavated areas, the characteristics of the west Mao Mountain tunnel can be summarized as follows:

- ultra-shallow overburden. The overburden mostly varies from a few meters up to a maximum of approximately 50 m. 80% of the tunnel route is under 50 m, especially, part of the section is

opencast (35 m length). The length of the overburden under 7 m of the downlink reaches 115 m.
- large-span, oblate shape.
- complex geological conditions and low classification of the surrounding rock. 52.7% of the surrounding rock is type II and 26.8% is type III.

Combined with the topography and the geological conditions, the west Mao Mountain tunnel was excavated and supported following the principles of the New Austrian Tunneling Method (NATM), except that the portal sections and ultra shallow overburden sections, where the strongly pre-support technology using large steel pipe shed or advanced grouting small pipe was applied. Moreover, at the opencast area, the covered excavation method (cover first and then excavated) is adopted. The composite lining structure consists of the initial support system and the inner reinforced concrete lining, the former structure includes rock bolts, wire mesh, shotcrete, and steel arch girder. The EVA waterproofing membrance are in the gap between the initial support and the inner lining. The excavation scheme is cross diaphragm (CRD) method. Fig. 1 shows its typical cross section geometry and the excavation steps.

3 GEOLOGICAL AND HYDROLOGICAL CONDITIONS

3.1 *Stratum and lithology*

The route of the west Mao Mountain Tunnel from west portal to east portal passes through many rock formations. These are gravel deposits, conglomerate, andesite and tuff formations. Among these formations, gravel information is a rare occurrence in tunneling, which makes the excavated workings difficult. The total length of this layer is more than 500 m and the maximal buried depth is greater than 30 m. The cause of gravel formation is eluvial on the piedmont. The color of the gravel deposits is mainly dust-color, or gray-purple. It is formed with loosely pebbles and gravels cemented by clay and sandy clay. The percentage of the gravel block is 20∼50% and with the depth increases, the percentage is reaching 50∼70%. The size of gravel particles is from fine to large coarse, the diameter of which is 5∼20 cm, some reaches 50∼80 cm. In general, the diameter of the block at the top of the deposits is smaller than that at the bottom. The gravel formation consists of mainly gray to white quartz sandstone and grey to purple clastic sandstone. Due to very high content of gravel particles, the original gravel formation behaves as generally hard and brittle. Moreover, the other rock stratums have large numbers of joints.

3.2 *Geological structural features*

The tunnel locates at the active Mao Mountain fault zone. However, there are few major faults crossing the tunnel alignment except in the vicinity of the east portal area, where an inverse fault locates between the Pu-kou group conglomerate and the Long-wang-shan group tuf. Correspondingly, many unrecorded small faults were found during tunnel excavating. Generally speaking, the geological conditions change along the tunnel route drastically.

3.3 *Hydrological conditions*

The groundwater is mainly porous phreatic water and bed rock fissure water. The underground water quantity is small controlled by rainfall mainly. However, in view of the characteristics of shallow overburden, particular area with weak structural plane combination is deserved to considering.

3.4 *Rock mass classification*

Considering the engineering geological and hydrogeological conditions, rock mass structure, RQD index and other influencing factors, the appropriate classification of the surrounding rock is proposed as Table 1. Class II, mainly consisting of gravel deposits, signifies very poor conditions. The excavation face is unstable without pre-supporting measures. Class III signifies poor conditions, mainly consisting

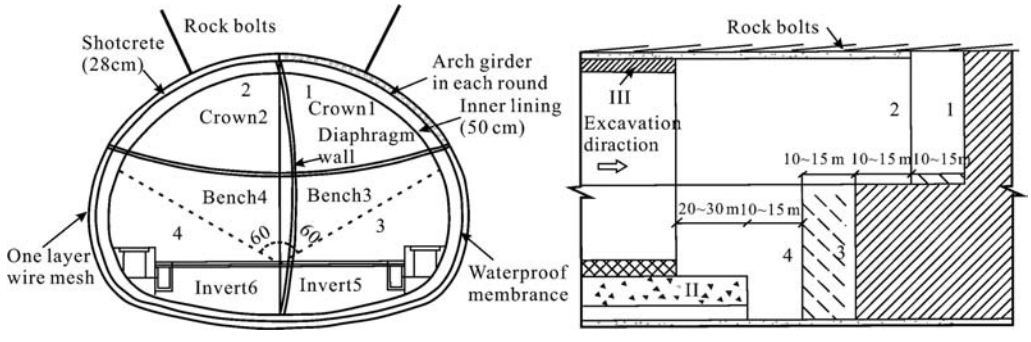


Figure 1. Typical cross-section of west Mao Mountain tunnel excavated by CRD method.

of strongly weathered conglomerate and tuff, which requires pre-supporting measures also. In Class IV, the underground conditions are to be considered good and the excavation face is always stable without pre-supporting.

4 MEASUREMENT AND ANALYSIS OF DEFORMATION BEHAVIOR OF WEST MAO MOUNTAIN TUNNEL

4.1 *Main monitoring scheme*

Systematic in-situ monitoring is an integral part of NATM. According to the geological conditions and surrounding environment, the original design sets up primary monitoring management value. During the excavation and support workings for the mined tunnel, the continuous measurements allowed the modification of the monitoring management value and to assess the original design assumptions. Three kinds of displacements are measured: ground surface settlement, vault settlement and horizontal convergence, shown as Fig. 2. In addition, monitoring of stress and strain on the rock-lining-structure contact has been carried out by installing rock pressure cells, strain gauges and steel bar gauges at main sections. So the stress distribution is studied by the measured surrounding rock pressure, shotcrete-lining stress, steel arch stress and inner lining stress.

The installation instruments, the locations and the space can be adjusted according to the actual engineering conditions. The monitoring frequency can also be changed according to the alert value and the measurement data. For the west Mao mountain tunnel, monitoring cross-sections for the ground surface settlement measurement were provided within the west and east portals area, the ultra shallow area, with an average space of 10 m. Moreover, the number of the sections at every monitoring area should be larger than 3. The cross-sections for vault settlement and horizontal convergence measurement were generally installed at regular intervals of about 5∼10 m at the class II or III surrounding rock area along the longitudinal axis. The monitoring sections consisted of five to seven displacement monitoring points for the three-dimensional (3D) monitoring of the tunnel.

Table 1. Summary of the rock mass classification results in the project area.

Route	Total length (m)	Surrounding rock type II	III	IV	Percentage of Class II and III
Uplink	452	215	62	175	61.3%
Downlink	582	330	215	37	93.6%

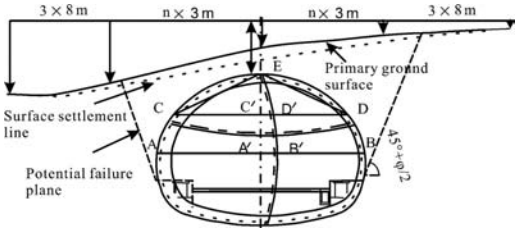


Figure 2. Scheme illustration of displacement monitoring system.

4.2 *Transverse surface settlement measurement and characteristic results*

Due to shallow overburden and poor geological conditions, the safety of tunnels itself and adjacent structures are subject to ground movements when constructing. In the beginning, the working field clearance in the west portals resulted in ground collapse, which signified the importance of the pre-support systems for gravel deposits. With the strongly pre-support system using large steel pipe shed or advanced grouting small pipe, which formated curtain effect, the ground settlements had been controlled to a range from 0 to 40 mm almost, and only few points reached to a maximum of approximately 50 mm. The results show that the deformation was controlled under safety and expected estimates. However, the settlements at the area with NATM system instead of strongly pre-support system were relatively larger, which also didn't reach the limit values. The transverse settlement range is about 36 m symmetrical relative to the tunnel axial line, which is influenced by the overburden. So the interaction between uplink and downlink tunnels is very weak at the space of 34.35 m to 51 m.

Just shown as Fig. 1, the tunnel cross-section has such sequential excavation and NATM supporting stages: crown 1, crown 2, bench 3, bench 4 and invert, reducing the open surface of each face, thereby decreasing the potential for collapse. The distances between crowns, benches and invert excavation were restricted by logistics and settlements monitoring. The measurement data showed that the settlements caused by crown 1, crown 2, and the rest stages were 11 mm, 7 mm, 5∼12 mm respectively (shown as Fig. 3). The longitudinal settlement scope along the route was about 10 m before the excavating face and 20 m after the excavating face, which was influenced by the production rata. That is, the sufficient space was required to at least 30 m for regular advances.

Such information indicated that the diaphragm wall, invert filling and arch support are very important for deformation control, and the strongly pre-support system and CRD method conforming to NATM principles were most appropriate and advantageous for such large-span tunnel in gravel deposits.

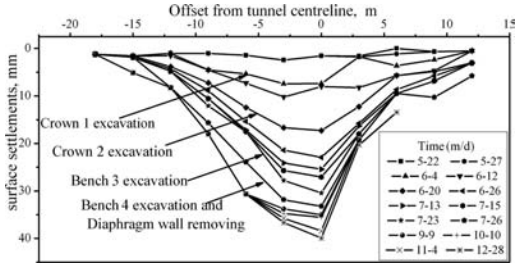


Figure 3. Measured ground surface settlements due to excavation of the different stage (cross section of FK24 + 797).

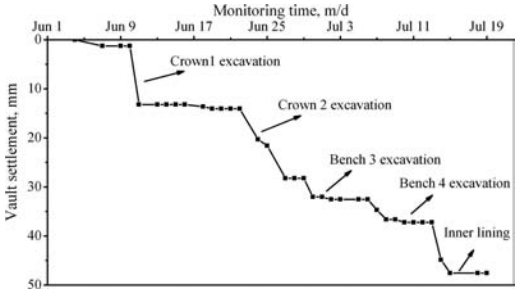


Figure 4. Vault settlements due to excavation of the different stage (cross section of FK24 + 797).

4.3 *Vault settlement measurement and characteristic results*

The characteristics of vault settlement were similar to that of the ground surface settlement. Moreover, the vault settlement value at the west portals supported by large steel pipe shed was 10 mm smaller than that at the cross-sections supported by normal NATM method. The maximum total vault settlement was approximately 33 mm. In fact, the actual value was approximately 50 mm because of the installation of monitoring points was slightly delayed. The measurement data showed that the vault settlements caused by crown 1, crown 2, benches excavation and diaphragm wall removing, were 5∼15 mm, 5 mm and 17 mm respectively (as shown in Fig. 4). The abrupt increase of the settlement after a period of apparent stabilization indicated that next excavation stage was beginning to process. The vault settlement results also indicated that the sequential excavation and predesigned support methods were most advantageous at the gravel formation.

4.4 *Convergence measurement and characteristic results*

The characteristics of horizontal convergence measurement were similar to that of the ground surface and vault settlements (as shown in Fig. 5). The maximum total convergence value was about 30 mm. The

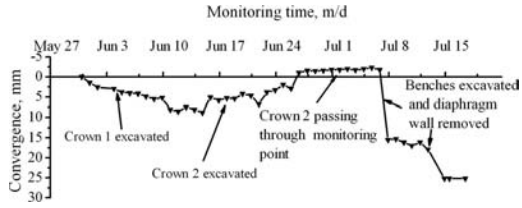


Figure 5. Convergence due to excavation of the different stage (cross section of FK24 + 797).

developing process can be described as: The convergence measurement was continually increasing at the crown1 steps; then, when the crown 2 was excavated, with the supporting of the diaphragm wall, the convergence was abnormally decreasing and when the latter crown 2 face passed through the crown 1 face, the value became inverse; After that, with the excavation processing, the convergence tended to stabilization until the benches were excavated and the diaphragm wall was removed; Finally, after the convergence was stabilized, the inner lining working was undertaken.

5 DISPLACEMENT-BASED BACK ANALYSIS AND EVALUATION OF THE RESULTS

According to the field measured displacements mentioned-above, the back analysis was carried out using the GeoFBA2d software, that is, the SHUGUANG FEM software designed by Tong-ji University, China. Several general optimizing methods are provided, including damped least square method, genetic algorithm, simulated annealing genetic algorithm, mixed genetic algorithm, and Simplex method. This paper selected the genetic algorithm for back analysis. The purpose of back analysis was to obtain the actual Young's modulus of the surrounding rock and to tell the engineers what would happen in subsequent construction stages by utilizing the information obtained in the former stages.

5.1 *Computational model*

A set of assumptions was made as follows:

- the gravel information can be considered as isotropic media, the constitute model of which is elastic-plastic Drucker-Prager model.
- the rock bolts can be simulated as cable element. The initial support system including steel arch and shotcrete can be simulated as beam element, just as the diaphragm wall. The contacts between rock bolt or initial support and surrounding rock, initial support and inner lining, can be simulated as Goodman element. The invert filling and inner lining concrete are simulated as solid element, parameters of which are C20 and C30 concrete, respectively.

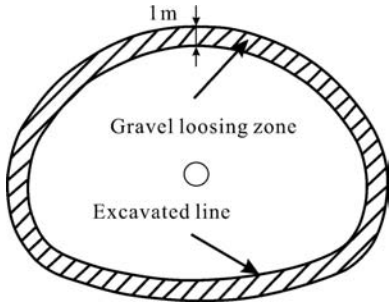


Figure 6. Illustration of two-medium model considering surrounding loosing zone.

- the release loading coefficient is introduced to simulate the three dimensional effect of the excavation in the 2-D model. In this paper, the coefficients pre and after the initial support system installed were 0.3 and 0.5 respectively. The residual 0.2 was for the inner lining.

Taking into account rock loosing zone in the surrounding rock due to tunneling, this paper presents the displacement back analysis based on the two-media model (shows as Fig. 6). The loosing zone is 1 m out of the excavated line. The modulus of the residual soil within the excavated line was the same as that of the loosing zone. The vault settlement was applied for back analysis.

Before back analysis, the measured data should be modified according to the following equation:

$$\mu=\mu_m+\mu_1+\mu_2 \quad (1)$$

where μ_m is the field measured value, μ_1 is the value caused by the delaying of the measuring points installation, μ_2 is the value caused by the former excavated faces which did not reach the measured point. In this paper, the modified scheme was to increase the measured data by adding the value measured at the first day.

5.2 *Strategy and process of back analysis*

The typical cross-section, FK24 + 797, was selected as an example for back analysis, the sequential excavation stages of which can be simplified as follows:

step1: crown 1 excavating; step2: crown 1 initial supporting and diaphragm wall setting; step3: crown 2 excavating; step4:crown 2 initial supporting; step5; bench3 excavating; step6: bench3 initial supporting; step7: invert5 lining; step8: invert5 concrete filling; step9: diaphragm wall removing; step10: bench4 excavating; step11: bench4 initial supporting; step12: invert6 lining; step13: invert6 concrete filling; step14: inner lining.

Table 2. Initial estimated material parameters for back analysis.

Material	Young's modulus (MPa)	Poisson's (ratio)	Unit weight (kN/m^3)	Cohesion (kPa)	Internal friction angle (°)
Gravel loosing zone	back analysis	0.35	25	100	35
Primary gravel formation	200	0.35	25	100	35
Invert concrete filling	26000	0.25	20	100	40
Inner lining	30000	0.2	25	5000	55

Table 3. Structural element properties for the back analysis.

Material	Young's modulus (MPa)	Unit weight (kN/m^3)	Cross section area (m^2)	Inertia moment (m^4)
Rock bolt	210000	78	0.000197	/
Initial support	28500	25	0.273	0.00173
Diaphragm wall	28500	25	0.174	0.0004378

5.3 *Results of back analysis*

As the gravel tunnel is generally conducted in stages, field measurement and back analysis are often associated with each of those stages. That is, what is found at stage *i* must or is expected to tell something about what might happen in stages $i+1$, $i+2$, and so on. The comparison between the field monitoring and the predicted displacements then can be conducted. According to the results, the parameters and even the models can be modified so as to obtain reasonably accuracy. The range of the pre-set Young's modulus of loosing zone is $0.05 \times 10^6 \sim 0.2 \times 10^6$ kPa.

Results of the analyses have been partly shown in Table 4. As can be seen from the Table, predicted vault settlement values based on step3 and 4 of the tunnel are in very close agreement with the field measurements. The Young's modulus predicted by the two-media model for gravel loosing zone are 82.35 MPa, 158.24 MPa and 121.76 Mpa respectively. Corresponding to the relative error analysis (shown as Table 4), the average Young's modulus of the loosing zone is 140 MPa. Compared to the primary elastic modulus, 200 MPa, the value decreased 30% due to excavating.

Table 4. Back analysis results based on vault settlement measurement of different excavated steps.

No.	Excavated steps	Modified field measurement (mm)	Predicted displacement (mm)	Relative error (%)	Predicted modulus (MPa)
Based-on step 2	Step-2	14.51	14.23	1.93	82.35
	Step-3	15.35	18.64	21.43	
	Step-4	22.48	24.21	7.70	
Based-on step 3	Step-2	14.51	10.21	29.63	158.24
	Step-3	15.35	15.33	0.13	
	Step-4	22.48	21.36	4.98	
Based-on step 4	Step-2	14.51	11.77	18.88	121.76
	Step-3	15.35	16.7	8.79	
	Step-4	22.48	22.63	0.67	

5.4 *Application of the results: forward FEM analysis*

Moreover, forward FEM analyses of typical cross-sections were conducted using the predicted Young's modulus, which was not included in this paper limited, but the detailed data can be seen in the reference (Li H.B., 2005). The deformation trends of ground surface and surrounding rock were predicted and analyzed along the total route of the tunnel. According to the characteristics of displacements and stress distribution, some advices should be presented as follows:

- corresponding to the sequential multi-stages construction of CRD method in gravel formation, the timely invert supporting and filling are important for deformation control. The installation of the diaphragm wall should also be considered as an essential support structure, the integrality of which should be insured at some sections with large deformation. The removing time of the diaphragm wall was also strictly controlled.
- some positions with large concentrated stress at special cross sections should be additional reinforced, such as the vault area, steel arch foot area, partially initial support, joints between vault and diaphragm wall.

6 CONCLUSIONS AND RECOMMENDATIONS

For successful tunneling in difficult geotechnical conditions or in sensitive environments, monitoring and evaluation techniques are indispensable. This paper provides a detailed insight and valuable experience in cycling for future large-span gravel tunnel and other underground spaces construction, particularly in urban area. The experiences gained from such complex geo-monitoring and back analysis workings can be summarized as follows:

- the deformation behavior of the large-span tunnel during constructing at gravel information is obtained by systematic displacements monitoring and back analysis workings. The results also showed that CRD method using the sequential excavation model could be used for the preliminary design of NATM tunneling for the conditions used in this research. Especially, at the shallow overburden sections and portals, the strongly pre-supported system using large steel pipe shed or advanced grouting small pipe is also recommended.
- displacement back analysis based on the two media model, which considering losing zone, is introduced. The predicted average Young's modulus of the gravel loosing zone is 140 MPa, which is decreased 30% compared to the primary gravel stratum. The predicted displacement also has good agreement to the field measurement data.
- finally, in order to preventing accidents and reducing maintenance costs, the excavation of this critical gravel tunnel should consider all things, such as the geological conditions, construction method, support system, field displacements and stress monitoring, working productivity, facilities, management approach and the overall performance.

REFERENCES

L.Q. Zhang, Z.Q. Yue, Z.F. Yang. Displacement-based back-analysis method for rock mass modulus and horizontal in situ stress in tunneling – Illustrated with a case study[J], Tunnelling and Underground Space Technology, 21 (2006) 636–649

H.B. Li (2005). Application of Displacement Back Analysis of Taking into Loosing Zone for Tunnel Engineering [D], Tong-ji University, China,2005

Y.C. Chen (2001). Engineering behavior of tunnel construction in gravel deposits[J], building and water conservancy, Institute of building and water conservancy in Taiwan, vol.28, no.2, pp.5∼1

Underground Space – the 4th Dimension of Metropolises – Barták, Hrdina, Romancov & Zlámal (eds)
© 2007 Taylor & Francis Group, London, ISBN 978-0-415-40807-3

EPB-Tunnelling control and monitoring in a urban environment: the experience of the "Nodo di Bologna" construction (Italian High Speed Railway system)

V. Marchionni
S. Ruffillo scarl, Bologna, Italy

V. Guglielmetti
Geodata S.p.A., Turin, Italy

ABSTRACT: The realisation of tunnels in a sensitive urban environment and complex geological conditions requires an accurate, integrated, excavation management approach. The mechanized tunnelling permits to minimize the impact of the excavation on the surface existing structures but it is mandatory to guarantee an accurate control of the face stability and a constant monitoring of the effects on surface. This paper puts in evidence that the choice of the optimal excavation methodology alone is important but not sufficient; only the rigorous application of excavation procedures, including the strict control of the EPB-machines parameters integrated to the continuous monitoring of the effects of the excavation on surface, in terms of settlements, is the key to the success of a tunnel project, specially in sensitive environment.

The realisation of the "lotto 5" of the High Speed Rail system in Bologna represents an example of the application of the above mentioned integrated methodology for the excavation of two 9.4 m diameter, 6.1 km long, twin tunnels using EPBs.

1 INTRODUCTION

The excavation of tunnels in an intensely urbanized context requires particular methodology in order to minimize the effect on the surface existing structure and facilities.

Mechanized tunnelling technologies have been developed, in the last decades, to control the face stability and that of the roof and to minimize surface settlements. Nevertheless, there are some ground and environmental conditions requiring not only the use of an appropriate excavation technique but also the application of a rigorous and integrated methodology that comprehends: the assessment of risk and development of a risk management plan, specific excavation procedures and real-time monitoring of excavation parameters and surface settlements, the "Plan of Advancement of Tunnel" (PAT), a method that allows to adjust the design and control parameters during excavation.

The aim of this paper is the description of the successful application of this integrated methodology for the realization of the "lotto 5" of the High Speed Rail system in Bologna.

2 THE "LOTTO 5" BOLOGNA HIGH SPEED RAILWAY PROJECT

2.1 *General description*

A section of the new High Speed Rail Line Milan-Naples, which crosses the city of Bologna, an intense urbanized area, is foreseen for the most part underground.

In 2000, the joint venture S.Ruffillo (Acciona-Salini-Ghella) was awarded the contract for realizing the Lot 6 of the Project, under passing the city of Bologna. The Project starts at the North abutment pier of the Savena Bridge (km.$0+000$), south of the city, and ends at the new Central Station (km.$7+375$); it consists of the following main structures:

1. A trench tunnel and a launch shaft (for the TBMs), double track, from km.$0+000$ to km.$0+958$;
2. Two EPB tunnels ("Pari" and "Dispari" tunnels), single track, 9.4 m diameter, starting from km.$0+958$ to km.$7+075$;
3. An Emergency Shaft ("Via Rimesse" Shaft) at km.$4+820$ and a Ventilation Shaft at km.$6+857$;

Table 1. Tunnels characteristics.

Total single tunnel length	6112 m
Start chainage	km.0 + 960
End chainage	km.7 + 072
Excavation technology	EPB
Tunnels axis distance	15 m
Overburden (min-max)	15–21 m
Inner lining diameter	8.3 m
Outer lining diameter	9.1 m
Excavation diameter	9.4 m
Excavation section	69.81 m^2
Max tunnel slope	1.5%

4. A transition shaft (TBM's exit and "Bologna" parking) from km.7 + 075 to km.7 + 235;
5. A conventional tunnel, double track, from km.7 + 235 to km.7 + 350, connecting the transition shaft to the Central Station.

The excavation of the first EPB tunnel started in July 2003 and the second excavation started in November 2003. The completion of the excavation was achieved for both TBMs at the end of may 2006.

2.2 *Geological layout*

Ground conditions are very heterogeneous and comprise soft marine clays, sands and alluvial deposit (mainly gravel).

In the first part of the alignment, up to km.2 + 150, the tunnels are excavated in sea clay and loose sandy deposits (Pliocenic Clay and Yellow Pleistocenic Sands) below the water table while the second part, in Savena river deposits, consisting of mainly gravel and sand layers with a high percentage of fines (lenses of clay and silt).

The heterogeneity of the ground excavated represented a critical aspect because the excavation conditions, in terms of surface settlement response and machine's behaviour, changed very rapidly.

2.3 *Choice of excavation methodology*

The two tunnels start at the S.Ruffillo quarter, south of Bologna, and from km.0 + 960 to km.1 + 500 underpass an electrical power plant and a recently built store. From approximately km.1 + 500 to km.7 + 075, the alignment runs below one of the main Italian railway roads, the Bologna-Florence line, that lies on an 8–12 m high embankment.

The average overburden thickness ranges from 15 to 21 m (at the bottom of the embankment), with a minimum value of 5 m in the first 100 m of excavation.

In order to minimize the impact on surface, the Client imposed a mechanized excavation methodology (EPB, Slurry shield or Mix shield), i.e. a technology to minimize the needs to modification of the ground and the disturbance to the ground water regime.

Table 2. Main characteristics of RME370SE machines.

Cutter-head diameter	9.377–9,402 m
Tail shield diameter	9.364 m
Shield length	10.7 m
Number of Thrust Jacks	36
Length of cylinders	2250 mm
Total machine length (w/ back up)	195 m
Max EPB pressure	3.5 bar
Max penetration rate	0.08 m/min
Max thrust force	100.000 kN
Max cutterhead Torque	24.000 kN*m
Cutting head opening ratio	34%
Number of earth pressure sensors	8
Number of longitudinal grouting lines	6
Number of foam injection lines	8

The Contractor has chosen two EPB Machines, due to the following:

– geological and geotechnical conditions (variable ground conditions, and the presence of gravel up to 100 mm diameter.);
– the respective experiences of the two lead Companies in the Contract J.V. for the underground works (Acciona in Madrid and Barcelona) and Ghella (in Valencia and Caracas);
– environmental problems related to the slurry disposal and the treatment plant.

The two tunnels are parallel for most of the alignment (up to km.6 + 650 approx), and the distance between the tunnels is only 5.6 m. The minimal distance between the tunnels represented one of the most critical aspects of the excavation.

The-twin tunnel solution was imposed by the Client and the Designer (TAV S.p.A. and Italferr S.p.A.) due to safety reasons for the train passengers and because the realization of a unique 14 m diameter double-track tunnel, with minimal overburden (1–1.5 diameter), would have caused critical differential settlements for the existing infrastructures, facilities and buildings on surface.

As a matter of fact, during the excavation it was verified that, due to the small distance between the 2 tunnels, the ground encountered by the 2nd EPB machine was more disturbed by the 1st tunnel excavation and presented lower geotechnical characteristics; as a consequence of this effect, during the EPB excavation it was necessary to apply more restrictive control parameters and a higher level of excavation control of the second tube.

2.4 *EPB machines characteristics*

For the excavation, two LOVAT Machines, RME370SE, 19600 (Emilia) and 19700 (Felsinea), were chosen. The main characteristics of the EPB machines are shown in Table 2.

3 EPB EXCAVATION MANAGEMENT

3.1 *First phase of the project*

The excavation was done in two distinct periods:

1 from July 2003 up to October 2004: from pk.0 + 980 up to pk 3 + 050 (1st TBM) and pk.2 + 440 (2nd TBM);
2 from May 2005 up to May 2006 (end of excavation – pk. 7 + 375).

A number of geotechnical complexities, contractual constraints and settlement problems stopped the excavation in October 2004 when 32% of the 1st tunnel and 23% of the 2nd one were completed.

With the aid of the opinion received by the Dispute Review Board, the excavation stoppage was resolved at the end of May 2005.

On resumption, the Contractor Acciona-Ghella set up a rigorous and extensive monitoring system, in terms of TBM parameters and effect on surface implemented with the assistance of a Consultant (Geodata Spa) responsible for EPB excavation operation control.

3.2 *The excavation control system*

The factors that were identified as essential to restart and strict control of the excavation, have been:

1. Production of a detailed TBM Advance Plan (PAT-Geodata Spa) for each 300 m of excavation and for each TBM, so that all the parameters and design issues related to tunnelling were effectively addressed before the excavation. During the excavation of every 300 m of tunnel, the Consultant back-analysed the main TBM parameters, the geotechnical conditions and effects on surface, to check the appropriateness of the used and recommended values. After that, they defined, also considering the interferences with the existing surface structures, the excavation procedures and TBM parameters for the next 300 m stretch;
2. The constant presence of a tunnel engineer in order to collect all the excavation parameters and control the respect of working procedures for all tunnelling phases to ensure that the TBM operations were carried out in a proper manner;
3. Setup of a Technical Desk for reviewing and analysing both the daily and weekly TBM excavation reports, in which the range of operating conditions, recorded parameters, and any significant events, and the relevant effect on surface (settlements, distortion on structures, Volume loss) were summarised.

A weekly meeting (attended by technicians from the Consultant, the Client and the Contractor), where the week's performance was reviewed and the draft PAT for the future excavations was analysed, completed the control procedures.

Table 3. Alarm and Attention Thresholds for controlling EPB pressure above water table.

	Attention threshold (bar)		Alarm threshold (bar)	
	Lower	Upper	Lower	Upper
TBM 1	1,2	1,6	1,0	1,8
TBM 2	1,4	1,9	1,2	2,1

3.2.1 *Parameters*

The fundamental parameters controlled during excavation were: Face Support Pressure, Muck "Apparent Density", Extracted Muck Weight, Tail Void Grouting volume and pressure.

Initially, on the basis of all geotechnical and general design data and using numerical simulation results, reference values for face support pressure were calculated and an operational range, between upper and lower levels (the so-called Attention Thresholds) were identified.

An Alarm Thresholds was also set, that when reached, the excavation would stop automatically (see an example in Table 3). The reference support pressure was defined and measured in the highest sensor located within the bulkhead, 1.5 m below the crown.

To keep the face pressure within the operational range, the TBM operators used the normal control devices, such as the machine advance speed and the screw conveyor rotation speed. During stops, either long, e.g. for maintenance, or short, e.g. for ring assembly, bentonite slurry was automatically injected into the excavation chamber. This operation was giving an immediate response in terms of re-lifting face pressure and was much more efficient than foams, used only for ground conditioning. During excavations it was verified the face pressure to be of paramount importance in controlling the surface settlements. In spite of the high advance rates, the EPB pressures, for both TBMs, were maintained above 1.5 bars, often 2 bars, minimizing the pre-subsidence phenomenon.

In order to minimize the risk of air bubbles in the chamber crown due to an excessive use of foam, an air valve was periodically opened to evacuate the air.

To control how full the plenum was, the "apparent density" parameter (Geodata 2003) was utilised. By measuring the face pressure at different heights and dividing by the height difference between them, calculated the apparent density of the muck inside the chamber. A vertical pressure gradient and an "apparent density" near or less than unit, identified the accumulation of air bubbles within the plenum.

Also the amount of extracted muck is fundamental for controlling the face stability and settlements; consequently an additional balance and one volumetric scanner were installed on the main belt conveyor of each TBM, before the restart. Data from only one of

the balances was used (the 2nd one being for reserve), and the values measured were compared in real time to the theoretical excavation volume, defined as the product of the section area of the excavation per advance speed multiplied by the in-situ density of the material.

The same control was also applied to the scanner measurement for a double check. To control the muck extraction, the TBM operators controlled the rotation of the screw conveyor (proportional to the muck extracted) and the TBM advance speed (proportional to the total excavated quantity of muck), maintaining the face pressure within the range of attention threshold values.

Backfilling around the segments, an important element for controlling surface settlements, was carried out using a longitudinal grouting system composed of 6 double-oval lines. During every excavation cycle, about 6.15–6.5 m^3 (theoretical value as a function of external teeth wearing) of grout was pumped up to a pressure value at the crown 0.5 bar higher than the measured EPB pressure. The quantity of grout pumped was automatically recorded and visualised. Furthermore, for double-checking the grout volume values recorded, a manual measurement of the grout level in the basin has been implemented before and immediately after the single excavation cycle.

3.3 *Monitoring system*

A specific monitoring system was developed in order to get all the required information in real time into a specific database on web-platform (GIDIE – Golder Associates Srl), to understand the soil behaviour and the potentially-affected-structures response during the different excavation phases and to decide for eventual countermeasures.

All the raw data (geotechnical, structural, topographical and TBM's) were stored in the job-site dedicated server, which was accessed periodically by the GIDIE web database for self-updating in order to allow for a real time on-line query by the authorized users (i.e. the Client, the on site TBM Consultants, the tunnel engineers).

In particular, the following measures and data were collected into the system:

Soil behaviour around the excavation area:

19 geotechnical sections with multipoint extensometers, in-place inclinometers and piezometers;

TBM Parameters:

Almost 200 EPB parameters were constantly recorded (every 5 sec) and made available in real time through the web site to the Client and the Consultant.

Real time surface areas and interferences response to excavation:

1. surface railway embankment, existing buildings and structures settlements and movements;

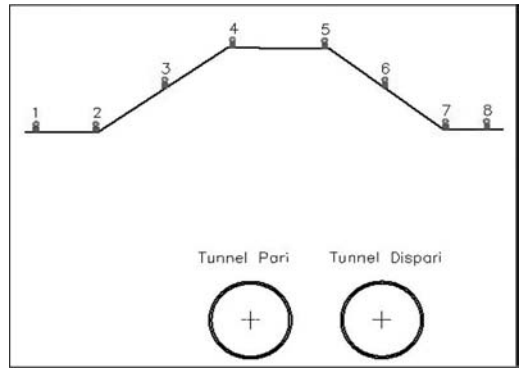


Figure 1. Typical settlement monitoring points through a section on railway embankment.

2. bridges and underpasses settlements and movements.

3.3.1 *Monitoring measurements and alarm levels*

Due to the sensitivity of the urban area above the excavation and in particular of the existing railway embankment, a continuous topographical monitoring system was necessary.

The system was realized through total stations (TS) and topographical prisms installed on the railway embankment, on the buildings and existing structures (bridges and underpasses), potentially affected.

All the measurements were recorded, real time transferred and processed in order to calculate the coordinates for each monitoring point.

Approximately, 150 buildings and infrastructures and 230 topographical sections, spaced at 25 m, perpendicular to the alignment of the tunnels, guaranteed the monitoring of the embankment and the potentially affected area.

Sections with 8, as in Figure 1, or 2 topographical measuring points succeeded one another:

For each tunnel 50 m ahead and 130 m behind the machines' face, the potentially affected area was constantly monitored and all the data automatically downloaded to a web site GIDIE every 3 hrs, with an accuracy of ± 2 mm.

Furthermore, the automatic calculation of Volume Loss (V_p) due to the excavation, according to O'Really and New '82, was performed every 3 hrs. All the data were then analyzed and automatically compared with the predefined alarm levels calculated by the Designer for the different kind of interferences (V_p for topographical sections, differential settlements for bridges and viaducts, distortions for buildings).

For every topographical section the followings graphs and values were automatically visualized on the web site:

– Single point settlements and movements vs. time and TBM advance rate;

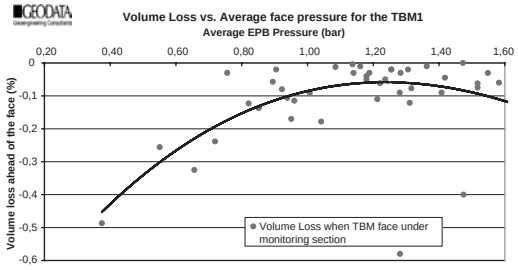


Figure 2. Relationship between Volume loss and average EPB pressure (Volume loss back-analysed from the portion of settlement occurred ahead of the face).

– Volume loss (V_p) vs. time or advance rate;
– Settlement profiles (longitudinal and transversal);
– Geotechnical and structural measurement vs. time.

3.3.2 *Monitoring results*

As a matter of fact, the back analysis of the surface settlements, compared with the excavation parameters, has proven to be the most efficient way to evaluate the response of the ground towards TBM excavation and the interferences of one TBM with the excavation by the other later on.

The excavation control consultant have continuously analyzed the settlements data to correlate volume loss and settlements with the EPB pressure (see Figure 2), taking in consideration also short/long stops.

As shown in Figure 3a, the implementation of stricter TBM excavation controls reduced significantly the settlements to a maximum value of 2 cm and the volume loss to values of about 1,2%, a result absolutely satisfactory considering that most of excavation was performed in granular soils. As already mentioned, even with these stricter controls it was not possible to limit settlements for TBM2 (see Figure 3b) as low as those for TBM 1 because of the stress changes in the ground as result of the 1st tunnel excavation.

3.4 *Compensation grouting operations*

For the excavation of the twin tunnels underneath the railway line in operation, a series of protective measures had to be implemented in order to minimize the effects of the tunnelling operation to the adjacent structures and in particular to railways bridges. These measures comprised of the conventional protection like consolidation grouting, as well as the active settlement control with compensation grouting where the potential damage was relatively high.

One important structure was the railway brick bridge called "Ponte Vecchio" which passes an important inner city street. The bridge spans 2 sections of railway embankment and is 130 m long (9 arches) and the axis of the twin tunnel were about 24 m below ground surface, which yields a cover between the

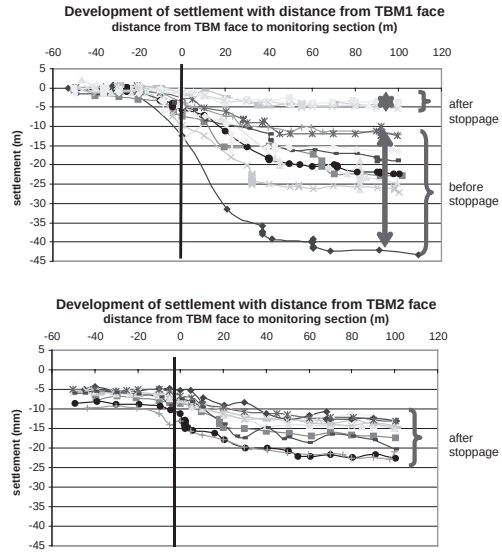


Figure 3. Development of settlements with distance from the face for TBM1: comparison between 1st phase and 2nd phase of the excavation (fig. 3a – top) and TBM2: 2nd phase of the excavation (fig. 3b – below).

footing and the top heading of the tunnel section of about 10 m. The differential settlement between two adjacent piers had to be limited to l/3000, where l denotes the free span of the arch. Moreover, this ultimate limit state has to be covered by a safety factor, reducing the before mentioned limit by another 30%.

As a consequence, the allowed differential displacement between the main arch piers was limited to 5,0 mm, whereas the maximum value for the standard arches was 2,7 mm. Due to these strict limit, compensation grouting was employed, in combination with strict control of TBMs excavation.

A JV of Trevi Spa and Keller Srl were responsible for the compensation grouting. Prior to the arrival of the TBMs, an array of 96 grouting pipes (maximum length of 68 m) in two layers with a spacing of 1,5 m were installed using directional drilling technology, creating a "semi rigid grout cushion" beneath the base of the piers and above the crown of the tunnels (see Figure 4).

The railway bridge was surveyed with a real time hydrostatic levelling system (measurement every 15 min). In order to get a comprehensive view of the deformations occurring on the structure, the hydrostatic levelling system (93 measuring points with a precision of ± 0.5 mm) was arranged at three levels of the bridge, as shown in Figure 5. During the TBMs, passages the differential settlements of the bridge piers were limited controlling the volume and pressure of grout injected through the appropriate

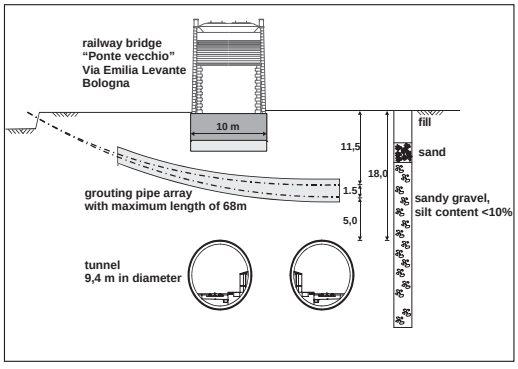


Figure 4. Typical cross section of the compensation grouting.

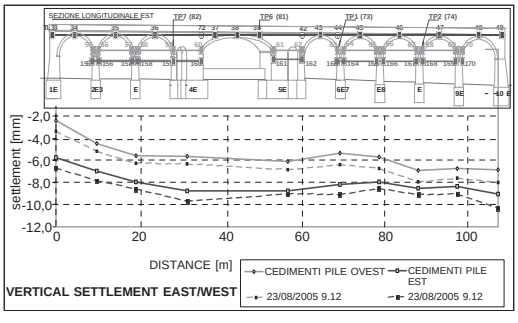


Figure 5. Final settlement profile for the "Ponte Vecchio".

grouting pipes-valves and by rigorously controlling the EPBM excavation parameters.

Continuous monitoring and observation of the settlements and TBM parameters indicated the amount of the lifting using compensation grouting during the excavations. In addition, due to the measured interference of the 1st tunnel on the 2nd one, it was necessary to increase the face pressure in TBM 2 by an additional 0.3bar and to decrease its operational range. After the 2nd TBM excavation, the bridge piers settled by 10 mm maximum with a differential settlement between 2 piers of 2 mm maximum (see Figure 5). The proper use of compensation grouting and excavation parameters demonstrated that settlements of a very sensitive structure could be well controlled.

3.5 *Results and performances*

The average performances of the two machines were 8.2 ring/day = 12.3 m/day (TBM 1) and 9.33 ring/day = 14.0 m/day (TBM 2), taking in account the working days. In the first phase of the excavation, the machines were operated 24 h/day, 5 days/week; the first one was stopped for some time to allow the excavation of the cross-connections by conventional method; the second phase of the tunnel (after the restart in May 2005) was excavated working 24 h/day, 7 days/week, without any planned stoppage (except maintenance and repair).

Best day for both TBMs: 25 rings per day (37,5 m/d)

Best month: 612 m/m for the first TBM (March 2006) and 635 for the second one (April 2006).

Best month for the two TBMs together: 1.182 m/ month in April 2006.

The performance of the two machines during the last three-month reached 3.200 m of twin tunnel!

All the impressive performances were achieved working strictly in EPB mode with the plenum always full of material and under pressure of 1.5 to 1.8 bars at the crown, following the design specifications.

4 CONCLUSIONS

Special technologies have been developed to control the stability of the face and roof of the tunnel in order to minimize surface settlements. The actual application of such technology for achieving the specified goals requires: appropriate ground characterization, risk assessment and development of a risk management plan, appropriate TBM choice, Plan for Advancement of Tunnel (PAT), specific excavation procedures and real time monitoring of excavation parameters and surface settlements.

The experience of the "Nodo di Bologna" construction has demonstrated that following this "design-monitoring-adaptation running method" in one word "the PAT Method", it is possible to control the face stability and the settlements level in urban areas and difficult ground conditions, without any consequences on the machine's performances: on the contrary, the recorded performances have been very near to the best results recorded in the world in similar conditions.

REFERENCES

Marchionni V., Minguez F., Breveglieri E., 2004. The High Speed Rail system in Bologna: an example of a complex urban EPB twin tunnel excavation. I*nternational Congress on Mechanized Tunnelling: challenging case histories* (Torino Nov 2004) – *Proceeding. S173-S180*;

Locatelli L., Ramelli E., Marchionni V., Borgonovo G., Perolo M., 2005. Progressing monitoring of tunnelling under railway embankment. *Les tunnels, clè d'une Europe durable – AFTES – Congres International de Chambèry* (Chambery 10–12 October) – *Proceedings S401*;

Marchionni V., Savignano L., Locatelli L., 2006. Lo scavo e le interferenze con la linea ferroviaria esistente: il monitoraggio della linea per la sicurezza in esercizio. *Gestione del Territorio e Sicurezza del Lavoro: il modello dei cantieri AV/AC di Bologna* (Bologna Feb 2006) – *Proceedings.*

Jacobs M., Kummerer C., Marchionni V., 2006. The application of a hydrostatic levelling system under extreme temperature conditions for the control of a protective measure for the tunnelling under a railway bridge in Italy. *Messen in der Geotechnik 2006 (Braunschweig Feb 2006) – Proceedings*.

Guglielmetti V., Grasso P., Gaj F., Giacomin G. Mechanized Tunnelling in urban environment. Control of ground response and face stability, when excavating with an EPB Machine. *ITA World Tunnelling Congress 2003, Amsterdam April 2003 – Proceedings, S645–652.*

Guglielmetti V., Minguez F., Gregori A., 2005. Best practice in EPB management. *Tunnels and Tunnelling International* (*November 2005, S 21–24*).

Guglielmetti V. Letter to the Editor Tunnels and Tunnelling International (June 2006 S 34)

This page intentionally left blank

Underground Space – the 4th Dimension of Metropolises – Barták, Hrdina, Romancov & Zlámal (eds)
© 2007 Taylor & Francis Group, London, ISBN 978-0-415-40807-3

Monitoring of structures and environment under construction and service of underground transportation projects in Russia

V. E. Merkin
Research Center "Tunnels and Metro", JSC TsNIIS, Moscow, Russia

S. N. Vlasov
Russian Tunneling Association

ABSTRACT: Basic tasks of monitoring are formulated. The information on the results of realization of the monitoring program when building large transportation tunnels in Moscow with regard to the state of underground constructions being erected and environment is presented.

In the package of works on construction of underground transportation projects in large towns of Russia the great emphasis is placed on systematic instrumental supervision (monitoring) of actual state of the structures under construction and natural and urban environment.

Such monitoring is aimed at provision of service reliability of tunnels, ecological safety and preservation of buildings and structures near by the tunnels under construction.

Monitoring is designed for definition of the following actual data:

- physical, mechanical and geometrical characteristics of the constructions under supervision and their comparison with the corresponding design requirements;
- components of stress-strain state of the structure, starting from the moment of erection up to stabilization of its loads. This makes it possible to introduce changes operationally into the design decision during the construction process and if the structure is under service to evaluate its carrying capacity reserve and durability and to propose, if necessary, reasoned measures for repair and rehabilitation works, accounting for the detected defects;
- deformation of ground surface, buildings and utilities;
- changes in groundwater level, air and soil composition.

Comparing the monitoring data with their allowable meanings and prediction, emergency situations might be avoided if timely to respond to the dangerous tendencies (to change the tunnelling mode, to take protective measures, etc).

The normative base for solution of the above problems is considered to be specifications for design and manufacture of constructions, being developed for each project, technological regulations, where sequence and methods for work performance are indicated, and a network of observation stations.

According to the recorded observation results of the latter and with consideration of geomechanical prediction, basing on solution of the problem of joint deformation of "underground structure-soil" system, the state and dynamics of stress-strain state change of the lining and soil during construction is evaluated. Besides are specified the range of devices, the places for their installation and measurement intervals.

The works performed on construction of a set of Lefortovo (1990–2002) and Serebriany bor (2003–2007) transportation tunnels in Moscow, designed by Public Joint Stock Company "Metrogiprotrans", may serve as the most obvious examples of full scale realisation of the monitoring program applied for the new projects.

The peculiarity of those tunnels construction was their location in nature reserve and historical areas of the great town, legislatively protected against man caused interference.

So, for construction of transportation lines in those areas was selected the most sparing method among the advanced ones – TBM boring with the use of precast waterproof lining.

To realise such method "Herrenknecht" Bentonite TBM "S-164" and "S-290" were used for construction of transportation tunnels of Ø14.2 m and a service tunnel of Ø6.28 m respectively.

Accounting for particular engineering and geological conditions of the tunneling route and the

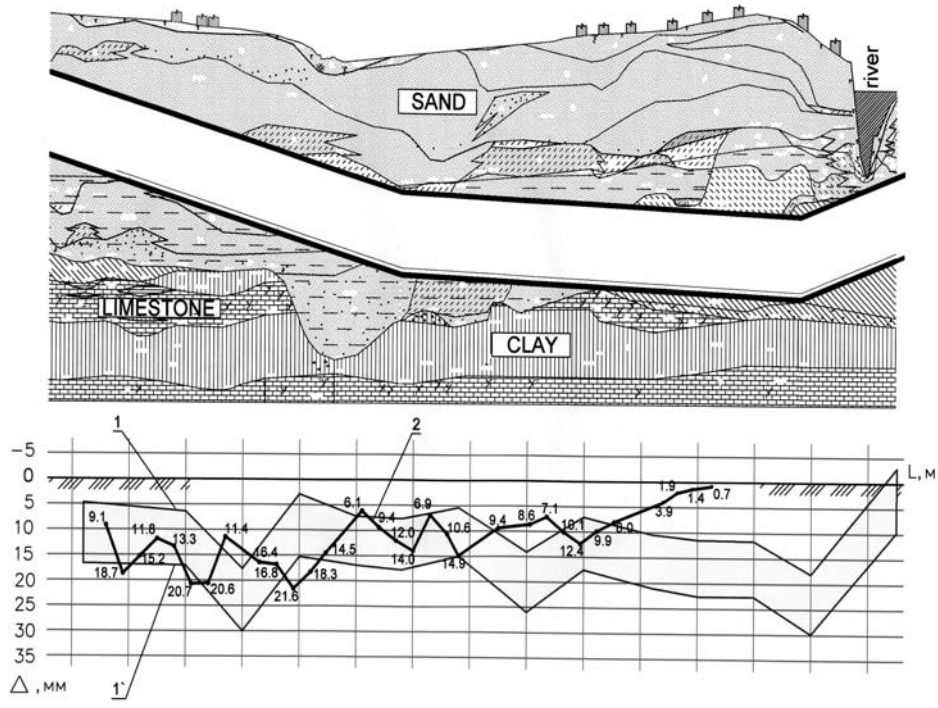


Figure 1. Design (1, 1′) and actual (2) surface settlements under construction of Serebriany bor tunnels in Moscow.

capabilities of TBM and on the basis of geomechanical calculations probable deformations of the soil massif were predicted, among them settlements of surface and bases of buildings and structures, located within the zone of tunneling works effect.

On the basis of such prediction and available results of primary inspection (before the construction start) on the state and ultimate allowable deformations of the structures under operation engineering measures were taken, if required, to ensure their safety (Figure 1).

The calculations assume that soil shift under bentonite shield tunnelling takes place due to size difference of the excavation and the lining to be erected with consideration of partial (pessimistic prediction, 1′) or complete (optimistic prediction, 1) filling of the generated gap by grouting mortar (see the design scheme in Figure 1).

Later on after tunneling of the first 150–200 m that prediction was corrected, accounting for actual measured settlements, which made it possible to raise significantly the prediction accuracy, to specify precisely the face pressure and, in some cases, to reconsider the measures designed for preservation of on-surface structures and utilities.

At present it can be already stated that the adopted technological decisions and work practice and procedures in combination with operational analysis of monitoring data have resulted in driving of Ø14.2 m tunnels by means of "Herrenknecht" bentonite shields with mean advance rate of 8–10 m per day under minimal (not more than 12 mm) surface settlement without emergencies and environment effects.

Measurements in the tunnel have also revealed a certain reserve of lining carrying capacity and showed that the influence of the moving shield on the forces in the lining had been recorded at the length from 100 to 150 m depending on the soil type and route curvature (Figure 2).

When constructing tunnel sections by cut and cover method, the data on the developing deformations of the cut enclosure structures were analyzed and compared with the data, obtained by "PLAXIS" program. As a result their failure has been prevented due to timely installation of additional braces. Besides, surrounding buildings and near by utilities have been saved due to soil strengthening by cementation.

The main task in the process of construction of various infrastructure projects (buildings, underground car parks and utilities) not far from the operating metro lines is to exclude or at least to bring to allowable minimum the construction effect on stress-strain state of the tunnel lining. So, before the work starts there shall be carried out inspection of the actual tunnel condition. The degree of its carrying capacity compliance (with

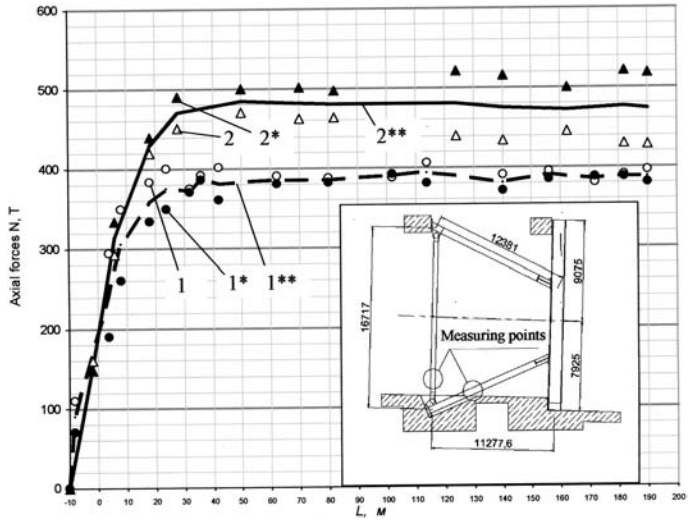


Figure 2. Forces in braces of start trust frame under TBM traveling.
1,1* and 1** – forces in the left brace, in the right brace and mean value in braces of Lefortovo tunnel, respectively.
2,2* and 2** – forces in the left brace, in the right brace and mean value in braces of Serebriany bor tunnel, respectively.

consideration of recorded defects) with the supposed effects of the new construction being defined, special protective measures shall be recommended.

In most cases they comprise compacting and filling cementation of voids and unpacked soil behind the lining, detected by geophysical methods, and monitoring of stress-strain state of metro structures during new construction. Monitoring is in particular stated in the metro instructive documents as the required control element for observance of agreement conditions with regard to the new construction project.

Operational information data on the compliance of the changes recorded in the tunnel state with the metro requirements, for example on permissible deformations of the lining and rail track in the tunnel, are considered to be the criteria for evaluation of the construction effectiveness.

Our large experience gained has proved the necessity in the above mentioned works. Thanks to the latter not only emergency but any extraordinary situations during underground construction in Moscow have been avoided.

This page intentionally left blank

Underground Space – the 4th Dimension of Metropolises – Barták, Hrdina, Romancov & Zlámal (eds)
© 2007 Taylor & Francis Group, London, ISBN 978-0-415-40807-3

Geotechnical monitoring of the excavation exploratory galleries for the Dobrovského Tunnel in Brno

D. Rupp & J. Pavlík & L. Klímek
GEOtest Brno, a.s., The Czech republic

ABSTRACT: Constantly unacceptable high density of traffic in Brno urgently requires relief in terms of large traffic structures. As part of the constructed Large City Ring Road in Brno, the cut – and – cover Husovický tunnel and mined Pisárecký tunnel on the highway feeder Prague Radial Road already been constructed. Preparation of the third structure – the Dobrovského tunnel has finished. The future tunnel construction what to be started this year.

Three exploratory galleries were completed in August 2003, whose purpose was to find optimal technology of excavation as well as total design solution of the construction.

Object of the exploration was the tunnel route consisting of two tubes in lengths of app. 1250 m from which more than 1000 m fall on the mined part. Commission for the exploration estimated the excavation of three exploratory galleries with approximately triangular cross section in the area of tunnel tubes at the bases of their vaults, which will be used during the future construction of the tunnel structure.

Geotechnical monitoring consisted of the measurement of gallery convergence, of deformation of rock mass during excavation of the galleries both in boreholes, both on the surface and pressure in lining. Geotechnical monitoring has continued even after finishing of the excavation to the present days.

Article evaluates results of the measurement during the excavation of the galleries and after excavation to the present days. Realized monitoring activity proved the possibility of construction of the designed tunnel structure and set the conditions for the design intent to be accomplished.

1 INTRODUCTION

Geotechnical exploration of the Dobrovského tunnel and engineering-geological conditions in the locality are described in the article "Geotechnical Exploration for the Dobrovského Tunnel in Brno" in section 2.

Excavation of exploratory galleries and geotechnical monitoring were done after completion of engineering-geological investigation. A consortium of companies Štoly Dobrovského was delegated to be the general contractor of the geotechnical exploration. It consisted of GEOtest Brno, a.s. – leader of the consortium guaranteeing the exploration results, and three construction companies Metrostav, a.s., Subterra, a.s. and ŽS Brno a.s. responsible for excavation of the galleries and connected engineering works.

Three exploratory galleries were completed in August 2003, whose purpose was to find an optimal technology of excavation as well as total design solution of the construction. The purpose of realization of the exploratory galleries and connected exploratory works are presented in the mentioned article in the section 2.

2 GEOMONITORING

Extensive geotechnical monitoring, realized both galleries and from surface in locations of the concentrated exploration was an integral part of the exploratory works. Four groups of geotechnical boreholes were installed in area of the IIB gallery in the line of the tunnel II and two groups of boreholes for geotechnical monitoring were installed in vicinity of the IB gallery (tunnel I).

Extensometric boreholes, observing vertical deformation of the massif in three depth levels based on distance from the face, were located in the tunnel axis. Original measurement was realized sufficiently in advance, still in times when the approaching excavation had no impact on the extensometer. The own measurement consisted of both manual measurement of distance between the extensometer anchors and its head and geodetic measurement of height of this head. Deformations of the lowest anchors, installed in the level of 0.5–1.0 above top of the calotte, after elimination of the surface settlement reached values of 5.0–29.5 mm based on geology and vicinity of the adjacent gallery.

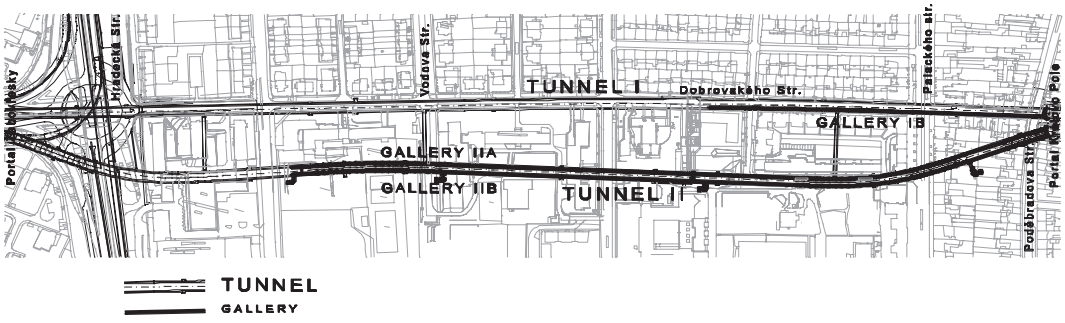


Figure 1. Exposure of galleries and designed tunnels in urban area of Brno.

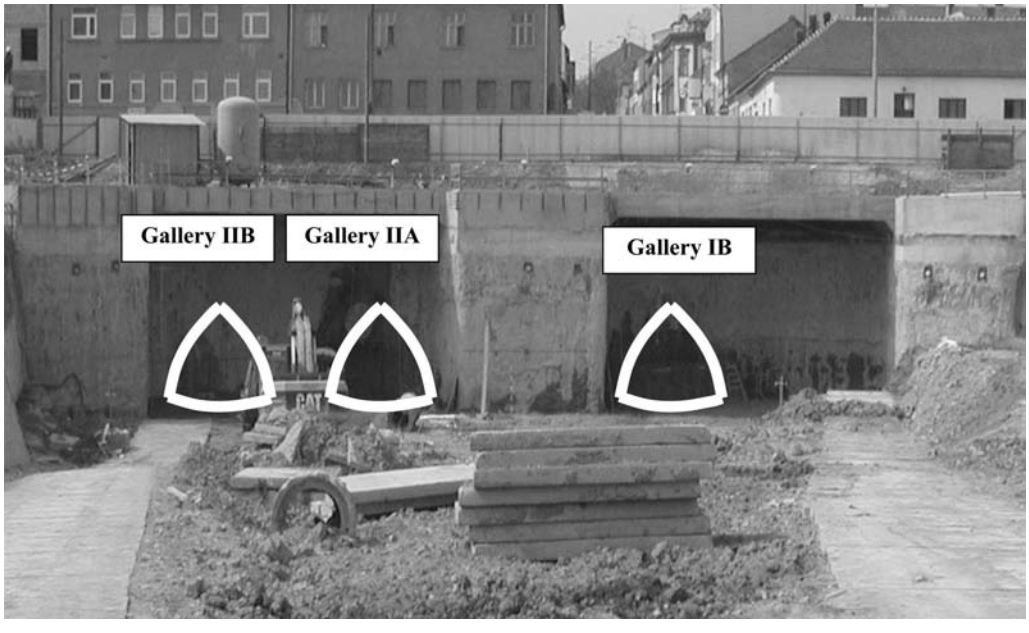


Figure 2. Schematic view at the mouth of the exploratory galleries in the provisory portal Královo Pole.

In distance of 1.0–1.5 m from lining, bores for precise inclinometry were carried out to observe vertical movements of the massif. Bore depths were designed for the measurement to encounter those parts of the rock massif where deformations are expected in connection with realization of the exploratory galleries, but also of the future tunnel tubes. Schematic position of the monitoring boreholes is shown on the Figure 3.

Vertical deformations reached, upon passage through the gallery and subsequent settling at the level of the underground work, values between 4.5–13.0 mm. Curves of vertical movement proved that even in depth of 23 m below the gallery floor the deformations are not yet entirely settled, which was

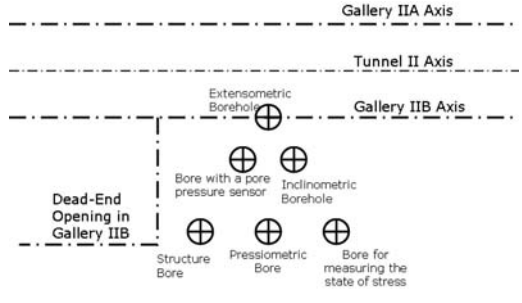


Figure 3. Schema of the position of the monitoring boreholes.

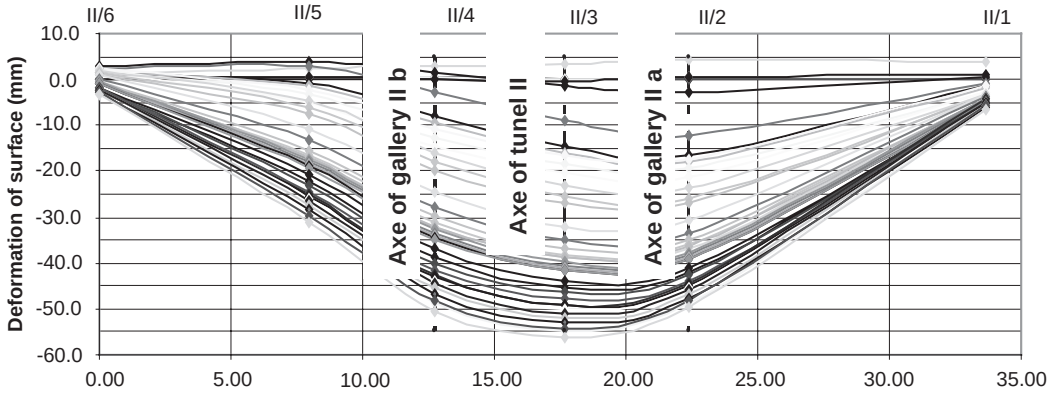


Figure 4. An example of deformation of surface.

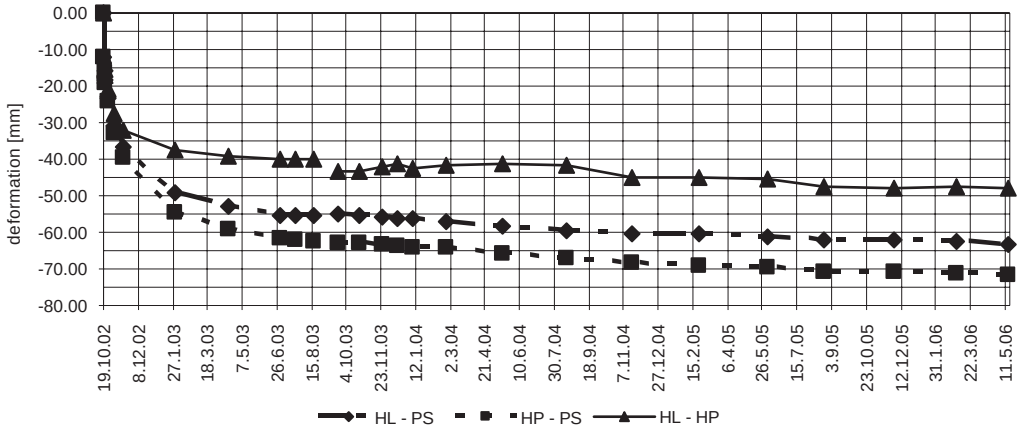


Figure 5. An example of results of convergence measurements.

obvious from the curves of deformation running from bore bases.

Close to the gallery lining, three bores were installed to measure changes in pore pressure we installed in bores in depth, where the floor of the exploratory gallery during the passing excavation was at the time. From the measurement was an apparent large decrease of pore pressures at the time of the passing gallery to less than 10 kPa.

Nets of bores for the geotechnical monitoring remained intact for future use within the frame of fully-profile excavation of the tunnel tubes.

The aforementioned measurements, realized by employees of Stavební geologie Praha, a.s., meant to analyze behavior of the rock massif based on passing of the underground work. Frequency of the measurement changed with approaching and retreating of face of the exploratory gallery to and from the measured bores.

Size and shape of the settlement through were observed from surface. Bores of depth 0.80 m served max) for stabilizing of points of precise leveling, which formed a network of profiles running perpendicularly to gallery axes. Vertical movement of points was measured based on the passing face of the gallery below profiles. These measurements were realized by INSET, s.r.o.

Monitoring in the galleries was mainly focused on the observation of deformations in the lining and leveling. Convergence profiles, which observed the mutual movement of three points, were equipped every app. 150 m. Leveling measurements of convergence profile points and profiles stabilized by surveyors that serve for guidance of the work were measured between 20–40 mm, in extreme cases, for instance given by unfavorable geology in initial sections of the excavation, up to 85 mm. As for leveling measurement of the lining, attention was focused namely on heaving of center of the floor (35 mm and settlement of bases of the mining support frames (app. 10 mm).

Sensors of pressure on the lining were installed behind the lining in three profiles so called pressure cells. The cells were installed at selected places as a contact between the rock and lining. The sensors, which submitted relevant values, recorded the increases of pressures behind the lining upon moderation between 120–400 kPa. Convergence measurements and measurements of pressure on the lining were commissioned by SG Geotechnika, a.s. geodetic measurements were carried out by employees of the measuring department of GEOtest Brno, a.s. and IGM s.r.o.

From the measured processes of length changes, observed by the convergence measurement and vertical movements, analyzed by the leveling measurement, it was possible to determine the progress of these movements in future. During the convergence movement, approximation of wall centers and the floor were observed – the following charts show observed lengths characterized as lines between the points designated HL – point in central section of the left-wall reinforcement, HP – point in central section of the right-wall reinforcement and PS – point on the center of the floor reinforcement. During the leveling measurement, vertical movements were observed beside the previous points also in the floors points at its ends. From these measurements it was possible to calculate inflexions of the floors (difference between measured movements of the floor center and average of measured movements at its end) and total movements of the gallery profile as an average of measured movements of centers of the reinforcing elements.

It was discovered that upon diminution of impacts of the proceeding excavation (advance of the face by 5–15 m from the measured profile), or of excavation of an adjacent gallery, deformations generally settled exponentially. Therefore, result of the measurement allowed determining regression of the deformation on time. Coefficient of the curves and final curves were determine by calculation using step-by-step approximation of the reliability coefficient to one, which was the quite a few times the case for the convergence measurement – measured values of the prediction interval thus lied directly on the curve of the theoretical deformations.

3 EVALUATION OF RESULTS OF THE GEOTECHNICAL MONITORING

As results of the realized exploratory activity and geotechnical monitoring showed, the tunnel structure will be excavated in an environment of overconsolidated Neogene clays with specific attributes that need to be respected during the design of its

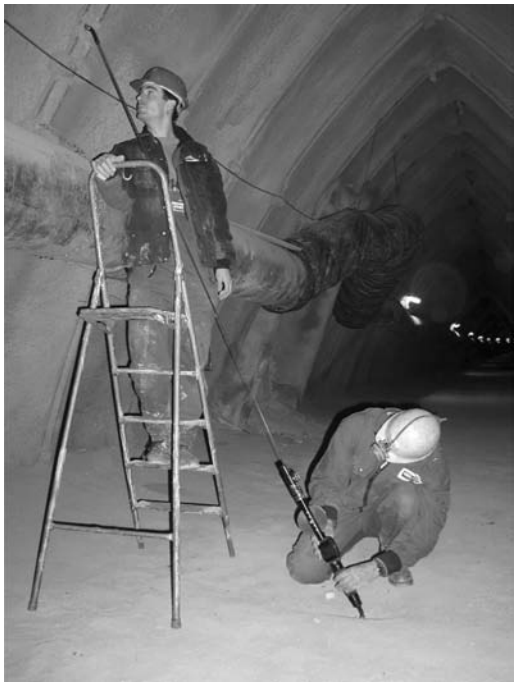


Figure 6. The convergence measurement in the exploratory galleries.

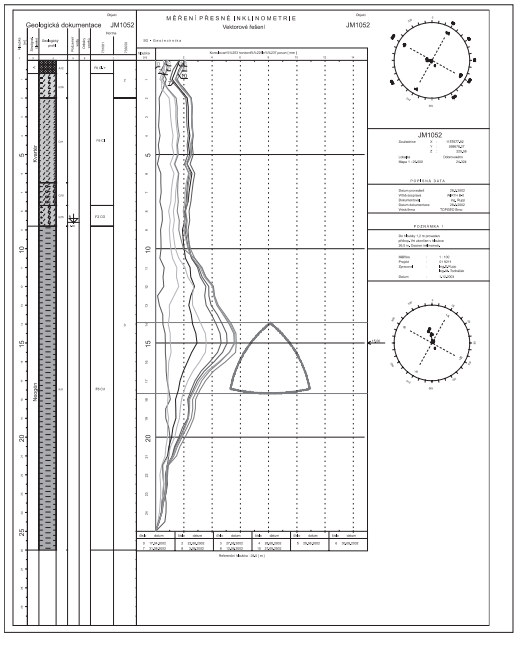


Figure 7. An example of results of inclinometric measurements.

dimensions as well as during the technology of realization. This environment is marked by relatively low strength, high contraction, slow creep and volume modifications due to changing water amount.

There is very positive factor in very low permeability of the clay massive, and therefore running groundwater will be unfavorably affecting the excavation only in sections adjacent to the exit portal, where the cut penetrates into Quaternary rocks. Nevertheless, the clay massive holds some water, which is discharged from the massive after longer disburdening by the excavation otherwise not secured by non permeable lining along the entire periphery. The described phenomenon was observed in most test galleries as well as those galleries where front bases of the lining experienced damp places.

4 CONCLUSION

The monitoring of behavior of rock massif during excavation of the exploratory galleries and three years after its finishing showed, that deformation of surface and underground openings had developed after assumption of the project. The results of the realized measurement thus proved possibility of construction of this designed tunnel as the significant transport structure very important to the life in the city of Brno.

REFERENCE

Pavlík, J. & Klímek, L. & Rupp, D. 2004. Geotechnický průzkum pro nejvýznačnější stavbu na Velkém městském okruhu v Brně – tunel Dobrovského. Geotechnical Exploration for the Dobrovského Tunnel, the Most Significant Structure on the Large City Ring Road in Brno. *Tunel. Magazine of the Czech Tunneling committee and Slovak Tunneling Association ITA/AITES, Vol.13 No.2/2004:2–12* Praha.

This page intentionally left blank

Underground Space – the 4th Dimension of Metropolises – Barták, Hrdina, Romancov & Zlámal (eds)
© 2007 Taylor & Francis Group, London, ISBN 978-0-415-40807-3

An optimised monitoring of critical buildings adjacent to tunnel construction in urban area

S.H. Shin, C.Y. Kim, K.Y. Kim, K.S. Jue & S.W. Hong
Korea Institute of Construction Technology (KICT), ilsan-Gu, Gyunggi-Do, South Korea

ABSTRACT: This paper presents a new strategy for determining an optimum position of monitoring point and criteria with which judgment is made if the settlement values at the point are critical or not for a significant structure adjacent to tunnel construction. The position and criteria are differently given to each structure by considering its geometry and exact position. It is unlikely to the conventional monitoring scheme undertaken by a fixed criterion applied at certain monitoring points that are also intuitively placed. The strategy proposed is based on an iterative scheme by incorporating the so-called Intelligent Tunnelling Information System (ITIS). Details of the iterative procedure are described with an illustrative example. In the example, the settlement criteria at three different damage levels are given at an optimum monitoring point.

1 INTRODUCTION

A number of urban tunnel constructions take place as the social demand for public transportation increases, in which the major concerns would be not only for safety of tunnels itself but also for safety of adjacent structures to the tunnels. The safety of the adjacent structures is subject to ground movements due to tunnelling. Intensive studies have been made to date in this topic (KICT, 2000; Kim et. al., 1998; Son, 2003). In general, a prediction of ground movements and potential damages of the adjacent structures are carried out, in which a number of damage parameters such as angular distortion, deflection ratio, etc. are involved (KICT, 2000). Monitoring on the adjacent structures is also undertaken for evaluating their damages during tunnel construction. The number of monitoring points might be limited because of economical reason, etc., at which ground settlements and tilts would be monitored periodically.

In the circumstance, a new strategy is proposed for determining an optimum location of monitoring point as well as evaluation criteria at various levels for assessing the monitored values of settlements. Such information is given for individual structure independently. The strategy is based on an iterative procedure of assessing the structures with respect to the gradually increasing ground settlements in various steps, which are automatically performed considering the exact location, geometry and mechanical properties of individual adjacent structure. An illustrative example for showing how the proposed strategy works is given.

1.1 *Typefont, typesize and spacing*

Use Times New Roman 12 point size and 13 point line spacing (Standard;text tag). Use roman type except for the headings (Heading tags), parameters in mathematics (not for log, sin, cos, ln, max., d (in d*x*), etc), Latin names of species and genera in botany and zoology and the titles of journals and books which should all be in italics. Never use bold, except to denote vectors in mathematics. Never underline any text. Use the small font (10 points on 11 points) for tables (Table tags), figure captions (Figure caption tag) and the references (Reference text tag).

Never use letterspacing and never use more than one space after each other.

2 STRATEGIES PROPOSED

2.1 *Determination of an optimum monitoring point*

With limited number of monitoring points, an attempt is made to determine an optimum monitoring point at which a maximum settlement may take place. The strategy is based on an iterative scheme. Considering a 3D trough of ground settlements, the shape and quantities of the trough will vary as the tunnel goes ahead. The deformation of the structure will progressively grows up, thereby leading to progressive change of its structural damages at certain levels. The progressive deformation of the structure can be check up by automatic calculation of 3-D settlements at the foundations of all the columns of the walls consisting

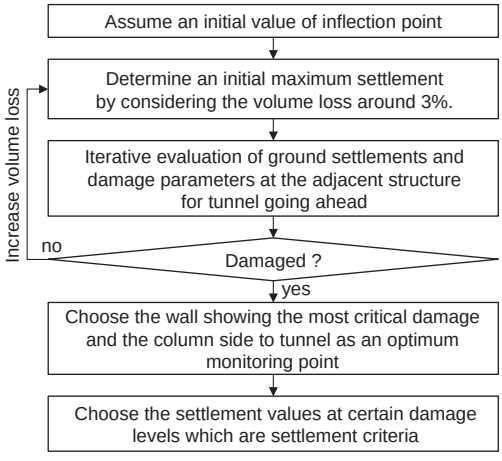


Figure 1. Plane view of the tunnel site concerned.

of the structure. From the results, conventional damage parameters of all the walls can be calculated at every stage of tunnel progresses. The theoretical background on the 3-D settlement trough and ITIS can be found in the literature in details (Kim, 1998).

A schematic diagram for determination of an optimum monitoring point is given in Figure 1. Based on the damage parameters for the walls calculated, one of the walls, which shows the most critical values at several excavation stages, can be chosen and then a column of the wall side to tunnel would be a suggested monitoring point for the structure. In progressive prediction of the deformation of the structure, initial values for a maximum settlement and inflection point, which are involved in 3D equations of the ground settlement trough (Kim, 1998), should be required *a priori*. The values will be arbitrarily chosen which should be big enough to make at least one of the walls damaged on purpose. An inflection point can be determined by a ground loss which is in general 1%∼3%. However, bigger values of the inflection points from assumption of about 6% ground loss, are fixed first in this study. Then a big maximum settlement of about 100∼200 mm is applied for the automatic progressive calculation of settlement tough. It is noted that the chosen values should be confirmed to be insensitive to determination of the monitoring point. This aspect has been confirmed by a number of verification tests that, however, is not given in this paper.

2.2 *Giving settlement criteria to the optimum monitoring point determined*

As shown in Figure 1, settlement criteria can be given to the optimum monitoring point determined by the manner addressed in previous chapter. A variety of the existing evaluation charts could be involved for the purpose (Son, 2003). In this study, the evaluation charts by lateral strain vs. angular distortion (Boscardin & Cording, 1989) is used, on which a number of line plots for all the walls under consideration can be made through all the progressive stages. One of the lines that reaches first to the boundary between the damage levels given in the Boscardin' chart can be easily determined by ITIS. On the line determined, the settlement value at the calculation stage of reaching to a boundary between damage levels becomes the settlement criterion at the damage level within the boundary. Note that settlement criteria at certain monitoring point of an adjacent structure vary depending on its geometrical characteristics and lateral distance from tunnel axis.

3 ILLUSTRATIVE EXAMPLE

The strategy proposed here was applied to the design stage of the Ban-Song Subway Line. Attempts for giving an optimum monitoring points as well as evaluation criteria at different damage levels has been made for total 18 significant buildings adjacent to tunnel construction. By page limitation, only an application case is given in this paper. The plane view of the tunnel site is shown in Figure 2, in which the building concerned in this paper is located on the 11th section in Figure 2. A brief field description at location of the building is given in Table 1.

First of all, the settlements parameters such as maximum settlement and inflection point and damage parameters of the building are predicted for safety evaluation by using ITIS system (KICT, 2000). The prediction is made by a neural network trained from a number of field monitoring data available in the system. The settlement parameters predicted are given in Table 1. The location of the building and variation of the damage parameters of its walls through construction stages are also shown in Figure 3.

As shown in Figure 3, all of the damage parameters predicted by the tunnel passed through seems to be within a safe domain so that no structural damage may take place. The 3D view of the damage assessment is also shown in Figure 4. Herein, the colours on the walls represent the level of damage parameters predicted for the walls, all of which are in safe range. However, the building is crucial for this site so that it is needed to place a monitoring point on the building for confirming the safety throughout tunnel construction.

By the strategy mentioned in previous chapter, another set of settlement parameters is assumed in which the settlement parameters are determined at around the ground loss of 6%. Then, the iterative calculation of ITIS is carried out again checking up the damage parameters varying on an evaluation chart. As a result, damage parameters of the 6th wall shows the

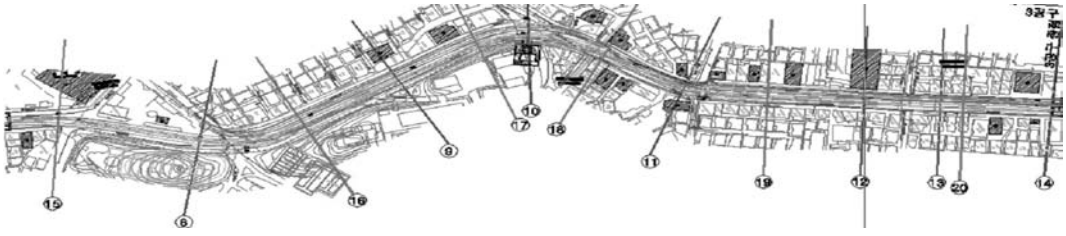


Figure 2. Plane view of the tunnel site concerned.

Table 1. The predicted and assumed settlement parameters with brief field description.

Tunnel depth	Water level	Pattern no.	Maximum settlement predicted	Inflection points predicted	Ground loss predicted	Maximum settlement assumed	Inflection point assumed	Ground loss assumed
15.71 m	6.23 m	PD-3A	15.1 mm	14.5 m	0.926%	100 mm	14.5 m	6.132%

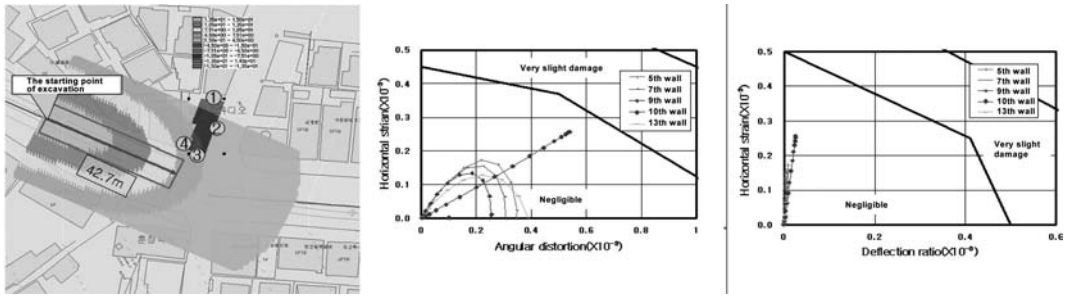


Figure 3. An adjacent building concerned and progression of damage parameters calculated.

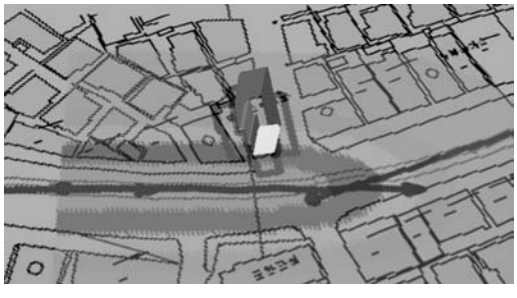


Figure 4. 3D view of damage assessments by ITIS.

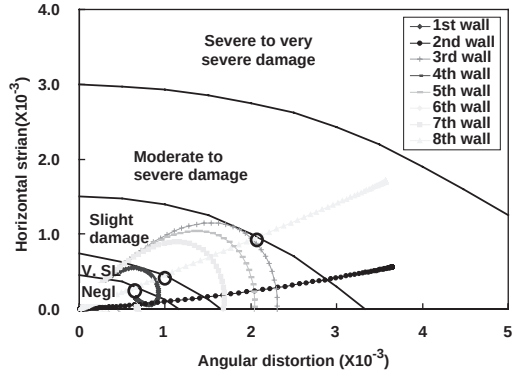


Figure 5. A chart used for determination of settlement criteria.

most fast progress as shown in Figure 5 so that the column of the wall side to tunnel is decided as an optimum monitoring point which can be seen in Figure 6 as an example. In addition, the ground settlements of the column are picked up at the stages circled in Figure 5. The stages are on boundaries between different damage levels. In this case, three settlement criteria have been given at three different levels of structural damages. The settlement criteria decided are 15.1 mm, 23.67 mm, 54.37 mm at damage level I, II, III, respectively. The damage level I, II and III represent to be very slightly damage, moderate to severe damage and severe to very severe damage, respectively as shown in Figure 5.

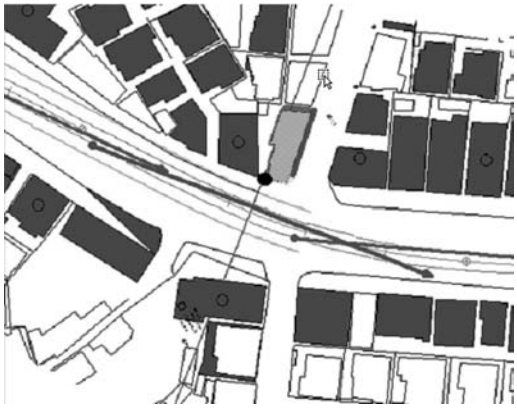


Figure 6. An optimum monitoring point determined by the proposed strategy.

4 CONCLUSIONS

This paper proposed a strategy to determine an optimum monitoring point and settlement criteria at the point for significant structure adjacent to tunnel construction. The criteria will be used for making an engineering judgement on deformation of the structure monitored at several levels of damages. It can be seen in the scheme that the strategy allows us to minimise installation of monitoring points but not to miss any severe symptoms of structural damages taking place on the structure. To date, monitoring point has been installed intuitively at which the same settlement criteria have been applied, even if the same settlement at the monitoring point can lead to the different damages on the wall. Therefore, the settlement criteria should be decided based on the damage parameters expected. As the damage parameters will depend on geometry and position of the adjacent structure, it is reasonable to give settlement criteria differently for each structure by taking into account the geometry and position of the structure which are achieved by the strategy proposed in this paper. An illustrative example has been given to show how to achieve the purpose. Moreover, more verification of the strategy and field application will be made, which will be reported again in future.

REFERENCES

Boscardin, M.D., Cording, E.J., 1989, Building response to excavation-induced settlement, Journal of Geotechnical Engineering, Vol. 115, No. 1, pp. 1∼21.

Kim, C.Y., 1998, A study on the prediction of ground movement and the damage assessment of adjacent structures due to tunnel excavation in urban area, Ph.D. thesis, Hanyang University, Seoul, Korea.

KICT, 2000, Development of the advanced information technology for tunnel design and construction, The final technical report, 2000-N-NL-01-C-137.

Son, M.R., 2003, The response of buildings to excavation-induced ground movements, Ph.D. thesis, University of Illinoies at Urbana-Champaign, USA.

Underground Space – the 4th Dimension of Metropolises – Barták, Hrdina, Romancov & Zlámal (eds)
© 2007 Taylor & Francis Group, London, ISBN 978-0-415-40807-3

Monitoring during the construction of a shallow urban tunnel and countermeasures

T. Solak & Z. Etkesen
General Directorate of Highways, Ankara, Turkey

A. Sirin
10. Distinct Directorate of Highways, Trabzon, Turkey

T. Düzgün
Zemtas A. S., Ankara, Turkey

ABSTRACT: A shallow urban tunnel has been constructed with conventional method at a residential area in Black Sea Region of Turkey. The excavation and support measures of the tunnel were designed considering soft rock conditions (highly weathered tuff-agglomerate) from site explorations. An extensive monitoring plan was performed to control the design considerations, interaction of the tunnel construction with surrounding structures and influence of the new tunnel excavation on the old tunnel under traffic. During the excavation near to the west portal of the tunnel, deformations and cracks were recorded at the ground surface, fortress masonry walls and one storey buildings inside the fortress area. By evaluating geological documentation, monitoring data and other records such as water discharge measurement, the mechanism of the instability problem was analyzed and required measures were determined. The measures comprised mainly grouting application in limited areas to prevent developing of the instability problems. This paper contains analyzing of data during the tunnel excavation and countermeasures to avoid adverse influence of the tunnel excavation.

1 INTRODUCTION

Design and construction of a shallow urban tunnel requires special considerations due to several reasons. During the determination of the alignment and site investigations local factors limit extent and quality of site investigation data. Changes in stratification and properties of layers in short distances are not unexpected facts. Empirical and analytical solutions or numerical modeling provide tools to determine support measures, predict deformations due to tunneling induced ground movement; surface, subsurface settlement, lateral deformation of the ground, longitudinal movement of the ground ahead of the tunnel face. However the prediction of those values depends on the quality of input data. Due to the nature of shallow tunneling, change in situ stress and hydrogeological conditions bring higher influence on surface buildings.

Design considerations should be checked during the construction with monitoring of both subsurface and surface movements, impact on nearby buildings and services. Geotechnical monitoring capabilities both at surface and subsurface provide early detection of negative effect of tunneling on nearby structures and taking measures on time. Improvements in evaluation methods suggested by Sellner et al 2004 and measuring devices such as chain inclinometer installed to the pipe roof systems explained by Volkman & Schubert 2006 increase those capabilities.



Figure 1. View from the west portal.

Kalepark Tunnel is a typical shallow urban tunnel with a maximum overburden of 21 m in a residential area. Tunnel with three lanes was planned to construct at a distance of 30 m from the axis of the old tunnel due to the traffic requirements (Figure 1).

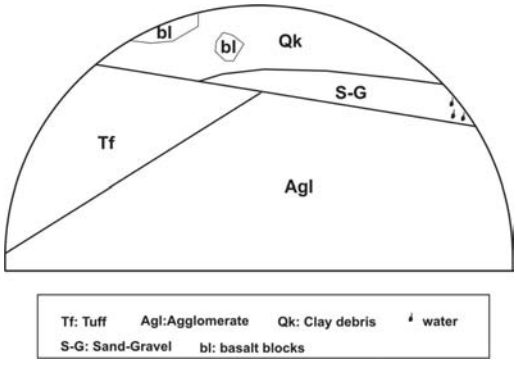


Figure 2. Face mapping from km: $0+549$.

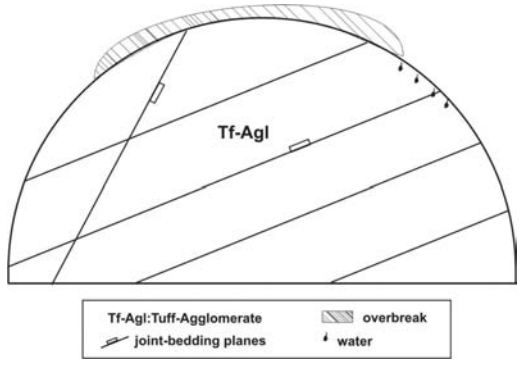


Figure 3. Face mapping from km: $0+567$.

Site investigation works consisting limited boreholes and geological mapping of outcrops could be realized and tunnel design was performed accordingly. Tunnel excavation was designed as sequential excavation; top heading, bench and invert. Support system includes fibre reinforced shotcrete, steel ribs, rock bolt, forepoling, shotcrete and rock bolting at the face if required Due to the high expenses for nationalizing works, structures with historical importance and varying types of buildings around the tunnel area, geotechnical monitoring and evaluation gained importance.

2 GEOTECHNICAL DESCRIPTION

The rock at the tunnel area is highly weathered tuff and agglomerate. Tuff and agglomerate is overlaid by clay debris containing basalt boulders. A layer of loose sand-gravel is encountered between tuff-agglomerate and clay debris at the first 25 m from the west portal. Highly weathered and water susceptible tuff-agglomerate has low strength. After 25 m advance from the west portal, tuff and agglomerate shows bedded structure. The bedding planes contain clay and calcite filling and rock mass is highly fractured. The water level was encountered at 10.5 m below the ground surface in the boreholes at the design level. During the tunnel construction the water income from the loose sand-gravel layer at the shoulders was observed as leakage in the first meters of the tunnel excavation. Water discharge increased with the tunnel advance. The rock mass conditions encountered during the top heading excavation are shown in two representative face mappings from km: $0+549$ and $0+567$. At km $0+549$ clay debris and loose sand-gravel layer were encountered at the upper part of the top heading. Water inflow from the sand-gravel layer resulted in overbreak at the shoulders (Figure 2).

At km: $0+567$ tuff and agglomerate at the face is highly fractured. Overbreak was observed at the crown. Water inflow from the right part of the face has a discharge rate of 0.4 lt/min (Figure 3).

3 MONITORING AND EVALUATION

An extensive monitoring program was performed both at the surface and inside of the tunnel. Measuring station in tunnel was established with a distance of 5 m and absolute measurements at five points in cross section were recorded during the construction. Before the construction, structures were examined; their type, actual condition and position relative to the tunnel were recorded.

The structures in a determined zone in portal area were nationalized. Topographic measuring stations at the ground and buildings were established. Strict acceptable limits for settlement values (absolute, differential settlement, rotation) were not determined due to varying characteristic of buildings such as reinforced concrete multistory buildings, masonry fortress walls etc. Extensometers were planned to set according to topographical measurement results.

When top heading excavation arrived km: $0+570$, cracks were recorded at the ground surface, fortress walls and one storey buildings inside the fortress area. Figure 4 shows measuring points at the ground and fortress wall, position of the structures and fortress walls relative to the tunnel and recorded cracks.

To evaluate the mechanism bringing failures at the ground surface and structures, the displacement measurements inside the tunnel, crack development and deformation measurements from surface stations were evaluated with combination of tunnel advance data and water discharge rates. The displacement amounts in the tunnel are less than 1 cm and no failure was observed at the support elements; no cracks at the shotcrete or sign of overloading in rock bolts.

The measurement result showed that the deformations at the ground surface and fortress wall increased with increasing discharge rate. Considering the



Figure 4. Plan view from west portal area showing measuring points, cracks and grouting areas.

deformation graphs and geological structure from face and surface mappings it is concluded that high water discharge due to tunnel excavation cause immediate settlement at the granular material. Tunnel support had required capacity to carry the additional load due to this fact. However masonry structures are sensitive to these movements and cracks occurred.

Damage in the masonry walls and buildings were evaluated according to the classification of visible damage of structures suggested by Burland 1995. The crack widths at four measuring stations were measured as 4–20 mm (Figure 6, Figure 7, Figure 8, and Figure 9). Typical crack widths of the masonry walls were 15–25 mm and classified as category of damage- 4, normal degree of severity-severe.

Because no other failure is observed in nearby structures and inside the tunnel, required measures were determined to rehabilite the structure and strengthen the foundation by cement grouting. This solution is also to prevent development of the failure with bench and invert excavation.

4 REMEDIAL MEASURES

Grouting application with vertical and inclined boreholes was planned in three zones (Figure 4). Location, inclination and extend of the grout holes were

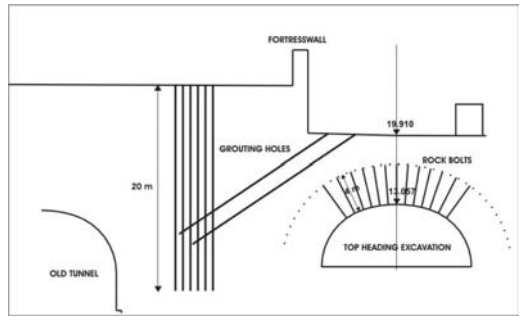


Figure 5. Grouting application at km: 0 + 560.

determined according to the crack measurements, position of the old tunnel, bolted area around the new tunnel, fortress wall and the buildings (Figure 5).

The benefits of the grouting were:

- to fill voids in formation,
- to increase resistance against deformation,
- to supply strength,
- to reduce conductivity,
- to control ground water table and seepage.

0.5 m*0.5 m square pattern is designed. But during construction according to monitoring records this pattern could be revised.

In cement grouting, the following principles are considered:

- Grouting is applied in 2 m levels
- Applied pressure (bar) is calculated from the following equation:

$$P=0.23*H \quad (1)$$

where H: distance between top of borehole and middle of each level (meter)

- Water cement ratio was decreased from 3:1 to 5:7 in stages. At the last stage sand (5%–20%) was added to the grout mix.

At Station A in Zone 2, crack width on the fortress wall was measured 20 mm before the grouting application within a month. Grouting at that region was completed in the next month. The deformation rate decreased during ground improvement and 5 mm deformation was recorded. After the completion of the grouting at that area no further deformation was detected (Figure 6).

At Station B in Zone 1, crack width on the fortress wall was measured 4 mm before the grouting application within 13 day period. During grouting lasting 19 days around Station B the deformation rate increased and deformations arrived 11 mm. After the completion of the grouting at that area deformations at Zone 1 stabilized (Figure 7).

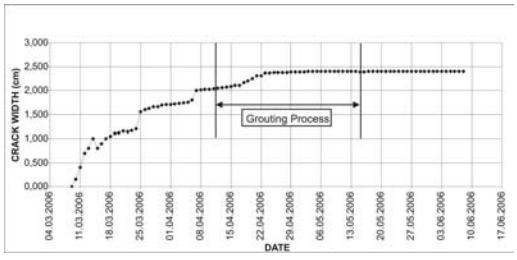


Figure 6. Crack width measurements from Station A.

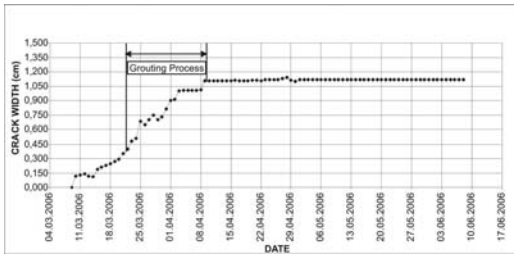


Figure 7. Crack width measurements from Station B.

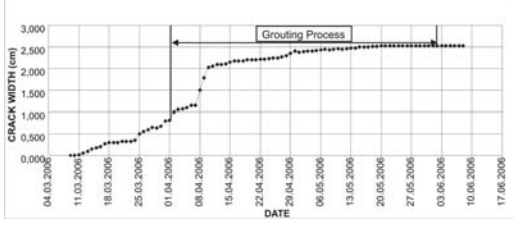


Figure 8. Crack width measurements from Station C.

At Station C in Zone 3, crack width on the fortress wall was measured 8 mm before the grouting application within 3 weeks. Due to the large size of that area grouting took 2 months. A sudden increase of 10 mm was recorded after start of the grouting. At the end of the application deformations was 25 mm. Stabilization of the deformation was achieved with grouting (Figure 8).

At Station D in Zone 1, crack width on ground surface was measured 4 mm before ground improvement within 2 week period. Grouting took 10 days near this Station. Similar deformation rate was observed during the grouting process. At the end of the grouting deformations reached to a final magnitude of 7 mm (Figure 9).

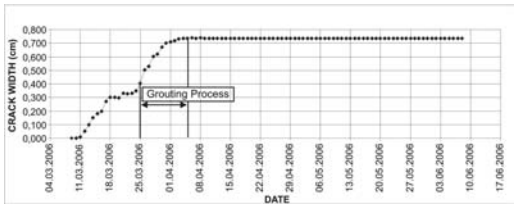


Figure 9. Crack width measurements from Station D.

Grouting was applied in three distinct zones to stabilize deformations on the fortress wall and ground. A close pattern of grout holes were applied. The success of the ground improvement was checked with the measurement of the crack widths at the measurement stations.

5 CONCLUSION

Due to characteristic of urban tunnels (soft rock/soil conditions, low overburden, groundwater level, nearby structures and services), monitoring of tunnel induced movements at the ground surface and buildings, change in ground water level are necessary to control negative influence of tunnel construction. Monitoring results should be analyzed with tunnel advance data and geological documentation to evaluate the mechanism of tunnel induced movements and failures at the surface. The measures to stop or limit deformations at the surface can be determined as stages. The effectiveness of the measures can be evaluated by continuous monitoring during all stages. The measures can be taken inside the tunnel or at the surface. For an economical solution type and extend of the measures should be determined considering failure mechanism.

REFERENCES

Burland J. B. 1995. Assesment of risk of damage to buildings due to tunneling and excavation. Invited Special Lecture in 1st Int. Conf. on Earthquake Geotech. Engineering 1995.

Sellner P., Grossauer K. & Leitner R. 2004. How to predict movements & prevent damages of the surface structures. In Wulf Schubert (ed.), 53rd Geomechnanics Colloguy & EUROCK 2004, *Salzburg, October 2004*.

Volkmann G., Schubert W. Opptimization of excavation and support in pipe roof supported tunnel sections. In Wulf Schubert (ed.), 53rd Geomechnanics Colloguy & EUROCK 2004, *Salzburg, October 2004*. Rotterdam: Balkema.

Underground Space – the 4th Dimension of Metropolises – Barták, Hrdina, Romancov & Zlámal (eds)
© 2007 Taylor & Francis Group, London, ISBN 978-0-415-40807-3

Longitudinal surface settlements induced by EPB tunneling in Bangkok Clay

S. Suwansawat
Department of Civil Engineering, Faculty of Engineering
King Mongkut's Institute of Technology Ladkrabang, Thailand

ABSTRACT: This research studied extensive data on ground surface settlement and shield operation collected at the MRTA Bangkok project where eight Earth Pressure Balance (EPB) shields were used. It was found that three distinct zones of longitudinal surface settlement were observed irrespective of soil conditions. Zone 1 originates ahead of the shield where the ground begins to deform. Zone 2, the largest portion of overall settlements, initiates a short distance in front of the shield face and develops largely over the shield body. Zone 3, begins after shield passing and after the tail void grouting has being performed. Operational parameters such as face pressure and penetration rate affect the magnitude of surface settlements within each zone. Large settlements found in Zone 1 are associated with low face pressure and low penetration rates. In contrast, if applied face pressures and penetration rates were very high, less surface settlements or even ground heave occurred in Zone 1. Face pressure and penetration rate also affect settlements in Zone 2 during shield passing. However, settlements occurred in Zone 3 were mainly influenced by tail void grouting.

1 INTRODUCTION

The Bangkok MRTA project is the first phase of an integrated transportation plan for Bangkok, to be implemented in conjunction with other schemes, by the Metropolitan Rapid Transit Authority (MRTA). The project of 20-kilometers of twin tunnels is subdivided into two main tunnel sections namely, the North Tunnel Section and the South Tunnel Section, which in turn are divided into Sections A, B and C, D, respectively (Figure 1). The tunnel alignment covers heavily congested areas of the city. Each of the twin tunnels is 6.3 meters in outer diameter and 5.7 meters in inner diameter. Each section uses two shields, one each for excavating the northbound and southbound tunnels. Hence, eight EPB shields were used in total for the entire project. Due to comprehensive arrangement of instrumentation both in the field and in the shields, the information is available so that the effect of tunneling variables on the development of ground deformations can be studied. Details of the project can be found in Suwansawat 2003.

There are two objectives in this research: (1) to evaluate the behavior of ground movements associated with EPB shield tunneling and (2) to investigate effects of EPB shield operational parameters on ground movements. Measurement results recorded from various types of instrumentation installed in the project including settlement markers and extensometers to measure maximum surface settlements above the tunnel centerline. Additionally, since readings were taken over time covering a period between before shield approaching and after shield passing, surface settlement markers also allow one to observe longitudidal surface settlement profiles and to study how they develop during shield passing.

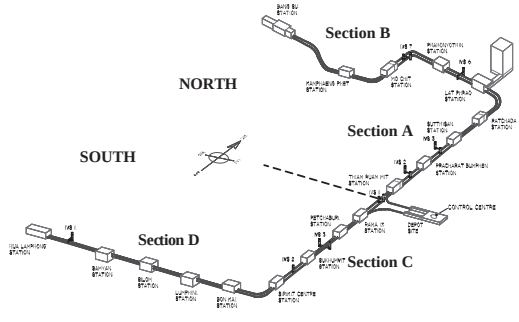


Figure 1. Bangkok MRTA route.

2 SUBSURFACE CONDITIONS

Bangkok lies in the Chao Praya delta plain. Its topography is low and flat being approximately 0.5 to 1 meter above sea level. For the MRTA project extensive field explorations and laboratory programs were carried out. Subsurface conditions along the MRTA

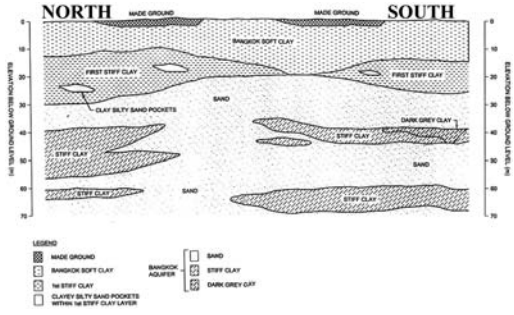


Figure 2. Subsurface conditions along the MRTA tunnel.

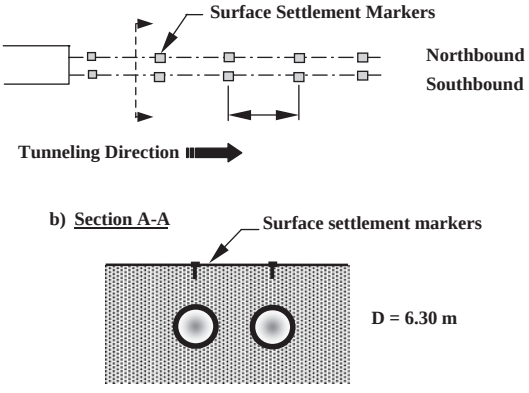


Figure 3. Instrumentation layout of the MRTA project.

project can be also subdivided into the North Tunnel section and the South Tunnel section.

For the North section, the soil profile is very uniform with soft clay underlain by stiff clay along the tunnel alignment. In this tunneling section, the horizontal-twin tunnel is excavated mostly within the stiff clay layer (i.e. about 15–25 m below ground surface) but with some parts in the sand. For the South section, most of the tunnel alignment is also mostly located within a stiff clay layer. However, in some part of the route, tunnels are stacked so that the lower tunnel is excavated in a sand layer.

3 GEOTECHNICAL INSTRUMENTATION

In the MRTA Project, large amounts of surface settlement markers and settlement arrays were installed to measure surface settlements during excavation. Typically, surface settlement markers were installed approximately at 50 meters intervals along the tunnel alignment as shown in Figure 3. The primary objective of the measurements with settlement markers is to measure maximum surface settlements above the tunnel centerline. Additionally, since readings were taken over time covering a period between before shield approaching and after shield passing, surface settlement markers also allow one to observe longitudidal surface settlement profiles and to study how they develop during shield passing.

Consequently, results from the instrumentation provide engineers with useful information to design appropriate measures for preventing damage to existing structures induced by EPB tunneling. Note that monitoring frequencies adopted in the MRTA project depended upon shield position. For example, readings were taken every day before and after shield passing but increased to higher frequency (i.e. every 2–4 hours) during shield passing in order to capture the development of surface settlements.

4 SURFACE SETTLEMENTS

4.1 *Tunnel Section A*

Section A is a part of the North Tunnel Section. Most of the tunnel in this section was excavated within the stiff clay layer. Note that only the first tunnel is studied since only the impact of the first shield on ground deformations is considered. The EPB shield used in this section was operated by controlling the amount of excavated soil that was extracted from the face by a screw conveyor. The face pressure was used as a control parameter during the excavation process. This pressure was monitored by pressure cells installed inside the earth chamber.

To allow a clearer relationship to be established between surface settlements and tunneling, settlement data were plotted against the shield face position as shown in Figure 5. As can be seen from the figure, the ground surface began to deform about 30 meters ahead of the shield. As the shield advanced close to the measurement section, larger settlements developed and accelerated over the shield body. Subsequently, the settlement ceased after the shield arrived at 15 m. behind the measurement section. Figure 5a shows the settlement measured at the ground surface over the lining ring no. 49 labeled "*a*" in Figure 4a. As the shield passed the section, the average face pressure was only 30 kPa. (Figure 4b). Large surface settlements occurred while the shield approached the measurement section particularly in the plane of the shield face. This observation is in agreement with laboratory experiment results shown in reported in earlier studies (i.e. Kimura and Mair; 1981, and Atkinson and Potts; 1977) in which ground tended to move towards the tunnel face in the centrifuge test. Additionally, large settlements significantly extend over the shield body but ceased about 15 m. (i.e. 2-shield diameter) behind the face. Subsequently, beyond this point, the settlement showed a small change after shield passing.

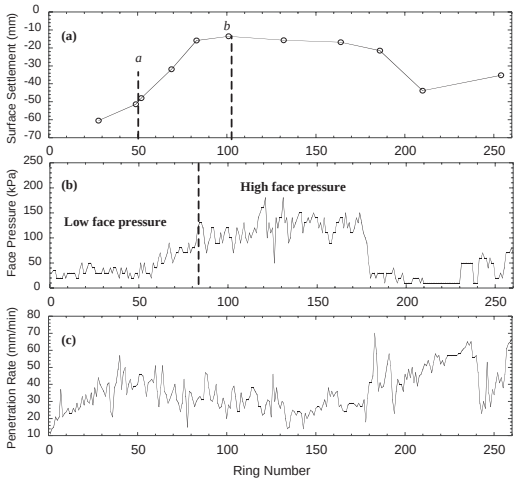


Figure 4. Surface settlements, face pressures, and penetration rates recorded in Tunnel Section A.

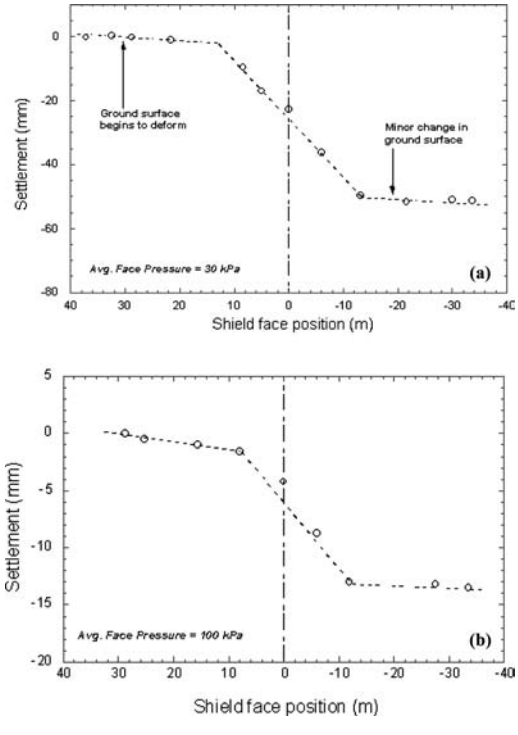


Figure 5. Surface settlements Longitudinal surface settlement profiles measured at location (a) "*a*" (Ring No. 49-SB), (b) "*b*" (Ring No. 101-SB).

After the SB shield was driven 72 m away from the launching station and 60 segmental rings were installed, the shield was stopped, equipment backup

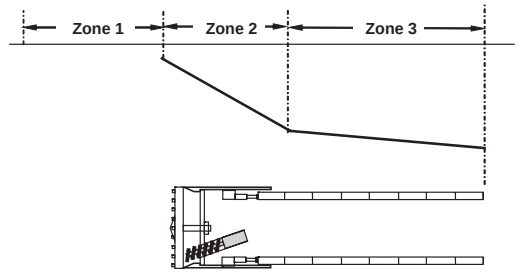


Figure 6. Schematic diagram of a typical longitudinal suface settlement profle.

trains were set up, and all temporary supports were removed. This was the end of the initial drive and the shield then resumed the excavation again. From this moment on, the SB shield was able to increase the face pressure up to 180 kPa (Figure 4b). To investigate the relationship between surface settlements and the shield progress, location "*b*" was selected for investigation. Average face pressures during shield passing were 100 kPa for location "*b*". The operation is in the "earth pressure balance mode," where surface settlements can be minimized by adjusting the face pressure equal to the surrounding earth pressure during excavation.

Surface settlements versus the shield face position in locations "*b*" is plotted in Figure 5b. In the figures, the maximum settlements were 13 mm. Obviously, the section has less settlement than section "*a*" (∼ 50 mm), where low face pressure was applied. This confirmed the assumption made previously that the face pressure applied during shield passing has a significant effect on the magnitude of surface settlements. Typically, shield operators need to drive the shield under a controlled face pressure to minimize the surface settlement.

Based on these observations, surface settlements induced by EPB tunneling can be divided into three zones regardless of face pressure level namely, (1) Zone 1, (2) Zone 2, and (3) Zone 3 as shown in Figure 6. The first zone originates approximately 30 m ahead of the shield, where the ground surface begins to deform. The surface settlement then continues to develop as the shield advances close to the measurement section. About 10 m in front of the shield, the surface settlement significantly increases and accelerates over the shield body. This stage of the surface settlement creates a clear inflection point separating "Zone 1" and "Zone 2". As observed in Section A, the surface settlement in Zone 2 is the largest portion of overall settlement induced by the EPB shield. After the shield tail passes the measurement section (i.e. about 15 m from the shield face), the settlement development begins to slow down; this is the beginning of Zone 3. The surface settlement in this final zone stops about 30 m after shield passing.

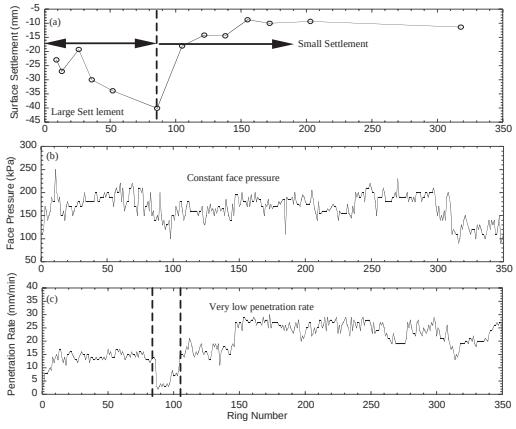


Figure 7. Surface settlements, face pressures, and penetration rates recorded in Tunnel Section B.

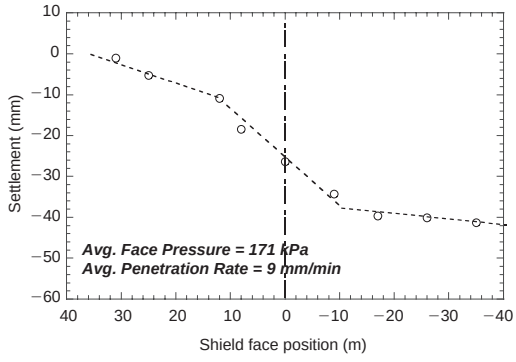


Figure 8. Longitudinal suface sttlement profile measured over ring No. 86-SB in Section B.

4.2 *Tunnel Section B*

Soil conditions of the tunnel in Section B are very similar to those of Section A, where most of the tunnel alignment was excavated within the stiff clay layer. Surface settlements measured in this section were recorded along the tunnel alignment as shown in Figure 3. At the beginning of the tunnel drive, relatively large settlements were observed even though the shield was operated at high face pressures (i.e. 150–200 kPa).

One of the factors that affect the ground response in the early stages of excavation is the inexperience of the tunnel crews. Furthermore, if one takes a detailed look at the shield penetration rates plotted in Figure 7c, it was found that the shield was driven at only 10–30 mm/min at the beginning of the excavation. In particular, between rings No. 80–100, the penetration rate was very low (i.e. less than 5 mm/min in some sections). Unlike other tunnel sections, a pipe transport technique was adopted instead of muck locomotives. This technique required the rate of pumping to be related to the shield advance/penetration rate or vice versa. Hence, this becomes a limitation in this tunneling section in that the shield cannot be shoved at high penetration rates. Evidently, such a low penetration rate was found to be associated with large surface settlements measured over the shield, particularly at ring No. 86 as shown in Figure 7a. To explore the behavior of ground response during shield passing, surface settlements recorded over the ring No. 86 were plotted against the shield position as shown in **Figure 8**.

The shape of the longitudinal surface settlement is similar to that of Section A with three distinct zones. Particularly Zone 2, settlement over the shield body is also the largest portion of the settlement. The surface settlement in Zone 1 appears to be relatively large (i.e. 11 mm at the transition point between Zone 1 and Zone 2), while the surface settlement in Zone 3, where the shield already passed the section has the smallest settlement. Based upon this observation, although the shield was operated at high face pressures during excavation in Section B, the surface settlements were still large as long as the penetration rate was very low. This suggests that penetration rate may also be a factor affecting the magnitude of surface settlements.

4.3 *Tunnel Section C*

Tunnel Section C is a part of the South Tunnel Section. Unlike other sections, the northbound shield was launched first. Most of the tunnel alignment was excavated entirely within the stiff clay and the very stiff clay layers. The shield used in this section is very similar to the machines used in Sections A, and B. However, each shield was operated differently depending upon each contractor's practices. Maximum surface settlements and operational parameters were also measured here along the tunnel alignment as shown in Figure 9. As can be seen in Figure 9b, very high face pressures were applied at the early stage of the excavation causing significant ground heave. Additionally, the applied face pressure was oscillated in the initial drive because the shield operator was determining an optimum pressure balance mode by trial and error.

Unlike Section B, although penetration rates recorded in the initial drive were relatively low (Figure 9c), the ground surface did not settle but heaved instead. It seems that the effect of very high face pressure dominated the behavior of ground response at this location. After the shield excavated the tunnel for a distance and the shield operators succeeded in obtaining an optimum operation, relatively constant face pressures and penetration rates were recorded. At this stage, the EPB shield can achieve low surface settlements during excavation.

Surface settlements were plotted against the distance from the shield face as shown in Figure 10. As

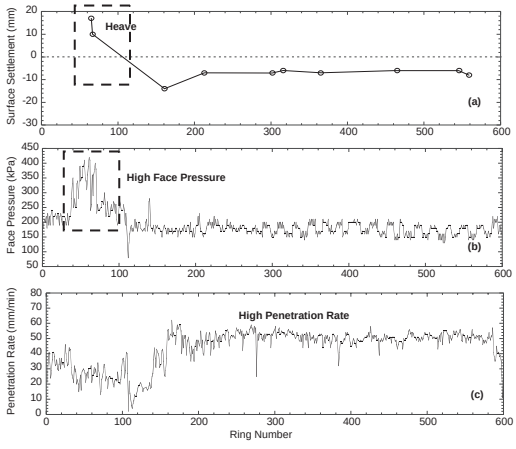


Figure 9. Surface settlements, face pressures, and penetration rates recorded in Tunnel Section C.

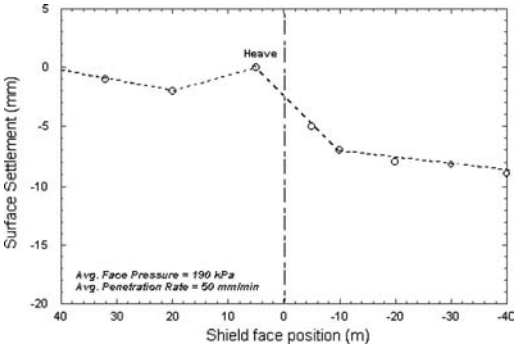


Figure 10. Longitudinal surface settlement profile measured over Ring No. 303-NB.

can be seen in the figures, the ground began to deform 30–40 m ahead of the shield. However, as the shield approaches the measurement sections at a distance of 3–5 m in front of the shield, the ground experienced a small heave before it subsided over the shield body. If one makes a detailed observation of the face pressures recorded in these sections, it was found that the applied pressure was relatively high during shield passing. Furthermore, penetration rates were also high (Figure 9c). Hence, the combination of these factors may have caused heave.

Based on the observation of Tunnel Section C, the face pressure and the penetration rate have impacts on the magnitude of surface settlements. It was found that if the face pressure is very high, ground heave will be observed regardless of the penetration rate. If the face pressure is low and the penetration rate is also low, relatively large settlements will be observed. Finally, if medium level face pressure and high penetration rate are used, some surface settlements will be found.

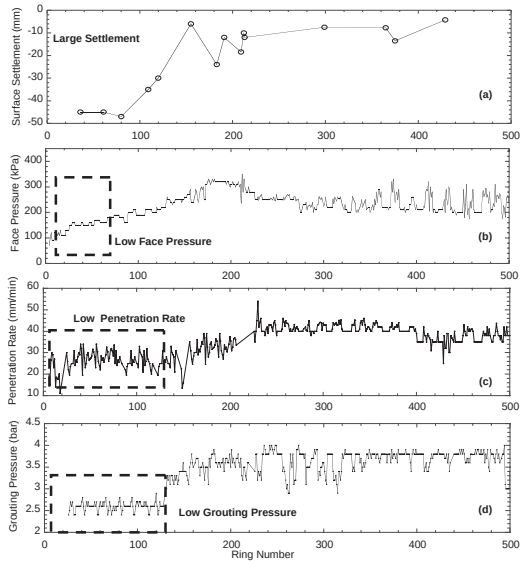


Figure 11. Surface settlements, face pressures, and penetration rates recorded in Tunnel Section D.

4.4 *Tunnel Section D*

In Section D, the southbound tunnel was excavated first and followed by northbound tunnel approximately one month later. Therefore, only the southbound tunnel is considered here. As in the other sections, surface settlement markers were installed along the tunnel alignment to measure the maximum and the development of surface settlements during excavation. Furthermore, extensometers were installed along the tunnel route in both the southbound and northbound tunnels to monitor subsurface settlements of the ground immediately above the tunnels in Section D.

Figure 11 shows maximum surface settlements measured along the southbound tunnel. Operational parameters including face pressure, penetration rate, and grouting pressure were also recorded. As can be seen in the figure, substantial surface settlements occurred within the initial drive zone. Within this zone, the learning curve of the crew may play an important role as well as operational parameters. For instance, Figure 11b shows low face pressures observed in the initial drive. After the initial drive, the shield developed greater face pressure that was built up to greater than 200 kPa. Obviously, in the pressure build up zone, smaller surface settlements were observed.

As can be seen in Figure 11c, in the early stage of excavation, penetration rates are relatively low. In addition, the grouting pressure applied at the early stage was also low (Figure 11d). Hence, the combination of low face pressures, low penetration rate, and low grouting pressure may also contribute to large surface settlements observed at the initial drive.

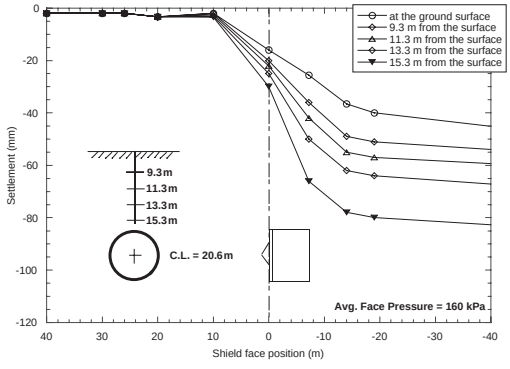


Figure 12. Subsurface settlements measured on RE-T5-001 over Ring No. 61-SB.

Within the initial drive zone, extensometer RE-5T-01 was located above ring no. 61. Large ground deformations were found over the shield crown at the monitoring depth of 15.3 m from the ground surface, and the magnitude of ground deformation decreases with decreasing monitored depth as illustrated in Figure 12. It was found that the ground began to subside approximately 10 meters ahead of the shield face and its deformation accelerated substantially over the shield body. The deformation then increased only slightly after the shield tail passed and no significant settlements were observed about 30 m after shield passing. Large ground settlements occurring ahead and over the shield may result from low face pressures and low penetration rates applied during shield passing.

Although very large ground deformation developed over the shield body as shown in the measurement section, the development appeared to slow down considerably as sharp inflection points of settlement curves were observed over the shield tail. Tail void grouting was performed at the segmental lining right behind the shield. This caused the inflection in the settlement curve. Note that tail void closure is a component causing ground deformation because of the gap between lining and ground. If no grouting was adopted to fill the void, the deformation in Zone 2 would extend further.

5 CONCLUSIONS

Based upon observations, in most cases, longitudinal surface settlements induced by EPB shield tunneling can be divided into three zones regardless of soil conditions namely, Zone 1, Zone 2, and Zone 3. Zone 1 originates ahead of the shield where the ground begins to deform. However, it should be noted that in the case of very high face pressures and high penetration rates, the ground might experience heave ahead of the shield in Zone 1. Zone 2 initiates a short distance in front of the shield face and develops significantly over the shield body. Also regardless of soil conditions, Zone 2 was found to be the largest portion of overall settlements. The final zone, Zone 3, begins after shield passing and after the tail void grouting has being performed. Operational parameters affect the magnitude of surface settlements within each zone. Large settlements found in Zone 1 are associated with low face pressure and low penetration rates. In contrast, if applied face pressures and penetration rates were very high, less surface settlements or even ground heave occurred in Zone 1. Face pressure and penetration rate also affect settlements in Zone 2 during shield passing and tail void grouting was found to influence settlements occurred in Zone 3.

REFERENCES

Atkinson, J. H., Potts, D. M., 1977. Subsidence above Shallow Tunnels in Soft Ground. *Proc. ASCE Geotechnical Engineering Division* 103(4): 307–325.

Kimura, T., Mair, R. J., 1981. Centrifugal Testing of Model Tunnels in Soft Clay. *Proc. 10th Int. Conf. of Soil Mechanics and Foundation Engineering* (1) : 319–322.

Mair, R. J., Taylor, R. N., 1997. Bore Tunneling in the Urban Environment. Theme Lecture, Plenary Session 4. *Proc. 14th Int. Conf. of Soil Mechanics and Foundation Engineering* (4): 2353–2385.

O'Reilly, M. P., New, B. M., 1982. Settlement above Tunnels in the United Kingdom – Their Magnitude and Prediction. *Tunneling 88*: 231–241.

Suwansawat, S., 2003. The Challenging Subway Project in Bangkok: New Hope of Thais in Solving Traffic problem. Keynote Lecture. *Proc. the 8th Conference of the Association for Computer Aided Architectural Design Research in Asia, Bangkok*.

Underground Space – the 4th Dimension of Metropolises – Barták, Hrdina, Romancov & Zlámal (eds)
© 2007 Taylor & Francis Group, London, ISBN 978-0-415-40807-3

Tunnel excavation by controlling water pressure in the ground with unevenly distributed water bearing strata

H. Takahara, J. Yorita & Y. Tuzuki
Iiyama Railway Construction Office, Japan Railway Construction, Transport and Technology Agency, Nagano, Japan

H. Takahashi
Kumagai Gumi Co., Ltd., Nagano, Japan

ABSTRACT: It is difficult to technologically assess the pressure and volume of the water in the ground near the excavating face. Therefore, long drainage boring has been adopted to reduce the pressure and volume of water on the assumption that the aquifer is evenly distributed. If high-pressure aquifers are locally distributed, however, it is difficult to reduce the pressure and volume of groundwater sufficiently by long drainage boring while stabilizing the cutting face. Therefore, the authors have developed a tunnel excavating method that combines long drainage boring and short drainage boring.

1 INTRODUCTION

The cutting face has been controlled in mountain tunneling by the NATM through evaluation of physical properties of the ground and deformations caused by excavation. In unconsolidated ground, it is very important to keep track of groundwater status in order to maintain the stability of the face.

Against this background, the authors have developed a new method for face control through confirmation of the presence of groundwater ahead of or near the face, and of groundwater pressure and volume, in the Tomikura sector of the Iiyama Tunnel. This paper reports a NATM tunnel excavation method that uses a new technique for water pressure control.

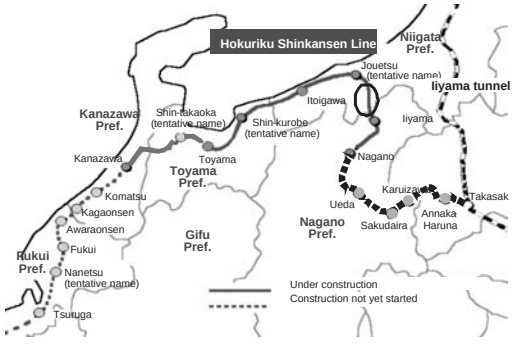


Figure 1. Hokuriku Shinkansen Line.

2 OUTLINE OF THE PROJECT

The Iiyama Tunnel is a mountain tunnel with an approximate length of 22 km that is located on the Hokuriku Shinkansen Line between Nagano City and Joetsu City, and connects Iiyama City in Nagano Prefecture with Myoukou City in Niigata Prefecture. The tunnel consists of six sectors and the Tomikura sector is the second sector counting from Nagano. Its total length is approximately 4,500 m. The overburden exceeds 200 m; the upward gradient from the beginning of the tunnel is 30 per mill, the highest point is approximately 152.700 km from Takasaki and the downward gradient at the end of the tunnel is 30 per mill. Construction work commenced in 1998, and a passage was successfully opened on the Joetsu side. At present, excavation is under way toward the Iiyama side, and the main tunnel excavation length exceeds 4,300 m.

The geology in the area of the Iiyama Tunnel is sediment formed in the process of elevation and subsequent terrestrial deposition of shallow sea regions at the end of the Tertiary Era and beginning of the Quaternary Era. In addition, the tunnel is located in the northern Fossa Magna, an area with advancing fold formations and prominent deformations in the geological structure. The ground of the Tomikura sector is made up of the Haizume Formation and the Nishiyama Formation of the Pliocene Era, and the Shiiya Formation and Teradomari Formation of the Miocene Era. Currently, excavation work is under way in the

Haizume Formation that is composed of alternate layers of sandstone, mudstone and conglomerate with a low degree of consolidation.

3 TECHNIQUE FOR CONTROL OF WATER PRESSURE

3.1 *History*

Unconsolidated sandstone layers make up the geology of the Tomikura sector, and surveys pointed out the possible presence of large volumes of groundwater under high pressure. Furthermore, though the groundwater level was confirmed to have been lowered after drainage boring, pressurized groundwater ingress was found in the face. There was therefore the fear that since the aquifer distribution would be uneven, ordinary drainage boring would be unsatisfactory to correctly grasp the existence of aquifer. In unevenly distributed aquifers such as in the construction sector in question, it is impossible to sufficiently reduce the pressure and volume of groundwater using long drainage boring alone and consequently it is very difficult to stabilize the face.

To deal with this problem, the authors have developed a tunnel excavation method that combines long drainage boring, to confirm the geology and groundwater volume and pressure ahead of the face, and short drainage boring, the purpose of which is to confirm the geology and aquifer status in the vicinity of the face, and to conduct drainage.

3.2 *Long drainage boring*

3.2.1 *Implementation method*

Long drainage boring is carried out at lengths in the range 100 to 200 m, with the objective to confirm the geological structure and the distribution of aquifers ahead of the face. In the event that aquifers are confirmed, groundwater volume and pressure are measured at the mouth of the bored hole, and the results are reflected in face control. The basic concept of long drainage boring is as follows:

1) In order to grasp the geology in the entire sector, it is necessary to implement core boring in such a manner that two succeeding borings overlap each other at their ends. They serve as drainage holes in the event that water ingress is found.
2) Construction positions that will enable prompt lowering of the groundwater level are selected with consideration to geological inclination and sedimentary status.
3) Borings are conducted so that they overlap on both sides of the face, even when water is not found.

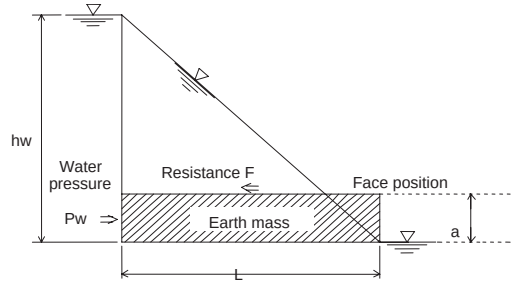


Figure 2. Schematic diagram of hydraulic.

3.2.2 *Control method*

In long drainage boring, a limit hydraulic gradient was taken into consideration as a control criterion in order to determine the pros and cons of excavation. The covering rock in front of the face was considered as a soil mass (width a × height a × depth L), and the balance between the water pressure (Pw) applied on the soil mass as described below and the resistance (F) of the soil mass to water pressure was taken into account and used as the control criterion.

$$PW = \gamma w \times hw \times a \times a$$

$$F = \gamma' \times (4\,hr + 2a) \times a \times L \times \tan\phi + 4a \times L \times C$$

a : sectional side length of soil mass (tunnel) (m)
L : soil mass length (covering rock length) (m)
γw : unit weight of water (1.0 t/m^3)
hw : piezometric head (m)
hr : thickness of overburden that contributes to resistance (m)
γ' : submerged unit weight of soil (1.0 t/m^3)
C : cohesion of soil mass (tf/m^3)
ϕ : angle of internal friction of soil mass (degrees)

In principle, the frictional force to the vertical load, which is equivalent to the overburden thickness, is estimated as resistance. However, consideration given to the possibility of loosening ground in the vicinity of the tunnel, or progressive failures starting from the face, the calculation was made conservatively, that is the overburden thickness hr is deemed to be zero, and only the dead weight of the soil mass is evaluated.

When Pw=F, the limit hydraulic gradient (iC = hw/L) is given as follows.

$$iC = (4C + 2a \times \gamma' \times \tan\phi)/a \times \gamma w$$

If C = 0 and $\phi = 30°$ assuming unconsolidated sediment ground, then the limit hydraulic gradient is approximately unity. Furthermore, a safety factor 1.5, the value that is used when exploring the possibilities for ordinary boring, is applied, and L/h = 1.5 is taken as the control criterion. However, considering the

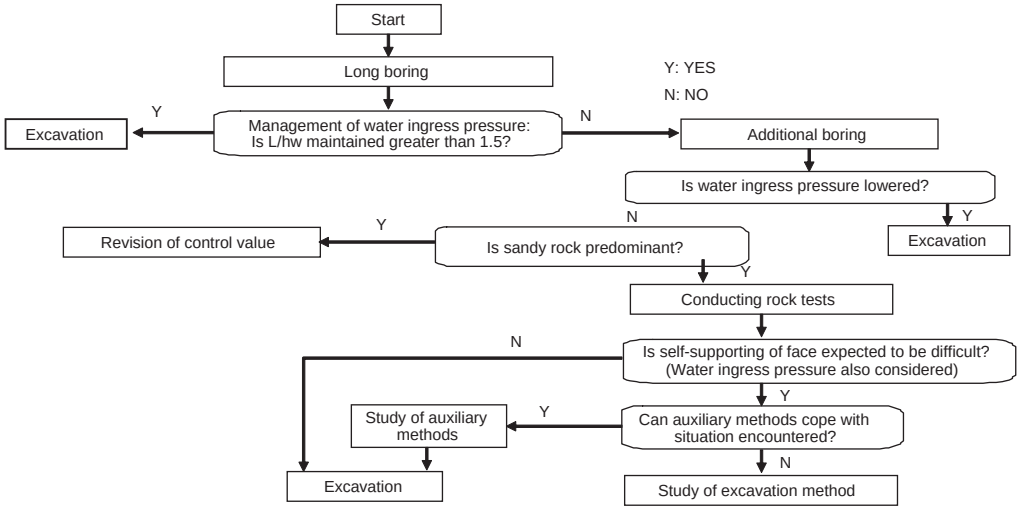


Figure 3. Flow of long boring management.

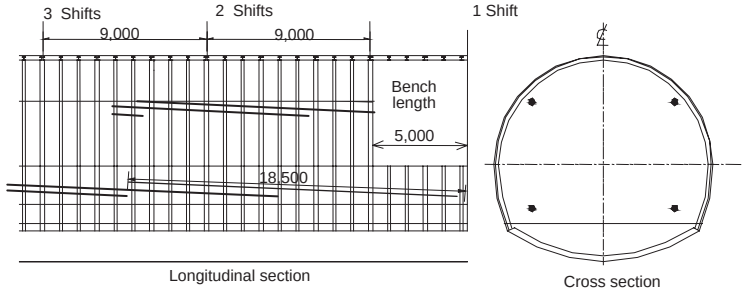


Figure 4. Schematic diagram of short boring.

ground status, the values for C and ϕ are revised and the control criterion is set anew. Figure 3 is a flowchart of the long drainage boring process.

3.3 *Short drainage boring*

3.3.1 *Implementation method*

The purpose of short drainage boring is to confirm whether there is locally distributed groundwater, which could not be found with the long drainage boring, around the face, and in the event that such groundwater exists, to lower the water level. Similar to the long drainage boring, it assesses the volume and pressure of groundwater and reflects the results in face control. The short drainage boring is carried out using FIT pipes that are used in forepoling, with a 9-meter pitch. The borings are made at a total of four points in the face – left and right shoulders and left and right on the bottom half (Figure 4). The length of the drilling is fixed to 20 m. The basic concept of short drainage boring is as follows.

1. It is implemented in order to confirm the presence of unevenly distributed groundwater that is associated with the inhomogeneous quality of the ground.
2. It is implemented also in places where water drips have been found.
3. The implementation position and frequency are modified more easily than those in the long drainage boring.
4. In the event that high-pressure groundwater is confirmed, excavation is terminated and necessary countermeasures are explored.

3.3.2 *Control method*

The control value was set such that a sufficient resting force could be ensured, maintaining face stability. In line with "Railway Structural Design Standards for NATM Tunnels in Urban Areas" and based on previous experience, the condition for application of this method in ground with sandy soil is that the pressure

Table 1. Results of long boring (∗L: face left, R: face right, T: crown)

No.	Distance	Bored hole length (m)	Water ingress volume (liters/min.)	Water ingress pressure (Mpa)	Necessary covering rock length (m)
1	151 km 840 mL	200	850.0	0.700	105
11	151 km 608 mL	200	173.0	0.340	51
16	151 km 475 mL	100	90.0	0.207	31
17	151 km 440 mL	120	340.0	1.500	50
18	151 km 428 mL	120	390.0	1.011	34
19	151 km 412 mL	116	930.0	1.513	50
20	151 km 396 mL	110	900.0	1.300	43
21	151 km 396 mR	165	209.0	1.043	35
22	151 km 385 mL	110	1,400.0	1.250	42
23	151 km 360 mL	200	5,000.0	1.100	37
24	151 km 360 mR	160	297.0	0.640	21
25	151 km 360 mL	100	1,740.0	0.820	27
26	151 km 335 mR	105	583.0	0.160	5
27	151 km 358 mT	100	7.5	–	
28	151 km 352 mR	136	1,500.0	0.310	10

head in front of the face should be less than +10 m from the face center. If the pressure head in front of the face is more than +10 m, a technique for lowering the water level should be considered in addition. Thus, water ingress pressure of 0.1 Mpa was set as the control criterion.

In the event that water-caused destabilization of the face is confirmed in the process of excavation, in which water pressure is controlled using the provisional reference value, auxiliary methods and drainage techniques are applied in order to stabilize the face and a downward revision of the reference value is studied. In the event of upward revision of the reference value, the resistance of the ground layers to water pressure is separately evaluated through core sample tests.

4 WATER PRESSURE MEASUREMENT RESULTS

4.1 *Long drainage boring results*

Part of the long drainage boring results are shown in Table 1.

The necessary length of the covering rock in this table is based on the control criterion, and the criterion was satisfied up to boring No.16. In boring No.17 a water pressure of 1.5 MPa was recorded, and the necessary length of the covering rock could not be attained under the initial control criterion. The core boring showed that the covering rock was made up mainly of mudstone. Referring to the properties of the ground, the authors revised the control criterion. As a result, covering rock length of more than 1/3 of the pressure head was set as the control criterion for this area (covering rock length of 50 m).

Determining the position where the preceding long drainage boring is to be implemented is extremely important in order to correctly grasp the geological conditions as soon as possible. The geological structure of the Tomikura sector is characterized by standing layers and there is a tendency for new layers to appear from the left on the face. Based on these geological conditions, a decision was taken to bore first the left of the face. Below is a description of the patterns of water volume in long drainage boring so far.

1. A large volume of water ingress was encountered through advance boring on the left side, while boring on the right side water ingress volume and pressure were not significant.
2. Large amounts of water ingress were confirmed in layers that had not been reached in the previous boring.

Based on the above findings, macroscopic lowering of groundwater level in the vicinity of tunnels was confirmed using the long drainage boring method.

4.2 *Short drainage boring results*

Water pressure has been measured 40 times so far. The measurement results are shown in Figure 5.

These results show that in some cases water pressure in the aquifer is relatively high even though the water ingress volume is small. Possible explanations for this are that the water bearing strata are of low permeability and have a high-pressure head, or that the groundwater is confined in an artesian condition.

Therefore, there is a high possibility that short drainage boring may prove efficient in reducing locally distributed groundwater level that cannot be lowered using the long drainage boring.

Distance	Upper half left①		Upper half right②		Lower half left③		Upper half right④	
	bolume (liters/min)	pressure (Mpa)	bolume (liters/min)	pressure (Mpa)	bolume (liters/min)	pressure (Mpa)	bolume (liters/min)	pressure (Mpa)
151km657m	17	0.033	0	0	9	0.003	34	0.019
151km639m	4	0.003	1.4	0.002	12	0.008	13	0.005
151km621m	2	0.001	47	0.076	4	0.001	10	0.002
151km612m	13	0.002	20	0.041	0	0	0	0
151km603m	0	0	10	0.048	25	0.012	25	0.010
151km567m	6.5	0.008	7.2	0.009	8.1	0.009	13.3	0.01
151km549m	0	0	53	0.075	13	0.001	5	0.001
151km537m	0	0	0	0	4.7	0.001	7.2	0.001
151km393m	1	0	0	0	11	0.005	18	0.013
151km366m	0	0	0	0	5	0.001	4	0.001
151km316m	0	0	0	0	0	0	0	0

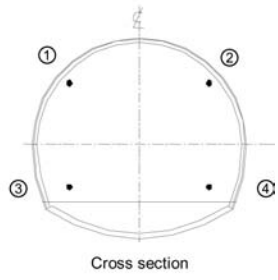


Figure 5. Results of short.

An example of this is a point located 151.541 km from Takasaki. There, water pressure exceeding the control criterion (0.1 MPa) was recorded in the upper right shoulder section during short drainage boring. The process implemented at this point was as follows.

1. In the course of excavation the rock bolts located few meters before the face have been pushed out approximately 20 cm.
2. After a water drainage hole was drilled again, there was a spurt of a large amount of water again.
3. Excavation was terminated and short drainage boring was performed. Water ingress was not found anywhere except for the upper right shoulder section, but high water pressure was confirmed in the course of drilling in the upper right shoulder section and drilling failed around the 12th meter.
4. Short drainage boring was performed again near the face, and water volume of 43 liters/min and water pressure 0.115 MPa were confirmed.
5. Water pressure exceeded the control reference value. Accordingly two drainage borings with L=30 m were made.
6. After confirming the reduction of water ingress volume and pressure following the drainage boring, a second short drainage boring was made in the upper right shoulder section at the point 151.541 km. Then, reduction of water ingress volume and water pressure was confirmed and excavation was resumed.

In short drainage boring made in areas other than the upper right shoulder, almost no water ingress was confirmed, which probably means that the geology was inhomogeneous. Also, long drainage boring performed in this area confirmed relatively high water pressure in the strata, and locally distributed aquifers, in which drawdown could not be sufficiently performed through long drainage boring, were recognized in advance using short drainage boring.

5 BENEFITS OF THE DEVELOPMENT

A system was constructed to constantly keep track of ground conditions in the vicinity of the face that is based on a systematic combination of long drainage boring and short drainage boring. This system enables early recognition of face status and determination of appropriate measures in advance.

Furthermore, since short drainage boring uses forepoling and face bolts to control water pressure around the face, it is not necessary to drill additional holes, and pressure is easily controlled as a part of the auxiliary processes. Thus, this development enables significant improvement of safety and economic efficiency by minimizing time required.

6 CONCLUSIONS

This development is particularly efficient in tunnel excavation in ground with a low degree of consolidation and large volumes of groundwater since it enables accurate evaluation of groundwater and water pressure around the face (a potential cause of collapse). It also sufficiently lowers groundwater level, and thus improves the safety of excavation operations. Therefore, it is recommended that in the future tunnels constructed under similar circumstances are excavated using the new control techniques developed in this sector that utilize the short and long drainage boring methods.

This page intentionally left blank

Underground Space – the 4th Dimension of Metropolises – Barták, Hrdina, Romancov & Zlámal (eds)
© 2007 Taylor & Francis Group, London, ISBN 978-0-415-40807-3

Prognosis of underground structures deterioration based on in-situ measurements

M. Vaníček, I. Vaníček & J. Pruška
Czech Technical University in Prague, The Czech Republic

M. Bubeníček & D. Jirásko
Ph.D. Students, CTU in Prague, The Czech Republic

K. Soga
University of Cambridge, Department of Engineering, UK

ABSTRACT: The stability of the underground structure is very important not only from the point of view of the structure itself, but also from the point of view of other structures. Therefore, the evaluation of the process of deterioration can help us very much. In the first part of the paper the ageing of the structures in the scope of their life cycle will be described. The whole process of deterioration is important but limited to certain time intervals and is able to give signals about changes in macro-scale. The second part of the paper is focused on the adaptation of new methods: micro technology of monitoring – such as MEMS (Micro Electrical Mechanical Systems) and wireless technologies for data transfer. It is obvious that such new technologies have to be assessed for the ability to deliver data continuously and for their safety and solidity. At the end of the paper the application of the measurements on the Prague metro's lining is mentioned.

1 INTRODUCTION

Recently a great attention is devoted to the problem of structure ageing. Relatively significant proportion of engineering structures were constructed during the last century, whereas an average service life in industrialized countries is roughly 50 years. Therefore there are two basic questions. The first one is dealing with problem of ageing generally and with the influence of this ageing on structural safety. The second one is connected with the most appropriate time when to carry on a small repair or complete reconstruction or substitution of the old structure by a new one. The decision-making process is also affected by an access to the structure. For example the quality of a motorway surface can be easily checked, while more complicated are checks of bridges and underground structures. The presented paper concentrates on underground structures, especially on metro systems and is one of the outputs from the European project "Ageing of underground structures". Hence the problems regarding the most appropriate time for remediation together with the possibilities and significance of monitoring are described here. The requirement for continuous monitoring is stressed as there are minimum demands on operating staff, especially when the signals from the underground are monitored with the help of wireless technology on the surface.

Monitoring of micro cracks can give us highly significant signals when some unexpected change is registered. Real time monitoring of continuous crack development together with the defined maximum allowable crack opening size can define more precisely the expected service life. For underground structures as for similar engineering structures a usual service life is nowadays about 120 years. Different certificates are required by the authorities for the materials to be used in such structures in order to guarantee the specified service (design) life. Nevertheless, for such important structures as metro is, it would be very useful to be able to predict the time at when this limit state will be reached. We would expect much longer time than is the usual expectancy. For many underground structures the result of monitoring will be very useful in this matter. Therefore some proposals how to approach this problem are described in more details. These proposals are part of the above mentioned common European research project.

2 AGEING OF STRUCTURES

Engineering structures require monitoring, expert inspections, and periodic maintenance in order to determine their state and define when is the best time to carry out repair works instead of expensive and time-consuming reconstruction, usually accompanied by closure of traffic in not to far distant future. The monitoring of the ageing process of underground structures has a substantial importance because signs of deterioration may remain unnoticed. Due to the complicated access, the identification of the signs of underground structures might be difficult. The subsequent repair works or even reconstructions are usually more complicated and more expensive in comparison with new construction.

The deterioration process of underground structures is mainly influenced by the surrounding aggressive environment, external or internal loading and traffic. The whole ageing process can be accelerated by defects of load bearing structure, which are stated for reinforced concrete in Table 1 (Soga et al., 2005).

The whole process of deterioration can be divided into four phases:

1. Latent period – this stage follows the construction of structure. The deterioration and decreasing of the quality doesn't occur.
2. Progressive period – the deterioration curve decreases with time, the first cracks and subsequent possible seepage can appear.
3. Acceleration period – the deterioration curve decreases rapidly, the cracks develop, the reinforcement rusts and concrete degrades. It leads to a loss of the section of the structural member.
4. Deteriorated period – the quality of structure permanently decreases, the strength of material looses, which results in collapse of structure.

The phases of deterioration and deterioration curve are demonstrated on Figure 1. It is evident, that effect of repair works depends significantly on time. If the reconstruction of the underground structure is done in the accelerated period, a suitable state can be achieved with minimum costs. In case of late reconstruction in the deteriorated period it will require much higher costs in order to achieve the same level of desired quality of reconstructed structure.

Table 1. Summary of deterioration categories for reinforced concrete.

Deterioration category	Seriousness
1. Progressive corrosion of steel reinforcement bars through continuous water seepage or repeated cycles of humidity and dryness. Rust and rust fluid is detected on the surface of the concrete.	The seriousness can be minor at this stage before this situation becomes one that requires urgent measures.
2. Cracks have been generated within the concrete as a result of corrosion of the steel reinforcement bars. An increase of rust fluid and swelling in the vicinity of the cracks is detected.	If swelling is identified in the vicinity of cracks, there is the possibility that exfoliation has occurred.
3. Diagonal and intersecting cracks	When cracks have been generated in a regular pattern or when the cracks are concentrated, this may indicate that the design mechanical strength has not been achieved.
4. Falling of concrete debris as a result of expansion of rust due to corrosion of the steel reinforcement bars.	This is a situation that is close to becoming an urgent one.
5. Progressive corrosion of the steel reinforcement bars that are exposed (phenomenon that occurs at the cross section of steel reinforcement bars).	The rate of corrosion of the steel reinforcement bars accelerates. If it is left unattended, there is every possibility that the situation will develop into an urgent one.

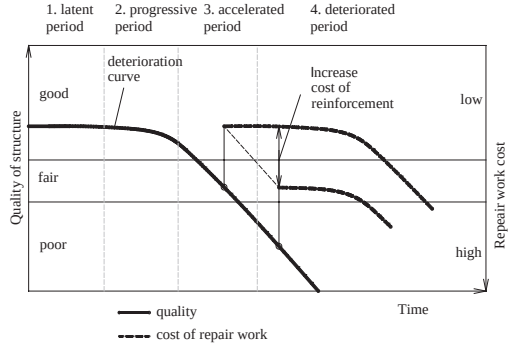


Figure 1. Life cycle of ageing structure.

3 THE PROJECT OF MONITORING

The main aim of the European research project is a development of a complex wireless monitoring system Underground M^3 that is to be able to provide data for assessment of tunnels ageing grade. The system is to be designed for cracks detection using a special computer vision and for monitoring using the latest advances in micro electrical mechanical systems (MEMS) and in wireless data transmition. This potentially cheap monitoring technologies can significantly reduce the costs of tunnels operation i.e. maintenance, renewals,

repairs and reuse planning. Underground M^3 system development consists of four stages:

- micro detection – real time damage detection using computer vision,
- micro monitoring – MEMS strain sensors,
- micro communication – in ground wireless systems with power harvesting,
- system integration, data management and decision making.

3.1 *Micro detection*

Due to public pressures to run metro systems for 24 hours as well as limited human resources, we expect that the current method of network-wide human visual inspection will be difficult to conduct in the future. Instead of network-wide visual inspection of underground infrastructure by means of direct inspection (in person) or remote measures using geometry inspection devices, there is a need to conduct inspection more rapidly and automatically. In the frame of this European research project it is proposed to develop a real-time damage detection system using new advances in computer vision compared to the existing surface imaging technologies. It is important to note that the currently available technologies are static camera-based, whereas the new system utilizes video camera for fast data acquisition during inspection. The proposed system will detect surface cracks and color changes. In the proposed "Micro detection" system, the images taken from a video camera that is carried by an inspector or a robot will be put together by image mosaicing and will be registered automatically into a spatial coordinate system using the real time Camera Pose System recently developed at Cambridge, see Figure 2.

This system allows the images to be registered independently of the camera position (that is, the inspector does not need to be at the same location for every inspection even under different light conditions). Using the "super-resolution" technique of multiple video images, the quality of images that show cracks and surface deteriorations is improved.

3.2 *Micro monitoring*

Once significant anomalies or cracks are detected, there is a need for more intensive monitoring. Pointwise strain measurements are often suitable for certain above-ground building components (such as column and beams) because the strains do not change rapidly within these components. In underground infrastructure, this is not the case; there is large change in strain within a short distance by the soil-structure interaction because the external ground forces vary spatially. We therefore propose that the solution for underground

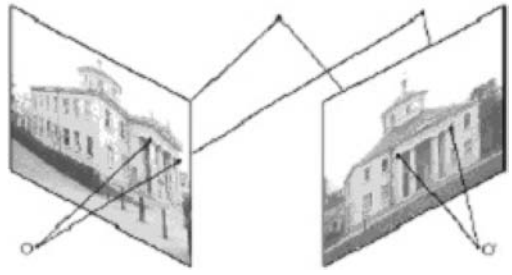


Figure 2. Camera pose system (Soga et al., 2005).

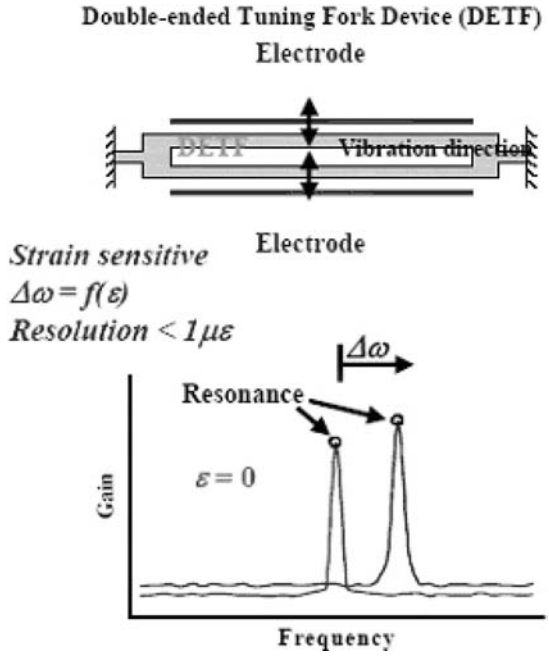


Figure 3. Schematic and principal of MEMS prototype.

infrastructure monitoring is the use of low cost sensors of a distributed nature. The project teams aim to develop low-cost MEMS strain or displacement sensors through the course of the project. Simultaneous readings from multiple sensors, possibly placed with diversity of space orientation, will allow for determining the spatial distribution of strains with high accuracy. An example of a MEMS resonant strain sensor that will be developed from existing prototype for the project is shown in Figure 3.

The basic principle is to couple the strains axially onto a vibrating beam. The added strain energy in the beam shifts its resonant frequency. The strain can be inferred by monitoring the shift in resonant frequency. Modeling of such an electromechanical resonator requires the inclusion of a stimulus and a

sensing transduction mechanism between the electrical and the mechanical domain. Electrostatic transduction is to be used in the project due to the good scaling properties with dimension and the relative ease of interface with control and detection electronics. Both parallel-plate electrostatic drive as well as comb-drive actuation principles will be explored. The controller electronics comprises of a sustaining amplifier that maintains resonant motion compensating for damping and other losses and accurately controls the amplitude and frequency of oscillation. Other types of low cost MEMS strain/displacement sensors will be investigated as well, including piezoelectricity as the transduction principle for silicon strain sensors. In all cases, technology fabrication processes would require either surface or bulk micromachining with proper etch-stop mechanisms.

3.3 *Micro communication*

The data obtained from the micro-monitoring sensors needs to be transmitted effectively to infrastructure owners. This also involves communication to other underground infrastructure owners since it is common that a failure or activity associated with one type of infrastructure impacts on or induces another failure in neighboring infrastructure. Problems also arise from the complex structure of monitoring and maintenance operations adopted by ageing infrastructure owners. It is often the case that discrete information and technical knowledge of circumstances surrounding pipeline or tunnel failures are scattered within a company. There is therefore a need to develop a common communication protocol (CCP) in which sensors in one type of infrastructure can effectively communicate with sensors in surrounding infrastructure. Recent advances in wireless communication allow us to do this easier than before when old fashioned hard wire communication was used. We propose the use of IMOTE/STARGATE technology (see Figure 4) currently developed by Intel.

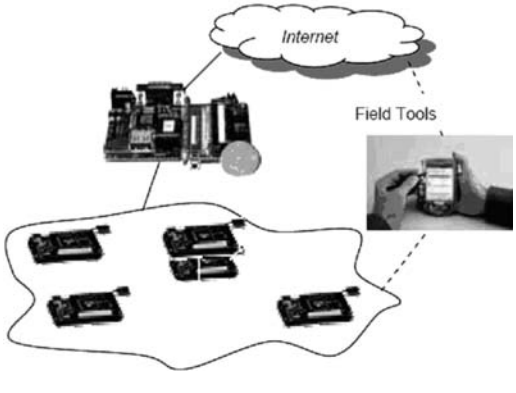


Figure 4. Network wide communication.

IMOTE is a generic wireless communication system and incorporates a small processor coupled with TinyOS that can perform data processing before sending the information to the main server. Since most available wireless technologies are limited to working in air, their use for underground infrastructure may be restricted, especially with regard to sending data between non-connecting underground infrastructures. This project will integrate IMOTE and in-ground wireless technologies, allowing the development of a trans-infrastructure network that transmits signals both through soil and air.

To ensure maximum efficiency and network life, the proposed micro-communication systems will operate under low power consumption conditions. In addition, we propose to develop an energy harvesting unit integral with MEMS/Wireless communication technology that will power these devices. This solution is practical as the sensors will be used for long-term monitoring and as a result will not be required to make measurements very frequently. It is proposed to use the energy available in the surrounding environment (e.g. harnessing energy from pressure fluctuations and wind flow while trains are running).

3.4 *System integration, data management and decision making*

Once the data are gathered, there is a need to interpret the data effectively to make appropriate decisions. The key for a successful development of Wireless Sensor Network systems with innovative sensors is identification of the fundamental causes of failures and associated warning signatures. This is often a difficult task due to the nature of the failure modes, involving complicated interactions between Internet Field Tools the underground structures and the surrounding ground. The monitored data will be used to update the understanding of the on-going soil-structure interaction and model parameters for future prediction needs to be selected through a parameter optimization process. The proposed research includes the following development of assessment tools for long-term performance prediction:

(a) Tool 1: Predicting deformation developments of underground infrastructure. The following aspects will be assessed: (i) Magnitude of cracks (including crack pattern analysis), (ii) Deformation of underground shape, and (iii) Load bearing capacity (including the corrosion of reinforcing bars/dowels and steel segments).
(b) Tool 2: Decision support system with automatic diagnostic capabilities. The tool will assess the subsequent impact on underground function based on the inspection and survey results, using past experience and numerical analysis.

In order to develop a data analysis and expert system for Underground M^3, the following three levels of data interpretation will be adopted.

- 1st level: Compilation of all data sensors, including a rough analysis of the measurements, in order to identify those sensors providing limit values. A simple comparison with limit strains would be a convenient procedure to identify potential critical zones. Post-processor software is required in order to manipulate the information in a user-friendly manner.
- 2nd level: Mechanical analysis of the potential critical areas. Only some zones would require further analysis. That includes a finite element analysis of the 3D geometry involved in the zone (i.e., the lining, the surrounding ground, any buildings affected by the underground structure, etc.). An optimization module should be used to identify parameters of the materials, in order to assess the integrity of the structural elements. Identification of models or geometry could be attempted as well, if the complexity of the problem requires such extension.
- 3rd level: Suggestion of actions to be undertaken by the manager, regarding the maintenance of the underground infrastructure. This task will be performed by an expert system software that integrates all the information provided by the preceding levels and also the experience accumulated from previous analyses.

3.5 *In-situ macro measurement*

In order to incorporate new technologies into existing underground infrastructure, it is proposed to install conventional monitoring devices so that the performance of the new technologies can be properly evaluated. The macro monitoring experiments proposed for deformation measurements are:

- tiltmeter, which can provide an accurate history of structure deformation – movement,
- tape extensometer, which is used to detect and monitor changes in the distance between two reference points,
- VW crackmeter, which is able to measure the deformation of cracks and joints.

Geophysical methods such as seismic tomography or geophones, which can give more information about changes in material properties with depth (of the tunnel lining) and it is planed to use them at selected field sites.

4 SELECTION OF APPROPRIATE PLACE FOR MONITORING IN-SITU MEASUREMENT

The choice of the appropriate locality with respect to the project aims and objectives was carried out and the Prague Metro was selected as the main location. In order to gather relevant information, the selection of the location for monitoring is very important. For this purpose selected sections of Prague's metro were visited and inspected. Figure 5 shows general view into a double track tunnel of Prague's metro. After checking through the chosen Prague metro's sections, few trial sites were selected.

On Figures 6, 7 and 8 are presented three examples of traced defects on selected trial sites. On these macro-cracks in-situ measurements – macro-monitoring will be realized and in parallel on nearby micro-cracks micro-monitoring will be performed. The final decision about monitored profiles will be compared with numerical modeling and specified as a result of the soil-structure interaction occurring at the sites.



Figure 5. General view into a recently finished double track metro tunnel in Prague.



Figure 6. First example of traced defects – transversal cracks and their simple monitoring using plaster tags.



Figure 7. Second example of traced defects – longitudinal cracks across one lining section.



Figure 8. Third example of traced defects – both transversal and longitudinal cracks.

5 CONCLUSIONS

The importance of the monitoring of underground structures behaviour is becoming very important nowadays as it can help us to understand the development of the structure in time. At the same time the monitoring is becoming a multidisciplinary matter as it is combined in expert system with theoretical knowledge of the structure and results from numerical models. Also the development of such micro-monitoring devices integrates knowledge from currently available techniques in in-situ measurements, advances in micro-technologies in electronic engineering and wireless technology.

ACKNOWLEDGEMENT

The authors wish to express their gratitude to the Grant Agency of the Czech Republic for research project GA 103/06/1257 "Research of Ageing of Underground Infrastructures with the Help of Micro-measurements and Monitoring" for allowing preparation and presentation of this paper.

REFERENCES

Bubeníček, M. and Záleský, J. (2006). New possibility in the underground structures ageing monitoring (in Czech), *Stavební listy, June 2006*, Vol. XII, no. 6, p. 24–25.

Gourvenec, S., Mair, R.J., Bolton, M.D. and Soga, K. (2005). Ground conditions around an old tunnel in London clay, *ICE Journal of Geotechnical Engineering*, Vol. 1, pp. 25–33.

Soga, K. et al. (2005). Micro-Measurement and Monitoring System for Ageing Underground Infrastructures (Underground M^3). *Eurocores Programme*, Full Proposal, Cambridge University. 117 p.

Yimsiri, S. and Soga, K. (2002). Application of micromechanics model to study anisotropy of soils at small strains, *Soils and Foundations*, Vol. 42, No. 5, pp.15–26.

Záleský, J. and Bubeníček, M. (2006). New microsensors for monitoring of geotechnical structures deformation (in Czech). *In Proceedings of international workshop Field Geotechnical Methods*, Ústí nad Labem. AZ Consult, spol. s r.o., pp. 155–158.

Záleský, J. and Bubeníček, M. (2006) Project of monitoring of underground structures ageing (in Czech). *In Proceedings of Conference Foundations 2006 Brno*.

Underground Space – the 4th Dimension of Metropolises – Barták, Hrdina, Romancov & Zlámal (eds)
© 2007 Taylor & Francis Group, London, ISBN 978-0-415-40807-3

Interaction between tunnelling and groundwater – Its impact on tunnel behavior and ground settlement

C. Yoo & S.B. Kim
Sungkyunkwan University, Suwon, Korea

Y.J. Lee
RIST, Hwaseong, Korea

S.H. Kim
Hoseo University, Chunan, Korea

H.T. Kim
Hongik University, Seoul, Korea

ABSTRACT: This paper presents the results of 3D numerical analysis on a case history in which tunnelling caused groundwater drawdown and associated ground settlements. The dynamics of the effect of groundwater on the tunnel behavior and the ground settlements are thoroughly investigated by analyzing the results of analysis. The results highlighted the role of groundwater drawdown on the ground settlements and on the tunnel behavior. Based on the results, the ground surface settlement characteristics associated with groundwater drawdown are identified. Practical implications of the findings from this study are discussed.

1 INTRODUCTION

In response to the demand for significant upgrade to existing infrastructures in Korea the subway system in Seoul (Seoul Metro) is being undergone a recent major expansion. One example is the construction of Line 9 which runs underground from Kimpo International Airport on the western part of Seoul towards the Gang-Nam business district, located in eastern part of Seoul. As the entire route is aligned in close proximity to Han River and under heavily populated areas, such as Yuido, Banpo, and Gang-nam business districts, the geotechnical aspects of tunnelling conditions are rather difficult with high groundwater table.

Tunnelling beneath the groundwater table causes changes in the state of stress and the pore water pressure distribution. In such tunnelling problems, the tunnelling work inevitably causes water inflows into excavated area, thus causing the change in the pore water pressure distribution. The direct environmental consequence of water inflows during tunnelling is the drawdown of groundwater level in the surrounding aquifer (Yoo 2005). The related ground subsidence occurring as a result of the reduction in water pressures in the soil layers can damage nearby structures/utilities (Figure 1). One of the major case histories illustrating damage due to ground settlement associated with tunnelling-induced groundwater drawn is perhaps the Romeriksporten tunnel in which the highspeed railway tunnel construction caused more 1 m of ground subsidence due to groundwater drawdown, raising significant technical and political issues pertaining to the effect of tunnelling on surrounding environment (NSREA 1995).

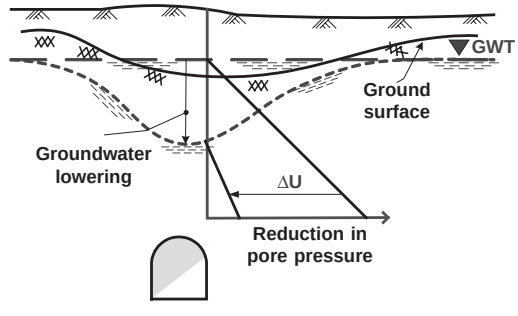


Figure 1. Illustration of ground settlement associated with tunnelling-induced groundwater drawdown.

This paper focuses on the interaction mechanism between tunnelling and groundwater in soft ground tunnelling. A 3D stress-pore pressure coupled finite element analysis was conducted on a tunnelling case

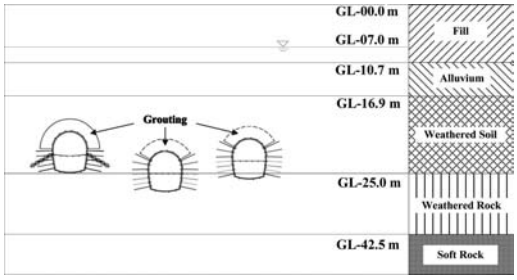


Figure 2. Transverse tunnelling condition.

of the Seoul Metro expansion project in which the tunnelling caused significant groundwater drawdown. Based on the results, the interaction mechanism between the tunnelling, groundwater lowering, and ground settlement was identified.

2 SITE CONDITION

2.1 *Subsurface condition*

The subsurface condition for the site under consideration is characterized by multi-layers of soil, including an alluvial deposit and a residual soil, with high groundwater table. Typical stratigraphy includes a 7∼10 m thick miscellaneous fill material including sand, gravel, and silty clay. Underlying the fill layer is a 7 m thick alluvial deposit followed by a 15 m thick decomposed granitic soil layer underlain by a weathered granitic rock layer having RMR values ranging 10 to 20. The weathered granitic rock layer is followed by a soft to hard granitic rock layer with RMR values ranging from 26 to 38. The hydraulic conductivity of the residual soil layer is on the order of 2×10^{-6}m/s. The groundwater table is relatively high at GL -3 m, located in the alluvial layer, thus leaving the entire tunnel is to be excavated through the water bearing weathered soil despite as shown in Figure 2. The geotechnical properties of the each layer are summarized in Table 1.

2.2 *Tunnelling condition*

The tunnel section considered in this study is approximately 350 m long and consists of three parallel tunnels with slightly varying elevation, as marked in Figure 2. The left most tunnel is returning (RE) tunnel, center and right most tunnel are west bound (WB) and east bound (EB) tunnels, respectively. The sequential excavation method (Eisentein & Sorensen 1986) was adopted. The cover depth of the tunnels is approximately 20 m on average, and therefore most of the tunnel sections run through the weathered soil deposit as mentioned.

Figure 2 illustrates cross sections of the tunnel with the standard support patterns adopted in the design.

Table 1. Geotechnical properties of ground.

Type	γ (kN/m^3)	c' (kPa)	ϕ' (deg)	E (MPa)	ν	K (cm/sec)
Fill	18	0	27	6	0.40	3.8×10^{-4}
Alluvial	25	25	30	10	0.40	3.8×10^{-4}
Weathered soil	25	15	33	50	0.33	2.4×10^{-4}
Weathered rock	25	50	35	120	0.30	8.8×10^{-5}
Hard rock	26	100	35	200	0.25	5.0×10^{-5}

Note: γ = unit weight, c' = cohesion, ϕ' = internal friction angle, E = young's modulus, ν = poisson's ratio, K = coefficient of permeability

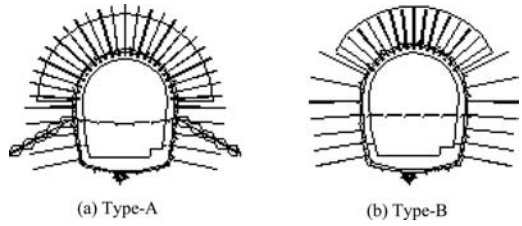


Figure 3. Standard support patterns.

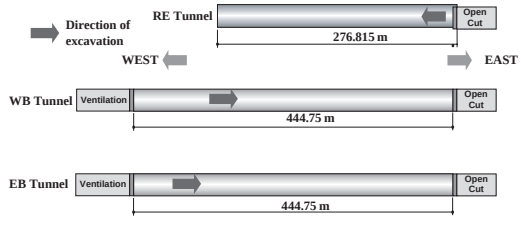


Figure 4. Excavation sequence.

The three tunnel sections has the same cross section of a maximum height and width of 8.4 m and 11.4 m, respectively, giving a net excavation area of approximately 100 m^2. The bench cut method was adopted with one segment excavation length of 0.8 m. The support system consists of a 0.16 m thick steel fiber reinforced shotcrete (SFRS) layer with 3 m long system rock bolts. In order to promote the face stability, the pipe roofing technique with fiber-reinforced pipes (FRP) of 60 mm in diameter was adopted. Note that the top heading distance between the EB and WB bound tunnels is kept approximately 20 m. The excavation sequence is that the WB and EB tunnels are excavated with the top heading distance of 20 m. Upon completion of the approximately 300 m long WB and EB tunnel, the RE tunnel is then excavated from the east, as given in Figure 4. Details of the tunnel design are summarized in Table 2.

Table 2. Support pattern summary.

Support pattern	SP-A	SP-B
Gound condition		
0.5D above crown	Residual soil	Weathered rock
Upper	Weathered rock	Weathered rock
lower	Weathered rock	Weathered to soft rock
Excavation method	Bench cut	Bench cut
Length of excavation (m)	0.8	0.8
Shot'c thickness (m)	0.16	0.16
Rock bolt		
Length(m)	3.0	3.0
Longitudinal spacing(m)	0.8	0.8
Transverse spacing(m)	1.6	1.6
Auxillary method		
Crown and face reinforcement	– FRP(MSG) roofing (L = 12.0 m, ϕ 60 mm) – Cover zone:180° overlap: 4 m	– FRP(MSG) roofing (L = 12.0 m, ϕ 60 mm) – Cover zone:180° overlap: 4 m

3 3D COUPLED FINITE ELEMENT ANALYSIS

3.1 *Fundamentals of stress-pore pressure coupled analysis*

The commercially available finite-element package ABAQUS (ABAQUS 2003) was used for analysis which is capable of simulating the stress-strain-strength behavior of ground in stress-pore pressure fully coupled manner. Note that the importance of carrying out the stress-pore pressure fully coupled analysis for tunnelling cases where the interaction between the tunnelling and groundwater takes place has been discussed by Yoo (2005).

A porous medium is modeled approximately in ABAQUS by attaching the finite element mesh to the solid phase. A continuity equation, equating the rate of increase in liquid mass stored at a point to the rate of mass of liquid flowing into the point within the time increment, is written in a variational form as a basis for finite element approximation as Eq. (1).

$$\int \sigma : \delta\varepsilon dV = \int t \cdot \delta v dS + \int \hat{f} \cdot \delta v dV \quad (1)$$

Where dv is a virtual velocity field, $\delta\varepsilon = sym(\partial\delta v/\partial x)$ is the virtual rate of deformation, σ is the true (Cauchy) stress, t are surface tractions per unit area, and $\hat{f}$ body forces per unit volume. For coupled analysis, $\hat{f}$ includes the weight of the wetting liquid.

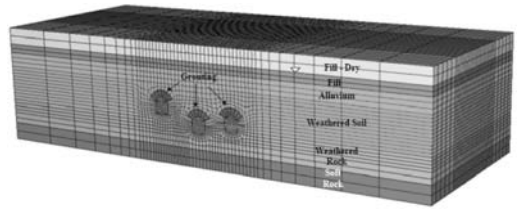


Figure 5. Finite-element model used in the analysis.

$$f_w = (sn + n_t)\rho_w g \quad (2)$$

Where ρ_w is the density of the wetting liquid and g is the gravitational acceleration, which we assume to be constant and in a constant direction. Considering this loading explicitly so that any other gravitational term in $\hat{f}$ is associated only with the weight of the dry porous medium. Equation (1) can be rewritten as Eq. (3):

$$\int_V \sigma : \delta\varepsilon dV = \int_S t \cdot \delta v dS + \int_V f \cdot \delta v dV + \int_V (sn + n_t)\rho_w g \cdot \delta v dV \quad (3)$$

where f are all body forces except the weight of the wetting liquid. The liquid flow is described by introducing Darcy's law or, alternatively, Forchheimer's law.

The continuity equation is satisfied approximately in the finite element model by using excess wetting liquid pressure as the nodal variable (degree of freedom 8), interpolated over the elements. The equation is integrated in time by using the backward Euler approximation. The total derivative of this integrated variational statement of continuity with respect to the nodal variables is required for the Newton iterations used to solve the nonlinear, coupled, equilibrium and continuity equations.

3.2 *Finite-element modeling*

Figure 5 shows the finite element model adopted in this study, consisting approximately 57,000 nodes and 53,000 elements. The finite-element mesh extends to a depth of two times the tunnel diameter (D) below the tunnel spring line and laterally to a distance of 8.0D from the returning and east bound tunnel centerline. At the lateral boundaries, displacements perpendicular to the boundaries were restrained whereas pin supports were applied to the bottom boundary.

With regard to the hydraulic boundary conditions and with reference to Figure 5, a no-flow condition was assigned to the vertical boundaries perpendicular to the tunnel drive. The pore water pressures on the left and right vertical boundaries are assumed to be constant throughout the analysis at the original

groundwater level of GL-3 m. The locations of the lateral and bottom boundaries are selected so that the presence of the artificial boundaries does not significantly influence the stress-strain-pore pressure field in the domain.

The ground and the shotcrete lining were discretized using 8-node displacement and pore pressure elements with reduced integration (C3D8RP). The rock bolts were modeled using the 2-node 3D truss elements. With regard to the material modelling, the soil and rock layers were assumed to be an elasto-plastic material conforming to the Mohr-Coulomb failure criterion together with the nonassociated flow rule proposed by Davis (1968), while the shotcrete lining and the rock bolts were assumed to behave in a linear elastic manner. The geotechnical properties for the ground given in Table 1 were used for analysis. The young's moduli of the shotcrete and rock bolts were chosen as 10 GPa and 21 GPa, respectively.

The actual tunnelling process consisting of a series of FRP grouting, excavation, and lining installation stages was closely simulated in the analysis by adding and removing corresponding elements at designated steps. After establishing the initial stress and pore pressure conditions with appropriate boundary conditions, the step-by-step tunnelling process pertinent to the bench cut excavation method, was then simulated. Note that the excavation sequence of the east and west bound tunnels as well as the returning tunnel was closely simulated as given in the design documents.

4 RESULTS AND DISCUSSION

4.1 *Ground settlement*

Figure 6 illustrates the development of ground surface settlement trough with the tunnel excavation. Also shown in this figure are the measured settlement values using the geodetic method. As seen in Figure 6, the tunnelling-induced ground surface settlement trough tends to become noticeable well before the WB tunnel heading reaches the section. The WB and EB top heading advance further deepens the trough causing a maximum settlement of 220 mm upon completion. One interesting trend is that the excavation of RE tunnel does not significantly increase the maximum settlement but tends to widen the trough.

The results of the total stress analysis without considering the stress-pore pressure coupled effect yields much smaller, less than 50% of that from the coupled analysis in terms of maximum settlement, and narrower settlement trough as shown in Figure 7, demonstrating the importance of carrying out stress-pore pressure coupled analysis when predicting the tunnelling-induced ground settlement.The effect of face advance on the ground settlement is better illustrated in Figure 8. As seen approximately 60% of the

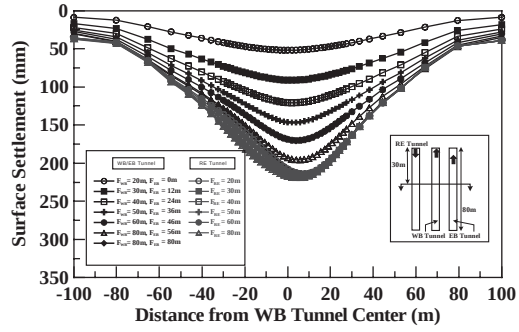


Figure 6. Ground surface settlement trough at various stages of tunnel.

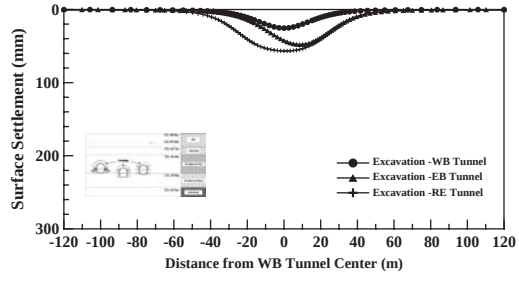


Figure 7. Settlement troughs from total stress.

maximum settlement at the measuring point A takes place before the top heading of WB tunnel reaches the section. The passage of top headings of the WB and EB tunnels further causes the rest 40% of the settlement as seen in this figure. The trend of which a significant portion of the total settlement occurs well ahead of the tunnel heading is a direct consequence of the groundwater drawdown caused by water inflow from the non-grouted excavated boundary. Note that the groundwater drawdown curve at the measuring point A, shown in Figure 9, resembles that of the surface settlement. In addition, as expected the settlement trough extends laterally approximately 80 m showing a larger inflection point ($i = 42$ m) than cases without groundwater drawdown. Again the groundwater drawdown is responsible for the trend shown in these figures as discussed by Yoo (2005).

4.2 *Tunnel deformation*

Figures 10∼12 illustrate the longitudinal crown settlement profiles for WB, NB, and returning tunnels at various locations of respective tunnel top heading. It is of worth noting that approximately 2/3 of the final crown settlement occurs before the top heading reaches the corresponding section. Compared to which typically 30 to 40% of final crown settlement occurs

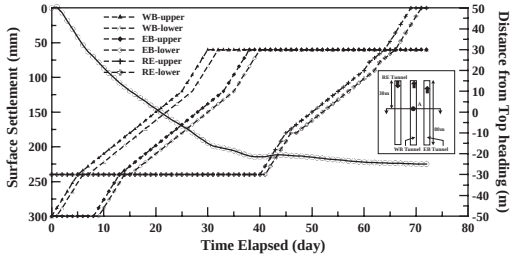


Figure 8. Development of settlement at point A with tunnel excavation.

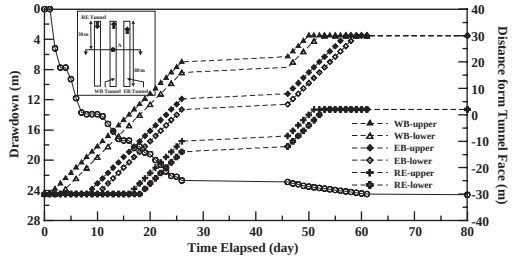


Figure 9. Groundwater drawdown with tunnel advance at point A.

before top heading reaches such pre-settlements values appears excessive and again such a trend is due to the groundwater drawdown ahead of the tunnel heading. It should therefore be expected that the traditional geodetic measurement technique being performed in-tunnel can only measure 30∼40% of final crown settlement. This may lead to unsafe-side estimate of tunnel stability in terms of the tunnel convergence. This is well illustrated in the measured data plotted in these figures as they represent only 20 to 30% of the final crown settlement predicted by the 3D analysis. Care should therefore be exercised when interpreting the tunnel deformation measurements for tunnelling cases where tunnelling accompanies groundwater drawdown.

Another of importance trend is that the final crown settlement for the RE tunnel is only 60% of those for the WB and EB tunnels. This is due primarily to that the RE tunnel excavation takes place under much lower hydraulic head as the WB and EB tunnel excavation significantly lower the groundwater level to the RE crown. The shear strength of the ground around the RE tunnel is thus expected to be greater than the WB and EB tunnel as the effective stresses are larger.

CONCLUSIONS

This paper presents the interaction mechanism between tunnelling and groundwater in soft ground. A 3D stress-pore pressure coupled finite element

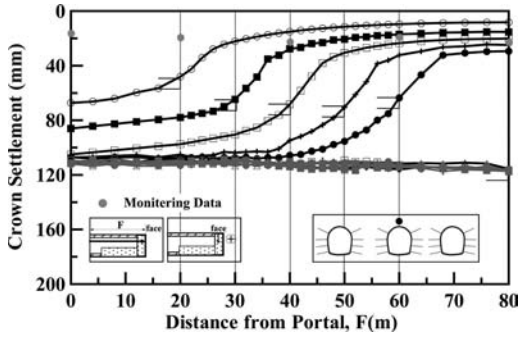


Figure 10. Longitudinal crown settlement at various stages (WB tunnel).

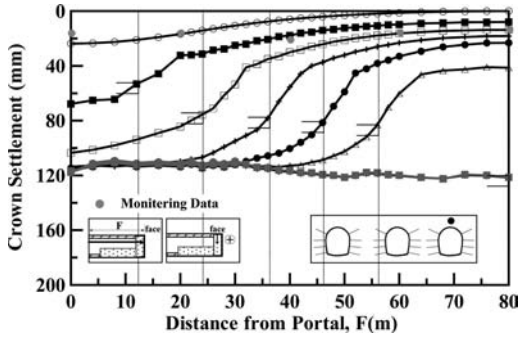


Figure 11. Longitudinal crown settlement at various stages (EB tunnel).

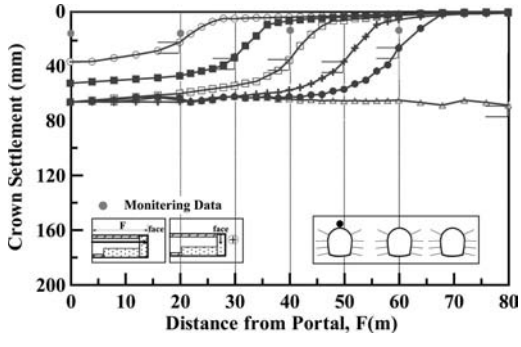


Figure 12. Longitudinal crown settlement at various stages (returing tunnel).

analysis was conducted on a tunnelling case of the Seoul Metro expansion project in which the tunnelling caused groundwater drawdown. Based on the results, the following conclusions can be drawn.

1. When tunnelling accompanies groundwater drawdown, a wider and deeper ground surface trough should be expected.

2. For cases where groundwater is lowered during tunnelling, significant portions, more than 50%, of the final crown and surface settlements may take place before tunneling heading reaches. Special care should therefore be exercised when interpreting the measured tunnel deformation data using the conventional in-tunnel geodetic method.
3. One way of improving tunnel stability during excavation is to lower groundwater level. This is well illustrated in the RE tunnel excavation.

REFERENCES

ABAQUS users manual, version 6.3. 2002. Hibbitt, Karlsson, and Sorensen, Inc., Pawtucket, Providence, R.I.

Davis, E. H. 1968. Theories of plasticity and the failure of soil masses. *Soil mechanics: Selected topics*, Butterworth's London, U.K., 341–380.

Eisentein, Z., & Sorensen, K.L. 1986. Tunneling for the south LRT extension in Edmonton: Alberta. *Canadian Tunnelling*. 19–30.

Norwegian Soil and Rock Engineering Association (NSREA). 1995. *Norwegian Urban Tunnelling*. Publication No. 10.

Yoo, C. 2005. Interaction between Tunnelling and Groundwater – Numerical Investigation Using 3D Stress-Pore Pressure Coupled Analysis. *Journal of Geotechnical and Geoenvironmental Engineering*, Vol. 131, No.2, ASCE.

Part 4.2
Conventional tunnelling

This page intentionally left blank

Underground Space – the 4th Dimension of Metropolises – Barták, Hrdina, Romancov & Zlámal (eds)
© 2007 Taylor & Francis Group, London, ISBN 978-0-415-40807-3

Integrated design and construction of Klashnice tunnels

P. Anagnosti
Civil eng. faculty Belgrade University, Serbia

D. Lukich
Civil eng. faculty Subotica, Serbia

ABSTRACT: Twin tunnels Klashnice in construction on the new highway E-661 in Republic Srpska (Bosnia) situated between Banja Luka City and its airport, have been designed basing on the contemporary tunneling construction procedure using primary support structure composed of reinforced spray concrete with radial ground anchors. The design and structure dimensioning was controlled using 2D "PHASE 6" software. The dominant rock mass along the tunnels consists of metamorphic rocks with flysh like structure with alternating marls and silica (chert) layers dipping at app. 30° along the tunnel axis. The max overburden is app. 50 m but the most of the tunnel length has its overburden thickness of the order of 30 m. The construction of the 375 and 480 m long tunnels is in progress, and the regular convergence measurements are used for control of the primary support behavior.

The paper describes the main points of the design and construction behavior of the primary support structure as the components of the unified procedure required for the optimum result in tunneling.

1 GENERAL DATA

Klashnice tunnels situated on the Highway E-661 Gradishka – Banja Luka in Republic Srpska consist of twin-tube dual carriage motorways. Each tube has the excavation cross section 11.70 m in its width and 9.25 m in its max height. The upper part of the profile is made with the radius of 5.85 m; the lower part is made as the rectangular with the height of 3.45 m. The traffic clearance is 9.50×4.80 m. The longitudinal slope of the invert is directed from the middle of the tunnel towards its portals, 1.66% towards the exit and 0.63% towards the entrance. The detailed design and construction works are contracted as the "turn key job" and at this date substantially performed by Integral Co. Banja Luka, The construction works started in 2004 year and substantial completion is expected in 2006 year.

2 GEOTECHNICAL CONDITIONS

The bed rock along the tunnel alignment consists of metamorphic "diabase – chert formation" that is predominantly composed of clayey and sandy schists, with sporadic inclusions of tectonized limestone and chert blocks. The basic clayey or marly rock constituents are irregularly weathered particularly in milonite zones. The overburden at the ground surface consists of gravelly – clayey colluvial deposit that may have thickness of 3 to 6 m. Another unfavorable feature is the shallow depth of the tunnel with overburden thickness above the tunnel crown that varies from 25 to 35 m for the most of the tunnel length. The very long gently sloping (app.15°) ground at the tunnel exit area, created unfavorable conditions for the stability of the long and deeply excavated slopes at the portal entrances.

The ground investigations consisted of 8 bore holes that provided the cores for visual examination and for laboratory tests on small sized monoliths. The performed bore holes thus provided mainly lithological and structural information of the rock mass along the tunnel alignment, and the ground water conditions. The geophysical soundings provided the most valuable data of seismic velocities ranging from $Vp = 3.8$ km/s and $Vs = 1.75$ km/s for the most competent rocks to $Vp = 1.8$ km/s and $Vs = 1.15$ km/s for the least competent rocks. The ground water presence has been attributed to its local percolation from the ground surface during rains and / or snow melting periods. The seismic impact which in the region of Banja Luka has PDE value of ground max acceleration of the order of 0.17 g has had minor influence to the support design of the tunnel structure. Its significance is however high for design of the surface structures

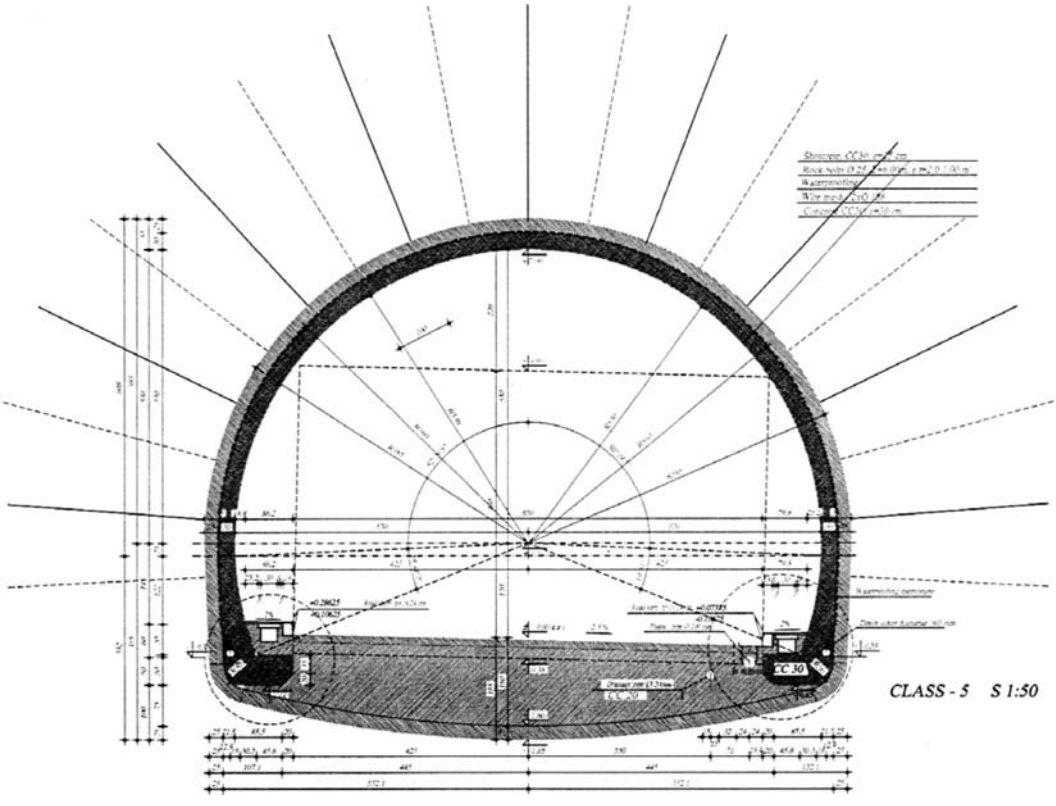


Figure 1. Klashnice tunnel tube type section.

and in portal areas. In general the design rock mass rating assessment (based on Bieniawski et. al. charts) resulted in RMR = 30 to 50 points for the most competent and RMR = 20 to 30 points for the least competent rocks. The design parameters (strength and deformability) for simulation of the rock mass and primary support behavior were derived from RMR rating. The additional empirical constants related to unconfined compression strength have been extensively used as the basic rock mass parameters. These constants have been then used for the estimate of mechanical properties of rock mass along the tunnel axis on the basis of the Hoeck – Brown contemporary empirical relationships between GSI and rock mass strength, and deformability. The cited "GSI" – Geological Strength Index has been recently extensively used as the basic rock mass parameter.

3 TUNNEL DESIGN AND CONSTRUCTION

Both tunnel tubes have been designed as "integrated rock – support" structure with rock support primary structure types classified in three basic support categories. It has been therefore anticipated that the rock competence is "good enough" to form the supporting ring around the excavation in jointed interaction with the primary support that allows the mobilization of the rock mass strength in vicinity of the supported excavation. The primary support has been designed to carry the rock mass pressures permanently i.e. without any interference with the final lining function. This approach resulted in the selection of the three classes of primary supports. In the most competent rock (RMR = 40 to 50 points), the primary support. consists of 15 cm thick sprayed concrete (with the compressive strength not less than 30 MPa), radial rock bolts at 2 m/2 m spacing, 4.5 m in length and standard reinforcement mesh of 4.2 mm bars at 10 cm spacing in both directions. This category however was used in the smallest length, of the order of 5 to 10% of the total tunnel length.

In the least competent rock (RMR = 20 to 30 points), the primary support consists of 25 cm thick sprayed concrete, radial rock bolts at 2 m/1.0 m spacing 5.5 m in length and two standard reinforcement meshes of 6 mm bars at 15 cm in both directions. The "inverted U" arched steel sections were placed

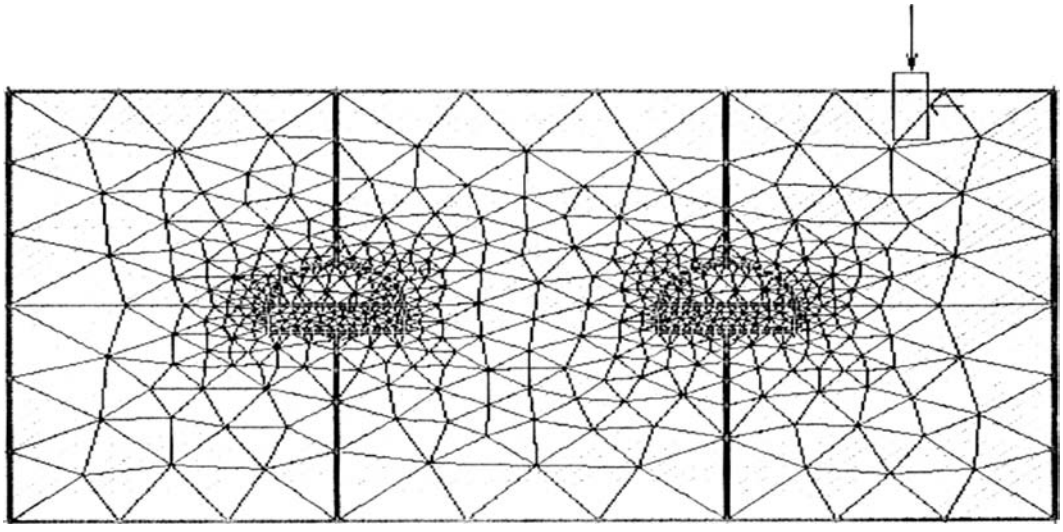


Figure 2. FEM modeling for twin tubes.

at the spacing from 0.5 to 1.0 m, as deemed necessary. This type of support has been used along app. 50 to 60% of the tunnel length. In the rock of intermediate competence (RMR = 30 to 40 points), the primary support consists of 20 cm thick sprayed concrete (30 MPa compressive strength), radial rock bolts at .0/1.5 m spacing 5.0 m in length, and two standard reinforcement meshes of 5 mm bars spaced at 15 cm in both directions.

The "inverted U" arched steel sections were placed at the spacing from 1 to 1.5 m, as deemed necessary.

After the completion of the primary concrete structure, the inner side of the sprayed concrete is covered first by the permeable geotextile liner and, then the waterproofing PVC membrane is fixed to prevent any ground water intrusion.

The permeable geotextile liner directs all eventual intruding waters to the collection pipe drains situated at the invert level at the both sides of the tunnel invert. This final lining is designed to carry the required infrastructure (lighting, fire protection, monitoring, traffic signs and other necessary facilities),and to provide adequate appearance inside the tunnel.

4 CONSTRUCTION PERFORMANCE

The excavation and primary support structure for the rocks of the cited competence usually applied within the sprayed concrete and rock bolting system (mainly quoted as NATM method), consists of the sequential excavation of the top heading following the excavation of the bench.

The cited procedure has been controlled by convergence measurements carried out in five points, one in the tunnel crown and two points on its left and right sides. At the installed marks the vertical and horizontal components of the inner sprayed concrete surface have been monitored for the period required for their stabilization. These measurements also indicated the requirements for forming up the section improving the support or to decreasing the length of unsupported excavation, and the possibility to compare the predicted values of primary support displacement to the actual ones. The original design provision of the cited procedure was based on the length of the fully supported top heading and bench section not less than 20 m in length before the start of the sequential excavation of the invert part. The excavations and primary support of the left tube was required to advance at least 30 m in front of the heading top of the right tube. The alignments of the tubes have been designed with inner (intermediate) rock mass space of app. 16 m thus providing the independent rock mass – support structure interactive relationship.

On the basis of performed numerical construction simulation (excavation and primary supporting) in 2D conditions by "PHASE V.6" software, the control of the actual displacements appeared reasonably well predicted for the better rock mass conditions and for the deeper parts of the tunnel.

This procedure was designed and performed in Klasnice tunnel, as no-blasting procedure, also with separate sequential excavation and the final – secondary lining consists of 30 cm thick reinforced concrete (30 MPa concreting of the lowest part of

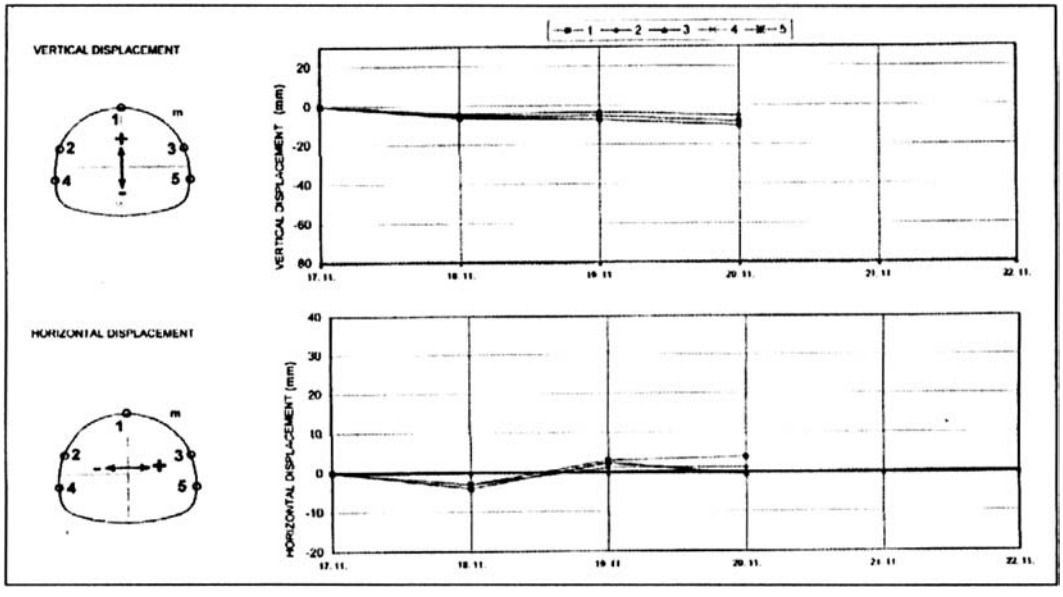


Figure 3. Type records for convergence measurements.

the invert as the latest step in CC) that is placed in conventional manner using movable formwork .

However the parts of the tunnel situated in the least competent rocks and being at the most shallow overburden thickness conditions, appeared less suitable for performed numerical simulation, that resulted in stronger support requirements and at the location app. 100 m from its exit the construction of the heading in the right tube was interrupted (in June 2006) by the rock fall in the length of app. 15 m forming the cave at the surface with the radius of app. 30 m at the collapse location the rock mass overburden thickness from the tunnel crown to the ground surface was app. 15 m thus indicating the limits of the reliable numerical simulation of the tunneling in the rocks of the low competency, such as appeared at the Klashnice tunnel.

The impact of this event on the construction timing and on the completion of the right tube required the fast and appropriate action for restoring the construction of the right tube. As the most adequate remedial procedure is envisaged the application of 20 m long fore poles – "umbrella" pre-support closely spaced steel tubes 4 inch dia, for forming up the complete arch above the designed excavation and primary support section. Then the step by step excavation of the collapsed rock mass and construction of 50 cm thick primary support ring fixed in the undisturbed rock mass at the lower part of the tunnel section is considered. The ground conditions at the tunnel exit have been considered in the design of the portal walls as "only conditionally safe" for a short period of time after excavation during dry season, the final stability had to be attained by backfilling of the excavated space above the tubes built as a "cut and cover" structures. The overall coordination of the works in this area was not fully performed to the cited requirements thus the development of instability of the area was prevented by retaining structure made of the row of closely spaced concrete piles made at the right side of the left tube.

5 LESSONS AND CONCLUSIONS

The "integrated design and construction" principle in tunneling often called by the acronym NATM, has been applied in the construction of Klashnice twin tube tunnel which substantial completion is expected in 2006. One of the basic requirements for the application of this tunneling procedure is the capability of the contractor to provide flexible and often very rapid modification of the initially designed excavation and primary support structure. The application of the cited flexibility is facilitated whenever the tunnel design is based on the already available experience in similar ground conditions, and previously performed estimates of the rock competence using RMR or some other reliable rating scale. The use of the available numerical simulation software is very helpful whenever the ground conditions correspond to the numerical models of rock mass used in the applied software, considering also the geometry limits of the model as important constituents to attain the proper

relationships with actual states. Nevertheless many important factors governing final stability of the primary support are to be learned during the construction period, and the changes of the rock mass competency associated with the size of the rock mass in question shall be constantly monitored and in an appropriate manner introduced into the structural reanalysis of the primary support. This is of the paramount importance particularly in case of the rock masses of low competence such as described in the case of tunnel Klashnice.

Still, even in inferior ground conditions, with accepting of occasional mishaps, such as local collapse of the top heading roof or/and front side, the "integrated design and construction" conceptual approach has its significant advantages comparing to the previously used firm design provisions for the primary support, that is inevitably linked to an overestimate of support requirements, particularly in poor ground conditions.

It is therefore, for the rocks similar to that were met in construction of Klashnice tunnel, the flexible approach in determination of final primary support dimensions, governed by the field experience gained during construction, shall be considered as fully appropriate. It is also important to stress that the geometry of the tunnel section and in particular its overburden rock thickness play very important role in selection of the excavation and support construction sequence and determination of necessary support strength.

The time factor, in tunneling is of primary importance, particularly in potential collapse situations, but also for the expedient completion of the already excavated or partially supported length. The monitoring of the performed support structure, was made mainly by convergence measurements, but also by monitoring of other important features such as cracks in sprayed concrete, appearance of percolating water etc.

All other records including the geotechnical rating of the rock mass during excavations are contributing to the timely completion of the tunnel structure, and provide the most reliable background for either improving support structure strength or decreasing its thickness, reinforcement number of anchors, etc.

REFERENCES

Hoek, E., Carranza-Torres, C.T., Corkum, B. 2002 . Hoek-Brown failure criterion – 2002 edition. *Proc. North American Rock Mechanics Society meeting in Toronto July 2002.*

Hoek, E., Brown, E.T. 1997 Practical estimates of rock mass Strength. *Int. J. Rock Mech.ˆMining Sci.ˆGeomechanics Abstracts. 34 (8), 1165–1186.*

Marinos, P. Hoek, E.2000 GSI – A geologically friendly tool for rock mass strength estimation. *ProcGeoEng 2000Conference, Melbourne*.

This page intentionally left blank

Underground Space – the 4th Dimension of Metropolises – Barták, Hrdina, Romancov & Zlámal (eds)
© 2007 Taylor & Francis Group, London, ISBN 978-0-415-40807-3

Tunneling in an urban critical area – A case study

J.M. Carvalho & A.T. Cavalheiro
Departamento de Engenharia de Minas – FEUP & CIGAR, Porto, Portugal

P. Teixeira
Golder Associate Portugal

ABSTRACT: A 700 m road tunnel crossing very heterogeneous granite formations within a critical area of the city of Porto, Portugal, in which around 400 m were excavated below groundwater according to NATM principles, has been open to public use in 2005. The average excavated section area is 100 m^2 with a cover varying between 2,7 m and 21 m. The concerned area is quite challenging from a geological/geotechnical point of view – very heterogeneous Porto granite rock mass overlaid by residual soil – as well as from a technical/environmental and social point of view – intense traffic, densely constructed and under construction area having some problematic old nearby buildings with delicate foundations. The question of whether or not explosives should be used in such an environment has been a very controversial issue. Following various geotechnical, geophysical, vibration surveys, reports and feasibility studies, the tunnel has been successfully excavated using mainly blasting techniques and, whenever necessary, mechanized means. During the tunnel excavation a comprehensive seismic vibration monitoring survey took place aiming at preventing damage risks as well as optimizing subsequent blasting diagrams. The present report, following a brief summary of some project key issues regarding namely the final feasibility study, adjusted in-situ strategies during the excavation works, monitoring procedures and safety measures, presents seismic vibration monitoring data treatment procedures and an example of the promising preliminary results aiming at improving the geological/geotechnical model inference along the tunnel alignment.

1 INTRODUCTION

In 2005 opened to public use a 700 m long shallow -cover varying between 2,7 m and 21 m – urban road tunnel in the city of Porto, putting an end to a several years long process. Although the initial geological/geotechnical site investigation program was concluded in 1995, throughout the following ten years several hindrances delayed the conclusion of the project namely doubts regarding whether or not explosives should be used, causing a two year interruption in the tunnel excavation.

In fact, the involved urban area is rather critical from a geological/geotechnical point of view – very heterogeneously weathered Porto granite rock mass overlaid by saprolitic soil – as well as from a social/environmental point of view – densely constructed and under renovation area, with some problematic nearby old buildings. Following some studies and technical advices pointing to the inadequacy of using blasting techniques in such an environment, a feasibility study was then undertaken (Carvalho et al., 2003) in order to assess the possibility of using explosives to excavate the 400 m mining tunnel sector.

The main conclusion of the study was the predicted adequacy of using explosives in a maximum of two thirds of the total length of the tunnel. Nevertheless, considering the critical urban area involved, it was advised a continuous cautious blast monitoring, beginning with a predicted initial advance of 1 m per blast. It was also expected that the monitoring would indicate the subsequent possibility of further advances reaching a predicted maximum around 2 m.

The tunnel excavation works, using mainly explosives, restarted in January 2004, the heading tunnel excavation finished in July 2004, and the complete excavation finished in October 2004.

Following a brief description of the mentioned feasibility study key points as well as of the tunnel project including, namely, excavation works, monitoring strategy and safety measures (Carvalho et al., 2005) the focus will be in the under development procedures, and some preliminary promising results, for the treatment of the seismic monitoring vibration data acquired during the opening of the tunnel, aiming at improving the geological/geotechnical model inference along the tunnel alignment.

2 SUMMARY OF FEASIBILITY STUDY

In order to assess the adequacy and advantage of using explosives along the tunnel excavation, vibration tests were carried out in two selected areas, taking advantage of at the time existing surface excavations. Several holes, drilled in the rock mass, were loaded with weighted ammonia gelatine 33% charges and data acquisition took place at the surface in selected representative places, namely close to foundations of nearby buildings.

Extensive exploration of the optimization algorithms especially implemented in MatLab language for this purpose allowed the selection of three sets of values, for the used Langefors & Khilstrom equation parameters, considered representative of the rock mass. Results pointing to the advantageous possibility of using explosives allowed the dimensioning of a drilling and blasting design adjusted to imposed legal constraints, namely by the 20 mm/s PPV threshold allowable by the Portuguese NP-2074 safety Standard "Evaluation of the influence in buildings of vibrations due to blasting or similar effects".

The mentioned three sets of optimized parameter values were then used in a particle velocity formula in order to obtaining tables of theoretical explosive charges for different distances from source, depending on the considered admissible PPV thresholds, according to Portuguese, Spanish and Swedish safety standards.

Based in the obtained tables for particle velocity thresholds – distance – maximum admissible charge, simulations were performed for the three considered data sets, considering different maximum admissible velocity scenarios. These simulations led to mapping of the tunnel susceptibility to being excavated by explosives, assuming a calculated drilling and blasting design.

The synthesis of many simulation results led to the conviction that using explosives in two thirds of the total tunnel length was an adequate solution.

The vibration tests allowed a good picture of time window lengths having higher peaks as well as determining relevant signal frequency bandwidths. This kind of analysis allowing namely an estimation of the minimum advisable time-delay between consecutive detonations, is rather important for the planning of micro-delaying in the blast global design, in order to minimize the total wave amplitudes resulting from the sum of effects due to sequential blasting.

It was suggested a blasting diagram based on the heading and benching method with fun cut central ring, comprising two main phases, respectively for the heading tunnel and for the bench, having the first phase three distinct sequential sub-phases.

As referred, the main conclusion of the study was the predicted adequacy of using explosives in two thirds of the total length of the tunnel with initial exploratory advances of 1 m.

3 TUNNEL OPENING

3.1 *Some generic project data*

The two-way road tunnel (Fig. 1) is part of an E-W traffic corridor of the town global traffic network. The tunnel has a total length of around 700 m from which 400 m were excavated in very heterogeneous granite formations according to NATM principles.

The average excavated section area is 100 m^2, the cover varied from 2.7 m to 21 m, the water load above the tunnel varied from 3 m to 12 m, and the volume of removed terrain was about 40.000 m^3. On the surface, along its alignment, are located several very sensitive old buildings.

The predicted geological/geotechnical conditions (Fig. 2) along tunnel alignment show a very heterogeneous underground formation changing from W1 massive granite to W6 residual saprolitic soil. This model was later up-dated namely in the less surveyed, by drilling, W6-W5-W4 zone.

3.2 *Tunnel excavation*

Based on available geological and geotechnical information it was possible to define six E-W geotechnical tunnel segments using a G1 to G5 geotechnical classification related to the conventional W1 massive granite to W6 residual saprolitic soil classification.

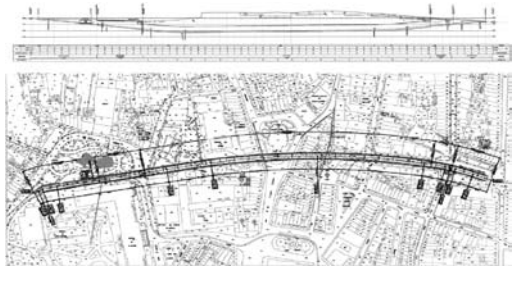


Figure 1. Tunnel alignment and cross section in top.

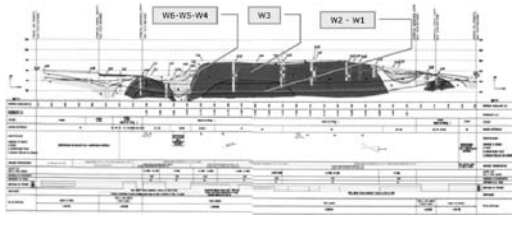


Figure 2. Predicted tunnel geological/geotechnical section.

The excavation was carried on using blasting techniques wherever possible and otherwise mechanical means were used, namely: roller-head, excavator bucket or hydraulic hammer. The excavation in poor ground is usually phased, accompanied by immediate shotcreting in order to minimize collapses of surrounding terrain and related surface settlements.

Excavation took place simultaneously from both sides, first for the total heading tunnel and next to the bench subdivided in two phases.

3.3 *Blasting*

In order to optimize the blast design constrained by Portuguese Standard NP-2074 PPV threshold, additional in-situ essays were carried on. Those results, combined with previously obtained ones in the mentioned feasibility study, lead to the finally adopted Langefors & Khilstrom equation parameters different from those previously obtained. Nevertheless the main conclusions of the feasibility study remained valid, namely the adequacy of blasting techniques use and the average advance per blasting event under the 20 mm/s PPV threshold adopted value.

The most advanced blasting control is presently, based on electronic detonators. In the present case the use of electronic detonators allowed optimizing the heading tunnel excavation method changing the initially suggested phased approach by a unique blasting event for the full front face (Fig. 3). The initially proposed phased approach has been adopted when mechanical excavation was used in weak clayish ground. In addition and among other advantages, electronic detonators allowed an excavation total time reduction of one month.

Figure 4 shows the blast diagram for second excavation phase, comprising the depicted two sub-phases "Bancada" and "Soleira" of the benching phase.

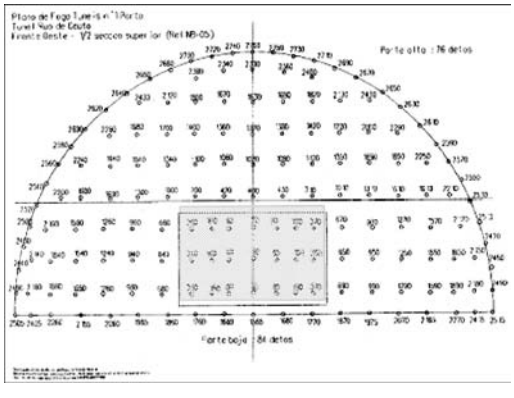


Figure 3. Heading tunnel: drilling design (blasting time sequence) with a 3 rows V shaped central ring.

The worst disturbance and possible danger in using explosives in an urban environment is due to induced propagating seismic vibrations. In order to monitor the attained vibration level at surface during excavation, before each blasting round was placed in the surrounding area a network of White Industrial Seismology, Inc. Mini-Seis seismographs that registered the ground induced vibrations. The analyzed results were used namely to tune the charges of the next blasting sequences and to identify and locate in the blasting diagram the charge responsible for exceeding the adopted PPV threshold, if this would be the case.

From more than a thousand of events, their PPV and predominant frequencies were registered in daily reports. The experimental distribution of PPV readings is very well fitted by a lognormal distribution as Figure 5 shows.

Presently, the mentioned acquired vibration data is being used in the subsequently presented methodology.

3.4 *Monitoring and safety measures*

Considering the very sensitive urban zone involved, a careful monitoring network has been installed at ground surface, buildings and underground. It has been controlled the displacements in buildings and terrain, the water level and the seismic and acoustic vibrations. All along the excavation geological/geotechnical characterization of crossed zones took place.

The monitoring campaign used the following equipments and procedures: accurate topographic survey at selected surface and in building locations; vertical

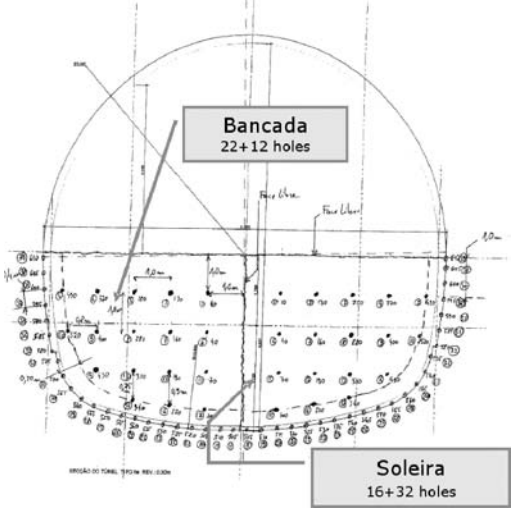


Figure 4. Two sub-phases of second excavation phase drilling design.

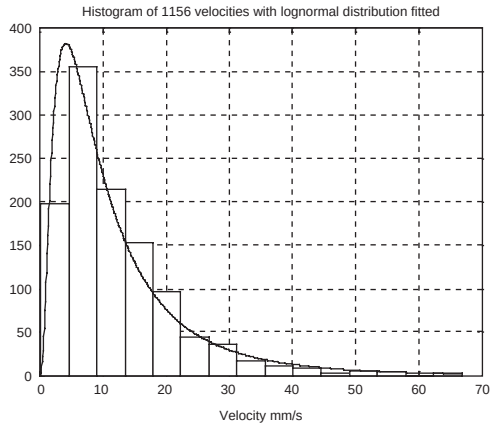


Figure 5. PPV histogram fitted by a lognormal distribution.

extensometers at surface; inclinometers for measuring horizontal deformation in depth; piezometers for water level control; tiltmeters for measuring displacements, namely rotational, in buildings; intensive survey of cracks was also made.

Every building considered in risk of damage during excavation was previously verified in order to establish adapted safety measures and, during excavation works, data from monitoring survey was analyzed in order to decide whether or not were necessary further safety measures.

4 VIBRATION DATA TREATMENT

Next will be presented a seismic monitoring vibration data treatment approach aiming at improving the ground characterization between the tunnel front, where blasting events take place, and the surface vibration monitoring detecting devices.

The fraction of the ground crossed by the generated seismic energy, between an underground single detonation and a receiver, may be considered a system/filter applied to an input signal, $s_i(t)$, whose output signal, arriving at the receiver, is $s_o(t)$. The Fourier transform of $s_o(t)$:

$$S_o(f) = \int_{-\infty}^{\infty} s_o(t) \cdot e^{-i2\pi ft} dt \qquad -\infty < f < \infty \qquad (1)$$

contains the amplitude and phase information of every frequency present in $S_o(f)$. Assuming an invariant receiver, the changes observed in $S_o(f)$, are mainly caused by the type and characteristics of the traversed ground and in a much minor degree by changes in the detonation characteristics.

In a blasting sequence, the recorded three component seismogram contains the information related to a number of different overlapping individual blasts whose overall frequency content is expected to vary with space or time.

The conventional Fourier transform of the registered seismogram does not allow establishing any correspondence between space or time and frequency domains. In order to establish such a correspondence will be used a windowed Fourier transform calculated by the Matlab function "specgram.m". This function splits the signal into overlapping segments, windows each with a Hanning window vector and calculates the spectrogram from signal, as a time-localized sequence of Fourier transforms.

In order to investigate the possibility of using this methodology to correlate the different ground characteristics/features along tunnel alignment with their distinctive associated frequency content, some seismograms were selected, corresponding either to different tunnel geotechnical sections or vibration monitoring positions.

In an ideal situation, the system impulse response i(t) or its equivalent, in the frequency domain, transfer function I(f), can be deterministically calculated.

Assuming an idealized input signal, $s_i(t)$, resulting from a detonation, as a Dirac impulse function, $k \times \delta(t)$ and the fraction of ground crossed by the seismic energy as a linear, stable system of constant parameters, the output signal, $s_o(t)$, reaching the receiver could be deterministically calculated as the convolution of $k \times \delta(t)$ by the ground impulse response, that is $k \times \delta(t)*i(t)$. In reality the recorded signal "results" from a sequence of partial convolutions associated with several crossed ground sections and overlapping seismic waves due to the sequential blasting events.

The preliminary results obtained with the referred approach are promising, pointing to the possibility of capturing, in the frequency domain, some geotechnical/geological relevant ground characteristics/features.

4.1 *Some preliminary results*

As an example, two seismic vertical component records, W432032 and W432036, were chosen corresponding to the monitoring at ground surface of the same blasting event, in which the heading tunnel excavation progressed 1,5 m eastwards and the maximum explosive charge in each of the 130 blasting diagram holes was 0,5 Kg. Figure 6 shows the partial geological/geotechnical predictive model section along tunnel alignment in which both blasting and monitoring took place. The blasting took place around PK 0+444 and the detecting devices were respectively located at surface around PK 0+443 for record W432032, almost vertically in respect to blasting, and around PK 0+473 for record W432036. The respective linear distance between blasting and detection was around 14,23 m and 32,27 m. Blasting took place close to an interface between two distinct grounds, corresponding to

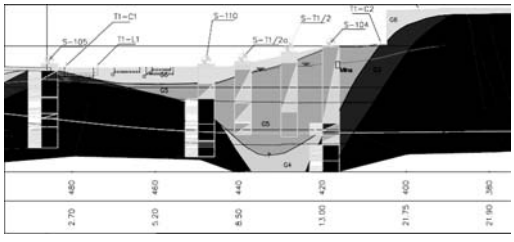


Figure 6. Predicted geological/geotechnical partial section.

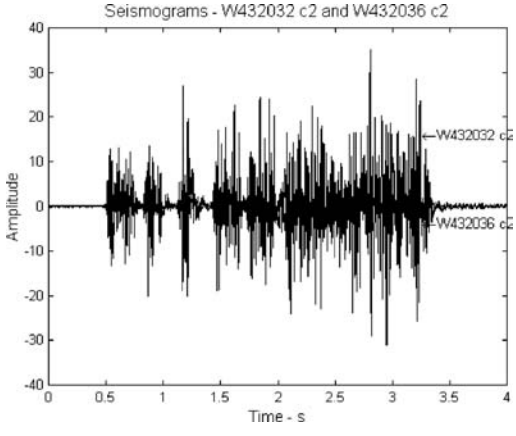


Figure 7. Seismograms W432032 and W432036.

different geotechnical predictive sections, G5 and G6 eastwards in the direction of tunnel progress and G2 and G1 westwards.

Figure 7 shows the two referred vertical detecting transducer records, W432032 and W432032.

The two seismograms amplitude spectra, after normalizing both spectra areas, are shown in Fig. 8 in which can be compared their global frequency content. The unit area normalization allows a clearly observable higher filtering effect of sections G5 and G6. In fact, although the traveled distance is significantly longer for record W432036, whose average trace amplitude is much smaller than for record W432032, the global filtering effect of the crossed ground is significantly less evident.

The referred effect is graphically put in evidence in Fig. 9 in which the difference between W432032 and W432036 amplitude spectra is shown, up to 275 Hz frequency. Negative frequency amplitude values correspond to the differential significantly higher filtering effect of the ground above the blasting event when compared with the predominantly G1 and G2 segments.

In Fig. 10 the phase spectra of both seismograms show the higher phase shift change rate global effect of sections G5 and G6 when compared with sections G1 and G2, accordingly to what could be expected.

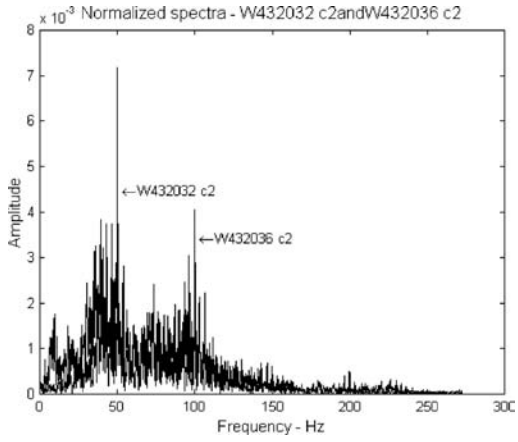


Figure 8. Signals W432032 and W432036 normalized amplitude spectra.

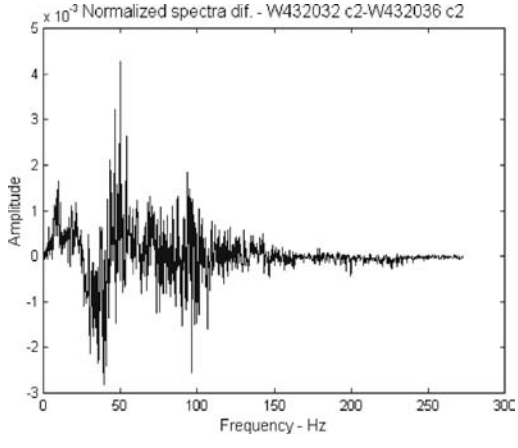


Figure 9. Signals W432032 and W432036 normalized amplitude spectra difference.

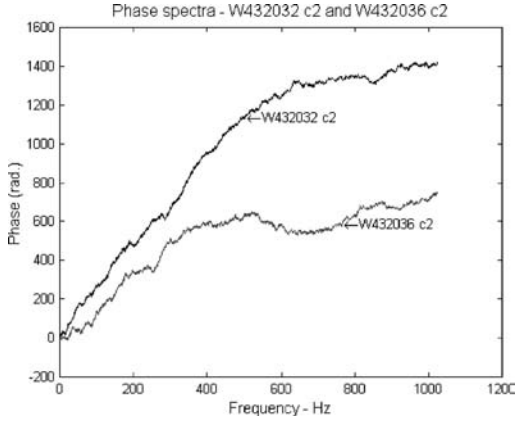


Figure 10. Signals W432032 and W432036 phase spectra.

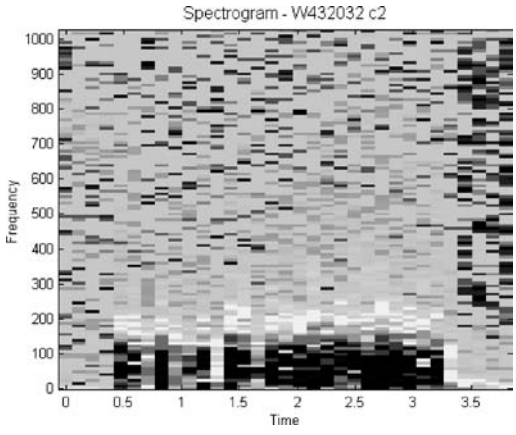


Figure 11. Spectrogram of W432032 seismic record.

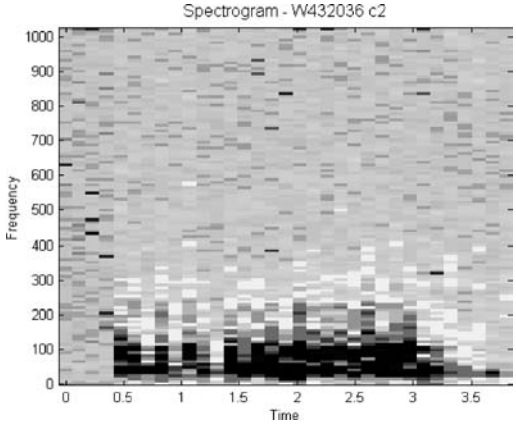


Figure 12. Spectrogram of W432036 seismic record.

As previously mentioned the conventional Fourier transform does not allow establishing any relationship between time or space domains and frequency domain. The next two figures showing the spectrograms of records W432032 and W432036 illustrate graphically the associated differential filtering effects in both cases as a function of time using a selected Hanning window. Its length may be adequately adapted in order to obtain a convenient spectra distribution along time.

In addition, to evaluate the relative energy absorption between both grounds, the following approach has been used.

The decrease of amplitude due to absorption for elastic waves in rocks and a given frequency appears to follow an exponential law with distance (Sheriff & Geldart, 1982):

$$A = A_0 e^{-\eta x} \tag{2}$$

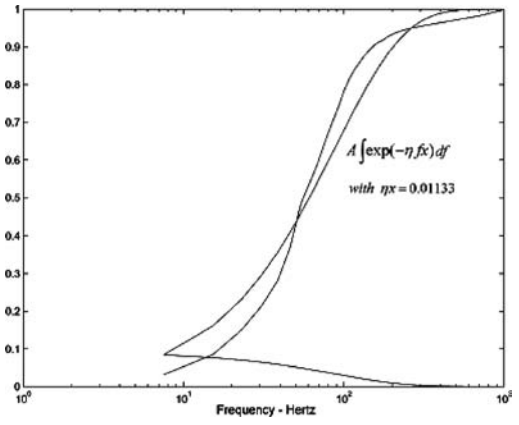


Figure 13. W432032 data fitted by the cumulative normalized module of Equation 3.

where A and A_0 are amplitude values of a wavefront at two points a distance x apart and η is the absorption coefficient. Experimental evidence suggests that the absorption coefficient η is approximately proportional to frequency, that is, $\eta \times f$ is roughly constant for a particular rock, so the final form that relates attenuation with frequency and distance is:

$$A = A_0 e^{-\eta . fx} \tag{3}$$

The adjustment of η, made with Nelder-Mead simplex search algorithm of Matlab Optimization Toolbox, on the records W432032 and W432036 normalized spectra cumulative curves, lead respectively to the following unit η values: $\eta_1 = 7,97 \times 10^{-4}\,\mathrm{m}^{-1}\mathrm{s}$ and $\eta_2 = 2{,}08 \times 10^{-4}\,\mathrm{m}^{-1}\mathrm{s}$, which means that attenuation in the first situation was, approximately, four times the attenuation in the other one. Figure 13 shows the obtained fit for record W432032.

5 CONCLUSIONS

Following a brief summary of the long process related to the opening of a road tunnel in the city of Porto, this report presents the preliminary results of vibration seismic data treatment. The generic aim of the present approach is to take advantage of data obtained during vibration monitoring surveys of underground excavation works with explosives in sensitive urban areas in order to gain a better understanding of the involved rock/soil mass formations. The promising preliminary results point to the possibility of reducing the uncertainty associated with the predictive initial geological/geotechnical model updating process.

The final objective of the described approach is to develop a methodology capable of capturing, in

the frequency domain, the "signature" of distinctive geological/geotechnical relevant ground characteristics/features allowing an optimized risk damage control.

ACKNOWLEDGMENTS

The authors are grateful to GOP-EM, a Porto townhall municipal enterprise for all the support, namely in providing information.

REFERENCES

Dowding, C.H., 1985, Blast Vibration Monitoring and Control. Northwestern University, Ontario.

Carvalho, J.M. *et al*, 2003 "Road Tunnel in Porto: Explosives or not, that was the Question – A Case Study", proceedings of the "EFEE 2nd World Conference on Explosives and Blasting", Prague, Check Republic.

Carvalho, J.M. *et al*, 2005, "Road tunnel excavation in Porto – successful experience using explosives ", proceedings of the "EFEE 3nd World Conference on Explosives and Blasting" Brighton, United Kingdom.

Gustafsson, R., 1973, Swedish Blasting Technique. Publ. SPI, Gothenburg, Sweden.

Langefors, U. and Khilstrm, B., 1973, The Modern Technique of Rock Blasting. 2nd. Edn. New York, Wiley.

Norma Portuguesa NP-2074, 1983, Avaliação da Influência em Construções de Vibrações Provocadas por Explosões ou Solicitações Similares. LNEC.

Olofsson, S.O., 1988, Applied Explosives Technology for Construction and Mining. Publ. Applex, Arla, Sweden.

Papoulis, A., 1962, The Fourier Integral and its Applications, McGraw Hill.

Santamarina, J.C. *et al*, 2001 Soils and Waves, John Wiley and Sons, Lda.

Sheriff, R.E. and Geldart, 1982, L.P. Exploration Seismology, Vol 1, Cambridge University Press.

This page intentionally left blank

Underground Space – the 4th Dimension of Metropolises – Barták, Hrdina, Romancov & Zlámal (eds)
© 2007 Taylor & Francis Group, London, ISBN 978-0-415-40807-3

Construction of city service tunnel in Ostrava without preliminary protection of surface

Karel Franczyk
Subterra, a.s., The Czech republic

Karel Dolinek
Tchas, a.s., The Czech republic

ABSTRACT: There is a long history in building city service tunnels in the Czech republic, especially in Prague and Brno. That tunnels are very sensitive to surface and protection of buildings. Therefore it is usuall to do a general protection of the surface facilities as a preliminary means before the construction starts. Those means (typically jet grouting, deep walls, etc) are however very expensive and not always are neccessary. During the city service tunnel construction in Ostrava, completed in 2003–2005 a very different way was chosen. The protection of surface was completed after precise measurements of settlements, ground water table changes, etc after decision of the group of experts. Thus the means were tailored to a specific problem and were limited in time, extend and cost. The way was very flexible and enabled to solve particular problems differently under specific conditions. The paper describes the observation methods, the decision making procedure, the protection means (grouting, chemical grouting, micropilots, jet grouting, bolting, etc), the final effect on the surface as well as the estimation of the cost saving, that has been significant towards the general protection method. The paper also briefly describes the project itself from the very beginning to the end, including the unique design of sewer positioning, and all experiences from the completion.

1 INTRODUCTION

The challenge that city of Ostrava in general,designers and contractors had been facing in 2002 was to build a service tunnel – nearly 2 km long – in the city centre conditions with many buildings close along, many of them disturbed by mining activities in a past, under heavy traffic roads and crossings, with gas explosion hazard due to methane occurrence and able to involve/apart from central heating, cables, water supply, etc.) a gravition sewer pipeline 1400 mm ID to 600 mm ID including all house connections.

2 IMPLEMENTATION OF TEAM DATA

Investor: Statutory City of Ostrava, Investment Department, Co-financed by the European Union, ISPA Fund, and Environment Ministry of the Czech Republic. Contractor: Ostavské kolektory consortium. Leader of the consortium: Subterra, a.s. Member of the consortium: Tchas, division Ingstav Ostrava. General designer: Hutní projekt Ostrava, a.s. Engineer : Consortium Technoprojekt – Halcrow JV. Building office: Ostrava.

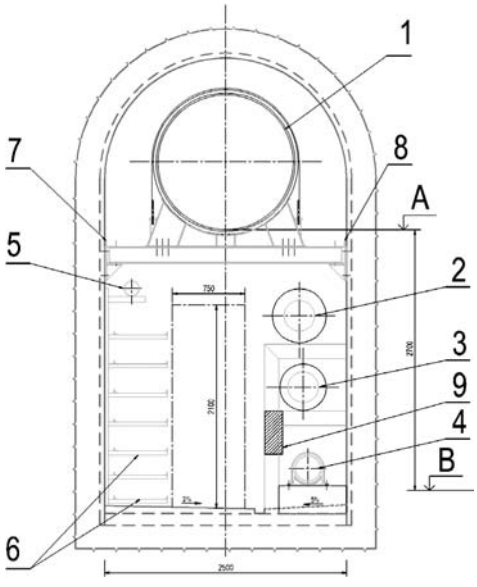
3 CONSTRUCTION DATA

Implementation period : 1. January 2003 to 30. November 2005. Tunnel length : 1769,57 incl. The 112 m of sewer gallery. Contract value : 702 mil CZK.

4 BRIEF CHARACTERISTICS OF THE CONSTRUCTION

It is a City service tunnel right in the historical centre of Ostrava that joins the service tunnel in Poděbradova Street, completed in 1999. Already during that construction it showed that when constructing the service tunnel network, the main difficulty will be the existing integrated sewer system deposited approx. 3 to 4 m deep under the street surface. In Poděbradova St., the sewer system renewal was solved using a new sewer pipe place in the excavation on both sides of the service tunnel.

The state of the City Centre sewer system resulted in a logical requirement by the City Council, that a problem-free rainwater and wastewater drainage be solved together with the service tunnel construction. The original study dealing with the City Centre service



LEGEND

1 Fibreglass tube of the main sewer
2 Central heating steel pipe – hot branch – DN 300 at maximum
3 Central heating steel pipe – return branch – DN 300 at maximum
4 Drinking water pipe – DN 150 to 250
5 Reserved for gas pipe – DN 150 at maximum
6 Cable racks
7 Cable trough for tunnel's own consumption
8 Cable trough for measurement and signalling
9 Socket box, approx. every 50 m
A Sewer bottom level
B Tunnel bottom level at axis Fibreglass pipe
Composite storage and supporting structures
Stainless steel bolted connections and fixing clamps
Reinforced concrete tunnel lining

tunnels proposed the placement of a new backbone sewer under the service tunnel. That, however, resulted in the following environmental problems:

- Repumping the wastewater and rainwater from the Ostrava City Centre
- Operating sewerage pumping station in the City Centre
- Operating costs of repumping the wastewater and rainwater reach the value of several million crowns during the tunnel lifetime

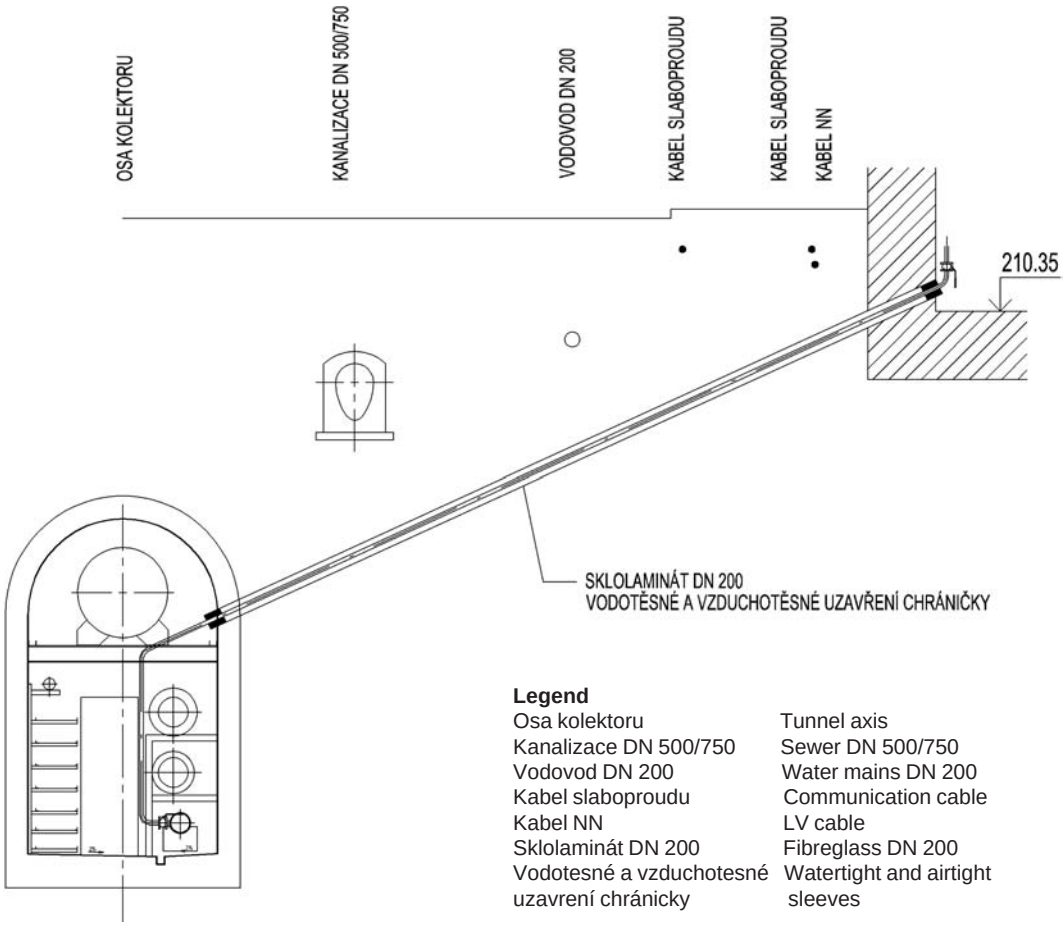
Therefore, during the Construction preparation, a goal was set that the tunnel provide also gravity drainage for the wastewater and rainwater away from the City Centre.

Such a requirement lead to verification of series of designs where the sewer pipe was placed on structures as well as in underground tunnels and finally a completely unconventional location of the sewer pipe was designed in the tunnel calotte. Since there is, from the urban point of view, a stabilised development in the City Centre around the tunnel, this enabled the long-term solution for a problem-free rainwater and wastewater drainage without the necessity of future excavations in the streets.

Geologically the tunnel was situated on the joint of two geological forms – neogene clays from the bottom and tercial gravels from the top. As clays have been waterproof whereas gravels are very permeable, the typical problem was dealing with huge water inflows. Another problem was changing character of the ground were both clays, as well as gravels changed many of its physical and geotechnical data very frequently.

The City Centre Service Tunnel is 1668 m long and along its whole length it was driven employing a mining method. 112 m long sewer tunnel – also driven – also forms a part of the Construction. The whole tunnel has a uniform width of 2.5 m and its height varies according to the diameter of the sewer pipe from 3.6 to 4.5 m. The driving was done classically, employing a new Austrian tunnelling method, mostly with two benches, in a lesser part in a full profile. The driving was done from six access points (shafts) simultaneously. After the tunnel was completed, five shafts were filled up and one created the Central Entry in the tunnel. Possible occurrence of methane under Ostrava could complicate the Construction; therefore some conditions applicable in coal mining had to be observed (methane indication, non-explosive design of electrical equipment, ventilation, etc.)

To connect surrounding buildings, local connecting sleeves have been constructed connecting the building to the tunnel. The sleeves, too, have been constructed using trenchless controlled drilling from the tunnel. Sleeves for heating and drinking water, gas connection, LV connection and telecommunication cable as well as sewer connection have been brought to every building along the tunnel. Sewer connections from the street gullies as well as from particular buildings are



Legend

Osa kolektoru	Tunnel axis
Kanalizace DN 500/750	Sewer DN 500/750
Vodovod DN 200	Water mains DN 200
Kabel slaboproudu	Communication cable
Kabel NN	LV cable
Sklolaminát DN 200	Fibreglass DN 200
Vodotesné a vzduchotesné uzavrení chránicky	Watertight and airtight sleeves

connected to new connecting manholes connected using trenchless technology to the sewer pipe in the service tunnel.

The new connecting manholes located in the pavement edge, or in the road, close to the kerb stone, allow a controlled connection of the house connections as well as street gullies. At the same time, such system provides for a possibility of connecting new sewer connections. Thus, 7518 m of connections have been constructed.

Gradually, the existing sewer branches, sloping towards the tunnel, were connected to the main sewer duct in particular intersections.

Drinking water mains, central heating, sewerage and some HV cables were placed in the completed service tunnel. Gradually, according to the needs, other HV cables, telecommunication cables, cable TV and others will be added. Supporting equipment and sleeves for houses, as well as in the intersections for connecting the adjacent streets, are prepared for all the energy distribution systems.

5 VERBAL DESCRIPTION OF THE CONTRACTOR'S CONTRIBUTION TO THE LIMITATION OF ADVERSE IMPACT OF THE CONSTRUCTION ON ENVIRONMENT

The Construction was implemented in the very centre of the City of Ostrava. In spite of that, apart from minimal occupation of land near the access shafts, the Construction in no way restricted the City traffic and transport. All the tramway, trolleybus and bus lines, as well as all the roads and walkways were preserved, even in the areas right above the large tunnel chambers (e.g. the K1 chamber's clearance is 7 metres and is situated mere 3 metres under the major intersection of Sokolská and Českobratrská Streets; during the construction, the intersection was fully operational). During the construction, all the requirements by the City concerning the noise, transport and dust were observed using the available technology (silencing the machine elements, using the continuous non-reload transport of concrete mixture with top panels over

the pouring areas, sprinkling when spraying concrete, removing the excavated materials only in the time specified by the City, etc.) In spite of a fact, that the tunnel goes in the city center all along buildings, none of the buildings had been stabilised before the construction to be preserved. There were measurements undertaken on all buildings as well as on the terrain itself, pointing the emergency as well as critical values of settlements for each of the buildings. The whole tunnelling was done under protection of roof bolting on a face. In case of touching the emergency points on measurements, other means were undertaken like jet grouting, micropilots and grouting of conventional materials. Thus – 6 buildings have been eventually protected by deep walls from the influence of the construction. This was however still much more economical solution as most of all buildings needed no protection at all. Even though some other 10 buildings have been repaired after the construction finished, these repairs were only cosmetic ones and the total costs of the construction remained considerabely lower compared to a possibility with uniform protection of buildings before the commense of the tunnel construction.

6 CONCLUSION

The project has won prices for "Environmental friendly construction of 2005" and "Water and sewer construction of 2005" in the Czech republic. It also applied for the International NO DIG AWARD on the ISTT conference in Brisbane in October 2006. At the time when this paper was written, no result on that was known.

Underground Space – the 4th Dimension of Metropolises – Barták, Hrdina, Romancov & Zlámal (eds)
© 2007 Taylor & Francis Group, London, ISBN 978-0-415-40807-3

Aspects of urban tunneling within the project of Sitina tunnel

M. Frankovský
Terraprojekt a.s., Bratislava, Slovakia

T. Aoki
Taisei Corporation, Tokyo, Japan

S. Choma
Národná dial'ničná spoločnost' a.s., Bratislava, Slovakia

V. Chomová
Dopravoprojekt a.s., Bratislava, Slovakia

V. Kotrík
Skanska BS, a.s., Prievidza, Slovakia

ABSTRACT: The 1,440 m long Sitina tunnel is the major structure built under the Lamacska cesta – Stare grunty section of the D2 Motorway project in Bratislava, the capital of Slovakia. The project is considered an extremely complicated as there is a number of aspects which had to be considered under the tunnel driving phase. In the first place, the tunnel was driven under the conditions of a highly weathered and altered granite formation and low overburden. The project also faced the challenge relating to the closeness of the site to the existing urban area. Driving work was executed downhill of and close to the research institute complex equipped with a number of sensitive measurement devices and the Zoo serving as the recreation zone for the inhabitants of the city.

1 INTRODUCTION

Bratislava, the capital of the Slovak Republic, is situated on the Vienna – Bratislava – Budapest line connecting three capitals on the river Danube. With its position close to Vienna and benefiting from the European TwinCity Bratislava – Vienna project, the town is facing the great development perspectives and hence necessitates for an intensive and complex solution in the field of transport infrastructure.

Moreover, the necessity to complete the basic infrastructure in Bratislava has sharpened due to the long-lasting failure to solve this problem.

Motorways D1 and D2 (Fig. 1) are the crucial lines of the transport infrastructure of the town. The Lamacská cesta – Stare grunty section including the Sitina tunnel is the last missing section of the D2 motorway connecting the Czech Republic and Hungarian borders, with a branch line to Austrian borders. The western part of the town currently suffers for the combined transit and urban traffic load concentrated to the Patronka junction area, the most heavily trafficked junction in Bratislava with the average number of 65 thousands vehicles daily passing through. The completion of the D2 Lamacska cesta – Stare Grunty motorway section would release the Partonka junction from the traffic burden and finally create the motorway section by-passing the centre of the town, which allows the urban roads to get released from the transit and outskirt urban traffic.



Figure 1. Project location on the city map.

2 LOCATION AND HISTORY OF PROJECT

The efforts aimed at solving the critical transport situation on the western road access to the town are more than 10 years old. First studies mentioning a tunnel-based solution were worked out in 1980s. In 1995, a technical study was developed for the Slovak road administration providing 9 alternatives of the connection of the Lamač D2 Motorway section to the Lafranconi Bridge. A number of alternative solutions, including 3 tunnel-based ones, were worked out in addition to the initial solution – the left by-pass underrunning the railroad and Patronka junction. The multi-criteria evaluation showed the solution including the 1.5 km long Sitina tunnel routed through the uphill bearing the same name to be the most advantageous. The land-use permit documentation for the chosen alternative was worked out in 1998 and the building-permit documentation in 1999–2001.

In the urban territory it was extremely hard to design a suitable corridor acceptable as the consensus considering all stakeholders' interests within the location concerned. Routing of this motorway section close to the Zoo recreation zone and the Slovak Science Academy buildings with a number of workplaces which could have been affected by the motorway section constructed and subsequently operated in their close neighbourhood raised the demand for specific solutions.

The first specific task included a thorough preparation of environmental and seismic monitoring. Based on the results of the noise, vibration and emission monitoring a number of measures including the adjusted working time and schedule aimed at minimizing the impact of the motorway construction, especially the necessary tunnelling works, onto the surrounding environment, were worked out and subsequently implemented under the construction phase.

Also, the noise and emission impact of the motorway in service had to be thoroughly considered. The anti-noise measures included the extension of the cut-and-cover section and location of the tunnel faces in from of the Academy area, and a system of anti-noise barriers behind the tunnel exit in Mlynská dolina close to the Zoo. The geographic situation of Bratislava and the local microclimate provide favourable conditions for the dispersion of emission in the atmosphere. Considering all the aspects, no additional measures were necessary to improve the tunel emission dispersion.

The tasks relating to the construction logistics and ensuring the smooth public transportation had to be faced in the design-preparation and construction phase too. The site included a number of heavy-trafficked public roads requiring a multiple traffic diversion and ensuring the site traffic access to both tunnel forefaces and minor sites of the structures designed on the existing road lines. Moreover, the time schedule of the project had to consider the traffic intensiveness on the adjacent roads varying in the course of day and organize the heavy site traffic so as to avoid the main traffic-peaks.

The tender for the project announced in the second half of 2002 awarded the contract to one of the three bidders, the Japan-Czech Joint Venture Taisei Corporation – Skanska. The total length of the motorway section is 3.3 km. The overpassing junctions and especially the first two-tube tunnel within the Slovak motorway network are the main structures within this section. The construction of the tunnel started in the summer 2003. The driving of both tunnel tubes was completed in the spring months of 2003. Building works on bearing structures ran concurrently with tunnel drilling. In 2005, the construction of the cement-concrete paved road was completed. The trial operation in the tunnel is expected to start after the installation of the tunnel operational and technology equipment is completed in 2007.

3 BASIC SPECIFICATIONS OF THE TUNNEL

The Sitina tunnel will be composed of two one-way tunnel tubes. In case of the traffic closure of one tunnel, the remaining tube will be used for two-way traffic. The transportation and engineering prognostic studies expect the traffic load in the tunnel to exceed 20,000 vehicles per 24 hours in both directions as soon as in the year of its putting into service. This is why no but the two-tunnel solution was acceptable for this project. The locations of both tunnel faces, as well as their elevation and directioning, were determined by the current use of the lots concerned and their development, and by the need to minimize negative environmental impacts as much as possible.

Basic technical specifications of the tunnel are as follows:

- Traffic area 7.5×4.8 m
- Excavation area: 79 – 98 m^2
- Tunnel length: 1,440 m; 1415 m
- Driven tunnel length: 1189 m, 1159 m
- Lay-byes: 1 lay-by in each tube
- Cross connections: 4 person passages, 1 emergency access passage
- Emergency niches: one per 150 m
- Fire niches: one per 90 m
- Tunnel ventilation: longitudinal

Both tunnel tubes have been divided into particular driven sections and cut-and-cover sections built in the open construction excavations at both tunnel faces. These sections were be filled after the construction was completed. A more than 200 m cut-and-cover tunnel section in the Academy area, which is actually built on the surface, was included into the project in order

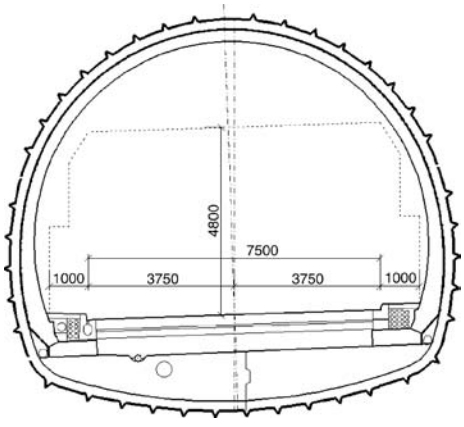


Figure 2. Typical cross-section of the driven tunnel with invert.

to protect the area concerned against the negative site-traffic impacts (noise, emissions).

The driven tunnel tubes (fig. 2) can be also divided into inverted tunnel sections built due to less favourable geological conditions and the sections without any invert built in generally more favourable conditions. The share of the inverted sections in the total driven tunnel footage reached 13%. The inverts are situated mainly in the face-adjacent sections and in the tectonically corrupted zones.

4 GROUND CONDITIONS

The Sitina tunnel was mostly driven in granitoid formations of the Sitina uphill situated in the meeting point of the Male Karpaty (Small Carpathians) Mts. and Lamacsky prielom valley. The uphill massif was characterized by heterogenous formation due to various tectonic fault zones along the entire tunnel. Rocks adjacent to tectonic fault zones were strongly altered, partially intensively mylonitized, creating a formation of mixed clay minerals and altered rock fragments. Except for granitoid formations, there were converted rock partings often intensively mylonitized, found along the tunnel route. Biotic paragneiss was the dominant type of converted formations. During tunnelling works, the massif was quite dry, underground water occurred mainly due to waterfall and was limited to weathered formation partings.

A relatively small height of the tunnel overburden varying from 4 to 32 m was also a significant tunnelling factor (fig. 4). The low overburden not exceeding 12 m was found in the portal sections and in two local depressions along the tunnel route. The rock arch over the tunnel excavation profile cannot be created in the sections with the low overburden.

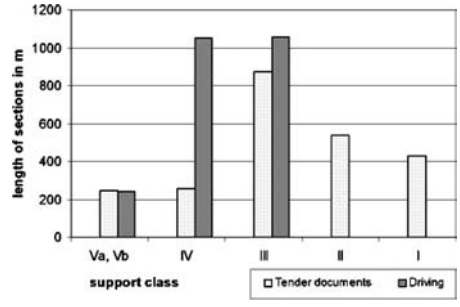


Figure 3. Comparison of total amount of expected and actual support class length for both tunnel tubes.

The tunnel lining structure had to be fully loaded by the overburden in these sections.

5 CONSTRUCTION METHOD

Construction work was launched in the summer in 2003. First, the tunnel faces were built in the south in the Mlynská dolina valley and in the north close to the SAV area. In the late 2003, both tunnel tubes started to be driven from the south face in the Mlynská dolina valley, and in the next year tunnelling works were launched on the north-face sites. The west tunnel tube was finally cut-through in March 2005 and the eastern tube in May 2005.

All tunnelling works were carried out in compliance with the New Austrian Tunnelling Method. The tunnel was vertically divided into the top heading, bench and invert, if appropriate. The applied 150 to 250 mm shortcrete primary lining was reinforced using one or two steel welded mesh and steel lattice girders. Also, the tunnel was systematically radially anchored using the 4 to 6 m long SN anchors. The stability of the tunnel roof was ensured using fore poles and 4 to 8 m long IBO anchors. The face and the tunnel roof were protected by a 12 m long micropile umbrella roof over the tunnel arch in the face-adjacent sections with a low overburden.

During tunnelling works in both tunnel tubes, the actual rock formation conditions showed to be less favourable if compared to the tender documents (Frankovsky & Snopko 2006). Support classes II and I with a 2.0 and 2.5 m advance could not be used. Moreover, the explosion works assumed in the tender documents have been significantly reduced since mechanical excavation could be used within a large portion of tunnel tubes. See Figure 3 and Figure 4 for comparison of assumed work and actual driving.

The system of geotechnical measurements applied during the Sitina tunnel construction have been applied in compliance with current driving practice according to the NATM principles using tunnel deformation

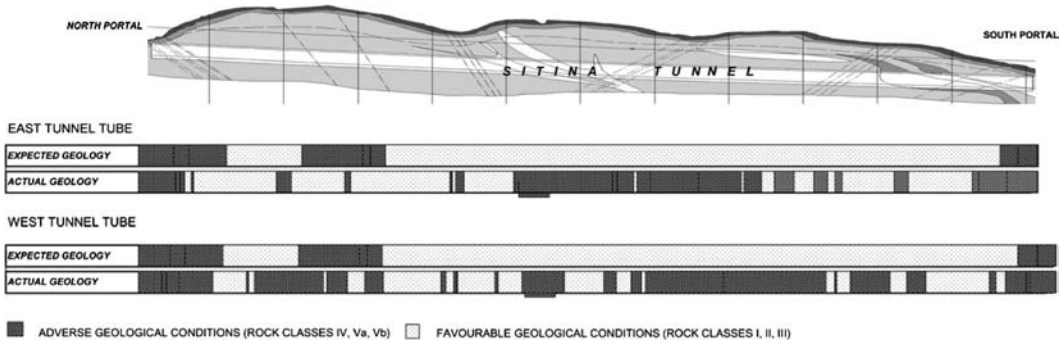


Figure 4. Longitudinal profile with comparison of expected and actual geologic conditions.

(convergences) measurement, surface deformation measurement, extensometric measurement, inclinometric measurement, face slope deformation measurement, measurement of the stress in the primary lining and contact stress values and measurement of then stress in the secondary lining concrete. Deformation progress of the massif formation was characterized by mostly limited, fast maturing deformations usually not exceeding 25 mm. Local maximum values of radial tunnel deformations did not exceed 76 mm.

The thickness of the final lining of the driven tunnel is 300 mm, or 350 mm in lay-byes. The standard length of the final lining blocks is 10 m. The reinforcement of the final lining was designed on the basis of the static calculation results assuming that the massif load will be partially borne by final lining and partially transferred by the primary lining. The reinforced lining blocks of the driven tunnel were applied along the face-adjacent sections with the low overburden, in the sections with a significant deformation performance or local failures of the tunnel roof stability, in lay-byes and in the blocks including emergency cross-connections. The total number of 56 fully reinforced blocks represents 24 % of the footage of both driven tunnel tubes.

6 DIFFICULTIES DURING TUNNEL DRIVING

There are many ambiguous factors, especially in tunnel construction, which could not be foreseen at the design stage. Therefore, it is important to workout the "Action-Measurement-Interpretation-Evaluation". The protocol considering the special urban tunnelling aspects has been developed for the Sitina Tunnel project (Zuzula et al. 2004).

Following the common procedure, the Geotechnical Committee was established at the first stage of the project in order to overcome any difficulties within the project. The Committee was created by the National motorway society (the Client) and was composed of designers, engineers, geologists and Contractor representatives. The project is located in the urban area and many factors relating to adjacent spaces had to be considered such as noise, vibration and ground settlement due to tunneling works.

The difficulties faced under this project included cave-ins occurring due to the adverse geological conditions under the blasting at cutting stage which required interruption of works resulting in delayed performance and representing potential danger to workers and people in the adjacent areas. The project considered 4 major cave-ins and procedures were worked out to eliminate the relating risks. These procedures enabled the implemented step-by-step solutions to be confirmed under the project execution stage. The developed procedures can be divided as follows:

- investigation of the reasons for cave-in occurrence;
- additional survey aimed at localization of potential cave-ins occurrences;
- identification of the cave-in occurrence mechanisms,
- respective support pattern changes.

The following characteristics have been detected and conclusions made on the basis of the rock formation surveying using the sample cave-in occurrences:

- the sufficient strength of the rock (80–160 MPa);
- the partial occurrence of clay in the rock joints;
- the cave-ins cannot be foreseen using the results of the cutting face surveying: the face was firm and stable before blasting;
- no symptoms were detected during the drilling of forepoles;
- difficulties in the cave-in localization based on the additional survey carried out from the surface.

The situation is similar to the so-called "domino effect". Several reports dealing with these issues have been already published in Japan. There are a number of cracks in rock formations which use to be stable under the internal stress conditions. Once the cutting face is uncovered, the unbalanced stress conditions result in the rock element slides along the existing cracks affecting the existing rock joins. The extension of the breakage is determined by the directioning and

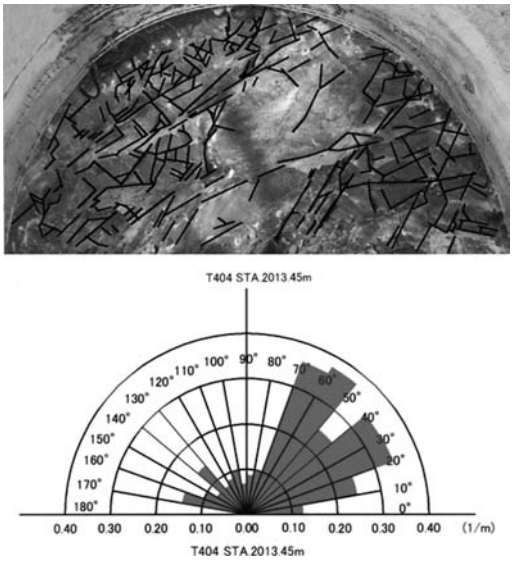


Figure 5. Observed joints in the cutting face.

strength of the face. The rock joint orientation and frequency was observed and more than 100 cutting faces have been examined to explain this mechanism and phenomena as shown in Figure 5. It was stated that the acceptable deformation falls within the range of 0.3–0.4% based on the allowed dilatancy. It means that the probability of sliding of the rock elements is reduced under the stable internal pressure conditions (Tanimoto et al. 2006).

Moreover, the 2-dimensional DEM (Distinct Element Model) simulation was carried out on the basis of the information on the orientation and frequency of joints (Fig. 6). This simulation proved that if the friction angle of joints is small (close to zero), huge sized cave-ins can occur easily (Iwano et al. 2006). Finally, the support pattern showed in Figure 7 has been adapted. The pattern is considered the combination of systematic forepoling and face boiling aimed at increasing the internal pressure of the rock elements.

Geological conditions, less favourable that expected, brought other problems. As geological conditions were worse, driving steps were shorter and the used support was required to be heavier. Moreover, the progress of work was interrupted several times due to the cave-in occurrence. Rock Classes I and II, which had been expected over 40% within of tunnel driving, did not appear at all (fig. 3). More adverse geological conditions than expected raised the necessity to apply a heavier support pattern to the same rock class. Finally forepoling and face-bolting was installed regularly, which resulted in the extension of working time.

Therefore, the Contractor, upon the Engineer's consent, introduced the following acceleration methods in order to keep the set scheduling of the project: the

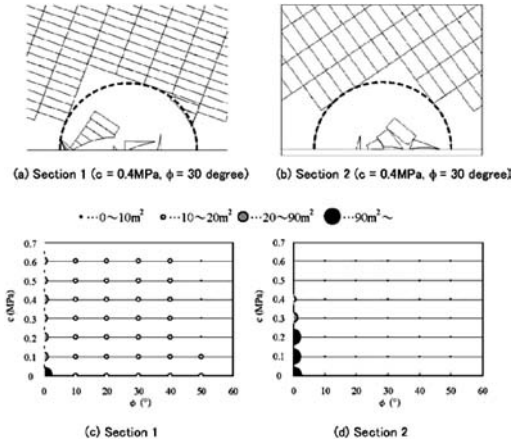


Figure 6. Simulation model for the mechanism of cave-in occurrences.

extension of working time; the increased frequency of noise and vibration measurements; the evaluation of the amount of the explosives used; the installation of the anti-noise barrier and reduction of the amount of explosives used; driving from the other portal demanding mobilization of additional resources, additional slip form.

The construction of the tunnel within the urban area laid considerable restrictions upon the progress of works. In this particular case, the following had to be considered:

- the Slovak Academy of Science performs various important experiments and vibration resulting from blasting works might influence the results;
- there is a horse riding school keeping horses and helping children with special needs located above the tunnel; horses might get shocked due to blasting works and injure some children;
- there is the ZOO area spread close to the tunnel portal and blasting works and/or heavy machinery might produce disturbing noise and vibration.

The following measures have been introduced to minimize the above listed undesirable impacts:

- test blasting: vibrations were measured ahead under the test blasting in order to evaluate the negative impact and determine optimal amount of explosives;
- anti-noise barrier: an effective noise barrier was built up in order to extend working hours to 24 hour a day;
- reduction of the amount of explosives (step blasting): the cutting face was divided into two or three parts form the point of blasting works in order to reduce vibration;
- pre-announcement: daily announcements of planned blasting times were issued and a special

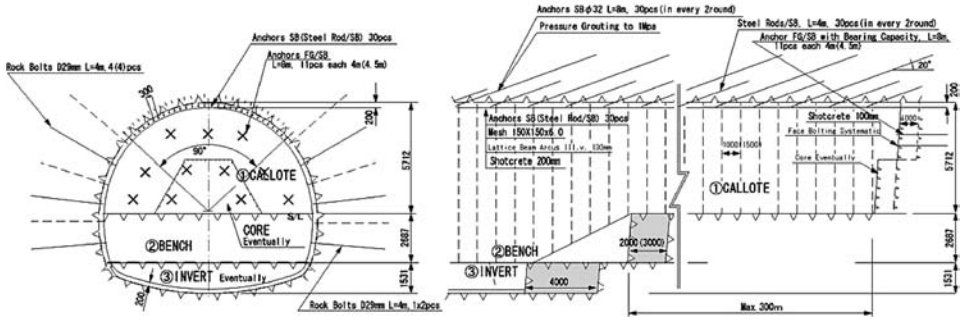


Figure 7. Support class IV with special measurements.



Figure 8. South portal of Sitina tunnel in september, 2006.

announcement was provided 30 minutes ahead of each explosion;

– accountability: regular communication and visits of particular subjects (institutions and inhabitants concerned) within the adjacent areas were introduced to explain conditions occurred under the project.

7 SUMMARY

The construction conditions of the projects located within urban areas are limited and special attention has to be paid to the adjacent areas and facilities. Definitely, the construction period is getting longer and the probability of work delay, interruption or stoppage is increased due to such restrictions. Moreover, if some difficulties occur within a highly developed area, the project costs may significantly increase and it takes a long time to remedy the damages. In addition, it is vitally important to enhance cooperation with particular subjects (institutions and inhabitants concerned) within the adjacent areas to assure proper progress of the projects. The accountability of project members, i.e. the Client, and the Designer and the Contractor is essential to ensure such cooperation.

The completion of the D2 Motorway section in Bratislava including the Sitina tunnel will significantly improve traffic conditions in the town. However, the entire region is under continual development and the capacity of the newly built roads will be exceeded soon.

Traffic conditions in Bratislava could be further improved by the construction of a "zero" by-pass of the town including an approximately 10 km long tunnel routed through the Malé Karpaty (Small Carpathians) Mts. massif. Nowadays, this project reached the technical surveying level. However, the expert public as well as the inhabitants of Bratislava believe that in the near future they will be able to find resources to implement this demanding engineering project.

REFERENCES

Zuzula, P. et al. 2004. Consideration Construction and Influence in Urban Area Tunnelling with Small Overburden, *Proceedings of Significance of tunnels in transport, STA.*

Frankovsky, M. & Snopko, J. 2006. Geotechnicky monitoring pri vystavbe tunela Sitina, *Geologia a zivotne prostredie, Bratislava, SGUDS.*

Tanimoto, C. et al. 2006. How to Define a Magnitude of Loosening in Tunnel, American Rock Mechanics association, *The 41st U.S. Symposium on Rock Mechanics (USRMS).*

Iwano, M. et al. 2006. Construction on Sitina Tunnel project in Bratislava, Slovakia Republic, *The 16th Tunnel engineering conference, JSCE.*

Underground Space – the 4th Dimension of Metropolises – Barták, Hrdina, Romancov & Zlámal (eds)
© 2007 Taylor & Francis Group, London, ISBN 978-0-415-40807-3

New Austrian Tunneling Method: Directly under an expressway on weak silt

K. Fujimoto, J. Yorita & Y. Sasaki,
Japan Railway Construction, Iiyama City, Nagano Pref., Japan

N. Yamaki & M. Okamura
Toda Co., Ltd., Iiyama City, Nagano Pref., Japan

ABSTRACT: The Takaoka Tunnel on the Hokuriku Shinkansen Line is a 6,918 m long tunnel built in the northern part of Nagano Prefecture using the New Austrian Tunneling Method (NATM). It was divided into the northern (3,990 m long) and southern (2,928 m long) sections. The tunnel crosses under an expressway at a vertical distance of about 15 m. Because the soil is soft silt with many fissures (N values: 10 to 30), it was concluded that ordinary tunneling methods could cause large settlement problems. Therefore, a pipe roofing (ϕ 812.8 mm) method was used in the planning stage as a countermeasure. This study reports on a newly developed method applying two-dimensional numerical analysis to three-dimensional phenomena incorporated in the structural design for the pipe roofing. Also reported is a monitoring system for excavation directly below the expressway, which feeds back the measuring results for surface ground settlement.

1 INTRODUCTION

The Takaoka Tunnel on the Hokuriku Shinkansen Line is located between 131 km 550 m to 138 km 490 m from Takasaki, the origin of the line. It is a double track tunnel (6,918 m long) running through the Nagaoka Hill area along the right bank of the Chikuma River flowing in the northern part of Nagano Prefecture.

The Nagaoka Hill area consists of a northern section, topographically relatively rugged hills over 400 meters above sea level, and a southern section of gently rolling hills 380 meters above sea level at Chausu Hill, the highest point.

The southern section of the Takaoka Tunnel is located on the southern block of the Nagaoka Hill area, and the tunnel length is 2,928 m. The earth covering varies from 1D to 5D. The tunnel crossed under or near many structures, including an expressway and power transmission towers, as well as blocks of apartments and houses.

This study reports on execution directly under the expressway routed in soft silt, a representative geological characteristic of this region.

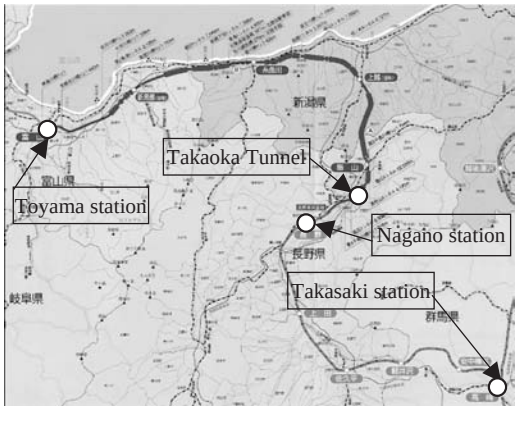


Figure 1. Location map.

2 OUTLINE OF GEOLOGICAL FEATURES

The geology surrounding the Nagaoka Hill area over the tunnel contains soils deposited on the bottom of a lake, including secondarily deposited pyroclastics, silts, sands and gravel coming from the Izuna volcano. These soils consist of the Sarumaru layer, corresponding to the Quaternary Pleistocene prophase, and the Toyono layer, corresponding to the metaphase, which are covered with the Nango layer, considered to be Pleistocene anaphase. Since the strata belonging to later generations are distributed throughout, it can be said that the geology is very soft and gently rolling. In addition, because the Nagaoka Hill area consists of risen hills formed by a strong diastrophism and the active Nagaoka Fault, the strike fault and slope of the

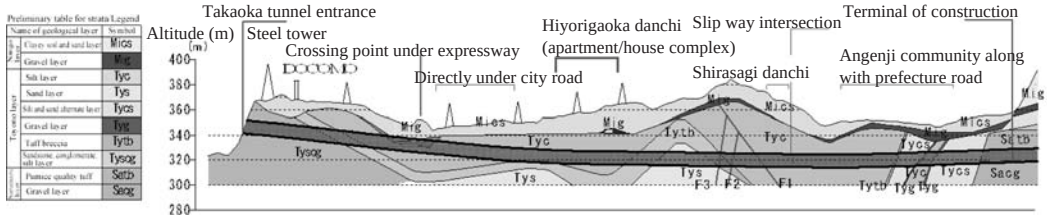


Figure 2. Longitudinal.

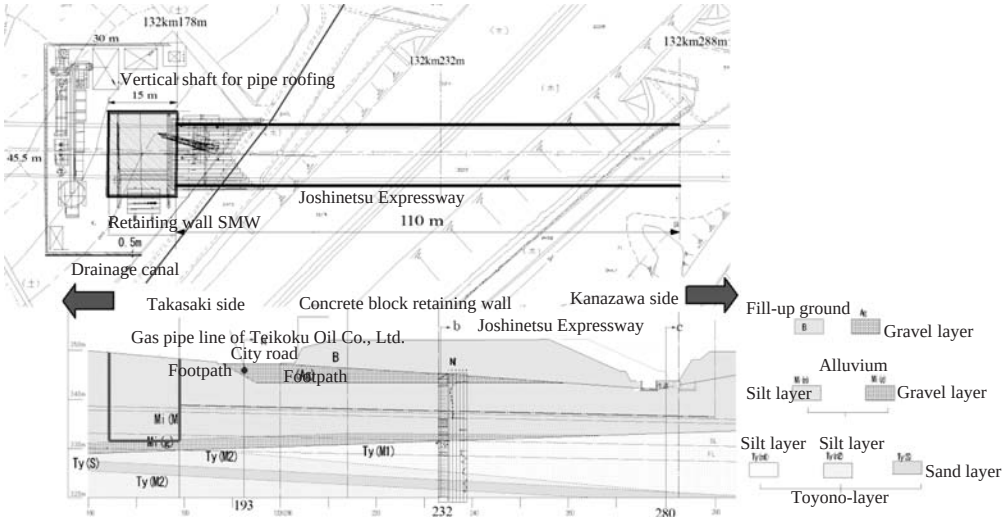


Figure 3. Interconnection with expressway: Plan view.

strata around the hill areas are complicated and varied over a short distance, as well, the silt layer has many fissures. Furthermore, since there is an aquifer sand layer and a gravel layer in a narrow area, an overflow of soil could occur, coupled with the multi-fissure silt. The silt layer, which is shown on the cross section of the tunnel, is the Toyono layer. Its unconfined compressive strength is as small as 0.8 Mpa (8.0 kgf/cm^2), and both the modulus of deformation and competence factor are also low level, around 20 MN/m^2 and Gn < 1.5 respectively (see Figure 2).

3 CROSS POINT WITH EXPRESSWAY

The Takaoka Tunnel crosses the Joshinetsu Expressway at a vertical distance of about 15 m (embarked ground: 7 m, natural ground: 8 m) and the level cross angle is about 45 degrees at around 132 km 230 m from Takasaki. The earth covering is less than 1D. Accordingly, there is the possibility of affecting the expressway, such as settlement caused by the tunnel excavation, resulting in obstacles to vehicle traffic. Therefore, it is necessary to minimize the effect on the ground structure of the expressway when the tunnel is excavated.

4 STUDY OF AUXILIARY MEASURES

From the soil test results and execution results achieved in the past, it is clear that the silt layer ranged on this area is of a younger generation. Therefore it becomes a high-level silt layer that is deformable because of the large influence of the fault. In the tunneling done so far, application of a long-distance end bearing method, long-distance end plate method, side wall preceding method, upper and lower halves shotcrete invert method, etc., controlled ground settlement and allowed successful excavation without problems.

For the crossing below the expressway, in order to ensure traffic safety, a management reference value has been established. It was determined that the extent of the ground settlement was 50 mm and the settlement gradient was 10/1000 rad. To establish the reference value, the road administrator was consulted, with reference to the “Guidance of Execution Technology

Table 1.

End bearing method:	Control effect for settlement	Economical efficiency	Execution properties	Evaluation in total
Modified high-pressure jetting method:	Δ	Δ	Δ	Δ
Long-distance steel pipe end bearing method:	Δ	○	○	Δ
Pipe roofing method:	◎	Δ	◎	◎

for Neighboring Construction" (Edit Committee for Guidance of Execution Technology for Neighboring Construction, March 1997).

In order to meet the management reference value, measures required for the tunnel excavation were studied. In the study, it was understood that the fill-up ground (about 7 m) had an interaction load with the tunnel. Accordingly, it became necessary to securely support the interaction load coming from the fill, as well as the crown protection.

First, the end bearing method was studied comparatively (Table 1). In addition, since the load directly above the tunnel is borne with the end bearing method, it needed to provide a certain length for end bearing. In addition, settlement at the legs was assessed, making it is necessary to study the natural ground around the legs. For the end bearing necessary to control settlement of the surface ground, the pipe roofing method was used. Steel pipes were arranged on the periphery of the tunnel. Before tunneling, a line of highly rigid pipes surrounding the natural ground was adopted, the result of a study looking into economic efficiency and execution properties. In addition, for constructing the pipe roofing, it was necessary to consider controlling settlement caused by piling the pipe roofing, because of the severe management reference value for where the expressway crosses. Therefore, an auger screw excavation method was not adopted. Instead, a small diameter pipe jacking method was used on the pile driving area. For the pipe diameter, the minimum diameter able to operate in the pipe, i.e., ϕ 812.8, has been selected to prepare for possible accidents.

5 VERIFICATION WITH TWO-DIMENSIONAL FEM ANALYSIS

A two-dimensional FEM analysis was applied to verify effectiveness for crown protection and settlement control of legs with the pipe roofing. Since a two-dimensional FEM analysis is an analysis to make

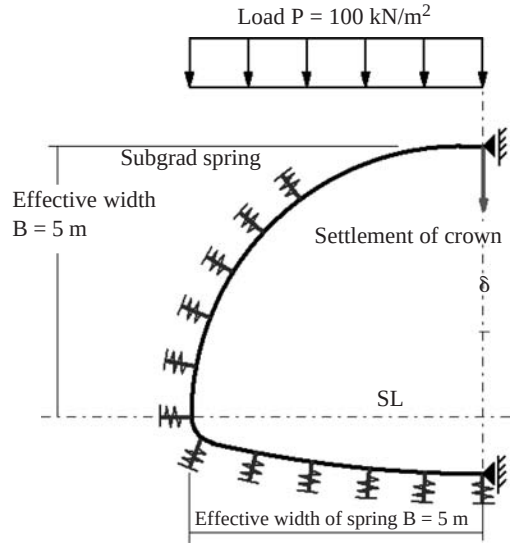


Figure 4. Calculation model for timbering spring.

traversal verification of the tunnel profile, it is difficult to gauge effectiveness in the longitudinal direction of the tunnel. Thus a method was studied for the two-dimensional FEM analysis with the longitudinal girder effect of the pipe roofing. Next, the number of roof pipes to be piled to achieve effective action, without affecting the soundness of the adjacent structures, was studied.

5.1 *Prediction of settlement by means of modeled girders*

Models of girders on an elastic floor were used to study the longitudinal effects. Taking modeled girders as roof pipes, and taking the modeled elastic floor (springs) as the natural ground between tunnel timbering and pre-excavation area, the settlement of pipe roofing for the upper half of the excavation phase was estimated.

For the spring value in the tunnel timbering, taking the modeled plane framework as the tunnel's transverse direction (upper-half profile) (Figure 4), the value of the spring for the tunnel timbering work was calculated from the crown displacement. This was done by measuring the loading unit (load) on the combined member consisting of steel timbering and shotcrete. For the spring value of the pre-excavation terrain, the ground spring obtained from geological data was set up. The rigidity of the roof pipe was converted by equalizing the numbers of piling under 150° (20 pipes) with piling intervals of roof pipes by using a combined member, and considering heating concrete.

The analysis was achieved with the modeled girder on the elastic floor by setting up the above-mentioned

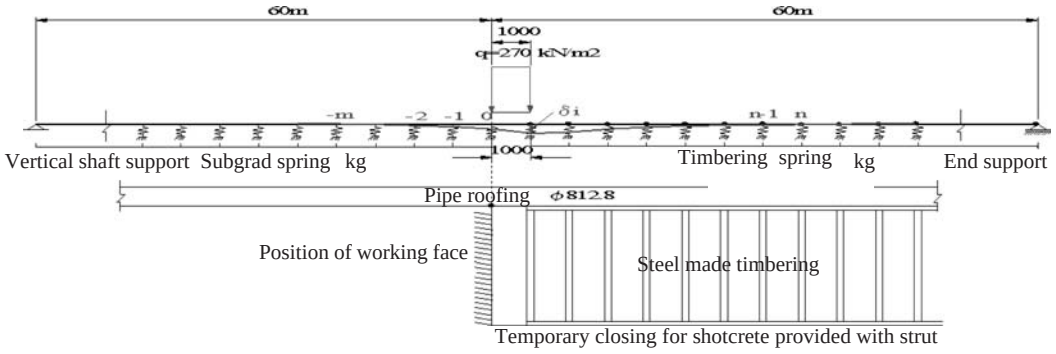


Figure 5. Model for girder.

conditions as shown in Figure 5. The analyzing method was such that all settlement values obtained at every point were summed (under a state that the center portion where the largest settlement of the roof pipes was estimated) and was excavated 1 m. The roof pipes lose sub-grad reaction by excavating 1 m, and the upper portion of the pipe roofing bears the load of the natural ground. In this analysis, both natural ground and fill ground loads were regarded as the total load to be applied.

As a result, the total settlement (accumulated settlement) became 31.0 mm. Since the result could be considered as settlement, including consideration for the longitudinal girder effect, the total settlement was regarded as the crown settlement at completion of excavation of the upper half of the tunnel.

5.2 *Two-dimensional model of pipe roofing*

The crown settlement at completion of excavation of the upper half of the tunnel obtained from the modeled girder was applied to the identical step in the two-dimensional FEM analysis. The two-dimensional FEM analysis model for the analysis was applied at piling work with 150°, also the case of the modeled girder. For rigidity of the pipe roofing, the converted rigidity calculated for the modeled girder was taken. In order to fit the crown settlement, the elementary width having a modulus of deformation equivalent to pipe roofing was studied. Further, material values, such as dead weight of natural ground portion and the pipe roofing portion and so on, were applied to each value.

In addition, in carrying out the analysis, non-linear elasticity analysis was applied to the dynamical model based on the actual results of this terrain in the past. Formalization of no-linearity was in accordance with "Non-linear model by means of destructive accessibility" (*NATM Design and Execution guidance*, Japan Railway Construction Public Corporation). For the classification of the natural ground according to geological time, the Toyono layer with a high concretion grade was classified into soft rock and Nango layer with low concretion grade was classified as earth and sand. The sub-grad physical properties values, such as initial coefficient of elasticity and shearing strength, were estimated by taking the N value as the parameter from analyses of the boring survey data, soil sampling test result and in-situ test results.

As the result of the analysis under these conditions, the tunnel crown settlement of the two-dimensional FEM analysis model was 35 mm. This was compatible with the total settlement of the pipe roofing of 31.0 mm derived from the study with the modeled girder.

5.3 *Comparative analysis of pipe roofing installation range by means of two-dimensional FEM analysis*

By using the elementary width of the pipe roofing and converted modulus of deformation acquired from the analysis, comparative analysis of the steel pipe installation range was achieved. There were four models for this study: upper and lower half models, 180° model, 150° model, and a model modifying 150° model with adding improvement of side wall preceding method. Each model was named from A to D. Table 2 shows the analysis result.

Next, acceptability of the analysis result was studied. Specifically observing the surface ground settlement of the last step for models A to C, which only incorporated the pipe roofing as the auxiliary measures method, there were differences in surface ground settlement among the models. It was considered for this reason that there was a gravel layer (Mi-g) on the Nango layer, of which the N value was higher than those of the others. It was considered that models A and B, where the pipe roofing piling areas reached to the gravel layer, suppressed settlement at tunnel legs, and that overall settlement was controlled. On the other hand, for model C, because it did not reach to the gravel layer, it was considered that the settlement at the tunnel legs was larger than those of the others. Consequently, the entire settlement would become larger.

Table 2. Analysis results.

Analysis model	A	B	C	D
	Degree(°)			
Piling range for pipe roofing:	Upper and lower halves			
		180		150
Auxiliary measures	–	–	–	
	Improvement of side wall			
	mm	mm	mm	mm
Settlement of crown:				
Upper half	2	14	35	35
Last	4	32	65	52
Settlement of surface ground:				
Upper half	1	12	30	30
Last	2	27	56	45

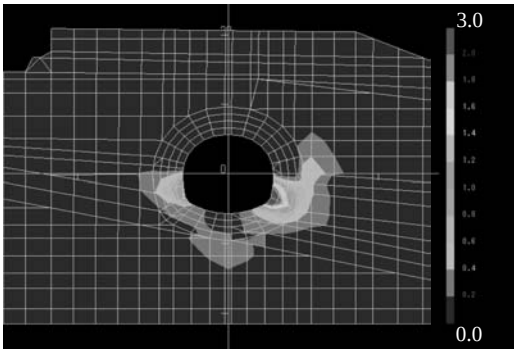


Figure 6. Analysis result for model B (Maximum principal strain).

From the value of the predetermined management reference value (50 mm), 30 mm, which was 60% of the reference value (50 mm × 60%), was taken as the primary management reference value. This was the result of a comparative study of models satisfying the primary management reference value, where model A showed 2 mm and model B showed 27 mm. It was clear that these two models, where the side walls were protected with the pipe roofing, were superior in controlling the effect of the surface ground settlement. On the other hand, even though the side wall of model C was protected by modification of the side wall preceding method in parallel (similar to model D), model C could not satisfy the 30 mm requirement. Furthermore, it was understood that the improvement with injection was not perfect.

As the result of studying the analysis results and problems occurred during actual execution, as well as considering economical efficiency, model B, where settlement control was reliable (piling range of pipe roofing was 180° and numbers of pipes are 22) was selected. In addition, before starting the tunneling work, studies were made for improving the lower half side wall preceding method, for upgrading the timbering work, and for improving the batholith as auxiliary tunneling practices for settlement larger than the estimation.

6 SCHEME OF EXECUTION OF PIPE ROOFING

It is necessary to execute the pipe roofing in advance of tunneling to protect the arched cross section of the tunnel, as preparation of a vertical shaft was considered as the execution base. The location of the vertical shaft was selected at the Takasaki side (around 132 km 170 m) across form the expressway where the geological stability was relatively high and a temporary site was easily available. The execution length of the pipe roofing was decided from 132 km 178 m to 132 km 288 m considering operability of the vertical shaft itself and protection of fill-up structure of the expressway at the Takasaki side (Figure 3). The tunneling was decided to start from the Kanazawa side to go to the Takasaki side.

The position of the vertical shaft adjoins a city road and also adjoins the fill-up ground of the expressway. Therefore it is necessary to consider not only the effect on the expressway but also the effect on the natural gas pipe line routed under the city road. Accordingly, a soil cement method involving high rigidity was planned for the earth retaining structure to be able to control deformation and looseness of peripheral natural ground. In addition, since building the pipe roofing in the vertical shaft requires enough working space inside the vertical shaft, an earth anchor method was adopted to retain the soil.

7 CONCLUSION

In this analysis, in order to consider the longitudinal girder effect of the pipe roofing, analysis was done using modeled girders, and equivalent rigidity for the pipe roofing was achieved in the two-dimensional analysis. In addition, by applying FEM analysis, where reproducibility was high with the many fissures shown in analyses in the past, the NATM measures at the crossing point at the expressway were studied. Furthermore, the scheme of execution was prepared, which included protective measures for the gas pipeline running along the expressway and the measuring plan, as well as temporary facilities, such as the vertical shaft necessary for the pipe roofing. We would like to proceed with the execution upon reflecting on the analysis results acquired in the past and the data obtained from the measurement to the execution, and by paying attention to ensure safety.

This page intentionally left blank

Underground Space – the 4th Dimension of Metropolises – Barták, Hrdina, Romancov & Zlámal (eds)
© 2007 Taylor & Francis Group, London, ISBN 978-0-415-40807-3

The Prague new connection tunnels

Michal Gramblička
SUDOP Praha a.s., The Czech Republic

David Cyroň
Metrostav a.s., The Czech Republic

Miroslav Chyba
Subterra a.s., The Czech Republic

ABSTRACT: As usual for large civil engineering projects, the history of preparation of the New Connection project is very eventful. Ways to replace the tens-of-years-old connection of the Prague Main Station from the north and east, being insufficient in terms of the capacity and technical level, have been sought from the fifties. As this railway connection has been possible via the Vítkov single-rail track connection only, a change of this condition is only viable by development of new railway lines between the Main Station and Masaryk Station on one side, and Libeň, Vysočany and Holešovice on the other side. This is the origin of the project name The New Connection. The works commenced in 2004, and the conclusion is scheduled for 2008. The tunnels consist of two cut-and-cover sections, where, in a joint construction trench, the individual rail lines are joined with the mined sections. The tunnels link to a four-track viaduct on the west and a double-track viaduct and a track in an open cut on the east. The year 2005 saw the excavation of the construction trenches. The year 2006 saw excavation of 100% of the length of the tunnels.

1 HISTORY OF THE PRAGUE RAILWAY JUNCTION

The network of railway tracks and stations in the Prague territory developed by connecting new railway lines from various directions, where each of the lines built its own station, without anybody to take care of proper interconnections. This is how the first Prague railway station originated in 1830, before the Bruska Gate, on the second horse railway line from Prague to Pilsen. Fifteen years later, the Northern State Railway Line from Olomouc to Prague was opened to traffic, and the area of the current Masaryk station was selected for its Prague station (to be shared in the future with the railway line to Dresden, which was in the planning phase then). Another Prague station originated in 1862 in the Smíchov district under the name of the Prague Station, in the framework of the construction of the Czech Western Railway Line from Prague to Pilsen. The Franz Joseph Railway Line from České Budějovice to Prague originated in 1871, simultaneously with Franz Joseph Station (the today's Main Station) at the bottom of Vinohrady hill. The modern history of the Prague Railway Junction started in 1910, when the Prague Railway Station Committee originated. Its task was to find a way to a comprehensive solution of the Prague railway network, with an idea of separation of the passenger service from the freight service and its centralisation to a central passenger station. The realisation of the first actions was suspended or delayed due to World War I. All complementary structures improved the traffic function, although, they were not able to remove the lack of conception in the historic construction development. In addition, the outdated railway facilities started to collide with the city's functions and requirements for development.



Masaryk Station 1850.

2 THE NEW CONNECTION – PART OF THE PRAGUE INTEGRATED TRAFFIC AND RAILWAY CORRIDORS

The first solution of this project was brought forward at the turn of the 1950s and 1960s when a redevelopment of the Prague Rail Junction was considered. Along with a change in social conditions at the beginning of the 1990s, an enormous increase in movement of persons took place, in the field of commuter traffic mainly. Most jobs, the attractive ones above all, are concentrated in the Prague conurbation. This fact is connected with a continually growing demand for daily transport of citizens. Not all of this demand can be satisfied by urban mass transportation and car traffic. It is therefore not a less important purpose of the New Connection project to get the suburb transportation to the city centre, and to incorporate the railway traffic into the integrated system of traffic in Prague (PIT) and its vicinity. This will be possible only when the construction of the New Connection and subsequent modernisation of the Main Station are completed.

As probably known today even outside the sphere of the professional public, there are sections of European railway corridors currently under construction passing through the Czech Republic. The Corridor I between Děčín and Břeclav, which was completed in 2002, passes through Prague, as well as the corridors III (from Cheb to Plzeň) and IV (from Horní Dvořiště and České Budějovice) which are in preparation.

This means that, in addition to inland trains, also new-generation interstate trains will arrive to Prague, reaching a velocity of 160 km/h in our conditions. It must be stated that the construction of the New Connection affects its surroundings too.

The existing railway connection between the Main Station and Libeň via the Vítkov tunnel and Hrabov track connection will be cancelled, and the land used today for the railway traffic will be abandoned. It is expected that a cycle and pedestrian track and connected quiet zones will be established on the track bed of the current Vítkov railway line. This solution will connect Vítkov hill with the adjacent buildings of Žižkov.

3 ENGINEERING, GEOLOGICAL AND HYDROGEOLOGICAL CONDITIONS

The configuration of Vítkov hill was changed in the past by quarrying and by the construction of the National Monument. The assumed location of quarries was situated to the area of the Army Museum, the southern and eastern edge of the National Monument, and to the area at the bottom of Vítkov hill on the south. The height of the quarries reached even 10 m. In addition to this large-scale quarrying activity, a lot of minor quarries existed in this series of the Skalec quartzites. The quarries were backfilled up to the surface level with materials containing mainly the rock (quartzite) dug during the construction of the National Monument.

Vítkov hill is a significant morphological element in Prague's landscape. Its ridge is formed by the denudation-resistant Skalec quartzites. The beds of the Skalec quartzites are about 100 m thick; in the south and north they are divided stratigraphically and tectonically from the overlying series of measures of the Dobrotivy shales or Šárka shales. The contact between the Šárka shales and Skalec quartzites found in the northern slope of Vítkov forms a geological profile which has been placed on the list of sites of nature conservation. The excavation will encounter the Palaeozoic, Middle Ordovician Šárka shales and the overlying Dobrotivy series of strata in a facies of the Skalec quartzites.



East portal of North tunnel.



East portal of South tunnel.

Originally the ground water table was restricted to the bedrock with relatively wide range of the levels, depending of precipitation. The original hydrogeological conditions have changed due to the construction of underground spaces under Vítkov (civil-protection shelters with ventilation systems and wells securing the cooling and supply systems, the pedestrian tunnel, railway tunnel, sewers etc.). Because a majority of the underground spaces are found under the alignment of the designed railway tunnels, it is obvious that the railway tunnels will be excavated under the standing level of the ground water table.

4 THE TUNNEL DESIGN

The southern Vítkov tunnel is 1,365 m long. Out of this length, 1,250 m was built by mining methods. The north tunnel is 1,316 m long. Out of this length, 1,151 m was built by mining methods. The tunnels are interconnected by four cross-galleries at an overall length of 100 m. In the final condition, they will be used as escape ways. They are equipped with fire-check doors with signalling, fans and fire dampers. Cable and hydrant lines are also interconnected through the cross-galleries.

The space before the entrance and exit portals of the tunnel are accessible for road vehicles; mustering areas for mobile fire appliances are prepared on both sides.

The layout of the areas is accommodated to the needs of the excavation work so that the movement of mining equipment and vehicles during the tunnel driving is possible.

The 0.20–0.30 m thick temporary lining is designed according to the NATM principles. It consists of sprayed SB20 concrete reinforced with two layers of steel mesh, friction bolts expanded by pressurised water and three-section lattice girders. The horizontal excavation sequence is applied, with the top heading vault having the shape of an ideal 6.05-radius semi-circle.

The advance per cycle ranges from 1.0 to 2.0 m. Steel forepoles are either driven or inserted into pre-drilled boreholes ahead of the face in the top heading sections where instability is a threat. The distance between the top heading and sidewall drift faces varies from 50m to 120m, depending on the rock mass quality.



West portals of tunnels.





Double- to triple-length rounds, i.e. 2.0 to 6.0 m long, are applied to the sidewall drifting or to the closing of the profile by the invert.

The excavated cross-section area grows from 96.22 m^2 at the excavation class III, through 97.51 m^2 at the class IVa, to a maximum of 106.84 m^2 and 108.13 m^2 at the higher classes IV b and V a (involving the invert structure) respectively. Percentage classification of the excavation along the mined tunnels was designed in accordance with the results of the geological investigation. The anticipated need for the application of the higher classes (V a about 36%, IV about 34%, III about 30%) was not confirmed.

The deciding lengths of the completed tunnel excavation were categorised as the easiest class III; only the pre-portal sections were driven in the excavation class V a. About the middle of their length, the tunnels are crossed by the pedestrian tunnel connecting Tachovské Square in Žižkov with Thámova Street in Karlín. The tunnels pass at a distance of 6.50 m above the pedestrian tunnel.

The pedestrian traffic was be protected during the excavation by means of steel frames and timbering placed between a frame and the lining.

The excavation of the Vítkov tunnels commenced on 27.5.2005 and 15.8.2005 in the southern tunnel and northern tunnel respectively. The situation at the southern tunnel excavation face was favourable in an extent that allowed Metrostav a.s., the contractor, to abandon the excavation sequence V a designed for the top heading, carry out a length of 90 m without blasting, and apply the easiest class III at a distance of 134 m from the portal.

The most important structures that were passed under by the tunnels with the overburden less than 40 m are the building of the National Monument and the equestrian statue of Jan Žižka of Trocnov. A FEM structural analysis was developed for the prognosis of the rock mass behaviour. The analysis resulted in a prediction of a total subsidence value of 12 mm following the passage of the two tunnels. The reality was different – 24 mm.

A seismic measurement system was designed and maximum charge weight limits were set to enhance the protection of the building and the statue.

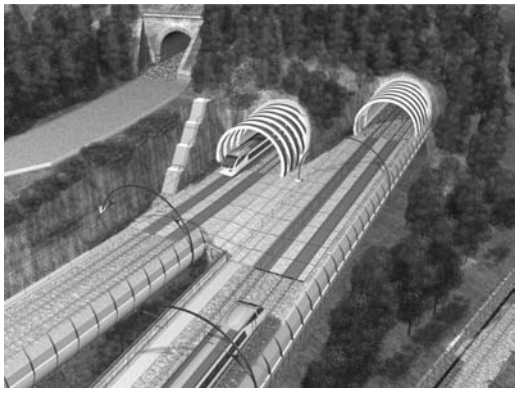
The cast in situ concrete final lining is designed both reinforced and unreinforced, 50:50 in proportion by the length of the sections.

Travelling formwork sets will be used for the casting. The length of the casting blocks of 12.50 m corresponds to a half of the 25 m distance between safety recesses. The horizontal alignment is determined by a rock crest of Vítkov Hill; the tunnel alignment follows its longitudinal axis. The distance between centres of the two parallel tunnels is of 30 m on average, with a minimum of 3 m and maximum of 42 m (under the National Monument grounds). The routes consist of straight sections and curves (648 m and 602 m radii for the southern tunnel and 902 m and 3602 m radii for the northern tunnel).

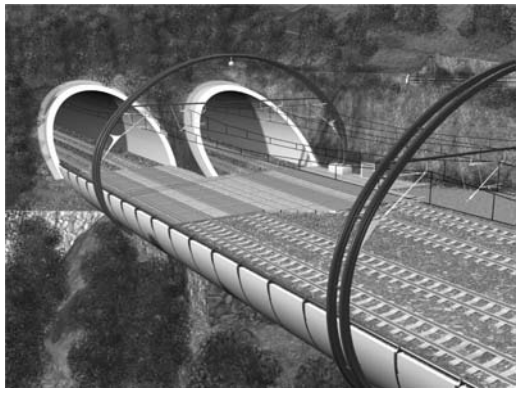
The alignment of the tunnels descends in the east-west direction on a gradient of 0.33%; downhill excavation will take place.

Survey of pre-construction conditions

In addition to low buildings at sports grounds, there is the National Monument on Vítkov hill with a monument to Jan Žižka found above the tunnel route. The structural condition of the building of the National Monument, that was used in the course of its life for various purposes (starting from a monument during the First Republic, through a Wermacht storage during World War II, and a mausoleum after the war) and was left more or less without systematic maintenance, is not good. Despite the fact that the tunnel excavation did not threaten the structural condition of the building, increased attention was paid to the structural elements, wall cladding and individual items of work of art. There is an equestrian statue of Jan Žižka of Trocnov in front of the building, above a grave of the Unknown Warrior. This statue, one of the world's largest equestrian



East portals.



West portals.

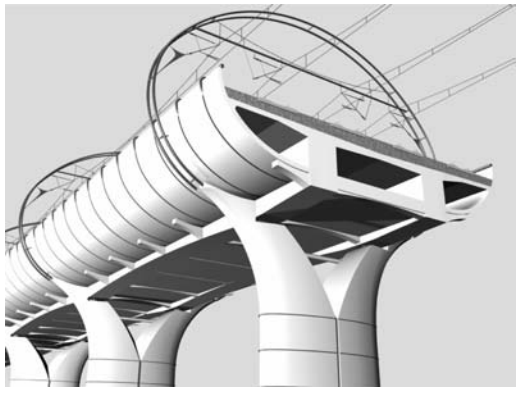
statues, was thoroughly observed in the framework of the geotechnical measurement program.

5 THE DESIGN OF PORTALS

The deciding length of the tunnels was be driven from the east portal, whose location is in the centre of the construction operations designed to improve the uncared northeastern slopes of Vítkov Hill. There will be a modern park in the final condition, connected with the city centre not only via transit tunnels but also via a cycle track. This track will link the park outside Prague Main Station with Balabenka via an existing single-track line (to be abandoned subsequently), and with a part of the Vysočany/Harfa location which is being newly developed. The construction works started in the autumn 2004 by the site preparation and development of access roads to the tunnel portals. New revetment walls allow the existing rail line to be operated until the moment of the opening of the new tracks running through the newly built tunnels to traffic. The muck is removed both by rail and road-based transportation.

The construction trenches at the portals are designed in a manner guaranteeing that rock pillars with a minimum width of 3.5 m to 10 m remain between the cut-and-cover and the mined tunnels. The walls of the pillars are supported by 15 m to 27 m high double-stage vertical anchored micropile walls consisting of 108/16 mm steel tubes. The walls are stabilised by permanent cable rock anchors 8.0 to 22.0 m long.

A 0.25 m thick layer is applied to the surface of the walls. The toes of the walls are keyed into the areas of vaults of the existing railway tunnel; therefore the condition of the vaults was paid extraordinary attention during the grouting operations. Once the cut-and-cover double-track tunnels are completed, they will be backfilled. A thorough condition survey of all above ground and underground structures was performed prior to the works commencement. A detailed monitoring system has been designed in compliance with the NATM principles.



The four-track railway trestle bridge over the locomotive depot of Masaryk station belongs undoubtedly among the very interesting structures of the project. It is connected to the western (entrance) portal of railway tunnels. It solves connection of the tracks to the northern gridiron of the Prague Main Station. It is a unique, 450 m long, pre-stressed concrete bridge structure for four running tracks.

6 CONCLUSION

The Vítkov tunnels solve the connection of Prague's centre with the future high-speed railway lines coming from the east and north of the Czech Republic. Apart from this, they will allow the suburban service and inter-urban lines to pass across the city in the east-west and north-south directions.

This page intentionally left blank

Underground Space – the 4th Dimension of Metropolises – Barták, Hrdina, Romancov & Zlámal (eds)
© 2007 Taylor & Francis Group, London, ISBN 978-0-415-40807-3

Development of rock fracturing method, and application of EG-Slitter Method to the tunnel

Toshiaki HARA & Mitsumasa OKAMURA
Toda Corporation, Tokyo, Japan

Tetsu KIMURA & Kouji ISHIYAMA
Nishimatsu Construction Co., Ltd., Kanagawa, Japan

ABSTRACT: The tunnel constructions, near the residential zone or the constructs, are increasing yearly. The conventional excavation methods are unsuitable in these areas, because it is becoming the critical issue for noise and vibration control engineering to excavate controlling the large shock wave, noise and the accident by falling rocks.

So we developed the new rock fracturing technique to be characterized by the non-blasting hard rock excavation. This new construction techniques are named the continuous Slit, EG-Slitter (Elastic Guide-rod Slitter) Method.

The process of the hard rock fracturing method in the tunnels is firstly cutting tunnel faces and periphery faces into the small blocks surrounding by cutting free faces with EG-Slitter, and next we break up the tunnel face extending continuous slit by oil wedges, finally we break the rocks with breakers.

In this paper, it was described the development of the new formation of continuous slit method, EG-Slitter , and the application of this method to the tunnel excavation.

1 GENERAL INSTRUCTIONS

Rock fracturing method is one of the tunnel construction methods. The first stage of this method is cutting of the faces and the periphery free faces. Second stage is quarrying stones on the cutting faces. This rock fracturing methods (EG-Slitter method) is available to the hard rocks of the unconfined compressive strength 100～200 MPa in the prohibiting Blasting method, but it is not efficiency as compared with Blasting method. The process of the EG-Slitter method) is shown in Figure-1.

The process of the rock fracturing method is as follows;

① Drilling the free faces
② Drilling the dividing holes
③ First fracture by the oil wedge, etc.
④ Second fracture by the breaker, etc.

The technical characters of the EG-Slitter Method are on the process ① and ②.

2 THE EG-SLITTER METHOD

The EG-Slitter Method is developed by the experiments in the tunnel sights and the testing of concrete blocks.

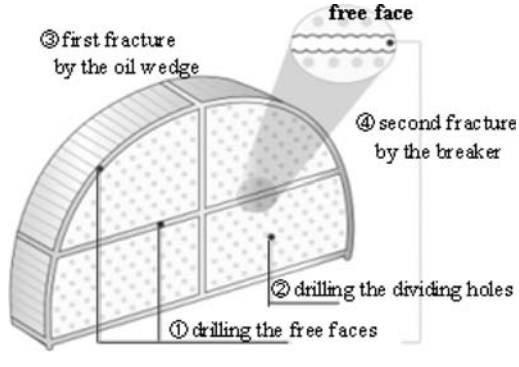


Figure 1. The outline of the Rock fracturing method.

2.1 *Characters of the system*

Figure-2 shows the EG-Slitter system. The system is composed by the hard rod and Elastic short guide rod attached on the guide cell of the tunnel faces drilling machine, jumbo. And Figure-3 shows the how to make drilling holes on the free faces. We make the pilot drill hole and dividing hole, contracting Elastic guide rod. After this the short and expanding guide rod is put into the pilot hole, and the next hole is digged by the bit supported with the hard rod and Elastic guide rod,

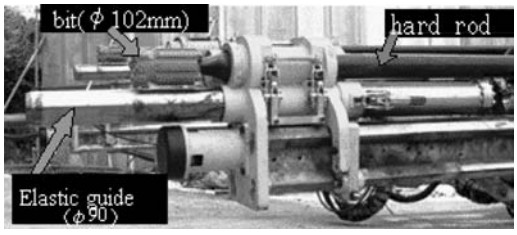


Figure 2. EG-Slitter system.

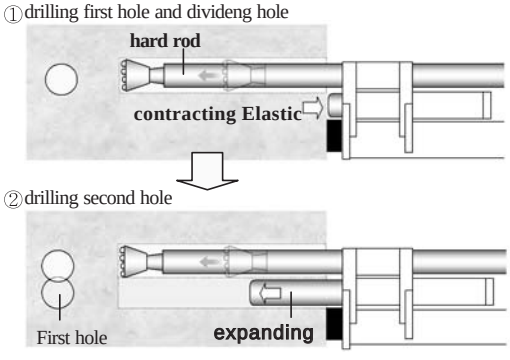


Figure 3. The system of the drilling free faces.

so we can excavate straight periphery free faces. We continue the work and it makes free face quickly.

Characters of the EG-Slitter system as follows:

① It is unnecessary the excursive machine.
The EG-Slitter system fits to guide cell of the drill jumbo which is the instrument used usually in the tunnel constructions, so it is unnecessary the excursive machine.

② It can excavate straight drilling used by the hard rod. And it is not curved to the next-hole by the hard rod, so we can excavate easily free faces on the tunnel face.

③ The length of the Guide rod is 50 cm.
In the case of short guide rod, the troubles of the drilling are increasing, and it is discharged rock powder simply. The other methods have a long Guide rod and many troubles in the pilot hole.

④ The Elastic guide rod is equipped.
The drill jumbo always have the elastic guide rod. The excavating efficiency on the free faces is higher than the common rock fracturing system.
The high drilling capacity of the EG-Slitter method is shown in Figure-4. It is more quick drilling compared with the usual drilling method used in the tunnel construction.

2.2 *The movement of the EG-Slitter*

We have the experimentation of the EG-Slitter movement on the concrete block.

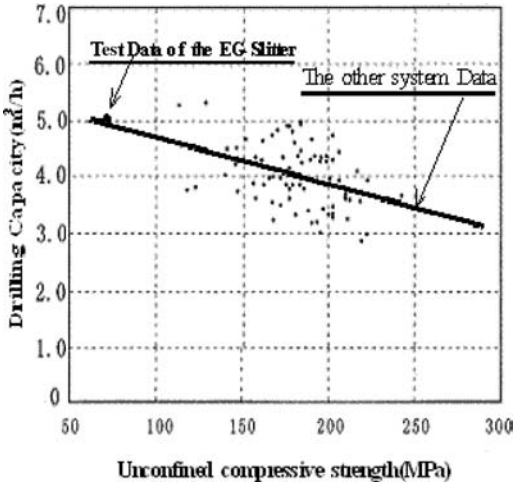


Figure 4. Drilling Capacity of the EG-Slitter system.



Figure 5. Experimentation on the Concrete Block.

Figure-5 shows the EG-Slitter system drilling the free face on the concrete blocks. It is smooth drilling and it can make the clear free faces.

3 EXAMPLE OF THE APPLICATION TO THE TUNNEL CONSTRUCTION

We applied the EG-Slitter Method to the tunnel excavation.

3.1 *Geology of the tunnel sight*

The extremely hard granite distribute with Vp value of 4.5 km/s which was measured by the seismic refraction method, and with unconfined compressive strength of 80~150 MPa, and rare crack. The geology of the tunnel is coved by the granite.

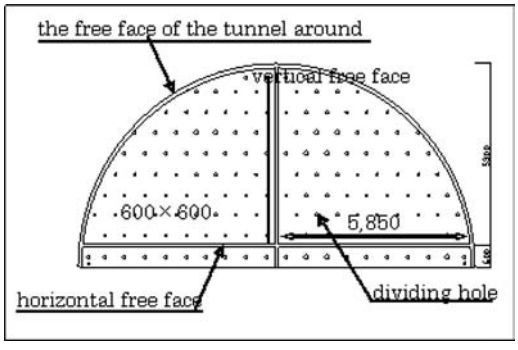


Figure 6. The drilling pattern of the free faces and dividing holes.

3.2 *The reason for development*

There are many homes around the tunnel portal, so we built soundproof shelter and soundproof doom in these cases surrounding the tunnel. In these areas, we cannot use the Blasting method. So we applied the EG-Slitter Method to the tunnel excavation.

3.3 *The drilling pattern of the EG-Slitter Method to the tunnel face*

The drilling pattern of the free faces and dividing holes is shown in Figure-5.

3.4 *The Excavation of the tunnel*

In Figure-6 and Figure-7, it means the free face and the dividing holes constructing by the EG-Slitter. That process of EG-Slitter operation is very smooth.

3.4.1 *The noise condition*

It is very silent and noise level is less than 55 dB in the near homes around the tunnel portal.

3.4.2 *Excavation by the EG-Slitter*

It can be very smooth and efficiency excavation of the free face and dividing holes, and powder is flow out easy.

Figure-7 shows the excavation in the tunnel face.

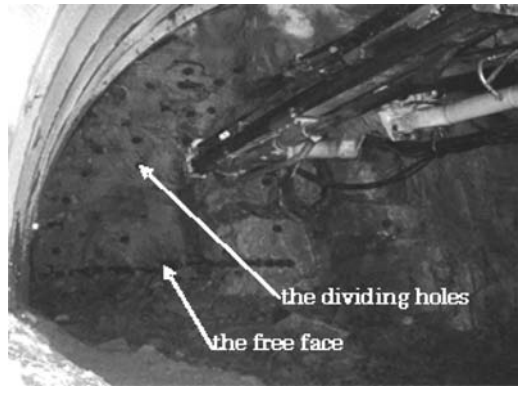


Figure 7. The free face and the dividing holes.



Figure 8. Free faces by the EG-Slitter system in the tunnel face.

The free faces digging by the EG-Slitter system is shown by Figure-8.

Vertical free faces, Horizontal free faces, and Incline free faces are drilled easily, and accurately by the EG-Slitter system.

4 CONCLUSION

The EG-Slitter method system was applied to the tunnel excavation, and it can drill very efficiency free face and dividing holes.

After this, we would like to applying the EG-Slitter system to many tunnels excavation.

This page intentionally left blank

Underground Space – the 4th Dimension of Metropolises – Barták, Hrdina, Romancov & Zlámal (eds)
© 2007 Taylor & Francis Group, London, ISBN 978-0-415-40807-3

The Sir Adam Beck II intake tunnels – homage to the builders

David Heath
Ontario Power Generation, Niagara Falls, Canada

Clair Murdock
Construction Consultant, Vancouver, Canada

ABSTRACT: The 1,280 MW Sir Adam Beck II Hydroelectric Project was constructed in the 1950's, at Niagara Falls, Ontario, Canada. The twin intake tunnels total over 17 kilometers in length and pass deep below the City of Niagara Falls. The tunnels were excavated using drill and blast methods, with a top heading and bench approach. The shot rock was loaded with electric shovels and transported to the five shafts with off-highway trucks. The tunnel muck was hoisted to the surface by skip and transported by truck to disposal areas. The volume of underground excavation for the 15.55 meter diameter tunnels and the shafts exceeds 3,500,000 cubic meters, then and now the largest underground civil works excavation by drill and blast in the Western Hemisphere. The lining required over 900,000 cubic meters of concrete. All of this work was completed in three years, remarkable progress, considering the technology of the day, comparing very well with the rapid excavation and tunnelling methods of the twenty-first century. Big, fast, and deadly- at least 20 lives were lost in construction accidents.

1 SIR ADAM BECK

1.1 *Beck's accomplishments*

Adam Beck was an early proponent of publicly owned electricity grids, opposing the privately owned companies which he felt did not adequately serve the needs of the people. With the slogan "Power at Cost", he was appointed in 1906 as the first chairman of the Hydro-Electric Power Commission of Ontario, better-known as Ontario Hydro, now called Ontario Power Generation. He created the Queenston Chippawa power station, which was renamed after him. The subject of this paper, the Sir Adam Beck II Project (SAB II) was also dedicated to his memory, to recognize his enormous contributions to the progress of the people of Ontario.

1.2 *Beck's life*

Adam Beck was born in 1857 in Baden, Ontario to German immigrants. Beck worked in his father's foundry as a teenager and later went into business with his brother William, manufacturing cigar boxes. Their business flourished and Adam Beck became a wealthy man. He was elected mayor of London, Ontario several times and also was elected to the Ontario legislature, where his public power campaign took flight. Knighted by King George V in 1914, Beck died in 1925.

1.3 *Beck's words*

Beck-"The gifts of nature are for the people". His statue still commands the intersection of University Avenue and Queen Street in downtown Toronto. "Nothing is too big for us. Nothing is too visionary."

The essence of Beck's leadership was in his vision.

2 THE NIAGARA RIVER

2.1 *Drainage area*

At Niagara Falls, the Niagara River drains an area in Canada and the United States of 583,000 square kilometers. This is larger than all of France (547,030 square kilometers) or greater than Germany, the Czech Republic, Austria and Slovakia combined (567,802 square kilometers).

2.2 *Flow*

The 140 year average instantaneous flow of the Niagara River is 5,876 cubic meters a second. Because of the modulating effect of the Great Lakes upstream (Lakes Superior, Michigan, Huron and Lake Erie) the flow at Niagara is very steady, as compared to other major rivers of the world. The maximum flow is less than triple the minimum flow, whereas other major rivers'

flow may vary by factors of 15 to 30, passing great torrents where there was previously only a trickle.

2.3 *The Falls*

Niagara Falls is, by volume, the world's greatest waterfall. The American Falls are 260 meters wide and carry 10% of the flow. The Canadian, or Horseshoe Falls are 670 meters wide, and carry 90% of the flow. The falls were formed some 25,000 years ago, as the retreating glaciers exposed the Niagara Escarpment, permitting the waters of Lake Erie, which previously flowed south, to flow northward into Lake Ontario. The falls have eroded the soft shales and limestones of the escarpment at an average rate of 1.2 meters a year and they now stand 11 kilometers from their origin at Queenston. The rate of erosion has been substantially reduced, due to hydro-electric diversions and riverbed remediation work.

2.4 *History*

Known to the Iroquois people for thousands of years, the name Niagara means, from their language "thunder of the waters". The awesome spectacle was described by explorer Father Louis Hennepin in 1678, who called them "a vast and prodigious Cadence of Water". Charles Dickens wrote "I seemed to be lifted from the earth and to be looking into Heaven". The first exploitation of the power of the falls came in 1759, when Daniel Joncairs built a small canal above the falls to power his sawmill. The first generation of electricity at Niagara Falls, in 1881, was sufficient to light the Village of Niagara Falls, New York, power a few local mills and illuminate the Falls at night, using 18 carbon arc lights.

2.5 *Tourists and tourist power*

Over 14 million people visit Niagara Falls each year. The 1950 Niagara River Water Diversion Treaty between Canada and the United States provides for the most beneficial use of the waters, with varying minimum flow requirements over the Falls, dependent on time of day and the time of the year. In the daytime, from April 1st to October 31st, the flow must be not less than 2,832 cubic meters per second.

For the remaining five months of the year and at night during the other seven months, the flow over the falls may be reduced to not less than 1,416 cubic meters per second. These figures represent roughly ½ and ¼ of the Niagara's average flow. Power production in Canada and the US is exactly tailored to fit water availability, with a very close compliance to the minimum flow requirements.

2.6 *Sharing the water*

Canada and the United States share the available water equally, with a small adjustment of 141 cubic meters per second in Canada's favour, recognizing two Canadian diversions into the Great Lakes watershed. The Long Lac and Ogoki Rivers originally flowed into the Hudson's Bay watershed.

2.7 *Installed hydroelectric capacity*

On the US side of the Niagara River, the Robert Moses Generating Station and the associated Lewiston Pump GS (pump-turbine) have a total capacity exceeding 2,575 MW. On the Canadian side, The Sir Adam Beck I and Sir Adam Beck II Generating Stations, along with the SAB Pump GS (pump-turbine) and two associated smaller plants at St. Catherines, Ontario have a total capacity of 2,235 MW. In total then, with 64 generators (18 of those being reversible pump-turbines), Canada and the US have 4,810 MW of generating capacity at Niagara. Recent upgrades to the US and Canadian generating units are reflected in the figures above. Excavation of the third intake tunnel for the Sir Adam Beck complex is now underway, to augment OPG's diversion capacity. A fourth tunnel remains under consideration, along with additional OPG generating capacity.

3 THE MAJOR COMPONENTS OF THE SIR ADAM BECK II PROJECT

3.1 *The Control Dam on the Niagara River*

The control dam extends 600 meters into the Niagara River from the Canadian shore. It has 18 sluices, each with a clear span of 30.5 meters, separated by piers 4.25 meters wide and 28 meters long. The 18 sluice gates are of the 'fish-belly type', hinged at the upstream sill, affording no obstruction to the passage of ice when in their lowered position. The Control Dam ponds the water, called the Grass Island Pool. This is the primary control of intake water levels for both the US and Canadian sides of the river.

3.2 *Two intakes of the Johnson-Wahlman type*

The Johnson-Wahlman design looks like a very long mouth-organ lying on its side. Ice on the Niagara River is of concern every winter. Following extensive model-testing, each intake was designed to be 152 meters long, with varying heights and depths for the slots. The sills for the intake slots are set 7.6 meters below river level, while the lintels vary from 5.8 to 2.4 meters below the water level. Behind the slots is a gathering tube of increasing cross section leading to the intake gates. The 180 tonne gates have a clear span of 13.7 meters and are 17.7 meters high.

3.3 *Two parallel concrete-lined tunnels*

The two tunnels are on 76 meter centres, excavated to a diameter of 15.55 meters and lined to a finished

diameter of 13.72 meters. The nominal thickness of the concrete lining is 0.91meters. Tunnel No. 1, which follows the longer outer course around the curving Niagara River, is 8,707 meters long, while Tunnel No. 2, following the shorter inner course, is 8,323 meters long. Each tunnel is designed to carry 565 cubic meters per second, although testing showed a possible capacity of 650 cubic meters per second. Water velocities at these two capacities are 3.8 meters per second and 4.4 meters per second respectively.

3.4 *An open canal*

As the tunnels approach the outlet portal, they rise at an angle of 30 degrees and converge, to discharge their flow into an open canal leading to the forebay. The portals are at the southerly side of the St. David's Gorge, a prehistoric river channel filled to a great depth with glacial drift materials and debris, unsuitable for tunnelling. (The third tunnel, now under construction and at greater depth goes under the Gorge). The canal is concrete lined through the Gorge section. The overall canal length is 3,622 meters, with a width of 61 meters.

3.5 *A forebay with headworks*

The forebay widens from the canal, reducing water velocity to about 0.9 meters per second. The headworks structure is 267 meters long, the entire width of the forebay. It is here that control of the water entering the penstocks is maintained. There are 32 openings on the upstream side of the headworks, two for each of the 16 penstocks.

3.6 *16 concrete-encased steel penstocks*

Each of the 16 penstocks is 5.8 meters in diameter and 152 meters in length, of welded steel construction. Plate thickness at the upper end is 16 mm, increasing to 36 mm at the lower end. Each penstock was built of 68 prefabricated rings, brought to the site by road. They were installed on the 60 degree slope of the excavated cliff face and welded in place, followed by an X-ray inspection of each circumferential weld. The penstocks were encased in 60 centimeters of concrete to protect them from rapid and extreme temperature variations.

3.7 *A 16 unit powerhouse*

The powerhouse is located on the left river bank in the Niagara Gorge, just upstream of the SAB I powerhouse. The SAB II powerhouse is 350 meters in length, 19.2 meters in width and 15.2 meters in height. The 16 turbines are of the Francis type, operating at a head of 89 meters. The main transformers which increase the generator voltage from 13.8 to 230 kV are located on an outside deck behind the powerhouse superstructure. Three single-phase transformers are provided for each pair of generating units, for a total of 24 transformers. Excavation for the draft tubes was carried out behind a cofferdam in the Niagara River, to a depth of 13 meters below water level.

3.8 *A 6 unit pumped-storage powerhouse*

The pumped-storage generating station pumps water into a storage reservoir during low demand periods, for reuse in heavy demand periods. The reservoir area is 304 hectares, with a drawdown of 7.6 meters. Usable storage is 19,000,000 cubic meters, equal to about 4 ½ hours of full flow from the two tunnels. The reservoir is bounded by a dike of about 7,400 meters in length, varying in height from 5 to 20 meters. The perimeter dike contains 2 million cubic meters of zoned fill, mostly built with tunnel muck. The reversible pump-turbines operate through head ranges of 18–27 meters in pump mode and 12–24 meters in generating mode.

3.9 *Overall cost and schedule for SAB II*

The final cost for the SAB II project was $343,742,000, giving a unit cost of $245.00 per kW of installed capacity, about 1/10th of today's hydroelectric costs. Construction started in April, 1951 and the first unit commenced production on April 30, 1954, just 37 months later. By mid-1955 12 units were on line, and all 16 units were producing power in early 1958. Ontario Hydro decided, in response to their mid-1952 forecast of sharply-increasing demand (and a year after work had started on the first tunnel) to add a second intake, a second tunnel and six more units, in addition to the six units originally planned. Later, in 1953, Hydro decided to add four more, bringing the final total to 16 units, plus adding the pumped-storage project. The availability of the last four units delayed the overall project completion into 1958, but all the 'original' 12 units were on line within 52 months of breaking ground.

3.9.1 *Employment, work regime and contracting*

Project employment peaked at 7,655 persons. The nominal work week was 5 days. Tunnel workers worked 9.6 hours a day, surface workers 8.8 hours, giving work weeks of 48 and 44 hours- the difference was for underground travel and cage time. Workers requiring accommodation were housed in three temporary camps- Chippawa Camp, near the intakes; Whirlpool Camp, near the downstream portals and Queenston Camp, near the powerhouse. Each camp had a cafeteria that would seat 600 men. All of the work (with the exception of the intake tunnels and the 5 shafts) was done by Ontario Hydro personnel. The tunnels were competitively bid, with each bid package comprising 2 shafts and about 3,600 meters of single tunnel. One contract was awarded to Rayner-Atlas, the other to Perini-Walsh. Ontario Hydro's mid-1952 decision

to add the second tunnel required negotiations with both contractors, as work was then under way on the first tunnel. The remaining portion of 1,100 meters of tunnel at the intake end was subsequently awarded to Perini-Walsh, who were out-performing Rayner-Atlas.

4 SHAFTS

4.1 *Locations*

Shafts are located midway between the two tunnels, which are at 76 meter centres. The five shafts range in depth to tunnel invert level from 60 to 101 meters.

The reasons for this range are three- the topography; the slope of the tunnel invert and the depth to the underside of the Irondequoit limestone. This is the most competent rock strata and it was decided to make the underside of the Irondequoit limestone the crown of the tunnel. The Irondequoit slopes up from the inlet end of the tunnels at a gradient of approximately 0.5%, with the tunnel crown following that relatively strong and consistent 2.4 meter thick band.

4.2 *Geology*

Following are the depths of various strata encountered in the excavation of Shaft #1, the deepest of the five shafts. The total depth is also shown.

4.3 *Dimensions*

Shafts #1 and #2, done by Rayner-Atlas, were sunk to rock using 9.75 meter inside diameter concrete caissons, with a wall thickness of 76 centimeters, giving an outside diameter of 11.27 meters. For Shafts #3, #4 and #5, Perini-Walsh chose to use sheet pile cofferdams, due to the lesser overburden depths at those locations. A tight international supply situation for steel sheet pile then prevailed, another factor for Rayner-Atlas in choosing to use concrete caissons. On reaching rock level the shafts were continued to tunnel invert grade at an excavated diameter of 9.75 meters. Temporary timber sinking head-frames were used, these replaced with steel head-frames of greater hoisting capacity, after the tunnel invert level was achieved. The muck loading pocket and the sump at each shaft were excavated a further 21 meters, at a diameter of 5 meters.

Table 1. Thicknesses of the strata encountered.

Strata description	Depth (m)	Total (m)	Notes/observations
Clay	7.3	7.3	From the surface
Sandy silt	16.8	24.1	Water table @ 14 m
Boulder clay, slabs	9.1	33.2	Top of rock
Lockport dolomite	12.2	45.4	Water-bearing rock
Dolomite/Gasport	8.5	53.9	Water-bearing rock
Gasport limestone	8.3	62.2	Water-bearing rock
Rochester shale	18.9	81.1	Tight- no water
Irondequoit limestone	2.4	83.5	>>Tunnel crown<<
Reynales dolomite	4.3	87.8	Tunnel horizon
Neagha shale	1.8	89.6	” ”
Thorold sandstone	2.4	92.0	” ”
Grimsby sandstone	12.5	104.5	” ”
		99.1	>>Tunnel invert<<
Power Glen shale	13.4	117.9	Muck pocket, sump
Whirlpool sandstone			Muck pocket, sump

4.4 *Overburden excavation methods- Rayner-Atlas*

The top few meters of soil inside the caissons was excavated by backhoe, followed by clamming. After the third lift of concrete was placed in the caisson, the total weight exceeded 1,100 tonnes but it just wouldn't go down. In addition, uncontrolled inflows of water under the cutting edge flooded the previously-dry excavation. Then ensued a series of ineffectual missteps, truly a comedy of errors, including: attempts to block the inflow from the inside of the caisson; placing 25 kilogram blocks of dry ice in pits dug inside the cutting edge, trying to freeze the soil, discontinued after five weeks because the carbon dioxide gas released by the melting dry ice became hazardous to the crew; grouting around the perimeter, this discontinued after 3 days of effort; driving an external ring of sheet pile, with this attempt much obstructed by the earlier grouting program, all of these measures with little success. It was then decided to continue with wet clamming but the caisson still wouldn't drop. Soil losses from the exterior piped to the surface, requiring backfill. The next effort required top-ballasting the caisson. With a top load of 562 tonnes of sheet pile, the caisson finally moved, bottoming-out on rock, and after 3 months of frequently-futile work. By contrast, Perini-Walsh, at their three shafts, and using the sheet pile rings proceeded uneventfully and in much less time.

4.5 *Rock excavation methods- Rayner-Atlas*

Work in each shaft was carried out on 8 hour shifts, working around the clock. Each shift had a 22 man crew. The average sinking rate achieved was 0.9 meters per day. Hand-held pneumatic pluggers, with drill steels of 0.9, 1.8 and 2.4 meters length were used to drill 65 holes on half the bench, with each round pulling about 1.9 meters. Drilling off half a bench took about 2.5 hours. A half bench took about 12 hours to muck, all done by hand. Crew access to the bench was by the muck buckets, rated at 1.4 cubic meters or 11 men. Mucking took over 70% of the total shaft-sinking time, exclusive of the timbering, which was done on Sundays by a special crew.

4.6 *Shaft bottom complications and hoisting*

Substantial structural steel arches and underpinning were required at the shaft bottom, to permit the safe excavation of the cross drifts to the main tunnels. The hourly-paid underground work force at Shaft #1 during this portion of the work totaled 240 men. During this period the permanent structural steel head frames and the electric hoists were installed. A typical shaft arrangement provided for 2 counter-balanced muck skips each of 10 cubic meter capacity and an 18 tonne capacity cage with counterweight. The cage was used for men, materials and the construction equipment, which included 15 tonne capacity Euclid Model 87FD off-highway trucks and 2 cubic meter Northwest Model 80 D electric shovels.

5 TUNNEL EXCAVATION

5.1 *Planning for the 15.55 meter diameter face*

Rayner-Atlas intended a full-face approach, using two multi-deck jumbos, one for the top portion and another for the lower, with mucking to be done with 0.7 cubic meter Eimco overhead loaders dumping onto a conveyor, to load 4 cubic meter muck cars, for locomotive haulage back to the shaft. This arrangement was shown to be inadequate, impractical, slow and unsafe. With Ontario Hydro's strong encouragement, Rayner-Atlas hastily adopted the more productive top heading and bench approach that Perini-Walsh was using, even copying the Perini-Walsh plans for the drill jumbo. That approach divided the face into a 9 meter high top heading excavated the full length of the section, followed by a 6.5 meter high bench, this work done on a second pass.

5.2 *Drilling and loading the heading*

For Rayner-Atlas' modified approach, the heading was drilled with a multi-deck rail-mounted jumbo fitted with 23 Ingersoll-Rand pneumatic drifters, 16 of which were column and bar mounted. Three drills on the top deck and four more on the rail bogeys were mounted on hydraulic booms which worked only in the vertical plane- the horizontal movement was manual. Jacklegs supplemented the four hydraulic booms for the bottom lifter holes. A round required 173 holes, drilled to 6 meters, using tungsten carbide bits. Electric blasting caps were used, with an overall powder factor of 1.6 kg/m^3. The toe of the muck pile was usually about 40 meters from the face, exceptionally as far as 55 meters. Considerable oversize was encountered, and the grizzly at the loading pocket was reset, from 60 cm × 60 cm to 90 cm × 90 cm openings. Rocks sometimes had to be hoisted off the grizzly by air tuggers and loaded into small trucks, for cage transport to the surface, when the grizzly became clogged with oversize. Up to 10 electric driven air compressors supplied as much as 212 m^3 of air per minute. In contrast, Perini-Walsh used fewer drills- 17 Joy drifters, but all on hydraulic booms and pulled rounds averaging 4.8 meters. A Perini-Walsh heading round produced 900+ cubic meters of muck.

5.3 *Scaling and rock support*

Scaling after the blast was difficult and dangerous, as much scaling was done manually from the jumbo decks. Additional scaling was done using the Northwest shovels and from the muck pile. Steel ribs (W8 × 20) 20 cm × 65 kg were set at 1.2 meter centres, blocked, and timber and steel lagging was installed. The ribs were in 4 pieces, hoisted by air tugger onto the drill jumbo decks and then man-handled into place. Several rock falls occurred in Tunnel 1 during August of 1952, requiring that 80 meters of tunnel be retimbered. Intermediate ribs were placed in some areas where the rock was suspect. On the breakthroughs between headings, the alignments compared within a few centimeters- on the money.

5.4 *Crew size and cycle times, for 2 headings*

After abandoning their fatally-flawed full-face approach and after copying the Perini-Walsh jumbo, Rayner-Atlas still didn't get it right and went cheap

Table 2. The Rayner-Atlas underground crew.

Category	Men	Notes and observations
Drilling	51	23 drills + jack-legs for lifter holes
Mucking	35	Drilling Hdg. A, Mucking on Hdg. B
Steel & timber	23	4+ steel sets required per round
Ventilation	4	1 shift only
Mechanics	19	
Total UG crew	128 men	(Add for electricians)

Table 3. Typical Rayner-Atlas cycle for a round.

Operation(s)	Time required		Notes and observations
Smoke out	0 hr.	30 min.	
Cleanup & scale	0	45	
Mucking	4	50	Perini-Walsh time- 4 hr 45 min.
Move in jumbo	0	30	Parked 60 m back from face
Drill, load, out	4	35	Road maintenance opportunity
Total cycle	11 hr.	10 min.	=2+ rounds in 24 hours

on their choice of drills, with higher labour costs as the result. Nonetheless, Rayner-Atlas excavated 173 meters of tunnel in 21 shifts, working two headings at once, during their best-ever 7-day production week. This required excavating 20,400 cubic meters.

5.5 *Mucking the heading and the bench*

Both contractors used similar equipment for loading and hauling- Northwest Model 80 D electric shovels and 10 cubic meter Euclid off-highway trucks. The shovel booms were cut down to give better clearance under the support ribs and lagging. Perini-Walsh, always the innovator, found a clever way to reduce truck turnaround time- they drove the empty Euclid onto a large steel plate resting on another steel plate and then rotated the truck around, to face in the opposite direction, with oil between the plates, and an air tugger used to spin the truck around- a steel-on-steel turntable. All Euclids were scrubber-equipped. Crews mucked one heading while drilling the other.

5.6 *Drilling the bench*

After cleaning the bench with compressed air and water jets, drilling proceeded using a rail-mounted vertical jumbo equipped with 17 drills, mostly Gardner-Denver. This jumbo ran on rails attached to the bottom of the ribs and it was moved forward with air tuggers. Each vertical hole was drilled to a calculated depth, producing a nearly circular invert shape.

The overall powder factor for the bench excavation was 1.45 kg/m^3, using packaged high explosives and electric caps. A muck pile about 15 meters long was left in place before blasting, to reduce fly rock. Rounds were loaded during drilling and were blasted at the end of each 8 hour shift. The average daily advance in Tunnel 2 was 30 meters, done over 3 shifts.

5.7 *Ventilation*

1.2 meter diameter steel ventilation ducts were brought up to within 60 meters of the top heading face. Reversible electric fans at the surface and at 250 meter intervals underground supplied 1,840 cubic meters of fresh air per minute to the tunnel. Reversing the fans expelled blast fumes. The duct and fans were removed for benching operations. Some supplemental unducted airplane-type fans were used to improve circulation while benching.

6 CONCRETE OPERATIONS

6.1 *Arrangement*

The nominal excavation size was 15.55 meters diameter, the finished size 13.72 meters. The 20 cm ribs and blocking are within the nominal 15.55 meters. With an average over-break of 25 cm, the concrete volume is 54 cubic meters per meter of tunnel. The lining was placed in 3 operations. First, two small curbs each 30 degrees above the invert, on which the concrete equipment would ride; secondly, the invert, covering the bottom 60 degrees of the circular lining; and finally, the upper 300 degrees.

6.2 *Concrete supply and delivery arrangements*

All concrete was supplied by Ontario Hydro from a wet mix central batch plant at Chippawa. This plant supplied much of the SAB II project. Rayner-Atlas used up to 17 three-axle dump trucks to haul the mix to delivery drop hoppers, at distances as great as 5 kilometers and on city streets. At intervals of about 150 meters, 25 cm diameter steel drop pipes were installed in holes that had been drilled in advance of the tunnel excavation. Hoppers in the tunnel caught the falling concrete. There were no re-mix facilities, but concrete segregation appears not to have been a problem. For the invert, concrete was transported to the placement location with a traveling and self-propelled pot gantry that rode rails set on the top of the curbs. The workers christened this gantry "The Queen Mary". For the arch concrete, a gantry was positioned under the drop hole and the dropping concrete was directed by chutes to twin Pumpcretes. 20 cm steel pump lines transported the concrete to the arch form, which was never more than 200 meters from the drop points. The form was fitted with numerous concreting access doors and a slick line filled the tunnel crown.

6.3 *Invert concrete*

Steel formwork panels were placed along the top sides of the invert section. The top of the side forms was the traveling surface for the drag screed and the finishers' access bridge. The drag screed was ballasted with rock and weighed about 11 tonnes. It was pulled ahead using a 3 tonne capacity air tugger on a 5 part line, anchored to steel pins set in the invert ahead. For batch plant and transport reasons, concrete placement was done on a single shift per day, although clean-up and form-setting went on around the clock. The record length placed in one 8 hour shift was 86 meters, while the average pour length was 40 meters. The Queen Mary was used to move the formwork and rails ahead. Stripping was started after a minimum 8 hours of curing. After the wood float and steel trowel finishing, the fresh invert concrete was covered with Fibreen bitumastic paper, for curing and protection. Richmond screw anchors were embedded near the top of the invert pour, as anchors for the arch form.

6.4 *Arch concrete*

Just before concrete placing, it was necessary to remove all the loose rock that had accumulated behind

the wood lagging, along with removing most of the lagging. This was done from a re-timbering gantry running on the curb rails. The arch forms were manufactured by Mayo, and as designed by Rayner-Atlas, who again got it wrong, by specifying forms that were too lightly-built and that blocked supply traffic on the completed invert, because the flimsy formwork required numerous bottom struts. The forms had to be reinforced underground, with doubling of ribs and replacement of inadequate steel members. The skin plate couldn't be changed underground and it became distorted, requiring continual repair work. Even the cast iron wheels carrying the arch form had to be changed to solid steel wheels, due to failure. Two arch forms were used by Rayner-Atlas, never one for anticipation or standardization. One form was originally bought at 18.3 meters length, the other at 24.4 meters length. Both were later lengthened by 3 meters, giving final form lengths of 21.3 and 27.4 meters. The forms ran on rails supported by beveled timbers resting on the curved invert. The forms were built in sections 6.1 meters long and these were the lengths moved ahead on shifting the form to the next pour. Vertical movement for stripping was 15 cm and each side panel could be swung in 22 cm- a two hinge form, with the hinges located just above the springline. It was generally possible to pour the form every day, with concreting done on a single shift, with 12 hours allowed for curing and then four hours to strip and move the forms ahead and prepare for the next pour. After moving the form into the new location and jacking it up to grade, the bottom edges of the two side flaps were bolted-in, using the Richmond screw anchor inserts that had been set into the top edge of the invert concrete. The average placing rates with the two Pumpcretes exceeded 100 cubic meters per hour.

6.5 *Grouting*

Following 60 days of concrete curing, the Cementation Company (Canada) Ltd., working as a sub-contractor to Rayner-Atlas, commenced their grouting operation. Cementation equipped the job with a C. F. Johnson surface batch plant and a Colcrete mixer. Grout was pumped in 40 mm steel lines to the underground injection plant. This consisted of three receiving agitator tanks for receiving and remixing grout from the surface and low and high pressure grout pumps, all equipped with pressure-limiting devices. All of this was mounted on a too-light gantry composed of sections of modular scaffolding. The gantry gave ongoing and completely avoidable aggravation and delay. Grout hole drilling off the gantry was with jacklegs and stoppers. For the invert, the drilling was done with wagon drills- wheeled undercarriages with mast-mounted drifters. After the low-pressure sequence using sand-cement grout, the high pressure grouting using cement-only grout was undertaken. This was followed by a series of test holes- drilling followed by grouting- very little grout was taken on the test sequences. The total job grout take was one third of expectations, due to the excellent filling at the crown of the tunnel with the air sluggers (a pneumatic placer) and the Pumpcretes. In Tunnel I, Rayner-Atlas gave very little attention to timely clean-up of excess grout in the invert and wound up chipping the pooled and hardened grout with pneumatic hammers. For Tunnel 2, timely grout clean-up was made routine, and at a lesser final cost.

ACKNOWLEGMENTS

The authors wish to thank the following engineers for their reviews, comments and other generous assistance in the preparation of this paper-

Mr. John Boots, BC Hydro, Vancouver, Canada
Mr. Bill Earis, BC Hydro, Vancouver, Canada
Mr. Scott Sylte, EBA Engineering, Vancouver, Canada
Mr. James Thomson, Oakville, ON, Canada

REFERENCES

Central Intelligence Agency World Fact Book

Hale, John (Mr. Hale was a Surveyor for the Hydro-Electric Power Commission of Ontario on the SAB II Tunnels) *Conversations in 2006 with the co-author*

Hearn, Richard L. 1956. (In 1956, Dr. Hearn was Chairman of the Hydro-Electric Power Commission of Ontario) The New Sir Adam Beck Generating Station at Niagara *Proceedings of the Institution of Electrical Engineers* Paper No. 2204 S- Pages 41–48: London

Norton, Dean (Public Affairs Officer- Niagara Plant Group) *Sir Adam Beck 2 G.S.- A Commemorative Retrospective- The First 50 Years- 1954–2004* Ontario Power Generation. Toronto. OPG

Ontario Hydro News- HEPC of Ontario- Various issues
January, 1954 *Pattern of Progress*
March, 1954 *Big Job*
July–August, 1954 *Romance of the Niagara*
September, 1954 *From Queenston's Cliffs*

Rayner-Atlas Limited- Description of Operations, June 1954
Volume 1- Excavation- Pages 1–86
Plates 1–69
Volume 2- Tunnel Lining & Services- Pages 87–160
Plates 70–111

Thomson, G. James (Mr. Thomson was an Engineer for the Perini-Walsh Joint Venture on the SAB II Tunnels) *A Ring of Urgency*: *An Engineering Memoir* Pages 58–77. Abbeyfield Publishers, Scarborough, ON *Conversations in 2006 with the co-author.*

This page intentionally left blank

Underground Space – the 4th Dimension of Metropolises – Barták, Hrdina, Romancov & Zlámal (eds)
© 2007 Taylor & Francis Group, London, ISBN 978-0-415-40807-3

Královopolský Tunnel in Brno, CZ

V. Horák, J. Pechman & J. Rožek
Amberg Engineering Brno, a.s., Brno, The Czech Republic

ABSTRACT: The paper deals with the design of two parallel road tunnels passing under a densely built-up area on a ring road in the city of Brno. Major critical parameters for the construction will be adverse ground conditions in neogenous clay, large excavation cross-section, low overburden and an overlying residential area. Thorough geotechnical investigation included driving of three exploration adits and extensive surface and underground monitoring. The twin-tube tunnel of approximately 1250 m in length will be driven using NATM principles and core method of excavation, with short cut-and-cover sections. Low overburden in portal sections will necessitate the use of supplementary measures, such as pipe umbrellas and jet grouting. Special attention is paid to evaluation of estimated subsidence and to minimization of possible damage to existing structures. The project costs are about 100 mil EUR (tunnels only). The opening of the tunnel is scheduled for 2011–2012.

1 INTRODUCTION

1.1 *The project*

Section Žabovřeská-Dobrovského of the city ring road (VMO) forms an important part of the traffic system of Brno, as well as the national road network (road I/42) and the international road network (road E461).

- the project will be incorporated in the radial ring traffic system, whose three ring roads have graded traffic functions
- the construction represents a substantial step towards closing of the third outer ring, which will help decrease traffic loads on parts of the intermediate ring road
- accordingly, completion of the outer city ring road (VMO) will contribute further to directing through traffic away from the city centre

A twin-tube tunnel, 1.25 km long, is the key component of the project (Figs 1–2).



Figure 1. Layout of Brno traffic system.

1.2 *Principles of town planning and architectural solution*

The objective is to consistently separate residential areas from the through traffic and city ring road (VMO) traffic. At the same time, the existing green areas are considerably enlarged (Fig. 3).

To improve pedestrian connection between residential districts on both sides of the city ring road, two new footbridges will be built.

Extensive planting of trees and climbing plants in border zones should not only set off the living areas from the traffic, but also enhance the overall structural design (soft landscaping of the roundabout area and the area above the tunnel openings, green foot bridge, earth walls, ground shaping). Accomplished planting design also helps to minimize the visual impact of the traffic structure, so that even inhabitants of the upper floor flats see as little of the finished construction as possible.

The immediate environment will be developed into park-like areas using soft landscaping, street furniture and small architectural elements, with the aim to create an impression of small piazzas connected by footpaths. Closing off open inner courtyards by high fencing with climbing plants and green roofing on new buildings should round off the picture.

1.3 *Environmental impact of the construction*

The endeavour to minimize major impacts of the construction work on the environment was focused in



Figure 2. The tunnel layout.



Figure 3. Computer image of the western portal.

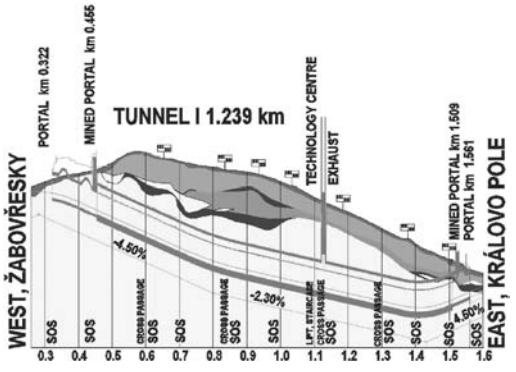


Figure 4. Longitudinal profile with geology.

particular on reducing noise and air pollution and on massive planting:

- Closing of the residential area of the streets Voroněžská and Záhřebská with noise barriers and earth walls, placing of the side ramps into covered galleries and their extension up to the bridge at Korejská street
- Noise protection walls and substantial green planting in front of the eastern tunnel opening
- Elimination or substantial reduction of exhalations around tunnel openings due to the use of controlled ventilation system in tunnels
- Sufficient height of the exhaust chimneys above the surrounding buildings in the area of technology and ventilation centre, installation of noise attenuators
- Forming of functional and achitecturally attractive areas for pedestrian traffic and recreation at Voroněžská street, Záhřebská street, Hradecká street – east and Královopolský tunnel opening
- Stabilization of the city floorscape in the new opening at the tunnel portal in Královo Pole

2 THE TUNNELS

2.1 *Layout overview*

The east-west tunnel tube – denoted Tube I – is located beneath Dobrovského street, the second tube – Tube II – is situated in parallel about 60 m to the south. Both tubes pass under a densely buit-up area, which means that the excavation will have to traverse under or near buildings up to seven storeys high. The tunnel is connected at both portals to large intersections with grade separation (see Fig. 2).

Tunnel tube I: total length 1237 m

The driven part is 1019 m long; cut-and-cover parts built in cased excavation pits are 168 m long in Žabovřesky and 50 m long in Královo Pole.

Tunnel tube II: total length 1258 m

The driven part is 1060 m long; cut-and-cover parts built in cased excavation pits are 149 m long in Žabovřesky and 49 m long in Královo Pole.

Both tunnel tubes are oriented in the west-east direction. The distance between the tubes varies between 6 and 70 m.

The longitudinal profile of both tubes had to be adjusted to the links to existing roads, while keeping two important trunk sewers in front of the Královo Pole portal intact. Moreover, the vertical alignment of tunnel axes is governed by the geology, more specifically the minimum necessary overburden thickness in clays (see Fig. 4). The resulting alignment has a sag vertical curve located in the bottom part, which means water will have to be pumped out of the lowest point both during construction and during operation of the tunnel.

2.2 *Geology*

The geological conditions in the area are monotonous. The top cover (3–10 m thick) is made up by fills and loess loams. Basis of the Quaternary cover is

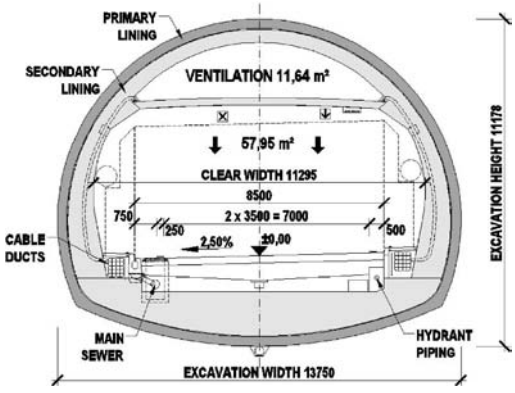


Figure 5. Standard driven tunnel cross-section.

represented in places by water-bearing gravel/sand terraces, which are not continuous. Its underlay is formed by limey, silty clays of Tertiary (Neogene) origin, so called Brünner Tegel in German. The thickness of the clay layer is several tens of meters – the bedrock was not reached by boreholes more than 60 m deep. Groundwater is bound to sandy gravel locations on upper Neogene horizon in the form of impoundments in the local depressions. The consistency of the Neogene clays is hard up to solid. From the point of view of plasticity the clays are highly plastic (MV or CV according to USC system) and in connection with groundwater highly squeezing. The cover thickness on both tunnels is approximately the same and ranges between 6 m up to about 21 m. The tunnels are vertically positioned in such a way that a minimum thickness of impervious Neogene clay cover of 2 to 3 m above the excavation is always secured.

2.3 *Design of the tunnel interior*

The standard driven cross-section is horseshoe-shaped with an arched invert (see Fig. 5). The excavation area is 125 m^2. The cross-section is divided by an intermediate ceiling into the traffic area and ventilation area. The tunnel lining is of double-shell type with intermediate waterproofing.

Primary excavation support is formed by steel arches and shotcrete reinforced with wire meshes. Steel plate girders are preferred due to their immediate bearing capacity. Total thickness of primary support is 350 mm. The tunnel is sealed with a closed waterproofing membrane. The final RC concrete lining has minimum thickness of 450 mm.

Tunnelling in areas with low overburden thickness or areas endangered by higher than permissible settlement will be supplemented with pipe umbrellas above the excavation roof.

Due to the confirmed groundwater corrosivity (concrete-aggressive action), the primary lining is considered to be a temporary structure. Long-term load-bearing capacity is fully ensured by the reinforced concrete inner lining.

Table 1. The tunnel profile – basic technical data.

Length / Area / Volume	Amount
Basic width of the traffic lanes in the tunnel	3.50 m
Clear headway	4.50 m
Clear width between curbstones	8.50 m
Area of the traffic space	57.95 m^2
Ventilation area (air exhausting)	12.0 m^2
Primary lining with the thickness of 350 mm	11.95 m^3/ running meter
Secondary lining (min. thickness 450 mm)	32.53 m^3/ running meter
Tunnel excavation area	125 m^2

2.4 *Tunnel ventilation*

The tunnel is designed with a semi-transverse ventilation system. The clean air will be drawn into the tunnel through the tunnel openings. The polluted air will be channeled through the air ductwork situated above the suspended ceiling and exhausted centrally into the tunnel technology and ventilation centre located in approximately one third of the tunnel length. The exhaust air will be blown into the atmosphere with an increased speed from two chimneys 25 m high above the surrounding terrain. The ventilation of both tunnels will be separated and entirely independent.

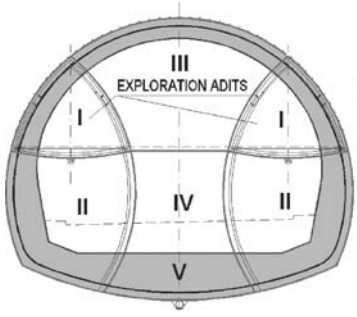
The excavated parts in Žabovřesky and also in Královo Pole will be completed with auxiliary axial flow fans for additional air suction from the tunnel openings to minimize the emission of polluted air from the tunnel openings into the area of the housing estate Žabovřesky or into the residential part of Královo Pole.

2.5 *Tunnelling method*

A tunneling procedure with vertically and horizontally sectioned heading (so called Ulmenstollen, Paramentstollen in German) is proposed. The sequential excavation method incorporates the existing exploration adits (Fig. 6). The excavation will proceed from the eastern portal towards Žabovřesky. The construction of secondary liner will follow approximately 200 m behind the invert closure of the excavation support.

The secondary lining is made of cast in-situ reinforced concrete. To speed up the construction, the central part of the tunnel floor is made of precast elements, which will provide more or less continuous access to the tunnel face.

The estimated settlement trough is relatively narrow. According to mathematical models and forecasts



Areas of partial excavations:

I	12 m^2
II	24 m^2
III	29 m^2
IV	20 m^2
V	4 m^2
Total	125 m^2

Figure 6. Division of excavation.

the width of the settlement curve extends – depending on the cover thickness – up to the maximum distance of about 25 to 30 m from the tunnel axis. The maximum subsidence value reaches up to ca 110 mm directly above the tunnel axis at the location with minimum overburden thickness, otherwise the maximum value reaches 70 to 80 mm along the tunnel route.

2.6 *Safety construction measures*

Both tunnel tubes are connected by four cross passages. One of them is linked to an escape staircase and evacuation lift, which enables to escape directly to the open space.

Both tunnels are equipped with a 40 m long emergency lay-by.

Each tunnel is furnished with six emergency (SOS) stations with standard equipment. The emergency stations are built in on the right hand side in the direction of travel, while the hydrant niches are situated on the left. The stations are spaced 150 m apart.

Both the tunnel tubes and the escape routes including the underground rooms of the technology centre will be equipped with fire hydrant mains. The looped water supply system enables to cut off individual branches of the supply system in case of a major accident and is completed with additional dry standpipes in tunnel cross-connections and escape routes.

The drainage system is designed to prevent fire and flammable liquids from spreading inside the tunnel. It includes slot gutters and fire protection manholes. A water sump with a pumping station is located at the lowest point of each bore. The pumping station has a 100% capacity reserve including back-up and protection of pump units and remote control.

2.7 *Safety equipment*

As far as the operational safety is concerned it can be said that the tunnel's safety equipment satisfies the standard of the other two Brno tunnels already in operation. It also meets the requirements posed by the European Directive 2004/54/EC on the minimum

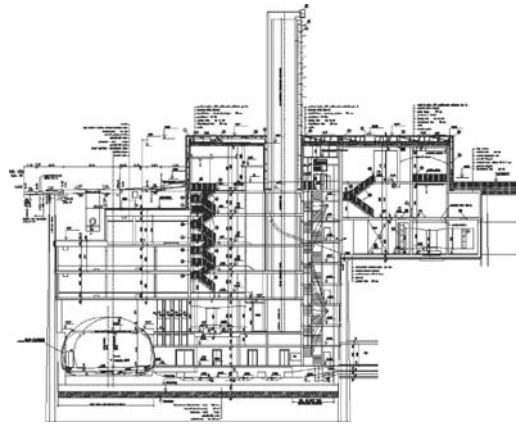


Figure 7. Cross-section of the technology centre.

safety requirements for tunnels in the trans-European road network. Since 1999 the city-owned company Brněnské komunikace operates a central tunnel control room (CTD) with round-the-clock service, to which all the systems of the new tunnel will be connected.

3 TECHNOLOGY AND VENTILATION CENTRE

It is necessary to provide corresponding room for the selected semi-transverse ventilation system (especially the ventilation fans) and for the other technological systems (lighting, power supply, traffic signals, communication) within the tunnel. The adequate space had to be fitted in the relative dense existing housing development. The underground object of the technology and ventilation centre will have the plan dimensions of 14×44 m, the depth of the escape route finish floor and the lowest floor level is 25.50 m under the terrain. The technology center will have altogether five underground floors and one ground storey, as well as two exhaust chimneys with the height of 25 m above the terrain.

The first tunnel tube passes through the bottom floor of the technology centre. This fact will be taken advantage of during the tunnel construction as the construction pit for the underground centre will give additional access for rock material removal and ventilation. The second tunnel tube – Dobrovského II – will be connected to the technology center by three adits – an escape route with cable duct and two ventilation tunnels. The ventilation tunnels will channel exhaust air through a separate air-handling plant (VZT) directly into the chimney. On the surface there will be only two relatively small buildings with an access road



Figure 8. Digital rendering of the surface buildings of the technology centre.

and two tall chimneys (see Fig. 8). The above-mentioned buildings will be architecturally integrated into the future multi-purpose building of the VFU (University of Veterinary and Pharmaceutical Sciences Brno).

4 EXPLORATION ADITS

4.1 *Objective*

The tunnel design has to cope with three main adverse consequences of the tunnel location: relatively difficult ground, comparatively low overburden and a number of existing buildings and utilities that could be affected on the surface. All this makes the construction an engineering task that is yet unparalleled in The Czech Republic.

A detailed technical survey of the endangered buildings and utilities was made. The documentation comprises records of about 260 buildings. Approximately 160 buildings will be monitored and measured during tunnelling.

The actual impact of the tunneling on the surface was verified during tunneling of the exploration adits. Three exploration adits with a total length of about 2000 m were driven. The adits are situated inside the future tunnel cross-section. They were driven by the same method as is assumed for the large tunnels so that valuable experience with working the rock could be gained. The results of the measurement programme and the monitoring of the adit excavation impact in the critical areas show that their implementation was more than justified.

4.2 *Construction of the exploration adits*

Two adits denoted IIa and IIb and 835 m long were driven in the tunnel profile of the tube Dobrovskeho II. One 365 m long adit with the designation Ib was excavated in the tunnel profile of the Dobrovského I tube. The adits were driven from the temporary tunnel



Figure 9. Temporary portal at Královo Pole in 2002.

portal in the Královo Pole construction pit. The temporary tunnel portal and the excavation pit at Královo Pole were designed and carried out so as to enable driving of both large tunnels.

The adits have the shape of isosceles triangles. The sides of the triangles are vaulted with the radius of the future tunnel lining. The invert is also arched. The lining is made of sprayed concrete with the thickness of 100 mm, which is reinforced with one layer of wire mesh and rigid frames made of mining sections K24 spaced in 1.0 m distance. The excavation area of each adit is 13 up to 15 m^2.

4.3 *Geotechnical investigation programme*

The geotechnical field tests were carried out in four short lateral drifts, which were driven from the IIa adit to the space outside of the future tunnel cross-section. The exploration boreholes, inclinometer, extensometer and levelling profiles were all situated near the lateral drifts. The locations of concentrated investigation were previously selected based on available data. Beside the above mentioned investigation techniques a detailed geological sequence was drawn up for each adit and several measuring cross-sections were set up, where convergence, change in shape and position of the lining and ground settlement were recorded in dependence on the excavation progress.

5 EXPERIENCE GAINED THROUGH TUNNELLING OF THE EXPLORATION ADITS

5.1 *Problems in the area of extremely low overburden*

Close to the tunnel portal in Královo Pole, about 50 to 80 m into the tunnel, the tubes have a very low cover thickness of 5 to 8 m. The most serious difficulties with respect to the settlement and deformations

of the overlying buildings were encountered here during tunneling of the IIa and IIb adits. A significant increase in the maximum settlement by ca 120% compared with the original assumptions occurred here. The maximum measured building subsidence was 56 mm and the inclination of the building exceeded the set critical limit.

The causes of the excessive subsidence can be summarized in the following items:

- A depression in the horizon of Neogene clays filled with gravel aquifer was reached without previous indication. That meant substantial, unexpected and long-term water ingress into the excavation of the IIa adit. It is interesting to note that the IIb adit, mere 6 m far from the IIa excavation, was almost dry.
- Two more stories were added to the former one-storied house – and the building permission for the extension was obtained – only a few months prior to the tunnelling start.

In spite of these problems the contactor managed to go through this critical locality without any further damage due to adopting additional technical measures and thanks to the combined effort of all interested parties.

The tunneling of the Ib adit, which is situated under the street, ran smoothly without unfavourable ground settlements. The assumed deformations were not exceeded.

5.2 *Mathematical modelling and prediction of the settlement trough development*

During tunnelling of the exploration adits a continuous evaluation of the obtained data took place. The exploration findings and measurement results were incorporated in a mathematical model created using the FLAC software. The results of the mathematical modeling were compared with the actually measured values. Subsequently the forecast of the tunnelling effects was elaborated. The predicted settlement troughs and ground deformations were determined for the entire length of both driven tunnels. A map of combined settlement trough for both tunnels was plotted using settlement contour lines. These forecasts were used as source data for the detailed evaluation and checking of the buildings in the settlement area of the future tunnels and for the design of their reinforcing measures.

5.3 *Evaluation of the acquired findings from the tunneling of exploration adits with respect to the engineering solution of the large tunnels*

Taking into account the findings from the tunneling of the exploration adits, the rock environment and the tunnel construction in the given area can be characterised in the following terms:

- The deformation development is long-term. The steady state is reached only a year after the passage of the tunnel face. The Neogene clay can be compared to a “viscous liquid” with respect to deformation effects.
- It was confirmed that deformations in the invert (invert heaving) influence substantially the overall displacement.
- Stiffness of the primary support has to be increased proportionally with the excavation area.
- Partial excavation steps have to be carried out and support has to be installed in the shortest time possible. Interruptions in excavation cycle result in increments in displacements and in settlement trough area.
- The settlement trough is relatively narrow. Points of maximum gradient lie approximately 20 m from the tunnel axis.
- Excavation in very shallow sections and under sensitive structures on surface requires additional measures, such as ground improvement, grout screens and pipe umbrellas, as well as the use of state-of-the-art boring techniques and grouting materials.

6 CONCLUSION

As of 2006, the construction work on the project has already started. The start of the excavation is planned for the spring of 2007. The authors are going to be involved in the detailed design as well as the building supervision and they hope they would be able to report on the projects headway at the WTC 2007.

Underground Space – the 4th Dimension of Metropolises – Barták, Hrdina, Romancov & Zlámal (eds)
© 2007 Taylor & Francis Group, London, ISBN 978-0-415-40807-3

Planning and design of the A3 Hindhead tunnel, Surrey, UK

T.J. Ireland & T.A. Rock
Mott MacDonald, London, UK

P. Hoyland
Balfour Beatty, London, UK

ABSTRACT: The A3 Hindhead project includes a 1.8 km long twin bore tunnel that is planned to commence construction in 2007. This paper describes the development of the tunnel design through the planning and design phases including the design for maintenance, and the innovative approach to tunnel support in the sand and 'soft rock' sandstone.

During the preliminary design period, the UK Health and Safety Executive (HSE) issued three Chemical Hazard Alert Notices (CHAN's) relating to a reduction in the allowable exposure levels of respirable silica and NO_x during construction. This caused us to compare SCL and TBM design and construction strategies and compare the risk profiles.

1 INTRODUCTION

The A3 Hindhead project located in Surrey, UK is a 6.7 km dual carriageway truck road that includes a 1.8 km tunnel being delivered under a Highways Agency Early Contractor Involvement (ECI) contract. This paper describes the development of the tunnel design through the planning and design phases including vertical and horizontal alignment, tunnel cross section, ground support measures, and the design of the tunnel structure to resist fire loading.

During the preliminary design phases both TBM and Sprayed Concrete Lining (SCL) methods were considered for construction, and a comparison between the designs is included. The differences in construction methodology including planning, and program are also discussed, and the different risk profiles outlined.

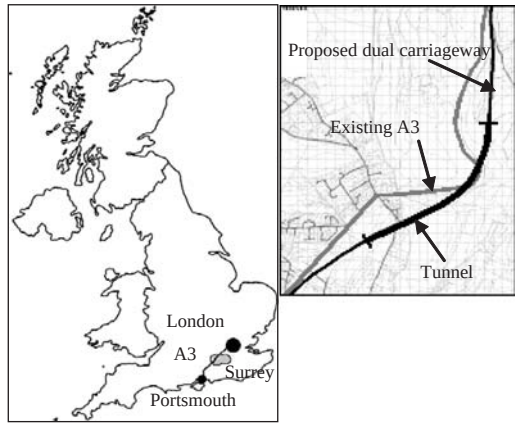


Figure 1. Project location.

2 PROJECT DESCRIPTION

The A3 Hindhead project is one of the schemes in the UK Government's Targeted Programme of Trunk Road Improvements. The project will complete the dual carriageway link between London and Portsmouth and remove a major source of congestion, particularly around the A3/A287 traffic signal controlled crossroads. Refer to Figure 1 for location details.

The project will deliver quicker, more reliable journeys on a safer road, and remove much of the present peak time "rat-running" traffic from unsuitable country roads around Hindhead. The centre of Hindhead will be freed from the daily gridlock that blights the area, with the result that the project will bring benefits to road users, local residents, and the highly prized environment.

2.1 *Planning phase*

The A3 Hindhead project has been planned since 1983 when it was included in the Government's Trunk Road program. The challenge for this project was balancing environmental impact with user economic benefits. Striking the right balance between these competing

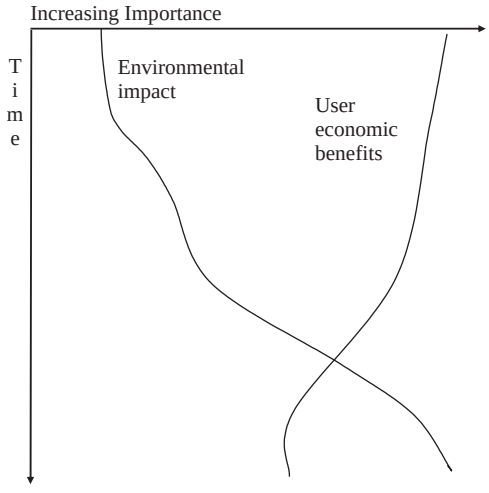


Figure 2. Change in approach to development of A3 Hindhead Scheme.

issues has taken over 20 years to resolve. Almost all the scheme lies within an 'Area of Outstanding Natural Beauty' (ANOB) with Site of Special Scientific Interest (SSSI) that are part of the Wealden Heaths SPA – an EU Designation that prohibits development except for "no choice" and national economic or safety considerations. The route passes through National Trust owned land which is classified as "in-alienable". It can only be compulsorily purchased against their wishes with the approval of the UK Parliament.

In the 19 years since the project was first mooted, and the commencement of the current phase of project development in October 2002 there has been a sea change in planning and approval thinking where economic benefits originally had primary importance and now environment damage mitigation is uppermost. This change in planning approach with time is shown on Figure 2. The key to a successful planning process in this case was to provide a tunnel under the environmentally sensitive areas, and to close the old A3 thereby reuniting sections of the SSSI/SPA. Other environmental benefits included the removal of intrusion and severance within the AONB, and the removal of air, noise and light pollution.

Part of the change in approach was the adoption by the Highways Agency of partnerships for scheme development. This was manifested on the A3 Hindhead project by the establishment of a Project Advisory Group (PAG) incorporating all the key stakeholders including the protectors of the environment such as National Trust, English Nature, Countryside Agency and English Heritage. The objective of the PAG was "*To assist in developing the tunnel scheme to minimize its impact on the built and highly prized natural environment, and one that is broadly acceptable to the local community, while ensuring that all impacts have been addressed*". Table 1 below outlines the project development timetable since inception in 1983.

Table 1. Project development time-line.

Date	Activity
1983	Enters Trunk Route Program
1987	Single Route Consultation
1988	Red Route confirmed as preferred
1992	Second public consultation
1993	Modified yellow route with bored tunnel announced as preferred route
1995	Work suspended
1998	Roads review – Road Based Study into tolling announced
1999–2000	Tolling Study
2001	Enters TPI
10/2002	ECI contract awarded
9/2004–2/2005	Public Inquiry
8/2005	Inspectors Report received
9/2006	Secretary of State decision
1/2007	Commence construction
7/2011	Open Tunnel
3/2012	Complete Scheme

2.2 *Early Contractor Involvement (ECI) contract*

The Highways Agency introduced the principle of "Early Contractor Involvement" in 2001. This new form of procurement is about bringing suppliers and designers together much earlier in scheme conception than previously occurred, allowing them to work together more closely. This allows more scope for innovation, improved risk management, better forward planning of resource requirements and minimization of long term environmental impacts, improved consideration of buildability and health and safety, shorter construction periods and reduced environmental impacts during construction. Overall, the early creation of delivery teams clearly offers the opportunity for better value and improved performance.

3 GEOLOGY

3.1 *Overview*

The geology of the Hindhead area comprises a sequence of fine grained sedimentary deposits laid down during the Lower Cretaceous period in near shore transgressive marine conditions on the margins of the subsiding Weald Basin. The tunnel is within the Hythe Beds – a 90 m thick sequence within the Lower Greensand Series formation.

The Hythe beds are variably sorted, highly glauconitic, variably bioturbated and cross-bedded sands and sandstones.

The Hythe bed unit is divided into 6 litho-stratigraphic subdivisions, 4 of which the tunnel passes through.

3.2 *Tunneling conditions*

The tunnel at the southern end passes through units Upper Hythe A and B which are similar units with an increasing number of sandstone bands with depth, described as '*medium dense thinly bedded and thinly laminated, clean to silty and clayey fine and medium SAND with subordinate weak to strong sandstone, cherty sandstone and chert*'.

The majority of the tunnel passes through the more competent Upper Hythe C and D, and Lower Hythe A units, described as '*Weak, locally very weak to moderately strong, slightly clayey fine to medium SANDSTONE with occasional thin beds of clayey/silty fine sand*'.

The remaining unit is Lower Hythe B which has been avoided by the tunnel as clays and sand become dominant in the lower half of the unit.

The sandstone within Upper Hythe C/D and Lower Hythe A has typical UCS values of between 2 and 5 MPa and is heavily fractured with 6 joint sets including the sub-horizontal bedding with mean fracture centers varying between 190 and 815 mm.

The tunnel is above the historically observed water table, with the maximum predicted water table exceeding the invert level in only 1 location. Refer to Figure 3 for geological longsection.

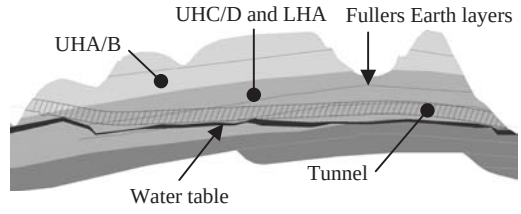


Figure 3. Geological longsection and vertical alignment (1H:4V).

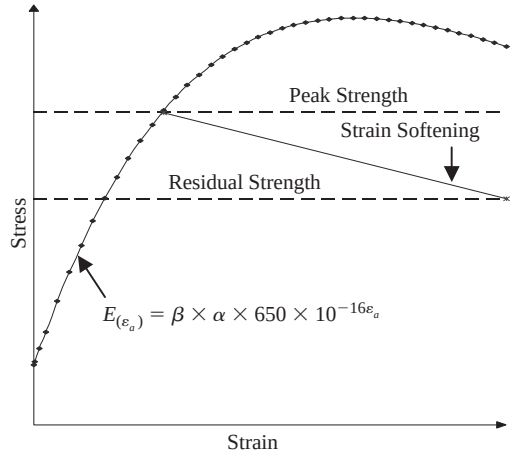


Figure 4. Ground model used for design.

3.3 *Ground behavior model*

A challenge for this project was to define a ground behavior model in an unusual material that has not been tunneled previously. The difficulties in interpretation stem from the weak to very weak nature of the sandstone material in combination with the content of up to 20% interbedded soil layers. A recurring challenge in tunneling is to determine the rock mass strength and stiffness, with empirical methods such as GSI, RMR or the Q-method (Bieniawski, 1984) often used. The strength and stiffness relationships that are the cornerstone of these methods are generally determined from data from significantly stronger rocks than the 2–5 MPa sandstone and do not take account of the influence from the soil layers leading to a significant overestimate of stiffness.

An extensive geotechnical investigation was undertaken with sonic testing, pressuremeters and triaxial testing all used to determine the Elastic Modulus of the rock mass. Pressuremeter testing was found to be the most reliable with the sonic testing over-estimating the stiffness, and the triaxial testing surprisingly under-estimating the stiffness in a number of cases. This was thought due to the difficultly in finding a 300 mm long specimen for testing in a material with 6 joints sets and an average bedding spacing of 190 mm. Fortunately some good quality rock joint shear box testing was undertaken that provided a lower bound for strength and stiffness interpretations.

The interpreted model used in design was a small strain stiffness model ($E_{(\varepsilon a)}$) that varied the stiffness of the rock mass with strain, and a Mohr-Coulomb strain softening model used for strength. Due to the large variation in cover from 16 m to 58 m the rock mass stiffness was also related to depth (α) in order to take advantage of the positive effect of larger insitu stresses as depth.

4 ALIGNMENT

The horizontal alignment for the tunnel was determined based on road design considerations and environmental constraints resulting in a reverse curve through the tunnel with a minimum radius of 1050 m.

The vertical alignment was determined based on geological constraints with the desire to minimize the length of tunnel through the sand at the southern end, to keep the tunnel above the water table and to also maximize the vertical clearance to the Lower

Hythe B material which has insufficient strength to carry horizontal stresses around the tunnel opening. The tunnel passes beneath the Devil's Punch Bowl which is a re-entrant, primarily spring-sapped valley system with erosion feeding backwards from the Hythe Bed/Atherfield Clay interface at the valley base. The crossing of the punchbowl provides a cover constraint to the tunnel, and the cover changes rapidly from around the minimum cover of 16m to the maximum cover of 58 m within a horizontal distance of 130 m.

The decision to follow the optimal tunnel material and to avoid the softer Lower Hythe B material results in a low point within the tunnel.

5 DESIGN

5.1 *Cross section*

The Hindhead tunnel consists of twin 2-Lane bores with cross passages at 100 m nominal centers. Refer to the typical cross section in Figure 5 below. Each bore has two 3.65 m lanes, with full batter curbs and 1.2 m wide verges on each side of the tunnel. The verges are required for sight-lines due to the horizontal curvature of the tunnel, to accommodate electrical services and also to provide wheelchair access to the cross passages and emergency points at 100 m nominal centers along the tunnel.

The vertical traffic gauge provided is 5.03 m with an additional clearance of 250 mm to the Equipment Gauge.

A continuous drainage system is utilised, located beneath the curb and verge with the cable duct bank. Other services such as the fire main, high voltage cables and pump mains are buried beneath the carriageway, with jets fans, lighting and communication cables contained within the crown.

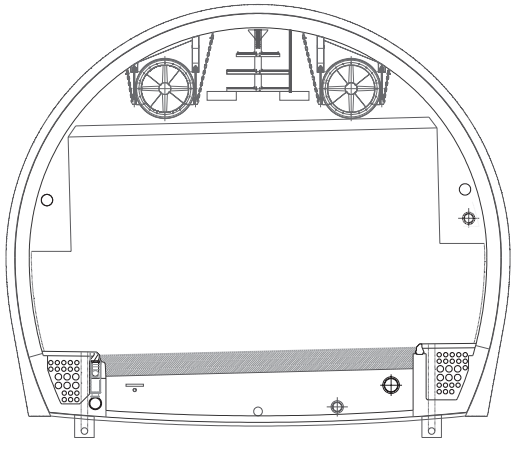


Figure 5. Typical SCL tunnel cross section.

These requirements result in a horseshoe shaped tunnel structure with an internal diameter of 10.6 m and an excavated diameter of 11.6 m.

5.2 *Fire and life safety provisions*

The tunnel has cross passages at 100 m nominal centers for escape to the non-incident bore. Cross passages include fire hydrants, dry pipe connections, fire extinguishers and emergency telephones. Emergency Points (EP's) are also provided at 100 m nominal centers located at the mid-point between cross passages. Each EP has an emergency telephone and fire extinguisher.

A longitudinal ventilation system comprising 20 jet fans per bore is provided for smoke control. Consideration was given during the preliminary design phase to the inclusion of a Fire Suppression system, however it could not be justified on cost benefit grounds. The decision was taken to make space provision for the future installation of a fire suppression system, should further evidence of the benefits become available or standards and or technology change.

5.3 *Design for maintenance*

Due to the life cycle cost of managing tunnel assets and more stringent health and safety regulations, the design team focused on minimization of whole life costs and the development of corresponding design details. Design for maintenance included:

- Minimization of unplanned maintenance interventions
- Consideration of the safety of maintenance
  - deletion of equipment where possible
  - selecting materials with the longest design life
  - Provision of safe maintenance access
  - Provision of replacement options for all infrastructure and equipment
- Maintenance risk assessments

Specific design initiatives incorporated in the works included:

- Provision of spare HV conduit and blind pits to allow replacement of HV cables in routine closures
- Modular hydrant connections allowing replacement in routine closures without disturbance of cable ducts and other services
- Relocation of in-tunnel sump to outside the tunnel by using a directional drilled gravity drain allowing maintenance access to sump without a tunnel closure

5.4 *Tunnel excavation and support*

The presence of the sand layers, in one location up to 2 m thick, led to the selection of sequential excavation

methods and support techniques commonly used in the Sprayed Concrete Lining (SCL) technique also known as the New Austrian Tunneling Method (NATM) where shotcrete is sprayed at the face following each excavation advance. Standard hard rock tunnel support techniques such as pattern bolting where not considered suitable due to the sand layers and the very low bond stress negatively impacting the effectiveness of rock reinforcement.

The tunnel is generally excavated with a full face heading followed at a distance by the bench excavation. Due to the generally stable nature of the ground and location above the water table, a closed invert is not required and the horse shoe shaped primary lining is supported on elephants feet. One main support type has been adopted through the sandstone with additional support measures such as spiling, face support wedges and/or face dowels to be triggered should an instability in the excavation occur. Refer to Figure 6 for details of the primary lining in the sandstone section.

In the sand section at the southern end the excavation will be carried out on dayshift only due to constraints on working hours and is made stable with the use of a steel pipe umbrella and face dowels. In this section three support types are required as the area of sand in the face transitions to a full sandstone face. Figure 7 shows a typical support type in the SAND section.

A principal innovation with the support measures is the design of primary lining as permanent. This is possible due to a number of advances in tunneling technology in recent years. Firstly, non-alkaline accelerators are now available with no loss in shotcrete strength with time. A recent innovation is the use of 3-D scanning survey equipment that provides excellent shape control for both excavation and spraying, and allows SCL tunnels to be constructed without lattice girders. This technique has been recently used successfully for the Heathrow T5 project (Williams et al. 2004). Historically the inclusion of lattice girders meant the primary lining had to be considered temporary due to the corrosion potential of the steel lattice girder within the primary lining. Spiling is envisioned in several locations due to adverse soil layers. This will be carried out with self-drilling Glass Reinforced Plastic (GRP) dowels, again with no adverse durability issues. The sprayed concrete will be reinforced with steel fibers as is required for safe installation, however the design does not rely on the flexural capacity of the steel fibers, and the lining is designed as plain concrete. This is possible due to the curved shape of the section with all moments resisted by axial forces within the lining.

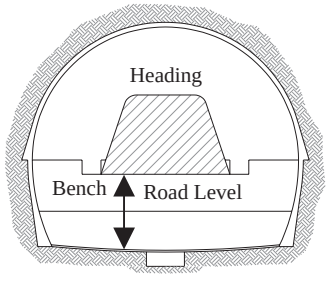


Figure 6. Typical primary lining through rock.

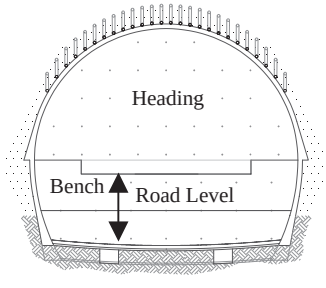


Figure 7. Typical primary lining through sand.

5.5 *Secondary lining design*

A secondary lining is provided to support the proposed sheet waterproof membrane, and also to provide fire resistance to the tunnel. The secondary lining is constructed from plain concrete, with all tensile loads in the lining resisted by the tensile capacity of the concrete. The main concern is to minimize the heat of hydration and shrinkage, and this is achieved with a 35% Pulverized Fly Ash (PFA) cement replacement mix design with low shrinkage. Fire resistance is achieved by adding 1–2 kg/m^3 of polypropylene fibers to the concrete mix in order to prevent explosive spalling. The precise dosage of fibers will be confirmed by fire testing.

6 COMPARISON BETWEEN SCL AND TBM TUNNEL OPTIONS

6.1 *Chemical Hazard Alert Notices (CHAN's)*

Towards the end of the preliminary design period, the UK Health and Safety Executive (HSE) issued three Chemical Hazard Alert Notices (CHAN's) relating to a reduction in the allowable exposure levels of Respirable Crystalline Silica (RCS) and NO_x during construction. The recommended changes to exposure levels are shown in the following Table 2.

All project development up to that stage has been based on excavation of the tunnel with diesel equipment. It was not possible to achieve these proposed limits with the diesel based construction methodology. The lower CHAN limits produced conflicting

Table 2. Details of Chan's

CHAN	Particulate	1989 COSHH regulations	Proposed limit (ppm)
28	NO	25 ppm	1 ppm
29	NO_2	3 ppm	1 ppm
35	RCS	0.3 mg/m^3	0.1 mg/m^3

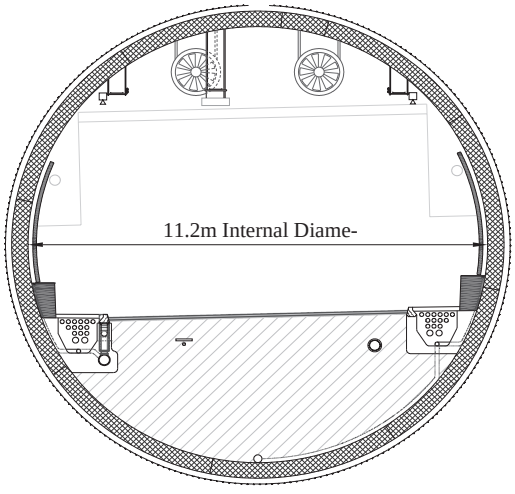


Figure 8. TBM tunnel cross section.

demands, as the lower NO_x limits require increased ventilation, but increased ventilation produces more dust causing problems with respirable silica.

This resulted in the consideration of an alternative method of construction, and a preliminary design prepared for a tunnel constructed using an Earth Pressure Balance (EPB) Tunnel Boring Machine (TBM).

6.2 *Comparison of SCL and TBM options*

The TBM tunnel cross section is shown in Figure 8 below. One of the benefits of utilizing a TBM was that it was no longer necessary for the vertical alignment to follow the optimal material for ground support. This meant that the tunnel could fall from south to north, allowing the deletion of the low-point sump. Another advantage of TBM construction was that a single-pass lining could be utilized. A fully gasketed segmental lining fire hardened with polypropylene fibers was proposed.

The main disadvantages with the TBM options were the openings required at cross passage junctions and for Emergency Points. The junctions are significantly more expensive for a TBM tunnel, and where the benefit cost ratio (BCR) for the Emergency Points was greater than 1 for the SCL tunnel, the cost of the opening for a TBM tunnel resulted in BCR < 1, however once a safety measure is proposed to the Emergency Services it is very difficult to withdraw it at a later date.

6.3 *Program*

There was a small benefit to the program for the TBM option however this was minimal due to the fact that the SCL tunnel is proposed to be excavated concurrently from 4 faces, whereas the TBM had to excavate 1 bore, and then be turned for excavation of the second bore. The total bore length of 3.6 km was insufficient to give the TBM option a significant program advantage. A tunnel of 2.5 km length would have been required to see a significant program advantage for the TBM.

Another disadvantage with the TBM option was the long lead time for the procurement of a 12.0 m diameter machine.

6.4 *Risk assessment*

A rigorous risk management procedure has been used through the project, and allowances for commercial risks are included in the project target cost. The assessed commercial risk for the SCL tunnel was significantly higher than for the TBM due to the larger potential impact from adverse ground conditions and the uncertainty of achieving the new exposure levels.

6.5 *Outcome*

An interim guidance note "Occupational Exposure to Nitrogen Monoxide in a Tunnel Environment" based on the ALARP principals applied to NO exposure limits has been prepared by the BTS (2006), was used to develop a modified SCL construction methodology such that NO limits of 3–5 ppm and the revised CHAN limits for NO_2 and RCS could be achieved. Additional measures include increased ventilation, more electric plant including an additional face conveyor and diesel plant conforming to the Stage III emissions standards in the Non-road Diesel Engines Directive. The modified SCL solution was still more economic than the TBM alternative.

7 CONCLUSIONS

The development of the planning and design of the A3 Hindhead project has been outlined in this paper. The main conclusions are:

- Projects through environmentally sensitive areas need to provide special mitigation measures in order to achieve planning consent.
- Tunnel details have been developed to avoid non-routine maintenance closures through the life of the tunnel.

- The design of the tunnel support includes a permanent primary lining possible due to:
  - Availability of non-alkaline accelerators
  - Use of 3-D laser scanning survey technology for control of robotic spraying equipment to achieve tight shape tolerances avoiding the need to use lattice girders
  - Use of self-drilling GRP spiles in areas of poor ground.
- Alternative designs have been prepared for an SCL tunnel and a TBM tunnel with the following conclusions:
  - Below a length of 2.5 km the TBM option had no program advantages
  - The TBM option had a lower assessed commercial risk due to the insensitivity to adverse ground conditions; however this was insufficient to overcome the increase in cost.
  - A modified SCL methodology that using ALARP principles for airborne pollutants in accordance with the BTS best practice document was developed.

REFERENCES

Bieniawski, Z.T. 1984. Rock Mechanics Design in Mining and Tunneling. Rotterdam: A.A.Balkema.

British Tunnelling Society. 2006. Occupational Exposure to Nitrogen Monoxide in a Tunnel Environment. London. http://www.britishtunnelling.org

Williams, I., Neumann, C., Jäger, J. & Falkner, L. 2004. Innovativer Spritzbeton-Tunelbau für den neuen Flughafenterminal T5 in London. In Proc. Österreichisher Tunneltag 2004, Austrian Committee of the ITA, Salzburg, pp. 41–62. Salzburg: Die SIGN Factory.

This page intentionally left blank

Underground Space – the 4th Dimension of Metropolises – Barták, Hrdina, Romancov & Zlámal (eds)
© 2007 Taylor & Francis Group, London, ISBN 978-0-415-40807-3

Geotechnical investigations and construction conditions for the tunnel "Strazevica" on E-75 motorway near Belgrade

B. Jelisavac, S. Jotic, S. Savic, V. Vujanic, M. Roljic, M. Jotic & S. Milenkovic
The Highway Institute, Serbia

ABSTRACT: Geotechnical investigations and design of double – tube tunnel through the mount Strazevica, under the suburban settlement Resnik near Belgrade on E-75 motorway, lasted from 1987 till 1992. The length of the left tube is 745 m and 686 m for the left one. Day profile opening is 90 sq.m whereas the distance between respective tubes is 25 m. The width of driving carriageways is 11.5 m each. Maximum height of the surcharge is 35 m. The works for the right tunnel tube at the exit portal started in 1992 when 186 m of the tunnel were completed. After a long interruption, the works have been resumed in 2004 and till nowadays 500 m have been completed. In view of the fact that the tunnel is located within the urban zone, specific requirements and techniques for the portal construction along unstable slopes have been elaborated. The excavation was carried out in the terrain of complex geologic structure and hydrogeological properties. There are alternating replacements of sandy clays, clayey debris, marls and sandy limestone. New Austrian Tunnel Construction Method has been implemented.

1 INTRODUCTION

Double-tube tunnel "Strazevica" of length 745 m, i.e. 686 m is under construction along future E-75 motorway bypassing Belgrade on Pan-European Corridor X and this facility is passing under the suburban settlement Resnik. The tunnel is located in the curve with radius R-1000. Tube width without bracing is 15 m, height amounts to 8 m, in other words the surface is 90 sq.m. Maximum height of the surcharge under the central part of suburban settlement is 40 m, and on portals 5–15 m. The excavation began in 1992 when 186 m were completed. After a long interval due to the U.N. sanctions imposed to Serbia, the works have been resumed in 2004 and till nowadays some 500 m, within the right tube, have been completed. (Fig. 1)

2 INVESTIGATIONS AND RESULTS

Geotechnical investigations were made in two different times, namely for Preliminary and Main civil-engineering design. Following works were undertaken: detailed geologic mapping of terrain, testing by refraction seismic method, exploratory drilling survey, installation and monitoring of piezometers, laboratory testing of soil samples and ground water.

By synthesizing gathered data, we have been able to form longitudinal and cross-section geotechnical profiles of terrain, whereof quasi-homogeneous zones and geotechnical models with parameters of physical–mechanical properties have been set aside along with the forecast of tunnel construction conditions.

Tunnel is passing directly through "Strazevica" mount and linking the valleys of Topciderska river and Rakovica stream.

Wider area is made of three geochronological units: on terrain base there are sedimentary rocks of Cretaceous flysch ($K_{1,2}F$), over which there are deposits of Miocene reef limestone set transgressively with layers of conglomerates (M_3K, Kg) or even marls (M_3Kl). On terrain surface there is rock waste of diluvial and diluvial-proluvial origin (d, d-pr), (Fig. 1).

Pre-Quaternary rock masses have tectonic properties and are divided by numerous fractures and faults into blocks of differing dimensions, thus making the forecast of tunnel construction conditions even more complex.

The assessment of physical–mechanical parameters of rock masses, necessary for dimensioning of structures, was made on the basis of analysis and synthesis of the results pertaining to: laboratory testing of rock samples, level of degradation, homogeneity, anisotropy, structural – texture properties, measurement of propagation speed of seismic elastic waves, and current empirical correlations between physical–mechanical properties and ratings of rock masses (Q, RMR), etc.

Forecast values of parameters of physical–mechanical properties of rock masses for quasi-homogeneous zones (geotechnical milieus), have been

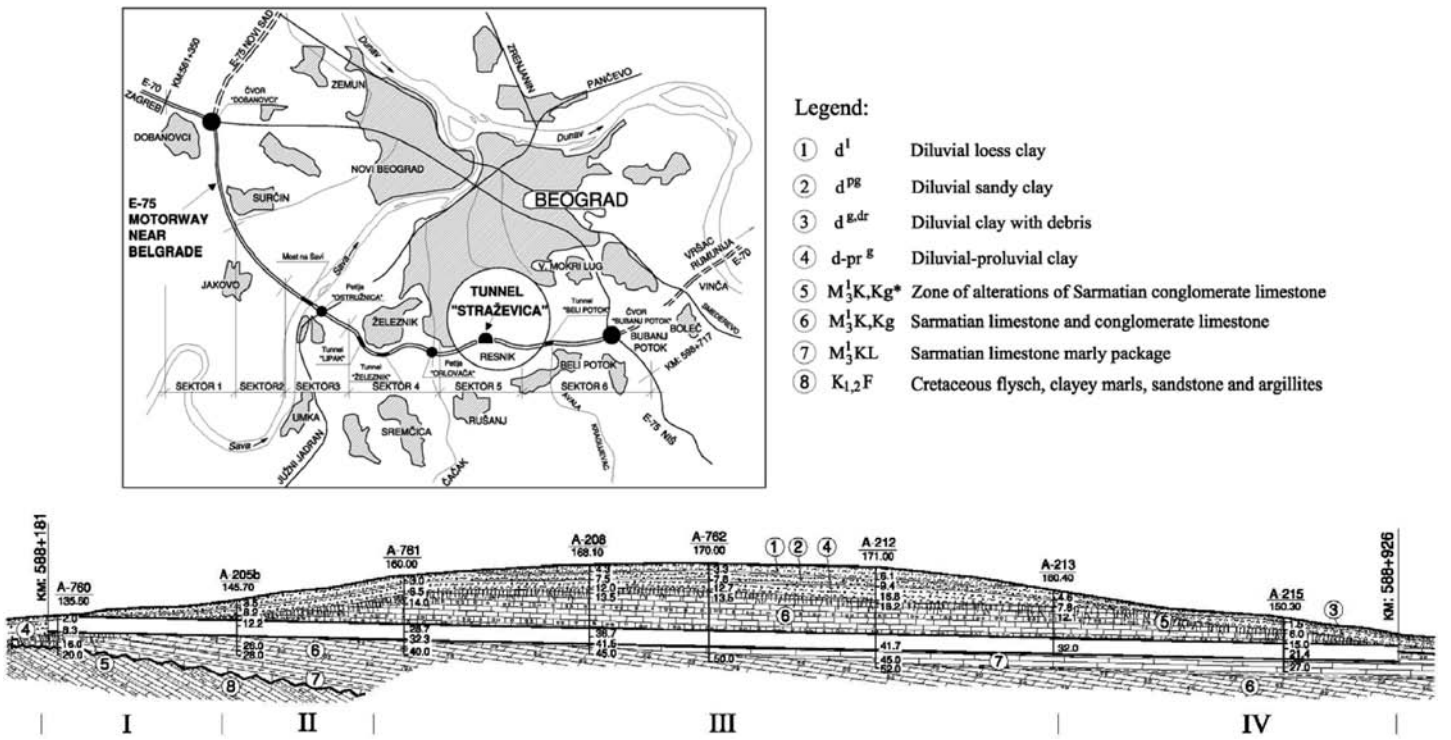


Figure 1. Engineering-geologic cross-section of terrain along the “Strazevica” tunnel route.

singled out along the profile of tunnel according to table 1 and geotechnical models (Figures 2, 3, 4 & 5).

Ground water as permanent aquifer has not been ascertained through investigation works, yet with the exception of entry portal, within the framework of surface alterations of limestone conglomerate deposits (M_3K,Kg^*), where ground water is gravitating towards the river Topciderska. There are some potentials of local and seasonal seepage of ground water on the contact of Quaternary and Tertiary deposits, as well as on the interface of marl interlayers with limestone layers within the limestone and marly deposits.

Table 1. Ruling physical–mechanical properties.

Milieu	γ (kN/m^3)	φ (o)	c (kPa)	Ms (MPa)	D (MPa)	μ
d^{pg},d-pr^g	19	20	25	7	–	–
$M_3{}^1K,Kg^*$	20	25	15	10	–	–
$M_3{}^1K,Kg$	22.5	40	100	–	2500	0.25
$M_3{}^1KL$	20	25	50	–	300	0.3

In view of continuous spreading out of Quaternary clayey deposits on terrain surface (elevated hydrogeologic insulator), there are considerably less possibilities of surface water infiltration into deeper terrain parts, yet no one is asking questions regarding essential collector function of limestone in the bedrock. Therefore, depending on seasonal conditions, there are potentials of diffuse aquifer occurrence within the deposits of limestone and conglomerates. Surface and ground water prevailingly gravitate towards the respective valleys of Topciderska river and Rakovica stream.

3 ANALYSIS OF GEOTECHNICAL CONDITIONS FOR THE TUNNEL CONSTRUCTION

Geotechnical zoning of rock masses along future tunnel excavation has been carried out in regard of complex geologic composition of terrain, with the purpose to define the tunnel construction conditions. Four quasi-homogeneous zones of similar properties, relevant in establishing the conditions of tunnel

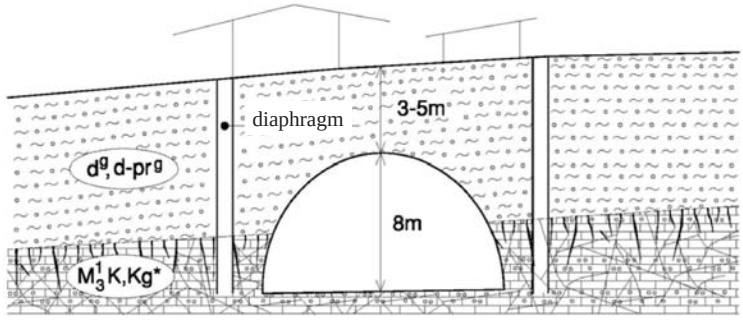


Figure 2. Geotechnical model of quasi-homogeneous zone I.

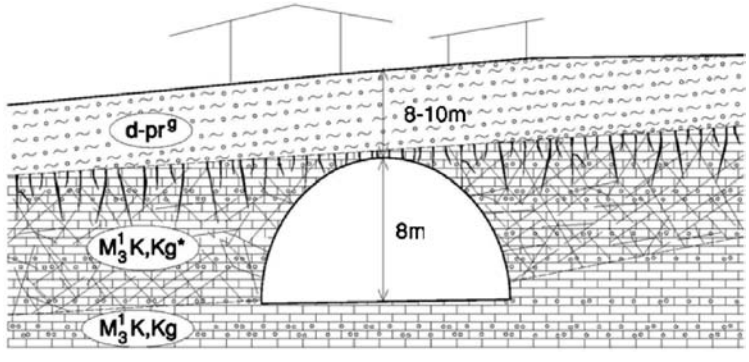


Figure 3. Geotechnical model of quasi-homogeneous zone II.

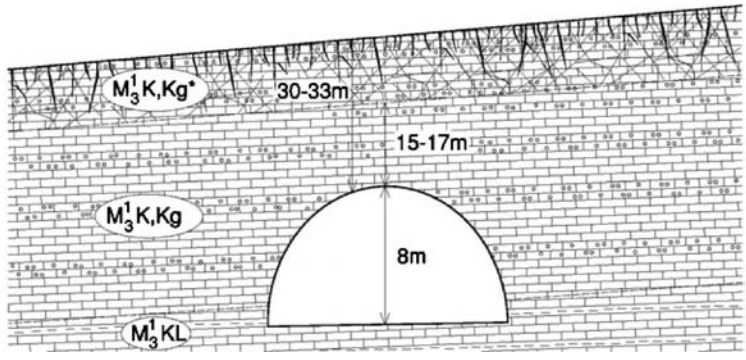


Figure 4. Geotechnical model of quasi-homogeneous zone III.

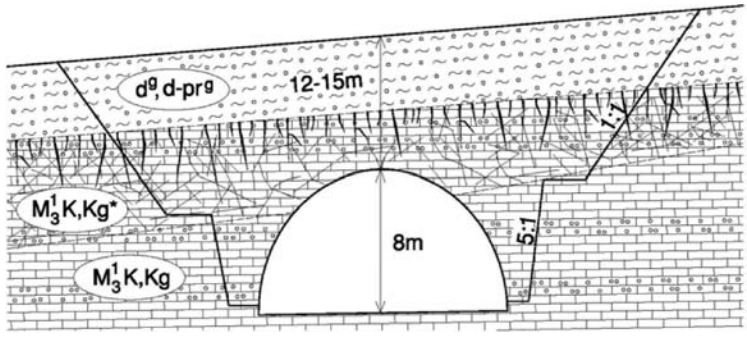


Figure 5. Geotechnical model of quasi-homogeneous zone IV.

construction, have been singled out. Zoning criteria have been as follows:

- lithologic composition in the excavation zone and interactions,
- surcharge thickness,
- structural, physical–mechanical and technological properties of rock masses,
- presence of ground water.

By taking into account the criteria thereof, the zones have been singled out within whose frame-work it has been made possible to implement uniform excavation technology and provide for tunnel profile stability.

3.1 *Quasi-homogeneous zone I/km 588 + 181 – 588 + 263*

Basic characteristics of this quasi-homogeneous zone are as follows: unfavorable physical–mechanical properties of rock masses within the excavation zone, unfavorable orientation of interfaces amongst lithologic members, small height of surcharge (3–5 m), high population density on the terrain above tunnel tube, etc. In the excavation vault there are occurrences of silty–clayey Quaternary deposits (d^g,d-pr^g), settled over degraded limestone (M_3K,Kg*). Interface of Quaternary and Miocene sediments, at the gradient of 30 degrees, is directed towards the entry portal, i.e. front of excavation. On this particular excavation stretch, in addition to unfavorable conditions, excavation categories III and IV, one cannot avoid the problem of deformations on terrain surface. Namely, a calmed down landslide has been recorded in the zone of portal.

A proposal has been made of resorting to open cut excavation in view of indicated properties of the zone thereof, with compulsory immediate protection of both excavation slopes and housing facilities located on the terrain surface. Stability of housing facilities must be provided prior to the commencement of works, for example, with diaphragms, by sinking of Larssen piles or with some other procedure.

3.2 *Quasi-homogeneous zone II/km 588 + 263 – 588 + 315*

In view of surcharge height and surface properties, geotechnical conditions for the tunnel construction in this specific zone are somewhat more favorable. It is prevailingly composed of rock masses ensuing from

the weathering of limestone being either clastic or even marly (M_3K,Kg* and M_3Kl*). There are potentials of local occurrence of alternating series of limestone and interlayers of marls. The appearance of ground water is possible in entire excavation zone. Average surcharge thickness amounts to 10 m, whereas the substratum above tunnel tube is densely populated.

Excavation conditions in this zone are very difficult and unfavorable, with excavation categories III and locally IV, so that it is required to build the profile with the provision of immediate stability of both excavation operations and facilities located on the terrain surface. In the course of excavation there are potentials that excess profile might occur on entire bulk of excavation.

3.3 *Quasi-homogeneous zone III/km 588 + 315 – 588 + 760*

This quasi-homogeneous zone is 450 m long and is typified by uniform lithologic composition with rather high surcharge (30–35 m). It is made of limestone with conglomerates and marls (M_3K,Kg and M_3Kl). They feature sub-horizontal interface and fall into excavation category V. Limestone materials appear prevailingly in the vault and flank, while marl and marly clays (excavation category III) are present in the underlying stratum of excavation.

Construction conditions assessments pertaining to procedure of excavation and bracing, temporary and permanent stability of excavation, subterranean pressures etc. have been made in accordance with: Bieniawsky (RMR), Barton et al. (Q), Louis and National civil-engineering norms GN-200. Classification results as per first two procedures have been presented on Tables 2 & 3.

This quasi-homogeneous zone can be typified as a suitable milieu as regards the stability of excavation, yet for the provision of permanent stability, it is required to provide a certain volume of bracing with the application of systematic anchors and sprayed concrete (gunite) with wire mesh. The appearance of interlayers of marl and marly clay in the flooring, on the foundation spot for abutments, is unfavorable. Therefore, in the process of founding the ground abutments, it is required to foresee eventual substitution of materials or deepening of foundation spot level, down to the first limestone layer. Interlayer thickness of marls is in the range from several cm to 3 m. One should not expect relevant occurrences of ground water, except for some minor wetting and seepage, at the interface of limestone and marl.

3.4 *Quasi I-homogeneous zone IV/km 588 + 760 – 588 + 926*

Rather thick surface weathering crust up to 18 m which is made of limestone and limestone – marly package has been ascertained on this tunnel section. Quaternary clayey deposits are thick up to 4 m. Surcharge height from 5 to 20 m, as well as absence of facilities on terrain surface, provide for open cut excavation with subsequent backfilling. Temporary slopes of cuts, of gradient 1:1, in clayey deposits and in zone of limestone surface alteration, are feasible with compulsory protection by wire mesh and gunite. It is possible to pursue to the excavation through younger lots of limestone under gradient 5:1 with the berm interfacing with the zone of limestone alteration, with minimum width of 3 m. Temporary slopes are considered as such provided that they shall not last longer than one building season.

Table 2. Classification according to Barton.

Parameters for classification						points
RQD	In	Ir	Ia	Iw	SRF	Q
80	3	3	4	1	5	3,99
Q	Class	Meaning of a class			Bracing type	

Table 3. Classification according to Bieniawsky.

Parameters		Points
σ (Mpa)	22	2
RQD (%)	80	17
Distance of fractures	0,6–2 mm	15
Properties of fractures	<1 mm	20
Ground water	wetting	10
Orientation of fractures	unfavorable	−12
Total – points	52	
Description	favorable milieu	
Class	III	
Type/Standing w/out	class: III	
Bracing	7 days for 5 m span	
Cohesion	200–300 Mpa	
Friction angle	25–35°	
Type of bracing	SS (systematic anchors 4 m long) at distance 1,5 – 2 m + T(gunite) = 5 – 10 cm	

4 INSTEAD OF CONCLUSION

Geotechnical conditions forecast as regards the construction of "Strazevica" tunnel, as presented in this paper, could have been either confirmed or not in the course of construction carried out so far. Authors of the project thereof are satisfied with the achievements attained in the previous activities of

building the prevailing tunnel's stretch 500 m long, in quasi-homogeneous zones III & IV, since the geotechnical supervision confirmed almost completely the forecast as regards the construction conditions.

Taking into account that these geotechnical conditions may refer also for some other areas, the investigation results during design and construction of tunnel "Strazevica", allow adequate professional generalization and geotechnical conditions forecast of building subterranean facilities in similar geologic milieus.

LITERATURE

Barton N., Lien R., & Lunde I. (1974): *Engineering Classification of Rock Masses for the Design of Tunnel Support,* Rock Mechanics, Vol.6. No 4.

Bieniawski Z.T. (1983): *The Geomechanics Classification (RMR System) in design applikacion to undergraund excavacion,* Int. Sy and mp. on Engineering – geology Undergraund Construction, Lisaboa, Portugal.

Šijaković J., Vujanić V., Lapčević R., & Lokin P. (1997): *Geotehnički uslovi izgradnje tunela Straževica na obilaznici Beograda,* Podzemni prostor u razvoju Beograda – II Savetovanje, Beograd.

Underground Space – the 4th Dimension of Metropolises – Barták, Hrdina, Romancov & Zlámal (eds)
© 2007 Taylor & Francis Group, London, ISBN 978-0-415-40807-3

The construction of tunnel "Lipak" within the framework of E-75 motorway on Belgrade city bypass stretch

S.Jotic, S.Savic, M.Jotic & V.Vujanic
The Highway Institute, Serbia

ABSTRACT: The tunnel "Lipak" is located on the fourth sector of Belgrade city by-pass. The right tube of the tunnel thereof is 665 m long, whereas its left tube is 660 m long. Structure of the tunnel is a double – frame construction with common party wall. It has separate carriageways with three driving lanes for every single driving direction. The lane width for one single driving direction is 11.50 m. The construction of tunnel was carried out in open cut excavation including also the part under the railroad line which was out of service due to the bridge tearing down during the bombing in 1999. The excavation was carried out through differing geologic milieus: in the peak parts there were silty – clayey rock masses, whereas in the deeper parts there were both thick – bedded, and thinly stratified rock masses of differing hardness (sandstone, clayey marls, argillites), and levels of damage (separated by fractures and folded). The greatest problems encountered referred to the provision of stability of temporary operating slopes, protection from ground water, excavation for foundation and backfilling of excavation over which the railroad line was set again.

1 INTRODUCTION

The tunnel "Lipak" is under construction within the framework of E-75 motorway on section Dobanovci – Bubanj Potok (Belgrade by-pass). It is located on the fourth sector, wherein the motorway alignment is in the transition from Sava river alluvion zone (Makis colony) into the rolling backing of Sumadija region, passing under triple track railroad for goods traffic. The right tube of the tunnel is 665 m long, whereas its left tube is 660 m long, thus the tunnel is staggered due to topographic feature of terrain.

Preparation of the design documentation for this facility began in 1987 and was completed in 1991. Framework of civil engineering design was composed by adequate geotechnical data base. From a series of variants taken into consideration, one variant was adopted which was affiliated with a problem of passing through two tunnel tubes directly under the railroad tracks on railroad station plateau, with a condition not to disrupt the railroad traffic. Due to exiguous thickness of surcharge it was anticipated to build the tunnel as open cut excavation except for the passage under the railroad tracks. Execution technique on this specific part included implicitly the operations under traffic and driving of three pilot shafts according to New Austrian Method (NATAM). They provide for the construction of tunnel abutments from the foundation up to the vault's beginning, as presented on Fig 2.

Operation with pilot shafts was made very difficult, primarily due to the fact that they are partly located within the railroad embankment with rather thin surcharge and with abundant inflow of ground water.

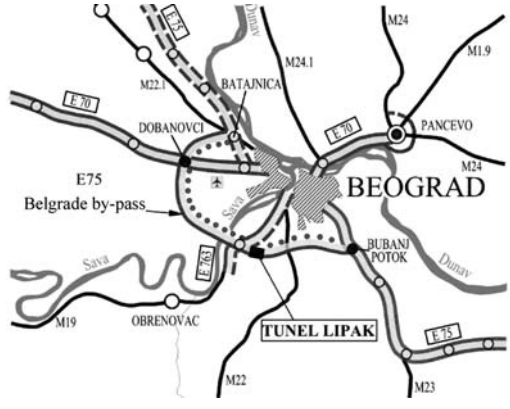


Figure 1. Belgrade city by-pass with the location of tunnel "Lipak".

The works on the construction of "Lipak" tunnel were carried out in the period 1991–1993, when they were interrupted due to the U.N. sanctions imposed to our country. In the latter period a number of activities have been undertaken on the approach cutting of exit portal towards Zeleznik colony and on entry approach cutting, i.e. on portal in the immediate zone of railroad station. Pilot shafts of midrange and left wall of tunnel tube were built on a short stretch within the scope of

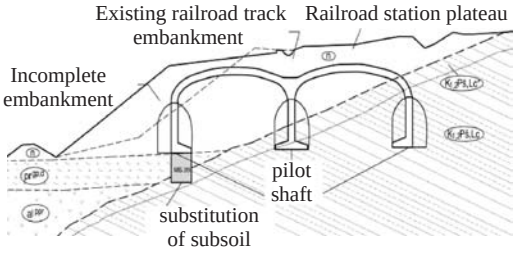


Figure 2. Pilot shafts on the stretch foreseen for tunneling.

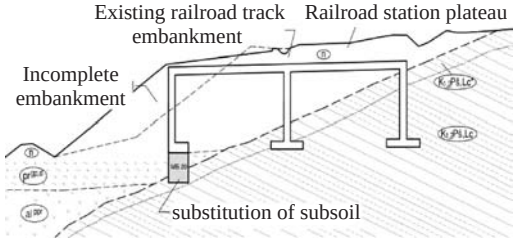


Figure 3. Tunnel's final solution.

these works. The substitution of silty – sandy (marshy) highly compressible alluvial deposit was carried out in the pilot shafts, under the foundations, down to the rock bed with good bearing capacity. This operation was carried out with the concrete grade MB 20.

Railroad bridge across the river Sava was demolished in 1999 during the aerial bombardment. Railroad line was put out of service for quite some time, thus providing the prerequisites to build the tunnel with an open cut excavation.

Arched tunnel profile was substituted by box-type construction through the rationalization process of the design itself as per Fig. 3. Final solution for building tunnel thereof is in fact referring to double-frame construction with common party wall with separate carriageways for respective driving directions. Pavement width for one driving direction is 11.5 m (three lanes for a single driving direction).

The subject matter of this paper is referring to geotechnical problem area of performing the open cut excavation and construction techniques for tunnel tubes.

2 BRIEF REVIEW OF TERRAIN'S GEOLOGIC STRUCTURE AND GEOTECHNICAL PROBLEM AREA

Geologic structure of terrain under study is made of flysch-like sediments of Cretaceous age represented by sandstones, marls and subordinately by argillites. Indicated rock masses are found in the tunnel zone at uneven depths, with outcrops on terrain surface down to the depth of 13 m. Their distinctive features are referring to layered and somewhat thick-bedded texture, yet the series in askance monocline is set towards SW under the angle of 20–25 degrees, which is suitable for major cutting (right side of open cut excavation). Cretaceous flysch-like products are divided by fractures and fissures into monoliths of cm-dm dimensions, physically and chemically altered and partly folded. They are covered by older Quaternary alluvial–lacustrine sediments of heterogeneous clayey, clayey–sandy and sandy–gravel composition. Surface terrain parts are made of the youngest Quaternary deposits, prevailingly of sandy–silty–clayey composition. From geotechnical point of view, these deposits present unfavorable resistance–deformation properties and as such are prone to landslides and erosion, particularly in the event of inadequate side-cutting.

From hydro-geologic aspect they also feature considerable heterogeneity. In this connection main problems are expected to occur at the appearance of free ground water within the framework of sandy-gravel deposits or seepage water through fractures in flysch-like sediments.

Complex geologic structure requires various geotechnical measures to be undertaken. This is referring primarily in providing the stability of temporary slopes of open cut excavation.

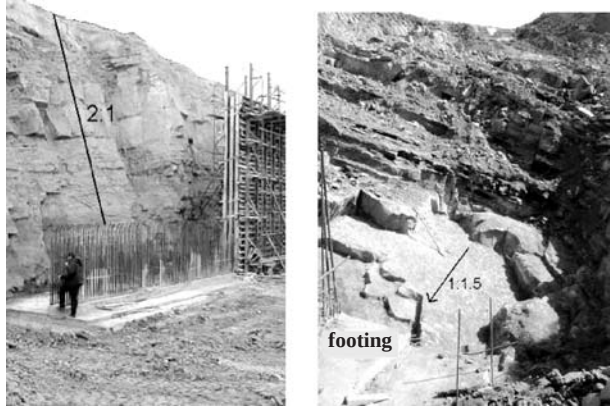
The appearance of several calmed down landslides with average depths of approximately 3.5–5.5 m has been recorded in the tunnel zone. There was a potential of activating the sliding process by every single side-cutting, thus requiring the necessity of undertaking a whole variety of repair measures in the tunnel zone.

The performance of works required the dismantling of existing railroad tracks, stripping of railroad embankment and excavation in phases up to the designed spot level. The design generally anticipated three phases, yet the same had to be broken down right on the spot into a series of sub-phases in accordance with geologic conditions and lythologic composition of terrain.

Part of the tunnel in railroad track zone is the most favorable for slope stability, since the hard rock base is present from the surface or is located at the minor depth. That part of widespread excavation served as *"trial section"* for remaining part of open cut excavation, which from stability considerations was far more risky, either due to the depth, or due to terrain structure. However, with the construction in phases and permanent professional monitoring of works, whereby prescribed sequence and schedule terms had to be strictly held on to, which provided for successful implementation of open cut excavation along the entire tunnel without structural protection. Labile parts of terrain were brought under control by resorting to the



Figure 4. Open cut excavation.



(a) right side of excavation; (b) left side of excavation;

Figure 5. Open cut excavation in hard rock mass.

experience attained in the previous tunnel liner for the subsequent one.

Open cut excavation was carried out within the scope of following conditions:

- excavation was carried out in the slope gradient 1:2 starting from terrain surface, through diluvial and diluvial-proluvial silty-sandy clay and alluvial lacustrine sands and sandy clays down to the contact with hard rock mass – Fig. 4.
- then the berm was built 2–3 m wide with the cross-fall of 4% towards the hill and with control grade meant for drainage of surface water catchment from slopes onto the berm – Fig. 4.

Through hard rock masses, i.e. sandstones, marls and argillites with the slope gradient 2(3):1 at the full excavation height, starting from the foundation engineering spot level. The right side of excavation was carried out with success due to the drop of layered structure (into the hill), whereas the left side, although at lesser depth, had to be carried out along with some alterations of originally designed slope gradient. Namely, the slope gradient 2(3):1 on the left side due to drop of layered structure (towards the excavation – Fig. 6) could not have been maintained under the conditions of required stability. Motions of blocks of major proportions were carried out along the surfaces of layered structure at the slope gradients 1:1.5 to 1:2. The only repair measures to be undertaken referred to permanent follow-up of excavation slope gradient with the progress at restricted scale and subsequent closure.

In the alluvial plain of Sava river there is a presence of ground water as permanently compacted aquifer. Its level is reaching almost the terrain surface. In the rolling zone of terrain there were frequent occurrence of ground water along the fractures as moisture, rather weak leakage or effluent seepage in a form of short-term springs of variable discharge linked with hydrological conditions.

Deadline schedule of operations was strictly complied with in regard to the excavation geometry thereof. The excavation was carried out in tunnel liners



Figure 6. Open cut excavation ring.

50 m long out of which 20 m referred to full profile, and 30 m in preparatory phase at higher spot levels – Fig. 6.

Every progression shift of excavation in an almost full profile meant also the building of tunnel construction in full profile with the closure of wide excavation in complete height of walls in the zone of both tunnel tubes.

Members of design and geotechnical supervision staff monitored the excavation on daily basis (harmonization with the Design of foundation pit protection and Design of tunnel construction).

3 REVIEW OF TUNNEL CONSTRUCTION AND PERFORMANCE OF WORKS

Tunnel construction has been carried out completely in a wide excavation, and later backfilled up to the designed spot level. The height of backfilling of the construction thereof is variable and is ranging from 1.80 m in the intersection zone with the railroad to 5.0 m in the deepest cut zone.

Operations regarding the tunnel construction have been carried out in semi-prefabricated manner, in view of the fact that some parts of the tunnel have been made by standard procedure (excavation, footing concrete works and walls), and then prefabricated reinforced concrete sheeting rails have been exposed to the process of obtaining monolithic properties. Aforementioned processed sheeting rails have been finally set upon hardened walls into proper designed position.

Performance of works has been carried out in phases as follows:

- Phase I – Concrete works – footing
  Reinforcement of the footing ceded for the length of anchorage (splicing for overlap), in order to link with the wall's reinforcement. Footing was made of impervious concrete MB 35, WDP6. Taking into account the terrain's structure, respective footings of the left and intermediate wall, within the zone of soft and highly compressible river load, have been driven into the incompressible rock bed (sandstones, marls) with the substitution made of "lean concrete", Thereby the prerequisite has been fulfilled that footings must be founded on incompressible rock bed.
- Phase 2 – Concrete works – walls
  Link of adjacent walls has been carried out according to the system "Tongue & Groove". Reinforcement has been drawn out and set aside in order to be processed to attain monolithic features for sheeting rails and walls. Concrete grade for walls – MB 30.
- Phase 3 – Setting of sheeting rails
  Setting of sheeting rails into the designed position is carried out after the attainment of 75% of hardness as specified by the design. Sheeting rails are prefabricated elements and they have to pass all required quality controls within their manufacturing facility, and only afterwards they are transported to the tunnel building site. Sheeting rails are delivered to the building site with drawn out bars meant to obtain monolithic features with walls. Quality of sheeting rails has reference to MB35, R.A.400–500.

  Sheeting rail has "T" shaped cross-section and is 160 cm high, with stem thickness of 18 cm. Upper flange width amounts to 90 cm, while lower flange has dimensions 35×26–36 cm, as presented on Fig. 10.

  Some five different types of sheeting rails have been installed in the tunnel thereof with various

a)



b)



Figure 7. Concrete works – walls.

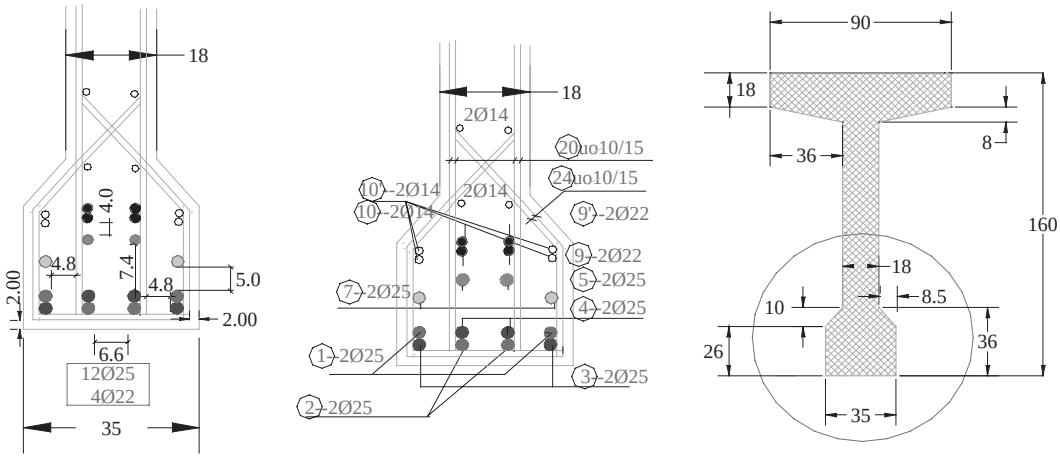


Figure 8. Reinforcement of sheeting rails.



Figure 9. Setting of sheeting rails



Figure 10. P.C.C. – Prefabrication of sheeting rails.



Figure 11. External drainage.

quantities of reinforcement thus to take into account the static impacts (train impact, height of potential backfilling, seismic impacts).

- Phase 4 – Monolithic properties of sheeting rails
  Monolithic properties of sheeting rails and walls both in longitudinal and transverse sense are obtained through reinforced concrete slab 10 cm thick. The latter also serves for laying of waterproofing elements.
- Phase 5 – Setting of external drainage pipes
  Pipes are made of PVC and perforated on upper side. Pipe diameter amounts to ϕ 250 and these pipes are laid in the MB20 lean concrete bed, 10–15 cm thick. Layer of coarse – grained gravel 1.2 m high is set above the pipes. This material with such particle-size distribution fills out the entire space from the wall's edge to the dug – out slope, while from outer side it is covered with geotextile. These pipes have chambers on every 25 m and from chambers thereof the water is overflown transversely into the collector which was designed to be on the interior tunnel's side, along with pavement's edge. Collector has also inspection chambers on every 25 m. Polyethylene pipe of high density HDPE ϕ 300 is set between

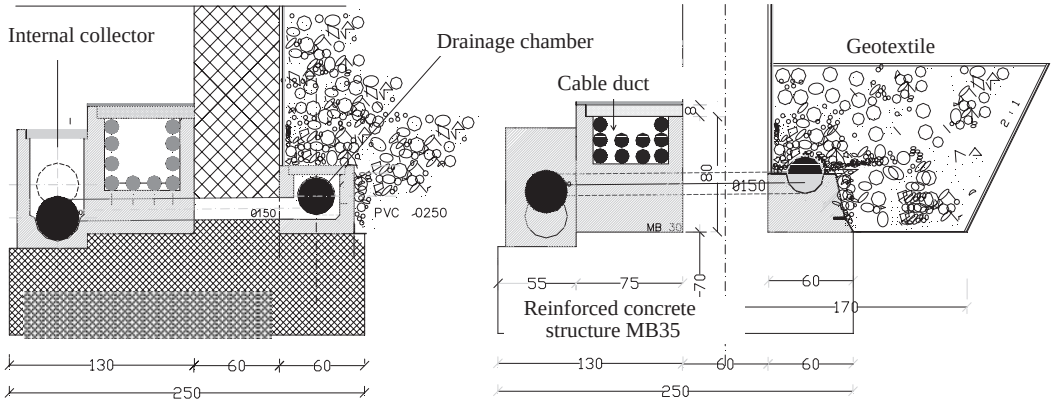


Figure 12. Canal details

inspection chambers, while the space around the pipe is filled with concrete MB300 and reinforced with wire-mesh reinforcement M.A.500–560.

- Phase 6 – Performance of waterproofing works Waterproofing foil was continually stuck to monolithic slab of sheeting rails. Waterproofing was carried out by polymer – bitumen tape hardened with non-woven fabric knitted with polyester fibers. Tape thickness amounts to 4 mm, denominated "Testudo 3" manufactured in Italy by the firm "Index". This tape has EU authoritative certificates of its quality, which was reconfirmed in Serbia by competent authorities (I.M.S., The Highway Institute, Department for building materials).
- Phase 7 – Protection of waterproofing foil Reinforced concrete slab 8 cm thick is cast horizontally over waterproofing. The latter is protected on the horizontal surface from sharp edges of backfilled material with bricking, and partly with proteflon foil.
- Phase 8 – Tunnel construction backfilling This was carried out symmetrically and on both sides up to the design spot level.
- Phase 9 – Performance of works on internal ducts for electrical and mechanical installations
  The tunnel "Lipak" was built by contractor "Planum" from Belgrade, while waterproofing works were carried out by the firm "Hidroizolacija", Belgrade as subcontractor. Prefabrication of sheeting rails was performed by the contractor "Ratko Mitrovic", Belgrade.

4 CONCLUSION

The works as regards "Lipak" tunnel facility was carried out successfully although in a series of several phases.

During the works it turned out that engineering-geologic and geotechnical investigations in all design phases provided sufficient and relevant data with high level of reliability in forecasting, which was confirmed in the operation of open cut excavation.

Thanks to full collaboration amongst the contractors, supervising agents and designers, wherein agreed deadline schedule and sequence of works were strictly held on to, thus providing great savings since the deep open cut excavation over 30 m was carried out without structural measures of protection which were considered as an alternative within the scope of design stage.

Despite all difficulties encountered in the performance of works, the tunnel was built with implementation of the most advanced techniques and materials utilized for protection.

One has to emphasize the operations carried out within the operating activities of two groups which are very sensitive (with unforeseeable negative consequences in case of error), which are specific for this methodology as follows:

– group of activities pertaining to the obtainment of monolithic features of sheeting walls and walls;
– group of activities as regards the protection of waterproofing in the backfilling process of tunnel construction.

LITERATURE

Fondovski materijal:

(a) Geotehnicka dokumentacija za Glavni projekat autoputa E-75, deonica: Dobanovci – Bubanj potok (Obilaznica Beograda), Institut za puteve a.d., Beograd, 1991. i 2003. god.
(b) Glavni izvodjacki projekat tunela "Lipak", Institut za puteve a.d., Beograd.

Underground Space – the 4th Dimension of Metropolises – Barták, Hrdina, Romancov & Zlámal (eds)
© 2007 Taylor & Francis Group, London, ISBN 978-0-415-40807-3

Settlement control during the construction of urban tunnels by NATM construction of Kitayama Tunnel on national highway 455

Toshihiko Komatsu, Hideyuki Kitamura, Ken Matsubara & Takaomi Sakurai
Maeda/Hazama/Nashi/Kitayama tunnel construction joint venture

ABSTRACT: The Kitayama Tunnel is constructed by the New Austrian Tunneling Method (NATM) through urban hills. The earth cover is thin throughout the tunnel alignment. It is necessary to control surface settlements according to the type of land use above the tunnel. The tunnel is stabilized by reinforcing the excavation face, tunnel crown and the foot of top heading, and giving priority to early closing of the ring. Ground stabilization ahead of the excavation face and the early reinforcement at the foot of top heading in particular were found to help control surface settlements.

1 INTRODUCTION

NATM, a way of excavating tunnels, has increasingly been applied in urban districts as well as in mountainous areas because it is an effective and economical tunneling method. Numerous issues, however, remain unsolved such as controlling surface settlements when adopting the method in urban areas.

In the Kitayama Tunnel, sections with an earth cover of less than the tunnel diameter occupy 50% of tunnel length. The tunnel penetrates hills with thin earth cover (refer to the earth cover shown in Figure 1 Longitudinal profile of the tunnel.)

The land over the tunnel is used for various purposes from houses to roads, fields and forests. Effective control of surface settlements and adverse effects of tunneling on structures is required. Geology at the site mainly consists of melange mainly composed of mudstones and melange composed of greenstones. Difficulty in geological prediction in melange and outstanding loosening of rock mass due to stress release during excavation make the control of surface settlements and adverse effects on structures even more difficult.

2 PROJECT OUTLINE

The Kitayama Tunnel is located in the north of the central part of Morioka with a population of 300,000 in Iwate Prefecture. It is an urban bypass planned to alleviate chronic congestion caused by commuter traffic from bedroom suburbs of Morioka. The tunnel has a length of approximately 1 km and be composed of two tunnels carrying bidirectional traffic. The tunnels are mechanically excavated and the muck is removed in dump trucks. The upbound and downbound tunnels have cross sections of 100 m^2 and 80 m^2, respectively.

Excavation was started in August 2004. The downbound tunnel was excavated throughout in July 2006. The excavation of the upbound tunnel will be over in December 2006 and the lining will be completed in July 2007.

3 GEOLOGICAL CONDITIONS AT THE SITE

The geology at the tunneling site belongs to one of the oldest zones composed of accretionary prisms on the islands of Japan, and mainly consists of melange mainly composed of mudstones and melange composed of greenstones. The majority of the rock mass at the site has been highly fractured and weathered into sand.

Melange is likely to suffer loosening along cleavage planes owing to stress release during tunnel excavation, and cause large-scale deformation. In preliminary surveys, seismic velocity is frequently measured to be relatively high because earth pressure acts. Rocks are distributed without forming layers, so geologic structure is difficult to grasp and the condition during tunnel excavation can hardly been identified. No serious deformations may occur during tunnel excavation in melange. Remedial measures are therefore sometimes taken only belatedly while economic construction

is given priority. As a result, deformation may be aggravated.

4 CHARACTERISTICS AND PROBLEMS OF CONSTRUCTION WORK

The tunnel is constructed in highly weathered rock mass with a thin earth cover with structures on the ground surface. Cut-and-cover construction is considered most reliable in view of the site conditions. The method, however, cannot be selected because the site is in a scenic area and because of the mode of land use. Excavation using shields is impracticable because of the existence of semi-hard rocks in tunnel cross section. That leaves NATM. The method, however, has the following problems.

(i) Tunnel excavation increases loosening, so no working face is freestanding.
(ii) The soil lacks sufficient bearing capacity at the foot of top heading to temporarily support the tunnel.
(iii) With a thin earth cover, excavation has direct impact on the ground surface.
(iv) Construction should be carried out without adversely affecting land use above the tunnel.

5 REQUIREMENTS FOR CONSTRUCTION

Requirements for tunnel construction in the project are listed below in descending order of priority.

(i) Safe construction work
  – The ground should be stabilized before the start of tunneling to create homogeneous conditions.
(ii) Consideration of effects and the environment
  – Adverse effects on the users of land, roads and water supply systems should be eliminated.
(iii) Economical construction
  – Rational remedial measures should be taken.

6 CONSTRUCTION

Reinforcement from the surface is generally effective during the construction of a tunnel with thin earth cover. In a 40-m section with an extremely thin earth cover of 2.5 m at a point 230 m from the portal, the tunnel was excavated after the ground was stabilized by applying mechanically agitated cement from the surface around the sidewalk (zone A in Figure 1).

In other sections, reinforcement was installed at the working face because the land above the tunnel was used for specific purposes and because no remedial measures could be taken from the surface.

6.1 *Division of cross section and increment of bench advance*

In tunnel construction in weak soils, division of the cross section and the increment of bench advance are important factors. In urban areas, attempts have been made to avoid danger by dividing tunnel cross section into numerous segments.

There were, however, concerns about high cost relative to the effectiveness for controlling adverse effects of excavation. At present, automation and mechanization of construction and use of general-purpose equipment are considered important. Heading and bench is therefore the most common approach, which has also been adopted in this project. The method requires appropriate reinforcement.

6.2 *Construction*

The increment of bench advance was set at 30 to 40 m for simultaneous construction of top heading and bench. Face collapsed frequently at the face of the heading. Settlement occurred 40 m from the portal with sectional cracks in shotcrete at the boundary between the heading and bench (zone B in Figure 1 and Figure 2.) Beyond the point, the increment of bench advance was shortened to 10 to 20 m, and the heading and bench were excavated alternately every 10 m. In the downbound tunnel, the top heading settled 1.5 m over a length of 20 m at a point 350 m from the portal (zone C in Figure 1 and Figure 3.) Prediction of the deformation was difficult because measured displacement satisfied the control levels. Reactive measures resulted in the aggravation of loosening. At the point, a technical review committee composed of experts was launched, and additional geological surveys were conducted to investigate the distribution and fracture of the melange of mudstones.

The committee confirmed that

(a) Tunnel cross section should be completed as early as possible including the invert by minimizing the increment of bench advance,
(b) Appropriate reinforcement should be installed at the face, tunnel crown and at the foot of the heading to ensure construction safety and control the progress of loosening, and
(c) Supports should have sufficient strength to carry overburden pressure.

The road administrator decided not to construct an emergency parking place that was initially planned at the midpoint of the tunnel alignment in view of the construction cost relative to the service function provided.

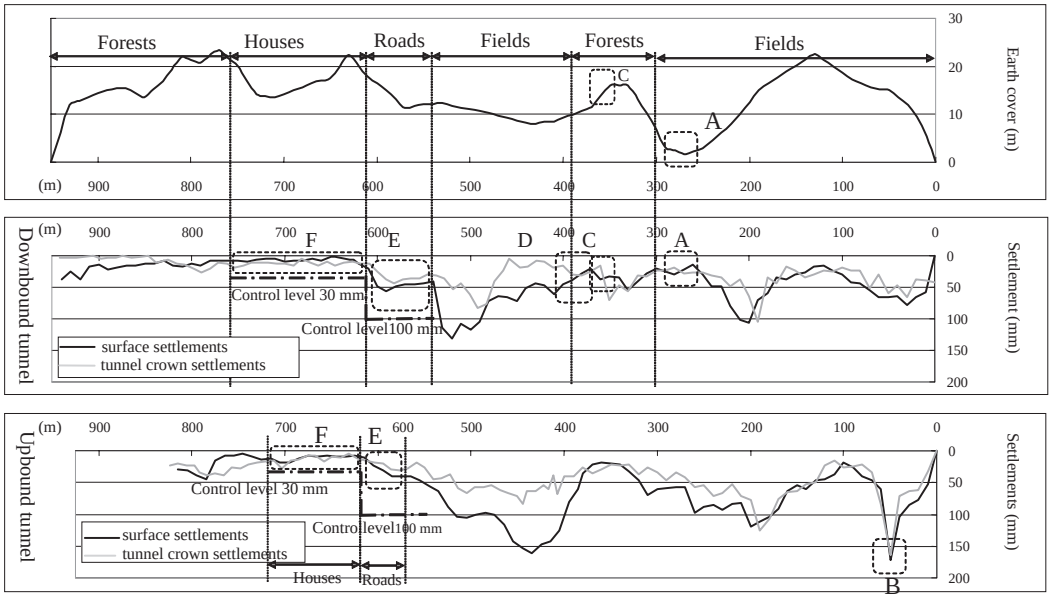


Figure 1. Longitudinal profile of the tunnel (earth cover, surface settlements and tunnel crown settlements).



Figure 2. Fall in a face.

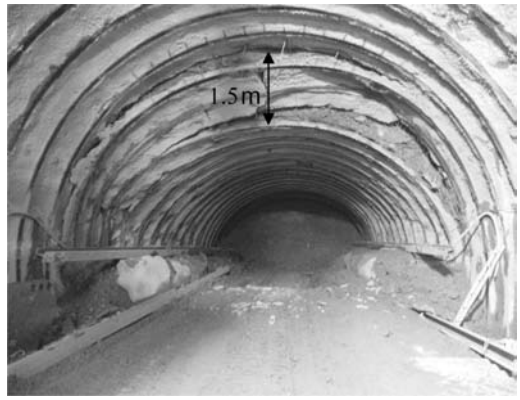


Figure 3. Deformation due to settlement.

The Road Structure Ordinance required no installation of parking places at the site.

7 APPROPRIATE INCREMENT OF BENCH ADVANCE AND REINFORCEMENT

With frequent collapses of the top heading, shortening the increment of bench advance and enlarging the cross section of the face were of concern from a viewpoint of safety. Actively stabilizing the ground and closing the ring early were expected to ensure the safety of work, keep the surrounding ground in sound conditions and increase the total quality of the tunnel.

7.1 *Early closing of the ring*

The increment of bench advance in the top heading was set at 3 to 6 m. The top heading, bench and invert were constructed alternately every 3 m. The distance from the face of the top heading to the point where the ring was closed by constructing the invert was set at 11 m or less (Figure 4.)

7.2 *Crown reinforcement*

The injection-type long forepoling method (umbrella AGF) was adopted. Steel pipes with a length of 12.9 m, a diameter of 114.3 mm and a thickness of 6.0 mm were driven at the tunnel crown. Urethane grouts were used that were expected to prevent the loosening on the cleavage plane (Figure 5.)

7.3 *Face reinforcement*

Injection-type long bolts were driven through the face. Steel pipes with a length of 12.5 m, a diameter of 76.3 mm and a thickness of 5.2 mm were driven at spacings of 1.5 m on the face (Figure 5.) Steel pipes were designed to have slits at spacings of 50 cm and cut by the boring machine and collected to separate them from the muck. Mortar grouts were generally injected. Where urethane grouts were employed, the muck had to be disposed of elsewhere.

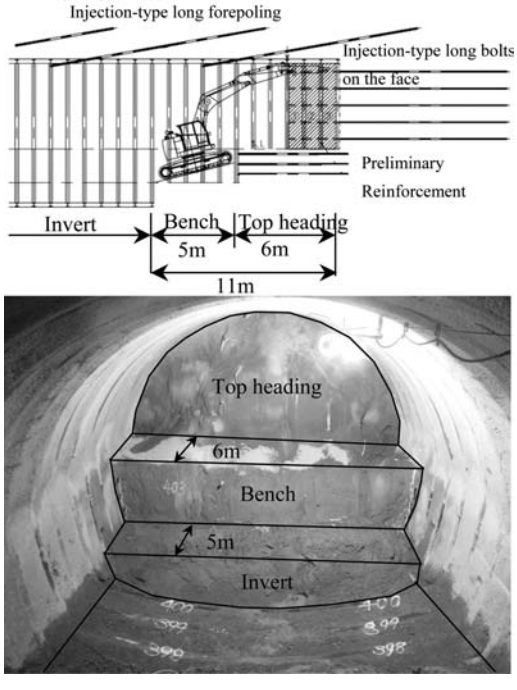


Figure 4. Outline of early closing of the ring.

7.4 *Preliminary reinforcement at the foot of the top heading*

Piles used to be driven from the top heading for reinforcement. Then, construction was delayed and it was doubtful whether they were actually effective or not. A method was therefore proposed and applied to install reinforcement at the foot prior to the excavation of the top heading.

Settlement of the top heading was expected to occur before the closing of the ring after the construction in the bench and at the invert. Closing of the ring was given priority wherever allowable. Whenever the settlement was determined to exceed the allowable level, reinforcement was installed. When the increment of bench advance in the heading was 3 m, the minimum level, 6-m-long steel pipes were driven from the outer circumference of the face in the bench to the foot of the top heading as in tunnel crown reinforcement (AGF). Thus, reinforcement could be installed at the foot of the top heading over a length of 3 m prior to excavation. Instability during the excavation of the bench could be avoided until the installation of supports (Figures 5 and 6.)

8 CONTROLLING OF SETTLEMENTS

No control levels were specified in areas with forests or fields as long as land was used without any problem. Water supply pipes that supply water to twenty thousand people were under the roads. The pipes were replaced with those resistant to settlement and the

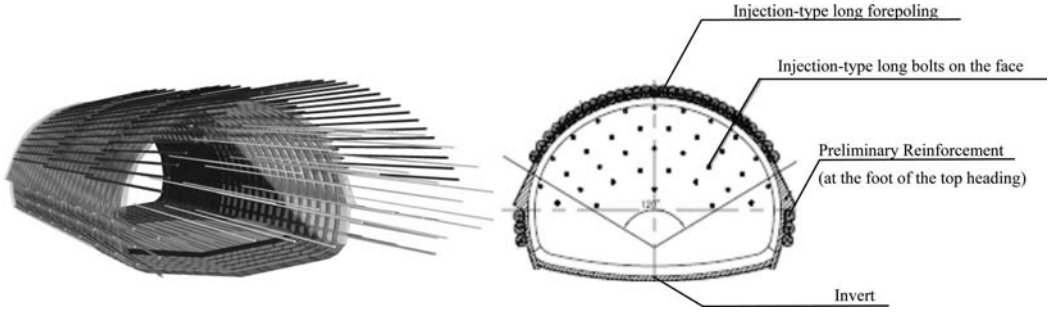


Figure 5. Outline of reinforcement.

control level was set at 100 mm. In sections with houses, generally 30 mm and 1/1000 were specified for settlement and slope of the ground that settled as generally applied.

Fortunately, the control level increased as the tunnel advanced from the areas with forests and fields to those with roads and houses. A few cases of surface settlements were found in the sections where the areas ahead of the face were stabilized with urethane grouts, based on the past construction data (zone D in Figure 1.) Urethane injection in some of the injection-type long bolts on the face resulted in satisfactory reinforcement (zone E in Figure 1.)

In sections with houses, the most strict control level was specified. Injecting urethane grouts for reinforcement contributed to the achievement of the control level (zone F in Figure 1 and Figure 7.)

9 RESULTS OF CONSTRUCTION

The findings obtained during construction are described below.

9.1 *Safe construction*

Appropriate reinforcement can help avoid the risk of face collapse due to early closing of the ring. Proper shotcrete application to the face and subsequent monitoring can ensure the establishment of a safe construction environment.

9.2 *Consideration of effects on surrounding areas and the environment*

Measurement revealed that control levels for settlement were satisfied according to the mode of land use: 100 to 160 mm for settlements under fields (no control levels specified), 30 to 55 mm for settlements under roads (control level: 100 mm), 3 to 19 mm for settlements under houses (control level: 30 mm) and 0.4/1000 to 0.7/1000 for the slope of ground that settled under houses (control level: 1/1000).

9.3 *Economical construction*

It has been determined based on the construction condition (9.1) and measurements (9.2) that rational reinforcement was installed.

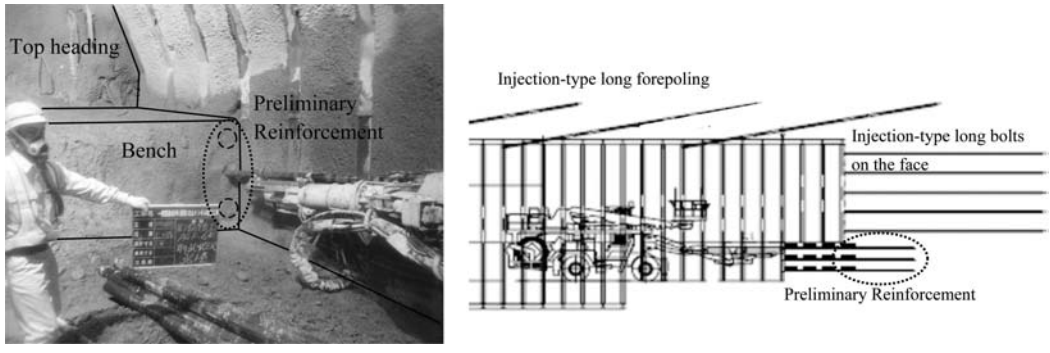


Figure 6. Preliminary reinforcement at the foot of the top heading.

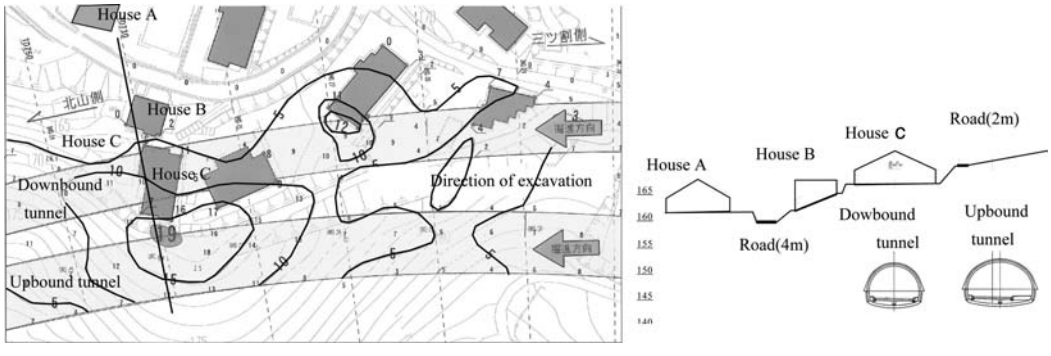


Figure 7. Ontour line of settlement under houses and cross section.

10 CLOSING REMARK

The basic idea that “Nothing is more important than early closing of the ring.” proved right when constructing tunnels in unconsolidated ground as in this project. Trouble can be prevented and high-quality tunnels can be constructed by actively installing reinforcement ahead of the face to keep surrounding ground in sound conditions and closing the ring early to stabilize the tunnel. This is ultimately a highly cost-effective choice in terms of maintenance after the tunnel is placed in service as well. It is hoped that this paper will be of some help in future implementation of NATM in urban areas.

Underground Space – the 4th Dimension of Metropolises – Barták, Hrdina, Romancov & Zlámal (eds)
© 2007 Taylor & Francis Group, London, ISBN 978-0-415-40807-3

Highways in the Czech Republic in terms of tunnel construction

Ing. Petr Laušman
Ředitelství silnic a dálnic ČR, Prague, The Czech Republic

ABSTRACT: The tunnel constructions are designed for new highways in 2006 and 2007 years. There are highways on route D3/R3 PRAGUE – Tábor – České Budějovice – state boundary, D11/R11 Prague – Poděbrady – Hradec Králové – Jaroměř – Trutnov – state boundary Czech Rep. / Poland, Route D8 Prague – Lovosice – Ústí nad Labem – state boundary Czech Rep. / Germany prepared.

1 ROUTE D3/R3 PRAGUE – TÁBOR – ČESKÉ BUDĚJOVICE – STATE BOUNDARY

Total length of route D3 + R3 between Prague and the Austrian border line is 171.40 km. The route is divided into 12 construction passages 0301 through 0312.

The tunnel constructions are designed just at the first construction passages, i.e. at construction sites 0301 and 0302 within the region of Middle Bohemia. The other construction passages feature no tunnel construction.

Let's have a look at the freeway project in terms of tunnel constructions. From big elevated crossing of the Prague Circle, where stationing of D3 starts off, the route is turning right, west of the town of Libeø. Here, between milestones of about 5.0–6.2 km, the first tunnel "Libeř" is proposed. Its technical solution and way of construction will be decided as late as in more detailed phase of project documentation, after precise level setting of the road. The tunnel will primarily serve as a protection of Libře's residents against adverse impact of the traffic and is to reduce the barrier effect between Libeř and Libeň, where hosing development is planned. The need of this tunnel construction itself will be verified through the EIA process and area management. Further on, another tunnel "Kamenná vrata" is placed at about 7.5 km milestone and being about 300–400 m long. This tunnel will be driven and will have deepened three-portal parts. In order of the stationing direction, third tunnel, "Svatováclavské lázně", about 200 m long is situated at 8.8 km mileage mark and is to preserve the above located forest area. Just after the elevated crossing Jílové, about 100 m long dug tunnel "V Obrázku", follows. Its main purpose will be to allow spreading a bio-corridor over the freeway body as well as recreationally used rural road. At the descending passage towards the river Sázava, driven tunnels "Kopanina" (at 10.8 km, 250 m long) and "Hůrka" (at 11.3 km, 350 m long) are proposed.

After crossing the lower watercourse of Sázava River via an architectonically and technically exceptional arched bridge of about 1000 m in length, the route gets to an area of extended forest complex near Lešany. Here, three short and dug tunnel constructions of length about 200 m are newly proposed. These are to reduce occupation of lands designed for fulfilling forest functions by reducing ground work cubage at trenches while passing through the local broken terrain as well as to allow as easy as possible migration of animals through this area, via given trails.

There is no doubt about realization of the freeway D3 among the professionals. Unfortunately, the progress of investor's preparation status quo in area of the Middle Bohemia region doesn't correspond to this need. In fact, all the preparation work has been stopped, partly due to having the ground plans of large territorial units of the Prague region and Benešovský region still not approved even though their acquisition moved on in 2006, after several years, but also due to a prolonged budget of preparation works at each building passages. Leading the route through a broken terrain south to Prague, with a dominant element – canyon of Sázava's lower watercourse will require a relatively substantial amount of underground passages of various functions, with regard to the high density of inhabitants, permanent and recreational.

In conclusion, it needs to be reminded that the sheer existence of tunnel constructions on route of the freeway D3 or only the technical data and characteristics of each tunnel are entirely orientating in that investor preparation status quo. The final status will be given after the final land order, preceded by environmental impact assessment as well as assessment of building impact on Natura2000 system. This and the wireline

loggings and analysis within the frame of area management documentation compiling, will lead to additional requirements of touched bodies of state administration and autonomy which may considerably affect the final technical solution of the freeway and thus even parameters of all proposed tunnel constructions.

2 ROUTE D11/R11 PRAGUE – PODĚBRADY – HRADEC KRÁLOVÉ - JAROMĚŘ – TRUTNOV – STATE BOUNDARY CZECH REP./POLAND

The total length of route D11, R11 between Prague and the state boundary with Poland, is 112.10 km divided into 9 construction passages 1101 through 1109.

Tunnel constructions are proposed at the last construction passage i.e. the building site 1109 within the are spread between Trutnov and the state border with Poland. The other building passages have no tunnel construction on them.

Route of the building site 1109 enters area of Východní Krkonoše Mts. after Trutnov and passing over so called Poříčský ridge. Here, the topographical and partly even ecological condition require two-tunnel proposal within locality of Poříčí and Zlatá Olejnice. In either case, building of two separated tubes in distance of 21 m is assumed.

The tunnel "Poříčí", 540 m long is proposed with longitudinal gradient 3.5%; in terms of direction, the tunnel is shaped in clockwise curve of 1000 m in radius.

The tunnel "Zlatá Olešnice", 375 m long is proposed with longitudinal gradient 3.2% and straight, in terms of direction.

Width arrangement equal in both tunnels – 2×3.5 m for lanes, 0.25 m for edge lines and servicing footpaths of width 1 m are assumed.

Tunnelling of both tunnels is assumed to occur in gneiss, stable rock setting.

The above stated data is drawn from a technical study and unfinished documentation of EIA, used as the groundwork of the Ground Plan of VÚC Trutnovsko – Náchodsko regions, approved by the region administration of Královéhradecký region in 10/2004. In term of Investor preparation, a point of crossing the state boundary was set at negotiations, held in 05/2004 in Warsaw and in 10/2004 in Český Těšín, at ministerial level, about interconnection of R11 and S3 within area of Královec-Lubawka. A proposition of "Agreement between Governments of Czech Republic and Poland about Interconnection of Czech Freeway R11 with Polish Freeway S3 on Czech/Polish State Boundary" was made and ratified. Subsequently, the "Agreement between Governments of Czech Republic and Poland about Interconnection of Czech Freeway R11 with Polish Freeway S3 on Czech/Polish State Boundary", was ratified on March 18 2005 in area between municipalities Královec-Lubawka with term of putting into service after year 2010.

Further preparation, admittedly, depends on amount of financial resources granted to this building. In the budget of SFDI for 2005, an amount of 0.00 CZK was reserved, for 2006 0.00 CZK was reserved. For those reasons, any investor preparation has been put on hold.

On the Polish side, situation is similar. A report on Polish preparation status was given away by director of the General Management of Routes and by director of Regional Development department in Wroclaw at international talks in Jaroměř, held on May 15 2006. From that report, it was made clear, that a programme of route building in years 2006–20013 was approved by Polish government in January 2006.

It contains building of S3 in direction towards Štětín with realization term set to year 2013. They pointed out that this program will not allow them to build up all routes as planned.

They confirmed the realization term of S3 at point of connection to R11 in 2013 and added, that the term depends on amount of granted financial resources. Further, they noted, 2-lane road has been prepared in the meantime, in regard to the current traffic intensity of 5,000 vehicles a day but will be adjusted as needed.

3 ROUTE D8 PRAGUE – LOVOSICE – ÚSTÍ NAD LABEM – STATE BOUNDARY CZECH REP. / GERMANY

Total length of route D8 between Prague and state boundary with Germany reaches 112.10 km, divided into 7 building passages 0801 through 0807.

3.1 *Building 0805 E tunnel Prackovice*

It is about a newly-built highway tunnel between mileage marks 58.280 km– 58.550 km. It goes through ridge massif of Debus hill (eastern hillside) at peak passage of Prackovický stonepit above municipality of Prackovice and comes out at the opposite hillside above the valley "Uhelné strouhy". The tunnel construction consists of tunnel tubes themselves, LTT (left tunnel tube) 270 m long and RTT (right tunnel tube) 260 m long, with maximal axis distance of 14 m, subcontrol office object and approach retaining wall. The tunnel tubes are proposed with inner clearance to allow for the highway surface inside the tunnel having width 9.5 m ($0.5 + 3.75 + 3.75 + 0.25 + 1.25$) with two footpaths on sides of width 1 m for passing profile according to norm ČSN 73 75 07 "Road Tunnel Design". The basic height of passing section

is 4.5 m – tunnel category T 9.5 (two-lane, one-way tunnel).

3.2 *Building 0805 F tunnel Radejčín*

It consists of a highway tunnel, newly built between mileage marks 58.760 km–59.380 km, highway bridge between tunnels and complex body of the highway of length 1080 m. Within the frame of the building, object required by the building itself are also realized. The highway tunnel Radejčín undergoes flat Radejčínský ridge of Českého středohoří (Czech Central Mountains) east to railway station in Radejčín. The tunnel construction includes tunnel tubes themselves, LTT (left tunnel tube) 600 m long and RTT (right tunnel tube) 620 m long, with maximal axial distance of 14 m. The tunnel tubes are proposed with inner clearance to allow for the highway surface inside the tunnel having width 9.5 m $(0.5 + 3.75 + 3.75 + 0.25 + 1.25)$ with two footpaths on sides of width 1 m for passing profile according to norm ČSN 73 75 07 "Road Tunnel Design". The basic height of passing section is 4.5 m – tunnel category T 9.5 (two-lane, one-way tunnel). The inside dimension also allows for placing of technological equipment of the tunnel (ventilation system, lighting, drainage system, cables, road signs, etc.). The highway bridge, of which support construction is designed as a beam, sandwiched steel-and-concrete continuous structure of 3 fields, has span of 132 m.

3.3 *Building 0805 G*

This project is a separate building of highway D8. It is a capacity traffic solution, connected to traffic of the current road network. It is a pilot work, required for safe base setting of the highway tunnel Prackovice, the main object of building 0805 E.

Control gallery deep goes through the ridge massif of Debus hill (eastern hillside) at peak passage of Prackovický stonepit above municipality of Prackovice and comes out at the opposite hillside above the valley "Uhelné strouhy". Access is proposed on current roads, requiring their modification, from Prackovický stonepit. As a reason of this construction is specifying detailed geologic-engineering probe, verification of factual geological and hydro-geological conditions, proving suitability and efficiency of construction elements used for securing the driven tunnels. The control gallery deep will be realized inside the right abutment of the left tunnel tube in length of 175 m.

This page intentionally left blank

Underground Space – the 4th Dimension of Metropolises – Barták, Hrdina, Romancov & Zlámal (eds)
© 2007 Taylor & Francis Group, London, ISBN 978-0-415-40807-3

Urban tunneling under existing structure

H.S. Lee, K.S. Jue, D.Y. Kim, W.H. Jung & Y.N. Lee
Hyundai Engineering & Construction Co., LTD, Seoul, Korea

ABSTRACT: This paper presents a design and construction case of an urban tunneling construction section carried out in the Seoul Metropolitan Subway. In this section, the tunnel was excavated under an existing overpass thus encountering a pile foundation of the overpass where cutting was unavoidable. In order to ensure the stability of both tunnel and overpass, the ground was reinforced using jet grouting from the surface. The steel pile reinforced step grouting was employed for inside tunnel reinforcement method. The total of 67 piles were exposed during excavation and all of them were properly cut, maintaining the stability of the overpass. The tunnel excavation was successfully complete without any problems for the area under the overpass.

1 INTRODUCTION

One of the major issues in urban tunneling is an underground excavation adjacent to existing structures in poor ground condition. In urban tunneling, unlike mountain tunnels, comprehensive and systematic evaluation and analysis on design, construction, and monitoring are required to ensure the stability of existing structures as well as that of tunnels. This paper presents a case of urban tunneling in Seoul, Korea where the tunnel passes under an overpass. Pre-investigation revealed that a total of 67 piles of the overpass foundation were located in the ground to be excavated. In this paper, the construction process and results of monitoring are presented as well as results of the numerical analysis on the stability of the tunnel.

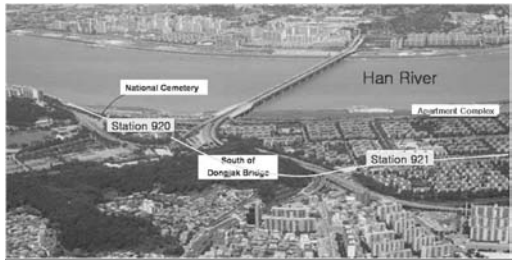


Figure 1. Overview of subway section 912.

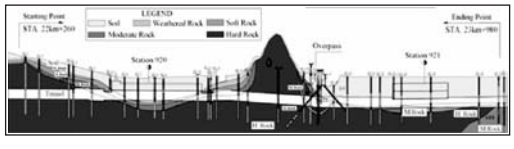


Figure 2. Geological map of section 912.

2 OVERVIEW OF CONSTRUCTION SITE

2.1 *General description of construction site*

Seoul metropolitan subway Line No. 9 (L = 38 km, total 37 stations) runs on the west-east axis of the southern part of Seoul, below Han River. The construction of Line 9 is divided into two stages. The 1st stage is between Gimpo airport and Gangnam (L = 25.5 km). The 2nd stage between Gangnam and Bangi(L = 12.5 km). The 1st stage is to be finished in 2008 while the construction of 2nd stage has not started yet. The 12th work section of the 1st stage, denoted as Section 912, will be discussed in this paper. The total length of Section 912 is 1,720 m (open cut 258.45 m, tunnel 1131.55 m, and 2 stations 330 m), and is excavated by NATM. Figure 1 displays the aerial photo of Section 912.

2.2 *Geological condition*

Banded biotite gneiss in Precambrian period is well developed as bedrock and alluvial soils in the Quaternary period are placed unconformably on top of the bedrock. The alluvial soils widely found in the area show characteristics of bed sediments of the Han River which consists of mainly silty sands with gravels. Figure 2 shows the geological map of Section 912.

2.3 *Overview of overpass area*

A 12-lane overpass consists of 3 bridges and one concrete covered structure. This overpass crosses over the E-Soo crossroad as shown in Figure 3. In this crossroad, the tunnel underpasses the overpass at a



Figure 3. Overpass on E-Soo crossroad.

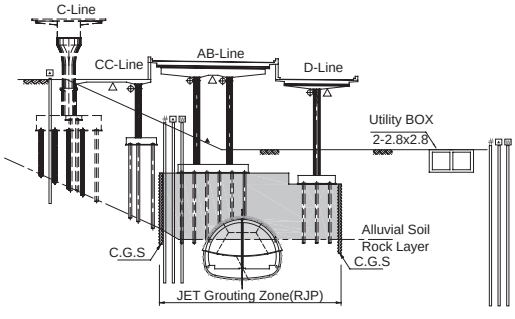


Figure 4. Cross section view of tunnel and overpass.

depth of $10 \sim 20$ m below the ground level at an angle of $30 \sim 45°$. This tunnel would contact the pile foundation of the overpasses along the length of 50 m.

As shown in Figure 4, the pile foundation of the existing structures is located near or inside the tunnel excavation section. The number of piles that would fall into the excavation section were expected to be a total of 67.

Table 1 shows the major structures near the excavation area, types of foundation, and each number of piles to be cut. The C-Line is a 4-span continuous steel composite box girder bridge and CC-Line is a 8-span continuous R.C. structure. Four-span continuous R.C. slab bridge is denoted as AB-Line while 8-span continuous R.C. lahmen structure is denoted as D-Line.

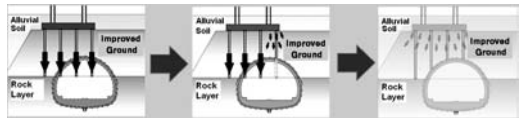
3 DESIGN OF TUNNEL

3.1 *Excavation and ground reinforcement*

As previously stated, the depth of the tunnel is $10 \sim 20$ m below the ground level. At this depth, the tunnel is to contact the pile foundation during excavation thus cutting of the piles that are exposed to the excavation section is unavoidable. In order to ensure the stability of the superstructure due to pile cutting,

Table 1. Major structures on E-Soo crossroad and foundations.

Structure number	Foundation type	Number of piles to be cut
C-Line	PHC pile (dia. = 500 mm, L = 11.0 m)	0
CC-Line	Steel pile (dia. = 406 mm, L = 11.0 m)	14
AB-Line	PHC pile (dia. = 400 mm, L = 11.0 m)	38
D-Line	PHC pile (dia. = 400 mm, L = 9.0 m)	15



End-bearing piles | Pile cutting Gradual load transfer to improved ground | Load transferred to block footing foundation

Figure 5. Load transfer mechanism due to ground reinforcement.

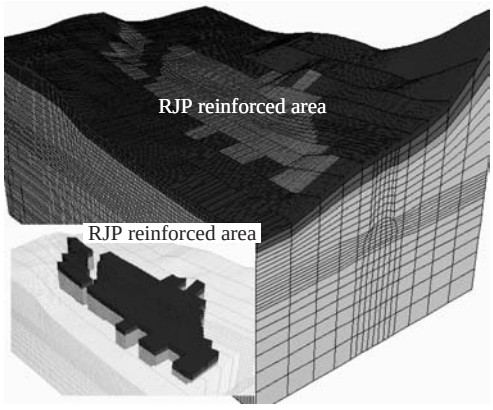
the ground reinforcement should precede prior to tunnel excavation. Jet grouting and enlargement of the pier foundation section have been carried out in the surface while steel pipe step grouting and forepolling have been employed for reinforcement inside the tunnel. Total length of the reinforcement area is 110 m along the tunnel.

RJP method (D2000 mm, C.T.C 1.8 m), employed for ground reinforcement, reinforces the ground by injecting the cement suspension of high pressure ($300 \sim 700$ kg/cm^2) using the triple rod. Basic concept of the ground reinforcement is transformation of foundation type. Since piles are trimmed step by step as the excavation proceeds, the load acting on the piles would be gradually transferred to the reinforced ground. Through this process, end-bearing pile foundation of the bridges would be changed to block-footing foundation eventually. Figure 5 shows the schematic diagram of the load transfer mechanism.

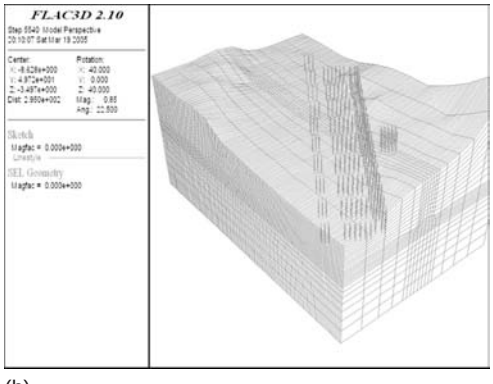
The reinforcement range has been decided to be two times of pier foundation width based on the result of stability analysis as illustrated in Figure 4.

3.2 *Analysis on stability of tunnel and overpass*

The numerical analysis has been performed to evaluate the stability of the tunnel and overpass for the range of excavation adjacent to pile foundation. Since numerous piles are located at the tunnel depth and ground reinforcements have been applied in this range, a careful consideration has been taken to appropriately



(a)



(b)

Figure 6. Analysis modeling of (a) the reinforced ground and (b) overpass piers.

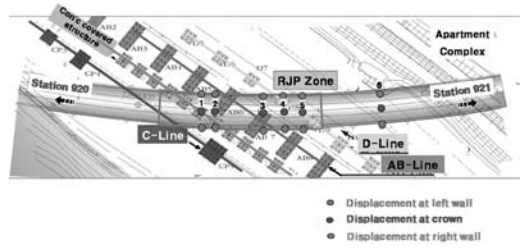


Figure 7. Measuring points for numerical analysis.

simulate the in-situ condition such as the characteristics of the reinforced ground and neighboring ground condition. Another numerical analysis on the superstructure (the overpass) has also been conducted. Both numerical analysis have been conducted using FLAC 3D. Figure 6 shows the analysis modeling of the reinforced ground and overpass piers.

Table 2 shows the material properties used in the analysis. Increased material properties have been used for the reinforced ground to simulate the effect of RJP. The pile elements in the reinforced ground are simulated to be eliminated in the appropriate step of excavation.

3.3 *Results of the numerical analysis*

The results of the numerical analysis are presented in this section. The displacements are investigated along three lines, which are the crown, the left wall, and the right wall of the tunnel. Six measuring points for each measuring line are displayed in Figure 7. Five points for each line are located inside the RJP reinforced zone while one point for each line is outside the RJP zone.

Table 2. Material properties.

								Reinforced ground with RJP			
	Landfill layer	Sand	Gravel	Weathered rock	Soft rock	Moderate rock	Hard rock	Land fill layer	Sand	Gravel	Steel pipe step grouting
Friction angle (°)	31	33	40	35	35	40	45	31	38	37	37
Cohesion (ton/m^2)	0	0	0	5	20	60	140	23	50	80	80
Unit weight (ton/m^3)	1.8	1.8	1.9	2.1	2.3	2.5	2.6	1.8	1.8	1.9	2.1
Modulus of deformation ($\times 10^3$ ton/m^2)	1.0	1.3	3.0	20	90	300	1200	36	47	48	50
Poisson's ratio (ν)	0.33	0.32	0.3	0.3	0.26	0.24	0.22	0.33	0.32	0.3	0.28

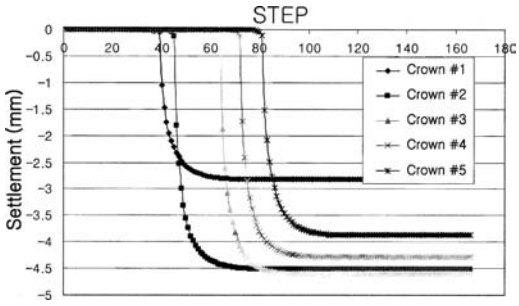


Figure 8. Settlement at tunnel crown.

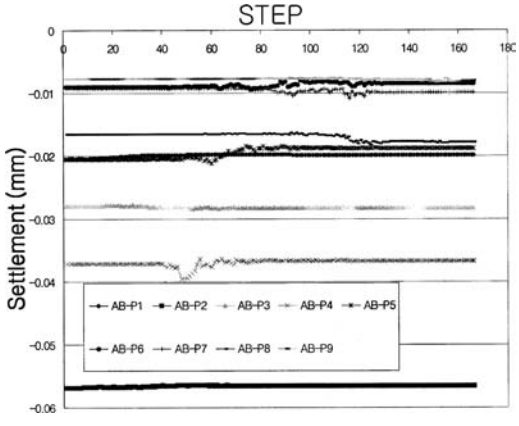


Figure 9. Settlement at overpass foundation (AB-Line).

The analysis results show that the maximum displacements are 4.6 mm for the crown, 0.04 mm for the left wall, and 0.02 mm for the right wall. It was observed that all the values are within the allowance thus was expected that the tunnel would be stable.

It was also observed that the settlements of the overpass foundation ranged from 0.01 mm to 0.19 mm, which were all within the allowance of 25 mm; influence on the foundation by tunneling would be very small. Figure 8 and Figure 9 show the settlement at tunnel crown and at overpass foundation, respectively.

4 TUNNEL EXCAVATION AND MONITORING

4.1 *Tunneling*

As previously stated, cutting of the piles that were exposed to the excavation section was unavoidable. As shown in Table 1, the total number of piles to be cut was expected to be 67. It was observed during tunneling that the location of piles agreed well with the expected location. It was notable, however, that several unexpected piles and different material type of piles also

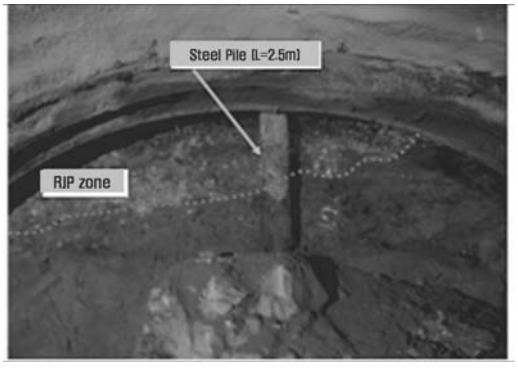


Figure 10. Exposed steel pile during tunneling.

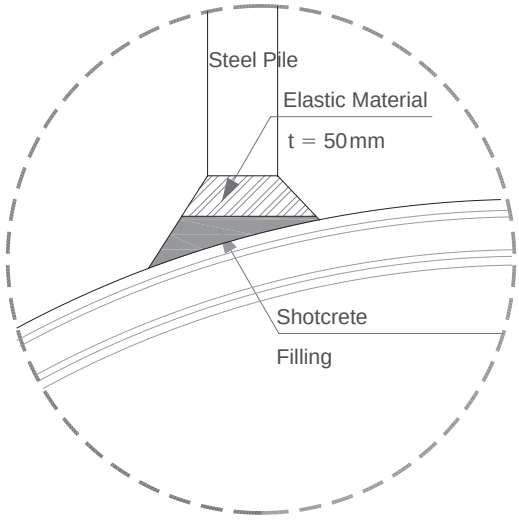


Figure 11. Pile cutting work.

appeared during tunneling, resulting in difficulties in excavation.

The tunnel was excavated as explained in Section 3.1; the ground was first reinforced by means of RJP and the width and height of the foundation were enlarged then tune tunnel was excavated. The sequence of the pile cutting was as follows; (1) once the pile was exposed as shown in Figure 10, the ground around the pile was excavated and the steel rib and shotcrete were installed, (2) pile was cut, (3) elastic material was installed between the pile end the shotcrete layer as in Figure 11, and (4) shotcrete was again installed at the cutting section, and the excavation was repeated.

4.2 *Monitoring and results*

In order to ensure the stability of the overpass and tunnel during both excavation and operation, a total of 98

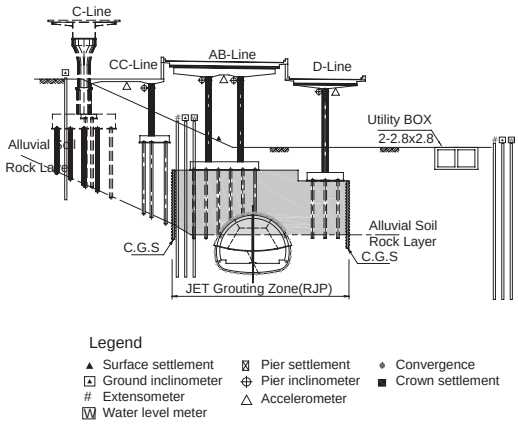


Figure 12. Monitoring plan.

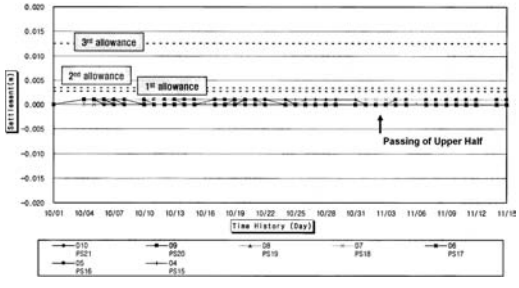


Figure 13. Monitoring result – pier inclinometer.

instruments were installed to determine the stability of the overpass, and to investigate the ground behavior. It included settlement for the ground and the overpass, inclinometer for the ground and the pier, extensometer, water level meter and so on. Inside the tunnel, crown settlement and convergence were measured at a spacing of 5 m, and ground movement and support stresses were measured at 5 points. Figure 12 shows the types of monitoring and location of the instruments.

The results of monitoring show that all the measured values fall within the allowance thus stability of both the overpass and the tunnel was obtained. Figure 13 shows a result of pier inclinometer.

5 CONCLUSIONS

A case study of urban tunneling under the existing structure was presented in this paper. Preliminary investigation showed that pile foundation of the overpass would fall into the tunnel excavation area. Therefore, ground reinforcement was applied to the neighboring ground and around the tunnel to ensure the stability of the overpass and tunnel. Jet grouting (RJP) was applied from the surface of the ground and the width and height of the foundation was enlarged. Steel pipe step grouting was also employed for reinforcement of the ground inside the tunnel. The reinforcement design was verified to be appropriate by the numerical analysis. Excavation of the tunnel was successfully performed without any problem. Monitoring results showed that all the measured values satisfied the allowance.

ACKNOWLEDGEMENT

This paper was funded by the Korean Institute of Construction and Transportation Technology and Evaluation and Planning under the Ministry of Construction and Transportation in Korea (Grant No. 04-C01).

REFERENCES

Jue, K. S. and Na, D. S. (2005), “A study on the construction of tunnel near the piles of foundation of an overpass”, KSCE tunnel committee special conference, Seoul, Korea

Seoul metropolitan government (2005), “Report on design change of construction of Seoul subway section 912 due to modification of design standard”, Seoul, Korea

Yoo, C. S et al. (2005), “Report on design and construction plan of tunnel for Seoul subway section 912”, Institute of science technology, Sungkyunkwan University

This page intentionally left blank

Underground Space – the 4th Dimension of Metropolises – Barták, Hrdina, Romancov & Zlámal (eds)
© 2007 Taylor & Francis Group, London, ISBN 978-0-415-40807-3

Large double adjoined binocular tunnels in shallow and soft ground Shoji Tunnel project

M. Mori & M. Nakano
West Nippon Expressway Company Limited, Osaka, Japan

K. Shirakawa
Shoji Tunnel Project, Taisei Corporation, Osaka, Japan

M. Koike & M. Iwano
Civil Engineering Division, Taisei Corporation, Tokyo, Japan

ABSTRACT: Large double adjoined binocular tunnels, which consist of four-linked tunnel system, are implemented in shallow and soft ground at densely populated area in Japan. From a view point of efficiency and safety, the tunnels are planed to be constructed by NATM method using machine excavation in combination with auxiliary methods such as diaphragm wall, soil improvement and AGF (All Ground Fasten) method. First of all, the soil improvement to surrounding soft ground is adopted to support the center pillar and to ensure the stability of the tunnel face in advance. Next, the diaphragm wall is constructed prior to the tunnel excavation not only for the site-work efficiency, but also for the environmental protection. Finally, the secondary linings of tunnels are designed with the following features; (1) center pillars are separated from secondary linings to ensure the structural stability. (2) secondary linings are designed as reinforced concretes to resist earthquakes and to endure external water pressure.

1 INTRODUCTION

1.1 *Outline of project*

Keihan No.2 Road is a expressway connecting Kyoto and Osaka as a bypass for National Road Route 1 to relieve the congestion of traffic on the existing roads, as well as to form a part of the area trunk road network in Kinki region. Figure 1 shows the network of the Arterial High-Standard Roadway in Kinki region.

This paper describes the construction planning and the design for Shoji Tunnel, located on the hillside in a dense residential district between Neyagawa-Kita IC an Neyagawa-Minami IC on Keihan No.2 Road, where an unprecedented construction method in the country is employed, i.e. the Large double adjoined binocular tunnels constructed by NATM in shallow and soft ground.

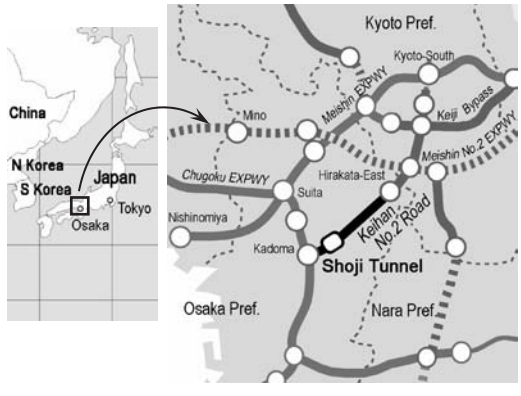


Figure 1. Network of the Arterial High-Standard Roadway in Kinki region and the tunnel position.

1.2 *Structural features of the tunnel*

Figure 2 shows a typical cross section of Shoji tunnel. The tunnel cross-section forms with four main tunnels (expressway: 2 tubes, $A = 170\,m^2$/national road: 2 tubes, $A = 85\,m^2$) connected with each other. The three center pillars placed between the main tunnels are to be built as SRC (steel framed reinforced concrete) structures in the drifts (3 tubes, $A = 40\,m^2$) that are to be excavated prior to the main tunnel excavations. The center pillars structurally bear only the primary

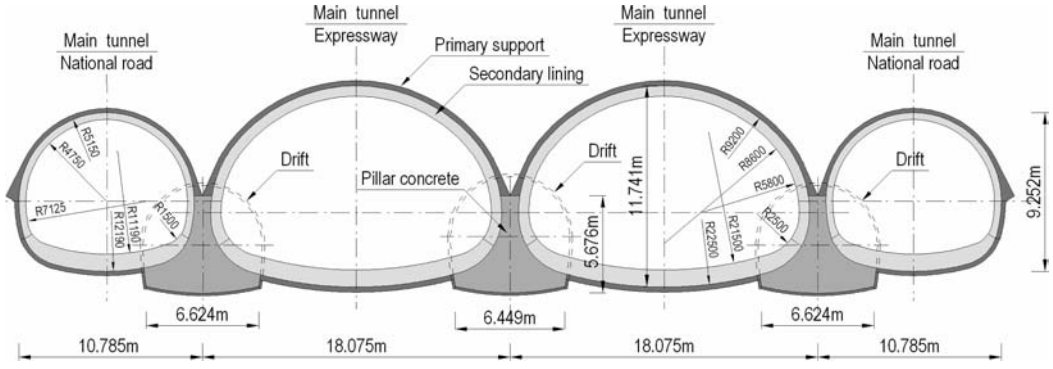


Figure 2. Typical cross section of Shoji tunnel.

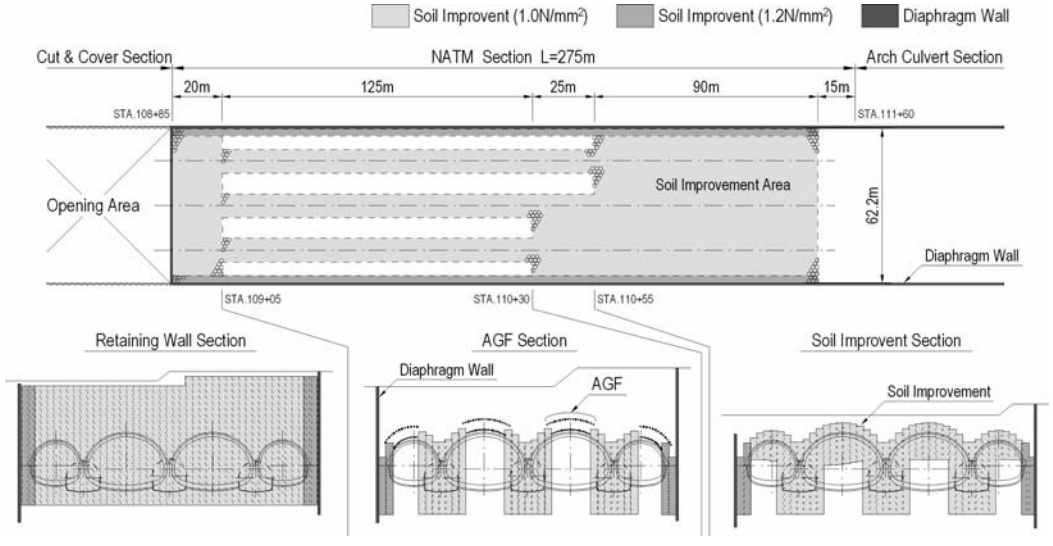


Figure 3. Schematic illustration for works of construction methods for countermeasures against ground surface settlement.

supports of the main tunnels, and are separated from the secondary lining. This is a measure for securing structural safety, and the secondary lining is designed to satisfy adequate safety for surrounding earth pressure, ground water pressure, and seismic loads.

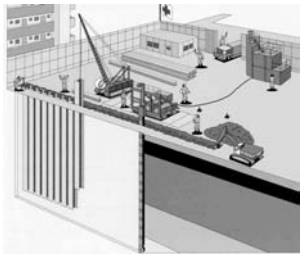
2 CONSTRUCTION PLANNING

2.1 *Outline of tunnel*

The tunnel is located in the Osaka Layer group consisting of alternate layers of unconsolidated sediment with cohesive layers, sandy layers, and gravel layers, and the overburden height is as small as 10 m at maximum with houses in close proximity. With these severe conditions, it has been determined to reinforce the surrounding ground using the following construction methods before excavating the tunnel, so that ground surface settlement in the private land area should remain as small as possible.

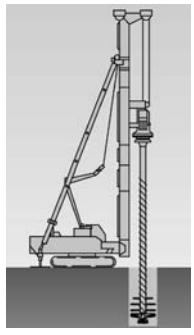
- Underground diaphragm wall
- Soil improvement
- Long pile fore pilling (so-called AGF method)

Figure 3 shows locations and bounds of the above described construction methods. The overall tunnel is roughly divided into three sections, i.e. (1) Soil improvement section, (2) AGF section, and (3) Retaining wall section adjacent to the Cut & Cover section, from the portal side, respectively.



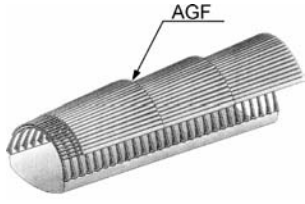
Specification
– Design strength
0.5N/mm^2
– Width of DW
550mm
– Steel rib
H400×200 ctc 1m

Figure 4. Schematic figure of construction of diaphragm wall.



Specification
– Design strength
1.0 ~ 1.2N/mm^2
– Improvement diameter
ϕ 1.6 or 2.0m
– Number
5227

Figure 5. Schematic figure of construction of soil improvement.



Specification
– Diameter of steel pipe
ϕ114.3mm (t=6.0mm)
– Injection diameter
ϕ450mm
– Number
19 (Expressway)
13 (National road)

Figure 6. Schematic figure of AGF method for tunnel.

First, the soil improvement section is the section where the soil improvement is applied to the upper half of the tunnel since the overburden height is very small and soft alluvial soil appears in the tunnel cross-section. Next, AGF section is the section that injection type long steel pipe fore piling at the tunnel crown is adopted instead of soil improvement, to prevent falling in at the tunnel crown during tunnel excavation. Lastly, retaining wall section adjacent to the Cut & Cover section is the section where the soil improvement is applied reaching the bottom of the tunnel for the purpose of reinforcing the retaining wall between the NATM section and the Cut & Cover section at which the tunnel arrives.

2.2 *Diaphragm wall*

Since the excavation is performed in the Osaka Layer group with high ground water level, it has been decided to build up an underground diaphragm wall prior to excavation, considering ease of works and attention for surrounding environment (noise, vibration, etc.). It is expected that the prior diaphragm wall have an effect to reduce ground surface settlement due to the tunnel excavation. Further more, it is also expected that the diaphragm walls prevent the tunnel itself from expanding in horizontal direction and also contribute to secure the tunnel stability as a whole. Figure 4 shows the outline of the diaphragm wall construction. In constructing the diaphragm wall, the following method has been adopted where the ground is cut toward lateral direction by a chainsaw-shaped cutter and both the cement milk and the in-situ soil are mixed and agitated.

2.3 *Soil improvement*

Soil improvement conducted from the ground surface has been applied, and its main purposes are as follows.

– Improving the face stability during excavation
– Bearing capacity of the center pillars
– Securing long-term permanence and aseismic safety of the secondary lining

As Figure 3 shows, three sections with different improvement methods are set up according to overburden heights and geological conditions. Required strength of the improved body has been determined basing on analyses and the like. Meanwhile in the adopted construction method, the in-situ soil and caking material are mechanically forced to be mixed and agitated with slurry like caking material that is pumped out into the in-situ ground, and after the bore hole reached the designed depth, the mixing and agitating device is pulled out, agitating soil and caking material once again, and thus the improved ground body are formed.

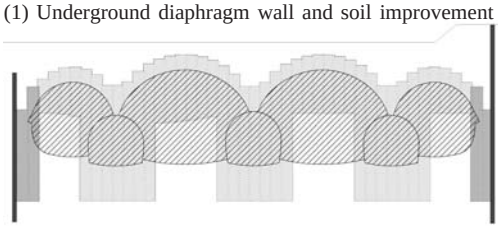
2.4 *AGF method*

For the main tunnel excavation in the section without soil improvement at the tunnel crown, it has been determined to carry out injection type long steel pipe fore piling to protect from falling in at the crown during tunnel excavation. It is a stressed point of this method that fore piling about 12 m beyond the face can be performed by placing steel pipes and grouting with a drill jumbo that is ordinarily used at tunneling works.

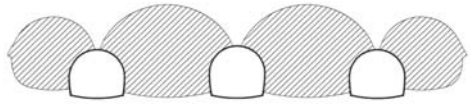
2.5 *Construction procedure*

Construction procedures in the soil improvement section are the followings.

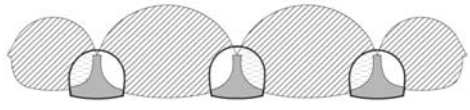
(1) Underground diaphragm wall and soil improvement



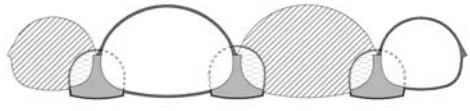
(2) Excavation of drift



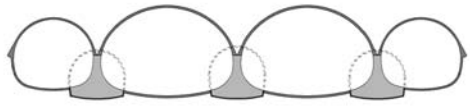
(3) Placing pillar concrete and air mortar



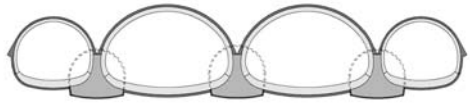
(4) Excavation of advance tunnel



(5) Excavation of following tunnel



(6) Placing lining concrete



3 TUNNEL DESIGN AND ANALYSIS

3.1 *Outline of design*

In general, it is required for tunnel excavation to make sure the surrounding ground stability and the tunnel deformation behavior associated with excavation before starting execution control. In this tunnel, excavation should be performed under difficult conditions such as small overburden height or neighboring private houses located close to the tunnel, and therefore it has been considered necessary to accurately predict deformation behavior of the tunnel and the like. For these reasons, three-dimensional excavation analyses have been carried out representing relative influences of face positions of the four tunnels or effects of three-dimensional geological and topographical structures. It has been decided to set the following specified control parameters necessary for excavation works on the basis of the results of three-dimensional analyses.

(1) Induced deformation in the private land area
This is an important control item for tunnel construction. Specified control parameters are determined through comparing predicted analysis results with allowable limits for the surrounding private land.

(2) Ground surface settlement above the tunnel and the tunnel deformation
Since these predicted deformations are considered to have a strong correlation with deformation in the private land area, the specified control limits are set up using the relative correlation obtained through the prediction analyses.

(3) Displacement of the pillar concrete
The pillar concrete is considered to play a very significant role in reducing ground surface settlement and securing the tunnel stability on the whole. Hence the deformation modes or displacements of the pillars shall be analytically predicted, and these should be determined to conduct the execution control during construction basing on these predictions.

3.2 *Three dimensional excavation analysis*

Three-dimensional excavation analysis is performed under the following conditions.

(1) Analysis code
FLAC3D version2.1

(2) Three-dimensional FDM (Finite Difference Method) analysis model
Figure 7 is an illustration for the three-dimensional FDM analysis model, which is prepared taking specifications of topography and strata, and structural conditions of the tunnel into account. In modeling, three-dimensional geological structures, such as ground surface, boundary of stratum, distribution of soft strata (alluvial clay) and others, have been faithfully represented basing on the boring survey results ($n = 12$), and also mutual positions of the tunnel, retaining wall, and soil improvement area are three-dimensionally incorporated.

(3) Ground model
A Mohr-Coulomb type perfect elasto-plastic model is assumed for the ground, by using solid elements. Ground physical properties in each layer are set through geological survey.

(4) Support system model
For the underground diaphragm walls, characteristics of bending and axial rigidity of soil cement and core material are taken into consideration, and it is decided to model the walls as solid elements composing those materials together.

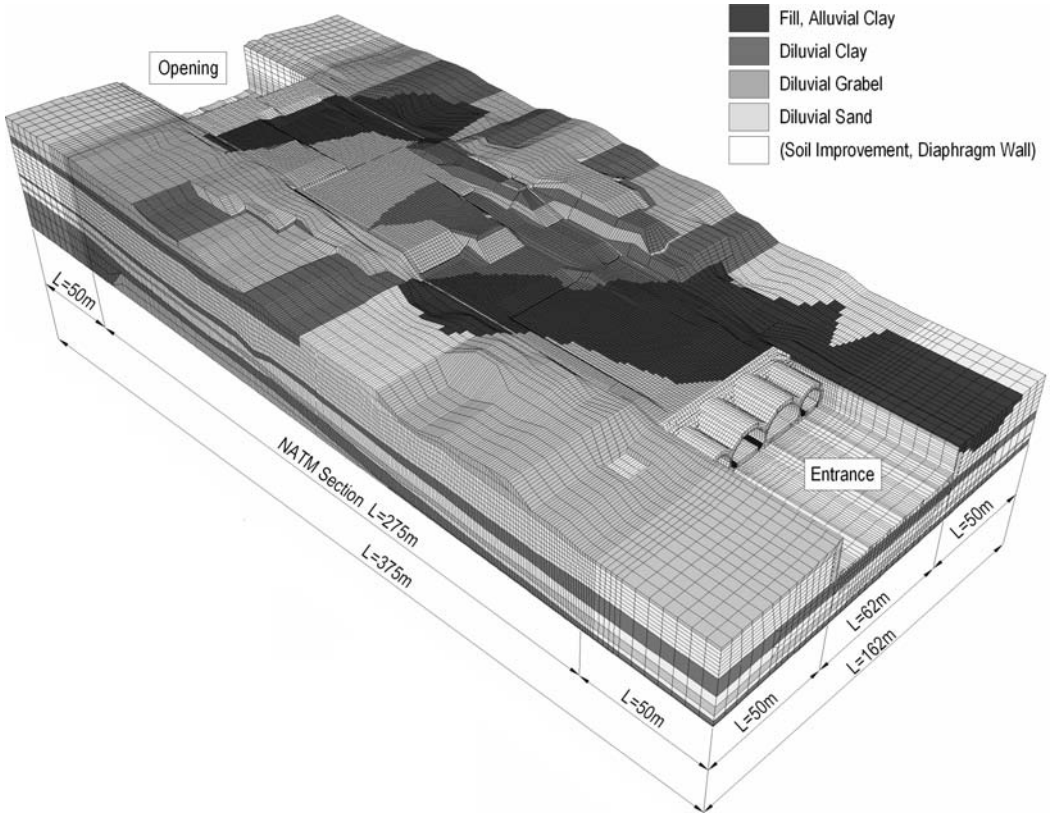


Figure 7. Analysis model.

Support members of the drifts are modeled to be shell elements where characteristics of bending and axial rigidity of shotcrete and steel supports are considered. Bending rigidity is set to be equivalent to that of steel supports, as bending rigidity of concrete has been neglected. While for axial rigidity, axial rigidity of shotcrete and axial rigidity of steel supports were added together.

Support members of the main tunnels consisted of shotcrete and steel supports, and shotcretes are modeled as solid elements and steel ribs are modeled as beam elements.

Figure 8 is an illustration for analysis steps.

3.3 *Distribution of ground surface settlement*

Figure 9 shows settlement distribution at the time of completion of excavation. Ground surface settlement directly above the tunnel is 20 mm at the soil improvement section and about 45 mm at the AGF section. Meanwhile, settlement at the border of the private land area, which is significant for execution control, is around 3 mm in the soil improvement section and 5 mm in the AGF section. On the basis of these predictions, it is planned to carry out an execution control during construction.

3.4 *Behavior and structure of the center pillars*

Figure 10 shows an example of deformation of the center pillars at the central part. The figure shows the result that horizontal displacement of 13 mm at the maximum appears at the top end of the center pillar with excavation of the pilot drift. The center pillars behave in a complicated manner during the following excavations, and displace about 10 mm in the reverse direction due to excavation of the following tunnel. On the other hand, reinforcements for the center pillar have been determined according to the following concepts.

(1) It is assumed to reinforce with steel material only for zone where tensile stress appears during construction, and the bottom of center pillars, where the analysis results for ordinary state show an appearance of tensile stress, has been decided to be reinforced by steel rib (H250 ctc 1.0 m).

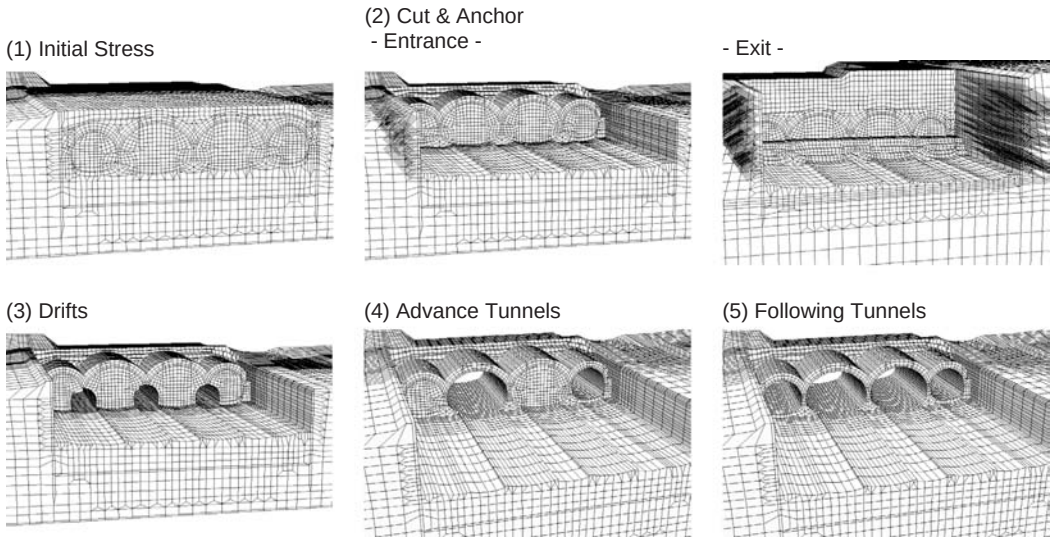


Figure 8. Analysis step.

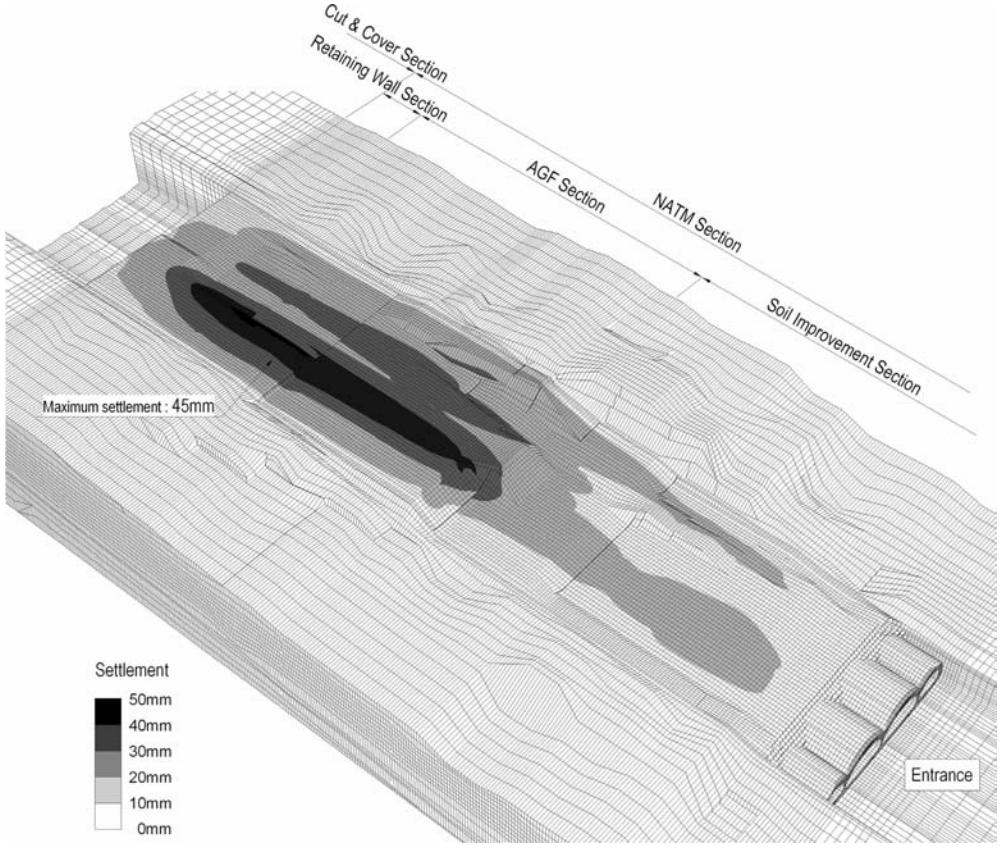


Figure 9. Settlement distribution diagram.

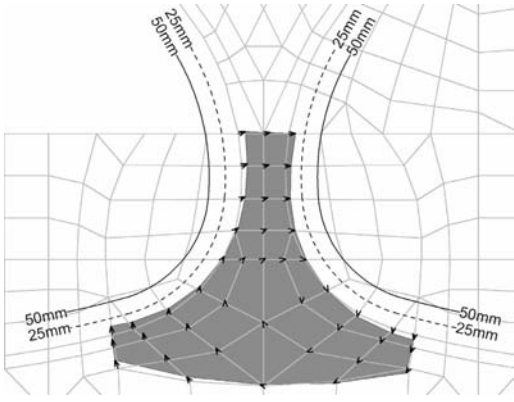


Figure 10. Deformation diagram for pillar concrete (at the time of completion of the upper half of the advance tunnel).

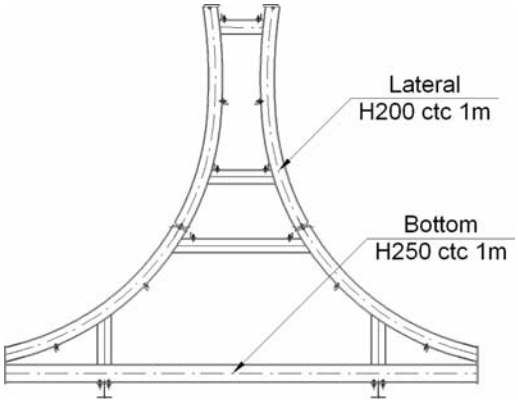


Figure 11. Schematic illustration for reinforcing steel frame layout.

(2) Considering the continuity with primary supports which contain steel rib with the spacing of 1 m, the reinforcements have been decided to execute by equivalent steel supports with the spacing of 1 m, and those effectiveness have been ascertained by both the seismic analysis and the three-dimensional excavation analysis.

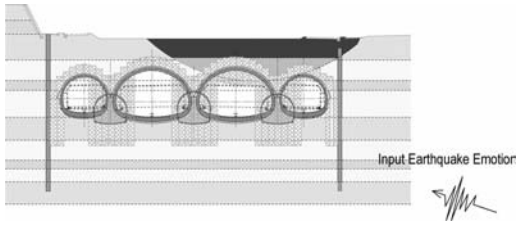


Figure 12. Schematic figure of dynamic analysis during earthquakes.

4 ASEISMIC DESIGN

Regarding seismic stability of secondary lining, it is designed basing on seismic dynamic analyses to secure the safety against the seismic movement in the level equivalent to the actual earthquake motions recorded at the famous Hyogoken-Nambu earthquake occurred in Japan in 1995. Figure 12 shows a schematic figure of dynamic analyses during earthquakes. The Japanese aseismic design codes require the addition reinforcements standing against the induced shear forces for arch and invert concrete.

ACKNOWLEDGEMENTS

Authors express here our deep gratitude to the committee members of the Construction Study Committee, which are organized by West Nippon Expressway Company Limited, who have cooperated with us in this project.

REFERENCE

M. Mori, M. Nakano, K. Shirakawa & M. Oshima. 2006. Method to support the center pillar of double adjoined binocular large tunnels in the shallow ground at densely populated area, *Proc. 61st JSCE Annual Meeting*. JSCE. VI-175: 349–350. (in Japanese).

This page intentionally left blank

Underground Space – the 4th Dimension of Metropolises – Barták, Hrdina, Romancov & Zlámal (eds)
© 2007 Taylor & Francis Group, London, ISBN 978-0-415-40807-3

Stability estimation method and analysis for pillar considering the reinforcement during twin-tunnel excavation

Sisam Park & S.W. Yoon
Senior Engineering Researcher, R&D Team, Technical Division, GS E&C Corp., Seoul, Korea

J.S. Hwang
Senior Researcher, Civil Design Part, Doosan Co. Ltd., Seoul, Korea

ABSTRACT: Recently, even though designing the twin tunnel is getting more common considering prevention of disasters and environmental disruption, research papers on the twin tunnel are not enough to examine it. Concentration of the vertical stresses and relaxation of the horizontal stresses in the pillar located in the twin tunnel gradually increase by deviation stresses, which causes instability of base rocks. This instability increases according to a decrease in the width of the pillar. In this study, the numerical analysis was carried out on the various conditions to analyze interference effects and behaviors of the stress variation in the pillar according to excavation of the twin tunnel. The induced stress estimation equation of the pillar through the regression analysis on the results of the numerical analysis was proposed. In addition, the quantitative method to estimate the stability of the pillar was proposed by application of Hoek-Brown failure criterion and the proposed equation. In order to enlarge the application of the proposed method, the analysis method was suggested considering reinforcement methods. Lastly, the efficiency of the proposed method was proved by the analysis of various variables.

1 INTRODUCTION

Recently, even though designing the twin tunnel is getting more common considering prevention of disasters and environmental disruption, research papers on the twin tunnel are not enough to ideally examine it. As stated above, the examination of causing stresses of the pillar considering the distance between the tubes and estimation of stability considering the strength of the pillar are very essential when the twin tunnel is designed because the twin tunnel has a progressive failure risk of the pillar by concentration of stresses. When the twin tunnel is designed, things that should be considered first are whether the failure of peripheral rocks comes out or not.

The in-situ ground before excavation balances in stresses, however deviation stresses gradually increase by concentration of vertical stresses and deliverance of horizontal stresses in the pillar between the tubes. As stated, increase in deviation stresses of the pillar by excavation causes the unstable condition of a peripheral rock consisting of the pillar. Hence, the distance of the pillar in behavior estimation of the twin tunnel is a very important factor. In this study, the analysis method to estimate the safety factor of the pillar without reinforcement considering strength parameters, the diameter of the tunnel, the distance from the surface to the crown and the distance between the tubes of peripheral rocks around the tunnel is proposed, and the method to consider a case applying the reinforcement method for the application enlargement of the proposed analysis method on the pillar without reinforcement is proposed.

2 ESTIMATING EQUATION OF THE PILLAR THROUGH THE REGRESSION ANALYSIS

The equation of the regression analysis is the equation 1 using non-linear fitting with the exponential function as the generating function. The estimating equation of the stress ratio (SR_{yp} & SR_{xp}) was determined to the function satisfying that in case strength was better than soft rock, an average square root error was under 5%, and in case strength was worse than weathered rock, an average square root error was under 10%.

$$SR_{ip} = a_i + b_i \cdot \exp[-c_i \cdot (P/D)] \quad (\text{where}, \quad i = x \ or \ y) \qquad (1)$$

Where, represents the stress ratio, and a_i, b_i, c_i represent constants according to the types of base rocks through the regression analysis. Furthermore, if i is equal to x, the equation 1 represents the horizontal direction, and if i is equal to y, the equation 1 represents the vertical direction. The values of constants by the regression analysis are summarized in table 1,

Table 1. The values of a_i, b_i, c_i applied to estimate stress ratio.

Section of base rock Types/Classification	Vertical stress ratio			Horizontal stress ratio		
	a_y	b_y	c_y	a_x	b_x	c_x
Hard / RMR II	1.79	3.18	2.68			
Medium / RMR III	1.79	3.30	2.94	0.93	0.49	1.34
Soft / RMR IV	1.68	2.57	2.65			
Weathered / RMR V	1.48	1.78	2.68	1.10	0.52	1.42
Com. Weatrd. / –	1.29	0.82	1.93	1.30	0.55	1.50

and the relation between stress ratio and regression curves of hard rock and weathered rock. In addition, the constant of horizontal stress ratio in table 1 was determined under the condition that the same constant values were applied to the estimation of stress ratio because the constant values according to the types of base rocks were similar in case strength was better than soft rock. Hence, in case of excavation of the tunnel, the stress ratio considering the types of base rocks, the width of the pillar and the distance from the surface to the crown can be determined by use of the equation 1 and table 1.

The applied stresses of the pillar changed in case of excavation of the twin tunnel are determined by the equation 2 and 3 based on the stress ratio of the equation 1.

$$\sigma_{1p} = SR_{yp} \cdot \gamma \cdot (H + D/2)] \tag{2}$$

$$\sigma_{3p} = SR_{xp} \cdot k_0 \cdot \gamma \cdot (H + D/2)] \tag{3}$$

(In case of $p \geq 2D$, in case of estimating SR_{xp}, $p = 2D$)

Where, σ_{1p} and σ_{3p} are maximum and minimum principle stresses of the pillar. The strength of the pillar that is minimum principle stress (σ_{1p}) of Hoek-Brown failure criterion corresponding to minimum principle stress (σ_{3p}) of the pillar is determined by the equation 4. Hence, the safety factor of the pillar considering the variation of stresses derived by excavation of the twin tunnel in the ground is determined by the equation 5 as the ratio between maximum principle stress (σ_{1p}) derived to the pillar and maximum principle stress estimated by the equation 5 from the Hoek-Brown failure envelope.

$$S_p = \sigma_1 = \sigma_{3p} + \sigma_c (m_b \cdot \sigma_{3p} / \sigma_c + s)^a \tag{4}$$

$$F_s = \frac{S_p}{\sigma_{1p}} = [\sigma_{3p} + \sigma_c (m_b \cdot \sigma_{3p} / \sigma_c + s)^a] / [SR_{yp} \cdot \gamma \cdot (H + D/2)] \tag{5}$$

Where, m_b is a Hoek-Brown quota considering the condition of in-situ ground and the types of rocks, s and a are constants depending on the condition of in-situ ground, and σ_c is the unconfined compressive strength of intact rocks. In this study, the strength of base rocks was estimated by use of initial Hoek-Brown failure criterion assuming that it was assumed that $m_b = m$, a = 1/2 because the strength characteristic estimation of base rocks was not a main purpose.

3 THE ESTIMATION METHOD OF STABILITY CONSIDERING THE REINFORCEMENT METHOD OF THE PILLAR

3.1 *Profile on the reinforcement of the pillar*

Overall, in case that obtaining the stability is difficult, the modification of the lines or the reinforcement of the pillar can be used for stability of the tunnel. However, in case of the linear structures like a railroad, road, etc., the modification of the lines is not easy. Generally, the modification of the lines designed first with economical efficiency derives a lot of construction expenses. Hence, the reinforcement method is required to obtain the stability of the tunnel. In this study, in order to increase application of stability estimation method on the pillar proposed, the analysis considering application of reinforcement method is proposed as follows.

3.2 *Estimation of stability in case of the reinforced method of the pillar*

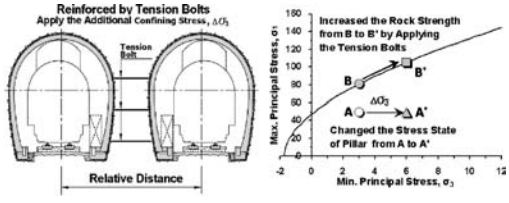
Of the reinforcement methods of the pillar proposed so far, the tension bolt and grouting method are available in administrative work, and then the profile and principle of reinforcement are illustrated in figure 1 and 2. In case of tension bolt to reinforce the pillar like a figure 1(a), the additional confined pressure causes by installation of tension bolt in the pillar. Therefore, as illustrated in figure 1(b), the additional confined pressure ($\Delta\sigma_3$) derived by the installation of the tension bolts has changed the strength of the pillar ($B \rightarrow B'$) and induced stresses ($A \rightarrow A'$), which increases stability of the pillar. The figure 2(a) describes the instance of grouting for reinforcement in the pillar. In case of grouting for reinforcement, the overall magnitude of the Hoek-Brown failure envelope increases according to an increase in unconfined compressive strength. Eventually, the safety factor of the pillar increases.

In addition, the estimation of the safety factor on the pillar with the reinforcement method can be estimated to the equation 7 based on the equation 5 and 6.

$$\Delta\sigma_3 = q_{tb} / (S_h \cdot S_v) \tag{6}$$

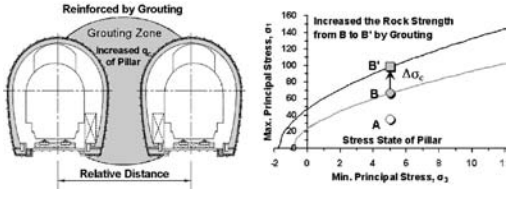
$$F_s = \{(\sigma_{3p} + \Delta\sigma_3) + (n \cdot \sigma_c)[m_b(\sigma_{3p} + \Delta\sigma_3)/(n \cdot \sigma_c) + s]^a\} / \sigma_{1f} \tag{7}$$

Where, q_{tb} is the strength of tension bolt, S_h is the vertical installation distance, S_v is the horizontal installation distance. And n is a quota that represents the degree of increase in unconfined compressive pressure of the pillar by grouting. Generally, it is reported that in case of soft rock, n increases up to 2 times, and in case of weathered rock, n increases up to 4 times,



(a) Tension bolt (b) Principle of reinforcement

Figure 1. The principle and profile of reinforcement by tension bolts.



(a) Grouting reinforcement (b) Principle of reinforcement

Figure 2. The principle and profile of reinforcement by grouting.

and in case of worse than strength of weathered rock, n increases up to 40 times. In this study, in case of application of proposed reinforcement methods, tension bolt can be applied in the condition of better than the strength of soft rock, and tension bolt + grouting or grouting method is more effective method in the condition of worse than the strength of weathered rock.

4 ANALYSIS AND CONSIDERATION

In this study, the trend of the variation on the safety factor of the pillar was analyzed according to the variation of unconfined compressive strength on the types of base rocks, the width of the pillar, and intact rock except hard rock by using the proposed methods.

When analyzing, unconfined compressive strength of intact rock was applied by use of the values proposed by Bieniawski(1979). The strength of base rocks was applied by use of initial Hoek-Brown failure criterion assuming that $a = 1/2$. m_b and s determined by the types and conditions of base rocks were applied by use of the proposed values on pelite, and the representative values proposed to the analysis are summarized in table 2.

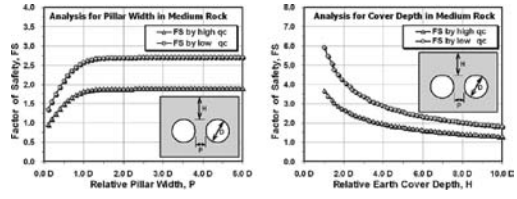
4.1 *Analysis according to the variation on the width of the pillar and the distance from the surface to the crown*

This analysis is about the variation of the safety factor on the pillar according to the variation on the width of the pillar and the distance from the surface to the crown. When analyzing, the compressive strength of intact rock was applied by use of the maximum value and minimum value in the range proposed in table 5. As a result, in case the width of the pillar is over 0.5D and the height of the shaded area is over 10D in hard rock, it is possible to secure the safety factor over 4.0 on the proposed strength of base rocks. However, in case of the completely weathered condition, the trend of the safety factor on analysis was almost same as weathered rock, so it wasn't stated in this study.

Table 2. Representative value proposed to the variable analysis.

Rock types	Compressive strength range (MPa)	H-B constant (pelite, 1980) m_b	s	H (m)	Unit weight (kPa)	Width pillar (P)
Medium	25∼50	1.0	0.004	7.5D	24.8	0.5D
Soft	10∼25	0.2	0.0001	5.0D	22.9	1.0D
Weatrd.	2∼10	0.05	0.00001	2.5D	20.5	1.0D
Com. W.	1∼2	0.01	0	1.25D	18.8	2.0D

Remark. (1) H: Distance from the surface to the crown; (2) D: Diameter of the tunnel (8.0 m); (3) k_0: 0.5; (4) q_{tb}: 98.0 KPa; (5) Compressive strength: refer to the Bieiawski, 1979.



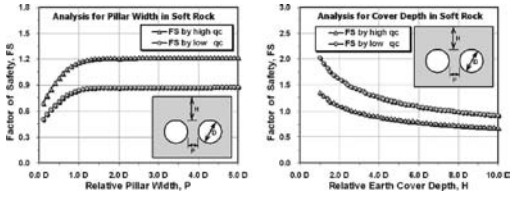
(a) Width of the pillar (b) Distance from the surface to the crown

Figure 3. The safety factor on the medium rock.

4.1.1 *Results of analysis on the rock*

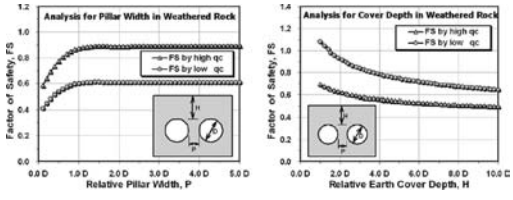
The results of the analysis are illustrated according to the width of the pillar, the distance from the surface to the crown and the strength of base rocks on the rock in figure 3. As a result of the analysis on the rock according to the unconfined compressive strength of intact rock proposed by Bieniawski, even though the strength of base rocks is 25 MPa that is under the given values, the safety factor according that the width of the pillar is 0.5D and the height of shaded area is 7.5D is 1.487 (Fig. 3(a)).

And even though the height of the shaded area increased up to 10.0D, the safety factor was calculated over 1.0 (Fig. 3(b)). Hence, it is turned out that the security of the safety factor on the pillar in the ground conditions of the rock was comparative easy. In addition, it is turned out that the safety factor was gradually convergent over 1.0D of the width of the pillar.



(a) Width of the pillar (b) Distance from the surface to the crown

Figure 4. The safety factor on the soft rock.



(a) Width of the pillar (b) Distance from the surface to the crown

Figure 5. The safety factor on the weathered rock.

4.1.2 *Results of analysis on soft rock*

The results of the analysis on soft rock were illustrated with figure 4.

As a results of the analysis on the rock by use of the unconfined compressive strength of intact rock proposed by Bieniawski, in case the strength of base rocks was under the given values (10 MPa), it is turned out that the safety factor of the pillar was under 1.0 (Fig. 4 (a)). Moreover, In case the height of shaded area increased up to 10.0D, it is turned out that all safety factors were under 1.0 (Fig. 4 (b)). Hence, it is turned out that the meticulous examination on the security of the safety factor on the pillar was required in the conditions of soft rock.

4.1.3 *Results of analysis on weathered rock*

The results of the analysis on weathered rock were illustrated with figure 5.

In case of weathered rock, it is turned out that all safety factors were under 1.0 on the strength of base rocks proposed (Fig. 5(a)). In addition, in case the strength of base rocks was over the given values (10 MPa), it is turned out that the calculated safety factor was under 1.0 as the safety factor of 1.4D on the distance from the surface to the crown is 1.01 (Fig. 5(b)). Through the results of this analysis, it is reasonable to take into consideration the reinforcement of the pillar on the ground conditions under weathered rock.

5 CONCLUSION

In this study, the regression analysis was carried out on the results of the numerical analysis examined with various variations of the strength of the ground, the width of the pillar and the distance from the surface to crown according to excavation of the twin tunnel. And the quantitatively estimation method of stability on the pillar was proposed by use of Hoek-Brown failure criterion and the induced stress equation of the pillar through the regression analysis. In addition, in order to enlarge application of the proposed estimation method for stability, the estimation method was proposed considering the reinforcement method of the pillar. The results of this study are as follows. First, the various factors influencing security of stability on the pillar were analyzed according to various variations of the strength of the ground, the width of the pillar and the distance from the surface to crown. Through this analysis, it was turned out that the careful examination on security of stability on the pillar was required in case of soft rock, and the reinforcement was required in case of the ground conditions below weathered rock. Then, the variable analysis was carried out according to application of reinforcement methods, and it was turned out that the reinforcement by grouting and tension bolts was effective. Lastly, it is possible for the proposed method to be widely applied to the stability examination of the pillar, application of the reinforcement method and the distance between tunnels in a step for the preliminary design on the twin tunnel. And when considering that the quantitative design method for the configuration of the pillar and reinforcement method is not properly erected, the proposed method in this study is one of the effective methods possible to apply in administrative work.

REFERENCES

Bienniawski, Z.T. (1979), “Engineering Rock Mass Classification”, John Wiley & Sons, New York.

Brown, E.T. (1970), “Strength of Models of Rock with intermittent Joints”, *J. Found. Eng. Div., ASCE*, SM6, pp. 1935∼1949.

Hoek, E. (1968), “Rock Mechanics in Engineering Practice”, John & Wiley, London.

Hoek, E., and Brown, E.T. (1980), “Underground Excavation in Rock”, Institution of Mining and Metallurgy,

Matsuda, T., Terada, K., Igarashi, M., and Miura, K. (1998), “Ground behavior and settlement control of twin tunnels in soil ground”, *Tunnels and Metropolises*, Vol. 2, pp. 1193∼1198.

Kikuchi, K., and Mito., Y. (1995), “Case Study on the Mechanical Improvement of Rock Masses by Grouting”, *Proceeding of Internatioal Workshop on the Rock Foundations*, Tokyo, pp. 393∼397.

Underground Space – the 4th Dimension of Metropolises – Barták, Hrdina, Romancov & Zlámal (eds)
© 2007 Taylor & Francis Group, London, ISBN 978-0-415-40807-3

Design and construction of the longest road tunnel with eight-lane in China

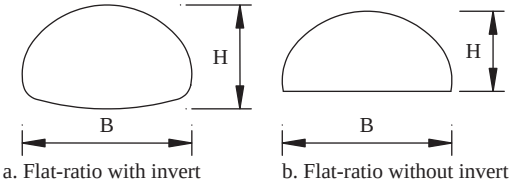
H.F. Qu, H.H. Zhu, Y.C. Cai & X.Y. Zhuang
Department of geotechnical Engineering of Tongji University, Shanghai, China

ABSTRACT: Longtoushan Tunnel is a two-way tunnel with eight-lane in either way located in Guangdong province of China. The tunnel has a maximum excavation width of 21.47 m and a maximum height of 13.56 m(including invert arch). Featured by a length of 1010 m one way and a cross-sections area of 230 m^2 in either way, it is the longest and largest tunnel so far in China. Therefore, rational design and construction method is required to assure the stability of surrounding rock and support structure. The paper mainly introduces the successful experience of design and construction on Longtoushan Tunnel. Firstly, the state of design and construction of eight-lane road tunnel in China is summarized. Secondly, design of cross-section, supports, construction, monitoring of Longtoushan Tunnel are presented and discussed in detail. Finally, difficulties and emphases of design and construction, economic benefits during construction are analyzed briefly. According to above experience and methods, the Longtoushan Tunnel has been completed successfully and collapse or accident never happened during the construction.

1 INTRODUCTION

The quick development of economy of China in recent years gave an enormous increase of traffic flow, the usual two-way tunnel with four-lane or six-lane in either way can no longer endure such a heavy traffic burdon. Therefore, eight-lane road tunnels gradually came into being in recent years. The first eight-lane road tunnel named Dageshan Tunnel was built in Guizhou province early in 1999. After that, the second one, Hanjialing Tunnel was built located in Dalian city of Liaoning province. At present, there are two eight-lane road tunnels under construction, one is Yabao Tunnel in Shenzhen city and the other is Longtoushan Tunnel in Guangzhou city. The Table 1 provides the eight-lane road tunnel statistics of China. Here, we defined the flat-ratio β as the ratio of height and span of tunnel ($\beta = H/B$) which is shown in Fig. 1. Height is the distance from the bottom of invert to the crown (if there is no invert, height is the distance from bottom of excavation line to the crown such as right column one of Fig. 1), Width is the longest distance of excavation of cross-section.

Although some experiences are accumulated from the formerly built eight-lane road tunnels, the design and construction of eight-lane road tunnel are still



a. Flat-ratio with invert b. Flat-ratio without invert

Figure 1. The definition of the flat-ratio.

Table 1. Construction statistic of eight-lane tunnel in China.

Tunnel name	Dageshan tunnel	Hanjialing tunnel	Longtoushan tunnel	Yabao tunnel
Length/m	496	521	1010	265
Span/m	21.04	21.242	21.47	20.9
Height/m	11. 5(exclude invert)	15.52	13.56	13.48
Flat-ratio	0.55	0.731	0.63	0.645
Excavation area/m^2	200	230	230	220
Construction method				Double Side Pilot Method
Type	one-way four-lane	one-way four-lane	two-way eight-lane	two-way eight-lane

faced many difficulties because of its characteristic of large-span and low flat-ratio. The paper describes the design and construction of Longtoushan Tunnel which is the longest eight-lane road tunnel in China. The article mentions to provide a reference for the design, construction and study of the extra-large cross-section and span road tunnel.

2 GEOLOGY OF LONGTOUSHAN TUNNEL

Longtoushan Tunnel is located in the eastern section of East-Ring expressway in Guangdong province. It is the longest two-way tunnel with eight-lane in either way ever constructed in China. The tunnel has a maximum excavation width of 21.47 m, a maximum invert arch height of 13.56 m a total length of 1010 m in one direction and a cross-sections area of 230 m^2 in either way. The running speed expected was 100 km/h, traffic flow forecasted was 58710(pcu/d) in 2027. The altitude of tunnel is between 30 m to 166 m along its axis, i.e., 136 m difference in elevation.

Most part of the Longtoushan tunnel crosses the micro-efflorescence monzo- granite. RQD of micro-efflorescence monzo-granite varies between 22% to 88%, ultimate compression strength is from 135.3 MPa to 151.6 MPa. The ground surface of tunnel roof is covered by lush arbuscle and natural grass. At entrance of the tunnel, geological condition is very bad because of serious efflorescence of granite, so it brings some difficulties for construction. In addition, construction is affected by rainfall which reaches 1600–1700 mm/year because of its subtropical marine monsoonal climate.

3 DESIGN OF CROSS-SECTION AND SUPPORTS

Currently, four eight-lane tunnels and tens of six-lane tunnels have been built or are now under construction in China. Usually, a three-centered arch or five-centered arch cross-section was adopted for these road tunnels.

For the first and the second eight-lane road tunnels in China, with reference to the design experience of six-lane road tunnels, three-centered arch cross-section has been adopted because of its well stability. However, a five-centered arch cross-section can reduce the excavation area and is more economic if the stability of tunnel can be assured. Thus, in 2003, five-centered arch cross-section was adopted for the design of Longtoushan tunnel as well as the Yabao tunnel which are the third and fourth eight-lane road tunnel built in China. In addition, the flat-ratio of Longtoushan tunnel is designed less than 0.65 (include the inverted arch) based on the design experience of the large cross-sectional tunnels of Japan(Katushi 2003). Fig. 2 shows the construction cross-section of the

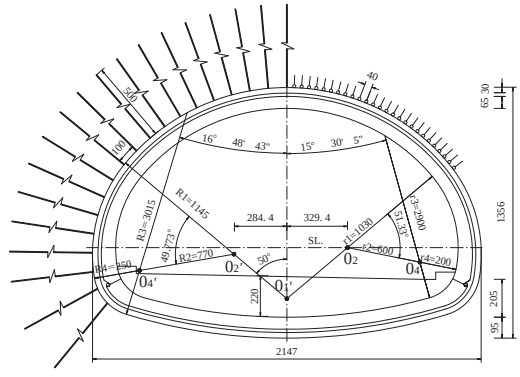


Figure 2. The cross-section of Longtoushan tunnel in V level shallow surrounding rock condition (cm).

Longtoushan tunnel in V level shallow surrounding rock condition. (Rock mass classification is based on *code for design of road tunnel of china*, it becomes worse from level I to VI.)

Support system of tunnel is composed of bolt, steel arch support, plain shotcrete and concrete lining. Hollow injected bolt is used in this tunnel to improve the tunnel stability. H-steel is adopted in steel arch support with the space of 0.75 m in V level shallow surrounding rock condition. C25 plain shotcrete is used during the construction. The C30 reinforced concrete is used to obtain a reducd design thickness of concrete lining. The parameters of support of Longtoushan tunnel are shown in Table 2.

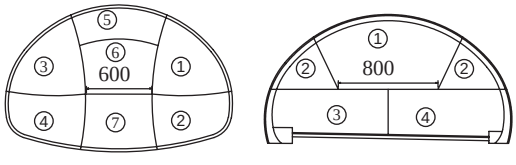
4 CONSTRUCTION AND MONITORING

NATM(New Austrian Tunneling Method) is used for Longtoushan tunnel construction. Two excavation methods have been adopted considering different ground conditions, which have been divided by *Code for Design of Road Tunnel of china* as shown in Fig. 3. The left one(a) of Fig. 3 was called *Double Side Pilot* excavation method which was used at the portal department or for poor surrounding rock condition such as V and IV levels, and the right one(b) was applied at the comparatively good ground conditions such as II and III levels. The Longtoushan tunnel was designed to minimize the damage to nature environment because it passes through the longtoushan-Mountain Park. Fig. 4 is the photo of excavation in entrance.

Huang Hailun (2005) discussed the rationality of excavation methods mentioned above. He studied the excavation method of eight-lane tunnels of poor conditions based on the physical model experiment and the two-dimensional FEM simulation. The scale of model is 1:5 and three excavation methods (Fig. 5) have been studied in the experiment. The experiment carried by *Integrated Test System for Surrounding Rock Mass of*

Table 2. Main parameters of complex lining of Longtoushan tunnel.

Item		Surrounding rock level				
		V (shallow)	V(deep)	IV	III	II
Thickness of shotcrete	C25/cm	30	27	22	15	10
Radial bolt	diameter/mm	25	25	25	22	22
	length/cm	500	450	400	350	300
	disposal/cm	100 × 75	100 × 80	100 × 100	120 × 120	150 × 150
steel arch	H-steel/mm	H200 × 200	H175 × 175	H150 × 150	/	/
	space/cm	75	80	100	/	/
Thickness of Concrete	C30 concrete	/	/	/	45	40
lining/cm	C30 reinforced concrete	65	60	50	/	/
Thickness of inverted	C25 shotcrete	30	27	22	/	/
arch/cm	C30 reinforced concrete	65	60	50	/	/
Advancing support	type	Φ108 pipe roof; Φ50 tremie pipe	Φ50 tremie pipe	Φ50 tremie pipe	/	/
	space/cm	40	40	40	/	/
	length/m	40	4.5	4.5	/	/



(a) (b)

Figure 3. Construction sequence of Longtoushan tunnel (cm).

Road Tunnel which is based on the idea of first loading and second excavation. The system adopts the inlay-jack and high accuracy displacement device in order to simulate and record stress response and change of displacement, and by using it, objective and true simulation of excavation of tunnel can be realized. The results of model experiment and numerical simulation show that *Double Side Pilot* excavation method has the minimum displacement and surrounding rock pressure among three methods, particularly in roof part of tunnel. Therefore, in poor ground conditions, the *Double Side Pilot* excavation is regarded as the most suitable method in China. If there is special poor conditions or urgency, temporary inverted arch can be used in side pilots as Fig. 4 and Fig. 5(b).

Monitoring, the essence of the NATM, was quite extensive after the designer's program. As there are some differences between the eight-lane tunnels and the conventional two-lane tunnels, therefore, monitoring scheme should be improved and perfected gradually in order to adapt to the eight-lane tunnels during the construction. Monitoring of Longtoushan tunnel consists of two parts, conventional monitoring and special monitoring.

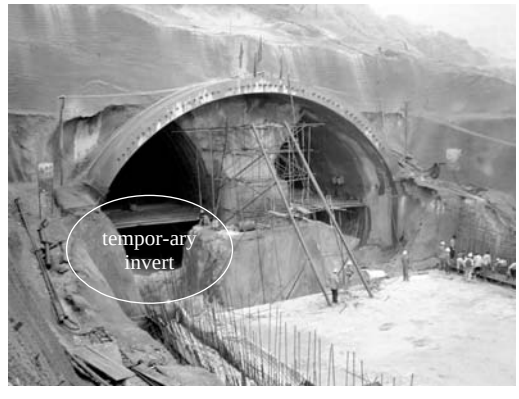


Figure 4. The photo of construction in entrance of Longtoushan tunnel.

Conventional monitoring includes the convergence and the crown settlement measurements. The purpose of conventional monitoring is to monitor the stability of surrounding rock and primary lining and to provide the guidance for construction of tunnel. Usually it is enough that there are three observation points of displacements and three lines of convergence measure per each measuring section in the primary lining of two-lane tunnels. However, as for Longtoushan tunnel, we disposed a lot of measure points and lines in order to seek the best optimum scheme. Through a lot of tests, we determined monitoring scheme of five points and five lines in which two of them monitor side pilots and three of them monitor the whole tunnel in V and IV levels, three points and three lines in II and III levels. Monitoring schemes are shown in Fig. 6.

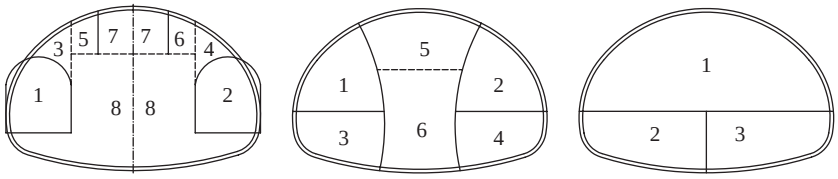
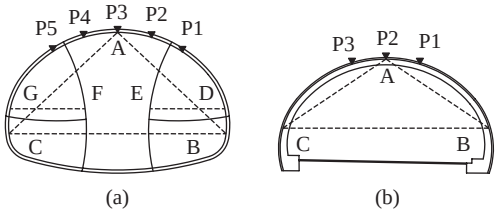


Figure 5. Three excavation schemes.



a. In poor ground condition b. In good ground condition

Figure 6. Monitoring schemes in different ground condition.

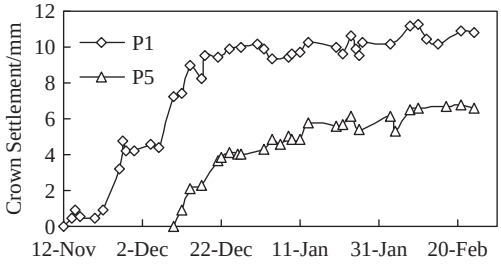


Figure 7. Crown settlement monitoring record of k5 + 859 in left lane in poor ground condition.

Fig. 7 and Fig. 8 are part measure results of crown settlement and convergence in k5 + 859 which is in poor ground condition. In Fig. 7 and Fig. 8, the maximum settlement of crown is only 11.8 mm, and the maximum deformation of convergence is only 22.5 mm. Both of them are less than the allowable value 55 mm. Measure results indicate that the *Double Side Pilot* excavation method is rational.

Special monitoring can provide the data for research topics such as structure optimization design of large cross-section, information construction, information-integration, structure durability and so on. It includes settlement of surface ground, contact pressure, axial forces acting on the steel ribs, axial force acting on the rock bolt, internal force of lining, multi point borehole extensometers(MPBX) as shown in Table. 3. In Longtoushan tunnel, according to the result of MPBX, the dimension of loose zone of V surrounding rock levels is about 10 m.

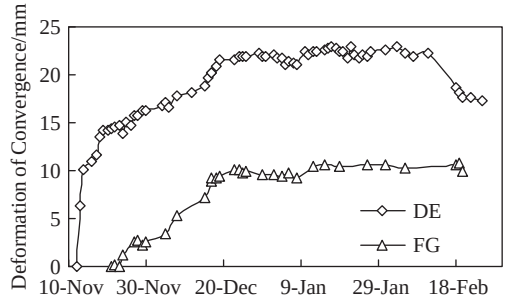


Figure 8. Convergence monitoring record of k5 + 859 in left lane in poor ground condition.

Table 3. Disposal of special measuring cross-section.

Surrounding rock levels	Position	Monitoring items
V level shallow and	YK5 + 870	1,2,3,4,5
Unsymmetrical pressure	YK5 + 885	
V level shallow	YK6 + 730	1,2,3,4,5
	ZK6 + 730	
	YK6 + 700	2,3,4,5
	ZK6 + 700	
V level deep	ZK6 + 665	2,3,4,5
	ZK5 + 870	2,3,4,5,6,7
IV level deep	ZK5 + 890	2,3,4,5,6,7
	ZK6 + 645	2,3,4,5
III level deep	YK5 + 960	2,3,4,5
	ZK5 + 960	
II level deep	YK6 + 000	2,3,4,5
	ZK6 + 000	
	YK6 + 095	
	ZK6 + 098	

Note: 1 = settlement of surface ground; 2 = contact pressure; 3 = axial force acting on the rock bolt; 4 = axial forces acting on the steel ribs; 5 = internal force of lining; 6 = MPBX; 7 = axial force acting on temporary support.

5 DIFFICULTIES AND EMPHASES OF DESIGN AND CONSTRUCTION

During the design and construction of Longtoushan tunnel, there are two distinct characteristics differed from other tunnels. One is adjacent design of oil store. The other is design and construction of unsymmetrical pressure of entrance in shallow ground condition.

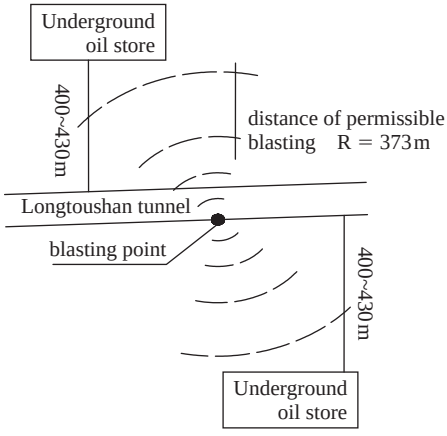


Figure 9. Plane figure of tunnel and underground oil store.

5.1 *Adjacent design and construction of oil store*

Along axes of tunnel, there are two large-scale underground oil stores 400 m distant from the tunnel respectively, which brings us challenge of technology construction. Controlled distance of permissible blasting is the key point in order to avoid the influence on oil stores as shown in Fig. 9. Therefore, techniques of smooth blasting and presplitting blasting are adopted during the construction so that safety shock velocity can be controlled within 1.2 cm/s which is equivalent to IV level earthquake intensity. The equation (1) is used to design parameters of blasting.

$$R = \left(\frac{K}{v}\right)^{\frac{1}{a}} Q^m \tag{1}$$

Where Q is the volume dynamite (kg), v is the safety shock velocity ($v <= 1.2$ cm/s), m is the factor of volume dynamite ($m = 0.5$), K and a are the parameter and decaying exponential which are decided by landform, ground condition and blasting layout and they can be acquired by looking up the table in *Data Ordinary Manual of Engineering Blast* (Yuan 2002).

Three macroseismographs of ALTUS-K2 produced by KINEMETRICS Co. of U.S.A. are adopted to monitor the blasting shock velocity. Table. 4 is the monitoring result of axial line of tunnel direction, vertical ground surface direction and vertical axial line of tunnel direction. In this testing, the volume dynamite is 180 kg, the distances between blasting point and monitoring points are 100 m, 200 m, 300 m separately. From the Table. 4 we can find that the maximum velocity is 1.184 cm/s, it is less than the allowable value 1.2 cm/s.

Table 4. Maximum shock velocity in different direction cm/s.

Distances of monitoring points from blasting point	Axial line of tunnel direction	Vertical ground surface direction	Vertical axial line of tunnel direction
300 m	0.374	0.047	0.609
200 m	1.090	0.209	1.054
100 m	1.184	0.594	0.874



Figure 10. The photo of unsymmetrical pressure in entrance.

5.2 *Design and construction in unsymmetrical pressure ground condition*

As we know that the effect of unsymmetrical pressure ground condition should be properly treated, especially for such a large cross-section tunnel. It usually affects the stability of tunnel directly and brings the potential danger to construction. The unsymmetrical pressure landform of Longtoushan tunnel is shown in Fig. 10. Three measures were applied consequently to avoid development of unsymmetrical pressure. The first one is reinforcement of ground surface injection and backpressure backfill. And then, concrete lining of unsymmetrical form is designed in order to adapt unsymmetrical inner force of lining structure by unsymmetrical pressure landform as shown in Fig. 11. Finally, length of 36 m Concrete lining is built outside mountain after excavation of 10 m distance to enhance the stability of tunnel entrance. Experience proves that above three methods are effectual to control the stability of tunnel entrance, and it ensures the trouble-free operation of construction.

6 ECONOMIC BENEFITS

6.1 *Parameter of support modification*

Steel fiber reinforced shotcrete (*SFRS*) is used in the initial design, however, it is difficult to be carried out

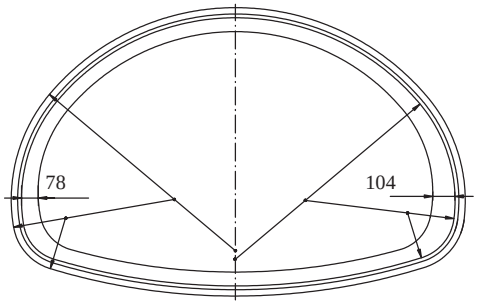


Figure 11. The cross-section of unsymmetrical pressure (mm).

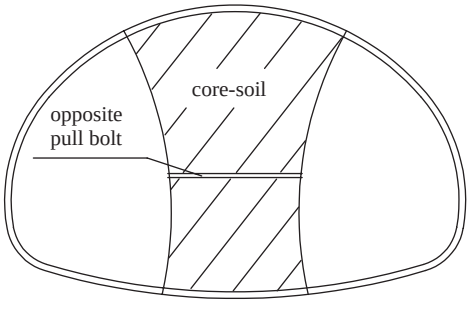


Figure 12. The technology of opposite pull bolt.

during the construction of tunnel because of high technology. Through field tests of 50 m, the plain shotcrete was adopted instead of *SFRS*. Experience proves that plain shotcrete not only meets the strength of design but brings about obvious economical efficiency.

6.2 *Opposite pull bolt instead of temporary inverted arch*

Without question, temporary inverted arch is very effective to control the stability of core-soil and side pilot, however, it also brings some negative effects such as limiting the vehicle running. Therefore, the technology of opposite pull bolt was put forward instead of temporary inverted arch in relative little deformation according to result of monitoring by 5.5 m length and Φ22 reinforcing steel bar in order to restrain the deformation of core-soil as shown in Fig. 12. The technology of opposite pull bolt not only curtails expenditures but shortens construction period.

7 CONCLUSIONS

The paper summarizes the status quo of design and construction of eight-lane road tunnel construction in China. Furthermore, design of cross-section, supports, construction, monitoring and economic benefits are analyzed and discussed in detail based on the Longtoushan tunnel. The building of extra-large cross-section tunnel is just threshold in China, however, with the acceleration of building of infrastructure, the eight-lane road tunnel must be the main design form and instead of four-lane or six-lane road tunnels. For example, a 300 m long eight-lane road multi-arch tunnel will be built in this year in Fujian province. Therefore, we hope that our efforts for the Longtoushan tunnel construction may contribute to the extra-large cross-section and span road tunnel technology in China.

REFERENCES

Karmen Fifer Bizjak, Borut Petkovă ek. 2004. Displacement analysis of tunnel support in soft rock around a shallow highway tunnel at Golovec[J]. *Engineering Geology*, 75: 89–106.

Katushi Miura, Hiroshi Yagi, Hiromichi Shiroma, etc. 2003. Study on design and construction method for the New Tomei–Meishin expressway tunnels[J]. *Tunnelling and Underground Space Technology*, 18: 271–281.

HUANG Lun-hai. 2005. A Study on Construction Schemes of Highway Twin Tunnel with Eight Traveled lanes[J]. *HIGHWAY*, 19:206–211(in Chinese).

Sang-lim No, Seung-Hwan Noh, Sang-Pil Lee, etc. 2005. Construction of Long & Large Twin Tube Tunnel in Korea-Sapaesan Tunnel[A]. *WTC*.

The Professional Standards Compilation Group of People's Republic of China. *Code for Design of Road Tunnel(JTG D70–2004)*[S]. Beijing: China Communications Press, 2004.(in Chinese).

Yangwen Yuan. 2002. *Data ordinary manual of engineering blast*[M]. Beijing: China Communications Press.(in Chinese).

Underground Space – the 4th Dimension of Metropolises – Barták, Hrdina, Romancov & Zlámal (eds)
© 2007 Taylor & Francis Group, London, ISBN 978-0-415-40807-3

Experiences from driving dual-rail tunnels on Prague metro's IV.C2 route

J. Růžička, M. Kochánek & V. Valeš
METROPROJEKT Praha, Prague, The Czech Republic

ABSTRACT: Two driven route sections with lengths of 977 m and 1,410 m have been carried out as part of building up the 2nd stage of the IV.C route to the Prosek and Letňany area. The paper describes the process of building the route tunnels and the evaluation of the effect of driving the tunnels on the existing structures situated on the ground. Attention will be paid to the spot where the Metro tunnel was driven under two prestressed road bridges traversing a high-speed road, and to the area where the tunnel was driven shallowly, under small residential buildings. To minimise the squeezing of the roof, driving the tunnel using vertical structuring of the stope, makeshift props when the stope was being extended and fixing the head by a system of long laminate fasteners was designed. The results of geotechnical monitoring prove that these measures were efficient.

1 METRO LINE IV.C2

In 2004, the phase 1 of the operational section of the metro line C was put into operation – from Nádraží Holešovice (railway) station to Ládví station. This section is followed by the 4.6 km long phase 2 of the construction IV.C to the area of Prosek and Letňany that will be completed in 2008 and include three new excavated stations Střížkov, Prosek and Letňany, a single excavated inter-station section, excavated manoeuvring rails behind Ládví station and two route sections, driven for their most part. These are sections between Ládví – Střížkov and Prosek – Letňany stations.

The first driven double-track tunnel joins from the west side the excavated manoeuvring rails behind Ládví station, it is 975 m long with a short section of a 80.7 long excavated tunnel, and leads to Střížkov station on the east side. Raising the double-rail tunnel was carried out from the excavation pit of manoeuvring rails, and underhand driving in the opposite direction from the east portal at Střížkov station was performed concurrently.

The second running double-rail tunnel is connected to Prosek station through a short excavated tunnel of 141.7 m. It is 1,287 m long and leads to Letňany station through two running single-rail tunnels of 63.3 m. The development of the running double-rail tunnel was realised from the construction site Klíčov. The access to the double-rail tunnel was provided by descend ramp and short access gallery. The raising to both sides was carried out from the inset point. The double-rail tunnel in the direction of Letňany station is 494 m long, and in the direction of Prosek station 793 m long.

2 GEOLOGICAL CONDITIONS OF THE LINE IV.C2

The bed sequence of the rock environment is similar for both driven lines of running tunnels on the line IV.C2, and it is formed from its top by quaternary sediments and landfills with thickness from 5 to 12 m. These are mostly loess, loess loams and clay-silt-sand loams with detritus (S, D+E). In addition, they are followed by cretaceous formations. The top layer is formed by marlstones (marls) with total thickness from 5 to 10 m. Marlstones (SL) are of various level of consolidation and variable strength. The rock is characterised by tabular and rectangular jointing. Under the marlstone layer, there is a layer of light grey clays (J), which merge into yellow-brown to yellow-grey mudstones. This layer is practically impermeable, it follows the undulating base of marls, and its stable thickness is ca 4 to 6 m. Below, there is a thin layer of glauconitic argillaceous sandstone (GL) with thickness from 1 to 2 m. Its strength is relatively low. Under the layer of soft glauconitic sandstone, there is a formation of quartz Cenomanian sandstones (P), mostly fine-grained. Locally softer layers are crumbly and slack easily into sand. The rock is characterised by tabular and rectangular jointing, with two main systems of fissures, almost perpendicular to each other. Basal chalk formation of clays and mudstones altered with sandstones is located in the sandstone bedrock. These are black chalks with local small coal beds that occur under tunnel bottoms.

In terms hydrogeology, this is an environment with 2 horizons of underground water. There is a turonian

groundwater body based on marlstones with the thickness up to several meters that in some places negatively affected stability of the extraction. This body at some points slightly declines into the layer of impermeable mudstones. In addition to this upper level of underground water, there is also a second (lower) level of underground water in sandstone layers above the grey-black mudstone level. This lower level of underground water revealed itself occasionally by minor outbursts at the bottom of tunnels.

Cenomanian sandstones (P) represented the best geological environment for metro line tunnels on IV.C2 construction. Extractions showed minimum distortion, and also subsidence was low. Increased distortion of extractions and subsidence occurred at the moment, when the tunnel profile started "emerging" from sandstones to the layer of soft mudstones, which tend to press into the extraction profile (confirmed by inclinometer). Problems increased as soon as water tightness of mudstones was disturbed and underground water from lower layers of saturated mudstones started leaking into the extraction. Mudstone layers located in the upper bed of the tunnel have one more negative feature – they create relatively very narrow sunken cauldron. As compared with driving of the same tunnel profile, for example in the environment of less strong Ordovician shalestones, subsidence in the extraction tunnel axis is comparable, but distortion in marlstones disappears quickly at extraction edges. This causes increased frequency of defects in buildings of the aboveground development, in particular when the building reaches above the tunnel extraction only partially.

3 DOUBLE-TRACK TUNNEL LINING

All cross-sections of the double-track tunnel have a shape of a closed flat oval, the dimensions of which respect metro's structure gauges, the arrangement of technical facilities of line tunnels, or eventual suspension of the rail body to reduce the noise and vibration effects on the aboveground development in sections with a low overdburden. Basic profile of the double-track tunnel is designed for the distance between line axes of 3.7 m, with the stope area of 62.20 m^2. For sections where continuous increase of the distance between line axes takes place, other increased profiles of the double-rail tunnel have been designed: 3.9 m, 4.4 m, 5.0 m, 5.8 m and 6.5 m. Jump increase of the tunnel profile is always carried out in these sections.

The double-rail tunnel lining is double-skin lining with closed intermediate foil water-proofing. The outside primary lining is made of shotcrete SB 25 with variable thickness from 200 mm to 350 mm, depending on the actual geological conditions. Water-proofing foil and the inside lining were carried out after a long time interval, after completion of the entire tunnel. The inside lining is made from the monolithic reinforced concrete C 25/30 with the minimum thickness of 400 mm.

4 DOUBLE-TRACK TUNNEL IN THE ROUTE SECTION LÁDVÍ-STŘÍŽKOV

In the most part of the driven tunnel, the distance between line axes is 3.70 m. Only before the portal of manoeuvring rails at Ládví station, the distance of tracks increases gradually up to 4.66 m. The tunnel was driven using a new Austrian tunnelling method (NRTM). Rock disintegration from the west portal was made by a jib cutter Eickhoff 380 with a cross-head. Driving was made in chalk siliceous sandstones with the upper bed of glauconitic sandstone, which with the progressive driving intervene with the extraction. The face of heading was mostly dry without underground water effects. Rock disintegration in driving process in the opposite direction from the east portal was made using a tunnel excavator Schaeff ITC 312. Blasting operations were used for stronger rock layers to a limited extent. Driving was carried out in complicated geological conditions, with rotten and fissured marlstones in the upper bed and the top section of the tunnel profile, and soft mudstones at the tunnel bottom. With respect to underhand driving, the face of heading was affected by underground water due to relatively permeable upper bed. In spite of that, distortions of the extraction were minimal, and also subsidence was small.

Tunnelling in the location, where the double-rail tunnel passes in the close proximity under foundations of bridges for the multilevel junction of Liberecká a Střelničná street was technically the most demanding and also the most interesting section. Within the driven double-rail tunnel, underpinning of medium bridge supports to minimise subsidence caused by tunnel driving, and a method of subsidence levelling at abutments were realised.

5 DESCRIPTION OF BRIDGE STRUCTURES

The bridge structure consists of two independent bridges. Each bridge contains two traffic lanes, 2×3.5 m of width, and a sidewalk, 3.5 m of width. In Liberecká street located under these bridges, there is a four-lane motorway with a central strip and slip lanes with total width of 25 m. The bridge in its longitudinal direction consists of three indeterminate structures of three fields with pairs of medium jugglers with split hinges in base footings. The bridge deck is embedded simply on steel friction bearings of arch abutments. The bridge deck span is $10.80 + 24.60 + 10.80$ m. Its

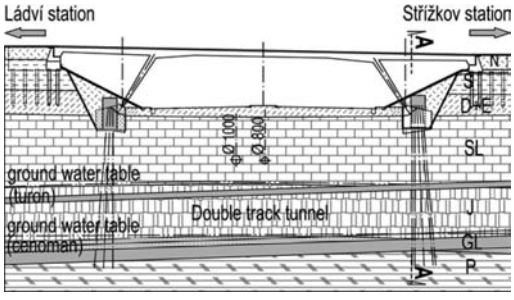


Figure 1. Longitudinal sections of bridges in Liberecká street.

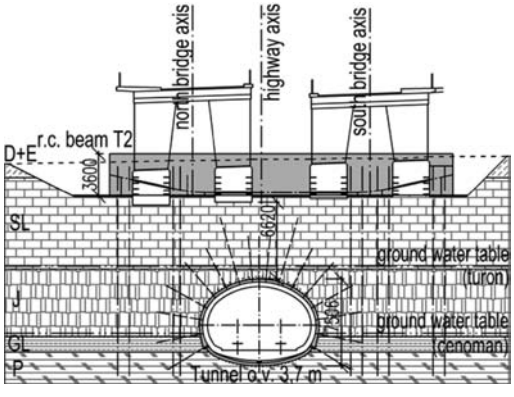


Figure 2. Cross sections of bridges in Liberecká street.

span at the level of base slabs of frame legs is 31.40 m. Arch abutments and bridge wings are embedded on 4.5 m long reinforced concrete piles.

6 TUNNELLING UNDER BRIDGE STRUCTURES

When driving the tunnel under these bridges without taking additional technical measures, subsidence up to 40 mm may occur according to results of mathematical modelling. Based on geo-monitoring results in the driving section outside bridge structures, we can retroactively state that actual subsidence would be up to 30 mm, the existing bridge structure is however not capable to transfer these distortions. To minimise this subsidence, the project designer have proposed underpinning of base slabs of central supports using two teaming pre-stressed reinforced concrete beams embedded on injected micro-piles, the base of which reaches under the bottom level of the metro tunnel. The coupled reinforced concrete beam, 1,600 mm of width and 3,600 mm of height, has connected all 4 base slabs of both parallel bridges. With the proposed method of bridges underpinning, the settlement of central supports has been calculated up to 8 mm at the most.

Subsidence of arch abutments have been levelled using hydraulic presses fitted between abutments and the lower face of the bridge deck. Base slabs plates inserted between the lower and upper bearing section have been used for adjustment.

Other measures have been taken in order to reduce subsidence of bridge structures when driving the tunnel under bridges in 80 m long section. Procedures and outfitting means have been selected so that there is minimum occurrence of distortions of the ambient rock environment. This applies in particular to the max. length of unfitted 1 m attack, the use of self drilling anchoring bolts, densification of 4 m long piles, increasing the thickness of consolidation coating of the extraction, providing the heading face with shot-concrete after each attack, etc. Bottom removal and closing the shell of primary lining was carried out in the distance of 4–6 m from the extraction head. Behaviour of the head in the course of tunnelling in mudstone layers was verified by monitoring before driving under base slabs of the bridge. When driving under sewer collectors in the middle of Liberecká street, it was necessary to proceed with shortened arch anchorage in the top section to avoid drilling in gullies. The entire section was driven using restricted blasting operations, while blasting was completely banned under sewers.

It was unconditionally necessary in the course of tunnel driving to monitor disruptions of the bridge structure by accurate differential levelling. Based on this measuring, it was then decided on subsidence levelling. At the point of arch abutments, subsidence up to 14 mm was observed. Since the limit differences of subsidence determined by the structural engineer were exceeded (max. 5 mm), rectification and levelling of the difference in elevation has been subsequently carried out.

Maximum subsidence measured on supports was 7.5 mm; maximum irregular settlement at the level of supports was 1:1064.

In conclusion, we can state that the measures taken to reduce the extent and irregularity of subsidence of pre-stressed reinforced concrete bridges of the multilevel junction of Liberecká and Střelničná streets were very effective. Project designer's assumptions corresponded well with the reality, and the proposed technical solution of bridge securing when driving the tunnel underneath was correct.

7 DOUBLE-TRACK TUNNEL IN PROSEK-LETŇANY ROUTE SECTION

Basic axial distance between lines of the running double-rail tunnel is 3.70 m and increases gradually in the direction towards stations up to the value of 3.931 m at Prosek station, and 6.559 m at Letňany station.

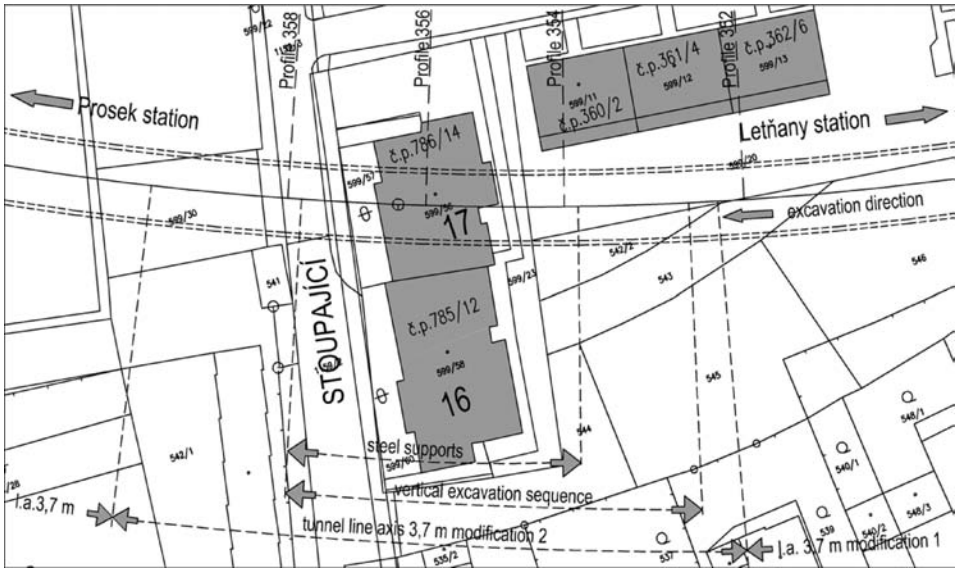


Figure 3. Situation of the metro tunnel under the development in Stoupající street.

The tunnel was driven also by NRTM. Disintegration of rock from the inset point towards Letňany station was carried out using a tunnel excavator Liebher with the assistance of blasting operations. Driving was carried out without difficulties, with minor inflows of underground water. Increased inflows into the underground work occurred at the end of the section, where part of the calotte reached the boundary between mudstones and marlstones. The extraction from driving showed minimum distortion and there was just minor terrain subsidence.

Driving in the direction of Prosek station was also carried out using a tunnel excavator, but without blasting operations. Except for the first 200 m of the tunnel, the driving was carried out in very difficult geological conditions, shallowly under the residential development. Increased disruptions of the extraction and terrain subsidence started occurring when shallow mudstones began to reach the calotte of the extraction. Passing under residential buildings in Stoupající street proved to be the most difficult section in terms of driving, where the horizontal arrangement of the extraction was changed to vertical arrangement. Driving was carried out in complicated geological conditions.

8 ABOVEGROUND DEVELOPMENT IN STOUPAJÍCÍ STREET

The tunnel route passes almost vertically under the building no.17 (č.p.786/14), with adjacent building no.16 (č.p. 785/12), see Fig. 3. The upper bed of the tunnel before the buildings mentioned is ca 12 m thick, and it is reduced to ca 10 m behind these buildings, where ca 3 m are formed by backfills and quaternary soils, and the rest by chalk marlstones (cretaceous marls). The tunnel route continues almost vertically under the local road in Stoupající street, where a sewer gully of 1,300 × 2,100 mm is located. The elevation of the upper bed up to the road level is ca 10 m, ca 6 m of which are formed by marlstones, and the rest upper layer by deluvial soils and sands covered with a loess layer.

Construction works in Stoupající street show many deficiencies. Although in terms of their layout these are two detached residential buildings, their structure is not separated. These are brick buildings with reinforced concrete ceiling panels. Buildings have 4 and 5 aboveground storeys; the floor of the lowest storey is with respect to the ground slope divided into several elevation levels. Buildings are founded on benched wall footings made of mass concrete. Soon after the final building approval, particularly the building no.16 encountered many defects of its structure. It was the case of breaks in building walls caused by movement of the lower building section down the slope. The following causes have been determined: inappropriate foundation method, inappropriate supporting construction, and inappropriate building layout. In 1999, the foundation of the building no. 16 was redeveloped using jet-grouting piles under wall footings. Redevelopment also included installation of linkages connecting both sections. After completion of this redevelopment, control measuring of subsidence was carried out showing stabilised condition of the building.

Table 1. Review of calculated values and actual values measured during tunnelling.

	Mathematical model		Real state	
Arrangement	Horizontal	Vertical	Horizontal	Vertical
Subsidence in tunnel axis [mm]	41.8	16.9	37	18
Max. cross gradient of the valley	1:170	1:800	∼1:300	∼1:600
Extraction arch crown decline measured [mm]	43.3*	18.7*	12–14	6–8

*Total subsidence of the point, incl. subsidence before completing the primary lining and fitting measuring points.

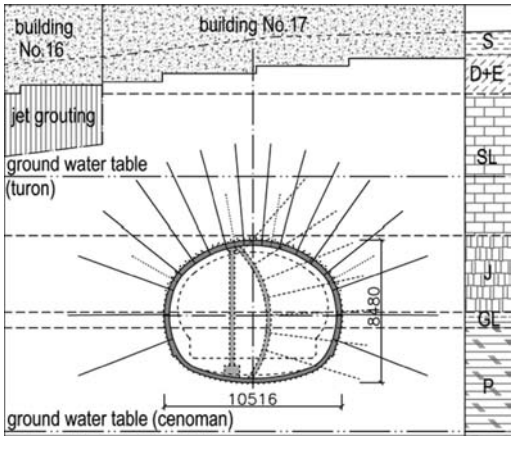


Figure 4. Cross profile of the tunnel under the building no. 17 in Stoupající street.

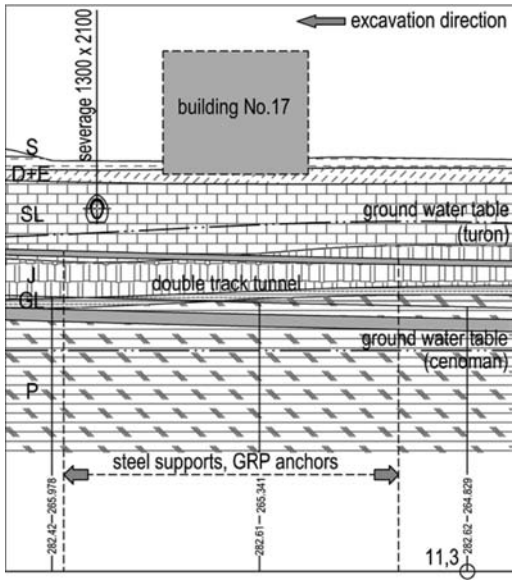


Figure 5. Longitudinal profile of the tunnel under the building no. 17 in Stoupající street.



Figure 6. Driving the left partial extraction.

9 TUNNELLING CONCEPT UNDER BUILDINGS ON STOUPAJÍCÍ STREET

During preparation of the building permit documentation (DSP), and in particular the documentation for the contractor selection procedure (DZS), the party preparing the construction-technical survey of the aboveground development warned about poor technical condition of buildings on Stoupající street. For these reasons, a 2D mathematical model (program MISES 3) was created at the beginning of 2003 using the Finite Element Method, where 2 methods of tunnelling were simulated in given geological environment. It is divided between regularly anticipated driving with horizontal arrangement and driving with vertical arrangement of the extraction. The purpose of this model was to compare the extent of maximum distortion of the terrain above the tunnel, synclinal valley width, and maximum cross gradient in the valley. Based on results of this mathematical model, technical condition of buildings and geo-monitoring results from previous sections of the driven tunnel, it was decided on driving with vertical arrangement of the extraction of 60 m in the area of Stoupající street. The table 1 contains a review of calculated values and actual values measured during tunnelling.

10 DRIVING PROCEDURE UNDER BUILDINGS IN STOUPAJÍCÍ STREET

For the primary lining design of the tunnel driven shallowly under the development, minimisation of rock mass distortions and thus maximum subsidence reduction of the terrain, incl. the aboveground development, is necessary. In our case, the lining was designed from reinforced shot-concrete SB 25 with 300 mm thickness. The temporary middle wall in case of vertical arrangement was 250 mm thick. Other outfitting elements include 9 m long piles from steel self-drilling bolts, and up to 6 m long rock anchors from steel self-drilling bolts. Piles and anchors that reached to the second partial extraction were made of laminated self-drilling bolts. Drilling from the access gallery towards Prosek station was carried out with horizontal arrangement. At the distance of ca 30 m before the building no. 17 (Fig. 3), drilling with vertical arrangement was applied, i.e. the left partial extraction was driven first.



Figure 7. Driving the right partial extraction.

Upon completion of ca 20 m long extraction, 35 m long longitudinal laminated anchors with grout were built in the upper section of the heading, where mudstones were encountered (ca 1 anchor/1.5 m^2 of the heading area, total of 11 anchors). This additional measure was to prevent against extrusion of mudstones into the extraction heading. Subsequently, it was followed by driving the remaining left partial extraction of ca 40 m with the maximum 1 m advance per attack. With respect to the size of driving mechanisms, it would not be possible to maintain the temporary middle partition wall during subsequent driving of the right partial extraction. Therefore another additional measure was proposed under the building no.17 in the length of 40 m to reduce building subsidence.

In the left partial extraction, a temporary wall footing was concreted at the bottom of the primary lining that was fitted with iron props (tubes with Ø279/8 mm) in the interval of 2 m. They were activated by filling the contact of the prop head and the primary lining with shot-concrete. When driving the right partial

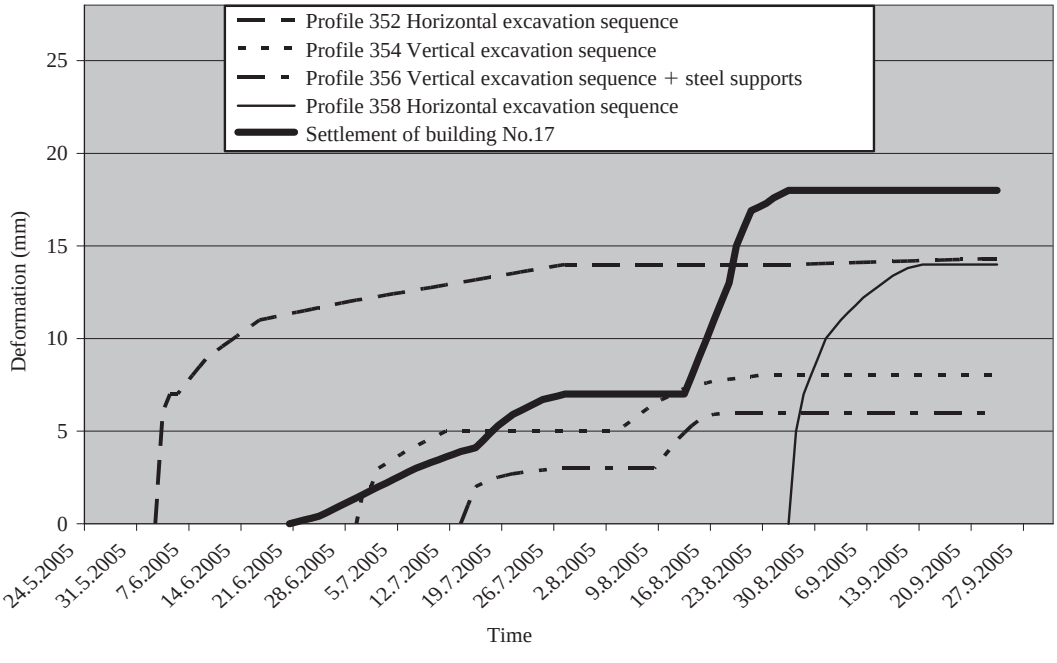


Figure 8. Diagram of the course of distortion of the tunnel extraction arch and settlement of the building no.17.

extraction, the temporary middle wall was gradually demolished and vertical load was transferred to metal props.

These were removed after the shot-concrete of the primary lining of the right tunnel side hardened to its required strength. Efficiency of this measure was verified by measuring of temporary props load. It ranged between 800 to 1000 kN, which corresponded very well with the static calculation. Distortions of the primary lining after props removal ranged between 1 to 2 mm, at the very border of measurability. This also indicates efficiency of this supplementary measure.

11 EVALUATION OF CONVERGENT MEASURING AND SETTLEMENT OF THE BUILDING NO.17

In that situation (Fig. 3), selected convergent profiles with measured extraction distortions are indicated. The diagram in Fig. 8 shows time-dependent vertical displacements of the tunnel arch top. For comparison, there are measured values of the maximum settlement of the building no. 17 stated in the diagram that correspond with respective convergent profile 356, installed in the same place. It is apparent that the measured vertical displacement of the top of the tunnel arch amounts to ca 30 to 40% of the total terrain settlement. Profiles 352 and 358 are in sections, where driving with horizontal arrangement is applied, profiles 354 and 356 are in sections, where driving with vertical arrangement is applied.

12 CONCLUSION

The measures taken to reduce subsidence of the critical building no.17 in Stoupající street were very efficient. They were however very demanding in terms of time and finances. Removing statically unimportant defects in the residential development in sections with horizontal arrangement of the tunnel extraction is naturally considerably easier. It is therefore necessary to always consider use of these procedures and to select them in urgent cases only, in particular if the static function of the building passed under is jeopardised, or eventual faults removal in the building would be unacceptable for financial or other reasons.

This page intentionally left blank

Underground Space – the 4th Dimension of Metropolises – Barták, Hrdina, Romancov & Zlámal (eds)
© 2007 Taylor & Francis Group, London, ISBN 978-0-415-40807-3

Development of grade separation structures with small cross-sections

M. Shimizu, A. Watanabe & T. Genjyun
East Japan Railway Company, Tokyo, Japan

M. Kurisu, Y. Hagihara & T. Maeda
TEKKEN CORPORATION, Tokyo, Japan

H. Watanabe
JTEC Co., Ltd., Tokyo, Japan

ABSTRACT: A technique of building structures that traverse under existing railways or roads has been developed to construct small section grade separation structures such as footpaths and channel boxes without using an open-cut method. This method allows construction of a structure with a rational section under a road or track protection composed of steel plates and steel supports. This paper outlines this method and reports on the series of verification tests conducted prior to practical application.

1 INTRODUCTION

In recent years, more cases have been seen in Japan of non-open-cut methods used for building structures that cross under roads or railway tracks.

Non-open-cut methods include several techniques. Crossing structures under roads and railway tracks that use conventional non-open-cut methods are intended mainly for large section roadway boxes and their direct application to small section structures such as footpaths and channel boxes may end up with disproportionately large protection (including auxiliary methods) for the scale of the structure. As has been pointed out, this method results in protective measures occupying an excessively large proportion of the construction costs. In element methods that do not require special road or track protection, the sizes of elements are limited by workability requirements, which results in construction work that is disproportionately large for small-scale structures and comparatively high prices. To address these issues, a method called COMPASS (COMPAct Support Structure) has been developed as a method of construction of small section grade separation structures that allows rational structural sections and is more economical than the conventional methods. In this method, a structure with a rational section is built under a road or track protection composed of steel plates and steel supports. Steel plates are pulled and inserted along the circumference of the planned structure that has been previously cut with an earth cutting wire. The steel supports are installed when the inside of the steel plates has been excavated with a cutting unit. These components function as part of the road or railway track protection and the plates and supports respectively provide the outer form for the building of the structure and part of the structure. This paper reports on the results of the series of construction tests conducted prior to practical application of the COMPASS method.

2 OVERVIEW AND CHALLENGES OF COMPASS METHOD

2.1 *Overview of COMPASS method*

Figure 1 shows the construction processes of the COMPASS method. In this method, two earth cutting wires (11 mm in diameter) are provided, with one over the other, to first cut the ground, steel plates (22 mm thick) for protection are inserted in the cut ground and the structure is built inside the steel plates. The supports erected when the inside of the steel plates has been excavated (the lower slab and sidewalls are wide-flange beam supports and the upper slab a truss support) are not removed and embedded in concrete, forming inside the steel plates an SRC (steel plus reinforced concrete) structure.

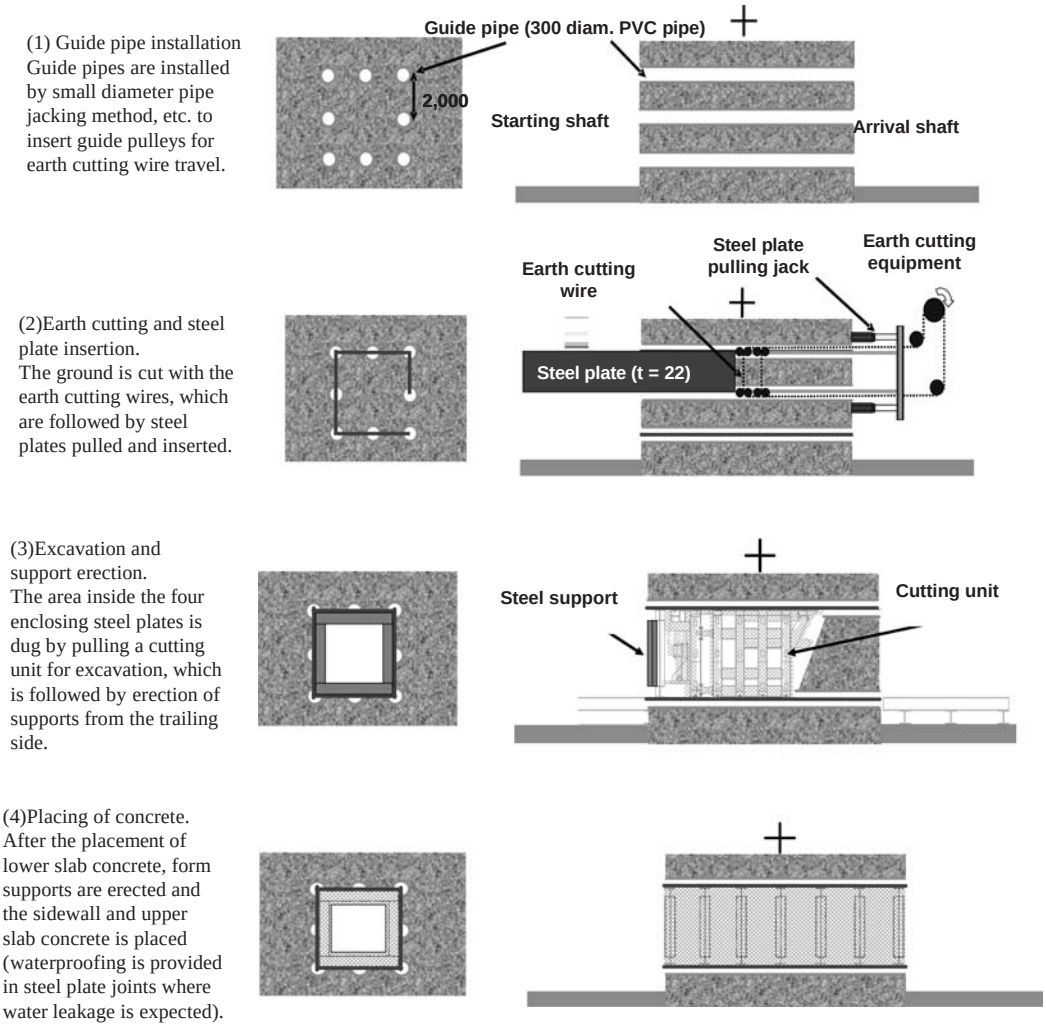


Figure 1. Construction procedure of COMPASS method.

2.2 *Challenges*

For the method to be put into practical use, the following issues have been found to require solutions:

(1) The friction between the ground and steel plates generated during the insertion of the plates may move the soil above horizontally.
(2) Because steel plates with lower rigidity than conventional pipe roofs (steel pipes) are used as protection, excessive vertical displacement may be generated.
(3) Insertion of steel plates must be possible in the ground with obstacles such as large gravel and cobble stones.

To address these issues, tests for earth cutting/inserting steel plate, for excavation of the inside of the steel plates with a cutting unit and for placing upper slab concrete have been conducted for verifying the practicability of the method.

3 TEST FOR EARTH CUTTING AND INSERTING STEEL PLATES

3.1 *Test overview*

Figure 2 shows an overview of the test and Figures 3 and 4 illustrate test conditions. For the test, simulated

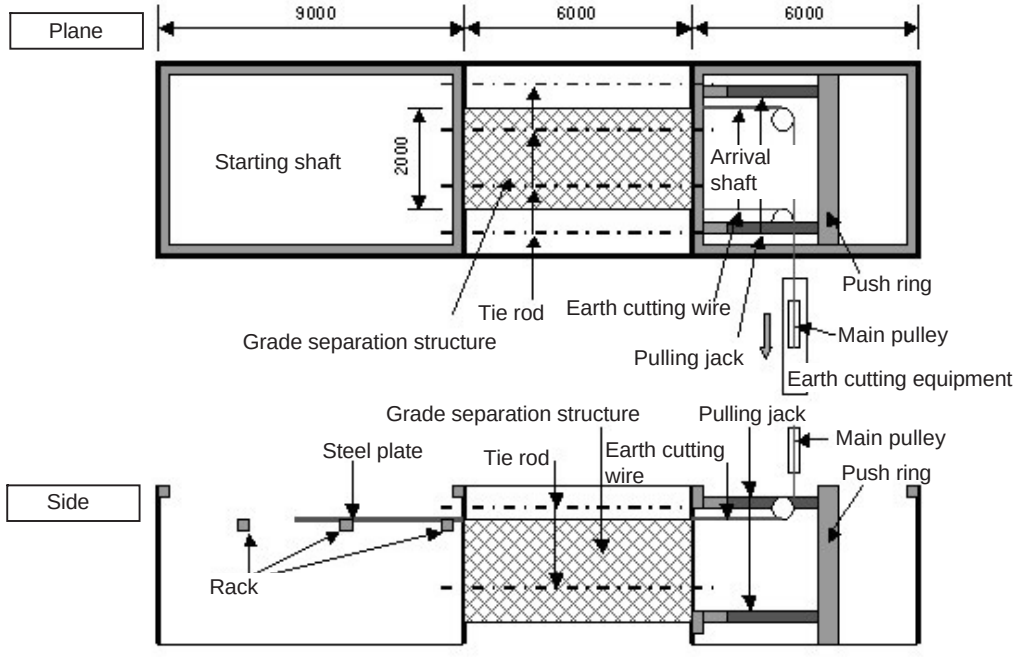


Figure 2. Overview of earth cutting and steel plate insertion test.

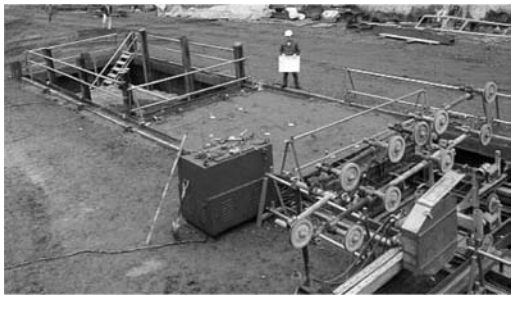


Figure 3. Test for earth cutting and inserting steel plates (full view).



Figure 4. Test for earth cutting and inserting steel plates (starting shaft).

ground of sandy soil was made by mixing 20 percent gravel of 80–350 mm diameter between the starting and arrival shafts (6.0 m in length). This sandy soil was cut by pulling the earth cutting wires with the earth cutting equipment installed beside the arrival shaft while a steel plate was pulled with a traction apparatus composed of a pulling jack and push ring. The steel plates measured 2.0 m in width and 22 mm in thickness. The plates were inserted starting with the upper slab and then the lower slab and vertical walls (left and right) in that order to form a square section of 2.0 m by 2.0 m. The simulated ground made was found to have an N value of approximately 5 as determined by a rapid dynamic cone penetration test. The N value distribution in the simulated ground is shown in Figure 5.

In addition to the vertical and horizontal displacements of the simulated ground, behavior of the wire drive unit was measured. Table 1 lists the items measured in this test, where the axial torque of main pulley refers to the torque of the hydraulic pulley that runs the earth cutting wires, and the value increases when gravel is cut or the pulling speed is rapidly increased[1)]. Figure 6 shows the plan of measurement points for vertical and horizontal displacements. The vertical and horizontal displacements are measured at positions of 0.3 m earth covering.

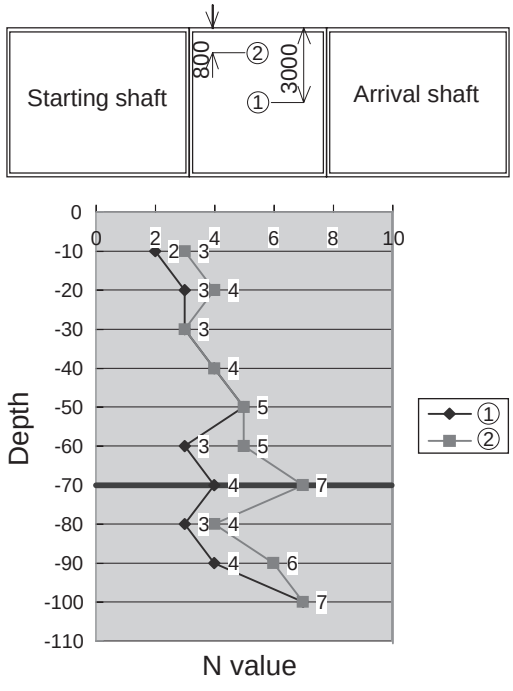


Figure 5. N value distribution in the simulated ground.

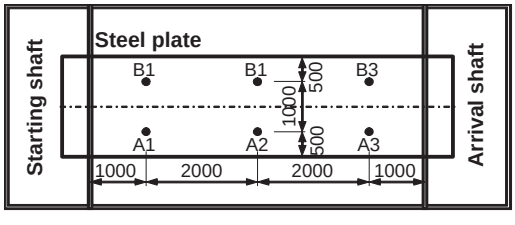


Figure 6. Plan of displacement measurement points.

3.2 *Test results*

3.2.1 *Steel plate insertion*

The appearance of the steel plates as their insertion is complete is shown in Figure 7. The plates were inserted as planned without being hampered by gravel and a square section was successfully formed. No rupture of the earth cutting wires occurred. Figure 8 shows gravel cut with an earth cutting wire.

3.2.2 *Vertical and horizontal displacements of the ground*

Figures 9 and 10 show vertical and horizontal displacements of the ground during the insertion of the upper slab. Horizontal displacement toward the arrival shaft is taken as positive and that toward the starting shaft as negative. While some variation was observed for either case depending on the point of measurement,

Table 1. Items measured.

Items measured	Measurement interval	Measuring instrument
Vertical displacement		
Upper slab	Per 100 mm advance of the steel plate	Level
Other	Per 500 mm advance of the steel plate	
Horizontal displacement		
Upper slab	Per 100 mm advance of the steel plate	Electro-optical measuring device
Other	Per 500 mm advance of the steel plate	
Pulling force of the steel plate	Per 100 mm advance of the steel plate	Load cell
Pulling speed of the steel plate	Per 100 mm advance of the steel plate	Stroke meter



Figure 7. Steel plate insertion completed.

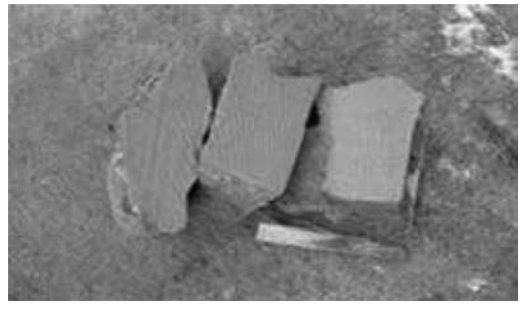


Figure 8. Cut gravel.

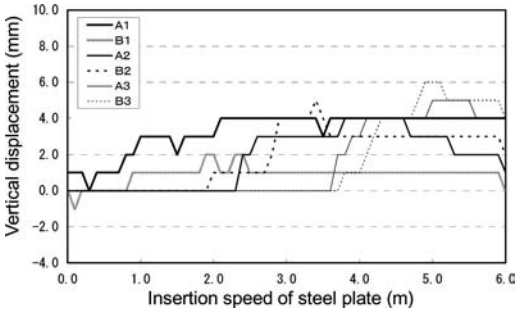


Figure 9. Vertical displacement (during insertion of upper steel slab).

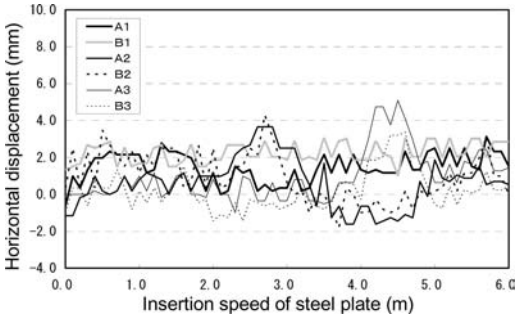


Figure 10. Horizontal displacement (during insertion of upper steel slab).

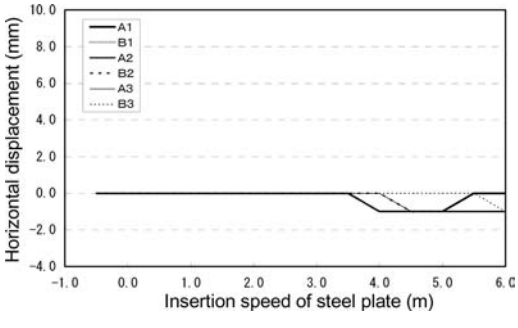


Figure 11. Vertical displacement (during insertion of lower steel slab).

vertical displacement of up to 6 mm was induced with an average of 3 to 4 mm and horizontal displacement toward the arrival shaft of up to 5 mm with an average displacement of 2 to 3 mm.

Almost no vertical or horizontal displacements were observed during the insertion of the sidewalls and lower slab. Figure 11 shows the vertical displacement during the insertion of the lower slab.

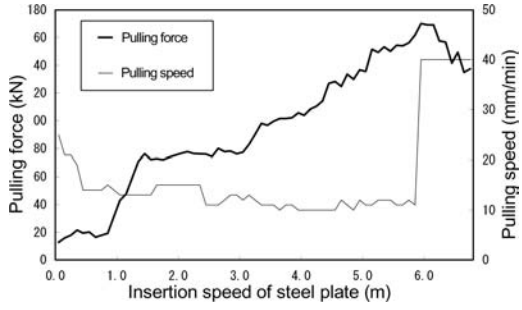


Figure 12. Pulling force vs. pulling speed (during insertion of lower steel slab).

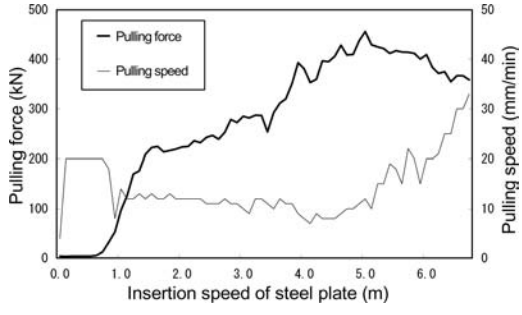


Figure 13. Pulling force vs. pulling speed (during insertion of vertical steel plate).

3.2.3 *Pulling speed and pulling force*

Figures 12 and 13 show the results of the measurements of the pulling speed and force during the insertion of the lower slab and vertical steel plate (on the right side as seen from the starting shaft). These figures indicate that, with a constant pulling speed maintained, the pulling force increases as the friction area between the steel plate and natural ground becomes larger.

The pulling force during the insertion of the vertical steel plate is larger in value than during the insertion of the lower slab. This is presumed to be because, for this test, the vertical steel plate was inserted as engaged via joints with the upper and lower slabs inserted earlier, which generated engaging friction.

4 TEST FOR EXCAVATION OF THE AREA INSIDE OF THE STEEL PLATES WITH A CUTTING UNIT

4.1 *Test overview*

The procedure of this test is shown in Figure 14 and the excavation conditions inside the steel plates in Figure 15. For this test, the inside of the steel plates which had been inserted in the test for earth cutting

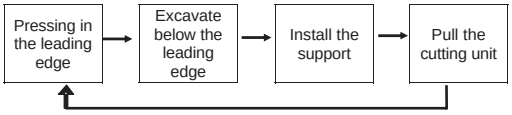


Figure 14. Test procedure.



Figure 15. Test (during excavation).

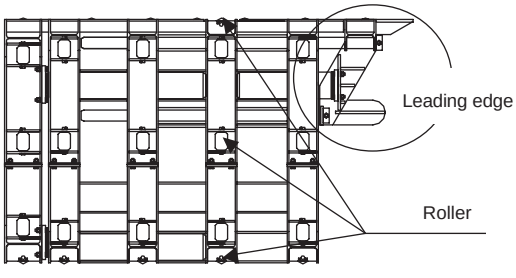


Figure 16. Cutting unit overview.

and inserting steel plates, was cut with the cutting unit specifically designed for excavation of the area inside the plates, and steel supports (H-250 ×250, 1.0 m spacing) were installed. Figure 16 and Figure 17 show the overview of the cutting unit. This unit has a leading edge that is extendable from the unit by means of hydraulic jacks, which makes it capable of being pressed into the ground first. The four sides of the unit that come in contact with the steel plates have rollers, which support the plates as the cutting unit moves forward, and contribute to the reduction of friction between the unit and steel plates. The cutting unit was pulled by pulling prestressing steel bars using the four hydraulic jacks installed on the arrival shaft. As with the test for earth cutting and inserting steel plates, vertical displacement was measured at positions of 0.3 m of earth covering on the upper slab for this test. Figure 18 shows the plan of measurement points.

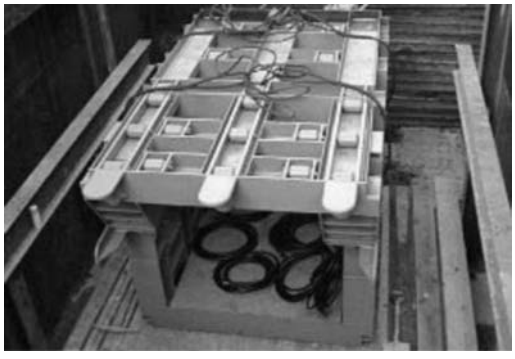


Figure 17. Full view of cutting unit.

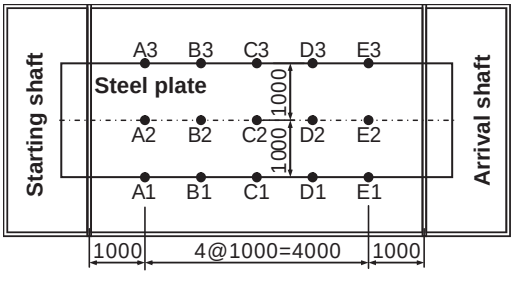


Figure 18. Plan of vertical displacement measurement points.

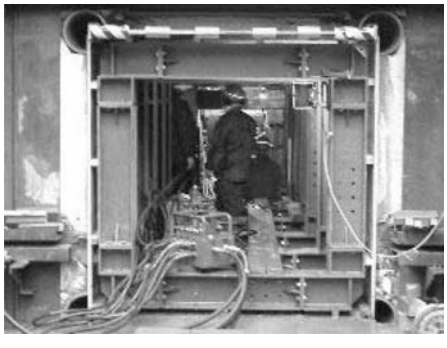


Figure 19. Test completed.

4.2 *Other results*

Figure 19 shows the view at the completion of the test and Figure 20 the results of the vertical displacement measurement at the end of the test. Settlement of up to 23 mm was observed in this test. Study of the settlement of the individual stages of the work reveals that there was a certain tendency toward heaving during the pressing in of the leading edge and erection of supports but almost no displacement was generated during the pulling of the cutting unit, which indicates that the settlement occurred during the excavation.

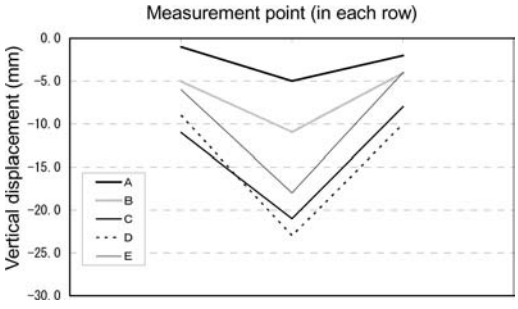


Figure 20. Results of vertical displacement measurements (at completion of test).

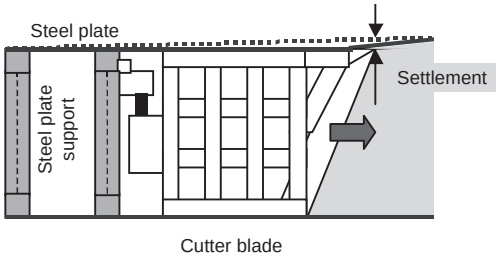


Figure 21. Schematic diagram of cause of settlement during excavation.

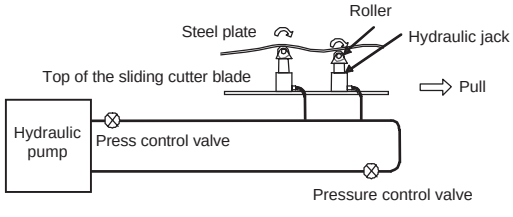


Figure 22. Overview of the adjustable height roller.

A possible cause of the settlement during the excavation is the slightly upward insertion of the steel plate that generated a gap between the plate and the cutting unit, which was horizontally pulled for digging, resulting in the settlement as large as the gap. Figure 21 is a schematic diagram of the cause of settlement during excavation. Regarding this problem, settlement is presumed to be controllable by replacing the roller mounted on the cutting unit with adjustable height units. Adjustable height rollers have also been tested and their ability to support flexibly according to the irregularity of steel plates has been verified. Figure 22 shows an overview of the adjustable height roller.

5 CONCLUSIONS

A series of tests of construction using the COMPASS method have been completed and the following conclusions have been reached. In addition, practicability of the technique has been verified:

(1) The mechanism of earth cutting and steel plate insertion used in this test allows insertion of a steel plate of 2.0 m in width and 22 mm in thickness into ground that contains gravel.
(2) During insertion of a steel plate, no displacement that is large enough to affect the track is generated.
(3) Although settlement of about 23 mm occurred during excavation inside the steel plates, settlement can be controlled by using adjustable height rollers on the cutting unit.

REFERENCES

Ota, Ito, et al., October 2003. Underground Steel Plate Insertion Test (Application to Gravelly Ground), *58th Annual Conference of the Japan Society of Civil Engineers*: VI-168

Arimitsu, Nagao, et al., October 2003. Underground Steel Plate Insertion Test (Application to Sandy or Cohesive Soil Ground), *58th Annual Conference of the Japan Society of Civil Engineers*: VI-167

Arimitsu, Nagao, et al., September 2004. Construction of Small Section Box Culvert by Earth Cutting No. 1, *59th Annual Conference of the Japan Society of Civil Engineers*: VI-217

Abo, Arimitsu, et al., September 2004. Construction of Small Section Box Culvert by Earth Cutting No. 2, *59th Annual Conference of the Japan Society of Civil Engineers*: VI-218

Shimizu, Fujisawa, et al., November 2004. Development of Construction Methods for New Small Section Underground Structures, *Proceedings of Tunnel Engineering Vol. 14, Japan Society of Civil Engineers*

This page intentionally left blank

Underground Space – the 4th Dimension of Metropolises – Barták, Hrdina, Romancov & Zlámal (eds)
© 2007 Taylor & Francis Group, London, ISBN 978-0-415-40807-3

Civil tunnelling with electronic blasting systems – Early experience from Korea

Young-Suk Song
Hanwha Corporation, Commercial Explosives Division, Korea

Dave Kay
Orica Mining Services, Australia

ABSTRACT: To meet the needs of South Korea's rapidly expanding economy, a large number of infrastructure project are under way to improve transportation efficiency within the nation. These projects include high speed rail links between major population centres and improvements to the road network. Being densely populated and geographically mountainous, infrastructure development in Korea requires a significant amount of tunnelling. Owing to the predominantly hard granitic nature of rock, Drill and Blast is the preferred method of tunnel advance. The Korean tunneller, however, faces the same pressures as those of his international counterpart; that both cost and production targets need to be achieved whilst meeting expectations of both community and regulator. The growing acceptance of electronic blasting systems now presents a number of opportunities to the civil tunnelling sector. Conventional initiation systems used for full face firing of large tunnels are hampered by limitation of delay periods and their firing accuracy. The availability of fully programmable and accurate delay systems now open a number of possibilities to the civil tunneller, opposite advance rate, excavation efficiency, perimeter control and environmental conformance. This paper details a series of blasts undertaken at the Kang Chon 1 Tunnel on the 7th Zone of the Kyung – Chun Railway Line Construction. A blast measurement program was undertaken to firstly benchmark two conventional blasts followed by three blasts fired with the i-kon™ Electronic blasting system. Key parameters were measured including rock mass evaluation, tunnel advance, blast fragmentation, perimeter control and vibration. The paper concludes with indications of improvements to perimeter control and a higher confidence level in vibration predication. It then points to further possibilities for electronic blasting systems in civil tunnel applications.

1 INTRODUCTION

South Korea is said to be one of the most mountainous countries in the world with 70% of land mass occupied by rugged terrain. It also has one of the highest population densities in the world. To meet the needs of growing population and industrial development, infrastructure projects are underway to improve transportation links between major population centres. Given the predominant terrain and populous nature of the nation, preference is given to a 'straight line' method requiring significant use of tunnel and bridge for both road and rail construction. Granite and limestone rock are dominant, thereby making drill and blast the preferred method for tunnel advance. Korean civil engineers and tunnellers are therefore faced by a number of challenges, not uncommon to their international counterparts – to complete projects on time, within budget whilst meeting the environmental expectations of both community and regulator. One such project is the Kyung-Chun Railway Line Construction which is providing a complete double track link between the South Korean city of Chunheon and the capital of Seoul.

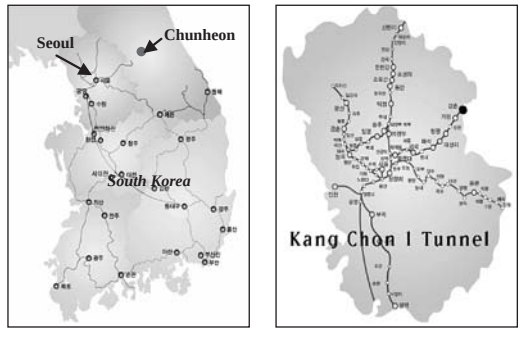


Figure 1. Rail network map of South Korea.

Opportunity arose to fire 3 'full face' tunnel rounds in the Kang Chon 1 Tunnel of the 7th Zone of the Kyung-Chun Line construction using the i-kon™ Digital Energy Control System and perform some preliminary assessment verses conventional pyrotechnic signal tube initiation. It also allowed for a fresh look at initiation timing possibilities for large civil tunnels. This paper is a summary of the results obtained from a series of 5 firings in the Kang Chon 1 Tunnel – 2 preliminary bench marking blasts using conventional non-electric (NE) initiation followed by 3 firings by electronic blasting system (EBS) and modified timings. It should be noted that the results were obtained under 'production conditions' whereby data collection and trial quality were dictated by operational needs. This paper will describe these limitations and attempts made to normalise the results to give performance indicators opposite key aspects of the tunnel cycle including: perimeter control, advance, fragmentation and vibration.

2 THE KANG CHON 1 TUNNEL

The Kang Chon 1 Tunnel is one of several on the 7th Section of the Kyang-Chun Line. It's completed length will be of 2500 m (8197 ft) with cross sectional dimensions of 10.6 m (34.6 ft) wide by 8.4 m (27.6ft) high and a face area of 88 m^2 (946 ft^2). The major rocks present are granite gneiss or banded gneiss with sporadic quartz dykes and scattered cubic jointing observed. A rock mass rating (RMR) gives a result of 66 indicating a medium hardness rock. A 12 hour cycle is worked which includes the following elements : mark-up, drill, charge, fire, excavate, scale, bolt and shotcrete. Typical blasting parameters give 116 (45 mm diameter – 13/4″) shotholes drilled with a V Cut (wedge), with a centre stab hole, for 3.5 m (11.5ft) round depth. Shotholes are charged with 32 mm (11/4″) dia. MegaMITE cartridge explosives and stemmed with wet sand plugs. Perimeter holes are charged with NewFINEX 17 mm (0.7″) pipe charge. Initiation uses a range of millisecond (20 ms) and long period (100 ms) HiNEL, non-electric (NE) detonators. To off-set the timings the face is fired in 4 bunches with the bunches fired with 0 to 42 ms trunkline delays. A conventional face timing is shown in Figure 2.

3 ELECTRONIC INITIATION DESIGN

Given the accuracy and flexibility of the electronic blasting system (EBS) it was decided to redesign the face timing based on a number of good blasting principles. The V Cut timing was left the same as conventional, thus to minimise risk related to cut failure, giving 3 holes firing at any one instant. Once outside the V Cut, timing was set to give single hole firing

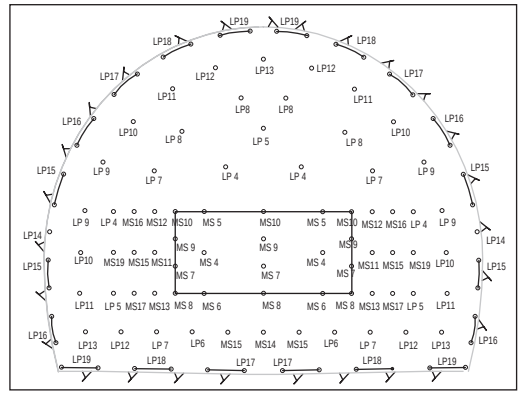


Figure 2. Conventional non-electric timings with MS and LP series detonators.



Figure 3. Change of rock quality in tunnel face.

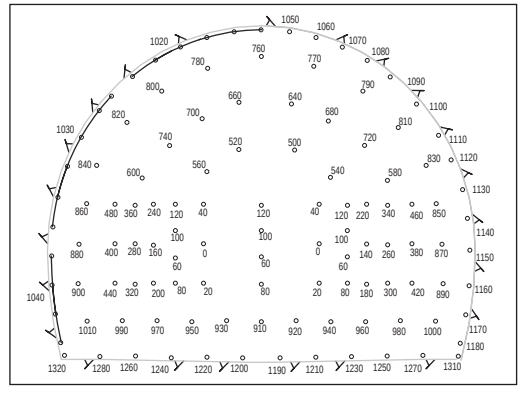


Figure 4. Generic electronic timing used in the blasts.

within a 20 ms window, working direct opposites from the initial cut. With the cut extension removed the face holes were set at 10 ms, off-setting either side of centre. The perimeter was to be fired in 2 halves. One

half was fired in instantaneous batches of 6 holes to gauge the effect of post-split perimeter control, whilst the other half was fired on 10ms delay interval. The delay verses batch firing sides were swapped on alternate firings to negate the effect of geology. The lifter holes were designed to fire on 10ms delay off-set either side of centre. Total blast duration was reduced from 3.2 seconds to 1.3 seconds.

4 TUNNEL CONDITION

During the trialing period a phorphory intrusion entered the left hand side of the tunnel face. This caused a number of poor rounds both with the two non-electric blasts and the first electronic blast. The tunnel contractor decided to increase the number of shot-holes drilled from 116 to 132. This change may have masked some results, however attempts were made to normalise the outcomes by swapping perimeter technique left and right and to compare results only in similar ground. Following is a summary of the results obtained.

5 VIBRATION ANALYSIS

All blasts were monitored for vibration and airblast. Up to 4 monitors were used for each blast spaced along the tunnel at distances of 131 m to 604 m from the tunnel face. To give statistical credibility a further two non-electric blasts were included that were monitored the week previous.

A regression analysis on the above data revealed the following

Furthermore a comparison of the near field vibration traces was conducted. The available vibration recording time was only 2 seconds therefore latter stages of the non-electric blast is missing.

The following conclusions can be drawn from the above data:

1. Comparison of the regression analysis shows that both systems gave similar results for the K (geological constant) and n (reduction level). This is expected in that all the results are taken in the same rock mass with similar explosive weight per delay and indicates that rock mass is not a significant factor for the difference in result. It can however be seen that regression line for the electronic blasts gives an r^2 value of 0.953 compared to 0.653 for the non-electric system. This indicates that the vibration prediction will be far more reliable with electronic blasting.
2. Comparing the vibration traces; it can be seen that the ppv generated in the Cut was slightly higher for the electronic blasting system. This is not surprising as the design allowed for 3 shotholes firing same delay and the accuracy of the EBS would guarantee

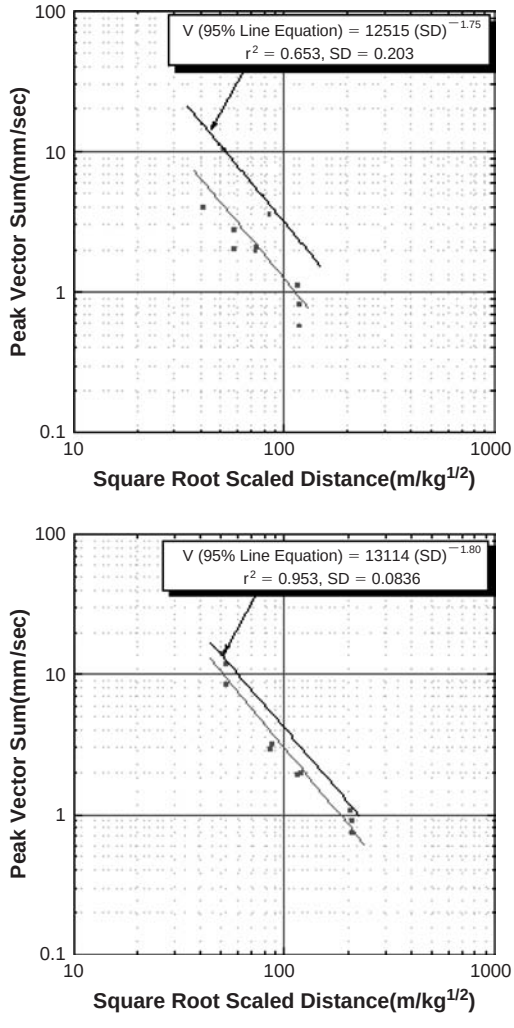


Figure 5. **Non-electric system** & Electronic Blastic System.

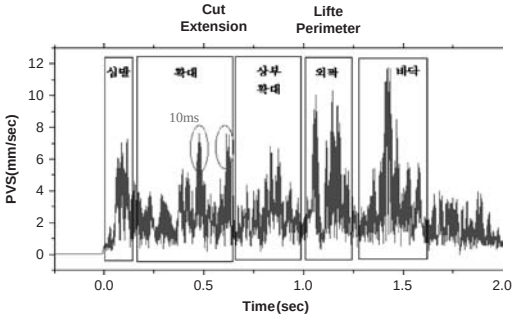


Figure 6. Vibration trace electronic firing.

Table 1. Non-electric vibration and airblast data.

Initiation	Distance (m)	Result: Vibration (PPV, mm/sec) V	T	L	PVS	Airblast dB(A)	Max. Charge wt/delay (kg)
NE 1	290	1.11	2.13	2.68	2.94	105.5	6.375
	131	9.91	4.95	3.67	10.2	108.0	
NE 2	216	2.83	3.37	2.46	3.57	108.0	6.375
	296	0.714	0.826	0.603	1.10	97.4	
NE 3	206	5.75	2.95	1.86	6.54	107	25.5
	291	1.62	1.24	2.22	2.73	74.4	(off-set
	371	1.71	0.92	1.16	1.98	96.0	bunching
	601	0.65	0.45	0.60	0.81	103	not used)
NE 4	209	3.18	2.35	3.38	3.98	107	25.5
	294	1.51	1.44	1.59	2.00	104	(off-set
	374	1.73	1.05	1.29	2.06	94.8	bunching
	604	0.35	0.35	0.52	0.57	101	not used)

Table 2. Electronic vibration and airblast data.

Initiation	Distance (m)	Result: Vibration (PPV, mm/sec) V	T	L	PVS	Airblast dB(A)	Max. Charge wt/delay (kg)
EBS 1	294	1.70	0.619	1.17	1.92	98.2	6.375
	524	0.984	0.667	0.746	1.05	100.0	
EBS 2	134	11.2	5.02	5.21	11.7	98.0	6.375
	219	1.38	2.67	2.56	2.92	102.0	
	299	1.41	1.17	1.75	1.87	98.0	
	529	0.476	0.540	0.873	0.905	101.0	
EBS 3	137	8.26	2.16	2.92	8.37	97.2	6.375
	222	1.51	3.02	2.49	3.13	103.0	
	302	1.48	1.13	1.21	1.94	99.8	
	532	0.460	0.381	0.667	0.730	99.6	

instantaneous firing of these holes. The non-electric system gave higher ppv in the cut extension, due to the fact of more shotholes firing within a tight time window, and the EBS now operating on true single hole firing at 20 ms interval. This is similar with the face where the EBS has true single hole firing and the NE system now operating with multiple holes firing at the upper end of the delay range. The EBS gave higher readings in the perimeter, probably due to multiple holes firing in batches on same delay compared to the NE system. The highest vibration came from the EBS lifter area firing on 10ms delay. The reason for this is not fully understood and needs more work to assess if this is related to reinforcement due to a tight time window. Opportunity exists to refine this in future tests.

6 FRAGMENTATION SIZE ANALYSIS

Fragmentation analysis was conducted for all five blasts using photographic image analysis. An example is shown in Figure 7. The non-electric detonator showed the average (P_{50}) fragmentation size of 34.9 cm verses 31.2 cm for the EBS, indicating a size reduction of 11% with the overall results showing a uniform distribution. No direct conclusion can be draw here.

7 PERIMETER CONTROL

A series of photo's were taken of the perimeter at the completion of each blast for digital analysis, by

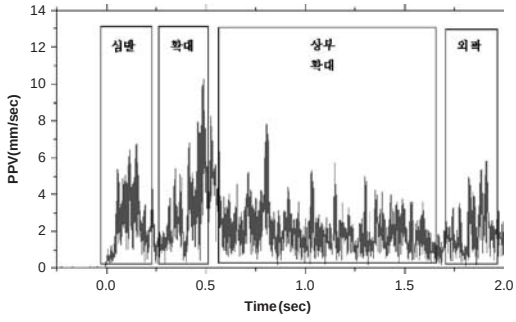


Figure 7. Vibration trace non-electric firing.

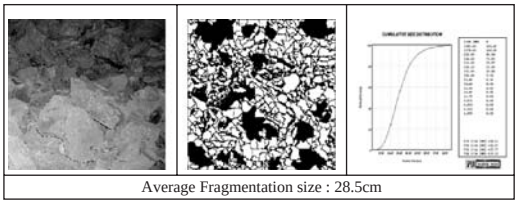


Figure 8. Example of fragmentation analysis.

Table 3. Fragmentation analysis results.

	NE		EBS		
Passing size	1st	2nd	1st	2nd	3rd
P_{20} (cm)	12.9	20.3	15.4	19.2	18.9
P_{50} (cm)	35.3	34.4	33.0	32.3	28.5
P_{80} (cm)	67.2	66.1	51.0	55.1	40.7
Top size (cm)	95.3	115.5	76.9	96.1	82.7

Table 4. HCF of all non-electric perimeters vs all electronic perimeters.

H.C.F Rating	0∼25 V.P	25∼50 P	50∼75 G	75∼100 V.G
NE				
EBS				

assessment of Half Cast Factor (H.C.F). An example of the technique is shown in Figure 8.

Owing to the change in rock type between left hand and right hand side, the results are presented as a series of comparisons between non-electric vs. electronic, simultaneous vs. delay, and the difference between simultaneous vs. delay in each side of the tunnel face.

The following comparisons were obtained using the above analysis technique.

Table 5. HCF of EBS Instantaneous batch vs delay fired perimeter.

H.C.F	0∼25 V.P	25∼50 P	50∼75 G	75∼100 V.G
EBS Instantaneous				
EBS Delay				

Table 6. HCF of EBS Instantaneous batch vs delay fired perimeter.

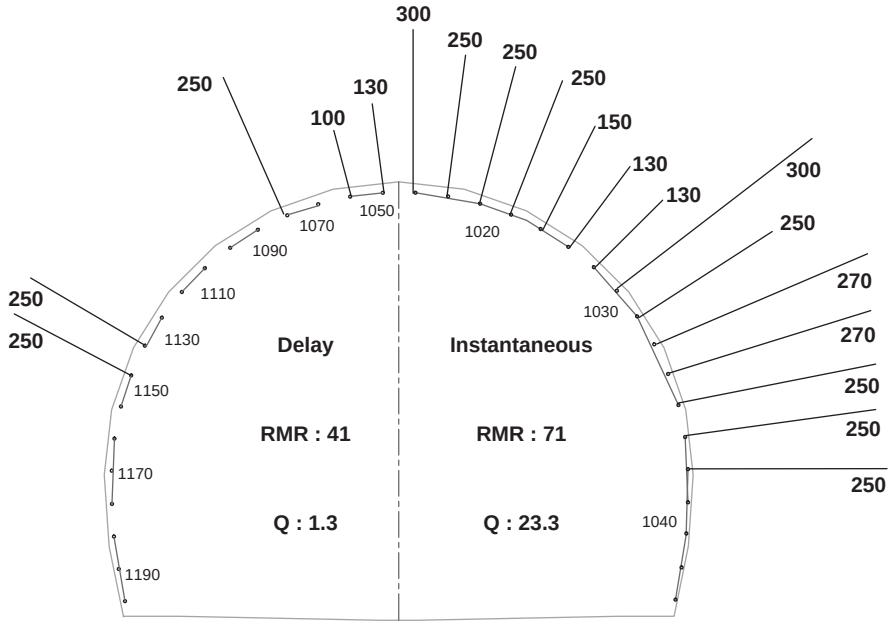
H.C.F	0∼25 V.P	25∼50 P	50∼75 G	75∼100 V.G
EBS Instantaneous				
EBS Delayed				

Table 7. Instantaneous firing vs delay firing in excellent ground (RMR:71).

H.C.F	0∼25 V.P	25∼50 P	50∼75 G	75∼100 V.G
EBS Instantaneous				
EBS Delayed				

Table 4 shows that all non-electric perimeters gave a HCF of 49.7% verses all electronic perimeters with 57.6%. This result is taken in both the left and right side of the tunnel face and with delayed and instantaneous firing. Table 5. compares EBS instantaneous firing with EBS delayed firing of perimeter in both sides of the tunnel. Overall instantaneous firing gave a HCF of 68.85% verses delay firing of 44.75%. Table 6. gives a comparison of instantaneous verses delayed firing in the right hand side of the tunnel where the RMR was 71 (classified as 'excellent' rock). Instantaneous firing gave 82.6% HCF verses 63.1% HCF with delay firing. Table 7. shows the difference between instantaneous and delay firing in the left hand side of the tunnel where the RMR was 41 (classified as 'good'). Instantaneous firing gave 55.1% HCF verses delay firing with 26.4% HCF.

From these results it can be concluded that EBS firing has a positive influence on perimeter control compared to NE firing. It is also concluded that instantaneous firing of perimeter yields better result than delayed firing. The HCF analysis technique confirmed



H.C.F (Half Cast Factor)

H.C.F = 1030/(300×13 holes) = 26.4%

H.C.F = 3220/(300×13 holes) = 82.6%

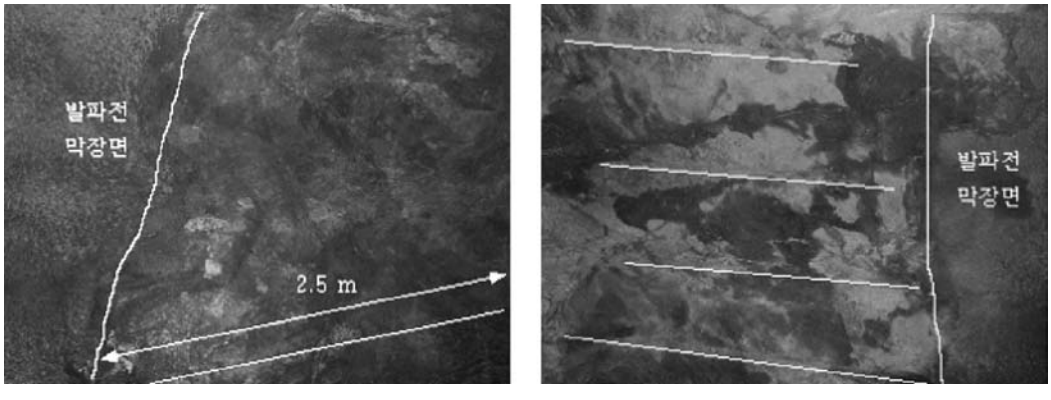


Figure 9. Example of Half Cast Factor analysis.

those observations made in the field where an obvious difference between system was noticed.

8 TUNNEL ADVANCE

Measurements were taken of tunnel advance for each firing. Unfortunately, after some disappointing result due to a change in geology, for both the bench mark blasts and the first electronic blast, more shotholes were added to the round. No direct conclusions can be drawn here, other than the addition of more shotholes is significant to face advance.

CONCLUSIONS

Whilst some of the measurements have yielded no positive result, there are a couple of good pointers to where Electronic Blasting Systems may offer some value to

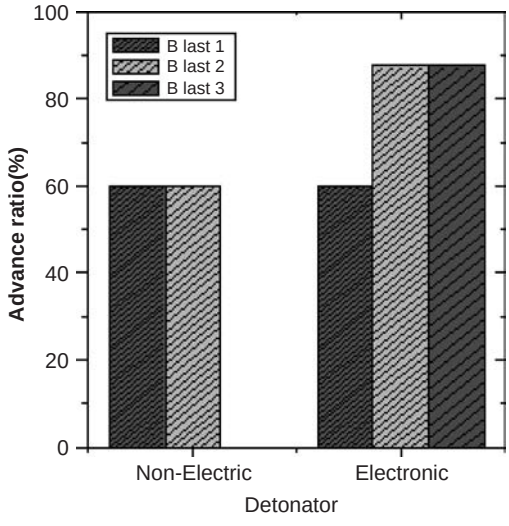


Figure 10. Advance ratio.

the Civil Tunneller. The firing and measurements were taken in a production environment. This meant that no special controls were taken opposite drill accuracy and charging. It could be said that the positive results are most powerful in that the sole change was initiation timing and accuracy.

Most obvious was the improvement to perimeter control. This is a critical aspect of civil tunnel in that the perimeter must conform to specification. Underbreak results in re-work and overbreak is at the expense of the project is terms of additional support material placement.

The fact that vibration prediction proved to be more reliable will have value to tunnellers operating in environmentally challenging locations. Often cautious limits are set for maximum charge weight to overcome variability in vibration results. Charge weight limitation usually results in shorter drill length and therefore reduced advance per cut. Being able to maximise advance for a given set of criteria is of enormous value.

The electronic timing designs were not optimised for vibration control. Opportunities exist to further refine these designs to give true single hole firing to minimise charge weight per delay.

This page intentionally left blank

Underground Space – the 4th Dimension of Metropolises – Barták, Hrdina, Romancov & Zlámal (eds)
© 2007 Taylor & Francis Group, London, ISBN 978-0-415-40807-3

Blanka tunnel complex in Prague

P. Šourek, L. Šajtar, F. Polák, J. Dvořák & A. Butovič
SATRA, Prague, The Czech Republic

M. Hadrava
METROSTAV, Prague, The Czech Republic

ABSTRACT: The largest underground construction being built at present in the Czech Republic is Blanka tunnel complex in Prague. This extensive construction is being realized within the construction of the north-west part of Prague City Ring the whole length of which is 6,382 km and the length of the tunnel part is 5,5 km. After completion of Blanka complex the operating lenght of the City Ring will be approximately 17 km including Zlíchov, Mrázovka and Strahov tunnels.

1 INTRODUCTION

The route of Prague City Ring goes through central part of the City, bordering the historic core and through the area of preserved natural monument Královská obora Park. The first studies, which were made at the beginning of 90 s in the last century, showed necessity for the most part of the route to go under the ground either in cut and cover or driven tunnels. The reason was to minimize the influence of the tunnel construction and then the traffic operation on to the environment. And thus continuous Blanka tunnel complex was created. It includes three tunnel sections which concur fluently from Malovanka intersection at the north portal of Strahov tunnel to Trója intersection by new Trója bridge across the Vltava River. The already operating western part of the City Ring Road continues in:

- Brusnice tunnel section goes from northern portal of Strahov tunnel under Patočkova Street at first through cut and cover tunnels. Behind the crossing Myslbek street the driven part of the route begins and ends in front of Prašný most intersection. There the cut nad cover tunnels route again continue. The aggregated length of this section is 1,4 km, out of which 550 m are driven.
- Dejvice tunnel section starts at Prašný most intersection and continues by the cut and cover tunnels under Milada Horáková Avenue up to the area of the future intersection U Vorlíků. The aggregated length of the section is 0,6 km.
- Královská obora tunnel section begins at the intersection U Vorlíků at first by short cut and cover section in Letná area. The adjoining driven section underpasses block of flats, Královská obora Park, a shipping canal, Císařský Ostrov, the Vltava River and then through other cut and cover section up to Trója portal. The aggregated length of the section is 3,43 km out of which 2230 m are driven. The length of the whole tunnel complex is 5502,20 m in the northern tunnel tube and 5489,14 m in the southern tube. The aggregated length of all driven tunnel tubes is 5,54 km, the aggregated length of all cut and cover tunnel tubes is 6,60 km. The opening of the tunnel complex is expected in 2011. This tunnel will be twice longer then the existing longest one in the Czech Republic.

2 HORIZONTAL AND SLOPE ALIGNMENT

The whole City Ring route is always divided in to two or three-lane tubes in both directions. The tunnels descend from Malovanka crossing upto under the Vltava River where they start to ascend to Trója portal. The maximum longitudinal gradient amounts to 5%. The level difference between the highest and the lowest point in the tunnel is 113,5 m. The minimal horizontal curve radius value is 300 m. The traffic lane width in the whole section is 3,5 m, the gauge limit height is 4,8 m. The designed speed is 70 km/h.

3 GEOLOGICAL CONDITIONS

Complex Blanka construction will be driven in a rock massif formed by sediments, which settled at the bottom of the cold Ordovician sea (lower Paleozoic)

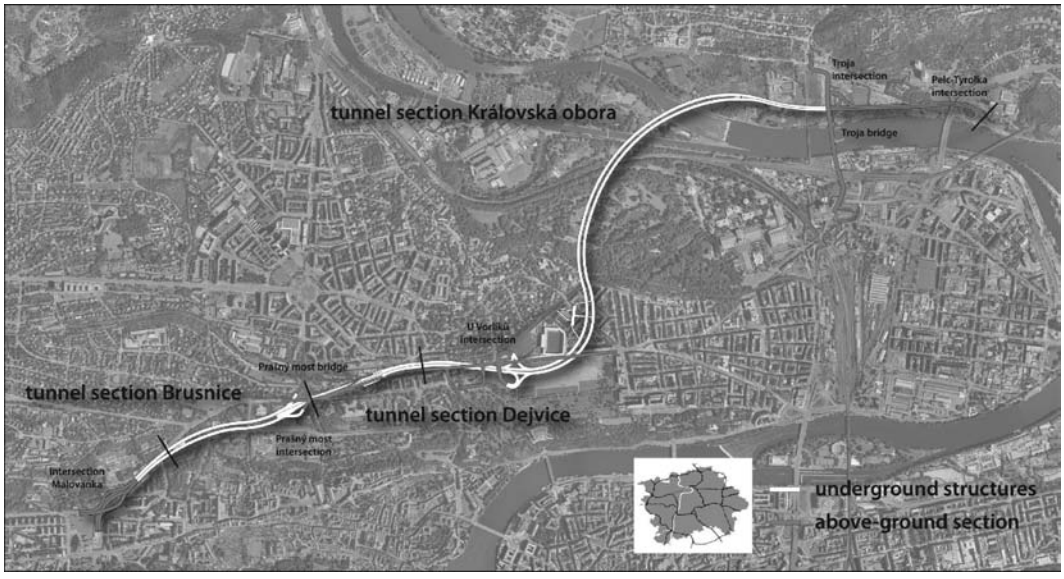


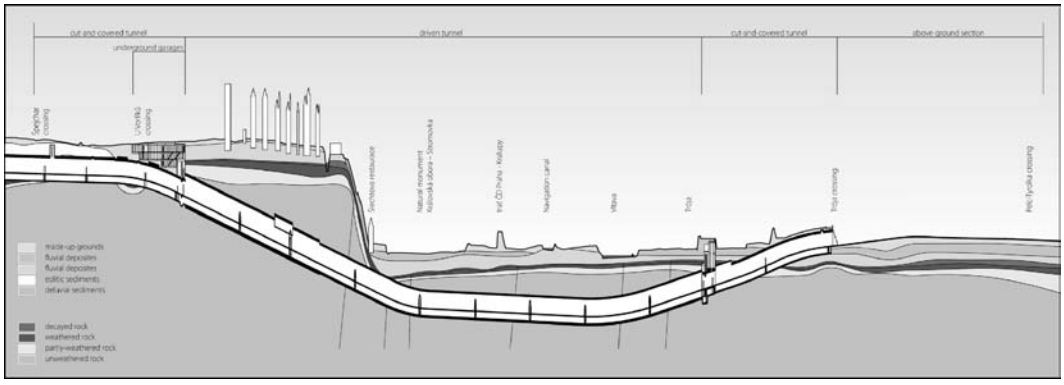
Figure 1. Situation of the Blanka tunnel complex.

in Prague basin, which is a part of the Barrandiene (a characteristic sedimentation basin of the Proterozoic Eon, reaching up to the Paleozoic Era, named in honour of a renowned French palaeontologist). Successively, those sediments were first folded during the Variscan orogeny (the Carboniferous, i.e. upper the Paleozoic), which manifested itself by pronounced synclinal or anticlinal structures (e.g. a quartzite anticline. Later on, these sediments were fractured along faults or local tectonic weaknesses into individual tectonic blocks.

The rock environment of Malovanka–Pelc Tyrolka package is very variable. It consists of Ordovician rock types represented, in the direction of chainage, from the starting point of the construction up to the foot of the slope from Letná by sandy shales of Letná Member (both monotonous and flysh types of sedimentation), which are replaced by clay-silty shales of Libeň Member at the slope from Letná (at a length approximately of 170 m).

A 60 m wide zone of Řevnice Quartzite of Libeň Member begins in the area of the Šlechta restaurant. Further on, in the section passing under Královská obora Park, there are sandy – silty shales of Dobrotiv member, which change to Skalec quartzite of Dobrotiv Member. The remaining section from Trója embankment on is found in clay-silty shales of Dobrotiv Member.

– monotonous development of Letna series
  sandy shales exhibiting an uniaxial compression strength of 20 to 35 MPa in a sound horizon, thus, medium strength (defined by σc within an interval 15 to 50 MPa). Thickness of weathered rock can be about 4–5 m, and sometimes higher (at one bore it was over 14,0 m).
– flysch development of Letna series
  sandy to greywacke shales prevail with a strength of 25 to 55 MPa which are mostly classified as medium strong rock. In a small extent, they come to the lower part with high strength. Quartzite and sandstone inter-beds have an average strength between 80 and 130 MPa. The above mentioned results refer to the difficulty in the rocks disintegration, and they are one of the input values rendering the assessment of suitability of particular types of possible driving equipment.
– Liben shales
  are in non – weathered state dark grey or black grey shales with silt admixture, in terms of excavation, a very important formation, as they are the worst rock material in the route of the tunnels. The clay-silty shales encountered have the strength of 10 to 15 MPa, and they are classified as the rock with low strength.
– Revnice quartzites excavating of the exploratory gallery. This face is created by dark to yellow–brown quartzites with tabular to bench bedding. The thickness of detailed layers is about 7–100 cm. It contains 96–99% quartz which creates slightly oblong corns of 0,06–0,02 mm size. In some places layers of clay siltstone shales with thickness up to 2,0 m can be found. The strength on average of the prevailing fine-grained quartzites is of 100 to 150 MPa, which means that this is the high-strength rock.


cut and covered tunnel
driven tunnel
cut and covered tunnel
above ground section
underground garages
Sedlčná crossing
Vrchlická crossing
Natural monument Královská obora - Šárovcová
Navigation canal
Vltava
Troja
Troja crossing
Prague - Kladno
Prague - Kralupy
Prague - Kladno
Prague - Kralupy
Prague - Kladno
Prague - Kralupy

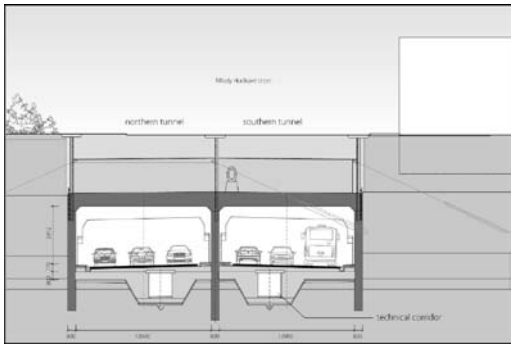


Figure 4. Typical cross-section of cut and cover tunnel constructed by "Milan method".



Figure 5. Model of the Malovanka intersection with southern portal.

fibres on 1 m^3 with fibre length of 6 mm and 0,018 mm diameter) in the upper vault will be used as a protection against entrance contraction and above all against influence of fire over the loss of capacity.

Cut and cover tunnel sections are according to their technical solution divided into classical tunnels and tunnels realized by frontal excavation by means of so-called "Milan method". The classical cut and cover tunnels are always designed into open excavation pit secured by either underground rider or micropile walls, eventually by sloping or anchored rock walls. Suporting structures of the tunnel are made from bottom slab with walls and roof or with upper vault. All constructions are monolithic reinforce concreted from the concrete C30/37 and C25/30. Polypropylene fibres are also designed in the construction of walls and roofs, eventually upper vaults. The classical cut and cover tunnel method is used above all in sections with complicated space layout. Waterproof isolation of these sections is supposed on the base of isolating bentonite mattres always with additional elements to make construction and daywork joints tight.

"Milan method" of the construction of the cut and cover tunnels is designed in the places with very narrow space conditions or where it is necessary to minimize traffic restraint time. Sequence of construction consists in the building of the underground monolitic walls from the surface or secured exavation pit. The finished roof construction will be concreted on the pit bottom. It will be filled up again after hardening and final finishing and traffic renewal can be made. Excavation of the proper tunnel profile is made after finishing the whole tunnel section . Cut and cover tunnels have common central wall for southern and northern tunnel tubes and roof floor will funcionate as continous one with two sections. The cross section of the tunnel tube consists of the bottom angle reiforce concrete board, underground walls 800 mm thick are fixed into hard floor and reinforced concrete roof. Roof and walls are designed from concrete C30/37 with adding PP fibers and hard floor is from concrete C25/30. The roof board is 1300 mm thick. The tunnel waterproofing is created by watertight bearing concrete constructions, with additional elements to make construction and daywork joints tight.

A lot of technical and constructional interesting solutions in demanding section are in Blanka complex. The most interesting ones are as follow:

- The portal tunnel part connecting intersection Malovanka is the first of them. It is made form reinforced conrete monolith two tunnel tubes and technological equipmet center between them. All this section (ground plan about 120×100 m) was divided into several dilatation elements, according to sequence of construction and with the influence of the necessity of keeping the public transport on the streets.
- More difficult conditions for design and construction are in three lane driven tunnel tubes between Myslbekova and Prašný most intersection. In the places where the geological conditions are worse the horizontal jet grouting column are designed to be made in advance over the upper tunnel vault.
- The intersection ramps, technological center and undeground garages (for 463 parking places) are situated in the open construction pit (Prašný most). The coordination of the sequence of construction, keeping the public transport on the streets mainly trams and maintaining excess to the construction of driven tunnels is a demanding task. This asks for special attitude for design of the reinforce concrete construction of the building.
- The situation of cut and cover tunnels near vestibule of the metro station and raliway station in Dejvice is other very complicated probelm, which demands special design. It will be necessary to reconstruct one part of the metro vestibul and build and new railway underpass.

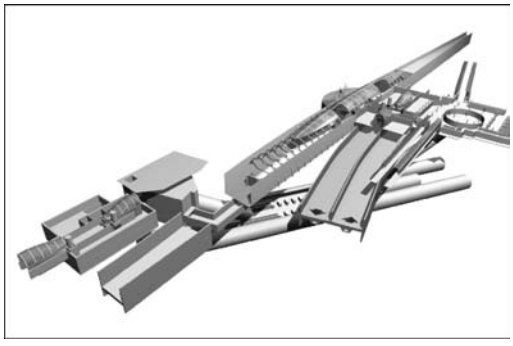


Figure 6. 3D animation of the Dejvice tunnel section in the area of metro station Hradčanská and railway station Dejvice.

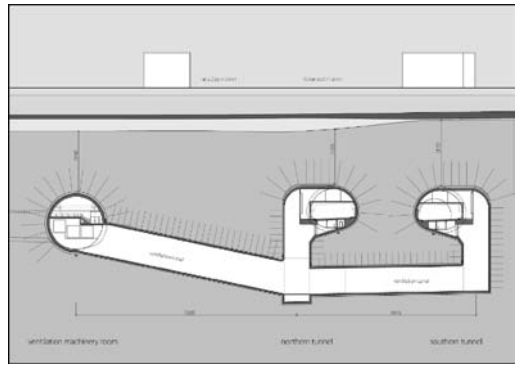


Figure 7. Longitudinal section through the ventilation duct.

– The construction coordination of cut and cover tunnels with individual and public transport is also necessary in Dejvice city district. The route is mostly situated in the track of Milada Horáková Avenue, which is in fact the only connecting road between west and east in all northen city segment. The construction cut and cover tunnels according to "Milan method" was used to minimize the partial closing of the street. The additional sectioning of some of bearing constructions in longitudinal direction is necessary to minimize the area of the closing. Complicated joning details of roof reinforcement construction above middle wall in the place of the maximum banding moment arises from this. The height of the filling above roof construction is extraordinarily even 7 m. It was not possible to make use of vault roof construction because the sanitary sewer was placed on the roof. That is why the horizontal roof slab is bearing all height of the filling. This asked for making the filling from light-weight concrete 3,5 m high with 600 kg.m^{-3} bulk density.
– Cut and covered tunnels end at Letná, where they continue three lane driven tunnels. Open construction pit (25 m deep) houses undergorund intersection, proper tunnel tubes, underground technological center and car park for 863 cars. The interesting solution is roofing of the place where three lane tunnels are widening by two merging or turning lanes lead into intersection U Vorlíků. The biggest span of the roof construction in this place is 26,4 m. The composite construction concrete/concrete prestressed bridge beam VSTI 2000 with reinforced concrete slab 300 mm thick was used.
– The driven tunnels begin in the construction pit at Letná go under Královská Obora Park and the Vltava river ending at the oposite bank in Trója. More dificult place from the point of driving will be at the bottom of the hill from Letná to Stromovka in the vicinity of the hisorical building Šlechta restaurant. Both tunnel tubes go through the lowest overburden on the border of the poor quality Liben shales and Řevnice quartzites layers.

  The overburden consists of 1,5 m high rock and 11 m high sandy gravel. This situation will be solved by jet and press grouting from the explorartory gallery. The driving will be realized afterwards under the protection of microplilot umbrellas with horizontal sequntions and temporal floor vault. This underpassing (120 m^2) the Vltava river will be the biggest ever done in the City of Prague.
– The underground ventilation machinery room at Letná consists of several paralel tunnels. The biggest of these have cross section cca 300 m^2 and length 125 m. The machinery room is conected with the tunnels by ventialtion ducts for fresh and exhust air. This sofisticated underground junction was designed only because of very good geological conditions in this area. The results of the final element method analysis confirm viability of the design solution of the machinery room and gave the information about supposed settlements, which should not be over 35 mm in the overhead built-up area.
– The last part of Blanka tunnel complex is cut and cover section on Trója bank. The influence of floods was one of the criteria for the design of it.

5 TECHNOLOGICAL EQUIPMENT

Technological and safety tunnel equipment of Blanka complex meets and in many cases is above minimal safety demands given by European Directive from 2004. The kind of equipment of Blanka complex is compatible with other Prague road tunnels because it will be controlled from the same Control Centers as it is now. One is for traffic control and the other one for monitoring, control and mainatnence of technological tunnel equipment. The great importance of all tunnel section, from the point of traffic in Prague



Figure 8. Vizualization of northern portal in Trója.



Figure 9. Vizualization of final driven tunnel.

and supposed high traffic intensity, specified demands on high reliability of design of technological systems with minimal operational and maintanence cost. Price of eletrical energy was one of the reasons why a great attention was given to the design of ventialtion system. Operational ventilation system makes use of piston effect of driving vehicles and combines longitudinal and semitransver ventilation systems with local exhaust and fresh air supply in one direction tunnels. Fresh air is mostly supplied by driving vehicles in entrance portals in combination with several hole air supplies. Polluted air is exhausted in a controlled way by ventilation machinery rooms into the chimneys and at the same time the portals are protected as much as possible against the polutant exhaust. Fire ventilation system in driven tunnel sections is designed as a smoke control exhaust into holes in the tunnel vault with remote control dampers each after 80 m. The smoke and heat from the fire will be exhausted in a controlled way by local ventilation machinery and by help of jet-fans to the portals.

6 SEQUENCE OF CONSTRUCTION

The elaborated coordination documentation was prepared for coordination. It solves sequence of construction from individual realignment underground services, individual and public traffic organization and time schedule up to trail run of the system. The construction is divided into 20 basic time periods, which are time and place connected. Three temporary bus lines and 1km long tram line will be opened to ensure public transport in the same way. The tunnel construction will be realized from five main construction sites. The construction of the driven tunnels will be realized always from both portals. Machinery or blast driving are supposed to be used according to the geological conditions. Waterproofing and secondary lining will be realized by flow-line process.

Part of Blanka tunnel construction besides the tunnels will be other adjoining city comunication e.g. new surface section of City Ring in Trója, new road bridges, one across the railway (Prašný most) and the other across the Vltava River (Trojský most).

The scope, number and type of the geotechnical monitoring is very large because of the place of the construction, which is found in these block of flats. It can not be compared with any other tunnel construction in the Czech Republic. To ensure safety sequence of the undeground construction and trail run, twenty six kinds of basic measuring are designed including proposal of the observation method.

7 CONCLUSION

The range of the whole Blanka tunnel complex construction is unique. The time of the design preparation and construction, number of other city investments and realignment underground services, temporal public nad individual transport restrictions and coordination and organization all construction are unique too. The preparation design works started in 1998 and the construction began in 2007. The improvement of the environment and traffic situation in the area of the boundry of historical center of the City of Prague, listed in the cultural and histotical UNESCO heritage will be reached after completion of it.

REFERENCE

Butovic A., Dvorak J., Šourek P.: The Blanka Tunnel on the City Circle Road in Prague. *Tunel* 2006/1, magazine of the Czech Tunnelling Committee, ISSN 1211–0728.

Underground Space – the 4th Dimension of Metropolises – Barták, Hrdina, Romancov & Zlámal (eds)
© 2007 Taylor & Francis Group, London, ISBN 978-0-415-40807-3

Study on the behavior of an ultra-large section tunnel project in unconsolidated ground-design and construction of the Minoh toll road tunnel

K. Taketomo
Osaka Prefectural Road Public Corporation, Minoh Site Office, Osaka, Japan

Y. Mitarashi, H. Shiokawa, S. Nishimura & K. Konishi
Kumagai Gumi Co., Ltd., Tokyo, Japan

ABSTRACT: This paper discusses the Minoh tunnel construction. The geology at its south portal is unconsolidated soil, with a high groundwater level. A significant amount of water inflow was therefore anticipated. In such adverse ground, this tunnel with a maximum excavation section of 313 m^2, which is one of the largest sections in Japan, was successively constructed using the side-drift advance method with various new techniques. During tunneling, informatics technologies were fully utilized, by feeding back various measurement results to design and construction, thereby enabling selection of suitable auxiliary stabilizing techniques and excavation methods. The auxiliary methods involved were pipe roof (812.8 mm in diameter, 90 m long), long steel pipe forepiling, and long face bolts. In addition, "quasi-high fluidity concrete" was used to place high quality lining.

1 INTRODUCTION

The Minoh toll road is an expressway about 7.3 km long extending north from Shin-Midosuji Avenue, providing a bypass of Route 423 linking central Osaka to northern Osaka and the city of Kameoka, Kyoto Prefecture, as well as providing an access to the Second Meishin Expressway (Fig. 1).

The Minoh toll road mountain tunnel construction project (south sector construction) covers 2.2 km on the south of the tunnel extending over about 5.6 km (main and evacuation tunnels). Its most significant feature is that the maximum excavation area reaches as large as 313 m^2 at the southern portal of the main tunnel, and is one of Japan's greatest ultra-large section tunnels in unconsolidated ground.

Prior to the excavation of the main tunnel, the construction project started with the work for a working tunnel (having an excavation section area of 41 m^2 and a length of 347 m) that would run in parallel with the main tunnel. In the course of this construction work, the project team encountered difficult problems on the heavily fractured shale bed in the Tanba belt, including extrusion, collapse and large deformation of the face. The construction team excavated the main tunnel by utilizing the data obtained during construction of this working tunnel; and they gradually enlarged the excavation section area from the back toward the portal.

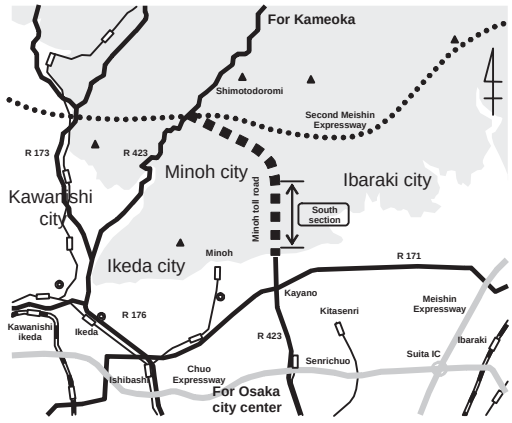


Figure 1. Site location map.

The tunneling team prepared for construction involving an ultra-large section area while re-examining the design and construction method and referring to the measurement results on the working tunnel and the construction results of the sections already excavated in the main tunnel.

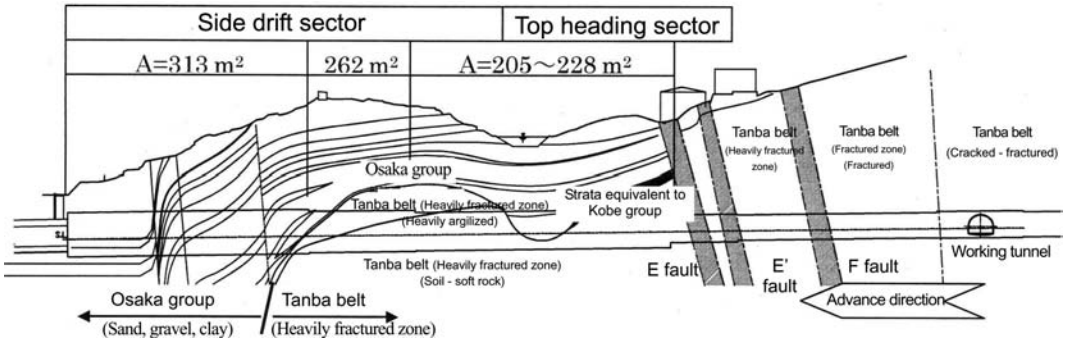


Figure 2. Longitudinal profile of the south portal.

2 GEOLOGICAL OVERVIEW

As shown in Figure 2, the soil around the southern portal contains distributed segments of the Mesozoic or Paleozoic Tanba belt (largely composed of shale) forming the Hokusetsu Mountains, covered with the Osaka group (of sand, conglomerates and clay).

In this construction section, the ground is vulnerable with high clay content as a result of heavily fractured shale beds while a number of branch layers of the Arima-Takatsuiki tectonic line.

The deformation modulus of ground at the southern portal was generally 80–100 MPa for the Osaka group and 55–70 MPa for the Tanba belt (fractured shale bed), according to simulation analyses involving data from various geological surveys and tests as well as measurements on tunnels under construction.

3 CONSTRUCTION OF A PORTION WITH AN ULTRA-LARGE SECTION

3.1 *Tunnel support pattern*

The support structures and section specifications are as shown in Figure 3 and Table 1, which do not include any special specifications but combinations of standard support members.

3.2 *Construction procedure*

Figure 4 shows a flow of construction work for a portion with an ultra-large section.

First, drifts were constructed on the right and the left, and then sidewall concrete was placed. Next, an arch section was excavated and arch concrete was placed.

This construction method succeeded in restricting settlement at the tunnel foot.

Last, the invert was closed to ensure permanent safety.

3.3 *Construction overview*

3.3.1 *Drift excavation*

As each of the sidewall drifts was vertically long with an excavation section area of 74 m^2 and a height of 11 m, the heading was divided into four sections: upper, middle, lower and invert sections.

One excavation round consists of consecutive driving of upper and middle sections, followed by cutting of lower half and invert, with early closure by shotcreting the invert.

Injection pattern forepoling was adopted as an auxiliary method.

Measures to control water inflow included drainage boring with long pipes in sandy aquifers that had been anticipated through the drift faces.

These drainage operations and the application of the auxiliary method enabled excavation of sandy soil (Fig. 5).

3.3.2 *Concrete placement on sidewalls*

Construction of 7.7 m-high sidewalls was divided into two segments: the foundation and the wall.

The bar arrangement specifications included two-tier using internal main reinforcement of D35 at intervals of 125 mm.

Moreover, considering the high density of corner-reinforcing bars and stirrups, the construction plan was streamlined, including [1] preassembly of main and distribution reinforcement bars into modules, [2] simplification of stirrup assembly work through adoption of wedge press-in type joints, [3] adoption of the screw-squeeze type joint (mechanical joint) for sections where the arch section was jointed to invert (Fig. 6).

3.3.3 *Main tunnel arch excavation work*

After the completion of concrete placement on sidewalls, arch excavation was started.

Efficient excavation was conducted using a large-scale breaker (with the long reach) with several back hoes (Fig. 7).

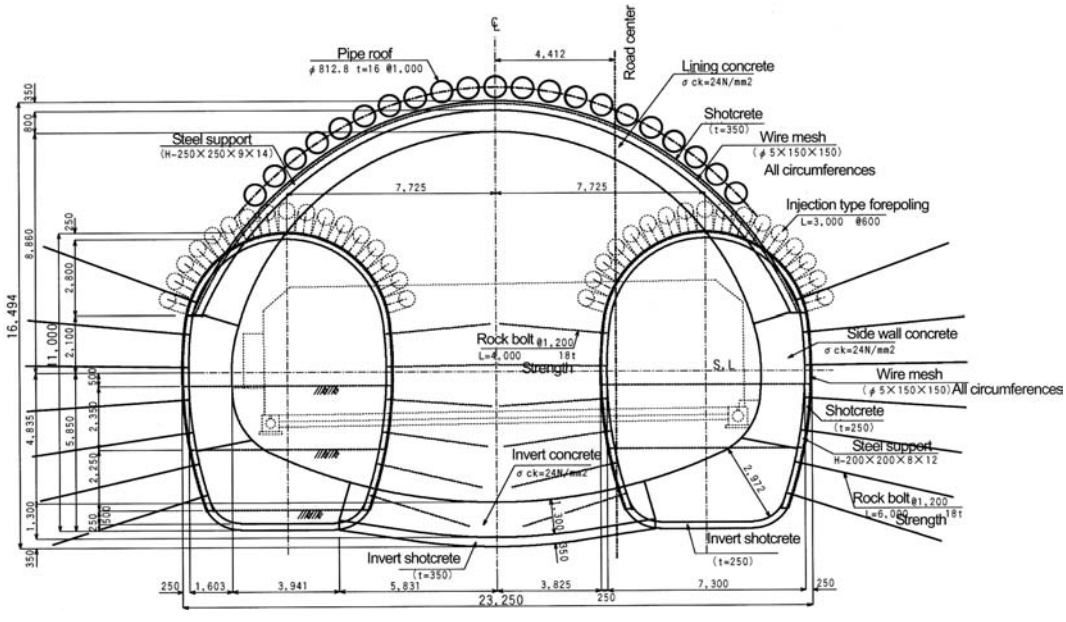


Figure 3. Support pattern.

Table 1. Support structure and section specifications.

Name	Division of heading: Drift	Division of heading: Main tunnel	Remarks
Shotcrete	t = 250	t = 350	σck = 18 N/mm^2
Steel arch support	H – 200	H – 250	SS 400
Rock bolt	L = 6 m / L = 4 m	Not provided	Ground side n = 7 / Cavity side n = 6
Excavation section area (designed)	Total cross section (m^2)		313
	Drift excavation (m^2)		74 (on each side)

Since the steel arch supports extend as long as 14 m on one side, four supports (two each) were jointed at the temporary storage to form two sets of supports for the left and the right sides and were installed using a support erector.

The pipe-roof protection method (ø812.8, about 90 m long) was adopted as an auxiliary method for the section with the maximum section area (313 m^2), considering the fact that the construction was in unconsolidated ground in the Osaka group.

Meanwhile, in the section with the second largest section area (262 m^2) in ground of heavily fractured rocks in the Tanba belt, the improved-type steel pipe forepiling not enlarging the cut section was used.

3.3.4 *Pipe roof*

When selecting a method for pipe-roof work, the following construction conditions were considered; [1] a long-distance (about 90 m) excavation was involved, [2] the ground contained soils with significantly different properties like sand with a low self-sustainability and hard clay, [3] groundwater inflow was likely to occur, [4] the working space was cramped, [5] reaction force generated from propulsion must be borne by an existing structure, [6] it would be impossible to recover the foregoing device (boring machine) on the arrival side and [7] high-precision propulsion was essential. Given those conditions, the sludge pressure type propulsion method (Fig. 8) was adopted, which enables recovery of the cutter and driving unit through the excavator duct.

When construction began, shafts were created on the portal side, from which boring proceeded toward the back of the tunnel. This method enabled us to maintain construction precision to about 1/2000.

3.3.5 *Arch lining concrete*

Concerning arch lining for the section in question, the following problems and challenges were anticipated:

[1] Occurrence of honeycombs, segregation and poorly filled portions with reinforcing bars arranged densely
[2] Poor filling in the crown of the arch, and
[3] Occurrences of thermal cracks associated with very large spans and very thick lining as well as cracks accompanying drying shrinkage.

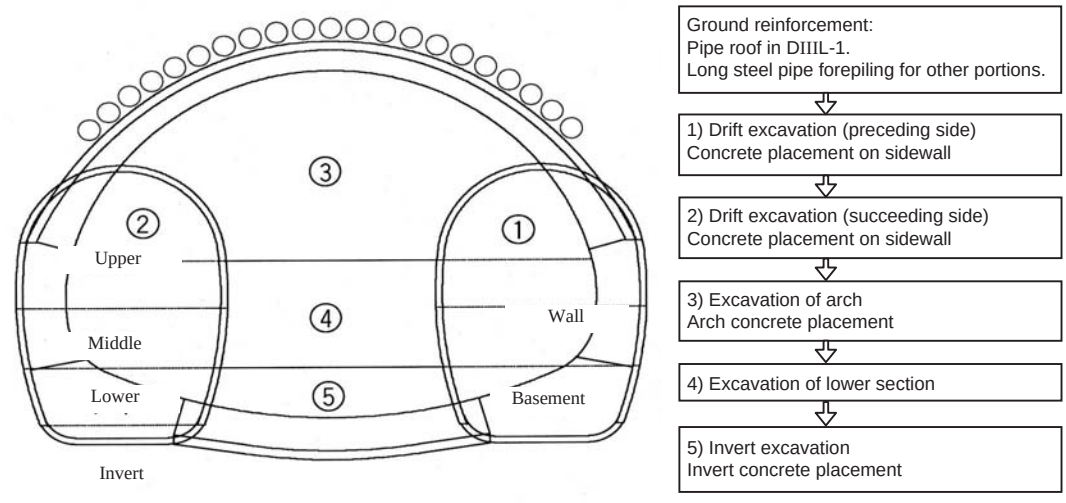


Figure 4. Construction sequence.



Figure 5. Drift portal.

In dealing with the above problems, high-fluidity concrete has been applied in a growing number of cases lately, but not without the following possible drawbacks:

[1] Insufficient strength relative to increases of side pressures,
[2] Concrete running out through the bulkhead,
[3] Higher unit cost of concrete.

For the above reasons, we judged high-fluidity was not an appropriate solution and opted to develop a new type of concrete.

In the development effort, various studies, mix design and trial mixing were repeated from two viewpoints: property improvement of fresh concrete such as workability and that of hardened concrete such as crack control.

Finally, a model was constructed using part of arch forms to verify the adaptability to actual construction.



Figure 6. Bar arrangement in the drift (for the foundation).

Thermal stress analysis of cracks using the three-dimensional finite element method confirmed that the minimum crack index for the crown, which was previously 0.7, was improved to about 1.3 as a result of addition of an expansive admixture, which we decided to use in our development project.

The properties and mix of the developed concrete are summarized in Table 2 and also actually achieved satisfactory construction results.

For reference, the construction span length of the lining concrete was basically 6 m so that one concrete

Table 2. Mix Table for Quasi High-Fluidity Concrete (with expansion additives added).

G max (mm)	Cement type	W/C (%)	s/a (%)	σck (N/mm^2)	Slump (cm)	Unit content (kg/m^3)						
						C	W	S	G	P	E	AD
20	N	57	48	24	23	287	175	796	890	100	20	5.29 / 1.3%

P: Fine limestone power E: Low hydration heat expansive admixture (ettringite-lime compound) AD: AE superplasticizer
*Slump flow was set at 42 cm as management reference.



Figure 7. Excavation of main tunnel arch.



Figure 8. Pipe-roof boring machine.



Figure 9. Invert concrete placement.

placement at a time could be controlled at a volume no more than 200 m^3.

3.3.6 *Construction of the lower and invert sections*
The lower section was excavated en masse while breaking the drift. The invert section was excavated and shotcrete was applied in sequence to close the section early.

Lastly, reinforcing bars were arranged and invert concrete was placed.

4 MEASUREMENT RESULTS

4.1 *In-tunnel measurements*

As a result of convergence and settlement measurements shown in Figure 10, the following observations were confirmed:

[1] The maximum crown settlement exceeded 100 mm for the preceding portion of the upper section. However, the settlement of the crown of the main tunnel's arch was no more than 30 mm or so in the preceding portion of the sidewall drifts. The distance over which the main tunnel arch converged was in the range from 35 m to 40 m in the preceding section of the sidewall drifts. This is equivalent to 1.5–2 times of the tunnel diameter.

[2] In the preceding portion of the upper section, settlement at the foot occurred in conjunction with crown settlement, also showing some correlation with the overburden. Meanwhile, in the sidewall drift sections, the settlement of the main tunnel's arch at the foot was contained within the ratio of an average 55% against the crown settlement. Moreover, no correlation with the overburden was recognized.

4.2 *Measurements outside the tunnel*

Figure 11 shows results of follow-up surveys on ground settlement at a point 2.5 m above the tunnel arch. According to this figure, the convergence displacement was 101.7 mm including bench excavation, indicating that the drift excavation brought about 50% displacement. The preceding displacement ratio for the upper arch excavation alone was about 27% relative to the initial value, i.e., the pre-excavation value for the upper arch.

Figure 12 shows an overall view of outside-tunnel measurements. In the working tunnel, a phenomenon

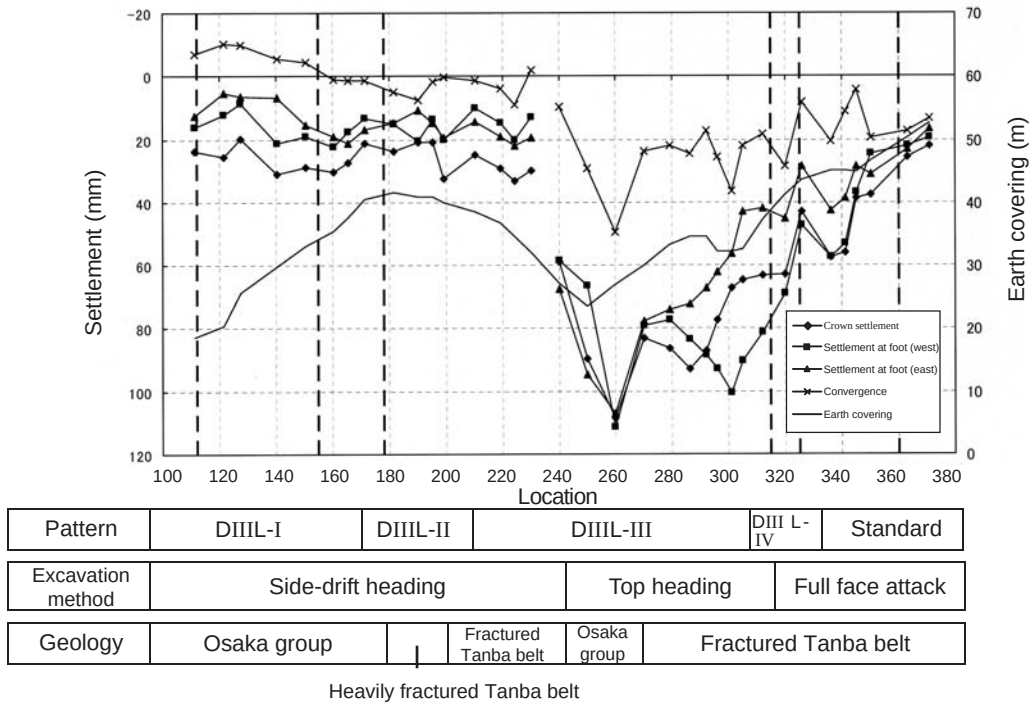


Figure 10. Longitudinal distribution of convergence and settlement measurement results (Data for drift sections represent measurements from excavation of the upper arch sections).

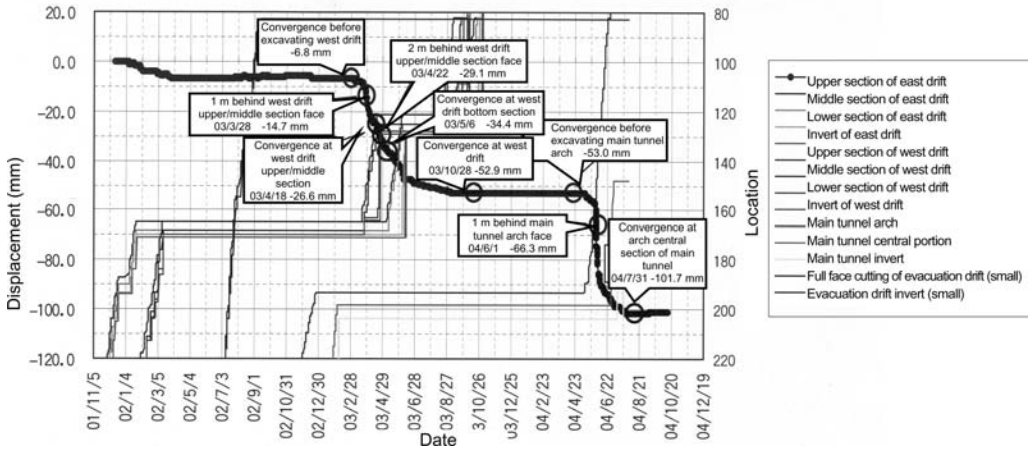


Figure 11. Change in ground displacement.

referred to as "accompanying settlement" was observed, in which settlement occurred across the entire scope from the tunnel arch to the ground surface. In the main tunnel, however, the surface settlement ratio against the underground settlement directly above the tunnel was about 60%, showing some reduction, and no accompanying settlement occurred. This can be attributed to the effect of restricting settlement at the foot that might have arisen from the presence of sidewall drifts.

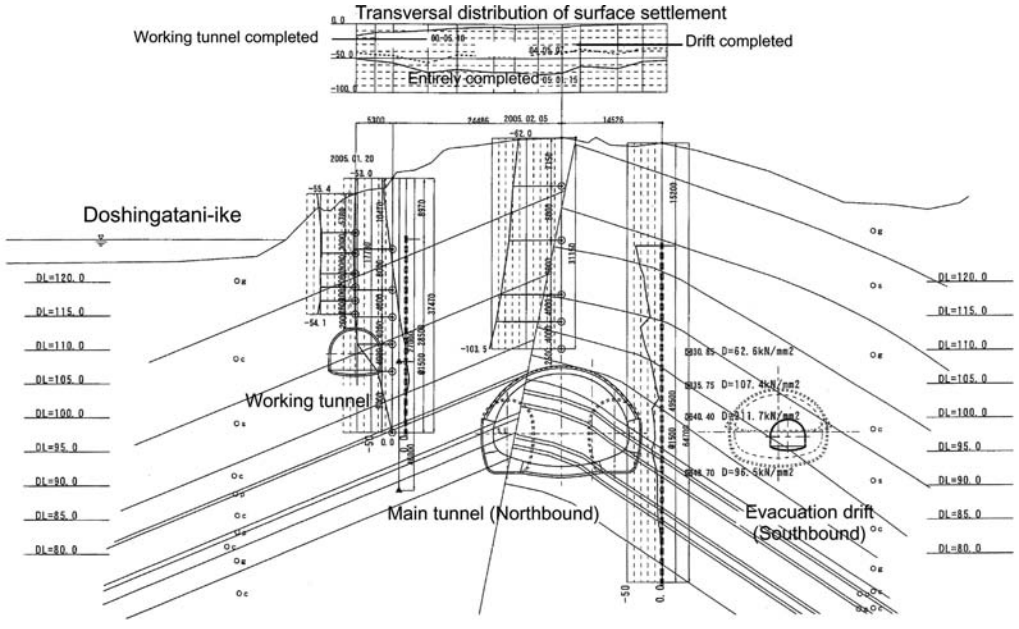


Figure 12. Overall view of outside-tunnel measurements.

5 CONCLUSIONS

This construction project was started in May 1999 with its invert closure for the portion with an ultra-large section completed in February 2005. During the course of construction, we faced numerous problems, for which solutions were sought and utilized in the subsequent construction stages. The following is a summary of findings and related comments.

- One of the challenges was to provide face stabilization measures during arch excavation the width of which reached 23 m. The solution made it clear that effective reinforcement ahead of the face including long face bolts enabled stable excavation.
- Settlement at the foot of the large-span arch was significantly limited by the presence of the side drift. This solution contributed to the prevention of accompanying settlement as well as to restriction of loosening.
- While a control criterion surface strain (1.2%), various measurement results and reproduction analysis results proved that excavation advance was stable with strain below the control criterion.

The project successfully completed an ultra-large section tunnel with the maximum excavation section reaching as large as 313 m^2 in unconsolidated ground.

This success should be attributed to the feedback of measurement results by the construction management based on information technology to the design and construction processes as well as to appropriate selections of auxiliary construction methods and excavation methods.

REFERENCE

Matsuo, M., Isozaki, K., Katoh, T., Mitarashi, Y., Fukui, T. & Nishimura, S. 2004. A challenge of an ultra-large section tunnel project in unconsolidated – design and construction of the Minoh toll road tunnel. *ITA - AITES 2004 Underground Space for Sustainable Urban Development*

This page intentionally left blank

Underground Space – the 4th Dimension of Metropolises – Barták, Hrdina, Romancov & Zlámal (eds)
© 2007 Taylor & Francis Group, London, ISBN 978-0-415-40807-3

Large deformations in squeezing ground in the Saint-Martin La Porte gallery along the Lyon-Turin Base Tunnel

J. Triclot
Scetauroute DTTS, Pringy, France

M. Rettighieri
LTF-SAS, Torino, Italy

G. Barla
Politecnico di Torino, DISTR, Torino, Italy

ABSTRACT: Within the context of the Lyon-Turin railway project, the excavation of the *Saint-Martin La Porte* inclined gallery (section 80 m^2 – length 2000 m) has encountered a highly fractured Carboniferous rock mass. Different ground support systems were implemented and convergence measurements confirmed the squeezing behaviour of the rock mass. Convergences of approximately two meters were observed as soon as the cover reached three hundred meters. As a result significant changes in the excavation and ground support systems were required. After setting up a ground support system adapted to the squeezing ground, the rate of convergence reached 40 mm per day in the zone of the face and 2 to 4 mm per day at a distance of approximately 60 metres from the face. Due to the difficulties encountered and with consideration given to the exploratory nature of the work, new support systems and organisation works were implemented, combined with an extensive monitoring programme.

1 INTRODUCTION

The Lyon-Turin railway programme requires the excavation of a 53 km long Base Tunnel. The dual national company Lyon Turin Ferroviaire (LTF), a subsidiary company of RFF and RFI, has been appointed to carry out preliminary studies and works involving the excavation of inclined galleries and exploration adits.

The Saint-Martin La Porte inclined gallery is the closest drive to the West portal of the base tunnel. It is to reach the level of the Base Tunnel situated at a distance of 2300 meters from the portal. The cross sectional area of the gallery ranges between 80 and 100 m^2.

The gallery is situated near an important zone of difficult ground and is designed to fulfil several objectives:

- provide additional geological and geotechnical data on the rock mass conditions to be encountered during the excavation of the main tunnel;
- quantify the uncertainties associated with the difficult ground to be excavated;
- provide access for the future tunnelling work.

When the tunnel will be in operation, this inclined gallery will be used for access by emergency teams and also for maintenance and ventilation purposes.

Participants in the programme are:

- Owner: LTF – Lyon Turin Ferroviaire SAS;
- Project management: Group Scetauroute (agent), Antea and Alpina;
- Contractor: Razel inter-company group (agent), Pizzarotti, Bilfinger Berger, Granulats Rhone-Alpes;
- Sub-contractor: Fondazioni Speciali/GD Test.

2 GEOLOGICAL AND GEOTECHNICAL CONDITIONS

The Saint-Martin La Porte gallery is situated near the contact between the Briançonnaise zone, composed of limestone, marl and dolomite, and the Briançonnaise Carboniferous zone, composed of schists, Carboniferous schist and coal (Fig. 1).

Between the two zones a transition zone is present comprising anhydrites (Fig. 1). The contact area between the Carboniferous and the Briançonnaise zone was found after excavating a tunnel length of 800 m and presented characteristics in line with predictions. Also encountered during excavation was a zone with fluvio – glacial alluvium under a cover of

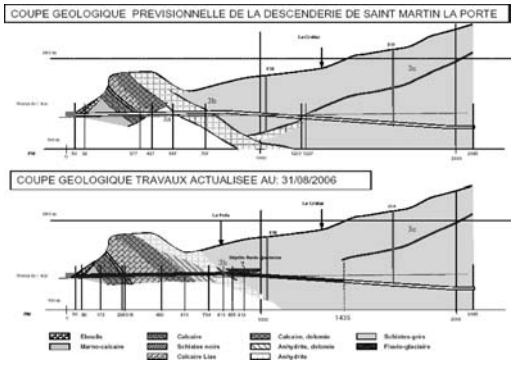


Figure 1. Geological profile.



Figure 2. Appearance of the Carboniferous rock mass at the face. Chainage 1414 m.

150 to 200 meters. This required staged excavation (top heading and bench) and pre-treatment of the ground.

Once the excavation of this latter zone was completed, the gallery encountered the Productive Carboniferous Formation, composed of schists, clays, highly tectonised sandstone and coal. A characteristic feature of the ground in this zone is the highly heterogeneous, disrupted and fractured condition of the rock mass, which exhibits extremely to very severe squeezing problems, Hoek, 2001, Barla, 2001 (see Figs. 2 and 3). As a crude approximation, the GSI (Geological Strength Index, Hoek and Marinos, 2000) is in the range 20–30 (short term conditions) down to 10–20 (long term conditions).

The conditions encountered made the different parties involved in the work to define first a support system based on heavy steel sets (HEB 180) with invert, combined with fibreglass dowel pre-reinforcement at the face, together with a concrete ring approximately 50 cm thick.

Under these conditions, the excavation resumed at a rate of 2 to 3 meters per day and was associated



Figure 3. Appearance of the Carboniferous rock mass during excavation. Chainage 1350 m.

with a specific monitoring programme. As the gallery became deeper, leading away from the valley (Fig. 1), the overburden increased. The tests carried out have confirmed the limitations of the support system adopted when subjected to the high stress conditions expected with an overburden depth in excess of 250 m.

3 SUPPORT SYSTEMS AND GROUND BEHAVIOUR

3.1 *Adoption of the yielding support system*

Several support systems were used following the initial application of a stiff support, as underlined above. It soon became apparent that a stiff support would not be feasible in the severe squeezing conditions encountered, with very high stresses developing in the concrete lining as the overburden increased.

Finally, the design concept chosen was to allow the support to yield in a controlled manner, with the following pre-reinforcement, full face excavation, and support sequence being adopted:

1. fibreglass dowel face pre-reinforcement;
2. full face excavation (1 m face advance);
3. use of yielding steel ribs with sliding joints (TH, Toussaint-Heintzmann type);
4. installation of rock bolts along the excavation perimeter, including the invert, requiring 400 linear meters of rock bolts per meter excavation.

3.2 *Considerations on the observed behaviour*

The excavation-support system, adopted over a length of approximately 100 metres, was marked by high convergences of up to 2 metres, with the radial strains of the tunnel wall ranging between 8% and 16% at a distance of 20 m behind the face. More specifically, with a progress rate of 1 m per day, convergence rates of

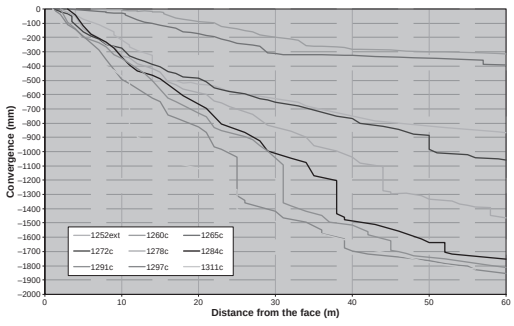


Figure 4. Tunnel convergences measured along the horizontal between chainage 1260 and 1320 m.

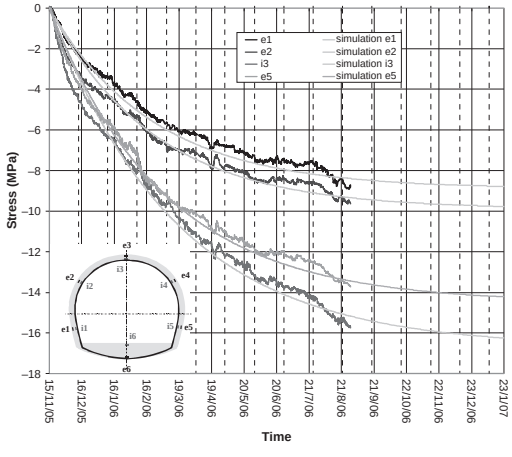


Figure 5. Stress distribution in the lining at chainage 1229 m.

approximately 40 to 50 mm per day were observed. These decreased when moving away from the face and resulted in values of 2 to 4 mm/day at distances between 80 m and 100 m from the face (Fig. 4).

In order to gain in the understanding of the deformational behaviour of the rock mass along the tunnel length, it is of interest to pay attention to the extensometer measurements carried out at chainage 1330 m. It is shown that the zone characterised by a significant strain gradient (say where the strain value is in excess of 0.5%) is un-symmetrically distributed around the opening, with the maximum extent (18 m) being attained at the right rib, in line with the rock mass anisotropic structure (Figs. 2 and 3).

Also to be emphasised, as a means for appreciating the severity of the squeezing conditions being encountered, is the state of stress in the concrete lining at chainage 1229 m as shown in Fig. 5. The vibrating wire strain-meters embedded in the concrete give tangential stresses in the lining, that are still increasing



Figure 6. Re-profiling operations of the opening to the original tunnel profile followed by concrete placing behind steel plates.

8 months following installation with a maximum long term value estimated up to 16 MPa.

The mechanical behaviour of the Carboniferous zone has been shown to be significantly less favourable than anticipated in the design documents. Based on the information gained so far through performance monitoring and back analysis (Barla and Panet, 2006) the ground was found to exhibit a unique deformational response distinguishing between a “short term” and a “long term” behaviour.

In the short term (just behind the face), if the face advance does not stop, the rock mass exhibits a negligible time-dependent behaviour. The tunnel and face deformation can be computed by using an elastic plastic constitutive law. In the long term, the time-dependent behaviour cannot be neglected and an elastic viscous plastic law needs be adopted in order to reproduce the deformational response satisfactorily (Barla and Panet, 2006; Sulem et al, 1987).

3.3 *Improvement of the yielding support system*

Due to the conditions being met, work progress was interrupted for long periods of time, as the reduction in cross section made it necessary to “re-profile” of the opening to the original tunnel profile. With systematic re-profiling operations taking place section by section up to chainage 1325 m, concrete behind the steel plates was placed as soon as possible after completion of the remedial work. Fig. 6 gives a clear view of the re-profiling operations being undertaken with adaptation of the cross section shape.

The observations made, associated with the experience gained during tunnelling in the squeezing ground conditions encountered, made it mandatory to consider a number of possible options for driving the tunnel. The aim was to be able to improve the previous phase of yielding support application, while seeking a different

work organisation in order to adapt to the increased cover and to the necessity to contain the residual deformations at a certain distance from the face.

The main objectives to be achieved were as follows:

- reduce/control, where possible, the amount of convergence in the tunnel and the disturbance of the surrounding rock mass;
- use excavation and support systems compatible with the increased overburden to be experienced in the future (up to 600 m) along the inclined gallery and in the base tunnel;
- optimise the pre-reinforcement, excavation and support sequence, including the distance from the face where to install the concrete lining;
- assess the residual deformations to be expected following support installation and the long term state of stress in the concrete lining.

3.4 *Main adaptations required*

Considering the consequences in terms of the tunnel excavation and support costs, including the time delays in completion of the inclined gallery, the following adaptations were made:

- reorientation of the gallery alignment in order to drive nearly perpendicular to the geological structure;
- change the shape of the opening to a near circular section;
- implementation of a pre-reinforcement, excavation and support sequence leading to avoid the need for important re-profiling to the original tunnel section;
- control of the extent of the disturbed zone around the tunnel, thus reducing the ground time-dependent deformations.

3.5 *Pre-reinforcement, excavation, and support sequence adopted*

The new pre-reinforcement, excavation, and support sequence finally adopted can be summarised as follows (Fig. 7):

Phase 0 – face pre-reinforcement, including a ring of grouted fibreglass dowels around the opening perimeter, designed to reinforce the rock mass over a 2 to 3 metres thickness.

Phase 1 – mechanical excavation carried out in segments of one meter length, with installation of support consisting of systematic bolting (length 8 m) along the perimeter, including the invert, and yielding steel ribs with sliding joints (TH, Toussaint-Heintzmann type).

Phase 2 – application of 20 to 30 cm shotcrete with 8 longitudinal slots fitted with HDC (High Deformable Concrete) elements designed to undergo a total tangential strain of 50%, while maintaining a support pressure of 8.5 MPa with controlled movement (Figs. 8 and 9).

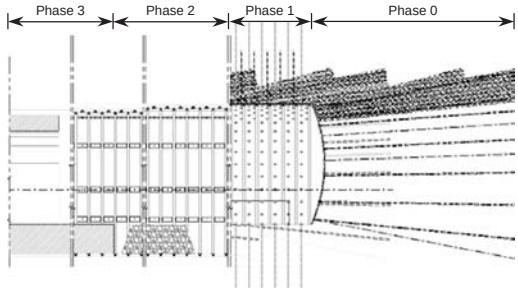


Figure 7. Schematic representation of the adapted pre-reinforcement, excavation, support sequence.



Figure 8. View of the deformable elements installed between the joints of the TH steel ribs.



Figure 9. Photograph taken during Phase 2 implementation.

Phase 3 – installation of a coffered concrete ring when the rate of convergence is low enough to allow this, and outside the zone of influence of the face (Fig. 10).

The guidelines followed for the selection of the excavation-support sequence above were developed



Figure 10. Concrete lining installation.

based on numerical simulations by using both elastic plastic and elastic viscous plastic constitutive laws, with rock mass parameters defined on the basis of performance monitoring. In this context, the support design needs be continuously reassessed according to the results of monitoring and experience feedback from the work site.

It is important to note that the distance from the face at which phase 2 is implemented will depend on the efficiency of the support measures adopted and on the convergence values observed at the face. Diameter reduction for this section is limited to 600 mm. Beyond these values, the shotcrete lining would be overstressed too soon and require repair work on the support structure.

3.6 *First lessons learned*

Use of monitoring equipment during the ongoing work makes it possible to perform back analysis and acquire the experience feedback required for the project. Systematic convergence monitoring takes place continually in both phases 1 and 2. So far also monitored in detail are the strains experienced by the HDC deformable elements installed in phase 2, in conjunction with the tangential stresses induced in shotcrete. The ground response around the excavation in both phases 1 and 2 is being monitored by using multi-point extensometers 24 m long.

Monitoring has shown that the pre-reinforcement and support measures implemented during Phases 0 and 1 have resulted in a better distribution of convergences, while maintaining a tunnel deformation (convergence/diameter ratio) of approximately 2% to 5% at a distance of 20 meters from the face.

Phase 2 (Fig. 9) has been first implemented at a distance of 35 m from the face. The shotcrete ring was rapidly under stress, with a maximum overall deformation being attained in the HDC elements of 20%, i.e. with a reserve for further deformation of up to 25–30% before reaching the limit design value. As a result, phase 2 is being moved closer to the face, to a distance of 15–20 m. Future observations of the overall system behaviour and response will allow one to decide if phase 2 could be implemented at a shorter distance from the face.

A special coffer was designed for the project. It was assembled inside the gallery and served to install the concrete lining in 5-metre long segments, as shown in Fig. 10.

4 CONCLUSIONS

The inclined gallery is currently under construction and is faced with exceptional difficulties over a significant length. This calls for a continuous reflection on the resources and methods to be used. The feedback from experience will be directly used for the excavation of the main tunnel, which is expected to be driven in similar conditions, with a cover close to that to be experienced at the bottom of the inclined gallery.

One of the main challenges ahead lies in the definition of the optimal time for installing the final lining ring, and also in the assessment of the long term state of stress for design. Consequently, particular attention needs to be paid in identifying the long term behaviour and the mechanical properties of the squeezing rock mass. The application of the interactive observational design approach, including design analyses and systematic performance monitoring, become essential for achieving this objective.

REFERENCES

Barla G. and Panet M., 2006, Avis sur les conditions de soutènement de la descenderie de Saint Martin La Porte dans les Schiste Houiller, Rapport interne LTF.

Barla G., 2001, Tunnelling under squeezing rock conditions. Tunnelling Mechanics. Eurosummerschool, Innsbruck, 2001, D. Kolymbas (Editor), pp.169–268.

Hoek E., 2001, Big tunnels in bad rock. Journal of Gotechnical and Geoenvironmental Engineering, vol. 127, 9, pp. 726–740.

Hoek E. and Marinos P., 2000, Predicting tunnel squeezing problems in weak heterogeneous rock masses. Tunnels and Tunnelling International, pp. 45–51: part 1; pp.33–36: part 2.

Sulem J., Panet M. and Guenot A., 1987. Closure analysis in deep tunnels. Int. Jour. Rock Mech Min. Sc. & Geom. Abstr., vol. 24, 3, pp.145–154.

This page intentionally left blank

Underground Space – the 4th Dimension of Metropolises – Barták, Hrdina, Romancov & Zlámal (eds)
© 2007 Taylor & Francis Group, London, ISBN 978-0-415-40807-3

Geotechnical conditions, methods, and issues of building the transportation tunnels in the wider area of Belgrade

V.Vujanic, M.Jotic, S.Milenkovic, J.Josipovic & B.Jelisavac
The Highway Institute, Serbia

ABSTRACT: Belgrade is the capital city of Serbia located southwardly from the rivers Sava and Danube on the final part of "Sumadija region crest", i.e. "Belgrade cape". Wider area of Belgrade relief is at the absolute altitude of approximately 70 m above sea level.

Geologic composition of the terrain thereof over basic mountain chain is composed of cohesive clastic sediments and carbonate-limestone, with subordinated presence of metamorphites – serpentinites and with drifts of volcanite – andesites and dacites of Jurassic and Cretaceous age. Almost entire area of Belgrade is covered by Quaternary alluvial, marshy, proluvial-diluvial and eolian sediments. Differing chronsotratographic and lithofacies units are brought into same hypsometric level by numerous faults, thus making even more complex geotechnical conditions for the construction of transportation tunnels.

This paper is presenting briefly spatial distribution of Belgrade area in accordance with geotechnical conditions of previous and forthcoming construction of transportation tunnels, applied methods of excavation and improvement of resistance – deformation properties of rock masses.

1 INTRODUCTION

Belgrade wider area is featuring three geomorphologic units, of higher rank (Figure 4):

- Alluvial plain of rivers Sava and Danube, at absolute altitude of 69–78 m above sea level, whereas the parts of "urban" and "loess" plains are at the altitude ranging from 80 to 115 m above sea level;
- "Sumadija region crest" and its final part – horst-anticline "Belgrade cape" are modified by fluvial erosion and storage, and by proluvial – diluvial processes at the altitude of 25–35 m above sea level, above alluvial plains, i.e. at the absolute altitude of approximately 100 to 200 m above sea level, being bordered by Avala mountain on the city south-side with absolute altitude of approximately 506 m above sea level.
- Neogene basin at Mokri Lug colony, diluvial-proluvial relief covered with loess, locally eroded in the valleys of surface flows. Absolute altitudes of this terrain range from 120 to 190 m above sea level, with certain peaks with absolute altitudes over 250 m above sea level.

Indicated geomorphologic units to the depths relevant for the construction of transportation tunnels are differing as regards the complexity of geologic structure.

Central part of Belgrade wider area in geotectonic sense is falling into the northern part of Central Vardar river sub-zone, i.e. "Sumadija region crest" and its final part denominated as "Belgrade cape".

The oldest discovered rock masses on terrain surface are composed of Jurassic-Cretaceous clastic rocks and limestone of basic mountain chain. Over Jurassic-Cretaceous rock masses, on prevailing part of terrain, there are cohesive, semi-cohesive, and cohesionless clastic (conglomerates, sandstones, clayey marls, argillites, clays, marls, gravels and sands) and carbonate (limestone) rock masses of Neogene. Almost entire area of Belgrade is covered by Quaternary alluvial, marshy, proluvial-diluvial, and eolian sediments. Differing chronostratigraphic and lithofacies units are brought into same hypsometric level by numerous faults with saltation ranging from 20 to 150 m (Figures 1 & 4).

Such lithological composition of terrain thereof predetermined complex, non-homogeneous and anisotropic, geotechnical features of rock masses: grain size distribution of non-cohesive rock masses, origins, and tropism within the system of fissures and fractures of solid rock masses, degradation of rock masses, mode of their interaction with ground waters (differing conditions and regime), as well as resistance – deformation properties of rock masses. Consequently, there is the presence of various

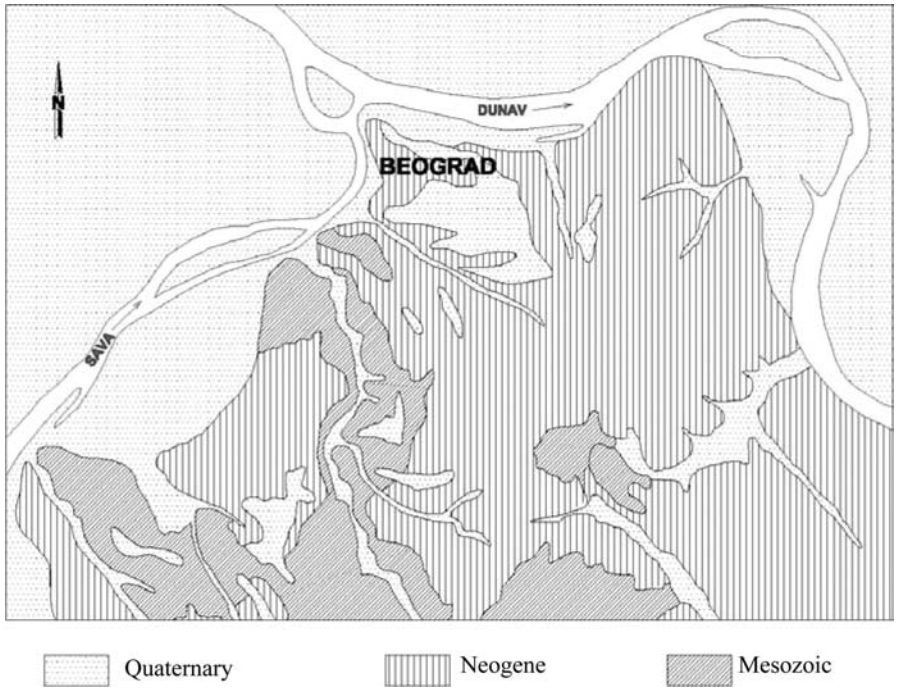


Figure 1. Geologic index map of Belgrade wider area.

geotechnical conditions for the construction and maintenance of transportation tunnels in certain parts of Belgrade wider area.

Until nowadays constructed transportation tunnels in the area thereof, were carried out within the terrains of various lithofacies structure, i.e. differing geotechnical features of rock masses and terrains. In this process, various problems came out which have not been foreseen on time, such as the problems of anchorage, breach of terrain at excavations, protection under ground waters within dusty "fluids", sands, issues of influent seepage of ground waters in already built tunnels, etc.

By analyzing these issues regarding the previous construction of transportation tunnels one came to a conclusion that certain problems occur primarily in terrain parts made of specific lithofacies and chronostratigraphic units. In the text hereinafter, there is a brief presentation of geotechnical features and conditions of transportation tunnels construction in basic lithofacies and chronostratigraphic units in Belgrade wider area, which is in fact the spatial distribution of Belgrade as regards geotechnical requirements, i.e. problems linked with the construction of these facilities. (Fig. 2, 3 & 4). This could be of particular interest for the professional audience, since in the area of Belgrade, there are anticipations for intense construction of transportation tunnels and other underground facilities, such as "LRT-Light Rail Transit" or full-fledged subway, tunnels pertaining "Internal arterial ring", along with the completion of works on tunnels within the framework of Belgrade by-pass motorway E-75.

2 GEOLOGIC COMPOSITION OF BELGRADE WIDER AREA

In geotectonic sense this area is falling into Central Vardar river sub-zone which is ending on this specific terrain with "Sumadia region crest" and "Belgrade cape". The oldest discovered rock masses on terrain surface are made of Jurassic sandstones, with hornstones, clays and marls, and then diabases, melaphyrs, and serpentines. There is a major strike of Jurassic massive and thick-bedded limestone, and Jurassic-Cretaceous flysch. Cretaceous formations, represented in zoogeneous-reef, thick-bedded and massive limestone of Urgon facies. Another lithofacies unit of Cretaceous, with large spreading, is made of Ostruznica flysch, represented by sandstones, marls, and silts in alternating sequence. Locally within their framework there are lenticular beds of breccia limestone and breccia itself. Cretaceous deposits have been ascertained by drilling in the inner urban area of Belgrade. Over Cretaceous and local Jurassic products, there are Neogene deposits set in discordant

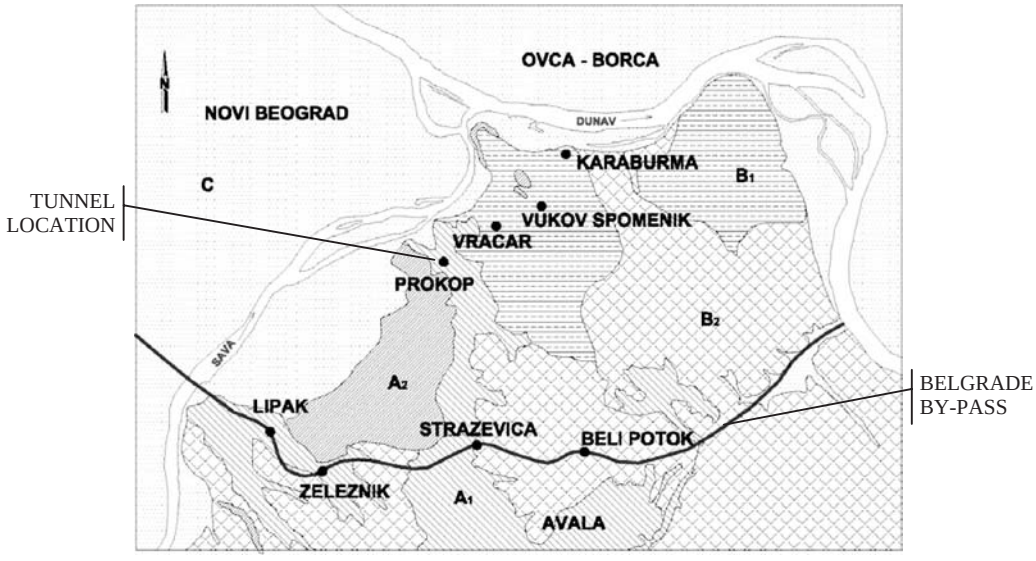


Figure 2. Spatial distribution of terrain as per geotechnical conditions for tunnel construction.

pattern. The oldest Burdigalian products, are represented by schistose, thinly layered clays, bituminous clays and sheet marls with interbeds of tuff and coal. Tortonian and Sarmatian sediments are represented by clays, sandstones, conglomerates and sands, and then by marly limestone, sandy limestone, sandstones and marls in alternating distribution pattern, and zoogeneous reef limestone. Over Sarmatian deposits on almost entire wider area of Belgrade there are Pannonian sediments concordantly set in the facies of marly clays, marls and clayey marls, (Figures 1 & 4).

Pontian sediments, are represented by clays, silts, and fine grained sands with interlayers of weakly cohesive sandstones, conglomerates and limestone.

Pre-Quaternary rock masses are split-up by tectonic motions into numerous faults as blocks set in motion vertically and horizontally, so that differing chronostratigraphic and lithofacies units are brought into same hypsometric level, (Fig. 4).

Quaternary deposits cover almost entire terrain, being represented by fluvial-lacustrine and river sands on the area of alluvial plains of rivers Sava and Danube, loess on the flat of Zemun municipality, diluvial – proluvial silt – clayey deposits on "Sumadia region crest" and Neogene basin in Mokri Lug colony.

3 GEOTECHNICAL CONDITIONS FOR THE CONSTRUCTION OF TRANSPORTATION TUNNELS

Based on previous experience in building transportation tunnels one may draw a conclusion that geotechnical features of rock masses and terrains in Belgrade wider area are very complex in view of heterogeneity and variability of lithofacies composition within the chronostratigraphic units. Thereby, such geotechnical conditions of construction and maintenance of present and future transportation tunnels have been predetermined within the spreading zones of certain lithofacies and chronostratigraphic units.

In the following text, there will be a brief presentation of geotechnical features of lithofacies units, i.e. material composition of terrains and geotechnical conditions for transportation tunnels' construction within their framework, (Fig.2), as per construction requirements, in accordance with following spatial distribution:

- Mesozoic rock masses, area "A_1" are spread out in the western and central part of "Sumadia region crest" and "Belgrade cape", main street Terazije, Tasmajdan park, then in riparian zones of Sava river and in wider area of Cukarica municipality. They are made of flysch sediments, Urgonian reef limestone, layered complex of sandstones, marls and limestone. Generally, these areas consist of highly heterogeneous material composition, differing levels of crystallization and diagenesis, tectonically deformed, with variable and non-uniform physical and mechanical properties along with differing porosity and weathering processes in the presence of water. Within these rock complex packages there are highly consistent and compact milieus, yet likewise with friable parts with undermined physical-mechanical properties which in the presence of water might become extremely unfavorable as operating environment. For such a reason,

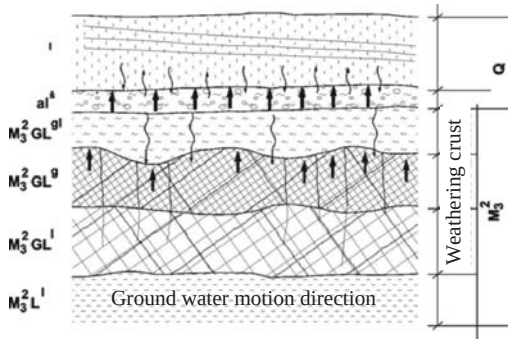


Figure 3. Diagrammatic geologic profile of terrain in narrow urban region.

Mesozoic products can be considered as suitable to restrainedly suitable for tunnel construction. In friable parts there is a possibility of occurrences of ground pressure and falling – in of excavated profile within the overlaying cover and flanks. According to excavation categories GN 200, strong compact parts fall into categories IV to VI, while friable and weathered lithologic units are encompassed by categories II to IV. As regards the conditions for tunnel construction (GN 206), this milieu falls into the category of semi-difficult tunnels with the appearance of minor vertical and lateral pressures. Adequate and thorough bracing is needed for profile heading for these facilities. Prevailing part of railroad tunnel "Dedinje", along with tunnels "Lipak" and "Zeleznik" on Belgrade by-pass motorway were built within these rock masses. New Austrian method (NATAM) can be applied successfully within their framework, with the exception for major distributed faults. This method provides for the excavation with machines or abrasive blasting, and utilization of anchors and prestressed concrete with steel fabric as bracing support. In this process it indispensable to adapt the blasting method to keep the rock mass properties as intact as much as possible and to protect the surrounding facilities.

- Tortonian and Sarmatian carbonate rock masses, area "A_2", are represented by reef limestone and lime- stone, sandstones and marls in an alternating pattern, above ground water level. It is appropriate for transportation tunnel construction. They are rather soft for excavation and stable during construction and maintenance of tunnel facility. In terrain parts where ground water storages are formed in these rock masses one may encounter major problems due to relevant inflow into the tunnel excavations. According to norms GN200, they fall into the category ranging from III to V, whereas regarding the tunnel construction GN 206 these fall into the category of medium difficult tunnels. Although, they provide for somewhat easier excavation conditions, generally speaking they are similar or same as previously described ones, which was proven in the construction of railroad tunnel "Vracar" and motorway tunnel "Strazevica" on Belgrade by-pass.
- Tortonian and Sarmatian marly rock masses, area "B_1", represent the milieus which after the excavation break-up and pulverize into debris and clayey material, thus having unsuitable properties as milieus for tunnel construction. The excavation within their framework must be carried out with particular caution, and excavated profile should be braced immediately, in order to prevent the surface weathering due to the relaxation of rock massif. According to GN 200, they fall into the category IV, while according to tunnel construction requirements GN 206, these fall into the category of difficult tunnels, where one might expect extensive pressures and scattered major falling out of materials above anticipated and required profile. The presence of ground water exerts a great influence onto the quality of rock mass. Adequate and thorough bracing is needed along with tight casing and cautious operations. The most efficient excavation in these milieus is carried out with cutting and milling machines (it can be performed with pneumatic tools), while for permanent bracing in these rock masses, one can utilize prefabricated concrete elements, standard cast reinforced concrete bedding, yet the advantage is obviously awarded to shotcrete, combined with anchors, steel centres and reinforced wire fabric.
- Pannonian marly rocks, area "B_2", represent the least suitable milieu for building transportation tunnels in "Sumadia region crest", i.e. "Belgrade cape", and within "Neogene basin" at Mokri Lug colony. Pannonian products are prone to fast weathering, particularly with the presence of ground water and formation of weathering crust with thickness over 20 m (Figures 3 & 4). In terrains made of Pannonian marls and clayey marls the construction of tunnels is followed by difficulties due to swelling, settlement and ground pressure occurrence, and not only in overlaying soil, but also in invert arch, which requires the construction of purpose-made structures. As regards the tunnel excavation, this milieu is featuring the same characteristics as Sarmatian marly sediments. Techniques of excavation and bracing is the same as in previously described milieus. Underground structures were built in these milieus such as: underground railroad station "Vukov spomenik", exit part of tunnel "Karaburma", whereas the future tunnel "Beli potok" will be built on E-75 motorway by-pass of Belgrade.
- Quaternary rock masses, area "C", represent the package of extremely differing geotechnical features and are made from:

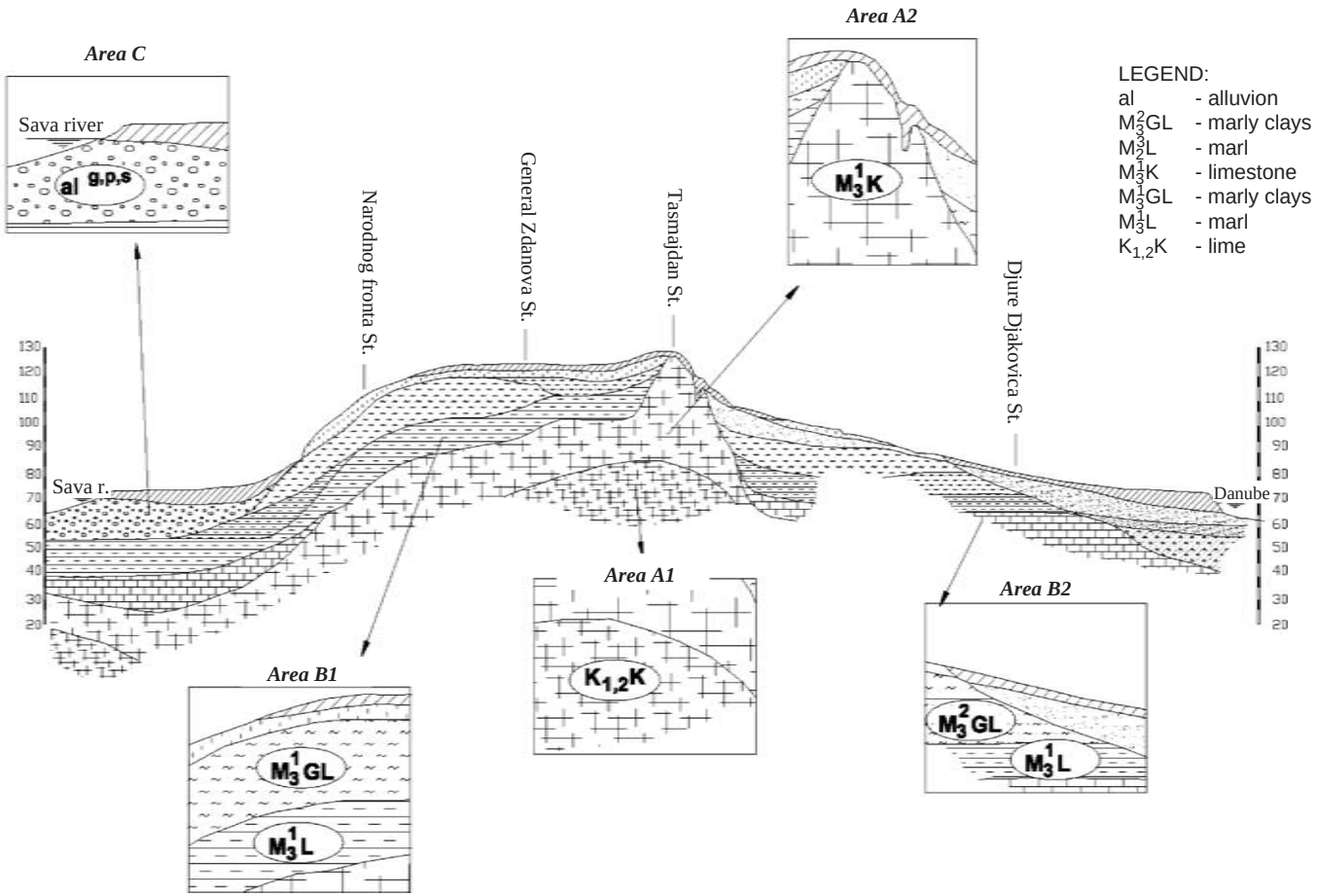


Figure 4. Geologic profile of narrow urban region with areas set apart.

– Diluvial-proluvial, silty-clayey deposits on "Sumadija region crest" and "Neogene basin" at Mokri Lug colony, with high to medium shrinkage, prone to alteration depending on the ground water presence. As regards the excavation (GN 206) they fall into the category of very difficult tunnels to make, with expected strong pressures, extensive overtopping of anticipated profile. Complex and strong bracing is required. Similar geotechnical features are found in boggy basin.
– On-shore loess, in parts above ground water level, as regards the excavation is placed in category I. According to GN 206, tunnels in loess are considered easy to build. Within the zone of ground water oscillations, loess is degrading itself and losing the typical tubular porosity and is becoming very shrinkable with potential breach of soil. In view of that, in the case of minor surcharge, it is advisable to build the tunnel as open cut mining.
– Fluvial-lacustrine and river sandy – gravel deposits, in the area of alluvial plains of rivers Sava and Danube, represent the milieu wherein the excavation can be classified in categories II and III and can be carried out with sophisticated protection from ground water by building watertight membranes, absorbing wells, etc. Tunnels in the area of alluvial plains of rivers Sava and Danube are classified in the category of very difficult facilities to build. Otherwise, conditions for tunnel construction within all these rock masses, are more or less identical, since anticipated severity of geotechnical issues is similar or identical.

4 CONCLUSION

Some of the conclusions should be drawn from the presented issues which are referring to the construction conditions, that is the excavation methods and solution of other problems to be tackled with during the construction of transportation tunnels in Belgrade wider area. The conclusions are as follows:

1. Belgrade wider area is specific by its geologic composition of terrain being highly diversified and complex, either on surface (locations) or deep down. Due to that, geotechnical requirements for the construction of underground facilities also vary within the range from highly suitable to very complex and difficult ones. Hence, the acquaintance with them in the project implementation of underground facility construction is having very high technical and economic relevance, among other things, because based on the results of geotechnical investigations, strategic decisions are being made as regards the viability of underground facility construction;
2. In addition, the construction of underground facility in such conditions must be controlled in view of its impact onto the environment, structures, buildings, streets, utilities, and installations as well. Consequently, one must provide for all necessary requirements meant for it, so that during its operation it can withstand all impacts;
3. Such a complex problem area, requires the creation of information system, and setting up of monitoring pertaining to parameters relevant for determining the construction requirements to which until nowadays insufficient attention has been awarded with;
4. In our view it is important to have at hand the permanent presence of design geologic-geotechnical supervision during the construction of underground facilities, since it has provided for very good results, particularly with reference to costs and target dates of construction.

LITERATURE

Bogdanović A. (2006): *Podvodni saobraćajni tuneli u Beogradu I i II deo*. Časopis «Izgradnja», br. 3–4 i 5–6, Beograd.

Božinović D. (1979): *Geotehničke osobine terena u području Beograda koje izgrađuju koherentni gornje miocenski sedimenti*, Beograd.

Josipović J., Vujanić V., Jotić M., Dangić A. (1996): *Podzemne vode i geotehnička svojstva panonskih sedimenata Beograda*. Međunarodni naučni skup "Pravci razvoja geotehnike 1880-1921-1996", Bgd.

Josipović J., Vujanić V., Jotić M. (1996): *Podzemne vode u kvartarnim i neogenim naslagama Beograda kao faktor uticaja na urbani prostor*. Zbirka referata XI jugoslovenskog Simpozijuma o hidrogeologiji i inženjerske geologije, Budva.

Krstić N., Sikošek B. (1984): *Prilog poznavanju tektonike Beograda,* Zbornik referata savetovanja »Geološka istraživanja u privrednom i prostornom razvoju Beograda«, Beograd.

Lokin P., Anagnosti P. (1997): *Geotehnički aspekti korišćenja podzemnog prostora u Beogradu*. II Savetovanje JUBa, "Podzemni prostor u razvoju Beograda", Beograd.

Marković R., Lokin P., Gojgić D., Jevremović M: *Inženjerskogeološke karakteristike terena i geotehnički uslovi građenja podzemnih objekata u Beogradu.* Zbornik referata savetovanja "Geološka istsraživanja u privrednom i prostornom razvoju Beograda", Beograd.

Studija o »premetrou« (1989), Beograd čvor, Beograd.

Studija »Razmatranje rešenja podvodnih saobraćajnih tunela« (1996), Beograd čvor, Beograd.

Stručna dokumentacija i publikacije Instituta za puteve, a.d. iz Beograda.

Zbornik radova sa I Savetovanja o podzemnoj izgradnji (1987), Beograd.

Vujanić V., Jotić M., Rokić LJ., Josipović J. (1997): *Uticaj podzemnih voda na geotehnička svojstva terena pri izgradnji podzemnih objekata na teritoriji Beograda*. II Savetovanje JUBa, "Podzemni prostor u razvoju Beograda", Beograd.

Underground Space – the 4th Dimension of Metropolises – Barták, Hrdina, Romancov & Zlámal (eds)
© 2007 Taylor & Francis Group, London, ISBN 978-0-415-40807-3

Construction of major trunk road tunnels in Moscow

B.I. Yatskov
Mosmetrostroy OJSC, Moscow, Russia

A.M. Zemelman
Metrogiprotrans OJSC, Moscow, Russia

S.N. Vlasov & I.S. Bubman
Russian Tunnelling Association, Moscow, Russia

ABSTRACT: Last years are characteristic with intensive growth of construction of major trunk road tunnels in Moscow. Data on ten largest tunnels are presented in table form. Detailed description is given to challenging Lefortovo and Serebryanoborski tunnels, the latter currently under construction. The Serebryanoborski tunnel system consists of two 2473 m long 14.2 m diameter transport bore barrels with 2060 long approach cut-and-cover sections, one 6.5 m diameter service bore barrel and five connection drifts built in mine techniques. Particular attention is given to safety and surface settlement issues.

During last ten years, general transport situation in Moscow has drastically aggravated. First of all, the streets of Moscow have got saturated with vehicles. From 1991 to 2005, car growth rate exceeded similar indices for previous periods 10 times.

The trend of previous Moscow Development General Pans to presumably develop the public transport modes, first of all metro systems, has resulted in the scope of road construction to lag far behind the city actual needs.

Three quarters of the city trunk roads and transport knots, particularly those in the central part of the city, are overloaded and operate at the upper capacity level.

Traffic jams and increased traffic intervals of surface public transport means have become common. The situation thus formed has considerably worsened the transport service and passenger travel comfort standards immediate solution of the problem was needed. This is why, in order to solve the transport problem and to rehabilitate the city central part, the "Third Transport Ring" program was adopted by the Government of Moscow in 1997–1998. The program stipulated creation of a new multi-purpose transport system as well as rehabilitation and development of areas adjacent thereto.

In order to provide for continuous traffic flows, interchanges must be built at the trunk road.

With this end in view, many structures of various types (bridges over the Moskva River, flyovers, tunnels under the trunk roads and under tracks Moscow Railway) are built along the alignment.

Implementation of this major project of Moscow is actively participated by Organizator Ltd., Corporation "Transstroy" OJSC, Moskapstroy OJSC, Misinzhstroy JSC, Mosmetrostroy OJSC, Moskomarkhitektura as well as Mosinzhproekt, Soyuzdorproyekt and Mosguiprotrans design institutes and many specialized design and construction companies.

While developing designs of the interchanges, it is always a matter of choice between the bridge and the tunnel options to be made with due account of site-specific city development, transport and environment considerations as well as of the availability and location of utilities. Quite often, in spite of higher costs and considerable underground utility rearrangement work, tunnels prove to be more preferable than flyovers, particularly in case of rolling relief.

Tunnel-type interchanges occupy relatively small areas. Their structural elements do not project above the surface, do not hamper visibility at intersections and do not destroy the previously formed architectural ensembles. Contrary to flyovers, tunnels are protected against adverse atmospheric impacts.

Road tunnels equipped with forced ventilation systems lower gas and dust contents in the tunnel environment; in case architectural/acoustic facing facilities (noise-dispersing barriers, hung-up ceilings, wall panels) are provided by the design, city environment will

be less subject to the noise. Vibration absorbing tunnel components and other facilities of similar action minimize the transition of vibrations to adjacent buildings and structures.

The transport infrastructure of Moscow has lately got enriched with several major road tunnels built the largest trunk road crossing sites and designed to separate road traffic flows using several levels. This resulted in higher traffic speeds, increased traffic capacity of the crossings, better traffic safety.

Among projects built by the end of 2007 there are:

- Kutuzovskaya Interchange representing a unique system of structures composed of 6 tunnels, total length 3065 m, flyovers, total length 758 m, and surface ramps, the five-level complex having made it possible to provide for the light-free traffic flows at the crossing; besides, the tunnel complex includes commercial/pedestrian zone, area 7000 m^2, and parking lots, area 5000 m^2;
- enormous interchange at Gagarin Square: 8-lane 900 m long road tunnel with exits towards Andreevski Bridge and Leninski Avenue; this major construction complex integrates 920 m long railway tunnel with transition center to Leninski Prospect metro station and two-level parking lots for 640 cars;
- 509 m long road tunnel for five traffic lanes at Volokolamskoye Chaussee under the Moscow Channel including one lane for trolley-buses; 160 m of this tunnel run immediately under the channel.

The largest underground project at the 3rd Ring optimally solving a set of transportation, ecological, architectural and historical problems is a tunnel in the area of Lefortovo designed for traffic intensity up to almost 4000 vehicles per hour in one direction at 60 km/h tunnel traffic design speed.

Main data on the largest Moscow tunnels are presented in Tables 1 and 2.

At present, construction of Serebryanoborski tunnels, one of most challenging and technically interesting tunnel complexes, is underway; the article is devoted mainly to these tunnels.

Serebryanoborski tunnels being built in the northwest part of Moscow make part of a section of Krasnopresnenski Avenue stretching from MKAD to Marshal Zhukov Avenue to join the central part of Moscow.

The tunnels were called “Serebryanoborski” since the route passes under Serebryanoborsk forestry, an ecologically protected region of Moscow.

The Moscow – Riga (“Baltiya”) up-to-date highway completed by the end of nineties ended at MKAD because it was not possible to directly join it with Marshal Zhukov Avenue and thus with the central part of Moscow. According to terms and conditions imposed by Serebryanoborsk Forestry, any highway surface route option was ruled out owing to ecology considerations.

This is why it was decided by the Government of Moscow to build Serebryanoborski tunnels using TBM with active face support purchased some years ago from Herrenknecht company (Germany) and available after completion of the deep Lefortovo tunnel.

Tunnel complex built by the closed methods consists of 3 tunnels and some drifts:

- two transport tunnels, excavation diameter 14.2 m, length 1514 m each;
- one service tunnel, excavation diameter 6.3 m, length 1514 m, located between the transport tunnels;
- the tunnels are interlinked with five drifts, length 21 m, excavation cross-section 6.5 m (span) × 9.0 m (height), spaced at 250 m.

In the transport tunnels structurally executed in two levels, combined traffic is arranged with road traffic at the upper level on three lanes each direction and trains of the Stroguinsko-Mitinskaya metro line at the lower level. This solution is as interesting from engineering viewpoint as sophisticated in execution, this is why it is seldom used in practice.

Given site specific climatic and ground conditions, it was decided to drive the tunnels using the active bentonite face support technology providing for minimum settlement of the surface, buildings, structures and utilities.

Bentonite slurry and compressed air based hydraulic face support technology was chosen since it makes possible to smoothly adjust hydraulic pressure values depending on changing geological conditions and technological parameters as well as to carry out objective instrumental control. These advantages were many times verified and successfully used while driving the Lefortovo tunnels using the same Herrenknecht TBM. TBM shield assemblage moment is fixed in Figure 1, while the moment of placing the machine into the dismantling chamber is shown in Figure 2.

By the moment, the left and the service tunnels are successfully driven; currently they are being equipped including construction of reinforced concrete carriageway slab and metro line compartment, application of fire-resistant coatings and installation of smoke-removing ducts and all utilities; the right tunnel is being driven.

The following results were attained while driving the above tunnels:

- maximum progress: 16 m/day (8 rings as wide as 2.0 m for the transport tunnel and 13 rings as wide as 1.2 m for the service tunnel);
- surface settlements fixed instrumentally in the course of monitoring made 8 – 12 mm;
- maximal connection accuracy: 8 mm for axis, 12 mm for stationing, 4 mm for height;

Table 1. Main data on road tunnels built in Moscow by end 2007.

Parameters	Unit	Tunnel title and location				
		Tunnel under Kutuzov Avenue	Gagarin tunnel under Lenin Avenue	Lefortovo deep tunnel	Lefortovo tunnels at the bypass of Lefortovo	Tunnel under the Channel of Moscow at Volokolamsk Chaussee
Traffic mode	–	road	road/rail	road	road	road/trolley
Tunnel traffic arrangement and direction	–	one level, two directions	one level, two directions	one level, one direction	one level, one direction	one level, two directions
Capacity	veh/h	6000	6000	3800	4600	3600
Number of lanes in main tunnels	pcs	3 + 3	3 + 3	3	4	3
Total length of main tunnels	m	3045	2030	3522	2969	150
Cross-section span × height	m × m	27.2 × 5.2	42.2 × 5.2	diameter 14.2	16.5 × 5.2	13.1 × 4.45
Structure (lining) type of main tunnels	–	precast/cast-in reinforced concrete	precast/cast-in reinforced concrete	precast reinforced concrete	precast/cast-in reinforced concrete	precast/cast-in reinforced concrete
Total length of entry and exit parts	m	707	918	1405	224	259
Structure (lining) type of entry and exit parts	–	precast/cast-in reinforced concrete	precast/cast-in reinforced concrete	cast-in reinforced concrete	precast/cast-in reinforced concrete	precast/cast-in reinforced concrete
Number of lanes at entry and exit parts	pcs	2 + 2	2 + 2	2	2	3
Total area for city infrastructure premises	sq m	7000	65,000	–	–	–
Total area for underground parking lots	sq m	5000	22,000	–	–	–
Location of ventilation ducts	–	upper part of the cross-section	central ventilation corridor	above the carriageway	upper part of the cross-section	–
Emergency exit	–	through portals	through 14 exits and central corridor	through corridor under carriageway	through portals	through portals
Construction method	–	“Milan” cut-and-cover	cut-and-cover	closed, TBM	cut-and-cover	closed, pipe screen
Construction period	years	1998–2000	1999–2001	2000–2003	2001–2003	1970–1972

– all rings were assembled within the tolerance (±50 mm).

Ground-cutting instruments were controlled, examined and changed under compressed air (caisson conditions) from the chamber adjacent to the face during shield operation stops.

Owing to perfected technological operations and high professional level of the personnel, no particular problems arose in the course of driving, excepting bentonite slurry separation in the course of simultaneous driving of the main and the service tunnels combined with operation under caisson conditions.

Connecting drifts, five in number, are spaced at 250 m station distance; they are multifunctional and destined to help effectively solve the following major tasks related to operation of main tunnels:

– supplying fresh air through service tunnel sections and its subsequent distribution over transportation zones of the main tunnels through the drifts;
– laying the required utilities (cables, pipelines, etc.);
– in case emergency situation occurs in any of the transportation tunnels, evacuating the passengers, drivers and operation personnel through emergency

Table 2. Main data on road tunnels built in Moscow by end 2007.

Parameters	Unit	Tunnel title and location				
		Tunnel at Sushchevsky Val Str.	Tunnel at Novaya Bashilovka Str.	Tunnel under Serebryanoborsk forestry	Tunnel under Begovaya Str.	Tunnel under Boris Galushkin Str.
Traffic mode	–	road/trolley	road/trolley	road/metro	road	road
Tunnel traffic arrangement and direction	–	one level, two directions	one level, two directions	two levels, two directions	one level, two directions	one level, two directions
Capacity	veh/h	4600	6000	7600	6000	8000
Number of lanes in main tunnels	pcs	2 + 2	3 + 3	3 + 3	3 + 3	4 + 4
Total length of main tunnels	m	237	124	4533	489	86
Cross-section span × height	m × m	9.7 × 5.0	23.6 × 5.2	diameter 2 × 14.2 + 1 × 6.2	20.2 × 5.2	37.9 × 5.2
Structure (lining) type of main tunnels	–	precast/cast-in reinforced concrete	precast/cast-in reinforced concrete	cast-in reinforced concrete	precast/cast-in reinforced concrete	precast/cast-in reinforced concrete
Total length of entry and exit parts	m	–	206	2060	190	495
Structure (lining) type of entry and exit parts	–	precast/cast-in reinforced concrete	precast/cast-in reinforced concrete	precast/cast-in reinforced concrete	precast/cast-in reinforced concrete	precast/cast-in reinforced concrete
Number of lanes at entry and exit parts	pcs	2 + 2	2 + 2	2 + 2	2 + 2	3 + 3
Total area for city infrastructure premises	sq m	–	–	–	–	–
Total area for underground parking lots	sq m	–	–	–	–	–
Location of ventilation ducts	–	–	–	in service tunnel	–	–
Emergency exit	–	through portals	through portals	through 5 connections and Service tunnel	through portals	through portals
Construction method	–	closed, pipe screen	closed, pipe screen	closed, TBM	closed, pipe screen	closed, pipe screen
Construction period	years	1962–1965	1966–1968	2004–2007	1966–1968	2001–2002

corridors in the service tunnel and providing for the flow of fresh ventilation air.

250 m distance was chosen proceeding from the condition that a person can stand fire and smoke no longer than for 1.0–1.5 minutes. Any person caught with emergency situation at maximal distance of 125 m from the nearest drift and moving at a speed of 6 km/h will escape within 1.0–1.25 minutes.

Most difficult was mine driving of drifts between the tunnels. The drifts pass in different ground conditions and the driving required various different special construction techniques to be used. Figures 3 and 4 demonstrate preliminary stabilization of the soil and driving of drifts between the tunnels respectively.

To drive the first (on move) drift passing through relatively dry sand below ground water table, horizontal jet techniques were used to stabilize the soil massive.

The second (on move) drift passes through water-saturated sand. Owing to this, two soil massive stabilization techniques were combined: injection of Microdur particularly fine mineral binder and horizontal jetting.

The third and the fourth drifts pass in most unfavorable natural conditions (ground water head approximately 1.6 bars, permeability coefficient from



Figure 1. Assembling Herrenknecht TBM shield rotor.



Figure 2. Moving the shield into dismantling chamber.

1 to 2 m/day). This is why it was decided to use horizontal freezing techniques, freezing station being installed in the left transport tunnel.

The fifth drift is built in relatively stable clay, protective screen of pipes driven above the tunnel vault being used.

All the five drifts are driven by means of partial excavation of the cross-section using the wall-supported vault techniques and temporary arch concrete supports.



Figure 3. Soil preliminary stabilization operations while driving drifts between tunnels.



Figure 4. Driving drifts between tunnels.

While executing every soil massive preliminary soil stabilization operation in each drift, thorough fulfillment of technological schedule requirements was observed and first of all, permanent multi-factor control and operation-vise acceptance.

Technological facilities as well as with life-supporting and project operation safety systems.

As soon as driving the transport tunnel whose general view is presented in Figure 5 is completed, the tunnel itself and drifts between its barrels will be equipped with permanent technological structures, life support and safe project operation systems.

Resulting from the tender and competitive bidding, the following main organizations were established:

- Client: Organizator Ltd.;
- General Contractor: consortium headed by Mosmetrostroy OJSC;
- Scientific and technical support: Tunnels and Metro Scientific Research Center, TsNIIS OJSC, and Russian Tunnelling Association;



Figure 5. General view of transport tunnel in the course of driving.

– Consultants: VINCI (France) and Herrenknecht (Germany).

In compliance with a decree of the Government of Moscow, the Serebryanoborski tunnel project is scheduled for completion and putting into operation along with the Stroguinsko-Mininskaya metro line at the end of 2007.

Construction of long tunnels demands that the following sophisticated operation systems absolutely reliable under emergency conditions be developed to provide for the safety of transportation flows: stable power supply systems; ventilation systems providing both for fresh air supply and for smoke evacuation in case of fire; water- and heat supply systems; systems of communication, signaling, information, telemonitoring, etc. Operation of various technological facilities must be concentrated in a single control post. Such systems do operate in the Kutuzovski, Gagarinski and Lefortovo tunnels.

Road tunnels are attributed to structures of increased responsibility level whose failure may result in serious economic, social and ecological consequences. Tunnel design and construction specifications stipulate that stain-stress condition of the tunnel lining be monitored both in the course of construction and during initial operation period. While driving the Serebryanoborski tunnels, special monitoring is being carried out including detailed control of surface deformation and condition of buildings and structures available within the tunnel driving possible influence area.

Underground Space – the 4th Dimension of Metropolises – Barták, Hrdina, Romancov & Zlámal (eds)
© 2007 Taylor & Francis Group, London, ISBN 978-0-415-40807-3

Selecting auxiliary construction methods for NATM tunnel excavation in urban areas

J. Yorita & Sasaki
Iiyama Railway Construction Office, Japan Railway Construction, Transport and Technology Agency, Iiyama city, Nagano, Japan

N. Yamaki & M. Okamura
Toda Co., Ltd., Chuo-ku, Tokyo, Japan

ABSTRACT: The Takaoka Tunnel on the Hokuriku Shinkansen Line is a tunnel 6,938 m long (north sector: 3,990 m, south sector: 2,948 m) under construction by the NATM in an urban area in northern Nagano Prefecture. The geology of the south sector is fractured cohesive soil (N-value 10 to 20) and silt (N-value 10 to 30) intercalating sand aquifer. Excavation is performed at small depths (tunnel diameter multiplied by about 2 to 3) directly below many existing structures. This paper discusses a technique for selecting auxiliary methods by statistical and FEM analyses, newly introduced for minimizing adverse impact of tunneling work upon nearby structures.

1 INTRODUCTION

The Takaoka Tunnel on the Hokuriku Shinkansen Line is a NATM tunnel 6,938 m long, longitudinally traversing the Nagaoka Hills on the right bank of the Chikumagawa River running in northern Nagano Prefecture, located at the Fossa Magna. The construction alignment is divided into two parts, north (3,990 m long) and south (2,948 m long) sectors. The south sector of this tunnel is located in the southern Nagaoka Hills, running just below many residences and other neighboring structures (Fig. 1). To minimize adverse impact of tunneling upon these structures, the primary requirement is to limit surface settlement. A technique was established for selecting auxiliary methods for limiting surface settlement. Statistical analysis was conducted as the first step, involving data obtained during the construction, to evaluate the auxiliary methods. Based on the results of the statistical analysis, auxiliary methods for numerical modeling were selected. Then, a numerical analysis model was created to mechanically evaluate the auxiliary methods.

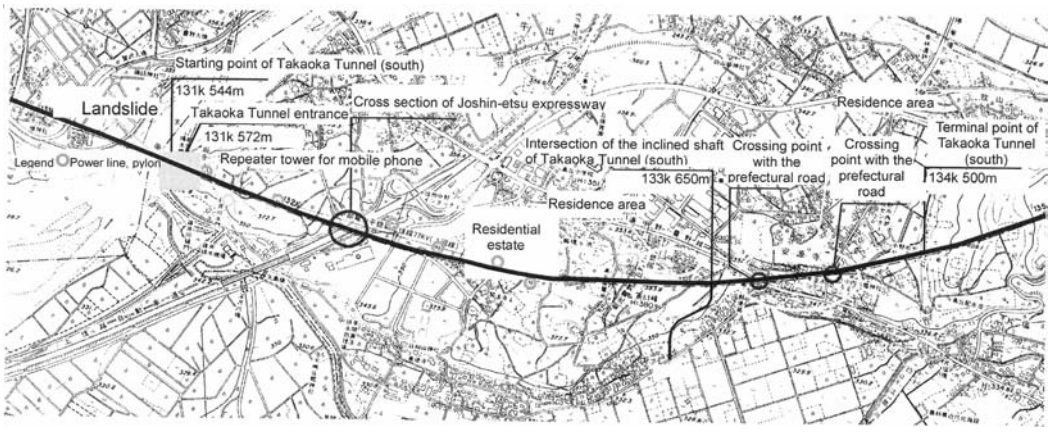


Figure 1. Plan.

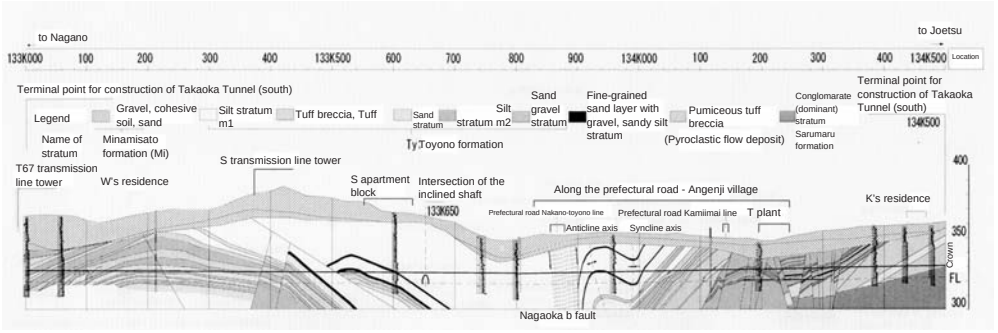


Figure 2. Longitudinal profile.

2 GEOLOGICAL OVERVIEW

The geology of the south sector is weak and unconsolidated. The tunnel is to be constructed at shallow depths just below many residences and important infrastructure. The Toyono stratum forming a large part of the ground of this sector is mainly composed of silt of 1.0 MPa in unconfined compressive strength. Settlement at the support foot and other parts is anticipated due to decrease of bearing capacity of the ground. The silt stratum contains intercalating or alternating sand and gravel layers. Where the ground contains water, there is fear of ground collapse because of water inflow with the soil. The geology is very complex with noticeable folds, dips and faults generated by active tectonic movements (Fig. 2).

3 EVALUATION OF THE AUXILIARY METHODS BY STATISTICAL ANALYSIS (MULTIVARIATE ANALYSIS)

Different auxiliary methods were evaluated in terms of their effect in limiting settlement by means of statistical analysis (multivariate analysis). Since the ground conditions of the tunnel (geology, existence of fault, folding, overburden, etc.) vary from section to section, it is difficult to evaluate each auxiliary method in a generic manner. However, the authors attempted generalized evaluation by multivariate analysis with plural samples of quantifiable data. By involving samples of multiple sections, it is possible to assess the effect of each auxiliary method in limiting settlement in typical geology in the south sector of the Takaoka Tunnel.

3.1 *Evaluation by regression analysis*

Ground surface settlement was taken as an objective variable, and ground condition, supports and auxiliary methods as explanatory variables, to quantitatively evaluate by means of regression analysis. Scarcity of available numerical data of tunnel excavation sometimes makes it difficult to develop a suitable model. Nevertheless, data were quantified as much as possible for analysis. The results of the regression analysis are summarized in Table 1.

Table 2 shows the effect each auxiliary method had in limiting settlement when used alone. This table demonstrates that each auxiliary method is similar in surface settlement effect. However, X(5) (closure with struts), X(3) (AGF: injection type long forepiling) and X(7) (sidewall pre-grouting) are comparatively more effective. Hence these variables should be involved in the modeling to develop an accurate FEM model.

3.2 *Correlation analysis*

Multicollinearity among variables (among different auxiliary methods) is found in the results of correlation analysis shown in Table 3. This is attributable to the fact that multiple auxiliary methods work in concurrence with each other to restrain surface settlement, that is to say, auxiliary methods combine to limit settlement.

Although the analysis used all the explanatory variables that could be quantitatively given, t-value (test of hypothesis concerning mean) is small for the variables, showing that they are not reliable as explanatory variables, except for closure with struts, foot reinforcement pile and sidewall pre-grouting (Table 3). This can be assumed to be due to multicollinearity among variables. The same holds for F-value (variance test).

3.3 *Evaluation by the statistical analysis*

The statistical analysis was capable of quantitatively analyzing the effects of the auxiliary methods. As shown by the analytical results, the effects of X(3) (AGF: injection type long forepiling) and X(7) (sidewall pre-grouting) are more effective for surface settlement. Hence these variables should be modeled for creating an accurate FEM model. In addition, the analysis on correlation among the different

Table 1. Results of regressing analysis.

No.	Variable	Regression coefficient	Partial correlation coefficient	F-value	t-value
X (1)	Steel support	−2.98	−0.15	0.54	0.73
X (2)	PASS	−8.35	−0.11	0.32	0.56
X (3)	AGF	−3.02	−0.18	0.78	0.88
X (4)	Top heading temporary closure	−0.33	−0.06	0.09	0.30
X (5)	Closure with struts	−2.31	−0.37	3.75	1.94
X (6)	Foot reinforcement pile	−11.28	−0.46	6.48	2.54
X (7)	Sidewall pre-grouting	−1.83	−0.23	1.34	1.16
X (8)	Face bolt	−1.41	−0.17	0.72	0.85
Constant	–	258.41	–	–	–

Multiple correlation coefficient: 0.85
Contribution ratio: 0.72
Number of samples: 33

PASS: Pre-Ach Shell Support
AGF: Injection type long forepiling

Table 2. Surface settlement limiting effect.

No.	Variable	Remarks	Reduction in settlement (mm)	Order
X (1)	Steel support	Use of higher grade: H200 instead of H150	15	7
X (2)	PASS	3 m PASS	25	4
X (3)	AGF	12.5 m long pile	38	2
X (4)	Top heading temporary closure	30 cm thick shotcrete	10	8
X (5)	Closure with struts	20 cm struts	46	1
X (6)	Foot reinforcement pile	Foot pile	23	5
X (7)	Sidewall pre-grouting	Grouting and reinforcement of steel pile	33	3
X (8)	Face bolt	1.25 m long fact bolt	18	6

Table 3. Correlation analysis.

		Steel support	PASS	AGF	Top heading temporary closure	Closure with struts	Foot reinforcement pile	Sidewall pre-grouting	Face bolt
X (1)	Steel support	1.00	–	–	–	–	–	–	–
X (2)	PASS	−0.36	1.00	–	–	–	–	–	–
X (3)	AGF	0.35	−0.98	1.00	–	–	–	–	–
X (4)	Top heading temporary closure	0.45	−0.80	0.79	1.00	–	–	–	–
X (5)	Closure with struts	0.54	−0.67	0.66	0.83	1.00	–	–	–
X (6)	Foot reinforcement pile	−0.46	0.47	−0.44	−0.67	−0.86	1.00	–	–
X (7)	Sidewall pre-grouting	0.71	−0.47	0.48	0.48	0.50	−0.37	1.00	–
X (8)	Face bolt	0.22	−0.61	0.69	0.49	0.40	−0.16	0.39	1.00
Y	Surface settlement	−0.47	0.67	−0.71	−0.61	−0.55	0.23	−0.58	−0.66

Table 4. Comparison of values obtained in the respective analytical steps.

	Surface settlement (mm)				Crown settlement (mm)			
	Step	Measurement	Elastic	Nonlinear elastic	Elasto-plastic	Measurement	Elastic	Non-linear elastic	Elasto-plastic
1	Dead weight analysis	–	–	–	–	–	–	–	–
2	Top heading excavation Stress release ratio 40%	–	29	38	31	–	90	117	94
3	Top heading support	–	–	–	–	–	–	–	–
4	Top heading excavation Stress release ration 60%	–	58	91	71	–	160	239	186
5	Bench excavation Stress release ration 40%	–	64	105	79	–	169	261	198
6	Bench support	–	–	–	–	–	–	–	–
7	Bench excavation Stress release ratio 60%	104–119	69	121	85	210–232	177	288	204

variables quantitatively revealed the fact that they exhibit expected effects by dependency on each other.

4 CREATING A NUMERICAL ANALYSIS MODEL

4.1 *Selection of an analysis model*

Referring to the results of statistical analysis, an FEM model was created, which is capable of accurately simulating the surface settlement aimed at curbing impact on structures in the vicinity.

Through study on the surface settlements in the sector already constructed, elastic analysis, nonlinear elastic analysis and elasto-plastic analysis were conducted, to select a prediction model capable of closely simulating the actual situation.

The geology of the section considered in the analysis was comparatively uniform, mainly composed of silt, located at 133 km 680 m, with modulus of deformation $E = 27\,MN/m^2$, internal friction angle $f = 20$ degrees, cohesion $C = 101\,kN/m^2$ and overburden depth of 35 m.

Comparison was made in the analytical section, between measured surface settlements and those given by direct analysis of each analytical technique, and between surface settlement and tunnel crown settlement at each analysis step (Table 4). In addition, studying the major principal strain distribution diagram of each model, the authors attempted to determine a model that can correctly express the deformation characteristics of the tunneling sector discussed here.

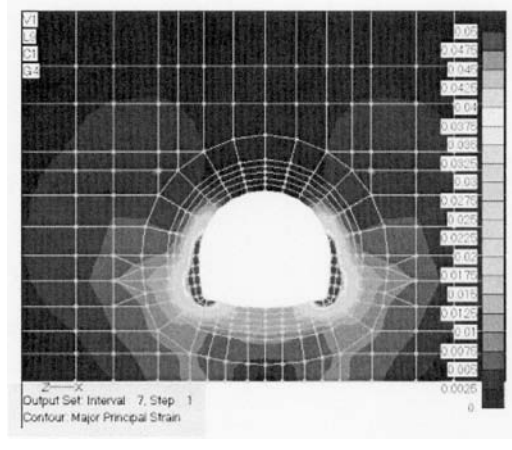


Figure 3. Distribution of major principal strain (nonlinear elastic analysis).

This comparative study confirmed that the nonlinear elastic analysis is capable of simulating the ground deformation characteristics of the tunneling sector in question, providing final surface settlement and crown settlement close to the measured values, and expressing, in the major principal strain distribution diagram, loosened zone in the crown and at the top heading. Consequently, the nonlinear elastic model was selected for analytical study of excavation patterns (Fig. 3).

The silt stratum is the main geology of the tunneling sector. It has a small modulus of deformation,

Table 5. Study cases and analytical prediction.

	Auxiliary method	Case 1	Case 2	Case 3	Case 4	Case 5	Case 6
Condition	Forepoling	–	○	○	○	○	○
	Foot reinforcement pile	–	○	○	○	○	○
	Top heading temporary closure	–	○	○	○	○	○
	Shotcrete thickness		15 cm	30 cm	15 cm	15 cm	15 cm
	Top heading struts	–	–	–	H150	–	–
	Shotcrete invert (20 cm)	-	○	○	○	○	○
	Sidewall pre-grouting	–	–	–	–	Bench	Top heading, bench
Result	Surface settlement (mm)	127	87	86	84	76	70
	Crown settlement (mm)	141	103	101	99	87	81

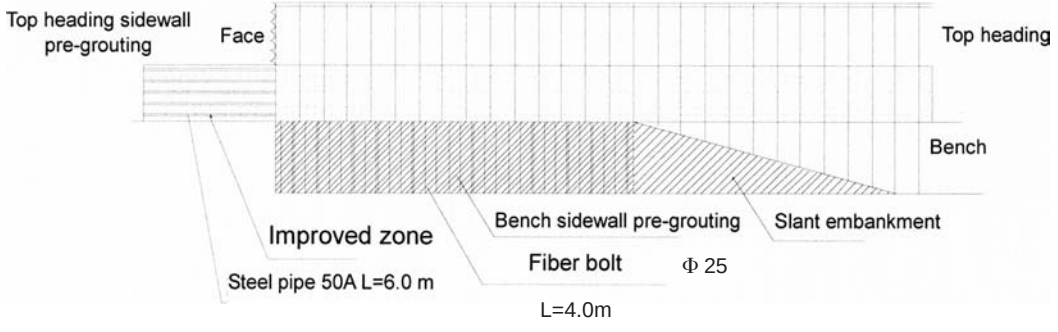


Figure 4. Longitudinal section of sidewall pre-grouting.

where fracture at the sidewall portion was assumed to partially progress along with excavation, causing the whole ground to deteriorate, decreasing the modulus of deformation of the ground around the tunnel, thereby increasing tunnel convergence and surface settlement. The nonlinear elastic analysis gives gradual decrease of modulus of deformation in response to increase in stress. Therefore, this analytical technique well expresses variation in modulus of deformation of ground in a wide range in ground mainly composed of silt.

4.2 *Selection of auxiliary methods using the analytical model*

By the use of the nonlinear elastic FEM model created for the section at 133 km 680 m, assuming the typical overburden depth and geological conditions of the tunneling sector, support patterns and support members were combined, to evaluate their effects in limiting surface settlement. The simulation study involved silt-dominant geology with N-value = 24, modulus of deformation E = 24 MN/m^2, internal friction angle $f = 18$ degrees, cohesion C = 94 kN/m^{2}and overburden depth of 25 m. Table 5 shows the analytically obtained surface and crown settlements with excavation patterns studied.

4.3 *Evaluation of sidewall pre-grouting*

In the tunneling sector, partial development of fractures in the cracked zone at the sidewall was anticipated, leading to deterioration of the whole ground, and resulting in lower modulus of deformation of the whole ground around the tunnel.

For preventing such adverse changes, it is essential to improve the ground strength before the modulus of deformation of ground begins to decrease, or more specifically, before the face arrives at the sidewall portion of top heading and bench, since ground deterioration is induced by fracture in those sections. Therefore, a new auxiliary method, i.e., sidewall pregrouting was adopted (Figs. 4 to 6). To validate the effect of this auxiliary stabilizing practice, numerical analysis was conducted on the preceding improvement with injection rock bolts and the succeeding improvement with injection rock bolts from the excavated cavity (Table 6). Comparison of the results shows that only the preceding improvement achieved surface settlements below control criterion (80 mm), proving the effectiveness of the sidewall pre-grouting. For verifying the improvement effect, sidewall pregrouting was tentatively implemented and bore hole load test was conducted. The test results showed cohesion of the top heading of 181 kN/m^2 and that of the

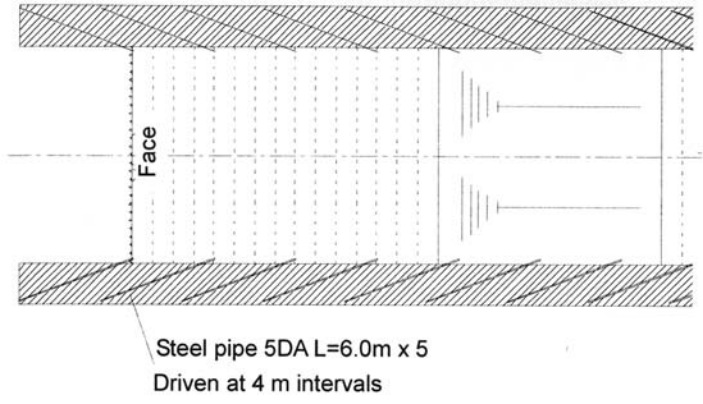


Figure 5. Plan of sidewall pre-grouting (top heading).

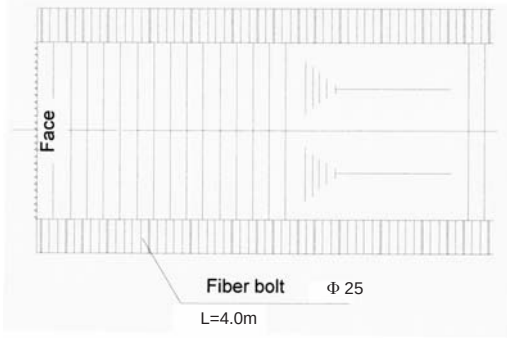


Figure 6. Plan of sidewall pre-grouting (bench).

Table 6. Effect of sidewall pre-grouting canalytical.

	Crown settlement (mm)	Surface settlement (mm)
Without improvement	173	86
Grouting at sidewall after excavation	154	84
Sidewall pre-grouting	138	75

bench of 185 kN/m^2 achieving the required strength level.

5 VALIDATION OF THE NUMERICAL MODEL

To validate the numerical model, comparison was made between analytical values and measured values of surface settlement with excavation patterns P-5 and M (Table 7). Good agreement was found between analytical and measured values, confirming validity of the numerical model.

Table 7. Comparison between analytical and measured values.

	Auxiliary method	P-5	M
Condition	Forepoling	PASS	AGF
	Foot reinforcement pile	x	x
	Top heading temporary closure	◯	◯
	Shotcrete thickness	30 cm	30 cm
	Top heading struts	x	x
	Shotcrete invert (20 cm)	◯	◯
	Sidewall pre-grouting	Top heading, bench	Top heading, bench
Result	Analytical	79	82
	Measurements	82	86

6 CONCLUSIONS

Tunneling in the sector discussed in this paper was planned at shallow depths in unconsolidated ground, with many vital infrastructure and residences on the surface just above. For minimizing impact of tunneling upon these structures, it was imperative to select an excavation method well suited to this project. First, various auxiliary methods were quantitatively evaluated in terms of surface limiting effect by means of statistical analysis. This analysis enabled quantitative expression of surface settlement effect. On the basis of the results of the statistical analysis, auxiliary methods to be involved in modeling were appropriately selected, thereby improving simulation accuracy of the numerical analysis model.

Part 4.3
Mechanizing tunnelling

This page intentionally left blank

Underground Space – the 4th Dimension of Metropolises – Barták, Hrdina, Romancov & Zlámal (eds)
© 2007 Taylor & Francis Group, London, ISBN 978-0-415-40807-3

Construction update and TBM excavation: Seymour Capilano Twin Tunnels Project, Vancouver, Canada

Dean Brox, Don Phelps & Brian Garrod
Hatch Mott MacDonald, Vancouver, B.C., Mississauga, Ontario, Canada

Tom Morrison
Greater Vancouver Regional District, Burnaby, B.C., Canada

Andy Saltis
Pacific Liaicon & Associates/SNC Lavalin, Vancouver, B.C., Canada

ABSTRACT: The Greater Vancouver Water District (GVWD) is currently constructing the Seymour-Capilano Filtration Project to enhance the quality of water supplied to the Vancouver area from the Seymour and Capilano reservoirs in North Vancouver. The project, designed by Hatch Mott Macdonald, includes major underground works comprising twin 3.8-m diameter, 7.1-km bored tunnels, the 11 m diameter, 180-m deep Seymour Shaft as the main construction access shaft, and the twin 4-m diameter, 275-m deep Capilano raisebored shafts. This work was tendered as a single contract, which was awarded to Bilfinger Berger (Canada) Inc. Construction started in early 2005 with the excavation of the Seymour Shaft by conventional shaft sinking methods through 30 m of dense glacial deposits followed by 150 m of granitic bedrock. Bilfinger Berger used lattice ring girders, mesh and dry-mix shotcrete for shaft support while sinking through the glacial deposits. Shaft support for the bedrock portion followed the Engineer's design, comprising pattern rock bolts, mesh and shotcrete. Shaft sinking was completed in early November 2005. Ancillary shaft-base excavations and structural, electrical and mechanical work were completed in May 2006. TBM excavation commenced in mid-2006 with the first TBM followed by the second TBM in September 2006. TBM excavation is scheduled to be completed in late 2007.

1 INTRODUCTION

The Greater Vancouver Water District (GVWD) is currently constructing the Seymour-Capilano Filtration Project (SCFP) to enhance the quality of water supplied to the Greater Vancouver area from the Seymour and Capilano reservoirs in North Vancouver. The main element of the SCFP is a 1,800-megalitre per day filtration plant, currently being constructed in the Seymour Valley. This plant, when built, will be the largest in Canada. Considerations of cost, community impacts and environmental issues resulted in the decision to build a single filtration plant in the Seymour Valley, connected to the Capilano reservoir by twin tunnels, rather than two separate plants adjacent to each water source. Raw water will be drawn from the Capilano reservoir and pumped through the Raw Water Shaft, Raw Water Tunnel and Seymour Shaft raw water riser pipe to the head of the Seymour Filtration Plant. Treated water will return by gravity through the Seymour Shaft treated water riser pipe, the Treated Water Tunnel and the Treated Water Shaft through an Energy-Recovery Facility and pressure-balancing tank to the Capilano distribution mains.

The Twin Tunnels component of the project comprises the 11 m diameter, 180-m deep Seymour Shaft as the main construction access shaft, twin, 3.8-m diameter, 7.1-km bored tunnels (the Twin Tunnels), and two 4-m diameter, 275-m deep raisebored shafts connecting the tunnels to surface at Capilano. Figure 1 shows the Laydown area of the Seymour Shaft in May 2006.

Investigations and preliminary design work for the SCFP date back nearly ten years. The GVWD selected Hatch Mott Macdonald (HMM) to participate in the preliminary design of the Twin Tunnels and awarded the detailed design to HMM in 2002.

The GVWD awarded the construction of the Twin Tunnels as a single contract, with lump sum and unit price components, to Bilfinger Berger (Canada) Inc. in August 2004. Pacific Liaicon and Associates/SNC Lavalin are responsible for construction management

and HMM are providing resident engineering services. The project is scheduled for completion in early 2009. The GVWD appointed a Technical Advisory Board in late 2004. Tenderers were provided with a Geotechnical Data Report and Geotechnical Baseline Report. The contract makes provision for Escrow Bid Documents and a Dispute Review Board.



Figure 1. Seymour Shaft laydown area.

2 PROJECT LOCATION

The GVWD decided early in the design process to connect the Capilano and Seymour sites entirely by tunnels, rather than by combinations of tunnels and surface pipelines. Length, routing and community impacts made this the best option.

Tunnelling, however, was affected by the existence of deep buried valleys at both ends of the tunnel alignment, eroded from the bedrock by glaciers and filled with mixed, water-bearing glacial materials. The horizontal and vertical alignments of the tunnels were both reached after considering many possible options.

The tunnels will be driven westwards from the Seymour Shaft, beneath the Lynn buried valley, passing beneath the slopes of Grouse Mountain and Mount Fromme and under the Capilano buried valley to a western terminus 275 m from surface immediately south of Cleveland Dam. There, the tunnels will be connected to surface by twin 4-m diameter raisebored shafts. Figure 2 shows the overall project layout.

The location initially selected for the Seymour Shaft was at the west side of the Filtration Plant. Drilling revealed water-bearing glacial materials to 100 m from surface with shattered bedrock conditions beneath.

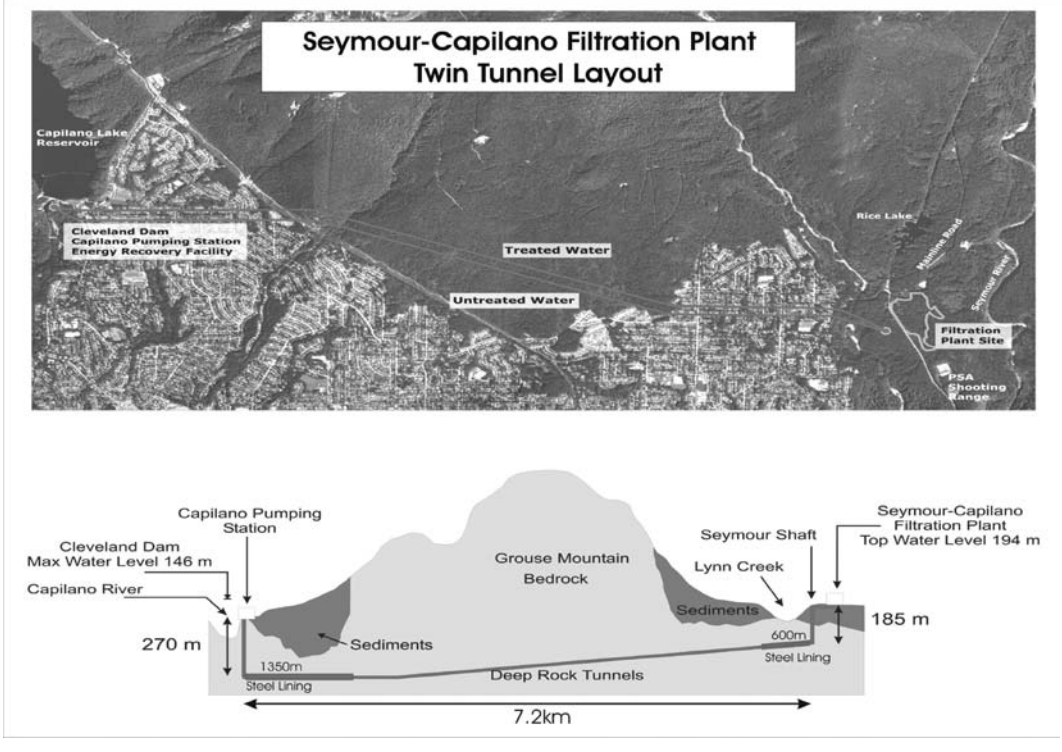


Figure 2. Project layout.

The GVWD and its consultants considered ten alternative shaft sites, taking into account technical, financial, social and environmental considerations. The site finally selected was about 200 m southwest of the original site, where seismic surveys and drilling proved the existence of a buried bedrock hump rising to within 30 m of surface. The Twin Tunnels contractor was provided with a cleared, leveled, drained and graded site; site operations began in the autumn of 2004.

3 SEYMOUR SHAFT CONSTRUCTION

3.1 *Shaft Excavation and Support in Overburden*

Bilfinger Berger Canada commenced construction of the project with the excavation of the 11 m diameter, 180 deep, Seymour Shaft in January 2005. The 30 m deep overburden portion of the Seymour shaft was excavated conventionally through dense glacial materials in approximately 1.0 m lifts using a CAT 308 excavator with mucking into 6 m^3 buckets. Shaft excavation was undertaken with two 12-hour shifts with shift changes at 6:00 AM and 6:00 PM daily.

Bilfinger Berger Canada proposed an acceptable alternative support system for sinking through the glacial deposits, consisting of lattice girders, mesh and 250 mm thickness of dry mix shotcrete and shown in Figure 3. The ground support was installed immediately upon completion of excavation of each lift. No raveling or any form of instability occurred during excavation in the overburden and the alternative shaft support system performed well. Sporadic, localized groundwater inflows were encountered during excavation and drainage holes were completed accordingly. The dry-mix shotcrete for the overburden portion mainly comprised a pre-manufactured product that included an accelerator. The strength of dry-mix shotcrete exceeded the project specifications based on results from test panels and from in situ cores.

3.2 *Shaft Excavation and support in bedrock*

The 150-m bedrock portion of the shaft was excavated by conventional drill and blast methods using two Atlas Copco R3 Crawler drill rigs. A typical blast hole production round varied from 1.5 m to 4.0 m deep. The blast design was based on 220 parallel-drilled blast holes with a typical perimeter hole spacing of 0.5 m. The blast design initially comprised a wagon-wheel cut comprising four reamer holes and a single middle blast hole. The blast design was later changed to a nine hole cut comprising five reamer holes with four surrounding blast holes, which produced significantly improved results.

Shaft support for the bedrock portion of the shaft followed the base design and comprised a combination of a pattern of 4.0 m long, 32 mm diameter, fully grouted and hand tensioned rock bolts at a typical 1.5 m square spacing, welded wire mesh and 150 mm minimum thickness of dry-mix shotcrete.

Welded wire mesh was installed around the full shaft perimeter for the full round depth following mucking. Shotcrete was then applied followed by the installation of pattern rock bolts. Shotcrete was applied to each excavation lift using a portable lifting assembly that was designed by Bilfinger Berger Canada and lowered to the shaft floor by a crawler crane. The portable shotcrete lifting assembly comprised 2–1 m^3 hoppers, 2–16 liter Aliva 252 shotcrete machines, and 2–150 liter pumps for injection of accelerator.

Shotcrete application was closely monitored and tested during excavation as per the project specifications with a testing frequency of three cores (from panels and/or in situ) for every 200 m^2 of applied shotcrete.

Both the pre-mix and on-site batch mix shotcrete provided consistently good strength results from the quality control and quality assurance testing.

Quality assurance testing of the shotcrete was carried out by AMEC of Vancouver on behalf of the GVWD. The quality assurance testing was typically



Figure 3. Shaft support in overburden.



Figure 4. Shotcrete lifting assembly.



Figure 5. Shaft support in bedrock.



Figure 6. Shaftbase excavation, early 2006.

carried out at a frequency of 10% of the quality control testing. The quality assurance testing always comprised in situ core testing.

Figure 5 shows the drilling of rock bolts using a single drill rig. On a few occasions a number of hollow-core self-drilling injection anchors were installed in closely fractured metavolcanic rock that prevented easy insertion of rock bolts following normal drilling. The support system for the bedrock portion of the shaft performed well and no form of any instability manifested along the shaft walls during excavation.

4 SEYMOUR SHAFTBASE CONSTRUCTION

The shaftbase excavation adopted for construction was not significantly dissimilar to the proposed base design. The shaftbase was allowed to be modified by the Contractor and Bilfinger Berger Canada elected to adopt the same excavation width for the starter and back chambers of approximately 14 m and 10 m respectively but extended the length of both the starter and back tunnels as well as the back chamber to facilitate the set up and launching of the TBMs and mucking logistics. The excavated lengths of the starter tunnels, back tunnel, and back chamber were about 35 m, 50 m, and 30 m respectively. The excavated heights of the starter and back chambers are 6 m and about 5 m respectively. Figure 6 shows the start of excavation of the starter tunnels in early 2006.

Excavation of the starter and back chambers were completed by drilling and blasting 1.5 m to 3.0 m full-face rounds. The initial rock support for the starter chamber was modified from the base design by Bilfinger Berger Canada to include lattice girders for the first 6 m. In addition, 6-m long rock bolts were installed for the first 4 m. The length of the rock bolts was subsequently reduced to 4 m for the remainder of the chamber excavations based on inferred good geological conditions and the initial results of the convergence monitoring.

Excavation of the starter and back tunnels were also completed in 1.5 m to 3.0 m full-face rounds. Spot rock bolts and full coverage shotcrete with mesh were applied for support.

The encountered rock conditions within the shaftbase excavation typically comprised mixed granitic and metavolcanic rock of varying quality. Groundwater inflows into the shaftbase excavation have been measured to date to be less than 20 l/min. The final excavation for the shaftbase comprised an 8 m deep pit to receive the mucking buckets and an 8 m deep sump.

5 SEYMOUR SHAFTBASE INSTALLATION

Substantial structural, mechanical and electrical work was needed in the Seymour Shaft and shaftbase chamber in preparation for TBM excavation. This work lasted from March to May 2006. The sidewalls at the heading of starter tunnels have been concreted to facilitate the bearing of the thrust pads of the TBMs. Rails have been laid out for the movement of rolling stock.

A Liebherr modular gantry crane was constructed at the shaft collar, equipped with two hoists, each capable of hoisting 70 tons as can be seen in Figure 1. These are being used for installing the TBMs and, once tunneling begins, will be used to hoist two 28 m^3 mucking buckets built to a Bilfinger Berger patented design. The gantry system is unique and equipped with electronic sensors for automatic muck removal operation.

An Alimak elevator with a capacity of 2,400 kg or 23 people was installed. The electrical facilities were installed to transmit power down the shaft at 12.47 kV for transformation at the shaft base to 4,160 V for supply to each TBM at 600 V. Two 100-kW ventilation fans were installed on surface with ducting down the shaft. In addition, a 400 m^3 capacity sump pit and two muck pits each having a volume of 125 m^3 have been

excavated at the shaft bottom. The pit for the rock buckets was covered with two hydraulically actuated doors. The chamber floor was concreted and track, switches, car dumps and muck chutes were installed. Concrete cradles and gripper walls were installed for the start of TBM excavation.

6 TBM SELECTION AND DESIGN

Bilfinger Berger Canada selected two new 3.8 m diameter, 1,260-kW TBMs that were built new for the project by Robbins at Solon, Ohio. These machines are high-powered, open-shield, hard rock machines with 483 mm (19-inch) cutters and support fingers immediately behind the shield. With trailing gear, each machine will be approximately 250 m long. The trailing gear will include pumping and grouting equipment and will also allow for passing of the mucking trains. Each TBM will be equipped with two drills for forward probing and pre-excavation grouting. A probe-hole will be maintained continuously ahead of the face.

Bilfinger Berger Canada has designed the TBM mucking arrangement such that each 1.5-m push by the TBM will fill a train of six Mühlhauser 5 m^3 side-dumping cars. A GAI diesel locomotive will haul each train from the TBM to the Seymour Shaftbase for tipping. One train will fill one 28 m^3 mucking bucket. The TBM muck will be hoisted to surface and trucked to the GVWD designated disposal site located 4 km away up the Seymour valley.

The Robbins TBMs were trucked from Ohio to Vancouver in 72 tractor-trailer loads, starting in early May 2006. TBM installation and commissioning, with the assistance of Robbins personnel, was carried out in the latter part of May and early June 2006. Figure 7 shows the first TBM assembled in the shaftbase. TBM tunneling is anticipated to begin in mid-June 2006.

7 TBM EXCAVATION PROGRESS

In mid-2006 TBM # 1 was advanced approximately 150 m in the Raw Water Tunnel using an umbilical cord with the back-up for this TBM placed in the Treated Water Tunnel. This procedure was adopted in order to allow for sequential set up of TBM # 2. TBM # 2 was set up in September 2006 and excavated the first 140 m in the Treated Water Tunnel. Figure 8 shows the first part of TBM excavation of the Raw Water Tunnel and Figure 9.

ACKNOWLEDGEMENT

The authors gratefully acknowledge the permission of the Greater Vancouver Water District and Bilfinger Berger (Canada) Inc. to publish this paper.



Figure 7. Installation of first TBM in shaftbase.



Figure 8. Start of TBM excavation.



Figure 9. Raw water tunnel.

REFERENCES

Brox, D.R., Rotzien, J., Genschel, C., Messner, Gupta, A. J. Morrison, T., and Saltis, A. Construction Update and TBM Excavation Planning, Seymour Capilano Twin Tunnels, Tunnelling Association of Canada Conference 2006. Vancouver, BC, Canada.

This page intentionally left blank

Underground Space – the 4th Dimension of Metropolises – Barták, Hrdina, Romancov & Zlámal (eds)
© 2007 Taylor & Francis Group, London, ISBN 978-0-415-40807-3

Stress–strain soil behavior during tunneling in soft ground: experimental study on 1g-earth pressure balanced shield model

D. Branque, C. Boutin & H.V. Doan
Ecole Nationale des Travaux Publics de l'Etat, Département Génie Civil et Bâtiment, Rue Maurice Audin, Vaulx-en-Velin cedex, France

ABSTRACT: Since several years, the ENTPE's Geomaterial Laboratory in Lyon (France) has started a large experimental project based on the so-called "Earth Pressure Balanced Shield" (EPBS) method adapted to tunneling in soft ground. Within the framework of the project, a specific reduced-scale physical model of the EPBS (1:10 approximately) was built. A first objective has been to perform a direct rational analysis at the model scale, aimed to understand the different mechanisms occurring during the EPBS method of tunneling. In a second stage, this analysis and the resulting data base will be used to elaborate a numerical modeling of this method. The present paper presents typical test results obtained with the EPBS model for frictional – cohesive material (humid fine silica sand). These results concern the stress-strain soil behavior during ideal tunneling rate. Moreover, the sensitivity of the main control parameters available on the command shield and the action of the cutter head are debated.

1 INTRODUCTION

Tunneling with the earth pressure balance shield (EPBS) originally appeared in Japan during the seventies in fine-grained alluvial soils suitable for this mechanical tunneling procedure. Since that time, several authors had described its theoretical principles in the literature (Kurosawa, 1981, Clough et al, 1983…). The fundamental idea of the EPBS method consists in balancing the hydrodynamic pressure and the earth pressure at the tunnel face by a controlled confinement of the excavated soil contained in a pressure chamber at the front of the shield. In theory, a perfect earth balance is obtained when the weight of discharged soil from the pressure chamber by the screw conveyor is equal to that of soil excavated and entering in the chamber during the same time. This balance between these two weights requires a good synchronisation between the tunnel boring machine (TBM) advancement rate and the screw conveyor rotation speed.

In practice, the EPBS method remains relatively complex. In Europe in particular, the technique is often confronted with very mixed and pervious grounds in which controlling the confinement pressure at the tunnel face remains difficult. Additionally, in some coarse and heterogeneous grounds, it is often observed that the torque required in order to ensure the rotation of the cutter head reaches high values and becomes a non-negligible limiting parameter of the machine advancement speed.

Other practical difficulties of the EPBS technique are revealed on the work site. For example, neither the weight of excavated material nor that extracted from the pressure chamber are usually measured with sufficient accuracy to allow a driving of the TBM uniquely based on the knowledge of these two weights. The definition of additional control parameters appears therefore essential to guarantee the safe driving of the machine.

Feedbacks from work sites also show that a confinement of the working face, though appropriately ensured, does not necessarily prevent large displacements of the ground surface. Other causes of volume loss around the TBM (displacement along the shield tail, ground convergence at its end…) shall be taken into consideration to control the displacement of the ground surface. More generally, it appears in practice that the action of the TBM on the surrounding ground is highly dependent on soil characteristics and tunneling rates. In consequences, the ground volume influenced by TBM during its advancement is generally difficult to define prior to tunneling.

The Geomaterial Laboratory of the "Ecole Nationale des Travaux Publics de l'Etat (ENTPE)" has started in 1998 a large research project devoted to Earth Pressure Balanced Shield method. The project aims to analyze and understand the main physical mechanisms occurring during EPBS method tunneling. The ambition is to provide technical support and guidance to overcome the different difficulties

encountered on work sites. In particular, these studies should lead to the development of an appropriate numerical tool in pressurized tunneling method modeling.

Within the framework of this research project, an experimental study has been carried out in laboratory. For this study, the Laboratory has built an original reduced scale model of earth pressure balanced shield. This model, with a geometric scale between 1/4 and 1/20, allows representing the principal stages of the EPBS tunneling process: excavation of the ground with a cutter head, confinement of the tunnel face with the excavated material, extraction of the material with a screw conveyor and immediate radial support of the excavated ground by means of a sliding cylindrical shield tail.

In a first stage, the analysis of the test is performed at the scale of the model. For this analysis, the excavated ground on the scale model is equipped with both internal stress and displacement sensors. This allows a simultaneous and comparative study on the data collected on the machine and in the ground. Besides, the choice of the material for the scale model and the design of the machine are justified by appropriate similitude laws, which control the transposition to the full-scale model (Mandel, 1962).

So, the present paper presents the details of the experimental set up and the monitoring system. Typical tests results obtained during the digging of frictional-cohesive soils are presented and discussed. These results concern the analysis of stress–strain soil behavior around the TBM during ideal rates of excavation, the identification of pertinent control parameters to guarantee the safe driving of the machine and the analysis of the cutter head action in function of the nature of the ground.

2 THE ENTPE EPBS MODEL

2.1 *Description of the experimental set up*

The ENTPE earth pressure balance shield model is presented Figure 1. The EPBS model consists of a 0.55 m cutter head (A), a conical working chamber (B), a screw conveyor inclined at an angle of 10° (C), a horizontal screw conveyor (D), a cylindrical steel shield tail (E), four thrust hydraulic jacks (F), a frame carrying the whole assembly (G), a stiff steel container placed in front of the TBM frame and containing the ground (H). The test ground dimensions were 2 m long, 1.3 m wide and 1.3 m high. Note that, the ground can be compressed vertically by means of ten air chambers (J) placed under the top of the container (K). This system can maintain a uniform pressure to represent an extra cover above the tunnel, up to four tunnel diameters.

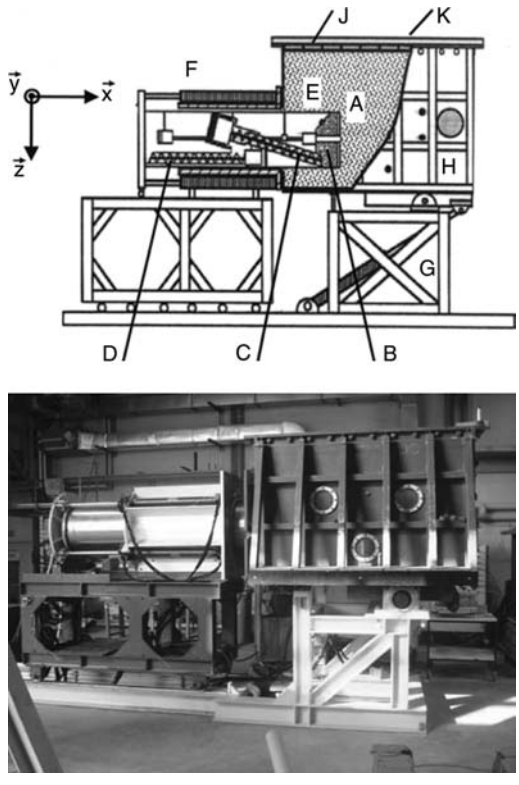


Figure 1. Earth Pressure Balanced Shield model of ENTPE: longitudinal section and photo.

During the test, the TBM enters the ground through a circular port in the container wall. The tunneling maximum length is 1 m. The shield tail forced forward behind the shield itself provides the radial support for the excavated ground. Two alternative cutter heads can be used on the test rig. A low opening ratio head (35%) is usually favored for purely frictional grounds, whilst a high opening ratio head (85%) is retained for cohesive–frictional grounds. To this date, the presence of water table and groundwater flows is not taken into account in our study.

2.2 *Instrumentation*

In our EPBS model, machine parameters alike soils characteristics are directly monitored in real time conditions. For this monitoring procedure, the TBM model is instrumented as follows: three total pressures cells fixed on the working chamber walls measure stresses at sides and roof of the chamber, four dynamometers fixed at the hydraulic jacks extremity measure the thrust cylinder total load, four hydraulic pressure cells provide the measurement of inclined screw conveyor and cutter head torque, an electronic scales deliver real

time measurement of the mass of materials discharged at the rear of the shield, and two precision comparators measure the shield penetration rate.

Simultaneously, the stress–strain ground evolutions are followed during tunnelling with several sensors laid in the excavated ground when the container is filled. The ground monitoring system is made up of:

- 8 internal total stress cells laid at fixed point to measure changes in the state of stress in different directions. During our tests, the measurement of frontal horizontal stresses (σ_{xx}) and vertical stresses (σ_{zz}) in various points of the ground are privileged. (Note that, the subscripts x, y, z relates to the directions $\vec{x}, \vec{y}, \vec{z}$ of the referential given at Figure 1.)
- 10 displacement sensors able to measure real time vertical displacements of the ground free surface.
- 8 internal displacement sensors, laid in the ground to measure internal vertical displacements (u_z), internal horizontal frontal displacement (u_x) and internal horizontal radial displacement (u_y) at the height of tunnel axis.

2.3 *The soil models*

The choice of the materials for the soil models has been led by considering the conditions of similitude (Branque et al, 2006). Cohesive–frictional grounds considered in this paper are made from humid fine ($d50 = 0.35$ mm) silica sand (S28 Hostun RF). Two water contents of the humid sand have been used during our tests: 0.5% and 3%. These are voluntarily taken low with the objective of avoiding gravity drainage and viscosity-driven phenomena.

The sand and water mixture is stirred and poured loosely in the container in uniform layers. Every layer is compacted with an iron roller until the required density is attained. Ultimately, a plastic film, so as to avoid any drying during the tests, covers the whole structured.

In these conditions, the resulting ground apparent cohesions, induced by capillary suction, are less then that 1 kPa for the water content of 0.5%, in the order of 3 kPa for the water content of 3%. If no additional pressure is applied on the ground surface, note that these two cohesions are sufficient to ensure the tunnel face stability without earth pressure acting on this face. However, in some tests, instability of the tunnel face is deliberately induced by means of uniform pressure developed by the chamber placed under the top of the container.

The other mechanical characteristics of the soil model, identified from series of axi-symmetric tri-axial tests performed under low levels of lateral stress ($5\,\text{kPa} \leq \sigma 3 \leq 40\,\text{kPa}$) are given on Table 1.

Table 1. Mechanical characteristics of soils models used on tunnelling tests and deduced from conventional tri-axial tests.

	Total unit weight, γ (kN/m^3)	Void ratio, e	Water content, w (%)	Tangent stiffness, E_t (Mpa)	Apparent cohesion, C (kPa)	Friction angle, φ (°)
Wet sand 1	13.3	1	0.5	10	<1	35
Wet sand 2	13.3	1	3	10	3	35

3 STRESS–STRAIN SOIL BEHAVIOR UNDER IDEAL TUNNELING RATES

3.1 *Identification of the ideal tunnelling rates*

Tests carried out with the EPBS model of ENTPE have shown that this last one is able to reproduce different excavation rates observed on work sites, which directly govern the stress–strain behaviour of the ground in front of the shield. In agreement with the theoretical principle of the EPBS method, the tests show that these rates are directly dependent of the ratio (R) between the mass flow of the material discharged from the pressure chamber (Qt) and the theoretical mass flow of excavated material (Qc). Note that in case of homogeneous ground, Qc is calculated on the model as the product of the ground volumetric weight (ρ_{ground}) times the machine advancement speed (v) and the tunnel section (S).

In this context, the ideal tunneling rate, which corresponds to a minimum of strains in front of the shield, is obtained in the model when Qt equals Qc. However, our tests show that this last condition is necessary but not sufficient to guarantee the stability of the tunnel face. In order to obtain and maintain this stability, it is also necessary in function of the geometrical and geotechnical tunneling conditions: (i) to apply a sufficient but not excessive relative pressure on the tunnel face, which limits the volume losses around the machine, (ii) to rotate the cutter head with a minimum rotation speed (dependent of the machine advancement speed) aiming to guarantee the homogeneity of the stresses at the tunnel face and to prevent the apparition of passive earth pressure in the ground which could cause plastic behavior in the soil.

3.2 *Surface Displacements under ideal tunnelling rates*

Under ideal tunnelling rates and for the different cohesive frictional ground tested on the model, the

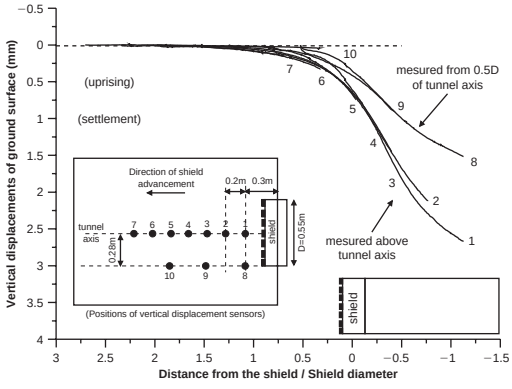


Figure 2. Stationary behavior of surface settlement observed on EPBS model under ideal tunneling rate.

displacement fields measured on the surface of the ground structure reveal a stationary behavior, which depends on the distance to the tunnelling machine. Figure 2 shows this stationary behavior for frictional cohesive material made from wet sand 1: vertical displacements measured at the same distance from the tunnel axis, range in the same zone in the figure. For the different tested materials, the settlements increase as the shield approaches. They are maintained afterwards in result of the friction stresses along the shield tail. Note that, this behavior is in good agreement with observations made on sites (Clough et al. 1993, Kastner et al. 1996).

Concerning the geometry of the settlement basins observed during tests on cohesive frictional material, the cross sections of these basins are consistent with the Gauss distributions usually considered (Fig. 3). The maximal settlements measured on frictional-cohesive grounds are close of 1 mm for a cover height of 1 diameter. By taking into account the displacement scale ratio u^* ($u^* = L^* = u_M/u_P \approx 0.1$), note that settlements measured on EPBS model (u_M) for this material appear in agreement with those observed in practice (u_P) (about 10 mm: Lee and al 1999).

3.3 *Internal Displacements under ideal rates*

As observed for the surface displacements, Figure 4 illustrates the stationary character of the horizontal radial displacements measured in the ground at the tunnel axis height under ideal tunnelling rates. This figure shows that the direction of soil displacements at a fixed point in the ground depends merely on the distance to the shield. Thus, as the shield gets closer, the ground structure is pushed away in the horizontal radial direction. This can probably explain a part of the vertical settlement observed on the ground surface ahead of the machine. Once the shield has passed, an inward movement takes place, driven by the shear

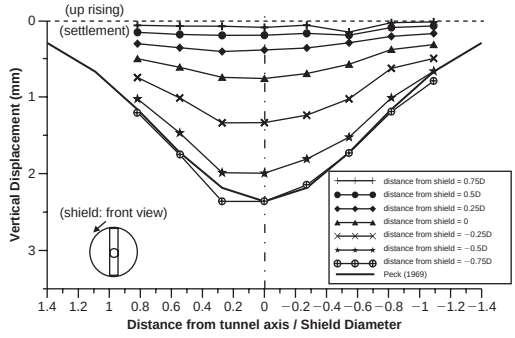


Figure 3. Surface settlement troughs at different distances from tunnel face.

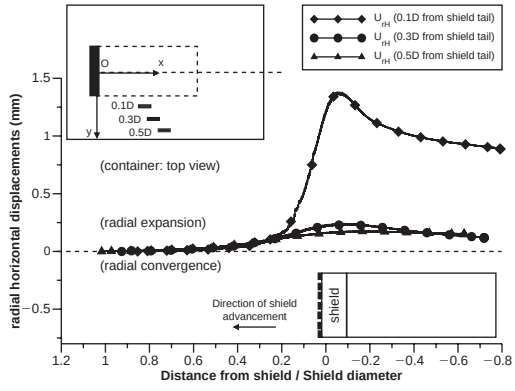


Figure 4. Horizontal radial displacements measured at the tunnel axis height during ideal tunneling rate.

stresses along the shield tail. The horizontal radial displacements revealed on the scale model are consistent with some measurements performed on sites. Those can be found in specific literature (Clough et al 1983, Lee et al 1999).

3.4 *Stress fields under ideal tunnelling rate*

In practice, it may happen that normal stresses on tunnel lining are monitored, but the evolutions of stresses in the soil volume around the machine are generally not well known. These stresses informations are however essential to analyze and to understand the different mechanisms occurring during the EPBS method of tunneling.

In the case of ideal tunneling rate, observations made on the EPBS model in this domain show that, the horizontal frontal and vertical stresses (σ_{xx} and σ_{zz} respectively) measured in the ground unveil a stationary behavior as well, with respect to the tunneling machine. This behavior can be visualised in Figures 5a and 5b, which show the vertical and the horizontal

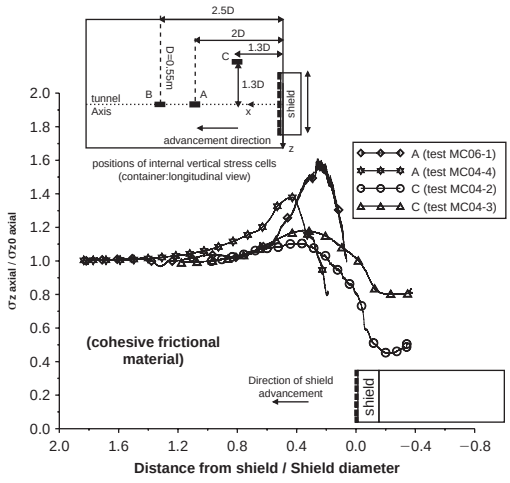


Figure 5a. Stationary behavior and decrease of vertical stresses (σ_{zz}) observed during ideal tunneling rate.

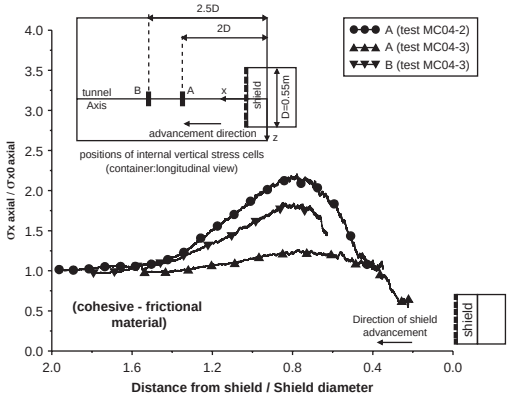


Figure 5b. Stationary behavior of horizontal frontal stresses (σ_{xx}) observed during ideal tunneling rate.

frontal relative stresses obtained in the tunnel axis (A, B) and above the tunnel arch (C). For frictional cohesive materials, the stresses look sensitive to the presence of the TBM up to 1.5 diameters in front of the shield. Moreover, the mean stress measured along the tunnel axes increases in a zone situated between 0.5 to 1.5 diameters ahead the shield, and tends to decrease in the close vicinity of the machine. This can probably illustrate a longitudinal arching effect ahead the machine. The volume of the low-pressure bulb has been partially identified on the scale model in case of frictional – cohesive material. If it is detected up to 0.5 diameters ahead the shield, it seems also spread up to 0.5 diameter above the tunnel crown. Note that, this vertical decompression, which can be associated with a rotation of the principal directions of stresses, remains once the shield has passed, especially above the tunnel crown (C).

4 TUNNEL BORING MACHINE DRIVING: CONTROL PARAMETERS AND ACTION OF THE SHIELD

4.1 *Identification of the "extreme" rates.*

Tests carried out on the ENTPE earth pressure balance shield model have shown that the apparition of large plastic strain in the soil is generally induced by particular conditions of TBM driving. These conditions correspond to the so-called "extreme" rates. These have the particularity to lead to a generalized ground failure if they are maintained for to long. Two kinds of extreme rates can be distinguished in the model:

- under-extraction regimes (in which the rate of material removed is less than the design rate: Qt < Qc) produce excessive confinement of the working face. These regimes involve the passive earth pressure causing plastic behavior in the soil and an upward flow of material in front of the shield.
- in the opposite situation, over-extraction regimes (in which the rate of material removed is greater than the design rate: Qt > Qc) cause a loss of confinement of the working face. In this latter case, the consequences of this extreme rate on the excavated ground vary depending on the soil mechanical characteristics. For purely frictional material, the transition to the over-extraction rates induces instantaneously a flow vertical chimney above the shield, leading progressively to sink holes at ground level. With the presence of cohesion, the apparition of large strains around the shield is delayed and the failure mechanisms imply more a kinematics of block failure rather than a process of soil flow.

4.2 *Sensitivity of driving control parameters*

In this context, tests on the EPBS model have been used to assess the sensitivity and the pertinence of the different control parameters, potentially available on the machine to identify in real time the nature of tunneling rate. As an example, Figure 6 shows the variations of these different control parameters measured on the EPBS model during a tunneling test on frictional cohesive material. The values of ratio R measured in parallel are also given.

Firstly, our tests unveil that the torque applied on the cutter head, the pressures measured at the middle of the working chamber and the horizontal thrust effort developed by the hydraulic jacks present variations that are interdependent and directly in phase with the variations of the ratio R. Thus, in case of homogeneous grounds tested on EPBS model, it can

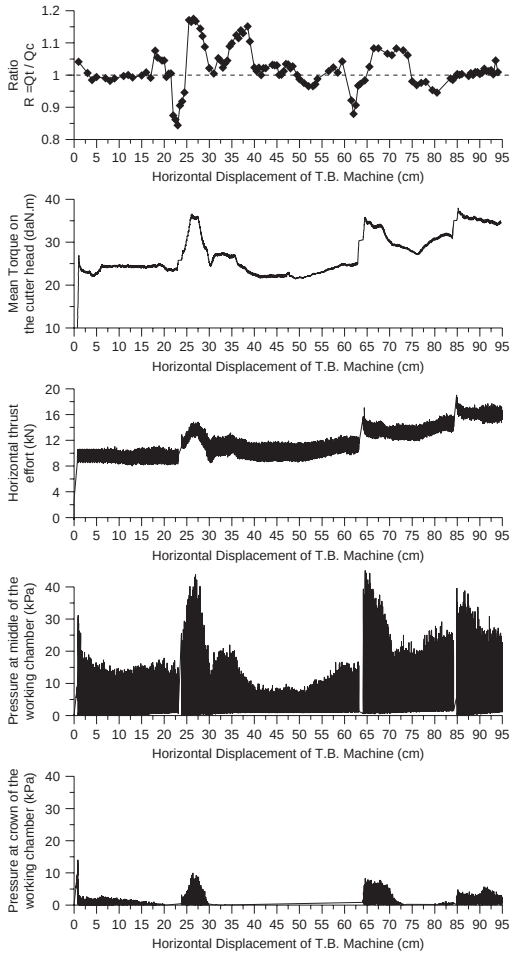


Figure 6. Sensitivity of the principal TBM control parameters to the relative changes in the driving regime.

be widely accepted that a stability of the torque on the cutter head (respectively a stability of the amplitudes of the pressure measured at the middle of the chamber, or a stability of the horizontal thrust effort) is typical of a tunneling phase led with a ratio R equal to 1. In opposite case, increase or decrease in torque on the cutter head (respectively in amplitudes of the pressure measured at the middle of the chamber, or in horizontal thrust effort) characterizes necessarily an extreme tunneling rate.

However, as indicated in paragraph 3.1, the condition of ratio R equal to 1 is not sufficient to guarantee the stability of the tunnel face. This stability depends of the confinement applied at the considered time. For this reason, it appears on EPBS model that informations given by the pressures measured at the crown of the working chamber are essential and complementary of those given by the other control parameters. Thus, if the variations of the torque on the cutter head give indications about the nature of the tunneling rate, pressures measured at the crown of the working chamber give informations about the filling state of the working chamber, and consequently about the quality of the confinement applied on the tunnel face. For example, pressure measured at the crown of the working chamber, and presented Figure 6, show that the tunneling phase occurring between the advancement positions of 30 cm and 64cm has been realized with a working chamber partially full. Note that this condition of tunneling is possible uniquely in case of grounds with a sufficient cohesion.

4.3 *Action of the shield*

It is commonly thought that the torque applied on the cutter head corresponds to the efforts required to cut the ground and to mix the excavated soil contained in the working chamber. Nevertheless, the tests on reduced scale model show that the shield action depends on the mechanical characteristics of the excavated ground. In the case of frictional – cohesive grounds for which the tunnel face is steady, the shield with the large open ratio is used merely for the cutting of the ground. On the contrary, for purely frictional material, the tunneling can be interpreted as a material flow through the wheel and the chamber. In this latter case, the shield with small opening is used as regulator of this flow and its role of mechanical support on the tunnel face cannot be neglected.

Tests on reduced scale model have also shown that the rotational movement of the cutter head appears like an essential parameter to guarantee the stress homogeneity at the tunnel face. Consequently, for the ideal rate ($Qt = Qc$), a reduction of the cutter wheel rotation speed can lead the apparition of passive earth pressures. In the same way, it was observed under extreme extraction rate ($Qt < Qc$) that the appearance of the plastic behavior is strongly accelerated in the case of cutter wheel lock.

5 CONCLUSION

Among the results of the tests carried out at ENTPE on a large 1g reduced scale model of earth pressure balanced shield, the direct rational analysis performed at the model scale has confirmed the existence of different rates of excavation directly governing the stress–strain behavior of the ground in front of the shield. Additionally, an analysis of the sensitivity of the different control parameters has unveiled that a real time control of the excavation rate must consider the complementarities between the different control parameters available on the tunnel-boring machine.

Besides, the same tests have shown that stress profile in front of the shield is directly dependent on the rotational movement of the cutter head.

REFERENCES

Branque, D., Doan V.H., Boutin C. 2006. Earth pressure balanced shield method: experimental study on a large reduced scale model. *Intern. Conf. on Physical Modeling in Geomechanics, Proceedings Rotherdam*, Balkema.

Clough G.W. 1983, Measured soil response to EPB Shield tunneling. *Journal of Geotechnical Engineering*, vol 109 (2), pp. 131–149.

Clough, G.W. & Leca, E. 1993. EPB Shield tunnelling in mixed face conditions. *Journal of Geotechnical Engineering* 119 (10): 1641–1656.

Kastner, R. & Ollier, C. 1996. In situ monitoring of the Lyons metro D line extension. In Mair & Taylor (ed). *Geotechnical Aspects of underground construction in soft ground, Proc. intern. symp.*: 701–706.

Kurosawa S. 1981, Earth pressure balanced shield tunneling, *Journal of the Construction Division, ASCE*, vol 107, n° CO4, pp. 609–618.

Lee, K.M. & al. 1999. Ground response to the construction of Shanghai metro tunnel – line 2. *Soils and Foundations, Japanese Geotechnical Society* 39 (3): 113–134.

Mandel, J. 1962. Essais sur modèles réduits en mécanique des terrains, étude des conditions de similitude. *Revue d'Industrie Minérale*, 9 : 611–620.

This page intentionally left blank

Underground Space – the 4th Dimension of Metropolises – Barták, Hrdina, Romancov & Zlámal (eds)
© 2007 Taylor & Francis Group, London, ISBN 978-0-415-40807-3

Conquering the construction challenges of the Arrowhead Tunnels

Brian Fulcher
Shea-Kenny Joint Venture and Shea Construction Co., Walnut, CA, USA

John Bednarski
Metropolitan Water District of Southern California, Los Angeles, CA, USA

Michael Bell
Hatch Mott MacDonald, Pleasanton, CA, USA

Werner Burger
Herrenknecht, AG, Schwanau, Germany

ABSTRACT: The Arrowhead Tunnels Project represents the final portion of a 70 km (44-mile) long water conveyance facility that will bring up to 28 m^3/sec (1,000 ft^3/sec) of water into Southern California. The 13 km (8-mile) tunnelling project is well underway and consists of two, 5.8 m (19-foot) diameter TBM bores through extremely variable geological conditions. The tunnels lie near the base of the San Bernardino Mountains and several significant faults including branches of the San Andreas Fault that run within one kilometer (0.5 miles) of the tunnel alignment. There are numerous other major active faults that cross the tunnel alignment and water pressures in the tunnel have been recorded as high as 20 bar (300 psi).

This paper will describe some of the problems encountered and the solutions implemented to advance the two hybrid TBMs under conditions that ranged from hard rock with no water inflows to full-face granular material under 10-bar pressure and 32 l/sec (500 gpm) inflows. Due to the range and severity of ground and water conditions actually encountered, the Owner-Contractor-Designer team adjusted the means and methods to be more responsive – virtually on a day-by-day basis – to suit the conditions actually encountered.

1 INTRODUCTION

1.1 *Project description*

The Arrowhead East and Arrowhead West Tunnels, both of which will have a finished inside diameter of 3.65 m (12 ft), will traverse the mountainous terrain north of the City of San Bernardino. The work includes completing the East Tunnel, constructing the West Tunnel, finishing the connections between completed portions of the pipeline and tunnels, and site restoration.

The remaining 6,840 m (22,440 ft) of the East Tunnel excavation must proceed in a down-grade drive from the Strawberry Creek Portal. This tunnel is being excavated beneath ground cover ranging from less than about 15 m (50 ft) to 630 m (2,065 ft). Construction of the 6,062 m (19,890 ft) West Tunnel is an up-grade drive from the Waterman Canyon Portal. This tunnel is being excavated beneath ground cover ranging from less than about 15 m (50 ft) to 335 m (1,100 ft).

1.2 *Purpose and design of the tunnels*

The Arrowhead Tunnels were designed to convey water from the California Aqueduct system to the Diamond Valley reservoir. They were also intended to provide a second source of supply for the Owner.

1.3 *Construction challenges to overcome*

This project required extraordinary cooperation and understanding from all parties and stakeholders involved and required that innovative methods be implemented to deal with the actual ground conditions encountered. The Arrowhead Tunnels Project was not by any measure a routine hard rock tunnel located adjacent to an urban development. It tested the resolve of the project team to meet and succeed in frequently difficult and challenging conditions to successfully pierce the mountain and complete the tunnel that at this stage is 50% complete overall.

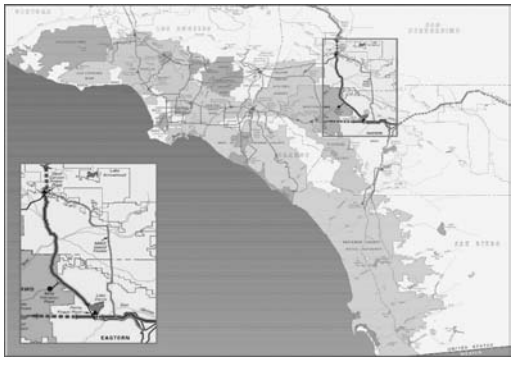


Figure 1. Project location in the San Bernardino National Forest, 100 km (60 mi) east of the city of Los Angeles, California.

2 GEOLOGY AND GROUND CONDITIONS

2.1 *Geological conditions – general*

The geology of the area is very complex and ranges from intact to highly weathered and altered gneiss, marble/calc-silica gneiss and granitic rocks. These conditions required the design of two, one-of-a-kind hard rock TBMs which were modified once experience with tunnelling was gained to better address specific geologic and water inflow conditions.

2.2 *Geological conditions – ground water*

A key construction requirement was to protect the water resources within the strata and neighboring private properties during tunnel construction. In order to protect these water resources, specific limitations on groundwater inflows into the tunnels were established by the U.S. Forest Service in a Special Use Permit. Ground water inflow control measures are mandatory and a key element to the success of the project. The tunnels excavated to date have encountered extremely variable ground conditions and high groundwater inflows due to high hydrostatic pressures. See Figures 2 and 4.

2.3 *Geological conditions – rock mass*

The rock and soil deposits encountered during the excavation of the West and East Tunnels in descending order of abundance include the following:

- Granite rocks including mainly quartz monzonite, quartz diorite, and granodiorite.
- Gneissic rocks including quartzo-feldspathic gneiss with amphibolite and biotite gneiss.
- Marble and calc-silicate gneiss breccia
- Fault gouge, crushed rock and breccia

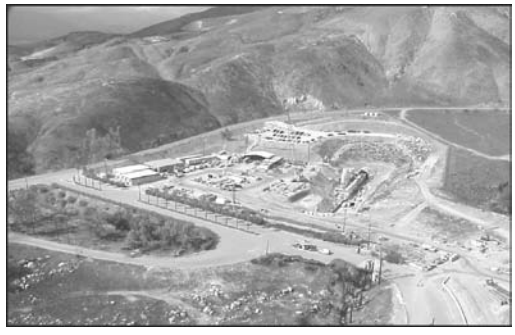


Figure 2. Aerial view of the Waterman Canyon portal (West Tunnel) showing the mountainous terrain and remote access.

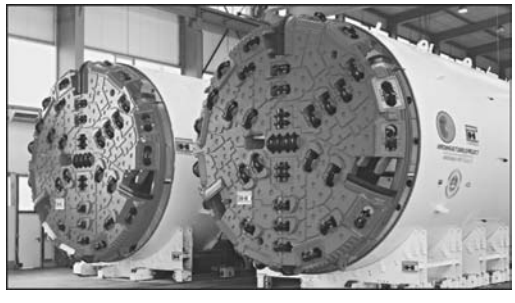


Figure 3. Herrenknecht 5.8 m diameter hard rock TBM undergoing tests in the fabrication shop in Schwanau, Germany.

Both tunnel alignments cross numerous faults that impact tunnel construction. Sixteen separate faults have been mapped and projected across the West Tunnel alignment, and five separate faults have been mapped across the East Tunnel alignment.

3 TUNNELLING PRODUCTION AND IMPACTS

3.1 *Tunnel Boring Machines (TBM)*

This is a unique tunnel that required not only specified tunnel excavation equipment but also a capability to perform repetitive pre-excavation drilling and grouting operations through various geological conditions. Accordingly the TBMs may be generally described as single-shield hard rock machines (cutterhead) with soft ground muck handling and segment erection capabilities. The drilling and grouting equipment included three drills (initially) and several grout plant/pumps. See Figures 3 and 6.

3.2 *Tunnel boring machine advance rates*

The tunnelling advance rates have varied substantially and are dependent on the ground and water conditions.



Figure 4. Aerial view of the Strawberry (East Tunnel) portal area showing the fully-assembled TBM and trailing gear.

Table 1. Tunnel lengths and overall advance rates.

Description	East Tunnel (AET)	West Tunnel (AWT)
Tunnel (total)	6,840 m (22,440 LF)	6,062 m (19,890 LF)
Tunnel (TBM)	6,765 m (22,195 LF)	6,023 m (19,760 LF)
Best month	361 m (1,185 LF)	201 m (660 LF)
Best week	102 m (335 LF)	61 m (200 LF)
Average month	113 m (371 LF)	58 m (189 LF)
Average week	18 m (59 LF)	10 m (33 LF)
Average day	3.6 m (12 LF)	2.0 m (6.6 LF)

Generally, the more water that is encountered at the face, the slower the overall mining advance rates. This is due to the need to perform additional pre-excavation drilling and grouting, water handling as well as the presence of excess quantities of fine material. Fault, gouge and shear zones have also contributed to slower advance rates, in addition to encountering "highly altered" rock that behaves poorly in the presence of ground water and a free face in front of the TBM. See Table 1 and Figure 5 for tunnelling production data.

The tables and charts below will summarize the average productions per month in both tunnels and the distribution of the productions since the start of the work. Overall mining is 50% complete at the time of this writing.

The actual performance of the mining work has averaged the following for both tunnels.

4 PRE-EXCAVATION DRILLING & GROUTING

Probing and grouting ahead of the TBM (probe hole drilling and pre-excavation grouting) was required for both tunnels. The U.S. Forest Service Permit limits groundwater inflows into the tunnel heading behind the advancing face back towards the portal to no more than 32 l/sec (580 gpm) inflow into the tunnel for more

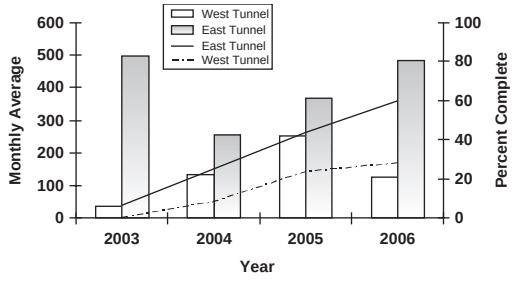


Figure 5. Average annual tunnel advance in the East and West Tunnels – including pre-excavation grouting operations.

than one week. Control of the groundwater inflows to this limit was accomplished by a combination of the following operations;

- Pre-excavation grouting to control water
- Ground improvement grouting
- Filling of discontinuities in the rock mass
- Installation of a watertight segmental lining
- Timely backfill grouting
- Installation of inflatable segment collars
- Installation of drain holes

As an initial criteria, probe hole inflow which exceeds 0.02 l/sec/m (0.3 gpm/ft) or an accumulated 2.0 l/sec (30 gpm) for a 30 m (100-ft) long probe hole represented the threshold at which pre-excavation grouting was considered necessary. Because of the uncertainty of groundwater inflows through a fractured rock mass, probe holes do not necessarily detect all potential groundwater inflows.

A minimum overlap of 6.5 m (20 ft) at the face between successive set-ups of probe/grout holes. Probe holes are limited to a maximum of 45 m (150 ft) in effective length and grout holes are limited to a maximum of 30 m (100 ft) in effective length due to the uncertainty in hole location for longer holes and the reduced effectiveness of grouting long holes.

5 OTHER WATER CONTROL MEASURES

5.1 *Water control grouting & drainage programs*

The Arrowhead Tunnels required the implementation of several grouting programs for the control of water inflows as the TBMs advanced. These included the following as briefly described below;

1. *Stage I Backfill Grouting* – Installed as the TBM advanced and filled the annular void surrounding the segment tunnel lining
2. *Stage II Contact Grouting* – Installed periodically as the TBM advanced and completed the filling of the void surrounding the tunnel

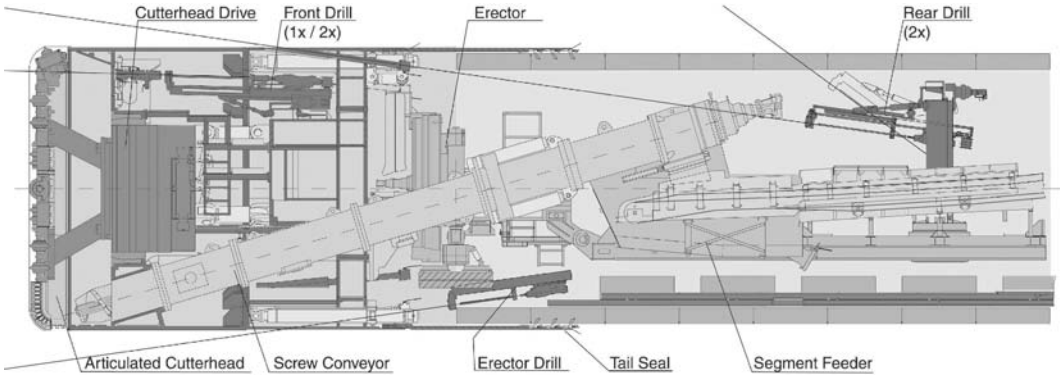


Figure 6. Section through the Herrenknecht TBM showing the principle components, auger and drills for grouting operations.

3. *Drainage Holes:* – Installed at 20° through the segmental tunnel lining to relieve hydrostatic pressure and inflows into the cutterhead.

Several grouting materials have been used with various success for the control of inflows and ground improvement. These have included the following.

- Chemical grout (sodium silicate)
- Polyurethane grouts
- Micro-fine cement
- Colloidal silica grout

A substantial (in excess of 70%) amount of time experienced to date has been consumed with pre-excavation drilling and grouting operations before the TBMs have been advanced. Notwithstanding, this was essential to successfully and safely mine the tunnels through highly variable strata with unknown geological and water bearing features.

5.2 *Segmental tunnel lining with gaskets*

A bolted and gasketed, precast concrete segmental lining is required as the primary support system for the entire length of both tunnels. This construction has been substantially addressed in the referenced papers and will only be briefly described here.

As a baseline for the design of the primary support system the maximum groundwater head during construction for the West Tunnel alignment is 170 m (550 ft) above the tunnel and for the East Tunnel alignment is 275 m (900 ft) above the tunnel.

5.3 *Final tunnel lining – RCCP pipe final lining*

A final lining will be installed in the tunnels to provide a hydraulically efficient system for conveying water, and to prevent infiltration and exfiltration of groundwater. In addition, the final lining must support long-term rock and hydrostatic loads, provide erosion protection, and facilitate dewatering and inspection of the tunnels. Reinforced Concrete Cylinder Pipe (RCCP) was chosen as the final tunnel liner. The annular space around the RCCP will be filled with cellular grout having a density of 330 kg/m^3 (65 lb/ft^3). This will fully envelope the RCCP and is critical to the long-term performance of the final lining. Welded steel pipe will be used also.



Figure 7. Interior of the East Tunnel transition from the starter to the bored tunnel – lined with precast gasketed segments.

6 GROUND BEHAVIOR IN TUNNELLING

6.1 *Actual ground behavior experienced to date*

While the anticipated ground conditions were as generally described in the GBR and variable, we have experienced a wide spectrum of ground types and behaviors. The rate of change from one type to another was very frequent to the extent that extremely hard material could be encountered on the same day as soft and raveling material. Periodically, acute geological features would release flush flows and even flowing ground resulting in the formation of a cavity that

Table 2. TBM basic specifications, weights and measures.

Description	Size or capacity	
1. Design parameters:		
• TBM design	single shield, articulated	
• Static pressure deign	10 bar	145 psi
• Operating pressure	3.0 bar	44 psi
2. Dimensions and weights:		
• Cutterhead diameter	5.820 m	19'-1"
• TBM total length	10.355 m	34'-0"
• TBM & trailing gear	142 m	465 ft
• TBM & trailing gear	820 t	906 tons
3. Power and thrust:		
• Cutterhead power	2,000 kW	2,670 HP
• Cutterhead torque	2,000 kNm	1.5 mil ft-lbs
• Thrust cylinder power	29,270 kN	3,300 tons
• Total installed power	3,600 kW	4,800 HP

required an immediate halt to the mining operations and then backfilling.

Occasionally to date we have encountered decomposed rock acting like sand and silt, blocky ground with large pieces dislodged from the face, both white and gray marble as well as very competent granitic material. High in-situ water pressures and flows have from time to time been enountered and have daunted the pre-excavation grouting program to the extent that this program is adjusted before each mining cycle and constantly assessed during the actual grouting program to be responsive to the conditions.

Shea-Kenny's crews together with the Owner's geological and grouting experts developed a toolbox of flexible means and methods to cope with a wide range of ground and water conditions with the goal to achieve effective pre-excavation grouting and to optimize the TBM advance rates safely.

7 MODIFICATIONS TO THE TBMS

7.1 *TBM design and features*

Two Herrenknecht TBMs were purchased for the project and included a full complement of supporting systems including power, segment handling, ventilation, waste water management, grouting material storage and mixing mounted on the trailing gear. The TBMs had the following specifications that were subsequently adjusted as described below.

7.2 *Unique characteristics of the TBMs*

The TBMs are hybrids in that they need to deal with rock from less than 2.0 MPa to more than 310 MPa (300 to 45,000 psi), in addition to ground water pressures up to 10 bar (145 psi). The TBMs are designed to continuously operate with 3.0 bar (44 psi) pressure based on the cutterhead bearing seal capacity in dynamic mode – in hard rock conditions.

7.3 *Improvements to the TBM and trailing gear*

Based on experience and performance in variable ground conditions and water inflows, several significant modifications were made to the TBM to cope with ground control and ground water inflows.

1. *Cutterhead Shroud*: Installed on the trailing edge of the cutterhead to close-up the gap with the forward shield.
2. *Cutterhead Bucket Closure:* This modification was needed to improve breasting of the face in poor and raveling ground conditions.
3. *Cutterhead Torque Increase:* The original cutterhead torque was 2,000 kNm, (1.5 million ft-lbs) but after several months excavating in variable geological conditions including "soft round", it was determined that the drive gearboxes should be changed resulting in a torque increase by 50% to 3,520 kNm (2.25 million ft-lbs) and cutterhead rotational speed was reduced to 7.5 rpm from 9.75 rpm.
4. *Thrust Pressure Increase:* Thrust was increased to provide improved ability to move the shield forward in squeezing ground conditions.. The total theoretical thrust on the shield was increased by two times from 29,270 kN to 58,540 kN (6,580 tons).
5. *Four-Degree Grout Holes:* An additional 19 grout holes were installed through the forward bulkhead and cutterhead to provide for additional and more effective grouting operations.
6. *Additional Drills – Total of Four:* Three drills were originally installed as per the TBM specifications – one front and two in the rear. One additional probe drill was installed.
7. *Slurry Handling System:* Developed on-site and installed and proved to be a major asset to improve mining production. This will be described below in more in detail.

8 SLURRY HANDLING SYSTEM

8.1 *Slurry handling system*

The Herrenknecht TBMs were not originally equipped with a slurry handling system. The TBMs did, however, have a powerful dewatering system in accordance with the specifications and was designed to pump a high volume of water from the heading out of the tunnel. These TBMs were truly hybrid rock cutting machines designed to operate with a screw auger for muck handling but not in closed mode as an EPBM with a pressurized plenum chamber. They were also not designed to handle high volumes of fines (sand

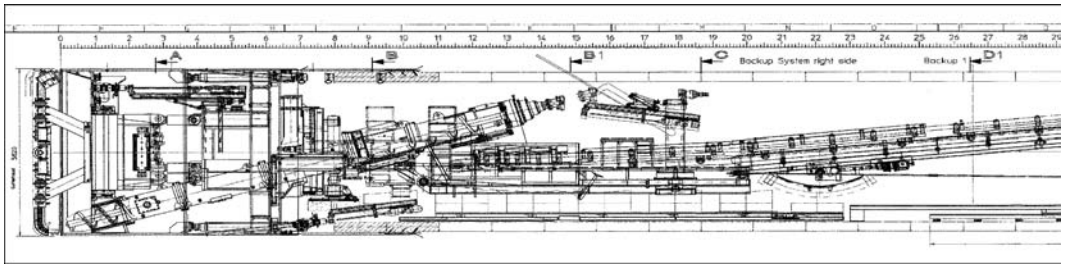


Figure 8. Longitudinal section through the Herrenknecht TBM showing the drilling, segment handling and mucking systems.



Figure 9. Interior of the East Tunnel at the end of the trailing gear and showing the arrangement of the segmental lining.



Figure 10. Interior view of the segment build area showing the TBM thrust jacks and erector mechanism.

Table 3. Slurry system design and operating characteristics.

Description	System characteristic or capacity
Peak flow	550 l/sec (850 gpm) Habermann pump
Nominal flow	32 l/sec (500 gpm) Habermann pump
Fines suspension	15% nominal (by volume) 20% maximum and dependent on flows
Slurry medium	Water in a closed re-circulation circuit
Solids separation	Brandt screens, clarifier and centrifuge

and silt-sized particles) that from time to time could be far in excess of 50% of the material excavated from the tunnel face.

In order to cope with the periodic excess fines and water inflows, a slurry handling system was designed by Shea-Kenny in conjunction with Herrenknecht's engineers. The system has the following characteristics in response to the ground and water conditions. See Table 3 above.

This innovative system was integrated into the TBM and trailing operating systems and equipment wherever possible so as to become a seamless function with the overall mining operations.

The water slurry system was working well whenever excess water and fines were encountered at the face. The system flow was regulated to suit the fines and/or water inflows generally to a maximum of 15% fines (by volume). But as the density of the slurry flow increased, resulting flow decreased substantially due to the maximum power available in the system – principally at the Habermann pump.

9 CONCLUSIONS & RECOMMENDATIONS

9.1 *Conclusions from to date performance*

The Arrowhead Tunnels Project could be considered one of the most challenging tunnel projects presently underway in the United States and it has taken considerably longer to excavate than planned. The ground and ground water conditions are extremely variable and could not be well predicted largely due to the extent of the ground cover as well as the degree and frequency of the alterations in the rock mass including the influence from nearby faults. The pre-excavation grouting program was originally intended to address and arrest ground water inflows into the tunnel and is an essential operation to successful mining.

The stout design and high quality manufacture of the precast segmental tunnel liner was also a hidden benefit and especially when it was tested in-situ with as much as 103 mN (23 million pounds) thrust from

the TBM in order to move the machine forward in very difficult squeezing ground conditions.

9.2 *Recommendations from to date performance*

An effective pre-excavation drilling and grouting program was absolutely essential to successfully mine the tunnel in the presence of high ground water pressures and flows. Optimization was a continuous task and just as the ground conditions were variable, the pre-excavation drilling and grouting program was equally flexible and changed frequently. The Owner, designer and Shea-Kenny constantly worked together to discuss and evaluate various means to drill and grout to control water (first) then to improve the ground (second) so as to be able to mine the tunnel faster and reduce risks. Ground water pressures and flows and their effects on the ground behavior became the "enemy" and were eventually treated in a manner that not only provided control of the inflows but improved the safety and production of the overall mining operations too.

ACKNOWLEDGEMENTS

This paper includes key contributions from a number of persons in addition to the co-authors. We would, therefore, like to acknowledge Stuart Warren of Hatch Mott MacDonald, Tom Hibner and Howard Lum of the Metropolitan Water District of Southern California as well as Robert Gordon and Stuart Lipofsky of Shea-Kenny for their assistance.

There have been many recent papers written on the design and development of the Arrowhead Tunnels Project as part of the Inland Feeder Program for the Metropolitan Water District of Southern California. While they generally pre-date to events of the site work described in this paper, they should be considered as useful preconstruction references.

REFERENCES

Henn, R., Davenport, J., Tzobery, S., Bandimere, S., 2005, Additional Test Results for Comparison of Penetration of Grout Made with Various Ultrafine Cement Products, *RETC 2005, Hutton and Rogstad (eds.), p. 1039–1050, 2005.* Littleton: SME.

Hibner, T., Shamma, J., Tempelis, D., 2003, Managing the Groundwater Impacts of Tunnel Construction, *RETC 2003, Robinson and Marquardt (eds.), p. 592–599, 2003.* Littleton: SME.

King, M., Ghazi, M., Hebert, C., 2003, The Design and Manufacture of the Arrowhead Tunnels Project Precast Segmental Lining, *RETC 2003, Robinson and Marquardt (eds.), p. 688–696, 2003.* Littleton: SME.

Lum, H., Crouthamel, D., Hopkins, D., Cording, E., Shamma, J., 2002, Behavior of a Single Gasket System for a Precast Concrete Segmental Liner Subject to High External Hydrostatic. *NAT 2002, Ozdemir, L. (ed.), p. 141–150, 2002*. Lisse: Swets & Zeitlinger.

Shamma, J., Tempelis, D., Duke, S., Fordham, E., Freeman, T., 2003, Arrowhead Tunnels: Assessing Groundwater Control Measures in a Fractured Hard Rock Medium, *RETC 2003, Robinson and Marquardt (eds.), p. 296–305, 2003.* Littleton: SME.

Swartz, S., Lum, H., McRae, M., Curtis, D., Shamma, J., 2002, Structural Design and Testing of a Bolted and Gasketed Precast Concrete Segmental Lining for High External Hydrostatic Pressure. *NAT 2002, Ozdemir, L. (ed.), p. 151–160, 2002*. Lisse: Swets & Zeitlinger.

Swartz, S., Tzobery, S., Hemphill, G., Shamma, J., 2005, Trapezoidal Tapered Ring – Key Position Selection in Curved Tunnels, *RETC 2005, Hutton and Rogstad (eds.), p. 957–969, 2005.* Littleton: SME.

This page intentionally left blank

Underground Space – the 4th Dimension of Metropolises – Barták, Hrdina, Romancov & Zlámal (eds)
© 2007 Taylor & Francis Group, London, ISBN 978-0-415-40807-3

Ground loss control in EPB TBM tunnel excavation

M.C. Gatti & G. Cassani
Rocksoil S.p.A., Milan, Italy

ABSTRACT: In urban tunnelling, EPB TBM excavation is recommended in soft ground and watery conditions, where there is very sensitive interaction between tunnel and surface. Ground loss control is the basic parameter that has to be considered in the design and construction phases for reliable prediction of surface settlement and the consequent risk of damage to buildings. Analyses of ground loss in EPB TBM excavation are presented in this paper and the tools to minimise it, chamber pressure control, soil conditioning and backfill injection pressures, are discussed. One new important aspect concerns the injection of foam or grout through the shields of modern EPB TBMs to control cavity stability until the lining is placed. Numerical approaches to investigate the problem and systems to monitor the operating parameters of EPB TBMs are presented, with particular reference to some new experiences on Italian construction sites.

1 INTRODUCTION

The increasing demand for transport infrastructures in recent decades has resulted in considerable growth in underground works, especially in urban environments where there is less surface space available. Mechanised excavation using EPB type TBM's is particularly recommended in these contexts where "unstable" face behaviour (Lunardi 2000) must be tackled in ground with particularly poor geotechnical characteristics, in order to minimise effects at ground level and to work in hydrostatic conditions when below the water table. The control of deformation induced in the ground by excavation plays a very important role at the design stage for assessing the risk of damage to existing structures, such as buildings and underground utilities, as reliably as possible. An examination of interference between the tunnel and existing structures must be performed by predicting expected deformation and by surveying the geometry and state of conservation of existing structures to define admissible absolute and differential settlement.

Empirical formulations are very useful for evaluating expected subsidence (Peck 1969, Rankin 1987, O'Reilly & New 1982). Developed on the basis of experimental findings taken from a very large number of case histories, these allow Gaussian subsidence curves to be quickly determined from simple parameters such as the geometrical data of the operation (tunnel diameter D and overburden H), the geotechnical characteristics of the ground (by defining a coefficient K, varying between 0.2 and 0.3 for granular soils and between 0.4 and 0.7 for cohesive soils) and the method of excavation (identified by a value for expected ground loss V).

From a comparison of expected values with subsidence considered admissible, determined for example by means of risk analyses by Mair et al. (1996) and damage classes by Boscardin & Cording (1989), it is possible to verify the compatibility of excavation with existing structures, or to identify corrective action such as revising excavation methods (with the assumption of a different value for V) or the adoption of structural ground improvement and reinforcement works to protect existing structures. The value assumed for ground loss in the process described is without doubt the key parameter in the analysis and it is therefore fundamental that it is accurately forecast at the design stage and that it is monitored during the construction stage.

2 GROUND LOSS IN EPB TBM EXCAVATION

The construction of a tunnel determines a change in the stress state of the ground at the face and around the excavation and generates deformation, the size of which depends on the strength and deformability properties of the ground, on the geostatic conditions and on the method of excavation. The development of deformation is governed principally by the stability of the core of ground ahead of the face (Lunardi, 2000): if the core remains in the elastic domain after excavation then modest deformation is to be expected at the face in terms of extrusion and preconvergence, with convergence of the cavity limited by the stiffening action performed by the face. If the strength of the ground

in the core is exceeded then substantial deformation and plasticisation phenomena will occur at the face, which will be followed by relaxation of the terrain and substantial convergence of the cavity. The deformation generated during excavation propagates towards ground level and constitutes the underlying cause of surface subsidence.

The deformation phenomena that occurs in the tunnel determines a value for "ground loss", defined as the volume of ground which on conclusion of tunnel advance is inside the theoretical excavation cylinder and which, given the propagation of the phenomena on the surface, is equal to the volume subtended by the curve for subsidence at ground level. Ground loss is generally expressed as a percentage of the area of the tunnel excavated ($V = V_L \cdot A_{exc}$, for 1 metre of tunnel) and varies greatly as a function of the excavation method employed, up to 2.0–3.0% with conventional excavation methods without adequate confinement and support intervention. The usual values for EPB TBM excavation are in the range of 0.3–0.6%, with maximum values of 1.0% when the operating parameters of the TBM are not regulated properly or in difficult unforeseen situations; the lower values of the range are typical of cohesive soils, while the higher values of 0.4–0.6% are expected for granular grounds, especially when under the water table. The technical specifications of the major Clients in Italy set the standard value for ground loss, for use in designs and monitoring during excavation, at 0.5%.

It is important to consider that given the deformation development described, the volume lost is the sum of various components which cumulate during the construction of a tunnel. As shown in figure 1, in the specific case of excavation using an EPB TBM, three main components can be considered:

- ground loss "at the face" (V_{Lf}) associated with extrusion and preconvergence which occur in the excavation chamber as a consequence of the behaviour of the core ahead of the face, as a function of the stabilisation pressure applied;
- ground loss "around the shield" (V_{Ls}) in the section of tunnel where the EPB TBM is present, associated with the closure of the excavation profile towards the extrados of the steel shield owing to the annular gap that is generally present between the external cutterhead and the TBM;
- ground loss "behind the lining ring" (V_{Ll}), as convergence of the cavity in the tunnel section where the precast segments are placed, in case the backfilling is not properly applied to guarantee a perfect fill behind the lining (e.g. if the injection pressure is too low, slow hardening mortar is used or it is washed away, etc.).

A fourth component associated with long term settlement (V_{Lt}) must then be added. It is a function

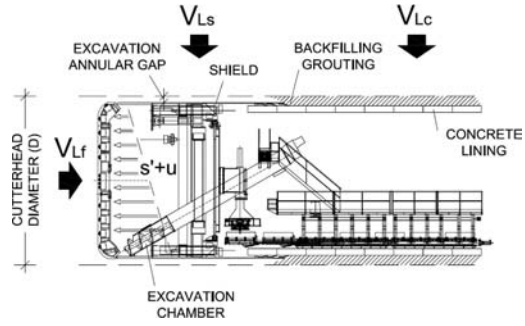


Figure 1. EPB TBM components of ground loss.

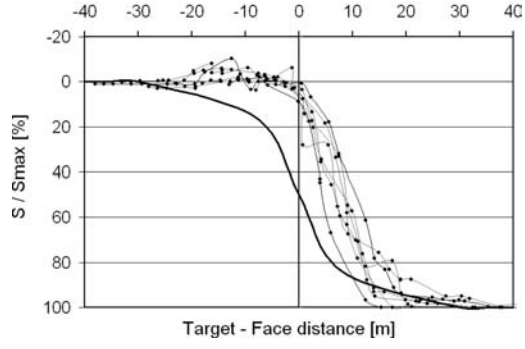


Figure 2. Castellanza railway tunnel – Longitudinal settlements.

of possible ground creep or decay in the strength and deformability characteristics of the ground or of consolidation processes connected with drainage of groundwater which occurred during excavation, especially in clays. Total ground loss can therefore be expressed by the following formulation:

$$V_L = V_{Lf} + V_{Ls} + V_{Ll} + V_{Lt} \quad (1)$$

Longitudinal subsidence curves from some case studies were examined to evaluate the effect of each component. The results obtained on the construction site of the Castellanza tunnel on the Milan-Malpensa railway line are presented in figure 2. In order to superimpose a number of subsidence curves, settlements are expressed as a percentage normalised to the maximum settlement, which is related to ground loss according to the well known equation:

$$S_{max} = (0.31\ V_L \cdot D^2) / (K \cdot (H+D/2)) \quad (2)$$

Figure 2 also contains the longitudinal subsidence curve obtained using Attewell's empirical formulation based on a cumulative probability function (Attewell & Woodman 1982). It can be seen that the settlements that

occurred at the face before the TBM arrival amount on average to 15–25% of total settlements (they are even less than 10% on some curves where ground is actually observed to rise by some millimetres), while the most substantial part accounting for around 60% occurs on the shield section, about 10 m in length, with a final 20% of the settlement occurring along the tail of the machine, during backfill and for long time settlements.

It is significant to observe that because of the stabilisation pressure exerted in the excavation chamber, settlements at the face are much lower than predicted according to Attewell & Woodman's (1982) empirical formulations and are generally less than or close to the value identified by Panet & Guenot (1982) for face convergence in terrains with elastic behaviour, equal to 27% with a stability factor $N = \sigma_o/c_u = 1$. Settlements of more than 27%, up to 50%, would indicate plastic behaviour which it is best avoided.

Furthermore it is important to consider that the problems connected with containing ground loss do not end with proper dimensioning of the stabilisation pressure at the face, but appropriate measures must be adopted for the entire excavation process. For the main components of ground loss, design and control criteria are discussed in the sections that follow.

3 FACE GROUND LOSS CONTROL

Face confinement in EPB TBMs is achieved by using the excavated earth itself (Earth Pressure Balance), which is accumulated through cutterhead openings in the excavation chamber and it is compacted, after additives have been introduced, by the thrust exerted by jacks when the machine advances. The pressure inside the excavation chamber is controlled by regulating the TBM advance rate and the screw conveyor extraction rate (hence the chamber filling rate). When the ground extracted by the screw conveyor is greater in quantity than the volume entering the head, the pressure decreases and vice versa when the quantity extracted is less, the volume increases. The balance is achieved when the conditioned ground reaches maximum density in the excavation chamber, since it can no longer be compacted further, and the volume extracted by the screw conveyor is equal to that excavated by the cutterhead. In these conditions the pressure in the excavation chamber tends towards the "at rest ground pressure", or otherwise it moves towards either an active or passive pressure condition depending on the ratio between the material extracted by the screw conveyor and the ground excavated, (Maidl et al., 1996; Russo, 2003). In order to control the face stability and consequently ground loss at the face, the correct pressure in the excavation chamber must be applied and especially it must remain stable during tunnel drive by controlling the EPB TBM operating parameters and the soil conditioning.

3.1 *Face stability pressure design*

In order to determine the correct excavation chamber pressure, different analysis approaches should be considered. First the minimum pressure needed to guarantee equilibrium in the wedge of ground at the face to avoid failures and collapse of the advance core must be determined. This pressure can be done by applying "limit equilibrium methods", the most indicated of these is that developed by Anagnostou & Kovàri (1996) specifically for excavation with EPB TBMs. The method is based on the silo theory according to the three dimensional failure mechanism proposed by Horn and it allows the effective pressure (s') to be determined in drained conditions by using the following compacted formula:

$$s' = F_0\gamma'D - F_1c + F_2\gamma'\Delta h - F_3c\,\Delta h/D \quad (3)$$

where F_i are dimensionless coefficients, given by normograms, dependent on the soil friction angle, on the overburden H and the diameter of the excavation D, on the ratio $(h_0-D)/D$ and the submerged weight γ'; c is the soil cohesion and

$$\Delta h = h_0 - h_f \quad (4)$$

is the piezometric difference between the level of the water table h_0 and the piezometric height in the excavation chamber h_f, as a function of which filtration forces are generated. Since it is advisable to avoid draining the water table during excavation, the piezometric difference must be nil ($\Delta h = 0$) and consequently the total pressure to be adopted in the excavation chamber to guarantee limit equilibrium conditions s_L, is:

$$s_L = s' + u = (F_0\gamma'D - F_1c) + h_0\,\gamma_w \quad (5)$$

the sum of the effective pressure and the hydrostatic pressure u, with γ_w the water specific weight.

However, the method described cannot be used to assess the face deformation state for the pressure s_L applied and does not therefore allow volume loss to be estimated. Further analysis must be performed to establish a correlation between the pressure in the excavation chamber and values for extrusion and preconvergence. One possible approach is to use axial-symmetric models which, quicker than the more laborious 3D analyses, are able to provide indications of how the stress-strain state is evolving at the face. The calculation is conducted in effective stresses employing finite element or finite difference calculation codes, using the geotechnical characteristics and the constitutive law most appropriate for the grounds concerned and considering the different geostatic conditions along the alignment of the tunnel. To simulate the conditions in the excavation chamber, the

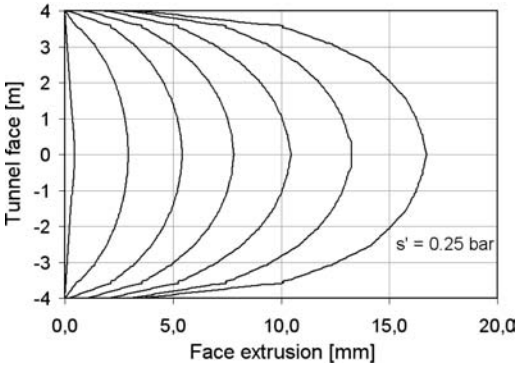


Figure 3. Axial-symmetric analyses – Extrusion vs face-pressure.

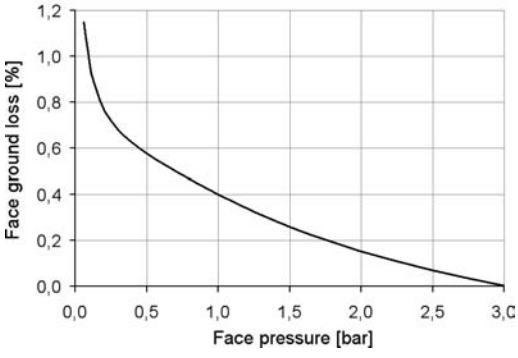


Figure 4. Face ground loss vs face-pressure.

pressure at the face is progressively reduced by the geostatic value to zero in steps of 0.5 bar (0.05 MPa), to thereby evaluate the relative development of extrusion. Figure 3 gives an example of the extrusion graphs calculated for the Castellanza tunnel (with excavation diameter of 8.0 m, in granular soil above the water table, specific weight of 20 kN/m^3, nil cohesion, friction angle of 40° and elastic modulus of 120 MPa), for face pressures varying between 3.0 and 0.25 bar.

Determination of extrusion values at the tunnel axis and at the edges of the face allows the shape of extrusion volumes to be identified (cylindrical, truncated cone, spherical dome) and calculated by using, for example, the formulas reported in Cassani & Mancinelli (2005). It is thus possible to diagram the ground loss at the face as a function of the pressure applied, as shown in figure 4, and select the correct face pressure.

Use of the diagram allows the correct stabilisation pressure to be identified; more specifically it allows to estimate the pressure which constitutes the limit of the core elastic behaviour (s'_E), below which the extrusion-pressure relationship is no longer linear and there is a progressive increase in volume loss as a result of plasticisation that is generated until the face becomes unstable. It should also be observed that the value for extrusion and as a consequence for ground loss is nil for pressures that are equal to the geostatic pressure, which therefore constitutes the upper limit of the pressure range to be applied at the face and can be easily determined with reference to the "thrust at rest" (s'_{ko}) by applying Jaki's formula, corrected in overconsolidated ground:

$$s'_{ko} = \gamma \cdot (H+D/2)\,(1-\sin\phi)\,OCR^{\alpha} \qquad (6)$$

where ϕ is the soil friction angle and OCR the over-consolidation ratio. Additional pressure rate could be considered for loads present on the surface.

In conclusion, the optimum effective pressure in the excavation chamber (s') lies within this range:

$$s'_L < s'_E < s' < s'_{ko} \qquad s = s' + u \qquad (7)$$

To estimate the total pressure (s) the hydrostatic pressure (u) must be added; moreover a linear development along the height of the face has to be taken into account.

3.2 *Soil conditioning*

The broad working range of modern EPB TBMs in terms of the soil granulometry and permeability means that the ground in the excavation chamber must be appropriately conditioned by means of foams and/or polymers. The conditioned ground must present good plastic deformation, soft consistency, low inner friction and low permeability so that it can be employed as a fluid to support the face, especially under the water table, and at the same time it must minimise drive torque and wear of the excavation tools; proper soil conditioning is essential for maintaining the pressure in the excavation chamber "over time". The ratio between the quantity of foam and the ground (FIR, Foam Injection Ratio), the quantity of air and water to be mixed with the foam (FER, Foam Expansion Ratio, and c_F, concentration of foaming solution), see Langmaack (2001), must be established at the design stage together with the chemical composition of the products employed. In granular soil with a low percentage of fines (<5–10%), foams that are capable of increasing the plasticity of the mix and reducing its permeability must be used with high FIR values (>35–45%, usually 10% higher than soil porosity); in cohesive soil, especially in sandy clay and pure clay, the use of dispersing polymers is advisable to prevent clogging of the cutting tools and screw conveyor and also wear resulting from strong adhesion to the cutterhead, with values for FIR of ~25–35%. The values for FER are generally within the 8–15 range, the higher values for granular soils.

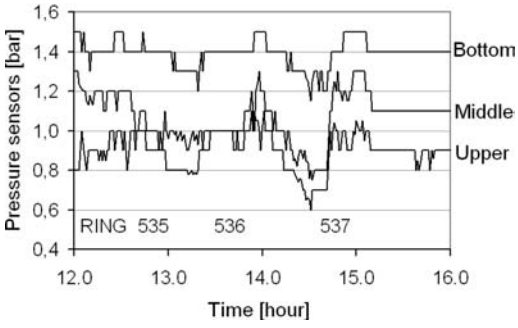


Figure 5. Excavation chamber pressure sensors vs time.

3.3 *Control of EPB TBM drive-parameters*

It is very important to control the operating parameters governing the advance of the EPB TBM, which are the thrust (kN) and the cutterhead torque (MN · m) in relation to the advance rate (mm/min) and penetration (mm/rpm); the control of the screw conveyor torque and rotation is important too.

The drive-parameters must be monitored to make sure that they remain within the specified range without any sharp variations or interruptions. It is also very important to record the length of work cycles and any machine down times. Measurements of pressure in the excavation chamber must be taken using sensors placed at different heights (bottom, middle and upper) to monitor ground loss at the face.

Figure 5 gives an example of tunnel advance, showing reductions in pressure during the installation of the 536 lining ring which it is best to avoid .

4 CAVITY GROUND LOSS CONTROL

The final confinement of the cavity is performed by placing a precasted segment lining in the zone protected by the shield, followed by backfill injections behind the lining performed from the TBM tail; maximum attention must be paid here too, with a view to containing ground loss components pointed out in figure 2.

4.1 *Shield zone*

The annular gap between the excavation diameter and the extrados of the shield, generally employed in TBM construction to reduce friction during tunnel advance (radial 10–15 mm), represents a critical element in controlling convergence of the cavity, especially in cohesionless soils under the water table where the cavity stand-up is negligible. The confinement of the excavation profile relies entirely on the flow behind the shield of the foam injected at the face,

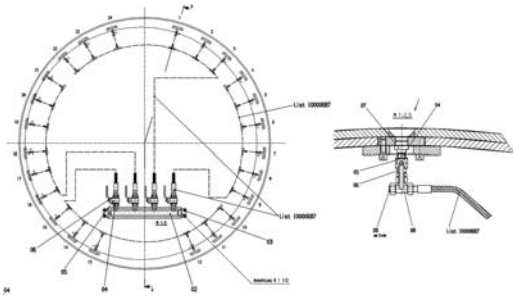


Figure 6. Wirth 816/H shield injection.

often without success. To reduce this problem some modern EPB TBMs have been fitted with systems for injections through the shield to fill the gap using special greases and plastic or expansive mixes capable of preventing the ground from closing around the shield.

The EPB Wirth 816/H TBM employed on excavation of "Channel Tunnel Rail Link" in London and on the Castellanza tunnel is equipped with 24 radial valves connected to a pressure and volume controlled injection system, as shown in Figure 6. Injection of special grouts on some sections of the Castellanza tunnel, where the presence of surface structures was most delicate, resulted in an appreciable reduction in settlements at ground level from 35–40 mm to 10–15 mm, revealing a potential that we feel it is worthwhile developing in future works.

4.2 *Lining placement, backfil and grouting stages*

The ground loss control is performed by defining the injection system and the quantities of grout mix to be injected, where the aim is to completely fill the annular gap between the extrados of the lining and the excavation profile. The EPB must be equipped with a number of injectors along the perimeter of the tail shield to allow good diffusion of the injected grout mix (generally 4–6 injectors fed by different pumping systems so that injections can be performed even if one of them breaks down) and it must also be fitted with a precision balance system to weigh the material excavated in order to calibrate the necessary volume of mix to be injected (V_{gr}) for each stroke by means of the relationship:

$$V_{gr} = (P/\gamma - D_{ext}{}^2 \cdot \pi/4 \cdot L) \qquad (8)$$

where P is the weight of the ground excavated in one boring stroke of length L (equal to the lining ring with diameter of the extrados D_{ext}) and γ is the ground specific weigth to be determined with laboratory tests to also take account of soil conditioning. Monitoring of the real volume excavated, $V = P/\gamma$, with the theoretical volume $V_{exc} = D_{exc}^2 \cdot \pi/4 \cdot L$ allows possible over-excavation or releases of ground to be identified

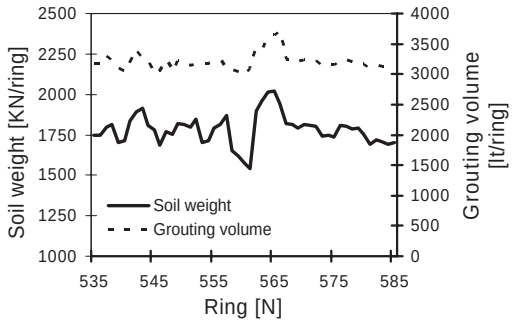


Figure 7. Excavation soil weight/Grouting volume.

so that they can be promptly filled at the injection stage. Figure 7 contains a monitoring graph prepared during tunnel advance, which can be used to "balance" the material excavated with the volume of mix injected.

The injection pressure (p_{gr}) must be a little greater than the geostatic pressure to avoid increasing the convergence of the cavity:

$$p_{gr} > (u + \gamma \cdot (H+D/2) \cdot K) \quad \text{with } K^{O} < K < 1 \qquad (9)$$

The grout mix design must ensure that the mix can be pumped and also that the hardening curve is adequate which avoids compressibility and does not allow it to be washed away. The authors have obtained very positive results using "bi-component" mortars, where a rapid hardening additive is added to a cement mix base in the tail of the shield, through a separate pipe, so that the mix sets immediately after injection but with no risk of clogging the injection systems.

5 CONCLUSIONS

The value for "ground loss" constitutes a key parameter for managing excavation using an EPB shield, because of its importance in assessing surface subsidence phenomena and building damage risk.

It is the sum of different components, which develop during the stages of tunnel advance at the face and around the cavity, in the tail zone and after the precsted segments lining is placed. Account must be taken of the specific aspects of design discussed in this paper for each step of operations: the correct stabilisation pressure to be kept constant in the excavation chamber must be defined (which will leave the core at the face in the elastic range and limit extrusion); the type of soil conditioning; the injection of special greases and mortars through the shield to prevent the cavity from closing in during the delicate stage of shield advance; monitoring the volume of ground excavated and the injection of backfill grout mixes to make sure there are no gaps in the ground.

The design of a monitoring system both in the tunnel by monitoring the operating parameters of the TBM and on the surface by setting up a network of topographical datum points to monitor settlements along the tunnel alignment and across it is an indispensable instrument for verifying and regulating excavation activities.

REFERENCES

Anagnostou, G. & Kovari K. 1996. Face stability condition with Earth-Pressure-Balance Shields. *Tunnels and Underground space Technology*, 11, 2, 165–173.

Attewell, J. H. & Woodman, J. P. 1982. Predicting the dynamics of ground settlement and its derivitives caused by tunnelling in soil. *Ground Engineering*, 15, 13–26.

Boscardin, M.D. & Cording, E.G. 1989. Building response to excavation-induced settlement. *Int. Geo. Egrg. Asce*, 115, 1, 1–21.

Cassani, G. & Mancinelli, L. 2005. Monitoring surface subsidence for low overburden TBM tunnel excavation: computational aids for driving tunnels. *Proc. 11th International Conference of IACMAG Symposium*, 631–638 Turin.

Langmaack, L. 2001. Application of new TBM Conditioning Additives. *Proc. 6th International BAUMA Tunnelling Symposium*, 27–37 Munich.

Lunardi, P. 2000. Design and construction tunnel – ADECO-RS approach. *Tunnels & Tunnelling International Special Supplement*.

Maidl, B., Herrenknecht, M. & Anheuser, L. 1996 Mechanised Shield Tunnelling. *Ernst & Sohn*, Berlin.

Mair, R. J., Taylor, R. N. & d, J. B. 1996. Prediction of ground movements and assessment of risk of building damage due to bored tunnelling. *Geotechnical aspects of underground construction in soft ground*. Mair & Taylor (eds) Rotterdam Balkema.

O'Reilly, M. P. & New, B. M. 1982 . Settlement above tunnels in the United Kingdom – their magnitude and prediction. *Tunnelling 1982*. IMM London 173–181.

Panet, M. & Guenot, A. 1982. Analysis of convergence behind the face of a tunnel. *Tunnelling 1982*. IMM London 197–204.

Peck, R.B. 1969. Deep excavations and tunnelling in soft ground: state of the art report. *Proceeding 7th Int. Conf. on soil mechanics and foundation engineering*. 225–290 Mexico City.

Russo, G. 2003. Una riflessione sui criteri di valutazione della pressione di stabilizzazione del fronte nello scavo con EPBS. *Gallerie e grandi opere sotterranee.* 71, 1–9.

Underground Space – the 4th Dimension of Metropolises – Barták, Hrdina, Romancov & Zlámal (eds)
© 2007 Taylor & Francis Group, London, ISBN 978-0-415-40807-3

City-Tunnel Leipzig, a challenge for the shield drive

W. Glitsch
DEGES, Deutsche Einheit Fernstraßenplanungs- und –bau GmbH, Berlin, Germany

T. Maidl
Ingenieurbüro Maidl & Maidl, Bochum, Germany

ABSTRACT: The City-Tunnel Leipzig project is the central part of the reorganization of the railway network within the Leipzig area. The subterranean double-tube connection beneath the centre of Leipzig is divided into six sections, with three interspaced stations, and has a total length of 2.94 km. Following the construction of the stations, the single shell tunnel will be constructed via a Hydroshield with a diameter of 9 m. The biggest challenges for the shield drive are the heterogeneous glacial ground conditions, which already proved challenging in the construction of the sealing blocks, and the very difficult structural boundary conditions.

Natural and non-natural obstacles are to be expected within the tunnel alignment. The tunnel route is below the ground water level, which has a maximum height of approx. 18 m above the tunnel invert. Due to the shallow ground coverage and under-passing of important buildings, a careful tunnelling technology was tendered. Additionally, several ground treatment measures have been executed in order to protect buildings within the settlement trough. Substantial compensatory grouting measures linked to the settlement data will actively counteract detrimental deformations to buildings.

The Hydroshield is designed and constructed based on the tender requirements and the special geotechnical boundary conditions. Innovative monitoring systems are installed to facilitate the excavation of the tunnel in the most sensitive way for adjacent buildings, and simultaneously to monitor at surface level the reaction to the tunnelling process.

1 PROJEKT DESCRIPTION

1.1 *The Projekt*

The City-Tunnel Leipzig project is the central part of the reorganization of the city's railway network, which will run under the city centre from the station Bayerischer Bahnhof via the stations Wilhelm-Leuschner-Platz and Markt to the Central Station.

The tunnel will be used by all suburban and regional train lines and will result in more frequent services and shorter journey times. Spring 2004, the project was put out to tender. On 10th January 2005, the consortium City-Tunnel Leipzig Los B – comprising DYWIDAG Bau GmbH as technical lead, together with ALPINE Bau Deutschland AG, Oevermann GmbH & Co. KG, Universale Grund –und Sonderbau G.m.b.H und STRABAG AG – won the contract to construct the main section between the station Bayerischer Bahnhof and the Central Station.

The total construction costs were estimated at 570 m Euros.



Figure 1. Horizontal alignment.

1.2 *Subsoil*

The City-Tunnel Leipzig will be excavated in glacially-formed, loose quaternary granular soil and a mixture of loose and cohesive tertiary sediments. From south to north, initially quaternary pebble (medium-grain sand and fine gravel) is encountered, then with decreasing alignment, tertiary medium to fine sand and, in places, soft to semi-solid clay in the cross-section of the tunnel. The hydro-geological conditions along the tunnel alignment are determined by two aquifers, which are separated by two aquicludes. The tunnel lies entirely below the ground water level and the maximum height

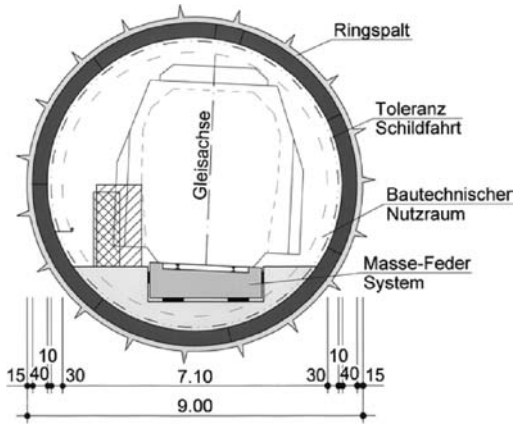


Figure 2. Standard cross-section.

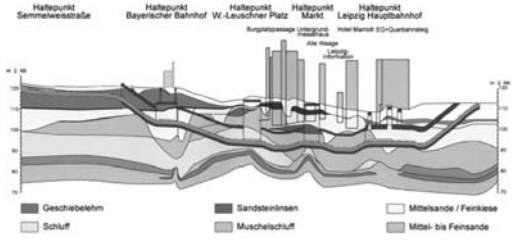


Figure 3. Vertical alignment.



Figure 4. Sandstones in the excavation pit of the Marriott-Hotel.

of the ground water is around 18m above the floor of the tunnel.

In the area of the tunnel tubes, natural and non-natural obstacles are to be expected. Next to the clay or marl deposits, for example, boulders up to 1m in diameter, and sandstone monoliths of up to 15 m^3 and a compression strength of up to 250 N/mm^2 are anticipated.

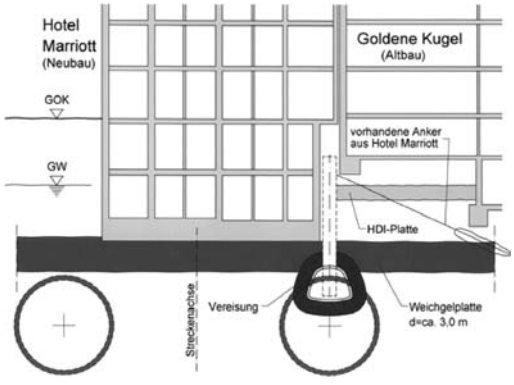


Figure 5. Tender design: salvaging the pile wall by means of mining and soil freezing technology.

Coal deposits are known to be present in the sand and silt, and fossilised tree trunks cannot be ruled out in the layers of gravel.

In this inhomogeneous subsoil, the building contractor must take into consideration the plugging nature of the malleable clay in the shell silt, as well as the abrasive impact of the quartz components of the loose formations.

In the built-up area in particular, non-natural obstacles are to be expected. The ground anchorage in the area of the tunnel between the stations Wilhelm-Leuschner-Platz and Markt was removed with considerable effort. However it cannot be entirely ruled out that further, as yet unknown, anchorages to the working face may have to be removed manually. Over and above this, inadequate or unfilled boreholes cannot be ruled out.

Below the Marriott Hotel, an intersecting bored pile wall remains in the ground, which served as a retaining wall to the adjacent building 'Goldene Kugel'. The partly reinforced piles reach into the roof area of the western tunnel tube and will be salvaged in advance, protected by soil freezing technology.

2 SHIELD ROUTE

Due to the subsoil conditions and the high ground water level, an economically viable under-passing of the centre of Leipzig with minimal settlement is only possible with a TBM with shield.

The excavation of the tunnel begins at the northern end of the station Bayerischer Bahnhof and finishes at the Central Station. It is planned that the machinery will be pulled through the excavations of the intermediate stations (planned in the cut-and-cover method of construction) and, upon reaching the Central Station, the machinery will be dismantled and put back



Figure 6. Moving the portico at the station Bayerischer Bahnhof.

together at the Bayerischer Bahnhof for the excavation of the second tube.

2.1 *Station Bayerischer Bahnhof*

The station Bayerischer Bahnhof is 197 m long. A special proposal from the ARGE suggested moving the 20 m tall, 30 m wide and 2800t heavy listed portico around 30 m to one side, to enable the cut-and-cover construction of the station. Following extensive strengthening of the foundations with HEB-steel girders and a coating of reinforced concrete, the construction was successfully raised and moved by pushing it on a slide bearing on 10th April 2006. Upon completion of the construction of the station, the portico will be returned to its former position.

2.2 *Construction of the stations Markt and Wilhelm-Leuschner-Platz*

The stations will be constructed using the cut-and-cover method (figure 7) with double shell walls. The retaining wall forms a diaphragm wall, which is a retained part of the construction and is attached rigidly to the ceiling. The approximately 26 m high diaphragm wall is embedded, or strengthened, for the duration of the construction, and is embedded in the watertight shell silt. In its finished state, an inner layer made of site-mixed concrete, calculated according to water pressure, guarantees the structure is watertight.

Due to existing constructions directly next to the upper end of the station Markt, the placement of the sealing blocks was only possible using jet grouting. Because the seal of the jet grouting blocks could not be guaranteed, in particular due to the extensive charcoal deposits, the seal is secured with an inner layer of cement blocks, through which the shield drive travels.

The sealing blocks at the other stations, which can be inserted from above without additional effort, take

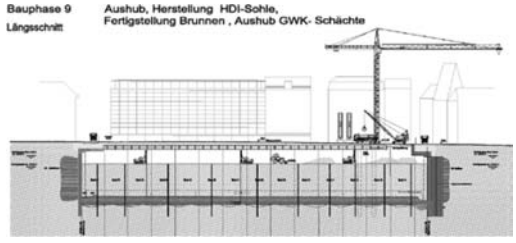


Figure 7. Cut-and-cover method at the station Markt with HDI floor and sealing blocks.



Figure 8. The station Markt on 07.09.06.

the form of a single-layered lamellated diaphragm wall.

2.3 *Sections of tunnel*

In the area of the city centre, numerous buildings and mains have to be under-passed, or are situated in the area affected by the settlement trough, which occurs when the shield drive removes the soil. Settlement of up to 20 mm for a single tube and 30 mm for both tubes were forecast. Under-passing a structure highly sensitive to settlement at a proximity of as little as 4 m requires measures to minimise settlement along the route.

It is planned to use the Compensation Grouting Process (CGV process), which stabilises the ground and – if necessary – with which an elevation is created ahead of the shield drive and occurring settlement can be compensated. The necessary injections of high pressure are delivered by means of valve tubes via shafts and an existing media duct.

The tunnel will be built as a single shell construction. One ring of precast segments consists of seven segments and a capstone with a clam connection where they adjoin. The segments are 40 cm thick and 1.80 m broad. They are prefabricated in a factory of the Max Bögl company and transported by rail to Leipzig.

To avoid the seal tread at the outer edges of the segments 'expanding' during the lifetime of the construction, the front ends and back ends of each section are joined to each other by means of prestressing tendons. The use of ducts for the cables, which run along the inside of the segments, requires an exact ring construction from the outset of the shield's journey.

3 SCHIELD DRIVE

3.1 *The concept of the shield drive*

The use of a Hydroshield with a fluid-supported working face was selected to best cope with the heterogeneous soil conditions and the difficult structural conditions present. With its chamber system, where the extraction and the pressure chamber are connected by a submerged wall opening, a precise, automatic control of the supporting pressure (to 0.1 bar) is possible via the compressible air cushion in the pressure chamber. This enables grain displacement and settlement to be reduced to a minimum. The technical specifications of the shield drive are based on the contractual agreements and the experience of the machine constructor, the Herrenknecht company.

In order to keep the grain displacement in the ground along the shield as minimal as possible, a rigid shield casing with a small shield conicity of 20 mm was chosen and a pressure and volume controlled grouting of the annular space is installed. In addition to this, an excavation control system, i.e. electromagnetic inductive throughput and radiometric density measurement plus a comprehensive operational datacapture, enables the interaction between the ground and machine to be recorded and monitored.

Due to the suspension-supported shield drive technology, the quality of the shield drive correlates, amongst other things, with the separation and bentonite technology, which must be deployed with equally great care and know-how.

Table 1. Technical specifications of the Hydroshield.

Drill diameter	9.0 m
Schield length	9.650 m
Weight	approx. 1,100 t
Total length of machinery	approx. 65.0 m
Max. driving force	65,000 KN
Cutterhead power (8 engines)	880 kW (electric)
Installed total power	2,500 KW
Torque	4,837,000 Nm
Max pressure of the 14 pairs of jacks	65 MN
Cutterhead equipment:	
176 cutters, 42 discs und 16 buckets	



Figure 9. Hydroshield of Herrenknecht.

3.2 *Drill-head area*

The cutterhead was adapted to the heterogeneous foundation conditions in Leipzig: its rim is relatively closed and its equipment includes cutters for areas of soil and rock and discs for boulders, bankings of sandstone and other obstacles. It turns in two directions, is axially moveable up to 400 mm and can be tilted by means of a swing bearing. By tilting the cutterhead, a minimal corrective radius of 300 m can be achieved. Additionally, a hydraulically-operated overcutter can increase the drilling diameter by 60 mm.

Due to the heterogeneous, abrasive ground conditions, the cutterhead is fitted with additional Hardox-wear plates. 6 cutters and 2 buckets are equipped with an electric wear-detection device while the remaining mining equipment can be visually monitored with an endoscope.

The rock discs are 17″ one and two ring rollers 100 mm apart, which can be replaced from the rear. For access to the working compartment, the Hydroshield has a double-chambered channel for people and one material channel, which can withstand a test pressure of 6 bar.

The hydraulically-steered stone crusher, designed for a grain of a maximum edge length of 800 mm, is situated in the floor. Larger boulders are initially broken up by the cutterhead until they fit through its openings. The spaces on the grill in front of the suction flange of the suspension pipe are 180 mm wide.

To avoid blockages in the area of the stone crusher, there is a swivelling suspension jet in the floor area. The extraction and pressure chamber are connected by a communicating vessel which ensures the circulation of the suspension in the event of excessive material deposits between the pressure and submerged wall.

According to the tender document, stone breaking tests took place in the machine constructor's plant to demonstrate its capacity to deal with boulders.

3.3 *Schield peripherie*

In order to be able to carry out ground strengthening measures in difficult construction conditions, for

example within areas of loose gravel or obstacles of any kind, there is an arrangement of 10 test drill channels of a nominal width of 100 mm and an angle of 7° in the roof area of the shield. This enables roof injections to secure the safety of the heading face to allow access to the work compartment. Due to the anticipated obstacles in the soil, the shield's cutting edge was designed to be relatively resilient at 80 mm.

The 2.5 m long carriage drill is mechanically fixed to the erector. Hydraulically-powered Topphammer drive the drill poles via a drill channel through the shield and into the ground.

The pressure grouting at the annular space takes place at the rear of the shield via 6 active pipes, with additional openings fitted with valves and preventer to enable the insertion of a high-pressure hose with rotating jet for cleaning the pilaster strips. To avoid risking settlement by delaying the grouting, a quick unloading of the cement container on the rear carriage is possible, which saves the time it would take to pump through.

To seal the gap between the rear of the shield and the lining, a three-row brush construction is present with 10 pipes per compartment for the sealant. Sealant consumption, flow and pressure are automatically registered.

3.4 *Backup system*

Due to space limitations and entering, transferring across and exiting the stations, the rear carriage is relatively short at 60 m. The rear carriages are designed to accommodate minimal approach and corrective radii. It is an enclosed framework construction set on hydraulically-steered Vulkulan castors.



Figure 10. Station Bayerischer Bahnhof in August 2006.

The key installations to operate the shield drive are situated on the rear carriage. The drill head is electrically powered by 8×110 kW engines.

The transportation and feeding cycle of the bentonite suspension is carried out using pipes of a nominal diameter of 350 and 400 mm with a maximum flow volume of 1844 m^3/h.

3.5 *Innovative measurement and data system*

In accordance with the tender documents, the operational data is centrally captured and made available to the TBM operator, as well as to the construction management above ground and the client in an easily comprehensible form. To guarantee a tunnel-drive with minimal settlement, particularly at the critical points where buildings are under-passed, a continuous cross-checking of the excavation parameters as well as with the actual measured soil displacements are essential.

- **Sonic Soft Ground Probing (SSP)**
  In order to reduce the risk of settlement and the negative implications of geological faults, the seismic pre-assessment system SSP is installed. 4 transmitters, located at the cutterhead, emit acoustic waves which are reflected when density changes or obstacles occur within the ground. By analysing the runtime, a prediction based on the reflection is possible. Specialised 3-D analysis software visualises the reflected signals, which enables a low-impact shield drive to take place, as demanded by the ground conditions.
- **Realtime process controlling system**
  As a result of latest developments, the TBM operator is in the position to directly assess the impact of the shield drive, due to the immediate availability of displacement data.

The recording, collation, evaluation and presentation of data is carried out by the contractor with the process-control system CBP. Closer monitoring,



Figure 11. Controlled Boring Process (CBP) System for low-impact tunnel drive.

within the predetermined boundaries, of data from the machinery directly responsible for settlement, showing, for example, confinement pressure, slurry circuit, bentonite level etc. is thus possible.

In addition to this, measurement data from the immediate surrounding area is fed into the CBP system so that the TBM operator is constantly aware of his exact position in relation to the current geological situation. Additionally a ring-based operational data evaluation takes place during the shield drive.

4 CONCLUSION

The City-Tunnel Leipzig represents an exceptionally demanding challenge in tunnel construction, due to the extremely difficult geo-technical and civil engineering conditions present. Therefore a technique was selected which guarantees low impact tunnel drive. Key to the successful delivery of this project are the collective experience of all people involved in the project, as well as a constructive working partnership and co-operation.

In contrast to the original timetable, the shield drive will not commence in 2006 and therefore information on the actual delivery of the project is unavailable at this time.

REFERENCES

Fechner, H. & Kleffner, H.-J. Konzeption und bautechnische Herausforderungen beim Bau des City-Tunnel Leipzig. *Forschung + Praxis, U-Verkehr und unterirdisches Bauen*, B. 41: Tunnel-Neue Wege-Neue Chancen. Bauverlag: 231–235

Glitsch, W. & Rehm, U. 2006. The conception of the shield-machine for the City-Tunnel of Leipzig under particular consideration of the local geological conditions, 17. Symposium Felsmechanik und Tunnelbau – Fachseminar Maschineller Tunnelbau, March 29.–30. 2006, Haus der Wirtschaft, König-Karl-Halle, Stuttgart, Germany

Handke, D. 2003. Prüfen der Schildmaschine auf Eignung und Abnahme auf Grundlage einer Risikoanalyse. Beitrag anlässlich des XI. Kolloquiums für Bauverfahrenstechnik, Tunnelbau und Baubetrieb, Bochum, Deutschland 16.09.2003. *Risikopotential und – bewältigung bei aktuellen Tunneln.* Essen: Verlag Glückauf

Ingenieurbüro Maidl + Maidl 1997. Tunnelbautechnisches Gutachten zur Vorplanung.

Ingenieurbüro Maidl + Maidl 2001. Bewertung der Kostenanschläge und Analyse der Risikopotentiale.

Ingenieurbüro Maidl + Maidl 2002. Variantenuntersuchung – Bewältigung der Baugrubenanker Juridicum Passagen.

Kleffner, H.J. & Mämpel, H. Bahnhofsverbindung in der Innenstadt von Leipzig – Bebauung und Hindernisse im Bereich der Schildstrecke. Beitrag anlässlich des XI. Kolloquiums für Bauverfahrenstechnik, Tunnelbau und Baubetrieb, Bochum, Deutschland 16.09.2003. *Risikopotential und –bewältigung bei aktuellen Tunneln.* Essen: Verlag Glückauf

Kleffner, H.J. & Maidl, R. 2004. Baugrundtechnische Herausforderungen beim Bau des City-Tunnels Leipzig im Schildvortrieb. *TIEFBAU* 12/2004: 754–758

Maidl, B., Herrenknecht M., Anheuser, L. 1994. *Maschineller Tunnelbau im Schildvortrieb*. Berlin.

S-Bahn Tunnel Leipzig GmbH. 2001. City Tunnel Leipzig-Entwurfsplanung (erstellt durch Ingenieurgemeinschaft Schüßler Plan / DE Consult).

Underground Space – the 4th Dimension of Metropolises – Barták, Hrdina, Romancov & Zlámal (eds)
© 2007 Taylor & Francis Group, London, ISBN 978-0-415-40807-3

Integral studies on mechanical functions of mudding agents and the properties of muddified soils in the EPB shield tunneling technology

T. Hanamura, J. Kurose & Y. Aono
Okayama University, Okayama, Japan

H. Okubo
Taisei Corporation, Tokyo, Japan

ABSTRACT: A key technology of EPB shield tunneling is the mixing of excavated soil with the conditioning agent called "mudding agent" to create the desirable mud state of soil called "muddified soil" having enough flow ability and plastic behavior. In this paper it is clarified the mechanical and chemical functions of mudding agents and the properties of muddified soil. Mudding agents are categorized and classified by the chemical analyses and confirmed by the experiment. The compatibility of mudding agent with soil to be excavated is discussed and clarified also by the experiment.

1 INTRODUCTION

1.1 *EPB shield tunnel and mudding agents*

The EPB shield tunnel is known to be the most economical shield tunnel method used in many parts of the world that was originally developed in Japan, and had been used mostly in Japan until around 1990. Difficulties were existed in the controlling of the excavated soils to keep mud states in order to make the excavated face stable and excavate smoothly in the cutter-head chamber. In the EPB system earth and water pressure can be balanced by the excavated soil pressure through the mechanical thrust from shield machine. One of the most crucial technologies is the method of excavated soils to keep mud states to counteract the earth pressure homogeneously in the face throughout the chamber and excavate smoothly in the cutter-head chamber. In most cases it is necessary to use the conditioning agent to have excavated soils created mud state to keep enough flow ability and plastic behavior. This conditioning agent is mostly the chemical agent of industrially produced or naturally produced and is defined as "mudding agent", for it makes the excavated soil into mud state. Since the soil was not the mud but the mud state soil, the excavated soil mixed with mudding agent can be defined as "muddified soil".

Mechanical functions of mudding agents in the muddified soils are to be required to have first, the bridging effects over soil particles to create mud as plastic and homogeneous and to cope with earth pressure from collapsing, secondly the flow ability to ensure the smooth excavation and to reduce cutting torques during excavation, thirdly the preventing ability of soil from sticking in the chamber by consolidation hardening that cause the stop of cutter-head rotation, fourthly the enough impermeability to ensure the prevention of the muddified soils from leaking into the ground, and fifthly smooth, inseparable and enough cohesive property to prevent muddified soils from gushing through screw conveyor and keep the transporting ability of excavated soils high in the screw conveyor, and on the belt conveyor, in the pipe or on the rail trucks.

1.2 *Purpose of the research*

There are numbers of mudding agents in the EPB shield tunnel market. However there are few explanations and classifications on the mudding agents. It is inevitable to understand the mechanical and chemical properties of mudding agents and muddified soils and to classify them according to the functions. It is also in need to select appropriate mudding agents with the soil conditions to excavate. Therefore the purposes of this study are set up as follows.

(1) Understanding the mechanical functions of the mudding agents in relation to chemical properties.
(2) Proposal of the classification of mudding agents.

(3) Selection of compatible mudding agents to different types of soils.
(4) Evaluation of plastic fluidity of muddified soil.

2 BASIC PROPERTIES OF MUDDING AGENTS

2.1 *Necessary functions of mudding agents*

Existing mudding agents can be roughly divided into two categories as polymer agents and mineral agents. Polymer agents can be also divided into the industrially produced and naturally made agents. The typical mineral type agent is bentonite or clay. These agents are mixed with excavated soils in the cutter-head chamber to modify the excavated soil into the mud state soils called muddified soils.

The required basic properties for the muddified soils are discussed in chapter 2 and can be summarized as "the muddified soils must have the properties of plasticizer, such as appropriate cohesion, inseparability, homogeneousness, impermeability and flow ability". Therefore the basic functions necessary for the mudding agents are as follows.

(1) Appropriate cohesiveness, plasticity and homogeneousness by bridging over the soil particles with polymer chain or by dispersing particles by polymers.
(2) Lubrication by polymers.
(3) Inseparability and impermeability by polymers or grade adjustment materials into the soil particles.

2.2 *Chemical interaction between mudding agents and excavated soils*

Chemical interaction occurs inter-phase between mudding agents and excavated soils. Therefore the mudding agents of high polymer are mostly kinds of surfactants acting on the excavated soil surface in the wide sense. Functions of mudding agents are the bonding, flocculation, dispersion and lubrication between soil particle phase and polymer liquid phase.

Mudding agents of high polymers have molecular weight from 10^5 to 10^7 and make the bridge structures by expanding their molecular chains, thus make the effects of water absorption, flocculation, dispersion and lubrication on the soil particles. Each category of mudding agent will be discussed hereafter. Typical types of industry produced high polymers as mudding agents are a water absorbent polymer, a flocculant polymer, a dispersion polymer and a lubricating surfactant. Furthermore there are other types of mudding agents of high polymer made from natural process. Bentonite is also can be considered as the mineral mudding agent. However bentonite mechanism is somewhat different from high polymer agents as discussed in 2.3.6.

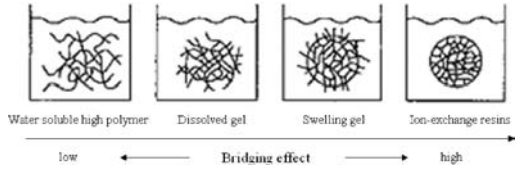


Figure 2.1. Increase of mechanical strength by bridging effect by water absorbent polymer (Revised from Fujimoto 1992).

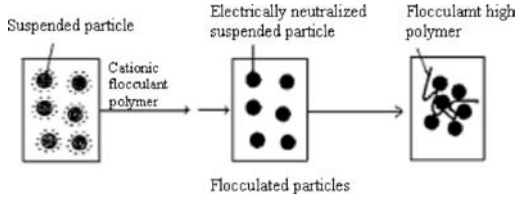


Figure 2.2. Agglomeration processes by the flocculant polymer (Revised from Fujimoto 1992).

2.3 *Typical mudding agent*

2.3.1 *Water absorbent polymer*

Water absorbent polymer absorbs water and swells, and produce the doughty gel. This gel increases in impermeability and inseparability, thus prevents soils from leaking into the ground and gushing in the screw conveyor. Water soluble polymer, especially electrolytic polymer increases the bridging effect with molecular chains. The more bridging effect increases, the more stiffness of gel increases. The mechanical property changes to be strong from a water soluble polymer to semi-soluble gel, swelling gel and ion exchange resin at the end as shown in Figure 2.1. The water absorbent polymer used as mudding agent has the property in-between semi-soluble polymer gel and swelling polymer gel. Water absorbent ability increases by the osmotic pressure and chemical attraction of water, and wraps the large size particles of soil. Typical types of these polymers are polyacrylate, amyloid, etc.

2.3.2 *Flocculant polymer*

The soil particle in the suspension water has an electric charge on the surface, repels each other and suspend without flocculation. Flocculant polymers have strong polymerization reaction, and thus flocculate and cohere to the soil particles by the bridging effect of high polymers. The flocculant polymers build high polymer chain bridges over the soil particles and have them flocculate. The flocculant polymers are effective to cohere to the suspended particles that are relatively small in size. Typical types of these polymers are polyacrylamide, sodium polyacrylate, polymethyl acrylamide, etc.

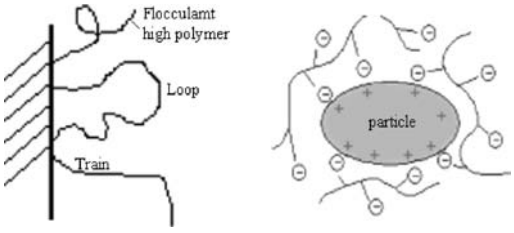


Figure 2.3. Polymer adsorption on the surface of particle (Revised from Fujimoto 1992).

2.3.3 *Dispersant polymer*

Small sized particles such as clay consolidate and have cohesion among them. These soil particles cannot be soluble in the water. By adding the dispersant polymer, the soil particles adsorb polymer on the surface called as the train state as shown in Figure 2.3. The surface of a soil particle is wrapped by the electric charge by polymer adsorption. Since the electric charge of the particle surface is opposite to that of dispersion polymer, each soil particle has the same electric charge and repels each other. The repellent forces enlarge the distance among particles and decrease cohesion of the soil. Therefore the dispersant polymer is effective to separate the cohesive soils like clay and silt. Typical types of these polymers are polycarboxylic acids, melamine sulfonic acid, polyacrylate, etc. Here polyacrylates are primarily used as dispersants and scale inhibitors in a wide range of industrial applications, but they are used as water absorbent polymers when they are used in large amount.

2.3.4 *Surfactant agent*

Surfactants are regarded as wetting agents that lower the surface tension of a liquid, allowing easier spreading, and lower the interfacial tension between two liquids by adsorbing at the liquid-air/liquid interface, thus reduce the interfacial tension at the liquid-soil interface by adsorption. Mudding agents of surfactants in the original meaning are mostly lubricating surfactants. There are two types of lubricating surfactants as follows.

a. Water-soluble type of surfactant
   These mudding agents are used to reduce the cutter torque and smooth excavation or to reduce transporting friction in the pipe flow.
b. Foam type of surfactant
   There is a foam type of EPB shield system. In this system the foam type of mudding agent is used. This agent is a foam type of surfactant agent that is foamed by blowing gas into the polymer liquid. A foam type of surfactant is different phase of high polymer surfactant, and has also same properties as water-soluble type surfactant.

2.3.5 *Natural high polymer*

There are some mudding agents called natural high polymer that are naturally made. They are water-soluble high polymers that increase cohesion, thicken or gelatinize water and wrap soil particles by the polymer bridge. At the same time these polymers are used for lubricating purpose by adjusting the water solution. They are chemically classified as polysaccharides that include starch, glycogen and cellulose. They are nonionic liquids. Typical mudding agents of naturally made polymers are guar gum, alginate, carboxymethyl cellulose (CMC), etc. Guar gum is a natural gum extracted from the guar bean. The alginate such as sodium alginate or alginic acid is a viscous gum extracted from seaweed. The carboxymethyl cellulose (CMC) is a water-soluble high polymer that is made from natural wood pulp and is synthesized by the alkali-catalyzed reaction of cellulose. Though it is produced in the industrial process, it is categorized here as the natural high polymer, for it is originally made from natural wood and is used for food science as a viscosity modifier or thickener.

2.3.6 *Mineral agent as the supplementary mudding agent*

Bentonite and clay can be categorized in the mineral mudding agent. Bentonite is an absorbent aluminium phyllosilicate generally impure clay consisting mostly of montmorillonite. *Swelling bentonite* that is sodium bentonite can be used for mudding agent. Clay is also used for the supplement for the soil. Main purpose of this type of agents is the grade adjustment of particle size of soil. Though bentonite or clay is sometimes used singly for soil additive in the EPB shield excavation, it is used only for soil supplement in order to increase the flow ability and impermeability by filling it into gaps among soil particles. However specially when bentonite is used together with the high polymer agent, the mixed mudding agent works well as good additives for EPB shield tunnelling. Therefore mineral material of bentonite and/or clay can be categorized not as the mudding agent but as the supplement for soils or mudding agents, and can be called as mudding agents supplement. They are categorized as a flocculant agent supplement and a protective colloid supplement.

a. Flocculant agent supplement
   Flocculant agent flocculates and coheres selectively to non-active soil particles such as silt and crushed debris as shown in Figure 2.4. Since the active material of bentonite is not flocculated, bentonite strengthens the bridge effect by polymers, thus increases viscosity and flow ability. These types of selective flocculant agents are polyvinyl acetate, maleic acid copolymer, etc. Since flow ability can be assured by the suspension of bentonite

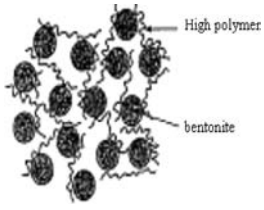


Figure 2.4. Bentonite as flocculant agent supplement (Revised from Fujimoto 1992).

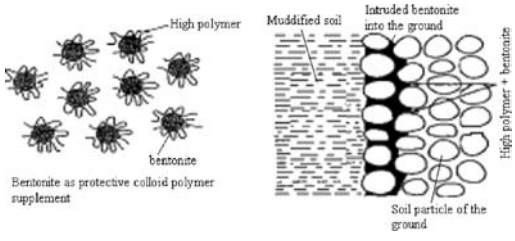


Figure 2.5. Bentonite as protective colloid polymer supplement for sealant (Revised from Fujimoto 1992).

and flocculation of crushed debris, the progress of excavation will increase.

b. Protective colloid polymer supplement Protective colloid polymer itself has hydophillic colloidal property and cover bentonite particles, thus maintains stable colloidal states. This bentonite colloid works as sealant to the soil of surrounding ground together with high polymer. Typical polymer of this type is carboxymethyl cellulose (CMC). CMC keeps the stable bentonite colloid and adsorbs to the calcium ion of soil particle of the ground by the ionic bond. Though the bentonite itself has a sealant ability, the protective colloid polymer accelerates the sealant ability shown in Figure 2.5.

3 EXPERIMENTAL EVALUATION OF MUDDIFIED SOIL

3.1 *Items to be evaluated and be experimented*

3.1.1 *Items to be evaluated*

Before selecting and using mudding agents for excavated soil normally mixing experiments of soil and mudding agents shall be done to evaluate items of mudding agents. The most important experimental item is the plastic flow ability called the plastic fluidity. However at the same time homogeneousness of the mixture; the muddified soil is also evaluated by the sense of touch. Other evaluating items of muddified soil are strength, inseparability. Impermeability of soil is generally not experimented beforehand.

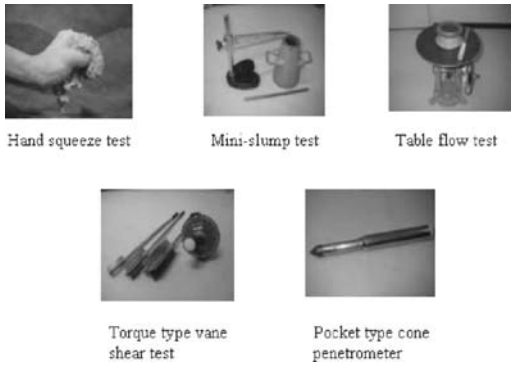


Figure 3.1. Experimental methods to apply.

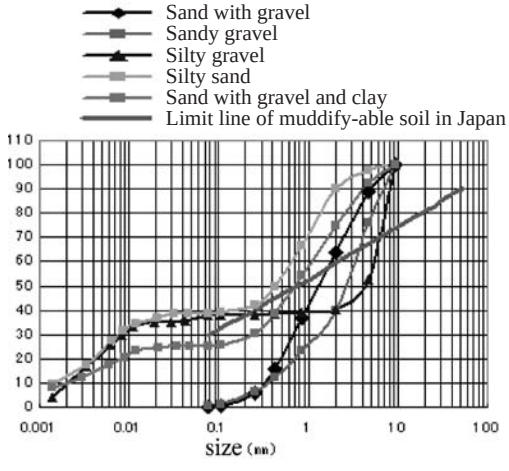


Figure 3.2. Size distribution curves of tested soils (Limit line adapted from Shield T. Assoc. of Japan 2006).

3.1.2 *Test methods to be used*

Conventional experimental test methods employed for the muddified soil are applied by those of fresh concrete. Slump test and table flow test are the most common test methods. Since the plastic fluidity cannot be evaluated directly from the above tests, the direct test of fluidity is evaluated by the hand touch test. The hand squeeze test can evaluate the homogeneousness and inseparability of the muddified soils. Strength of muddified soils is normally evaluated by vane shear test and by cone penetrometer. These test methods are shown in Figure 3.1.

3.2 *Experimental soils to be evaluated and mudding agents to be used*

3.2.1 *Experimental soils to be evaluated*

Five types of soils are tested and their size distribution curves are in Figure 3.2.

Table 3.1. Five types of mudding agents used with different density of agent.

Mudding agent	Density				
A	4 kg/m^3	6 kg/m^3	8 kg/m^3	10 kg/m^3	12 kg/m^3
B	2 kg/m^3	4 kg/m^3	6 kg/m^3	8 kg/m^3	10 kg/m^3
C	500 ml/m^3	1500 ml/m^3	2500 ml/m^3	3500 ml/m^3	4500 ml/m^3
D	10 kg/m^3	12 kg/m^3	14 kg/m^3	16 kg/m^3	18 kg/m^3
E	8 kg/m^3	10 kg/m^3	12 kg/m^3	14 kg/m^3	16 kg/m^3

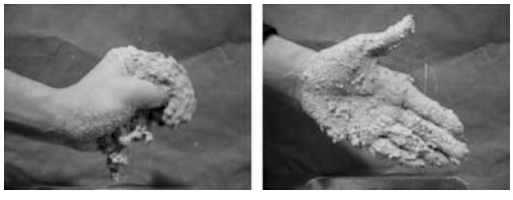


Figure 3.3. Hand squeeze test.

3.2.2 *Experimental mudding agents to be used*

Five types of mudding agents are used as shown in Table 3.1.

Mudding agent A is a complex mix agent of polyacrylamide; a flocculant polymer, and a polyacrylate type of water absorbent polymer. This is recommended to use for sand and gravel soil in the commercial brochure. Mudding agent B is a complex mix agent of a cellulose type of natural high polymer and a polyacrylamide of flocculant polymer, and is recommended to use for sandy soil. Mudding agent C is a dispersant agent of polyacrylate and is recommended to use for clayey soil. Mudding agent D is a natural high polymer of CMC with bentonite as a protective colloid polymer supplement and is recommended to use for sand and gravel soil. Mudding agent E is a natural high polymer of derived mainly from vegetable fiber and is also recommended to use for sand and gravel soil.

3.3 *Mudding agent compatibility with soil*

3.3.1 *Evaluation of plastic fluidity by the hand squeeze test*

Most effective way to understand the property of the muddified soil such as plastic fluidity, homogeneousness and inseparability, is the hand squeeze test with very primitive way as shown in Figure 3.3. The results are shown in Table 3.2 and the circled mudding agents showed good compatibility with the plastic fluidity by the hand squeeze tests.

3.3.2 *Compatibility evaluation of mudding agent with element material of soils*

a. Water absorbent polymer
   This polymer absorbs a large quantity of water and form a gel state. The gel wraps around the soil particle of gravel or sand, and gives the plastic fluidity. This polymer is effective for sand and gravel with high density.
b. Flocculant polymer
   Long chains of high polymers flocculate multiple soil particles with bridge effects and give the cohesion and plastic fluidity. Flocculant polymer is effective for silt and fine sand portion of the sand.
c. Dispersant polymer
   This polymer adsorbs single soil particle and adsorbed particle repels each other. In this way soil particles separate and give the plastic fluidity of the sticky soil of clay. This is effective for sticky type of fine particle of soil such as clay or silt.
d. Natural high polymer
   Natural high polymers of CMC and vegetable fibers in mudding agents D and E have no chemical ingredients to react to soil particles. However the more density of agent increase, the more bridging effect of high polymers increases and wraps soil particles. High density of natural polymer accelerates to be the gel state and gives the plastic fluidity not only for fine particle but also coarse particle of soil such as gravel. In this sense, natural high polymers are considered to be density adjusting agents. These mudding agents can be used for wide range of soil particle size with the quantities to use as additives. Furthermore mudding agent D has bentonite as protective colloid polymer supplement in it and gives good compatibility to large size particle of soil like gravel to increase sealant ability.

3.3.3 *Compatibility result of mudding agents*

Compatibility of mudding agents to excavated soils can be summarized as follows.

(1) For sticky clay or silt, dispersant high polymer agent is good to loosen soil particles.
(2) Flocculant mudding agent represented by polyacrylamide is good to cohere fine and coarse sand particles and easy to handle in mixing process.
(3) Water absorbent polymer increases cohesion to the large size particle of soil such as gravel by making high polymer bridges and wraps gravel particles with high density use of agents.

Table 3.2. Compatibility of mudding agents with four types of soils by hand squeeze tests.

Mudding agents		Sandy soil			Gravel soil	
Type	Density	Salty sand	Sand with clay and gravel	Sand with gravel	Clayey gravel	sandy gravel
A	4 kg/m^3		○			
	8 kg/m^3		○	○		
	12 kg/m^3	○	○	○	○	○
B	2 kg/m^3	○	○			
	6 kg/m^3	○	○			
	10 kg/m^3	○	○			
C	500 ml/m^3	○	○			
	1500 ml/m^3	○	○			
	2500 ml/m^3	○	○			
D	10 kg/m^3	○	○			
	14 kg/m^3	○	○		○	
	18 kg/m^3	○	○		○	
E	8 kg/m^3	○	○		○	
	12 kg/m^3	○	○		○	
	16 kg/m^3	○	○		○	

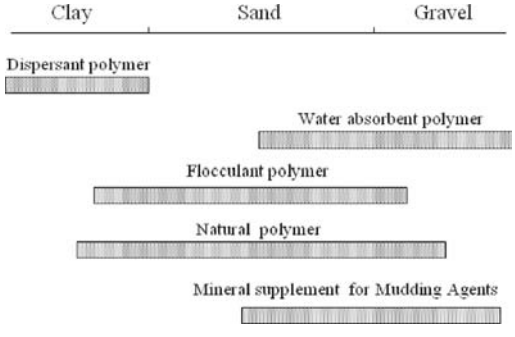


Figure 3.4. Compatibility chart of mudding agents to excavated soils.

(4) Natural high polymers also make other type of bridges over the soil particles with their fibers. Since natural high polymers with high density can wrap not only fine sand particles but also gravel size particles of soil, they can be called density adjusting agents. Above results can be drawn in Figure 3.4 as compatibility diagram of mudding agents to soils.

3.4 *Results of instrumental tests*

3.4.1 *Mini slump tests*

Mini slump cone is the half size of normal concrete slump cone and has a dimension of 150 mm in height, 50 mm of upper inner diameter and 100 mm of lower inner diameter. Results are shown in Figure 3.5. Slump values with the good plastic fluidity are diversified in no particular orders. Therefore mini slump cone values cannot be the evaluating indexes of good plastic fluidity.

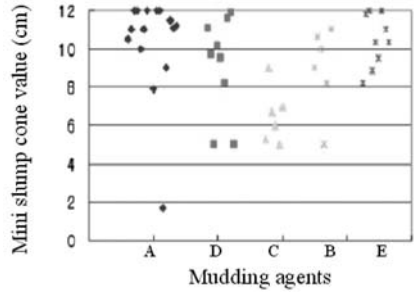


Figure 3.5. Mini-slump values of different mudding agents.

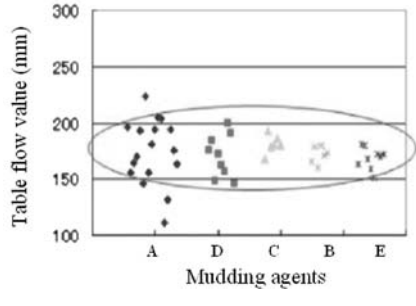


Figure 3.6. Table flow values of different mudding agents.

3.4.2 *Table flow tests*

Table flow test is the same testing method used in concrete test. Table flow values of good compatibility values with good plastic fluidity are between 150 mm and 200 mm and can be good indexes for the good plastic fluidity as shown in Figure 3.6.

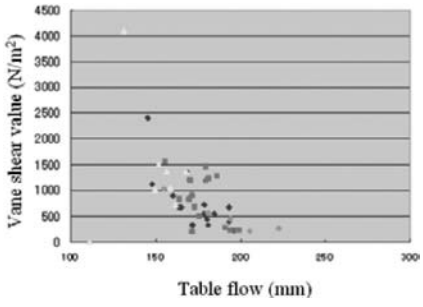


Figure 3.7. Relation between vane shear and table flow test.

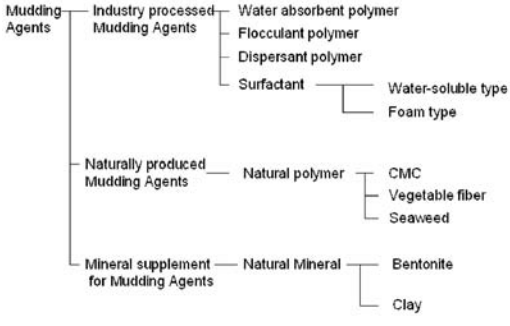


Figure 3.8. Classification of mudding agent.

3.4.3 Relation between Vane shear test and table flow test

Vane shear test and table flow test has some relation. Two groups of values have a hyperbolic relation as in Figure 3.7.

3.4.4 *Cone penetrometer evaluation*

All the penetrating values showed zero, thus pocket type of cone penetrometer cannot be used for evaluation of muddified soils.

4 CLASSIFICATION OF MUDDING AGENTS AND DESIGN MIX EVALUATION

4.1 *Classification of mudding agents and soil conformity*

Through the chemical and physical analyses in Chapter 2 and experimental results of Chapter 3, the mudding agents can be classified as follows.

5 CONCLUSION

(1) Mudding agents for EPB shield tunneling were categorized and classified. Mudding agents could be classified as three types of industry produced high polymers and naturally made high polymer.
(2) Compatibility of mudding agents with the soils was roughly evaluated. Furthermore detailed evaluation of compatibility should be studied in the near future.
(3) Most reliable way of evaluating mudding agents and muddified soils were hand squeeze test. However it is necessary to find good way and to evaluate mudding agents by the digital way.
(4) Table flow values can be a good index for evaluating the good plastic fluidity.

REFERENCES

Fujimoto, T. 1992. *New Introduction to Surface Active Agents*, Tokyo: Sanyo Chemical Industries (in Japanese)
Shield Tunneling Association of Japan 2006. *Technical archives of EPB shield tunnel 2006*: 14–15 (in Japanese)

This page intentionally left blank

Underground Space – the 4th Dimension of Metropolises – Barták, Hrdina, Romancov & Zlámal (eds)
© 2007 Taylor & Francis Group, London, ISBN 978-0-415-40807-3

North-South Urban Light Railway Cologne – a challenge for planning and construction – technical solutions for the accomplishment of the upcoming tasks concerning the tunnels

Dr.-Ing. Dieter Handke
Maidl & Maidl Consulting Engineers, IMM, Bochum, Germany

Dipl.-Ing. Lutz Tempel
Kölner Verkehrs-Betriebe AG (KVB), Cologne, Germany

ABSTRACT: The building of the North-South Urban Light Railway Cologne takes place in an extremely sensitive environment; extensive requirements have to be met in order to construct the tunnels. The main part of the 2×3860 m long tunnel route is being built underneath the densely populated city of Cologne parallel to the river Rhine, using slurry shield tunnelling machines. The single shell lining is installed ring by ring covered by the shield of the tunnelling machines. Exemplary for the challenging environment are the building structures in the area of the central station, which are highly sensitive to surface subsidence damages (roofs, railroad embankments, abutment structures), the tunnelling underneath an existing metro tunnel, the philharmonic concert hall, museums, historical buildings and numerous up to four-storey buildings, both business and residential. The tunnels are mainly located in the water bearing quaternary Rhine deposits consisting of sands, gravel sands and gravels. In the northern section the fills of a Roman port have to be passed, and historical relicts can be encountered. The overall project consists of seven underground and one over ground station. Three shield tunnelling machines with a diameter of 6.80 m and 8.40 m are used. The machines, complying with the newest state-of-the-art, have systems to investigate the geological conditions in front of the cutting wheel and to detect unknown wells or relicts of buildings. In addition, equipment is used, which allows the grouting of soil in front of the cutting wheel and the identification of abrasions. Computer data logging systems deliver continuous information about the stability of the heading face, the stabilisation of the lining ring and the deformation of the subsoil. On the basis of failure analyses extensive soil improvements and stabilisations of the buildings have been performed in the run-up of the shield drive in order to minimise the risk. The tunnelling will be accompanied by a permanent supervision of the building structures, the subsoil and the machine data. The determination of boundary and warn values as well as technical failure notifications for the machine allows an early reaction in the case of unexpected failure situations. After starting the tunnelling with all three machines in the middle of 2006, the main report at the conference will be about the experiences of the shield drives – after a short overview of the planning phase. A comparison is made to determine whether the machines and the concept of tunnelling were adequate to cope with the numerous challenges.

1 INTRODUCTION

The beginning of the shield drive in summer 2006 has marked a decisive step for the realisation of the project Urban Light Railway Cologne. After completion the overall building project includes seven underground and one over ground stop and its total length is 2×3860 m. The predominant part will be excavated as tunnel tube in shield advance mode. Thus, after finishing the project, the central station will be connected to the Southern city.

The project is divided into two contract sections. The consortium of the companies Bilfinger Berger AG, Wayss & Freytag Ingenieurbau AG and Ed. Züblin AG (joint venture contract section South) has been assigned with the execution of the southern section in November 2003 and the consortium of the companies Hochtief Construction AG, Bauer Spezialtiefbau GmbH, Keller Grundbau GmbH und Brückner Grundbau GmbH (joint venture contract section North) with the execution of the northern section.

Special requirements will not only demand a thorough technical implementation of the project underneath a, over centuries historically evolved, major city, but will also focus on the logistics within a city centre with high traffic density. Because of the two

thousand years of history in Cologne, special attention is put on the archaeological land conservation, as numerous discoveries from Roman, medieval and Prussian times are expected. The available knowledge had already been considered in the documents of the planning approval. Furthermore, in coordination with the Romano-Germanic Museum of Cologne, timeframes had been agreed upon in the run-up, which then had been integrated in the various construction phases.

Shield machines with slurry-supported face of heading excavate the two, one-track, parallel tubes of the southern section. They both start in the southern part at the starting shaft at Bonner Wall and end in the reception shaft at Kurt-Hackenberg-Platz, south of the philharmonic concert hall.

The two tubes will be excavated parallel to each other, but delayed in time, by two shield machines which are identical in construction. During their course they cross under large parts of the old Roman town and abut on the ancient Roman harbour.

The East tube, which runs away from city, has a length of approximately 2462 m and the West tube, which runs into the city, a length of approximately 2456 m. The internal diameter of the tubes has a value of 7.30 m. The start of the first shield machine for section South (East machine) was on 6 June 2006, the West machine has started early on 2 August 2006.

For the tunnel tubes of the northern section, which will be excavated in opposite direction from the stop Breslauer Platz to the North side of the philharmonic concert hall, only one shield machine is in use. Because of the eminently shorter tunnel, 2×260 m, one machine is sufficient to keep to the timetable. After the machine has excavated the first of the two tubes, the internal machine technology will be dismantled and transported back through the completed tunnel. The shield skin remains in the subsoil. After that, the parallel tube will be excavated from the second starting shaft at Breslauer Platz in the same way. The internal diameter of these tubes has a value of 5.85 m. The tunnelling works have started on 10 July 2006 with the excavation of the eastern tube.

In the run-up extensive requirements had been determined for the logistics of the shield drive in order not to strain the inner city too much. Therefore, an area at the goods station Bonntor has been rented for the building site equipment of the southern section, from which the ground excavations can be taken away via rail. The lining segments can also be delivered via rail, so that the number of heavy goods vehicle transports in the heart of the city can be reduced immensely.

The building site equipment of the northern section is located in the area of the Central Station, also on premises of the German Railway. For this reason old buildings of the Railway had been knocked down. After finishing the procedures, the square Breslauer Platz in front of the station will be completely renewed with regard to urban development.

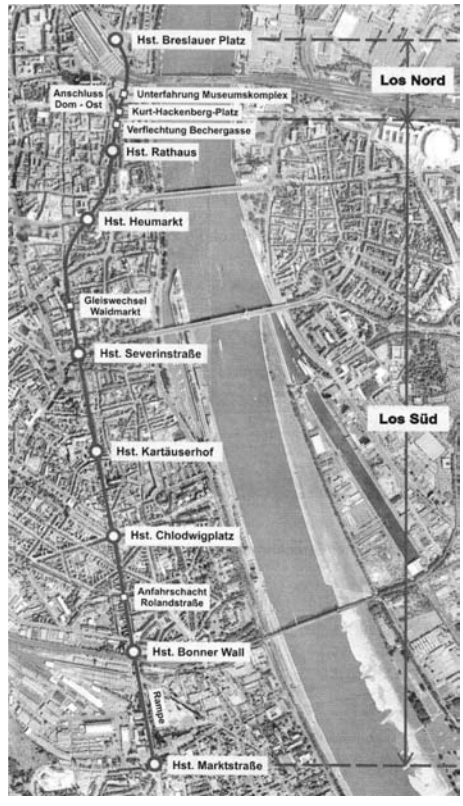


Figure 1. Alignment and special buildings of the North-South Urban Light Rail (Thon, Spohr 2003).

For further information on the total project it is exemplarily referred to the publications (Reinarz 2005), (Thon, Spohr 2003) & (Trier, Tempel 2005).

2 GEOLOGY

The predicted soil conditions, which are located in the sphere of influence of the shield drive are characterised as follows:

Near the surface level, approximately 1 to 2 m of massive filling is encountered. The fillings are either of natural or of anthropogenic type.

Below the fillings, the quaternary Rhine sediments are situated, which are under influence of ground water – here the main parts of the tunnels are being excavated. The sediments consist of sands and gravels in which benches of stone exist. The bedding of these layers varies between loose and dense, whereas medium-dense bedding dominates.

The quaternary layers are located below the tertiary layers. They are characterised as silty fine to middle-grained sands, clayey silt and brown coal.

The tertiary layers are bedded densely and nearly impermeable.

The tunnel cross-sections are located mainly in the water bearing Rhine sediments consisting of sands, gravel sands and gravels. Over a short distance they are crossing the fillings of the Roman port basin.

The tunnel has, in the main part of the alignment, an overburden of 15 to 20 m to surface level. In the area of buildings, foundation distances are minimal in parts.

3 MECHANICAL ENGINEERING AND PROCEDURAL REQUIREMENT PROFILE OF THE SHIELD DRIVE OF THE SECTIONS

Primarily, the planned urban drive requires an advance procedure that guarantees a minimum of subsidence to avoid the damaging of buildings. The total construction method including machine technology has to be suited to this. Simultaneously, the geological conditions have to be mastered with the machine concept.

The mechanical engineering and procedural requirement profile of the shield drive of the sections will be determined basically by the following main demands:

- Maintenance of urban infrastructure (road traffic, public transport), restrictions, respectively partial barring, is conceded only in areas of cut-and-cover methods.
- Conservation of the substance of the buildings, bridges, or rail tracks, which are directly affected by the shield drive.
- Securing of working order of cables and other supply systems installed underground, which have to be crossed under.

These highly difficult infrastructural conditions are overshadowed by the, in parts, extremely unfavourable in-situ subsoil conditions with regard to the advance works and stability and usability of the tunnels.

In addition to the passage of the Roman port basin, where subsoil layers with low load-carrying capacity and deposited obstacles can be found, other obstacles can be expected in the subsoil due to former construction activities: old wells, rests of buildings, anchors, sheet pile walls or piles.

There is no expected arching in the subsurface for the buildings that are crossed under with little foundation distance. Therefore, in many parts of the project, subsoil and foundations of buildings have been improved (jet grouting walls, compensation injections, holdings, shorings, stiffenings) as additional building protection before starting the shield drive. Further details to the forerunning protection measures see publication (Trier, Tempel 2005).

While excavating the tunnel track brown coal layers can furthermore be found in the tertiary layers. Granular structure, compactness or texture could be very diverse in the alignment, which requires precautions as to guarantee the stability of the face of heading.

In the alignment a maximum water pressure of up to 2.5 bar can be expected in the shield invert. Such heights of water pressure are, quoting references, controllable without difficulties using present-day technology.

In order to satisfy the requirements of the sensitive environment within the city, a shield advance procedure is the method of choice for excavating the tunnel tubes.

The most important requirements for the machine as stated in the invitation of tenders are described as follows. The consideration of standard equipment of a shield is obvious and will not be extended further.

- Means to create a grouting area in the top section for preceding stability of subsoil, e.g. as additional security while inspecting the face of heading or for interception and reduction of subsidence of the buildings, which have to be crossed under.
- Development of cutting head with the possibility of giving access to the complete area of the face of heading to remove existing and non-sliceable obstacles.
- Integration of a stone crusher for fragmentation of boulders and building remains to a transportable size for minimisation of inspection states under compressed air.
- Possibility for complete sealing of the face of heading, in order to guarantee the stability of the face of heading during a stop and to avoid postfailures with the consequence of harmful subsidence at surface level.
- Integration of systems for pre-investigation of the expected obstacles in the subsoil, in order to manage necessary procedures on time.
- Possibility of longitudinal displacement of cutter head in order to create a limited area in front of the shield, in which preparatory measures can be taken for removing obstacles.
- Integration of systems for control of mass balance, which are especially important in the lower steady soils for control of volume constancy, therefore for the limitation of subsidence.
- Limitation of conicity of the shield machines and over-cut for minimisation of settlements.
- Possibility for change of main bearing from within the shield for areas in which the construction of caverns for the change of main bearing from the surface level is not possible, e.g. underneath buildings.
- Continuous registration of data of grouting pressures and grouting amounts for the backfilling, to get a nearly cavity-free grouting, which reduces subsidence.

– Systems for automatic registration of annular gap in order to guarantee the building of an ideal ring and to avoid bending of the ring, which could result in damages.
– Distribution of semi-trailer loads for minimization of bending on the freshly grouted lining segment ring.
– Control of operation for all essential components of the machine by optical and acoustic warning facilities as well as limit switch for observation of flow, liquid levels, developments of pressure and temperatures, e.g. in oil circulation, to clear faults as quickly as possible.
– Installation for data registration to observe all data of the shield drive using on-line transmission to the client as well as the engineering offices involved in the building observation.

Superficially this serves as self-observation for the contractor. Furthermore the foreign observation consciously aims at a psychological effect on the contractor.

Due to a demanded risks – hazards analysis in the invitation of tenders for critical advance situations (e.g. crossing under of objects, failure of machine components, accident situations) the tenders were sensitised to the project's specific problems while constructing the tunnels in order to let that knowledge influence the conception of the shield machine.

The shield concept, which has been commissioned and put into action in the end, will be presented exemplarily for section South, on the basis of the essential technical facilities.

4 TECHNICAL SOLUTION FOR THE SHIELD MACHINES OF CONTRACT SECTION SOUTH

Finally, shield machines using the principle of slurry-supported face of heading (Hydro-shield) had been proposed and commissioned concurring to the conditions of the invitation of tenders. All shield machines have been delivered from producer Herrenknecht AG, Schwanau, Germany.

4.1 *Basic principle of shield machines with slurry supported face of heading*

The principle of shield machines with slurry supported face of heading is based on the fact that a pressurized liquid, in this case bentonite suspension, counteracts the extrinsic forces of subsurface, ground water and surrounding buildings to hold the balance of pressure. The liquid is located in a special chamber of the shield machine, in which the cutter head, which excavated the soil, is also situated.

The excavated material at the face of heading is mixed with the supporting liquid in the chamber and extracted to the surface through pipes. The liquid is then separated from the soil and, in a cycle, conveyed to the chamber again.

Only in special situations – e.g. when the tools, which are assembled on the cutter head for excavating the soil, have to be changed – the supporting liquid will be released and substituted by compressed air to render possible the lock in of personnel.

The structurally complete tunnel tube is constructed under the cover of the shield skin behind the chamber. For building the tunnel, lining segments (single re-enforced concrete segments) will be connected to one ring using special bolting and sealing.

While moving forward the shield machine, the annular gap between shield skin and lining segment is grouted with a special mortar, so that no cavities remain in the soil in order to avoid damages to buildings.

The machine moves forward with jacks that press hydraulically against the lining segments. This way, lining segment for lining segment, meter for meter, the final tunnel is constructed.

The complete process using Hydro-shield machines corresponds to the current state of technology. It represents a procedure that is, on the basis of application for more than 30 years, extremely secure, environmentally beneficial, and to the highest degree safe for the personnel involved.

The control of the supporting pressure using a compressed air bubble allows a very sensitive reaction to possible pressure fluctuations at the face of heading, resulting from irregularities in the subsoil in order to reduce subsidence to a procedural technical minimum. Alternative advance methods using compressed air or the EPB-principle are not suitable in the subsoil conditions.

4.2 *Technical data of the shield machines*

Some facts and figures of the machines give an insight into the dimensions and the technical construction of the shield machines.

Shield machines contract section South:

Length of advance machine:	76000 mm
Total weight including semi-trailer:	11000 KN
Length of shield:	9500 mm
Weight of shield machine:	6200 KN
Excavation diameter:	8430 mm
Thickness shield skin front section/middle section/shield tail:	80/50/50 mm
Number of double jacks:	14 pairs
Maximum thrust:	60300 KN
Installed total power:	2800 KW



Figure 2. Shield machine – southern section.



Figure 3. Longitudinal displacement of cutting wheel of shield machine southern section.



Figure 4. Tools equipment cutting wheel of shield machine southern section.

4.3 *Constructive features of the shield machines*

In the design phase of the machines the contractor had been actively accompanied by the client and his consultants. In addition to the technical construction of the shield machines according to the contract, the client proposed, supported by his consultants, recommendations, many of which have been included and put into action by the contractor.

One of the essential requirements was to implement the demand of minimal subsidence.

The closed cutter head is equipped with a total of 174 cutting knives, 19 disk chisels and 16 reamers, whereas the cutting knives are used primarily for the excavation of sands and gravels and the disks for tackling grouted areas and obstacles.

The open parts of the cutting wheel provide enough space to reach all places of the face of heading in order to remove possible obstacles manually if required.

A skew at the flanks of the cutting wheel has a positive effect to the material flow to the back. Four hydraulic extensible over-cuts with copy-cutter function are integrated in the cutting wheel in order to enable the capacity to navigate curves.

In order to control possible signs of agglutination and optimising the material flow, the cutting area has been equipped with an extensive wash-up system. For that purpose, four nozzles and one additional nozzle in the centre have been installed at the cutter head. Separate flushing facilities have been installed in the area of the stone crusher to keep it clear and also to the left and right of the opening in the diving plate for supporting the material flow at the exhaustion.

The power transmission of the cutting wheel works longitudinally moveable as centre-free ring drive. Displacement cylinders support themselves axially at the supporting frame in the middle section. In order to minimise subsidence the cutting wheel can move back within the cutter head. In order to excavate the grouted areas, the cutting edge has a massive design of 80 mm.

In the upper area of the circumference of the shield skin, seven conductors with a nominal diameter of NW 100 for the boring rods are welded to facilitate forward drillings and injection bodies.

The middle section has injection canals in the upper area at the circumference of the shield skin, so that, when required, bentonite suspension can be injected for reduction of skin friction.

An additional gap in the diving plate renders possible the inspection of the face of heading, respectively of the cutter head by means of an endoscope or a camera.

A pressure sealed diving plate gate valve allows working under atmospheric conditions between diving plate and pressure bulkhead when closed.

The machine is equipped with a total of fourteen pressure pairs on the circumference. The jack pairs are divided into six groups. Each group has a cylinder for determining the amount of stroke, using a position measuring system.

The shield tail at the end of the shield skin is equipped with a two chamber brush sealing to counteract the ground water pressure.

The pipes for grouting the annular gap and for the sealing mass of the brush sealing are also integrated in the shield tail skin.

The pressure and volume controlled back-filling is carried out using grouting pipes. Pressure sensors measure the pressure of the grouting pipes. The grouting amount is recorded by the piston stroke of the grouting pumps as well as an ultrasound sensor at the mortar tank. Now the system is switched over to load cells in order to register continuously the temporal change of weight of the grouting amount.

The erector, which is steered from a user interface, places the single lining segments. The air gap (distance outer edge lining segment to inner edgeshield skin) is measured semi-automatically using so-called distometers (measurement of distance through laser beam and wireless data transmission to the data registration plant), which will be installed manually at the relevant place.

The semi-trailers are situated behind the machine. They consist of one bridge and four semi-trailers, which are closed-platform carriages, equipped with steerable wheels. The wheel loads of the semitrailers are distributed evenly on the lining segment rings, so that concentrations of load are avoided.

The data registration is synchronised. The data is visualised and saved for each advance, including ring number, date and time.

The control system determines the position and height of the machine at any time. This laser controlled navigation system shows the shield driver the actual position of the machine in graphical and numerical form on a monitor in the control cabin.

The observation of the bentonite level is carried out using two independent systems. The suction gate valve can close the suction pipe over the first level measuring point automatically. The second level measuring point activates the feed gate valve for automatic closing of the feeding line.

For mass control, a comparison of the flow measurement in the pipes of the feeding line and the transport line is used.

The seismic pre-investigation is carried out by the help of the SSP-System (Sonic Soft Ground Probing) for mechanised shield tunnelling with bentonite supported face of heading. In order to do so, 4 transmitters and 1 receiver are installed at the cutter head. Geological in-homogeneities and obstacles up to a distance of approximately 40 m in front of the cutter head reveal themselves using a seismic reflection method. Cross-hole measurements at the beginning of the tunnelling served as an early calibration of the system.

The direct wear observation, parallel to the excavations, is carried out through conductor loops integrated into six excavation tools. The cut gives information about wear of tools. The other tools are checked visually using an endoscope. The material flow from the face of heading into the excavation chamber is unhindered due to, in parts, conic gaps and due to the cutter head that is 34% open.

5 STATE OF PROJECT AT DATE OF DRAWING UP THE REPORT AT THE END OF SEPTEMBER 2006

5.1 *Contract section south*

The first shield machine under the Bonner Straße has started the advance of the East tube on 6 June 2006.

At date of preparing this report (end of September 2006), approximately 700 m of the East tube and 350 m of the West tube of section South had been excavated.

The average rate of advance was approximately 6 m/day and the maximum rate was 14 m/day.

The subsidence that occurred largely corresponded to the prediction of total subsidence. Continuous supervision and optimisation of confinement pressure in the upper third of the sphere of tolerance, as defined according to static calculation, resulted in a considerable reduction of predicted forerunning subsidence. The forerunning settlements had an average value of 5 mm. The medium total settlements were approximately 15–20 mm, whereas, caused by the procedure, the predominant share of subsidence occurred at the length of the shield. The subsequent settlements were approximately 15–20%, which indicates that the back-filling was adapted ideally to the subsurface conditions.

The advance is accompanied by an extensive measuring system. With this innovative system, a demand in the invitation of tenders, the shield driver has, at any time, an extensive view at:

- Machine data, e. g. jack forces, confinement pressures,
- Functional disorders in the machine system, e.g. leakages, failure of components
- Survey and control system of machine, e.g. position of machine at nominal axis
- Deformations of subsoil (e.g. measuring points in the soil, extensometers), building bolts, hydrostatic tube balance measuring system.

At regular distances measuring points in the soil and so-called main measurement cross-sections (fitting with soil-points and extensometer points in cross and longitudinal direction of advance) are installed at surface level. Additionally, measurement bolts have been installed at every building for which, before the start of the advance, warning and alarm values had been determined.

The segmental lining completely fulfils the requirements of the invitation of tenders with regard to the density. Wet places and spallings have appeared only secondarily at single places. At the same time, this documents the perfect interaction of machine technology and lining segment design regarding the underground conditions.

5.2 *Contract section north*

The shield machine for the northern section has started the advance for the East tube on 7 July 2006 and reached the final position on 9 September 2006.

While excavating the approximately 260 m long section, several buildings had to be crossed under, partly with very low distances.

The average rate of advance in this section was 4.5 m/day and had been characterised especially by the reduced rates of the advance while driving through the Jet grouting walls.

The measured average settlements were 10 mm and can be interpreted as a confirmation of the prediction.

6 CONCLUSION

The systems used for tunnelling have proved successful. They met all requirements. For the future we hope that the accident-free advance continues and situations will be mastered as securely as before.

REFERENCES

Handke, D. 2003. Prüfen der Schildmaschine auf Eignung und Abnahme auf der Grundlage einer Risikoanalyse. Lehrstuhl für Bauverfahrenstechnik, Tunnelbau und Baubetrieb (ed.), *Risikopotential und-bewältigung bei aktuellen Tunneln. Tagungsband zum XI. Kolloquium für Bauverfahrenstechnik*: 27–42. Essen: Verlag Glückauf GmbH.

Handke, D., Maidl, B. 2006. Bauverfahrenstechnische Prozessabhängigkeiten als Steuerungselemente zur Risikominimierung bei der Realisierung von Schildprojekten – Vorstellung einer Risikostrategie auf der Basis baupraktischer Erfahrungen. *Tunnelbau Taschenbuch (30)*: 189–220. Essen: Verlag Glückauf GmbH.

Reinarz, W. 2005. Die Nord-Süd Stadtbahn Köln – ein Ingenieurbauprojekt mit höchsten Anforderungen. Teil 1: Verkehrspolitisches Konzept der U-Bahn-Neubaumaßnahme. *Deutscher Bautechnik-Tag*: 1–3.

Ruttkamp, J., Wahrmund, H. 2005. Die Nord-Süd Stadtbahn Köln – ein Ingenieurbauprojekt mit höchsten Anforderungen. Teil 2: Bauausführung Los Süd *Deutscher Bautechnik-Tag*: 4–15.

Thon, R., Spohr, I. 2003. Nord-Süd Stadtbahn Köln, Teil I – Das Projekt. *Tunnel* 22 (8): 26–40. Gütersloh: Bauverlag BV GmbH.

Trier, Dr. M., Tempel, L. 2005. Nord- Süd Stadtbahn Köln, Teil II – Die Archäologie. *Tunnel* 24 (7): 32–43. Gütersloh: Bauverlag BV GmbH.

This page intentionally left blank

Underground Space – the 4th Dimension of Metropolises – Barták, Hrdina, Romancov & Zlámal (eds)
© 2007 Taylor & Francis Group, London, ISBN 978-0-415-40807-3

The latest technology in mechanized tunnelling – the design of the world's largest EPB and slurry shield TBMs

Dr.-Ing. E.h.Martin Herrenknecht & Dr.-Ing. K.Bäppler
Herrenknecht AG, Germany

ABSTRACT: The general increase in growth is a result of a worldwide growing need for an efficient infrastructure in the areas of transport, supply and disposal services. Topographical conditions in large cities and towns encourage tunnelling solutions, particularly by mechanized methods. The mechanized tunnelling process has captured the attention of the public sector. As a safe, settlement controlled tunnelling process it offers a beneficial alternative to other tunnel excavation methods. Innovative solutions are increasingly required for tunnelling projects with a high level of difficulty in terms of construction, such as large diameter inner-city tunnels in heterogeneous grounds with high water pressures or the construction of long-distance tunnels integrating combined traffic systems in the tunnel cross section. Mechanized tunnel excavation moves into new dimensions especially regarding complexity of ground conditions, diameter, length and depth of underground constructions where the feasibility of other tunnelling methods is limited. This paper focuses on the design and technical challenges of the three largest soft ground tunnel boring machines, two Slurry Shields (ø15.4 m) for the Shanghai River Crossing project and one Earth Pressure Balance Shield (ø15.2 m) used for a road tunnel project in Madrid in Spain.

1 INTRODUCTION

The tendency of the tunnel projects of today show the innovative move of using full-face TBMs with diameters larger than 14 metres.

The resulting larger effective tunnel cross sections enable the possibilities of integrating more than 2 lanes of traffic or more than one traffic system in the tunnel or as shown with the example of the Storm Water Management and Road Tunnel project in Kuala Lumpur in Malaysia that the tunnel can take over more complex service functions.

With the example of the two largest soft ground tunnel projects in the world the latest technology in mechanised tunnelling will be described. The current largest Earth Pressure Balance Shield (Ø15.2 m) was in use for a road tunnel project in Madrid. The tunnel takes three lanes of traffic side by side on one level in the tunnel cross section. The two largest Mixshields (Ø15.4 m) designed for the Shanghai River Crossing Project in Asia are in use for the construction of a road tunnel carrying three lanes of traffic on one level and a safety passage and a rescue lane in the bottom of the tunnel cross section.

2 LARGEST EARTH PRESSURE BALANCE SHIELD (Ø15.2 M) USED FOR THE M30 ROAD TUNNEL PROJECT IN MADRID

Within the framework of the project Calle M30, the largest Earth Pressure Balance Shield (EPB) was in use for the construction of the north tunnel of the south bypass on Madrid's highway M30.

The tunnel route passes through a densely populated area and crosses beneath several structures such as three metro lines and railway tracks with minimal cover. The lowest distance from the tunnel crown to the structure is only 6.5 meters and this with an inside diameter of the tunnel of 13.37 m.

The tunnel is constructed with reinforced concrete segments. One tunnel ring is composed of $9 + 1$ segments and has a length of 2.0 m.

The EPB-Shield with a diameter of 15.2 m has been designed to suit the prevailing cohesive soil conditions, which have been predicted along the designed tunnel alignment. Clay and gypsum of stiff to hard consistency are characteristic of the geological conditions at tunnel level.

Large diameter EPB machines, and very large diameter EPB machines such as the one used on the south bypass tunnel for M30, require a very high cutting wheel torque compared for example to slurry TBMs.

Machine technical and process technical factors such as drive unit and bearing unit, cutting wheel design and rotational speed have a relevant effect on the torque of the cutting wheel. The EPB-Shield for the Calle M30 project has a very high cutting wheel torque which amounts to 125,000 KNm. Therefore the cutting wheel is equipped with two concentrically arranged cutting wheels.

The inner cutting wheel is installed in the free centre of the outer cutting wheel as a flat disc-type wheel. It is installed in the working surface of the outer cutting wheel and it is longitudinally displaceable relative to the outer cutting wheel.

The rotational drives of both cutting wheels are completely independent with different rotational speeds in both directions of rotation.

Part of the high torque is consumed in the mixing chamber, which is neutral with respect to the rolling of the machine. The torque is consumed between the cutting wheel and the tunnel face, it is the active part regarding the rolling of the TBM and can be resisted in loose soil by means of the skin friction or by transfer into the tunnel lining (reinforced concrete segments). If the torque rises beyond the value which can be resisted by the moment of friction of the shield shell, the machine will show a tendency to roll.

With a diameter of 15.2 m and a torque of 125,000 kNm the Herrenknecht EPB Shield beats all dimensions which have up to now been available on the mechanised shield tunnelling market.

The drive unit of the inner cutting wheel comprises 10 motors with a total power of 2,000 kW. To summon up the required power of 12,000 kW for the outer cutting wheel a new design was conceived. Altogether 50 motors are necessary for the outer cutting wheel drive. They have been distributed around the main drive in two rows of 29 motors and 21 motors.

The double cutting wheel design also improves the excavation process and the soil conditioning. The material excavation in the outer and inner area of the tunnel face can to a large extent be carried out at an optimised cutting tool speed. This is achieved by adjusting the differences in peripheral speeds, which can be applied to the cutter tools.

The design of the outer cutting wheel area facilitates the arrangement of various cutter positions, which is normally not possible at all in the inner area as a favourable opening ratio must be maintained. A great difference in the cutter penetration depth between the outer and the inner area can be avoided by a higher rotational speed in the inner area, which has also the effect of reducing wear on the cutting tools.

With regard to the soil conditioning with the double cutting wheel design and in particular with respect to the material removal and kneading or mixing effect, the mixing chamber can be divided into two zones. Both can be handled independently from each other.

The areas of the inner and outer mixing chamber are in direct contact with each other so that an exchange of material between both zones is possible but not necessary. Because of the individual handling of the outer and inner mixing chamber, a homogenous consistency of the material in the chamber can be achieved.

The cutting wheel is equipped with eight independent injection points at the front face of the centre cutting wheel and with 14 independent foam lances installed in the outer cutting wheel. Thus the injection of plasticizing agents such as foam is possible. Thereby 36% of the total volume will be injected through the injection points, which are provided on the front face of the centre cutting wheel and the remaining 64% will be injected in the outer ring section.

The start-up of the excavation process of the currently largest EPB-Shield begins when the inner cutting wheel starts rotating. The soil will be conditioned with foam through the rotary union, which is attached to the centre cutting wheel and above the stators. The stators are positioned in the centre area behind the cutting wheel in order to reduce the friction on the inside. To increase the mixing effect in the centre area, the displacement cylinders will be slowly extended.

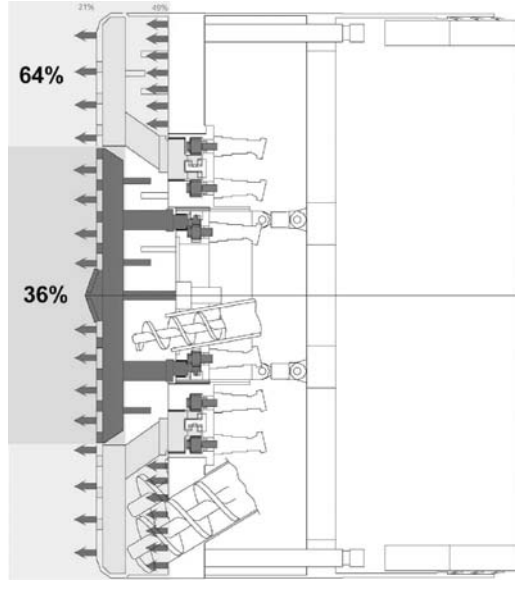


Figure 1. Injection of plasticizing agents through the two concentrically arranged cutting wheels of the EPB-Shield (Ø15.2 m) for M30.

It can be assumed that the soil will be well-conditioned up to a diameter of approximately 9 m and this will considerably reduce the starting torque of the outer cutting wheel.

As soon as the centre area is conditioned, the outer cutting wheel starts turning and simultaneously adding foam. Thus, the complete excavation area will be homogeneously conditioned and the advance process can commence.

The excavated material is transported out of the excavation chamber via three screw conveyors, which are integrated in the shield. They handle an excavated volume of 565 solid cubic meter per ring. There are two parallel screw conveyors (Ø1,250 mm), which are located in the lower part of the shield to remove the excavated material from the outer cutting wheel and to transport it back to the belt conveyor. The third and smallest screw conveyor (Ø600 mm) is arranged in the lower third of the central cutting wheel. It will remove the excavated material from this area and convey it back to the belt conveyor.

The complete transport of the TBM from the manufacturing factory to the jobsite took two months. The main components of the Shield TBM were first transported with a river boat to the port of Rotterdam and then with two ships to Spain. For unloading the components a crawler crane with a capacity of 600 tons was necessary. The transport on the road lasted approximately nine days (50 km per night accompanied by the police).

The excavation of the 3,525 m long north tunnel of the south bypass on Madrid's highway M30 started on November 15, 2005 and could successfully be completed, on July 12, 2006, by the team of the contractors Acciona Infraestructuras S.A. and Ferrovial-Agroman S.A. in cooperation with Herrenknecht AG, after only 8 months of construction time.

During advance the giant boring machine achieved convincing performances, which could be increased week by week and pushed to a best weekly performance of 94 rings or 188 m. The best daily performance amounted to 18 rings or 36 m and the strongest monthly performance could be reached in May 2006 with considerable 758 m.

After the assembly and learning phase, weekly performances, which were clearly higher than 50 rings or 100 m, could be achieved permanently. The tunnelling cycles were 30 minutes and the construction of a ring, consisting of 10 concrete segments, 13.9 tonnes each, could be carried out in approx. 50 minutes. During tunnelling a cycle time of less than 100 minutes could be achieved for the advance and the installation of a 2,000 mm long ring. The TBM supplier's and construction firms' skilled personnel helped to reduce learning curve effects.

After approx. 1,000 m, 2,000 m and 3,000 m of tunnelling, a standstill of approx. 4 days was each scheduled in order to inspect the cutting tools, install tunnel belt boosters and carry out other maintenance operations that could not be done parallel to the advance. The target construction time of 12 months could clearly be underrun, and the 8-month tunnel construction time equals an excellent TBM performance of more than 450 m per month.

3 LARGEST MIXSHIELD (Ø15.4 M) IN OPERATION IN SHANGHAI

With the construction of the gigantic project "Shanghai Changxing Under River Tunnel" the region of the Yangtze delta near Shanghai will be further opened.

The Yangtze is Chinas biggest river. Its yearly flow of 951.3 billion cubic metres of water amounts to approx. 52% of the total yearly quantity of all Chinese rivers.

The greatest challenge of this project is the connection of the two river banks from the Pudong mainland with the island of Chongming. Two parallel motorway tunnels with a length of 8,950 m each will be built between the mainland Pudong and the island of Changxing. A bridge will connect the island of Changxing with the island of Chongming.

Since the waterway between the mainland Pudong and the island Changxing is a very busy main shipping route, the tunnel solution was preferred instead of a bridge construction.

With a length of 80 km and a width of 20 km, Chongming is the third biggest island of China. The island Changxing with a population of about 30,000 is characterised by the establishment of industries with three large shipping services.

The two parallel tunnels will run beneath the largest river of China with the currently largest two tunnel boring machines. The Mixshields have a shield diameter of 15.43 m. Each of the tunnel tubes will integrate two levels, of which the upper level will contain three lanes for motor traffic and the lower level is planned to integrate a rescue lane in the centre and a safety passage.

The planned construction period of the Chongming Yangtze River Crossing Tunnel near Shanghai amounts to four years.

The challenges for the design of the two largest Mixshields for the river crossing were on the one hand the large shield diameter of 15.43 m and on the other hand the predicted geological and hydrological conditions. Each tunnel will have a total length of approx. 7,170 m with a gradient of ±2.9%.

The two Mixshields are adapted to the local geological and hydrological conditions featuring clayey formations and very high groundwater pressures. The entire tunnel will be built in very weak, clayey soils below the groundwater table. Characteristic of the



Figure 2. World's largest Mixshield Ø15.4 m for Shanghai.

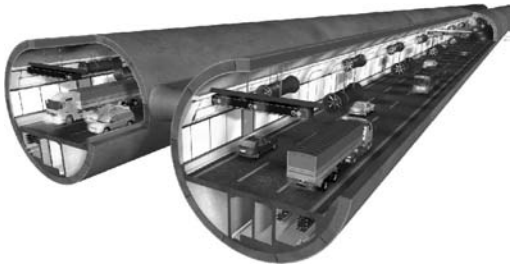


Figure 3. Changjian under River Tunnels, Shanghai.

expected geology are local intercalations of silty and sandy layers and shell residues.

Due to a ground-water level of up to 47 m above the centre of the tunnel, the TBMs are designed for a maximum working pressure of 6.5 bar. At the deepest point the tunnel will run about 65 m below the surface.

The tunnel lining consists of precast reinforced concrete segments with an inside diameter of 13.7 m. One tunnel ring consists of $9 + 1$ segments and has a length of 2 m. For both tunnels altogether 7,500 segment rings are needed. They will be delivered with two special trucks from the segment fabrication yard, which is about 1.5 km away, to the jobsite.

A feature of the cutting wheel design are six accessible main spokes, which are sealed against the water pressure. To avoid adhesion of sticky clay at the cutting wheel, the centre area is equipped with an own slurry circuit. Large openings in the cutting wheel optimise the flow of material and reduce the risk of blockage of material in the centre.

In order to get reliable information about the condition of the soft ground tools and buckets, especially in the loaded outer area of the cutting wheel, ten cutting tools (2 buckets and eight soft ground tools) are equipped with an electronic wear detection system.

The system generates online data on the state of the selected cutting tools and gives early warning of possible wear to the TBM staff.

With this electronic wear detection system maintenance works can be planned and the service life of the tools can be optimised, thereby minimising costly chamber accesses under compressed air.

The heart of the system is a new tool support with integrated sender electronics. This is permanently connected to the soft ground tool through induction loops and "detects" whether the wear limit is reached. For this purpose the sender is electrically connected with a power supply. If the probe is intact a certain current flows but if the probe is destroyed due to wear of the tool this is "sensed" by the sender through a significantly higher fault current. The sender is inductively connected with the receiver and the tool probe through a small gap. A LED informs the machine driver of the wear. With this automatic method of wear detection unnecessary maintenance could be avoided.

The design of the cutting wheel was conceived in order to allow man access to its interior space under atmospheric air pressure, sealed from the ground water pressure outside.

Tool change devices, which are integrated in the cutting wheel, allow the personnel to replace tools under atmospheric conditions from the interior of the cutting wheel.

The tool change device has two functions:

1 To serve as receptacle for the tools.
2 To allow the outward and inward airlock transit of the tools.

In order to flush the devices there are flushing connections installed on the rear case.

This tool change device consists of the following main components:

1 Front casing. This forms the connection to the steel structure of the cutterhead and is circumferentially welded to it.
2 Rear casing. It is flange-mounted to the front casing and assumes in connection with the front casing the guidance of the slider and of the sliding pipe.
3 Slider.
4 Sliding pipe. The sliding pipe receives the cutting tool.

The sliders are opened in the working position. In this position the cutting wheel is made water tight by the front seal. In case of damage of this seal, the circumferential profile seal located around the slider and the rear seal would assure the leak tightness.

A further feature, which has to be mentioned, is the installation of road elements by the back-up of the Mixshield. The back-up is composed of three trailers. The first one contains all necessary equipment and supply material for the functioning of the excavation

process. The second trailer is a bridge construction to allow free space of ±20 m for placing the road elements, which are precast concrete parts of 2 m length in dimension, 4.30 m in width and 4.56 m in height. Each element has a weight of approx. 35 tons.

Supplies will be delivered to the TBM with trucks. They will drive along these rectangular road elements which are placed along the centre of the bottom of the tunnel. The trucks will be unloaded in the back-up trailer number 3.

Back-up number 1 will run on invert slabs. These are placed on the already built segment ring and will be taken out and moved to the front as soon as the first back-up trailer passed this section. Back-up trailer number three runs on auxiliary rails.

The tunnel excavation for the about 7,170 m per tunnel tube is expected to take about 34 months. The commissioning of the BOT-tunnels is planned for 2010.

4 CONCLUSION

The two cited Shield TBM projects are characteristic of demanding conditions like the under river crossing near Shanghai and the inner-city tunnelling for the M30 project in Madrid. Both projects illustrate the feasibility of large diameter tunnels and are pointing the way for future projects regarding the excavation of even larger tunnel cross sections, long-distance bored tunnels and even deeper excavations.

In general, it is important to have a good understanding of all the conditions of a project already in the planning stage. The geological information is of particular interest because the machine design will be adapted to the predicted geological conditions. It is increasingly important to avoid possible risks when tunnelling in urban areas and also in the open country when underpassing existing structures or rivers and to further adapt the technology to make it even more safe and efficient.

This page intentionally left blank

Underground Space – the 4th Dimension of Metropolises – Barták, Hrdina, Romancov & Zlámal (eds)
© 2007 Taylor & Francis Group, London, ISBN 978-0-415-40807-3

Compressed air work with tunnel boring machines

E.h. Martin Herrenknecht & K. Bäppler
Herrenknecht AG, Germany

ABSTRACT: In general diving and compressed air works are associated with works on offshore drill rigs and production platforms in the North Sea and Baltic Sea, national and international recovery operations, refurbishments of dams and works in contaminated waters, e.g. treatment plants. The use of divers in tunnelling first seems to be unusual. For more than one hundred years, however, compressed air works have been carried out on large construction sites during tunnelling works below groundwater level and nowadays, in particular, during river crossings at very high water pressures. The diving techniques employed in conjunction with mechanized tunnelling have included diving to depths of more than 50 m using mixed-gas or saturation diving. The tasks undertaken by the divers have included welding and cutting underwater; or in a bentonite suspension; surveying, welding inspections, removing and replacing tools on the cutting wheel. This report gives detailed information on the use of divers as well as the latest developments in construction and diving technology during very complex tunnelling projects at overpressures of more than 4 bars, referring to tunnelling projects such as the '4th Elbe Tunnel' in Hamburg (Germany), the 'Wesertunnel' (Germany) and the 'Westerscheldetunnel' (the Netherlands).

1 DIVING AND COMPRESSED AIR WORK IN TUNNEL BORING MACHINES

1.1 *General information on TBM design and diving operations*

The use of professional divers in mechanized tunnel excavation is usually limited to those machines that are deployed in very complex heterogeneous geological conditions at high water pressures: Mixshields. They can safely support the tunnel face by using a pressurized liquid. Here water-bentonite suspensions are often used for the support of the tunnel face. The bentonite is used because of its geomechanical characteristics, its plasticity and its swelling capacity in the support liquid. The pressurized suspension penetrates the ground and seals the tunnel face with a possibly thin, impermeable film, the so-called filter cake that is used to generate the support pressure. This process is carried out within a relatively short time span of 1 to 2 seconds. The support pressure balances the encountered ground and water pressure and avoids uncontrolled collapses and stabilizes the tunnel face.

The regulation of the support pressure in the excavation chamber is not directly carried out via the suspension pressure but via an air cushion between bulkhead and submerged wall. Fully automatic circuits, permanently controlling the pressure conditions at the face and generating the relevant counter pressure via the support media, allow for a precise support pressure control. Thus settlement or heave is avoided between the machine and the surface, which is especially important where there is low overburden.

In this operating mode, the bentonite suspension not only serves as a stabilizing support medium but also as a slurry transport medium to remove the material excavated at the tunnel face. The spoil is pumped through a slurry line to a separation plant that is normally located outside the tunnel, where the ground and the suspension are separated and the treated suspension is fed back to the slurry circuit.

Within the protection of the tailskin of the shield, the tunnel lining of precast reinforced concrete segments are put into position by the segment erector. For excavation, the tunnel boring machine is advanced by hydraulic thrust cylinders which push against the last-built segmental ring. The gap between the extrados of the segmental ring and the ground is continuously grouted as the tunnel boring machine advances to secure the ring and to support the surrounding ground.

1.2 *Compressed air works during mechanized excavation*

Work in compressed air (compressed air work) is carried out at an air pressure above atmospheric pressure. The compressed air work at overpressure in the excavation chamber can present serious health hazards to the personnel. Thus medical checks are mandatory prior to the works to ensure that the workers are fit for this type of work. Important health and safety regulations must be observed and complied with.

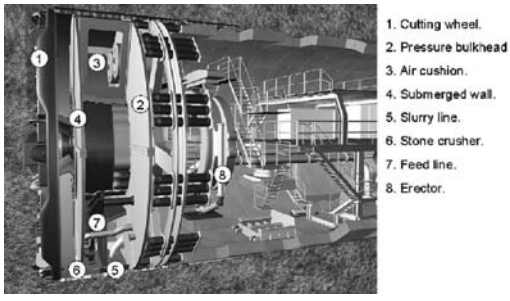


Figure 1. Functional Principle Mixshield (Shield Tunnelling with liquid supported tunnel face).

Divers also work under hyperbaric conditions as soon as they move below the water surface. The exposure to overpressure implies serious health hazards to the personnel even if the compressed air works are appropriately organized and monitored. According to the 'Regulations for Compressed Air Works – ('DruckluftV' of 1972) – the staff must not carry out works at an overpressure of more than 360 kN/m^2 (3.6 bars/52.2 PSI).

From 4.0 bars/58 PSI overpressure (40 m (131 ft) water column) upwards, the extended decompression times for the compressed air personnel and the reduced working time reaches a levels where it is no longer viable to carry out compressed air works in the conventional way. Here the use of divers is required. There is no pressure limit for diving. With compressed air as breathing air, the diving depth is limited to 50 metres (500 kPa or 5.0 bars overpressure). Breathing-gas mixes allow diving depths of more than 100 meters (328 ft) and operation times of several days or weeks using saturation methods.

Based on three prestigious projects, compressed air works and diving, that have become vital for mechanized excavation, will be explained in more detail.

1.3 *Compressed air works and diving during the '4th Tunnel under the River Elbe project'*

During the construction of the '4th Tunnel under the River Elbe', a Mixshield was deployed with a liquid supported tunnel face. The TBM was 14.2 m diameter and the special requirements of the project (an overburden of only 7 m between the top section of the tunnel and the river bed of the 'Elbe' at the most critical point) put the personnel and the technology to the test.

The geological conditions, in particular, the presence of large boulders, required a cutting wheel equipped with mixed cutting tools consisting of cutter discs as well as soft-ground cutting tools. The possibility to excavate boulders with sizes of 0.8 m up to 1 m with groups of cutter discs has been proven in practice.

The cutting wheel consists of five main and five additional spokes and is equipped with 120 soft-ground cutting tools as well as 31 cutter discs.

Due to the low overburden at pressures of up to 5 bars, a conventional access to the working chamber (lowering of the compressed air support) was considered critical. Since a cutting tool change had to be expected, a complete set of cutters was installed on two levels.

The first level comprised soft-ground cutting tools that were arranged correlatively with the cutter discs. The latter could only be exchanged after a conventional access.

The second level was equipped with cutting knives (scrapers) that could be exchanged from within the accessible spokes without lowering the slurry in the excavation chamber. This also applied for the cutter discs.

Additionally, the machine was equipped with all installations required for diving operations in the excavation chamber.

The cutter tools can partially be exchanged under atmospheric pressure from the five accessible main spokes and, in part, from the tunnel face under overpressure conditions.

To allow for a cutting tool change without lowering (fully maintaining the liquid support), another step (cutting tool change in the arm with exchange unit) was inserted between the conventional cutting tool change and the diving.

This was achieved through accessible spaces within the cutting wheel and depressurization valves located behind the cutters. The spaces within the cutting wheel could be accessed via the cutting wheel center, at atmospheric pressure or under hyperbaric conditions. Here the cutting tool change under atmospheric pressure in the cutting wheel arm was carried out as follows:

Each cutting disc is mounted in a pressurized housing with a hydraulically operated gate valve. The cutting disc is held in position by a hydraulic cylinder whilst the mounting bolts are removed. The cutting tool is then withdrawn and the gate valve is closed sealing the housing off from the face.

A crane attachment is then used to remove the worn cutting disc to be replaced with a new disc.

The same method is used for the replacement of scraper tools located in the five main cutting wheel spokes.

This development is part of the safety concept.

The tools on the first level could only be exchanged after a conventional access. Thus a new method for 'works in compressed air' was, for the first time, implemented during the construction of the project '4th Tunnel under the River Elbe'. During the planning phase, the use of divers was already considered for maintenance and repair works to the cutting wheel equipment. An operation program for potential diving

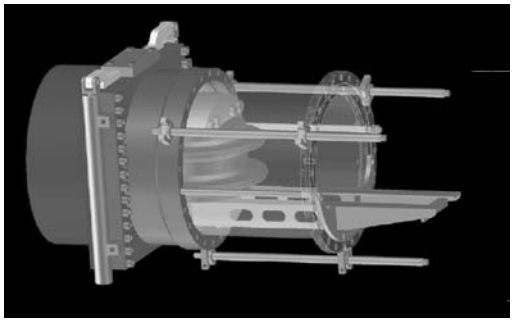


Figure 2. Cutting tool change under atmospheric conditions.



Figure 3. Emergency/Transport chamber to evacuate injured personnel from the pressurized zone to the surface.

works in bentonite as well as compressed air works at overpressures up to 5.5 bar was formulated in cooperation with the joint venture partners: 'Bilfinger + Berger', 'Hochtief AG', 'Wayss & Freytag AG', 'Philipp Holzmann AG', 'Dykerhoff und Widmann AG', 'Züblin AG', 'Heitkamp GmbH' (construction companies), the 'Amt für Arbeitsschutz' (Occupational Health and Safety Authority), the 'TBG' (The Employer's Liability Insurance Association for Underground Works) and the 'Nordseetaucher GmbH' (diving company).

A special team of nine divers was formed and prepared for the diving operations.

The tunnel boring machine was equipped with additional technology and a rescue system for the diving operations specially adapted to the machine. Claus Mayer working with 'Nordseetaucher GmbH' was senior manager in charge of this special operation.

Since the available decompression tables for works under hyperbaric conditions were insufficient, the works were partially based on the 'Druckluftverordnung für die Taucherarbeiten' (Regulations for Diving Operations in Compressed Air) and the French tables 'Air Oxy 12 M'.

For the diving operations, a special container with control and supply units was located on the tunnel boring machine, equipped with an individual air supply and communication system, independent from the Mixshield.

For the first time, a supply flange, specially adapted to the diving operations, was mounted on the bulkhead for:

- the supply of breathing and reserve air,
- the communication and lighting cables,
- the video and depth control units as well as
- the water and hydraulic connections for tools (impact drill, FLEX grinder and split-type drill rigs)

When accessing the excavation chamber for maintenance and repair works, the divers used specially adapted offshore diving helmets (Kerby Morgan 27), fitted with a water flushing system to prevent the breathing membranes of the air regulator from sticking together in the bentonite suspension.

The TBM is equipped with three man locks to pressurize the operating personnel and the divers, two man locks Ø2, 000 mm in the top section of the shield and one man lock in the center Ø1, 640 mm. The man locks consist of two independent chambers that are sequentially arranged (prechamber/main chamber). The prechamber serving all locks provides space for two persons, the main chamber (lock DN1600 mm) is designed for three persons and the main chambers (locks DN 2000 mm) for 5 persons each.

The prechambers are normally not be pressurized to allow additional personnel to access the main lock to assist with the evacuation of injured persons from the working chamber.

A door connects the main chamber to the working chamber in the cutting wheel. Each lock is equipped with a clock, a thermometer and the pressure gauges that display the pressures required for pressurizing and decompression. Each lock chamber can be pressurized or depressurized from the inside or the outside. A full-stroke safety valve limits the pressure to 5.5 bars.

Outside the man lock, additional pressure gauges are installed to display the air pressure measured in the pre- and the main chamber as well as in front of the bulkhead. A multi-band recorder registers the different pressures.

Optionally a transport chamber (with a Nato-connection flange) can be docked on to these locks during the works in compressed air to evacuate injured persons via the transport system (train) on the machine and out of the tunnel in an emergency. Above ground, the transport chamber can then be docked on to a recompression chamber where the necessary measures can be taken that are required for treatment. However, no emergencies occurred during the entire period of



Figure 4. Soft rock tunnel face – tool change at 3.5 bar at the 4th tube Elbe Tunnel (Hamburg, Germany).

the tunnelling works. The emergency chamber is part of the safety concept in order to safely evacuate injured persons from the pressurized zone to the surface.

During the tunnelling works on the site '4th Tunnel under the River Elbe' in Hamburg, a total of 10,920 hours were worked in compressed air, 6,603 of which in the pressure and excavation chamber. A total of 2,738 pressurizations of personnel were carried out, 237 pressurizations of which above 3.6 bars, 21 cases of decompression sickness occurred, all in a pressure range up to 3.6 bars.

Regarding the cutting tool change times, it needs to be mentioned that, approx. 13 hours were initially required for a cutting tool change under atmospheric conditions in the accessible spokes without particular complications. Since this time effort was considered too costly, several options were evaluated to reduce the working time. Through organizational improvements and modifications in terms of the existing cutter exchange design, the assembly time could be reduced from 13 to 6 hours.

With divers conventionally accessing the pressurized working area, approx. 8 cutter discs could be changed within about two hours compared with 2 to 3 hours required for a double disc cutter, depending on the type and volume of the muck to be cleared.

1.4 *Works in compressed air during the crossing of the river 'Weser' project in Mixshield mode*

In Dedesdorf, Germany, a Mixshield ø 11.67 m was deployed during the crossing of the river 'Weser'. Two parallel road tunnels, each with a length of approx. 1,635 m, were driven in very varying ground with heterogeneous formations.

The Wesertunnel is the first onshore traffic link north of Bremen crossing the river 'Weser'. Before, ferries connected the cities 'Nordenham-Blexen' and 'Bremerhaven', 'Kleinsiel' and 'Dedesdorf' as well as 'Brake and Sandsted'.

The shielded tunnel boring machine was designed for an operational pressure of 5.5 bars.

In this tunnelling mode, the support pressure is generated via an air cushion in the working chamber. The pressure communication between the chambers is carried out through the submerged wall opening. Even in case of clogging at the submerged wall opening, the pressure communication can still be maintained. This is achieved by additional compensation lines, connecting the invert area of the working chamber with the excavation chamber. The regulation of the air-cushion pressure is carried out through a redundant compressed-air regulator.

The 'Mixshield concept' allows for a pressure compensation from the atmospheric zone behind the bulkhead or from the working chamber, when the suspension level is lowered for accessing the excavation chamber.

Requirements such as low overburden and high water pressures, during projects with large TBM diameters, led to a situation where the suspension level can often be lowered by only one third in order to access the excavation chamber. In this case, it is mandatory to close the submerged gate valve. By closing the submerged wall gate valve, the principle of 'communicating pipes' is suspended. Additional units in form of pressure basins that are connected separately to the excavation chamber then serve as air cushion to support the tunnel face.

Maintenance and inspection works below the partially lowered bentonite level or at pressures higher than 3.6 bars were carried out by divers. The working chamber could be accessed via two double-chamber manlocks.

Regarding the diving operations, the following difficulties occurred during the compressed air works:

- tide-related pressure variation up to 0.4 bar per tide,
- compressed air works up to 4.5 bars for operations on the cutting wheel,
- compressed air works up to 5.0 bars for operations in the shield invert,
- use of divers up to 5.0 bars for operations in bentonite.

During the construction of the two 'Wesertunnel' tubes, the maximum admissible limit for compressed air works of 3.6 bars was exceeded at the deepest point due to compressed air operations at approx. 5 bars. Since the tunnel had to be driven 4 m below the planned tunnel alignment due to a modification of the operating program, the 'Druckluftverordnung für Arbeiten in Druckluft' (Health and Safety Regulations for Works in Compressed Air) and the H & S regulations 'VBG 39' (now 'BGV C 23') could, at times, no longer be observed. To be able to carry out compressed air works above the maximum admissible working pressure of 3.6 bars, a special authorization was required.

In cooperation with the responsible 'Occupational Health and Safety Authorities' 'TBG' and 'GAA-Oldenburg' as well as the 'Nordseetaucher GmbH' (diving company), a method was developed to comply with H & S regulations during compressed air works or diving operations at overpressure by the JV 'Wesertunnel' consisting of the companies 'HOCHTIEF AG', 'Philipp Holzmann AG', 'Ludwig Freytag GmbH & Co. KG', 'Heinrich Hecker GmbH & Co. KG' and 'Martin Oetken GmbH & Co. KG'.

During works at pressures of up to 5 bars, that had to be faced during this project, the ratio between the efficient working time at overpressure and the required decompression time has already now become uneconomical and borderline, e.g. reaching the physical limits of the personnel. Thus the involved parties ('Nordseetaucher GmbH', 'TBG' and 'GAA-Oldenbug', JV 'Wesertunnel', the hyperbaric doctor) issued the following framework regarding health and safety regulations for staff working at overpressure:

- common charts based on the 'Regulations for Works in Compressed Air' up to 3.6 bars and 'Air Oxy 12 M up to 5.0 bar'.
- in principle, depressurization with oxygen.
- an oxygen break of five minutes after a maximum of 30 minutes in compressed air.
- use of a 'hyperbaric assistant' as link between the personnel and the hyperbaric doctor.
- additional 'trial pressurizations' of the entire staff in the emergency chamber prior to the first operation above 3.6 bars.
- Reduction of the maximum working time at overpressure:
  - for the first exposure
  - after a longer working break
  - for extreme physical works.
- regular training of the tunnelling staff for operations at overpressure up to 5.0 bars.
- training of the doctors on call by the hyperbaric doctor.
- training and test of the personnel as to the appropriate conduct before, during and after pressurization/decompression.
- training of the lock attendant by the hyperbaric assistant and the hyperbaric doctor.
- regular assistance by the hyperbaric doctor of the compressed air works
- extension of the waiting time on site to 2 hours after an operation at an overpressure of more than 3.6 bars.
- a prophylactic 30-minute oxygen treatment at 0.9 bar in the emergency chamber for travel distances of more than 100 km after work.
- alarm system for the operating personnel, the doctors on call as well as the divers.



Figure 5. Special flanged connections installed at the bulkhead to allow manned interventions to be carried out in the bentonite.



Figure 6. Diving helmet for diving in bentonite.

This concept for Works in Compressed Air has been proven in practice and needs to be adapted to the information and conditions determined by the project requirements and the operation. Thus it is possible to safely access the working chamber at overpressure without exposing the 'compressed air personnel' to serious health hazards.

For diving in bentonite, special flange connections are installed at the bulkhead of the tunnel boring machine (figure 5), providing the divers and the personnel under hyperbaric conditions with breathing and reserve air, communication, lighting, video and data transmission as well as drinking water for the air regulators in the diving helmets.

The diving equipment consists of a diving helmet supplied through an 'umbilical'.

With pressures of up to 5 bars, the works were similar to offshore works. Thus a diving helmet (figure 6), comparable to those used during offshore diving, was specially adapted for the operations in bentonite. To make it easier for the divers to breathe in the bentonite suspension, the diving helmet was fitted with a water-flushing unit for the air regulator. The drinking

water prevents the breathing membranes from sticking together. The diving helmet is designed as hard hat that is connected with a diving suit. The air volume within the helmet and suit is constantly flushed with compressed air.

The 'umbilical' (figure 7) is the 'umbilical cord' for divers consisting of hoses and cables for the supply of air, emergency breathing air, drinking water, communication, lighting, video and data transmission.

For works in the working chamber, the diving equipment and the required tools are pressurized via a material lock in the working chamber. Following this, the operating personnel are pressurized. The latter consists of two divers, one 'signal person' and one assistant. Prior to the works, the excavation chamber is inspected for possible overhangs and cloggings at the cutting wheel for risk prevention. The maintenance and repair works then start and the cutting tools are inspected for potential faults or damage. If a cutting tool change becomes necessary the required equipment, tools and auxiliaries are mounted on the submerged wall and the cutting wheel and the worn or defective cutting tools are exchanged and depressurized. Figure 7 shows a diver during a maintenance and inspection operation below the partially lowered bentonite level. After completion of the works, the required tools and auxiliaries are disassembled and the connection door to the excavation chamber is closed. The divers return to the lock, where they are depressurized.

At pressures between 4 and 4.2 bars, a cutter disc was changed within approx. 2 to 3.5 hours. The change of 12 soft-ground cutting tools could be carried out within 2 hours, depending on the type and volume of the clogging.

1.5 *Excavation with saturation diving during the construction of the 'Westerscheldetunnel'*

The most demanding diving operations in tunnelling were carried out during the project 'Westerschelde' in the Netherlands. Here the experiences gained during the projects '4th Tunnel under the River Elbe' and 'Wesertunnel' could be used. While pressures up to 5 bars had to be mastered on the 'Elbtunnel' site and overpressures of up to 5.5 bars during the 'Wesertunnel' project, hyperbaric conditions of up to 8.5 bars were expected on the 'Westerscheldetunnel'. During works at an overpressure of up to 8.5 bar, compressed air can no longer be used, since the nitrogen contained in the breath causes narcosis with increasing depth. The nitrogen is replaced by helium. During the design phase, the use of mixed gases was already planned. Mixed gases consist of oxygen with different inert gases. Depending on the pressure ranges that had to be expected, operation times of several days and weeks (saturation method) are possible. To smoothly carry out saturation diving, the TBM technology and



Figure 7. Use of divers for maintenance and repair work in the working chamber.

logistics needed to be designed in compliance with the requirements for saturation diving and rescue technology, already in the planning phase. The required technology was successfully designed and implemented by the diving company 'Nordseetaucher GmbH'.

Saturation diving is a long-term stay at overpressure. All tissues are 100% saturated with inert gases, i.e. an increase of the diving time leads to a longer decompression phase. This technology makes diving operations at depths of more than 150 m more efficient, since the divers can stay pressurized (depending on the working depth) until the completion of the works.

To allow the divers during the project 'Westerscheldetunnel' a long-term stay under hyperbaric conditions, a chamber system was planned, consisting of two pressurized living chambers outside the tunnel. This chamber system, containing all the necessary facilities such as berths, showers and toilets, can take on a maximum 12 divers and technicians.

Since it was not possible to install the saturation unit in the tunnel and to dock it on to the tunnel boring machine, a mobile transport system (shuttle) was manufactured. The shuttle can transport up to 4 divers under hyperbaric conditions. The shuttle collects the divers at the living chambers outside the tunnel (figure 8, right) prior to their diving operations. It transports the divers into the tunnel and docks on to the left manlock (DN 2000), in direction of advance (figure 9). This lock is equipped with a 'NATO' flange which allows the transport shuttle to dock on and also provides access to the working chamber.

In contrast to the 'Elbtunnel and Wesertunnel' projects, it was impossible to work at pressures of more than 4.5 bars with compressed air. Mixed gases were used instead, consisting of helium, nitrogen and oxygen. The special gas mixes reduce the absorption of the dangerous nitrogen in the blood. The oxygen content of these gas mixes is higher and its nitrogen content lower compared with normal breathing air.



Figure 8. Transport shuttle.

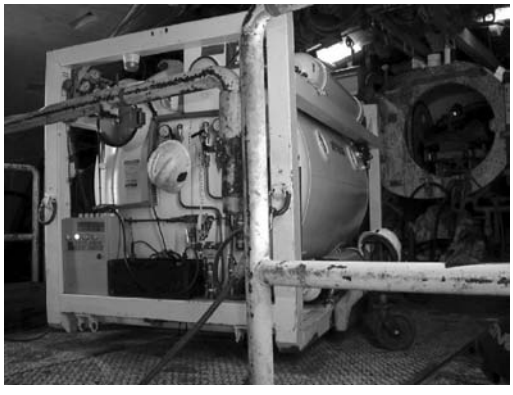


Figure 9. Transport shuttle before docking on the manlock.

The diving equipment is similar to the equipment that has already been successfully used during other tunnelling projects. For the works in the partially lowered conditions under the river 'Westerschelde', lightweight diving helmets used in the chemical industry were provided, specially adapted for this task. The special diving helmet is equipped with two air regulators and a controllable cooling system, since the temperature at the tunnel face can reach up to 60 degrees centigrade. All necessary tests prior to the works, were carried out at the Belgian Navy's Hyperbaric Center in Zeebrugge.

During the operation in the bentonite suspension, about 7 to 10 soft-ground cutting tools could be changed within 3 to 4 hours during one diving shift. The change of a double disc could be carried out in approx. 1.5 diving hours.

In total, five excursions in saturation were performed with a total saturation time of more than 40 days. The decompression time at working pressures



Figure 10. Special diving helmet (hyperbaric helmet) for application in hyperbaric conditions at 6.9 bars.

up to 6.9 bars was 4 days each time. In addition, six excursions were performed with mixed gas and 1,652 hours with compressed air involving 546 transfers. Five cases of decompression sickness (DCS) occurred, all of which could be treated in the on-site emergency chamber.

2 CONCLUSION

The above stated projects are exemplary for diving operations and compressed air works under extremely complex conditions at high pressures. Due to their technical profile, the qualified professional divers are an integral part of the day-to-day operations on a mechanized excavation site. The divers are permanently exposed to dangerous pressurization and depressurization transfers during their work in order to provide a smooth excavation process. State-of-the-art equipment is deployed, in accordance with the latest technologies in construction and diving and in compliance with national as well as international health and safety requirements. Good qualifications of the divers and compressed air workers involved, the permanent training as well as the adaptation of the tunnel boring machines to new requirements, make it possible to carry out technically challenging projects with success.

The experiences, that we have gained up to now, show that new methods for compressed air works in tunnelling were found that pave the way for increasingly complex projects with growing requirements in terms of TBM and diving technology. Only through a close cooperation between all parties involved in such a complex project, we will be able to continue a successful and innovative implementation of difficult projects.

This page intentionally left blank

Underground Space – the 4th Dimension of Metropolises – Barták, Hrdina, Romancov & Zlámal (eds)
© 2007 Taylor & Francis Group, London, ISBN 978-0-415-40807-3

Stormwater management and road tunnel (SMART)

Gusztáv Klados & Yeoh Hin Kok
MMC – Gamuda JV, Kuala Lumpur, Malaysia

David R. Parks & Derek T. Tavender
Mott MacDonald JV, Kuala Lumpur, Malaysia

ABSTRACT: Kuala Lumpur, the business and commercial hub of Malaysia has of late often been inundated by the floods from the Klang River as development has canalized the river. Over the years the intensity of the floods increased with each incidence, causing financial losses and inconvenience to the city folk. With cars submerged and traffic grinding to a standstill, the city was in urgent and immediate need for flood mitigation.

The SMART Project provides a stormwater diversion scheme including floodwater storage and a 10 km, 11.8 m diameter bypass tunnel, sufficient to save the city from flooding in the foreseeable future. With no major flood event most of the year the tunnel a dual use was engineered, with double road decks built into the central three kilometre section, relieving traffic congestion by providing 2×2 traffic lanes for cars connecting the city centre to the southern gateway, the KL – Seremban highway.

The flood water is diverted at the confluence of the Klang and Ampang rivers into a Holding Pond. From there the water passes through the tunnel into the Taman Desa Attenuation Pond and via a box culvert discharges into the Kerayong River.

The government accepted the innovative proposal of two Malaysian companies, MMC and GAMUDA, to reduce the cost of the scheme for the Government. The firms proposed to build the road tunnel section at a cost to be recovered by a toll collection Concession from the Government thus providing a dual purpose usage and offsetting the overall Government costs as a Concession.

1 MAIN PROJECT COMPONENTS

Besides the 9.7 km long, 11.8 m internal diameter stormwater tunnel the project also comprises of a number of other major structures associated with river diversion, intake to the tunnel, road structures and outfalls. The main project components are as follows:-

- River Klang Offtake Structure
- River Klang Diversion Weir
- Holding Pond
- Tunnel Inlet Structure
- 9.7 km, 11.8 m internal dia. bored Tunnel
- Emergency Escape Passages
- North Ingress/Egress Road Box ramps
- North Junction Box
- North Ventilation Shaft
- South Ventilation Shaft
- South Junction Box
- South Ingress/Egress Road Box ramps
- Tunnel Outlet Structure
- Attenuation Pond
- Twin Box Culvert
- River Kerayong Outfall Structure

The overall scheme provides storage for some 3,000,000 m^3 of water and allows water to be transferred through the system whilst utilizing the upper and lower road decks for traffic at the same time. Three operational modes are envisaged.

2 ORGANISATION OF THE SMART PROJECT

The project owner, the Government of Malaysia is represented by JPS the Public Works Department, DID the Drainage and Irrigation Department and by LLM, the Highway Authority.

The project design and supervision Consultants are Sepakat Setia Perunding (SSP) in association with Mott MacDonald of the UK.

The project promoter is the MMC – GAMUDA Joint Venture. MMC – GAMUDA Joint Venture also set up the Concession holder company for the road operation called Syarikat Mengurus Air Banjir & Terowong Sdn Bhd (or SMART Sdn Bhd). The EPC Contractor for the whole project is the MMC – GAMUDA Joint Venture.

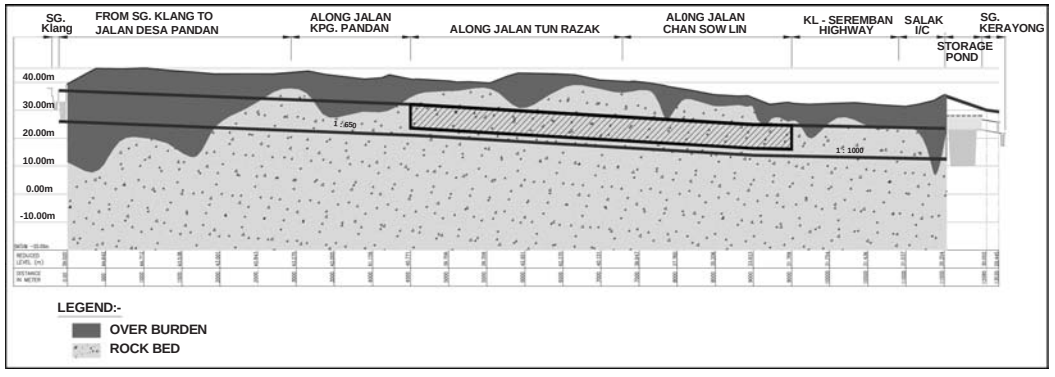


Figure 1. Sub surface conditions for the SMART tunnel.

3 GEOLOGICAL PROFILE

The tunnel traverses the Kuala Lumpur limestone formation at shallow depth (Figure 1). The mature karstic formation is covered by loose silty sand, peat or, at some places, mine tailings, the remnants of the extensive but now historic tin mining in the region.

The quaternary alluvial deposit is generally 4–5 m thick. However in karstic areas and at granitic dykes the unpredictable rockhead may suddenly drop 20–30 m due to eroded solution and cliff formations.

The groundwater table is 1.5–2.0 m below the surface. The permeability of the rock is generally low although groundwater movement through the soft alluvial overlay and karstic features can be extensive and lead to water drawdown hundreds of metres away from a disturbed area.

From north to south the tunnel runs in alluviums, or in mixed face conditions with frequently changing rockhead. The overburden is natural alluvium or mine tailings. The central section is predominantly in limestone with karstic features. The south section being with shallow rockhead, covered by soft alluvium or mine tailings. The last 200 m is in residual soils of the Kenny Hill Formation. Typically, the rock cover is around 3–7 m but in areas of depressed rockhead, a full face of soil or a mixed face of soil and rock were encountered.

The karst is very sensitive to groundwater drawdown. The reduction of groundwater level is known to activate existing sinkholes in karstic areas.

4 TUNNEL AND SHAFT CONSTRUCTION METHOD

Four major shafts were constructed to house ventilation structures and gate house structures for the central 3 km section of the tunnel which accommodates the double road deck. These shafts were at the quarter points along the road section at the North Junction Box, the North Ventilation Shaft, the South Ventilation Shaft and the South Junction Box.

On consideration of having the majority of the tunnel in karstic rock or mixed soil/rock face conditions and the paramount need to control groundwater it was considered appropriate to select slurry TBMs. Two identical Mixshields were purchased from Herrenknecht. The first TBM was delivered within 12 months and the second machine within 15 months of order. The cutterhead was designed for mixed face conditions. The double rotational head had to be able to effectively excavate medium rock and soft soil or mixed face conditions.

The shaft excavation experience has shown that ground treatment including grout curtains, prior to open excavation was essential in controlling ground water lowering which may trigger sinkholes some distance from the works. At the deeper karstic features bored piling with tie-back anchors was necessary to support the excavation. These areas were extensively ground treated to control ground water before excavation by drill and blast methods continued. Overall more than 600,000 m^3 of rock was successfully excavated by controlled blasting in a city environment for the four major shafts and for the egress-ingress ramps construction. The rock surface was secured by rockbolts and shotcrete where necessary.

5 TUNNEL LINING

The tunnel segmental lining consists of an 11.8 m internal diameter precast lining with 500 mm thick segments. The ring is in effect a universal taper of 110 mm, but the rings are used as left and right tapers to keep the keystone above the axis level for ease of erection. The ring is made up of 6 standard plates, 2 counter keys and a keystone. The rings are 1.7 m long and

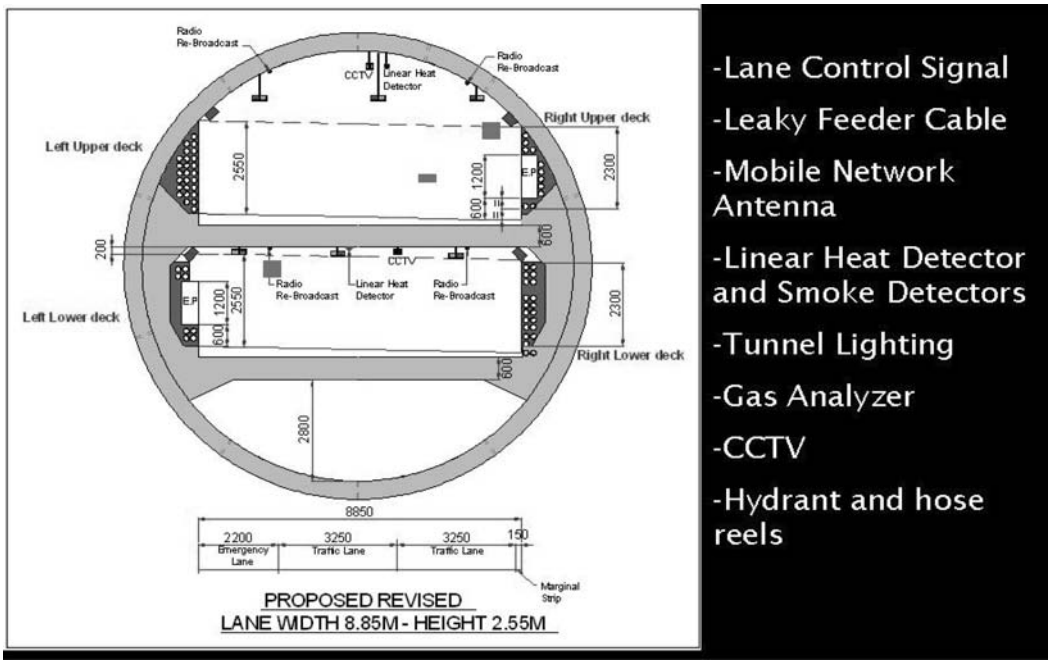


Figure 2. Road Deck Configuration in Tunnel with E&M equipment indicated.

weigh 82 tons each. The segments were produced by local subcontractors at two precast segment factories to the required high quality.

6 ROAD DECK

Within the central 3 km of tunnel the dual purpose facility of double deck roads is included between the North and South Junction Boxes, parallel to an existing notorious traffic bottleneck. These Junction Boxes provide the bifurcation arrangement where the stormwater and road systems merge together with provision of the road and flood gate systems which provide the control and safety of the operation of the scheme.

The road decks were constructed in two pours. Firstly the lower deck and secondly sidewalls and upper deck (Figure 2). The original design and anticipated construction method was modified to that using precast planks, 100 mm thick carrying the lower reinforcement cage, introduced, similar to the 'Omni' system used in bridge decks. To achieve programme the work progressed at the same time that TBM tunnelling continued while deck construction proceeded above the TBM service railway.

Provisions for hydrant, cables and openings to cross passages are provided within the secondary mass concrete placed inside the structural walls.

7 CROSS PASSAGES

Escape staircases are provided at a nominal 250 m spacing along the tunnel to facilitate passenger escape to a 'place of safety' in the event of an emergency. These comprise cross passages connecting the lower and upper road decks and at the ventilation shafts locations, escape staircases and fireman's lifts to grade. The cross-passages are not considered as a 'place of safety' in themselves but provide a passenger escape route to the non-incident road deck. These provisions together with fire detection, alarm and extinguishing equipment, smoke control by the tunnel, ventilation system designed to handle a 10 MW fire and an extensive Emergency Response Plan co-ordination with the Highway Authority and the Fire Brigade, ensures public safety.

Extensive grouting from the surface preceded the construction of the cross passages to prevent groundwater drawdown. Drill & blast method with shotcrete temporary support and spot rockbolting was used. Sprayed on water insulation membrane was followed by the shotcrete permanent lining.

8 M&E COMPONENTS

Integrated within the major structural components detailed above are significant mechanical and

electrical services. These facilities are similar to those incorporated in modern road tunnels but adapted and supplemented to allow for dual usage of the structure, as a road and water tunnel. The design challenge was to enable the road decks to be periodically flooded to facilitate full use of the cross section for flood relief of Kuala Lumpur.

The main mechanical and electrical components comprise:

- HV/LV electrical supply and distribution systems
- Tunnel lighting
- Fire alarm, detection and extinguishing facilities
- Communication and control systems
- Building services for the ancillary structures and buildings
- Tunnel Ventilation
- Pumping
- Flood detection system
- Flood gates, watertight doors and transits

9 HV/LV ELECTRICAL SUPPLY AND DISTRIBUTION SYSTEM

2 No. 33 kV independent incoming supplies are available to supply the SMART project from the TNB grid. Each of the 2 No. 33/11 kV transformers feed one side of a ring mains such that should one source/side of the ring fail, supply can be reinstated via the other. From the load centres the supplies are again transformed and distributed at LV. The essential and very essential loads are backed-up by LV gensets and the very essential loads like the emergency lighting are also backed-up by UPS.

10 TUNNEL LIGHTING

The tunnel lighting is designed to CIE 88:2004 2nd Edition. The ingress/egress tunnels contain the threshold, transition and exit zones boost lighting with the luminiares IP65 rated. The bored tunnel section basically encompasses the interior zone lighting and as this section is flooded all the luminaries are rated at IP 68++ designed and tested to maintain their integrity and withstand a hydrostatic pressure of 2.5 bar with a hydrodynamic force equivalent to a flow of 5 m/s for 24 hours. The IP 68++ luminiare is designed around a 70 W ceramic metal halide lamp. Cable glands were specially designed integral with the body of the luminaire.

11 FIRE ALARM, DETECTION AND EXTINGUISHING FACILITIES

A comprehensive system has been installed throughout the project that is independent of but linked to, the SCADA system and comprises alarm system, detectors, hydrants, hose reels, portable extinguishers and fixed gas extinguishing systems. Within the tunnel an emergency panel is located every 90 m containing a hydrant, hose reel and dry powder portable extinguishes. The cross passages also have a hose reel at each level. There is a fibre optic type, zoned linear heat detector installed throughout the tunnel monitoring temperature and rate of temperature rise with smoke detectors, break-glass points and emergency telephones in the cross passages. All data is fed back via intermediate fire alarm panels to the manned Motorway Control Centre.

12 COMMUNICATION & CONTROL SYSTEMS

The main components comprise:-

- SCADA System for the Tunnel Control System
  The SCADA system incorporates redundancy throughout the whole design. The use of a single fibre provides an acceptable level of redundancy and capability due to the unique arrangement provided by the network supplier.
- Communications Network
  The main communications network is a ring structure using latest techniques from a well known system supplier.
- Radio System
  A leaky feeder is installed within the tunnel to provide for incident, emergency and maintenance communications.
- Closed Circuit Television (CCTV)
  CCTV coverage of the whole tunnel is provided with cameras spaced at every 55 m. Coverage of the cross-passages and escape stairways is also provided.
- Public Address/Telephone System
  A pubic address system is installed in the cross-passages and the escape stairs.
- Access Control and Intruder Detection
  Proximity card readers will be used for access to all controlled areas.
- Variable Message Signs and Lane Control Signs
  Variable message signs are provided at the tunnel approaches to advise and control traffic with lane control signals over the 2 No. traffic lanes spaced between 90 and 135 m according to the curvature of the tunnel.
- Automatic Incident Detection (AID)
  Road tunnel Automatic Incident Detection based on the use of video detection units from fixed camera along the length of the tunnels.
- Video Wall
  The Video Wall is a very comprehensive system being provided by a well known supplier and is installed in the MMC.

- TMCS and FDS Interface
  The Tunnel Management Control System and the Flood Control System are two separate systems. When the FDS notifies the Controller that a flood is imminent, the Controller will check the status and notify the Tunnel Operator accordingly using a secure communication mode.

13 BUILDING SERVICES FOR THE ANCILLARY STRUCTURES AND BUILDINGS

Comprise small lighting and power, ventilation and air conditioning and water supplies and drainage in the ventilation buildings, cross-passages, Motorway Control Centre, Toll Supervision Building, Maintenance Workshop, Stormwater Control Centre and other ancillary buildings.

14 TUNNEL VENTILATION

There are four ventilation shafts covering the bored section each containing axial fans supplying and extracting air. The supply fans deliver air to Saccardo nozzles located in the walls of the lower deck and the roof of the upper deck with adjacent extract ducts. During normal operations, tunnel ventilation is by the piston effect of the vehicles only. During congested operations ventilation is by half the operational axial fans and the ingress/egress jet fans, activated as necessary by air quality monitoring units installed throughout the tunnel. For incident operations, smoke control is provided by the manual operation of all fans serving the incident deck, in response to input from the linear heat detector, CCTV, comms., etc.

15 PUMPING

Sumps and pumps are provided for road tunnel drainage during normal operations.

Following flooding of the tunnel the water will be gravity drained as far as possible and then the tunnel gates will be lowered and a considerable amount of residual water in the flooded road tunnel will have to be pumped into the water tunnel and then, to maintain the reservoir, from the stormwater tunnel into the attenuation pond.

The pumps at the tunnel outfall are designed to be able to drain the water tunnel within 21 hours.

16 TUNNEL OPERATION MODES

The tunnel can operate in three modes: with the whole tunnel dry (Mode I); with the tunnel upstream and downstream of the highway section flooded, and with water flowing beneath the invert of the lower deck, but with the road decks open for traffic (Mode II); and with the highway decks closed to cars and open to water flow (Mode III) (see Figure 3).

During a flood event (Modes II or III), flood flows are diverted from the Sg. Klang into the SMART system to store the flood water before returning it to the Sg Kerayong when conditions in that river allow.

17 FLOOD DETECTION SYSTEM

At the side of the Sg, Klang within the Holding Pond area is the Stormwater Control Centre which monitors information provided by the Flood Detection System (FDS). This is an early warning system utilizing river level and rainfall information from 28 gauging stations in the Sg. Klang and other catchment areas. If the event is significant enough the Motorway Controller is instructed to close the road and a shutdown sequence is initiated.

18 ROAD AND FLOOD GATES

The Junction Boxes are configured to allow bifurcation between the tunnel road facility and stormwater. Within the stormwater section of the junction box sits the Gate House which houses the service gates separating the road, and thus public, from stormwater section where water will be flowing a number of times per year without the need to close the road section. The service gates which seal each road deck at either end of the tunnel are backed up by an emergency gate.

In the other leg of the junction boxes sits the road gate housing which is built into the road slab. This houses the road gates which rise up radially and seal the ingress/egress ramps from flooding when the tunnel is used for stormwater control.

19 PROGRESS ACHIEVED

The first 0.7 km section of the 5.2 km long North Tunnel drive from the North Ventilation Shaft to the North Junction Box holed through in December 2004. The TBM was relaunched on the 4.5 km long second drive towards the Holding Pond to the north in March 2005. Completion is anticipated in March 2007.

The TBM of the South Tunnel was launched in August 2004, having passed through two shafts, the final breakthrough of the 4 km long drive was in April 2006.

The entire dual use tunnel section including the nine Cross Passages has been completed, including the road decks. The shaft building structures have been completed. M&E installation will be completed in January 2007. Ingress/Egress works are substantially complete

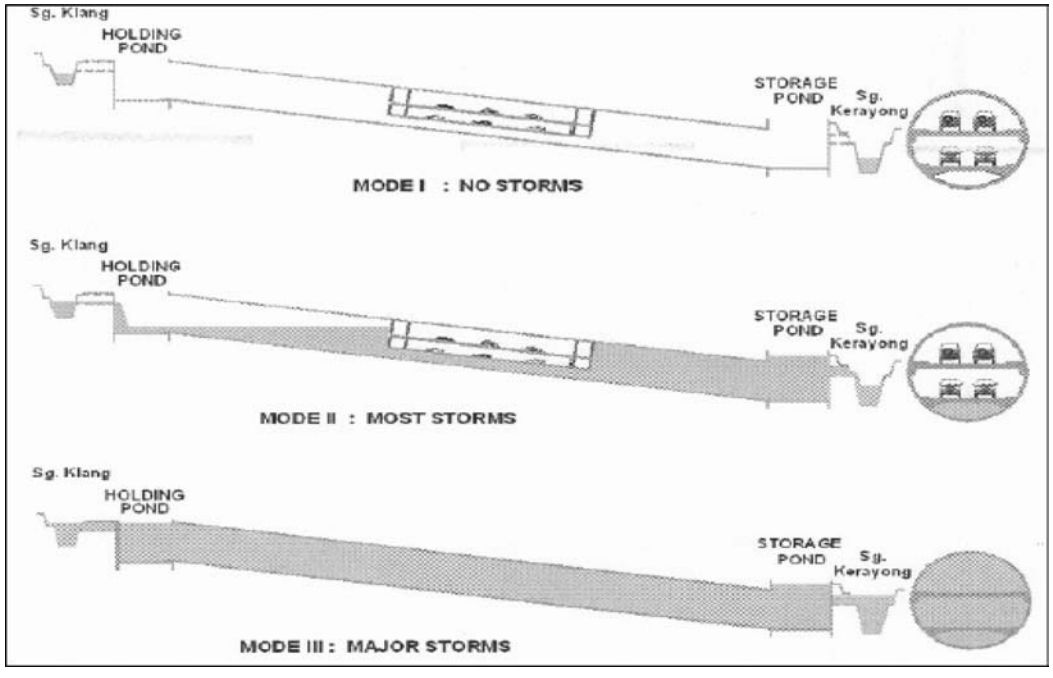


Figure 3. Tunnel operation modes.

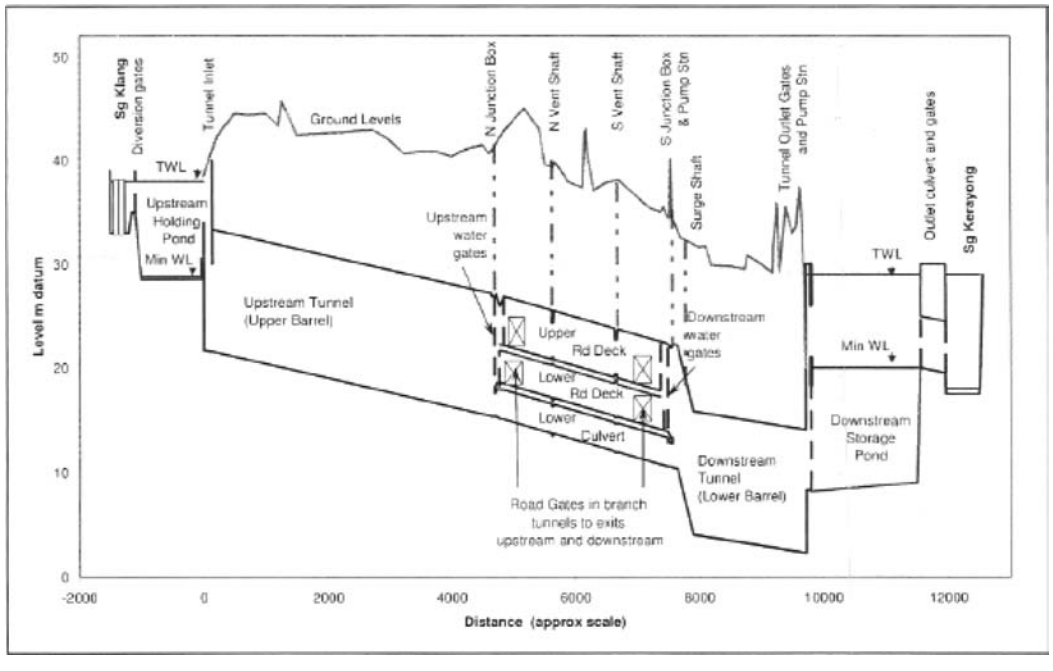


Figure 4. Longitudinal section of SMART system.

with Toll Plaza, Toll Supervision Building, Motorway Control Centre, Maintenance Depot completed.

Overall SMART project progress is on schedule at 92% as of November 2006. The full Stormwater Management facility will be open in July 2007.

20 SUMMARY/CONCLUSION

The Stormwater Management and Road Tunnel scheme is unique but has demonstrated that with some innovative thinking dual usage of major infrastructure works are feasible from an engineering perspective. The submersible road facility is a first of its kind and needed a new level of engineering for the fixtures and fittings within it.

Despite concerns about the variable nature of the karstic limestone in Kuala Lumpur before embarking on the project the choice of TBM type has been vindicated and the project has shown that tunnelling in this type of ground is possible, although considerable care is needed to maintain optimum TBM parameters and slurry properties.

Large scale shaft excavations have also been achieved with minimal settlement using carefully designed ground treatment strategically located to control groundwater in geological features and avoid sinkholes, a common event in this type of ground.

This page intentionally left blank

Underground Space – the 4th Dimension of Metropolises – Barták, Hrdina, Romancov & Zlámal (eds)
© 2007 Taylor & Francis Group, London, ISBN 978-0-415-40807-3

Wienerwaldtunnel – a challenging tunneling project

Hans Köhler
Porr Tunnelbau GmbH, Vienna, Austria

ABSTRACT: Work is under way on the Wienerwald Tunnel contract, which is part of the new railway route between Vienna and St. Pölten, currently Austria's largest tunnel project. By 20012, this new rail link will reduce travel time between Vienna and St. Pölten from 40 to 25 minutes. The technical challenges of the project include conventional tunneling in large cross sections on a length of 2,35 km, as well as the use of two tunnel boring machines with a diameter of 10,68 m on a length of 10,7 km each. Challenging geological conditions call for experienced tunneling crews and immediate reaction to actual conditions. On site segment casting and hauling of large material quantities over major distances need sophisticated logistics.

1 THE PROJECT

The Wienerwald Tunnel, approximately 13,35 km long, will form an important part of the Vienna to St. Pölten high-capacity rail link in eastern Austria and, passing under the Vienna Woods, will connect the Lainz Tunnel at the western border of the city of Vienna with the Tullnerfeld plain in Lower Austria.

The client of this important infrastructural project, ÖBB-Infrastruktur Bau AG awarded the contract to ARGE Wienerwaldtunnel, a joint venture sponsored by Porr Tunnelbau GmbH, in July 2004.

The Wienerwald Tunnel route passes mainly through Molasse and Flysch formations.

The contract sum is app. 340 million Euros at 2004 prices. The contract period is from July 2004 to August 2009, the project is scheduled to be put into service in 20012.

The project (figure 1) is composed of four different sections, each of which presents a number of technical challenges:

- Section "East", 2,35 km long, driven by conventional tunneling.
- Section "West", with two tubes, 10,7 km each, driven by two tunnel boring machines.
- Taglesberg landfill and mucking gallery.
- A 10,5 km long above ground section west of the tunnel, involving earth- and concrete works.

The paper concentrates on the main tunnel works in section east and west.

2 SECTION "EAST"

The East Drive starts underground from its eastern end, in the Hadersdorf-Weidlingau shunting hall.

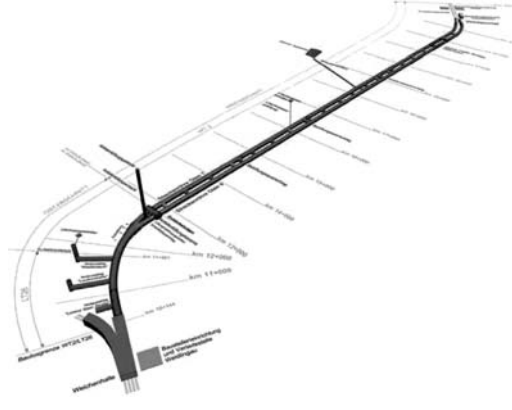


Figure 1. Project overview.

A length of some 2,35 km is being driven by conventional excavator and drill&blast tunneling, passing through the changing flysch sequences of the Vienna Woods, thus resulting in frequent changes of rock support classes.

The drive starts with a cross section of app. 120 m^2 for the twin track tunnel, is then enlarged to a maximum of 250 m^2 in several steps and continues in two single track tubes to the emergency ventilation chamber, where the east drive ends. This chamber will as well be the disassembly chamber for the two TBM's of the west drives.

The East Drive includes several special features, which are "firsts" at least for Austria.

- The site installations are, except offices, completely situated underground (figure 2) to avoid causing nuisance to residents in the densely populated area.



Figure 2. Underground site installations.



Figure 3. Top heading and bench.

- The wet mix for the shotcrete is produced according to the so called mixed-in-car system. Aggregates, cement, plasticizer, water and retarder are loaded into the drum of the remixers by a fully automatic filling station, the mixing is done in the remixer drum while driving into the tunnel. The availability of shotcrete in the tunnel at any time on short notice is essential for this drive with shallow overburden and buildings above the tunnel.
- The entire muck of the tunnel is removed by train, the train loading station is located underground and presently two mucking trains are loaded with 800 tonnes of excavated material each per day.
- The top heading as well as bench- and invert drifts proceed simultaneously at a distance of 80 to 130 m, by use of the "island" system, which means there is no connection to the top heading by a ramp (figure 3). All material supply to the top heading is to be reloaded at the bench, all top heading equipment stays up there for the whole drive and has to be serviced and repaired there.

The secondary lining will be installed after completion of the tunnel driving operations and will be made of a special fire resistant concrete. The part beneath existing buildings will be equipped with a reinforced inner lining combined with a heavy mass- and spring system in the invert.

3 SECTION "WEST"

The Section "West" is a twin tube tunnel with 10,75 km in length and an excavation diameter of 10,68 m. The drives proceed slightly uphill with a gradient of 2,8 ‰, a 2000 m long molasse section is followed by varying formations of flysch.

The tubes are driven by two single shield tunnel boring machines, rock support is provided by reinforced concrete segments, which are erected under protection of the tail shield. All necessary equipment, invert erection and logistics for the drives are provided on the 240 m long back up trains. Material to the machines is provided by rail bound equipment, muck transport is handled by continuous conveyors.

The two single track tunnels are connected by 23 cross cuts at an average distance of 500 m. These connection galleries are constructed behind the main drives by drill and blast method.

3.1 *Site installations*

The site installations are located app. 700 m west of the tunnel portals. The main parts are the segment factory, concrete mixing plant, filling station for mortar, cement and pea gravel, workshops, storage facilities, muck handling and intermediate storage as well as offices.

The segments are produced in a field factory. One segment ring is 2,25 m long, 35 cm thick, and consists of 5 large segments and one small key stone which is always situated in the invert. The segment reinforcement is a welded steel cage, which is completed in the field factory. After pouring, the segments are left to set in the heating tunnel for 6 hours. Following a 24-hour intermediate storage within the factory hall, the segments are stored in the open. The rail bound segment cars are loaded by two gantry cranes which are covering the entire open-air storage area.

The batching plant is during tunnel excavation needed mainly for filling concrete for the invert, the full capacity will be required later on for the inner lining of the tunnel.

The logistics for material supply to the TBM's is set up to transport all material for two segment rings on one train and a cycle time of two hours, therefore an automatic filling station for pea gravel, sand and cement has been installed.

The intermediate muck storage is capable to store 38000 m^3 of muck from each tunnel and to separate different quality of material to be used for different



Figure 4. Site installations at the west portal.

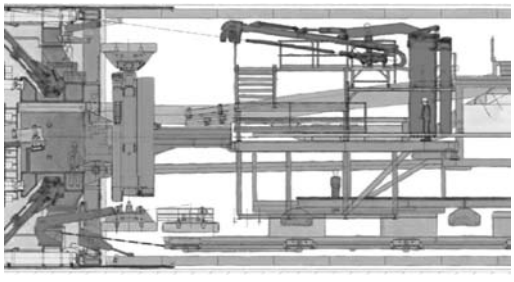


Figure 5. TBM and back up.

purposes on the above ground section of the new railroad line.

3.2 *The tunnel boring machines*

The two tunnel boring machines and their back up trains have been newly built by Herrenknecht for this project to fulfill the specific demands for these particular drives.

The single shield machines are equipped with a closed hard rock cutter head with 64 disc cutters. The cutter head has an electrical drive with 14 motors with 350 kW each, the cutter head speed from 0 to 5 rpm is controlled by frequency converters.

In the shield, just behind the cutter head there are two feeds mounted, capable to bore in an angle of 45 degree upwards for bolting or grouting, behind the shield there is one more feed installed with which exploration holes or grouting holes in an angle of 8 degree off the tunnel axes can be bored to a maximum depth of up to 80 m.

The segment erector is designed to set up one complete ring in app. 15 minutes. The segments for one complete ring are stored in the segment feeder behind the TBM in the invert of the front part of the back up, from where they are picked up by the erector and installed in the tail shield. Simultaneously to boring operation the annular gap is filled with mortar through

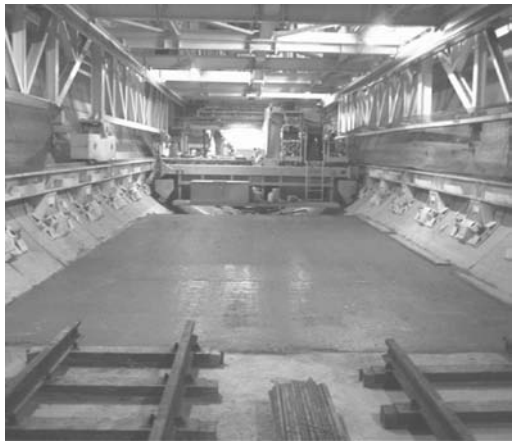


Figure 6. Invert concrete in the back up.

channels in the tail shield in the invert (app. 120°), the upper part is filled with pea gravel through openings in the segments.

Technical data of the tunnel boring machines:

Length of shield:	10,40 m
Total length incl. back up:	248 m
Total weight:	1750 to
Excavation diameter:	10,68 m
Cutter head power:	4900 kW
Cutter head speed:	0–5 rpm
Torque:	29532 kNm
Installed thrust:	156260 kN
Total installed power:	8400 kVA
Number of cutters:	64 pcs
Size of cutters:	17 inch

The capacity of the back up train is designed for a complete cycle time of one hour.

In the front part of the back up all necessary electrical and hydraulic equipment and components which are needed to operate the TBM are placed. Furthermore there are the silos for pea gravel, sand and cement storage, as well as mortar batching plant, mortar pumps and shotcrete pumps for filling the annular gap with pea gravel.

Behind these decks there is the invert concrete installation area which is designed to pour the invert of one daily production within the four hours maintenance shift with the aid of a concrete finisher which is installed in the back up.

In the rear part of the back up there is the train unloading station. The supply train is parked there and a fully automatic crane transports the segments and other material to the point of destination in the front part of the back up.

At the rear end of the back up, ventilation tube magazine, high voltage cable reel and installation area for the structure of the continuous conveyor are placed.



Figure 7. Train unloading station.

3.3 *Assembly of tunnel boring machines*

The two machines have been completely installed at the west portal before they have been moved into the 20 m long starting chamber, which had been constructed by conventional means before.

Since there was space enough available we took advantage of the possibility to start with completely ready units without the necessity to interrupt tunneling operations for additional assembly stages.

The biggest parts to be handled had a weight of 280 to, accordingly heavy cranes were needed.

For start of boring the thrust cylinders of the TBM pushed against a steel ring which transferred the forces into the rock via 16 heavy pretensioned rock bolts.

The second TBM was erected 3 months after the first one. So the same assembly crews could work on both machines. To have a certain distance is required by the project for geotechnical reasons and the advantage for the contractor is, that experience from start of the first unit can be utilized for the second start.

3.4 *Tunneling and cross cuts*

Tunneling works are done in two shifts 10 hours each per day and a 4 hours maintenance shift, seven days per week.

Both tunnels are equipped with a double track rail system in order to secure continuous supply to the tunnel boring machines and to construct the cross cuts parallel to boring operations.

A total number of 23 connection galleries between the two tunnels have to be constructed, most of them parallel to boring the main drives due to the fairly short overall construction period.

There are works for at least four cross cuts simultaneously in operation. First the segments of the main tunnels are secured by bolting them into the rock and the rings are connected to each other to transfer the forces from the opening to the neighbor rings before cutting the opening with diamond saws. The second stage is excavation works by drill and blast, and then the invert concrete is installed. The final stage is the inner lining of the connection gallery.

The supply to all four worksites of the connection galleries has to be arranged so that the supply to the tunnel boring machines is not interrupted.



Figure 8. Mounting of the cutter head.



Figure 9. TBM assembly at the west portal.



Figure 10. Mucking installation connection gallery.

4 CONCLUSION

The tunneling works, currently in full swing both at the east and the west drives present substantial logistical and technical challenges. The drives will meet in the emergency ventilation cavern towards the end of 2007.

At the time of the world tunnel congress app. 70% of the excavation should be completed, the presentation at the congress will include more details about performance and progress rates of excavation works.

End of 2007 the concrete works for the permanent lining are scheduled to start, to be completed by summer 2009.

The total high-capacity rail link project between Vienna and St. Pölten is scheduled to be put into service in 2012.

This page intentionally left blank

Underground Space – the 4th Dimension of Metropolises – Barták, Hrdina, Romancov & Zlámal (eds)
© 2007 Taylor & Francis Group, London, ISBN 978-0-415-40807-3

The construction of shield tunnel crossing right under Shinkansen station

Atsushi Kojima[1], Takashi Inoue[2], Atsushi Sano[3], Mitsuru Shimizu[4] &
Shiroh Suematsu[5]
[1,2,3]*East Japan Railway Company Tohoku Construction Office, Sendai, Japan*
[4,5] *East Japan Railway Company, Tokyo, Japan*

ABSTRACT: AKITA-CHUO road is a road only for the high standard car from the center part of Akita City to express highway interchange of AKITA-CHUO. Among these, extend about 178 meters sections of the part where the East Japan Railway company Akita Shinkansen line Akita Station premises right under are crossed is a part that East Japan Railway was received the consignment from Akita Prefecture and constructed with the shield method because it is necessary to cross the station building and 11 lines in the railroad line. In this paper, we describe the result of the obstacle paling removal by the JC&R method of construction, and the railroad line right under crossing of the shield machine.

1 INTRODUCTION

This construction was the one to cross the shield machine right under the railroad line after the obstacle things such as the foundation piles of Akita station building were removed and to construct the underpass tunnel as for the underpass where the Akita Station east to west was connected. Especially, the JC&R (Just Cut and Reduce) method of construction that was able to cut and remove the obstacle part foundation piles to the shield section by operating on the ground was developed to achieve the construction time saving and cost reduction, and the station building obstacle pile removal was applied to the practice construction. Moreover, the pipe roofing was executed as the track guard method because it was large section shield tunnel in soft ground construction for the railroad line right under crossing of the shield machine, and construction was executed while quantitatively managing the influence on the railroad line. In this paper, we describe the result of the obstacle paling removal by the JC&R method of construction, and the railroad line right under crossing of the shield machine.

2 OBSTACLE THING REMOVAL CONSTRUCTION ACCORDING TO SHIELD TUNNEL CONSTRUCTION

The problem of this construction was to be going to exclude the factor that might become the trouble of construction surely by the time the shield machine reached because it constructed the shield tunnel by the shortest days.

The pile in this construction for the removal was four of the following.

CASE I : The cast in place RC pile. (The foundation pile of present station building)
CASE II : The cast in place RC pile. (The foundation pile of Akita Station escalator pit)
CASE III : The timber pile. (The foundation pile of Shinksen platform)
CASE IV : The hollow PC pile. (The foundation pile of old station building)

In this paper, we describe the case I (The cast in place pile. (The foundation pile of present station building)) that applied JC&R method of construction.

2.1 *JC&R method of construction*

The construction space is limited because there is an existing structure on the removed pile when the pile is removed, and in general, there is a lot of strict construction conditions, and the construction method is limited. The conventional method is Chicago method. This method were attended by many risks due to removal works by manpower excavation and manpower demolishing. Moreover, the soil improvement work for water stops is needed and a high cost generally. Another method is that pile of full length is pulled out after cutting the skin friction of the pile with steel casing. Where the overhead clearance is very small, the pile of full length cannot be pulled out. Thus it is necessary to cut the pile short enough for the clearance and connect

each short casings many time. This method required a long period of time.

Therefore, we have developed a new method, cutting a pile horizontally below the existing structure by operating wire sawing system on the ground and pulling up only the upper pile to the ground above the cutting depth. As for the application of this method, the length of the obstacle pile is long, and the range of the removal targets the case only in the top of the pile to cross section of shield tunnel.

The order of constructing JC&R method

1. The CD machine(the machine of overall casing method) inserts the casing to the removal pile. (In this case, the casing shaves off the removal pile to 1000 mm in diameter.
2. The cutting device of the JC&R method is descended. (photograph-1)
3. The removal pile is horizontally cut with Wire saw by the ground operation at the position.
4. Inserting steel bar for pulling up the pile and the power jack for the pile lifting up, and the pile in the ground part is cut and removed with wire saw.

The advantage of the JC&R method to the conventional method (Chicago method) is as follows so far.



Photograph 1. The cutting device of the JC&R method.



Photograph 2. The CD machine inserts the casing.

1. It is possible to cut it by the operation from the ground.
2. The soil improvement work for water stops is no necessity.

The advantage of the JC&R method to the conventional method (the casing as for the total length of the pile) is as follows so far.

1. The frequency of casing build and pull off casings pile decreases because building of the casing is by the cutting position.
2. The cutting removal frequency of pile decrease in the ground part.
3. To break off top of pile is unnecessary.

Safe and time saving construction became possible compared with the conventional method by JC&R method on the above mentioned reasons.

2.2 *Construction condition*

Objects of removal piles were foundation pile of station building. The removal pile received design load 275 t per pile. The bearing layer of foundation piles of station building were siltstone. This work took the isolation of 2.0 m from the bottom of the shield tunnel for the pile of eight obstacle of the existing pile that receive a present Akita station building, cuts in the ground. Then only the upper part is removed from the cutting plane. The underground cutting position is G.L.-30.8 m. The pile cutting length is 20.5 m. The plane and the cross section are shown in Figures-1 and 2.

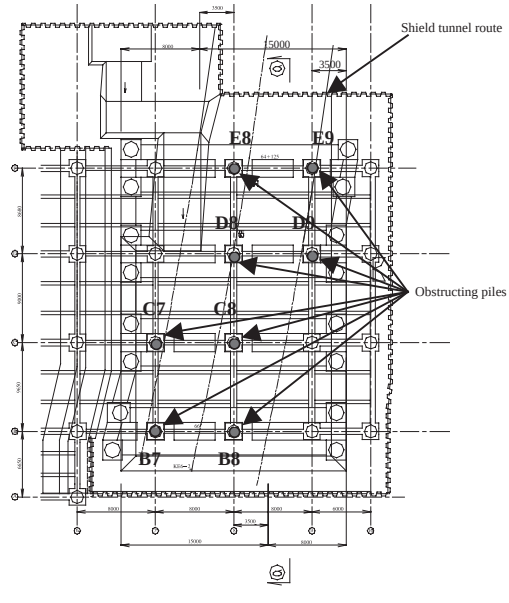


Figure 1. Ground Plan of AKITA station building.

The load of the station building that operated on eight existing piles was received with the beam and the pile of new built by the underpinning process. Before this work, the relation between the station building and the existing pile was cut. The construction environment was an underground plane space 19 m × 30 m, and the overhead clearance was 4.3 m above the excavation bottom. The existing pile removed by this work was the cast in place pile pf earth drill of 1000∼1300 mm in diameter. The construction accuracy of the amount of eccentricity and the shape of drilling, etc. was not able to be understood though parameters such as the lengths of the pile and the arrangement of bar were able to be understood beforehand.

2.3 *Problem and verification in construction*

2.3.1 *Casing built and shaving of existing pile*

The problem of this work shaved the existing paling without twisting off the pile, and built the casing. There was a possibility that reaming cutter cuts a main reinforcement of the pile when the pile has inclined, and the pile was twisted off when falling below the torque reading of CD machine that the endurance force on the twist of the pile was transmitted from the casing to the pile. Therefore, we managed to setting the upper bound value of the shaving torque to be 400 kN · m from the result of the examination construction, and so as not to cause a rapid torque rise.

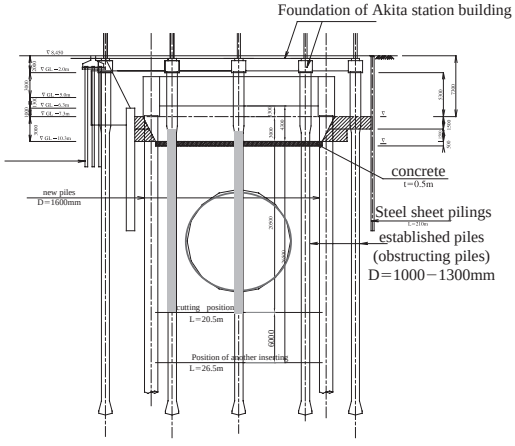


Figure 2. Section of AKITA station building.

The construction result at built of the casing is shown in Table-1. B-7 and B-8 were upper bound values 400 kN · m or less, cannot twist off the pile though were bad vertical accuracy, and were big compared with another the shaving torque, and built of the casing ended safely. The time that had been required to cut 1 m for the pile other than B-7, B-8, and D-8 became 130∼160 minute. Be able it to cut well, and it to be built though it took some time the much more before this construction than as a result of the full-scale shaving examination done beforehand (about 120 minutes).

2.3.2 *Cutting of pile and built of cutting device*

The problem of this work was to avoid an impossible cutting by the wire saw moving intensely. Therefore, when the full-scale cutting was examined, we arranged the pulley for the wire saw was prevented from intensely moving, and improved cutting device. Then we adopted an endless wire on a no edge without connection parts so that prevented the wire saw from breaking while cutting it.

The construction result when the pile was cut is shown in Table-2.

The cutting position was changed once in E-9 for cutting. This reason was because cutting became impossible on the way. The cutting plane had hoop ties, main reinforcements, and the reinforced ring when the removed pile was seen, and it tried just to cut the part in the top of the reinforced ring (photograph-3).

Table 1. The result of construction (The building the casing).

		The building the casing			
Pile no.	The order of constructing	The length of excavation (m)	The time of excavation (min)	Time a meter in excavating length (min)	The maximum cutting torque (kN · m)
B-7	1	23.5	5439	231	371
B-8	6	22.5	5827	259	371
C-7	7	24.5	3732	152	202
C-8	4	22.6	3313	147	202
D-8	5	22.5	6503	289	202
D-9	8	20.5	3320	162	202
E-8	2	24.5	3698	151	202
E-9	3	22.5	2942	131	168
Average		22.9	4347	190	

Table 2. The result of construction (The cutting pile).

Pile no.	The order of constructing	The cutting pile: The time of building the cutting device (min)	The cutting pile: The time of cutting (min)
B-7	1	285	45
B-8	6	550	31
C-7	7	330	35
C-8	4	225	39
D-8	5	290	75
D-9	8	400	41
E-8	2	250	51
E-9	3	240	45
Average		321	45



Photograph 3. Cutting plane of pile.

Therefore, we guessed that the wire saw was not able to cut the pile because it tried to run away to the weakness or more and the side that the reinforced ring was no and the cutting plane lost planarity on the way. Then, about 200 mm was cut again in the lower side.

Cutting when the cutting position was changed ended without trouble. A steady cutting was able to be done about other pile both building the cutting device and cutting in the ground. Wire speed was low, about 4∼5 m/sec, and we could not confirm the moving of wire intensely. It took about 45 minute on the average to cut the pile.

3 RAILROAD LINE RIGHT UNDER CROSSING OF SHIELD MACHINE

Right under the railroad line, besides, the construction results of the large section shield with the soft ground are little. This large section shield tunnel was rare construction also in Japan. The shield machine adopted the closed type shield machine of slurry from the construction of the soft ground. We adopted inside concrete placing type ductile segment from the necessity for supporting the train load. (12.2 m in diameter, 1200 mm in width, and beam height 400 mm, when inside concrete is included, it is 500 mm.)



Photograph 4. The shield machine.

The earth covering in the range of our construction was about 13.0 m. The sandy clay of soft alluvial deposit and the cohesive soil were distributed in the alternation of strata, and the cohesive soil formed the soft ground of the subject, and the surface layer was the humus, and the groundwater level was high with about G.L.-2.0 m. Moreover, the bedrock layer decreased rapidly from the vicinity of west area of Akita station, and was a drowned valley of about 40 m in depth.

3.1 *Technical feature*

3.1.1 *Track guard method*

As for this construction, for the soft ground and the large section shield, the generation of the track displacement because of loosening of the forward ground of proceeding to excavate the shield was feared.

Therefore, the result of comparing the chemical grouting method, the pipe roofing method, and the high-pressure jet stir mixing method as the track guard method, we adopted the pipe roofing that indicated the value with the smallest amount of the track displacement We placed the pipe roof to be gate type arrangement by 1.2 m in diameter and 70.5 m in length. (Figure-3) We adopted the excavator of closed type that the chemical grouting method used an unnecessary so that construction might prevent groundwater from flowing in the pipe roof that became the factor of the track displacement (photograph-5). As for the yard that constructed the attainment shaft, securing the yard was difficult because it was adjacent to the station building, and overlapped with construction yard of the underpinning of the station building. Therefore, we adopted that the excavator was pulled to the start shaft after construction, and the excavator of the return type that was able to be collected. The water stop of 3 m in total thickness and protective layer was formed by the soil improvement, and about the face stop of the pipe roof in the attainment part, the pipe roof was intrusive and fixed to this part. The pipe roofing was aiming at another of the track defense and the investigation of the obstacle of underground laying thing moreover, the obstacle thing did not exist from among this when there was an obstacle thing by any chance though it was scheduled to remove it.

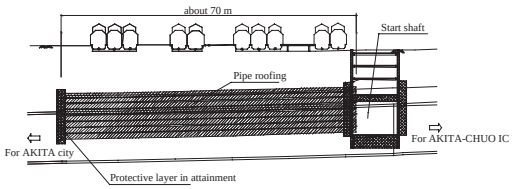


Figure 3. Longitudinal section of the pipe roofing.



Photograph 5. Track guard method.

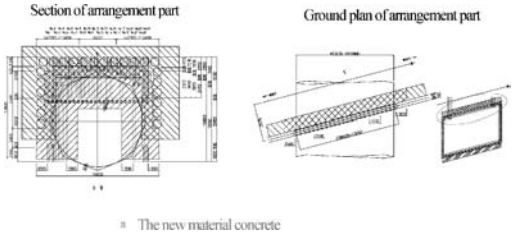


Figure 4. Arrangement part of the new material concrete.

3.1.2 *The new material concrete (improvement type of the NOMST material) is adopted for the pipe roof start shaft of earth retaining structure*

In this construction, we adopted the new material concrete that the coarse aggregate was the lime aggregate that can be cut with cutter of shield, and the reinforcement was high strength and the big carbon fiber reinforced plastic of the modulus elasticity, so that the pipe roofing start shaft of earth retaining structure of soldier piles were obstacle to the shield proceeding to excavate. This new material concrete was the NOMST method. (NOMST : Novel Material Shield cuttable Tunnel-wall System) (Figure-4) In a past construction case, it transmitted of soldier piles (H steel) set up in the NOMST section by shield passing over the NOMST section, and the vibration in the ground level was confirmed. Therefore, the vibration when the shield machine passed over the NOMST section was feared. This time, we adopted the new material concrete that was improvement type of past NOMST method. This type improved the shape of the grid reinforced that made from the carbon fiber reinforcement.

3.2 *Problem and verification in construction*

3.2.1 *Influence on track according to shield machine proceeding to excavate*

The problem of this work was to understand the influence on the track by proceeding to excavate the shield machine by the track measurement. We adopted the track measurement by the hand because there was no passing train in the station premise, and constructed the track guard of pipe roofing. As the management value, the maintenance standard value was adopted to be a limit value, and the 70% was adopted to be a construction discontinuance value. Moreover, to prevent the ground level from subsiding along with excavating, a simultaneous filling injection method was adopted for the shield machine to reduce the influence on the track as much as possible. The simultaneous filling injection method was a method of inject beginning at the same time as excavating beginning from the injection tube set up by the shield machine. Therefore, the possibility of loosening the ground while proceeding to excavate even if it was the ground that collapsed was high was small. In this construction, necessary filling quantity was calculated from the proceeding to excavate data of the shield machine automatically, and the injection material was injected from the hole in four places in the machine upper part at the same time as generating tail void.

The construction management of the filling injection executed it using the injection pressure management together with the injection quantity management. The target value of the injection pressure set the face slurry pressure from past construction results in the lower bound, and the upper bound value added face slurry pressure to 200 kPa. Moreover, the target value of the quantity of the injection was adopted to be 100～150% of the quantity of the calculation void.

The relation between the track displacement and the top position of the shield machine in the vicinity of the section of the crossing under the railway track beginning position is shown in Figure-5. The amount of the maximum track subsidence on the shield center became 3 mm. This amount of the subsidence was a value that was smaller than 5.94 mm that was the amount of the assumption subsidence requested beforehand by two dimension FEM analysis. The change in the amount of the track subsidence on the shield center showed the subsidence tendency immediately after proceeding to excavate, and showed the tendency to the rise after passing the shield machine. When the distance from the measurement part to the top of shield machine exceeded about 30 m, the upside converged. Moreover, all were below the construction discontinuance value as for track measurement by the hand.

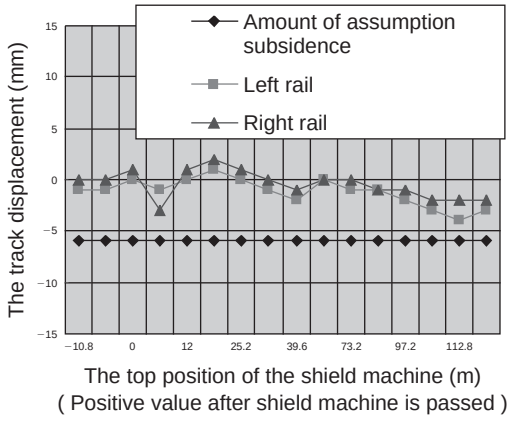


Figure 5. The relation between the track displacement and the top position of the shield machine in the vicinity of the section of the crossing under the railway track beginning position.

3.2.2 *Vibration and noise measurement when new material concrete was proceeded to excavate of shield machine*

We measured the vibration that generated cutting the new material concrete so that cutting the new material concrete that adopted the new NOMST material for the wick material with the shield machine of the prototype became the first construction this time.

The feature of this measurement management was a point to set the vibration acceleration level of the convertible acceleration to the management value. The purpose of this was to prevent the emergency's stopping of elevator (ELV) set up in the station premises. The vibrograph was set up in ELV set up at Akita Station, and when 10 gal (correspond the vibration acceleration level 80 dB) were measured, ELV was stopped. Therefore, when the vibration measurement member was arranged in the shinkansen platform, and the vibration acceleration level exceeded 75 dB, we adopted by lowering the proceeding to excavate speed. The plan proceeding to excavate speed was usually adopted 20 mm/min, but the plan proceeding to excavate speed of the new material concrete section was 2 mm/min.

The relation between the shield proceeding to excavate time above the new material concrete and the vibration acceleration level was shown in Figure-6. Proceeding to excavate the new material concrete section began proceeding to dig at first according to schedule of 2 mm per minute. The value of the vibrograph showed 30∼40 dB. This measurement value showed the tendency to the value similar to before it began to proceed to excavate. Moreover, before it began to proceed to excavate and after it began to proceed to excavate, the tendency to a similar value was shown about the noise meter set up in the Shinkansen

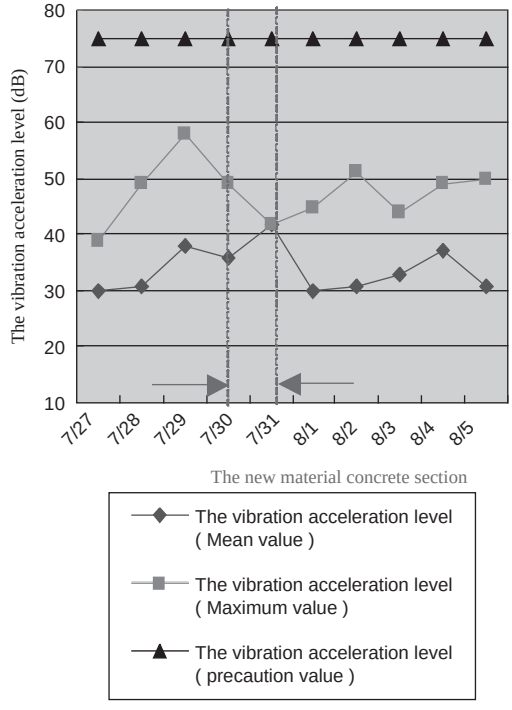


Figure 6. The relation between the shield proceeding to excavate time above the new material concrete and the vibration acceleration level.

platform. We managed the proceeding to excavate speed while confirming the value such as vibrograph by the result of the above-mentioned measurement, and the proceeding to excavate speed was executed up to 13 mm maximum per minute. The value of the vibrograph became 40∼55 dB along with proceeding to excavate. It became a result with room enough for 75 dB set as a precaution value. Moreover, the rounds were executed at Shinkansen platform, therefore there were no swing of the overhead wires, and the vibration that became unpleasant of the customer was not generated.

We considered the reason why the value of vibration in the NOMST section that compared with the case cut in the all sections of the cutter face was small so that the new material concrete was cut by part of cutter face because a new material concrete wall was diagonally arranged for the shield machine. The problem that the NOMST material blockaded the sludge pipe was assumed about cutting the NOMST material along with proceeding to excavate a new material concrete section. However, the result of excavating the new NOMST material (GRM), the NOMST material discharged from the low head screen was cut by the size of about 100 mm. (photograph-6) Therefore, the blockage of the sludge pipe that depended on the NOMST



Photograph 6. A piece of the reinforcement of the new material concrete.



Photograph 7. Tunnel interior of completion.

material was not caused. We considered that it was one of the factors to decrease the vibration and the noise that cutting improved like this.

4 SUMMARY

This construction was extremely rare construction that passed the large section shield in the section of the crossing under the railway track in the soft ground for an intense heat period after removing the various obstacle things to the shield section.

We stopped the minimum influence on the station building, and completed proceeding to excavate that not causing spurts of slurry neither the track subsidence nor the road subsidence.

This page intentionally left blank

Underground Space – the 4th Dimension of Metropolises – Barták, Hrdina, Romancov & Zlámal (eds)
© 2007 Taylor & Francis Group, London, ISBN 978-0-415-40807-3

Non-circular full face tunnel boring machines –21st century challenge

M. Krčík
Geotechnical Design Office, Bojnice, Slovak Republic

ABSTRACT: Rapid development of Full Face Tunnel Boring Machines admits using very large units, often more than 14 metres in diameter. However, only two thirds of those excessive cross-sections are utilised efficiently. Therefore, development of Tunnel Boring Machines is focused to excavating ideal cross-section works, similar to cross-section typical for the New Austrian Tunnelling Method (NATM). The mentioned development takes place mostly in countries such as Japan, Germany but also in Slovakia supported by private resources. Several concepts of these machines are introduced herein describing both their advantages and disadvantages.

1 INTRODUCTION

Tunnel boring machines in excess of 14 metres in diameter are commonplace. In Madrid there is a machine with a 15.2 m diameter. This is an EPB SHIELD manufactured by Herrenknecht. In Niagara Falls there is a machine with a 14.4 m diameter; this is HARD ROCK TBM, produced by the ROBINS Company. In Switzerland there is a machine with a 14.4 m diameter made by WIRTH, whilst in the Netherlands is a machine with a 14.87 m diameter from the French manufacturer NFM.

A disadvantage of such big tunnel boring machines for traffic tunnels, road, railway or subway tunnels with two or three lanes is that the excavation in the bottom part of the profile is not utilised and often filled with material again (see Fig. 1 and Fig. 2).

In different tunnels driven by means of tunnel boring machines the road pavement is supported by piers in the full length, similarly to the bridge deck (see Fig. 3 and Fig. 4).

Concepts of non-circular full face tunnel boring machines with the cross section aiming at the profile

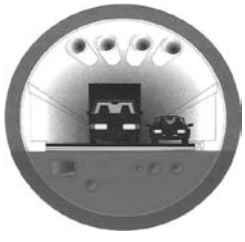


Figure 1. Cross section of 14,2 m diameter motor way TBM.

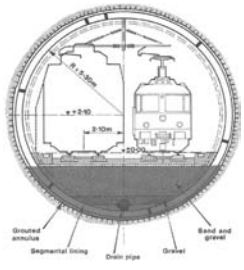


Figure 2. Cross section of 11,62 m diameter railway TBM.

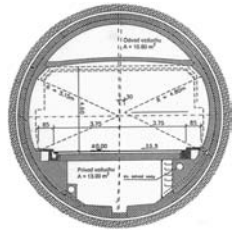


Figure 3. Cross section of 11,8 m diameter.



Figure 4. Cross section of 15,2 m diameter.

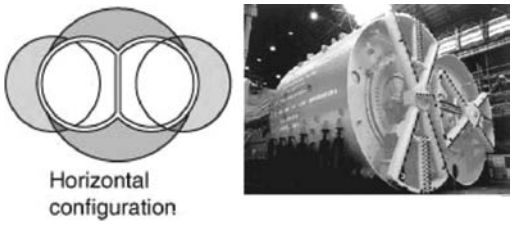


Figure 5. Cross section and DOT (Double-O-Tube) shield.

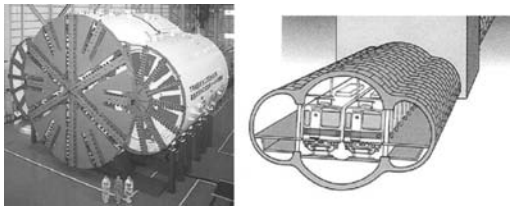


Figure 6. A horizontal triple-circular shield tunnelling machine excavated two railways and a platform.

used in the drill and blast method, and the NATM method, solve the above disadvantage.

2 MANUFACTURED AND SUCCESSFULLY USED NON-CIRCULAR TUNNEL MACHINES

The Japanese are well advanced with the concept of tunnel boring machines with non-circular profile.

Nevertheless, these are generally machines designed for soft sedimentary ground. It is probably due to the fact that all big industrial cities in Japan are situated along the Japanese shore, which is the typical location for this type of sedimentary rocks.

An advantage of DOT (Double-O-Tube) tunnel boring machines consisting of circular cross sections is that they cover less space than two tunnel tubes next to each other as to the width, but also less space as to the height, with low overburden, than one circular tunnel tube, especially in the rural built-up areas (see Fig. 5).

Their disadvantage is that the pillars must be supported in the place in which the circles are interconnected due to the static reasons.

It is similar with the multi-circular Shield machine, which was successfully used for subway stations. (see Fig. 6)

Various cross-sectional shapes (Fig. 7) is Shield machine with a circular disc cutter at the center of the face and multiple planetary cutters, as shown in Figure 8.

The orbit of planetary cutters can be changed freely by adjusting the angle of swing arms attached to them.

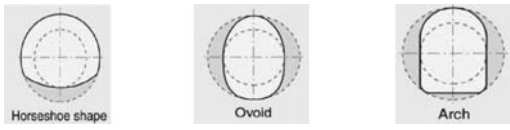


Figure 7. Variations of cross section.

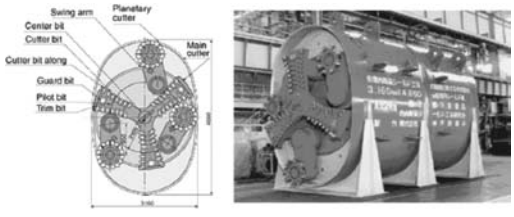


Figure 8. Three – part articulated OK (muddy soil pressure) shield.

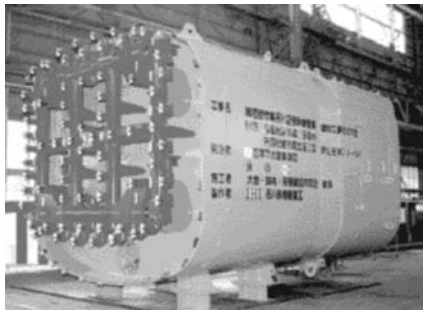


Figure 9. DPLEX shield: 4 m wide in Narashino City.

Thus, various cross sections can be created easily such as a rectangle, oval and arch.

DPLEX (Developing Parallel Link Excavation) shield method is used in Japan by the HITACHI Company for the construction of Subway line No. 11 in Tokyo.

3 PLANNED NEW CONCEPTS OF NON-CIRCULAR TUNNEL MACHINES FOR SOFT GROUND

3.1 For SOFT GROUND there are two interesting concepts of shields designed for full face. It is the DPLEX shield for a three-lane motorway tunnel with economy cross section being 17.2 m wide and with the total length of 12.8 m. (Fig. 10)

Four division cutter head – has for stabillity the face pre EPB with rotational speed of the screw conveyoe.

The TMB concept with combination of the rotation cutter method and the sliding cutter method is also interesting. The TBM is of the slurry shield type.

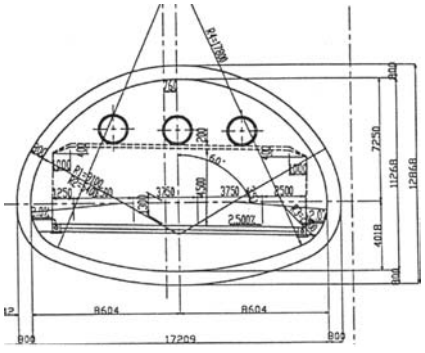


Figure 10. Cross section of the three-lane motorway tunnel in soft ground.

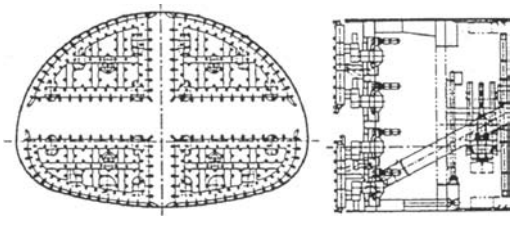


Figure 11. Developing parallel link excavating 4-division type.

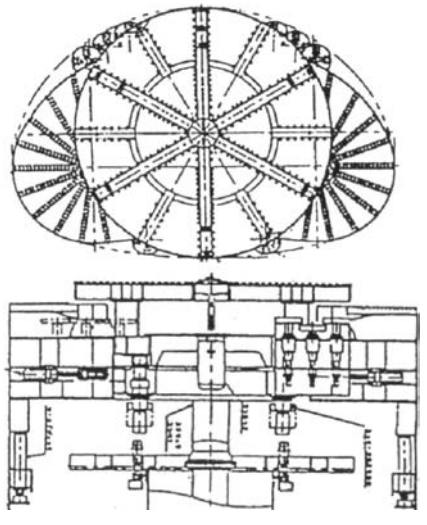


Figure 12. Combination of the rotation cutter method and the sliding cutter method.

4 SUCCESSFULLY USED NON-CIRCULAR TUNNEL MACHINES FOR HARD ROCKS

This area has been the main focus of the WIRTH for the past 15 years and of the ROBBINS Company for the past 20 years. Since 1991 WIRTH has developed and manufactured the Continuous Miner Machine successfully used in Canada. Profiting hereof the undercutting technique distinctly increases the excavating performance per cutter, whilst this technology was applied for a Continuous Miner. (Fig. 13)



Figure 13. Continuous undercutting miner.

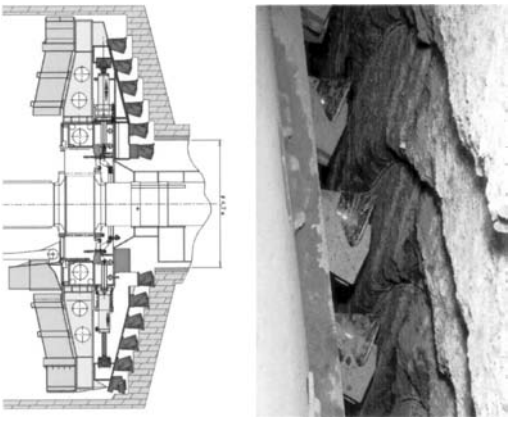


Figure 14. Reaming tunnel boring machine.

This technical development has now been applied for the first time for teaming principle. The WIRTH TBE 500/1440 H-HST is a Reaming Tunnel Boring Machine (Fig. 14)capable of boring diameters up to 14.4 m.

It was used with success to drive the UETLIBERG Tunnel in Zurich, Switzerland last year. Its profile is slightly elliptical being 14.4 m wide and 14.2 m high.

The American tunnelling machine – a mechanical hard rock excavator (Fig. 15) manufactured by the ROBBINS Company, and which belongs to the machines with conventional radial chisels, was used with success.

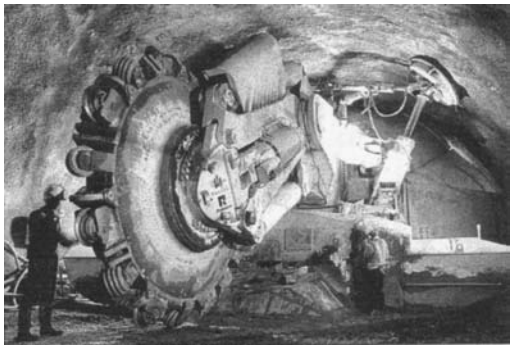


Figure 15. Mobile Miner ROBINS MM 130.

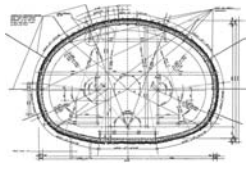


Figure 16. Profile of the two-track railway tunnel driven by means of NATM in Prague.

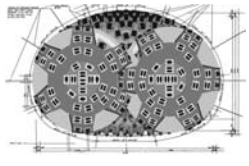


Figure 17. Profile driven by means of NATM with the use of the "two plus two face" TBM.

5 SOME PLANNED CONCEPTS OF NON-CIRCULAR HARD ROCK TBMs

The idea of developing such technology which would enable us to excavate the economical profile in a rapid manner is based on the fact that the construction of more than 50 km of motorway tunnels is necessary in Slovakia. As there is no need for the invert in the majority of long Slovak tunnels the horse-shoe shaped economical profile seems reasonable enough and advantageous indeed.

The "Two plus two face TBM" concept consists of four rotary cutting heads. (Fig. 17) The front two of them have the same circular shape. Behind them two other cutting heads are situated. The upper of them, barrel shaped, excavates the crown and the lower one, which may have barrel or drum shape according to quality of rock, excavates the invert of the tunnel. Such configuration enables to excavate full economy cross section at the same time.

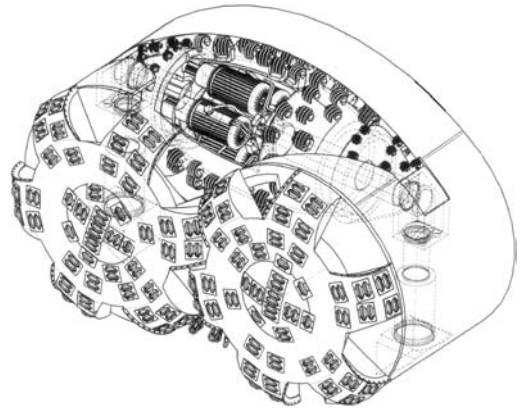


Figure 18. View 3D of the TBM with partial section throught upper barrel shaped cutting head.

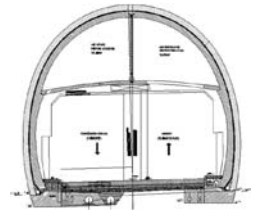


Figure 19. Cross section of the Planneed motorway 7 km Višňové Tunnel for the NATM 7 km long for NATM.

The additional advantage of the "Two plus two face TBM" concept, comparing with circular one, is possibility to lower the upper head by means of mighty hydraulic jacks in case of geological dislocation. (Fig. 18) This feature enables access to the space "over the barel heads" without necessity to make additional excavations. Two possible tandems can be attached behind the "Two plus two face TBM" cutting head system:

a) TBM with expanding hydraulic jacks leaning against tubing lining
b) TBM with extruded concrete lining system, enabling rapid tunnelling, well-known mainly from Japan.

The concept of TBM consists of one non-circular head only which has two additional finishing cutting pear-shaped heads (Fig. 20) to excavate the horse shoe-shaped profile well-known from the NATM.(Fig. 19)

Power supply of the finishing cutting head is situated inside the barrel which provides for electricity and cooling by means of a non-rotating shaft.

In soft rocks it is possible to use the version TBM with the shield and the tubbing lining.(Fig. 22)

The concept of TBM which has only one non-circular head and two finishing cutting pear-shaped

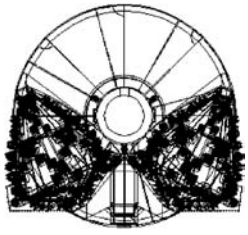


Figure 20. Profile of NATM driven with use the full face TMB with the finishing pear-shaped cutters.

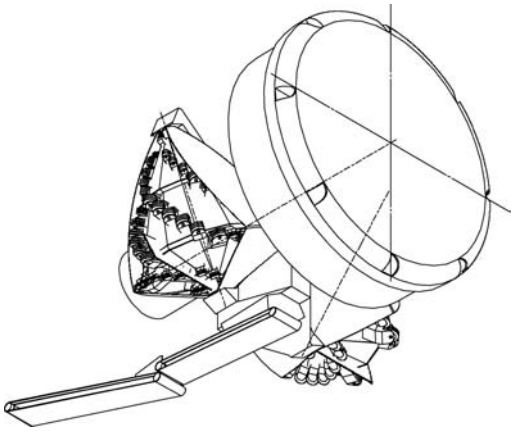


Figure 21. Undersight of the TBM principle with the finishing cutters.

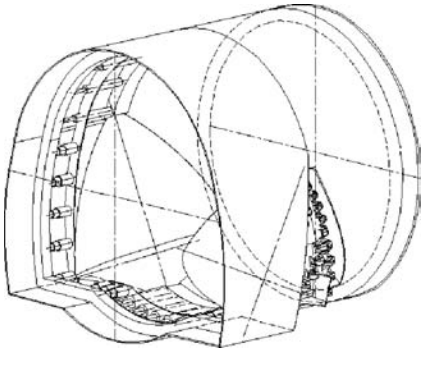


Figure 22. Rear view of the shield type TBM with the finishing pear-shaped cutters.

heads behind which excavate a horse-shoe shaped profile well-known from the NATM.

The power supply of the finishing cutting head is inside a barrel in which electricity and cooling is provided by means of non-rotating shaft. Both TBM concepts have patent protection.

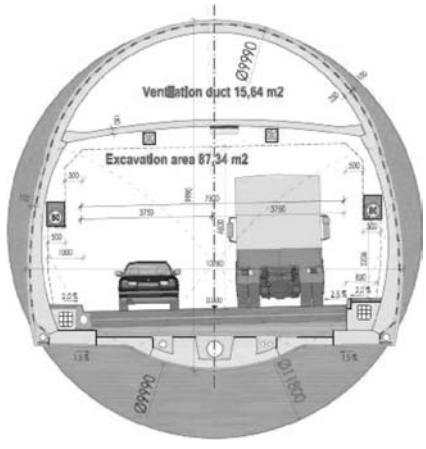


Figure 23. Sample cross section of the motorway tunnel by means of the non-circular TBM with a smaller area compared to the circular TBM.

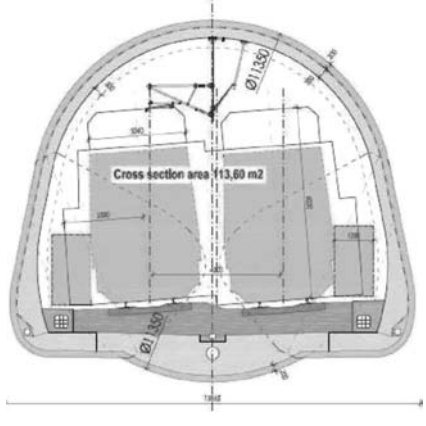


Figure 24. Sample cross section of the railway tunnel driven by means of the TBM.

In softer rocks it is possible to use the concept with a shield and tübing lining. Apart from the use of pear-shaped cutters for the TMB gripper it is possible to use the finishing cutters for the shield type TBM. Hydraulic jacks for pressing of tubings, adjacent to the finishing cutting heads have telescopic design. (Fig. 22)

6 CONCLUSION

The economical advantage of non-circular TBM with horse-shoe profile is especially convenient from long full face traffic tunnels.(Fig. 23 and Fig. 24) The cost

of a tunnel excavated by means of a non-circular TBM is lower if compared with a circular TBM, namely:

- cost of rock excavation is lower by 20% to 30% due to the smaller profile, i.e. lower costs for electric energy and exchange of cutting discs
- construction of lining with the tunnel circumference smaller by15% to 20%
- backfilling and compacting of the space beneath the road pavement or railway yard which increases the speed of driving.

The disadvantages of the non-circular TMB are as follows:

– initial higher cost for the manufacturing of a complicated TBM
– higher number of tübings for the tübing lining.

In case of tunnels which are longer than 3 km the above disadvantages are minor and the advantages of non-circular TBM prevail.

REFERENCES

Yukihiko ISHIKAWA 1998 *Attachment Type Three-Centered Station Shield*

Ing.Marián KRČÍK 2002 *A possibility of designing TBM for economy cross section tunnels Geotechnics 2002 Bratislava*

HITACHI CONSTRUCTION MACHINERY Co., Ltd. 2006 *Activitie 2006s*

Underground Space – the 4th Dimension of Metropolises – Barták, Hrdina, Romancov & Zlámal (eds)
© 2007 Taylor & Francis Group, London, ISBN 978-0-415-40807-3

Toulouse Metro Lot 2: soil conditioning in difficult ground conditions

Alban Martinotto
Campenon Bernard SA (Group Vinci), Paris, France

Dipl.-Ing. Lars Langmaack
BASF Construction Chemicals (Europe), Zürich, Switzerland

ABSTRACT: The JV of Campenon Bernard TP (VINCI Group) & Eiffage TP was working on the Metro Line B, Lot 2 Project in Toulouse, together with BASF Constructions Chemicals for the soil conditioning and annulus grout admixtures. The machine used was the Herrenknecht S-208 7,75 m diameter EPB TBM. The TBM was driven under a housing area leaving the TBM launch shaft, continuing under a railway and houses with foundations lower than the tunnel alignment, coming then under the «Canal du Midi» and crossing old archaeological sites and sewers that were in a poor condition. Therefore the correct and stable face pressure was a prerequisite in order to prevent surface settlements and uncontrolled water & soil ingress. In addition, the clogging risk at the cutterhead and in the working chamber of the TBM caused by the tertiary molasses was fairly high, especially taking into account that the molasses were disturbed by sand lenses and large sections of the tunnel were below ground water level.

1 THE PROJECT

In June 1997, SMAT (Societé du Métro de l'Agglomération Toulousaine) got the task to construct the metro extension Line B from north to south through the city centre (Figure 1), a natural complement to Line A with the common station being Jean Jaurès.

Line B consists of 20 stations and a total length of 15.000 m, where 2.000 m represent cut and cover sections and 13.000 m bored tunnel.

The main Lots were:

- Lot 2: Herrenknecht EPB TBM, 4.731 m
- Lot 3: CSM Bessac compressed air TBM, 1.000 m
- Lot 4: FCB Slurry TBM, 3.700 m
- Lot 5: FCB EPB TBM, 3.400 m

Campenon Bernard TP & Eiffage TP were responsible for Lot 2, using a Herrenknecht EPB TBM S-208 named «Carlos Gardel». The TBM had a shield length of 8,50 m; a shield diameter of 7,750 m and a cutterhead diameter of 7,785 m. About 200 excavation tools were installed on the cutterhead and its rotation speed was adjustable from 1–3 RPM. The TBM speed was designed to reach 80 mm/minute with and EPB pressure of up to 3 bar. The installed power was 2.000 kW, resulting in a driving force of 55,75 kN and a jack force of 6.000 tons.

The tunnel inner diameter was designed reach 6,80 m with a $5 + 1$ Segment structure of 1,40 m length and 340 mm thickness. The total number of placed segments reached 26.000 and the muck excavation of 225.000 m^3 or 517.000 tons.

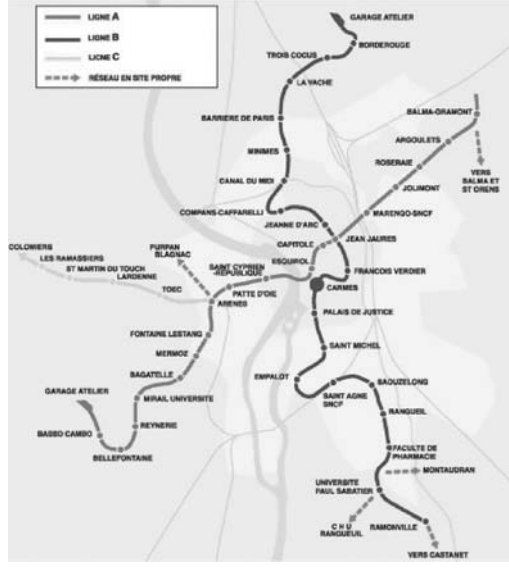


Figure 1. Metro plan Toulouse.

The tunnel alignment was placed under a housing area just leaving the launch shaft «Trois Cocus», continuing under a railway and houses with foundations lower than the tunnel, coming then under the

«Canal du Midi» and crossing old archaeological sites and sewers in a poor condition. Therefore correct and stable face pressures were a must in order to prevent surface settlements and uncontrolled water & soil ingress. In addition, the cutterhead clogging risk of the tertiary molasses was fairly high, especially taking into account that large sections of the tunnel were below ground water level. Furthermore, sand strata were present at the TBM crown level.

2 SOIL CONDITIONING BACKGROUND

EPB tunnelling is used in homogeneous as well as heterogeneous ground conditions. Famous examples for EPB drives in very heterogeneous geological formation are BPNL Lyon with a 10,98 m diameter NFM machine (Bentz et al 1997) and Barcelona Metro L9 with a 12,06 m diameter Herrenknecht machine (Gabarró et al 2003). The soil distribution of these two projects is indicated in.

As a consequence of the soil heterogeneity, the TBMs cannot be designed for the optimum of a specific geology, but for the overall optimum (Rehm 2004). This implicates a compromise from the machine technology point of view which has to be optimized by using different soil conditioning agents. The 3 most important factors for soft ground tunnelling – apart from the hard rock geology – are the

- Soil permeability
- Ground water pressure
- Risk of clogging and adhesion

The soil permeability for EPB drives can reach values of up to $k = 10^{-3}$ for the most porous soils (BPNL Lyon, Turin) and comes down to practically impermeable clay (Heathrow T5).

The TBM drives in clay soil – either full face or mixed face – often face clogging and adhesion problems. In porous soils, the faced problems are very instable tunnel face, uncontrolled soil and water income as well as loss of face pressure through the soil. These problems were lately described for the Milan Metro project (Grandori et al 2003). Important for a successful TBM drive is the mechanical adaptation of the TBM itself including shield opening factor, number and choice of tools and finally the right soil conditioning with foams and polymers combined with a complete filled working chamber. The use of pure foams will not be successful.

Another important influence for the EPB drives in soft ground is the ground water pressure. The higher the water pressure, the more difficult to handle will be uncontrolled water ingress and subsequent settlement risk. From the machine technique point of view only few things can be done like very long screw conveyors, dual screws with intermediate water release or the installation of piston pumps after the screw conveyor. The most important and successful factor to control the water and the soil income is to fill the TBM working chamber completely with a homogeneous and impermeable soil paste by help of Foams and Polymers. Site examples are Botlek Tunnel and Aviles Sewage Tunnel as described in the literature (Fernandez et al 2002).



Figure 2. Clay clogging in Toulouse Line B Lot 2.

EPB drives in clay formations – either full face or mixed face – often run into clogging and adhesion problems: as it was the case in Toulouse. Even working in dry mode with compressed air in the working chamber resulted in huge problems.

Figure 2 shows how easily the cutterhead centre can be plugged, openings can be closed and cutterhead tools can be turned ineffective by clogging clay. The problem of clay clogging and adhesion will always lead to difficult TBM guiding, slow advance rates and extensive cleaning. From the machine technique point of view few things can be done like the design of an open cutterhead – especially in the centre – and well placed mixing devices in the working chamber. Again one of the most important factors to reduce successfully the clay clogging and adhesion is the use of highly effective Foams and/or special anti-clay Polymers. Site examples are Madrid MetroSur (MBT Online) and Roma 4 Venti (MBT Online) or Toulouse Metro as described in chapter 3.

2.1 *Foam*

The main demand of foam as a conditioning additive is to obtain the suitable rheology of the soil in order to build up and to maintain the necessary support pressure in the working chamber and to prevent high pressure variations. Foam incorporated in the earth paste has got the same effect as the big air bubble in slurry machines. The reduction of torque and abrasion are very important additional effects too. Foam is produced by turbulent mixing of a surfactant solution with air (Langmaack 2000).



Figure 3. Clay behaviour without and with anti-clay polymer.

The main surfactant properties are:

- fluidising effect on soils because of the decrease of surface tension. Soil particles are no longer bound to each other by linked water.
- electrostatic repulsion effect which can separate two particles attracting each other by electrostatic forces.

Laboratory tests as well as the site experience show, that often each soil type, from stiff clay to sandy gravel, requires more or less an own type of foam to reach its best effectiveness. The reduction of the angle of internal friction as well as the cohesion is important. In clay soil, the reduction of cohesion is one of the main tasks of foam. The type of surfactant used for a specific site has to be determined by preliminary laboratory tests with the original in situ type of soil.

Generally, the use of only foam reaches its limits when it comes to clay containing soil as well as soil with high porosity and low cohesion. In these cases, the dual use of foam and polymers is necessary, as described in chapter 2.2 and 2.3.

2.2 *Polymer for clay soils*

As indicated already in chapter 2.1, soil conditioning additives shall decrease the clogging and adhesion characteristics of clay soil. Therefore anti-clay polymers have to adsorb on the clay particle surface. They have to carry a high charge density to separate the soil particles and they should furthermore be able to create a steric barrier in order to avoid reagglomeration effects. These demands can be fulfilled by surfactants and anti-clay polymers, but anti-clay polymers are much more efficient.

Anti-clay agents are mainly used to support the destructuring properties of the foam, but they might be introduced without foam, too. Figure 3 illustrates the effect of those polymers in clay soil.

Using only foam and water, the clay particles agglomerate immediately and show extensive adhesion to metal surfaces (figure 3 left part or figure 2). Using a TBM in this mode, the cutterhead as well as the working chamber will get plugged. Only the additional use of anti-clay polymer results in separated clay lumps and decreases to a minimum their adhesion (figure 3 right part). A proper EPB mode with a reasonable TBM speed and regular maintenance work is only possible under these conditions.



Figure 4. Comparison of original pure dry porous soil and as homogeneous paste after mixing with foam and polymer.

2.3 *Polymer for porous soils*

In contrast to the anti-clay polymers, the polymers for porous soil have to create cohesion in order to obtain a pasty soil rheology. This was important for the partially existing sand strata at the TBM crown, preventing an uncontrolled inflow of sand or uncontrolled squeeze-out of foam.

A couple of polymers can be used in porous soils:

- water binding polymers
  to dry out (liquid) soils.
- soil structuring polymers
  which are useful in loose, coarse soils to change the soil rheology and which prevent sedimentation.
- foam stabilising polymers.

Some polymer developments are based on hydrocarbon chains and are produced by bacterial fermentation. These polymers are water soluble, biodegradable and compatible to the foam surfactants. Well designed, both of them are safe for the foaming generator and consequently they can be mixed with the foaming solution and pass through the foam generator. Polymers also induce a more stable support pressure in the working chamber during boring and when stopping the machine.

All polymers should preferably be in liquid form to avoid dosing problems and additional installation to get a solution or suspension out of the powder.

3 PROJECT TOULOUSE LINE B LOT 2

After the start on 5th August 2002, the TBM advanced slowly in the initial face. With in average 10 m of cover, the TBM had no general problems in zones of pure (full face) stiff & dry clay, but the numerous encountered sand lenses with pressurized water made the machine advance quite difficult. Despite the air pressurized working chamber, water and fine soil came into the TBM in an uncontrolled way, causing clogging & adhesion problems on the cutterhead (see figure 5), huge



Figure 5. Problems working in dry compressed air mode.

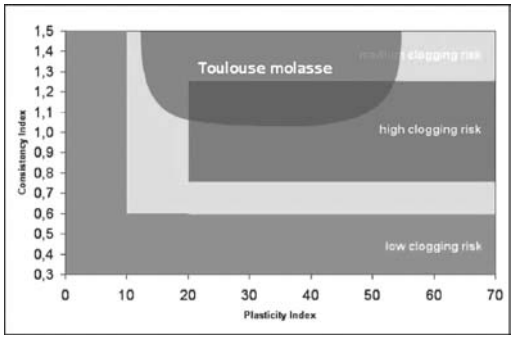


Figure 6. EPB mode (Babendererde 2003).

cleaning problems and last but not least causing doubts on abrasion, face stability and surface settlements.

The only way to successfully counterbalance the soil and water pressure on the tunnel face is a completely filled and pressurized TBM working chamber (Herrenknecht et al 2003, Steiner et al 1994). Therefore the soil must be treated during excavation with soil conditioning agents either separately or in combination:

- Foams
- Polymers for porous soil
- Polymers for clay soil

Their use enables filling of the TBM working chamber with excavated soil and reducing simultaneously the TBM torque and abrasion. No other modes of advance are suitable for instable, water bearing ground and sensitive surface areas as Babendererde 2003 has shown in figure 6.

In order to advance the TBM quickly and safely, the in-situ soil must be transformed into a non-adhesive and non-clogging soil paste in order to completely fill the working chamber and work in EPB mode.

This soil transformation called «soil conditioning» has to be pre-tested in laboratory scale in order to determine suitable products and their quantity.



Figure 7. Clogging soil in the laboratory.

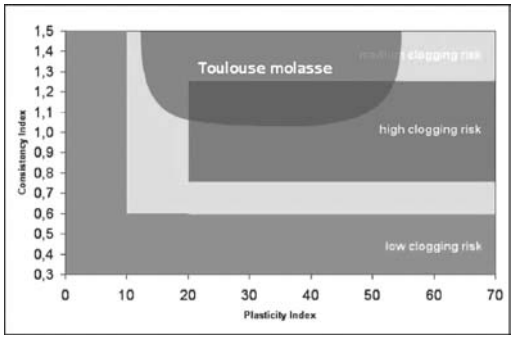


Figure 8. Clogging soil in the laboratory.

3.1 *Laboratory tests*

The first step in the laboratory is to reproduce the difficulties encountered on site. Therefore, original soil was used together with the soil conditioning systems originally used. The result is shown in figure 7, indicating quite well the difficulties encountered on site.

Scientifically, the clogging and adhesion capacity of the Toulouse molasses can be explained by their atterberg limits, showing a wide plasticity index between 15–55 combined with a high consistency index of >1 as indicated in figure 8 after Thewes 2004. In order to achieve the desired pasty and nonclogging soil rheology, numerous trials had been carried out. The best results were achieved with simultaneous addition of water, foam and Rheosoil® anti-clay agent. The result is shown in figure 9.

3.2 *EPB mode using SLF30 and Rheosoil®*

The soil conditioning concept determined in the laboratory had to be translated into the site system with a 6 line foam generator, serving 5 injection points on the cutterhead, 2 in the working chamber and 2 into the screw conveyor. An example of the TBM setting is shown in figure 10, demonstrating full EPB advance with 54 mm per minute and 2,6 bar medium earth pressure.



Figure 9. Correct EPB conditioning in the laboratory.

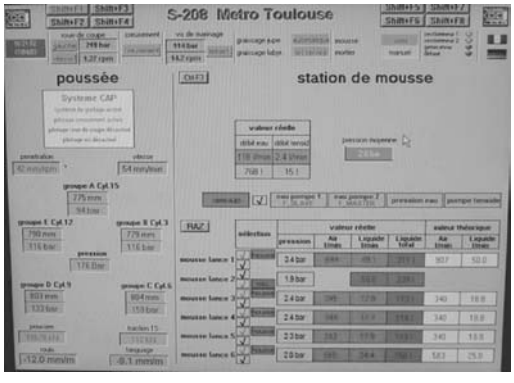


Figure 10. Foam generator screenshot.

The setting details were the following:

- Foam concentration SLF 30: 2–3%
- Expansion Ratio FER: 8
- Foam Injection Ratio FIR: 70% (+30% for the chamber)
- Rheosoil® 211: 0,8–1,0 kg/m^3 soil in situ
- Water (in case of dry soil): 5–20 m^3/ring

This soil conditioning system could be handled in a very flexible way:

- advancing with low torque and low abrasion values in compressed air mode, in case of homogeneous dry soil
- quick change to EPB advance with completely filled working chamber within minutes, in case of geology change

Figure 11 indicates the TBM parameters just after switching from air to earth pressure, mainly decreasing the pressure of the cutterhead centre (reducing the clogging risk). Graphs show also an increasing TBM speed with simultaneous decrease of torque values, indicating a highly efficient soil treatment. Figure 12 illustrates the soil conditioning quality, creating a plastic and non-clogging earth paste.

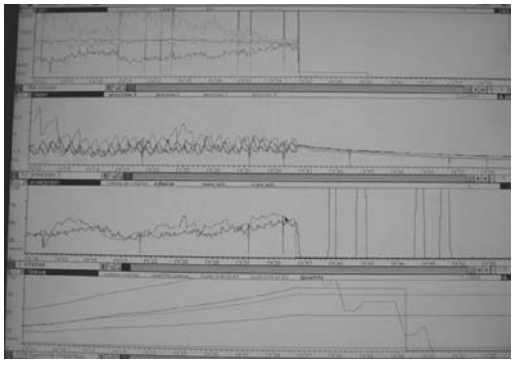


Figure 11. TBM data working EPB mode.



Figure 12. Plastic & non clogging excavated soil.

Once this soil conditioning concept was established, the TBM showed reasonable advance rates of 40– 50 mm/min also in the EPB mode, no water ingress occurred any more and the face support could be secured. Figure 13 shows the clean cutterhead after the TBM breakthrough.

3.3 *Sand strata above TBM*

From ring number 2758 onwards, a sand strata was located in the crown of the TBM and on top of it. In order to avoid uncontrolled sand flow-in, a polymer (MEYCO Fix SLF P2) enriched foam with structuring effects was injected into the TBM crown. This system turned out to be quite effective, but due to increasing sand strata and collapse risk it was decided to undertake surface injection with cement and silica gel in order to stabilize this geology (ring 3095–3120).

3.4 *Ecotoxicology*

In the beginning of the project, also ecotoxicological questions were raised concerning the landfill of the excavated soil (see figure 14).



Figure 13. Clean cutterhead after breakthrough.



Figure 14. Landfill of conditioned soil.

After switching to the BASF soil conditioning concept, all additives used including the anti-clay polymer passed a strict risk assessment study to ensure minimum impact on the workers and the environment. Neither during construction nor on the disposal sites negative influence of the soil conditioning additives could be observed.

The lixiviation data (1×24h, DIN 38-414 4) and following acute toxicity tests on Daphnids (NF EN ISO 6341) showed no dangerous potential of the treated soil from day 1 on. This enabled the contractor to avoid costly pre-stocking of the soil and to achieve a low general cost level for the landfill disposal.

4 CONCLUSION

As demonstrated by various site examples including Toulouse Metro Lot 2, it is possible to drive a TBM successfully and quickly through difficult geologies. In addition to the choice of a well adapted TBM machine, the use of the right soil conditioning additives is vital – for very permeable soil under ground water table as well as for clay rich soils with high clogging and adhesion potentials.

With an average daily TBM speed of 16,20 m and a significant best day advance of 37,80 m, the tunnel Lot 2 in Toulouse was finished within the foreseen time schedule with the final breakthrough on the 30th August 2004, 25 months after the start.

REFERENCES

Babendererde 2003 *TBM mit Slurry- oder Erddruckstützung – Einsatzbereiche und Zuverlässigkeitsanalyse* Felsbau 21 (2003), No.5, p. 155 ff

Bentz et al 1997 *Optimierung des schaumgestützten EPB-Vortriebs, Boulevard Périphérique Nord de Lyon* STUVA Tagung Berlin 1997, Alba Verlag Berlin, 1998, Volume 37, p. 88, ISBN 3 87094 636 9

Fernandez 2002 *Aviles Sewage Tunnel, a tunnel below sea water level* AFTES 2002 Toulouse, p. 131 ff, Specifique ISBN 951 04 16 2 4

Gabarró et al 2003 *Metro Barcelona Linea 9 – Europe's greatest metro project with tunnel boring machines of large diameter* ITA 2003 Amsterdam, p 637 ff, Balkema ISBN2: 90 5809 542 8

Grandori et al 2003 *Turin Metro Systems – Design and operation of EPB TBMs beyond the limits of this technology* Felsbau 21 (2003), No.6, p. 34 ff

Herrenknecht et al 2003 *Geotechnische und mechanische Interaktion beim Einsatz von Erddruckschilden im Fels* STUVA Tagung 2003, Dortmund, p. 175 ff, Bauverlag ISBN 3 7625 3602 3

Jancsecz et al 1999 *Advantages of soil Conditioning in shield tunneling: Experiences of LRTS Izmir* ITA 1999 Oslo, p. 865 ff., Balkema ISBN 90 5809 063 9

Langmaack 2000 *Advanced Technology of Soil Conditioning* North American Tunnelling Congress, Boston 2000, A.A. Balkema, Rotterdam, Brookfield, 2000, p. 525 ISBN 90 5809 162 7

Langmaack 2001 *Application of new TBM Additives* BAUMA 2001, 6th int. symposium for tunnel construction Verlag Glückauf GmbH, Essen, 2001, p. 27, ISBN 3 7739 5964 8

Langmaack 2004 *EPB-Vortrieb in inhomogenen Böden: Möglichkeiten neuer Konditionierungsmittel* Tunnel- und Tiefbautagung 2004, Györ, p. 121 ff

Marchionni et al 2002 *Galleria Quattro Venti in Rom* Tunnel No.8, 2002, p. 8 ff

MBT Online Madrid MetroSur www.degussa-ugc.com

MBT Online Roma 4 Venti www.degussa-ugc.com

Rehm 2004 *maschineller Tunnelvortrieb unter sehr schwierigen geologischen Verhältnissen* Tunnel- und Tiefbautagung 2004, Györ, p. 99 ff

Steiner et al 1994. *Face support for a large Mix - Shield in heterogeneous ground condition* Proc. of Tunnelling '94. London: Chapman & Hall

Thewes 2004 *Clogging risks for TBM drives in clay* Tunnels & Tunnelling International, June 2004, p. 28 ff

Underground Space – the 4th Dimension of Metropolises – Barták, Hrdina, Romancov & Zlámal (eds)
© 2007 Taylor & Francis Group, London, ISBN 978-0-415-40807-3

Upper bound solutions for tunnel face stability considering seepage and strength increase with depth

Jun Kyung Park, J. Tanner Blackburn, & Jae-Hun Ahn
Zachry Department of Civil Engineering, Texas A&M University, College Station, TX, USA

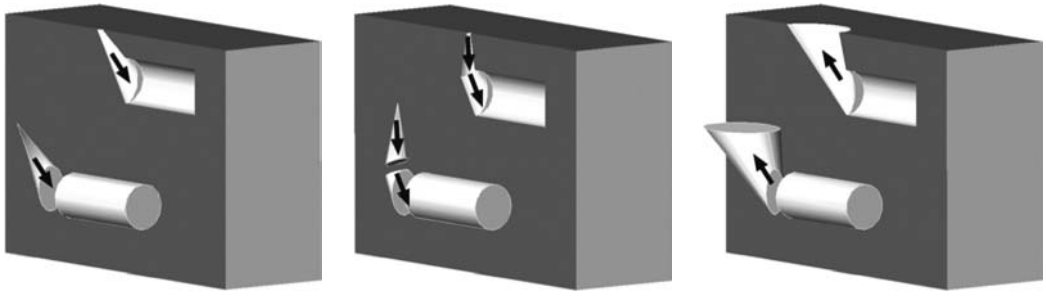
ABSTRACT: The upper bound method of limit analysis theory can be employed to calculate the active and passive limit pressures for maintaining tunnel face stability when using pressurized shield methods. The influence of seepage forces and depth-dependent effective cohesion was investigated for a dual-cone failure mechanism (MII, as defined by Leca et al., 1990), using the upper-bound method implemented by numerical analysis. The upper bound analytical derivation for depth-dependent effective cohesion and corresponding numerical results are presented and compared to those presented by previous authors. The analysis illustrated that the required face supporting pressure decreases when the depth-dependent rate in increase of effective cohesion increases. In addition, the numerical analysis demonstrated the influence of tunnel diameter on required face supporting pressure. Lastly, the upper bound limit analysis was employed to compare the relative importance of seepage force on cohesive and cohesionless materials, illustrating that the effect of seepage force is less prominent for cohesive materials.

1 INTRODUCTION

Face stability analyses are required to determine the proper pressure to be used for pressurized shield construction of shallow circular tunnels. Analytical, limit based methods have been developed (Atkinson et al., 1977; Davis et al., 1980) to calculate the optimum supporting pressure, which avoids face collapse (active failure) and surface 'blow-out' (passive failure).

Active failure of the tunnel face is caused by surcharge and self weight exceeding the frictional resistance and tunnel face pressure. Under passive conditions, the roles are reversed and the face pressure causes blow-out with resistance being provided by the surcharge, frictional resistance, and self-weight. Three failure mechanisms which involve the movement of solid conical blocks with circular cross sections, proposed by Leca et al. (1990), are shown in Figure 1. MI and MII failure mechanisms are single-cone and dual-cone systems, respectively; where the cones move into the excavation. An MIII failure mechanism is a single-cone, passive mechanism, where the cone moves outward to the surface.

In this paper, the MII collapse failure mechanism, which is most common failure pattern in shield tunneling (Chambon et al., 1994), is investigated by the upper-bound theorem. Recently, Lee et al. (2001) proposed that the seepage forces acting on the tunnel face under steady-state flow conditions should be considered if the tunnel is located under the groundwater table. However, general solutions which combine the



(a) M I (b) M II (c) M III

Figure 1. Failure mechanisms.

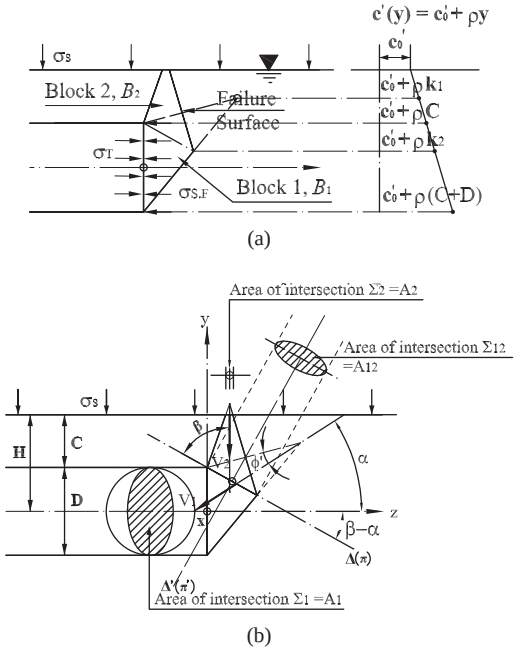


Figure 2. Collapse mechanism of tunnel face by the two conical blocks (modified from Lee et al., 2001).

depth-dependence of the effective cohesion (c′) of NC clays and the influence of seepage have not been reported.

In this paper, the influence of seepage forces and changes in shear strength with depth will be investigated for a Mohr-Coulomb material (c′, ϕ') based on the upper-bound method.

2 KINEMATIC APPROACH TO FACE STABILITY ANALYSIS BASED ON UPPER BOUND THEOREM

2.1 *MII failure mechanism geometry*

The MII active failure state can be idealized by considering a circular rigid tunnel of diameter (D) driven under a depth of cover (C) in soil with an effective cohesion (c′) increasing at rate, ρ with depth. A surcharge (σ_s) is applied at the ground surface and a constant retaining pressure (σ_T) is applied to the tunnel face.

Figure 2(a) shows a schematic cross-section of the MII failure mechanism geometry. Kinematically admissible failure mechanisms must be considered to obtain upper-bound solutions, initially developed by Leca et al. (1990). An MII failure occurs as two conical blocks move vertically and into the tunnel face, as shown in Figure 2(b). The two conical blocks consist of:

- **B_1**, a cone truncated by plane π, which is perpendicular to the page and represented as line $\Delta(\pi)$ in Figure 2(b)
- **B_2**, a cone corresponding to the removed, upper section of the cone B_1, mirrored about a plane π', such that the axis of B_2 is vertical. The mirror plane, π', is also perpendicular to the page and passes through the center of the ellipse created by the intersection between B1 and B2.

As such, the orientation of initial plane, π, is defined by the requirement that the axis of B_2 be oriented vertically and that π' pass through the center of the ellipse formed by the intersection of B_1 and B_2. Therefore, the MII failure mechanism geometry can be characterized by the angle of the axis of B_1 from horizontal, α, as shown in Figure 2(b).

For all three failure mechanisms, the intersection of the tunnel face and the adjacent block forms an ellipse, Σ_1, with a major axis length equal to $D/2$. For the MII failure mechanism, the intersection between blocks B_1 and B_2 is an ellipse, Σ_{12}, in plane π.

2.2 *Derivation of upper bound solutions*

This section summarizes the kinematic upper bound solutions to the MII failure mechanism, as originally reported by Leca, et al. (1990) and modified by Lee, et al. (2001). However, a new solution is derived to account for an increasing effective cohesion with depth.

The upper bound limit analysis solution is found by comparing the power of external applied loads, P_e, to the dissipation power caused by system movement, P_V. When the external power exceeds the dissipation power, an upper bound state exists. The following sections describe the derivations of the upper bound solution, as introduced by Leca et al. (1990), along with the modifications for increasing soil strength. The reader is referred to Leca et al. (1990) for additional geometric derivations.

2.2.1 *Dissipation power*

The dissipation power associated with the MII failure is calculated from the integration of plastic energy dissipation per unit area along block interfaces,

$$P_V = P_{1V} + P_{2V} + P_{12V}, \tag{1}$$

where P_{1V} is the contribution of the surface between B_1 and the surrounding soil, P_{2V} is the contribution of the surface between B_2 and surrounding soil and P_{12V} is the contribution of the interface between B_1 and B_2, represented as Σ_{12}. The dissipation is a function of the resistance along the interface surface and the block

velocity, therefore the dissipation power of the three interfaces are given as:

$$P_{1V} = \left(c_0{}' + [\rho y]_{y=k_1}^{y=C+D}\right) V_1 \cos\phi' \cdot S_{B1}, \tag{2}$$

$$P_{2V} = \left(c_0{}' + [\rho y]_{y=0}^{y=k_2}\right) V_2 \cos\phi' \cdot S_{B2}, \tag{3}$$

and

$$P_{12V} = \left(c_0{}' + [\rho y]_{y=c}^{y=k_2}\right) V_{12} \cos\phi' \cdot A_{12}, \tag{4}$$

where S_{B1} and S_{B2} are the perimeter surface areas of B_1 and B_2, respectively, A_{12} is the area of Σ_{12}, V_1 and V_2 are the velocities of B_1 and B_2, and V_{12} is the relative velocity between B_1 and B_2. Leca et al. (1990) derives the geometry of the surface areas and the velocity fields with the following equations:

$$S_{B1} = \frac{\pi D^2}{4}\left(R_A \frac{\cos\alpha}{\sin\phi'} - R_C R_D \cos(\alpha+\phi')\right), \tag{5}$$

$$S_{B2} = \frac{\pi D^2}{4}\left[R_C R_D \cos(\alpha+\phi') - \frac{\sin\phi'}{\cos^2\phi'} \cdot \left(\frac{\cos^2\phi'}{\sin\phi'}\frac{R_C{}^2}{\cos(\alpha+\phi')} - \frac{2C}{D}\right)^2\right], \tag{6}$$

$$A_{12} = \frac{\pi D^2}{4}\frac{\cos^2(\alpha+\phi')}{\cos\phi'}\frac{\sqrt{\sin(\beta-\phi')}}{[\sin(\beta+\phi')]^{3/2}}, \tag{7}$$

$$V_1 = \frac{\sin(\beta+\phi')}{\sin(\beta-\phi')}V_2, \tag{8}$$

$$V_{12} = \frac{\cos\alpha}{\sin(\beta-\phi')}V_2. \tag{9}$$

where R_A, R_C, and R_D are simplified geometric coefficients, introduced by Leca et al. (1990):

$$R_A = \frac{[\cos(\alpha-\phi')\cos(\alpha+\phi')]^{\frac{1}{2}}}{\cos\phi'}, \tag{10}$$

$$R_C = \frac{\cos(\alpha+\phi')}{\cos\phi'}\left[\frac{\sin(\beta-\phi')}{\sin(\beta+\phi')}\right]^{\frac{1}{2}}, \tag{11}$$

$$R_D = \frac{\sin\beta}{\sin\phi'\sin(\beta+\phi')}. \tag{12}$$

β is the angle between the intersection of B_1 and B_2 and vertical, and can be shown as:

$$\beta = 45° + \frac{\alpha}{2}, \tag{13}$$

2.2.2 *Power of external loads*

The power of the external loads, P_e, can be calculated as

$$P_e = P_T + P_S + P_\gamma + P_{S.F.}, \tag{14}$$

where,

$$P_T = -\sigma_T V_1 \cos\alpha A_1, \tag{15}$$

$$P_S = \sigma_S V_2 A_2, \tag{16}$$

$$P_\gamma = \gamma V_1 \sin\alpha V_{B1} + \gamma V_2 V_{B2}, \text{ and} \tag{17}$$

$$P_{S.F.} = \sigma_{S.F.}\frac{\pi D^2}{4}\frac{R_A}{R_C{}^2}\frac{\cos\alpha\cos^2(\alpha+\phi')}{\cos^2\phi'}. \tag{18}$$

P_T is the power of the tunnel face pressure(σ_T), P_S is the power of the surcharge(σ_s), P_γ is the power of the soil unit weight(γ), and $P_{S.F.}$ is the power of seepage force. The contact areas A_1 and A_2 correspond to the surface Σ_1 and the area of the intersection between the B_2 and the ground surface, respectively. The areas are defined as:

$$A_1 = \frac{\pi D^2}{4}\frac{\sqrt{\cos(\alpha-\phi')\cos(\alpha+\phi')}}{\cos\phi'}, \tag{19}$$

$$A_2 = \frac{\pi D^2}{4}\left[\frac{\sin\beta\cos\alpha}{\sin\phi'\sin(\beta+\phi')} - \left(\frac{2C}{D}+1\right)\right]^2 \tan^2\phi'. \tag{20}$$

The soil unit weight component of the external power depends on the volume of the failure blocks, V_{B1} and V_{B2}, which are given as:

$$V_{B1} = \frac{\pi D^3}{12}\left(R_A R_B - R_C{}^3\frac{\cos\phi'}{2\sin\phi'}\right), \tag{21}$$

$$V_{B2} = \frac{\pi D^3}{12}\left[R_C{}^3\frac{\cos\phi'}{2\sin\phi'} - \frac{\sin^2\phi'}{2\cos^2\phi'} \cdot \left(\frac{\cos^2\phi'}{\sin\phi'}\frac{R_C{}^2}{\cos(\alpha+\phi')} - \frac{2C}{D}\right)^3\right], \tag{22}$$

where R_A and R_C are given in equations (10) and (11) and R_B is defined as:

$$R_B = \frac{\cos(\alpha-\phi')\cos(\alpha+\phi')}{\sin(2\phi')}. \tag{23}$$

2.2.3 *Upper bound theorem*

Using the upper bound theorem, an MII failure mechanism will be avoided if the external power is below the dissipative power, shown as:

$$P_e \leq P_V \tag{24}$$

Substitution of equations (1) through (23) into equation (24) will give an upper bound solution in the following form:

$$N_S Q_S + N_\gamma Q_\gamma \le Q_T + \frac{\sin\phi'}{\cos\alpha}\frac{R_F \cdot R_c^2}{R_A}. \quad (25)$$

The three loading parameters (Q_S,Q_T,Q_γ) and the coefficients (N_S,N_γ) are given in equations (26)–(30) as defined by Leca et al. (1990) and Lee et al. (2001). A new parameter (R_F) is introduced which accounts for the increase in soil effective cohesion, and is given in equation (32):

$$Q_S = (K_p - 1)\frac{\sigma_S}{\sigma_C} + 1, \quad (26)$$

$$Q_T = (K_p - 1)\frac{\sigma_T - \sigma_{S.F}}{\sigma_C} + 1, \quad (27)$$

$$Q_\gamma = (K_p - 1)\frac{\gamma D}{\sigma_C}, \quad (28)$$

$$N_S = \frac{1}{\cos\alpha\cos^2\phi'}\frac{\sin(\beta-\phi')}{\sin(\beta+\phi')}\frac{{R_E}^2}{R_A}, \quad (29)$$

$$N_\gamma = \frac{1}{3}\left[\begin{array}{l}\tan\alpha R_B + \dfrac{\cos\phi'\cos(\beta+\phi')}{2\sin\phi'\sin(\beta+\phi')}\dfrac{{R_C}^3}{R_A} \\ -\dfrac{1}{2\sin\phi'\cos\alpha\cos^2\phi'}\dfrac{\sin(\beta-\phi')}{\sin(\beta+\phi')}\dfrac{{R_E}^3}{R_A}\end{array}\right], \quad (30)$$

$$R_E = \frac{\cos^2\phi'}{\cos(\alpha+\varphi')}R_C - \frac{2C}{D}\sin\phi', \quad (31)$$

$$R_F = \cos\phi'\cdot\left\{\begin{array}{l}\left[\dfrac{\cos\alpha}{\sin\phi'}\dfrac{R_A}{{R_C}^2} - \cos(\alpha+\phi')\dfrac{R_D}{R_C}\right]\rho(C+D-k_1)+ \\ \left[\dfrac{\cos^2\phi' R_C R_D}{\cos(\alpha+\phi')} - \dfrac{{R_E}^2}{\sin\phi'\cos^2(\alpha+\phi')}\right]\rho(k_2)+ \\ \left[\dfrac{2\cos\beta\sin 2\phi'\cos(\alpha+\phi')}{\sin\beta}\cdot\dfrac{{R_D}^2}{R_C}\right]\rho(k_2-C)\end{array}\right\}, \quad (32)$$

where, σ_c is the unconfined compression strength, K_p is the Rankine passive earth pressure coefficient, $\sigma_{S.F.}$ is the seepage pressure acting on the tunnel face, γ is the unit weight of the soil, D is the tunnel diameter, k_1 is the apex of block 1 (B_1), and k_2 is the lowest point of the intersection between B_1 and B_2.

Relation (32) provides the best upper bound associated with an MII failure mechanism when N_s and N_γ are maximized by optimizing α.

The parameters Q_S and Q_γ are imposed geometric and loading conditions, and the supporting pressure σ_T should be chosen such that failure of the tunnel during construction is prevented. The selection of supporting pressure corresponds to:

$$Q_T = N_S Q_S + N_\gamma Q_\gamma - \frac{\sin\phi'}{\cos\alpha}\frac{R_F \cdot R_c^2}{R_A}. \quad (33)$$

which can be rewritten, after substitution, as:

$$\left[(K_P - 1)\frac{\sigma_T - \sigma_{S.F.}}{\sigma_C}\right] = N_S Q_S + N_\gamma Q_\gamma - \frac{\sin\phi'}{\cos\alpha}\frac{R_F {R_C}^2}{R_A} - 1, \quad (34)$$

$$\sigma_T = \frac{\left[N_S Q_S + N_\gamma Q_\gamma - \dfrac{\sin\phi'}{\cos\alpha}\dfrac{R_F {R_C}^2}{R_A} - 1\right]\sigma_C + \sigma_{S.F.}}{(K_P - 1)}. \quad (35)$$

The parameters in equations (33)–(35) correspond to geometry and Mohr-Coulomb soil properties except for the seepage pressure acting on the tunnel face. To calculate the seepage pressures acting on the tunnel face, the failure surface must be pre-determined from the limit analysis. Given this failure surface, seepage pressures acting on the tunnel face can be obtained from the difference of total head between the tunnel face and the failure surface. The average predicted seepage pressure has been calculated using numerical analyses by Lee et al. (2003). The analysis conducted by Lee et al. (2003) demonstrated that seepage force seriously affects tunnel face stability, but effective overburden pressure is reduced slightly by the arching effect during tunnel excavation, the seepage pressure remains the same.

The variation of the effective cohesion (c′) of NC clays with depth has not been included in previous numerical analyses and model tests. However, the seepage analysis results will not change due to added cohesion, because the hydraulic head will be the same. Therefore, the seepage analysis results reported by Lee et al. (2003) were employed for the calculation of upper bound supporting pressure (σ_T) in this research.

3 CASE STUDY OF TUNNEL FACE STABILITY

The optimal upper bound solution that accounted for the influence of seepage force and the depth-dependence of effective cohesion (c′) of NC clays was calculated using a spread sheet program created for this research.

As shown in Figure 3, when the depth-dependent rate of change (represented as ρ) of effective cohesion increases, the required face supporting pressure decreases. A value of $\rho = 0$ corresponds to a homogenous soil, with constant cohesion. In Figure 3, negative supporting pressure values indicate that additional face supporting pressure is unnecessary. In this case, the surcharge (σ_s) will have very little influence on face collapse because the tunnel is deep enough ($C/D = 2$). This is because the results of failure shape and support pressure have the same values when the depth ratio (C/D) was greater than 0.2 as shown in Figure 4.

Figure 5 shows the required face supporting pressure as a function of tunnel diameter and effective cohesion. As the tunnel diameter increases, the

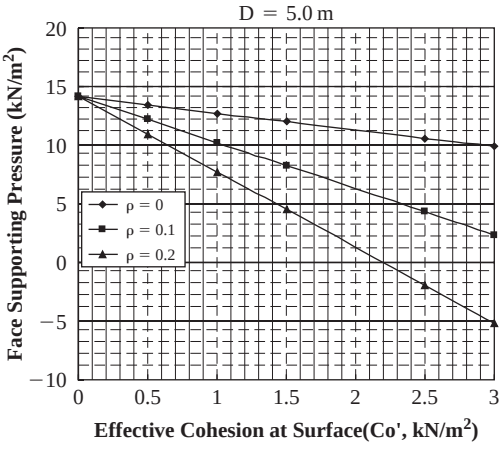


Figure 3. Change of support pressure with variation of the rate of change of c′ with depth (In case of $\phi' = 35°$, $\gamma = 15.2(\text{kN/m}^3)$, C = 10 m, Water Level (Hw = 5 m), D = 5 m).

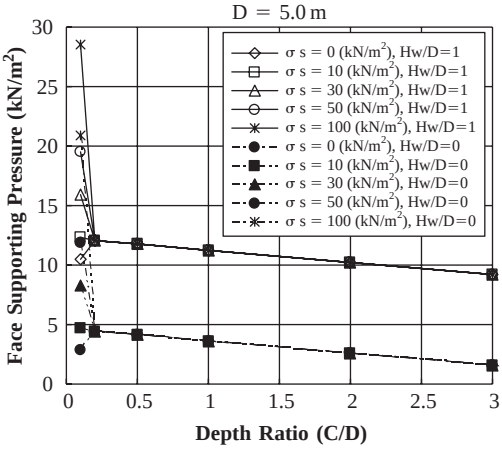


Figure 4. Change of support pressure with variation of surcharge (σ_s) and depth ratio (C/D) (In case of $\phi' = 35°$, $\gamma = 15.2(\text{kN/m}^3)$, $\rho = 0.1$ (kN/m^2/m), $c'_o = 1$ (kN/m^2)).

required face supporting pressure will also increase. Even if the failure happens in the very shallow depth when depth ratio is larger than 0.2, the effect of surcharge (σ_S) is very small compared to the changes in the required supporting pressure by other parameters such as tunnel diameter, cover depth, effective cohesion as previously shown in Figure 4.

4 COMPARISON WITH OTHER PREVIOUS RESEARCH RESULTS

The relationship between groundwater depth, tunnel depth, tunnel diameter, and required tunnel support

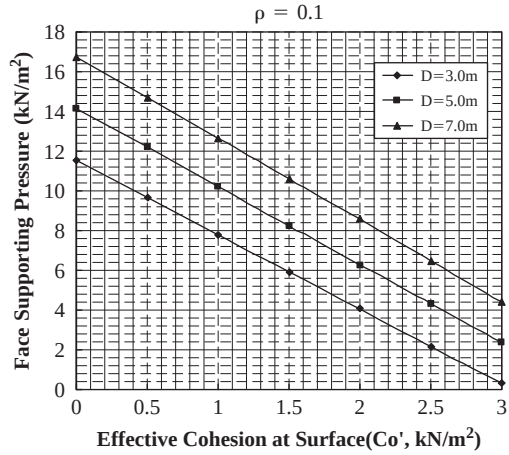


Figure 5. Change of support pressure with variation of tunnel diameter (D) (In case of $\phi' = 35°$, $\gamma = 15.2(\text{kN/m}^3)$, C = 10 m, Water Level (Hw = 5 m), $\rho = 0.1$ (kN/m^2/m)).

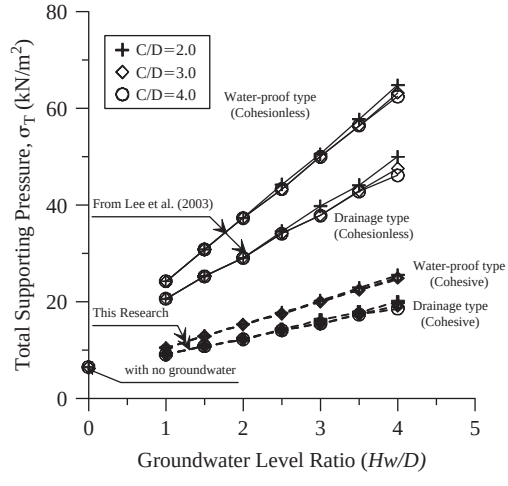


Figure 6. Change of support pressure with variation of the Hw/D.

pressure for a sand and an NC clay material is shown in Figure 6. The cohesionless sand results are those reported by Lee et al. (2003) ($\phi' = 35°$, $c' = 0$). The cohesive material results were computed using the spreadsheet, based on the derivation described herein ($c'_o = 10\,\text{kN/m}^2$, $\phi' = 35°$, $\rho = 0.5\,\text{kN/m}^2\text{/m}$).

Figure 6 illustrates the large influence of groundwater conditions on required tunnel face supporting pressure for both soil types and for drained and waterproof tunnel construction methods. Although, the influence of seepage pressure on the upper bound required supporting pressure is less for an NC clay material, this effect must be considered for this material type.

5 CONCLUSIONS

In this study, an upper bound solution that will address both the influence of seepage forces in front of tunnel face and the depth-dependence of effective cohesion was derived for the collapse failure mechanism (MII). A spreadsheet program was developed to investigate the influence of seepage forces and changes in cohesion for a general Mohr-Coulomb material (c', ϕ') based on the upper-bound method with an assumed seepage pressure. The new upper bound solution was used to calculate the effective support pressure in steady-state groundwater flow condition. The results of this study lead to the following conclusions.

- When the depth-dependent rate (ρ) of change of effective cohesion (c') increases, the required face supporting pressure will decrease. Negative supporting pressures indicated that, in some cases, no additional face support pressure is necessary.
- As the tunnel diameter increases, the required face supporting pressure will also increase.
- The surcharge (σ_S) will have very little influence on face collapse when the depth ratio (C/D) is larger than 0.2. Even if the failure happens in the very shallow depth, the effect of surcharge (σ_S) is very small compared to the changes in the required supporting pressure by other parameters such as tunnel diameter, cover depth, effective cohesion.
- Seepage force is a key factor for maintaining stability of the tunnel face in non-cohesive material as mentioned by Lee et al. (2001). However, the effect of seepage pressures on the upper bound supporting pressure (σ_T) is decreased in a cohesive material. This difference implies that this effect should be considered in weathered soil having both c' and ϕ' properties.

REFERENCES

Atkinson, J.H. & Potts, D.M. 1977. Stability of a shallow circular tunnel in cohesionless soil. *Geotechnique* 27(2): 203–215.

Chambon, P. & Corte, J.-F. 1994. Shallow tunnels in cohesionless soil: stability of tunnel face. *Journal of Geotechnical Engineering; ASCE* 120(7): 1148–1165.

Davis, E.H. 1973. The effect of increasing strength with depth on the bearing capacity of clays. *Geotechnique* 23(4): 551–563.

Davis, E.H., Gunn, M.J., Mair, R.J. & Seneviratne, H.N. 1980. The stability of shallow tunnels and underground openings in cohesive material. *Geotechnique* 30(4): 397–416.

Leca, E. & Dormieux, L. 1990. Upper and lower bound solutions for the face stability of shallow circular tunnels in frictional material. *Geotechnique* 40(4): 581–606.

Lee, I.M. & Nam, S.W. 2001. The study of seepage forces acting on the tunnel lining and tunnel face in shallow tunnels. *Tunnelling and Underground Space Technology* 16(1): 31–40.

Lee, I.M. Nam, S.W. & Ahn, J.H. 2003. Effect of seepage forces on tunnel face stability. *Canadian Geotechnical Journal* 40(2): 342–350.

Underground Space – the 4th Dimension of Metropolises – Barták, Hrdina, Romancov & Zlámal (eds)
© 2007 Taylor & Francis Group, London, ISBN 978-0-415-40807-3

Gotthard Base Tunnel: Work progress at the five construction sections

M. Rehbock-Sander & A. Gerdes
Amberg Engineering Ltd., Regensdorf-Watt, Switzerland

ABSTRACT: The 57 km long Gotthard Base Tunnel (GBT) is scheduled to be opened in the year 2015, the preparatory work started in 1996. When completed the GBT will be the longest railway tunnel in the world. This paper gives an overview on the five construction sections of the tunnel and shows the status of work of each. The overcome of the problems with the blocked tunnel boring machine (TBM) in Amsteg, the successfully applied yielding rock support in Sedrun and Faido and the occurred rock burst phenomena in Faido are described in more detail.

1 GOTTHARD BASE TUNNEL – OVERVIEW

1.1 *General*

Today modern traffic infrastructures have to ensure faster and more reliable connections. Switzerland's New Alpine Transversal (NEAT) will provide a high-speed rail link for passenger and freight trains passing through the Alps between northern and southern Europe. It will enable much of the traffic to be shifted from road to rail. There are two NEAT lines: the Lötschberg axis in the west and the Gotthard axis in the east.

The heart of the Gotthard axis is the 57 km long GBT. The initial preparatory work for the Base Tunnel started in 1996, it is scheduled to be opened in the year 2015. After completion, the GBT will be the world's longest railway tunnel.

1.2 *Design*

The GBT is designed to handle high speed passenger trains travelling at speeds of up to 250 km/h and freight trains travelling at up to 160 km/h. This will be achieved with an alignment with a minimum radius of 5,000 m and a maximum slope of 1%. It will have an elevation of approx. 500–550 meters above sea level and a maximum overburden of approx. 2,300 m.

The GBT stretches from Erstfeld in the north to Bodio in the south. It consists of two parallel single track tubes with a diameter varying from 9.0–9.5 m, which are linked by cross-passages every approx. 300 m. Multifunction stations (MFS) are located at two locations one-third and two-thirds along the length of the tunnel. These will be utilized for the diversion of trains to the other tube via crossover tunnels, to house technical – infrastructure and equipment, and as a emergencystation for the evacuation of passengers.

To shorten construction time and for ventilation purposes, the tunnel has been devided into five sections and will be excavated from several sites simultaneously. Excavation will take place from the portals as well as from three intermediate attacks, by access tunnels in Amsteg and Faido and by two vertical shafts in Sedrun (Fig. 1).

1.3 *Geological conditions*

From north to south, the Gotthard Base Tunnel passes through mostly crystalline rock, the massifs which are interrupted by narrow sedimentary tectonic zones. The three crystalline rock sections include the Aare massif to the north, the Gotthard massif and the Pennine gneiss zone to the south (Fig. 2). These massifs consist mainly of high strength igneous and metamorphic rock. More than 90% of the total tunnel length consists of these types of rock.

The most difficult section of the new tunnel from the viewpoint of geology is expected to be the (old crystalline) Tavetsch intermediate sub-massif (TZM) in the Sedrun section, located between the Aar-massif and the Gotthard-massif. Beneath this section there are about 90 different isolated short fault zones along the 57 km.

The Tavetsch intermediate massif consists of a steeply-inclined, sandwich-like sequence of soft and hard rock.

The initial planning phases concentrated – beneath other aspects – on aligning the tunnel through the various fractured zones at their narrowest points wherever possible.

The high mountain overburden of up to 2,300 m means that rock temperatures in the tunnel can reach

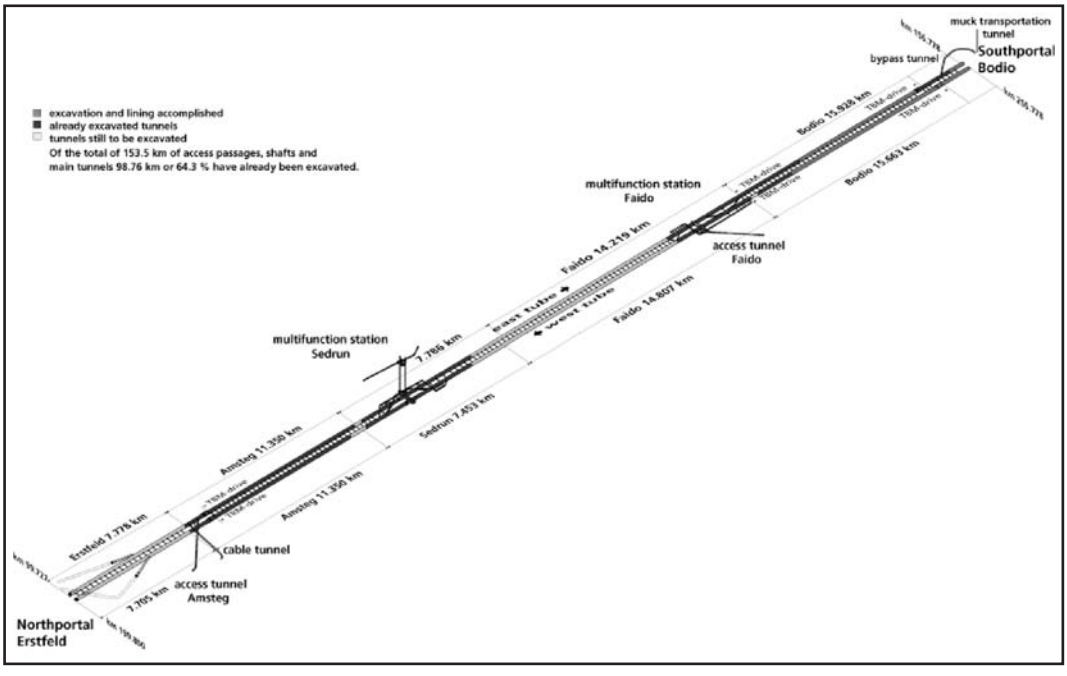


Figure 1. System of the GBt and construction status as of September 2006.

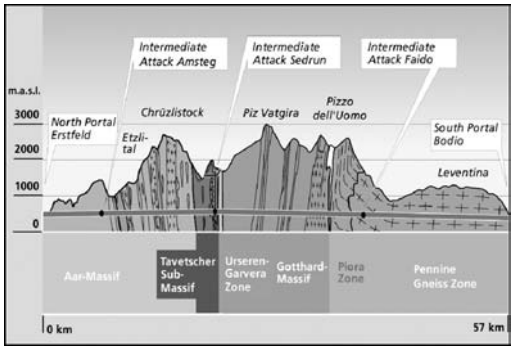


Figure 2. Longitudinal geological profile of the GBT.

more than 50–55°C. In order to maintain the required air temperature in the various working areas, an air conditioning system is required.

2 THE FIVE CONSTRUCTION SECTIONS

2.1 *Erstfeld*

Preparatory work started at the north portal at Erstfeld in July 2004.

The works for the construction lot Erstfeld contain the driving of the two single-track tubes of the 7.8 km long section from Erstfeld to Amsteg, the excavation of the 23 connecting galleries and the construction of an underground fork. The work contract is not yet awarded. This will happen in 2007.

2.2 *Amsteg*

In Amsteg, the heading of a 2 km long horizontal access adit to the GBT along with construction of the processing plant and conveyor belt equipment for muck removal began in December 1999.

In autumn 2003, the two tunnel boring machines (TBM) in the Amsteg section with a diameter of 9.58 meters each, were installed in underground assembly caverns. In April 2004, the first zone predicted to contain difficult geological conditions (Intschi Zone) was penetrated successfully and without the expected time delays.

The muck is transported with conveyor belts from the back-up of the TBM to the material processing plant on the construction site, where a part of it is recycled to produce concrete aggregates. Tunnel trains only provide transportation of rock support materials, concrete, miners, staff members, and some visitors. The rest of the muck from the Amsteg and Erstfeld sections will be transported by rail and boat to the nearby Reuss river mouth , where it will be used for restoration of the natural conditions of the river delta.



Figure 3. Restart of Gabi II.

In June 2005, the Amsteg tunnellers came across a fault zone with hydrothermally influenced rock below the Chrüzlistock mountain. The TBM in the eastern tube, Gabi I, penetrated this roughly 50 m long zone without any problem. The TBM Gabi II in the western tube, however, was brought to a halt, as a mix of loosened rock and groundwater flooded the cutterhead. In order to ensure Gabi II could function properly again, the soft area in front of the machine's cutterhead was consolidated with cement via a 15 m long grouting gallery from the parallel running eastern tube. At the same time, a 50 m long gallery leading to the western tube was excavated from the eastern tube, and the TBM's cutterhead subsequently exposed by November 15th, 2005. Thanks to the counter-drive, it was possible for Gabi II to resume excavation in the western tube towards Sedrun (Fig. 3).

In mid-June 2006, Gabi I reached the Sedrun section in the eastern tube nine months ahead of schedule. The tunnellers of Amsteg and of Sedrun are separated by only 700 m of rock mass. This rock, where in some places highly squeezing conditions prevail, will be excavated mainly from the Sedrun side. Breakthrough is expected by summer 2008. The TBM Gabi II is expected to reach Sedrun by the end of 2006.

In the coming months, Gabi I will be completely dismantled underground, and its individual parts then transported out of the tunnel by the service train.

2.3 *Sedrun*

Sedrun is the most complex section of the base tunnel due to logistical and geological reasons. The adit (1 km), the inclined ventilation shaft (450 m), the cavern at the top of the first shaft and the 835 m-deep vertical access shaft were completed in several preparatory construction lots since 1996. The entire logistic supply for the heading of a total tunnel length of 2×6.8 km (four simultaneous tunnel drives, together with others minor drives) has to be conducted through the access tunnel and the double shaft system. Up to 6,000 tonnes of excavated material have to be handled every day. Shaft drives were installed for a double floor hoisting cage with a 5 MW rating, providing a 60 km/h hoisting speed for an 80 t load.

Because of the complex geological conditions, different auxiliary support measures are to be applied during excavation, e.g. investigations ahead of the tunnel face with geophysical systems and/or percussion and core probe drillings. The drillings must be preventer-protected against water inflow and debris under high pressure. In the GBT Sedrun, for example, the core drilling rigs must be equipped to water pressure strikes as high as 200 bar. The triple preventer systems used offer three independent systems. If water under high pressure is struck unexpectedly, the drilling rod can be clamped (pipe ram) or even cut off (shear preventer). The third system, Roto Pac, makes it possible to keep on drilling even in zones with high water pressure. This preventer technology was developed for the oil and gas drilling industry.

In the TZM since May 2005 both tubes were driven in squeezing rock. With regard to deformations, the geotechnical behaviour of the kakiritic gneisses and slates encountered turned out to match the forecast. Some 30 m behind the face the deformations converge. Here the first shotcrete lining is applied and the flexible lining changes to the resitance principle. The friability is extremely high in some areas. In this regard, the influence of the strike of the layers vis-à-vis the tunnel axis is of major significance. In the case of vertical and perpendicular layers towards the tunnel axis there is a higher need for supporting the face (shotcrete with net reinforcement, excavation in stages, and installation of spiles), whereas in the case of flat lying layers, the danger at the edge of the excavation is increased. All situations occurring so far have been mastered by adapting the means of support and the length of advance.

The deformations in squeezing rock occur radially at the anticipated average magnitudes of 20 to 80 cm. The deformations in the cross section can occur in a very different manner (asymmetrical deformations). These asymmetrical deformations are reacted by corresponding additional supports (grouted anchors).

Rates of advance in TZM North have increased since the start of drives after the learning phase of the contractor had set in relation to the various excavation phases and the optimisation of construction measures. Apart from these phases, optimisations also concerned project aspects such as adapting the length of advance, the spacing between steel arches and the application of spiles.

To counter the immense rock pressure, Alp Transit Gotthard Ltd. and the Engineering Joint Venture have pioneered a new method of tunnel construction for this kind of deep tunnels. Two steel rings are

installed, one inside the other. Each of the two rings is composed of eight segments which are connected together by slightly compressible joints. When the rock pressure starts to take effect, the rings slowly close in on themselves until the maximum supporting force is reached.

This technology is used in German coal mines, but nowhere in the world has it ever before been applied with these dimensions. The system has proved itself in recent months: driving is within budget and on schedule from the clients point of view.

The cross section of the single tubes increases from about 80 m^2 up to more than 130 m^2. The installed steel mining arches have the capacity to deform to the permissible 80 cm radial deformations as planned. The large -in some cases asymmetrical -deformations that occur have so far been mastered thanks to the proposed supporting measures.

The southern drives in both tunnel tubes in the Gotthard Massif gneisses have been undertaken by means of highly mechanized excavation and transport installations with drill and blast since spring 2005. The driving operations for both single-track tunnels are more than 6 months ahead of schedule as compared with the contract construction program. This is due to the technically easier penetration of the Urseren Garvera Zone, which was tackled prior to entering the Gotthard Massif in summer 2005. Further driving operations will run until the middle/end of 2008 towards the north and south. Starting in the second half of 2006, vault supporting work in the core area of the MFS will commence in the tunnel change-over enlargements followed by the lining operations for the adjoining single-track tubes. Emergency stations follow in the first quarter of 2007.

An interesting project to be mentioned for the section Sedrun is the project "Porta Alpina". During the operation of the Gotthard Tunnel the Porta Alpina intends to use the MFS Sedun as an underground train station which allows passengers to leave the train. From there the passengers can reach the 800 higher village Sedrun and the Gotthard region by using lifts. The Alp Transit Gotthard has awarded the order for the preparatory construction works. The costs of this project are estimated to be about 50 Million CHF.

2.4 *Faido*

In Faido, the GBT is accessed up via a 2.7 km long sloped tunnel (declination of 12.7%). Construction of this tunnel began in December 1999 and was constructed by conventional drill and blast methods. Close to the access tunnel portal, extensive material processing plants for recycling of a part of the muck and for the production of concrete aggregates as well as conveyor belt systems for the transportation of debris were installed. A 5 km long conveyor belt transports the muck for permanent disposal in an old quarry.



Figure 4. Breakthrough MFS Faido, September 2006.

The contract for the main lot has been awarded in combination with the southern Bodio section at a sum of 1.1 billion US$.

The first tunnel boring machine (TBM) in the Gotthard Base Tunnel started out in the east single-track tunnel from Bodio in November 2002. Two months later, the second TBM started driving in the west tunnel. A number of different geological zones had to be overcome along the approximately 15 km route to the multifunction station at Faido.

In September an important milestone was reached in Faido: the first breakthrough by a tunnel boring machine was done (Fig. 4).

It took place with the expected precision. Continuous measurements showed that the specified accuracy was maintained along the entire length of the drive. At breakthrough, the deviation of the TBM was only 2 cm vertically and 5 cm horizontally.

2.4.1 *Fault zones in the MFS Faido*

The MFS Faido lies at the end of the Faido access tunnel. It consists of the two tunnel tubes that are connected with each other by two tunnel crossovers in the MFS, the cross cavern for housing the railway infrastructure equipment, the cross-cuts required for construction operations, the cavern for handling logistics in the construction phase, the two emergency train stops that are connected by side galleries, and a ventilation tunnel system.

Altogether there are about 6 km of tunnels and galleries with cross-sectional areas ranging from 40 m^2 to more than 300 m^2.

The MFS Faido was planned according to the geological prediction of favourable rock conditions. The different types of galleries, tunnels and caverns are excavated by drill and blast.

In summer 2002 an intensive fault zone was tunnelled into unexpectedly. It passes through the large caverns of the multifunctional station at a very acute angle. An intensive investigation program was carried

out to define the best location of the large cross over caverns with cross sections up to 260 m^2. An intensive investigation program was carried out. The risk of constructing the large cross-section in the middle of a fault zone was judged to be too high. Based on the results of these investigations, it was decided to adapt the layout of the MFS Faido with the aim of placing the large caverns in good rock conditions in the southern part.

Besides the layout of the MFS the geology encountered also made it necessary to carry out a critical review of excavation support means to be applied in the relevant cross-sections.

In the meantime in the MFS Faido a yielding support system with steel arches with friction clutches and convergency slits is being used successfully (Fig. 5). This yielding arches allow deformations of the ground (principle of yielding). Depending on the result of deformation the slits are filled with shotcrete and the support system becomes rigid (principle of resistance). Additionally to the steel arches different other support elements are applied and they are adapted according to the requirements of the heading. At the MFS Faido the yielding steel arches in addition with staggered anchoring and shotcrete are being applied. The launched task force interpreted the geological conditions encountered as a combination of loosening and squeezing behaviour. Currently the overall rock support system is always adapted and optimised based on the geotechnical computations, the continuous observations of geology on site and the experiences (observations, measurements) from the last excavation steps.



Figure 5. Yielding steel support with convergency slits.



Figure 6. Rock burst in the MFS Faido, June 2005.

2.4.2 *Rock burst phenomena in the MFS Faido*

The excavation of cavities associated with mining and tunneling works lead to the disturbance of the primary stress conditions of rock. Redistributions of stress result in some cases to stress concentrations which exceed the material strength. A rock burst is the immediate failure of the rock under which large amount of stored energy is released. In hard rock tunnelling and mining as a rule, as the compactness of rock and overburden increases, the probability of rock bursts increases. Rock bursts are extremely difficult to predict or to prevent. In order to ensure occupational safety at tunnelling sites, steps must be taken to predict as much as possible the probability of rock bursts and to minimize their effects upon workers and the structure.

During construction of the Faido MFS frequent and often massive rock bursts or rock burst phenomena have occurred since March 2004. According to geologic prognosis and the above described phenomena of rock bursts in hard rock tunnels, rock bursts are to be expected in the massive gneiss of the Gotthard Massif. In the layered, highly faulted gneiss of the MFS Faido, these phenomena were not expected.

An extremely heterogeneous geology is present and could be regarded as a possible cause. Hard, brittle Leventina gneisses are situated next to more ductile Lucomagno gneisses. Through the nearly parallel orientation of the tunnel axis and the fragmented Lucomagno-gneisses, narrow rock wedges of Leventina-gneiss are locally formed. These competent wedges take on loads from the Lucomagno-gneiss which causes local stress concentrations that increase as excavation proceeds. At the same time the incompetent sections of Lucomagno-gneiss are prevented from unhindered pressure relief by the competent Leventina-gneiss. Stress concentrations in the Leventina-gneiss can lead to loads which exceed the rock strength accompanied by rock burst-type pressure release.

A prognosis of the rock burst risk was undertaken along with the envisioned measures for the entire MFS Faido. A rock burst information sheet and lists of progressive measures have been prepared. Specific dangers and the necessary actions are being determined in advance and are continually adapted as new knowledge is obtained during tunnelling operations.

In addition, excavation support measures are altered to meet the different levels of rock burst risk. Special yielding support elements are used to absorb dynamic loading, such as rock bolts (Swellex or Yielding Swellex bolts) and flexible steel arches.

The most powerful rock burst experienced at that time occurred on June 1, 2005 north of the cross-cavern. At the same time, instruments at the ETH Zurich Earthquake Service registered seismic activities that were not perceptible on the surface. This prompted efforts to investigate the correlation between the construction of the GBT and the resulting rock bursts as well as mini-tremors.

A work group "Mini-tremor" was formed. The goal of the work group is to develop measures for the tunnel to address the risks associated with mini-tremors.

A seismic monitoring programme with a total of ten seismometers around the MFS including one station on the surface above the MFS and one in the MFS is now attempting to determine whether there is a correlation between the MFS Faido tunnelling operations, pressure relief phenomena in the rock and the weak earth tremors in the Leventina. On March 25, 2006 an earthquake with a magnitude of 2.4 was recorded and at the same time a very heavy rockburst occurred in the MFS.

Important is to determine which dynamic and static loads are to be expected for the tunnel from the seismic events. The goal is to maintain the highest possible safety for tunnel construction and tunnel operations.

Based on the available results and the strength of previous tremors, the specialists believe that until now it was not possible to justify whether further reaching actions are necessary or not.

2.5 *Bodio*

Extensive construction work was realized at the southern Portal in Bodio before autumn 2002 in preparation for the heading of the main tunnel section. These were e.g. a bypass-tunnel (1.2 km) to bypass the very delicate and time-consuming loose rock zone at the portal, a 3.2 km long mucking tunnel and processing plants that recycle muck into concrete aggregates.

The past year was marked by good rates of advance. The lining operations are also forging ahead parallel to the excavations. In 2003 the roughly 600 m of equipment for the rear "inner vault" construction site assembled at the Bodio yard in front of the tunnel. The concreting of the lining support and of the lining itself was started in the west tube in April 2004. A specially designed vault formwork, which possesses some degree of adaptability, is being utilized. It is used to optimize the support taking into account any TBM deviations and the actually installed supporting elements.

After driving some 13.5 km and almost four years after starting out from Bodio the first TBM reached the MFS Faido in September 2006.

3 CONCLUSIONS

Construction of the GBT is preceding full speed ahead. Up to now all challenges were successfully managed. The unpredicted fault zones in Faido and Amsteg caused delays in the schedule but in the meantime they were overcome by applying suitable rock support systems.

As things stand today the GBT should be completed on schedule in the year 2015 and it will be a milestone for the realization of the New Alpine Transverse in Switzerland.

Amberg Engineering is member of the Engineering joint venture Gotthard Base Tunnel South with the partners Pöyry Infra Ltd. and Lombardi SA. We like to thank the AlpTransit Gotthard AG for the allowance to present this paper and to use some pictures from their homepage.

Underground Space – the 4th Dimension of Metropolises – Barták, Hrdina, Romancov & Zlámal (eds)
© 2007 Taylor & Francis Group, London, ISBN 978-0-415-40807-3

Innovative design and construction in Sydney's newest underground rail line

J. J. Rozek
Parsons Brinckerhoff, Sydney, Australia

ABSTRACT: The new Epping to Chatswood rail line will consist of 12.5 km of fully underground rail, constructed between 15 and 60 meters below the ground, and include four new underground stations. The project is the largest publicly funded infrastructure project to be built in New South Wales, Australia. The project represents an important precedent in Australia for underground rail and station design and construction in an urban environment. All four stations were excavated as mined station, three of them, Macquarie Par Station, Macquarie University Station and the Delhi Road station were excavated as caverns. The cavern stations were constructed with unique architecturally established asymmetrical arched roofs, with one side flatter than the other. This paper discusses many of the design and construction challenges and innovative solutions that were utilised to perform the excavation of this complex urban project enroute to meeting the project requirements and a 2008 opening.

1 INTRODUCTION

Sydney is the largest city in Australia, with a population of some five million people. Today, there are 1,000 people coming to Sydney every week. The need for transportation mobility is an ongoing challenge. There have been a number of underground transportation projects since the early nineties. The Epping to Chatswood is one of the most significant and is the first new rail start in Sydney in 80 years.

The 12.5 km AU$880 million (civil works) Chatswood to Epping underground rail link is the largest publicly funded projects in New South Wales history. The project is significant for its shear size and the rate at which design and construction was required to be performed. There was a need for close control of settlement and groundwater as the rail line excavation passed under residential, commercial, public areas and water bodies. Three of the most notable features are the underground stations at Macquarie Park, Macquarie University and Delhi Road. Each of these stations is excavated as caverns below significant urban activities at the surface. The excavated spans are amongst the largest performed to date in Sydney and probably internationally, and despite excellent Sydney Basin geology, posed significant challenges to the detailed design, including significant bedding and subvertical features in the sandstone, high insitu stresses up to 6 MPa, a lack of precedence of near surface wide span arch excavation in high stresses, a tight schedule and stringent surface settlement criteria.

2 GEOLOGY

The new rail line is located within the Sydney Basin. The majority of the route lies within well known Sydney geological formations – the Mid Triassic Ashfield Shale, Mittagong Formation and Hawkesbury (Sydney) Sandstone. Ashfield Shale is a dark grey to black shale and siltstone, which weathers to produce high plasticity clays. The Mittagong Formation marks the transition between the marine sequence of Ashfield Shale and the fluvial sequence of the Hawkesbury Sandstone. This formation is characterised by interbedded shale, laminite and medium-grained quartz sandstone. Hawkesbury Sandstone is a medium to coarse grained quartz-rich sandstone, typically with a strength of 35 MPa, with occasional minor shale and laminite lenses. The Hawkesbury Sandstone comprises massive, thick-bedded and cross-bedded strata in near horizontal layers. Most of the tunnelling occurred in Hawkesbury Sandstone, while the dive structures will be excavated predominantly in Ashfield Shale.

3 RUNNING TUNNELS

The tunnel TBM excavation works for the project were completed in July of 2005. It took almost two years to complete the excavation of the 12.5 km long, 7.2 m diameter twin tunnels, during which time over two and a half million tones of Hawkesbury sandstone were

excavated. One of the TBMs set a world record by excavating 92 meters in one day.

Design of the tunnel support system considered the risks of potential variations in geology in the development of the range of tunnel support systems. One of the most significant parameters providing an impact on design was the pre-existing in situ stress fields which influence tunneling conditions, and post excavation induced ground movements. Rock mass and rock defects, including shear strength, cohesion and friction values were developed on the basis of geotechnical information, data and testing. Published information and geological experience in the Sydney Basin were also used to develop rational design parameters.

The running tunnel support consisted of initial or temporary support. An array of six 2.7 meter long, 310 kN capacity, temporary full-resin-encapsulated rock bolts generally made up the temporary support. They were installed approximately 6 metres back from the face directly behind the TBM cutting head. About 110,000 bolts were used in the excavation of the two running tunnels. Sets were used as the excavation crossed the North Ryde fault zone, as very poor ground conditions were encountered. Ground support did not change from TBM No. 1 to TBM No. 2. However, from the detailed information of the geologic structures encountered by TBM No. 1, the geotechnical team was able to provide TBM No. 2 crew an accurate forecast on impending ground conditions.

The permanent lining for TBM excavation, was a circular formed, unreinforced concrete, nominally 200 mm thick, with a design strength of 32 MPa at 28 days. The concrete lining was the same for drained and undrained tunnels. The formwork consisted of six shutters, 15 metres long.

Waterproofing was achieved by installing hydrophilic waterstops in the joints. The long term steady state condition of the ground water was established by investigation and analysis, to meet the maximum inflow criteria of 0.1 L/sec/100 m of running tunnel and no visible water spotting on the interior of the lining. About 75% of the tunnel was constructed as drained. As the three creeks and the Lane Cove River were approached, forward probing was required to determine if grouting was required. The effects on ground water and settlement were monitored.

4 STATIONS

The distinctive station configuration for Macquarie Park, Macquarie University and Delhi Rd stations consists of an asymmetrical arched roof defined by the architects, with one side having a flatter arc than the other. It was designed to not only meet functional requirements, but also to enhance aesthetic qualities. The stations consist of 190 m long platform caverns that were 14 m high and 20 m wide. For these cavern stations, there is also a 50 meter long concourse caverns excavated adjacent to the platform caverns, also excavated as a arch. At either end of the Mac Park and Mac University stations, there is a 32 by 18 meter large service shaft about 30 meters below the ground. See Figure 1. The Delhi Road station has a slightly different configuration. The stations were located as close as 15 m below the existing ground surface.

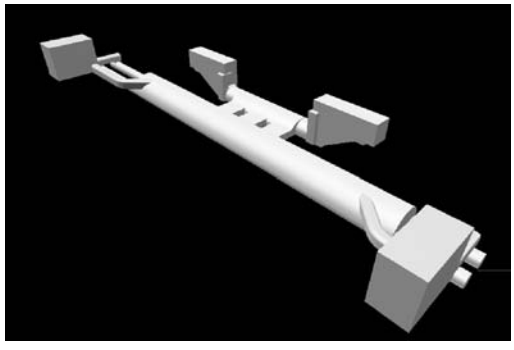


Figure 1. Isometric view of Macquarie Park station.

Each of the station cavern detailed design was developed which included excavation layout and dimensions, excavation sequencing, as well as permanent and temporary support of cavern excavations, shafts and related tunnels. Permanent waterproofing was performed for the caverns, shafts and related tunnels, including associated drainage was developed. Permanent lining of the station caverns, shafts and related tunnels, was also developed, including provisions for fixing points for subsequent works.

4.1 *Cavern design*

The design methodology for the principal components of the station caverns at Macquarie Park, Macquarie University and Delhi Road included an initial study of cavern shapes to determine the feasibility of large span arched caverns in these geologic conditions, and the relative costs when compared with the precedent practice of flat roof or trapezoidal sections. The study indicated that despite no precedence for long span arched construction in the Hawksbury sandstone, the architectural arch shape was technically and economically feasible. Numerical modeling was performed to investigate the rock mass response. The modelling was performed for the platform cavern alone, for typical and adverse rock conditions, and included excavation and support sequencing. Numerical modelling of the adjacent cavern configuration was performed to measure overall cavern stability and compliance with all relevant criteria. Analytical and numerical studies of secondary openings, junctions, passageways and service shafts were also undertaken. Permanent anchor

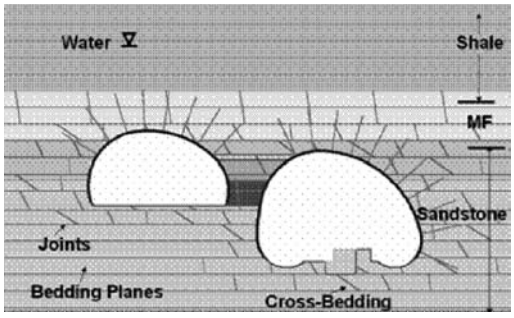


Figure 2. Simplified cross section of caverns in geology.

support and passive shotcrete arch construction were compared.

Preservation and utilisation of inherent rock strength were explicitly considered while analysing the cavern arches, the cavern and shaft interactions, the pillars, the excavation sequence with 3DEC and Phase2 software. Staged top heading excavation and timely installation of temporary and permanent rock reinforcement bolts combined with the observation and monitoring were the core principles of the design strategy for establishing a stable crown arch and haunch. Extensive numerical modelling was performed during the detailed design using state of the art practice 2D and 3D finite element and discrete element programs to evaluate rockbolt loads, bedding shear displacements, crown displacements, surface subsidence and shotcrete loads under various combinations of rockbolt types, (end anchored versus grouted), horizontal stresses, local bedding geology, and excavation sequence.

4.2 *Insitu stresses*

The natural insitu stress state of the rock mass had a significant impact on both tunnelling conditions and induced ground movements in the immediate area of the tunnelling works. The existence of significant and variable virgin stress field within relatively shallow rock is well established in Sydney.

A strategy was developed to deal with the potential for high loads and shearing stresses. The risk could best be managed through an observation approach, by establishing sufficient instrumentation from the surface and within the tunnel (in addition to normal convergence and surface monitoring), and to closely monitor the ground behaviour as the excavation progressed. The designers defined criteria upon which additional ground support would be triggered.

4.3 *Rock support*

In general, the station caverns were excavated in mainly competent, horizontally bedded sandstone and shales, although weaker weathered sandstone, and some shale, occurred above the crowns of the caverns at MP and MU Stations.

Precedent international and local practice indicated that large-span excavations in these conditions could be permanently supported using composite linings consisting of specified rock reinforcement in the form of rock bolts and shotcrete. The particular cavern geometries required the architectural arched profile be followed in order to minimise excavation. The proximity of adjacent major caverns required the station caverns to have specific detailed designs. See Figure 2, for a simplified cross section of the excavation. The bedding characteristics of the sandstone, and the potentially high local insitu horizontal stresses could be expected to lead to a rock mass response that developed predominantly horizontal crown beams, rather than conventional arching action. The crown beam response was strengthened where high horizontal stresses existed. Consequently, where large curved haunches were formed, the haunch rock and sidewalls could potentially experience significant shearing on the bedding planes, and fallout of blocks and wedge-shaped corbels released by the bedding planes and sub-vertical jointing. The roof support concept began with the basic assumption that the horizontal crown beam response was developed within the rock mass above the caverns. To retain the rock haunches, early support was required to sustain self-weight loading. The primary crown beam acts over the top of the haunches.

4.4 *Permanent lining, drainage and waterproofing*

The caverns were fully lined, as the internal surfaces of the permanent linings were required to be essentially dry. Since the caverns long term structural support was provided by permanent rockbolts, there was very little transfer of rock load to the linings. The permanent lining of the station caverns could therefore be of minimum thickness, consistent with constructability requirements, support of its own self-weight, the hydrostatic head of less than a 100% efficient drainage system and other considerations such as cover to rock bolt face plates and nuts. From consideration of the scale of the cavern roofs, the profiles, and programme requirements, the final cavern linings were determined to be shotcrete. The thickness was established at 120 mm thick for the platform caverns. The lining was integrated with the rock support elements by means of mechanical connections ('spiders') and which provided long-term security against minor rock fall from between the elements. The caverns were designed as drained structures, *i.e.* not subject to significant groundwater pressure. This was accomplished by a drainage system, which includes continuous

waterproofing membrane on the extrados of the lining so the internal surface of the lining remains dry throughout the design life. A sprayed membrane was selected over sheet membranes due to the requirement for architectural penetrations. The approach adopted for the caverns included a drainage fleece over the full excavated area supplemented by vertical strip drains at regular close spacings.

4.5 *Macquarie Park station*

The Macquarie Park station cavern design began in September 2002. It was carefully studied and was the proto type for the subsequent Mac University and Delhi Rd stations. Its design was based on modeling moderate and worst case geotechnical scenarios both as bedded and joined ground types, typical and adverse conditions. Results of insitu stress testing received January 2003 indicated stresses some 50% greater than had been anticipated at tender preparation time. Following careful consideration by the design team and external experts and specialists, it was determined that these unusually high results could not be ignored, and the design had to be adapted to accommodate the stresses and to investigate their impact. The higher stresses resulted in higher predicted ground displacements, particularly along thin beds of clay and other weaknesses in the rock which acted as shear planes. Of critical concern was the timing of the installation of the permanent rock bolt support. As the platform cavern was some 14 meters high, the cavern was excavated in a series of levels stating from the top. Installation of the permanent bolts was preferred from the top heading as the roof was easily accessible, however, there was the significant risk of having to rebolt the roof at a later date, as shear movements could occur during the subsequent lower bench excavation, or from the excavation of the significant service shafts or entry shafts adjacent to the caverns. As a result, the issue of rock bolt design and the timing of permanent rock bolt installation was a critical issue.

Permanent, corrosion-protected, fully grouted end anchored two stage and single stage rock anchors were the primary support mechanism for the MP cavern design. Over 1000 permanent rock anchors were installed in the platform area including some 340 two stage rock anchors. The array of rock anchors comprised 310 kN and 600 kN anchors. The approach taken for the MP cavern support design incorporated local precedence for example rockbolt lengths, and used a combination of numerical modelling, observation and monitoring, field adjustment as required and mandatory excavation and support sequence to arrive at the overall construction solution. See Figures 3, 4 and 5 for the excavation sequence at Macquarie Park station.

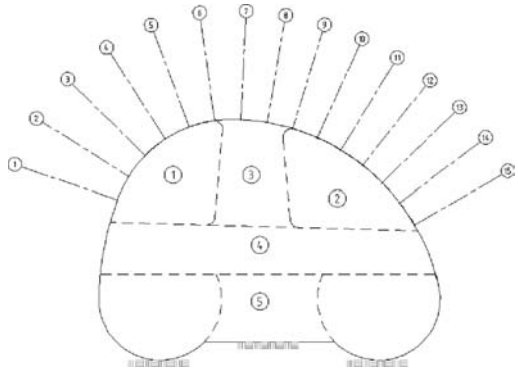


Figure 3. Sequence of exaction of platform cavern.



Figure 4. Excavation of first top heading drift.



Figure 5. Excavated top heading and intermediate bench.

4.6 *Macquarie University*

The initial design of the excavation sequence and ground support at Macquarie University station, was carried out using a geotechnical model developed in the light of geotechnical information available in the early stages of design. Further geotechnical investigations were conducted during the detailed design. There

were significant differences between Macquarie Park and Macquarie University stations, including the presence of significant clay beds in adverse locations in relation to the cavern crown and the permanent support at Macquarie University. These beds, in conjunction with the inferred high insitu principal stress across the caverns, were identified as shear movement concentrators which had the potential to either rupture the rock anchor anchorages or shear the anchors in the free length and to develop large extensional loads within the anchors themselves. The numerical modelling indicated that the primary agent mobilising these shear movements was bedding plane displacement associated with the stress relief induced from sinking of the shafts and the concourse excavation adjacent to the platform cavern after installation of the permanent support.

Because of the concern over the impacts on the cavern support, from both stability and anchor durability standpoints, there was a design prerequisite to dissipate stress relief if the shafts were sunk before the platform cavern excavation was supported with permanent anchors. The permanent rock support could be designed to take advantage of the reduced shears and anchor demands. However, based on schedule and access factors, and in order to avoid schedule delays to the cavern construction (which was driven by the need to have excavated and supported the crown before the TBMs came through), the decision whether to sink the shafts first was important. Equally important, the experience at the adjacent Macquarie Park station suggested that the ground behaviour might be more "benign" than the modelling had indicated and the support design had assumed. A relatively large amount of data had been collected from ground movement monitoring at Macquarie Park and it was considered appropriate to reassess the geotechnical design parameters used for the Macquarie University station modelling based on back-analysis of that data. Further to these considerations, the shafts were excavated first to minimise the risks.

The material costs of the rock bolts for the Macquarie University and Delhi Road station were reduced as the 2-stage bolts were replaced with single stage bolts as the service shaft excavation was performed before the cavern excavation so the permanent bolts did not experience the shaft excavations shear. As such, a "most probable" ground model was developed. This predicted lesser shear which allowed simpler anchors but required closer observation to ensure that corrective action could be taken if movements greater than predicted actually occurred.

4.7 *Delhi Road station*

Delhi Rd design was based on analysis of further stress testing (in late July, early August 2003), a re-assessment of the stress regime, an incorporation of observed movements, and a detailed geological mapping from 'exploratory' adits.

Although the Delhi Road station geology had the highest insitu stresses of the three stations, its geology was massive. The pervasive clay beds in Mac Uni station were not present at Delhi Road. As such the high stresses were locked in as they had no defined shear planes. Single stage bolts were also used pervasively as the permanent support.

4.8 *Monitoring*

The complexity of the geology and the possibility of higher insitu stresses than have been allowed for in the design led to the adoption of an observational approach to the construction and support of the works. An essential part of this process was the feedback, assessment and possible re-analysis based on monitoring the performance of the works as the station is constructed. Elements of the performance monitoring included:

- geological mapping to confirm the nature of the ground, i.e. exposed rock type, quality, prevailing jointing, shears and discontinuities;
- endoscopic inspections of proposed permanent bolt anchor zones in those areas where the design predicts significant localised shear displacements;
- ground movement monitoring in the form of convergence monitoring within the excavations, multipoint borehole extensometer monitoring in the crown, inclinometers and extensometers in the rock pillars and surrounding the shaft and cavern excavations, to monitor horizontal shear and vertical ground movements, and surface settlement monitoring;
- rock bolt load cells and/or strain gauges;
- endoscopic, up-borehole inspections to assess crown geology and to determine the locations and magnitudes of bedding shear movements in the rock anchor zones; and
- piezometers and groundwater inflow measurements to monitor groundwater drawdown and compliance with Deed requirements.

5 STATION DESIGN POSTSCRIPT

The three 'brain' caverns, although similar in appearance, were significantly different in the aspects that affect rock support.

The design of the three underground cavern stations was based on precedent design, factual geotechnical data, 2 and 3 dimensional computer modelling, empirical design, as well as the knowledge obtained from the ongoing construction, which allowed back analysis and refinement of design elements. The results

show that the work was highly successful. The surface settlement has been within the allowable levels permitted by the Deed and there was close correlation between the predicted movements and the actual movements. A key component of the design was the use of the observational method. It enabled the design to be implemented rapidly but required specific action, when pre-set trigger values were exceeded.

There was some appropriate conservatism in the Mac Park design, as exampled by the design of the rock bolts to accommodate the ground movement through any of four possible scenarios (moderate case, worst case, bedded and jointed) even though only one of which could occur at any one location. This approach was modified for Macquarie University station, based, based on back analysis of ground behaviour at Macquarie Park station. Instead, the design was based on a most probable scenario but with distinct clay beds, there was the higher risk of re-bolting. As the ground was behaving better than anticipated, the risk taking was successful. The observational method allowed the designers to specify bolts that would be lower in cost than ones that would be required to fully take the modelled loads and shears. Importantly, the allowable trigger levels for rock bolts were exceeded at both Mac Park and Mac Uni Station, which resulted in 108 temporary rock bolts were replaced in Mac Park, and a lesser number of permanent bolts in Macquarie University station. There were about 1500 temporary rock bolts installed in each of the three cavern stations, and about 2500 permanent rock bolts installed. In all, an appropriate design was provided at each of the cavern station. Adjustments were made based on the geologic conditions of the exposed rock, additional borehole data, back-analysis of measured deformations and movements observed during the initial works.

The Macquarie Park station design was successful. The measured settlement at the surface was 10 mm, well within the maximum allowable settlement of 40 mm. The maximum shear displacement was 14 mm. Macquarie University Station had a maximum measured shear of 29.5 mm. The largest shear seen by bolts was 16 mm. Delhi Rd. Station has had a maximum measured shear of 5 mm.

6 CONCLUSIONS

The design was successfully completed for the very large multiple arched profile spans of up to 20 metres and with relatively low covers which have never before been attempted in the jointed and bedded rock of Sydney Sandstone. The designs had to cope with the high horizontal residual rock stresses and planning consents which required minimal surface settlements and strict constraints on ground water ingress to the structures. As of July 2006, the concrete work was complete at Macquarie University Station. The station M&E is being outfitted. Concreting works at Macquarie Park and Delhi Road stations will be complete in early 2007 for the platforms, escalator shafts and stairwells, and work is progressing at the interchange station at Chatswood and at Epping to meet the 2008 opening.

In 2008, the Epping to Chatswood rail project will move more than 250,000 people a week and bring public transport to new suburbs housing 1 million people.

As a reflection of the success of the project, and the need for more rail service, the New South Wales Government announced it would invest $8 billion between 2005 and 2020, for the biggest expansion in Sydney's rail network since the 1930's. 25 kilometers of the 38 km expansion will be in tunnel, including stations.

Underground Space – the 4th Dimension of Metropolises – Barták, Hrdina, Romancov & Zlámal (eds)
© 2007 Taylor & Francis Group, London, ISBN 978-0-415-40807-3

Evaluation of the effects of shield tunneling on the historical Sio-Se-Pol bridge piles

H. Saghaeian Nejad
Esfahan's Urban Railway Organization, Esfahan, Iran

H. Hashemol Hosseini
Esfahan University of Technology, Mining Engineering Department, Esfahan, Iran

R. Rahman Nejad
Bahonar University of Kerman, Mining Engineering Department, Kerman, Iran

ABSTRACT: Sio-Se-Pol bridge, built 500 years ago in Esfahan, is one of the most popular and historical bridges in the world. Due to this important fact the effects induced by probable subway tunneling during the passage of the tunnels under the bridge are studied in this paper. In Esfahan's jobsite two parallel tunnels with the diameter of 6.88 is under the process of excavation with two earth pressure balance TBM machines. Settlement is one of the most important effects that occur during underground excavation that may cause sever damage to the construction. In this study the tunnels and the bridge will be simulated by a two and three dimensional Finite element package (Plaxis 7.2 and 3D Tunnel) and then the effects of shield tunneling on Sio-Se-Pol bridge piles will be discussed.

1 INTRODUCTION

Esfahan is one of the historical cities of the world. Several historical monuments such as the ChaharBagh School and the Sio-Se-Pol Bridge are located in the centre of it where Esfahan's metro North-South line passes through. Esfahan's North-South line consisting of 21.2-km of twin tunnels is subdivided into two main tunnel sections namely the east tunnel (S-228) and the west tunnel section (S-227). There have been serious discussions between the City officials and the Cultural Heritage Organization on the tunnels alignment. The Cultural Heritage Organization is concerned about the tunnel's construction under the ChaharBagh Street and the Sio-Se-Pol Bridge. In this paper the effects of shield tunneling on the Sio-Se-Pol foundation are discussed using a three dimensional Finite analysis.

Many innovations have been introduced to improve tunneling in soft ground. At Present, the earth pressure balance (EPB) shield tunneling Method, which first was developed in Japan (Stack 1982; Maidl et al.1996), has become one of the most popular methods for soft ground tunneling. With this tunneling technique, ground movement can be, in theory controlled by balancing the pressure inside the earth pressure chamber relative to the outside ground pressure during excavation.

Two Herrenknecht Earth Pressure Balanced Shields are used for twin tunnel drives. The excavation diameter is 6.88 m (without over cut). The lining is pre cast concrete, composed of six segments plus one key



Figure 1. Esfahan Metro line network.

element. The inner diameter is 6.00 m and the exterior diameter is 6.60 m.

In order to analyses the stability of the overburden and to determine confinement pressures, model presented by (Mohkam 1989) has been used, the model considers a three dimensional potential failure surface. The phenomenon of arching effect, soil's mechanical parameters and physical characteristics, as well as muck conditioning in the working chamber have been taken into account.

2 GEOMETRICAL, GEOLOGICAL AND HYDROGEOLOGICAL CONDITIONS

The overburden is more or less uniform and has about 8 to 8.7 m thickness. The soil formation is:

Fill; on top composed of fine materials with some coarse particles and building waste. The fill thickness lies in the range of 1.5 to 2.5 meters.

Fine Grained Alluvium; comprised of clay and silt of low to high plasticity. These deposits have brown to light brown color, and are mostly homogeneous and firm in place. Among the fine grained deposits, there are some lenses of coarse grained gravely deposits, which may be encountered at the tunnel face.

Coarse Grained Alluvium; predominately consisting of clean well graded/poorly graded (gap graded), very sandy gravel and/or very gravely sand. The soil particles are mostly rounded with 60 mm maximum grain size. These deposits are water bearing and dense in place.

According to the geotechnical investigation results, the following design data of the soil layers have been considered in designing of the tunneling parameters. In the section studied, tunnel's heading would run in the Coarse Alluviums.

The groundwater elevation is mainly related to the Zayandeh-Rud River. Records, since 1997, show the highest level on April and May of 1998 and lowest level at January 2002. The recent level (August 2006) is situated at some 2 meters above the surface.

3 SHIELD OPERATION FACTORS AFFECTING SURFACE SETTLEMENTS

Based upon case history reviews (Clough and Leca, 1993; Finno and clough, 1985; and Matsushita et al., 1995) and extensive observations in Esfahan Project, the shield operation factors causing settlements can be listed as bellow:

- Face Pressure
- Penetration rate
- Pitching Angle
- Tail void Grouting Pressure
- Percent Tail void Grout Filing
- Thrust Forces
- Soil Conditioning Agent
- Foam Expansion Ratio
- Foam Injection Ratio
- Polymer Presence in Foam

In this paper only the Tail void grouting pressure and the percent tail void grout filing is discussed.

4 TAIL VOID GROUTING

Quality of tail void grouting contributes to the extent of the ground settlement. As the shield is jacked forward, a tail void around the outside of the lining is created. Tail void grouting is necessary in order to prevent ground moving towards the void. In general practice, grouting pressure should be sufficient enough to guarantee the flow of grout material and to resist the ground moving into the void. Another criterion to check the grouting performance is percent grout filling that has

Table 1. Esfahan's Soil Parameters.

Soil type	Total unit weight KN/m^3	Horizontal coefficient of permeability m/s	Mohr-Coulomb shear strength parameters*	
			Cohesion KN/m^2	Angle of internal friction deg
Fill	18	10–5	15	23
Fine grained alluvium	19	10–8	30	25
Coarse grained alluvium	20	10–3	0	35

* Strength parameters are in terms of effective stress.

to be maintained at a level higher than the theoretical void. Another parameter is the grout mix. The grout mix should be given according to the geometrical, geological and Hydro geological Conditions of the region. Tunneling operation with an appropriate grouting pressure and sufficient percent of grout filling and also an appropriate grouting mix can considerably reduce settlements developed after the shield passing (examples: the WMTA project; Leca 1989; MRTA project; Suwansawat, 2002 and Esfahan project). Figure 2, shows an example of the actual grout pressure and executed grout pressure applied in Esfahan jobsite.

5 INSTRUMENTATION AND SURFACE SETTLEMENTS

Few surface settlement markers and extensometers were installed to measure settlements during excavation. The primary objective of the measurements with extensometers is to measure surface and subsurface settlements above the tunnel axes. Additionally, since readings were taken over time covering a period between shields approaching and after shield passing, extensometers also allow one to observe longitudinal sub surface settlement profiles and to study how they develop during shield passing.

From ring number 860 in the tunneling direction, arrays of settlement markers were installed to measure settlement troughs developing during and after shield passing. The layouts of arrays on one hand, concentrates the instrumentation above the tunnel alignment because this is where shield operators wanted to check on settlements, and on the other hand, place instrumentation adequately distant from the alignment to determine a zone of influence.

Thus, the main objectives of surface settlement array measurements are (1) to measure the extent of settlement during excavation, (2) to observe the shape of settlement troughs and the magnitudes of the displacements. Therefore, results from the instrumentation provide engineers with useful information to design appropriate measures for preventing damage to existing structures induced by EPB tunneling. Note that monitoring frequencies adopted in Esfahan project depended on the shield position. For example readings were taken everyday before and after shield passing but increased to higher frequency (i.e. every 2–4 h) during shield passing in order to capture the development of surface and sub-surface settlements. Note that large settlements occurred over the shield body behind the face. Subsequently, beyond this point, the settlement showed a small change after shield passing.

On ring number 866 (4147.2 kilometer of the alignment) a sewage pipe was observed at the depth of 6 meters. The sewage system of Esfahan was built 40 years ago by the Russians. Due to this critical situation for monitoring the settlements an eight meter long extensometer was installed before the sewage pipe. The extensometer has 4 rods that are in the depth of 1, 4.76, 6.76 and 7.76. Figure 3, shows the settlement recorded by the extensometer during the tunnels construction.

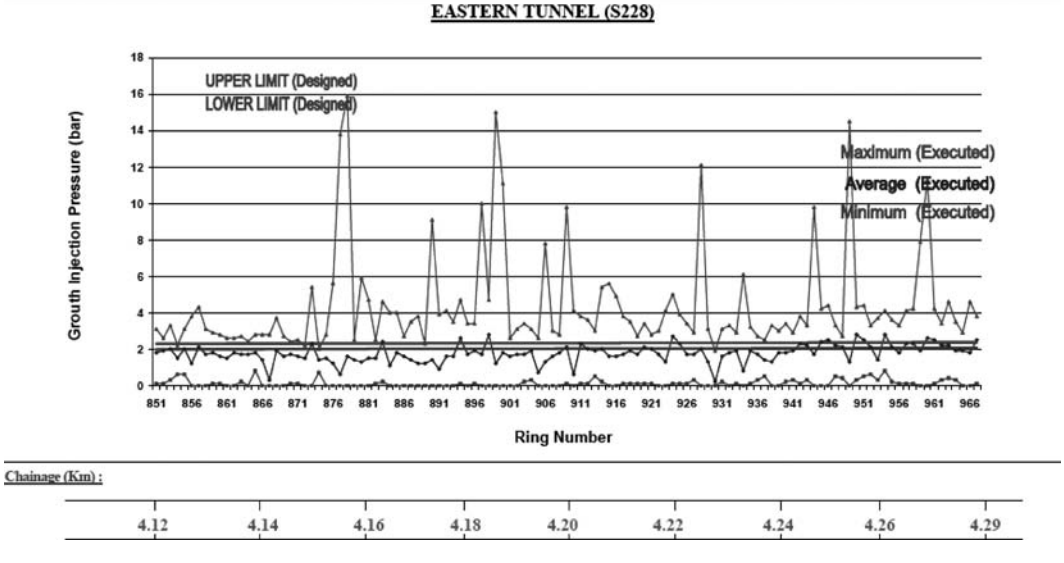


Figure 2. The Designed and executed grout pressures group 2.

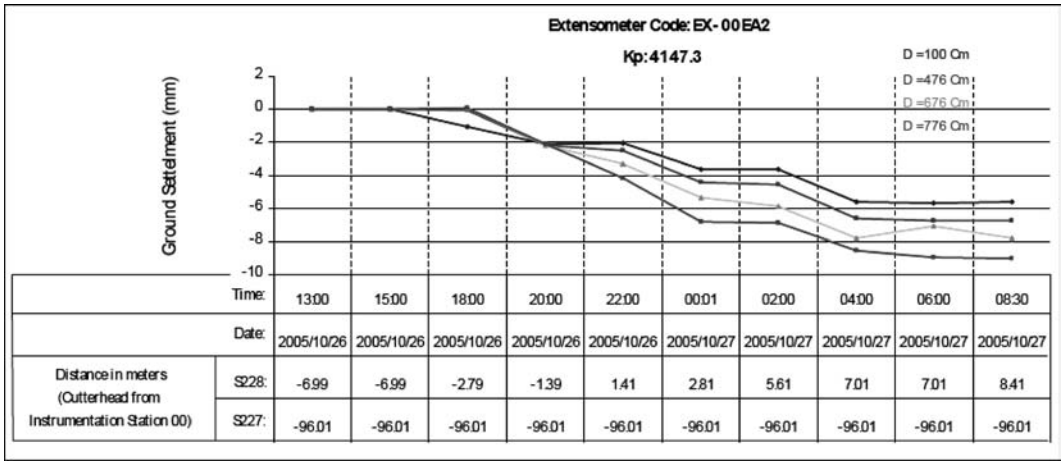


Figure 3. Settlment recorded by the extensometer.

Table 2. TBM properties used in 3D model.

Axial stiffness	Flexural rigidity	Equivalent thickness	Weight	Poisson ratio
KN/m	KNm^2/m	m	KN/m/m	–
8.2×106	6.17×104	0.3	32.7	0

Table 3. Segment properties used in 3D model.

Axial stiffness	Flexural rigidity	Equivalent thickness	Weight	Poisson ratio
KN/m	KNm^2/m	m	KN/m/m	–
9.4×106	7.06×104	0.3	7.2	0.15

6 SIMULATION OF EPB TUNNELING IN 3D TUNNEL PLAXIS

This model takes into account the following parameters: geometry, geology, the hydrological conditions, the TBM machine, the lining, excavation of the tunnels, applying the Tail void (Contraction), And the face support pressure. The TBM and Segment properties used in 3D Tunnel Plaxis are listed in Table 2 and Table 3.

7 BACK ANALYSIS ON THE MODEL

To calibrate the parameters of the calculations on the main model and to have an outlook of what exactly is happening in practice, a primary model was made based on the location where the extensometer was installed on ring number 866 (4147.2 kilometer of the alignment).

Several values of contraction are applied to the model and the settlement results are then compared to the settlement results obtained from the extensometer. The face pressure applied is exactly the same as the value used for excavation. Also a sensitive analysis was made on the soil strength parameters, cohesion and the frictional angle(C and Φ). Figure 4, shows the designed and executed face support pressure in the Instrumentation region.

7.1 *Back analysis results*

Due to the back analysis results the value of contraction should be near zero. This is achieved with an appropriate grout pressure injection and sufficient grout quantity for the tail void. Also it is shown that the strength parameters of the soil are in acceptable ranges.

8 SIMULATION OF SIO-SE-POL BRIDGE IN 3D TUNNEL PLAXIS

The Sio-Se-Pol Bridge built on the Zayandeh-Rud River is a 295 meter long 14 meter wide structure. It is constructed on a $295 \times 35 \times 2$ meters foundation. According to some resources it is built on a shallow foundation while due to some other resources it is possible that some kind of well foundation has been used for its construction .However the nature of the Sio-Se-Pol Bridge foundation is not clear. The bridge is made of stones and old bricks. It has been repaired several times.

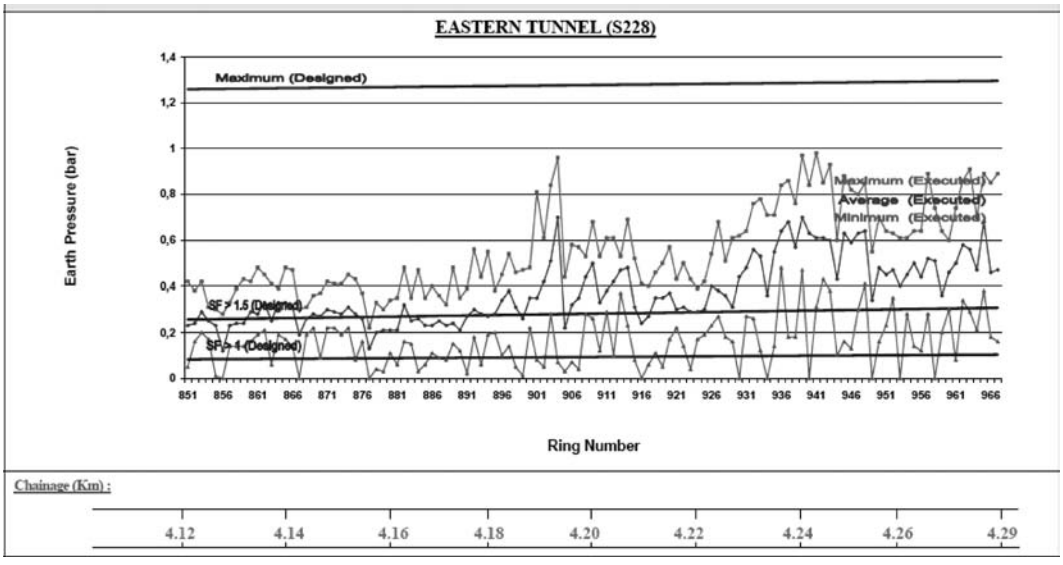


Figure 4. The designed and executed face support.

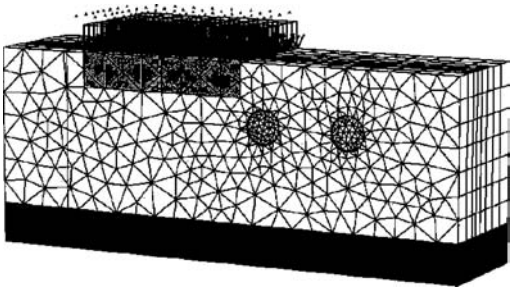


Figure 5. Sio-Se-Pol Bridge designed with a rigid foundation.

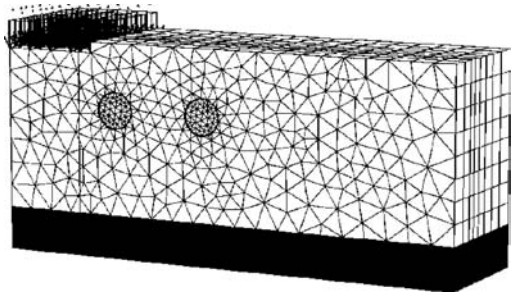


Figure 6. Sio-Se-Pol Bridge designed with a shallow foundation.

According to the above argument two different model of foundation has been used. First a rigid foundation with 7 meters depth Figure 5. And second a shallow foundation with two meters depth Figure 6. A 75 KN/m^2 force is applied on the rivers surface as the structures weight. The actual designed distance between the tunnel's axes and the bridge is 93.5 meters. This distance is reduced to the point where the settlements under the foundation are allowable. According to Iran's Heritage organization's principles for historical monuments the maximum allowable settlement amount for historical monuments is 2.5 mm. Also the contraction applied to the front plane is 1%. As mentioned before this amount could be reduced to near zero with an appropriate grout injection pressure and a sufficient amount of grout quantity. The earth pressure applied to the face for the crown of the tunnel in this section is 110 KN/m^2. The soil model used is Mohr-Coulomb Elasto-Plastic. The distance between the two tunnels axes is 17 meters.

It should be mentioned that all the parameters used for the modeling are selected in high ranges of conservative senses. Therefore the results achieved can be compromised.

After applying all the parameters to the model the distance between the foundation and the eastern tunnel axes is decreased each 10 meters from 93.5 meters (the actual designed distance) to 5 meters where the settlements exceed allowable values.

Four points are selected under the foundation. Point D is the nearest point to the tunnel axes. And point A is the most far. The settlement of these points is monitored in the software.

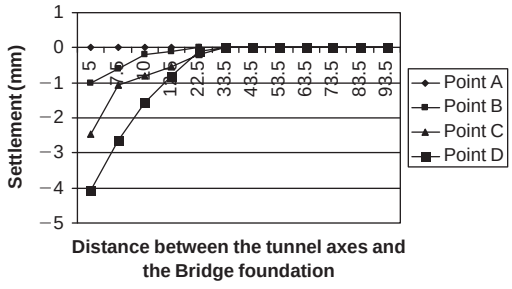


Figure 7. Settlement results of the rigid foundation.

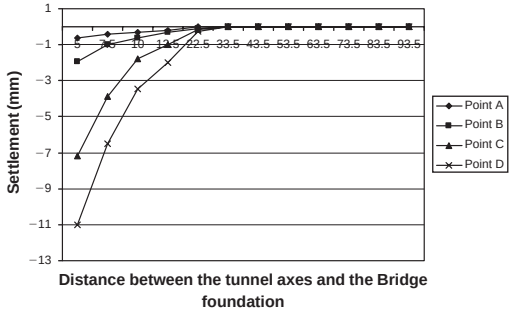


Figure 8. Settlement results of the shallow foundation.

9 RESULTS

9.1 *Settlement results of the rigid foundation*

In this case the results show that there is no significant settlement until the distance of the Eastern tunnel axes and the Bridge's foundation is 22.5 meter. From this point the settlements start to show up but they are in the allowable range until the distance is decreased to 7.5 meters. On this point, point D shows -2.629 mm of settlement which according to the limits is out of range and is not acceptable.

9.2 *Settlement results of the shallow foundation*

In this case as predicted before, the settlements are more intensities than the first case. The results show there is no significant settlement until the distance of the Eastern tunnel axes and the Bridge's foundation is 27.5 meter. From this point the settlements start to show up but they are in the allowable range until the distance is decreased to 12.5 meters. On this point, point D shows -2.5 mm of settlement which according to the limits is out of range and is not acceptable.

10 CONCLUSION

The back analysis method shows its capabilities to provide some vital parameters such as the contraction for evaluating the damage risks due to the excavation process by shield tunneling. As shown in this paper using a prediction and correction method based on a finite element method during the excavation makes a safe tunnel construction possible in very sensible and critical conditions. Also the closest safe distance of excavation near Sio-Se-Pol Bridge is determined.

ACKNOWLEDGMENTS

The authors thank Esfahan's Urban Railway Organization for providing unlimited accesses to all data used in this paper.

REFERENCES

Clough,G.W., Leca, E. 1993. EPB shield tunneling in mixed face conditions. Journal of geotechnical Engineering 119(10): 1640–1656.

EFNARC, April 2005. Specification and Guidelines for the use of specialist products for Mechanized Tunneling (TBM) in Soft Ground and Hard Rock.

Finno, R.J., Clough, G.W. 1985. Evalutaion of soil response to EPB shield tunneling. Journal of Geotechnical Engineering 111 (2): 155–173.

Maidl, B., Herrenknecht, M., Anheuser, L., 1996. Mechanised shield Tunneling. Ernst &Sohn, Berlin.

Mohkam, M., Taheri, A. 2005. Esfahan Mass Rapid Transit System Line 1- Middle Section from PK 3 + 800 to PK 4 + 265 tunneling parameters design Report number one.

Mohkam, M., Taheri, A. 2005. Esfahan Mass Rapid Transit System Line 1- Middle Section from PK 4 + 265 to PK 4 + 965 tunneling parameters design Report number two.

Mohkam, M., Wong, Y.W. 1989. Three dimensional stability of the tunnel faces under fluid pressure. Numerical Methods in Geomechanics. Innsbruck, Swaboda(ed.).

Suwansawat, S., Einstein, H.H., 2005. Artificial neural networks for predicting the maximum surface settlement caused by EPB shield tunneling. Tunneling and underground space Technology 21(2006): 133–150.

Underground Space – the 4th Dimension of Metropolises – Barták, Hrdina, Romancov & Zlámal (eds)
© 2007 Taylor & Francis Group, London, ISBN 978-0-415-40807-3

Review of the project Uetliberg Tunnel

A. Sala
CEO Amberg Engineering Ltd. and Deputy Overall Project Manager Uetliberg Tunnel,
Civil Engineer FH, Amberg Engineering Ltd., Regensdorf-Watt, Switzerland

ABSTRACT: On May 18, 2006 the tunnel bore extender (TBE) finished successfully the enlargement of the second pilot tunnel. This signified that all excavation work had been successfully concluded for the Uetliberg Tunnel. Also the interior lining work has already been finished by now. At the moment all the electromechanical equipment is being installed. This is an ideal point of time for a review, first of all about the TBE driving.

1 PROJECT OVERVIEW AND GEOLOGY

1.1 *Project overview*

The Uetliberg Tunnel in Switzerland is the longest tunnel in Zurich's new Western Bypass Expressway.

The project comprises two parallel tubes, each about 4.4 km long. The two tunnel tubes are connected every 300 m by a transverse walkway and every 900 m by a transverse roadway. The SOS niches are spaced 150 m apart. The total cost will be about CHF 1.12 billion (price basis October 1994).

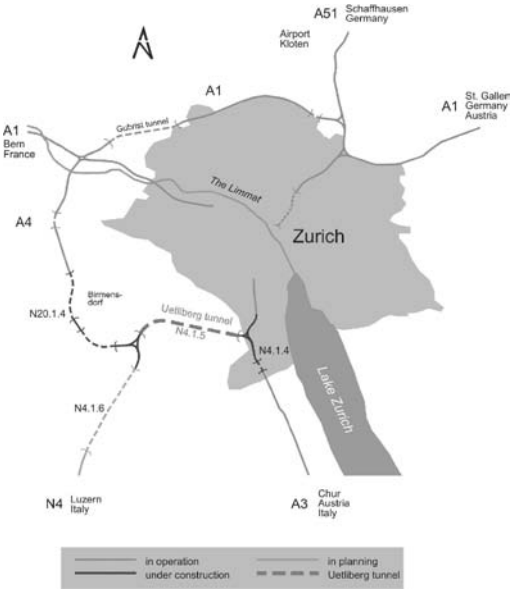


Figure 1. Project overview of the Uetliberg Tunnel.

1.2 *Geology*

From west to east, the Uetliberg Tunnel passes under two parallel ranges of hills (Ettenberg and Uetliberg) with the Reppisch Valley in between. The core of both ranges consists of flat layers of the upper fresh water molasse and alternating deposits of sandstone and soft marl. Maximum overburden of the tunnel under the Uetliberg is about 320 m.

Before the molasse sections of Eichholz (500 m) and Uetliberg (2800 m) were reached, three sections of soft ground (Gjuch, Diebis and Juchegg) had to be driven.

2 CONSTRUCTION PROGRAM AND PROCEDURES

From the Reppisch Valley construction site, the rock tunnel excavation was driven downwards under the Uetliberg to the Zurich-South motorway interchange.

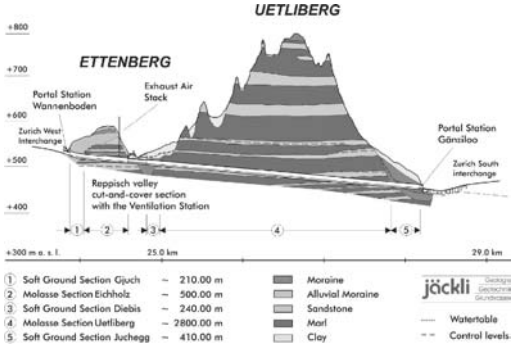


Figure 2. Geologic profile along the Uetliberg tunnel.

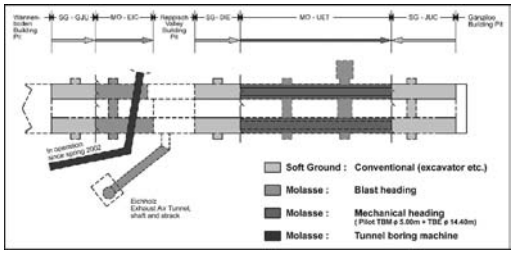


Figure 3. Heading methods of the Uetliberg tunnel.

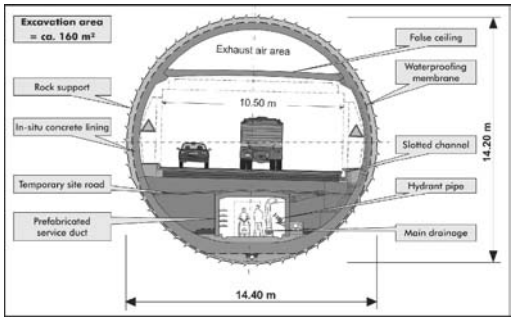


Figure 4. Standard cross-section of the TBE-section.



Figure 5. Core method for all soft ground heading.

This work was preceded by the excavation of soft ground sections using the core construction method in both tubes over distances of 250 m and 350 m from April 2001 to May 2002. At the end of the soft ground excavation at Diebis, starting caverns were excavated in the molasse under the Uetliberg for the tunnelling machine operations to follow in both tubes.

At the beginning of April 2002 an open pilot tunnel boring machine (TBM) Type Wirth TB III 500 E (diameter 5.00 m) was installed in the first tube. After starting in the middle of May 2002, the TBM drove the entire Ueltiberg molasse section. Since the beginning of May 2003, a tunnel bore extender (TBE) Type Wirth TBE 500/1440 using the undercutting technique has been traversing this entire molasse section under the Uetliberg to extend the centered pilot tunnel bore to the final profile of 14.10 to 14.40 m. Simultaneously with this bore extension, work has proceeded on driving the other pilot tunnel in the second tube untill the end of 2003. Afterwards this pilot tunnel was enlarged to its final profile by the same bore extension procedure.

Starting from the Gänziloo pit, excavation has been proceeding since February 2002 in the two 450 m long rising tubes through the soft ground of the Juchegg section. In both tubes, the first 50 m were driven through Uetliberg loam with pipe screen protection, likewise using the core construction method.

Since the beginning of April 2002, work has also proceeded on the downward tunnel starting at the west portal (Wannenboden) and leading under the Ettenberg towards the Reppisch Valley excavation site. The first hurdle here was the Gjuch soft ground section with a length of 220 m. It is followed by the 500 m long Eichholz molasse section, which was excavated by drill and blast and ripping.

3 TUNNEL CROSS-SECTIONS

3.1 *Soft ground sections and Eichholz molasse section*

The horseshoe cross-section used in all of the soft ground sections (SG) and for the drill and blast excavation in the Eichholz molasse section (MO-EIC) is about 14.70 m wide and about 12.70 m high. The face area is roughly 143 to 148 m^2.

3.2 *Uetliberg molasse section (TBE)*

The standard cross-section for the Uetliberg molasse section (MO-UET) is 14.40 m wide and 14.20 m high. The face area is about 160 m^2. Figure 4 shows in detail the elements of the tunnel cross-section.

Waterproofing, concrete invert, service duct (prefabricated elements), a cable conduit block and side backfilling were installed beneath the back-up equipment behind the TBE suspended from rock bolts in the ceiling. The concrete ring of the inner shell and the intermediate ceiling were installed successively later on in the rear areas.

4 SOFT GROUND HEADING WITH THE CORE METHOD

All soft ground sections were driven with the core construction method, shown in Figure 5.

Normally, temporary support measures consisted of steel arches (HEM 180 girders spaced 1 m apart) and a 25 cm thick layer of steel fiber reinforced shotcrete.



Figure 6. Excavation of the Eichholz molasse section.

After about two years of construction and the installation of 10,000 tonnes of steel, it is now possible to issue a positive progress report. During this two year period, about 1800 meters of tunnel has been driven successfully through soft ground. The excavation rate specified in the contractor's bid, 1.2 m advance per day over the entire cross-section was achieved and even exceeded. The systematic installation of steel supports has made it possible to organize efficient and predictable tunnelling progress practically free of unpleasant surprises and complications (first of all without a cave-in) despite these exceptionally heterogeneous geological formations. Overall support at the working face and support of the partial cross-sections was insured at all times with face anchors and cement injections.

5 DETAILED DESCRIPTION OF DRILL AND BLAST AND MECHANICAL HEADING IN THE UETLIBERG TUNNEL

5.1 *Drill and blast excavation of the Eichholz molasse section*

The 500 m long Eichholz molasse section was excavated by drill and blast with round lengths of 3 m, divided into crown, bench and base. Rock support generally consisted of mesh reinforced shotcrete and rock bolts. Initially, the tunnel crown was driven over the entire length of the molasse stretch. As soon as breakthrough of the crown was achieved, work started on excavation of the core and the base (by pneumatic pick and roadheader).

5.2 *Pilot tunnel in the Uetliberg molasse section*

The TBM for the pilot tunnel bored two 5.00 m diameter tunnels in both tubes.

Rock support used consisted of steel fiber reinforced shotcrete and glassfiber reinforced rock bolts



Figure 7. TBM-excavation of the pilot tunnel.

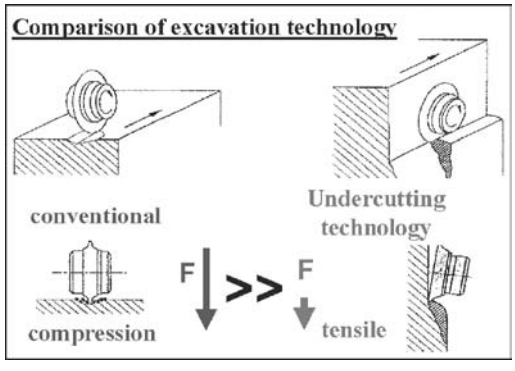


Figure 8. Principle of the undercutting technique.

2.5 m long. The peak rate of advance was 42.6 m/workday in three shifts. The average rate over the entire section was 20 m/workday.

5.3 *Tunnel bore extender (TBE) in the Uetliberg molasse section*

Starting in November 2002, the TBE was assembled in the Diebis soft ground section and in the starting pit. The rock was excavated with the undercutting technique, known to be an effective cutting method ever since the early days of tunnel boring machines. With this technique, the cutting rollers worked against the rock's tensile strength, which is much lower than its compressive strength.

The TBE enlarged the pilot tunnel of 5.00 m to a diameter of 14.10 to 14.40 m. The head of the TBE consisted of a two piece cutterhead body with six cutter arms. It rotated on the inner kelly, which was braced and positioned in the pilot tunnel and in the extended tunnel cross-section. The cutters, which were offset both axially and radially from the tunnel axis, were mounted on radially movable slides on the cutter arms.

When the six arm boring head rotated, the rollers were shifted from an inner to an outer boring diameter. When the nominal boring diameter was reached, the

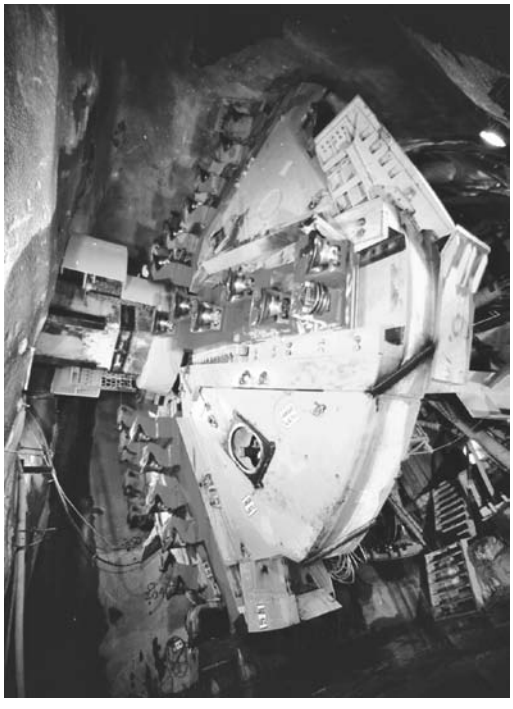


Figure 9. The TBE boring head.

slides were retracted. Then the continuously rotating head was shifted by one 20 cm advance towards the face, and boring of the next round could begin.

Excavation support, comprising cable bolts, Swellex rock bolts, nets and shotcrete, was installed right behind the cutting head.

The erection of the TBE with its back-up equipment had a total length of about 180 m.

6 EXPERIENCES WITH THE TBE-DRIVING

6.1 *Back-cutting technology*

The successful enlargement of the two tubes showed that the back-cutting technology functions well. It was possible to reduce the energy output by some 50% through working against the rock's tensile strength rather than its compressive strength. When passing a previously excavated cross-passage it was possible to observe the back-cutting process (Figure 10).

The offset traces of the cutter rollers could clearly be identified on the face as well as the exact removal of material in accordance with the profile. Dust, vibrations and water meant that the complex electronic control facilities in the cutterhead, which were installed for the back-cutting technology, had to be maintained intensively. Even when individual cutterhead components failed, which meant that only three of



Figure 10. TBE-cutterhead passing an accessible cross-passage.

the six cutter arms could be extended, it was still possible to continue excavating. Through ensuring that the diverse technical components for the cutterhead were set up in a redundant manner for the second tunnel tube, the TBE's availability could be constantly geared to a high level albeit with a substantial maintenance requirement. As the forces in each case act in a diametrically opposed manner when the slides with the roller bits are extended radially and consequently nullify each other, only slight forces are generated from the main bearing. The abolition of the major contact forces (thrust) and the related high torque loads on the tunnel boring machine was also positive.

6.2 *Block-form of the excavated material*

The block-form of the backcut excavated molasse material (flat lying sandstone and marl layers) differed considerably from the chip form of traditional TBM drives. The grading curve of the material is more similar in fact to that of a drill and blast operation. On account of its larger block-form the material had to be reduced at the end of the back-up by means of a crusher in order to adhere to the maximum permissible edge length of 30 cm for conveyor belt transportation. A powerful dedusting plant together with its casing was installed at the crusher to protect the crew's health. The resultant block-form made it possible to reutilise the excavated material for backfilling at both sides of the service duct after sieving and adding a hydraulic binder.

6.3 *Possibility of overcutting*

A circular profile of 7.0 m radius was excavated by the roller bits on the six radially extendable cutterhead slides. Thanks to the three additional extendable roller bits (Figure 11) installed in the cutterhead an overbreak with a maximum radius of 20 cm could be attained in order to provide more room for supporting the



Figure 11. Overbrake roller bit on the TBE cutterhead.



Figure 12. Excavation support in L1 of the TBE (with spalling above the cutterhead).

excavation. The overbreak was only required in the vault area because the completed base invert was placed some 80 m behind the face so that the temporary excavation support there could be reduced. Thanks to targeted overbreak, it was on the one hand possible to save on material transport and on the other on concrete and backfill requirements.

6.4 *Applied supporting media*

The supporting friction bolts that were used for overhead protection could be installed at the earliest some 4 m behind the face slightly inclined forwards and 4.5 m behind the face vertical to the tunnel axis.

In zones with geological overbreak for example on account of the molasse's horizontal bedding, it was possible to react flexibly at local level to spalling thanks to the chosen support system (friction and rope anchors, netting and shotcrete, Figure 12). In this connection, the anchors and netting were placed in the cavities that ensued and subsequently filled with shotcrete. Where potential areas of spalling were identifiable (e.g. coaly base levels) additional anchors with $l = 3.60$ m were placed in addition to the anchorage system ($l = 5.0$ or 6.0 m in a 1.20×1.20 to 1.50×1.50 m grid).They were set up in such a way that they penetrated possible areas prone to spalling that were identified in order to additionally nail the fissured zones. A row of the anchor system was installed every 1.20 tm in such geologically tricky zones and a row of additional anchors offset by 0.60 m placed every 1.20 m.

This flexible system of rock support did stand the test. However it demanded of all the involved a high attention and a professional competence to react correctly and in time to the identified hazard scenarios.

6.5 *Deformations of the rock support*

The deformations measured (3D convergence measurements following installation of the support means

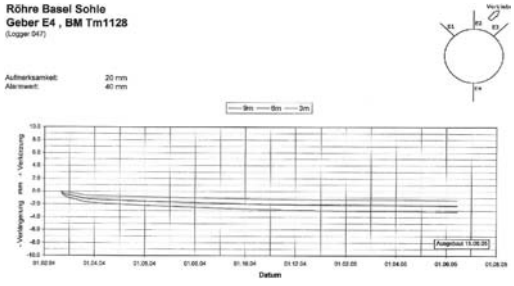


Figure 13. Maximal deformations of the base in the molasse (extensometer).

were of about 1–2 cm. The deformation occurred around the entire vault periphery, mostly radial to the excavated surface towards the cavity.

Extensometers in the base showed normally about 1 mm of enhancement, at most 3 mm because of swelling after contact with water (Figure 13).

6.6 *Ventilation*

As far as the TBE application was concerned the prior production of the centric pilot tunnel represented a prerequisite in order to provide pre-tensioning for the enlargement. Alongside some invaluable geological findings from the pilot tunnel excavation, the pilot tunnel served for surveying purposes during the TBE drive and especially for ventilation. The dust that occurred during the drive or rather during the drilling of the anchors (dry) was suctioned off by fans stationed at the end of the pilot tunnel, cleansed by means of dedusters and released into the open. As a result, it was possible to largely minimize dust nuisance in all TBE working sectors.

6.7 *Rates of advance*

In 2003, the TBE drive was executed by means of a two-shift operation (driving 7.00 a.m. till noon and 1.00 till



Figure 14. Service duct and backfilling behind the TBE.

10.00 p.m.) with residual supporting and maintenance taking place from 11.00 p.m. till 3.00 a.m.) during a five-day week. Weekly rates of some 20 m were attained. The maximum daily rate amounted to 12 m.

Since early 2004, work was carried out on a three-shift basis (for schedule reasons), with supporting and maintenance operations being undertaken during the reduced third shift (driving from 6.00 a.m. till 10.00 p.m. continuously, with residual supporting and maintenance jobs taking place between 10.00 p.m. and 6.00 a.m.). As a result of this measure, average weekly rates of advance of some 40 m were arrived at, with maximum weekly progress of 63.5 m. The maximum daily rate of advance amounted to 16.5 m per work day. At the same time the entire base area was tackled in the back-up zone simultaneously with the drive (base invert, service duct and backfilling).

On the basis of the three-shift operation, the average rate of advance for the entire cross-section amounts to approx. 29 m/week (including the pilot tunnel and the completion of the base area in the back-up zone).

7 OUTLOOK

At the moment all the electromechanical equipment is being installed in the tunnel. Finished this installations the functioning will have to be checked.

It is planed to open the Uetliberg Tunnel for traffic at the end of 2008.

For further information, click on:
www.westumfahrung.ch (client)/
www.uetlibergtunnel.ch (project designer and coordinator)

Underground Space – the 4th Dimension of Metropolises – Barták, Hrdina, Romancov & Zlámal (eds)
© 2007 Taylor & Francis Group, London, ISBN 978-0-415-40807-3

Completion of a trans-Tokyo Bay long-distance undersea shield tunnel

Shinichi Shirai, Tomoaki Takeuchi
The Tokyo Electric Power Co., Inc. Construction Department, Tokyo, Japan

Shigeru Kurosaki
The Tokyo Electric Power Co., Inc. Higashi Ohgishima Thermal Power Station, Kawasaki, Japan

Motoi Takebayashi
The Tokyo Electric Power Co., Inc. Futtsu Thermal Power Plant Construction Office, Chiba, Japan

Tatsuya Tomidokoro
The Tokyo Electric Power Co., Inc. Nuclear Quality Management Department, Tokyo, Japan

ABSTRACT: The Tokyo Electric Power Company (TEPCO) planned the construction of a gas pipeline connecting a TEPCO LNG base located on the east shore of Tokyo Bay with another on the west shore, in order to supply LNG to its thermal power stations on the Tokyo Bay coast more flexibly and efficiently. As part of this project, a shield tunnel was built to house the 18-km section of the pipeline that crosses Tokyo Bay. The construction of shield tunneling was that each slurry shield machine starts tunneling from each side of shore of Futtsu and the opposite Higashi-Ohgishima, and the two shield machines meet midway beneath the seabed of Tokyo Bay. Each shield machine is required to tunnel a distance of 9.0 km, of world-class long tunnel. This paper reports on the planning and construction of the shield tunnel.

1 INTRODUCTION

The location and cross section of the tunnel are as shown in Figure 1. The internal and external diameters of the shield tunnel are 3.0 m and 3.44 m, respectively.

The following is a chronological summary of the construction of the tunnel:

- In November 2003, shield tunneling from the Chiba side (east side) was started (called the "Futtsu" section).
- In February 2004, shield tunneling from the Kawasaki side (west side) was started (called the "Ohgishima" section).
- The shield machine from the Chiba side completed the excavation of the Futtsu section (9,030 m) and reached the docking point in March 2005, and the shield machine from the Kawasaki side completed the excavation of the Ohgishima section (9,030 m) and reached the docking point in July 2005.
- After 5 months of underground docking work, the tunnel was completed in December 2005.

The most challenging parts of the construction of the tunnel were (1) to ensure that the shield machines could withstand excavation of 9.0 km tunnel, (2) to ensure high-speed tunneling at a steady rate of more than 500 m per month and (3) to successfully complete the mechanical underground docking operation under a high water pressure of 0.6 MPa.

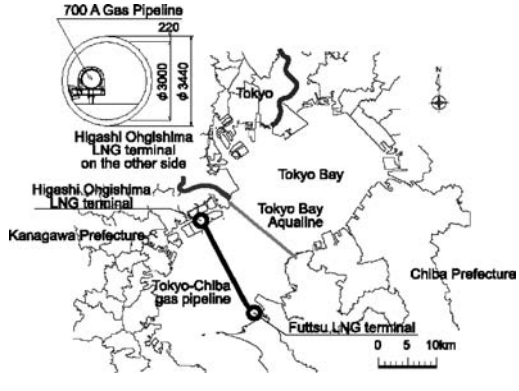


Figure 1. Location and cross section of the tunnel.

The following chapters describe the planning and construction of the shield tunnel in detail, focusing on these three points.

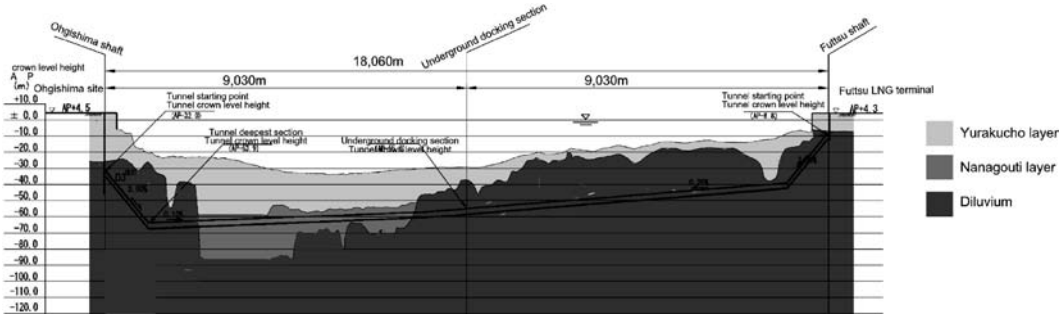


Figure 2. Supposed geological structure of the construction site.

2 OVERVIEW OF THE GEOLOGICAL STRUCTURE AND THE TUNNEL PROFILE

Figure 2 shows the geological structure of the construction site, which was estimated by the past survey records in surrounding areas including "the Tokyo Bay Aqua-Line" and the periphery of this and sonic prospecting conducted in Tokyo Bay. An estimated profile is used because it is difficult to conduct boring surveys in the construction area due to the heavy sea traffic in Tokyo Bay.

To ensure the stability of the tunnel against earthquakes, the tunnel profile was designed so that the tunnel run through the Nanagohchi layer and diluvium and no part of the tunnel is located in the soft Yurakucho layer. As a result tunnel gradients are ranging from 0.1% to 0.3%. In addition, it was expected that this profile design would subject the shield machines to a water pressure of 0.67 MPa at its deepest part. This was a tough environment for shield tunneling. The alignment of the entire tunnel is a straight line, except for one curve with a radius of 4,000 m located in the Futtsu section.

3 PLANNING AND CONSTRUCTION OF THE LONG-DISTANCE SHIELD TUNNEL

It was expected at the outset of the project that the construction of the tunnel would involve many risks, because (1) each of the two shield machines would be required to excavate a 9.0-km section of the tunnel, (2) most of the two sections of the tunnel had to be constructed in a high water pressure condition beneath the seabed, and (3) There would be uncertainties in geological condition. In addition, the specified construction period required high-speed tunneling at a rate of 500 m or more per month.

All possible risks associated with the design and construction phases were identified and measures were taken to minimize or eliminate these risk. In addition, backup measures were prepared in case of a critical problem. The following sections describe the durability enhancement measures taken for the cutter bits, which is easy to be worn away and damaged when used continuously in long-distance tunneling difficult to be repaired or replaced.

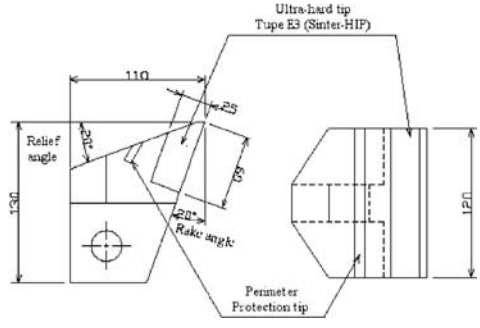


Figure 3. Shape and dimensions of main bit (Futtsu section).

3.1 *Durability design of cutter bits*

Because the shield tunnel is a small-diameter tunnel with an external diameter of 3.6 m, it was practically impossible to equip the shield machines with a cutter bit replacement mechanism. It was therefore decided to plan and implement measures to allow the shield machines to excavate the respective 9-km tunnel sections without bit replacement.

Tips made of a type E3 material (equivalent to Sinter-HIP), which has high abrasion resistance (hardness) and shock resistance (transverse rupture strength), were attached to the cutter bits. Figure 3 shows the shape and dimensions of the main bit for the Futtsu section. The tips were attached to the bits using the plate-style attachment method, which allows a larger surface area as the cutting edge.

The leading bits were deployed on the same path, to reduce the abrasion load on the main bits. Multi-tier shell-type leading bits, which are highly durable and suitable for excavation of hard soils and gravel layers,

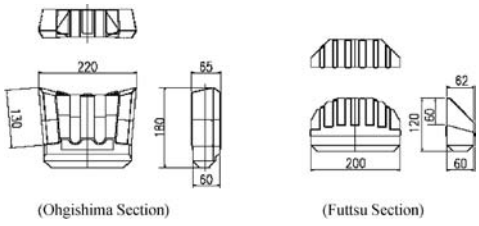


Figure 4. Shape and dimensions of leading bit.

were attached to the shield machine for the Futtsu section, and large-sized leading bits were attached to the shield machine for the Ohgishima section (Fig. 4).

The expected amount of abrasion of a cutter bit can be calculated from the following formula:

$$\delta = k \cdot \pi \cdot D \cdot N \cdot L/V$$

where, δ: expected amount of abrasion (mm), k: abrasion coefficient (mm/km), D: external diameter of the shield machine (mm), N: number of revolutions of the cutter (min^{-1}), L: tunneling distance (km), V: tunneling speed (mm/min).

The abrasion coefficient was determined individually for each soil type from bit shape-specific records of past tunneling projects, taking into account the height difference between the leading bit and the main bit. This resulted in lesser calculated expected amounts of abrasion of the outermost main bits (with the largest sliding length) than the allowable amounts of abrasion (26 mm, 30 mm), which meant that the designs would allow the shield machines to excavate the respective 9-km sections without suffering excessive abrasion.

3.2 *Other measures*

Although the calculated expected amounts of abrasion were based on records of actual past tunneling projects, they were still estimates, and so the actual amounts of abrasion could have turned out to be significantly different from the estimated amounts. It was also possible that unexpected abnormal abrasion might occur. To protect against these risks, the following measures for the bits were taken in addition to backup measures.

To prevent cutter bit abrasion due to excessive sliding, a system was adopted which could automatically adjust the cutter revolution speed to the tunneling speed to keep the bit penetration depth constant.

In addition, the design of the shield machines was modified to allow the excavated material to be taken in more efficiently (including elimination of the cutter perimeter rings), because the amount of abrasion of a bit is closely related to the amount of excavated material that remains on the cutter disk surface. As a result of these modifications, a cutter aperture rate of 42 to 43% was achieved, which was higher than that of existing slurry shield machines.

Table 1. Measured maximum amounts of abrasion of the outermost bits.

		Leading bit		Main bit	
		Expected	Measured	Expected	Measured
Futtsu section	Amount of abrasion (mm)	61.3	31.0	18.6	4.0
	Abrasion coefficient ($\times 10^{-3}$ mm/km)	14.8	6.61	4.48	0.85
Ohgishima section	Amount of abrasion (mm)	80.1	19.0	15.7	0
	Abrasion coefficient ($\times 10^{-3}$ mm/km)	23.2	3.72	4.55	0

3.3 *Results*

After completion of tunneling, the shield machines were disassembled and the bits were inspected to confirm the amounts of abrasion. Table 1 shows the results. The abrasion coefficient values in the table are averages over the tunneling distances. The actual amounts of abrasion of the leading and main bits of both shield machines were significantly smaller than the expected amounts of abrasion. This is due to the fact that considerably larger portions of the lengths of the two sections (than originally estimated) lay in soil layers consisting predominantly of cohesive soils. It is also considered that the main bit protection effect of the large-sized leading bits, as well as the design modifications to allow the excavated material to be taken in more efficiently, helped reduce abrasion by reducing the cutting load.

4 MEASURES TO ENSURE CONSTANT HIGH-SPEED TUNNELING AND RESULTS

To achieve an average tunneling rate of more than 500 m per month, measures were taken to enhance the levels of performance and availability of individual systems and facilities.

4.1 *Performance enhancement measures for the shield machines and individual systems and facilities*

The tunneling capacity of a shield machine is largely determined by its advancing speed. The shield machine for the Ohgishima section was designed to be capable of advancing at a speed of 70 mm/min. and that for the Futtsu section at 90 mm/min. Table 2 shows the specifications of the shield machines.

Measures were also taken to enhance the performance levels of individual systems to help the shield

Table 2. Summary specifications of the shield machines.

		Ohgishima section	Futtsu section
External diameter		ϕ3,590 mm	ϕ3,620 mm
Total length		11,645 mm	12,180 mm
Shield jack	Thrust × Number of jacks	1,680 kN/jack × 20	1,225 kN/jack × 18
	Length	2,550 mm	2,000 mm
Jack extension/contraction speed (when all jacks are in operation)	Pushing	70 mm/min	90 m/min
	Pulling	1,500 mm/min*1	450 mm/min
Cutter torque		560–805 kN•m ($\alpha = 12.1$–17.3)	674–1,013 kN•m ($\alpha = 14.2$–21.4)
Number of revolutions of the cutter		1.93–3.0 rpm	0.6–3.0 rpm
Driving system		Hydraulic	Hydraulic

*1: When 7 jacks are in operation.

machines constantly advance at the design speeds. The system to transport segments through the tunnel was designed to be capable of running three battery-driven trucks coupled together with each truck carrying segments for two rings or six battery-driven trucks coupled together with each truck carrying segments for one ring, at a maximum speed of 11 km/h. In addition, a facility capable of fully loading a train of trucks with segments/slabs at a time and a facility capable of fully unloading a train of trucks of segments/slabs at a time were constructed under the vertical shaft in the Futtsu section and at the face areas, respectively.

The slurry transport and slurry treatment systems were designed to be able to handle both a 100% sandy soil cross section and a 100% cohesive soil cross section, in order to accommodate uncertainties in geological condition of the construction site. In addition, the slurry transport systems were designed to have two or three intermediate bypasses to reduce losses in the event of a start-up failure, etc.

4.2 *Segment type*

Efficient segment assembly is also essential for high-speed tunneling. To achieve a highly efficient segment assembly process, segments for the Futtsu section were designed so that six segments comprise one segment ring with a segment length (along the tunnel axis) of 1.35 m, and the segments for the Ohgishima section were designed so that five segment comprise one segment ring with a segment length (along the tunnel axis) of 1.2 m. Segment joints for both sections were designed such that the segments could be easily joined together just by operating the erecting system. Table 3 shows the shapes of the segment joints.

4.3 *Availability*

Apart from enhancing the capabilities of facilities and systems, ensuring a high level of availability of the shield machines is also essential for high-speed tunneling. The best way is to reduce failures of the shield machines. In this project, maintenance of the shield machines was performed monthly and parts were replaced systematically according to a meticulous replacement plan, to reduce failures. In addition, spare equipment and parts including an ample stock of segments were kept in the tunnel against an unexpected failure or problem.

These availability improvement measures resulted in an availability of higher than 93%, which was much higher than the target availability of 80%.

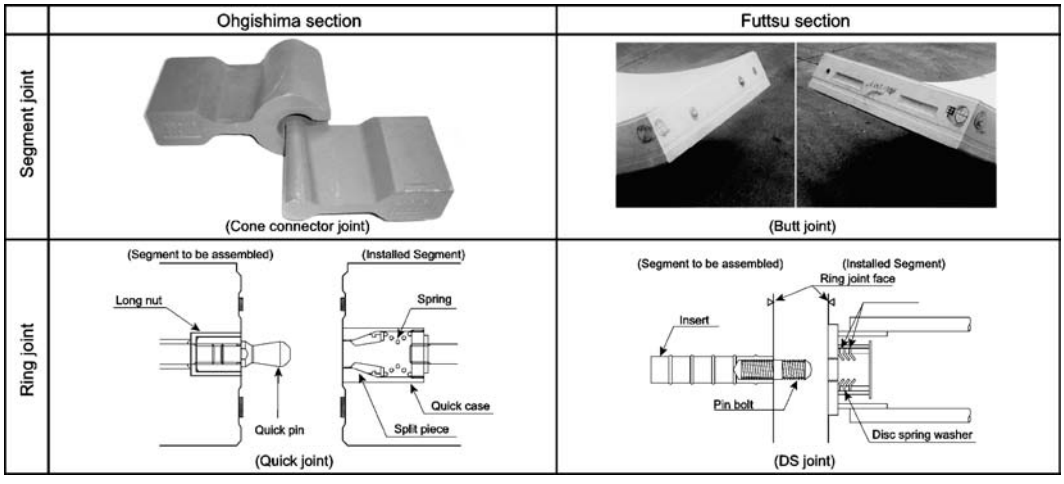
4.4 *Results*

Figure 5 shows a graph of the distances tunneled by the two shield machines, both on a monthly basis and on a cumulative basis, with the above-mentioned measures implemented. The shield machine for the Futtsu section excavated at an average monthly rate of 665 m and that for the Ohgishima section at 605 m. Although the rates of tunneling varied from month to month because of unexpected encounters with gravel layers, steady high-speed tunneling was achieved overall. The maximum monthly distance was 1,168 m in the Futtsu section and 830 m in the Ohgishima section. The shield machine for the Futtsu section achieved the maximum distance on 23 days in a month, and the average daily distance for that month was approximately 50 m. To sum up, both shield machines performed better than expected, successfully tunneling as long as 9 km at a high tunneling rate of more than 600 m per month without any major failure or safety-related problem. The Ohgishima section was tunneled in three shifts for the entire tunneling period, and the Futtsu section was tunneled in three shifts until July 2004 and in two shifts thereafter.

5 MECHANICAL UNDERGROUND DOCKING

The two shield machines started from opposite sides of Tokyo Bay and docked with each other beneath the seabed of Tokyo Bay after each completing 9 km of tunneling. In this project, a mechanical docking

Table 3. Shapes of joints.



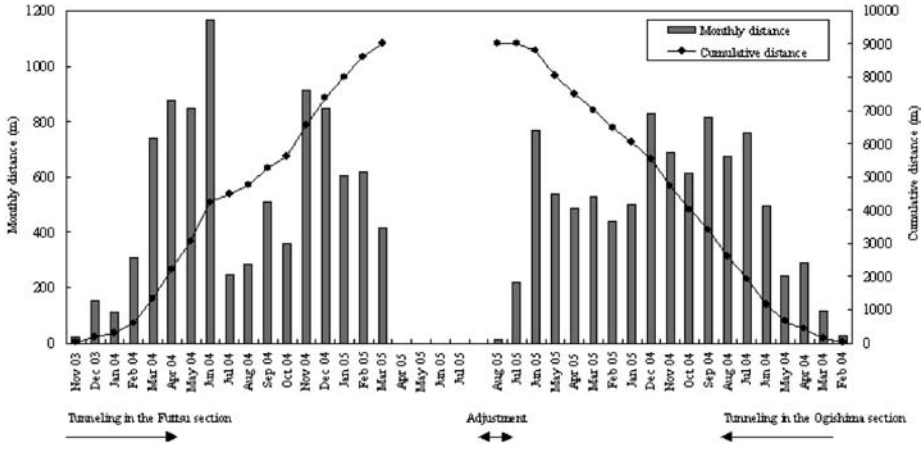


Figure 5. Distances tunneled by the two shield machines.

method was adopted whereby the shield machines were directly docked with each other. This method had been used in more than 10 projects, but never in an environment under a high water pressure of 0.6 MPa anticipated for this project. Therefore, effective sealing of the connection section to prevent infiltration of water was a major challenge.

5.1 *Overview of the underground docking work*

Figure 6 illustrates three steps of the docking work. As can be seen in Step 3, both shield machines have an inner cylinder comprising a cutter head and a bulkhead, which slides in the outer cylinder (i.e. the shield machine body). The shield machines are directly docked by sliding backward the inner cylinder of the receiving shield machine (the Futtsu shield machine) and sliding forward the inner cylinder of the entering shield machine (the Ohgishima shield machine).

5.2 *The three steps of the docking work*

In Step 1, the entering shield machine is advanced until the center bit of the entering shield machine reaches the point exactly 50 mm away from the center bit of the receiving shield machine (the relative positions of the machines are continuously checked throughout the process). After the entering shield machine reached the point exactly 50 m away from the receiving shield machine, the relative positions of the shield machines are confirmed by horizontal boring utilizing magnetic sensors and RI radiation sources. The allowable arrival error for the entering shield machine was $\pm$50 mm and $\pm$1 degree.

In Step 2, the inner cylinder of the receiving shield machine is slid backward using the articulation jacks with its spokes contracted and the face water pressure maintained at the appropriate level. After this, the entering shield machine is advanced using the shield jacks until its hood reaches the point exactly 50 mm away from the hood of the receiving shield machine with the entering shield machine's spokes contracted. Minimizing the distance between the hoods is an effective means of ensuring the stability of the soil surrounding the shield machines.

In Step 3, the inner cylinder of the entering shield machine is slid forward by 510 mm. Then, the tube seal system to prevent infiltration of water is activated to seal the gaps in the connection section. The tube seal system expands the rubber film tubes attached on the inner surface of the outer cylinder of the receiving shield machine by injecting water into the tubes, so that the seal plates are strongly pressed against the outer surface of the inner cylinder of the entering shield machine.

After this, the spaces behind the seal plates are filled with grout material and iron seal plates are welded (all-around welding) to complete the docking.

5.3 *Results of the docking work*

In each of the three steps, all the relevant mechanisms, including the spoke contraction mechanism and the inner cylinder sliding mechanism, functioned as expected. The water leakage rate with the tube seal system in operation was less than 0.1 l/min., indicating that the tube seal system effectively prevented infiltration of water. The mechanical docking operation under the high water pressure of 0.6 MPa was completed successfully despite the fact that it was a highly complex process in terms of both mechanisms and procedures. In addition, no human errors were made during the docking operation, thanks to the constant communications and efforts of the teams of both sections.

6 CONCLUSIONS AND ACKNOWLEDGEMENT

The construction of the 18-km trans-Tokyo Bay undersea tunnel was successfully completed in spite of many tough challenges, including accurately estimating the geological structure by means of sonic prospecting from above the water surface, ensuring that each of the two shield machines would withstand as long as 9.0 km of shield tunneling beneath the seabed of Tokyo Bay, ensuring high-speed tunneling at an average monthly rate of more than 500 m per month and successfully completing mechanical underground docking of the two shield machines under a high water pressure of 0.6 MPa.

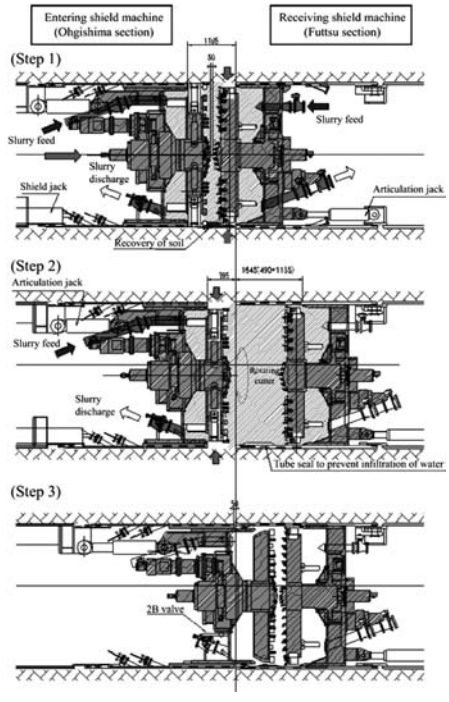


Figure 6. The three steps of mechanical underground docking.

The main reasons for the success of the project were the development of a meticulous construction plan, the rigorous control of construction work and the rigorous implementation of measures to resolve the challenges.

We would like to express our gratitude to many people who supported the project in its design and construction phases by providing valuable guidance and advice, including Emeritus Professor Toru Konda, Professor Atsushi Koizumi and Mr. Yukinori Koyama. The basic plan for the Futtsu section was developed based on a proposal by a joint-venture team comprising engineers from Kajima, Nishimatsu and Obayashi Corporation and the basic plan for the Ohgishima section was developed based on a proposal by a joint-venture team comprising engineers from Taisei, Shimizu and Hazama Corporation (because the project was a "design-and-build" project). We sincerely thank all people who provided great assistance to the project including staff of the above-mentioned construction companies who participated in the project.

REFERENCES

T. TOMIDOKORO et al. 2006 Special Feature – Construction of trans-Tokyo Bay gas pipelines. *Tunnels and Underground* 37(7)

Underground Space – the 4th Dimension of Metropolises – Barták, Hrdina, Romancov & Zlámal (eds)
© 2007 Taylor & Francis Group, London, ISBN 978-0-415-40807-3

Behavior of the shield studied with 3D geological structure models

M. Sugimoto
Nagaoka University of Technology, Nagaoka, Niigata, Japan

H. Sasao
Tekken Corporation, Tokyo, Japan

Y. Ootsuka & T. Ogawa
OYO Corporation, Tokyo, Japan

K. Harada
Kawasaki Geological Engineering Co., Ltd., Tokyo, Japan

E. Kondo
Kansai Electric Power Company, Oosaka, Japan

ABSTRACT: To predict shield behavior correctly, understanding geological structure around the tunnel is important. Therefore, this paper examines the 3D geological structure using data obtained from boring and investigates the relationships among the 3D geological structure, the shield operation and the shield behavior. Furthermore, the effect of 3D geological structure on the shield behavior was confirmed, comparing the simulation results of the shield behavior with actual observations. As a result, not only macro geological structure but also micro geological structure have an effect on shield behavior and shield operation.

1 INTRODUCTION

Shield behavior depends on geological structure, soil properties, tunnel alignment, tunnel dimensions, shield dimensions, and shield operation. Therefore, understanding geological structure around the tunnel is important to predict shield behavior more precisely (Sugimoto et al. 2003). This paper examines the 3D geological structure using data obtained from boring around the tunnel, and investigates the relationships among the 3D geological structure, the shield operation, and the shield behavior. Finally, the effect of 3D geological structure on the shield behavior is confirmed, based on the results of shield behavior simulation by applying the inferred 3D geological structure to the shield kinematic model (Sugimoto and Sramoon 2002).

For a case study, Hon-chou Tunnel in MM21 Line in Yokohama, Japan was adopted as the test site. Since this tunnel is located along the seashore and the sand spit existed close to this tunnel more than 100 years ago, it is expected that the geological structure around the tunnel is complicated. This tunnel is a twin tunnel, which was excavated by EPB type DPLEX shield. The out bound tunnel and the in bound tunnel are constructed on the seaside and land side respectively by using the same shield machine. The dimensions of the tunnel and shield, and the geological profile around the tunnel are shown in Table 1 and Figure 1 respectively.

Table 1. Dimensions of tunnel and shield.

Item	Component	Value
Tunnel	Horizontal radius	Straight
	Vertical gradient	0.2% up to 1.2% up
	Overburden depth	16.7 m to 15.4 m
	Groundwater level	14.7 m to 12.3 m
	Outer radius of segment	3.5 m
	Width of segment	1.2 m
Shield	Outer radius	3.575 m
	Total length	7.485 m
	Self-weight	3.1 MN
	Open ratio of cutter face	54.4%
	Radius of cutter face	3.583 m

2 GEOLOGICAL STRUCTURE OF GROUND

2.1 *Geological cross section*

Figure 1 shows the geological cross-section along the tunnel. The geological structures drawn in the figure

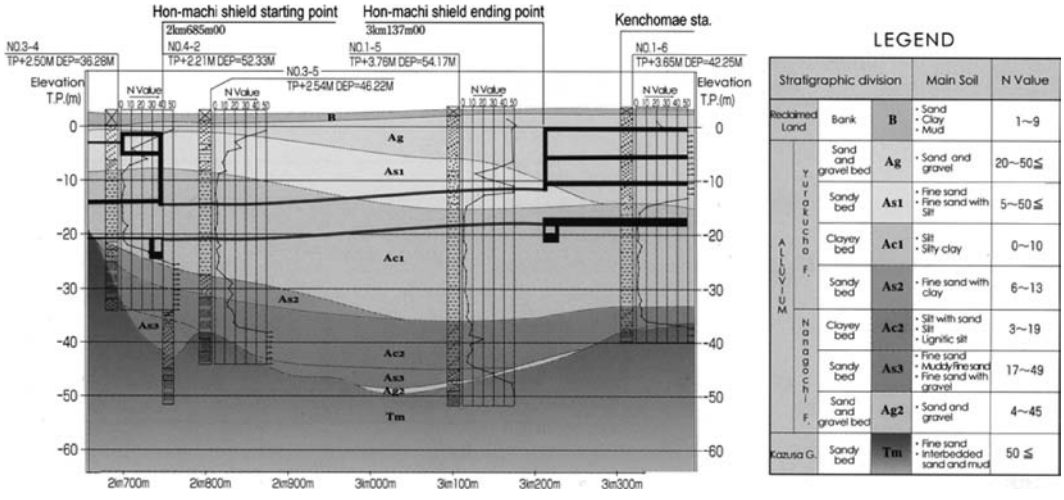


Figure 1. Geological profile at test site location.

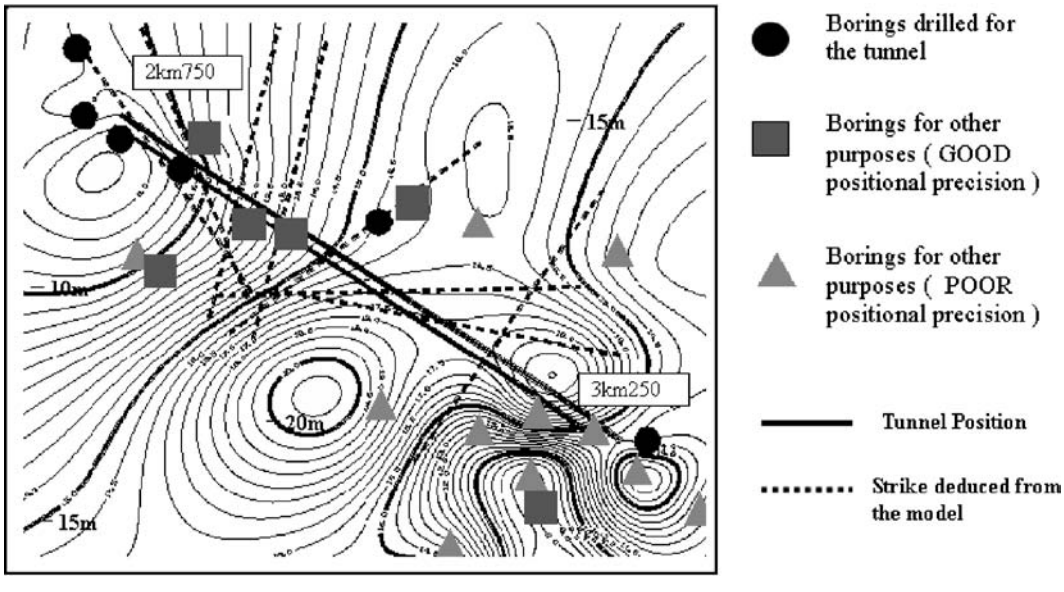


Figure 2. Contour display of Ac1/As1 boundary.

were inferred from data obtained from the four holes drilled along the tunnel. The composite log displays of the data obtained from boring are drawn on the figure. The tunnel position is also shown with two solid lines. The geological structures in this area appear to be simple layered ones in the alluvial formations, As1, Ac1, etc. above the base rock Tm, although the shape of the in boundary of the basement rock is a little rough.

In the simulation of shield behavior, several parameters relating geological structures along the tunnel are used, such as, soil properties, elevations of geological boundaries along the tunnel axis, and dip and strike of the geological boundaries. These parameters, especially strike of geological boundary, are very sensitive to the detailed shape of the geological boundary when the geological boundary has a low angle as is often the case with alluvial formations. To infer these parameters more precisely, the 3D geological structure was investigated utilizing more data obtained from boring nearby the tunnel in addition to those in Figure 1.

2.2 *3D geological structure*

Figure 2 shows 1 m contour lines of Ac1/As1 boundary by the Convergent Gridding method (Schlumberger

Ltd, 2000). In this figure, the circles, the triangles and the squares denote the drilling locations used for modeling this Ac1/As1 boundary. The triangle marks mean slightly less precision of the boring head location, compared with the other borings. The two solid lines in the figure from upper-left (NW) to lower-right (SE) denote the tunnel location.

From this figure, it is obvious that the geological boundary is rough in orthogonal direction to the tunnel axis. This also proves the importance of 3-D geological modeling since it is difficult to grasp such geological boundaries only from geological cross-sections.

3 SITE DATA

In this section, the site data are examined, taking account of the above 3D geological structure. Figure 3 shows the soil component, the horizontal jack moment during tunnelling, and the deviation of the segment in the horizontal direction. The three upper figures show the data along the out bound tunnel, and the three lower figures show the data along the in bound tunnel. The distance between the two tunnel centers is 10.650 m. The horizontal jack moment (here after called as M_{3p}) has a positive sign for right turn in direction of excavation. Therefore, the opposite sign of M_{3p} along the out bound tunnel and the upper one means the same rotation direction, since the excavation direction of each line is reversed. The soil components were obtained by sieving the mucking soil at each ring. The horizontal deviations of segments were surveyed after the completion of the shield tunneling work.

3.1 *Soil component*

The tendency of soil component distribution around the out bound tunnel and the in bound tunnel corresponds in range A, range B, and range C in the figures. Considering the geological profile in Figure 1, the out bound tunnel from 2800 m to range B is located in Ac1 layer, and the sand content in the in bound tunnel is about 10% higher than that around the out bound tunnel. The thickness of As1 layer in the upper part of the tunnel cross section increases in the area between range B and range C, since the sand content in this range is about 60%. In range C, Ag layer almost covers the tunnel cross section gradually, since the gravel content increases from 0% to about 95%. These facts coincide with the above 3D geological structure. On the other hand, in area A, the sand content increases up to about 60%, and in area B, half of the tunnel cross section is in the gravel layer, since the gravel content is about 50%. These ground configurations can not be observed in the above 3D geological structure. It is considered that this comes from the scarcity of information about soil conditions in this area, since data from boring near this area are at the distance 2809 m and 3077 m only. Furthermore, considering that the sand content of As1 and Ac1 layer is about 75% and 16% respectively, it is supposed that the sand layer appears in the tunnel cross section at the range between the distance 2800 m and range B.

3.2 *Horizontal deviation of segment*

Along the out bound tunnel, the segment positions are changed to the sea side near points a and b, to the land side after point c, and to the sea side gradually at the other range. Along the in bound tunnel, the segment positions are changed to the sea side after points d, e, and f. The deviation of segment position usually appears due to the following reasons: 1) shield control is difficult due to a sharp curve; 2) shield operation, such as, jack pattern, copy cutter length and range, and articulated angle, is changed; 3) ground reaction force is not symmetric due to inclined ground layer or twin tunnel; and 4) shield has a special characteristics due to the center of gravity or the manufacturing accuracy. Therefore, it is considered that the deviation at points a and f comes from the tunnelling at the curve alignment, the deviation at points b, c, and d comes from the inclined soil layer, and the deviation at point e is caused by the shield operation so that a taper segment is installed near the distance 2890 m.

3.3 *Horizontal jack moment*

From Figure 3, it is found that the horizontal jack moment M_{3p} is not equal to zero at some range, even if the planned horizontal tunnel alignment is a straight line, and the tendency of the fluctuation of M_{3p} along both tunnels has a certain relation with the distribution of the soil component. Furthermore, M_{3p} in range D except for range A is applied to the land side continuously, M_{3p} in range E is applied toward the opposite tunnel, M_{3p} in range F is applied to the sea side, and M_{3p} in range G shows fluctuation. These shield jack operations were carried out to prevent the wriggle motion of the shield. Taking account of the soil component distribution, these phenomena can be explained as follows: 1) in ranges D and F, the shield excavates the boundary of the inclined soil layer; 2) the soil layer with high gravel content like seam exists in range E, which corresponds to the gravel content in range B; and 3) the shield meets Ag layer in range G.

Assuming that M_{3p} is applied continuously when the shield excavates the boundary of the inclined soil layer in a transverse direction of the tunnel, strike direction angle can be estimated by connecting the points on both tunnel centers where M_{3p} is changed. Figure 4 shows the estimated strike line using the above assumption. Figure 5 shows the strike direction angle along the distance. In this figure, Ag-As1 and As1-Ac1

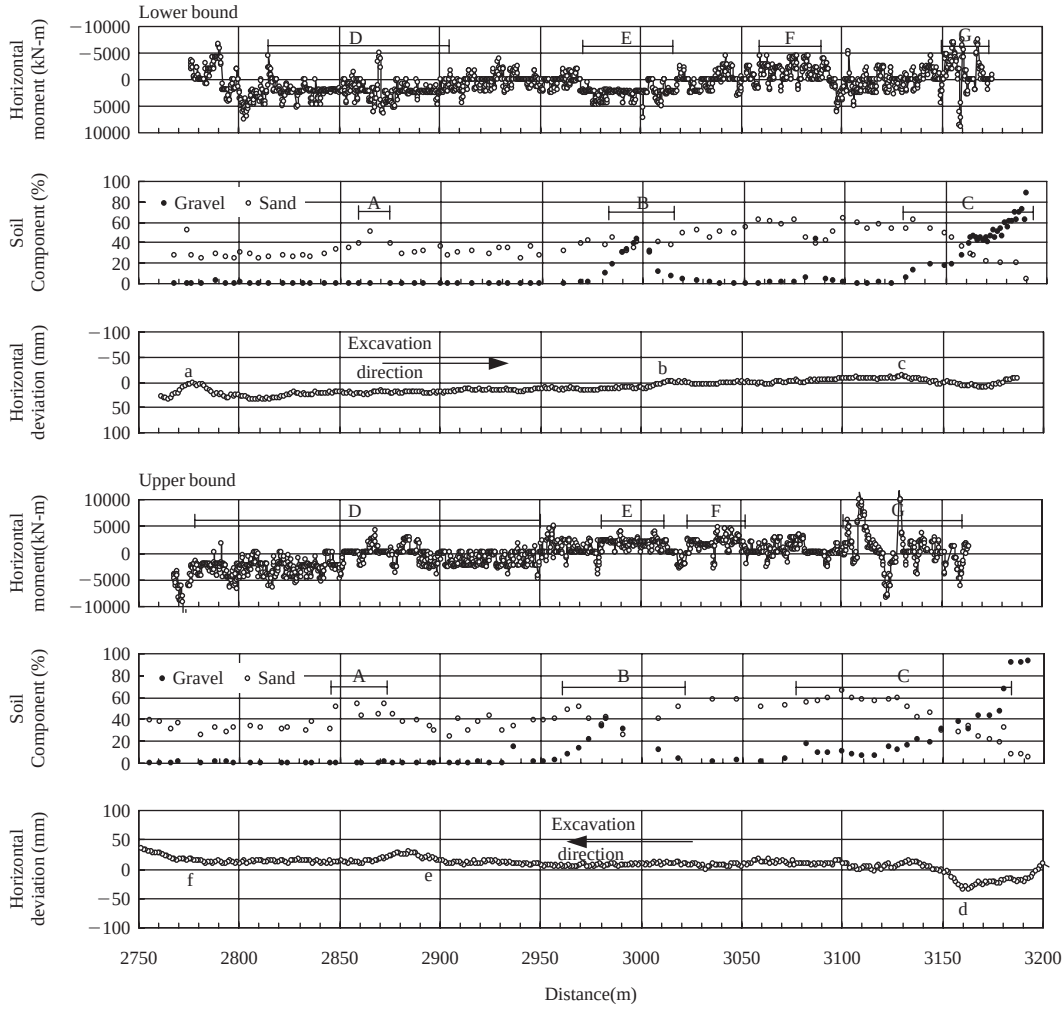


Figure 3. Horizontal jack moment, soil component, and horizontal deviation of segment.

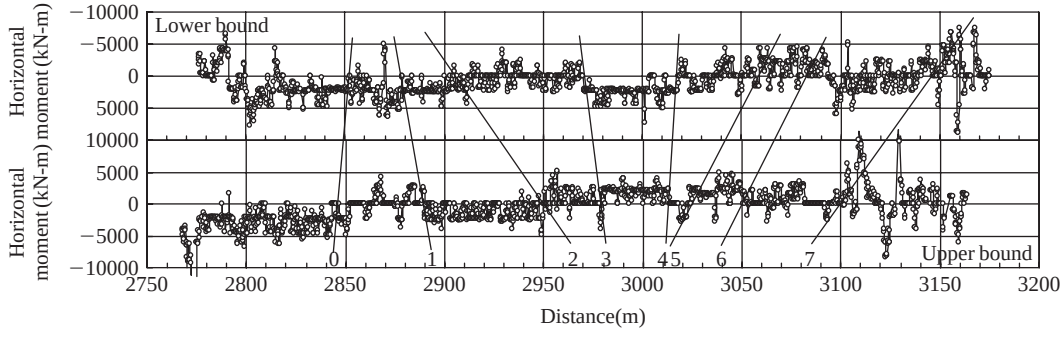


Figure 4. Strike direction by horizontal jack moment.

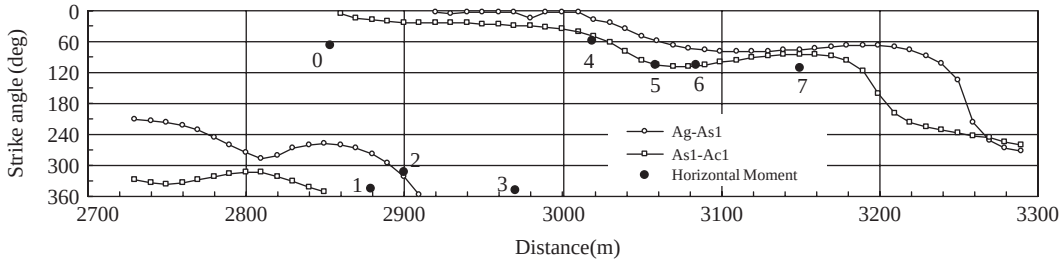


Figure 5. Strike direction angle along out bound tunnel.

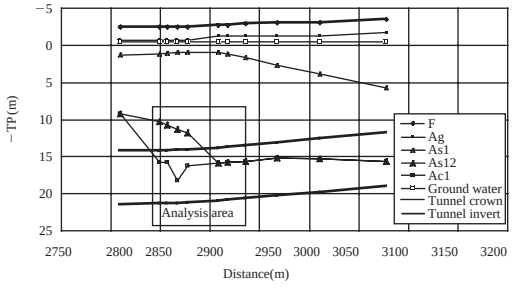


Figure 6. Geological profile used in the analysis.

Table 2. Ground properties.

Ground layer	As1	As12	Ac1
Unit weight (kN/m^3)	19.0	19.0	15.1
Cohesion (kN/m^2)	0	0	172
Internal friction angle (°)	32.4	33.8	0.0
K_{ho}	0.464	0.444	0.621
K_{vo}	1.000	1.000	1.000
k_h (MN/m^3)	16.2	900	16.2
k_v (MN/m^3)	16.2	900	16.2
Coeff. of dynamic friction	0.05	0.10	0.00
Dynamic adhesion (kN/m^2)	0.0	0.0	2.1
Equivalent *SPT N*-value	16	45	4

show the strike direction angle on the planned horizontal alignment of the out bound tunnel, which are obtained from the 3D geological structure as shown in Figure 2, and the black circle points are obtained from the line in Figure 4, of which the number corresponds to the number in Figure 4.

From this figure, it is found that the strike directions at points 2 and 4–7 coincide with that of As1-Ac1. This means that the geological structure affects M_{3p} directly. On the other hand, the strike directions at points 0, 1 and 3 are different from that of As1-Ac1. This fact indicates that a certain 3D geological structure exists around these points, irrespective of the above 3D geological structure, since the above 3D geological structure can not represent the change of the soil component along the tunnel.

4 SIMULATION OF SHIELD BEHAVIOR

4.1 *Analysis conditions*

The dimensions of tunnel and shield have already been described in previous sections. Based on the above examination of the 3D geological structure, the 3D geological structure was inferred as shown in Figure 6. Here the depth of As12 is estimated by calculating the thickness of sand layer at the tunnel cross section based on the soil component in Figure 3. Table 2 shows the ground properties used in the analysis. The values of the dynamic friction were adjusted so as to fit the calculated shield behavior with actual observations.

Figure 7 shows the input measured data, which were measured continuously by the automatic measurement system. Here, observed data were summarized at 20 cm intervals, i.e. one segmental ring is about six excavation steps. The operational control data are the jack thrust F_{3r}, the horizontal jack moment M_{3p} (+: right-turn), the vertical jack moment M_{3q} (+: downward), and the cutter torque CT (+: counter-clockwise direction, view from shield tail). The observed shield behaviors are the yawing angle ϕ_y (+: right-turn), the pitching angle ϕ_p (+: downward), and the rolling angle ϕ_r (+: clockwise direction, view from shield tail). The excavation conditions are the shield velocity v_s, the slurry pressure σ_m, and the slurry density γ_m in the chamber.

The initial excavated area, which is long enough for the whole length of the shield, i.e. from Ring Nos. 72 (Distance 2846.507 m) to 90 (Distance 2868.768 m) was set up by using the observed position and rotation of the shield. The shield behavior was then simulated up to Ring No. 141 (Distance 2929.307 m), based on the operational control data and the excavation conditions in Figure 7, using the shield kinematic model.

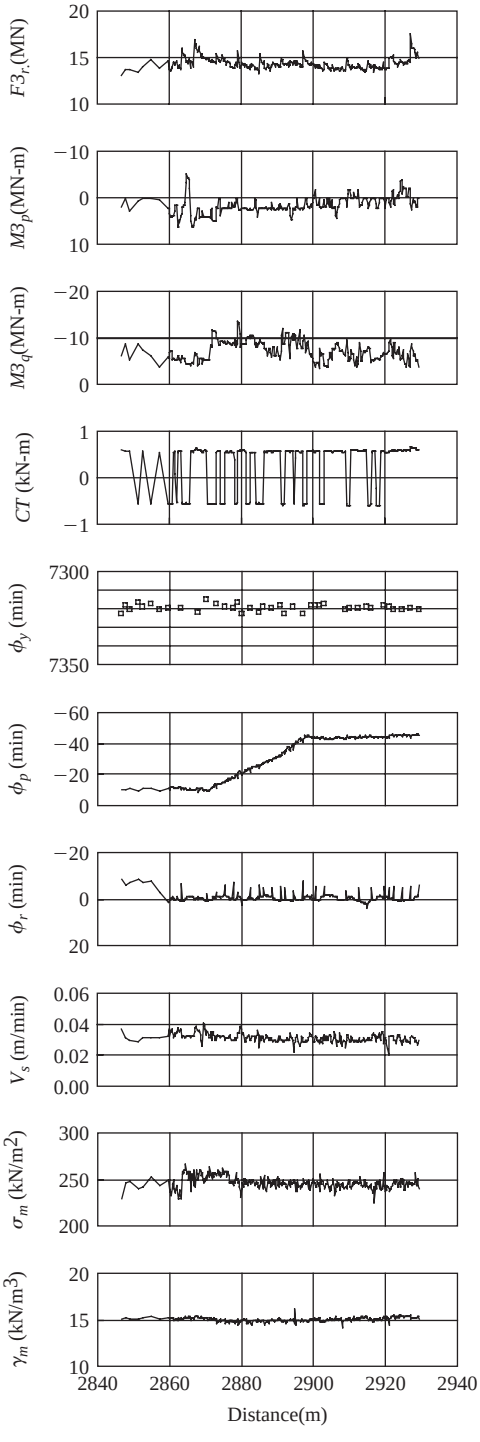


Figure 7. Shield tunnelling measurement.

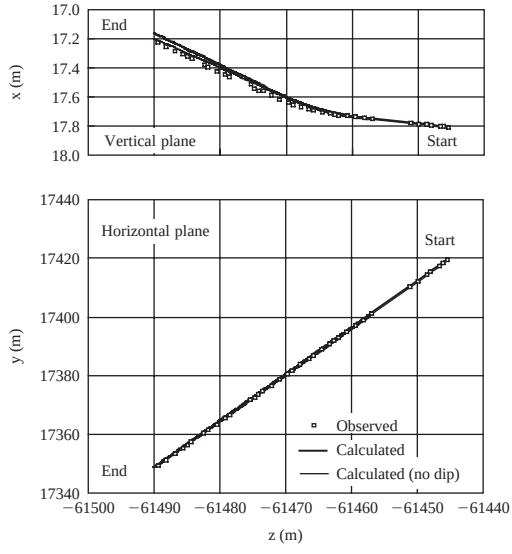


Figure 8. Shield traces.

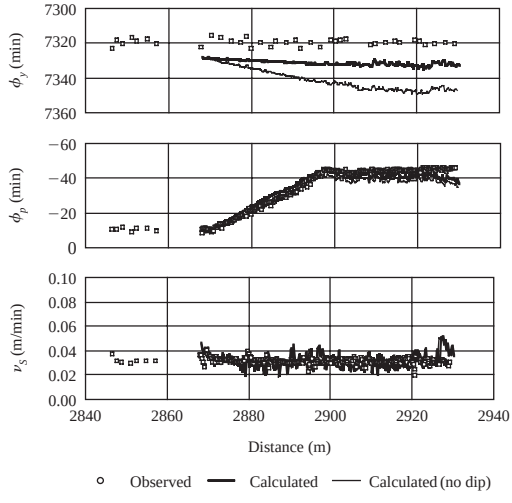


Figure 9. Shield behavior.

4.2 *Analysis results*

Figure 8 shows the shield traces on the vertical and horizontal planes, and the time dependent parameters ϕ_y, ϕ_p and v_s are shown in Figure 9. These figures include the observed data, the calculated data taking account of the 3D geological structure (called Case 1), and the calculated data without the consideration of the 3D geological structure (called Case 2), where the other parameters are the same as those of Case 1. Here, the observed shield position and the observed yawing angle were surveyed after excavation, whereas

the other observed data were measured continuously by the automatic measurement system.

These figures show overall good agreement between the calculated shield behavior of Case 1 and actual observations. As a comparison between calculations and observations, the maximum differences are 3 cm for the vertical position, 12 cm for the horizontal position, 5 min for ϕ_p, and 1 cm/min for v_s. The calculated ϕ_y of Case 1 has a slight parallel shift to the right about 6 min and 12 min from the planned ϕ_y and the observed ϕ_y respectively. This is because the observed ϕ_y were surveyed after the excavation, i.e. after relieving the jack thrust, while the calculated ϕ_y shows ϕ_y during excavation.

On the other hand, the calculated ϕ_y of Case 2 increases up to the distance 2910 m. This is because M_{3p} is applied to the right turn in the excavation direction as shown in Figure 3. This fact indicates that it is important to take account of 3D geological structure to simulate shield behavior precisely.

5 CONCLUSIONS

The 3D geological structure was obtained using the data obtained from boring around the tunnel, the relationship among the 3D geological structure, the shield operation, and the shield behavior was discussed. Finally, the effect of 3D geological structure on the shield behavior was confirmed, comparing the simulation results of the shield behavior with observations. As a result, the following conclusions can be drawn:

1. When geological structure is complicated, 3D geological modeling is important, since geological cross section does not provide adequate information.
2. Horizontal jack moment and shield behavior depends on not only macro geological structure, which is obtained from 3D geological modeling using data obtained from boring, but also micro geological structure due to soil component change, seam etc..
3. The shield kinematic model can simulate the shield behavior in the inclined soil layer in transverse direction.

ACKNOWLEDGEMENTS

The Japan railway construction, transportation and technology agency and Hazama Co. are gratefully acknowledged for providing the test site data.

REFERENCES

Schlumberger Ltd. 2000, GeoFrame3.8.1 online manual.

Sugimoto, M. & Sramoon, A. 2002. Theoretical model of shield behavior during excavation I: Theory. *Journal of Geotechnical and Geoenvironmental Engineering*. 128(2): 138–155.

Sugimoto, M., Sramoon, A., Maeda, K., Konishi, S., & Sato, Y. 2003. Simulation of slurry shield behavior during excavation at Ootsu tunnel, *Reclaiming the Underground Space* 2: 715–720. Rotterdam: Balkema.

This page intentionally left blank

Underground Space – the 4th Dimension of Metropolises – Barták, Hrdina, Romancov & Zlámal (eds)
© 2007 Taylor & Francis Group, London, ISBN 978-0-415-40807-3

Lining response of twin tunnels affected by EPB shield operation

S. Suwansawat
Department of Civil Engineering, Faculty of Engineering
King Mongkut's Institute of Technology Ladkrabang, Thailand

ABSTRACT: In the Bangkok MRTA project, some parts of the tunnels were designed to run close to each other due to the limitation of underground space. To investigate the lining response when an EPB shield was driven very close to another tunnel, convergence bolts were installed to measure changes in the tunnel shape. The convergence bolts were observed relative to the advance of the second shield. Additionally, shield operational parameters were monitored to determine effects of shield operation on tunnel linings. It was found that the first tunnel lining was deformed during the passing of the second shield as the second tunnel can induce stresses acting on the first tunnel. The stresses can cause inward deflections in the tunnel lining particularly at the location between springline and invert. The deflection magnitude of the first tunnel appeared to be proportional to the face pressure and the grouting pressure levels of the second shield. This paper describes the behavior of tunnel lining as affected by the shield operation.

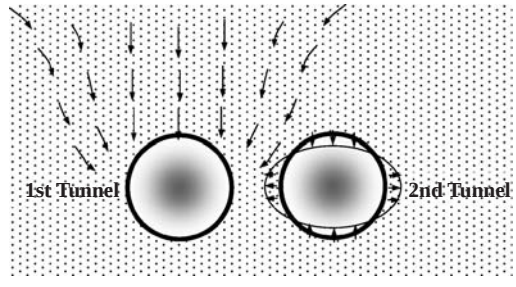
1 INTRODUCTION

In recent years, many tunneling projects have been built in congested urban environments which often involve the tunneling of twin tunnels in close proximity to each other. Furthermore, in many cases, the new tunnel is often excavated adjacent to existing tunnels. Hence, in the design of new tunnels, it is crucial to understand the interaction mechanism of the twin tunnels and their effect on the surrounding ground. Furthermore, from the structural engineering point of view, one needs to ensure that excessive bending moments or displacements are not developed in the lining of the tunnel which is built first.

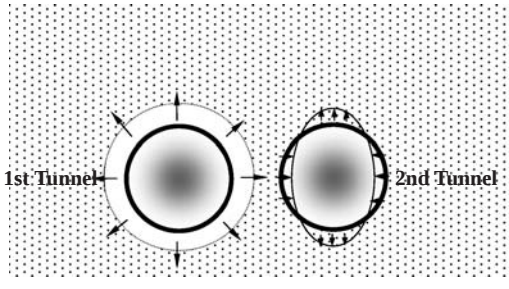
This research observed the behavior of the tunnel lining of the first tunnel as affected by the construction of the second tunnel in Bangkok MRTA project. Operational parameters applied during excavation of the second tunnel were also recorded and analyzed to study if they have effects on the existing tunnel lining.

2 EFFECTS ON EXISTING TUNNEL

Several authors observed the interaction occurring between closely spaced tunnels. For instance, as reported by Terzaghi (1942) and Ward and Thomas (1965), a set of field instrumentation records on tunnels excavated in Chicago Clay and London Clay indicated that significant lining deformations occurred in the first tunnel as the second tunnel was being excavated causing ground loss toward the tunnel (Figure 1a).



(a) Ground loss toward the 2nd tunnel



(b) Ground pushed out of the 2nd tunnel

Figure 1. Effect of the second tunnel on the first tunnel.

Physical tests were also conducted to investigate the response of the first tunnel's lining on the approaching

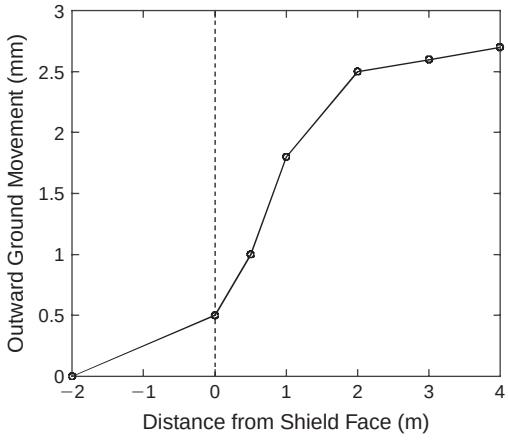


Figure 2. Maximum lateral deformations relative to the shield.

of the second shield. Kim et al. (1996 and 1998) performed laboratory tests using a miniature shield to simulate the effect of tunneling on an existing tunnel. The results of their model tests showed that the interaction effects are greatest in the springline and crown of the existing tunnel. However, the interactions between tunnels are unlikely to be significant unless the spacing between the tunnel centerlines is less than about two tunnel diameters (Kim et al., 1996). Additionally, numerical analyses of this interaction problem were carried out by Leca (1989), Addenbrooke and Potts (1996), Yamaguchi et al. (1998). Their results were similar in that the influence of driving of a second tunnel on the previously installed lining of the first tunnel depends upon relative tunnel position and on the spacing between two tunnels.

Effect of a second tunnel was also found to depend on shield operation. Suwansawat (2004) illustrated that the arrival of the Earth Pressure Balance (EPB) shield used in the construction of twin tunnels in the Bangkok MRTA project can cause outward ground movement during shield passing (Figure 1b). The magnitude of the outward movement depends on distance from the shield face as shown in Figure 2. It was found that the maximum outward movement occurred at the position corresponding to the shield tail. In other words, it was affected by tail void grouting. Additionally, the magnitude of outward deformations also appeared to correspond to the magnitude of the applied grouting pressure and the distance from the shield. This ground response mechanism can affect lining of existing tunnels nearby.

Therefore, it is clear that the problem of interaction between adjacent tunnels is complex, and the interaction depends on the geometry of the tunnels, the shield operation, lining properties, soil

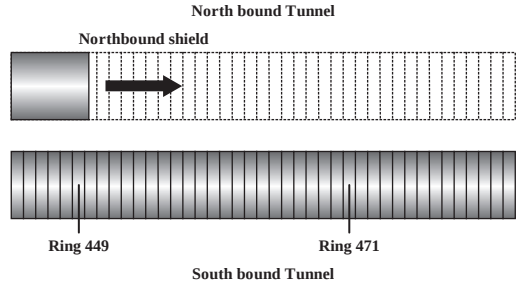


Figure 3. Schematic diagram of the twin tunnels and installed locations of convergence bolts in the Bangkok MRTA project.

characteristics, and relative stiffness of soil and lining. Operational parameters such as face pressure and grouting pressure are among the most significant factors. Nevertheless, although many studies on the interaction between two tunnels excavated side by side were carried out, very few were based upon field instrumentation and operational parameter records.

3 BANGKOK MRTA PROJECT

This research specifically copes with the Bangkok MRTA Project. The project of 20-kilometers of twin tunnels is subdivided into two main tunnel sections namely, the North Tunnel Section and the South Tunnel Section. The tunnel alignment was excavated underneath heavily congested areas of the city. Each of the twin tunnels is 6.3 meters in outer diameter and 5.7 meters in inner diameter. Eight EPB shields were used in total for the entire project.

Bangkok geological profile is quite uniform with soft clay underlain by stiff clay along the tunnel alignment. In most tunneling section, a horizontal-twin tunnel was excavated mostly within the stiff clay layer (i.e. about 15–25 m below ground surface). The tunnels have to be excavated within sand layer only at the mid-point between stations and also in the case of stacked tunnels. Details of the project can be found in Suwansawat (2003).

In the South Tunnel Section, some parts of the tunnels were designed to run close to each other due to the limitation of underground space in Bangkok. The southbound (SB) tunnel was excavated first and followed by the northbound (NB) tunnel approximately one month later. In some locations, the spacing between two tunnels is less than 3 m. To investigate the lining response when an EPB shield was driven very close to another tunnel, convergence bolts were installed (Figure 3) to measure changes in the tunnel shape.



Figure 4. Measuring lining deformation using tape extensometer.

4 CONVERGENCE BOLTS

The tape extensometer (Figure 4) is used to detect and monitor changes in the distance between two reference points. By comparing the current reading to the initial reading, the operator can calculate the change in distance between the two reference points where convergence bolts were installed. In this research, the monitoring was designed to correspond to the position of the second shield in order to study effects of the second shield operation on the first tunnel lining. Results of the monitoring are shown in Figure 5 and Figure 6.

5 LINING RESPONSE

The installed convergence bolts were observed relative to the advance of the second shield and the data were all plotted in the polar graphs (i.e. it is also recommended to look at the plots of lining deflection versus distance from the second shield face). It was found that the first tunnel lining was deformed during the passing of the second shield. It is evident that the second tunnel can induce stresses acting on the first tunnel. The stresses can cause inward deflections in the tunnel lining particularly at the location between springline and invert as clearly shown in Figure 5 and Figure 6. However, the pattern of the lining deflection observed in the MRTA project is not a typical result. Theoretically, the most significant inward deflection was expected to occur at the springline. As the second shield approaches the measurement section, it should induce inward movement at the springline and outward movement at the crown and the invert of the existing tunnel.

If one takes a detailed look at the plots of lining deflection versus distance from the second shield face (Figure 5), it was found that the lining begins to deform about 10 m ahead of the shield. As the second shield face approached the ring equipped with the convergence bolts, the lining deflected. However, the deflection decreases or the lining moves toward its initial shape shortly after the shield face passes the section. Therefore, based on this observation, it was suggested that the first tunnel lining was affected by the approaching second shield. However, this effect only occurred during the second shield passing. The shape of the tunnel lining rebounded back as the second shield passed away about 10 m from the measuring point.

The deflection magnitude of the first tunnel appears to be proportional to the face pressure level and the grouting pressure of the second shield applied during passing. For example, in Figure 5, during the northbound shield (i.e. the second shield) arrival at SB ring 449 where the first series of convergence bolts were installed (see also Figure 3), the shield was operated at high face pressure up to 200 kPa and at high grouting pressure up to 4 bar. As a result, the first tunnel lining deflects significantly (i.e. 11 mm at the 298 degree location or at between springline and invert). Thus, shield operators had to reduce face pressure to 150 kPa and maintain this pressure level until the end of the tunneling drive. Also, the grouting pressure was reduced to 3 bar in order to ensure that no significant deflection takes place at the lining of the southbound or the first tunnel. Accordingly, as the northbound shield continued to excavate to the end of the tunneling drive, other series of convergence bolts installed in the first tunnel measured smaller deflection compared to that installed in ring 449.

For the other section studied in this research, converge bolts were installed at SB ring 471 to measure effects during NB shield passing. There is only 2.5 m spacing between two tunnels. Figure 6 showed plots of lining deflection and also operational parameters recorded at the NB shield. It was found that the first (SB) tunnel lining begin to deform at 5 m ahead of the shield face and continues until the shield passed approximately 10 m away from the measurement point. During the shield passing, the face pressure was applied at earth pressure balance mode (i.e., somewhat equal to external ground pressure). However, the grouting pressure was still high up to 4 bar. This lining behavior recorded at this section is very similar to that of the section measured at SB ring 449. The tunnel lining tends to deform during shield passing but recovers after shield passing.

6 CONCLUSIONS

The behavior of tunnel lining relative to the second shield operation was studied. It was evident that the second shield can induce deflection at the first tunnel lining particularly between springline and invert. The deflection magnitude of the first tunnel appeared to be related to the face pressure and the grouting pressure

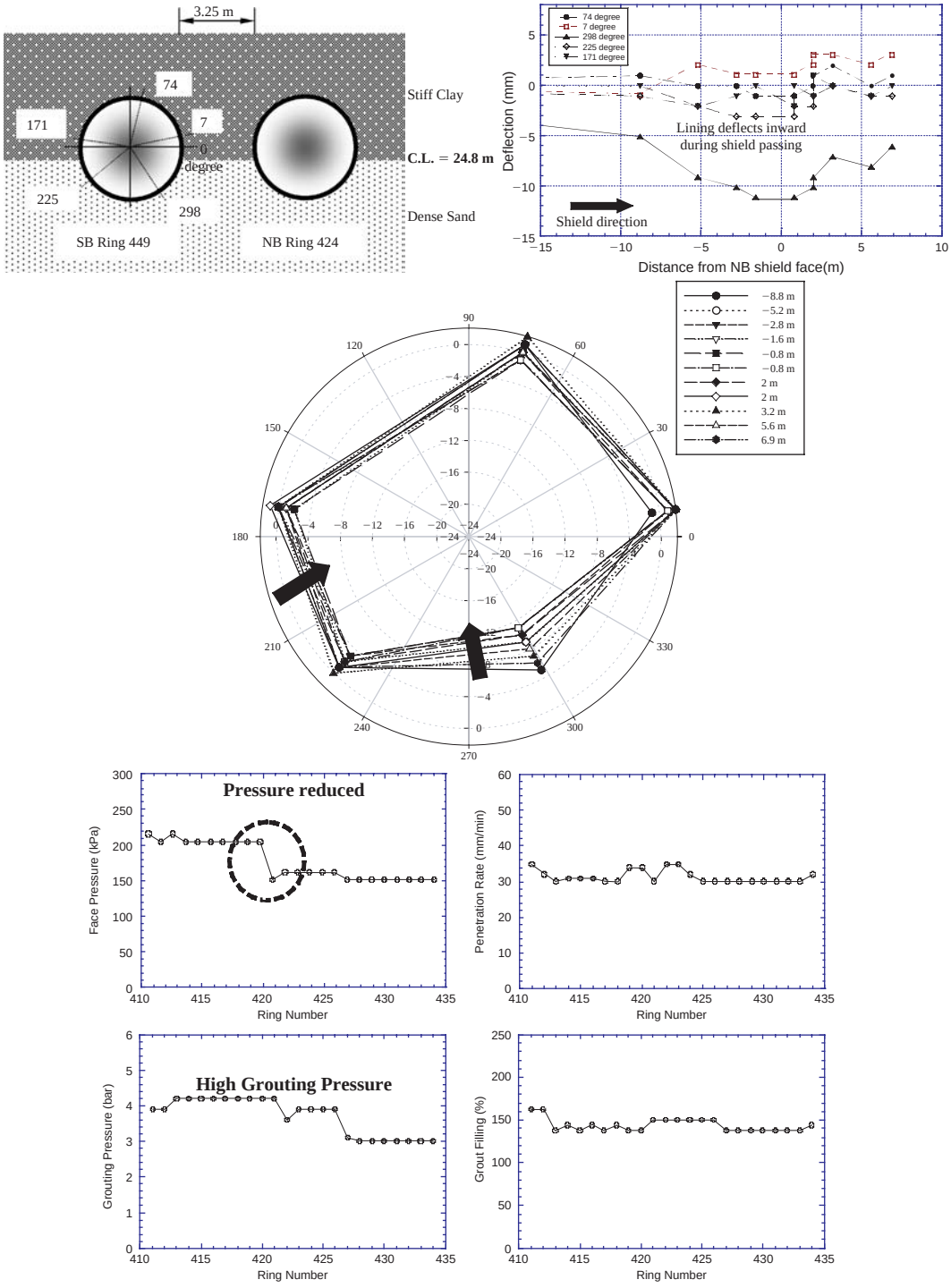


Figure 5. Deflection of SB tunnel Ring 449 during the passing of NB shield and operational parameters recorded in NB shield corresponding to the NB Ring 424.

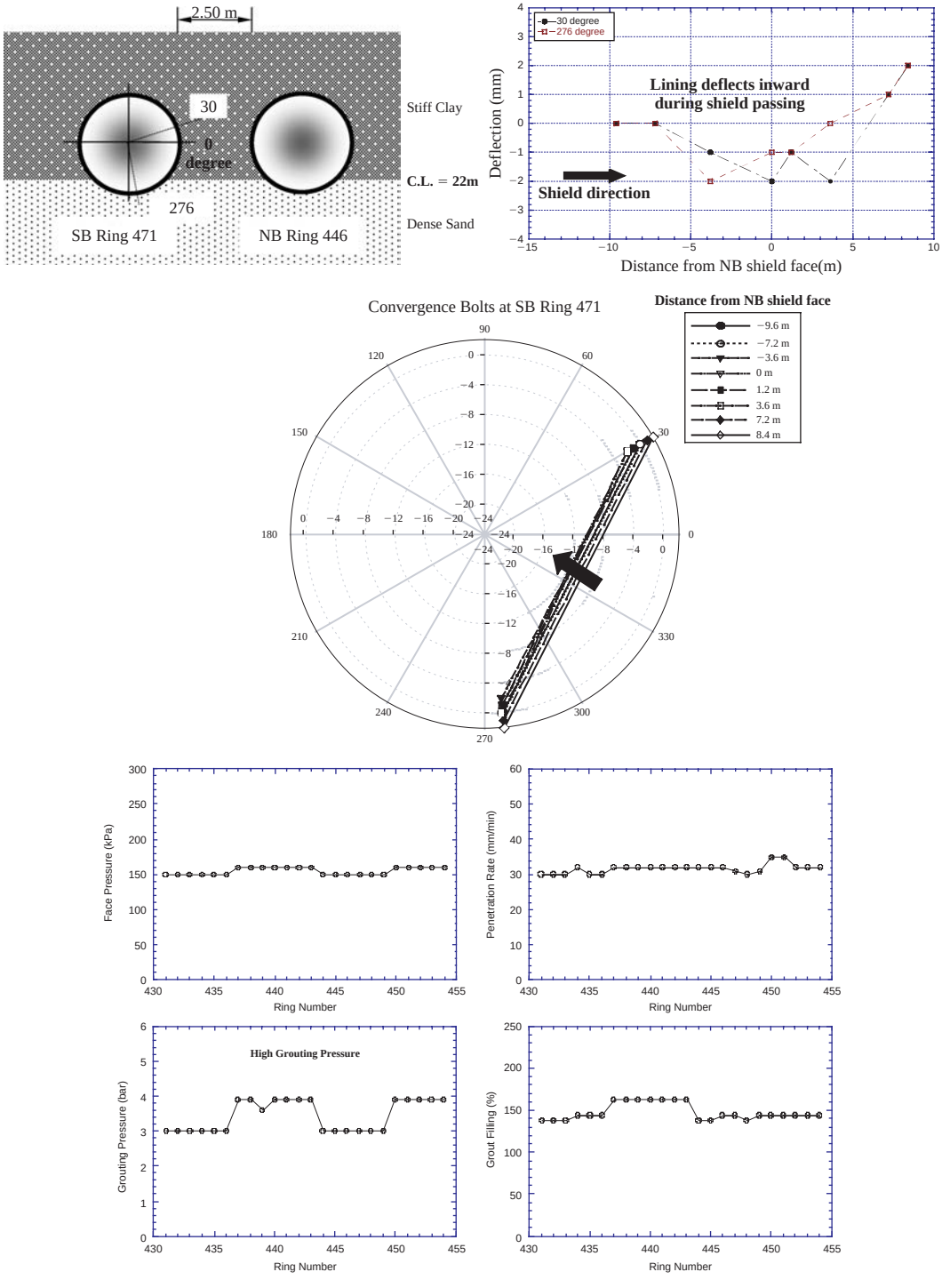


Figure 6. Deflection of SB tunnel Ring 471 during the passing of NB shield and operational parameters recorded in NB shield corresponding to the NB Ring 446.

levels of the second shield. In other words, at close distance, if applied face pressure or grouting pressure is high, the lining of the nearby existing tunnel can be affected. However, the monitoring showed that the effect only occurred during shield passing (i.e. from about 10 m ahead of the shield face to 10 m behind the shield face.

This suggests that to minimize the lining deformation in case of twin tunnels in close proximity to each other, the second shield have to be operated carefully to maintain operational parameters at suitable level. Also, this study showed that tunnel lining should not be only designed to withstand overburden pressure from surrounding ground, but also has to consider the pressure induced by the second shield operation. Safety of the lining should be calculated that excessive bending moments or displacements are not developed. Otherwise, the lining can be exposed to the risk caused by the construction of the second tunnel.

REFERENCES

Addenbrooke, T. I. and Potts, D. M., 1996. Twin tunnel construction – Ground Movements and Lining Behaviour. *Proc. International Symposium on Geotechnical Aspects of Underground Construction in Soft Ground*: 441–446.

Kim, S. H., Burd, H. J. and Milligan, G. W. E., 1996. Interaction between Closely Spaced Tunnel in Clay. *Proc. International Symposium on Geotechnical Aspects of Underground Construction in Soft Ground*: 543–548.

Kim, S. H., Burd, H. J. and Milligan, G. W. E., 1998. Model Testing of Closely Spaced Tunnels in Clay. *Geotechnique*, 48(3): 375–388.

Leca, E., 1989. Analysis of NATM and Shield Tunneling in Soft Ground. Ph.D. Thesis, Virginia Institute and State University, Blacksburg, Va.

Suwansawat, S., 2003. The Challenging Subway Project in Bangkok: New Hope of Thais in Solving Traffic problem. Keynote Lecture. *Proc. the 8th Conference of the Association for Computer Aided Architectural Design Research in Asia*. Bangkok.

Suwansawat, S., 2004. Influences of Tail Void Grouting on Lateral Ground Deformations Conducted with Shield Tunneling. *Proc. the 15th SEAG Conference*. Bangkok.

Terzaghi, H., 1942. Liner-Plate Tunnels on the Chicago Subway. *Proc. ASCE* 68(6): 862–899.

Ward, W. H. and Thomas, H. S. H., 1965. The Development of Earth Loading and Deformation in Tunnel Linings in London Clay. *Proc. 6th Int. Conf. of Soil Mechanics and Foundation Engineering Vol. 2*: 432–436.

Yamaguchi, I., Yamazaki, I. and Kiritani, Y., 1998. Study of Ground-Tunnel Interactions of Four Shield Tunnels Driven in Close Proximity, in Relation to Design and Construction of Parallel Shield Tunnels. *Tunnelling and Underground Space Technology* 3(3): 289–304.

Underground Space – the 4th Dimension of Metropolises – Barták, Hrdina, Romancov & Zlámal (eds)
© 2007 Taylor & Francis Group, London, ISBN 978-0-415-40807-3

A86-West Paris ring road-a bi-mode TBM

J.L. TORIS
Socatop JV, VINCI Company, Paris, France

ABSTRACT: The East tunnel of the A86 project is a 11.65 m external diameter tunnel, excavated in a very sensitive environment composed of forest parkland, historic sites and residential areas .This tunnel has been bored through thirteen different geological grounds (chalk, clay, limestone, sands . . .), three water sheets with a bi-mode TBM (Slurry and Earthpressure mode). This TBM has been driven with only 10 m below railway tracks and 15 m below a motorway. All the equipments needed by these two excavation modes have been installed on the TBM and only two days were necessary to change the boring mode. The TBM selection, the technical description of all the equipments and the monitoring will be exposed in details.

1 INTRODUCTION

The A86, the outer Parisian ring road has been built mostly in 1990s. Its west section is not complete yet, a ten kilometers section is still in works. This part is located in a very sensitive environment composed of forest parkland, historic sites (Versailles and Petite Malmaison castles) and high residential areas. The current project consists of building the link between Rueil Malmaison and Versailles with a bored tunnel. This tunnel has an innovative design with two superimposed traffic spaces, each level receive one way traffic composed by two traffic lanes of 2.8 m wide and one hard shoulder for emergency lane .It only accommodates vehicles with maximum 2 meters high. Each traffic space is equiped with two ventilation tubes, one for fresh air, the other for emergency/fire ventilation.

The east tunnel of A86 is the largest tunnel ever bored in France with a Tunnel boring machine. It has an external diameter of 11.6 m and an internal one of 10.4 m which allows 2.55 m clearance on each traffic level. Along the tunnel, the overground moves between a minima of 10 m and a maxima of 70 m and two specific areas are encounted. The first one is when the tunnel is located under the railways of Butard with only 10 m of overground and the second one when the tunnel drive beneath the A13 with a cover of 157 m.

2 DESIGN OF THE TBM

The first part of this tunnel, of 4.5 km long, starts near the seine river in Rueil Malmaison and goes up until the plateau of Vaucresson where the interchange with the A13 is located, 150 m higher. During this drive, the TBM crosses almost all the différent geological grounds which can be found in the Parisian area. Only few are missing and we encount successively the following families of grounds:

- Chalk : soft rock with inclusion of flint
- plastic clay : clay with some inclusion of sands
- limestone : the easiest soil to excavate
- marl and gravel layers : ground with mostly marl and some limestone
- Beauchamp sands and sandstone: On this first part of the east tunnel we mainly met sands without water
- the sandwich of marl, sannois limestone and green clay : this is the impermeable layer supporting the water table of the Fontainebleau sands
- marl with inclusion of shells : this is a mixed of limestone and marl with permeable lines where we were in contact with the water table of the Fontainebleau sands under a pressure of 3 bars
- Fontainebleau sands: Thickness of 50 m with 20 to 25 m of water

As we can see we did not have a sole dominant geological formation. We also notice that we had to manage a big diameter tunnel boring machine (excavation diameter of 11.6 m) with several different thin layers of ground (1 to 3 m per layer) and three separate water tables. The behaviours of these sandwiches of different grounds in the front face of the machine always moved during the excavation of the tunnel and needed an adaptable machine.

The TBM had also to manage with the surface settlements to minimize them specifically when the tunnel was bored beneath the building areas, the butard railways and the A13 traffic lanes.

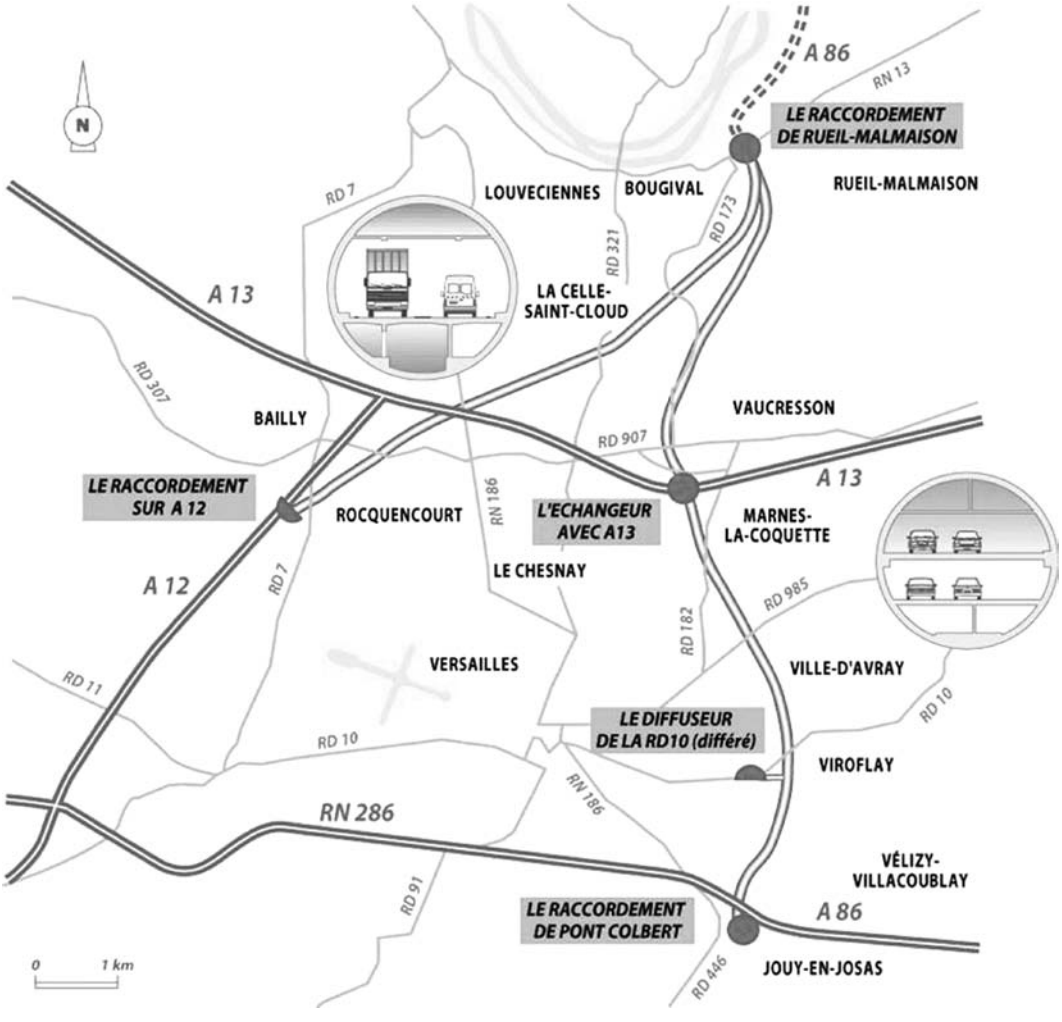


Figure 1. General project layout.

The conception of the tunnel boring machine had also to take into account the general schedule of the project and the target to excavate the first 4.5 kilometers of the east tunnel in 24 months.

To excavate in the cohesive grounds and soft rock, the technical committee of Socatop agreed with a choice of an earth pressure boring machine which permits to work in open mode, compressed air mode and in EPB mode. High speed of excavation can be expected in these grounds with this kind of machine and with the depth of cover available, settlements were managed.

The question was: How did an EPB machine drive in sand layers with or without water table?

To check this point, tests have been done on a reduce model composed with a pressurised tank, a reduce spoil extraction screw and a discharge gate. All these equipments were monitored with pressure captors. The target was to simulate the behaviour of the mucking with a screw in sands, to check the possibility to plug it enough to manage a pressure in the front at a maximum of 3 bars. To be representative, the tank was filled with sands extracted in a shaft near the future project and several tests have been driven with varying pressure, using different additives with varying concentration. These tests have shown that it was not possible to manage in the Fontainebleau sands, a high pressure in the front with a spoil extraction screw. A slurry machine had to be used in this layer which was met on 30% of the length. With this mode of excavation, a better face control was possible in this unstable formation and a higher level of limited settlements could be guaranteed. The problem was that a slurry machine can not

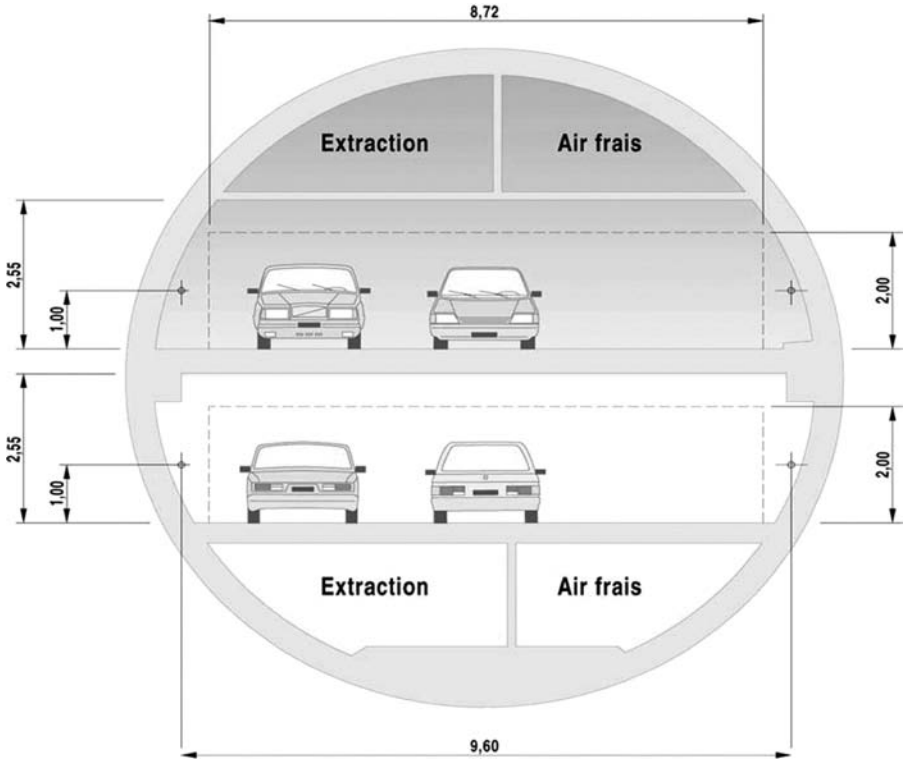


Figure 2. East tunnel – Transverse profile.

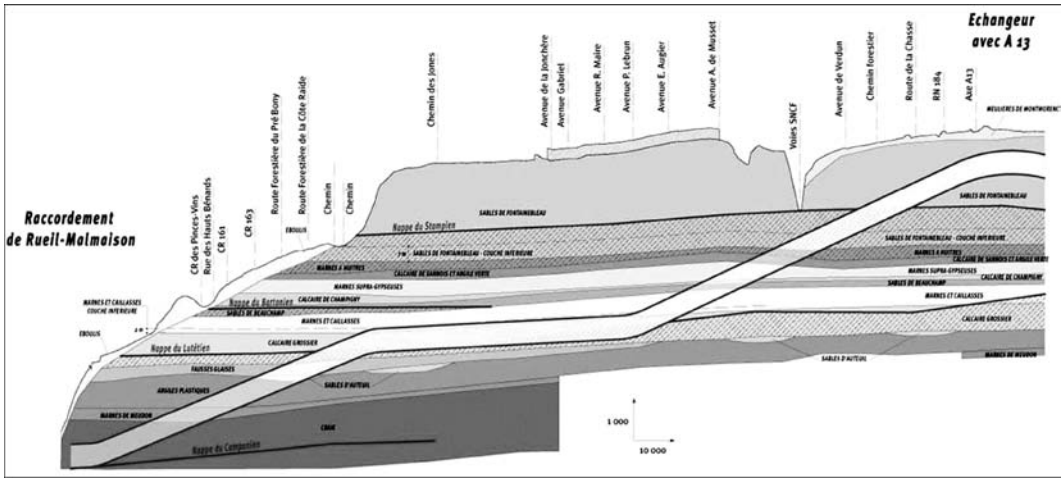


Figure 3. Tunnel East – Geological profile.

be used in grounds with high level of thin particles as clay, chalk, marl (Slurry treatment too long and expensive).

After these studies and tests, Socatop went through a design of a bi-mode tunnel boring machine, able to drive in every mode described above. On the first part of the east tunnel between Rueil-Malmaison and A13, it was foreseen to start the excavation in EPB configuration until the junction with the Fontainebleau sands where the slurry mode had to be used.

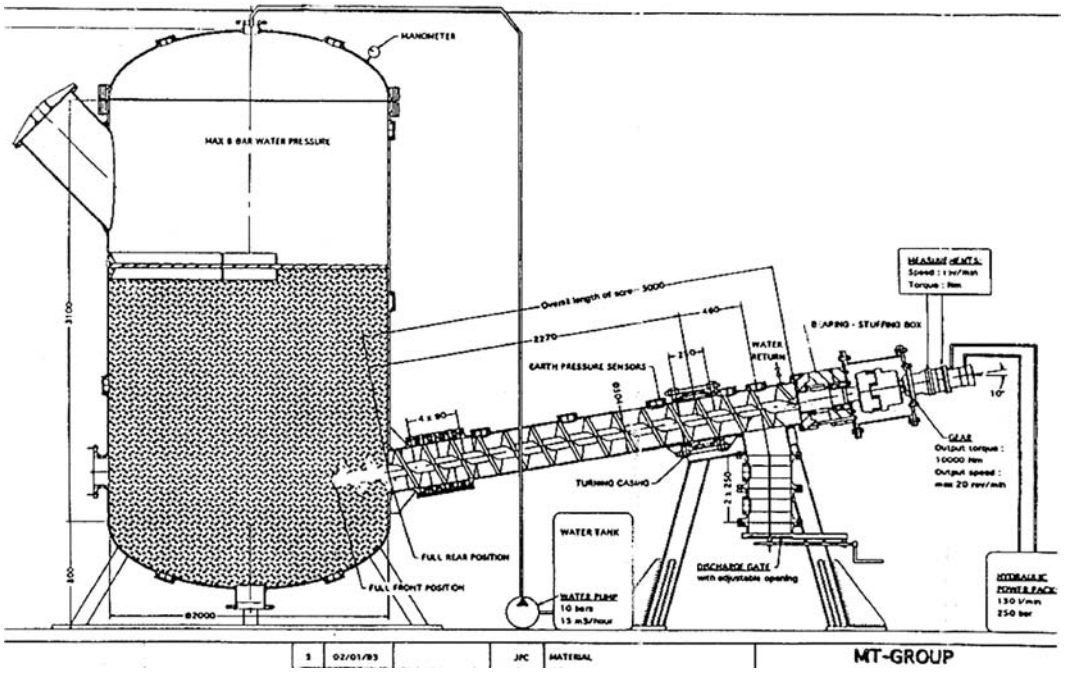


Figure 4. Test layout.

To be able to have a short time modification between these two modes, we design with the supplier, a tunnel boring machine with all the equipments necessary for both modes, installed at the beginning. So only 48 hours were needed for the modification of the configuration of the TBM, and one week for training in the new mode of excavation.

In the different grounds, the excavation modes were the following:

- Fontainebleau Sands : slurry mode – Hydraulic mucking
- Chalk, Limestone, marl and gravel: open mode – mucking with the spoil extraction screw and a belt conveyor
- Clay : compressed air mode – mucking with the spoil extraction screw and a belt conveyor
- Beauchamp and Auteuil sands between clay layers: Earth pressure mode – mucking with the spoil extraction screw and a belt conveyor

3 DESCRIPTION OF THE TBM

The figures 5 & 6 show the configurations of the shield of the TBM in the EPB and the slurry modes.

In the EPB mode a 1.25 m diameter and 22 m long spoil extraction screw takes the excavated material behind the cutter head in the bottom of the excavation chamber. This material is carried by this screw until a discharge gate and then fall on a belt conveyor installed on the TBM. Further, at the back of the back up of the TBM, this conveyor is connected with a belt conveyor installed in the tunnel on the precast concrete segments.

To pass in the slurry mode we had to move back the casing and the screw to liberate the bottom area of the air bubble chamber where we were pumping out the slurry. After this modification, we injected clean slurry in the top of the excavation chamber and we pumped out the heavy slurry (clean slurry + excavated material) in the bottom of the air bubble chamber. These slurries were carried through 450 mm diameter pipes and five 750 kw pumps to go to the slurry plant installed on the outside yard. In this station, the excavated material was separated from the slurry and the cleaned slurry was re-used and sent to the TBM.

The capacity of the slurry circuit was 2 000 m^3/hour.

4 TBM DRIVE BENEATH BUTARD RAILWAY

On the first part of the east tunnel, the TBM had to cross a specific and very sensitive point.

At this point the tunnel is located beneath the butard railways (two traffic lanes) with a cover of 10 meters. At this point the front face is on its upper half in the

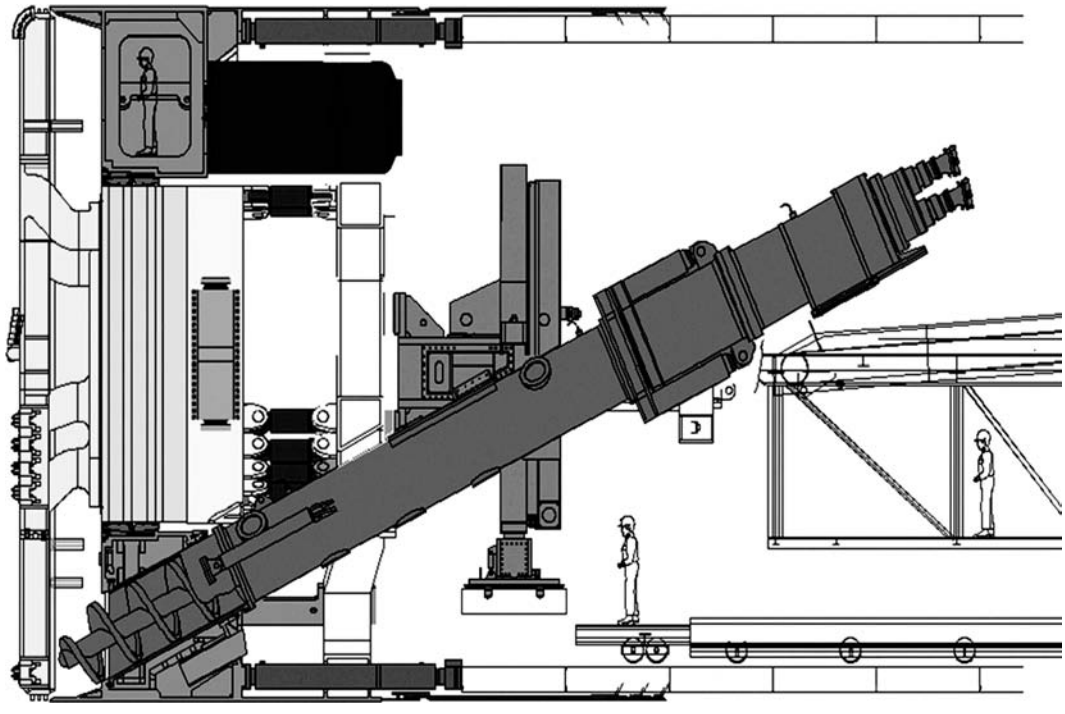


Figure 5. EPB shield configuration.

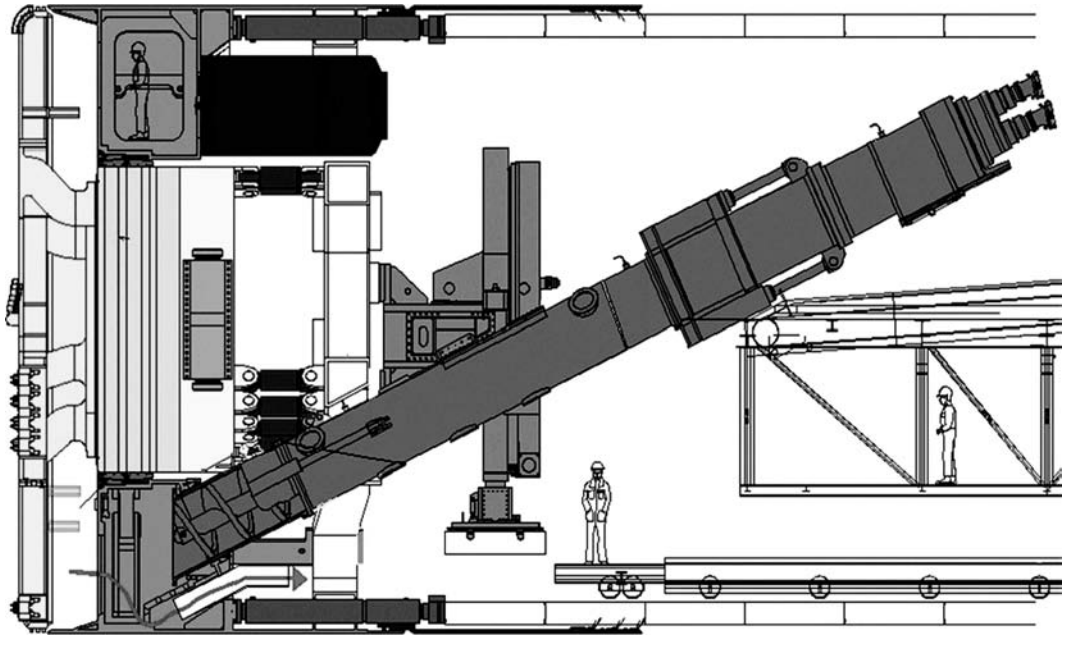


Figure 6. Slurry shield configuration.

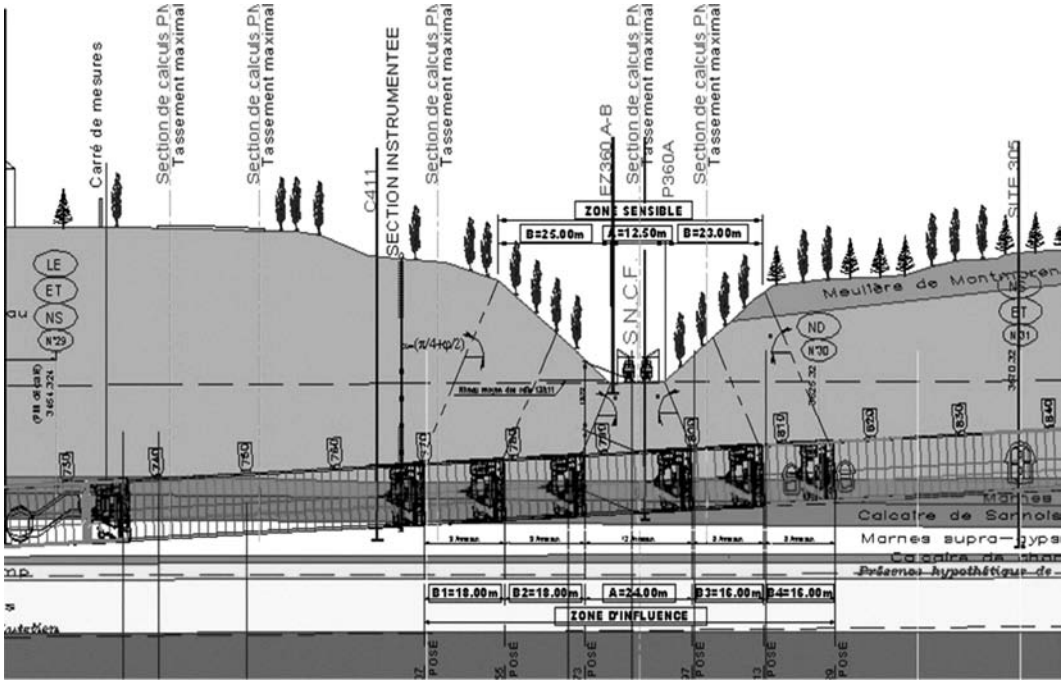


Figure 7. Butard profile.

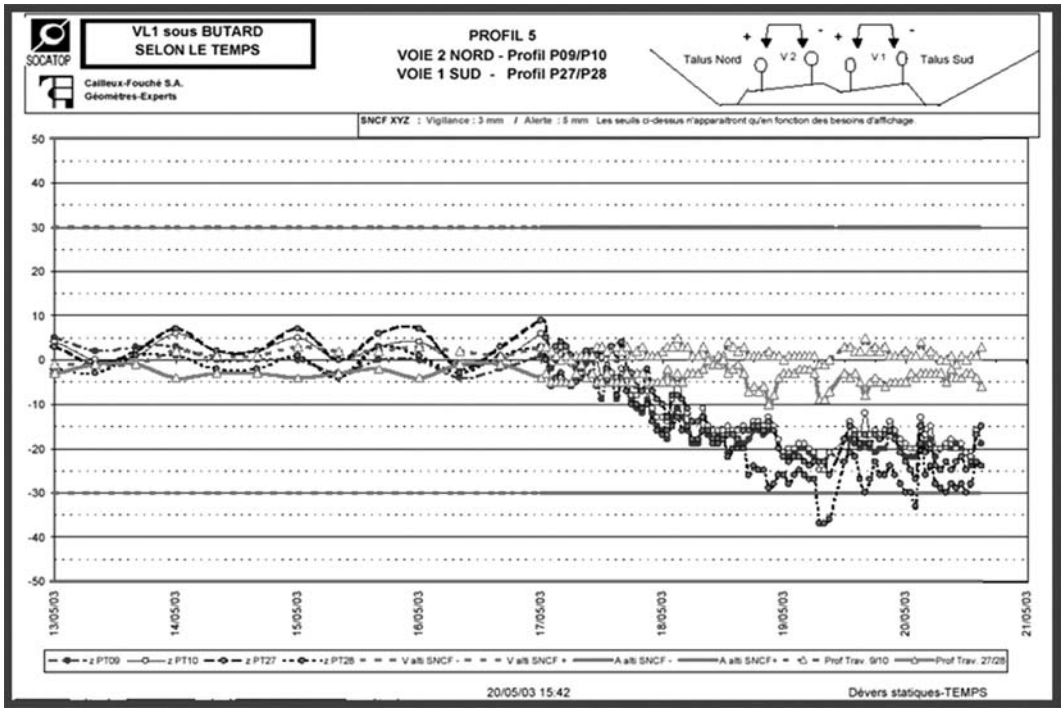


Figure 8. Monitoring results.

Fontainebleau sands and under a water table, and on its bottom half in a sandwich of marl, clay and limestone.

The project had to manage with several other difficulties:

These railways were located in the bottom of a valley and on 60 m of tunnel, the cover first decreased from 40 m to 10 m then grew to 35 m.

- These railways were under a tunnel just 20 meters before crossing the east tunnel.
- The TBM had only a 50 m training period in the slurry mode before this point.
- The traffic of the trains could not be stopped during the crossing of the TBM.

A three dimensions modelisation has been done to define the levels of slurry pressure to use.

A permanent and full automated monitoring has been installed to survey the railways and the settlements in the area. The results were available on a website for the work company and the railway company and a coordinated emergency plan had been done in case of too high settlements.

The TBM drive, in a continuous way, beneath this point during a week end when the train traffic was lower and when it was possible to reduce their speed.

It has been a great success for the project and the highest settlement measured was 3 mm for a maximum authorised of 5 mm.

5 CONCLUSION

On the A86 project, the TBM technology has climbed one more step with a machine able to use all the excavation modes, and therefore be compatible with very different ground formations and a high level of guarantee in the management of settlements.

This page intentionally left blank

Underground Space – the 4th Dimension of Metropolises – Barták, Hrdina, Romancov & Zlámal (eds)
© 2007 Taylor & Francis Group, London, ISBN 978-0-415-40807-3

RandstadRail Rotterdam – Experiences with tunnelling in difficult ground conditions

D.C. van Zanten
Engineering department Rotterdam Public Works, The Netherlands

Dr.-Ing. Dieter Handke
Maidl & Maidl Consulting Engineers, IMM, Bochum, Germany

M.C. Braam
Engineering department Rotterdam Public Works, The Netherlands

ABSTRACT: RandstadRail is a light-rail link between the cities of Rotterdam, The Hague and Zoetermeer. It connects the local transportation systems in aforementioned cities in such a way that travelling between the inner cities is possible without transfer.

In Rotterdam RandstadRail will be connected to the existing North-South metro line at Rotterdam Central Station. At present time a tunnel of 3 kilometres length is being realised of which 2,4 kilometres is constructed using shield tunnelling for two single track tunnels. Halfway the alignment the underground station Blijdorp is constructed 17 meters below reference level at the transition of soft clay and Pleistocene sand.

The two bored tunnels both have an outer diameter of 6,5 metres. The tunnels are mainly placed in the deep Pleistocene layers. However adjacent to the starting shaft, the receiving shaft as well as the station the tunnels are placed in soft Holocene layers.

When the bored tunnels are placed for more than 50% in the soft Holocene clay additional measures have to be taken as the clay does not support the tunnel lining enough. If possible a ground improvement is used. However instead of a concrete lining with additional ground improvement a steel tunnel lining is used under the railway track near Central Station and adjacent to the station Blijdorp.

The boring process takes place in different ground conditions:

i. Regular ground conditions (clay, sand);
ii. Ground improvement (jet grout, soil deep mixing, gel);
iii. Wooden piles;
iv. Low strength concrete and diaphragm walls with glass fibre reinforcement.

The tunnel boring machine has a length of 68 metres. The shield has a joint for making the curves in the alignment ($R_{min} = 240$ metres). The tunnel boring machine crosses a highway, a channel and a railway line at two locations. Near Central Station over 16 railway tracks have to be crossed.

This article gives an overview of the project and will give insight in the boring process in different ground conditions as well as the boring process at sensitive locations regarding settlement.

1 INTRODUCTION

RandstadRail is a light-rail concept with the aim of realising a high quality public transport system in the southern part of the urban area called "Randstad". RandstadRail connects the local public traffic network of Rotterdam, The Hague and Zoetermeer. In Rotterdam RandstadRail will be linked to the local North-South metro line which now ends at Rotterdam Central Station.

For the connection between Rotterdam and The Hague an already existing railway line, Hofplein line, is used. This heavy railway line has been transformed for light-rail use in 2006. For the connection between Rotterdam Central Station and the Hofplein line the Engineering Department of Rotterdam Public Works has worked out a design using the shield driving method.

This was namely the best method regarding the surrounding conditions. This results out of the crossing



Figure 1. Map of the Netherlands.



Figure 2. Horizontal alignment.

of the different traffic systems, such as railway lines, roads and a channel. Also the shield driving method gave the best results regarding construction time and cost criteria. Now the link between Central Station and the Hofplein line is under construction. In 2008 RandstadRail connects to the North-South metro-line.

Alignment

The alignment has a length of 3 kilometres and is more or less u-shaped (Figure 2). The alignment follows the run of the road Statenweg in north-south-direction. Starting in the northern part the alignment turns west and crosses the "infra bundle", consisting of a railway (Rotterdam-Utrecht), a local tram line, highway between Rotterdam and Utrecht, a channel including the yacht harbour.

In the southern part the alignment turns to the west starting from Rotterdam Central Station crosses a railway embankment consisting of 16 tracks.

Shield tunnelling is used over a total length of 2,4 kilometres which is divided in two sections by "Station Blijdorp". The alignment is constructed as two single-track tubes with an outer diameter of 6,5 m. The thickness of the tunnel lining is 0,35 metres.

2 SOIL CONDITIONS

An extensive soil investigation has been performed along the alignment of the tunnel. Over 60 geotechnical borings and 600 CPT's have been executed to determine the geological build-up of the soil layers. The build-up along the alignment primarily consists of a Holocene overburden and a Pleistocene sand layer underneath. Over 500 laboratory tests regarding strength and stiffness have been done. This intensive research has given detailed insight in the soil parameters.

Directly at the surface, above the Holocene layers a man made sand layer with a varying thickness of 2–5 m is found. Underneath this layer Holocene soil layers, consisting of clay and peat (Hollandveen) are present. The boarder layer to the Pleistocene layer normally consists of a less thick basic peat layer.

Under the Holocene overburdens a 20 metres thick Pleistocene sand layer is present. This layer is the foundation level for the built-up area.

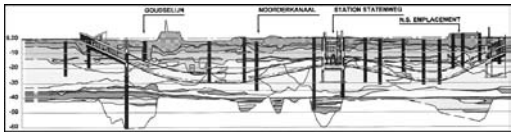


Figure 3. Vertical alignment.

3 VERTICAL ALIGNMENT

The bored tunnels are placed mainly in the Pleistocene sand layers. However adjacent to the building pits the tunnels lie in the Holocene clay which is above the Pleistocene sand layer. Reason for this is that the total building costs of the project reduce when the bored tunnels are placed in clay adjacent to the building pits. So the building pits are made as shallow as possible.

Figure 3 shows the vertical alignment of the tunnel as well as the geological profile.

4 CHALLENGES

For realising the bored tunnels in Rotterdam two aspects are special:

i. Bored tunnel in Holocene clay;
ii. Surrounding conditions.

Bored tunnel in Holocene clay
The Holocene clay does not support the tunnel lining very much. The Holocene soil layers are also effected by extremely strong settlements resulting from consolidating and creep effects (Pachen et. al, 2002). The surface settlements expected for the future are about 1,5 cm per year. The long-term settlement leads to additional loads on the tunnel lining (Zanten et. al, 2002). During the engineering phase it was found out that due to these additional loads it was necessary to use ground improvement techniques when the bored tunnels are placed for more than 50% in the Holocene clay. However on two locations these ground improvement techniques were not desirable as the surface is in use for train and car traffic. On these locations a steel lining is used instead of a concrete tunnel lining.

Surrounding conditions
The surrounding conditions of the project are difficult that is why the goal of driving the TBM is to be able to handle the settlement. As it is necessary to cross the abovementioned railway lines, highway, channel as well as roads. Above this it is necessary to consider obstacles in the tunnel alignment, such as wooden piles with a diameter of 0,2 to 0,3 metres. These pile foundations are not in use as the buildings were already demolished. The design philosophy is that the piles have to be removed before the tunnel boring process. However at the crossing with the railway tracks this was not possible. So the TBM has to pass through the wooden piles. Additional ground deformation due to the presence of the wooden piles has to be avoided. Taking all factors of influence into account the tunnelling conditions are complex.

5 DEALING WITH RISKS

The overall aim of the project was to find out all risks, evaluate them and examine as well as evaluate technical solutions.

The requirements to guarantee a life-span of hundred years have to be regarded with low running costs.

On account of the extremely difficult surrounding conditions Rotterdam Public Works decided to prepare an own design in order to gain an insight in the problems that could occur.

Settlement
With regard to the settlement the performed analyses led to:

- The use of a ground improvement technique (gel) in the railway embankment Rotterdam-Utrecht for realising a crossing with a low risk profile (Zanten et. al, 2003);
- Definition of maximum values for settlements (gradient, torsion angle) for buildings and tracks;
- Insight in sensitivity of settlement in respect to buildings, tracks, pipes and surface level;
- Well defined monitoring program.

Machine-technological aspects:
With regard to machine-technological aspects the analyses led to detailed information on:

- steering of the machine in soft soil;
- stability of the face even while men entering the drilling chamber;
- obstacle removal.

Construction-technological aspects:
With regard to construction-technological aspects the analyses led to:

- use of ground improvement techniques, e.g. jet grouting, mixed in place;
- segmental lining with reinforced concrete elements with a high content of reinforcement;
- segmental lining with steel segments.

6 CONTRACT

To attain in the following steps the best project safety, Rotterdam Public Works decided to take the already worked out technical solution (final design) as basis of the tender documents. Within the final design feasibility results, cost criteria and risk profile studies were

considered. In formulating the technical minimum requirements, which the bidder has to adhere the level of the quality is defined. The danger of receiving "less serious tenders", meaning tenders which carry high risks for the principal is eliminated.

Machine- technological:
The following demands are specially given in respect to the TBM:

- minimum thickness of sheet metal of the shield skin to secure the correct form;
- limitation of the conicity and of the overcut;
- integration of injection possibilities for hood injection and stabilisation of the steering gap;
- alarm secured control for support of the face, annular gap grouting, shield tail seal and mass balance;
- data capture devices with notice of disturbance messages for the most important functions of the shield machine;
- pre-checking systems for the ground;
- wear measure systems.

Segmental lining:
The following demands are specially given in respect to the tunnel lining:

- minimum thickness and minimum reinforcement amount for reinforced segments;
- steel segments for critical sections with permanent prestress to the reinforced segments;
- quality assured fabrication and installing of the segments;
- minimum requirements for the design of the segments;
- performance of tests to cover the limit support behaviour;
- the integration of measuring facilities for the surveillance of load and deformation behaviour.

On the basis of these requirements the contractor has free room for a solution of the technical concept with a manageable risk:

- detailed design tunnel lining;
- design TBM;
- boring parameters.

7 GROUND IMPROVEMENT

The contract was awarded in February 2004 to the contractor Saturn v.o.f. Works started at the starting shaft and the ground improvements near the starting shaft. These ground improvements consist of:

- soil removal for sand;
- mixed in place;
- gel.



Figure 4. Ground improvement mixed in place.

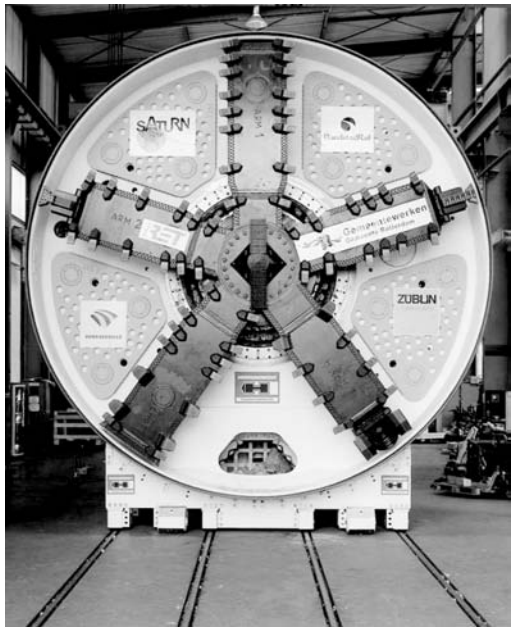


Figure 5. TBM.

The minimum strength of the mixed in place was 0,6 MPa. However testing showed that strength values over 2 MPa were realised as well.

Adjacent to the receiving shafts jet grouting is done. Approximately 2000 columns are made. The strength is varying between 2 and 8 MPa.

8 TBM

The tunnel sections are driven using a shield machine with fluid-supported face. The TBM has a total length of 68 meters. The length of the shield is 9,8 meters. In June 2005, the shield machine was approved at the factory in the presence of the client and consultants. In the process, the functional capacity of the entire machine together with all components was demonstrated and verified. The shield started operating in December 2005. Figure 5 shows the TBM at the factory.

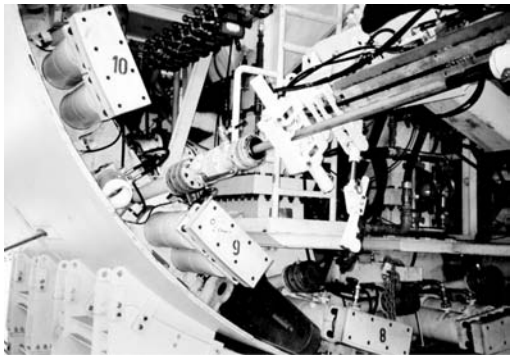


Figure 6. Drilling ports.

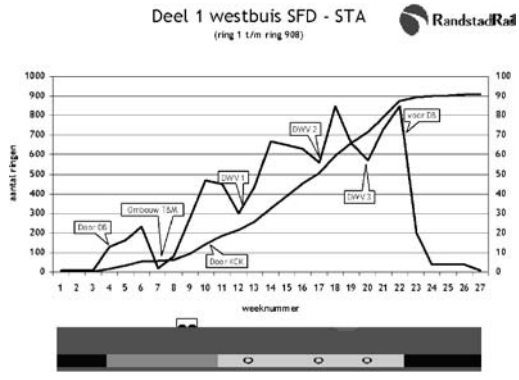


Figure 7. Building speed.

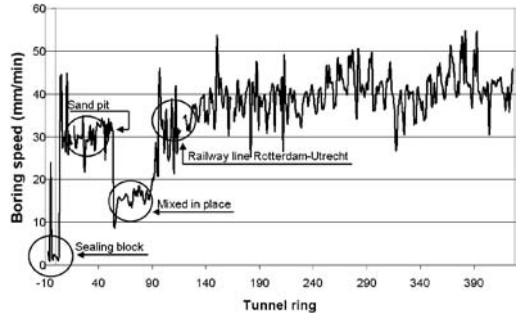


Figure 8. Boring speed.

The machine possesses an external diameter of 6,78 m and a 5-arm cutting wheel.

The curves in the alignment have a small radius (240 meters). So a joint between the middle shield and the tail shield is constructed.

The cutting wheel is equipped with cutters, overcutting tools, a central device and special wear measuring systems. The transmitters and receivers integrated in the cutting wheel serve geological advance exploration purposes. On six cutting tools measurement tools for wear are placed.

A rock crusher is installed in front of the intake screen. Drilling ports integrated in the shield skin facilitate the production of a ground improvement.

The cutting wheel can be shifted in longitudinal way over a length of 0,4 meters. So over cutting is possible. Shifting can be helpful by overcoming a blocking of the cutting wheel as well.

9 BORING PROCESS

In June 2006 the TBM reached the station Blijdorp. For the first section between the starting shaft at the "St. Franciscus Driehoek" and station Blijdorp 908 tunnel rings are placed. Each tunnel ring has a length of 1,50 m. The average speed was approximately 8 m/day. It can be seen that due to building segments for the cross passages the building speed is lower.

The concept using a hydro shield with a 5-arm cutting wheel worked out well. The settlement along the alignment was on average 15 mm. When crossing the railway track Rotterdam-Utrecht surface settlement of 10 mm was registered. This had little influence on the tracks. No influence on train service was encountered. The wooden piles which were in the tunnel alignment were taken care with the cutting wheel without problems. No problems with the bentonite cycle were encountered.

Boring speed

Starting the boring process it was found out that the sealing block adjacent to the starting shaft was very hard. The strength of the concrete was 15 MPa. This led to substantial wear of the cutting tools. So it was necessary to change the cutting tools several times. The type of cutting tools was also changed. A cutting tool with a better cutting behaviour was used. When crossing the ground improvements it was found out the boring speed was somewhat lower than regular speeds.

In August 2006 the boring process restarted from the building pit of the station Blijdorp. In this restart the tunnel had to cross diaphragm walls with glass fibre reinforcement. The strength of the diaphragm wall was on average 45 MPa. The boring speed was very low, approximately 1 mm/minute.

Directly after the building pit the tunnel is placed in Holocene clay for more than 50% of the cross-section. So over a length of 40 meters a steel tunnel lining had to be placed. Figure 9 shows the building of a steel tunnel ring. Due to the many bolts building a tunnel ring takes approximately 12 hours.

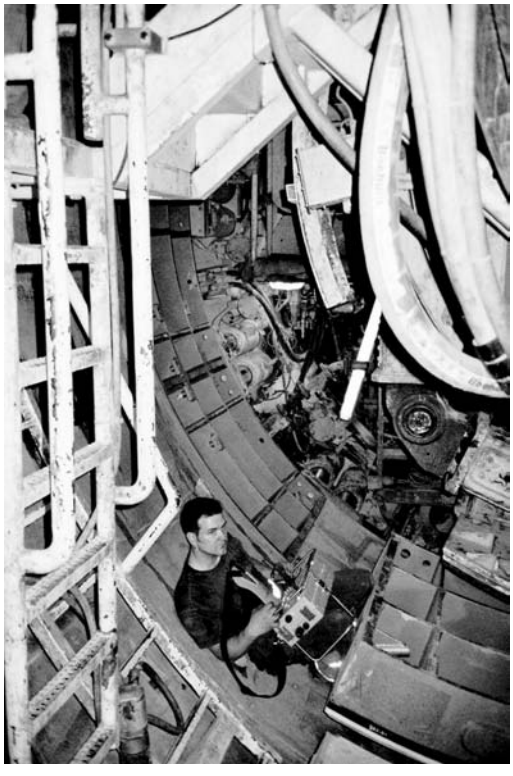


Figure 9. Steel tunnel lining.



Figure 10. Tunnel rough structure.

Tunnel lining
The quality of the tunnel lining until now is good. The tunnel is very dry. The requirements of the contract are met. Only a small amount of damages are encountered (<0.5**%**). The maximum tunnel deformation is 5 mm (measured at radius).

Monitoring
The boring process was accompanied with a extensive monitoring program. With this innovative monitoring system the TBM driver has on line insight on:

- TBM data, e.g. boring pressure;
- Faults in system, e.g. leakage;
- Surveying system tunnel and shield, e.g. position of shield;
- Deformation of sub soil, e.g inclinometer, extensometer.

The actual position of the TBM with respect to the measuring points, the buildings, geology is shown to the TBM driver. Also a sonic system was used (SSP-System). With this system it is possible to "look" in the ground over a length of 40 meters. So large obstacles can be seen in advance.

10 CONCLUSION

The hydro shield has been proved yet totally. The requirements to them were fulfilled. For the future one can hope that the accident-free advance will go on and possible situations will be mastered securely as before.

REFERENCES

Handke, D., Jonker, J. 1999. Innovationen für Schildvortriebe an der Betuwelinie in den Niederlanden. *Bauingenieur 74 (2)*: *59–66*. Düsseldorf: Springer VDI Verlag.

Pachen, H.M.A., Brassinga, H.E., Bezuijen, A. 2003. Geocentrifuge tests to predict the loading conditions on a bored tunnel due to consolidation settlements. *ITA World Tunnelling Congress 2003*.

Pachen, H.M.A., Zanten, D.C. van. 2002. Prediction of long-term settlement of a bored tunnel in soft soil. Geotechnical aspects of Underground construction in soft soil Ground. Lyon.

Zanten, D.C. van, Vries, M. de. 2003. Railway crossings for RandstadRail in Rotterdam. *ITA World Tunnelling Congress 2003*. Amsterdam.

Zanten, D.C. van, Pachen, H.M.A., Feijen, T.A. 2002. Tunnelling for RandstadRail in Rotterdam. *ITA World Tunnelling Congress 2002*. Sydney.

Section 5
Underground constructions executed from surface in built-up areas

This page intentionally left blank

Underground Space – the 4th Dimension of Metropolises – Barták, Hrdina, Romancov & Zlámal (eds)
© 2007 Taylor & Francis Group, London, ISBN 978-0-415-40807-3

Analysis of long-term deformations of an earth-covered tunnel

J. Barták
Czech Technical University, Faculty of Civil Engineering, Prague, Czech Republic

ABSTRACT: A road tunnel leading to the active face of a stage-working limestone quarry is being continually covered with an inner dump consisting of inert material, which will restore the landscape to the pre-existing contours once it has been reforested. The final depth of the dump will amount to some 60 m. Continual monitoring of the contact stress on the external surface of lining, of deformations of the tunnel sub-base and deformations of the tunnel lining allows a control analysis of the tunnel lining to be conducted during the course of the tunnel covering.

1 INTRODUCTION

The five-stage Hvížd'alka limestone quarry, which is situated on the south-eastern periphery of Prague on a slope of the Radotín brook valley, forms a distinct "scar" in close proximity to the border of the Český Kras (Czech Karst) Protected Landscape Area. The years shortly after 1990 saw the beginning of the process of searching for environmentally friendly and technically suitable disposing of a significant amount of the spoil and waste cement rock. The system of gradual development of a disposal site inside the quarry, which would not only require no extra land but would even reinstate the ground to its original profile, was adopted as a solution advantageous in all respects. But the excavation of the first quarry stage required a permanent access to the bottom of the quarry. The access was provided by building a horseshoe shaped profile road tunnel with the cross section area of 30 m^2. The tunnel was 332 m long in the first stage and it can be gradually extended up to a length of 400 m.

The tunnel, with a roadway for Terex-type cross-country lorries inside, is continually covered in the waste material forming the inner dump with the depth over the tunnel roof reaching up to 60 m. The depth followed both from the requirements for the volume of the soil and rock to be dumped and from a structural analysis, which was developed within the framework of the dump management using the Finite Element Method.

The dimensions of the final lining with the thickness of 0.85 m allow the thickness of the cover to achieve 60 metres starting from 104 m chainage (measured from the entrance portal). The safe angle of 29° for the front slope of the dump was calculated and verified on a physical model. This slope angle allows the full height of the dump of 60 m to be achieved. At the cover height of 60 m and the tunnel length of 332 m, the Hvizdalka quarry will be able to hold 960,000 cubic metres of the spoil material and unusable stone from the quarry.

The tunnel covering process is continually monitored, with the focus being on deformations of the tunnel sub-base, convergences of the tunnel lining and development of pressures exerted by the dump on the external surface of the lining. Owing to the observation of these quantities it is possible to observe actual stresses in the tunnel structure, to compare them with the design loading capacity of the tunnel lining, and to trigger a timely response to unexpected irregularities in the development of the tunnel deformations and the state of stress.

2 GEOLOGICAL CONDITIONS

In terms of the geological structure, the Hvizdalka location is part of the eastern part of the Silurian-Devonian zone of the Barrandiene formation, a part of the eastern edge of a tectonic-structural unit called the Choteč Syncline. The underlying bed of the deposit consists of the Slivenec Limestone. The cement rock deposit body is a complex of the Dvorec-Prokop limestone, which represent the bulk of the sedimentation complex. The greatest thickness of the deposit that was determined by a survey amounts to 160 m. In terms of hydrology, the massif is characterised by movement of ground water along open fissures and dislocations. The circulation of the water is very irregular and heavily dependent on precipitation.

In terms of tectonics, the area is significantly folded and affected by slip faults. The typical feature of the deposit area is a flat synclinal structure with the wings dipping at 30°–40°. At the south-eastern edge of the deposit, the layers are stretched out at 50°–80° as a result of dip-slip faulting.

The faulting of the rock environment at the bottom of the Hvizdalka shelf quarry is mainly of endogenous origin. It is a result of equalisation of the endogenous pressures and forces that formed the current block faulting and folding system during the geological development of the area. The rock massif can be assessed as mostly significantly broken.

Anthropogenic effects are considered a nonnegligiblecause of disturbance to the rock mass at the quarry bottom level. They comprise the breaking of the deposit block by blasting operations (bench blasting and chamber blasting) and also the discharge of the load acting on the quarry bottom due to the removal of the overburden; the discharge has resulted in opening of fissures within the existing discontinuity systems. The geotechnical characteristics of the rocks (physical-mechanical properties, alterations and intensity of the rock mass disruption by discontinuity surfaces) significantly influence the magnitude of the rock compression (even irregular) in the active zone under the quarry bottom in the course of the placement of the backfill forming the inner dump.

3 THE TUNNEL OBSERVATION MEASUREMENTS

The observation measurements taken on the tunnel leading inside the Hvizdalka quarry have the aim of long-term monitoring the deformational behaviour of the tunnel lining and the tunnel sub-base during the process of the tunnel covering with the spoil. The monitoring allows observation of the relationship between the actual stress state of the lining and the stress values obtained by the design structural analysis (according to the original structural analysis [1] and sizing [2], the tunnel lining can safely carry the loading by the cover up to 60 m thick).

The observation comprises the following tasks:

– To quantify deformations of the sub-base generated by the continual addition of the load acting on the rock massif on which the tunnel structure is founded.
– To follow changes in the shape of the tunnel lining.
– To monitor the distribution of changes in the contact stress on the outer surface of the lining attributable to the growing thickness of the tunnel cover.

The following three methods were utilised to meet the above tasks:

– monitoring of the settlement of the tunnel sidewalls using precision levelling,
– measurement of deformations on the inner surface of the tunnel lining,
– measurement of the contact stress on the outer surface of the lining using hydraulic pressure cells.

3.1 *Vertical survey of the tunnel*

The vertical survey of the side walls of the tunnel during the process of covering with spoil has been performed since 1996; till 2000 at regular 4-month intervals, since 2000 every even year at 6-month intervals [3]. A schematic longitudinal section through the 25 m thick cover existing at the end of 2005 is shown in Fig. 1. The measurement results from the mid 2006 are documented for individual measurement profiles No. 1 to 9 and for both tunnel sidewalls (R-L) in Fig. 2.

The assessment of the vertical survey clearly shows that differential settlement has been affecting the tunnel tube both in the longitudinal and transversal directions. While the differential settlement in the longitudinal direction is not dangerous for the tunnel lining because the individual 5 m long tunnel blocks are not interconnected and do not interact in terms of the structural analysis, the differential settlement of the side walls of the tunnel lining in the transversal direction significantly affects the magnitude of internal forces in the lining of the individual tunnel blocks.

The majority of differences in the settlement values fluctuate under 5 mm; nevertheless, the actual difference in the settlement of side walls at the profile No. 5 amounts to 6.7 mm and the largest value of the

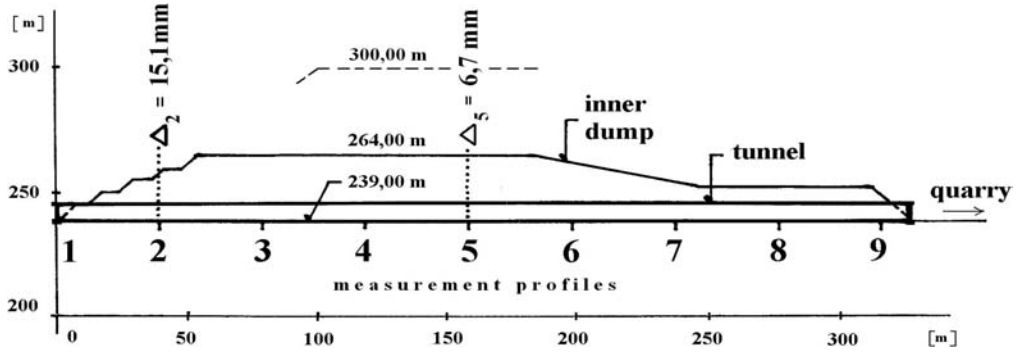


Figure 1. Schematic longitudinal section through the tunnel and earth cover.

differential settlement at the profile No. 2 amounts to 15.1 mm.

3.2 *Measurement of the contact stress*

The measurement of the contact stress on the outer surface of the tunnel lining is carried out at the same intervals as the levelling. Three pressure cells of the 6 installed ceased to measure due to irremovable causes of unclear origin.

It follows from the assessment of the contact stress measurements that the vertical stresses registered by the remaining three cells are nearly identical. They change continually and always closely correlate with the weight of the cover. The conclusion that follows from this fact is that the common theoretical assumption that, in this particular case, the concentration of the loads acting on the relatively rigid tunnel structure found inside a continually built high embankment has not been confirmed by direct measurement of pressures on the outer surface of the tunnel lining. The most probable reason is the fact that the material covering the tunnel was being improved, even if only imperfectly, by waste cement up to the top of the tunnel and roughly up to a distance of 10 m from the outer surface of the side walls. Owing to this treatment, the differences in the subsidence of the rigid reinforced concrete structure and the settlement of the surrounding cover material considered at the level of the tunnel top are insignificant, thus no surcharge is imposed on the structure.

3.3 *Measurement of the tunnel lining convergence*

The measurements of the tunnel lining convergence have been conducted at the same intervals as the

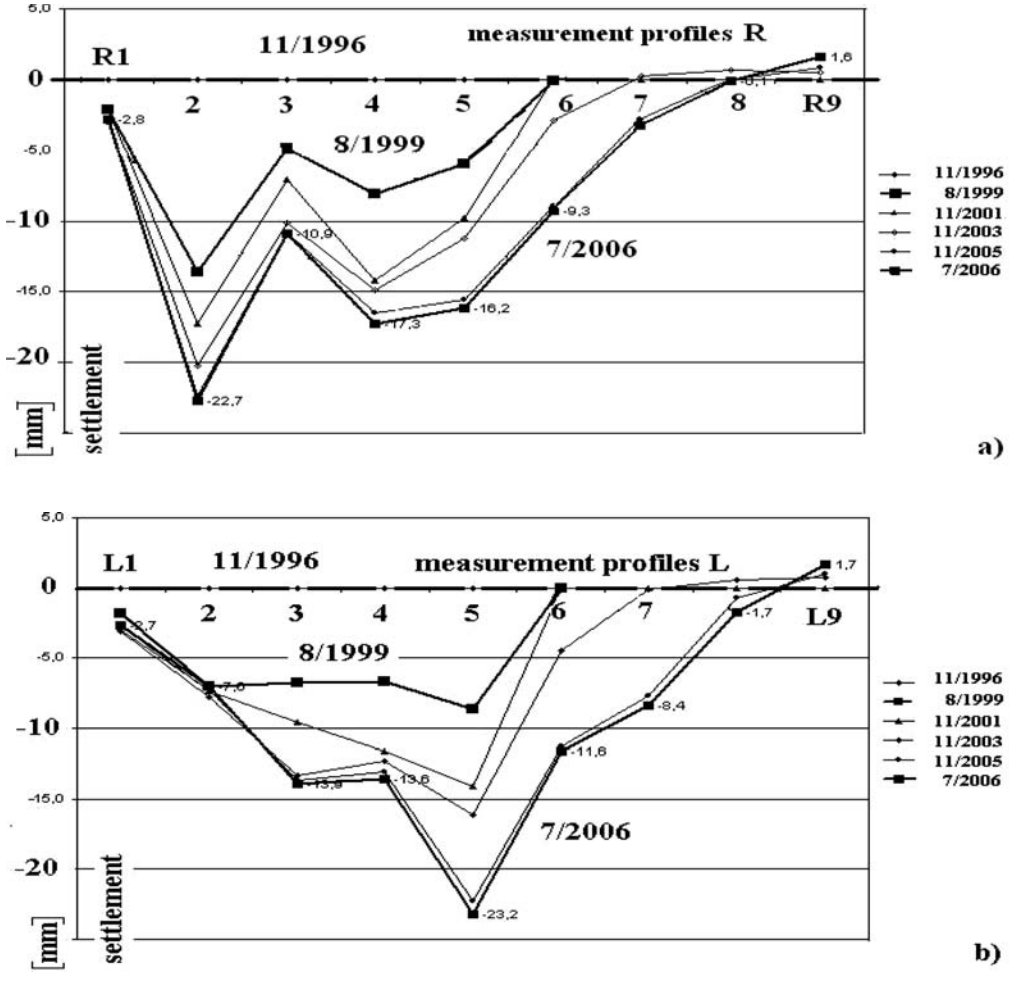


Figure 2. Settlement of the tunnel right (a) and left (b) side walls in the longitudinal direction.

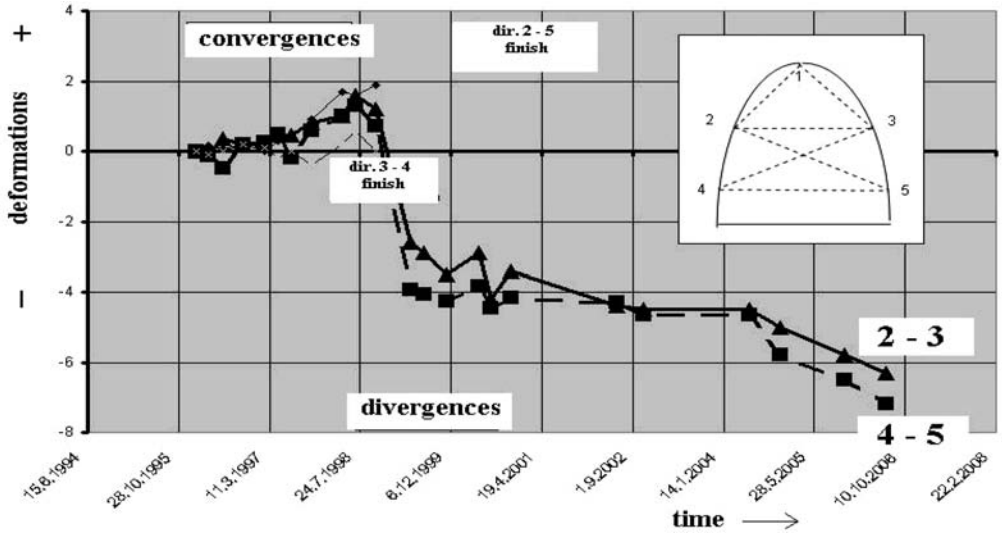


Figure 3. Convergences (divergences) of the tunnel lining at the profile No. 3.

levelling and the measurement of the stress on the outer surface of the tunnel lining. The measurement have been performed by means of a tape extensometer.

The graphical representation (see Fig. 3) shows relatively considerable horizontal divergences of the lining. It is obvious that the cross section of even a relatively rigid tunnel tube formed by the 0.85 m thick reinforced concrete lining is changing under the pressure; the width of the cross section is growing while the height is diminishing. The good structural function of the lining therefore depends on deformational properties of the cover material along the tunnel sides; those properties can be expected to be improving to a certain extent during the course of the continual placement of the cover.

4 MATHEMATICAL MODELLING OF THE DIFFERENTIAL TUNNEL SETTLEMENT

Inhomogeneities in the bedrock of the quarry caused differential settlement of the side walls of the tunnel structure. Differential settlement of supports of a statically indeterminate system of a tunnel liner causes significant increase in the internal forces, primarily the bending moments. These conditions require regular structural back analysis of the lining based on the measured values. The reason is the fact that larger values of transversal differential settlement induce additional stresses in the tunnel liner for which the liner has not been designed and which could cause damage to the structure. If necessary, technical construction measures can be implemented (e.g. grouting under the foundation of the tunnel side walls) which will prevent excessive deformations of the sub-base. Mathematical modelling of the state of stress and deformations of the covering body and its sub-base, but primarily the structural analysis of internal forces and deformations of the tunnel lining are carried out using the Finite Element Method. The PLAXIS program simulates the interaction of the two elements of the system (the lining and the cover) on the basis of a constitutive relationship for the contact zone (the Mohr-Coulomb failure condition for tensile stress in tension cut-off conditions).

The largest value of the differential settlement at the end of 2005, at the actual depth of the cover of 25 m, amounted to 12.4 mm in the exposed profile No. 2 and 6.7 mm in the profile No. 5. In the other profiles, this value is somewhere under 5 mm.

The completed calculations proved that the design loading capacity of the reinforced concrete profile has not been exceeded even in the profile No. 2; however, the final depth of the cover is only of 12 m because the profile position is under the inclined front slope of the cover body. The final state of the thickness and shape of the cover body in the profile No. 2 was reached as long ago as 2000; the differential deformations of the lining slightly grew by 2005 as a result of the increase in the cover thickness in the adjacent parts of the tunnel.

Actual internal forces acting in the profile No. 5: max $M_5 = 726$ kNm, $N_5 = 2780$ kN (see Fig. 4); the corresponding lining failure moment amounts to 1400 kNm, therefore, the cross section is perfectly satisfactory for the time being. Nevertheless, the final depth of the inner dump will grow by 35 m. Because the increase in the differential deformations has a continually growing character, the tunnel cross section must be paid permanent attention.

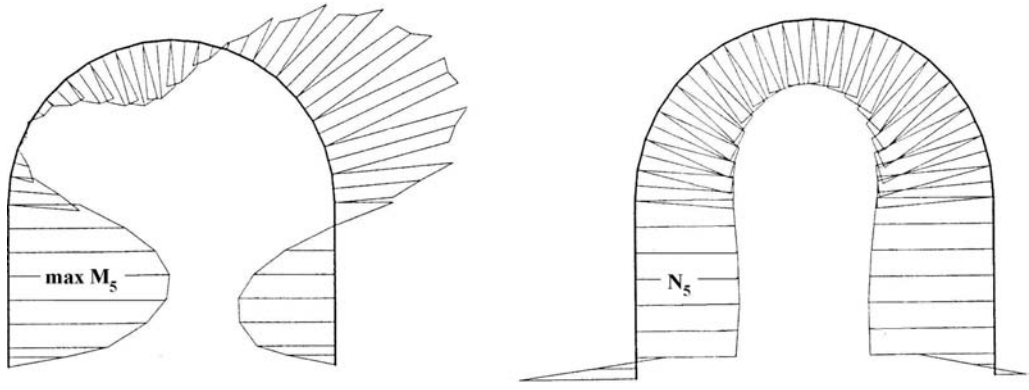


Figure 4. Internal forces in the lining (end of 2005, pr. No. 5 – max $M_5 = 726$ kNm, $N_5 = 2780$ kN).

5 CONCLUSION

The observation measurements conducted on the Hvizdalka covered-over tunnel allow continual checking on the deformation of the rock mass under the tunnel and analysing of the behaviour of the tunnel structure.

The so far obtained results, i.e. results for the years 1996 to 2006, in principle correspond both with the knowledge about the tectonic structure and geotechnical properties of the sub-base and the cover and with the assumptions about the behaviour of a thick-walled vaulted structure in terms of the structural analysis. The situation is, however, complicated by quite significant differential settlement of the tunnel side walls. If the current trend in the differential settlement continues in the course of the increasing of the cover thickness, internal forces acting in the liner that will exhaust the load bearing capacity of the most stressed cross sections will originate at smaller thickness of the cover than assumed. The adverse consequences of this state on the final thickness of the cover are obvious: smaller thickness would mean smaller capacity of the inner quarry dump.

REFERENCES

Klokner Structural Laboratory of the Czech Technical University in Prague, 1993. Assessment of the design of the tunnel in the Hvizdalka quarry in Radotin. Prague.

Subterra A.S., 1993. The design documents for the "New concept of the dump management for the Hvizdalka quarry". Prague.

Barták J. et al. 1996–2006. The package of reports "The performance and analysis of observation measurements on the Hvizdalka earth-covered tunnel".

Barták , J. et al. 2000. Measuring of the earth-covered traffic tunnel in the quarry Hvizdalka. *Tunel* 8(1): 6–10.

The analyses describes above have been conducted within the framework of the research project of the faculty of civil engineering No.1MSM 6840770001 "Functional capability of civil engineering structures".

This page intentionally left blank

Underground Space – the 4th Dimension of Metropolises – Barták, Hrdina, Romancov & Zlámal (eds)
© 2007 Taylor & Francis Group, London, ISBN 978-0-415-40807-3

Underpinning of live MRT piers for Singapore's new Circle Line Interchange Station

T.F. Lim
Design Manager, Land Transport Authority (LTA), Singapore

B.S.C. Tan
Deputy Project Manager, LTA, Singapore

K. Kozo
Senior Project Manager, LTA, Singapore

W.A. Chang
Design Manager, Nishimatsu-Lum Chang Joint Venture

C. Rintu
Project Manager, Nishimatsu-Lum Chang Joint Venture

ABSTRACT: The construction of the underground Circle Line Paya Lebar Interchange Station requires two existing viaduct piers of an operating Mass Rapid Transit (MRT) line to be underpinned. The loads from each viaduct pier were transferred from their existing piled foundation to a new support system using hydraulic jacks and a transfer beam supported at both ends on barrette piles. This paper describes the design of the underpinning works, its construction and the monitoring of the nearby existing MRT viaduct structure including the measures that were implemented to minimize movements.

1 INTRODUCTION

The underpinning works described in this paper is the first such operation carried out in Singapore on a live railway viaduct. As land scarce Singapore extends its transit infrastructure, companies and developers will find it commercially attractive to build future projects around the existing MRT structure. Underpinning would be a method that can be employed to incorporate the new developments with the existing MRT. The information in this paper would be useful to the developer and the contractor who undertakes such a project.

The proposed underground Circle Line (CCL) Paya Lebar (PYL) interchange station is situated west of the existing East-West Line (EWL) Paya Lebar Station. It will serve as an interchange station for the new Circle Line and the existing East-West line. CCL PYL station is being constructed under Circle Line Stage 2, comprising five fully underground stations, namely Old Airport Road Station (OAR), Tanjong Katong Station (TKT), Paya Lebar Interchange Station, Macpherson Station (MPS) and Upper Paya Lebar Station (UPL). Figure 1 shows the location of these stations in relation to the whole Circle Line.

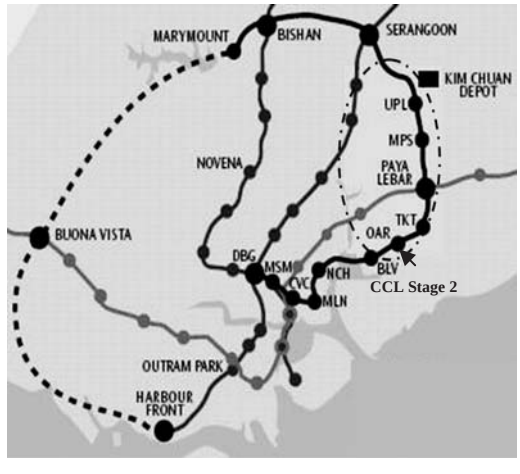


Figure 1. Singapore's circle line stage 2.

Nishimatsu-Lum Chang Joint Venture (NLC) was awarded the Contract 823 to build three of the CCL Stage 2 stations (OAR, TKT and PYL) with 1.66 km of bored tunnels and about 150 m of cut and cover tunnels.

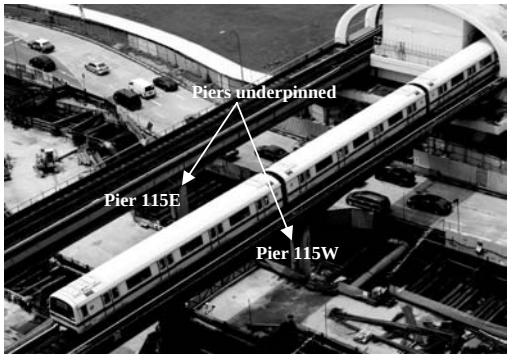


Figure 2. Viaduct Piers underpinned.

At the CCL PYL station two existing viaduct piers (identified as Pier 115E and Pier 115W on Figure 2) were underpinned as its piled foundations were in the way of the new underground station.

The new PYL station is constructed using the conventional cut and cover and bottom-up approach in soft marine clay. The underpinning was carried out by casting a transfer beam beneath the pile cap of each of the piers. Hydraulic jacks were used to transfer the pier load to the new support system before cutting the piles.

The following sections of the paper will describe this underpinning work which highlights the design of the structural elements of the underpinning, the construction, the jacking system and the monitoring of the nearby existing MRT structure. The paper also discusses the risks assessed and the measures that were implemented to minimise movements to the existing Piers 115E and 115W during excavation and underpinning. At the time of writing this paper, the Project had successfully underpinned the piers.

2 DESIGN CONSIDERATIONS

The underpinning is the main risk on this project. Redundancies were intentionally designed into the system to cater for any contingencies. One of these measures was providing 'spider' struts to resist horizontal loads of the piers during the construction stage. A second measure was the provision of six rows of lean concrete walls in the marine clay layer to minimise the deflection of the temporary earth retaining structure. Another measure was to provide additional capacity in the jacking system.

2.1 *Ground conditions*

The site investigation shows the following geological formations:

a) Fill
b) Kallang Formation, comprising F1 (Fluvial Sand), F2 (Fluvial Clay) and M (Marine Clay)

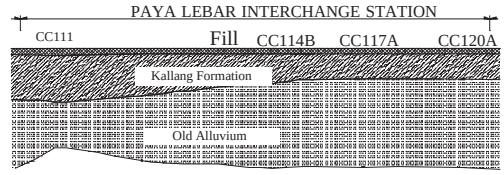


Figure 3. Interpreted longitudinal soil profile.

c) Old Alluvium.

A longitudinal soil profile along the station is shown on Figure 3. The Kallang Formation layer is deeper at the southern side of the station than at the northern side. The depth varies from approximately 25 m below ground level at the southern side to about 13 m at the northern end. An intensive soil investigation with boreholes every 20 m along the rectangular outline of the station box provided a good basis for design.

2.2 *Underpinning design*

The two existing EWL MRT piers were designed to be underpinned by transfer beams spanning between barrette piles. The loads from the existing MRT piers were to be transferred to the new transfer beams using hydraulic jacks. Figure 4(a) shows the cross section of the underpinning area. The 8 m (L) × 1 m (W) barrette piles provide support for the 18 m (L) × 8 m (W) × 3.1 m (D) transfer beams. To allow adequate working space for jacks set-up, the transfer beams were located 1 m below the soffit of the pile caps.

The design intent was to cast in the jacks to mitigate the risk of jack removal. The gap between the soffit of the pile cap and transfer beam will be grouted to ensure structural durability and stability. The bored piles were separated from the new transfer beam by a gap to ensure that they could slide easily during jacking.

At the design stage, an alternative approach of post-tensioning the transfer beam (without jacks) was studied. Finally, the hydraulic jack option was chosen as it allowed the flexibility for adjustment until the station structure is completed. The jacks could also be activated in a configuration that could correct any tilt of the piers.

2.2.1 *Lean concrete walls*

The six rows of lean concrete walls acting as in-ground struts were provided to limit the inward deflections of the temporary retaining system during excavation. These proved to be effective.

2.2.2 *'Spider' struts*

Spider struts were installed between the piers and the temporary earth retaining system to resist the lateral forces of the piers and any additional loads arising during construction.

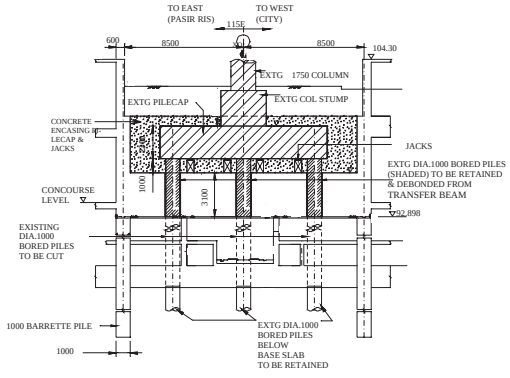


Figure 4(a). Sectional View of Underpinning.

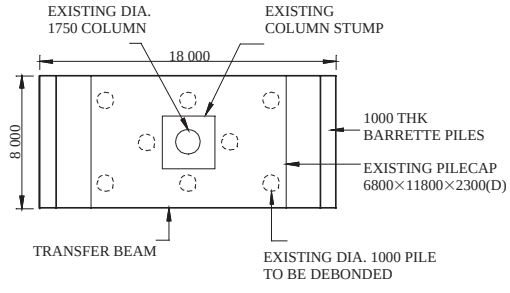


Figure 4(b). Plan View of Underpinning.

To provide sufficient rigidity, a minimum steel section of H350 × 350 × 137 kg/m, was specified. A plan view of spider struts is shown in Figure 5.

2.2.3 *Corbels*

Concrete corbels were introduced as 'guides' at four corners of each pile cap to restrict movement in the:

a) horizontal plane
b) vertical plane during and after pile cutting. Vertical restraint was provided by wedging the top of the corbel using steel plates after jacking.

This mitigates the risk of movement during jacking and the holding period before finally encasing the pile cap and jacks in concrete, i.e. when the piers are being supported off the jacks.

2.3 *Transfer beam and barrette pile design*

The barrette piles and transfer beams were analysed as a 2D sub-frame. The vertical and horizontal stiffness of the barrette pile supports were modeled in the analysis. The effective width of the transfer beam in the design was reduced to 4 m due to the bored piles, although the overall width is 8 m. Depth of the transfer beam (3.1 m) was selected by checking the amount of space available and structural performance to limit deflection during load transfer.

Figure 7 (a) to 7 (c) illustrates the design sequence of load transfer.

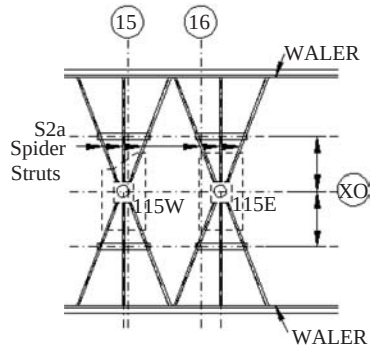


Figure 5. Spider Struts.



Figure 6. Corbel.

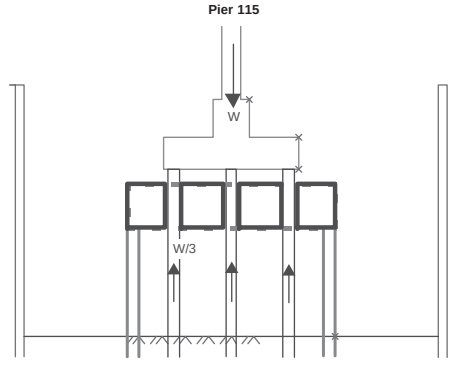


Figure 7(a). Initial condition.

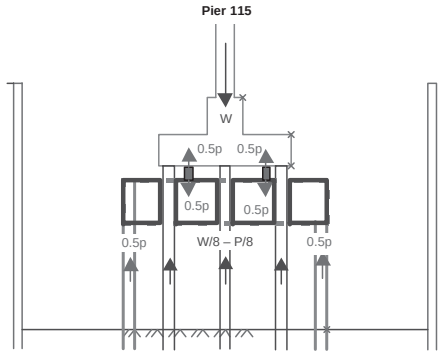


Figure 7(b). Pre-loading of jacks by a total force of "P".

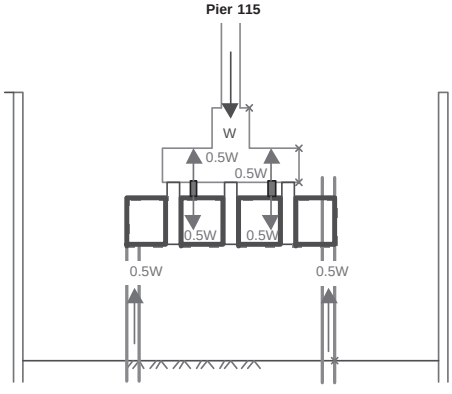


Figure 7(c). After cutting off the existing bored piles.

This construction sequence with pre-loading was chosen as it serves to 'load test' the new support system. At this stage, with the existing bored piles still in place, any unforeseen problems could be detected.

In order to derive the optimum percentage of jack pre-loading, a sensitivity study was carried out using different percentages of pier dead load. The predicted vertical movements of the pier and new transfer beam are plotted on Figure 8 (a) and (b) respectively.

From the sensitivity analysis, a jack pre-loading of 50% of pier dead load is optimal as it limits the vertical movement of piers to <0.5 mm. This also caters for:

a) Minimum effect on the EWL tracks
b) A preview of the effects of load transfer and opportunity to make adjustments, if necessary
c) Adequate buffer to prevent jacking beyond the actual load

Pre-loading of jacks to 50% of the existing pier dead load was then adopted.

The structural analysis of the sub-frame was modelled in 4 stages in the design:

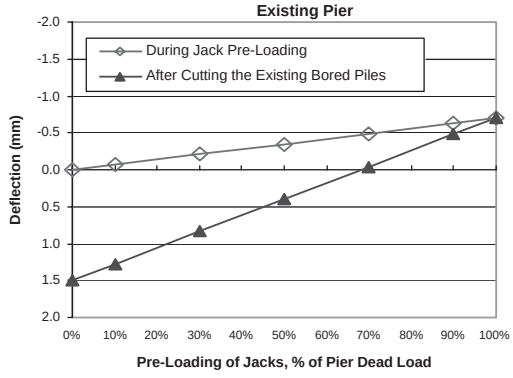


Figure 8(a). Existing piers.

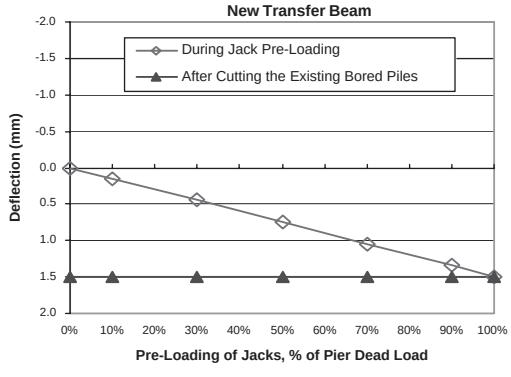


Figure 8(b). Center of transfer beam.

Stage 1 – Casting of the transfer beam (first loads introduced to the barrettes)
Stage 2 – 50% of pier loads (through pre-loading of jacks)
Stage 3 – 100% of pier loads, after cutting the existing bored piles
Stage 4 – Final Stage (when underpinning frame has been integrated with station structure).

2.4 *Predicted movements*

From the results of the sensitivity analysis shown on Figure 8(a), the predicted movement of the pier during jacking is about 0.3 mm (upwards) and 0.4 mm (downwards) after cutting of bored piles.

From Figure 8(b), the predicted movement of the transfer beam during jacking is about 0.75 mm (downwards) and 1.5 mm (downwards) after cutting of bored piles.

The predicted movements are well within the allowable limits imposed by the Code of Practice for Railway Protection (see Table 1) and rail operator (see Table 2).

Table 1. Allowable limit for the movement of structure.

Total movement in any direction	Differential movement in any plane
15 mm	15 mm or 1:1000

Table 2. Operating limits for track.

Twist	Vertical dip or peak
1:500	5 mm (measured over 5 m chord)

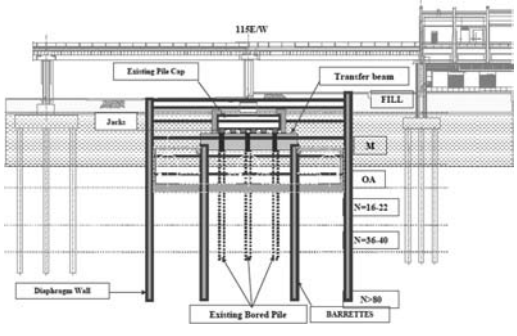


Figure 9. Construction sequence.

3 CONSTRUCTION

3.1 *Construction sequence*

The sequence adopted for underpinning construction is as follows:

a) Installation of barrette piles to about 50 m below ground level
b) Installation of lean concrete walls to about 15 m below ground level
c) Strutted excavation in 4 layers to 10 m below ground level (completed in July 06)
d) Construction of the transfer beams across the barrette piles with de-bonding of the existing piles (completed on 11 Sep 06)
e) Construction of corbels at four corners of each pile cap (completed on 20 Sep 06)
f) Excavation to 2 m below transfer beams to allow deflection by self-weight (completed on 14 Oct 06)
g) Installation of jacks and jacking (completed on 15 Oct 06)
h) Cutting of 8 nos of 1m diameter bored piles at each pier (completed on 29 Oct 06)
i) Continue strutted excavation to formation level (about 5m) (in progress at the time of writing this paper)
j) Cast station base slab and build up structure in stages up to roof level (expected to complete in Aug 07)
k) Encasement of pile cap and jacks (scheduled in Sep 07).

Table 3. Major risks.

Risk	Remedial measures
Pier movement due to uneven excavation	• Controlled excavation in layers not exceeding 2 m
Lateral stability of piers	• Spider strut provided
Soundness of barrette piles	• Confirmed by Pile Integrity Test
Uneven load distribution of existing bored piles due to eccentricity/as-built condition	• Checked as-built condition • Jack arrangement derived with nearly zero center of gravity
Inaccuracy of jack load	• Jacks re-calibrated one month before installation
Uneven movement of pile caps/piers during jacking	• Controlled by adjusting individual jacks • Jacking done during non-revenue hours
Unforeseen deflections during pile cutting	• Symmetrical cutting of piles

3.2 *Risk assessment*

The entire underpinning work is carried out below the operational viaducts of the EWL. Adverse effects of the construction activities could cause significant movements or unforeseen settlements to the piers and viaducts. Thus, risks that could lead to suspension of rail operation were assessed for every construction activity.

Prior to the commencement of underpinning work, a detailed risk assessment was undertaken; the major ones are listed in Table 3.

3.3 *Monitoring plan*

Existing piers, viaducts and pile caps were inspected to assess the condition of bearings and concrete quality.

Monitoring of the piers comprises (see Figure 10):

a) 3D prisms and electrolevels mounted on viaduct beams and piers that provide real time information on three-dimensional behaviour.
b) Weekly monitoring of EWL track twist and dip.
c) Daily monitoring of absolute levels of piers, pile caps and transfer beams.
d) Dial gauge monitoring of relative movement between pile cap and transfer beam (implemented only during jacking and pile cutting).

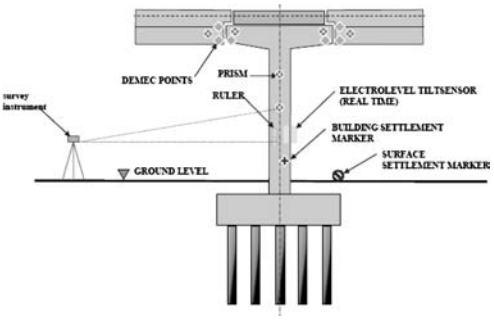


Figure 10. Monitoring schematic.



Figure 11. Installation of Barrette piles.

3.4 *Structural elements*

The biggest challenge was to build the structural elements (viz: barrette piles and lean concrete walls) under the viaduct with headroom less than 6 m. Special low-head equipment was required to carry out the work, especially the barrette piles and lean concrete walls (see Figure 11). Also, mini-excavators were used for all excavation work ensuring little impact on the operating EWL.

3.5 *Jacking*

Based on the calculated loads, a combination of jacks of rated capacities 100T, 150T and 200T were used (see Figure 12).

Typically, a pair of jacks (positioned so as to maintain almost zero centre of gravity) was used to support each pile; thus requiring 16 jacks per pier. Loading of jacks was done using three pumps serving the three jack groups (see Figure 13).

Jacking was carried out during non-revenue hours between 0130 hours and 0430 hours. In order to



Figure 12. Jack installation.

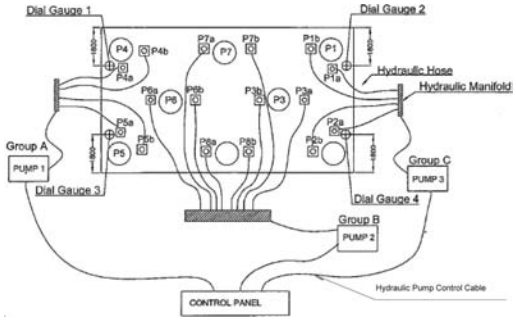


Figure 13. Jack layout schematic.

complete the whole jacking sequence in incremental steps within this time frame, it was essential to pre-plan and trial run the command and communication protocol (see Figure 14).

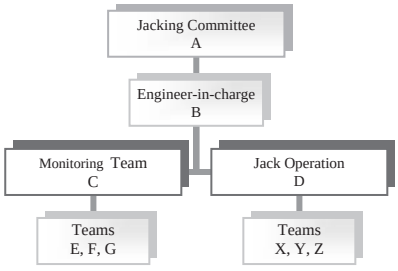
The dial-gauges were monitored at every 10% load increment, other survey readings were taken at 20% load increment.

3.6 *Pile cutting*

Cutting of piles was carried out during non-revenue hours using low-vibration diamond wire-saw cutter in a symmetrical sequence, see Figure 15 (a) to (c). In order to work within the available time of 3 hours, setting-up of the cutting rig and pre-cutting preparation were done in advance during revenue hours. Three cutting machines were deployed to complete the cutting operation in four consecutive nights.

3.7 *Monitoring results*

The same monitoring plan used during jacking was implemented to measure settlements and deflections during pile cutting.



A: Comprised project stake-holders to manage the jacking operation
B: Coordinator of all jacking related activities
C: Coordinator of Monitoring Teams
D: Coordinator of Jacking Teams
E: EWL Track survey team
F: Team to survey transfer beam, pile cap and pier
G: Team to monitor real-time data
X,Y, Z: Teams on individual pumps and dial gauge readings

Figure 14. Jacking operation control.



Figure 15(a). Pile Cutting Set-up.

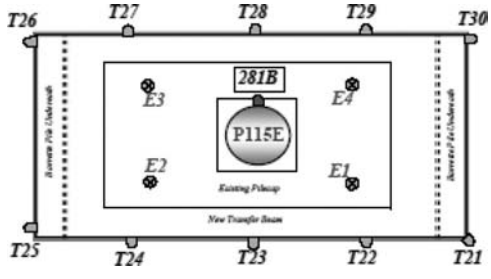


Figure 15(b). Close-up of wire saw set-up.



Figure 15(c). After pile was cut.

Table 4. Settlement values (mm).



Date	T25	E2/ T24	281B/ T23	E1/ T22	T21
15 Oct (aft jacking)	0.0	0.0/ 0.0	0.0/ 0.0	0.0/ 0.0	0.0
Predicted	–	–	−0.75	–	–
01 Nov (aft pile cutting)	−1.0	−2.5/ −1.5	−1.5/ −1.5	−2.0/ −1.0	−0.5
Predicted	–	–	−1.5	–	–

At the end of jacking, no measurable movement was observed on the piers. At the end of pile cutting, 1.4 mm settlement of the pier was recorded. Table 4 graphically presents the settlements observed on the transfer beam (T21 to T25), pile cap (E1 to E2) and pier (281B).

4 CONCLUSION

Based on the monitoring results, the actual performance of the new transfer beam is close to the design analysis. The settlement at mid-span of the transfer beam after pile cutting was measured at 1.5 mm, which is consistent with the design prediction.

The risk mitigation measures implemented to control the pier movements were effective in restricting the pier settlement to 1.5 mm.

The track twist and the pier tilt measurements during underpinning showed very little change and remained well within the operating limits.

Thus the underpinning was carried out successfully and safely without any impact to the EWL operation.

REFERENCES

Min, Cai & Boey S. 2003. *Design Consideration for Paya Lebar Interchange Station, Circle Line: RTS Conference*, Singapore.

Public Works Department. 1976. *Geology of the Republic of Singapore.* Singapore.

Land Transport Authority. 2004. *Code of Practice for Railway Protection.* Singapore.

Underground Space – the 4th Dimension of Metropolises – Barták, Hrdina, Romancov & Zlámal (eds)
© 2007 Taylor & Francis Group, London, ISBN 978-0-415-40807-3

Design and construction of a cofferdam for a sub-sea tunnel on The Palm Jumeirah, Dubai

J.S. Gahir
Kellogg Brown & Root, Leatherhead, UK

A. Mochizuki
Taisei Corporation, Tokyo, Japan

N.O. Othman
Parsons PTG, Washington, USA

M.A. Qamzi
Nakheel, Dubai, UAE

ABSTRACT: The paper presents design, construction and performance of a sheet piled cofferdam required to construct a 1.4 km long sub-sea vehicular tunnel in dry conditions. An overview of the challenges faced whilst piling and how these were overcome are presented. Measures taken to maintain the cofferdam during tunnel construction are included.

1 INTRODUCTION

The Palm Jumeirah in Dubai, United Arab Emirates, involves the reclamation of land to form the shape of a palm tree comprising of a crescent, 16 Fronds, Spine and Trunk. Reclamation extends some 5.5 km into the Arabian Gulf and the artificial island is protected at the seaward side by a rock armoured semi-closed elliptical Crescent (Figure 1). The resulting development increases the Dubai shoreline by 75 km and when completed will provide for a community of about 100,000 people.

To cross a body of water some 500 m wide a sub-sea vehicular tunnel connects the Spine to the 11.5 km long Crescent. The tunnel cross-section comprises 3 cells, the outer cells carrying 3 lanes of traffic in each direction while the central cell is reserved for services and emergency evacuation.

The construction methodology adopted was cut and cover in dry conditions which required a 2.4 km long sheet piled cofferdam as temporary works, with the sheet piles acting as cut off to reduce seepage into the cofferdam to manageable levels. Offshore and onshore operations were undertaken to install 30 m long steel sheet piles into the crest of temporary dykes and into the recently reclaimed islands where the tunnel portals are located. The construction sequence was to dredge, form dykes, install sheet piles and drain the cofferdam. After draining, the dykes provide construction access to the Crescent, a significant advantage over an immersed tube approach. The cofferdam constitutes some 30% of the total project cost of the tunnel works.

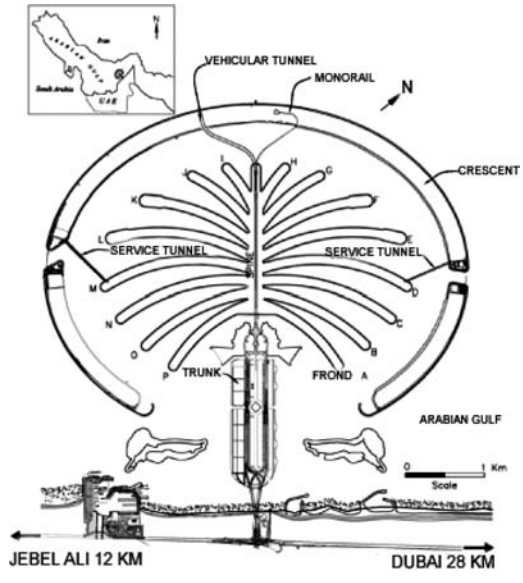


Figure 1. Overall view of The Palm Jumeirah.

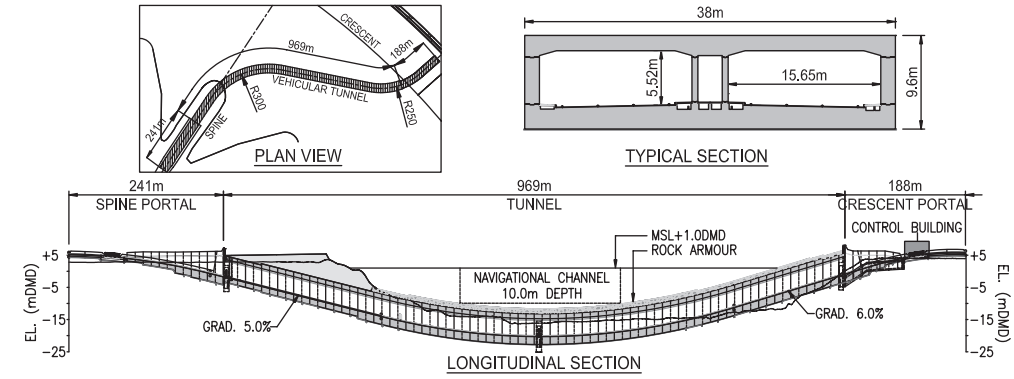


Figure 2. Tunnel alignments.

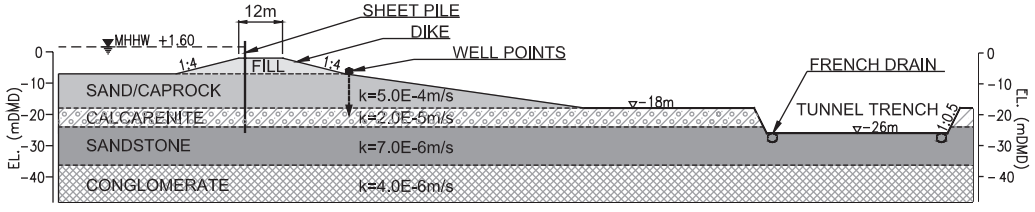


Figure 3. Typical cross section and ground conditions.

2 PROJECT DESCRIPTION

The total length of the tunnel structure is 1398 m and comprises of a 241 m long Spine portal approach, 969 m of reinforced concrete box section and 188 m of Crescent portal approach.

The horizontal and vertical alignments were dictated by a maximum grade of 6% for a 60 kph design speed, in compliance with Dubai Municipality Geometric Design Manual for Dubai Roads (1999), and the need to ensure that the tunnel was sufficiently deep to maintain a 125 m wide arc-shaped navigation channel with a minimum draft of 10 m, above the 1.5 m thick layer of armour protection on the roof slab. The vertical alignment and the horizontal alignment, which is a reverse curve with a central straight section, are shown in Figure 2.

Mean sea level is +1.0 mDMD (Dubai Municipality Datum, which is 0.09 m below Admiralty Chart Datum) with a tidal range of 1.2 m between MHHW and MLLW. The reclaimed islands are at +3 m and +4 mDMD at the Spine and Crescent, respectively. Seabed elevations before The Palm reclamation were in the range −11 m to −12 mDMD. Pre-construction surveys indicated that the minimum seabed elevation along the tunnel alignment and the cofferdam region was −15 m and −19 mDMD respectively, in areas where materials had been won for breakwater construction.

A Design and Build contract was awarded to Taisei Corporation in 2004 for the construction of the vehicular tunnel.

3 GEOLOGY AND GROUND CONDITIONS

The local geology in the vicinity of the project site has been shaped by the current hot arid climate and by fluctuations in sea level and is described by Gahir *et al*. (2006).

Ground conditions were determined by sinking 13 offshore boreholes to a depth of 30 m into the seabed and 3 boreholes up to 30 m depth on the onshore reclamation. The minimum elevation explored is −45 mDMD. The offshore boreholes were drilled along the alignment of the dykes and are offset up to 230 m from the tunnel centre line. All boreholes were grouted after completion.

The boreholes revealed that under a 12 m thick recent fill a 1 m to 2 m thick band of weak caprock is present which in turn is underlain by 2 m to 4 m thick layer of medium dense sand. The sand overlies an 18 m to 22 m thick sequence of very weak to weak interbedded calcarenite and sandstone. A conglomerate layer whose upper horizon is some −35 mDMD is present across the site (Figure 3). The UCS of rock encountered is in the range 1 to 3.5 MPa. In isolated boreholes a thin layer of soft silt was recorded

under the fill, and is suspected to be the original seabed.

In-situ permeability of the rock units, measured using standard Lugeon tests and variable head permeability tests, indicated k values ranging from 4×10^{-6} to 5×10^{-4} m/sec with lower values at depth.

4 DESIGN CONSIDERATIONS

The cofferdam is required for some 17 months and at peak periods a workforce of about 1000 was expected within its confines and thus safety was of paramount consideration in the design process.

The cofferdam outline was dictated by the following considerations (a) the dykes have a 12 m wide crest at −2 mDMD; an elevation adopted after a soil-structure interaction analysis was undertaken for different pile sections and various crest elevations, to provide a balance between the fill available and the structural performance of the piles (b) the sheet piles were planned 2 m from the seaward edge so that a 10 m wide corridor was available for a 2 lane temporary road inside the cofferdam after draining (c) the tunnel trench at its deepest is −26 mDMD and the trench slopes, located in interbedded sandstone and calcarenite, were planned at 1 V:0.5 H (d) a 15 m minimum clearance was maintained from the top of the trench excavation to the toe of the dyke thus avoiding surcharging and undermining the stability of the trench slope and (e) a dyke slope of 1 V:4 H from crest to −10 mDMD and 1 V:7 H thereafter, was adopted from slope stability considerations based on recent experience gained in the construction of The Palm. A 2.4 km long cofferdam outline was thus identified having a plan area of some 300,000 m^2 and a maximum width of about 400 m. This outline involved 1550 m of offshore piles and 850 m of onshore piles. Local filling adjacent to the recently formed islands was undertaken to maximize land based operations.

Both marine and land driven sheet piles are up to 30 m long and the top of the piles were planned at +3.3 mDMD for minimal overtopping under storm surge and wave conditions, and the toe at −26 mDMD based on seepage analyses which required 1 m minimum penetration into the lower less permeable sandstone which underlies the calcarenite. Bending stresses and deflections complying with Technical Standard and Commentary for Port and Harbour Facilities (2001) indicated that pile sections SX27 (section modulus, z = 2700 cm^3/m) for the offshore piles, and PU25 (z = 2500 cm^3/m) for onshore piles were appropriate. The estimated maximum deflections at the top of the marine piles, after draining, was calculated to be about 200 mm and the relative deflection between +3 m and −2 mDMD i.e. the cantilevered section, to be about 150 mm. These estimates are based on a sea level of +2.45 mDMD, to take account of storm surge, and a horizontal modulus of subgrade reaction of 10,000 KN/m^2/m based on an empirical relationship to an SPT-N value of 5.

Seepage analysis using 2D FLOW with an average k value determined for each substrata indicated that some 820 m^3/hr could be expected under the cofferdam once steady state conditions had established. French drains at the base of the tunnel trench, with pits and submersible pumps of sufficient capacity, and lines of well point systems were designed to collect the inflow (Figure 4). The collected inflow was directed to two locations, one either side of the tunnel trench, before being pumped back to the sea over each dyke with due care taken not to erode the outer slope.

5 CONSTRUCTION METHODOLOGY

5.1 *Dyke construction*

Cutter suction dredgers were used to excavate the tunnel trench, one for shallow and one for deep dredging below −15 mDMD, with operations commencing at the end of the alignment i.e. at the newly formed islands and progressing towards the centre where the trench is deepest. The dredgers lowered the seabed elevation by some 2 m in a single step until the desired elevation along the tunnel alignment was achieved within 0.5 m of the invert elevation, with the final grade being achieved using earthworks equipment in dry conditions. Seabed elevations were constantly monitored by surveying equipment on the dredger and from a survey boat.

The dredged material was sucked into the dredger holds and placed at the dyke locations using a spread pontoon positioned by GPS and controlled by anchors and winches. Both dykes were built up concurrently and care was required to achieve the 1 V:4 H slope by considerably reducing the volume discharged through the pipe. Total volume for the two dykes was 920,000 m^3 of which 660,000 m^3 was obtained from the tunnel trench excavation and the balance was obtained from a borrow source nearby, with a small quantity purchased from a supplier. A larger volume than had been estimated at the tender stage was necessary due to the flattening of the dyke slopes from 1 V:4 H to 1 V:7 H below −10 mDMD as already described in Section 4. Bathymetric surveys were carried out after filling to either confirm that the desired dyke profile had been achieved or identify local areas requiring additional fill.

5.2 *Sheet pile procurement and preparation*

Procurement of the 12,500T of sheet piles was a lead item due to a shortage on the world market. Some 9500T of new SX27 sections in 15 m lengths were

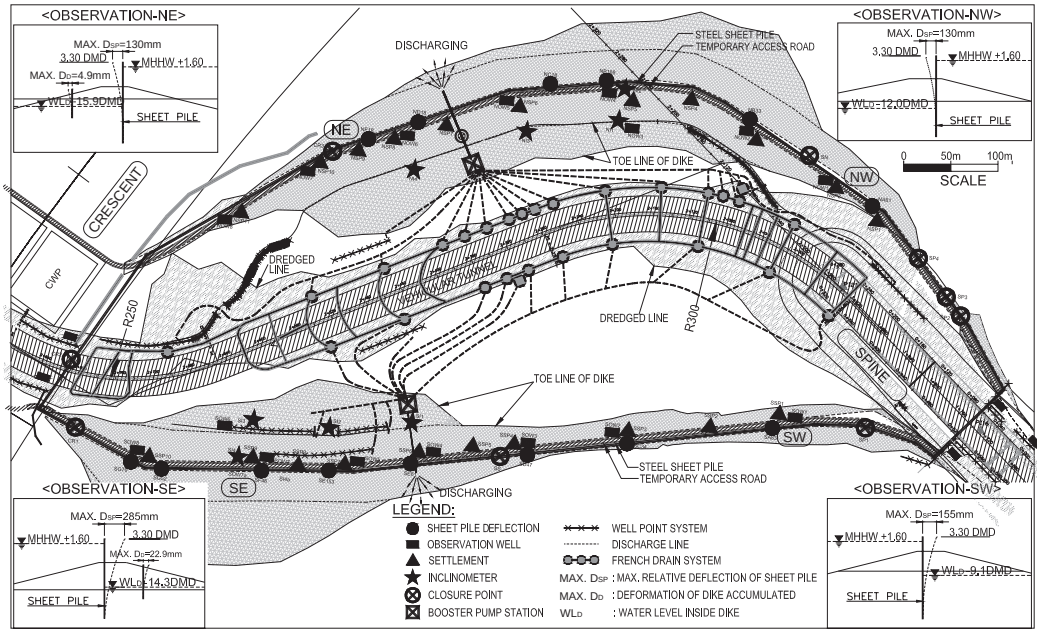


Figure 4. Dewatering regime and cofferdam monitoring points.

procured from Japan and had a 2 to 3 month delivery time. Used PU25 sections of some 10 m length were purchased locally and taken to an onsite yard at the top of the Spine where 20 m lengths were assembled. To determine the sheet pile drivability a trial was undertaken near the Spine portal close to a borehole location using PU series. The piles were spliced and driven to depths of 33 m using vibrohammer ICE815C (1250 kN max centrifugal force) without difficulty.

The newly purchased SX27 sections were taken to Hamriya Port, about 35 km east of the project site, where they were chamfered and welded to form 30 m lengths. Hyperseal DPS-1000 was applied to the pile clutch. This material can expand up to 10 times its original volume in fresh water but its performance offshore is curtailed due to the salinity of sea water and it expands to half the figure. The piles were paired to form 1.2 m wide panels, so that each prepared offshore panel comprised of 4 sheet piles, before being barged to site.

5.3 *Onshore sheet piling*

Sheet pile sections, 20 m long and 0.6 m wide, were pitched into a guide frame capable of accommodating 16 sheet piles and driven one by one with a 1.5 m stick up. Longer sheet piles could not be accommodated due to limitation of the crane boom. Ten metre long pile sections were hooked through the guide frame and spliced to the driven piles. Driving recommenced using vibrohammer ICE815C and progress was slow due to difficult driving. Some hard nodules present within the calcarenite and the wear and tear on the used piles were felt to contribute to difficult driving. Additionally two splices in the desired pile length did not always provide a plumb vertical section and this led to an increase in the frictional force in the pile clutch.

At some locations especially on the Crescent piles were terminated 5m short of the required design penetration due to refusal with the driving system. A reassessment of the seepage inflow into the cofferdam was undertaken using k of calcarenite 2×10^{-5} m/s which indicated that the anticipated inflow in this area increased 9 times locally with the nett effect that the overall infow into the cofferdam after draining increased from 820 m^3/hr to 1600 m^3/hr. To cope with the additional inflow contingency measures were put in place and comprised of (a) drive secondary short length sheet piles in local areas at the top of the tunnel trench excavation (b) increase the number of wells and (c) increase pump capacity.

5.4 *Offshore sheet piling*

Offshore piling was undertaken from 2 barges, each with a 150T crane, and the prepared panels 30 m long and 1.2 m wide, were driven through a guide frame using a double clutch vibrohammer ICE1412 (2300 kN max centrifugal force). The contractor reported difficult driving conditions which required greater effort

in getting the necessary penetration than had been anticipated initially. On average 2 to 3 panels were being achieved in a 12 hour shift. When the second barge, operating a week later on the opposite dyke, also experienced similar difficulties it was recognized that the problem was not local.

Piling records indicated that the penetration rate decreased significantly below −17 mDMD in the second calcarenite layer. A review of the unconfined compressive strength results indicated weak rock and that although the presence of hard nodules may explain some of the driving difficulties, something fundamental had been overlooked. Pairing the piles doubled the area at the cutting edge and also doubled the friction from the fill and underlying rock, and this resistance could not be overcome by simply doubling the hammer capacity required for a single pile section. The decision to pair the piles was taken after discussion with a local piling contractor who had successfully driven paired piles but not to the depth required for this project. An offshore pile driving trial may have revealed the problem earlier, and more work in this area would have been useful.

To overcome the difficulties in the short term predriving was undertaken with a panel connected to a water jetting system to −25 mDMD and withdrawn, and the final 1 m was driven with the permanent pile. Following the initial success with water jetting, a decision was taken to weld four 25 mm diameter steel pipes in the corners of all the sheet piles along its total length and connected to 2 mm diameter jetting nozzles located near the toe of the sheet pile. The pipes were hooked to a high pressure pump capable of delivering 250 l/min at 40 bar pressure. Simultaneous water jetting and driving with the same hammer overcame the driving difficulties. To make up for lost time a third barge was mobilized and a night shift introduced. In 86 working days 1290 paired sheet piles were successfully driven to the desired toe elevation. Towards the end a production rate of 5 to 6 pairs was being achieved in a single shift.

5.5 *Cofferdam closure*

Seven onshore and 2 offshore closures were necessary to complete the perimeter. Sheet pile sections driven from the opposite ends were overlapped so that an open box was formed. A uPVC tube was inserted from the top of the piles to key into the top of the dyke and grouted, thus sealing the open box. After setting, a borehole was drilled through the grout, the dyke and into seabed extending to the same elevation as the toe of the sheet piles. A rapid setting chemical grout, colloidal silica with sodium chloride, was then injected at 0.5 m centres working from the bottom up. The colloidal silica when set has a very low permeability, thus effectively sealing the closure point.

The offshore closure was undertaken during a Neap tide within a 4 hour window. Due to an increased flow velocity some scouring of the dyke, up to 2 m deep over an 8 m long section, was observed by divers deployed periodically during the course of the works. The dyke was repaired after closure.

5.6 *Draining*

Some 4,350,000 m^3 of water inside the cofferdam (excluding seepage) was pumped out in stages to reduce the water level from +1 m to −23 mDMD. This was undertaken using 9 high capacity pumps each fitted with a flow meter, of which 7 were operational at one time, connected via valves and manifolds to the discharge pipes and over the northern cofferdam wall and to sea. The pumps were located on two floating pontoons placed centrally at the deepest section of the trench excavation. Discharge was completed in 45 days and the rate of water level drop was maintained at less than 1 m/day. Some leaks in the sheet piles joints were sealed using underwater welding and sealants.

6 IN-SERVICE PERFORMANCE AND MONITORING

6.1 *Summary of instrumentation installed*

To provide information on sheet pile deflections, the deformation of the dykes, and water levels in the cofferdam 6 total station targets with a mirror attachment, 8 inclinometers, 16 observation wells with ground water loggers, and settlement monitoring stations were installed at strategic locations and depths. Base readings were established on top of the sheet piles before draining and the instruments were installed shortly thereafter. Temporary bench marks were installed at 50 m intervals on the shoulder of the dyke for monitoring settlements. Trigger and action values were identified for each item along with an action plan should the values be exceeded, and to provide an early warning system in the event that unanticipated conditions arise. Typical results are included on Figure 4 and an aerial view of the cofferdam is shown on Figure 5.

6.2 *Strengthening works*

A maximum total deflection of some 1000 mm and a relative deflection of 285 mm was recorded along a 200 m long section at the end of draining, which were in excess of the action values set. The measured deflections, which incorporates pile rotation, is in an area where the original dredged channel was the deepest and the dyke height maximum. CPT testing indicated the presence of very loose material with entrapped silty clay for which a horizontal modulus of subgrade reaction of 2000 $KN/m^2/m$ was appropriate. A best fit analysis using a 2D FEM analysis with



Figure 5. Aerial view, December 2005.

the surveyed dyke geometry and the lower modulus value was undertaken to simulate the actual condition, and indicated that the stresses in the steel piles were within tolerances. As a result, the trigger values for sheet pile deflection were revised up to 1250 mm at the top of the sheet pile as an absolute deflection and 335 mm between +3.0 m and −2.0 mDMD as relative deflection to reflect yield stress situation. Vibrotreatment works on 2.5 m grid spacing and to a depth of 15 m were undertaken in this portion of the dyke fill to densify the material and the crest level was raised by 2 m to 0 mDMD and the dyke widened locally to limit further deflections.

6.3 *Maintenance*

In addition to visual inspections the instruments are monitored daily. Once steady state conditions had established there was no further deformation of the dyke or additional deflections of the sheet piles, other than minor cyclic fluctuations due to tidal variations. The measured discharge averages 1650 m^3/hr and compares very favourably with the calculated inflow estimate of 1600 m^3/hr indicated by the seepage analysis.

Corrosion of the sheet piles due to seawater aggressivity was observed along the perimeter. Ultrasonic testing revealed that the rate of corrosion was 0.8 mm/yr at the upper half, where tidal fluctuations occur, and 0.3 mm/yr at the lower end of the cantilever section. A couple of moist areas were observed on the dyke slope and standpipes were installed in these areas which recorded water level at a depth of 3.5 m below the dike slope. The moist spots are related to the capillary rise in the area and the capillary fringe is consistent with the results reported by Fookes *et al*. (1983) for sandy silts.

7 PROGRAMME

The overall project schedule is shown on Figure 6.

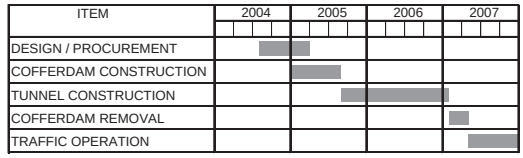


Figure 6. Overall schedule.

8 HEALTH, SAFETY AND ENVIRONMENT

A plan was prepared to evacuate the cofferdam in an emergency and drills undertaken at periodic intervals demonstrated that the work force could be safely evacuated in 8 minutes. Discharge water quality was visually monitored on a daily basis with water quality samples analysed weekly.

Whilst draining the cofferdam local fishermen were engaged to catch fish trapped within its confines using wire net traps of different sizes, up to 2 m in diameter. The trapped fish were removed and placed in oxygenated cool boxes before being returned to sea. Almost 1900 fish comprising 35 species were safely returned to open waters.

9 CONCLUSION

The successful completion and draining of the cofferdam has resulted in a safe environment enabling cut and cover tunnel construction to proceed. At the time of writing in September 2006, 85% of the tunnel structure is complete and the tunnel will be operational in December. Difficulties encountered whilst pile driving were successfully overcome with additional effort and within programme constraints, without compromising safety.

ACKNOWLEDGEMENTS

The authors are grateful to Nakheel for their kind permission to publish this paper.

REFERENCES

Dubai Municipality Geometric Design Manual for Dubai Roads. 1999 Edition.

Gahir J.S., Radwanski R. and Hafez T.A. 2006, “Design and Construction Challenges of Sub-sea Directional Drilled Crossings on the Palm Jumeriah, Dubai. ITA congress, Korea.

Technical Standard and Commentaries for Port and Harbour Facilities in Japan (The Overseas Coastal Area Development Institute of Japan). 2001 edition.

Fookes P.G., French W. J. and Rice M. M. 1983. The influence of ground and groundwater geochemistry on construction in the Middle East. Quarterly Journal of Engineering Geology, London, 18, 101–128.

Underground Space – the 4th Dimension of Metropolises – Barták, Hrdina, Romancov & Zlámal (eds)
© 2007 Taylor & Francis Group, London, ISBN 978-0-415-40807-3

Flood Protection of Prague Metro after the 2002 flood

M. Jakoubek
Metroprojekt Praha, Prague, The Czech Republic

ABSTRACT: About one third of the length of operating lines of the Prague Metro found in the central area of Prague were inundated during the flood in August 2002. The construction of a new flood-protection system commenced immediately, when the damage caused by the flood had been repaired and the metro lines operation had resumed. Analyses and the assessment of the flood impacts showed that the flood wave threatens most of all cut-and-cover structures of the metro lines which are founded near to the surface, namely by increased external hydrostatic pressure and/or the hydrodynamic effects of this pressure. Mined metro sections are virtually unthreatened in these cases. Protection of the cut-and-cover structures is provided by several basic types of traditional construction measures. The structural parts found in the flooded zone are reinforced or thickened, permanently anchored, braced or supercharged. Structures which are selected with respect to their design and local hydrogeological conditions are provided with elements relieving the hydrostatic pressure on the outer surface of stations and concourses. This paper describes the function of the relieving elements in detail.

1 INTRODUCTION

The oldest line of the Prague Metro has been in service since 1974. Since then, 54 stations have brought into service, on three lines. Before 2002, all threatened sections of the Prague Metro had been protected against inundation from the surface up to the level of the Vltava River peak flood calculated in a 100-year cycle. The water surface level exceeded the 100-year flood level by more than 2 metres in the vicinity of some stations during the August 2002 flood. The metro entrance spaces were inundated by surface water; it was impossible then to prevent the water from rushing into the stations. At the same time, the flood wave was running through the metro tunnels. This is how the inundation affected the total of 17 stations (6 stations – primary inundation, 11 stations – subsequent inundation through running tunnels and cross-passages). Even though the flood wave did not affect integrity of structures, it caused extensive damage to the structural parts and equipment of the metro.

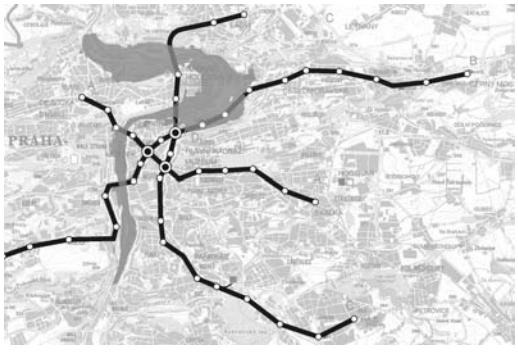


Figure 1. Plan map of the Prague Metro showing the extent of the surface inundation during the 2002 flood.

2 HYDROLOGICAL CAUSES OF THE FLOOD

The flood that passed through Prague in August 2002 had not been recorded before since 1827 when systematic hydrological monitoring started. It was probably the greatest flood in the history starting in 1432, when a flood destroyed five pillars of Charles Bridge, which was at that time the only stable connection between the Vltava River banks in Prague.

The peak flow was assessed statistically as a 500-year recurrence flood. Nearly 3 km^3 of rainwater fell during a single August week in 2002 in southern and south-western Bohemia. The amount of precipitation exceeded the precipitation totals for many months in some locations. The ground, which had been saturated by previous rains, did not receive other water, therefore nearly all this amount flew directly to streams and rivers. Virtually the entire above-mentioned area is part of the Vltava River catchment basin, therefore this amount of water had to flow through Prague in the course of several days.

The volume rate of flow, which is referred to as "100-year flood discharge" in statistical terms (3700 $m^3\,s^{-1}$) was exceeded roughly by 1500 $m^3\,s^{-1}$.

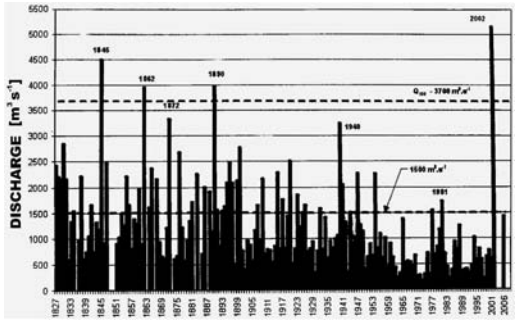


Figure 2. Time series of culmination flow capacity on the Vltava River – maximum annual flow capacity.

3 FLOOD PROTECTION SYSTEM DESIGN

3.1 *Parameters specified for the new flood protection system*

The catastrophic effect of the flood brought about a need for development of a new system of the Prague Metro flood protection. This is why the city authorities subsequently decided that the height of flood barriers be raised up to the level of the inundation experienced in 2002 in the given profiles of the particular stations, with a safety margin of 0.6 m. This level was further considered to correspond to the design protection height $Qn_{2002+0.6\,m}$.

The underground railway protection system is designed as a system independent of the systems protection individual districts of Prague; it protects the underground railway even in the case of the water spilling over barriers installed along the Vltava River. The primary task of the project is to prevent a flood wave from getting inside the metro spaces from the surface, in the case of inundation, to prevent water from spreading into other spaces of the metro, and to provide resistance of load-bearing structures of the metro against hydrostatic and hydrodynamic effects of the flood wave; The load bearing capacity of the metro structures is adequate to the height of all completed barriers.

3.2 *The summary of implemented measures*

The inundation of metro entries is prevented at the surface level by fixed walls and new lines where mobile barriers can be erected are prepared. When the flood wave is stemmed by barriers surrounding a metro station, the hydrostatic pressure on the station envelope will increase. Individual expansion blocks of cut-and-cover structures founded near the surface are, with respect to hydrogeological conditions threatened by heaving due to the buoyancy forces, or by a structural failure due to the hydrostatic pressure. The mined sections of the underground railway are not directly threatened by the flood.

The recently completed system of flood protection of the stations consists of implementation of several basic types of traditional construction measures. The load-bearing structures found in the flooded zone are reinforced or thickened, permanently anchored, braced and supercharged. Elements relieving the hydrostatic pressures on the outer surface of envelopes of stations and concourses are installed in some parts of the structures in the flooded zone, with respect to the design of these parts and local hydrogeological conditions. The construction measures that are implemented either remain hidden from passenger sights or they are incorporated into the architectural design of the stations.

The work on the flood protection system was carried out without any interruption to the underground railway operation. If the design protection height ($Qn_{2002+0.6\,m}$) is exceeded, the internal spaces of the metro stations found in the flooded zone will be automatically inundated. Elements of the civil defence system of the metro, namely pressure-resisting gates and other barriers, are also incorporated into the system preventing a flood wave from spreading.

In two cases (Florenc interchange station and the concourse of Invalidovna station), the implementation of the complete set of protection measures to reach the unified level is so complex and difficult that it will require much longer time than that required at the other stations. In the short run, organised inundation of the internal space of the metro is designed for these stations, to begin when a lower water surface level is reached for which the load-bearing capacity of the structures has been verified. The inundation of the internal space of the protected structure is a simple flood protection method. In this case, the pressures are equalised, thus damage to the structures is prevented. It has been proven that the damage due to the forced organised inundation would be lower by an order of magnitude and significantly faster to be compensated for than the damage resulting from contingent destruction of load-bearing structures.

4 TYPES OF THE CONSTRUCTION MEASURES IMPLEMENTED

4.1 *Permanent fixing of a concourse structure with anchors*

The system of protection against inundation from the surface level was provided for the concourse of Vltavská metro station, which had been originally built in an open trench. A line of permanent walls and mobile barriers up to 1.8 m high as a maximum was erected at the surface level. The barriers were

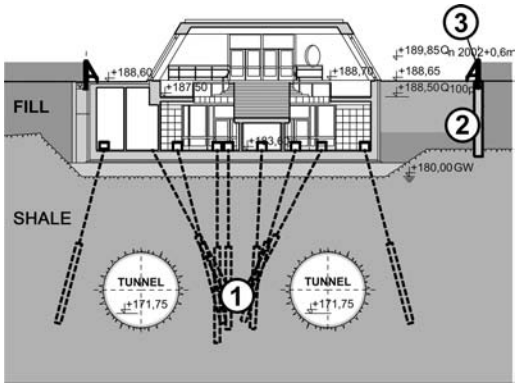


Figure 3. Permanent anchoring of Vltavská station to the bedrock. 1. Permanent anchors, 2. Jet-grouted pillars, 3. Mobile barriers.

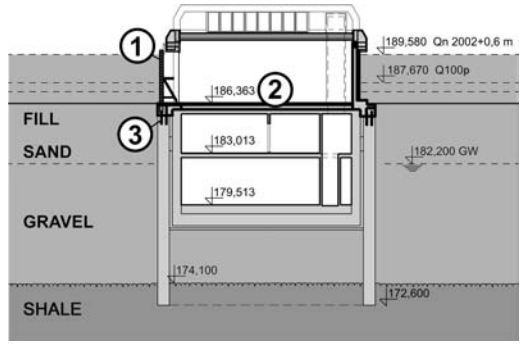


Figure 4. Incorporation of the weight of the diaphragm walls into the weight of concourse structure – Křižíkova metro station. 1. Mobile barriers, 2. Thickening of the roof structure, 3. Sills joining the diaphragm walls to the concourse structure.

founded on newly installed jet-grouted pillars keyed into bedrock consisting of shale.

The protection of the concourse structure against floating was provided by a system of permanent anchors (see Fig. 3). The structural analysis assumed full hydrostatic pressures exerted as a result of the design flood flow; the environment surrounding the concourse structure consists, according to the hydrogeological survey, of permeable man-made ground. The foundation slab of the concourse, which is found at a depth of 5.0 m under the surface, was tied to the bedrock with anchors; in terms of the structural analysis, this system even reduces the span of the slab carrying the hydrostatic forces. The ground plan of the grid of anchors was adjusted to operational requirements. The ends of the 500 (800) kN capacity anchors were provided with steel face plates. The openings where the anchors passed through the slab and the waterproofing layers were made watertight by grouting. The heads of the anchors found on the floor of the public area of the concourse were masked by visible benches. The hinged upper part of the benches allows an easy access to the anchor heads, where the pre-stress can be checked. The benches were incorporated into the architectural design of the concourse.

4.2 *Reinforcing and/or thickening of the structures; incorporation of diaphragm walls weight into the weight of the concourse structure*

The whole height of the original light-weight glazed external walls of the Křížíkova station concourse, from the floor to the roof, are designed to be replaced by 300 mm thick reinforced concrete walls. The walls will be structurally connected with the existing reinforced concrete underground part of the station and tied to the at grade steel structure of the concourse.

The newly constructed reinforced concrete sills are tied to the original diaphragm walls for the purpose of protecting the concourse structure against the buoyancy effects (spliced reinforcement bars). The incorporation of the weight of the diaphragm walls into the weight of the overall structure is shown in Fig. 4. Additional elements of the at-grade part of the concourse structure were built and this part of the structure was extended to cover the entire ground plan area of the underground part within the framework of the flood protection works. Openings and entrances to the concourse are protected up to the height of 3.0 m by means of mobile barriers. The architectural design maintains the features of the original design. The new external walls are a combination of stone cladding with opaque glazing.

4.3 *The drainage system for lowering of the ground water table during a flood emergency*

The technical solution to the flood protection system around Malostranská station is based on the idea of preventing inundation of the underground railway from the ground surface by means of mobile barriers and, at the same time, lowering of the ground water table in the immediate proximity to the concourse structure to a level specified by a structural analysis. The at-grade atrium space will be closed during a flood from all sides: from three sides by means of new lines of mobile barriers; from the west, the barrier is provided by the building of the Waldstein Riding-School built in 1630. The mobile barriers are founded on jet-grouted pillars. There are drainage galleries in the area surrounded by the barriers driven along the external wall of the concourse. Dewatering wells are at the ends of the galleries (see Fig. 5). The gallery houses a DN 250 mm horizontal drainage pipeline installed

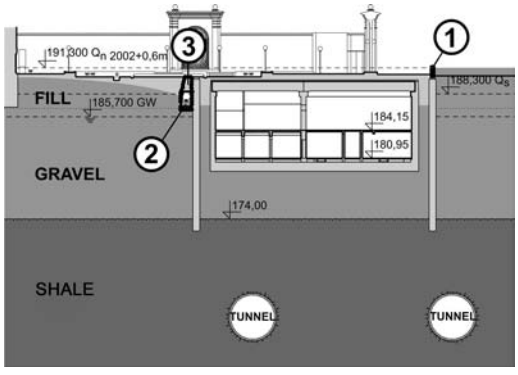


Figure 5. The drainage system along the concourse of Malostranská metro station. 1. Mobile barriers, 2. Drainage gallery, 3. Dewatering pump.

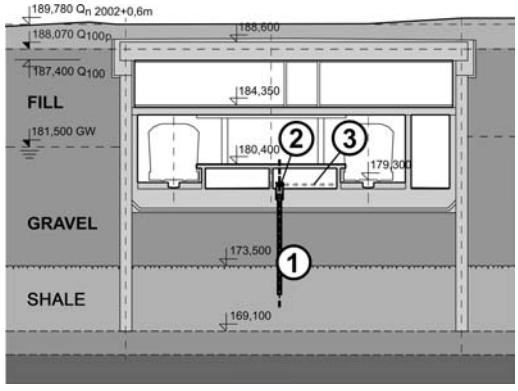


Figure 6. The pressure-control element passing through the foundation slab of Florenc metro station. 1. The cased hydrogeological borehole, 2. The head of the pressure-control element, 3. The pipeline draining water away.

on a 1 per cent gradient falling toward the dewatering well. The remaining space of the gallery around the pipeline is filled with gravel-sand, which guarantees that the stability of the environment being dewatered will remain unimpaired. The ground water that will seep to the galleries during a flood will be collected by the drainage and led to the wells; it will be pumped from the wells behind the barrier line, to the raised Vltava River. Thus the ground water table level in the atrium will be lowered and the hydrostatic pressure on the concourse structure reduced. The design has allowed for requirements for the stability of the Waldstein Riding-School subbase to be secured. The flow of water in the closed atrium space was verified by a hydrogeological survey and mathematical model.

4.4 *Pressure-control elements passing through the foundation slab*

The inventive solution to the problem of protecting the foundation slab against the buoyancy effects is based on pressure-control elements passing through the foundation slab of Florenc interchange station on the Line C (Fig. 6). The station was cut-and-cover top-down box excavation between slurry diaphragm walls. The foundation slab of the station consists of a single 221.0 m long expansion block. The design of the station (diaphragm walls braced with the bottom and roof slabs) does not allow overloading during the design flood.

The original structural analysis from 1970 assumed the 100-year flood level to be lower by 2.38 m than the current design level of the flood wave. This criterion is hard to satisfy by implementation of the above-mentioned traditional measures because of the existing intensity of operation of the interchange station. This is why a non-traditional solution to the problem of protection of the station substructure was adopted.



Figure 7. Drilling of the hydrogeological borehole through the hermetically embedded gate of the pressure-control element, with the seeping water drained away to a branch pipeline. A temporary extension piece is attached to the pressure-control element making it possible to cope with the inflows during the drilling operation.

Two hydrogeological boreholes passing through the foundation slab and reaching the bedrock were carried out inside the station to be used for pumping tests; additional two monitoring boreholes were drilled. As described in detail below, the drilling rods passed through special gates hermetically embedded in the foundation slab, with an intention to use them after the completion of the hydrogeological survey as parts of the pressure-control elements (see Fig. 7).

Based on the results of the hydrogeological survey, the function of the pressure-control elements can be described in the following simplified way: In a flood emergency, the hydrostatic pressure in the closed space under the bottom of the station and in the vicinity will

grow as a result of the rising ground water table level combined with an increased rate of seepage through the external diaphragm walls. The ground water table level around the station is bound to the level of the Vltava River surface. The installed pressure-control elements will allow controlled relieving of the hydrostatic pressure under the foundation slab of the station. When the valves installed on the heads of the pressure-control elements are opened, the pressure ground water will flow to the interior of the station and, at the same time, the hydrostatic pressure will be reduced in a controlled manner to the level verified by the structural analysis. Considering the completed measurements and on the basis of a model calculation, we can expect that the rate of the inflow which will be drained away into the existing sufficiently capacious non-faecal sump found in the metro station and pumped over back to the swollen Vltava River will amount to $5.0\,l.s^{-1}$. The efficiency of the protection of the foundation slab using the pressure-control elements was verified by hydrodynamic pumping tests within the framework of the survey activities, both in normal condition of the ground water table and, subsequently, using a mathematical model, which assumed the flow of the ground water during a flood emergency situation. The results of the model analysis resulted in addition of two elements to the existing four pressure-control elements so that gradual and steady process of reducing the hydrostatic pressure under the entire area of the foundation slab was possible. The filtration stability in the situation of ground water flowing from under the foundation slab of the station to the interior of the station is guaranteed owing to the hydraulically tested perforated casing of the boreholes and the fill around the casing pipes.

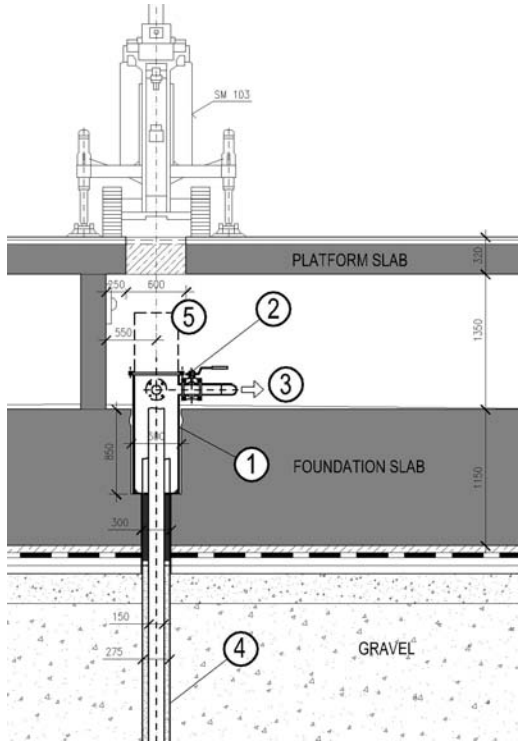


Figure 8. Vertical section through the pressure-control element. 1. The head, 2. The ball valve, 3. The pipeline draining water away, 4. The cased borehole, 5. The temporary extension piece allowing the drilling while ground water flows in.

5 SOME ASPECTS CONCERNING THE INSTALLATION OF THE PRESSURE RELIEVING ELEMENTS

5.1 *The design*

The additional incorporation of the pressure-control elements into the load-bearing structure is an innovative solution, which has been applied neither in Czech probably nor foreign construction practice. The design followed pre-set requirements to be met by the pressure-control elements, first of all the viability of drilling through the foundation slab, which is exposed to a permanent hydrostatic pressure, and handling the subsequent flow of ground water into the station space. Further, the elements had to allow installation of equipment necessary for the pumping tests to be carried out within the framework of the hydrogeological survey, waterproof embedment into the foundation slab, and had to meet requirements for long-term resistance against pressure.

The work was complicated by the fact that the drilling of the cored boreholes had to be carried out through the reinforced concrete platform slab, during overnight traffic closures. The pressure-control elements were incorporated into the foundation slab using the following procedure (see Fig. 8):

1. Ø500 mm core drilling down to a depth of three quarters of the foundation slab depth (approximately 850 mm),
2. gluing of stainless steel prefabricated head of the pressure-control element into the foundation slab using an epoxy sealant,
3. a check test of hardening of the epoxy sealant,
4. checking on the sealing of the head by means of a pressure test (see below),
5. Ø300 mm core drilling through the remaining portion of the slab and the waterproofing layers, drainage of ground water away to the pumping station,
6. the final hydrogeological borehole extending to the bedrock; a pumping test,

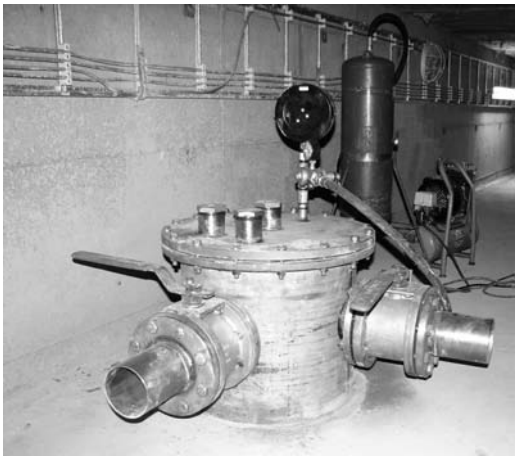


Figure 9. The complete pressure-resistant head embedded in the foundation slab.

7. installation of the equipment of the head, installation of closing ball valves,
8. closing of the pressure-control element

The valves are closed in the condition of common operation. These elements, which interconnect the external and internal environment, even allowcontinuous monitoring of the ground water pressure under the foundation slab.

5.2 *Testing of quality of the gluing and sealing of the heads of the pressure-control elements*

The tests carried out during the installation of the stainless steel heads of the pressure-control elements consisted of pull-out tests performed to verify the process of setting of the epoxy glue and pressure tests checking the tightness of the glued sealing and individual components (the valves, flanges) of the head of the pressure-control element. The testing set is shown in Fig. 9.

6 NOTES

6.1 *Other measures implemented within the framework of the flood prevention system*

The flood protection structures were built concurrently with installing permanent instruments monitoring the hydrostatic pressures in selected structures as a part of the survey operations. The load-bearing capacity of roof decks of the stations was tested using loads corresponding to the expected extent of the surface inundation. The services penetration points were inspected and the openings provided for the services in external walls were protected against leakage.

6.2 *Mined sections of the metro and the flood*

In terms of the condition of tunnel structures, we can say that the mined sections of the Prague metro survived the 2002 flood without any damage. The metro was in full service even during the initial hours of the flood while the water surface level had risen by several metres. No increased leakage was observed, let alone operational safety threatening defects caused by the adequately increased hydrostatic pressure on the tunnel lining. Despite the fact that speculative notions that the inundation happened due to a collapse or holing of the main load-bearing structures which were expected to withstand the water pressure, the inspection carried out after the water pumping had been completed and the condition of the structures checked conclusively proved that the tunnel lining passed this test undamaged.

7 CONCLUSIONS

The solutions described in this paper regarding the problem of protection of load-bearing structures are generally applicable to other structures located in a flooded zone or threatened by increased level of the ground water table.

The above-mentioned method of diminishing the hydrostatic effects by means of additional incorporation of the pressure-control elements can be conveniently utilised in other cases, after a thorough analysis of the condition of the lining and of the potential rate of water inflow from the outer environment. A hydrological survey of the outer environment and subsequent verification of the function of the pressure-control element are advisable.

Regarding the existing underground structures exposed to one-off effects of increased hydrostatic pressures, for instance during a flood, the application of the pressure-control elements is not only a highly effective but also highly economic solution compared with traditional conventional methods.

A catastrophic flood, similar to the flood which hit Prague and inundated the metro, can also affect other cities where underground railway lines are within the reach of a river. We can recommend a responsible solution of the flood protection system to be developed in such a case.

REFERENCES

Jakoubek, M. 2005. The flood protection of the Prague underground – the projekt and constructional layout, *Zakládání 4/2005*: 24–27.

Jakoubek, M., Hrabánek, M. & Kolísko, J. 2006. The flood protection of metro station Florenc – investigation of structures and emergence spillway elements, *Beton 2/2006*: 28–33.

Underground Space – the 4th Dimension of Metropolises – Barták, Hrdina, Romancov & Zlámal (eds)
© 2007 Taylor & Francis Group, London, ISBN 978-0-415-40807-3

Underpinning using pipe-roof

Kawakami Kazutaka
Waseda Work Office of the Construction Department, Tokyo Metro

Sumino Takaaki
Shinjuku 7-chome work Office of Konoike, Aoki Asunaro, Siraishi Kensetu Joint Venture

ABSTRACT: The Tokyo Metro Line No. 13 of is a north-south line between Kotake-Mukaihara and Shibuya, of which the 8.9 km section from Ikebukuro to Shibuya is currently under construction for scheduled opening in June 2008. (Figure 1). The project includes building the Shinjuku 7-chome Station (tentative name) at an average excavation depth of 37 m and with a length of 373 m immediately below Meiji Street, which has one of the largest traffic volumes in Tokyo. The section discussed is located in the first section on the Ikebukuro side (199 m long). The approximately 20 m length portion of this section, which is under the Okubo Intersection where Meiji Street and Okubo Street cross, has major underground lifelines, including two NTT tunnels, a Tokyo Electric Power tunnel, and a main sewer (Figure 2). As it is difficult to proceed with excavation while protecting these existing buried utilities through suspension, it was decided to employ the cut-and-cover method for each section on Ikebukuro and Shibuya sides from the intersection, except that the section immediately below the intersection was to be excavated according to the non-cut-and-cover construction method. This paper provides a summary of the underpinning method using pipe-roof to protect the intersection structures.

1 SUMMARY OF GEOLOGICAL FEATURE

The geological profile of the section includes, from the top downward, subsurface soil, Kanto loam (with the N-value of around 5), terrace gravel (with the N-value of around 2), Tokyo formation (with the N-value ranging from 10 to 50) and Kazusa group (with the N-value of 50 or more). The clayey soil is hard and the sandy soil is extremely compacted. Figure 4 shows the soil boring log.



Figure 1. Work location map.

2 OUTLINE OF THE WORK PROCEDURE

To avoid impacting the large buried utilities during excavation according to the non-cut-and-cover construction method for the approximately 20 m section

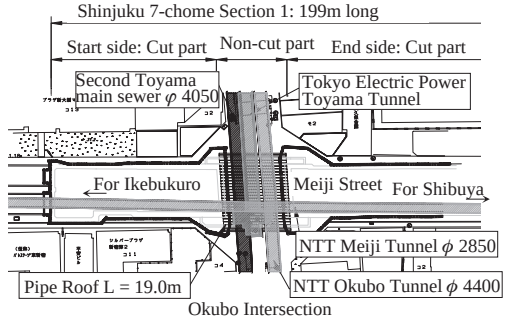


Figure 2. Plane view.

below the Okubo Intersection, the pipe-roof was constructed under the buried utilities, followed by its underpinning with bearing piles and finally by tunnel excavation and construction of tunnel structures. Figure 3 shows a plan view, Figure 4 provides a cross sectional view, and Figure 5 a longitudinal profile.

2.1 *Construction work sequence*

Figure 6 provides an outline of the work.

2.1.1 *Shaft excavation*

Using a cut-and-cover method a shaft was excavated at both ends of the intersection to be used as a base for constructing the pipe roof.

2.1.2 *Pipe-roof*

From inside the shaft, 26 horizontal pipes and 13 vertical pipes were driven to form the pipe-roof for temporary support. Explanation on how this was done will be made later.

2.1.3 *Excavation of the portion protected by pipe roof and driving of bearing piles*

The portion (5.6 m high) protected by the pipe-roof was excavated in steps of every 2.5 m depth. Each time such excavation was completed, bearing piles were driven from inside the shaft, support beams were installed, and jack-up (preloading) was done. By supporting the pipe-roof through sequential steps in this

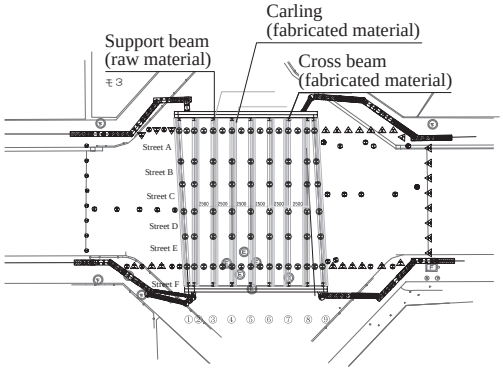


Figure 3. Plane view.

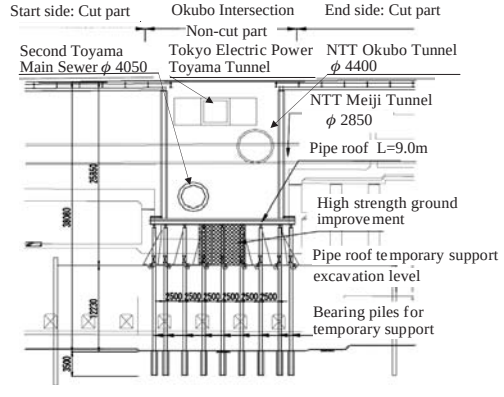


Figure 5. Longitudinal profile.

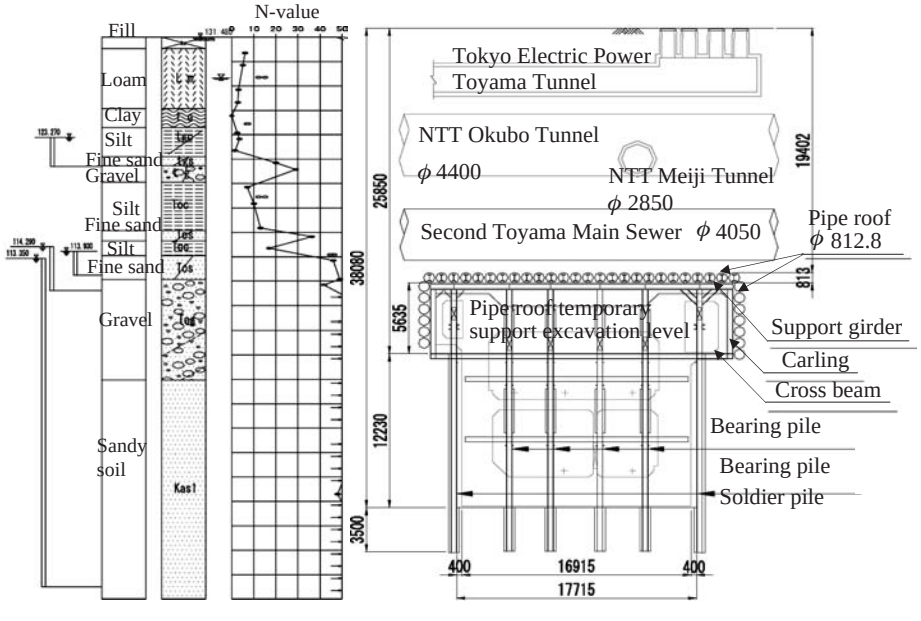


Figure 4. Cross section.

way, temporary underpinning was provided under the intersection. Concurrently, earth-retaining piles were also placed on both sides.

2.1.4 *Excavation of the main tunnel*
Under the protection of the pipe-roof, subgrade excavation of the tunnel was made in two stages (double-deck support).

2.1.5 *Building the tunnel structure and backfilling*
After completion of subgrade excavation, the tunnel structure was constructed.

3 ENGINEERING CHALLENGES

3.1 *Excavation under the pipe-roof protection*

As the pipe-roof was to be provided immediately below the important structures, the superfluidity (??) balance semi-shield method (mud density shield method) was employed, which can prevent ground collapse and groundwater inflow and minimize the extent of the ground loosening during excavation (Photograph 1). To protect launching and arrival of driving under pipe-roof protection, chemical grouting for water cut-off was made in advance from inside the shaft and also for the excavated portions to minimize any impact on the buried utilities from excavation under pipe-roof protection.

3.2 *Pipe-roof members*

Preliminary study was made on the displacement of the pipe-roof, the axial force of the bearing piles and the effects on the buried utilities expected during excavation of portion protected under the pipe-roof. Since the result proved that the initially designed members would exert substantial effects on buried utilities, members were changed to those with higher rigidity.

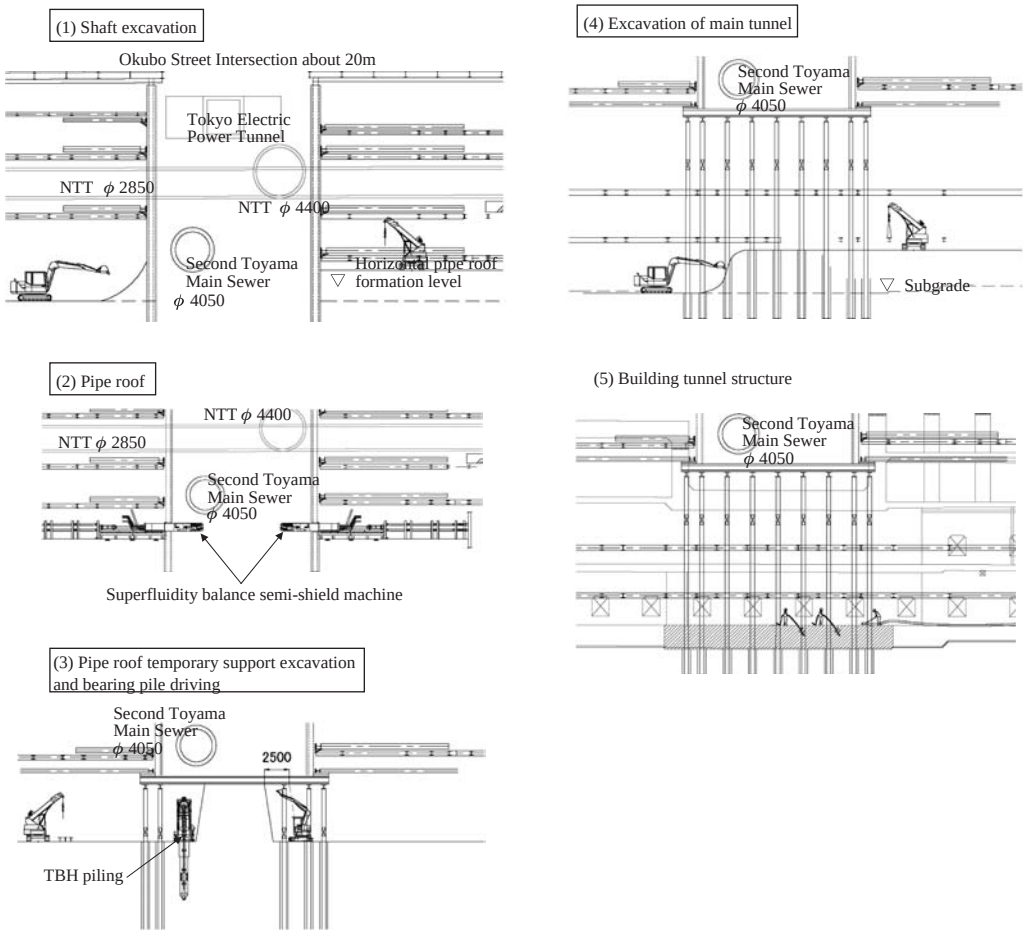


Figure 6. Construction outline.



Shield machine



Horizontal pipe roof



Vertical pipe roof

Photograph 1. Completion of pipe roof protection.

– Before change Horizontal steel pipe φ812.8 mm t = 12 mm (Mortar filled)
– After change Horizontal steel pipe φ812.8 mm t = 22 mm (Mortar filled) Insert a core material H-488 × 300 in a steel pipe

For analysis, the sequential stress analysis method was employed, in which the excavation sequence and ground plasticization were studied by applying the surcharge to the elasto-plastic beam spring model comprising the beam for the pipe-roof, the elastic foundation for the ground, and the elastic support for bearing piles. Figure 7 shows the analysis model.

3.3 *Bearing piles*

The pipe-roof carries the overburden load of about 130,000 kN (13,000 tf). The maximum load burden per pile is 5000 kN in case of temporary support and 3000 kN after completion of the temporary support. Therefore, TBH piles that are advantageous in easy treatment of their edges were used to secure the bearing capacity and to reduce pile settlement under load (Photograph 2).

3.4 *Preloading method*

Initial preloading was done each time one row of support beams had been installed and adjustment preloading was done after completion of temporary support protection (completion of installation of all support beams).

3.4.1 *Initial preloading*

The load of 100% or more of the dead load was introduced during initial preloading after laying the support beams, so as to enable monitoring load measurements during construction without fastening the safety nuts of jacks.

Loading was made as follows: the load expected in the future was applied, as the hysteretic load*1, stepwise in advance, followed by unloading to the preload*2 after confirmation that there was no abnormality in the pile settlement and pipe-roof behavior. Figure 8 shows the initial preloading steps.

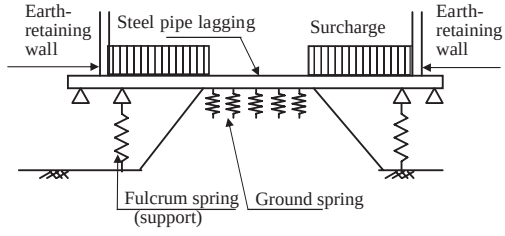


Figure 7. Analysis model.



Photograph 2. Pipe roof temporary support, TBH piles.

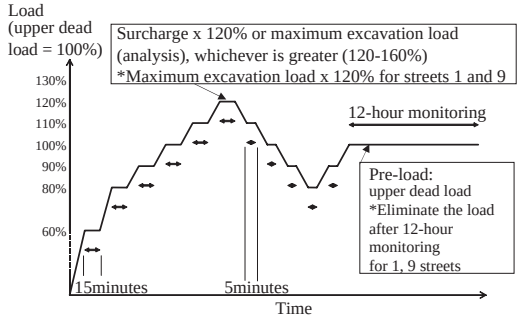


Figure 8. Initial preload loading steps.

*1. *Hysteretic load*

In the preliminary elasto-plastic analysis, the maximum load applied during excavation or the preload (surcharge) × 120%, whichever is larger, is introduced as the hysteretic load. Preliminary loading to provide

hysteresis enables prevention of further settlement of bearing piles.

*2. *Preload*
Unit surcharge x assigned area, which is determined by calculating the overburden load and by taking into account the tare of pipe-roof and the tunnel. Displacement of the pipe-roof is prevented by applying the loads to the bearing piles before excavation.

3.4.2 *Adjusted preload*
It was decided to adjust the load balance when any variation was observed in the load of support beams that had already been subjected to initial preload after installation of all beams.

The adjusted preload to be applied was set as the total of preloads on piles.

3.5 *Subgrade excavation of the main tunnel*

Skin friction resistance that is reduced by excavation is thought to migrate into the pile embedment, causing settlement. Therefore, a vertical load test using the driven piles was made to confirm the distribution state of pile bearing capacity and skin friction resistance and to estimate the increased load migrating to the pile embedment.

3.6 *Measurement control*

Various measuring instruments were installed to identify the conditions of buried utilities and temporary support protection members during construction, so that excavation can be made concurrently while comparing measured values with the predicted values. (Table 1)

3.7 *Bidirectional excavation*

As it was necessary to shorten the construction period to open the tunnel in June 2008, bidirectional excavation was employed, instead of the originally designed unidirectional excavation. As deformation of the pipe-roof in bidirectional excavation was greater than that in unidirectional excavation, attempt was made to achieve high ground strength by grouting chemicals of a design strength of 1.0 N/mm^2 (10.0 kgf/cm^2) in the center of the pipe-roof to restrain deformation of the ground and the pipe-roof.

4 VERTICAL LOAD TEST

4.1 *Bearing capacity*

By multi-cycle tests, maximum 6000 kN was loaded, resulting in observation of some change against a load of 5000 kN or more. It was thought that the value would not reach a first limit resistance . We judged that the ultimate bearing capacity would be 6000 kN or more and the allowable bearing capacity 5000 kN or more (safety factor of 1.2).

Table 1. Measurement control items.

	Subject	Measurement item	Measurement method
Buried utilities	NTT Okubo Tunnel and Meiji Tunnel	Distortion and convergence	Optic fiber strainmeter in the tunnel
	Second Toyama Main Sewer	Settlement	Placed settlement bar in the sewer and surveyed level of the crown of the sewer pipe
	Tokyo Electric Power Toyama Tunnel	Settlement	Entered the tunnel and surveyed level of the lower floor
Temporary support	Horizontal pipe-roof	Settlement	Placed pressure-type settlement gauges in the pipe-roof steel pipes
	Bearing pile jacks	Jack pressure	Placed pressure converters in the hydraulic cables of jacks
	Bearing piles	Axial power	Placed strainmeters on the bearing piles. Converted the measured strain to the axial force
		Settlement	Placed electronic staff in the bearing piles and measured the levels with an automatic level

4.2 *Skin friction resistance*

Figure 9 shows the distribution of axial force as measured by strainmeters attached to the piles. The strainmeters were not placed at the subgrade level but, judging from the distribution state (red dotted line), a load of some 2500 kN was carried near the subgrade under the load of 3000 kN after completion of temporary support. It was estimated that the incremental load at the embedment by subgrade excavation would be about 500 kN.

5 MEASUREMENT CONTROL RESULTS

5.1 *Measurement of the buried utilities*

We were able to complete the excavation within the controlled values, although some effects were seen

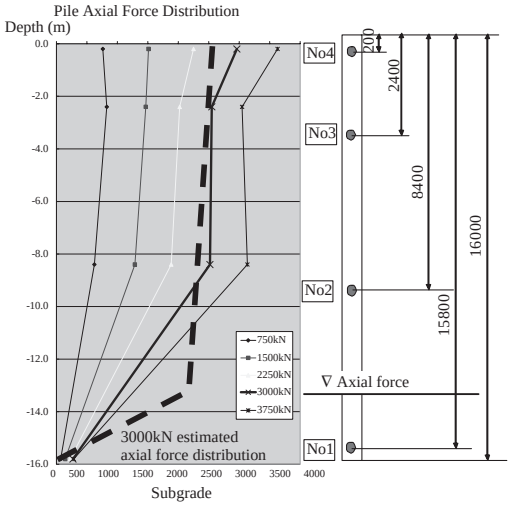


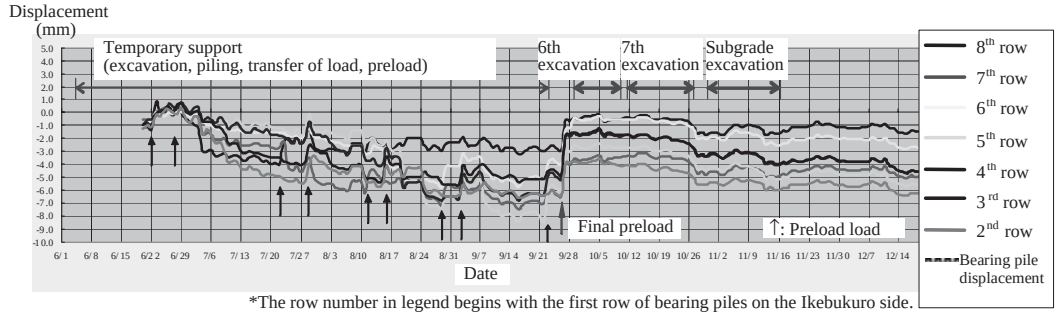
Figure 9. Pile axial force distribution.



Photograph 3. Completed pipe roof temporary support.



Photograph 4. Subgrade excavation upon completion.



*The row number in legend begins with the first row of bearing piles on the Ikebukuro side.

Figure 10. Chronological change in pipe roof pressure-type settlement gauge and bearing pile electronic staff.

during the pipe-roofing. Upon establishing temporary support and subgrade excavation, the protective structures such as the pipe-roof effectively worked and caused no increase in displacement.

5.2 *Pipe-roof settlement*

5.2.1 *When excavating pipe-roof temporary support for temporary support*

The settlement at maximum was 9 mm as compared to the projected value of 8.5 mm, but it was 4 mm at maximum upon final preload (Photograph 3).

5.2.2 *Subgrade excavation*

The settlement increased by about 2 mm as compared to the incremental predicted value of about 5 mm, but the maximum settlement was about 6 mm (Photograph 4).

5.3 *Bearing pile settlement*

Like the pipe-roof settlement, there was an increase of about 2 mm between completion of the final preload and subgrade excavation. Figure 10 shows the chronological changes of the pipe-roof pressure type settlement gauge and the bearing pile electronic staff.

6 CONCLUSION

We conducted non-cut-and-cover construction of a station site for a subway line in an important traffic node in central Tokyo by using a temporary support with pipe-roof underpinning to reduce the effects on large buried utilities. We hope this example can serve as a reference for similar projects.

Underground Space – the 4th Dimension of Metropolises – Barták, Hrdina, Romancov & Zlámal (eds)
© 2007 Taylor & Francis Group, London, ISBN 978-0-415-40807-3

Mathematical modelling of arch-shaped cut-and-cover structures

K. Kunc
Radioactive Waste Repository Authority, Czech Republic

J. Pruška & J. Barták
Czech Technical University, Faculty of Civil Engineering, The Czech Republic

ABSTRACT: This project has completed a thorough review and evaluation of the state of the art in design and construction of large-span corrugated metal and reinforced concrete Arch-Shaped Cut-and-Cover (ASCC) structures. Through full-scale field tests the behaviour of investigated structures was made. Indeed, the extensive computer modelling took an important role within this research to extend the understanding of ASCC structures behaviour under different conditions. Both the corrugated metal and reinforced concrete ASCC structures are the main interest of this work. Two comprehensive computational models were developed using finite element package PLAXIS and validated by field measurements of tunnel profiles at different stages of backfilling procedure. Firstly, the replacement of the soil by two different kinds of plasticity models is conducted. Secondly, the response of the numerical models without and with compaction process is analysed. Finally, several parametric studies are performed by means of the numerical model with the closest results to the field measurements.

1 INTRODUCTION

The general aim of the research presented here is to update the construction specifications for metal and concrete ASCC structures which do not reflect current knowledge. Because large span Arch-Shaped Cut-and-Cover (ASCC) constructions depend on soil support for proper performance, it is imperative that the construction procedures must be carefully specified and implemented.

The main findings of this work are twofold. Firstly, a comparison between the results from the finite element analyses by means of two material models for non-linear soil behaviour; the Mohr-Coulomb model (perfect plasticity) and the Hardening-Soil model (deviatoric and volumetric hardening with plastic strains); and observed field measurements from real arch-shaped corrugated metal as well as reinforced concrete cut-and-cover structures are made. Secondly, parametric studies are carried out using the numerical models with the closest computed results to the real case. Three main objectives are analysed within parametric studies. Namely relevancy of using more sophisticated material models, behaviour of ASCC structures in different geological conditions and behaviour of ASCC structures in extreme unfavourable situations. The results of the parametric studies are used to develop generalised simplified expressions for predicting design forces for both the corrugated metal and reinforced concrete ASCC structures. Factors such as the influence of different types of subsoil, arch structural material, cover depth and extreme situations are reviewed.

2 STATE OF THE ART OF ASCC STRUCTURES

Flexible and rigid ASCC structures, ranging in span from 3 m to occasionally more than 15 m, are often a practical structure for short to intermediate span crossings, especially on local road systems. The use of these structures is growing; however, the available design and construction specifications have not been updated for many years. Current design of metal ASCC structures is largely experience based, and, with the exception of thrust, design forces are not computed. Current design of large-span concrete ASCC structures is less empirical than that of metal constructions. However, several key parameters are still not defined, and the result is that designs may vary because of reasonable interpretations of the code.

Over the past 30 years, the development of ASCC structures in the Czech Republic has been quite significant. The first structures of this type were constructed in the middle of the 1970's these constructions were abandoned in the 1980's. The advantages of ASCC structures and today's more advanced technology concerning the construction process and monitoring as well as a fundamentally different economic approach

to led further substantial development of these constructions in the Czech Republic in the second half of the 1990's.

3 FULL-SCALE FIELD TESTS

The results presented below are related to cases with small heights of backfill cover. The opportunity to compare calculated and measured behaviour of these structures was afforded at two full-scale field tests conducted at the University of Massachusetts at Amherst within the framework of the National Cooperative Highway Program to investigate the structural behaviour of large-span ASCC structures under shallow fills. The test investigated the ASCC structures response to forces resulting from erection, placement and compaction of backfill as well as from live load. During field measurements ASCC structures behaviour, soil behaviour, structure-soil interaction during backfilling and live loading were monitored. The ASCC structures were installed end to end in a single trench, see Figure 1. The span and rise of both test structures were approximately 9,3 and 3,6 m, respectively. The concrete ASCC structure was precast and delivered to the site in 1,8 m segments. The metal ASCC structure was assembled on site from corrugated structural plates. Two sets of tests were carries out. The first installation used a well-graded, clean sand backfill compacted to 92% Proctor Standard. The second test used the same backfill but without compaction. In this second test, the material achieved about 85% Proctor Standard density.

In both tests, the crown continued to rise until earth was placed over the top of the structure, at which point the movement was reversed. In test with the backfill compacted to 95 percent of maximum dry density, crown peaking deformation exceeded the subsequent downward movement during overfilling. Maximum peaking during backfilling was about

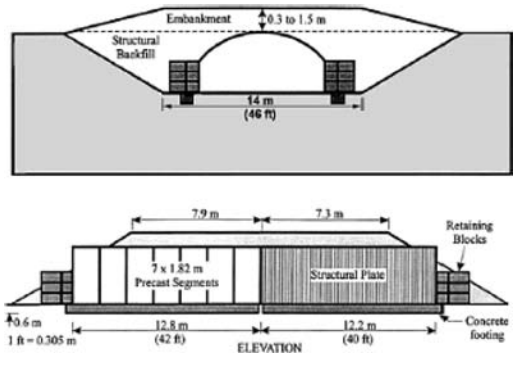


Figure 1. Installation of the arches (McGrath et al., 2002).

80 mm, respectively. Both tests showed fairly similar trends for movements of the curvature points.

Horizontal changes in top chord measurements for both investigated structures during backfilling operation were obtained. The reinforced concrete arch showed very little movement between the curvature points for both tests. The metal arch produced similar changes in top chord measurements during top loading for both tests (inward movement of the curvature points and thus contraction). More over, the concrete arch did not significantly deform during backfilling procedure. Measurements indicate a maximum downward movement of the crown of less than 2 mm at the end of backfilling operation. Also, maximum outward movement (spreading) of the arch legs was less than about 2 mm.

4 NUMERICAL MODELLING

The finite element package PLAXIS v. 7.2 (Plaxis Reference Manual, 1998) was chosen for developing comprehensive computational model of both the corrugated metal and reinforced concrete ASCC structures, presented in this project. In this project the lining of the cut-and-cover construction was assumed to be linear-elastic and for the soil continuum two different soil models were used. Firstly, the soil continuum was assumed as Mohr-Coulomb model (perfect-plasticity) for a quick and simple first analysis of the problem, and secondly Hardening-Soil model (deviatoric and volumetric hardening with plastic strains) was used as a more sophisticated constitutive model.

5 DEVELOPED NUMERICAL MODELS

On the whole eight numerical models were developed and adopted to approximate the actual construction processes as closely as practically feasible. First set (four) of numerical models represent the corrugated metal structure and the rest reinforced concrete structure. Two soil constitutive models (Mohr-Coulomb and Hardening-Soil) are applied into numerical model of each investigated structure. More over, each of used numerical models based on different soil constitutive models was calculated in respect of the construction process without and with compaction procedure.

6 DEVELOPED NUMERICAL MODELS

The database of obtained data from the full-scale field tests was used to compare the response of four constitutive models for both concrete and steel ASCC structures. Selected results of the constitutive models are examined, in order to achieve a better understanding of the cut-and-cover system behaviour. Most

observations refer to horizontal and vertical displacements, internal forces (bending moments and thrust) and the development of earth pressures in time on the contact of tunnel lining and backfill. In additional, the construction phase where the tunnel structure was built up was taken into the comparison as an initial state with zero displacements and/or pressures.

6.1 *Metal ASCC construction*

6.1.1 *Comparison on displacements*

Deformation measurements were made with the laser, digital level, structural extensometers and the manual tape extensometer. The measurement locations are summarised in Figure 2 for the metal structure, respectively. A total of 26 locations around the circumference of the metal construction were selected for detailed laser measurements. A conventional level survey with a digital level was used to obtain level measurements of crown and points of radius change. Structural extensometers were used to measure relative horizontal movement between points of radius change.

Table 1 summarises the calculated and measured response of the crown using values of total uplift movement to the point where the backfill reaches the crown and the subsequent downward movement as the earth is placed up to 0,9 m above the structure. Again, these demonstrate that the values calculated by HS and MC are the most similar ones to demonstrations measured in the tests.

6.1.2 *Comparison of internal forces (bending moment & thrust)*

Sets of four weld able electrical resistance strain gauges were installed at each of 25 locations on the inside wall of the metal lining (circumferential and longitudinal directions on inside crest and valley locations). In Figure 3 is clearly visible the exact locations of strain gauges. However, the thrust strains were small and are believed to be in error. The computed bending moments are believed to be correct and, therefore, only bending moments obtained from the full-scale test are reported here. Wall thrusts were estimated from measured radial pressures. In addition to computing strain thrusts from the measured radial pressures, additional strain gauges were installed just before removal of the backfill at the centroidal axis of the wall section at seven locations around the arch circumference. These locations included the arch springlines, curvature, shoulders and crown. After the centroidal strain gauges were added, the structures were uncovered, and the load on metal arch could thus be obtained from unloading.

Bending moments at the crown and shoulders are summarised in Table 2. Calculations at other locations were also reviewed and yield similar trends. Peak negative moments occur at the crown, as a result of lateral earth pressures and compaction induced deformation during placement.

Results obtained with the compaction models provide conservative bending moments for this shallow buried structure. Bending moments would eventually change sign as the structure was buried further. From that point, the analysis without compaction would yield conservative values of bending moments.

6.2 *Concrete ASCC construction*

6.2.1 *Comparison on displacements*

The same equipment for measure deformations was used as for corrugated steel ASCC structure (the laser, digital level, structural extensometers and the manual tape extensometer). The measurement locations are summarised in Figure 4 for the reinforced concrete structure, respectively. A total of 23 locations

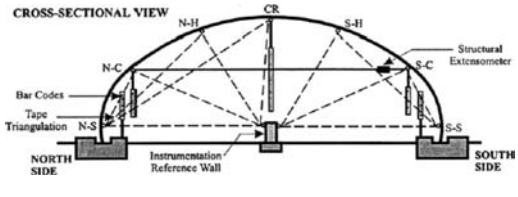


Figure 2. Instrumentation for monitoring deformation in metal structure (McGrath et al., 2002).

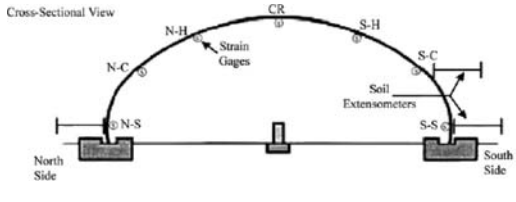


Figure 3. Strain measurement locations in metal ASCC structure (McGrath et al., 2002).

Table 1. Comparison of calculated and measured crown displacements (uplift of crown and subsequent downward movement).

Direction	Measured [mm]	Uncompacted MC [mm]	Uncompacted HS [mm]	Compacted MC [mm]	Compacted HS [mm]
Upward	77,2	57,1	45,8	76,9	81,7
Downward	5,4	9,9	8,4	12,33	8,2

Table 2. Comparison of calculated and measured moments: metal arch.

	Location	Measured [kNm/m]	Uncompacted MC [kNm/m]	Uncompacted HS [kNm/m]	Compacted MC [kNm/m]	Compacted HS [kNm/m]
Min.	Shoulder	−2,97	−3,86	−3,57	−3,97	−4,15
	crown	−6,85	−8,19	−7,53	−10,3	−10,7
Max.	Shoulder	1,41	0,62	0,58	2,15	1,72
	crown	−0,42	2,56	3,22	1,57	1,54

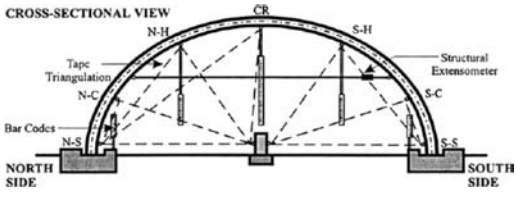


Figure 4. Instrumentation for monitoring deformation in concrete structure (McGrath et al., 2002).

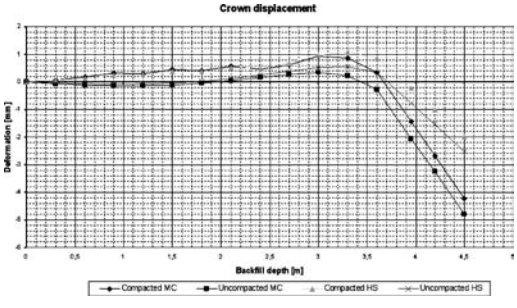


Figure 5. Crown deformations of concrete arch during backfilling procedure.

around the circumference of the metal construction were selected for detailed laser measurements. A conventional level survey with a digital level was used to obtain level measurements of crown and points of radius change.

The reinforced concrete ASCC structure showed very little movement between the curvature points during the test. For the concrete arch, compaction test produced slightly more inward movement (contraction) of the curvature points compare with test without compaction. The concrete arch did not significantly deform for either of the tests during backfilling procedure. Field measurements indicate a maximum downward movement of the crown less than 2 mm at the end of backfilling. Also, maximum outward movement (spreading) of the arch legs was less than about 2 mm. For the reasons mentioned above no results obtained from field measurements were presented. Figure 5 presents crown movement of the concrete arch

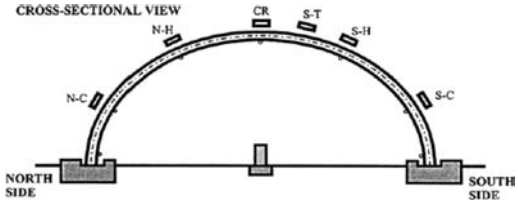


Figure 6. Interface pressure cells for reinforced concrete arch (McGrath et al., 2002).

during backfilling calculated by code PLAXIS. From the plot is visible the upward movement of the crown within all analyses less than 2 mm since the fill reached the top of the arch. Then movement changed direction and at the end of backfilling crown moved downward up to 5 mm, respectively.

6.2.2 *Comparison on displacements*

The transverse locations of installed earth pressure cells around the reinforced concrete ASCC structure are shown in Figure 6, respectively. Sixteen earth pressure cells were installed around the arch.

Analysis of the reinforced concrete field tests focused on the interface pressures, as these pressures are commonly used as a basis for simplified design. As for the metal ASCC structure test, the results were evaluated with two-dimensional computer model.

Table 3 compares field data with mathematical calculations with and without compaction for earth loads. The table shows that calculated pressures by the code PLAXIS at all measured points are somehow slightly lower compare to field measurements and the calculations at the crown are also less than measurements at both locations. In this case, the field data may be in error, as the vertical pressure at the crown should be essentially geostatic, which is consistent with the computer predictions. The field data might be also affected by the low cover and low stress levels.

These comparisons also highlight an important discrepancy between measurement and calculation near the arch crown. The soil at this location likely experiences a vertical earth pressure distribution close to geostatic values. Using a bulk unit weight of 20 kN/m^3 implies vertical stress of 18 kPa at 0,9 m depth. This

Table 3. Comparison of calculated and measured earth pressures.

		Measured	Uncompacted		Compacted	
	Location	[kPa]	MC [kPa]	HS [kPa]	MC [kPa]	HS [kPa]
SC-NC	North	51,93	39,67	42,12	40,19	40,47
	South	48,01	41,42	38,93	41,73	42,11
SH-NH	North	31	27,6	28,58	28,59	29,25
	South	27,85	28,01	29,12	28,64	29,42
ST		26,9	22,29	22,71	23,28	24
CR		23	16,69	16,93	17,18	17,3

is consistent with the finite element calculations and implies that either the stress distribution at the crown of the arch is not geostatic or, more likely, that the stress cells overestimate earth pressures when the stress is low.

7 PARAMETRIC STUDIES

The finite element analysis used the mathematical models with compaction were giving closer results to the field measurements throughout the whole procedure compared to other numerical models without compaction. That is why the analyses using the finite element models with compaction are chosen for further investigation.

A comparison between the results obtained from the finite element analyses by means of two material models for non-linear soil behaviour; the Mohr-Coulomb model (perfect plasticity) and the Hardening-Soil model (deviatoric and volumetric hardening with plastic strains); is made. Moreover, the seven different types of subsoil are used to get comprehensive understanding of investigated constructions and their behaviour during backfilling procedure. The types of subsoil used within individual analysis represented the whole spectrum of geological conditions (from good grained sands through overconsolidated clayey soils to soft clays) where ASCC structures could be constructed on.

The main findings of the parametric studies are threefold:

1. To investigate the relevancy of using more sophisticated material models in the case of mathematical modelling and design of the ASCC structures.
2. Recommendations of the most suitable usage for both metal and concrete ASCC structures within different geological conditions are made.
3. To observe the influence of extreme antisymmetrical earth load as well as the extreme local force load with and without interaction of backfill soil on the behaviour of both the corrugated metal and reinforced concrete ASCC structures.

Table 4. Extreme displacement differences of metal and concrete arches in respect of dissimilar geological conditions. A – Berlin Sand, B – Frankfurt Clay, – Percentage [%].

	Metal			Concrete		
	NC-SC	NS-SS	CR	NC-SC	NS-SS	CR
A	−18,42	−57,13	40,25	−0,66	−0,79	0,911
B	−14,82	−56,91	37,23	−0,35	−0,66	0,694
C	−19,5	−0,4	−7,5	−46,9	−16,1	−23,8
A	−41,39	−56,85	74,61	1,97	0,917	−1,69
B	95,10	15,14	−50,37	30,87	11,74	−24,93
C	−329,7	−126,6	−167,5	1467	1180	1373,8

Note: All values are in [mm], negative values = inwards and/or downwards movements of the arch. Negative percentage values represent higher deformations reached on Berlin Sand subsoil.

8 SUMMARY AND CONCLUDING REMARKS

Comparative analyses have shown that, although simple models generally provide realistic values of lining movements and distribution of internal forces, only the most complex model accurately predict soil displacements. The first part of parametric studies is aimed to analyse the relevancy of using more sophisticated material model in respect of large span ASCC structures. From results reached within first part is clearly visible that in both cases, corrugated metal and reinforced concrete arch, is recommended to use more sophisticated material model if:

- the quality of subsoil layer is poor (very soft clays),
- the overburden layer is higher than rise of the arch.

The behaviour of ASCC structures built on varied spectrum of different subsoil layers were introduced in the second part of parametric studies. On the whole, seven types of subsoil were analysed. From obtained results can be seen that for worth subsoil layers is suitable to use more flexible constructions in this case corrugated metal arch. Deformations calculated on the reinforced concrete arch built on different subsoil

Table 5. Maximum thrust differences in metal and concrete arches in respect of dissimilar geological conditions. A – Berlin Sand, B – Frankfurt Clay, – Percentage [%].

	Metal					Concrete				
	NC	NS	CR	SS	SC	NC	NS	CR	SS	SC
A	−165,7	−83,8	−135,9	−153,3	−167,9	−9,5	−129,9	−111,3	−129,9	−27,3
B	−167,2	−84,0	−135,7	−156,1	−164,8	−11,4	−128,3	−108,6	−128,3	−27,8
C	0,9	0,2	−0,2	1,8	−1,8	20,0	−1,2	−2,2	−1,3	1,9
A	−169,7	−157,3	−135,9	−156,3	−133,7	−155,8	−129,9	−111,1	−129,9	−155,2
B	−163,1	−131,5	−114,3	−143,5	−144,6	−113,3	−115,5	−134,9	−118,0	−114,5
C	−3,9	−16,4	−15,9	−8,2	8,1	−27,2	−11,1	21,5	−9,2	−26,2

Note: All values are in [kN/m], negative values represent pressure and positive tension. Negative percentage values represent higher thrusts reached on Berlin Sand subsoil.

Table 6. Maximum bending moment differences in metal and concrete arches in respect of dissimilar geological conditions. A – Berlin Sand, B – Frankfurt Clay, – Percentage [%].

	Metal					Concrete				
	NC	NS	CR	SS	SC	NC	NS	CR	SS	SC
A	2,9	2,9	−3,4	7,0	7,0	−7,2	−3,2	−5,3	−2,9	−1,1
B	2,7	2,7	−3,3	7,3	7,3	−8,9	−4,4	−4,0	−3,9	−2,0
C	−8,4	−5,8	−3,4	3,4	4,1	22,7	40,4	−25,5	34,3	85,0
A	2,1	5,7	6,7	6,7	3,7	−7,2	−3,2	8,7	−2,9	−7,2
B	−6,5	2,1	2,7	2,7	−10,7	14,4	62,2	96,8	60,9	13,5
C	−404,9	−62,1	−58,9	−58,9	−386,9	−299,5	−2045	1001	−2185	−287,5

Note: All values are in [kN/m], negative values represent pressure and positive tension. Negative percentage values represent higher thrusts reached on Berlin Sand subsoil.

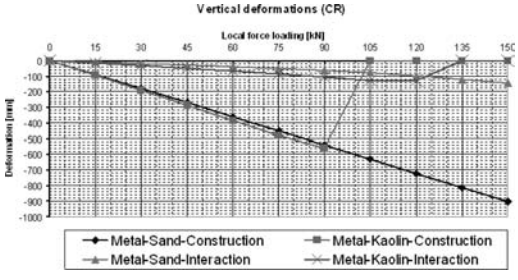


Figure 7. Vertical movement of the top of the metal arch built on different subsoil considering interaction with surrounding soil.

were approximately ten times higher compare to the corrugated metal arch, see Table 4.

Analyses of internal forces showed the same tendency and approve the conclusion remark reached by study of deformations, see Tables 5 and 6. This part of parametric studies demonstrated high sensitivity of stiffer constructions on geological conditions especially on subsoil layer.

As it is mentioned above the third part is focused on behaviour of ASSC structures on extreme unfavourable situations. In the case of antisymmetrical earth loading was the behaviour of the metal arch almost identical within different foundation conditions compare to concrete arch. More over, deformations calculated in the metal arch were significantly higher and had opposite tendency with respect of the concrete arch during antisymmetrical loading.

Second unfavourable situation was concentrated on vertical deformations of the top of both metal and concrete arch loaded by local force. The influence of structural interaction with surrounding soil on construction behaviour was studied. In the case of metal arch considerable effect of displacement occur when the interaction was taken into account, see Figure 7.

9 ACKNOWLEDGEMENTS

The authors wish to express their gratitude to Ministry of Education of the Czech Republic for research project *MSM 6840770003* "Developments of the Algorithms of Computational Mechanics and their Application in Engineering" for allowing to develop this article.

REFERENCES

Kunc, K. 2002. Numerical modelling of a cut-and-cover construction. A dissertation submitted in partial fulfilment of the requirements of the degree of Master of Science in Geotechnical Engineering, Glasgow.

Kunc, K. 2005. Mathematical modelling of Arch Shaped Cut and Cover Constructions. *doctoral thesis*, Prague.

McGrath, T. J.; Moore, I. D.; Selig, E. T.; Webb, M. C.; Taleb, B. 2002. Recommended Specifications for Large-Span Culverts. *NCHRP Report 473*, National Academy Press, Washington, D. C.

PLAXIS Reference Manual 1998. Version 7 for Windows 95/NT. A.A. Balkema, Rotterdam, Brookfield.

Sandsford, T.C. 2000. Soil-structure interaction of buried structures. A2K04: *Committee on Subsurface Soil-Structure Interaction*, Transportation in the New Millennium, University of Maine.

Vaslestad, J.; Arkadiusz, M.; Janusz, L. 2002. Field Measurements of Long-Span Corrugated Steel Culvert Replacing Corroded Concrete Bridge. Transportation Research Record 1841, pp. 163–170, *Transportation Research Board*, Washington DC.

This page intentionally left blank

Underground Space – the 4th Dimension of Metropolises – Barták, Hrdina, Romancov & Zlámal (eds)
© 2007 Taylor & Francis Group, London, ISBN 978-0-415-40807-3

Numerical modelling of the interference between underground structures and aquifers in urban environment. The Turin subway – Line 1

G. Ricci, R. Enrione & A. Eusebio
Geodata S.p.A. Turin, Italy

R. Crova
GTT S.p.A. Gruppo Torinese Trasporti, Turin, Italy

ABSTRACT: A case study is presented where the construction of underground structure is expected to interfere with unconfined aquifer: the design of the Metro Line 1 in Turin (Italy), where deep retaining structures have to be built for the stations. A full range of water table monitoring data were collected and analyzed. In addition to this a hydrogeological modelling approach has been developed, to simulate the groundwater-structures interference. A site investigation program provided the model geometry data (geological inputs) and intrinsic hydrogeological properties for the aquifer. Firstly, a regional modeling was performed, to obtain the starting conditions for the local model (works scale). Subsequently, with the local model, the interference between groundwater flow and structures was computed. The results were coupled with the long-term data monitoring and the information on the historical groundwater table level in order to allow the designer to define the appropriate countermeasures and interventions to be taken for both the construction and the exploitation phase.

1 INTRODUCTION

The city of Turin is an urban environment where new infrastructure and transport network (local railway, parking and metro line) are being increasingly developed underground. Such development is increasingly occupying a space never or poorly used before. The first metro line (Line 1) has been designed and constructed in the last five years. The line is crossing the city from east to west passing through a heavily urbanized area where both existing and new underground works are present.

Logistical and functional needs were considered to choose the alignment (in plan), on the other hand (in depth), such choice had to cope with critical constraints that the project design had to properly face and solve. One of these critical issues is the hydrogeological scenario, because the metro works are interfering with an unconfined aquifer.

2 THE LINE 1 OF THE TURIN SUBWAY NETWORK

The Line 1 is the first Metro Line ever constructed in the city of Turin and is divided into two sections (Fig. 1). Section I connects the town of Collegno, on the city's western outskirts, to the Porta Nuova railway station in the city centre. It includes 9.5 km of running tunnels, 15 stations and 15 ventilation and emergency-access shafts in-between stations. Section II runs entirely in the urban area of Turin with 4 km tunnel length and 6 stations.

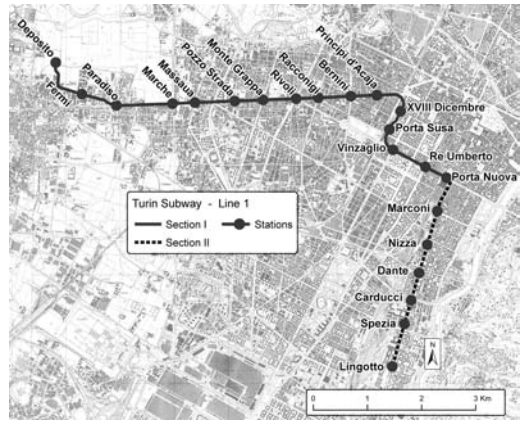


Figure 1. The Turin subway Line 1.

This article will refer to Section II and particularly to the problems due to the interference between the underground works and the unconfined aquifer.

3 GEOLOGICAL AND HYDROGEOLOGICAL SETTING

3.1 *Geology*

The town area of Turin is placed in an alluvial plain built up by numerous contributions of alluvial fans located at the Alpine valley mouths of Dora Riparia and Stura di Lanzo rivers. Alluvial fans are composed by outwash deposits that were partially reshaped by the fluvial activity of the rivers that cross the town area (Po, Stura di Lanzo, Dora Riparia e Sangone).

Geological stratigraphy (Bonsignore et al. 1969) of the area shows the following units described starting from surface:

- outwash and Quaternary fluvial deposit (Riss Glacial Period): gravels, pebbles and sands in a silty matrix. The deposit is from 30 m to 40 m thick and is generally loose except for some cemented lens of conglomerates.
- lacustrine and fluvio-lacustrine deposit of Villafranchiano (Sacco, 1886): clayey silts with sandy gravel lens poorly cohesive. The thickness of the deposit varies from 40 m to 150 m.
- neritic marine deposits from Pliocene: clayey silts, silty sands and fine blue and grey sands moderately cohesive. Maximum thickness is about 40 m–50 m.

While the first Quaternary deposit (outwash and fluvial deposit) is wide-spread and represents the first unit in the town area, both the Villafranchiano and the Pliocene deposits are underlying the Quaternary outwash and fluvial deposit. This is due to local uprising and differential erosion of the Villafranchiano at the beginning the Quaternary Period. As a result, both Villafranchiano lacustrine and fluvio-lacustrine deposits and neritic marine deposits from Pliocene can be found under the outwash and Quaternary fluvial deposits.

3.2 *Hydrogeology*

With reference to tunnel depth, that varies from −12 m to −25 (railway level), the hydrogeological setting shows an unconfined aquifer located in the outwash and fluvial quaternary deposits. This aquifer is confined below by a thick layer of low permeability deposit (clayey silts located at the top of Villafranchiano) and has a saturated thickness from 15 m to 25 m. In the area of the Section II of the Metro Line, depth to water ranges from −12 m to −15 below ground level. The unconfined aquifer is recharged from the west side while direct infiltration (from rainfall) in the urban area is almost totally intercepted by the city water drainage system. In the town area the Po river bed is located at a lower level and acts as a drain to the groundwater of the unconfined aquifer. This role is confirmed by the relationship between the water table contour lines and the river water level, which

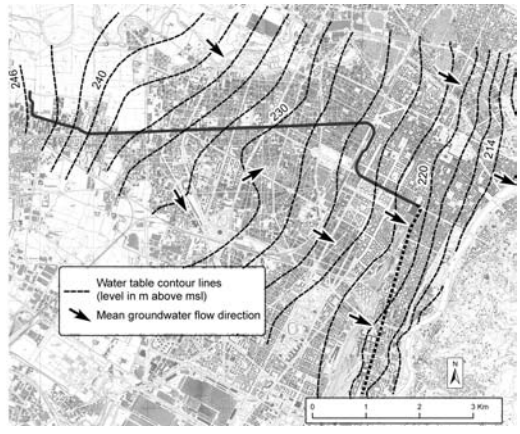


Figure 2. Water table contour in the Turin area (level in m above msl) and mean flow direction.

crosses the town flowing from South to North-East. Groundwater mean flow direction is oriented ESE (120° N) and locally diverges because of permeability anisotropies that creates converging and diverging flow paths. Hydraulic gradient varies from 0.25% (mean value in the centre of the town) to 0.7%–0.8% approaching the Po river bed (Fig. 2). Piezometric level is located at about – 15 m from ground level and the natural phreatic fluctuation is about of ±1.5 m as response to rainfall input.

It must be pointed out that during ancient times (Eighteenth Century) phreatic level was probably about from 4 m to 5 m higher than current level. This fact is confirmed by the presence of ancient adits of the underground defence system of the city (excavated just above water level) and by some historical water well found below the old town building foundations. Moreover, in the last five decades the unconfined aquifer has been exploited for industrial purposes, causing a widespread lowering of the water table. In the last twenty years the displacement of many industrial factories from the town has decreased water extraction rate and, consequently, this fact has allowed the water table to slowly rise back towards the "unexploited" level. Nevertheless, water table monitoring data collected in the last twenty years have clearly shown that the water table uprising rate, due to the cease of industrial exploitation, has notably dropped especially in the last 10–15 years. This evidence suggests that current water table will probably never reach the pristine level referred to the ancient times. An explication to this could be the urbanization of the town area that has practically led to a minimum groundwater recharge from precipitation that is now canalised in the main drain system and discharged in the Po river.

By the way, the design of such an important underground work has to deal with very long time scenarios,

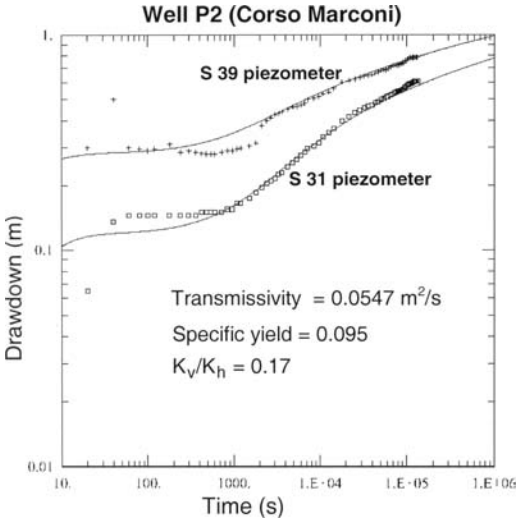


Figure 3. Water pumping test in water well P2 (Corso Marconi). Drawdown vs Time chart with interpolation curve (Neuman, 1975) and hydraulic properties.

therefore the "historical" level of the water table has to be considered and then taken into account in the design of the infrastructure.

4 HYDROGEOLOGY TESTING AND WATER HEAD MONITORING

4.1 *Water test*

A full range of permeability tests were performed during the site investigation campaigns carried out in the design phase of project.

- over 50 Lefranc permeability tests were performed in 25 boreholes (core boring drilling), distributed along the Section II. Water tests were performed at different depths in order to investigate hydraulic properties both in the outwash and fluvial deposits and in the low permeability Villafranchiano deposits.
- n. 2 long-time water pumping tests (Fig. 3) were performed in the outwash and fluvial deposit with ad-hoc excavated wells. Each well had water table drawdown monitoring devices installed in two piezometer located at close distance.

The water test results have showed that the Quaternary deposits have medium to high permeability while the underlying Villafranchiano top layer has low to very low permeability. Table 1 below summarises the permeability range for both units.

These permeability test results clearly show that the aquifer in the Quaternary outwash and fluvial deposits has good permeability while it is confined below the by

Table 1. Hydraulic properties of hydrogeological units.

Unit	Outwash and fluvial Dep. (Quaternary)	Fluvio lacustrine Dep. (Villafranchiano)
k (m/s)	$1.0E^{-05} \div 3.0E^{-03}$	$5.0E^{-06} \div 1.0E^{-08}$
k_v/k_h	$0.1 \div 0.01$	n.d.

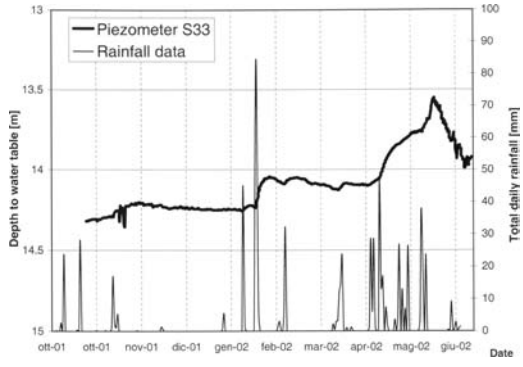


Figure 4. Groundwater table monitoring data (continuous recording) and daily rainfall data recorded in piezometer S33.

low permeability layer of the top of the Villafranchiano deposit.

4.2 *Water head monitoring*

Water head monitoring on the Metro Line 1 wide area has been systematically carried out starting from the beginning of the design phase. Open pipe piezometers were installed in most of the drilled boreholes, where a monthly monitoring activity was initiated. Some piezometers were instrumented with continuous monitoring devices set to 12 hours data recording (Fig. 4), in order to monitor little water table fluctuations in response to recharge input.

Moreover, together with the site investigation campaign and water table monitoring activity, an extensive research of all piezometric level data has been carried out on the whole urban area of Turin. More than 250 data were acquired, referring to water wells or piezometers drilled in different times (from '60s to '90s); most of them are now destroyed and not measurable anymore. Anyway, the significance of the data is important to the understanding of the long-term water table fluctuations.

This activity has also comprised the reconstruction of the "ancient" water table level, determined on the level of the ancient water wells discovered in the old part of the city. These data together with 3D reconstruction of the underground defence adits network (excavated just above water table level) has indicated that the historical groundwater level (referred to XVIII century) could have been some 4–5 m above current level. It must be said that this hypothesis is

based on few observations and on the assumption that water table geometry and mean flow direction hasn't drastically changed over the times.

All the monitoring data have allowed to delineate with a great accuracy the current groundwater table which was used as a reference for the numerical modelling.

5 DATA MANAGEMENT

In order to have a unique platform to store, analyse and manage all the different data, a GIS was implemented. Such a common platform has allowed to analyse in 3D the design data such as the tunnel alignment, deep founded stations and other existing underground infrastructures together with geological and hydrogeological features such as the bottom of the highly permeable unit and the groundwater table. The aim was to highlight the potential critical scenarios where a numerical model should be employed in order to quantify the interference between the underground works and the groundwater table.

GIS data file formats were fully compatible with numerical modelling software so as to allow a fast setting of input parameters. The same GIS platform has already been employed in the construction management of the Section I to collect and manage excavation parameters (TBM) together with externally collected monitoring parameters (settlements, vibrations and water table fluctuations).

6 NUMERICAL MODELLING

6.1 *Problem statement*

When an underground structure is constructed below water table it may cause a partial or total reduction of groundwater flow. Considering that the structure is totally impermeable it acts like a "barrier" to the flow. This causes (Fig. 5) an uprise of the water table along the side of the structure (upflow side) and a symmetrical lowering of the water table on the other side (downflow side). The entity of this interference is proportional to some factors such as the length of the structure, the angle of incidence between groundwater flow direction and the structure, the thickness of the free hydraulic section under the structure, the permeability of the media and the aquifer recharge condition.

The design of Section II of the Metro Line foresees interferences with groundwater table for most of its total length. The tunnel direction is perpendicular to mean flow direction causing, theoretically, the maximum possible interference. Some stations (Marconi and Spezia) have deep foundations that are driven so deep almost reaching the low permeability layer, causing a reduction of the hydraulic section.

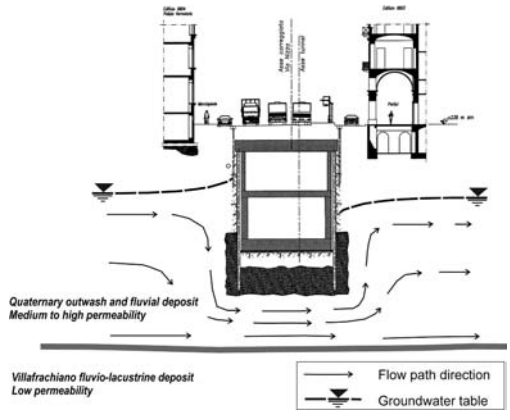


Figure 5. Partial obstruction of groundwater flow caused by a deep founded structure (not in scale).

The potential interference of the deep structures with the aquifer created some concern to the client because potential significant increase of water level in the long term may require heavier design with consequent cost increase. Hence, it was necessary to estimate the real, expected entity of this potential increase of water level. To respond to this need, the 3D numerical modelling was naturally the best approach.

The numerical code employed was MODFLOW (McDonald e Harbaugh, 1988 & 1996) a finite difference model with a user-friendly interface (GMS 3.1 Groundwater Modelling System, Boss International, 2001) able to perform geostatistical data treatment of input parameters.

The model applied was suitable to the hydrogeological setting because the aquifer is a typical porous media characterised by a fair homogeneity. In addition, the two hydrogeological units have little inclined surfaces and moreover, the metro line alignment is easily reproduced by finite difference models that are constrained to a rectangular grid.

6.2 *Large scale numerical modelling*

A groundwater numerical model must reproduce, in practical terms, the groundwater flow conditions as highlighted by the conceptual hydrogeological model, based on field observations.

In this case, the numerical modelling of small and localised scenarios, useful to quantify critical interferences, requires, as a first step, the set up of a larger scale numerical model able to simulate the general setting of groundwater circulation in a big area.

Such model was implemented in order to verify the correctness of the boundary conditions that are:

– lateral recharge prevailing on direct infiltration that is almost annulled in an urban environment.

– drainage towards the river with consequent increase of hydraulic gradient towards and in coincidence of the slope that connects to the river bed.

The area considered for the general model is a rectangle of 6300 m × 4200 m regular grid spacing and with 6300 cells. Total depth is set to 60 m and the model is divided into two layers to simulate the different hydraulic properties of the two hydrogeological units (Quaternary aquifer/Villafranchiano aquiclude). The top surface of the second layer (aquiclude) has been obtained by kriging the core boring results of deeper site investigations. Specifically, the boundary conditions are:

– "constant head" applied on the NW boundary to simulate lateral recharge.
– "no flow" along the sides of the model where flow direction is parallel to model sides.
– "head dependent flux boundary" (drainage) condition along the river boundary. This condition is reproduced by specific draining cells that simulate water drainage from the model. Their efficiency is ruled by a factor (conductance "C" that is dimensionally a L^2/T) that will be calibrated.

Given the reference scenario, a calibration process has been done in steady state, trying to reproduce measured water table contour lines. The calibration process is carried out by varying cell by cell the values of k_h and k_v (horizontal and vertical permeability) in order to obtain a good comparison (Fig. 6) between modelled water table contour (performed by the model) and measured water table (obtained by on-the-field measured data). In addition, the efficiency of the drain cells was calibrated along the riverside of the model.

The permeability range assigned to the model cells is coherent with the range obtained by water permeability tests carried out during the site investigation campaign.

6.3 *Numerical modelling of the interferences*

As a second step in the numerical modelling approach, some localised models were implemented. The aim was to quantify with greater accuracy the entity of possible water table uprising caused by the deep founded structures.

Based on the results of the large-scale model, two local detailed models were implemented to simulate the construction of underground structures (cut&cover stations) and the tunnel below the water table.

Specifically, two critical scenarios were taken into account:

1. the interference due to by cut&cover structures that partially obstruct (almost perpendicularly) groundwater flow.
2. the interference created by the running tunnel itself.

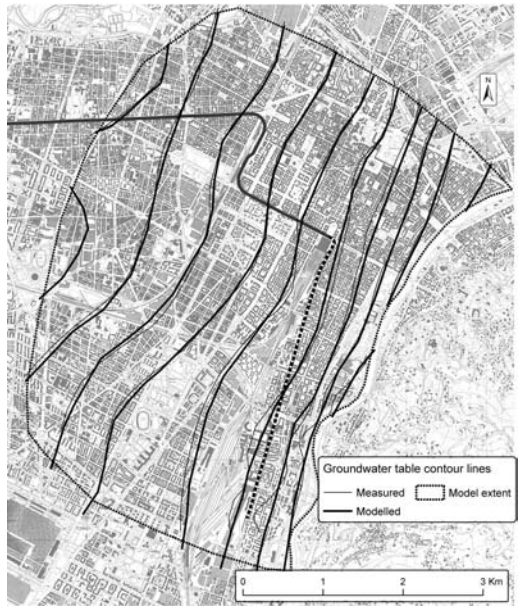


Figure 6. Calibration result of large scale model.

The first scenario refers to the train deposit and nearby Marconi Station and also to Spezia Station. All these structures will be constructed with cut&cover technology. In both cases the model area was about 1200 m × 900 m and wide enough to avoid the influence of boundary conditions on the simulation results.

Grid dimension was variable (cell dimension ranging from 5 m to 25 m) with cells refinement around the structures. Total cell number was about 5200 per layer. Total depth was again set to 60 m and divided into three layers.

Constant-head boundary conditions were employed on opposite sides of the modelled area to simulate inflow (lateral recharge) and outflow (discharge) of groundwater. Lateral sides had no flow conditions.

Calibration process was carried out with reference to a measured water table situation and the final results showed a good agreement between measured and modelled groundwater table. The barrier effect of the cut&cover structures was introduced by assigning very low permeability ($k = 1E^{-08}$ m/s) to the cells referred to the geometry of the structures. Once calibrated, the model was used to simulate the presence of the structure and other scenarios such as a higher groundwater level (up to +2 m from current groundwater level).

The model results were presented in terms of iso-anomalies (differential rising or lowering of the groundwater table with respect to undisturbed situation) due to the interference of underground structures (Fig. 7).

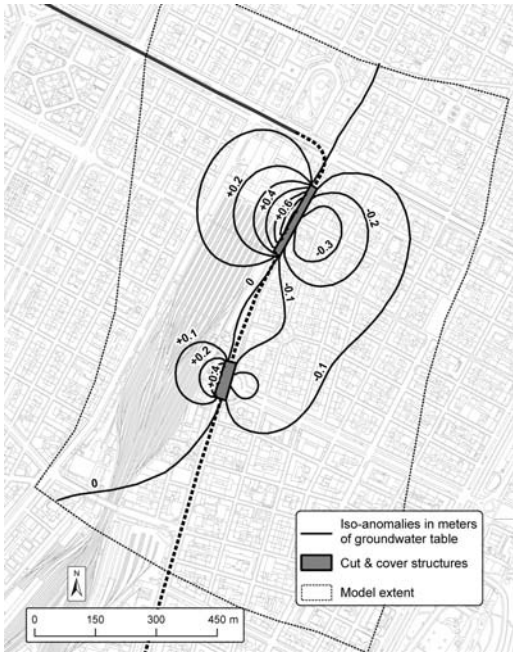


Figure 7. Iso-anomalies (m) generated by the interference of train deposit and Marconi station structures.

6.4 *Results*

The model results have highlighted that the interferences created by cut&cover obstructing structures generate a local variation on the groundwater table. This variation rises up to $+1$ m on the upflow side of the structure and a lowering on the opposite side that is a little less than a metre. In addition, the tunnel itself is responsible for a small rise of the water table that is quantified to be about $+0.2$ m. The choice of some conservative parameters employed in the numerical simulations (i.e. aquiclude deep surface level) indicates that the results obtained can be considered as fair and reasonable.

7 CONCLUSIONS

The design and construction of an underground work like a subway line under the groundwater table have to deal with some geotechnical and hydrogeological problems. These problems mainly refer to the groundwater level to be adopted as reference for the design of the works. Moreover underground structures, when located under groundwater table, cause an interference that create a rising of the groundwater table on the upstream side of the structures that act as a barrier to flow direction.

With reference to these issues, the design of an underground works have to take into account the evaluation of all the interferences caused by the works on all surrounding underground structures.

In the reported case of the Turin metro the problems were faced and solved by collecting and evaluating, in a common GIS platform, all possible data available on the field, in order to highlight all potentially critical scenarios. Then, a numerical model was implemented for chosen situations in the aim of quantifying the interferences. The modelled results have shown that the water table rise on the upstream side of the deep structures is quite small ($+0.2$ m due to the running tunnel and about $+1.0$ m due to the deep stations) in comparison with the long-term potential natural recover of water table of the aquifer.

This can be explained by two reasons:

– high permeability of the unconfined aquifer in which the structures are inserted.
– the deep cut&cover structures, even in the worst scenario, didn't reach the low permeability layer at depth, leaving the hydraulic connection under the structure.

Model simulations were performed in steady state, reproducing, in same way, the long-term scenario. It is reasonable to expect that during the construction phase only a limited amount of these interferences will occur. They will be easily faced with common on-the-site countermeasures. The specific numerical modelling approach proved to be effective and efficient, for the following reasons:

– the numerical model applied was suited to the hydrogeological setting because the aquifer is a typical porous media characterised by a fair homogeneity. In addition, the two hydrogeological units have little inclined surfaces.
– a full range of data (from historical evidences to continuously monitored water table) were available to define, as much as possible, the wider possible scenarios.
– the metro alignment is easily reproduced by finite difference models that are constrained to a rectangular grid. In these scenarios the models are simple but reliable and provide good results in reasonable computing time.

The modelled results together with the data from long-term monitoring and the information on the historical groundwater levels have allowed the project designer to define the appropriate design countermeasures and interventions to be taken for both the construction phase and the exploitation phase.

REFERENCES

Bonsignore, G., Bortolami, G., Elter, G., Montrasio, A., Petrucci, F., Ragni, U., Sacchi, R., Sturani, C. & Zanella, E. 1969. Note illustrative della Carta Geologica d'Italia, fogli 56 e 57 (Torino e Vercelli). Servizio Geologico d'Italia, Roma.

Mcdonald, M.G. & Harbaugh, A.W. 1988. Modflow, 1988. A modular three-dimensional finite difference ground-water flow model. *U. S. Geological Survey Techniques of Water-Resources Investigations*, Book 6, Chapter A1, 586 p.

Mcdonald, M.G. & Harbaugh, A.W. 1996. User's documentation for MODFLOW-96, an update to the U.S. Geological Survey modular finite-difference ground-water flow model: U.S. *Geological Survey Open-File Report* 96–485, 56 p.

Neuman, S.P. 1975. Analysis of pumping test data from anisotropoic unconfined aquifers considering delayed gravity response . *Water Resources Research*, 11:329–42.

Sacco, F. 1886 Il Villafranchiano al piede delle Alpi. *Boll. R. Comit. Geol. It.* , 7, 421–449, 1t.

This page intentionally left blank

Underground Space – the 4th Dimension of Metropolises – Barták, Hrdina, Romancov & Zlámal (eds)
© 2007 Taylor & Francis Group, London, ISBN 978-0-415-40807-3

Application of corrugated structural plates to a cut & cover tunnel

Y.W. Shin
Tunnel & Geotech. Div., Hakyong Eng. Co., Korea

W.R. Yu
Candidate, Hanyang University, Korea

B.S. Chun
Hanyang University, Korea

K.Y. Kim
Samsung Engineering Co., Korea

ABSTRACT: Application of various materials has been increased in construction. The design and construction cases of corrugated structural plates instead of reinforced concrete for a cut & cover tunnel construction are described in this paper. A large slope near the tunnel portal is cut and tension cracks are produced in the slope face during construction. Because a large amount of cut soil and rock have to be dumped in this field, the counterweight fill after cut & cover tunnel construction is adopted as an optimal alternative plan. It is estimated that application of the corrugated structural plates contributes to 70% decrease in construction period and 30% decrease in construction cost.

1 INTRODUCTION

The interest of the protection of environment has been increased because of natural environmental damage by construction of social overhead capital such as road and railroad. Therefore, tunnel construction has been increased in order to minimize the damage of mountains and forests in construction of a new road, in widening a road, and in improvement of an old road alignment. However, even if the tunnel has been constructed, a formation of a portal slope is inevitable. Therefore, the minimization of cut area is very important. In this paper, the first application of corrugated structural plate instead of a reinforced concrete for a cut & cover tunnel of a portal is introduced in Korea. The considering site is located in Ulsan. The portal slope had collapsed and was expected an additional collapse. The purpose of this design is to perform the site investigation and field tests, to estimate the stability of the slope and to work out a countermeasure. Considering site is located in the portal of tunnel planed for widening a existing road. For all that, a portal is planed in a valley and a high slope is come into being inevitably. The geological features of this site are gray green shale and hornfels. Rocks are much crushed and faults are distributed in place. So, stability of slope isn't guaranteed for original slope. Also, the slope slides off after some snow and rains. On the investigation, abandoned soil of the site is very much. Therefore, a counterweight fill after constructing cut & cover tunnel is more profitable than slope reinforcement in slope stability and economical efficiency.

Corrugated structural plate is used instead of a reinforced concrete to reduce of a term of works and construction costs. Reasons of selecting the counterweight fill as an alternative for the slope stability are described in this paper. In addition, the design and construction of the corrugated structural plate applied as a cut & cover tunnel are described.

2 TOPOGRAPHY AND GEOLOGY

The site is located in a small valley that surface water and ground water are concentrated. A great deal of surface water flows down in the whole year. A bed rock of the site is grey green shale and sandstone of the Cretaceous period. The slope concerned is located in a valley with complex geological features and an irregular metamorphism. Faults are composed of an intrusive clay and gravel. The gravel layers have been

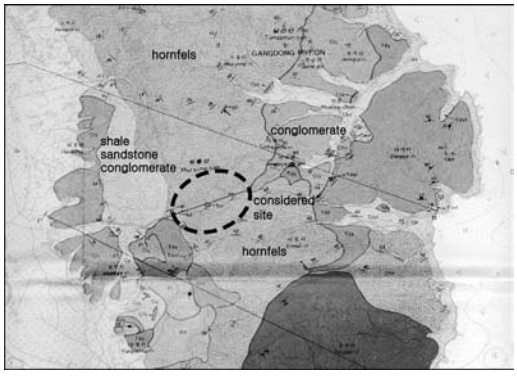


Figure 1. Geological map.

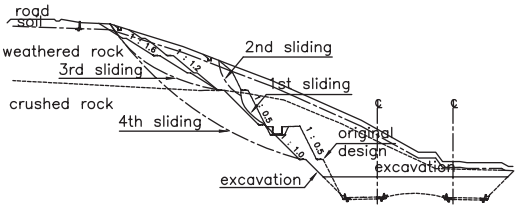


Figure 2. Slope section.

hardened. The gravel sizes are 2∼30 cm. Faults are dense and a groundwater flows out. A small quantity of ground water flows, even valleys are located in the left and right sides of the tunnel exit. Therefore, the water flow will be increased as increasing of surface water in the rainy season.

3 A SLOPE STATUS

The geology of the slope having a height of 54 m and length of 140 m is grey shale and severely cursched hornfels. The upper part of the slope has a thickness of 5 m and is completely weathered or highly weathered. The lower soft rock is a metamorphic fallow hornfels and is highly crushed by crust movements. A joint spacing is very narrow and a joint orientation is irregular. The highly crushed lower soft rock has been collapsed a few times in a small scale. A viscous soil between the rocks of 10 cm diameter exists. The tension cracks are caused at the upper parts of the slope after snowing in winter. Surface water flown in a valley penetrates into the slope in the start points of the slope.

The 31st national road is located in the upper part of the slope. Therefore, if it slides on a large scale, the confusion by transportation interruption is expected. A inclination of the slope is 1:1.2∼1.5 in a soil, 1:0.7 in a weathered rock, and 1:0.5 in soft and hard rock in a design stage. Figure 2 shows the inclination of the slope when tension cracks were caused.



Figure 3. Slope scene.

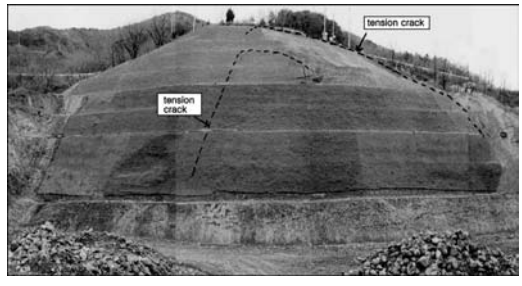


Figure 4. Tension cracks.

4 INVESTIGATION OF AN ALTERNATIVE

The suitable reinforcement methods for slope are examined. The alternatives suitable for the slope are investigated for a long-term stability, a convenience of construction and construction costs in priority. A site investigation and field tests are carried out for the slope, and the stability of it is evaluated and the alternatives are examined. The counterweight fill is chosen. The upper part than 30 m from the formation level is cut with an easy slope 1:1.8 and water drainage pipes are installed. The lower part than 30 m from the formation level is backfilled. In general, the counterweight fill is more expensive than the slope reinforcement owing to cut & cover tunnel. However, the waste rocks cut in this site is very much. So, if the waste rocks are reused, the construction costs are reduced. If a vehicle is dropped from the 31st national road located in the upper parts of the slope, a large scale accident can be aroused. In conclusion, the counterweight fill after constructing the cut & cover tunnel is chosen for stabilizing the slope.

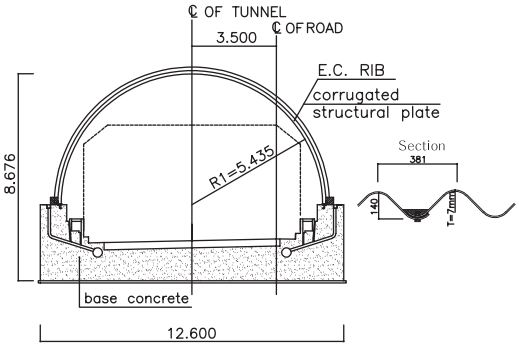


Figure 5. Cut & cover tunnel section.



Figure 6. Ditch excavation.



Figure 7. Rebar assembling.



Figure 8. Base concrete construction.

5 CONSTRUCTION METHOD OF A CUT & COVER TUNNEL

The reinforced concrete and the corrugated structural plate as the construction method of a cut & cover tunnel are examined. A cut & cover tunnel should be backfilled as soon as possible because the slope will be collapsed when it rains heavily. A corrugated structural plate is selected to construct a cut & cover tunnel because a construction period is reduced by 70% and a construction cost is curtailed by 30%.

6 DESIGN OF A CORRUGATED STRUCTURAL PLATE

A design of a corrugated structural plate is based on CHBDC (Canadian highway bridge design code) method. Thereafter, a finite element analysis is executed with the program CANDE89 for verification. The finite element analysis is useful when an overburden of a corrugated structural plate is inclined because the CHBDC method can't consider a tilted backfill. A behavior of a corrugated structural plate is dependent on the compression forces. So, a buckling, a compression yield failure, and the shear failure of longitudinal bolts should be estimated. An failure index is whether a plastic hinge is aroused or not, because the internal forces in the member of a corrugated structural plate are compression forces and moments. A finite element method is another method that can be used in design of an corrugated structural plate. A finite element method can consider the various ground conditions and the inclined backfill, therefore it can be used to verify the results by CHBDC design method. The maximum compression force is 2,037 kN/m. The maximum bending moment is 18.74 kN.m/m at the roof. A plastic hinge is not occurred in the finite element analysis.

7 CONSTRUCTION SCENES

Figure 6∼figure 11 show the construction scenes described as above. Construction sequence is a ditch



Figure 9. Fabrication of the corrugated structural plate I.



Figure 10. Fabrication of the corrugated structural plate II.

excavation, rebar assembling, base concrete construction, fabrication of a corrugated structural plate and backfill.

8 CONCLUSIONS

This paper presented the construction of a corrugated structural as a cut cover tunnel.

(1) A portal is planed in a valley and a high slope comes into being inevitably. A local sliding failure and large tension cracks are occurred during the construction. On investigation, there is a lot of abandoned soil in the site.



Figure 11. Backfill.

(2) Counterweight fill after constructing cut & cover tunnel is more profitable than reinforcing cut slope in slope stability and economical efficiency.
(3) A cut & cover tunnel should be backfilled as soon as possible because when it rains heavily, a cut slope can be collapsed. Hence, a corrugated structural plate instead of a reinforced concrete is adopted as a substitute.
(4) A corrugated structural plate is selected to construct a cut & cover tunnel because a construction period is reduced by 30% and a construction cost is curtailed by 30%.
(5) The stability of a cut slope is preserved when it rains in 400 mm for 3 days

REFERENCES

Abdel-Sayed et al. 1993, Soil-Steel Bridge : Design and Construction, McGraw-Hill

Canadian Standard Association, 2001, Canadian Highway Bridge Design Code, CAN/CSA-S6-00, Rexdale, Ontario

Kim, N.Y. et al. 2002, An analysis for application of a corrugated structural plate in the tunnel entrance, '02 conference of Korean tunneling association, pp.172∼188

Pusan National Territory Management Office, 2002, The report for a test construction and an alternative for a slope stability of Ulsan tunnel

Seoul national university, the Korean highway corporation, 2001, Research report to put to practical use of a corrugated structural plate

Underground Space – the 4th Dimension of Metropolises – Barták, Hrdina, Romancov & Zlámal (eds)
© 2007 Taylor & Francis Group, London, ISBN 978-0-415-40807-3

Evaluation of the stability of anchored diaphragm wall basing on acceptance tests of anchors

A. Siemińska-Lewandowska & M. Mitew-Czajewska
Warsaw University of Technology, Warsaw, Poland

ABSTRACT: The paper describes acceptance tests of anchors performed during the execution of 17.5 m deep excavation in Warsaw. The main issue of the investigation was to estimate the real value of an average extension of the tendon Δs as well as to calculate the change of the value of L_{app} within the limits given by the Code EN1537. Considerable variations of the free anchor lengths observed in the 1st and 2nd anchoring levels caused significant changes in the estimated stability factors. Revisions to the detail design had to be introduced.

1 INTRODUCTION

The case was 800 mm thick and 17.5 m deep anchored diaphragm wall joined in upper part to a soldier pile wall. Due to the depth of the excavation and its width (42 m), stability of the wall was provided by 5 levels of ground anchors with the resistance of 500–600 kN. Total length of anchors varied between: 25 m in the first level, 20.50 m and 19.50 m in the second level, 19.50 m, 18.00 m, 17.00 m in the third level and 15.0 m in the fourth and in the fifth level. Fixed anchor length was constant for all levels and equalled 8.5 m. Anchors were spaced 2.7 m centres in the first level and 1.35 m in the other levels. The tendons in the first four anchoring levels consisted of 6 cables, 40.5 mm diameter. Each cable consisted of seven 5 mm diameter wires made of high yield steel. Tendons of the fifth (lowest anchoring level) were made of 7 cables. Grout body of anchors was formed using double cement grout injection. Fixed length of the anchors was separated from its free tendon length. Plastic PVC sheaths, sealed against ingress of water, were used to provide protection against corrosion of the tendon free length and to allow for the movement of the tendon in the borehole. All anchors were executed in a very complex geotechnical conditions, going through soils such as Pliocene clays, silty to medium sands, moraine clays.

According to the geotechnical investigations report, following geotechnical layers were specified:

- layer I – manmade fills, 1–3 m thick, in some places up to 4 m;
- layer II – moraine deposits reaching depth of 8–11 m below ground level (bgl), consisted of medium and stiff sandy clays and clayey sands of Warta glaciation in upper part, deeper - stiff sandy clays of Odra glaciation;
- layer III – continuous layer of sand deposits about 15 m thick represented by fine and medium sands;
- layer IV – cohesive soils (clays and silty clays) 1–5 m thick;
- layer V – sand deposits (medium and coarse sands as well as gravels and sandy gravels, 10–15 m thick).

There were two levels of ground water table observed. The main water table was stabilizing around 14.5 m bgl. Due to the technology of underground works and considering the stability of the bottom of excavation, water table was lowered during construction. Figure 1 presents typical cross-section of the structure including geotechnical conditions and detailed data concerning anchors.

2 DESCRIPTION OF ACCEPTANCE TESTS

Until the year 2002 in Poland there was no code specifying methods of ground anchors testing – today the situation has changed and the translation of European code PN EN 1537 is obligatory. All tests described in the paper, finished before 2002, were performed in accordance with German code DIN4125. Figure 2 presents the chart resulting from loading of anchors during testing.

All working anchors were subjected to an acceptance test. The objectives of acceptance test were: determining the apparent tendon free length L_{app} and demonstration that a proof load of 120% or 150% of load capacity can be sustained by anchor. At each loading level displacements of free tendon length were measured in the 1st, 2nd, 3rd, 4th, 5th, 10th and 15th

minute of loading. In addition one in ten anchors was overloaded to the 150% of the value of it's calculated bearing capacity. Basing on the values of the elastic extension of tendon Δs measured on site the elastic displacements curve was plot as well as limits of the elastic extension of tendon were calculated. Elastic displacements curve of the properly executed anchor should fit the area limited by two lines describing upper (1) and lower (2) limits of the elastic extension of tendon. According to DIN 4125 these limits are defined as follows:

$$S_{up} = \frac{P_p - P_0}{E_t \cdot A_t} \cdot (L_{tf} + 0.5 \cdot L_{tb}) \quad (1)$$

$$S_{low} = 0.8 \cdot L_{tf} \cdot \frac{P_p - P_0}{E_t \cdot A_t} \quad (2)$$

where: P_p is the proof load
P_0 is the datum load
L_{tf} is the tendon free length
L_{tb} is the tendon bond length
A_t is the cross-sectional area of anchor tendon
E_t is the elastic modulus of anchor tendon

These limits are equivalent to upper (4) and lower (5) limits of apparent tendon free length L_{app} (3) defined in EN 1537 as follows:

$$L_{app} = \frac{A_t E_t \Delta s}{\Delta P} \quad (3)$$

$$L_{app} \le L_{tf} + L_e + 0{,}5 L_{tb} \quad (4)$$

$$L_{app} \ge 0{,}8 L_{tf} + L_e \quad (5)$$

Where L_e is external length of tendon measured from the tendon anchorage in the anchor head to the anchorage point in the jack, which was not considered in calculations described in the paper.

It may be assumed that the method of calculation of L_{app} used in the discussed case was compliant with the recommendations of PN EN 1537.

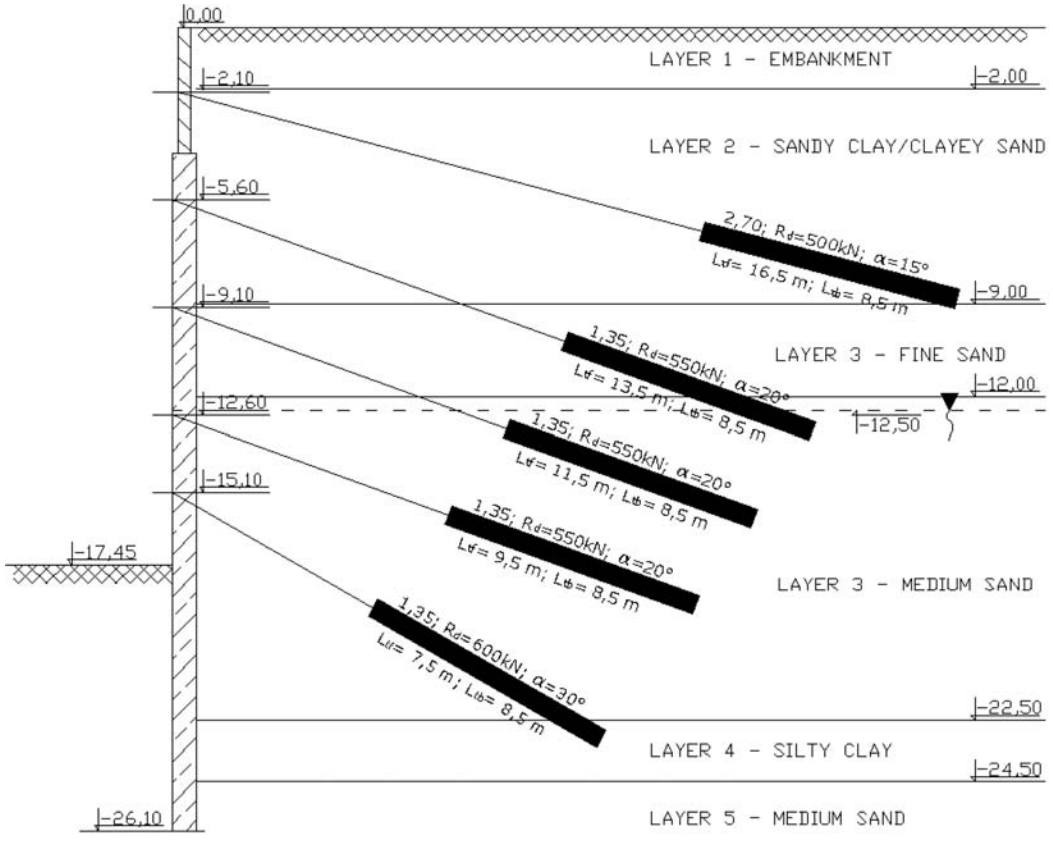


Figure 1. Typical cross-section.

In the paper, in next section, the results of acceptance test of first and second levels of ground anchors are described.

- 1st level – L_a = 25.00 m, L_{tf} = 16.50 m, R_d = 500 kN, $\alpha = 15^{\circ}$, number of tested anchors - 44;
- 2nd level – L_a = 22.00 m, L_{tf} = 13.50 m, R_d = 550 kN, $\alpha = 20^{\circ}$, number of tested anchors - 89;

Values of upper and lower limit of the elastic extension of tendon Δs are presented in table 1.

3 RESULTS

The technology of the execution and also the make-up of the separator were the main reasons that the carried out apparent tendon free length (L_{app}) varied from the one assumed in the design. In order to estimate real values of the free anchor length (L_{free}), the results of 1241 anchor acceptance tests were analysed. Taking into account measured values of the elastic extension of free tendon length (Δs) real values of apparent tendon free length L_{app} were calculated. Two sets of results for the first two anchoring levels (statistic samples) of acceptance tests consisting of 44 and 89 real values of Δs were analysed. Normal distribution curves, average values as well as standard deviations were calculated.

Figures 3 and 4 present normal distribution curves of both statistic samples. Average values, standard deviations and L_{app} are compiled in table 2.

It was assumed that proof load (P_p) amounts to 120% R_d, and datum load (P_0) is 15% of R_d. Were R_d is the value of design resistance of an anchor.

The results of acceptance tests proved that tendon free length L_{tf} had shortened. Taking it into consideration, after execution of the 1st and 2nd anchoring levels additional analysis of the stability of the wall-soil-anchor system was performed using Kranz method.

The objective of the calculation was to verify the stability factor of the wall (Fs) taking into account the value of tendon free length L_{tf} equal to L_{app}. In the calculation the average value of Δs was considered. There was a potential risk that due to the shortening of tendon free lengths (L_{tf}) of 1st and 2nd anchoring

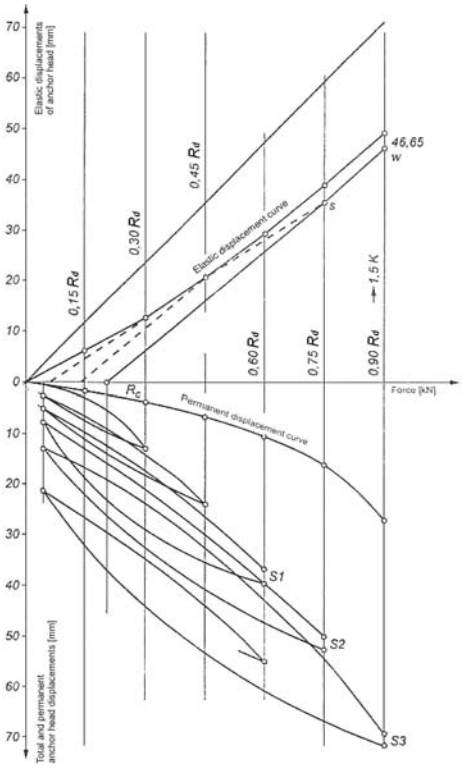


Figure 2. Loading chart.

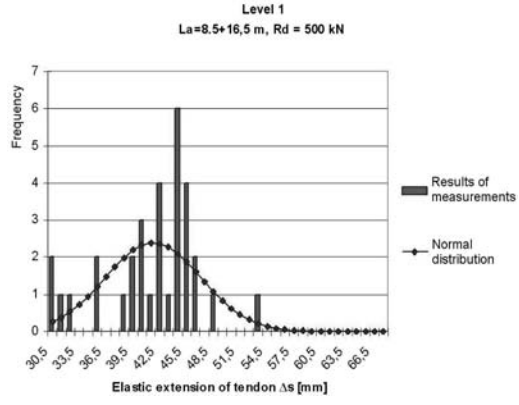


Figure 3. Results of acceptance tests of 44 anchors, 1st anchoring level.

Table 1.

level	R_d [kN]	L_a [m]	L_{tf} [m]	L_{tb} [m]	120%R_d S_{low} [mm]	120%R_d S_{up} [mm]	150%R_d S_{low} [mm]	150%R_d S_{up} [mm]
I	500	25.00	16.50	8.50	42.96	67.53	55.24	86.83
II	550	22.00	13.50	8.50	38.66	63.55	49.71	81.70

levels the wall might loose its stability asset in the design stage.

Parameters of 3rd, 4th and 5th anchoring levels were considered unchanged (equal to values used in the basic design), Figure 1. Minimum permitted value of stability factor was Fs = 1,50. Values of calculated stability factors (Fs), for each of anchoring levels were as follows:

1st level $Fs_1 = 3,1$
2nd level $Fs_2 = 1,88$
3rd level $Fs_3 = 1,20 \leq 1,50$

Too small stability factor was found in the 3rd anchoring level.

4 NUMERCIAL VERIFICATION

Authors decided to verify numerically values of safety factors calculated years ago using Kranz method. Numerical analysis were carried out using Geo5 software, programs: Sheeting check and Slope stability. Construction stages were modelled in accordance with the basic design and with real phasing performed on site. The value of tendon free lengths of first two rows of anchors L_{tf} were considered equal to average value of L_{app}, consequently the L_{tb} lengths were extended. Calculation of internal stability of the system considering the stage after the installation of the 3rd anchoring level showed that Fs values did not satisfy requirements (Fig. 5) and they were as follows:

1st level $Fs_1 = 3,61$
2nd level $Fs_2 = 1,71$
3rd level $Fs_3 = 0,93$

Second calculation run was performed with the input of extended tendon free lengths of the 3rd row of anchors (change from 11,5 m to 13,0 m). Resulting stability factors were as follows:

1st level $Fs_1 = 3,61$
2nd level $Fs_2 = 1,71$
3rd level $Fs_3 = 1,55$

In addition, analysis of overall (global) stability was performed using the method of Bishop. Global

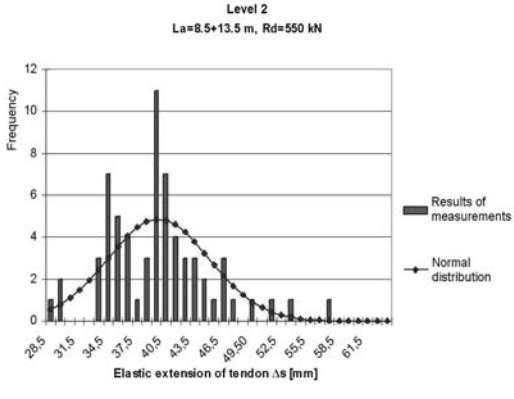


Figure 4. Results of acceptance tests of 89 anchors, 2nd anchoring level.

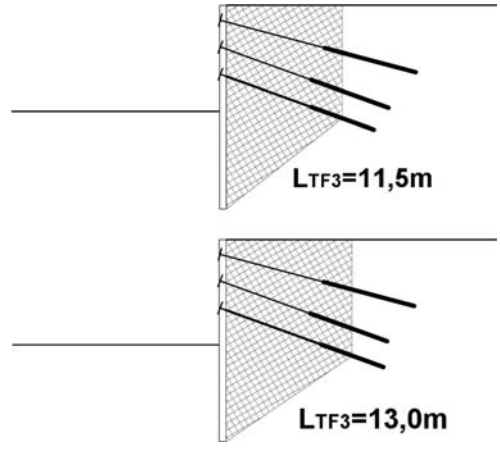


Figure 5. Verification of internal stability – 3rd anchoring level.

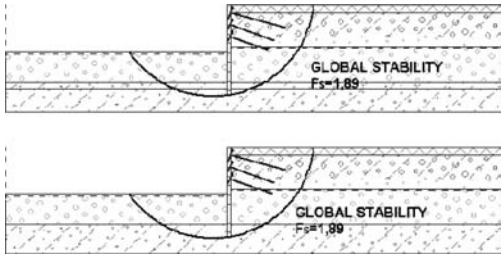


Figure 6. Verification of global stability – Bishop.

Table 2.

	R_d [kN]	L_a [m]	L_{tf} [m]	L_{tb} [m]	ΔS [mm]	σ	E_tA_t [kN]	ΔP [kN]	L_{app} [m]
I	500	25	16.5	8.5	41,74	+/−5,327	161310	525	12,82 +/−1,63
II	550	22	13.5	8.5	39,71	+/−5,325	161310	577,5	11,09 +/−1,48

stability factor in both cases (before and after extending tendon free lengths of the 3rd anchoring level) amounted to Fs = 1,89.

Figure 6 shows both models and estimated slip surfaces.

5 CONCLUSIONS

It was stated that due to a fault technology of the separator of the 1st and 2nd anchoring levels shortening of tendon free lengths of anchors in these rows occurred. This lead to a change in geometry of forces acting on the wall and in consequence caused lowering stability factors estimated using Kranz method. The length of anchors in the 3rd anchoring level determined in the basic design (L_a = 20.00 m, L_{tf} = 11.50 m, L_{tb} = 8.50 m, R_d = 550 kN, $\alpha = 20°$) proved to be to short for satisfying the minimum permitted value of stability factor (Fs). As a result, decision of incorporating changes into the basic design was made. Tendon free lengths of anchors of the 3rd level were extended. Redesigned tendon free lengths were set to 13 m causing anchor's total length to be 21,5 m.

Numerical verification proved that decisions made basing on on-site measurements and simple "by-hand" calculations were right and rational.

The case discussed in the paper proves the importance of acceptance tests and necessity of determination of apparent tendon free lengths (L_{app}) on-site, in accordance with the recommendations of European code. Special attention should be paid in case of multi level anchoring systems. Even small mistakes made in the first construction stages may lead to serious consequences especially in terms of safety in subsequent stages of construction.

REFERENCES

Siemińska-Lewandowska, Anna 2001. *Displacements of anchored diaphragm walls* (in polish). *Prace Naukowe, Budownictwo, zeszyt 139.* Warsaw: Oficyna Wydawnicza Politechniki Warszawskiej.

B.P. Metroprojekt 1996. *1st Metro line in Warsaw. Technical design of A13 station* (in polish). Warsaw.

B.P. Metroprojekt 1996. *Technical requirements for the design of Warsaw metro – section: station A13 Centrum – station A15 Ratusz. Geotechnical conditions of A13 station* (in polish). Warsaw.

B.P. Metroprojekt 1996. *Geotechnical conditions and soil parameters of soils along 1st metro line in Warsaw* (in polish). Warsaw.

PN-EN 1537. 2002. *Execution of special geotechnical works: Ground anchor* (in polish). Warsaw. Polski Komitet Normalizacyjny.

DIN 4125. 1990. *Kurzzeitanker und Daueranker, Bemesung, Ausfürung und Prüfung*.

This page intentionally left blank

Underground Space – the 4th Dimension of Metropolises – Barták, Hrdina, Romancov & Zlámal (eds)
© 2007 Taylor & Francis Group, London, ISBN 978-0-415-40807-3

London Heathrow Terminal 5 – Construction and monitoring of Piccadilly Extension Junction

A. Stärk & J. Jäger
Beton- und Monierbau Ges.m.b.H, Innsbruck, Austria

ABSTRACT: The new Terminal 5 of London Heathrow's Airport had to be connect to the existing airport terminals by means of seven tunnels in the vicinity of sensitive structures such as runways, fuel mains, and terminal buildings.

The final element of the overall tunnelling projects, the Piccadilly Extension Junction, should complete the connection of the existing Piccadilly Line with the Piccadilly Extension to the new Terminal 5. From a cut and cover box four tunnels have been excavated using Sprayed Concrete Lining (SCL) and LaserShell™ method of construction. The tunnels were built alongside existing running tunnels, with a minimum distance of less than one meter. To prevent existing tunnels from excessive movement they have been plugged with foam concrete over some length. An extensive monitoring regime and a careful selection of trigger limits were also required.

This paper shows how the existing tunnels reacted due to SCL excavation and gives a comparison of measured to predicted deformations. It also explains the SCL construction process, with particular attention paid to the principles of the LaserShell™ method of construction.

1 PROJECT OVERVIEW

The Airport London Heathrow is being upgraded by a new Terminal. This Terminal 5 (T5) is constructed separately from the Central Terminal Area and had to be connected to the existing terminal buildings and to downtown London by means of a total of 7 tunnels. The running tunnels were constructed by Tunnel Boring Machines; all the connecting constructions, such as headshunts, shafts, emergency exits, ventilation openings, cross passages etc. were constructed using Sprayed Concrete Lining (SCL). In total more than 40 SCL structures with an overall length of more than 1100 m had to be built (Hilar et al. 2005, Williams et al. 2004).

The tunnelling work has been successfully completed in 2006 and T5 is about to open in 2008.

This paper focuses on the PiccEx Junction as the last part of T5's SCL tunnelling work and probably the most difficult and interesting one.

London Underground provides public transport to London Heathrow via the Piccadilly Line, which had to be extended to serve the new T5. To connect the T5 Piccadilly Line Extension (PiccEx) with the existing Piccadilly Line, the so called PiccEx Junction had been constructed – in the middle of the heart of one of the busiest airports in the world (Fig. 1).

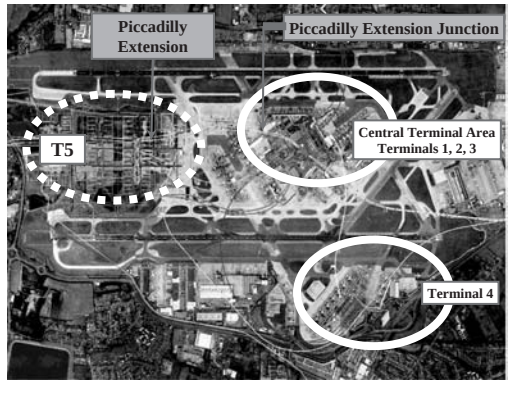


Figure 1. Airport London Heathrow overview.

2 BOX

A box has been excavated, approximately 20 m deep, 50 m long, and 20 m wide, to allow access to the existing tunnel systems.

The box structure consists of 1.2 m thick reinforced retaining 'diaphragm' walls. Half way down it is stiffened by a gallery-like intermediate slab. Two concrete pillars in the middle of the box provide additional



Figure 2. The box.

support. All machines, gear, equipment and material had to be lifted down the box opening by means of a crawler crane. For the first few weeks this included also the shotcrete supply until a permanent shotcrete pipe had been installed to the bottom of the box.

At the openings for the tunnels one meter thick and heavily reinforced headwalls have been cast to support the portal.

3 CONSTRUCTION OF SCL-TUNNEL

To enable trains to reach new T5 a turnout from the existing Piccadilly Line had to be built.

East of the box the existing Piccadilly running tunnels needed an enlargement to provide enough space for the necessary switches for the Piccadilly Line Extension turnout, resulting in Eastbound and Westbound Turnout Tunnel (Fig. 3).

On the West side of the box the connection to the previously built Piccadilly Extension had to be completed, creating a need for Eastbound and Westbound Stub Tunnel.

Table 1 gives a brief overview of all four SCL tunnels at the PiccEx Junction.

3.1 *Ground condition*

The only ground encountered was London Clay, which appeared homogeneous, with almost no water. A layer of scattered clay stones up to Ø 300 mm followed all four headings, approximately at tunnel axis. Occasional greasy backs were of no harm since the excavation followed the principles of the LaserShell™ method.

3.2 *LaserShell™*

Until now, it has been common when using shotcrete support, to enter the unsupported heading to install

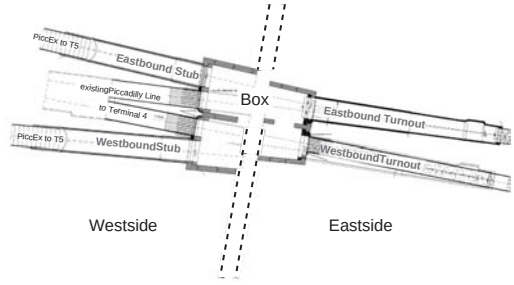


Figure 3. PiccEx Junction overview.

Table 1. Tunnels at PiccEx Junction (in order of construction).

Tunnel	Length (m)	Diameter (m)
Eastbound Turnout	52.9	$Ø_a$ 6.755 – 4.850
Eastbound Stub	26.7	$Ø_a$ 5.500/4.500
Westbound Turnout	52.9	$Ø_a$ 6.755 – 4.850
Westbound Stub	30.1	$Ø_a$ 5.500/4.500

girders and steel mesh. This is a fundamental aspect of the support system in soft ground. Girders provide immediate support and are required to fix the first layer of mesh. In addition, the girders are used to control the profile. Both, mesh and girders can only be installed manually, which includes the necessity to enter the unsupported heading. However, due to British health and safety regulations, no one is allowed to enter under the unsupported or even not completely supported heading. But no access to the heading implies no installation of girders and hence no tunnel construction.

Thus, a tunnelling method had to be developed which could satisfy the British health and safety regulations, does not need any girders and steel mesh, and is applicable in London Clay. LaserShell™ was born (Eddie & Neumann 2003, Eddie & Neumann 2004).

The most obvious feature of LaserShell™ is the inclined and domed face (Fig. 4). The inclined face guaranties that nobody stands under exposed ground at any time, but under the already hardened shotcrete of the previous advance. In addition, the inclination is contribution to a more stable face rather than a vertical one. As permanent support steel fibre reinforced shotcrete is used with a 75 mm initial layer, and a minimum of 200 mm structural layer. A 50 mm finishing layer without steel fibres covers up the steel fibres of the previous sprayed structural layer and provides a smooth finish comparable to shuttered concrete surface. There is no inner lining.

Another less obvious feature: The structural layer is been sprayed circumferential in one go, including



Figure 4. LaserShell™, inclined face.

the invert. This reduces the joints to the absolute minimum, to the radial joints between advances, with the added bonus of increased quality.

3.3 *TunnelBeamer™*

Another issue under rigid British health and safety regulations is profile control. Since profile can only be controlled from a distance, the TunnelBeamer™ is pushed to paramount importance. The TunnelBeamer™ – a laser theodolite – is connected to a laptop. The latter contains all relevant information with respect to geometry. I.e. the chainage of each advance and shape of its face (inclined and domed); furthermore the geometry of the unsupported heading as well as the geometry of every layer of shotcrete. During excavation the profile of the heading and during the spraying process, the thickness of each layer of shotcrete is monitored – continuously, easily and in real time. All as-built profiles are stored on the hard disc for conservation of evidence.

4 MONITORING

4.1 *Existing Piccadilly Tunnel Eastside*

On the Eastside of the PiccEx Junction the existing Piccadilly tunnels had to be enlarged (see Fig. 3 for location). The first half of the existing Piccadilly Eastbound was plugged with foam concrete; the second half remained unplugged during excavation. That gave the unique opportunity to monitor the unplugged area ahead of the SCL-face once the plugged area had been left behind (Fig. 5). Information to be obtained from monitoring the existing tunnel should help to determine the amount of stress re-distribution ahead of the current SCL heading and thus to assess that part of the displacements acting already on the shotcrete lining before the base reading could be done.

It was possible to take readings until the approaching heading was within just one width of a ring, which was 600 mm. Although the database was complete



Figure 5. View into existing Piccadilly Eastbound.

from that point of view, no evidence was given of any deformation ahead of the face. Two conclusions can be drawn from this surprising result:

1. It confirms previous observations that displacements in advance of the heading are small or negligible. This is not a general statement to London Clay, but it applies to this particular condition at the PiccEx Junction.
2. Under common circumstances some time goes by from applying shotcrete, installing the monitoring array, and taking the base reading. During this period of time the freshly applied shotcrete is already loaded and displaced by the stress re-distribution around the heading. Due to this inevitable delay in taking the base reading, this pre-displacement cannot be read and this information is lost. With the knowledge of the results discussed above, it is clear that the unreadable pre-displacement must be very small, so that the ordinary monitoring provides a nearly complete picture of the total displacement and hence of the load acting upon the shotcrete lining. Again, this is not a general statement to London Clay, but it applies in these particular conditions at the PiccEx Junction.

4.2 *Existing Piccadilly Tunnel Westside*

Before this particular part of the monitoring will be discussed some general information on the existing Piccadilly Line tunnels should be given.

The lining of the existing Piccadilly Eastbound Tunnel is made of Spherical Graphite Iron segments (SGI-segments). The joints between the segments were filled with plywood or similar to cope with curves and changes of the gradient. No gaskets have been used to prevent water from intruding through the joints. The London Clay at T5 in general is technically watertight, but somehow water find its way down to the tunnels and through the joints. As a result plenty of stalactites



Figure 6. Stalactites on SGI-segments, exist. Piccadilly Line.



Figure 7. LHS existing Piccadilly, RHS SCL Eastbound Stub.

growing upon the lining and also rusting of the iron segments is visible (Fig. 6).

The distance between the existing Piccadilly tunnels and the SCL Stub Tunnels was very small (Figs. 3, 7). The remaining ground pillar between the tunnels varied from 0.4 m at the box to approximately 3 m at the end.

The integrity of the existing structures during SCL-work had to be ensured; therefore monitoring of the existing Piccadilly Line tunnels was inevitable. Of particular interest was the performance of the existing Piccadilly Line Eastbound during the excavation of the SCL Eastbound Stub Tunnel which was the first SCL Stub tunnel to be constructed.

The existing Piccadilly Line Eastbound is approximately 20 m long (before it unifies with the existing Piccadilly Line Westbound, Fig. 3), of which the first 8 m, measured from the box, have been plugged with foam concrete to enhance stability during excavation of the adjacent SCL Eastbound Stub. In the remaining

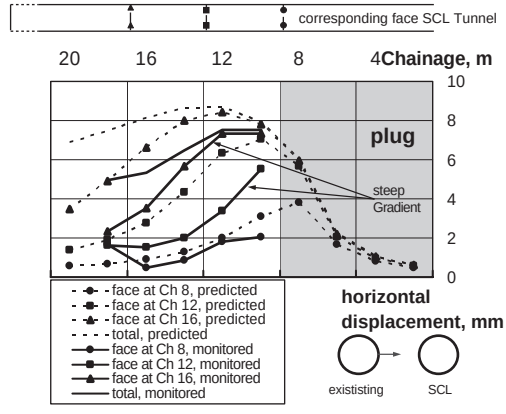


Figure 8. Horizontal displacements exist. Piccadilly.

unplugged part four monitoring arrays have been installed. Access was given through the neighboured Piccadilly Line Westbound Tunnel.

The existing Piccadilly Line Eastbound Tunnel experienced 3 to 5 mm vertical displacement in the crown, and 5 to 7 mm horizontal displacement at axis level directed towards the SCL Eastbound Stub, indicating clearly an ovalisation. All displacements were limited to the crown and that side of the lining where the SCL Eastbound Stub passed by (Fig. 8).

Significant displacements could be observed approximately only 2 m ahead of the current SCL face and continued 4 to 5 m after the SCL face had passed the relevant monitoring array (equivalent to half a tunnel diameter before and one tunnel diameter after passing the monitoring array, or in terms of time equivalent to approximately three days altogether).

Although the overall displacements in the existing Piccadilly Line Eastbound were 2 mm smaller than anticipated in the design (see also companion paper Jäger & Stärk 2007), the gradient appeared steeper, creating a larger longitudinal 'bending' of the SGI lining towards the SCL Stub Tunnel.

This information was important with respect to the stability of the neighboured tunnel, the existing Piccadilly Line Westbound, during the upcoming excavation of the SCL Westbound Stub. It was decided to extent the foam concrete plug in the existing Piccadilly Westbound to full length (instead of only 8 m). Thus any movement of the expanded lining and any further opening of joints were prevented.

5 CONCLUSION

The civil engineering and tunnelling works at PiccEx junction have been completed successfully (Fig. 9). A contributor to that success was the collaboration between contractor and designer. Through this



Figure 9. Completed SCL-work Eastbound turnout Tunnel.

collaboration, new designs and methods were realized and these reduced both cost and construction risk while at the same time ensuring high quality in the finished works.

REFERENCES

Eddie, C & Neumann, C 2003. LaserShell™ leads the way for SCL tunnels. *Tunnels & Tunnelling*, June 2003.

Eddie, C & Neumann, C 2004. Development of LaserShell™ Method of Tunneling. *Proc. North American Tunneling Conference 2004, Atlanta*. Rotterdam: Balkema.

Hilar, M et al.: 2005: The latest Innovation in Sprayed Concrete Lining – The LaserShell™ Method. *Tunnel* 4/2005 *(Czech Edition).*

Jäger, J & Stärk, A 2007. London Heathrow T5 – Deformation prognosis for new Piccadilly Extension Junction. *Proc. ITA-AITES World Tunnel Congress 2007, Prague, 5–10 May 2007*. Rotterdam: Balkema.

Williams, I et al. 2004. Innovativer Spritzbetontunnelbau für den neuen Flughafenterminal T5 in London. *Proc. Österreichischer Tunneltag, Salzburg, 6. October 2004.*

LaserShell™ and TunnelBeamer™ are registered Trade-Marks by Beton- und Monierbau and Morgan = Est. The TunnelBeamer™ has been patented by Beton- und Monierbau and Morgan = Est.

This page intentionally left blank

Underground Space – the 4th Dimension of Metropolises – Barták, Hrdina, Romancov & Zlámal (eds)
© 2007 Taylor & Francis Group, London, ISBN 978-0-415-40807-3

Effect of moving load to foundation excavation support configuration

Chi Xiuwen[1], Luo Yuanfang[1], Qin Ying[1], Lin Chi[2] Cai Guanghuang[3], Wang Shuping[3], Chen Zhoupin[4] & Huang Zhangjun[4]

[1] *Wuhan University of Technology, Wuhan, China*
[2] *Group of Urban Construction Investment Development Ltd, Wuhan City, Wuhan China*
[3] *Mechanization Co. of Wuhan Civicism, Wuhan, China*
[4] *Erchu Co., LTD of China Railway Tunnel Group, Beijing, China*

ABSTRACT: Support problem of complicated loading deep excavation pit at underground engineering are analytically investigated. Through support engineering, advanced technology should be used to assure stability of the slop and safety of the establishment around excavation pit. Subway on YueMa Square grade separation works of Wuhan city receives dense traffic, which suffers from the effect of moving load obviously, for example from buses, cars etc, and surrounds with many buildings. Selection of supporting configuration, with the consideration of change of excavation pit depth, geological environment, traffic demand and situations of the buildings around excavation pit at different area, take different supporting project. In this project, many support styles are used such as retaining wall, pile, bolt and so on. Through monitoring to the support configuration, analyzing the monitor result, evaluating the effect of moving load to the support configuration.

1 INTRODUCTION

Yuema Yard fly-over locates the south of Snake Mountain, Shouyi Square and periphery. The yard, which is around by Yellow Crane Building, Shouyi Square, Hubei Theater and Hubei Library, comes through Shouyi Square from west to Changjiang Bridge, connects Wuluo Road from east to Da Dongmen fly-over. Yuema Yard fly-over tunnel project, which is consisted of west lead path, main tunnel and east lead path, the tunnel adopted open excavation method, tunnel foundation pits move along with change of working face. The situation around foundation pit is complicated, there are five eight-floors concrete structure residential buildings in the right of K0+320∼K0+500, which is 5 m away from top slop of the foundation pit, and key cultural relic Red Building is on the left of K0+565∼K0+605, which is 5 m and 3.2 m respectively apart from top slop of the foundation pit. And there are brick mix structure house on the left of east section of main tunnel and high-level construction on the left. Meanwhile, adopting single side excavation on the east section of K0+720, traffic wouldn't be brought to a standstill under the foundations construction. Cars put an uncertain moving load to the foundation supporting and slope for running close to the pit. Due to great stream of people and traffic at the cross of Yuema Yard and Shouyi Square, and serious disturbance, adopting reasonable supporting form and monitoring supporting structure play an important role in assurance of safety construction. This paper focuses on the monitoring situation of k0+720∼k1+060 section foundation pit to inspect effect of moving load on support.

1.1 *Construction program and supporting form*

With open excavation method adopted in Yuema Yard tunnel Project, the k0+780∼k1+060 section use single side excavation in order to ensure constant traffic. And cars put an uncertain moving load to the foundation supporting and slope for running close to the pit. In the process of excavation, if supporting structure is unstable and validable, the foundation pit and soil would fall into extra-big displacement and settlement even slipping as a result of unstable or ineffective supporting structure, which would bring about destruction of construction and establishment or damage to builders. Therefore, it is necessary to carry out completely systematic monitor and control on supporting form, soil distortion and displacement, change of groundwater, give monitoring information back in time to achieve informational construction.

Because of adopting row piles and prestressing steel supports in this section, row piles use C30 RC perfusion pile, whose diameter is 900 mm, length is 112.0 m, with 0.5 m height C30 RC coronal girder connected each pile. Adopting two horizontal prestressing steel supports, which changes according to depth of foundation pit, the first one is in the position of

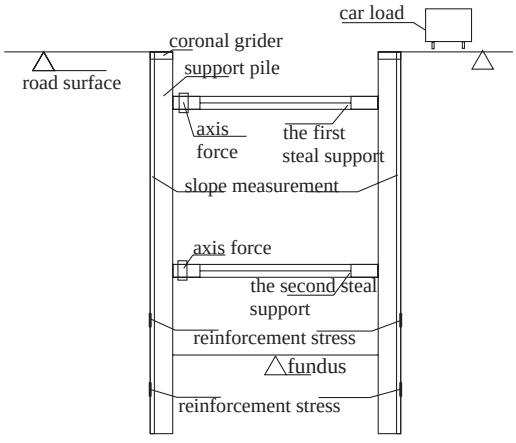


Figure 1. Monitoring measurement disposal of k0+820 Section.

coronal girder while the second one is 6 m away from top of the pit. Middle girders use general hot-rolling I-shape steel.

1.2 *Monitoring program*

1.2.1 *Monitoring item*

Following are the main items: a slope instrument to observe deep-layer level displacement; b. axis force monitoring to inspect force situation of prestressing steel support; c. suffering force monitoring of supporting pile to test suffering force situation of supporting pile by using reinforcement stress buried in it.

1.2.2 *Collocation of measuring point*

According to geological condition, surrounding situation and supporting structure, collocation program of measuring points in k0+780~k1+060 section include: (1) measuring point of slope measurement: dispose a pipe of slope measurement at space between 20 m (space out the pipes 20 m apart); (2) measuring point of reinforcing steel internal force: dispose two reinforcement stress in pile every 40 m; (3) measuring point of axial force: dispose axial force meter on two supports separately every 40 m. Specific disposal position of instrument was shown as figure 1.

2 ANALYSES ON MONITORING RESULT

In k0+780~k1+060 sections, which hold traffic thoroughfare, two section construction method was adopted to avoid blocking traffic. That is carrying out the north side construction first. Meanwhile, the south side keeps transportation and starts construction till the north side is completed and resumes transportation. Considering Yuema Yard project which holds traffic

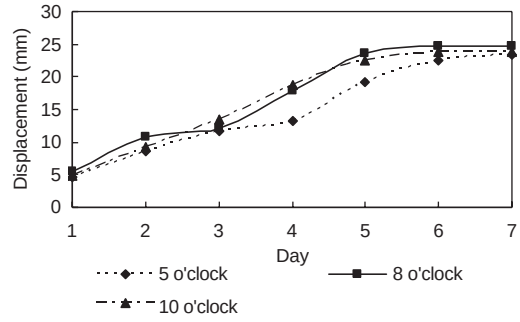


Figure 2. Pile top horizontal displacement-time curve.

thoroughfare and great cars flux, would bring about certain effect on foundation pit supports. Therefore, apart from routine monitor methods, three different break surface were used in the process of foundation excavation for supervising suffering force , level displacement of pile body and pile top of supporting pile under the effect from moving load at different period of time and vary traffic flux.

In foundation pit excavation, three sections would be monitored at 5 o'clock (min vehicle flux), at 8 o'clock(max vehicle flux), at 10 o'clock (average vehicle flux) and three sections (k0+820~ k1+140~k0+360) respectively for a week.

In the position of k0+820, support fashion was cantilever pile and steel support. In this section, pipe of slope measurement and Reinforcement Stress measurement were fixed into support pile, and axis-force measurement was fixed into steel support. Excavation began on Aug.19th and finished on Aug.24th. Monitoring result illustrate in table 1 below:

According to the early monitoring results, we found that horizontal displacements, stress of supporting pile, axis-force of steel supports all rise along with the depth of pit excavation and reach the max in 2 or 3 days after the excavation completed. But then the index value would go down and be stable.

The following three figures express variety rules of displacement, stress in each time for one week. Synthesizing the three sorts of curve, we can see that the variety rules of monitoring result are consistent with early dates in other sections, and stress of supporting piles reach maximal as well as displacement.

The figure 2 expresses variety rules of horizontal displacements of supporting piles top along with time when foundation pit was excavating. From the curve, it is clear that the horizontal displacement is always minimal when the vehicle flux is minimal (5 o'clock); and the horizontal displacement is always maximal when the vehicle flux is maximal (8 o'clock). After 2 days of the excavation is finished, the displacement is consistent in three times. The most discrepancy of horizontal displacement between maximal and minimum

Table 1. Monitoring result of k0+820 section (1).

Day	O'Clock	Excavation schedule(m)	Displacement of pile to(mm)	Max displacement of pile body(mm)
1	5	4	4.7	4.7
	8	4	5.6	4.9
	10	4	4.8	4.8
2	5	6	8.5	8.5
	8	6	10.7	9.7
	10	6	9.3	9.8
3	5	8	11.6	12.7
	8	8	12.1	13.6
	10	8	13.5	15.7
4	5	10	13.2	14.1
	8	10.5	17.9	20.2
	10	finished	18.7	23.5
5	5	–	19.2	22.7
	8	–	23.5	25.4
	10	–	22.6	25.1
6	5	–	22.5	26.4
	8	–	24.7	27.3
	10	–	23.8	26.7
7	5	–	23.3	26.2
	8	–	24.6	27.1
	10	–	23.9	26.6

Table 2. Monitoring result of k0+820 section (2).

Day	O'Clock	Excavation schedule(m)	Force of reinforcing steel bar in pile(Mpa)	Force of steel support (Mpa)
1	5	4	14.3	–
	8	4	15.7	–
	10	4	15.6	0.5
2	5	6	18.5	1.3
	8	6	19.3	1.8
	10	6	19.7	2.1
3	5	8	20.9	3.5
	8	8	22.7	4.7
	10	8	25.1	5.6
4	5	10	24.3	7.3
	8	10.5	26.7	8.9
	10	finished	24.8	10.6/0.3
5	5	–	25.5	9.9/0.5
	8	–	25.1	10.1/0.9
	10	–	24.9	11.3/1.6
6	5	–	26.3	10.2/2.1
	8	–	27.7	10.5/1.9
	10	–	25.6	10.4/2.3
7	5	–	26.1	11.1/2.2
	8	–	25.8	10.0/2.5
	10	–	26.4	9.4/2.1

vehicle flux was happened on Aug.24 and Aug.25. The maximal discrepancy is 6.5 mm.

Figure 3 expresses variety rules of stress of supporting pile body along with time when foundation pit was excavating. From the curve, it is apparent that stress rises rapidly in the early days of excavation, but the rising trend goes slowly and steadily with the completion of excavation. In the three different times, the discrepancy of stress is not very high.

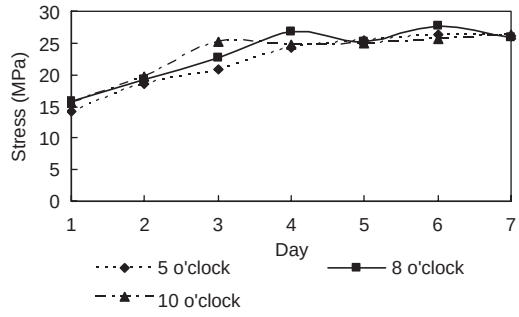


Figure 3. Support pile force-time curve.

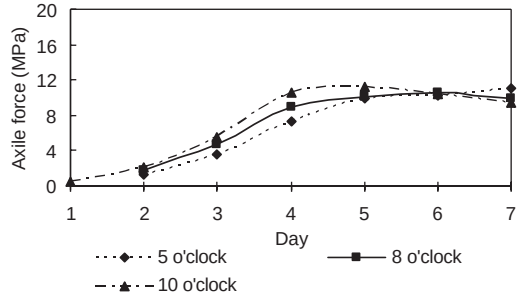


Figure 4. Steel support axile force-time curve.

Figure 4 expresses variety rules of steel support axis-force along with time when foundation pit excavating. From the curve, it is obvious that axis-force rose rapidly in the early days of foundation pit excavation, but the rising trend goes slowly with the completion of excavation. The maximal discrepancy of axis-force between maximal and minimum vehicle flux is 2.5 MPa which was happened on Aug.24. The variety rule is consistent with the horizontal displacement of pile top.

Synthesizing the three results of monitoring, we can see that with the foundation pit excavating, the rising trend of stress of supporting pile and horizontal displacement of pile top go slowly after the first steel support is fixed. It means that the steel support took effect. The position of horizontal max-displacement of pile body is moving down slowly, which is between the two steel support (4∼6 m) after the second steel support is fixed. For different time, vehicle flux is different, as well as the monitoring result. But the discrepancy is not very distinct because of the effective support configuration. On account of

the special geographical position, design unit chose a high safety sector to calculate for the sake of project safety when deciding the support fashion. Furthermore, the support fashion of monitoring section is row pile and steel support, and the support effect of support configuration is very good. So the effect of moving load to support configuration is not very remarkable.

3 CONCLUSIONS

Through monitoring analysis of foundation pit supporting configuration in different time, we can see that the effect of moving load to foundation pit is existed and restricted by many other factors such as supporting configuration, geologic condition, geographic situation, environments, ground water and so on. It is necessary to monitor support configuration in the process of deep foundation pit excavation. Through analyzing the monitoring results to reflect construction effect, it can make for carrying construction organization into execution and choosing economical and rational supporting.

REFERENCES

[1] P.S.K. Ooi and T. L. Ramsey. Curvature and Bending Moments from Inclinometer Data. INTERNATIONAL JOURNAL OF GEOMECHANICS,2003(9)

[2] Donghyun (Don) Kim, Richard B. Langley, Jason Bond, Adam Chrzanowski
Local deformation monitoring using GPS in an open pit mine: initial study. GPS Solutions, 2003(7)

[3] Richard.J.Finno, J. Tanner Blackburn. Automated monitoring of supported Excavations. Geotechnical Applications for Transportation Infrastructure, 2006(5)

[4] S.F. Su, H.J. Liao, Y.H. Lin. Base stability of deep excavation in anisotropic soft clay. Journal of geotechnical and geoenvironmental engineering, 1998(9)

[5] J.P. Turner, J.A. Steele, W.F. Maher, M.R. Zortman, J.R. Carpenter. DESIGN, CONSTRUCTION, AND PERFORMANCE OF AN ANCHORED TANGENT PILE WALL FOR EXCAVATION SUPPORT. GEO-Support, 2004

[6] Gordon T.K. Lee and Charles W. W. Ng. Effects of Advancing Open Face Tunneling on an Existing Loaded Pile. JOURNAL OF GEOTECHNICAL AND GEOENVIRONMENTAL ENGINEERING, 2005(2)

[7] D. Matthew Stuart. Project-Specific Steel Sheet Piling Applications. PRACTICE PERIODICAL ON STRUCTURAL DESIGN AND CONSTRUCTION, 2004(11)

[8] Charles W.W. Ng. STRESS PATHS IN RELATION TO DEEP EXCAVATIONS. JOURNAL OF GEOTECHNICAL AND GEOENVIRONMENTAL ENGINEERING, 1999(5)

[9] H.F. Thurner. Non-destructive Test Method For Rock Bolts. International Society for Rock Mechanics, International Congress on Rock Mechanics, Montreux(Suisse), 1979

[10] Vrkljan I, Szvarits Nossan A, Kovacevic M S. Non-destructive procedure for testing grouting quality of rockbolt anchors. Proceedings of the 19th international congress of the international society for rock mechanics 1475–1478, Aug25–28, 1999

Section 6
Concrete in underground construction

This page intentionally left blank

Part 6.1
Sprayed concrete

This page intentionally left blank

Underground Space – the 4th Dimension of Metropolises – Barták, Hrdina, Romancov & Zlámal (eds)
© 2007 Taylor & Francis Group, London, ISBN 978-0-415-40807-3

Finite element analyze single shell lining based on contact mechanics

Junru Zhang & Wenge Qiu & Huijian Zhang
School of Civil Engineering, Southwest Jiaotong University, Chengdu,Sichuan, China

ABSTRACT: For the moment, there are mainly three mechanical models (load-reaction model, nonindividual body model, convergence-constraint model) used to calculate tunnel structure. Because of discontinuous section existed in the single shell lining, the above three models can not analyze. Therefore single shell lining mechanical model based on contact theory has been proposed. This model introduced non-thickness contact element to simulate the interaction between surrounding rock and support, support and structure, then used non-linear finite element analysis to study the mechanical property of single shell lining. The study results indicate that under the same conditions single shell lining produced 50%∼80% the internal force of composite lining producing. Another saying is that to produce the same internal force, the thickness of single shell lining could be reduced four times than that of composite lining. In a word, single shell lining used could reduce excavation and concrete amount. Consequently, the cost of the engineering is dropped.

1 INTRODUCTION

Single shell lining is date back to 1970s and the first country who used it is Norway. Compared with composite lining, it is chiefly characterized by canceling repelling board, so shearing force can function in lining[1]. At present, many countries use single shell lining as final lining, such as China, Germany, Switzerland, France, America, Japan and so on. Although single shell lining has been extensively applied in our country, its design method is mainly aiming at concrete reinforced with shot steel fiber. For instance, there are Q system method, limiting state method and energy theory method[2]. Among the three, Q system method is based on experience, the other methods is rarely used due to their small scope of application. Therefore, to find a better mechanical model for single shell lining is greatly significant.

2 MECHANICAL MODELS OF TUNNEL AT PRESENT

2.1 *The existing mechanical models of tunnel*

The tunnel deign model group of ITA sum up in three mechanical models as load-reaction model, nonindividual body model, convergence-constraint model[3]. These three models all have some assumptions and restrictive conditions added, so they have different scope of application.

2.1.1 *Load-reaction model*

Load-reaction model is characterized by its simple calculation method and definite safety coefficient, so it is recommended in tunnel design code of our country[4]. This model mainly considers that surrounding rock loose load and elastic resisting force combined composed on lining at the same time, then calculates the inner force of lining, consequently evaluates whether it is safe or not. It is obvious that how to determine load model and surrounding rock elastic resisting force is the key to accuracy of calculation.

2.1.2 *Convergence-constraint model*

Convergence-constraint model is also a important method. It uses the crossing point of surrounding rock characteristic curve and support characteristic curve to determine the best condition of balance, as shown in Fig. 1 [5]. But in the application of this model, there are several difficult problems. On one hand, the surrounding rock and support characteristic curves are hard to exactly determined, on the other hand, the influencing factors of characteristic curve can not be described with fixed quantity. Therefore this model still stays in the phase of qualitative.

2.1.3 *Nonindividual body model*

Nonindividual body model is based on interaction of support and surrounding rock, which bear the loads together. The surrounding rock is seen as main load-bearing structure, while support is as like as a stiffening

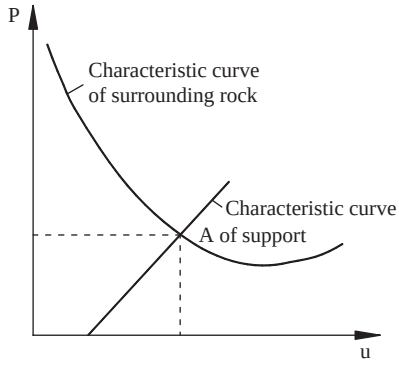


Figure 1. Convergence-constraint model illustration.

ring inlaid in the hole located at semi-infinite body [6]. In the practice of this model, the major work is to analyze the redistribution of ground stress caused by excavation, and then the induced deformation, establishment of surrounding rock and stress in support can be gotten. Afterwards whether the tunnel is safe or not is known. At present, there are two calculation methods for the nonindividual body model. These two methods are analysis method and numerical method. The former can obtain solution only in analyzing few tunnel with regular shape because of difficult in the aspect of math, and the latter can simulate all the features of rock and structure, even it can simulate the construction course. So it is gotten more and more used in underground engineering.

2.2 *The proposing of mechanical model for single shell lining based on contact theory*

For each mechanical model, only when it exactly reflected real state of surrounding rock and how to contact between surrounding rock and support can get the reasonable result [1]. Because it is discontinuous between surrounding rock and structure, structure and structure in the single shell lining, the above three model can not reflect this discontinuous surface. Thus to improve mechanical model to suit the feature of single shell lining is highly required. Substantially to simulate discontinuous surface belongs to contact issue of solid mechanics. When solving the contact issue, more exact deformation and stress feature of contact plane are taken into account, so the calculation result is more like practical situation [7]. This paper introduced non-thickness contact element to simulate the interaction between surrounding rock and structure, structure and structure on the base of regular nonindividual body model, and then using non-linear finite element method to analyze the stress in single shell lining. Consequently the theory for single shell lining design can be provided.

Table 1. Calculation cases.

case	Lining style	Thickness of primary support (C20 shotconcrete)	Thickness of final lining (C25 cast-in-place concrete)
1	Composite lining	15	35
2	Single shell lining	15	35
3	Single shell lining	10	25

3 NON-LINEAR FINITE ELEMENT ANALYSES FOR SINGLE SHELL LINING

3.1 *General situation of engineering*

This analysis took NO.2 inclined shaft of Da-bie-shan Tunnel which located at high-speed railway from He-fei to Wu-han as background. Da-bie-shan Tunnel, which is the longest tunnel in the high-speed railway from He-fei to Wu-han, spans 13.256 kilometers. NO.2 inclined shaft locates at right of line, and its longitudinal gradient is 8.2%, with spanning 1077 meters. The midline of railway is orthogonal to midline of tunnel. Three different support parameters are listed in Tab. 1 The surrounding rock is IV rank. Through analyzing these three cases to compare the stress in structure, then optimum design can be carried out.

3.2 *Finite element analysis*

3.2.1 *Model and parameters for calculation*

ANSYS is used in this analysis and elasto-plastic plan strain model is taken as calculation model. Surrounding rock employed four nodes plane isoparametric element, and its yielding criterion is Drucker-Prager criterion [8]. Beam element is served as primary support and final lining. Face to face contact element of two-dimension (targe169 and conta171) is used to simulate interaction between surrounding rock and primary support, primary support and final lining. Normal displacement of lower boundary is restricted. Horizontal direction restraint is imposed on right and left boundary, while upper boundary is free. The calculation model is shown in Fig. 2. The corresponding physical mechanics parameters are listed in Tab. 2.

3.2.2 *Contact element and its yield criterion*

Face to face contact element of two-dimension is able to simulate bonding, separating and gliding. In ANSYS program, it is realized by targe169 and conta171 sharing one real constant [9]. This element is shown in Fig. 3. Each node has two degree of freedom as moving along X axis and Y axis in the node

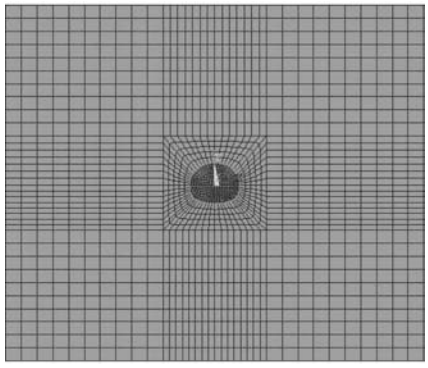


Figure 2. Model and finite element mesh.

Table 2. Physical mechanics parameters.

Stratum and material	Elastic ratio E/GPa	Poisson ratio/μ	Weight γ /kN·m^{-3}	Cohesion force c /MPa	Internal friction angle ϕ/°
IV degree wall rock	1.3	0.35	20.0	0.20	27
C20 shotconcrete	21.0	0.20	22.0	–	–
C25 cast-in-place concrete	28.0	0.18	23.0	–	–

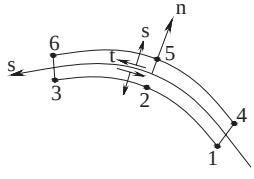


Figure 3. Contact element.

coordinate system. Unknown quantities of this element contain nodal displacement and contact stress, while geometrical condition and static balance condition is considered as additional equation contained in the stiffness equation. Due to this, equivalent stiffness matrix and load vectors of contact element can be established, then to add the contribution of contact element to the total equation by regular method. With that the solution can be done.

Contact element takes maximum shear stress criterion and Mohr-Coulomb criterion as criterion for contact state. Discriminant equation follows:

$$\tau \le [\tau], \quad \tau \le C + \mu\sigma \tag{1}$$

Where τ and $[\tau]$ are the equivalent shear stress and maximum shear stress allowed respectively; C and μ are the cohesive strength and friction coefficient of the material respectively, and σ is normal stress of contact.

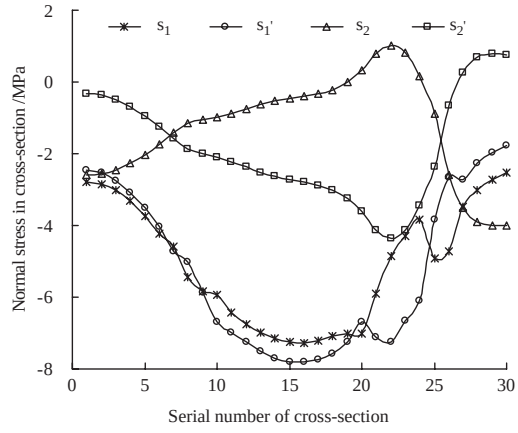


Figure 4. Stress distribution in cross-section in calculation case 1.

3.2.3 *Simulation of tunnel excavation*

Simulation of tunnel excavation is realized by killing corresponding elements, namely to set the stiffness and load of died element to a small value (for example 10–6). To active corresponding elements and modify their attribution can be used to simulate applying lining. Release ratio of stress due to excavation is determined by ratio of surrounding rock displacement at the time of applying lining to total displacement [10].

$$\bar{\delta} = W^{\lambda} \tag{2}$$

Where δ and W are the stress release ratio and displacement release ratio of surrounding rock respectively, and λ is one parameter related to geological condition and construction method (this paper take 0.7 for calculation).

According to the arch crown settlement of NO.2 inclined shaft observed in site, the average stress release ratio is worked out as that: 40% when applying primary support and 60% when applying final lining.

3.3 *Calculation result*

From calculation result, it is seen that relative slip occurred between primary support and final lining under Case 1, while not do Case 2 and Case 3. In order to find out the feature of normal stress distribution under each case, the normal stress distribution map is employed, as shown in Figs 4, 5 and 6. Where horizontal ordinate indicates serial number of cross-section showed in Fig. 7; and vertical ordinate expresses the normal stress in corresponding cross-section. In these figures, the details of σ_1, σ_1', σ_2, and σ_2' are shown in Fig. 8.

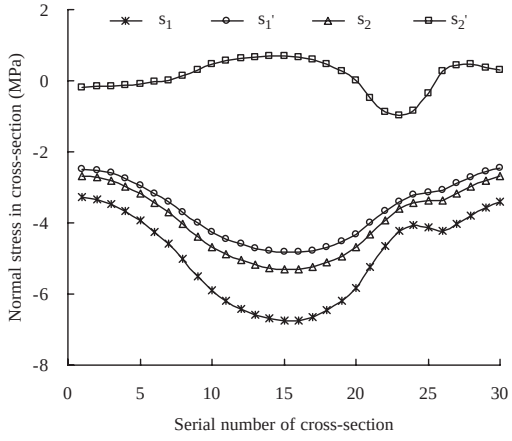


Figure 5. Stress distribution in cross-section in calculation case 2.

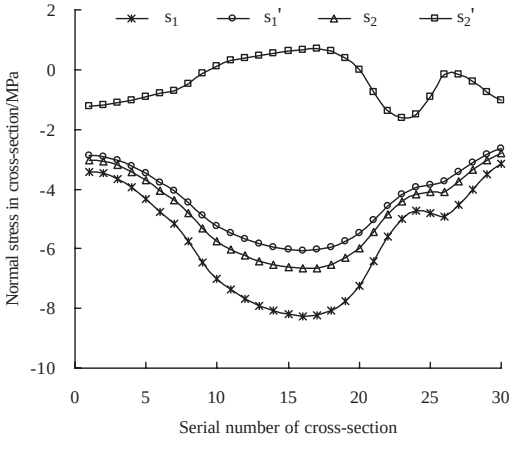


Figure 6. Stress distribution in cross-section in calculation case 3.

The conclusion can be drawn follows:

(1) In Case 1, lining could be seen as composite beam because the friction existed between primary support and final lining is very small. As Fig. 4 illustrating: primary support is totally in compression, and the majority of final lining is in compression except basement and invert. The maximum compression stress locates at side wall (NO.16 section), inside of primary support with -7.81 MPa; and the maximum tension stress locates at basement (NO.22 section), outside of final lining with 1.03 MPa.

(2) In case 2, lining appears deforming entirely, because shear stress can be transferred between primary support and final lining. As shown in Fig. 5, primary support is totally in compression,

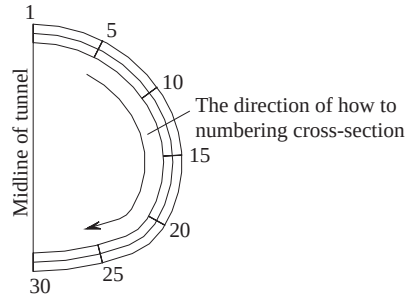


Figure 7. Serial number of cross-section.

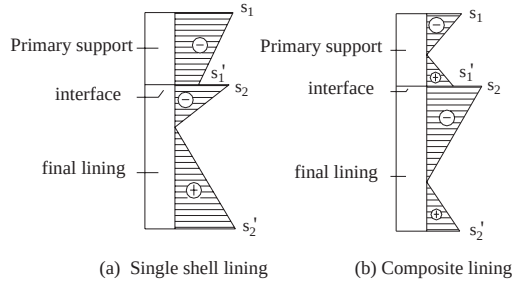


Figure 8. Normal stress distribution in cross-section.

but for final lining, the parts of arch springing, side wall and invert are in tension, the other parts in compression. The maximum compression stress locates at side wall (NO.15 section), outside of primary support with -6.75 MPa; and the maximum tension stress also locates at side wall (NO.15 section), inside of final lining with 0.68 MPa. In addition, normal stress on the interface of primary support and final lining jumped because elastic ratios of the two are different.

(3) Compared to case 2, in case 3 the thickness of primary support is reduced 5 centimeters, and that of final lining decreased 10 centimeters. However, the mechanical feature and vary tendency in case 3 are similar to those in case 2, only the value of normal stress have some difference. Just shown from Fig. 6, the maximum compression stress locates at side wall (NO.16 section), outside of primary support with -8.25 MPa; and the maximum tension stress also locates at side wall (NO.16 section), inside of final lining with 0.68 MPa.

(4) The compression strength and tension strength of C20 shotconcrete are 10.0 MPa and 1.1 MPa respectively, and those of C25 cast-in-place concrete are 12.5 MPa and 1.33 MPa respectively [11]. The above calculation results all feasible. But under the same condition, the maximum compression stress in case 1 is 1.2 times of that in case 2;

Table 3. Economic comparison between composite lining and single shell lining.

Case	Item	Amount of per meter	Unit	Unit price/ *yuan*	Price/ *yuan*	Total price/ *yuan*
1	Excavation	62.76	m^3	98.0	6150.5	13248
	C20 shotconcrete	4.18	m^3	375.9	1571.3	
	f 22 mortar bolt	57	m	23.0	1311.0	
	C25 cast-in-place concrete	9.23	m^3	283.4	2615.8	
	Repelling board	58.58	m^2	27.3	1599.2	
3	Excavation	58.58	m^3	98.0	5740.8	10593
	C20 shotconcrete	2.72	m^3	474.1	1289.6	
	f 22 mortar bolt	51	m	23.0	1173.0	
	C25 waterproof concrete	6.51	m^3	367.0	2389.2	

while the maximum tension stress is 1.5 times. But the maximum tension stress in case 3 is agree with that in case 2, and the maximum compression stress in case 3 is 1.3 times of that in case 2, but all less than allowable value. Therefore, the lining style in case 3 is reasonable and economical.

3.4 *Comparisons of composite lining and single shell lining in economics*

On account of space limitation, only comparison of case 1 and case 3 is illustrated in Tab. 3. The contents in Tab. 3 are quantities of work and construction cost per meter.

From Tab. 3, it is clear that single shell lining can save 2655 yuan per meter without consideration of economic benefits caused by increasing work efficiency.

4 CONCLUSIONS

(1) A mechanical model for single shell lining based on contact theory is proposed in this paper, namely to introduce non-thickness contact element to simulate the interaction between surrounding rock and structure, structure and structure on the base of regular nonindividual body model, and then using non-linear finite element method to analyze the stress in single shell lining. Consequently the theory for single shell lining design can be provided.

(2) For composite lining, the maximum compression stress locates at side wall, but maximum tension stress at basement. For single shell lining, both the maximum compression and tension stress locate at side wall.

(3) under the same conditions, single shell lining produced 50%∼80% the internal force of composite lining producing. Another saying is that to produce the same internal force, the thickness of single shell lining could be reduced four times than that of composite lining. Therefore, single shell lining used could reduce excavation and concrete amount. Consequently, the cost of the engineering is dropped.

REFERENCES

[1] GUAN Bao-shu. *Collection of Design Consideration for Tunnel [M]*. Beijing: China Communications Press, 2003.

[2] ZHANG Jun-ru, QIU Wen-ge. Present status and comment of tunnel single shell lining study[J]. *Chinese Journal of Underground Space and Engineering*, 2006, 2(4): 693–699.

[3] WANG Jian-yu. *Technical Progress in Tunnel Engineering [M]*. Bejing: China railway Publishing House, 2004.

[4] LUO Yan-jian. Problem Existed in The Theory and Method of Railway Tunnel Design [J]. *The World Tunnel*, 1997, (5): 8–12.

[5] GUAN Bao-shu. *Generality of tunnel mechanics [M]*. Chengdu: Southwest Jiaotong University Press, 1993.

[6] LI Zhi-ye, ZENG Yan-hua. *Theory and Method of Underground Structure Design [M]*. Chengdu: Southwest Jiaotong University Press, 2003.

[7] MAO Jian-qiang. A Finite Element Approach for Contact Problems and Its Application in Geotechnical Engineering [D]. *Southwest Jiaotong University Doctor Degree Dissertation.* 2002.

[8] GAO Xin-qiang, QIU Wen-ge, GAO Yang. Plane numerical analysis of mechanical behaviors of lining structure under high hydraulic pressure in mountain tunnel[J]. *Rock and Soil Mechanics.* 2005, 26(3): 365–369.

[9] WANG Guo-qiang.*Practical numerical simulation and how to fulfill by ANSYS [M]*. Xi'an: Northwestern Polytechnical University Press, 1999.

[10] ZHOU Shun-hua, GAO Qu-qing, CUI Zhi-jian. The Algortihmic Model of the Release [J]. *Shanghai Journal of Mechanics.* 1997,18(1): 91–98.

[11] TB10003-2005. *Code for Design of Railway Tunnel [S].*

This page intentionally left blank

Underground Space – the 4th Dimension of Metropolises – Barták, Hrdina, Romancov & Zlámal (eds)
© 2007 Taylor & Francis Group, London, ISBN 978-0-415-40807-3

The development of early-high-strength shotcrete and the evaluation of improved tunnel support system

Hiroshi Kanazawa & Takahiko Nishi
Japan Railway Construction, Transport and Technology Agency, Yokohama, Japan

Tsutomu Kiuchi, Shoushi Nishizaki & Yukihiro Furuto
Shimizu Corporation, Tokyo, Japan

ABSTRACT: With an aim of further improvement of high-quality shotcrete, JRTT-Japan Railway Construction, Transport and Technology Agency-has developed high-performance shotcrete showing that its rebound and dust during being placed are remarkably reduced on account of the increased viscosity of the shotcrete owing to the mixture of fine powder and the separation resistance developed by separate mixing. The new high-performance shotcrete is successfully evaluated through its application to more than 120 actual tunnel construction sites for the bullet train, so called Shinkansen. This paper addresses the development of high-performance-early-high-strength shotcrete exhibiting increased strength at young ages based on the accumulated technologies on high-quality shotcrete and the trial construction for the evaluation of improved tunnel support system employing it.

1 INTRODUCTION

Lately the growth of social request for reduction of construction cost for infrastructures in Japan, without exception to the area of railway construction, has strongly encouraged the JRCTT-Japan Railway Construction, Transport and Technology Agency-, who takes charge of railway construction in Japan, to have made effort on saving the cost for construction of Japanese bullet train, so called "Shinkansen". As a means for fulfilling the purpose, development of high-performance shotcrete has been processed to make tunnel supports more effective. The high strength at an early age for the newly developed high-performance shotcrete exhibiting $3\,N/mm^2$ of 10-minute compressive strength has been expected to be capable of simplifying tunnel supports on account of the rapid development of early-age strength. This paper addresses the development of rapid high strength shotcrete at length. Again, developed with an aim of promoting fast tunnel excavation, the high-performance shotcrete has been applied to the trial construction for verifying the appropriateness of fast tunneling employing it. In addition, for the purpose of examining the difference between the conventional shotcrete and the newly developed one with respect to load-carrying capacity, a dense package of monitoring has been implemented to investigate the behavior of tunnel supports under the various patterns of tunnel excavation.

2 DEVELOPMENT OF HIGH PERFORMANCE SHOTCRETE EXHIBITING HIGH STRENGTH AT EARLY AGE

2.1 *Background and process for the development*

High-quality shotcrete is created to reduce the rebound during its installation by separate mixing with the use of silica fume and fine lime powder. This study aims the enhancement of tunnel support in a way that development of high strength at an early age on the basis of the preceded technologies puts high-performance shotcrete into practical use.

Regarding the method for gaining early-age high strength, a high-strength admixture is added to base concrete so that the accelerator mainly consisting of extra accelerating cement minerals is utilized to facilitate quick setting. This principle for gaining the high-early-strength can be accomplished in such a way that the structure of cement concrete is densified by the help of ettringite which is fine needle-like crystals created owing to the hydration between the high-strength admixture and the accelerator. In this study, the practical mix designs for high-early-strength shotcrete are suggested based on the optimum mix proportion of

concrete for the target strength of 3/Nmm^2 after 10 minutes. The procedure for the development can be summarized as the following three steps;

(1) Indoor mortar test
(2) Shotcrete test at outdoor model tunnel
(3) In-situ field shotcrete test at actual tunnel site

2.2 *Indoor mortar test*

With an aim of concentrating achievement of a practical mix design for shoctrete as well as the required strength, flow values, setting times and strength characteristics of mortar with varying design mixes have been evaluated.

Table 1 and Table 2 shows the materials used for the indoor mortar tests and range of mix designs, and the results from the indoor mortar tests, respectively.

From Table 2, it is easily understood that the compressive strength at the 10-minute age demonstrates a good correlation with the accelerator added to the mixture, and as the amount of accelerator is increased, the compressive strength also appears to increase. Although it is shown by the test that a few of design mixes can achieve 10-minute compressive strengths greater than 3 N/mm^2, the pursuit of economical design imposes adoption of a dosage of (Cement and Silica fume) 400 kg/m^3, 12% of high strength admixture and accelerator as the mix design for the shotcrete test planned in the next step.

Table 1. Materials used in mortar tests for high early strength shotcrete.

Item	Specification
Cement (C)	Ordinary Portland cement
Silica fume (SF)	$SiO_2 \geqq 9$ % Specific surface area $\geqq 15$ m^2/g
Lime fine powder (LM)	Grain size $\leqq 0.147$ mm
High-strength admixture (H)	Ettringite admixture
Accelerator	Extra accelerating cement minerals

2.3 *Shotcreting test in model tunnel*

The shotcreting test has been implemented as well to examine the pumpability of mixture, pulsating motions of conveying hose, rebound and so forth as to verify the reproducibility of shotcrete designed with reference to the indoor mortar tests. The mix designs in Table 3 obtained from the indoor mortar tests are utilized for the test.

The shotcreting has been executed at the model tunnel with 5.5 m in width, 4.5 m in height and 20 m in length.

Table 4 describes the compressive strengths of concrete. Every specimen from each mix design has shown approximately 5 N/mm^2 in compressive strength at the age of 10 minutes which is greater than that of the mortar in the indoor tests. This result could be attributed to the existence of coarse aggregate and accelerator well mixed in the concrete.

2.4 *Field in-situ testing of shotcreting at Mineyama tunnel*

A series of field in-situ shotcrete tests have been carried out to examine the reproducibility of model shotcrete test using the material and equipments in an actual working tunnel which is a part of Mineyama

Table 2. Results from mortar tests.

Mix	Cement kg/m^3	Silica fume kg/m^3	High-strength Additive %*1	Water kg/m^3	Water/ binder*2 %	Accelerator %*1	Compressive strength N/mm^2					
							10 minutes	1 hour	3 hours	1 day	7 days	28 days
1	408	22	10	200	42.5	10	2.8	7.8	12.1	15.3	59.3	74.0
2	408	22	8	200	43.2	8	2.4	6.4	10.4	11.1	60.3	75.6
3	408	22	10	190	40.3	10	3.9	10.5	13.9	17.7	66.8	76.0
4	408	22	8	190	41.1	8	2.9	7.0	11.7	11.4	58.6	65.3
5	380	20	12	200	44.9	12	3.4	9.2	11.6	17.8	54.3	62.6
6	380	20	10	200	45.7	10	2.7	6.7	8.9	12.3	53.0	62.0
7	380	20	12	190	42.7	12	3.8	11.2	14.0	19.0	58.7	68.1
8	380	20	10	190	43.5	10	2.9	7.0	10.4	14.7	59.0	67.0
9	361	19	12	200	47.3	12	2.7	8.1	10.8	15.1	48.8	56.7
10	361	19	10	200	48.1	10	2.0	6.5	10.0	11.4	50.3	55.2
11	361	19	8	200	48.9	8	1.4	3.6	6.2	6.9	48.1	56.2
12	361	19	12	190	44.9	12	3.0	9.8	13.9	18.5	53.2	63.5
13	361	19	10	190	45.7	10	2.4	6.8	10.8	13.0	55.6	60.2
14	361	19	8	190	46.5	8	1.7	4.4	8.4	8.5	53.8	62.1

*1: Ratio to (Cement + Silicafume), *2: Binder = Cement + Silicafume + Additive.

tunnel construction site. With a viewpoint of economical aspect, the optimum mix proportion with accelerator and high-strength admixture has been adapted for the in-situ field tests for shotcrete.

Table 5 shows the mix design of shotcrete. Because the Mineyama tunnel employed three types of mixed cements consisting of cement, silica fume and lime fine powder with varying dosages, the same materials have been utilized in the in-situ filed shotcrete test.

To achieve an economical mix design, characteristic of strength development, construction efficiency and spraying nature are evaluated with the dosages of high strength admixture and accelerator changing as 12%, 10%, 8% and 12%, 10%, 8%, 6% for each, as shown in Table 6.

Table 7 indicates the re-testing results. Comparing the two mix proportions, it can be found that the Mixes A_{12-8} with a large content of high-strength admixture come to produce high strength at the age longer than 7 days while the Mixes B_{11-10} with a large content of accelerator come to yield high strength at the age not longer than 1 day.

Considering these characteristics of the high early strength shotcrete, the shotcrete test was carried out again under varying temperature, on the dosage of accelerator 9% against a fixed high-strength admixture content of 11%. This test provided approximately

Table 6. 10-minute compressive strength of shotcrete (N/mm^2) with variation of mix proportion in Shotcrete test.

Mix	High strength additive (%)	Accelerator (%) 12	10	8	6
A	12	3.84	3.25	3.07	1.95
		3.78	3.01	3.60	2.36
		4.24	3.72	3.25	2.48
B	11	3.54	2.95	2.53	2.48
		3.83	3.42	2.93	2.24
		3.71	3.07	3.13	2.18
C	10	2.71	2.48	2.54	1.86
		3.30	3.07	2.83	2.10
		3.13	3.07	2.48	2.46

Table 3. Mix designs in simulation tests for shotcreting.

Mix	Sand/ aggregate %	Water/ binder %	Water kg/m^3	Cement kg/m^3	Silica fume kg/m^3	Limestone powder kg/m^3	Sand kg/m^3	Coarse aggregate kg/m^3	High-strength additive kg/m^3 (%*)	Accelerator kg/m^3 (%*)
1	80	44.6	200	380	20	141	1232	345	48 (12)	48 (12)
2	70	42.4	190	380	20	125	1094	525	48 (12)	48 (12)

*: Ratio to (Cement + Silicafume).

Table 4. Compressive strength of concrete in shotcreting test.

Mix	Shotcreting equipment	Pullout test 10 minutes	1 hour	3 hours	1 day	Core sample test 7 days	28 days	Base concrete 7 days	28 days
1	Pump type	4.9	5.6	7.7	21.3	33.6	47.0	33.3	58.7
2	Rotor type	6.3	–	6.8	25.1	36.5	50.7	35.1	60.7
2	Pump type	5.4	–	6.4	25.8	43.5	58.2	35.1	60.7

Table 5. Mix designs in in-situ shotcrete at Mineyama tunnel site.

Mix	Sand/ aggregate %	Water/ binder %	Water kg/m^3	Cement kg/m^3	Silica fume kg/m^3	Limestone powder kg/m^3	Sand kg/m^3	Coarse aggregate kg/m^3	High-strength additive kg/m^3 (%*1)	Accelerator kg/m^3 (%*1)
A	70	44.6	200	380	20	127	1070	529	48 (12)	24–48 (6–12)
B	70	45.0	200	380	20	127	1073	530	44 (11)	24–48 (6–12)
C	70	45.5	200	380	20	127	1076	531	40 (10)	24–48 (6–12)

*1: Ratio to (Cement + Silicafume).

Table 7. Compressive strength of shotcrete at various ages in the in-situ shotcrete test at Mineyama tunnel site.

Mix	Additive %	Accelerator %	Compressive strength (N/mm^2) 10 min.	3 hours	1 day	7 days	28 days
A_{12-8}	12	8	2.83	4.30	20.2	39.6	50.4
			3.43	5.50	20.2	43.3	–
			3.33	6.00	21.2	42.0	–
B_{11-10}	11	10	3.54	6.06	20.2	35.2	41.4
			3.33	4.34	21.7	35.7	–
			3.54	6.57	21.2	32.3	–

constant compressive strength reaching more than 3 N/mm^2 for every mix proportion including even the case with a dosage of accelerator reduced by 9% under varying temperature.

Based on the above results, the mix B with 11% of high-strength admixture and 9% of accelerator has been adopted for the main tunnel at the Mineyama tunnel site.

3 APPLICATION OF EARLY-HIGH-STRENGTH SHOTCRETE TO JOB SITE

High-performance early high strength shotcrete is applied to the Mineyama tunnel in the section between Joetsu and Toyama of the Hokuriku Shinkansen, promising a rapid transportation means in the Hokuriku Region. The geological profile are shown in Figure 1. The rock masses of the tunnel section consist mainly of soft rock on the basis of mudstone in the Noudani Formation of Neogene (Miocene to early Pliocene) age. The tunnel is driven by the large partial tunnel face excavation machine. To improve the efficiency and speed of construction, this site has employed the machinery facilities which required appropriate tunnel supports corresponding to the updated driving speed. For that intention, a new tunnel support combined with high-performance early high strength shotcrete has been suggested and its applicability has been verified. The length of the section employing the new tunnel supports extends up to 3,790m out of total length of 7,090 m accounting for approximately 65%. The other section of tunnel has been driven with the conventional supports utilizing steel supports. The driving speed in the new support section has exhibited 304 meters per 1 month, which is recorded as the highest speed of mechanical tunnel driving with NATM.

4 TRIAL CONSTRUCTION

The trial construction has been executed to estimate the different driving methods for a certain part of the Mineyama tunnel. It is intended to evaluate the practical applicability of newly suggested tunnel support employing high-performance-early-high-strength shotcrete through investigating the behavior of rock mass and tunnel supports according to the varying driving speeds and patterns of tunnel supports. Figure 1 shows the geological profile of Mineyama tunnel.

4.1 *Outline of trial construction*

In the trials, the pattern of tunnel excavation described in Table 8 are prepared to compare the effects of varying driving speeds and tunnel supports on the behavior of surrounding rock mass.

In the section of trial construction, monitoring has been carried out as shown in Figure 2. Detail of the monitoring is shown in Table 9.

4.2 *Monitoring during trial construction*

4.2.1 *Behavior of inner section*

Figure 4 and Figure 5 show the settlement at crown and convergence of inner section monitored during 140 days from the beginning of trial construction. The convergence of inner section has been obtained by monitoring the horizontal line at S.L.+1.5 m.

The results of monitoring provide the findings as follows;

- The ordinary advancing with the A tunnel support shows larger settlements at crown than those of the fast advancing with the A tunnel support and the ordinary advancing with the B tunnel support. This behavior, on the contrary to performance of the shotcrete strength, may be due to the local change of the ground condition.
- By the way, regarding the convergence, the ordinary advancing with the A tunnel support comes to produce relatively small convergence compared with the fast advancing with the A tunnel support and ordinary advancing with the B tunnel support.
- From the results of settlement and convergence, in spite of the smaller thickness of shotcrete, it is understood that the new tunnel support can decrease the settlement and convergence of the tunnel comparing to the conventional high performance shotcrete combined with steel support.

4.2.2 *Behavior of tunnel support*

Figure 5 shows the monitoring results about stresses developed in shotcrete, which provide the following findings;

- The measured stresses in the early-high-strength shotcrete adopted in the A tunnel support appears to be relatively higher than that in the conventional shotcrete employing high-quality shotcrete.

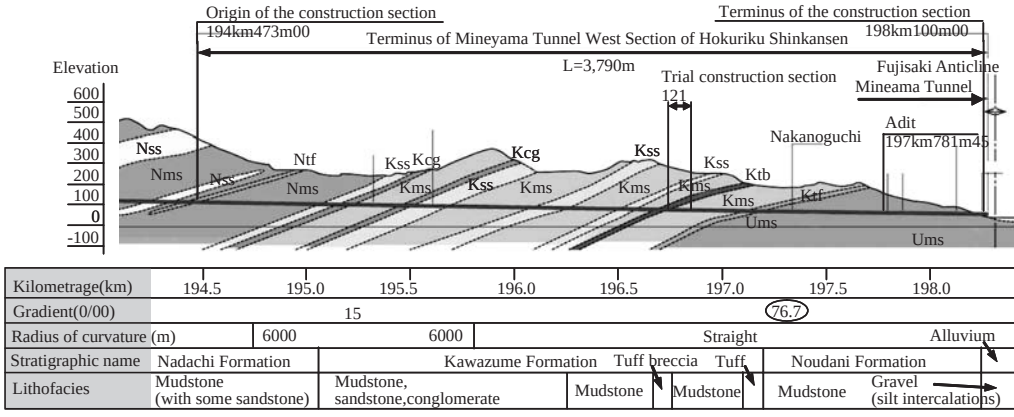


Figure 1. Geologic profile.

Table 8. Patterns of tunnel excavation at trial construction.

Pattern	Speed of advance m/month	1 cycle length m	Pattern of tunnel support			
			Type	Shotcrete	Rockbolt	Steel support
Fast advance Support-A	250	1.5	A tunnel support	High-performance early-high strength t = 10 cm	L = 3 m n = 14	–
Ordinary advance Support-A	100	1.0			ctc = 1.0 m	
Ordinary advance Support-B	100	1.0	B tunnel support	High-quality t = 15 cm	Same as above	H-125 ctc = 1.0 m

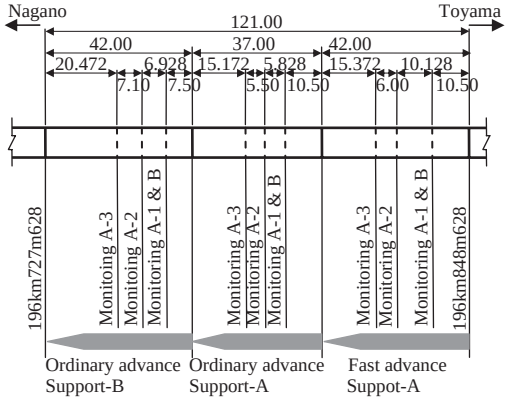


Figure 2. Location of monitoring.

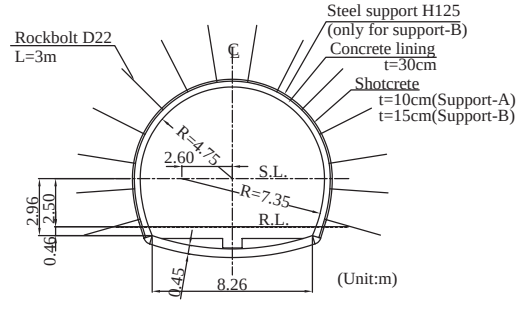


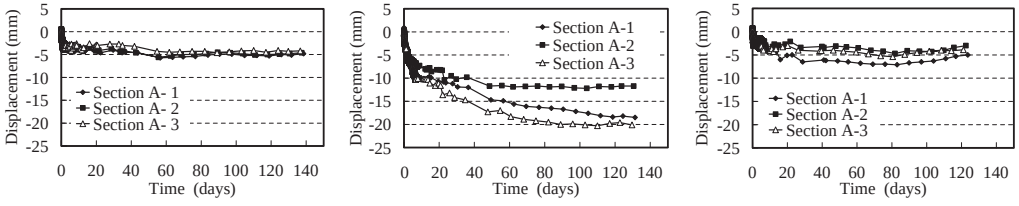
Figure 3. Tunnel support pattern.

- Although the stresses in the B tunnel support combined withsteel support show a steady increasing tendency for all measuring points, those in the A tunnel support appear to decrease after a certain point in elapsed time, moreover some of them falldown under the zero, which means occurrence of tensile stress. This observation indicates that the shotcrete without steel support is supposed to behave in conjunction with structural changes accompanied by cracks caused by drying shrinkage and ground pressure. while that with steel support appears to steadily behave without abrupt change by virtue of stiffness of the steel support imposing restraint of deformation.

Table 9. Detail of monitoring.

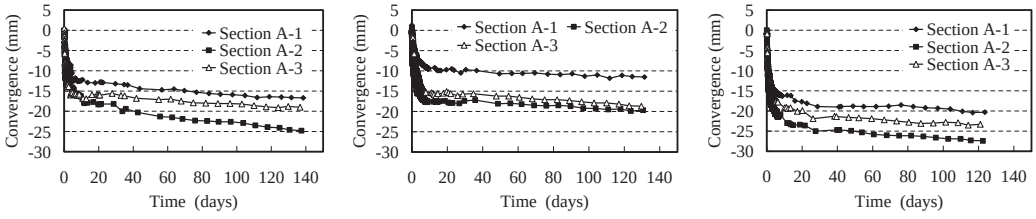
Monitoring	Measurement
A	Convergence Settlement of crown and foot
B	Shotcrete stress Shotcrete strain Axial stress of Rockbolt Stress of steel support Ground displacement Displacement of ground ahead of face

- The large resultant stress of shotcrete observed may be due to the high stiffness of early-high-strength shotcrete at young age. It indicates early load-carrying capacity as a tunnel support, and may be considered as a substitute for steel support having function of support against ground pressure until the conventional shotcrete takes effect in accordance with time passed. Furthermore, it is expected that its high strength at early age, strongly required to increase advancing speed of tunneling, can make a contribution to assure safe excavations, which has been quite difficult because of the weak strength at young ages for the conventional shotcrete.



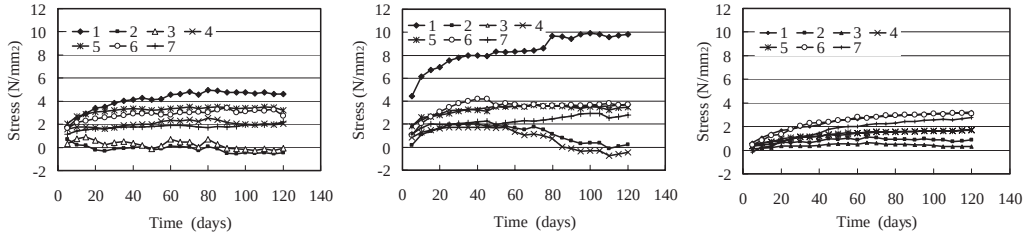
(a) Fast advance, Support -A (b) Ordinary advance, Support-A (c) Ordinary advance, Support-B

Figure 4. Crown settlements.



(a) Fast advance ,Support -A (b) Ordinary advance ,Support-A (c) Ordinary advance ,Support-B

Figure 5. Convergences at S.L. + 1.5 m.



(a) Fast advance ,Support-A (b) Ordinary advance ,Support-A (c) Ordinary advance ,Support-B

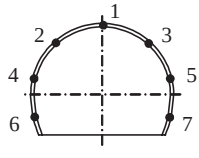


Figure 6. Stresses developed in shotcrete.

5 CONCLUSION

- The high-performance-early-high-strength shotcrete showing a compressive strength of 3 N/mm^2 after 10 minutes has been developed in this study, and suggested is the mix design that satisfies the requirements from both applicability to job sites and economical aspect.
- The application of high-performance-early-high-strength shotcrete to the Mineyama tunnel has clearly shown that the newly suggested tunnel support employing the high-performance-early-high-strength shotcrete without steel support can be appropriate for a practical use with sufficient safety, at the same time, for enhancement of advancing speed of NATM tunnel.
- The characteristics of tunnel supports have been successfully investigated through the trial construction providing comparison of the behaviors of the conventional tunnel support combined with steel support and the new tunnel support employing early-high-strength shotcrete without use of steel support.
- The comparative trial construction has informed that the new tunnel support has load carrying capacity no less than that of the conventional tunnel support, furthermore can make a contribution to increasing speed of tunnel excavation by virtue of its early-high strength facilitating safe excavation of tunnel face within a short time after installation of the shotcrete.

This page intentionally left blank

Underground Space – the 4th Dimension of Metropolises – Barták, Hrdina, Romancov & Zlámal (eds)
© 2007 Taylor & Francis Group, London, ISBN 978-0-415-40807-3

Study on a strength characteristic and a quality control of the high-quality shotcrete which aimed at single-shell structure of a tunnel lining

T. Tosaka
Japan Railway Construction, Transport and Technology Agency(JRTT), Yokohama, Japan

T. Asakura
Kyoto University, Kyoto, Japan

T. Abe
Railway Engineering Co., Ltd, Tokyo, Japan

Y. Ito
Ishikawajima Construction Materials Co., Ltd, Ayase, Japan

M. Suenaga
Sumiko Consultant Co., Ltd, Tokyo, Japan

ABSTRACT: Japan Railway Construction, Transport and Technology Agency (JRTT) has applied High-Quality Shotcrete (HQSC) to a supporting member of the tunnel for the New Bullet Train Projects (Hokkaido, Tohoku, Hokuriku, and Kyushu) since fiscal 1997. The number of construction sites using HQSC is beyond 120. The feature of HQSC makes rebound and dust lower, and improves the quality of lining. In this papers, various studies on HQSC such as the site mix, the strength of the ages, the physical properties of fine aggregate are described. Furthermore, the FEM analysis is conducted in order to estimate the stress distributions in and around shotcrete lining. On the basis of the results, it is proposed that the selection method of natural ground and the lining applied the single-shell structure with HQSC.

1 INTRODUCTION

Japan Railway Construction, Transport and Technology Agency (JRTT) has applied High-Quality Shotcrete(1) (HQSC) to a supporting member of the tunnel for the New Bullet Train Projects (Hokkaido, Tohoku, Hokuriku, and Kyushu) since fiscal 1997. The number of construction sites using HQSC is beyond 120. HQSC is a advanced shotcrete, which limestone powder and silicafume are used, and made with two stage mixing method(2). The more powder is mixed in concrete, the higher viscosity and strength becomes. This feature of HQSC makes rebound and dust lower. Furthermore, HQSC helps to keep the quality of lining constantly and to save the cost of tunnel construction.

In this research, various studies on HQSC such as the site mix, the strength of the ages and the physical properties of fine aggregate are studied. These studies clarify the characteristic of the fine aggregate effecting to the performance of HQSC. Furthermore, the results of the strength test of the core samples gathered from construction sites indicate the large value of 27.2 N/mm^2 and the small variation of 8.6% in average. This fact suggests that there is a possibility of raising the conventional design strength of 18 N/mm^2 up greatly.

It is judged that the tunnel lining by using good quality shotcrete allow the design of the single-shell structure with HQSC. Therefore, the FEM analysis is conducted in order to estimate the stress distributions in and around shotcrete lining. On the basis of the results, authors propose the selection method of natural ground and the lining applied the single-shell structure with HQSC. The adoption of a single-structured tunnel lining, which would eliminate the need for secondary lining, would be immensely profitable since it would allow smaller excavation cross-sections, improve the execution cycle, and would not require the use of the centering for a secondary lining. Therefore, it should contribute significantly to the reduction of costs for

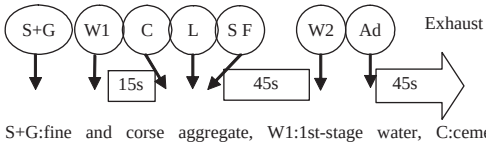
constructing new tunnels, as well as for renovating existing tunnels.

2 OUTLINE OF HIGH-QUALITY SHOTCRETE

HQSC is a Shotcrete of a new type characterized by substituting a part of the fine aggregate by a lime stone powder, and mixing silicafume. The feature of HQSC is the mix proportion with much binder. Therefore, plastic viscosity of concrete can be increased. Other features are low rebound and decrease of dust, increase of strength, stabilization of quality, and reduction in construction cost.

About the specified mix proportion, 5% of the weight of cement is substituted by the silicafume, and total weight of binder are set on 360 kg/m^3. The weight of a limestone powder was set for weight in which the fine aggregate of the particle size 0.15 mm or less was added to become 15% of the all up weight of the fine aggregate.

Moreover, about HQSC, two stage mixing method are introduced in concrete mixing process, to promote a viscous effect of a fine powder. The feature of two stage mixing method is to be poured into concrete by dividing into the first water to which water is provided by the examination beforehand and the water of the remainder (the second water). As the results, the mixed powder (cement, silicafume, and limestone powder) is dispersed by the first water and the paste film of a low water cementitious material ratio consisted by is formed around fine aggregate. Example of the mixing flow chart is shown in Figure 1, and example of mix proportion at the site is shown in table 1 respectively.



S+G:fine and corse aggregate, W1:1st-stage water, C:cement, L:limestone powder, SF:silica fume, W2:2nd-stage water, Ad:superplasticizer

Figure 1. Example of the mixing flow chart.

Table 1. Example of site mix proportion.

Gmax (mm)	Slump (cm)	W/(c + SF) (%)	s/a (%)	Content(kg/m^3) Water	Cement	Silica fume	Fine aggregate	Limestone powder	Corse aggregate	Admixture
10	8 ± 2	59.7	61.7	215	242	18	994	87	689	2.124

3 INFLUENCE OF FINE AGGREGATE PROPERTIES ON STRENGTH OF HIGH-QUALITY SHOTCRETE

3.1 *Fine aggregate properties and mix proportion classified into regional*

The distribution situation of the kind of the fine aggregate in Tohoku, Hokuriku, and Kyushu various places are shown in Figure 2. According to this Figure, as for the fine aggregate in the Kyushu region, the crushed sand is a main source, and also as for the fine aggregate in the Tohoku region, the crushed sand including mixed sand is a main source. On the other hand, in the Hokuriku region, natural sand such as the river and the mountain sand is a main source, and the lime stone is used as a raw material for the crushed sand.

Regional comparisons with physical properties of fine aggregate are shown in Table 2. In the fine aggregate properties, it was confirmed that there were differences in the mean value and the coefficient of variation. The cause is difference of distribution situation of kind of fine aggregate. The weight of a limestone powder (L) was set for weight in which the fine aggregate of the particle size 0.15 mm or less ($S_{0.15}$) was added to become 15% of the all up weight of the fine aggregate. Therefore, the amount of the unit of L can be decreased when $S_{0.15}$ is large.

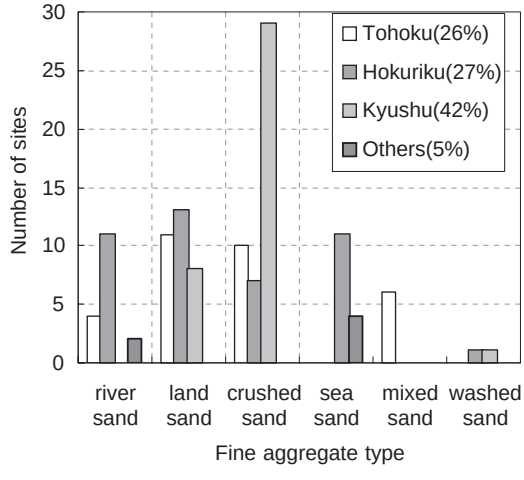


Figure 2. Regional distribution of fine aggregate type.

The regional mixing factor of HQSC is shown in Table 3. $S_{0.15}$ and β_{OH} are different according to the difference of a regional fine aggregate property, and unit weight of binder (B) and the first water cement ratio (W1/B) have varied greatly. The change in these mixing factors exerts a large influence on plastic viscosity, workability, and the mechanical properties of HQSC.

3.2 *Mechanical properties l*

Daily quality control for strength of HQSC was analyzed from the construction results of three Shinkansen tunnel group in Tohoku, Hokuriku, and Kyushu. Results of daily quality control for strength are shown in Table 4. The site data is classified by the site, and also had been calculated to average strength, standard deviation, the coefficient of variation, and design strength, according to the material age. The calculation of design strength of concrete is determined by the method of Japanese Society of Civil Engineers (JSCE), which requests the lower bound value that satisfies the dangerous rate 10% for the mean value (see equation (1)).

$$f'_{ck} = f'_{m} - 1.64 \times \sigma \quad (1)$$

where f'_{ck} = Design strength; f'_{m} = Average strength; and σ = Standard deviation.

According to Table 4, the average concrete core strength at 28day (core f′c(28)) of all sites was 27.2 N/mm^2, and this value was higher than the ordinary shotcrete. Therefore, average value of design strength calculated by JSCE method was 22.3 N/mm^2. Moreover, the coefficient of variation of core f′c(28) is 8.6%, and it corresponds to the value in the general ready mixed concrete plant. Even if the region of site and kind of fine aggregate are different, when same aggregate is used on each site and when the daily quality control in the plant is suitable, it is considered that the change is small.

Table 3. Regional mixing factor of HQSC.

Region	Item	Mean value	Maximum value	Minimum value
Tohoku	α(%)	23.7	26.0	22.0
	L(kg)	90	110	55
	B(kg)	450	470	415
	W/B(%)	48.1	52.0	46.0
	W1/B(%)	29.4	40.8	21.6
	$S_{0.15}$(%)	7.0	10.0	5.0
	β_{OH}(%)	2.5	8.0	0.1
Tohoku	α(%)	22.9	26.0	22.0
	L(kg)	103	118	90
	B(kg)	463	478	450
	W/B(%)	45.2	48.0	38.0
	W1/B(%)	26.0	28.8	24.3
	$S_{0.15}$(%)	5.9	7.0	5.0
	β_{OH}(%)	1.6	2.4	0.8
Kyushu	α(%)	22.4	25.0	21.0
	L(kg)	76	97	40
	B(kg)	437	458	400
	W/B(%)	49.9	55.8	47.0
	W1/B(%)	28.5	32.7	24.3
	$S_{0.15}$(%)	8.4	12.0	6.0
	β_{OH}(%)	2.8	7.7	1.3

Table 4. Results of Daily quality control for strength.

Item	Target strength*1 (N/mm^2)	Mean strength (N/mm^2)	Standard deviation (N/mm^2)	Design strength*2 (N/mm^2)
3hr	1.5	2.4	0.5	1.7
24hr	8.0	11.1	1.5	8.7
28day(core)	18.0	27.2	2.4	23.3
28day (Controled)	18.0	34.1	3.0	29.0

*1:Indicated in Ref. (1), *2:Calculated by JSCE method

Table 2. Regional comparisons with physical properties of fine aggregate.

Region	Item	Density under saturated surface dry (g/cm^3)	Absorption Q(%)	Percentage of solid volume (%)	Content rate of particle size 0.15 mm or less (%)	F.M.	β^{*2}_{OH} (%)
Tohoku	Mean value	2.66	2.4	63.8	7.0	2.58	2.5
	V*1(%)	1.0	26.4	2.8	13.3	7.44	67.5
Hokuriku	Mean value	2.59	2.1	65.6	5.9	2.84	1.6
	V*1(%)	1.5	30.5	2.8	13.1	3.65	28.5
Kyushu	Mean value	2.63	1.4	62.8	8.4	2.64	2.8
	V*1(%)	3.4	29.1	5.9	14.0	6.47	38.4

*1:Coefficient of variation, *2:Bind water ratio of fine aggregate

4 STRESS ANALYSIS OF SINGLE-SHELL STRUCTURES USING HIGH-QUALITY SHOTCRETE

In the NATM, execution management is carried out by field monitoring, which consists of measurements taken as a routine procedure for the estimation of ground properties, and detailed and concentrated measurements taken in areas of relatively unfavorable ground conditions that are generally carried out separately from the former. The routine monitoring for estimation of ground properties combines the crown settlement measurement and horizontal relative convergence measurements taken near the springline with several other convergence measurements. These data are utilized for determining the appropriateness of the supports in the vicinity of the cutting face and auxiliary construction methods, as well as for making the decision on the timing of concrete lining. Therefore, the measurements are taken at extremely short distance intervals, regardless of the ground property conditions, and continued until the convergence subsides. Thus, authors have decided to use the field monitoring data as the basic data for investigating the applicable range of shotcrete as the permanent structure. In the first step of the investigation, the relationship between the tunnel convergence and soundness of the shotcrete was determined based on the field monitoring data. Then, a back analysis was performed to calculate the physical properties, or the applicable range, of the shotcrete and the ground properties. Furthermore, the results were used to determine the applicable range, proposed later in this paper, of the shotcrete that could withstand use as the permanent structure for a given tunnel convergence.

4.1 *Results of field measurements and soundness of the shotcrete*

The measurement data used here are those from the 21.498 km stretch for which excavation has been completed for the Iiyama Tunnel, which is the longest tunnel between Nagano and Toyama prefectures in the Hokuriku Shinkansen (bullet train) railway that should measure 22.225 km when completed. The thickness of the shotcrete is either 15 or 20 cm, with nearly the same number of data points for each. Note that the ground properties for the tunnel displays expansive characteristics, and that the data for sections with steel-fiber-reinforced shotcrete (SFRSC) or which have undergone additional shooting have not been included. Of the measurement data taken for routine field monitoring, the data for horizontal relative displacement measurement taken near the springline and the crown settle measurement are used in the investigation due to their stable data acquisition conditions and availability of data from the earliest stages in the construction.

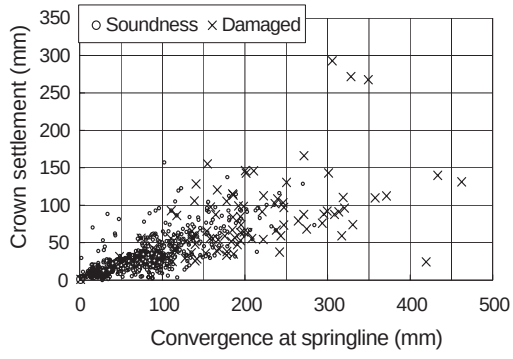


Figure 3. Relationship between horizontal relative displacement and crown settlement.

Figure 3 shows the relationship between the horizontal relative displacement and crown settlement, with symbols representing the soundness of the shotcrete evaluated from the observation records of the tunnel walls. The range of measurement includes a total of 899 data points for horizontal relative displacement up to 500 mm and crown settlement of 300 mm. The open circles in the figure denote sound concrete conditions, and crosses denote points where some form of damage to the concrete had been reported. It can be seen from the figure that damage to the shotcrete appears with increasing frequency. However, there seems to be no clear boundary between soundness and amount of damage, and a gradual loss of soundness and conversion to the damaged state occurs in the shotcrete with progressive convergence. To clarify this point, the convergence data were divided into groups and the proportions of data points with damaged shotcrete out of all data points in each group were calculated. In analyzing the data, the damaged states were categorized by cause of the damage, i.e. whether they were due to the horizontal convergence or crown settlement. Taking into consideration that the horizontal convergence is the sum of displacements of the right and left tunnel wall surface, the threshold value for the horizontal convergence can be regarded as twice that of the crown settlement.

The result of the horizontal convergence is shown in Figure 4. It can be seen from Figure 4 that nearly all data points for the group having horizontal convergence smaller than 100 mm (or crown settlement less than 50 mm) belong to the group of sound concrete condition. If the ratio of displacement between the horizontal convergence and crown settlement is taken into account, then it can be concluded that the point at which the concrete loses its soundness is consistent in both cases.

Figure 5 shows the details for horizontal convergence, which has more data points than crown

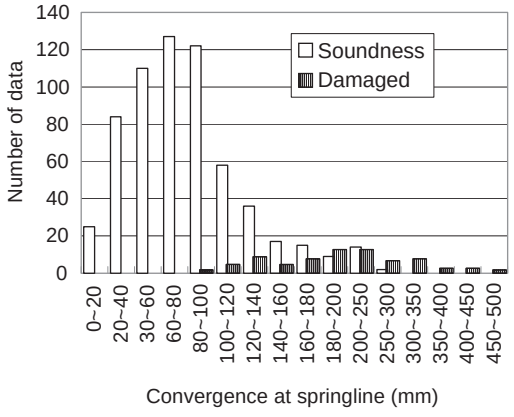


Figure 4. Relationship between displacement and soundness of shotcrete.

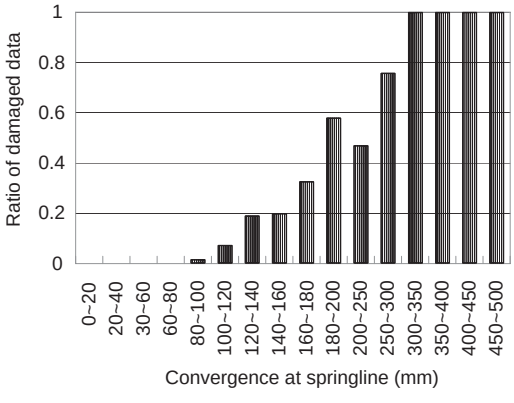


Figure 5. Relationship between convergence and ratio of damaged data.

settlement. For data points where the horizontal convergence is less than 100 mm, damage to concrete occurs in only several percent of the cases. At a convergence larger than 100 mm, there is a sharp increase in the rate of damaged concrete, and at a convergence exceeding approximately 300 mm, all of the data points fall into the damaged state. These results imply that the soundness of shotcrete may be maintained up to a horizontal convergence of 100 mm.

4.2 *Evaluation of the physical properties of shotcrete as support*

It is widely known that the physical strength of shotcrete as tunnel supporting structures must be evaluated lower than those of concrete structures at an age of 28 days. One of the reasons for this is that the occurrence of displacement is restricted to the relative vicinity of the excavation point, except in rare cases where ground properties results in strong temporal dependency in displacement.

Based on the theory of elasticity, it is generally believed that dominant displacement occurs within the 2D range (distance) from the cutting face. In the case of a tunnel for a double-track bullet train having an inner radius of about 10 meters, the 2D range is normally excavated in two to five days. Thus, the shotcrete suffers the effects of displacement during the early age of extreme weakness, resulting in decreased rigidity, including time-dependent rigidity. Also, there is the reduction in effective rigidity caused by drying shrinkage, etc., and so the rigidity of shotcrete must be estimated to be smaller than the rigidity at 28 days. Furthermore, tunnels are often excavated by dividing the cross section of the tunnel, such as in the short bench method, and phenomena such as subsidence of the entire structure caused by the subsidence of the foot and displacement resulting from the small resistance before lining closure are often experienced. There are also structural problems such as the absorption of displacement by the plasticity on the backside of the support, and so the overall rigidity of the shotcrete as a structure must be estimated to be smaller than in normal conditions.

In the present case, the rigidity of the shotcrete will be employed for the single-shell structure, so the structural rigidity was evaluated based on the relationships between concrete strength, convergence, and concrete damage. As stated in Section 3.2, the failure strength of shotcrete is about 27 MPa. On the other hand, the displacement at which shotcrete begins to suffer damage is about 100 mm in the case of horizontal convergence, as stated above. Therefore, using the values of horizontal convergence and crown settlement at which concrete damage is initiated, the modulus of elasticity for when the maximum stress acting on the shotcrete reaches the failure strength was calculated by back analysis and evaluated.

In Figure 6, the two points at which damage to the shotcrete is initiated are extracted, and the effective modulus of elasticity of the shotcrete was calculated by back analysis. The horizontal axis represents the modulus of elasticity of the ground. It can be seen from this figure that there is a tendency for the modulus of elasticity of the shotcrete to decrease with increasing rigidity of the surrounding ground, even for the same amount of convergence. However, the amount of reduction is small, and when combined with the fact that the single-shell method is applied only to regions of relatively good ground properties, it can be concluded that the effects of rigidity of the surrounding ground may be ignored and only the convergence needs to be considered. As a result, the effects of rigidity of the surrounding ground may also be ignored in assessing the soundness of the shotcrete.

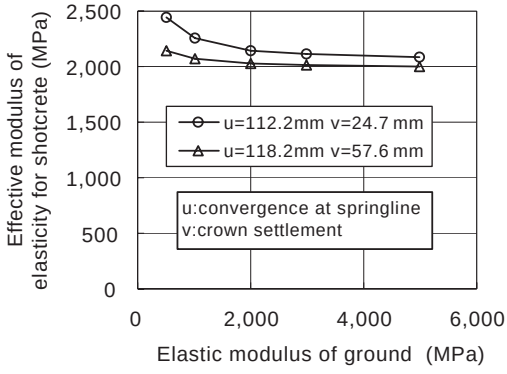


Figure 6. Effective modulus of elasticity for shotcrete.

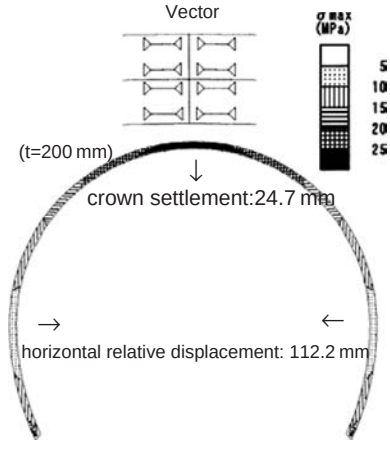


Figure 7. Results of stress analysis.

When determining the applicable range for the single-shell method based on convergence, the deformation capacities of the shotcrete must be taken into account, and so the larger effective modulus of elasticity must be chosen. When a modulus of elasticity of 500 MPa is assumed for grounds with relatively small rigidity, the effective rigidity of shotcrete should be about 2,500 MPa. For a more realistic range of application in which the ground condition is hard rock having a modulus of elasticity of 2,000 MPa, the effective modulus of elasticity of the shotcrete should be about 2,200 MPa. There is no significant difference between the two values, and the latter value is selected for the discussions that follow.

4.3 *Stress of the shotcrete and applicable range of the single-shell structure*

The single-shell structure is required to satisfy the function of the primary support that handles the conventional load placed by excavation, as well as the function of the secondary concrete lining, which is a permanent structure. Thus, it must sufficiently withstand the applied load, and at the same time, a simple management method must be developed for the safety assessment of the single-shell structure. Generally, the safety single-shell structures are assessed mainly by the horizontal relative convergence and crown settlement measurements taken during routing field monitoring practices. Thus, no additional measurements are made for the purpose and judgments are made based on the information available in conventional routine monitoring works. Needless to say, visual inspection compliments the above assessment. On the other hand, damage to shotcrete is initiated at a convergence exceeding 100 mm, as shown in Figure 5. However, damage to the entire structure does not appear until the convergence exceeds 300 mm, and between 100 and 300 mm, there is a gradual increase in the probability of damage to the concrete. Therefore, by assuming that the breaking point of concrete had been reached when the damage is initiated, calculations can be made on the safe side. Furthermore, by setting an appropriate value for allowable stress and carrying out the design based on such, it is believed that the safety factor may be secured.

The inverted part was not included in the range of the singe-shell structure, and the ends at which stress concentration occurs were excluded from the range of stress investigation. However, in the results of the present survey, these ranges are included in the inspection and judgment for damage to shotcrete. In the previous section, it has been shown that the effective modulus of elasticity, failure strength, and allowable stress for the shotcrete used in the investigation of the applicable range and convergence of single-shell structure were about 2,200 MPa, 27 MPa, and 23 MPa, respectively.

Figure 7 shows the results of stress analysis using these data. It can be seen from the figure that the single-shell structure is thin, and that the displacement in the applicable range is small. Furthermore, it can be seen that within the target range of the investigation of the single-shell structure, there exists a stable stress condition in which the axial force predominates due to the lack of excessive unsymmetrical earth pressure. However, note that that the generation of a bending moment is observed at the ends due to stress concentration.

Based on these results, the relationship to the applicable ranges of horizontal relative convergence and crown settlement for failure strength and allowable stress were determined and presented in Figure 8. It can be seen from the figure that the applicable ranges for the allowable stress for single-shell structure may be set up to 90 mm and 55 mm for horizontal relative convergence and crown settlement, respectively.

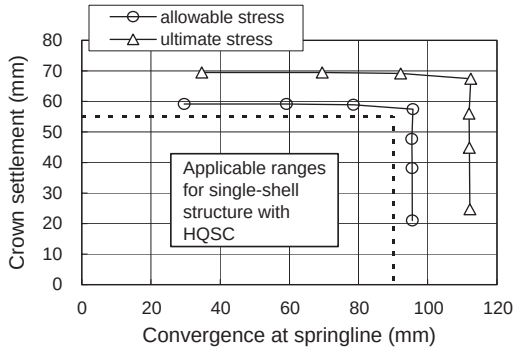


Figure 8. Applicable area to single-shell structure with HQSC.

5 CONCLUSIONS

In this study, execution management data for over 120 locations under the jurisdiction of the Japan Railway Construction, Transport, and Technology Agency were analyzed in order to clarify the effects of fine aggregates which affect the quality of the HQSC, and estimations of ground properties for which the single-shell structures made of HQSC may be applicable were estimated using measurement data for convergence and crown settlement in tunnels. The following conclusions were made in the present study.

(1) The minute particle content of the fine aggregates significantly affects the quality of the HQSC. Especially, the use of crushed sand results in low concrete strength due to the high minute particle content and low limestone powder content.

(2) The average strength of HQSC is large at 27 N/mm^2, and so the design strength may be set at 23 N/mm^2 (conventionally 18 N/mm^2). Furthermore, the variation of core strength is 8.6%, with is comparable to those produced for commercial use by ready-mixed concrete plants.

(3) Based on the analysis results of convergence in the Iiyama Tunnel, it was concluded that the soundness of shotcrete may be maintained up to a horizontal relative convergence of 100 mm.

(4) When evaluating the modulus of elasticity or stress of shotcrete based on convergence, the effect of the rigidity of the surrounding ground on the applicable range of single-shell structures, although present, are small and may be ignored in the evaluation.

(5) The effective modulus of elasticity for shotcrete calculated using the measurement data for convergence in the Iiyama Tunnel is about 2,200–2,500 MPa.

(6) Based on the results of stress analysis of single-shell structures using the above values, it may be concluded that single-shell structures may be applicable for ground conditions having horizontal relative convergence below 90 mm and crown settlement below 55 mm.

REFERENCES

Japan Railway Construction Company. 1997. Recommendation for Design and Construction of High-Quality Shotcrete: 3–4.

Yukikazu, T. et al, 1987. Improvement in Quality of Concrete Structures by Two-stage Mixing Method, IABSE Symp., Paris, 1987. 333–338.

This page intentionally left blank

Underground Space – the 4th Dimension of Metropolises – Barták, Hrdina, Romancov & Zlámal (eds)
© 2007 Taylor & Francis Group, London, ISBN 978-0-415-40807-3

Applications of a shotcrete robot for creating an immediate comparability of mix designs

M. Thewes & G. Vollmann
Institute for tunneling, pipeline construction and construction management, Bochum, Germany

ABSTRACT: Shotcrete tests under edge conditions that are repeatable at any time can provide important and unique decision criteria for specific fields of application of shotcrete as a securing mean. Nowadays the emphasis of interest is lying more and more on particular questions of the consistency and adherence of mixture and the possibility of reaching a certain strength level depending on the mix-design. It happens more frequently that for example certain cements or supplements are allowed by a client, whose usabilities for shotcrete have not always been assured completely. Nowadays spray experiments are conducted on site which are restricted to the common spray boxes. Samples gained by this method are only feasible to a limited extent. This paper illustrates how experiments with little deviation among the measurement results can be achieved in comparison to current construction site testing methods. For the purpose of comparison the most important parameters are contrasted and classified with respect to their reproducibility. Therewith the test results are valued in reference to their significance as empiric measurement. Concluding a prospect on the necessary progresses of shotcrete technology is provided and a possible spectrum of application of a set-up under laboratory conditions is developed.

1 INTRODUCTION

Shotcrete is an indispensable building-material for the production of temporary supports for conventional tunnelling methods. The shotcrete-method facilitates according to the concept of flexible rock support the development of a natural structural arch while simultaneously protecting the workers in the tunnel. Therefore, the early achievement of a specific strength of the shotcrete is of particular importance.

The desired strength of concrete can bee guaranteed by standard concrete parameter testing. Test procedures which offer a fast availability of the early strength results while being highly reliable are, however, necessary for tunnel constructions and their specific boundary conditions. Therefore different test procedure were developed in the past, as provided by the Austrian shotcrete guideline (Austrian Society for Concrete- and Construction Technology, 2004) or the preEN 14488-2 (penetration needle method, bolt firing method).

A thorough and reliable comparison of different mix-designs for shotcrete prior a construction project can be problematic, as for example for the finding of mixture with the most favourable strength features or the lowest rebound. Often so-called shotcrete boxes are used for the production of testsamples on the construction site. It can, however, not be made sure that every shotcrete test production is produced under equal conditions. The comparability of shotcrete samples may therefore not be given. Differences in nozzle guidance during the shotcreting for the test samples, differences of the air quantity during spraying or also changing humidities of the concrete aggregates are only a few of the production parameters of the shotcrete which have direct influence on its quality and therefore on strength development and rebound.

In the decision making process for a shotcrete mix it is a considerable advantage if the suitability of particular mix can be tested in examinations which are independent and which are executed under controlled, identical laboratory conditions. For this a special experimental setup is required which guarantees on the one hand the reproducibility of the essential boundary conditions and on the other hand provides for an exact data acquisition of all parameters with significant influence on the shotcrete quality. These requirements are for example fulfilled by the experimental shotcrete test rig at the Institute for Tunnelling, Pipeline Technology and Construction Management at the Ruhr-University Bochum.

In the following the general influences on the quality of the shotcrete are initially discussed and the precision of shotcrete tests performed onsite are discussed. As an alternative the set-up of the laboratory shotcrete testing equipment is described and its possibilities outlined exemplarily. In conclusion, an executed performance test for various competing

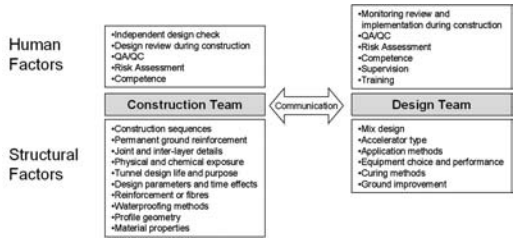


Figure 1. Influences on quality and sustainability of sprayed concrete structures (Melbye & Dimmock).

shotcrete mixes to be used at a large tunnel project is described and further possible options for testing are highlighted.

2 SIGNIFICANCE OF BOUNDARY CONDITIONS FOR THE RESULTS OF SHOTCRETE TESTS

2.1 *Initial situation*

Contemporary requirements on constructions made of shotcrete are focussing on its quality and its durability, as for example provided by the EFNARC-Guidelines (EFNARC, 1999). These attributes are determined in their development by all sorts of influencing factors, which can be divided in human factors and structural factors. These factors further have to be differentiated regarding the two areas of "design" and "construction". *Melbye* and *Dimmock* (Melbye & Dimmock) illustrated this effect in the following image:

Assuming that the choice of a suitable construction method and the accompanying constructive concept has been made according to the state-of-the-art, the influence on quality and durability of the shotcrete caused by application method, the mix-design and primarily also the type of the accelerator becomes recognizable. If furthermore one assumes that the processing of the shotcrete during the construction phase also meets demands of the quality assurance, the choice of an optimized shotcrete mix is finally a question of profitability but primarily of the safety on the construction site.

Therefore a mix-design must be found with an optimized performance regarding the desired strength level and under consideration of minimal possible production costs. Even small differences between different mix-designs, e.g. the development of strength or the rebound, can already show a clear influence on the cost of shotcrete on the construction site depending on the dimensions of the tunnel project and the according quantities of shotcrete being processed. For this reason performance comparisons of mix designs in the preparation phase of a tunnel project can provide an important contribution to the cost reduction related



Figure 2. Creting of a shotcrete box.

to the overall project. A mandatory requirement for a comparative performance test is that the test results are obtained in a test environment under comparable and reproducible boundary conditions.

2.2 *Significance of comparative performance tests under construction site conditions*

Often, performance comparisons of different shotcrete mixes are executed with shotcrete boxes on the construction site. These shotcrete boxes are sprayed manually and serve subsequently as specimen for quality and strength tests (Fig. 2).

It is obvious that such a setup for shotcrete tests results in a fairly high variance of the examined parameters. Different control of the nozzle movements, varying distances of the nozzle to the shotcrete box, changing weather conditions or also fluctuations in the air supply of the shotcreting machine are providing fluctuating conditions which cause scattering of the test results. Furthermore, the geometry of the shotcrete boxes hinders the achievement of a solid shotcrete structure, similar to the quality achieved at the tunnel face. This is due to the fact that rebound partly is included within the shotcrete sample in the area of the side walls of the shotcrete box.

The scattering of the test results and the low reliability and reproducibility of such comparative examinations with shotcrete boxes can also be statistically measured (Fig. 3).

Assumed (3A) that a certain test parameter (e.g. the rebound of a dry spraying method) has a value of 30% at a coefficient of variance of 25%. If, as shown in (3B), a reduction of the rebound to 20% were achieved by using a mixture with a variance of 5%, it is obvious to (3C) that this does not represent any confirmed statement. The apparent obtained improvement still lies within the normal variation range of both parameters. A reduction of the scattering, as for example in (II) on 8%, provides reliable results.

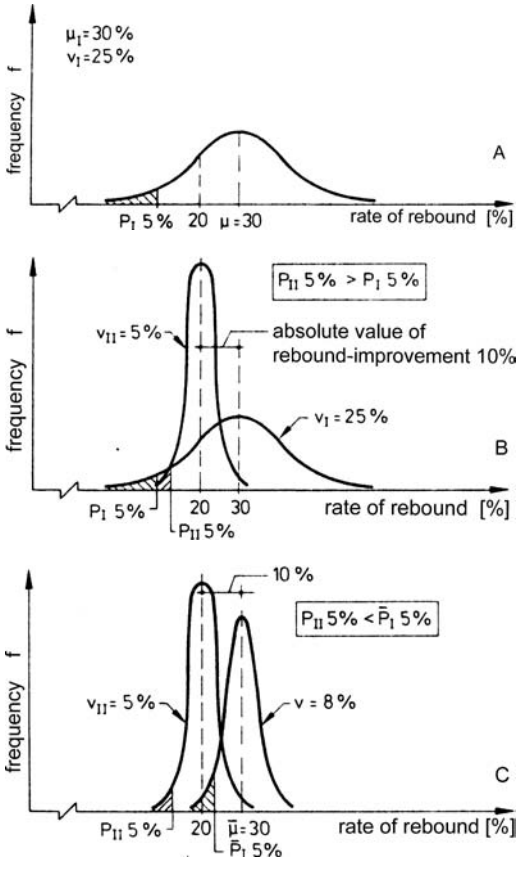


Figure 3. Significance of single results derived from examinations with high variance.

2.3 *Conclusion*

The considerations presented above show that the choice of the mix-design for shotcrete constructions can have an significant influence on profitability and efficiency. However, this circumstance often is not being considered appropriately. When making a choice a suitable design of shotcrete mix test results with highly scattering results are consulted. This can be improved considerably by performing laboratory shotcrete tests under reproducible boundary conditions to provide more reliable test results and to close existing knowledge gaps.

Accordingly, key parameters can be listed which for reliable test results of a performance comparisons are to be kept constant or at least at the lowest possible fluctuation. These important parameters are in particular:

- a quality-assured application method for the shotcrete
- air-flow rate with the necessary quantity

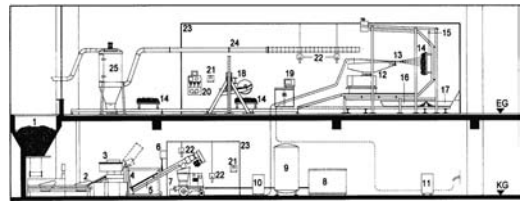


Figure 4. Configuration of the experimental shotcrete equipment.

- the composition of the mixture
- the flow rate of the mixture
- the quantity of the accelerator
- the quantity of water added with the dry spraying method

3 THE SHOTCRETE LABORATORY EQUIPMENT AT THE INSTITUTE FOR TUNNELING, PIPELINE TECHNOLOGY AND CONSTRUCTION MANAGEMENT

3.1 *History and configuration of the experimental equipment*

The experimental shotcrete equipment at the Institute for Tunnelling, Pipeline Technology and Construction Management is part of the experimental facilities of the faculty of civil engineering at the Ruhr-University Bochum. Figure 4 provides an overview of the test rig.

Central unit of the test rig is a modified industrial roboter (12) with which defined and controlled motions of the nozzle (13) can be carried out. The batch mix sprayed with this unit is produced exactly according to a defined recipe in the mixing unit (1–5). The mix is transported with a shotcrete pump (7) to the mixing nozzle. In this section air and the accelerator is added to the mixture and the shotcrete is sprayed on a prepared surface. This way large-sized samples are produced at a minimum of disturbing influences. A test specimen is produced with realistic nozzle motions. As a consequence such test bodies provide better and more reliable results since the boundary conditions of the test are controlled close by. Also, a typical and realistic structure development of the shotcrete sample is realized.

With this test rig numerous important findings for for shotcrete research were reached in the past, for example in the field of dust development (Handke, 1987), in the field of nozzle geometries and nozzle guidance (Gutthoff 1991) or in general process engineering for shotcrete (Halhege 1985).

3.2 *Realisation of an experiment*

During a shotcrete test all significant data for the description of the shotcrete parameters are recorded and the properties of the fresh-mixed concrete are

documented. The weights of the complete mixture before the test of the spraying test specimen and of the rebound are recorded. Thus the quantity of the rebound can exactly be monitored. Furthermore, the consumed amount of accelerator, the air-flow used and the stream of air are measured and evaluated in the mixing nozzle. By exact control of these parameters the creation of constant boundary conditions for shotcrete-tests can be realized. Single selected parameters of the mix-design, such as cement, aggregates or particular admixtures, can be varied while all other parameters remain unchanged.

Moreover, to be able to guarantee least possible deviations of the parameters, which remain unchanged, and to compare the achieved results, it is required that the tests are performed in a defined order with defined time-steps. The individual production steps of a shotcrete test are divided as follows:

(1) Production of the concrete mix
(2) Testing of the properties of the fresh concrete
(3) Starting of the test rig
(4) Beginning of the experiment: Spraying aided by the robotic arm
(5) Completion of spraying and beginning of early strength testing
(6) Cleaning of the test rig and retrieving of the sprayed specimen
(7) Drilling of sample cores and performing of strength and integrity testing

The sprayed samples are treated for curing in the following of the experiment (between step (6) and (7)), to be able to guarantee an optimal hydration-process. For this purpose the samples are kept in a humid environment and stored at a temperature of about 20 degrees Celsius before they are brought to further processing, e.g. the drilling of cores for compressive strength examinations.

3.3 *Conclusion*

The described experimental shotcrete equipment delivers the reproducible boundary conditions demanded in chapter 2, so that protected and reliable statements can be made with regard to single parameters of a mix-design and their influence on the construction process. In the following chapter this is demonstrated with results from a real series of experiments.

4 SELECTION OF AN OPTIMIZED MIX-DESIGN BY COMPARATIVE TESTING

4.1 *General*

For a tunnel project described in the following a temporary lining had to be created by shotcrete, using the wet spraying method. Moreover, the client required the use of a mix-design with certain features, documented in table 1. The use of a cement type required by the client with a comparatively slow hydration rate, which is unfavourable for the production of shotcrete, proved to be problematic.

Table 1. Required features of the mixdesigns.

Task	Target	Test Method
w/c-ratio	$\leq$0,50	Mix design/drying
Workability		
– consistency	Good Slumplife (200 to 220)	Slump-test
– open time	Open time up to 12 h	Penetration
Pumpability	Good pumpability	Mix design -> visual inspection
Cohesion	Good cohesion	Mix design -> visual inspection
Additives	Chemical risk assessment	Approval
Shotcrete rebound	Reduce to minimum	Spraying-tests
Early-Age strength	J2 area (EN 14487-2)	prEN 14488-2
Compressive strength (28d)	C 25/30	EN 12504-1

For the realisation of the lining one of three possible shotcrete mixes had to be applied in a comparative test, in which the focus of attention laid on initial strength and rebound development. Comparative tests were issued for the determination of the respective performance. The fresh concrete properties as well as the development of the compressive strength after 7 days and after 28 days were also to be tested.

The three mixes were developed by the use of different accelerators and different grain fraction distributions. They are called mix A, B and C in the following. Their exact compositions were provided by the manufacturer of the various accelerators under the requirements to use the aggregates which are available on the construction site.

4.2 *Test procedure and evaluation*

4.2.1 *Production of the specimen*

Using the test scheme described in chapter 3, one large-sized specimen was produced with every mix and examined with regard to the mentioned properties of the shotcrete. Figure 5 shows one specimen, out of which several core $d = 100$ mm have already been taken.

The required fresh concrete parameters were obtained by all mixes. All mixes A, B and C were characterized by a good pumpability and by an optical impression of low rebound. This impression was



Figure 5. Example for a shotcrete specimen.

Table 2. Rebound according to different mixdesigns.

Mixdesign	Ø Rebound [%]
A	4,8
B	3,7
C	3,8

verified by analysing the test-data. Table 2 shows the rebound-development:

4.2.2 *Early strength testing*

The following diagram shows the early strengths found out in the comparison.

The test results show, that none of the mixes delivers a young shotcrete which is conform with the strength standard J2 according prEN 14488-2. The shotcrete made with mix B seems to be the most favourable since it delivers the highest early strengths directly after spraying the shotcrete, which will also make over head spraying possible. Mix C achieves the desired strengths after 6 hours, shows however very low strength in the first minutes after spraying. In view of the scheduled application, which also requires overhead spraying, such a low early strength development was judged to be unsuitable.

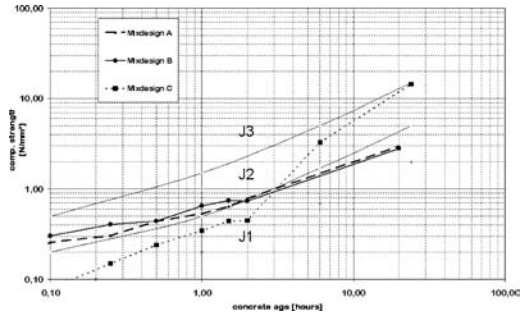


Figure 6. Results of the early strength testing.

4.2.3 *Evaluation*

The available results show that none of the three suggested mixes delivered a shotcrete which entirely meets the requirements. Although the demanded fresh concrete parameters and the long-term strength development were achieved by all mixes (all specimen fulfilled the strength tests after 7 or 14 days with results above the values demanded in Table 4.1), none of the mixes achieved the demanded early strength of the shotcrete. According to the applied standards prEN 14488-2 the shotcrete should develop a strength within the first 24 hours according to J2. This level is obtained by the mixes A and B within the first three hours, both shotcretes, however, fall back to the strength area of J1 after this. Mixture C achieves the demanded strength in the J2 area for the time-span from 4-24 hours, but remains below the necessary strength within the first four hours.

Due to the fact that one of the three mixes was definitely to be used for the construction lots to be driven in shotcrete, mix B was recommended to use. The shotcrete created with this mix delivered the highest strength directly after spraying and thereby made overhead spraying possible. Moreover, mix B reached the highest strength after 7 and 28 days and, compared to the other mixes, it produced the lowest rebound. Furthermore the use of formula B supplied a fresh concrete with very good, long-termed processing features and a high degree of flowability.

4.3 *Possible secondary examinations*

By using shotcrete mix B, a successful implementation of the temporary lining works was executed on the construction site. The optimization potential of the shotcrete was, however, still not exhausted. Secondary examinations could have realized an optimized fine-tuning of the mixture, a reduced addition of accelerator or further optimization of the rebound for example. To achieve this goal it would be possible to vary single parameters, such as the cement content or the amount of plasticizer, to achieve test results with a low variance in a series of low-cost tests.

5 CONCLUSION AND PERSPECTIVE

The details of this article have shown, that modern constructions made of shotcrete are subject to a high degree of requirements regarding durability and quality. In the future, this might become, by further establishing final shotcrete linings, even more common. An optimization of the performance of shotcrete is important to the profitability of the construction site, for the structural concept in general, but also (in case of final shotcrete linings) for the maintenance efforts during operation.

To optimize the performance of a shotcrete mix, examinations are required which provide reliable and reproducible results. To realize such results at a construction site is a complex effort with many sources of errors. Controlled variations of single parameters often are not possible. For this reason facilities like the described shotcrete testing rig can provide an important input for the application of shotcrete with improved performance and quality contributing to the technical and economical success of tunnelling projects.

REFERENCES

Austrian Society for Concrete- and Construction Technology. 2004. Austrian shotcrete guideline. Austrian Society for Concrete- and Construction Technology. Vienna

prEN 14488-2. 2002. Testing of shotcrete Part 2: Compressive strength of young sprayed concrete

EFNARC. 1999. European specification for sprayed concrete. Surrey

Melbye, T.A. & Dimmock, R.H. Sprayed Concrete: A Modern, Holistic Approach. Internet distribution. Zurich: UGS

Handke, D. 1987. Kriterien zur Beurteilung und Verminderung der Staubentwicklung bei Spritzbetonarbeiten. Technical Reports Nr. 87–3. Bochum: Institut für konstruktiven Ingenieurbau

Guthoff, K. 1991. Der Einfluss automatischer Düsenführung auf die Herstellung von Spritzbeton. Technical Reports. Nr. 91–7. Bochum: Institut für konstruktiven Ingenieurbau

Hahlhege, R. 1985. Der Versuchsstand für Spritzbetonarbeiten an der Ruhr-Universität und seine Nutzungsmöglichkeiten. Technical Reports. Nr. 85–6. Bochum: Institut für konstruktiven Ingenieurbau

Underground Space – the 4th Dimension of Metropolises – Barták, Hrdina, Romancov & Zlámal (eds)
© 2007 Taylor & Francis Group, London, ISBN 978-0-415-40807-3

Sprayed concrete for primary tunnel lining

P. Polak & D. Cyron
Metrostav a.s., Prague, The Czech Republic

J. Vlasimsky
Sika CZ s.r.o., Brno, The Czech Republic

V. Mika
Beton Bohemia s.r.o., Prague, The Czech Republic

ABSTRACT: The process of adding accelerators to sprayed concrete of the primary lining applied by Metrostav during the course of the Vítkov tunnels excavation has been monitored in a systematic manner. In addition to the customary check testing carried out to verify whether the set/hardness build-up curves prescribed are maintained, also other relevant quantities were monitored and recorded, e.g. the concrete mixture temperature, ambient temperature, consistency of the mixture and dosage of additives. Also the concrete application by the nozzle operator was monitored, with a view to the correctness of the procedure. The results are currently being assessed and should be used not only as a basis for the development of modified sprayed concrete formulas to be applied in the conditions of production in a certified concrete mixing plant but also for the determination of the minimum theoretical and practical requirements for qualification testing of nozzle operators.

1 INTRODUCTION

Sprayed concrete primary support should be a slender system deforming in a controllable manner, which, owing mainly to experience empirically obtained in the particular rock environment and a properly designed shape and manner of anchoring into the rock massif, properly interacts with the rock massif, forming a higher-level load-bearing system consisting of the primary support itself and the surrounding rock ring. The "skill" of the manager, a tunneller, is therefore based primarily on knowledge of local geotechnical and hydrological conditions, combined with sensitive assessment of whether the deformations of the lining, which depend above all on the dimensions of the tunnel cross section and the excavation technique, will reach the values specified by the design as limits or other possible values. Limiting deformations are determined primarily according to the degree of their transformation to the ground surface with respect to the density and character of surface buildings. The deformations may even significantly affect underground structures, both existing or under construction. Recorded values of deformations measured on the internal surface of the primary lining characterise the presence of earth pressures or hydrostatic pressures. Primary deformations at the lining-rock interface are followed by favourable equalisation of the state of stress along the circumference of the opening. They should, however, approach zero, usually within 72 hours of the first measurement. In the opposite case it is necessary to implement measures leading to reinforcement of the support system. Zero deformations measured on the internal surface of the lining imply high load bearing capacity of the lining-rock system. To follow the economic aspect of excavation, the support should be modified to correspond to a less demanding excavation class, i.e. application of primary support with lower supporting power or even with smaller number of elements providing the interaction with the surrounding rock mass. The "reasonable" degree of the convergences of primary lining should be exhausted as a proof that the performance of the operations is economic. Because of the variability of geological and hydrological conditions, the determined applicable measures and their sequence during the excavation are not intended to apply "forever". However, the scope of proposed measures may be limited due to the inexperience of the parties involved in the construction in tunnelling in the particular geological conditions. The fact remains that, in the Czech Republic, a primary support system is considered to be a temporary element in terms of structural analyses, and its load bearing capacity is not at all taken into consideration once the final lining has

been completed. This opinion is incorrect and the function of primary support will have to be re-evaluated, mainly where hydrological or other conditions do not cause rapid degradation of the primary support. Our dilemma remains: to build a primary support system as cheaply as possible, but never with savings which would lead in a worst-case scenario, to a collapse of the underground excavation, which would result into increased cost of the works and threatened safety of crews, other structures or the public.

The construction of the New Connection tunnels under Vítkov Hill in Prague was selected as a suitable site where some new information about the dominant element of primary lining structures, sprayed concrete, should be obtained. This information had not been sought in the Czech Republic till that time.

Table 1. Main dimensions of the New Connection tunnels.

	STT (m)	(m^2)	NTT (m)	(m^2)
Total length	1365		1316	
Mined sect. Length	1250		1150	
cut-and-cover length				
eastern sect.	70		107	
western sect.	45		58	
excavation width	12,7		12,7	
excav. height		9,52–10,38		9,52–10,38
excav. c.s. area – tunnel		96–108		96–108
excav. c.s. area – chamber		125,8–173		125,8–173

2 BASIC DATA ON THE CONSTRUCTION

2.1 *The New connection*

The New Connection project will interconnect railway stations Praha – Hlavní Nádraží and Praha – Masarykovo Nádraží with stations in the Libeň, Vysočany and Holešovice districts, thus the overall reconstruction of the Prague railway junction will be completed. The user, České dráhy, s.o., hired Nové Spojení Praha, a group of companies consisting of Skanska, a.s., Metrostav a.s. and Subterra, a.s., as the contractor. The works started in 2004 and the completion is planned for 2008.

The design of the alignment of the new railway line across the Žižkov and Karlín districts contains two tunnels under Vítkov Hill. This variant of the railway traffic passage through the given terrain configuration proved to be the most suitable with respect to the noise protection of both urban districts.

2.2 *Dimensions of the New Connection tunnel tubes*

Apart from new railway routes, grade-separated intersections and diversions, the extensive railway construction project New Connection comprises construction lots 801.1 "The Southern Tunnel of the New Connection" (the southern tunnel tube – STT) and construction lot No. 800.1 "The Northern Tunnel of the New Connection" (the northern tunnel tube – NTT), which will, when complete, consist not only of mined sections, but also of shorter cut-and-cover sections. The tunnels run along the longitudinal axis of Vítkov Hill. The horizontal alignments are partially straight, with adjacent curves with diameters of 602 m and 648 m for the southern tube and 902 m and 3602 m for the northern tube. The vertical alignments of the tunnels descend from the east towards the west at a minimum gradient of 0.33%. The mined tunnels, together with 4 cross passages and 6 overhead line tensioning chambers represent an excavated space volume of 244 800 m^3; the volume of the wall-in space of the cut-and-cover sections amounts to 26 750 m^3. The most important data regarding the lengths and cross sectional areas of the mined tunnels of the New Connection is shown in Table 1.

2.3 *Geological conditions*

The excavation of the Southern Tunnel of the New Connection project encountered the Šárka Member and Dobrotiva Member rock types. The Šárka Member strata were assessed from the geological viewpoint at the very beginning, during the excavation of construction pits for portals and portal sections of the tunnels. This type of rock developed in the area in so-called "monotonous" sedimentation processes, resulting in facies of black-grey, clayey to sandy bituminous shales to siltstones. These rock types are relatively firm and compact, with platy to heavy-bedded jointing; the rock disintegration requires blasting operations. Further from the portals, the Šárka Member strata were replaced with the Dobrotiva Member, which is characterised by alteration of two lithofacies – the Skalec Quartzite facies and the Dobrotiv Shale facies. The Skalec Quartzite forming the Žižkov massif is characterised by alteration of plates or thick beds of whitish, ochre- or red- tinted siliceous sandstone. The quartzites are medium jointed, locally tectonically disturbed. Discontinuities are tight, coarse, mostly limonitised and hematitised. The shales are quartziferous, grey to grey-black, locally tinted by limonite and hematite. They mostly exhibit platy jointing. The excavation passed through a relatively dry environment. The inflows encountered by the

excavation were only local, weak, in the order not exceeding 0.01 l/s.

2.4 *Excavation technique*

The two tunnel tubes were driven using the New Austrian Tunnelling Method (NATM), with the exception of portal sections, where a horizontal excavation sequence was adopted. The specification of the excavation support for the anticipated geotechnical conditions was determined by application of excavation classes 3, 4a, 4b and 5. The classes defined in more detail the division of the cross section, number of partial advances and their length, the height of the top heading, bench and bottom or invert, thickness of primary lining, spacing of lattice girders, length of rock bolts and method of the supporting the face. Excepting short sections at both portals, the entire length of the tunnels was driven by drill and blast. Standard survey, geological, deformational and other check measurements covered by the general term of "monitoring" were inseparable part of the operations.

Driving the tunnel under the National Monument building and the equestrian statue of Jan Žižka of Trocnov on Vítkov Hill was a unique operation. The overburden height reached nearly 40 m in this location. The seismic measurement design, which was carried out for this section, set out limits for the charges to be used. The aggregate surface settlement value, which was assessed in advance of the work, was determined at 12 mm. This value was exceeded during the excavation of the second tunnel in the location of the monument, therefore eight 108/16 mm grouted micropiles, with the lengths between 12 and 15 metres, had to be installed under peripheral footings of the building.

2.5 *The lining of the New Connection tunnels*

The design of the tunnel lining consists of traditional two shells. The structure of the primary lining of each mined double-rail tunnel is traditional, consisting sprayed concrete reinforced at both surfaces with welded mesh. Lattice girders and friction rock bolts expanded by pressurised water were added to the lining (plus steel needles along the circumference of the top heading in the sections threatened by instability). The thickness of the primary lining varied within a range of 30–20 cm, depending on the determined excavation class.

The final lining design comprises both reinforced and unreinforced cast-in-situ concrete sections. The lining will be cast using a 12.5 m long travelling form set (a half of the spacing of safety recesses). An intermediate waterproofing membrane is installed between the primary and secondary lining. The final lining is designed at a 35 cm thickness.

3 OBSERVATION AND TESTS

3.1 *Observed items*

The construction of the primary lining is one of the most demanding operations of the tunnel driving cycle. The success of the tunnelling method in the particular geotechnical conditions depends on whether the lining is built in due time and good quality, and the dimensions are designed adequately. The design prescribed the sprayed concrete to be of the SC25 (C20/25/II/J_2/8 mm) grade, with the layers 200 mm, 250 mm or 300 mm thick, depending on the excavation class. The design concrete mix formula had to satisfy the required parameters and the early strength development in concrete had to conform to the J_2 curve. Shotcrete was placed using the wet process, with a manipulator coupled with a Meyco-Potenza piston pump. Other observation items and procedures were selected for the southern tunnel of the New Connection project to be added to the set of preconstruction and checking tests; they were intended to help to improve the work process or to achieve the required final quality of the shotcrete primary lining.

To summarise, the following main observation items were introduced:

1. Regular checking on consistency and temperature of the concrete mix supplied to the site
2. Concrete setting and the early strength development to be within J_2 range within 24 hours of application
3. Standard testing of strength at 28 days
4. Measurement of ambient air temperature at the working place during application
5. Temperature measurement during the tests
6. Measurement of consumption and dosage of the accelerator additive relative to the set output of the machine
7. Regular inspection of the manner and procedure of application of shotcrete, including the personnel training.

3.2 *Selected results of the shotcrete testing*

The consistency of the mixture supplied for the construction of the primary lining was prescribed by means of slump values to vary between 180 and 240 mm. These values were the primary criterion for production of the mixture in the certified batching plant. The temperature of the mixture and air and properties of aggregates affected the dosing rates of the SikaViscoCrete 305 superplasticising additive, which was used also for regulation of the application life on site. It was possible to extend the application life even to 4 hours from the moment of mixing. The usual dosage of the superplasticising additive was about 1% of the weight of the binder contained in the concrete mixture. The influence of the consistency of the

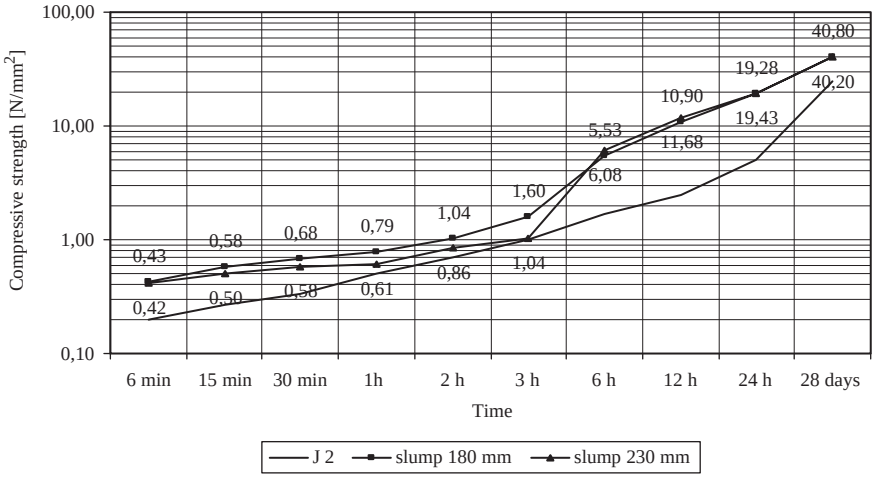


Chart 1. The influence of differing concrete consistency on the development of compressive strengths at the accelerator dosage of 6% (31.8.2005).

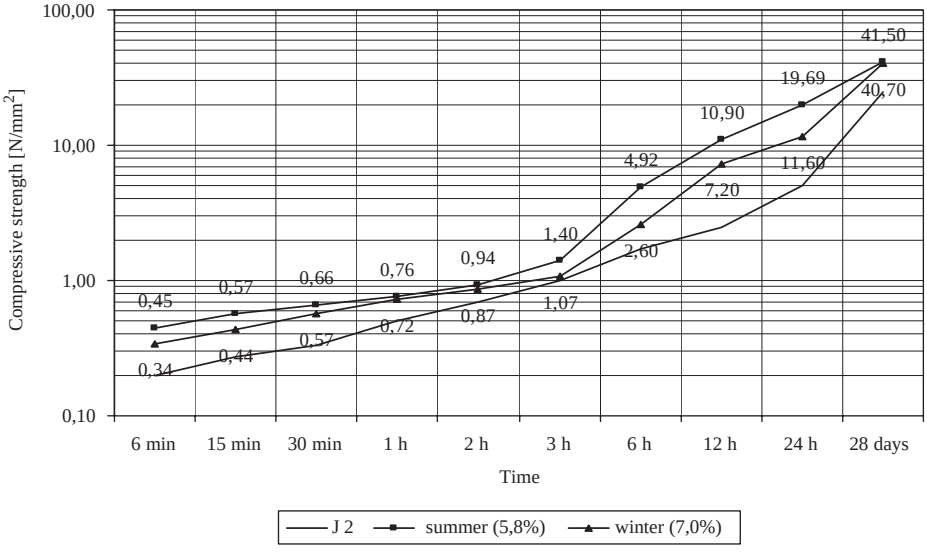


Chart 2. The differences between the time-strength curves in the “summer period” (May – September; accelerator dosage 5,8 %) and “winter period” (November – February; accelerator dosage 7,0 %).

supplied concrete on the development of setting is obvious from the Chart 1 above.

The rate of setting and early strength development in concrete was regularly monitored for the entire time of the STT excavation, once in a month being the minimum frequency. At the ambient temperatures distinguished for the summer period (from May to September) and winter season (from November to February), the most significant difference was observed 3 to 24 hours after the application. The time-setting curves for the summer and winter could get closer to each other when the average dosage of the accelerator additive was increased to 7% in the winter period compared to the summer period value of 5.8%. The average temperatures of concrete mix supplied to the site were 17°C and 26°C in the winter and summer periods, respectively. The strengths of the samples at 28 days were virtually identical. The differences between the time-strength curves are obvious from the Chart 2.

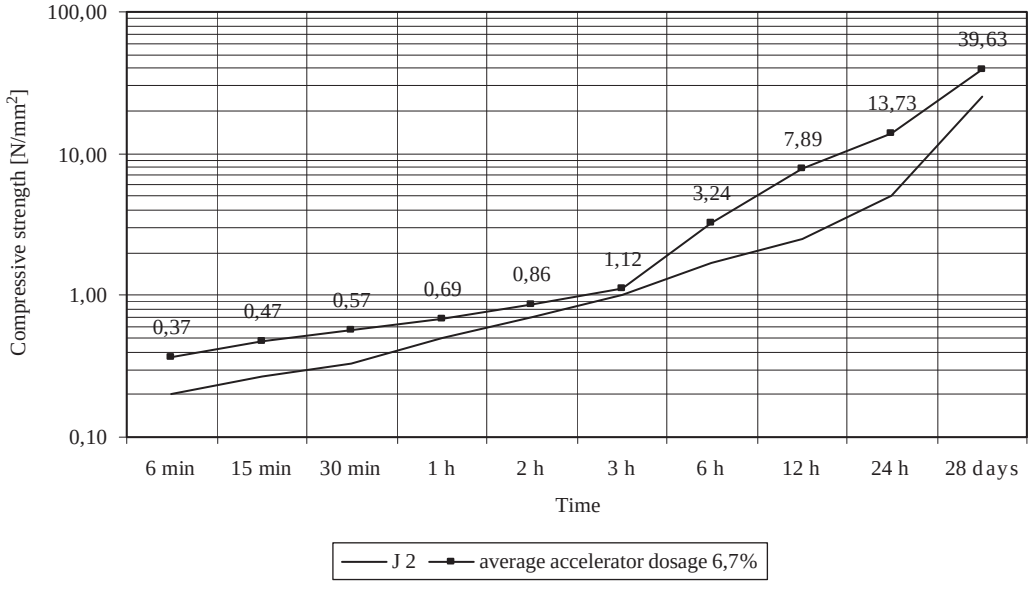


Chart 3. Average values of the time-strength curves for sprayed concrete measured from May 2005 to May 2006.

The Chart 3 shows the average values of the time-strength curve for the primary lining shotcrete during the entire time of the STT construction. The amount of 430 kg of Portland cement per 1 m^3 of the concrete mixture, together with the accelerator additive, guaranteed that the time-setting curves remained within the J_2 range for the entire construction time. The experience was gained that the amount of cement had to be maintained mainly so that the above-mentioned time-setting curve was achieved, despite the fact that the final strength of the sprayed concrete at 28 days substantially exceeds the strength of the required SC 25 concrete grade.

The dosage of the Sigunit L-53AF accelerator additive was observed simultaneously with the measurements of concrete and ambient air temperature at the excavation face. When the several results significantly differing owing to the influence of the human factor during the processing are left out, the relationship between the consumption of the accelerator additive and temperature is obvious from the Charts 4 and 5. The reaction of the accelerator with the concrete applied to the substrate manifested itself after six minutes through temperature of the sprayed concrete increasing in the range of 1°C to 4°C. The temperature after 15 minutes was even higher, approximately by 1°C, then the temperature started to gradually decrease and stopped at the value of the ambient temperature, approximately 24 hours after the application.

Another part of the observation was the assessment and improvement of the manner of spraying concrete by individual nozzle operators. In addition

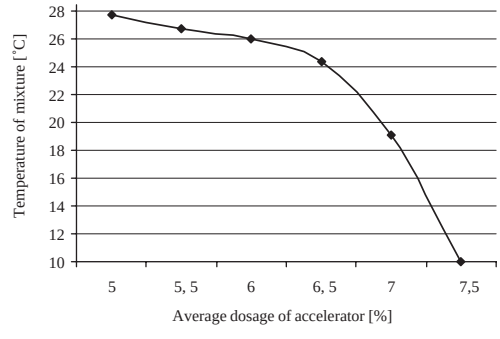


Chart 4. The relationship between the dosage of accelerator and the concrete temperature.

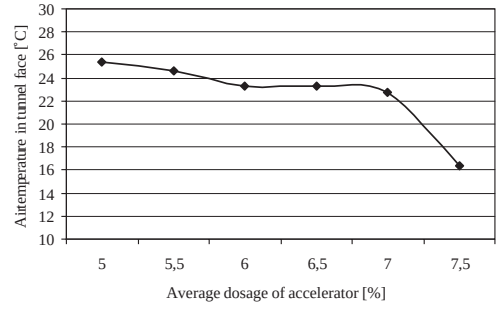


Chart 5. The relationship between the dosage of accelerator and the ambient air temperature at the excavation face.

to the standard rules for an optimum spray application, the theoretical and practical training taught the workers about mistakes made during the last passes of the nozzle. The application rules were delivered in the form of presentations.

4 CONCLUSIONS

There were many measurements carried out during the construction of the Vítkov tunnels of the New Connection project, which exceeded the previous standard scope of checking tests. Apart from consistently observed temperatures of the ambient air and the concrete mixture, even the performance parameters of the Meyco-Potenza pump were recorded, including the rates of dozing and consumption of the accelerator additive. However, to achieve satisfactory results of application of the primary lining shotcrete, it was necessary to continuously work on improving practical working habits of the nozzle operators and broadening their knowledge in terms of both operation of the equipment set and properties of concrete mixtures used. To maintain the quality of sprayed concrete, the process of increasing the level of competence of nozzle operators and the entire crew must be a permanent task.

REFERENCES

Polák, P. & Mika V. 2006. Primární ostění ze Stříkaného betonu; Proceedings of the conference: Beton v podzemních a základových konstrukcích – 2. konference. Praha

Štefan, I. & Vlašimský J. 2006. Stříkané betony ražených tunnelů a příprava definitivních ostění Nového spojení v Praze; Proceedings of the conference: Beton v podzemních a základových konstrukcích – 2. konference. Praha

Underground Space – the 4th Dimension of Metropolises – Barták, Hrdina, Romancov & Zlámal (eds)
© 2007 Taylor & Francis Group, London, ISBN 978-0-415-40807-3

Concrete and shotcrete with crushed aggregates: experience from the AlpTransit construction site Mitholz

R. Weiss
VSH – Hagerbach Test Gallery Ltd., Sargans, Switzerland

ABSTRACT: For reasons of ecology and economy, efforts are made at large tunnel construction projects to optimally recycle excavated material.

Tunnelling specialists at the construction site Mitholz of the Lötschberg Base Tunnel utilized over 800,000 m^3 of concrete produced with aggregates processed from tunnel excavation material. The use of broken aggregates from excavated material affected the concrete production process in several ways.

The experience gained from the construction site Mitholz proved that high-quality concrete can be produced from aggregates processed from tunnel excavation material. Additional constraints do result, however, that demand that all affected parties are very willing to cooperate.

The experience from construction site Mitholz serves as a valuable basis upon which future structures can be designed in accordance with the latest standards, especially those such as the performance-based design process of SN EN 206–1.

1 INTRODUCTION

Both of the large transalpine railway links in Switzerland, the Gotthard and Lötschberg Base Tunnels, are currently under construction. Both lines will be part of the European high-speed rail network.

The official opening of the 34.6 km long Lötschberg Base Tunnel on June 16, 2007 will complete the first construction phase consisting of two one-way single-track railway tubes.

The northern section of the base tunnel (construction site Mitholz) was constructed between 2000 and 2006 starting from the intermediate point of attack Mitholz, which was reached through an access gallery. The tunnel was driven both to the north and to the south. The construction site Mitholz included the excavation of 23.5 km of single-track tunnel with cross sections of 61 to 64 m^2 and 1.6 km of connecting galleries. Tunnelling was conducted from preliminarily constructed caverns that were accessible through the 1.5 km long 12% sloped access gallery. The entire excavation volume equaled 1.8 million m^3. Tunnelling work was conducted by the construction consortium ARGE Satco, consisting of the contractors Strabag, Rothpletz, Lienhard + CIE AG, Walo Bertschinger AG, VINCI GP and Skanska International Civ. Eng. AG, using drill and blast together with shotcrete support, system rock bolting, waterproofing and an inner lining in the equipped "east tunnel".

The concrete and shotcrete needed for the structure was produced by Mobilbaustoffe AG on site. In total, the ARGE Satco handled 800,000 m^3 of concrete and shotcrete.

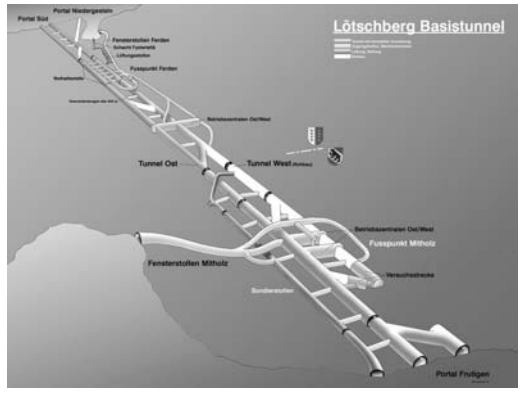


Figure 1. Project layout (Source: BLS AlpTransit AG).

2 CONCRETE SPECIFICATIONS

The concrete type and specifications were defined by the project engineering team. The most common types are presented in Table 1.

Die ARGE Satco defined additional requirements related to fulfilling the client's requirements:

- Production (delivery performance, safety of supply and availability)

Table 1. Specifications included in tender documents.

Utilization	Shotcrete lining	Invert concrete	Concrete lining
Name	Class C/D, SIA 198, wet-mix shotcrete	B 35/25 SIA 162	B 35/25 SIA 162
Compressive strength	B 35/25	B 35/25	B 35/25
Early strength		12 h ≥ 10 N/mm^2	12 h ≥ 10 N/mm^2
Water penetration	<50 mm	<50 mm	<50 mm
Sulfate resistance	if >250 mg/l	if >250 mg/l	
Freeze-thaw resistance	to 2000 m below ground	to 2000 m below ground	to 2000 m below ground

- Workability (oven time to 3 h, pumpability of max. 100 bar pump pressure, low risk of variability)
- Early compression strength, formwork removal resistance (work and tact)
- Total costs

In addition to the requirements of the tender documents, additional constraints which in some cases decisively affected the concrete mix, production, working and quality were establish.

The most important include:

- Procedures regarding AAR-resistance when utilizing AAR-reactive aggregates
- Effects upon supply safety of aggregates (material processing)
- Variations of the aggregate in connection with the processing of the excavated material

3 CONCRETE PRODUCTION AND QUALITY CONTROL

Concrete production for the construction site Mitholz was carried out by the firm Mobilbaustoffe AG. The custom-built concrete production plant was located underground in a cavern of the intermediate point of attack Mitholz. A plant with a twin shaft mixer from SIMEN (batch size 2.25 m^3) with maximum hourly performance of 80 m^3 was installed for the production of concrete and shotcrete. Three cement silos were available per mixer each with a capacity of 100 tons and 14 silos for aggregates each with a volume of 80 m^3.

The quality control tests of the concrete production were conducted by the Hagerbach Test Gallery. The Hagerbach Test Gallery has several construction materials testing laboratories at its disposal throughout Switzerland. For on-site tests in Mitholz, a mobile laboratory was set-up very near the concrete plant. The monitoring of concrete production was realized with systematic testing of fresh concrete. The on-site mobile laboratory was equipped with instruments for determining the early compression strength of shotcrete and concrete. Separately produced test specimens (cubes, cylinders, shotcrete test boxes) and intermittent specimens from the structure itself were tested at the Hagerbach Test Gallery to ensure that hardened concrete requirements were met.



Figure 2. Fresh concrete test at on-site lab.

4 AGGREGATES FOR CONCRETE PRODUCTION

For reasons of ecology and economy, efforts are made at large tunnel construction projects to optimally recycle excavated material.

The excavated material of the Lötschberg Base Tunnel generated from drill and blast operations was therefore assigned a recycling classification and processed accordingly. From the processed muck at the Mitholz site, enough aggregates were obtained to enable self-sufficiency of the site. Surplus material was passed on to third parties. Missing grain sizes were bought according to need.

After each round, the geologist from the overall project management team classified the excavation material in accordance with its recycling class.

In addition to the petrographic evaluation, the suitability of the raw material K1 was verified as deemed necessary with physical tests.

From the K1 material, the material processor prepared the following aggregates for concrete:

- Sand 0–4 mm, unwashed
- Sand 0–4 mm, washed
- 4–8 mm, 8–16 mm, 16–22 mm

Table 2. Recycling class.

Class	Rock type	Utilization
K1	Good rock quality, relatively homogeneous rock formations, e.g. limestone, sandstone, granite with small slate fraction (≤10%)	Material suitable for production of aggregates for concrete, gravely sand for foundations, crushed stone, gravel and drainage gravel
K2	Medium to good quality rock, heterogeneous rock formations, e.g. marl, Triassic dolomite, alternating layers of clay slate, marl and limestone	Material suitable for production of gravely sand. If necessary, it is possible to use K2 material as raw material for Class K1 after preliminary sieving and removal of fines (K2S)
K3	Poor rock quality, e.g. kakirite, anhydrite, flysch	Material suitable for filling of gravel pits and quarries, embankments, backfill, terrain modifications

The quality of the prepared aggregate sizes was monitored and documented by the material processor in accordance with a testing plan within the framework of production control.

Independent of the production tests by the material processor, specimens were systematically taken from the silos of the concrete plant by the contractor ARGE Satco and their grain size was determined.

4.1 *Aggregate variations*

During processing of aggregates of varying composition from tunnel excavation material, the uniformity of the material and its handling is critical, especially of sand.

During the rock crushing process, the raw material behaves in different ways depending on the geology and moisture content of the excavated material. The effects were especially apparent in unwashed sand.

During the start phase in Mitholz, one sand was delivered by the material processor that consisted of both washed and unwashed sand. The large fines fraction <0.125 mm of approx. 16% and large variations affected the amount of water needed for the concrete mix and made concrete production more difficult. The high water content limited the early strength development of shotcrete to an unacceptable level and the w/c ratio was considerably higher than 0.50. After a phase with approx. 13% <0.125 mm, the delivery was modified to the originally planned ratios of unwashed and washed sands so that varying site requirements and the shotcrete mix could be better accounted for.

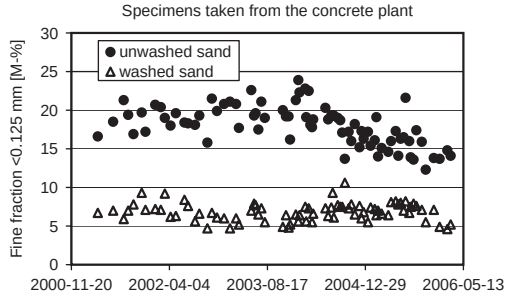


Figure 3. Fine fraction <0.125 mm in sands.

The following graphic shows the subsequent fraction of fines in the sand, as determined from over 80 specimens taken regularly from the concrete plant.

The fine fraction <0.125 mm of unwashed sand was on average 18.0% with a standard deviation of 2.5%. For washed sand, an expectedly lower average value of 6.8% and a smaller standard deviation of 1.2% could be measured.

The handling of unwashed crushed sand was a critical factor. The sand was susceptible to decomposition and often settled at the bottom of the silos of the concrete plant. It therefore had to be re-loosened with much effort. Concrete production workers were permanently attending to water requirements and mix consistency during production.

Visible variations in the consistency of the shotcrete mixes (in area designated for concrete work) increased the risk of changes to the mix through uncontrolled addition water into the mix. The quality of the concrete would thereby be reduced.

4.2 *Ensuring supply*

In addition to the suitability of the excavation material, the supply of enough aggregates to the site had to be ensured. The mix design for concrete and shotcrete therefore had to take the rate of material extraction into account as much as possible. In an initial phase in which much more shotcrete than cast concrete was required, an insufficient amount of grain size 4–8 mm was available. During this phase, approximately one-third of the aggregate of size 4–8 mm was procured externally. The lack of 4–8 mm aggregates was accounted for within the mix design by limiting its use as much as possible. The cast concrete mixes (mainly invert concrete) during this phase were therefore poured without the 4–8 mm grain size. The shotcrete mixes however could not be applied by reducing the 4–8 mm fraction through substitution of 0–4 mm sand, because the quantity of water in the mix was already high and further increases could not be tolerated (see chapter 4.1).

The petrographic composition, the aggregate form and the size distribution of aggregates produced on site differed from the externally procured aggregates. The deliveries of the externally procured aggregates to the concrete plant were carried out without prior notice. The concrete mixes were robustly designed so that resulting variations could be tolerated.

4.3 *Alkali aggregate reaction (AAR) resistance*

The aggregates to be used for concrete production (mainly silicic limestone) were classified to be reactive to highly AAR reactive (microbar values over 0.2%).

With the limitation of the alkali content in the concrete mix and the limitation of the amount of cement, the client made allowances for the AAR reactivity of the aggregates.

For shotcrete, Portland composite cement CEM II/A-M 52.5 with 10% limestone filler and 8% microsilica was utilized. The cement content was limited to 420 kg/m^3. The limitation of the cement content (420 kg/m^3 instead of the usual 460 kg/m^3 in Switzerland) with smaller maximum grain size decisively affected the workability and early-strength development of the shotcrete. The fines content of the shotcrete was approximately 590 kg/m^3, 170 kg/m^3 of which was 100 % crushed aggregates.

In instable areas, a mix with 520 kg/m^3 cement for face support and support in the area L1 was therefore specified to ensure sufficient early strength development.

In cast concrete, Portland cement CEM I and flyash of the ratio 70/30 % to 80/20 % was used.

The testing of the resistance to AAR of the mixes was conducted by the client with LCPC performance tests.

5 CONCRETE

5.1 *Test methods*

The verification of the strength classification was conducted in accordance with SIA 162 on cubes for cast concrete and SIA 198 on drill cores for shotcrete.

The water penetration depth under pressure, tested in accordance with DIN 1048 and SN EN 12390–8, served for verification of impermeability.

The sulfate resistance was tested in accordance with the Swiss standard SIA 262/1, Appendix D.

For the test of the sulfate resistance, six drill cores of diameter Ø 28 ± 2 mm with a length of 150 mm were taken from test cubes, shotcrete testing boxes, or directly from the structure. Cycle of drying and saturation can lead to the transport of significant quantities of sulfate into a test specimen. The sulfate reacts with the constituents of the specimen resulting in an increase in volume and destruction of the concrete matrix. For the evaluation, the changes in length and mass are determined. Initial experience from the test method is available, especially from the site Mitholz and other AlpTransit Gotthard sites.

Table 3. Mixtures.

	Shotcrete	Cast concrete	Cast concrete
Utilization	Sealing/ support	Invert construction	Lining
Max. grain	8 mm	22 mm	22 mm
Cement	CEM II/A-M 52.5 420 and 520 kg/m^3	CEM I 42.5 285–305 kg/m^3	CEM I 42.5 320–340 kg/m^3
Flyash		95–75 kg/m^3	110–80 kg/m^3
Liquefier	1.2–1.4%	1.5–1.8%	1.8–1.9%
Accelerator	0 and 5.5%		



Figure 4. Test for sulfate resistance.

5.2 *Shotcrete*

Image 5 shows that the shotcrete fulfils strength requirements of the classification B35/25. The average value of 290 tests was 49.2 N/mm^2 with a standard deviation of 9.8 N/mm^2. In comparison with cast concrete, the values for shotcrete deviated more widely, which is characteristic for the material.

Table 4. Fresh concrete values for shotcrete.

315 measured values	Slump [cm]	Water content [kg/m^3]
Average value	49	221
Standard deviation	4	10

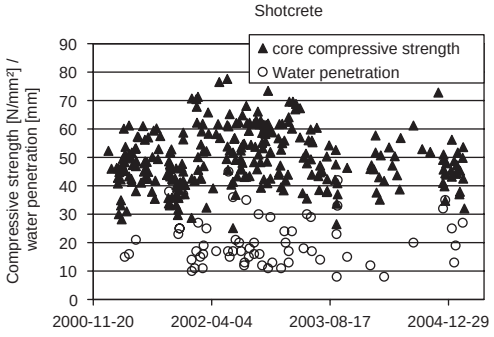


Figure 5. Shotcrete results.

Table 5. Fresh concrete values invert construction.

292 measured values	Slump [cm]	Water content [kg/m^3]
Average value	45	195
Standard deviation	7	13

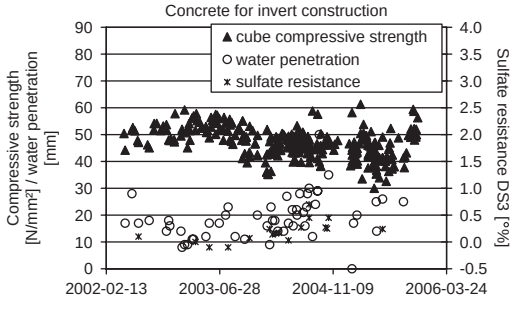


Figure 6. Concrete for invert construction.

The average of 66 tests of water penetration was 21 mm. The amount of reserve to the limiting value was good at three standard deviations (9.1 mm).

5.3 *Concrete for invert construction*

The cube compressive strength reached an average of 47.0 N/mm^2 with a standard deviation of 5.4 N/mm^2. The strength classification requirements for B35/25 were fulfilled. The requirements for impermeability were also fulfilled by with a good amount of reserve with a water penetration on average of 19.4 mm with a standard deviation of 7.7 mm.

For sections with a sulfate concentration of over 250 mg/l, concrete with a high sulfate resistance was required. The Δl(DS3)-values from Mitholz were on average 0.2‰ for 17 tests. As a reference value for concrete with high sulfate resistance, SIA 262/1 requires a series value Δl(DS3) of 0.5‰.

Table 6. Fresh concrete values for inner lining.

313 measured values	Slump [cm]	Water content [kg/m^3]
Average value	53	196
Standard deviation	6	10

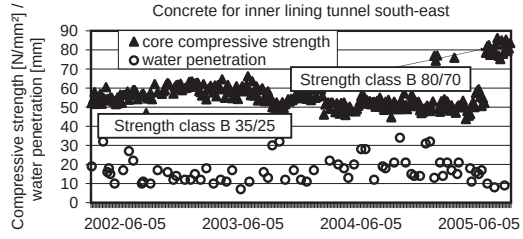


Figure 7. Concrete for inner lining.

5.4 *Concrete for inner lining "south-east"*

The demands on strength (B35/25) and impermeability (water penetration <50 mm) could be met with the average compression strength of 54.5 N/mm^2 (standard deviation 4.5 N/mm^2) and an average water penetration of 17 mm (standard deviation 6 mm) with sufficient reserve. The mixes were tolerant against construction variability and were therefore of little risk for the construction consortium.

For approx. 20 sections in a zone with very unfavorable rock conditions, the strength requirements were significantly increased to B80/70. The concrete mix was adapted. Instead of the cement CEM I 42.5, the cement CEM II/A-M 52.5 with 400 kg/m^3 and a maximum grain size of 16 mm was utilized. The quality control of the production was intensified. This difficult phase could be realized with a impressive compression strength on average of 80.8 N/mm^2 with a very good standard deviation of 3.2 N/mm^2. The average value of water penetration in this concrete was 9 mm.

6 CONCLUSIONS AND OUTLOOK

The experience gained from the construction site Mitholz proved that high-quality concrete can be produced from aggregates processed from tunnel excavation material.

The special constraints demand however that all affected parties are very willing to cooperate. For the

constructive and excellent cooperation at the Mitholz site, gratitude must be passed on the participating personnel of the construction consortium ARGE Satco, the concrete producer Mobilbaustoffe, the representatives of the client and the material processors. Thanks also to the site supervision team, who generously provided the test data used in this report.

The experience gained from construction site Mitholz serves as a valuable basis upon which future structures can be designed.

Engineering design work conducted in accordance with the Swiss standard SIA 260 must incorporate the choice of suitable construction materials as a measure for dealing with hazards of structural members. For concrete, this means that the design engineer must determine the exposition class of the concrete, and accordingly, any further necessary requirements and procedures. Because the expected service life of tunnels usually exceeds 50 years, a performance-based design process in accordance with SN EN 206–1 is to be applied. In Switzerland, many recognized testing methods and assessment values (sulfate resistance, frost and frost salt resistance, water penetration, water conduction) can be utilized by the design engineer.

Underground Space – the 4th Dimension of Metropolises – Barták, Hrdina, Romancov & Zlámal (eds)
© 2007 Taylor & Francis Group, London, ISBN 978-0-415-40807-3

Certification of shotcrete nozzlemen around the world

C. Larive
CETU, Bron, France

K. Gremillon
DIR IdF, Créteil, France

ABSTRACT: Quality of shotcrete works is deeply linked with the nozzlemen know-how which results from a long experience combined with strictness. That also implies the knowledge of the equipments and the appreciation of the supports, the evaluation of the incidence of the climatic conditions, the knowledge of the rules concerning the mixes and the additives, the respect of health and safety conditions. It is necessary, as well for the owner and for the engineering company, to be able to guaranty the quality of the work. The ITA WG 12, shotcrete Use, has thus decided to study the existing certification procedures and try to establish an all-over-the-world state of the art on that subject. This paper also enlightens the mains points to check to assess the know-how of the nozzlemen.

Shotcrete is being more and more used in the construction industry and it has taken real importance in civil engineering nowadays. It may be seen all around, for instance in:

- tunnels and underground car parks,
- houses and swimming pools,
- repair and reinforcement of concrete structures,
- soil nailing and slope stabilization.

That is why it has become important to propose a way to ensure a good quality of work. It is also suggested in the Eurocode 2 – "Design of concrete structures".

In every country, standards provide guides to obtain high quality projects but one usually recognizes that this is not enough; well-mixed concrete and standardized machines are not sufficient to provide superior quality by themselves, because, hidden behind all these material aspects, people work and a good job needs qualified operators.

In some countries, such as Brazil, Canada, France, Norway and the USA, certification programs for nozzlemen have been established. They tend to recognize the know-how of the workers, and of course, to give a proof that they are capable of providing a good job. Another organisation, the EFNARC, is trying to elaborate a certification which could be used as a reference in the whole Europe, mostly based on practical issues. This certification should be available in 2007. Sweden is also being preparing a certification procedure.

Information available in this paper have been gathered via exchanges with the ITA WG12 members. It may still not be exhaustive. Any comments or additions will be welcomed.

Currently the most well-known and used certification in the world is the North-American one, prepared by the American Concrete Institute (ACI). The first *Guide to certification of shotcrete nozzlemen* was dated from 1991 and has now been withdrawn by ACI. A new nozzleman certification program developed by ACI Committee C 660 is outlined in publication CP-60, "Craftsman Workbook: ACI Certification Program for Shotcrete Nozzlemen". Around 550 nozzlemen are now certified in America (both North and South) and this certification is world-wide delivered. Some countries, for example the United Kingdom, also use it whereas others take it as a starting point for their own certification process, France for example. The documents available in other countries are dated from 1996 for Brazil and 2004 for France.

1 TYPE OF CERTIFICATION

Different types of certification are to be considered: those for « manual » nozzlemen and those for « robot-aided » nozzlemen. In each one, the process (wet- or dry-mix) can be distinguished. Certification can also deal with only one type of position (vertical) or both (vertical and overhead).

Table 1 summarizes the situation.

Table 1. Different types of certification today.

	Type		Process	
	Robot	Manual	Dry	Wet
Brazil		x	x	
France	x	x	x	
Norway	x	x		x
Sweden	x	x	x	x
ACI		x	x	x
EFNARC	x		x	
	Experience		Position	
	Theoretical	Practical	Vertical	Overhead
Brazil			x	
France	x	x	x	x
Norway	x			
Sweden	x			
ACI	x	x	x	x
EFNARC	x	x	x	x

Note: French examinee has to shoot both vertical and overhead panels during the certification. ACI proposes to be certified in vertical position only or in both vertical and overhead position.

As there are two ways of spraying (aided or not), there must be two types of certifications. Today, the only country that proposes a complete (theoretical and practical) certification for robot-aided nozzlemen is France but the EFNARC will elaborate an other one in 2007 and Brazil also will. In this paper, emphasis is put rather on ≪manual≫ nozzlemen certification but indications are also given on the future EFNARC procedure and on the specificities of the French procedure for robot certification.

Note: ACI is discussing about robotic certification. Many in ACI believe now that a nozzleman must first be certified for manual shotcrete before he/she can be certified for robotic.

Concerning wet- and dry-mix process, some countries chose to separate certifications, judging the process is different enough, because wet-process nozzlemen need to regulate only the amount of air while dry-process nozzlemen need to regulate both air and water to produce good shotcrete.

Norway and Sweden have merely theoretical examinations today. Anyway, it is commonly considered that both theoretical and practical parts of the certification are useful to ensure the operator works well and safely, understands concrete technology, and is able to sort out a problem *in situ* if necessary.

Practical tests are about the same in every country although there are small differences. Theoretical requirements vary depending on the country: it can be an oral or a written exam and the amount of required knowledge is not the same.

Shotcreting on a vertical panel is easier than on an overhead panel. That's why ACI International proposes two different certifications for nozzlemen: one for vertical shotcreting only, and another one for both vertical and overhead shotcreting. However, France for instance proposes only one certification taking into account both positions. The EFNARC will probably propose only one certification, done on a construction site, with both vertical and overhead panels to shoot.

According to an article from *Shotcrete for underground support VIII* dated April 1999, Brazil has only one certification, for dry-mix process and manual nozzlemen. But now another one is in preparation, for wet-mix process and robot-aided nozzlemen.

2 BACKGROUND AND PREPARATION

Is there a "background" needed before having the right to apply for the certification? Here, background means professional experience as well as technical knowledge, diploma, or so.

- Brazil: according to the paper mentioned above, there is no need to have a specific experience to have the certification but the examinee has "to give a proof that he is able to take the test",
- France: there is no need to have any proof of professional background; both practical and theoretical knowledge are tested during an oral examination,
- Norway : the examinee has to attend a one week course specially dedicated to nozzlemen,
- ACI International: a minimum 500 hours of professional experience is needed to apply for the certification and there is a written test in which you have to prove that you not only know how to work safely and how to prepare your work but also that you have a basic theoretical knowledge about concrete.

Concerning the preparation, in Canada and the USA, the American Shotcrete Association (ASA) provides training courses as well as France but they also enable people to learn by themselves with a book: Craftsman Workbook, ACI Publication CP-60 (02).

Some documents published by ASQUAPRO (Association for the Quality of Spraying Concrete and Mortar) are also available in France, for example the technical guide *Mise en oeuvre des bétons projetés* (Shotcrete implementation). The book *Projection des bétons, mortiers & plâtres* is not specific for the preparation of the test but is also helpful. We are not aware of any documents of that type in other countries.

Note: ACI publishes ACI 506R-05, "Guide to Shotcrete", which is used in training sessions and is very helpful to nozzleman candidates.

The EFNARC should propose to send self-study pack to applicants before they take the jobsite test.

3 THEORETICAL CERTIFICATION

There are two different ways of passing the theoretical certification: an oral examination or a written one. This latter implies that the worker can read and write which may not be the case of every nozzlemen, even skilled ones but one can consider that it gives a better impartiality. However, an oral test allows more flexibility, and the inspector can re-direct his questions in order to better evaluate the nozzleman's knowledge, or ask him to precise his answers.

The theoretical part of the certification is closed book in every country (no documents allowed). As other documents are not available yet, here is what the *Craftsman Workbook* from the ACI expects from nozzlemen. This document is divided in 2 sections:

- Basic concrete technology, describing what concrete is made of and how it behaves.
- Shotcrete, section with 10 chapters in it:
  - What is shotcrete?
  - Equipments
  - Materials
  - Environmental conditions and precautions
  - Inspection and preparation of surfaces
  - Shotcrete placement, principles, and techniques
  - Communication (between nozzleman and either the gunman or the pump operator)
  - Finishing and tolerance controls
  - Safety
  - Testing/Quality

The test is made of 60 to 90 multiple choice questions. An oral examination instead of the written one can be permitted in special cases when conducted in accordance with ACI guidelines.

Note: the CP 60 Workbook and ACI Examination are now available in English and Spanish.

What the ACI certification expects from nozzlemen in this theoretical part is probably the highest amount of theoretical knowledge a nozzleman can be asked, along with the Norwegian certification.

The nozzlemen course in Norway has about the same program as ACI, including knowledge on concrete and shotcrete, construction site preparation, health and safety, environmental and strength classes, and so on. A written examination of 45 questions is administrated after the one week training.

In France, inspectors ask questions about machines set-up, substrate preparation, visual control of quality, health and safety, basic knowledge on shotcrete formulation – more specifically on admixtures, but not on other types of concrete. This is because good nozzlemen are expected but they will not be asked to design their own concrete mix.

In Brazil, the examination can be either written or oral. The field of required knowledge seems to be about the same as in France.

Finally, the EFNARC will probably ask questions on practical issues, such as the correct way of spraying, or the conditions of health and safety. This theoretical part should consist of a multiple choice questions test, oral or written.

It can be noted that, even where there is no need to give a proof of a minimum professional experience to take the certification, it is in fact necessary to pass.

Sweden is at the start of a development phase designed not only to raise (via the certification of personell) the competence of shotcrete nozzlemen, but also to increase the understanding of all staff involved in shotcreting. The post-treatment of shotcrete is an important element in this. The main ideas are:

- The results of shotcreting are highly dependent on the skills of nozzlemen. Many elements in the work cannot be subsequently checked. Complete trust has to be placed in such elements being correctly executed in any given situation.
- The results of shotcreting carried out by contractors are also highly dependent on work supervisors, consultants and customers having the necessary knowledge. Because standstill costs in general are considerable in tunnel projects, correct decisions must often taken under great time pressure.
- For shotcrete workers, the Shotcrete Centre and Vattenfall Utveckling shall develop course packages that can be used for licensing. The Shotcrete Centre and Vattenfall Utveckling shall also develop training materials for work supervisors, consultants and organisations buying shotcreting services.

4 PRACTICAL CERTIFICATION

According to ACI, after passing the theoretical test, nozzlemen are allowed to take the practical one. It is usually held in this order, first theoretical, then practical, so that if the first one is failed there is no need to set up the installation.

The practical part usually consists of shooting two panels, both vertical and overhead, except in Brazil where only vertical panels are sprayed. For the ACI program, the examinee chooses whether to shoot only vertical, or both. In France, there is no possibility to take the test only for the vertical panels.

The certification in France is taken either at the end of a training course or on a construction site. In that latter case the examinee's equipment is provided by the company. In the former case, a hard hat, security boots and protective clothings are brought by the examinee. In North America, nozzlemen should have their own equipment to take the test. No information is available for Brazil.

In every country where the certification can be taken, as part of the practical examination, the

examinee has to check that the machine is properly set-up, then he has to shoot a vertical panel.

After this,

- In North America, he is allowed to shoot an overhead one if the first panel has been estimated good by the inspector.
- In France, he shoots the overhead panel without waiting for the inspector to look at the first panel.
- In Brazil, he shoots another vertical panel.

In France, if a nozzleman thinks that he failed his panel, he is allowed to shoot another one.

Those panels are examined by the inspector at least 24 hours later in France. A furrow is sawn in the back face of the panel, perpendicular to the steel bars. A measurement of the voids behind the bars is then performed. In North America, five core samples are drilled through the reinforcing bars and graded from 1 (best quality) to 5 (worst quality).

In France, when the certification is taken after a training course, the concrete used for the test is standardized, otherwise it is the mix used on the construction site. In North America the shotcrete mixture is one in common use in the geographic area of the test site. This information is not available for Brazil.

The test panel has standardized dimensions, in France and in North America. France chose to reduce the dimensions of test panels from $75 \times 75\,cm^2$ to $60 \times 60\,cm^2$, judging it would be enough (the sides of the panels are semi-open) and easier to manipulate. No information from Brazil is available.

The EFNARC will probably only propose to take the test on the construction site. It should consist of shooting sample panels and check the results on cores.

The aim to shoot those panels is obviously to evaluate nozzlemen. A lot of criteria are examined during this test, depending on the country in which the examinee takes the test. In Brazil, the main criterion is the homogeneity of concrete, in order to check that the nozzleman is able to reproduce shotcrete with minimum variations. So the factor water/dry material shall not vary of more than 1% between the two panels, and volume of void shall not vary of more than two 2%. There is also a limit value not to reach: wastes ought to be inferior to 35%.

However, in France and North America, there is no criterion of homogeneity. In France, the main criteria are voids behind steel bars, which represents 60% of the mark; then come the surface quality, which represents 10% of the mark, framed edges quality (10% of the mark) and strength at an age of 7 days (20% of the mark).

In North America, a lot of criteria are also examined, divided in three steps, preplacement, start up, and placement. The examinee has to identify people and machines, to check the installation, and to use proper positions during the spraying, then 5 cores are examined, in which the inspector will detect laminations, sandy areas, shadows and voids.

Note: for the French "robot-aided" nozzlemen certification, the dimensions of the test panels are modified: 1000 mm × 1000 mm × 150 mm. 9 cores are extracted to analyse the compressive strengths at the age of 7 and 28 days and the homogeneity of concrete. Other particularities, not described here, are to be taken in account. For instance, if the examinee uses of fibre reinforced concrete, the amount of fibre should be controlled in situ.

5 NOTATION

Concerning the theoretical part, in Brazil the examinee has to give the correct answer to ten questions out of twenty to pass the test. In the ACI exam, the nozzleman has to give the correct answer to 75% of the proposed questions. In France, each type of question is evaluated between 0 to 4. The examinee must have no marks less than 2 for the five types of questions, which gives a minimum of 10 out of 20 but without any real lack of knowledge in any field.

The percentage of good answers to pass the theoretical exam in Norway is not available.

A lot of points are examined by the inspectors to evaluate the practical part, as seen in the previous chapter.

In France, the way to give a mark is quite complicated:

- Basically, the idea is first to measure the section of voids behind the five steel bars, and to give a mark (on 5, one point per bar). If a mark of 0 is given for one armature, or if the total is 3 or less, the test is failed. So examinee is given a mark on 12 for the two test panels (two marks on 5, multiplied by a factor of 1.2). The way to measure those voids depends on the diameter of steel bars (reference: 16 mm) and can easily be adapted if the steel bars used on the construction site are different.
- The quality of framed edges is marked on 2; the examinator eliminates 5 cm at each extremity and reduces the maximum mark by 0.1 when a default is seen on 1 to 5 cm. The mark 0 to this part means failure of the entire certification.
- The quality of surface is also marked on 2, but a mark of 0 here does not mean failure of the certification.
- Finally, compressive strength at an age of 7 days is marked on 4. The test is done on three cores. The maximum mark is given when the measured compressive strength is greater than 90% of the compressive strength at an age of 28 days. A mark of 0, meaning failure of the certification, is given when the measured strength is below 65% of the compressive strength at an age of 28 days.

Table 2. Notation for ACI certification.

	Grade (%)(a)	Weight (b)	Score (a*b)
Step A		0.25	
Step B		0.20	
Step C		0.55	
Total weighted score (Minimum passing = 75%)			

- The French certification is granted when the total mark is 12 or above.

In the ACI system, the examinee must have more than 15 correct out of 19 points observed in step A, preplacement. Then, more than 7 correct out of 9 points is needed in step B: start up. For step C: placement, each point is given a mark from 0 to 4. The total gives a mark on 36 (overhead panels) or 44 (vertical panels). If two or more 0 are given, the certification is failed. Finally, five cores are examined, and given a mark from 1 (best quality) to 5 (worst quality). If any one individual core is graded higher than 3, the entire test panel is failed, or if more than 2 cores are graded 3 or higher the entire test panel is failed.

To pass the ACI certification, the examinee must have:

- « Pass » for the core grading part
- a minimum of 75% of correct answers for steps A, B and C, with the following calculations

For example, assuming the examinee has taken the exam for vertical shotcreting only, and got 16/19 for step A, 8/9 for step B, and 30/44 for step C, that means 84.2% for step A, 88.9% for step B, and 68.2% for step C.

$$84.2 * 0.25 + 88.9 * 0.2 + 68.2 * 0.55 = 76.3\%$$

The examinee passed his certification.

The way to grant the practical part of the certification in Brazil is not available.

6 VALIDITY AND RE-EXAMINATION

This certification is usually granted for a limited period of time. In the ACI program, it has a validity period of 5 years. After that, nozzlemen have to take another certification examination which includes an oral interview and the practical examination

In France, the system is even harder. The first time you pass the certification, its validity period is 3 years and after you have to renew it every 5 years, as in North America. To lighten this system, heavy for both nozzlemen and companies, ASQUAPRO, that has designed the French certification, thinks about asking for proof that a certified nozzleman has been practising during the period of validity of his certificate, instead of asking him to take the exam again. The main problem is that proof must not be easily falsified. No information is available for Brazil and Norway.

Concerning the re-certification process when one has failed once, the North American certification proposes to retake only the failed part during the same year. For example, if the examinee failed the written exam, but passed the practical test, he will be allowed to retake only the theoretical examination for one year. Otherwise he has to retake the entire certification.

The process is about the same in France. The examinee can even choose to re-shoot a panel during the practical test if he thinks he failed the first one. The theoretical examination can be retaken if failed. The criteria to retake the tests are the same as in the ACI system.

7 CONCLUSION

Certification for shotcrete nozzlemen positively contributes to the good quality of work by insuring that the craftsmen are capable of constructing shotcrete structures in the proper manner.

This paper reflects the existing procedures. It can be updated by sending comments to the author[1] and it should be soon available on the ITA WG12 website.

It would certainly be good to adopt a common certification in every country but it is probably impossible to achieve because of the specificities of the already existing certifications. At least, it should be possible, inside the ITA WG12 “shotcrete Use”, to discuss on minimum adjustments so that foreign certifications could be accepted abroad.

REFERENCES

Shotcrete for Underground Support VIII. 1999, Shotcrete – Standardization in Brazil, www.asce.org

ACI International, Farmington Hills, MI, 2002, 69 – ACI CP-60(02), Craftsman Workbook: ACI Certification Shotcrete Nozzleman, pp, www.conrete.org

American Shotcrete Association (ASA), www.shotcrete.org

ACI International, Farmington Hills, MI, 2005, 39 – ACI 506R-05, Guide to Shotcrete, pp., www.concrete.org.

Hawk, C. Oral and written communication (Norway)

ASQUAPRO, 2005. Mise en oeuvre des bétons projetés, www.asquapro.asso.fr

[1] catherine.larive@equipement.gouv.fr

This page intentionally left blank

Underground Space – the 4th Dimension of Metropolises – Barták, Hrdina, Romancov & Zlámal (eds)
© 2007 Taylor & Francis Group, London, ISBN 978-0-415-40807-3

Robotic application of a unique sprayable membrane for the waterproofing of a subsea tunnel

S.L. Lamhauge
Nordöytunnilin PF, Tórshavn, Faroe Islands

K.G. Holter
BASF UGC Europe, Zürich, Switzerland

C. Ziegler
MEYCO Equipment, Winterthur, Switzerland

ABSTRACT: An innovative sprayable membrane was applied by a state-of-the-art computerized spraying robot for the waterproofing of a 6.2 km long road tunnel. The finally applied waterproofing system consisted of a thin composite liner with a 3 mm thick watertight spray applied membrane in a sandwich structure between the sprayed concrete for rock support and a final protective layer of sprayed concrete. This was the first time a completely computerized and mechanized method for the application of a waterproofing system in tunnels has been employed. The robotic application of the membrane included precise scanning of the surface to be sprayed as well as very controlled application of the membrane. This enabled the consistent application of the required thickness at a high speed.

1 BACKGROUND

1.1 *The project*

The Nordöy road tunnel connects the two islands of Eysturöy and Bordöy in the Faroe Islands with a fixed road connection. The second largest town Klaksvik, located on Bordöy, with 5000 inhabitants is thereby linked to the rest of the archipelago. The tunnel is entirely located in rock and passes under the fjord between the two islands.

The design of the tunnel was done according to the standards of the Norwegian Road Authorities. The tunnel was excavated by traditional drill-and-blast methods with rock support based on the single shell lining method with sprayed concrete and rock bolts. For control of the water seepage into the tunnel, a scheme with exploratory percussive drilling ahead of the tunnel face was carried out in the entire tunnel length.

Action criteria based on seepage into the tunnel measured in the exploratory holes defined the use of cementitious pre-injections ahead of the tunnel face in order to reduce the seepage into the tunnel to a cost-effective level.

The length of the tunnel is 6155 m with a cross section of 64 m^2 (two lanes). The maximum depth under the sea is 150 m with a minimum rock cover of approximately 40 m.

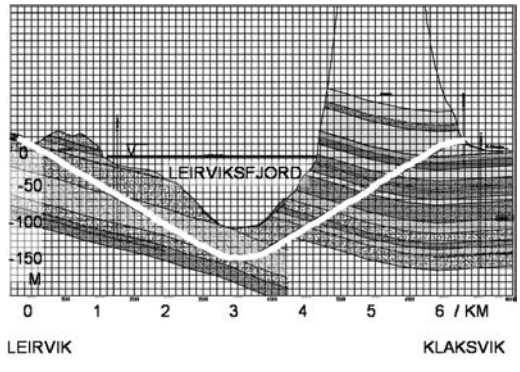


Figure 1. Geological section of the tunnel with main features. The strata indicated with the dark shade on the right (Klaksvik) side represent the weakest basaltic rock which were encountered. The light colored strata represent the competent basalt types.

1.2 *Geological conditions*

The Faroe Islands consist of volcanic deposits which are typical for the North Atlantic basaltic area. The rock types found are mainly extrusive basalts approximately 50 million years old.

The rock mass consists of a stratigraphy of basaltic rocks in which distinct layers can be identified with

thicknesses that vary from a few meters up to approximately 50 m. Each layer represents an event of a lava flow. One basaltic layer which was encountered in about 700 m of the tunnel length had a relatively soft and porous character and required extensive need for pre-injections and continuous rock support with sprayed concrete and rock bolts.

Otherwise the rockmass encountered in the tunnel consisted of very competent and massive basalts with compressive strengths in the range of 80–90 MPa.

2 REQUIREMENTS FOR THE WATERPROOFING OF THE TUNNEL

The original design and the tender documents required a waterproofing system based on Norwegian standards which basically consisted of a drainage shield with polyethylene (PE) foam sheets covered with sprayed concrete. The total cost of the waterproofing of the tunnel made up approximately 10% of the total project cost. The main reason for the waterproofing of the tunnel was to avoid drips on the actual road and to protect the different installations from humidity.

The experiences from the first subsea tunnel built in the Faroe Island, the Vaga Tunnel, completed in 2002, were that water seepages tend to diminish significantly over time. The first four years after opening of this tunnel, the seepage into the tunnel had been reduced by 20%. This was caused by minerals in the groundwater which deposit on the joints, and hence reduced the conductivity of the rock mass.

For this reason the main requirement for the installation of waterproofing was changed to 6 drips per minute from the original requirement of 3 drips per minute in an area of one square meter.

The Faroe Islands has a relatively mild climate. Significant freezing occurs only under adverse weather conditions. The waterproofing was therefore designed with frost insulation in only 200 m of the tunnel from both portals.

In the last few years there has been a trend to avoid flammable materials in underground construction. The flammable PE foam sheets were therefore not in accordance with a modern design philosophy with non-flammable materials. For this reason the owner was interested in alternative technical solutions for the waterproofing which could fit in with the single shell tunnel lining design. The goal was to reduce the amount of the PE foam waterproofing with more than 50%.

Several alternative technical solutions were considered. A technical solution with a sprayable waterproofing membrane in a composite liner based on sprayed concrete was chosen. Favourable experiences with sprayable waterproofing membrane had recently been made in Switzerland (Meier et al. 2005) and in the United States (Blair et al. 2005). This system could be made an integral part of a single shell tunnel lining based on sprayed concrete and rock bolts. Hence, this technical solution offered significant financial benefits over a technical solution with PVC sheet membrane and cast-in-place concrete lining.

The owner and the contractor reached an agreement in which the contractor was to make final decisions as to which waterproofing to apply. The criteria for this decision were based on seepage types and seepage intensities. In addition the cost-effectiveness based on the required amount of additional sprayed concrete was to be taken into account. Both the contractor and the owner had a financial benefit of utilizing the sprayable waterproofing membrane instead of the traditional PE foam waterproofing.

3 THE WATERPROOFING SYSTEM

3.1 *Properties of the chosen waterproofing system*

This waterproofing system is basically a composite liner which consists of a spray applied membrane in a sandwich structure between two sprayed concrete layers. The membrane has a normal thickness of 3 mm and a minimum thickness of 2 mm.

The main property of this membrane is that it bonds to both the substrate and the concrete which is applied onto it. This again leads to the important technical feature that the two interfaces between membrane and concrete on either side are impermeable. Hence, no water can migrate along these interfaces. Figure 2 below shows a core taken through the composite liner with spray applied waterproofing membrane and sprayed concrete.

The membrane-concrete interface has a tensile bonding strength of 1–1.2 MPa when completely cured. The curing of the membrane starts immediately after the spray application. The curing process consists of hydration of the cement part of the product and evaporation of the excessive water. Through this process a continuous waterproof film is formed. The curing process is irreversible. Hence, a subsequent feeding of water onto the membrane after curing, will not lead to a change of the waterproofing properties.

It is essential that the membrane thickness does not exceed approximately 5 mm thickness (other than local spots). Excessive membrane thickness might lead to very slow curing and if exposed to water from the substrate, the bonding and waterproofing properties might be compromised.

Waterproofing with a sprayable membrane embedded in a composite liner creates an undrained surface impermeabilisation. This might lead to local build-up of groundwater pressure immediately behind the membrane. When designing the waterproofing of the tunnel

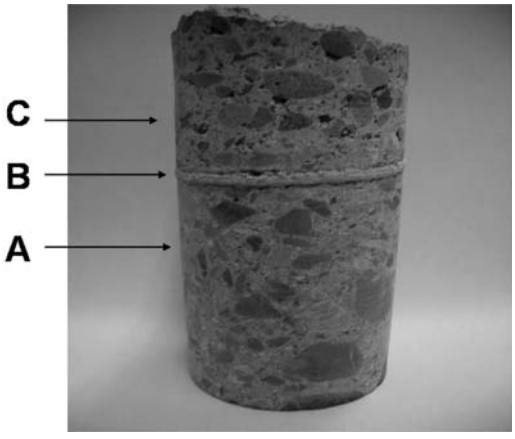


Figure 2. Composite liner, with sprayable waterproofing membrane in a sandwich structure between two sprayed concrete layers. The membrane (B) is applied onto the sprayed concrete substrate (A) with a thickness of 3 mm. Subsequently the membrane is covered with a covering layer of sprayed concrete (C) with minimum thickness 4 cm. (Meier et al. 2005)

one therefore had to bear in mind that a part of the tunnel contour had to remain drained, or a drainage measure had to be considered based on the actual situation.

In most cases, cracks and joints in the rock behind the membrane/concrete sandwich will drain to the invert ("umbrella" solution) without any significant pressure build-up.

4 APPLICATION OF THE WATERPROOFING SYSTEM

4.1 *Sequence of operations*

In order to provide suitable conditions for the spray application it was necessary to establish a proper substrate. The two main issues of the substrate preparation were substrate roughness improvement and removal of wet spots.

After the substrate had met the specified requirements, the application of the waterproofing membrane could commence.

4.1.1 *Improvement of the substrate roughness*

Achieving a continuous membrane with the required thickness between 3 and 5 mm, depends heavily on the quality of the substrate. An acceptable roughness in the cm order is achieved by utilizing a sprayed concrete with maximum grain size of 4 mm. A good substrate can also be achieved with 8 mm if the aggregate is very well graded and the actual application of sprayed concrete is particularly aimed at achieving a sufficiently good surface finish.

The surface characteristics regarding edges, holes and other irregularities were important to improve in a way that a thin continuous membrane was feasible. This involved the filling and smoothening out of holes and "trenches" as well as edges, sharp points and major irregularities in the substrate surface. Additional sprayed concrete had to be applied locally to the substrate for this purpose.

In several areas in the tunnel it was therefore necessary to apply an additional thin coat of sprayed concrete in order to achieve the proper substrate characteristics.



Figure 3. Handling of wet spots prior to the spraying of the waterproofing membrane. Manual application of a rapid curing priming membrane in progress to cover areas with installed drainage half-pipes.

4.1.2 *Handling of wet spots*

The wet areas which occurred where the sprayable membrane was intended had to be treated before the application of the membrane. Basically wet spots had be drained or injected. Only drips in the order of 3–4 drips per minute could be accepted.

The methods which were utilized for removing surface water ingress points were installation of drainage half pipes, polyurethane injections, drainage holes with drainage hoses and priming of the surface immediately before the application with a special rapid curing membrane.

Figure 3 shows the application of a rapid curing membrane as a primer in an area with drips and moisture where drainage half-pipes have been installed.

4.2 *Mechanical application*

The mechanical application of the sprayable waterproofing membrane utilized a state-of-the-art robotic (fully automatic) spraying machine.

This machine was originally designed for the robotic application of sprayed concrete with a very precise layer thickness.

The features of this machine, in particular the scanning of the substrate and the possibility to achieve a constant speed of the nozzle over the surface, made it suited for the robotic application of the waterproofing membrane.

4.2.1 *Scanning of the substrate surface*

Scanning is a digital distance measurement with a laser scanner of the detailed substrate contour. The scanner is located at the very front of the boom just behind the spraying head.

The operator defines the boundaries (corner points) of a square area on the tunnel contour to be scanned. The scanner then records the surface with a predefined grid density. In this case one used a 20 cm square grid density. The file with the scanned area was then in turn used for the robotic spraying of the area.

4.2.2 *Robotic spraying of the membrane*

The actual application of the membrane took place with the dry spraying method. That means the product was delivered using a rotor machine and transported pneumatically in a powdered state through a 32 mm diameter hose to the nozzle. The nozzle for membrane spraying is a standard nozzle for dry mortar spraying. Water is added in the nozzle through the precise adjustment possible with a needle valve. The equipment used for the application is very similar to that of dry sprayed shotcrete, but with minor modifications in order to achieve a low output which could be also be varied.

The robotic spraying of the membrane took place in the area which was scanned immediately in advance. In the given tunnel dimensions with a cross section of about 64 m^2, it was possible to spray sections of 3 m tunnel length covering the entire tunnel contour. The robotic part of the spraying process was the automatic movement of the boom and the nozzle. Feeding of air, water and the output of the product had to be adjusted manually.

The constant speed and smoothness of the spray manipulator movement and the ability to follow the surface topography made it possible for all given points in the scanned area to receive the exact same amount of membrane. These machine parameters had to be defined in advance. This was done in an initial exercise in order to optimize the mechanized part of the application.

When, during the application some irregularities on the surface were encountered, the necessary adjustments of the machine parameters could be carried out online with subsequent immediate response of the machine and consequential best results.

When starting spraying on each shift, one only had to fine-tune the air, amount of water (in order to achieve to correct mixture ratio) and the output of the dry spraying machine. When the crew had gained sufficient experience with the equipment, capacities of approximately 800 m^2 per twelve-hour shift were realized.

4.2.3 *Application of the covering layer of sprayed concrete*

The completion of the composite liner consisted of the final inner layer of sprayed concrete. The minimum thickness of the inner layer sprayed concrete was 4 cm. Steel fibre reinforced sprayed concrete was used for this purpose. This layer was applied after the curing of the membrane, which took 10–14 days under the given temperature, humidity and ventilation conditions.

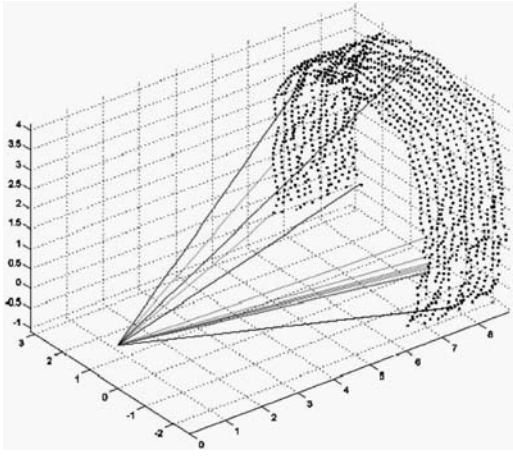


Figure 4. Principal sketch showing a 3D representation of a scan of the tunnel substrate surface prior to the application of the membrane.



Figure 5. Robotic application of the sprayable waterproofing membrane in progress.

The curing state of the membrane was measured indirectly by measuring the hardness of the membrane surface (Shore A hardness). Criteria based on measured Shore A hardness values were specified for the application of sprayed concrete onto the membrane.

4.3 *Quality control issues*

In order to assure that the proper preparations were undertaken and that the actual application of the membrane was done correctly a detailed procedure for the practical works was made. The procedure required the proper preparation works like substrate roughness improvement with sprayed concrete, different surface treatment of seepage points in order to assure feasible conditions for the membrane application.

Furthermore, the details in the application of the membrane were described, in particular how to achieve the correct sprayed thickness on the wall. This included thickness control measurements and the monitoring of the membrane powder consumption. The procedure also specified remedial measures to deal with seepages which occurred through the membrane after application.

5 EXPERIENCES

The composite liner with the sprayable membrane proved to be a successful waterproofing system. The main experience gained was that the importance of preparing the substrate properly cannot be underestimated. It was absolutely essential to have a smooth substrate with a limited roughness in order to achieve a continuous membrane. In this way a continuous regular composite liner was achieved. (Figure 7)

In areas where the waterproofing system was applied only locally in the tunnel contour or in smaller areas, the result was good. No effects of migrating water seepages to adjacent areas causing a possible need for waterproofing in a previously dry area were observed. (Figure 6)

The robotic application of the membrane proved to be cost-effective regarding overall application speed as well as reaching optimum material consumption. With the robotic application a consistent membrane thickness within the intended range was achieved. This again depended much on the substrate quality.

In areas with large substrate irregularities the robotic application could not be successfully completed so an additional application of the membrane with the same robotic equipment in manual-mode together with computerized support had to be done. The areas which were sufficiently treated with drainage measures showed no or only very little need for remedial works.

Some difficulties with the system during the application were experienced. These were mainly seepages penetrating through the lining in areas where a continuous membrane was not achieved during the spray application. This partially resulted in need for remedial local injection works. One important experience is that seepages through the membrane occur within the first day after application. These cases were targeted directly in a simple manner with local injections since the water seeping points in the membrane could be easily found.



Figure 6. Complete tunnel with the composite liner waterproofing system applied locally in one of the walls and half of the crown.



Figure 7. Complete tunnel with waterproofing with the composite liner of sprayable membrane and sprayed concrete in both walls and the entire crown area.

6 CONCLUDING REMARKS

The cost-effectiveness of the waterproofing system with a composite liner with sprayable membrane depends mainly on two main issues; creating a smooth enough substrate and the extent of wet areas which impose a need for wet spot treatment prior to the application of the membrane.

The experienced advantages with robotic spraying definitely favour this application method. Particularly the consistent membrane thickness which can be achieved with the lowest possible material consumption is a significant advantage. High application capacity with low demand on amount of manpower was realized.

REFERENCES

Blair, A.J. & Lacerda, L.L. 2005. Construction of the Wolf Creek Upper Narrows tunnel waterproof membrane – a comparison of tunnel projects utilizing the spray-on waterproof membrane. *Rapid excavation & tunnelling conference 2005, Seattle*. Littleton, USA. SME.

Meier, W. & Holter, K.G. & Häusermann, S. 2005. Waterproofing of an emergency escape tunnel by employing an innovative sprayable membrane: the Giswil highway tunnel project, Switzerland. *Proceeding of the 31st ITA-AITES world tunnel congress 2005, Istanbul Turkey pp 571–575*. Leiden. Balkema.

Part 6.2
Cast in situ and precast concrete

This page intentionally left blank

Underground Space – the 4th Dimension of Metropolises – Barták, Hrdina, Romancov & Zlámal (eds)
© 2007 Taylor & Francis Group, London, ISBN 978-0-415-40807-3

Study on cracks control of tunnel lining concrete at an early age

Hirofumi Takayama, Masaichi Nonomura & Yasuo Masuda
Japan Railway Construction, Transport and Technology Agency, Tokyo, Japan

Takashi Nakayama, Mikio Takahashi & Yoshiyuki Kojima
Railway Technical Research Institute, Tokyo, Japan

ABSTRACT: In Japan, cast-in-place plain concrete has been generally used as the secondary lining of mountain tunnels. In many cases, the small cracks induced by the thermal, autogenous and drying shrinkage were occurred at an early-aged concrete. It can be considered that an overall tunnel stability would not be reduced by this kind of crack, however, in the long term it could cause concrete spalling if cracks run cross one another.

In this study, firstly, the site observations were carried out for investigating the influences of concrete material, construction method and climate on the occurrence of cracks at the tunnels of the Kyushu Shinkansen line (in the southwest area) and the Tohoku Shinkansen line (in the northeast area). Secondly, the specimen tests were performed for observing the temperature and strain of concrete at an early age. Moreover, the model tests of concrete lining were carried out to investigate effects of the factors that detected from site observations. From these results, the methods of controlling crack are proposed and discussed.

1 INTRODUCTON

1.1 *Early-aged cracks on a second lining*

In Shinkansen project, NATM (New Austrian Tunneling method) is mainly used for constructing the tunnel in mountainous area. In this method, cast-in-place plain concrete has been generally used as a secondary lining (Fig 1). In many cases, the small cracks induced by the thermal, autogenous and drying shrinkage were occurred on inner surface (contact with air) at an early age. It can be considered that this kind of cracks would not reduce an overall tunnel stability, but it could cause concrete spalling in the long term if cracks run cross one another and could affect to the safety of a bullet train.



Figure 1. A secondary lining of NATM.

1.2 *Purpose of this study*

In the past, many studies had been carried out to find out the methods of controlling these cracks.

Some of studies focused on the reduction of friction between concrete and ground, because the occurrence of cracks mainly due to difference in strain between inner surface (contact with air.) and outer surface (contact with ground.). As a result, the following methods were developed, and applied widely in Japan.

- Usage of the isolation sheet by placing it between concrete and ground
- Installing of seam controlling cracks

However the above studies were carried out at the beginning of NATM technology that there were few preliminary case studies. Furthermore, the previous reports had a little discussion about the reduction of the thermal, autogenous and drying shrinkages at an early-aged concrete in a quantitative way.

In this study, firstly, the site observations were carried out for investigating the influences of variables on the occurrence of cracks at the tunnels of the Kyushu Shinkansen line and the Tohoku Shinkansen line before operating.

Table 1. Results of site investigation.

Tunnel	Division	Number of span	Ratio of cracks occurred (%)	Month	Temperature	Unit cement content (kgf)	Unit water content (kgf)
A	1	351	12	1∼12	19	271	160
	2	222	19	1∼12	18	273	163
	3	336	38	1∼12	16	273	163
	4	54	13	1∼3, 8∼12	16	276	164
	5	234	24	3∼12	21	272	161
	6	286	22	1∼12	18	279	164
	7	244	59	1∼12	18	298	179
B	1	68	37	2∼11	19	268	162
	2	334	43	1∼12	18	267	160
C	1	57	81	11∼12	–	312	181
D	1	44	39	6∼8	–	312	181
E	1	102	25	1∼12	20	268	155

Next, the specimen tests were performed for observing the temperature and strain of concrete at an early age. Then, the model tests of tunnel concrete lining were carried out to investigate effects of the factors that detected from site observations. From these results, the methods of controlling crack are proposed and discussed.

2 SITE INVESTIGATION

2.1 *Methodology of investigation*

The site investigations focus on the six variables; the ratio of the occurring cracks per span, the month and temperature when placing concrete, unit cement content, and unit water content. They are under concerned because, they have the high possibility to affects the thermal, autogenous and drying shrinkage. The information and data were collected from both northern and southern parts of Japan.

2.2 *Results*

The data of 2,332 construction span (span length = 10.5 m) were collected from 12 divisions of 5 tunnels. Table-1 shows the occurrence of the early-aged cracks in each division and construction variable, and Figure 2 shows the occurrence of cracks per division. The maximum ratio of crack occurrence is 40% and most of all cracks occurred at the tunnel crown.

2.2.1 *Concrete placing month*

The ratio of crack occurrence with month is shown in figure 3 and figure 4. In Tohoku region (table 1, tunnel A and B), the ratio is low in the summer. Whereas, in Kyushu region (table 1, tunnel C, D and E), the ratio is low in October and December.

2.2.2 *Concrete placing temperature*

The ratio of crack occurrence with temperature is shown in figure 5 and figure 6. The ratio was very low when the temperature less than 16°C for Tohoku region (table 1, tunnel A, B). In the case of Kyusyu region (table 1, tunnel C, D, E), the ratio is very low when the temperature is about 22°C.

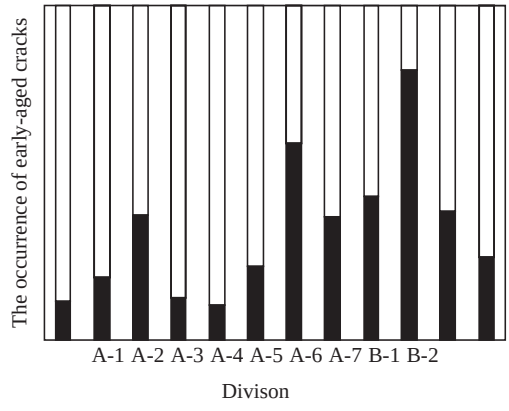


Figure 2. The occurrence of cracks per division.

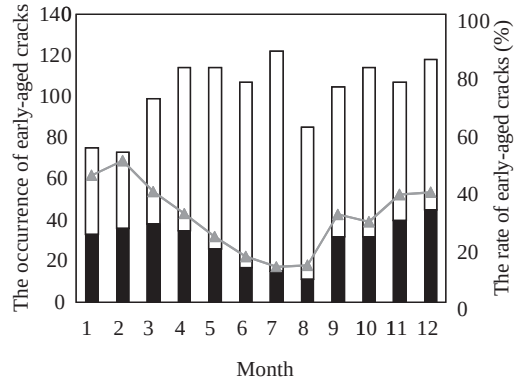


Figure 3. The occurrence of cracks with month in Touhoku region.

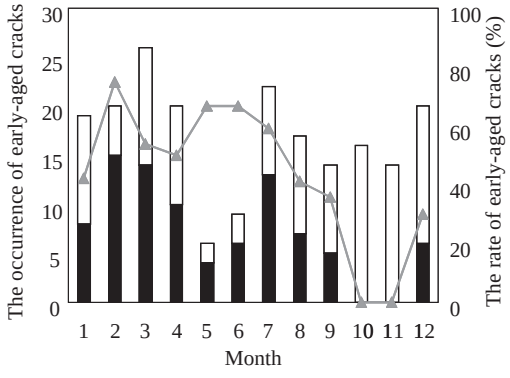


Figure 4. The occurrence of cracks with month in Kyusyu region.

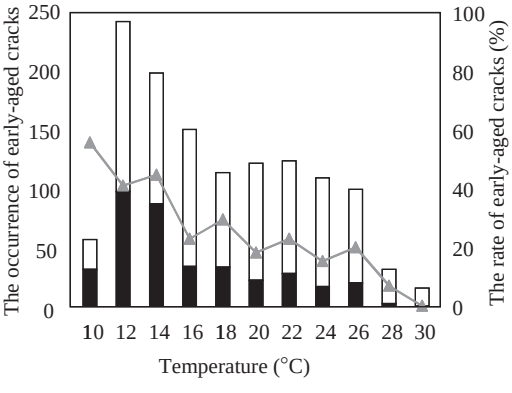


Figure 5. The occurrence of cracks with temperature in Touhoku region.

2.2.3 *Unit water content*

The ratio of crack occurrence with unit water content is shown in figure 7. As the unit water content increases, the ratio also increases.

These investigation results show the effects of the concrete placing month that can be implied to the ambient temperature, placing temperature and the unit water content on the occurrence of crack in tunnel concrete lining. However, there are many unknown factors such as the friction between concrete lining and ground, the amount of shrinkage strain that are very difficult to evaluate by site investigation.

Thus, in order to evaluate and the effects of each factor individually, it is necessary to investigate through the specimen tests and model tests.

3 SPECIMEN TEST

Specimen tests were carried out to investigate the effects of thermal and drying shrinkages on the occurrence of early-aged cracks by neglecting the friction between concrete and ground.

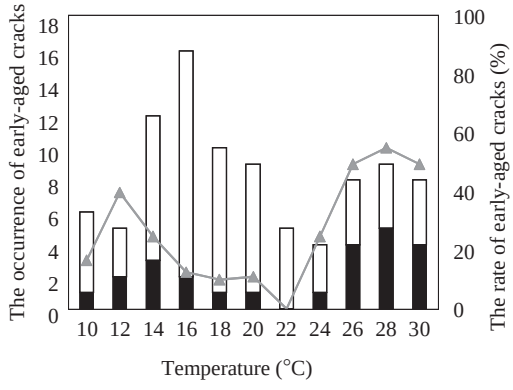


Figure 6. The occurrence of cracks with temperature in Kyusyu region.

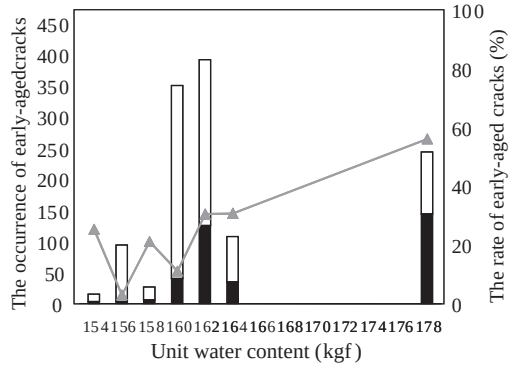


Figure 7. The occurrence of cracks with unit water content.

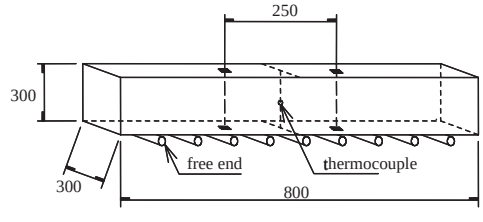


Figure 8. Test specimen.

3.1 *Methodology of test*

Figure 8 shows the specimen which has a pillar shape with 300 * 300 * 800 mm (300 is equal to lining thickness). Strain gauge and thermocouple were installed

Table 2. Mix proportion of concrete specimens.

W/C (%)	s/a (%)	Unit content (kg/m^3) W	C	S	G	Slump flow (cm)
60	48	180	300	847	941	15

Table 3. Test cases.

Case	Drying	Thermal dissipating
①normal	○	○
②No drying	×	○
③Partial drying	○ (only one surface)	○
④Insulation	×	×

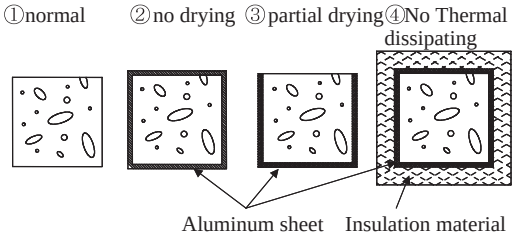


Figure 9. Wrapping conditions of each case.

within the center of specimen. Table 2 shows the mix proportion of concrete.

Table 3 shows the cases adopted in this test and Figure 9 shows image of each cases. Case①is normal type that has drying and thermal dissipating. Case②is no drying type that does not have both drying but has only thermal dissipating. Case③is partial drying type that has only one drying surface, same as the concrete lining. Case④is insulation type that does not have drying and dissipating surface.

All cases were testes under temperature 20°C, humidity 60%, constantly.

3.2 *Results of tests*

3.2.1 *Effects of drying*

Figure 10 shows the strain curves which show effects of drying between Case①and Case②. The strain of Case②is 200μ larger than Case①at about 50-day age. Figure 11 shows the strain curves which show the differences between a drying surface and a non-drying surface drying of Case③. The strain on a drying surface is 200μ larger than the other at about 50-day age.

Comparing with the concrete lining, the drying surface is the inner side of a lining, whereas, the non-drying surface can be implied as the outer side of a lining. Thus, these results show the difference of shrinkage strain between the inner and outer side of a lining that cause the cracks at concrete surface.

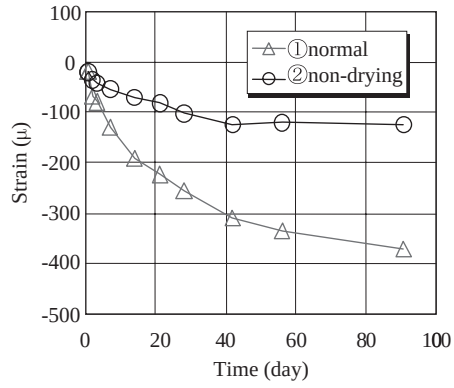


Figure 10. Effects of drying (Case①and Case②).

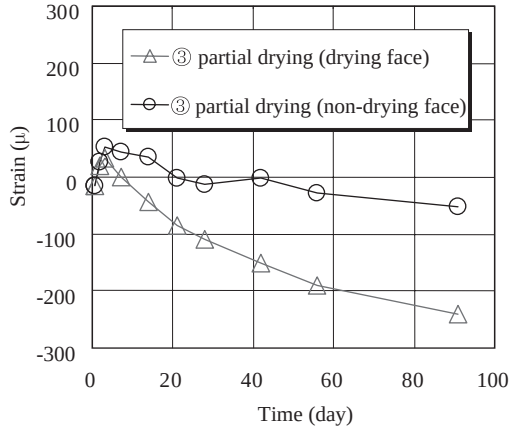


Figure 11. Effects of drying (Case①and Case③).

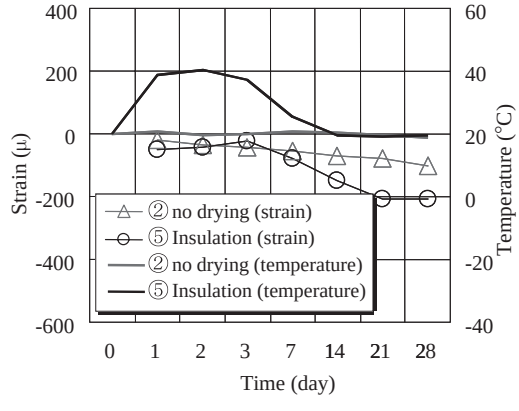


Figure 12. Effects of thermal state (Case②and Case④).

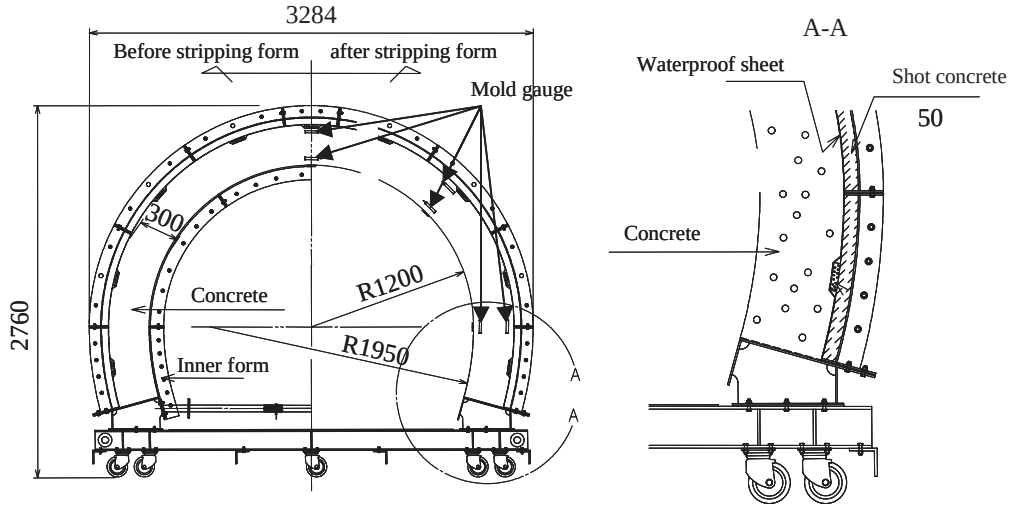


Figure 13. Test piece of tunnel model.

3.2.2 *Effects of thermal state*

Figure 11 shows the strain which show the effects of thermal dissipating between Case② and Case④. The strains of Case④ is 200μ larger than Case② at about 50-day age.

From these results, the outer surface that contacts to a ground were significantly affected by the thermal state while the inner surface that contacts to an air were significantly affected by the drying. The strains at both surfaces differ about 200μ, that is possible to make cracks on concrete lining. Thus it can be concluded that only the thermal and drying can cause the cracks on concrete lining.

Table 4. Test case.

	Material		Condition	
Case	Cement	W/C	Stripping time	Atmosphere
①Normal	Normal	60%	18 h	60%
②Type of cement	Flyash			
③W/C		70%		
④stripping Time	Normal	60%	12 h	
⑤atmosphere			18 h	50%

4 TUNNEL MODEL TEST

To connect the results of site investigation and the results of specimen test and find out the methods of controlling an early-aged crack, the tunnel model test were performed. The test was mainly focused on the following problems.

- The differences of strains between the outer and inner of lining, that show the effects of tunnel shape.
- The differences of construction method and concrete material, that show the relation between drying and thermal dissipating.

4.1 *Methodology of test*

Figure 13 shows the tunnel model that has a horse-shoe shape with 1200 mm and 1950 mm in inner radius and 300 mm in thickness. The mold gauges (combination of strain gauge and thermocouple) were installed at the inner side and the outer side of tunnel crown, springline and 45° from the crown.

Table 4 shows the conditions for each case and Figure 14 shows picture of form. Case①is the normal type that based on the common construction method and normal environments. Case②is the flyash cement type. Case③is the W/C type with high water content and little high concrete placing temperature. Case④is the stripping time type that has shorter time for curing. Case⑤is atmosphere type that was placed in low humidity environment. All of parameters were varied in the range of real tunnel conditions in Japan.

4.2 *Results of test*

4.2.1 *Effects of tunnel part*

Figure 14, 15, and 16 show the strain curves with time of Case①. These results show that outer strain is larger than inner strain at tunnel crown. At the springline, the outer strain decreases and becomes constantly.

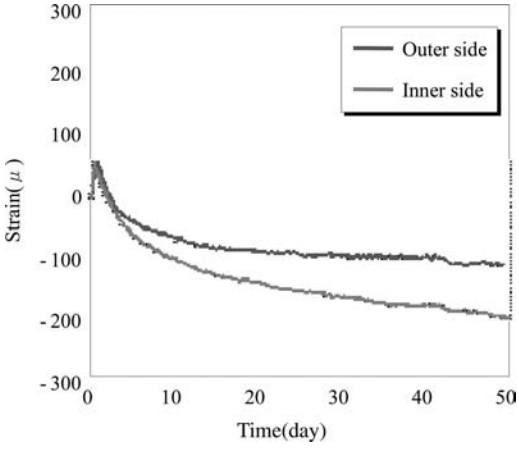


Figure 14. Strain curves at Tunnel Springline.

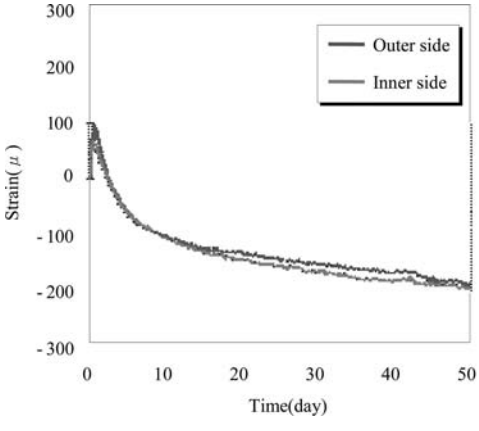


Figure 15. Strain curves at 45° from Tunnel Crown.

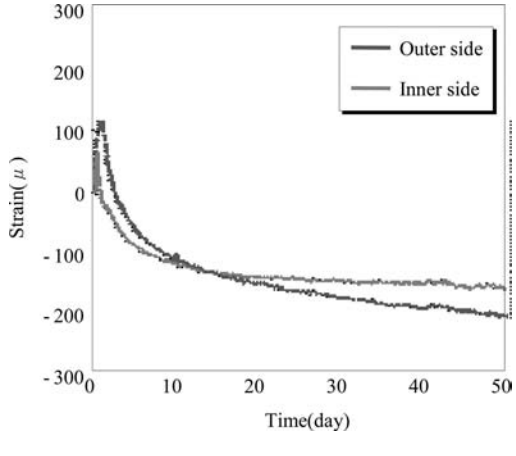


Figure 16. Strain curves at Tunnel Crown.

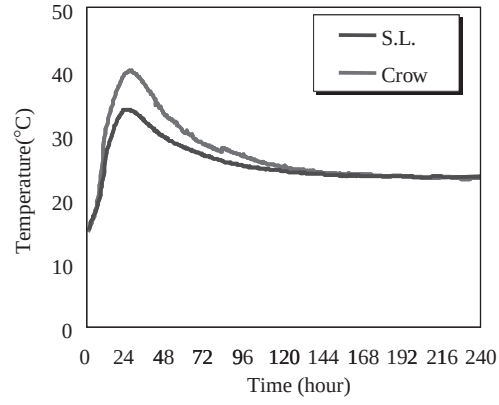


Figure 17. Temperature curves of Case①.

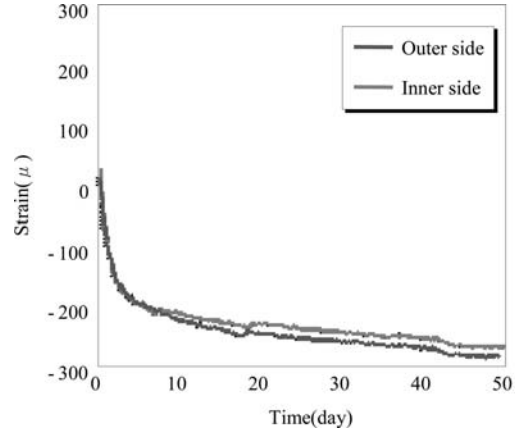


Figure 18. Strain curves of Case③.

Figure 17 shows the temperature curve with time of Case①. This change can be explained at the thermal viewpoint.

The effects of autogenous and drying shrinkage on each part of tunnel lining, do not show the remarkable different. However, about the temperature change, the thermal of hydration increases from tunnel springline to crown.

4.2.2 *Effects of construction method and material*

Figure 18, and 19 shows the strain curves with time of Case③ and Case⑤. The results of Case②, Case④ and Case③ are nearly same and it do not show the remarkable between the inner and outer strain. It can be assumed that there is no remarkable influence on

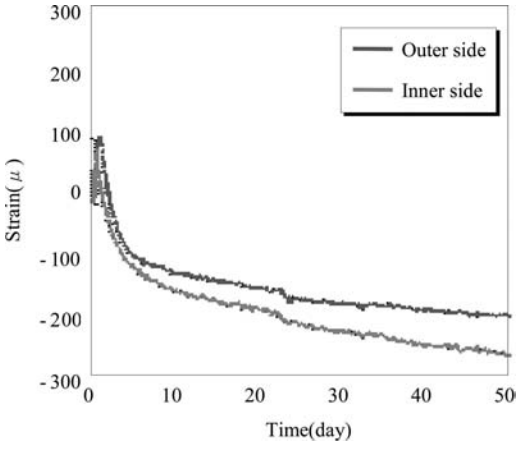


Figure 19. Strain curves of Case⑤.

the occurrence of cracks because both inner and outer sides shrink at the same amount.

For Case⑤, the inner strain is larger than the outer, and that has a possibility to make the occurrence of cracks in this test.

5 CONCLUSION

In this study, site investigation, specimen test and tunnel model test were carried out. The results can be concluded as followings.

- Drying and thermal dissipate have remarkable effects on causing cracks on lining.
- Tunnel crown generally does not have possibility to cause the occurrence of cracks only due to thermal state.
- Only atmosphere, especially the humidity, has the possibility to affect the occurrence of cracks due to drying.

Now, we plan to develop the method of control atmosphere, and the in-situ test to identify its effects.

This page intentionally left blank

Underground Space – the 4th Dimension of Metropolises – Barták, Hrdina, Romancov & Zlámal (eds)
© 2007 Taylor & Francis Group, London, ISBN 978-0-415-40807-3

A study on fire resistant segment using short fiber resin

Sinji Seki
Manager, Civil Engineering Technology Division, Shimizu Corporation

Toru Goto
General Manager, Civil Engineering Technology Division, Shimizu Corporation

Takeshi Morita
Dr., Institute of Technology, Shimizu Corporation

Yugo Hayashi & Takuya Nakagawa
Chief, Civil Engineering Technology Division, Shimizu Corporation

ABSTRACT: A fire in the current shield tunnel on a highway or railway would cause explosive spalling of concrete lining due to high temperature that mostly result in significant damages to the tunnel structure. The conventional fire protections for the tunnel structure have utilized separate ceramic panels being attached or spraying fireproof materials on the surface of the lining. However, the ceramic panels are rather costly, and the spraying induces poor working conditions. As a substitute, the concrete segments with enhanced fireproof performance have been developed by the use of short fiber resin. A series of fire tests were conducted to verify their fireproof performance. This paper mainly reports on the results of fire tests.

1 INTRODUCTION

A fire in the tunnel on a highway or railway would cause breakages of concrete lining due to high temperature that mostly result in significant damages to the tunnel structure. The conventional fireproofing methods for shield tunnels have so far employed second lining over the primary lining, or utilized fireproof coating being pasted or sprayed to the surface of primary lining, any of which protects the primary lining by the use of additional fireproofing materials. However, these conventionl foreproofing methods have been not so beneficial with respect to econical efficiency, working efficiency and construction periods as to satisfy every requirement for the current construction conditions.

Thereupon, this study, encouraged to impose fireproof performance on concrete segments themselves, has focused on the Polyacetal (hereinafter PA) fiber in addition to the PP that conventionally developed with reference to the AFR concrete employed to practical use of very high strength concerete. And the fireproof performance, manufacture and repair of short fiber reinforced concrete has been experimentally examined on the basis of the concerete used in the RC segments.

The elementary experiments have investigated difference of heat-induced breakages according to the existence of short fiber resin and distribution of temperature. The experiments for practical use have then implemented a series of heating tests with the employment of the specimens reflecting the situation in actual use and manufacture process, which provided an examination of characteristics and performance required to the practical design guide. This paper presents the experimental results that facilitate new development of fireproofing structure for shield tunnels.

2 ELEMENTARY EXPERIMENTS

The favourable effect of AFR concrete has been already verified with the very high strength Concrete (design strength $> 80\,\mathrm{N/mm^2}$) for building construction. However, the elementary experiemts were conducted in the necessity of examining acquisition of similar effect even for the segments showing a low design strength and different mix proportions, and occurrence of heat-induced breakage under the RABT heating curve.

2.1 *Testing methodology*

a) *Materials and mix proportion in base concrete*
Table-1 demonstrates the mix design of base concrete.

Table 1. Mix design of base concrete.

Maximum size of coarse aggregate(mm)	Slump (cm)	Air content (%)	W/C (%)	Sand percentage s/a (%)	Unit weight (kg/m^3)				
					Water	Cement	Fine aggregate	Coarse aggregate	Additive
20	3 ± 1.5	1.5 ± 1.0	36.4	43.5	150	412	804	1059	16.9

Table 2. Type and quantity of concrete and heating test.

Mix design	Fiber	Specimen for heating: Mixing Ratio of fabric *1 (%)	Specimen for heating: Small speciment*2	Specimen for heating: Panel
N36.4	–	–	3	2
N36.4-PP0.1	PP	0.1 (1.0 kg/m^3)	3	–
N36.4-PP0.3	PP	0.3 (3.0 kg/m^3)	3	2
N36.4-PP0.5	PP	0.5 (5.0 kg/m^3)	3	1
N36.4-PA0.1	PA	0.1 (1.5 kg/m^3)	3	–
N36.4-PA0.3	PA	0.3 (4.5 kg/m^3)	3	2
N36.4-PA0.5	PA	0.5 (7.5 kg/m^3)	3	2

*1 ( ) indicates the mixing weight per 1 m^3 of concrete (mass)
*2 plain concrete specimen of which the end face is 100×100 mm, 400 mm in length.

b) *Type of concrete and specimen*
7 types of concerete were used in the experiments according to the type of fiber and its mixing ratio as shown in Table-2. Using this concrete, the specimens for heating test, compressive strength test and water content test were prepared.

For the heating test, small specimens with a dimension of $10 \times 10 \times 40$ cm and panel-type specimens as shown in Figure-1 were employed. The small specimens were manufactured without reinforcement, whereas the panel-type specimens were reinforced with single rebar of D10@100 (the depth from the surface to the center of distribution reinforcement: 50 mm).

c) *Procedure for heating test*
The heating tests were conducted with two sets of specimens grouped by curing ages of 36 days and 41 days due to limited space of the heating furnace. The heating temperature was given following the RABT temperature curves for tunnel fire test. According to the capacity of heating furnace, the maximum temperature was maintained for a duration of 25 minutes which had been readily proved to be valid for inspection of heat-induced breakage. Figure-2 illustrates the RABT curves employed to the tests. Also, the figure simultaneously demonstrates the internal temperature of the member (40 cm in thickness, no heat-induced breakage) that was calculated based on the Fininte Difference Scheme.

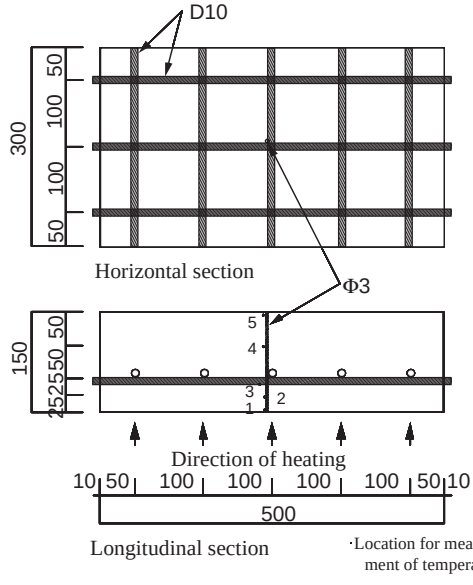


Figure 1. Panel-type specimen for heating.

Both of the end parts 5 cm long from each end of a specimen in the direction of long side are located right above the supporting frame for the specimen, those parts are not directly heated. Hence the heated area of the specimen with a dimension of $10 \times 10 \times 40$ cm (hereinafter $10 \times 10 \times 40$ cm specimen) actually becomes 10 cm $\times$ 30 cm, and that of the panel-type specimen becomes 30 cm $\times$ 40 cm.

The heating temperature and internal temperature of specimen were measured during the heating test. (the internal temperature is limited to panel-type specimen). Besides, the depth of heat-induced breakage was also inspected by the use of a vernier caliper before and after the heating test. As for the $10 \times 10 \times 40$ cm specimen, the depth of heat-induced breakage was measured across the heated area (10 cm $\times$ 30 cm) in the form of grid whose vertical and horizontal spacings were identically 2 cm, as for the panel-type specimen, it was measured at a spacing of 5 cm in both the horizontal and vertical directions over the heated area (30 cm $\times$ 40 cm). Photo-1 thru 2 show the situation of specimen after the heating test.

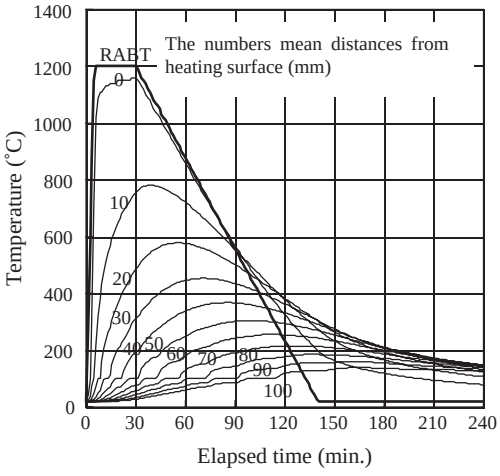
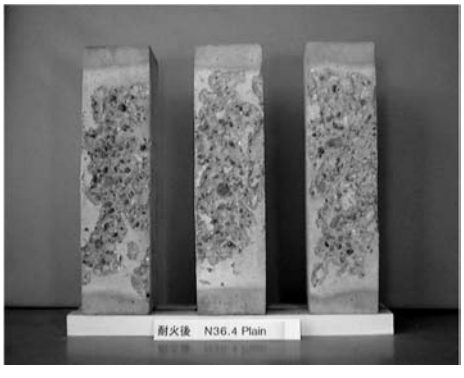


Figure 2. RABT temperature curves and internal temperature of panel specimen (Calculated).



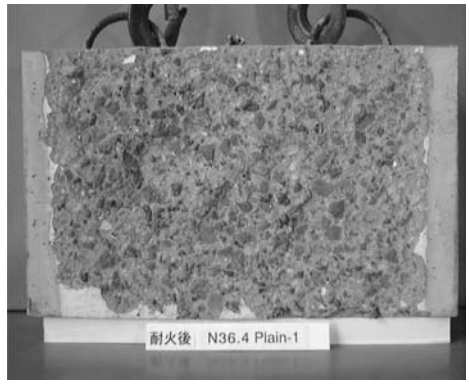
<Without fiber mixed (Mixed design:No.36.4)

Photo 1. Situation after heating test with small specimen.

2.2 *Summary of elementary experiment*

In order to obtain the elementary data regarding fireproof performance (resistance against heat-induced breakage) of AFR concrete for tunnels, a series of heating tests had been implemented with the various specimens prepared by changing mixing ratio of the PP and PA fiber reinforcement to the base concrete with a W/C value of 36.4% that was usually adopted to RC segments in shield tunnels. These testing results provided some findings as follows;

– As for the specimens without fiber reinforcement, heat-induced breakage occurred in all the specimens, regardless of the existance of steel reinforcement in the concrete, showing greater depth of the heat-induced breakage with the reinforced panel-type specimen which resulted in the maximum depth of 13.5 mm.
– No heat-induced breakage could be observed in the specimen prepared with the mixing ratio of 0.1∼0.5 vol% for PP fiber and PA fiber.
– Since the experimental results acquired from this study had shown perfect prevention of heat-induced breakage, it might be valid to cut down the mixing ratio of fiber reinforcement.
– The FDM calculation provided quite suitable estimation of the internal temperatures up to the depth of 50 mm from the heated plane in a concrete specimen, whereas those at deeper depths appeared to become greater than the calculation due to the effect of excessively high heat transmission of the embedded steel rod.



<Without fiber mixed (Mixed design:No.36.4)

Photo 2. Situation after heating test with panel specimen.

3 EXPERIMENT FOR PRACTICAL USE

Product of concrete segments for shield tunnels need to rely on the machinery facilities belonging to the manufacturer. Again, once the segments got assembled in underground space, they would become subjected to large axial forces which are unfavourable to heat-induced breakage.

Therefore, the experiments were set to focus on productability of the segments in conjunction with the facilities at a factory and achievement of the optimum mixing ratio under the axial loadings. In addition, the vital necessity of establishing the repairing methods for application of the AFR concrete to practical use imposed investigation into its repairing performance.

Thereupon, a series of heating tests had been conducted using the specimen manufactured to be subjected to axial forces at a factory. Additionally, the reheating tests were employed to examine the fireproof performance for both of the repaired and



Photo 3. Addition of short fiber at factory facilities.



Photo 4. Compaction of specimen at factory facilities.

non-repaired segments. In addition to the heating tests, situation of heat-induced breakage during being reheated, distribution of internal temperature of a specimen, compressive and adhesive strengths of repair material before and after heating, neutralization depth before and after heating and neutralization depth by accelerated neutralization were measured.

3.1 *Testing methodology and testing specimen (situation of manufacture; Photo-3 to 4)*

Four specimes with an identical dimension of 600 mm wide, 900 mm long and 550 mm thick were prepared as shown in Figure-3. And four mixing ratio of fiber were PA0.1, 0.2, 0.3%, PP0.1% were adopted. Totally 20 thermo couples were installed at every specimen as indicated in Figure-4. As initially heated, the specimen was subjected to 13 N/mm^2 of compressive stress by means of the PC strands. After the initial heating had been terminated, the reheating test was executed with the PC strand eliminated in light of safe core sampling.

Photo-5 thru Photo-6 show the situation of heat-induced breakages in the specimens mixed with PP0.1%, PA0.1, 0.2, 0.3% in conjunction with axial

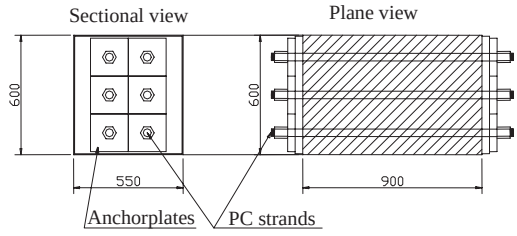


Figure 3. Dimension of specimen.

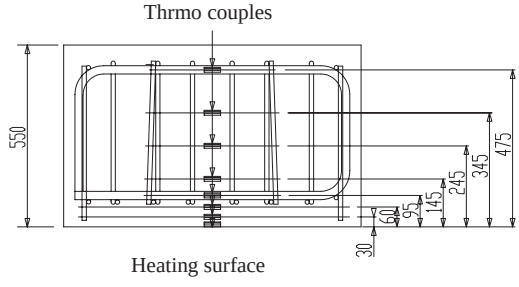


Figure 4. Installation of thrmo couples.

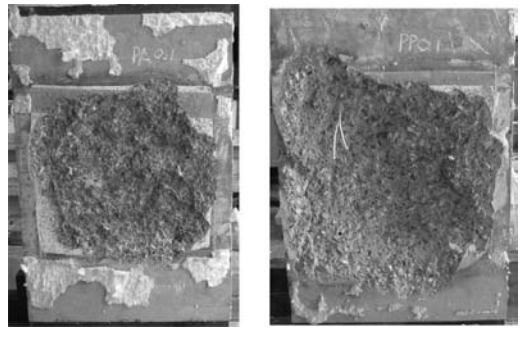


Photo 5. Heat-induced breakages under axial loads (1).

loads. Photo-7 shows the situation of heat-induced breakages after reheating.

3.2 *Summary of experiments for practical use*

At first, summarized are the mixing ratio of short fiber in case of factory manufacture and charge of axial force which was the primary goal of these experiments.

It appears that the mixing ratio up to 0.3% hardly makes any influence on mixing process in factory facilities, even while producing excellent quality. No further machinery is thus required to production of segements. Besides, the mixing ratio of 0.2% enables prevention of heat-induced breakage, which can lead to enhancement of fireproof performance of segments.

Secondly, it appeared from the reheating tests that even the non-repaired specimen hardly created

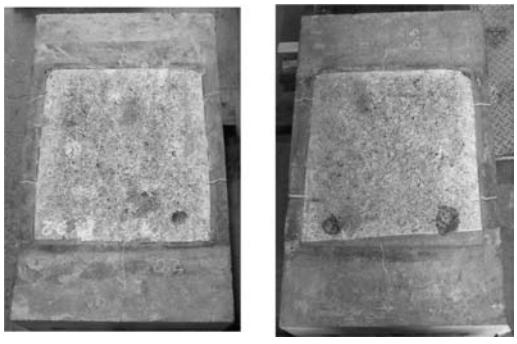


Photo 6. Heat-induced breakages under axial loads (2).

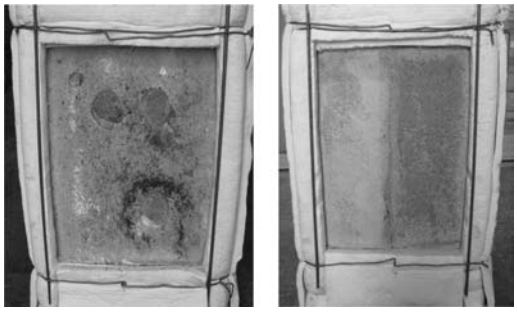


Photo 7. Heat-induced breakages after reheating (None).

heat-induced breakage, and the strength of concrete kept exceeding the design strength at the depth deeper than 25 mm, even under reheating.

In order to prevent decrease of the compressive strength of concrete due to fire in a structural member, an additional thickness of 25 mm that reflects a round of coated cover is considered to be in need. This additional thickness extends to increase of cover thickness above the primary reinforcement by 25 mm which facilitates restraint of increasing internal temperature at the reinforcement, and then enhancement of fireproof performance as a sturctural member. On the contrary, it also appeared that the porous surface caused by heating, made the rate of heat transmission increased so as to make the maximum temperature even higher.

In case that the specimens got repaired, they all hardly showed heat-induced breakage. And their internal temperature appeared to reach no more than 150°C at the depth of reinforcement, the insulating performance of repair materials was also favourably evaluated.

Comparison of the two repair materials informed that the mortar mixed with 0.2% of PA could achieve greater compressive and adhesive strengths, and better performance in service against the inner pressure from surrounding ground and wind pressure due to traffic.

As a result, the following findings have been newly recognized in this study;

- In addition to the polyprophylen fiber well known for its restraining effect against heat-induced breakage from the existing studies, the optimum mixing ratio for poly acetyl fiber has been suggested.
- The manifacture of short fiber-mixed concrete has been successfully verified.
- The serviceability of segments having suffered fire has been clearly evaluated in terms of the existence of repair.

4 CONCLUSIONS

The elementary tests and tests for practical use in this study have successfully demonstrated that the segments employing short fiber-mixed concrete could exhibit excellent fireproof performance and be supplied simply as factory products holding a required fireproof performance with the aid of the existing segment manifactureres. In addition, the applicability of the segment to repair works after a fire has become worthy of consideration in this study.

It can be noted that improvement of fireproofing performance of the segments themselves has considerable influence that the segments enable saving the cost as well as the construction time through eliminating the process of fireproofing panel installation. For the purpose of practical application, despite an additional cover of 25 mm required to avoid reduction of strength due to the increasing temperature of heated surface, given the thickness of currently used fireproofing panel saying 50 mm, the use of fireproofing segments might further lead to saving of the excavated area of tunnels.

Not a small number of shield tunnels is currently being planned for expansion of motor roads passing underground space in Japan. The authors hope that the useful findings and suggestions obtained from this study shall be effectively incorporated to construction of such tunnels from now on.

This page intentionally left blank

Underground Space – the 4th Dimension of Metropolises – Barták, Hrdina, Romancov & Zlámal (eds)
© 2007 Taylor & Francis Group, London, ISBN 978-0-415-40807-3

Basic studies on earthquake-resistance of tunnel linings

H. Miyabayashi, T. Tosaka & A. Isogai
Japan Railway Construction, Transport and Technology Agency, Tokyo, Japan

K. Yashiro & T. Aruga
Railway Technical Research Institute, Tokyo, Japan

ABSTRACT: New Austrian Tunneling Method (NATM) has been increasing in unconsolidated ground and shallow covering by progress of construction technology. In general, tunnel has well seismic resistant as compared to other structures on the ground. However, it is a fact that tunnels are susceptible to a large-scale damage where the seismicity is great and the distance is not far from the focus of seismic activity. On the other hand, there is no evaluation method, which can explain the deformation behavior and the mechanism of suffering quantitatively when earthquake. Therefore, we prepared model tests of 1/4 scale of existing tunnel lining. Moreover, we performed a numerical simulation of model test by non-linear FEM analysis. As a result, we confirmed that lining does not collapse but only cracked, and the analysis evaluates ductility of lining.

1 INTRODUCTION

In October 2004, the Mid Niigata Prefecture Earthquake occurred and many railway tunnels suffered damages (see Fig. 1). Some of the tunnels located adjacent to a focus of seismic activities suffered especially serious damages. Eventually two or more months were required to restore the tunnels that adversely affected reopening of a Shinkansen line or conventional lines. In railway system where many tunnels exist, it is an essential subject to minimize earthquake damages to tunnels. On the other hand, due to recent rapid progress of tunnel construction technology, the New Austrian Tunneling Method (NATM) has increased for unconsolidated grounds and shallow covering in diluvium, which are susceptible to suffer from earthquake damage. For example, NATM tunnels constructed at 60 percent in approximately 80 km of total length on Tohoku-Shinkansen under construction (see Fig. 2). Most of them constructed at shallow covering in the ground that is composed of diluvium. Conventional mountain tunnels are normally constructed in stabilized bedrock, and they are seismic resistant structures compared with other structures on the ground. However, it is a fact that even such mountain tunnels, where the seismicity is great and the distance is not far from a focus of seismic activities, are susceptible to large-scale damages. In order to suppress severe damage of the tunnels to the minimum, it is important to evaluate correctly a mechanism of damages and an earthquake resistance of tunnel, and to make them reflect suitably for design, construction,



Figure 1. A railway tunnel suffered damage by the Mid Niigata Prefecture Earthquake.

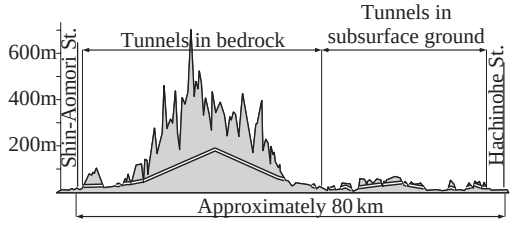


Figure 2. Railway profile of Tohoku-Shinkansen.

and maintenance. However, the method has not suggested that enables to explain deformation behavior or suffering mechanism quantitatively, although suffering conditions by earthquake of the mountain tunnels are experientially arranged. Therefore, we performed

model tests and numerical analyses to elucidate behavior of NATM tunnel lining in the unconsolidated ground and shallow covering.

2 ASSUMPTION OF A DAMAGE MECHANISM

The unconsolidated ground and shallow covering is comparatively soft with ordinary bedrock, thus the ground deformation tends to grow by amplifying earthquake activities. It is conceivable that shearing deformation adversely affects NATM tunnels under such ground condition. The deformations are identical to cut and cover tunnels or shield tunnels. Since a unit-weight of a mountain tunnel is less than one of surrounding ground or equivalent, and hence the structure does not cause a natural vibration. The relative displacement of surrounding ground controls behavior of tunnel during earthquake. It is imaginable that cracks occur on shoulders of tunnel lining due to such shearing deformation (see Fig. 3).

It is preferably to perform an experiment of seismic damages in soil. It considers the interaction between ground and tunnel by modeled tunnel lining and ground because the tunnel is an underground structure. However, the experiment has some problems that are many uncertainties of modeled ground. On the other hand, the NATM tunnel lining is a method of construction applicable after the tunnel become stable by the interaction of ground and tunnel supports, thus an ordinary loading is inactive on the lining in the stable ground. In addition, waterproof membranes or isolation sheets separate the lining and shotcreting. For that reason, the experiment is possible that a seismic loading acts only on a modeled lining without modeled ground. The shearing deformation acts on the modeled lining with one-point loading in horizontal direction in air, based on the above concepts.

3 MODEL TEST OF 1/4 SCALED TUNNEL LININGS

3.1 *Outline*

The object of the test model is to clarify the deformation characteristic and destruction behavior of tunnel lining. A tunnel section for the test model is on the assumption of a double track tunnel driven on Tohoku-Shinkansen Line (see Fig. 4). The test lining model was made as a 1/4 scale of the existing tunnel as shown in Figure 4 by the constraint of the size of the test apparatus. Fig. 5 shows its size and Fig. 6 shows an image of the lining model.

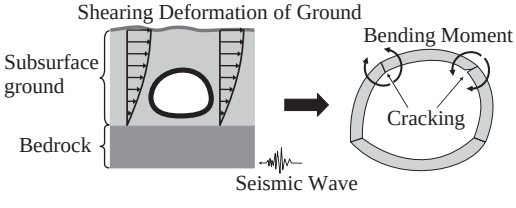


Figure 3. Seismic behavior of tunnel in unconsolidated ground and shallow covering.

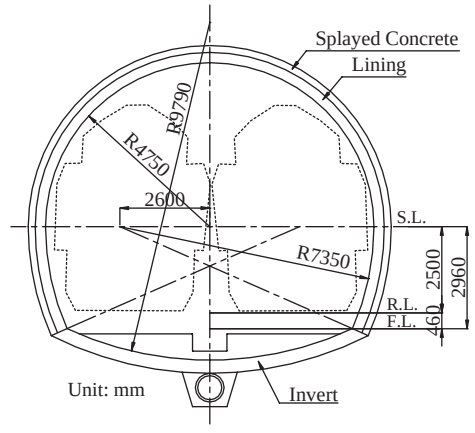


Figure 4. Section of Tohoku-Shinkansen.

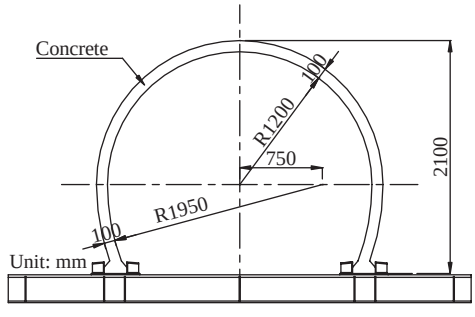


Figure 5. Size of the lining model.

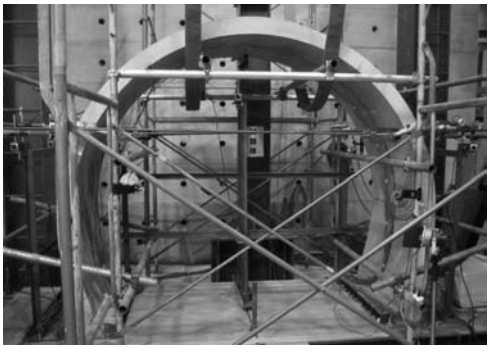


Figure 6. A lining model.

3.2 *Test method*

Table 1 lists the test cases. Case-1 is a test of lining model made of plain concrete as a basic case. Case-2 is a test of lining model made of fiber reinforced concrete that polypropylene fiber mixed. The mixing rate of polypropylene fiber is generally 0.5% per unit volume. However, the mixing rate was 1.0% per unit volume by upper bounds of construction in this test.

The composition of concrete for the lining model was identical to one of the existing lining. Only, coarse aggregates of small grain sizes were used because the thickness of the model lining was 100 mm. Table 2 lists the material properties of the models.

The loading method was alternate loading, thus it assumed the shearing deformation of tunnel lining by ground displacement during earthquake. Tow loading plates were set on outside of lining model and 2/3 of height of the model. The loading plates connected a reaction wall with threaded steel bars. The displacement of lining model was controlled at 0.2 mm/min with rotating the steel bars. Figure 7 shows the location of the loading plates. The specific way was as follows: the displacement was added in one direction still the first crack occurred on the lining model. After it cracked, the displacement was added to right and left alternation to increase gradually amounts of displacement. The displacement of one-step was the displacement ($=\delta$) when the first crack occurred. In the following step, displacement changed to $\pm\delta\times1$, $=\pm\delta\times2$, $\pm\delta\times3\cdots$. Figure 8 shows a conceptual diagram of loading step. We visually identified the progressive of crack, and measured the loading and displacement of the crown to make a load-displacement curve (see Fig. 7).

Table 1. Test cases.

No	Material	Mix ratio Vol.%	Remarks
1.	Plane concrete	0.0	Basic case
2.	Fiber reinforced concrete (Polypropylene Fiber)	1.0	L = 48 mm

Table 2. Material property of concrete.

Cement	Portland cement
Unit volume of cement	294 kg/cm^3
Water cement ratio	61%
Coarse aggregate	Gmax :15 mm
Strength at test	24 ~ 25 MPa (14 days)

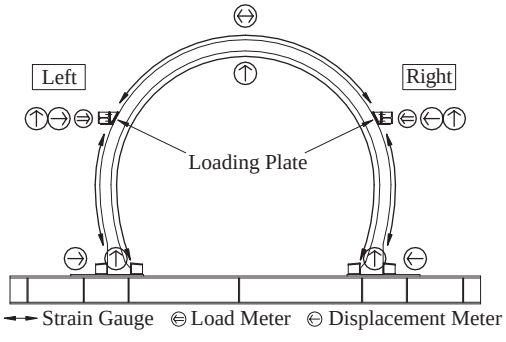


Figure 7. Loading plates and measurement items.

3.3 *Cracking situation*

(1) *Case-1: plain concrete*
At STEP-1 ($\delta=4$ mm), when a load was added rightward, a bending crack occurred on inside of the lining at the left upper loading plate and another crack occurred on the outside of lining at the upper right loading plate (see Table 3). At STEP-2 ($\delta=-4$ mm), when loading was added leftward, the crack closed at the upper right loading plate, and a new crack occurred on the opposite side of that crack. From STEP-3 to STEP-8, the situation of cracks repeated the same as Steps 1 and 2. The situation shows as follows: the number of cracks did not increase; the crack width became large as the displacement of the crown increased. Finally, loading was added until STEP-12 ($\delta=-40$ mm). The lining model has kept the shape of arch and it has not collapsed although it was greatly deformed.

(2) *Case-2: In case of fiber reinforced concrete*
At STEP-1 ($\delta=4$ mm), when a load was added rightward, a bending crack occurred on inside of lining at the right loading plate. It was not passing-through crack. At STEP-2, when loading was added leftward, other bending crack occurred on inside of the lining at the left loading plate. Furthermore, the first crack closed at upper the right loading plate, and new crack occurred on the opposite side of that crack. From STEP-3 to STEP-8, the situation of cracks repeated

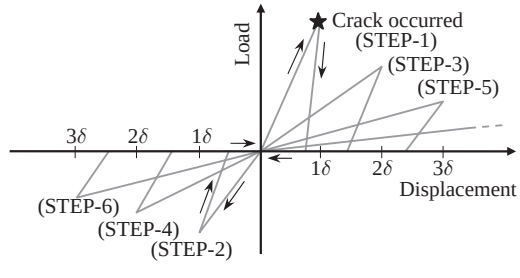


Figure 8. The conceptual diagram of loading step.

Table 3. Cracking situation on Case-1.

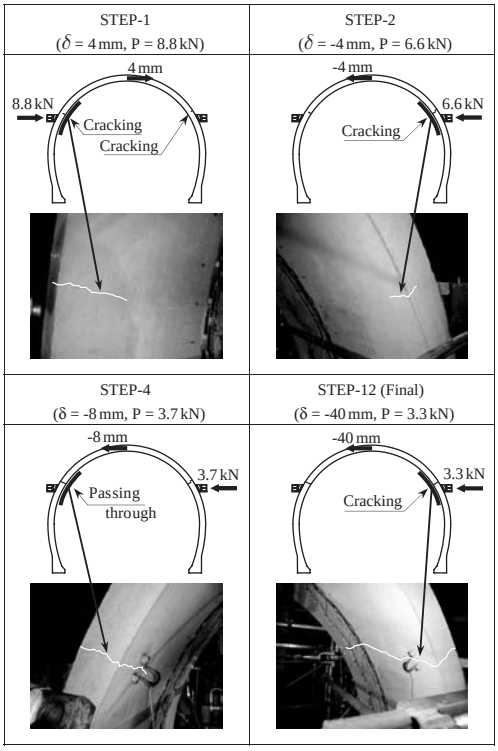
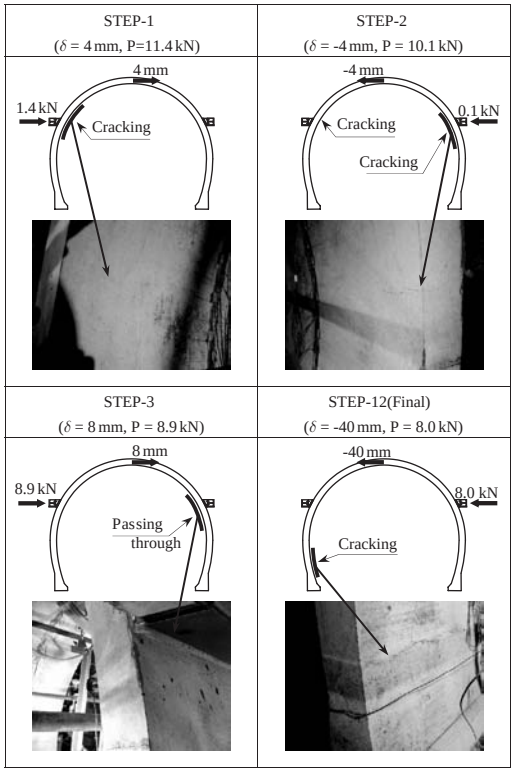


Table 4. Cracking situation on Case- 2.



the same as Steps 1 and 2. Finally, loading was added until STEP-12 ($\delta = -40$ mm). The lining model has kept the shape of arch and it has not collapsed although it was greatly deformed.

3.4 *Load-displacement curve*

Figure 9 and Figure 10 respectively show Load-Displacement Curves of each case. As shown in the Figures, the horizontal displacement of crown of the lining is as shown as a horizontal axis, and the load value at loading point is as shown as a vertical axis. In both cases, it is the maximum load simultaneously with the first crack occurred. The cracking load was approximately 10 kN in both cases. In generally, even when the reinforcement fiber are mixed with concrete, the tensile strength that is the strength for cracking is almost same compared with the plain concrete. In this test, the fracture mode was the flexural and tensile failure by pure bending of a member in both cases. For the reason, it is conceivable that the cracking load as a structural system is almost equal. After cracking, the decline of load and the increase of displacement occurred suddenly in the CASE-1. On the other hand, they occurred gradually in the CASE-2. It is conceivable that the reinforcement fiber (polypropylene fiber) improved the ductility of the lining.

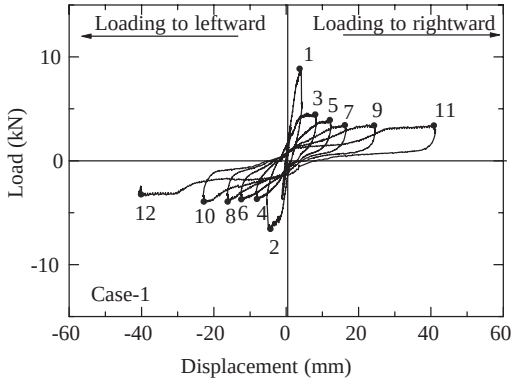


Figure 9. Load-displacement curve (Case 1).

3.5 *Test result*

(1) *Case 1: plane concrete*

The model lining was deformed approximately 40 mm (actual tunnel conversion 160 mm). As a result, the lining model itself did not collapse in brittleness or any concrete flaking did not occur, although the bending crack took place only. Therefore, we observed that

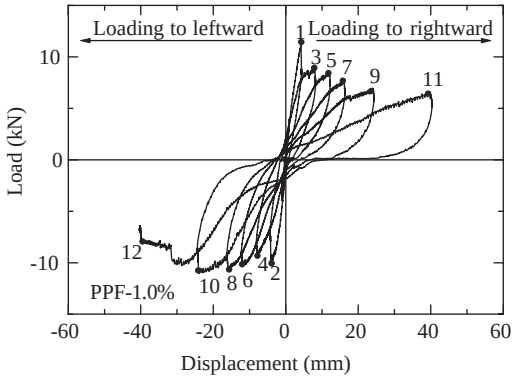


Figure 10. Load-displacement curve (Case 2).

the effect of shape of arch enable the model lining to withstand the large deformation.

(2) *Case 2: fiber reinforced concrete*
The model lining was deformed approximately 40 mm (actual tunnel conversion 160 mm). As a result, the lining mode itself did not collapse in brittleness or any flaking of concrete did not occur, although the bending crack took place only. The crack load was similar to the plain concrete. Therefore, we observed that the effect of mixing of reinforcement fiber improved the ductility of the lining model compared to the plain concrete.

4 SIMULATION ANALYSIS OF MODEL TEST

4.1 *Outline*

The object of numerical simulation is to confirm the behavior of a model test by numerical analysis method in consideration of material nonlinearity. We performed the numerical simulation for the fiber reinforced concrete. Because, it is difficult to analyze appropriately the deformation behavior of the lining made of plain concrete. The loading declines suddenly after cracking, in case of the plain concrete. The numerical simulation has used Non-Linear FEM code WCOMD that took account of the occurrence and progress of crack. Softening behavior of concrete element after cracking is expressed by several parameters: a tensile strength, a cracking strain (εtu) and a softening coefficient (c). Figure 11 shows the conceptual diagram of softening behavior after cracking. This code is applicable mainly for a structure analysis of reinforced concrete. The softening coefficient is 0.4 in case of common RC structure. When the softening coefficient is large, it tends to become large the extent of the decline in stress. However, the softening coefficient has not been defined in case of the fiber reinforced concrete, and thereby we

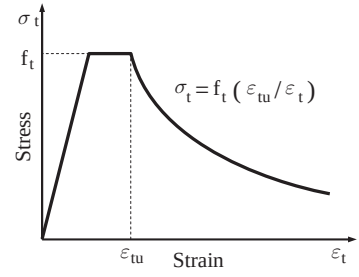


Figure 11. Conceptual diagram of softening behavior after craking.

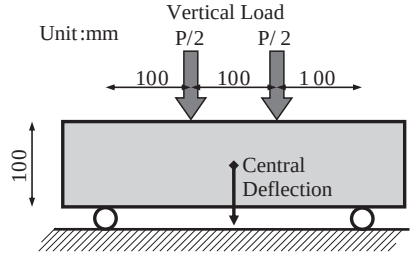


Figure 12. Conceptual diagram of the element test.

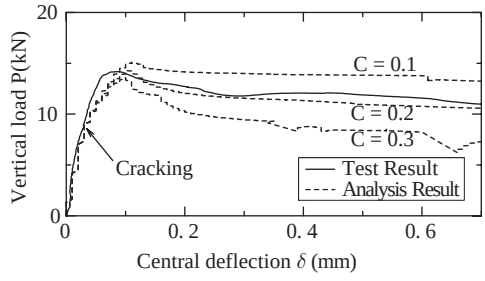


Figure 13. Results of identification analyses.

performed bending test of fiber reinforced concrete and identification analysis to determine the softening coefficient.

4.2 *Element test and identification analysis*

We performed the element test to obtain the load-displacement curve to identify the softening coefficient. Figure 12 depicts the conceptual diagram of the element test. The size of the test specimen was $100 \times 100 \times 400$ mm (loading span: 300 mm) as a shape of beam. The height 100 mm was identical to the thickness of the model lining. The material and strength of concrete was also identical to the model test. Figure 13 shows the load-displacement curve as the result of the element test.

As a result, we performed the fiber reinforced concrete that the bending moment declined slowly

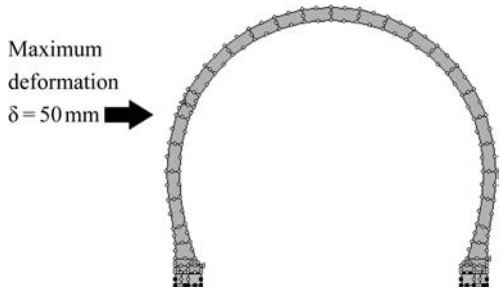


Figure 14. Analysis model.

Table 5. Parameter for analysis.

Compressive strength	$f'_c = 24.9(N/mm^2)$
Tensile strength	$f'_t = 0.23f'c^{2/3} = 1.96(N/mm^2)$
Cracked Strain	$\varepsilon_{tu} = 102.9f'^{1/6}_c = 175\mu$
Softening coefficient	$c = 0.2$

and sustained to some extent after cracked. Next, we performed the identification analysis with that load-displacement curve. Figure 13 shows the results of the element test and the identification analysis. The result of the identification analysis shows that the softening coefficient is between 0.1 and 0.3. When it is 0.2, the analysis result is equivalent to the test result. Accordingly, $C = 0.2$ applies the softening coefficient in this study.

4.3 *The analysis model and material properties*

Figure 14 shows the analysis model. Each element has eight nodes element. This analysis used the joint element on the both feet of lining to allow rotation of the feet. Table 5 lists the material properties for analysis. In addition, the numerical simulation applied a pushover analysis in one direction, although the model test used alternate load.

4.4 *Result of simulation analysis*

Figure 15 indicates the result of numerical simulation of the model test. The Figure shows the test result of a comparison of both results. By comparing the two graphs in Figure 15, the analysis result almost corresponds to the test result. As a result, WCOMD enable to express appropriately the decline of load of lining after cracked. However, the rigidity to the peak in the analysis result, it is in a small tendency as compared with the test result. It is similar to the identification analysis by the element test. The cracking displacement of analysis result was smaller than the one of test result. It is conceivable that the rigidity of the analysis result decreased earlier than the one of the test result.

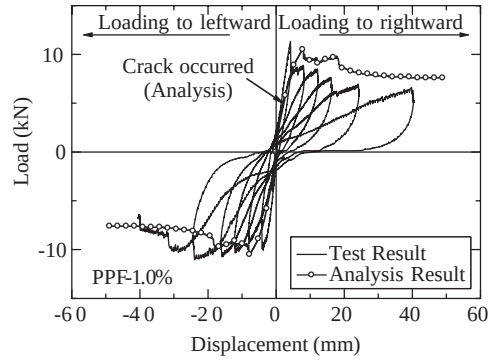


Figure 15. Load-displacement curves.

5 CONCLUSIONS

(1) *Model tests of 1/4 scaled tunnel linings*
Under this test condition, even the lining made of plain concrete did not collapse, although cracks occurred under large shearing deformation. From the previous instances, the deduced shearing deformation is approximately 100 mm when an earthquake occurred. To convert it into the model is approximately 25 mm. The lining of an existing tunnel will only crack, and it will not collapse during seismicity consequently. In addition, to mix reinforcement fibers with concrete improve the ductility of the lining.

(2) *Numerical simulation of model test*
When the softening coefficient used for the analysis of WCOMD is $C = 0.2$, the analysis result is equivalent behavior of fiber reinforced concrete after cracked. WCOMD is possible to analyze behavior of lining made of fiber reinforced concrete under shearing deformation during earthquake.

6 ASSIGNMENTS

We verified that the progress of crack on the lining and the failure mode of the lining during seismicity by the model test. We are preparing to analyze the behavior of lining in ground deformation during an expected earthquake. It is to examine the seismic resistant properties of an existing tunnel and to apply fiber reinforced concrete to an existing tunnel. We will also examine a suitable method to analyze occurrence of cracks on lining constructed of plain concrete.

REFERENCES

Asakura, T., Matsuoka, S., Yashiro, K., Shiba, Y., & Oya, T. 2001. Damage to mountain tunnels by earthquake and its

mechanism. IS-Kyoto 2001. Modern Tunneling Science and Technology, Kyoto: Japan.
East Japan Railway Company. 2006. Record of Disaster Recovery of Railway Structure, Mid Niigata Prefecture Earthquake. (In Japanese)
Kitagawa, T., Goto, M., Isogai, A., Yashiro, K. & Matsunaga, T. Analysis on Behavior of Soft Ground Tunnels with Low Earth Covering. Proceedings of Tunnel Engineering, JSCE. Vol. 15. 2005. (In Japanese)
Miyabayashi, H., Nonomura, M., Oku, T., Yashiro, K. & Aruga, T. 2005. Basic Tests on Earthquake-Resistance of NATM Tunnel Linings. Proceedings of Tunnel Engineering, JSCE. Vol. 15. 2005. (In Japanese)
Okamura, H. & Maekawa, K. 1991. Nonlinear Analysis and Constitutive Models of Reinforced Concrete. Gihodo Shuppan Co.,Ltd.
Shimizu, M. Damages of Railway Tunnels by Niigata Chuetsu Earthquake. Tunnels and Underground. vol.36. No.5. pp.37–44. 2005. (In Japanese)
Yoshikawa, K. 1981. Investigations about Rast Earthquake Disasters of Railway Tunnels. Quarterly Report of RTRI. Vol. 22. No. 3. pp. 103–107. 1981

This page intentionally left blank

Underground Space – the 4th Dimension of Metropolises – Barták, Hrdina, Romancov & Zlámal (eds)
© 2007 Taylor & Francis Group, London, ISBN 978-0-415-40807-3

A study on the seismic design methods for precast concrete lining (PCL)

Du-Hwa Lee, Yeong-Tae Choi & Dong-Hyun Kim
Sambo Engineering Co. Ltd, Seoul, Korea

Byung-Wan Jo
Hanyang University, Seoul, Korea

ABSTRACT: A method of assembling and installing the precast concrete lining (PCL) at the spot in factory was developed and invented in Norway. Earthquake behavior of PCL is different from that of extrude concrete lining (ECL) because it is installed apart from excavation line. Accordingly, we carried on the shaking table tests with one fifth reduced structure model for dynamic behavior analysis of PCL. We found out, through comparing and analyzing the shaking table tests for numerical results, that it is reasonable to apply connecting condition between PCL panels to internal hinge. Stress of PCL is stable at the level of acceleration (0.154 g) provided by the national earthquake criteria but unstable in max acceleration (0.3 g) in case of shallow tunnel depth (less than 1.0D).

1 INTRODUCTION

The construction of road and railway increased for fundamental facilities and improvement of line alignment. Having mountainous landscape, Korean tunnel construction is processed by NATM. The concrete lining in NATM do a primary role of supporting earth pressure by a part of tunnel structure, durability and maintenance of beautiful view. But extrude (cast in place) concrete lining method has some problems, such as construction capability, long-term durability also crack occurrence, increase instability by remained water pressure. As a result, precast concrete lining (PCL) method has been developed in Norway to overcome these problems. PCL method is a part of NMT (Norwegian Method of Tunneling) that uses shotcrete and rockbolt in eternal supports on good rock. PCL method installs PC (Precast) instead of cast in place concrete lining. At the time when PCL method was invented in Norway, there was no study on earthquake resistance design. But as the consideration of earthquake increases recently, Korea needs to research the behavior of PCL during earthquake and develop earthquake resist design from these results to adopt PCL method.

Accordingly, we carried out the shaking table tests with one-fifth reduced structure model for dynamic behavior analysis of PCL. The dynamic behavior of PCL is expected to be different from that of extrude concrete lining (ECL), because PCL is installed apart from excavated surface. We adopted modeling technique comparing the results of shaking table test with numerical analysis. Earthquake resistance capacity of PCL is evaluated from numerical analysis for various conditions. And we evaluated the applicability of simple analysis, comparing simple structural analysis (pseudo dynamic analysis, response spectrum analysis) with accurate analysis (time history analysis).

2 PCL METHOD

NMT is a new tunneling method that uses shotcrete and rock-bolt by eternal supports which adopts precast panel that is made in factory instead of extrude concrete lining of which thickness is about 30∼40 cm. The features of NMT are shown in figure 1 that support

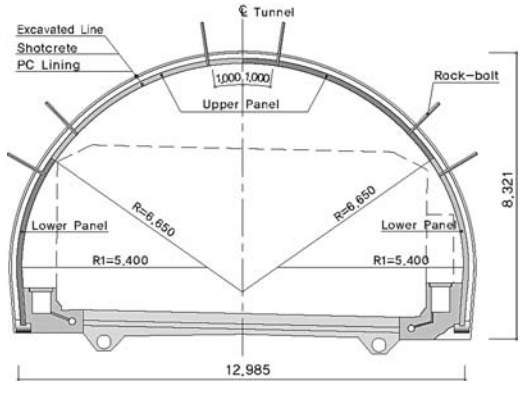


Figure 1. Draft of PCL (Highway tunnel).

good rock with first support (shotcrete, rock-bolt) and then install precast panel. Precast panel performs a role of surfacing in tunnel supporting self-weight and additional facilities.

PCL method is economical and provides good constructional ability because this method uses precast panels that are made in factory. But joins between panels are inevitable. PCL endures self-weight, windy load that occurred by vehicles, collision load, roof fall load, and so on in normal time. But PCL shows complicated behavior during earthquake because PCL is installed apart from tunnel surface. During earthquake, inertia force of PCL is expected to play an important role and we consider stress transfer in joints between panels. Because of these reasons, simple structural analysis is not capable to analyze earthquake behaviors of PCL.

3 EVALUATION METHODS OF EARTHQUAKE RESISTANCE CAPACITY OF PLC

Evaluation methods of earthquake endurable capacity of PCL are divided into two parts.

3.1 *Test schemes*

3.1.1 *Modal test*

Modal test is the method that obtains dynamic properties of structural system from the dynamic results, by applying dynamic forces to structure. Transfer function or Response function can be calculated from the known applied force and measured response results. Then dynamic properties of structure are calculated from obtained modal variable. Modal test is usually used in analysis on resonance of upper-structures, so it is not suitable to analyze dynamic properties of underground structures.

3.1.2 *Pseudo dynamic test*

Pseudo dynamic test obtains similar results with dynamic test by analyzing static test results. This test enables to grasp structural dynamic properties performing static tests. After applying static load corresponded with earthquake wave, the evaluation of dynamic properties, i.e. structural acceleration, velocity etc., by use of measured responsible force. The disadvantage of this method is that it does not simulate soil-structure interaction.

3.1.3 *Shaking table test*

Shaking table test is the method that evaluates dynamic properties of structure applying earthquake force to a real scale or a reduced model on shaking table. This method is used for determine dynamic properties of upper structure (bridge, architecture, etc), underground structure (tunnel), embankment, dam and retaining wall generally. Shaking table test is better for evaluating soil-structure interaction effect during earthquake than pseudo dynamic test and modal test. Therefore, this paper adopts shaking table test for understanding dynamic properties of PCL.

3.2 *Numerical analysis method*

3.2.1 *Simple analysis method*

Simple analysis method is divided into pseudo dynamic analysis and response spectrum analysis. Pseudo dynamic analysis is suitable for earthquake resistance design of upper structure. In the case that inertia force is an important roll for earthquake. Static load which is converted from inertia force of structure is added to structure, and we analyze structure behavior but don't consider the change of SSI (Soil Structure Interaction) and acceleration according to depth. Assumption of response spectrum analysis method is that deformation of underground structure is induced by deformation of outskirts ground. From this assumption, we can calculate displacement by analyzing response spectrum and apply the displacement to structure compulsively to evaluate stress of structure. This method is more exact than pseudo dynamic test but does not represent structure behavior according to time variation and SSI.

3.2.2 *Time history analysis*

Time history analysis method shows the most precise results and can analyze liner, nonlinear behavior of structure during earthquake. But it is not economical method because calculation takes a long time. Time history analysis method is divided into time history method (direct integration method, mode superposition method) and frequency domain analysis method. Time history analysis is the method that input time history earthquake wave to calculate dynamic characteristics of structure, can consider nonlinear behavior and mode damping.

4 EVALUATE DYNAMIC BEHAVIOR OF PCL BY SHAKING TABLE TEST

4.1 *Similitude rule for reduced model*

We executed an experiment by reducing model of highway 2 lanes tunnel section to analyze behavior of PCL during earthquake and applied similitude rule for manufacturing. Roscoe (1698), Kagawa (1978) and Iai (1989) proposed two important concepts. First, it is mechanical behavior of model to represent prototype, as shown in figure 2. We made use of stress-strain relationship that is applied similitude rule with a similitude ratio to evaluate the behavior of prototype from that of model (Iai, 1889). Second, ground and structure are considered not separate but as one. Eq (1)∼(3) is about equilibrium equation and constitution equation of ground, Eq (4)∼(5) is equation that proposed

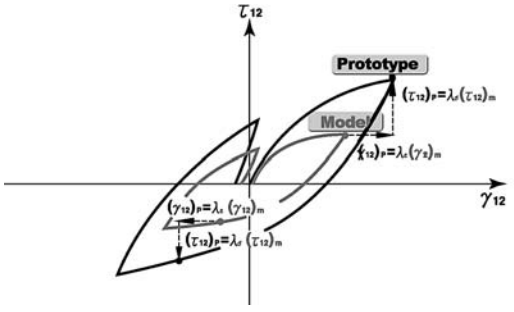


Figure 2. Stress-strain relationship between prototype and model.

similitude ratio for each parameter from relationship of ground and structure that are combining governing equation.

$$L^T f + \rho g = \rho u'' \quad \text{(Equilibrium Eq.)} \tag{1}$$

$$d\varepsilon = L\,du \quad \text{(Strain)} \tag{2}$$

$$d\sigma = Dd\varepsilon \quad \text{(Constitution Eq.)} \tag{3}$$

$$EI\frac{\partial^4 n^T u}{\partial n^4} + \rho_b n^T u'' - \rho_b n^T g + n^T Sf = 0 \tag{4}$$

$$EA\frac{\partial^2 t^T u}{\partial s^2} + \rho_b n^T u'' - \rho_b n^T g + t^T Sf = 0 \tag{5}$$

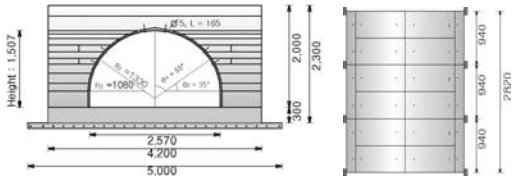
In this thesis, we adopted similitude ratio 5 consideration of shaking table size and tunnel scale. And Iai's similitude rule is chosen because soil structure interaction is an important factor. Type III among Iai's similitude rule is applied in this thesis because we cannot manufacture the model that has similar density of tunnel outskirt ground.

4.2 *Resource and manufacturing reduced model*

We manufactured reduced model applying type III among Iai's similitude rule.

4.2.1 *PCL panel*

In the case when PCL panel is made of concrete, the thickness of lining is so thin that it is not able to manufacture the lining. Therefore, aluminum is chosen to satisfy flexibility ($EI = 2.03 \times 109 \mathrm{N \cdot mm^2}$) of the model, it is easy to assemble and install, besides, ductility is so high that it can represent soil-structure interaction exactly. Connection of PCL panels completely separates longitudinally and upper panel leaves lower panel simply. As a result the connection of prototype reappears exactly. The 2 strain gauges are adhered on every crown, shoulder part and side wall in lower panels to measure stress and strain of PCL.



a. Front view b. Plan view

Figure 3. Model.

Table 1. Shaking table test results (Unit : Strain $\times 10^{-6}$).

Wave	PGA	Crown	Shoulder	Side	Rock-bolt
El Centro	0.1 g	17	20	13	9
	0.2 g	19	22	14	10
	0.3 g	30	32	22	16
	0.35 g	34	40	28	20
Artificial	0.15 g	22	24	12	11
Northridge	0.1 g	16	20	11	7
	0.2 g	18	20	13	10
	0.32 g	28	34	26	18

4.2.2 *Rock-bolt*

Rock-bolt supports PCL panel by connecting PCL ground. It also transfers earthquake wave to PCL panel during earthquake. Steel rod is used to manufacture model for shaking table test by material of rock-bolt. In this thesis we used steel rod that is reduced by one fifth to execute more exact test.

4.2.3 *Ground*

PCL is installed in good ground condition (more than hard rock), so relative displacement in environs ground of tunnel almost do not occur. Therefore timber is applied to represent environs ground of tunnel as shown in figure 3. Timbers are tightened not to move separately but to behave together.

4.3 *Test conditions*

Input earthquake waves are artificial (0.154 g) and measured waves are El Centro (0.35 g) and Nothridge wave (0.32 g). Artificial wave agrees with Korean design criteria which PGA (Peak Ground Acceleration) is 0.154 g. El Centro wave is the earthquake that occurred in California and its predominant period is from 0.08 seconds to 0.85 seconds. Northridge wave is the earthquake that occurred in Los Angels and its predominant period is form 0.18 seconds to 0.32 seconds.

4.4 *Test results*

In the case input acceleration is over than 0.2 g, strains of PCL panel and rock-bolt increased rapidly

(figure 4). The reason is the effect of inertia due to PCL mass is small below 0.2 g, but the effect of PCL inertia is so important that stress of PCL panels and rock-bolts grow up rapidly over 0.2 g which increases ground acceleration. PCL is weaker that extrude concrete lining for strong earthquake. It needs attention in earthquake endurance design.

5 EVALUATE OF PCL BY NUMERICAL ANALYSIS

We studied connection condition between PCL panels comparing shaking table test results and numerical analysis. And we evaluated earthquake resistance capacity of PCL by performing numerical analysis for tunnel depth, earthquake waves.

5.1 *Analysis conditions*

We performed numerical analysis with highway 2 lanes tunnel section that is applied in shaking table test. Analysis conditions are same as that of shaking table test. Additional condition is tunnel depth change i.e. 1.0D, 1.5D, 2.0D (D: tunnel diameter). We adopted transmitting boundary condition to avoid reflecting input waves on boundary of model. Numerical analysis programs are AFIMEX 2D, PENTAGON 3D that can analyze non-linear behavior. Other analysis conditions are shown in Table 2.

5.2 *Connection condition of PCL*

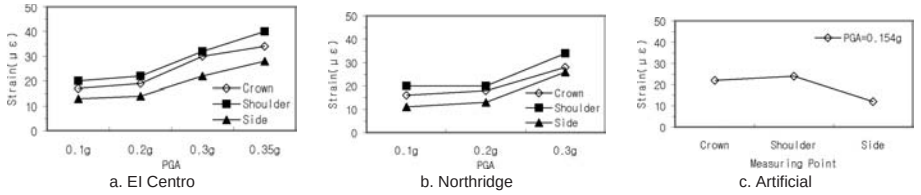
Connection condition between PCL panels can affect PCL behavior in earthquake, so we chose most proper condition comparing shaking table results with 2D, 3D numerical analysis results. As shown in figure 5, stress of PCL occur higher in fixed condition than in internal hinge approximately and internal hinge condition show similar results with shaking table test results. This is a reason that PCL panels move separately because PCL is connected panel to panel that is different from extrude concrete lining. Therefore it is reasonable that connection condition of PCL panels is applied to internal hinge in the case of analyzing dynamic behavior. We take 2D, 3D numerical analysis applying internal hinge condition to estimate earthquake resistance of PCL.

5.3 *2D, 3D dynamic behavior of PCL*

Applying internal hinge condition, we performed 2D, 3D numerical analysis. Figure 6 shows relationship of 2D and 3D results. Correlation of 2D and 3D is very high ($R^2 = 0.78$) and 2D results is about 24% higher than 3D. This is the reason why resistance force is estimated lower than 3D because 2D analysis can't consider longitudinal behavior of PCL like 3D analysis.

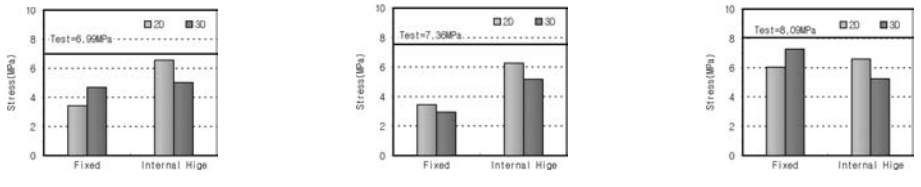
Table 2. Analysis conditions.

	Thickness (m)	Unit weight (kN/m^3)	Elastic modulus (MPa)
PCL	0.15	24.5	27,468
Shotcrete	0.05	23.1	24,525
Rock-Blot	D25	68.7	206,010
Ground	–	24.5	5,600



a. El Centro b. Northridge c. Artificial

Figure 4. Max. response of PCL(Shaking table test).



a. El Centro b. Northridge c. Artificial

Figure 5. Comparison between shaking table test and numerical analysis.

But 3D behavior can be estimated from 2D analysis because of high relationship, Therefore 2D analysis is chosen to evaluate earthquake resistance capacity of PCL in this thesis.

5.4 *Earthquake resistance capacity of PCL*

5.4.1 *Dynamic behavior of PCL*

As shown in figure 7 max. moment, shear force and axial force tend to decrease as tunnel depth increases. This is why behavior of ground amplified that of PCL by connecting rock-bolt. That is to say that inertia force of PCL is main factor for earthquake because PCL panels are installed apart from ground. Therefore stability of PCL increases as tunnel depth increases. The behavior for artificial wave is similar with that of El Centro, the decreasing ratio of stress grows with depth increasing for Northridge wave. It shows that properties of these waves are similar. For Northridge wave, in the case of max. acceleration and tunnel depth of 1.0D, PCL stress is over the allowable stress level. But PCL stress is below the stress for the other conditions. PCL is unstable for shallow tunnel depth (below 1.0D) and strong earthquake. Therefore we consider countermeasures for these conditions.

5.4.2 *Dynamic behavior of shotcrete*

Moment and shear force of shotcrete decreases as tunnel depth increases. This trend is a reason that confining stress of ground that increases in proportion to tunnel depth restrains oscillation of shotcrete and ground. This result coincide with underground structures are affect for earthquake little.

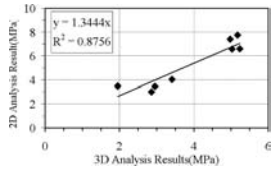


Figure 6. Relationship between 2D and 3D.

5.4.3 *Dynamic behavior of Rock-bolt*

Stress of rock-bolt must be considered at exposed part between shotcrete and PCL panels. So we evaluate stress of rock-bolt at the exposed part. Compressive and tensile stress of rock-bolt decrease with tunnel depth increment as shown in figure 9. Similar with shotcrete, it is estimated that confining stress restrains relative displacement of ground with tunnel depth increment.

Behavior of PCL is similar with rock-bolt but different from shotcrete somewhat. That's why movement of shotcrete is affected directly by ground because shotcrete adheres to excavated surface, PCL and rock-bolt installed apart from ground are affected by inertia force than ground deformation on the other hand. Therefore not only the effect of outskirt ground but also dynamic behavior due to inertial force are considered for earthquake resistance design of PCL. Analysis method that is able to represent these phenomena is applied to evaluate capacity of PCL.

Rock-bolt rust when exposed for a long time. Accordingly rock-bolt needs constant management (epoxy coating etc).

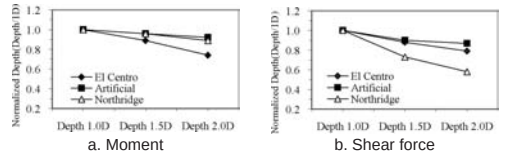


Figure 8. Stress of shotcrete(0.514 g).

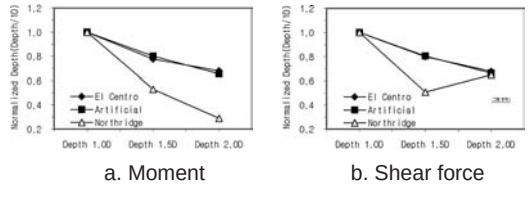


Figure 9. Stress of rockbolt.

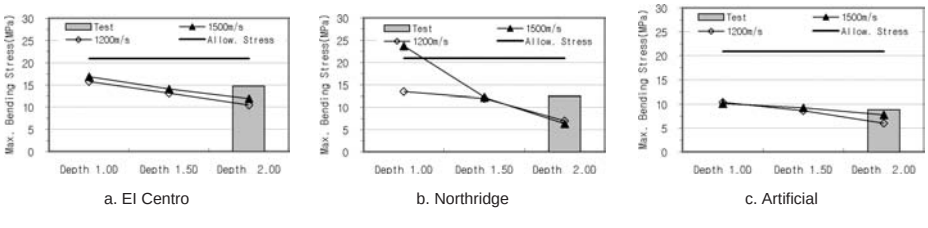


Figure 7. Behavior of PCL according to tunnel depth at max. acceleration.

6 APPLICABILITY OF SIMPLE ANALYSIS METHOD FOR EARTHQUAKE DESIGN

Simple analysis method is divided into pseudo dynamic analysis and response spectrum analysis. Pseudo dynamic analysis is applied in the case that inertia force is important, response spectrum analysis considers dynamic response characteristics. Simple analysis method has disadvantage not to represent SSI but is so simple that is used broadly. Therefore we study applicability of simple analysis method for earthquake resistance design comparing accurate analysis methods.

6.1 *Pseudo dynamic method*

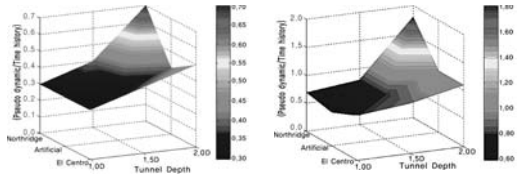
Comparing pseudo dynamic with time history analysis, moment in PCL is about 1.3 ∼ 1.0 times higher in time history than pseudo dynamic method. Shear force is 1.0∼2.4 times higher in pseudo dynamic method. This trend is a reason that pseudo dynamic method can't reproduce dynamic behavior of ground to analyze fully. Axial force of rock-bolt is higher than time history analysis approximately. That is, if tunnel depth is deep (over 1.5D), pseudo dynamic analysis is conservative design except moment. But pseudo dynamic method can't estimate stress of PCL partly and in detail, so pseudo dynamic method is not reasonable for earthquake resistance design. Figure 10 shows normalized stress ratio (coefficient = pseudo dynamic method/time history method).

6.2 *Response spectrum analysis method*

Response spectrum analysis is used to evaluate earthquake resistance of PCL. Design response spectrum is shown in figure 11.

Comparing response spectrum and time history method, moment is about 3∼4 times in time history method higher than in spectrum method. Shear force is about 1.4∼2.0 times higher in response spectrum method like pseudo dynamic method. That is, if tunnel depth is deep (over 1.5D), pseudo dynamic analysis is conservative design except moment. But response spectrum method can't estimate stress of PCL partly and in detail, so this method is not reasonable for earthquake resistance design. Figure 12 shows normalized stress ratio (coefficient = pseudo dynamic method/time history method)

As shown above, simple analysis methods show conservative results in deep tunnel depth but PCL is unstable for moment in 2.0D. Therefore simple analysis method is not applicable for earthquake design inspite of deep tunnel depth. Stress of PCL itself and connecting part are so important that time history method is reasonable to analyze behavior of PCL for earthquake.



a. Moment b. Shear force

Figure 10. Comparison between time history and pseudo-static method.

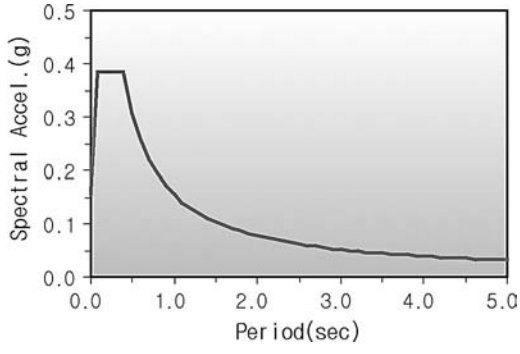
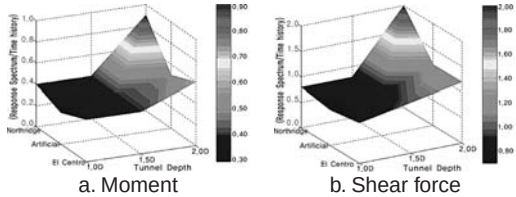


Figure 11. Design response spectrum at S_B ground condition.



a. Moment b. Shear force

Figure 12. Comparison between time history and response spectrum method.

7 CONCLUSION AND FURTHER STUDIES

In this thesis, we evaluated dynamic behavior of PCL that is different from general concrete lining of tunnel. Performing and comparing shaking table test and numerical analysis, earthquake resistance capacity of PCL is studied and applicability of simple analysis methods is evaluated. Summary of studies is as follows.

(1) Comparing shaking table test with one fifth reduced model with 2D, 3D numerical analysis results, it is reasonable to apply internal hinge to modeling condition between PCL panels.
(2) From results of various numerical analysis with internal hinge, stress of shotcrete and PCL decrease according to tunnel depth increment. It is a reason that earth pressure increase with tunnel

depth so increasing earth pressure confine oscillation of ground. Variation of PCL stress is larger than shotcrete. It is because inertia force plays an important roll in PCL installed apart from ground so ground behavior amplifies PCL behavior.

(3) Performing numerical analysis for various conditions, PCL is stable for Korean criteria (0.154 g) but unstable over 0.3 g in the case that tunnel depth is below 1.0D. Therefore minimum tunnel depth must be over 1.0D to satisfy stability requirement of PCL for strong earthquake (acceleration is over 0.3 g).

(4) In applicability of simple analysis methods, moment for simple analysis methods is lower than time history method. Therefore simple analysis method underestimates PCL stress for earthquake, this method is not proper to apply earthquake resistance design.

REFERENCES

Ministry of construction & transportation, 1997, Earthquake resistance design criteria research.

Lee Du Hwa. 2004. A study on the seismic design methods for precast concrete lining, PhD Thesis, Hanyang university.

Lee Yong Jun. 2001. The dynamic behavior of cut-and-cover tunnel by seismic waves, Ph.D Thesis, Hanyang university.

Chung Hyung Sik, Bae Gyu Jin, Lee Yong Jun. 2001. A study on the seismic performance evaluation and the seismic analysis method for pre-cast concrete lining, Korean Geotechnical society, Vol. 17, No. 5, pp. 197–207.

Dowding, C. H. and Rozen, A., 1978. Damage to Rock Tunnels from Earthquake Shaking, Journal of the Geotechnical Engineering Division, ASCE, Vol. 104, No. GT2, pp. 175–191.

Iai, S., 1989, Similitude for Shaking Table Tests on Soil-Structure-Fluid Model in 1g Gravitational Field, Soils and Foundations, JSCE, Vol. 29, No. 10, pp. 109–118.

Iai, S. and Sugano, T., 1999, Soil-Structure Interaction Studies through Shaking Table Tests, Earthquake Geotechnical Engineering, Balkema, Vol. 3, pp. 927–940.

Meymand, P. J. 1998. Shaking Table Scale Model Tests of Nonlinear Soil-Pile-Superstructure Interaction in Soft Clay, Ph.D. Dissertation, University of California, Berkeley.

This page intentionally left blank

Underground Space – the 4th Dimension of Metropolises – Barták, Hrdina, Romancov & Zlámal (eds)
© 2007 Taylor & Francis Group, London, ISBN 978-0-415-40807-3

Design of inner lining at the Gotthard Base Tunnel, approach for the evaluation of loads, the different types of lining

R. Stadelmann, A. Pfeffer & Z.Q. Wei
Amberg Engineering AG, Regensdorf-Watt, Switzerland

ABSTRACT: The following article deals with the approach for the determination of rock loads based on hazard scenarios, rock pressure and additional design loads that have to be taken into account for the inner lining of the Gotthard Base Tunnel. The decisions for single and double lining as well as cost-reductions were discussed.

1 THE GOTTHARD BASE TUNNEL

1.1 *The purpose*

The 57 km long Gotthard Base Tunnel (GBT) is a key part of the project AlpTransit for the new high speed railway through the Alps in Switzerland. The designed maximal train speed is 200 to 250 km/h so the route must be very flat with gradients no higher than 1%. It is currently under construction and will be put into operation in 2015.

1.2 *The design*

The tunnel consists of two parallel single-track tubes, which are connected by crosscuts at about 300 m intervals. Because it is very long and very deep with a mountain cover up to 2500 m thus the detailed geology is mostly unknown, which gives rise to too many uncertainties in the design and greater risks during the construction: unexpected bad geology, instability, the safety of workers and equipment, logistic plan, construction time and overall costs.

In order to reduce these uncertainties and risks, the tunnel was divided into five sections from the North to the South: Erstfeld, Amsteg, Sedrun, Faido and Bodio. It is being driven simultaneously from both portals Erstfeld and Bodio and from three intermediate points of attack by access tunnels in Amsteg and Faido and by combined access tunnel and two vertical shafts.

Sedrun and Faido sections each has a multifunction station (MFS) with complicated tunnel and adit systems due to the requirements of construction, emergency, ventilation and technical niches.

The two main tunnels have a circular profile and most of them are excavated by Tunnel boring machines. The method of drill and blast is used for the two stations as well as the section of the main tunnel in Sedrun due to expected bad geology in Sedrun.

The major part of the tunnel is designed with double shells. The inner lining is normally not reinforced. The approach for the evaluation of lining loads will be discussed using the examples.

2 OBSERVATION METHOD AND EFFECTIVE LOADS OF ROCK MASS

The loads on the tunnel lining are composed of rock pressure and additional mechanical, physical and technical effects. But the critical part for tunnel stability is the rock pressure and therefore must be correctly determined.

2.1 *Observational method*

The geology in the section Faido is completely different from the prediction. The rock mass contains complicated boundaries of different rocks, folds, a few joint sets and fault zones. Even with many core drillings and boreholes ahead of tunnel faces, the prediction of the rock mass behaviour ahead of the tunnel faces was not very good. In order to obtain realistic geology, it is required to observe tunnel faces and make records. Figure 1 is an example of tunnel face sketch and description at Tm 1152.5 of the Emergency Tunnel West in the MFS Faido. From the sketch, one obtains not only the detailed geology but also the likely loosening rock pressure in the area around this tunnel cross section. With the regional geology and the information from core drillings and boreholes, one tries to get a three dimensional geological structures like rock boundaries, foliations, joint sets, fault zones and groundwater conditions as well as some insight about tectonic activities. These are fundamental information for predicting the short and long term behaviour of the rock mass.

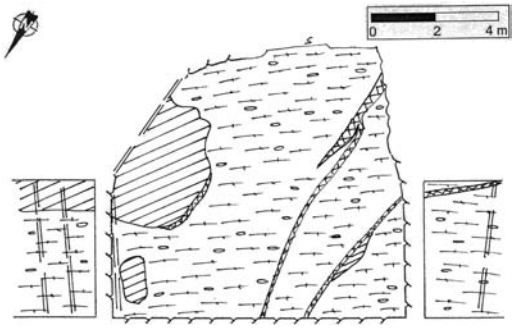


Figure 1. An example of tunnel face sketch and description at Tm 1152.5 of the Emergency Tunnel West in the MFS Faido.

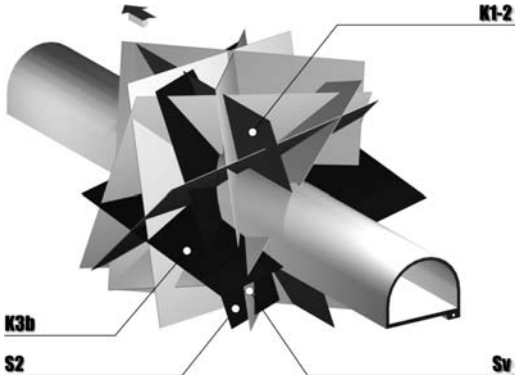


Figure 2. Rock joint systems in Sedrun.

With the information from the tunnel faces, geologists, contractors, construction supervisors, engineers and the owners have to work together to quickly find solutions for the details of construction methods and tunnel support. Rock mass displacements and the reaction of the tunnel support have to be observed, measured and interpreted by existing and possible new computations.

Based on the geological and hydrogeoligical information and the interpretation of rock mass deformation and the reaction of tunnel support, plus long term consideration, one can determine the profile types of inner lining and rock loads.

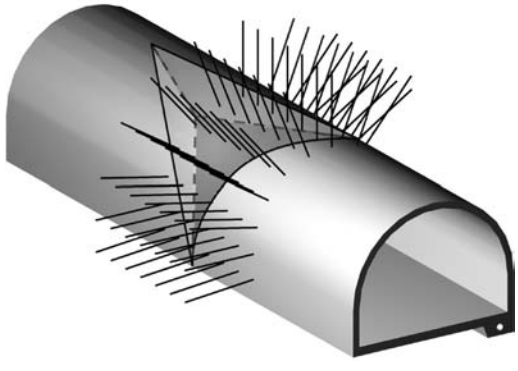


Figure 3. Pattern bolting of wedges.

2.2 *Effective loads carried by rock support*

Due to the importance of the project AlpTransit, it has been assumed that the structural effects of the rock support would not be considered in the tunnel lining design and that the tunnel (inner) lining must alone maintain the stability and functionality of the tunnel. This leads to an assumption that the loads carried by rock support like anchors, shotcrete and steel sets will be transferred onto the tunnel lining. In order not to be too conservative, one has to find out the effective loads carried by rock support.

One possibility to find out the theoretical loads in hard rock is to take the orientation of joints and frictions into account. This method has been used to define loads of loosening zones in hard rock.

Special investigations have been made to find out the joint orientation within the enlarged section of the branch-off structure. Their orientation defines the possible size of wedges that must be fixed. The Figures 2 and 3 are the examples of the MFS Sedrun. After deformations have come to an end the length of actually used anchors limits in a more precise way the real height of these wedges which otherwise would have an unrealistic high and long peak. By that the maximum size of wedges for the caverns has been limited.

As far as excavation has already taken place the measured deformations also give an answer to the question about the real load that the excavation support received. One priority objective of the excavation support is to guarantee security for the workforce under rather unknown rock conditions. After the excavation has been carried out, the geologic documentation and the observation of deformation give much more precise information about the rock behaviour. The check of the inner lining is based on this documentation, which leads to more precise load estimations. Narrow local fault zones can mostly be excluded. Based on the chosen rock support and the measured deformation the effective loads on the vertical closure at the end of the branch-off were identified and compared with the design-loads based on the predicted geology.

During excavation a massive unexpected fault zone was detected within the multifunctional station Faido (MFS). For this part the effective loads could be defined by the characteristic line method. A lot of geological information was collected and evaluated by the Geological Strength Index Method (GSI). This

method gave a vague impression of the parameter. But at least the minimum E-modulus could be defined. To define the necessary rock support a 3D-analysis was carried out to verify the results of the characteristic line method. After the completed excavation and based on the data obtained by the observation numerical calculations followed in order to estimate the rock loads for the permanent lining. This was based on the effectively chosen rock support. The calculated deformation is compared with the measured deformation. By back-Analysis the geotechnical parameter and the lateral pressure coefficient were assigned.

3 DESIGN LOADS FOR THE INNER LINING

3.1 *Design loads of rock mass for the inner lining*

The tunnel is designed for a service time of 100 years. The excavation support needs not to fulfil any long term durability criteria such as being protected against corrosion or against sulphate attack. 100% of the effective loads on the excavation support are taken into account for the inner lining. Remaining supporting effects of the excavation support will not be considered in the calculation for the inner lining.

Pattern bolting and steel arches to ensure safe working conditions loose their importance after the finished excavation. Due to the project importance, the primary supports are neglected by the design of the inner lining.

In the determination of the reaction forces of rock support to rock deformation and transferring them into the design loads of rock mass on the inner lining, the records of observation in Section 2.1 play an important role. Figure 4 is an example of breakout and fractures in the Main Tunnel West South around Tm 228 in the MFS Faido. This photograph shows us that the overall rock pressure is low but the local weak zone and rock joints lead to an asymmetrical distribution of rock pressure.

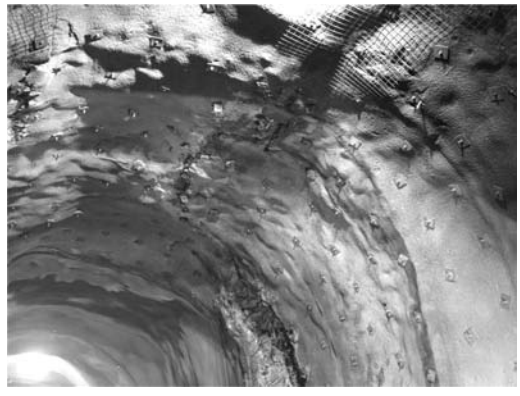


Figure 4. An example of breakout and fractures in the Main Tunnel West South around Tm 228 in the MFS Faido.

Table 1. Design considerations for primary tunnel support and final tunnel inner lining.

Load	Excavation support	Structural safety/ serviceability
Safe working conditions	x	0
Dead load of structure	x	x
Shrinkage	0	x
Effective loads of rock mass	x	x
Fixation of cantilever	0	x
Shock pressure and suction	0	x
Difference of temperature	0	x
Flexible drainage system	0	x

Table 2. Total design loads for the inner lining of the tunnels in the MFS Faido.

Load	Structural safety/ serviceability
Dead load of structure	25 kN/m^3
Shrinkage	0.2 [‰]
Vertical loads of rock mass	90 to 1200 kN/m^2
Horizontal loads of rock mass	0 to 1000 kN/m^2
Fixation of cantilever	4 [kN]
Shock pressure and suction	+/− 10 kN/m^2
Difference of temperature	+/− 20 [°]
Thickness of drainage layers	20 mm

3.2 *Total design loads for the inner lining*

The inner lining of the Gotthard Base Tunnel has been designed for dead load of structure, shrinkage, effective loads of rock mass, fixation of cantilever wire, shock pressure and suction due to train passing, difference of temperature and flexible drainage system (Tab. 1 and 2). Water pressure could be excluded because of the design of an effective and durable drainage system.

4 SINGLE SHELL OR DOUBLE SHELL

4.1 *Operation demands*

Corrosion and malfunction of electric equipment because of humid climate had to be avoided. Therefore the ingress of water had to be limited according to the requirements of the owner, the Swiss railway company. Water sealing was necessary on the whole length of both single-track tunnels. A second important demand represents the limitation of the roughness of the surface. Both demands led to the design of a double



Figure 5. An example of primary drainage of groundwater by half pipe shells in the Main Tunnel East South around Tm 750 in the MFS Faido.

shell tunnel. Nevertheless parts of the ventilation tunnels for the emergency case and small service tunnels within the multifunctional station could be designed with single shells.

4.2 *Advantages of double shells*

Due to the high water pressure a water drainage system is necessary. As mentioned above a double shell system with water sealing leads to an effective minimization of water inflow. The drainage can easily be built between inner and exterior shells. Figure 5 is an example of primary drainage of mountain water by half pipe shells. They will divert most of mountain water into drainage canals but cannot keep lining dry like in Figure 6. After certain time the mountain water may also redistribute. If water pressure builds up, it will crush the tunnel. Figure 7 is an example of high water pressure in the MFS Faido. In the core borehole in the Emergency Tunnel West at Tm 1320 the measured water pressure was 41.5 bars, that is 415 m water column.

The inner shell can be built by in-situ concrete, which is cheaper than shotcrete. The surface can be built smoother and therefore aerodynamically more



Figure 6. A Section with cracks and wet spots of the Main Tunnel West South from Tm 950 to 970 in the MFS Faido.



Figure 7. Measuring of groundwater pressure (41.5 bars, after Volpers) in the core borehole in the Emergency Tunnel West at Tm 1320 in the MFS Faido.

favourable (Fig. 8). Widely ramified cracks, typically for single shells, can be also avoided.

4.3 *Advantages of single shells*

The exterior part of a double shell is very similar to a single shell (Fig. 9). The main difference concerning the design control lies in its missing durability. This can easily be completed by adopting the concrete composition. So why should it be built twice? The cost reduction effect is obvious. In addition, the construction of single shells is much easier compared to double shells, especially when the geometry is changing as in cross-over caverns. In some cases the high requirements can also be fulfilled with low-cost single shells. That will be done in completely dry sections with no or very little reinforcement as well as in short sections with complicate geometry and limited water inflow.



Figure 8. Double shell lining concept.

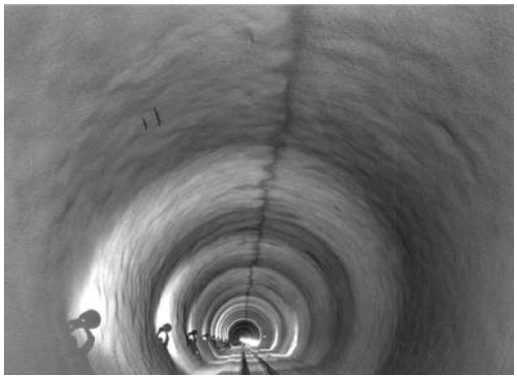


Figure 9. Single shell lining concept.

5 REINFORCEMENT

5.1 *Unreinforced inner lining*

The tunnel geometry will influence the decision concerning the reinforcement. Though this depends on the results of a general design check, the question of the tolerable crack width has to be answered. Concerning the serviceability and the durability cracks have to be checked. It is obvious, that in case of reinforced concrete cracks have to be limited according to the climate because of the possible corrosion. In contrast unreinforced concrete will not rust. Therefore, whenever the inner lining can be dimensioned without reinforcement, corrosion-problems can be avoided. On the other hand wider cracks have to be accepted. Depending on the maximum allowed size of cracks, the inner lining can be dimensioned without reinforcement. Steel reinforcing takes time and costs more, and also requires complicated logistic plan and high quality control to achieve a uniform concrete. When there is no steel and no steel corrosion in the lining, the risk of the railway operation interruption by maintenance work will largely be reduced. Not only the construction costs but also the maintenance costs will be reduced. As mentioned at the beginning this was one main target of the design for the Gotthard Base Tunnel.

6 CONCLUSIONS

The Gotthard Base Tunnel is the most important part of the AlpTransit Project. Advantages and disadvantages of single and double shell tunnel lining were discussed. Due to the importance of the Project, most sections of the tunnel were designed with double shells. Only parts of ventilation and service tunnels have a single shell.

The methods for the determination of lining loads were discussed under consideration of load bearing capacity of anchors and shotcrete, possible wedges and loosening zones, and the effective deformation. The role of the observational method was enlightened.

In accordance with stability, serviceability and durability and under control of allowable cracks, major sections of the tunnel inner lining were designed without reinforcement. This will avoid corrosion problems and therefore have less maintenance work and interruption of tunnel operation, and largely reduce the risk of railway interruption and the construction and operation costs.

This page intentionally left blank

Underground Space – the 4th Dimension of Metropolises – Barták, Hrdina, Romancov & Zlámal (eds)
© 2007 Taylor & Francis Group, London, ISBN 978-0-415-40807-3

Final lining of the Valík Tunnel on D5 express highway – the vault construction

Z. Vozarik
Metrostav a.s., Prague, The Czech Republic

J. Svoboda
Pragoprojekt a.s., Prague, The Czech Republic

ABSTRACT: The Valík tunnel is located on the Plzeň city motorway by-pass which is the part of D5 express highway connecting Prague with German border. It was the last section opened to traffic to complete the entire route. The tunnel is designed as a twin-tube connected by central cast-in-situ pillar within the primary lining. The length of the southern tunnel bore and northern tunnel bore is 380 and 390 m respectively, width of the roadway from curb to curb is 11.5 m and clearance height above the roadway is 8.2 m. Concreting of cut-and-cover tunnels begun before the definitive linings of the driven tunnels. Casting in of the driven tunnel's cross section was realized in two stages – bottom vault and ceiling vault. The basic technology consisted in pumping the concrete behind travelling steel form on rails.

Express highway D5 connecting the capital of Czech Republic Prague with German border is a part of trans European express highway network. Requirements of Czech tunneling directives namely regarding tunnel technological equipment were respected in the tunnel's design. Based on the tunnel's technological equipment and expected traffic intensity in one direction, 18125 cars per 24 hours, the Valík tunnel is ranked into the highest tunnel category TA.

1 GEOLOGICAL CONDITIONS

The slopes of Valík are covered with quaternary era sediments of 0.5–2.0 m thick. Under the layer of about 0.2 thick there are brown to reddish brown clay sands containing humus in some places more clayey with sharp fragments of strongly weathered porphyry. The tunnel itself is routed through moderately metamorphic proterozoic schist. The schist is strongly weathered and the strongest is 3 to 20 m deep along the entire length of the tunnel. A very detailed geological survey was carried out using a survey tunnel in the early stages (Fig. 1).

2 TUNNEL DESIGN

The Valík tunnel is a motorway tunnel with two bores. Each bore has two lanes, each is 3.75 m wide, and one emergency lane 3.25 m wide, the road is 11.5 m wide form curb to curb and the footpaths are 1 m wide (Fig. 2).

The bores are located next to each other with no rock pillar and they share a central pillar made of reinforced concrete. The central pillar was constructed inside the provisory middle tunnel (Fig. 3). This design was chosen because of the requirement to take as little land as possible for the tunnel.

The tunnel bores were made by driving uphill (inclination about 4%) from the temporary Rozvadov entrance. The structural calculation allowed the distance between both fronts from 10 m to max. 30 m. Tunnelling was mainly done without blasting using only mechanical disintegration of the rock and the use of explosives was exceptional.

The subdivision of the excavation area was mainly vertical and only a small scope was horizontal. The primary lining consist of sprayed concrete, braced arches, meshes and bolts.

3 SECONDARY LINING

3.1 *Cut-and-cover tunnel*

The tunnel mouths have shape of canted tubes and are provided with protective attic. The tubes themselves are made of watertight concrete with no outer isolation, only on the contact with the driven tunnel, an isolation membrane GSE – LDPE 3 mm thick was laid on the tubes (Figs 4,9,10)

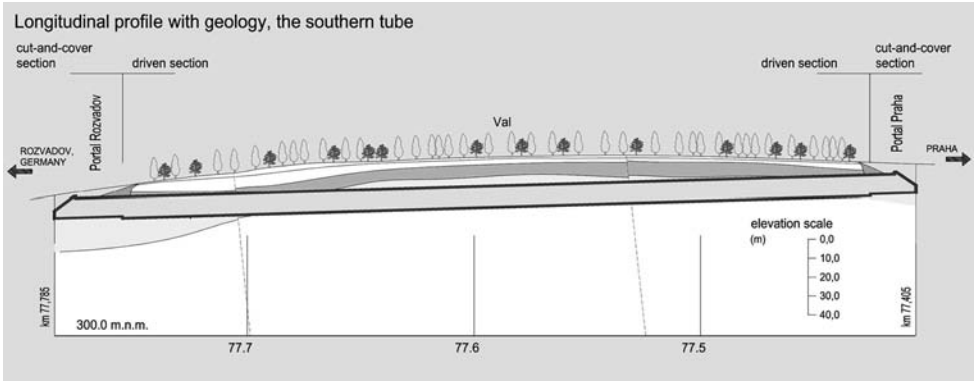


Figure 1. Longitudinal profile with geology, the southern tunnel bore.

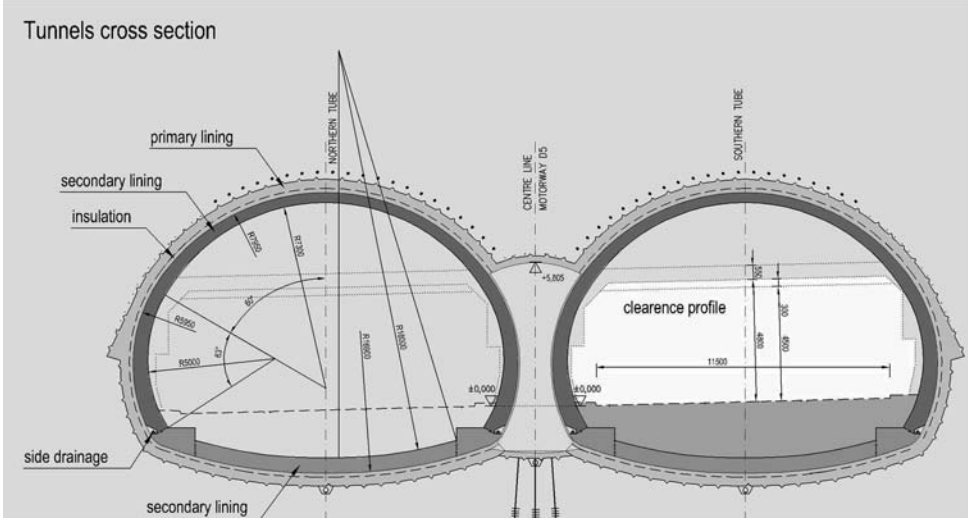


Figure 2. Cross-section of the driven tunnels.

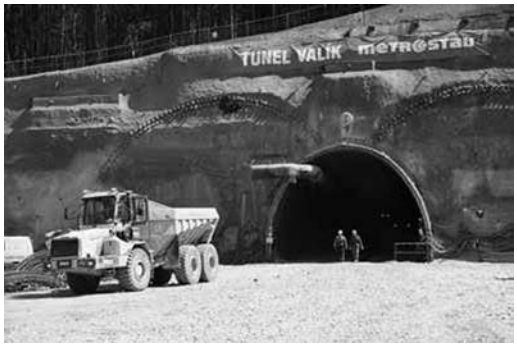


Figure 3. Entrance to the temporary middle tunnel, Rozvadov portal.



Figure 4. Cut-and-cover tunnel formwork at Rozvadov portal.

The cut-and-cover tunnel is a compact vault construction firmly connected with foundations. Minimum thickness of the concrete shell is 550 mm at the top of the vault and broadens down to the foundations. Casting in of the cut-and-cover tunnel was done using travelling steel form (specially made for the cut-and-cover tunnel) by 10 m segments and was begun before secondary lining of the driven tunnel. The steel formwork was made with DOKA system materials using chipboard sheets as facing (Fig. 4).

For the compact vault, reinforced concrete C 30/37 XF4, XD3 was used with maximum water ingress value equal to 20 mm. The foundations were cast of reinforced concrete C 25/30 XA1.

Filling of the tunnel form was done evenly at both sides of the tunnel through several filling windows on outer side of the form, so that the concrete mixture did not fall from height greater than 1.5 m. Compaction of fresh concrete was carried out by pervibration and in lower sections using form vibrators placed to the form.

3.2 *Driven tunnel*

The driven tunnel cross-section was designed having upper and lower compact vault. The tunnel vaults are combined of circular arches, the actual shape of the tunnel cross-section resulted from given clearance profile (Fig. 2). Connection between bottom and ceiling vault was carried out by flat joint. Minimum thickness of the tunnel's definitive lining is 400 mm at the top of the ceiling vault and broadens down to the bottom vault where it is cca. 600 mm thick. Concrete class used for the ceiling vault was C 25/30 XF4, XD3, for the bottom vault was used concrete class C 25/30 XA1, the minimum ingress value for both classes was limited to 20 mm.

Curvature of routing in the tunnel was replaced with polygon of short straight segments where the tunnel lining was longitudinally divided by admitted stop end and key every 10 m. The design of the steel form was subjected to this. Connection between neighboring segments (subblocks) at each polygon break was realized by contact concrete-concrete. Only at the touch between the cut-and-cover tunnel and the driven section, a dilatation joint with inserted polystyrene was carried out.

Static calculations were performed using elastic computational model. Dimensioning was done for the stability limit state and serviceability limit state (structure deformation, width of cracks in concrete). Calculations of crack widths in concrete were performed for the cut-and-cover tunnel and the driven tunnel's definitive lining. Following loads were regarded in the static calculations:

- Load by own weight
- Load by rock pressure (isotropic and anisotropic rock environment)
- Shrinking of concrete and creeping
- Temperature strain by non-uniform warming (summer) and cooling (winter) on the surface of the lining
- Influence of decreased friction between primary and secondary lining (by inserted hydro isolation)
- Influence of deterioration of bearing capacity and other deformational characteristics of the primary lining

By the cut-and-cover tunnel, an impact of car was regarded in the combination of loads. Load by hydrostatic pressure was not included into calculations.

Casting in of the driven tunnel's cross section was realized in two stages. In the first stage, the bottom vault was completed in tunnel's full length. After cleaning the surface of the primary lining, steel formwork was erected at the head of the concreted segment and on vertical sides. Length of each segment in bottom vault was 10 m, width was equal to 14 m. A mobile concrete pump was applied. To prevent extrusion of material by higher laying masses of concrete in the sides, casting in was done in successive layers, starting with lower bottom parts. For doing this, right composition of concrete mixture had to be secured.

After the completion of the bottom vault, works on the ceiling vault could begin. These were done from four working platforms spaced along the height of the tunnel with the use of special car moving on shared rails (Fig. 5). Works included treatment of the basis for hydro isolation, installation of hydro isolation, reinforcement assembly and concreting.

As a hydroisolation, 2.5 mm layer of GSE (LDPE) with signal coat was applied and transverse seams of isolation were covered with strengthened strips. Steel reinforcement consisted of truss frames positioned 1 m apart and steel nets, supplemented with bound steel rods. This design helped to reduce time needed for reinforcement assembly. Concrete cover specified by realization documentation was 50 mm.

Casting in of the upper vault was done into travelling steel formwork (by company OSTU Stettin) which was equipped with hydraulic control, pneumatic vibrators and safety overpressure components (Fig. 6). Construction of the form enabled fixing of additional steel forms for concreting of SOS shelters, tunnel bore connection and for hydrant, cable and drainage inspection niches as well. Concrete mixture was pumped into the divider by stable pump placed in front of the formwork. The mixture was deposited into the form evenly through several filling inlets so the difference between the levels of concrete on both sides of the form did not exceed 120 cm. Compaction of fresh concrete was performed by set of form vibrators. Casting the 10 m segment took cca. 7–8 hours during which approximately 180 m^3 of concrete mixture were laid. After 18 hours since the end of concreting, the



Figure 5. Car travelling on rails, hydro isolation installation, reinforcement assembly.



Figure 6. Steel form used for concreting the driven tunnel secondary lining.

steel form could be removed. Corresponding compression strength of the concrete at this moment reached 14 MPa (as detected by Schmidt impact hammer).

Immediately after the form removal, treatment of concrete against drying out was undertaken. The concrete treatment and other measures were adjusted depending on momentary climatic conditions.

3.3 *Finishing tunnel paintings*

For the surface finishing of the tunnel's secondary lining, protective and reflective paintings were used. Up to the 4 m level above the tunnel sidewalk, protective and reflexive light ochre paint was realized (for this tone a light-technical calculations were performed). Green stripe with the icon of moving walker inside, indicating the direction of evacuation, is running approximately 1 m above the ground (Figs 7–8). Remaining space of the vault above the 4 meter level is covered with uniting gray paint. The cut-and-cover tunnels are finished with uniting light ochre tone from both sides of the lining.



Figure 7. Architectural rendering of the tunnel interior, middle tunnel connection and SOS niche.



Figure 8. Tunnel interior, reflective part of paintings with icons.

The architectural solution of the inner paintings had been subject of discussions with Plzeň region citizens. The designer had prepared three proposals, and the winning design had to be passed by the Fire Department and also by the Police of Czech Republic. Inner architectural concept of the tunnel is purposely adjusted so that it facilitates maximally orientating of tunnel users during any emergency situation (Fig. 7).

Special attention was paid to the selection of the most suitable painting material which had to comply with various mechanical, physical and chemical requirements. The requirements included, for example, resistance to various harmful agents (exhaust emissions, road chemicals, detergents by regular tunnel washing, etc.) resistance to abrasion, flame resistance, resistance to changing temperature, freezing cycles, health harmlessness, color durability and many other factors.

Requirements for reflective part of paintings were best fulfilled with epoxy-based dispersion (Sikagard Wallcoat) applied in two layers – first penetration spray ($0.15\,kg/m^2$) and then finishing spray application ($0.20\,kg/m^2$), total thickness of the paint was 100 μm.

Uniting paint in upper vault was done with two layers of acrylate dispersion (Elastocolor by Mapei).

Before starting painting, quality of the concrete basis was tested on spotlighted referential area with applied paint. Thickness of the paint was regularly checked at 30 evenly spaced out points every 250 $m^2$of finished area, or after ending the day progress.

Inner tunnel painting works could be carried out only after all dusty activities in the tunnel had ended.

4 CONCRETE ROADWAY

An asphalt concrete roadway construction with reinforced joints in both directions was designed in the tunnel. Cement-stabilized aggregate road base is 200 mm thick, the subbase, 250 mm thick, is made of crushed stone (grading 0–32 mm). Filling of the bottom vault was done with two layers of crushed stone (grading 0–32 mm and 16–32 mm) instead of originally intended concrete filler. Under the roadway construction, the calculations regarded subgrade soil with $E_{def,2} = 60$ Mpa, and on crushed stone layer, $E_{def,2} = 110$ Mpa .

Tunnel sidewalks are cast of concrete, class C 30/37-XF4, 120–150 mm thick. Width of the sidewalk is 1 m. Joints in the pavement were cut every 5 m (Figs 7–8).

5 GEOLOGICAL MONITORING (GTM)

The construction was done in line with principles of the observation method when the basic structural design is reviewed on regural basis and can be modified in the course of the construction. There were clearly defined responsibilities for parties involved in the project and they all were provided with technology for fast communication.

As part of the geological monitoring of the structure behavior, selected parameters of all structures affected were monitored in terms of alerts, limit values and trends. In case of deviation from the desirable trends or when the alerts and limit values were exceeded, a signal was received upon which the required action, already incorporated in the design, was initiated.

6 TUNNEL EQUIPMENT

The tunnel is equipped with the traffic control and technical systems that provide more or less automatic control of all operating modes of the tunnel. The equipment of the Valík tunnel meets the requirements of the European parliament an Council on the minimum safety standards in tunnels of the trans European network (C00M 2002/0309-000) and complies with the latest European standards (amatic ventilation, monitoring system, SOS cabinets, CCTV surveillance, weighing of vehicle, spead reading, etc.).

The necessary documentation for operation, management and maintenance of the Valík Tunnel was developed, consisting of a set of documents covering the organization, responsibilities and activities related to tunnel operation. The operation of Valík Tunnel will be controlled by the Police of ČR, from a control room at Svojkovice; the tunnel equipment is maintained and upgraded by the operator who also provides services to the Police of ČR.

7 FIRE SAFETY IN THE TUNNEL

Practical understanding of effects of actions taken during any emergency situation is an essential requirement for choosing a right solution to the situation. This applies especially for the case of tunnel fire. Before opening the tunnel to traffic, in May 2006, a set of test fires with heat release rate equal to 5 MW (corresponding to burning a larger automobile) was performed. During these tests, the influence of tunnel self-venting and forced ventilation on smoke spread in the tunnel was examined.

Findings of the tests offer useful ground for better understanding the principles of spreading of hot smoke in short tunnels. Besides that, the tests are meaningful contribution to the improvement of the tunnel's fire safety. Findings of the tests can be further generalized and implemented into existing codes of practice.

8 CONCLUSION

Great attention was paid by all interested parties, ahead with the chief designer Pragoprojekt a.s. and the contractor Metrostav a.s., to the construction of the tunnel's secondary lining and to choosing the best composition of used concrete mixtures. The result is building work of high quality which is the credit of collective effort of all construction participants.

By construction of definitive linings, adding up of various unfavorable deviations could result in diminishing of the clearance profile. The design of the tunnel regarded these effects, nevertheless it was absolutely indispensable for the contractor to secure working technology as best as possible.

Monthly opened excursions for local public were regularly organized on the building site and local press kept constantly bringing information on progress of the construction. The clearing-house served for the public informedness and informational brochure was issued on starting the construction of the tunnel. The public contributed to the overall architectural concept of the tunnel and its surroundings in terms of public



Figure 9. Cut-and-cover tunnels, Rozvadov portal.



Figure 10. The tunnel entrance, Rozvadov portal.

inquires arranged by local daily paper. The outcomes of the inquires were respected in the design of the tunnel operation building, the tunnel portals, portal cuttings and also inner tunnel paintings (Figs 7–10).

The Valík Tunnel was designed and constructed so it is friendly and safe to its users. At the same time it meets all requirements of local administration as well as of ecological organizations. The hill Valík is, from the environmental point of view, an important landscape element. All actions in this space were therefore closely watched by an expert and general public.

Underground Space – the 4th Dimension of Metropolises – Barták, Hrdina, Romancov & Zlámal (eds)
© 2007 Taylor & Francis Group, London, ISBN 978-0-415-40807-3

Development in pre-cast concrete segmental circular tunnel linings

Y.K. Vimalanathan
Mott MacDonald, London, UK

ABSTRACT: In the past, the number of segments in a ring was kept high to reduce handling loads and to improve articulation of the ring there by reducing bending moments.

However, to speed up construction the segments in a ring got fewer and larger and this was made possible by strengthening the segments with reinforcing bars and by using stronger erector arms in TBMs so that the weight of segments was no longer a problem.

This now seems to have gone a full circle with the introduction of steel fibres in place of reinforcing bars. The Channel Tunnel Rail Link tunnels in the UK contained nine segments per ring. These segments have low bending strength and therefore required an increase in the number of segments per ring.

Segmental linings from recent projects will be compared to highlight the current trends in segmental lining design.

1 INTRODUCTION

Pre-cast concrete tunnel linings were first used in the 1930's. The designs used un-reinforced pre-cast concrete segments. The number of segments in a ring was kept high to reduce handling loads and to improve articulation of the ring there by reducing bending moments.

Many were used for lining tunnels in clay and the ring of segments was expanded against the ground, rather than bolted and grouted.

Since then design and construction methods have changed significantly.

There are a number of factors which affect segmental tunnel lining design. Some of these are listed below. Each of these will be examined in relation to recent projects to see how they affected that particular design.

- Segmentation
- Segment geometry
- Segment reinforcement
- Radial joints
- Circumferential joints
- Bolts & dowels
- Fire resistance

2 SEGMENTATION

For almost all linings the moment capacity of the joint is much less than that in the body of the segment. Therefore the flexibility of a lining is increased significantly and its 'average' inertia (I) reduced as the number of joints increases. The most common formula used for calculating the equivalent stiffness of the lining is:

$Ie = Ij + I\ (4/n)^2$ (Muir Wood 1975)
$Ij \ll I$ for an expanded and articulating lining
Ij = Second moment of inertia of the joint
Ie = Effective inertia of the ring
n = Number of segments in a ring

Ij is an extremely difficult quantity to calculate, as it is a function of the hoop thrust as well as the geometry of the joint, but usually it would be expected that Ij would be close to zero.

To benefit from a flexible lining that attracts a lower bending moment the number of segments in a ring should be greater than 5. This assumption comes out of studies for the Channel Tunnel (UK) project in the 1970's, which showed that the maximum bending moment (BM) in a 5-segment ring is very close to that of a 4-segment ring. The studies also showed that if the joints in a 4-segment ring coincided with the vertical and horizontal axes, where the maximum BMs occur in a rigid ring, the maximum BMs are not significantly reduced.

The projects listed below have followed this basic principal and the minimum number of segments in a ring is always 5 or greater. It should also be noted that where steel fibre reinforcement is used the linings have 8 or 9 segments in a ring. This is done in order to increase their flexibility as steel fibre reinforced concrete has reduced flexural strength compared to segments reinforced with steel bars.

Segmentation is also dependent on the position of the Tunnel Boring Machine's (TBM's) rams. Segment sizes are chosen to avoid ram positions coinciding with radial joints, but if the rings are rolled to prevent cruciform joints this may be unavoidable. Where this happens the circumferential joints should be detailed to prevent edge damage.

Segments are also sized to allow maneuverability within the confined spaces of a tunnel.

To minimize moments therefore, there are advantages in having a large number of segments. However a balance has to be struck between speed of erection and an economic design. For many projects one of the key costs is overall duration of the tunneling. There in many cases a balance is struck between many segments, which would require low bending stiffness and fewer segments which can be installed more quickly but require heavier reinforcement.

3 SEGMENT GEOMETRY

Most segments built are rectangular in plan with the Top and Key segments having radial joints which are inclined to the long axis.

Trapezoidal tunnel linings as the name implies have trapezoidal shaped segments. The inclined radial joints in these segments make the rings very much more rigid (stiff) than conventional segments which have the joints parallel to the tunnel axis. There is some evidence that trapezoidal segments are easier to erect and assist in ensuring that the lining rings are circular prior to grouting.

There are two disadvantages of the trapezoidal form. The lining has to resist a larger bending moment as the joints do not allow the longitudinal rotation of the more conventional lining. Also the geometry of the lining means that more space is required to erect each individual ring. This in turn means that for any given ring the tunnelling machine erection area and the length of the jacks have to be longer.

4 SEGMENT REINFORCEMENT

As noted above, when pre-cast concrete segments were first used, the individual segments were small to allow manual handling within the tunnel.

As tunneling machines, and in particular the erectors became more sophisticated it became much easier to use larger segments.

Until relatively recently the standard approach was to use steel bars for reinforcing segments to prevent failure or excessive cracking .

In designing this reinforcement the following are the key load cases-

- During de-moulding, handling and stacking
- At radial and circumferential joints due to tensile and shear stresses induced by local stress concentrations
- In the body of the segment due to bending moments generated by non uniform ground pressures and joint eccentricities

However in the past decade steel fibres have been used as an alternative to steel bars. Three projects are listed in Table 1. Since the use of steel fibres on the prestigious Channel Tunnel Rail Link (CTRL) project momentum has grown for its wider use.

Steel fibres give the concrete segments ductility and help withstand high shove loads by its enhanced tensile strength.

Due to the minimal thickness of steel fibres their expansion during corrosion does not cause concrete spalling. Therefore steel fibre reinforced segments would be classed as durable. With steel bars, corrosion of reinforcement can cause early durability problems. Therefore it is essential to have sufficient cover to

Table 1. Segmentation on some of the recent tunnel projects.

Project	Internal diameter (m)	Thickness (mm)	Aspect ratio length/thickness	No. of segments	Year detail
Channel Tunnel, UK, Undersea, Type 1	7.6	270	13.7	8 + key	1988 rebar
Storebaelt Eastern Railway Tunnel, Denmark	7.7	400	10.6	6 + key	1989 rebar
Heathrow Baggage Handling Tunnel, UK	4.5	150	13.9	7 + key	1993 fibre
Heathrow Express Tunnel, UK	5.675	220	12.6	5 + key	1994 rebar
Airside Road Tunnel, Heathrow, UK	8.1	350	10.8	7 + key	2001 rebar
Delhi Metro, India	5.7	280	13.4	5 + key	2002 rebar
Dublin Port Tunnel, Ireland	10.84	350	15.9	6 + key	2002 rebar
SMART Tunnel, Malaysia	11.83	500	9.7	8 + key	2003 rebar
Channel Tunnel Rail Link, UK	7.15	350	7	9 + key	2004 fibre
Heathrow Express Extension to T5, UK, expanded lining	5.675	220	12.6	9 + key	2005 fibre
Durban Harbour Services Tunnel, South Africa	4.4	250	11	5 + key	2005 rebar

reinforcing bars. However high cover in what are often relatively slender concrete segments can compromise the strength of the segment, and in particular allow damage to corners and other areas which, because of the cover requirements, are effectively un-reinforced. This problem does not arise with steel fibres provided that they are uniformly distributed through the segment thickness.

Although steel fibres are proving to be popular in Europe that is not the case in other areas of the world where steel fibres are not locally produced and the cost of labour intensive activities such as steel fixing is low.

Reinforcement density for reinforced segments is unlikely to be less than 75 kg/m^3 and a normal average figure would be about 90 kg/m^3. A typical dosage of steel fibres is 30 kg/m^3, but the actual figure will depend on the type of fibre used as well as the loads imposed on the lining.

5 RADIAL JOINTS

Radial joints are either designed as curved or flat. Curved joints were developed for expanded linings where convex/convex contact surfaces allow improved articulation at joints when the ring expands against the ground as the key is wedged in.

However the radii required for an efficient joint are large, requiring extremely high tolerance steel moulds for casting the segments. Usually the patterns used for casting the curved joints have to be machined from large steel blocks and then installed very accurately within the main body of the mould. Segment casting tolerances are always, or should be, tighter than the tolerances listed in codes of practice for pre-cast components such as bridge beams.

Therefore the preferred radial joint detail for a bolted gasketted lining which sits within a grout annulus is flat. With flat joints proper consideration needs to be given to the joint geometry to avoid damage due to large eccentricity in the joints due to poor build of the ring. No ring can be built perfectly circular and the design must allow reasonable construction tolerances, particularly at the joints. If contact is a line at or close to a corner of a joint, damage is inevitable, if the forces normal to the joint are anything but trivial.

In the past plywood packers have been specified in flat joints to improve articulation, but more recently flat jointed segments have been constructed satisfactorily without packers. This is due to the increased concrete strength, elastic/plastic deformation of the concrete at the joints and tight construction tolerances now achievable.

The radii given in Table 2 were calculated using design rules derived from the results of tests made on knuckle joints in reinforced concrete test pieces and from other published data.

Although curved joints reduce eccentricity and improve articulation, flat joints sustain a higher load at failure, assuming the flat joints are in full contact (Woods 2003). However with joint rotation the maximum sustainable load for flat joints reduces rapidly but rotation has little impact on the capacity of curved joints.

The present trend appears to be to use curved joints with expanded rings and flat joints with bolted rings.

6 CIRCUMFERENTIAL JOINTS

Circumferential joints are designed and detailed to resist TBM ram loads and to contain gaskets. Of the 11 projects listed in Table 1, 9 have flat circumferential faces, whilst two have a cam and socket coupling system as shown in figure 2. The intended purpose

Table 2. Curved joint radii on recent projects.

Project	Convex/convex joint radius (mm)	Lining types
Channel Tunnel, UK	3200	Expanded
Storebaelt, Denmark	2500	Bolted
Heathrow Express, UK	1375	Expanded & bolted

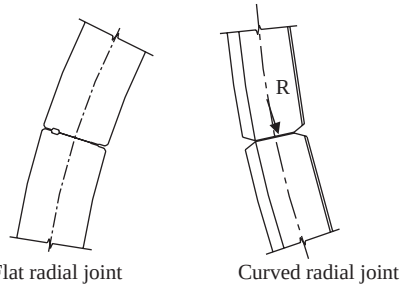


Figure 1. Flat and curved joints.



Figure 2. Cam and socket detail.

of the cam and socket is to assist the TBM driver to locate the segments into position. The other means of positioning segments accurately would be to use laser targets, which is possible with the modern TBMs.

6.1 *Cam and socket coupling*

The beauty of segmental lining is that it creates a flexible tube which can accommodate a small amount of movement. Therefore when a cam and socket is used as shown in figure 2 it is essential that there is sufficient tolerance in the coupling that rings can be installed without damage.

The tolerance in the coupling has to allow for the following:

- Casting and construction tolerances
- Differential deformation of adjacent rings due to ring roll and non coinciding longitudinal joints
- Frictional resistance created between the mating surfaces due to the pre-stressing effect of the ram forces

When all these effects are added together it is possible that the clearance between the cam and socket is exceeded inducing additional load on the joint causing it to crack.

Cam and socket arrangements, therefore, would not be recommended, unless the tunnel is in very soft ground and requires stiffening effect from these couplings. It may then be necessary that additional reinforcement is provided to make the connection work as a shear key. At the same time the rings need to be built to an accuracy which is greater than is usually achieved.

6.2 *Circumferential reinforcement*

Very often segmental lining thickness is determined by the short term TBM ram forces rather than by the long-term ground and water loads. It is therefore imperative that the circumferential joint is designed adequately to resist the large bearing and bursting stresses induced by the TBM rams.

Empirical results obtained from studies for the Channel Tunnel project in the 1980s (Eves & Curtis 1991) shows that the major part of the anti-bursting capacity of a joint comes from the inherent tensile strength of the concrete. However steel reinforcement is also very often required close to the joint face to compensate for the shortfall between the imposed ram load and the concrete strength.

For the Delhi Metro and the Durban Harbour services tunnel projects as shown in figure 3, German contractors introduced closed links adjacent to the circumferential face as anti-bursting steel. These designs were based on the assumption in most concrete design codes that the concrete tensile strength should not be included in determining the ultimate joint load capacity.

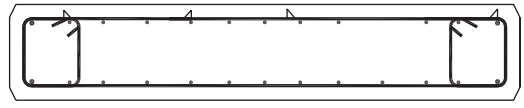


Figure 3. Example of links along circumferential joint.

7 FIRE RESISTANCE

Several major fires in European tunnels have raised awareness about how high strength concrete performs in fire situations. A significant loss of cross-sectional area in the tunnel lining can occur due to the spalling of concrete when exposed to very high temperatures.

Explosive spalling occurs when moisture in the concrete vaporizes under intense heat causing pressure build up within the concrete which is greater than its tensile strength.

The addition of polypropylene fibres at a dosage of 1 kg/m^3 has been shown in tests to significantly reduce this spalling. The basic reasoning behind this reduction is that, as the concrete is heated, the polypropylene fibres melt and create voids for pressure relief. The Airside Road tunnel at Terminal 5 Heathrow UK and the CTRL segmental linings contain polypropylene fibres.

8 BOLTS & DOWELS

8.1 *Bolts*

The purpose of bolts in a segmental lining is only to provide temporary support until the grout annulus hardens. The bolts are required in the short term to keep the radial joint gasket compressed and the circumferential joint gasket compressed when the TBM ram is released. They also assist in supporting the segment weight whilst a TBM ram is removed to install the next segment.

In the 1980s curved bolts were favored as they required smaller pockets in the concrete segments. But with the reliability of plastic cast in sockets now demonstrated spear bolts have become more commonly used in linings of 200 mm thickness and greater. The advantage of spear bolts is that it only requires a single pocket although the pocket size is larger than for a curved bolt.

8.2 *Dowels*

Dowels are very often proposed for circumferential joint connections. Unlike bolts, dowels require no pockets, which is an advantage. However once two segments are joined together with dowels it is nearly impossible to pull them apart.

In gasketted linings the circumferential joint dowels have to not only work in shear but also in tension as they keep the gaskets compressed whilst the TBM rams are

released to insert the next segment. Hence dowels have to fit snugly. Therefore great care has to be taken in choosing the right type of dowel. Dowels made with plastic sockets and push fit steel rods can cause the circumferential joint to crack if there is insufficient room for expansion as the steel rod is hammered into the cast in socket.

9 CONCLUSIONS

This paper summarises very briefly some of the current trends in segmental lining design and discusses some of the issues with the present day designs.

Innovations in TBM design and the need to build deep tunnels in poor ground conditions will lead the way in which segmental tunnel lining design has to develop in the future.

ACKNOWLEDGEMENTS

I wish to thank Mott MacDonald for permission to publish this paper, and John Curtis and Tony Deane for their assistance.

REFERENCES

Muir Wood, A.M. 1972. The circular tunnel in elastic ground, Geotechnique 25, No. 1, 115–127

Woods, E. 2003. Design decisions for CTRL 2's bored tunnels, Tunnels & Tunnelling international supplement September 2003

Eves, R.C.W. & Curtis, D.J. 1992 Channel tunnel lining design and procurement, ICE proceedings, UK

Behnen, G. & Hesterman, U. May 2006. Load bearing capacity of segment couplings, Tunnel, Official journal of the STUVA

This page intentionally left blank

Underground Space – the 4th Dimension of Metropolises – Barták, Hrdina, Romancov & Zlámal (eds)
© 2007 Taylor & Francis Group, London, ISBN 978-0-415-40807-3

Design of replaceable structural lining segments

Wenge Qiu, Junru Zhang* & Dongmei Li
School of Civil Engineering, Southwest Jiaotong University, Chengdu, Sichuan, China

ABSTRACT: To resolve the problems about waterproofing of single shell lining and surface evenness, the paper put forward a sort of new "flue lining structure" matching the single shell lining – replaceable structural lining segments. Study minutely about characteristics of structure, classified principia of precast lining segments, joint of members and waterproofing and the manufacturing and assembling of the members. The purpose is to gain the types of single shell lining to resolve the problems in practice and to base for the development and popularity.

1 INTRODUCTION

Since 1960, single shell lining, an advanced tunnel supporting structure, have been applied far-ranging at home and abroad. Such as the underground ice hockey rink of Gjolasvik in Norway, the tunnel of Vereina in Switzerland[1], and the project of underground storage of liquefied petroleum gas in Shantou (a city of China)[2], and the most arrestive is the Scandinavian . But single shell lining is mainly used in certain instances without notable deformation of the surrounding rock, gushing water, and water seepage and leakage. The Waterproofing of lining and surface evenness are major factors limiting the further popularize of single shell lining[3–4]. The experts of domestic and international have done a lot of research about the two problems, and the results can conclude thus: the waterproofing method of a structure is self-waterproofing achieving by put some admixture into shotcrete (such as silica power etc)[5]; the actualize of surface evenness achieves by construction technology (such as moulded shotcrete and shotcrete surface reprocessing etc) or decorating the surface of lining. On this foundation according to highway or railway tunnel cross section, the paper put forward a sort of new "flue lining structure" matching the single shell lining – replaceable structural lining segments, to resolve the problems of structure waterproofing and surface evenness. We will introduce the design essential of this new structure.

* Communication of Junru Zhang:
Tel: 86-28-86465636
E-mail: zhuangjunru_1@163.com
ADD: 301#, School of Civil Engineering, Southwest Jiaotong University, Chengdu, Sichuan, 610031, China

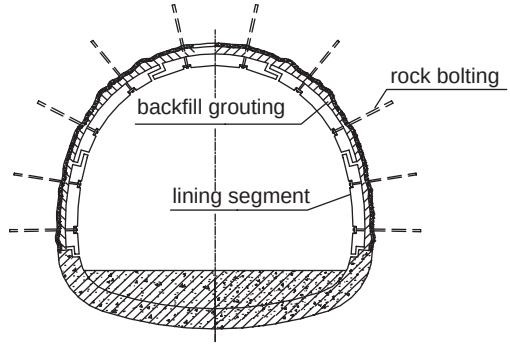


Figure 1. Structure of single shell lining.

2 STRUCTURAL CHARACTERISTICS

A single shell lining supporting system is shown in Fig. 1, carrying on shotcrete and rock bolt support to the arch wall of excavation, and cast-in-situ concrete to inverted arch and bedplate according to loaded of structures after excavation. Besides, a sort of replaceable structural lining segments is installed inboard shotcrete lining to resolve the problems of structure waterproofing and surface evenness. The following are characteristics about this sort of structural:

- The segments are structure lining only, take no account of supporting in principle;
- The segments are prefabrication, guaranteeing and raising the quantity index of the structure, such as strength, durability, corrosion proofing, and waterproofing etc. Besides, construction project time can be contracted;
- The segments are made of reinforced concrete of C30, with 20 cm of thickness, 0.3% of reinforcement ratio, and S8 of waterproof degree.

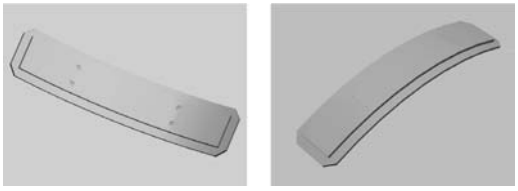


Figure 2. The forms of segments.

- The longitudinal and circumferential joint of segments are connected by ordinary bolt erecting together with radial rock bolting ;
- Do some backfill grouting between segments and shotcrete shell to make them forming a firm and impervious integral structure after completing installation of segments.
- It is convenient for segments to assemble, disassemble and repair.

3 CLASSIFICATION OF PRECAST LINING SEGMENTS

The following factors are considered in classification of precast lining segments[6]:

- Reduce the types of the members possibly to produce on a large scale.
- View to loading, it's better to dowel the joint of segments on the place of zero bending moment or plus bending moment approaching to zero;
- Considering the convenient of producing and assembling , it's better to limit the weight of each member. The weight of a member shouldn't exceed 2.5t∼3.0t if the width is 1.2 m;
- It's should be in favor of processing of joint, the evenness of surface and operation ventilation.

Therefore, it's better to adopt the following classification for lining segments of single-track railway tunnel: the part of arch needs 2∼3 blocks + each of side wall needs 1 + the bedplate or inverted arch. The form and classification of segments are shown in Fig. 2 and Fig. 3.

4 JOINT OF MEMBERS AND WATERPROOFING

The construction of joint and waterproofing are the key technologies of precast effecting usage and durability.

4.1 *The construction of joint*

The joint of members include longitudinal ones and transverse ones, and view to the construction of joint used it include joint by cast-in-situ-concrete, bolted

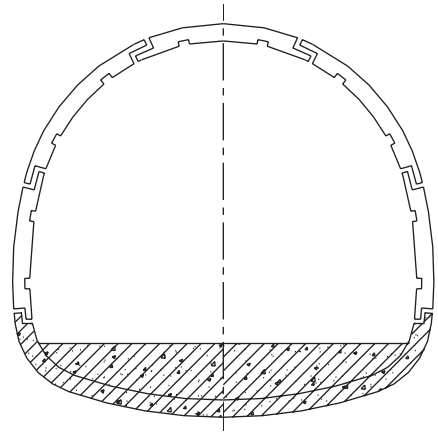


Figure 3. The classification and assembling of precast.

joint by pre-clamping, mortised joint by self-clamping and joint by bolt connection etc. When selecting, whichever, the following terms should be satisfied:

- With shear-bearing capacity of required;
- With waterproofing capacity of required;
- Convenient to combine and locate;
- With certain universality and durability.

Considering convenient to assemble and disassemble, the replaceable structural lining segments mentioned in the paper are jointed by bolt connection.

4.2 *Waterproofing of structures*

4.2.1 *Waterproofing of segments*

The waterproofing of segments carries on self-waterproof by the using of watertight concrete. Quality can be completely guaranteed for it's prefabrication, and the gradation of waterproofing is first-order.

4.2.2 *Joint and joint seal*

Rubber sealing strip, sealing combined around the segment, is adhered to the interface for waterproofing, and it's shown in Fig. 4 and Fig. 5. Considering assembly accuracy and construction, it's made by the material with water-expansion quality the mixture of a kind of polymer material with water-absorbing quality and neoprene rubber. The material can proof the intrusion of water and resist certain water pressure for volume expansion and the counter force produced by the bind of groove when reacts with water.

4.2.3 *Waterproofing of bolt hole*

For the joint of bolt connection, the following is the process of waterproofing of bolt hole: first, set the sealing gasket collar made by water expanded rubber; second, screw the nut tightly; third, put on the helmet;

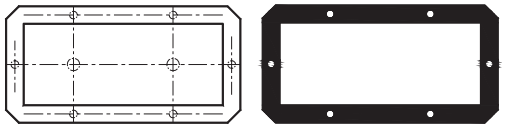


Figure 4. Precast segment and rubber sealing strip.

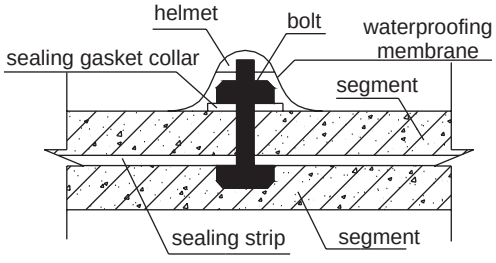


Figure 5. Connection between segments.

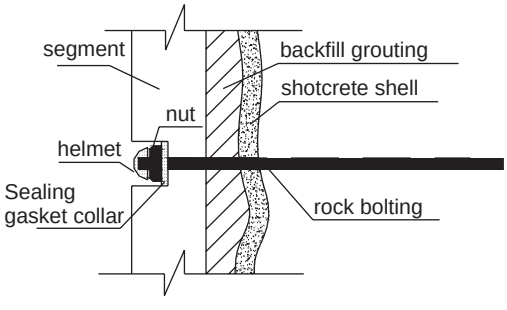


Figure 6. Connection between segment and rock bolting.

the end, coat waterproofing membrane around the nut. That is shown in Fig. 5 and Fig. 6.

5 THE MANUFACTURING AND ASSEMBLING OF THE MEMBERS

The manufacturing of structural segments must guarantee the accuracy required together with the convenient of assembling and the development of the follow-on work. Therefore every segment sets two preformed holes for pressure grouting whose flue lining are steel tube of 85 mm with screw thread on the innerface enclosed when grouting concrete. Screw a special of hook in the holes for hoisting. The following is the particular assembling of structural segments:

- Clearing the bed;
- Grouting inverted arch and bedplate of concrete.
- Installing segments of both sidewall;
- Installing segments of the part of arch;
- Screwing bolt tightly and waterproofing of joint;

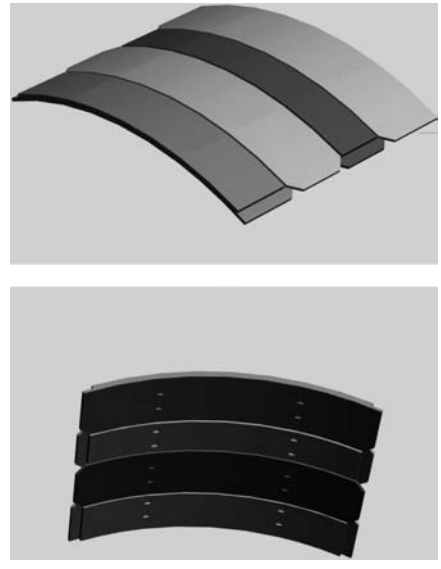


Figure 7. Assembling segments of local.

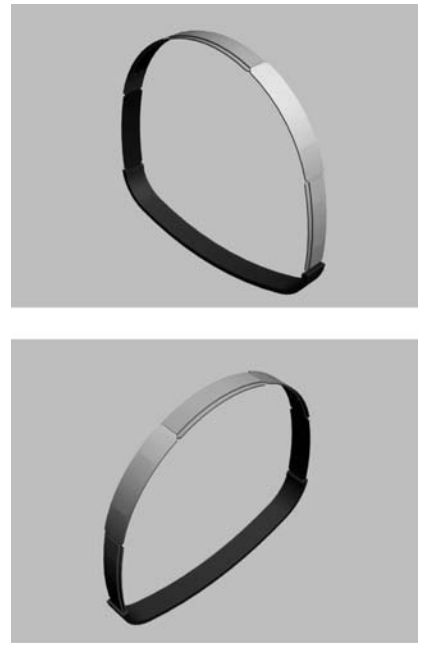


Figure 8. Assembling segments of signal ring.

- filling and grouting from the back;
- Constructing the ditches and cable trenches;

Figure 7 to Fig. 9 displays the process and outcome of assembling the structural segments.

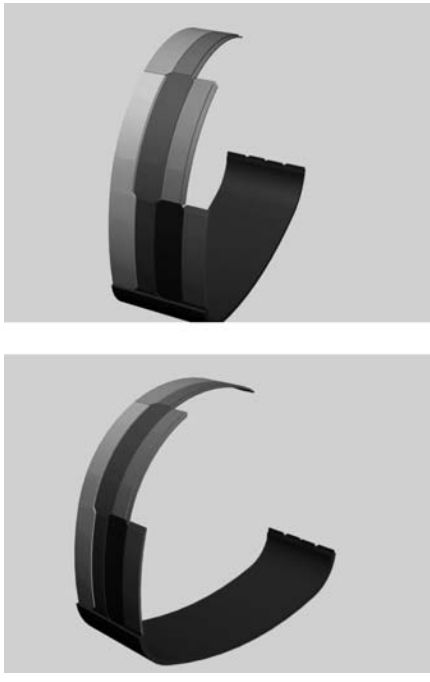


Figure 9. Assembling segments of integral.

6 CONCLUSIONS

The paper put forward a kind of new "flue lining structure" matching the single shell lining – replaceable structural lining segments, it's writers' sum-up about the study of single shell lining, to resolve the problems about waterproofing of single shell lining and surface evenness. Study minutely about characteristics of structure, classified principia of precast lining segments, joint of members and waterproofing and the manufacturing and assembling of the members. Certainly, it needs a process to pullulate for anything, so it's hard to avoid some insufficiencies, pleasing point them out to perfect.

REFERENCES

[1] Bin Wang. Project Of Vereina Tunnel [J]. *Journal of tunnel translations*. 1994 (7): 22–26.

[2] Youqiang Li. The Used Of NTM In The Project Of Underground Storage Of Liquefied Petroleum Gas In Shantou (a city of China) [J]. *World Tunnel*. 2000(6): 17–23.

[3] Jianyu Wang. *Progresses Made By Technology Of Tunnelling [M]*. Beijing:Railway Publishing Company, China. 2004.

[4] China Association for Engineering Construction Standard. *Technical Specification For Fiber Reinforced Concrete Structures(CECS 38: 2004)[S]*. Beijing:China Planning Press. 2004.

[5] Chengsan Wu.Master The Technology Of Single Shell Lining In Time To Reducing The Cost *[J]*. *Railway Standard Design*.1996.(12): 1–3.

[6] Baoshu Guan. *Outlines Of Tunnelling Design[M]*. Beijing: China Communications Press. 2003.

Underground Space – the 4th Dimension of Metropolises – Barták, Hrdina, Romancov & Zlámal (eds)
© 2007 Taylor & Francis Group, London, ISBN 978-0-415-40807-3

Structural behavior of SFRC tunnel segments during TBM operations

R. Burgers & J. Walraven
Delft University of Technology, Delft, The Netherlands

G.A. Plizzari & G. Tiberti
University of Brescia, Brescia, Italy

ABSTRACT: The paper addresses precast tunnel segments for the new Line 9 of Barcelona Metro. After the experimental determination of the material properties, non-linear analyses allowed to study the structural behavior of the tunnel segments under TBM thrust jack forces during construction process. The paper focuses its attention to the advantages coming from the use of Steel Fiber Reinforced Concrete (SFRC) in terms of crack control and bearing capacity. Finally, Ultra High Performance Concrete (UHPC) has been investigated to study if this material is suitable for the application in tunnel segments.

1 INTRODUCTION

After more than 40 years of research, interest in Fiber Reinforced Concrete (FRC) is continuously growing in many application fields. FRC is already widely used in structures where fiber reinforcement is inessential for integrity and safety, such as in slabs on grade or in first phase linings.

For structural purposes, steel fibers are becoming widely utilized since fibers enhance toughness of the concrete matrix (which involves the ability to resist stresses after cracking), improve impact and fatigue resistance and make the crack pattern more distributed with cracks having a smaller crack width.

Among the structural applications of steel fiber reinforced concrete (SFRC), there is a growing interest in precast tunnel segments to be used with the Tunnel Boring Machines, TBM (Blom, 2002, Plizzari and Tiberti, 2006). These segments are generally made of ordinary reinforced concrete; however, the addition of fibers is gaining considerable attention among designers and producers due to the enhanced toughness that allows a partial or even total substitution of the conventional reinforcement that, in such members, is characterized by a curved geometry. Fibers also guaranties a reinforcement in the corner of the segment or in the large covers that are often required for fire resistance.

In the present paper, the structural behavior of the segments for the Metro Line 9 of Barcelona (Spain) are numerically simulated with non-linear analyses (Plizzari and Cominoli, 2005).

The TBM-excavated tunnel of Barcelona has a diameter of approximately 12 m, a length of more than 40 km and is located from 30 to 70 m below the surface. Every ring is made of 7 segments with a length of about 4.70 m and 1 key segment of half that length (Fig. 1).

Experiments have been performed to determine the materials properties and the constitutive laws of SFRC for use in tunnels.

Numerical analyses have been performed by using a finite element model based on Non Linear Fracture

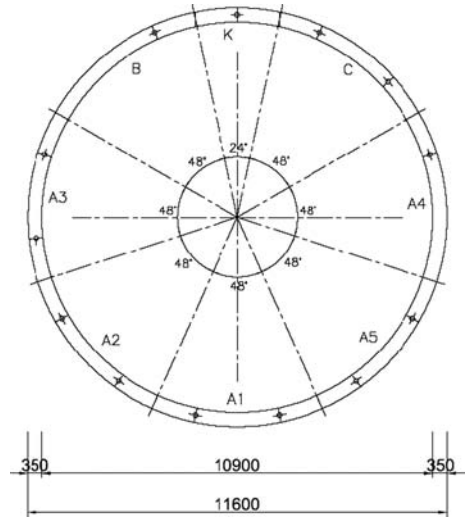


Figure 1. Transverse section of the tunnel for the line 9 of the Barcelona Metro with evidenced the eight precast segments (Gettu et al., 2004).

Mechanics (NLFM; Hillerborg et al., 1976) with a smeared crack approach. The numerical model has been validated by using the experimental results of splitting tests performed on SFRC specimens (Schnütgen and Erdem, 2003). During the validation, different concrete crack models have been tested and compared.

2 MATERIALS

The experimental characterization of the material properties of SFRC was performed on a concrete matrix having the same mix-design of the one used for the Line 9 of the Barcelona Metro.

Segments were reinforced with steel fibers Wirand FF1 having a length L_f of 50 mm, a diameter ϕ_f of 1.0 mm and an aspect ratio L_f/ϕ_f equal to 50. These fibers are cold drawn, have a hooked shape, a rounded shaft and a tensile strength higher than 1100 MPa. Fibers were used with the volume fractions (V_f) equal to 0.58% (45 kg/m^3).

Fracture properties of FRC were determined by using eight notched beams ($150 \times 150 \times 600$ mm) tested under 4-point bending according to the Italian Standard (UNI, 2003; Fig. 2). In addition, 4 beams of plain concrete were used as reference specimens. The slump of the fresh concrete was always greater than 150 mm. Specimens were stored in a fog room (R.H. $> 95\%$; $T = 20 \pm 2°C$) until 24 hours before testing. The mechanical properties of concrete (average values), as determined after about 60 days of curing are the following: tensile strength (determined from cylinders having $\phi = 80$ mm and $L = 240$ mm) $f_{ct} = 4.10$ MPa, compressive strength (from cubes with a side of 150 mm) $f_{c,cube} = 64.1$ MPa and Young's modulus (from compression test on cylinders $\phi = 80$ mm, $L = 240$ mm), $E_c = 37000$ MPa.

Fracture tests were carried out with a closed-loop hydraulic testing machine by using the Crack Mouth Opening Displacement (CMOD) as control parameter, which was measured by means of a clip gauge positioned astride a notch at midspan, having a depth of 45 mm. Additional Linear Variable Differential Transformers (LVDTs) were used to measure the Crack Tip Opening Displacement (CTOD) and the vertical displacement at midspan and under the load points (Fig. 2).

Inverse analyses of the bending tests, based on NLFM (Hillerborg et al., 1976), allowed to determine the best-fitting post-cracking law (σ-w) for the SFRC adopted in the present research (Roelfstra and Wittmann 1986). The Young's modulus (E_c) was the one experimentally measured from the cylinders while the Poisson ratio (ν) was assumed equal to 0.2. The softening law was approximated as bilinear where the first steeper branch can be associated with the

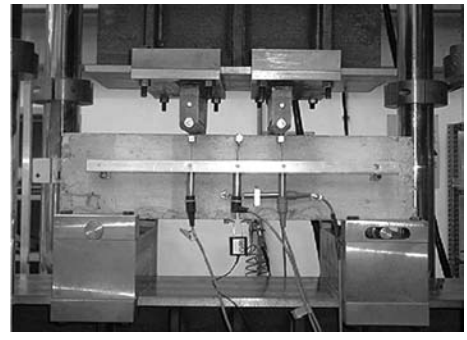


Figure 2. Instrumentation for the notched specimen used for the 4 point bending beam tests.

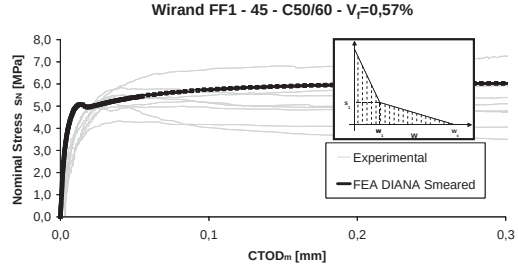


Figure 3. Experimental and numerical results obtained from SFRC beams and the bilinear law adopted.

bridge action of concrete between microcracks while the second branch represents the residual stress due to fiber bridging (Fig. 3). The numerical analyses were performed by assuming both a discrete crack and a smeared crack approach with Diana ver. 9.1 (2005); the latter was also used for the numerical simulations of the tunnel segments.

The material parameters identified from the bending tests are the following (see Fig. 3): $f_{ct} = 4.10$ MPa, $\sigma_1 = 2.134$ MPa, $w_1 = 0.023$ mm, $w_{cr} = 5.35$ mm. The best-fitting numerical curves obtained with Diana are compared with the experimental ones in Figure 3.

Firstly, numerical analyses of tunnel segments were carried out with different amounts of steel fibers; secondly, the response with Ultra High Performance Concrete (UHPC) has been investigated. The post-cracking properties of concrete with different fibers contents were assumed starting from the bi-linear law "experimentally" determined from concrete C50/60 with 45 kg/m^3 of steel fibers.

The stress–strain relations and the values of UHPC were obtained according to den Hollander (2006). The stress-strain diagram for UHPC is given in Figure 4.

UHPC was made with two types of fibers: micro and macro ($l = 50$ mm) fibers; the latter govern the ultimate tensile strain. The characteristic values of the stress–strain diagram are given in Table 1.

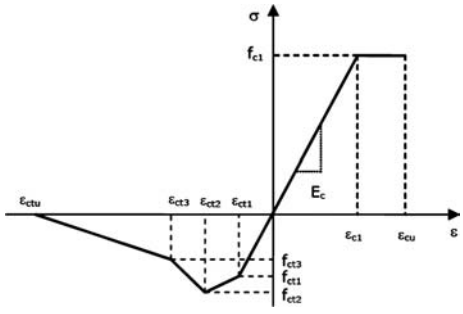


Figure 4. Stress–strain diagram for UHPC with strain hardening (den Hollander, 2006).

Table 1. Material properties for the adopted UHPC mixture.

Material property	Symbol	Value
Compressive strength	f_{ck}	200 MPa
Design comp. strength	f_{c1}	120 MPa
Design tensile strength t_1	f_{ct1}	8 MPa
Design tensile strength t_2	f_{ct2}	9 MPa
Design tensile strength t_3	f_{ct3}	5 MPa
Yield compressive strain	ε_{c1}	1.75‰
Ultimate compressive strain	ε_{cu}	3.00‰
Ultimate tensile strain	ε_{ctu}	10.00‰
Specific weight	ρ_c	28 kN/m^3
Young's modulus	E_c	55000 Mpa

3 DESIGN ASPECTS

An open question for the construction companies and the designers concerns the reinforcement for these precast elements. Generally, reinforcement is designed according to the design actions on the tunnel segments, resulting from segment transportation, placing process and soil pressure in the final state.

In particular, during construction, the thrust forces and the grout pressure are the most critical factors. Cracks often appears in the tunnel lining in the phase in which these forces occur. Some examples of cracks that have been observed in Line 9 of the Barcelona Metro are shown in Figure 5. Possible causes of these cracks could be: eccentricity, inclination of the thrust jacks. Also a number of phenomena due to the trumpet shape as the torsional deformation or an uneven support of the ring joint cause these cracks.

It is desirable to mitigate or reduce these cracks as much as possible since they determine a loose of quality and leakage and high repair costs. Cracking phenomena can be limited by introducing a change in tunnel design by using, for example, an opportune configurations of the thrust jacks and supports. Alternatively, they can be reduced by using FRC.

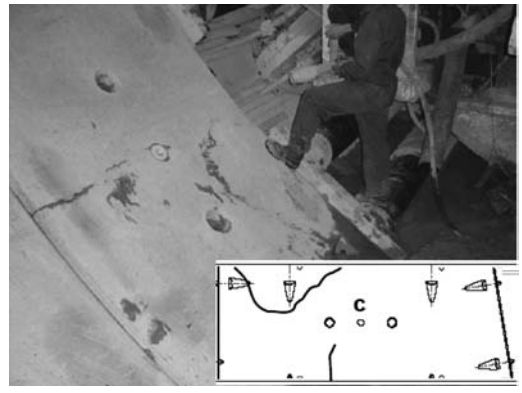


Figure 5. Spalling cracks observed during construction of Line 9 of the Barcelona Metro.

The research work presented herein focuses on the last topic. In order to verify the influence of steel fibers on the crack development in segmental linings during construction, several non-linear analyses were carried out.

Based on the material properties described in § 2, the total strain rotating crack model provided by DIANA was adopted for FE simulations of the SFRC tunnel segments. The numerical analyses were carried out by adopting a 3D solid model with 5184 first order hexahedral elements (eight nodes brick elements HX24L). The constitutive law for concrete under compression was assumed according to Thorenfeldt (1987) that is a suitable model for a concrete grade C50/60. Moreover, the increase of compressive strength due to lateral confinement has been implemented according to Selby and Vecchio (1993).

During excavation process, 30 TBM actuators act on the Barcelona Metro lining. The average service load applied by a single actuator is 3 MN. The load configuration used in Barcelona is a combination of the French and Japanese jack configuration. In practice, two pairs of thrust jacks act on each tunnel segments whereas four bearing pads are positioned in the rear face of the tunnel segments (ring joints).

One single segment with his two pairs of actuators was considered and its boundary conditions (i.e. presence of adjacent segments) were simulated by elastic springs whose stiffness was previously calibrated. Noticing that also ring joints have been simulated by using "no-tension" elastic springs positioned on the bearing pad surfaces (Fig. 6).

Figure 6 shows the loading scheme when thrust jacks are exactly placed in position and the support of the ring joint is uniform.

Figure 7 shows the numerical results in terms of load (from the actuators) versus the average longitudinal displacement under the loading surfaces. The segment collapses at a total load of 30.7 MN; since the service

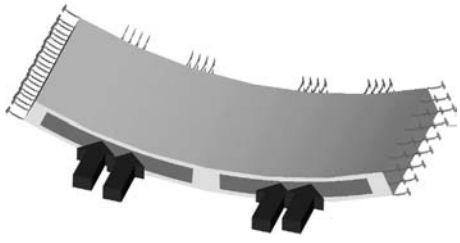


Figure 6. Scheme of a segment with the load from the two pairs of jacks, four rear bearing pad supports and spring representing the stiffness of the neighbor segments.

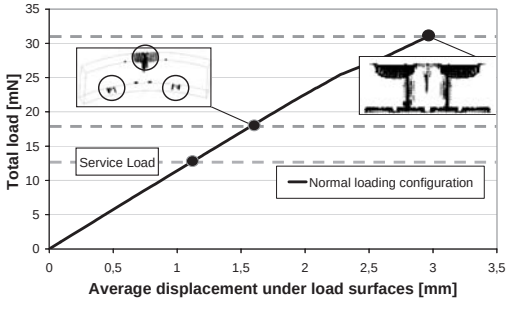


Figure 7. Load displacement curve with the nominal load scheme.

load is 12 MN, the safety factor is 2.58. The compressive strength of concrete is almost reached in longitudinal stresses under loading surfaces ($\sigma_c = 55$ MPa, $f'_c = 58$ MPa). As shown in Figure 7, the first cracks appear between the loading surfaces, due to spalling, at approximately 6.0 MN (0.5 times service load). The spalling cracks develop with an increase of load and penetrate more deeply in the segment.

Splitting cracks appear under the loading surfaces at 17.5 MN, due to splitting stresses in radial direction (σ_r). In the classical elastic solution, the depth of the disturbed zone is approximately the width of the structure that means, in this case, the thickness of the lining.

After cracking, the splitting stresses decrease in the cracked zone and are redistributed over a larger area with respect to the classical elastic solution. Because of the concrete toughness provided by fibers, cracks develop in a stable way.

Figure 9 shows the development of the splitting crack width under the load. The graph represents the relative displacements of two nodes: one located inside of segment and the other on the outside. Three pairs of nodes are taken on 20, 30 an 40 cm along the longitudinal direction from the TBM side of the segment (Fig. 8). The graph evidences that there exists a redistribution of stresses after cracking.

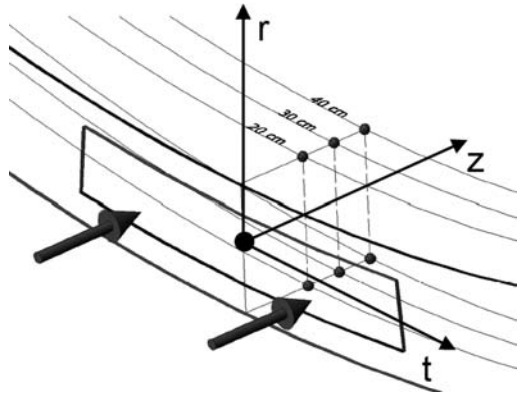


Figure 8. Scheme of the measurements of the splitting cracks.

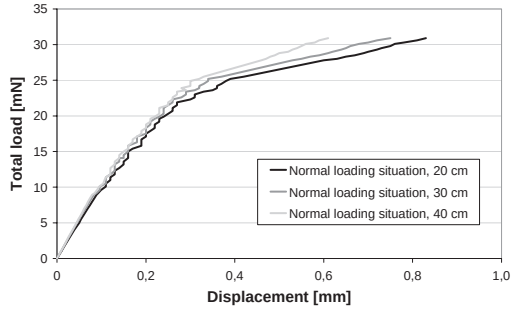


Figure 9. Development of splitting crack width under the load.

However, a number of irregularities can occur in practice. As a consequence, the ring joint may not be plane and the thrust jacks may be not exactly on place. For this reason, a possible eccentric placement of the thrust jack, its orientation and an uneven support in the ring joint have been investigated. In particular, numerical results of and eccentric load are presented herein in comparison with normal load conditions.

Eccentric placement of thrust jack in radial direction has been considered because it will increase the spalling stresses and can damage the segment. The eccentric placement has been modeled in FE analysis as a triangular pressure distribution on the loading surface. This provokes an eccentricity of 37.3 mm (Fig. 10).

When the above mentioned eccentricity is present outward (Fig. 10b) the ultimate load decreases significantly. In fact, the numerical analyses show a maximum load of 23.6 MN, that corresponds to a safety factor of 1.97 (Fig. 11). Spalling cracks initially appear between the thrust jacks; they start with a load of 5.0 MN and significantly influence the segment collapse.

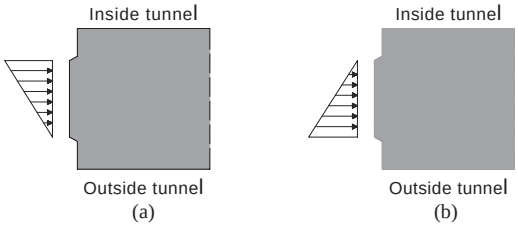


Figure 10. Eccentric pressure of the thrust jack inward (a) and outward (b).

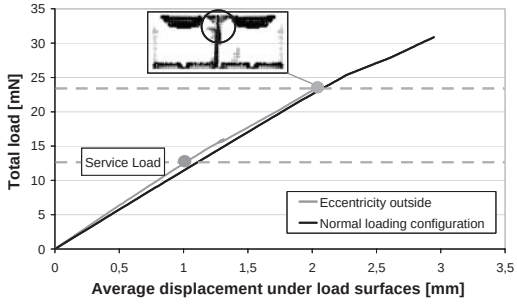


Figure 11. Load–displacement curve with and without eccentricity.

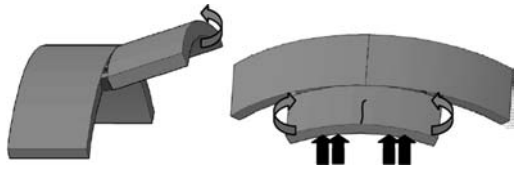


Figure 12. 3D scheme to of the dominant mechanism in the case of the outward eccentricity due to spalling cracks and bending moments.

Because of the eccentricity, the segment tilts outward providing a non-smooth support. Consequently, a bending moment occurs, as shown by the 3D model in Figure 12.

Splitting stresses initiate at an earlier load level (11.4 MN instead of 17.5 MN without eccentricity); this is probably due to higher local stresses in the longitudinal direction. The development of these splitting cracks under the load is schematically shown in Figure 13.

The cracks between the loads develop over the total depth of the segment due to the increased bending moment for the outward tilting. It can be noticed that similar deeply penetrating cracks between the thrust jacks have been observed in the Line 9 of the Barcelona Metro. Figure 14 exhibits the location of the cracks of the segment as well as the crack patterns obtained by

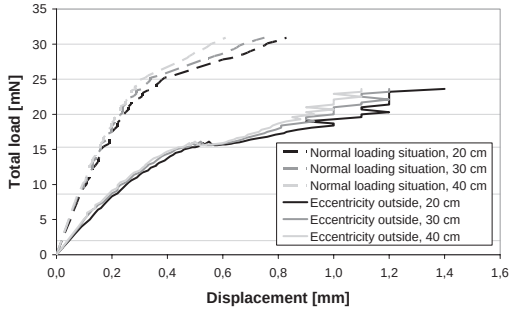


Figure 13. Development of splitting stresses under the load.

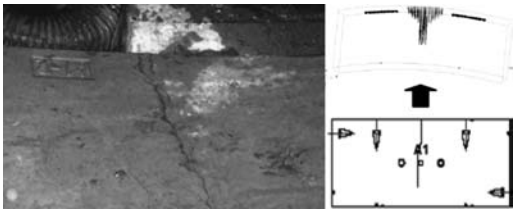


Figure 14. Cracks between the jack loads observed in the Line 9 of the Barcelona Metro and FE crack patterns.

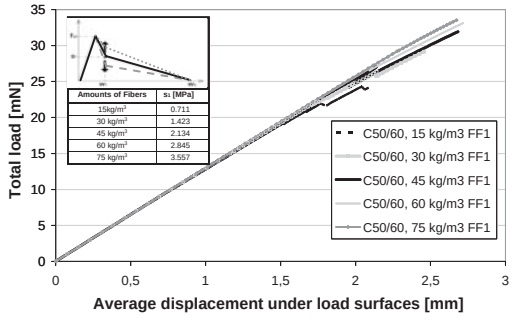


Figure 15. Load-displacement curves for a segment with different amounts of steel fibers.

numerical simulations. In the Barcelona Metro tunnel these cracks appeared when 9.3 MN were applied by the jacks (corresponding to 0.78 times the target load) whereas the numerical crack patterns refers to a load of 11.4 MN. Looking at the similarities between the numerical and the actual cracks in the tunnel, eccentricity could explain the presence of these cracks.

The normal load situation has been simulated by considering also SFRC with a different amount of steel fibers. The adopted fiber contents are 15, 30, 45, 60 and 75 kg/m^3. The numerically obtained ultimate load ranges from 24.3 MN (for 15 kg/m^3) to 33.5 MN (for 75 kg/m^3; Fig. 15). The constitutive post-cracking laws for the different fiber contents are shown in Figure 15.

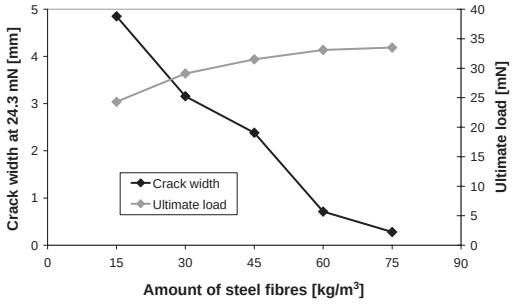


Figure 16. Influence of the amount of steel fibers on the ultimate load and on the maximum crack width.

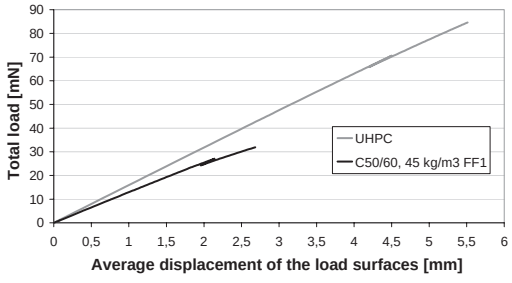


Figure 17. Total load vs. average displacement of loading surfaces for UHPC and C50/60 with 45 kg/m^3 FF1 steel fibers.

Numerical results show a significant increase of bearing capacity of the segment for fiber contents up to 45 kg/m^3; beyond this dosage, fibers has not effect in this tunnel (Fig. 16).

The maximum crack width (at 24.3 MN) for the different amounts of steel fibers is shown in Figure 16. It can be observed that the maximum crack width significantly decreases with larger fiber contents and that fibers play a major role on cracking phenomena; this also emphasizes the role of fibers on structural durability. By comparing a concrete with 60 kg/m^3 and with 75 kg/m^3, it can be noticed that 25% of extra fibers does not increase the bearing capacity but reduces the maximum crack width by a factor of 2.5. This can be explained by the two major cracks in the analyses with 60 and 75 kg/m^3 and by the presence of one mayor crack in the analysis with 15, 30 and 45 kg/m^3.

Finally, the behavior of a tunnel segment made of UHPC has been investigated. Numerical results gave an ultimate load of approximately 85 MN, corresponding to 2.66 times the ultimate load of a C50/60 concrete with 45 kg/m^3 of fibers (Fig. 17).

By using UHPC, the crack width at ultimate load is approximately 7.1 mm. The maximum crack width present with a load of 68.6 MN is 2.375 mm, which is similar to the one with a C50/60 concrete with 45 kg/m^3 of steel fibers with a total load of 24.3 MN.

4 CONCLUDING REMARKS

The present paper shows results of a numerical study of precast tunnel segments for the Line 9 of the Barcelona Metro. The numerical model shows reasonable results in terms of bearing capacity and crack development in a segment during TBM operations.

Eccentric placement of the thrust jack is one of the possible explanations of longitudinal cracks that are often present the in tunnel linings, including the one of the Barcelona Metro. In fact, the presence of eccentricities is one of the possible unfavorable conditions that causes higher stresses in the lining. In this loading situation, it has been demonstrated that the ultimate load reduces significantly and larger cracks are present.

The bearing capacity of the segment under jack load increases with the fiber content up to a maximum value (45 kg/m^3 in the considered case) that depends on the collapse mechanism.

The crack width gets benefits from the presence of fibers and continuously reduces when the fiber content increases. This results underlines the importance of fibers in concrete or r.c. structures for the durability aspects.

Because of the enhanced compressive and tensile strength as well as the higher toughness, a tunnel segment made of UHPC with steel fibers can carry very high thrust forces and only small cracks occur. As a consequence, by using these materials, for a given thrust force the lining thickness could be reduced.

ACKNOWLEDGEMENTS

The research project was financed by Officine Maccaferri S.p.A. (Bologna, Italy) whose support is gratefully acknowledged.

REFERENCES

Blom C.B.M. 2002, *"Design philosophy of concrete linings in soft soils"*, ISBN 90-407-2366-4, Delft.

Bloemhof, K.C. 2001. *"Geometrical tunnel model; damages on a shield tunnel"*, Delft.

Burgers, R.A. 2006. *"Non-linear FEM modelling of steel fibre reinforced concrete for the application on tunnel segments in the thrust jack phase"*, Delft.

Den Hollander, J. 2006. *"Technical Feasibility Study of a HUPC Tied Arch Bridge"*, Delft.

Diana v. 9.1. 2005. *Material Library.* TNO DIANA BV, Delft (The Netherlands).

di Prisco M. & Toniolo G. 2000. *"Structural applications of steel fibre reinforced concrete"*, Proc. of the international workshop. Milan, April 4, CTE publ., 126.

Gettu, R., Barragán, B., García, T., Ramos, G., Fernández, C. & Oliver, R., 2004. *"Steel Fiber Reinforced Concrete for the Barcelona Metro Line 9 Tunnel Lining."*

In BEFIB 2004, Proceedings of the 6th RILEM Symposium on FRC, Varenna (Italy), September 20–22, RILEM PRO 39, pp. 41–156.

Kooiman, A.G. 1996. *"Steel fibre reinforced concrete in shield tunnel linings, a state of art"*. Stevin report 25.5-96-10. Delft University of Technology.

Plizzari G.A. & Cominoli L. 2005. *"Numerical Simulations of SFRC Precast Tunnel Segments."* In Proceedings of ITA-AITES 2005, Underground space use: Analysis of the past and lessons for the future, Erdem Y. and Solak T. Eds., Istanbul (Turkey), May 7–12, pp. 1105–1111.

Plizzari G.A. & Tiberti G. 2006. *"Steel fibers as a reinforcement for precast tunnel segments"*, in the *World Tunnel Congress* ITA AITES 2006, Seoul Corea, April 22–27.

Roelfstra, P.E. & Wittmann, F. H. 1986. *"Numerical method to link strain softening with failure of concrete"*. In Fracture Toughness and Fracture Energy of Concrete, Wittmann F.H. Ed., Elsevier, Amsterdam, 163–175.

Schnütgen B. 2003. *"Design of Precast Steel Fibre Reinforced Tunnel Elements"*, in "Test and Design Methods for Steel Fibre Reinforced Concrete – Background and Experiences", Proc. of the RILEM TC 162-TDF Workshop, Bochum (Germany), March 20–21, 145–152.

Selby, R. G., & Vecchio, F. J. 1993. *"Three-dimensional Constitutive Relations for Reinforced Concrete"*. Tech. Rep. 93–02, Univ. Toronto, Civil Eng., Toronto, Canada.

Thorenfeldt, E., Tomaszewicz, A. & Jensen, J.J. 1987. *"Mechanical properties of high-strength concrete and applications in design"*. In Proc. Symp. Utilization of High-Strength Concrete (Stavanger, Norway).

UNI 11039. 2003. Steel fibre reinforced concrete – Part I: Definitions, classification specification and conformity – Part II: Test method for measuring first crack strength and ductility indexes. Italian Board for Standardization (UNI).

Waal R.G.A. de. 1999. *"Steel fibre reinforced tunnel segments"*, Delft, ISBN 90-407-1965-9, Delft.

This page intentionally left blank

Underground Space – the 4th Dimension of Metropolises – Barták, Hrdina, Romancov & Zlámal (eds)
© 2007 Taylor & Francis Group, London, ISBN 978-0-415-40807-3

Development of damage detection method on the tunnel lining from the laser scanning data

Jong-Suk Yoon
Inha university, Incheon, S. Korea

Myung. Sagong and J.S. Lee
Korean Rail Research Institute, S. Korea

ABSTRACT: Laser scanning is an emerging non-destructive technology to monitor surface condition of structures from various applications. High density of laser scanning points, point clouds, allows detecting the morphological features and surface conditions of structures. In order to extract useful information from laser point clouds, an adequate and effective approach should be applied. This study proposes a method to detect damaged parts from laser scanned tunnel data using radiometric and geometric properties of laser points. The scanned tunnel data includes all of accessories attached to a tunnel as well as tunnel liners. To apply a mathematical model to tunnel liners, the accessories are first separated and eliminated, and then the damaged parts on the tunnel liners are ultimately detected. The method proposed in this study verifies the capability of a laser scanner to detect physical condition of tunnel lining surface and also expands the usage of laser scanning technology. Furthermore, the developed process of tunnel lining inspection will facilitate the tunnel inspection process and increase efficiency on the tunnel inspection and accuracy of the results.

1 INTRODUCTION

Underground structures, for example tunnels, undergo regular inspection process to ensure the safety and to estimate the remaining life cycle of the structures. Due to aging process, the tunnel supporters, rockbolt and shotcrete, can be deteriorated and lose a portion of their supporting strength. The deterioration could be an initial step to induce deformation of a tunnel. The occurrence of deformation on a tunnel can cause cracking, spalling and leaking of water on the concrete liner. Therefore, the regular inspection process will investigate the detailed conditions of tunnel such as strength of concrete liner, cracks and spalls on the lining, leaking spots and approximate volume, tunnel deformation etc.

Regular inspection scrutinizes the surficial characteristics of tunnel liners. Since the traditional tunnel inspection method relies on the visual and hammering method, the task is time-consuming and labor intensive. Recently, with advance of technology various inspection techniques have been introduced such as the use of line-sensor camera for image capturing (Asakura and Jokima, 2003, Sasama, et al. 1998), and radar technology (Davis et al, 2005). Detailed technical review of the tunnel inspection methods can be found from Haack et al. (1995) and Richards (1998).

Among the others, image and laser scanning technologies show sufficient applicability of surficial tunnel inspection aspect. Existing tunnel scanners using image processing technique acquire images by line camera or video recorder. The images will undergo image processing to detect the cracks and spalls on the concrete liners. This method has high accuracy and resolution depending upon the camera capacity and running speed of the vehicle mounting the image capture devices.

Generally, compared to the image scanning method, laser scanning technology has lower resolution and accuracy even with the laser scanner with high sampling rate. However, the laser scanner collects three dimensional (3-D) data from which restriction boundary of tunnel can be checked. In addition, from the data, the longitudinal and cross-sectional drawings can be extracted for old tunnels, which do not have CAD drawings. In consequence reverse engineering for old tunnel is possible. Furthermore, a comparison between the sets of scanned data for each scanning allows the laser scanner functioning as a member of Intelligent Tunnel Maintenance System (ITMS). From the comparison between the scanned data sets, the overall behaviors of tunnels can be checked: deformation trend at the certain location of tunnel, development of cracks and spalls and conditions of tunnel accessories.

In this study, we developed a filtering method to detect tunnel accessories and damaged part on the concrete liners from the laser scanned data. First, this process can filter tunnel accessories such as electric pipe lines, catenary for railway tunnels and brackets. In conclusion, the laser scanning technology has been expanding its application with the advantage of the high density data and accuracy. This study will provide the potentiality to inspect the underground facilities using radiometric and geometric characteristics of laser technology.

2 METHOD

Laser scanner data has an advantage to provide high density and accurate 3-D information. However, an effective method should be applied to extract useful information from numerous laser point clouds. The method proposed in this study is mainly composed of two steps to discover damaged part of liners (Figure 1). The laser scanned data includes all of accessories attached to tunnel liners such as pipe lines, catenary, etc. The points from the accessories are necessary to be separated and eliminated for the detection of the damaged parts. Subsequently, remaining data showing the state of tunnel liner is mathematically fitted as a plane and the damaged parts are detected based on the residuals of the fitting.

2.1 *Scanned tunnel data*

A laser scanner, Acuity AR-4000 LIR with line scanner, scanned a tunnel for this study. The scanner scans an object far from 0 to 16 m range with 2.5 mm accuracy. The scanner moves forward and scans by 80 cm in a profiling manner. The scanner recorded and stored 245,006 points for 80 cm in width as shown in figure 2. The scanned data contains X, Y, Z coordinates and intensity value. The origin of the coordinates is the location of the scanner. x axis is the horizontal, y axis is the direction to the crown of the tunnel and the z axis is along the tunnel. The intensity is recorded by the backscattered signal power in the 8 bits. Figure 2a illustrates the scanned tunnel data and the axis of the coordinates, and figure 2b is the digital image of the real tunnel at the inset of figure 2a. The black and white color of figure 2a represents the intensity value. The scanned tunnel in figure 2 is one of railway tunnels in Korea.

2.2 *Separation of tunnel accessories*

The data points from the tunnel accessories will be detected and eliminated to fit the points as a plane. Since the scanned data is high density, it will be effective to find the tunnel accessories first rather than processing the whole data. The detection of the tunnel

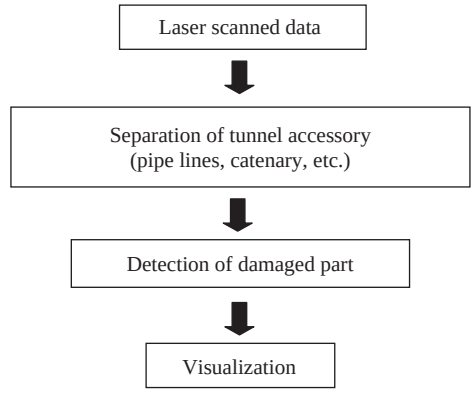


Figure 1. The conceptual flowchart of the processing.

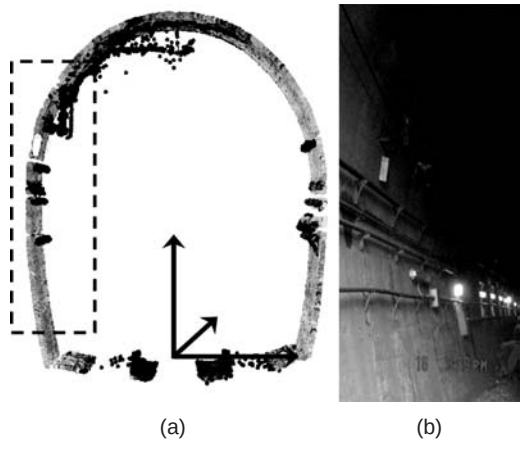


Figure 2. Scanned tunnel data illustrated by intensity value.

accessories uses the calculation of correlation coefficients between x and y coordinates. Since the cross section of tunnel will change where pipes locate, the correlation between x and y directions will be quite low at this location. On the other hand, the data from tunnel liner will have certain type of correlation between x and y directions depending on the tunnel shape. The tunnel profile is separated into several segments to calculate the coefficient of correlation. Once the correlation coefficient of x and y is under 0.92, the part is considered to hold accessories and following steps are conducted to separate the tunnel accessories.

This study proposes to use intensity of laser scanner data for the separation tunnel accessories because intensity is strongly influenced by materials' reflectance (Ahokas et al., 2006). Due to different material types, intensity values of tunnel accessories are quite different compared to the intensity of the

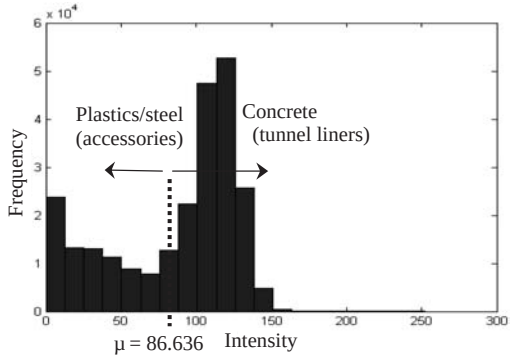


Figure 3. Intensity histogram of the entire scanned points.

tunnel liner as illustrated in figure 2a. The accessories attached to tunnel liners are mainly made of plastics and steel while the tunnel liners are made of concrete. Intensity backscattered from tunnel liners is much higher than that of the accessories as shown in figure 2a and figure 3. Figure 3 shows the intensity histogram of the scanned tunnel data in figure 2a. In figure 3, the pattern of histogram is bimodal with two peaks from accessories (plastics/steel) and tunnel liners (concrete). Based on figure 3, the entire dataset can be initially divided by two groups based on the intensity values. If the intensity of a point is higher than average of intensity value of whole points which is 86.636, then the points are initially considered from tunnel liners. In other case, when the intensity values are less than the average value of intensity, the points are regarded to represent tunnel accessories. The average of each group is used as representative points to calculate Euclidian distance in the following step.

Along with intensity, x coordinates are the complimentary factor to separate accessories since all of accessories are attached inside tunnel. Therefore, the distinctive factors to separate accessories from the tunnel liner are intensity and x coordinates. The separation of accessories is processed a scanned tunnel profile by a section of 50 cm in height (in y axis). If a section holds accessories as explained, the Euclidian distance between a point and each representative point of accessories and tunnel liners is calculated using x and intensity. Since the intensity and x coordinates are the distinctive characteristics, the distance is calculated by the two factors. Depending on the distance, the point is assigned to a closest group, and the group of accessories is separated from the group of tunnel liners.

Figure 4a shows the section with under 0.92 correlation coefficient where the points from accessories are included. Figure 4b is an enlarged plot of inset of Figure 4a. The several points from the accessories which seem to be representing pipe lines are plotted at some distance from the tunnel liners. Figure 4c is the plot of the data within one section illustrated in

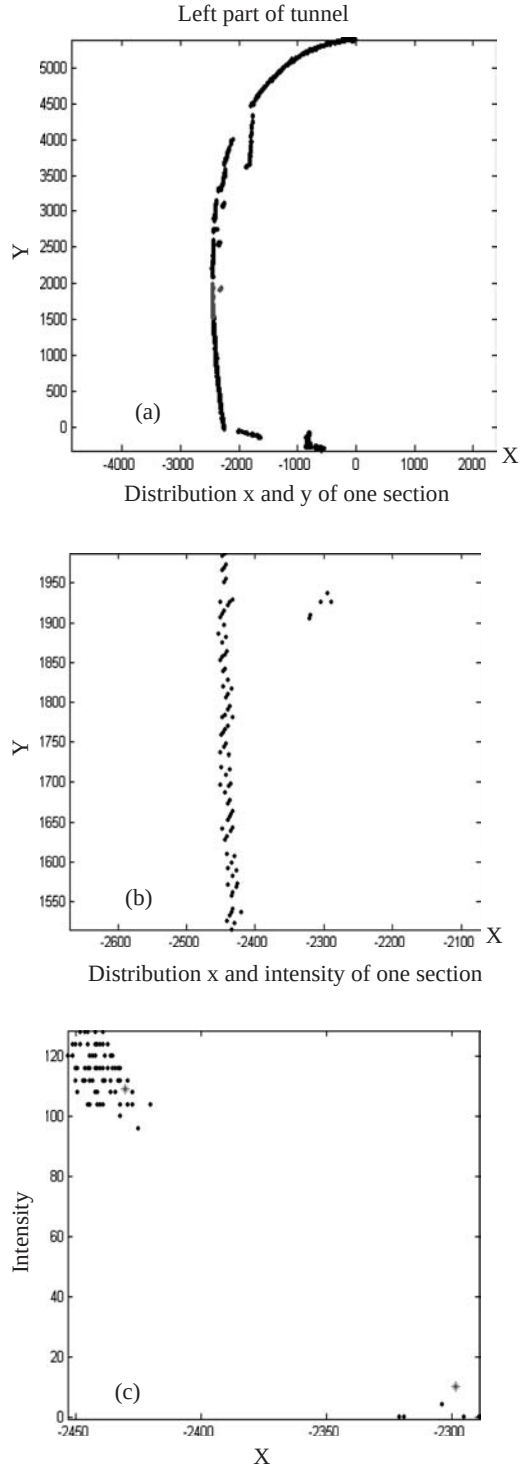


Figure 4. The procedure of tunnel accessories separation.

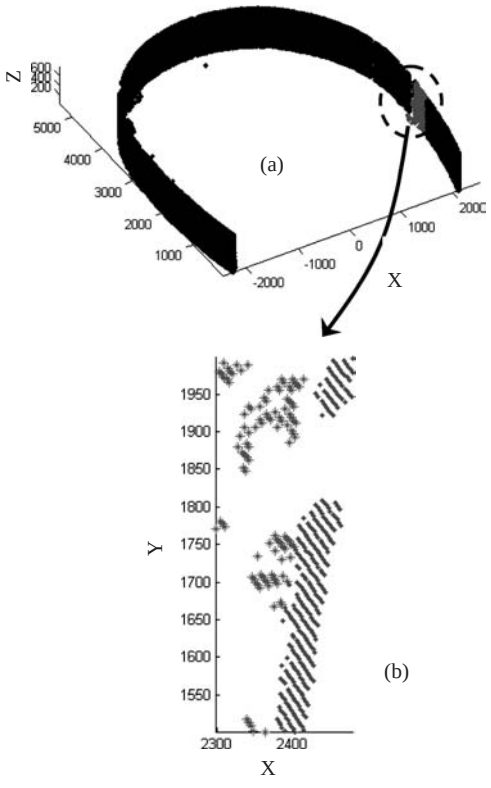


Figure 5. A section to detect damaged part on tunnel liner (a) and the result of plane fitting (b).

figure 4b in x coordinates vs. intensity of the points. The figure shows apparent separation of concrete liner and the accessories. The points from accessories are far distant from the group of tunnel liners' points in the plot of x coordinate vs. intensity (figure 4c). Figure 4c clearly explains the x coordinate and intensity are distinctive factors to discriminate facility from tunnel liners.

2.3 *Detection of damaged part*

Since the tunnel scanning data is in the form of 3-D aspect, 80 cm long tunnel scanned data can be segmented into 2-D data. In this study, the scanned tunnel is segmented in 50 cm in y direction (see figure 5a). The figure shows the section characterized as a plane. Data segmentation process is carried out to identify the data points of tunnel accessories and damaged part on the liner. The tunnel accessories and damaged parts are determined from the distance between the plane and a point. If the distance is greater than a threshold value, the point is determined as a point from the damaged or accessories part. Equation (1) is a formula of a plane, and equation (2) is the calculation of distance between a point and the plane. A plane with equation (1) is established by the points composed of a section of the tunnel liners. Equation (3) shows the decision making process of a point belong to tunnel accessories and damaged part of liner or undamaged part of liner.

Identification of tunnel accessories and damage of liner is conducted by using the normal direction of the points from the plane. The directions of accessories and damaged parts are reverse from the plane because the accessories locate inside of tunnel liner and damaged part can be detected outside of the tunnel cross section. Therefore, the opposite sign of threshold value should be applied for the detection of accessories and damages.

$$ax + by + cz + d = 0 \tag{1}$$

$$d_i = \frac{|ax_i + by_i + cz_i + d|}{\sqrt{a^2 + b^2 + c^2}} \tag{2}$$

$$P_i = \begin{cases} \textit{tunnel liner} & \text{if } d_i < \text{threshold} \\ \textit{damaged or accessories} & \text{otherwise} \end{cases} \tag{3}$$

where, $P_i = i_{th}$ *point*

3 RESULT

Most points backscattered from accessories are eliminated in the first step, using radiometric and geometric characteristics of laser points through the proposed procedure of this study. However, the points are not completely removed, because some part of tunnel liners are mixed with accessories' points because of moisturized dark intensity. As the second step, calculating normal distance from a point to a plane, is performed, the accessories attached to tunnel liners are completely eliminated.

Once a threshold value of equation (3) is set, tunnel accessories, liner and damaged part can be separated as shown in figure 5b. The points (.) in figure 5b are the plane characterized as equation (1), while the asterisks are the points of accessories. The accessories' points are completely eliminated through the second step (figure 6). Figure 6a is the raw data of scanned tunnel and figure 6b plots only tunnel liners after elimination of accessories points.

The detection of damaged part is sensitive to the threshold value used in equation (3). The threshold value is depending on the density of a scanner. If the scanned data is highly dense, the threshold value can be small to detect fine damage such as cracks. In this research, several threshold values are tested. Figure 7 shows the damaged part detected on the tunnel liners with a digital image taken by a digital camera. On the digital image of figure 7, two driven nails on the tunnel liners are within a circle. The two areas are

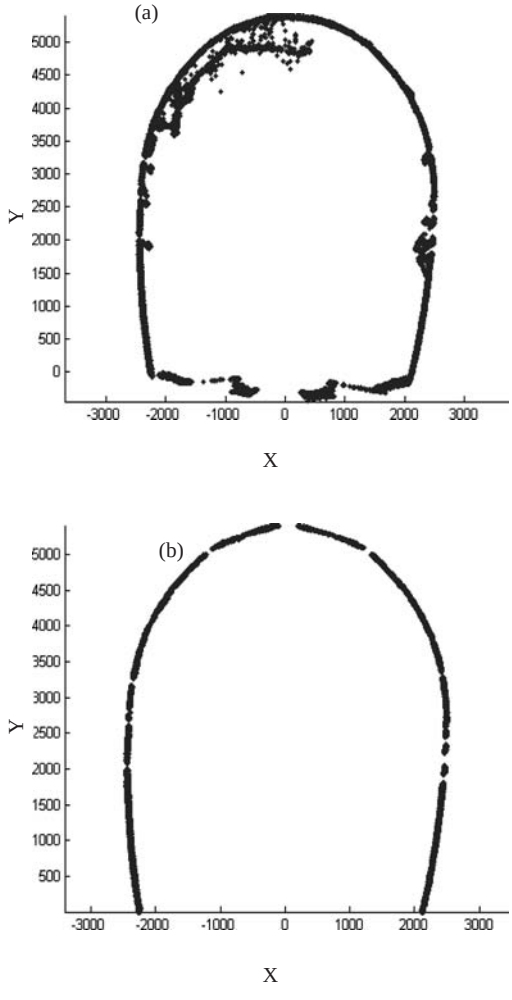


Figure 6. The laser scanned tunnel (a) and the tunnel liners eliminated facility points (b).

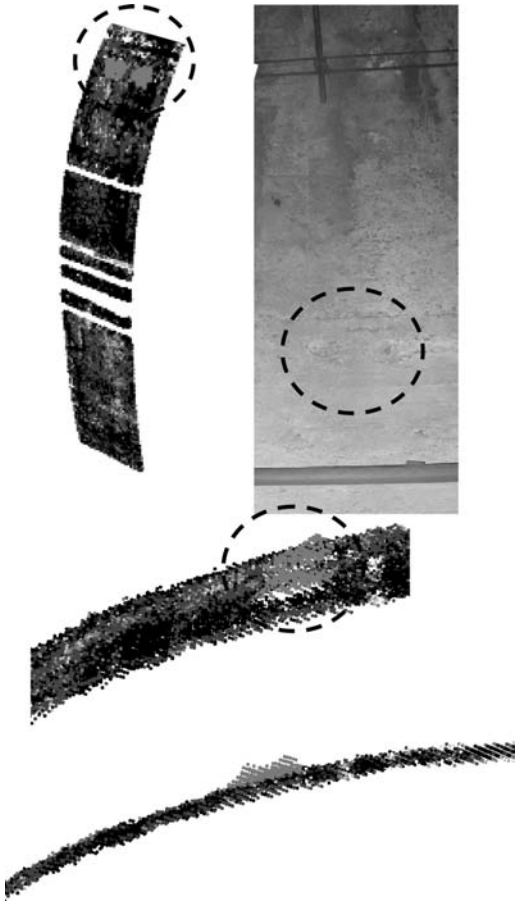


Figure 7. Detected damaged part on the tunnel liners.

physically damaged by the driven nails and detected by the proposed method. In this case, the threshold value is set to 20 mm. If the threshold value was set to smaller, then finer parts would be detected.

4 CONCLUSIONS

This study proposes an approach to detect the tunnel accessories and damaged part of tunnel liners from the laser scanned data. The laser scanned data with high-density and accurate point clouds is composed of three dimensional (x, y and z) coordinates and intensity which is another benefit of laser scanners. For the use of laser scanning technology on the tunnel maintenance, the specific and effective approach is required to extract useful information from laser point clouds.

The approach employed in this study is as follows. First, the proposed method separates points backscattered tunnel accessories from tunnel liner. The intensity and x coordinates are used to separate the points reflected from the tunnel accessories from the entire laser scanning data. As the intensity of laser data is mainly affected by the target materials, concrete of tunnel liners and plastics and steel of accessories are contrast with bright and dark intensity values in the scanned tunnel data. Second, the points from tunnel liners within a section are fitted as a plane. The scanned three dimensional data can be segmented in two dimensions. The segmentation is conducted along the y axis, direction to the crown of the tunnel. By using the threshold value of geometric distances between the plane and points, tunnel liners and accessories are complete separated.

This study provides a preliminary work on the use of laser scanned data to identify the different types of material in the tunnel: concrete liners and tunnel accessories such as pipe lines and catenary. Nevertheless, further work must be required to adopt the laser scanning technology as a key of automated tunnel monitoring system. Detailed works will be on the assessment of accuracy, generation of highly dense point clouds, and data processing techniques.

REFERENCES

Ahokas, E., Kaasalainen, S., Hyyppä, J. and Suomalainen J., 2006. Calibration of the Optech ALTM 3100 laser scanner intensity data using brightness targets, International Archives of Photogrammetry & Remote Sensing, Paris, 2006, Vol. XXXVI, Part 1 A+B, CD-Rom.

Asakura, T. & Kojima, Y. 2003. Tunnel maintenance in Japan. *Tunnelling and Underground Space Technology* 18(3–4): 161–169.

Davis, G.A. Lim, M. K. & Petersen, C.G. Rapid and economical evaluation of concrete tunnel linings with impulse response and impulse radar non-destructive methods. *NDT&E* 38(): 181–186.

Haack, A. Schreyer, J. & Jackel, G. State-of-the-art of non-destructive testing methods for determining the state of a tunnel lining. *Tunnelling and Underground Space Technology* 10(4): 413–431.

Richards, J.A. (1998), Inspection, maintenance and repair of tunnels: international lessons and practice, *Tunnelling and Underground Space Technology* 13(4): 369–375.

Sasama, H. Ukai, M. Ohta, M. & Miyamoto, T. Inspection system for railway facilities using a continuously scanned image. *Electrical Engineering in Japan* 125(2): 1345–1354.

Underground Space – the 4th Dimension of Metropolises – Barták, Hrdina, Romancov & Zlámal (eds)
© 2007 Taylor & Francis Group, London, ISBN 978-0-415-40807-3

The MASW method for testing tunnel lining integrity

René-Michel Faure
Centre d'étude des Tunnels, Bron, France

Guy Lefebvre, Mourad Karray
Université de Sherbrooke, Sherbrooke, Canada

Gérard Hémond
Solem SA, Carouge, Suisse

ABSTRACT: The MASW method (Modal Analysis of Seismic Waves) has been developed by the Sherbrooke University for the last ten years. It is now frequently used for soil investigation. In a cooperation with CETU (France) and Solem (Switzerland) the Sherbrooke University has adapted the method for checking the lining integrity of tunnel. The first in situ experiment was in the Mont Blanc tunnel after fire and the obtained results were confirmed by sampling. Since, other experiments were achieved and a 88 square meters slab was built with lot of well defined anomalies in it. The paper, after a reminder of the method will present the last results and will develop the how to use this non destructive, easy to use, in situ method.

1 INTRODUCTION

The big fire that occurred in the Mont Blanc tunnel caused 39 fatalities and destroyed all the equipments of the tunnel. For safety engineers lot of questions raised and for civil engineers the main question was the concrete vault integrity. With other classical investigations, new one were tested, the MASW method, applied for the first time for estimating the damaged concrete.

2 THE MASW METHOD FOR TESTING LINING COMPETENT STRUCTURE

On March 24 1999, a fire was declared in the Mont-Blanc tunnel starting from a truck stationed near the garage 21 (6550 m from the French entry). The fire lasted 53 hours and was equivalent to 200 tons of burnt fuel. Very high temperature was developed, 39 people died and 34 vehicles burnt including 23 lorries.

The damages to the concrete vault (not armed) were limited and rescue teams were delayed only by heat. The length of tunnel the most exposed to the fire lies between garages 19 (5950 m) and 23 (7150 m from the French entry) on approximately 1200 m. Comparatively to other fires (Manche, Storebelt, Tauern) where important chipping (spalling) occurred, concrete in the Mont-Blanc tunnel remained in place. Only some small repaired zones provided falling concrete. Extend of damages to the concrete vault was an important question to be examined after the fire. Faure and Hémond (2001) and Faure et al. (2002) presented the different methods used for the investigation of the vault. Because burnt concrete have a modulus increasing with depth, we decided to use the Modal ASW method that was set first, for soils.

In March 2000, a team from Sherbrooke University (Québec) did the MASW measurements. By performing MASW tests in continuous, profiles of elastic shear modulus can be determined at closely space location in such a way that the results can be presented as a kind of tomography, allowing a good appreciation of spatial variability.

We obtained 15 profiles and several maps (80×80 cm) of speed waves in concrete. As these measures were the first we obtained, we were very doubtful about them. At this time, lot of people believed that all the concrete was destroyed after a 53 hours fire, and the profiles show that only some centimetres of concrete was burnt. Later, other investigations with different methods confirmed the MASW results.

MASW method was used again in 2004 to characterize a modern concrete lining in the newly built Fontain tunnel in Franche-Comté, France.

3 THE MASW METHODS

The shear wave velocity (V_s) is a direct expression of material rigidity since the elastic shear modulus (G_{max}) is related to V_s as:

$$G_{max} = \rho V_s$$

where ρ is the density of the material. For this reason, there has been since a long time interest in evaluating V_s by means of surface waves.

The Spectral-Analyses-of-Surface-Waves (SASW) was developed in the early eighties. The SASW testing procedure was designed to minimize the contribution of higher Rayleigh modes since it assumes that the average dispersion curve is representative of only the fundamental Rayleigh mode. A number of numerical studies first demonstrated that this basic assumption was valid only when the shear wave velocity varies regularly with depth. However, Karray and Lefebvre (2000) have demonstrated, based on numerical simulations and experimental cases that the multi-Rayleigh modes problem can occur in various situations even if the shear wave velocity increases regularly with depth.

The MASW method (Modal Analysis of Surface Waves) was developed in order to identify and separate the energy of higher modes (Karray, 1999).

Other MASW method exists (Multichannel Analysis of Seismic Waves), not so accurate due to not taking in account higher modes. (Park et al, 1999)

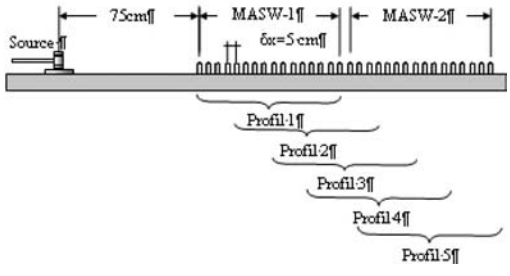


Figure 1. Configuration of the MASW method.

3.1 *Test procedures*

In the MASW method, an array of 16 sensors placed at constant intervals, are excited at the same time using an impact source (figure 1). Several tests can be done successively to establish a mapping of the medium in terms of shear wave velocity. It is indeed possible to combine 16 signals of two or more adjacent tests using the same source Bruel & Kjaer sensors with a natural frequency of 25 kHz were used for the characterization of the concrete tunnel liners.

3.2 *Analysis of the signals*

In the MASW method, the recorded signals are interpreted in series of 16 by carrying out an analysis in time-space domain using a wavelet technique. For each frequency, an energy spectrum is established in the phase travel time and group travel time plane.

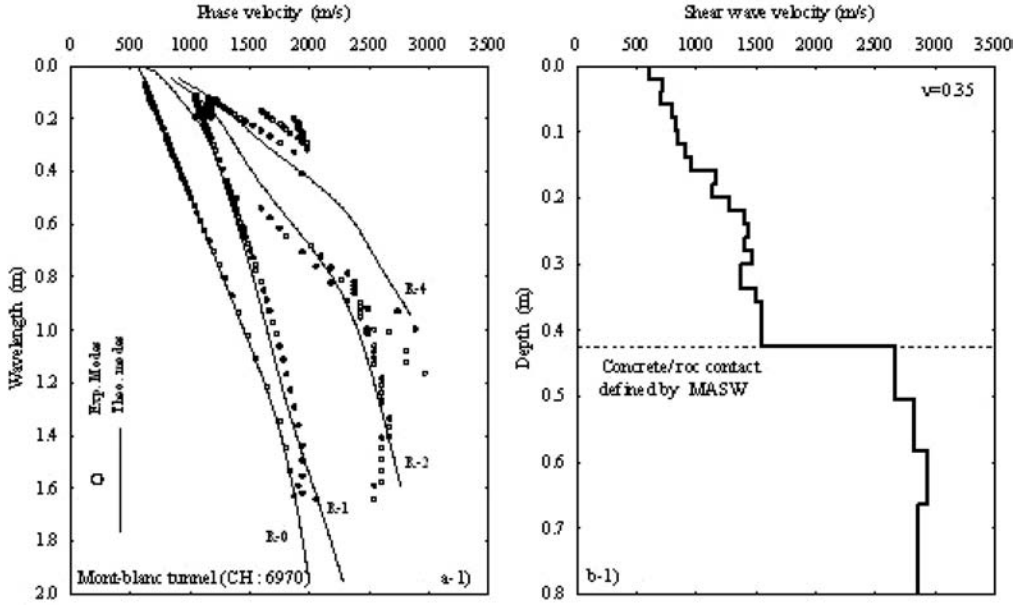


Figure 2. Dispersion curves and V_s profile at the Mont-Blanc tunnel.

The presence of more than one peak of energy indicates the existence of different wave groups. The phase velocity and group velocity of each peak of energy are then computed for each frequency and the dispersion curves of the different Rayleigh modes are established. (Figure 2)

3.3 *Inversion process*

The MASW inversion process is automated and the match between the theoretical and the experimental curves is minimized not only in terms of difference in phase velocity, but also in terms of the shape of the dispersion curve, allowing a more rapid convergence in the automated process and also a better detection of the weaker or stronger layer at depth (Karray, 1999).

4 MONT BLANC TUNNEL TESTS

The Mont-Blanc concrete lining lies on bedrock without any reinforcement or impervious membrane. In terms of surface wave propagation, these conditions are similar to geotechnical formation where the rigidity is generally greater at depth than close to surface. For this reason, the MASW algorithms could be used directly without modification.

Seven series of MASW tests were carried out in April 2000 in the zone affected by the fire.

The average shear wave velocity profiles obtained at each site tested by the MASW method are presented in figures 3 (a and b). The shear wave velocity profile obtained at location 7070 (1120) is repeated in figures 11a and 11b, because located at the limit of the fire zone.

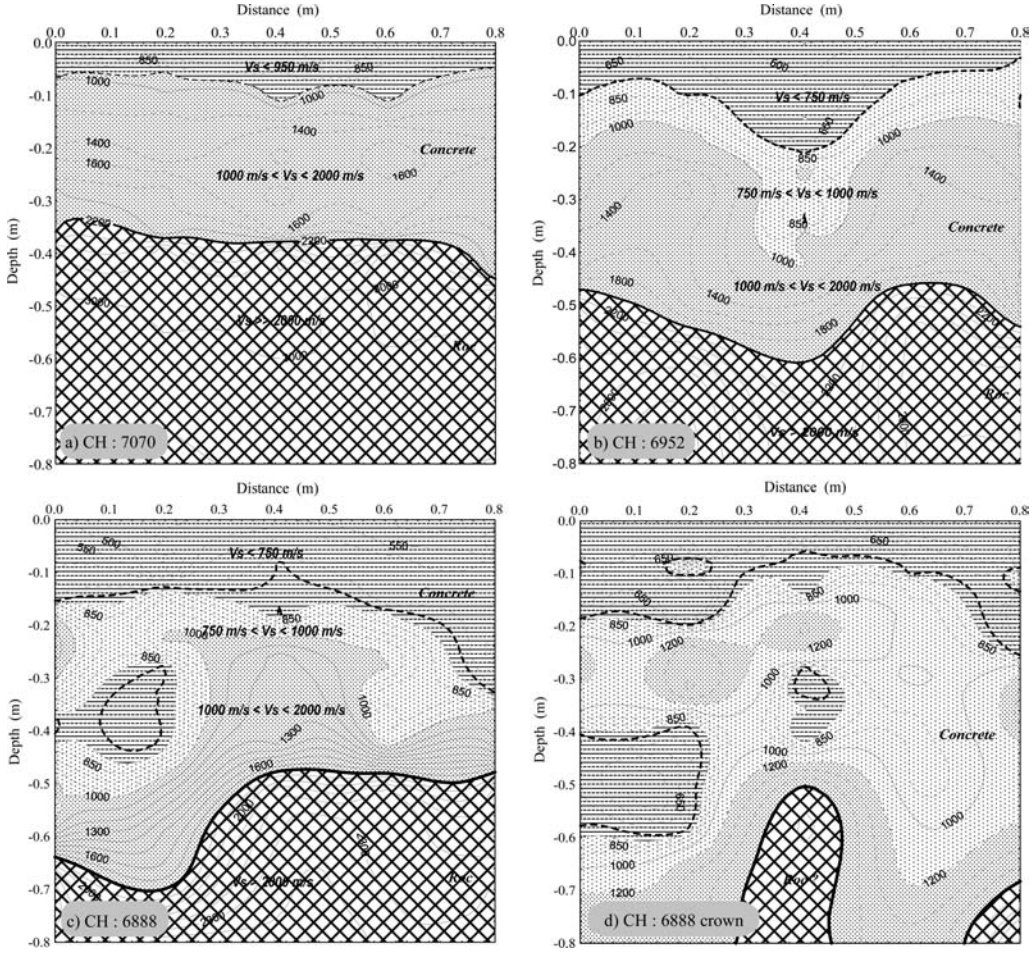


Figure 3. Vs tomography in the Mont-Blanc tunnel a) location 7070, b) location 6952, c) location 6888 and d) location 6888 crown.

Figures 3 a,b,c and d, show contours of shear waves velocity determined at location 7070, 6952, 6888 (wall and crown).

The contact between the lining and the bedrock is easily detected by a jump in V_s of about 1500 m/s in the concrete to values close to 3000 m/s in the bedrock. The thickness of the concrete lining is irregular and varies generally between 350 and 700 mm (Fig. 3a to 3c) except in the crown where over thickness and irregularities are more important (Fig. 3d). V_s values, as low as 500 m/s, were observed near the surface of the lining.

5 MASW TESTING AT THE FONTAIN TUNNEL

MASW tests were performed in March 2004 in the new Fontain tunnel before it was opened to traffic. The modern concrete liner in the Fontain tunnel differs from the Mont-Blanc liner because it was built with high performance (HP) concrete and because it contains an impervious membrane made of a 5 mm geotextile and a 2 mm PVC membrane between a shockcrete layer applied on the bedrock and the high strength concrete. In some areas, the impervious membrane was placed on 2 mm steel plates held by metallic supports. In these areas, a filling concrete was placed between the bedrock and the impervious membrane.

The data acquisition procedures like in the Mont-Blanc tunnel with 100 mm spacing between the accelerometers was used. A total of 154 V_s profiles were determined, spaced at 200 mm on 7 different lines, for a total of 29 m. This impervious membrane incorporated in the concrete lining creates particular conditions for the propagation of surface waves, acting as a discontinuity in the propagation of the shear component of the surface wave. These conditions were totally different of the geological model considered in surface wave testing. New algorithms had to be developed and incorporated in MASW. (Figure 4) For only 7% of the V_s profiles, the surface wave propagated across the impervious membrane. Examples of these profiles, interpreted with the geological model approach are presented in Figure 5. The contact between the HP concrete lining and the shotcrete layer is easily identified on these profiles by a drop of V_s. Behind the shotcrete layer, V_s increases to about 3 000 m/s in the bedrock. It is only in these few profiles (7%) that the material behind the HP concrete liner could be characterized in terms of V_s.

In most cases, the surface wave propagation was limited by the impervious membrane and the V_s profile characterized only the HP concrete liners. The thickness of the HP concrete liner as determined by MASW has varied from 220 to 660 mm except at one location where over thicknesses of 1 100 mm were detected. The thickness determined with MASW were, in general, in good agreement with construction records except occasionally where steel arches were incorporated in the filling concrete to support the impervious membrane. The additional rigidity of the zone of the filling concrete in which were embedded the steel arches made more difficult to differentiate between the filling concrete and the HP concrete, if by chance the surface wave did propagate across the impervious membrane at such location.

The few V_s profiles (11 or 7%) which extended beyond the HP concrete indicate V_s generally between 2 500 and 3 200 m/s in the bedrock. Slightly lower values in a few instances near the rock-concrete contact possibly indicate some dynamiting related fissuring.

6 SLAB FOR CALIBRATION

The Solem society built a large slab (88 m^2) with great number of defaults or inclusions allowing a good calibration of the Modal ASW method. Tests will be performed soon. (Figures 6 and 8).

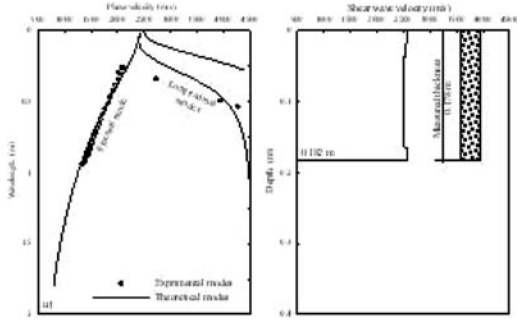


Figure 4. Example of MASW investigations for a concrete slab a) Experimental and theoretical dispersion curves; b) V_s profiles and measured thickness.

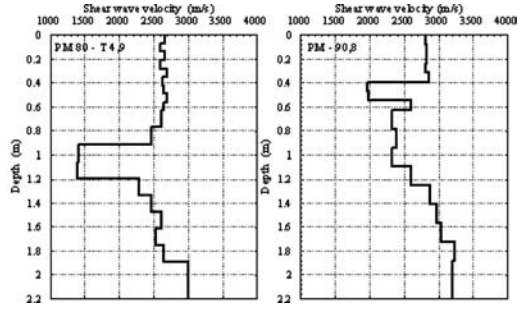


Figure 5. Examples of V_s profiles extending through the impervious membrane.

7 CONCLUSION

Conditions of a tunnel concrete lining can vary rapidly from point to point, particularly its thickness, due to the irregularity of the rock profile after excavation (blasting). A continuous method of investigation allowing a tomographic type of representation is consequently desirable to appreciate thickness variation or inside anomalies. The direct measurement of mechanical parameters (modulus) is also important when the lining investigation has the purpose to detect defect in the lining, the state of degradation of the concrete or simply to determine when the concrete has the necessary strength to support itself after placing.

The MASW results are in good agreement with results obtained in intrusive investigations, namely penetration velocity during drilling and compression wave velocity measured in the laboratory on drilled cores. The contact between the concrete liner and the rock was clearly identified in MASW testing in addition to the characterization of the rock in terms of V_s.



Figure 6. Solem testing slab: setting for Modal ASW test.

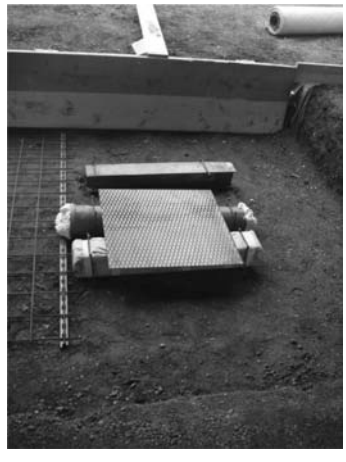


Figure 8. Solem testing slab: detail of an inclusion.

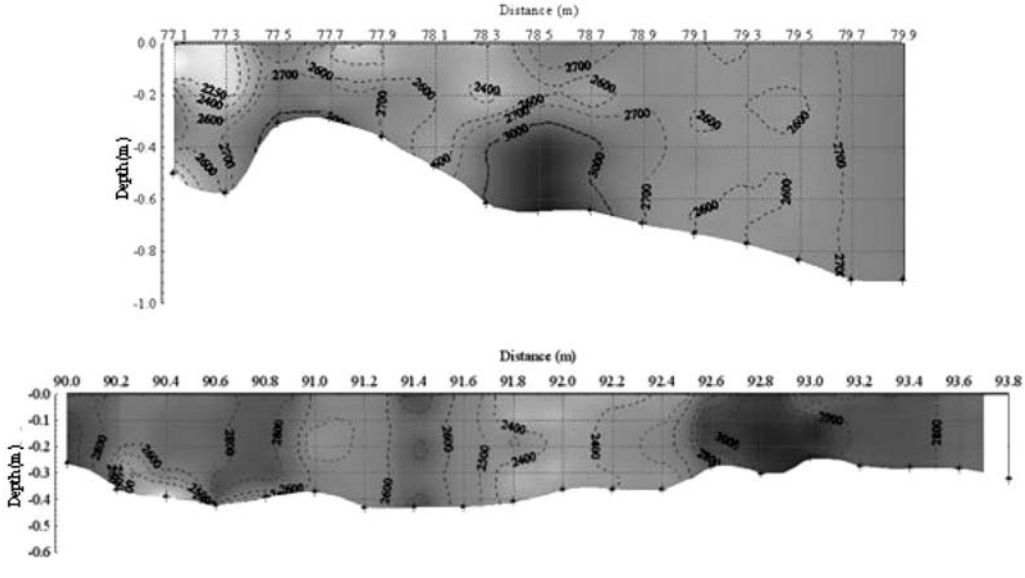


Figure 7. Examples of V_s contours for two segments of the Fontain tunnel liner.

REFERENCES

Faure R.M., Hémond G., 2001. Reconnaissance de l'état du béton du tunnel du Mont-Blanc après l'incendie de Mars 1999, Proc ITA Milan.

Faure, R.M., Pozzi, V., Trasino, C., Hémond, G., 2002. Colour and speed drill measurement for risk mitigation of a lining after a fire. The experience of Mont-Blanc tunnel. Proc ITA.

Karray, M., 1999. Utilisation de l'analyse modale des ondes de Rayleigh comme outil d'investigation géotechnique in-situ, Thèse de doctorat en génie civil, Département de génie civil, Université de Sherbrooke, Sherbrooke, (Québec), Canada, 275 p.

Karray, M., Lefebvre, G., 2000. Identification and Isolation of Multiple Modes in Rayleigh Waves Testing Methods,. Use of Geophysical Methods in Construction, Proceedings of the sessions of Geo-Denver 2000, ASCE, Denver, Colorado, USA, pp 80–94.

Karray, M., Lefebvre, G., Faure, R.-M., 2004. Results of surface waves testing in the investigation of the Mont-Blanc tunnel after the 1999 fire, Proc. 2nd Int. Site Characterization conference (ISC'2) Porto, Portugal.

Park, C.B., Miller, R.D., Xia, J. 1999. Multichannel analysis of surface waves, Geophysics, vol. 64, no 3. p. 800–808.

Underground Space – the 4th Dimension of Metropolises – Barták, Hrdina, Romancov & Zlámal (eds)
© 2007 Taylor & Francis Group, London, ISBN 978-0-415-40807-3

Design of the strengthening of tunnel linings under localized pressures

A.R. Marí & C. Molins
Technical University of Catalonia, Barcelona, Spain

ABSTRACT: Strengthening tunnel linings by means of placing a new interior lining (relining) built with self compacting high strength concrete, connected or not to the existing one, is a feasible solution that can be constructed in a reasonable period of time. This solution is well adapted to resist uniform pressures distributed along the perimeter. However, sometimes severe pressures have limited extension, encompassing merely an arch. Such a loading leads to significant bending moments concomitant with axial forces that have to be resisted. This paper presents and applies a methodology to design such strengthening.

1 INTRODUCTION

The rising number of tunnels under construction in new transport infrastructures increases the probability of crossing hazardous sections with problems related to the expansion of the ground or to cavities filled of water or mud. This is possible in spite of previous ground investigation and geotechnical characterisation. Extraordinary ground movements or water flows can eventually appear and have to be restrained by the lining. In such cases, the overloading of the lining can be far away of its maximum capacity. Because of that, different solutions have to be appraised taking into account the tunnel serviceability, mechanical strength, water tightness, environment and economy. Sometimes the structural strengthening becomes the best possible solution.

Strengthening the tunnel lining by means of placing a new interior lining (relining) built with self compacting high strength concrete, connected or not to the existing one, is a feasible solution that can be constructed in a reasonable period of time. This solution is well adapted to resist severe uniform pressures distributed along the circumferential perimeter. However, ground heterogeneity produces that severe pressures sometimes have limited extension, encompassing merely an arch of circumference instead of the whole one. Such a loading leads to significant bending moments concomitant with axial forces that have to be resisted.

The moment and axial force ratio depends on the radius of the strengthening ring and on the length of the loaded arch, defined by its angle. In addition, there exist multiple axial/moment ratios that can be resisted by a reinforced concrete section with a determinate amount of steel. This leads to an uncertainty on the worst angle of loading that would provide the largest amount of reinforcement.

This paper presents a methodology to design the strengthening of tunnel linings subjected to severe ground pressure of known maximum value but of unknown length and position on the perimeter. The method was used in the design of the strengthening of a Spanish high speed railway tunnel (HSRT) that was subjected to severe ground expansion. In that case, strengthening works were carried out before the tunnel had its first service. The paper describes the design of the strengthening, the analyses performed to find out the worst loading angle using nonlinear finite element models, some features related to its construction and monitoring.

2 DESCRIPTION

In 2002, during the ending work of the linings of three consecutive HSRT: Lilla, Camp Magré and Puig Cabrer (with a total length over 3000 m), abnormal deformations on the base and severe cracking were observed in all of them. Such tunnels belong to the HSR line Madrid-Barcelona-French border, nowadays under construction, and they are close to the city of Montblanc (Tarragona province). Damages in the lining were attributed to unexpected expansions of the surrounding ground consisting of sulphate-bearing clays. The tunnels under construction were bored by NATM, using sprayed concrete and bolts as a preliminary lining, and a final lining of 0.30 m of plain concrete was placed using conventional moulds. Figure 1 shows its typical cross section and its main measures.

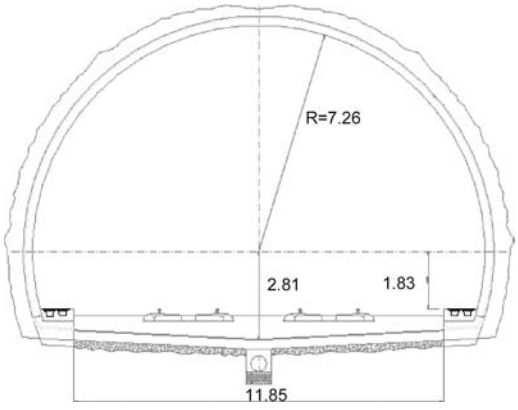


Figure 1. Cross section of the original lining that was under construction in the Lilla HSRT. Distances in m.

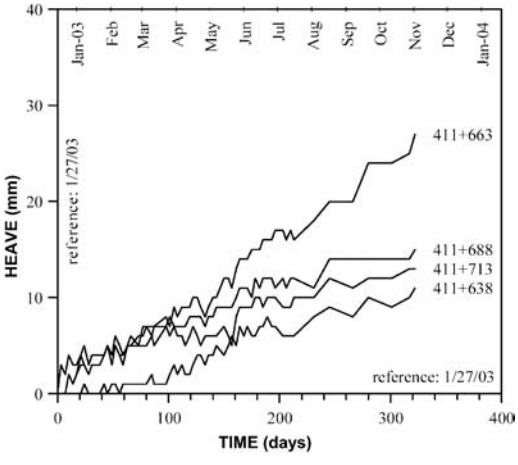


Figure 2. Floor heave in sections with invert (Alonso *et al.*, 2005).

Figure 2 shows the evolution of the floor heave. A team led by the Department of Geotechnical Engineering of the Technical University of Catalonia studied the origin and the nature of the ground expansions. Such studies included laboratory tests to analyse the expansive phenomena, *in situ* measurements of actual pressures in different sections by means of pressure cells placed in the invert-arch and in the vault (Figure 3), and testing of several solutions in experimental sections. Field data and laboratory tests results showed connections between some mechanisms of degradation and the swelling behaviour of the foundation material (Alonso *et al*., 2005). The authors concluded that the safer solution was to build a retrofit system consisting of an inner ring, relining, connected to the existing vault. This relining had to be capable of bearing the pressures of ground expansion,

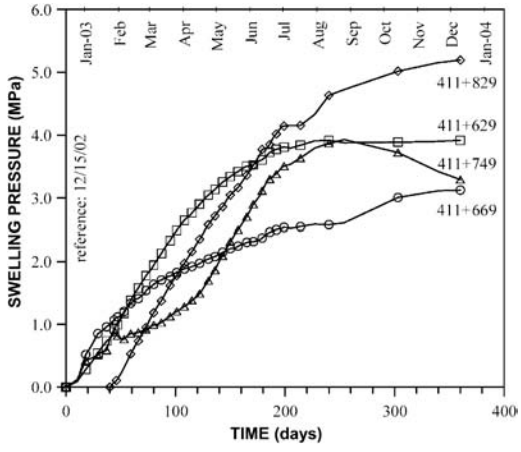


Figure 3. Swelling pressures in sections with invert (Alonso *et al.*, 2005).

which reached maximum values of 4250 kPa on the invert-arch and 1360 kPa on the vault. Such pressures overpass the capacity of conventional relining of tunnels based on steel trusses and concrete. Because of that, the public company responsible of the project management of the Railway Infrastructure, Gestor de Infraestructuras Ferroviarias (GIF), commissioned the developing of a technical solution to the Department of Construction Engineering at the UPC. The solution had to be economically and technically feasible for that challenging problem.

3 PROPOSED SOLUTION

3.1 *Geometry and loads*

Design loads were chosen according to the *in situ* measurements: 4500 kPa on the grade invert-arch and 2500 kPa on the vault. To resist such amount of load a ring shape was selected for the relining. In addition, experimental pressure measurements showed that the distribution was far from been uniform in the transverse direction neither in the longitudinal direction. So, the design pressure could be applied in the worst position and extension. Another condition to be satisfied was that the inner radius had to be at least 6.00 m and better 6.50 m, owing to the required dimensions for HSR traffic.

Lilla tunnel presents two main different sections: section 1 had the tunnel support of sprayed concrete and a lining of 30 cm of concrete, while section 2 had the tunnel support of sprayed concrete with no additional lining. In the Camp Magré and Puig Cabrer tunnels there were always lining. This was taken into account in the overall response of the support of the new lining because these additional stiff layers

Table 1. Thicknesses and deformation properties of the existing support.

Tunnel	Lilla		Camp Magré & Puig Cabrer
	Sect. 1	Sect. 2	
Thickness of tunnel support (cm)	15	15	15
Thickness of lining (cm)	30	–	30
Available thickness (cm)	46	76	126
Ground deformation modulus (GPa)	250	250	120
Ground Winkler modulus (MN/m^3)	334	160	160
Winkler modulus including linings (MN/m^3)	664	444	490

improve the support condition. Table 1 shows the thicknesses of the lining in the different sections and the deformation properties, mainly radial Winkler moduli, used in the analyses. Tangential Winkler moduli were approached by one third of the radial one.

A first approach to the problem showed that the solution had to be built in high strength concrete (HSC) with a significant amount of steel rebars. Because of pressures could present any limited extension, the strengthening had to resist significant bending moments concomitant with large axial forces.

To solve that problem, nonlinear finite element analyses were performed to obtain the worst loading condition on the vault and on the invert-arch.

3.2 *Design analyses*

In-plane nonlinear material and geometric analyses of the lining were carried out using the model of Marí (2000). Assumptions for the nonlinear plane analysis of the ring were: (1) longitudinal contribution of the lining is neglected, (2) the interaction with the ground is simulated by a unilateral Winkler model in both radial and tangential directions, (3) loads acting on the ring are self weight and design pressures, which can act in an arbitrary extension.

The moment and axial force ratio depends on the radius of the strengthening ring and on the length of the loaded arch, defined by its angle. In addition, there exist multiple axial/moment ratios that can be resisted by a reinforced concrete section with a determinate amount of steel. This leads to an uncertainty on the worst angle of loading that would provide the largest amount of reinforcement.

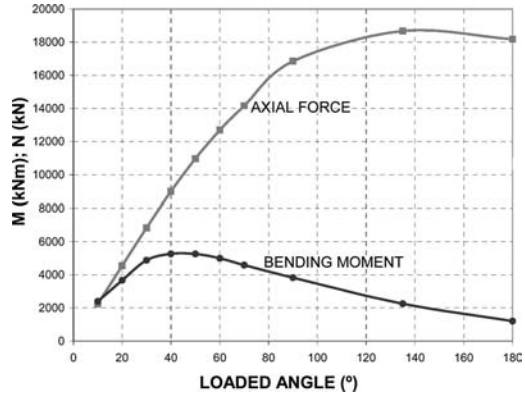


Figure 4. Bending moment and axial force, as a function of the loaded angular extension.



Figure 5. Total amount of steel as a function of the loaded angular extension.

In this case, to obtain the worst loaded angular extension in the invert-arch, an study varying the extension of design pressure (4500 kPa) on a cylindrical lining with a constant depth of 76 cm of reinforced concrete ($f_{ck} = 50\ N/mm^2$ and $f_{yk} = 500\ N/mm^2$) was developed. Figure 4 show the sectional forces obtained. Maximum bending moment was achieved with a loading angle of 40° while maximum axial force was obtained for 135° of loaded extension. However, maximum reinforcement, supposing a mechanical cover (d') of 10 cm, is produced by a loaded extension of 60° as Figure 5 shows. That preliminary result allowed to define the worst loading extension in approximately 60°. More details of the numerical predictions can be found in Marí & Pérez (2003).

Sensitivity analyses were also performed to select the concrete strength. They showed that concrete with a compressive characteristic strength of 60 N/mm^2 was unable to bear the loads. It was possible to use a 70 N/mm^2 concrete but it produced a huge amount of reinforcement. An 80 N/mm^2 concrete was selected

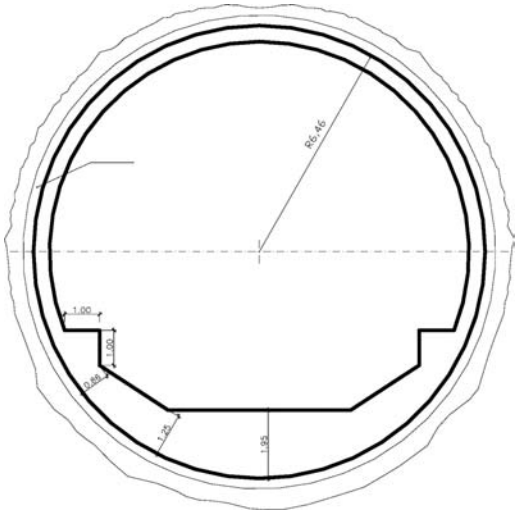


Figure 6. Geometry of the relining designed for section 1 of Lilla Tunnel.

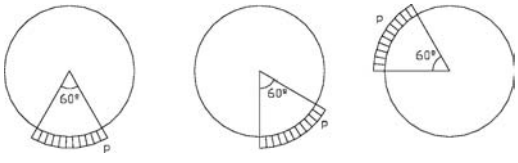


Figure 7. Loading cases considered in final design.

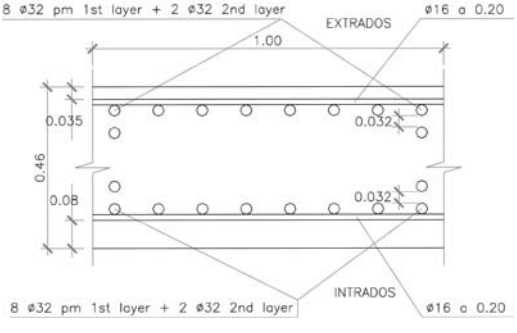


Figure 8. Reinforcement in the vault at the Section 1 of Lilla tunnel.

because the amount of reinforcement, in spite of being very large, was viable.

For final design purposes, three main loading cases with an extension of 60° were considered (Figure 7). The first two cases correspond to a load of 4500 kPa acting symmetrically and asymmetrically on the invert-arch. The last case in Figure 7 corresponds to a lateral unsymmetrical loading of the vault with a pressure of 2500 kPa.

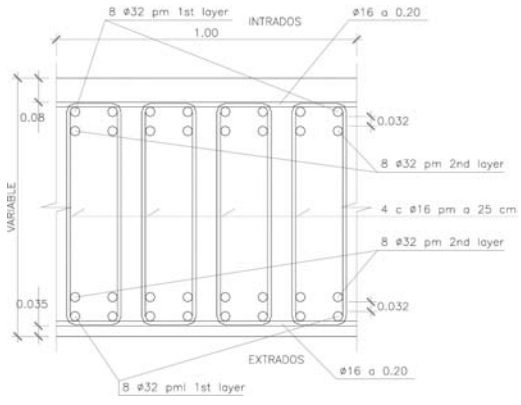


Figure 9. Reinforcement in the base at the Section 1 of Lilla tunnel.

3.3 *Final design*

The final design with the geometry shown in Figure 6 included an amount of steel of 80 cm^2/m in the vault and 128 cm^2/m in the invert-arch. Figures 8 and 9 show the cross section of the vault and of the base, respectively, including the reinforcement. All of them are symmetric.

Reinforcement of the invert-arch presents stirrups, as shows Figure 9.

4 CONSTRUCTION

The amounts of reinforcement, in both base and vault, make difficult placing conventional concrete. To improve the placing of a HSC in such conditions, self compacting concrete was finally chosen.

The composition of the mix deserved a careful design (Barragan *et al.*, 2005) because many factors had to be taken into account: a temperature range from 5°C to 35°C during the construction time, curing by spraying water was not possible owing to the deficient drainage of the tunnel during construction, a transport time of thirteen minutes, a high pump speed and a high initial strength required to reuse moulds. The resulting mix is shown in Table 2.

The construction process of the strengthening presented three main phases. Firstly the demolition of the grade slab and the excavation of the invert-arch were done. Secondly, the reinforcement cage of the whole invert-arch was placed in only one operation because it was prefabricated. Then, it was filled of concrete (Figure 10). Thirdly, the semicircular vault was built. Figure 12 shows the springing of the vault.

The construction of the relining was finished in 2005 (Figure 12). At this stage, vertical boreholes were drilled on the base and horizontal ones on the walls to extract samples for testing in the lab. Tests

Table 2. Composition and test results of the concrete.

Composition		(kg/m^3)
Cement		500
Micro-silica		50
Water		165
Lime sand (0–5 mm)		576
Natural silica sand (0–5 mm)		411
Granite aggregate (6–12 mm)		658
Superplasticer		11.0
Viscosity modifier agent		2.0
Test results		
Slump flow	D_f (mm)	610
	T_{50} (sec.)	4
Funnel V	T_V (sec.)	11
U box	ΔD (mm)	40

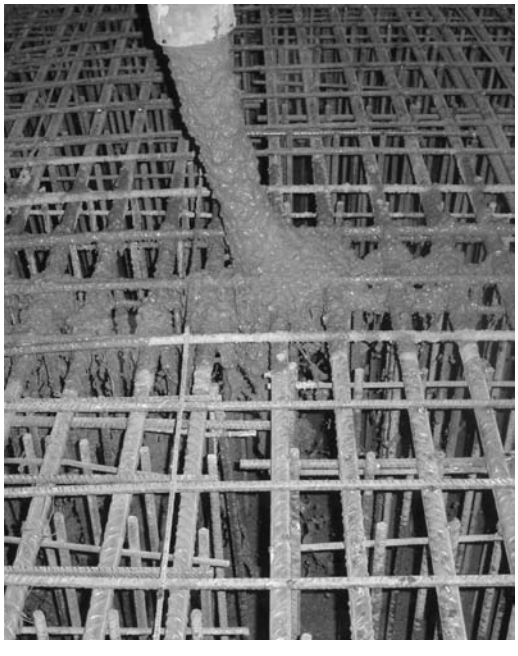


Figure 10. Placing concrete at the base of Lilla tunnel.

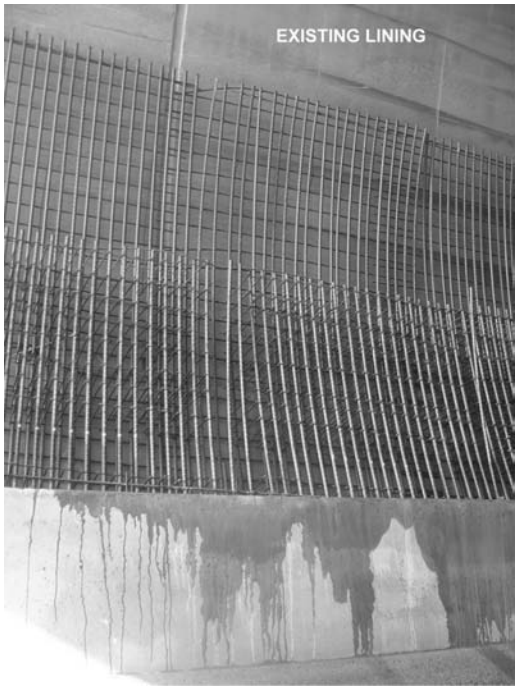


Figure 11. Reinforcement at the springing of the vault. The invert-arch is completed.

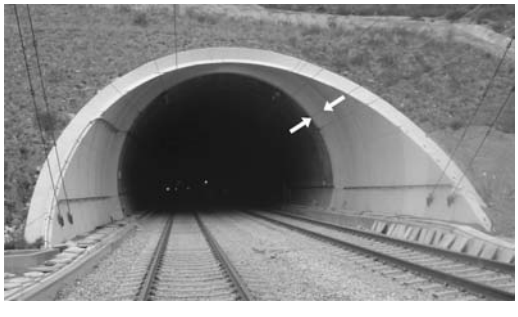


Figure 12. Lilla tunnel after finishing the works. It shows the change in the cross section after the initial section.

on more than twenty specimens provided information on the actual compressive strength of concrete, that was over 100 MPa. The actual deformation modulus (E_c) was 44 GPa. Water tightness was also tested and segregation was visually checked in all extracted cores.

5 MONITORING

Since the construction was finished, monitoring has provided data about both the behaviour of the structure and the pressures acting on the lining. Figure 13 shows the typical layout of instruments, placed at twenty one cross sections in the Lilla tunnel and seven more sections in the Puig Cabrer and Camp Magré tunnels. One pressure cell and two extensometers welded at the reinforcement of the intrados and of the extrados were placed in selected angular positions.

In addition, three cross sections in the Lilla tunnel have instruments on the vault, where much lower pressures were expected and are actually measured.

Since 2005, the instruments show an overall upward trend that it is not uniform along the time. In September 2006 it is not stabilized yet. Lilla tunnel presents the

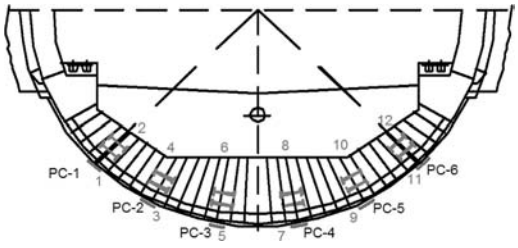


Figure 13. Typical layout of pressure cells and extensometers for the monitoring.

highest values (IIC, 2006). In four sections one of the six pressure cells place in the base has measured more than 3000 kPa and the highest value is 4980 kPa. However, pressure cells on the vaults measured a maximum value of 40 kPa.

6 CONCLUSIONS

A technical solution for strengthening of tunnel linings by placing a new interior lining (relining) to resist severe non uniform pressures along the circumferential perimeter has been described.

In the case presented, relining was built with high strength self compacting concrete, not connected to the existing lining. The use of such a concrete allows good final serviceability conditions, mechanical strength and water tightness. It is a robust solution, environment friendly and at a known final cost. In addition, it was constructed in less than one year.

Monitoring of the pressures acting on the lining and the strains in the steel reinforcement close to the intrados and to the extrados are showing an adequate response of the lining subjected to localized pressures over 4000 kPa. So that, the design and the construction process were appropriate for the considered problem.

The methodology has recently been applied to another HSRT that was subjected to huge water pressures, over 400 m, in a karstified mass rock. In that case, there were also serious doubts about the uniformity of the pressure distribution (corroborated by measurements).

ACKNOWLEDGMENTS

The authors thank *ADIF* (formerly GIF), the public company responsible of the design and construction of the HSR network in Spain, for funding the structural studies developed at the Department of Construction Engineering of UPC (Technical University of Catalonia), as well to the firm INOCSA and the construction companies Ferrovial-Agroman and Corsan-Corviam for their technical support.

REFERENCES

Alonso, E.E., Gens, A., Berdugo, I., Romero, E. 2005. Expansive behaviour of a sulphated clay in a railway tunnel. In: *Proceedings of the 16th International Conference on Soil Mechanics and Geotechnical Engineering*. 1583–1586. Rotterdam: Millpress.

Barragán, B., Gettu, R., Pintado, X., Bravo, M., Rodríguez, R. & García, J. 2005. Self compacting high strength concrete for tunnel lining strengthening (in Spanish). In: *III Congreso de Puentes y Estructuras de Edificación de la ACHE 14 al 17 de noviembre de 2005, Zaragoza* 1: 599–611. Madrid: Asociación Científico-Técnica del Hormigón Estructural.

Ingeniería de Instrumentación y Control, S.A. IIC (unpublished) 2006. HSR line Madrid-Barcelona-french border. Section Lleida-Martorell. Lilla tunnel. Monitoring of the strengthened lining (in Spanish). (Report n° 14). Madrid

Marí, A.R. 2000. Numerical simulation of the segmental construction of three dimensional concrete frames. *Engineering Structures* 22: 585–596.

Marí, A.R. & Pérez, G. (unpublished) 2003. Informe: Strengthening of the lining of the Lilla, Camp Magré and Puig Cabrer tunnels in the high speed railway line Madrid-Zaragoza-Barcelona-french border. Section Lleida-Martorell, Tarragona province (in spanish). Barcelona: UPC.

Mekano Instrumentación, (unpublished) 2006. Final Report: HSR line Madrid-Barcelona-french border. Strengthening of tunnels. (in Spanish) Madrid.

Underground Space – the 4th Dimension of Metropolises – Barták, Hrdina, Romancov & Zlámal (eds)
© 2007 Taylor & Francis Group, London, ISBN 978-0-415-40807-3

DeCo Grout – Innovative Grout to cope with rock deformations in TBM tunnelling

B. Billig, B. Ebsen, C. Gipperich, A. Schaab, M. Wulff
HOCHTIEF Construction AG, Essen, Germany

ABSTRACT: In order to extend the field of application of precast segmental lining in rock tunnelling, efforts were made by HOCHTIEF to develop a flexible segmental lining system which allows moderate rock deformations. The system comprises a defined compressible zone around a segmental lining system. This compressible zone may be made up of compressible grout, a compressible substitute for pea gravel or a compressible layer on the back side of the segment. Different materials were tested in laboratory for the different applications. Very good results with respect to the required stress-strain behaviour were obtained with the so-called DeCo grout – a cement-based mortar with EPS pearls and foam. In a confined compression test the material behaves initially in a linear-elastic manner. When the so-called compression limit is reached the material behaves more or less plastically, i.e. the stresses remain but the specimen is compressed. Compression rates up to 50% of the initial volume are possible. The innovative material opens up new chances for mechanised tunnelling in moderately squeezing rock.

1 STATE OF THE ART: TUNNELLING IN SQUEEZING ROCK

1.1 *NATM vs. TBM*

The New Austrian Tunnelling Method (NATM) as a method for the excavation of tunnels in rock has a long tradition. But in the course of the years TBM tunnelling has gained more and more importance in rock tunnelling. Apart from high advance rates this method provides further advantages. Due to the high degree of mechanism the working conditions for the personnel have been well improved. TBM tunnelling is especially suited and economic for very long tunnels with no possibility of intermediate starting points for tunnelling.

TBM tunnelling in rock generally allows two different kinds of primary tunnel linings:

- shotcrete in combination with reinforcement, anchors, bolts and steel arches according to the principles of NATM or
- precast segmental tunnel lining.

The shotcrete support can be adapted to the existing rock conditions. But in many cases it is not possible to make the most of the TBM power, because the installation of the primary lining is the limiting factor. High advance rates can only be achieved with a precast segmental tunnel lining. But the application of a segmental lining system is limited up to now due to rock deformations.

1.2 *Design of segmental lining*

The design of the segmental lining for tunnels in soft and granular soils with a low overburden height is driven mainly by the loads resulting from the water pressure and the overburden earth pressure. Due to the small overburden only small reductions of the earth pressure are possible. Ground deformations which could allow a redistribution of loads are mostly not acceptable, so the tunnel lining is designed in many cases for the complete overburden pressure.

For deep lying tunnels in rock the circumstances are fundamentally contradictory: The design of a tunnel lining for the entire vertical forces resulting from the overburden rock is in the majority of cases technically not possible. Therefore the tunnelling method must allow for the possibility of deformations. Due to these deformations the acting rock stresses will be reduced so that the tunnel lining can support the remaining acting ground forces.

This principle has been known and successfully realized in the NATM for a long time. On the one hand side the primary tunnel lining with shotcrete and anchors allows the stabilization and the support of the surrounding rock immediately after blasting. On the other hand side the thin layer of shotcrete and the time-delayed development of the compressive strength and stiffness enable a further progression of rock deformation in the tunnel until casting the inner lining with in-situ concrete. Using a precast segmental lining system requires the installation of the first ring under the

protection of the tail shield of the TBM. On the one hand side this gives directly a support and a protection against falling rock fragments but on the other hand side the support is effective with 100% of it's stiffness from the moment of installation. In comparison to a primary lining made of shotcrete a precast segmental lining is more stiff, because the concrete has gained the full strength and stiffness at the moment of installation and the complete ring is erected at once.

In squeezing rock deformations may therefore limit the use of a precast segmental lining.

1.3 *Project examples in the past*

In the past the question of the feasibility of TBM tunnelling in combination with a precast segmental lining came up several times during the tender phase. So the swelling potential of Shale led for example to significant rock deformations which had to be considered in the design of the precast segmental lining. Also when tunnelling in rock with high overburden one is confronted sometimes with large plastic rock deformations. Time dependant rock deformations of very weak or strong weathered rock make the use of a TBM doubtful.

These cases document the interest in and demand for a compressible annular grout. For the future we expect miscellaneous projects especially for tunnels in the Alps with high overburden pressure or tunnels in swelling rock.

2 COMPRESSIBLE TUNNEL LINING

2.1 *Theoretical idea*

The difficulties of tunnelling in squeezing rock have been known since the beginning of underground construction. The theoretical solution to this problem is even known, but only realized so far in the NATM. The following diagram shows the correlation between rock stresses and the stiffness/resistance of the tunnel lining.

The rock loading is found as the intersection point of the characteristic rock line with the respective support line. The earlier installation and the higher stiffness of a conventional precast segmental lining leads to increased rock loads, which are in many cases economical not justifiable. Obviously an initial linear-elastic behaviour followed by a plastic branch allows to decouple rock deformations from rock loads acting on the lining and to reduce rock loading significantly. Such a deformation behaviour may be reached by a "defined compressible precast segmental lining".

On the basis of the theoretical idea of a compressible precast segmental tunnel lining a lot of different ideas were developed and patented in the past, but in the majority the described solutions are very vague

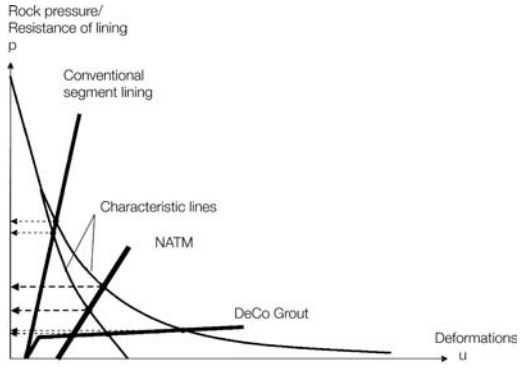


Figure 1. Characteristic line for NATM and precast segmental linings (Principle sketch).

and the actually required compressible materials which could accommodate rock deformations do not exist. Furthermore these patents mostly refer to the preliminary ground and rock support and not to the final tunnel lining, because of the close connection to the developments in mining.

2.2 *Executed projects*

According to our information and a study of literature only a few projects – most of them with pilot character – exist where a compressible lining was executed. One project was the mine in Ibbenbüren, Germany (Maidl et al. 2001). To deal with the expected high deformations tangential compressible elements have been installed between the joints of the segmental lining. In some rare cases tangential compressible elements have been used within the scope of a primary shotcrete lining, for example Gotthard-Basis-Tunnel, Los Faido (Brux 2004) or in the Strengener Tunnel (Budil et al. 2004).

3 RESEARCH AND DEVELOPMENT BY HOCHTIEF

In order to develop a defined compressible lining system R&D works were focussed on two approaches: tangential or radial deformable systems.

3.1 *Tangential compressible elements*

The idea of a tangential deformable system is to decrease the circumference of the lining while deformations take place. Due to the limited deformation capacity of concrete the shortening of the circumference requires special elements which are placed within the longitudinal joints between the segments. With the installation of the tangential compressible elements

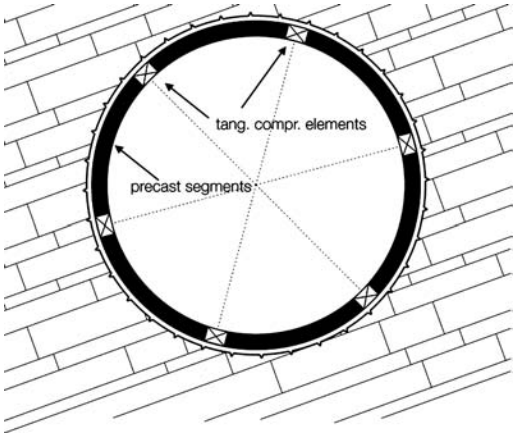


Figure 2. Tangential compressible element.

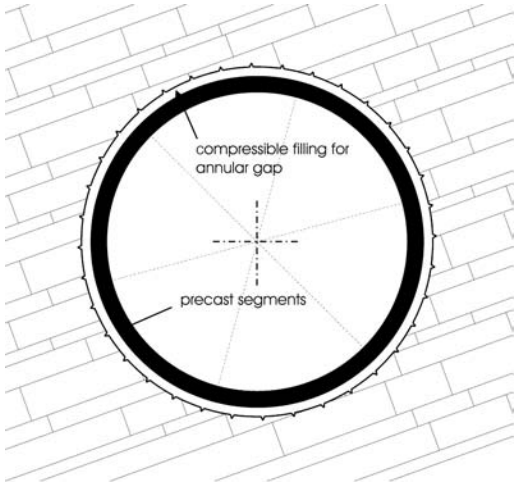


Figure 3. Radial compressible element.

only in the longitudinal joints of the segments the deformations are concentrated in 6 or 7 points according to the number of segments. The following figure serves as an example for the layout of a tangential compressible precast lining system.

Some structural studies about tangential compressible systems indicate that the accommodation of rock deformations is generally possible, but the bending moments in the precast segments are still very high so that thick segments with a high reinforcement ratio are required. Other disadvantages of these elements are especially the high labour costs for their installation and the time delay for the tunnel drive. Furthermore this system of precast segments and tangential elements does not provide a water proof tunnel lining. So this system can only be used in dry rock. All these arguments show that the development of tangential compressible elements are only qualified for temporary tunnel linings in combination with a subsequent final lining.

3.2 *Radial compressible systems*

More promising however seems to be the concentration on radial compressible systems. Generally it is distinguished between three different kinds of installation a compressible layer between the segmental lining and the surrounding rock:

- Filling the annular gap with a pumpable cement-based compressible grout
- Filling the annular gap with a compressible granular material by means of compressed air (compare backfilling procedure of pea gravel)
- Adding of a compressible layer fixed on the back side of the segments before the installation of the ring in combination with a traditional annular grouting or a compressible grout (sandwich)

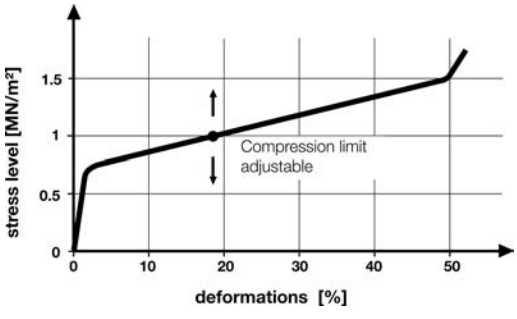


Figure 4. A spired nearly ideal plastic material properties.

In the beginning qualified materials had to be searched for and improved. The definition of a target corridor for the material properties was set up to assess the test results. Figure 4 illustrates the demands concerning the stress-strain properties for a nearly ideal plastic material. In the first part of the stress/strain relationship a stiff reaction with a fast increase of the stresses and low deformations at the same time is aspired. With reaching the so-called compression limit the material shall react more or less plastically, i.e. the stresses remain but the specimen is compressed until approximately 50%.

Although in relation to other well known materials like concrete or mortar the aimed compression limit is quite low but from the point of view of a lining designer rock loads in the range of 700 to 1500 kN/m^2 are quite high.

3.2.1 *Testing apparatus and testing procedure*

In order to compare the mechanical behaviour of different materials an adequate test setup had to be

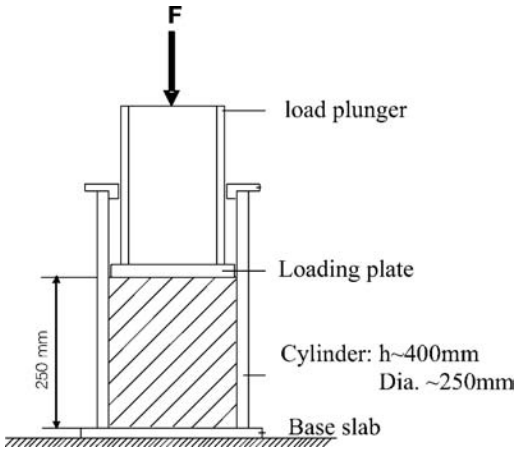


Figure 5. Measuring apparatus.

developed which reflects the restrained deformation conditions of the material in the annular gap.

Finally a test apparatus as shown in Figure 5 was chosen which allows to test the material with full lateral constraint. The loading speed was chosen with 0,2 mm/s.

To analyse the effect of the pot wall's friction on the results a series of tests with varying heights of specimens was executed. The comparison of the stress-strain behaviour showed a slight influence of the pot wall's friction increasing when smaller specimens were used. Even the velocity of testing was varied in several experiments but without any recognizable decisive influence.

3.2.2 *Test results*

The choice of materials tested in the first phase of the research project covers a large range of materials and corresponds to the different kinds of use, as a grout, a granular material or sandwich segment.

For a pumpable annular grout different super lightweight aggregates, several combinations of foam and EPS pearls and varying water-cement-values were tested. To find a granular compressible substitute for pea gravel mainly expanded clays and cellular glasses were analysed. Furthermore material combinations and the addition of other more elastic materials like vulcanised rubber were tested. For the third way – a so-called sandwich segment – plenty of thermal isolating materials and stones of lightweight gas concrete were put to tests.

The results are as well different as the materials. Figure 6 shows a selection of typical stress-strain curves. Some very light weight materials (a) show a more or less linear relationship between stresses and strains but on a quite low level. A typical material for this group is e.g. vermiculite. The initial stiffness is

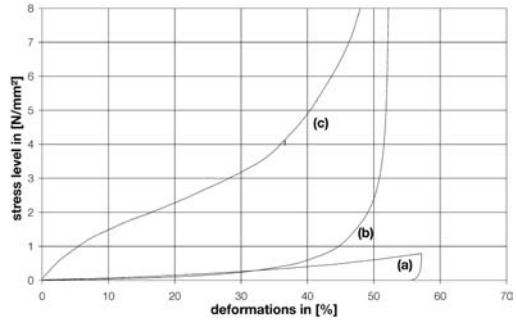


Figure 6. Stress-strain relationship for different materials.

very small as it is for material marked (b) in the beginning. Material (b) is a granular recycling rubber. With increasing compression the stresses increase initially very slowly. As soon as the internal pore volume is used up the stiffness of the material increases drastically. In this state the material behaviour is determined by the material behaviour of the particles. Without any internal pore volume the material is getting incompressible and the stresses grow beyond any limits.

Curve (c) shows a typical stress-strain relationship of light weight concrete aggregates. After an initial elastic branch the stiffness decreases which is typically caused by local crushing of the particles. With increasing compression the internal pore volume is used up and the same mechanism as described above determines the stress-strain behaviour of the specimen.

Although type (c) is most like the aimed behaviour the second branch of the stress-strain curve is to stiff and on a stress level which is too high.

Outstanding results with respect to the aimed stress-strain behaviour (Fig. 4) were achieved with a self created cement-based grout – a further development of the compressible concrete developed by HOCHTIEF some years ago. The development and the characteristic of this grout are described in detail in the following chapter.

4 DECO GROUT – A COMPRESSIBLE ANNULAR GROUT

4.1 *Further development of the compressible concrete*

Some years ago HOCHTIEF developed a damping concrete with an accommodation of approximately 50% of the starting volume for shock absorber slabs in the management of nuclear power plant waste. These test results form the basis for the further development of DeCo Grout. The following diagram documents the good starting position for the optimisation of the material.

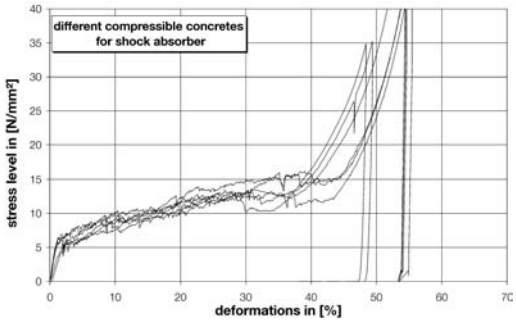


Figure 7. Test results of compressible concrete.

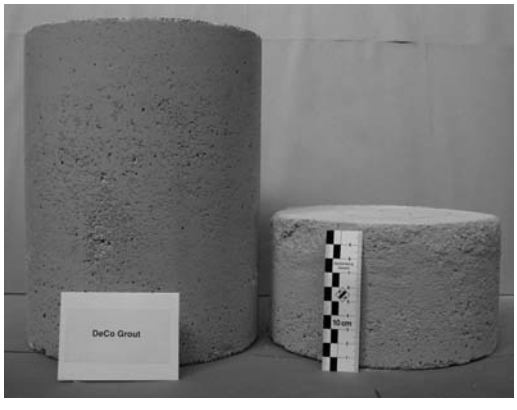


Figure 8. DeCo Grout before and after compression test.

The necessary modifications starting from the above described compressible concrete had to concentrate on four items:

- Reduction of the compression limit
- Improvement of the plastic behaviour
- Increase of the maximal compressibility
- Maintenance of the initial elastic modulus until reaching the compression limit

Tests to replace expanded polystyrene pearls with other lightweight aggregates like expanded clay or glasses were not successful, because these materials own a compression limit which is significant too high. Even with a maximum of expanded polystyrene pearls the stress level was too high and the compressibility not sufficient. To increase the compressibility it was necessary to enlarge the pore volume in the mortar. This was achieved by adding foam.

The result was a pumpable mortar with outstanding compression properties. This can excellently be documented with Figure 8, showing a specimen of DeCo Grout before and after the compression test.

In the meantime this grout has been applied for patent. More material tests have been continued to analyse the qualities of different kinds of cement and relationships of water and cement.

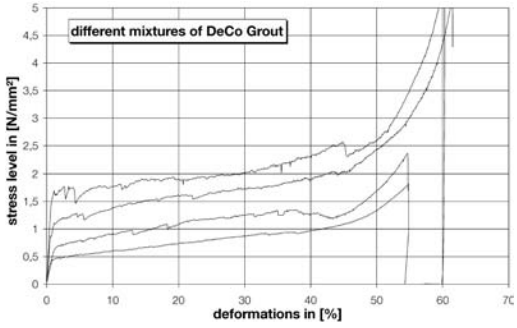


Figure 9. Test results for different mixtures of DeCo Grout.

4.2 *Adjustment possibilities of DeCo Grout*

Under the scope of this R&D project (Dorgarten et al. 2005) a number of tests were done. The numerous test results form the basis to assess the effects of the different materials added to the mix. Figure 9 shows test results from different mixtures of DeCo Grout.

The gained experiences allows now to modify the material properties as required by project specific needs.

4.3 *Defined compressible lining*

The enormous deformation capacity of DeCo Grout of nearly 50% allows with typical dimensions of the annular gap of approximately 15 cm the compensation of 75 mm radial deformations, i.e. 150 mm in diameter. Sensitivity studies showed that beside regular radial deformations also deformations in oval shape or local deformations can be accommodated.

Using this new and innovative material will of course require extensive monitoring during construction. The new system can be used in combination with conventional support methods in order to cope with local zones with increased rock deformations.

5 CONCLUSION

The new materials offer new chances in mechanized tunnelling in hard rock. With the development of a compressible material allowing moderate rock deformations the field of application of precast segmental lining in rock tunnelling can be extended. In the experiments done by HOCHTIEF the compressible DeCo Grout with an adjustable stiffness has shown extraordinary qualities.

The planned tunnels in the Alps with high overburden are an opportunity of using DeCo Grout. From

the comparable projects it is known that due to the high overburden rock deformations will occur and can prohibit common TBM tunnelling with a segmental lining. With the new compressible grout mortar it is possible to deal with moderate rock deformations.

A further example of the use of DeCo Grout is swelling rock for instant in Gypsum Keuper. The rock deformations are time-delayed and sometimes the stopping of deformations is very slowly and the temporary shotcrete lining have to support the ground for a long time until the final reinforced concrete lining can be installed. Here again the DeCo Grout can accelerate the progress of construction work. The time-delayed deformations will be accommodated by the compressible grout even when the final lining is installed.

These two cases are only a part of the complete application list telling where DeCo Grout can make tunnelling possible or easier within the scope of TBM tunnelling.

REFERENCES

Brux, Gunther. 2004. Deformierbarer Stahleinbau im Gotthard-Basistunnel. In Der Eisenbahningenieur 37–38.

Budil, A., Höllrigel, M., Brötz, K. 2005. Strenger Tunnel – Gebirgsdruck und Ausbau. In Felsbau, Rock and Soil Engineering Nr. 1 2004 39–43: Essen: Verlag Glückauf GmbH.

Dorgarten, H.-W. et al. 2005. Tunnelbauforschung in Europa. In Taschenbuch für den Tunnelbau 2006: 273–306. Essen: Verlag Glückauf GmbH.

Maidl,B., Schmid, L., Ritz, W. Herrenknecht, M. 2001. Tunnelbohrmaschinen im Hartgesteins, Berlin: Ernst & Sohn Verlag.

Underground Space – the 4th Dimension of Metropolises – Barták, Hrdina, Romancov & Zlámal (eds)
© 2007 Taylor & Francis Group, London, ISBN 978-0-415-40807-3

Immersed tunnels state-of-the-art

L.C.F. Ingerslev
Parsons Brinckerhoff, New York, U.S.A.

ABSTRACT: The ITA Immersed and Floating Tunnels working group issued the second edition of their state of the art report in 1997. This paper looks at recent tunnel design and construction to see changes that have occurred since then. There is still very much a place for immersed tunnels in today's sustainability world and they should be included as an option considered for any water crossing. Design requirements have become much more specific, focusing much more on project specific requirements. Available software has changed significantly analysis methodology and consequently how much can sensibly be presented to reviewing engineers and clients. Interesting new techniques are appearing on the construction side too. Concepts of some of these changes are presented here.

1 INTRODUCTION

It is now 10 years since ITA Working Group 11 Immersed and Floating tunnels issued the second edition of its State-of-the-Art Report (ITA 1997). Where has the state of the art gone in that period? Perhaps the most important changes affecting immersed tunnels are the environmental regulations affecting changes in water quality and concerns about existing fauna and flora, and the handling of contaminated material. In many countries, these are not necessarily new concerns, just that the requirements have been made more stringent and that increases costs.

Technology too has advanced. In the same way that bridges were made to fit the highways instead of highways made to fit bridges, immersed tunnels today are no longer necessarily straight tunnels with a constant cross-section. Much of this may be due to the much greater computing power available at our fingertips on the desktop and the great sophistication of software with user-friendly interfaces. The majority of immersed tunnels today are rectangular, shaped to provide ideal layouts for roads and railways with little wasted space. Immersion and final joint design has also improved. Noteworthy is that TBMs are to bore directly into the Bosphorus immersed tunnel to form the final joints in deep water.

Though there are still no design codes for immersed tunnels, guidance on design can be obtained from the ITA State-of-the-Art Report and in Japanese from the Coastal Development Institute (2002). Many papers have also been published, particularly in the proceedings of the ITA annual congresses.

Reasons for selecting an immersed tunnel (ITA 1999) have still not changed. For crossing a waterway, immersed tunnels are often viable alternatives and should be considered along with other options. Attributes to consider include:

- Immersed tunnels are shallow tunnels, often reducing the overall length of tunnel and enabling flatter approach gradients than would be possible for bored tunnels.
- Immersed tunnel cross sections are highly versatile, making them particularly suitable for wide highways and combined road/railway crossings.
- Most immersed tunnels have been built in water depths between 5 m and 30 m, although schemes have been postulated for 100 m depth. The deepest constructed is in 40 m of water to the underside of tunnel, and 60 m is under construction.
- They are suitable for most types of ground, including soft alluvial materials and conditions often unsuited to tunnel boring machines.
- Many immersed tunnels are in earthquake zones and have been shown to survive undamaged.
- Immersed tunnels can be prefabricated remote from the final immersion site, allowing placement in tight (e.g. urban) locations with little working space.
- The required dredging can generate material for new land reclamation.
- Construction can take place on many fronts simultaneously.

Contract packaging also varies considerably from the traditional design, bid and build, tending much

more towards design-build with the contractor also providing independent design verification. Project management for the owner's side is becoming more of a compliance-with-requirements role coupled with construction monitoring.

2 STRUCTURAL DESIGN

2.1 *Foundations*

Other forms of foundation besides sand and gravel are also used (Ingerslev 2001). Grouting in various forms is a much favored method of filling voids beneath immersed tunnels in seismic prone Japan after setting the tunnel to the design level. Formulations are possible that resist penetration of any underlying gravel layer that might be required to dissipate excess pore water pressures and thus reduce risks of liquefaction.

Ground failure as a result of seismic shaking can include liquefaction, post-liquefaction settlements, slope instability (landslide) and fault displacement. Some of these can result in horizontal and vertical displacements of the tunnel, which, if not taken into account in design, may require mitigation. No matter what kind of soil there is, some movement following a major seismic event is inevitable, but this is acceptable as long as such movements are within design tolerances. The effects of liquefaction and liquefaction-induced ground deformations can include the following:

- Uplift, buoyancy, and flotation;
- post-liquefaction settlements and deformations (total as well as differential settlements);
- lateral sliding stability of the tunnel;
- loss of bearing capacity;
- down-drag and reduction in lateral/vertical resistance of deep foundations.

To ensure that such movements do fall within acceptable limits, some soils susceptible to liquefaction may be improved sufficiently to ensure movements are limited to acceptable values; it may not be necessary to eliminate liquefaction altogether. Methods have included placing free-draining coarse aggregates around the tunnel structure to minimize the uplift potential, and installing sand or grout compaction piles below the tunnel invert to improve the soil properties. For liquefaction potential evaluations, SPT and CPT data requires careful evaluation, taking into account sampling procedures, depths and soil layer thicknesses.

2.2 *Minimizing fabrication facility depth*

For a number of projects, the temporary dry dock has been arranged so that perhaps only a small portion of the dock is deep enough to float out elements when the gate is opened. Elements are moved into that deeper location by pumping water in to a higher level than outside, enabling the remaining elements to float and be moved. This may result in additional flooding operations, though this cost and time may be offset by reduced excavation requirements.

Steel tunnels can have a very low draft when launched empty. For the Bosphorus concrete tunnel, a similar concept was used to minimize dock depth; only the lower half of each element was concreted in the dry dock; a braced steel waterproofing membrane was used as outer formwork for the remaining wall and roof construction. Bracing girders above roof level are later to be removed for reuse or disposal.

2.3 *Closure or final joints*

Where the final element to be placed has to be inserted between two elements or surfaces rather than merely appended to the end of the previous element, space is required to enable insertion. When tunnel ends are vertical, a marginal gap will be necessary at the secondary end. This short length of tunnel will need to be completed using special methods and is known as the closure or final joint. Several methods have been used to complete such joints in the past. It is important that axial and shear capacity of the tunnel is also achieved through the closure joint.

With the terminal block method, a short length of prefabricated tunnel is contained within the structure adjacent to the closure joint, outside a temporary bulkhead. This section can then be jacked or pulled out to meet the adjacent tunnel element and fill the gap. Seals similar to the immersion joints can be used on the end face of this moving section. The gap between the moving section and the oversize tunnel surrounding it must also be capable of being sealed, perhaps using inflatable seals and grout. This method has been used for the Tamagawa and the Kawasaki Fairway Tunnels in Japan. The use of divers is not required.

With the wedge-shaped block method, Figure 1, the width and shape of the closure joint must be fairly accurately known in advance. Sloping ends to the adjacent elements are required. Rubber compression seals permit the joints each side of the wedge to be dewatered and the joint to be completed from within. This method has been used for the Osaka Sakishima and

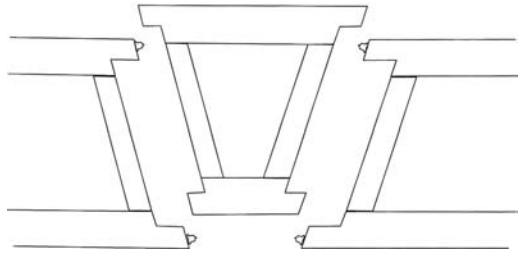


Figure 1. Wedge-shaped block final joint.

Kobe Minatojima Tunnels in Japan. The use of divers is not required.

More traditionally, a temporary external seal can be fitted around the marginal gap, dewatered and the joint completed in the dry. Plates with rubber seals may be attached to the adjacent tunnel elements so that upon placement a seal is obtained. Alternatively, divers have been used to place such plates. Once a seal is achieved, the joint is dewatered and completed in the dry from within. This type of joint has been used extensively, but may need diver support to obtain the initial seal. It may also be difficult to achieve in deeper tunnels.

Tremie joints have been used extensively in the past. Temporary forms are used to minimize the quantity of tremie concrete to be used around the joint. It is also recommended to lower into the gap "biscuits" of weak material to fill the areas that will later be removed to become tunnel voids. The tremie operation has in the past always been an external operation requiring diver assistance. The tremie joint will require waterproofing from within, since it may leak with time.

The need for a closure joint will depend primarily upon schedule, for it is not unusual for the abutting structures to require early completion. These may therefore both be built before the complete immersed tunnel can be laid, and therefore for both terminal elements to be laid early. Laying outwards from both ends results in a closure joint being needed. The immersed tunnel is considerably simpler if the tunnel can be laid from one end to the other without a closure joint. For the first transit tunnel in Hong Kong, connection to the land tunnels was achieved by TBMs boring into prepared ends of the terminal immersed tunnel elements. This method is also proposed for the Bosphorus crossing.

It may also be necessary to provide a flexible joint in the vicinity of a final joint since some forms of this joint are rigid. For Western Harbour Crossing in Hong Kong, completed in 1997, the element to one side of the final joint included a pre-compressed immersion joint containing a Gina-type gasket, and the first few meters of the adjacent element, while the element to the other side was missing the first few meters and the width of the closure joint. The end temporary bulkheads for those two elements were obviously located slightly differently from other elements. A rigid final joint was therefore made from within a temporary external seal and the pre-compressed immersion joint released, creating an element approximately the same length as the others (between Gina-type flexible joints).

2.4 *Applied loadings*

Design of immersed tunnels uses different load factors to those usually considered in design codes. Loads can be characterized as: dead or permanent loads; live or variable loads; exceptional loads that probably occur once during the design life that must be survived without damage; extreme loads that the structure must survive perhaps with limited amounts of damage to be defined; and construction loads. Extreme loads would include sunken or stranding ships, anchor impact, ship collision, flooded tunnel, train derailed with collision, explosion (e.g. vehicular), fire, the design basis earthquake (DBE) predicted for the location, and the resulting movement of soils.

Load cases to be analyzed can be similarly grouped into normal, abnormal (the after-effects of an extreme load, which might include changed soil conditions), extreme and construction. Although Japanese practice is to use partial factoring, when these partial factors are combined, the resulting load factors match those given in Figure 2. Extreme loads should only be combined after taking into account their probability, for example, 100-year storms, tsunamis and earthquakes do not all occur simultaneously. It should be noted that earthquakes have occurred during construction and should therefore be considered; since the construction period is relatively short, it would be appropriate to consider a smaller or more frequent event than the DBE.

2.5 *Watertightness*

The concept of watertightness needs to be associated with a rate of leakage that is acceptable; trivial

Loading / Design Loading Conditions	Normal	Abnormal	Extreme	Construction	Life Safety
Dead load & permanent ballast	1.4/0.9	1.2/0.9	1.05	1.1	1.0
Train/traffic load:					
Normal	1.6/0	1.2/0	_	_	_
Centrifugal	1.6/0	1.3/0	_	_	_
Braking load	1.6/0	1.3/0	_	_	_
Wind and waves	_	1.2	1.05	1.2	_
Current	1.4	1.2	1.05	1.2	_
Water level variation	1.4/0.9	1.2/0.9	1.05	1.2	1.0
Surge, etc	_	1.2/0.9	1.05	1.2	_
Backfill pressure:					
Horizontal	0.9/1.6	0.9/1.4	1.05	1.3/0	1.0
Vertical	1.6/0.9	1.4/0.9	1.05	1.3/0	1.0
Creep and shrinkage	1.3	1.3	1.05	1.1/0.9	_
Temperature, prestress	1.3	1.3	1.05	_	_
Sunken ship	_	1.2/0	1.05	_	_
Earthquake	_	1.2	1.05	1.2	1.0
Other extreme loads	_	_	1.05	_	_
Construction	_	_	_	1.3	_

Note: Where two values are given, such as 1.4/0.9, the more critical value shall be used.

Figure 2. Ultimate load factors and combinations.

leaks can often be ignored. Tunnels may be considered watertight when:

- Above road or track slab level and in all areas where the structure forms part of a ventilation duct, there are no drips or moving films of water;
- Below road or track slab level, there are no single leaks indicating a high pressure by jetting or spraying;
- The average water intake is below 5 ml/hour/m^2 of internal surface of the external structure.

2.6 *Fire protection*

Within those areas of the tunnel where inundation could occur as a result of fire and material degradation, fireproofing should be applied. The level of protection should be sufficient to evacuate tunnel users and for fire services to attempt to extinguish the fire. It is essential to prevent explosive spalling of concrete that might otherwise prevent fire services from approaching the fire.

3 DESIGN OF TYPICAL TUNNEL SECTIONS

Tunnel Types and concrete construction joints are discussed in some detail in an earlier paper (Ingerslev 2003) and are therefore not repeated here. Nevertheless, since steel sandwich tunnels (Figure 3) seem to be the most popular type in Japan recently and are not widely known elsewhere, a brief note is included here.

Structural steel plates are used on both the inner and outer faces of a steel sandwich tunnel, connected by web (shear) plates that divide the structure into a number of closed cells, each perhaps 10 cubic metres in volume. These are filled with unreinforced non-shrink self-compacting concrete. The concrete takes compression loads and, through embedded stiffeners on the steel plates, acts to stiffen the steel plates and prevent buckling (Japan Society of Engineers 2002). For the Bosphorus tunnel, the collar area of the tunnel elements (the 3 m adjacent to the joints) is designed as a sandwich type, while the remainder of each element is designed as a concrete tunnel.

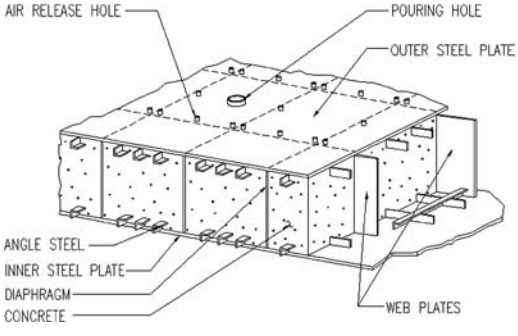


Figure 3. Typical sandwich tunnel.

Since the external plates are structural, they require protection against corrosion; existing tunnels have used sacrificial anodes with a design life exceeding 100 years.

In the seismically active areas of California, Japan and Turkey, shear reinforcement using head bars is becoming more commonly used. They are relatively easy to install and allow a higher density of shear reinforcement to be used. One end is a hook and the other terminates in a friction-welded plate.

4 DESIGN PROCEDURES

For the majority of contracts, design is still a three-stage procedure, namely concept, preliminary and final designs, though they might go under different names. For the Bosphorus tunnel, site response analyses to seismic loading on the tunnel had to be based on site specific response spectra; the spectra were developed by local experts and issued together with the bidding documents to ensure that all bids were based on the same seismic criteria.

The Bosphorus tunnel contract was awarded to a design-build joint venture led by Taisei; an early document produced was a design manual that incorporated the design assumptions, data and the concept design. Material properties and applied loading were defined, including ultimate design factors. Rigid frame models on elastic foundations were used in the structural analyses. The design used finite elements to model the soft ground and bedrock formations. The results provided response acceleration waveforms, velocities, displacements, stresses and strains. For the response analysis of the tunnel in the longitudinal direction, the immersed tunnel was modeled as a single line with each tunnel element subdivided into seven members. In order to determine appropriate ground spring constants at each location, 3-dimensional fiber models of representative tunnel cross-sections were developed. These were divided into elements and provided with ground springs; the backfill and existing ground were modeled and dynamic loads from the response analyses were applied to each section. Sensitivity analysis was included in each case to cover potential variations in soil properties.

Basic or preliminary design should define and analyze every procedure and stage of construction, as well as site-specific material properties for use in the design. Calculations should consider both serviceability and ultimate conditions. All failure modes must be ductile; failure due to shear should not be permitted. Foundation stability and settlement should be checked. Floating stability and buoyancy calculations are essential at each stage of construction. Any

locked-in stresses during construction must be included, both while supported and while afloat. Requirements for achieving the design life should also be defined, such as cathodic protection, waterproofing, joint details with associated gaskets, and fireproofing. Model testing may be needed to verify procedures such as immersion in strong currents. Full scale test construction may be needed for complex areas.

Transverse analyses for the Bosphorus tunnel assumed rigid frames concentrated at member centroids. Reinforcement was determined at serviceability limit state. The non-linear relationship between bending moments and curvature was recalculated and checked at ultimate. Seismic effects were incorporated at ultimate limit state after site response analysis was repeated with new data and new coefficients of subgrade reaction. Increased member forces that occur during a seismic event were determined using a two-dimensional FEM analysis (seismic response coefficient method); non-linear relationships between bending moment and curvature were calculated for each member for the loads applied. Allowance for slip at the surface of the tunnel was a requirement. Locked-in stresses due to stage construction were considered. Longitudinal analyses used three-dimensional beam elements for the tunnel and spring elements for the ground. Seismic effects were input by imposing ground deformations. Additional local analyses were used in the vicinity of the access shaft immersion joint where sandwich construction was used, and in the vicinity of the access shaft where holes are provided in the tunnel roof.

Detailed design essentially firms up on the basic design and should allow for tolerances, wall penetrations, sumps, etc. Design of construction items such as the bulkheads, lifting hooks and bollards, etc., and their effects on element design must be included. For the Bosphorus tunnel, a finite element model was used to verify stresses around the cross-section, especially at the corner haunches. A three-dimensional shell analysis was carried out to determine forces in the vicinity of the immersions and terminal joints due to local variations in stiffness and geometry. Heat transfer analyses verified that effects during a fire met requirements. Ductility was demonstrated by imposing excessive seismic deformations.

Computer analyses have become very much more user friendly, but with this come complications. The volume of input data can become very large and complex, much of it visual and not easy to check. While the computations are essentially the assembly of matrices and their inversion, post processing into useable results can involve methodology and assumptions that may be ill defined and perhaps in some cases inappropriate, being based on assumptions or codes for a different type of structure. This has the result that the sheer volume of input data and output data can be difficult for independent checking. Great care must be taken in verifying that the correct assumptions are used and that results match those obtained independently by other methods.

5 TUNNEL IMMERSION & PLACEMENT

Many immersed tunnels are placed in canals where water velocity is relatively low or in tidal waters where low velocities occur as the tide changes. A few tunnels are placed in rivers where currents do not change, so that methods of controlling tunnel elements during immersion and placing must match conditions perhaps far from ideal. Such conditions exist, for example in the East River of New York, not really a river at all but primarily a stretch of water in which water velocity is controlled primarily by the difference in tidal water levels around Long Island, with a fresh water contribution from the Hudson River through the shallow Harlem River. Here, as in many estuarial waters, variations in salinity with depth exist, resulting in contra-flowing currents with depth so that at no time is the water still; times of tidal changes for surface waters is very different for waters at depth.

The Bosphorus, a narrow river-like channel joining the less-saline Black Sea to the more-saline Sea of Marmara and eventually to the Mediterranean, also has contra-flowing currents driven by the difference in level of the two seas and their variations in salinity. These currents are often 4 knots at the surface southbound and half that value northbound at depth, though both do sometimes reach speeds half as much again. Immersing and placing procedures are based upon infrequent windows of opportunity with lesser currents. Mooring and adjusting cables will need to take into account current reversal during the lowering process, according to depth. Furthermore, the catamaran barges to be used for this operation will initially be aligned parallel to the current while the element is lowered to a region of less current, only then are the barges and element rotated to the placement orientation. Element position will be monitored and controlled remotely without the use of divers. Additional water ballast may be added remotely during immersion as water density increases and again after placing. The elements will be placed on pads equipped with jacks for horizontal and vertical position adjustment. After dewatering the joint between the most recently placed elements, the element position is checked from within and adjusted as required.

For the Fort Point Channel in Boston, a very shallow tunnel in a location with poor access by water, clusters of buoyancy tubes placed on top of the elements allowed controlled placement by ballasting (Figure 4). Elements could be winched into position



Figure 4. Fort Point Channel Tunnel buoyancy cylinders.

from the adjacent fabrication facility located within the alignment.

6 DEEPER WATERWAYS

While immersed tunnels are buried below the waterway, concept, preliminary and detailed designs have been prepared for a few projects where the tunnels would not be buried but would pass instead through the water. This would make the water depth irrelevant. In its simplest form, an immersed tunnel could be supported on piers like an underwater bridge. Other support options considered include hanging the tunnel from floating pontoons and using tension-legs similar to those of tension leg oil platforms together with a buoyant tunnel. All these options passing through the water are known as "floating" tunnels (ITA 1997); none have yet been built.

Where would such tunnels be used? Recent studies have considered deep lakes, fjords and straits such as Høgsfjord and Storfjord in Norway, Lake Lugano and Lake Zurich in Switzerland, the Straits of Messina and Lake Como in Italy, Jintang Strait and Qiandao Lake in China, Funka Bay and others in Japan, Elliot Bay and Lake Washington by Seattle in USA, and out to Vancouver Island in Canada.

If a tunnel has to cross an active fault, a floating tunnel would be capable of providing the necessary flexibility to avoid fracture.

Another serious concept for the future that has been presented employs dynamic positioning and has been proposed for trans-oceanic tunnels.

REFERENCES

Coastal Development Institute of Technology August 2002, Library No. 10, *Technical Manual for Immersed Tunnels, Revised Edition*, Japan.

Ingerslev, L.C.F. June 2001, *Immersed Tunnel Foundations*, AITES-ITA 2001 World Tunnel Congress.

Ingerslev, L.C.F. April 2003, *Understanding immersed and floating tunnels*, AITES-ITA 2003 World Tunnel Congress.

ITA Immersed and Floating Tunnels Working Group April 1997, *State-of-the-Art Report, Second Edition*, Great Britain, Pergamon www.ita-aites.org/cms/166.html

ITA Immersed and Floating Tunnels Working Group May 1999 ,*Immersed Tunnels: A Better Way to Cross Waterways?* Tribune, www.ita-aites.org/cms/159.html

Japan Society of Engineers Oct 2002, *Guidelines for Performance-Based Design of Steel-Concrete Hybrid Structures*, Structural Engineering Series 11.

Underground Space – the 4th Dimension of Metropolises – Barták, Hrdina, Romancov & Zlámal (eds)
© 2007 Taylor & Francis Group, London, ISBN 978-0-415-40807-3

Immersed tunnels continue to meet the challenges of water crossings

Walter C. Grantz
Senior Consultant, Parsons Brinckerhoff, Istanbul, Turkey

Vahan Tanal
Senior Vice President, Parsons Brinckerhoff, New York, New York, USA

Christian Ingerslev & Jaw-Nan Wang
Senior Engineering Manager, Parsons Brinckerhoff, New York, New York, USA

Donald P. Richards
Senior Engineering Manager, Parsons Brinckerhoff, Portland, Oregon, USA

ABSTRACT: The concept of an immersed tunnel is relatively simple and also time tested. More immersed tunnels are being built today than ever before. Every project has its challenges and this paper describes how many of these issues have been met. Many of these innovations are the product of collaboration involving multiple engineering disciplines, including geotechnical, civil, structural, mechanical, hydraulics, marine and environmental. Seismic events also impact tunnels and methodologies had to be developed to address seismic risk.

1 INTRODUCTION

An immersed tunnel is often the most economical method for an underwater tunnel crossing. These structures are made up of prefabricated steel or concrete sections or "tubes" usually constructed off-site, floated to the site, and placed inside a predredged trench. Steel or concrete construction is used for the elements. Operationally, there is no difference in how the final product functions, and for the same internal space, they weigh the same.

2 GEOTECHNICAL ISSUES OF IMMERSED TUNNEL CONSTRUCTION

Geotechnical risks are always a challenge in any underground project, but for underwater projects, the risks are often higher due to site investigation limitations as well as restrictions in addressing ground and/or groundwater control problems during construction. Geotechnical risks that must be identified and accounted for during the investigation, design, and construction planning include:

- Profiling of the subsurface conditions beneath the open water
- Properties and character of sediments to be dredged and in which the immersed tunnel will be placed
- Slope stability during construction of the immersed tunnel dredged trench
- Environmental restrictions on water turbidity during dredging
- Environmentally sustainable disposal of contaminated dredged materials
- Long term total and differential settlement of tunnel sections
- Liquefaction potential during the service life of the facility

Due to the expense and technical difficulties involved in off-shore drilling, vertical borings must be supplemented by other methods such as marine geophysics.

Geophysics can be useful not only in establishing a reliable bottom profile, but also sediment depth above bedrock, the character of the sediments, and the presence of buried obstructions within the shallow sediments to be dredged.

Conventional offshore site investigation techniques include Standard Penetration Testing (SPT) and cone penetration testing (CPT) for in-situ determination of strength and deformation characteristics, as well as variations in material properties. Laboratory testing

of soil and rock samples are necessary to establish engineering design parameters.

3 IN THE BEGINNING . . . THE DETROIT-WINDSOR TUNNEL (1927–1930)

In 1927, Parsons Brinckerhoff (PB) was retained for a monumental job—the design and construction of a 2.4-kilometer-long, single tube, two-lane immersed tunnel under the Detroit River from Detroit, Michigan, USA, to Windsor, Ontario, Canada. It was a challenging task for the primary reason that underwater vehicular tunnels were still a new concept—this would be only the third subaqueous vehicular tunnel constructed in the US, and the country's second immersed vehicular tunnel. Additionally, the project—the first vehicular tunnel to connect two countries—was to be delivered similar to a current design-build-operate project, a revolutionary concept at the time (and still noteworthy today).

The project, which employed a pioneering combination of construction techniques, including immersed, shield-driven and cut-and-cover tunneling, included a number of other innovative aspects, such as an improvement in installing tunnel elements by concreting them as they floated—rather than using sand or water to ballast the elements and then concreting them in place in the river-bottom trench. Additionally, the Detroit-Windsor Tunnel set the pace for a new procedure in tunneling that used welding for the first time in a double-shell immersed tunnel. The octagonal outside form plates and circular inner lining (Figure 1), together with welded steel construction, captured the imagination of tunnel designers and has been copied for many subsequent tunnels.

Not only were the tunnel's construction techniques innovative, but completion in just 26 months was unprecedented for a project of this scale and complexity; in fact, it is a construction record for immersed tunnels that has yet to be surpassed!

4 BART TRANS-BAY TUBE—PROVIDING STABILITY IN SHAKY GROUND (1953–1970)

Studies for the Trans-Bay Tube Project began in 1953 and the tunnel opened in 1970. This crucial link in the Bay Area Rapid Transit (BART) system provides a subaqueous rapid transit connection between San Francisco and Oakland, California. The 5.8-kilometer tunnel is 15 meters wide and 7 meters high. Binocular in cross-section, the tunnel provides two track compartments, an inspection gallery and space for utility lines. It is made up of 57 elements averaging 100 meters in length plus one short connector element. Each prefabricated element consists of a structural steel shell, generally 9.5 millimeters thick, with a 0.6-meter-thick concrete internal lining. The elements were immersed and joined in a trench dredged to depths of 41 meters below the water surface. This deepest immersed tunnel in the world will be surpassed by the Bosphorus Tunnel, currently under construction.

Since the Trans-Bay Tube was to be located in a seismically active zone, the development of design criteria for earthquake resistance merited special consideration. Much of the research on earthquake effects was unprecedented, resulting in pioneering engineering design. To meet seismic criteria, the immersed tunnel was designed to move as a flexible tube during an earthquake. To rest on soft alluvial soils, conform with the profile of the San Francisco Bay bottom, and accommodate navigational channels, the tunnel alignment changes direction twice horizontally and six times vertically along its length. Beneath the Oakland shipping channel, concrete slabs protect the top of the tunnel.

Teflon-lined, sliding seismic joints were designed for the landfall connections to allow longitudinal, transverse, and rotational movements during an earthquake (Figure 2). These special joints faced their first major test in October 1989 when an earthquake



Figure 1. Detroit-Windsor Tunnel tube under construction.

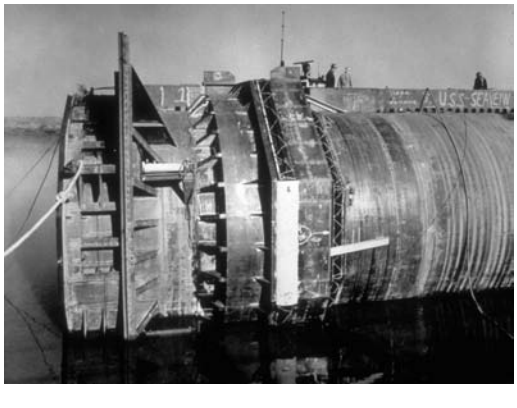


Figure 2. BART Trans-Bay Tube seismic joint.

measuring 7.1 on the Richter scale shook the San Francisco area. Interestingly, BART was one of the few major transportation (life line) links that was fully operational after the disaster struck.

The Trans-Bay Tube is the longest and deepest immersed tunnel in service, and was the first time a single shell tunnel was protected by impressed current cathodic protection. The patented triaxial seismic joints at the landfalls performed successfully during the earthquake when area bridges did not. The tunnel features the first US use of a double gasket system (American version of GINA), as well as ventilation buildings constructed in huge hydraulic caissons with built-in seismic joints.

5 CREATING ISLANDS IN THE SEA—THE HAMPTON ROADS CROSSINGS (1954–1976)

In 1954, the state of Virginia initiated the design for a crossing of the strategically significant Hampton Roads ship channel. Just three years later, the First Hampton Roads Bridge-Tunnel opened, across the James River, a major military and shipping channel. Twelve years later, in 1969, our firm was once again tapped to provide design and construction inspection services for a parallel second crossing to meet increasing traffic demands. Both of these crossings are noteworthy for several reasons.

The original 6.4-kilometer crossing, joining the cities of Hampton and Norfolk, is a combination bridge and tunnel. Engineers solved the problem of minimizing the length of the tunnel under the busy ship channel by terminating it on artificial islands on each side of the channel. Concrete trestle bridges connect the mainland with each island, and for the first time in the history of vehicular tunnel design, an immersed tunnel was constructed with portals emerging on man-made islands. The islands were constructed from suitable hydraulic fill placed within stone dikes built in stages as the islands rose out of the water (Figure 3). The south island had to be constructed on soft ground, heavily testing the soil mechanics technology of the time. The tunneling operation also took great care not to negatively impact nearby shellfish beds. When completed, the First Hampton Roads Crossing was the second deepest immersed tunnel in the world, reaching a trench depth of more than 36 meters; was one of the longest at 2.4 kilometers and 23 elements in length; and featured state-of-the art "tremie joints," whereby the joints between elements featured overlapping steel collars and hoods buried and sealed in tremie concrete.

The Second Hampton Roads Crossing is composed of a 1,930-meter southern approach trestle; a 965-meter northern approach trestle; 600 meters of open approaches on the two enlarged portal islands; and a 1,920-meter immersed tunnel under the channel.



Figure 3. Second Hampton Roads Crossing south island under construction.

It opened to traffic in 1976. Constructing the second parallel crossing involved some unique challenges never faced before. The alignment had to be a compromise between being close enough to the first tunnel to limit the footprint of the crossing, while not being so close as to cause settlements or displacements of the existing tunnel or ventilation buildings.

The existing islands had to be substantially widened to accommodate the new open approaches, while avoiding settlement issues. The North Island widening was mostly over sandy strata. Because some of the strata were fairly loose, vibrocompaction was used for densification. During the South Island sand-drain/surcharge construction program, settlements, displacements, and pore pressures were continuously monitored using deep settlement points, inclinometers, and piezometers.

The centerline of the second tunnel trench was kept a minimum of 75 meters away from the first tunnel to assure that there would be no influence on its stability. The dredging of the trench was carried out by a cutterhead suction dredge until reaching its maximum operational depth. Then a large bucket dredge using split barges for disposal was used to complete the trench. The joining of the tunnel elements benefited from earlier experiences gained on the BART Trans-Bay Tube in the form of a double gasket hydraulic immersion joint.

6 GROUNDBREAKING ENVIRONMENTAL SENSITIVITY—THE FORT McHENRY TUNNEL (1979–1985)

This massive eight-lane facility in Baltimore was the single largest interstate project in the US when it opened to traffic in 1985.



Figure 4. The Fort McHenry Tunnel west approach and wetlands mitigation site over the tubes.



Figure 5. The Fort McHenry Tunnel near shore CDF was later developed into the Seagirt Marine Terminal.

This tunnel was conceived and constructed as two four-lane, twin-bore immersed tunnels installed side-by-side in a 54-meter-wide common trench. Each tunnel consists of 16 double steel shell elements about 105 meters long for a total length of about 1,646 meters. There are 32 elements in total. The geometry was complicated by the fact that both tunnels had to be constructed on concentric curves while also featuring vertical curves.

It was constructed with the side-by-side elements only 5 meters apart at the ends where the elements were the widest (Figure 4). For the first time, a special folding wedge system was used that allowed for quick, simple alignment corrections at the gaskets.

The dredging was one of the most environmentally sensitive undertakings ever attempted in the US, as the first 2 meters of the Patapsco River bottom contained the residue of centuries of industrial wastes, including oils and heavy metal deposits. An environmental task force with representatives from the joint venture, federal environmental agencies, and city and state governments, worked together to identify acceptable alternatives. After a year of study, it was decided that a 59-hectare decommissioned open water disposal site in neighboring Canton/Seagirt would be used as a nearshore confined disposal facility (CDF). The contaminated sediment would be contained within a sealed cofferdam separately from a larger cofferdam area for cleaner sand and stiff clay material. Most of the dredging of the wide trench was carried out by a very large cutterhead suction dredge that pumped the material about 4 kilometers through a booster pump to one of the two containment areas. The overflow was treated with flocculants and allowed to settle in a 210-meter-long basin before being released to the harbor.

After project completion, the CDF was turned over to the Maryland Port Administration and developed into the modern Seagirt Marine Terminal, a major container port in Baltimore Harbor (Figure 5). The aquatic habitat lost to the CDF site was mitigated by the development of a tidal wetland between the historic park site and the west ventilation building.

7 THE BIG DIG—THE TED WILLIAMS TUNNEL (1987–1995)

The Ted Williams Tunnel, Boston's newest harbor crossing to Logan International Airport, opened to traffic in 1995, as part of the Central Artery/Tunnel Project, a massive program to upgrade the area's transportation infrastructure. Named for the legendary American baseball player, the tunnel doubles Boston's cross-harbor tunnel capacity from four to eight lanes.

The 1.2-kilometer underwater portion of the 2.6-kilometer tunnel is made up of 12 binocular-shaped steel tunnel elements, which were assembled in a shipyard in Baltimore and barged to Boston. Each element consists of two circular tubes set over a flat base. One tube holds the eastbound traffic, the other westbound traffic. They are each approximately 12 meters in diameter and over 91 meters long.

The project was environmentally sensitive due to the dredging of contaminated sediments from the tunnel trench. Commercial fisheries were concerned about potential impacts, especially during certain seasonal migrations. Mitigations included real-time monitoring of silt during dredging; sealed dredge buckets; a lined, sealed and fully enclosed upland CDF for contaminated sediments near Logan Airport; some disposal at designated underwater locations outside the harbor; and a specially designed common disposal site at Spectacle Island, south of Boston Harbor.

This project broke ground in many areas of state-of-the-art engineering applications, including the solidification/stabilization of contaminated dredged sediments. For the first time anywhere, this project involved processing 53,000 cubic meters of contaminated dredged material in an upland CDF, chemically solidifying the material, and compacting the CDF for future use (Figure 6).



Figure 6. The Ted Williams Tunnel upland CDF where contaminated sediments were chemically amended for solidification/stabilization.



Figure 7. The Fort Point Channel Tunnel Construction site.

8 TUNNELING IN EXTREMELY TIGHT QUARTERS—THE FORT POINT CHANNEL TUNNEL (1988–2002)

Although not very long, the Fort Point Channel Tunnel in Boston is noteworthy for several reasons, including its placement only 2 meters above two operating century-old transit tunnels. This is also the first immersed vehicular tunnel in the US to use a rectangular reinforced concrete configuration.

The tunnel carries 11 lanes of highway traffic from South Boston to Logan International Airport. Crossing the Fort Point Channel in this vicinity was extremely challenging given the site constraints—poor access from the harbor, and busy rail lines crossing the alignment of Interstate 90 just west of the project area. In addition, a large industrial plant and US Post Office facility were located close to the site (Figure 7). Because of these constraints and the shallow water depth, a rectangular immersed tunnel was selected as the preferred approach.

The crossing comprises six tunnel elements, each approximately 99 to 127 meters long, 7.9 meters high, with widths varying between 21 and 47 meters. The tunnel features side ventilation inlet and exhaust ducts, providing full transverse ventilation. The elements were placed three in each direction in two close parallel lines across the channel, with cut-and-cover approaches on the east and west. The foundation of the ventilation building and 12 piers for the new Dorchester Avenue Bridge were built integral with the elements that were placed at the west end of the tunnel—the first time this has been done on an immersed tunnel. This approach eliminated the need for expensive cofferdams to build the bridge and building foundations in the channel.

Drilled shaft caissons 2 meters in diameter extend as much as 56 meters into the bedrock below the channel to support tunnel elements that were placed only 2 meters above the crown of the existing Red Line subway tunnel, which remained in service during construction. These subway tunnels, constructed by "sand hog" methods with un-reinforced concrete, needed to be treated very carefully. If uncovered, they might have become unstable and collapsed, flooding most of Boston's subway system.

9 CONNECTING TWO CONTINENTS—THE BOSPHORUS TUNNEL (2004–2010)

Split in two by the Bosphorus Strait, the city of Istanbul has always sought ways to move people and goods across this narrow and busy waterway separating Europe and Asia. In 1985, a consortium led by PB conducted feasibility studies, planned and performed the preliminary design of a rail tunnel beneath the strait. In 2002, the Ministry of Transport & Communication, General Directorate of Railways, Harbours and Airports Construction, commissioned Avrasya, a joint venture led by Pacific Consultants International of Japan, to assist the Ministry in implementing the project as its general engineering consultant. Subsequently, in 2004, a design/build contract was awarded to a joint venture of Taisei, Kumagai, Gama and Nurol.

The project, involving the world's deepest immersed tunnel as well as related improvements to 63 kilometers of at-grade rail lines, is one of the most ambitious and complex undertakings of its kind. It features a 1.5-kilometer-long tunnel in more than 50 meters of water below one of the busiest waterways in the world. The complex hydrology of the Bosphorus will be a challenge to placing tunnel elements: bi-directional currents are not tidal but vary according to the hydraulic gradient between the Black Sea and the Sea of Marmara. The currents vary rapidly and can reach 6 knots southbound at the surface and 2 knots northbound. Tunnel elements will be placed when surface currents are below 1.5 meters/second (3 knots). The shallowest element will be 40 meters deep—twice the depth of most immersed tunnels in

Europe and Japan—while the deepest will reach a depth of 58 meters.

The immersed tunnel starts and ends in deep water. At these locations, after each terminal element is placed, a soil mix fill will be used to form a weak concrete-like connection to the rock. Starting from Sirkeci Station excavation on the European side and Üsküdar Station on the Asian side, tunnel boring machines (TBMs) will bore two circular running tunnels—one each for eastbound and westbound tracks—out to two receiving sleeves fabricated at the ends of the terminal elements. Until then, access for constructing the immersed tunnel will be limited to one shaft to be installed on the first element to be placed, located offshore, upstream of KizKulesi (Leander's Light)—the famous ancient lighthouse. This access shaft will be reached by a trestle and bridge constructed to it from the Asian shore.

The tunnel is designed to resist seismic events. Ground conditions in the tunnel subgrade vary considerably. A zone from Element 11 (Asian end) to Element 8 was found to have a risk of liquefaction during an earthquake. To counter this risk, the area has been treated by compaction grouting (CPG). Nearly 2,800 grout columns spaced on a 1.7-meter grid have been injected into the seabed below tunnel level to compact the deep foundation soils.

Dredging is being carried out by a large grab dredge with a capacity of 28 cubic meters. In a zone near the European side, about 136,000 cubic meters of contaminated soil has been dredged and transported in barges to the port of Kartal, approximately 30 kilometers to the southeast, where it was trucked to a specially constructed upland CDF. The use of a CDF for contaminated dredged sediments is unprecedented in Turkey (Figure 8). The clean materials were loaded into split barges and transported to a designated deep open water disposal site in the Sea of Marmara 25 kilometers from the tunnel trench.

The design of the tunnel is based on a rectangular concrete box with a central wall dividing the trackways. The base and sides are made watertight by a 7-millimeter-thick steel membrane. The roof slab is covered with a special PVC membrane that is protected with a reinforced concrete slab. The ends of the elements are steel/concrete sandwiches structurally tied to the longitudinal reinforcing steel in the concrete section. These "end shells" support the temporary GINA gasket of the immersion joint and the watertight bulkheads. The casting yard at Tuzla consists of two specially built drydocks each large enough for two elements and deep enough to allow about half of the concrete cross section to be placed before the drydock must be flooded and the element towed to an outfitting pontoon within the adjacent harbor. The elements remain moored at the pontoon while the concrete and waterproofing work are completed.



Figure 8. The Bosphorus Tunnel upland CDF.

After final outfitting, a placing barge with the element will be taken upstream of the trench where the first anchor will be run out on a windlass. As the barge nears the trench, this operation will be repeated with a second anchor placed the same way. The barge and element will be end on to the current to limit drag forces. More anchor lines will then be attached using a tender and the element will be lowered to a regime of acceptable current where it will be rotated to its alignment in the trench. As the final lowering proceeds, the inboard end of the element being placed will engage centering guides installed on the tunnel already in place. The outboard end will sit on an alignment correction frame that will rest on prepared bedding. A jack will be extended from the existing tunnel to pull the element being placed and obtain an initial seal by compressing the soft nose of a GINA-type gasket. The immersion joint will then be fully activated by lowering the water pressure in the joint space by pumping it out. The bulkhead doors can then be opened to permit position survey of the new element and any adjustment thereto using jacks on the alignment correction frame.

As the tunnel progresses, backfilling over the elements will take place, which will return the bottom of the Bosphorus to its original contours. The Bosphorus Tunnel is scheduled to open to rail traffic in about 2010.

10 CONCLUSION

Seven case histories spanning over 75 years have shown that innovative engineering is necessary in immersed tunnel projects. Environmental issues are more challenging today than ever before. Close coordination of multiple disciplines with an open-minded, teamwork approach is a common denominator for success.

Underground Space – the 4th Dimension of Metropolises – Barták, Hrdina, Romancov & Zlámal (eds)
© 2007 Taylor & Francis Group, London, ISBN 978-0-415-40807-3

Case study for the deterioration of lining in vehicular tunnel based on ventilation system

J.H. Choo, H.S. Ryu, Y.S. Shin & S.R. Ahn
Tunnel Division, Korea Infrastructure Safety and Technology Corporation, Goyang, Korea

ABSTRACT: The ways of tunnels ventilation system are classified as natural, semi-transverse, full-transverse according to the place of duct. Most of aggressive causes in deterioration on the tunnel lining are as follow: water, smoke, atmospheric conditions, impact damage, overburden, etc. In this paper, the distribution of deterioration on concrete lining is investigated as a part of precise safety diagnosis in 8 service-in vehicular tunnels in South Korea. Three methods have been implemented to measure the range and trend of deterioration; Schumidt hammer test (NR-type), ultrasonic test, and carbonation. Depending on the ventilation system, the trend of deterioration is compared with the way of ventilation system within each vehicular tunnel and examined the mutual influence between the distribution of deterioration rate and ventilation system. The output of this paper is demonstrated that the tendency of deterioration rate is bigger along the exit. Also, the depth of deterioration rate is high on the duct slab primarily, then lining inside duct, beneath the duct slab in sequence at the same section.

1 INTRODUCTION

Depending on the construction situation, the shapes of the tunnel can be presented functionally as follow: circle, horse shoe, ellipse, oval, etc. Most of the shapes in vehicular tunnels are flat horseshoe or circular section. One of schematic characteristics in general shape of vehicular tunnel is the duct, which is adapted to evaluate the capacity of ventilation. With or without duct, ventilation system can be classified with natural, semi-transverse, and full-transverse, etc.

Most structures related to the precise safety diagnosis (government regulated it since 1995 in South Korea) have shown problems in structure or non-structure by the change of tunnel circumstances and deterioration of lining as the years of use for tunnel goes by.

In this study, the deterioration of lining in vehicular tunnel based on ventilation system have been inspected by three conventional NDT(Non-Destructive Test) methods such as Schumidt hammer test (NR-type), ultrasonic test, and carbonation. These mostly preferred NDT methods in precise safety diagnosis are well researched and conducted by over 500 companies since those NDT methods have been introduced in precise safety diagnosis field.

The general procedure of precise safety diagnosis in vehicular tunnel is shown in Figure 1. This study aims for discerning the amount of deterioration of the surface on lining concrete depending on what kinds of ventilation system has been adapted in vehicular tunnel. Also, the purpose of this study is to suggest how to arrange and analyses the previous data in re-diagnosis (precise safety diagnosis which is repeatedly conducted in every 5 years in South Korea).

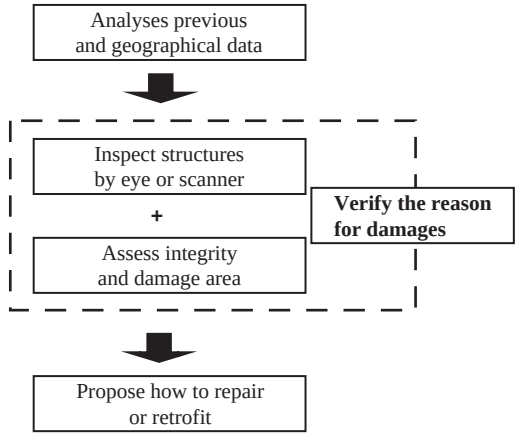


Figure 1. General procedure of precise safety diagnosis in vehicular tunnel.

2 TUNNEL EXPLANATION

Three methods for assessing the deterioration on lining concrete have been implemented in 8 service-in vehicular tunnels. Two major fields of precise safety

diagnosis are the strength and integrity. Schumidt hammer Test (NR-type) and ultrasonic test are well known for estimating the strength of lining. To assess the area of deterioration on lining, carbonation is a mandatory test item especially in reinforced concrete structure such as duct, ventilation ways in vehicular tunnel. Conventional cross-section of vehicular tunnel for this study is shown in figure 2. Natural system is applied for mountain area or low traffic zone, which is not required of ventilation supplies. Either semi-transverse or full-transverse system can be applied in urban area or heavy traffic zone depending on the geological level, fan capacity, and maintenance fee, etc. The specific information of 8 tunnels is detailed in table 1.

3 CHARACTERISTICS OF CARBONATION ON LINING SURFACE

One of primary considerations of design step in vehicular tunnel is to sustain the airflow steadily for the safety for tunnel user and evaluation for efficiency. The carbonation of lining concrete is mostly affected by CO_2 (carbon-dioxide) which is major combustion products of vehicular while the car is passing through. According to this study of carbonation classified by ventilation system, the depth of carbonation in natural system is not progressed as much as its extent and speed compared to the semi-transverse or full-transverse system. The depth of carbonation on slab in the duct is faster and deeper than its wall in the road at same section in semi-transverse system.

Also, the same extent of carbonation on slab is investigated in the road area in full-transverse system. In particular, the extent of carbonation on exhaust duct is severely progressed than supply duct. These outputs for carbonation can be shown in figure 3 as in order: natural, semi-transverse, and full-transverse.

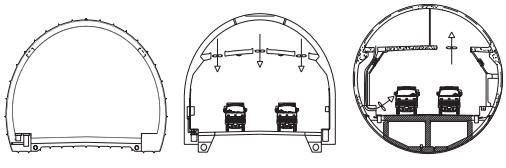


Figure 2. General cross-section of vehicular tunnel.

4 CHARACTERISTICS OF SCHUMIDIT HAMMER ON LINING SURFACE

The general trend of the rebound number by Schumidt Hammner in this study is getting lower compared to

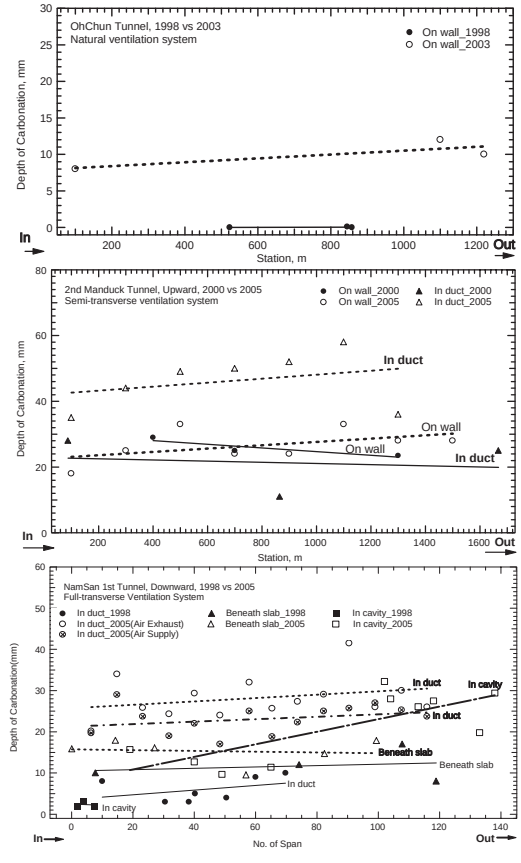


Figure 3. The outputs of carbonation as ventilation system.

Table 1. The detailed tunnel information in this study.

Name of tunnel	Location	Length (m)	Ventilation system	Construction method	Completed year
OhChun	KwangWonDo	1,296	Natural	NATM	1990
HaeSan	KwangWonDo	1,986	Natural	NATM	1980
NamSan 1st	Seoul city	1,532	Semi/Full transverse	ASSM/NATM	1980/1994
NamSad 3rd	Seoul city	1,280	Semi transverse	ASSM	1988
KwangAhn	BuSan city	1,136	Semi transverse	ASSM	1980
Gudeok	BuSan city	1,880	Semi transverse	ASSM	1984
ChangWon	ChangWon city	2,340	Semi transverse	NATM	1993
Manduk 2nd	BuSan city	1,840	Semi transverse	ASSM	1988

the result in 5 years ago due to its deterioration of the lining surface. Shortly, the difference of range in rebound numbers for estimating the strength is bigger in semi/full-transverse than natural system. As we can see in figure 4, the discrepancy of extents in rebound numbers for strength is greater on slab in the duct than on wall in the road at the identical section in semi-transverse system. Also, the fluctuation of rebound numbers is larger on the exhaust duct than the supply duct in full-transverse system.

5 CHARACTERISTICS OF ULTRASONIC WAVE VELOCITY ON LINING SURFACE

There is another well-performed testing method for estimating the deterioration of lining surface in precise safety diagnosis field. Ultrasonic test is one of useful techniques in NDT scopes for detecting the depth of crack and for evaluating of the penetrating sonic velocity through concrete lining. In this study, indirect technique has been implemented on lining surface along with Schumidt hammer test and core sampling for acquiring the coefficient of correlation and evaluating the range of lining deterioration.

The velocity through lining is influenced by the extent of deterioration and the quality of construction. The more poor quality and bad deterioration, the later sonic wave velocity due to the long propagation time is elapsed.

Considering the fresh air condition and less traffic, the difference between 5 years with sonic wave velocity in natural system is determined with a general aspect. As we can see in figure 2, the basement in full-transverse system is conventionally used for drainage of water, passage of power or communication cable, etc. Due to the convection and moisture in full-transverse basement, the lining surface is constantly moisturized so that the discrepancy of the determined velocity by ultrasonic test is larger than dry condition. In semi-transverse, the determined velocity by

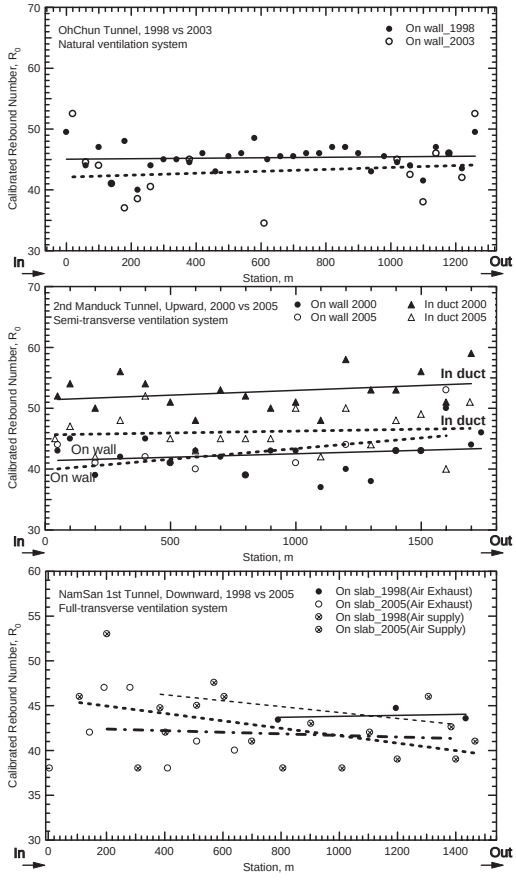


Figure 4. The outputs of rebound numbers in Schumidt Hammer test as ventilation system.

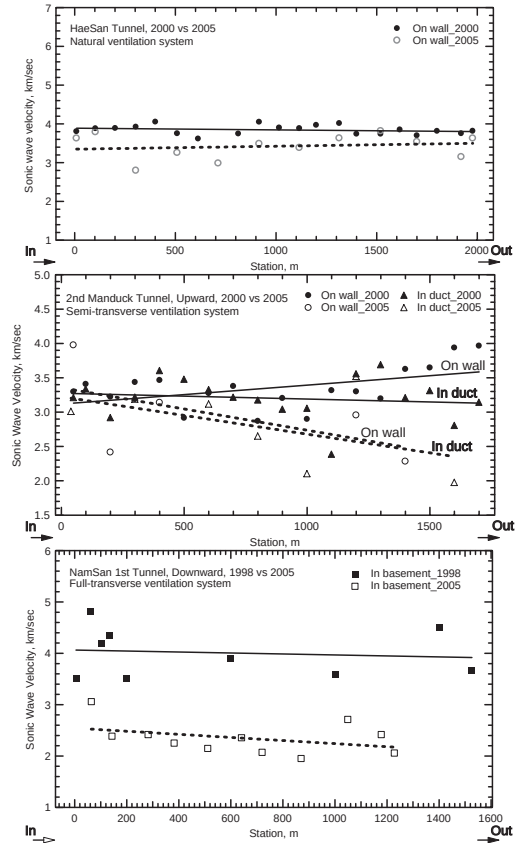


Figure 5. The outputs of ultrasonic wave velocity test as ventilation system.

indirect technique is gradually decreased on slab in duct area far from the fan because the slab surface is badly deteriorated by the accumulated combustion product depending on the distance from the fan.

6 CONCLUSION

In this study, the deteriorations of lining in vehicular tunnel based on ventilation system have been investigated by three conventional NDT methods such as Schumidt hammer test, ultrasonic test, and carbonation. The aims for this study are estimating the extents of the deterioration of lining concrete and verifying the validity of three NDT methods depending on the types of ventilation system. Also, the goal of this study is to suggest how to arrange and analyses the previous data in re-diagnosis.

First, three conventional indexes for assessing the deterioration of lining surface such as depth of carbonation, number of rebound, velocity of sonic wave is well-matched with the same pattern and one another.

Second, three NDT methods validate to estimate the deterioration of lining surface depending on the three ventilation system; natural, semi-transverse, and full-transverse.

In conclusion, the deterioration of lining is severe in semi/full-transverse system rather than natural system. The depth of carbonation, decrease of rebound number and sonic velocity is deeper and larger in semi/full-transverse system than natural system. Especially, the badly deteriorated part in vehicular tunnel is on slab in the duct because of the accumulation of combustion products. The output of this paper is demonstrated that the tendency of deterioration rate is bigger along the exit. Also, the depth of deterioration rate is high on the duct slab primarily, then lining inside duct, beneath the duct slab in sequence at the same section.

To maintenance properly, like in the basement in full transverse system, dry condition should be sustained not to progress the deterioration of lining and damage the convenient supplies.

REFERENCES

1. Guian Sin Kwa, 2004, The Design of Tunnel Ventilation System for a Long Vehicular Tunnel, *ITA*, Singapore (CD).
2. 2003, *Guideline of the precise safety diagnosis, Tunnel field (Korean)*, KISTEC.
3. 1998 & 2003, *Report of precise safety diagnosis on NamSan 1st tunnel (Korean)*, KISTEC.
4. 1996 & 2001, *Report of precise safety diagnosis on NamSan 3rd tunnel (Korean)*, KISTEC.
5. 1999 & 2003, *Report of precise safety diagnosis on KwangAhn tunnel (Korean)*, KISTEC.
6. 2000 & 2005, *Report of precise safety diagnosis on HaeSan tunnel (Korean)*, KISTEC.
7. 1998 & 2003, *Report of precise safety diagnosis on OhChun tunnel (Korean)*, KISTEC.
8. 1997 & 2004, *Report of precise safety diagnosis on GuDuck tunnel (Korean)*, KISTEC.
9. 1997 & 2004, *Report of precise safety diagnosis on ChangWon 1st tunnel (Korean)*, KISTEC.
10. 2000 & 2005, *Report of precise safety diagnosis on ManDuck 2nd tunnel (Korean)*, KISTEC.
11. Choo, J.H., Maeng, D.Y., Ryu, H.S. & Ahn, S. R. 2006, A study on the carbonation of the lining of vehicle tunnel based on ventilation system, *Tunnelling and Underground Space Technology, Vol. 21. p324*.
12. John O. Kickel, T.R. Kuesel, 1982, *Tunnel Engineering Handbook; tunnel ventilation, pp.483–563*, Van Nostrand Reinhold Company, Inc, USA.
13. Peter H. Emmons, 1995, *Concrete Repair and Maintenance Illustrated*, R.S Means Company, MA, USA.

Underground Space – the 4th Dimension of Metropolises – Barták, Hrdina, Romancov & Zlámal (eds)
© 2007 Taylor & Francis Group, London, ISBN 978-0-415-40807-3

Březno Tunnel Shaft

E. Stehlík
IKP Consulting Engineers s.r.o. Prague, The Czech Republic

J. Heřt
Metrostav a.s. Prague, The Czech Republic

T. Parák
IKP Consulting Engineers s.r.o. Prague, The Czech Republic

ABSTRACT: The Březno Railway Tunnel is located in the North of the Czech Republic, near to the town Chomutov. The construction of 1.8 km long single track railway tunnel started in May 2000 and was interrupted in May 2003 due to the large collapse while tunnelling with pre-cut method using Perforex machine. After resuming the works in 2004, an emergency escape shaft was sunk in the collapsed area, just above the buried machine. The shaft lining was formed by secant piles, supported by reinforced concrete ring beams and shotcrete rings, respectively. The paper describes the main features of the unique shaft design and its construction.

1 INTRODUCTION

1.1 *Brief history*

The tunnel construction started in 2000, the tunnelling using pre-cut method with Perforex machine started in March 2002. In May 2003, after completion of approximately 800 m, the primary lining created by non-reinforced shotcrete sprayed into the pre-cut slot, collapsed. The collapse started at the face, followed by collapse of approximately 100 m of the primary lining behind the tunnel face. The collapse created a depression on the surface and completely buried the Perforex machine.

1.2 *Construction after collapse*

Due to the legal and financial problems caused by the tunnel collapse, the tunnel construction was stopped for more than year, and restarted in October 2004. The works started from the other portal, using sequential excavation method with initial lining consisting of shotcrete, lattice girders and bolts. During the entire stretch of the tunnel from the portal towards the collapsed area, the overlapping steel pipe umbrellas were applied. The tunnel face was reinforced by overlapping fibre glass bolts.

1.3 *Emergency escape shaft*

The planning process of the Březno Tunnel started well before the year 2000. At that time, according to the valid safety regulations, the emergency escape shaft was not required for the Březno Tunnel.

Due to the relatively long planning process and delay due to the collapse, the updated safety regulations valid in the time of works restarting in 2004, already required an intermediate emergency escape shaft for the tunnel length of 1.8 km. The Client decided to build the emergency escape shaft to comply with all the latest safety regulations.

2 SHAFT DESIGN

2.1 *Shaft location*

After careful consideration, it was decided to locate the shaft directly above the buried machine and in this way to make the removal of the machine much simpler than would be from the mined tunnel.

The shaft was not located directly above the tunnel axis; shaft axis was shifted approximately 1.5 m of the tunnel axis.

2.2 *Geological conditions*

The entire area in which the shaft construction took place was a part of former tunnel collapse. Immediately after the collapse few boreholes were drilled in the collapse area and basic tests performed. The results gave relatively low geotechnical parameters, as could be expected.

Because the time period between the collapse and the shaft construction was more than two years, it

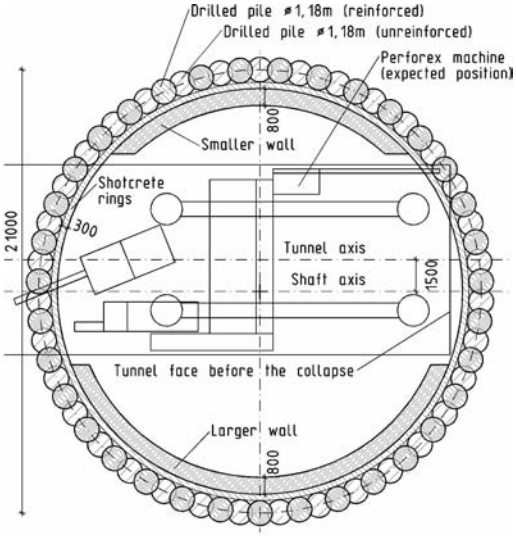


Figure 1. Shaft cross section.

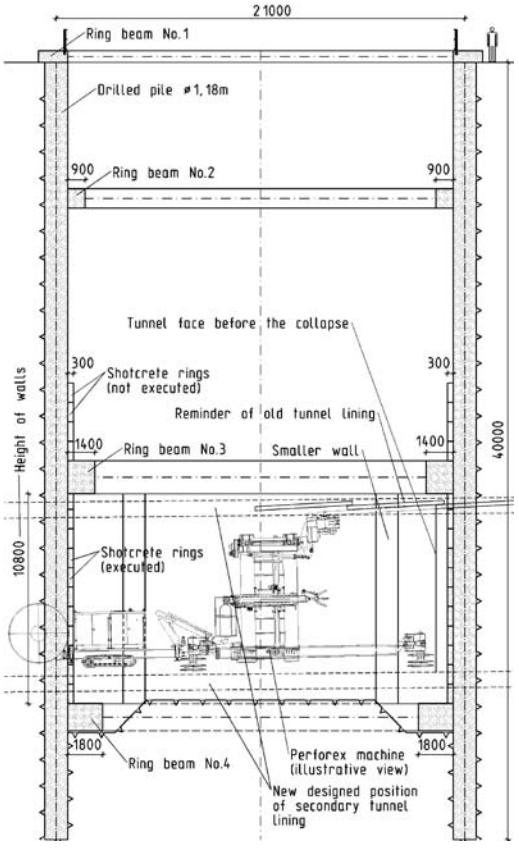


Figure 2. Shaft longitudinal section.

was decided to verify the geotechnical conditions by one borehole (core drilling), located inside the shaft. Besides gaining samples for basic laboratory tests, the aim was to find eventual voids or larger empty spaces. The ground water conditions were also a concern.

Naturally, the conditions for shaft construction were considerably affected by presence of buried Perforex machine, together with utility lines and collapsed primary lining.

The results of core drilling were surprisingly good, the material in the area was "consolidated" and dry. This was also confirmed by piles drilling.

2.3 *Secant piles*

The shaft lining consists of 70 secant piles, with diameter of 1.18 m, distance of their axes 0.942 m and piles' length 40 m. The diameter of the shaft is 21 m (measured to the piles' axes) and depth of the shaft is 35 m. Every second pile is reinforced by 32 mm rebars. The shaft cross section is shown on Figure 1.

For the successful construction process the verticality of piles was of paramount importance; a tolerance of 1% of the drilled length was given to the contractor as a maximum allowed deviation.

In some areas it was obvious that the pile will during the drilling hit steel parts of buried machine; in such case the drilling was supposed to be stopped and the space between two adjacent piles filled by steel braces and shotcrete.

2.4 *Grouting*

Before pile drilling a total number of 29 grout holes (diameter 50 mm) provided by PVC pipes was drilled in the shaft area and grouted with approximately 750 cubic meters of cement grout. Obviously, some open spaces around the machine and collapsed lining contributed to the relatively large grout consumption.

2.5 *Other structural members*

The need to consider construction tolerances (especially piles deviations from the vertical) and construction of two large tunnel openings after shaft completion, led to the design of other structural members; namely four large cast concrete reinforced ring beams (No. 1 to 4), reinforced shotcrete rings and two walls between the ring beams No. 3 and 4 (see Figure 2).

The large reinforced ring beams (height 1.7 m, thickness 1.4 m), were designed to support the pile lining. Their installation was proposed as part of shaft excavation process, after reaching ring beam bottom level.

Shotcrete rings installation was depending on vertical tolerances of piles. Their height was 1.0 m and thickness 0.30 m. Their installation during the



Photo 1. Shaft lining – piles and ring beams.

construction was proposed to start 4 m above the ring beam No. 3.

Two heavily reinforced walls, between the beam rings No. 3 and No. 4 were designed to be cast after the shaft excavation completion. Their purpose was to provide support to the shaft lining (secant piles), after its integrity is disrupted by two large tunnel openings.

2.6 *Structural analysis*

The structural analysis presented extremely difficult part of the shaft design process. The reasons were complicated geological conditions in the space of former collapse, unique construction scheme (e.g. no possibility to use anchors) and not predictable positions of piles with increasing shaft depth. To ensure the safe function of the whole system, a probability model of piles' position was prepared and based on the results the specified deviation for the pilot drilling was established max. 1%. The standards for pile drilling use the value 2%.

The analysis took relatively long time, before it was possible to prove sufficient safety margins of the shaft lining design. Considerable help with the analysis came from A. Zapletal (Metrostav a.s.) and J. Masopust (Zakládání staveb a.s.).

3 SHAFT CONSTRUCTION

3.1 *Pile drilling*

The construction of the shaft was subcontracted by Metrostav a.s. Prague to the Zakládání staveb a.s. Prague, Czech Republic.

The pile drilling was performed by AU BG25 machine; the subcontractor made a very good job resulting in minimum deviations of piles from vertical direction (see Photo 1).

The drilling started in February 2006 and was completed in March 2006. Totally 3 piles hit the steel structures of Perforex machine and were not drilled to the full prescribed depth.



Photo 2. Ring beam No. 3 – heavy reinforcement.



Photo 3. Buried Perforex machine and remainder of collapsed tunnel lining.

3.2 *Shaft excavation*

After piles completion, the ring beam No. 1, located on top of the piles was built.

The shaft excavation started in April 2006. After reaching the bottom level of ring beam No. 2, relatively heavy reinforcement was installed, followed by formwork installation. The same procedure was re-peated during the shaft excavation for beam rings No. 3 and 4 (see Photo 2).

Below the level of ring beam No. 3 was the buried Perforex machine, which considerably complicated the excavation works (see Photo 3).

Because of minimum deviations of piles from the vertical direction, shotcrete rings were installed as late as 3 m below the ring beam No. 3 and their installation continued until the shaft bottom was reached.

The last construction members built were two walls, fixed to the beam rings No. 3 and 4, located on the sides of future tunnel opening. Due to the shaft eccentricity towards the tunnel, one wall was larger than the other one.

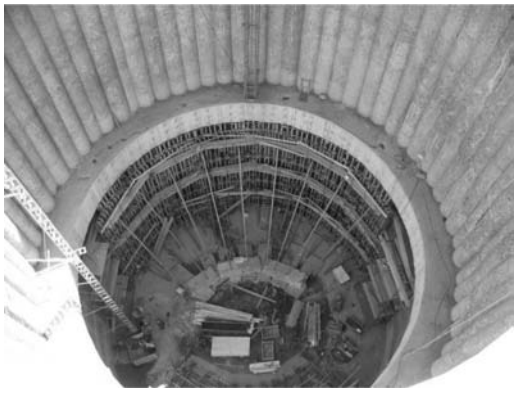


Photo 4. The formwork of the larger wall.



Photo 5. Tunnel breakthrough to the shaft.

Difficult technical task was to provide formwork and find the optimum procedure for casting the concrete of the walls between the ring beams No. 3 and 4. The walls are relatively high (10.8 m), the designer insisted on casting the entire wall without horizontal cold joint; later was agreed to cast one of the walls in two parts. Walls construction presented problems with support of formwork and concrete casting.

Two different methods were applied. Larger wall was cast using self-compacting concrete, with precise timing of casting, depending on the sufficient strength of previously cast layer, but still not creating cold joint. This wall was cast without cold joint (see Photo 4).

For the smaller wall one cold joint was allowed and one-sided formwork was used.

The first opening for the tunnel mined through the previously collapsed tunnel was broken through in July 2006, the breakthrough of the second one for the tunnel mined from the opposite portal was in October 2006 (see Photo 5).

3.3 *Geotechnical monitoring*

To monitor the behaviour of the shaft lining during the construction, six inclinometers were installed in the piles; eight of measuring points in five levels for geodetical measurements were installed on ring beams and piles. Based on construction progress, inclinometers and measuring points were regularly monitored during the whole construction period.

The measured values were very small, no significant movements were monitored during shaft excavation; after tunnel breakthrough expected small deformations on sides of openings were monitored.

3.4 *Main problems encountered during construction*

The shaft construction went relatively smoothly, without any significant problems.

Few problems were encountered during the start of the shotcrete application to build shotcrete rings, which were fixed immediately.

As already mentioned, the buried Perforex machine made the excavation in its vicinity relatively complicated.

4 CONCLUSION

The design of 21 m diameter and 35 m deep shaft in the area of collapsed tunnel proved to be a difficult task, with many unknown features.

The designer had to deal with complicated structural analysis, in some cases using non conventional approach. But even in such circumstances the designer used flexible approach and provided the possibility to change the construction process and the designed structural members, depending on actual conditions, namely geological conditions and accuracy of piles drilling.

Thanks to high quality pile installation there was possibility to take advantage of mentioned flexibility and reduce some of the proposed measures, which would complicate the construction process. The shaft construction was therefore shorter by 2.5 months than was expected according to the original construction schedule.

Underground Space – the 4th Dimension of Metropolises – Barták, Hrdina, Romancov & Zlámal (eds)
© 2007 Taylor & Francis Group, London, ISBN 978-0-415-40807-3

Repair and reinforcement of damaged tunnel by Acid Mine Drainage (A.M.D.)

Lee Yu-Seok, Yoon Tae-kook, Shin Yong-Suk & Han Ja-Jung
Manager, Korea Infrastructure Safety & Technology Corporation(KISTEC), KOREA

ABSTRACT: This study was carried out in order to figure out the effects of Acid Mine Drainage (A.M.D.) generated from abandoned mines on the adjacent Bam-Je tunnel which is located in Kang-Won province, Korea. To complete this study, visual inspection and G.P.R as well as geological, geographical, water analyses are implemented, and these methods enabled us to identify how influx of A.M.D. cause damages on the tunnel. In addition, based on various experimental supports, we have set up and displayed how to repair and reinforce the damaged areas of the tunnel caused by A.M.D.

1 INTRODUCTION

There are more than 900 metal and mines in Korea, which are currently being mined or exist as abandoned mines. It's reported that hard coals are mainly produced from the coal mines, and gold, zinc and copper are mined from the metal mines. These mining activities, however, cause some serious problems that undermine surrounding environment and we call the result of the problems as "The mine damage" This mine damage is usually caused by some factors which are contaminated water generated from mines, acid mine drainage, and collapse in abandoned mines.

This study was carried out in order to figure out the effects of Acid Mine Drainage (A.M.D.) generated from abandoned mines on the adjacent Bam-Je tunnel structure which is located in Kangwon province, Korea. To complete this study, visual inspection and G.P.R as well as geological, geographical, water analyses are implemented, and these methods enabled us to identify how the influx of A.M.D. cause damages on the tunnel. In addition, based on various experimental supports, we have set up and displayed how to repair and reinforce the damaged areas of the tunnel caused by A.M.D.

Table 1. Specifications of tunnel.

Location	Kang-Won province, Korea.
Shape	Horseshoe-shaped section
Type	Railroad tunnel
Construction method	Conventional method(ASSM)
Length	1,825 m
Year of completion	1963



Jung-Dong-Jin Way



Abandoned Mine and A.M.D.

2 BAM-JE TUNNEL

The Bam-Je Tunnel is located between Ok-Ge and Jung-Dong-Jin in Kang-Won province and was completed in 1960. It is a horseshoe-shaped single track railroad, and its lining is made up of concrete. It was built by means of a conventional method (ASSM). Since the completion, its concrete lining has repaired and reinforced the damaged areas of the tunnel caused by cracks and leakage 10 times for 40 years. Thus, the repaired areas with liquid water proofing and powder water proofing in its interior structure are found. Furthermore, cracks, leakage and exfoliation exist over its whole interval since the concrete lining was built with hand work a long time ago.

3 ΔΔ MINING STATION

3.1 *Y-Y region*

Y-Y region of the ΔΔ mining station is an area including the start point of the Bam-Je tunnel.

Its surrounding geological layers are tilted about 20–40 degrees toward northeast. The "7th Y-Y pit",

the central area of Y-Y region, has repeating an anticline and synclinal structures, and the axis of fold is toward northeast. This area had been developed until the year of 1989, and now abandoned mine as a coal industry promotion policy. Total 6 pits including "Y-Y developing pit (103 ml)" have been built, and coal are mined. While the time of mine development, totally 4,400 tons were produced and it has been reported that the coal quality was 4,000 kcal/kg, which is good.

3.2 *H-H region*

The surrounding geological layers of H-H region are inclined at approximately 50 degrees toward northeast. It had been mined until the year of 1989, producing 1,800 tons, and then abandoned mine as a coal industry promotion policy.

3.3 *Bam-Je tunnel and ΔΔ mining station*

A number of abandoned mines in ΔΔ mining station was detected and for the effect of that, abandoned mines in ΔΔ mining station and cross section of a geological stratum, <fig. 1, 2> are shown. Also, <fig. 1> is shown the pH about ground water, which is the neighborhood tunnel. The Bam-Je tunnel is located within "Hong-jum series". Carboniferous period in Paleozoic Erathem and there is an expressway above the tunnel of which ground level from the tunnel is 40 m. The tunnel is at intervals of 130 m far from a planned Dong-He expressway route and 260 m far from the nearest abandoned mine.

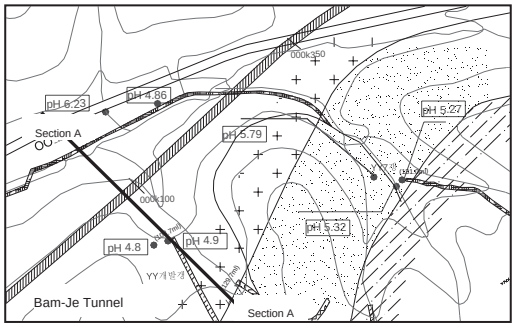


Figure 1. Bam-Je tunnel and surface water pH around ΔΔ mining station.

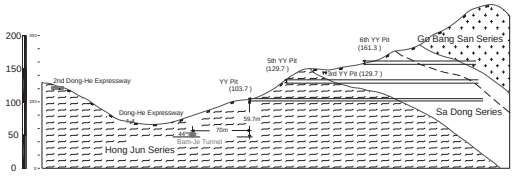


Figure 2. Bam-Je tunnel and ΔΔ mining station (Section A-A).

4 MINE DAMAGE

"The mine damage" is an environmental pollution caused by mining or development of underground natural resources. The mine damage happens due to lack of consideration for natural environments while developing mines or after closing mines. The significant is that the mine damage lasts for a very long time and has seriously unpleasant effects on natural environments and human living circumstances. In addition, the mine damage occurs more often in inactive mines and closed mines rather than the ones under mining.

The mine damage is mainly classified as follows

- The influx or leakage of acidic water containing heavy metals
- Wash away of gobs and efflux of poisonous sludge
- The ground settlement around the mine
- Scattering of fine aerosols or dusts in dry seasons

If we don't take an action for restoring or repair on the areas where the mine damages happen, it's certain that the impact of mine damage will expand and result in serous environmental and social problems.

4.1 *The mine damage caused by mine drainage and wastes*

A sulfide of iron is one of main factors that compose of many metalic mineral, and it is contained with significant amount in a layer that has a lot of organic compounds such as coal. The sulfide of iron mainly consists of sulfur and metal elements that are combined to the sulfur. These would be preserved consistently as long as there is no material interchange with the exterior surroundings and little change in temperature and pressure. However, the metalic mineral and sulfide in coal layer can be dissolved or oxidized when contacted with the air or water that contain dissolved oxygen. This matter usually happens while building a pit mouth or removing an upper-level layer in order to mine metalic mineral or to develop coal layer.

Among sulfide, pyrite has the most effect on the acidification of wastewater produced from mines. pyrite is often observed in metalic ore and is contained a lot in coal layer. If there is a significant activity of microorganisms in the interaction between water and pyrite and in the oxidation between those two, the consistent oxygen supply needed in the interaction between pyrite and underground water and the residence time for the interaction play a very crucial role in the acidification of the wastewater. In fact, the wastewater around abandoned mines shows very low pH. It's because while the underground water that has dissolved oxygen runs along with abandoned mine, the

water is allowed to have enough time to interact with pyrite. However, the acidification of the wastewater is little in active mines since the reaction time between pyrite and the underground water is relatively short due to an artificial drainage.

The theoretical chemical procedures of acidic wastewater containing heavy metals are like followings:

$$2FeS_2 + 2H_2O + 2FeSO_4 + 2H_2SO_4 \quad (1)$$

$$4FeSO_4 + 2H_2SO_4 + O_2 \rightarrow 2Fe(SO_4)^3 + 2H_2O \quad (2)$$

$$Fe_2(SO_4)^3 + 6H_2O \rightarrow 2Fe(OH)_3\downarrow + 3H_2SO_4 \quad (3)$$

$$7Fe_2(SO_4)^3 + FeS_2 + 8H_2O \rightarrow 15FeSO_4 \quad (4)$$

The hydroxide generated from the procedures produces yellow, brown or red sediment along with the wastewater way. We call the sediment "yellowboy." If wastewater is once produced, even though there is no oxygen, the oxidation of pyrite can be proceeded. From the oxidation procedures of pyrite above, Fe^{2+} or SO_4^{2-} saturated wastewater occurs and the quality of the wastewater is various depending on the kinds of pyrite and the magnitude of chemical reaction with surrounding materials.

4.2 *The mine damage caused by ground settlement*

The mining activity produces underground cavity . If cavity doesn't fill back and a balance between pressures and stress forced from upper-level layers is lost, cavity is subject to collapse. If the stress working in the upper-level is less than a ground strength at cavity roof or pillar, there would be no damage. However, the damage or destruction of cavity can happen due to a reduction of the ground strength, a creep transformation of ground and a water migration caused by seepage pressure with the passage of time after the start of mining. Specifically, over a short or long time interval, high humidity of cavity changes the strength of rocks and causes deformability. Also, the underground water in fragmental zone of fault which is a weak part in geological structures weakens the strength of ground.

5 INSPECTION (DIAGNOSIS)

Topographical, Geological inspection, Boring test and non-destruction test etc. were carried out to figure out the condition of tunnel and area around the tunnel.

5.1 *Visual inspection*

Some damages such as cracks, leakage and exfoliation are observed over the whole tunnel including the original concrete lining and the repaired and reinforced concrete lining. In the Figure 3, we can see a water leakage at the boundary between original concrete lining and repaired area on the ceiling where it was built with liquid water proofing. Specifically, the leakage in the right-side wall is very serious. Furthermore, a large amount of efflorescence is produced along with the right-side wall. Considering the tunnel's location close to abandoned pits such as y-y developing pit, y-y 3rd pit and 5th pit, water examination was also carried out.

5.2 *Water experiment*

In order to analyze and figure out the effects on the concrete lining durability of the tunnel, we took surface water and incoming water that leaks into the side of concrete lining at three places and implemented tests on the content of harmful ions. The focus of the test was pH, dissolution evaporation residue, SO_4^{2-}, Cl^-, Na^+, Mg^{2+}, K^+ and Ca^{2+} etc. Figures from the test were compared with the ones from lakes and swamps. The results are shown in the Table 2.

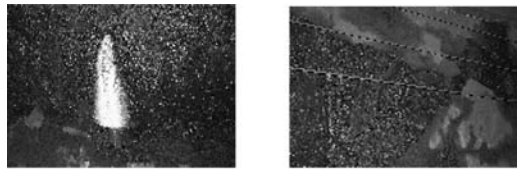


Figure 3. Leakage (Left: the influx of acid mine drainage(pH 4.7), Right: normal leakage).

Table 2. Water experiment (mg/ℓ).

Station	pH (20°C)	Dissolution evaporation residue	SO_4^{2-}	Na^+	Ca^{2+}	K^+	Cl^-	Mg^{2+}
000k030-RW	6.3	420	373	3.14	91.9	2.42	6.60	28.3
000k189-LW	7.8	4.27	54.4	1.93	32.3	2.12	6.57	4.27
000k350-LW	4.7	3.01	56.3	1.16	11.3	3.26	6.83	3.01

The pH of 6.3 and 7.8 at the locations of 000k030 and 000k189 respectively don't seem to harm or damage the tunnel's concrete lining. It is also regarded that the small content of Mg^{2+} and SO_4^{2-} would not harm the concrete lining. However, the 4.7 pH at 000k350 may have a harmful effect on the concrete lining. Thinking about nearby abandoned mines and geological state, we assume that pH is affect by abandoned mine drainage.

5.3 *pH test for abandoned mine water and surface water*

Since A.M.D. was observed, to figure out how the A.M.D. flew in and the acidity of the interior of the closed abandoned mines, we had taken the pH test with ph-meter on the leakage area in the tunnel, closed mines around the tunnel, and surface water. The test results in tunnel and out are listed in the Table 4 and Figure 1.

The pH range of abandoned mine entrance and of surface water around the entrance was recorded at between 4.8 and 5.79(Figure 1). The pH of incoming water leaking to the tunnel and the one of surface water above the tunnel were compared. In case of Y-Y developing pit, mine drainage has reached the entrance of the pit mouth and leakage and efflorescence have been observed over the tunnel areas to which it's assumed that mine drainage leaks. From this observation, A.M.D seems to have harmful effects on the tunnel structure. There is a feasibility that concrete lining might be damaged or ground slackness would happen due to continuing influx of A.M.D. So, we need to take an immediate action for solving the A.M.D. problem.

Table 3. pH and influence on concrete.

pH	Influence on concrete	Decision
∼ 4.0	Melting Cement	Danger
4.1∼5.0	Unevenness on surface	Danger
5.1∼6.0	Infirm onsurface	Caution
6.1∼7.9	Caution early age	Safety
8.0∼	Safety	Safety

Table 4. pH in tunnel.

Station	pH	Station	pH
000k080	4.99	000k441	7.45
000k341	7.52	000k502	7.64
000k350	5.56	000k571	6.18
000k353	7.26	000k735	7.53

6 HOW TO REPAIR AND REINFORCE THE DAMAGED AREAS

In order for A.M.D. not to flow into the tunnel, the tunnel concrete lining has to prevent a water leakage incoming into some areas of the tunnel where waterproof is not applied. In addition, a proper method of the injection for cavity usually happening on the ceiling of the tunnel between bedrock and tunnel concrete linings should be considered carefully. We need to take some considerations for first, the works of grouting on the leakage areas and cavity areas, and second, for selecting inorganic cement needed in injection. Among many considerations, the most important one is to check out the change of concrete strength and the decreasing rate of weight caused by loss of cement element. Ordinary Portland cement (C1), Sulphate Resistance Portland cement (C5), Blast Furnace Slag cement (SC), and Blast Furnace Slag cement and fine powder mixture 55% (SM) were taken for the experiment and the results are as follows.

6.1 *Considerations about acidity*

The experiment was implemented by putting the 4 cement samples into sulfuric acid. The focus of this experiment was to find out the most effect of the strength of concrete and mass ratio on the stability of the tunnel. In the experiment, it was found that the decreasing compressive strength of C1 and C5 had been very steep as the time had gone by, while the compressive strength of SC and SM had showed an increase for 28 days, and then had decreased after that.

We also examined the change of weight ratio in order to figure out weight change of cements caused by acidic erosion. In the exam, we observed that mass of C1 and C5 had decreased rapidly along with soaking acid while the one of SC and SM had showed a very slight change or even had increased. From the X-ray experiment, it's found that $Ca(OH)_2$ is produced less, has more resistance against sulfuric acid. In the following list, $Ca(OH)_2$ is produced less in a order respectively: C1, C5, SC, and SM. Thus, category such as SC and SM which produce the least amount of $Ca(OH)_2$ has the most resistance against acidity.

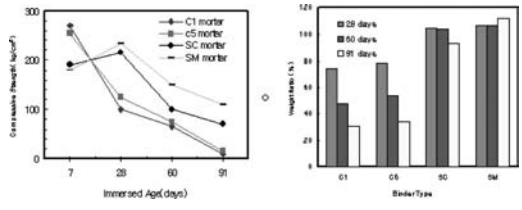


Figure 4. About acidity (Moon, ph.D., 1996).

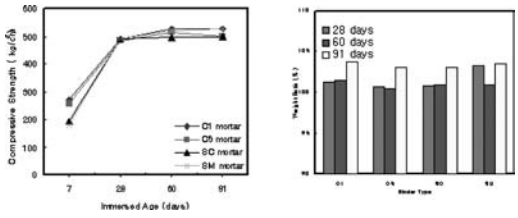


Figure 5. About SO_4^{2-} (Moon, ph.D., 1996).

6.2 *Considerations about SO_4^{2-}*

We took another experiment, putting the 4 cement samples above in sulfate solution. This experiment showed that there had been little change in compressive strength. And regardless of time, in the experiment of weight ratio change against sulfate, the weight of mortar has a little heavier than the one of water curing.

6.3 *Method of repair and reinforcement*

Leakage usually happens in places of crack, construction joint, and insufficient waterproof, and its magnitude depends on the conditions of layers and a structure. So how to repair the leakage relies upon the condition of leakage. Considering concrete's erosion and harmful effects on surrounding layers due to A.M.D. incoming from abandoned mines in ΔΔ mining station adjacent to the tunnel, it seems that the damaged areas are need to be repaired and reinforced with Sulphate Resistance Portland cement grouting that fights well against acidity and Blast Furnace Slag cement and fine powder mixture 50–55%. Also, adding an liquid water proofing to cement during construction helps to prevent water leakage behind concrete lining. As a sub-method, it's recommended that the drainage channel method on the face of concrete lining should be applied.

About cavities of lining, Lightweight form grouting is recommended to prevent stress by self weight, which is caused by mass above the tunnel's ceiling while filling back.

And about affected A.M.D. cavities, Sulphate Resistance Portland cement grouting and Blast Furnace Slag cement and fine powder mixture 50–55% is recommended.

6.4 *How to select areas influenced by A.M.D.*

To find out the areas influenced by A.M.D. in the tunnel, we have used the results of geological, topographical and water examinations. Using these results, we have selected two places close to an abandoned mine in the east of □□ mountain and another area (extended length 340 m) where acidic water incomes into the tunnel. From the observation showing that the leakage was concentrated more seriously on the right side of the tunnel and acidic water was also found there, it's been assumed that the path of A.M.D. is surface water way along with valleys rather than a path along with fault of bedrock.

7 CONCLUSIONS

In order to find out effects of A.M.D. from abandoned mines around the objective tunnel, visual inspection, water experiment, G.P.R, geological and topographical inspection were taken, and from the examinations results, we have found conclusion.

(1) The result of visual inspection, leakage was concentrated seriously on the right side of the tunnel. The result of water examination pH is 4.7 and specifically, as supposing, influx of A.M.D. section is produced a large amount of efflorescence and some erosion with leakage. For such reason, we have conclusion A.M.D. seems to have effects on leakage and the tunnel structure.

(2) The distribution of bedrock in the tunnel goes through the interior of "Hong-Jum series" consisting of limestone. And with an analysis of geology around the tunnel and a place of leakage it's been assumed that the path of A.M.D. is surface water way along with valleys rather than a path along with fault of bedrock and determined its influencing area.

(3) There are some main solutions for A.M.D. are like followings, as prevent generation of A.M.D., neutralize A.M.D. which is already generated and prevent A.M.D. from influx to a tunnel.

For the third solution above, on the basis of experimental results, it's suggested about leakage and cavity that grouting with mixed cements of Sulphate Resistance Portland cement grouting and Blast Furnace Slag cement and fine powder mixture 50–55% need to be applied.

REFERENCES

1. Jung-youp, kim and two others. 1995. Neutralization Process of Acid Mine Drainage from the Abandoned Donghae Coal Mine. *Journal of the Korean Society of Groundwater Environment* Vol2, No.1: pp.38–47.
2. Korea Railroad. 1998. *A study on the damaged tunnel.* Seoul: Korail.

This page intentionally left blank

Section 7
Distribution and management of risks and accidents during tunnelling

This page intentionally left blank

Underground Space – the 4th Dimension of Metropolises – Barták, Hrdina, Romancov & Zlámal (eds)
© 2007 Taylor & Francis Group, London, ISBN 978-0-415-40807-3

Data management for highly mechanized shield tunnelling in the construction of the Line 9 Metro Barcelona

Ing. Carme Deulofeu & Dipl.-Ing. Henning Schwarz
Gestió d'Infraestructures S.A. (GISA), Barcelona, Spain

Dr.-Ing. Ulrich Maidl & Ing. Marc Comulada
Maidl Consulting Engineers, Bochum, Germany

ABSTRACT: In shield tunnelling in urban areas a rapid reaction to unexpected situations requires an efficient data management. Practical experiences have shown how an optimum management, processing and evaluation of the available data provide a tool to react against initially unforeseen situations. Furthermore, data management allows optimizing shield tunnelling from the point of view of all the parties involved in the construction. The factors concerning safety, settlement minimization, tunnel lining quality, production maximization and cost minimization are taken into account. Since the planning phase of Line 9 Metro Barcelona, special attention has been focused on the management of the large amount of monitoring and shield machine operational data, as well as of the ground information from the soil investigation programs. The tunnel is built with three different shield machines under very dense urban areas and in heterogeneous ground conditions.

1 INTRODUCTION

To comply with the present safety standards and with demands on risk minimization, tunnelling methods are developing by the improvement of more realistic calculation models and also by the introduction of more efficient and safer construction methods. However, these factors have to be complemented by efficient controlling systems during construction.

The Metro Line 9 in Barcelona is a reference tunnelling project due to the large variety of geological and hydrological conditions which it encounters. Furthermore, the vast figures which characterise this Metro Line with a total length of shield driven tunnels of more than 40 km, large tunnel excavation diameters of 9,4 m and 12,0 m and the use of two earth pressure balanced (EPB) shields and one convertible shield TBM, give an idea of the magnitude of this project.

In a project of these dimensions it has become clear that Process Controlling needs to be part of an efficient Data Management system.

2 PROCESS CONTROLLING IN SHIELD TUNNELLING

In shield tunnelling a particular machine technology is applied to deal with ground conditions, which may be variable and partly uncertain.

Not only are the underground conditions determinant in shield tunnelling. Specially in urban areas, the surface conditions, with the presence of different types of structures and pre-existing underground infrastructures, also condition the performance of the tunnelling process.

Taking these facts into consideration, it becomes clear that any controlling system in shield tunnelling should be continuously oriented to the construction processes. Such a controlling system must also help to improve and accelerate the decision taking processes.

As well as in other construction methods, the complex shield tunnelling process is formed by a series of partial processes. Specially in shield tunnelling, these partial processes interact with each other, in order to successfully perform the ground excavation and to provide a safe ground support.

The control of the partial processes and their interactions is defined as Process Controlling.

2.1 *Process Controlling circuit*

The Process Controlling system has to be fed with data to provide the basis for a founded analysis.

Presently most shields are equipped with a large number of sensors which record the main operational parameters of the machine. This makes shield tunnelling specially adequate for highly automatised Process Controlling systems with an important number of

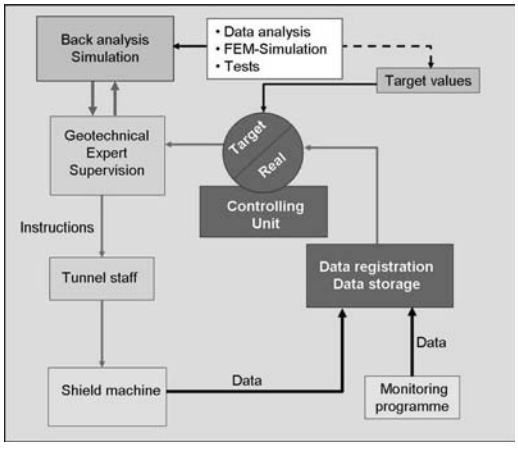


Figure 1. Scheme of the Process Controlling circuit in shield tunnelling.

treated data. The more significant data is provided, the more efficient will the Process Controlling system be.

The typical control circuit for state-of-the-art shield tunnelling is schematically represented in Figure 1.

The operational data from the shield machine are electronically registered and recorded. Additionally, the external monitoring programme provides data about the influence of the tunnelling process on the ground and on other infrastructures and buildings.

On the other hand, previously to the tunnel construction, the theoretical values for the machine operational parameters and for the interaction between the machine and the ground are determined. These theoretical values are set as initial target values for the shield drive.

On the basis of the estimations, previously to the TBM drive start, the first decisions can be taken concerning both, the shield machine operation parameters and the execution of additional measures. Such measures comprise ground improvement treatments and protective measures for buildings and infrastructures located in the influence area of the tunnel construction.

Once the tunnelling process has started, the controlling circuit is principally based on the comparison of the measured real values with the target values. This comparison is generally performed by the board of experts on-site, taking into account the geological and geotechnical characterisation of the ground, as well as other external conditions. The aim of this comparison is, to be able to take the appropriate decisions in order to adapt the construction process to the really encountered conditions.

A permanent check of whether the tunnelling process is behaving as expected has to performed through the comparison analysis. Then, if necessary, specific countermeasures have to be decided and carried out. Such countermeasures comprise changes in the machine operational parameters, as well as additional ground treatments or protection measures.

2.2 *Determination of the target values*

The expected theoretical values of the shield operation parameters and of the ground movements are obtained by calculations based on the existing ground models, theories and experiences in previous projects, Burland (2001). The simulation of the shield drive in complex conditions by means of numerical models is particularly convenient for the determination of the theoretical values.

As discussed in Maidl (2005), numerical models provide a realistic simulation of the tunnelling process, as well as a good estimation of the interaction between the shield machine, the ground and the buildings or other infrastructures. Thus, it is possible to obtain realistic values for the expected settlements under different assumptions concerning the shield machine operation and the ground conditions.

3 DATA MANAGEMENT

One of the main sources for the Process Controlling are the data from the construction process and from the monitoring program. Additionally, a great amount of information from the soil investigation programs is generated in tunnelling projects, before and during the construction phase.

Shield tunnelling is characterised by high production rates. Thus for the Process Controlling to be able to provide rapid responses to the needs of the shield drive, it is firstly necessary to have an organised and interconnected data management system.

3.1 *Monitoring data*

The monitoring data becomes an essential tool when tunnelling in urban areas. Only by monitoring the external effects of the tunnelling works, can any decisions concerning the TBM operation be taken. Therefore a georeferenced monitoring data system has to be installed and connected to other databases. Extensive information about monitoring is included in Dunnicliff (1993).

3.2 *TBM data*

The machine operational parameters measured by the different sensors installed in the shield machine are continuously registered and recorded. These data are generally available by real-time transmission, as well as in digital format in data files. By this way, both a real-time as well as a post-process access to the TBM data is possible at any time.

The number of registered parameters and the coding and structure of the data is different depending on the TBM manufacturer. From the experience of working

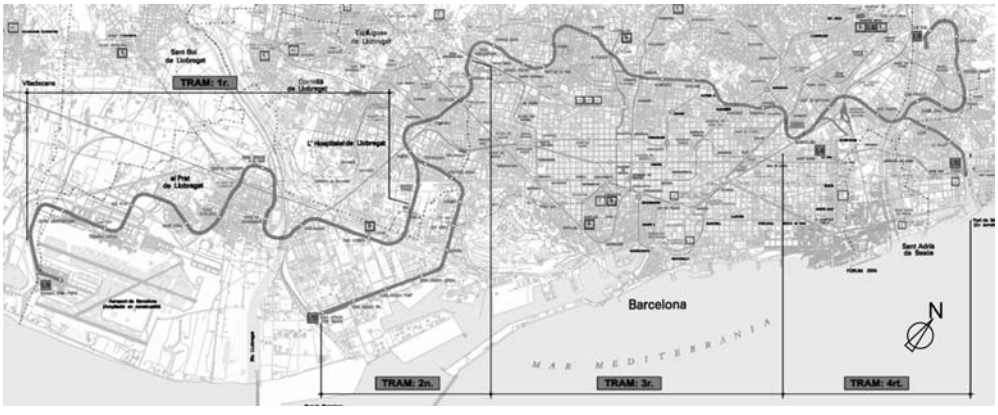


Figure 2. Ground plan of the Metro Barcelona Line 9.

with different TBM manufacturers, it has also become clear that a unified coding system for the machine parameters should be attained in future.

Taking into account that about 400 parameters or more are registered and stored in frequencies comprised between 10 to 60 seconds, it becomes clear that the management and processing of these data must be prepared to efficiently provide the required information for the Process Controlling.

3.3 *Geotechnical ground parameters*

The analysis of the interaction between the shield machine and the ground has to be based on the geotechnical characterisation of the excavated ground.

The geotechnical ground parameters are obtained from the soil investigations programs generally performed before the start of the works. However, new boreholes and tests are sometimes performed also during the construction phase, in order to provide additional ground information.

In large and complex projects, all this information ought to be easily available as well as updatable at any time, to allow an efficient and rapid analysis, as it has been done in the Barcelona Metro Line 9 project.

4 BARCELONA METRO LINE 9

4.1 *Project description*

The Barcelona Metro Line 9 project comprises a total tunnel length of approximately 45 km and the construction of 47 underground stations. As it is shown in Figure 2, through this completely new Metro line, Barcelona will be provided with new connections to the metropolitan area, north-west and south-east of the city of Barcelona. By this way the public transport system will take a new structure within the Barcelona Metro network. Additionally, new public transport connections will be created to strategic areas such as the airport, Barcelona's industrial area or the new high-speed railway station.

Most of the tunnel length is being built by means of shield machines. The construction methods for the rest of the stretch are the shotcrete method and cut and cover. Part of the Line 9 runs on a viaduct.

In total three shield machines take part in the construction of the tunnel sections. A 12 m EPB shield is in charge of the construction of about 11 km of the line, in different areas formed respectively by stiff Miocene conglomerate, Miocene marl, soft Quaternary alluvium soils and Pliocene claystones and siltstones. A second 12 m diameter convertible TBM shield has already excavated along 4,5 km through fresh to highly weathered granodiorite. About 10,5 km still have to be driven through different kinds of rock with several fracturing and weathering grades and also through faulted areas. Finally, a 9,4 m EPB shield is driving southwards for about 15 km, through the fine sands and silts of the Llobregat river alluvium. For more extended descriptions about the Line 9 project, please refer to Boté (2004a,b) and Tersol (2005).

The Client of the project is the public enterprise Gestió d'Infraestructures, S.A. (GISA).

Due to the length of the line and to the vast amount of information related to the project, GISA has implemented a Data Management system, including the Process Controlling software.

4.2 *Data Management in the Line 9*

This section describes the way that the Data Management is being performed for all the tunnelling construction lots of the Line 9.

To start with, there are two main groups which ought to be distinguished. On one hand there are data which are updated only in frequencies of several months, such as the geology, the topography or the information about the buildings and infrastructures.

On the other hand, there is a group of data which are regularly updated. These are, for instance, the monitoring data or the machine operational data.

The most representative data, the ground information, the monitoring data and the TBM operation parameters, and its management are described in this section.

4.2.1 *Geotechnical ground parameters*

All the existing borehole information and test results from the soil investigation program of Line 9 have been introduced in a database, named DINS-L9. Additionally, since the ground investigation program is being extended also during the construction phase, this database is continuously updated with new information.

The Contract to develop the access to this information through a Geographical Information System (GIS), has been awarded by GISA to the engineering consultant Eurogeotècnica.

Specially in such a large project as the Line 9, the possibility of accessing all the project data in one organised database allows to save time and to increase the analysis capacity of the engineering teams involved in the project.

4.2.2 *Monitoring data*

With the purpose of having a unified monitoring system for the whole length of the Line 9 project, GISA has grouped in one single contract the monitoring of all the construction lots which comprise the Line 9. The monitoring Contractor is a joint venture formed by Sol-Data Iberia, Applus and IIC.

Most of the monitoring performed in the Line 9 construction is oriented to the shield drive. However, extensive monitoring programs have also been developed for the construction of the station shafts. Additionally, the tunnel lining's deformations and stresses are monitored by means of instruments installed in the concrete lining segments and 3D-LADAR survey. Details of the monitoring program are provided in Bono (2004) and Soteras (2005).

The monitoring database allows all the data to be georeferenced, clearly identified and easily traceable. From the moment when the data are introduced into the database, this information is available at any moment via the Internet to each of the Contractors and Site Supervisors. In the case of the Line 9, the access to this data is performed through a project specific software developed by the monitoring Contractor.

GISA has also developed its own database, named MIDA-L9, to extend individual monitoring data into groups and to provide pre-analysis tool as well as connections to other databases.

4.2.3 *Process Controlling of the TBM drive*

The TBM operational data are automatically stored in the form of files on a computer at the jobsites. For the TBM data management, GISA is applying for the Line 9 a Process Controlling software (ProCon) developed by Maidl Consulting Engineers. This software reads the TBM data in the format given by the respective TBM manufacturer.

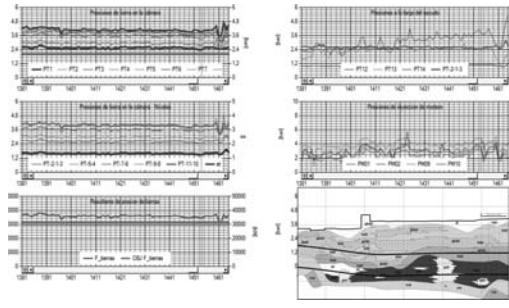


Figure 3. Process Controlling surface for the TBM data and correlation with the geological profile.

The way in which the data are processed and provided to the user for its assessment, is based on the premise stated earlier about the decomposition of the global shield tunnelling process in a series of comprehensible partial processes. The behaviour of each of the partial processes and their interactions shall be recognised as soon as possible by the site engineers.

This software is organised in a series of surfaces. Each single surface graphically represents the data for a given partial process of the shield drive. The surfaces for each of the partial processes are organised in a series of graphics, which allow to visually follow the correlations between different machine operational parameters. Figure 3 shows the general graphical distribution of the Process Controlling surfaces when working with the ProCon software.

Aiming to provide a global assessment which does not only include the TBM operation itself, but also the assessment of the interaction with the excavated ground, additional calculation parameters are also processed by the software. These additional parameters help to provide more complete information about important aspects of the shield tunnelling, such as the quality of the material flow in the excavation chamber, the pressure communication between the tunnel face and the ring gap behind the shield or the ground conditioning.

Additionally, the target values which have been set for specific TBM operational parameters along the tunnel alignment, are also represented on the corresponding surfaces in order to control that the tunnelling process is following the theoretically expected behaviour.

Since the interaction with the ground is one of the main aspects which has to be assessed, the software allows to superpose the geological profile on the graphical representation of the TBM data, as it is also shown in Figure 3.

For a complete analysis of the TBM drive and of its influence on the surface and on the surrounding structures and infrastructures, the Process Controlling software also allows to show selected data of the monitoring program to directly contrast it with the TBM operation.

Through the Process Controlling software, the time costly processing and organizing of the TBM data are avoided. This helps to react more rapidly when deviations of the expected behaviour in the tunnelling process occur. Process Controlling aims to be an effective decision-taking tool, by making a rapid processing and use of all the information available concerning the shield tunnelling process.

4.3 *Process Controlling case studies in Line 9*

Through the case studies presented here it can be seen how Process Controlling helps to understand the behaviour and interaction between the shield drive and the ground.

The case studies correspond to the 12 m EPB shield drive in the soft alluvium soils of the Besòs River delta. In this area difficult heterogeneous ground conditions were expected and have been encountered. The ground is characterised by the interbedding of sediment layers with a high variety of grain particle distributions. The tunnel face is variably composed by layers of medium grained sands (Qb2), gravels and blocks in a sandy matrix (Qb2g), clay and silts (Qb3) and coarse sands and gravel (Qb4). The tunnel is driven below a high groundwater table.

4.3.1 *Face pressure control and ground conditioning*

The settlement curve in Figure 4 shows how, around ring 1000, a gradual increase of the surface settlements has been measured. The control of the TBM operational parameters shows a coincident gradual decrease of the earth pressure in the crown area in the excavation chamber. This correlation between the supporting pressure decrease and the increase of the surface settlements seems clear, however the causes for the loss of control of the supporting pressure are complex.

Additionally, around ring 1000 an increase of the cutterhead torque between 25% to 30% occurs. Generally the magnitude of the cutterhead torque is related to the properties of the excavated ground. Once the tunnel geological profile is superposed, it can be seen that at the point when the torque increase occurs, the clay and silt layer (Qb3) disappears from the tunnel face. This means that the plasticity of the ground in the excavation chamber has reduced and, thus, its internal friction increases. This is directly related to an increase of the cutterhead torque.

After some rings, a drastic reduction of the injected foam flow occurs. This is reflected by the FIR (Foam Injection Rate) parameter shown in Figure 4.

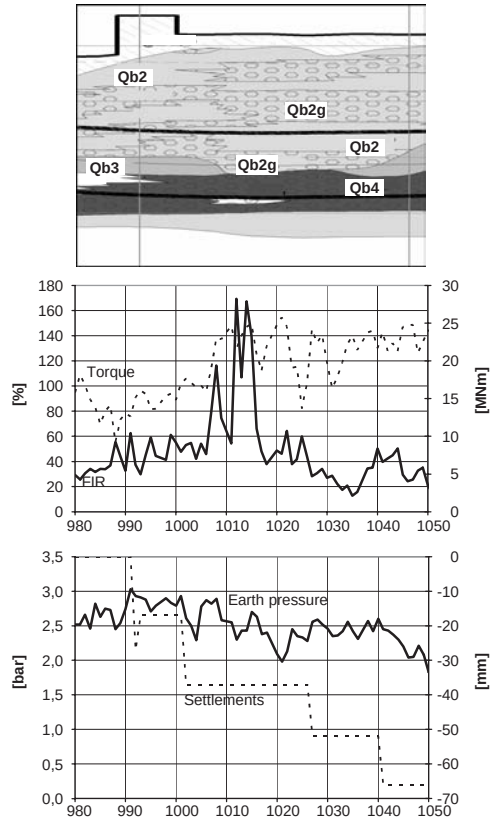


Figure 4. Application of the Process Controlling for the analysis of the TBM-ground interaction (Case study 1).

Generally, in EPB tunnelling the combination of reduced ground plasticity, together with a decrease of the conditioning of the excavated material automatically yields the hindrance of the material flow from the tunnel face to the screw conveyor. At the same time this complicates the control of the supporting pressures in the excavation chamber. Eventually, the supporting pressure becomes too low and the surface settlements increase, as the tendency between rings 1000 and 1050 shows.

After the corrective measures were adopted, i.e. improvement of the foam ground conditioning, the supporting pressure and thus, the settlements could be controlled.

4.3.2 *Improvement of the ground support pressure between the tunnel face and the ring gap*

In comparison to conventional EPB shield technology, the shield machines of the Line 9 are equipped with an additional injection system around the shield shell. This system allows injecting a grout or bentonite suspension between the shield and the ground. The aim of

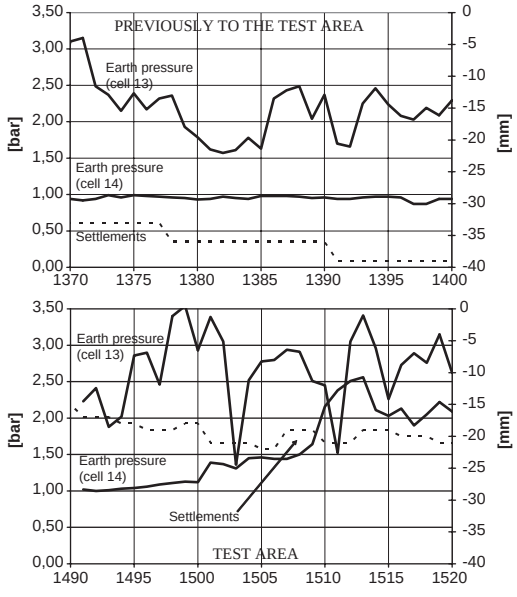


Figure 5. Application of the Process Controlling for the analysis of the TBM-ground interaction (Case study 2).

this system is to provide a more active control of the ground support along the shield.

The active control of the pressure from the tunnel face until the grout injected ring gap should allow to control the ground decompression and the ground deformation. Eventually, this should result in a reduction of the surface settlements.

For this reason a test stretch was performed where a controlled injection of a bentonite suspension around the shield shell was carried out.

Figure 5 shows the pressures measured by the pressure cells 13 and 14 which are installed on the outside of the shield shell at the crown area.

Before the test stretch, settlements generally lied between 30 mm and 40 mm, as it can be seen in Figure 5 between rings 1370 and 1400. In the test area however, a reduction of the ground settlements of up to 50% was measured between rings 1490 and 1520 (Figure 5), in comparison with the previous section.

The analysis of the TBM operation data shows a correlation between the reduction of the settlements and an increase of the pressures measured by cells 13 and 14. Cell 13 is located closer to the tunnel face and therefore it is more influenced by the face support pressure. This shows that the shield shell injection has improved the pressure communication along the shield. This has resulted in a better support of the tunnel profile ground, i.e. lower decompression of the ground stresses, and an improved grouting process in the ring gap behind the lining segments. Consequently, the final surface settlements have been reduced.

5 SUMMARY

The data related to tunnelling projects, which includes the monitoring data, the TBM operational data and the results of the soil investigation programs are a valuable source of information. All these data should be used and updated during all the different phases of a project.

Data Management is the tool to provide all the available and necessary information for Process Controlling in shield tunnelling.

Shield tunnelling is characterised by high tunnel production rates. In order to satisfy the needs of the construction process, one of the main aims of Process Controlling is to allow processing the large amount of available data rapidly, so as to reduce the reaction time against any deviations from the expected conditions and behaviour. This way, the decision taking process for the performance of countermeasures can be accelerated.

The application of Process Controlling in the Metro Barcelona Line 9 project, in combination with an organised Data Management system, is providing positive results as it has been shown in two case studies in this paper.

REFERENCES

Bono, R. 2004. Barcelona New Line 9 Metro. *Proceedings International Congress on Mechanized Tunnelling: Challenging Case Histories, Turin, Italy, 16–19 November 2004*. Torino: GEAM-Associazione Georisorse e Ambiente.

Boté i Frech, R. & Schwarz, H. & Comulada, M. 2004a. Erfahrungsstand im Tunnelvortrieb mit zwei 12 m Schilden für die U-Bahn Linie 9 in Barcelona. Bauingenieur 79. 253–263.

Boté i Frech, R., Schwarz, H. & Maidl, U. 2004b. U-Bahn-Linie 9 in Barcelona. *Tunnel* 8: 8–20.

Burland, J.B., Standing, J.R. & Jardine, F.M. 2001. *Building response to tunnelling. Case Studies from Construction of the Jubilee Line Extension*. London: Thomas Telford Publishing.

Dunnicliff, J. 1993. *Geotechnical Instrumentation for Monitoring Field Performance*. New York. Wiley-Interscience.

Maidl, B., Maidl U. & Ruse, N. 2005. Erfahrungen mit der FEM-Simulation im Rahmen des Prozesscontrollings beim Schildvortrieb. *Bauingenieur* 80: 337–342.

Soteras Aras, M., Ema Domingo, C. & Schwarz, H. 2005. Instrumentación y auscultación durante la construcción de túneles y estaciones de la futura Línea 9 del Metro de Barcelona. *Ingeopress* November: 40–47.

Tersol, M. & Schwarz, H. & Comulada, M. 2005. Doppelstöckig ausgebauter U-Bahn-Tunnel mit grossem Durchmesser für die Linie 9 in Barcelona. *Bauingenieur* 80: 387–394.

Underground Space – the 4th Dimension of Metropolises – Barták, Hrdina, Romancov & Zlámal (eds)
© 2007 Taylor & Francis Group, London, ISBN 978-0-415-40807-3

Tunneling in water-bearing unconsolidated ground according to specifications for auxiliary methods revised to reflect varying soil conditions – Construction in the north work section of the Takaoka Tunnel on the Hokuriku-Shinkansen railway line

F. Furukawa, Y. Hino & H. Inoue
Maeda Corporation, Nagano, Japan

H. Inoue
Maeda Corporation, Tokyo, Japan

K. Asari & J. Yorita
Japan Railway, Construction Transport and Technology Agency, Nagano, Japan

ABSTRACT: The 3,990-m-long north work section of Takaoka Tunnel, is being excavated using the short bench cut method based on NATM. The ground is unconsolidated throughout the tunnel length and the groundwater level is above the tunnel. Excavating the tunnel in the water-bearing unconsolidated ground was required. Disturbances were therefore of concern such as the failure of tunnel face or tunnel crown and large-scale liquefaction. In order to avoid such risks, auxiliary methods were adopted such as long forepoling for tunnel crown with a multiple packer sleeved pipe system using water glass grout and long forepoling for supporting tunnel face. A decision was made to flexibly adopt according to the soil condition with a view to achieving high cost effectiveness, because the geology consists of alternate layers of sand, gravel and silt and transverse folding and anticlines were found.

1 INTRODUCTION

Auxiliary methods including those with long forepoles have recently been used for tunneling in water-bearing unconsolidated ground on an increasing number of occasions. Unconsolidated ground with shallow depth frequently consists of alternate layers of sand, gravel and other materials and exhibits a lens-shaped body owing to the mode of sedimentation. The characteristics of the ground never remain unchanged over a long distance. In such a soil condition, adopting the pattern of an auxiliary system and materials that have been determined in the design phase without any modification would be detrimental not only to the effectiveness of soil stabilization but also to cost performance. Flexibly applying materials and determining the length of drilling a steel pipe per shift according to the soil condition would be important. In the north work section of the Takaoka Tunnel, construction is being carried out varying the material to be injected for soil stabilization, injection specifications and the range of injection according to ever changing soil conditions regardless of the predetermined design. Tunnel excavation has been progressing smoothly without any serious accidents. It has been found although the construction is still in progress that the twin tube double packer system is highly effective for making the best use of long forepoling in water-bearing unconsolidated ground and that downward cutoff from the upper half of the working face using injection piping used by the system is effective for controlling water seepage. This paper describes the process of implementation of auxiliary methods.

2 PROJECT OUTLINE

The Nagano-Kanazawa section of the Hokuriku-shinkansen railway line is being constructed by the Japan Railway Construction, Transport and Technology Agency based on the National Shinkansen Railway Development Law. The length of construction between Nagano City and Kanazawa City via Joetsu, Uozu, Toyama and other cities is approximately 230 km (Figure 1).

The Takaoka Tunnel on the Hokuriku-shinkansen railway line has a length of 6,938 m and penetrates a hill between Takaoka and Nagaoka in the city

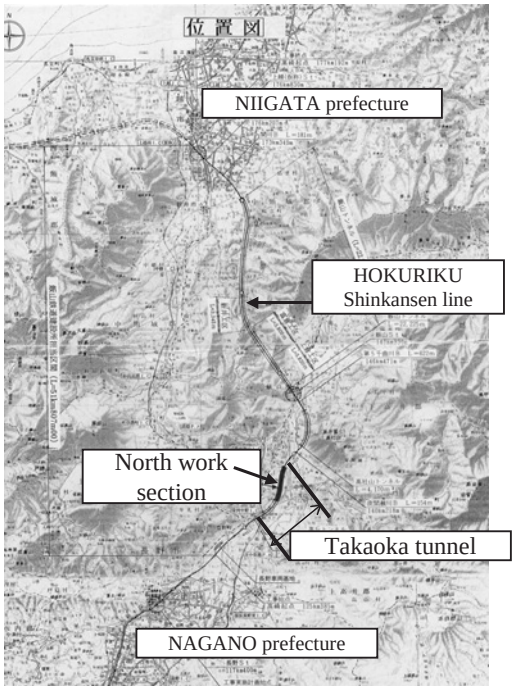


Figure 1. Location map.

of Nakano, Nagano Prefecture. Construction over a length of 3,990 m will be carried out in the north work section on the side of Joetsu. The tunnel cross section will be 80.1 to 83.3 m^2. The top heading is being constructed first by mechanical excavation. A road haulage system has been adopted for muck removal.

Construction of an inclined adit for working space (sectional area: 26.8 to 54.2 m^2, length: 656 m and slope: 2.8%) was started in March 2001. The excavation of the tunnel was commenced in November 2001. The tunnel is being excavated to both portals. Excavation has been completed over a length of 2,720 m at the end of May 2006.

3 GEOLOGICAL AND TOPOGRAPHIC OUTLINES

The geology at the site consists of lacustrine and estuarine sediments of the Pliocene epoch of Neogene period through the Holocene epoch of Quaternary period such as gravel, sand, silt and volcanic ash. The ground is unconsolidated throughout the tunnel length and the groundwater level is above the tunnel. The excavation site in the north work section is in the Sarumaru formation at a relatively great depth and composed of gravel, tuff breccia, sand and silt. The Sarumaru formation is composed mainly of well graded large conglomerates, but is not so much consolidated in the matrix and likely to become vulnerable when subjected to wetting and drying. Tuff breccia is composed of pumiceous tuff breccia mainly consisting of pumiceous gravel, and andesite tuff breccia containing hard andesite gravel, and is assumed to be in the water-bearing formation. Sand and silt exist in narrow areas in thin layers of a few meters. In some sections, coarse sand particles with few fine particles and a low uniformity coefficient are widely distributed. Occurrence of quicksand is therefore of concern. Figure 2. shows a geological profile in an area with a thin earth cover drawn based on the results of pre-construction borehole exploration.

At the working face, layers composed predominantly of 20- to 30-cm-diameter gravels, those composed only of sand and of sandy silt alternately appear although all are classified as sand and gravel layers. Folding of rocks and formations of anticlines are also found perpendicular to the tunnel alignment (Photograph 1).

4 SELECTION OF AUXILIARY METHODS ACCORDING TO THE GEOLOGICAL PROPERTIES

The water-bearing unconsolidated ground detected in the tunnel as described above was likely to cause disturbances such as the collapse of working face or tunnel crown, or large-scale quicksand or deteriorate the bonding of shotcrete.

Before excavating the tunnel, a study was made to select the method for controlling water seepage. Installing deep wells from the ground level was considered because there was a relatively shallow depth. The method was, however, found to have limited effects because of drastically varying soil conditions. It was decided instead to drill dewatering boreholes from within the tunnel regularly.

Long forepoling methods were selected as listed in Table 1. from among those that had an excellent track record in water-bearing unconsolidated ground. Then, screening was made in view of the effectiveness for chemical grout injection in sand or sandy gravel layers. As a result, long forepoling with a twin pipe double packer system using water glass grout (AGF-R method) was adopted.

For supporting the working face, methods listed in Table 2. were examined. To use the same material and maintain the uniformity of construction cycle with the forepoling method, the long face grout method (FG method) using water glass grout and AGF-R steel pipes was adopted.

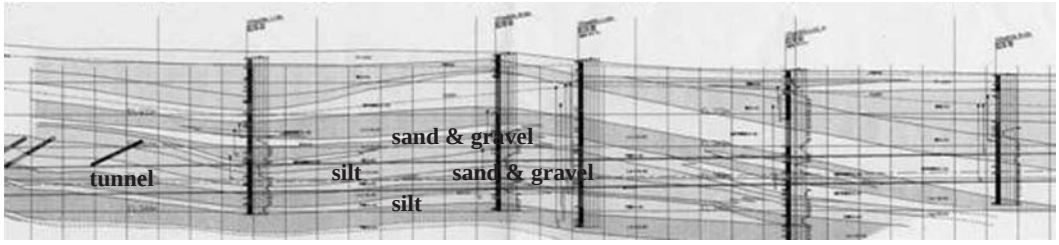


Figure 2. Geological profile in an area with thin earth cover.



Photograph 1. Condition of tunnel face.

Table 1. Long forepoling methods.

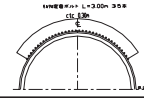
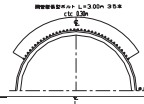
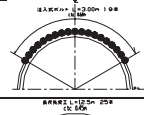
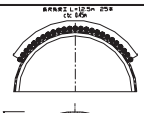
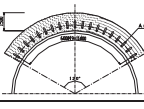
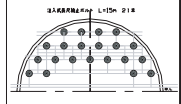
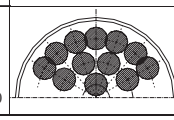
Method	Outline	Effect		
		Low consolidated conglomerate	craked silt	sand
Bolt with mortal (L = 3 m@30 cm)		×	×	×
Frictoin anchored bolt (L = 3 m@30 cm)		O	Δ	×
Bolt with injection (L = 3 m@60 cm) drilled every face (silca resin injection)		Δ	O	×
AGF method (L =12.5 m@45 cm) drilled every face (silca resin injection)		Δ	O	Δ
AGF–R method (L = 12.5 m@60 cm) drilled every (silca resin injection) or (Denka S Pack injection)		Δ	Δ	O

Table 2. Supporting method at tunnel face.

Method	Outline	effect		
		Low consolidated conglomerate	Craked silt	Sand
Face bolt with injection (L = 4 m) drilled every 2 m (silca resin injection)		Δ	Δ	×
Face bolt with injection (L = 12 m) drilled every 9 m (silca resin injection)		O	O	×
Face grout method (L = 12 m) drilled every 9 m (silca resin injection) or (Denka S pack injection)		Δ	Δ	O

5 OUTLINES OF SELECTED AUXILIARY METHODS

The AGF-R method is a long forepoling method. Steel pipes with injection nozzles equipped with a check valve are drilled into the ground. A grouting sleeve is formed around the steel pipe, and then highly flowable grout is injected by the twin pipe double packer grouting method. Composite ground composed of the steel pipe and cylindrical soil-grout column is intended for soil stabilization or improvement.

Forming solid soil-grout columns is extremely difficult in collapsible sedimentary ground. Conventional AGF methods have frequently caused soil collapse between steel pipes. The AGF-R method adopted in this project injects highly flowable grout into steel

pipes in steps using the twin pipe double packer grouting method to consolidate the ground between steel pipes.

6 IMPLEMENTATION OF AUXILIARY METHODS

6.1 *Basic pattern*

The diameter (thickness) of the soil-grout column for soil stabilization either at the tunnel crown or on the working face was set at 1.5 m where there was water seepage or at 1.0 m otherwise.

The injection rate was set at 35% : 10% in the primary injection (rough injection of Denka S Pack) and 25% in the secondary injection (penetration injection of Silicarizer). Where alternate layers of silt and gravel were found in the soil stabilization area, primary injection was carried out throughout the area but secondary injection only in the gravel layer. The range of implementation of the AGF-R method was basically 160 degrees, but reduced to 120 degrees depending on the soil or seepage conditions. The length of drilling a steel pipe per shift was set at 9 m. Figure 3 shows a basic flow of steps of the AGF-R method. Figure 4 provides a typical cross section in the case without any seepage.

At the tunnel site, the ground consists of alternate layers of sand, gravel and silt and folding of rocks and formations of anticlines are also found perpendicular to the tunnel alignment. In order to obtain the greatest effect possible of soil stabilization and cost performance under ever changing soil conditions, therefore, the construction specifications such as the length of drilling a steel pipe per shift, grout material, injection rate and grout pressure were modified wherever required during construction.

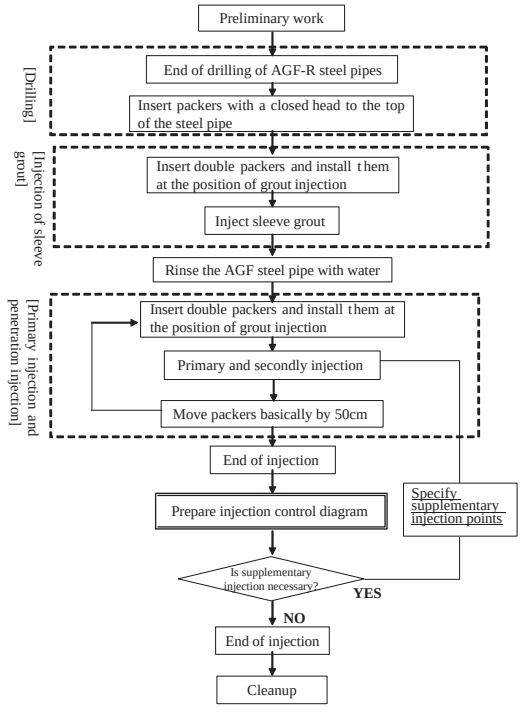


Figure 3. Basic flow of AGF-R method.

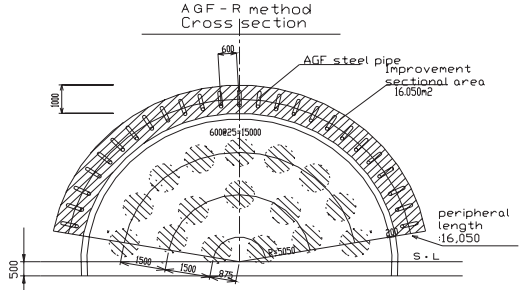


Figure 4. Typical cross section in the case without any seepage.

6.2 *Construction in sandy soils*

Ground collapsed between steel pipes in a sandy soil section. It was determined that the collapse occurred probably because drastically changing grading of sandy soil particles caused the chemical to easily run out resulting in insufficient stability (Figure 5). Then, the following changes were made to construction conditions.

(i) In order to ensure soil stability between steel pipes, steel pipes were drilled at a pitch of 45 cm instead of 60 cm perpendicular to the tunnel alignment and the longitudinal length of injection was increased from 10 m to 11 m.

(ii) Material for primary injection was changed to cohesive cement-bentonite grout to enhance the effectiveness of primary injection.

(iii) Both volume and pressure of grout were controlled. Final pressure in each step was verified at the end of grout injection. For the step in which grout pressure was below the requirement, supplementary grouting was carried out.

Modifications to specifications are listed in Table-3. Construction to the revised specifications contributed to the prevention of collapse of unconsolidated sandy layers and smooth progress of tunneling.

6.3 *Construction in sections with alternate layers*

In sections with alternate layers of gravel and silt, soil-grout columns of varying shapes were formed in respective types of soil, so they were not uniform

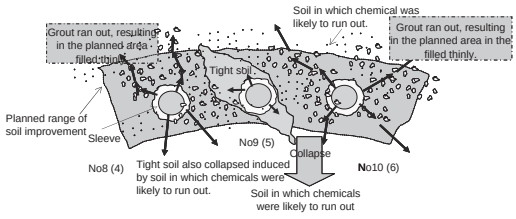


Figure 5. Conceivable reason for soil collapse in the sandy soil section.

Table 3. Modifications to specifications in a sandy soil section.

Item	unit	137 km502 m ～	～137 km511 m	remarks
Pitch of steel pipe	m m	600	450	
Sift length	m	9.0	9.0	
Length of injection	m	10.0	11.0	
Material of sleeve		Denka-s-pack (5 L/m)	Denka-s-pack (5 L/m)	
Material for primary		Denka-S-pack 5～10%	Cement bentonite	
injection (Required grout pressure)			5% (less than 1.0 Mpa)	
Materia for secondary injection (Required grout pressure)		Silicarizer 25～30%	Silicarizer 30% (less than 1.7 Mpa)	
Layer boundary measure		non	2 m lap	Secondary injection to silt layer

throughout the section. As a result, soil-grout columns suffered spalling at the bottom edge of AGF-R steel pipes. To solve the problem, soil-grout columns were restrained in the sandy layer by forepoling with silica resin grout injection during excavation following the implementation of the AGF-R method. In silt layers where penetration injection (secondary injection) is inapplicable, only primary injection was carried out. Forepoling was adopted during excavation. Where the ground was composed of silt layers throughout the section, the AGF method was employed that involved the injection of silica resin grout. Figure 6. shows examples of forepoling in different types of soils.

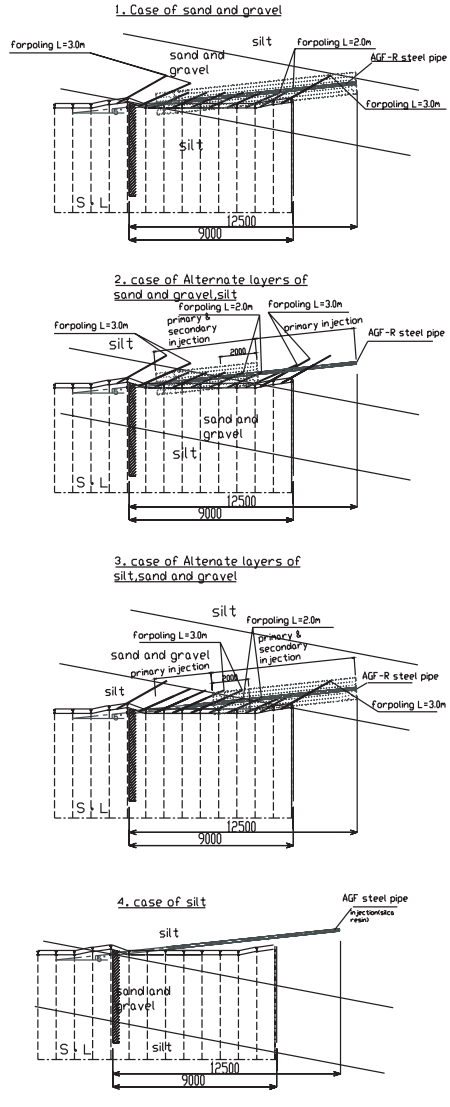


Figure 6. Examples of forepoling in different types of soils.

6.4 *Construction in seepage sections*

In sections with seepage, drilling a dozen of FGs with a design diameter of one meter at the working face inevitably resulted in gaps being left, so no sediment runoff was likely to be prevented. Grout injection was therefore applied at the working face using the twin pipe double packer system to stabilize the soil throughout the face (provide a water cutoff).

At the bottom of the top heading, no FG steel pipes could be drilled by a drill jumbo. Manchette tubes instead of FG steel pipes were drilled by a drilling machine. Ground over a length of 18 m was stabilized (water cutoff was provided) in a shift for higher

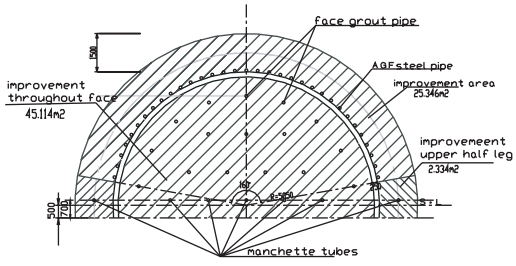


Figure 7. Pattern on face stabilization in the case with water seepage.

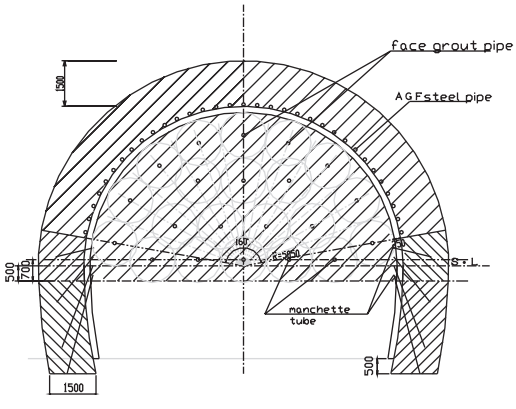


Figure 8. Face improvement pattern in the case with seepage throughout the section.

efficiency. Figure 7. shows a pattern of working face stabilization in the case with water seepage at the working face of top heading.

Sandy layers with seepage also appeared in the bench and runoff of the sandy layers occurred during excavation. Soil improvement was therefore necessary as in the top heading. In sections where top heading face advanced, only side walls of the bench were improved over a length of 18 m in a shift using manchette tubes at the bench face.

Both top heading and bench were improved from the top heading face ahead of the top heading face to shorten the cycle. The length of drilling a steel pipe per shift at the bottom of the top heading was reduced to 9 m from 18 m as in bench excavation. Soil-grout columns for the side walls of bench were constructed diagonally downward ahead of the top heading face. Figure 8. shows a face improvement pattern in the case with seepage throughout the section.

7 CONCLUSIONS

Basic soil stabilization patterns were defined before excavation in water-bearing unconsolidated ground.

Construction has taken place according to the basic patterns only over a length of approximately 40 m so far. Patterns have been modified continuously in response to changing soil conditions. Table-4 lists major modifications to the specifications for auxiliary methods.

The following findings have been obtained.

(a) In order to achieve a sufficient level of soil stabilization by long forepoling in water-bearing unconsolidated ground, the AGF-R method employing twin pipe double packer grouting system is very effective.
(b) Downward cutoff from the top heading working face using the twin pipe double packer system with manchette tubes is effective for controlling water seepage.
(c) In sand and gravel layers, chemicals are likely to run out. Cohesive materials are therefore effective in primary injection.
(d) Controlling both quantity and pressure of grout is effective during the injection in sand and gravel layers.
(e) In alternate layers of sand and silt, soil-grout columns are formed in varying shapes and are not uniform, so restraining soil-grout columns by forepoling during excavation is effective.
(f) In the case where considerable seepage is found and sediment runoff is likely to occur, injecting grout throughout the working face (providing a water cutoff) is necessary.

Large-scale soil collapse has been prevented during the excavation so far by predicting varying ground conditions by exploratory drilling and making modifications to specifications in the next shift accordingly.

8 FINAL REMARK

In sections with drastically changing soil conditions, predicting changes is difficult and whether an auxiliary method selected suits the ground or not cannot be determined without identifying the soil deformation or stress acting on supports after excavation. Constantly monitoring the process of construction and making improvements based on the determination of effects of excavation are therefore important. Then, the auxiliary method will have the minimum effects on construction progress and be more cost effective.

In the north work section of the Takaoka Tunnel, the above principle was applied and specifications for auxiliary methods have been modified frequently. Nearly optimal specifications have been identified for auxiliary methods under respective soil conditions. It is hoped that similar applications will increase and that specifications for auxiliary methods will be established.

Table 4. Modifications to specifications and tunnel sections.

Tunnel sector distance(m)		137 k466 m–137 k511 m 45	137 k511 m–137 k520 m 9	137 k520 m–137 k556 m 36	137 k556 m–137 k562 m 6	137 k562 m–137 k568 m 6	137 k568 m–137 k592 m 24	137 k592 m. 24
Geology		Alternate layers of sand and gravel, sandy silt and sand	Sandy soil mixed with gravel and coarse sand in a complicated manner	Mainly composed of sand, and congested with sand and gravel, and silt	Same as stated to the left	Composed predominantly of sand and gravel with seepage	Same as stated to the left	Sandy layer mixed with gravel
Modifications to specifications for auxiliary method	Tunnel crown	Basic specifications – Length of drilling a steel pipe per shift: 9 m – Pitch of steel pipes drilled: 60 m – Depth of grout injection: 10 m – Grout for primary injection: Denka S Pack – Grout for secondary injection: Silicarizer – Controlling the volume of grout – Required thickness of soil-grout columns: 1.5 m(with seepage) or 1.0 m (without seepage) – No secondary injection overlapped the silt	– Pitch of steel pipes drilled: 45 cm – Depth of grout injection:11 m – Change of grout in primary injection (to cement bentonite) – Secondary injection overlapped the silt layer 2 m from the layer boundary. – Grout pressure (during supplementary injection) is also controlled.	Soil stabilization according to the soil type – Sand and gravel area: Addition of 2 m-long friction bolts with silica resin injection – Silt area: Only silica resin injection was adopted but secondary injection overlapped the silt area over a length of 2 m.	– Length of drilling a steel pipe per shift changed to 6 m (Steel pipe length changed from 12.5 m to 9.5 m)	– Increase of injection rate in primary injection from 5% to 10% – Increase of injection pressure	– Reduction of injection pressure and reduction of volume of supplementary grout (50%)	– Reduction of injection rate in primary injection from 10% to 5% – Reduction of injection pressure
	Tunnel face	Basic specifications – Length of drilling a steel pipe per shift: 9 m – Pitch of steel pipes drilled:1.5 m – Grout for primary injection: Denka S Pack – Grout for secondary injection: silicarizer – Controlling the volume of grout – Required diameter of soil-grout column: 1.5 m(with seepage) or 1.0 m (without seepage) – No secondary injection overlapped the silt.	– Change of grout in primary injection (to cement bentonite) – Secondary injection overlapped the silt layer 2 m from the layer boundary. – Injection pressure (during supplementary injection) is also controlled.	No modifications.	– Length of drilling a steel pipe per shift changed to 6 m (Steel pipe length changed from 12.5 m to 9.5 m)	– Soil improvement throughout the working face – Injection using manchette tubes at the bottom of the top heading – Increase of injection rate in primary injection from 5% to 10% – Increase of injection pressure	– Reduction of injection pressure and reduction of volume of supplementary grout (50%) – To resist injection pressure, ordinary shotcrete was changed to steel fiber reinforced concrete.	– Reduction of injection rate in primary injection from 10% to 5% – Reduction of injection pressure
Reason for modification		– Tunnel crown collapsed at 137.510 km. – No chemicals found in the soil mass that collapsed – Chemicals ran out due to drastic changes of soil conditions.	– Spalling of the soil-grout column at the bottom end of an AGF-R steel pipe	– Frequent spalling of the soil-grout column in later stages in a shift of drilling a steel pipe – The length of drilling a steel pipe per shift was long, and soil-grout columns were broken due to the displacement at the end of the steel pipe	– Quicksand occurred at lower part of face at 137.559 km. – An unconsolidated sandy layer with seepage was expected to appear at the working face.	– Tunnel deformation during injection – High injection pressure in secondary injection led to excessive injection	– Soil was stabilized by improvement throughout the section. – For higher cost performance	

This page intentionally left blank

Underground Space – the 4th Dimension of Metropolises – Barták, Hrdina, Romancov & Zlámal (eds)
© 2007 Taylor & Francis Group, London, ISBN 978-0-415-40807-3

Use of risk management plan for urban mechanized tunnelling projects: From the establishment of the method to the successful practice

P. Grasso, E. Chiriotti & S. Xu
Geodata S.p.A., Turin, Italy

N. Kazilis
Geodata S.p.A., Thessalonica, Greece

ABSTRACT: Tunnelling in urban environment demands for particular methods and flexibility to guarantee minimum impact on whatever already existing above the tunnel, on the daily activities of the city, as well as on the routine life of its inhabitants. The method of mechanized tunnelling can permit to realize the work and minimize at the same time the undesirable interferences. However, mechanized tunnelling is not a risk-free technology. Encountering geological conditions different from those foreseen, or a non ideal performance of the shield machine itself will all open the way to a series of risks, which are often disastrous to the project if not properly managed. Most risks can be effectively managed through the use of a Risk Management Plan (RMP). The RMP was integrated and successfully applied in recent years to a series of important urban transformation projects like the Turin Metro (Italy), Porto Metro (Portugal) and the Bologna Railway Link (Italy).

1 INTRODUCTION

The design and construction of tunnels in urban areas are often associated with risks that can arise from different factors such as: inadequacy of the geotechnical information; geological and hydrogeological conditions locally different from those foreseen for the design; inappropriate choice of the construction method; in case of mechanized tunnelling, non ideal performance or behaviour of the shield machine itself or deviation of the actual ground-machine system behaviour from the theoretical one; etc. The various potentially critical scenarios will all open the way to a series of problems and risks, which are often disastrous to the project if not properly managed.

We strongly believe that the first response to risk is the selection of the appropriate construction method. Considering the huge technological improvements achieved in the last decades, the method of mechanized shield tunnelling can permit to realize the work and minimize at the same time the undesirable interferences. However, mechanized shield tunnelling is not a risk-free technology, even though it is a modern and advanced technique.

Risks cannot be ignored, they have to be managed, reduced, shared, transferred, or simply accepted once they are known. Nowadays within the international tunnelling community (ITA) there is an agreement that Risk Management is the key of success for all kind of tunnelling works, including urban mechanized tunnelling.

In the last decade we developed and applied in various urban mechanized tunnelling projects (Turin Metro Line 1, Italy; Porto Metro, Portugal; Bologna High Speed Railway Junction, Italy; reconstruction of the Lesnaya-Muzhestva section of the St. Petersburg Metro, Russia; Santiago Metro Line 4, Chile; SMART Project, Malaysia) the concept of RMP - Risk Management Plan, a robust and transparent risk management methodology made of clearly identified steps that aims not only to manage risks but also guaranteeing safety, quality, cost and duration limits by:

- systematically quantifying residual risks which has to be known, communicated and further reduced or controlled;
- extending the concept of risk management from the design to the construction phase;
- offering specific tools for facilitating the decision-making process in the management of both initial and residual risks during design and construction.

The following sections are devoted to specifically address the concept of RMP for urban mechanized tunnelling, giving the background of the suggested methodology and practical examples from the Designer perspective.

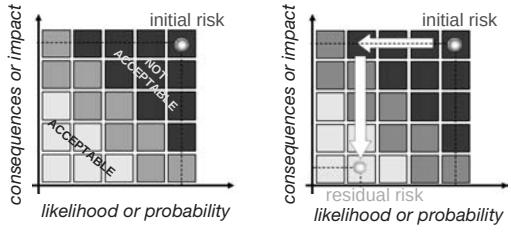


Figure 1. Risk as a combination of probability and impact: from initial risk to residual risk through mitigation.

2 APPROACH FOR RISK MANAGEMENT

2.1 *Definitions*

'Hazard' is an event which may give rise to elements of uncertainty or the property of a situation that has a potential to cause damage. Each hazard is associated to a probability of occurrence, P, and an impact (consequences), I, in terms of safety, time, and cost. The risk, R, associated to an identified hazard is defined as the product R = PxI, and is called 'initial risk' (figure 1).

Hazards are something we can do little about except identifying them. The risks they pose can be (and should be!) reduced. A project-based 'acceptability criterion' has then to be set, allowing to define if a certain initial risk in a certain context can be assumed or has to be reduced through specific mitigation measures at the design and/or construction phase. The 'mitigation measures' usually consist of a set of predefined measures to be systematically implemented at the various stages of a project in order to reduce each single, unacceptable initial risk within the acceptability criteria by acting on its probability and/or its impact.

Risk remaining after the implementation of the mitigation measures is called 'residual risk' (figure 1). It consists of the acceptable risk and the risks that have not been properly assessed or the risks that have not been identified. Initial risks have to be constantly updated during the project life, while residual risks have to be constantly controlled through key-parameters and re-assessed.

2.2 *Sources of risk in urban mechanised tunnelling*

The main sources of risk in a urban mechanized tunnelling project are related to geology and hydrogeology, design, construction (finance and exploitation risks are not specifically addressed in this paper).

– Geology and hydrogeology related risks can include, *inter alia*: limited investigations at design and/or construction phase; inappropriate on site and/or lab tests; insufficient understanding of the peculiar mechanisms of failure and of rock mass/soil behaviour; availability of resources and equipments; lack of site accessibility; lack of systematic face mapping during construction; lack of validation/update of the geological and hydrogeological model during construction; etc.
– Design related risks can include, *inter alia*: insufficient experience of the Designer; uncompleted analysis of the potential risk scenarios; evaluation of loading conditions acting on the lining is not complete; low or difficult constructability of proposed solutions; lack of design flexibility vs. actual ground conditions; inadequate method for predicting settlements and assessing potential damages on existing buildings/utilities; inadequate monitoring system and/or readings; no threshold limits or operational ranges for the monitored parameters or TBM key-parameters, respectively; poor or missing definition of countermeasures and related triggering criteria; etc.
– Construction related risks can include, *inter alias*: poor management of the 'learning curve' period; lack of Contractor experience; lack of personnel training; inadequate procedures; incompatibility of the machine with the ground; major mechanical failures; inadequate logistics; inadequate face pressure; inadequate injection of the tail void; lack of TBM's parameter controls and/or review and interpretation; insufficient probing ahead; etc.

2.3 *The first step of a Risk Management Plan: the Risk Register*

The objective of a RMP is to reduce as low as reasonably possible all the risks identified in each phase of the Project life. The activation of the RMP assures the timely identification of the potential problems and initial risks, the implementation of the appropriate measures for risk mitigation, and the control of the residual risk. Hence, the RMP should be implemented as soon as possible and integrated in all phases of the project from conceptual design to exploitation.

The main principle of a RMP (Grasso et al., 2002) is that risks have to be identified, quantified and reduced for every single investigation, design and construction discipline involved in the project. Once the Designer has identified the basic requirement of the Owner and his tolerance to the risk, the process of risk identification should go through the following: (a) formation of a group of specialists according to the size and complexity of the project; (b) collection of published data on the regional and local geological conditions, to be complemented later on by adequate investigation; (c) production of a geological model and estimate of the likely ground conditions and their variability; (d) identification of the possible construction techniques; (e) use of workshops and engineering judgment based on previous experience for identifying the risks, using 'checklist'; (f) preparation of a formal Risk Register which should be used as a base for selecting the optimum project alternative.

The Risk Register should be structured to include: the families of hazards and, within each family, the list of hazards and their causes; the quantification of their likelihood and impact and hence of risks; the indication of unacceptable initial risks; the identification of a specific strategy to reduce each initial risk (mitigation measures); the quantification of residual risks through a re-assessment assuming that mitigation measures have been implemented. The Risk Register has to be updated constantly during the project life and used to communicate and share risk policy and residual risk acceptance.

2.4 *Use of the Risk Register and further steps in the RMP*

If properly used, the Risk Register becomes the real guideline for the development of the project, since it allows to track in a 'tabloid' the proposed action plan in terms of organisation, investigations, design and/or construction needs to reduce the identified risks. If seen from the Designer perspective, the Risk Register highlights various requirements not only related to the level of detail of the design or to the correctness and state-of-the-art implementation of the construction procedures, but also to the effective management of the interface issues among the involved disciplines. As a matter of facts, urban mechanized tunnelling is generally related to huge infrastructure projects such as metros, urban railways, storm-water conveyance tunnels, service tunnels for utilities, sewerage or roads. Consequently, urban mechanized tunnelling is part of a complex process where different disciplines have to converge to deliver the final result in time and within budget. The method for successfully ensuring this convergence is explained in the next section.

2.4.1 *Management of interfaces*

According to our experience, being aware of the importance of managing interfaces is a real added value that the Consultants can bring to a project, either acting as Designers or as Supervisors, provided that the Consultant can suggest effective solutions to problems before they rise thus preventing blockages of works.

We suggest the use of a 'Centralised Design Management' involving all project disciplines (geology, geotechnics, structures, monitoring, construction techniques, as well as architecture, electrical and mechanical, etc.) to ensure that design fulfils primary objectives of completeness, availability, compatibility, buildability and maintenance, additional to the 'basic internal correctness' of each design element. The check of the 'basic internal correctness' (consistency with Technical Design Specifications and to local and international norms and codes of practice, correctness of assumptions and calculations, completeness of drawings, etc.) is the easiest part to deal with, since it is based on a sort of routine checks. Setting a strategy to ensure the achievement of the primary objectives in a complex project is the real challenge.

Since 1998, when the idea of the Turin Automatic Metro Line 1 (9.6 km of double-track, single-tube mechanised tunnel) started to become reality, we experimented with success a way to make the Centralised Design Management happen; the establishment of an 'Exchange Table' (ET) within a 'Group of Permanent Coordination' (GPC). The GPC is set by the Owner, through his Consultants and Supervisors or can be promoted by the Designers. The group is in charge of guaranteeing the coherent and integrated development of the project, of leading the onset of the interfaces among the disciplines and of organizing and running a common system for sharing documents and information. This involves the specialists of tunnelling (geologists and engineers), architects, urban planners, system engineers, etc., according to the type of infrastructure being developed. The group acts through the overall implementation period of the Project in a continuous effort of mediating among the various needs, that could be in conflict. The ET is not only a physical place of interface coordination, but also the expression of a shared working methodology that permeate all the Actors, no matter of their level of involvement and responsibility in the Project.

2.4.2 *Management of tunnel design risks*

The Designer of the underground works should be able of managing all kind of design risks related to geology, hydrogeology, load conditions and impact at the surface from the conceptual design to the follow-up of the construction. Risks related to tunnel design that are identified at the Risk Register stage generally emphasize the need for the following RMP components:

- Planning investigations that are adequate for the level of geotechnical risks of the project.
- Recognizing that the deterministic approach may be less accurate and give preference to sensitivity and risk scenarios analysis and to probabilistic approaches;
- Design through risk scenarios: for example, not only the most likely load condition or the average geotechnical parameters should be considered. Especially in a urban area the consequence of encountering even locally the most unfavourable situation must be analysed and designed for.
- Adopting a flexible design for taking into account unfavourable situations. It entails, for each critical key mechanism: defining countermeasures to manage adverse trends during construction; identifying parameters and key events to be controlled and monitored during construction; defining the relevant operational ranges or threshold limits;

predefining triggering criteria for activating countermeasures, if ranges/limits are exceeded.
- Adopting a transparent risk mitigation policy through the design process: from the design of segmental lining to the design of the consolidation works to avoid damages due to tunnelling-induced settlements, each identified initial risk has to be dealt with through adequate design choices (tracked in a transparent way!).
- Quantifying and communicating any residual risk affecting the design choices, e.g., using the probabilistic methods to assess the design reliability: average factors of safety (of the support, prescribed face pressure to be applied by the TBM, etc.) are replaced by the probability of a negative event (e.g., face instability) to occur, and the probability has to be reasonably low.

When tunnelling in urban areas, special care has to be used for establishing a Building Protection Strategy. This is based on: survey all identified buildings in the construction-influence zone before construction starts (BCS – Building Condition Survey); use the BCS results for assessing the vulnerability of buildings to damage; establish a specific damage classification system for the project; perform settlement-sensitivity analysis for each identified building and define its tolerance to tunnelling-induced movements; classify all identified buildings into different risk categories; single out those buildings at risk and requiring protection; identify those buildings requiring survey and special monitoring during construction; perform BCS post-construction, independent of whether damage occurred or not; archive and maintain all relevant data in a dynamic and relational database for use by all Actors.

2.4.3 *Management of tunnel construction risks*

We already addressed the role of the right choice of the excavation method as the primary response to risk. However, the complete effectiveness of the RMP is achieved if the appropriate excavation method is accompanied by culture and training of personnel and by the establishment and implementation of procedures to guide all the relevant construction processes, to govern the key events and to address all the potential anomalies with a proper and predefined action plan. Within the RMP framework the Designer plays two important roles during the construction phase:

- The Designer must have the capacity to interact with the TBM manufacturers in order to contribute in suggesting new ideas for technological innovations, with the aim to assure safety and improve the production in terms of advancement in all kind of geological context.
- The Designer must validate the design hypothesis during construction and make use of the construction feedback to match the design prescriptions to the real encountered conditions and to optimise the design, also in terms of costs. We were the first to introduce in 2000 for the Porto Metro, Portugal, the concept of the iterative design through the use of a TAP – Tunnel Advancement Protocol (or PAT, in Portuguese). The TAP is a low-cost, easy-to-implement practical procedure for the designer-contractor-engineer team to continuously update the risk scenarios and the corresponding mitigation plans as construction proceeds. TAP facilitates the management of residual risks. It is a detailed and dynamic design document produced for each 200 to 500 m of the tunnel to be excavated, prepared prior to the actual excavation of that section and based on the construction feedback from the previous section(s).

In addition, all the Actors of the Project have to be conscious of the importance of using the 'learning curve' section (e.g., first 300–500 m of TBM excavation) to validate the TBM procedures and to collect all the monitoring data to start validating the majority of the design assumptions (a special monitoring section has to be designed and implemented and a strict follow-up made).

2.5 *Tools to support the RMP*

Properly managing risks in urban tunnelling projects demands for special thinking, particular approaches and innovative tools. We mentioned the probabilistic design approach and the TAP as being the answer to quantification and follow-up of residual risks (mainly related to geology, design and construction). However, additional risks are related to the likelihood of exceeding scheduled planning and budget and to the availability and integrity of information in real time. This is why we commonly and systematically use, within the RMP, two additional tools:

- DAT (Decision Aids for Tunnelling), and
- GDMS (Geodata Master System) used for managing information in real time via web.

DAT is used to simulate the process of underground construction in a probabilistic manner and was developed by the MIT (Massachusetts Institute of Technology, USA) and the EPFL (Ecole Polytechnique Fédérale de Lausanne, Switzerland) and was used by Geodata on various tunnelling projects around the world resulting in further development of the software (Einstein et al., 1998). DAT simulates the construction cycles of a linear infrastructure by following a predefined construction sequence along a probabilistic geological model that stochastically changes for each complete simulation process, for a probabilistically relevant number of times. The output of DAT is a probabilistic cost and time distribution. DAT allows

Table 1. Recent examples of successful application of the RMP in urban mechanized tunnelling projects.

Project description	RMP elements used in the project	Benefits to the project
PORTO METRO, Portugal  Double-track, single-tube tunnel (L = 7.0 km; D = 8.7–8.9 m), 3 access ramps, 2 EPB-TMBs. Excavation end: 2003. Geodata role *: FD, CD, CS	– Identified Risks: heterogeneous rock mass; residual soil with local metastable structures sensitive to hydraulic gradient; brittle rock mass behaviour; – Organisation: Designer on site, Resident Engineer and Follow-up Team after severe problems occurred during the TBM 'learning curve'. – Design: Risk Register; risk-scenarios-driven design; statistical geotechnical characterisation; BCS and BRA; provision of a procedure to calculate required face pressure and operational ranges of TBM key-parameters; activation of TAP. – Construction: adoption of TAP; development of GDMS for managing monitoring and TBM data; new TBM procedures; new TBM devices ('secondary face support system'; alarm system in the TBM-driver cabin); systematic interpretation of TBM data (Gaj et al., 2003: Chiriotti et al., 2003).	No accidents; average settlements of 5 mm even in low cover areas (3–4 m); production: 40–50 m/ week; reduction of foreseen consolidation works; optimisation of monitoring instruments (numbers and readings). BCS/BRA method adopted as standard by station designers, by LNEC, used for technical specs of Athens Metro extensions and now in use by the Tel Aviv Metro Owner.
TURIN METRO Line 1, Italy.  Double-track, single-tube tunnel (L = 9.5 km; D = 6.8 m), 15 stations, 15 ventilation shafts, 3 EPB-TBMs. Excavation end: 2005. Geodata role *: PD, FD, CS	– Identified Risks: Politically sensitive project (risk of not meeting 2006 Winter Olympics deadline in presence of damages and adverse public opinion); difficult ground (abrasive rock, blocks up to 1 m3, high permeability, locally less than 5% of fines). – Organisation: Activation of PCG and ET. – Design: Risk-scenarios-driven design; standardisation of stations to smooth cw/e&m interface issues and improve industrialisation; BCS; BRA; GDMS for sharing data/documents; – Construction: TBM procedures (Porto); use of GDMS for real time management of monitoring and TBM data; systematic interpretation of TBM data; special consolidation works ('Cittadella' historic tunnels); additives in the TBM chamber to correct natural soil grain size (Grasso et al., 2006).	Impressive result of conceiving, design, tender, built and operate a completely new metro line in less then 6 years, thanks to a huge coordination effort, a special attention to risk management. Construction value of the tunnels – 15% than design budget. Construction value of the tunnels plus stations, finishes and e&m works exceeding only 4% the available budge, equal to 50% of the total.
BOLOGNA RAIL LINK, Italy.  Twin-bore, single-track tunnels (L = 6.1 km; D = 8.3 m), 2 EPB-TBMs. Excavation end: 2006. Geodata role *: CD, TC on TBMs restart after stoppage.	– Identified Risks: alignment right beneath existing surface railway (strict limitations on settlements); soft marine sands and clays to be excavated also under water table; close proximity of the 2 tunnels (TBM2 runs through disturbed soil). – Organisation: consultant responsible for TBM added to allow restarting the TBMs excavation. – Design: preparation of TAP as in Porto Metro. – Construction: adoption of TAP; new TBM procedures and controls; new TBM devices ('secondary face support system'; two balances and a volumetric scanner to control the extracted muck weight; systematic interpretation of TBM data (Minguez et al., 2005).	Since the excavation restart dramatic reduction of settlements (from 10–45 mm before stoppage to 1–5 mm up to the end of tunnel excavation). Best daily performance for both TBMs: 25 rings (37.5 m). Best monthly performance: 612 m in March 2006 for TBM1 and 635 m in April 2006 for TBM2.

*PD – Preliminary Design; FD – Final Design; CD – Construction Design; TD Tender Docs preparation; CS – Construction Supervision (the Engineer); TC TBM Consultant for technical assistance during construction.

comparing the effectiveness of different risk mitigation strategies or plans, and identifying the optimum solution with minimal residual risks in terms of time and cost.

According to the authors' experience, a typical RMP for a urban tunnelling project should also include a real-time data-sharing and management system accessible to all parties involved (Owner, Contractor, Designer, Engineer, Consultants, etc.) to facilitate the communication and support the decision-making process. GDMS is based on the modern GIS (Geographical Information System) and web technologies (accessible via Internet) to give an answer to the need of real-time management of design documentation, construction records, monitoring data, TBM parameters and back-analysis.

GDMS started to be developed in 1999, to be used in parallel in Porto and Turin Metros. Then it underwent continuous software improvements and was supplied in various urban projects such as the Santiago Metro (Chile) and the SMART Project (KL, Malaysia). The aim of GDMS include: (a) to collect in a database and geo-referring all the *ante operam* information and to the design data (e.g., geology, alignment, etc.), including additional investigations during construction, within a unique reference system; (b) to collect and geo-referring all the information related to BCS and BRA; (c) to manage the manual and/or real-time acquisition of the geotechnical and structural monitoring data, doing standard graphical representation, comparing readings with thresholds, identifying adverse trends and automatically sending warning messages to pre-selected responsible people in the organisation by SMS, e-mail, etc.; (d) to make the TBM parameters available by direct connection with the TBM acquisition system; (e) to guarantee data integrity; (f) to permit extractions and analyses of data to allow correlations and cross-checks (e.g., TBM parameters vs. geology; building monitoring vs. TBM parameters; etc.); (g) to produce factual data reporting.

3 FROM THE ESTABLISHMENT OF THE METHOD TO THE SUCCESSFUL PRACTICE

In Table 1 examples of successful RMP application in urban mechanized tunnelling are given. Details can be found in the reference documents.

4 CONCLUSIONS

The geotechnical risk, in the form of unforeseen or unforeseeable geologic conditions, together with design and construction risks are a decisive factor in controlling the time, cost, and safety of all major civil engineering projects, especially in urban areas. Experience have shown that even with mechanized tunnelling such risks cannot be avoided. Hence, all phases of the Project need to be developed with due attention to the sources of risk and their identification, quantification, and reduction. This requires a risk management culture from all the Actors in all phases of the Project. The enforcement of this culture could be greatly facilitated by adopting a RMP. The implementation of RMP needs operative tools, and probabilistic design, DAT (Decision Aids for Tunnelling), TAP (Plan for Advancing the TBM) and GDMS (GIS-based system for the management of monitoring and TBM parameters) are just some example tools developed by Geodata in recent years. The recent case histories of RMP application in urban mechanised tunnelling show how management of risk can only provide benefit to the overall community.

REFERENCES

Chiriotti, E., Grasso, P., Xu, S. 2003. Analyses of Tunnelling Risks: State-of-the-art and Examples. *Gallerie*.

Einstein, H.H, Xu, S., Grasso, P., Mahtab, A. 1998. Decision Aids in Tunnelling. *World Tunnelling, April '98.*

Gaj, F., Guglielmetti, V., Grasso, P., Giacomin, G. 2003. Experience on Porto EPB follow-up. *Tunnels & Tunnelling International*, Dec. 2003.

Grasso, P., Mahtab, M.A., Kalamaras, G.S., Einstein, H.H. 2002. On the Development of a Risk Management Plan for Tunnelling. *28th ITA General Assembly and World Tunnel Congress*, Sydney.

Grasso, P., Fornari, E. 2005. Turin Metro Line 1: an example of successful use of EPB-TBM for tunnelling in unfavourable groind conditions and vulnerable context. P*roceedings of the AFTES Congress*, Chambery.

Minguez, F., Gregori, A., Guglielmetti, V. 2005. Best practice in EPB management. *Tunnels & Tunnelling International*, Nov. 2005.

Underground Space – the 4th Dimension of Metropolises – Barták, Hrdina, Romancov & Zlámal (eds)
© 2007 Taylor & Francis Group, London, ISBN 978-0-415-40807-3

Risk analysis and evaluation considering geotechnical stability and environmental effect in tunnel design

Do-Hyung Kim, Chang-Rim Choi & Sea-Joon Oh
Sambo Engineering Co.LTD, Seoul, Korea

Young-Geun Kim
Samsung Corporation, Seongnam, Korea

Jun-Kyung Park
Texas A&M University, Texas, USA

ABSTRACT: The risk analysis of geotechnical stability factors were performed by classifying the factor of safety calculated SSR method, the damage of neighboring structure due to settlement, the groundwater inflow rate into the tunnel and the potential damage by the certain earthquake. Also, the social environmental factors can be grouped into two aspects such as the construction stage and the operation stage; vibration, noise and the drawdown of the groundwater level caused by tunnel construction. Each risk factor was evaluated as a classified term to be the fixed quantity based on various probabilistic and statistic technique, then it was analyzed the distribution characteristic of risk along tunnel line. Finally, the impact was evaluated that how much each risk factor influences on the construction cost with a tunnel construction period by analyzing social charge, so it is possible to perform reasonable tunnel design which was capable of minimizing the risk in the construction stage as well as the design stage.

1 INTRODUCTION

The concept of safety factor was used mainly in the design of underground structure. Such safety factor could be expressed with the ratio of the resistance and the load. It is the most important disadvantage that the conventional design must assign the representative value about the design parameters although the ground itself has the variation and the uncertainty. Therefore, in the conventional design method, estimating the relative reliability of the underground structure is unreasonable. The risk analysis which is referring in this research is the method to use the various probabilistic technique and statistical data.

To complement the traditional design performed by the analysis of the mean ground behavior, the risk analysis considers the uncertainty of ground investigation result and environment element of circumference rationally. Risk factors, which will be able to occur in the design and construction stage of the underground structure must be selected, and quantitative analysis about the risk factors must be performed. The risk about each risk factor can be represented as follows:

$$RISK = \Sigma P_f \times C_f \quad (1)$$

where P_f = the probability of failure; C_f = the cost of failure.

In risk analysis, the assessment about the probability of failure which has the reliability is most important. We estimated the uncertainty of soil parameter and failure model using probabilistic techniques. But, risk factors such as environmental problems are very difficult to be evaluated by probabilistic techniques, so we evaluated the environmental risk using verified statistical data within the related laws and ordinances.

2 SELECTION OF RISK FACTORS IN TUNNEL DESIGN

With a case of the railroad tunnel design in the urban area, we try to explain the method for the analysis and assessment of risk factor in tunnel. As shown in figure 1, the railroad tunnel is comprised of a 3,516 m long main tunnel with two inclined shaft. The residence areas of large scale are located at the tunnel portals and the vicinity of tunnel section with shallow soil-depth. And, the road tunnel intersects at the middle part of tunnel. Risk factors in that tunnel can be categorized by

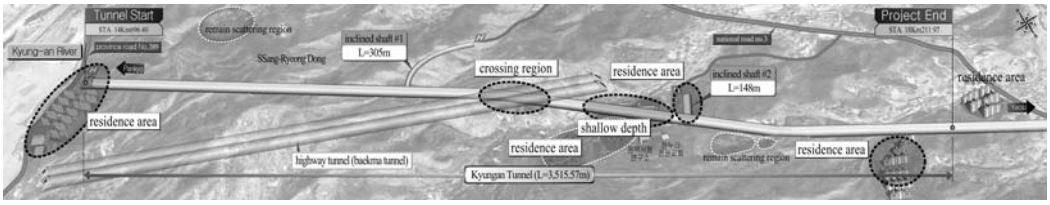


Figure 1. The overview of tunnel region.

geotechnical stability factors and social environmental factors.

2.1 *Risk factors for geotechnical stability*

(1) Support capacity of ground: Tunnel stability is analyzed by using shear strength reduction method (SSR), which is repeatedly calculated the safety factor of tunnel for quantitative evaluation in according to reduction of shear strength (c, ø) of soil and rock.
(2) Ground settlement: Influence on adjacent buildings in tunnel excavation is evaluated by numerical analysis. In this study, maximum strain and settlement of buildings are analyzed for the stability of adjacent buildings.
(3) Inflow of groundwater: Ground water flows into tunnel due to ground excavation and affected the stability of tunnel. In this study, seepage and flow analysis are conducted for the evaluation of groundwater inflow into tunnel.
(4) Earthquake: It is important of influence of earthquake in urban subway. Thus, tunnel stability for earthquake is evaluated by dynamic analysis using amplification of earthquake vibration.

2.2 *Risk factors for social environment*

(1) Vibration and noise by blasting under tunnel construction: Estimation the compensation amount for mental and property damage by tunnel blasting and noise
(2) Vibration and noise by operating train: Estimation the compensation amount for mental damage and property damage by train operation
(3) Drawdown of groundwater: Estimation the compensation amount for damaged wells by tunnel excavation

3 RISK ANALYSIS FOR GEOTECHNICAL STABILITY

3.1 *Support capacity of ground*

The risk for support capacity is analyzed by evaluating the probability of failure due to uncertainty of

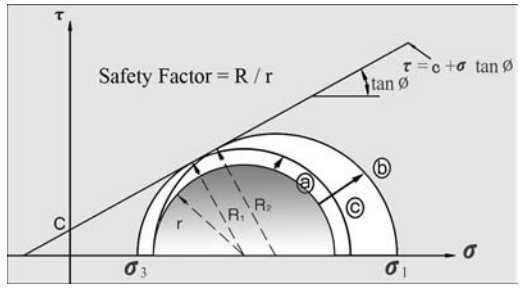


Figure 2. Evaluation safety factor by SSR method.

ground characteristics. Although the sufficient site investigation was performed, the characteristics of the ground behavior couldn't be grasped perfectly. Therefore, strength parameters of the ground include certain level of uncertainty.

The coefficient of variation is the quotient of the empirical standard deviation and the expected value:

$$C_v = \sigma / m \tag{2}$$

The safety represent support capacity of ground itself is evaluated by using shear strength reduction method. Figure 2 shows the concept for evaluation safety factor by SSR method.

The probability of the failure may be expressed by the central safety factor v_c. In the case of normal distribution

$$P_f = 1 - \Phi[(v_c - 1)/\sqrt{v_c^2 C_{vR}^2 + C_{vQ}^2}] \tag{3}$$

where C_{vR} and C_{vQ} are the coefficient of variation of the resistance and the load respectively.

The corresponding relationship for the lognormal distribution is as follows:

$$P_f = 1 - \Phi\left[\frac{\ln v_c \sqrt{(1+C_{vR}^2)/(1+C_{vQ}^2)}}{\sqrt{\ln(1+C_{vR}^2)(1+C_{vQ}^2)}}\right] \tag{4}$$

The risk is evaluated by multiplying the unit cost of tunnel construction with the probability of failure obtained by equation (4).

Table 1. Assessment criteria for the inclination and settlement.

Grade	Management	Inclination	Deg. of damage
A	Normal maintenance	<1/750	0%
B	When the continuous careful observation is needed, normal maintenance after simple repairing.	>1/750 <1/500	5∼10%
C	Partial repairing, reinforcement; the continuous observation	>1/500 <1/300	20∼40%
D	Judgement of the utility limit; overall large scale reinforcement	>1/300 <1/200	40∼60%
E	The utility prohibition, emergency reinforcement; the dismantle and reconstruction	>1/200	60∼100%

Table 2. Groundwater parameter in RMR rock classification criteria.

Parameter		Range of values				
Inflow per 10 m tunnel length (ℓ/min)		0	<10	10∼ 25	25∼ 125	>125
Ratio	Joint water pressure	0	<0.1	0.1∼ 0.2	0.2∼ 0.5	>0.5
	Major principal stress					
Rating		15	10	7	4	0

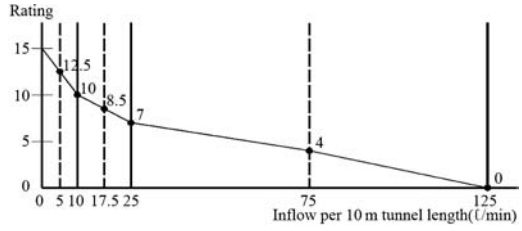


Figure 3. The Continuous graph of RMR rating.

3.2 *Settlement of ground*

The damage of the structure in proximity, which is happens to the ground settlement due to tunnel excavation is important factor in risk analysis. The equal settlement and the inclination of the structure are computed by the numerical analysis and empirical equation, and the damage degree of each structure is estimated. The risk of ground settlement can be evaluated from the damage degree and the unit cost of construction.

3.3 *Inflow of groundwater*

As the failure probability according to the reduction rating from a groundwater inflow at the tunnel face is computed, uncertainty of rock classification is considered in risk analysis. RMR rock classification is computed to the sum total of the assignment rating to be composed of five parameters. Because the rating to be assigned is represented by an unity rating about the case of the schedule range of the parameter, the assignment of continuous rating is impossible and the assessment rating is overestimated or underestimated about a specific parameter.

Charging the rating against the center-value vicinity for the groundwater parameter is performed using interpolation method in consideration of the corresponding RMR value of the phase which is good. As the rating is continuously charged by the stage, the continuous RMR value against the parameter value is expressed as shown figure 3.

The continuous RMR graph of groundwater parameter represent the rating to zero, but in the case which the inflow quantity is large, the rating has a negative value. The continuous RMR rating for tunnel inflow can be expressed by numerical equation as like equation (5).

$$\text{Reduction rating} = -8 \times (\text{inflow quantity} - 0.125) \quad (5)$$

The probability density of an each interval in figure 2 can be evaluated as shown table 3 and the probability density of RMR reduction rating can be expressed in normal distribution as shown figure 4.

The probability of failure for each RMR reduction rating is represented in table 4. The risk for groundwater is evaluated by multiplying the unit cost of tunnel construction with the probability of failure obtained.

3.4 *Earthquake*

At the sections where the computed earthquake acceleration exceed the acceleration criteria based on the coefficient of the earthquake area, it is assumed structures in that dangerous area are collapsed when the earthquake occurs. There, the risk for earthquake is evaluated by considering the damage repair cost for the structure which the collapse is predicted.

4 RISK ANALYSIS FOR SOCIAL ENVIRONMENT

4.1 *Vibration by tunnel blasting*

The estimation criteria of compensation follow the related laws and ordinances and the risk (social cost) by the vibration is divided by mental and property damage. The compensation amount for mental damage can be represented as follows:

$$D = E_{vt} \times P \tag{6}$$

$$E_{vt} = \Sigma(V_e - V_t) \times T \tag{7}$$

where $D =$ damage, \$; $P =$ unit compensation cost, \$/dB·day; $E_{vt} =$ total over exposure of vibration, dB·day; $V_e =$ evaluated vibration level, dB(V); $V_t =$ threshold vibration level, dB(V); $T =$ exposure time, day.

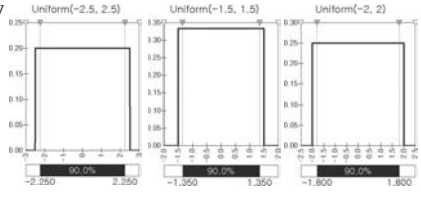
The compensation amount for damage of property can be represented as follows:

$$D = C_{st} \times V_c \tag{8}$$

$$V_c = \frac{V_o}{(15 - S_{st}) + V_o}, \qquad C_v = \frac{V_{pr}}{V_{cr}}^{1.5} \times 4 \tag{9}$$

where D = damage, \$; $C_{st} =$ estimated cost of structure, \$; $V_c =$ vibration contribution; $V_o =$ operation vibration level; $S_{st} =$ status estimation of structure; $V_{pr} =$ presumption value of vibration; $V_{cr} =$ vibration velocity criterion.

Table 3. The probability density of RMR rating.

Inflow	0 ~ 10	10 ~ 25	25 ~ 125
Rating	10 ~ 15	7 ~ 10	0 ~ 4
Probability density graph			

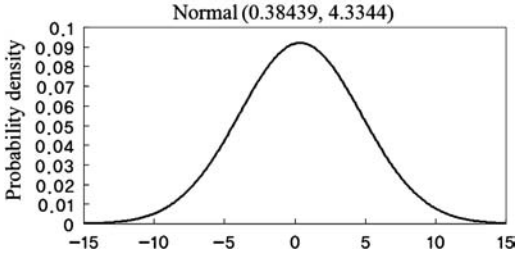


Figure 4. Probability density graph of RMR reduction rating.

4.2 *Noise by tunnel blasting*

The risk of mental damage by blasting noise is evaluated with deductive equation (eq.10) through regression analysis based on the cases of actual damage compensation.

$$M = 12.5D - 102.5 \tag{10}$$

where $M =$ damage amount per a person, \$; $D =$ value in damage conversion table.

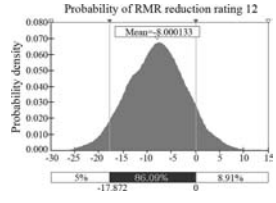
The noise by excavation blasting can be estimated as follows:

$$dB\,(A) = -16.02 \log\,(d/W^{1/3}) + 95.195 \tag{11}$$

where $d =$ distance of the object point, m; $W =$ charging amount of the explosive, kg/delay.

Table 4. The probability of failure for RMR reduction rating.

Rating	Probability of failure	Rating	Probability of failure (%)
12	8.91%	6	0.93
11	7.04%	5	0.65
10	5.12%	4	0.42
9	3.47%	3	0.22
8	2.62%	2	0.22
7	1.76%	1	0.07



The noise by blasting can be predicted by equation (11) based on the charging amount of general blasting in tunnel. And, the compensation amount by general blasting method can be estimated by multiplying the unit compensation cost from equation (10) with the number of residents.

4.3 *Vibration and noise by operating train*

The noise by operating train can be calculated by Lange equation (11) assuming the design life of the tunnel in 30 years.

$$La = 59 - 20 \log d \quad [dB(A)] \tag{12}$$

where d = distance of the building in tunnel

The vibration by operating train can be calculated by Tokita equation (13) through the correction of the vibration level, the transfer characteristic of the vibration wave and the correction about the interaction with structures, etc.

$$L_v = L_o - [A_1 \log (r / r_o) + A_2 r] \tag{13}$$

It is assumed that the noise increases as shown in equation (14) than the initial value as the period to be happened the noise increases.

$$\Delta L = 5 / \log 3 \times \log T \, [dB] \tag{14}$$

Because the damage by the operating train has many continuance periods relatively, the risk by the operating train has very big value than the risk by the blasting.

4.4 *Drawdown of groundwater*

The risk against wells of the neighborhood area which is caused by the tunnel excavation is evaluated. Groundwater levels at each bore hole are measured by groundwater flow analysis before and after the excavation, the influence range which the drawdown of the groundwater is happened is computed. And, the damage compensation cost is estimated by grasping the number of wells in the range of the damage influence.

5 RESULT FOR RISK ANALYSIS

As it is explained from the preceding paragraph, from the risk assessment for risk factors, the relative distribution of the risk in tunnel can be obtained as shown in figure 6 and figure 7. Tunnel engineers can select danger zones and consideration items in the design stage. And, the risk to be inverted to the cost of the failure or the compensation can be expressed as shown in figure 8 and figure 9. The risk amount is very high at the tunnel portals and at the vicinity of tunnel section with shallow soil-depth. Therefore, various design solutions to lower the risk amount were examined in such danger zones.

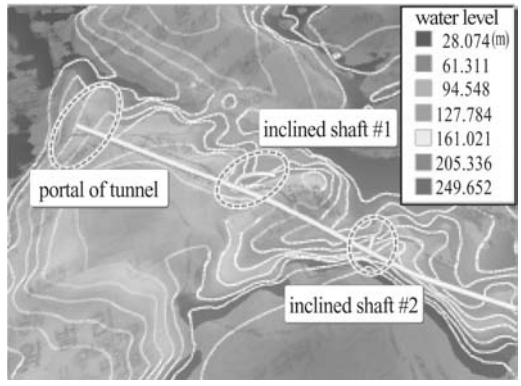
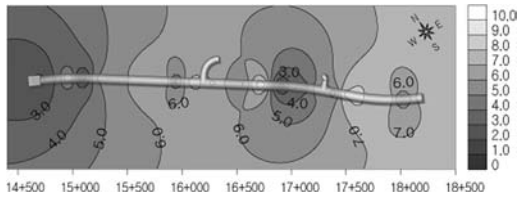
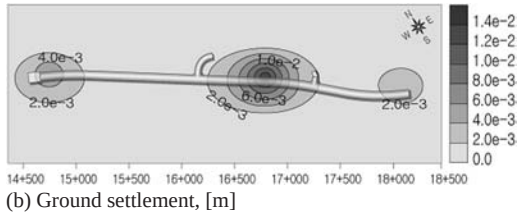


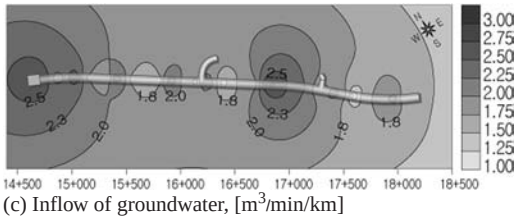
Figure 5. 3-dimensional groundwater flow analysis.



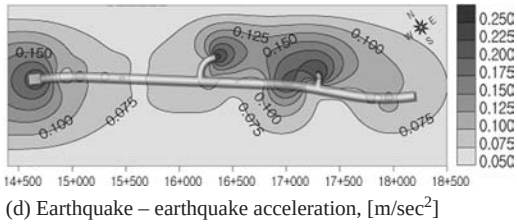
(a) Support capacity of ground – safety of ground



(b) Ground settlement, [m]

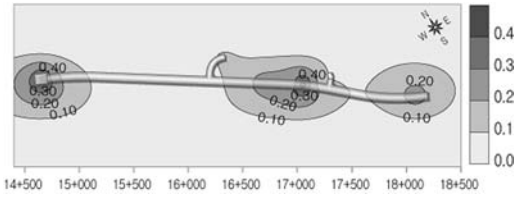


(c) Inflow of groundwater, [m^3/min/km]

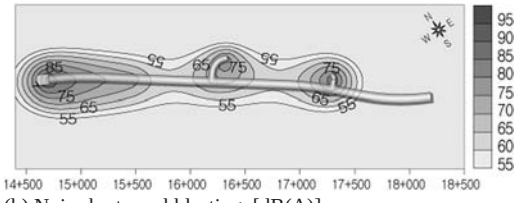


(d) Earthquake – earthquake acceleration, [m/sec^2]

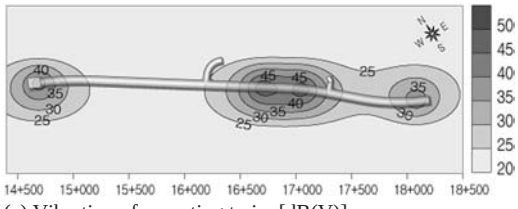
Figure 6. Distribution of risk factors for geotechnical stability.



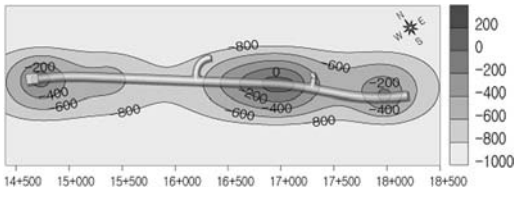
(a) Vibration by tunnel blasting, [cm/sec]



(b) Noise by tunnel blasting, [dB(A)]



(c) Vibration of operating train, [dB(V)]



(d) Drawdown of groundwater – damage range, [m]

Figure 7. Distribution of risk factors for social environment.

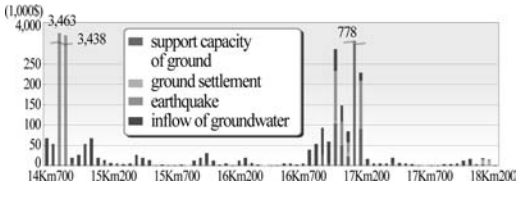


Figure 8. Result of the risk analysis for geotechnical stability.

6 APPLICATION OF THE RISK ANALYSIS IN TUNNEL DESIGN

With application for the evaluation grade of 5 phases for each risk factor, the holistic design index (HDI) system based on the risk analysis is developed in tunnel design.

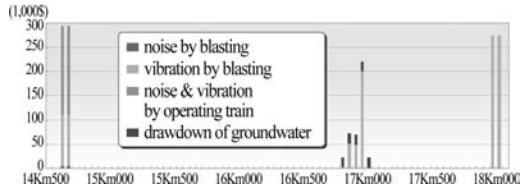


Figure 9. Result of the risk analysis for social environment.

HDI-T represents the relative risk for the geotechnical stability, and HDI-E represents the relative risk for the social environment. The holistic design index of two kinds to be obtained is expressed in figure 10 with the class of rock mass. In the selection of excavation method, the application of reinforcement method and the decision of region for water-proof grouting, the holistic design index offer rational data which can come down the judgement to tunnel engineers.

For example, from comparing the compensation cost due to general blasting method with the increment of the construction cost due to controlled-blasting or non-blasting method in the selection of excavation method, economic design having the rationality is possible.

In the event, we suggested the design method which supplement to the conventional tunnel design based on the class of rock mass through the application of the risk analysis in tunnel design.

7 CONCLUSION

As the tunnel construction increases, there have been risen many environmental issues as well as the stability of the tunnel itself caused by the tunnel excavation. Because tunneling works have many risk factors in both design and construction stage due to the uncertainty characteristics of the ground, the risk assessment and its control is very important for the tunnel construction. In this research, risk factors in tunneling distinguished into two groups such as geotechnical stability factors and the social environmental factors. Each risk factor was evaluated as a classified term to be the fixed quantity based on various probabilistic and statistic technique, then the distribution characteristic of the risk along tunnel line was analyzed. The impact was evaluated that how much each risk factor influences on the construction cost with a tunnel construction period by analyzing social charge, so it is possible to perform reasonable tunnel design which is capable of minimizing the risk in the construction stage as well as the design stage.

With applying the assessment technique for the risk to the conventional tunnel design which be dependent on the class of rock mass preponderantly, we

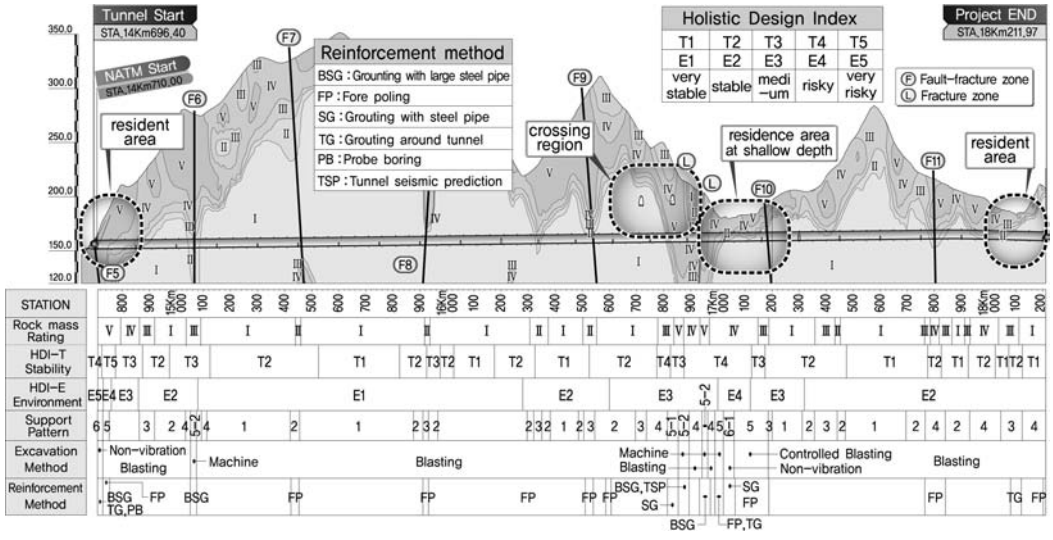


Figure 10. Application of HDI-system for tunnel design.

attempted the rational design for tunnel which considers both the geotechnical stability and the social environment.

In the future, it is needed that the supplementation between the predicted risk in design stage and the actual risk which will occur in the construction stage through the risk management in the construction stage.

ACKNOWLEDGEMENTS

This work was supported by the Korea Science and Engineering Foundation Grant funded by the Korea government (MOST) (No. 2005-D00346). The authors express their appreciation to the KSEF for financial support.

REFERENCES

D.H. Kim, Y.G. Kim, C.S. So, S.J. Oh, K.B. Kim and J.K. Park. 2006. Risk analysis and evaluation considering geotechnical stability and environmental effect in tunnel design; *The Proceedings of Korean Society for Rock Mechanics and Engineering*: 21–38.

C.R. Choi, J.K. Park, D.U.You, Y.G. Kim and D.H Lee. 2003. Development and Application MI System for Tunnel Design; *The Proceedings of Korean Tunnelling Association*: 260–261.

Y.G. Wye, J.K. Park, S.K. Jwun and Y.G. Kim. 2002. Development and Application Multiple Index for Reasonable Tunnel Design; *The Proceedings of Korean Society for Rock Mechanics and Engineering*: 31–42.

The Report for Tunnel Design for Seongnam-Yeoju Double Track Railway Construction Lot. 5. 2005; Korea Rail Network Authority.

László Rétháti. 1988. *Probabilistic solutions in geotechnics, Developments in Geotechnical Engineering 46*: Elsevier.

Milton E. Harr. 1996. Reliability-based design in civil engineering: Dover Publications, INC.

E.M. Dawson et al. 1999. *Slope Stability Analysis by Strength Reduction*; Geotechnique Vol. 49, No. 6: 835–840.

This page intentionally left blank

Underground Space – the 4th Dimension of Metropolises – Barták, Hrdina, Romancov & Zlámal (eds)
© 2007 Taylor & Francis Group, London, ISBN 978-0-415-40807-3

Third party safety issues in international urban tunnelling

Guy Lance & John Anderson
Consultants, UK

Donald Lamont
Health and Safety Executive, UK

ABSTRACT: The worldwide expansion in the development of civil engineering infrastructure has led to a major increase in the numbers and types of tunnels constructed for road, railways and water supply/sewerage schemes. This development has seen significant innovation in design, construction and procurement methods which often involve balancing the commercial risk of new forms of construction against proven methods while maintaining effective control over workplace and third party risks. However a number of identified tunnel failures have led to incidents involving loss of life and damage to property resulting also in substantial underwriting losses. As a number of major tunnelling projects are planned for London, the UK Health and Safety Executive (HSE) commissioned a world-wide research study to obtain a better understanding of the risks posed by urban tunnelling which would also contain conclusions and recommendations.

1 INTRODUCTION

In the development of urban infrastructure over the last thirty years there has been significant innovation in the development of tunnel linings, tunnelling machines, specialist equipment, ground investigation techniques, methods of procurement and in contractual relationships between parties. The evolutionary process of developing innovative design and construction often involves balancing the commercial risk of newer forms of design and construction against proven methods while maintaining control over workplace and third party risks during construction. However a number of tunnel failures have led to ground and sub-surface impacts involving loss of life and damage to property. These events have also resulted in substantial underwriting losses. Consequently, in the UK these events have resulted in an increased awareness of societal risk issues; prosecutions for health and safety offences; and a requirement for risk-based management systems for all independently insured tunnelling projects.

The HSE therefore commissioned a study (Lance and Anderson, 2006) to research a list of the incidences of internationally occurring "emergency events" in urban soft ground tunnelling construction. The term "emergency event" included tunnel collapse, tunnel lining failure, fires, floods, excessive surface settlements (such as surface craters) and significant damage to third party surface and subsurface infrastructure. The study also drew upon the information obtained to produce findings on causes of such emergency events and sought to identify preventative measures that might be adopted.

The methodology of this study was to establish databases on the size of the world market and on numbers of emergency events that have occurred during recent world wide tunnel soft ground construction projects and to draw out conclusions from this information. Published data was collected for all soft ground tunnel types and construction methodologies, and, where sufficient information was available, the primary and underlying causes of emergency events were pinpointed. This information was then used to consider what recommendations might usefully be made to improve the delivery processes of urban soft ground tunnelling projects in order to minimise the risk to third parties arising from construction work. The report has been posted on the HSE website and readers are invited to consult the full text for a more comprehensive report of the research findings and recommendations.

2 INTERNATIONAL MARKET

There is no centralised international database on the number of tunnels that are constructed around the world each year. A few countries regularly publish data regarding their own tunnelling statistics, but these are not presented in a common format that would aid the collation of all international data. The UK, for example, does not publish data on its tunnelling output. In order to establish reliable information on the

Table 1. Length of worldwide tunnels projected by GNP (US$ per Capita).

	Worldwide tunnels – length (km)					
GNP (US$)	1999	2000	2001	2002	2003	2004
>9386	801	840	1039	1080	931	1028
9386–3036	34	144	62	89	86	81
3036–766	236	408	442	404	225	163
<766	97	123	125	47	76	9
Total	1168	1515	1668	1620	1318	1461

Table 2. Number of tunnel emergency events per decade.

	Tunnel emergency events				
	1970s	1980s	1990s	2000s	Total
NATM	0	9	12	4	25
Other	2	2	9	6	19
Total	2	11	21	10	44

size and rate of growth of the world market, a number of web sites listing current and planned tunnel projects were interrogated. The accuracy and completeness of the available information cannot be fully verified and needed to be taken at face value.

From these sources a substantial data set was abstracted, which lists the lengths of tunnel projects that have been announced in each of over 100 countries for the last six years in each of these countries. The database has also been interrogated and re-classified to include the GNP (Gross National Product, per capita, using the World Bank definition) of the countries listed.

3 SOFT GROUND TUNNEL INCIDENTS

The specific focus of the research report was urban tunnelling and, given this objective, further research of the published literature was undertaken to identify and list the numbers of tunnel projects around the world that had experienced emergency events during such construction. These data sets on historic projects have been divided into two main categories, i.e. The New Austrian Tunnelling Method and other tunnelling methods (non-NATM). Both sets of data were then interrogated to identify projects where emergency events had taken place in urban areas sited in soft ground, and the results are shown in Tables 2 and 3.

It can be seen that Table 3 demonstrates a consistent rise per decade in the proportion of emergency events in soft ground urban tunnels to the number of emergency events in all types of tunnel world-wide.

Table 3. Breakdown of tunnel emergency events by ground environment.

Tunnel emergency events	1970s	1980s	1990s	2000–2005
In soft ground	22%	32%	46%	53%
Other ground types	78%	68%	54%	47%

3.1 *NATM incidents*

The HSE report on the Safety of NATM tunnels (HSE, 1996), published in 1996 following investigations after the Heathrow Express tunnel collapse, identified over 100 incidents recorded during NATM tunnelling. Table 1 of this 1996 document describes 39 significant NATM incidents and collapses throughout the world in both urban and rural environments. That information was obtained from an extensive literature search and was supplemented by other sources including private correspondence. Table 2 of this document classified the primary cause of each identified collapse. It was emphasised that, for a range of reasons, most incidents that occur are not reported in any 'official' way and therefore the data must be considered as incomplete. In addition to these listed incidents, the HSE report (see Para. 48 page 16) also identified that 71 incidents had been reported in 65 tunnels constructed in Japan between 1978 and 1991 at unspecified locations. These ground collapses ranged from the 'quite small' through volumes of between 50–500 m^3 of ground (15 Incidents.) to volumes of over 1000 m^3 of ground (3 Incidents.). Additional research undertaken by the authors since 1996, and for the 2006 study, has extended the HSE 1996 list of NATM incidents from 39 to 66 including two incidents that occurred in early 2005.

A feature of the data obtained for the 66 NATM tunnel incidents was the high number of "*failures that were recorded in the area between the tunnel face and the first completed ring of the sprayed concrete lining*". These types of failure were classified as Type A in the 1996 HSE Report. Of the total number of 66 incidents, 44 have a reported failure type, and from those 44, 39 are of the Type A. Of the total number of 25 incidents in soft ground urban tunnelling, 22 have a reported cause of which 20 are of the Type A. Of the total number of 22 with a reported cause, 12 of those incidents also reported the incidence of a surface crater. Other features of the 66 incidents include, (1) the overall ratio of urban incidents to rural incidents as reported by HSE (1996, Para. 47) remains at 2:1, and (2) high levels of consequences, in terms

Table 4. Numbers and causes of non-NATM incidents.

Cause	All	Urban soft ground
Unpredicted ground	20 (63%)	10 (52%)
Fire	3 (10%)	2 (11%)
Compressed air explosion	2 (6%)	1 (5%)
Methane gas explosion	1 (3%)	1 (5%)
Defective workmanship	2 (6%)	2 (11%)
Temporary works failure	2 (6%)	2 (11%)
Flood	1 (3%)	0
Unknown (despite investigation)	1 (3%)	1 (5%)
Total	32	19

of disruption to construction work and to third parties, were associated with the incidences of craters in urban areas.

3.2 *Non-NATM tunnels*

A list of identified incidents that have taken place since 1970 on Non-NATM tunnels in all types of ground and environments has been researched, and totals 42 emergency events. As before, this list has been examined to extract details of those urban projects that were constructed in soft ground. The 42 incidents demonstrate a wider range of primary causation and consequence than for the NATM data. This is demonstrated in the following breakdown and analysis of the information from 32 of the most reliable data sets. The list of causes for "all incidents" and for "urban soft ground" incidents is as follows:

At least half of the above incidents have been recorded as being caused by "unpredicted ground conditions". In general terms, unpredicted ground conditions may arise from poor or inadequate site or ground investigations and for other reasons. In these non-NATM emergency events there are few recorded instances of collapses at the tunnel face. Within the 19 incidents listed above there were 8 instances of surface craters. A further feature of the data set of 32 incidents is that they are randomly distributed in terms of country of location.

Following surface crater incidents in UK involving closed face Tunnel Boring Machines which reflected other incidents that had taken place in other countries (Shirlaw et al, 2003) the British Tunnelling Society (BTS) set up a Working Group to research the backgrounds to these events and draw conclusions. Their Report (BTS, 2005) brought together information on over 100 incidents including 14 incidents associated with Slurry Machines, and 47 incidents relating to Earth Pressure Balance Machines. None of the incidents whose data are included in the BTS Report are specifically identified, but the Authors of this paper are aware that at least three of the UK incidents are also included in the summarized data on non-NATM incidents included in this paper.

4 CONCLUSIONS AND RECOMMENDATIONS

The main conclusions of this research were that quantification of third party risk could not easily be undertaken because of a lack of sufficient and reliable data on a world- wide basis.

Information on the number of tunnel emergency events recorded in the last four decades indicated that both the total number of emergency events and the proportion of these events taking place in urban areas with soft ground tunnels, increased in the three decades since 1970. The latter trend has continued into this part decade.

There were differences between non-NATM and NATM tunnel failures. In non-NATM tunnels there was a tendency for surface craters to form some distance behind the tunnel face and there was greater diversity in the primary causes for such incidents which could involve engineering, management, procurement, organisational, competence, resource or communications issues.

NATM tunnels exhibited different failure characteristics, with surface craters forming above the tunnel face whilst the primary cause of failure was attributed to unpredicted ground conditions.

Urban projects introduced additional risks to tunnelling work due to the density of the existing infrastructure and the close proximity of aging and unfavourably sited infrastructure that was not met on rural sites.

Incidents and emergency events that occurred during underground construction did so as a result of failures of the engineering and health and safety systems devised and put in place to prevent such happenings. It follows that effort should be put into devising, implementing and continuously improving the overall management systems tailored to fit the specific circumstances of the particular underground project. No safety management system, by itself, can eliminate all risk of danger and harm, and some hazards and risks have to be effectively managed on a day-to-day basis by competent persons and organisations. This needs commitment and input from the workforce right through to the higher management levels of key organisations within the specific project structure.

Because of the diversity of underground design and construction work there is no single management methodology for all projects. The authors believe that the factors listed and described below, together with existing published information and guidance, provide a strategic framework of approach that can lead

to a satisfactory safety management system for any underground construction project in any location.

- *Effective Project management*
- *Organisational, procurement and contractual arrangements*
- *Specific Engineering systems*
- *Specific Health and safety systems*
- *The consideration of human factors, and*
- *Availability and use of "enforcement" action*

Effective Project management

Each of the parties needs to project manage effectively his particular input to the development of an integrated safety management system – starting with the client and his initial outline considerations for his project. Consideration of the whole-project risk spectrum from the beginning is appropriate and there are significant advantages to be gained from, for example, integrated management teams, early contractor involvement; early supplier involvement and early operator involvement.

Organisational, procurement and contractual arrangements

Organisational, procurement and contractual arrangements, such as between the client and his chosen design teams, can be crucial to the quality and effectiveness of the overall safety management systems (ITA Working Group No.2. 2004). Project organisational systems also need to relate to those third parties who may be affected by the works. The internal contractual arrangements provide an opportunity to emphasise the importance of cooperation, coordination and communication in the effective identification and control of hazards and risks throughout the project by all parties and the responsibility of all parties to expend the necessary competence and resources to ensure 'best practice' approaches. There is no other field of civil engineering where the integration of design and construction is more important or necessary. Poorly drafted procurement and contractual arrangements can conflict with statutory obligations; impose unfair and unreasonable conditions; create ambiguity, misunderstanding and doubt; and cloud areas of responsibility.

Specific Engineering systems

Much of both design and construction on underground projects relies on the choice and implementation of the engineering systems that are commonly applied to this type of construction work. This could range from the overall design, specification, layout and detailed design of the tunnel lining to the specification and manufacture of complex tunnel boring machines to work effectively in the tunnelling medium of the particular project. The inappropriate choice of, for example, computer analysis software; persons to fill key safety-critical engineering management positions; open or closed face tunnel boring machines; the wrong type of ground stabilising technique; the tunnel lining/surrounding ground monitoring system or the depth of the construction work within the ground in urban situations etc., can compromise the effectiveness of the overall safety management system.

Specific Health and safety systems

The provision and effective implementation of specific systems for the purposes of health and safety are essential (Anderson and Terezopoulos 2000). These range from the provision of specialist advice on health and safety and risk management to those working in both design offices and construction sites and to the provision of persons with special expertise on project expert advisory panels. The prompt, thorough and timely investigation of any accidents, incidents and 'near misses', together with the downloading of the information and conclusions obtained to all who need to know, is of the first importance. Also important is the auditing and review of the elements of the safety management systems with the objective of seeking ways of improvement. Health and safety standards never stand still, and there needs to be the flexibility, coupled with appropriate leadership, to seek to apply higher health and safety standards where this is both practicable and appropriate whether or not required by law.

The consideration of human factors

In large projects it is almost inevitable that safety management systems will be complex and diverse, but they will have to be implemented and managed by persons with a range of skills, experience and knowledge. Some persons will also be given the task of exercising judgments in both engineering and in other contexts – in other words aspects of the overall safety management system will be dependent on 'human factors'. The question then arises, when and where might 'human errors' of one kind or another be made, and, if so, what the possible consequences of these 'errors' might be. It is undoubtedly the case that some 'emergency events' have also been caused by persons intentionally violating work systems and procedures that have been correctly set out, and it is also the case that high level 'errors' can play a major part in creating the circumstances where others might make errors at the workface. The potential for human failure, error or misjudgment is almost everywhere within the system, and as such merits careful consideration by all parties.

Availability and use of "enforcement" action

Where shortcomings in the safety or engineering management systems have been pinpointed, there needs

to be a mechanism by which, if appropriate, effective corrective action can be taken. In some cases it may be necessary to stop the construction work so that the necessary remedial measures can be given priority. This power exists within the statutory enforcement body for health and safety, but should also exist within the contractual arrangements. The sanction of ultimately stopping construction work on health and safety grounds or for deviation from the design could be retained by the client – if necessary on being properly advised about the proposed course of action. Alternatively, the client could retain an organisation with the appropriate competence, skills and knowledge to exercise the role of construction supervision on his behalf.

REFERENCES

Lance, GA and Anderson, JM. (2006), The risk to third parties from bored tunnelling in soft ground. HSE Research Report RR453 downloadable from www.hse.gov.uk/research.

Health and Safety Executive, (1996), Safety of New Austrian Tunnelling Method (NATM) Tunnels, HSE Books.

Shirlaw, NJ., Ong, J., Rosser, H., Tan, C., Osborne, N. and Heslop, P. (2003), Local settlements and sinkholes due to EPB tunnelling. Geotechnical Engineering 156. Issue GE4. Pg. 193–211. Thomas Telford, London.

British Tunnelling Society, (2005) Closed-Face Tunnelling Machines and Ground Stability. A Guideline for best practice. Closed face working group of the British Tunnelling Society, Thomas Telford, London.

International Tunnelling Association Working Group No.2 Guidelines for tunnelling risk management. Tunneling and Underground Space Technology 19(2004) 217–237.

Anderson JM and Terezopoulos NG (2000) Safety in tunnelling is far too important to be left only to safety officers. Proceedings International Tunnelling Conference, Singapore (Nov) pages 567–572 AA Balkema.

This page intentionally left blank

Underground Space – the 4th Dimension of Metropolises – Barták, Hrdina, Romancov & Zlámal (eds)
© 2007 Taylor & Francis Group, London, ISBN 978-0-415-40807-3

Risk management in connection with execution of underground structures and surface development securing

A.J. Lossmann
SG-Geotechnika, a.s., Brno, The Czech Republic

B.V. Motyčka
University of Technology, Brno, The Czech Republic

ABSTRACT: The characteristic features of modern management are comprised of the ability to work successfully in risky conditions. Technically and organizationally complicated engineering structures are usually also demanding from the financial perspective. This applies also to execution of underground structures – tunnel advance and the related securing of the surface development. Application of risk management with utilization of the observation method enables quality, safe, and cost-efficient execution of such structures. At the same time, environmental burden of the construction site surroundings is minimized.

1 INTRODUCTION

Risk management is connected with various areas and it is also understood that way (natural disasters and accidents, environmental risks, financial risks, design risks, commercial risks, organizational risks, technical risks).

However, there are also general regularities of risk management which jointly apply to all areas. The main goal always is to limit the effects of both existing and future risks and to propose solutions which will help to eliminate the consequences of such effects. The process of risk management always comprises the decision making process based on the risk analysis.

Assessment and management of technical (engineering) risks usually consists of the following parts [1]:

- Identification, quantification (determination of quantity) of existing risks
- Risk evaluation (acceptable risk level definition)
- Design and implementation of a program aimed at existing risks reduction
- Monitoring of the implemented program's efficiency
- Possible corrections of the risk reduction program

The above-mentioned parts of the technical risks management process must be carried continuously during the entire course of construction for all significant projects.

2 GEOTECHNICAL RISK MANAGEMENT

Modern projects incorporate certain risk level into underground structures and surface development securing designs. The risk is expressed by the probability that an undesirable effect with certain economic consequences will occur in case of a given project solution in the assessed conditions. The value of acceptable risk is defined, which must be acceptable for all parties involved in the construction and the agreement must clearly stipulate who will bear what part of such risk. The purpose of all this is to achieve a fair saving of work equipment, means, labor force, and of course also time, i.e., in a final context, the saving of construction costs. **At the same time, the quality of the completed work must not be affected.**

This procedure is based on the fact that the rock massif behavior during the tunnel advance can be foreseen less or more successfully, however, it can not be determined precisely. That is why the geotechnical risk of tunnel advance is defined. The geotechnical risk is understood to be a coincidence of the probability of an undesirable development of rock massif interaction with the tunnel lining and resulting impact on the construction. Such negative development would have a negative impact on the economy of the entire project.

Prerequisites for the geotechnical risks management therefore comprise monitoring and evaluation of the interaction between the rock massif and the tunnel lining so that the undesirable development of such an

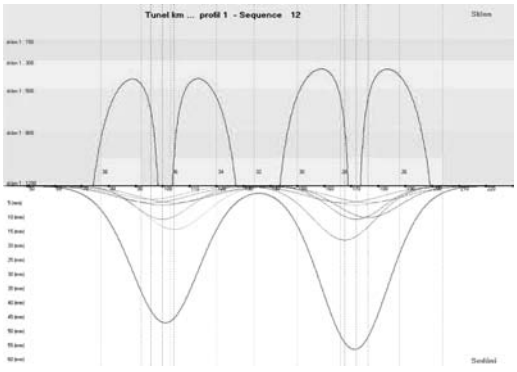


Figure 1. Example of subsidence though prediction for tunnel.



Figure 2. Tunnels often pass below densely developed areas which must be properly secured against the effects of tunneling.

interaction is envisaged and clearly defined in a timely manner.

A group of activities aimed at rock massif condition determination, monitoring of its development, and directing its further behavior is collectively referred to as control monitoring. The control monitoring is based on a measurement design, which comprises a hypothesis of the rock massif deformation, technical and economic analysis of the geotechnical risks and determination of the control monitoring goals, i.e., forecast of the rock massif behavior and related measures. A major part of the control monitoring is comprised of extensive measurement and monitoring of pre-defined quantities (monitoring) within the entire area of the construction (both below and above the terrain level) both during the tunnel advance and after its completion.

3 OVERGROUND DEVELOPMENT SECURING USING THE OBSERVATION METHOD

The so called observation method represents a special control monitoring method. This monitoring method was first described in geotechnics in 1969. The principle of the method is that the initial construction project including the selected execution technology is adjusted and further corrected during the construction process depending on additional information identified regarding in particular the rock massif behavior, its interactions with the tunnel lining, and depending on the real impact of the tunnel construction on the surface development. The construction phase thus provides large amounts of information which was not obtained by previous (although detailed) geological survey.

The structures executed on the basis of traditional design methods (based on geological survey and high safety level) are considerably more expensive when compared to those using the observation method. This method is therefore used in particular to reduce labor demands, material and time saving during the construction execution (including securing of the surface development and therefore the total costs of such construction).

Monitoring thus represents a significant component of the observation method. This in principle comprises measurement and monitoring of selected quantities – their values changing during the construction and their partial evaluation. First of all, these measured values represent the groundwork for verification of correctness of the designed structures and technological procedures or new technical and organizational measures are adopted in order to ensure an uninterrupted and safe course of the construction. Such measures can comprise, for example, tunnel lining modification or changes in surface development securing, etc.

Monitoring relating to tunnel advance and to surface development securing is usually comprised of the following activities:

- Geotechnical assessment of the tunnel
- Convergence measurement of tunnels deformations
- Measurement of stress in the tunnel lining and in the adjacent rock massif
- Extensometric and inclinometric measurements for identification of rock deformations
- Geotechnical surveying of points on the surface and on buildings
- Observation of cracks and deformations of the development
- Dynamic and acoustic measurement of the effects of tunneling on the surface development

The main goal of monitoring and of the observation method is to enable safe execution of construction on the basis of continuously identified values of monitored quantities while minimizing related financial



Figure 3. Methods of sub-basement ceilings securing ribbon vaults in masonry buildings.



Figure 4. Detail of reinforced ribbon vault ceiling securing in subbasement of a residential building.

costs of construction and obtaining the data necessary for passportization and re-passportization of surface development after tunnel advance; this data also serves as the groundwork for possible litigation regarding faults and damages caused by the construction on the surface structures.

Observation method utilization thus relates to the underground structure and, at the same time, to the surface development securing. It is important to emphasize that the securing of surface structures against dynamic effects and subsoil displacements caused by tunnel advance represents the key part of the tunneling process. It is important in particular to secure those structures located in the subsidence trough, for which subsidence, deformations, and inclination are supposed.

4 PRACTICAL APPLICATION OF THE OBSERVATION METHOD DURING CONSTRUCTION OF TUNNELS IN BRNO

The countries of Central and Eastern Europe have been recently subject to a steep increase in individual road transport. In particular in the post-communist countries, where changes in the economic environment have influenced the behavior of most people, the number of cars has doubled during the past fifteen years and this number is still increasing. High loading of transport systems is common in particular in large and medium sized cities, which become jammed during rush hours several times a day.

This unfavorable transport situation has also had to be solved in the Czech Republic, in particular in Prague but also in other major towns including the second largest city – Brno. Due to high technical and technological demands, there has been a long search for a solution, which would be acceptable for the city from an economical perspective.

In the end, it was decided to build the Large Municipal Ring which will be comprised of several long tunnels. It is expected that the entire structure will be executed with geotechnical risks management system utilization. This method of construction should enable significant economic savings for the city and also for the state budget.

This project is based on Brno's new transport organization concept, which consistently enforces protection of private property and environment in the city. This was the reason why tunnel sections have been incorporated into the basic municipal communication system. Two of these tunnels are already in construction – Pražská radiála tunnel below Strážný Hill, which forms part of the western link road and Husovický tunnel, which forms part of the Large Municipal Ring. The third tunnel structure will consist of two tunnel tubes – Dobrovského I and Dobrovského II tunnels (their axial distance reaches up to 100 meters in some places), which are located in Královo Pole and Žabovřesky municipal districts. These municipal districts will be interconnected by the tunnels. They represent the biggest project of its kind in Brno area.

The municipal circuit section passing through these tunnels is approximately 1.2 kilometers long and the tunnels pass below densely built-up area with numerous residential and communal facilities. This places high demands on securing of the surface structures which are subject to vibrations and subsequent subsidence as a consequence of tunnel construction.

Vertical arrangement of both tunnels has been determined with respect to the limitations given by portal sections of the tunnel, municipal main sewer lines, and by the geological conditions in the given area. Surface layers of loess loans and backfills with thickness between 3 and 10 meters with gravel and sandy terraces underneath occur at the construction site. The subsoil of these terraces consists of Neogene clays, so called



Figure 5. Basic Dobrovského drift lining structure consisting of shotcrete C 20/25 (thickness of 100 mm) with mesh size from 60×60 to 150×150 mm and with stiff steel frames from K24 profiles with spacing of 1.0 or 0.5 meter.

"tégly". Vertical positioning of the tunnels has been proposed to ensure minimal thickness of these non-permeable clays between two and three meters above the stope. In order to keep the underground water above these clays in the gravel sand layers. The total overburden thickness varies between 4 and 21 meters in these tunnels.

5 DOBROVSKÉHO TUNNELS – DRIFTS

In order to obtain detailed information about geotechnical parameters of the rock environment along the Dobrovského I and II tunnels route, a project named Silnice I/42 Brno, VMO Dobrovského A, Tunely DOBROVSKÉHO – PRŮZKUMNÉ ŠTOLY (Road I/42 Brno, Dobrovského A City Ring, DOBROVSKÉHO TUNNELS – DRIFTS) has been carried out. It is comprised of three drifts which comprise approximately 20% of the total volume of both tunnels.

These drifts have also been constructed for other reasons:

- verification of the tunneling technology in the environment of Neogene clays,
- identification of previously unspecified problems which could occur during tunnels construction,
- verification of tunnel advance effects on municipal development in order to provide for subsequent extrapolation of these effects on advance of full tunnel profiles.

The construction of the Dobrovského tunnels is currently at the phase where work on drifts has been completed. Work relating to surface structures securing still continues and construction of the tunnels is being prepared.

The Roads and Motorways Directorate of the Czech Republic (Brno Branch) is the investor in this project. Design has been prepared by Amberg Engineering Brno, a.s.

Tunnel advance is expected to start in 2007.

6 CONCLUSIONS

The securing of surface structures against the dynamic effects and subsoil displacements caused by tunnel advance represent an important part of drift and tunnel construction. It is in particular important to secure those buildings which are located in the subsidence trough, and for which subsidence, deformations, and inclinations are therefore expected.

Complicated geological conditions caused by the rock environment of Brno's Neogene clays (tégly) and dense surface development consisting of residential and communal facilities, utility networks, and roads, make the construction of the Dobrovského tunnels a unique engineering project within the whole Czech Republic. This is reflected in modern construction methods comprising the risk management system, which enables significant economic savings to be achieved for the entire project.

The aim of geotechnical risks management is therefore to ensure timely technical and organizational response to an undesirable interaction development including any consequent deformations of structures on the surface and to ensure a continuous, economic, and safe course of construction.

LITERATURE / REFERENCES

[1] Rozsypal A. 2001: Kontrolní sledování a rizika v geotechnice (Control Monitoring and Risks in Geotechnics) Jaga group Bratislava, Slovak Republic.

[2] Bažant Z., Klusáček 2001: Static During Reconstructions, Brno University of Technology, Faculty of Civil Engineering, Brno, Czech Republic.

[3] Zemánek I., Lossmann J., Socha K. 2003: Impact of exploration galleries for the Dobrovského Tunnel on surface development in Brno; Application of the observation method, Tunnel magazine 3/2003, Czech Republic.

[4] AMBERG Engineering, 2003–2006: Comprehensive Information – Roads I/42 Brno, Czech Republic.

[5] Smejkal V., Rais. K. 2003.: Řízení rizik (Risk Management), Grada Publishing a.s., Czech Republic.

[6] Barták J. a kol.: Tunel Mrázovka (Mrázovka Tunnel) , Satra spol.s r.o., Praha, 2004.

[7] Lossmann, J. 2004: Řízení rizik – vliv ražby tunelů (štol) na objekty povrchové zástavby, konference Zakládání staveb Brno 2004 (Risk Management – Impact of the Tunnel Heading (Drifts) on the Buildings of the Surface Housing, Conference for Foundation of Buildings – Brno, Czech Republic.

Underground Space – the 4th Dimension of Metropolises – Barták, Hrdina, Romancov & Zlámal (eds)
© 2007 Taylor & Francis Group, London, ISBN 978-0-415-40807-3

Contracting issues for conventional tunnelling

Nasri Munfah
Parsons Brinckerhoff, New York

ABSTRACT: Conventional tunnelling, also referred to as the New Austrian Tunnelling Method (NATM) is different from other tunnelling methods because of its dependency on the means and methods and the qualifications of the contractor and his work force. In addition, conventional tunnelling is often used in unknown or difficult ground, and has high construction risks. The main issue that overrides all aspects of underground construction and particularly conventional tunnelling is risk. The level of risk sharing between the owner and the contractor is a major factor in deciding the type of procurement practices and the contractual terms and conditions to be implemented.

1 GENERAL

1.1 *Conventional tunnelling*

The International Tunnelling Association (ITA) Working Group 19 defined Conventional Tunnelling as: the construction of underground openings of any shape with cyclic construction process of:

- Excavation, by using the drill and blast methods, or mechanized excavators except for full face TBM
- Mucking
- Placement of primary support elements such as steel ribs or lattice girders; soil or rock anchors; or sprayed or cast in situ concrete.

In this context the conventional tunnelling, also referred to as the New Austrian Tunnelling Method (NATM) is different from other tunnelling methods because of its dependency on the means and methods and the qualifications of the contractor and his work force.

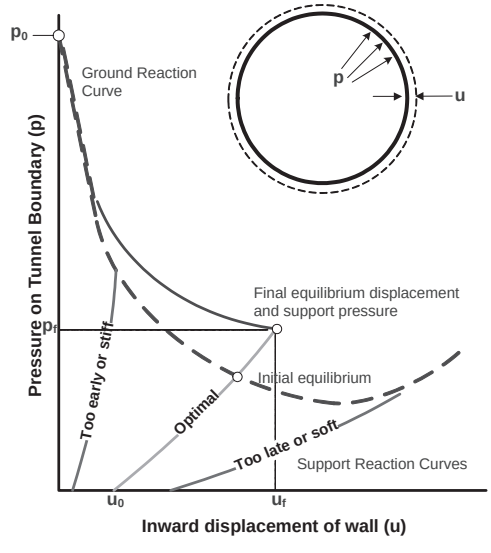


Figure 1. Ground reaction curve concept.

1.2 *Principles of conventional tunnelling*

Conventional tunnelling is used for long and short tunnels, of constant cross section or irregular shape; it is used for large opening such as storage caverns, rail stations, or complex intersections; it is used in rock, soft ground, or mixed face and difficult ground; in dry and wet conditions; it can be used for deep excavation as well as in the case of low overburden.

The design philosophy is based on mobilizing the inherent ground strength to the maximum extent possible through controlled deformation of the ground (see figure 1). Therefore, it is critical for the success of conventional tunnelling that the stiffness, the strength and the timing of the initial support are compatible with the ground deformation. Hence conventional tunnelling is dependent on a rigorous instrumentation and monitoring system to verify the ground stability and the adequacy of the support.

The principles of conventional tunnelling consist of:

- Sequential excavation
- Curvilinear profile (cross section)
- The ring must promptly be closed
- Initial support using shotcrete in combination with steel fibres or welded wire mesh and lattice girders or steel ribs
- Stability confirmed by rigorous monitoring of stresses and deformations.

In addition, conventional tunnelling has a variety of tools to improve the performance of the ground by increasing its stand-up time, limit deformations, control ground loss at the face, create ground arch and increase the ground inherent strength. Some of these tools include:

- Ground reinforcement such as rock bolts
- Pre-support including spiles, pipe umbrellas, horizontal jet grout, etc…
- Vacuum dewatering
- Face support by earth berm, fibreglass bolts, and shotcrete
- Abutment piles to increase the lateral stability
- Adjustment to the geometrical configuration and sequence of excavation.

Conventional tunnelling is a flexible tunnelling system and depends on the observational method and the qualifications of the workers; therefore its contractual terms should also be flexible to be able to compensate for variations in ground condition encountered and its performance, and be able to address potential construction risks.

The main issue that overrides all aspects of underground construction and particularly conventional tunnelling is construction risk. The level of risk sharing between the owner and the contractor is a major factor in deciding the type of procurement practices to be implemented.

1.3 *Construction risks in conventional tunnelling*

Conventional tunnelling imposes risks on the owner, the contractor, the designer, and potentially the public. There could be the risk of unknown and unanticipated ground and groundwater. There could be risk of delay and cost overrun and potentially environmental risks. In urban areas, there is the risk of subsidence and potential damage to third party properties or persons. In addition, public opposition of the tunnelling project due to its disturbance to the neighbourhood, noise and vibration, and other issues could result in significant delay.

In a study conducted by the US National Committee on Tunnel Technology (USNCTT) in 1988, it was documented that over 55% of construction claims in tunnelling projects are related to unforeseen ground conditions, with over 95% of these claims relatively substantial in value and a significant percentage of these claims are settled for their full (or almost full) values. It is no surprise that most cost increases in tunnel projects are related to unforeseen geotechnical conditions. These generally include type and behaviour of the soil and rock; ground water conditions; presence, size, and nesting of boulders; contamination of the soil or the ground water; presence of methane gas or other hazardous materials; etc. Therefore it is essential to have a complete and comprehensive geotechnical exploration program. However, it is more important to properly interpret the geotechnical parameters and the anticipated behaviour of the ground and document such interpretation in the contract documents.

Undocumented abandoned foundations, uncharted utility lines, uncontrolled rubble fills, and man-made obstructions buried underground are some of typical construction risks. These elements add to already difficult ground conditions and may increase construction risks and cost, and negatively impact the project schedule.

Generally tunnelling projects need the approvals of various public and private entities, each with its requirements and interests. Approvals from environ mental agencies, funding agencies, and project stakeholders are critical. Public opinion and the approval of citizen groups especially in well-established communities and cities where such organizations have significant political influence are critical. Typical concerns related to construction are impact on property values, disruption to businesses and daily routine activities, emission of dust, noise and vibration, working hours, and the potential increase in pests and rodents. Buy-in of construction methodologies and approaches by the public in the early stages of the project is critical for its successful completion. Agreements reached with the public should be reflected in the construction contract documents. Continual interfacing with the public during construction is important to assure the people that agreements reached are being implemented, and also to address new concerns that might develop after the start of construction.

2 RISK MANAGEMENT

Traditionally construction risks have been managed indirectly through the design process often resulting in conservative design that would lead to higher contractor contingencies in his bid price. ITA Working Group 2 developed guidelines to manage construction risks using systematic risk management techniques from the project conceptual development through implementation in the construction phase.

As stated above, most claims in underground construction are related to unforeseen conditions. Therefore, the underground construction industry in the United States tried to provide a viable trigger by means of the Differing Site Condition (DSC) clause, culminating in the use of the Geotechnical Baseline Report (GBR) and Geotechnical Data Report (GDR). It is important from a risk-sharing perspective that the contractual language in the DSC and the GBR is harmonized.

2.1 *Risk allocation/sharing*

The allocation of risk between the owner and the contractor will have a direct relationship to the contractor contingency as part of the contractor's bid. Therefore, it is important to identify a risk sharing mechanism that is fair and equitable and that will result in a reasonable contingency by the contractor and sufficient reserve fund to be provided by the owner to address unforeseen conditions. For example unforeseen conditions due to ground conditions are paid for by the owner if certain tests are met, while means and methods are generally the contractor's responsibility and his inability to perform under prescribed conditions are risks to be absorbed by the contractor.

2.2 *Contractor's contingency/owner's reserve*

With proper contracting form and equitable allocation of risks between the owner and the contractor, the contractor contingency, which is part of its bid price, will be reduced. Similarly, the owner's reserve will be used only if certain conditions are encountered, resulting in an overall lesser cost to the owner.

3 CONTRACTING PRACTICES

Generally, two categories of delivery methods have been used in the past for underground construction, with various levels of success. They are:

- Design-Bid-Build
- Design-Build

The contractual terms of these two delivery methods vary widely. The most common is the fixed price approach, although for conventional tunnelling unit prices approach is the most suitable and prevailing. However, other contract terms used include:

– Fixed Price lump sum
– Low bid based on unit prices
– Quality based selection
– Best and Final Offer
– Cost plus fixed fee
– Negotiated Compressed Process (NCP)
– Quality based selection

The following discussion addresses the advantages and disadvantages of these methods with respect to conventional tunnelling.

3.1 *Design-Bid-Build with fixed price contract*

The form of contract known as Design-Bid-Build is traditionally for a firm fixed price. In this contract form the work must be performed as shown and specified in the contract documents, and may not be qualified or conditioned. Generally, the owner engages a design engineer to provide a complete design and document it in contract documents consisting of drawings and specifications, obtain all approvals, secure right-of-ways and easements, obtain third party and stakeholders approvals, and obtain required permits. In this form of contract, it is presumed that the owner is getting the fixed price and the contractor will have the benefit of profit and accept the full responsibility of losses. As such, the contractor is assuming the full risk, and therefore he adds high contingency to his bid. This form of contract is easy and straightforward. It delineates clearly the roles and responsibilities between the owner and the contractor, the owner provides a complete design and obtains all approvals, while the contractor executes the work with the best means and methods it sees fit; it provides strong owner control, as a result potentially higher quality is achieved, although it will often cost more; in this form of the contract, the owner should have a complete identification of the geotechnical issues and resolutions to the environmental issues prior to bid otherwise, they are added cost. However, this method of procurement has its disadvantages, including: higher contractor contingency. Since the contractor is assuming all the risks, he would place a high contingency in his bid, regardless of whether such risks materialize or not. The owner will have no input on the contractor's means and methods in order not to assume the contractor's risk, however if the means and methods selected by the contractor are not suitable, the owner will suffer by having a delayed schedule or a lesser quality product. Because the contractor is bidding on a completely pre-established design with no provisions for qualifying the bid, the contractor will have little incentive to be creative or to deviate from the prescribed design. In this form of the contract, the contractor's qualifications are established post bid opening which might result in a selection of inexperienced or unqualified contractor to perform conventional tunnelling which is highly dependent on the workmanship and the qualifications of the workers.

3.2 *Design-build project delivery method*

In this process, the project is awarded to the low responsive and responsible bidder to prepare the design and construct the project. The owner's engineer usually prepares bidding documents based on preliminary design level identifying the owner's requirements. For conventional tunnelling projects, the geotechnical and environmental investigations are generally advanced to a higher level of completion to provide better information. The selected contractor then prepares the final design and constructs the project. This process is gaining interest among owners for underground projects in order to reduce the overall time required to complete the project, avoid dealing with disputes over changed conditions, and avoid lengthy and costly litigations.

The procurement options of the design-build approach vary based on the project goals and the owners objectives. Examples of the procurement options include: Competitive Bid (low price), Competitive Bid with High Responsibility Standards (cost and qualifications), Competitive Bids with Alternative Proposals, Price and Other Factors, Price after Discussion including "Best and Final Offer", Quality Based Selection, or Sole Source Negotiation.

The intent of the design-build process is to accelerate the schedule by shortening the time of the design, to develop the design to meet the construction means and methods, and to advance the procurement of long lead items.

It is imperative in a design-build process for tunnelling projects that the owner obtains all right-of-ways and easements, and necessary approvals and permits. It is also important to carry the geotechnical investigation to a high level of completion and to identify and resolve all interfacing with adjacent properties, private and public organizations, and other stakeholders prior to awarding the contract in order to avoid potential delays and unanticipated cost.

The advantages of this procurement process are: potential accelerated schedule; contractor's input in the design, which may result in better details for construction and implementation of less costly methodologies; early interaction with the designer to identify and address constructability issues; it encourages innovation and allows creative construction approaches; it provides a simplified accountability and responsibilities process; and it may shelter the owner from potential construction claims and changes.

The major disadvantage is the overall loss by the owner of the control of the project during the final design and construction. While owners are concerned about the long term performance of the project and about peripheral yet critical issues such as maintenance of existing operations, adjacent utilities, environmental issues, and the long term maintenance and operation of the facility, the design-build contractor is often less concerned about these issues. Although owners try via this process to shift the risk of unforeseen site conditions to the design-build contractor, unless a full geotechnical investigation is performed and a baseline is established, such shifting of risk is usually unsuccessful. Other disadvantages include: a potentially lower quality product, it requires complete definition of the project requirements early, and it may result in higher overall cost.

It is recommended that for conventional tunnelling projects where design-build delivery method is to be used the geotechnical and environmental investigations are completed, all right of ways and easements are acquired, all approval processes be completed, and all permits obtained prior to awarding the contract. It is also recommended that a GBR be included as part of the bid documents.

3.3 *Qualification based selection*

Qualification based selection is suitable for conventional tunnelling but seldom used. The contact is modelled similar to Construction Manager/General Contractor (CM/GC) approach using a qualification based process. In this contract the cost is established either as a guarantee maximum price, or as an estimated reimbursable (the Portland Model) which is the sum of the anticipated cost reimbursable plus a fixed fee. Labour, equipment and materials are paid on cost reimbursable while contractor overhead, superintendent, management, general conditions costs and profit are parts of the fixed fee.

The selection process is modelled after the two-step selection process similar to procuring professional services. A key element of this process is an interview in which contractors would have the opportunity to demonstrate their understanding of the project and highlight their experience.

In this form the selected contractor would review and comment on the design and would perform constructibility reviews, value engineering, and risk assessment and jointly with the designer and the owner establish baseline values and the contract's general provisions. The estimated reimbursable cost (ERC) would be developed and negotiated. The goal of the ERC is to establish a baseline budget and a cash flow plan. The intent is to establish a reasonable construction cost without contingencies. The contingency would be separately established based on the risk analysis and would be held by the owner. The estimated reimbursable cost plus the fixed fee becomes the contract value. To accurately track and control the cost an accurate cost control program would be needed.

The advantages of this approach are: the selection is based on the best value rather than the lowest cost; it provides evaluation of the contractor's qualifications, techniques, and processes; it provides the ability for the contractor to be involved in the design, including constructibility review, value engineering, provisions for means and methods, etc. . . . These are important factors for a successful project. It also provides opportunities for creativity and innovation. In addition, the determination of contractor responsiveness is made prior to award, and the contingency is held by the owner and would be used only if conditions are different than stipulated in the contract.

However, this approach has disadvantages: it may not be able to protect confidentiality of means and methods, resulting in contractors' reluctance to fully disclose their means and methods prior to award; it may invite protests from bidders identified as unqualified,

or from bidders challenging the technical ranking of the various proposals; it requires significant oversight by the owner and an elaborate project control program, without it may result in uncontrolled project cost; and it is difficult to implement.

Variations of this approach is the Two-Envelope approach in which the selection is made purely based on qualifications; and the Negotiated Compressed Process (NCP) which elements include pre-qualification of contractors, establishment of a technical working group, and execution of a technology acceptance agreement.

4 CONTRACTUAL MEASURES FOR CONVENTIONAL TUNNELLING

Using conventional contracting, design build, or qualification based selection, it is important to establish measures to manage construction risks in conventional tunnelling. These measures may include prequalification of contractors, full geotechnical disclosure, Dispute Review Board (DRB), the use of differing site condition clause, escrow bid documents, unit prices and contingent bid items, value engineering, owner controlled insurance program, and partnering. Some of these provisions are discussed here.

4.1 *Prequalification of contractors*

This involves technical and financial qualifications of the potential bidders to ensure their ability to perform the work effectively, economically, and to a high quality. The pre-qualification would include the company's or the joint venture's technical ability to perform the work. Items to be evaluated include: approach, experience with similar projects, with similar ground, and similar proposed methodology. Pre-qualification of the key staff, such as the contractor project manager, the field manager or superintendent, the senior staff, and he workforce is critical for a successful project. In addition the bidder's financial ability to obtain bonding and its solvency, its history of completing projects on time and within budget are factors in the bidder financial qualifications. Pre-qualification should extend to major subcontractors and major suppliers.

4.2 *Unit prices and contingent bid items*

It is recommended that for conventional tunnelling unit prices be the basis of the bid. The unit prices should reflect the various anticipated ground conditions and their support systems. They should also reflect the various "tools" in the conventional tunnelling tool box such as spiling, forpoling, pipe umbrella, horizontal jet grouting, vacuum dewatering, rock bolts, face stability measures, abutment piles, and changing in the excavation sequencing. In addition providing contingent bid items to supply some of the conventional tunnelling tools in the field is recommended. Some of these tools may not be anticipated but their provisions in the field would be beneficial to address unanticipated conditions. The unit costs of these items would be established as part of the bid and would be used only if needed and if approved by the engineer.

4.3 *Full geotechnical disclosure*

Experience has shown that full disclosure of geotechnical information would reduce the risk to both the owner and the contractor and thus the project cost. Therefore it is important for owners to invest in a comprehensive geotechnical program. The information should be included in the contract documents in the Geotechnical Data Report, Geotechnical Interpretive Report, or Geotechnical Baseline Report. The intent of the disclosure of geotechnical information is to share and allocate construction risk between the owner and the contractor.

The Geotechnical Baseline Report establishes quantitative values for selected conditions anticipated to have great impact on construction. These values are established through technical interpretation of the data and commercial considerations of risk allocation and sharing. The advantages of this report are ease of administration of contractual clauses, unambiguous determination of entitlement, clear basis of contractor's bid, and clear allocation of risk between owner and contractor.

4.4 *Dispute Review Board (DRB)*

The dispute review board process started in the United States in the mid-1970s as a result of accelerated claims and disputes in underground construction and expanded dramatically in the 1980s and 1990s. In this process a board of independent, experienced, and impartial members is selected to hear and address disputes. Generally the board consists of three members, one representing the owner, one representing the contractor, and the third, who will act as the chair of the board, selected by the other two members. The board provides recommendations to resolve disputes that participants are unable to make. It was found that this process has resulted in lower bid prices, better communication and less animosity at the job site, fewer claims, and more timely and cost effective resolutions.

4.5 *Partnering*

Recently, partnering clauses have been included in tunnelling contracts. The goal of partnering is to minimize disputes and to prevent them from escalating in time and value by resolving them at the lowest possible level

in the project organization. It attempts to establish a win-win attitude between the project participants. This process encourages dialogue among the various participants and relies on reasonable people to resolve disagreements reasonably. It seeks to eliminate adversarial posturing and positioning that often develop when disputes and claims arise.

4.6 *Differing Site Conditions clause (DSC)*

The Differing Site Condition clause was established as a measure of allocation of risk between the owner and the contractor relative to the ground condition.

There are two categories of DSCs: Category 1 governs when subsurface conditions differ from those indicated in the contract documents. Category 2 applies when conditions which were not known to the contractor at the time of contracting, differ from those normally encountered in the area. It is generally related to unusual conditions and not based on contract documents. It is important to note that to recover on the DSC clause the contractor must show impact on cost and time and must show causality.

4.7 *Escrow bid documents*

In this process the lower bidder bid documents are placed in an escrow, that is, held in trust by a third party and turned over to the grantee only upon fulfilment of a condition. These documents would then be utilized if needed to assess a fair entitlement and adjustment for additional work, differing site condition issues and claims. However, in this process owners fear that the contractor could condition its bids and contractors fear that they could lose confidentiality of means and methods. This process has not been used extensively.

5 CONCLUSION

The need for a creative, progressive, and fair contracting form is critical to control the rising costs of underground construction. The contract form should address the uncertainty of conventional tunnelling work and its associated risks. It is important that conventional tunnelling be preformed only by qualified contractors with fair contracts that would allocate risks equitably between the owner and the contractor, in order to have safe, on time, and high quality underground projects.

REFERENCES

American Society Of Civil Engineers: '*Avoiding and Resolving Disputes during Construction*', 1991

G. Brierley And G. Smith: 'Going Under? How About Urban Design/Build!', *World Tunnelling*, November 1998

P. Gribbon et al 'Portland, Oregon's Alternative Contract Approach to Tackle a Complex Underground Project' RETC Rapid Excavation and Tunneling Conference Proceedings, 2003

ITA/AITES 'Guidelines for tunnelling risk management: international Tunnelling Association, Working Group No.2', 2004

ITA/AITES 'Conventional Tunnelling: Report of the working Group 19', 2006

A.A. Mathews, R. Matyas, P.E. Sperry and R. Smith: 'Dispute Review Board – Current Status and Recommendations', Rapid Excavation Tunneling Conference (RETC) Proceedings, 1995

N. Munfah 'Contracting methods for underground construction' NAT 06 Proceedings, Chicago, 2006

R. Robinson, M. Kucker and J. Gildner: 'Levels of Geotechnical Input for Design-Build Contracts', RETC Proceedings, 2001

R. Robinson et al 'Application of Design Build Contracts to Tunnel Construction', North American Tunneling Conference Proceedings, 2002

J. Stolz: 'Proposed Revisions to the Differing Site Condition Clause', North American Tunneling Conference Proceedings, 2002

Underground Technology Research Center (UTRC): 'Geotechnical Baseline Reports for Underground Construction', Technical Committee for Geotechnical Reports, Randall Essex ASCE, Editor, 1997

Underground Space – the 4th Dimension of Metropolises – Barták, Hrdina, Romancov & Zlámal (eds)
© 2007 Taylor & Francis Group, London, ISBN 978-0-415-40807-3

Development and application of the new TBM risk management system

K. Murakami
Kajima Corporation, Tokyo, Japan

M. Murayama & K. Terada
Kyoto Prefectural Road Public Corporation, Kyoto, Japan

Y. Fuke & Y. Miyajima
Joint venture of Miyazu No.12 Tunnel Project, Kyoto, Japan

K. Aoki
Kyoto University, Kyoto, Japan

ABSTRACT: The TBM Excavation Control System developed by authors has already been put to practical use. It can monitor the drill energy coefficient calculated from the drill logging data as an index of rock properties and the TBM driving data during the excavation. In this paper, the new TBM risk management system is developed to realize the automatic, real-time prediction of the rock properties ahead of the tunnel face with good precision. The core feature of this system is to analyze data by means of the geostatistical methods such as the Kriging and the Sequential Indicator Simulation. It allows us to use outputs as a form of risk management. This system is put into practical use and validated in the ongoing construction site.

1 INTRODUCTION

The TBM method is used because of its potential for high-speed excavation. However, if there is some ground trouble such as collapse, it hinders the progress, making it impossible to fully achieve the high-speed excavation capability of the TBM. It is important, especially in countries like Japan that have complex geological conditions, to have a detailed information of ground conditions and to be able to take appropriate action as soon as necessary to avoid trouble.

For this purpose, the authors have developed the TBM excavation control and monitoring system (Shirasagi et al. 2000), which can combine the results of the drill logging (Aoki et al. 1990), TBM driving data, an amount of muck measured by conveyer belt scales (Inou et al. 2001), a ground evaluation method based on the state of muck (Inou et al. 2000) and display in one system so as to predict geological conditions ahead of and surrounding the tunnel face and to help an operator control TBM excavation.

However, all these data are independently used for ground evaluation and it is difficult to link them to make real-time geological prediction. Thus, the authors have developed comprehensive geological evaluation methods that could coordinate these data and process more data with highly accuracy. One of the methods statistically describes ground information such as the drill energy coefficient obtained from the drill logging, TBM driving data and the observational rock mass grade as a regression equation derived from multivariate analysis, calculating the rock mass grade at cutting face by means of the regression equation (Yamamoto et al. 2003). The other analyzes the drill energy coefficient and TBM driving data by means of geostatistical method such as the Kriging and the Sequential Indicator Simulation (Mito et al. 2003), creating distribution maps of rock mass properties and maps showing the distribution of the probability of weak rock emerging.

This paper reports on the results of the new TBM risk management system which can conduct real-time geological assessments using multivariate analysis and geostatistical methods. The method, which is applied to the TBM construction of an evacuation tunnel in the Miyazu No. 12 Tunnel, is found to be able to make more accurate predictions of geological conditions than previous methods. This paper also reports that construction could be undertaken while conducting accurate risk management because of this system.

2 OVERVIEW OF THE MIYAZU NO. 12 TUNNEL

2.1 *Description of the construction*

This project is to construct the main tunnel which is 3,660 m in length and the accompanied evacuation tunnel which is 3,692 m in length. The length of 3,457 m of the evacuation tunnel has already been excavated by the 5.0 m-diameter open-type TBM as you see in Figure 1. The TBM was equipped with a percussion-drilling machine used in drill logging and in reinforcement in loose ground.

2.2 *Topography and geology*

The geology is composed of granites of the Mesozoic-Cretaceous. However, because this base rock is intruded by other types of granites, the geology is more complex than that of ordinary granitic ground. The maximum overburden depth is approximately 280 m.

2.3 *Support pattern*

Table 1 shows the structure of each support pattern, while Figure 2 shows a comparison between the designed support proportions and adopted ones. The actual ground conditions were about one or two ranks worse than the designed. Furthermore, the support patterns were often changed because of the ground conditions changing every few meters to every few dozen meters.

The steel liner (SL) as you see in Figure 3 was developed by Kajima so as to support tunnel walls by means of wire net coupled to two ribs of C-100 steel beams. It is adopted as a special support for well-fractured and continuously collapsing ground condition in order to quickly prevent the rock around the tunnel from loosening. It is built up in the TBM roof in advance, and then pressed against tunnel walls as soon as they appear.

Although it is initially designed for a shielded hard-rock TBM, it is expected that the main ribs are bent because the wire net, which is rigidly welded to ribs, is pushed out against walls by TBM main grippers of the open-type TBM. Consequently, the buffer spring

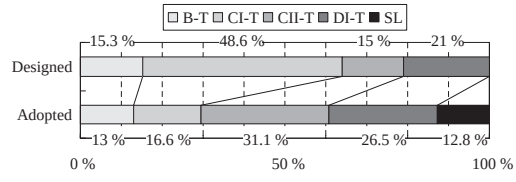


Figure 2. Comparison between designed support proportions and adopted ones.



Figure 1. 5.0 m-diameter open-type TBM.



Figure 3. Installed steel liner supporting walls with wire net.

Table 1. Structure of support patterns.

Support pattern	Geological evaluation score	1 stroke (m)	Fiber shotcrete		Steel support size, intervals
			Angle (°)	Thickness (mm)	
B-T	65∼100	1.5	–	–	–
CI-T	55∼70	1.5	120	20	–
CII-T	35∼60	1.5	180	20	H-100, 1.5 m
DI-T	0∼40	1.0	180	30	H-100, 1.0 m
SL	0∼40	1.0	–	–	C-100, 1.0 m

coupling the wire net with the ribs loosely is developed as you see in Figure 4.

3 NEW TBM RISK MANAGEMENT SYSTEM

The New TBM risk management system sorts out and processes various data automatically, such as TBM driving data, drill logging data, and wall rock mass grade. And it applies them to a multivariate analysis and the geostatistical methods. Thus, this system can visualize the geological conditions ahead of the tunnel face in real time, and provide feedback on the geological conditions for the next excavation.

3.1 *Characteristics of the new TBM risk management system*

Figure 5 and Figure 6 show flow charts of the conventional geological evaluation method and the New TBM risk management system respectively. As shown in Figure 5, in the conventional method, drill logging and TBM driving data and observational rock mass grade have been collected as the excavation progresses, and the ground conditions have been evaluated separately.



Figure 4. Buffer spring connecting rib and wire net.

On the other hand, in the new TBM risk management system (shown in Figure 6), when data are collected to some extent (e.g. when the face reached 700 m from the portal at this site), a multivariate analysis is conducted using drill logging and TBM driving data as explanatory variables and rock mass grade as criterion variables to derive a regression equation. The regression equation can thereafter calculate the rock mass grade at the cutting face for the next excavation automatically in real time, using drill logging and TBM driving data.

Using the geostatistical methods, the drill energy coefficient obtained from drill logging and the predicted rock mass grade are processed, creating a drill energy coefficient map ahead of the tunnel face as well as a probability map of collapse occurring ahead of the tunnel face. The latter map, in particular, largely contributes to risk management during the construction, as it helps to grasp a risk of the occurrence of collapse as probability. Moreover, these maps are updated along the progress of TBM excavation, therefore, it is expected that the precision of geological prediction will be improved.

3.2 *Components of the new TBM risk management system*

The new TBM risk management system consists of five components.

First is the TBM driving data. Its components such as the penetration rate, torque, revolutions, excavating

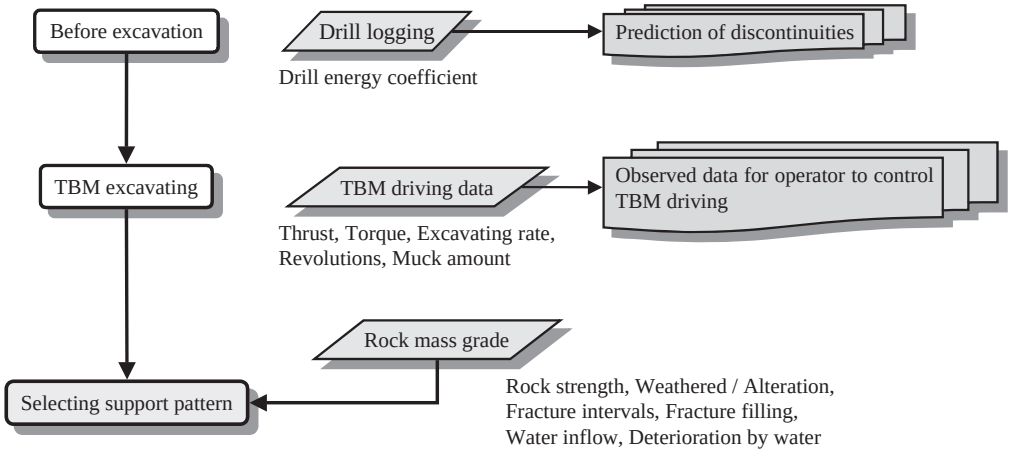


Figure 5. Flow chart of ordinary evaluation system.

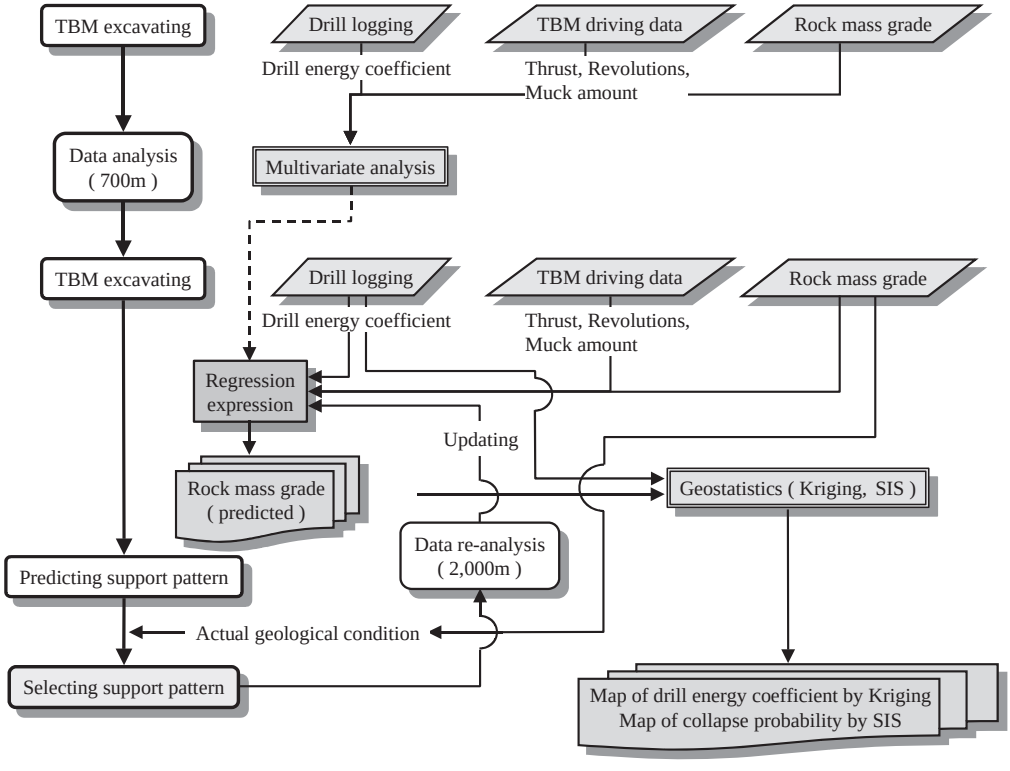


Figure 6. Flow chart of geostatistical evaluation system.

rate, thrust, and muck amount are recorded in the TBM excavation control and monitoring system. The real-time monitoring of these data is of great help to TBM operators.

Second is the drill logging system. It aims to calculate a drill energy coefficient based on drilling data. To collect the drilling data, a percussion-drilling machine installed on the TBM bores about 40 m ahead. A drill energy coefficient is defined as the energy required for crashing a unit volume of rock and shows good correspondence with rock mass quality.

Third is the rock mass grade (RMG). The geology behind the TBM tail is observed and six items, such as rock strength, alteration due to weathering, joint spacing, joint condition, water inflow and deterioration by water, are graded 4, 5 or 6 ranks. Every tunnel support pattern is decided predominantly based on a such weighted averaged rock mass grade and stability of tunnel wall.

Fourth is the multivariate analysis to set of a regression equation for predicting rock mass grade. This project has two regression equations. One is obtained from another site which was under similar condition. The other is calculated after the excavation progressed to 700 m and 2,000 m from the portal. The second regression equation applied to the depth of 2,000 m or below is shown as Equation 1

$$S = 3.3\ R + 0.0034\ T_h - 0.36\ M + 35 \quad (1)$$

where S = predicted RMG; R = revolutions; T_h = Thrust; M = Muck amount.

Finally, the geostatistical methods for prediction of geological conditions ahead of the tunnel face are the core features. One of the major objectives of geostatistics is to estimate with high precision the spatial distribution in a broader area using limited sample data from limited sections. In such cases, it is notable that spatial random structure is estimated based on probability. In the prediction of geological conditions ahead of the tunnel face using the geostatistical methods, two distribution maps are created: one is a rock property distribution map by Kriging, and the other is a probability map, which describes a probability of rock property exceeding a certain threshold by the Sequential Indicator Simulation (SIS). The procedure is shown below:

(i) To estimate spatial property (spatial structure) of the target physical values from a mean value, variance and covariance showing spatial random

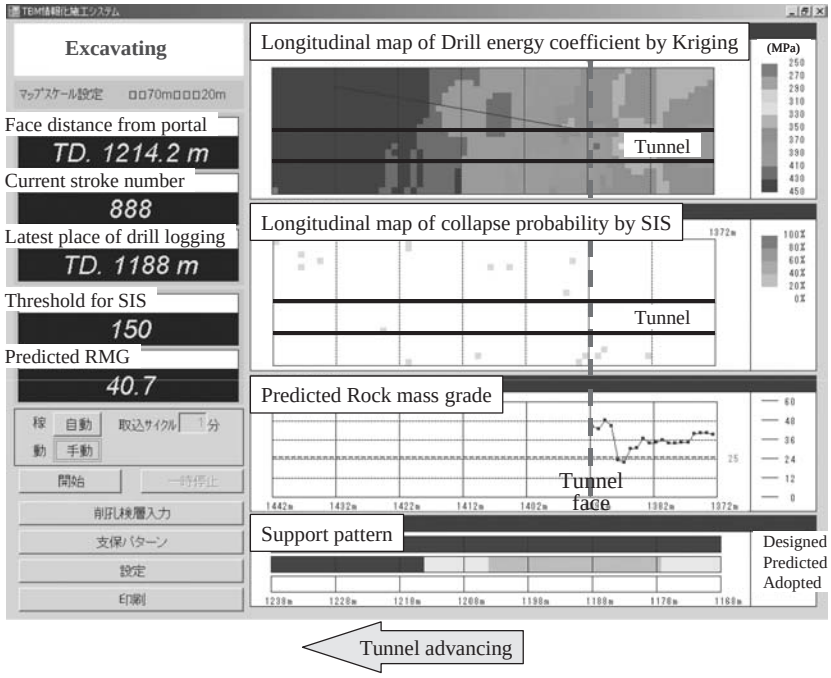


Figure 7. Monitor display of the TBM risk management system.

structure of observation values, and create a random field model (Calculating Variograms).

(ii) To estimate values at somes point with no observation values as linear sums of the observation values, using a modeled spatial structure (Kriging).

(iii) To use an estimated value for a point with no observation value as an observation value (as a known value) in sequentially estimating the next value, and develop an estimation map.

(iv) To develop a number of estimation maps by changing the order of estimation points based on random numbers, and evaluate and output the probability of an estimated value at each point (SIS).

3.3 *Observational construction using this system*

Figure 7 shows a screenshot. On the left side of the screen, the basic status of TBM is displayed, such as the present position of the face and a stroke number, whereas on the right, the results of comprehensive geological evaluation are shown. These indications can be analyzed and updated at every stroke of excavation (every 1.0 to 1.5 meters) with one click. In such a way, the geological evaluation using various data and geostatistical methods can be conducted easily at a site, enabling observational construction to be promptly implemented.

The window at the top shows the drill energy coefficient map by Kriging. Based on drill logging and TBM excavation data, drill energy coefficient is mapped using Kriging to show ground conditions ahead of and surrounding the tunnel face.

The window under that shows the probability map of collapse occurring by SIS. This is useful to estimate the probability of collapse occurring and to show particularly risky place. At this project site, the probability of a drill energy coefficient of 150 J/cm^3 or below is mapped using SIS.

The window under that shows the predicted rock mass grade as a graph. It is obtained by substituting a drill energy coefficient and TBM driving data into the Equation 1.

The window at the bottom shows the support patterns. It is possible to display a designed tunnel support pattern, a predicted one based on a predicted rock mass grade and the adopted one.

4 RESULTS OF APPLICATION TO THE ACTUAL CONSTRUCTION

Figure 8 shows the application results of the new TBM risk management system to 3,320 m to 3,370 m from the portal. A longitudinal geological profile based on the observation is shown at the top, followed by a comparative graph of the designed and adopted tunnel support patterns. Below this graph, a drill energy coefficient map, a probability map of collapse occurring,

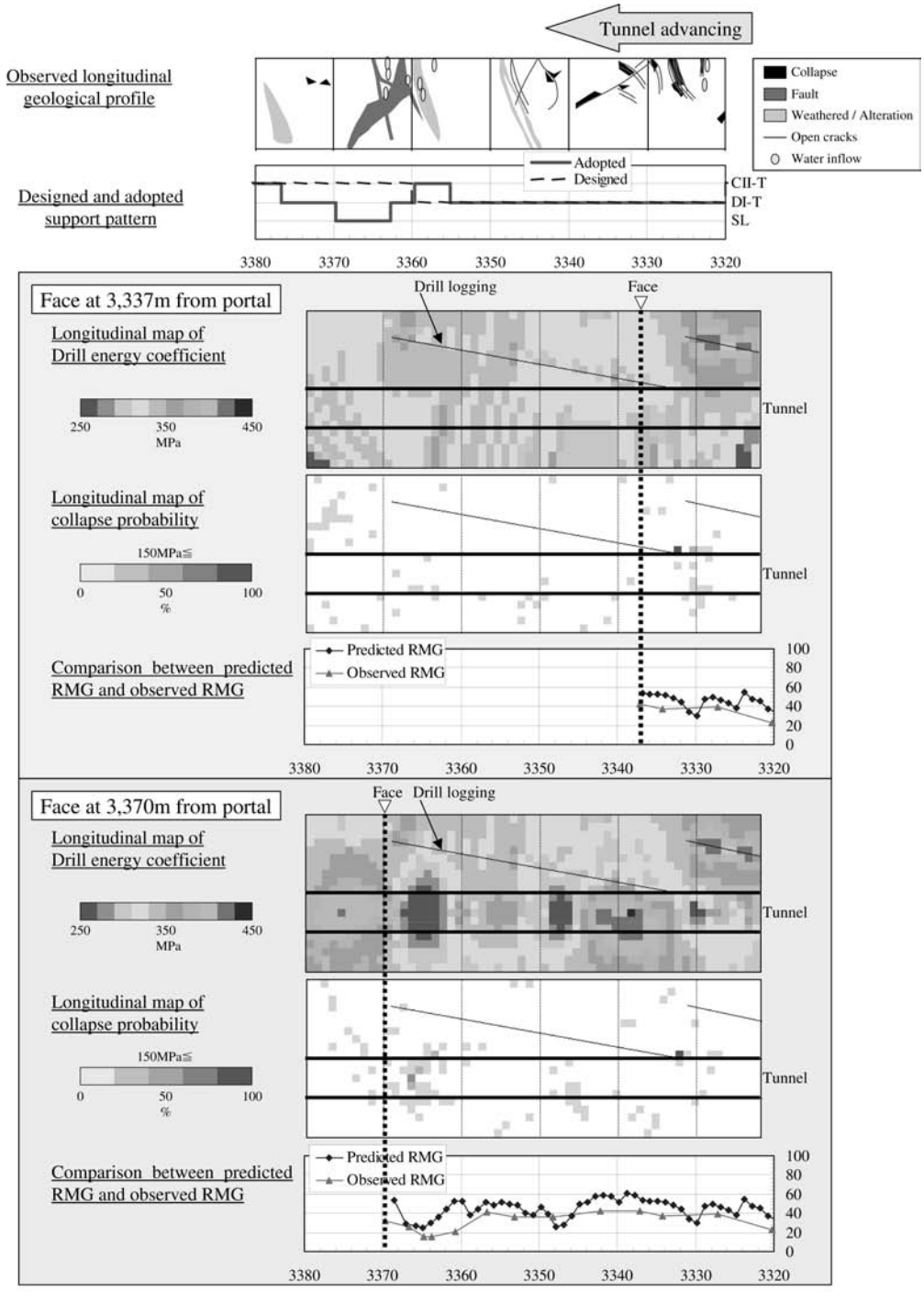


Figure 8. Application results of the new TBM risk management system.

and a comparative graph of the predicted and observed rock mass grade output from this system when the tunnel face was at 3,337 m are shown as the initial value; then, similar graphs for 3,370 m are shown as the final results.

It is clearly shown by these maps and graphs with the progress of the excavation that the distribution of low drill energy coefficient, high probability of collapse occurring and low predicted rock mass grade are around 3,348 m, where a weathered or altered layer exists, and around 3,365 m, where much amount of weathered granite falling off was observed. Because the probability map of collapse showed that the blocks with high probability of collapse accumulated around 3,363 m, it became possible to change the tunnel support pattern to the steel liner. Thus, a probability map, in particular, could largely contribute to the risk management against collapse, by changing the tunnel support patterns or examining the auxiliary methods.

Although the predicted rock mass grade fluctuates more frequently than the observational one, the former almost correspond to the latter on the whole. The rock mass grade at the tunnel face that cannot be observed can be estimated in advance, making it possible to decide the tunnel support pattern before the TBM roof passes.

Moreover, these analytical results will provide important data for confirming whether or not the construction on the ground with severe geological changes has been implemented appropriately, too much, or not enough.

5 CONCLUSION

In this paper, the outline of the new TBM risk management system is given in the beginning; that is, this system introduces a multivariate analysis and the geostatistical methods to visualize the geological conditions ahead of the tunnel face in real time using TBM driving data, drill logging data, and rock mass grade, then feedbacks the geological conditions to the next excavation. Then, this system was installed on the TBM used for the excavation of the Miyazu No. 12 Tunnel, and the results of application to the actual construction were examined. As a result, the following points are validated: (1) The rock mass grade at the tunnel face that cannot be observed visually can be estimated with high precision, (2) The geological conditions ahead of the tunnel face can be estimated as a rock property map with high precision, and (3) The blocks where collapse is likely to occur can be predicted from a probability map. Thus, this system has been proved to be a geological evaluation system that largely contributes to the implementation of the reasonable TBM construction method. Moreover, it can also provide important data to verify after the construction whether the adopted tunnel support pattern is appropriate, too much, or not enough for the actual ground.

In the future, we aim to make this system more sophisticated by analyzing data again more precisely. Furthermore, by applying the geostatistical methods to the main tunnel construction of this project, we hope to establish this system as a risk management system for the main tunnel accompanied by an evacuation tunnel.

REFERENCES

Aoki, K., Inaba, T., Shiogama, Y., Tezuka, Y. 1990. Evaluation of geological conditions by "Drilling Logging System" (in Japanese). *Proc. of the 8th Japan Symp. on Rock Mech.* pp.67–72.

Inou, M., Yamamoto, T., Shimodera, S. 2001. Evaluation method for tunnel face using muck weight by TBM's excavation (in Japanese). *Proc. of the 56th JSCE annual meeting 2001*. pp.104–105.

Inou, M., Miura, S., Yamamoto, T., Kuronuma, I., Tanaka, H. 2000. Development of Evaluation Methods for Tunnel Face using Muck by TBM's Excavation (in Japanese). *Proc. of the 55th JSCE annual meeting 2000.* pp.116–117.

Shirasagi, S., Yamamoto, T., Inou, M., Yamamoto, S., Mito, Y., Aoki, K. 2000. Development of Intelligent TBM excavation control system. *Proc. of the ISRM Regional Symp. Eurock 2001, Espoo, Finland, 4–7 June 2001*. pp.615–620.

Yamamoto, T., Shirasagi, S., Mito, Y., Yamamoto, S., Aoki, K. 2003. Observational construction using the TBM excavation control system. *Proc. of the Sixth Intern. Symp. on Field Measurements in Geomechanics, 15–18 September 2003, Oslo, Norway.* pp.401–407.

Mito, Y., Yamamoto, T., Shirasagi, S., Aoki, K. 2003. Prediction of the geological condition ahead of the tunnel face in TBM tunnels by geostatistical simulation technique. *ISRM 2003 – Technology roadmap for rock mechanics, Proc. Intern. Symp., Johannesburg, 8–12 September 2003.* pp.833–836. South African Institute of Mining and Metallurgy.

This page intentionally left blank

Underground Space – the 4th Dimension of Metropolises – Barták, Hrdina, Romancov & Zlámal (eds)
© 2007 Taylor & Francis Group, London, ISBN 978-0-415-40807-3

Risk assessment of discharge due to tunnel excavation using Simplified Seepage Analysis System (SWING)

Yuzo OHNISHI
Dept. of Urban and Environment Engineering, Kyoto University

Hiroyasu OHTSU
Dept. of Urban Management, Kyoto University

Kenji TAKAHASHI & Toru YASUDA
Dept. of Tunnel Engineering, Pacific consultants Co., Ltd, Osaka

ABSTRACT: Excavation of tunnel in Japan recently faces a lot of difficult conditions such that very complex geology, interaction with adjacent structures and groundwater problems in relation to environmental impact. In addition, the large amount of groundwater that happens in the tunnel construction is an important problem of the tunnel construction. That is, Groundwater is one of the important risks in the tunnel construction. Moreover, the risk evaluation technology that is related to groundwater is an indispensable technology to construct the tunnel of the economy and the high quality. This paper describes a new evaluation method executed in the mountains tunnel intended to carry out construction with higher reliability, including methodology of risk evaluation method that is related to groundwater.

1 INTRODUCTION

Groundwater poses problems for the construction of mountain tunnels in that measures to prevent or control face collapse and tunnel drainage are needed due to the large quantities of water inflow that result from the discontinuous nature of the ground. Groundwater problems in the surrounding environment include the chain reaction of damage to the surrounding water environment that occurs due to the drainage of groundwater and the impacts of groundwater on existing water resources. There have been many cases in which such problems have inevitably led to enormous cost overruns and missed deadlines. Numerical analysis has been a primary method to evaluate such groundwater problems, but it requires the time and effort of preparing ground models of a certain scale and processing the data. For this reason, in almost all cases, the evaluation of groundwater problems has relied on preliminary evaluation throughout, and reverse or verification analysis rarely been performed during the construction. Moreover, even with current analysis tools it is difficult to conduct impact evaluations that reflect the preceding excavation data. This study proposes a new observational system for mountain tunnel construction, the Simplified Seepage Analysis System ("SWING"), which enables streamlined construction with risk evaluation for cost fluctuations while at the same time considering measures to deal with groundwater problems.

2 DEVELOPMENT OF THE SWING SYSTEM

Groundwater poses problems for tunnel construction in that measures to prevent or control face collapse and tunnel drainage are needed to deal with large quantities of water inflow, as well as measures to ensure safety during the construction process. The damage to the surrounding water environment due to groundwater drainage and the impacts on existing water resources of a drop in the groundwater level also pose problems in the surrounding environment, and conservation of the natural environment is an important issue for tunnel construction.

Groundwater analysis has been used to evaluate such groundwater-related problems. However, existing groundwater analysis methods require the preparation of ground models of a certain scale, and even with the improved calculation performance, analysis and data processing are still both time-consuming and labor-intensive. As a result, unlike deformation analysis, groundwater analysis has rarely taken the form of reverse or verification analysis based on preceding data collected during actual tunnel excavation work, and thus has conventionally been performed as

preliminary analysis in almost all cases. As such, it is difficult even using current analysis tools to conduct, in accordance with the progress of tunnel excavation, an impact evaluation that reflects preceding data gathered during the construction process. Given this, a new evaluation system called the Simplified Seepage Analysis System (SWING) is proposed here, which is easy to use and is capable of making accurate predictions for the conservation of water environments in the area around tunnels and groundwater problems in tunnel work.

This paper presents an overview of the SWING system, which has been developed to enable economical, streamlined tunnel construction while considering hydrologic systems, as well as the development of related analysis methods and evaluation techniques. The tunnel used as a case study for analysis here was running under a water system inhabited by rare hydrophilic species and waterfalls that are tourist attractions, which required environmental conservation considerations. Behind the development of the SWING system, there was the need for development of a groundwater analysis method that satisfied the following basic principles of dealing with water inflow during construction and the impacts on the surrounding water environment.

3 HYDROLOGICAL BALANCE ANALYSIS MODEL IN THE CROSS-SECTIONAL DIRECTION USING THE SWING SYSTEM

The SWING system is not a numerical analysis method using a ground model, as represented by seepage flow analysis or the modified tank model. Based on the water inflow incurred by actual tunnel excavation, modeling is conducted with a unit slice volume of 50 meters in the excavation advance direction, and a hydraulic equation is applied within this slice volume to determine the coefficient of permeability and the effective porosity. Furthermore, based on the hydraulic constant determined from preceding data, the range and volume of the drop in groundwater level and the drop in the quantity of marsh water are determined for the slice volume. Then, during tunnel construction, it is used to validate the results of predictions made against site measurements (marsh water flow and groundwater level) and the current impact of droughts.

In the case of this study, the pre-construction input values consisted of the seismic velocity in the tunnel longitudinal direction, the specific resistance, and other results of physical exploration which were used to determine the hydrological categories in the tunnel longitudinal direction. The SWING system was used to make predictions based on these initial settings. As the construction progressed, the excavated sections were reviewed based on the preceding construction data, and continued estimates of the as-yet-excavated sections were made. In the case study here, identification of the excavated sections and predictive evaluation for the as-yet-excavated section (with respect to the tunnel water inflow, the range of the drop in the groundwater level, and the marsh water reduction) was done in about 2–3 hours, including correction of the input data. In some cases, the results of drain boring at the face were retrieved rapidly and determination of the quantity of water inflow during the main shaft excavation and predictions of the effect of the accompanying drought were done instantaneously. The equations used to assess the hydrological balance elements in the SWING system are shown below.

3.1 *Assessment of tunnel water inflow and drop in groundwater level*

The one-dimensional unsteady flow shown in Figure 1 was considered in order to determine the basic nature of tunnel water inflow accompanying excavation and the mechanism of groundwater flow in the event that water inflow is produced. In short, it was assumed that a tunnel with a sufficiently small diameter with respect to the ground size had been constructed within an aquifer above horizontal impermeable ground. With the passage of time following excavation, the groundwater level for which the initial water level H is constant drops gradually starting from directly above the tunnel. At this time, the groundwater flow is a two-dimensional unsteady flow. In the SWING system, this is replaced with Dupuit's quasi-uniform flow analysis. Other methods that take the similar approach as the SWING system in which groundwater during tunnel excavation is analyzed using a slice coordinate system include the methods proposed by Nishigaki et al[1)] and by Sato et al[2)]. As shown in Figure 1, assuming that the groundwater level in the aquifer accompanying rainfall seepage ε is level for an initial value of $t = 0$, the groundwater level at $t = 0$ can be derived from Dupuit's quasi-uniform flow equation. Thus, the tunnel water inflow quantity q(t) considering time-history is given by Equation (1).

$$q(t) = \frac{k(H_0^{\,2} - h_0^{\,2})}{2\left[\frac{k(H_0^{\,2} - h_0^{\,2})}{2\varepsilon}\left\{1 - e^{-6\varepsilon t / \lambda e(H_0 - h_0)}\right\}\right]^{\frac{1}{2}}} \quad (1)$$

where, ε: Rainfall seepage, K: Permeability, H_0,h_0: Groundwater head, q(t): Water inflow per unit of length, R(t): Length of section in which groundwater level has dropped, h(x,t): Water level at arbitrary point, λe: Effective porosity. This enables the characteristics of the reduction in tunnel water inflow quantity within each slice volume to be calculated. However, here it is necessary to take into consideration the rainfall seepage ε as a hydrological cycle element.

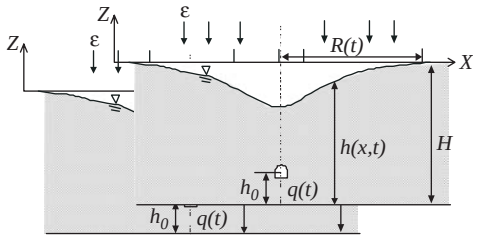


Figure 1. Flow of groundwater accompanying tunnel water inflow.

Here, a rainfall seepage value that matches the amount of rainfall is adopted, using the critical storage height at the surface and a one-dimensional tank model that recreates the Horton's uniform flow. This value is determined for each tunnel excavation slice, and the tunnel excavation distance is calculated successively as a time-history parameter. Naturally, the tunnel water inflow within existing work sections continues to decline over time. The accumulated quantity of water in each slice volume is the amount of water inflow at the tunnel entrance.

In addition, the degree and range of the drop in groundwater level will increase along with the amount of tunnel water inflow, but these values can be determined for each slice volume using the hydraulic equation shown in Eq. (1). Tunnel water inflow is closely related to the geological conditions and the groundwater in the surrounding ground, and fluctuations in tunnel water inflow over time and rainfall response constitute extremely important information regarding ground conditions.

In addition, because face water inflow gushes out from the face at the front of the excavated section and the surrounding uncovered sections, it will usually fluctuate in sequence with the progress of the construction.

3.2 *Evaluation of impacts on surface water*

This section will show the procedure used in the SWING system to assess the impact on surface water. The base flow in the valley topography shown in Figure 3 will be considered. Because "base flow" is normally synonymous with groundwater runoff in the river basin, based on the shape of the valley topography, the base flow component of surface water can be approximated using a hydraulic equation for impenetrable wells and open channels. Accordingly, the drop in groundwater level caused by tunnel excavation can be substituted with the drop in groundwater level in the river basin, and that reduction can be used to assess the decrease in base flow. In other words, in this procedure the average drop in groundwater level is calculated based on the drop in groundwater level within the river basin, followed by the calculation of decrease in base

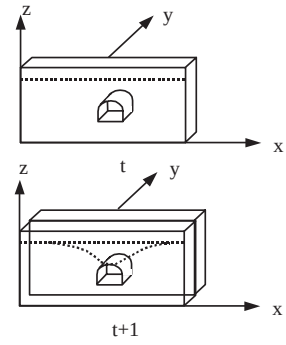
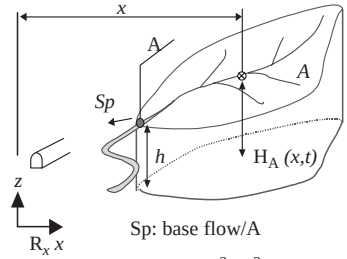


Figure 2. Cumulative unit slice volume accompanying progress in tunnel excavation.



$$Sp(t) = \frac{\pi K (H_A^2 - h^2)}{Ln(R/r)} \cdot \frac{\theta}{360} \cdot \frac{1}{A}$$

R: Width of river basin
r: Width of river channel
θ: River basin angle of aperture
A: Area of river basin

Figure 3. Assessment of effect on surface water.

flow for an arbitrary river basin. Surface water fluctuates considerably along with rainfall, and the impact on base flow will be different from the flow of surface water observed directly in site surveys. Given this, tank models for each flow monitoring site are linked and the fluctuations in flow are determined from the original surface water hydrograph accompanying the reduction in base flow. Figure 3 shows the hydraulic equations for each hydrological cycle element used in the SWING system. The figure shows the equations used to assess the water inflow mode and the drop in groundwater level in the slice volumes for the increased tunnel progress length, as well as the drop in groundwater level at an arbitrary point and the marsh water impact.

4 EVALUATION OF CONSTRUCTION COSTS NEEDED FOR GROUND RISK AS DETERMINED USING THE SWING SYSTEM

This section deals with the additional study of ground risk, which is defined as the anticipated loss (the

probability of occurrence multiplied by losses due to preventive measures) for events that are assumed to cause groundwater-related damage, based on the statistical models considering the uncertainty of ground during tunnel excavation and the remedial work cost by incorporating ease of use, one of the SWING system's characteristics, and its impact evaluation technique. Ground risk incurred by tunnel excavation includes construction-related risks (such as face collapse and unexpected water inflow gushing out during construction) as well as the impact on the surrounding water environment. However, this evaluation will focus on the risks to the surrounding water environment as a result of tunnel excavation.

4.1 *Assessment of tunnel water inflow quantity and drought impact using the SWING system*

The tunnel boundary conditions were applied to the aforementioned analysis conditions and an assessment was conducted of the quantity of water inflow expected to be produced inside the tunnel, as well as the drop in groundwater level and the reduction of marsh water. As was mentioned earlier, all of the water inflow produced in the tunnel is the result of physical properties in the tunnel longitudinal direction, and the values are calculated for each slice volume using the SWING system. With regard to the prediction of specific water inflow quantity and impact estimates, assume that the number of Monte Carlo simulations is noted as N and a permeability distribution in the tunnel longitudinal direction is created for each realization. In this case, a tunnel water inflow quantity and degree of impact will be calculated for each realization using the SWING system. Estimates of water inflow quantity, groundwater level and marsh water reduction that are in accordance with N will also be assessed.

4.2 *Risk of cost fluctuations for measures to deal with water inflow and droughts*

Based on existing references and interviews with specialists with regard to the control of and countermeasure against water inflow to deal with the quantity of water inflow, the cost Ci of water inflow and drought measures with respect to the results of analysis of realization i are assessed from countermeasure scenarios for the drop in groundwater level and the reduction in marsh water and the relationship between the degree of impact and the quantity of water inflow for realization number i. Therefore, the cost of water inflow and drought measures that indicate the estimation method will be discrete probabilities derived from the Monte Carlo simulations. Accordingly, a risk curve is used with an evaluation of costs in which the vertical axis is the exceedance probability and the horizontal axis is the cost of water inflow and drought measures. The risk curve is used primarily in the fields of finance and engineering to evaluate the uncertainty of income (loss) from the relationship between income and exceedance probability. The main characteristic of the risk curve is the advantage of being able to visually judge income (loss) in accordance with exceedance probability.

4.3 *Case study*

This section will present a case study using the SWING system. Here, as shown in Figure 4 , there is an important marsh water river basin directly above the tunnel route, and the need to preserve the amount of water in this river basin is a prerequisite for the tunnel excavation. Figure 5 shows the permeability model in the tunnel longitudinal direction. Table 1 shows the scenarios for countermeasures to deal with the reduction in marsh water, based on existing references and interviews with specialists[3)]. The specific scenarios for countermeasures are to provide additional wells if the impact is slight; if the impact is considerable, it will not be possible to preserve the quantity of water through the placement of new wells alone, and in such cases tunnel water inflow will have to be used, and addition of catchment pits inside the tunnel shaft and application of high pump head pump-up will be needed.

Monte Carlo simulations were conducted 50 times and the values were assessed using the marsh water reduction histogram shown in Figure 6. In addition, by applying the countermeasures scenarios shown in Table 1 in accordance with the reduction in marsh water, the cost of drought measures needed to preserve the water quantity can be assessed for each realization. Figure 7 shows the risk-curve indicating the relationship between exceedance probability and the cost of countermeasures.

5 CONCLUSIONS

The objective of this study was to develop a method for quantitatively evaluating the risk of cost fluctuations with regard to the control of water inflow and drought incurred by tunnel excavation. The findings of the study can be summarized as follows.

(a) A method of quantitatively evaluate the cost of water inflow and drought measures in ground of highly uncertain nature using a risk curve has been developed. Through introduction of the financial engineering theory, risks can be proposed as one of decision-making factors even when the owner is outside the civil engineering discipline.

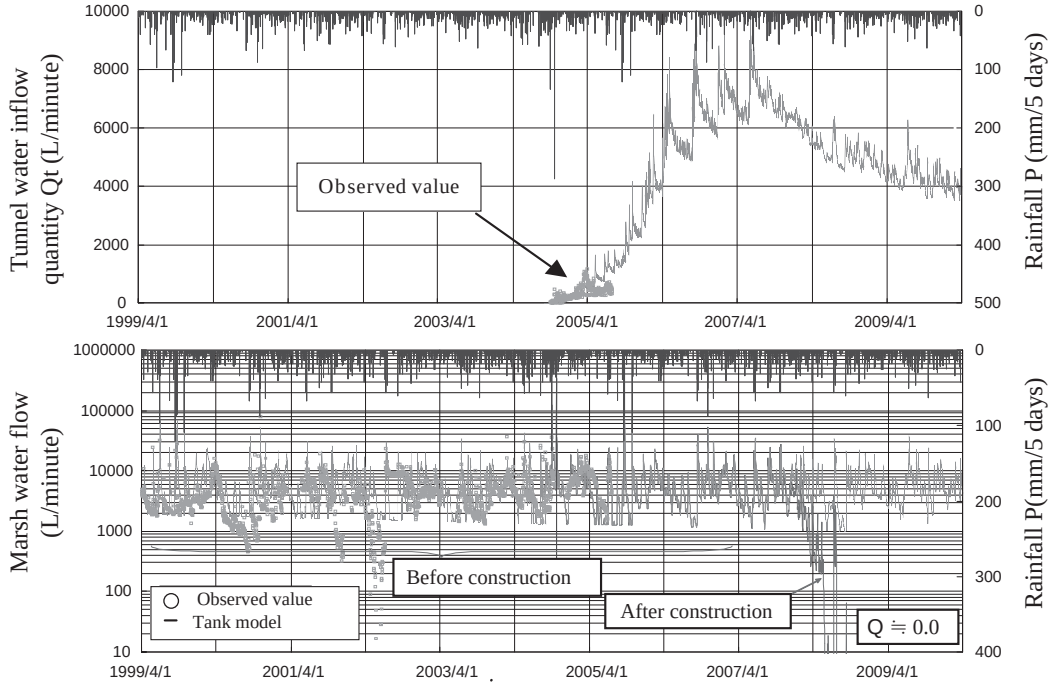


Figure 4. Prediction of tunnel water inflow and fluctuations in surface water as determined using the SWING system.

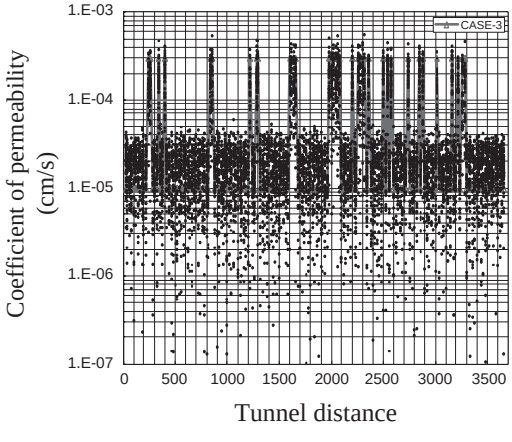


Figure 5. Prediction of tunnel water inflow and fluctuations in surface water as determined using the SWING system.

(b) It was shown that the uncertainty of preliminary surveys could be expressed in the cost dimension by means of the risk of cost fluctuations for water inflow and drought measures. Moreover, it is anticipated that the ease of use of the SWING system will make it possible to express in the cost dimension the tunnel excavation results and, in the event that additional surveys are implemented, the incentives

Table 1. Drought measures scenario.

Impact (m^3/min)	Conservation measure	Cost (JPY)
0.0–0.5	No measures	0
0.5–1.0	Add new well (one location)	98 million
1.0–3.0	Add new wells (three locations)	150 million

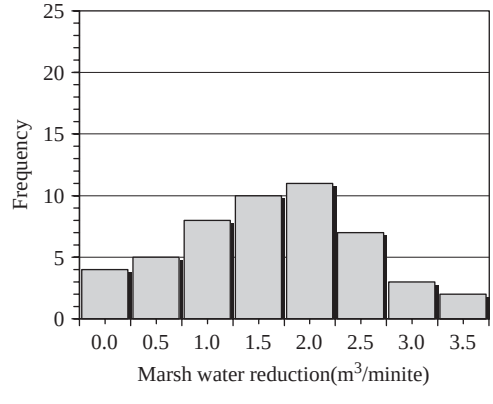


Figure 6. The marsh water reduction histogram.

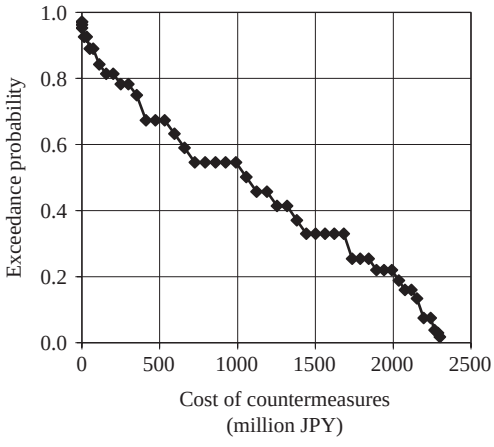


Figure 7. The risk curve indicating the relationship between exceedance probability and the cost of countermeasures.

for conducting the survey in terms of the reduction of cost fluctuation risk.

(c) Introduction of financial engineering theory makes it possible to propose risk evaluation as one of the tools in the decision-making process even the project personnel are outside the civil engineering discipline. For example, one example of specific decision-making using these risk evaluation techniques is expected to be the expression, in the dimension of the cost of water inflow and drought measures, of the value of reducing the uncertainty of the ground from the standpoint of computerized construction that takes into consideration preliminary surveys and the results during the construction process.

REFERENCES

Sato, K.: *Groundwater modeling for mountain tunnels and application* of simulation techniques, Applied Geology 23, No. 3, 1982, pp. 50–56.

Development of a simplified seepage analysis system (SWING system) for the construction of the Mino Tunnel, Japan Society of Civil Engineers 58th Annual Conference, III-016.

Study of methods used to investigate tunnel water inflow, Japan Tunneling Association, 1990, p. 128.

Underground Space – the 4th Dimension of Metropolises – Barták, Hrdina, Romancov & Zlámal (eds)
© 2007 Taylor & Francis Group, London, ISBN 978-0-415-40807-3

Driving of shallow tunnel in uncertain geological boundary conditions – A case history

R. Pöttler, F. Thum & W. Jöbstl
Feldkreuzstraße, Innsbruck, Austria

ABSTRACT: In the course of the new Nuremberg – Ingolstadt high-speed railway line, the 7-km long Irlahüll Tunnel was driven mainly through karstified chalk marl. In the southern section of the tunnel the chalk marl is covered by Tertiary. For a length of about 500 m the tunnel traverses a transition zone of chalk marl, weathered chalk marl and Tertiary. The tunnel was constructed according to the principles of NATM with heading, bench and invert. Between tunnel metre 300 and 400 of the southern section the deformation in the heading did not cease and exceeded the predicted values considerably. To prevent a total collapse of the tunnel, additional measures had to be carried out. After the shotcrete invert had been placed, the work on site was stopped for about 1.5 years. One year after the construction works had been stopped, cracks occurred in the invert and additional settlements occurred. The settlements could only be stopped when the tunnel was partly refilled with material and the shotcrete lining of the heading was supported by wooden columns. Extensive numerical calculations were performed, aiming at detecting the reason for this failure. 12 different possible scenarios with different numerical methods and models were investigated to define the reason for the failure and thus to be able to design the inner lining in an optimum manner. The outcome of the investigation was that none of the investigated scenarios was the reason for the failure. Therefore the dimensioning of the inner lining was done in a very conservative way.

1 PROJECT AND GEOLOGIE

The Irlahüll Tunnel, connecting with its length of 7260 m the Altmühl valley and the plateau of the southern "Fränkische Alb", is part of the new Nuremberg-Ingolstadt high-speed railway line. The tunnel was planned according to NATM principles, with heading, bench and invert. Between shotcrete lining and cast-in place inner lining a waterproofing membrane was installed. A drainage system prevents any water pressure from acting on the lining. The inner lining has to take over the loads resulting from the traffic in the tunnel, the loads of the electrical–mechanical installations of tunnel and of the deterioration of shotcrete, as well as the loads of the primary shotcrete lining and of the anchors which will corrode with time.

The tunnel was driven mainly through karstified chalk marl. In the southern section of the tunnel the chalk marl is covered by Tertiary. The prognoses of the geological situation were done based on the well known geological mapping and additional drillings spaced over the course of the tunnel.

In this southern section discussed, the tunnel traverses a transition zone of chalk marl, weathered chalk marl and Tertiary for a length of about 500 m. In that area the overburden is about 25 m thick. According to the prognosis, the interface was predicted to be monotonous, both in longitudinal and transverse direction. The foundation of the shotcrete lining of the heading was prognosed to be situated on rock mass.

Numerical analyses for verifying the stability of the tunnel were done prior to the construction based on the geotechnical report. The geotechnical parameters were verified and improved by back analyses. The main input parameters, for the finite element calculations, modulus of elasticity E, and the undrained parameters cohesion c_u and angle of friction ϕ_u could be determined quite well. Supervision of the tunnel drive was done by comparing and interpreting the geotechnical measurements on site with the calculated displacements.

2 EXCAVATION OF HEADING, BENCH AND INVERT

The FE model used for calculation is shown in Figure 1. The material law of Tertiary and of the rock mass is Drucker Prager. Differentiation in the chalk marl (TER1 to TER3) takes into account that the weathering of rock mass nearer to the surface was expected to be higher.

The thickness of the shotcrete lining was 280 mm. In addition to the lattice girders, anchors with a length

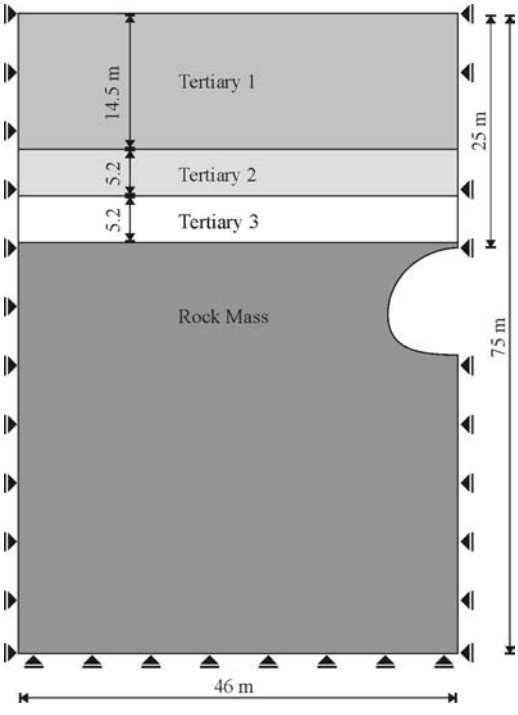


Figure 1. Numerical model for FE calculation.

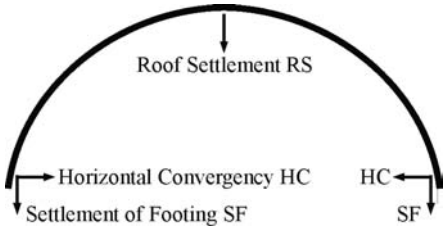


Figure 2. Observation of displacements.

of 6 m spaced every 2 m × 2 m were installed. For the excavation of the heading the following ranges of displacements were calculated (Figure 2):

- Roof settlement (RS) 45 mm–50 mm
- Horizontal convergence (HC) 10 mm
- Settlement of footing (SF) 25 mm–30 mm

As there was no prognosis on long-term behaviour of the ground it was expected that displacements due to tunnel drive would cease 1–2 tunnel-diameters behind the face. The normal force in the shotcrete lining was 2,1 MN/m, resulting in stresses of 3,5 MN/m^{2}in the footing of the lining. Although these stresses are well below the sustainable stresses of the rock mass, additional numerical analyses were performed to investigate the influence of an enlargement of the shotcrete lining at the footing ("elephant

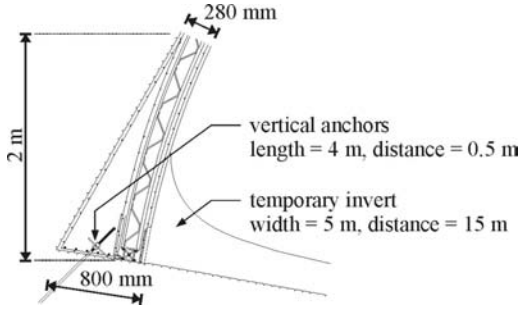


Figure 3. Additional support measures (elephant footing, vertical anchors).

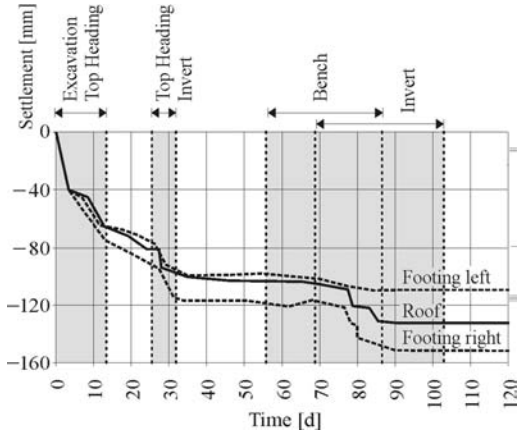


Figure 4. Measured displacements.

footings" – Figure 3) up to 800 mm to reduce the stresses in the footing of the heading.

Enlargement of the shotcrete lining at the footing had only minor influence on the stress-strain behaviour of the tunnel. The same investigation was done for the placement of additional vertical anchors at the footing. This additional support measure also had no major influence on the overall stability of the heading. Therefore there was no reason to carry out both support measures from an engineering point of view.

In the course of the tunnel driving, the measured displacements became bigger than the calculated displacements (Figure 4). This was mainly because the transition zone of Tertiary and rock mass was located lower than in the prognosis. Numerical analyses with reduced values for the geotechnical parameters resulted in higher allowable displacements.

For the excavation of the heading the following adapted ranges of displacements were calculated:

- Roof settlement (RS) 75 mm–85 mm
- Horizontal convergence (HC) −10 mm–60 mm (- .. divergence)
- Settlement of footing (SF) 65 mm–80 mm

As said before, it was assumed that the displacements would cease 1–2 tunnel-diameters behind the face. But the results of the measurements showed no abatement of displacements at that distance (Figure 4). As the geotechnical parameters of the weathered rock mass had been assumed to be almost the same as of the Tertiary, from a geotechnical point of view the ground behaviour could not be explained. Additional support measures had to be installed based on engineering judgement to prevent a collapse of the tunnel. In a 1st step these consisted of enlarging the shotcrete lining at the footing, in a 2nd step of installing vertical anchors at the basement and in a 3rd step a temporary invert of the heading, 5 m wide and at a distance of 15 m. The 1st and 2nd step did not have any influence on the deformation behaviour of the heading. Thus the numerical investigations done at the beginning, showing no major influence of these support measures, have been proved. Deformations only ceased after installing, a temporary invert arch in a 3rd step in the relevant section. Also, in the invert a shotcrete lining with a thickness of 250 mm was installed.

3 STOP OF CONSTRUCTION WORK – ADDITIONAL GROUND INVESTIGATIONS

After the shotcrete invert had been placed, the work on site was stopped for about 1.5 years. During this time additional ground investigations were performed in the karstified zones of the tunnel. Geological anomalies due to karst phenomena located in the vicinity of the tunnel, that may have an influence on the permanent stability and serviceability of tunnel for a service life of 100 years had to be detected. These investigations were done by geophysical measurements and drilling in an area of about 15 m around the tunnel (Pöttler 2004). So all in all, the geological and hydrogeological boundary conditions of the relevant surroundings were investigated in more detail than for any other tunnel.

Using these investigations, it was possible to generate a realistic geological 3D model. The 3D model of the area under discussion is shown in Figure 5. A major discrepancy between the geological model in the prognosis stage and reality is evident. A main discrepancy is that the weathered rock mass is not situated in the area of the heading but under the invert. The surface of the weathered rock mass is quite irregular both in longitudinal and transversal direction.

4 UNPREDICTED EVENT

During this period of no construction, regular inspections of the shotcrete lining were undertaken by the site management. One year after the construction works had been stopped, cracks appeared in the invert lining

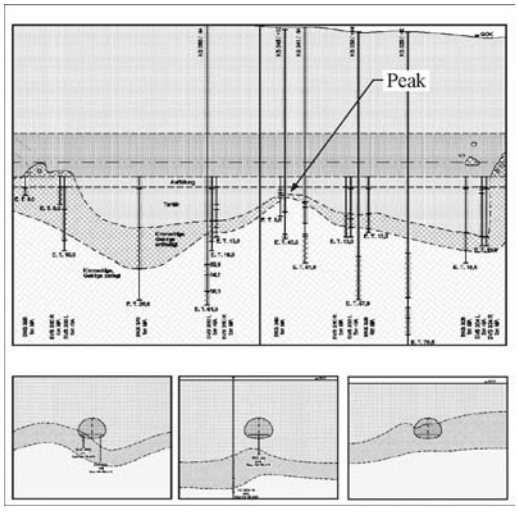


Figure 5. Geological situation in reality.



Figure 6. The wooden support.

and additional settlements occurred. The settlements could only be stopped when the tunnel was partly refilled with material and wooden columns placed to support the shotcrete lining of the heading (Figure 6). Due to the large settlements of up to 150 mm, the tunnel lining had to be reconstructed again to provide enough space for installing the inner lining. Additional drilling had been performed to get even more information on the ground in this area. The main questions to be answered were:

- What was the reason for the unpredicted restart of movements?
- What is the realistic load on the inner lining caused by shotcrete deterioration?

Different scenarios to explain the behaviour of the tunnel have been discussed:

Scenario 1: Change of location of geological strata: The tunnel is situated in Tertiary and the weathered rock mass is about 10 m below the invert. The reduced

Table 1. Comparison of numerical analyses and geotechnical measurements.

	RS [mm]	HC [mm]	SF [mm]
Numerical analysis	114	75	100
Measurements	125	80	125

values of the geotechnical parameters have been used for the numerical analyses. Taking account of the excavation sequence, the numerical analyses yielded the same results in terms of displacements which were measured (Table 1), therefore it could be assumed that the ground behaviour and the excavation process were modelled realistically.

But the numerical analyses showed no failure of the shotcrete lining in the invert section. The stresses in the shotcrete lining were considerably lower than the sustainable stresses. The actual location of the geological strata differed from the prognosis, but this could not be the reason for the unpredicted event.

Scenario 2: Influence of rock "peak": As can be seen from Figure 5, the weathered rock mass forms a peak in the vicinity of the area where the crack in the shotcrete lining appeared. This geological situation was also analysed, assuming a great difference in the stiffness behaviour between Tertiary and rock mass. The modulus of elasticity of the rock mass was assumed to be 300 MN/m^2. The influence of this rock "peak" on the stresses in the shotcrete lining was minor. No failure of shotcrete lining occurs.

Scenario 3: Influence of the rock "peak" and additional weathering of ground in the invert. It was assumed that the Tertiary under the shotcrete lining of the invert weathers due to water ingress from inside the tunnel, cohesion decreases to zero and the modulus of elasticity is considerably lower. This scenario is rather unrealistic as no water was in the tunnel and only a small wet zone of Tertiary of about 100 mm was detected when the shotcrete lining in the invert was replaced. The numerical analyses based on this model (Figure 7) showed that a failure of shotcrete lining would occur only if the weathered zone was very large.

Scenario 4: Influence of excavation procedure of the heading: The heading was driven without applying an enlarged footing of the shotcrete lining. Scenario 4 shows that because no enlarged footing was constructed, the amount of vertical displacement of the heading was so great that a loosening of the Tertiary at the crown occurred, resulting in the total load of overburden resting on the lining. The geotechnical parameters of the Tertiary have been proved and the numerical analyses based on these parameters made it possible to model the overall behaviour very realistically. These numerical analyses also showed that the influence of an enlargement of the footing of the lining has only minor influence on the behaviour and

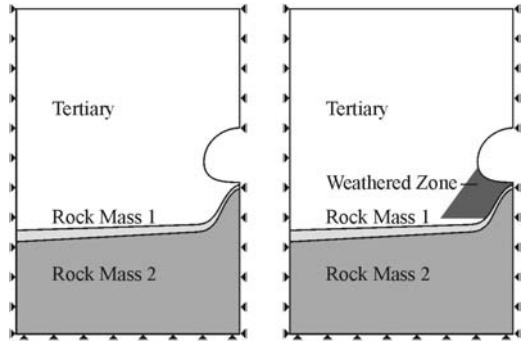


Figure 7. Numerical Model for FE calculations.

on the factor of safety. This was in addition proved by geotechnical measurements.

Scenario 5: Long-term behaviour of rock mass: The geological formation of the Tertiary and Chalk Marl does not show any aspects of creeping or swelling. The tunnel is situated well above the permanent groundwater level. No change in groundwater conditions occurred in the relevant period.

Scenario 6: Pore water pressure: The change of stresses and strains due to the excavation process also changes the pore water pressure and thus the effective stresses of the ground. In case of low permeability this process takes a long time. The permeability of the Tertiary is high so that this process, even if it had had occurred, would have taken only a few days. From this point of view, the change of pore water pressure as the reason for the unpredicted event can be excluded.

Twelve different possible scenarios with different numerical methods and models were investigated to ascertain the reason for the failure and thus to be able to answer the two questions above in a satisfactory manner. Some of these scenarios are more unrealistic than the one described, such as heave of the tunnel due to groundwater and change of temperature. But every scenario that was brought up by an involved expert was discussed. None of the investigated twelve geotechnical models could answer the question in a satisfactory manner. So the client and the engineer had to face the question of additional geotechnical and geological investigations. Both came to the conclusion that it was not possible to do more – neither in terms of extent nor accuracy – as had already been done.

5 SOLUTION

In the heading additional injection rock bolts were installed to support the shotcrete-lining during the time of removing the temporary support and constructing the inner lining. The transition zone of weathered chalk marl and Tertiary below the invert was grouted to homogeneous the basement of the tunnel.



Figure 8. Construction of the inner lining.

The dimension of the inner lining was done very conservative so that it could sustain the entire loads of overburden. The thickness of the lining is 550 mm, concrete grade B45 (DIN 1045) and reinforced by 23.2 cm^2/m on both sides. The arched invert-lining was replaced by massive monolithic blocks of about 400 m^3 of concrete, which had to be cooled while casting – sometimes even with nitrogen, depending on the weather situation – because of the high setting temperature. The wooden support of the heading and the filling of bench and invert were replaced step by step shortly before constructing each single block of the inner lining (Figure 8).

In summary, the discussion and investigation showed that a reason for the unpredicted event could not be identified, not even after a lot of additional numerical analyses and additional ground investigations.

6 CONCLUSION

The prognosis of the geological situation was done based on the well-known geological mapping and additional drillings spaced every 500 m over the course of the tunnel. After problems as described appear, "experts" may state that a greater number of ground investigations have to be carried out before tunnel driving. It goes without saying that the better the ground investigations are before the construction starts, the lower the risk of an unpredicted event is. The amount and quality of ground investigation representing the state of the art is found in the relevant standards. But even if the standard is met, like in the described case study, unpredicted events may occur. In this case study, the reason for the unpredicted event could not be defined in a proper way, although a far greater number of ground investigations were performed than ever done in a tunnelling project and although the geological situation was well known.

As numerical analyses were used to a great extent, and as there was time for a lot of discussion and meetings after the completion of the tunnel, at the end of the process one had to become aware that, for the present, the limit of understanding and numerical modelling has been reached. It becomes evident that tunnelling in such ground conditions can be done only by an experienced team. The numerical analyses are helpful but not the only tool for success.

There was no complete collapse of the tunnel and no loss of life. This section of the tunnel was expensive, but all in all economic with regard to other possible and realistic scenarios. This was thanks to the proper work done on site by the client, construction company, site supervision and designer.

REFERENCE

Pöttler, R. 2004. Die Beherrschung der Karst- und Erdfallproblematik bei Tunnelbauwerken. *Veröffentlichung des Instituts für Geotechnik der Technischen Universität Bergakademie Freiberg.* Freiberg.

This page intentionally left blank

Underground Space – the 4th Dimension of Metropolises – Barták, Hrdina, Romancov & Zlámal (eds)
© 2007 Taylor & Francis Group, London, ISBN 978-0-415-40807-3

Geotechnical risk management for tunneling beneath open water

D.P. Richards
Parsons Brinckerhoff, Portland OR, USA.

B. Nilsen
Norwegian University of Science and Technology (NTNU), Trondheim, Norway

ABSTRACT: Tunnel construction beneath open bodies of water presents certain types of risks not encountered when tunneling beneath "dry land". If major problems develop with tunnel equipment, ground control, or ground water control, construction personnel are exposed to risk of catastrophic flooding in the tunnel and recovery operations from the surface are generally not possible. Under these construction conditions, management of geotechnical risk during construction is of paramount importance. This paper addresses some of the more critical risks that must be considered and evaluated for such tunnel construction, starting with the planning process, and continuing through design and construction. Due to the increased difficulty and expense of geotechnical site exploration under water, the extent of the site investigation is sometimes decreased rather than increased, increasing the geotechnical uncertainty, requiring more detailed planning of construction methods and sequences, and appropriate redundancies and contingencies. The paper discusses the investingation, planning and construction processes for both soft ground and hard rock tunnels, and both conventional and machine excavation.

1 INTRODUCTION

The planning, design and construction of underground facilities beneath open water is always a challenge. In contrast to on-shore tunnel operations, when ground and/or ground water control problems are encountered, the physical constraint of no access from above for recovery operations when problems are encountered, introduces a higher degree of risk during construction, requiring an increase in the level of effort in the site investigation, design detailing and construction planning.

2 GEOTECHNICAL RISKS

Geotechnical risks are always a challenge in any tunnel project, and must be accounted for to minimize risk during construction, but for under water projects, the risks are often higher due to site investigation limitations and restrictions in addressing ground and ground water control problems during construction. Geotechnical risks that must be identified and accounted for in the investigation, design, and construction planning include:

- General profiling of the bottom surface
- Identification of low spots in the bottom profile
- Depth and character of sediments
- Variations in type and character of bedrock
- Location and extent of geological weaknesses
- Identification of rock structure patterns
- Characterization of the in-situ permeability

Potential risks associated with construction of hard rock subsea tunnels may be illustrated by the following examples from Norwegian projects (Blindheim et.al., 2005):

- The Bjorøy tunnel (1996), where a more than 10 m wide fault zone filled with clay, sand and coal fragments quite unexpectedly encountered. This was a zone of extremely high permeability and very poor stability, and a very time-consuming procedure involving stepwise grouting, drainage, spiling and shotcrete arches was necessary to tunnel through it.
- The North Cape tunnel (1999), where flat lying, broken sedimentary rocks caused very poor stability, resulting in slow progress and requiring shotcrete and concrete lining at the face. The difficult conditions were not realized from the pre-investigations due to the relatively high seismic velocity of the flat lying layers (4,500–5,500 m/sec).
- The Oslofjord tunnel (2000), where a deep cleft filled with Quaternary soil was encountered, necessitating ground freezing to tunnel through. A distinct weakness zone was detected prior to tunnelling. Despite very comprehensive pre-investigations

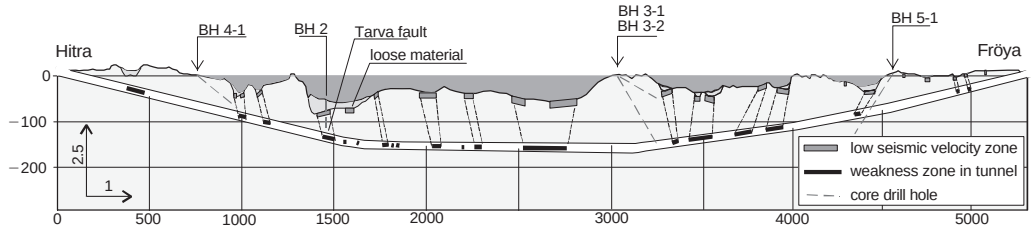


Figure 1. Longitudinal section illustrating low velocity/weakness zones in the Frøya tunnel (from Nilsen & Palmstrøm, 2001).

including traditional refraction seismics as well as directional core drilling and seismic tomography it was not found that the zone was eroded to a deep cleft. A by-pass tunnel was prepared to allow continued tunneling under the fjord. The soil filled section was frozen (at 120 m water pressure) and excavated through.

- At one of the most recent Norwegian projects, the Frøya sub sea tunnel, a pattern of very distinct, regional faults was identified by pre-construction investigations. Some of these faults could be followed over a distance of more than 200 km. Challenging ground conditions were documented, including high permeability zones as well as weakness zones containing very loose, sandy material and extremely active swelling clay. The locations of the main weakness zones are shown in Figure 1. In the planning of the Frøya tunnel, great benefit was gained from the previous construction of the nearby Hitra tunnel, where the major fault in the fjord was found to consist mainly of a mixture of heavily crushed rock and clay minerals (including swelling clay). The water seepage through the zone was minimal, and a combination of short blast rounds, spiling, steel fiber reinforced shotcrete, straps and conventional rock bolts, was used for getting through it.

The risks noted above for conventionally excavated drill and blast tunnels are similar for hard rock TBM tunnels, but they are sometimes more difficult to cope with using a TBM, due to limited access to the face for grouting or other ground improvement procedures, as well as problems in getting around a TBM if it becomes stuck. Aside from ground water inflows being a potential risk, other geological risks such as unanticipated faults or intrusions, either associated with an increase in fracture frequency, increases (or decreases) in rock strength, and increased abrasion also become more significant for a TBM excavation.

Significant risks for soft ground tunnels are mostly related to pressurized face TBM driven tunnels, since compressed air as a ground and/or ground water control technology is being replaced by improvements in soft ground TBM technology. Considering this though, there are still significant risks, mainly related to the presence of unanticipated ground conditions such as higher permeability, higher/lower cohesion, presence of boulders, buried obstruction, abandoned exploratory boreholes, extremely weak (or strong) materials, increased abrasiveness etc.

3 SITE INVESTIGATION AND PLANNING

3.1 *General*

A comprehensive site investigation is critical to the successful planning and execution of a tunnel beneath open water. Due to the additional expense and technical difficulties involved in off-shore drilling, vertical borings penetrating to tunnel level are often limited, and are often supplemented by directional drilling beneath the water, and by the use of marine geophysics. Geophysical techniques often considered for such off-shore investigations include:

- Hydrographic surveys: River, lake, or ocean floor bathymetric mapping
- Multibeam sonar: Multichannel hydrographic surveying that records a wide swath of data
- Sub-bottom sonar profiling: Detection of layering beneath the floors of rivers, lakes, or oceans
- Marine Seismic Reflection: Multichannel profiling of sediment and rock layering beneath the floors of rivers, lakes, or oceans
- Marine Seismic Refraction: For mapping of thickness and character of sediments, rock mass characterization and faults/weakness zones based on seismic velocity (see also Figure 1)
- Seismic tomography: Investigation of rock mass character between drill holes or between drill hole and sea floor
- Marine Magnetometry: For mapping of rock type boundaries and weathering
- Electrical Imaging: Two-dimensional (cross-sectional) imaging of sub-bottom electrical properties to detect and delineate sand, clay or gravel lenses, bedrock fractures – sensitive to water salinity.

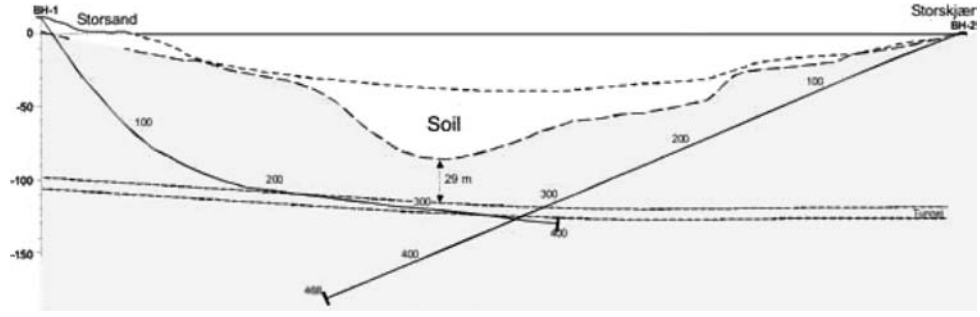


Figure 2. Conventional and directional core drilling at critical part of the Oslofjord tunnel (after Palmstrøm et.al., 2003).

In addition, conventional site investigation requirements are applicable, including sampling for determination of strength, weathering, mineralogy, deformation characteristics, porosity, abrasion potential, as required to make decisions with respect to applicable construction methods. For hard rock this would be a decision between tunnel boring machine and conventional excavation by drill and blast techniques. For soft ground, this would be a decision between types of pressurized closed face tunnel boring machines – slurry shield or EPB technology.

3.2 *Norwegian hard rock practice*

As a supplement to normal geological surveys, seismic investigations are crucial in the first stages. Acoustic profiling is first carried out for a large area to determine the most suitable corridor. Extensive refraction seismics is then carried out to select the best alignment and to provide information about soil deposits above the bedrock and about weakness (low velocity) zones in the bedrock. If possible, directional core drilling as illustrated in Figure 2 is used from shore to the critical deepest points of the alignment, which typically also could be the location of major fault zones. Core drilling from drilling ships has been applied in a few cases in Norway, when other drilling has not been feasible.

The costs for the site investigations for Norwegian sub sea tunnels typically amount to 3–7% of the construction costs. The established practice of site investigations has proven to be reliable, but exceptions have occurred as noted above.

Optimizing the minimum rock cover is crucial for safety as well as economy. Increased rock cover makes the tunnel unnecessarily long, representing extra construction costs and increased operating and traffic costs over the project's lifetime. Too little rock cover may cause severe stability problems, unacceptable work safety, heavy water ingress, and need for excessive grouting and high pumping costs.

A minimum rock cover of 50 m is basically required. A rock cover of less than 50 m can be accepted when detailed site investigations have demonstrated fair rock mass conditions (taking into account the typical occurrence of fault zones at the deepest point). This is left open to interpretation and rock cover less than 20 m has been used, but is then typically restricted to shallow waters and for good rock conditions.

3.3 *Hard rock TBM tunnels*

Investigation requirements for TBM tunnels in hard rock are similar to those for conventional excavation, since the risks are similar. However, as noted above, ground and/or ground water control problems are often more difficult to cope with for a TBM excavation, often making the understanding and reliability of geological conditions a bit more critical.

3.4 *Soft ground tunnels*

Soft ground tunnels passing beneath open water are usually relatively shallow. For example, transportation tunnels passing beneath rivers or shallow bays or channels usually have the depth restricted by the gradient of the approaches to the tunnel.

While site investigation practices for such soft ground tunnels are very similar to those identified above for hard rock tunnels, they must also include adequate material property characterization to allow informed decisions to be made with respect to soft ground TBM technology. The usual material property tests contributing to the ability to make these decisions include density, permeability, gradation, and plasticity.

For these applications, conventional sampling by both Standard Penetration Testing (SPT), and recovery of "undisturbed" samples are both commonly used, in addition to CPT (Cone Penetration Test). For such shallow soft ground applications in historic urban areas, it is often required to identify buried obstructions such as sunken ships and abandoned foundation piles, both of which can often be detected by geophysical techniques.

4 CONSTRUCTIONAL ASPECTS

4.1 *General*

It is during the construction planning phase, that final decisions must be made for the appropriate selection of means and methods of construction best suited to the subsurface geological conditions identified during the site investigation phase. These selected means and methods of construction must be an integral component of the risk management process, and must be chosen to best satisfy the intent of the mitigation measures for reducing risk exposure.

Key considerations in selecting construction means and methods for hard rock tunnels include:

- Rock types, distribution, and conditions
- Rock properties; strength, hardness, abrasiveness
- Discontinuity characteristics; frequency, orientations, continuity, roughness
- Major structural features; fault number, orientation, thickness, character

Key considerations in selection of construction means and methods for soft ground tunnels include:

- Thickness of overburden cover
- Soil type, layering, stiffness/relative density
- Soil properties; plasticity, gradation, permeability
- Hard inclusions; boulders, cemented zones
- Hydrostatic water pressure
- Ground water chemistry

4.2 *Hard rock conventional excavation tunnels*

The Norwegian hard rock sub sea tunnels have all been excavated by drilling and blasting. This method provides great flexibility and adaptability to varying rock mass conditions and is cost effective.

Systematic percussive probe drilling with the drilling jumbo is most critical for safety. By applying criteria related to inflow per probe hole on when to pre-grout, the remaining inflow can be controlled and adapted to preset quantities for economical pumping, which is normally 300 liters/min per km. Grouting against water pressures of 2∼3 MPa can be efficiently achieved with modern packers, pumps and grouting materials. Grouting pressures up to 10MPa are today quite common. Follow-up at the tunnel face by well qualified engineering geologists (and rock engineers) is of great importance.

In the Norwegian projects, all rock support structures are drained, whether they are made of cast-in-place concrete (mostly horseshoe) lining, sprayed concrete ribs or sprayed concrete. Sprayed concrete is dominantly applied as wet mix steel fiber reinforced. Extensive testing demonstrates that, if the thickness of the sprayed concrete is above a minimum of 60–70 mm, and the concrete quality is good (C45), corrosion of steel fibers is not a problem. Rock bolts have extensive corrosion protection. Rock support is always adjusted to the actual rock mass conditions, with heavy support applied only in very poor stability conditions. The use of spiling and shotcrete ribs has mostly replaced a concrete lining.

4.3 *Hard rock TBM tunnels*

Although numerous rock TBMs are operating around the world, many below the static ground water table, not all of these pass beneath open water. As with any rock TBM, good ground conditions usually allow good TBM excavation rates. However, as noted by McLearie et.al. (2001) for bored rock tunnels recently completed in Hong Kong, tunnel excavation success was largely dependent upon ground and ground water conditions, with intensely fractured zones (faults and dikes) often introducing large amounts of ground water infiltration, requiring extensive cut-off grouting before the TBM could progress, delaying the schedule and increasing the costs.

At the opposite end of the spectrum, was the Channel Tunnel, where ground conditions were ideal for TBM excavation in the relatively consistent chalks and chalk marls (Varley et.al., 1992 and Barthes et.al., 1994a). As noted by Barthes et.al., (1994b), although the chalks were relatively consistent on both sides of the channel, the French side was more faulted, with higher in-situ permeabilities, and these factors influenced the selection of TBMs as well as other means and methods of construction.

4.4 *Soft ground tunnels*

A fairly recent example of a large diameter soft ground tunnel excavated by a pressurized face TBM beneath open water, was the crossing beneath the Nile River by the Cairo Metro Line 2 bored tunnels in Egypt (Richards et.al., 1998). This was excavated by a 9.43 meter diameter slurry shield TBM in dense saturated sands and crossed two separate branches of the river. A subsurface profile is shown in Figure 3.

Prior to starting the tunnel bore beneath the river, a risk assessment was performed, addressing both design, construction, and long term performance issues. Based upon this risk assessment, a number of design issues were double checked to ensure adequate construction term and long term performance of the tunnel. This risk assessment was also used for construction planning, in which emergency response plans, contingency plans and appropriate redundant construction systems were identified and implemented.

Key issues identified to minimize risk while tunneling beneath the river included: maintenance of face stability, lining ring shape, ring position, reduce blowout risk, avoid bridge foundation, avoid TBM

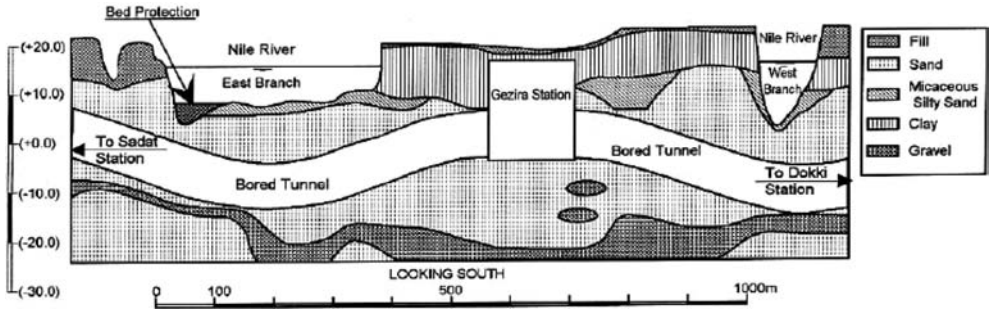


Figure 3. Nile crossing subsurface profile (Richards et.al., 1998).

break downs. Construction related contingency measures put into place to achieve these goals included: back-up electrical power, back-up compressed air supply, back-up locomotives, redundant slurry pumping equipment, extra reserve supply of bentonite, TBM improvement and/or modifications before passing beneath the river channel, and redundant communications between underground and topside personnel.

The tunnel beneath the river was completed in two separate tunnel drives, with continuous operation until the TBM had safely passed beneath the open water portion of the alignment. Both were completed without mishap, with no problems encountered which could not be handled by the contingency measures put into place prior to starting the excavation beneath the river.

5 RISK EVALUATION AND MANAGEMENT

To better control the complexity of underground projects, new codes and guidelines for design, modern quality systems and special methodologies for risk analyses have been introduced. Such tools provide a better basis for planning of investigation as well as construction and time/cost estimation.

The basic principle for determining the extent of investigation should always be related to the type and complexity of the project, and to the prevailing geological conditions.

A risk analysis may be divided into the following steps (Nilsen et.al., 1999; Pennington, et.al., 2006):

1. Identification of hazards and damage events
2. Assessment of probabilities for hazards and damage events identified
3. Description and valuation of consequences including analysis of initiating events
4. Calculation of pre-mitigation risk rating
5. Identification of appropriate mitigation measures for each risk
6. Calculation of post-mitigation risk rating

Within a project, risk analysis and quality control/assurance should be focused upon:

- Identifying and elimination or reducing hazards
- Reducing the probability of initiating events
- Finding barriers to stop damage events
- Reducing the consequence of possible damage
- Implementation of mitigation measures

The types of geotechnical risks to be considered include:

- Hard rock tunnels
  - Geology more complicated than anticipated
  - Weathering deeper than anticipated
  - Rock stronger or weaker than anticipated
  - More/wider fault zones than anticipated
  - Rock more fractured than anticipated
  - Rock more abrasive than anticipated
  - Rock mass (including fractured/faulted zones) permeability higher than anticipated
  - More voids (e.g. karst) than anticipated
- Soft ground tunnels
  - Bottom profile more irregular than anticipated
  - Sediments softer/harder or stiffer/denser than anticipated
  - Soils more granular /cohesive than anticipated
  - In-situ permeability greater than anticipated
  - Soil profile more irregular than anticipated
  - More boulders or inclusions than anticipated

Hazards and uncertainties are not only related to the soil or rock, but also with people involved in a project. A major task within risk analysis is to understand, describe and handle uncertainties. The Frøya sub sea tunnel case may be used to illustrate this. Here, the refraction seismic measurements showed more low velocity (weakness) zones than for any of the subsea tunnel previously constructed in Norway. In addition, the core drillings penetrated long sections of rocks with weakness zones having a higher degree of alteration than is normal in Norwegian hard rocks. The results

of the investigations indicated that the Frøya tunnel required thorough evaluations to assess its feasibility, and that special routines be implemented during planning and construction.

As a part of this, two groups were established to evaluate the feasibility of the tunnel. In their two independent reports excavation methods and rock support were analyzed, supported by a cost estimate and risk assessment. Construction time and cost estimates were based on a detailed prognosis of the expected ground conditions, and the estimate proved to correspond quite well with reality (Palmstrøm et.al, 2000).

6 DISCUSSION AND CONCLUSIONS

Tunneling beneath open water is usually more challenging them landside operation, often with a higher degree of uncertainty and risk. The following lessons of general relevancy for the planning of future projects are applicable.

- The extent of ground investigation and planning should always reflect the complexity of the geology, the type of project, and the degree of risk.
- Risk assessment should start in the planning phase and carry on in design and construction.
- The results from the investigations should be properly documented and their use in calculations and assessments shown.
- The geological setting and understanding of the tectonic are vital for all large tunnel projects.
- Ground investigations where the extent is based on bidding, may cause vital information to be lost, and should never be accepted.
- Sufficient time must be allocated for necessary investigations and testing.
- The ground investigations should continue through the entire construction period. Tunnel mapping and following up should be done by experienced engineering geologists representing owner as well as contractor.
- Risk analysis, assessment of uncertainties and development of mitigation measures are critical.
- The tender documents, including geological/ hydrological/hydrographic reports, should be thoroughly prepared, with full quality control.
- An independent reference committee should be established. For the construction period, strict requirements should be put on the engineer's and contractor's competency and qualifications.
- Planning and investigation should always carry risk assessment forward to the detailed design and construction phases, since residual risk remains, even after significant and relevant site investigations.

REFERENCES

Barthes, H., A. Bordas, D. Bouillot, M. Buzon, Ph. Dumont, J. Fermin, J.-C. Landry, J.-P. Larive, J.-J. Morlot, L. Szypura, Ph. Vandebrouck and B. Vielliard. 1994a. "Tunnels – Geology", Paper # 10486, Proceedings Institution of Civil Engineers, Supplement to Civil Engineering, Vol. 102, Special Issue No. 1 – The Channel Tunnel, Part 3: French Section, ICE, London.

Barthes, H., A. Bordas, D. Bouillot, M. Buzon, Ph. Dumont, J. Fermin, J.-C. Landry, J.-P. Larive, J.-J. Morlot, L. Szypura, Ph. Vandebrouck and B. Vielliard. 1994b. "Tunnels – Tunnel Boring Machines", Paper # 10489, Proceedings Institution of Civil Engineers, Supplement to Civil Engineering, Vol. 102, Special Issue No. 1 – The Channel Tunnel, Part 3: French Section, ICE, London.

Blindheim O.T., Grøv E. & Nilsen B. 2005. Nordic sub sea tunnel projects. Tunnelling and Underground Space Technology, 20:570–580.

CEN 1997. Geotechnical design – Part 1: General rules. European Pre-standard ENV 1997–1, Comite Europeen de Normalisation, 123 p.

McLeary, D.D., W. Foreman, W.H. Hansmire and E.K.H. Tong. 2001. "Hong Kong Strategic Sewage Disposal Scheme Stage I Deep Tunnels", Proceedings Rapid Excavation and Tunneling Conference, Society of Mining Engineerrs, pp. 487–408, Littleton, CO, USA.

Nilsen B. & Palmstrøm A. 2001. Stability and water leakage of hard rock subsea tunnels. Proc. Int. Symp. IS-Kyoto, 2001, Balkema, pp. 497–502.

Nilsen B., Palmstrøm A. & Stille H. 1999. Quality control of sub-sea tunnel project in complex ground conditions. Proc. ITA World Tunnel Congress Oslo, June 199. Balkema, pp. 137–145.

Palmstrøm A., Stille H. & Nilsen B. 2000. The Frøya tunnel – a sub sea tunnel in complex ground conditions. Proc. Swedish Rock Mechanics Meeting, Stockholm March 2000, BeFo, pp. 19–30.

Palmstrøm, A., Nilsen, B., Pedersen, K.B. & Grundt, L. 2003. Optimum extent of site investigations for underground facilities. Publ. No. 101, Directorate of Public Roads, 116 p. (in Norwegian).

Pennington, T.W., R.F. Cook, D.P. Richards, J. O'Carroll, and T. Cleys. 2006. "A tunnel case study in risk management", Proceedings, North American Tunneling, Chicago, Illinois, Taylor & Francis, London.

Richards, D.P, P. Ramond, and O. Ezzeldine. 1998. "Design and construction of the first bored tunnel across the Nile River", Proceedings, ITA Congress, Tunnels and Metropolises, Sao Paulo, Brazil, A.A. Balkema, Rotterdam.

Varley, P., A. Darby and E. Radcliff. 1992. "Geology, Alignment and Survey", Paper # 9932, Proceedings Institution of Civil Engineers, Supplement to Civil Engineering, The Channel Tunnel, Part 1: Tunnels, ICE, London.

Underground Space – the 4th Dimension of Metropolises – Barták, Hrdina, Romancov & Zlámal (eds)
© 2007 Taylor & Francis Group, London, ISBN 978-0-415-40807-3

Impact of a geological incident on the construction of a land sewer outfall in Ferrol, northwest Spain

J. L. Sánchez Fernández
EPTISA, Grupo EP, Spain

B. Antuña Álvarez
North of Spain Water Agency, Spain

I. Pardo de Vera Moreno
Road, Canal and Harbour Engineer, North of Spain Water Agency, Spain

ABSTRACT: The land sewer outfall tunnel in Ferrol is 7,344 metre long and has an excavated diameter of 3.70 metres. It forms part of a large scheme including four interventions to depurate and clean up the waters in the town of Ferrol. The total investment of the project is about 125 million euros. The excavation of the tunnel began at the end of August 2004, with an open face Robbins TBM 1215–265. The project required to go through the Cariño Fault, located between chainage 3 + 210 and chainage 3 + 400, spanning a length of approximately 200 metres. However, at the beginning of July 2005, a geological incident occurred at chainage 2 + 746.077, which led to halt the excavation of the tunnel until November 2005. This article describes the geological and geotechnical conditions in the area, as well as the technical solution used to carry on with the excavation of the tunnel. The effects of this geological incident are also analyzed, both from the contractual point of view and the time frame of the project.

1 BACKGROUND

Construction of La Malata-Cape Prioriño land outfall commenced at the end of August 2004. To bore the tunnel, an open face ROBBINS tunnel boring machine is used, model 1215–265.

The selection of excavation by TBM was based on the fact that the rock was predominantly granodiorite. The grain size is medium to fine, with feldspar mega crystals. In general, it can be considered very hard rock with a high quality index.

Nevertheless, the bedrock that the tunnel crosses includes a major fault, the Cariño Valley Fault, where substantial weathering process can be observed, with kaolinization and oxide zones associated with water. This fault will be crossed by the tunnel between chainages 3 + 210 and 3 + 400, as can be seen in the geological profile in Figure 1.

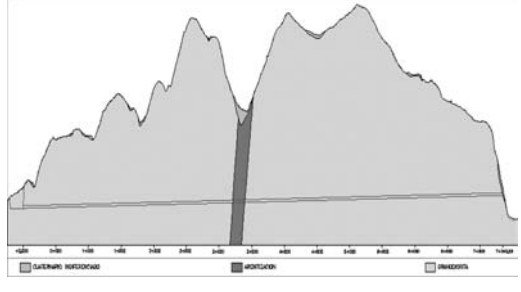


Figure 1. Geological profile.

2 WORK SCHEDULE

Tunnelling commenced at a slower pace than initially planned. This was partly due to the need to train the personnel to the tunnelling method and to delays in organizing continuous work shifts.

The achieved work advance can be seen in the next diagram.

As can be observed in Figure 2, the best monthly progress was achieved in April 2005, with advance of about 600 metres/month.

3 ENCOUNTERING A GEOLOGICAL INCIDENT

In early July 2005, tunnelling was seriously affected from chainage 2 + 746 by the presence, at the tunnel face, of some very fine porphyry dikes.

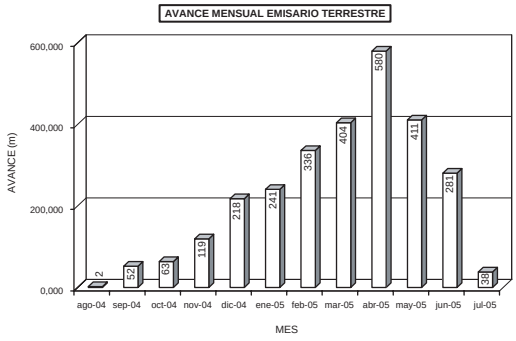


Figure 2. Achieved work advance.

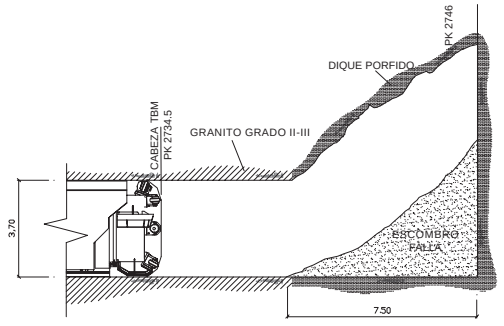


Figure 3. Overbreak height.



Figure 4. Overbreak.

The highy fractured material encountered and its poor geotechnical quality, together with substantial meteorization of the contact zone between the granodiorite and the porphyry and the presence of water, caused the tunnel face to become totally instable.

As a first option, it was decided to try to cross the area, performing short advances and installing TH-16.5 steel arches and Bernold sheets, immediately behind the TBM shield, given the own limitations of the TBM, which does not have special equipment to treat the face.

This progress option did not have good results, since the rotation of the cutterhead was often blocked and the TBM had to stop due to saturation of material on the conveyor belt.

Similarly, as a consequence of the poor stability of the face, the initial overbreak quickly became a big chimney.

Before that situation and with the objective of avoiding that overbreak worsened, it was decided to halt tunnelling with the TBM and to find out alternatives to be able to cross the area the earliest possible, by minimizing risks for the personnel and the TBM.

With the TBM method, access to the tunnel face is practically restricted, since it is limited to a manhole for the maintenance and change of disc cutters.

The manhole is a hole of approximately 60 centimetres, that is situated on the TBM cutterhead and can be accessed from the lower part of the conveyor belt. Such a restriction limits very much the possibilities of intervention to consolidate the face because nearly all the face is occupied by the cutterhead.

Faced with the impossibility to be able to access to the tunnel face to do any work, it was decided to try to fill the overbreak with concrete, by sealing the face and pumping concrete into the overbreak area. To do it, it was necessary to move the machine backwards, approximately six (6) metres.

Such an intervention could be achieved because in the area before where the geological incident occured, no support had been installed, thanks to the fact that the ground before the fault was of good quality. Had crews installed some type of support, then it would have been necessary to stabilize the area beforehand to be able afterwards to take the machine backwards, because placing supports behind the TBM shield reduces the inner diameter of the tunnel and it is therefore not possible to try to have the machine to move backwards.

Once the TBM could be moved to the back, a timber plug was installed at the tunnel face, that played the role of a formwork. That step was followed by the subsequent drilling of the face to install steel pipes to pour concrete into the overbreak. The mentioned overbreak can be seen in Figure 4.

It is important to stress that, since the tunnel has a small diameter (3.70 metres, outer diameter), the equipment and device limitations extremely restrict the implementation of efficient and rapid solutions. The concrete pump had to be placed in the California switch rail of the TBM (at approximately 235 metres from the face) and the steel pipes for concreting had to be carried through all the TBM back-up, then through the manhole to finally reach the face where was the overbreak.

The steel pipes were installed at approximately three (3) metres above the crown level, with the objective of

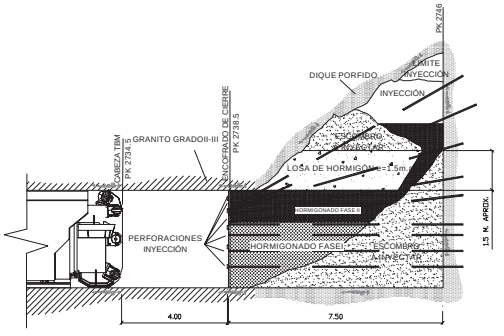


Figure 5. Alzado de la solución planteada.

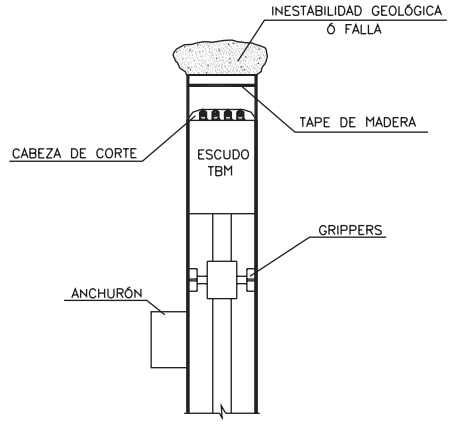


Figure 6. Construction of the lateral siding.

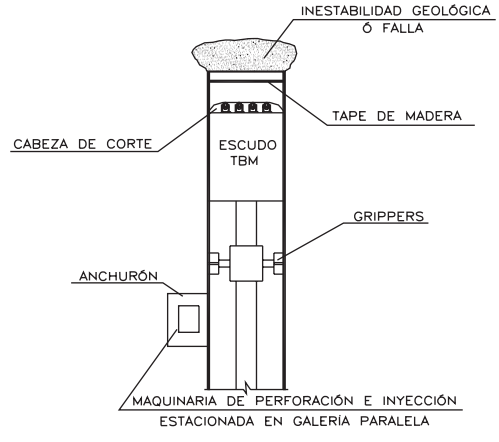


Figure 7. Placement of the TBM parts in the siding.

making sure that a concrete cushion would be poured on the tunnel vault in the overbreak area.

Altogether, 66 cubic metres of concrete has been pumped.

Once the concrete pouring operation ended, crews waited for the setting of the concrete. After that, they removed the timber formwork and reinstated the TBM at the face into its initial position to resume tunnelling.

It is also important to underline that the adopted solution, though it did not fully guarantee stability of the area, aimed at consolidating the ground to overcome the problem with the resources available at the site and reduce to the minimum the stoppage of tunnelling.

When tunnelling resumed, it was found that the alternative used did not overcome the problem since material continued to collapse from the crown and walls.

As an alternative solution to the geological instability, it was then decided to perform injections into the face and drill a canopy of steel pipes around the tunnel vault.

Such intervention, which was not chosen at the beginning to avoid a long stoppage of tunnelling works, required the use of equipment that was not available at the site and obliged to analyze how to bring them to the face to be able to do the reinforcement works.

To be able to bring the drill rig to the face ahead of the TBM cutterhead, two (2) alternatives were analyzed. The first consisted in boring a by-pass tunnel while the second consisted in building a siding in one of the tunnel walls.

For cost and time reasons, engineers decided to build the siding. Its construction, performed by means of hydraulic jack hammers, included a small lateral tunnel in one of the tunnel walls, approximately 2.50 metres in length and 2 metres deep. It was not possible to use the drill and blast method for lack of permit to use dynamite and also to avoid any damage to the TBM.

The siding was bored immediately after the grippers of the TBM since it is in that area that the largest room is available to manoeuvre the excavation equipment.

Once the siding was completed, the drilling equipment was placed in it further to its partial disassembly so that workers could carry the parts through the TBM back-up.

Once the drilling rig pieces were stored in the siding, the TBM was moved backwards to approximately 20 metres behind the face, far enough to place the cutterhead downstream the siding just built. It then was possible to reassemble the drill rig to proceed to the reinforcement works.

It is important to emphasize that during the backward movement of the TBM, it was necessary to take away the precast concrete segments placed on the floor by the machine as it progresses.

Once the teams finalised all the necessary handling prior to the reinforcement stage, they commenced to

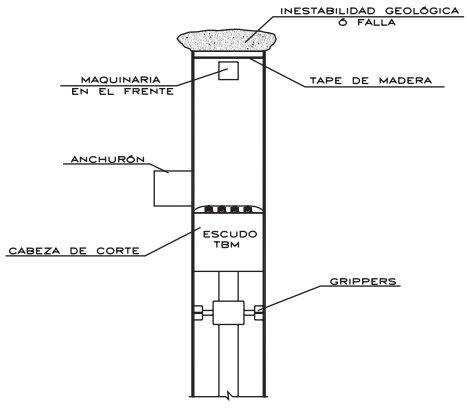


Figure 8. Access of the drilling rig to the face.

consolidate the subsoil collapsed from the vault at chainage 2 + 746.

The consolidation programme basically comprised the following phases:

3.1 *Concreting of the face*

Concreting was performed for the purpose of sealing the caved-in face and guaranteeing the confinement of the cement grout to be injected in the zone to be stabilised.

3.2 *Consolidation*

Given the heterogeneous materials that had to be grouted, shallow drilling was first carried out, then deeper drilling later on. In addition, the drilling time for all the drill holes was monitored, with the aim of trying to collect some information on the quality of the rock mass, according to the resistance to penetration of drilling rods.

The drilling and grouting process was started at the tunnel invert and continued up to the top heading, to try to guarantee the confinement of the rock to be treated.

Cement grout was first injected with a dosing of 1.25:1 and dosing even varied up to 1.5:1 according to the consumption observed on the spot.

The maximum grouting pressure applied by crews was 5 kg/cm^2.

Altogether, approximately 65 tonnes of cement was used for these reinforcements.

3.3 *Consolidation of the tunnel periphery*

As a final consolidation, project managers decided to install a canopy of approximately four (4) metres, concentric with the outer contour of the tunnel.



Figure 9. Drilling to reinforce the face.

This canopy was installed by tubes a manchettes (TaMs) and the grouting pressure utilized ranged from 10 to 20 kg/cm^2.

During that phase, approximately 26 tonnes of cement was injected.

3.4 *Forepoling*

When the injection process ended, the forepoling technique was implemented, consisting in the construction of a canopy (umbrella) of sub-horizontal steel beams. The implementation of the technique was decided to consolidate even more the tunnel crown.

The drilling diameter applied to form a supporting arc in the rockmass was 133 millimetres, with a space between each forepole piles of 15 centimetres.

The incline angle varied from 6 to 9 degrees.

The forepoles are formed by 114.3 × 6.3 mm steel pipes.

It is important to remember that, since the intervention with forepoles was applied inside the cross section excavated by the TBM, it was necessary that all the forepoles – in the first metres of the drive – be applied using plastic pipes, until the forepoles could be applied outside of the cross section excavated by the TBM, to avoid any damage to the disc cutters when the TBM was going to resume tunnelling.

Altogether, approximately 13 tonnes of cement has been injected in the steel pipes.

The length of the steel pipes drilled sub-horizontally ranges from 15 to 18.70 metres. These forepoling lengths were mainly conditioned by the capacity of the drill rig. Miners attempted to drill the longest holes possible to avoid having to drill another umbella vault after resumption of tunnelling, which would have obliged to move again the TBM backwards and bring back the drilling rig to the siding.

When the consolidation process ended, the drill rig was taken back to the siding and stored there. The TBM could therefore be moved forward to the tunnel face.

Once the TBM grippers had moved forward ahead of the siding, the drilling rig was taken out of the tunnel

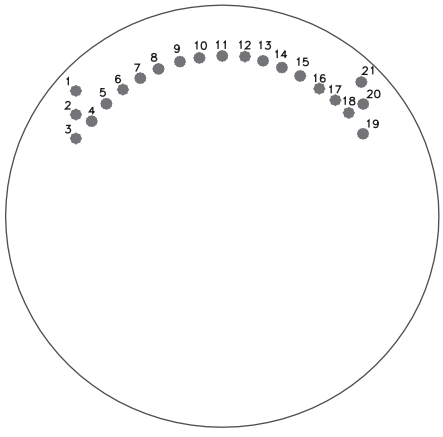


Figure 10. Location of the forepole piles.

Table 1. Summary of the reinforcement works.

Number of drills	Drilled metres	Kg injected
90	680.60	91,525

and tunnellers started preparatory works to cross the reinforced segment with the TBM.

Tunnelling resumed in early November 2005 very slowly, in order to evaluate the behaviour of the reinforced ground.

The zone disrupted by the geological incident had a length of approximately 15 metres. Beyond that zone, it was not necessary to do any additional work further to the reinforcements already achieved and tunnelling continued at normal pace.

In all, tunnelling was halted for four (4) months while reinforcement works were under way.

4 CONSEQUENCES

The occurrence of a geological incident of such a magnitude during construction of the tunnel has important consequences for the project, not only from the financial point of view and the time frame but also socially and politically.

The consequence of the fact that tunnelling has been halted for such a long time is that the project will be behind schedule.

From the social point of view, the project forms part of a complete programme that includes wastewater treatment and discharge facilities in Ferrol. The future wastewater treatment plant will be built in the area currently occupied by the tunnel worksite. Therefore, the fact that the targeted completion of the tunnel is behind schedule may greatly impact on the commencement of construction of the wastewater treatment plant.

Regarding the project time frame, the delay compels to carry out an in-depth analysis of what happened so far and find out mechanisms that restore the project within its initial schedule.

From the financial point of view, the consequences affect both the main contractor and the project owner (the North of Spain water agency). They are linked by contractual relationship that allows to determine the responsibilities for such events.

5 RECOMMENDATIONS

It is well known that tunnel construction entails great risks. The latest advances gained in recent years in tunnelling technology have considerably mitigated those risks. Nevertheless, there still are projects around the world affected by problems similar to the one described in this paper.

For that purpose, we consider it is convenient to do efforts to try to resolve such problems and keep the construction of tunnel projects with the budget and time frame determined during the design phase.

To reach that goal, we consider it is important to suggest the following recommendations:

- Contracts must include clauses that enable to share the risks incurred by the geology of a tunnel, above all for projects where unpredicted adverse geological conditions appear.
- Designers and public administrations must be aware that more investment is required during the initial geological investigation phases, which will contribute to reduce surprises during tunnelling.
- The process to choose a tunnelling method must be reinforced.
- It is necessary to include in the decision-making process all the persons and organizations linked to the project, by establishing real mechanisms of participation.

BIBLIOGRAPHY

Keller Terra. Memoria de ejecución para la consolidación del desprendimiento en el P.K. 2 + 746 en el túnel del Emisario Terrestre La Malata-Ferrol. August 2006.

Mendaña, Felipe. Túnel Emisario Terrestre A Malata – EDAR Cabo Prioriño. Visitas a Obra. September 2005 to January 2006. January 2006.

Pardo de Vera, Ignacio et al. Experiencias constructivas en la construcción del túnel del Emisario Terrestre a Malata-Cabo Prioriño. Proceedings Tunnelling for a sustainable Europe. Chambéry. October 2005.

Proyecto Constructivo del Emisario Terrestre a Malata – EDAR de Cabo Prioriño. (Depuración y vertido de Ferrol). Saitec Ingenieros. September 2002.

This page intentionally left blank

Underground Space – the 4th Dimension of Metropolises – Barták, Hrdina, Romancov & Zlámal (eds)
© 2007 Taylor & Francis Group, London, ISBN 978-0-415-40807-3

Sub-sea Microtunnel by Pipe Jacking Method – Construction challenges

Syed Shakil Ahmed
Assistant Construction Manager, Parsons Brinckerhoff (Middle East) Ltd.

Sam Alfaour
Construction Manager, Parsons Brinckerhoff (Middle East) Ltd.

Mohammad Al Ghanem
Project Manager, Parsons Brinckerhoff (Middle East) Ltd.

ABSTRACT: The paper describes the challenges faced during the construction of sub-sea microtunnel. The method of construction was pipe jacking and excavation was done by Tunnel Boring Machine (TBM). During jacking operation an abnormal point load condition to the section of the pipe string were observed creating obstacles to the jacking operation that required high jacking force and resulted in tension as well as compression cracks to the pipe. This paper explains the possible causes for the increase in jacking forces encountered during jacking operation and remedial works carried out to remove the obstacles. It also describes the steps taken to overcome this construction difficulties starting with the investigation conducted, risk assessment for restart of jacking operation after cracks occurred, and culminating in successful completion of the jacking drive.

1 INTRODUCTION

Two sub-sea microtunnels were recently constructed by a private developer in the Middle East region. The concept of microtunnel by pipe jacking method of 3.0 metre diameter precast concrete pipes at an elevation of −26 metre below sea level was a challenging task for designer, contractor and the project management team.

2 PROJECT DESCRIPTION

The construction of sub-sea microtunnels had numerous design and construction challenges. Al Naboodah Engineering Services (ANES) was awarded to design and build two microtunnels, one to the west and one to the east of the main arterial. The design of these tunnels was performed under the supervision of Dr. Mikhail Ryjevski of ANES. The design build contract in a fast track delivery within 16 months, consisted of installation of a 3.0 metre outside diameter tunnels, 750 and 675 metre in length, at an elevation of approximately −26.0 metre below sea level, in mainly sandstone ground conditions.

The west tunnel which was 750 metre long is the focus of this paper. The challenges faced by the developer, contractor, and project management team and risks associated with it during the jacking operation are discussed.

3 GROUND CONDITION

Based upon 14 exploratory bore holes drilled to 35 metre depth, the existing subsurface condition comprised of loose to very loose, to medium dense to dense, gray, silty fine to coarse sand from the existing ground (±4.0 metre) level up to 12 metre (fill material); underlain by weak to moderately weak, fine to medium grained calcareous sandstone, sandy siltstone, and conglomerate up to −35 metre depth.

4 MAJOR TUNNEL COMPONENTS

The major components of the microtunnel works were; launching and receiving shafts, precast concrete pipe, and TBM. The shafts were necessary to be constructed before commencing with the jacking operation to attain the required elevation of approximately −26 metre below sea level, to reach sandstone and maintain the required design profile of the tunnel. This section summarizes these three key components used for the construction of the microtunnel.

4.1 *Launching and receiving shafts*

The launching shaft was constructed on frond up to a depth of approximately −27 metre and having an

internal diameter of 12 metre. This shaft was used to lower the TBM to the bottom of the shaft.

Receiving shaft was constructed on the crescent side up to a depth of approximately −20 metre and having an internal diameter of 9 metre. This shaft was used to recover the TBM from the bottom of the shaft, after the completion of the drilling and pipe jacking operations. Each shaft was made of three main components: secant pile wall, base slab and capping beam.

Both shafts were constructed using secant pile method of shoring of 1.2 metre diameter piles. These piles were drilled to about 2 metre below the base slab level of the shafts. Initial design of the secant pile wall required excavation depth of toe level to −33 metre for the launching shaft, however to control seepage and avoid soil collapse due to high external water pressure the length was increased to −34 metre. A capping beam was constructed at each shaft at top of the secant piles to provide lateral support.

Both shafts also had permanent reinforced concrete liner of 0.35 metre thickness over two layers of water proof PVC membrane and inner protection layer of geotextile.

4.2 *Precast concrete pipe*

The reinforced concrete pipes that have been used for the tunnel drive were off site factory precasted of 3.0 metre length and having 3.0 metre outside diameter, transported to the site, lowered in the launching shaft and jacked by means of a hydraulic jacking frame system. Inside diameter of each pipe was 2.4 metre with wall thickness of 300 millimeter and concrete design compressive strength was 45 N/mm^2. There were three types of pipes manufactured and used for the tunnel; standard pipe of 3 metre length, pipe with Injection Port (IP Pipe) of 3 metre length and inter jack station pipes of 0.5 metre and 1.5 metre. The weight of each standard pipe was 20 ton. Figure 1 shows a typical standard precast concrete pipe used in the tunnel drive.

Every fifth pipe jacked was an IP pipe, which was used for lubrication during the drive and for grouting after the completion of jacking operation. Four inter jack pipes were installed to serve as an intermediate jacking station due to extraordinary length of the tunnel, as during excavation the jacking force generated by the main frame could not fulfill the required force to push the pipe and TBM.

4.3 *Tunnel Boring Machine (TBM)*

TBM used was Herrenknecht AVND2500 mix shield slurry machine. Prior to installation of TBM and commencement of the jacking, all components of TBM which include thrust block, TBM launch rails, and seal pipe brake along with the main jacking cylinder were installed. TBM consisted of 6 parts, a total of



Figure 1. Standard precast concrete pipe.

approximately 12 metre in length, which were installed in 3 phases due to space limitation at the launching shaft.

The TBM was controlled by remote control from the control cabin. Guidance System was installed in the control room having graphical and numerical display of TBM axis position against the design tunnel axis.

4.3.1 *TBM operation*

The TBM was equipped to operate in slurry mode in which water was pumped from the separation plant to the face and mixed with the cuttings produced by the cutting wheel. This mixture was then pumped back to the separation plant and treated, by separating the solids and allowing cleaned water to be recycled.

The excavation procedure consisted of 2 phases; excavation cycle in which the pipe line and TBM was advanced through the ground at a distance of 3 metre and pipe change during which a new pipe was lowered and positioned for jacking. During this phase the slurry circuit was closed off at the shaft via gate valves in the shaft bottom. The pipe brake was tensioned and the thrust ring pulled back. All slurry lines and services were then disconnected from the previous pipe. A new pipe was dropped onto the guide rails and then pushed into the seal of the preceding pipe. All services and slurry lines were then reconnected and the pipe brake relaxed and the excavation cycle begin again.

4.3.2 *Intermediate Jacking Stations (IJS)*

The intermediate jacking stations are pipes adapted to hold hydraulic cylinders and are placed periodically during the advance. Due to the length of the pipe line 4 intermediate jacking stations were installed as the force generated by the main jacking station was not sufficient to move the pipe line. The IJS allow the pipe line to be moved in sections. The IJS pipes were installed using the same procedure as for a standard pipe.

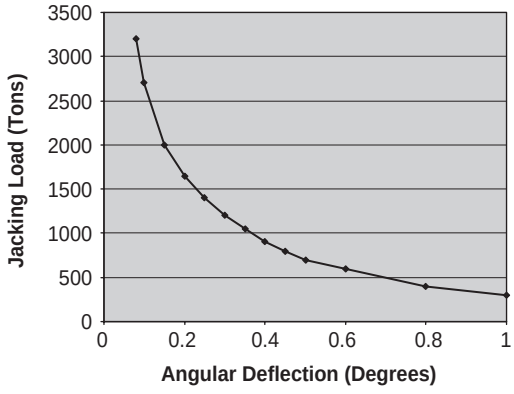


Figure 2. Permissible load at various angular misalignments.

4.3.3 *Pipe line lubrication*

The annulus between the outside of the product pipe and the excavation profile was filled with bentonite to prevent the collapse of the excavated ground onto the pipe thus reducing friction forces.

The bentonite mix was Baroid Tunnel Gel mixed with water to a ratio of 3–5%; in addition Baroid PAC-R polymer was added to the bentonite mixture at approximately 0.5%. The polymer was used to reduce water loss from the bentonite mixture. The bentonite mixture was constantly monitored and adjusted during the jacking operation depending on jacking forces experienced.

Injection of the bentonite was done through injection ports which was cast into the concrete pipe and was controlled by the Herrenknecht Automatic Lubrication System 80.

5 JACKING FORCE AND INTERJACK STATION

Jacking operation involves pushing pipes through ground surface and therefore exposes them to high loading during the construction. The critical area is at the pipe joints where the risk of stress concentration from pipe misalignment and or angular deflection is very high. Therefore, it was extremely important to control and monitor the alignment during jacking operation to ensure allowable angular deflection is not exceeded. Jacking load was assessed and the designer had recommended allowable jacking force of 900 ton, while maximum permissible force at joints with 0.5 degree deflection was 730 ton. Figure 2 shows allowable jacking force with respect to angle of deflection.

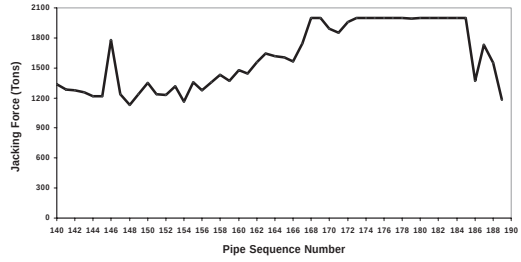


Figure 3. Maximum jacking force for the West Tunnel.

It was also recommended to use inter jack stations when the jacking force reaches 66% of the permissible load.

5.1 *High jacking pressure*

During initial jacking operation, a maximum jacking force applied to a pipe was around 900 ton or less which was below the allowable pressure and drive was running smoothly with a rate of production of around 9–10 metre per day. A sudden increase of jacking pressure was noticed during driving operation at the main jacking station and jacking force went as high as 1550 ton causing minor cracks to few of the jacked precast concrete pipes (pipe number 142, 143 and 146) located approximately 504 metre from the launching shaft.

Figure 3 shows the maximum jacking force applied to each of the jacked pipe between 420 metre (pipe sequence number 140) and 567 metre (pipe sequence number 189) of the tunnel drive. A meeting was immediately called with the designer and contractor to discuss this issue. The contractor and the designer explained that in their opinion there was an obstruction outside the pipe and they plan to push through and grind away obstruction and they expect damage up to 10 more pipes. It was also believed that jacking is a time related operation; therefore usually it is not a good practice to keep TBM idle for 3 days or more and lubrication must be maintained all along.

The question remained what would be the line of action if pipes continue to get damaged after jacking 10 more pipes? It was agreed by all that washing out material under the pipe would be the next option. It was also noticed that the contractor has to apply maximum jacking force to allow the material underneath to grind away, which could be as high as 2100 ton, which was also the ultimate capacity of the main jacking station.

After discussion with the contractor, designer, tunnel experts and the project management team, it was agreed to continue with the jacking operation at a much slower pace and monitor jacking force and survey pipe for damages every 20 cm of push. Damaged pipes were repaired by epoxy injection and concrete patching and



Figure 4. Damaged pipe number 146.

jacking operation was restarted after suspension of 3 days.

5.2 *Failed attempt to restart jacking operation*

During subsequent drive the jacking pressure continued to increase and reading went up to approximately 2050 ton and production rate decreased to 4.5 metre per day. After jacking approximately 66 metre tension and compression cracks appeared in 5 pipes (pipe number 143, 144, 145, 147 and 148) and deformation was noticed in one of the pipe (pipe number 146). Thus, it was obvious that condition has worsened and appeared that above solution of grinding away the hard material underneath the pipe with high jacking force had failed. It was decided that jacking must immediately be stopped, remedial measures be assessed, viable solution agreed by all and risk assessment should be carried out to determine the safety of the crew and tunnel itself as there was a very strong opinion that worst case scenario of complete failure of the pipe was a real possibility. Figure 4 shows damaged pipe number 146.

5.3 *Possible Causes of High Jacking Pressure*

Based upon detail investigation and field survey it was concluded that the prime reason of the cracks and deformation of the pipes was misalignment of the pipes resulting in non symmetrical loading condition. There could have been several factors for these pipes to be misaligned.

A field survey of the damaged pipes revealed that the pipes moved in the upward direction during the jacking operation resulting in grinding with the rock above it and small size (4–5 cm) rock fragments kept falling under the pipe and get accumulated which tend to push the pipes in upward direction. These deposited materials beneath the pipe became compacted and hard when jacking operation was stopped (ranging from 1 to 5 days) on number of occasion during the drive, due to maintenance works, and to control leakage at the inter jack stations.

Few cores were drilled through invert of the pipes to investigate the conditions underneath the pipe and it was observed that soil, very elastic in nature almost glue like material was found which was contributing to the excessive jacking force and misalignment. It appears that the use of polyurethane, bentonite mixed in with seawater could have resulted in chemical reaction ending up in a sticky elastic material which could have caused the pipes to slide horizontally and with continuous high jacking pressure applied these pipe instead of moving forward was forced to move upward resulting in misalignment.

It was also investigated whether steel collar of the concrete pipe has detached which might have caused the pipes to crack. This theory was rejected as no water was found leaking at the joints, no cracks at joint were visible and no crushing of pipe was noticed.

6 REMEDIAL MEASURES AND RESTART OF JACKING OPERATION

By now, it was clear that there was some obstruction which was creating these pipes to deflect and misalign. Pipes 143 to 148 have deformed and seemed unstable and there was a strong possibility of a total failure, therefore a procedure was worked out which included installation of steel in-liner to stop deformation, grouting between damaged pipes and the steel liner, and flushing out materials underneath the pipes which was believed to be causing high jacking forces for pipes 143 to 148.

6.1 *Installation of steel liners*

The steel in-liner was installed in all six damaged pipes which were designed to take the form of a segmental structure consisting of 6 segments with bolted flange joints. There was a provision in the steel in-liners to accommodate gate valves to be used for drilling of core holes and flushing the materials from behind the pipe. After the installation of the in-liners the area between the damaged pipe and steel liner was grouted using high strength non shrink grout. The grouting operation was done in three stages, starting from the bottom third. This sequence was necessary to reduce any uplift forces during the grouting operation.

6.2 *Flushing out of hard material*

100 mm drilled openings were made through the invert of each damaged pipes, 25 degree offset to the 6 o'clock vertical position in each of the lined pipes followed by the installation of gate valves in each of the

openings. Once gate valves were installed, jetting of materials under pipe was done by controlling the flow of material through these valves, material removed by natural water pressure and by suction methods. It was noted that approximately 27 cubic metre of material was flushed out.

6.3 *Safety and risk*

Prior to restart of the jacking operation it was agreed by all that the use of high pressure water for removal of material is highly risky operation and all protective equipment must be in place and used by all crew member working inside the tunnel and shaft. A comprehensive briefing and drill was conducted for the risk associated with this work. Minimum number of crew was allowed to work inside the tunnel and it was decided that no personnel should be inside the tunnel when jacking is in progress. In this respect, CCTV, pressure and length monitoring devices were installed in the damaged area inside the tunnel to monitor the movement of the pipes from the control station.

Trigger values and hold points for monitoring the pipe movement were discussed and implemented which included maximum length reduction of 10 mm for the steel in-liner, maximum jacking load of 1500 tons, and increase of pressure on any single cylinder gauge of a maximum of 150 bar.

7 CONCLUSION

The remedial measures performed on the damaged pipes described above helped in reducing the jacking pressure. Continuous monitoring of the jacking pressure was done and when there was an increase in jacking pressure from the hold point values, flushing was performed and jacking recommenced. This flush and push operation was a success and the jacking of the pipes continued till the completion of the tunnel and approximately 180 metre of jacking was done with an average of 6 metre per day.

It is a known fact that the success of TBM operation depends on many factors, which includes type of TBM selected, experience of the steering crew of the contractor, control and supervision and proper use of mix design for lubrication. TBM will not move in a straight line due to change in ground condition, grade, gravity and extreme water pressure might tend to move the TBM from straight path, they can create misalignment of the tunnel which would result in high jacking force resulting in severe damage to the tunnel itself. Proper and constant supervision of the work is also essential and any abnormalities noticed during initial stage must be addressed immediately to avoid major damage. It is also important to note that lesson learned from this tunnel drive was successfully applied to the east side tunnel and east microtunnel was completed with an average of 12 metre per day and jacking force was well within the allowable limit through out the drive of 675 metre in similar soil condition.

ACKNOWLEDGEMENT

The authors wish to express their appreciation to Dr. Mikhail Ryjevski of Al Naboodah Engineering Services for his assistance in the preparation of this paper. Useful comments made by colleagues in reviewing this paper are also acknowledged.

This page intentionally left blank

Underground Space – the 4th Dimension of Metropolises – Barták, Hrdina, Romancov & Zlámal (eds)
© 2007 Taylor & Francis Group, London, ISBN 978-0-415-40807-3

Geotechnical safety management on site

W. Schubert
Graz University of Technology, Austria

ABSTRACT: The uncertainties in the ground model and consequently the design of tunnels call for an observational construction approach. To allow for safe and economical tunneling a safety management plan has to be implemented. Basis for the safety management plan is the design, which continuously is updated, as information increases. The contribution deals with following topics:

- Targets of the Safety Management
- Basic elements and structure of the Safety Management Plan
- Parties involved and their responsibilities
- Determination/Definition of the expected behavior; definition of warning and alarm levels/criteria
- Monitoring program; layout and frequency of monitoring in accordance with expected behavior and boundary conditions
- Information and communication flow
- Action plan; organization, and mitigation measures in case observed behavior deviates from the expected
- Management of a crisis

A key element for establishing realistic warning and alarm criteria is a profound understanding of geotechnical processes and the ground-structure interaction. Thus a meaningful plan can be only established in close cooperation between designers, geotechnical experts, and the site management. Advanced tools for monitoring data evaluation and interpretation assist in establishing expected behaviors and check the monitored values against the warning and alarm criteria. The implementation and execution of safety management plans on site will be shown with case histories from the Wienerwald railway tunnel in Austria.

1 INTRODUCTION

Even with an excellent investigation, testing, and ground characterization program, as well as the application of up to date design methods, uncertainties with respect to geological conditions and ground reaction remain during construction. To obtain safe and economical tunnel construction, an observational approach is required.

Rules, methods, definition of responsibilities, etc. are laid down in a safety management plan, which is basis for all safety relevant actions on site. The procedures outlined here reflect the practice, as executed by the Austrian Federal Railways (OeBB, 2004).

2 TARGETS OF A SAFETY MANAGEMENT PLAN

The targets of the Safety Management Plan are:

– Allow for safe and economical tunneling in not completely known conditions
– Definition of preparatory steps, methods, and procedures for the implementation of the observational method
– Definition of responsibilities and procedures to prevent unfavorable effects or stability problems
– Definition of required procedures and measures in the case of a crisis to avoid damage, in particular to third parties

3 BASIC ELEMENTS

The geotechnical safety management plan consists of following basic elements:

– Definition of the parameters to be observed
– Definition of the expected behavior of the underground structure during construction
– Definition of monitoring methods, locations, amount, and reading frequency
– Definition of warning and alarm levels
– Organisation required to conduct monitoring, data handling, evaluation and interpretation and

communication structure between the paties involved
- Procedures and measures in case the behaviour deviates from the expected one
- Procedure for the case of a crisis, including alarm criteria, organisation, and protection priorities
- Framework construction plan
- Updating of the prediction made during the design, as new information is available

The geotechnical safety management plan consists of two parts, the first being valid fort he whole project, the second part containing the detailed regulations for different sections with different ground or boundary conditions.

4 PARTIES INVOLVED AND THEIR REPONSIBILITY

In the general part of the Safety Management Plan the function, addresses, phone and e-mail numbers of all parties involved in the project are listed. Also listed are the contact details of institutions and organizations, which have to be informed in the event of a crisis, where third parties are at risk.

In addition the general part contains a detailed description of the responsibilities of the individual positions in the project.

5 DEFINITION OF EXPECTED SYSTEM BEHAVIOUR AND WARNING AND ALARM CRITERIA

The designer defines the expected system behaviour of the tunnel during the excavation and the influence of the tunnelling works on surface and subsurface structures being influenced for the single sections of the tunnel. This serves as a basis for the geotechnical engineer on site, who has to evaluate the monitoring results.

Following details have to be given:

- Deformations of the tunnel
- Surface settlements and settlement trough
- Deformations of the ground in the vicinity of critical objects
- Deformations in the influence area of retaining structures
- Influence of tunnel works on utility lines and indication of advance mitigation measures

6 MONITORING PROGRAM

The monitoring methods have to be selected to capture the parameters relevant for the safety. The monitoring intervals shall be frequent enough to detect unfavourable developments in time, and the evaluation of the monitoring results has to be sufficiently rapid in relation to the possible evolution of the system.

Monitoring includes observation of the geological and water conditions, measurements of displacement on the surface, the ground, and the tunnel, as well as measurement of vibrations if required.

Type and amount of monitoring, as well as minimum reading frequency for the single sections of the tunnel are put down in the Framework Construction Plan.

6.1 *Specification of monitoring criteria and control measures*

For the single parameters observed, following is specified for each section:

- Expected behaviour
- Method of observation evaluation of data
- Criteria for attention level
- Criteria for the warning levels 1 to 3
- Mitigation measures
- Alarm criteria for the warning levels 2 and 3
- Method of intervention in case of an alarm

6.2 *Warning levels*

In case the actual behaviour deviates from the predicted one, one of the four warning levels is applied, depending on the severity of the deviation.

The attention level applies, when the actual behaviour, respectively the predicted actual behaviour exceeds the expected one or is close to the limits specified by the authorities.

The criteria for warning level 1 are set at significant deviations from the expected behaviour, but with a reasonable safety margin against failure.

The criteria for warning level 2 are reached in case of progressive deformation development, low margin of safety, or local failure. When level 2 is reached, alarm is announced. Warning level 3 applies, when warning level 2 is reached and third parties are affected.

Conditions for resetting a warning level are the stability of the tunnel, or when observation results show that objects or utilities are not influenced, as well as, when the mitigation measures have proven to be effective.

6.3 *Monitoring methods and extent*

Monitoring methods in general include documentation of geological and hydrological conditions and interpretation, visual observations in the tunnel and on the surface, displacement measurement, and vibration measurement, measurement of water and gas quantity/concentration.

Displacement monitoring includes measurement of surface points and objects, inclinometers, extensometers and 3D displacement monitoring of the tunnel itself.

The basic monitoring layout and minimum reading frequency is determined by the designer and the geotechnical on-site engineer, and is shown in the Framework plan. Detailed adjustments of the program are made by the on-site geotechnical engineer according to the requirements.

6.4 *Execution of measurements*

The owner usually takes the responsibility for making the geotechnical measurements, while the contractor is responsible for the correct position of the tunnel.

The survey team receives the instructions for the type of measurements and minimum reading frequency from the geotechnical engineer. The evaluation of the data has be done in a way, that the results are available for the geotechnical engineer within the same day of the reading.

7 INFORMATION FLOW

In general everybody involved has to report unusual observations immediately to the Engineer and the geotechnical on-site engineer, as well as the contractor.

To allow for an efficient flow of information and up to date access to evaluated data, a ftp-server is installed. The parties involved in the evaluation of data have to store the evaluation results on the server immediately after evaluation. All parties involved in the project have access to the data stored on the server.

Preferably a daily joint site visit of the representative of the contractor, the Engineer, the geotechnical on-site engineer and the geologist is made. After evaluation of the monitored data, a meeting among the parties mentioned above is held, where information is exchanged, and necessary measures are decided.

In case of deviations from the routine, for example due to an increased or changed reading frequency or unusual events requiring a change of the routine, the geotechnical engineer informs the Engineer and the external expert about the storage of out of routine data by email or phone.

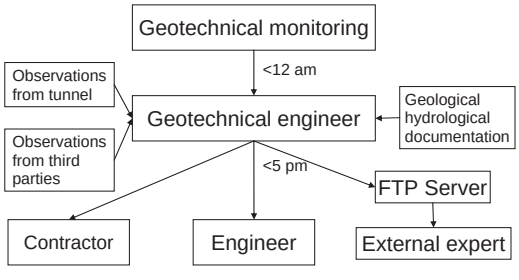


Figure 1. Routine safety relevant information flow.

8 PRACTICAL APPLICATION

Besides the stability of the tunnel itself, the effects of the tunnel works on other objects and utilities is of particular importance. In the design those issues have been addressed, and consequently the design form the initial basis for the geotechnical safety management plan.

All critical objects and utilities are listed in a table as well as the acceptable impact on those structures by the tunnelling works. The expected "normal" behaviour of the tunnel, its influence on the surface and objects is quantified. For a timely detection of deviations from the normal behaviour it is not enough to define final deformation values, but also the timely and spatial development. It has shown beneficial to specify expected deformations in relation to the face distance, for example in distances of 1/2 diameter and 2 diameters in addition to the final displacements. Thus it is possible to detect deviations in time to initiate strengthening or mitigation measures.

The table also includes the methods of observation and evaluation of the safety relevant parameters. For example for the assessment of the stability of the face usually only visual inspection is available, while for the deformations of the tunnel and the surface geodetic and geotechnical instrumentation can be used. The method of evaluation in this case can reach from simple plots of displacement histories (time-displacements plots) to more sophisticated ones, like the trend of the displacement vector orientations.

Following the definition of the expected behaviour the warning and alarm criteria are listed. For the tunnel displacements or surface settlements, the trigger for the attention level might be taken at the expected values, while the criterion for the warning level 1 might be an increase of deformations in the order of 20% above the expected values. The mitigation measures in this case would be an increase in the support if only the tunnel displacements exceed the warning level. If the warning criterion is reached also on the surface, additional face support, a decrease in the round length and the excavation rate might be the recommended mitigation measures. In the case of houses and other objects in general the criteria are admissible distortions. The observation of trends, as the tunnel progresses allows a timely detection of unfavourable developments, provided that appropriate tools are used for the data evaluation.

While the attention level and warning level 1 are considered to be managed with relatively low level mitigation measures, levels 2 and represent serious hazards for the structure or third parties. Top priority

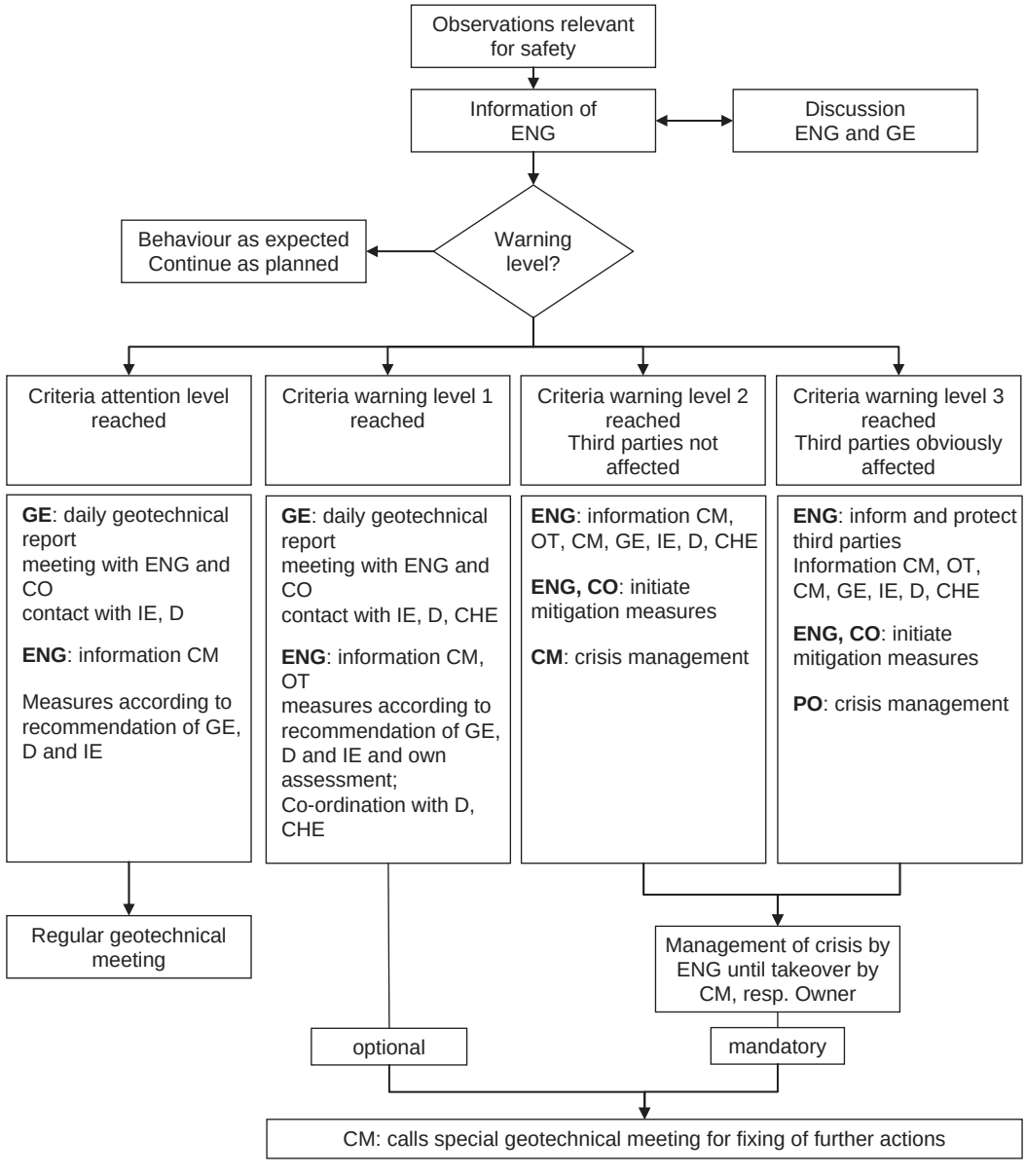


Figure 2. Procedure in Geotechnical Safety Management Plan; Abbreviations: GE – Geotechnical Engineer on site, ENG – Engineer, CO – Contractor, IE – Independent Expert, D – Designer, CHE – Checking Engineer, CM – Construction Management, OT – Owners technical representative, PO – Owners Project Representative.

in those cases has the public safety, followed by the safety of those involved in the project, and finally the stability of the structure.

Naturally in the case of a crisis also parties are involved, which are not familiar with the details of the construction and the evolution of the system. Thus a good routine documentation of all facts is essential to quickly convey the critical developments, and to arrive at mitigation measures appropriate to the situation. All parties involved must be aware, that in the case of a crisis, appropriate decisions can only be made if the data basis is excellent. As a crisis usually is unexpected, the monitoring and data quality have to be at a top level at all times.

Good preparation therefore is essential. A list of all those to be protected, as well as the contact details of all parties and organisations to be alerted has to be prepared well in advance. Also means, methods, and equipment required to conduct appropriate mitigation measures must be available on site at al times.

9 APPROPRIATE TOOLS FOR DATA ACQUISITION AND EVALUATION

It can be observed, that on many sites the methods of monitoring and data evaluation have not developed beyond the status of the 1970ies. Still convergence tape measurements seem to be the state of the art, while the only evaluation method is a plotting of the displacements versus time.

Since more than twenty years geodetic 3D displacement measurement techniques allow to gain much more information. Parallel to the advance in measurement technique, methods of data evaluation have been improved. Plotting of displacements versus time nowadays is only one method of visualizing the results of monitoring. Deflection line diagrams, trends of displacements, or ratios of different displacement components, allow a much better assessment of the mechanical processes during tunnelling, than was possible with the traditional methods.

Efficient software for the data processing and evaluation is available (Tunnel:Monitor, 2006; GeoFit, 2005). In particular the possibility to predict the development of the displacements in relation to face advance and time after a few readings allows a timely detection of unfavourable developments (Grossauer et al., 2005).

10 CASE HISTORIES

Two case histories from the Wienerwaldtunnel, a double track railway tunnel located at the western outskirts of Vienna shall illustrate the practical application of the safety management plan.

On November 21st, 2005 the geotechnical engineer on site detected, that the development of the surface settlements at the measuring sections 390 and 400 reached the criteria of warning level 1 (criterion 37,5 mm). Via e-mail he informed the Engineer, the construction management, the technical representative of the owner, the contractor, and the external tunnel expert. As a building is located close to the face and the displacement trends showed an increasing tendency, the geotechnical engineer proposed to change the excavation and support sequence, with a shortening of the ring closure distance of the temporary top heading invert. In a site meeting in addition the thickness of the shotcrete in crown and invert was increased, as

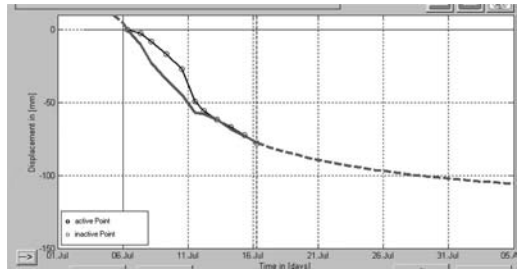


Figure 3. Predicted development of settlements (dashed line).

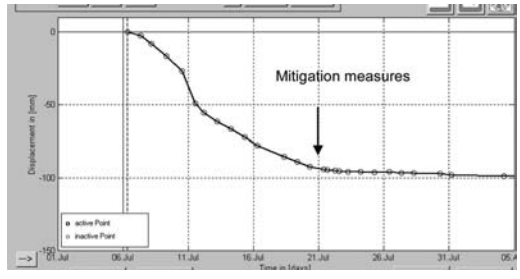


Figure 4. Development of displacements after mitigation measures were put into effect.

well as the number of bolts starting from station 422. The increase in support and the reduced ring closure distance reduced the amount of the displacements in the tunnel.

Another unfavourable development was observed at the same tunnel around station 1.000. Obviously due to the influence of a fault zone outside the right sidewall, displacements increased in a progressive manner in measuring section 997 (see figure 3). The situation was assessed by the geotechnical engineer, the designer and the external expert. As the tunnel is located outside built up areas, no immediate action was required, but increased attention paid to the further development. Additional bolting was ordered and executed on a length of around 20 m. In addition, the tolerance for deformation was increased to 20 cm. As a local phenomenon could have caused the increase, it was decided to continue with the excavation, while simultaneously mitigation measures were evaluated, should the additional bolting not show the desired effect. With the data available from July 16th, it was clear that the tunnel is in the process of stabilization, but total displacements would most probably exceed the deformation allowance (figure 4). Thus in an extraordinary geotechnical meeting, the previously discussed mitigation options were fixed. Those consisted of additional bolts, and the installation of three stripes of temporary invert with a length of 4 m each. The excavation was stopped and the strengthening measures put into effect.

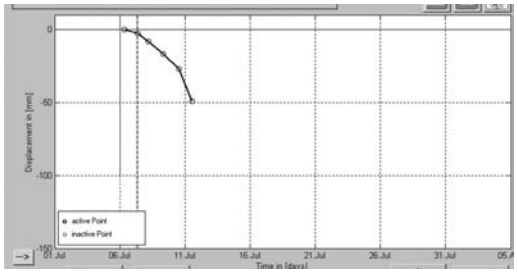


Figure 5. Development of vertical displacement of the right footing of the top heading.

Figure 5 shows, that the displacements came to a complete stop, as the strengthening measures became effective. No further problems were encountered in this section, even when the bench and invert were excavated, and the total deformations were within the tolerance.

11 CONCLUSION

Especially when tunnelling in sensitive areas with adjacent buildings and utilities, increased attention is required to minimize adverse influences caused by the tunnel works. A thorough planning and preparation is required to allow for quick and appropriate action in case of unfavourable developments.

For a successful establishment and execution of a safety management, all possible hazards have to be assessed prior to construction. Limitations of surface settlements, as well as criteria of serviceability have to be observed. A well structured plan of communication and action has to be fixed to allow for efficient response to unexpected or unfavourable developments. In addition the site has to be equipped with experienced staff, and appropriate software for efficient data evaluation. Up to date displacement monitoring evaluation software should have features to predict displacements with a few readings only in relation to time and tunnel advance, as well as the possibility to assess the degree of utilization in tunnel linings.

IT nowadays allows that also off site experts are fully informed about the performance of the project at all times, and can give advice whenever required, based on a sound information level. A precondition for complete information of all parties involved besides of the installation of a server is the continuous feeding of quality data and evaluations.

It has to be stated, that a safety management plan is not rigid, but requires updating, as more information about the ground and the system response is acquired during construction.

REFERENCES

OeBB, 2004. Geotechnischer Sicherheitsmanagementplan Wienerwaldtunnel, Ostabschnitt

GeoFit, 2005. www.geofit.3-g.at

Grossauer, K., Schubert, W., Sellner, P. 2005: *The Importance of Displacement Prediction*. In Erdem, Y., Solak, T.(eds), Underground Space Use – Analysis of the Past and Lessons for the Future; Proc. of the 31st ITA-AITES World Tunnel Congress, Istanbul, Turkey, 9–12 May 2005: 1239–1244. Great Britain: A.A. Balkema Publishers

Tunnel: Monitor, 2006. www.tunnelmonitor.com

Underground Space – the 4th Dimension of Metropolises – Barták, Hrdina, Romancov & Zlámal (eds)
© 2007 Taylor & Francis Group, London, ISBN 978-0-415-40807-3

NATM tunnelling at Dulles airport

Ermin Stehlik
Tunnelling Consultant for D2 Consult Prague, The Czech Republic

Martin Srb
D2 Consult Prague, The Czech Republic

ABSTRACT: Tunnel collapse in 2000 during excavation of connection tunnel at Dulles airport causing fatal injury raised the Client's (airport authorities) concerns about construction safety. Ambitious expansion of the airport foreseen for the next decade with airport capacity increase up to 50 mil passengers/year when expansion completed, requires numerous underground facilities to be partly located in mined (both conventionally and TBM driven) tunnels under the airport. All consequent tunnelling works have been set under new systematic supervision scheme including position of a "NATM Engineer" as a part of contractor's team to be present during all excavation & support works. This position has specified strict requirements on experience and qualification of individual experts. Since 2004 to 2006 several conventionally mined (NATM) tunnels have been successfully completed. Paper briefly describes specifics and procedures of some of these drives as well as an experience with the "NATM Engineer" role as part of the Contractor's team.

1 INTRODUCTION

1.1 *Brief summary*

Washington Dulles International Airport (WDIA) is at present undergoing ambitious expansion, which is enabled by availability of land around the existing airport facilities thanks to the Client – Metropolitan Washington Airports Authority (MWAA) policies in the past. Long term planned modernization includes the construction of a new runway, air traffic control tower, new terminals and service buildings, and also service and transport tunnels.

Construction aspects of these tunnels with emphasis on New Austrian Tunnelling Method (NATM) application and especially on the NATM Engineer role are the main features of the paper.

1.2 *Tunnelling contracts*

The tunnel construction involves all kinds of tunnelling methods; there are many open cut construction sites serving as starting or receiving pits for either TBM or NATM tunnelling contracts. NATM was used in parts with complicated geological conditions or in tunnel stretches with difficult horizontal alignments and small radiuses.

Construction of mined tunnels started in 2000 with so called "Walkway Tunnel" between the Main Terminal and Terminal B, using NATM tunnelling method. In November 2000 a tunnel collapse, causing death of one worker, happened. The accident and following investigations delayed the construction process; construction of another contract – "West Utility Building Tunnel (WUBT)" was awarded to the Kiewit construction company and construction started in 2004. The part of the contract was 348 m long horse-shoe shaped tunnel with 6 m wide cross section, excavated according to the NATM principles.

Following contracts included the construction of Automatic People Mover (APM) tunnels, with total length of more than 3 km with four stations built in open cuts, divided into several contracts and awarded to the Clark/Shea JV (east) and Atkinson/Clark/Shea JV (west). These included open cut, TBM and NATM tunnelling. NATM tunnels were circular, 6.5 m outer diameter tunnels, divided in east and west part (see Fig. 1, 2).

1.3 *Contract stipulations – NATM Engineers*

Due to the problems experienced with the first contract, the Client's requirements defined specific position as a part of the Contractor's team designated as "NATM Engineer". Contract stipulations called for permanent presence of NATM Engineers, with sufficient experience of the method application.

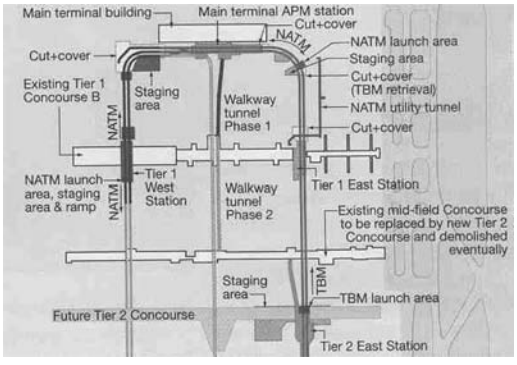


Figure 1. General Dulles airport layout.

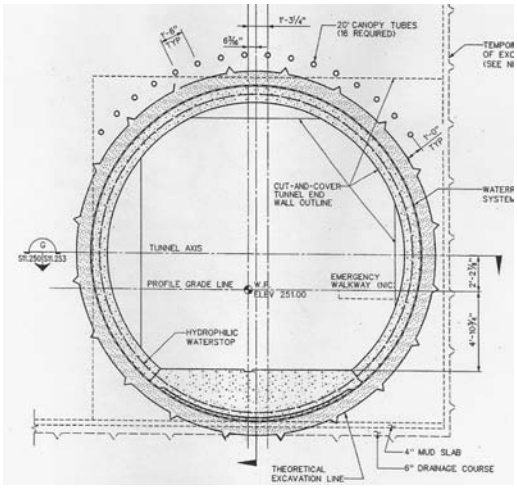


Figure 2. Typical cross section of NATM APM tunnel.

The situation in the US tunnelling market driven by the low cost rule, with few NATM tunnels, resulted in shortage of suitably qualified engineers and tunnel workers. Even the largest companies are commonly hiring external specialists for tunnelling contracts.

Position of NATM Engineers for both mentioned contracts were subcontracted to the Austrian tunnel consultants D2 Consult, and through its daughter company D2 Consult Prague, several Czech tunnel engineers worked on the project as a part of the contractor's teams.

2 TUNNEL CONSTRUCTION

2.1 *Geological and Hydrological conditions*

Geological conditions for the tunnel construction are relatively favourable. The bedrock, in which the tunnels have been predominantly mined, consists mainly of competent hard mudstone and claystone, with few sets of joints and UCS range between 20–40 MPa. Only at limited locations rock weathering process created softer soil with clay characteristic.



Figure 3. Typical face conditions.

The earlier conventional tunnelling at the airport was performed using drill&blast excavation technique, with large amount of explosives used, significantly disturbing the surrounding rock. As a result, when crossing in the vicinity of previous construction works with newly built tunnels, excavation and support installation have to consider earlier affected broken rock conditions.

Massive mudstone and claystone were during excavation relatively dry, the water penetrated into the excavation only through joints and was related to surface precipitation.

2.2 *TBM tunnelling*

There were several contracts, in which TBM tunnelling with bolted precast segmental lining assembled in the TBM shield has been used. The latest technology for the segment production has been introduced; for the tunnel lining water tightness the modern sealing systems with rubber sealing gaskets have been applied.

2.3 *NATM tunnelling*

2.3.1 *Generally*

Designed support classes (I–III) for the tunnel excavation and support were applied according to the NATM Engineer's decision.

Both, horseshoe and circular tunnels were excavated in two steps. Firstly, the top heading was excavated and support measures as specified for the initial lining applied. In the second step the invert was excavated and initial lining completed.

2.3.2 *Excavation*
The excavation in all contracts was done by roadheaders, blasting was strictly prohibited. There were several types of roadheaders, mostly Voest Alpine models AM 75 for large profiles and AM 50 for e.g. invert and final profiling.

2.3.3 *Support Classes*
The following description is related to the APM contract.

The round length was corresponding to the applied Support Class. In the Support Class I, which was used for massive sound rock, this length was 1.5 m; and at the same distance lattice girders were erected. Initial lining was formed by 15 cm thick shotcrete with steel fibres.

In the Support Class II, applied for jointed rock, 4 m long spiles were installed in each round to prevent loosening of the rock blocks and their falling from the excavation roof. Round length was 1.2 m, shotcrete thickness 20 cm, lattice girders at 1.2 m distance. Probing ahead of the face was performed every fourth round, the length of probe drill hole was 12 m.

Support Class III was applied when the tunnel profile entered into the area of heavily weathered rock having character of clay. The round length was 0.9 m and the pre-support measure consisted of grouted steel pipe umbrella length of 9.0 m. In some cases the Support Class III was applied during tunnelling under other structures or utilities as a safety precaution measure.

Bolting was considered as an additional measure, bolts installation was based on NATM Engineer's decision. SN bolts installed into boreholes fastened with resin cartridges have been applied.

2.3.4 *Shotcrete*
There were batching plant directly on the site; mixing of the wet shotcrete mix was done in truck-mixers. From the trucks the shotcrete was delivered to the stable pump located on the surface. From the pump the shotcrete was pumped by delivery line (slick line) to the shotcrete spraying robot with remote control, close to the tunnel face. Accelerator was delivered to the nozzle by small pump at accelerator storage tank.

2.3.5 *Final lining*
Final lining was made of reinforced cast in situ concrete of 30 cm thickness. Specific feature was universal use of corrosion protection coat of all reinforcement bars. Between shotcrete and final lining a waterproofing membrane was installed.

2.3.6 *Problems during tunnelling*
The biggest problem encountered during tunnelling was shotcrete delivery to the tunnel face. Due to the pump location on the surface, the delivery lines were long, with many bends. They were also exposed to the heat or cold conditions and as a result there were many blockages on the lines, leading to delays in shotcrete delivery. Very often the problems with accelerator dosage caused delays during shotcrete application.



Figure 4. Finished final lining of east APM tunnel.

The biggest problem, from the NATM Engineer's point of view was long time period required for shotcrete support application in the cases of unstable rock conditions.

Another problem was presence of water in the tunnel, affecting the conditions of the temporary top heading invert. The water was mainly technological water from the roadheader spraying the face during cutting; the water used for cleaning and in some cases the water coming from the portal areas. As a result there was permanently thick layer of mud on the tunnel invert, making the working conditions difficult.

Application of roadheaders for the tunnel excavation did not allow for partial suitable excavation of the face. In some cases, it would be advantageous to excavate only top part of the face and apply shotcrete layer to support unstable rock. With the roadheader, the excavation had to start at the lower part to create the space for roadheader apron, to allow cutting boom reaching the top of the face.

Typical tunnel worker has not NATM tunnelling experience and is trained for required specific skills before project starts. Also Trade Union labour rules make it rather difficult to use available labour force in tunnel with required flexibility and efficiency.

3 NATM ENGINEER POSITION

The NATM Engineer is a specific position, present in the moment only on the USA tunnelling market, therefore brief explanation of his position and role follows, together with few comments based on experience gained on the Dulles Airport contracts.

Generally, the NATM Engineer could be characterized as bearer of NATM know-how, who is responsible for effective and safe application of the method. There are strict criterions stipulated in the contract documents as far as the NATM Engineer qualification and experience is concerned (years of experience, type of works done, both design and site experience requirement, etc.).

Actual role of the NATM Engineer on Dulles Airport tunnelling contract encompassed few more tasks. NATM Engineer provided also geological mapping of tunnel faces and monitored probe drilling in relevant support classes. He was taking decision on what support class will be applied for given conditions and also about any additional measures required (additional shotcrete, bolting). Part of his responsibility was evaluating the results of geotechnical monitoring (deformation measurements) and proposing relevant measures to react on the results.

NATM Engineer was an important partner during technical discussions and negotiations with the Client's Representative, who was at Dulles Airport project called Project Management Consultant (PMC). In the PMC team there was highly qualified international staff with long term experience regarding NATM tunnelling.

Two years project experience demonstrated importance of the newly established position. Responsibility of the NATM Engineer was quite high and his activity significant, especially in the case of worsening geological conditions and a need to take and imply quickly the decisions in respect of changing to another support class or to apply additional support or excavation measures. Although a part of contractor's team, quite understandably sometimes the priorities of both subjects (NATM Engineer vs. Contractor's management) were slightly different. This fact was also confirmed at the meetings with PMC an/or Client, where NATM Engineer's position and reasoning were considered by the parties as rather neutral and objective, not much affected by project economical interests.

From the personal experience, a serious problem for the NATM Engineer was to get support measures done as fast as possible and in required quality. This is valid mainly for the timely shotcrete delivery in the case of unstable rock conditions. To improve and accelerate this process was beyond the NATM Engineer capability and competence, although he was generally responsible for proper and timely application and safe and stable conditions.

4 CONCLUSION

The presence of "NATM Engineers" on the Dulles airport tunnelling contracts definitely contributed to safe realization of WUBT and APM conventionally driven tunnels. European tunnelling experts experienced working in different contractual environment and different working conditions with respect to local workforce experience with NATM, tunnelling qualification, and local practises. It is probable that on follow up tunnelling contracts on Dulles extension, the same or similar model of NATM expert working directly for contractor shall be applied.

Underground Space – the 4th Dimension of Metropolises – Barták, Hrdina, Romancov & Zlámal (eds)
© 2007 Taylor & Francis Group, London, ISBN 978-0-415-40807-3

Risk Management of the construction of tunnels using Tunnel Boring Machines (TBMs)

A.H. Thomas & J.P. Banyai
Mott MacDonald, London, UK

ABSTRACT: As one stands inside one of the new hi-tech closed face TBMs one could almost believe that everything is computerised and all risks are completely under control. Sadly the truth is that, not only do surface collapses sometimes occur above TBM tunnels, but also the costs associated with the collapses are increasing rapidly. This has caused a crisis in the insurance industry and prompted the publication of a Code of Practice for Risk Management of Tunnel Works in the UK. Insurers are demanding that contractors adopt the code of practice if they are to be given project insurance. An international version of this code is being prepared. This paper will discuss the risks associated with TBM tunnels and how risk management can be applied to TBM tunnelling. This paper will illustrate how these general procedures can be applied by describing a recent project where TBM tunnels have been driven successfully in a high risk urban area.

1 INTRODUCTION

Tunnelling is a risky business. Unlike other types of civil engineering, tunnelling is exposed to greater risks, primarily because of the limited knowledge about the ground ahead of the tunnel and how it will behave. In tunnels under mountains or water the knowledge is limited because of the natural obstacles to site investigations. In tunnels in an urban environment there is uncertainty over how the tunnel will interact with surrounding buildings. Throughout the history of tunnelling engineers have developed informal ways of handling these risks.

However, these have not always been successful. High-profile tunnel accidents highlight the dangers (e.g. T&TI 2003, Forrest 2006). Coupled with some notable financial failures in the 1990's, this refocused attention on how risks are managed in tunnelling. Coming from different viewpoints, several groups have concluded that one answer to these problems is an improved management of the inherent risks.

In line with European Union health and safety directives, risk management has been introduced into safety legislation (e.g. the CDM regulations in the UK (HMSO 1994)). This affects all aspects of life from theatre performances to civil engineering. In the context of tunnels in the UK the CDM regulations have had a pronounced effect on the design process. While it may be difficult sometimes to identify how the final designs are different because of CDM, the formal process of risk management is clearly visible on all projects. The same applies during construction.

Often the financial consequences of a major problem end up being carried by an insurance company. Insurers in several countries have become so concerned about the impact of large losses on the handful of projects which go wrong that they are threatening to refuse to insure the projects. This would expose clients and contractors to huge financial risks and planned projects could be cancelled. To address this, the British Tunnelling Society (BTS) teamed up with the Association of British Insurers and published a Joint Code of Practice on Risk Management of Tunnel Works in the UK (BTS/ABI 2003). The International Tunnelling Insurance Group, in conjunction with the BTS and supported by the International Tunnelling Association (ITA), is currently developing an international version of this code of practice.

In parallel, tunnellers themselves have promoted the use of risk management too. Various organizations have published guidance on the subject (e.g. the BTS/ABI (2003) the German Committee for Underground Construction (DAUB) – outlined in (Naumann & Brem 2004) and the ITA (2004).

2 RISK MANAGEMENT IN TUNNELLING

2.1 *A general overview*

"A plan is nothing" General Eisenhower is reputed to have said "but planning is everything" he continued. This quotation – to a degree – could be applied to risk management. The act of a project team sitting down to

consider everything that could affect the tunnel and the actions that result from this can be more important than the mere fact that documents called risk assessments are produced.

Risk management can be used at all stages of a project – during concept design and planning, detailed design, tender evaluation and construction, as well as during operation and maintenance. The concept can be applied to safety, environmental, financial and contractual risks. In each context the details of the approach differ but the underlying theory is the same. To avoid creating a negative atmosphere, this process is sometimes called "hazard and opportunity" management. There may be beneficial conditions – opportunities – which could occur and steps can be taken to maximise the chance of the benefit being realised. Risk management in tunnelling has been discussed in detail in many other papers so the general principles will not be repeated here.

The overall philosophy is to reduce the risks to As Low As Reasonably Practicable (ALARP). At least in the UK there is a preferred hierarchy of mitigation measures.

- remove
- mitigate
- protect

First, one should try to remove the hazard completely. If this is not possible, one should use mitigation measures that protect everyone exposed to the hazard. Finally, one can provide protective measures that individuals can use. There is also a preference for "passive" protection – i.e. something which protects a person without them having to do anything – rather than "active" protection. A handrail beside a deep excavation is an example of passive protection whereas a safety harness is an active protection measure.

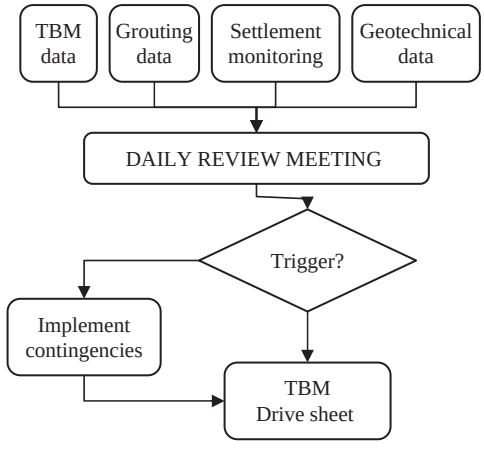


Figure 1. Typical flow of information through Daily Review Meeting.

During construction, the best way to manage these risks is, firstly, by monitoring the performance of the tunnel – to verify that it is behaving as intended by the designer – and, secondly, to have a representative of the designer (or a person with sufficient understanding of the design) on site to assist in the review of proposed changes in construction method and the interpretation of the monitoring data. This process has been successfully implemented on many SCL tunnelling projects (e.g. Hilar & Thomas 2005b).

In addition to helping to manage risks, a benefit of the presence of the designer on site is that he can help to realise opportunities and with them come cost and programme benefits for the client. The ideal situation is one in which a "single team" culture is created and the client, designer and contractor work together for their mutual benefit.

The process outlined above is not just applicable to SCL tunnels. It can also be applied successfully to tunnels constructed using Tunnel Boring Machines (TBM). In urban environments it is important to monitor how the TBM is being operated, how surrounding buildings are responding and how the tunnelling is interacting with other works, such as compensation grouting. As before it is important that all parties are at the Daily Review Meetings (DRM) to interpret and react to the monitoring data as each one brings with him an understanding of his own activity and its influence on the others. Figure 1 illustrates the typical flow of information. The output of the DRM can be formally recorded in a TBM Drive sheet which is then sent to the TBM pilot. This is analogous to the Excavation Support sheet in SCL tunnelling (Hilar & Thomas 2005b).

2.2 *Opportunities*

A pint of beer that looks half empty to one person appears half full to another. There is a danger with this subject of focusing solely on all the things that could go wrong. One should not forget that the regular systematic review of a project can just as easily throw up opportunities to improve a project as it can highlight deficiencies that must be resolved. The same processes and tools that are commonly labelled "risk management" can be applied potently to the search for improvements to a project.

3 APPLICATION TO TBM TUNNELLING

3.1 *Scope of application*

TBMs are often perceived as a lower risk option, particularly when a closed face TBM is compared against the open face sprayed concrete lined (SCL) tunnelling method. Although well established in practice, it is arguable that the development of closed face TBMs

has outstripped the understanding of how they operate. As a result, despite their capabilities, failures do occur. For example, accidents in London (T&TI 2003) and Porto metro (Forrest 2006) – both involving closed face TBMs served to demonstrate the huge impact that failures can have. Apart from such visible problems, there is a litany of projects that have suffered delays and cost overruns due to difficulties with TBMs (e.g. see Barton 2000). This has even prompted some to argue that TBMs are a higher risk option in the case of long tunnels in hard rock (Barton 2000).

Research is ongoing in many places to close the gaps in understanding – e.g. on soil conditioning and EPBMs at Cambridge and Oxford Universities (Nattrass 2003) or face and grouting pressures at Ruhr University Bochum (Kasper & Meschke 2006).

Publications such as the British Tunnelling Society's guidance on closed face TBMs (BTS 2005) have echoed the call for the application of active risk management to TBM tunnelling.

3.2 *Hard and soft risk management*

One could differentiate between the "hard" and "soft" application of risk management. Where there are legal imperatives or strong demands from a client or third parties, one can observe a formal and systematic application – a "hard" usage of risk management. This could be characterized by mandatory procedures such as daily reviews, a fixed programme of activities such as workshops and an explicit desire to document the process. The latter is in part for the benefit of the project team but often largely so that an audit trail is generated to serve as proof to others that the project is being well managed. This approach is often used for SCL tunnels but less frequently applied to TBMs.

A "soft" application could be characterized by the adoption of risk management as an ethos for the project that suffuses its activities. Common tools such as risk workshops and live risk registers appear just as in the more formal approach but these are used on a more ad hoc basis. The project team applies them as and when it feels a need, as opposed to a predetermined timetable. For example, as a tunnel approaches a high risk area, such as the under-passing of another tunnel or a river valley, the team might decide to gather – the client, design and construction teams – to review the possible risks and the planned mitigation measures.

The case study below illustrates an example of a "hard" application. If one takes the example of a TBM in Iceland that became mired in a series of fractured zones (T&TI 2006), one could speculate that this was the type of situation that would have benefited from a "soft" application of risk management. The TBM was stuck for more than 3 months, causing huge disruption to the programme. While the contractor and supervision team discussed at length the options and hazards, the rigorous, dispassionate forum of a risk workshop might have helped to highlight the perils of certain strategies and to identify one which would have been more successful. When faced with an obstacle there is always a temptation to hope for the best and try to battle through it. However, sometimes it is more prudent to take a more cautious approach. In the case above, one could hypothesize that applying systematic pre-treatment ahead of the face from the point when the first fractured zone was encountered could have saved time, despite the time that such grouting would have required. Such is the benefit of hindsight but how is tunnelling to progress if not by learning from past failures?

4 CASE STUDY – THE AIRSIDE ROAD TUNNEL, HEATHROW, UK

4.1 *Project description*

The Airside Road Tunnel (ART) is a 1.3 km long twin bore tunnel constructed under London's Heathrow Airport (Williams & Audureau 2005, Hilar & Thomas 2005a). The 8.1 metre diameter pre-cast concrete segmentally lined tunnel, passes under taxiways, with as little as a 7 metres cover to the ground, and passes over the Heathrow Express (Hex) tunnel with a clearance of 3 m. The tunnel carries a road for airport vehicles moving between the Central Terminal Area and the new Terminal 5. To link these areas, the tunnel must traverse a large area of taxiway as well as sensitive and important structures such as fuel pipelines and fire mains.

In general settlement had to be kept below 25 mm and trigger levels were set for the important structures – see also Table 1.

The tunnel is located in the stiff overconsolidated London clay which is overlain by 6 to 8 m of waterbearing granular material.

Sprayed Concrete Lined (SCL) tunnelling was used to build cross-passages for emergency egress and to house equipment (Hilar & Thomas 2005b).

This work will not be discussed here as it was managed in the normal fashion for SCL tunnelling.

4.2 *Risk-based design*

The key risks were excessive ground movements resulting in unacceptable settlement and encountering

Table 1. Examples of trigger limits on settlement for ART.

Structure	Slope	Deformation
Taxiways	1 in 100	
Aircraft stands	1 in 60	
Hex tunnel	(change in diameter)	34 mm

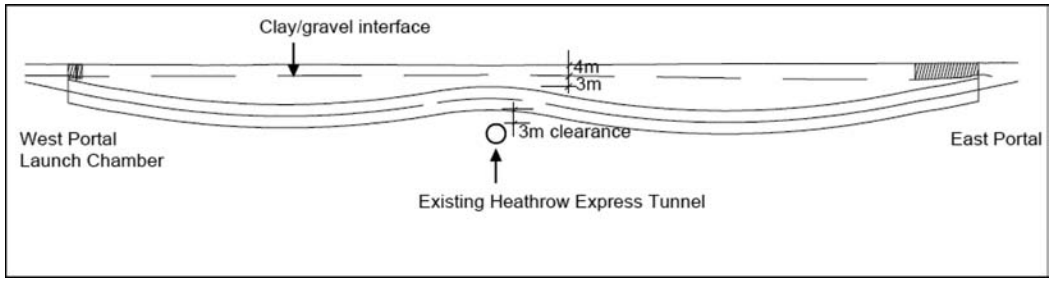


Figure 2. Vertical alignment.

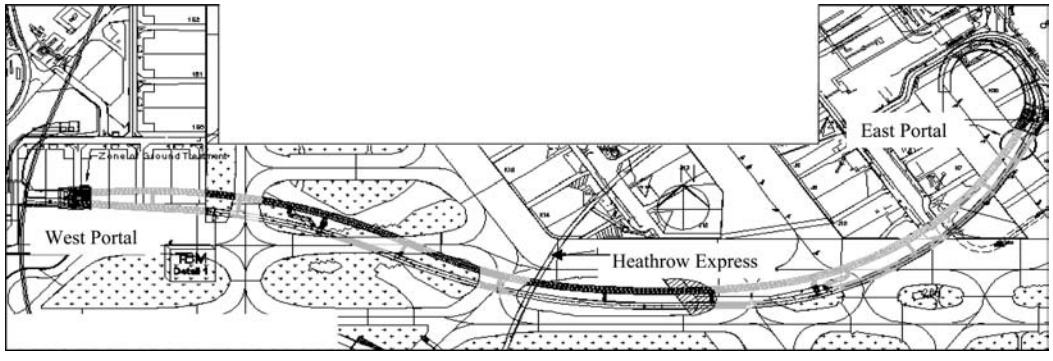


Figure 3. Horizontal alignment.



Figure 4. Cutterhead being lowered into place.

the water-bearing gravels, resulting local face collapse and again unacceptable settlement. These risks were explicitly addressed in the design.

Within the constraints of the design (e.g. existing structures, maximum gradients for the road vehicles, etc.) the vertical alignment was set to reduce the risk of encountering the clay-gravel interface (see Figure 2). Additional site investigation using cone penetration tests was done to map the interface.

As far as possible the horizontal alignment avoided sensitive areas such as taxiways (see Figure 3).

A closed face Tunnel Boring Machine (TBM) was chosen as the lowest risk option (see Figure 4). A hybrid TBM that had both an earth pressure balance (EPB) system and a compressed air system was developed with the manufacturer, Herrenknecht. This allowed the TBM to excavate rapidly through the large amount of London Clay using the compressed air, but also deal effectively with any gravel or mixed ground encountered during the excavation. Closed-face TBMs are renowned for their ability to control settlement.

Despite all these risk mitigation measures, significant residual risks remained for the construction team to manage.

4.3 *Risk management during construction*

A feedback loop of monitoring and modifying TBM operations was used to control the risks during construction.

The TBM was fitted with a data logger which allowed the engineers to monitor the performance on a real time basis. This recorded several critical parameters for controlling settlement, namely the air pressure/face pressure, the pressure of the bentonite in the annulus around the TBM and the grout pressure. These could then be compared directly within the logger to the tunnel excavation and ring building sequence.

Based on the detailed examination of performance over the first 300 m of the drive, the design parameters for the TBM operation were refined. The optimum combination was found to be: 0.5 bar air pressure in the TBM cutterhead; bentonite pressure of 1.0 bar in the annulus around the TBM and a grout pressure of 90% of the overburden pressure at the crown plus 0.5 bar (up to a limit of 2.85 bar).

Each tunnel bore was excavated continuously – 24 hrs a day, 7 days a week – over a period of almost 6 months. The only exceptions were the routine maintenance shifts. This programme was chosen to reduce the time the TBM was at a standstill, which also helped minimise settlement.

The monitoring of the TBM as well as settlement continued throughout construction. When the information from the data logger is examined in conjunction with the relevant settlement data and TBM shift report, the monitoring team have a far better understanding of why settlement may be occurring, and with this information, can make a judgement on the best way forward to halt the settlement, and prevent further settlement in the future.

The monitoring team was assembled from representatives from the Client (BAA), the Designer (Mott MacDonald) and the Contractor (Morgan Vinci Joint Venture) and met routinely every day to discuss the current data available.

The benefit of the daily review meetings (DRM) lay not necessarily just in spotting any gross errors or the identification of individual problem areas in the tunnel excavation, but the DRM could highlight any trends that have occurred, and to flag up any warning signs. This proactive approach not only reduced the severity of settlement that might occur, but also helped to reduce the frequency of more significant settlements.

4.4 *Performance*

The majority of the tunnel bores were constructed in compressed air (semi-open mode), with EPB mode only being utilised at the portals.

The success of this method of construction management is clear when we consider that, while face loss was predicted to be 1.0%, an average of 0.2% (7.5 mm settlement) was achieved, with a maximum of 0.35%. All surface settlements were less than than the maximum limit of 25 mm.

Due to aircraft operations, the surface settlement over the entire route could only be measured once a day (not real time), which meant the TBM face pressure and other parameters could only be adjusted on a daily basis. Real time monitoring would have had the benefit of observing any settlement trends faster, enabling the construction team to react faster to the movement on the surface.

5 CONCLUSIONS

Despite the advances in TBM technology, tunnelling remains a risky business and the consequences of failures can be very serious.

Formalized risk management offers one way to handle these risks. This can be applied in a "hard" or "soft" manner. As illustrated by the case study, this rigorous approach to examination of the TBM excavation parameters and assessment of the monitoring results, it is possible to achieve better control the effects of tunnelling. In particular, this method can assist in reducing the likelihood (risk) of those undesirable effects, such as settlement.

This method of continual assessment of the excavation movement and using the results to tune the excavation technique is more commonly used when constructing using sprayed concrete, but the application used on the ART shows how it can be effectively used on TBM excavated tunnels too.

ACKNOWLEDGEMENTS

The authors would like to contributions of numerous colleagues to discussions of this subject, in particular those of Mike Talliss.

REFERENCES

Barton, N. 2000. TBM Tunnelling in Jointed and Faulted Rock, Taylor & Francis, London.

BTS 2005. Closed-Face Tunnelling Machines and Ground Stability – A guideline for best practice. Thomas Telford Ltd, London.

BTS/ABI. 2003. Joint Code of Practice for Risk Management of Tunnel Works in the UK, British Tunnelling Society / Association of British Insurers, London.

Forrest, M. 2006. Porto Pressure. Materials World, July 2006, pp 31–33, www.iom3.org.

Hilar, M. & Thomas, A. 2005a. Tunnels Construction under the Heathrow Airport. Tunel – Magazine of the Czech Tunnelling Committee and the Slovak Tunnelling Committee ITA/AITES, Vol 3, pp. 17–23.

Hilar, M. & Thomas, A. 2005b. The Latest Innovation in Sprayed Concrete Lining – the LaserShell Method. Tunel – Magazine of the Czech Tunnelling Committee and the Slovak Tunnelling Committee ITA/AITES, Vol 4, pp. 11–19.

HMSO. 1994. The Construction (Design and Management) Regulations, (1994, amended 2000), HMSO, London.

ITA. 2004. Guidelines for tunnelling risk management, (S. Degn Eskesen et al.), Tunnelling and Underground Space Technology 19, pp 217–237.

Kasper, T. & Meschke, G. 2006. On the influence of face pressure, grouting pressure and TBM design in soft ground tunnelling. Tunnelling and Underground Space Technology 12 (2006) pp 160–171.

Nattrass, H. 2003. Easing the way – soil conditioning.

Tunnels & Tunnelling International, June 2003, www. tunnelsonline. info.

Naumann, J. & Brem, G. 2004. Empfehlungen des Deutschen Ausschusses fur Unterirdisches Bauen e.V. (DAUB) zu Planung und Bau von Tunnelbauwerken, Tunnel 4/2004, pp 73–79.

T&TI. 2006. Robbins TBMs all go in Iceland. Tunnels & Tunnelling International, February 2006, www. tunnelsonline.info.

T&TI. 2003. Ground collapse above CTRL. Tunnels & Tunnelling International, March 2003, www. tunnelsonline.info.

Williams, I. & Audureau, J-L. 2005. Large diameter TBM for tunnelling shallow tunnels beneath Heathrow Airport, UK. Felsbau 23 (2005) Nr. 5, pp 71–75.

Underground Space – the 4th Dimension of Metropolises – Barták, Hrdina, Romancov & Zlámal (eds)
© 2007 Taylor & Francis Group, London, ISBN 978-0-415-40807-3

Assessment of ecological safety in the process of underground development on the example of a big Russian city

V. Umnov & N. Vorozheykina
Moscow State Mining University, Moscow, Russia

ABSTRACT: The intensive development of underground construction in a big city is inseparably linked with its ecological safety. This paper deals with the effect of underground construction on the environment, as well as the impact of surface infrastructure on the underground space. The analysis of the situation has been performed for the biggest city of Russia – Moscow. The characteristics of basic reasons causing emergencies linked with the use of underground space are presented. The paper includes the methods for the assessment of potential damages.

1 INTRODUCTION

The majority of urban population in Russia (73%) is subject to ecological, economic and social problems caused by the growing density of construction and population. One of the most effective ways to address this problem with regard to Russian cities is to develop underground space. However, the growth of underground construction increases risks of underground and surface catastrophes, pollution of underground waters and other consequences that threaten health and lives of people and their property. Due to the lack of appropriate economic tools, administrative structures, methodical basis and legal norms the regulation of underground space usage in Russian cities is not adequate.

2 DESCRIPTION OF THE UNIT

Moscow has been chosen as an object for investigations since it is a city with well-developed and growing underground infrastructure. Underground space of Moscow from surface to 20 m is stable (= competent rock) in character, below there are unstable Jurassic clays and floating earth under which it is limestone. So the underground units are being build either close to the surface in depth of less than 20 m or at a considerable depth >80 m.

The conditions of the city with respect to geology are considered unfavourable. Incompetent rock and watering create engineering difficulties. Sedimentary rocks are not very fit for the construction of heavy tall buildings. General geological risks on the territory of Moscow are connected with the development of such geological processes as karst-suffosion, subsidence, landslides, flooding of the territory and soil compressibility.

Ecological safety is an urgent problem for Moscow. There are a number of emergencies occurring in Moscow every year and some of them are connected with the use of undergrounds space. Large accidents of product pipelines with human victims were recently made public and naturally caused considerable economic and ecological damage. The problem of terrorism has intensified.

The state of underground space in Moscow, its usage and ecological safety has been analysed and the characteristics of possible emergency situations provided. The method for the assessment of ecological risks and consequences of emergency situations occurring in the use of underground space has been developed along with economic estimation of measures intended to prevent possible emergencies.

There is one of the biggest in Europe underground commercial-recreation complexes "Okhotni ryad" (a museum, offices, commercial centre, restaurants, parking etc.) in Moscow. Moscow international business centre "Moscow city" that is under construction is designed to be three levels deep under the surface. One of the largest constructions is an underground part of Atrium on the square of "Kurskaya" railway station. The construction of section of the 3-rd transport ring road is being completed underground with a cross-section of 17.5 m × 5.2 m.

3 ANALYSIS OF ECOLOGICAL SAFETY IN THE USE OF UNDERGROUND SPACE

There is a considerable impact of the city over subsoil that leads to instability. Main reason is the inadequate

calculation for loads not taking into account the condition of subsoil in the process of design and construction. Under the pressure of surface units, changes in hydrogeological conditions, pollution caused by water, soil erosion, and damage of subsurface and surface. Surface pressure, vibration and underground water contamination effect the underground units and the impact is actively noted at the depth of up to 60–100 m.

Surface units (buildings, constructions, and embankments) put significant pressure upon the surface of the ground (from 0.01 to 2 N/mm^2 and more). Compacting of strata under the weight of tall house of the Moscow University caused 4.7 cm of soil settlement in the centre and created depression of settlement to the distance of 50–120 m along the perimeter of the construction (situation is the same round other tall buildings of the city). Change of topsoil upsets evaporation. This leads to settlement and shift of surface and subsurface. Dynamic loads by mainly transport tighten (compact) porous grounds and destroy insubstantial thixotropic grounds. Buildings along the streets with intensive traffic have settled on average to 3–8 mm (up to 5–20 cm) compared to those situated in side streets or blind alleys.

The conditions for surface waters change as well and result in excessive moistening and flooding of territories. This in its turn destroys foundations, lowers toughness, complicates location of technical collectors and pathways, intensifies corrosion of pipelines and steel structures, which are assembled in the ground without appropriate electrochemical protection. In the result of flooding there are cases of collapse and subsidence that destroy surface and underground units. Because of floating earth it was necessary to suspend the construction of new lines of Moscow underground (Metro). As a whole the flooded territories make about 40% of the surface area of Moscow which houses over 30 large enterprises. Approximately 500,000 m^3 of water is annually infiltrated to the subsurface of Moscow. Half of this quality is leakage from underground pipeline for water supply and sewerage, ponds and water reservoirs.

Dehydration of karst carbonate solid monolith, ingress of acid surface water and other factors lead to subsidence of rock and surface. Within last 25 years in the Northwest of Moscow there were 42 cases of crater formation with diameter of up to 40 m and depth up to 8 m, which resulted particularly in the destruction of residential constructions.

As subsurface waters get depleted they become chemically and bacteriological polluted due to the pulling of overlying and surface water. For example, in some points of water inlet in Moscow (Centre, Paveletski railway station, Lyublino-Nagatino, Dorkhimzavod, Ostashkovki highway) the concentration of mercury, lead, zinc, cadmium and chromium in subsurface water exceeds maximum allowable concentration several times.

Washout and suffusion processes restore their activity along the route of underground communication and in the bulk of filled-up soil, slope development renews landslide processes especially along Jurassic clays in the lower parts of Moscow River valley. Landslides occupy about 3% of the territory of the city. In Moscow there are 15 large areas with deep (up to 100 m) landslides and 200 small (1–5 m) surface landslides in quaternary sediment (overburden). The number of landslides doubled within last ten years. In some regions of Moscow the deep landslides mainly caused by man's activities move with the speed of 5 to 30 cm a year.

4 INFLUENCING FACTORS AND METHOD OF THEIR ASSESSMENT

Analysis of factors that influence origination of extraordinary situations and their consequences allowed forming a cause-and-effect model of extraordinary situations in the course of underground space usage (fig. 1). According to the model the environment in which the extraordinary situations are being developed is divided into three parts: *A* –an underground object itself, *B* – surrounding solid monolith of rock, *C* – earth surface. Factors that cause extraordinary situation or determine its development (upper part of the chart), and influence the consequences of this event (lower part of the chart, indices with quotation mark) are presented for each of them.

where: *C*1 – mechanical effect of the objects on the surface, *C*2 – availability of resources, *C*3 – surface water bodies (reservoirs), *C*4 – atmosphere, *C*5 – type and work load of the territory; *B*1 – depth, *B*2 – rock mechanical properties, *B*3 – watering, *B*4 – gas composition of the solid monolith, *B*5 – adjacent underground objects, *B*6 – confining pressure, *B*7 – courses that connect with surface; *A*1 – access to surface, *A*2 – power supply, *A*3 – dewatering,

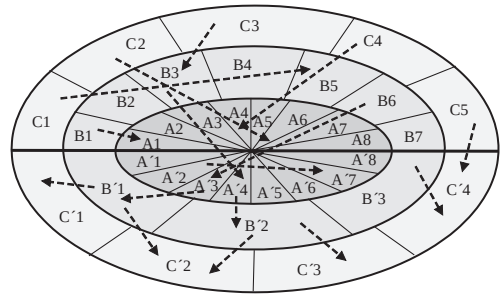


Figure 1. Cause-and-effect model of extraordinary situations in the course of underground space usage.

$A4$ – ventilation, $A5$ – maintenance of solid monolith, $A6$ – fire fighting, $A7$ – space workload, $A8$ – location of objects (processes); $A'1$ – fire, $A'2$ – explosion, $A'3$ – monolith fall, $A'4$ – flooding, $A'5$ – ventilation damage, $A'6$ – failure of electric power supply, $A'7$ – equipment fault, $A'8$ – hazard caused by located objects and processes; $B'1$ – damage of solid monolith, $B'2$ – failure of geological conditions, $B'3$ – pollution of underground waters; $C'1$, $C'2$, $C'3$, $C'4$ – impact on atmosphere, aquatic environment, territory, soil.

This model allows creation of possible scenarios for extraordinary situations that occur in the use of undergrounds space and their consequences.

Basic elements of emergency situation and their characteristics have been identified in order to assess the size of damage caused by extraordinary situation in the use of underground space and efficiency of measures directed to reduce the consequences (Table 1).

Measures on the reduction of damages are intended to change one or several characteristics of the extraordinary situation elements. The above mentioned elements have been taken into consideration in the development of the method for the assessment of the consequences of extraordinary situations and efficiency of measures intended to reduce them, which is based on the following criteria:

Table 1. Elements of extraordinary situation in the use of underground space and their characteristics.

Elements of extraordinary situation	Characteristics
Source	– type (ignition, flooding, mechanical impact, etc.)
	– location
	– probability of occurrence
	– duration of event
	– strength of event
Propagation medium	– extend to which the source of impact propagates
	– size of the zone of propagation
Factors of consequences	– mechanical
	– chemical
	– electric
	– electromagnetic
	– impact on climate
	– changes in the composition of atmosphere, air, water, etc.
Consumers	– people
	– material and spiritual values
	– natural environment
Damage	– ecological
	– economic
	– social

$$D=P\cdot W\cdot\sum_{i}^{I}(F_i\cdot T_i\cdot\sum_{j}^{J}(S_j\cdot k_{ij}^{s}\cdot\sum_{l}^{L}(Q_{jl}\cdot D'_{il})))\rightarrow\min \qquad (1)$$

where D – damage caused by extraordinary situation, \$; P – probability of initiation of the source of extraordinary situation, fraction; W – strength of the source of extraordinary situation, un.1, i – index of the type of negative factor that arises in the result of the effect of the source, $i\in I$; F_i – power of the factor of consequences caused by the source of extraordinary situation, un.2 /un.1; T_i – duration of hazardous factor, sec.; j – index of the zone of territory affected by the factor of consequences, $j\in J$; S_i – area of the territory affected by the factor of consequences, m^2; k_{ij}^{s} – coefficient of the factor of consequences propagation i in zone j, fraction; l – index of the type of consumers of the factor of consequences, $l\in L$; Q_{jl} – number of objects of the type l, situated in the zone j, pieces/m^2; D'_{il} – average damage caused to the object type l by factor i, \$/(un.2·pieces·sec); un.1 – unit for the power of the source of extraordinary situation (for example, earthquake magnitude); un.2 – units of negative factor arising in the result of extraordinary situation (for example, content of harmful substances in atmosphere).

Recommendations on the improvement of legislation relating to the use of urban underground space that allow to regulate the underground activities more effectively and thus to reduce possible damages caused by emergencies have also been developed.

5 CONCLUSION

This paper considers interrelation of underground usage and ecological safety in a big city. Moscow has been used as an example for performing analysis of major factors of underground units that effect the environment and vice versa. As a result the paper suggests systematization of reasons causing damage in emergency situations in the course of underground space usage. Assessment of major damages and measures for their mitigation are given.

This page intentionally left blank

Underground Space – the 4th Dimension of Metropolises – Barták, Hrdina, Romancov & Zlámal (eds)
© 2007 Taylor & Francis Group, London, ISBN 978-0-415-40807-3

Managing risk – successful project delivery, underground infrastructure for Terminal 5 Heathrow Airport, UK

O.I. Williams
BAA plc, London, UK

ABSTRACT: Terminal 5 (T5) will open in March 2008 and ultimately provide Heathrow Airport with an additional 30 million passenger annual capacity, giving a total annual capacity of about 90 million passengers. T5 is one of the largest construction developments in Europe with an estimated outturn cost of £4.3 billion. The Terminal's infrastructure includes approximately 14 km of tunnelling to provide road and rail links.

Managing risk is vital to the success of any project and in particular with those involving tunneling. In the last 15 years there has been a number of projects where their overall success was affected when the consequence of risk became a reality.

Fundamental to the success of T5 was the contract strategy developed by BAA and the implementation of risk management. The strategy was a non-adversarial contractual approach based on relationships and behaviours with risk management as a core activity. This paper describes BAA's contract strategy and the processes developed and implemented by the Team.

1 INTRODUCTION

1.1 *The Project (T5)*

The T5 project consists of a main terminal building and two satellites, additional 56 aircraft stands, car parking for 5000 vehicles and road and underground rail infrastructure. The key element of T5's infrastructure is approximately 14 km of tunnelling to provide the terminal with road and underground rail links, Figure 1 shows an aerial view of the T5 project and Figure 2 the plan location of the tunnel projects. The tunnels range in length from 1.3 km to 4.1 km and from 3 metres to 8.1 metres in diameter. The majority of the tunnels were constructed using Tunnel Boring machines (TBMs) and innovative developments of the single shell shotcrete lined method, Lasershell™, (Eddie et al 2003) for the construction of the numerous short, complex underground structures such as shaft and cross passage complexes. The specific details of the projects are described in detail by Hilar et al (2005).

1.2 *Why manage risk?*

In the last 15 years there has been a large number of UK and international projects were overall success was affected when the consequence of risk became a reality. These consequences ranging from cost and time overrun, technical failures (tunnel excavation and

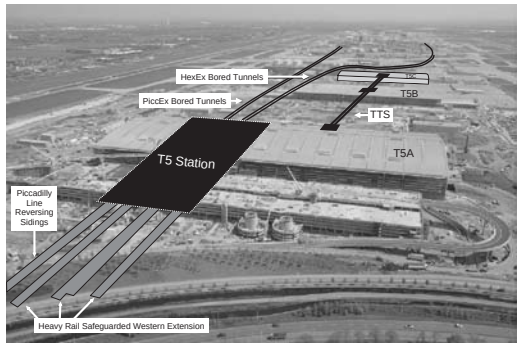


Figure 1. Aerial view of the T5 project.

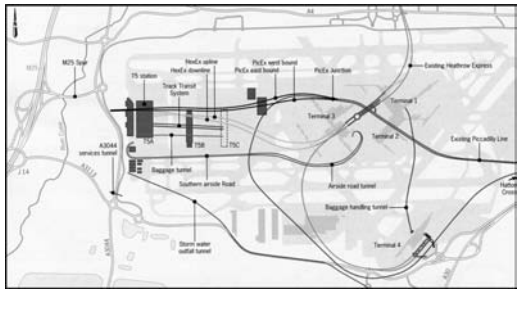


Figure 2. T5 project and the location of the tunnel projects.

collapses for example), injury to people, damage to property, and, corporate and industry credibility.

Notable tunnelling project examples include the Jubilee Line Extension (UK), whilst being a technical success, significant time and cost overruns occurred, Heathrow Express (UK) tunnel collapse in 1994 (HSE 1996), Munich (Germany) tunnel collapse in 1994, and most recently in 2004 the Nicoll Highway excavation collapse in Singapore (Magnus et al 2005). There are other worldwide instances too numerous to mention (Lance et al 2006).

It is generally accepted that all risks cannot be removed but it is also accepted that identification of risks and their proactive management can decrease the probability of occurrence, and in the event that they do occur, the severity of the risk event can be minimized with robust control processes and mitigation in place.

Given historical events, the delivery of T5 presented BAA with a challenge in respect of the tunnelling risk. The key factors contributing to this were: £4 billion plus project privately financed by a private company, the scale of project not undertaken previously by BAA, ambitious technical challenges to be delivered in the environment of the world's busiest airport. BAA's objectives from T5 were to deliver on time, within budget, compliant with specifications, safe and meeting customer needs and expectations.

From the experience of other projects and BAA's own experience of the Heathrow Express tunnel collapse in 1994, BAA recognised to meet its objectives they needed to develop a procurement and project delivery strategy that was able to meet the challenges of delivering a complex project. BAA accepted that to achieve different future results it was necessary to do something different to what was historically done by the construction industry. BAA recognized that to successfully meet these objectives BAA needed exceptional performance from it's suppliers. BAA considered the key success criteria for the strategy would be a non-adversarial contractual approach, based on relationships and behaviours with cost reimbursement as a cornerstone rather than conventional contractual approaches. Furthermore, BAA acknowledged that the risk of not achieving a successful T5 was so large that to achieve exceptional performance BAA would need to be for the time and cost risks all the time. These factors led to the T5 Agreement.

2 MANAGING PROJECT RISK

2.1 *The T5 Agreement*

The T5 Agreement is a unique contract which outlines processes and strategies to manage successful project outcomes in an uncertain environment and not contractual positions when things go wrong. It focuses on principles such as behaviours and relationships, risk management, performance and success, and, people as individuals contributing to integrated teams to achieve a common goal. The consequences of conventional contractual risk of cost and time are not shared, they are held by BAA. Suppliers' actual costs are reimbursed with a guaranteed element of profit and an incentive target payment to reward exceptional performance, and if achieved, shared between the suppliers and BAA.

2.2 *T5 tunnel projects delivery team*

BAA put together a single, multi-company integrated team to deliver the tunnel projects, this included: BAA (client and project leadership), Morgan Vinci (tunnel constructors), Mott MacDonald (overall civil and tunnel designer), and Beton-und Moniebau (Sprayed Concrete Lining [SCL] design and on site specialist support).

2.3 *Risk management*

The strategy of managing risk was through integrating risk and delivery management. Initially the process involved exposing the risks through project risk reviews and thereafter regularly updating and reviewing 'live' risk registers and live risk response plans within the framework of a project execution plan. Each of the specific tunnel projects presented a number of challenges. The two most significant physical challenges were controlling ground movement (and eliminating tunnel collapse), and workforce safety. It was considered that if these two areas were managed successfully, the other key risks of time and cost would directly be influenced positively. The Team adopted the fundamental principle of providing control measures not consequence control measures as a basic risk management approach to achieve the optimum solution. Specifically, the Team concentrated on eliminating the risk, for example ground movement, face collapse etc. by implementing control measures thereby preventing or minimising the hazard happening in the first instance rather than rely on a consequence control measure.

Notwithstanding that risk management was a core objective to the Team. UK legislation also imposes duty on parties to address risk. The legislation and its relation to risk are well documented by Lance et al (2006). The Project Team implemented these obligations and whilst not mandatory, the Team, through commitment to adopting best practice, followed the guidelines of the Joint Code of Practice for the procurement, design and construction of tunnels and associated underground structures in the UK. (ABI & BTS 2003).

3 MANAGING SAFETY RISK

3.1 *Incident & Injury Free program (IIF)*

A central project risk objective was ensuring workforce safety. A number of innovations and initiatives were developed and followed on T5 to meet this objective. Adoption of cause control measures and targeting attitude to personal safety were the two key elements of the strategy. It has long been considered that significant improvement in safety can only be achieved if a positive safety culture exists in everyone. To address this, a behavioural safety imitative was introduced, the Incident and Injury Free program (IIF). The key element of the program was to make safety a personal commitment, moving safety to a core value and creating a vision and expectation that all incidents and injuries are avoidable.

3.2 *Technical innovations*

The Team investigated and developed methods and techniques to reduce workforce exposure. One of the main innovations involved further developments with the sprayed concrete lining (SCL) technique. The Lasershell™ method was developed to improve safety by eliminating the need for miners to enter an unsupported face area and to mechanise the process to reduce injuries. Other key factors in the development were fast ring closure with minimum joints in the shotcrete lining and its suitability for complex structures. The application of the method at T5 is described in detail by Williams et al (2004).

A typical advance for SCL works in soft ground consists of a top heading, bench and invert. Girders and mesh are used for support along with the shotcrete and require miners to work in the face area. The basic concept of the innovative Lasershell method is a circular cross section with an inclined domed face and rapid shotcrete ring closure and eliminating the need for lattice girders. Figure 2 illustrates a typical cross section of Lasershell™. Traditionally lattice girders are used to aid shape control. To eliminate the need for lattice girder, the TunnelBeamer™ survey tool was developed which could accurately guide the excavation and spraying process. All excavation is carried out by machine and the shotcrete has a permanent load function, with no girders or mesh, no horizontal joints and only one circumferential joint.

4 MANAGING GROUND MOVEMENT RISK

4.1 *Ground movement risk management process*

The tunnels crossed beneath Heathrow airport infrastructure consisting of one of the runways, aircraft taxiways and stands, buildings, strategic fuel and fire mains and two existing underground railway tunnels. Despite having appropriate tunnelling methods, ground movement was inevitable. A holistic approach to the control of ground movement was developed which covered the full spectrum from selection of tunnel excavation method through to a robust geotechnical and TBM data output monitoring and review cycle, Figure 3.

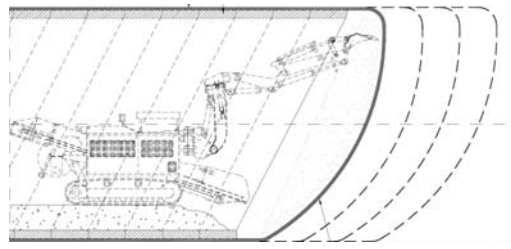


Figure 3. Cross section of typical Lasershell™ method.

This process did not prevent ground movement but provided the Team with a robust framework in which to manage the consequence with third parties. Whilst the emphasis was on cause control measures, detailed emergency and recovery plans were prepared in partnership with third parties to address the prevention of the occurrence of consequence escalation.

4.2 *Technical solutions – appropriate tunnelling methodology*

The Airside Road Tunnel (ART) presented the most significant ground movement risk to the project. The diameter of the twin tunnels (8.1 m inside diameter) and its need to remain shallow from an operational requirement had potential ground movements which could severely damage the existing airport infrastructure and existing railway. Whilst the tunnel horizon was anticipated to be stiff clay (London Clay), the possibility of encountering the overlying water bearing gravels existed. To meet the challenge the Team worked closely with Herrenknecht and Putzmeister to develop a TBM which had specific features to address the tight ground movement criteria (less than 25 mm), low cover and ground conditions (Williams et al 2005).

The solution developed consisted of a closed face TBM (9.18 m external diameter) capable of applying low air pressure to the face and to address the risk of encountering the water bearing gravels the TBM also had the capacity to convert to Earth Pressure Balance (EPB) mode. Tests confirmed London Clay would not form a plug in the screw conveyor, capable of reliably maintaining 2 bar pressure, therefore a mechanical method of maintaining pressure had to be developed. Following a significant development and testing program, a Putzmeister twin piston pump screw conveyor airlock system, consisting of two 750 mm diameter

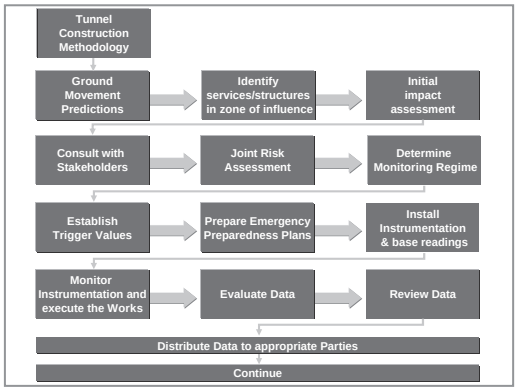


Figure 4. Ground movement management process.

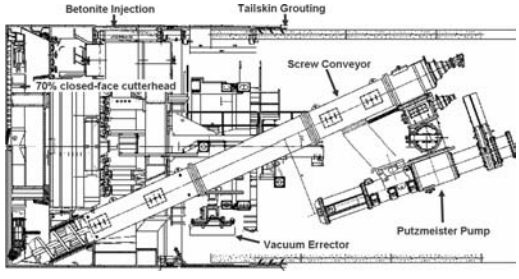


Figure 5. Cross section through the ART TBM showing the main components (Williams 2005).

pistons with an output of 400 tonnes/hour was fitted to the end of the screw conveyor. This allowed material to travel along the screw conveyor and then drop into the pump, where its two piston pumps acted as airlocks to control the air pressure in the chamber of the TBM, Figure 4.

Other features incorporated into the TBM, to aid the control of ground movement, included: keeping the cutterhead within the extrados of the TBM so that the front edge of the shield acted as a cutting edge; limiting the conical shape of the TBM; bentonite injection around the tailskin to provide ground support and maintain the face air pressure and simultaneous automated pressure controlled tailskin grouting.

4.3 *Tunnelling performance*

The surface monitoring data for the ART tunnels show that ground movements were kept within the maximum range and in most areas the actual ground movement was in close correlation to predictions. Figure 6 (Williams et al 2005) summarises the ground movement along the centreline of ART. In summary, the ground movement for over 36% of the drive length was between −5 and +5 mm, for 90% of the drive the

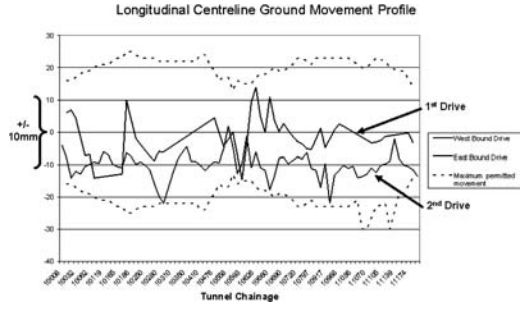


Figure 6. Ground movement along the ART tunnel drives (Williams et al 2005).

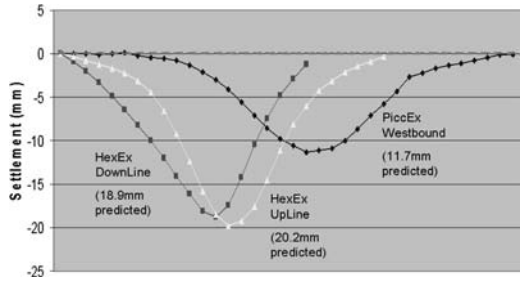


Figure 7. Existing rail tunnel movement caused by tunnelling.

movement was in the range of −10 and +10 mm and there was no significant movement greater than 20 mm was recorded.

The significant challenge for the Piccadilly Line and Heathrow Express tunnels was crossing beneath the existing Piccadilly line railway tunnel. Figure 6 shows the vertical movement recorded in the existing railway tunnel as a result of three tunnel crossings. The movement recorded was about 20 mm for the Heathrow Express tunnels (5.75 metres diameter passing 5 metres beneath the existing and the tunnel) and 12 mm for the Piccadilly Line tunnel the tunnel (4.5 metres diameter passing 4 metres). In both cases the actual movement was within 5% of the prediction value.

In all cases, tunnel construction proceeded without affecting the operation of the existing railway infrastructure and that of the airport.

5 CONCLUSIONS

14 km of incident free tunnel construction was completed on T5. The fundamental factors which underlined this achievement were the contract BAA developed and implemented, the T5 Agreement, and acceptance that the risk and its consequence rested with BAA. The principles of the Agreement focused on

success with all parties having aligned objectives and using risk management as a tool to support decision making, enhancing workforce safety, and eliminating unforeseen events. The implementation of the principles enabled the project to be delivered within the cost and time targets. Successful risk management was also supplemented by the introduction of IIF, a comprehensive behavioural safety program and the development of technical innovations.

ACKNOWLEDGMENTS

The author thanks the many individuals and companies who were fully committed to the principles of the T5 Agreement, these being of Trust, Commitment and Teamwork, without it none of the successes would have been achieved. Notwithstanding the commitment of individuals the author acknowledges the courage of BAA to implement the T5 Agreement.

REFERENCES

Eddie C & Neumann C. 2003. Lasershell leads the way for SCL tunnels. Tunnels & Tunnelling International, June 2003

Hilar M & Thomas A. 2005, Tunnels construction under the Heathrow Airport, Tunnel, 14 Rocnik – C/2005

Lance G & Anderson J. 2006. The risk to third parties from bored tunnelling in soft ground, Health & Safety Executive Research Report 453, HMSO, London

Magnus R, The Cee Ing & Lau Joo Ming. 2005, Report in the incident at the MRT Circle Line worksite that led to the collapse of the Nicoll highway, Ministry of Manpower, Singapore

The Association of British Insurers & The British Tunnelling Society, 2003. A Joint Code of Practice for the procurement, design and construction of tunnels and associated underground structures in the UK, Thomas Telford publishing, London

Williams I, Neumann C, Jager J & Falkner L. 2004. Innovative shotcrete tunnelling for London Heathrow's new Terminal 5, 53rd Geomechanics Colloquy and Austrian Tunnelling Day, Salzburg, Austria

Williams I & Audureau J.L., 2005. Large diameter TBM for tunnelling shallow tunnels beneath Heathrow Airport, UK, 54th Geomechanics Colloquy, Austria

The collapse of NATM tunnels at Heathrow Airport. A report on the investigation by the Health and Safety Executive into the collapse of New Austrian Tunnelling method (NATM) tunnels at the central Terminal area of Heathrow Airport on 20/21 October 1994. HSE Books. 2000

This page intentionally left blank

Underground Space – the 4th Dimension of Metropolises – Barták, Hrdina, Romancov & Zlámal (eds)
© 2007 Taylor & Francis Group, London, ISBN 978-0-415-40807-3

Development and application of process-oriented shield tunneling risk management system

Tang Xuan, Wu Huiming & Bob Chow
Shanghai Tunnel Engineering Co., ltd. (STEC), China

ABSTRACT: Based on the risk management flow suitable to construction enterprises, the paper creates a set of risk analysis structure for shield tunnel construction risk management. Moreover, combined with the platform of knowledge management in construction enterprises, a risk knowledge management system for shield tunnel construction is developed. The system helps to optimize the allocation of resources within enterprises and promote the efficiency of overall control in risk and construction cost.

1 INTRODUCTION

Risks can be divided into two types, pure risk and speculative risk. Pure risks cause only losses, while speculative risks may bring profits if the risk control measures are properly taken. The paper mainly concerns about pure risks caused by the uncertainty of staff capability, equipment performance, materials, accuracy of construction schemes and environment factors during shield tunnel construction. At present, researches in most domestic construction enterprises in this field still pause on the level of contingency plans. A systematic leap is anticipated in domestic construction risk management to effectively reduce the possibility of construction risk and the resulting losses during construction.

In that background, fully considering the needs of STEC in shield tunnels construction, we've set up a research group and worked out a practical process-oriented risk management system structured on the platform of knowledge management. Practices show that the combination efforts of construction risk management and knowledge management in construction enterprises helps to continuously promote its ability of risk control during construction, and also has great significance in enhancing its core competence.

2 FLOW DESIGN OF CONSTRUCTION RISK MANAGEMENT

2.1 *Construction risk analysis*

2.1.1 *Risk identification*

Risks in construction stage of a project come from either inaccurate evaluation of its resources by the construction enterprises, or the uncertainty of environmental conditions surrounding. Those risks will eventually cause several kinds of losses. Thus, at the beginning of risk identification, Risk classification in construction should first be done. Generally speaking, construction risks can be classified into four categories according to what kind of losses they induce (see Table 1).

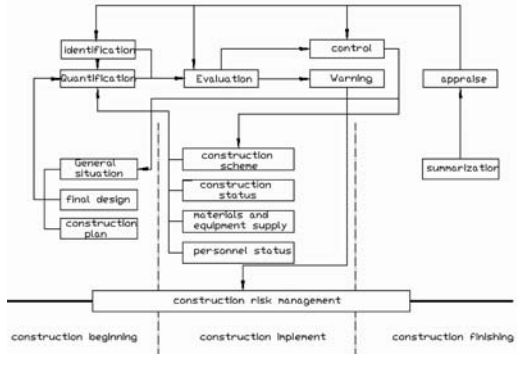


Figure 1. Flow design of risk management.

Following the sequence of construction procedures, we can analyze these four kinds of risks by identify their influencing factors during construction from different angles of view, such as staff, technology, equipment, materials, and environmental conditions, etc. Then, a primary risk factors hierarchical structure comes out for further analysis.

2.1.2 *Risk quantification*

In this process, we need determine unified evaluation criteria. Then proper appraisal indicators should be chosen or created to fully reflect the current status of

every risk influencing factor. In doing so, make sure that the value of chosen parameters should be easy to get and have enough representation. On that base, expert investigation or statistical methods from history cases can be used to determine the membership function of each risk factor corresponding to the evaluation criteria.

2.1.3 *Risk evaluation*

Use Analytical Hierarchy Process (AHP) to get the weighs of levels of risk influencing factors required in the evaluation of the objective hierarchy. Then second-order Fuzzy Comprehensive Evaluation (FCE) model can be presented to evaluate construction risk.

2.2 *Risk control*

According to whether the risk events have already occurred, risk control can be classified into pre-control and post-control. Pre-control measures including risk early warning are needed when the evaluation result of a certain risk in the objective hierarchy exceed the expected warning line. In such situation, the relating measures should be taken in advance to prevent losses. Post-control measures are taken when some risk events and their resulting losses have been inevitably detected. Such measures are taken to control existing losses from deteriorating or restrict other losses. The knowledge of both kinds of measures can be accumulated and improved by experts or case investigations.

2.3 *Evaluation after risk management*

In the progress of construction, the validity and effectiveness of the risk analysis model and risk control measures can be optimized continuously during construction by analyzing the difference between actual risk status and the forecast one, the difference between actual risk control schemes and the proposal ones, or the effects of the proposed scheme if it is taken.

Table 1. Classification of construction risks.

No.	Risk category	Resulting losses
1	Project quality risk	Project quality reduces.
2	Environmental safety risk	Personnel casualty, equipment destroy and environmental disasters such as destroy of buildings, underground utilities, etc.
3	Economic risks	Construction cost increases.
4	Time risk	Time of project completion delays, duration of the project is prolonged.

3 RISK EVALUATION SYSTEM OF SHIELD TUNNEL CONSTRUCTION

3.1 *Evaluation criteria*

Risk evaluation in shield tunnel construction can follow the criteria in Table 2. Standard get from index function provides a conservative choice for projects with more critical restricts to construction.

3.2 *Risk analysis model*

Through the process of risk identification according to Table 1, we can set up the shield tunnel construction risk factors hierarchical structure based on seven objective risks. These seven risks consist of two risks of Project Quality (Axis Deviation, Liner Deformation), three risks of Environment and Safety (Surrounding Structure Destroy, Personnel Casualty and Equipment Destroy), one economic risk (Cost Overrun) and one Time Risk (Construction Delay). Take the Axis Deviation Risk for example, its influencing factors hierarchical structure is shown in Table 3.

Indicators, which can reflect the status of risk influencing factors, can be divided into qualitative indicators and quantitative ones. The quantitative indicators consist of design parameters and construction variables. Design parameters can be determined before construction, while construction variables should be frequently updated during construction. In the process of risk evaluation, if the current value of some construction variable is unavailable, then a historical value or statistical predictive value will be used to get a predictive result.

4 RISK KNOWLEDGE MANAGEMENT OF SHIELD TUNNEL CONSTRUCTION

4.1 *Methodology*

The process of risk knowledge management in shield tunnel construction enterprises can be described by 3-level circle (see Figure 2).

Table 2. Criteria of shield tunnel construction risk evaluation.

Risk ranking	1st	2nd	3rd	4th	5th
Linear function	0∼0.20	0.20∼0.40	0.40∼0.60	0.60∼0.80	0.80∼1.00
Index function	0.1∼0.13	0.13∼0.29	0.29∼0.48	0.48∼0.71	0.71∼1.00
Risk descriptions	Can be neglected	Give early warning in some key projects	Attention give early warning	Take pre-control measures	Unacceptable take post-control measures

In Figure 2, the outer circle of risk knowledge gained from many separate construction projects shows the diversity and specialty of risk knowledge. After absorbing by technicians, the risk knowledge of shield tunnel construction becomes tacit knowledge in experts' brain (in the middle circle).

The knowledge in the middle circle still needs further regularization and integration to become the core competence of construction enterprises. So a risk knowledge management system with the function of self-improvement is needed to accumulate risk knowledge like human brain during construction processes. The function of self-improvement can be realized by adding new cases to case base, gaining new rules from risk control measures and optimizing the model of risk evaluation, etc.

4.2 *Management platform and system frame*

The risk knowledge management system of shield tunnel construction is developed based on Browser/Server mode and can store the instructional content in databases and release it on the network.

The system includes five domains: Project Data Management, Risk Management, Risk Knowledge Learning, System Management and Case Management.

4.2.1 *Project data management*

The value of key parameters determined in final design and construction scheme can be imported

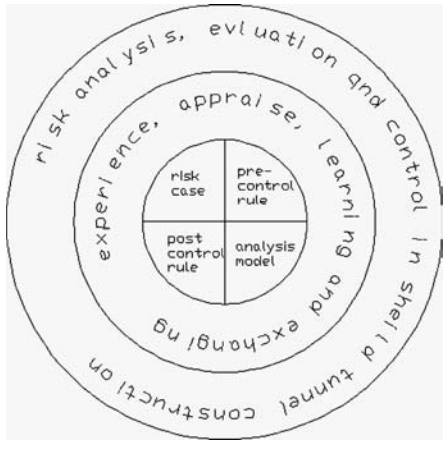


Figure 2. Three-level circle of risk knowledge.

Table 3. Risk influencing factors hierarchical structure (Axis Deviation Risk).

Objectives	Influencing factors I	Influencing factors II	Indicators	Type
Axis Deviation	Starting attitude of the shield	Position-setting of basement	Direction, slope, horizontal and vertical position	Construction variable
		Supporting system	Structure's safety factor ε	Design parameter
			Deformation of rear supporting structure	Construction variable
		Soil strength after foundation stabilization	Strength of sample	Construction variable
	Accuracy and efficiency of surveying	Equipments error	Error of equipments	Design parameter
		Surveyors' ability	Experience, qualification	Design parameter
		Efficiency of control measures	Accuracy of control points	Qualitative indicator
			Accuracy of orientation	Qualitative indicator
			Fitting of the curve	Construction variable
	Shield attitude control	Instability of excavation face	Pressure of cutting face	Construction variable
			Volume of discharged soil	Construction variable
			Driving speed	Construction variable
			Ground Settlement at cutting edge	Construction variable
		Rectification control	Degree of rectification per ring	Construction variable
		Soil condition	Value of Penetration N, water content	Design parameter
	Stress and attitude of lining	Efficiency of synchronous Injection	Injection Volume	Qualitative indicator
			Materials proportion	Construction variable
		Axis of segmental ring during erection	Settlement of segments	Construction variable
			Accuracy of lining axis direction	Construction variable
	fault of equipment	Jacking system	Accuracy of journey position	Qualitative indicator
		Regional pressure Control	Pressure deviation	Qualitative indicator

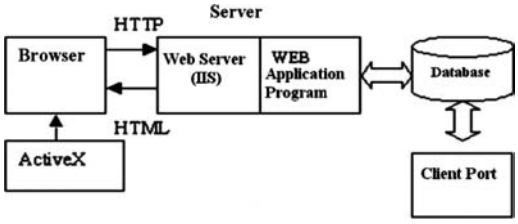


Figure 3. Structure of knowledge management systém.

before constructions, including information of tunnel length, tunnel lining, construction period and cost, geology parameters, embedded depth of tunnel, and surrounding conditions, etc, which are the basis of risk management.

4.2.2 *Risk management*
Main part of shield tunnel construction risk management, including five processes (risk identification, risk quantization, risk evaluation, risk control and evaluation after risk management) as previous discussed.

4.2.3 *Risk knowledge learning*
Provide a platform for learning and exchanging knowledge by forum, experts map and connection to the Case Base.

4.2.4 *System management*
It is the core of whole system, stored with all users and knowledge information including case base, rule base and risk analysis models. The system authorizes different users with different levels of rights to ensure safe operation and no leakage of core information.

4.2.5 *Case management*
History Cases can be accessed by matching algorithm based on risk categories, shield type, environment or geology characteristics and construction process when risk events occur, etc.

4.3 *Application in construction*

The system has applied in a certain shield tunnel project in the process of tunneling beneath a building. Before construction, parameters determined by design proposal and construction scheme should be input into Project Database. During construction, engineers can make risk identification with the help of system. The accuracy of this process is close related to the accuracy of input data or system prediction (if lack of input data). On this basis, the system goes further to evaluate every risks of seven.

If the result of any risk evaluation exceeds the expected line, the precaution warning and pre-control measures or post-control measures according to current risk status will be proposed based on the data base of rules and risk analysis model. But if the value

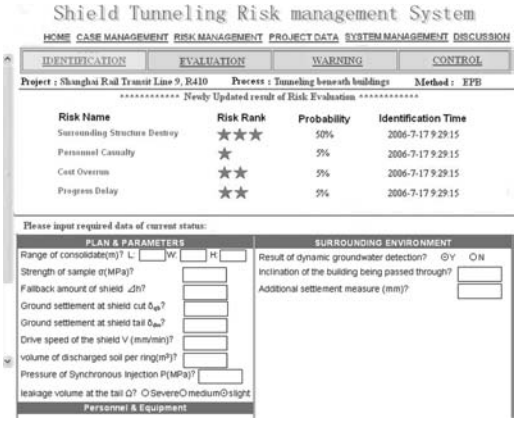


Figure 4. System interface of risk identification process.

is lower than warning line, the system only records current information for future references.

5 CONCLUDING REMARK

The system runs well during trail application in the process of tunneling beneath a building. The function of system evaluation after each cycle of risk management makes the risk knowledge management system an open one to continuously optimize itself in applications. It helps to promote efficiency of risk management. It can be anticipated that with the continuously improvement of the system, it will play an important role in optimizing the allocation of resources within enterprises by comprehensively consider the factors of personnel, materials, equipment and environment.

On the other hand, risk-cases occurred in application will be constantly imported into Case Base for further study. These cherish data is helpful for further understanding of the distribution and induction of construction risk during shield tunneling.

REFERENCES

Storey J. and Barnet E. Knowledge management initiatives learning form failure. *Journal of knowledge management* Vo1. 4 No. 2 145–156

Li Bing, Robert Lee-Kong Tiong, 1999. Risk Management in International Construction Joint Ventures. *Journal of Construction Engineering and Management*, 125 (4) 277–284

Zhang Fengxiang, 2004. *Shield Tunneling Method* [M] China Communications Press

Wu Xianguo, Wang Feng, 2005. Gradation Evaluation of Underwater Shield Tunnel Construction Risks Using $R = P \times C$ Method [J]. *Journal of Huazhong University of Science and Technology Urban Science*, 4. 44–46, 57

Huang Tao, 2006. Analysis on Reasons for Quality Defects of Shield-driven Tunnels and Their Prevention Measures [J] *Tunnel Construction*, 4. 58–60

Underground Space – the 4th Dimension of Metropolises – Barták, Hrdina, Romancov & Zlámal (eds)
© 2007 Taylor & Francis Group, London, ISBN 978-0-415-40807-3

Evaluation of tunnel behavior and decision making of counter measures in weak zones

Hiroshi Yagi & Masaaki Hashimoto
Central Nippon Expressway Co., Ltd., Japan

Yasutoshi Yoshida, Kouji Tamamura & Atsushi Uneda
Kajima Corporation, Japan

ABSTRACT: The Kanaya tunnel on the New Tomei Expressway is a large-section tunnel 4.6 km long with an excavation section of about 190 m^2. This tunnel is constructed by driving a drift 5 m in diameter using TBM, then enlarging the section. For the area in weak geological conditions, suitable support structures for main tunneling were determined by in-depth preliminary investigations to correctly grasp the ground properties, including studies on data obtained during excavation by TBM, various surveys and tests, and numerical analyses. During enlarging the section in the poor ground primarily composed of mudstone that lies near the center of the tunnel sector, convergence reached around 200 mm, rock bolts broke and cracks were induced in the shotcrete. Ultra-strong rock bolting (with prestressing steel bars) was selected to solve these difficulties through analyzing data of various measurements and conducting numerical analyses. This support worked effectively to reduce displacements. In this tunnel, an efficient and economical construction is aimed at by feeding back the construction results to the construction of the following section.

1 INTRODUCTION

Central Nippon Expressway Co., Ltd. is currently constructing the sector in Shizuoka prefecture of the New Tomei Expressway. A mudstone stratum lies in the line of the Kanaya tunnel where the competence factor (ratio of unconfined compressive strength to earth covering) is 2 or less with a large earth covering. In this sector, rock bolts broke and cracks occurred in the shotcrete, inducing excessive convergences and settlements at the tunnel foot. As countermeasures against such difficulties, rock bolts of prestressing steel of 748 kN in tensile strength were driven, aimed at limiting displacements and providing stronger supports. This solution was proved to be effective. Prestressing steel bars have generally been used for prestressed concrete. Table 1 shows the properties of the prestressing steel bar and rock bolts widely used. This paper discusses the results of studies on the deformation behavior of ground in large-section tunnels and applicability of prestressing steel bars to tunneling supports, referring to construction records of the west sector of the Kanaya tunnel in a mudstone stratum.

Table 1. Features of prestressing steel bar and rock bolt.

	Prestressing steel bar	High strength bolt	Normal bolt
Diameter	32 mm	24 mm	24 mm
Strength	748 kN (930 kN/mm^2)	297 kN (685 kN/mm^2)	180 kN (510 kN/mm^2)
Cross section	804.2 mm^2	433.1 mm^2	353 mm^2
Elastic modulus	210 kN/mm^2	210 kN/mm^2	210 kN/mm^2

2 OVERVIEW OF THE TUNNEL

2.1 *Construction summary*

The Kanaya tunnel is the longest tunnel on the New Tomei Expressway. It is located in Kakegawa City of Shizuoka Prefecture, including eastbound lanes spanning 4,527 m and westbound lanes spanning 4,667 m. The tunnel shape is a slightly flattened oval, with excavation sectional area of about 190 m^2 and width

of about 18 m (Figure. 1). The tunneling technique selected is TBM drift accompanied by enlargement, i.e., a drift is cut by a tunnel boring machine, then the tunnel cavity is enlarged by the top heading method for the westbound lanes first.

The main tunnel of the Kanaya tunnel is divided into east and west sectors. The westbound lane length in the west sector are 2,540 m. The top heading of this length took 36 months, comprising weak ground zone about 920 m long. Since measures were provided against various adverse changes in this weak ground zone, top heading took about 16 months. As of July 2006, the construction of the westbound lane tunnel (preceding tunnel) had been completed, and the eastbound lane tunnel (succeeding tunnel) is under construction.

2.2 *Geology*

The geology of the Kanaya tunnel site is composed, as shown in Figure 2, of Kurami group of Miocene Epoch of the Neogene Period and Setogawa group of Oligocene Epoch of the Paleogene Period. The boundary of these groups is located at the tunnel center. The west Kurami group is roughly divided into Matsuba formation, Towata mudstone stratum and Amagata sandstone stratum. Although the Matsuba formation is relatively hard Neogene mudstone, it is composed of significantly cracked sandstone. The Towata mudstone and Amagata sandstone strata are more brittle than Matsuba formation. The Towata mudstone stratum is especially weak, prone to slaking. In the zone from the Towata mudstone to Amakata sandstone strata, there were problems with TBM excavation of the westbound lane tunnel, such as significant convergence and crown settlement of the drift, constraint of the TBM movement and collapse of the crown. The ground in the Towata mudstone zone is liable to deformation after excavation due to their geological properties, with a large earth covering of approximately 250 m.

The east Setogawa group is alternately composed of sandstone and shale that has slickenside due to strong folding, with many cracks exhibiting noticeable spalling.

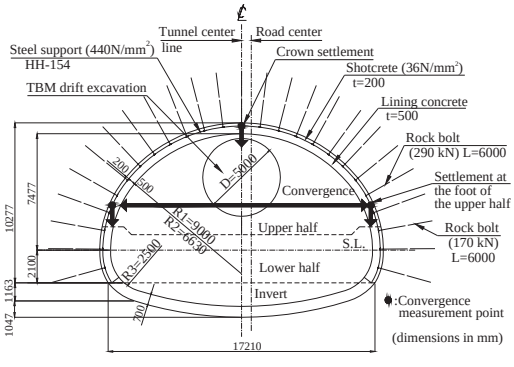


Figure 1. Standard cross section.

3 DEFORMATION CHARACTERISTICS OF THE LARGE-SECTION TUNNEL

On the basis of the measurement data obtained in this tunnel construction, a study was conducted to identify the deformation behavior of the large-section tunnel in mudstone ground, by determining relationships between convergences, crown and foot settlements with different support patterns.

3.1 *Relationship between crown settlement and convergence*

Figure 3 shows the relationship between final crown settlement and final convergence after invert closure. The ratio of convergence to crown settlement is 1 to 0.5 almost regardless of support pattern. As demonstrated by this result, the convergence is large in comparison with crown settlement.

3.2 *Relationship between foot settlement and crown settlement*

Figures 4 depicts the relationship between final foot settlement and final crown settlement. Strong correlation exists between foot settlement and crown settlement independent of the support pattern, the ratio being 1 to 1. As can be seen from this result, the crown subsides with the foot.

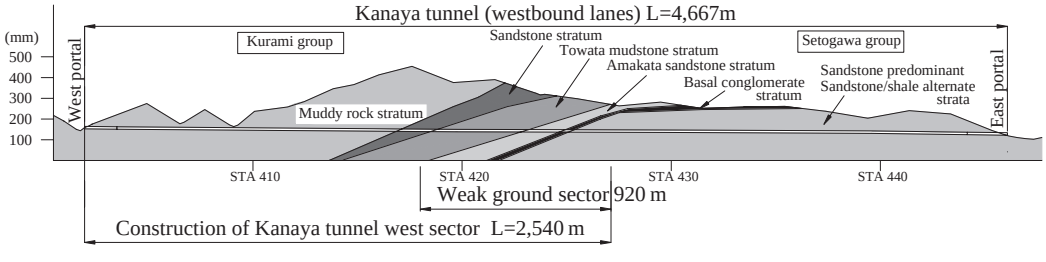


Figure 2. Geological overview of Kanaya tunnel.

3.3 *Relationship between value of crown settlement minus foot settlement and convergence*

Figure 5 illustrates the impact of crown-foot settlement relationship upon convergence after invert closure, by showing the relationship between the value of crown settlement minus foot settlement and convergence. In the region where this value is negative, that is, crown settlement exceeds foot settlement, convergence is not so large, 70 mm or less. In contrast, in the range where the value is positive, that is, the foot settlement is greater than the crown settlement, the convergence is larger as the absolute value of crown settlement minus foot settlement increases. These facts demonstrate that measures against foot settlement are essential to reduce convergence.

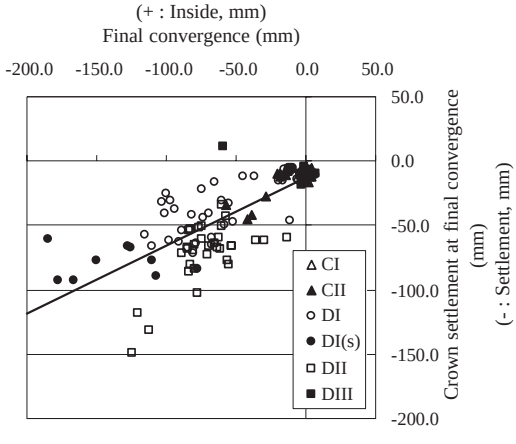


Figure 3. Relationship between crown settlement and final convergence.

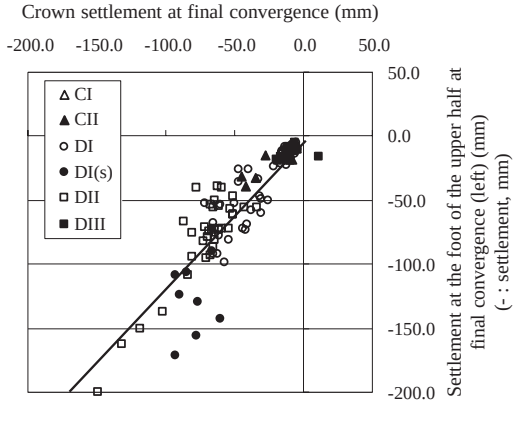


Figure 4. Relationship between foot settlement and final crown settlement.

4 MEASURES IN THE WEAK GROUND ZONE

In the study on the relationship between convergence and measures against foot settlement, focus was placed upon the zone from STA418+50 to 420+58.1 in the Towata mudstone sector greatly affected by ground displacements. For this zone, Figure 6 summarizes the ground data, support states and magnitudes of displacements with different support patterns. TBM excavation had revealed relatively poor geological conditions in this sector.

Therefore, geological surveys and FEM analyses were used to study support structures in advance. However, the geology turned out to be poorer than anticipated, and there were problems with supports along with increased displacement, such as cracks in shotcrete and deformation of rock bolt washers. Consequently, additional measures had to be taken and the support pattern had to be changed. In the following, support structures, measures against troubles and displacements are described for each ground zone.

4.1 *DI zone (STA418+50.5~STA419+32.1)*

Referring to the construction record of the tunneling project in question, the standard support pattern (DI) for road tunnels was adopted. However, the convergence reached around 80 mm at maximum during top heading near STA418+90. Since deformation occurred in plates of rock bolts at the foot and cracks in crown shotcrete, additional high strength bolts (strength: 297 kN) were driven to reinforce the rock bolts at the foot. When excavating the lower half section, a support pattern was used, with 6 m long prestressing steel bars (strength: 748 kN) placed into the lower half section. Consequently, the crown settlement increased very little during excavation of the lower half

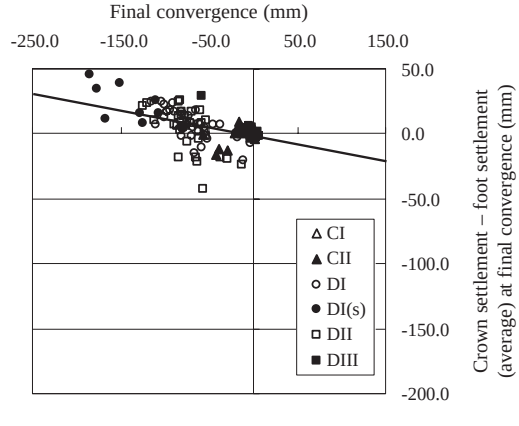
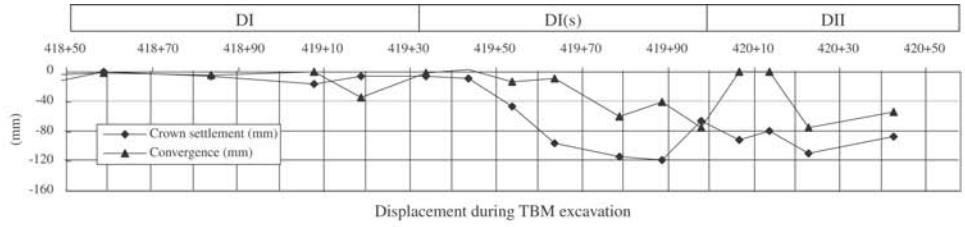


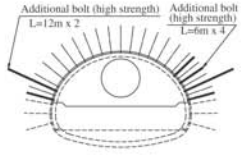
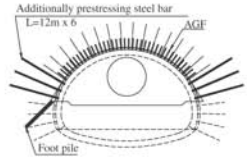
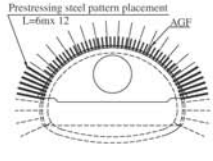
Figure 5. Relationship between value of crown settlement minus foot settlement at final convergence.

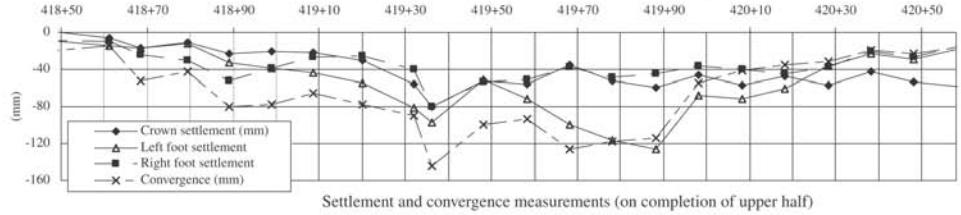


Displacement during TBM excavation

<Construction records of upper half >

Steel support (440N/mm^2), Shotcrete (36N/mm^2)

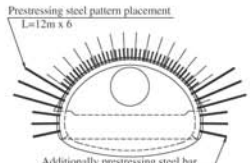
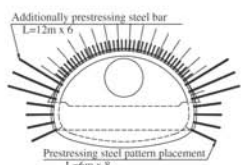
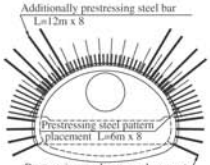
Steel support	HH-154		HH-200	HH-200 (Wing rib)		HH-200 (Wing rib)
Shotcrete	t=200		t=250		t=300	
Rock bolt	19 (High strength, 290kN)		6 (170kN)	6 (290kN)	20 (290kN) 26 (290kN)	14 (290 kN) 12 (Prestressing steel bars, 748kN)
Others	ñ		Foot protection concrete (Both sides)	ñ		
	ñ		AGF D=114.3, L=12.5m@500			
Additional counter measure construction	Additional bolt (High strength), 1 ~7 (L=6m, 9m or 12m)		20 (L=6m)	6 (L=6m)	ñ	ñ
	ñ	Reinforcement concrete of supports legs	ñ			ñ
	ñ		Foot pile (D=114.3mm, L=3.77m)			ñ
	ñ		Prestressing steel bar (L= 12m x 6)			ñ
Diagram of main pattern (during excavation of upper half)						

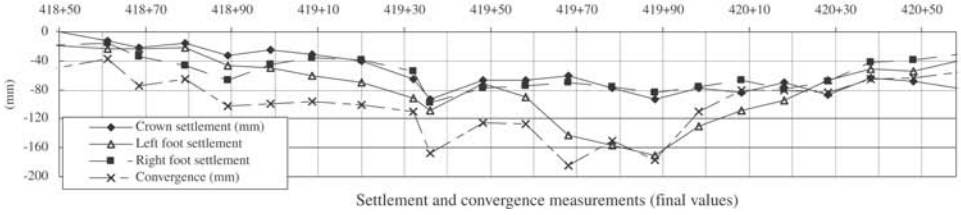


Settlement and convergence measurements (on completion of upper half)

<Construction records of lower half >

Steel support (440N/mm^2), Shotcrete (36N/mm^2)

Preliminary stabilizing measures before excavation on lower half	Additional prestressing steel bars (Side) L=12m x 6		ñ	Additional prestressing steel bars (at shoulder) L=12m x 8
Steel support	HH-154	HH-200		
Shotcrete	t=200	t=250	t=300	
Rock bolt	6 (Prestressing steel bars 6 ~ 12m long)	8 (Prestressing steel bars 6m long)		
Diagram of main pattern (during excavation of lower half)				



Settlement and convergence measurements (final values)

Figure 6. Construction data of Towata mudstone section (STA 418+50.5 – 420+58.1).

and invert, and increase in convergence was limited to about 20 mm.

4.2 *DI (s) zone (STA419+32.1∼STA420+01.1)*

From the result of the preliminary investigation from the TBM drift, the ground in the DI(s) zone was predicted to be poorer than the DI zone. The supports selected for upper half excavation in the DI(s) zone were steel arch supports with wing ribs and 25 cm thick shotcrete. However, near STA419+30 as shown in Figure 6, settlement at the left foot increased and the induced force exceeded the strength of the rock bolts at the foot. At first, additional high strength bolts were placed, but they did not exhibit a satisfactory effect.

Then, since measurements with extensometers at STA419+71 revealed displacements up to about 9 m from the tunnel wall, measures were taken, including reinforcement of the foot portion with 12 m long prestressing steel bars and piling at the left foot.

As a result, displacements were confined, but the convergence reached approximately 120 mm at maximum in the upper half excavation. During the lower half excavation, a support pattern was used with 6 m long prestressing steel bars driven into the lower half section. This pattern enabled increase of convergence due to lower half and invert excavation to be limited to around 60 mm. However, in this DI(s) zone, the final convergence was 180 mm at maximum since the convergence had already exceeded 100 mm in upper half excavation. These results prove how it is important to provide an appropriate amount of supports during upper half excavation to confine final displacements.

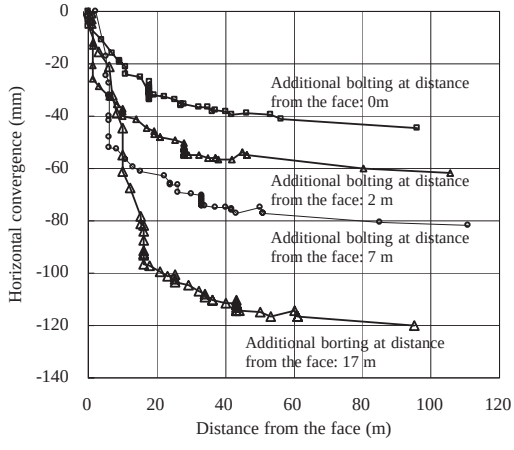
4.3 *DII zone (STA420+01.1∼STA420+58.1)*

Since ground in the DII zone was weaker than the preceding zones and satisfactory reinforcing effect of prestressing steel bars at the tunnel foot had been confirmed in the preceding zones, the support pattern in this zone used 6 m long prestressing steel bars at the foot of the upper half during upper half excavation. Consequently, the convergence was not more than 40 mm and the settlement at the foot was 60 mm or less. Measures against foot settlement such as foot piling were therefore unnecessary. However, because the upper half foot was constrained by prestressing steel bars in the area beyond STA420+02, ground extrusion concentrated at the shoulder of the tunnel, which induced cracks in the shoulder shotcrete. To accommodate further stress increase due to lower half excavation, 12 m long prestressing bars were driven into the shoulder as preliminary reinforcement, then 6 m long prestressing steel bars were placed as pattern bolts into the lower half section. As a result, beyond STA420+00, convergence increase was limited to about 20 mm in the lower half and invert excavation, and the final convergence was within about 100 mm.

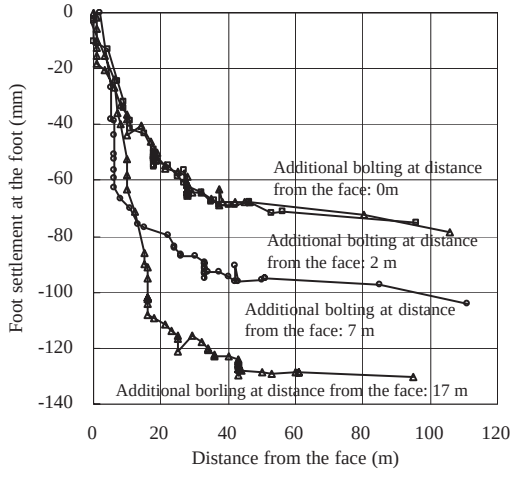
5 VERIFICATION OF ROCK BOLT EFFECT USING PRESTRESSING STEEL BARS

5.1 *Displacement confining effect of prestressing steel bars*

Figure 7 illustrates the relationship between placement timing of prestressing steel bars and convergence/foot settlement of this tunnel. The graphs in this figure reveal the fact that the smaller the distance between the face and the rock bolting position, the higher the convergence confining effect. Judging from the change in gradient of displacement graph before and after rock bolting, restriction of ground with prestressing steel bars contributed to prevention of settlement at the foot.



(a) Horizontal convergence



(b) Settlement at the foot

Figure 7. Position of prestressing steel bolting and convergence (during excavation on upper half).

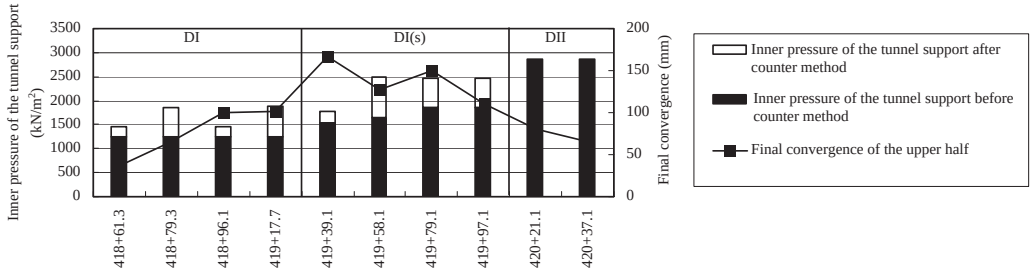


Figure 8. Inner pressure of the tunnel support vs. final covergence.

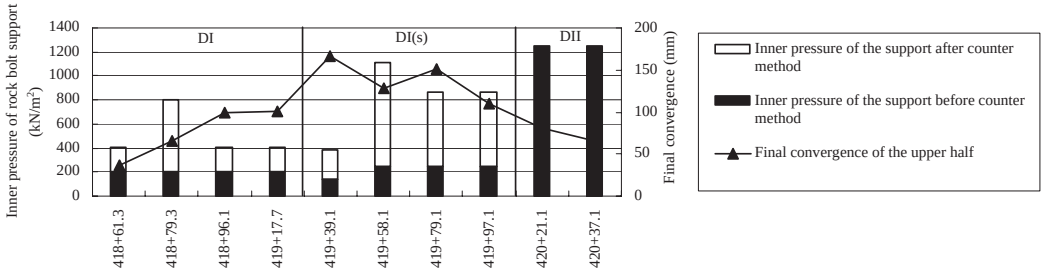
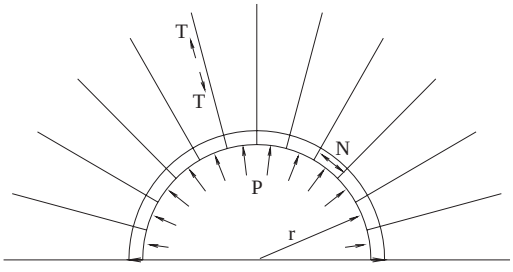


Figure 9. Inner pressure of the support (rock bold only) vs. final convergence.



$P=P_1 + P_2 + P_3$ (kN/m^2)
P=Total inertial pressure of tunnel
P_1: Inertial pressure of shotcrete
P_1=Axial force in shotcrete/ radius
P_2: Inertial pressure of steal support
P_2=Axial force in steel support/ radius
P_3: Inertial pressure of rock bolts
P_3=Tensile force in rock bolt/ shear area

Figure 10. Relationship of the acting force to the tunnel support and inner pressure.

5.2 *Relationship between tunnel deformation and supports*

The relationship between convergence and support inner pressures (Figure 10) is graphed in Figures 8 and 9, which will help investigate relationships between tunnel deformation behavior and support



Photo 1. Rock bolts with prestressing steel bars.

structure. These graphs demonstrate that the support pattern provided in the very vicinity of the face exhibits higher convergence confinement effect, and that pressures in the rock bolts effectively work to confine convergence.

The record of the Kanaya tunneling, in the sector with larger earth covering and lower ground strength, confirmed that rock bolts of prestressing steel bars were very effective to confine settlement at the foot and convergence. With this type of rock bolt pattern driven immediately near the face (shorter bolts were satisfactory in this case), tunneling could be performed highly efficiently and less costly compared

with the case where additional measures were taken from time to time referring to the measured data of displacement.

6 CONCLUSIONS

In large-section tunneling projects such as the tunnel discussed in this paper, the displacement speed is high in the initial stage of excavation, with plastic regions expanding rapidly. It is therefore essential to rapidly compile and evaluate the results of observation of the face and measurements, in order to select the best solutions suited to the ground mechanical properties. The experience of the Kanaya tunnel project proved that it is important to place a suitable support structure at an early stage after excavation, for fully utilizing the sustaining capability of the ground. Especially in large-section tunneling projects, ground reinforcement at the foot of the upper half section is vital to stabilize the whole of the tunnel. It can be concluded that prestressing steel bars are very effective supports that effectively confine ground maintaining triaxial compressive state.

This page intentionally left blank

Underground Space – the 4th Dimension of Metropolises – Barták, Hrdina, Romancov & Zlámal (eds)
© 2007 Taylor & Francis Group, London, ISBN 978-0-415-40807-3

The measures for preventing acid rock drainage through the results of acid rock drainage assessment and contamination transport numerical analysis

Yeong-Il Yoo, Jeong-Bae Oh & Du-Hwa Lee
Dept. of Geotechnical Eng., SAMBO Engineering Co. Ltd., Seoul, Korea

Jae-Gon Kim
Geotechnical & Environmental Hazards Division, Korea Institute of Geoscience & Mineral Resources, Daejeon, Korea

Hae-Pyo Chun
SAMDOO Co., Ltd., Seongnam, Korea

ABSTRACT: The exposed sulfide minerals contained in rocks are easily oxidized, when they contact with oxygen in air and water during tunnel excavation. The oxidation generates acid rock drainage (ARD) contaminating soil and water and corrodes tunnel lining and support such as rockbolt and shotcrete. This phenomenon has a bad influence on environment and tunnel. When a construction work plans in the area with high ARD potential, a proper evaluation for ARD should be conducted in advance. The potential of acid rock drainage could be judged from rock crop survey and geological maps and guideline for the estimation of acid rock drainage risk was presented through the results of acid rock drainage assessment and numerical analysis of contaminant transport modeling.

1 INTRODUCTION

There were a lot of cases that surface and ground water were contaminated during constructing tunnel. Three tunnels (Tunnel A, Tunnel B1and Tunnel B2) were designed at Kim-Hae City, Kyeung-Nam province, Korea in 2005. The key issue was that Hwa-Po wetland located within 250 m near tunnel portal should be preserved during tunnel excavation. We found that rocks containing sulfide minerals were scattered in the site and might cause severe environment contamination on Hwa-Po wetland.

We accomplished the site investigations, the Acid-Base Account (ABA) test, the Net Acid Generation (NAG) test and numerical analysis of contaminant transport modeling to analyze the environmental impact on Hwa-Po wetland and to set up long-term management strategies. We reports novel strategy for the protection of environment, tunnel support and portal slope from ARD.

2 SULFIDE MINERALS AND MECHANISM OF ARD GENERATION

2.1 *The minerals which can generate ARD and reaction process*

There are thousands of known minerals. But the most common minerals to generate ARD are pyrite (FeS_2), marcasite (FeS_2), and pyrrhotite ($Fe_{1-X}S$, where $x = 0$ to 0.17). Among those minerals, Pyrite is present around Kim-Hae City, Korea. The oxidation of pyrite starts with exposure of pyrite to oxygen (in air) and water (rain, snow, humid air). Pyrite is less reactive if submerged in water. It is reactive because of repeated wet/dry cycles and the action of bacteria present at the earth surface that generates acid drainage. Some of the generalized chemical reactions used to describe the cycle of pyrite oxidation are described below.

$$FeS_2 + 3.5\ O_2 + H_2O \rightarrow Fe^{2+} + 2\ SO_4^{2-} + 2H^+ \quad (1)$$

Ferrous iron released from initial pyrite oxidation is oxidized to ferric iron by bacteria that are ubiquitous in the environment. There are several aerobic autotrophic bacteria that can obtain energy from oxidation of sulfide minerals, such as *Acidithiobacillus ferroxidans*. The oxidation of ferrous iron by bacteria is much faster than abiotic oxidation. The oxidation of ferrous iron is described by the reaction:

$$Fe^{2+} + 0.25\,O_2 + H^+ \rightarrow 0.5\,H_2O + Fe^{3+} \quad (2)$$

Once formed, ferric iron is a powerful oxidant that can attack pyrite and release significant amounts of ferrous iron and acidity that can further propagate the cycle of pyrite oxidation:

$$14\,Fe^{3+} + FeS_2 + 8\,H_2O \rightarrow 15\,Fe^{2+} + 2\,SO_4^{2-} + 16H^+ \quad (3)$$

Note that the initial reaction (1) produced 2 moles of H^+, but the propagation reaction with ferric iron as the oxidizing agent produces 16 moles of H^+. Sulfide minerals that have metal/sulfur ratios = 1 such as sphalerite (ZnS) and galena (PbS) are not strongly oxidized by oxygen, but are affected when ferric iron presents as the oxidant:

$$ZnS + 8\,Fe^{3+} + 4\,H_2O \rightarrow Zn^{2+} + 8Fe^{2+} + SO_4^{2-} + 8H^+ \quad (4)$$

Unless the acid (H^+) generated by these reactions is counteracted by a neutralizing agent, a serious acid-drainage problem can develop. Most metal ions that behave as cations are more mobile at low pH.

2.2 *Sulfide mineral distribution*

In Korea, There are lots of sulfide minerals that might cause acid rock drainage as shown fig 2. Generally, they are rich in the Mesozoic volcanic rocks and the tertiary volcanic rocks. They are rich around Kim-Hae city.

The area for tunnel A mainly consists of tuff with quartz porphyry dyke at entrance. Sulfide minerals are not found in tuff. But they are found only in quartz porphyry.

The bedrock of tunnel B1 consists of sandstone. Several dykes with high content of sulfide minerals such as pyrite and sphalerite also occur at the entrance of tunnel B1 and between tunnel B1 and tunnel 2. The bedrock of tunnel B2 mainly consists of sandstone and granite. The granite contains a significant amount of pyrite.

2.3 *The mechanism of ARD in Tunnel Portal*

Sulfide minerals which exist in subsurface can hardly react oxygen in atmosphere and water. But, in excavating tunnel portal, exposed sulfide minerals can easily react with oxygen and generate sulfuric acid. The

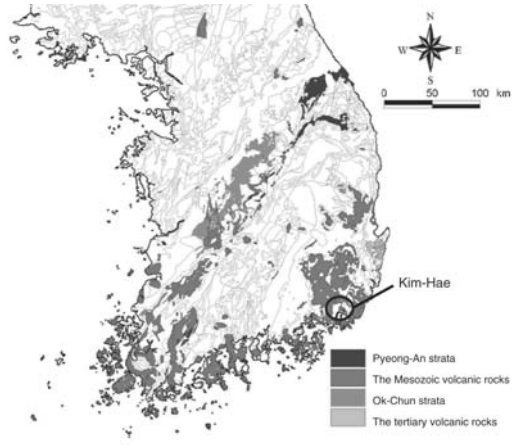


Figure 1. The sulfide mineral distribution map in Korea.

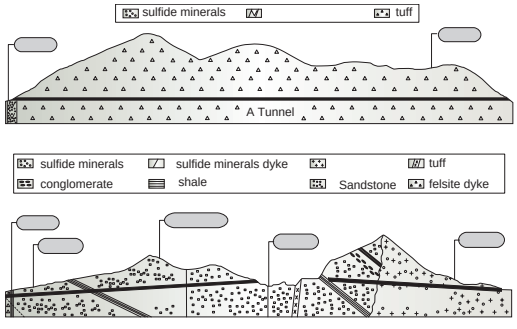


Figure 2. Sulfide mineral distribution in tunnel.

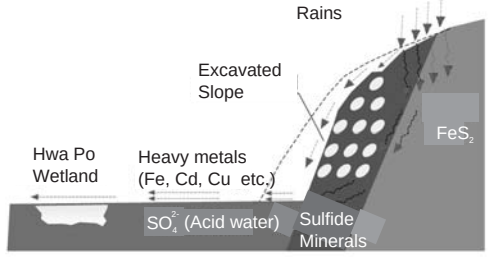


Figure 3. The mechanism of acid rock drainage.

oxidation of sulfides loads heavy metals contained in them.

3 ACID ROCK DRAINAGE ASSESSMENT

3.1 *The acid base account test*

The Acid-Base Account test (ABA test) is the most commonly applied method to acid rock drainage assessment. The results of ABA test in this site were

Table 1. The results of ABA (acid base account) test.

Sample no.	Sample location	Total S (%)	MPA ($KgCaCO_3/t$)	NP ($KgCaCO_3/t$)	NAPP ($KgCaCO_3/t$)	NAG (KgH_2SO_4/t)	(NP/MPA)	NAG* (pH)
TB-1*	A tunnel entrance	0.023	0.712	−0.037	0.749	0.521	−0.053	3.56
TB-1**		0.079	2.477	−0.200	2.677	3.060	−0.081	2.77
TB-1***		0.173	5.400	−0.162	5.562	2.450	−0.030	2.56
TB-6	A tunnel center	0.001	0.027	19.338	−19.311	0.000	728.863	6.78
TB-9	B1 tunnel entrance	3.710	115.800	1.988	113.813	46.062	0.017	1.97
TB-12		0.013	0.406	36.725	−36.319	0.000	90.542	6.91
TB-13-2	B1 tunnel center	0.208	6.492	18.225	−11.733	0.000	2.807	7.24
TB-15	B1 tunnel exit	0.001	0.025	1.975	−1.950	0.000	79.591	5.02
TB-20*	Between B1 & B2 tunnel	6.630	206.942	33.400	173.542	98.147	0.161	1.65
TB-20**		0.000	0.052	2.338	−2.338	0.000	45.387	5.22
TB-22	B2 tunnel exit	0.027	0.844	14.850	4.006	0.000	17.598	6.49

shown as table 1. The Maximum Potential Acidity (MPA) may be indirectly estimated by determining content of Sulfur (S) in a sample, assuming the S occurs as pyrite form

$$\text{MPA} = \text{total Sulfur (\%)} \times 31.213 \quad (5)$$

The MPA that can be generated by a material is expressed as a positive value. This value is usually expressed in Mg of lime equivalence per 1000 Mg of material tested. The convention of using Mg/1000 Mg is equivalent to kg/ton.

The Neutralization Potential (NP) of a sample represents as carbonates or other acid neutralizers in a sample. Negative NP values may occur when a sample contains weathering products, such as certain sulfate minerals, that produce acidity upon dissolution. If the resulting value is negative the material should produce acidic water upon complete and kinetically balanced reaction. Positive results indicate water drainage will be alkaline.

The Net Acid Producing Potential (NAPP) is calculated with following equation

$$\text{NAPP} = \text{MPA} - \text{NP} \quad (6)$$

3.2 *The net acid generation test*

This approach to determining acid potential is used in hydrogen peroxide (H_2O_2) method. The basis of the method is that H_2O_2 oxidizes sulfides and generates sulfuric acid, which presumably will react with alkaline components if present. The net acid generation (NAG) is determined by final titration with NaOH.

3.3 *The acid rock drainage assessment*

The possibility of acid rock drainage according to NAPP-NAG Chart was shown as fig 4.

The samples of TB-1, TB-9, TB-20 were classified as potential acid forming (PAF) It highlights one possibility that excavated slope surfaces are likely to react with water and generate ARD.

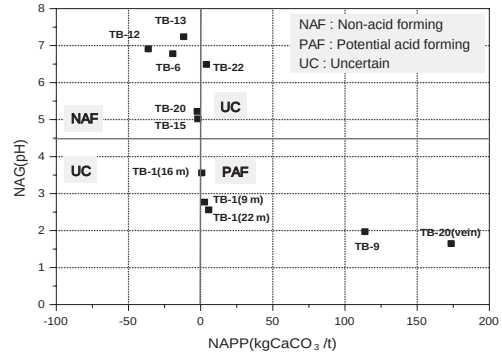


Figure 4. Acid base account assessment according to NAG and NAPP.

Table 2. Risk grade of acid rock drainage according to NP/MPA.

Risk grade	NP/ MPA	Sample no.	Remedy on acid rock drainage
dangerous	<1	TB-1, TB-9, TB-20(vein)	needed
warning	1-2 or 3	TB-13-2	needed if necessary
safe	>2	TB-6, TB-12, TB-20, TB-22	Not needed

The risk grade of acid rock drainage according to NP/MPA was shown as table 2. The possibility of ARD was very high in TB-1, TB-9 and TB-20 (vein) like the results of NAPP-NAG chart.

3.4 *The heavy metals leached by ARD*

The concentration of major cations and heavy metals was shown as table 3, after rock powder sample

Table 3. The concentrations of major cations and heavy metals after the reaction of sample and 15% H_2O_2 solution.

sample no	Mg	Ca	Na	K	Al	Mn	Fe	As	Cd	Ni	Zn	Pb	Cr	Co	Cu
	----mg/L(ppm)----							----------μg/L(ppb)----------							
TB-1*	0.17	2.24	0.96	2.84	568	1230	190	8	25	12	3070	1250	5	7	218
TB-1**	0.15	1.11	1.21	2.49	1520	40	492	1	65	11	1490	208	6	8	42
TB-1***	0.21	1.93	1.23	2.58	1700	38	477	1	6	12	56	56	7	7	15
TB-6	0.64	54.5	0.96	1.93	83	128	6	7	5	11	4	2	7	6	10
TB-9	6.16	10.1	2.35	4.01	9190	1220	33000	92	14	38	14	114	11	212	84
TB-12	0.84	52	1.13	0.21	102	129	8	7	5	11	5	4	5	11	13
TB-13-2	0.59	39	1.06	0.2	101	86	6	6	5	10	5	4	5	5	17
TB-15	1.11	2.64	1.13	0.17	73	88	67	28	2	5	2	2	10	6	6
TB-20	1.2	5.06	1.3	0.21	58	248	47	7	5	12	5	5	7	6	8
TB-20V	27.4	135.8	1.5	0.61	24304	3640	136350	256	43	173	43	43	10	429	83
TB-22	0.41	52.8	0.9	0.63	44	34	35	51	2	5	2	2	8	5	4
Environmental standard					300	2000	200	100	20		1000	200	500		500

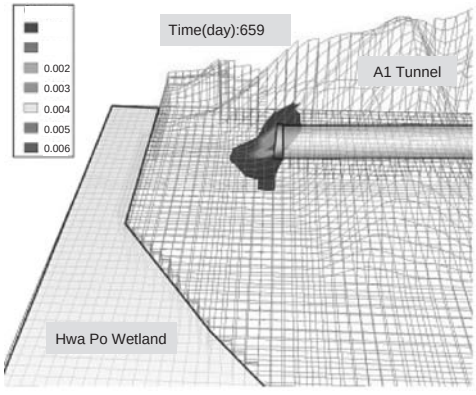


Figure 5. The Cd concentration of A Tunnel at the end of excavation.

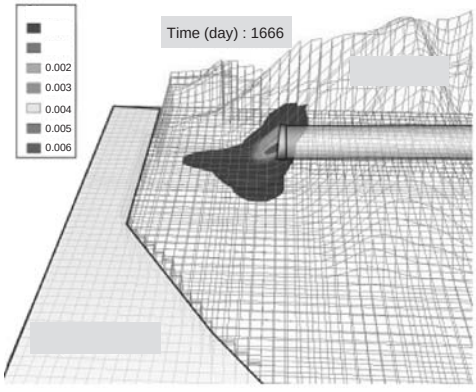


Figure 6. The Cd concentration of Tunnel A after 3 years of excavation.

reaction to 15% H_2O_2 solution (1 solid : 100 solution). Heavy metals (Cd, Fe, Mn, Al) concentrations of TB-1, TB-9 and TB-20 (vein) samples were high. So, remediation on not only neutralization of acid rock drainage but also removal of heavy metals should be made.

4 THE CONTAMINANT TRANSPORT MODELING

4.1 *The tracer of pollutants*

Considering heavy metal concentrations in the study area and ecological impact of heavy, cadmium (Cd) was selected as tracer of pollutant because the rock samples contains high concentration of Cd and Cd could cause very significant harm on men and ecological environments. We predicted Cd transportation behavior through groundwater flow induced by tunnel excavation.

4.2 *The contaminant transport analysis*

In analyzing Cadmium (Cd) transportation through groundwater flow induced by tunnel excavation, the regional groundwater flow was calculated as non-steady state flow using MODFLOW. The results of MODFLOW analysis showed that the groundwater head went down because of tunnel excavation and went up after installing tunnel lining.

In case of A Tunnel, excavation was planed to start from tunnel portal near Hwa-Po wetland and acid rock drainage would be caused and heavy metals could be transported into wetland.

In case of B1 Tunnel and B2 Tunnel, excavation was planed to start between B1 and B2 tunnel, could be transported into the valley between B1 and B2 tunnel.

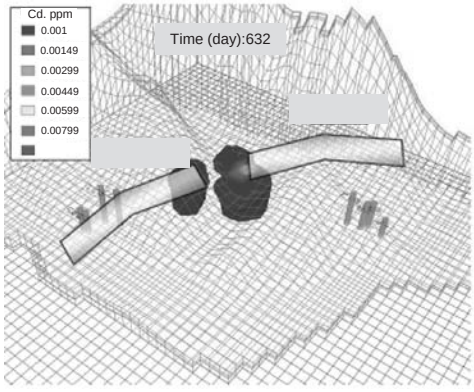


Figure 7. The Cd concentration of B1 & B2 Tunnel at the end of excavation.

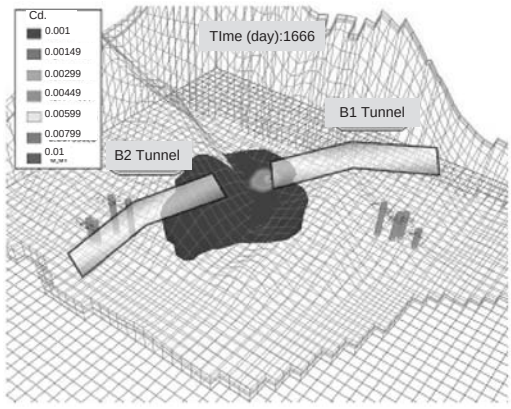


Figure 8. The Cd concentration of Tunnel B1 and Tunnel B2 at 3 years of excavation.

In the end of excavating A Tunnel, contamination area of Cd which excess 1.0 ppb spreads from tunnel portal to 10 m. After 1000 days, the area of Cd concentration below 0.1 ppb spreads to Haw-Po wetland. Vertical spreading of Cd reaches to depth 6 m. According to the standard Cd concentration of water which can be used in life and agriculture, 10 ppb, the Cd concentration which occurs in A Tunnel have no harmful effect on environment.

In the end of excavating B1 Tunnel and B2 Tunnel, contamination area of Cd which excess 1.0 ppb spreads from tunnel portal to 1000 m. The characteristics of Cd concentration in B1 Tunnel and B2 Tunnel are that Cd spreads far through valley. Vertical spreading of Cd reaches to depth 1.5 m.

5 THE TREATMENT ON ACID ROCK DRAINAGE

5.1 *The environmental protection strategies for Hwa-Po wetland*

The results of contamination transportation analysis show that there is low potential of heavy metal inflow into Hwa-Po wetland from the proposed site except the entrance portal of tunnel A.

The counter-measurement of acid rock drainage are chemical treatment, artificial wetland, and limestone channel. The artificial wetland is applied for acid rock drainage with high concentration of and strong acidity. This is relatively expensive and needs large space.

The limestone channel neutralizes acid rock drainage and removes heavy metals by passing through. However, it is effective for a short period and should be replaced worn limestone by new limestone.

The chemical treatment using NaOH is adopted because it has low maintenance cost and small site. This treatment is that NaOH is added to polluted water treatment settling tank and it neutralize acid rock drainage and precipitate heavy metals.

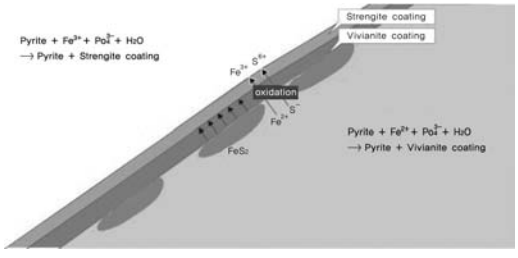


Figure 9. The surface coating that block acid rock drainage.

5.2 *The preventing strategy for tunnel lining and support deterioration*

Acid rock drainage that flows into tunnel portal even accelerates deterioration of constructed tunnel. It is important that acid rock drainage be interrupted before sulfide minerals of tunnel portal slope that are exposed to air and water are oxidized. The strategy is that excavated slope is covered by surface coating and anti-acid cement mortar (Fig. 9) and is installed by the double-casing rockbolt for long-term safety.

Tunnel portal structure is made of anti-acid cement to prevent lining from being impaired.

5.3 *The treatment of excavated rock fragment*

Generally, excavated rock was crushed and used as road base and fill. If rock fragments include sulfide minerals, metal-laden acidic (pH < 3) drainage cause surface water and ground water contamination.

The quartz-porphyry that exists in entrance portal of tunnel A include lots of sulfide minerals. So, It

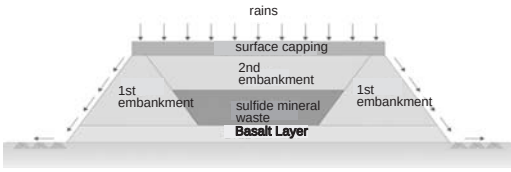


Figure 10. The proposed embankment slope encapsulation for preventing ARD.

is not good to use excavated rock fragments into roadbed-filling and aggregates. Though they are used into roadbed-filling, they should be encapsulated for preventing ARD.

6 CONCLUSION

During tunnel excavation, the exposed rocks containing sulfide minerals are easily oxidated, when they contact with oxygen in air and water. They generate ARD to contaminate ground and water environment and to corrode tunnel lining and support such as rockbolt and shotcrete, sometimes.

But, this phenomenon has a bad influence on environment and tunnel itself. As the chances of acid rock drainage through acid base account test(ABA test) is high, the measures are prepared in advance.
The results of ABA test shows that acid rock drainage contains lots of heavy minerals (Cd, Fe, Mn, Al etc.).

The results of contamination transport numerical analysis shows that cadmium (Cd) is not distributed into the ecosystem of Hwa-Po wetland. But, NaOH that can neutralize ARD was added to settling tank.

Anti-acid shotcrete, double casing rockbolt and surface coating were applied to portal slope to prevent sulfide mineral from contacting oxygen in air and water. Anti-acid cement is applied to portal structure of tunnel not to prevent deterioration of tunnel.

REFERENCES

Jeong,Yeong-Uk, 2005.5, The counter-measurement on the water drainage of Hoi-Buk I/C.

J.W. Molson, O. Fala, M. Aubertin and B. Bussière, 2005, Numerical simulations of pyrite oxidation and acid mine drainage in unsaturated waste rock piles, Journal of Contaminant Hydrology, Volume 78, Issue 4, Pages 343–371.

Lee,Kyu-Ho & Kim, Jae-Gon, 2005.7, The damage and assessment of excavated slope by acid rock drainage, Korean Geotechnical Society.

U.S. Department of the Interior U.S. Geological Survey, 2004. Acid Rock Drainage at Skytop, Centre County, Pennsylvania, USGS.

U.S. Environmental Protection Agency, 1994, Acid Mine Drainage Prediction.

Wolfgang Sand, Peter-Georg Jozsa, Zsuzsanna-Maria Kovacs, Nicolae Săsăran and Axel Schippers, 2006, Long-term evaluation of acid rock drainage mitigation measures in large lysimeters Journal of Geochemical Exploration.

Zenah Wilson Orndorff, 2001, Evaluation of Sulfidic Materials in Virginia Highway Corridors, Virginia Polytechnic Institute and State University Doctor of Philosophy in Crop and Soil Environmental Sciences.

Underground Space – the 4th Dimension of Metropolises – Barták, Hrdina, Romancov & Zlámal (eds)
© 2007 Taylor & Francis Group, London, ISBN 978-0-415-40807-3

State of the art tunnelling technologies

Ž. Žderić, G. Pervan & Đ. Radić, CE
Konstruktor inženjering, Split, Croatia

ABSTRACT: Intensive motorway construction, as a crucial infrastructure project, has inevitably led to intensive road tunnel construction as well. Various organizational and technical specific details that had to be dealt with in an extraordinarily short time have given rise to a specific tunnel construction method that was used in Croatia. The paper discusses construction methods and construction problems caused by greatly varying ground properties along the excavation path, as well as applicability and effects of new technologies and application of new materials in tunnel construction. The demand for speedy construction called for most efficient adjustment of existing and construction of new facilities and equipment needed for construction. Co-ordinating project planning and actual excavation and construction has proven to be an extremely important pre-requisite for achieving the best possible result. Only the most competent construction companies have been able to fully address the demands set forth regarding organization and quality of work carried out.

1 INTRODUCTION

Fast paced construction of motorway network connecting northern and southern parts of Croatia has been set as one of the priorities for the 1995–2007 development of the Republic of Croatia.

Such investments have led to development of modern construction facilities and equipment that is capable of executing highly demanding construction.

It is also important to note that it was the introduction of new construction methods and modern equipment that made possible construction of all required tunnels in extremely short time. This is greater achievement still considering that each of those tunnels had different and very specific plan as well as different geological properties of various excavation sites.

This paper provides an overview of the specific details of various tunnels along with an emphasis on the importance of simultaneous investment in equipment and human resources development.

2 WORK METHODS AND TECHNICAL SOLUTIONS

Construction of the tunnels has been carried out using the most recent equipment with optimum work effect, depending on the type of tunnel and the type of rock. Some of the solutions regarding excavation, support in freshly excavated areas and lining of the tunnels built so far are as follows:

1. Excavating the tunnels with common methods (boring and mining) in its full cross-section where rock properties permit that, resulting in faster progress of tunnel excavation.
2. Using smooth blasting with non-electric charge detonation system.
3. Applying rock improvement system, using anchors, shotcrete, steel mesh and arches (NATM), allowing greater efficiency of modern equipment, faster and safer work progress.
4. Using rotary equipment, i.e. milling excavation in softer types of ground being excavated.
5. Applying complete waterproofing of rock and primary substructure using two-millimetre thick PVC foil lined with geotextile.
6. Using dumpers in either full or half of cross-section of the excavation in order to facilitate faster removal



Figure 1. Computer guided rock boring.

of excavated material from the working face of the tunnel.
7. Protecting the primary substructure excavation using steel fibre micro-reinforced shotcrete and execution of non-reinforced secondary concrete lining using polypropylene fibres.
8. Using design solutions such as wheeled and telescopic hydraulically adjustable formwork that has been used for concreting more complex portions of tunnels (turnarounds, transformer stations, power niches).
9. Construction of vibration platforms used for continuous vault concreting.

3 A REVIEW OF EXCAVATION PROTECTION REGARDING CAVERNS

In motorway tunnel construction, various in situ plans and solutions have significant role where the excavation is carried out in rock that has limited load-bearing capacity and in rock containing cavern systems. Although these zones present a danger for workforce and equipment used in tunnel construction, using proper equipment and built-in support systems can help avoid serious problems.

In excavations carried out so far, one can distinguish several basic methods of excavation protection in zones containing cracks and caverns, depending on the way a cavern intersects excavation path:

1. excavation protection in crack systems through enlarged crack opening
2. excavation protection using substructure through filled caverns
3. excavation protection using substructure through unfilled caverns
4. excavation protection using substructure through caverns intersecting lateral portion of the excavation path
5. excavation protection using substructure in places where excavation path enters top of a cavern
6. excavation protection using substructure in places where excavation path passes through a cavern or on the bottom of a cavern

Technical solutions and experience used for safely excavating through faults and caverns have a very important role in tunnel construction and require expert knowledge and responsibility of technical staff. Because of those reasons, quick and quality solutions bring about cost cuts and safer working conditions.

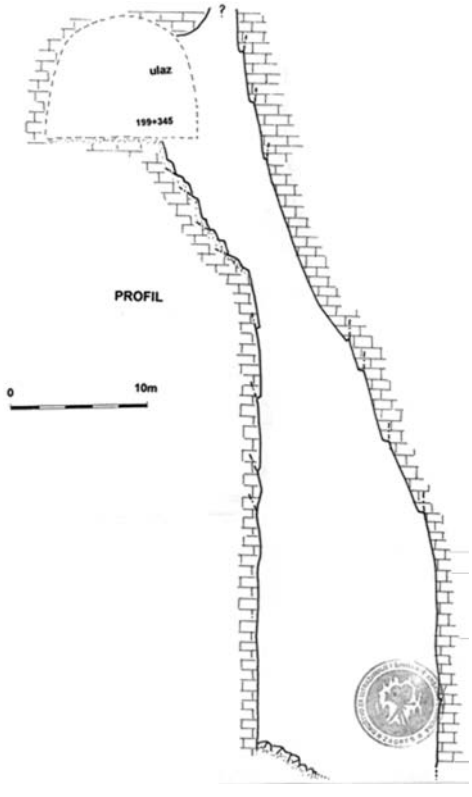


Figure 2. Cross-section of cavern system intersecting lateral portion of the excavation path.

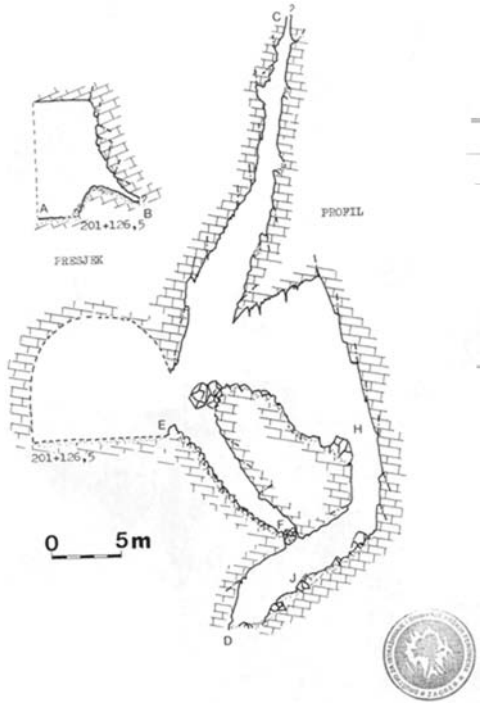


Figure 3. Cross-section of cavern system that is tangential to the excavation path.

4 TYPES AND A BRIEF DESCRIPTION OF EXECUTED TUNNELS

During the period between 1991 and 2007, "Konstruktor-Inženjering" d.d. alone has executed 24 tunnels. Three of those are hydro-technical tunnels, while the rest are road tunnels. As the most of the tunnels are a part of motorway network, they have been built as dual carriageway tunnels. Apart from the distinction by type, here is the breakup of the tunnels by various other criteria:

1. By length:
   a) medium length tunnels between 500 and 2000 metres long.
   b) very long tunnels with length exceeding 4000 metres.
2. By type:
   a) road tunnels.
   b) hydro-technical tunnels.
3. By cross-section size:
   a) small cross-section size, up to 20 m^2.
   b) medium cross-section size, up to 60 m^2.
   c) large cross-section size, up to 120 m^2.
   d) sections of "Sv. Rok" tunnel – turnarounds and vehicle emergency areas (approximately 1000 m^2).
4. By excavation type:
   a) single carriageway excavation: "Sv. Rok", "Javorova kosa", "Stupe", "Grude".
   b) simultaneous excavation of dual carriageway: "Sv. Rok" (central portion), "Ledenik", "Dubrave", "Vrtlinovec", "Konjsko".
5. By type and technology of excavation protection:
   a) tunnels with standard NATM substructures: "Sv. Rok", "Ledenik", "Dubrave".
   b) "Stupe", "Grude", "Konjsko".
   c) tunnels with additional protection "pipe roof" in geologically soft materials: "Vrtlinovac", "Konjsko", "Javorova kosa", "Rožman brdo".

Review of several tunnels executed so far contained in this paper therefore discusses tunnels that are generally defined in terms of these five divisions.

5 EXECUTED TUNNELS

As it has already been mentioned, the most important tunnels that "Konstruktor-Inženjering" d.d. has executed over the last ten years can be divided into two categories.

Those are road tunnels (with two or four lanes for traffic) and hydro-technical tunnels.

Road tunnels are further divided into two groups by length:

a) very long tunnels – exceeding 4000 m in length
b) medium length tunnels – 500 to 2000 meters long

According to the construction difficulty, the tunnels are normally divided into:

c) intermediately difficult construction
d) difficult construction
e) very difficult construction

6 SV. ROK TUNNEL

Among the very long tunnels, "Sv. Rok" tunnel is most notable. "Sv. Rok" tunnel is a part of the Zagreb – Split motorway and it is the longest road tunnel in the Republic of Croatia. Also, it is entirely Croatian product. It runs through Velebit massif under Tulove grede peak. It has been planned as a dual carriageway tunnel, with carriageway axes 35 m apart. The carriageways are 5.685,00 m and 5.766,00 m long respectively including portal structures.

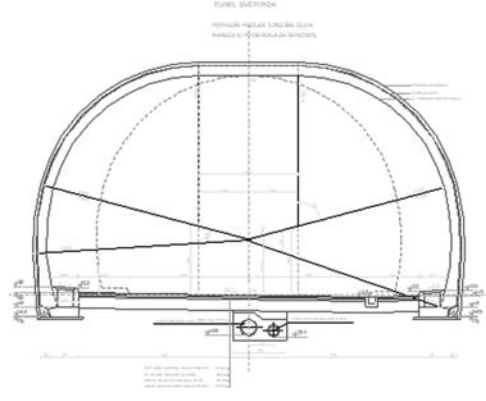


Figure 4. Cross-section of widening section.



Figure 5. Excavation using hydraulic drilling equipment.

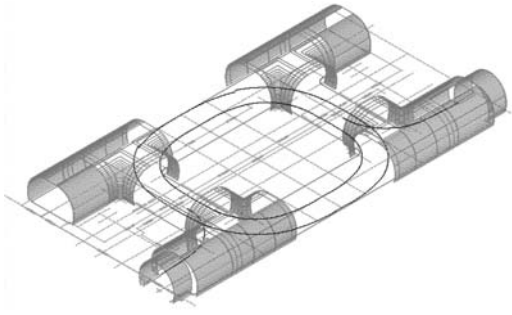


Figure 6. Sv. Rok tunnel turnaround schematic.



Figure 7. Formwork joint, concreting a part of a turnaround.

One of the carriageways is open for traffic and is a part of the motorway, while the other one is completely excavated and rough-in completed.

One particular speciality of this tunnel is the fact that it has been excavated sequentially, i.e. with partial progress on one work face and in the inner section, with excavation on several work faces simultaneously.

During the excavation of this tunnel, non-electric charge detonation system was used (it provided enhanced safety and greater efficiency of the excavation). This type of charge detonation system has been used in all tunnel excavations in Croatia since.

It should be also noted that this tunnel has twelve (12) vehicle emergency niches and four (4) turnarounds with two transversal passages connecting the left and the right carriageway. For concreting secondary lining in those locations, special formwork had to be obtained in addition to the standard cross-section (58,09 m^2) formwork.

Those portions of the tunnel are very complex regarding their construction.

Sv. Rok tunnel is a very long tunnel, while its construction is defined as intermediately difficult in fissured Karst with light substructure. Sv. Rok tunnel, like other tunnels has been executed in NATM tunnelling method.



Figure 8. A view of Sv. Rok tunnel right hand side carriageway portal.

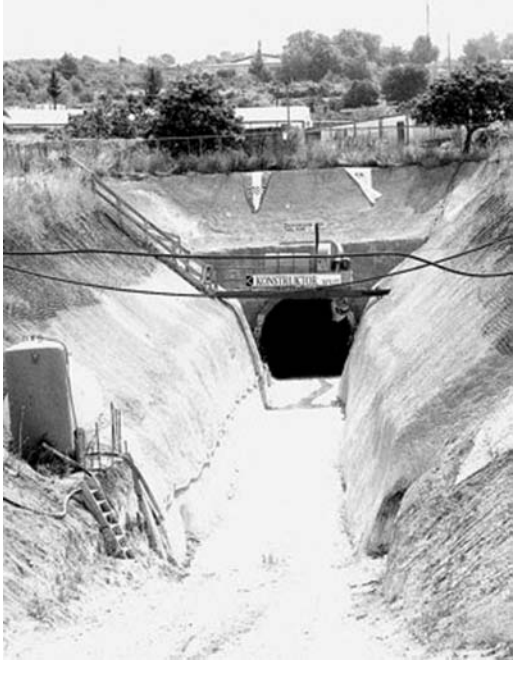


Figure 9. A view of a portal of hydro-technical tunnel "Stupe", a part of Kaštela environmental protection system.

7 TUNNELS UP TO 1000 M LONG

In this paper, tunnels of medium length (500 to 2000 metres long) will also be discussed. Among those tunnels, "Ledenik", "Dubrave", "Konjsko", "Rožman brdo", "Pod Vugleš", "Javorova kosa", "Bisko" and "Stražina" tunnels are distinguished by their construction difficulty. All of the listed tunnels are road tunnels.

"Ledenik", "Dubrave", "Bisko" and "Stražina" tunnels construction is defined as intermediately difficult in fissured rock with light and heavy substructure.



Figure 10. A view of northern portal of "Ledenik" tunnel.



Figure 11. A panoramic view of Ledenik, Čelinka and Bristovac tunnels.

"Stupe" tunnel, a part of Kaštela environmental protection system, is another tunnel of medium length that should be well noted. "Stupe" tunnel has been built for waste water transport from northern parts of Split and Solin with coastal environmental protection in mind. Also there is tunnel "Grude", which is a part of hydro-electric power plant and tunnel "Peć Mlini" in neighboring Bosnia and Herzegovina, both built using special technology.

"Ledenik" tunnel that is a part of motorway section between Sv. Rok and Maslenica, has 748,00 m long left carriageway and 764,00 m long right carriageway, both including portal structure, falls into category of tunnels with thin rock layer above (40 m on average) and has been excavated in geologically unfavorable rock. Its specific detail was simultaneous work on both sides, i.e. on four work faces at the same time. Excavation and concreting work carried out in this tunnel was organized as two separate construction sites with all required equipment for each site.

It is important to stress that the tunnel has been completed, starting with initial excavation through to completion of construction in nine and a half months



Figure 12. A view of completed portal of Dubrave tunnel.

(9,5), which represents a record performance as far as tunnel construction in Croatia is concerned.

"Čelinka" and "Bristovac" tunnels have been executed on the same motorway section, in very demanding and poorly accessible Karst as well.

Another one tunnel in this series is "Dubrave" tunnel, which is a part of motorway section between Vrpolje and Prgomet. This tunnel falls into same category as "Ledenik" tunnel, with average thickness of rock layer above tunnel of merely 25 m, and carriageway axes spaced 47 m apart. Its carriageways are 810,50 m and 779,50 m long respectively. It is also well noted that it has been completed quickly. Construction was completed in nine (9) months.

8 TUNNELS EXCEEDING 1000 M IN LENGTH

It is also necessary to mention "Konjsko" tunnel which, in terms of geological structure, falls into all intermediately difficult, difficult and very difficult construction category. It is a part of Zagreb – Split motorway section between Prgomet and Dugopolje. It has been planned and executed with two carriageways 1.265,80 m and 1.137,90 m long respectively, including portal structure. Pipe-roof construction technology has been used for this tunnel, i.e. excavation was carried out in extremely fragmented and porous rock with underground flows of water.

9 TUNNELS IN GEO-MECHANICALLY EXTREMELY WEAK MATERIAL WITH PIPE- ROOF CALOTTE PROTECTION

Tunnel excavation in geo-mechanically weak material is very complex. Instability of such material after excavation requires fast construction of primary substructure, with stabilization of tunnel calotte. Pipe-roof



Figure 13. Using laser to determine direction of excavation.

method development as additional reinforcement of calotte has very effectively addressed stabilization of calotte and it has made excavation work significantly safer and efficient.

Pipe-roof represents a grouting system in tunnel calotte. The pipes are generally 15,0 m long, spaced 30–35 m apart, while grouting is carried out with pressure of 20 bar. Usual overlap is 3,0 m long, which means that 12 m of excavation is carried out under one pipe-roof. Bore holes for the pipes are drilled at an angle (up to 5°) and radially in order to gain enough space for another pipe-roof to be drilled after next 12 m. The direction of bore holes is usually determined by surveyors and in combination with laser set in focus.

After the pipes are in place and pipe-roof is executed, excavation and primary substructure is carried out step by step. Excavation is usually carried out in 1,0 m increments and in several phases (usually 3: calotte, bench and base of the vault). Primary substructure consists of cross-bar steel arches, reinforcing steel mesh and 30 cm thick layer of shotcrete. This reinforced concrete substructure is radially drilled and anchoring and grouting is carried out. Special care is taken of continuous tunnel convergence monitoring by surveyors in order to detect any shifting (direction, amount, growth) and compare it to the planned values. This method has been applied in excavations of "Javorova kosa", "Konjsko" and "Vrtlinovec" tunnels.

"Vrtlinovec" tunnel is an example of tunnel in material of extremely poor properties with large excavation cross-section (approximately 123 m^2), what places it into the most difficult category to execute. According to Eurocode 7 (Geo-technical category 3, which includes the most complex structures and technological procedures in execution). Pipe-roof consisting of 35 pipes was applied. The overlap was 3 m long, and the pipes were made of 3 m long sections connected to each other and installed using existing equipment.

In static sense, pipe-roof functions as permeable substructure and acts as an unbroken reinforced concrete load carrying element supported by elastic bearings at each cross-bar steel arch (spaced 1,0 m). However, at the place where new set of bore holes are drilled and 3 m long pipes overlap, that part of structure acts as a cantilever allowing for greater deformation and shifting.

Equipment and personnel numbers were scaled for optimum work in both carriageways excavations, with a phased shift in each, in order to make best use of all resources. Extraordinarily demanding time scale set for excavation has been met by means of good site management, excellent execution and good effort, and the tunnel was opened for traffic before the deadline.

It is very important to stress that all of the tunnels, and especially the ones that are part of Zagreb – Split motorway, have been excavated using most recent technology and the very short terms for their completion did not affect quality of work carried out.

10 CONCLUSION

During the last ten years, tunnel excavation as a part of civil engineering has taken an important place in the economy of the Republic of Croatia.

Most of the tunnels concerned are road tunnels within motorway network, starting with the northernmost "Vrtlinovec" tunnel near Varaždin to the last – "Stražina" tunnel near Omiš, passing through "Sv. Rok" tunnel, for which it is fair to say that it has determined the course of Zagreb – Split motorway. The tunnels were of various cross-sections (from small to large cross-sections), of various lengths (medium length and very long), with one or two carriageways and running through material of varying geomechanical properties. NATM method has been used for excavating all of the tunnels, which is consistent with the tunnel excavation practice throughout the world.

Two long hydro-technical tunnels have been excavated during this period as well, with specific organizational and technological requirements due to their relatively small cross-section.

Extremely short terms have been met with preservation of high quality of work carried out.

Equally important is new generation of civil engineers that has developed in this period and forms the basis for development of Croatian tunnel excavation.

And finally it should be well noted that a special care must be given to tunnel excavation, especially on motorways, since the tunnels are time critical parts of all motorway sections making them objects of extraordinary importance. The point is that excavation of tunnels cannot be hurried (unlike the motorway route itself) because of specific technology and practice of work around the clock, while achieving completion term and preserving safety and quality of work carried out.

Section 8
Tunnel equipment: fire and operational safety

This page intentionally left blank

Part 8.1
Safety equipment

This page intentionally left blank

Underground Space – the 4th Dimension of Metropolises – Barták, Hrdina, Romancov & Zlámal (eds)
© 2007 Taylor & Francis Group, London, ISBN 978-0-415-40807-3

Safety analysis of the Branisko tunnel ventilation

M. Bettelini
INELMEC Ltd., Minusio, Switzerland

M. Bakoš
Amberg Engineering Slovakia, s.r.o., Bratislava, Slovak Republic

N. Seifert
ASIT Ltd., Berne, Switzerland

ABSTRACT: The Branisko tunnel in the Slovak Republic is in operation since 2003. The tunnel system consists of a single tunnel tube of nearly 5 km length with bidirectional traffic and a parallel emergency escape gallery transversally connected to the main tube.

This paper is mainly devoted to the detailed analysis of the performance of the semi-transverse ventilation system. This investigation was carried out in the framework of the safety analysis conducted by the authors for the administrator of the Branisko tunnel (National Motorway Company, Slovakia).

As expected the ventilation system proved to be critical for the overall safety of the infrastructure. The existing system is generally well suited for the Branisko tunnel. The main improvements proposed are related to an increase of the smoke-extraction rate and the implementation of an automatic system for mastering the longitudinal velocity of the tunnel air in case of fire. Both requirements are necessary for a proper smoke confinement.

1 INTRODUCTION

The Branisko tunnel, the first motorway tunnel in the Slovak Republic, was set in operation on June 29, 2003. The tunnel system consists of a single tunnel tube, 4,975 m long, with bidirectional traffic. The ventilation is of the semi-transverse type. Escape is allowed by means of a parallel safety tunnel with 13 cross connections to the main tunnel.

A safety analysis was conducted by the authors for the administrator of the Branisko tunnel (National Motorway Company, Slovakia). This effort included the following elements:

- Identification of relevant hazards and scenarios.
- Qualitative risk analysis.
- Quantitative risk analysis based on the OECD/PIARC model QRAM (Quantitative Risk Analysis Model).
- In-deep analysis of the ventilation system.

The present paper illustrates the analysis of the performance of the ventilation system, with focus on the following aspects:

- Performance in normal operating conditions.
- Safety in case of fire.
- Protection of the users in the safety tunnel and in the cross connections.



Figure 1. The west portal of the Branisko tunnel.

Further aspects of the safety investigation are described in a companion paper by the same authors (Bakos et al. 2007).

2 METHODOLOGY

The main steps of the investigation were:

- Gathering of tunnel documentation and operational experience.
- Normative comparison.
- Verification of normal operation, based mainly on analysis of the available data from tunnel operation.
- Analysis of fire scenarios by means of one-dimensional (1D) and three-dimensional (3D) simulation.

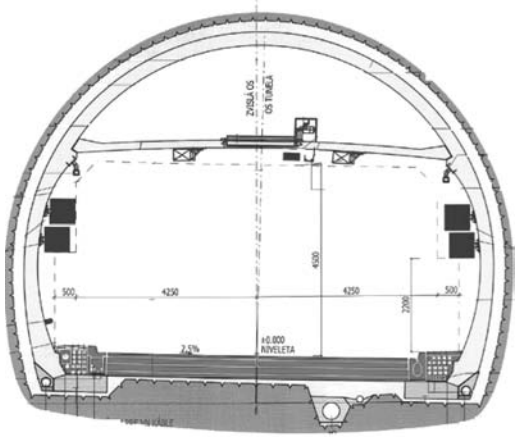


Figure 2. Tunnel cross section.

– Experimental verification of the performance of the fire-ventilation system.
– Assessment of operational safety.
– Formulation of recommendations.

A similar structure will be followed in the present paper.

3 THE BRANISKO TUNNEL AND ITS VENTILATION SYSTEM

The key data of the Branisko tunnel are as follows:

– Tunnel length:	4,975 m
– Slope (West → East):	+1.2% (4,550 m)
	– 1.65% (425 m)
– Length of ventilation	2,161 m (West)
sectors:	2,814 m (East)
– Current traffic	6,000 vehicles/day
– Expected traffic	10,000 veh./day
– HGV ratio	25%.

In spite of the expected increase after completion of the E50 highway, the expected traffic volume is comparatively moderate.

The Branisko tunnel is equipped with a semi-transverse ventilation system. From the operational point of view its key characteristics are as follows:

– Natural ventilation in case of normal operation with low traffic intensity.
– Central extraction during normal operation, with the additional possibility of fresh-air injection from one or from both portal stations, depending on needs.
– Concentrated smoke extraction through 6 dampers in case of fire, with the additional possibility of fresh-air injection in the opposite tunnel half.

The key components of the ventilation system are (Figure 3):

– Two exhaust fans (V_{A1}, V_{A2}) in the intermediate ventilation station, on top of the vertical exhaust shaft. Total capacity up to 215 m^3/s.
– One fresh-air fan in each portal station (V_{ZO}, V_{ZW}). Capacity: V_{ZO} 238 m^3/s, V_{ZW} 182 m^3/s.
– Ventilation duct used for both fresh-air supply and exhaust.
– 90 remotely-controlled dampers (K_{L1} . . . K_{L90}, surface 2 m^2) installed every 50 m in the false ceiling.
– 8 dampers (K_{A1} . . . K_{A8}, surface 6.5 m^2) for the intermediate extraction.
– 2 dampers separating the ventilation ducts from the ventilation station (K_{KO}, K_{KW}).

The available smoke-extraction rates for different locations are:

– Central part 215 m^3/s
– Portal zone 110 m^3/s.

As shown in chapter 8 the large reduction of the available smoke-extraction rate close to the portals is partly due to leakages.

4 NORMS AND RECOMMENDATIONS

4.1 *Applicable norms*

The national guideline for tunnel ventilation and safety in the Slovak Republic is still in preparation and not yet officially available. The Directive 2004/54/EC of the European Parliament and of the Council of 29 April 2004 on minimum safety requirements for tunnels in the Trans-European Road Network is fully applicable to the Branisko tunnel, which is part of the E50.

While the European Directive provides the basic elements, several modern national guidelines provide much more detailed specifications on minimum requirements. The following national guidelines were accounted for, as a part of the documentation of the international state-of-the-art:

– The German RABT (2006).
– The French Circulaire n° 2006–20 of March 29, 2006.
– The Swiss Guideline on tunnel ventilation (FEDRO/ASTRA 2006).

4.2 *Choice of ventilation system*

The requirements for the Branisko Tunnel are clearly stated in the European Directive (Annex I, Section 2.9.5):

"For tunnels with bi-directional traffic, with a traffic volume higher than 2,000 vehicles per lane, longer than 3,000 m and with a control centre and transverse and/or semi-transverse ventilation, the

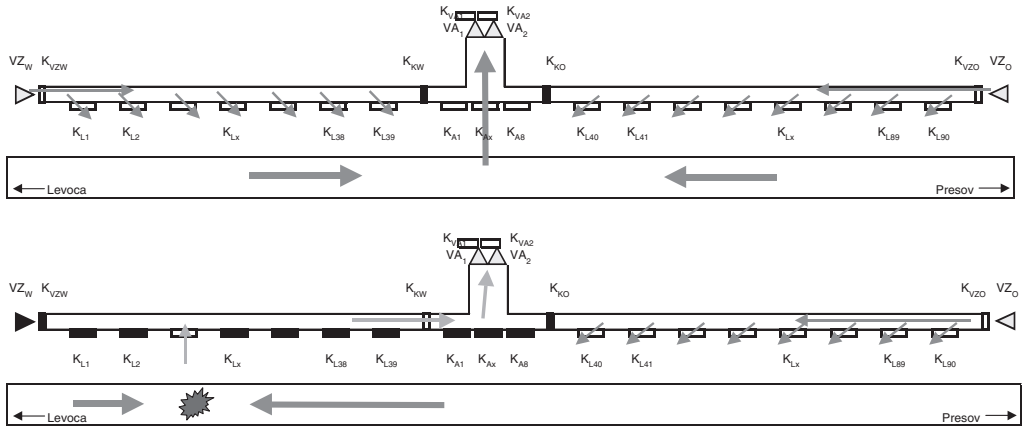


Figure 3. Ventilation in normal operating conditions (upper picture) and in case of fire (lower picture).

following minimum measures shall be taken as regards ventilation:

– air and smoke extraction dampers shall be installed which can be operated separately or in groups,
– the longitudinal air velocity shall be monitored constantly and the steering process of the ventilation system (dampers, fans, etc.) adjusted accordingly."

These requirements are confirmed by all the national guidelines considered. The choice of ventilation system in the Branisko tunnel is basically correct.

The goal of the two requirements contained in the EU directive, concentrated smoke extraction close to the fire and mastering of the longitudinal velocity, is to generate on both sides of the fire a sufficiently high longitudinal velocity directed towards the fire, which can effectively prevent smoke propagation outside the smoke-extraction zone. It is therefore essential to verify, for real-life fire scenarios, how far these conditions are satisfied.

4.3 *Smoke-extraction rate*

The national guidelines mentioned above contain detailed specifications on minimum smoke-extraction rates, Table 1. The available smoke-extraction rate in the central part of the Branisko tunnel is in line with these national requirements. Conversely, the available smoke-extraction rate in case of fires in the vicinity of the portals is significantly lower.

4.4 *Smoke management in case of fire*

The main goal of fire ventilation is the correct management of smoke propagation. An appropriate combination of concentrated smoke extraction near the fire origin and control of longitudinal velocity shall ensure that, after the initial transient phase, smoke propagation is confined to the exhaust zone with open dampers, see e.g. AIPCR/PIARC (1999) or Bettelini (2006).

Table 1. Smoke-extraction rates based on national guidelines (leakages not included).

Country	Minimum Smoke-Extraction Rate
Germany	180 m^3/s (300 m^3/s for a 100 MW fire)
France	155 m^3/s (110 m^3/s with control of longit. velocity)
Switzerland	191 m^3/s (143 m^3/s until July 2006)

The managements of longitudinal velocity is most commonly realized by means of jet fans. In the case of the Branisko tunnel this fundamental task can be accomplished only by means of the fresh-air injection through the portal stations. The available airflow is substantially sufficient, but this functionality needs yet to be implemented in an automated manner and thoroughly tested.

5 NORMAL OPERATION

The analysis of normal operation was based on 1D simulation (Figure 5) as well as on the analysis of the operational data collected since tunnel opening, between January and December 2005. The available data included detailed record of the following parameters: operation level of the exhaust and fresh-air fans, 14 opacity measurement stations and one CO measurement station. The series were quite detailed and encompassed 2,881 CO-values/day and 8,640 values/day for all further parameters.

The analysis of the data showed a number of short episodes with excessive pollutant concentration,

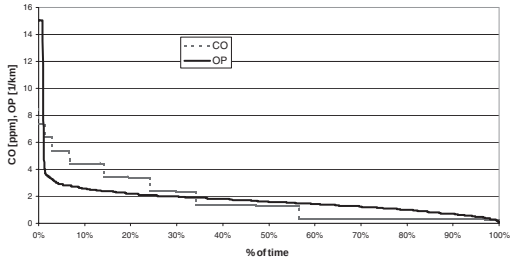


Figure 4. Pollutant levels distribution (06.04.2005).

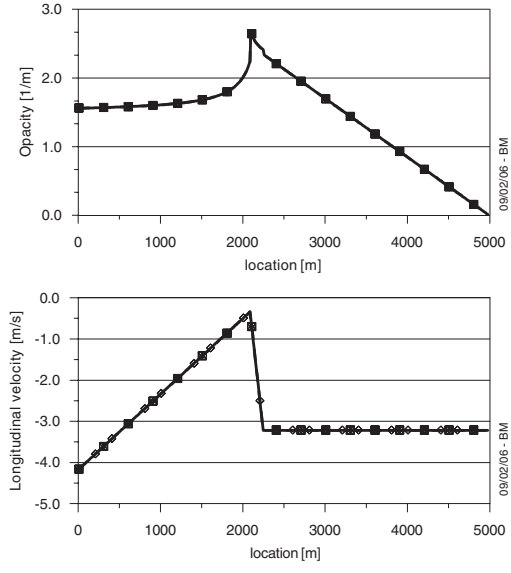


Figure 5. Ventilation in normal operating conditions (asymmetric traffic, exhaust in the middle of the tunnel, fresh-air injection from the western portal (left in the pictures).

resulting locally in very low visibility levels, which are mainly related to a relatively small number of highly polluting vehicles. The analysis showed that the automated system response is mostly appropriate, but that the ventilation system reaches its performance limit. These issues can be solved by iterative adjustments.

6 ONE-DIMENSIONAL SIMULATION OF FIRE SCENARIOS

The events in case of fire are intrinsically transient. The very first minutes are decisive for saving lives and for getting control of the fire. It is therefore important, not only to know the asymptotic state of the ventilation, but to simulate with sufficient detail its development. The analysis has therefore to be carried out based on a large number of particular fire scenarios, chosen as to be representative for all relevant potential fire conditions. Thereby it is possible to identify potentially critical conditions to be investigated in more detail.

By means of 1D simulation it is possible to investigate in short time a large number of fire scenarios. All relevant real-life effects, including traffic volume, composition and evolution, fire development, fire detection as well as ventilation and traffic management, can be accounted for in a very realistic manner. A description of the particular model used herein can be found in Bettelini (2006). Its peculiarity is the capability of modeling smoke propagation due to thermal stratification in an approximate manner, which increases significantly accuracy and reliability in simulation.

Two illustrative results are presented in Figure 6. It was shown that the fire ventilation performs generally in a satisfactory manner in case of “standard” 30 MW fires. In case of atmospheric pressure differences between the portals or increasing fire intensity smoke confinement is not complete anymore and part of the smoke “escapes” from the 600 m long smoke-extraction zone. As stated in chapter 4, this is a consequence the combination of the limited smoke extraction rate and the lack of an effective mastering of longitudinal velocity.

7 THREE-DIMENSIONAL SIMULATIONS OF FIRE SCENARIOS

CFD (Computational Fluid Dynamics) is an advanced simulation technology, which allows for very detailed three-dimensional simulations of fire scenarios. In the design-verification phase, CFD can offer an invaluable help in assessing the effectiveness and relative merits of different smoke-management options. The additional insight to be gained is in particular related to:

– Visibility conditions;
– Concentration of smoke and poisonous gases;
– Temperature and radiation.

In the case of the Branisko tunnel CFD was used for verifying the assessment on smoke-confinement capabilities originally based on 1D simulation. In this case 3D simulation fully confirmed the previous results, therefore providing an excellent confirmation of the capabilities of the 1D technology adopted for this investigation.

8 EXPERIMENTAL VERIFICATION OF SMOKE-EXTRACTION RATE

Because of the importance of smoke-extraction rate for tunnel safety and because of some uncertainties related to leakages, it was decided to conduct a specific measurement campaign in the Branisko tunnel.

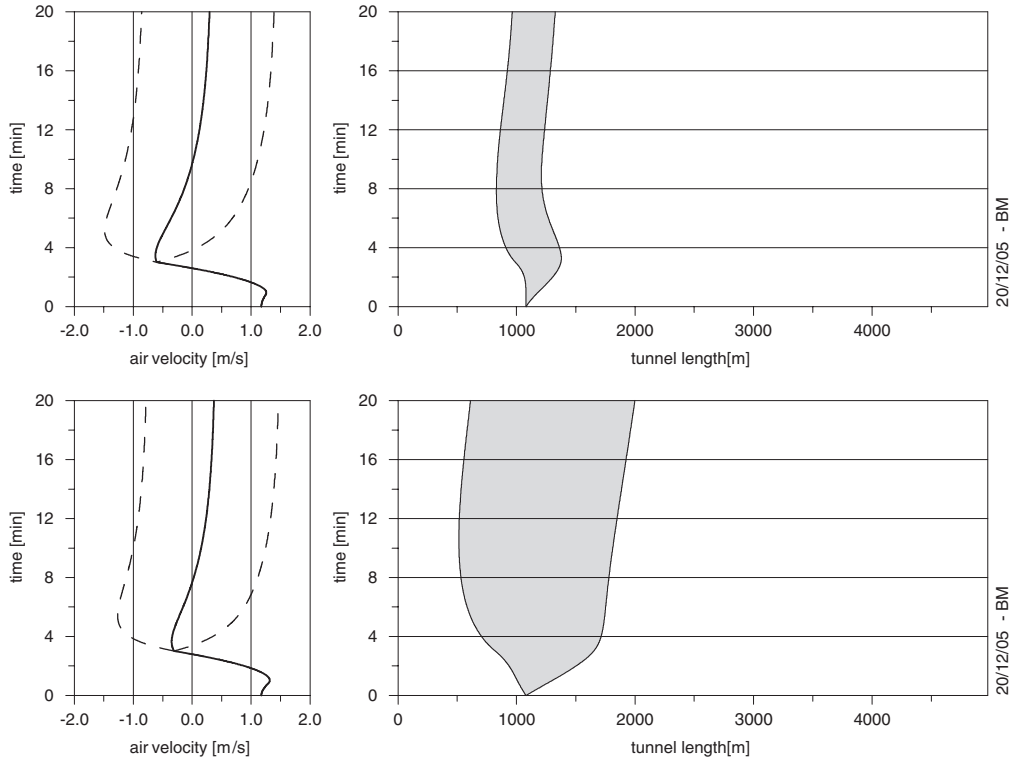


Figure 6. 1D simulation of fire scenarios. Fire location 1,080 m from the western portal, smoke extraction over 600 m, no fresh air, 600 vehicles/h in every direction, 25% HGV, no atmospheric pressure difference, fire detection after 3 minutes. Top: fire intensity 30 MW; Bottom: fire intensity 100 MW. The pictures on the left show the evolution of the longitudinal velocity (fire location as well as 300 m aside) with time. Smoke propagation is presented in the pictures on the right.

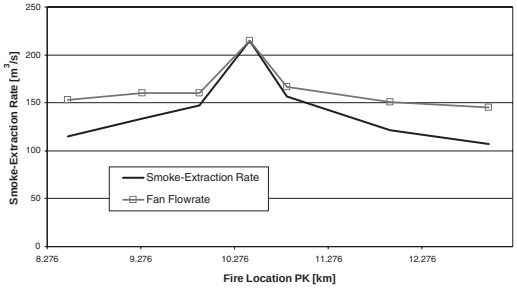


Figure 7. Results of the measurements of smoke-extraction rate (15–17 May 2006).

The measurements were carried out based on SF6 injection and concentration measurements, precision anemometers, pressure gauges and the built-in fan flowrate measuring devices.

The results presented in Figure 7 allowed for an accurate determination of the effectively available smoke-extraction rate. They also allowed confirming the presence of very substantial leakages, of the order of 25% for fire locations in the vicinity of the portals.

9 EMERGENCY EXITS

The main tunnel is connected to a parallel emergency escape gallery by means of 13 cross connections located every about 360 m. Fire doors separate the main tunnel from the cross connections.

The ventilation consists mainly of two fans installed at the entrances, where interlocked doors are installed for preventing pressure losses in case of transit.

The ventilation system is simple but effective and allows for an adequate safety level. Because of its fundamentals safety role, thorough periodic verifications are a key element of the whole safety system.

10 CONCLUSIONS AND RECOMMENDATIONS

The safety analysis of the Branisko tunnel included a thorough investigation of ventilation performance in normal operating conditions and in case of fire. The main findings are summarized below.

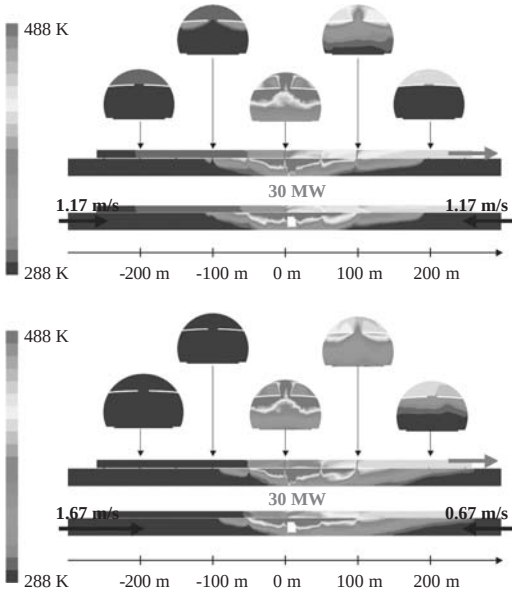


Figure 8. 3D simulation of fire scenarios. Fire intensity 30 MW. Top: full control of longitudinal velocity; Bottom: partial control of longitudinal velocity.

The comparison with the EU directive and with some leading European national guidelines showed that:

– The layout of the ventilation system is correct.
– The currently available smoke-extraction rate is in line with the national guidelines for fires in the central part of the tunnel, but is significantly lower close to the portals. This is partly due to leakages.
– The longitudinal velocity in case of fire cannot yet be properly controlled in an automated manner.

The smoke-extraction rate could be verified by means of dedicated test campaign. This allowed confirming the high leakage rate.

The performance analysis of the ventilation system in normal operating conditions was based on numerical simulation and on the analysis of the operational data. It can be concluded that:

– The system's layout and key design parameters are basically correct.
– Isolated episodes with locally very high opacity values occur periodically. They are mainly related to a small number of highly pollutant vehicles.
– Because of the heterogeneity of the vehicle park, the requirements on ventilation control in normal operating conditions are very high.
– In normal operating conditions large amounts of fresh air are injected through the dampers, in the upper part of the tunnel. In case of fire this could lead to a rapid loss of smoke stratification.

The system's performance in case of fire was evaluated by means of the simulation of a large number of fire scenarios, using both 1D and 3D (CFD) simulation techniques. This part of the investigation led to the following conclusions:

– Under ideal conditions the fire ventilation performs satisfactorily.
– The comparatively low smoke-extraction rate, coupled with the inadequate mastering of longitudinal velocity lead to an incomplete management of smoke propagation.
– "Disturbances", such as atmospheric pressure differences, high fire intensities, particular fire locations etc.) can have a dramatic impact on system performance.
– Initial "disturbances", such as highly asymmetric traffic volumes or slow fire detection, lead to a rapid smoke propagation in the very first phase of the fire, whose compensation is slow.

The main recommendations issued from this investigation are as follows:

– Ad-hoc adjustments to the control algorithms for normal operation can help reducing frequency and amplitude of the high-pollution episodes observed during 2005.
– Leakages shall be reduced.
– The currently available smoke-extraction rate is too small and should be increased to about 200 m^3/s.
– The implementation of an automated tool for mastering the longitudinal air velocity in the tunnel in case of fire is highly recommended.

Globally the Branisko tunnel risk analysis showed that the tunnel represents a minimum risk. The ventilation represents clearly the weakest link in its safety chain. If this deficiency is removed and some other minor measures are put into operation the Branisko tunnel shall fully comply with the up-to-date safety requirements.

The ventilation verification presented goes well beyond a mere normative comparison. The results showed that only a very focused analysis of the effectiveness, based on a large number of realistic fire scenarios, allows for a realistic assessment of ventilation performance.

The Branisko tunnel risk analysis has been the first risk analysis prepared for a Slovak road or railway tunnel. It contains a suitable methodology to be used in Slovakia in the future.

REFERENCES

AIPCR/PIARC 1999. *Fire and Smoke Control in Road Tunnels*, Lyon, May 1999.

Bakoš, M., Seifert, N. & Bettelini, M. 2007. Risk analysis of the Branisko tunnel. Paper presented at the *ITA-AITES*

World Tunnel Congress 2007, "Underground Space – the 4th Dimension of Metropolises". 5–10 May 2007, Prague, Czech Republic. Balkema Publishers, Rotterdam, The Netherlands.

Bettelini, M. 2006. *Tunnel Fires – Active Risk Reduction*. January 2006.

Circulaire interministérielle n° 2006–20 du 29 mars 2006, relative à la sécurité des tunnels routiers d'une longueur supérieure à 300 mètres (France).

European Union 2004. Directive 2004/54/EC of the European Parliament and of the Council of 29 April 2004 on minimum safety requirements for tunnels in the Trans-European Road Network.

FEDRO/ASTRA (Switzerland) 2006. Lüftung der Strassentunnel – Systemwahl, Dimensionierung und Ausstattung. Auflage 2004, Version 1.2 of 31.07.2006.

RABT – Richtlinien für die Ausstattung und den Betrieb von Strassentunnel, Ausgabe 2006 (Germany). Forschungsgesellschaft für Strassen- und Verkehrswesen.

This page intentionally left blank

Underground Space – the 4th Dimension of Metropolises – Barták, Hrdina, Romancov & Zlámal (eds)
© 2007 Taylor & Francis Group, London, ISBN 978-0-415-40807-3

Safety doors in the world's longest tunnel under the Gotthard: Outstanding requirements and performance. Feed-back from the bidding phase and results from the testing phase on selected prototypes

Davide Fabbri & Christina Strassl
Lombardi Engineering Ltd., Minusio, Switzerland / Mechanical Equipment GBT
member of the Joint-Venture Gotthard Base Tunnel South (Lombardi Engineering Ltd., Amberg Engineering Ltd., Pöyry Infra Ltd.)

Simon Peggs
AlpTransit Gotthard Ltd., Lucerne, Switzerland / Mechanical Equipment GBT

ABSTRACT: The 57 km Gotthard Base Tunnel (GBT) will be the world's longest railway tunnel. The tunnel is the central part of the new transalpine rail line in Switzerland. The two single-track tubes are linked by 178 cross passages approximately every 325 m, and two multifunctional stations with an emergency stop station for each tube located one-third and two-thirds along the base tunnel.

During regular operation, high speed passenger trains with a top speed of 250 km/h as well as slower freight trains (160 km/h) will run through the tunnel. In the worst case scenario e.g. a fire on a passenger train, the doors of the cross passages and those of the emergency stations will be essential elements of the safety concept.

This paper gives a short presentation of the safety concept in the case of fire on a passenger train and an overview of the most important requirements of the different door-types. It also includes the state of progress of the special procedure for the commissioning and feed-back from the tests on selected prototypes.

1 INTRODUCTION

A high safety level is a very important premise for the operation of a railway tunnel and as well an economic exigency. After tragic fatalities in existing long traffic tunnels public opinion is especially sensitive to tunnel safety: clients and project managers were called upon to undertake every reasonable effort to increase tunnel safety.

In order to ensure long service (long durability, no revision of the doors in the first 20 years after the installation), the required fire protection (90 minutes at a temperature of 1,000°C) and efficiency in the case of evacuation, very high and stringent regulations have been set for the delivery of doors for the cross passages of the Gotthard Base Tunnel.

Based on former experience, especially on the commissioning of the doors for the Lötschberg Base Tunnel (34.6 km long, also part of the New Alpine Transverses in Switzerland) and in consideration of the unique, extremely harsh conditions of the Gotthard Base Tunnel, the development of a special technical solution is essential; these doors will not be a "standard" product.

The client – AlpTransit Gotthard Ltd. – decided to adopt a special procedure for the commissioning as well as for the evaluation by means of prototypes. A selective bidding procedure with pre-qualification was started on January 2005.

The Joint-Venture Gotthard Base Tunnel South has been charged to carry out the bidding procedure.

2 HIGHLIGHTS OF THE SAFETY CONCEPT

2.1 *Safety requirements*

A fire on board a passenger train in the Gotthard Base Tunnel is the "worst case": the probability of such an incident is very low. However, the following requirements have to be met in the case of an accident:

1. Availability during an event. In the case of fire on board a passenger train, the safety of passengers has first priority. In order to ensure this, the availability of the tunnel has to be maintained as long possible, as passengers should be able to reach a safe place.

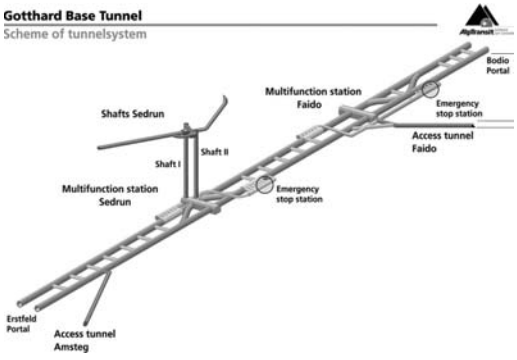


Figure 1. Gotthard Base Tunnel (GBT), the tunnel system [7].

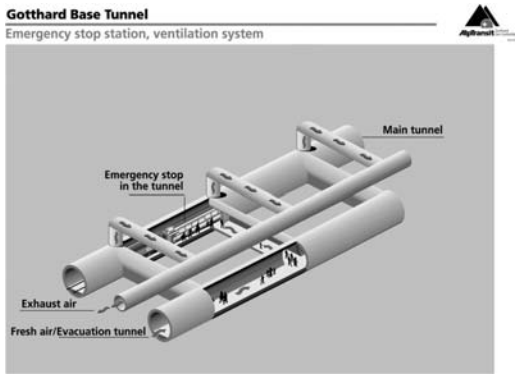


Figure 2. GBT, evacuation in an emergency stop station [7].

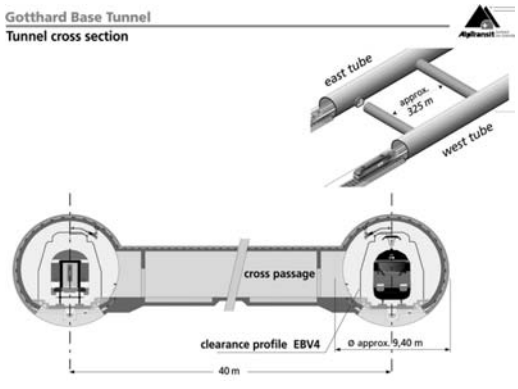


Figure 3. GBT, evacuation through a cross passage [7].

This is a must! In consideration of the fire/life safety system this means:

The tunnel has to maintain operation for 90 minutes after an alarm.

2. Availability after an event. In the case of fire, the interruption of tunnel traffic has to be as short as possible. After evacuation, the reopening of the railway line has first priority. In order to ensure this, constructive fire-protection measures have to be taken:
   - To exclude major damages or collapse of the safe tube,
   - To reduce resulting damages, time and costs for the repair of the burned tube.

2.2 *Overview of the fire/life safety system*

The tunnel system (Fig. 1) mainly consists of two single track tunnels with two train-crossover sections in the so called multifunctional stations. Along the tunnel, cross passages are located approximately every 325 m; the horizontal distance between the tube axes varies between 40 and 70 m.

In the case of a fire on board a passenger train, the procedure of the safety concept depends on the position of the train in the tunnel. Three cases have to be taken into account:

1. The train is running in the last section of the tunnel (after the second multifunctional station): the train has to reach the portal and stop outside the tunnel.
2. The train is running in the first or in a intermediate section of the tunnel: the train has to reach the next multifunctional station and stop there to let passengers be evacuated (Fig. 2). After the fire-alarm, prior to the arrival of the train, the lights of the emergency station will be turned on, the sliding-doors of the escape ways will be automatically opened and the ventilation system will start the extraction of exhaust air from the traffic tube trough the middle of the seven fire dampers. The passengers reach the "sheltered area" of the emergency stop station within 3 to 5 minutes.

   After evacuation from the train – without using stairways or elevators – passengers will wait at the emergency stop station of the opposite tube for evacuation by train.
3. Fire occurs on board a train and it is not able to reach the next multifunctional station or to exit the tunnel. In this case the train will stop at any position in the tunnel and evacuation will have to take place there. On a 1 m-wide side walk escaping passengers will be able to reach the next cross passage through which they will reach the safe tube (Fig. 3). In the opposite tube the speed of the trains is immediately reduced after the alert. In this case, the process of the external rescue proceeds in the same way as if the train had stopped in an emergency stop station.

For case nr. 3, object of the present paper, doors will provide fire-protection of the escape way and the technical equipment inside the cross passages. The ventilation system will ensure overpressure

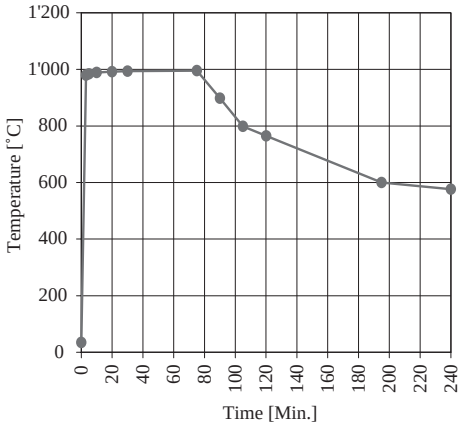


Figure 4. Goods train fire curve ATG (direct flame application).

conditions in the safe tube to avoid smoke entering the safe tube.

3 REQUIREMENTS FOR THE DOORS

3.1 *Main requirements*

According to the stringent requirements of the safety concept and for durability of the tunnel system, very high requirements have been set for the doors of the cross passages. The most important ones are:

- Resistance in case of fire: 90 minutes with AlpTransit temperature-time-diagram (Fig. 4), maximal average inside temperature of the door-panels of 200°C.
- Resistance for high pressure/suction loading due to the passage of trains: ±10 kPa in each running tube, resulting pressure difference on the door of 20 kPa.
- Serviceability: a conceptual solution for the guarantee of operational safety and impervious sealing is especially requested. A maximal necessary force for manual door opening of 100 N (mechanical support driving mechanism permitted) and serviceability in case of interruption of energy supply, as well as a max. air-leakage rate through the door sealing of 50 m^3/h (according to the ventilation system) are fundamental requirements.
- Durability: 100 years for the structure, minimum 20 years for electronic devices and for replaceable parts.

3.2 *Other requirements*

A 16 page long list of requirements, properties and conditions divided into 45 relevant themes, including the main requirements. Every single requested property or prescribed condition has to be fulfilled: some of them are now the object of direct verification with selected tests on prototypes doors. All others have to be certified or plausibly described in the offer.

4 THE BIDDING PROCEDURE

4.1 *The lots*

For the commissioning of the doors of the cross passages AlpTransit Gotthard Ltd. decided on the procurement of 2 separates lots:

- Lot A "Doors for the cross passages of the GBT" for the development, staggered fabrication, delivery and possible installation of steel doors in the tunnel.
- Lot P "Tests and verifications of prototype steel doors for the cross passages of the GBT" for the examination of the proposed solutions of lot A.

4.2 *Selective bidding procedure for Lot A*

The suitability of the contractor had to be determined by a selective procedure based on weighted suitability criteria in accordance with the Swiss Federal Law on Government Procurements (BoeB). For this reason, the selection procedure for Lot A is currently carried out according to the following 9 stages (at the time of the submission of the paper to the editor, stage 5 has been reached):

1. Invitation to tender / Invitation to participate at the prequalification. On January 10th 2005.
2. Prequalification of applicants according to the weighted suitability criteria. Reduction of the number of bidders to a maximum of 8.
   AlpTransit Gotthard's decision was published on June 9th: 2005, the applicants were admitted to the next stage.
3. Bidding phase. From Mai to September 2005: five bids were handed in.
4. Choice of offers based on the additional criteria: reduction of bidders to a maximum of 4. Based on the evaluation of the Engineers-JV, on December 7th 2005 AlpTransit Gotthard Ltd. called all 5 bidders for prototyping and testing.
   Facilities for testing the prototypes are carried out by an accredited testing institution chosen by AlpTransit Gotthard Ltd. This stage started on March 2006 and is in progress at the present time (September 2006).
5. After testing phase: discussions with the individual bidders for the improvement of the technical solution based on the results of the examination. Expected in Winter 2006/2007.
6. Revision of the submission documents.
7. Technical and financial revision of the offers. Expected in Winter/Spring 2007.
8. Revised evaluation of offers and supplements based on the additional criteria.

9. Opening of the supplements / Conclusion of the procedure / Signing of contract. Expected in Summer 2007.

4.3 *Suitability criteria for Lot A*

Suitability criteria were used at stage 2 to evaluate the basic qualifications of a contractor or a bidding consortium to carry out the project. Only suitable bidders were invited to submit an offer. The following suitability criteria were applied:

- Criterion 1: Experience with the production of doors with high technical requirements and with the installation of doors under difficult conditions (weighting: 60%, minimum score 3).
- Criterion 2: Sufficient personnel and technical capacity to fulfill the scheduling and qualitative requirements (weighting 20%, minimum score 3).
- Criterion 3: Sufficient financial capacity for the execution of the job (weighting 20%, minimum score 3).

4.4 *Additional criteria for Lot A*

To evaluate the offer of a contractor or a bidding consortium, the following additional criteria were applied at stage 4 and will be applied again at stage 8:

- Criterion 1: concerning a plausible declaration that the required quality, serviceability and durability will be guaranteed (weighting 30%, minimum score 3 / score scale: 1 to 5, scale division 0.5), i.e.:
  - Fulfillment of fire resistance requirements (partial weighting 10%).
  - Fulfillment of the requirements for high pressure/suction loading due to the passage of trains (partial weighting 10%).
  - Fulfillment of the requirements for serviceability, especially: conceptual solution for the guarantee of operational safety and impervious sealing (protection from dust and noise) (partial weighting 5%).
  - Fulfillment of the requirements for durability (life expectancy) (partial weighting 5%).
- Criterion 2: Price level (weighting 30%, minimum score 3).
- Criterion 3: Appropriateness of the installation concept (weighting 20%, minimum score 3), i.e.:
  - Appropriateness of the underground installation concept. Conceptual solution to guarantee simple and timely installation deadlines (partial weighting 5%).
  - Appropriateness of the underground storage concept (partial weighting 5%).
  - Appropriateness of the packing concept (partial weighting 5%).
  - Appropriateness of the underground transport concept (partial weighting 5%).
- Criterion 4: Guarantee of meeting deadlines (weighting 10%, minimum score 3), i.e.:
  - Reliability of the planned underground installation schedules (partial weighting 4%).
  - Flexibility of the delivery of the doors (high availability and large capacity during production, adjustment of the production schedule as a function of modified deadlines in the tunnel lots) (partial weighting 3%).
  - Plausibility of the tendered services (production and delivery times) (partial weighting 3%).
- Criterion 5: Guarantee of appropriate maintenance (weighting 10%, minimum score 3), i.e.:
  - Maintenance concept. Conceptual solution to guarantee simple and timely maintenance during the construction phases and in service (partial weighting 5%).
  - Possibility for replacements (partial weighting 5%).

5 TESTS ON SELECTED PROTOTYPES

5.1 *Installation tests under tunnel conditions*

To observe and evaluate the installation of the prototype doors – manufactured and mounted by the bidder of the separate Lot A – the contractor of Lot P (the joint-venture PQ: VSH Sargans & Berner Fachhochschule Biel) has been commissioned for the establishment of the conditions corresponding to the simulated tunnel conditions (Fig. 5 and 6).

5.2 *Functionality tests under tunnel conditions*

For the verification of the prototype doors according to the prescribed requirements (i.e.: observance of

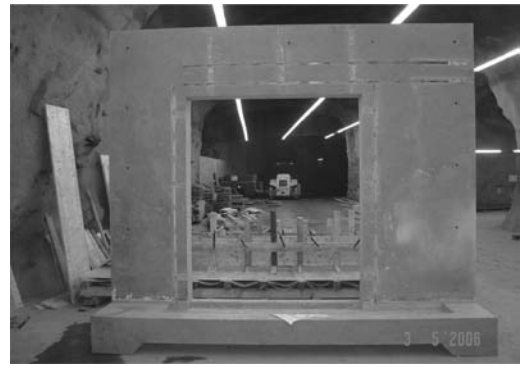


Figure 5. Simulation of the tunnel conditions: the wall [7].

the maximum permissible weight and dimensions for transport, door operation and opening, duration of the opening and closing operations, maximum necessary force for manual door opening of 100 N, verification of the door surveillance apparatus, verification of the function and storage capacity of the mechanical support driving mechanism) the contractor of Lot P has been commissioned for the establishment of the conditions corresponding to the simulated tunnel conditions:

- Execution of opening and closing operations with an overpressure of 0.5 kPa, performed by a robotic arm (Fig. 7), under similar tunnel climatic conditions (temperature and humidity).
- Verification of the air-leakage rate through the door sealing (max. 50 m^3/h during 24 hours, difference of pressure inside/outside of 100 Pa). The fulfillment of this condition is very important to allow the cooling effect inside the cross passage by the ventilation system (air recirculation). Operational equipment requires a max. air temperature during service of 35°C.



Figure 6. Simulation of the tunnel conditions: the lining [8].



Figure 7. Functionality tests, robotic arm [8].

5.3 *Endurance test under tunnel conditions*

For the verification of the prototype doors according to the prescribed pressure and suction loading during train passage and simulation of single pressure shocks (resulting pressure loading of 20 kPa and suction loading of 10 kPa, 500,000 loading cycles, 1 cycle every 2 seconds, 1 cycle = 1 pressure + 1 suction loading, functionality tests every 100,000 loading cycles and at the end of the endurance test) the contractor of Lot P has been commissioned to design and assemble a testing facility (Fig. 8, the so called "Mjöllnir"), to simulate the tunnel conditions:

- Loading by air pressure (no mechanical contacts between testing equipment and prototype doors), verification of the behaviour of the doors including the sealing.
- Very quick increase of the loading (shocks).

5.4 *Fire tests under tunnel conditions*

For the verification of the high fire protection resistance prototype doors the contractor of Lot P has been commissioned to design and assemble a testing facility (Fig. 9), corresponding to the simulated tunnel conditions in the case of a fire in front of the door:

- Freight train fire (250 MW, max. air temperature 1,000°C after the first few minutes, 90 minutes resistance required, see Fig. 4). After a major fire in the tunnel the functionality of the door is no longer required and a replacement is necessary.
- Overpressure on the side of the cross passage of about 100 Pa (reduced amount vs. real conditions) to simulate the air-leakage through the sealing to the "burning tube" during the fire, avoiding smoke and significant heat propagation in the cross passage. Overpressure is assured by the ventilation system in emergency mode.



Figure 8. Endurance tests equipment, the "Mjöllnir" [8].



Figure 9. Fire tests equipment [8].

A maximum average temperature of the inside face of the door during the fire load of 200°C is a must. A single sensor on the inside face of the door should not measure more than 240°C. These requirements are a condition to limit the inside air temperature of the cross passage at 45–50°C, permitting the functionality of the electrical equipment during a fire.

During an evacuation the functionality of the doors of the cross passage has to be assured up to an air temperature of 90°C in the "burning tube". This requirement can be tested in a preliminary phase of the fire test.

6 FIRST FEED-BACK FROM THE TESTS

At the present time (September 2006) the installation test, the functionality tests and the endurance tests have been completed. In October 2006 the fire tests will be carried out and the final reports of the tests should be completed before the end of the year. According to the bidding procedure, and respecting the copyright of the prototype doors disclosure of the results of the tests is not yet permitted.

First feed-back from the tests confirm the correct decision of the AlpTransit Gotthard Ltd. and of the engineers for a selective bidding procedure, with separate procurement of an independent certified contractor for the design and assembling of the testing equipment as well as for test processing. The extreme loading in the Gotthard Base Tunnel, endurance test and the verification of the air-leakage rate through the door sealing represent a real challenge for each bidder. After the completion of the tests, the following revision of the submission documents and technical / financial revision of the offers, based on the very interesting and significant results of the tests, will represent the next important challenge for the choice of a central element of the fire/live safety system of the Gotthard Base Tunnel.

7 CONCLUSIONS

The Gotthard Base Tunnel (GBT) will be the world's longest railway tunnel, with a length of 57 km. It will be unique. This is the reason why no standard solution or products can be adopted to reach the prescribed requirements in the case of an accident. Only "on mass tailored" solutions or products are able to meet all requested properties and prescribed conditions: The know-how of some of the best door manufacturers and the chances given by the new technologies are the mixture for success.

ACKNOWLEDGMENT

The authors would like to thank the AlpTransit Gotthard Ltd for permission to publish this paper.

Information on the outcome of the remaining phases of the selective bidding procedure for the Lot A "Doors for the cross passages" can be obtained under: www.alptransit.ch. http://www.alptransit.ch/pages/e/portrait/submission.php

REFERENCES

H.-P. Vetsch, C. Kauer – "Safety of the Gotthard Base Tunnel" – SIRRT Safety in Road and Rail Tunnels, Conference (Madrid) Spain, April 2001.

D. Fabbri – "The Gotthard Base Tunnel: Fire / Life Safety System", The 6th Annual Tunnelling 2004 Conference, Sydney (Australia), August 30th & 31st 2004.

AlpTransit Ltd./JV- Gotthard Base Tunnel South – "Publikationstext Los A", SHAB, January 10th 2005.

D. Fabbri, S. Pedrazzini – "The importance of the safety ASPECTS during the construction works for the new major Alpine tunnels related to the safety during the regular service phase. Parallelisms and differences", AFTES 2005 Conference, Chambery (France), October 10th–12th 2005.

AlpTransit Ltd./JV- Gotthard Base Tunnel South – "Publikationstext Los A", SHAB, October 11th 2005.

D. Fabbri, Ch. Strassl – "Rough work Equipment Part-Section", Tunnel 4/2006.

Pictures provided by AlpTransit Gotthard Ltd., client.

Pictures provided by the Joint-Venture PQ (VSH Sargans & Berner Fachhochschule Biel, contractor of Lot P.

Underground Space – the 4th Dimension of Metropolises – Barták, Hrdina, Romancov & Zlámal (eds)
© 2007 Taylor & Francis Group, London, ISBN 978-0-415-40807-3

Mechanical equipment in long, high-speed rail tunnels – Specification and operational experience of doors, cabinets, containers and other elements in the Loetschberg Base Line

R. Haldimann, S. Nyfeler & P. Reinke
HBI Haerter Ltd., Consulting Engineers, Berne, Switzerland

ABSTRACT: The Loetschberg Base Line (LBL) includes the 35 km long Loetschberg Base Tunnel (LBT) and the 3 km long Tunnel Engstlige. Several elements of the mechanical equipment of these tunnels were newly designed. "Non-catalogue" solutions were needed to meet the specific requirements of these long, high-speed rail tunnels. The specific requirements are characterized by uncommon climatic conditions, by the need for safety and reliability during normal and emergency operation, by the specific requirements of single-track, double tube tunnels with cross-passages and by the need for cost-efficient maintainability and fast and simple installation. The special features for a variety of elements such as the doors in the cross-passages, the large doors in the rail tunnel, the cabinets in the cross-passages and the containers in the technical equipment caverns are presented. The methodology to define, to select and to test the equipment during the tendering phase (prototype-based selection and utilisation of a test site in the tunnel) is illustrated. The requirements to manage the various technical interfaces of these elements with other lots of equipment in the tunnel are shown. The experience gained from the design, installation and commissioning phase of the LBL are presented.

1 INTRODUCTION

1.1 *Tunnel system LBL*

The Loetschberg Base Line (LBL) is a principal element of the new cross-alpine rail links (NEAT) in Switzerland which are an integral part of the European high-speed rail network. Central parts of the LBL are the Loetschberg Base Tunnel (LBT; drill and blast, TBM) with a length of approximately 35 km and the Tunnel Engstlige (TE; cut and cover) with a length of approximately 3 km.

The Loetschberg Base Tunnel will be built in stages. The first stage will be taken in operation in 2007. During this first stage, only the southern part of LBT will be a single-track, double-tube system. The northern section will be operated using one tube in bi-directional mode (see Figure 1). At the final stage, the tunnels consist of 2 single track tunnels which are connected with accessible cross-passages approximately every 330 m or emergency exits. In addition, the base tunnel system will include multifunctional stations (MFS) with crossovers and emergency train stations.

During normal operation, passenger trains will run at velocities of up to 250 km/h and freight trains at max. 160 km/h. Freight trains can reach a length of up to 1,500 m.

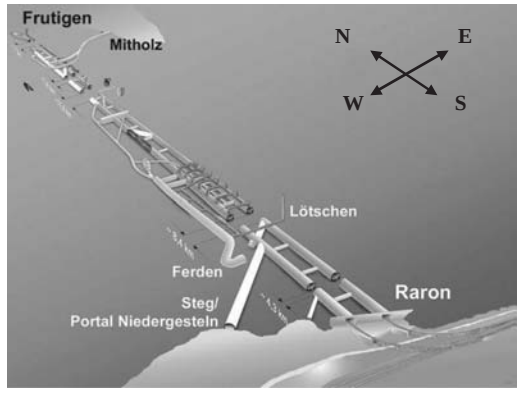


Figure 1. System overview of the Loetschberg Base Tunnel.

There are demanding requirements regarding the lifetime reliability, availability, maintainability and safety of the mechanical equipment. Several "non-catalogue" solutions were needed to meet the specific requirements of these long rail tunnels. These tunnels are characterized by extreme climatic conditions (e.g. significant pressure fluctuations, wide range of temperatures, humidity, dust, salt), by an extended need for safety and reliability during normal and

emergency mode, by specific requirements of single-track, double-tube tunnels with cross-passages, by the need for high availability and durability, by efficient maintainability and the requirement for fast and simple installation (see Ravn & Reinke, 2004).

1.2 *Rail equipment of LBL*

Numerous rail technology systems are needed to ensure smooth rail operations throughout the Loetschberg. Well over a quarter of the total project costs are related to the rail technology. Rail technology as defined for the Loetschberg project includes lots such as:

- track way
- train power supply (16.7 Hz) and catenary
- train control (ETCS 2)
- power supply of the electrical equipment (50 Hz)
- operational control and communication
- mechanical equipment
- ventilation (preliminary and permanent)
- logistics of installation and of rail technology

Above all, the rail technology must meet stringent safety requirements and guarantee reliable operation of the railway. To minimise failures, only the most essential equipment is installed in the rail tubes. All other systems are housed in air-conditioned technical rooms and containers, in the cross-passages or outside the tunnel system.

1.3 *Mechanical equipment*

Mechanical equipment as defined for the Loetschberg project includes elements as listed in Table 1. They make up approximately 15 to 20% of the costs of all rail equipment.

Other elements could be considered as "mechanical equipment" as well. However, these were allocated to other lots (ventilation fans, dampers, cross-passage ventilation, fire water supply, several steel structures, etc.).

Table 1. Mechanical equipment of LBL (approximate quantity refers to first stage of operation of LBL).

Mechanical equipment of LBL	Approx. quantity	Prototype lot	Part of this paper
Doors in cross-passages and emergency exits	173	Yes	Yes
Electrical cabinets	1443	Yes	Yes
Containers for electrical equipment in the operation centres inside the tunnel	136	Yes	Yes
Large doors (in tunnels for train operation)	2	No	Yes
Various other doors for air locks, equipment rooms, entrances of tunnels, etc.	>100	No	No
Heating, ventilation, air-conditioning of equipment rooms (HVAC-systems)	12 caverns	No	No
Handrails	56 km	No	No
Signage	3000	No	No
Various stairways, railings, crane systems, false floors	Various	No	No

2 REQUIREMENTS AND BOUNDARY CONDITIONS FOR MECHANICAL EQUIPMENT

The requirements of the mechanical equipment result from various domains:

- train operation in tunnel
- protection of equipment during normal, maintenance and emergency mode
- escape route network
- tunnel ventilation (see Rudin & Crausaz, 2005)
- connection to power supply (50 Hz)
- connection to tunnel and train control system
- civil design
- logistics of installation

In the following, only an overview of the requirements can be given, highlighting the specific requirements of a rail tunnel such as the LBT. Such tunnels are characterised by the following features:

- single track, double tube
- high-speed trains
- mixed traffic (passengers, freight and shuttle trains)
- increased tunnel length
- high rock overburden
- intense traffic load
- stringent occupational health regulations
- increased requirements for fire safety

These boundary conditions apply to various other rail tunnels as well, for example to Brenner, Ceneri, Gotthard, Guadarrama, Koralm, Loetschberg, Lyon-Turin and Pajares which are being planned or built at the moment. However, none of these are in operation yet, i.e. at the beginning of 2007. Some of these boundary conditions are new in comparison to existing long rail tunnels (Channel tunnel, Seikan tunnel, Simplon tunnel) or existing high-speed rail tunnels (e.g. in Japan, France, Germany, Italy, Spain).

The specific boundary conditions of the LBT, which lead to consequences as illustrated with the examples in Table 2, may apply only locally and/or temporarily.

Further to the specific requirements of the Loetschberg project, various other non-tunnel specific requirements need to be fulfilled. However, these will not be further addressed here.

Table 2. Boundary conditions and interacting consequences for mechanical equipment of LBT.

Boundary conditions of LBT	**Consequences for mechanical equipment**
Long tunnel	– Restricted access due to dense traffic – Long distances for installation and maintenance – Limited air-exchange resulting in accumulation of heat, humidity, salt and dust over a long distance
Limited space	– Demand for detailed transport planning and scheduling throughout the rail equipment installation phase and operation phase – Stringent requirements on the logistic and maintenances – Fast replacement of standardised elements necessary (e.g. cabinets)
Limited access for service and maintenance	– As few as possible equipment in tunnel – High availability and reliability of equipment and short maintenance times necessary
Extreme pressure fluctuations due to high speed trains and single-track tunnels	– Robust, pressure-tight elements or pressure compensation in equipment (e.g. for cabinets) – Extreme pressure difference between tubes, i.e. robust design required (e.g. on cross-passage doors)
Extreme temperatures due to heat release from trains (increased traction power in tunnel, many trains), heat release from technical equipment, heat ingress from rock	– Temperature robust design – Passive or active cooling of equipment
Increased humidity due to ingress from tunnel lining, trains and drainage; humidity accumulation due to tunnel length	– Non-corrosive materials – Air-tight design of certain elements
Reduced air-quality (dust and salt accumulation due to tunnel length)	– Design insensitive to dust, salt or pollution
Handling of fire and other incidents	– Fire-resistance or fail-safe behaviour – Requirement for remote monitoring and operation
Tunnel ventilation	– Remote operation of certain mechanical equipment (doors of cross-passage) to provide proper ventilation functionality – Support of ventilation objectives by pressure resistance, reduced leakage rates, etc. – Necessity for doors in rail tunnels – Adapted design of cross-passage ventilation/closures

3 DESCRIPTION OF THE VARIOUS ELEMENTS OF THE MECHANICAL EQUIPMENT

In this chapter, the doors of cross-passages, the large doors in the rail tunnel, the electrical cabinets and the containers for electrical equipment in the operations centres inside the tunnel are described.

3.1 *Doors of cross-passages – Requirements*

At the entrances to the cross-passages, emergency exits and escape tunnels, a total of 173 sliding doors are being installed. Cross-passage doors play an important role among the tunnel equipment elements:

– In the case of emergency operation cross-passage doors provide the interface to the safe non-incident tunnel. Any problems concerning the doors will have a major impact to safety and may harm the escape conditions.
– The doors help to capsulate the cross-passages and to protect all the equipment inside against aggressive and dusty tunnel air.
– The doors provide a safe egress along the escape route, particularly, with respect to taking into account the risks of incidents in one tube and high-speed traffic in the parallel tube. The doors protect maintenance staff.
– The doors support ventilation especially during the emergency operation. The lack of cross-passage doors would cause a major air short-circuit and disable for certain emergency ventilations concepts.
– The doors help to provide adequate climatic conditions in the tunnel system since they prevent

internal re-circulation of warm air within the tunnel.

Hence, the choice of an adequate cross-passage door is of particular importance.

3.2 *Doors of cross-passages – Specifications*

As a consequence of the above mentioned requirements the doors of the cross-passages need to fulfil major specifications as listed in Table 3.

The door system chosen for the LBL is shown in Figure 2.

3.3 *Doors in rail tunnels – Requirements*

Large rail tunnel doors are installed in both tubes of the base tunnel. These allow for the closing of the rail tunnels (partially or completely). Closing the rail tunnel allows the air-exchange conditions inside the tunnel system to be optimally controlled and monitored. This helps to provide a regulated tunnel climate during service and maintenance work.

The following specific functions need to be fulfilled by the rail tunnel doors:

- robust to aerodynamic forces (pressure, wind loads)
- robust to climatic boundary conditions (temperature, etc.)
- highest reliability class for locking of doors (SIL 4), i.e. part of the rail safety equipment
- connected to the tunnel and train control system
- minimum maintenance requirements and complete maintenance possible in "open"-position

3.4 *Doors in rail tunnels – Specifications*

The improper use of doors in rail tunnels may endanger the train traffic significantly. Hence, it has to be ensured imperatively that no rail traffic occurs when the opened door is not locked in the "open"-position or even closed. This safety requirement leads to control systems between the large doors, the door driving system and the train signalling system.

In addition, any door needs at least one separate escape route in order to ensure a safe escape route towards the exterior of the tunnel. This is of major importance, if trains stop in the vicinity of the door.

As a consequence of the above mentioned requirements, major specifications for the large doors need to be fulfilled as listed in Table 4.

The door system chosen for the LBL is shown in Figure 3 and Figure 4.

3.5 *Cabinets in tunnel climate – Requirements*

The cabinets, being exposed to the tunnel climate, contain equipment for the power supply system, working and emergency lighting, data transmission, door controls, fire detection systems, and safety and radio systems. They are mainly placed in cross-passages, which are not air-conditioned. For safety and maintenance reasons all of the electronic equipment will need to be capsulated, hence, it must be installed inside a cabinet.

Cabinets have to fulfil several basic functions, such as:

- fitting different technical equipment inside
- enabling a safe and reliable railway system and operation

Table 3. Major specifications of the doors of cross-passages.

Construction	– Sliding door (one part) mounted inside cross-passage – Pressure resistance 30 kPa in both directions (mainly due to anticipated shuttle trains) – 2 m wide and 2.2 m high in cross-passages (3 m wide in emergency station) – Lock and unlock mechanism working error-free, also during electrical power cuts – Uninterruptible power supply for the driving system and control technology – Reliable operation in a temperature range of $-15°C$ to $45°C$ and sudden temperature changes (partly temporal or local)
Fire protection	– Fire resistance of the door for 90 min (T90) – Reduced heat transfer through door in order to prevent heat-up of cross-passage during fire – Air-tight design to prevent leakage of smoke – Air-tight design to prevent leakage of false air, i.e. unnecessary air-losses of the ventilation system
Maintenance	– Easy replacement for parts suffering mechanical wear – Quick replacement of a whole door should be possible
Operation	– Default position closed and locked – Local and remote controlled door operation (lock and unlock) – Local door operation prioritised – 'Jam protection'; if automatic operation effort exceeds a certain force – Opening and closing time at automatic operation shorter than 15 s – Force to open the door manually <100 N – Position monitoring of the doors – If trains approach at high speed: Doors locked on cross-passage side – If the doors are unlocked or open: Train speed limitation to 40 km/h



Figure 2. Door of cross-passage.



Figure 3. Large door in rail tunnel partly closed.

– protecting electronic equipment against dust, salt, thermal and aerodynamic loads, humidity, smoke and heat
– providing flexibility concerning number and size of cables entering cabinet

For maintenance reasons only one type of cabinet is used in the tunnel (i.e. outside air-conditioned spaces). However, this type is flexible with respect to mounting of different equipment inside and different cooling requirements of the electrical equipment.

The cabinets have to withstand similar climate and aerodynamic conditions as the cross-passage doors, particularly with regards to:

– extreme temperatures, humidity
– rapid variations in the temperature
– dry environment

Table 4. Major specifications of the large doors in rail tunnel.

Construction	– Sliding door (two part) mounted in niches outside free tunnel envelope – Pressure resistance 30 kPa in both directions (mainly due to shuttle trains) – Uninterruptible power supply – Reliable operation in a temperature range of 10°C to 45°C
Fire protection (only if used to separate tubes)	– Fire resistance of the door for 90 min (T90) – Air-tight design to prevent leakage of smoke – Air-tight design to prevent leakage of false air, i.e. unnecessary air-losses of ventilation system
Maintenance	– Easy replacement for parts suffering mechanical wear – Quick replacement possible
Operation	– Default position closed and locked – Local and remote controlled door operation (lock and unlock) – Local door operation prioritised – 'Jam protection'; if automatic operation effort exceeds a certain force (probably a person is jammed)

– train induced pressure variations and wind loads
– high dust and salt concentration and iron particles in the air
– depending on installation and maintenance concept: allowing rapid installation and replacement and repairs outside tunnel

In addition, each cabinet should have different sensors for local and remote signalling of the cabinet internal temperature and humidity, status of air conditioners (if applicable) and the cabinet door status (open, close). In case of exceeding heat or humidity limits, as well as in case of electronic failures, a local and remote alarm shall be provided. Hence, the maintenance staff can rapidly locate the affected cabinet.

3.6 *Cabinets in tunnel climate – Specifications*

Major specifications of the cabinets are listed in Table 5.

Different equipment and temperatures depending on the location in the tunnel lead to different thermal power losses. Additionally, the temperature range for the equipment inside the cabinet might vary. Hence, different ventilation and cooling equipment might be used, preferable at the back of the cabinets.

A deepened socket provides space for a cable entry system. With the deepened socket combined with

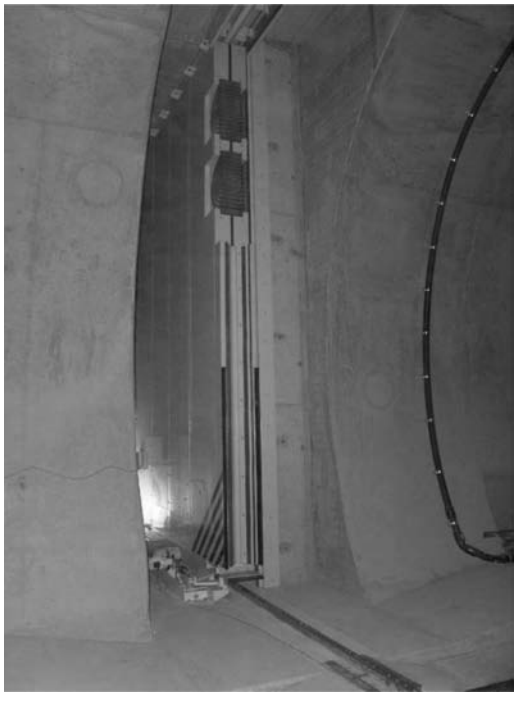


Figure 4. Large door in rail tunnel: Opened door in niche of tunnel.

a flexible system of the cable entry the following mounting procedure can be achieved:

1. installation of socket in cross-passage
2. installation of all cables
3. fitting the cables with plugs
4. placement of cables in sockets and closure of the socket with preliminary cover
5. final installation of cabinet, which is open at the bottom, on the socket and connection of cable plugs with the sockets in the cabinets.

The cabinets chosen for the LBL are shown in Figure 5. The cable entry in the socket mounted in the false floor is shown in Figure 6. The system allows for the pre-installation of cables and sockets before the instalment of the cabinets.

The cabinets were assembled and fitted with the electronic equipment outside the LBL, in order to provide unnecessary site traffic. The cabinets were assembled and pre-tested at a central place.

3.7 *Containers – Requirements*

The mechanical equipment also includes 136 containers, equipped with various control systems, which are installed in the technical caverns. Similarly to the cabinets, the containers protect equipment for the power

Table 5. Major specifications of the cabinets in tunnel climate.

Construction	– Simple and durable construction – Protection against corrosion – 19″ fixtures and fittings to fit standardised equipment – Cabinet dimensions depth/width/height 600/800/2000 mm (including socket) – Single placement on false floor – Maximum pressure loads +/−5 kPa – Air tight design (no filters) – Thermal power loss per cabinet to be specified [kW] – Protection class IP 65
Fire protection	– Temperature control inside – Air-tight design
Maintenance	– Parts suffering by mechanical or thermal wear shall be replaced easily – Simple and fast mounting and exchange procedure – All cable connections by sockets/plugs
Operation	– Simple lock and opening mechanism – Local display of the cabinet interior temperature – Local display of the cabinet interior humidity – Error warning sign exterior of the cabinet (e.g. lamp, diodes, etc.)



Figure 5. Cabinets in cross passage exposed to tunnel climate.

supply system, working and emergency lighting, data transmission, fire detection systems and safety and radio systems. They house the systems required for train control and air-conditioning as well.

Containers have to fulfil several basic functions, such as:

– fitting of different technical equipment inside
– enabling a safe and reliable railway system and operation

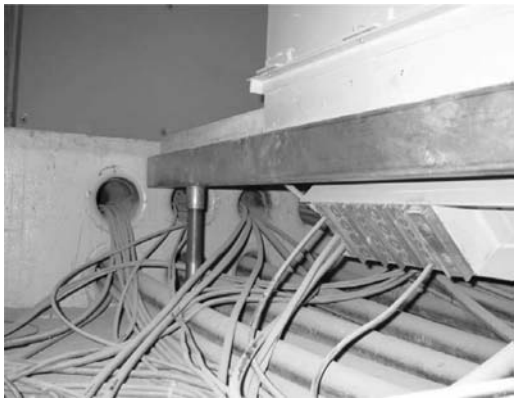


Figure 6. Flexible cable entry system at the cabinet socket.

Table 6. Major specifications of the containers.

Construction	– Simple and durable construction – Transportable 20' ISO-container on road and rail – Different assembly and connection possible – Walls insulated – Pressure resistance ±2.5 kPa – Protection class IP 65 – Equipped with false floor if necessary – Air tight design and air-conditioned
Fire protection	– Fire resistance F30 of walls – Fire extinguishing systems
Maintenance	– Parts suffering by mechanical or thermal wear shall be replaced easily – Simple and fast mounting and exchange procedure – All cable connections by sockets/plugs

– protecting electronic equipment against dust, thermal and aerodynamic loads, humidity and smoke
– providing flexibility concerning number and size of cables entering the container.

For maintenance reasons only one type of container is used in the tunnel.

3.8 *Containers – Specifications*

Major specifications of the containers are listed in Table 6.

The container system chosen for the LBL is shown in Figure 7. A technical cavern where containers are installed is shown in Figure 8.

The containers were manufactured, pre-assembled and equipped outside the tunnel (see Chapter 4.3).



Figure 7. Containers for technical caverns.



Figure 8. Underground technical cavern with containers.

4 SPECIAL METHODOLOGIES AT LBL

Some specialities of the methodology to select, to test and to install the mechanical equipment in the LBL are highlighted in the following sections:

– Prototypes as part of tendering process and evaluation
– Test section in tunnel and tests
– External pre-assembly of equipment in containers and tests in assembly hall
– Management of interfaces of mechanical equipment with other lots (rail equipment, civil, further lots).

4.1 *Prototypes as part of tendering process and evaluation*

In difference to the other equipment, in lots of the mechanical equipment the manufacturing of prototypes was an integral part of the tendering and selection process. The cross-passage doors, the cabinets and the containers were selected in this way. The choice of

the contractor for these elements was organized in 3 stages:

1. Offer for equipment based on written documents
2. Pre-selection of 2 to 3 companies and order to manufacture, deliver and test of prototypes
3. Final selection of company for delivery of the most qualified and economical solution

Reasons for test of prototypes were as follows:

– The components are of major importance for the availability, economy and for the safety of the tunnel system.
– The components are built in large number, i.e. deficiencies of these elements of large number must be firmly excluded.
– Regarding the expected specific boundary conditions in the tunnels of the Loetschberg, no "catalogue solutions" of the above elements (doors, cabinets, containers) existed and experience was lacking.

The objectives for the production of prototypes were:

– to collect systematically suitable solutions for the different elements
– to test selected solutions
– to optimize the prototypes
– to choose from optimized solutions the most economical offer

4.2 *Test section in tunnel and tests*

At a central base point of the LBT, one section of the west tunnel, still at the carcass construction stage, was used as a test section. The test section is hundred metres long. Of this, 62.5 m have the profile of drill and blast excavation and the remaining 37.5 m have the tunnel boring machine profile. The test section also incorporates a cross-passage.

In the test section, the entire interior was applied on a trial basis, in order to obtain important findings on the construction technology and rail technology systems at an early stage. All the constituent elements of the equipment which were finally installed in the tunnel and in the cross-passage were "test installed" in the test section and checked for the installation methodology and ease of maintenance.

4.3 *Pre-assembly of equipment in containers*

The equipment in the technical caverns inside the tunnel was installed in containers, pre-tested and only then installed in the tunnel. Once the rail equipment was installed in the tunnel, it was tested before the actual commissioning work started. Figure 10 illustrates the container installation and assembly of containers for the different technical caverns in the tunnel.



Figure 9. Test section of LBT.



Figure 10. Pre-assembly and installation of equipment in containers in assembly hall outside of the tunnel.

The major advantages of using containers and preparing them outside the tunnel are as follows:

– shortening of actual installation time in tunnel
– allowing tests of various complete electrical systems before installation in the tunnel
– facilitated access to work space – containers of all technical caverns in one hall

4.4 *Management of interfaces to other lots (rail equipment, civil, further lots)*

As in any other complex infrastructure project, civil design, the construction works and the various lots of the technical equipment need to be co-ordinated. This is true for both, the planning and the execution of the works. Since several companies were contracted for the various lots, special measures were required to arrange and control the interface schedules.

Among other measures, an extensive and permanently updated list of interfaces was established. The list identified for example:

– the content of the interface
– the lots being involved
– the responsible lot
– the technical solutions of the interface

During the detail planning phase of the contractors, these several hundred interfaces became systematically addressed and defined. For every single technical interface a document was created stating the technical solution and responsibilities. Each document had to be signed by the two or more contractors who were involved in the interface.

5 CONCLUSIONS

The particular features of modern, long, high-speed, single-track, double-tube rail tunnels lead to new challenging demands for the mechanical equipment being installed in such tunnels.

Technical solutions were found in interdisciplinary teams. Prototypes and extensive tests allowed for a smooth transition from installation to operation of the LBL.

ACKNOWLEDGMENT

The authors wish to thank BLS AlpTransit Ltd for permission to publish this paper.

REFERENCES

Ravn, S. & Reinke P. 2004. Twin tube, single track high-speed rail tunnels and consequences for aerodynamics, climate, equipment and ventilation, *Tunnelling Asia, New Delhi, India*.

Rudin, C. & Crausaz B. 2005. Der komplexe Übergang von der Baulüftung, Ausrüstungslüftung zur Lüftung für den Betriebszustand im LBT, *Swiss Tunnel Congress, Luzern, Switzerland*.

This page intentionally left blank

Underground Space – the 4th Dimension of Metropolises – Barták, Hrdina, Romancov & Zlámal (eds)
© 2007 Taylor & Francis Group, London, ISBN 978-0-415-40807-3

Study on the behavior of smoke from a train fire based on the track gradients in railroad tunnels equipped with a forced ventilation system

D.-H. Kim, Y.-J. Jang & J.-J. Moon
Korea Railroad Research Institute, Kyounggi-Do, Korea

ABSTRACT: This study carried out three-dimensional computerized numerical interpretation for some cases of fire outbreak in tunnels whose inner section measures 70 m^2 and with a 0.75 km extension. Specifically, numerical interpretation was conducted in each of the three cases of varying tunnel gradients after installing and operating a ventilation hole near the entrance and exit of the tunnel under the same conditions.

1 INTRODUCTION

The realignment of railroad tracks and use of the existing railroad lines for the high-speed train service resulted in the growing demand for long railroad tunnels in Korea. A train will likely be unable to get out of a long tunnel in case it catches fire; hence the need to examine the safety of passengers trying to escape in a situation wherein the train stops at a certain location deemed to be most dangerous in the tunnel in case of train fire.

This study sought to derive the design factors for the concept design of new tunnels incorporating disaster prevention facilities such as guide routes, escape routes, service tunnels, etc., through which all train passengers can escape safely from the toxic smoke in case of fire in a tunnel with a track gradient and equipped with a forced ventilation system. The behavior of hot air rising from a fire in a railroad tunnel has been studied intensively by conducting a variety of experiments and computational numerical analysis. Kajiyama and Tanemoto (1998) examined the relationship between the tunnel gradient and speed of hot air in case of fire in a railroad tunnel using model experiments and numerical simulations. On the other hand, Miles & Kumar (1999) verified the results of a full-scale fire experiment conducted on the Memorial Tunnel in the United States through computational numerical analysis and performed research on the behavior of hot air rising in case of fire in road tunnels based on the results. In Korea, Kim et al. (2002) conducted research on the behavior of smoke from a train fire based on the tunnel gradients. Likewise, Lee et al. (2002) conducted at a reduced scale a model experiment on smoke behavior under the influence of natural ventilation in case of fire in a tunnel.

This study examined the behavior of smoke from a train fire in single-bore double-track tunnel whose inner cross section measures 70 m^2 and equipped with a ventilation hole at the 1/5 and 4/5 points of its extension and gradients of −10‰, 0, and +10‰. The examination of smoke behavior per case aimed at understanding the spreading direction of smoke and its characteristics by distance and including them in the design concept of disaster prevention facilities such as escape routes for passengers, etc.

2 SUBJECT TUNNELS FOR THE ANALYSIS AND FIRE SCENARIOS

For the numerical analysis, tunnels whose inner cross section measures 70.0 m^2 and whose design has recently been applied to newly built single-bore double-track tunnels and with a 0.75 km extension (refer to Figures 1 and 2) were considered. Numerical analysis was performed by applying computational fluid dynamics based on the assumption that a fire broke out in a train car on one of the double tracks. Specifically, three-dimensional numerical analysis was performed for the fire simulations on a real-time basis, covering the outbreak of a fire and

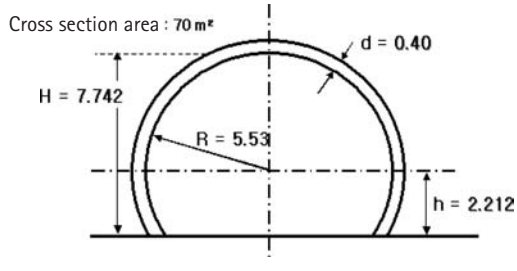


Figure 1. Specifications of the cross sections of the subject tunnels for interpretation.

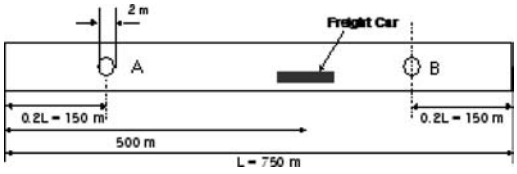


Figure 2. Specifications of the vertical ventilation hole.

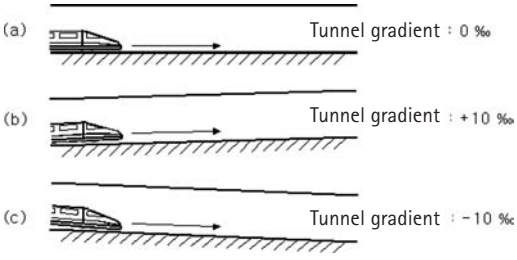


Figure 3. Analysis conditions for tunnel depending on track gradients.

Table 1. Classifications for numerical analysis in tunnel fire.

Classification	Tunnel Extension	Cross Sectional Area	Tunnel Gradient	Operating Condition for the Ventilation Hole
Case 1	0.75 km	70.0 m^2	0‰	A: Air supply B: Air exhaust
Case 2	0.75 km	70.0 m^2	+10‰	A: Air supply B: Air exhaust
Case 3	0.75 km	70.0 m^2	−10‰	A: Air supply B: Air exhaust

its progress given track gradients of −10‰, 0‰, and +10‰ as shown in Figure 3. Table 1 lists the conditions for each case.

The height from the bottom of each subject tunnel to its ceiling was 7.742 m; for purposes of calculation, the concrete lining of its inner wall was assumed to be 0.4 m (Figure 1). The physical properties presented in Table 2 were used for the calculation under the assumption that the inner wall of the tunnel was made of concrete.

2.1 *Source of train fire and heat release rate*

For purposes of calculation, the fire was assumed to have come from a train car located at the 2/3L point from the entrance of the tunnel. Figure 5 shows the specifications of the train fire as used for this study. Ota & Horiuchi's report (2001) suggests a fire-size design of 5 MW for cars, 20 MW for buses/trucks, 30 MW for vehicles used to transport heavy goods, and 100 MW for petroleum tank lorries. Assuming that the fire-size design is the largest for the vehicle

Table 2. Physical properties for numerical analysis.

Classification		Physical Properties
Tunnel Extension		750 m
Air	Density	1.198 kg/m^3
	Viscosity	1.82 × 10^{-5}kg/m·s
	Specific Heat	1000 J/kg·K
	Conductivity	0.02637 W/m·K
Concrete	Density	2300 kg/m^3
	Specific Heat	840 J/kg·K
	Conductivity	1.6 W/m·K
Heat Release Rate		30 MW

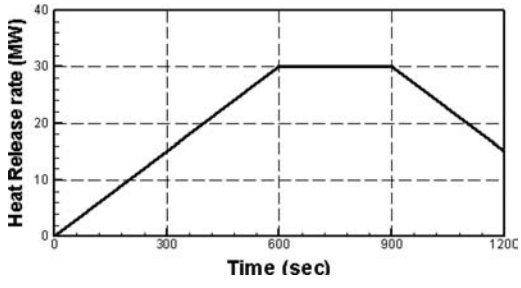


Figure 4. Heat release rate used for numerical analysis.

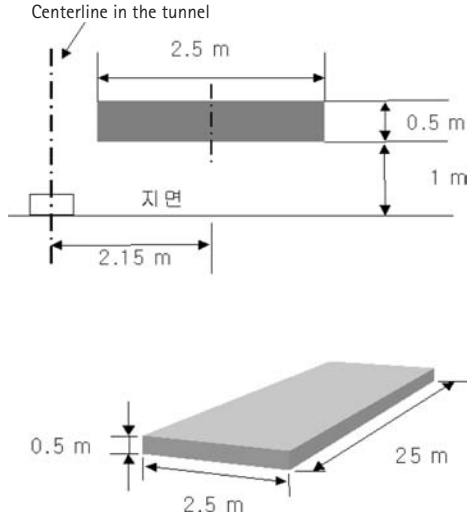
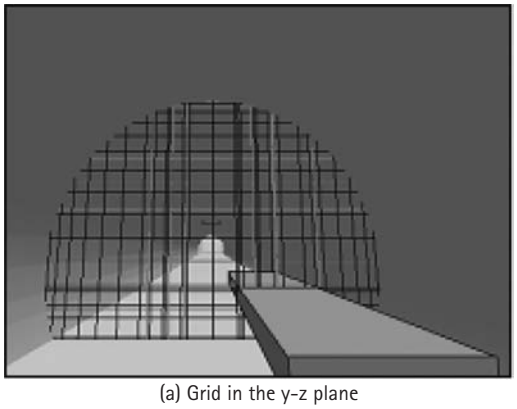
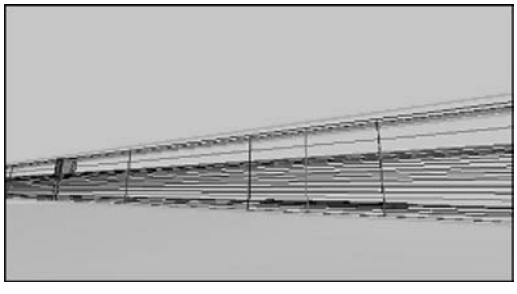


Figure 5. Specifications of the fire source for one unit of train car.



(a) Grid in the y-z plane



(b) Grid in the x-z plane

Figure 6. Grid system used for three-dimensional, computational numerical analysis.

transporting heavy goods, this study assigned a heat release rate of 30 MW for the numerical analysis as shown in Figure 4.

2.2 *TUNFIRE fire simulation code and grid generation*

This study used TUNFIRE Code (2001) the computational analysis program for tunnel fires developed recently by a British fire experiment and research institute. The program enables designing fire safety using the numerical method of computational fluid dynamics for the quantitative prediction of the flame spread and smoke flow in the tunnel.

The same grid system was used for the respective conditions for the numerical analysis of Case 1 ∼ Case 3 (Table 1). Figures 6(a) and (b) show the grid system around the source of the train fire. The direction of x denotes the progress direction of the tunnel, with y and z defined as the directions of its width and height, respectively. The number of grids used for the computational numerical analysis in the entire area of analysis was $46 \times 37 \times 35$, which is equivalent to 59,570.

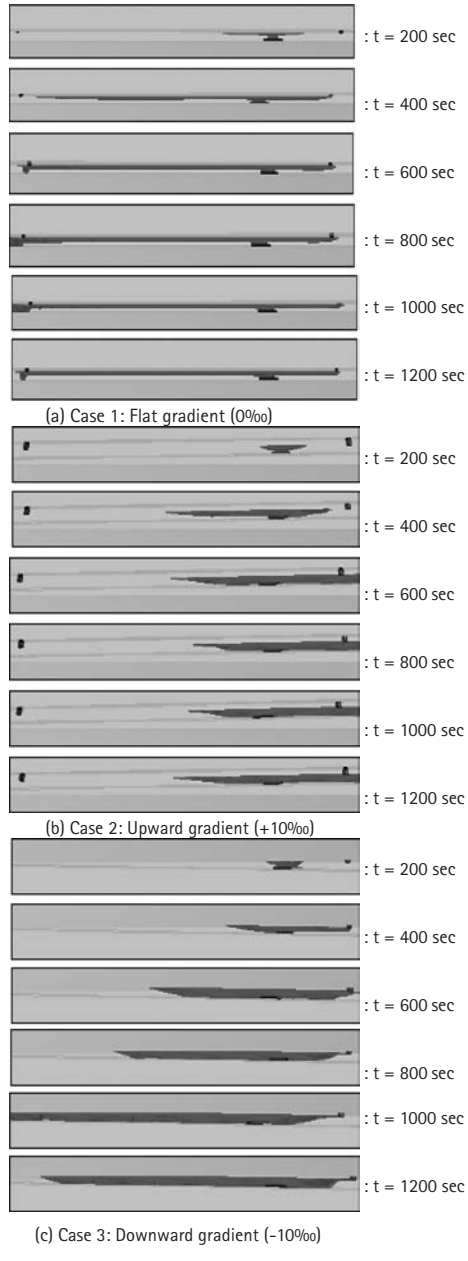


Figure 7. Smoke distribution inside the tunnel over time.

3 RESULTS AND DISCUSSION

The study performed three-dimensional computational simulations for the case wherein a train was unable to get out of the tunnel and was forced to stop inside it after a fire occurred. Figures 7(a) ∼ (c) each show the smoke distribution inside the tunnel on a

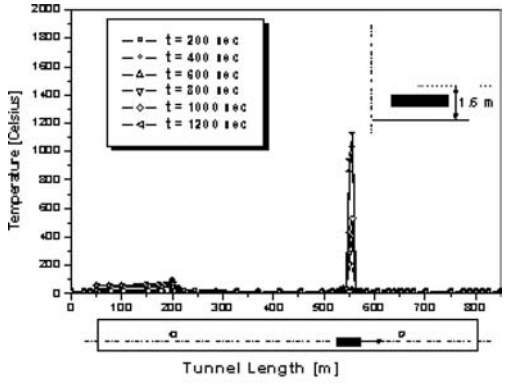
real-time basis following the outbreak of a fire, accounting for the result of each numerical analysis.

Only the distribution of smoke at 65°C or higher is shown in Figures 7(a)∼(c) in accordance with the NFPA (National Fire Protection Association) standards, i.e., exposure to smoke at 65°C for more than five minutes is fatal to the human body. In particular, Figure 7(a) shows the smoke distribution inside a tunnel with a flat gradient over time in case of fire. Note that the smoke consistently spread toward the entrance and exit of the tunnel because of the flat gradient. As shown in the figure above, smoke had already occupied over two thirds of the tunnel 400 seconds after the outbreak of fire and spread to most areas of the tunnel 800∼1000 seconds later. 1200 seconds after the occurrence of fire, however, the amount of smoke decreased. The smoke started to spread around the vertical ventilation hole located at the entrance of the tunnel 600 seconds after the outbreak of fire, suggesting that it spread toward the tunnel ground due to the outside air coming into the tunnel through the ventilation hole in air supply mode. In this case, passengers are likely to feel discomfort when they try to escape through the tunnel entrance due to the smoke spreading from the entrance area to the entire section of the tunnel. Figure 7(b) shows the smoke distribution inside a tunnel with an upward gradient of +10‰ over time in case of fire. Note that most of the smoke spread toward the exit of the tunnel under the influence of the upward gradient, starting to move down to the ground near the fire source around the tunnel exit 400 seconds after the outbreak of fire and to the ground almost everywhere around the exit 600 seconds later. On the other hand, minimal smoke spread toward the entrance not only because of the upward gradient but also due to the vertical ventilation hole in cool air supply mode installed at the entrance. Specifically, the outside cool air coming into the tunnel through the ventilation hole pushed the smoke toward the exit. In this case, if a jet fan is installed in the middle of the tunnel, an escape route can be easily secured at the entrance. As shown in Figure 7(c), a much larger amount of smoke spread toward the exit under the influence of the downward gradient. 400 seconds after the outbreak of fire, the smoke had already moved down near the ground in the direction of the entrance, moving down slightly to the middle height of the tunnel in the direction of the exit. 600 seconds later, the smoke moved down to the ground both before and behind the fire source and continued to spread toward the entrance and exit of the tunnel. Note, however, that the smoke already moved down to the ground and continued to spread almost everywhere toward the entrance 400 seconds after the outbreak of fire, moving down to the ground in only a small area toward the exit. The distribution area of smoke at more than 65°C near the tunnel entrance gradually decreased 1000 seconds after the outbreak of fire. Therefore, if a downward gradient is installed, the ventilation hole at the entrance should be set to air exhaust mode instead of air supply mode.

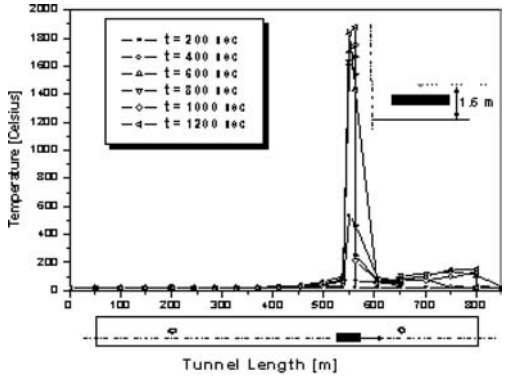
Figures 8(a)∼8(c) each show the temperature distribution inside the tunnel over time in case of fire for each case. The reference point for the temperature comparison was the point 1.6 m high from the ground, i.e., the tunnel bottom, passing the center of the track where the fire source was located. Note that the height for temperature comparison was set at 1.6 m based on the assumption that the average breathing height of Oriental people is 1.6 meters. Figure 8 (a) shows the temperature distribution inside a tunnel with a flat gradient. As shown in Figure 7(a), the temperature distribution was relatively low everywhere at a height of 1.6 m from the tunnel bottom except around the fire source owing to the minimal smoke moving downward. Note, however, that the temperature of about 100°C was distributed between the tunnel entrance and the ventilation hole, possibly due to the spread of smoke under the influence of air coming through the ventilation hole (Figure 7 (a)). Figure 8 (b) shows that the temperature around the tunnel exit was much higher than that around the tunnel entrance. In particular, the temperature around the fire source was about 2000°C, although an almost normal temperature was distributed around the entrance of the tunnel. As shown in Figure 8(c), the temperature around the tunnel entrance was much higher than that around the exit due to the influence of the downward gradient. 400 seconds after the outbreak of fire, the temperature around the fire source was about 2100°C; around the exit of the tunnel, smoke at high temperature spread by moving along the tunnel ceiling before it was released from the tunnel through the ventilation hole. In this case, the temperature fell, resulting in the distribution of an almost normal temperature. Around the entrance of the tunnel, high temperature (about 200°C) was distributed up to the ventilation hole area through which outside air entered, contrary to the tendency shown in Figure 8(b) wherein distribution at about 200°C was concentrated around the exit due to the influence of the tunnel gradient.

Figures 9(a)∼(c) each show the concentration distribution of carbon dioxide (CO_2) inside the tunnel over time in case of fire for each case. Note that the same reference point for comparing the temperature was used to compare the concentration distributions of carbon dioxide, i.e., 1.6 m from the ground. A carbon dioxide concentration of 4.3% or higher is considered hazardous to the human body as shown in Feizlmayer (1976).

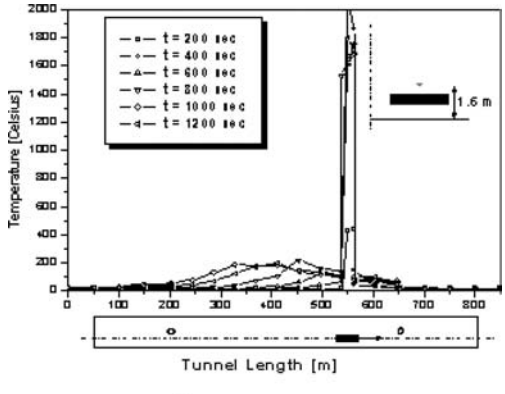
Figure 9(a) shows the concentration distribution of carbon dioxide produced from a fire makes up about 1% of the entire tunnel in case of the flat gradient of a tunnel. As shown in Figures 7(a) and 8(a), smoke did not move downward to the height of 1.6 m from



(a) Case 1 : 0 ‰

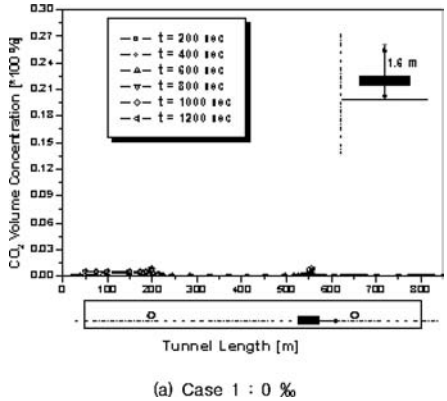


(b) Case 2 : +10 ‰

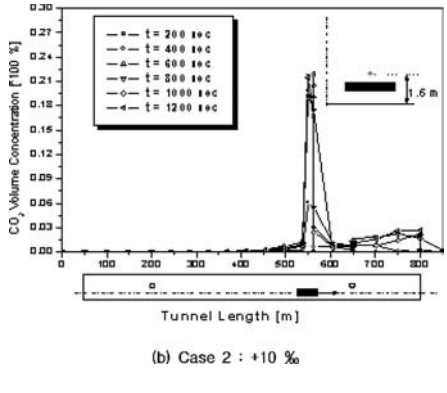


(c) Case 3 : -10 ‰

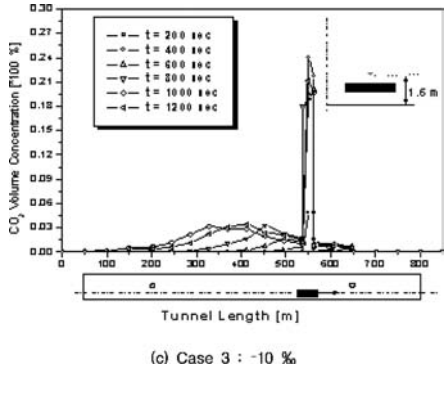
Figure 8. Temperature distribution inside the tunnel over time.



(a) Case 1 : 0 ‰



(b) Case 2 : +10 ‰



(c) Case 3 : -10 ‰

Figure 9. Concentration distribution of carbon dioxide (CO_2) inside the tunnel over time.

the ground 1200 seconds after the outbreak of fire in the tunnel with a flat gradient. Carbon dioxide concentration was slightly over 20% around the fire source in the tunnel with the upward gradient (Figure 9(b)); note, however, that the temperature distribution was about 3% around the tunnel exit due to the influence of the upward gradient. For the tunnel with a downward gradient as shown in Figure 9(c), carbon dioxide distribution tended to be similar to that in the tunnel with an upward gradient around the fire source. Around the tunnel entrance, however, carbon dioxide distribution was about 4%, which was the opposite of the case of

the tunnel with an upward gradient. Therefore, for tunnels with gradients installed based on the results of the abovementioned numerical interpretations, there is a need to set up an escape route in the direction of the entrance in the case of a tunnel with an upward gradient and in the direction of the exit in the case of a tunnel with a downward gradient. This way, loss of lives can be minimized.

4 RESULTS AND DISCUSSION

This study carried out three-dimensional computerized numerical interpretation for some cases of fire outbreak in tunnels whose inner section measures $70\,m^2$ and with a 0.75 km extension. Specifically, numerical interpretation was conducted in each of the three cases of varying tunnel gradients after installing and operating a ventilation hole near the entrance and exit of the tunnel under the same conditions.

First, in terms of the smoke behavior based on the tunnel gradient, more smoke was found to spread toward the tunnel exit due to the effect of buoyancy in the case of the upward gradient (+10‰). Likewise, the smoke moved down to the tunnel bottom faster around the exit than around the entrance. In the case of the tunnel with a downward gradient (−10‰), however, a lot of smoke spread toward the tunnel entrance. Moreover, a lot of toxic gas was distributed around the entrance rather than the exit of the tunnel. In addition, this study found that smoke usually moved down to the tunnel ground 400∼800 seconds after the outbreak of fire. Carbon dioxide (CO_2) distribution also reached a height of 1.6 m from the ground, which is the breathing height of passengers.

This study applied the same ventilation conditions for air supply and exhaust to the two ventilation holes, i.e., one installed at the tunnel entrance and the other at the tunnel exit. In the case of the tunnel with a flat gradient, smoke was likely to have spread already throughout the tunnel 600 seconds after the outbreak of fire due to the air entering through the ventilation hole at the entrance; thus possibly hindering passengers from escaping out of the tunnel. In case of the tunnel with an upward gradient, however, the air entering through the ventilation hole at the entrance prevented the smoke from spreading toward the entrance, thereby helping passengers escape out of the tunnel.

During a train fire inside a tunnel, the most serious problem is about the ventilation of toxic smoke generated from the fire. The results of the three-dimensional computational numerical interpretations imply that the movement of smoke and toxic gas in a tunnel with a gradient varies based on the direction of the gradient. Based on such information, how an escape route should be set up in the tunnel can be predicted.

The results of this study suggest the need to equip each tunnel with ventilation and smoke control equipment suitable for its conditions as well as to develop ways of securing a proper time period for passengers to escape safely from the tunnel in case of a train fire.

REFERENCES

Feizlmayer, A. H. 1976. Research on Tunnel Fire in Austria. *Second International Symposium on the Aerodynamics and Ventilation of Vehicle Tunnels, paper J2, pp. 19∼40, March.*

Jasmine, A. 2001. 3-D CFD Smoke Movement (TUNFIRE). *General Manual, KWC Fire Dynamics Research Centre.*

Kajiyama, H. & Tanemoto, K. 1998. Behavior of smoke and hot gases in a long railway tunnel: a literature review, *RTRI REPORT* Vol.12, No.12, Dec.

Kim, D.H., Moon, J.J. & Shin, M.H. 2002. A study on the behavior of smoke from train fire based on the track gradients inside double-track tunnels, *Journal Academic Presentation Meeting of the Korean Society of Civil Engineers*.

Lee, S.R., Park, Y.T., Kim, C. I. & Yoo, S. H. 2002. An experimental study on the smoke behavior based on natural ventilation in case of a tunnel fire, *Thesis Collection of Equipment Engineering, Vol. 14, No. 3, pp. 247 ∼ 253.*

Miles, S. & Kumar, S. 1999. CFD modeling fires in longitudinally ventilated tunnels.

Ota, Y. & Horiuchi, K. 2001. Thermal analysis for tunnel structures in case of fire, *Proceedings of the Fourth International Conference on Safety in Road and Rail Tunnels, pp. 151–160, 2–6, Madrid, Spain, April.*

Underground Space – the 4th Dimension of Metropolises – Barták, Hrdina, Romancov & Zlámal (eds)
© 2007 Taylor & Francis Group, London, ISBN 978-0-415-40807-3

An experimental study on the tunnel pressurization for smoke control

A. Lee, Ho Seok
Building and Tunnel Technologies. Inc, Seoul, Korea

B. Oh, In Seok
Esco Consultants, Seoul, Korea

C. Lee, Kun Chai & Kim, Won Keun & Kim, Woo Joon
Daelim Industrial Co., LTD, Seoul, Korea

ABSTRACT: In road tunnel safety design, most important factor is safe evacuation of people. In case of road tunnel fire, for the sake of smoke control ventilation fan must be operated. But in such a case cross passage doors are opened for egress to opposite tunnel, tunnel pressure balance easy to break. So this phenomenon cause failure of smoke control or smoke influx to opposite tunnel through cross passage. To avoid this phenomenon proper smoke control fan operating mode must be developed. Generally, it is difficult to estimate of tunnel pressure distribution curve by calculation on various cases. In this study, an experimental method is used to assess the proper fan operating mode. This result will use effectively in long tunnel smoke control system by basic data.

1 INTRODUCTION

Road construction is important part of nation's industrial competition. So, new road construction is occurred consequently. Tunnel occurs by a road network expansion. With this fact, it is coming to be long by excavation technique and maintenance management technique gradually.

As length of tunnel is longer, frequency for fire accident in tunnel is coming to be increased. Tunnel fire accident is brought about serious material-human damage. When initial countermeasure and fire preventing equipment is insufficient, social expense loss will come to be increased.

If fire break out in tunnel, evacuation of drivers or passenger occur firstly, and fire extinguishing works is progressed.

If fire were to break out in tunnel, for the sake of safe escaping uni-directional traffic tunnel, cross passages are installed every 200–300 m. Fire door should be equipped as a cross passages. Generally, cross passages are classified with two types; for only passenger, for vehicles and passengers.

In case of fire accident, safety designer must assumed that all fire door behind of fired car will opened to escape to opposite tunnel. With this situation, pressure balancing could be broken because both tunnels are connected with each other. Also fans in fire tunnel are operated to evacuation of passenger safety, and opposite tunnel fans are operated for prevent a fire smoke inflow.

When fans in opposite tunnel operate for pressurization, there is a possibility of fire smoke inflow. It is necessary to prevent a smoke control mode to prevent a smoke inflow to opposite tunnel.

The purpose of this study is to develop a smoke control mode system through the scale model test.

2 FIRE SAFETY DESIGN IN TUNNEL

2.1 *Smoke movement in tunnel*

In such case that fire accident of running vehicles in uni-directional road tunnel is occurred, the initial smoke flows to running direction of vehicles. If ventilation fans should be stopped, inertia force of air movement will lower after the lapse of time, and smoke should be divided to bi-directional flows.

The back-layering velocity of smoke is varied according to slope, tunnel cross-section and fire heat release rate. As fire heat release rate is larger over time, also back-layering velocity of smoke is faster.

The smoke what flows upper part of tunnel crown that goes down to bottom of tunnel by both heat loss and a turbulent flow, and to height of breath level.

An appropriate control is to regulate the smoke so that passenger could escape safety and to prevent a smoke inflow in opposite tunnel.

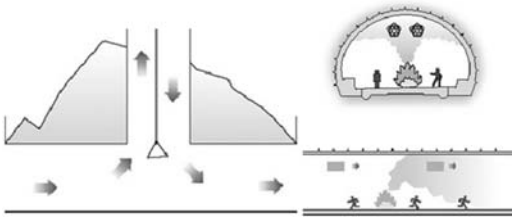


Figure 1. Longitudinal system.

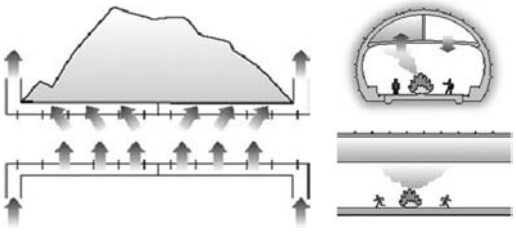


Figure 2. Transverse system.

2.2 *Smoke control system*

The effective smoke control is accomplished controlling through sufficient air volume and pressure. The smoke control must use mechanical equipment. Also long tunnel generally is furnished by operating fan for normal ventilation. Accordingly this ventilation fan is also used to smoke control.

Therefore there is correlation between smoke control system and ventilation method of tunnel. Consequently it uses method of smoke extraction or smoke control is used to type of ventilation system.

2.2.1 *Longitudinal system*

Longitudinal system is method that itself of tunnel is used for smoke moving pathway. If fire accident occurs, main evacuate direction is backward of running direction of vehicles. Also control direction for fire smoke has a same direction of vehicles. Namely, passengers must evacuate to entrance of tunnel, and smoke will be extracted to opposite direction.

2.2.2 *Transverse system*

Transverse/Semi-Transverse System is method that the duct of tunnel crown is used for movement of smoke. When fire break out, transverse system can use a duct port for smoke extraction, so smoke path-way is duct itself. The passengers can evacuate through both side.

3 MODEL EXPERIMENT

3.1 *Characteristic of model experiment*

It's very important to understand that how fire grows in tunnel fire. For the purpose of predict fire condition, full-scale test, model test, and numerical methods are available. Full-scale test is restricted actually. Accordingly, model test can be a best method to predict, and proper method to measure an inside pressure distribution, in safety design.

Such as model test need to be applied right scaling rule to output the correct data. And it is important to install a measure-sensor on the proper point to observe airflow.

Table 1. Applied specification in the scaled model.

Item	Actual size	Scaling size
Extension (m)	880 m(220 m × 4 blocks)	17.6
Cross section (m^2)	72.03	0.028812
HRR	30 MW	1.70 kW
Velocity (m/s)	3.17	0.448
Time proportion	7.07 sec	1.00 sec

3.2 *Scaling*

3.2.1 *Scaling of heat release rate*

The model and full-scale heat release rates Q_{model} and $Q_{full\text{-}scale}$ are related by eqn(1)

$$\frac{Q_{model}}{Q_{full-scale}} = \left(\frac{L_{model}}{L_{full-scale}}\right)^{5/2} \quad (1)$$

Where H_{model} and $H_{full\text{-}scale}$ are the respective length scales, in this case the heights of the model and full-scale tunnels. It is relatively easy to see that the scaling must have this form if one considers the low velocity limits. In this case, dimensional arguments suggest that the distance from the fire at which the temperature takes a given value is proportional to $Q^{2/5}$.

3.2.2 *Scaling of velocity*

The model and full-scale inlet velocities V_{model} and $V_{full\text{-}scale}$ are related by eqn(2)

$$\frac{V_{model}}{V_{full-scale}} = \left(\frac{L_{model}}{L_{full-scale}}\right)^{1/2} \quad (2)$$

3.2.3 *Geometrical scaling*

In this study, the scale of reduced scale model is applied to 1/50.

3.3 *Test model and condition*

3.3.1 *Test model*

In this study, production of model and installation of measuring instrument is composed by Figure 1.

Sensors are adopted anemometer, thermocouple, manometer in this model.

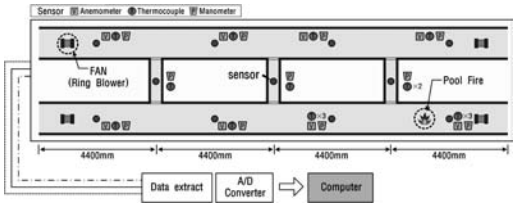


Figure 3. Description of model.

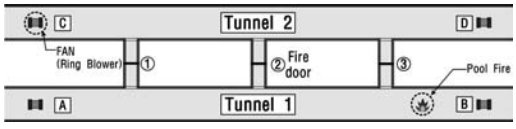


Figure 4. Description of test.

Table 2. Case of test.

	Test condition					
					Fire door	
Case	Tunnel 1		Tunnel 2		①	②	③
1	A:→	B:→	C:×	D:×	closed	closed	closed
2	A:→	B:→	C:×	D:←	closed	closed	opened
3	A:→	B:→	C:→	D:←	closed	opened	closed
4	A:→	B:→	C:→	D:←	opened	opened	opened
5	A:×	B:×	C:→	D:←	opened	opened	opened

3.3.2 *Realization of fire situation*

VVVF inverter(Variable Voltage Variable Frequency Inverter) is applied to control inside velocity of tunnel, which can control an aim velocity exactly. In this experiment, the fire source is applied by Pool Burner which fuel is gasoline. And burning efficiency of fuel is 0.7. It is because that the evaporated fuel doesn't burn in 100%.

4 RESULTS

4.1 *Experiment case*

When the fire breaks out, normal fan operating system can has a possibility that happen to smoke inflow opposite tunnel. Accordingly, experiment cases are selected to prevent smoke inflow to opposite tunnel 1 by the pressurization effect the experiment cases are selected.

4.2 *Case 1*

Fire on/off test is done under all fire doors closed to estimate how much pressure rise by fire in tunnel.

According to experiment results, when the fire break out, pressure is higher than opposite tunnel 1.

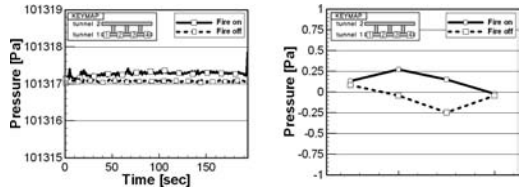


Figure 5. Tunnel pressure of Case 1.

Table 3. Pressure data of Case 1.

Pressure [pa]	1	2	3	4
Tunnel 1	0.1332	0.2733	0.1515	−0.0206
Tunnel 2	0.084	−0.0423	−0.247	0.0432

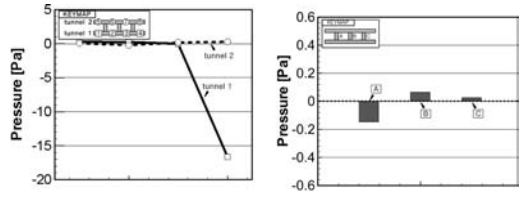


Figure 6. The tunnel pressure of Case 2.

Table 4. The pressure data of Case 2.

Pressure [pa]	1	2	3	4
Tunnel 1	0.2966	0.2437	−0.024	−16.6356
Tunnel 2	0.0706	−0.2254	0.188	0.2856

Table 5. The pressure difference data of Case 2.

Pressure [pa]	A	B	C
Pressure Difference	−0.1499	0.0642	0.0259

It's because of heat buoyancy made by fire. If it has opened doors, it suppose that smoke can inflow into opposite tunnel.

4.3 *Case 2*

Fan D is operated operation under fire door ③ opened in order to prevent spreading smoke into opposite tunnel. In order to know of smoke controlling capability, this test are performed.

According to the experiment result, pressure difference where both side of opened fire door ③ is 0.0259[pa]. The smoke spreading is stopped. It's

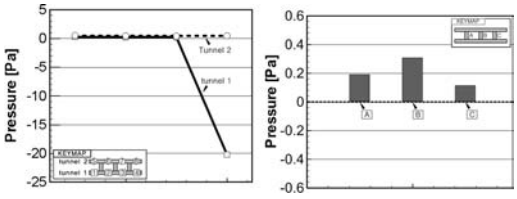


Figure 7. The tunnel pressure of Case 3.

Table 6. The pressure data of Case 3.

Pressure [pa]	1	2	3	4
Tunnel 1	0.2716	0.2404	0.2498	−20.1893
Tunnel 2	0.5159	0.4551	0.4368	0.466

Table 7. The pressure difference data of Case 3.

Pressure [pa]	A	B	C
Pressure Difference	0.1901	0.3073	0.1143

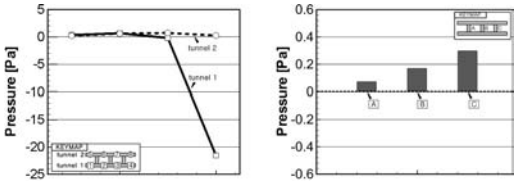


Figure 8. The tunnel pressure of Case 4.

because that the pressure in opposite tunnel is a little high.

4.4 *Case 3*

Fan C and D is operated pressurization under fire door ② opened in order to prevent spreading smoke into opposite tunnel. It's in order to know whether the fan can prevent smoke spreading into ② fire door.

In order to maximize of tunnel pressure, new fan operating mode is tested. Namely it is operated to fire point of tunnel both side.

The differential pressure through cross passage is 0.3073[pa]. Accordingly smoke inflowing is prevented. Because of pressure in tunnel 2 is higher than tunnel 1.

4.5 *Case 4*

All of cross passage is opened. And then Fans are operated pressurization.

Table 8. The pressure data of Case 4.

Pressure [pa]	1	2	3	4
Tunnel 1	0.3468	0.6726	−0.1821	−21.5364
Tunnel 2	0.2351	0.6135	0.7336	0.2519

Table 9. The pressure difference data of Case 4.

Pressure [pa]	A	B	C
Pressure difference	0.0718	0.1697	0.2975

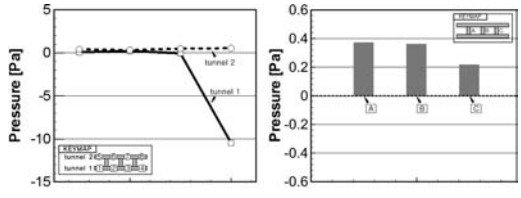


Figure 9. The tunnel pressure of Case 5.

Table 10. The pressure data of Case 5.

Pressure [pa]	1	2	3	4
Tunnel 1	0.0687	0.2159	−0.0572	−10.4422
Tunnel 2	0.4098	0.3166	0.4873	0.5363

Table 11. The pressure difference data of Case 5.

Pressure [pa]	A	B	C
Pressure Difference	0.3733	0.3629	0.2187

The pressure difference the opened fire doors is measured positive. So it is estimated that opposite tunnel pressure is higher than tunnel 1. Therefore smoke doesn't spread to opposite tunnel.

4.6 *Case 5*

Case 5 is assumed that fan in tunnel 1 can't be operated. And opposite tunnel fan is operated the pressurization under all cross passages are opened.

The smoke back-layering occurs constantly. Because the fired tunnel fans can't be operated. But, the possibility of smoke spreading is few. Due to the pressure is more than opposite tunnel.

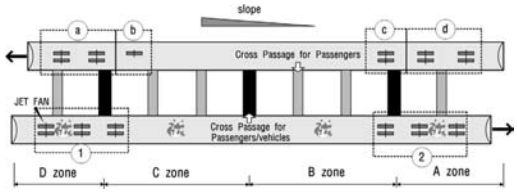


Figure 10. Description of fan operating matrix.

Table 12. Operating matrix 1.

Fire Zone	Fire tunnel ①	Fire tunnel ②	Opposite tunnel a	Opposite tunnel b	Opposite tunnel c	Opposite tunnel d
A	→	→	×	×	×	←
B	→	→	→	→	→	←
C	→	→	→	×	×	←
D	→	→	→	×	×	×

4.7 *Result of experiment*

The road tunnel fire model experiment is performed by many cases of scenario. The purpose of this test is to select and examine the pressurization mode.

It is examined that the differential pressure of cross passage to establish basic data. When it is pressurized by control operating mode, the differential pressure is accomplished. Accordingly, the smoke spread toward opposite is prevented.

Fire experiment is performed for various fire scenario. And the smoke flow is estimated by these fire scenarios.

Finally, the level of differential pressure which is made by pressurization is different by the length between cross passage and fan.

5 FAN OPERATING MATRIX

On the base of these test results, fan operating matrix for smoke control are developed by fire zone in tunnel. And these operating matrix can prevent of smoke spread through cross passage, so it is possible to escape to safety area.

5.1 *Fan in fired tunnel: able to operate*

This operating matrix is supposed that the fan in fired tunnel is not operated.

Table 13. Operating matrix 2.

Fire Zone	Fire tunnel ①	Fire tunnel ②	Opposite tunnel a	Opposite tunnel b	Opposite tunnel c	Opposite tunnel d
A	×	×	→	×	×	←
B	×	×	→	×	×	←
C	×	×	×	←	←	←
D	×	×	→	→	←	←

5.2 *Fan in fired tunnel: unable to operate*

It is supposed that the fan in fired tunnel can not be operated. Namely, this matrix is composed that is only using fan in opposite tunnel.

6 CONCLUSION

Experimental fire test study carried out to establish proper fan operating mode to prevent a smoke spread to opposite tunnel. Results of this study are as followed;

In order to analyze a pressure distribution of tunnel in case of vehicle fire, Scaled model test are used.

Owing to buoyancy effect of fire, pressure of fired tunnel is higher than other tunnel. So in order to prevent a smoke inflow to opposite tunnel, higher pressure are necessary than fired tunnel. As Pressure in tunnel is changeable due to fire-time situation, through various tests, analyzing is performed in case of various pressure patterns.

As a result of this test, fan operating matrix which satisfies the condition is developed. On the base of these results, fan operating matrix guidelines for road tunnel are developed. And this matrix can be adapted in road tunnel safety design and maintenance.

REFERENCES

SFPE Handbook of Fire Protection Engineering(3rd Edition), 2004.

Recommendations of the group of experts on safety in road tunnels, UN Economic and Social Council, 2001.

Ingason, Haukur., *"An overview of Vehicle Fires in Tunnels"*, SP Swedish National Testing and Research Institute, Sweden.

Ingason, H., Gustavsson, S. and Dahlberg, M., *Heat Release Rate Measurements in Tunnel Fires*, SP Report 1994:08, Swedish National Testing and Research Institute.

Fire in Transport Tunnels: Report on full-scale tests, EUREKA-Project EU499;Firetun, Studiengesellschaft Stahlanwendung elV.D-40213 Dusseldorf,1995.

Underground Space – the 4th Dimension of Metropolises – Barták, Hrdina, Romancov & Zlámal (eds)
© 2007 Taylor & Francis Group, London, ISBN 978-0-415-40807-3

Effectiveness of critical velocity method for evacuation environment in a railroad tunnel at fire situation

Seung-Chul, Lee[1], Seung-Ho, Lee[2], Jae-Heon, Lee[3]
[1] *School of Fire and Disaster Prevention, Samcheok National University, Samcheok, Korea*
[2] *Dept. of Civil Engineering, College of Science and Engineering, Sangji University, Wonju, Korea*
[3] *School of Mechanical Engineering, College of Engineering, Hanyang University, Seoul, Korea*

ABSTRACT: The effectiveness of one dimensional critical velocity method for evacuation environment at 10MW fire size in a railroad tunnel has been investigated in this paper by three dimensional CFD method. It was performed to evaluate the evacuation environment in terms of temperature distribution, visible distance distribution and CO concentration at some tunnel inlet velocity, 1 m/s, 2 m/s(near critical velocity), and 3 m/s. At all inlet velocity, passenger should give away downward the flow direction because the inlet velocity can not afford to sufficient evacuation environment for passengers. In case of 3 m/s inlet velocity, however, the evacuation environment for passengers is better than the other cases. To provide more safe evacuation environment on fire situation, tunnel inlet velocity should be larger than critical velocity.

1 INTRODUCTION

Korea is a country surrounded by sea on three sides. Approximately 70% of its land is steep mountainous with great geological variation. Tunnels play an important role in developing new road networks and the number of road tunnels in Korea has continually increased rapidly over many years. This is because of recent developments of road networks through mountainous ranges, and also because of the reduction of tunnel construction costs. In addition, with improving construction technology, tunnels have been adopted as an increasingly cost-effective engineering solution to traverse urban areas with minimum local environment impact.

Fires in tunnels occur no more often than elsewhere, but because of the restricted space and enclosed atmosphere, the consequences can be far more severe. Indeed, a fire may result in extremely damaging situations (e.g. Channel Tunnel fire) or even dramatic events, such as the fire which occurred in March 1999 in the Mont-Blanc Tunnel.(1–3)

When a fire occurs in a tunnel, the most hazardous factor for the users is not fire itself, but the combustion smoke is likely to spread into the tunnel rapidly. That smoke will reduce visibility and can cause deaths by asphyxiation.(4,5)

In case of a fire in a tunnel, the major concern then consists in controlling the smoke propagation by using the ventilation systems set up in the tunnels as efficiently as possible. The essential objective of fire ventilation in tunnels with longitudinal ventilation systems is that of ensuring smoke-free conditions throughout the tunnel cross-section upstream the fire to permit safe escape and rescue of persons and safe fire-fighting. With an inadequate air velocity, however, the smoke layer would also spread against the direction of air flow. A minimum air velocity must be assured, in order to avoid this. Knowledge of such so-called critical air velocities is therefore necessary for planning and design of the fire ventilation in tunnels. Wu etc(6). carried out experimental tests of tunnel fires using tunnels of different cross sections. They reported that different cross sections of tunnel have a small effect on critical velocity. Also, Tetzner(7) etc. pointed out the error for critical velocity equation by Kennedy(8) and proposed beta coefficient, which make up for the weak points in its equation. In case of a fire in a tunnel, however, it is important to consider the distribution of air flow, temperature and smoke in evacuation environment.

Therefore, the purpose of this paper is to identity the availability of one dimensional critical velocity method applied in design of disaster prevention system using three-dimensional Computational Fluid Dynamics. And then we would evaluate that the ventilation equipment designed by the critical velocity equation ensure the safe evacuation environment of passengers throughout the distribution of air current, temperature, visible distance and harmful gas.

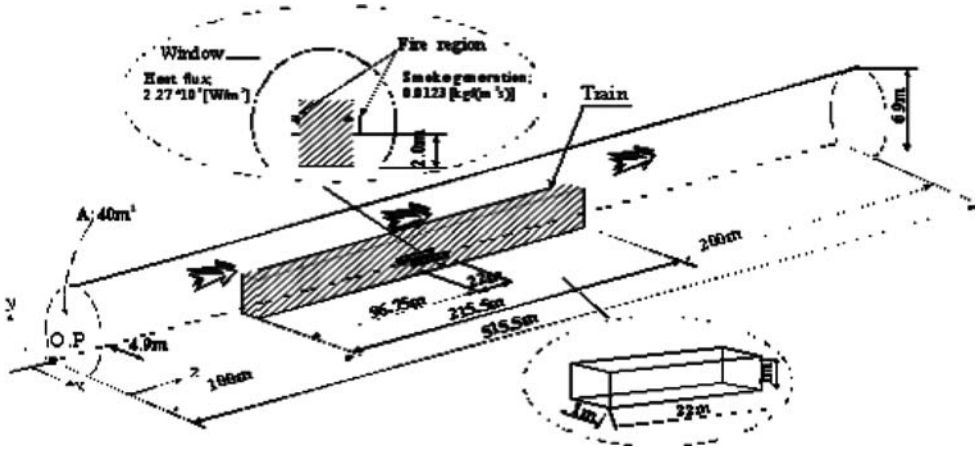


Figure 1. Approximation of tunnel model.

2 THE SAFETY STANDARDS OF EVACUATION ENVIRONMENT

This study checked the safety by applying following details considering foreign standards because there is no Korean standard for stability of evacuation environment.

(i) Air temperature: It must be sustained average temperature below 60∼80°C[9,10] for safe evacuation of passenger. And it must be sustained average temperature below 49°C for the case below 60°C within maximum some seconds or after the lapse more than 6 minutes.[11]

(ii) CO concentration: It must be sustained the density below 200 ppm within maximum some seconds, 1500 ppm within 6 minutes, 800 ppm within 15 minutes and 50 ppm after 15 minutes.[11]

(iii) Visible distance: It must be able to distinguish at least 10 m of wall and door.[11]

3 ANALYSIS MODEL

To investigate the inside environment of railroad tunnel by a train fire in this study it analyzed the case that the train of 210 m stopped by fire as shown in Figure 1. For convenience, it set the origin point to the lower left of the figure, the z-axis to the moving direction of the train, the x-axis to the bottom of tunnel, the y-axis to the height. The entrance of tunnel is the lower left of the figure. The fresh air is flowed into the tunnel through the entrance by the ventilation system. The cross section area of tunnel, A is 40 m^2, the height of tunnel, H is 6.9 m and the hydraulic diameter D_h is 6.88 m. The analytical range is total 515.5 m inclusive of train length[gear train(22 m) + passenger train(176 m) + power train(17.5 m)] and 200 m of the front and 100 m of the rear. The center position of the both windows in fired train is 2.5 m away from y-axis and 207.75 m away from z-axis. And the cross section area of that is 22 m^2. The heat of 10 MW fire size is delivered into the tunnel through the both windows of train in constant heat flux. It assumed the smoke is generated from the virtual volume space of 22 m^3 adjacent to the both windows.

4 THE COMPUTATION OF ONE-DIMENSION CRITICAL VELOCITY

It serves the evacuation of the passenger by sending the fresh air to fired space at fire situation. The phenomenon which the fresh air returns to the inflow direction names back layering. And that is unsafety. The minimum of inflow velocity to prevent back layering names critical velocity, and following equation is the computed equation of Kennedy's one-dimensional critical velocity $V_c^{(8)}$ that applies generally.

$$V_C = K_g\left(\frac{gHE}{Fr_C \rho_\infty c_P A T_f}\right)^{1/3} \quad (1)$$

$$T_f = \frac{E}{\rho_\infty c_P A V_C} + T_\infty \quad (2)$$

$$K_g = 1 + 0.0374\gamma^{0.8} \quad (3)$$

A : cross section area of tunnel [m^2]
C_p : specific heat of air [J/(kg·k)]c
E : fire size [W]
Fr_c : critical Fr number [4.5][12]
g : acceleration of gravity [m/s^2] Fr_c
H : height of tunnel [m]
ρ_∞ : air density except fire range [kg/m^3] k_g

This page intentionally left blank

Table 1. Governing equations.

Continuity equation;

$$\frac{\partial}{\partial \chi_i}(\rho u_i) = 0$$

Momentum Equation;

$$\frac{\partial}{\partial x_i}(\rho u_j u_i) = -\frac{\partial p}{\partial x_i} + \frac{\partial}{\partial x_j}\{(\mu + \mu_t)(\frac{\partial u_j}{\partial x_i} + \frac{\partial u_i}{\partial x_j})\} + \rho g_i \beta (T - T_m)$$

Turbulent Kinetic Energy Equation;

$$\frac{\partial}{\partial x_i}(\rho u_i k) = \frac{\partial}{\partial x_i}\{(\mu + \frac{\mu_t}{\sigma_k})\frac{\partial k}{\partial x_i}\} + G_k + G_b - \rho\varepsilon$$

Dissipation Rate Equation of Turbulent Kinetic energy;

$$\frac{\partial}{\partial x_i}(\rho u_i \varepsilon) = \frac{\partial}{\partial x_i}\{(\mu + \frac{\mu_t}{\sigma_\varepsilon})\frac{\partial \varepsilon}{\partial x_i}\} + C_{1\varepsilon}\frac{\varepsilon}{k}(G_k + C_{3\varepsilon}G_b) - C_{2\varepsilon}\rho\frac{\varepsilon^2}{k}$$

Energy Equation;

$$\frac{\partial}{\partial x_i}(\rho u_i T) = \frac{\partial}{\partial x_i}\{(\frac{\mu}{\sigma_l} + \frac{\mu_t}{\sigma_t})\frac{\partial T}{\partial x_i}\}$$

Concentration Equation;

$$\frac{\partial}{\partial x_i}(\rho u_i C_s) = \frac{\partial}{\partial x_i}\{(\frac{\mu}{S_l} + \frac{\mu_t}{S_t})\frac{\partial C_s}{\partial x_i}\} + S_c$$

$$\rho = (\rho_{ref} T_{ref})/T$$

$$\nu = -0.49467910^{-5} + 0.45839410^{-7} T + 0.8097410^{-10} T^2$$

where,

$$\mu_t = \frac{c_\mu \rho k^2}{\varepsilon},\ G_k = \mu_t(\frac{\partial u_j}{\partial x_i} + \frac{\partial u_i}{\partial x_j})\frac{\partial u_j}{\partial x_i},\ G_b = \frac{\mu_t g_i \beta}{\sigma_t}\frac{\partial T}{\partial x_i}$$

$$C_\mu = 0.09,\ C_{1\varepsilon} = 1.44,\ C_{2\varepsilon} = 1.92,\ C_{3\varepsilon} = 1.0,\ \sigma_k = 1.0,\ \sigma_\varepsilon = 0.9,\ \sigma_l = 1.0.$$

$$\sigma_t = 1.0,\ S_t = 0.68$$

T_f : combustion gas temperature [K] T
$\boldsymbol{T}_\infty$: air temperature except fire range [K]
γ : slope of tunnel [%]
K_g : grade factor [-]

Critical velocity is computed by iterating both equation (1) and (2). In this study that is computed at 2.0 m/s on the assumption that air temperature is 17°C.

5 GOVERNING EQUATION AND BOUNDARY CONDITION

5.1 *Governing equation*

The flow under consideration is three dimensional and turbulent, and has a steady state. The governing equations solved include those expressions for conservation of mass, the momentum, the turbulent kinetic energy, the dissipation rate of turbulent kinetic energy, and the thermal equations are illustrated from table 1. Energy equation and density equation is governing equation for analyzing each distribution of temperature and pollutant in table 1. It selected the sign of each equation by the example of general literature, it selected k-ε model[13] considered buoyancy to analyze turbulent flow.

5.2 *Boundary condition*

To obtain the physically meaningful solution to the problem in question, we must specify the thermal and flow conditions of tunnel inlet, outlet, wall and fire informations. Boundary conditions in this calculation to solve governing equation is illustrated from table 2. u, v and w is the velocity for the direction of x, y and z in table 2.

Heat release rate, the generation value of smoke and the generation value of CO by fire size supposed

Table 2. Boundary condition.

Tunnel inlet	$u=0,\ v=0,\ T=290K,\ C=0,\ w=1m/s,\ 2m/s\ and\ 3m/s$ $k=0.015\times w^2,\ \varepsilon=C_\mu\times k^{1.5}/(0.5\times D_h)$
Tunnel outlet	$\frac{\partial u}{\partial z}=\frac{\partial v}{\partial z}=\frac{\partial w}{\partial z}=0,\ \frac{\partial k}{\partial z}=0,\ \frac{\partial \varepsilon}{\partial z}=0,\ \frac{\partial C}{\partial z}=0,\ \frac{\partial T}{\partial z}=0$
Tunnel wall	$u=v=w=0,\ \frac{\partial T}{\partial x}=\frac{\partial T}{\partial y}=\frac{\partial T}{\partial z}=0,\ \frac{\partial C}{\partial x}=\frac{\partial C}{\partial y}=\frac{\partial C}{\partial z}=0$

to 10 MW, 0.541 kg/s and 0.055 kg/s from previous study[3,14]. It supposed that heat is delivering to tunnel inlet for heat flux $2.27\times 105\ W/m^2$ through right and left window at the fire part of train from that. Also it supposed that the smoke and CO is generated 0.0123 [kg/(m^3.s)] and 1250 ppm from the virtual volume space adjacent to the both windows.

It analyzed three case of tunnel inflow velocity, 1 m/s, 2 m/s(critical velocity) and 3 m/s in this study. The temperature of inflow air is 17°C.

The exit of the tunnel applied for outflow condition and the wall applied for viscosity condition and adiabatic.

5.3 *Numerical analysis method*

In the present study, PHOENICS[15], a general-purpose commercial code, was used to analyze the air flow, the temperature distribution, the CO distribution, and the tunnel environment in the space. To fit the irregular shape of the tunnel, the body-fitted coordinate system was adopted; i.e., the grid lines were arranged to match the physical bounding surfaces. There are $15\times 16\times 90$ grid cells used in the present study.

6 RESULT AND CONSIDERATION

It may ensure to sufficient evacuation environment for passengers at the aspect of flow distribution, temperature, visible distance and harmful gas distribution, to evaluate the effectiveness of one dimensional critical velocity method applied to design disaster prevention system for railroad tunnel.

On fire situation, the passenger got on the upward flow direction from the fire position can evacuate to the upward without passing the fire position. But the passenger got on the downward should pass through the fire position to evacuate to the upward. In fact, it is impossible. Therefore the downward passenger should evacuate to the downward, it must be evaluated the stability for evacuation environment of the downward. For that, it investigated each distribution for x-z section (the region of 186 m~400 m for z direction) that is 1.5 m away from y direction for the bottom of tunnel. This section is breathing height of passengers, it expected to influence on the evacuation of passengers at fire situation. It called breathing section in this study.

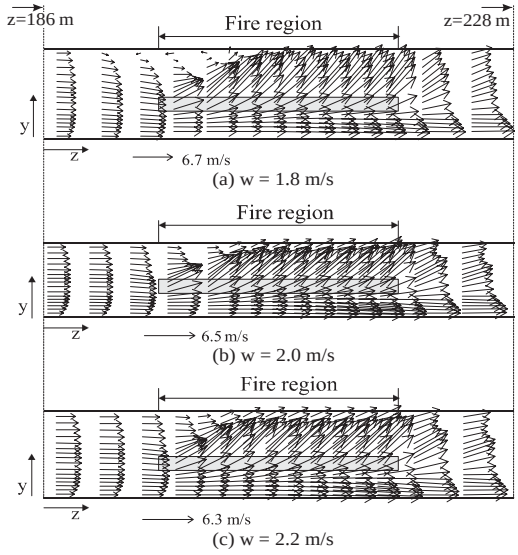


Figure 2. Tunnel inlet velocity distributions by changing inflow velocity.

6.1 *Consideration effectiveness at the aspect of air distribution*

It considered the air flow of the evacuation route (x = 1 m) section to verify the effectiveness of computing critical velocity(2 m/s) by equation (1) with changing inflow velocity, 1.8 m/s(90% of the critical velocity) and 2.2 m/s(110% of the critical velocity).

To check generation of the back-layering at the fire zone, Figure 2 show the flow distributions of the y-z section at the around fired train. Figure 2(a) shows that back-layering generate from fire zone to the evacuation direction of passengers. It generate maximum 6.5 m/s updraft from fire zone, it does not generate back-layering in Figure 2(b). Also it generate maximum 6.3 m/s updraft from fire zone, it does not

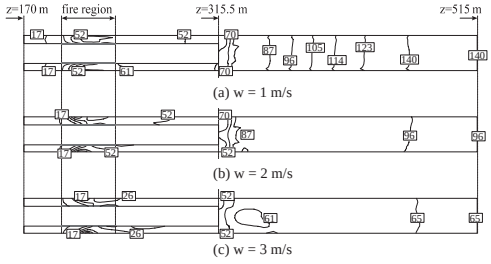


Figure 3. Tunnel inlet temperature distribution by changing inflow velocity [unit. °C].

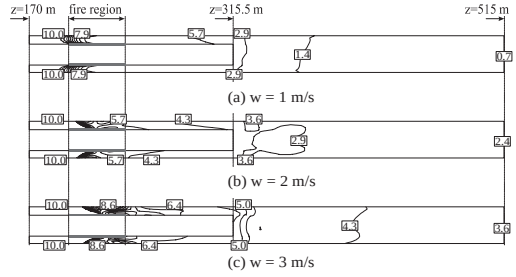


Figure 4. Tunnel inlet visible distance distribution by changing inflow velocity [unit in].

generate back-layering as the occasion of inflow velocity, 2 m/s in Figure 2(c). Therefore, it is considered that one dimensional critical velocity method applied to predict back-layering is comparatively appropriate.

6.2 *Consideration for availability at the aspect of temperature distribution*

Figure 3 shows the temperature distributions of breathing section by changing inflow velocity. In occasion of inflow velocity in tunnel is 1 m/s, the temperature of air is illustrated maximum 140°C by gradually rising from fire zone to inflow downward in Figure 3(c). It is considered that the evacuation environment of passengers at the downward is very poor. It shows that maximum temperature of downward direction is 96°C higher than allowable standard temperature 80°C in Figure 3(b) of inflow velocity 2 m/s. Indeed, it shows that the evacuation environment of passengers is ever poor though tunnel inflow velocity is kept 2 m/s by one dimensional critical velocity equation.

It is considered that the evacuation environment is not appropriate though critical velocity is minimum velocity to prevent back-layering.

Figure 3(c) of inflow velocity 3 m/s shows that the maximum temperature in the downward direction of fire zone is 65°C ower than allowable temperature. It is considered that 150% of critical velocity makes the sufficient evacuation environment for safe evacuation of passengers.

6.3 *Consideration availability at the aspect of visible distance distribution*

It is illustrated visible distance distributions computed by the smoke concentration distribution of at Figure 4 to evaluate the evacuation stability of the passengers. The visible distance distribution applied for following empirical formula and coefficient proposed by Steiner.

$$L_v[m] = \frac{D_s \cdot \ln(A)}{K \cdot Y_s \cdot C_s \cdot \rho_\infty} \tag{4}$$

A : Sight insurance distance [=10 m]
C_s : Smoke concentration of pollutant [-]
D_s : Optical density [-]
K : absorption area [m^2/kg]
L_v : Visible distance [m]
Y_s : Solid particle ratio [-]

Figure 4(a) shows that visible distance being lower suddenly to less than a meter by generating smoke at the place 150 m away from fire zone to flowing downward. It is considered that it need the additional ventilation equipment to make sure visible distance for evacuation because it is very poor for evacuation environment of passengers. Visible distance is elevated as compared with Figure 4(a) in Figure 4(b) increased to 2 m/s. However, it does not provide the visible distance to ensure safe evacuation environment of passengers. Although visible distance increased to 3∼4 m as Figure 4(c) increased to 3 m/s, it doesn't also ensure safe evacuation environment of passengers.

It is expected that it does not provide safe evacuation environment of passengers at the aspect of visible distance, in occasion of choosing ventilation equipment by critical velocity as visible distance distribution. Accordingly it considered to need additional ventilation equipment to ensure safe evacuation environment of passengers.

6.4 *Consideration availability at the aspect of harmful material distribution*

Figure 5 shows CO concentration distributions at the height of breathing section to evaluate stability of evacuation environment of passengers at the aspect of concentration distribution. It shows that CO concentration increase to 350 ppm by moving to downward direction in Figure 5(a) of inflow velocity 1 m/s. Considering Figure 5(b) Inflow velocity is 2 m/s, the maximum concentration of tunnel exit range is 300 ppm. and it doesn't be large different for the case of inflow velocity 1 m/s. however, it shows 225 ppm at the large range by the rising mixing of CO and air with increasing air velocity.

In Figure 5(c) of inflow velocity 3 m/s, the maximum concentration for evacuation road downward range is 250 ppm. And CO concentration greatly

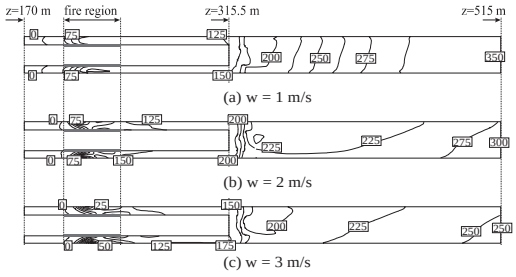


Figure 5. Tunnel inlet CO distribution by changing inflow velocity [unit: ppm].

decreases than the two case. It is considered to be able to provide some time in fire situation required prompt action. In the case of three inflow velocities, CO distribution is far lower than 800 ppm, average concentration for 15 minutes. But it is considered that passengers must evacuate to the position supplied fresh air within 15 minutes. Because CO distribution is far higher than 50 ppm required in evacuation over 15 minutes.

7 CONCLUSION

It studied that the ventilation equipment designed by one dimensional critical velocity equation can ensure to sufficient evacuation environment for passengers at the aspect of air distribution, temperature, visible distance and harmful material distribution, to evaluate the effectiveness of one dimensional critical velocity method applied to design disaster prevention system for railroad tunnel. It is obtained following conclusion.

(1) It is considered that one dimensional critical velocity method at the aspect of air current is reasonable because it doesn't occur back-layering at more than 2 m/s.
(2) It indicate that evacuation environment of passengers is poor at the aspect of temperature distribution in occasion of 1 m/s or 2 m/s. Consequently it is able to provide safe heat evacuation environment in occasion of 3 m/s.
(3) Visible distance is made better by increasing inflow velocity at the aspect of visible distance distribution. However, it is considered to need additional ventilation equipment to make better visible distance because it is expected that it doesn't provide enough visible distance.
(4) It is considered that passengers must evacuate to the position be supplied with fresh air within 15 minutes because CO distribution is far higher than 50 ppm required in case of evacuation time more than 15 minutes, though it is far lower than 800 ppm of average concentration for 15 minutes at the aspect of CO distribution.

REFERENCES

[1] Favre P. et al., 1997, Detailed simulation of smoke movement due to a train fire in the context of general safety considerations for the gotthard base tunnel, Proc. 9th Int. Symp. Aerodynamics & Ventilation of Vehicle Tunnels, Aosta Valley, Italy, BHR Group, pp. 245–254.

[2] Miles. S., and Kummer, S., 1997, Validation of a CFD model for fires in the memorial tunnel, Proc. 9th Int. Symp. Aerodynamics & Ventilation of Vehicle Tunnels, Aosta Valley, Italy, BHR Group, pp. 159–168.

[3] Eureka Project EU 499: FIRETUN, Nov. 1995. Fires in transport Tunnels, Report on full-Scale Tests, Editor: Studiengesell schaft Stahlanwendung e.V., D-40213 Dusseldorf.

[4] Shin, H.J. and Yu, J.O., 1999, Railway tunnel ventilation system design, J. of SAREK, Vol. 28, No. 6, pp. 463–466.

[5] Lee, S.I., 2000, A study on the environment inside a railroad tunnel on fire, MS thesis, Hanyang University, Seoul, Korea.

[6] Wu, Y., Baker, M.Z.A., Atkinson, G.T. and Jagger, S., 1997, A study of the effect of tunnel aspect ratio on control of smoke flow in tunnel fires, The 9th International Conference on Aerodynamics and Ventilation of Vehicle Tunnel, pp. 573–587.

[7] Tetzner, D., Pollak, R., Foit, W., and Sippel, M., 1999, Critical Velocity-Comparative Assessment of Test Results and CFD Simulation, International Conference Tunnel Fires and Escape from Tunnels, pp. 181–190.

[8] Kennedy, W.D., 1997, Critical Velocity Past, Present and Future, One Day Seminar, ITC Ltd., London, 1997.

[9] Meacham, B.J., 1998, "NIST GCR 98-761: Evolution of Performance-Based Codes and Fire Safety Design Methods", NIST, 65p.

[10] Chow, W.K. and Li, S.M., 1999, Safety Requirement and Regulations Reviews on Ventilation and Fire for Tunnels in the Hong Kong Special Administrative Region, Tunnelling and underground space technology, Vol. 14, No. 1, pp. 18–20.

[11] NFPA 130, Standard for Fixed Guideway Transit and Passenger Rail Systems, National Fire Protection Association, USA 2000.

[12] Lee, C.K., Chaiken, R.F., and Singer, J.M., 1979 ,"Interaction between Duct Fires and Ventilation Flow: An Experimental Study", Combustion Science and Technology, Vol 20, pp. 59–72.

[13] Rodi, W., 1984, Turbulence Model and Their Application in Hydraulics, pp. 27–31.

[14] Lacroix, D., 1997, "New French Recommendations for Fire Ventilation in Road Tunnels", Proc. 9th Int. Symp. Aerodynamics & Ventilation of Vehicle Tunnels, Aosta Valley, Italy, BHR Group, pp. 103–123.

[15] CHAM development team, 1991, The PHO-ENICS manual, CHAM.

Underground Space – the 4th Dimension of Metropolises – Barták, Hrdina, Romancov & Zlámal (eds)
© 2007 Taylor & Francis Group, London, ISBN 978-0-415-40807-3

Numerical simulation in effect of compartmentalization with Water Screen (WS) in a tunnel fire

M. Murakami, H. Kurioka, O. Imazeki, H. Kuwana
Kajima Corporation, Tokyo, Japan

R. Amano
Visiting Professor University of Tokyo, Kajima Corporation, Tokyo, Japan

ABSTRACT: A fire disaster prevention system using a water screen(WS) was developed for potential fires in underground spaces. This system is aimed at securing the occupants' evacuation from the fire by partitioning the fire zone using a water screen and also at the safety of a structure by reducing damage due to the fire. Because WS is composed by fogged drop of water discharged from the special nozzle continuously arranged under the ceiling, WS is possible to be a compartment of the fire zone even in a large and complex space. Moreover, because WS doesn't disturb the traffic of the people and the vehicle, it is suitable for in the subway station, the road tunnel and so on where a lot of passengers use.

To understand the performance of WS, fire experiments were conducted by using 1/2-scale models of a road tunnel. As a result, it was quantitatively confirmed the performance of WS for cooling the hot flow and washing soot particle off. Additionally, a numerical simulation method by CFD that was able to analyze the effect of WS was developed through the verification with results of the experiments. By this developed method, it has been possible to predict the flow of heat and smoke when WS operated. In addition, the occupant' safety at a fire can be confirmed by considering their behavior.

By this method, the fire safety was analyzed in two kinds of structures. 1st analytical case was assumed a fire in the road tunnel with the section having two lanes and the longitudinal slopes of 6%. The sprinklers and WS were assumed as disaster prevention equipments. The origin of fire was assumed 20 MW (corresponding to one large-scale bus) with gasoline in the center of the road. The distance from the fire origin to the shelter entrance as a safety zone was assumed to be 400 m. As a result, in the case of no equipment and only sprinklers, it was concerned that occupants' view was interrupted with the diffusing smoke before they got to the shelter entrance. By operating WS at the early stage of fire, occupants' was able to get to the entrance safely. 2nd analytical case was assumed a fire in the subway station. The fire origin was assumed 5 MW with gasoline in a train(corresponding to an arson). A smoke curtain (A small wall hung from the ceiling, height of 50 cm) and WS were assumed as equipment that prevented smoke spread at the evacuation route. As a result, in the case of no equipment and only a smoke curtain, it was concerned that the smoke was filled in not only the platform but also the evacuation route. But by operating WS, occupants' view was secured if they passed through WS.

1 INTRODUCTION

With big fires such as those which broke out in a tunnel in Daegu city in Korea (2003), the Mont Blanc Tunnel (1999) in Europe and the Tauern Tunnel (1999), interest in fire disaster prevention in tunnels has increased. The occurrence of fires can be attributed to various causes such as arson, accidental ignition and human error. Regardless of the cause, the common result is that a number of people may be killed or injured and that a great deal of time and labor is required for restoration work. With the promotion of highly developed utilization of such deep underground spaces as the Aqualine, the Metropolitan Expressway Shinjuku Line and the Outer Loop, how to secure safety in cases where fires break out in tunnels is an important problem which must be confronted. We have been developing water screens (hereafter referred to as WS) as well as investigating their applicability to the civil engineering field since 2002. The basic performance of the WS was established in large-scale fire tests using a 1/2 scale tunnel model. At the same time, a numerical analysis system for estimating the behavior of heat and smoke was developed in order to influence the compartmenting effects of the water screen.

Furthermore, evacuation simulation during a tunnel fire has been made possible by combining the predicted movements of occupants during evacuation and the safety standards for the occupants. This paper describes the effectiveness of the WS as well as introduces examples of the evacuation simulation for the road tunnel and the subway station.

2 WATER SCREENS

Waterdrops with a diameter of 200 μm which are sprayed from special nozzles arranged in rows on a wall create water screens. This fire disaster prevention system can restrain the diffusion of heat and smoke and secure the safety of occupants by collecting and washing out harmful floating particles. Moreover, this system can minimize the degree of damage to structures. Photo. 1 shows the WS when activated.

3 CFD (COMPUTATIONAL FLUID DYNAMICS)

The CFD, which is a system for a numerical analysis of the behavior of fluids and gasses such as water and air, has recently been applied in the field of fire safety design in tunnel spaces. Although fire tests are effective for the understanding of physical phenomena, a great deal of expense and labor are required in order to satisfy conditions for different sectional shapes according to structures, ventilation wind speed and fire source types. It is also difficult to carry out measurements and visualize flows. On the other hand, the CFD can help us understand any fire's behavior changing according to the aforementioned conditions quickly and from different angles. In our development, the FDS (Fire Dynamics Simulation: Developed by the National Institute of Standards and Technology of US Department of Commerce), which has been employed in many evacuation safety inspections around the world, was selected from among a number of CFD systems in order to build a function for analyzing the effects of the WS. The analysis accuracy of the FDS has already been verified through comparing the analysis results with the fire test results.



Photo 1. WS which are activated.

4 EVACUATION SIMULATION

In order that occupants may take refuge in safety during a fire in a tunnel, they must reach an emergency exit while avoiding fire induced heat and smoke. The evacuation simulation is carried out so as to judge whether or not the environment for the occupants satisfies the established safety standards until they reach the exit by comparing the behavior of heat and smoke obtained from the CFD with occupants' evacuation speed.

4.1 *Evacuation speed*

In inspecting the safety of evacuation, speeds at which occupants can escape are established according to different conditions in various literature references. The walking speed for a person who can walk unaided on a level surface (without stairs) is set at 1 m/s in most cases. In this study, it is assumed that occupants escaping from a fire source reach an exit with a walking speed of 1 m/s just after the occurrence of a fire.

4.2 *Safety standards*

4.2.1 *Safety standards for heat*

One literature reference indicates that humans can tolerate a temperature of 50°C and a humidity of 100% in the atmospheric condition surrounding their bodies for a period of only several minutes. Therefore, a temperature of less than 50°C at the height of an average human body can be regarded as a safe condition.

4.2.2 *Safety standards for smoke*

The light limiting smoke concentration under which occupants can take refuge in safety without missing visual directions is regarded as $Cs < 0.1 \sim 0.4$ for an attenuation coefficient of light. According to a literature reference, it is simpler and more straight forward to specify an evacuation direction for a tunnel structure than for an ordinary structure. Therefore, in the case of the attenuation coefficient of light at the height of an average human body being $Cs < 0.4$ occupants can be evacuated in safety. And for a subway station, in the case of the attenuation coefficient of light at the height of an average human body being $Cs < 0.1$ occupants can be evacuated in safety.

5 ANALYSIS EXAMPLE

5.1 *The cases of the road tunnel*

5.1.1 *Analysis conditions*

Analyses were carried out for a two-way traffic tunnel corresponding to class 2 for the Road Standard Type 1. The vertical section gradient of the tunnel was set as 6% in order that a traffic accident could easily occur and heat and smoke may rapidly spread. The fire protection rating for this traffic tunnel equipped with an emergency exit as well as water sprayers was classified as AA. Analysis conditions are shown in Table 1 and Fig. 1.

Table 1. Analysis conditions.

Fire source	Gasoline (Heat release rate 15 MW) (corresponding to one bus)	
Tunnel structure	Sectional shape	Inside diameter ϕ 10.8 m (Upper part of the road surface for the circular shield tunnel)
	Longitudinal length	L = 740 m
	Vertical section gradient	6% (maximum gradient of the subjective tunnel)
Water spraying equipment (WSE)	Nozzle	5 m/each (150 L/each/min)
	Compartment	Sprayed in two compartments with a length of 50 m (Sprayed in a 100 m length)
Compartmenting equipment (WS)	Nozzle	20/section (10 L/each/min)
	Compartment	50 m/each (Sprayed to both end sections in a WS compartment)
Ventilation equipment	Natural ventilation (primary wind speed 0 m/s)	
Emergency exit	510 m away from a fire source	

5.1.2 *Analysis cases*

Analyses were carried out in 6 cases shown in Table 2.

5.1.3 *Analysis results*

The results in both cases of S-2 and S-3 where the noticeable effects of the WS were discernible among all analysis results are compared with each other in Fig. 2,3. In the case of S-2 where the WS was not activated, smoke with Cs $\geqq$ 0.4 (red color in the figure) descended to the height of a human body 7 minutes after a fire broke out. On the other hand, in S-3 where the WS was activated 3 minutes after the outbreak of fire smoke concentration decreased and the smoke did not fall to the height of a human body even after 8.5

Table 2. Analysis cases.

Case no.	Analytical object	WS	Water spraying equipment (WSE)
T-1	Heat (Temperature)	Without	Without
T-2		Without	Activated 10 min after a fire broke out
T-3		Activated 3 min after a fire broke out	Activated 10 min after a fire broke out
S-1	Smoke (Attenuation coefficient of light)	Without	Without
S-2		Without	Activated 10 min after a fire broke out
S-3		Activated 3 min after a fire broke out	Activated 10 min after a fire broke out

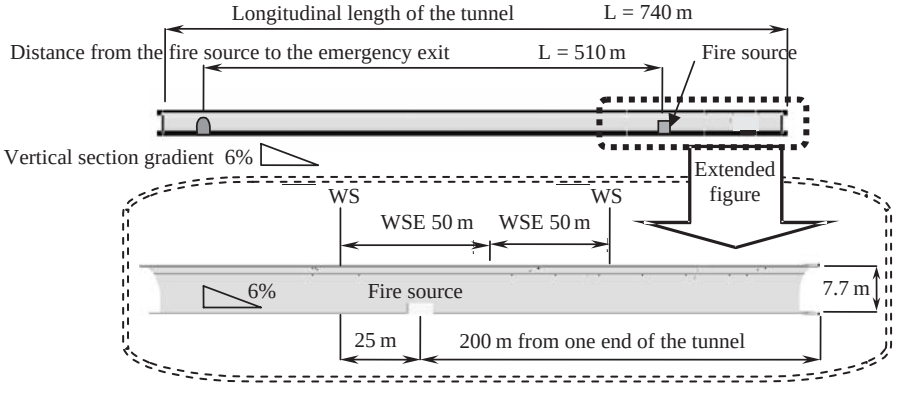


Figure 1. Analysis model.

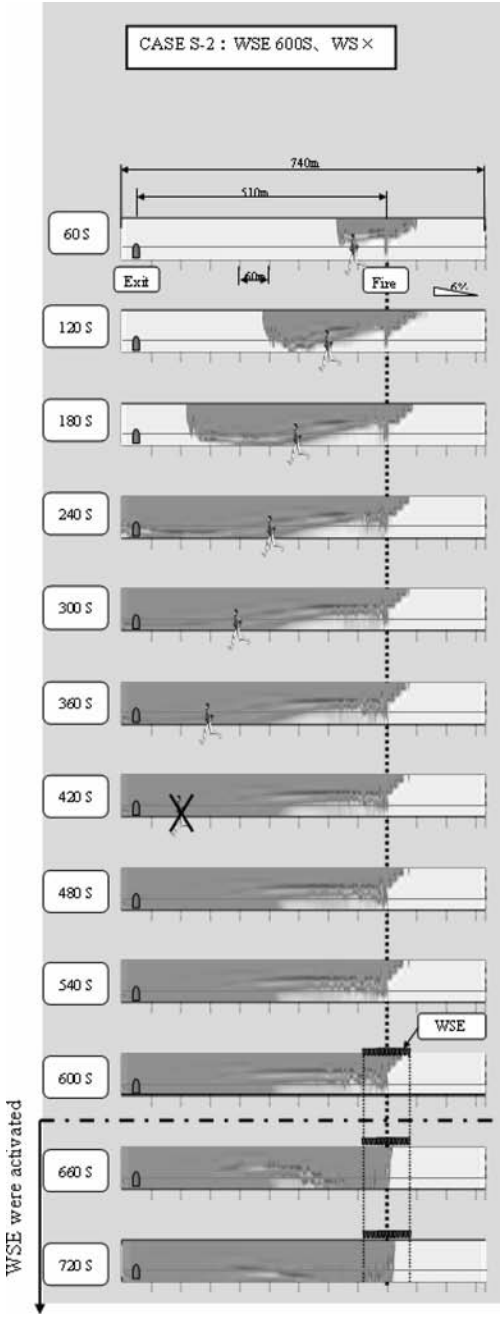


Figure 2. Evacuation simulation results for smoke (S-2).

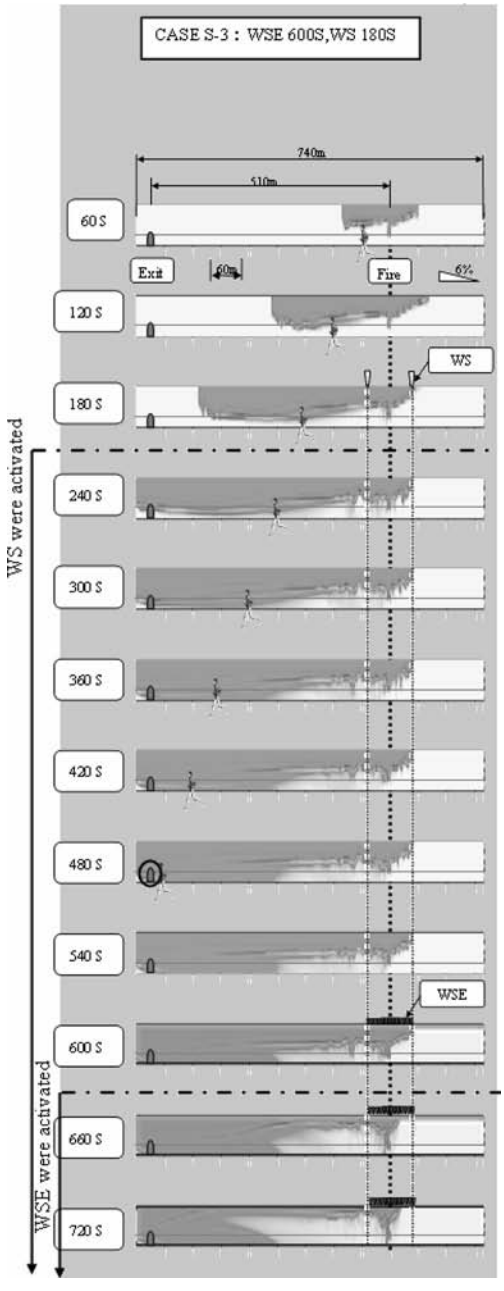


Figure 3. Evacuation simulation results for smoke (S-3).

minutes, in which time occupants reached the emergency exit. It was made clear that the WS contributes to the improvement of the safety for evacuation from fires. The same results were obtained from the WS for heat.

With regard to fire disaster prevention systems for tunnel spaces, the criteria prescribed after the occurrence of a fire in the Nihonzaka Tunnel are still applied. However, it can be thought that new studies on WS and evacuation simulation will be regarded as important in the future.

Table 3. Analysis conditions.

Fire source	Scale	A fire of a train caused by an incendiary: gasoline fueled large fire source * Calorific value Q: 5 MW * Burning time t: 3 min * Burning area A: 5 m^2 [1]
	Fire position	On the train in front of the ticket gates
Evacuation	Evacuation passageway	Trains → Platform → Ticket gates → Stairs → Stairs above the surface
	Time to finish evacuation	7.8 min (To refuge on stairs above the surface)[2]
Environment	Wind	Windless
	Temperature	20°C

[1] On the assumption that a fire breaks out in trains and flames as well as smoke are emitted from windows. (The total window area is 5 m^2 with 3 m^2 windows on the side of the platform and 3 m^2).
[2] According to the method for calculating the time required to take refuge prescribed in the "manual for evacuation safety in the case of fires breaking out in subway stations."

5.2 *The cases of the subway station*

5.2.1 *Analysis conditions*

Analyses were carried out for a subway station. Analysis conditions are shown in Table 3 and Fig. 4.

- Smoke extraction equipment of both up and down lines are activated simultaneously with the outbreak of a fire according to the judgment made by station service room staff.
- Water is sprayed simultaneously with the outbreak of a fire.
- Water is sprayed over 10 minutes.

5.2.2 *Analysis cases*

Case 1: Without any countermeasure
Case 2: Installation of smoke curtains
Case 3: Installation of WS (Water Screens)

5.2.3 *Analysis results*

Smoke flows and evacuation conditions are shown. It was confirmed that smoke is prevented from flowing compartments due to the effects of water out of fire screens and that the water screens functions the same as fire doors and fire shutters. Smoke easily climbs

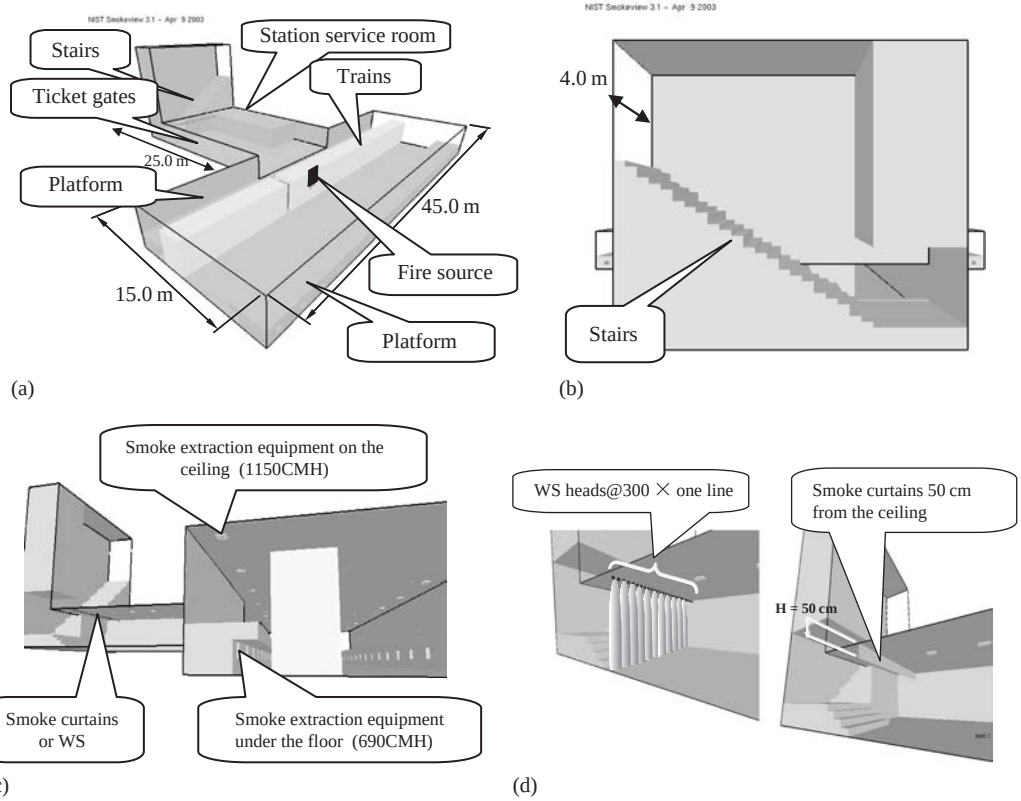
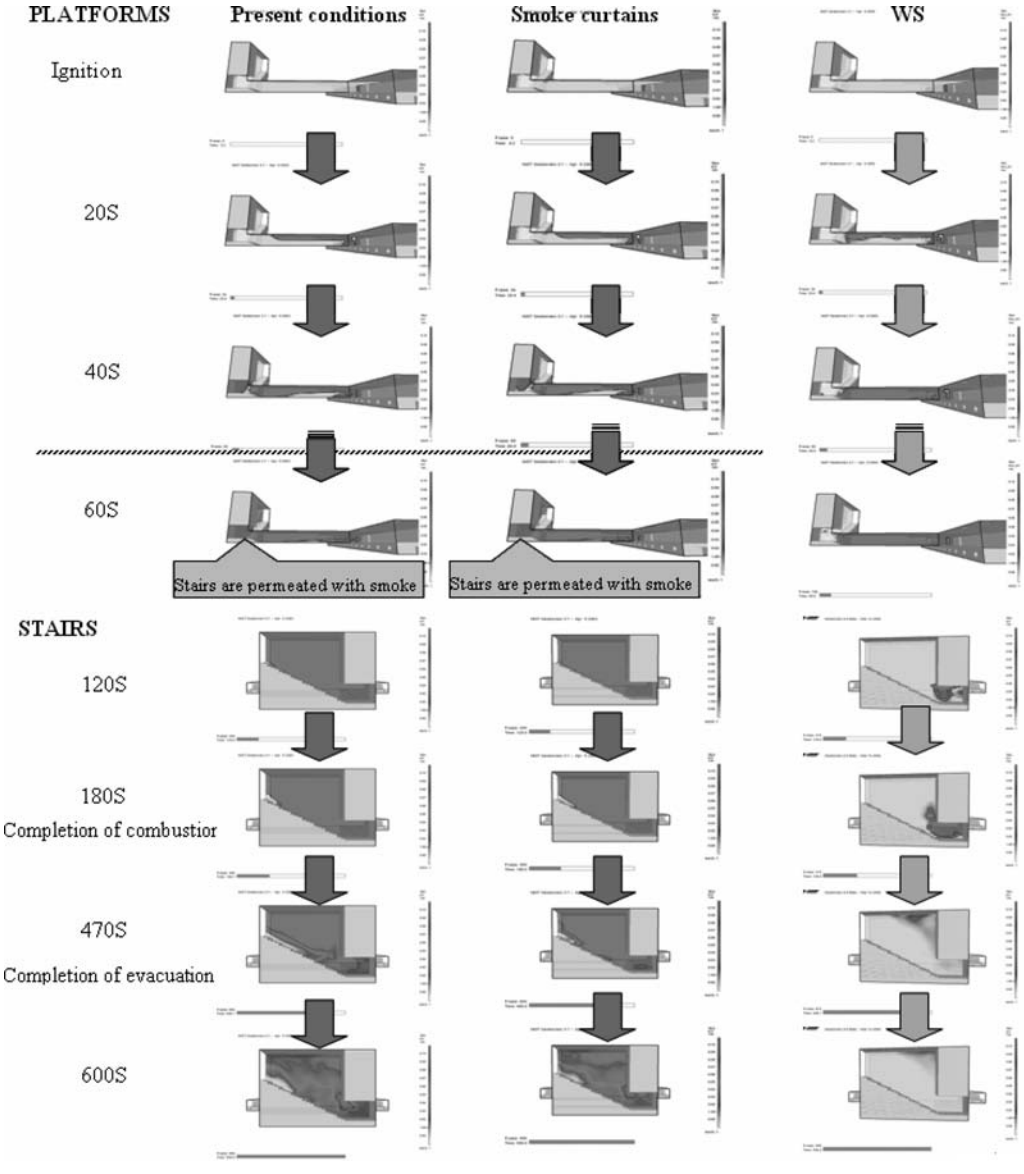


Figure 4-1. (a) The layout of the subway station. (b) Stairs. (c) Emergency facilities (Smoke extraction). (d) Emergency facilities (Smoke spread prevention).



over the smoke curtains in a shaft. Outflow conditions of smoke are not so different from the present conditions. It can not truly be said that smoke extraction equipment functions effectively in the case of explosive combustion immediately after the outbreak of a fire caused by a large fire source.

REFERENCES

R. Amano, Prevention Measures against Fires in Road Tunnels and Water Screen Fire Prevention System; *The International Symposium on Management Systems for Disaster Prevention* at Kouchi on March 9–11, 2006 Japan

R. Amano, Computational Fluid Dynamics Simulation of Thermal Behavior under Working Water Screens in a Tunnel; *the Fourth International Symposium on New Technologies for Urban Safety of Mega Cities in Asia* at Nanyang Technological University on October 18–19, 2005 Singapore

Underground Space – the 4th Dimension of Metropolises – Barták, Hrdina, Romancov & Zlámal (eds)
© 2007 Taylor & Francis Group, London, ISBN 978-0-415-40807-3

Road tunnel equipment

M. Novák, V. Misárek & D. Benda
Metroprojekt Praha, Prague, The Czech Republic

ABSTRACT: The article deals with equipment which is installed in road tunnels. The development of new motorways, expressways and the Prague City Ring Road cannot cope without construction of road tunnels. Road/motorway tunnels pose an increased risk for drivers, primarily in the case of a fire due to an accident in the tunnel. Road tunnel equipment improves operational safety and reduces potential consequences of accidents to a minimum. The designing of tunnel equipment in the Czech Republic is controlled by TS 98 Technical Specifications: Road Tunnel Equipment, which was issued after a revision in 2004. The other regulation with which tunnel equipment must comply is the EU 2004/54/EC Directive of the European Parliament and of the Council on minimum safety requirements for tunnels in the Trans – European road network. The structural design and requirements for safety equipment of road tunnels are solved in ČSN 73 7507 standard: Design of Road Tunnels (reissued in 2005). The requirements for safety equipment of road tunnels were incorporated into the design of new tunnels on the D8 motorway, namely the Panenská tunnel and the Libouchec tunnel, which were opened to traffic at the end of 2006.

1 INTRODUCTION

A design of a road/motorway tunnel must solve the equipment which provides for uninterrupted and safe traffic in the tunnel. In addition, the equipment significantly reduces the risk for drivers in the case of an accident and a fire in the tunnel, and makes safe escape of passengers from the tunnel to the surface possible. Designers working in the Czech Republic must conform mainly to the following fundamental regulations:

TS 98 Technical Specifications: Road Tunnel Equipment (revision 2004)

EU 2004/54/EC on minimum safety requirements for tunnels in the Trans – European road network (2004 issue)

ČSN 73 7507 standard: Design of Road Tunnels (reissued in 2005).

A total of four tunnels have been designed for the D8 motorway leading to neighbouring Germany via northern regions of the Czech Republic: the 2115 m-long Panenská tunnel and the 535 m-long Libouchec tunnel in the motorway section between Trmice and the border with Germany; the 620 m-long Radejčín tunnel and the 270 m-long Prackovice tunnel in the section between Lovosice and Řehlovice. The Panenská and Libouchec tunnel were opened to traffic at the end of 2006. The Lovosice – Řehlovice motorway section containing the Radejčín and Prackovice tunnels found in the České Středohoří highland are under preparation; the completion is planned for 2009–2010.

2 EQUIPMENT OF THE PANENSKÁ TUNNEL ON THE D8 MOTORWAY

The 2115 m-long Panenská tunnel on the D8 motorway section between Trmice and the border with Germany is currently the longest motorway tunnel ever brought into service in the Czech Republic. It is a twin-tube tunnel with two traffic lanes in each tube. The western tunnel tube is on a 3.22 per cent longitudinal gradient; the eastern tube is on a 3.28 per cent gradient. The traffic flow is anticipated at 12,500 vehicles per 24 hours per one tunnel tube; of that, 15 per cent is made up by lorries. The maximum speed allowed in the tunnel is 80 km/h; the average tunnel altitude is 590 m a.s.l.

The tunnel tubes are interconnected by ten cross passages, escape routes for passengers, every 200 m. The cross-passages No. 3 and 7 in addition allow the passage of small emergency vehicles, and the cross-passage No. 5 is passable for big vehicles of rescue units. Eight cross passages house small distribution substations for electrical equipment installed in the tunnel. The substations are fire separated from the respective escape routes.

2.1 *Tunnel ventilation*

A longitudinal ventilation system has been designed for the uni-directional tunnel tubes, with jet fans installed under the tunnel vault. The designed longitudinal ventilation, which is operated in the direction of the traffic, guarantees that the required limits

Table 1. Typical values of limits for noxious substances set for various traffic states.

Traffic state	CO-concentration [ppm] y. 2000	CO-concentration [ppm] y. 2010	Opacity Coefficient K $[10^{-3} . m^{-1}]$
Fluent peak traffic v = 50–100 km.h	100	70	5
Daily congestion, Stop and Go	100	70	5
Exceptional congestion	150	100	7
Longer maintenance work under traffic	30	30	3
Tunnel closure	250	200	12

of concentration of noxious substances produced by vehicles will be met. The limits have been set for Carbon Monoxide (CO), Nitric Oxide (NO_x) and opacity in the tunnel. The allowable concentrations of the noxious substances, which have been set on the basis of the Technical Specifications TS 98, are contained in the above table.

The recommended nitric oxygen maximum allowable concentration value is 20 $mg.m^{-3}$.

It follows from results of calculations that, at normal traffic volume and the speed of vehicles ranging from 30 km/h to 80 km/h, both tunnel tubes are sufficiently ventilated by the piston effect of vehicles passing through the tunnel. The jet fans installed under the tunnel crown are step-by-step started up in the case of traffic congestion in the tunnel or extraordinary climatic conditions (weather inversion, fog, windstorm etc.), depending on the situation, on the basis of the data provided by CO and opacity sensors, measurement of velocity and direction of airflow in the tunnel. When traffic in the tunnel is stopped, drivers are asked through a message sign to turn the engines off.

The complete ventilation system will be automatically switched on in the relevant tunnel tube in the case of an accident, a fire in one tunnel tube, approximately 6–7 minutes after the fire initiation. During this time the smoke is kept by the heat under the tunnel crown and an about 2.5 m high zone above the roadway remains free of smoke (under the condition that the longitudinal velocity of the airflow in the tunnel is less than 2 m/s). The fans are run in the direction of traffic so that escape of passengers found before the accident scene in the tunnel is possible. The fans are switched on stepwise, from the exit portal toward the entrance portal. Fresh air flows counter the direction of escape of passengers. Passengers found ahead of the fire can get out of the tunnel in their vehicles. The ventilation system in the other tunnel tube which is not affected by the fire is run in the reverse direction so that the airflow direction is identical with that in the tunnel tube with the burning vehicle. A total of four fans are switched on at the front end of the tunnel (viewed in the airflow direction – the reverse direction) and run in the reverse direction, whereas two fans on the opposite end of the tunnel are run counter the airflow (the main direction); thus the fans create positive pressure in the tunnel tube, which prevents drawing of the smoke which blows from the portal of the incident tunnel. The ventilation of the cross passages is also switched on, in the respective direction. The purpose of the ventilation is to allow passengers to escape to a smoke-free space via the cross passages or through the portal to the open air. The jet fans are capable of providing longitudinal airflow at the minimum velocity of 3 m/s even if as many as four fans fail to work.



Figure 1. Jet fans under the Panenská tunnel crown.

The fire ventilation is designed according to TS 98, to a norm fire size of 30 MW; the fans must keep operating at a temperature of 400°C for 90 minutes.

According to the design, the western (descending) tunnel tube will contain seven pairs of jet fans (14 pieces in total). Six pairs of jet fans are designed for the eastern (ascending) tunnel tube (12 in total). Parameters of one jet fan:

A high-pressure axial-flow fan, size 1000, with silencers, reversible, suited for temperatures until 400°C/90 min. The thrust produced by the fan in the main/reverse direction is 875 N; a 30 kW/400 V electric motor.

The ventilation system will be controlled from the tunnel control centre and locally, from respective switchboards.

2.2 *Tunnel lighting*

2.2.1 *Adaptation lighting of the tunnel*

The adaptation lighting of the tunnel is designed to illuminate the threshold and transition zones in the entrance section of the tunnel at a luminance level corresponding to the ability of driver's eye to adapt. In the tunnel entrance section, it consists of two rows of counter-beam asymmetric discharge lamps installed

below the ceiling of the respective tunnel tube. The rows of the luminaries are installed above the centre lines of both traffic lanes. The adaptation lighting is divided into zones; it corresponds to the maximum speed limit set for the tunnel at 80 km/h. The adaptation lighting is fed partly from an uninterruptible power source and partly from a source without a backup.

2.2.2 *Stand-by lighting of the tunnel*
Stand-by lighting of the tunnel is activated during extraordinary operating states, for example in case of a failure of normal power supply. The stand-by lighting consists of selected sections of luminaries of the adaptation lighting, which are fed from the uninterruptible power source. In the case of a failure of the normal power supply, the stand-by lighting keeps working; the maximum operating speed is reduced to a maximum speed limit of 60 km/h.

2.2.3 *Interior tunnel lighting*
The interior tunnel lighting is designed for the illumination of the internal part of the tunnel; it consists of one row of double-source symmetric discharge lamps installed below the ceiling, on the centre line of the respective tunnel tube. The lights are fed from an uninterruptible power source.

2.2.4 *Emergency lighting of the tunnel*
The emergency lighting of the tunnel is designed to illuminate escape routes in the case of a fire in the tunnel. The emergency lighting consists of LED-type luminaries with a source, which are embedded in recesses provided in the lining. With a view to the possible smoke logging of the upper space of the tunnel, the luminaries are installed at a height of 90 cm above the walkways. The luminaries are installed at 12 m spacing. The intensity and variation range of the emergency lighting must meet the values prescribed. The emergency lighting is fed from an off-line backup source.

2.3 *Electrical installations – the heavy current distribution system*

2.3.1 *Distribution substations, 22 kV*
The 22 kV distribution substations are divided into an inlet part with a separate entry for SČE (the power supplier), and an outlet part with a separate entry for the ŘSD (the tunnel operator). The inlet part of the substation in the Operating and Technical Services Building (OTSB) South will be built as a part of the tunnel construction. The inlet part of the substation in the OTSB North will be built as a part of a separate subsequent structure. The substations have been designed in the metal-clad version, with SF6 insulation. The inlet part of the substation in the OTSB South consists of three cabinets with disconnecting switches. The inlet part of the substation in the OTSB North consists of four cabinets with disconnecting switches. The outlet parts in both OTSBs consist of three cabinets (cabinet 1 – measurement (air space insulation); cabinets 2 and 3 – outlets to transformers with motor-actuated disconnecters and trip coils and fuses. Cabinet 2 contains, in addition, a capacitance voltage sensor with a remote signalling transducer. The inlet parts have been designed in a way allowing the use of T-connectors for cable connections; they are equipped with surge voltage protectors.

2.3.2 *Transformers*
Each OTSB will contain two 1000 kVa transformers; each transformer will be installed in a separate cell. The transformers are of the oil-cooled, air-tight type. Part of the supply of the transformers will be index pointer thermometers with contact outlets: temperature lower – warning, temperature lower – shutting down.

2.3.3 *Measurement of power consumption*
Each OTSB will have an independent commercial measurement system. Universal measuring boxes will be installed in the inlet part of each 22 kV distribution substation. The ratio of the current measurement transformers in the consumer's (ŘSD) outlet parts of the 22 kV substations corresponds to the agreed technical maximum, i.e. 25/5A.

2.4 *The traffic and equipment management system*

The management system controls traffic in the tunnel in relationship with an external motorway information system. It consists of switchboards fitted with programmable logic controllers, input and output circuits, and a link to the management and stand-by control centre. The stand-by control centre is located in the portal building, and the management centre, which is common for the Libouchec tunnel and Panenská tunnel, is in the SSÚD Řehlovice.

2.5 *The fire alarm and detection system*

The fire alarm and detection system (FADS) comprises FADS switchboards located in the portal buildings, fire sensors, manual call points and a linear heat detection system including cable connection. The FADS switchboards are connected to the management system and, via a direct communication line, to the fire rescue management centre and the other elements of the Integrated Rescue System. The following equipment will be controlled on the basis of the assessment of the FADS signals:

– emergency lighting
– fire ventilation
– traffic signs
– CCTV camera system



Figure 2. An SOS cabin in the Panenská tunnel.

– public address
– wireless communication

2.6 *Emergency announcement system*

SOS cabins are provided at maximum intervals of 150 m. The fundamental requirement for the SOS system is that nonverbal announcing of an emergency must be possible by pressing a relevant button (medical aid, Police, fire, defective vehicle). In addition, verbal communication with the police controller is possible. First aid tools and means (rescue tools, fire extinguishers and a first aid kit) are stored in SOS niches.

2.7 *The closed circuit TV camera system*

The video surveillance is solved by means of an independent closed circuit TV camera system (CCTV), which allows the police and technical-administrative controllers to visually check traffic in the tunnel. In addition, the CCTV system allows automatic video detection of specific traffic states. The CCTV control centre including the automatic video detection switchboard are located in the portal building, and are interconnected with the tunnel management system. The locations of the cameras guarantee that the entire tunnel is monitored, with a special focus on the SOS cabins and their neighbourhood, entrances to the escape galleries and their interior. The video surveillance is used by the traffic operators to check the traffic in the tunnel, and allows them to timely respond to an emergency situation in the tunnel or in front of tunnel portals. The automatic video detection system further improves effectiveness of the performance of traffic controllers and, in the case of an exceptional failure of the human factor, provides an automatic response to the emergency state detected in the tunnel, including a vehicle fire. This system is currently the fastest to detect crisis situations originating in the tunnel. Part of the CCTV system is the recording of the video signal provided by the cameras.

2.8 *Wireless communication*

The wireless communication system spreads radio signal inside the tunnel for selected users, as for example:

– the SSÚD
– the Fire Rescue Service
– Ambulance
– the Police of the Czech Republic
– mobile operators' services (an independent investment project organised by mobile operators)
– local FM radio providing traffic information broadcasting and the RDS.

2.9 *Public address*

In the case of emergency in the tunnel, drivers can be informed through the Public Address system. In principle, it is a low frequency signal distribution between the switchboard and loudspeakers installed in the tunnel and escape galleries. The public address system makes an entry of controllers possible, according to the allotted priorities (the Police, a traffic controller, the person in charge of a rescue intervention).

2.10 *Telephone for controllers*

The system of telephones for controllers is installed to make co-ordination and communication between the tunnel maintenance and operation control system components possible. The telephones are installed in all technical services rooms existing in the tunnel.

2.11 *Traffic lights and signs*

Traffic in the Panenská tunnel is controlled by means of variable traffic signs. The signs are used for the control of traffic in individual traffic lanes. The entry to the tunnel is closed by means of double-chamber light signs. The variable traffic signs are controlled by command signals from the tunnel traffic control room on the basis of control algorithms.

2.12 *Road signalling system*

The road signalling system must be understood as a complex consisting of fixed and variable traffic signs, including traffic lights, both in the tunnel and on the adjacent road sections (usually the intercrossing sections).

There are four gantry structures carrying variable traffic signs before each tunnel entrance, which make gradual reduction of speed of vehicles possible, to the speed at which the vehicles can be stopped by a red light. The gantries are further used for informing drivers about emergency situations in the tunnel.

2.13 *Vehicle height checking*

The height of vehicles is measured on carriageways of the motorway, at a distance from the tunnel portal

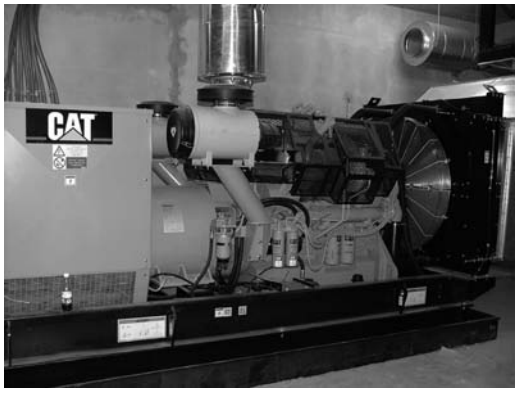


Figure 3. A 900 kVA diesel generating set – the stand-by power source in the northern portal building at the Panenská tunnel.

sufficient for stopping an oversize vehicle. The dimensions are checked by a detector based on the principle of and infrared barrier combined with an inductive traffic loop detector. The signal is transmitted from the infrared barrier to processor stations through the control system, which actuates the variable traffic signs in front of the tunnel. At the same time, the control system sends a message to the traffic control centre.

2.14 *The stand-by power source*

The supply of power for selected items of equipment in case of a failure of power supply from the public network is provided by rotary stand-by sources (SBS), i.e. diesel generating sets. The appliances for which the uninterrupted operation is required are backed also by rotary UPSs (RUPSs).

The sets of stand-by power sources, including the RUPSs, are installed in a common machine room, in the respective Operating and Technical Services Building (OTSB) at both portals. The OTSB North houses a 900 kVA SBS + a 250 kVA RUPS. The OTSB South houses a 750 kVA SBS + a 250 kVA RUPS. The sets are in the version comprising a frame, with elastic support of the motor and the generating set. The SBSs will be switched on automatically at a power failure, or on a command from the control room. The operation of the diesel generating set is interconnected with the RUPS, which guarantees uninterrupted operation of selected items of equipment and, in addition, aids the starting system of the diesel generating set, thus enhances reliability of the equipment.

3 CONCLUSION

The Panenská tunnel equipment guarantees a maximum possible level of the required safety of traffic and safety in the case of an accident and a fire in the tunnel. Early detection of an emergency situation, a fire etc. gives passengers a good chance of escaping to protected spaces and out of the tunnel. Early intervention of the elements of the integrated rescue system will not only protect the health of passengers, but it also will diminish a contingent damage to tunnel structures and equipment.

This page intentionally left blank

Underground Space – the 4th Dimension of Metropolises – Barták, Hrdina, Romancov & Zlámal (eds)
© 2007 Taylor & Francis Group, London, ISBN 978-0-415-40807-3

Site ventilation of a long deep tunnel: The lot Bodio of the Gotthard base tunnel

M. Oberaigner
Lombardi Engineering Limited, Minusio, Switzerland

F. Romerio
Consorzio Tunnel AlpTransit – Ticino, Bodio, Switzerland

ABSTRACT: In the future several very long tunnels with a high overburden are going to be built in Europe and all around the world. These structures mostly consist of two parallel running tunnels plus cross passages at regular distances. Generally all of these constructions are divided into several lots and consist of a combination of TBM or shield drives together with NATM drives. The automated drives tend to achieve 10,000 meters in length and beyond, cross passages or other special cross sections are usually carried out by NATM.

Thus they comprise a huge challenge regarding the supply of fresh air. Fumes of the drill-and-blast-sections, exhaust gases, any dust created through excavating or mucking, etc. have to be extracted and fresh air has to be brought up to the TBMs heads. Due to the extreme lengths and the need to simultaneously casting the inner lining the application of flexible ventilation ducts to carry the fresh air from the exterior to the tunnel head is almost impossible. Therefore a recirculation ventilation system is established during construction.

1 INTRODUCTION

1.1 *Short review of tunneling in the Alps*

The construction of tunnels with lengths of 10,000 m and beyond have a long tradition in the European Alpine countries. The first of these was the Mont-Cenis-Railway-Tunnel (also-called Fréjus-Tunnel) under the Franco Italian border between Modane and Bardonecchia in the Western Alps. Construction period of this originally 12,233 m long tunnel last from 1857 through 1871. The estimated construction time of some 25 years could be cut to around half by the introduction of pneumatic drill-hammers.

Based on the innovations made on the Mont-Cenis-Railway-Tunnel the Swiss Confederation decided to build the 14,982 m long Gotthard-Railway tunnel from 1871 through 1881. Ventilation was accomplished through the compressed-air ducts. After blasting the fumes of the explosives were cleared away by the air supplied by these ducts.

1.2 *The simplon tunnel*

After the completion of the Gotthard-Railway tunnel the Swiss decided for another railway line further west, connecting Brig in the Vallais canton in Switzerland and Iselle di Trasquera in the Italian Piemont region. For military reasons an alignment with the national border exactly in its half was chosen. This alignment led to a length of tunnel of almost 20,000 m, thus being one of the longest tunnels in the world until the late 1970s. An overburden of up to more than 2000 m at the highest summits, drive lengths of some 10,000 m and rock temperature of up to 42°C presented new challenges to the engineers.

For ventilation purposes two parallel tunnels were driven for the first time in history. While the eastern tunnel was excavated to its final cross-section, the western parallel drive was redimensioned to a small adit of some 2.5 m in diameter, which generally did not dispose of any inner lining. These two tubes were linked by cross passages at regular distances of 200 m. Fresh air for the main drive, the supply with pressurized water as well as the draining of seepage water happened through the parallel-adit, while the main drive was used for mucking.

This very advanced concept of having two parallel drives – one of which brings the fresh air to the tunnel head, the other evacuating the used air – is also applied for the long drives of the Gotthard base tunnel.

2 THE GOTTHARD BASE TUNNEL

2.1 *Gotthard base tunnel project overview*

The Gotthard base tunnel of 57 km consists of five sections, with a variable length between 7 km and 16 km. It is a system with two parallel single-track tubes with

an excavated diameter varying from 8.8 m up to 9.5 m. There is no parallel safety gallery, but 180 cross passages, with some 300 m of distance between one and another, link the two tubes. Considering all accessory works like access tunnels, shafts, multifunctional stations and by-passes, the whole length of excavation totals 153 km. Almost two thirds of it have been achieved by August 2006.

To shorten construction time and for ventilation purposes, the tunnel is driven from several sites simultaneously. Excavation in the five sections takes place from the two portals as well as from three intermediate attacks.

2.2 *The Bodio section*

The Bodio section is the very southernmost lot and consists of an open cut section, an excavated section under a rock-fall mass at the portal and the drill-and-blast section until the assembly-caverns, which was driven from an by-pass adit. This by-pass adit joins the main tunnel at a so-called crossing-cavern and was driven in order to evade the rock-fall mass situated at the portal zone of the tunnels' alignment, thus allowing an earlier start of the assembly works an launching of the TBMs. This latter TBM-section is the so-called main-lot.

This main-lot comprises the construction of the two running-tunnels starting at the assembly-caverns of the open TBMs some one and a half and two and a half km from the tunnel portal for the western and the eastern tube respectively. The eastern drive reaches a chainage of 15.97 km, the western one has its break-through point at 15.70 km from the portal. Furthermore a total of 50 cross passages have to be constructed.

The inner lining is cast some way behind the TBMs at the so-called "worm" installations on either drive of the tunnel. This installations are some 600 m long and encompass the revision of the excavated cross-section, laying of the seepage water drainage pipes and impermeability sheet, casting and curing of the vault concrete and all the necessary auxiliary equipment.

2.3 *Ventilation of the main lot in the Bodio section*

The SUVA (Swiss Accident Insurance Fund) defines clear rules for underground work in a hot and humid climate. The air temperature in and around the main working places must never exceed 28°C dry temperature (given 100% air humidity). In this way, acute heat affected diseases during an 8-hour shift of hard underground work can be avoided.

The site ventilation system ensures that maximum working point concentrations are retained by replacement of the used air and dilution of the toxic substances produced underground – although not air conditioning as such. The cooling function produced by the construction ventilation system does, however, represent a welcome side effect.

A recirculation system is set up in the Bodio section to provide fresh air for the parallel tunnel drives and the cross passage drive. For all work sites a total of 120 m^3/s of fresh air has been determined.

2.4 *Function of the recirculation system*

The tunnel's mouths are situated at some 30 m one from each other. The west portal is hermetically closed with a sliding door in it to allow passage to the train traffic. Two fans extract the air from the western tube and create a depression in the full section of the this tube, sucking the air from the interior of the tunnel. In order to avoid recirculation at the portals the fresh air is blown until the crossing-cavern through the by-pass adit, having its mouth some 200 m from the main portals.

From the crossing-cavern the air flows into the eastern tunnel in its full section, passing by the worm east, where the final lining of the eastern drive is cast.

Past the worm east the air passes on to the ventilators situated at the cross-passage QSx-3 (Figure 1), thus supplying the to TBMs with fresh air by means of flexible ventilation ducts. 45 m^3/s are delivered to each TBM, the remainder of the 120 m^3/s continue to the ventilator at the cross-passage QSx-2. This ventilator the blows the rest of the fresh air straight into the western tube, thus diluting the used air of the TBMs passing at this position an going further on to the worm west, where the inner lining of the western tube is cast.

The ventilator at the cross-passage QSx-1 evacuates the used air returning from the TBM-East to the western tube, where it joins the used air from the TBM-West. The exhaust air from the TBM-East jointly clears the fumes of the drill-and-blast drive at QSx.

These ventilators at the last cross passages care for a depression in the eastern tube, thus helping to suck in the fresh air from the outside of the eastern tunnel, and create an over-pressure in the western tube, pushing the waste air towards the ventilators at the portal of the western tube. These two ventilators help to strengthening the system and maintain it more reliable.

To granting the full flow of air to the deepest of the tunnel and obstructing ventilation short circuits all the cross passages have to be equipped with hermetically

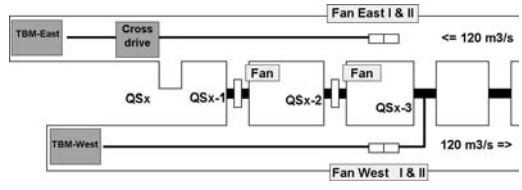


Figure 1. Overview sketch of the ventilators in the cross passages at the deepest of the tunnels.

leak-proof locks with a door in it, allowing staff to cross from one tube to the other when necessary.

2.5 *Work in progress*

Steady advance of the different work sites creates the necessity of disassembling and substituting these locks.

The first type of lock is mounted on the eastern side-wall of the western tube, right after the break-through of the new cross passage QSx. Once the invert of this cross-passage is finished a steel lock is mounted in the center of it. This lock later allows the attachment of the ventilators providing for the flow of air from the eastern to the western tube at QSx-1 and QSx-2.

After completion of a further cross passage these ventilators have to be advanced to the next cross passage. Thus this they give way for the worm west to proceed.

The western mouth of the cross passages is cast at the worm west, which is some three cross passages ahead of the worm east. Given an advance rate of some 500 m per month, casting of a mouth of a cross passage takes place every 20 days. The impermeability sheet and the seepage water drainage pipes have to be laid in the cross passage.

Therefore the lock in the center of a cross passage has to be dismantled and the cross passage is sealed with a different type of lock on the western side-wall of the eastern tube. When the shutter is needed the lock is placed aside, the shutter for the mouth is inserted from the eastern side of the cross passage and the lock is set back in place.

When the shutter is needed for casting the mouth of the next cross passage the lock has to be moved aside again. The shutter is moved to the eastern tunnel, loaded onto a train and transported to the next cross passage, where the before mentioned procedure is repeated. The lock at the cross passage the shutter stood before is closed with an again different type of lock on the eastern side of the cross passage adit.

By the time the worm east is ready to cast the mouth of that same cross passage the shutter is moved in form the western tube. A lock on the western edge of the cross passage is mounted, the lock on the eastern side is dismantled and the shutter is pulled in place through the cross passage.

When the shutter is needed for casting the mouth of the next cross passage the lock on the western side is dismantled, the shutter is loaded onto a train on the western tube and transported to the next cross passage, where the before mentioned procedure is repeated. The lock on the eastern edge of the cross passage is reestablished and the inner lining of the cross passages is cast at a later stage of work.

These locks will be only removed when the two final lock-wall will be cast on each side in a later work stage.

3 CONCLUSIONS

Maintaining the recirculation ventilation system functioning – assuring that all the work sites may advance in its pace – is a complex task, however it is inevitable to ensuring that the limits for the maximum working point concentrations are observed.

In the current project the depicted procedures guaranteed to keeping concentrations to the lowest possible and warranted good working conditions for all the staff involved.

This page intentionally left blank

Underground Space – the 4th Dimension of Metropolises – Barták, Hrdina, Romancov & Zlámal (eds)
© 2007 Taylor & Francis Group, London, ISBN 978-0-415-40807-3

Ventilation of cross-passages in long rail tunnels: Requirements and possible solutions with a passive or an active ventilation system for the Gotthard Base Tunnel

D. Portmann, P. Reinke, B. Hagenah & A. Busslinger
HBI Haerter Ltd., Consulting Engineers, Berne, Switzerland

ABSTRACT: The Gotthard Base Tunnel will be a main part of the new railway links crossing through the Swiss Alps. It will have a length of 57 km. A total of 180 cross-passages will connect the two single-track tubes. The cross-passages provide escape routes in case of emergency to the parallel tube and they house technical equipment for the operation of the train traffic. Due to the heat release of this equipment and the high rock temperatures, the cross-passages need to be ventilated. A passive ventilation system ("pitot-tubes") and an active ventilation system are described within this paper. Both concepts may provide an adequate cross-passage climate. In the specific case of the Gotthard Base Tunnel, the active ventilation is to prefer because of the demanding reliability and availability requirements and the challenging climatic conditions. However, the passive system was found to be suitable for many cross-passages with the advantage of low maintenance, low failure risk and low operation costs.

1 INTRODUCTION

1.1 *General*

The Gotthard Base Tunnel (GBT) forms a major element of the new Swiss alpine rail tunnels. It consists of 2 single track tunnels of 57 km each which are connected with accessible cross-passages (CPs) approximately every 330 m. In addition, the base tunnel system includes 2 multifunctional stations (MFS) with 2 crossovers and 2 emergency train stations each, see Figure 1.

Three different modes of operation must be distinguished for the GBT:

- normal operation
- maintenance operation
- emergency operation

During normal operation, the trains run from north to south in the eastern tube and from south to north in the western tube. The tunnel ventilation system is not in operation, since the train-induced airflow is sufficient to provide an adequate tunnel climate. The air-exchange of the CPs must be considered separately. Since the CPs accommodate equipment with considerable technical heat release (up to 7 kW per CP) and the initial rock temperatures reach up to 50°C, specific ventilation measures have to be provided.

Maintenance operation in the GBT takes place during the night time in one tube while in the other tube trains run alternately from south to north or from north to south. The tunnel ventilation system will provide fresh air for the maintenance teams. The ventilation of the CPs is needed during this phase.

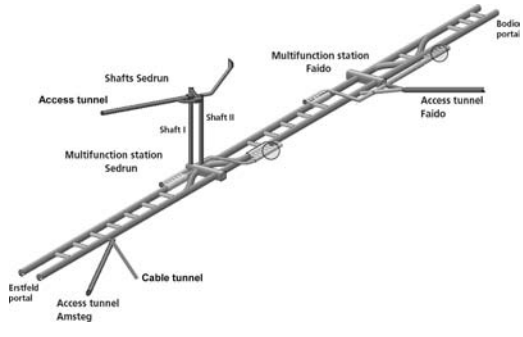


Figure 1. System overview of the Gotthard Base Tunnel.

In the case of an emergency in the tunnel, the incident train is supposed to leave the tunnel or to stop at a MFS. The tunnel ventilation system will provide smoke-free areas for escaping passengers along the rescue paths in the MFS. In the unlikely event of a train stopping in the tunnel but outside a MFS, the tunnel ventilation system will provide an overpressure in the non-incident tube. This results in a smoke-free non-incident tube, even if escaping passengers open the CP doors. During an emergency the CPs that are not opened by passengers must be ventilated to protect the equipment enabling the evacuation of the passengers.

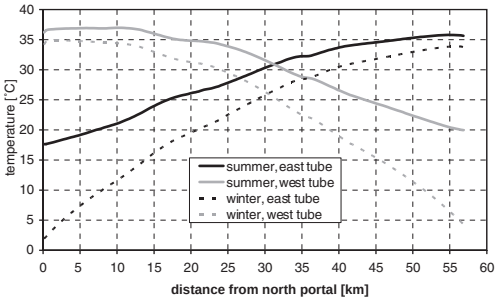


Figure 2. Expected tunnel temperature in the GBT from Busslinger et al.

Table 1. Classification of warmer and cooler tunnel sections.

Tunnel	North portal – km 30	km 30 – south portal
East	Cool	Warm
West	Warm	Cool

1.2 *Tunnel climate*

In order to ensure the proper operation of the base tunnel, an acceptable tunnel climate must be maintained. If the tunnel air is too warm or too humid, technical installations may fail or their lifetime will be reduced. Additionally, maintenance teams shall meet acceptable working conditions.

The expected temperatures along the base tunnel are shown in Figure 2. The temperature will rise from the entrance portals to the exit portals.

Figure 2 allows a classification of the tunnel into warmer and cooler sections. These are shown in Table 1.

While the climate in the train tunnels is mostly relevant for passenger comfort (air-condition systems on board depend on the outside temperature) and the maintenance teams the CP climate is crucial to the reliability, since they include most of the technical equipment. Additionally, the CP climate must fulfill requirements for maintenance teams. Tunnel and CP climate are strongly connected to each other because the fresh-air supply of the CPs will be provided from the tunnels.

1.3 *Cross-passage ventilation*

The CPs are located approximately every 330 m and are connecting the two single-track tubes. Their length is about 40 m, the free cross-sectional area is about 11 m^2. Each end of a CP is equipped with a door that separates the CP from the adjacent tube. For maintenance reasons or during an emergency the doors may be opened.

The CPs have two purposes:

- The main purpose is to provide evacuation paths in case of an incident with stop of the incident train in the tunnel but outside a MFS
- house technical equipment important for the operation of the tunnel

The technical installation in the CPs consists of:

- transformers
- telecommunication equipment (fix, mobile)
- traction current supply
- 50 Hz power supply

This equipment may emit during peak-times waste heat of up to 7 kW per CP.

2 OBJECTIVES OF CROSS-PASSAGE VENTILATION

To provide a safe, reliable and economic tunnel system, basic climate requirements must be fulfilled in the CPs. In the following sub-chapters the ventilation objectives of the CPs are stated for the different modes of operation.

2.1 *Normal operation*

The ventilation objectives for normal operation in the CPs of the GBT are as follows:

- temperatures shall not exceed 35°C
- relative humidity shall not exceed 70%

An exception of this rule is given for the CPs in the vicinity of the portals where meteorological conditions dominate and can not be controlled.

2.2 *Maintenance*

During maintenance the climatic conditions in the tunnel system including CPs have to meet the regulations of the Swiss Accident Insurance Fund (SUVA), i.e.:

- The maximum temperature shall not exceed 28°C (preliminary requirement which, possibly, will be changed to 28°C WBGT-temperature in the future).

Furthermore, the maintenance teams in the CPs must not experience severe pressure changes generated by trains travelling in the non-maintenance tube:

- The maximum pressure fluctuation during a 4 s-time period shall not exceed 1.5 kPa.

2.3 *Emergency*

During an emergency, most of the CP equipment is supposed to work reliably enabling the trains in the tunnel to leave the system and, at a later stage, allow

the entrance of an evacuation train. This results in the following requirement:

– The temperatures in the CPs shall not exceed 40°C for at least 90 min after the beginning of an emergency.

Furthermore, if CP doors are opened by escaping passenger, the following objective shall be met:

– The velocity of air in open CP doors shall inhibit smoke propagation into the non-incident tube (>2 m/s) and allow a safe escape (<11 m/s).

3 POSSIBLE CONCEPTS

3.1 *Basic principles*

To accomplish the objectives as defined above, some basic principles for the CP ventilation of the GBT may be introduced.

During normal and/or maintenance operation the following principle is favourable for the CP climate:

– Both, the fresh air supply and the waste air removal are achieved with the cooler tunnel tube.

One side of the CP is closed (closure to the warmer tube) and an aerodynamic decoupling of the tubes is established. This arrangement reduces non-favourable pressure fluctuations across the CPs and internal re-circulation of waste air. Additionally, it supports the efficiency of the tunnel ventilation system during emergency (less leakage).

During an emergency, another principle is taken into account:

– Air-supply is provided from the non-incident tube (not necessarily the cooler).
– Air removal is directed to the incident tube.

In this case, an air flow from the non-incident tube to the incident tube will result. Thus, the propagation of hot, smoky air into the CP can be prevented, even if a burning train is located just in front of a CP.

In the following sub-chapters, two selected solutions based on these principles will be described.

3.2 *Passive cross-passage ventilation*

The passive CP ventilation is driven by the train traffic. The trains in the GBT travel with speeds of up to 250 km/h and induce during normal operation a mean air velocity of about 7 m/s along the tunnels.

Parts of this air flow are guided into and out of the CP by “pitot-tubes” as shown in Figure 3.

The main principle of this ventilation concept is as follows: Due to the dynamic pressure there is a pressure difference between the tunnel openings of pitot-tube 1 and 2. This pressure difference generates an air-flow through the CP.

The pitot-tubes have a length of 2 m (tube 1) or 40 m (tube 2) and a diameter of 0.4 m. They will be installed

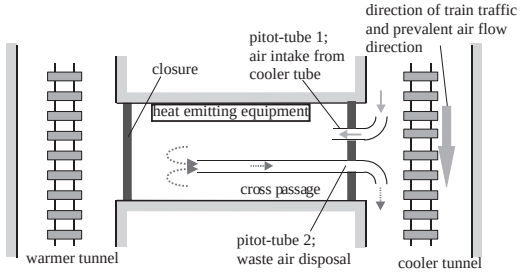


Figure 3. Ventilation of cross-passages with pitot-tubes during normal operation.

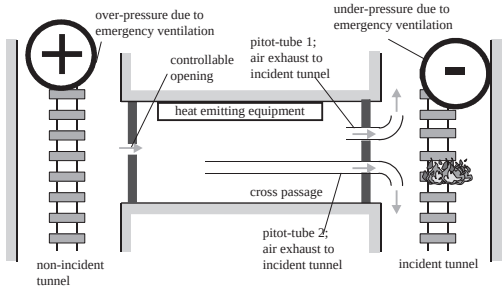


Figure 4. Passive cross-passage ventilation during an emergency in the cooler tunnel.

above the CP door to exclude any constraints for passenger escape (cf. Figure 6). The warm waste air will be guided through the longer tube 2 in the vicinity of the warm ceiling climate of the CP to increase the cooling efficiency. The length of tube 2 provides longitudinal flow of air along the whole CP. The concept allows for both flow directions in the rail tunnel even though the opposite of the presented flow direction leads to a smaller air-exchange.

Figure 3 is typical for normal operation and maintenance (if maintenance is taking place in the warmer tube). Three more modes have to be addressed therefore. These are:

– maintenance in the cooler tunnel
– emergency in the cooler tunnel
– emergency in the warmer tunnel

During maintenance in the cooler tunnel, no train traffic will induce air-flow. However, the maintenance teams have to be supplied with fresh air. In this case, the air will be supplied by the tunnel ventilation system. So, an air-flow will be guaranteed.

Due to the symmetric arrangement of the pitot-tubes on the tunnel side, air will be lead into the CP independently of the flow direction in the rail tunnel.

Figure 4 shows the situation during an emergency in the cooler tube. The tunnel ventilation system generates an over-pressure in the non-incident and an under-pressure in the incident tunnel, mainly to

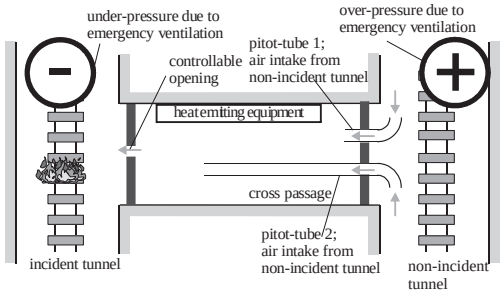


Figure 5. Passive cross-passage ventilation during an emergency in the warmer tunnel.

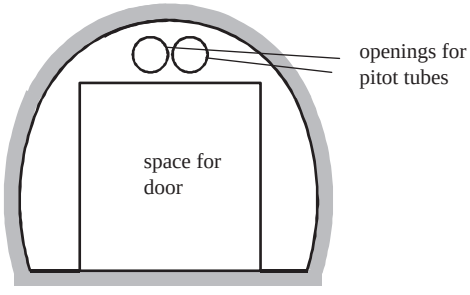


Figure 6. Front view of cross-passage with arrangement of openings for pitot tubes.

provide an air-flow through the opened CPs (by escaping passengers). CPs with closed doors would be endangered to be filled with warm and smoky air via the pitot-tubes, if no further measures would be taken. Dampers in the pitot-tubes might prevent this, but on the other hand, no more cooling air-circulation in the CP would take place. Additionally, they would reduce the ventilation power due to additional flow resistance. As a consequence, overheating and failure of equipment in the CP, especially with a train fire nearby, can be assumed. Therefore, a damper in the wall opposite the wall with the pitot-tubes of the CP must be foreseen. During an emergency, the damper will be opened. The pressure difference between the tunnels will lead to an air-flow through the CP and provide a minimal ventilation to enable the tunnel operation until all the passengers are evacuated.

In the case of an incident in the warmer tunnel as depicted in Figure 5, one could keep the controllable damper closed, since no warm air could enter the CP via the pitot-tubes. For the following reasons it still is advisable to open the damper:

- No decision of the operator concerning opening of the dampers is necessary, independently in which tunnel the incident takes place.
- The CPs are always minimally ventilated.

The installation of the pitot-tubes will preferably be above the CP doors (see Figure 6).

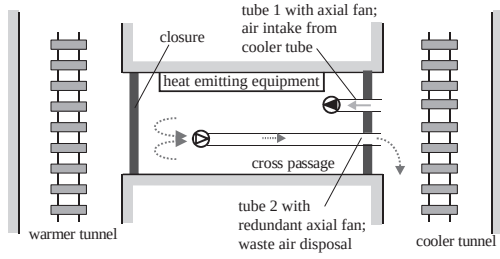


Figure 7. Active cross-passage ventilation during normal operation.

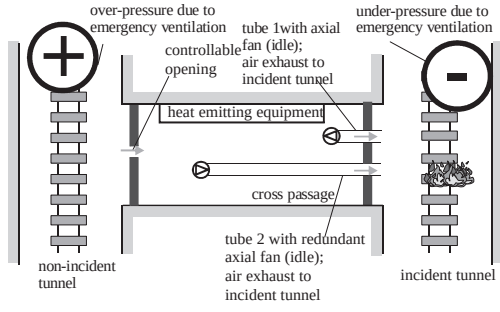


Figure 8. Active cross-passage ventilation during an emergency in the cooler tube.

3.3 *Active cross-passage ventilation*

In contrast to the passive CP ventilation, the active CP ventilation is only sparsely dependent on train traffic in the tunnels. The concept of the active CP ventilation system is shown in Figure 7.

A fan mounted on tube 1 will lead air from the cooler tunnel in the CP. The waste air will be disposed via tube 2 by the idle redundant fan. The situation just described is valid for normal operation and maintenance.

During an emergency, the tunnel ventilation system will create an over-pressure in the non-incident tunnel and an under-pressure in the incident tunnel. The fans in the CPs will be turned off and the above described damper on the opposite side of the CP will be opened. This allows a pressure driven ventilation of the CPs, automatically in the right direction, as shown in Figure 8 and Figure 9.

4 SIMULATION RESULTS

In this chapter, it will be shown that the described concepts are feasible.

4.1 *Passive cross-passage ventilation*

The following parameters determine the air-flow in a passively ventilated CP:

- air velocity in the railway tunnel

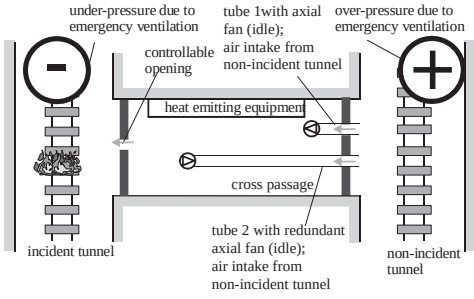


Figure 9. Active cross-passage ventilation during an emergency in the warmer tube.

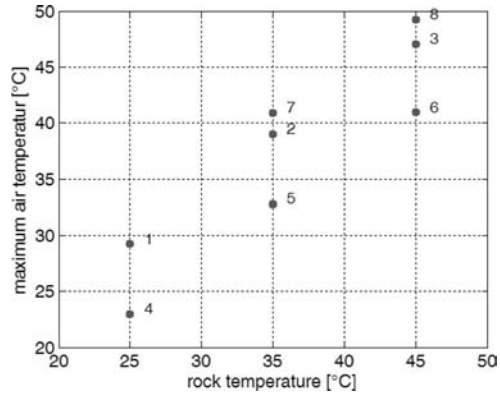


Figure 10. Maximum air temperatures in cross-passages for different rock temperatures, heat release rates and tunnel air temperature.

Table 2. Air temperature calculation results for selected cross-passages.

No.	Heat release into CP from equipment [kW]	Tunnel air temperature [°C]	CP volume [m^3]	Resulting maximum temperature [°C]
1	5	15	315	29
2	5	25	315	39
3	5	33	315	47
4	2.5	15	315	23
5	2.5	25	315	33
6	2.5	33	315	41
7	5	25	630	42
8	5	33	630	49

Table 3. Volume flow calculation for selected cross-passages.

No.	Heat release into CP from equipment [kW]	Tunnel air temperature [°C]	CP volume [m^3]	Necessary air volume flow to maintain 35°C [m^3/s]
1	5	15	315	<0.37
2	5	25	315	0.6
3	5	33	315	2.4
4	2.5	15	315	<0.37
5	2.5	25	315	<0.37
6	2.5	33	315	1.5
7	5	25	630	0.6
8	5	33	630	2.5

– diameter of the pitot-tubes, i.e. the flow resistance of the system CP and pitot-tubes
– position of the pitot-tube in the tunnel

Based on aerodynamic predictions for the GBT it is known, that the mean air velocity in the tunnel during normal operation will be about 7 m/s (mean value during normal schedule). The inner diameter of a pitot-tube is supposed to be 450 mm. Measurements carried out in a CP test site have shown, that a volume flow of about 0.4 m^3/s can be achieved with an optimal position of the pitot openings in the tunnel.

To estimate the cooling effect of the passive CPs ventilation, the subsequent parameters need to be known:

– air temperature and humidity of tunnel air
– heat release of CP equipment and rock
– size of CP, i.e. air that has to be replaced and CP surface in contact with the air
– water ingress through CP lining

In Table 2 and Figure 10 the results for the air temperature calculation are listed and depicted, respectively. The initial rock temperature has a major influence on the temperature in the CPs. Furthermore, the expected heat emission by technical equipment is of relevance. For the calculations, a minimal water ingress through the CP lining was assumed.

It is apparent, that as soon as the rock temperature is in the region of 45°C, the passive ventilation system will no longer be effective.

4.2 *Active cross-passage ventilation*

With active CP ventilation the volume flow through a specific CP can be chosen by installing an adequate fan.

In section 4.1 it was shown, that not for all thinkable combinations (rock temperature, heat emission, tunnel air temperature, etc.) the requirements to the CP air temperature can be met. In the Table 3 and Figure 11 is shown, what air volume flow is required to meet the design objectives for the CPs.

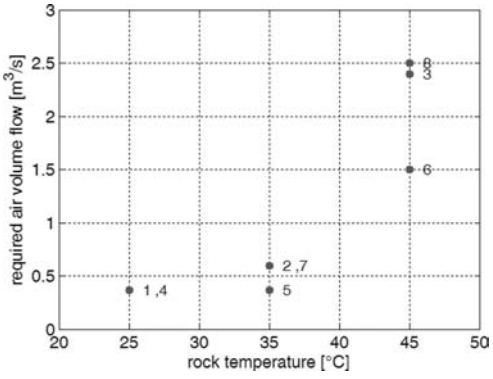


Figure 11. Required air volume flow to keep cross-passage below 35°C.

5 COMPARISON

The passive and the active CP ventilation should be compared on a qualitative level. The following criteria are relevant:

- During normal operation or maintenance:
  - *Climate control*: Low temperatures and low relative humidity shall be achievable in the CPs.
  - *Ingress of dust*: Ingress of dust in the CPs shall be as small as possible.
- During maintenance:
  - *Maintenance availability*: The ventilation of the CP shall also be possible during maintenance.
- During an emergency:
  - *Escape path*: The CPs shall be kept smoke free. Furthermore, no obstacles shall constrict the path of escape.
  - *Robustness*: The CP ventilation elements shall be operable as long as possible.
  - *Operability of CP equipment*: The temperature increase shall be as small as possible.
- Special conditions and general aspects:
  - *Ventilation during special situations*: The effort for the CP ventilation during situations that differ from normal schedule shall be as low as possible.
  - *Reliability and availability of CP ventilation*: The probability of failure or malfunction of the CP ventilation as well as the maintenance effort shall be as small as possible.
  - *Life-cycle cost*: The investment, the maintenance costs as well as the energy input shall be as low as possible.

In Table 4 the passive and the active CP ventilation were compared to each other, whereas "+" means good, "0" means neutral and "−" means poor.

Table 4. Comparison of passive and active cross-passage ventilation.

	Ventilation type	
Criteria	Passive	Active
Climate control	+	+
Ingress of dust	0	+
Ventilation during maintenance	0	+
Escape path	0	+
Robustness	−	−
Operability of CP equipment	+	0
Ventilation during special situations	−	+
Risk of CP ventilation failure	+	−
Life-cycle cost	0	−

Table 4 shows that for the GBT, the active CPs ventilation features more positive aspects. On the other hand, the passive system shows fewer weaknesses.

6 CONCLUSIONS

Depending on the specific boundary conditions of each tunnel, the active, the passive ventilation or a combination of both concepts are thinkable.

In the case of the GBT, a tunnel with high heat loads in the CPs and high rock temperatures, an effective control of the CP climate may not be guaranteed at all locations and at all operating conditions with a passive system. To achieve homogenous CP ventilation in all situations, an active CP ventilation system is required. It allows reliable CP ventilation in all possible operation modes, at the costs of frequent maintenance intervals and a non-optimal cost-benefit ratio.

The passive CP ventilation represents a robust solution, depending on adequate rock temperatures and moderate heat releases in the CPs. It is not suitable for the GBT. In case of uni-directional traffic, i.e. a specific air-flow direction in each tunnel tube, the passive CP ventilation is a feasible and cost-effective solution.

ACKNOWLEDGEMENT

The authors wish to thank AlpTransit Gotthard Ltd for permission to publish this paper. AlpTransit Gotthard Ltd decided for the active CP ventilation in 2004. In December 2006 the tendering for the Lot B1 "CP Ventilation" will be published. For information regarding the current active CP ventilation design contact AlpTransit Gotthard Ltd.

REFERENCE

Busslinger, A. & Zbinden, P. 2001. Current State of Climate Prediction for the Gotthard Base Tunnel and Further Steps, *International Tunnels Forum, New Technology in Tunnel Management Systems*, Basel.

Underground Space – the 4th Dimension of Metropolises – Barták, Hrdina, Romancov & Zlámal (eds)
© 2007 Taylor & Francis Group, London, ISBN 978-0-415-40807-3

Fire test in the Mrázovka tunnel and its impact on the ventilation control systems in tunnels Mrázovka and Blanka

J. Pořízek, M. Hanfová & L. Šajtar
SATRA, spol. s r.o. Prague, Sokolská, The Czech Republic

ABSTRACT: Risks, which are related with fires in road tunnels, will be always decisive for the choice of technological systems that enable a safe escape from tunnel. The biggest life hazard is the hot toxic smoke that is released during combustion of hydrocarbon fuels and flammable materials. Considering smoke behavior and laws of conservation, then the system of forced ventilation, which exhaust heat and smoke from tunnel, is the most effective method. It is possible to predict the smoke behavior in tunnel of a concrete geometry and location by the appropriate choice of initial and boundary conditions. One of the most effective methods for understanding the smoke behavior and for design of safety measures is the real fire test in tunnel with the using of the hot smoke. On the basis of results of these fire tests it is possible to determine or modify the strategy of ventilation control system. Several tests with cold and hot smoke were realized in the Mrázovka tunnel. The heat release during the combustion of hydrocarbon fuels was always only 5 MW. Different methods of forced smoke exhaust and other safety equipments in the tunnel were examined during fire tests. Fire tests in the Mrázovka tunnel proved the efficiency of the designed system and they have produced new knowledge about the smoke behavior. In the SATRA engineer's company these results are integrated into algorithmic rules of ventilation control systems.

1 INTRODUCTION

Especially in cases of long tunnels there are necessary devices for smoke exhausting. In urban tunnels, there can be increased a number of users during fire so it is necessary to provide smoke exhaust from short tunnels too. Potential sources of fire inside tunnel are vehicles, materials and equipments in tunnel or in technical area.

The most dangerous for tunnel users are fires of vehicles. Fire can arise anywhere in tunnel and for every type of vehicles and loads. Fire characters are very different from case to case. Heat release of real fire is in range from 2 to 200 MW (and sometimes even more).

For determination of temperature resistance of construction it is possible to issue from normative curves showed in figure 1.

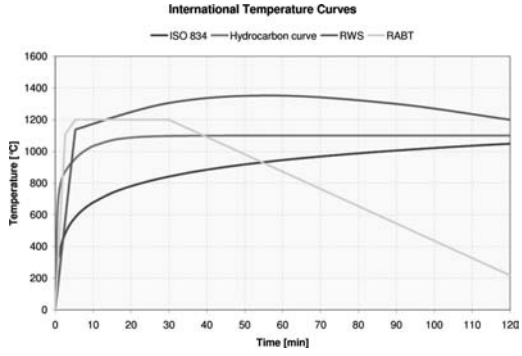


Figure 1. Temperature fire curve.

Normative temperature curve ISO 834 was derived for fire in underground buildings and it can be used for examination of the fire resistance in tunnels.

Hydrocarbon temperature curve is used where can be fire of cistern with petrol, crude or chemicals.

RABT temperature curve was derived in Germany within the bounds of several research plans. This curve corresponds with heavy goods vehicle fire.

RWS temperature curve is based on assumption of the worst fire with heat release 300 MW. The curve is result of many tests executed in the Netherlands in the late seventies of previous century. The RWS curve describes burning in closed area where a chance of smoke and heat spread to outside area is minimized.

The most used characteristic of fires for design of the ventilation systems are showed in table 1. These fires were chosen on purpose, because they include majority of real incidents.

The most important for determining of smoke volume, which is needed to exhaust from road tunnel is a

Table 1. The most frequently design parameters of fires.

Vehicle type	Heat release [MW]	Smoke production [$m^3 \cdot s^{-1}$]
1 Passenger car	5	$\leq$20
2 to 3 Passenger cars	8	$\leq$30
Heavy lorry (bus) without dangerous goods	20–30	60–80
HGV with fuel and oil (petrol tanker)	$\geq$200	>300

fire of heavy goods vehicle that cannot be extinguish by users and whose heat release exceed 20 MW is [7].

If a normative fire has been defined, than it has to be determined the exhausted flow of the air (smoke) from a tunnel during fire. The theme of this article is the fire test in the Mrázovka tunnel and some examples of requirements on determining of volume flow, which has to be forcedly exhausted from tunnel, according to directives of some EU states are shown here. These volume flows were determined for fires of heat release 20 to 30 MW. Documentation published by association PIARC issues from these nationally directives and it shows, that positive exhaust flow rate can set like three-fold of tunnel cross section. By fire with heat release higher than 100 MW it may be until fifth-fold.

Basic indicators for determining capacity of ventilation system are: type and length of tunnel, traffic density and first of all conceptual design of ventilation (longitudinal, transverse, semi-transverse or their combinations).

France
For design capacity of transverse system with eliminated dangerous goods vehicles is assumed fire heat release from 20 to 30 MW. In the case of tunnels with clearance profile over 3.5 m it is taken into account with 80 $m^3 \cdot s^{-1}$ of smoke volume. In the case of concentrated smoke exhaust from tunnel, the minimal volume flow can be determined like volume of produced smoke plus 1.5 multiply of longitudinal velocity in tunnel.

Germany
In ground of solution the minimal exhaust volume is determined like 1.5 multiply of smoke production.

Austria
This directive report that the minimal exhausted volume flow rate during fire must be at least 120 $m^3 \cdot s^{-1}$ over the length 150 m

Czech republic
In this directive, the flow extracted from three-lanes tunnel (cross section 65 m^2) in the case of transversal exhausting is determined to 195 m^3/s through a length,



Figure 2. Stratified smoke layer during fire test in tunnel Bruyères [13].

which is not defined. This value is based on the older Swiss directive [8].

Switzerland
In the directive of 2004, the minimal flow of extracted air has to be counted as three-times of the tunnel cross section. In the case of forced air supply, the flow of supplied air has to be added to this exhausted volume.

Following documents are obligatory in most of cases for the design of technological equipments in road tunnels and their operating in Czech Republic:

- TP98 – Technological equipments of road tunnels: 2004
- TP154 – Operation, management and maintenance of road tunnels
- ČSN 73 7507 – Road tunnels designing
- European Directive 2004/54/EC – minimum safety requirements for tunnels in the trans-European road network.

2 ABOUT THE VENTILATION SYSTEM IN THE MRÁZOVKA TUNNEL:

The smoke extraction in Mrázovka tunnel was designed for the fire of one heavy goods vehicle and for no danger goods vehicles. According to data that were used for the design, the heat power of a heavy goods vehicle fire will be 20–30 MW and flow of smoke will be 60 m^3/s [3]. In that time, requirements on extraction of 80 $m^3/s \cdot km$ for two-lanes section [4] seemed to be insufficient. Opinions on increasing of extraction were different for different theories 110–190 m^3/s.

The system of the transversal smoke exhausting, with slots in ceiling, was designed additionally for the fire in tunnel in the case of congestion. This method consists in prolonging of the time, in which the extracted smoke stays under the ceiling and when users may safely escape the tunnel. This system shall ensure zone of stratificated smoke (see Fig. 2) and thus the efficiency of longitudinal ventilation will be higher.

Transversal fire exhausts in cut and covered sections, which have shorter distance between the ceiling and the road, are other elements of the ventilation system in the Mrázovka tunnel, that increase security of users in the case of fire.

The power for transversal extraction was designed 150 m^3/s through the length 400 m. This value has been verified for specifics conditions in the Mrázovka tunnel on 3D model by means of CFD simulation, where was different traffic densities, different fire locations and different operating modes simulated.

3 THE FIRE TEST IN THE MRÁZOVKA TUNNEL

The aim of the fire test was to verify the designed system of ventilation, fire detection EPS etc. Test was realised in two localities in Eastern tunnel according to the location of smoke outlet and according to the technical equipment in airways for the smoke extraction.

On the basis of the requirement of Prague's firebrigade, which follows from their attitude to the project of the Operating documentation for the Mrázovka tunnel, there had to be the test of smoke extraction completed before putting the tunnel into operation. This test had to be completed with the participation of representatives of Prague's fire brigade. According to realisations of fire test in new or reconstructed tunnels, the attitudes to methods of fire tests are becoming unitary in EU. Examples of these tests are: Mont Blanc tunnel (France-Italy), Platsbush (Austria) and Rennsteig tunnel (Germany). Fire tests of real fires (5 MW) were realised in all these tunnels. The power 5 MW was achieved by lighting up of 20 litres of petrol in containers with the area about 2–4 m^2.

The method of realization of the fire test in the Mrázovka tunnel is based on the results of the project of EU: COST N˚ OC G3.40 "SMOKE SPREAD IN THE CASE OF FIRE IN ROAD TUNNEL", which worked out SATRA company in co-operation with VUT Brno in 1999–2003.

This project was aimed to problems of smoke spread in road tunnels immediately after ignition of fire. Problems were studied by means of Euler-Lagrange model of CFD.

The project of fire test, which came out from results and recommendations of fire tests in tunnels Mont-Blanc, Platsbush and Rennsteig, was modified and filled in after the consultation with KRASO company and Technical Institute of Fire protection, who were participated in fire test.

3.1 *Test preparation*

Fire tests with cold and hot smoke in Mrázovka tunnel were effected in 13. -15.8. In all cases was the fire of passenger car simulated and it correspond to heat

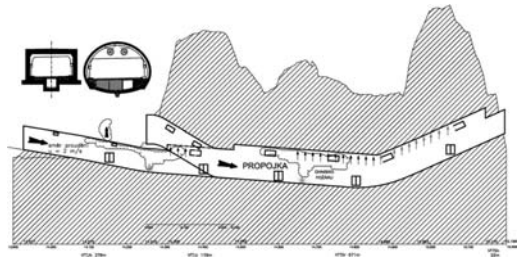


Figure 3. Scheme of fire tests (fire on the left – cut and covered two-lanes section – cross section 56 m^2, fire on the right – driven three-lanes section – cross section 93 m^2).

power about 5MW. For the test were used 40 l of petrol and 10 l of oil for visualisation of the thermal field with the smoke. This mixture was lighted up in the tank with the area about 2 m^2. The container was situated in the axis of cross section at a height 1,5 m under the road.

3.2 *Preventive measures*

The surface of the road round the tank was protected at the distance 2 m on both sides (cca 30 m^2) with panels of insulating material ROCKWOOL, which are made of miner wool. Protection of distribution system (lighting, EPS, antenna, cables) on ceiling was ensured at the distance 25 m on both sides with material of ROCKWOOL with an ALS foil LAROCK 65 ALS at thickness 120 mm.

4 COURSE OF THE FIRE TEST

4.1 *Initial conditions*

Before igniting of the fire the similar conditions to those, which are in the tunnel during the normal operation (average flow velocity 2 m/s and more) were simulated by means of jet fans. The flow velocity was measured by the air flow sensor FLOWSIC 200 (in the three lane section – u_{VTS}, in connected entrance ramp – u_B).

4.2 *Fire test in the three-lanes section*

The seat of the fire for the first test was chosen in the downward part of three-lanes section in the driven tunnel (see fig. 3 – Fire in the right part), before the section with the slope 4,5% in the direction of upward.

This test was effectuated to verify the efficiency of the exhaust slots in the ceiling of the driven tunnel and assurance of the smoke stratification under the ceiling.

Slots are end elements of the channels, which are in the tunnel lining and which joins to the smoke duct under the road (see Fig. 7). It is possible to close every channel with the remote control damper, which is situated at the connection with the smoke duct. The distance of the slots is 20 m. In the case of



Figure 4. *The test with a hot smoke* (driven three-lanes section).



Figure 5. The test with a cold smoke.

fire detection in the section with transversal smoke exhaust, 20 dampers are opened at the length of 400 m and 150 m^3/s of the hot smoke is exhausted.

The test with a hot smoke (see Fig. 4) was repeated more times. Before the ignition of the fire the exhaust ability of slots was several times tested (see Fig. 5). Behaviour of the cold smoke was and will be for every time different from the hot smoke.

The cold smoke starts to fill the whole section and fall towards the road immediately after the ignition, whereas the hot smoke rise up and form a stratificated zone of the smoke "pillow".

The cold smoke was spread in the whole section of the tunnel. Exhaust range of the slots is substantial only in their proximity and thus the cold smoke was not almost exhausted. During this test it could seem, that the system is ineffective. In the case of hot smoke test, the smoke stay under the ceiling and slots exhaust nearly all the smoke.

4.3 *Fire test in the two-lanes section*

The aim of the second fire test was to verify ability of the system to avert the back layering and assurance of the smoke stratification in the downward part. The other aim was to verify functionality of the natural exhaust of the smoke by the flue, which is situated at

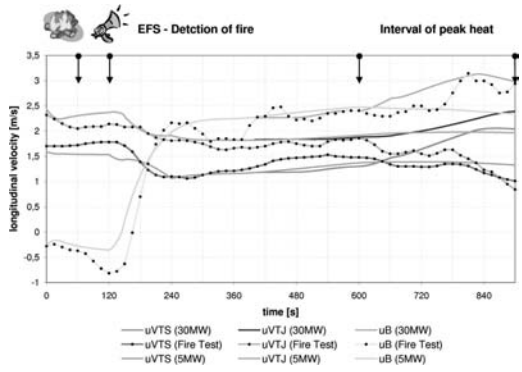


Figure 6. Behaviour of the longitudinal velocity.

the boundary of the driven and cut and covered part. And the last aim was to verify the efficiency of the parallel functioning of transversal smoke exhaust by the slots and control of the longitudinal flow. The seat of the fire was chosen in two-lanes cut and covered section of the Eastern tunnel with the slope −2% (see Fig. 3 – Fire in the left part).

4.4 *The airflow in the tunnel*

On the Fig. 6 is the shape of longitudinal velocity in the three-lanes section during the fire test. The direction and the size of longitudinal velocity are decisive factors for assurance of conditions for the save evacuation of users during the first phase of fire. On the figure is the velocity in the section with a fire (u_VTS) and the velocity in the connected entrance ramp (u_B). On the figure, there are the shapes of measured velocities and shapes of velocities, which were numerically calculated during the simulation of the 5 and 30 MW fires. The shape and the size of the flow velocity for the 5 MW fire correspond satisfactorily to values, which were measured during the test. If there will be a fire in upward part of the tunnel (represented by the calculation of 30 MW fire), the flow velocity will increase about twice. In the case of downward unidirectional tunnels, there is the danger of the back layering of the smoke above cars and users, which are escaping the tunnel.

For the calculation was used the development of a passenger car fire with power about 6 MW (according to results of fire tests of Eureka project) and the development of a fire of goods vehicle with flammable load with power about 30 MW (according to [9] or by modification of results of the fire test in Runehamar tunnel).

The mathematical calculation was based on the solution of the system of dynamic equations of the one-dimensional non-stationary flow of incompressible fluid and on the solution of continuity equations.

During the simulation of the fire in tunnel it is important to include the pressure loss, which is induced by the fire, into the calculation. This pressure loss depends on the heat power, on the shape of cross section and on many others factors. This loss can be correctly calculated only by the numerical calculation of three-dimensional models by means of CFD. By the analysis of results of many studies, realised in CETU and during which the velocity was between 1,5 and 3,5 m/s, the following approximate relation was founded:

$$\Delta p_F = c.\frac{Q.10^6}{u.D_H^2}\,[\mathrm{Pa}] \qquad (1)$$

where $c \approx 9.10^{-5}$.

5 ASSESMENT OF THE RESULTS OF THE TEST

In all cases the fire was detected between 55 and 60 seconds by means of thermo line detector Cerberus® FibroLaser II. Thus the requirement for fire detection in one minute was verify. Immediately after the detection the relevant emergency sequence, whose part is the smoke extraction too, was putted into action.

Immediately after the detection of the fire all the equipments of the ventilation are stopped and at the same time, jet fans or fans of the transversal exhaustion by slots, are put into operation according to the location of the fire. The power for exhausting may be concentrated into the area, where the smoke is going and where it could endanger escaping users, thanks to the possibility of closing or opening of dampers of the slots.

The highest temperatures, which were measured by the thermo line detector during the test, were 60–70°C in the three-lanes section and 80–90°C in the two-lanes section. (the highest expected temperature on the ceiling is 150°C in the case of fire in three-lanes driven tunnel and 250°C in the case of fire in the two-lanes cut and covered tunnel). At these conditions the smoke stayed under the ceiling of the tunnel. In the three-lanes driven section, the smoke filled the space in tunnel, because of low temperatures of the smoke and because of fast getting cool of diluted smoke in the cross section (93 m^2). In the two-lanes cut and covered section (about 56 m^2) the smoke formed an ideal layer of stratification under the ceiling, which has never get cool so that it started to fall into the escape zone.

5.1 *It can be claimed that*

1. The fire will be detected in one minute and since the stopping/starting of partial equipments the airflow in the tunnel will be steady in 3–4 minutes. During this time the smoke's behaviour is natural and the smoke stays safely under the ceiling.
2. At the using of the thermo line detector FibroLaser II, the reliability of EPS is very high.
3. When the heat rate of the fire is higher and the conditions are similar, the smoke temperature will be higher and the time for getting cool of smoke will be longer, so the smoke will stay at the ceiling for longer time and the space under the smoke will be diluted sufficiently.
4. For ensuring of smoke stratification, it is necessary to keep the move of the smoke in one direction and the flow velocity in the first phase of evacuation should be 1,5 m/s. This can be achieved by the control of the flow by means of jet fans.
5. Its suitable simplification and particularization of others eventualities of ventilation control system by nonscheduled smoke behavior.
6. It is important to differentiate between the faze of evacuation and that of firefighting. During the evacuation is the ventilation in automatic smoke control mode, when is desirable not to stir the smoke with high air flow velocities. During the fire fighting faze the ventilation is in the manual control, operated according to the needs of firefighters.
7. Algorithm design methodology of automatic ventilation system must be make on events passing in the time before and after fire detection.

Results of the COST project are available on www.satra.cz.

6 SYSTEM OF VENTILATION IN THE OTHER TUNNEL IN PRAGUE CITY RING

The Prague's City ring is very important part of traffic infrastructure of Prague. The main object of City ring is to ensure the fluid transit through Prague. One of the most important parts of the City ring is the Blanka tunnel considered. Length of this tunnel is about 6 km and the system of smoke and heat exhaust is nearly the same like in the Mrázovka tunnel (combination of exhausting from cut and covered and driven sections.

6.1 *The ventilation control in the case of fire*

A few minutes after outbreak of fire it is important to keep the visibility in tunnel as long as possible. In the case of non-exhausting of smoke, the whole cross section is filled with smoke in 3–5 minutes. This time can be lengthen by longitudinal velocity and smoke extraction regulation.

The smoke extraction from driven sections is by means of slots in the ceiling. The shape of slots was designed to minimize a non-uniformity of extraction (see Fig. 7). The transversal system exhausts the volume, which corresponds to three times cross section and its value is 240–300 m^3/s. The distance of slots is about 85 m. It is possible to close every channel with

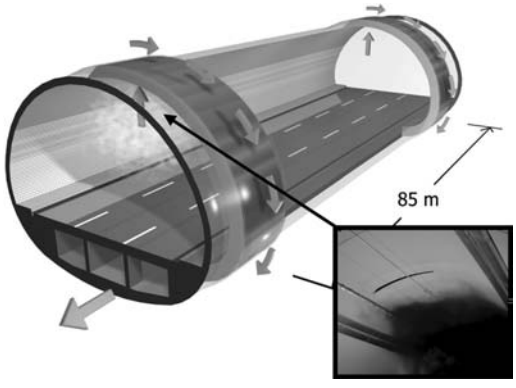


Figure 7. The channel in the lining of the driven tunnel with a detail of the slot in the ceiling.

the remote control damper, which is situated at the connection with the smoke duct, this enable to concentrate the power for exhausting.

The level of security in cut and covered sections (extraction in every 300–500 m) is lower than in driven sections (extraction every 85 m) in the case of fire during the congestion in the tunnel. In that case, jet fans in cooperation with local exhaust have to control the longitudinal velocity in value 1,5 m/s (according to the location and power of fire) during the phase of evacuation and it is necessary to exhaust the smoke according to the flow in the tunnel in order not to increase longitudinal velocity of the flow and smoke. Every increase of the longitudinal velocity may disturb the smoke stratification, which enable the visibility near the ground also behind the fire (in the sense of flow).

REFERENCES

Ventilation Report from Permanent International Association of Road Congresses (PIARC); Marrakesh 1991

Jícha, Katolický; *Modelování šíření ohně v automobilovém tunelu Mrázovka a návrh odsávacích vyústek*; Brno květen 1999

Fire and smoke control in road tunnels; PIARC Committee on Road Tunnels; August 1998

Lacroix D.; Le désenfumage des tunnels routiers en cas d'incendie, *Révue Générale des Routes et des Aérodromes*, v.n. 723, 727; novembre 1994

COST – průmyslové větrání; Modelování šíření kouře v automobilovém tunelu; Brno prosinec 2002

TP98/2004 *Technologické vybavení tunelů pozemních komunikací-Technické podmínky*; Ministerstvo dopravy a spojů; Odbor pozemních komunikací;

Dossier pilote des tunnels équipements, sectiton 4.1, Ventilation; CETU; novembre 2003

ASTRA; *Lüftung der Strassentunnel – Richtlinie*; 2001

ASTRA; *Lüftung der Strassentunnel – Richtlinie*; 2004;Bern

Richtlinien für die Ausstattung und den Betrieb von Strassentunneln, 2003; Bonn

Österreichische Forschungsgesellschaft für das Verkehrs- und Straßenwesen, Projektierungsrichtlinien Lüftungsanlagen, Grundlagen RVS 9.261

Andräss S., Mayr R., Rudolf A., Seitz P., *Fire Test and Safety Concepts in the Rennsteig Tunnel. Tunnel Safety and Ventilation* – 2nd Symposium edited by Sturm P., Minarik. S., Verlag Gratz University of Technology: 2004, s.149–156, ISBN 3-901351-95-7

Prezentační CD-ROM firmy: Tempest Technology, *Mobile ventilation unit* ver. 1.0

UPTUN, TNO, Promat; *Summary of Large Scale Fire Tests in the RUNEHAMAR Tunnel in Norway, conducted in association with the UPTUN Research Program*; September 2003

Federal Highway Administration: *Memorial Tunnel Fire Ventilation Test Program*, November 1995

NOMENCLATURE

VTT	Eastern tunnel
EPS	electronic fire-warning device
u	velocity of the longitudinal flow [m/s]
$u_{_VTS}$	velocity of the flow in the three-lanes section [m/s]
$u_{_VTS}$	velocity of the flow in the two-lanes section [m/s]
$u_{_B}$	velocity of the flow in the connected entrance ramp [m/s]
$\Delta\ p_F$	pressure loss induced by fire [Pa]
Q	convective heat power of the fire in tunnel [MW]
D_H	hydraulic diameter of area of flow cross section of tunnel [m]

Underground Space – the 4th Dimension of Metropolises – Barták, Hrdina, Romancov & Zlámal (eds)
© 2007 Taylor & Francis Group, London, ISBN 978-0-415-40807-3

Optimization of tunnel system based on ITS architecture

P. Přibyl
ELTODO EG, Prague, The Czech Republic

ABSTRACT: Road tunnels consist of several very complex sub-systems (safety, ventilation etc.), which have to be integrated in terms of transport telematics principles. The article describes a web-oriented tunnel safety architecture based on the European KAREN project and standards elaborated in the CEN/TC278 technical committee. Upon the choice of a user needs connected with tunnel safety (non mandatory equipments or systems) is generated automatically a set of functions and information flows between them in a form of ITS architecture. This system restricts both any useless functions to be implemented and any failure to install important functions and tunnel is equipped on an optimal way.

1 INTRODUCTION

The tunnel and its technological equipment is surely a very comprehensive system consisting of many sub-systems and equipments. As a scheme the tunnel may be shown as an equilateral triangle with corners "Safety", "Economy" and "Ecology" in the focal point of which is traffic. It concerns a transport system, which must be reasonably safe, appropriately built in terms of cost and ecological considerations as may be required. As regards ecology, there is almost never any problem because a tunnel usually replaces a longer and serpentine road on which drivers brake and accelerate more frequently. From the safety point of view it is much complicated because there is not only the cost of the original safety systems investment but also the cost of operation. This is the reason why a balance between a safety and a price of safety systems shall be searched.

This article describes the tunnel system in connection with and from the viewpoint of transport telematics. And the tunnel is really such a system because by using methods usual in transport telematic systems it integrates a number of heterogeneous systems in one target function, which is safe and smooth traffic. We can see very often that there are several equipment and systems installed in tunnels, which are not interoperable in full and thus their characters may be not used to the fullest. In order to provide for full integration of complex systems it is useful to model them in the form of architecture, which precisely defines functions and information flows of all sub-systems and equipment. Within several European projects (KAREN, FRAME) frameworks and rules for the establishment of architecture have been prepared. Similar processes are even standardised at the European level in technical committee CEN/TC278 "Road Transport and Traffic Telematics" and its working group WG13 "Architecture and Terminology".

The article describes the architecture of tunnel systems, which is to be used for the optimisation of any tunnel. The recommended procedure has been developed and tested within the national project of science and research OPTUN (Road Tunnel Optimisation) supported by the Ministry of Transport Czech Republic.

2 TUNNEL AS A TELEMATIC SYSTEM

A road tunnel, both in a city and in a rural area, is a component of a communication network, and traffic conditions in a tunnel correspond to traffic conditions on any road. The tunnel is, however, a specific traffic structure in terms of higher investment and operating costs. Tunnels must be viewed as integral parts of the communication system. It is always necessary to seek optimisation of economic, social and environmental impacts. An investor also has to pursue relations beyond the scope of a simple cost-benefit analysis.

These technical systems work with a large quantity of data which is often very different because a group of traffic parameters is measured as well as weather and ecological conditions, and besides, it is necessary to transmit verbal information reliably, for example from SOS boxes or telephones of road users while TV supervision is of great importance. A large data file is connected with safety and security systems in use (emergency buttons, fire alarms) and in addition,

there is a large group of data to control and monitor the technological systems such as ventilation, lighting, and charging batteries etc.

The tunnel must be seen as a part of the transport system in the area given and that is why it is necessary to communicate mutually with transport centres, police, rescue service and fire department hot lines but it is also necessary to provide for respective relations and links from the viewpoint of controlling, e.g. traffic signals near the tunnel have to react to any queuing in the tunnel.

The road tunnel equipped with the respective technology is a typical telematic system and, as such, must be integrated into a more general transport-telematics system of a city, region or district. There are several definitions of telematics, the first is from 1997, Pribyl 2003, see the simplified form below:

> The systems which may be classified as telematic systems used for the improvement of population mobility both *tele*communication and infor*matics* equipment. All necessary information is available for both any sub-system and equipment because everything is connected in one global telecommunications environment.

However, the sole connection of telecommunications and transmission is not enough because these systems are launched just and only for the purpose to ensure the common target function which, in case of a tunnel, may be providing for "smooth and safe traffic with minimum ecological impact and optimisation of operating costs". It means that e.g. to install a proper tunnel regime requires a transport sub-system with a ventilation sub-system so that tunnel users benefit from optimum conditions and that tunnel is operated safely and effectively. All co-participating sub-systems are connected at the information level so that they execute just such functions which are necessary. In case of fire in the tunnel other functions, prepared in advance, are activated which execute other processes. As the tunnel is to be deemed as a telematic system its model in the form of an ITS architecture can be prepared.

2.1 *Approach to tunnel system model preparation*

Before the approach to the preparation of architecture is described it is necessary to define the term "system" because the definition of the system is a basis for creating architecture. A real object which is a general transport telematic system and which is subject to "investigation" is composed of a number of entities mutually connected. The investigation may be understood in many ways. However, the preparation

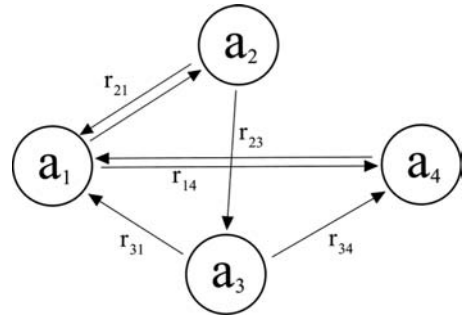


Figure 1. System structure of relations between elements.

of architecture is characterized by grouping entities into *elements* while a set of *relations* is established between them. The selected point of view concurrently determines the degree of investigation, which is a distinguishing level. Generally it applies that system S is made of a couple of sets A and R

$$S = [A, R]$$

Where A is a set of elements and R is a set of relations (links) among them:

$$A = \{a_1, a_2, ..., a_i, ..., a_n; n \in N\},$$
$$R = \{r_{ik} | r_{ik} = (a_i, a_k), \quad a_i, a_k \in N\},$$

this has certain characteristics (N is the set of natural numbers). Elements are particular fundamental entities of the system, Figure 1.

Interaction of elements is to be interpreted also that each element a_i fulfils within the system as a whole certain functions $f_{i1}, f_{i2}, \ldots, f_{ij}; j \in I$, which constitute a basis for creating architecture making. Graph G(A, R) is a structure of system S. Thus the term system is an abstraction which is the form in which the object is shown. In our conception the term system is understood as transport-telematics object which provides for the pointing out of his system characteristics. A realistic system is then a system installed in a concrete real object, for example concrete tunnel. Thus the real system becomes a model which the observer creates in the process of monitoring, investigating and describing the object given.

2.2 *Definition of architecture*

The tunnel system is a typical transport-telematics system because in addition to its primary function – transport it must provide for suitable lighting, good ventilation, safe traffic etc. It is a heterogeneous system consisting of several sub-systems of which each executes its macro-function. All macro-functions

execute one target function. The architecture of the tunnel system enables the complex sets to be described, which cannot be designed by exact methods, for example a safety system via a model which is sufficiently available to persons who are not extra specialists in the field given. The tunnel system architecture is to be defined as set out below:

From the transport telematics point of view the tunnel system architecture is described on the basis of user needs in the form of complex model made by a functional, information, physical, organisational and telecommunication model.

In making a model of telematic system in the form of architecture it is necessary to use suitable methods. The basic method how to approach the preparation of architecture is its breakdown into simpler pragmatic models. Their structure and division arise from experience of the European architecture KAREN, lit. Franco 2000 or at the level of the Czech Republic from the "ITS Architecture CR" lit. Svítek 2002. The architecture of systems in transport telematics is to be classified as:

Functional – creates and defines particular functions of elements, modules and subsystems including relations between them and thus it enables applications to be made.

Information – defines the principles of creating the structure of the respective information sub-system including requirements for allocation, encoding and transmission of information.

Physical – defines physical devices, which perform particular functions so that functions of applications are ensured i.e. allocation of particular elements, modules and sub-systems defined in functional architecture by relevant physical equipment.

Communication – describes transmission of information in the system in relation with physical architecture.

See graphical form of this breakdown on Figure 2. The tunnel system at the bottom level is presented by physical reality: own tunnel, communication, buildings, building sites. . .

In the second layer more detailed breakdown into physical systems and equipment is to be distinguished: transport system is made of sensors and actors, the control system consists of computers in the tunnel and control room etc. Based on this breakdown it is possible to form a vision how a physical model may look like. But it should not be connected with concrete elements or suppliers but should be as general as possible. The abstract description is placed at the highest layer, where functions (function architectures) are allocated to physical entities, relations between functions are defined (information architecture), information flows help define communication architecture and the whole activity is ensured by organisation layout, from which information architecture is formed.

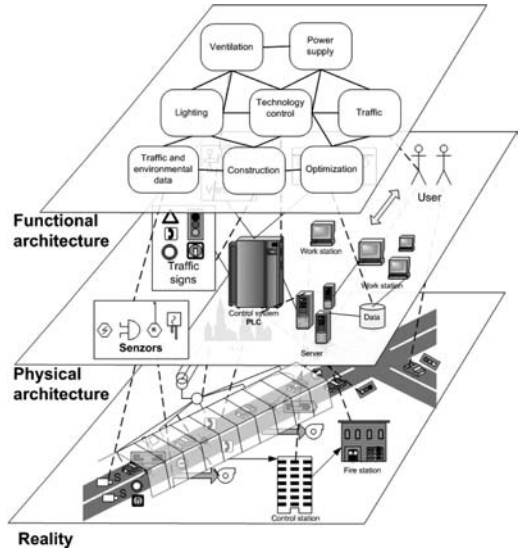


Figure 2. Distinguishing the architecture of systems in transport telematics.

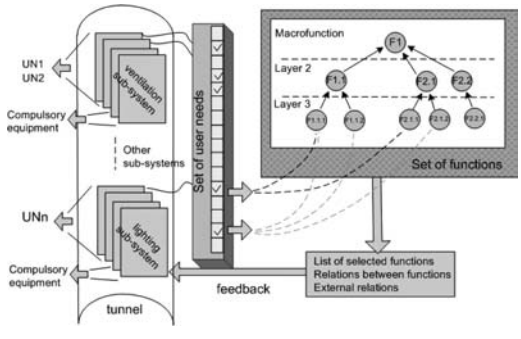


Figure 3. Making architecture scheme.

3 MAKING THE ARCHITECTURE OF THE TUNNEL SYSTEM

The conception how to develop the architecture is shown by scheme, see Figure 3. It is evident there from that the tunnel is divided into *n* sub-systems (Lighting, Ventilation etc.). Part of technological, transport or safety and security equipment in the tunnel installation is compulsory because it is stipulated in standards and given by technical conditions (in the Figure 3 it is marked as "compulsory equipment", which may include, for example, accommodation lighting or the position and performance of ventilators. There are accurate methodological instructions how to design them. Thus the tunnel may be equipped with devices which are not unambiguously required but are recommended or proven to be good in other tunnels. This

equipment required by the user (investor, future operator, security technician, IES units etc.) is marked as User Need/UN., see Chap. 3.1.

The user will specify user needs, which he would like to be satisfied in the tunnel and functions, which execute them, are allocated just to these selected needs. They are accurately defined and concurrently information flows between functions are unambiguously defined, or between functions and ambient conditions. The whole process is automatically executed within a database and web oriented interface.

Fundamental benefit is that a user who does not need to be any extra specialist in the field will get a list of functions and relations, which execute his needs and thus it cannot happen that any function or relation is forgotten or vice versa that he does not buy also functions which are not necessary for its execution. To get orientation in all functions which the chosen system is to execute or in relations which must exist in order to be integrated into the tunnel system in full is nearly impossible for the "lay person" or ordinary user. In particular in such cases various lobby pressures start to occur which may cause the system to be disproportionately much expensive or complicated. Just in these situations the role of architecture of the tunnel system is not substitutable.

3.1 *User needs*

As regards a general tunnel system user needs have been defined such as a set of functions (macro functions) providing for higher security of operation, improvement of comfort for the user, improvement of the quality of processes etc. As a representation of user needs for a security sub-system of the tunnel is Table 1. The main User Need *U*1 *Security* is broken down into fifteen concrete user needs ($U1.1 - U1.15$), which specify optional requirements for the equipment of the tunnel in detail.

The user chooses one or more User Needs from the list offering just those which will help him solve the problem given.

3.2 *Function and information architecture*

Thus the function architecture "fulfils" user needs. The user need is executed via functions, which belong to it. Functions of the system are divided into several group according to their character. There are functions which provide for security, ventilation, lighting, control etc. Functions are organised in hierarchy at three levels, at the lowest level there are the so-called elementary functions, see Figure 4.

Functions of the first level are the global functions (macro-function), functions of the second level give more details and only the functions of basic level of the function tree execute concrete requirement(s) of the system, execute user needs in part (measurement, control etc.) An example how to describe a function for a subsystem security is available at Table 2.

A sub-output of the program is an automatically generated list of all functions of one or several user

Table 1. Example of user functions of the sub-system "Security".

U1	Security
U1.1	Section speed control
U1.2	Car distance measurement
U1.3	Measurement of car temperature
U1.4	Verbal connection with dispatcher
U1.5	Push buttons signalization to dispatcher
U1.5.1	Safety guard connection
U1.6	Broadcast transmission
U1.6.1	Dispatcher entry to broadcast
U1.7	GSM telephone network
U1.7.1	All mobile networks
U1.8	Sound distribution in tunnel
U1.9	Registration of emergency situation
U1.10	Icing tunnel
…	…

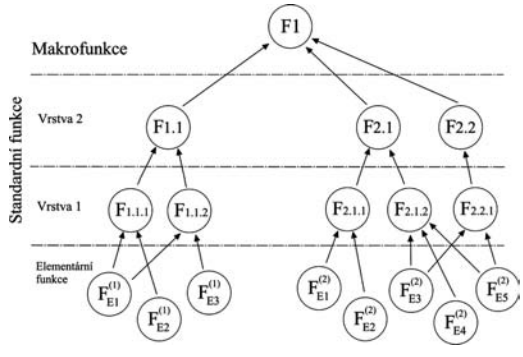


Figure 4. Hierarchy function architecture showing relations between functions.

Table 2. Description of functions for User Need "Section speed control". Example for 3rd level function F2.1.1 "Licence plate recognition".

F1	Section speed control
F1.1	Identification of car
F2.1.1	License plate recognition
	Description of the function: This function provides identification of European cars based on LPR. Process is speed and daily light independent until 200 kilometres and function returns to the process alpha-numeric text
	. . .

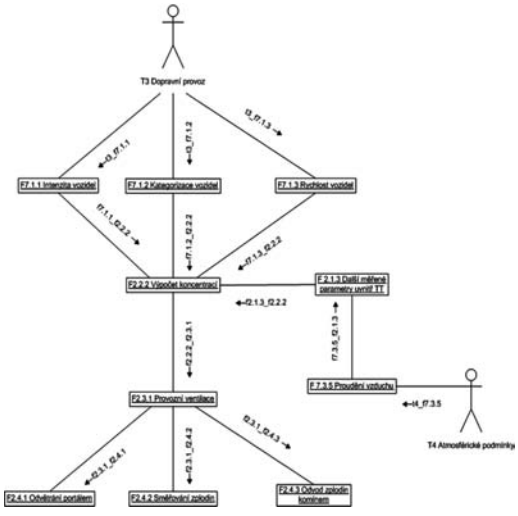


Figure 5. Function and information architecture-example.



Figure 6. Display web application for user needs definition.

needs. In the next step automatically all relationships between functions *UP*, between functions of the tunnel and external relations are defined while convention UML is used, all to be shown in Figure 5.

3.3 *Presentation of architecture*

The architecture of tunnel systems is presented at interactive websites. The display and keeping defined architecture is based on the XML language. The document in XML represents both the databases maintaining descriptive information about the architecture of tunnel both with use of suitable templates shows architecture in the required form. The application platform for web application is ASP. NET with programming language VisualBasic. The architecture is available in Czech at www.eltodo.cz.

4 CONCLUSION TO THE ARCHITECTURE OF THE TUNNEL SYSTEM

The tool developed within the OPTUN project is an interactive environment for co-operation of the investor or future operator in the preparation of a conception of the tunnel system. The user may potentially select the equipment or systems according to actual needs of the tunnel. The architecture of the tunnel based on user needs reliably generates functions and their relations for optimum design of the subsystem given. Thus it is guaranteed that the system is not equipped in excess, or on the other hand is not insufficiently equipped. The equipment and systems are unified to a certain extent, independently of suppliers. In addition, the system outlined as said above meets the conception of tunnel as telematic system.

REFERENCES

Pribyl, P. 2003. Definition of the traffic-telematics system, Traffic and telecommunication for 3rd millennium; Proc. of international conference, Faculty of Transportation Sciences, Prague, 26–27 May, Prague, Faculty of Transportation Sciences CTU

Franco, G. at all. 2000 European ITS Framework Architecture-Models of Intelligent Systems, *Deliverable D3.7, Report*, TR4108, KAREN

Svítek, M. 2002, ITS in the traffic-telematics conditions in the Czech Republic, *Technical report 2002*, Prague, Faculty of Transportation Sciences CTU

This page intentionally left blank

Underground Space – the 4th Dimension of Metropolises – Barták, Hrdina, Romancov & Zlámal (eds)
© 2007 Taylor & Francis Group, London, ISBN 978-0-415-40807-3

Increasing industrial safety and climatic conditions by the use of spray nozzles

A. Rudolf & O. Gloth
ILF Consulting Engineers SA, Switzerland

P. Schürmann
AxEnergy Ltd., Switzerland

ABSTRACT: One system can cope with fire safety, dust separation and cooling requirements at once: waster mist. These requirements must be considered thoroughly during construction, installation and later for operation of a tunnel in order to meet modern standards for health and safety. It is claimed that a water mist system is a multi-purpose system which should be incorporated as a fixed part in the basic construction of a tunnel structure such as cable ducts and drainage systems already are. Further, it is claimed that a water mist system is an uncommonly versatile and cheap system which requires only little installation space.

In this paper, the basic guidelines for design and dimensioning of such a system are outlined. In particular, the required water flow rates, the distance of water mist installations, droplet size as well as systemic requirements are discussed.

1 INTRODUCTION

During the construction of a tunnel, fire safety, dust separation and cooling are important aspects to meet modern standards for health and safety at work. Later, during the installation phase and during operation these aspects continue to be important in order to meet security standards and ambient requirements. In long alpine tunnels, these issues are particularly critical.

Fire and smoke are usually dealt with by a ventilation system. If no escape path is nearby, fire suppression systems and shelter areas are required additionally.

Dust is typically deposited by mechanical filters or water sprays where solid particles adhere to water droplets.

Cooling is most commonly achieved by heat exchangers with heat dissemination by water pipes. These pipes are large, thus they incommode installation works and hamper logistics. Besides, the mere temperature increase of the backflow water represents an environmental problem, which is sometimes difficult to overcome.

The required systems are often temporarily installed, even though their costs are in the same order of magnitude as the final installations. In this paper, it is shown that fire suppression systems may be used for cooling and dust separation during construction. In some cases, they may even be planned so that their use can be continued after regular operation has commenced.

A system which combines all the three functions is based on the use of spray nozzles which produce water mist with varying properties suitable for the specific function. It is a cost efficient, versatile, low profile and extremely effective measure.

The paper outlines the advantages of the use of spray nozzles during tunnel construction and thereafter in order to increase the safety level as well as the environmental conditions during construction and operation. It is also emphasized that cost effective synergies may be sought between different phases of the constitution of a tunnel if such a system is included in the basic tunnel structure as draining systems and cable ducts are nowadays.

2 SUGGESTED INSTALLATIONS

There are several possibilities to position pumps and nozzles and to provide the required infrastructure. After careful consideration of these options, the suggested configuration is outlined below.

2.1 *Water supply*

It is suggested to install a low pressure water pipe in the side-strip of the tunnel tubes with sufficient capacity to

cover fire and smoke suppression in an incident as well as to settle dust and to cool during normal operation.

2.2 *Central high-pressure pumps for fire suppression*

For the fire suppression system, high pressure pumps should be installed section-wise to cover larger tunnel portions or the entire tunnel. It should be considered to integrate a high pressure tube with regular T-pieces in the concrete lining as well in order to avoid hindrance of further installations works. Optionally, the high pressure pipe can be positioned along the tunnel lining.

2.3 *Distributed installation of high pressure pumps for dust suppression and cooling*

For dust suppression and cooling applications, the high pressure pumps should feed on the low pressure water line. They are positioned at the locations of the atomizing water nozzles. The dust suppression and cooling applications can be installed at arbitrary locations along the entire tunnel.

2.4 *Electricity*

The standard power supply can be used, as the high pressure pumps have fairly low power consumption (ca. 1–4 kW). If required, remote control data cables can be placed in cable ducts along the tunnel shoulder.

3 CHARACTERISTICS OF A DROPLET

In the sequel, the most popular mean and characteristic diameters, their definitions, and their most appropriate uses, are discussed (see Figure 1). Drop size terminology can be found in ASTM Standard E1296–92 [2,3].

DV0.5: Volume Median Diameter (also known as VMD or MVD). A means of expressing drop size in terms of the volume of liquid sprayed. The VMD is a value where 50 percent of the total volume of liquid sprayed is made up of drops with diameters larger than the median value and 50 percent smaller than the median value.

DV0.9: is a value where 90 percent of the total volume of liquid sprayed is made up of drops with diameters smaller or equal to this value. This diameter is best suited when complete evaporation of the spray is required.

*D*32: Sauter Mean Diameter (also known as SMD) is a means of expressing the fineness of a spray in terms of the surface area produced by the spray. The SMD is the diameter of a drop having the same volume to surface area ratio as the total volume of all the drops to the total surface area of all the drops. This diameter is best suited to calculate the efficiency and mass transfer rates.

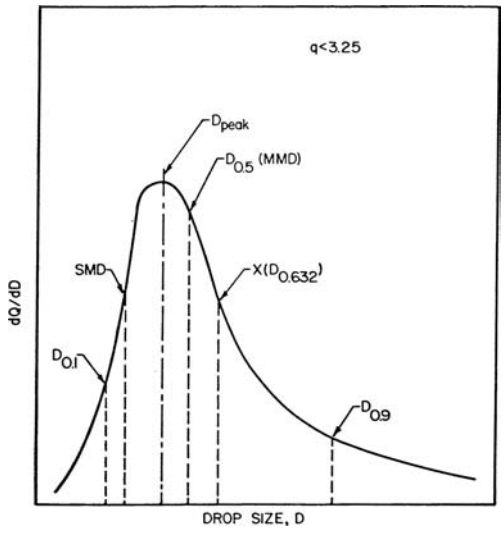


Figure 1. Statistical droplet distribution in water spray according to Rosin Rammler with indication of characteristic sizes of the droplet spectrum.

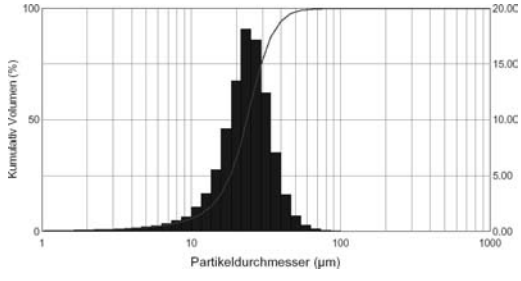


Figure 2. Volumetric distribution over particle size.

The typical droplet distribution of a high pressure atomizer is best described by the 2 parameter Rosin Rammler Function:

$$Q = 1 - \exp\left[-\left(D/X\right)^{q}\right] \quad (1)$$

where:

Q	::	fraction of total volume contained in drops smaller than D
X	::	empirical constant
q	::	empirical constant indicative of spread of drop sizes

Figure 2 shows a typical volumetric droplet distribution of a high pressure water atomizer nozzle, with a DV0.9 of 40 µm & D32 of 17 µm.

4 FIRE AND SMOKE SUPPRESSION

In the sequel, several advantages of a fire and smoke suppression system using water mist are discussed.

4.1 *Reduction of heat load*

With the beginning of the water discharge, the fire development can be significantly delayed, the spreading of the fire to other vehicles or combustible material avoided and thus the maximum heat load reduced. Consequently, the smoke production rate is, particularly in the first minutes, reduced.

The reduction if the smoke is of utmost advantage for the self-rescue, which is still a major key to tunnel security.

As the heat load and the smoke production rate are determining the sizing and the control of the ventilation system, additional security margins are generated.

4.2 *Reduction of structural damage to the tunnel*

The adiabatic cooling of the surrounding of the fire results in significantly reduced surface temperatures. As Wetzing and Reichsthaler, 2003 have shown, the following temperature criteria can be met or undercut:

- $<50°C$ at a distance of 20 m from a burning truck, this way the fire brigade can close in on the fire.
- $<250°C$ at a distance of 5 m from a burning truck; this avoids spreading of the fire to combustible material nearby.
- $<100°C$ at 10 mm depth in the concrete structure; this ensures stability of the concrete.

5 DUST SUPPRESSION

To get an efficient dust suppression system the water droplet spectrum has to be in the proper range. As shown in Figure 3, the droplet should be in the same magnitude as the dust particle to get a maximum effect for dust suppression.

Experience gained over the years with water sprays has established the following facts:

- for a given spray nozzle, the collection efficiency for small dust particles increases as the pressure increases.
- at a given pressure, the efficiency increases as the nozzle design is changed so as to produce smaller droplets.

The conclusion is clear-cut: the smaller the water droplets, the better dust particles adhere to them.

This can be demonstrated by considering a water droplet about to impinge on a dust particle, or what is aerodynamically equivalent, a dust particle about to impinge on a water droplet (see Figure 3).

If the droplet diameter is much greater than the dust particle, the dust particle simply follows the air stream

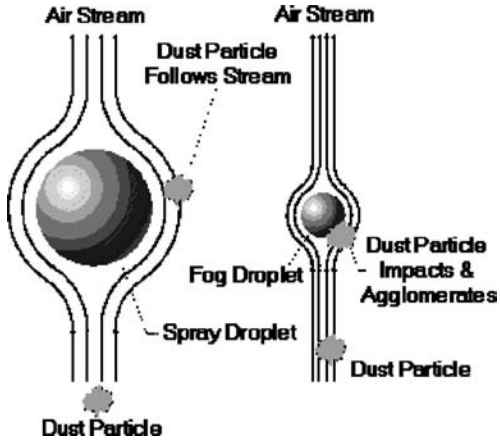


Figure 3. Airflow around a large water droplet prevents dust particles from colliding with water droplet. Flow around smaller droplets allows dust particle to cross the streamlines and to adhere to the water droplet.

lines around the droplet. Little or no contact occurs. In fact, it is difficult to impact micron-size particles on anything. This is the whole reason why inertial separators do not work well at these sizes. If, on the other hand side, the water droplet is of a size comparable to that of the dust particle, contact occurs as the dust particle tries to follow the streamlines. Thus the probability of adherence increases with smaller water spray droplets.

With these facts in mind, we are led through the logical extension of our approach to smaller droplet sizes, all the way to the vapor phase, extending the relative humidity above 100% and condensing the water directly onto the dust particles. In this way, the particles can be made to grow, under the proper conditions, to a size where they will either fall out or can be removed by sprays.

As soon as we take this step, we are in an area of physics known as “cloud physics” and can draw on the tremendous volume of scientific research results that exists in this area. For example, for over 20 years, the US Atomic Energy Commission has studied the basic processes by which radioactive fallout from bombs and reactor accidents is naturally removed from the atmosphere. The fundamental processes involved are nucleation and condensation.

Nucleation is the process by which raindrops are formed in clouds. There are two categories: homogeneous, where no foreign particles are present; and heterogeneous, wherein the droplet formations take place on foreign particles. The efficiency of the latter depends on many factors, such as particle solubility, wettability (hydrophobic or hydrophillic), the presence of hygroscopic salts, temperature, electric fields, charge and others.

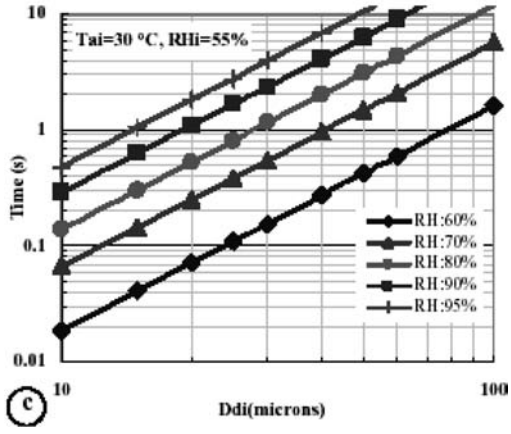


Figure 4. Time for evaporation over droplet size with relative humidity as a parameter (Chaker, 2003, p. 11).

6 COOLING

For a fast and efficient cooling effect, the water mist has to fulfil the following criteria.

6.1 *Duration of evaporation:*

The water droplets have to be small enough to evaporate in a given time. This time depends on the available evaporation distance and air velocity in the evaporation duct as shown in Figure 4.

At 30°C and 55% relative humidity a droplet starting at 20 μm diameter will need approx 2s to evaporate to a target humidity of 95%.

6.2 *Droplets must follow the air flow*

The water droplets have to be small enough not to collide with any obstacles within the evaporation duct. For a typical diameter of 10–20 μm, the viscous forces acting on a water droplet dominate the inertia forces. Thus, a droplet of this size will follow the air stream and will not collide with any obstacles.

The droplet size for large industrial adiabatic cooling units is in the order of 20 μm. With high pressure pumps capable of delivering up to 200 bar operating pressure and ceramic nozzles, a long life time for the industrial applications (up to 8700 operating hours per year) can be guaranteed. Only stainless steel materials are being used in these systems to meet the demanded service life of more than 25 years.

6.3 *High water quality*

The water quality has to meet high quality criteria. For most applications, a reverse osmosis water treatment system is recommended resulting in a conductivity of less than 1 μS/cm. This water quality guarantees the least amount of deposits left over from evaporated water, that the system will not be clogged by impurities in the water and that it is also safe for humans to breath in the cooled humidified air. Especially when used in a working environment, the absence of bacteria, especially Legionella, and respirable dust from minerals must be ensured.

Table 1. Yearly running costs for adiabatic cooling versus mechanical chillers w/ cooling power of 15 MW.

Adiabatic Cooling		
Needed cooling power	15'000	kW
Amount of water needed (approx.)	23	m^3/h
Electrical power rating of the system	120	kWe
Power factor (cooling power/ power consumption)	125	–
Operating hours per year	8,700	h/a
Electrical cost: CHF/kWh	0.30	CHF
Water cost: CHF/m^3	1.00	CHF
Cost of power consumption (power rating * operating hours)	1,044,000	kWh/a
Cost of water consumption (water cost * operting hours)	200,000	CHF/a
Total running costs	1,244,000	CHF/a
Mechanical Chiller		
Needed cooling power	15,000	kW
Electrical power rating of the system	5,000	kWe
Power factor (cooling power/ power consumption)	3	–
Operating hours	8,700	h/a
Electrical cost: CHF/kWh	0.30	CHF
Power consumption (power rating * operating hours)	43,500,000	kWh/a
Total running costs	13,050,000	CHF/a

6.4 *Life cycle costs*

In order to evaluate the life cycle costs, the running costs must be added to the installation costs of all required equipment.

The cost of the equipment is in most cases clearly in favor of adiabatic cooling as no backflow pipe is required and the water flow is significantly lower than the backflow of the mechanical chillers. Also, the required electrical installations and machinery is much smaller.

This is why in Table 1, only the typical yearly running costs for a total cooling power of 15 MW of an adiabatic system is compared to the costs of mechanical chillers.

The water costs have been estimated to 1 CHF/m^3, a rather high value as compared to actual projects. It



Figure 5. Fogging of air intake at gas turbine.

may vary depending on the conditions how water can be obtained. It must be added that only little costs for waste water treatment is necessary for cooling, as most of the water evaporates.

No water costs are considered for mechanical chillers as the water is circulating in this case and is not consumed.

Thus, from Table 1 it becomes obvious, that life cycle costs are in favor of adiabatic cooling.

6.5 *Typical cooling applications*

6.5.1 *Cooling of intake air for gas turbines*

A minimum in droplet size is recommended due to the very short evaporation time given in the air intake systems.

Not evaporated droplets may impinge on the turbine blades causing erosion.

6.5.2 *Adiabatic cooling system for tunnels*

For applications in the tunnel a compromise in droplet size (respectively in visibility) and evaporation efficiency (resp. in droplet travelling distance) had to be made. A typical droplet size if 40–50 μm was selected to be the optimal choice.

This first choice has been based on simplified estimates for particle traveling distances and visibilities. The falling velocity and hence the traveling distance for given tunnel conditions can be computed with (2).

$$v_{fall} = \frac{D^2 \rho_W g}{18\eta} \tag{2}$$

The visibility in meters can be estimated by equation (3), where LWC is the liquid water contents in g/m^3 and N_d the number density in 1/cm^3.

$$Vis = \frac{1002}{(LWC \cdot N_d)^{0.6473}} \tag{3}$$

This equation can be found in Gultepe a.o., 2006.



Figure 6. Water mist station in a tunnel environment with high ambient rock temperatures and significant technical heat.

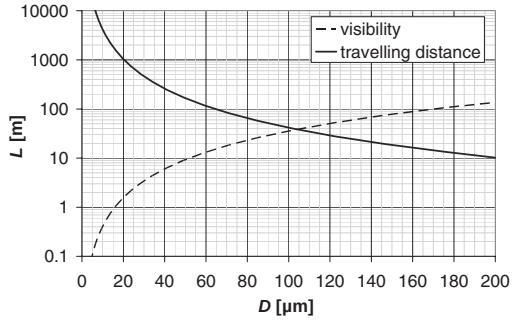


Figure 7. Distance traveled and visibility for different particle diameters (2.5 m/s flow velocity and 5 m ceiling height).

7 OPTIMAL DROPLET SIZE

Based on an air velocity of 2.5 m/s and ceiling height of 5 m, with nozzles located in the tunnel ceiling, Figure 7 illustrates the dependency of visibility and traveling distance on the particle diameter for a flow velocity of 2.5 m/s and a ceiling height of 5 m.

For droplet sizes of 40–50 μm a good compromise between visibility and traveling distance is expected from this simplified approach. Measurements of both, the traveling distance and the visibility, have to be carried out in order to gain confidence in the choice of droplet size.

(a) The visibility is in the order of 10 m, which is sufficient for the self rescue for the people trapped in the fire zone.
(b) The droplets in the range of 40–50 μm will travel at least 200 m within the tunnel.

8 CONCLUSIONS

This paper covered the combined use of a water mist system for fire and smoke suppression, dust separation and cooling during construction, installation and operation of a tunnel.

Due to its unique versatility and low expenses, it is suggested to incorporate a low pressure water tube in the basic design of a tunnel cross-section and to add a high-pressure tube in sections where fire suppression is required.

Based on travel distance and visibility, an optimal droplet size of 40–50 μm is suggested, subject to project-specific verification.

REFERENCES

Wetzing, V. und G. Reichsthaler. 2003. Wassernebelanlagen zur Brandbekämpfung. Versuchsstollen Hagerbach/ Aquasys GmbH. aus tec-21 1–2/2003.

Marshall, W.R., 06/1954. Atomization and Spray Drying. Department of Chemical Engineering. University of Wisconsin, Madison, pp 50–56.

Annual Book of ASTM Standards, 1996. General Methods and Instrumentation, Volume 14.02, pp 810–812. E1296–92: Standard terminology relating to liquid particle statistics.

Chaker, Mustapha A. 2003. Inlet fogging of gas turbine engines – experimental and analytical investigations on impaction pin fog nozzle behaviour in Proceedings GTC 2003/38801.

Gultepe, I., J. Milbrandt and S. Belair, 2006. Visibility parameterization from microphysical observations for warm fog conditions and its application to the Canadian MC2 model. AMS meeting, January 2006, Atlanta (USA).

Underground Space – the 4th Dimension of Metropolises – Barták, Hrdina, Romancov & Zlámal (eds)
© 2007 Taylor & Francis Group, London, ISBN 978-0-415-40807-3

Towards tunnel facility management: Applying asset management to the operation and maintenance of tunnels within infrastructure networks

J. Ruiter
Centre Applied Research Underground Space (CARUS) Zeeland University, Vlissingen, The Netherlands

ABSTRACT: Until now rational maintenance of tunnel constructions was not the foremost field of research due to which insufficient information was available to professionalise Tunnel Facility Management. Tunnel Owners (managers) have in the past underestimated the complexity of maintenance and related costs. A managerial approach is needed to professionalise the maintenance of tunnels.

The main objective of this paper is the professionalising of current maintenance practice towards Tunnel Facility Management so decisions can be taken based on facts rather than on implicit knowledge. The theoretical approach takes as starting point the managing of the asset and tries to learn from asset management. The Asset Management Theory can be used for the model creation of Tunnel Facility Management. Tunnel Facility Management will provide the framework within which the information can be used to take sound and economic based decisions as part of a total lifecycle approach to managing and maintaining tunnels as important assets within infrastructure networks.

1 INTRODUCTION

Until now rational maintenance of tunnel constructions was not the foremost field of research due to which insufficient information was available to professionalise Tunnel Facility Management. Tunnel Owners (managers) have in the past underestimated the complexity of maintenance and related costs. A managerial approach is needed to professionalise the maintenance of tunnels. In this paper the related fields of tunnel facility management will be discussed.

1.1 *Developments*

A recent study undertaken by the Centre Applied Research Underground Space (CARUS), concludes that the need to professionalize maintenance management of tunnels (and underground installations) will become more and more important from a social perspective. Also the introduction of private ownership of tunnels rather than public ownerships calls for a rethink on inspection and maintenance as part of often lifecycle based investments. Both developments underline the necessity to study Tunnel Facility Management with practice or action-based research so that maintenance of tunnels can develop into a more professional and economic based profession in the future.

There are also a number of developments in the public domain which have increased the awareness for a rational and economic based approach to maintenance. The focus nowadays moves from new development to maintenance of infrastructure because:

- Infrastructure networks are growing as economies worldwide continue developing
- Infrastructure networks are constantly ageing
- Requirements to be met by infrastructure networks are growing
- The impact of bad maintenance practice and management on the total network is enormous

1.2 *Objective paper*

The main objective of this paper is the professionalising of current maintenance practice towards Tunnel Facility Management so decisions can be taken based on facts rather than on implicit knowledge. The theoretical approach takes as starting point the managing of the asset and tries to learn from asset management. The Asset Management Theory can be used for the model creation of Tunnel Facility Management. The operation of a tunnel is part of the operation of an infrastructure system. It is impossible to see tunnel operation and infrastructure network operation in general as separate entities. The operation of the infrastructure network provides the framework and prerequisites of the operation of the tunnels. In reverse, the operation and the availability of tunnels has a major impact on the operation and availability of the total infrastructure network.

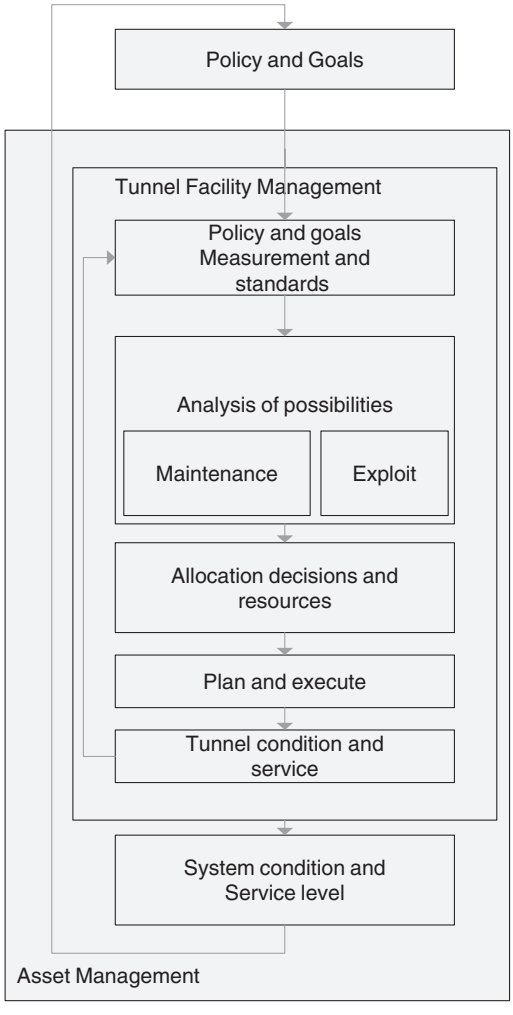


Figure 1. TFM model.

1.3 *Modelling Tunnel Facility Management*

The theoretical approach takes as starting point the managing of the asset (asset management). The asset management theory can be used for model creation of Tunnel Facility Management. During the study figure 1 is used.

1.4 *Policy*

The integral policy for infrastructure addresses on the infrastructure system as whole. The integral policy encompasses the mission, the policy view, the goals and the strategy. The most important part of the integral policy is formed by the mission. The mission will indicate the direction what the infrastructure system is going to achieve. In the policy's view is indicated how the manager handles with the developments that are outlined by the influences of the environment. The mission and policy's view will be worked out in integral objectives. Finally the strategy will be set up.

To make steering on functionality and quality possible, there has to be a link between the present policy and the to maintain objects.

- Environmental influences; a part of the policy is formed by the environment influences, i.e. influences from outside the organisation. The environmental influences will indicate which (future) developments need to be considered by the tunnel manager.
- The integral policy will be divided into feasible goals per object and the way to achieve these object specific policies.
- The object goals with the accompanying standards have to meet the following requirements:
  - Specific
  - Measurable
  - Acceptable
  - Real
  - Time dated

Both the objectives and complying standards have to be SMART.

The object specific policy needs to be checked against the functional requirements of the current policy goals. The core activity of maintenance is to maintain the quality during the rest of the lifecycle at a desired level. Measures are necessary when the desired goals and standards can not be met. RAM(S) thinking is introduced from the industry sector. No longer only safety and technology are important. Under societal pressure a shift is taking place towards availability and reliability as criteria to be met in the operation of infrastructure. In other words the optimisation of the RAM(S)-indicators is the goal which needs to be achieved. RAM(S) stands for the terms Reliability, Availability, Maintainability and Safety.

- Reliability is the probability that an object fulfils its function during the operational phase.
- Availability is the interval where an object fulfils its functions in both a normal operational situation and during emergencies.
- Maintainability can be divided into two categories:
  - Minimizing the maintenance by optimizing during the design phase.
  - Achieving accessibility for maintenance works.
- Safety can be divided in four categories:
  - Fulfilling Health & Safety requirements.
  - Structural safety.
  - Detection (gas, water electricity).
  - Unauthorized access.

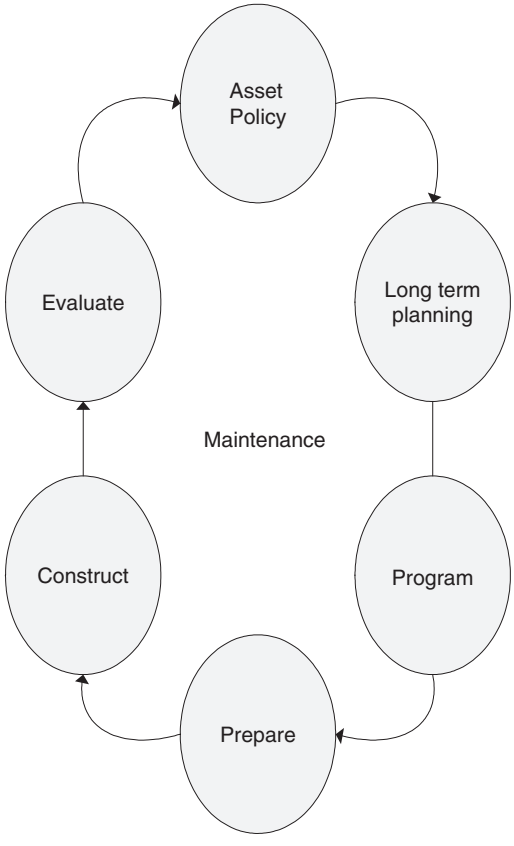


Figure 2. Maintenance Cycle.

1.5 *Maintenance & RAMS*

Maintenance has to focus on functionality and quality. The steering on functionality: Reliability, availability, maintenance and safety (RAMS), is based on checking the current asset to the expected and desired functionality. The maintenance of the asset has to be set from a technical approach to a managerial approach. The aim of this approach is to achieve accountability of maintenance based on budgeting and forecasts (see figure 2).

The maintenance process is top-down. Although there is also feed back to the policy level. This is necessary for self reflection of the policy maker and to ascertain if the goals are achieved.

1.6 *Operation*

The operation of a tunnel is part of the operation of an infrastructure system. It's impossible to see tunnel operation and infrastructure separate. The operation of the infrastructure provides for frameworks and preconditions for the operation of the tunnels. The operation of tunnels has influence on the operation of the infrastructure.

Successful accomplishment of the operational task relies on accurate and recent information on the condition of the tunnel.

- traffic management is aimed at an optimal flow of the traffic within the boundaries of the capacity of the infrastructure and the number of traffic participants.
- traffic information management consists of managing the traffic by monitoring the traffic.
- incident management consists of the multi-stage-plan and co-ordination process to signal traffic accidents.
- weather conditions management consists of acquiring information about current and up-coming weather conditions. Composing information about current and upcoming road conditions to support managers in their task to plan and execute maintenance. Prediction of traffic flow and giving traffic information. As well as formulating strategies for emergencies.
- Work location management consists of formulating strategies and adjusting to minimize obstruction as a result of maintenance works and to assure the safety traffic participants and workers.
- Emergency management consists of assuring an effective response of the infrastructure network in case of emergency, such as natural disasters, large traffic incidents and terrorist attacks.
- Transport management consists of activities which assure an efficient, safe and guaranteed transport of all categories.
- Ventilation management consists of activities which assure an efficient and safe air circulation.

1.7 *Life cycle management*

Life-cycle-management is a tool for decision support for the accomplishment of the policy-goals. "Sufficient Life Cycle Management" is not an autonomous goal. With regard to Life Cycle Management (LCM) it is not possible to set any functional requirements with exception of one, which is that for all decisions during the lifespan a LCM-analysis must be used for decision support. Therfore we can conclude that LCM is a tool and not a goal for policy decisions.

2 CONCLUSION

Successfully managing the operation of tunnels depends first and foremost on accurate and current information on the condition of the tunnel. Tunnel Facility Management will provide the framework within which the information can be used to take sound and economic based decisions as part of a



Figure 3. Tunnels form an integral part of modern infrastructure networks.

total lifecycle approach to managing and maintaining tunnels as important assets within infrastructure networks.

REFERENCES

Ministerie van Verkeer en Waterstaat Directoraat-Generaal Rijkswaterstaat Bouwdienst Rijkswaterstaat (ed.) (2004). Veiligheidsrichtlijnen Deel C. Utrecht: Bouwdienst Rijkswaterstaat. Versie 1.0.

Van Gestel, P.J. (1998). Reliability-Cent(e)red Maintenance. In: Nederlandse Vereniging voor Doelmatig Onderhoud. Onderhoudsmanagement: Handboek voor verantwoordelijken voor en betrokken bij de technische functie binnen organisaties Alphen aan den Rijn: Kluwer. ISBN 90 6500 780 6.

Van Wamel, J. en Van Gestel, P (2003). Het verhogen van bedrijfszekerheid door onderhoudsoptimalisatie. In: Nederlandse Vereniging voor Doelmatig Onderhoud (ed.). Onderhoudsmanagement: Handboek voor verantwoordelijken voor en betrokken bij de technische functie binnen organisaties. Alphen aan den Rijn: Kluwer. ISBN 90 6500 780 6.

Ter Brake, J.H.M. (2003). Inleiding tot Reliability-centered Maintenance. In: Nederlandse Vereniging voor Doelmatig Onderhoud. Onderhoudsmanagement: Handboek voor verantwoordelijken voor en betrokken bij de technische functie binnen organisaties Alphen aan den Rijn: Kluwer. ISBN 90 6500 780 6.

Federal Highway Administration, Federal Transit Administration (2003). Highway and Rail Transit Tunnel Inspection Manual. Gannett Fleming, Inc. Contract # DTFH61-01-C-00067.

Federal Highway Administration, Federal Transit Administration (2003). Highway and Rail Transit Tunnel Maintenance and Rehabilitation Manual. Gannett Fleming, Inc. Contract # DTFH61-01-C-00067.

Federal Highway Administration (2004). FHWA Asset Management Position Paper. Cambridge Massachusetts: Cambridge Systematics, Inc.

Federal Highway Administration (2004), FHWA Infrastructure and Asset Management. Cambridge Massachusetts: Cambridge Systematics, Inc.

Underground Space – the 4th Dimension of Metropolises – Barták, Hrdina, Romancov & Zlámal (eds)
© 2007 Taylor & Francis Group, London, ISBN 978-0-415-40807-3

International Tunnel Control System – Introduction and experiences from realization

Jiří Řehák
ELTODO dopravní systémy s.r.o.

ABSTRACT: International Tunnel Control Central (ITCC) was developed by international group of engineers inside Siemens Intelligent Traffic System Division. Engineers were originally from Czech Republic (ETODO dopravni systemy s.r.o.), Germany, Austria, Switzerland and Nederland. The main goal of the system is to unify tunnel control system software approaches used in each involved country to improve efficiency and reliability of new system together with increasing of total tunnel safety. The structure of ITCC system and system features is demonstrated including examples of software control modules. Special consideration is focused on traffic, mechanical and electrical modules. The experiences with ITCC on real project are presented. The approach to design and realization of complex tunnel control system on Sitina tunnel in Slovak Republic is discussed as the first example and the control systems for Turkish highway tunnels Bolaman-Persembe and Giresun-Espiye as the second example.

1 INTRODUCTION

Up to date road tunnels matching to requirements to mechanical and electrical system safety resulting from requirements of tunnel standards have to be equipped by tunnel control system. A tunnel control system represents the key integration component in the tunnel. In case of occurring of emergency situation the control system is a component which failure less functionality can decide about seconds needed for evacuation and safety of endanger people inside of tunnel. Proper functionality of control system turns on many factors. Between most important factors defining overall reliability of control system belong especially:

(a) design
(b) used components
(c) reliability of software equipment
(d) testing

This article will discuss in the following text new approach to design of software equipment of tunnel control system. On the beginning of article there will be a short prompt to basic requirements to tunnel control system. Recommendation of Czech standards TP98 – "Tunnel technological equipment" will be shown as example requirement. Czech standard TP98 in parts of tunnel safety equipment and control system belongs to one of the sharpest standards in the world. This standard has been taken as one of the fundamental standards for architecture proposal of new tunnel control system ITCC.

2 TP98 STANDARD REQUIREMENTS FOR TUNNEL CONTROL SYSTEM

The requirement of TP98 for integration of all control system components to one integrated system is one of the fundamental stones of the standard. This requirement applies mainly for controlling of traffic and mechanical & electrical tunnel equipment.

As it is shown on the Figure 1 TP98 standard defines control system as one entity to which has to apply also system of control. The systems of control of traffic and mechanical & electrical equipment has so shared set of common data that splitting of control of traffic and mechanical electrical equipment into two separated systems could lead to significant decreasing of overall system reliability.

Next TP98 define in detail requirements for hardware and software architecture of control system. Both these standpoints have been taken into account during ITCC system development. Hardware architecture of control system according TP98 defines hierarchical organization of control system from point of view of its structure in frame of high level telematical system as it is for example city or large regional traffic control management. The standard defines for each control level basic functional assumptions including definition of types of communication protocols. Main emphasis is focused on optimal usage of redundancy. Control system response and reaction time is required in real time with minimum system delay.

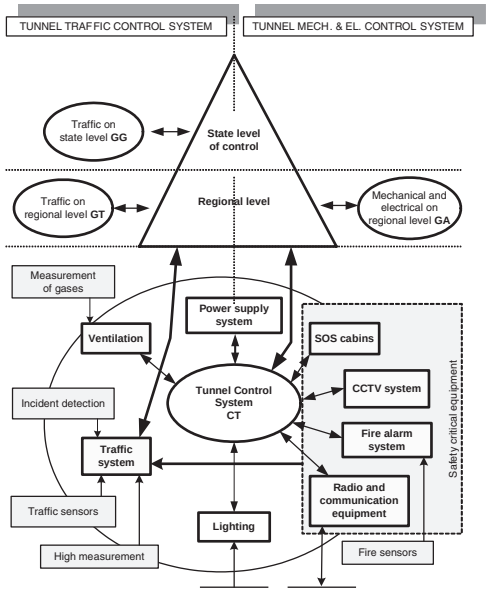


Figure 1. Integrated tunnel control system according TP98.

Table 1. List of tunnel operational status according TP98.

Name of tunnel status
Normal mode
Exceptional mode without necessity of emergency units
Exceptional mode with necessity of emergency units

TP98 takes into special account requirements to software design. For each level of control the standard defines a set of functions, which have to be implemented for proper function of tunnel control system. From operational point of view it is important that TP98 has direct reference to other Czech standard TP154 – "Operating of Road Tunnels". Both standards work with the same set of basic tunnel statuses. The set of tunnel status as it is described in TP98 is very important input for designing of software equipment of tunnel control system (Table 1).

3 TUNNEL CONTROL SYSTEM IN SIEMENS BEFORE 2003

In the frame of SIEMENS group number of software application for tunnel control has been developed in 90th of last century. Regional groups in SIEMENS has been pressed for development of own systems because of absence of central product. These systems have been prepared according local standards of each

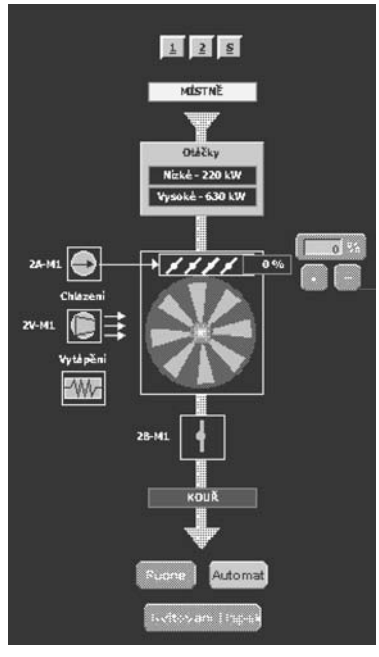


Figure 2. Sample of Kerberus GUI.

region. In the Czech Republic this development has been provided by ELTODO dopravní systémy s.r.o. ELTODO dopravní systémy s.r.o. developed complex tunnel control system with the name Kerberus. Kerberus is software equipment consisting from number of universal control modules intended to different control levels (for example SCADA level, level of main redundant PLC, level of field PLC) – see Figure 2 as example. Each successively tunnel application is than build from these modules step by step to required software structure.

Similar systems as Kerberus were also realized in Austria, Germany, Netherland and Switzerland. All of these systems were incompatible and were mostly related to national (regional) standards. Each system had different style of Graphic User Interface (GUI) and different style of control mode. The algorithms inside of software modules were prepared in different style, documentation to systems was written in different languages. Exchange of information and sharing of experiences between regional development teams was not possible.

4 ITCC – INTERNATIONAL TUNNEL CONTROL SYSTEM

The idea to realize new product built on base of existing regional software products arouse in year 2003.

Table 2. Overveiw of ITCC responsibilities.

Country	Responsibility
Austria	Traffic Manager (TM)
Czech Republic	Electrical and Mechanical Equipment
Germany	Project Coordination, Automatic Incident Detection
Netherland	Documentation
Switzerland	Traffic Manager (TCE)

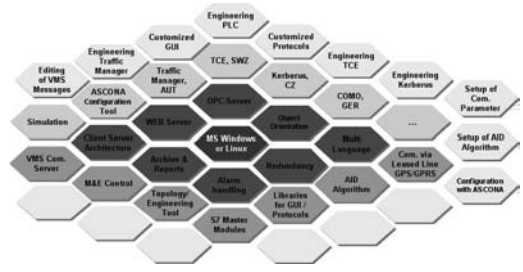


Figure 3. ITCC system structure.

Detail functional analyze of particular systems preceded technical realization of new system. The goal was to use maximum knowledge from existing systems. Special benchmark method for evaluating of existing system was used. Technical and economical parameters were used as inputs for evaluation. Based on the result of evaluation the development of new system was split to regional groups of developers as it is shown on Table 2.

Development of new control system had following main targets:

- Jointly coordinated development in five countries (Austria, Germany, Czech Republic, Switzerland and Netherland) with optimum utilization of know-how and account being taken of the requirements of all regions and customers
- Use of tried-and-tested industrial middleware and thus concentration on the know-how of Siemens ITS in the area of traffic and operations control
- Modular design of the software blocks with defined communications interfaces
- Centrally developed and updated software modules as product building blocks for the core functions of all tunnel systems
- Creation and configuration of the control centers from the product building blocks and the middleware in the region – therefore flexible in design to satisfy local customer needs (for example: graphic user interface, logs and statistics, control model)
- Platform-independent use under Windows and Linux
- Integration of different control models enables selection according to country-specific requirements.

5 ITCC KEY-FUNCTION BLOCKS

ITCC system was split to four different levels (Figure 3). The 1st level is the level of operating system – Microsoft Windows or Linux. On the 2nd level there is so called middleware i.e. SCADA system (in case of ITCC it can be PVSS or WinCC), database engine, system of redundancy and OPC interface. The 3rd level consists from developed control modules of ITCC system. It is for example module for Traffic Control (Traffic Manager and Traffic Control Engine), automatic incident detection module (AID) and software modules for controlling and monitoring of mechanical and electrical equipment. The integration software intended to particular realized tunnel is on the 4th level.

6 ITCC – STANDARDIZATION OF FUNCTIONAL BLOCKS

Maximum standardization of particular software modules was one of main targets during development of new ITCC system. Detail preparation preceding implementation of modules was necessary. For particular software block detail design specification was prepared – i.e. functional specification and specification of communication interfaces (Figure 4). Interface was defined in the way to ensure compatibility between software modules. Each module was split to two parts – Graphic User Interface part (GUI) and Programmable Logic Controller part (PLC). The list of elementary ITCC functional modules developed during the first stage of development is summarized in Table 3.

In the frame of ITCC Architecture listed elementary function modules are controlled in manual mode or are grouped to upper level function modules as it is for example Traffic Manager. Mechanical and electrical modules are grouped according particular requirement of realized application to complex algorithms on the level of PLC (for example automatic lighting functions, automatic ventilation functions, reaction of tunnel equipment on fire etc.). Standardization of software modules during ITCC development phase significantly increase speed of realization of final software equipment for tunnel control system.

7 SYSTEM TESTING

Testing phase of final ITCC system was a part of development. Special simulation environment for simulation of responses of real tunnel was prepared for this purpose. Special design documentation describing

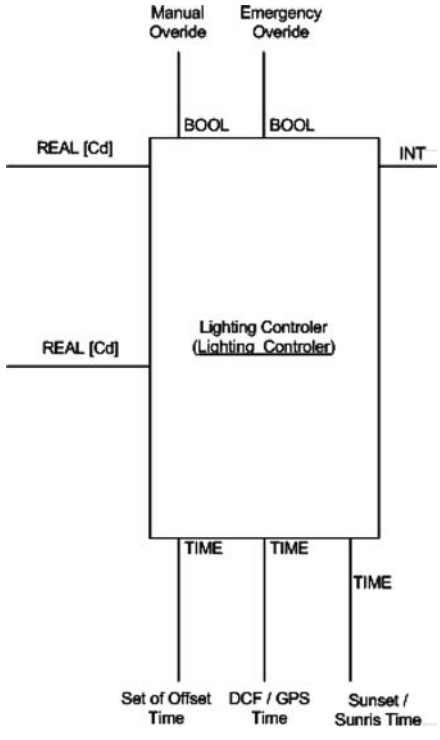


Figure 4. Sample of ITCC elementary module.

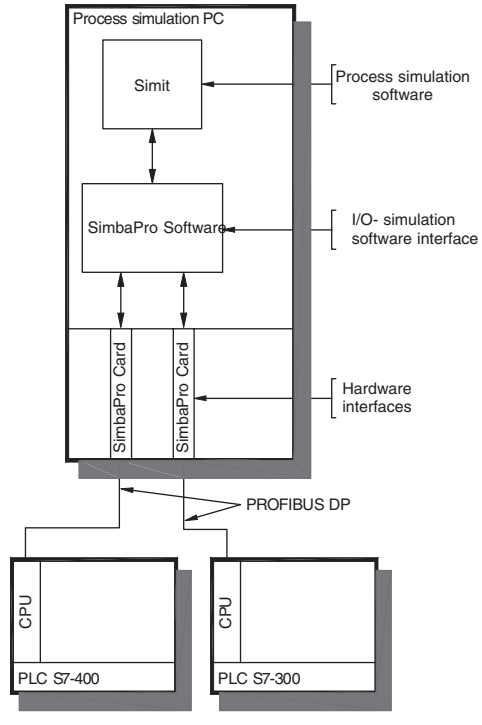


Figure 5. Simulation environment.

Table 3. List of ITCC elementary modules.

Function group	ITCC module
Lighting	Controller Astro Clock Contact Conversion
Power	Breaker Forecast KWH conversion
Ventilation	Selector Jet Fan Damper
Pump	Comparison
Fire detection	Fibro Laser CERBERUS
Traffic	LD4 Variable prismatic sign Lane Use Sign Traffic light

simulated tunnel was created. Simulated tunnel was implemented to process simulation PC, which was connected on PLC of ITCC system. Structure of simulation environment is shown on Figure 5. Simulation process was provided according prepared time schedule. Results were recorded to protocols and were subsequently evaluated. Several diagnosed failures were fixed and simulation process repeated. This process ensured 100% functionality of software modules in case of safe critical events in tunnel.

8 EXAMPLES OF REALIZATION OF ITCC CONTROL SYSTEM

ITCC system was at first time used in Sitina tunnel in Bratislava in Slovak Republic and next time in projects Bolaman-Pershembe and Gyreshum-Espyie in Turkey.

8.1 *Tunnel sitina*

Construction of two tube 1,4 km length tunnel Sitina in Bratislava in Slovak Republic started in 2004. The central control system is delivered as the part of mechanical and electrical equipment. The system is designed in ITCC environment. Sitina control system consists from four redundant layers (lighting, ventilation, traffic, power supply + auxiliary), which are fully integrated on level of SCADA system. Sitina control system is based on SIAMTIC S7 PLC, SCADA system PVSS is used.

8.2 *Bolaman-Pershembe and Gyreshum-Espiye tunnels*

System of two tube tunnels Bolaman-Pershembe and Gyreshum-Espyie in Turkey is constructed on the highway on Black Sea seaside near towns Samson, Odru and Trabzon. Control system is distributed into huge area. Control system manages 23,5 km highway including 9 tunnels. The longest controlled tunnel is 3,8 km length Neffise Akcelik Tunnel. Control system is based on SIAMTIC S7 PLC, SCADA system WinCC is used.

9 CONCLUSION

The new tunnel control system approach has been introduced in the article. The new tunnel control system with the name International Tunnel Control Central (ITCC) has been developed by joined group of engineers from five countries using their experiences with tunnel control systems. The system structure has been shown on all levels of control. Problems of development and testing of new universal tunnel control system has been described. Two examples of tunnel control system based on ITCC control system from tunnel realization in Slovak Republic and Turkey have been shown.

REFERENCES

Přibyl P., Svítek M. 2000. *Inteligentní dopravní systémy.* Prague: BEN

Přibyl P. 2003. *TP98 – technologické vybavení tunelů.* Prague: MDSČR

Sachse T. 2005. *Modular Control Center for Tunnel Systems.* Munich: Siemens ITS Magazine

Seitel T. 2004. *ITCC System Specification.* Munich: Siemens Document

This page intentionally left blank

Underground Space – the 4th Dimension of Metropolises – Barták, Hrdina, Romancov & Zlámal (eds)
© 2007 Taylor & Francis Group, London, ISBN 978-0-415-40807-3

System of traffic control on Prague inner city ring

Jiří Štefan
ELTODO dopravní systémy s.r.o.

ABSTRACT: This article describes the system of traffic control of the inner city ring in Prague with emphasis on control systems of tunnel constructions. A new control system is introduced, which is responsible for safe and continuous traffic flow, not only on highway parts of the ring, but also on adjacent roads. The main emphasis is put on safe operation of the tunnel in conditions of city environment. The Mrázovka tunnel – the key component of the inner city ring – was opened in August 2004 after six years of construction. The Mrázovka tunnel is the middle section of the tunnel system, which can be used by drivers for easy and safe passage between northwest and south part of Prague. The Mrázovka tunnel is one of the best technologically equipped tunnels, which is controlled by a sophisticated control system integrating automatic control algorithms for traffic, mechanical and electrical equipment. As a part of the construction of the Mrázovka tunnel, the integration of control of existing tunnel constructions to one "Supervising control system" had to be solved. This "Supervising control system" was developed by the Czech engineering group of the ELTODO dopravní systémy s.r.o. The system was put into operation at the same time as the Mrázovka tunnel.

1 INTRODUCTION

Fundamental decisions of tunnels are made already in the design phase, where the following matters have to be optimized: the building part and the technological equipment. Generally, the cost of technological part is much smaller than the building part, but the technology is able to significantly improve safety in the tunnel. The Mrázovka tunnel is one of the best technologically equipped tunnels and one part of its technological equipment – the section of speed control – has improved the discipline of drivers to an extent that cannot be reached by means of the building part, e.g. by building "sleeping policemen".

2 THE MRÁZOVKA TUNNEL AS THE COMPONENT OF THE TRAFFIC FLOW IN THE INNER CITY RING

The Mrázovka tunnel (the nickname ATM) is in the middle of the tunnel system of the Prague inner city ring. It is connected with the Strahov tunnel on its northern end, and with the Zlíchov tunnel on its eastern end. The Strahov was built as the first tunnel in the city ring.

The Mrázovka tunnel, especially its control system, has to make allowance for the traffic in these adjacent tunnels. In addition, all tunnels are placed close to the city center, on a built-up area. There are several multilane roads and traffic lights are placed close to the tunnel portals.

Let us spend a few words about the philosophy of the tunnel control systems. According to the Czech technical conditions (TP 154), each control system of tunnels involves, apart from the technology inside the tunnel, also further technological parts outside of the tunnel and traffic signs in the clearway (the space in front of tunnel). The technology on these clearways is controlled and powered from the tunnel. Especially the power system uses interrupt power supply. Clearways are equipped with variable traffic signs, traffic lights and pikes. In case of emergency, this technical equipment must be able to stop vehicles in front of the tunnel portals and switch to a state allowing for the fastest possible evacuation of the tunnel.

Because these tunnels are in the city, the case of gated tunnel (or tunnel with restricted operation – this condition occurs much more frequently than tunnel out of order) have influence to the urban traffic in the neighborhood. Traffic lights outside of the tunnel and their key elements – traffic controllers – have direct connection to the control system. One of the most difficult tasks was the design of the intersection 573. As can be seen on the picture nr.1, the traffic controller receives commands from the two tunnels – Mrázovka and Strahov. Furthermore, close to this intersection there is the shopping centre Tesco (KOC) with its big parking place. The commands that are created in the control system of the Strahov tunnel (SAT), Mrázovka

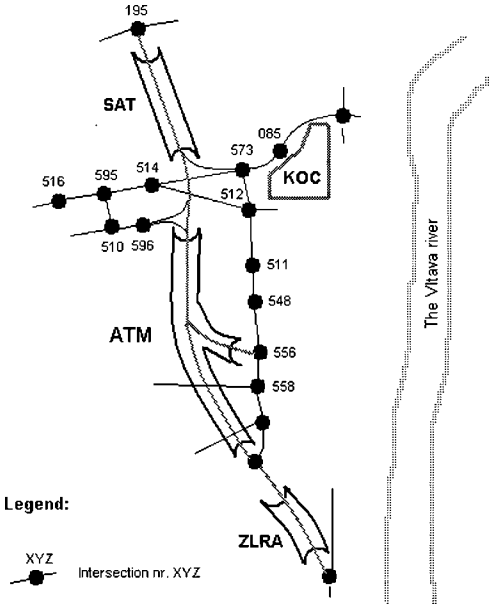


Figure 1. General situation.

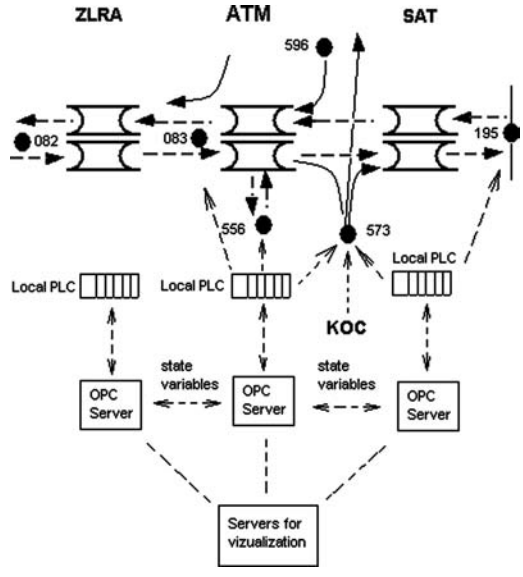


Figure 2. Relationships.

tunnel (ATM) and in the control system of the Tesco parking place are transmitted to the traffic controller nr. 573 are summarized in the following table.

I suggest, to implement a dynamic control system of the intersections placed on the inner Smíchov circle that would allow for the preference of public transport vehicles and high priority vehicles, and that would be connected to the central traffic control system.

The second problem was the interfacing between the control systems of these tunnels. The Strahov tunnel has used the control system made by G.E. Fanuc and tunnels Mrázovka and Zlíchov have used the Siemens control system. Therefore designers made a proposal to use a hardware-independent solution. The data exchange system is based on the OPS technology.

These state variables represent the states of the variable traffic signs. It can be seen that a small amount of state variables can represent all possible traffic situations in the tunnels.

On this chapter I would like to show that the traffic problems are much more complicated if the tunnel is built in the city than if it is built out of the city area. On the other hand, there is no problem with a sufficient electric power supply.

3 CONTROL SYSTEM OF MRÁZOVKA TUNNEL

The base conception of this control system is determined according to the category of the tunnel. In the Czech Republic, there are 3 categories: TA, TB and TC. The Input criteria are the length of the tunnel tube, and the traffic load (in vehicles per day). Tunnel Mrázovka has two tunnel tubes and the maximum length of 1300 m (the west tunnel tube). The traffic density has been over 4 000 vehicles per day. Therefore the tunnel Mrázovka belongs to the most intensive category TA.

4 WHY DO WE NEED A CONTROL SYSTEM?

From time to time, people ask this question. The Mrázovka tunnel contains 14 440 input/output points – sources of information or commands to action elements. Analyzing these amounts of information in each second is only if we use the computerized control system. The system analyzes the current events in the area of the Mrázovka tunnel, and issues commands to the underlying technology, but the human dispatcher has the higher priority to control. The regulation of such stochastic systems is increasingly dependent on computers, but a human dispatcher still has his own place in this process.

The base element of control system is a Programmable Logic Console for industry use (located in the control room) and the distributed I/O modules located by the technology. This solution was designed with regard to physical dimensions of this control system, according to the Czech regulations and, at least, to make the cost acceptable by the investor.

But this solution request to use very safe communication lines. We designed dual optical ring to connection among main control system and distributed I/O modules.

Table 1. List of variables to the intersection 573.

ATM	SAT	KOC	Description
x			Exit ATM across the 573: steady green.
	x		Exit SAT across the 573: steady green.
	x		Entry SAT across the 573: steady red.
	x		Entry SAT across the 573: green reduction 60%.
	x		Entry SAT across the 573: green reduction 30%.
	x		Entry SAT across the 573: green reduction 10%.
		x	Entry KOC across the 573: steady red (fire in the KOC).
	x		Entry SAT across the 573: steady green, exit SAT across the 5.573 : steady red.
	x		Entry SAT across the 573: steady green, exit SAT across the 5.573 : green reduction.
	x	x	Exit SAT across the 573: steady green, entry KOC over the 5.573: steady red.
	x	x	Entry SAT across the 573: steady red, entry KOC over the 5.573: steady red.
	x	x	Entry SAT across the 573: green reduction, entry KOC over the 573: steady red.
	x	x	Exit SAT across the 573: steady green, entry SAT across the 573: steady red, entry KOC over the 5.573: steady red.
	x	x	Exit SAT across the 573: steady green, entry SAT across the 5.573: green reduction, entry KOC over the 5.573: steady red.
x	x		Exit SAT across the 573: steady green, exit ATM across the 573: steady green.
x	x		Entry SAT across the 573: steady red, exit ATM over 573: steady green.
	x	x	Entry SAT across the 573: green reduction, exit ATM over 573: steady green. Exit ATM: steady green, entry KOC: steady red.
	x	x	Exit SAT across the 5.573: steady green, exit ATM across the 5.573: steady green, entry KOC across the 5.573: steady red.
	x	x	Entry SAT across the 573: steady red, exit ATM across 573: steady red, entry KOC across the 573: steady red.
x	x	x	Entry SAT across the 573: green reduction, exit ATM across 573: steady red, entry KOC across the 573: steady red.

Table 2. List of general variables between ATM and SAT.

State variables transmitted from Strahov tunnel to Mrázovka tunnel	State variables transmitted translated from Mrázovka tunnel to Strahov tunnel
SAT east tunnel tube right line closed:	ATM west tunnel tube right line closed:
SAT east tunnel tube left line closed:	ATM west tunnel tube left line closed:
SAT east tunnel tube closed:	ATM west tunnel tube closed:

Two optical rings are laid in the different cable shafts. As can be seen on the figure 3 there are 4 communication ways. The decision of which way has to be used is made fully automatically. The operator obtains only warning information in case of a defect. The second key element, the main station, has been built as hot standby redundant system. Both main PLC station (the first PLC operates as a master and the second PLC as a backup) are located in the different rooms, in the different fire segments. The optical synchronization bus guarantees the on-line data synchronization between master and backup PLC systems.

The problem of power supply is important as well. The power supply system uses two equivalent inputs for each important cabinet and the switchover is controlled by the control system. Each cabinet containing

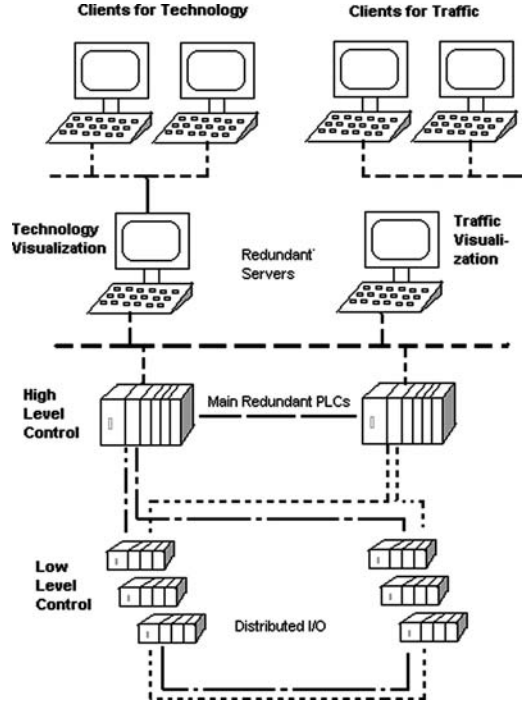


Figure 3. Structure of ATM control system.

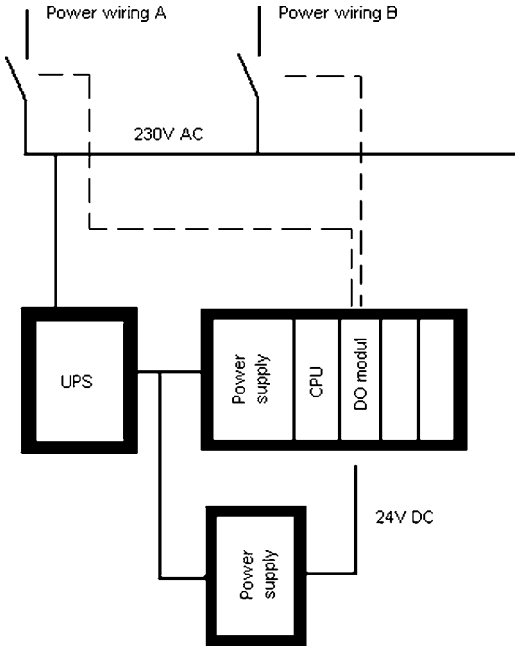


Figure 4. Layout of process station.

involving components of the control system has a dedicated UPS. Its capacity is 30 min. It is sufficient time for a service team to reach this locality and to fix the defect.

The control system is divided into two parts – transport control (dispatching Praha 2. ul Na bojišti – police works as traffic dispatchers) and control room of technology (Strahov, the civil staff). During ordinary operation the main control centre of ATM communicates with the superior control centers of tunnel and technology. The traffic flow in the ATM is controlled based on the received information (video control, traffic lights, phone communication, SOS and video-detection). The control system Kerberus was used. Its product has been developed for more than 10 years. It is a product of ELTODO dopravní systémy and has been used in 7 tunnels in the Czech Republic and in 4 tunnels in Turkey. It is independent on the type of the PLC equipment and also the tools for the integration with the city system (bindings to traffic information centre etc.) are available.

Table 3. Main features of Kerberus system.

Mode	• On – line Control • Simulation
Control	• Automatic Sequential • Manual
Options	• User Defined Traffic States and Sequences • Check Conflict Before Command

This system has these main features:

As was said before, the traffic system is of a high complexity. Therefore it is very useful to use the Simulation mode and options Check Conflict Before Command for the training and preparing of the human dispatchers.

REFERENCES

[1] Tichý Tomáš, 2006. Ověřování výsledků funkčnosti adaptivního řízení dopravy. Brno, Brněnské komunikace, Dopravní dny Mikulov 2006.

[2] SATRA spol. s r o, 2006. Tunel Mrázovka. Praha, Satra spol. s r.o.

[3] Přibyl Pavel a kolektiv, 2003. TP98 – technologické vybavení tunelů. Praha, MDSČR.

[4] Řehák Jiří, 2007. International Tunnel Control System, WTC Praha.

Underground Space – the 4th Dimension of Metropolises – Barták, Hrdina, Romancov & Zlámal (eds)
© 2007 Taylor & Francis Group, London, ISBN 978-0-415-40807-3

Facility management methods for an improved serviceability of traffic tunnels and their application to tunnel drainage problems

M. Thewes
Institute for tunneling, pipeline construction and construction management, Bochum, Germany

F. Heimbecher
Federal highway research institute (BASt), Bergisch Gladbach, Germany

G. Vollmann
Institute for tunneling, pipeline construction and construction management, Bochum, Germany

ABSTRACT: In order to be long-term effective and cost-effective for the operator transportation infrastructural buildings need very high service availabilities. This applies especially to tunnel buildings in the context of road networks and railway systems. Service availability problems often result from design errors or from inadequate realisation during the construction phase but may also occur as a result of wrong planned maintenance and refurbishment. A definition that is adapted to modern requirements therefore must include all three classic phases of the life cycle – planning, construction and operation – on an equal footing. In addition a precocious acquisition of specific data and its transfer through all phases of the life cycle has to be guaranteed in order to secure the service availability of the building. In the paper the problem, which has been introduced before, will be pointed out considering German traffic tunnels as example and in the progression of the paper a method of resolution will be presented that is identifying the possibilities of effective facility management for the international tunnel operators. Subsequently first genuine realised methods of resolution are presented on the basis of the problem of "tunnel drainage", which may lead to large expenses on traffic tunnels for the operating companies. Concluding, the mechanisms that form the basis of the developed concept are transferred to other sectors of tunnelling and tunnel operation and thus the specific possibilities of TFM are demonstrated.

1 INTRODUCTION

Traffic tunnels usually are located where no adequate alternatives for traffic are available or at least are connected with considerable disadvantages. Independently of the traffic mode they are used in, they in most cases represent highly needed key elements of the infrastructure network they belong to. That said high service availability is always a main target for the operator. Securing high service availability is thereby strictly connected to an efficient operating strategy, whereas methods of facility management are a useful help in the way they are exercised in the modern real estate economy. Especially taking a holistic approach for evaluating a specific building – thus regarding all phases of a lifetime, as there is planning, construction and operation up to the dismantling of the building – has to be considered as a reasonable method.

Regarding German road tunnels these reflections do not only have an influence on the German national economy. Because of Germany being a country which is highly frequented by transit traffic, especially regarding its location for the European community, these problems are of a serious concern for the EU-wide infrastructural network. Therefore a conclusive and efficient lifecycle strategy has to be carried out to insure high service availabilities for those buildings. In addition, it can be expected that the fields of operation and maintenance will in future take up a far greater share of the pending tasks for research and development. (Thewes, 2006).

In this paper, possible strategies for generating an efficient facility management for tunnels are described while taking German road tunnels as an example. During operation of such structures a large variety of factors has to be considered, out of which within this paper a first focus is given to the detail aspect of permanent drainage systems. Throughout the last years there has been a significant progress regarding draining systems, determined by a large amount of analyses and research (Maidl et al. 1999, Maidl et al. 2002, Maidl et al. 2004 unpublished). As a result a new guideline for planning, construction and operation of draining systems for road tunnels has been issued, which will

be released in the near future by the BASt, on behalf of the German Ministry for Traffic, Construction and Urban Development.

After a short and general introduction regarding methods of facility management and after some remarks concerning the operation mode of road tunnels, some of the methods of the guideline for drainage will be introduced to the reader. Those methods provide a holistic and lifecycle oriented approach to operation of drainage system.

2 FACILITY MANAGEMENT AS A METHOD TO REDUCE LIFECYLCE COSTS

Facility management (FM) regards a building in holistic way and relates to its complete lifecyle.

Thereby the main target is to reach a higher level of benefit, a higher productivity, more profitability and a conservation of the facility's value throughout its whole lifetime. During this process the benefit of the specific building should be increased, while the expense for maintenance will be constantly reduced. This fundamental approach to operating a facility is increasingly necessary due to the fact that in the last years an obvious change regarding the ratio of new constructions to the refurbishment of existing ones occurred. This development is shown in figure 1.

It can be assumed that this trend will proceed throughout the next years. Therefore it is obvious that maintenance and repair of a specific building will furthermore be a vital part of its operation phase and therefore needed expenses will rather increase then diminish. That said two central perceptions can be derived:

1. According to the higher meaning of the lifetime of a specific building and its extension due to sustainable refurbishment, an operation strategy has to be derived that allows to optimize the lifecycle costs by reducing the maintenance effort and the resulting expenses.
2. Thereby the operation strategy has to include methods of maintenance and repair which are preventive and proactive and allow an extension of the lifetime and a decrease of efforts for maintenance and – in a long term view – efforts for repair and refurbishment (Figure 2).

For determining the profitability of a specific building all influences on the facility from outside and from within have to be considered in the scope of an extensive analysis, while reduced expenses due to proactive measures have to be included. Generally therefore the following procedures need to be evaluated and to be included in the calculative approach:

– aspects of sustainability
– actions on structures

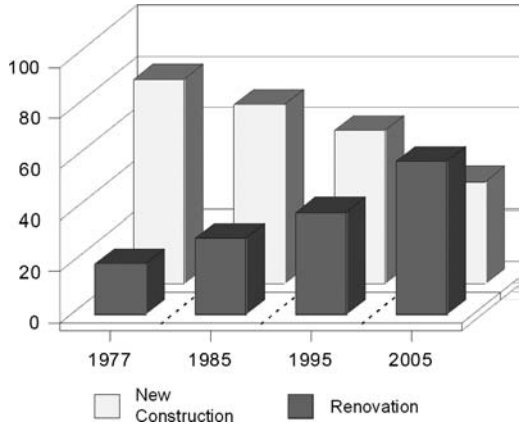


Figure 1. Ratio of new construction compared to renovation in Germany the last 30 years (Peil & Hosser, 2005).

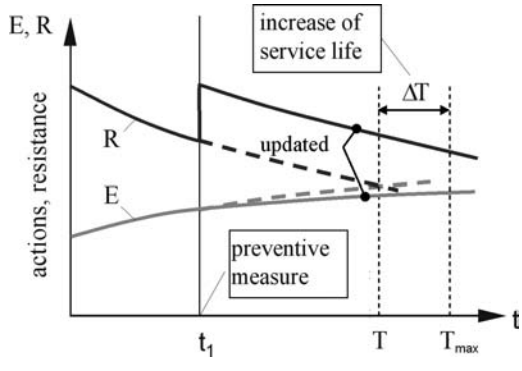


Figure 2. Increase of service life through protective and proactive measures and actions.

– accessibility and exchangeability of individual components or entire structures (inspection-oriented design and construction)
– component and structure characteristics
– lifecycle costs
– risk analysis
– energy and environmental performance over the entire lifecycle.

3 FACILITY MANAGEMENT OF TUNNELS: POSSIBLE AREAS OF APPLICATION AND PERSPECTIVES

3.1 *Points of operation of traffic tunnels and their influence on the cost structure*

Due to the specific common carriers traffic tunnels feature different points of operation, which are of vital importance regarding to the facility's function

within the transport network. A structured and efficient facility management needs to be focussed on these points. Regarding road tunnels the following points of operations can be pointed out:

- Ventilation
- Lighting
- Communication technology
- Systems for fire safety
- Systems for traffic surveillance, traffic guidance and signalling
- Drainage installations for road surfaces and (in case of permanently drained tunnels) for ground water.

In addition, the integrity of the inner lining and i.e. the roadsurface needs to be inspected frequently. However, the before labelled points of operation are subject to a higher frequency and intensity of maintenance and repair and naturally do have a shorter span of lifetime. This applies especially if the inner shells or the tracks of a tunnel are built due to high requirements regarding construction and durability.

All these points of operation do have in common that they first require an initial investment during the construction phase and that they generate operational costs during the operational phase of the building of a non substantial amount. This also includes costs for energy supply and cleaning. During later phases of the facility's lifecycle parts and components of theses systems need to be exchanged due to ageing, failure or wear. The influence of these matters on the facility's cost structure needs to be considered for generating a lifecycle cost-model (LCC-model) for road tunnels.

Furthermore all points of operation do have in common that their maintenance and repair, even if it's only on parts of the structure, will generate obstacles and handicaps for the utilization of the building, which results in a decrease of the facility's service availability. This has to be factored into the considerations. At some point the blocking of one track is necessary, at another point a complete tube or the tunnel as a whole has to be taken out of service. Expenses for the general public result here from.

In addition costs of general upkeep will occur, for instance due to cleaning of the inner shells or the track marks.

3.2 *Inspection, monitoring and damage detection*

For being able to maintain all points of operation efficiently, a substantial surveillance and detection of deterioration is needed. At this time mostly visual inspections and failure detection which is inherent to the specific system (for instance as function control for ventilation or illumination) is used for German road tunnels.

Naturally visual inspections are subject to fluctuations which depend on the conducting person. A deterioration, for instance to a draining system, isn't necessarily categorized in the same way by two different persons. On this account visual inspections need to be standardized as far as possible. To achieve this goal deterioration categories can be developed based on experiences from the past, which can be consulted during an assessment. In doing so the variance is reduced. However visual inspections do always have the disadvantage that only deterioration which has already und fully occurred can be recognized and not their development process. Therefore visual inspections in many cases only allow reactive and not preventive measures and actions.

Another large part of deterioration detection is carried out by non-destructive testing methods, for instance as a measurement for the integrity of the inner shell. The procedures with the biggest area of applications are the Impact-Echo-Method and the Ultrasonic-Method, which are already used to a large extent for inspections during the acceptance period of a construction and for the surveillance of existing facilities.

In a long term view it has to be expected that a surveillance of tunnels with monitoring-systems and -procedures will be exercised more widely. Especially deformations of the inner shell (convergence measurement) allow being collected and displayed by sensorial measurement and data logging. But even other applications are imaginable, for example tension detection on rock anchors, measurement of bedrock pressure, leakages, corrosion of the concrete or the range of sight and the exhaust development inside the tunnel. Hereby the advantage of monitoring procedures is that every measurement value logging can be conducted without any interference of traffic and therefore without any decrease of the service availability of the facility. The amount of data has to be collected and archived centrally in a control centre, and has to be used for optimizations of the operation.

3.3 *Measures of facility management as guidelines for planning, construction and operation*

As already mentioned, the primary centre of action of an efficient facility management has to be the operation phase of the lifecycle. This is essential for tunnels in comparison to other engineering works, due to the length of their lifetime, which has already reach about 150 years for some rail tunnels. In addition several points of operation are in need of maintenance with high intensity and frequency. The aimed quality of maintenance has to be clearly defined and to cope with adequate measures during the cause of action. Especially for the example of tunnel draining system studies have shown impressively, that wrong facilitated maintenance could be followed by an increase of maintenance costs (Maidl et al. 2002, Maidl et al. 2004

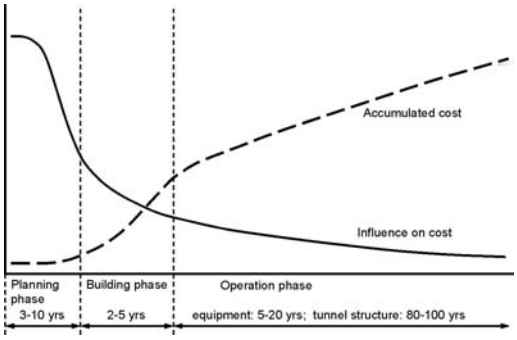


Figure 3. Tunnel project phases: Accumulated cost and corresponding influence on cost (PIARC, 2005).

unpublished). In addition, maintenance and repair are no static processes, but the necessary extent of maintenance changes throughout the lifetime due to wear of operational items or the change in operational boundary conditions of the building. Therefore a continuous adaptation of the extent of maintenance to the change in boundary conditions has to be carried out based on expertises from the phase of maintenance.

That said it doesn't cope with the problem to create a basis of action with modern methods surveillance, on which the operation staff may act in an arbitrary manner. Strictly defined maintenance measures are vital, as far as an accurate definition and description of maintenance documentation during its operational phase. This is essential especially for recognizing changes in boundary conditions at an early stage and for realizing an adequate reaction. The formulation of such clear guidelines for instance could be implemented by a explicit building management system, such as it is established by the BASt in Germany at the moment. (Haardt, 2004).

But also during the phases of planning and construction maintenance and repair have to be a vital part of the considerations in terms of a holistic approach. Studies of the PIARC have proven that a substantial part of expenses for maintenance and repair are determined by mistakes and errors which have occurred during design and construction phases. Most of the time this is influenced by the fact that those who are involved in the design and construction process have only little experience with the problems of maintenance and its costs. This becomes furthermore problematic, because the possibilities of taking an influence on matters during the operational phase, whose cost developments are directly linked to decisions taken in the planning or the construction phase are quite limited. The relationship between the cost of maintenance and the level of influence exercised on these costs can be depicted diagrammatically, as shown below (Figure 3).

4 INFRASTRUCTURE MONITORING AND OPTIMIZATION OF OPERATIONS WITH THE EXAMPLE OF TUNNEL DRAINAGE

4.1 *General*

In the following it is shown how a sustainable cost reduction can be achieved with methods of facility management, by following a holistic strategy, which comprises the design, the construction and the operation of particular details. Using the example of a drained tunnel, a problem which is specific for drainage systems is shown, which can is encountered at new road tunnels in Germany with a holistic strategy. This strategy is described by specifying measures from the areas of planning, construction and operation.

4.2 *Operational problems with drainage systems*

The permanent draining of tunnels during the operation phase is a solution, which is easier to build and which considerably reduces the construction costs in comparison with a tunnel with waterproofing. Over the service life of a tunnel, however, the effort for maintenance caused by a permanent drainage can become quite large. The result of a comparative LCC-analysis might therefore be that a waterproofing of the tunnel in spite of higher construction costs still is the more cost-efficient solution over the tunnels lifecycle. The main cause for this outcome could be lime deposits, which have to be cleared from the drainage pipes requiring a high technical and logistical and therefore costly effort. The mentioned lime deposits develop from precipitating calcium carbonate ($CaCO_3$) previously dissolved in the drained ground water and they partially are quite tough and resistant against cleaning. The $CaCO_3$ either originates from the temporary lining, where it is eluted from the groundwater contact with the shotcrete, or it caused by geologic limestone formations, which are passed by the drained ground water. Depending on the applicable case of origin for the $CaCO_3$ the lifecycle-oriented strategy for the design of a drained or undrained tunnel has to be developed. The main factors in this consideration are that the lime deposits caused by shotcrete linings are likely to become less with time whereas geologically caused lime deposits could continuously be problematic during the whole service life of the tunnel.

The mentioned causes for lime deposits principally can be differentiated regarding their hydrochemical and their hydromechanical origins. The hydrochemical causes have been extensively been investigated (Maidl et al. 2004 unpublished, Vollmann 2005, Girmscheid et al. 2003) and will not be discussed further at this point. However the hydromechanical causes of lime deposits always are closely depending on decisions and actions from the design, construction and operation phase of a tunnel (Maidl et al. 2002,

Maidl et al. 2004 unpublished, Vollmann 2005) and can be summarized as follows:

a) design: conception of the drainage system regarding the use of unsuitable components, i.e. unsuitable drainage pipes or filter materials
b) construction: placement of the drainage system with a lack of quality, i.e. placement of defect pipes or destruction of components of the drainage system
c) operation: application of unsuitable inspection and maintenance methods, unfavourable maintenance intervals

Together, these factors can cause a substantial maintenance and repair effort, which in the past in many cases was largely underestimated. In order to illustrate the resulting operational problem there are three main areas of influence which have a significant effect on the development of the operational cost:

a) the removal of deposits (i.e. with high pressure cleaning vehicles) and the resulting cost for the operator of a tunnel
b) the reduction of the service life of drainage pipes caused by the highly abrasive cleaning methods and the resulting cost for repair and for early replacement
c) the necessary (partial) closing of the tunnel for cleaning of the drainage system and the necessary traffic diversions and the resulting cost for the operator including a possible reduction of toll income

These factors have to be covered by a LCC-analysis even though the economic effort caused by the removal of deposits (a) is very difficult to quantify during the design phase of a tunnel. This is due to the difficulty of making a prognosis for the development of lime deposits before the tunnel actually goes in operation. The enormous problems caused in this context are illustrated by the decision of the German Railways (Deutsche Bahn) who in their building regulation, RiLi 853 (Deutsche Bahn AG, 2003) do not normally allow for the application of drained tunnels anymore but require full waterproofing of new tunnels. This is mainly due to the fact that train tunnels during maintenance are not available for service, causing the delay of trains at high cost because the rail network usually does not allow for equivalent detours.

4.3 *Constructive and operational solution approaches*

For the application field of German road tunnels extensive research has been performed on behalf of the Ministry for Traffic, Construction and Urban Development resulting in constructive and operational solution approaches aiming at the reduction of all deficits from design and construction which correlate with the development of lime deposits. The chosen approach

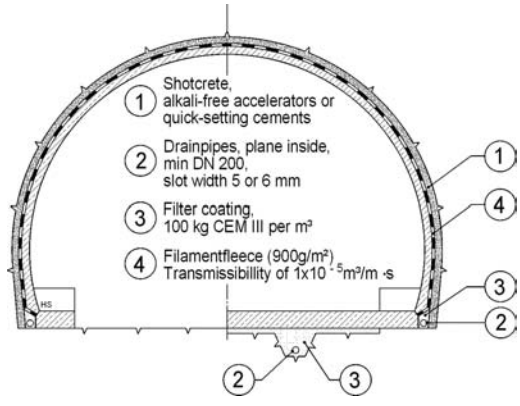


Figure 4. Deposit depleted ground system according to ZTV.-Ing.T5 (BMVBW, 2006).

led to the development of basic system of individual components with a reduced disposition towards developing lime deposits (Figure 4) proven by research projects (Maidl et al. 2002, Maidl et al. 2004 unpublished, Vollmann 2005). This basic system became mandatory in the national building regulation for road tunnels, ZTV-Ing. part 5 [11].

In case of a strong tendency towards the development of lime deposits, the basic system project-specifically can be enhanced by using components with an even further reduced disposition towards lime deposits. These components can be studded sheets in case of high local water inflow or uncemented gravel filters in connection with a special drainage pipe. Other solutions for handling drainage water with a high inclination towards lime deposits are available.

Finally, all data about the development of lime deposits will have to be collected and transferred to the operator for evaluation and for prognosis of deposit development during the operation phase. With this data it will become possible for the operator to optimize the strategy for inspection and maintenance and thereby reduce the operational cost for permanent drainage substantially.

4.4 *Proactive measures for maintenance and documentation*

Based on the data from the construction phase the operator can develop an optimized maintenance program for an individual drainage system adapted to its specific need for inspection and cleaning. Further, guidelines for the concept of a maintenance programme have been developed, consisting of the following points:

– data collection about the disposition toward the development of lime deposits at the inspection shafts

– camera inspection of the drainage system for the detection of the development of lime deposits using a unified classification method
– general recommendations for suitable cleaning methods of drainage systems in case of lime deposits
– tools for the collection, representation, evaluation and the archiving of data about the drainage system.

The use of a standardized method for classification and evaluation of inspection data the chance for arbitrary inspection results has considerately been lowered and the data becomes valid for long-term comparative evaluation of different tunnels and different drainage systems. This approach aims at the development of a central database for the drainage of German road tunnels leading to improved recommendation in future.

5 CONCLUSIONS AND OUTLOOK

It was shown that by a specific examination of the deterioration mechanisms and by the development of adequate measures a structured general program for operation and maintenance of a drainage system of a traffic tunnel can be developed. This on one hand will facilitate a reduction of the life cycle costs and on the other hand guarantee the highest possible availability of this individual point of operation and the whole tunnel. Further it was shown, that these systems can be flexible enough to be adapted to specific requirements of particular tunnels.

Similarly programs for the operation and maintenance of other points of operation are developed and will be integrated in a holistic overall approach for the facility management of traffic tunnels. For this a particular goal will be the collection of all relevant data for operation over the whole lifetime of tunnels and the subsequent optimization of adapted concepts for operation and maintenance regarding future changes of boundary conditions.

REFERENCES

Thewes, M. 2006. Zunkunft der Forschung für den Tunnelbau (Future of Research for Tunnelling). *Tunnel* 5/2006 P. 34–39.

Maidl, B., Kirschke, D., Schockemöhle, B. & Heimbecher, F. 1999. Abdichtungs- und Entwässerungssysteme bei Verkehrstunnelbauwerken, *Forschung Straßenbau und Straßenverkehrstechnik.* 773 Bonn: BMVBW.

Maidl, B., Abel, F., Karroum, A. & Stein, V. Untersuchungen zur Bestimmung des Versinterungsverhaltens unterschiedlicher Dränageelemente, *Forschung Straßenbau und Straßenverkehrstechnik.* 858 Bonn: BMVBW.

Maidl, B., Abel, F. & Vollmann, G. Empfehlungen für den Entwurf, die Herstellung und den Betrieb von Entwässerungssystemen im Straßentunnelbau. Abschlussbericht zum FE-Vorhaben im Auftrag des Bundesministeriums für Verkehr. Bochum: unpublished.

Peil, U. & Hosser, D. 2005. Life cycle assessment of structures via innovative monitoring. SFB 477 – Brochure.

Haardt, P. 2004. Bauwerks-Management-System (BMS) – Werkzeug zur Substanzerhaltung für Verkehrsbauwerke. *Bautechnik* 82, S. 794–798.

PIARC. 2005. Good Practice for the operation and maintenance of road tunnels. La defense cedex: AIPCR – Association mondial de la route.

Vollmann, G. 2005. Zur Härtestabilisierung als versinterungsreduzierende Maßnahme. Göttingen: Cuvillier Verlag.

Girmscheid, G., Gamisch, T., Klein, T. & Meinlschmidt, A. 2003. Versinterung von Tunneldrainagen – Mechanismen der Versinterungsentstehung. *Bauingenieur* 78. 292–300.

Deutsche Bahn AG. 2003. Richtlinie 853: Eisenbahntunnel planen, bauen und instand halten, Stand September 2003.

Bundesministerium für Verkehr, Bauen und Stadtentwicklung. 2006. ZTV-Ing. T5 – Zusätzliche technische Vertragsbedingungen – Abschnitt 5 “Tunnel”. Dortmund: Verkehsblattverlag.

Part 8.2
Fire protection measurement

This page intentionally left blank

Underground Space – the 4th Dimension of Metropolises – Barták, Hrdina, Romancov & Zlámal (eds)
© 2007 Taylor & Francis Group, London, ISBN 978-0-415-40807-3

Fire protection concept for the Ceneri Base Tunnel

S. Čufer
Edy Toscano AG, Engineering & Consulting, Chur, Switzerland

ABSTRACT: The Ceneri Base Tunnel, two single-track tunnels with the length of 15.4 km, is the south continuation of the Alptransit Gotthard transalpine rail route. This tunnel will allow, together with Gotthard Base Tunnel, fast and economical freight and passenger transportation service trough the Swiss Alps and assure optimal connections in both the Swiss and European timetable systems. In the same time, in the built-up areas, the regional rail system (TILO) will cut journey times to half of today's duration.

Report "Safety in Swiss railway tunnels" of BAV (Swiss traffic state authority) from 2001 shows that safety in the railway traffic is considerable bigger then safety in the road traffic. Although the probability of an accident in the railway tunnels is small, the consequences of the damages are massive and the rescue conditions, especially in the long tunnels, are very limited. The safety level in the newest base tunnels in Swizerland meets requirements of the European high-performance traffic routes.

This paper deals with the concept of the tunnel safety and fire protection system for Ceneri Base Tunnel based on the experience of the AlpTransit Gotthard. To meet fire protection requirements, the safety and protective measures have to be defined. These measures include railway facilities, ventilation system, drainage and tunnel structure. The focus of this paper is on the requirements for the fire protection of the tunnel inner lining.

1 CENERI BASE TUNNEL

The Ceneri base tunnel stretches from Vigana in the north to Vezia in the south. It consists of two parallel single-track tunnels which are linked by cross passages approx. every 320 meters. The rock cover of the tunnel is 400–800 m in the north and approx. 100–300 m in the south, see Fig. 1/Fig. 2.

The tunnel is embedded in the crystalline bedrock of the Southern Alps. The zone is complex and heterogeneous, which consists of various geological rock layers. Bedding of different rock formations runs inclined to the tunnel axis, see Fig. 1. The axis-center distance of the 2 single-track tunnels is approx. 40 m. Multifunctional analysis has shown that this tunnel system is the most suitable for long alpine tunnels. The Sigirino intermediate point of attack represents the central logistic base for the construction of the tunnel. It mainly embraces the Sigirino access tunnel (2.5 km), and the existing Sigirino exploratory tunnel (2.9 km), as well as the installation caverns located at the foot of the access tunnel.

The Sigirino access tunnel represents the main opening for the excavation of the installation caverns during construction phase and in the operation phase will be used for ventilation purposes. The installation caverns will be excavated in part sections by drill and blast method. Sigirino access tunnel will be excavated by open TBM. The main tunnels will be driven from the installation caverns in both directions. The Ceneri north tunnel section will be excavated by drill and blast method.

The southern section of the tunnel will be driven parallel with the construction work in the northern part of the tunnel. The south tunnel tubes will be excavated by drill and blast method over a distance of approx.

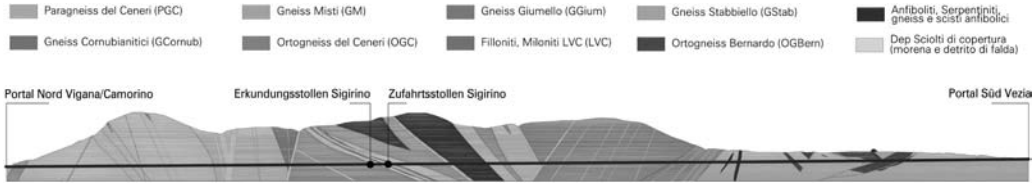


Figure 1. Geological longitudinal section.

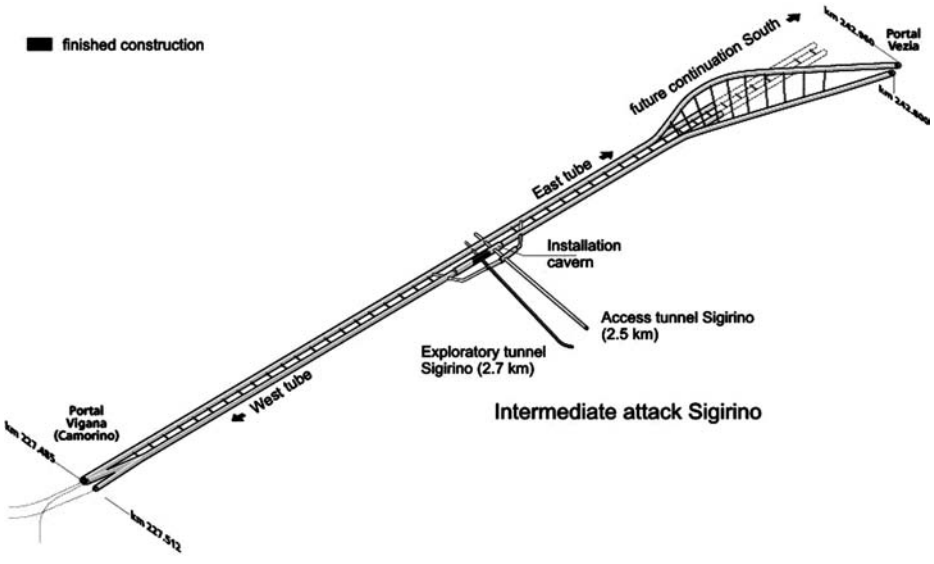


Figure 2. Ceneri base tunnel, length 15.4 km.

2 km to "Linea Val Colla" (LVC, approx. length of 600 m), one of the most geological challenged zones of the entire Ceneri Base Tunnel. The section after LVC will be excavated by TBM. The bifurcation caverns in Saré are located approx. 2 km from the southern portal, which provides the prerequisite for a future extension of the AlpTransit line to the south, in direction Milan, see Fig. 2.

2 PURPOSE AND FOCUS OF THIS PAPER

The aim of this paper is to provide a better understanding of a tunnel safety and fire protection design of the long railway tunnels. The following subjects will be discussed:

- Tunnel safety concept,
- Fire protection concept,
- Use of the fire protection standards,
- Fire scenarios,
- Concrete behavior during the fire,
- Requirements for the fire resistant inner concrete lining

3 SAFETY CONCEPT

The main elements of the Ceneri Base Tunnel are shown in figure 2.

The tunnel system is based on a twin tube system. Tunnel tubes are connected by cross passages approx. every 320 meters.

In emergency case the passengers can escape through the cross passages to the opposite tube where the evacuation measures from the tunnel take place. It is not planed to use the access tunnel in Sigirino for evacuation purposes. Since the evacuation of the passengers in an emergency case is based on the rail transport, the access route in the opposite tube must be free. To control traffic in the tunnel in the regular and incident mode, the Ceneri Base Tunnel will be equipped with modern signaling system.

In case that the burning passenger train can't reach the portal and has to stop in the tunnel, following operational regulations have been defined:

- All trains outside the tunnel have to be stopped before they enter the tunnel,
- Trains in front of the incident train leave the tunnel with normal speed,
- Trains behind the incident train have to be stopped immediately,
- Speed of the trains in the opposite tube is reduced generally to 80 km/h,
- Evacuation of the passengers is carried out using a rescue train in the opposite tube.

4 REQUIREMENTS FOR FIRE PROTECTION CONCEPT

The fire of the passenger or freight train in the Ceneri Base Tunnel can cause large damage of the tunnel structure following by extreme costs of the renovation works. Service breakdown in one or both tunnel

tubes can last several months. This subject have been analyzed by the safety department of the AlpTransit over the last years and following main requirement is defined: "During fire of the passenger or freight train in one tunnel tube, the operation safety in the other tube shall be as high as realistically possible."

Additional to this main requirement following requirements are defined:

– Availability during fire (passenger safety): The safety of the passengers during the fire has to be ensured. The tunnel must be in the service until the evacuation of the passengers is finished (compelling criteria).
– Availability after fire: A service breakdown of the tunnel shall be as short as possible.

5 CONSTRAINTS

5.1 *Availability during fire*

Following requirements for the availability during fire are determined:

a. Fire of the passenger train: availability of the accident tube: 45 min
b. Fire of the passenger train: availability of the opposite tube: 90 min
c. Fire of the freight train: availability of the opposite tube: 90 min

First requirement ensures that the passengers leave the burning train and accident tube through the cross passages. This requirement is valid for tunnel areas in the accident tube near to the source of fire. In these areas, explosive spalling of the concrete elements is not allowed.

Second and third requirement ensure that the trains, which are located in the tunnel and not affected by the fire, can leave the tunnel without damage, including evacuation of the passengers from the burning train. These requirements can be also applied for tunnel areas in the accident tube which are not in the immediate vicinity of the source of fire.

5.2 *Availability after fire*

In regard to reduce total renovation costs, protecting measures have to ensure that after fire, service in at least one tunnel tube begins as soon as possible. Evaluation of the protecting measures is based on their efficiency and costs.

The conditions for the service of the one tunnel tube after fire are determined as follows:

– Passenger traffic in not affected tube is possible if the ventilation system is in the service; one or two cross passages and the accident tube in the area of these cross passages may not be available.
– Freight traffic in not affected tube is possible when maximum four cross passages or ventilation system are not in service. It is not allowed to use an accident tube in the area of the damaged cross passages.

6 APPLICABILITY OF STANDARDS

The temperature-time curves for the case of the burning passenger or freight train in the long railway tunnels are not yet developed and standardized. Therefore, safety department of AlpTransit developed own temperature-time fire curves which are used for the fire protection design of Gotthard and Ceneri Base Tunnel. These temperature-time fire curves widely correspond to the international standardized curves, but they show longer duration of the fire.

– Fire of the passenger train with maximum value of the fire power* of 40 MW,
– Fire of the freight train with maximum value of the fire power* of 250 MW.

*The actual fire is described in terms of the rate of heat (or "fire Power") expressed in Mega-Watts (MW) which depends upon the rate at which the combustible materials burn. For example, in a tanker, the fire power depends very much upon the opening produced by an accident through which the fuel leaks, as well as on the capacity of the tunnel drainage system.

7 FIRE SCENARIOS

Following assumptions for the calculation of the fire temperature are defined:

– Basic air flow in tunnel is 2 m/s in the direction of travel,
– When train stops, the fire is already developed (20 min after begin of fire),
– Train burns down from the end to the begin of the train composition,
– Passenger train has 10 cars (250 m),
– Freight train has 32 cars (750 m),
– Temperature is evenly distributed in the tunnel cross section (simplified assumption).

7.1 *Fire of passenger train*

Maximum fire power is 40 MW. The source of fire is 125 m long (a part of the burning train). Each part of the train is exposed direct to the fire for 120 min and after 6 hours entire train is burnt down. A reverse current of the hot air is not expected, whereby, upstream of the source of fire, the air will be not heated. Downstream of the source of fire, the air will be cooled down through the heat exchange with the tunnel wall.

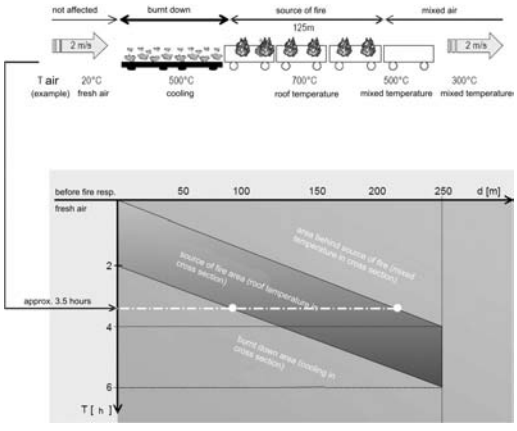


Figure 3. Assumption of the fire of the passenger train.

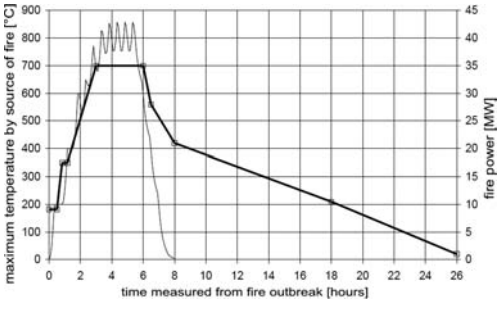


Figure 4. Maximum temperature of the passenger train by the source of fire incl. cooling. Right scale and fine diagram curve: fire load based on the fire standards.

Figure 4 shows a temperature flow in the tunnel cross section in the source of fire, in case of passenger train fire. During 6 hours, the source of fire moves along the entire train.

7.2 *Fire of freight train*

Maximum fire power of 250 MW will be used for all kind of freight trains, incl. the trains transporting dangerous materials. The source of fire is 200 m long (a part of the burning train). Each part of the train is exposed direct to the fire for 45 min and after 4 hours entire train is burnt down. Hot air can flow back 150 m against the basic air flow. Further upstream, the air will be not heated. Downstream, 25 m behind the source of fire, the air will be cooled down through the heat exchange with the tunnel wall.

Figure 6 shows a temperature flow in the tunnel cross section in the source of fire, in case of freight train fire. During 4 hours the source of fire moves along the entire train.

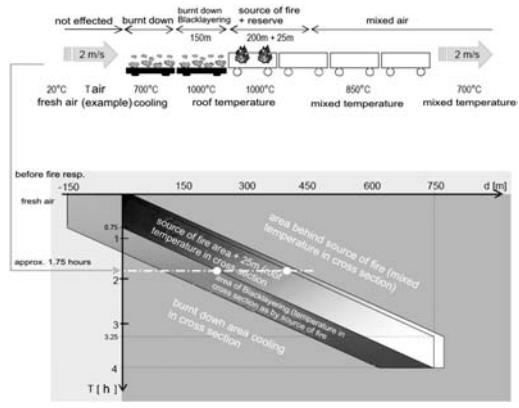


Figure 5. Assumption of the fire of the freight train.

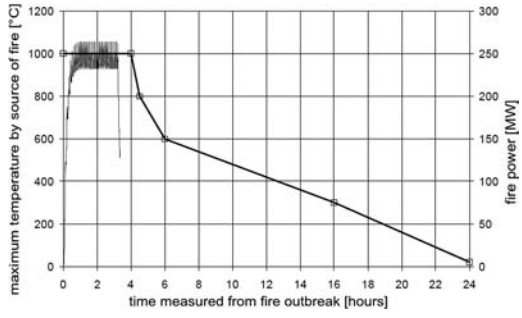


Figure 6. Maximum temperature by the fire of the freight train by the source of fire incl. cooling. Right scale and fine diagram curve: fire load based on fire standards.

8 CONCRETE BEHAVIOUR DURING FIRE

Fire impacts upon concrete structures insofar as it generates a heat flow into the concrete's exposed surface, producing temperature, moisture and pore pressure gradients within the concrete mass. Thermal strains, stresses and cracking develop within the heated structure and explosive spalling of the concrete takes place. The concrete and steel, as well as the bond between them, experience strength losses.

There are two problems of concrete in fire. These are: deterioration in mechanical properties as temperature rises, caused by physicochemical changes in the material during heating; and explosive spalling, which results in loss of material, reduction in section size and exposure of the reinforcing steel to excessive temperatures. Consequently, both the separating/insulating and load-bearing functions of the concrete member could be compromised.

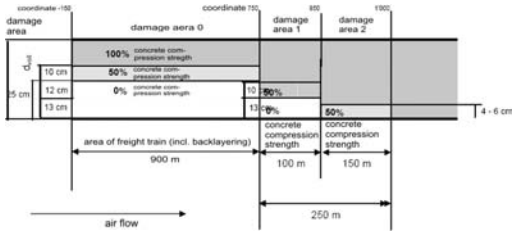


Figure 7. Damaged model of the concrete element without fire protection.

Table 1. Simplification of the damages in different areas of the concrete element.

Damage area	Distance (m)	Destroyed (cm)	Damaged (cm)
Area 0	−150 to +750	25	10
Area 1	+750 to +850	13	10
Area 2	+850 to +1000	0	5

8.1 *Concrete failure model without fire protection*

Explosive spalling:
Explosive spalling takes place when the concrete reaches temperature of 180°C. Based on the temperature-time fire curve and progress of the source of fire, the concrete element in the area up to 100 m downstream of the burning freight train, will be heated to 180°C in 6 cm concrete depth.

Strength loss:
By temperature of 380°C, the concrete strength decreases, caused by physicochemical changes in the material. Based on the temperature-time fire curve and progress of the source of fire, the temperature of 380°C occurs in 10 cm depth of the concrete element. Damaged model of the concrete element without fire protection measures is shown in Figure 7.

Damaged model:
Damaged model of reinforced concrete:
– Concrete cover of 5 cm is assumed,
– Explosive spalling will occur in the depth of the reinforcement,
– Reinforcement will be badly damaged (strength loss caused by high temperature),
– Damaged reinforcement stabilizes first fully weakened concrete layer, which ensures the thermal isolation of the underlying concrete layers,
– Strength loss and destruction influence can not go deep into the concrete element,
– Behind the reinforcement, first concrete layer of 10 cm is 100% and following 10 cm, 50% weakened.

Temperature- time process in source of fire:
(a) 45 min. after begin of the fire:
  – Heating of the concrete surface to the temperature of 930°C. With temperature rise of 3°C/min, the critical limit of the explosive spalling will be reached in 10 cm depth of the concrete element. In humid environment and under consideration of the progressive damage of material, 10–15 cm deep explosive spalling occurs in non-reinforced concrete areas,
  – Temperature of the inner reinforcement (in the areas of the fault gauges and by the cross passages) is min. 450°C (causes a significant strength reduction in the reinforcement).

(b) 90 min. after begin of the fire:
  – Temperature on the concrete surface is still approx. 900°C,
  – In 6 cm depth of concrete element the temperature reaches max. value of 500°C,
  – In the depth of 10 cm is the temperature approx. 270°C (still rises). It comes to the additional spalling, indeed with lower intensity as in the first 45 min. Total spalling is in the range of 10–20 cm. It comes to significant strength reduction in the following 5 cm of the remained structural concrete,
  – Temperature in the area of the inner reinforcement exceeds 600°C and the reinforcement shows only an insignificant bearing capacity.

(c) 16 hours after begin of the fire:
  – Slow cooling to the temperature of 250°C in the whole concrete cross section,
  – Additional spalling of the weakened area as a result of the temperature expansion,
  – After cooling: Strength loss as a result of the spalling in the whole cross section of the non-reinforced concrete element. In the reinforced areas, demolition of the concrete, caused by spalling, will be reduced (presence of the reinforcement).

(d) Banquets and cable protection pipes:
  – Cable protection pipes located in the banquets are exposed to the temperature of 150°C after 45 min. and to the temperature of 280°C after 90 min. The cable protection pipes have no fire protection function.

9 FIRE TESTS

Objectives of the fire tests are to:
– verify assumed depth of the spalled and weakened areas of the concrete lining in consideration of the project specific constraints incl. high compression stresses in the concrete element section,

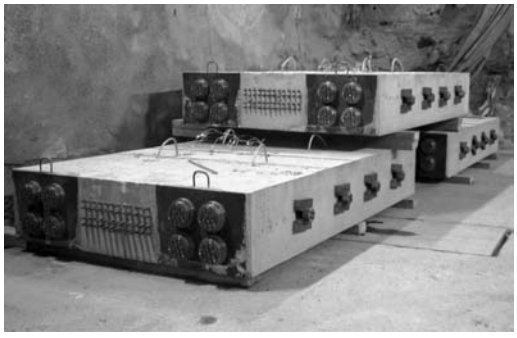


Figure 8. Test samples for the fire tests.

– optimize concrete cover in the bending tension stressed structural member,
– determine the temperature spread in the concrete cross section in order to verify used calculation models,
– optimize the concrete mix (aggregate, cement, W/C factor, mixing time,…),
– determine fire protection measures.

10 CONCLUSIONS

With planned fire protection concept described in this paper, the key principles of the safety philosophy related to the Ceneri Basis Tunnel can be achieved.

General requirements for the fire resistant concrete:

– Fire resistant concrete must have the same mechanical characteristics as a conventional concrete. Strength, strength development, long-term behavior (shrink, creep), frost resistance, tightness have to comply with given requirements,
– Fire resistant concrete must show high fire resistance, i.e. concrete may not show tendency of production of the deep spalling, based on the fast increasing and longer acting of the heat ($>1000°C$).

Special requirements:

Concrete strength:
Fire resistant concrete must reach the strength characteristics given by the Engineer based on the structural requirements.

Heat penetration after 45 minutes:
During the fire tests it has to be proven, that at the minimum cover depth (5 cm), the temperature after the first 45 minutes of fire exposure will not exceed 350°C.

Explosive spalling:
During the fire tests explosive spalling of the fire resistant concrete isn't allowed. After the fire tests the maximum depth of the concrete spalling should be at maximum 3 cm.

Cracking, resp. concrete surface condition after the fire:
Based on the temperature-time fire curve of the AlpTransit, the concrete surface after the fire has to be solid ("knockproof"). Cracking has to be fine distributed (crack size max. 0.3 mm). In the next 24 hours after the fire tests the concrete surface may not be changed.

REFERENCES

S. Cufer, EDY TOSCANO AG 2006: Economical aspects of the geological risk analysis for the construction of the road and railway tunnels, *PEMT '06, 5th Pan-European conference on planning for minerals and transport infrastructure, Proceedings first book:* 143–150

L. Lardi, M. Dolfini, ITC ITECSA-TOSCANO 2006: Brandschutzkonzept Einspurtunnel

O. Pini & S.Skaanes, ITC ITECSA-TOSCANO 2006: Ceneri Base Tunnel, *Tunnel: 4/2006:*44–47

AlpTransit 2006. The Ceneri Base Tunnel – the logical continuation, *www.alptransit.ch*

Underground Space – the 4th Dimension of Metropolises – Barták, Hrdina, Romancov & Zlámal (eds)
© 2007 Taylor & Francis Group, London, ISBN 978-0-415-40807-3

Newest issues of integrated road urban tunnel fire protection system

N.F. Davydkin
INTERSIGNAL Scientific/Production Coordination Centre, Moscow, Russia

S.N. Vlasov
Russian Tunnelling Association, Moscow, Russia

ABSTRACT: Brief analysis of fire danger, fire load quantitative and qualitative indices, ignition sources, fire temperature regimes, as well as time needed to safely evacuate people from the tunnel is provided in the article. Integrated road urban tunnel fire protection system developed in INTERSIGNAL and discussed in the article consists of the following sub-systems:

– fire prevention;
– passive fire protection;
– active fire protection;
– management and technical measures;
– fire liquidation and people rescue by operative teams.

The system makes it possible to duly provide for the safety of people, to preserve material values, to reduce fire risks and to liquidate fires at minimal losses.

In spite of considerable progress, contemporary engineering does not have absolutely safe construction and operation techniques or methods and means that would make it possible to forecast certain probable emergency situations determined as outwardly sudden events characteristic with uncertainty and difficulty of decision-taking and associated with sharp conflicts and stresses experienced by people, with social, ecological and material losses, especially life losses, resulting in considerable manpower, material and time expenses required to carry out evacuation and rescue activities and to liquidate the catastrophic consequences.

In case of fire in a road tunnel, transport vehicles, steel structures and equipment of the works become metal thrash. Structural components including tunnel lining (steel, reinforced concrete, etc.) get broken, loose their carrying capacity and collapse. This is particularly dangerous in case of urban tunnels running under existing structures, since tunnel collapse may result in forming a major surface cavity with catastrophic consequences (Davydkin et al. 1998; Strakhov et al. 2000; Koshmarov 2002; Haak 1999; Welzig 2000).

Well known are tragic consequences of fires in Baku metro (1995), under Mont Blanc 25 March 1999, in Capron funicular tunnel (11 November 2000) with more than 150 lives lost, in the approach part of the Freju tunnel (28 May 2001), in the 17 km long Sent Gotthard tunnel (24 October 2001) (Domke 1999).

Any fire in a tunnel results in operation of the whole transportation system of an urban region, a major city or even a country's part paralysed.

It is a strategic task to provide for safety of the people, for normal operation of road underground tunnels in major cities.

Since tunnels are long confined space structures of variable depth containing a good deal of flammable substances and materials as well as various ignition sources, they are much more dangerous in terms of fire rise and development in comparison with surface highways.

In case of a jam at the tunnel exit, quantities of flammable materials concentrated. In the space of a 3 km long three-lane tunnel, and attributed only to cars (6 m long with intervals, no gas vehicles) will make as follows (Davidkin et al. 2004; Davydkin 2002; ADAC 2000; Brux 1999):

– petrol: 61200 l;
– flammable liquids: 15300 l;
– rubber: 91800 kg;
– plastic: 30600 kg;
– synthetic materials: 61200 kg.

The figures may increase provided mixed traffic is taken into account.

As a matter of fact, tunnels are huge underground storages of easily ignitable liquids, flammable substances and materials with each vehicle being a bomb stuffed with incendiary mixture ready to ignite or blast any moment.

In case of fire, burning temperature of easily flammable liquids, plastic and other materials may reach 1100–1300°C an to last for a long time (up to 2–3 days) (French-Italian Commission 1999). For people happened to be in the tunnel, the situation becomes critical in 3 to 5 minutes from the moment of fire beginning (Shoigu et al. 1997; Grushevski et al. 1985), the figures determining the required people evacuation time.

Given the above mentioned temperature levels, it becomes practically impossible for emergency and rescue teams to enter the tunnel to liquidate the fire, provided this was not stipulated by design solutions beforehand.

Smoke escaping in the course of fire contains up to 70 types of chemical compositions poisonous for people (Shoigu et al. 1997; Davydkin et al. 1997 a, b, c, d, e; Toudos 2001; Day 1999).

Professor Pokrovsky and other researchers have established that combined impact of temperature and toxic gases to people increases as temperature rises. Carbon dioxide toxicity increases as fume and humidity of the environment rise resulting in synergic effect when combined impact of the factors exceeds that of the same individual factors.

Psychologically, the impact of fume is expressed in the form of fear people experience to enter into the visible fume environment.

If traffic jam gets formed at the tunnel exit, minimal number of people present in the vehicles and subject to be evacuated in case of fire will make approximately 2 thousand. This is why provision for people safe evacuation in case of man-induced catastrophes and fires in road tunnels is of priority while taking fire safety design solutions. Given psychological condition of a person facing emergency situation, the process proves to be fairly challenging.

Vitality of fire safety issues for operation of road tunnels determines the fact that in the course of their design and construction, sophisticated engineering solutions should be developed.

Having examined respective standards and codes of practice effective in Russia, USA (*Fire Protection Engineering*, SPPE, 2002), France, Germany, Italy, Switzerland, Japan, etc., and having generalised practical world experience gained in the course of road tunnel design, construction and operation, INTERSIGNAL RPCC supported by Russian Tunnelling Association and research and design companies developed an integrated road urban tunnel Fire Protection System (FPS) (Davydkin et al. 1999; Davydkin et al. 2000; Davydkin 2001; Davydkin 2002; Davydkin et al. 2002; Davydkin et al. 2004). Authors' rights for FPS integrated system development are protected.

FPS is an amalgamation of different interrelated most complex engineering solutions grouped in the following individual sophisticated autonomous systems: Fire Prevention System, Passive Fire Protection System, Active Fire Protection System, Management and Engineering Measures System, Fire Fighting and People Rescue System.

Described approximately, Fire Prevention System provides for elimination of one of the three main fire causes (that is for prevention of forming any fire situation), i.e. combustion and ignition sources, fire load (flammable substances and materials), entry of oxygen or other oxidizing agent. This is a very brief explanation of a broad complex of fire prevention and protection measures. Among subsystems there are:

- prevention of forming an inflammable environment;
- prevention of forming ignition sources in inflammable environments;
- elimination or restriction of oxidizer to inrush;
- making it inadmissible to arrange A and B fire/blast danger category premises in tunnels;
- gas (CO, CO_2, NO_3, etc.) control;
- lightning protection for buildings and structures.

Passive Fire Protection System is optimised for design and estimation documents made at various project development stages by all design process participants (Client – Designer – Examination body – State supervision bodies – Contractors).

PFPS comprises a complex of technical fire-protection solutions and determinations related to architectural and structural parts of the design including:

- solutions related to plans and master plans;
- solutions related to external water supply for fire-fighting needs;
- transportation and pedestrian flow ways;
- fire-protection space and plan parameters;
- allowable area of fire niches and sections;
- required (normative) and actual fire-resistance properties of tunnel structures;
- fire-protection membranes;
- blast-protection measures;
- integrated smoke-protection measures;
- fire-fighting technical measures;
- structures and plans of evacuation ways/exits/emergency staircases;
- fire-protection power-supply technical measures;
- distribution and transformer substations;
- continuous power supply facilities.

Calculation of fire resistance and fire protection properties of tunnel structures is a key fire safety

factor, since structures used for road tunnels at present are usually large and complex in terms of their design and space form.

For example, fire-protection technical solutions to be taken while developing plans and master plans will relate to:

- tunnel alignment;
- junctions to rail projects as well as to coach terminals and to parking lots;
- availability and parameters of: gas pipelines and underground reservoirs;
- oil product pipelines grouped to those carrying quickly inflammable, carrying inflammable liquid products or raw oil;
- other objects dangerous in terms of fire and blasting;
- underground storages of liquefied gas/flammable liquids/oil/petrol stations' tanks;
- other product pipelines;
- special-purpose underground works;
- other strategic utilities;
- routes of emergency and rescue teams.

Active Fire Protection System **(**AFPS) is an information and management part of FPS used to automatically implement the functions, examine information parameters, take adequate decisions on fire detection and warning subsystems, warn people on the fire and manage their evacuation from the tunnel, exercise running of integrated smoke-protection and automatad fire-fighting systems operated on the basis of foam, water, powder or gas devices.

Three priority levers are distinguished in AFPS Automated Management System (AMS) (Topolski 1997):

- top priority is given to subsystems providing for fire and blast prevention and to those responsible for continuous/discrete operation of the automated management system;
- first priority level is attributed to subsystems providing for safety of the people, of the project and of the personnel of emergency and rescue teams;
- second priority level is attributed to subsystems responsible for fire and blast safety of individual premises and works, provided their putting out of operation results in no catastrophic consequences and no danger for people.

Algorithm and software shall be developed for each subsystem, integrated algorithm and integrated software being developed then for AFPS AMS on the whole.

Central AFPS AMS remote control desk usually placed in the central master station together with AMSs for life-support and for road tunnel operation is a sophisticated complex of engineering and technical devices centrally operated in automatic regime.

Here is a list of main AFPS subsystems:

- automatic fire detection and warning;
- TV supervision over transportation and tunnel safety zones;
- people warning and evacuation from transportation and tunnel safety zones;
- telephone and radio communication of emergency and rescue teams;
- management of integrated smoke-protection system;
- internal fire-fighting water pipeline/taps;
- automatic foam fire extinguishing in the tunnel traffic carriageway space;
- drainage of water used for fire-fighting;
- automatic gas-type fire extinguishing in service premises;
- automatic powder fire extinguishing into power cable pipelines;
- aerosol fire extinguishing;
- robotic fire-fighting devices.

Management and Engineering Measures System comprises several algorithms and software sets developed and used to integrate AFPS AMS with other AMS (life-support, traffic control, unsanctioned approach, etc.) as well as with other algorithms, texts, manuals, maintenance schedules, etc. Other main components of the system are listed below:

- AFPS subsystems operation manual;
- testing and maintenance schedules for AFPS subsystems;
- technological automatics;
- manual on fire safety measurements;
- creation of fire safety supervision committees;
- creation of voluntary fire-fighting teams;
- instructive documents on fire danger.

Fire Fighting and People Rescue System serves as basis for mathematic simulation of parameters of probable fires in road tunnels and for two-dimensional calculation of fire areas at different points along the tunnel alignment. The calculations make it possible to assess tactical capabilities of fire-fighting teams and rescue services as well as to determine the types and the number of special equipment and the number of personnel required to extinguish the fire (Broushlinski et al. 2000). The fire liquidation and people rescue system makes it possible to comply as much as possible with recommendations regarding development of fire fighting and people and valuables rescue plans.

The system of liquidation of emergency events and fires and people rescue by efforts of mobile subdivisions consists of the following basic components:

- operative extinguishing plan;
- people rescue plan;

– provision for people rescue technical solutions and means;
– provision for fire fighting technical solutions;
– interface between fire-fighting teams and traffic police services while fighting the fire;
– automatic redistribution of traffic flows;
– automatic and remote control of traffic flows using traffic lights;
– restriction to park vehicles, to place equipment and devices near fire hydrants and tunnel exits;
– interface with other emergency and mobile services in conformity with fire-fighting plans.

The integrated FPS system developed by INTERSIGNAL SPCC has been approved in the course of design, construction and operation of the Volokolamsky, Kutuzovsky, Soushchevsky and Gagarinsky road and rail tunnels as well as the Lefortovo complex of the deep tunnel and the tunnel/viaduct route options.

Professional interest has been shown towards the integrated FPS for road tunnels on the part of leading foreign specialists in tunnel design and construction.

At present, INTERSIGNAL SPCC cooperates with many foreign companies in examining fire-protection technical solutions needed to provide for the safety of people and property in existing and future tunnels in Europe.

The integrated approach makes it possible to bring design, assemblage and start-up of a fire protection system of the whole project to higher standards, to duly provide for safety of the people and safe-keeping of the property, to optimise the expenses, to diminish the risk of catastrophes and to liquidate their consequences at minimal loses if occurrence took place in an operated tunnel.

– Taking into account the major functional aim of the integrated fire protection system, its importance in terms of provision for the safety of people and the works on the whole, the multidirectional nature of the tasks, the complexity of its social and engineering instruments, the authors are well aware of the fact that it is hardly possible to cover the problem in a single article.

REFERENCES

ADAC, 2000. Every third tunnel is dangerous. *ADAC – Motorwelt* (5): 42–46.

ADAC, 2002. Horror vision: car fires. *ADAC – Motorwelt* (5): 30–35.

Broushlinsky, N.N. & Sokolov, S.V. 2000. Simulation of fires in cities. *Proceedings of research works on issue "Simulation of fires and blasts in cities". Pozhnauka*: 447–474.

Brux, G. 1999. Safety aspects of long road tunnels. *Schweizer Baublatt* 59/60 (7): 7–8.

Davydkin, N.F. 2001. *Fire protection system for underground structures.* Moscow: Fort.

Davydkin, N.F. 2002. Emergency situations in urban road tunnels and their consequences. *World Underground Space* (2–3): 47–51.

Davydkin, N.F. 2002. Road tunnel fire protection system. *Proceedings of "Tunnel in Megalopolises" Round Table carried out in Moscow State Mining University on 30.10.02 within the frames of "Miner's Week". Session "Scientific and technical problems of urban tunnel construction projects":* 12–14.

Davydkin, N.F. & Kopylov, N.P. & Krivosheyev, I.N. 1997a. *Smoke protection of underground structures, adjacent territories, buildings and micro-districts.* Moscow: TIMR.

Davydkin, N.F. & Krivosheyev, I.N. & Kopylov, N.P. & Ostrand, L. 1997e. Particular features of ecological safety of confined spaces (garages, tunnels, etc.) under emergency situations. *Proceedings of "City and Automobile" scientific and technical workshop:* 65–70.

Davydkin, N.F. & Krivosheyev, I.N. & Kopylov, N.P. & Warshavski, V.Ya. & Skvortsov, L.S. & Ostrand, L. 1997b. Safety of underground structures under emergency situations. *Ecology and industry in Russia* July: 38–41.

Davydkin, N.F. & Krivosheyev, I.N. & Vostrotin, V.A. & Ostrand, L. & Warshavski, V.Ya. 1997c. Filtering of smoke and absorption of toxic components from gas/air mix formed in congested premises (garages, tunnels, etc.) under emergency situations. *Proceedings of "City and Automobile" scientific and technical workshop:* 71–76.

Davydkin, N.F. & Krivosheyev, I.N. & Vostrotin, V.A. & Warshavski, V.Ya. & Skvortsov, L.S. & Ostrand, L. 1997d. Cleaning of toxic gas/air mixes formed in congested premises under emergency situations and fires. *Ecology and Industry in Russia*: 23–26.

Davydkin, N.F. & Meshalkin, E.A. 2000. *Project fire safety flexible design technologies. FGU VNIIPO, RF MVD* (3): 94–99.

Davydkin, N.F. & Meshalkin, E.A. 2004. Integrated fire protection system for emergency situations in urban road tunnels. *World Underground Space.*

Davydkin, N.F. & Strakhov, V.L. 1998. *Fire resistance of underground works*. Moscow: TIMR.

Davydkin, N.F. & Strakhov, V.L. & Meshalkin, E.A. & Solntsev, N.D. 2004. Fire danger of urban road tunnels and integrated system of their fire protection. *World Underground Space* (5).

Davydkin, N.F. & Strakhov, V.L. & Meshalkin, E.A. & Solntsev, N.D. & Partsevski, V.V. 2002. Integrated fire protection system for urban road tunnels. *Proceedings of the "Tunnel construction in Russia and in CIS countries at the beginning of the millennium: experience and prospects" international scientific and practical conference:* 279–284.

Davydkin, N.F. & Strakhov, V.L. & Shourin, E.T. & Plotnikov, A.N. & Davydkin, A.N. 1999. Regarding development of fire safety system for underground structures. *World Underground Space* (5–6).

Day, J. 1999. Tunnel Safety and ventilation design and specifications. *Tunnel Management International* 1 (1): 8–11.

Domke, J. 1999. Fire in Mont Blanc Tunnel. *Brandschutz. Deutsche Feuerwehrzeitung* 53 (8): 722–73.

Fire Protection Engineering, SPPE 2002. *Handbook of Fire Protection Engineering, third edition.* Quincy, Massachusetts: National Fire Protection Association.

French-Italian Commission, 1999. Joint Report on technical investigation of fire catastrophe on 24 March. In Mont Blanc Tunnel 6.7.99.

Groushevski, B.V. & Yakovlev, A.I. & Krivosheyev, I.N. & Shurin, E.T. & Klimusgin, N.G. 1985. *Fire prevention in the field of construction.* Moscow: VIPTSh RF MVD.

Haack, A. 1999. Fire protection system made of perforated steel plate lining coated with insulating material. *Tunnel* 18 (7): 31–37.

Koshmarov, Yu.A. 2002. New calculation methods for fire resistance and fire protection of buildings and structures. *Fire safety* (2): 91–98.

Shoigu, S.K. & Davydkin, N.F. 1997. Russian MChS asserts: people mass parish may be prevented. *Life and Safety* (2–3): 74–98.

Strakhov, V.L. & Kroutov, A.M. 2000. *Fire protection of structures.* Moscow: TIMR.

Topolski, N.G. 1997. *Fundamentals of automated fire and blast protection systems for projects.* Moscow: MIBP RF MVD.

Toudos, S. 2001. Shoigu has heard us. *Za Rouliom.*(12): 11.

Welzig, V. 2000. Destruction mechanisms of concrete in the event of fire and protective systems. *Tunnel* 19 (7): 19–27.

This page intentionally left blank

Underground Space – the 4th Dimension of Metropolises – Barták, Hrdina, Romancov & Zlámal (eds)
© 2007 Taylor & Francis Group, London, ISBN 978-0-415-40807-3

Creation of advanced technologies in the generation of electrically safe flows of finely dispersed water for fire protection of underground installations

A.S. Chirko
"Mosinzhproekt", Moscow, Russia

A.V. Karpyshev & M.D. Segal
The Research Institute of Low Temperatures at the Moscow Aviation Institute (NIINT), Moscow, Russia

ABSTRACT: Specificity of fires in underground installations provides rigid requirements to fire fighting systems: fire extinguishing agents must be safe to people, fire fighting system shall provide a quick temperature drop and combustion products precipitation, fire suppression must not result in flooding of installation and engineering compartments. Special attention should be paid to fighting fires in alive electrical equipment which is of great importance for cable collectors and underground subway installations. Experts believe that the most effective way of fire fighting in specific conditions of underground facilities is use of finely dispersed water. Moscow specialists have made fundamental investigations in the field of generation of finely dispersed flows and experimental study of their conductivity on special electric stands. As a result of these researches, the advanced fire fighting systems based on finely dispersed water have been successfully tested and implemented, among them there are portable units and fire extinguishers for alive electrical equipment.

Improvement of city underground infrastructure safety system is aimed at fighting of technogeneous disasters and mitigation of high fire risk related with possibility of massive deaths, failures of city life support systems and transport communication lines.

Fires occurring at megapolis underground installations are especially hazardous. They are characterized by fast temperature growth, lockout of evacuation ways from underground facilities, adjoining ground areas and buildings by toxic combustion products, structural damage and their possible collapse.

Specifities of underground installation fire impose strict requirements to fire extinguishing systems: extinguishing agents shall be safe for people, fire protection systems have to ensure fast temperature decrease and combustion product deposition, fire extinction shall not result in installation and engineering room flooding. Special attention should be paid to a possibility of extinguishing live equipment, which is very important for metro cable collectors and installations.

According to expert opinion, atomized water application is one of the most efficient ways to extinguish underground infrastructure items. Specialists of Moscow Aviation Institute made fundamental research of atomized water flow generation, determination of their extinguishing capacity and dielectric test performance at special authorized electric test bench. On the basis of these investigations, they developed, successfully tested and reduced to practice advanced atomized water fire protection systems, both portable and mobile, able to extinguishing live equipment.

United metro tunnel network, high day and night passenger traffic that makes about 40% of the total city population results in dramatic negative consequences escalation caused by fire, electric trains tunnel blocks , and passenger evacuation prior to megapolis transport collapse.

Fire evolution in metro train carriages, at passenger platforms, escalators, railways and metro installations of vital importance is characterized by the following features:

- space restriction, great number of people present, and passenger evacuation difficulties caused by the above reasons;
- high degree of general fire load different for every carriage series exceeds 50 kg/m^2 and may include a great amount of materials releasing toxic combustion products;
- great number of $\sim$10 kV power cables in metro tunnels;

– presence of live equipment fastened on metro trains;
– impetuous temperature growth up to thousand degrees and even higher; actually in 3–5 min after a fire starts, the situation for the people becomes critical, therefore several hundreds of people have to be promptly evacuated from the tunnel;
– possibility of fast spread of smoke over the evacuation ways and the metro underground space;
– great difficulties and sometimes impossibility to deliver extinguishing agent supply to the underground installation fire;
– possibility of general panic arising among passengers.

Smoke pollution is admitted to be the major hazard for metro passengers in case of fire. People, as a rule, die of asphyxia and intoxication with combustion products dangerous for breathing.

As it has been already mentioned, the specificity of fires in underground installation and tunnels puts strict requirements at extinguishing systems:

– extinguishing agents applied in carriages, passenger platforms and escalators shall be safe for the people;
– fire-fighting system shall provide fast operation including tunnel traffic lockout;
– fire protection system shall ensure people's safety on trains, at platforms and escalators;
– fire protection system shall provide fast temperature decrease and combustion product fall out;
– fire extinction technique shall not result in flooding of metro tunnels, cable cradles and engineering rooms;
– fire protection system shall lockout smoke release areas, absorb smokes and fire heat emission;
– negative consequences of false actuation shall be negligible.

Similar problems are typical for other megapolis underground infrastructure items – motor transport tunnels, particularly of great length, underground parking lots, and trading centers.

Higher degree of fire hazard and difficulties of people evacuation from the city underground transport systems and metro facilities require fast operating and highly efficient fire protection system, safe for the passengers operating staff, and environment.

Atomized water fire protection technology application allows to extinct fires with utmost efficiency, faster operation and minimum water consumption. The greatest advantage of these systems is fire extinction with no current shutdown.

On the basis of the latest aerospace technology achievements, specialists of Moscow Aviation Institute developed efficient atomized water fire protection technologies superior to prior art devices and designed number of functioning well-proven units .

At present, there is some experience of implemention of atomized water in fire protection systems design, manufacture and service as part of automatic, portable, mobile and fixed fire extinguishing systems protected by dozens of patents issued in industrial countries of Europe, the USA, and Japan.

In recent years, a backpack firefighting unit RUPT-1-0.4 designed at the Institute for timely suppression of solid combustible, inflammable liquid and gas fires as well as live equipment fires has come to light.

Functioning of the unit is based on gas dynamic principles of atomized two-phase water-and-air flow acceleration, with an average water droplet diameter of 100 microns that allows to suppress fires fastly and efficiently.

The unit features small dimensions and modest weight (its gross mass is less than 20 kg); it is easy and reliable in service, always ready for operation. The extinguishing liquid is water or water and additives of about $9 \cdot 10^{-3}$ m^3 capacity. The unit operation is activated by pressurized air bottle of 30 Mpa operating pressure and $2 \cdot 10^{-3}$ m^3 capacity used in fire fighters' breathing systems. The RUPT unit operation is particularly efficient for suppressing fires in metro tunnels and engineering communication collectors. A curtain of fine water spray allows to block a smoke-filled area of up to 4 m diameter in the tunnel and ensure fire fighters' way to the fire. The second mode of extinguishing agent delivery allows to obtain atomized water jet up to 12 m long.

While running unit approval tests in Russia and abroad, it was confirmed that the unit could be used for the following purposes:

– Class 55A solid combustible fire extinction (under EN-3) that corresponds to fire area of approximately 60 m^2 including smoldering fires;
– Class 233 B inflammable liquid fire extinction (petrol, kerosene, heptane, different oils, etc.), herewith in the course of the unit approval tests it was shown that $9 \cdot 10^{-3}$ m^3 water and foam capacity was sufficient to extinguish about $200 \cdot 10^{-3}$ m^3 of burning petrol or heptane;
– up to 36V live equipment fire extinction from the distance of more than 1 m (approved by a jet breakthrough test at special electric test bench).

These features of the system make its application highly promising for underground infrastructure installations due to the following effects obtained:

– timely beginning of the fire suppression prior to fire crew arrival;
– exclusion of tunnel or any other room flooding by great quantity of water and complete avoidance of collateral damage;

– extinguishing of fire with personnel present in the fire area;
– extinguishing of fire with no voltage preswitched off.

Special firing tests conducted showed that a burning car was completely suppressed within 165 seconds by $3{,}5 \cdot 10^{-3}$ m^3 of extinguishing liquid only.

On the basis of statistical data on fire area by the moment of fire crew arrival, we may believe that 90% of all fires may be successfully suppressed by RUPT unit allowing to avoid great damage to property.

The design was patented in several industrially developed countries of the world, awarded Golden Medals at the 49th World BRUSSELS-EURIKA-99 Exhibition and the 28th International Exhibition (April 2000, Geneva), and the Prize of Government of Russian Federation for the year 2000. License for its manufacture was bought in Germany.

One of the latest designs is an air-emulsion extinguisher generating a jet of atomized extinguishing agent (EA) for timely suppression of initial comparably small fires.

Extinguisher EA capacity ($6 \cdot 10^{-3}$ m^3) is sufficient to suppress Class 34À fire under EN-3 (burn area is about 32 m^2) or Class 183B fire (approximately 180 litres of any inflammable liquid on a 2,7 m diameter tray). The gross weight of this extinguisher is 9 kg. An atomized EA jet range is 5–7 m, liquid flow rate is $0{,}3 \cdot 10^{-3}$ m^3/sec.

In the course of special approval tests at the electric test bench it was confirmed that the extinguisher could be reliably used to suppress Class E fires (live equipment) with the voltage up to 1 kV.

These features of the extinguisher allow to suppress such fires typical for metro and other underground infrastructure item fires as sleeper fire (including smoldering burn), tunnel cable fires as well as car fires.

To confirm a possibility of reliable extinguisher application for Moscow Metro installation, series of firing tests was conducted under the operating voltage on 825 V direct current rail. A kerosene cloth prepreg (50×40 cm in size) was ignited directly under the contact rail.

Fire suppression was effected by an operator at the distance of 2–3 m from the fire. The operating voltage of the contact rail at the end of fire suppression was 825 V.

In the process of test fire suppressing by the above extinguisher the operator wearing cotton gloves on his hands did not experience any discomfort related to the high voltage effect. The fire was completely suppresseds within 15 seconds.

An actually recorded atomized agent jet breakthrough value at each operating mode of the extinguisher amounted to 0,2 microampere, which is considerably less than the tolerance admitted by Russian Standards in force.

One of the most important objectives of stable functioning and evolution of a megapolis is communication collector fire protection improvement. City collectors house important communications vital for city life support, e.g., power cables, communication and telecommunication cables.

According to the current Standards, collector fire suppression may begin only on official information receipt of the voltage switch off. This procedure may take a few hours. Hence, the most actual systems are those of collector fire protection engineering design requiring no voltage switch off.

Analysis showed that special spray nozzles generating atomized water streams may serve as the above systems.

Specialists of Moscow Aviation Institute developed and tested highly efficient atomizers, their performance considerably surpassing the best foreign analogs, the application of which is desirable to consider while designing collector fire protection systems.

Apart from other systems, the spray nozzles with an operating water delivery pressure of about 8 MPa, MAI-designed highly effective atomizers operate at water delivery pressure of about 0,6–1,2 MPa and generate an atomized water stream, an average size of droplets being 150–200 mcm.

Electric tests at special test bench under the operating voltage of 36 kV showed that the atomized water jet of the above parameters had a break-through value considerably less than those admitted by the Standard requirements.

It should be noted that gas, powder and aerosol fire protection system application is very dangerous in a closed space with the people present. Atomized water application is not only efficient bur also safe for people. Fine water droplets intensively absorb heat release and adsorb chemically harmful and toxic substances, thus protecting people from hazardous fire factor effect and creating local safety areas.

In long tunnels with rare evacuation exits and joints it is advantageous to use SAFE-POINT unit that means group protection equipment in tunnel facilities. This joint development of MAI and “Mosinzhproekt” is especially efficient in the city deep tunnels as a compensation and additional safety measure designed to protect people who were not evacuated from the fire point. tests showed that the SAFE-POINT provides heat release protection from the surface area of not more than 65 kWt/m^2 and maintains oxygen contents in the protected area not less than 15%. The unit is easy to assemble, remotely and manually controlled. The SAFE-POINT is fitted with an advanced audible and light beacons system allowing to detect fire within the visual range not less than 0.8 m at the distance of

50 m. The unit is of high functional level, it may be integrated with automatic fire protection systems.

Hydraulic and fire tests of this equipment have shown their high efficiency in fire extinguishing, ability to decrease the fire temperature within the shortest possible time (of the order of a few seconds) and deposit the combustion products.

REFERENCES

Both, C. and Haack A. 2004. *Present-Day Design Fire Scenarios and Comparison with Test Results and Real Fires*: *Structures & Equipment. Safe & Reliable Tunnels. Innovative European Achievements*. Prague: First International Symposium, P. 73–87.

Bordakov V.N., Karpyshev A.V., Segal M.D. et al. 2005. *Safe Application of an Extinguisher at the Underground Railways with a Live Contact Rail.* Moscow: Problems of Safety and Emergency Situations, No 5.

Karpyshev A.V., Dushkin A.L., Yershov A.V., Segal M.D. 2006. *Metro Passenger Safety System Improvement at Fire Incidents.* Moscow: Metro and Tunnels, No 1.

Underground Space – the 4th Dimension of Metropolises – Barták, Hrdina, Romancov & Zlámal (eds)
© 2007 Taylor & Francis Group, London, ISBN 978-0-415-40807-3

Modeling of blasts and fires accidents in tunnels

A.S. Chirko
"Mosinzhproekt", Moscow, Russia

P. Efremov, V.E. Fortov, V.V. Golub & A.V. Zibarov
Institute for High Energy Density Russian Academy of Sciences, Moscow, Ru

ABSTRACT: Methods for physical modeling and experimental investigations for fire tunnel accident are described. Development of experimental and numerical techniques in the IHED RAS allows reproducing most part of blast and fires impacts in laboratory experiments.

Urban structure development is followed by expansion of tunnels and communications system. Fires and explosions in the communications may cause significant victims and damages. Reasons of initial fire may be very different, for example, electro explosion of conductor. Now development of experimental and numerical techniques in the IHED RAS allows reproducing most part of blast and fires impacts in laboratory experiments.

The first facility [1] consists of a diaphragm shock tube with 72×72 mm square cross section with length of 5 m., connected to a vacuum chamber (Fig. 1). This shock tube is equipped with optical windows and piezo-electric pressure transducers. Different tunnels can be angle mounted at the end of the shock tube. It is possible to obtain images in two directions of view perpendicular to each other. The post shock flow pattern can be recorded by IAB-451 schlieren device. The schlieren movie will show the time evolution of the process with intervals of 5–10 μs. The exposure is 1 μs. The single frame size is 60×60 mm^2. To obtain 72 images in one experiment, a high-speed opto-mechanical device VSK – 5, with the frame size 16×22 mm^2 can be used. New electronic device is used to obtain the high-speed digital imagines.

The detonation formation in front of the propagating flame in channel with the combustible gas mixture can be observed (Fig. 2). Flame front turbulisation leads to its acceleration and shock wave formation.

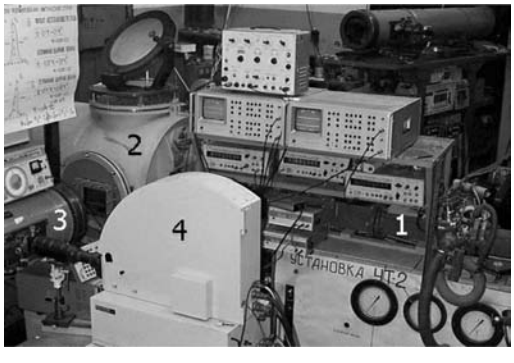


Figure 1. Experimental set up for explosion in tunnels investigation. 1 – Detonation/shock tube, 2 – Receiver/Vacuum chamber, 3 – IAB-451 schlieren device, 4 – High-speed photo-registration camera.

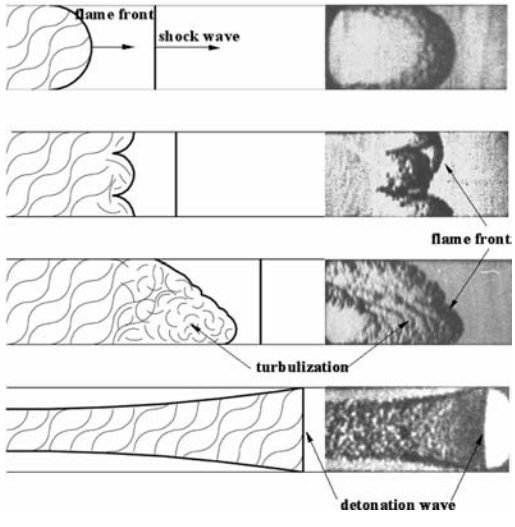


Figure 2. The detonation formation in front of the turbulent flame.

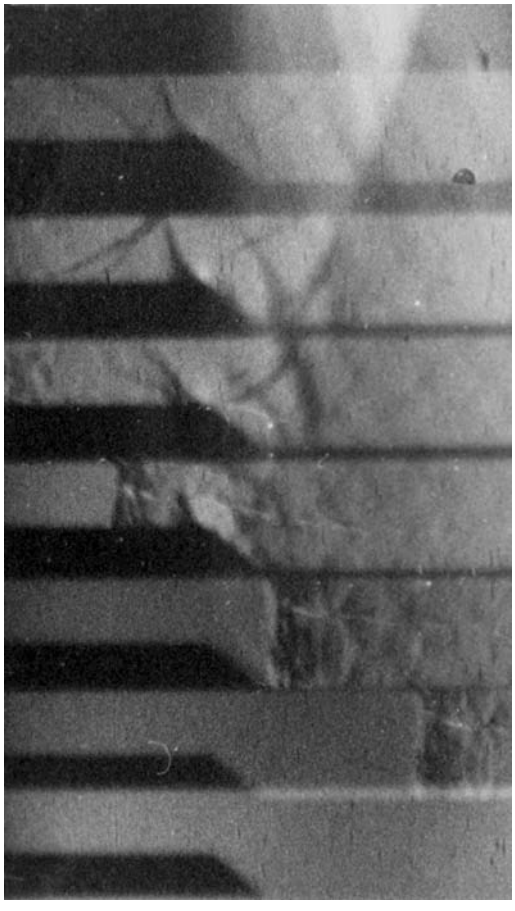


Figure 3. Gas ignition at the convex step.

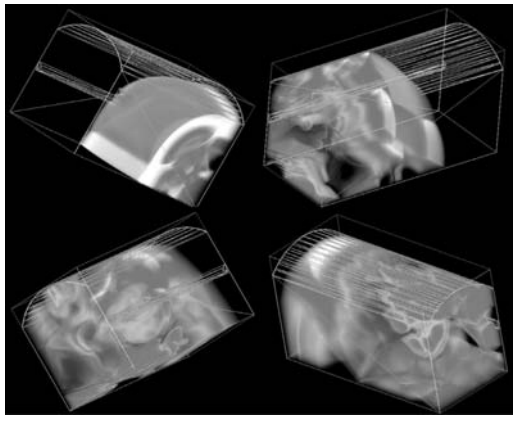


Figure 4. Pressure distribution after 3 kg TNT-charge explosion.

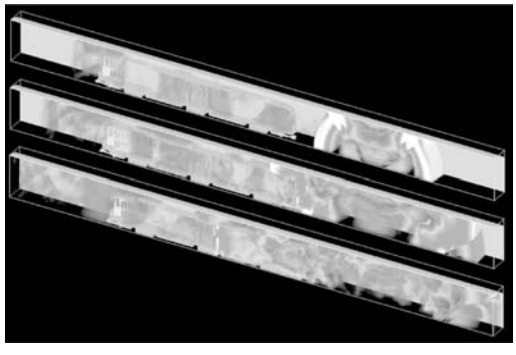


Figure 5. 3D-Pressure distribution after TNT-charge explosion in the railway tunnel.

The shock wave intensity is high enough to generate the detonation. In the channel.

The weak shock wave can initiate the detonation of the combustible mixture near the channel wall with a convex step (Fig. 3). The intensity of weak shock wave is not sufficient to ignite the gas. Near the step the reflected wave is formed, producing an additional sharp temperature rise in the gas. Ignition accompanied by bright gas glow is initiated.

The attenuation of shock wave produced by explosion of hexogen charge after sand-cement barrier destruction was observed.

The second shock tube allows us to carry out the large-scale experiments by exploding a massive charge to generate a powerful blast wave. The shock tube is of about 100 m in length and it consists of four sections with different lengths and diameters up to 5 m. Explosive charges of up to 20 kg TNT may be used for the blast wave generation. The object under investigation is located in the shock tube channel. The test complex is equipped with piezo-electric pressure transducers mounted along the wall. Moreover, the complex possesses a video observation system.

A high-performance CFD-code that provides a non-stationary 3D explosive problem solution has been developed [2].

The code allows operation with a number of explosive types: FAE (Fuel-Air Explosives), HE (High Explosives), LDE (Low Density Explosives), multiphase compositions (CHON-type fuel and metal particles).

For example in Figs. 4 and 5 the pressure distribution after 3 kg TNT-charge explosion and after TNT-charge explosion in the railway tunnel are shown. Euler equations for dilute-limit two phase flow with solid and gas phase chemical reactions are solved. There are three submodels differing by chemical reaction peculiarities of solid and gas phases: (1) metals reacting according to the type of aluminum; (2) metals reacting according to the type of magnesium; (3) metals reacting according to the type of aluminum boron.

The code is available on both SP, multiprocessor and cluster systems with Linux and Windows operating systems. The number of cells in domain is up to 50 million for a conventional PC with 2Gb of RAM. This enables calculating complex shock wave phenomena with the domain geometry close to the real one. Results of blast and fires impacts in laboratory experiments are necessary for fire and blast safety improvement of existing and projected tunnels. Also it allows designing effective emergency rescue system and elaborate new procedures of tunnels testing and maintenance directed to exploitation safety enhancement.

1 CONCLUSION

Development of experimental and numerical techniques allows reproducing most part of blast and fires impacts in confined volumes in laboratory experiments. Investigation of initial reasons of fire with following 3D-scenario of tunnel accident also is possible.

BIBLIOGRAPHY

Bazhenova T.V., Golub V.V. et al. 2006 *Self-ignition of a fuel gas upon a pulsed efflux into an oxidative medium* // Tech. Phys. Letters, V, N 3, p. 268–271.

Okhitin V.N., Selivanov V.V., Zibarov A.V. 2002. *Shock-Wave Calculation Model for Detonation of Multicomponent Energy Carrier Containing Combustible Phase*. New York Combustion of Energetic Materials.: Begell House, P. 1072–1089.

This page intentionally left blank

Underground Space – the 4th Dimension of Metropolises – Barták, Hrdina, Romancov & Zlámal (eds)
© 2007 Taylor & Francis Group, London, ISBN 978-0-415-40807-3

Fire test to characterize fire-induced damage of concrete lining in NATM tunnel

Soon-Wook Choi, Soo-Ho Chang & Gyu-Jin Bae
Korea Institute of Construction Technology, Goyang, Gyeonggi, Korea

Jong-Wook Kwon
NOWENG Co., Ltd., Seoul, Korea

ABSTRACT: Since the NATM (New Austrian Tunnelling Method) is the most popular tunnelling method in Korea, the fire-induced damage of the concrete lining or secondary lining should be assessed to propose the optimum fire-proofing method and the repairing method after a fire accident. This study is to evaluate the fire-induced damage of concrete lining by using a laboratory furnace. The concrete specimens were tested under the RABT fire scenario in which the maximum temperature was 1,200°C and a RWS fire scenario in which the maximum temperature was 1,350°C. From the tests, the loss amount of concrete materials under the RWS scenario was slightly bigger than under the RABT fire scenario. Especially, under the RWS fire scenario, the loss of concrete materials was mainly induced by melting. In contrast, it was proved that the material loss under the RABT fire scenario was mainly induced by explosive spalling.

1 INTRODUCTION

As tunnels and underground facilities become longer and deeper, the disaster management in underground spaces becomes more important. Especially, fire in an underground space can cause severe structural damage as well as heavy casualties (Haack, 1998). It is very essential to characterize the fire-induced damage of construction materials in underground structures to protect the underground structure and passengers from fire. However, it is almost impossible and uneconomical to carry out a full-scale fire test in a tunnel that is in use. Moreover, fire in underground space has rapid temperature gradient and relatively long duration time.

In this study, a high-temperature furnace was manufactured to easily evaluate the fire-induced damage of underground structure materials. Its biggest advantage is the capability to simulate fire situations in underground space, and to carry out fire tests on various construction materials at the laboratory. By using the furnace, it was intended to characterize the fire-induced damage in an un-reinforced concrete lining used in a NATM (New Austrian Tunneling Method) which is the most popular tunneling method in Korea. Fire scenarios applied in this study included the RABT (Richtlinien für die Ausstattung und den Betrieb von Straßentunneln) and the RWS (RijksWaterStaat) fire curves used in Germany and Netherlands respectively (Beard and Carvel, 2005). It was also intended to compare different fire-induced damage characteristics of NATM concrete lining materials under the RABT with those under the RWS scenarios.

2 FIRE TEST

2.1 *Fire scenarios*

Khoury(2002) pointed out that the structural behaviors after a fire are governed by the characteristics of a fire such as temperature gradient, maximum temperature, fire duration time and cooling time. Those characteristics can be expressed by the time-temperature curve applied in the surface of a structure.

In general, since a tunnel is a structure isolated in underground space, the maximum temperature during the fire in a tunnel is much higher than in other conventional structures. Moreover, a fire accident in a tunnel continues much longer because it is not easy for fire fighters to have a rapid access to the accident location. As a result, a fire scenario in a tunnel should be different from a general fire curve (ISO 834) used in conventional structures (Beard and Carvel, 2005). Figure 1 shows two representative fire scenarios in a tunnel. In the RABT scenario, the temperature reaches 1,200°C only after 5 minutes elapsed since the fire ignition, and is maintained for 30∼90 minutes. The scenario is known to be very close to a real fire situation in a tunnel. In the RWS scenario, the temperature

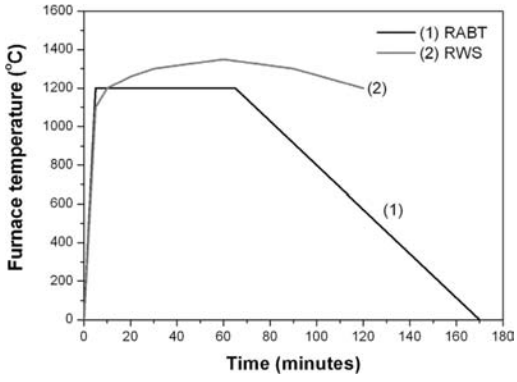


Figure 1. RABT and RWS fire scenarios.

reaches 1,100°C and 1,350°C after 5 minutes and 60 minutes elapsed since the fire ignition respectively. The RWS scenario is generally applied to simulate a catastrophic accident in a tunnel. In this study, it was intended to compare different fire-induced damage characteristics of NATM concrete lining materials under the RABT with those under the RWS scenarios.

2.2 *High-temperature furnace and specimens*

The maximum capacity of the two burners on the furnace was set to 580,000 kcal/hr enough to simulate the rapid temperature increase in the initial heating stage of RABT and RWS fire scenarios. The furnace also had the two-way directional windows for observing the states of the fire room and the specimen surface during the fire tests (Figure 2(a)).

Table 1 shows the mixing proportion of the concrete with the design strength of 24 MPa. The maximum size of aggregates, water/cement ratio, slump and air content were 25 mm, 50%, 15 cm and 4∼6% respectively. The concrete specimens for fire tests were 1,400 mm long, 1,000 mm wide and 500 mm thick.

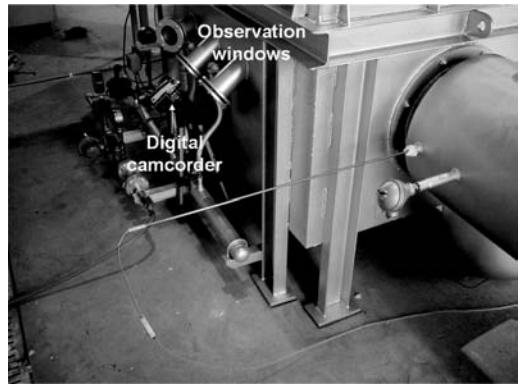
For each concrete specimen, seven K-type thermocouples with the diameter of 6.4 mm were embedded in the depth of 5 cm, 10 cm, 15 cm, 20 cm, 25 cm, 30 cm and 40 cm from the initial specimen surface. The used K-type thermocouple was a sheathed thermocouple with the maximum range of 1,370°C and the accuracy within ±2.5°C.

In addition, a number of cylindrical specimens were used to measure the changes of mechanical properties of concrete at different temperature conditions. The diameter of the cylindrical specimen is 100 mm and the ratio of the diameter to the length was set to 1:2.

2.3 *Experimental procedures*

After installing the concrete specimen as shown in Figure 2b, the specimen was tested under a RABT and RWS fire curves. During a test, the acquired temperature data from each thermocouple were saved at an interval of one second. Simultaneously, the surface of the specimen was observed with a digital camcorder.

For the cylindrical specimens to evaluate the alteration of mechanical properties at different temperature conditions, the maximum target temperature was from 300°C to 1,000°C at the interval of 100°C. The heating gradient to each target temperature was 450°C/min, which was almost as close as to the initial heating gradient of RABT and RWS fire curves. The target temperature was kept during one hour as soon as the room temperature reached it. After one-hour heating



(a) Two way-directional windows



(b) Furnace and Specimen

Figure 2. Furnace and specimen.

Table 1. Mixing conditions of concrete specimens (unit: kg/m^3).

Water	Cement	Fine aggregate	Coarse aggregate	Plasticizer
167	334	739	1,048	1.002

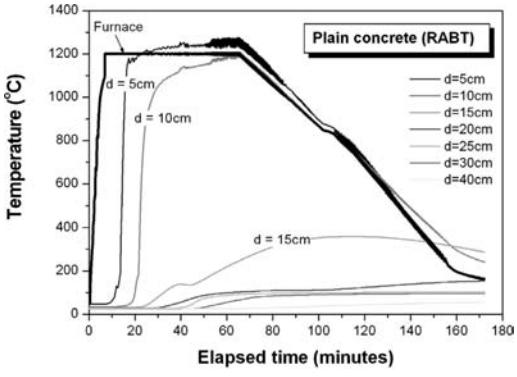


Figure 3. Temperature distribution in a concrete block under RABT fire scenario.

and successive natural cooling, mechanical properties and loss weight of the damaged concrete specimens were measured.

3 RESULTS OF FIRE TESTS

3.1 *Time-temperature histories*

Figure 3 shows the measured temperatures in the concrete under the RABT fire curve. Furnace temperature was shown to correspond to RABT fire curve well. In the initial stage, it was deduced that the concrete up to 10 cm from the surface exposed to fire was fallen off at intervals of about ten minutes. After 90 minutes elapsed, the maximum temperature at the depth of 15 cm from the surface exposed to fire reached 360°C by the heat accumulated in the concrete block. It is generally well known that concrete can experience significant strength loss at temperature above 300°C and is unable to carry sustained load at temperature in excess of 550∼600°C (Khoury, 2002). From such a reason, it was judged that the concrete nearby 15 cm from the initial surface exposed to fire should be investigated more precisely.

Figure 4 shows the severely damaged concrete surface after a fire test under the RABT fire scenario. The maximum depth of concrete loss amounted to 11.76 cm. It was observed that the original concrete block was grey but the surface exposed to the fire turned brown. In addition, the melting on the concrete surface was rarely observed.

Figure 5 shows the measured temperatures in the concrete during a RWS fire test. Furnace temperature was well controlled and corresponded with the RWS fire curve well. The loss of concrete material under the RWS fire curve was larger than that under the RABT fire curve. However, the speed of concrete loss up to the depth of 10 cm from the surface exposed to fire was slightly lower than that under RABT fire curve.



Figure 4. Damaged surface after fire (RABT).

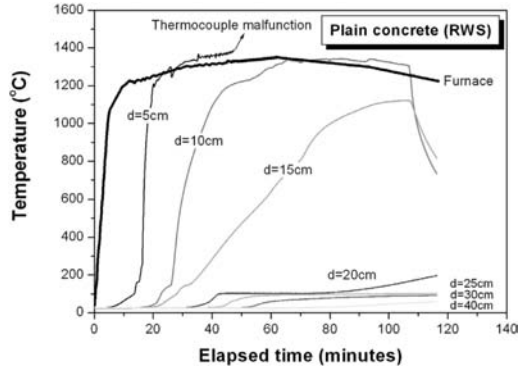


Figure 5. Temperature distribution in a concrete block under the RWS fire scenario.



Figure 6. Damaged and melted surface after fire (RWS).

Figure 6 shows the fire-induced damage after a RWS fire test. The maximum depth of concrete loss was 13.76 cm. We easily found the evidence that the whole area exposed to fire melted. Through a digital camcorder recording during a test, it was verified that

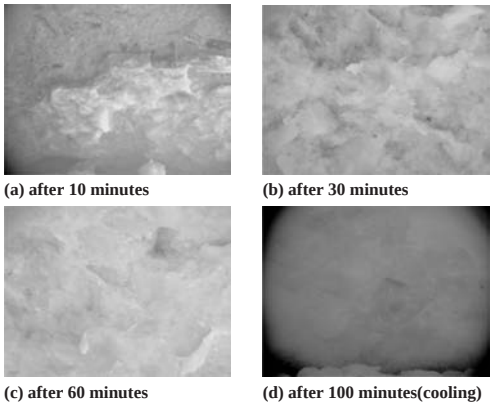


Figure 7. Concrete surface exposed to fire (RABT).

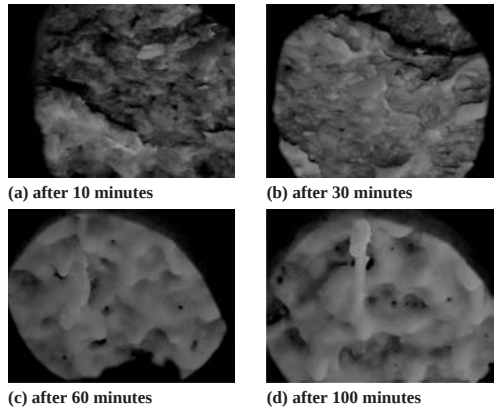


Figure 8. Concrete surface exposed to fire (RWS).

concrete materials became to melt just after the room temperature within the furnace reached over 1,200°C. The reason is why the melting temperature of concrete materials is 1,200°C or more (Khoury, 2002).

It is analogized that the melted material influenced the loss of concrete during the test and the transmission of heat. In other words, it is regarded that a layer of melted concrete materials interrupted the transmission of heat to the remaining concrete part. Nevertheless, the reason why the loss of concrete under RWS fire curve was larger than that under RABT fire curve is that high temperature over 1,200°C accelerated the loss of concrete materials by melting them rapidly.

Figure 7 and Figure 8 show the states of an exposed surface at different recording time conditions under RABT and RWS fire scenarios respectively. From them, it is possible to easily verify the effects of temperature levels on the deterioration and the loss of concrete materials.

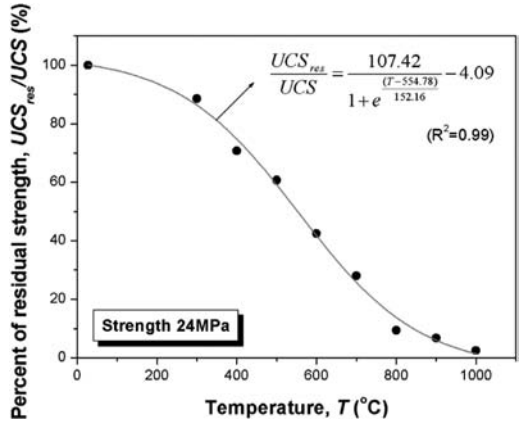


Figure 9. Relationship between residual strength and temperature.

3.2 *Alteration of mechanical properties under high temperature*

Extracting cylindrical core specimens from the large concrete block is inconvenient, time-consuming, and able to do damages on them during coring procedures. Therefore, specimens cured in the cylindrical moulds were used to evaluate mechanical properties of concrete under high temperature condition. They have the same mixing proportion as concrete blocks used in fire tests.

Figure 9 shows the average uniaxial compressive strength of concrete specimens after heating to each target temperature. As the temperature increases, the uniaxial compressive strength is prone to decrease. The relationship between temperature and uniaxial compressive strength can well regressed by the Boltzmann function. It is also found that uniaxial compressive strength rapidly decreases at the temperature range between 300°C and 700°C. In other words, uniaxial compressive strength starts to decrease at the temperature near 300°C. Therefore, the temperature of 300°C can be considered as a critical temperature level and a threshold for fire-induced damage on concrete.

Figure 10 shows the average elastic modulus of concrete specimens after heating to each target temperature. It is shown that as the temperature increases, the elastic modulus also decreases proportionally. Similar to uniaxial compressive strength, the critical temperature where the elastic modulus starts to decrease rapidly is considered as 300°C. At the temperature conditions over 600°C, residual elastic modulus after fire becomes less than 20% of the original property.

From the results, it is suggested that the critical temperature to judge whether concrete is damaged or not should be 300°C. In addition, it is considered that the recovery or the structural ability of a concrete material cannot be expected at the temperature level over 600°C

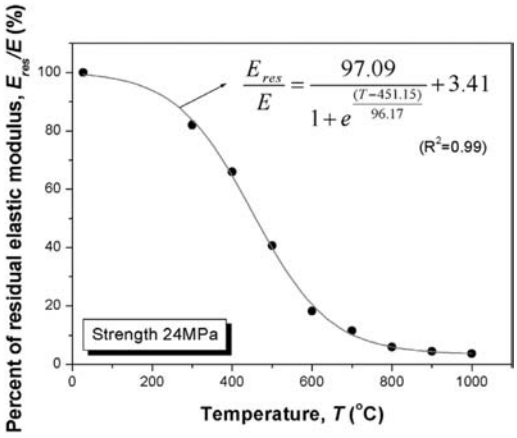


Figure 10. Relationship between residual elastic modulus and temperature.

or 700°C. It is highly expected that these two critical temperature thresholds can be utilized usefully for the optimum rehabilitation works after a fire accident.

3.3 *Proposal of a simple damage prediction model*

In this study, it was intended to propose a simple experimental model for the prediction of a temperature history within a concrete lining and its corresponding damage characteristics.

First, based on the experimental results shown in Figure 3 and Figure 5, the relationships between the elapsed time and the distance from the initial exposed surface were regressed. From the regression analyses, it was revealed that the relationships could be well approximated by the negative exponential functions:

$$T = a + b \times e^{(-t/c)} \quad (1)$$

where T = the temperature within a concrete lining; t = elapsed time after fire ignition; a, b, c, d = regression constants.

Figure 11 and Figure 12 show the regression models to predict the temperature distribution within a concrete lining at RABT and RWS fire scenarios respectively. The prediction results depend upon the distance from the initial exposed surface.

Finally, two simple diagrams (Figure 13) to predict temperature distribution within a concrete lining as well as its corresponding mechanical properties were proposed by combining Figure 9, Figure 10, Figure 11 and Figure 12.

It is expected that when the application of CFD(Computational Fluid Dynamics) analysis is limited or impossible, the diagrams can be usefully utilized to approximately estimate time-dependent

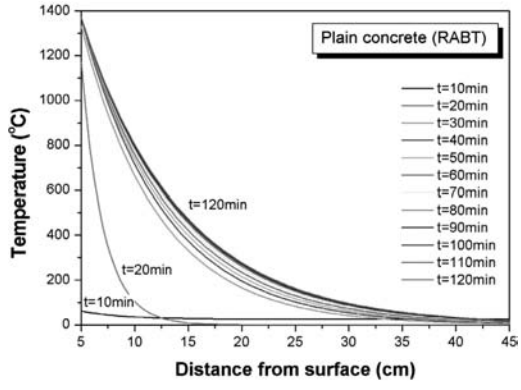


Figure 11. Temperature distribution within a concrete lining depending on the distance from the initial exposed surface (RABT).

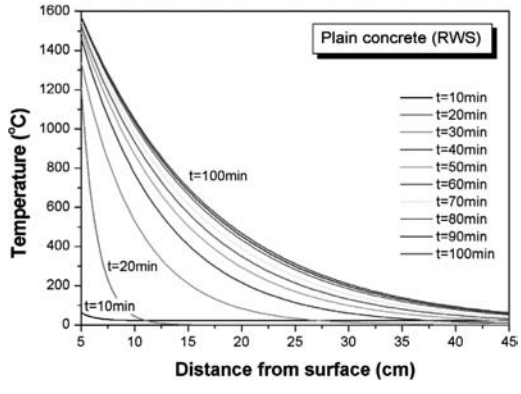


Figure 12. Temperature distribution within a concrete lining depending on the distance from the initial exposed surface (RWS).

temperature distribution within a concrete lining as well as its corresponding mechanical properties.

4 CONCLUSIONS

In this study, a high-temperature furnace was utilized to easily evaluate the fire-induced damage of underground structure materials. The concrete specimens simulating the concrete lining used in a NATM tunnel were tested under the RABT and the RWS fire scenarios. Under the RABT scenario, the maximum depth of concrete loss amounted to 11.76 cm and the maximum temperature at the depth of 15 cm from the initial surface exposed to fire reached 360°C. Under the RWS scenario, the maximum depth of concrete loss was 13.76 cm. In addition, it was easily found that the whole area exposed to fire melted. From a real-time camcorder recording, it was verified that

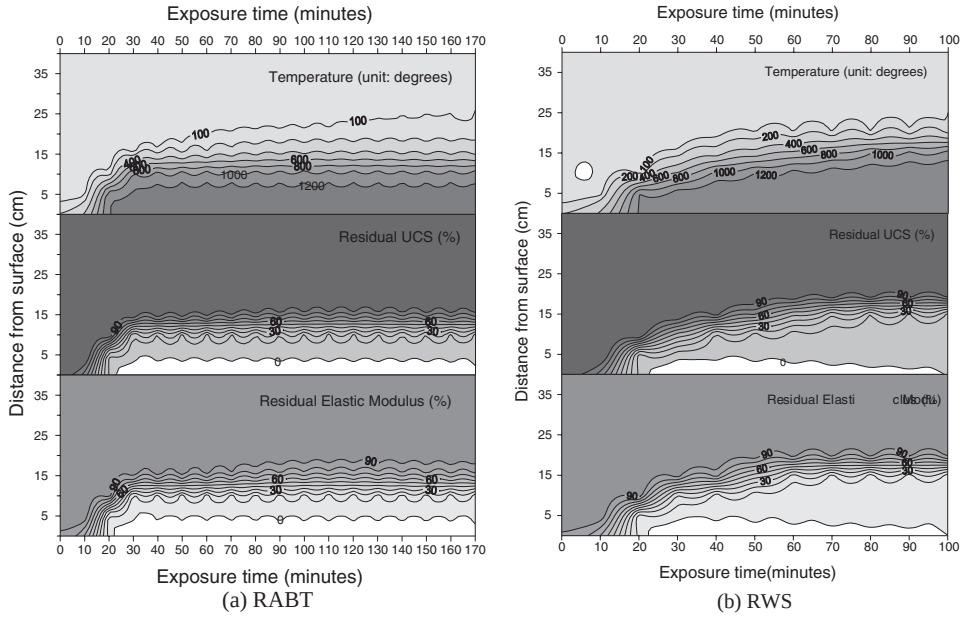


Figure 13. Proposed diagrams to predict temperature distribution and mechanical properties.

concrete materials became to melt just after the room temperature within the furnace reached over 1,200°C. The reason is why the melting temperature of concrete materials is 1,200°C or more.

The deterioration of mechanical properties of the concrete material was measured between 300°C and 1,000°C at the interval of 100°C. From the experiments, it was suggested that the critical temperature to judge whether concrete is damage or not is 300°C. In addition, it was considered that the recovery or the structural ability of a concrete material cannot be expected any more at the temperature level over 600°C or 700°C. It is highly expected that these two critical temperature thresholds can be utilized usefully for the optimum rehabilitation works after a fire accident.

Finally, two simple diagrams to predict temperature distribution within a concrete lining as well as its corresponding mechanical properties were proposed. It is expected that when the application of CFD analysis is limited or impossible, the diagrams can be usefully utilized to approximately estimate time-dependent fire-induced damage to concrete lining.

REFERENCES

Beard, A. & Carvel, R. 2005. *The Handbook of Tunnel Fire Safety*. London, U.K.: Tomas Telford.

Haack, A. 1998. Fire Protection in Traffic Tunnels: General Aspects and Results of the EUREKA Project. *Tunnelling and Underground Space Technology* 13(4): 377–381.

Khoury, G.A. 2002. Passive protection against fire. *Tunnels & Tunnelling International* November: 40–42.

Underground Space – the 4th Dimension of Metropolises – Barták, Hrdina, Romancov & Zlámal (eds)
© 2007 Taylor & Francis Group, London, ISBN 978-0-415-40807-3

Large scale fire tests with different railway overhead systems – experience by the test center

Sven J. Seirer & Volker Wetzig
VSH – Hagerbach Test Gallery Ltd., Sargans, Switzerland

ABSTRACT: Numerous tunnel fires in recent years in Europe ended in disaster and sensitized politicians and the public. It resulted in a high level of safety in tunnels. In a railway tunnel the probability of a fire disaster, caused by an accident, is far smaller than in a road tunnel. Authorities, railway companies and the industry are asked to appropriate measures to limit the risk of fire in rail tunnels or to cut one's losses. The most important task is to bring the train out of the tunnel, and this is (only) possible if the train wagons are operational and if there is an electric power supply as long as possible. Caused on the thermal impact and the load (tension) a conventional overhead wire elongate, and if the temperature is to high the probability of a failure is very high. An overhead conductor rail, without any tension load, should have a quit better behavior in case of fire in a tunnel. In summer 2004 Furrer + Frey Ltd., Bern, Switzerland, commissioned the VSH-Hagerbach Test Gallery Ltd. (www.hagerbach.ch) to carry out large scale fire tests to verify that assumption.

1 INTRODUCTION

The catastrophic fire disasters in European tunnels during the very recent past have raised awareness of tunnel safety among policymakers and the general public. Although the probability of accidents in a rail tunnel is lower than in a road tunnel, the consequences can also be catastrophic in a rail tunnel. This creates particular requirements for the authorities, the rail operators and industry. These sectors are seeking active and passive measures to prevent fire accidents in tunnels or to limit their consequences. One of the most pressing and important points is that the burning train must travel out of the tunnel whatever the circumstances. Most important of all, as well as rolling stock that is capable of functioning, the power supply from the overhead line must remain guaranteed for as long as possible. Under the influence of heat, the contact wires (- tensioned with a force of 10 to 30 kN -) become elongated, and it is even possible for constrictions or line tears to occur at the location of a fire.

On the basis of the installation method without tensile force for roof-mounted conductor rails developed by Furrer + Frey, and the substantially larger cross-section (8 to 12 times) as compared to the overhead lines, it was supposed that a roof-mounted conductor rail would remain functional for substantially longer.

In order to confirm this, Furrer + Frey Ltd. commissioned VSH-Hagerbach Test Gallery Ltd., to carry out large scale fire tests. The aim was to provide experimental confirmation of the theoretical consideration that the roof-mounted conductor rail from Furrer + Frey retains its mechanical functioning capability for longer than the conventional contact wire systems.

2 OVER HEAD SYSTEMS

2.1 *General*

All the systems were installed approx. 95 cm above the carriage roof, with a length of approx. 20 m each. In addition to the interception and securing fixtures at the ends, each system was additionally secured in the middle of the carriage.

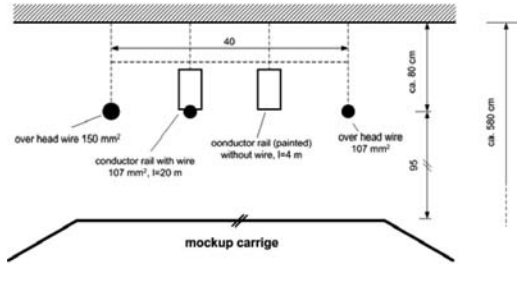


Figure 1. Cross-section from the test set up (not drawn to scale).

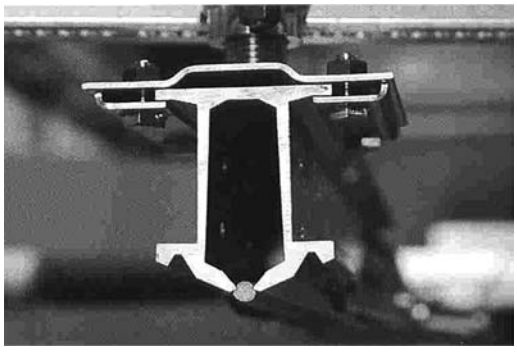


Figure 2. Conductor rail by Furrer + Frey Ltd.

Only the ≪fourth system≫ had a length of just 4 m and was fixed solely by the securing fixture in the middle of the carriage. The two overhead line wires were tensioned with a transmission ratio of 1:2. No power flowed through the lines during these tests.

2.2 *Conductor rail*

This is a box-shaped aluminium profile with a contact wire inserted without tensile force. It is a positive-type connection and both copper and aluminium of up to 161 mm^2 can be used as the contact wire. For this series of tests, a contact wire of 107 mm^2 was used.

The standard length is 12 m, and the system can be used for track radii ≥120 m without any special measures.

2.3 *Overhead wire*

Contact wires of 107 mm^2 and 150 mm^2 were used in these tests. In test 1, both cross-sections were tensioned with 900 kg and in tests 2 and 3 the weight was increased to 1250 kg for the 150 mm^2 cross-section. The transmission ratio was 1:2 for both cross-sections.

3 DESCRIPTION OF THE TESTS

3.1 *Test location at VSH*

The tests were carried out in an access tunnel of the ICST in the VSH-Hagerbach Test Gallery Ltd. (www.hagerbach.ch). The test area was approx. 25 m long and approx. 6.9 m wide, and it had an average height of approx. 5.8 m. The walls in the test area had a rough surface of rock or sprayed concrete.

3.2 *Mock-up carriage*

The mock-up carriage, manufactured from steel profiles and steel plate, was built by VSH according to the client's specifications. Up to a height of 2.62 m, the dummy was left open at the sides, thus simulating the window glass which is present in a railway carriage. Above 2.62 m, the entire surface area of the dummy was sealed with steel plate (t = 2 mm).

After test 1, it emerged that the steel plate represents a very major thermal barrier in the upward direction, in relation to the overhead line systems. For this reason,

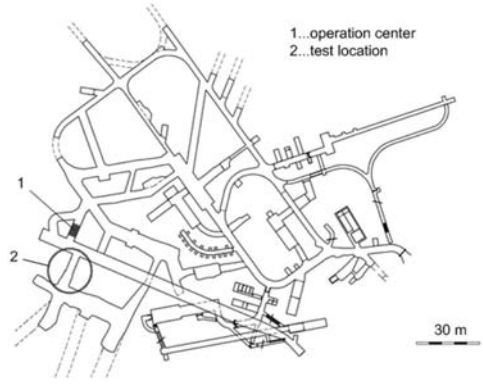


Figure 3. Plan of the tunnel test facility VSH-Hagerbach Test Gallery Ltd.

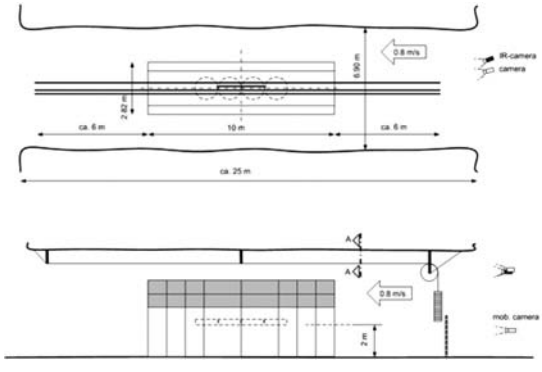


Figure 4. Sketch of the test location (not drawn to scale).



Figure 5. Construction of the mock-up carriage.

after consultation with the client, twelve openings were cut in the horizontal area of the carriage roof prior to test 2. Each slit was 70 cm long and 15 cm wide, providing an open area totalling 1.3 m^2. The distance between the slits was also 15 cm.

3.3 *Pool fire*

In order to carry out the tests, a fire seat was set up with four circular pools. These pools, with an internal diameter of 1.15 m and a height of 0.3 m, were manufactured from steel plate. The total area of combustion was therefore approx. 4 m^2. The fuel used was normal commercial heating oil with the following characteristics. The average heating capacity of one fire trough was approx. 1.4 MW, with a pyrolytic decomposition of some 0.034 kg/s. The total heating capacity of all four fire troughs was approx. 5.4 MW. The fire troughs were secured to the dummy carriage with a steel frame. In tests 1 and 2, the height of the fluid level at the start of the test was approx. 2 m, and for test 3 this figure was approx. 2.4 m.

3.4 *Test procedure*

The same climatic conditions prevailed in the test area for all three tests. An air flow is present in every tunnel due to differences in air pressure at the portals, mechanical ventilation or traffic (piston effect). As the tests were to be conducted under the most realistic conditions possible, an air flow of approx. 0.8 m/s was created in the test area.

For each test, one litre of heptane was added per fire trough as a fire accelerator, in order to speed up the ignition process.

3.5 *Data recording*

The MDA-600 multi-channel measuring and monitoring system was used for central recording of the measured data. One or more limit values can be assigned to each channel. All the data are stored in an indelible, error-proof memory.

The MDA-600 was accommodated in the central measurement technology unit and was protected against power failures by a UPS.

3.6 *Temperature sensors*

Due to the fuel used and a minimum air flow in the test area, maximum temperatures $<1000°C$ could be assumed. For this reason thermo couples of type K (NiCr-Ni) were used. These allow temperatures of up to 1200°C to be measured.

A total of 16 sensors (nos. 11 to 26) were affixed – four to the carriage roof and 12 to the overhead line systems. The positioning of the sensors is shown in Figure 8. The measuring point for the sensors was



Figure 6. Picture from the infra-red (IR) camera at test 1.

fixed on the underside of the copper wire in all the systems. One exception was the short rail (no overhead line); in this case, the sensor was fixed laterally on the aluminium.

All the sensors were designed as cased thermo couples with a diameter of 3 mm. Each sensor was connected with the data recording system in the operation centre via a shielded type K compensating data line.

3.7 *Video recording*

To provide optical monitoring of the overhead line systems during the testing, three cameras were installed in the fresh-air zone. The special camera and the thermal imaging camera were connected with analogue recording devices in the operation centre.

A special camera (fixed installation) for tunnel light conditions was used at a height of 4.5 m. This camera was designed for a minimum illuminance of 2 Lux and was equipped with a variable focus (7.5–75 mm). A thermal imaging camera (fixed installation) was also mounted at a height of 4.5 m and on approximately the same optical axis as the normal imaging camera. A Bullard® TIx thermal imaging camera, as normally used by fire brigades for fire- fighting, was used for the tests. Independently of the other two cameras, a DV Handy-Cam was installed at a height of approx. 1.3 m. The time progression of the elongation of the contact wire was recorded optically with the mobile video camera and a vertical yardstick next to the tensioning weights.

4 RESULTS

4.1 *Elongation*

Based on an optical evaluation of the video recordings, the reduction of the tensioning weights (Δs) for the two overhead line wires was determined. Since all the



Figure 7. The elongation was measured by a yardstick and video records.

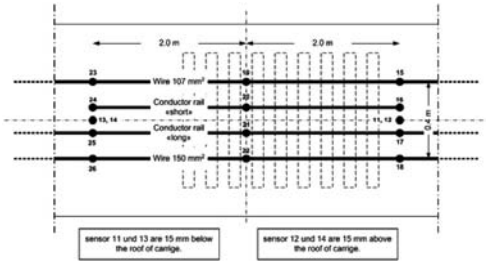


Figure 8. Location of the thermo couples. The sensors were fixed direct on each overhead system.

contact wires were tensioned with a transmission ratio of 1:2, the change in length (Δl) of the contact wire was half of the reduction in the tensioning weights (Δs). In test 1, both contact wires were tensioned with 900 kg, so the different cross-sections also gave rise to different tensions in the wire. In tests 2 and 3, the tensioning force on the 150 mm^2 contact wire was increased so that the tensions were the same.

In test 1 (closed carriage roof), the change in length (Δl) for the two contact wires – despite the difference in cross-section – was approx. 4 cm. None of the contact wires tore during this test.

In test 2 (slits in the carriage roof), the maximum elongation (Δl) of the 107 mm^2 contact wire was approx. 36 cm and the figure for the 150 mm^2 contact wire was approx. 16 cm. The wire with a 107 mm^2 cross-section tore 6 minutes and 35 seconds after ignition.

In test 3 (slits in the carriage roof, fire troughs at 2.4 m), the maximum elongation (Δl) of the 107 mm^2 contact wire was approx. 20 cm and the figure for the 150 mm^2 contact wire was approx. 36 cm. The contact wire with the 107 mm^2 cross-section tore 3 minutes and 18 seconds after ignition, and the contact wire with the 150 mm^2 cross-section tore 7 minutes and 12 seconds after ignition.

4.2 *Temperatures*

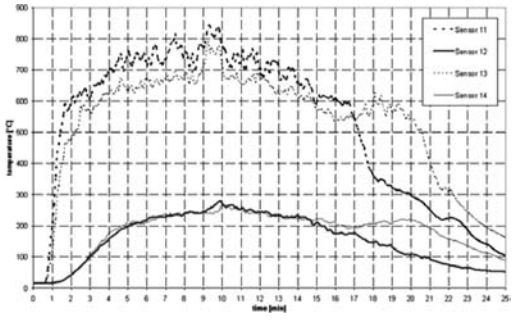


Figure 9. Temperature plot (example) from sensors 11, 12, 13 and 14. The peak at the end of the test is due to wind velocity change.

5 CONCLUSION

- The test results basically confirm the supposition that the conductor rail stays intact for longer than the conventional contact wire systems in case of a fire.
- The tests were not conducted with electrical power.
- The conductor rail heats up more slowly than overhead wire, probably due to its larger cross-section and its consequently higher heat conductivity.
- The conductor rail also remained mechanically intact at temperatures of 450°C.
- The results are valid for rail carriage made of steel.
- Test 1 showed that the closed steel roof shields temperatures in such a way that temperatures of "only" the level occurring during normal operation were measured on the overhead line systems. Slits were cut in the carriage roof for tests 2 and 3.
- Verification of electrical functioning capability was not a subject of this investigation.

6 OUTLOOK

All the system components used in the tests were dismantled and were subjected by the client to further testing in the laboratory (material technology and electrical).

Special attention should be focused on the carriage material, because it has a decisive influence on the progression of the fire. Modern carriage systems, of the sort that are already in frequent use and which will probably be used even more often in future, consist of aluminium or composite materials (plastics). The importance of tests with materials of these kinds is very great, and they would lead to highly relevant and important findings.

Another question which must be answered is: How does the locomotive system behave during a fire in a tunnel? An overhead wire system that is able to function is of little use if the power cannot be taken off by the locomotive, for example because the power take-off system is no longer functioning.

A further highly important aspect is the functional behaviour of the systems which separate the current carrying components from those which do not carry current (isolators) because here too, a failure leads to an interruption of the power flow.

The tests which were conducted were of great importance. In turn, however, the systems that were examined form a module in a larger and even more complex system, and the expected behaviour of a subsystem cannot be used as the basis for conclusions about the behaviour of the higher-level system.

The requirement specified by the rail operators, the authorities and the safety experts is that the train must travel out of the tunnel. In order to meet this demanding requirement, it is necessary for the entire system to be able to function.

For these reasons, we regard more extensive fire tests on system components as highly appropriate, or rather we consider tests on the complete system to be indispensable.

ACKNOWLEDGEMENT

The authors would like to express their gratitude to Mr B. Furrer, CEO from Furrer + Frey Ltd. (www.furrerfrey.ch), Bern, Switzerland, for his permission of publishing this paper. Special thanks also to all staff of VSH for their total commitment during this project.

This page intentionally left blank

Underground Space – the 4th Dimension of Metropolises – Barták, Hrdina, Romancov & Zlámal (eds)
© 2007 Taylor & Francis Group, London, ISBN 978-0-415-40807-3

The research on countermeasure of fireproofing and rescue for long highway tunnel

Wang Yong-dong; Xia Yong-xu; Deng Nian-bing
Highway College, Chang'an University, China

ABSTRACT: In view of laws of the occurrence and development of fire, countermeasure system of fireproofing and rescue for long highway tunnel can be divided into eight parts such as its guiding ideology, fire safety grade, propagandas and education, traffic management, ventilation control, monitoring and fire control, building materials and ancillary establishments, and system of fire rescue. Each subsystem has a detailed fireproofing countermeasure. Based on each fire safety grade, the fireproofing facilities and traffic control table to transport dangerous goods are put forward. Organizational process of fireproofing and rescue for highway tunnel is improved, and the principle, the content and the material program of studying the counterplan are put forward.

1 INTRODUCTION

With the rapid development of transportation in the world in the last 20 years, the grade of highways becomes higher and higher, the scale of highway tunnel becomes bigger and bigger, and the length becomes longer and longer. Nevertheless, many traffic safety problems have also emerged, and fire is one of them.

We can see from a large number of statistics[1][2], the probability of highway tunnel fire is 20–25% more than railway tunnel; there is one fire each 50 million vehicles per kilometers in the tunnel, in view of the Component of Common vehicles in the tunnel. Although the trucks only take 15% of the all highway transport vehicles, 30% of the fires were caused by trucks. In China, there was about one fire each 70 million vehicles per kilometers in shanghai Dapu Highway Tunnel from 1981 to 1988. In addition, to resume operation after the tunnel fire would take a very long time. For example, to resume the operation of Austria's Tauern tunnel after fire spent three months. France & Italy's Mont Blanc tunnel takes three and a half years to resume, and resuming the operation of the Swiss St. Gotthard tunnels takes one and a half year. Therefore, when a fire happened in the tunnel, economic losses were incalculable, it will also have a serious impact on society. Based on the analysis of available information of the world and the development trend of the tunnel safety, with the increase of traffic and the transportation of hazardous materials, number and the length of tunnels year by year, and the serious increase of terrorism, it can be sure that the probability of highway tunnel fire will go upward, therefore the traffic fire in tunnel has become an international concern.

Although China has built many long highway tunnels, but there are no management standards of long highway tunnel. Research of fireproofing and rescue for long highway tunnel is also still in its infancy, Many management departments do not know much about the relief and fire countermeasures. Therefore, it is important to research on countermeasure of fireproofing and rescue for construction, management and the constitution of management plans in fire of long highway tunnel.

2 CHARACTERISTICS AND CAUSES OF FIRE IN HIGHWAY TUNNEL

2.1 *The characteristics of fire in highway tunnel*

According to a large number of investigations and studies of fire in highway tunnel, there are several distinctive features:

(1) Randomness. The time, location, scale, morphology of fire is random.
(2) Disaster time is short. The time of fire broke out from vehicles generally between 5 and 10min, and the fire development process is quickly. The fire duration, which has relation to the environment of the tunnel, is generally between 30 minutes and a few hours.
(3) Smoke, and high temperature. Because of the tunnel is confined to a airtight space, in case of fire, smoke can not be ventilated naturally, so a lot of smoke inside the tunnel, the tunnel can not disperse heat easily. Fire makes the temperature inside the tunnel rise quickly, usually amounted to hundreds

or even thousands centigrade, for example, the fire temperature of Tauern tunnel is above 1300°C.

(4) To fight the fire is hard. The fire in tunnel may undermine the tunnel lighting system greatly which makes the fighting difficult. Moreover, because of the high temperature, to put out the fire source is difficult to the firemen.

(5) Difficulties in evacuation. Because the section of tunnel is small, it is almost impossible to evacuate personnel and material completely.

(6) To cause serious harm. As the fire in tunnel developed quickly, to put out the fir is difficult, it often causes huge casualties and property losses and has a bad effect on the society.

2.2 *The causes of the fire in highway tunnel*

There are many causes of the fire in highway tunnel. Common causes of the fire are : ① the burning of car carburetor; ② the brakes catches fire when the emergency brake; ③ traffic accidents; ④ inflammable goods in vehicle catch fire; ⑤ electrical lines or electrical equipments are short in tunnel.

3 THE COUNTERMEASURES OF FIREPROOFING AND RESCUE FOR HIGHWAY TUNNEL

3.1 *The guiding ideology of the countermeasures of fireproofing and rescue for highway tunnel*

The countermeasures of fireproofing and rescue in highway tunnel should follow the principles that prevention is primary combining with rescue. The basic idea should be to make people escape mainly and to protect property supplement. It mainly depends on the firemen of management department of tunnel.

3.2 *Fire safety grades of highway tunnel*

Considering the importance of the tunnel in traffic network and harm extent of fire, the tunnels are divided into several grades based on a certain safety standard system. Because of the different safety grade, the countermeasure of fireproofing and rescue, and fire safety equipment are different. Based on the technology development of highway tunnel and the national conditions, fire safety grade of highway tunnel in China is given, which can be divided into five grades: I, II, III, IV, V, the minimum length of the tunnel corresponding to the fire grade is 0.5 km, the characteristic lengths of tunnel of different fire grades safety are 1.0 km, 5.0 km and 10.0 km, the minimum traffic of each section is 10000 veh/d, Fig.1.

3.3 *Propagandas and education*

Propagandas and education are primary work to prevent fire of highway tunnel. The objects of education

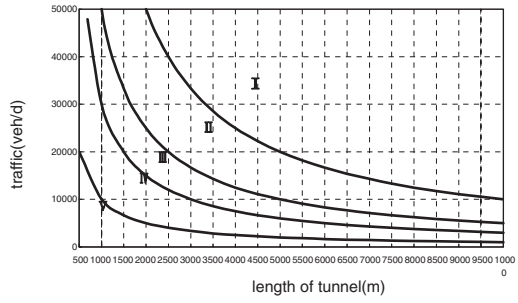


Figure 1. Fire safety grade of highway tunnel in China.

are users, tunnel maintenance and management staffs. Through education people can help themselves and minimize fire hazards. The means of propagandas and education are training, the dissemination of pamphlets and VCD. Education include: ① the characteristics of highway tunnel structure; ② the regulates of vehicle speed, overtaking and the distance between vehicles through the tunnel; ③ the alarm system of highway tunnel; ④ the extinguish facilities of highway tunnel; ⑤ the fire law of highway tunnel; ⑥ fire hazard of highway tunnel; ⑦ the escape system of highway tunnel; ⑧ the fire countermeasures of highway tunnel.

3.4 *Traffic management of highway tunnel*

3.4.1 *Normal operation and management of highway tunnel*

The main task of normal operation and management of highway tunnel is to control the traffic inside the tunnel, and limit the smallest distance and the maximum speed of the vehicle, so that to prevent congestion and accidents.

3.4.2 *Fire grade of vehicle in tunnel*

Fire grade of vehicle indicates the capability of fire resistance of vehicle. Fire grades of vehicle are classified A1, A2 and B by France. In those standards, only vehicle with A1 can be allowed to go through the tunnel. Fire grades of vehicle are classified A-A, A and B by Japan's transport department. The fire grade of vehicles through tunnel must be reached the highest-grade A-A. In management and operation of the tunnel, limiting the low grade vehicles to go through the tunnel or taking some control measures (such as escorting, allowing at night) will greatly reduce the probability of the fire occurrence of the highway tunnel.

3.4.3 *Management of dangerous goods in highway tunnel*

Currently, there is no corresponding standards and management system for the transport of dangerous goods in China. But with the increase in highway tunnel, these problems have to be resolved. The work must

Table 1. Traffic control table to transport dangerous goods in highway tunnel.

Traffic control	Grades				
	I	II	III	IV	V
Speed(km/h)	Design data-20	Design data-20	Design speed	Design speed	Design speed
Vehicle distance(m)	500 ~ 1000	400	300	300	300
Ultrahigh	Prohibit	Prohibit	Prohibit	Prohibit	Prohibit
Overweight	Prohibit	Prohibit	Prohibit	Prohibit	Prohibit
overlong	Escorting passed at night	Escorting passed	Escorting passed	Escorting passed	Escorting passed
Flammable liquid	Escorting passed at night	Escorting passed	Escorting passed	Escorting passed	Escorting passed
LPG	Escorting passed at night	Escorting passed	Escorting passed	Escorting passed	Escorting passed
Chemical item	Escorting passed at night	Escorting passed	Escorting passed	Escorting passed	Escorting passed
Explosives	Prohibit	Escorting passed at night	Escorting passed at night	Escorting passed at night	Escorting passed at night

Notes : If it is motorcade with dangerous goods, the distance must be kept at 1 ~ 2 km, or only allow one go through tunnel at a time.

be do to Enact strict transport laws about noxious, inflammable and explosive goods, which clearly regulate that which kinds of vehicles are permitted, limited or prohibited to use the tunnel. Management department can also consider the problem that which kinds of Vehicles carrying inflammable or explosive goods can be allowed to go through the tunnel or bypass the tunnel from the economic, security, society and other aspects.

Based on specific circumstances of highway tunnel in China, traffic control table to transport dangerous goods in highway tunnel with corresponding fire safety grade is put forward, Tab.1.

3.5 *Fire ventilation control of highway tunnel*

Fire ventilation control of highway tunnel is particularly important in the extinguishing process. Ventilation system of highway tunnel must be achieved aim: ① offering the minimum wind speed to prevent smoke going in the opposite direction; ② ventilating the smoke from the tunnel as soon as quickly; ③ lowering the temperature inside the tunnel; ④ providing fresh air for escape channel and refuge; ⑤ providing fresh air for firemen.

3.6 *Monitoring and fire control system of highway tunnel*

3.6.1 *The monitoring system of the highway tunnel*

The purposes of setting up monitoring system in highway tunnels are to make full use of the traffic capacity of the tunnel, ensure safety, meet environmental requirements and reduce disasters in highway tunnel. Tunnel Monitoring System is composed of the following parts: ① tunnel traffic control signal; ② ultrahigh -detection device in the both entrances; ③ detection loop of vehicle in the tunnel; ④ fire and smoke alarm device; ⑤ CO concentration detector; ⑥ visible detector in smoke; ⑦ brightness monitor in the both entrances; ⑧ closed-circuit television surveillance; ⑨ computer Auxiliary control system.

3.6.2 *Fire alarm system of highway tunnel*

(1) Fire detection system
There are three types: ① emergency phone; ② manual annunciator; ③ fire detector.

(2) Emergency alarm devices
There are three types: ① alarm display ② flash light, alarm light; ③ audio signal generator.

3.6.3 *Tunnel fire facilities*

There are four types: ① fire extinguisher; ② extinguishing hydrant; ③ water offering hydrant; ④ spraying facility.

3.6.4 *Other facilities*

In order to provide security for staffs and vehicles in emergency, other facilities are installed. Other facilities should include: ① some ancillary facilities to ventilate smoke; ② transfer channel and refuge for escape; ③ the car park in emergency situations; ④ asylum-oriented facilities used for evacuation of vehicles and staffs in disaster; ⑤ I.T.V; ⑥ emergency lighting facilities; ⑦ emergency power-supply facilities.

3.6.5 *Selection and installation of fireproofing facilities in the tunnel*

See Table 2

Table 2. Fireproofing facilities with corresponding fire safety grade.

Emergency facilities		Grades I	II	III	IV	V
Fire detection equipment	**Manual annunciator**	○	○	○	○	△
	Fire detector					
	Smoke detector	○				
	Temperature detector	○	○	△		
	Radiation detector	○	△			
	Emergency telephone	○	○	○	○	
Alarm equipment	*Alarm display*					
	Entrance	○	○	○	○	△
	Inside the tunnel	○	○	○	○	△
	Flash and alarm light	○	○	△	△	
	Audio signal generator	○	○	△	△	
Fire equipment	**Fire extinguisher**	○	○	○	○	△
	hydrant					
	Indoor fire hydrant	○	○	○	△	△
	Outdoor fire hydrant	○	○	○	△	
	Water hydrant	○	△	△		
	spraying facility	○	△	△		
	Fire engine	○	○	△	△	
Other facilities	**Refuge hole**	○	△			
	Asylum channel	○	○	○	○	△
	Emergency parking space	○	○	○	○	△
	Escape orientation Facilities					
	light show	○	○	○		
	Wall color sign	○	○	○	○	○
	Lineate broadcasting	○	○	○	△	
	Wireless broadcasting	○	○	○	△	
	I.T.V.	○	○	△		
	Emergency lighting	○	○	○	△	
	Smoke ventilating facilities	○	○	○	△	
	Emergency power facilities	○	○	△		

Note: need ○; choice △

3.7 *Fireproofing of construction materials and ancillary facilities of tunnel*

3.7.1 *Fireproofing of construction materials*

Fireproofing of construction materials mainly includes the fire-resistance of waterproof material, fireproofing of concrete and other burning-retardant lining material such as fireproofing paint layer.

3.7.2 *Fireproofing of ancillary facilities*

Fireproofing of ancillary facilities includes fireproofing of the fan, the lamps, detection equipment, monitoring equipment, power supply facilities.

3.8 *Fire rescue system of highway tunnel*

3.8.1 *Rescue echelon of highway tunnel*

Rescue echelon of long highway tunnel can be divided into three teams, the first team is composed of vehicle drivers and passengers in fire areas, the second team includes tunnel management staffs, non-professional firemen and policemen, and the third team includes professional firemen and doctors. The early tunnel fire fighting work is implemented by the first and second teams, and the latter part of work is finished by the third team. Based on some typical examples and the fire experiments, the time of the arrival of the professional rescue team should not exceed 10 minutes, otherwise they will lose the best chance to rescue and putting out the fire.

3.8.2 *The organizational process of putting out fire in highway tunnel*

Once the tunnel is on fire, in order to avoid of the deterioration of the rescue environment, it must be put out the fire as soon as possible to prevent the tunnel full of smoke. At the same time, the fire alarm must be provided to prevent vehicles driving to the scene of the fire and give the right guidance to the drivers so that they can leave the fire tunnel. Fire rescue work can be organized and implemented according to the Fig. 2.

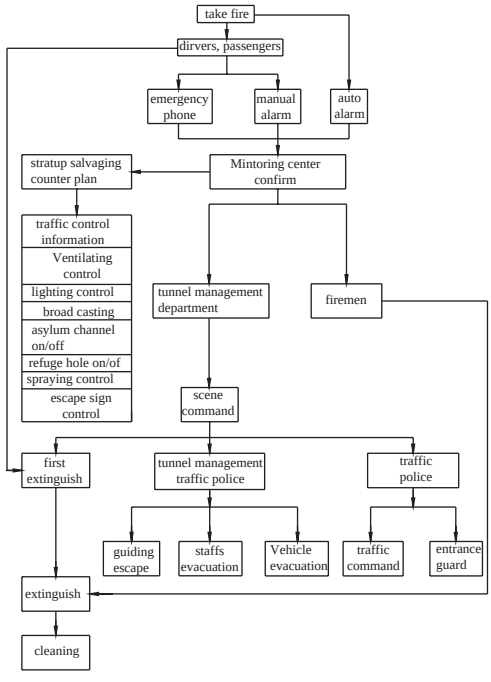


Figure 2. Organizational process of putting out fire and rescue in highway tunnel.

3.8.3 *Salvaging counterplan for fire of tunnel*

Salvaging counterplan for fire of tunnel is a kind of plan which is carried out when the tunnel is on fire. Various countermeasures are given based on different fire conditions (fire scale, the location, the type of fire, etc). If the tunnel is on fire, it is the important guiding principles to reduce greatly the time and prevent confusion and mistakes in operation.

Salvaging counterplan for fire of tunnel should be formulated based on safe, feasible and economic principles. The counterplan includes: tunnel sections divided in the fire, traffic control, lighting control, ventilating control, communication control, fire extinguishing, escape, evacuation and rescue. The startup model is an important step of the counterplan, if it is not carried timely after the fire, the counterplan will lose its meaning. The best way is to store the counterplan in the computer. If the tunnel is on fire, the monitoring equipment will judge the specific circumstances and corresponding countermeasures will be initiated. Of course, the fire condition also can be judged by the tunnel management operators, but the startup process should be simple to operate. Salvaging counterplan for fire of tunnel should be researched specially with numerical simulation, physical simulation and field experiment.

4 CONCLUSION

The research on fireproofing and rescue for long highway tunnel is a long-term and arduous task. This article presents basic countermeasure of fireproofing and rescue, the fireproofing facilities and traffic control table to transport dangerous goods based on each fire safety grade. Organizational process of fireproofing and rescue for highway tunnel is improved, and the principle, the content and the material program of studying the counterplan are put forward. These productions establish theoretical and technical basis for construction and research of counterplan of long highway tunnel.

REFERENCES

[1] Alfred Haack. 2001. Fire safety Conception in Vehicle Tunnel. Proceedings of Highway Tunnel Technical Communion of 2001' China-Switzerland.

[2] DENG Nian-bing. 2003. Research on Countermeasure of Fireproofing and Rescue for Long Highway Tunnel. Xi'an: Chang'an University.

[3] WANG Yong-dong; XIA Yong-xu. 2002. Numerical simulation of longitudinal ventilation of highway tunnel. China journal of highway and transport 15(1): 82–85

[4] XIA Yong-xu; WANG Yong-dong; ZHAO Feng. 2002. Ventilation scheme of Zhongnanshan highway tunnel in Qinling. Journal of chang'an university (natural science edition) 22(5):48–50

[5] XIA Yong-xu; WANG Yong-dong; DENG Nian-bing; ZHAO Feng. 2006. On safety grade of highway tunnels. Journal of safety and environment 6(3):44–46

This page intentionally left blank

Underground Space – the 4th Dimension of Metropolises – Barták, Hrdina, Romancov & Zlámal (eds)
© 2007 Taylor & Francis Group, London, ISBN 978-0-415-40807-3

Experimental study on mechanical behaviors of tunnel lining under and after fire scenarios

Z.G. Yan & H.H. Zhu
Tongji University, Shanghai, China

ABSTRACT: To evaluate the fire safety of tunnel lining under and after fire scenarios, a series of reduced-scaled experiments on mechanical behaviors of tunnel lining were carried out. Three types of concretes that are reinforced concrete, steel fiber reinforced concrete and polypropylene fiber concrete are employed in the experiments. The results indicate: a) mechanical properties of lining materials especially uniaxial compressive strength, elastic modulus and impermeability deteriorate significantly after high temperature; b) comparing with normal temperature condition, high temperature result in significant decrease of load-bearing capacity and significant increase of displacement of segments and joints; c) because of material deterioration, thermal damage and thermal stress due to high temperature, the load-bearing capacity and reliability of tunnel lining system decrease heavily. Moreover, large displacement of lining system may affect the safety of surrounding substructure and surficial buildings.

1 INTRODUCTION

There are a number of fire accidents with high peak temperature, rapid heating velocity and long duration in traffic tunnels. These fire accidents resulted in not only lose of property but also severe damage to tunnel linings in term of concrete spalling, deterioration of physical-mechanical property and reduction of load bearing capacity. For example, the Mont Blanc Tunnel fire in 1999 and St. Gotthard Tunnel fire in 2001 both cause severe damage to tunnel lining (Haack 2002).

To evaluate the fire safety of tunnel lining under and after fire scenarios, a series of reduced-scaled experiments on mechanical behaviors of tunnel lining, which include three levels tests i.e. lining material testing (FT1), segment (joint) testing (FT2) and lining system testing (FT3) were carried out in Tongji University. The scopes of the researches involve: a) the variation of uniaxial compressive strength, elastic modulus and impermeability with high temperature; b) mechanical behaviors of lining segments (joints) under and after different thermal-mechanical conditions; c) mechanical behaviors of lining system under and after different thermal-mechanical conditions and d) method to protect lining concrete from spalling without large decrease of impermeability durability.

This paper briefly introduces the experiments and main results from these experiments.

Table 1. Parameters of the Concrete, steel fiber and polypropylene fiber used in the experiments.

Items	Properties
Concrete	C50
Steel fiber	Hooked steel wire fiber, L = 50 mm, L/d = 55, Blend capacity = 60 kg/m^3
Polypropylene fiber (PP fiber)	Dispersed monofilament fiber, L = 12 mm, d = 18 μm, Melting point = 160°C, Blend capacity = 2 kg/m^3

2 EXPERIMENTAL SETUP

Three types of concretes that are reinforced concrete(RC), steel fiber reinforced concrete (SFRC) and polypropylene fiber concrete (PPFC) are employed in these three tests, as shown in Table 1.

In FT1, the temperature varies in the range of 20°C–1100°C, and the heating velocities are 50°C/min and 5°C /min in the testing furnace. In FT2 and FT3, two thermal-mechanical conditions i.e. Load case 1 and Load case 2 are considered (Fig. 1). And a standard HC curve with duration of 0.5 h or 1 h is used to simulate defined fire scenarios (Fig. 2). At the same time, in order to simulate the surrounding environment of tunnel lining, single face heating are conducted and the lining are covered by soil layer (Fig. 3, 4).

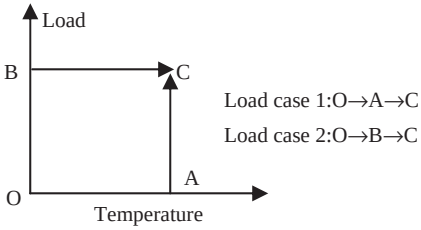


Figure 1. Two thermal-mechanical conditions in the FT2 and FT3.

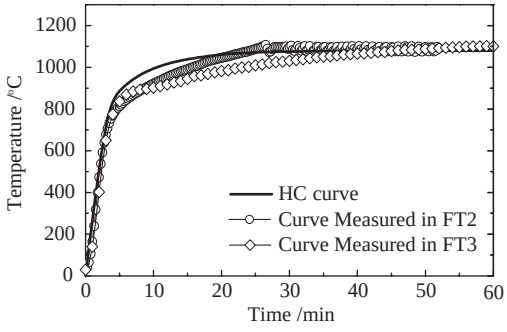


Figure 2. Temperature-time curves measured in the fire experiments.

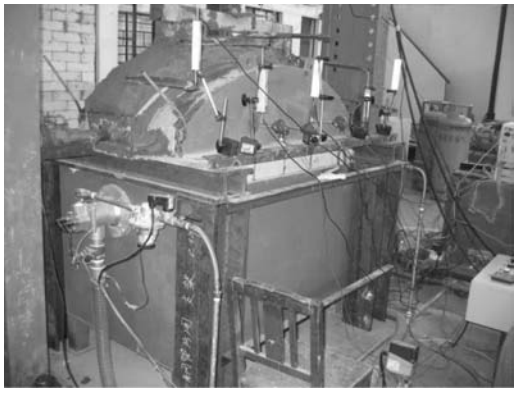


Figure 3. Experimental setup on mechanical behaviours of segments and joints during and after high temperature (FT2).

3 EFFECTS OF HIGH TEMPERATURE ON PHYSICAL-MECHANICAL PROPERTIES OF TUNNEL LINING MATERIAL

As shown in Figure 5, both uniaxial compressive strength and elastic modulus of three types of concretes decrease with suffered temperature after fire because of dehydration of cement paste, disharmony of heat expansion between cement paste and aggregate and



Figure 4. Experimental setup on mechanical behaviours of lining system during and after high temperature (FT3).

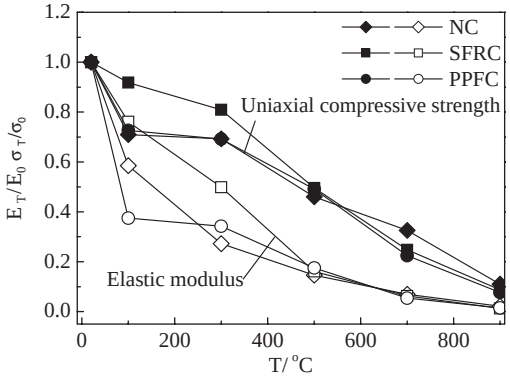


Figure 5. Variation of relative elastic modulus and uniaxial compressive strength of three types of concretes after high temperature.

cracking of aggregate. Owing to long duration of tunnel fire and high peak temperature, heavy damage to tunnel lining will occur in terms of deterioration of mechanical characteristics and reduction of load bearing capacity. These deteriorations may seriously affect the safety of tunnel lining.

Figure 6 shows variation of permeability of three types of concretes after high temperature, which is represented by relative permeability coefficient S_k. It shows that all the relative permeability coefficients of three types of concretes increase significantly after high temperature. Especially for PPFC, the relative permeability coefficient after high temperature of 300°C increases by 259 times of the value in 20° C. The increase of relative permeability coefficient means deterioration of impermeability durability of tunnel lining concrete. Because tunnel linings are embedded in surrounding soil and water, it is important to maintain sufficient impermeability durability in their lengthy service period.

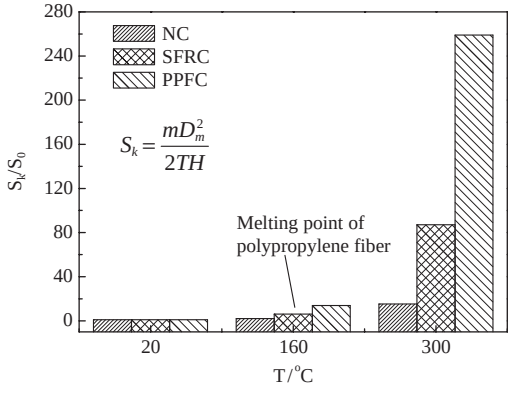


Figure 6. Variation of the relative permeability coefficient S_k of three types of concrete after high temperature.

It is noticed that addition of polypropylene fiber will results in severe decrease of impermeability durability of concrete although concrete spalling can be avoided successfully.

4 MECHANICAL BEHAVIORS OF LINING SEGMENTS (JOINTS) AND LINING SYSTEM UNDER AND AFTER HIGH TEMPERATURE

Because of material deterioration, thermal damage (e.g. concrete spalling), asymmetric thermal-stress, asymmetric deterioration of material properties within tunnel lining (result from asymmetric temperature distribution, as shown in Fig. 7) and resisting force of surrounding ground, the load-bearing capacity and reliability of segments (joints) or tunnel lining system deteriorate heavily. And comparing with the SFRC lining the load bearing capacity of RC lining is higher at same thermal-mechanical condition (Fig. 8).

Furthermore, because of recovery of strength and elastic modulus of reinforcement bar, the load bearing capacity of RC lining after high temperature is higher than the value during high temperature (Fig. 8). However, for SFRC lining the load bearing capacity after high temperature is lower than the value during high temperature because of development of cracks during cooling process.

At the same time, comparing with normal temperature condition, high temperature results in significant increase of displacement of segments (joints) or lining system besides significant decrease of load-bearing capacity. For example, the rotation angle and expending distance of joint increase significantly because of deterioration of mechanical properties of concrete and bolt (Fig. 9, 10). This increase of displacement of segments (joints) or lining system may affect the safety of surrounding substructure and surficial buildings.

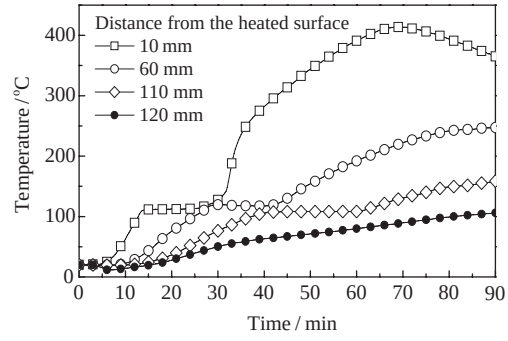


Figure 7. Temperature distribution in the section of segment in HC curve.

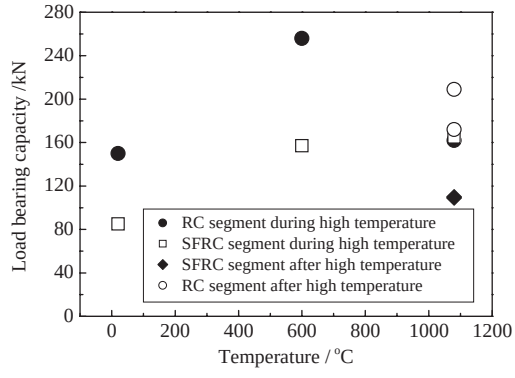


Figure 8. Load bearing capacity of segments under and after different thermal-mechanical conditions.

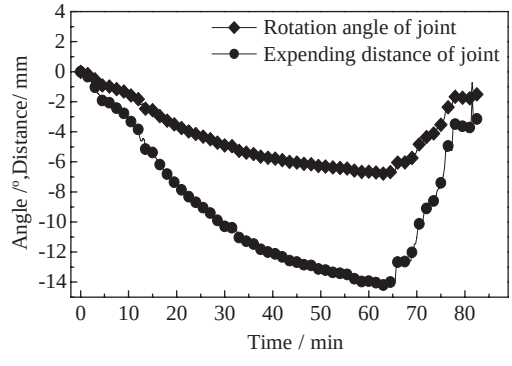


Figure 9. Rotation angle and expending distance of joint owing to high temperature.

Moreover, it is noticed that rubber sealing rod may be destroyed by high temperature if expending distance of joints reach to a certainvalue under fire scenario.



Figure 10. Large expending distance of joint owing to high temperature.

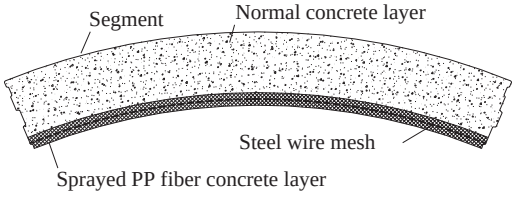


Figure 11. Schematic view of the new segment with ability to prevent spalling during high temperature.

5 A NEW METHODS TO PROTECT TUNNEL LINING FROM SPALLING

Because of rapid heating velocity, high compressive stress and low permeability of tunnel lining concrete, numerous fire accidents indicate that spalling is one of the most severe damage to tunnel linings (Kirkland 2002). Furthermore, due to continuous spalling reinforcement bar may be exposed to high temperature and quickly lose strength and elastic modulus leading to collapse of lining system.

Adding polypropylene fiber to entire concrete mixture is a general method to prevent lining concrete from spalling during high temperature. However, as shown in Figure 6, this method will make the impermeability durability of concrete reduce significantly.

A new method is established in the experiment of FT2 and a new prefabricated segment is designed. In this new method, polypropylene fiber is just mixed in defined thickness near to the inner side of the lining (Fig. 11). And based on spalling temperature of 250°C–420°C and spalling time (generally within the extension of 20 min from fire ignition) (Hertz 200, Khoury 2000), the required thickness of polypropylene fiber concrete layer is summarized in Table 2 according to temperature of hot smoke and time from ignition through FEM simulations. As shown in Figure 12, no spalling is found in the inner surface of the specimen

Table 2. The required thickness of the sprayed PP fiber concrete layer according to temperature of hot smoke/mm.

	Temperature of hot smoke/°C				
Time/min	600	800	1000	1200	1400
15	9–22	17–28	22–32	26–35	29–38
20	10–25	19–32	25–37	30–40	33–44
25	12–28	21–36	28–41	33–46	37–49
30	12–30	24–40	31–45	36–50	40–53

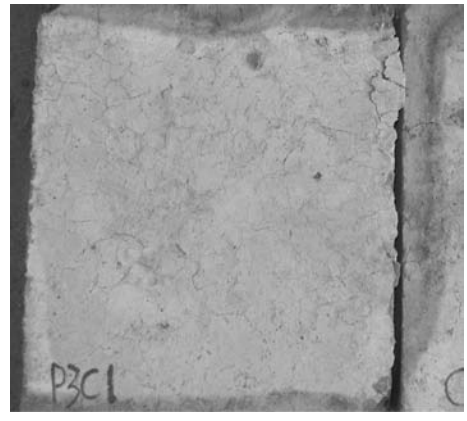


Figure 12. No spalling in the surface of the testing specimens.

with 3 cm polypropylene fiber concrete layer. These results indicate that adding polypropylene fiber to partial concrete mixture is feasible to prevent spalling and to prefabricate segments of shield tunnels.

Comparing with adding polypropylene fiber to entire concrete mixture, this new method will not reduce impermeability durability significantly because polypropylene fiber just is mixed in the thin concrete layer near the inner surface of lining.

6 CONCLUSION

Based on the experiments i.e. FT1, FT2 and FT3, the conclusions can be summarized as follows:

1. Mechanical properties of lining materials, which include uniaxial compressive strength, elastic modulus and impermeability deteriorate significantly after high temperature. This deterioration will seriously affect the safety and reliability of segments (joints) and lining system.
2. Because of material deterioration, thermal damage and thermal stress due to high temperature, the load-bearing capacity and reliability of segments

(joints) and lining system decrease heavily. Moreover, large displacement of lining system may affect the safety of surrounding substructure and surficial buildings.

3. It is important to reduce the deterioration of impermeability durability of lining concrete by high temperature besides preventing spalling. According to the results of the fire experiments mentioned in this paper adding polypropylene fiber to partial concrete mixture is a feasible method to prevent lining concrete from spalling and to control deterioration of impermeability durability.

REFERENCES

Haack, A. 2002. Current safety issues in traffic tunnels. *Tunnelling and Underground Space Technology* 17:117–127.

Hertz, K.D. 2003. Limits of Spalling of Fire-exposed Concrete. *Fire Safety* 38(2):103–116.

Khoury, G.A. 2000. Effect of Fire on Concrete and Concrete Structures. *Progress of Structure Engineering Material*. (2):429–447.

Kirkland, C.J. 2002. The fire in the Channel Tunnel. *Tunnelling and Underground Space Technology* 17(2): 129–132.

This page intentionally left blank

Part 8.3
Risk analysis of the Branisko tunnel

This page intentionally left blank

Underground Space – the 4th Dimension of Metropolises – Barták, Hrdina, Romancov & Zlámal (eds)
© 2007 Taylor & Francis Group, London, ISBN 978-0-415-40807-3

Risk analysis of the Branisko tunnel

M. Bakoš
Amberg Engineering Slovakia, s.r.o., Bratislava, Slovak Republic

N. Seifert
ASIT Ltd., Berne, Switzerland

M. Bettelini
INELMEC SA, Minusio, Switzerland

ABSTRACT: The Branisko tunnel is the first motorway tunnel in Slovak Republic. It was put in operation on June 29 2003. The tunnel system consists of a single tunnel tube with bidirectional traffic and a parallel emergency escape gallery transversally connected to the main tube. The administrator of the Branisko tunnel decided to conduct a risk analysis according to the EU and EC Directive 2004/54/EC on minimum requirements for tunnels in trans-European road network. The final report of the safety analysis includes the applied definitions, descriptions, assessment methods, safety and risk analysis results and recommendations for measures (structural, technical and organizational measures) to improve the safety of the tunnel Branisko. Future risk analysis and safety assessments for road tunnels in the Slovak Republic can apply the mentioned methodology, which fulfils the requirements of the EU/EC 2004/54/EC directive and has been used in other European countries as well.

1 INTRODUCTION

The nature of traffic tunnels and road traffic as such predetermines risk occurrence resulting in critical situations. Due to constantly increasing traffic density it is vital to monitor the current status of traffic safety, although, based on statistical data the accident rate in tunnels is lower that in open roads. Any traffic problems in relation to the confined space in the tunnel induce risk. As the most fatal result of such risk is fire, the fire safety is crucial. Safety assessment includes a variety of factors, therefore, a risk analysis using mathematical statistical methods and theory of probability seems a suitable tool for an objective and systematic assessment.

National Motorway Company, a.s. (NDS, a.s., Bratislava) as the administrator of the Branisko tunnel authorized the consortium Inžinierske združenie AGB which comprises AMBERG Engineering Slovakia, s.r.o., ASIT AG, INELMEC SA and BUNG Ingenieure AG as an independent consultant to perform the following task: "Preparation of risk analysis including ventilation simulation of the Branisko tunnel" a part of which has been the task to prepare tunnel safety documentation and a proposal of a detailed and appropriate methodology, for future use on a national level, corresponding to the best applicable practices (according to the EU and EC Directive 2004/54/EC on minimum requirements for tunnels in trans-European road network).



Figure 1. Western portal of the Branisko tunnel.

2 THE BRANISKO TUNNEL

The Branisko tunnel is the first motorway tunnel in Slovak Republic. It was put in operation on June 29 2003 (Fig. 1).



Figure 2. Escape exit.



Figure 3. SOS-box in an emergency lay-by.

Basic data typical for the tunnel structure:

- Total length of the tunnel: 4974.626 m (including the portals),
- Tunnel system: a single tunnel tube with bidirectional traffic; a parallel emergency escape gallery (clearance profile 2.50×2.50 m) transversally connected to the main tube,
- Longitudinal gradient: (from the west) $+1.2\%$ in length 4550 m, -1.65% in length 425 m,
- Transverse gradient: 2.5%,
- Traffic surface area: 47.68 m^2,
- Width of roadway between curbs: 7.50 m (2 traffic lanes),
- Left and right shoulder (service walkways), each 1.0 m wide,
- Transverse connections to the tunnel tube (Fig. 2) and emergency escape gallery (total number 13, each 360 m apart), whereas one transverse connection in the middle of the tunnel is designed for motor vehicles,
- Lay-bys: 6, out of which 4 single-sided and 2 double-sided (each 700 m),
- Emergency stations each 240 m,
- Ventilation shaft at a distance of 2050 m from the West Portal.

Technological equipment of the tunnel consists of the following devices:

- Ventilation devices: half-transversal system of ventilation with fresh air supply through axial ventilators located in the portal objects or longitudinal ventilation with fresh air supply through portals with ventilation shaft exhaust; louver ventilation flaps controlled by electric actuator are located each 50 m in the ventilation shaft (total number: 90, flow profile: 2.0 m^2);
- Technological equipment of the escape gallery: fire-proof doors with supervision, air condition indication, smoke detectors, lighting equipment, ventilation, wireless radio connection;
- Safety devices in the tunnel: emergency call system by means of emergency box (Fig. 3), system of closed video monitoring, system of wireless radio connection;
- Central controlling system;
- Measurement of physical quantities: opacity measuring devices, CO concentration measuring devices, air circulation speed and direction measuring devices, pressure differential measuring devices;
- Electrical fire signalisation (EPS): automatic fire alarms (point and linear thermal alarm), button fire alarms, stationary fire extinguishing devices;
- Lighting devices – standard, substitute and fire emergency.

3 BRANISKO TUNNEL SAFETY AND RISK ANALYSIS

Component parts of the analysis were the following:

(a) Identification of relevant hazards and scenarios, definition of the relevant operation scenarios at different operational regimes, during maintenance and other incidents, as well as the definition of traffic loading and the assessment of the procedures in case of emergency.
(b) Comparison of actual and prescribed safety measures, with regard to all relevant safety issues and standards in relation to substantial documents, such as Slovak and European safety regulations with particular reference to the Directive of EU and EC 2004/54/EC concerning essential issues of the various parts of the tunnel.
(c) Ventilation analysis (the actual state in relation to the air supply and comparison of the prescribed and actual state), simulation with regard to relevant operational and emergency scenarios, ventilation assessment.

Table 1. Typical values of vehicle fires.

	Min (%)	Max (%)	Special cases
Motor cars	2.0	2.0	2.0
Trucks/buses	1.5	4.5	13.5
Out of this not under control	0.5	1.5	4.5
Vehicles transporting hazardous goods	0.5	1.5	4.5
Out of this not under control	0.2	0.6	1.8

(d) Proposal of a detailed and appropriate methodology, for future use on a national level, corresponding to the best applicable practices. Due to the fact that at the time of developing of the risk analysis, an appropriate methodology valid in Slovak Republic was not yet selected, the task of the author of the risk analysis was also to propose a detailed and appropriate methodology in cooperation with all the concerned parties (i.e. the Ministry of Traffic, Posts and Telecommunications of the Slovak Republic, the Ministry of Internal Affairs, the Fire Brigade and Rescue Head Office, etc.).

(e) In the Branisko tunnel risk analysis, the OECD/PIARC model QRAM (Quantitative Risk Analysis Model) was used whose application is recommendded by PIARC and EU. The QRAM model has been evaluated by several national road and motorway authorities. The risk is visualized by means of a F-N-curve (frequencies versus consequences). The QRAM simulation considers also (apart from the traffic data) various structural and technical features of the tunnel in addition to the air-supply conditions and the smoke extraction of the tunnel ventilation system.

(f) Preparation of the final report as well as the "safety documentation" according the EU-Directive with all definitions, descriptions, assessments results, safety and risk analysis results, with recommendation of additional measures (i.e. structural, technical and organizational measures) and further proposals for improvement of safety and minimization of risks.

3.1 *Qualitative analysis of hazards and risks*

Basically fires in the tunnels are rare. Table 1 gives typical values for vehicles fires per 100 million kilometers (according to CETU 2003).

The minimum value is valid for motorway tunnels and/or municipal motorway tunnel without any specific gradient of access roads. The maximum value is valid for the sections with high longitudinal gradient and turnings or for state roads. The ratio of special cases is valid for tunnels with difficult access roads. So-called "fires not under control" represent such cases when the drivers were not able to extinguish the fire, thus the vehicle and the load was completely destroyed.

Table 2. Vehicle fires after collisions.

	Motorways	State roads
Motor cars	0.007	0.2
Trucks/buses	0.05	4.5
Vehicles transporting hazardous goods	0.5	1.5

Table 3. The most important hazards for persons and environment.

Hazard indicator	Hazard	Cause
Inhabitants (road users, other inhabitants)	Mechanical hazard	Collision, crash, stay in the tunnel
	Danger of fire or explosion	Fire, explosion after accident, technical defect
	Contact with chemical and substances dangerous to life	Leakage of chemicals, smoke after collision, technical defect or fire
Environment: Ground water/ Surface water	Pollution due to leakage of chemicals	Leakage of dangerous substances after collision, technical defect or fire

Only a small number of vehicle fires in the tunnels were primarily caused by a collision (only one vehicle fire out of ca. 30). Table 2 shows the values for fires in the tunnels after collisions for different types of roads (value for 100 million kilometers, CETU 2003).

Based on the CETU values the following fire frequency rates are valid for the Branisko tunnel for traffic frequency 6 000 vehicles per day and a length of 4 975 m:

- Motor cars: 0.7626675×10^{-3}/year.
- Trucks/buses: 5.447625×10^{-3}/year.
- Vehicles transporting hazardous goods (ADR): Transport of hazardous goods is not allowed.

As a part of analysis there are defined relevant hazard scenarios based on the potential hazard assessment. They are to be incorporated into the concept safety documentation/safety management of motorways in Slovakia. Subsequently the most important hazards and risks were determined.

The most important hazards for persons (road users, personnel or inhabitants) and environment adjacent to the D1 Motorway in the Branisko tunnel area are stated in Table 3.

Based on the CETU 2003 methodology the following significant trigger reactions were determined for

the Branisko tunnel (road tunnel with allowed passage of trucks, however, not allowed transport of hazardous goods):

(a) Truck fire (e.g. 20 MW) -> B1
(b) Truck fire transporting liquids or slightly liquefied substances with high heating power (e.g. 100 MW) -> B2

3.2 *Hazard and risk assessment*

The frequency of dangerous events occurrence is displayed in Table 4 (see CETU 2003 for categories) and the extent of the damage is shown in Table 5.

Qualitative risk categories as to the acceptability of risk:

– Unacceptable risk: must be excluded.
– Undesired risk: can be accepted if reduction of risk rate is not practically feasible and the approval by a competent safety authority has been submitted.
– Tolerable risk: accepted subsequent to control and approval by the tunnel administrator.
– Acceptable risk: acceptable without any further approvals by the tunnel administrator.

Subsequently the risks have been evaluated as to the risk acceptance.

Based on the above risk assessment it is possible to scale serious events such as a truck fire (B1) and a fire of a truck with big heating capacity (B2) as follows:

a) B1: C (occasional occurrence) – III (critical extent) = undesired (risk category);
b) B2: D (infrequent occurrence) – IV (serious extent) = undesired (risk category).

The risk for both fire scenarios is considered as undesired based on the proposed system. Therefore it is necessary to implement such measures in order to minimize the risks and the risk is to be monitored (periodic review and evaluation by the safety management).

Table 4. Frequency of dangerous events occurrence.

	Category	Definition	Frequency per km of tunnel/year
A	Very frequent	Very frequent occurrence	>0.1
B	Frequent	Frequent occurrence	0.1–0.01
C	Occasionally	Occasional occurrence	0.01–0.001
D	Infrequent	Infrequent occurrence	0.001–0.0001
E	Very infrequent	Very infrequent occurrence	0.0001–0.00001
F	Unlikely	Occurrence is unlikely but possible	<0.00001

Table 5. Extent of damages.

	Category	Definition	Quantity
I	Insignificant or zero	Material damage, minor injuries only, no death cases	0 dead, a few minor injured
II	Significant	A single death case and/or serious injury	0–1 dead, <5 injured
III	Critical	Several death cases and/or several injuries	2–10 dead, 5–10 injured
IV	Serious	Numerous death cases and numerous injuries	10–50 dead, 10–20 injured
V	Catastrophe	Great many death cases and injuries	>50 dead, >20 injured

3.3 *Quantitative risk analysis with QRAM*

3.3.1 *Introduction*

The OECD methodology was used for personal risk quantification using the software tool QRAM. Thus it is possible to determine individual risks for users due to the transport of dangerous goods (based on model scenarios) in tunnels and in the open route (risk cumulative curve). In addition it is possible to calculate two purely fire scenarios (for 20 MW and 100 MW fire). The individual risk for people is documented in the risk cumulative curves (F-N curves, frequency/fatalities). Environmental risks cannot be analyzed with QRAM.

It is to be emphasized that the QRAM software has been developed to mutually compare the risks of various alternative routes (including tunnels) for the transport of dangerous goods. The model has not been designed for assessment of specific measures to be taken for risk reduction. In the present risk analysis the QRAM version 3.5.1. was used. The QRAM model is partially restricted as to the simulation of certain parameters optimally. Ventilation parameters, for example, have a relatively considerable impact on the results of the model. Based on the hitherto experience with simulations using QRAM (for Swiss tunnels) the results for traffic roads seem correct and acceptable.

3.3.2 *Individual risk quantification for the Branisko tunnel*

The average daily traffic frequency rate in the tunnel is 6 000 vehicles per day, out of which 25% are trucks. The following crisis situations were used for QRAM analysis:

- Perfect fire scenarios:
  – 20 MW fire,
  – 100 MW fire.

- Despite the fact that the transport of dangerous goods is not allowed in the Branisko tunnel at present, three scenarios for dangerous goods were calculated:
  – Fire (pool fire),
  – Explosion (BLEVE propane),
  – Leakage of dangerous gas (e.g. ammoniac).

Calculations of the scenarios with dangerous goods were based on the distribution of ADR classes according to the "Handbook III, Transport routes" of the Swiss ordination "Protection against major accidents" for the transport of dangerous goods (DG).

The diagram in Figure 4 shows the cumulative curve of the fire scenario risks (20 MW and 100 MW fire) in the Branisko tunnel (probability per 100 m of a reference section in one year).

Figure 4 gives risk assessment criteria from Switzerland and Austria. Limit 1 represents the limit of acceptance; limit 2 represents the limit of insignificancy. It is obvious that considerably stricter risk criteria apply in Switzerland.

A 20 MW fire does not mean any substantial hazard according to the QRAM calculations; therefore it is not displayed in the diagram. The ventilation simulation for the Branisko tunnel showed that a 30 MW fire is normally (no pressure differences between the portals) without any problems. A 100 MW fire in the tunnel can be fatal (more than 15 death victims), e.g. the Gotthard tunnel fire (October 2001). Such fire, based on a high frequency rate, represents a considerable potential risk. If compared with the Swiss regulations such risk is not acceptable. If compared with the Austrian regulations the measures are to be inspected.

The transport of dangerous goods is not allowed in the Branisko tunnel. For the sake of completeness three other scenarios for the transport of dangerous goods in the Branisko tunnel were modelled.

The diagram in Figure 5 shows the cumulative risk curve for the scenarios with dangerous goods in the Branisko tunnel, apart from the Swiss and Austrian risk assessment criteria (limit 1 represents the limit of acceptance and limit 2 represents the limit of insignificancy).

Figure 5 shows the cumulative curves of risks of the respective crisis situations with dangerous goods and also the total cumulative curve of risks for the Branisko tunnel. The quantitative risk analysis clearly proves that when transporting dangerous goods the collective personal risk curve (total cumulative risk curve) for the current ventilation system does not fall within the acceptable scope of the Swiss assessment criteria for the Ordination "Protection against major accidents" (OPMA). Similarly it does not fall within ALARP scope of the Austrian assessment criteria.

The location of the overall cumulative curve of risks is dominant as to the "pool fire" scenario: it clearly expresses that for the current traffic frequency rate and for the current ventilation system such a situation constitutes a great risk. The tunnel user in case of a fire has a restricted chance of escaping to the protected or safe area in time. A high number of death victims is to be assumed. The previous modelling of a 100 MW fire without any transport of dangerous goods came to similar conclusion. The cumulative curve of a crisis situation when considering an explosion shows a high number (up to 60) fatalities and it passes through a transitory area according to the Swiss ordination. In such situation there is no chance to escape (short time factor).

The cumulative risk curve points to the fact that the Branisko tunnel is not without fault when assessing personal risk. Most significantly, the ventilation system based on the cumulative risk curves of a 100 MW fire (e.g. truck fire with high fire power without any transport dangerous goods involved) and a pool fire (in case of DG scenarios to be considered) has negative effects on fire scenarios.

In this regard it is also very important to implement recommendations as to the rescue planning and (operational) rescue plans.

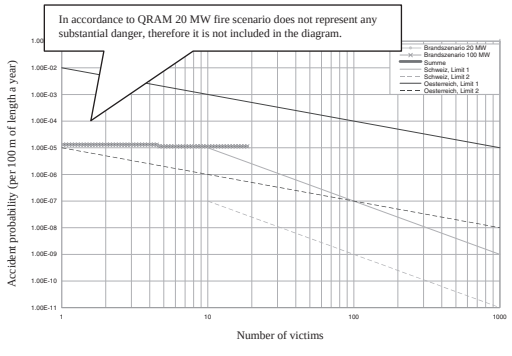


Figure 4. F-N curves of fire scenarios without DG for the Branisko tunnel.

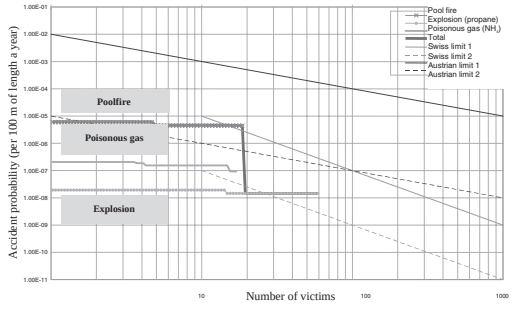


Figure 5. F-N curves of dangerous goods scenarios for the Branisko tunnel.

QRAM modelling demonstrated that the 100 MW fire scenarios and those of pool fire with dangerous goods show similar F-N curves results.

Safety measures are designed to remove a high potential risk in case of major fire events. In particular in case of fires with high radiation (more than ca. 100 MW) the insufficient output of exhaust fans has a negative impact on the cumulative curves of risks for fire scenarios.

3.4 *Level of measures assessment*

A system of assessing the level of the existing safety measures (level of safety measures) with reference to the safety technology condition (STC) has been proposed, using four categories:

1. Very good level of safety measures + STC fully attained (fully-fledged/total conformity with the EU Directive or with the practice of other states).
2. Good level of safety measures + STC partially but prevailingly attained (partial conformity with the EU Directive or partial conformity with practice of other states).
3. Critical level of safety measures + STC prevailingly not attained (low conformity with the EU Directive or only partial conformity with practice of other states).
4. Bad level of safety measures + STC not attained (no conformity with the EU Directive or no conformity with practice of other states).

Additionaly the real conditions and effectiveness of safety measures regarding risk relevance were assessed too and additional measures were recommended for the relevant issues regarding infrastructure (construction, technology equipment) and tunnel operation.

4 CONCLUSION

The Branisko tunnel risk analysis has been the first risk analysis prepared for a Slovak road or railway tunnel. It contains a suitable methodology to be used in Slovakia in the future.

The Branisko tunnel risk analysis showed that the tunnel in general represents minor risks. However is has to be pointed out that the current ventilation system is insufficient for adequate safety conditions for all operational regimes of the tunnel. This is due to its exhaust capacity in case of a fire. If the above deficiency is removed and some other minor measures are put into operation the Branisko tunnel shall fully comply with the up-to-date safety requirements.

REFERENCES

AIPCR / PIARC (C5) 1999. Fire and Smoke Control in Road Tunnels. World Road Association.

Bundesamt für Strassen ASTRA 2000. Tunnel Task Force.

Bundesamt für Strassen ASTRA 2004. Richtlinie Lüftung der Strassentunnel, Systemwahl, Dimensionierung und Ausstat-tung. Tunnel & Elektromechanik.

Bundesamt für Strassen ASTRA 2004. Richtlinie Branddetektion. Tunnel & Elektromechanik.

Bundesamt für Strassen ASTRA 2003. Richtlinie Verkehrs-fernsehen. Tunnel & Elektromechanik.

Bundesamt für Strassen ASTRA 2003. Richtlinie Funsysteme in Tunnels, Tunnel & Elektromechanik.

Bundesamt für Strassen ASTRA 2003. Richtlinie Signalisation der Sicherheitseinrichtungen.

Bundesamt für Strassen ASTRA 2002. Richtlinie Normalprofile, Rastplätze und Raststätten der Nationalstrassen.

Bundesamt für Strassen ASTRA 1999. Richtlinie Projektierung und Ausführung von Kunstbauten der Nationalstrassen.

Bundesamt für Strassen ASTRA 1998. Richtlinie Überwa-chung und Unterhalt der Kunstbauten der Nationalstrassen.

Bundesamt für Strassen ASTRA / BUWAL 2002. Richtlinien Nationalstrassen, Sicherheitsmassnahmen gemäss Störfallverordnung bei Nationalstrassen.

BUWAL 2001. Richtlinien, Beurteilungskriterien zur Störfall-verordnung StFV.

BUWAL 1992. Handbuch III zur Störfallverordnung StFV, Richtlinien für Verkehrswege.

CETU (Centre d'Etudes des Tunnels) 2003. Guide des dossiers de sécurité des tunnels routiers, Fascicule 4, Les études spécifique des dangers (ESD).

EUREKA Forschungsprojekt EU 499. Brände in Verkehrstunneln, Studiengesellschaft Stahlanwendung e.V., 1998.

EU 2004. Richtlinie 2004/54/EG des europäischen Parlements und des Rates vom 29. April 2004 über Mindestanforderungen an die Sicherheit von Tunneln im transeuropäischen Strassennetz.

Khoury, G.A., Both, C. (Kees) 2003: Fire Safety in Tunnels, *Fire & Rescue*.

OECD / PIARC 2001. Highlights: Safety in Tunnels, Transport of dangerous goods through tunnels.

OECD / PIARC 2001. Transport: Safety in Tunnels, Transport of dangerous goods through tunnels.

RABT 2003. Richtlinien für die Ausstattung und den Betrieb von Strassentunneln, Forschungsgesellschaft für Strassen- und Verkehrswesen, Arbeitsgruppe Verkehrsführung und Verkehrssicherheit.

Underground Space – the 4th Dimension of Metropolises – Barták, Hrdina, Romancov & Zlámal (eds)
© 2007 Taylor & Francis Group, London, ISBN 978-0-415-40807-3

ITA-Committee on operational safety of underground facilities – COSUF: Role and objectives

A. Haack
STUVA e.V., Cologne, Germany; Former President of ITA

ABSTRACT: The tragic tunnel fires of the past years have lead to discussions of experts in Europe and around the world. In many European countries they have caused a complete revision of the national safety guidelines for road and rail tunnels. The European Commission has developed directives concerning the minimum safety equipment of road tunnels as well as of railway tunnels. This action is supplemented by intensive domestic and international research activities. The Second International Symposium on Safe & Reliable Tunnels gives special focus on the objectives and important findings of this most recent research programme. The two projects UPTUN and SafeT being just in their final stage form together with COSUF – the ITA Committee on Operational Safety of Underground Facilities the main topic. The Committee is joining 8 research and network projects launched within the 5th and 6th Research Programme of the EU. It is aiming at a world-wide exchange of views, ideas and experience in the field of safety and security regarding traffic tunnels and other underground facilities.

1 INTRODUCTION

Fires in transport tunnels can cause catastrophic disasters. The accidents in the French/Italian Mont Blanc Tunnel (March 24, 1999), in the Austrian Tauern Tunnel (May 29, 1999), in the Swiss Gotthard Tunnel (October 24, 2001; Fig. 1), in the subway system in Daegu/South Korea (February 18, 2003; Fig. 2), in the Swiss Baregg Tunnel (April 14, 2004), in the French Fréjus Tunnel (June 4, 2005; Fig. 3) and most recently in the Swiss Via-Mala-Tunnel (September 16, 2006) have made this more than clear. The detailed analysis of the cause and progression of these fires have yielded new insights that had not been expected or calculated to this extent before. The only comparable experience before has been the fire in the Nihonzaka Tunnel in Japan of 1979, which involved a total of 189 vehicles.

One insight pertains to the extremely rapid development of truck fires with an enormous rise in temperature of up to 1000 degrees Celsius and above. Experience has also shown that large amounts of fire gases are released within a short time, starting in a very early phase of the fire development.

The fire in the Mont Blanc Tunnel also showed that heated gases are capable of setting other vehicles on fire even at distances of 200 meter and more with no vehicle in between. The third and especially frightening aspect is the behaviour of the tunnel users. Too many of them did not recognize the danger they were exposed to. When they finally realized what was happening, it was frequently too late for a successful escape. In the context of subway fires, the example of Daegu also showed how crucial the impact of railcar engineering and equipment, operational organization and safety training of train conductors and station managers can be. Severe shortcomings in these criteria were a crucial factor in the tragic outcome with 196 fatalities.



Figure 1. Burning lorries in the Gotthard Tunnel (Switzerland) on 24.10.2001.



Figure 2. Arson attack in the subway of Daegu/South Korea on 18.2.2003.



Figure 3. Fire accident in the Fréjus Tunnel (France) on 4.6.2005.

2 SAFETY RELATED EUROPEAN RESEARCH

In consequence of the devastating fire accidents the European Commission issued in April 2004 directives regarding the minimum fire prevention equipment of road and rail tunnels. In addition, a number of important research projects were initiated. These are seven multinational projects that have already been awarded and funded in conjunction with the fifth and one project with the sixth Research Framework Programme of the EU briefly described by Haack in 2005 and as follows. They are more or less linked with each other as well as with national projects like a puzzle.

- **DARTS** (**D**urable **A**nd **R**eliable **T**unnel **S**tructures) started in March 2001 and ended in early 2004. The initiative included eight European partners and was structured into six technical work packages. It was primarily dedicated to the problem of exceeded cost during the construction of underground transport facilities. Furthermore, the quality and lifetime of tunnels as the most cost-intensive component of the entire traffic infrastructure was to be improved. For more information see www.dartsproject.net.
- **FIT** (**F**ire **I**n **T**unnels) was established in March 2001 and limited to four years. This "thematic network" included 33 partners from twelve European countries. The project was to gather information from all over Europe and around the world about existing research results and general experiences with fire prevention and mitigation in transport tunnel facilities. For further details visit: www.etnfit.net.
- **UPTUN** (Cost-effective, sustainable and innovative **UP**grading methods for fire safety in existing **TUN**nels) is a RTD project, running from 2002–2006. UPTUN is being performed by 42 partners from 18 European countries. UPTUN comprises research work of approx. 950 man months. Detailed information on UPTUN and its partners can be found at www.uptun.net.
- **Safe Tunnel (Safe**ty in Road **Tunnel**s) began in September 2001 and was designed for a project term of three years. The project involved nine partners. The main focus was to reduce the extent and number of fire accidents in road tunnels. The web address of this project is: www.crfproject-eu.org.
- **SIRTAKI (S**afety **I**mprovement in **R**oad& Rail **T**unnels using **A**dvanced Information Technologies and **K**nowledge **I**ntensive Decision Support Models) was initiated in September 2001 for a term of three years. The initiative was shared by twelve European partners. The main focus of the project was to reform operative concepts with regard to safety and emergency management. Further details are available at: www.sirtakiproject.com.
- **Virtual Fires** (**Virtual** Real Time Emergency Simulator) was started 2001 for a duration of three years with eight partners from five European countries. The objective was to develop a suitable and practical simulator to train firefighters in confining and fighting fires in tunnels. A computer model is used to create virtual simulations of fires in tunnel situations. For more information visit: www.virtualfires.org.
- **Safe-T** (**Safe**ty in **T**unnels) represents another thematic network with a three-year term that was started in the fall of 2003. The primary objective is

to harmonize the European requirements regarding tunnel safety. Experiences gathered at the national level are to be compiled and assessed in such regulations. Given the background of the negative experience with the former operative concept of the Mont Blanc Tunnel, special emphasis will be on cross-border operative concepts. The experience of regional authorities, firefighters and emergency rescue services are of special importance for this project. Further details are available from the website at: www.safetunnel.net.

– L-SURF (Design study for a Large Scale Underground Research Facility on Safety and Security) as a research project on safety and security in enclosed underground spaces is of outstanding importance as most recent incidents (tunnel fires, terror attacks in metros etc) have shown. However currently the competence related to safety and security in Europe is largely unstructured, fragmented and mostly national oriented. Especially missing is a large scale research facility. For more details see www.L-Surf.org.

3 STEP INTO FUTURE

These eight projects mentioned before came to the conclusion that their joint capacity and the momentum gained by the intensive research work conducted during the last couple of years present a great chance for an ongoing future research work and global exchange of knowledge. They therefore looked for a worldwide well reputed international umbrella organisation which could offer a basis for coming activities to develop a better safety level for all kinds of underground facilities. ITA – the International Tunnelling Association – with its 53 member nations worldwide was ready to play that role in close cooperation with PIARC – the World Road Association. Finally the eight projects came to an agreement with ITA and established the ITA **C**ommittee on **O**perational **S**afety of **U**nderground **F**acilities (COSUF; Fig. 4). This committee was installed in May 2005 at the occasion of the ITA World Tunnel Congress 2005 in Istanbul, Turkey. Although starting from the 8 European projects listed above COSUF is open for all institutions, companies, consultancies, governmental organisations etc. world-wide which are active and interested in the field of safety and security regarding underground facilities.

4 SCOPE AND OBJECTIVES

The scope of COSUF concerns safety in tunnels and other underground facilities. It is limited to safety in operation and not during construction This subject is covered by ITA Working Group No. 5: “Health and Safety”. Security will also be covered and is considered as part of safety.

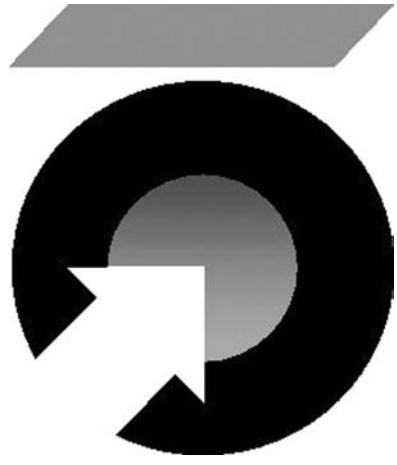


Figure 4. Logo of COSUF.

Within this scope the following objectives as basis for all the future activities of COSUF are defined:

– maintain and develop a network to:
  - exchange knowledge
  - encourage collaboration
  - facilitate the creation of dedicated teams and groups to perform specific (research) activities
– facilitate cooperation worldwide
– enhance research and development activities through combining of national, European and international funding and promoting support
– promote safety (and security) by:
  - fostering innovation
  - raising awareness of current and newly developed safety (and security) issues amongst decision makers, professional end-users, financers, risk managers, international forums and other stakeholders
– supporting the development of improved regulations

5 ACTIVITIES AND BASIC STRUCTURE

Considering the aforementioned objectives COSUF will follow the below listed activities as described by Haack in 2006. The list gives examples but does not claim to be complete. In detail the activities will include:

– networking and coordination meetings, at least once a year, possibly linked with other events
– to take part in international standardisation

– actions towards focussing international research programmes to include tunnel and underground safety (and security), e.g. in the EU framework programmes, European Technology Platforms or other international activities
– developing and maintaining a website, based on the FIT-website, which will promote its activities and disseminate its findings
– (co-)organising workshops and conferences
– to form groups and ad-hoc task forces inside the Committee to address issues related to the scope of the Committee and its objectives

For conducting the manifold activities COSUF has formed three Activity Groups (AGs):

– *Activity Group 1*: Interaction with European and international initiatives; coordinated by Ben van den Horn, Rijkswaterstaat, The Netherlands
– *Activity Group 2*: Regulations and best practice; coordinated by Dr. Marc Tesson, CETU -Centre d'Etudes des Tunnels, France
– *Activity Group 3*: Research and new findings; coordinated by Prof. Dr.-Ing. Markus Thewes, Ruhr University of Bochum, Institute for Tunnelling, Pipeline Technology and Construction Management, Germany

These AGs are described to more details further down. They generally aim at collection of information, creation of syntheses and recommendations, dissemination of information, identification of current and future needs for research and development giving direction as well as specific initiatives, and other related activities.

The AGs themselves do not carry out studies, research or similar activities of commercial value which could be done by institutes or companies. Instead of that they should develop to be centers of excellence for exchange of information and know-how with regard to safety and security of tunnels and other underground facilities.

The general objectives of the AGs are:

– sufficient safety and security for tunnel users, employees and rescue personnel
– cost efficient solutions for safety and security
– a strive for optimality taking into consideration life-cycle cost and socio-economy and societal demands
– improvements of tunnel safety and security by fostering innovation and with a vision of future possibilities and needs

The three AGs must interact to avoid duplication in their work. Thus their activities have to be coordinated by the SB. The AGs will establish task groups and ad-hoc groups which shall deal with specified sub-items.

The Activity Groups are controlled and receive advice in a strategical and political sense by the Steering Board (SB) of COSUF, which consists of representatives from the 8 research projects. The SB is chaired by a chairman as representative of ITA – the International Tunnelling Association and a vice chairman as representative of PIARC – the World Road Association. Both are responsible to the annual General Assembly of ITA.

6 WORK PROGRAMME OF THE ACTIVITY GROUPS

6.1 *Activity Group 1: Interaction with European and international initiatives*

AG 1 will take and keep contact with other external institutions, groups and projects in order to receive relevant information, to co-operate for avoiding duplication of activities, to give information about activities in COSUF to external groups and possibly influence the initiatives.

The relevant external groups and initiatives can include for example:

– European Construction Technology Platform, Focus Area Underground Construction (as far as COSUF is concerned)
– European Technology Platform on Industrial Safety "ETPIS"
– other international committees like: ACUUS, ISO, ISTT, ITP, PIARC, fib, RILEM, UIC etc.
– national or international organisations funding research
– existing and completed European research projects others than the projects founding COSUF, for example EuroTAP and TUNCONSTRUCT
– other research, commercial, national or international projects
– testing programmes
– large construction projects
– other relevant initiatives, groups or similar

The areas considered in Activity Group 1 are complementing those mentioned below for Activity Groups 2 and 3. The activities in Activity Group 1 consist e.g. of:

– identifying relevant initiatives outside COSUF
– attracting COSUF members from the initiatives or appoint liaison responsible COSUF members
– liaison with initiatives outside COSUF
– reporting to Activity Groups 2 and 3 about the results and findings of activities outside COSUF
– reporting transparently to relevant external groups and initiatives about the ideas and results of COSUF
– ensuring that safety and security is given proper priority in initiatives concerning underground facilities
– influencing initiatives to include safety and security aspects in line with the ideas of COSUF

– bringing COSUF ideas to life as projects either as part of existing initiatives or as new separate projects

Participants should come from the 8 projects, but should also be representatives from projects, committees, groups, and institutions outside of COSUF. If not otherwise possible a COSUF member could be appointed to be the liaison officer for those projects.

6.2 *Activity Group 2: Regulations and best practice*

AG 2 will cover regulations, the state-of-the-art and best-practices in various countries world-wide. The state-of-the-art can monitor the current practice and experience with various design methods for different tunnel systems. This includes discussion and comparison of regulations and best-practice procedures from different owners, networks, projects and the experience gained by them.

By doing this it is aimed to collect and distribute information on existing national and international regulations and recognised recommendations as well as to establish the best-practice for tunnel safety (and security). As a result it can be identified that

– there is a need of improvement or harmonisation considering regulations in different countries, between networks, between different projects etc.
– the regulations are not up-to-date compared with the recent activities and achievements in practice
– state-of-the-art or state of practice is deviating significantly from region to region, from industry to industry or from institution to institution.

The findings can result in requirements for new regulations; they can also contribute to disseminate the knowledge from region to region or from industry to industry, from institution to institution and identify areas for which new research is needed.

Ideally the work in this Activity Group is part of establishing a global state-of-the-art for tunnel safety (and security) and the regulatory tools to control that an adequate safety (and security) level is achieved.

All underground facilities are covered by these activities. This includes underground facilities for transportation like road, rail and metro tunnels, as well as underground facilities such as underground shopping malls, underground stations, places for other purposes e.g. for concerts, sports, exhibitions, production facilities, underground technical facilities, etc. For these areas there might be a need for establishing the best practices and the necessary up-to-date regulation.

The activities should cover all safety related aspects such as (at least):

– safety objectives
– basic methods of technical approach (prescriptive and performance-based approaches)
– protection of the structure
– methods for risk assessment
– safety systems and equipment
– interaction with human behaviour
– operation and maintenance
– intervention

These above-mentioned activities may be distinguished for the different types of underground facilities (road, rail, metro and other underground use) or may be considered together. For all activities it will be relevant to discuss both the side of best-practice and the side of regulations and to compare the two sides.

The area of security may be highlighted specifically, since there may be a need for establishing the state-of-the-art also in this field. Security deviates from safety particularly with respect to the prevention, whereas the reaction consequence side may be similar to those which are resulting from evaluation and analysis of accidents or so. These prevention activities will involve regulations of control, enforcement, and similar.

The participants will be mainly engineers, scientists, fire brigades, rescue teams, and other professionals with experience concerning safety in design, operation and rescue in various areas related to underground facilities. For security the professionals may include the police. Public servants and others involved (on project, regional, national, supranational (EU) and international basis) in developing and reinforcing regulations can significantly contribute to these activities. Also researchers and other professionals with knowledge of the most recent achievements and findings may contribute to the identification of needs and demands for the design process and its regulation.

The participants should also include representatives from Activity Group 1 and of current research projects, committees, organisations involved in developing and studying tunnel safety and security.

6.3 *Activity Group 3: Research and new findings*

The scope of AG 3 is to motivate to research and to use research results and other new findings for the benefit of safety (and security) in underground facilities in general. The activities include.

– collection of results of research and collection of new findings
– evaluation of events, results and new findings
– dissemination of the results and new findings among COSUF members
– synthesis of results and new findings into best practices (in collaboration with AG 2)
– collection and evaluation of ideas for research
– identify needs for the future and give directions for future research

The actual launch of new research projects is initiated outside COSUF by liaison through AG 1.

The aim is to make aware all relevant professionals of new findings and recent results of research in the safety and security related activities regarding underground facilities, to discuss these results and other ideas and to process them into specifications of needs of new research into recommended best practices.

In order to fulfil these aims it is necessary to:

- identify safety (and security) related activities for underground facilities
- identify relevant research activities and their results
- identify relevant new findings
- process into best practices (in cooperation with AG 2)
- evaluate the results and the findings
- receive and develop ideas for research
- communicate the results and findings
- identify new needs and requirements for research
- outline the basis of new ideas for research
- liaise with Activity Group 1 for the launching of projects outside COSUF

The sub-items considered cover all safety (and security) related activities. These areas could include the following, but the list may be modified and extended during the work, depending on the available information and the interests and qualification of the members of AG 3:

- new/innovative equipment in tunnels and new materials
- processes, analyses and design procedures integrated design procedures, risk analyses as part of the design, fire design techniques etc.
- IT tools in the tunnel design and operation
- test programmes using standardised techniques
- operation and maintenance monitoring
- safe intervention, evacuation, fire fighting etc.
  planning
  training
  simulation
- interface tunnel, users, operators and rescue services (human behaviour etc.)
- experience from tunnel incidents, accidents and near misses
- tunnel safety related data collection
- specific security related problems for underground facilities

For research and new findings it may be also relevant to divide into the types of underground facilities: road, rail, metro and other underground use, as mentioned for AG 2.

The possible number of a crosswise combination of items, sub-items, activities and types of facilities is high. The AG will have to organise itself and to prioritise the activities.

The participants in the activities are mainly researchers with activities in the field of safety (and security) of underground facilities and engineers, scientists and other professionals with experience in safety design in various areas related to underground facilities. Furthermore, other professionals involved in design, operation, rescue etc. of tunnels, and particularly the safety (and security) related side of these activities can significantly contribute to the activities. Public institutions and representatives of formulating research and funding institutes would also be highly relevant as participants in the work.

In addition representatives from AG 1 and of current research projects, committees, organisations involved in developing and studying tunnel safety and security outside of COSUF should also become participants of this AG.

7 MEMBERSHIP

COSUF invites all parties world-wide interested in the field of operational safety and security of tunnels and other underground facilities to become member and to co-operate within COSUF. There will be exceptionally corporative members, no individual ones. The membership in COSUF has to be confirmed by the General Assembly of ITA, but is not bound to membership in ITA or vice versa. Of course, a membership in both is possible and welcome.

The annual membership fee will be as follows:

- public organisations and educational institutes: EUR 250
- all others: EUR 500

Interested parties can subscribe membership at the occasion of the 2nd International Symposium Safe & Reliable Tunnels on May 30-31, 2006 in Lausanne, Switzerland or online using the form given on the ITA webpage www.ita-aites.org.

A numerous and wide-ranging membership will certainly help to improve and standardise the safety and security level in traffic tunnels and all other underground facilities.

8 OUTLOOK

The tremendous research efforts of the European Commission described here to improve the safety in traffic tunnels are an essential prerequisite for the highly needed all-European harmonization in this field. Here COSUF forms a platform to continue the activities even after finalising the research projects and in the same time presents a forum for a world-wide exchange of views, ideas and experience in the field of safety and security regarding underground facilities. This appears especially important as tunnels are an indispensable

part of the trans-European traffic network. Given this background, the research activities are delivering a crucial contribution to guarantee the mobility of persons and goods, which represents a high political priority.

REFERENCES

Directive 2004/54/EC of the European Parliament and of the Council, 29. April 2004 on minimum safety requirements for tunnels in the trans-European road network. In: Official Journal of the European Union L 201/56 pp; published 7.6.2004

Directive 2004/49/EC of the European Parliament and of the Council, 29. April 2004 on safety on the Community's railways and amending Council Directive 95/18/EC on the licensing of railway undertakings and Directive 2001/14/EC on the allocation of railway infrastructure capacity and the levying of charges for the use of railway infrastructure and safety certification (Railway Safety Directive). In: Official Journal of the European Union L 164/44 pp; published 30.4.2004

Haack, A. 2005. European Research and Development on Safety in Road Tunnels; 3rd International Congress – Traffic and Safety in Road Tunnels – HBV-Verkehrsconsult, Hamburg, 18–20. May 2005 in Hamburg

Haack, A. 2006. ITA-COSUF Work Programme; Paper presented at 2nd Symposium on Safe & Reliable Tunnels, Innovative European Achievements & ITA – COSUF Inauguration; 29/30.May 2006, Lausanne, CH

This page intentionally left blank

Underground Space – the 4th Dimension of Metropolises – Barták, Hrdina, Romancov & Zlámal (eds)
© 2007 Taylor & Francis Group, London, ISBN 978-0-415-40807-3

Optimisation of road tunnel safety based on risk analysis

M. Holický
Klokner institute, Czech Technical University in Prague, The Czech Republic

J. Smolík
SUBTERA, Ltd., Prague, The Czech Republic

L. Šajtar
SATRA, Ltd., Prague, The Czech Republic

ABSTRACT: Optimisation of operational safety of road tunnels is based on the probabilistic methods of risk analysis taking into account societal and economic consequences and possible safety measures contemplated in design. The total consequences of alternative tunnel arrangements are assessed using Bayesian networks supplemented by decision and utility nodes. It is shown that the optimization of the total consequences may provide valuable information enabling a rational decision concerning effective safety measures. A general procedure is illustrated by the optimization of a number of escape routes considered in design of road tunnels. It appears that the optimum number of escape routes is significantly affected by the discount rate and specified life time of a tunnel. Further investigation of relevant input data including societal and economic consequences of various hazard scenarios is, however, needed.

1 INTRODUCTION

Tunnel structures usually represent complex technical systems that may be exposed to hazard situations leading to unfavourable events with serious consequences. Minimum safety requirements for tunnels in the trans-European road network are provided in the Directive of the European Parliament and of the Council 2004/54/ES. The Directive also gives requirements concerning risk management, risk assessment and analysis.

Methods of risk assessment and analysis are more and more frequently applied in various technical systems (Melchers 1999, Steward & Melchers 1997) including road tunnels. This is a consequence of recent tragic events in various tunnels and of an increasing effort to take into account societal, economic and ecological consequences of unfavourable events (Holicky & Šajtar 2005, 2006). Available national and international documents (NS 5814 1991, CAN/CSA 991, ISO 2394 1998, ISO/IEC Guide 73 2002, ISO/IEC Guide 51 1999, ISO 9000 2000) try to harmonise general methodical principles and terminology that can be also applied in the risk assessment of road tunnels.

The submitted contribution, based on previous studies (Brussaard & Kruiskamp 2004, Ruffin et al. 2005, Vrouwenvelder et al. 2001, Vrouwenvelder & Krom 2004, Kruiskamp et al. 2001, Worm et al. 1998) and recent PIARC working documents, attempts to apply methods of probabilistic risk optimization using Bayesian networks supplemented by decision and utility nodes (Jensen 1996). It appears that Bayesian networks provide an extremely effective tool for investigating the safety of road tunnels.

2 PRINCIPLES OF RISK ASSESSMENT

Risk assessment is an essential part of the risk management as indicated in Figure 1 (based on CAN/CSA 1991). The diagram in Figure 1 indicates the main components of risk management and relevant basic terms. The whole process of risk management includes the risk assessment and risk control. The risk assessment further consists of the risk analysis and risk evaluation. The risk control consists of the risk decision and risk monitoring. Figure 1 also indicates an important part of the whole risk management, i.e. risk communication concerning an unavoidable exchange of data between the risk assessment and risk control. Obviously other types of risk communication may be required in case of the risk management of complex tunnel systems.

The main components of the whole risk management consist of the risk assessment and risk control.

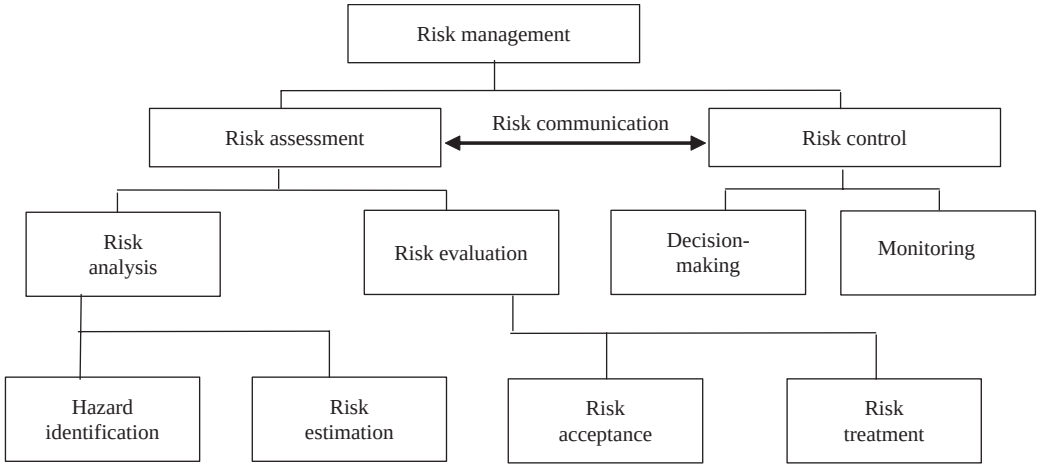


Figure 1. A framework for risk management (adopted from CAN/CSA 1991).

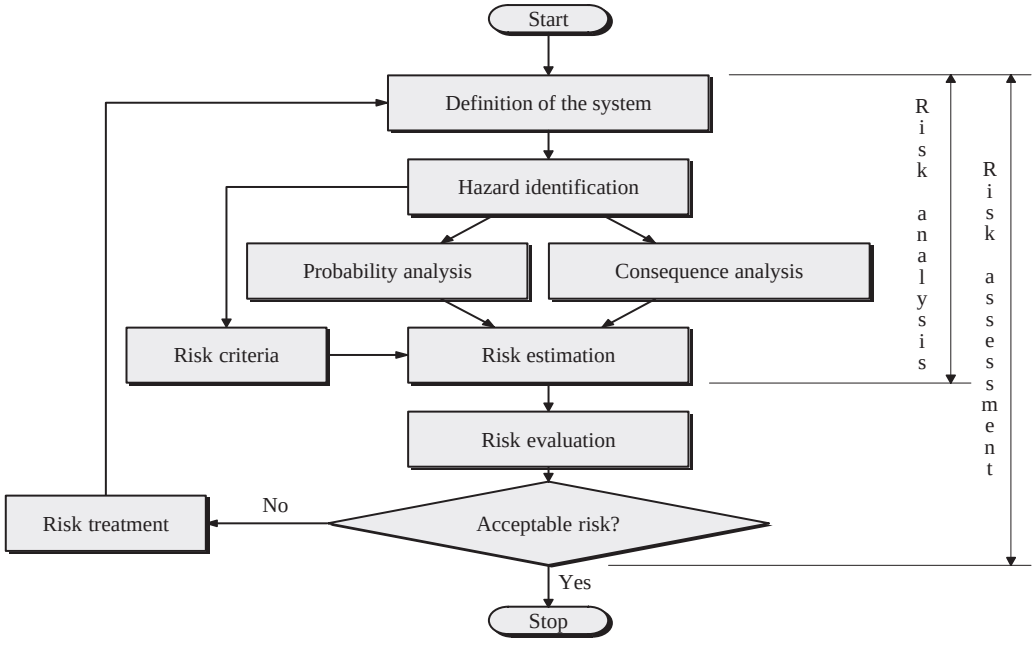


Figure 2. Flowchart of iterative procedure for the risk assessment (adopted from ISO 1999).

The risk control is outside the scope of this paper. A general procedure of risk assessment is shown in Figure 2 indicating the main steps. The flowchart is adopted from ISO 1999 and recent working materials of PIARC/C3.3/WG2. Two key steps of the risk analysis, probability and consequence analysis, and subsequent risk estimation are shortly described below.

3 PROBABILITY ANALYSIS

Probabilistic methods of risk analysis are based on the concept of conditional probabilities $P_{fi} = \mathrm{P}\{F|H_i\}$ of the event F providing a situation H_i occurs (Melchers 1999). In general this probability can be found using statistical data, experience or theoretical analysis of the situation H_i.

If the situation H_i occurs with the probability $P(H_i)$ and the event F during the situation H_i occurs with the probability $P(F|H_i)$, then the total probability P_F of the event F is given as

$$P_F = \sum_i P(F \mid H_i) P(H_i) \tag{1}$$

Equation (1) makes it possible to harmonize partial probabilities $P(F|H_i)$ $P(H_i)$ related to the situation H_i.

The main disadvantage of the purely probabilistic approach is the fact that possible consequences of the events F related to the situation H_i are not considered. Equation (1) can be, however, modified to take the consequences into account.

4 RISK ESTIMATION

A given situation H_i may lead to a set of events E_{ij} (for example fully developed fire, explosion), which may have societal consequences R_{ij} or economic consequences C_{ij}. It is assumed that the consequences R_{ij} and C_{ij} are unambiguously assigned to events E_{ij}. If the consequences include only societal components R_{ij}, then the total expected risk R is given as

$$R = \sum_{ij} R_{ij} P(E_{ij} \mid H_i) P(H_i) \tag{2}$$

If the consequences include only economic consequences C_{ij}, then the total expected consequences C are given as

$$C = \sum_{ij} C_{ij} P(E_{ij} \mid H_i) P(H_i) \tag{3}$$

If criteria R_d and C_d are specified, then acceptable total consequences should satisfy the conditions

$$R < R_d \text{ and } C < C_d \tag{4}$$

that supplement the traditional probabilistic condition $P_f < P_{fd}$.

When the criteria are not satisfied, then it may be possible to apply a procedure of risk treatment as indicated in Figure 2. For example additional escape routes may be provided. Such measures might, however, require considerable costs, which should be considered when deciding about the optimum measures.

5 RISK OPTIMIZATION

The total consequences $C_{tot}(k, p, n)$ relevant to the construction and performance of the tunnel are generally expressed as a function of the decisive parameter k (for example of the number k of escape routes), discount rate p (commonly about $p \approx 0,03$) and life time n (commonly $n = 100$ let). The decisive parameter k usually represents a one-dimensional or multidimensional quantity significantly affecting tunnel safety.

The fundamental model of the total consequences may be written as a sum of partial consequences as

$$C_{tot}(k,p,n) = R(k,p,n) + C_0 + \Delta C(k) \tag{5}$$

In equation (5) $R(k, p, n)$ denotes expected societal risk that is dependent on the parameter k, discount rate p and life time n. C_0 denotes the basic of construction cost independent of k, and $\Delta C(k)$ additional expenses dependent on k. Equation (5) represents, however, only a simplified model that does not reflect all possible expenses including economic consequences of different unfavourable events and maintenance costs.

The societal risk $R(k, p, n)$ may be estimated using the following formulae

$$R(k, p, n) = N(k)\ R_1\ Q(p, n),$$
$$Q(p, n) = \frac{1 - 1/(1+p)^n}{1 - 1/(1+p)} \tag{6}$$

In equation (6) $N(k)$ denotes number of expected fatalities per one year (dependent on k), R_1 denotes acceptable expenses for averting one fatality, and p the discount rate (commonly within the interval from 0 to 5%). The quotient q of the geometric row is given by the fraction $q = 1/(1 + p)$. The discount coefficient $Q(p, n)$ makes it possible to express the actual expenses Z_1 during a considered life time n in current cost considered in (5). In other words, expenses Z_1 in a year i correspond to the current cost $R_1 q^i$. The sum of the expenses during n years is given by the coefficient $Q(p, n)$.

A necessary condition for the minimum of the total consequences (5) is given by the vanishing of the first derivative with respect to k written as

$$\frac{\partial N(k)}{\partial k} R_1 Q(p, n) = -\frac{\partial \Delta C(k)}{\partial k} \tag{7}$$

In some cases this condition may not lead to a practical solution, in particular when the discount rate p is small (a corresponding discount coefficient $Q(p, n)$ is large) and there is a limited number of escape routes k that can not be arbitrary increased.

6 STANDARDIZED CONSEQUENCES

The total consequences given by equation (5) may be in some cases simplified to a dimensionless standardized form and the whole procedure of optimization may be generalized. Consider as an example the optimization of the number k of escape routes. It is assumed that

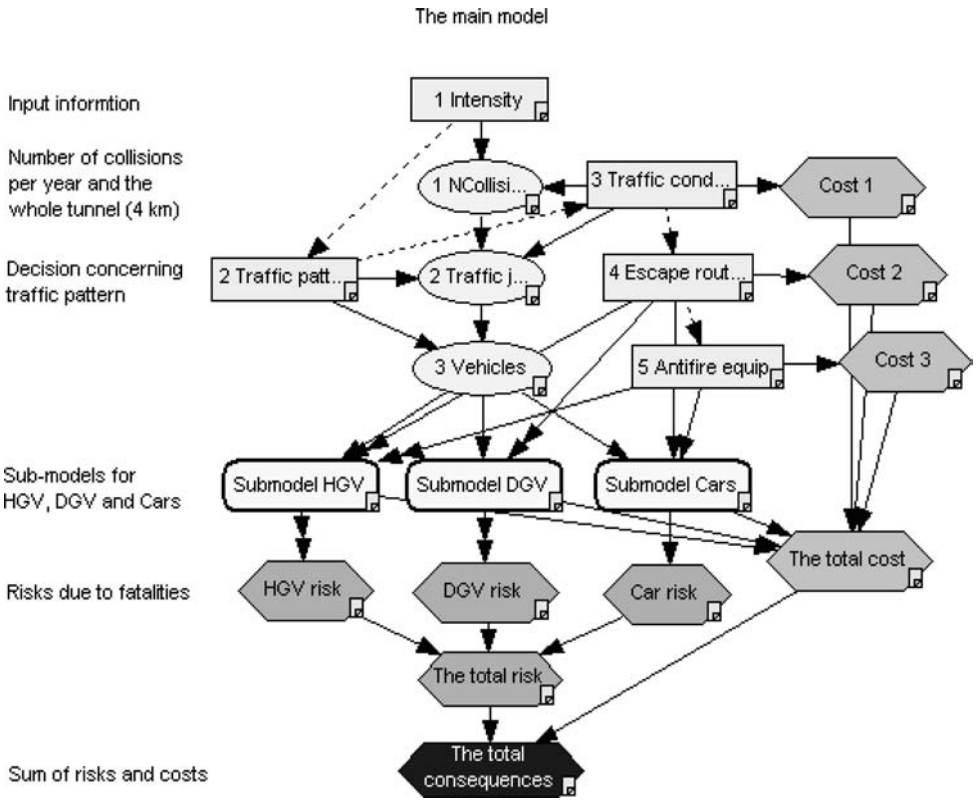


Figure 3. Main model of the tunnel.

involved additional costs $\Delta C(k)$ due to k may be expressed as the product $k\ C_1$, where C_1 denotes cost of one escape route. If C_1 is approximately equal to R_1 (assumed also by Vrouwenfelder & Krom 2004), equation (5) becomes

$$C_{\text{tot}}(k,p,n) = N(k)\ C_1\ Q(p,n) + C_0 + k\ C_1 \tag{8}$$

This function can be standardized as follows

$$\kappa(k,p,n) = \frac{C_{tot}(k,p,n) - C_0}{C_1} = N(k)Q(p,n) + k \tag{9}$$

Both variables $C_{\text{tot}}(k,p,n)$ and $\kappa(k,p,n)$ are mutually dependent and have the extremes (if exist) for the same number of escape routes k. A necessary condition for the extremes follows from (7) as

$$\frac{\partial N(k)}{\partial k} = -\frac{1}{Q(p,n)} = -\frac{1-1/(1+p)}{1-1/(1+p)^n} \tag{10}$$

An advantage of standardized consequences is the fact that it is independent of C_0 and C_1. It is only assumed that $C_1 \approx Z_1$ is a time invariant unit of the total consequences.

7 MODEL OF A TUNNEL

The main model of a road tunnel is indicated in Figure 3. The tunnel considered here is partly adopted from a recent study (Vrouwenfelder & Krom 2004). It is assumed that the tunnel has the length of 4000 m and two traffic lanes in one direction. The traffic consists of heavy goods vehicles HGV, dangerous goods vehicles DGV and Cars.

The total traffic intensity in one direction is 20×10^6 vehicles per year (27 400 vehicles in one lane per day). The number of individual types of vehicles is assumed to be HGV:DGV:Cars = 0,15:0,01:0,84. The frequency of serious accidents assuming basic traffic conditions (that might be modified) is considered as 1×10^{-7} per one vehicle and one km (Vrouwenfelder & Krom 2004), thus 8 accidents in the whole tunnel per year. The Bayesian networks used here need a number of other input data. Some of them are adopted from the study (Vrouwenfelder & Krom 2004) (based on event

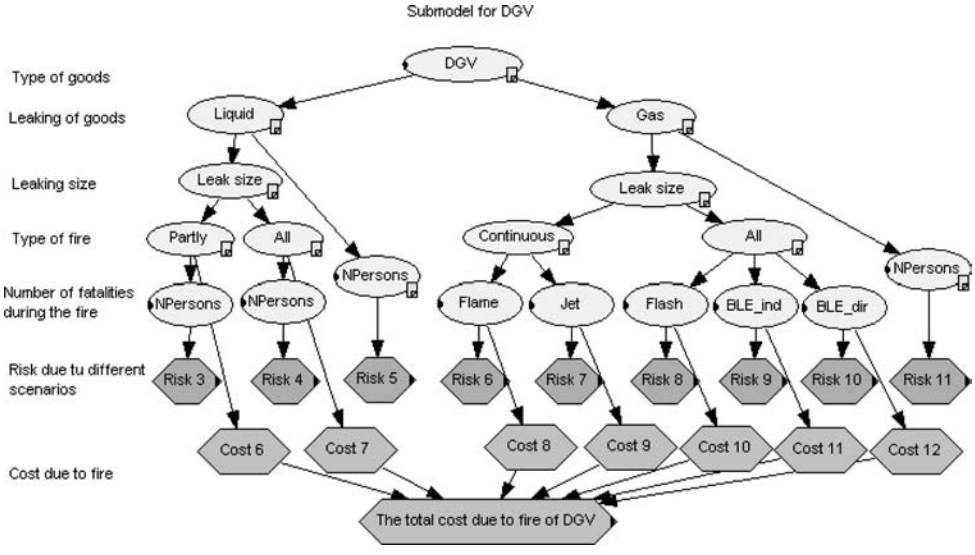


Figure 4. Sub-model for dangers goods vehicles DGV.

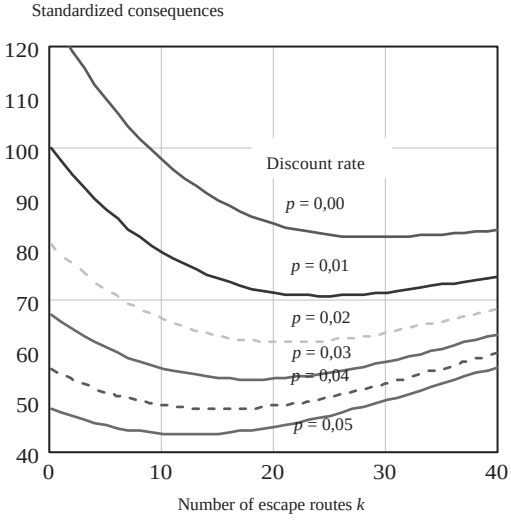


Figure 5. Variation of the standardized total consequences $\kappa(k, p, n)$ with k for selected discount rates p and the life time $n = 50$ years.

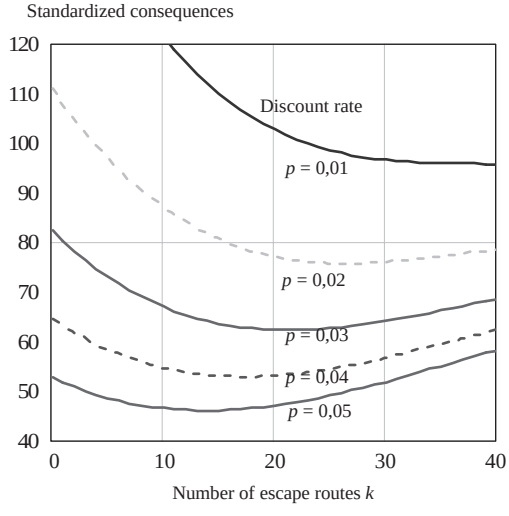


Figure 6. Variation of the standardized total consequences $\kappa(k, p, n)$ with k for selected discount rates p and the life time $n = 100$ years.

tree method), the other are estimated or specified using expert judgement.

The main model includes three sub-models for heavy goods vehicles HGV, dangerous goods vehicles DGV and Cars. Figure 4 shows a sub-model for dangerous goods vehicles DGV. Note that different types of hazard scenarios are distinguished as they may cause different consequences. Similar sub-models are used also for heavy goods vehicles HGV and Cars. Detailed description of the main model, sub-models and required input data is outside the scope of this contribution.

8 RISK OPTIMIZATION

Risk optimization of the above described tunnel is indicated in Figures 5 and 6 showing variation of

the standardized total consequences $\kappa(k, p, n)$, given by equation (9) with number of escape routes k for selected discount rates p (up to 5%) and life time n (=50 and 100 years).

Figure 5 shows the variation of the standardized total consequences $\kappa(k, p, n)$ with k for selected discount rates p and the life time $n = 50$ years only. Figure 6 shows similar curves as Figure 5 but for the expected life time $n = 100$ years (common value).

Figures 5 and 6 clearly illustrate previous finding that the discount rate p affects the total consequences $\kappa(k, p, n)$ more significantly than the number of escape routes k.

9 CONCLUSIONS

Similarly as in case of other technical systems the risk assessment of road tunnels commonly includes

- definition of the system
- hazard identification
- probability and consequences analysis
- risk evaluation and possible risk treatment

Probabilistic risk optimization based on the comparison of societal and economic consequences may provide valuable background information for a rational decision concerning effective safety measures applied to road tunnels. However, as tunnels are commonly design for a long life time (100 years), discount rate must be taken into account. It appears that assumed life time and the discount rate may affect the total consequences and the optimum arrangements of the tunnels more significantly than the number of escape routes.

The following conclusions may be drawn from the submitted study of probabilistic risk optimization of road tunnels using Bayesian networks:

- The optimum number of escape routes may be specified from the requirement of the minimum total consequences covering both the societal and economic aspects.
- The optimum number of escape routes depends generally on discount rate, required life time and the ratio between the cost for one escape route and acceptable expenses that a society is able to afford for averting one fatality (societal compensation cost).
- The total consequences are more significantly affected by the discount rate than by assumed life time, cost ratio and the number of escape routes.
- Bayesian networks supplemented by decision and utility nodes seem to provide an effective tool for risk analysis and optimization.

Correct specification of discount rate and required life time is essential for making proper decisions. Further investigations of input data concerning conditional probabilities describing individual hazard scenarios and models for their societal and economic consequences are needed. In particular cost of various safety measures and acceptable expenses for averting a fatality are required for advanced optimization of road tunnels.

ACKNOWLEDGEMENT

This study is a part of the project GAČR 103/06/1521 "Reliability and Risk Assessment of structures in Extreme Conditions" supported by The Grant Agency of the Czech Republic.

REFERENCES

Brussaard L.A. & Kruiskamp M.M. & Oude Essink M.P. 2004. The Dutch model for the quantitative risk analysis of road tunnels, *Proc. of the ESREL conference, Berlin*.

CAN/CSA-Q634-91, 1991 *Risk analysis requirements and guidelines*.

Directive 2004/54/EC of the European Parliament and of the Council of 29 April 2004 on minimum safety requirements for tunnels in the trans-European road network. *Official Journal of the European Union L 201/56 of 7 June 2004*.

Holický M. & Šajtar L. 2005 Risk Assessment of road tunnels based on Bayesian network. *Proc. of the ESREL conference Advances in Safety and Reliability, Taylor & Francis Group, London*, pp 873–879.

Holický M. & Šajtar L. 2006 Risk Assessment of road tunnels based on Bayesian network. *Proc. of the ESREL 2006 conference on Safety and Reliability for Managing Risk, Estoril, Portugal*, pp.

ISO 2394. 1998. *General principles on reliability for structures*.

ISO/IEC Guide 73. 2002. *Risk management – Vocabulary – Guidelines for use in standards*.

ISO/IEC Guide 51. 1999. *Safety aspects – Guidelines for their inclusion in standards*.

ISO 9000. 2000. *Quality management systems – Fundamentals and vocabulary*.

Jensen Finn.V. 1996. *Introduction to Bayesian networks.* Aalborg University, Denmark.

Knoflacher H. & Pfaffenbichler P.C. 2004. A comparative risk analysis for selected Austrian tunnels, *Proc. of the 2nd International Conference Tunnel Safety and Ventilation*, Graz.

Kruiskamp M.M., Weger D. de & Hoeksma J. TUNprim: A Spreadsheet model for the calculating road tunnels risk, *Tunnels Management International*, Volume 5, Number 1, pp. 6–12, 2002.

Melchers R.E. 1999. *Structural reliability analysis and prediction*. John Wiley&Sons, Chichester, pp 437.

NS 5814. 1991. *Requirements for risk analysis.*

Ruffin E. &. Cassini P. & Knoflacher H. 2005. Transport of hazardous goods, Chapter 17 of Beard A and Carvel R. *The Handbook of Tunnel Fire Safety*. Thomas Telford Ltd, London.

Stewart M.S. & Melchers R.E. 1997. *Probabilistic risk assessment of engineering system*, Chapman & Hall, London, pp 274.

Vrouwenvelder A., Holický M., Tanner C.P., Lovegrove D.R. & Canisius E.G. 2001. *Risk assessment and risk communication in civil engineering*, CIB Report Publication 259.

Vrouwenvelder A.C.W.M. & Krom A.H.M. 'Hazard and the Consequences for Tunnels Structures and Human Life', *Proc. of the 1st International Symposium Safe and Reliable Tunnels in Prague*, CUR, Gouda, The Netherlands, 2004.

Worm, E.W. and Hoeskma, J. 1998. The Westerschelde Tunnel: Development and application of an integrated safety philosophy, *Safety in Road and Rail Tunnels*, 3rd International Conference organized by University of Dundee and ITC Ltd., Nice, France.

This page intentionally left blank

Underground Space – the 4th Dimension of Metropolises – Barták, Hrdina, Romancov & Zlámal (eds)
© 2007 Taylor & Francis Group, London, ISBN 978-0-415-40807-3

Austrian risk analysis for road tunnels development of a new method for the risk assessment of road tunnels

B. Kohl & K. Botschek
ILF Consulting Engineers, Linz, Austria

R. Hörhan
Ministry of Traffic, Engineering and Technology, Vienna, Austria

ABSTRACT: For the Austrian Risk Analysis for Road Tunnels (TuRisMo) a set of different methodical tools are used to analyse the whole system of safety relevant influencing factors; the method consists of two main elements:

- Quantitative frequency analysis: event tree approach for calculating the frequencies of defined accident scenarios
- Quantitative consequence analysis:
  - mechanical accidents: estimation of consequences based on tunnel accident data
  - fire accidents: modelling of consequences by combining a ventilation model with an evacuation simulation model

The risk model covers the personal risks of tunnel users. The result of the risk analysis is the expected value of the societal risk of the tunnel investigated.

Risk evaluation is done by relative comparison of the tunnel investigated to the risk of a reference tunnel (tunnel of the same length, type and traffic characteristic, fully complying with the minimum safety requirements as per EC Directive).

Keywords: Tunnel safety, quantitative risk analysis, risk reducing effects, safety measures.

1 BACKGROUND

In April 2004, the EC Directive on road tunnel safety (Directive 2004/54/EC) was issued. Article 13 of this Directive obliges every member state to develop a method for a risk analysis on a national level. Therefore, the Austrian ministry started a design process to develop a methodology which meets the specific requirements of Austrian Road Tunnels. The work process was coordinated with an expert group of tunnel safety and ventilation experts.

The Austrian Risk Model focuses on frequently occurring mechanical accidents and fire accidents with small and medium sized fires. For a more thorough investigation of accidents involving hazardous goods, the DG-QRA model developed by OECD/PIARC shall be used in Austria.

2 TuRisMo – TUNNEL RISK MODEL FOR ROAD TUNNELS

2.1 *Database of risk analysis*

Due to the great number of tunnels in Austria and the extensive collection of data on accidents, the risk analysis is done based on Austrian data and experiences.

Data were collected from accidents with personal injury in tunnels on motorways and expressways for the years 1999–2003. In addition to Austrian data, foreign data sources are used for comparison and completition.

2.2 *Methodical approach*

2.2.1 *General consideration*

The risk analysis aims to investigate the risk to tunnel users (personal injuries and fatalities); as relevant

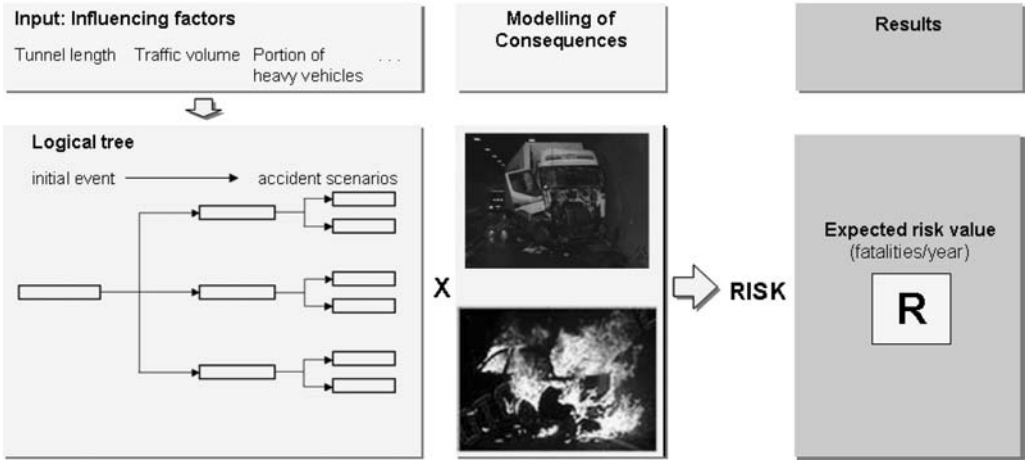


Figure 1. Sequence of risk analysis.

reference value the societal risk (fatalities per year) of the tunnel is calculated.

The methodical approach consists of two basic elements:

– a quantitative frequency analysis (event tree approach) and
– a quantitative consequence analysis (evaluation of statistical accident data for mechanical accidents and modelling of fire accidents)

The sequence of the risk analysis is shown in Figure 1.

2.2.2 *Influencing factors*

The following main influencing factors and their interrelations were identified and taken into account in

– traffic volume
– uni-directional or bi-directional traffic
– additional points of conflicts such as ascending and descending ramps
– dangerous goods (amount and composition – general approach only)
– portion of heavy vehicles (> 3.5 tonnes)
– portion of busses
– tunnel length
– ventilation system
– length of escape route to emergency exits
– operational components (fire detection, etc.)
– longitudinal gradient in tunnel
– longitudinal gradient in front of tunnel
– frequency of traffic jams
– cross section type

2.2.3 *Event tree analysis*

An event tree analysis is performed to calculate the frequency of defined accident scenarios. The event trees distinguish between accidents (with personal injury) and breakdowns. Starting from an initial event leading to a set of damage scenarios, possibly ensuing damage events are developed through the individual branches of the event tree. These damage scenarios differ significantly from each other as regards type of accident, vehicle involvement, involvement of dangerous goods and influence of fire. Taking into account the framework conditions of the tunnel infrastructure (e.g. distance between emergency exits), the extent of damage is estimated for the respective damage scenario.

The level of detail for an event tree is defined in such a way that the available data material can be used appropriately.

The input data of the event tree – accident rates and relative frequencies – are calculated based on an evaluation of data from 81 Austrian motorway tunnels (60 with uni-directional, 21 with bi-directional traffic). The accident rates are modified in dependence of tunnel length and traffic volume.

Table 1. Basic values of accident rates (own evaluation board upon Robatsch et al. 2003).

	Bi-directional tunnel [fat./Imio. vechicle-km]	Uni-directional tunnel [fat./Imio. vehicle-km]
Accident rate in Austrian road tunnels (on motorways)	0,077	0,112

2.2.4 *Consequence analysis*

For each damage scenario in the event tree the corresponding extent of damage is estimated.

– Estimation of extent of damage of mechanical accidents:



Figure 2. Part of event tree the risk analysis.

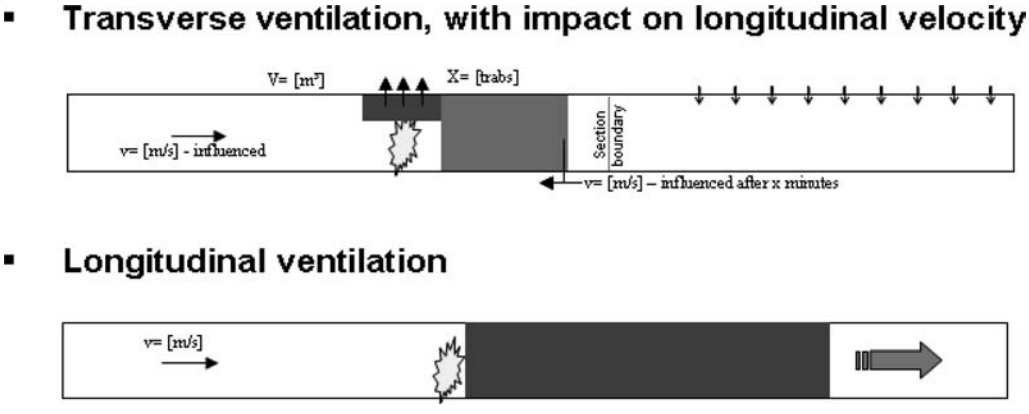


Figure 3. Basic principle of ventilation model.

The damage scenarios differ in terms of type of accident and vehicle involvement. The consequences of each damage scenario are estimated based on an evaluation of accident consequence data of 447 tunnel accidents with personal injuries (same database as for frequency calculation).

– Estimation of extent of damage of accidents involving fire:

The extent of damage of fire is estimated with the support of an evacuation simulation model in combination with a one-dimensional ventilation model.

2.2.4.1 *Ventilation model*

In the ventilation model two different scenarios (5 MW, 30 MW) und two different ventilation regimes can be selected (Fig. 3)

– longitudinal ventilation
– transversal ventilation, with impact on longitudinal air velocity

They are valid for standard situations. However, the model also makes it possible to investigate non-standard ventilation systems and non-standard situations, but this requires more work to compute this data.

The smoke release rates of fires are defined and smoke concentrations in dependence on time and location in the tunnel are calculated. The design of the model allows a detailed investigation of the performance of the ventilation system in combination with the corresponding evacuation procedures.

2.2.4.2 *Evacuation simulation model*

For the evacuation simulation the software package "buildingExodus 4.0" (Galea 2000) is used, which takes into account the effects of smoke gases according to the FED model (FED – Fractional Effective Dose) of Purser [2]. The influence of temperature, HCN, CO, CO_2 and lack of O_2 is included. The calculation is done for individual persons with individual characteristics.

In the evacuation simulation model, the location of the accident in the tunnel, the location of the emergency exits, the constellation of the vehicles on both sides of the accident, the propagation of smoke, the reaction of the people and their evacuation in the tunnel towards an emergency exit (a tunnel portal) are taken into account. This approach makes it possible to

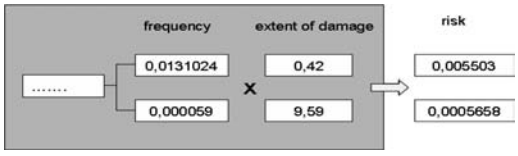


Figure 4. Combination of frequency and extent of damage.

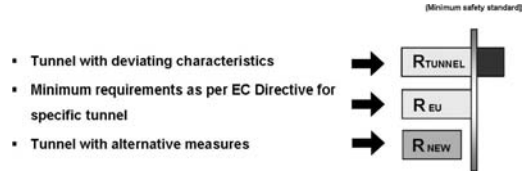


Figure 5. Risk evaluation in accordance with EC Directive (assessment through relative comparison).

investigate all influences, which may effect the lapse of time concerning the interaction of propagation of smoke and self rescue, such as

– fire alarm/start of ventilation
– reaction of people
– walking velocity with/without smoke
– walking distances
– congestion effects, etc.

The results of the evacuation simulation show, depending on the time elapsed, how many persons reach the "safe area" and how many persons are unable to get to safety due to the given framework conditions (length of escape route, start of evacuation, atmospheric conditions).

Based on these results, various accident locations in the tunnel are investigated, and an expected value of the extent of damage for every damage scenario is calculated; this expected value is implemented in the event tree.

This element of the risk model can be used for the consequence assessment of defined fire scenarios (calculating a risk value) as well as for a detailed scenario investigation.

2.2.5 *Risk calculation*

As reference value the expected value of societal risk (fatalities/tunnel and year) is calculated by combining incident frequencies and consequence values for defined scenarios in the event tree; a distinction is made between risks from car accidents with mechanical effects only, from fires and from accidents involving hazardous goods.

2.3 *Results of risk analysis and strategy of risk evaluation*

In Austria no quantitative risk criteria are defined. The EC Directive defines the minimum safety standard of a tunnel by laying down requirements for tunnel design and tunnel equipment in a prescriptive way. But the EC Directive allows limited derogations for these requirements, on the condition that the same safety level can be achieved by alternative risk reduction measures. For this reason risk evaluation is done by relative comparison of the risk of the tunnel investigated with the risk of a reference tunnel. A tunnel of the same length, type and traffic characteristic, fully complying with the minimum safety requirements as per EC Directive, is used as reference case. The identified divergences can be assessed in terms of risk. Alternative measures to offset the divergences can be evaluated; the risk reducing effects of the different safety measures can be investigated in a similar way. The safety assessment of safety measures can be completed by a cost-effectiveness analysis.

3 EXPERIENCE IN PRACTICAL APPLICATION

3.1 *Case study*

Design and equipment of an existing tunnel are in line with the requirements of the EC-Directive, only the share of heavy goods vehicles exceeds the reference value of 15%; according to Annex I, article 1.3.2 the respective additional risk has to be assessed.

The additional risk shall be compensated. Therefore several possibilities of upgrading of the existing tunnel by additional safety measures shall be investigated by calculating their effects on risk.

Definition of the system:

– Existing single tube tunnel, length 5,5 km
– Bi-directional traffic, 9.500 vehicles per day, 25% heavy goods vehicles
– Emergency exits: every 500 m
– Ventilation: transversal ventilation, extraction openings with dampers every 100 m – in line with Austrian guide lines
– Automatic fire detection system

Additional safety measures to be investigated:

– cross passages every 250 m to an already existing parallel evacuation gallery
– reduction of velocity of heavy goods vehicles from 80 km/h to 60 km/h
– construction of a second tunnel tube

As reference value the expected value of the societal risk is calculated (fatalities/year); a distinction is made between risk due to car accidents with mechanical effects only, due to fires and due to accidents involving hazardous goods.

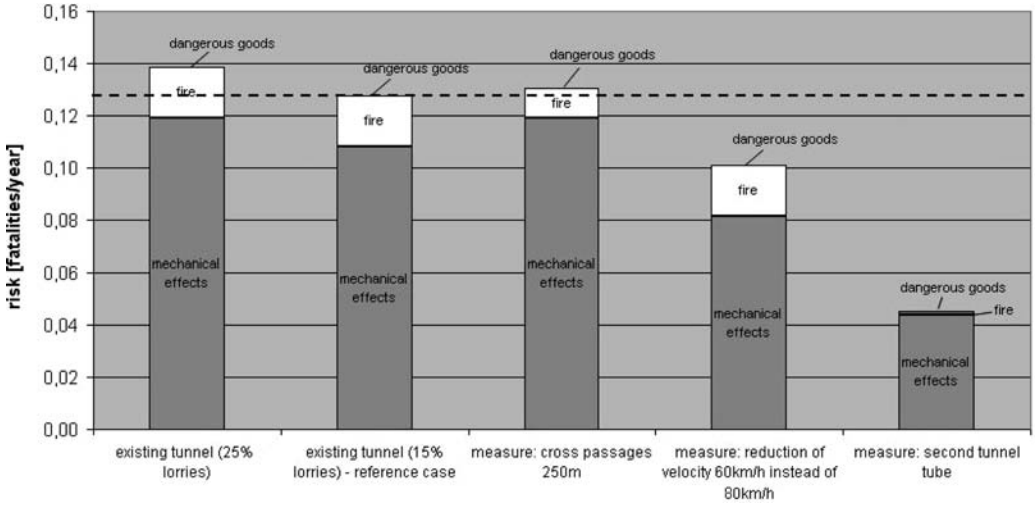


Figure 6. Graphical survey of results of case study.

Table 2. Results of risk analysis.

	Societal risk – expected value (fatalities/year)	Relative share in risk		
		Mechanical effects (%)	Fire (%)	Hazardous goods (%)
Existing tunnel (25% heavy goods vehicles)	0,139	86	14	< 1
Existing tunnel (15% heavy goods vehicles reference case	0,128	85	15	<1
Measure: cross passages every 250 m	0,131	91	9	<1
Measure: second tunnel tube	0,045	97	<1	3
Measure: reduction of velocity 60 km/h instead of 80 km/h	0,101	81	19	<1

For the tunnel investigated the following results are obtained (Figure 6):

Risk evaluation is done by relative comparison, mainly by comparing the tunnel as it is to the situation as it should be (reference case).

– The high portion (25%) of heavy goods vehicles causes an increase of risk of about 9% compared to the reference value according to the EC-Directive

The additional safety measures envisaged contribute to risk reduction as follows

– cross passages every 250 m can reduce risk by about 6%; this is almost the same order of magnitude as the additional risk, caused by the high portion of heavy goods vehicles; however, this measure considerably reduces fire risk but does not influence the risk portion due to accidents with mechanical effects
– reduction of velocity of heavy goods vehicle from 80 km/h to 60 km/h can reduce risk by about 38%, thus reducing it far below the risk value of the reference case. This measure considerably influences the risk due to mechanical effects of car accidents (which is dominated by the heavy goods traffic), but influences fire risk only to a small extent
– a second tunnel tube considerably reduces the risk level of the tunnel to about one third of the initial value, strongly influencing both, the fire risk as well as the risk due to mechanical effects.

The measure reduction of velocity of heavy goods vehicles can be realized within short term and causes only low costs, whereas additional cross passages are much more expensive and much more time consuming in terms of realization. Although very effective in terms of risk reduction, for cost-benefit reasons a second tunnel tube can only be justified, when the traffic volume is expected to increase considerably (up to 20.000 during the next 15 year – with reference to the EC-Directive, Annex I, article 2.1.2).

Therefore – if the effects on traffic flow are acceptable – the speed limit for heavy goods vehicles is recommended for cost benefit reasons as short term measure. If the traffic flow increases considerably, as long term measure a second tunnel tube should be envisaged.

3.2 *Range and limitations of application*

In general the model is applicable to all tunnels with mechanical ventilation; for specific situations (e.g. unconventional ventilation systems) the model can be used, but must be adapted. The advantages of the model are

- the high flexibility of the individual methodical elements, so that it is applicable to almost every tunnel, ventilation or traffic configuration
- the possibility of changing the most relevant input data very easily; thus new information can be implemented quickly in many cases
- its capability to include the effects of almost every important safety relevant influencing factor in a quantitative way; one of its key elements is the modelling of the complex interaction of smoke propagation in the tunnel and the procedure of self rescue in the situation of a fire, which allows the investigation of all influences on the lapse of time within this process
- its simply, clearly understandable and easy comparable results.

The model can be used for a wide field of different applications, such as safety assessment of new or existing tunnels, support of the decision-making process for a selecting safety measures (new tunnels) or upgrading measures (existing tunnels), definition of priorities for upgrading measures, etc.

However, the results of the model (expected value) do not include information about the distribution of different accident consequence classes (such as F-N-curves); therefore the model is not suited to specifically investigate accidents with very low probabilities and very high consequences. Hence, the model is not suitable for a more thorough investigation of the effects of accidents involving hazardous goods.

REFERENCES

Directive 2004/54/EC 2004, on minimum safety requirements for tunnels in the Trans-European network

Robatsch K., Nussbaumer C. 2003. Comparative Analysis of Safety in Tunnels, Vienna: Ministry of Traffic, Engineering and Technology

Galea E.R., Gwynne S. 2000. Principles and practice of evacuation modelling, Greenwich: University of Greenwich

RVS 09.02.31 2006, Austrian design code for road ventilation, Vienna: FSV

RVS 09.03.11 2006, Tunnel Risk Model, Vienna: FSV

Underground Space – the 4th Dimension of Metropolises – Barták, Hrdina, Romancov & Zlámal (eds)
© 2007 Taylor & Francis Group, London, ISBN 978-0-415-40807-3

Safety requirements of the 53 kilometer railway tunnel through the Alps between Italy and France

Mr. J.E. Nieuwenhuis M.Sc. & Mrs. F. Quezel Ambrunaz
ARCADIS Infra BV, Amersfoort, Netherlands & Scetauroute Tunneling Division, Pringy Cedex, The France

Mr. E. Verbesselt
Safety manager, LTF, The France

Mr. E. Boisguerin
Scetauroute Tunneling Division, Pringy Cedex, The France

Mr. P. Piepers & Mr. A. van der Giessen
ARCADIS Infra BV, Amersfoort, The Netherlands

ABSTRACT: Integration of the safety requirements for the Lyon-Turin Rail link project.

1 INTRODUCTION

The Lyon-Turin rail link between France and Italy, crossing the Alps, is one of the major projects in Europe. This high speed link is an important connection in the pan-European railway network. In 2015 the first trains will run. The link will be used by high speed passenger trains, freight trains and "Autoroute Ferroviaire" (trucks on the train) and will consist of a 53 km long tunnel crossing the border between France and Italy as well as the 12 km long Bussoleno tunnel. For such a project, the safety expectations are very high. Before starting the detailed design of the tunnel, it is therefore of importance which safety measures are to be integrated in the tunnel to meet the defined safety principles.

2 INCIDENT TREATMENT PRINCIPLES

Different kinds of incidents have to be potentially treated on the LTF section. They have to be identified and the specific constrains of the project have to be considered, in order to face them.

The topic of "Incident treatment principle" specific study is a global one which includes a lot of parameters and hypothesis coming from other studies.

The following paragraph details only the principles. Specific topics concerning equipment, dangerous goods and railway motorway are described below.

2.1 *Reminder of the project previous phases conclusions*

The two single-track tubes will be linked by cross passages every 400 m. A safety station will be provided at each extremity of the link (in the open air), in the middle of the tunnel (underground space close to Modane) and also on the Val Cenischia viaduct between the main tunnel and the Bussoleno tunnel. These emergency stations will be able to receive every type of train (AF, freight or passenger) and will be built for dealing with the possible incidents. Three additional underground intervention stations will be situated in the main tunnel for dealing with the incidents concerning the railway motorway and freight trains only. These emergency and intervention stations are to be designed and equipped to ensure the safety of users, even in the case of an incident.

2.2 *Events to take into account*

The identification of the events to take into account has been carried out in collaboration with the studies in charge of the global risk analysis of the project called "Safety principles". The main elements for identifying the potential incidents are:

- The infrastructure has to be designed for several kind of trains (passengers, freight, railway motorway);
- The infrastructure will consist of a 53 km long tunnel crossing the border between France and Italy

as well as the 12 km long Bussoleno tunnel and a viaduct;
– The freight train and the railway motorway may carry dangerous goods.

Consequently, the following events have been studied:

– Breakdown of each type of train in different locations;
– Fire on a passenger train in several locations in the tunnel or in the open air;
– Fire or explosion on a freight train or a railway motorway in several locations in the tunnel or in the open air.

2.3 *Major elements concerning incidents treatment*

In case of an incident, the goal for the concerned train is to reach an adapted place in order to treat the event (emergency station or intervention station). However, in case of a breakdown in the current section of the tunnel, the safety concept has to also to allow the treatment of this incident.

The trains behind the stopped train will have to stop and to reverse. The trains in front will have to continue their route with an adapted speed.

The behavior of the trains in the other tube will depend on the nature and the position of the incident train.

2.4 *Use of ventilation means*

In case of a fire on a train, there are two possibilities:

– All people on board are on the same side of the train;
– People on board are separated by the fire.

In the first case, the ventilation system is used in order to push all the smoke on the side where nobody is present. The minimal distance between two trains has been calculated in order to maintain the following trains free of smoke.

In the second case, the ventilation system is used in order to provide an environment compatible with an evacuation of the train passengers.

2.5 *Procedure in case of a fire on a freight train*

In case of a fire on a freight train, the driver has to stop the train in a safety or intervention station.

The ventilation system and the fire mitigation system are switched on in order to protect the train driver. He goes down the train and waits emergency services in a safe place.

In case of stop inside the tunnel, he waits in a cross passage.

2.6 *Procedure in case of a fire on a railway motorway train*

In case of a fire on a railway motorway train, the driver (located in the "Sonia" with all the truck drivers on board) has to stop the train in a safety or intervention station.

The ventilation system is switched on in order to protect the "Sonia". The driver start the diesel propulsion and separate the "Sonia" from the rest of the train in order to drive away from the burning convoy and exit the tunnel.

2.7 *Procedure in case of a fire on a passenger train*

In case of a fire on a passenger train, the driver has to stop the train in a safety station.

In the open air, users are directly taken care of by rescue teams.

In the tunnel, the train passengers wait for an evacuation train in the not-affected tube, which will bring them outside.

2.8 *Elements concerning rescue teams*

Elements concerning rescue teams are specific to the infrastructure:

– First line of intervention, with a very rapid response, because they are located permanently nearby the access to safety and intervention stations;
– Second line of intervention, which is organized by the public services.

Their vehicles will be both "road-rail"-vehicles together with traditional rolling stock for the more heavy logistics. The road-rail engines are rapidly put on rail and can operate in bad conditions (presence of smoke or high temperatures).

3 EQUIPMENTS

In order to provide for the required level of safety in the tunnel, several security systems and security equipment has been foreseen in both tunnels (Tunnels du base and the Tunnels du Bussoleno).

3.1 *Emergency philosophy*

The emergency philosophy for trains with a fire onboard has to, if possible, continue to a "safe haven" and to evacuate all passengers there. For all other trains not directly involved in the incident the rule is to a) leave the tunnel(s) as quickly as possible or to b) stop before entering the tunnel.

3.2 *Emergency installations and equipments*

The following emergency installations are used in the tunnel and connected areas:

- Detection equipment for:
  - Smoke and fire
  - Derailment
  - Train stop
  - Gage
  - Fumes and gasses
- Containment and extinguishing equipment in case of fire:
  - Ventilation systems in tunnels, inter tube tunnels
  - Ventilation of safe areas
  - Ventilation of technical rooms
- Control systems:
  - Lighting system
  - Video system (CCTV)
  - Central command post (PCC)
  - Communication equipment
  - Telephone system
  - HF communication system

The following equipment is foreseen in the tunnels, intervention stations and safety stations and surrounding elements:

- Evacuation of passengers:
  - Emergency platforms:
    - In the tunnels (min. 1.2 m width)
    - In the emergency stations and station (3.0 m width, 750 m length)
  - Cross passages (every 400 m, in Modane station every 50 m)
  - Collection rooms for the injured in every intervention and emergency station
  - Directions signs for emergency escapes
  - Audio system
- Accessibility and equipment for emergency services:
  - Emergency accesses at the highest point of every emergency tunnel, connecting to local infrastructure. The accesses are provided with a helicopter platform, parking space, and a command post
  - Emergency tunnels
  - Fire extinguishing equipment:
    - Hydrants (6–10 bar, every 133 m, French and Italian system)
    - Fire mitigation system in every intervention station and in the safety station
  - Automatic fire extinguishing system in technical rooms

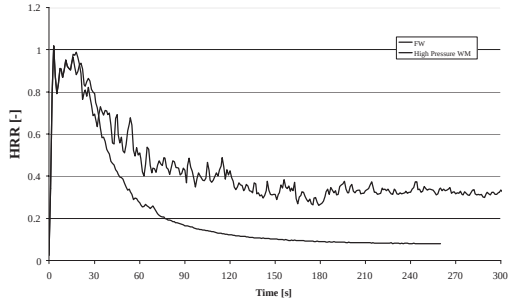


Figure 1. Test results from Foam Water and high pressure Water Mist systems to a 50 MW fire.

  - Emergency water reservoirs (with a capacity of 120 m^3) in each station.
  - Central command post (PCC), one in France and one in Italy.
  - Drainage system liquids (alpine water, extinguishing water)
  - Storage tanks for dangerous liquids (6 in total, storage capacity 240 m^3 per tank)

Three systems in particular will be described in following paragraphs, namely the foam water system, the emergency tunnels and the drainage system.

3.3 *Fire mitigation system*

Fires with a capacity of 50 MW can occur in the tunnel, due to the properties of transported goods and air speeds in the tunnel. These fires cannot be reached physically by fire fighters and therefore cannot be put out in a traditional way. For this reason, all goods trains will have to make a safety stop at an intervention station or safety station when exiting the tunnel is not an option. Each intervention and emergency station in the tunnel is provided with a sprinkler like system, using a specific mixture with water onto the fire from nozzles located on either side of the tunnel roof. Two systems have been modeled and tested: a Foam Water system and a high pressure Water Mist system. With a ventilation speed of 2 m/s, the following results are found.

The figure shows that the FW system reduces a fire to 20% of its original intensity within 70 sec and to 10% within 150 sec. The WM system mitigates a fire to 40% and 35% for the same time intervals respectively. These results are obtained when the system is called into action immediately after the start of a fire. There are however scenarios in which it takes up to 15 min before a train is located in an intervention station provided with a FM or WM system and the system is switched on. This way, 100 MW fires cannot be excluded.

3.4 *Emergency tunnels*

The intervention stations of Saint-Martin, La Praz and Venaus, as well as the emergency station of Modane are connected to the outside world by means of emergency tunnels. In total there are 4 emergency tunnels, with a diameter of 10 m and lengths varying from 500 to 4,500 m. The emergency tunnels will be used by emergency services in case of an emergency. The enormous length of the emergency tunnels led resulted in a one-way regime for traffic, with passage sites every 400 m, dividing each emergency tunnel into sections. The passage sites have a length of 200 m and a width of 20 m. Traffic lights will be used to indicate a free passage per section.

3.5 *Drainage system*

In the tunnel, a drainage system is applied to drain the alpine water from the tunnel the slope of the system is 2%, following the tunnel slope. In case of fire in a goods train leaking dangerous liquids, extinguishing efforts with water will result in a pool fire, possibly increasing the capacity of a fire. Therefore, the drainage system consists of lateral and longitudinal canals that collect in central collection points with siphons, to prevent progression of a fire in the closed drainage system. The liquids are collected in storage tanks, located at every station and at the heads of the tunnel.

4 DANGEROUS GOODS

One of the reasons the tunnels are being constructed is the transport of freight. From current transport of freight we know that a substantial part of the international transport can be classified as dangerous goods. Effects of an incident with dangerous goods in the tunnel may be serious for both persons present and the structure of the tunnel. Before allowing transport of dangerous goods in the tunnel, it has to be determined whether the possibility of an accident in relation to the effects is acceptable.

4.1 *The methodology*

The UN working group WP15 on the transport of dangerous goods has been developing a methodology to categorize tunnels. Through tunnels of different categories, different groups of dangerous goods are allowed for transport. For the LTF project this methodology has been the base to define safety measures and to determine whether transport of dangerous goods can be allowed in the tunnels. For each group is determined whether the possibility of an accident in relation to the effects is acceptable and if safety measures can be taken to ensure that the required safety level is reached.

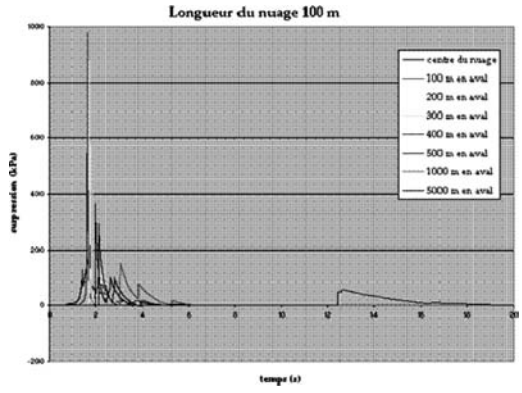


Figure 2. The blast effects after ignition of a cloud with a length of 100 meter.

4.2 *Possible effects and proposed safety measures*

4.2.1 *Group A*

Dangerous goods in this group are prohibited for transport and are therefore not analyzed in the studies for the project Lyon Turin Ferroviaire.

4.2.2 *Group B*

4.2.2.1 The effects

Dangerous goods in this group can provoke a big explosion. LPG is the product most transported good within this group. For this reason the effects of an accident with LPG are taken as normative to analyze the effects of a possible incident with goods of this group.

Two types of incidents have been considered: a leak of limited size leading to a vapor cloud explosion after ignition and a catastrophic failure of a LPG vessel leading to a BLEVE (Boiling Liquid Expanding Vapour Explosion).

A combination of a steady leak and steady ventilation flow may result in a homogeneous cloud in the tunnel downstream of the leak. For stoichiometric clouds of 10, 20, 50 and 100 meter length (it is never certain when a cloud may be ignited), the blast effects up to a distance of 5000 meters on either side of the cloud have been modeled.

A vapour cloud explosion as simulated can generate a blast that can cause victims up to 4200 metres.

4.2.2.2 Proposed safety measures

The prognostics show a large amount of possible transport of flammable gases. For this reason, both protective and preventive measures are proposed for the tunnel.

Since effects of an explosion reach up to 4,200 meters in the tunnel, the first measures is to keep a distance of at least 4,200 meters between a train carrying this products and a train with passengers. Furthermore the truck train combination is not allowed for

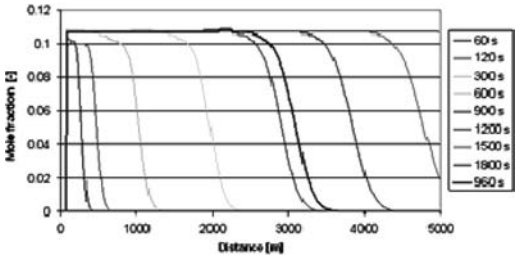


Figure 3. Dispersion of chloride in the tunnel after a leak (50 mm) of a vessel (ventilation speed 3 m/s).

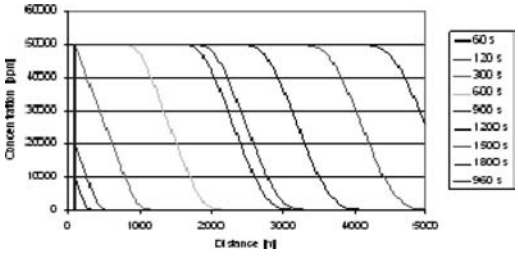


Figure 4. Dispersion after a leak (50 mm) of ammonia (taken ventilation speed 3 m/s).

this group since there are too many drivers present in the train, thus within the 4,200 m range.

4.2.3 *Group C*

4.2.3.1 The effects

Dangerous goods in group C are goods that can provoke an explosion or a toxic leak in the tunnel.

To analyse possible effects of possible incident with goods in this group, dispersion of ammonia and chloride in the tunnel is modelled.

With the probit function (probit functions give the mortality rate depending on concentration and exposure time) for chloride it is calculated the toxic cloud reaches up to 3,500 meters from the incident after 16 minutes.

The lethal concentration of ammonia will not reach as far as the chloride cloud.

Toxic vapour clouds from toxic liquids have also been analysed. Since evaporation from a liquid pool is a lot slower than evaporation of a pressurized gas, effects will not carry as far as the effects of pressurized gases.

4.2.3.2 Proposed safety measures

Since some of the goods in this group can provoke an explosion, a distance of at least 4,200 meters (3,500 m for truck-trains) between a train carrying this products and a train with passengers is introduced.

To reduce toxic effect of gases, the ventilation system should be able to influence the velocity and the direction of a toxic cloud.

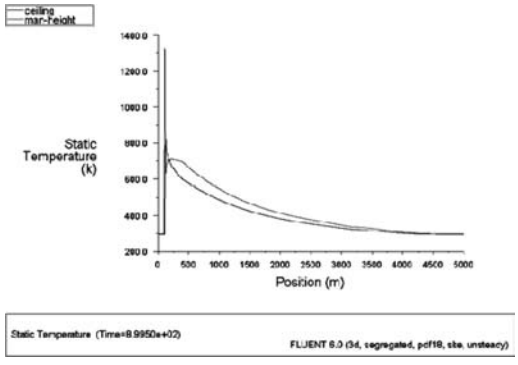


Figure 5. Temperature of 100 MW in relation to distance in the tunnel.

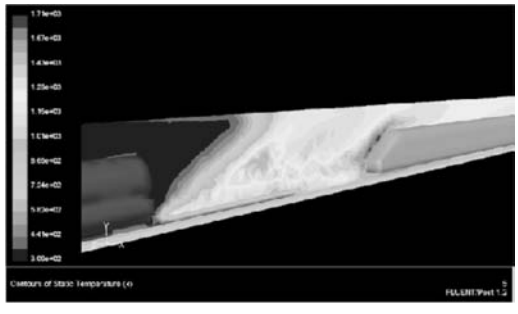


Figure 6. Simulation of a major fire next to a passenger train.

To reduce the effect of toxic liquids it is proposed to limit the surface of a possible pool to minimise evaporation. As for the flammable liquids a maximum of 100 m^2 is proposed (see above). The evacuation system has the possibility to separate toxic liquids and water (they can provoke a chemical reaction in some cases).

Further on, the ventilation systems of trains passing through the tunnel should be closed unless toxic clouds can be detected before trains with groups of passengers enter the tunnel.

The Sonia vehicle does also have this possibility to ensure that drivers of the trucks can get away in this vehicle.

4.2.4 *Group D*

4.2.4.1 The effects

Dangerous goods in groups D are those that can provoke a major fire. To analyse possible effects of possible incident with goods in this group, the effects of a fire of 100 and 200 MW in the tunnel have been modelled.

Furthermore the effect of a fire in case of another train present was analysed.

It has been concluded that the temperature reaches up to 50°C at 3,500 meter after 15 minutes. Since the air in the tunnel will be moist, this the level which can be dangerous to persons present in the tunnel.

4.2.4.2 Proposed safety measures

Since temperature and smoke can reach dangerous levels up to a distance of 3,500 meters, this distance should be kept between a train carrying flammable products and a train with passengers. The interdistance of 4,200 m caused by group B makes this one oblivious.

To prevent a fire from growing to fast and to limit effects, the ventilation system should be able to influence the velocity and the direction of the air in the tunnels.

To make sure a pool fire will be limited in magnitude, the surface of a possible pool should be limited to a maximum of 100 m^2 (gasoline generates about 2 MW/m^2).

The Sonia vehicle must be able to leave as fast as possible after an incident, before the effects of a fire reach the vehicle where the drivers are present.

4.2.5 *Group E*

Since the products in group E are either less dangerous or transported in smaller quantities this group has not been analysed. Measures taken to reduce risks for the other groups are supposed to be efficient enough to take away the risks of this group.

5 RAILWAY MOTORWAY

5.1 *Introduction*

The rail-motorway has to allow the HGV transport between France and Italy by rail. It should offer a new service that goes beyond conventional carriage and combined transport. The principle is that complete heavy goods vehicles (tractor + semi trailer) are carried through the Alps on wagons. The service includes a comfortable carriage for drivers.

The railway motorway trains to be designed to link Lyon and Turin are a new type of rolling stock compare to existing trains (Eurotunnel, *Modalohr* in France and Italy, *Petites roues* in Switzerland and Italy). According to the current rules, it is necessary to demonstrate the safety level of this new type of train by risk analysis. With this study the choice of the most adapted prevention and mitigation measures, to reach the safety level required, was taken.

5.2 *Description of the rail motorway*

A dense traffic of rail motorway trains per day is supposed to circulate in each direction. It allow the transport of 600 000 to 1 200 000 PL.

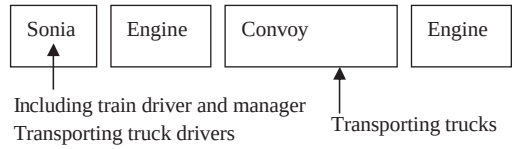


Figure 7. Composition of a railway motorway train.

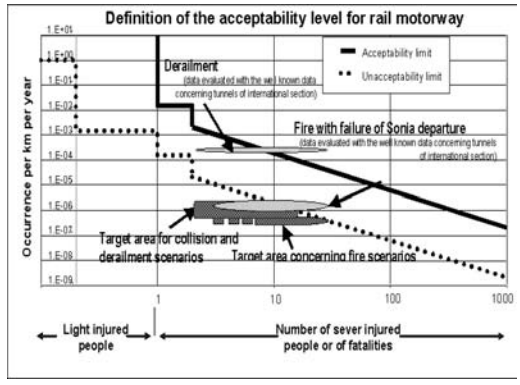


Figure 8. Safety level.

Trains are 750 meters long. The possibility to design 1,500 meters long train has been studied.

The train will be compound of several elements:

In this configuration the first vehicle, the "Sonia", is transporting all people on board and is equipped with a diesel propulsion to drive away from the burning convoy in case of a fire on a truck or on an engine. The complete safety procedure in case of an incident is described in paragraph 2.

5.3 *Result of the risk analysis*

5.3.1 *Prevention and mitigation measures to take into account*

Prevention and mitigation measures are introduced on several fields, like rolling stock, infrastructure, exploitation and emergency interventions.

Some of them are additional to measures concerning dangerous goods. The main conclusions are the following:

- The Sonia vehicle will necessitate a lot of adaptation of rolling stock;
- Because of the configuration of the train (with the Sonia vehicle in front of it), special care is required concerning collisions;
- A lot of verification will have to be proceeded before the departure of the train;
- Rolling stock will have to be tested frequently and safety elements will have to be used during maintenance;

– The distance between 2 trains have to respect the elements given by the “Safety principles” and the “Dangerous Goods” studies.

5.3.2 *Safety level*

The demonstration of the safety level has been carried out by the way of scenario analyses including failures, collision or fire events. The grid was elaborated by the “Safety principles” study. The target level was validated by the international governmental commission (CIG).

6 CONCLUSION

The safety studies have been carried out in order to determine the Functional Requirements Specifications of all safety measures in the tunnels to minimize the risks. The outcomes have been served as input for further technical studies of the project.

This page intentionally left blank

Underground Space – the 4th Dimension of Metropolises – Barták, Hrdina, Romancov & Zlámal (eds)
© 2007 Taylor & Francis Group, London, ISBN 978-0-415-40807-3

Operational safety of road tunnels: Safety reviews of tunnel projects and existing tunnels

N. Seifert
ASIT Ltd., Berne, Switzerland

R. Siegenthaler
ASIT Ltd., Berne, Switzerland

ABSTRACT: Proprietors/operators of road tunnels are responsible for the safe operation. Therefore the safety of road tunnels has to be reviewed in all life cycles.

Regarding the new Swiss regulation SIA 197/SIA 197/2 the safety planning in a tunnel project is performed as a stand-alone process. This concept is briefly introduced on the basis of an application example.

The safety assessment and planning for existing tunnels in exploitation can be performed using the approach described in the EU-directive 2004/54/EC. Using the example of the Bransiko tunnel in Slovakia a two-step approach combining different elements of safety and risk analysis methods is shown.

From the experience of the expert the conclusion can be drawn, that the integration of the safety analysis issue in the early stage of a tunnel project will have advantages also for the exploitation phase.

1 INTRODUCTION

1.1 *The responsibility of the proprietors or operators*

The proprietors and operators of motorways have the responsibility of a safe operation of the infrastructure. During the life cycle of roads and tunnels the safety measures have to be kept up-to-date under consideration of the economic constraints.

The users of road tunnels, the public and also political institutions demand a high level of safety for tunnel operation. It is necessary to control the relevant aspects for the operational safety for road infrastructure and particular tunnels directly in the design phase and periodically during exploitation.

The need to establish a safety management, which is responsible for the safety planning and the implementation of all necessary safety measures, is obvious. In practice the lead of the safety management refers directly to the top management of the responsible operational organization.

1.2 *Regulations and guidelines*

For the accomplishment of the operational safety of roads and road tunnels, the most important fundamentals are prescribed in the according regulations and guidelines (e.g. national technical regulations, national guidelines, EU directive 2005/54/EC for TERN roads), in laws (e.g. Swiss ordinance on the protection against major accidents) as well as in management system regulations (e.g. EN ISO 9001).

Theses prescriptions give the most important design and safety requirements for roads and road tunnels and are based on technical experience, safety and risk assessment results and research.

1.3 *Safety standards versus state-of-the-art of safety*

On one hand the operator of a road tunnel has to fulfill all design requirements, which are given by safety standards, which are updated in the range of several years. They can be considered as the common “Rules of Technology” (Engineering rules).

On the other hand there may be (legal) requirements to be followed as well, which claim the implementation of a so-called “State-of-the-Art of Safety Measures”. The latter represents a higher safety level becoming necessary because of a special risk situation and also depends on the risk acceptance of the public opinion. The level of the “State-of-the-Art of Safety Measures” can be higher than the rules of technology (Fig. 1). In the course of time, the gap between the levels of the rules of technology (safety standards) and the state-of-the-art of safety measures increases and can become considerably high.



Figure 1. Rules of Technology versus State-of-the-Art of Safety Measures.

Therefore a periodic review of safety and risk aspects is advisable.

It is important that the responsible proprietor/ operator distinguishes the mentioned aspects and is aware of the necessary relevant level of safety.

1.4 *Safety analysis in all life cycles of a tunnel*

The safety of road tunnels has to be reviewed and assessed in all life cycles of the infrastructure (design – realization – exploitation/operation/maintenance – removal). Reviewing the relevant safety aspects already in the planning phase of the project has considerable advantages, e.g. regarding cost – benefit considerations for later life cycles, especially for the operational phase.

Basically, the safety assessment/safety review of tunnels has to be carried out:

- During the design in the different project planning stages (preliminary studies, general project, detail project, regulatory approval project),
- In the construction (detail) project,
- During tunnel exploitation/operation and maintenance (e.g. prior to restoration)

The important means of the safety assessment/review lead to an optimization of the planning and are a decision support for the decision makers in the safety management on side of the tunnel proprietor or operator.

2 THE SAFETY CONCEPT AND SAFETY MANAGEMENT

Due to the fact that the proprietor/operator is responsible for the safe operation of the road or the tunnel, he would be well-advised to constitute a safety management, which works according to the principles of a safety concept or safety case and is the basis for all safety related activities. It comprises:

- The safety policy and the objectives;
- The safety organization (the management units, and the description of responsibilities, tasks, and interfaces to other players);
- Safety analyses (various studies and levels of detail adapted to the needs at the actual stage);
- Comprehensive and transparent documentation of all basis information, organizational framework, all analyses and assessments, planning material as well as concepts relevant for the safe operation of the road and tunnel infrastructure.

For the improvement of the operational safety of motorways and motorway tunnels it is essential and indispensable to establish an institutionalized collaboration between the safety management of the operator and the safety experts, road design experts and electromechanical experts. Only like this the operators can attend to their responsibilities in a complex environment with constantly changing boundary conditions and effectively protect the tunnel users from the consequences of catastrophic event scenarios.

3 SAFETY REVIEW AND PLANNING IN THE DIFFERENT STAGES OF A TUNNEL PROJECT

3.1 *The Swiss standard regulation SIA 197 and SIA 197/1 for tunnel projects*

The standard SIA 197 is the superior regulation concerning the design of tunnels and is amended by two more standards: SIA 197/1 for railway tunnels and 197/2 for road tunnels.

Amongst the documentation of project elements, constructive fundamentals, design issues, safety relevant issues, safety measures for different tunnel types and informative basics (e.g. exploitation duration, fire characteristics and curves, examples of normal tunnel profiles) the principle is described how a safety analysis with stage-specific content during all stages of a tunnel project has to be executed.

3.2 *Application example*

In the Swiss project of a new motorway exit and feeder road to the city of Geneva, the “Tunnel des Nations” has been assessed concerning the safety aspects even in a very early first preliminary study.

In this stage, the line management of the feeder road and the tunnel had been discussed in different possible variants, taking into account the connection with the city road network and the urban characteristics of housing in the area. It was crucial to consider the possible tunnel length with the requirements concerning escape routes for tunnel users, ventilation system and access for fire fighters from outside.

The design of the connection to the motorway A1 with its passage near the Geneva exhibition center and the Geneva airport area (with high density traffic in rush hours) was also introduced regarding the specific risks.

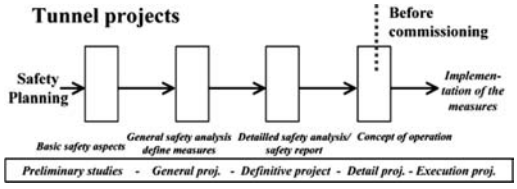


Figure 2. SIA 197 regulation – Safety planning during the different design stages.

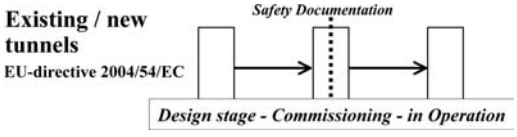


Figure 3. EU-directive – Risk analysis and safety documentation during the different stages.

In the next stage of the project the selected variants will be investigated more in detail till in further stages a complete and detailed safety analysis (safety report) will be available (Fig. 2).

4 SAFETY ASSESSMENT AND PLANNING FOR AN EXISTING TUNNEL IN EXPLOITATION

4.1 *The EU-directive 2004/54/EC for TERN roads*

The mentioned directive gives a prescription about the minimum safety requirements for tunnels in the trans-European road network (TERN) for tunnel design and tunnels in exploitation.

Different positions of the safety management and their tasks have to be defined: the administrative authority, the tunnel manager, the safety officer and the inspection entity.

Also it is required to execute a risk analysis and to elaborate the elements of the safety documentation in the design stage, the commissioning and the operation of the tunnel (Fig. 3) including among others a dangerous goods transport risk assessment, a hazard investigation and an emergency response planning.

4.2 *Application example*

For the existing tunnel of Bransiko (motorway D1, Slovakia: one tube – bidirectional traffic, safety gallery) a two-step analysis was carried out:

1. Prescriptive safety analysis: A wide set of different safety relevant issues had been investigated concerning the conformity of the existing safety measures with the safety level required by the EU-directive. If for specific issues a gap had been recognized between the current condition and the required safety level, recommendations were made together with an evaluation of the found safety level (1 = very good; 2 = good; 3 = critical; 4 = bad). All results are documented in a large listing to be the base of the decisions concerning safety measures planning.
2. Risk based analysis: A qualitative hazard analysis was carried out based on distinct incident scenarios. The frequencies and consequences were analyzed and a risk acceptance criteria matrix was proposed. The base results were also introduced to the safety documentation (see EU-directive).

   Then using the QRAM model of OECD/PIARC fire scenarios (20, 100 MW) were simulated for the Bransiko tunnel under consideration of the existing tunnel ventilation. It can be shown that with the 100 MW fire scenario the FN-curve reaches a zone, which, based on Swiss acceptance criteria, will be nearly unacceptable. Regarding other acceptance criteria however (ALARP) the risk curve reaches the transition zone.

   Also three DG-scenarios (pool fire, explosion, toxic gas release) have been simulated. The FN-curve of the pool fire scenario corresponds with the 100 MW fire.

The safety and risk analysis of the Bransiko tunnel has shown a modern tunnel with a mostly good safety level concerning the EU-directive requirements. There are however some improvements to be implemented. With the results of the detailed analysis the responsible safety management of the proprietor/operator has the necessary evaluation basics available to take decisions about additional safety measures.

5 EXPERIENCE AND CONCLUSIONS

ASIT has a great experience with safety and risk analysis of road tunnels. Tunnels of different types have been assessed or reviewed in the last years (one tube with bi-directional traffic; double tubes with one-directional traffic) and during different project stages or exploitation (Table 1).

Our experience clearly indicates that a well-organized safety management of a road tunnel who takes the responsibility seriously can avoid safety lacks and protect tunnel users from severe consequences. Introducing the safety analysis issue early in project stages can economize the financial resources in the later project stages and even in the exploitation phase.

Table 1. ASIT experience on road tunnel safety/risk analysis.

	Project/Exploitation			
Tunnels	1	2	3	4
Bransiko (SK)	x			
Vernier, Confignon, Chevres (Geneva; CH)	x			
Sonnenberg, Reussport (Lucerne; CH)	x			
Kirchenwald (Nidwalden; CH)	x			
Lopper (Nid-/Obwalden; CH)	x			
Les Vignes (Fribourg/Berne; CH)	x			
Hergiswil, Stansstad (Nidwalden; CH)		x		
Routes des Nations (Geneva; CH)		x		
Galgenbuck (Schaffhausen; CH)			x	
Flüelen (Uri; CH)				x
Libouchec, Panenska (CZ)				x

1 = tunnel in operation
2 = first preliminary studies/preliminary project
3 = definitive project
4 = construction project

REFERENCES

Directive 2004/54/EC of the European Parliament and of the council of 29 April 2004 on minimum safety requirements for tunnels in the trans-European road network, *Official Journal of the European Union L167 of 30 April 2004*

OECD/PIARC (2001): *Transport: Safety in Tunnels, Transport of dangerous goods through tunnels*, ISBN 92-64-19651-X

SIA, Norm 197 (2004): *Projektierung Tunnel, Grundlagen*, SN 505 197

SIA, Norm197/2 (2004): *Projektierung Tunnel Strassentunnel*, SN 505 197/2

Underground Space – the 4th Dimension of Metropolises – Barták, Hrdina, Romancov & Zlámal (eds)
© 2007 Taylor & Francis Group, London, ISBN 978-0-415-40807-3

Experiences and (in)effective application of QRA for assessing tunnel safety in The Netherlands

C.J. Soons [1,2], J.W. Bosch, P.H.A.J.M. van Gelder & J.K. Vrijling
[1]*Delft University of Technology, Faculty of Civil Engineering, Delft, The Netherlands*
[2]*Horvat & Partners, Rotterdam, The Netherlands*

ABSTRACT: Since 2006, it is compulsory in the Netherlands to use Quantitative Risk Assessment (QRA) for assessing tunnel safety. But previous to this legislative directive, risk analysis had already been applied to new tunnels for about ten years, but not all for the same reason or in the same manner. Therefore it is investigated in what manner QRA had been applied and what can be improved, all in order to eventually value QRA as an effective application for assessing tunnel safety. This research ends with a list of recommendations, from which can be concluded that QRA, up till now, has not been applied appropriately, some exceptions left.

1 INTRODUCTION

1.1 *Background*

Since the Alp fires around 2000, tunnel safety has become a major point of interest in the Netherlands. In May 2006, new legislation regarding tunnel safety has become valid. Safety standards for road and rail tunnels are set. In the legislation, the methods (i) scenario analysis and (ii) quantitative risk analysis (QRA) are referred to as the obligatory methods to use. But these methods to calculate the safety level in order to compare them to the set standards, are not established yet (2006).

There are some problems regarding these proposed risk analysis methods. For scenario analysis in road and rail tunnels, directives are set up in 2005/2006. These are obviously not completely finished (first set-up), but it is decided to review the documents in 2008, using comments/remarks from practice to develop an accepted scenario analysis method. Regarding QRA-modeling in road tunnels only the Rijkswaterstaat QRA-model is present for assessing tunnel safety. But for rail and metro tunnels no such method is present; only project based QRA-models exist. Further some stakeholders involved in the tunnel safety process (local government, emergency services etc) think the Quantitative Risk Assessment of tunnel safety is an ineffective application to approach tunnel safety. The question can be asked whether the stakeholders are right.

Therefore the goal in this research is to make sure the QRA method can be valued as an effective tool for assessing tunnel safety. To reach this goal the current use of QRA for assessing tunnel safety will be researched leading to a list of improvements.

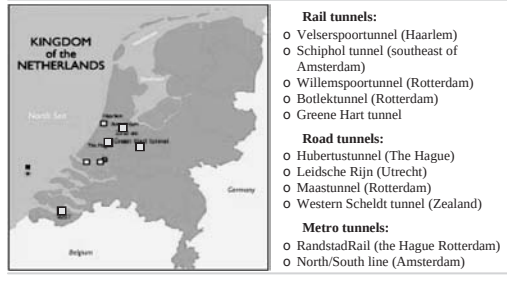


Figure 1. Dutch tunnels investigated.

Further the remarks must be made that the QRA-model is focused on the internal safety of personnel and passengers and that QRA should always be used together with Scenario analysis (SA) in order to assess tunnel safety thoroughly.

1.2 *Investigated Dutch Tunnels*

In this research several Dutch tunnels were assessed (road, rail as metro, both old as new tunnels), as shown in figure 1.

1.3 *Reader*

The analysis of the use of QRA for tunnel safety has been executed by applying an evaluation framework, see chapter 2. The analysis of each tunnel (type) is

described in chapter 3. At the end, the conclusions and recommendations for further research are provided.

2 EVALUATION FRAMEWORK FOR QRA

In order to evaluate the applied QRA in tunnel projects, a (theoretical) evaluation framework needs to be set. Then it is possible to compare the use of QRA in Dutch tunnels to the theoretical approach. The demands for a thorough QRA-model, can be divided in three aspects; (i) input, (ii) model and (iii) output. But to make sure the QRA-model is applied properly, also demands must be set for the organization and the process. In order to make all stakeholders (including politicians) understand the QRA-modeling and increase the confidence in QRA-modeling, it should be insightfully set up.

This results in the following evaluation framework:

A. Input (data)

Conditions to the input of the QRA-model are that (i) the data must be valid and (ii) the input must be as complete as realistically possible (f.i. human factors or tunnel technical systems).

Data are considered valid if the source (guarantee transparency), the context (correct use) and reliability (prevent 'wrong/filthy' data), are known. Input can be considered complete, if all input variables are identified and if the uncertainty of the parameters is known and clear.

B. Model

To make sure the QRA-method is valued as an effective method to determine the safety level of a tunnel, also the modeling itself is point of attention. It should be reliable ('comparable/usable' for the real situation), clear (no black box), flexible (future use) and complete (as possible).

Regarding the completeness of modeling the following issues should be taken into account, (i) all scenarios, (ii) modeling steps taken in each scenario, (iii) modeling steps taken for self rescue/emergency services/fire departments/human actions and (iv) relation QRA-model and procedures.

C. Output (Results)

The results of the model must be presented in such a way that they are understandable (for all stakeholders), unambiguous (to prevent discussions) and reproducible (increases confidence).

D. Organization

In QRA-modeling with 'THE organization' is meant all involved stakeholders. They should be aware of the limitations of QRA-modeling and have the knowledge in what manner the QRA-model is set up. Further should they be aware of the connection between the QRA-model and the procedures to be drawn and executed by personnel (driver, maintainers, operators).

Table 1. Overview of QRA studies per tunnel.

	QRA? (year)	stage
Rail tunnel		
Velserspoor-tunnel	Yes, to determine and improve safety level before a change of owner. (LREHC, 2003)	expl.
Schipholtunnel	No, evacuation study	expl.
Willemsspoor tunnel	No, qualitative risk analysis for changing security system	expl.
Botlektunnel	Yes, for external safety (1997), and sprinkler discussion (RWS, 2003)	design/ construction
Greene Hart tunnel	Yes, for assessing internal safety (2000)	design
Road tunnel		
Hubertustunnel	Yes, for assessing internal safety but QRA under embargo	design
Leidsche Rijn	Yes, for deciding on design alternatives (location of explosion holes) (RWS, 2002)	design
Maastunnel	No.	expl.
Western Scheldt tunnel	Yes, distance in between cross passages (Bouwdienst (1999)) & safety level during maintenance (TNO, 2005)	const/ expl.
Metro tunnel		
RandstadRail	Yes, for assessing internal safety (GWR, 2002)	design
North/South line	Yes, for assessing internal safety (North/Southline 1998/2002)	design

E. Process

To determine whether the QRA-process has been executed thoroughly and accurately, the following points should be addressed: (i) stage, (ii) reason to execute a QRA, (iii) relation to scenario analysis and (iv) decision process.

3 SAFETY ANALYSIS OF DUTCH TUNNELS

3.1 *Introduction*

The safety approach applied in several Dutch tunnels is researched. In table 1 an overview is provided of the use of QRA (reason, stage).

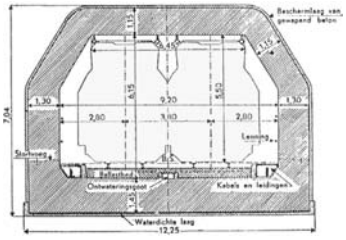


Figure 2. Cross section of Velserspoortunnel (crossing the NorthSea channel, west of Amsterdam).

In the following sections, it will be explained in what manner QRA has been applied in rail, road and metro tunnels together with the safety process.

3.2 *Rail tunnels*

The ownership and exploitation of the Velserspoortunnel (passenger/(dangerous) freight transport, opened in 1957), was transmitted from Rijkswaterstaat to ProRail in 2001. Therefore it was necessary to determine the safety level before handing over the tunnel. Another reason was that the existing safety level of the tunnel in the exploitation stage needed to be improved. QRA is used to make a comparison between three alternatives (LREHC 2003). SA is also executed by other stakeholders (RailNed 2003). Self rescue is the main focus in this studies.

Considering the input of the QRA study, the remarks can be made that there is a good overview of input parameters, the uncertainty of variables is clear, but the background of probabilities of failure is not clear.

Considering the model, it can be noted that all incorporated and remaining scenarios are clear. But the modeling of consequences, smoke and heat development is not explicitly taken into account. The uncertainty of QRA-modeling is clear when looking at the output (framework).

Finally it can be concluded that the QRA approach is clear, but the consequence modeling and background of probabilities of failure is not elaborated.

For the Schipholtunnel (opened in 1978/1990s) no QRA study has been executed, solely an evacuation study (ProRail 2006a) after an incident in 2001. Four trains were stopped inside the tunnel for several hours, due to a fire in the power supply room. This incident was researched by the Safety Board (RVTV 2003), issuing the improvement of the cooperation of all stakeholders.

It can be concluded that the evacuation study is a bit meager because not the complete system (rolling stock, organization, infrastructure) is taken into account, only the route is taken into account and no link was made to possible smoke and heat development, for instance the possible safety measures to prevent haltering of trains in the tunnel or to improve the organization.

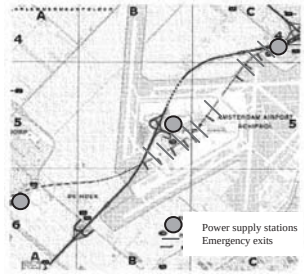


Figure 3. Overview of Schiphol rail tunnel underneath Schiphol airport, including emergency exits (two rail tunnels with each two tracks), (∼7,5 km)).



Figure 4. Interior Botlektunnel [S1].

The Willemsspoortunnel (crossing the river Meuse ∼3 km, opened in 1993) is used for both passenger as freight transport (dangerous goods). From 2007 this tunnel will also be used by HSL-trains. Because of current and future capacity problems, a qualitative risk analysis has been executed (ProRail 2006b) in order to provide a base on which the decision can be made that the security regime could be changed.

It can be concluded that not the whole system is assessed (capacity, type of transport etc.), no integral safety approach is conducted while changing the security regime (trias, stages and scenarios).

In the Botlektunnel (two bored tunnels part of the Betuweroute, open in 2007), two QRAs were executed; one in the design stage to assess the external safety and one in the construction stage (Bouwdienst 2003). The influence of sprinklers, heat resistant plaster, ventilation and detection on the safety level and the related costs were assessed in this study, issued by political discussion.

Further primarily qualitative safety studies were executed, due to the fact only personnel is involved in the tunnel. Most of the studies are executed in the construction stage and are described in the Integral Safety Plan of the Betuweroute (V&W 2004).

It can be concluded that the QRA is more used as a verification tool, rather than a design tool. The process of safety related studies is non-transparent, ad hoc and is not executed in the design stage but mostly in the construction stage. When considering the fact that the Green Book (BZK and V&W 1997) is set as a condition for gaining a construction permit it can be said



Figure 5. Cross section Green Hart (land tunnel) – one tube divided by wall (∼7 km) [S2].

that there was bad communication and cooperation amongst stakeholders.

The Green Hart tunnel is bored underneath the Green Hart (rural centre of the Randstad) and is solely used for public transport . It is part of the High Speed Line, and will be opened in 2007.

The QRA was used in the design stage as a design tool. Several safety committees were set and safety plans were set., including an integral safety plan (HSL-Zuid 2000, 2001), of which the QRA was part of (TNO-MEP 1998, 2000b).

It can be concluded that there was good communication from the design stage involving all stakeholders, setting up several safety committees. The QRA was used as a design tool and is executed in an integral manner (including SA).

Further all possible variables are implemented into the QRA model (trias), including human factors. The background of probabilities of failure is described. Several scenarios are considered (complete modeling), the modeling is clear and the steps taken are understandable. Good consequence modeling has been applied because the relation between the fleeing speed of the passengers and the smoke-heat development is taken into account.

But maintaining the designed safety level during the construction stage is a difficult issue.

Finally, considering rail tunnels, it can be concluded that in existing rail tunnels no/little attention is paid to the present safety level of the tunnel. Most of the safety studies are problem steered instead of a thorough integral approach. In rail tunnels owned by ProRail, uptill 2006, no integral QRA is executed in order to assess the safety level in the exploitation stage.

In new tunnels, attention is being paid to safety, but this has been worked out better in the Green Hart tunnel than in the Botlektunnel, probably having to do with the communication in the safety process. For rail tunnels no standard QRA approach is available.

3.3 *Road tunnels*

For the Hubertustunnel (two bored tunnels underneath rural and residential area, currently under construction) both SA and QRA were executed. The safety process already started in the design stage and several stakeholders were involved from the start and a safety concept is set-up. The QRA is under embargo and the SA is a qualitative research (Haaglanden 2005), so no valuation of input variables, but 9 scenarios have been analyzed qualitatively. The required time of each incident is compared to the demands set for self rescue, emergency services, traffic development and control of incidents.

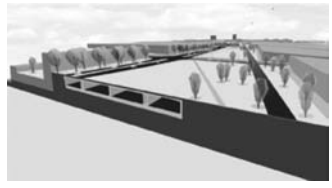


Figure 6. Cross section of Leidsche Rijn tunnel (land tunnel, in order to prevent barrier in between two urban areas).

It can be concluded that the start of the safety process is good (organization, safety studies), but the follow-up is unknown. And considering the scenario analysis the following remark can be made that whether each scenario complies to these set criteria is vague, due to the assumptions made of which no background is available.

For the Maastunnel project (immersed tunnel crossing the river Meuse) no QRA was executed. It is the oldest road tunnel in the Netherlands (1942).

Still TNO has executed a safety study (after the Alp fires), but this is under embargo. But all recommendations made are taken along in a maintenance plan for many years. The safety level of the Maastunnel will be as high as possible, but it must be taken into account that it is impossible to change the lay-out of an existing tunnel. It is built in a time, there was no policy regarding tunnel safety, therefore it is impossible to reach the safety level as set in the tunnel safety Directive (Tunnelsafety 2003).

In the Leidsche Rijn, both QRA as SA were executed in the design stage. The tunnel is designed according to the VRC-directives (Bouwdienst 2004) and this is the base of the RWS-QRA model. By executing a QRA a comparison is made between the design alternatives.

It is noted that not all safety measures are implemented in the QRA model, because the safety measures described in the VRC-directive are seen as 0-alternative. But human factors are incorporated (minimal).

The model itself incorporates 4 scenario types and the steps taken are clear. But the consequence modeling is inadequate and not the complete system incorporated in the modeling. Both internal as external risk are calculated due to multiple space use. But still there is no clear consideration between the two.

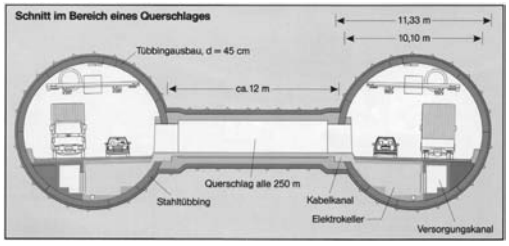


Figure 7. Cross section of Western Scheldt tunnel [S7].

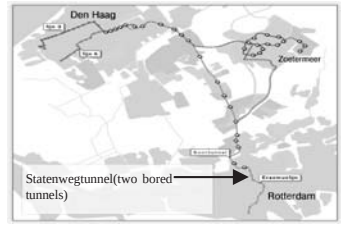


Figure 8. Layout of RandstadRail track [S5].

RWS executed the QRA and TNO executed the SA. In the SA it is mentioned that a partially opened tunnel is better for the internal safety compared to a completely closed one. Both studies had different conclusions regarding the alternatives. But these studies were not used in parallel, because in the decision-making process, only the QRA study was shown to the Committee Tunnel Safety and the SA was left out. Due to limited access of documents in the decision-making process, 'wrong' decisions are made (non transparent process).

In the Western Scheldt project (two bored tunnels opened in 2001) two QRA were executed; one in the design stage (to determine the hart-to-hart distance between the cross section – RWS-QRA) and one in the exploitation stage to compare alternatives of traffic diversion routes during maintenance of one closed tube (TNO 2005). This study was executed after an lethal accident has happened in 2001 during maintenance works (RVTV2004). In the design stage several stakeholders were involved. But this could not prevent the discussion on the distance in between the cross passages (500/250 m), for which the first QRA was executed by the Bouwdienst.

It can be concluded that no QRA is executed in the exploitation stage to assess the safety level integrally. The interaction with the fire department in the exploitation stage is good and the procedures are (regularly) updated and communicated.

In the TNO study, several scenarios are incorporated, but the validity of data is unknown. The modeling itself is not completely described, so it is not transparent. In the safety study the best possible alternative of traffic diversion routes during maintenance of one tube (closed) can be chosen.

Finally it can be concluded that in Dutch road tunnels mostly the QRA-RWS model (Rijkstunnels) Not all safety measures are implemented in the QRA model, because the VRC-directive is seen as 0-alternative. QRA is not properly used as a design tool, and in the exploitation stage it is not used in an integral manner. In municipal tunnels and old tunnels no such studies are executed.

3.4 *Metro tunnels*

The RandstadRail LightRail project is currently under construction and the Statenwegtunnel is being bored in Rotterdam. QRA is executed in the design stage to determine the safety of the Statenwegtunnel in case of fire. In this QRA study not all scenarios are incorporated, but the set up is clear. The uncertainty of the probabilities of failure is clear because of the division in classes. The QRA is used to determine the effect of distance between the cross sections, and therefore it is not used in an integral manner.

Further several other safety studies have been executed in the construction stage (RandstadRail 2004a, 2004b, 2004c, 2005, 2006a, 2006b). In these safety studies not a QRA approach is applied but it is solely based on existing frequencies without taking into account possible other causes which has not occurred until now. But SA is also executed.

Early on in the design stage, several stakeholders are involved. A safety concept is drawn, in which the main focus of self rescue and the Safe. Local government accepts the safety demands officially; increasing the compliance. And at the finalizing stage of the construction a Safety Case is executed.

It can be concluded that the safety process has started in the design stage, setting up an integral safety study. Several safety studies have been executed, but the QRA is not executed in an integral manner as a design tool incorporating all scenarios. And the safety studies are executed in the construction stage to check the safety level instead of in the design stage to gain a good design.

The North/South line metro project is currently under construction in the city of Amsterdam (two bored tunnels, underneath the old city centre).

Early on the design process several stakeholders are involved, evaluating safety studies. But there are people opposing the metro line and questioning the safety. The question is whether it is not communicated well or people do not want to understand. The Safety concept is an integral qualitative study in which the Safe-haven principle and self rescue are main focus (North/Southline 1998 and 2002a).

QRA for tunnel safety (North/Southline 2002b and TNO-MEP 2000a) is used to determine the effect of

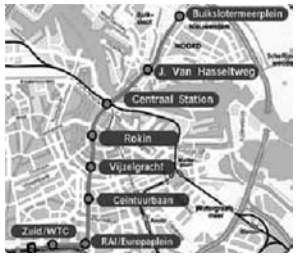


Figure 9. North/Southline track [S3].

distance between the cross sections. Besides the QRA for fire safety inside the tunnel, also a QRA for the underground station is executed. QRA is not used in an integral manner.

As input of the modeling the trias is applied (organization, infrastructure and rolling stock), including human factors. Not all scenarios are incorporated, but the set up of the model is clear. Consequence modeling takes relation between fleeing speed and smoke development into account.

It can be concluded that in metro tunnels, QRA is being used, but not in the integral manner as set in the evaluation framework. The safety process has been set up early on in the design process, but the safety documents do not all contribute to a thorough design. Some are more execute to verify the eventual safety level.

4 CONCLUSIONS

In this chapter, conclusions can be drawn on the use of Quantitative Risk Assessment in Dutch tunnels. As said in the evaluation framework, QRA can be valued as an effective application tool if:

- An integral approach is applied (trias, all scenarios).
- QRA is used as a design tool (comparing alternative designs, safety measures etc.)
- QRA is used together with Scenario Analysis (SA) in a probabilistic way to guarantee that all issues (traffic handling, self rescue, emergency services) are covered.

However, after the analysis in chapter 3, on the use of QRA in Dutch tunnels, it can be concluded that:

(A) No integral approach is used for executing QRA-modeling:
  (1) Tunnel safety is often assessed in a more *problem steered way* instead of a systematic approach, resulting in a shredded approach.
  (2) The *modeling of QRA* for assessing tunnel safety is inconsistent (trias, incorporated scenarios, elaborating each scenario, probabilities of failure, human factors, evacuation).

(B) The reason for executing quantitative analysis varies, increasing the suspicion of stakeholders;
  (1) Verification tool instead of design tool
  (2) Resolving problems ad hoc instead of systematically.

(C) Difference between internal and external safety is rather difficult, when considering multiple space use projects causing difficulties in decision-making:
  (1) The dividing line between internal and external safety is rather thin.
  (2) Are all effected areas taken into account for each main scenario; these can vary per scenario.

(D) As-built problems; After the construction stage the structure must eventually comply to the demands set in the design stage, but because several stakeholders are necessary to reach that goal this is a rather difficult issue.

(E) Process; good initial cooperation in several new projects, but in few projects it leads to a thorough and structured process. And the responsible stakeholder for safety is not always clear.

5 RECOMMENDATIONS

It is recommended to further investigate the use of QRA of the mass-transit systems and not of road tunnels, because in the Netherlands this field is already covered by the Bouwdienst of Rijkswaterstaat (RWS-QRA model). By developing QRA for mass-transit systems enables to make comparisons and as a consequence improve the trust of stakeholders in QRA-modeling.

But it is recognized that no standard QRA-model for 'all' tunnels should be developed, but a standardized QRA-approach. Several divisions need to be made because of the project specific conditions, location (land/water tunnel), type of tunnel (bored/immersed tunnels/in situ), geometry, multiple space use, type of transport.

By setting a standardized approach the modeling will be flexible for all locations and for future use. Therefore the goal is to incorporate all possible input variables, forcing the analyst to make considered choices (and describe those as well), resulting in a fit for purpose QRA-model for different types of underground mass-transit systems.

In the following sections recommendations are made regarding the improvement of the safety process, the organization and regarding the QRA-modeling itself.

5.1 *Recommendations regarding QRA application in Dutch tunnels*

(1) Use QRA and SA together; QRA should be used to check whether all steps are taken along in the SA and if all needed safety measures are taken. But then again, QRA should be used to determine safety level and as input for CBA.
(2) Create a link between the initial and actual conditions to guarantee the safety level in (i) the construction and (ii) the exploitation stage.
(3) Determine the stage and the situation in which QRA can be applied. QRA must be used as a steering tool for designing the tunnel and to maintain the safety level in the exploitation stage.
(4) Responsible stakeholder should be known and should manage the safety process structurally.
(5) The standards set for tunnel safety should be researched (background, relation to costs like dike safety, unit, relation to other safety related fields).
(6) Develop QRA approach for multiple space use.

5.2 *Recommendations regarding QRA modeling in Dutch tunnels*

To improve QRA-modeling the following issues should be improved:

(1) Classification of probability of failures: Ascribe each safety measure to a certain class (a/b/c).
(2) Prevent black box modeling.
(3) Incorporate human factors in a groupwise manner (professionals or not)
(4) Improve the modeling of self rescue (smoke and heat development and related consequences).
(5) Fully incorporate rolling stock.
(6) Incorporate the link between the QRA and the procedures (calamity plan, safety control plan).

If all these recommendations are researched, hopefully the stakeholders will recognize the effective application of QRA-modeling.

LITERATURE

Bouwdienst. (2002). "In Dutch: 'Leidsche Rijn – Risicoanalyse interne en externe veiligheid'." A2/LR/RA-R-02.001, Bouwdienst, Rijkswaterstaat, Utrecht, the Netherlands.

Bouwdienst. (2003). "In Dutch: 'Tunnel Technische Installaties Betuweroute'." 6917-2002-0050, Steunpunt Tunnelveiligheid, Bouwdienst, DG Rijkswaterstaat.

Bouwdienst. (2004). "In Dutch: Veiligheidsrichtlijnen Deel C – Basismaatregelen." Steunpunt Tunnelveiligheid, DG Rijkswaterstaat, Utrecht, the Netherlands.

BZK, and V&W. (1997). "Green Book (In Dutch: 'Beveiligingsconcept spoorwegtunnels uitsluitend bestemd voor goederenvervoer')." The Hague, the Netherlands.

Haaglanden. (2005). "In Dutch: Hubertustunnel Scenario's." Dienst Stadsbeheer – the Hague, the Netherlands.

HSL-Zuid. (2000). "In Dutch: Beveiligingsconcept HSL-Zuid Deel B: Boortunnel onder het Groene Hart." 00HSL210, the Netherlands.

HSL-Zuid. (2001). "In Dutch: Integraal Veiligheidsplan HSL-Zuid." versie 9, the Netherlands.

LREHC. (2003). "In Dutch: Optimalisatie veiligheidsniveau Velserspoortunnel.", Rotterdam, the Netherlands.

North/Southline. (1998). "In Dutch: Een concept voor een aanvaardbaar veiligheidsniveau voor de Noord/Zuidlijn." Amsterdam, the Netherlands.

North/Southline. (2002a). "In Dutch: Definitie Veiligheidseisen o.b.v. Safe Haven principe." Amsterdam, the Netherlands.

North/Southline. (2002b). "In Dutch: Kwantitatieve Risicoanalyse Baanvakken Noord/Zuidlijn; Toets brandscenario's enkel en dubbelsporige baanvakken Noord/Zuidlijn." Amsterdam, the Netherlands.

ProRail. (2006a). "In Dutch: Evacuatiestudie Schipholtunnel." IO-MJ-050060328, ProRail, Utrecht, the Netherlands.

ProRail. (2006b). "In Dutch: Veiligheidsverantwoording aanpassingen X/G regime Willemsspoortunnel." SpO-BaBe-PvG-XG-FO, Utrecht, the Netherlands.

Railned. (2003). "In Dutch: Veiligheidsstudie Velserspoortunnel – Probabilistische en deterministische analyse." *RvV/02/S12.018.033*, Utrecht, the Netherlands.

RandstadRail. (2003). "In Dutch: Integraal veiligheidsplan RandstadRail." Rotterdam, The Netherlands.

RandstadRail. (2004a). "In Dutch: "Gebeurtenissenboomanalyse Statenwegtunnel – Beoordeling RandstadRail-systeem in het kader van het Safe-Haven principe"." Rotterdam.

RandstadRail. (2004b). "In Dutch: Veiligheidsconcept RandstadRail – Rotterdamse deel." Rotterdam, The Netherlands.

RandstadRail. (2004c). "In Dutch: Veiligheidsanalyse In- en uitstappen – versie 7.0." Rotterdam, The Netherlands.

RandstadRail. (2005). "In Dutch: Veiligheidsanalyse RandstadRail – Risicoanalyse botsen perceel 1." Rotterdam, The Netherlands.

RandstadRail. (2006a). "In Dutch: Veiligheidsanalyse RandstadRail – Aanpassing risicoanalyse overwegen en oversteken." Rotterdam, The Netherlands.

RandstadRail. (2006b). "In Dutch: Veiligheidsanalyse RandstadRail – Risicoanalyse ontsporen perceel 2." Rotterdam, The Netherlands.

RVTV. (2003). "In Dutch: 'Brand in de Schipholtunnel'." Raad voor Transportveiligheid, The Hague, the Netherlands.

RVTV. (2004). "In Dutch: 'Tweerichtingsverkeer in een tunnelbuis tijdens geplande werkzaamheden' – ongevallen in de IJtunnel (1999) en Westerscheldetunnel (2003)." Raad voor Transportveiligheid, The Hague, the Netherlands.

TNO. (2005). "In Dutch: 'Risicoanalyse verkeersveiligheid tijdens onderhoudswerkzaamheden in de Westerschelde tunnel'." B&O-A R 2005/377, TNO Bouw en Ondergrond, Apeldoorn, the Netherlands.

TNO-MEP. (1998). "In Dutch: 'HSL-Zuid: Analyse veiligheid tunnel – Kwantitatief risicoanalyse model brand in de boortunnel'." TNO, Apeldoorn, the Netherlands.

TNO-MEP. (2000a). "In Dutch: 'Contra expertise Noord/Zuidlijn'." Apeldoorn, the Netherlands.

TNO-MEP. (2000b). "In Dutch: 'Veiligheidsanalyse brand in HSL tunnels – modelbeschrijving'." 30448, TNO-MEP, Apeldoorn, the Netherlands.

Tunnelsafety. (2003). “In Dutch: ‘Beleidsnota Tunnelveiligheid – Deel A Proceseisen’.”, the Hague, the Netherlands.
V&W. (2004). “In Dutch: ‘Integraal Veiligheidsplan Betuweroute’.” Ministry of Traffic & Public Works, The Hague, the Netherlands.

WEBSITES

S 1. www.betuweroute.nl
S 2. www.hslzuid.nl
S 3. www.noordzuidlijn.amsterdam.nl
S 4. www.n14-norah.nl (Hubertustunnel)
S 5. www.randstadrail.nl
S 6. www.rws.nl/rws/bwd/home/www/cgi-bin/index.cgi?site=2
S 7. www.westerscheldetunnel.nl

ABBREVIATIONS

LREHC	Lloyds Register and E. Horvat Consultants
RWS	Rijkswaterstaat
SA	Scenario Analysis
QRA	Quantitative Risk Assessment
TNO	In Dutch: “Nederlandse Organisatie voor **T**oegepast-**N**atuurwetenschappelijk **O**nderzoek (TNO)” – the Netherlands Organisation for Applied Scientific Research
TTI	Tunnel Technical Installations

Underground Space – the 4th Dimension of Metropolises – Barták, Hrdina, Romancov & Zlámal (eds)
© 2007 Taylor & Francis Group, London, ISBN 978-0-415-40807-3

Emergency egress provisions and their guidelines

Magdalena Vasilovska
Parsons Brinckerhoff, Sydney, Australia

M. Reedman
Parsons Brinckerhoff, Brisbane, Australia

ABSTRACT: The paper provides an overview of the egress provisions currently applicable in various countries around the world, and the recommendations by PIARC, NFPA, and the recently published Directive 2004/54/EC of the European Parliament. Presently, egress locations vary from 100 m up to 500 m, and with egress door widths varying between 0.815 to 1.4 m. If the guideline recommendations are strictly followed without limited performance based assessment, tunnel designs are at risk of ending up with either inadequate emergency egress facilities or surplus facilities that affect the sustainability of road tunnel projects, especially tunnels of relatively short length (<750 m). This paper mainly focuses on egress passage locations and dimensions as required by various guidelines for two-tube unidirectional urban tunnels. Egress analyses using SIMULEX have been performed for selected representative scenarios to compare the egress time of various international designs, with commentary on the results provided.

1 INTRODUCTION

1.1 *General*

The frequency of egress passages has an impact on the occupants egress time and safe evacuation, and the rapid implementation of fire fighting activities by the fire brigade required for extinguishing fires to save life and provide property protection in case of a fire incident within a road tunnel. On the other hand, they add considerable costs to the construction, fit-out, and maintenance of road tunnels.

Historically, there has been considerable debate within the fire-protection and tunnel engineering communities on the provision of acceptable fire prevention and protection facilities in road tunnels, including frequency of egress passages. Currently, there is no uniform position on the distance between egress passages in road tunnels internationally.

In addition to a brief overview of the egress passage requirements as defined in the internationally accepted guidelines such as PIARC, NFPA, EU Directive, and AFAC, this paper also provides a brief overview of the adopted guidelines in selected countries. Comparison of the predicted egress times in each tunnel by performing egress analyses using PB's version of the computer program SIMULEX has been performed. The egress time referred to in the paper is the actual movement time measured from the time the occupants decide to evacuate to the time when occupants have reached a place of safety The delay time (measured from the start of the fire until the time when occupants decide to evacuate) has not been included in the egress times as there are no set values and is another complex research topic.

2 GUIDELINES FOR ROAD TUNNELS

2.1 *PIARC 1999 recommendations (PIARC, 1999)*

Section VI.2.3.2 Tunnels with unidirectional traffic (two tubes or more):

> *. . .The most common escape route in two-tube tunnels is a connection (cross passage) between the two tubes. The distance between connections should depend on traffic density and emergency rescue scenarios, for instance 100–200 m in cities. This distance should be designed so that people can walk to the nearest exit before smoke reduces visibility.*

2.2 *Fire safety guidelines for road tunnels 2001*

AFAC (AFAC, 2001)

> *. . .It is not possible to provide a general recommendation for the distance between egress points and such details should be developed for each individual case after consideration of the conditions within the tunnel.*
> *. . .Required exit points depend on a number of factors such as the types and volumes of vehicles*

and the ventilation and smoke management systems within the tunnel. . . . Occupants must be provided with a means by which they can escape to a place of safety prior to smoke reducing visibility or creating untenable conditions.

2.3 *PIARC (PIARC, 2007)*

A second, or new report entitled 'Systems and Equipment for Fire and Smoke Control in Road Tunnels' is being prepared by PIARC Working Groups 6 and 2. This report is yet to be published and will complement the 1999 report and supplement, not replace the material contained in the earlier publication. Its view on egress provisions is:

. . .Emergency exits in enclosed road structures addresses the issue of emergency exits for evacuation, escape and rescue including consideration of the types and characteristics of emergency exits in road tunnels including how to deal with disabled people. Also included is the consideration of the necessary spacing between exits according to people behaviour and tunnel ventilation including escape modelling.

2.4 *NFPA 502 (NFPA, 2004)*

Section 7.17.7 Cross Passageways:

. . .Where tunnels are divided by a minimum of 2-hour fire-rated construction or where tunnels are in twin bores, cross passageways between the tunnels shall be permitted to be utilized in lieu of emergency exits. The following requirements shall be met:

(1) Cross passageways shall not be further than 200 m apart. . .

(3) An emergency egress walkway with a minimum clear width of 1 m shall be provided on each side of the cross passageways.

2.5 *DIRECTIVE 2004/54/EC of the European Parliament, 29 April 2004 (European Parliament, 2004)*

Section 2.3: Escape routes and emergency exits:

. . .In any event, in new tunnels, emergency exits shall be provided where the traffic volume is higher than 2000 vehicles per lane. . . Where emergency exits are provided, the distance between two emergency exits shall not exceed 500 m.

2.6 *Summary of egress requirements*

The egress provisions as defined in the guidelines above are summarized in Table 1 below:

Table 1. Summary of international guidelines egress provisions.

	Spacing (m)	Passage Width (m)	Door-width (m)
PIARC	100–200	1	0.8
AFAC	N/A	N/A	N/A
NFPA 502/101	200	0.915	0.810
EU-Directive	<500	N/A	N/A

3 EMERGENCY EGRESS REQUIREMENTS IN SOME INTERNATIONAL GUIDELINES

Various countries around the world have developed and adopted their own national guidelines that define the minimum safety provisions applicable to new tunnels including maximum distance between egress points. In some cases, they even define the minimum passage and door widths. Egress passage requirements defined in various national guidelines and considered in the egress analyses in this paper are summarised in the table below:

Table 2. Selected International Road Tunnel Cross passage Requirements*.

	Spacing (m)	Passage Width (m)	Door-width (m)
Australia^	120	1	0.8
France^	200	1.8	1.4
Germany	350 m	N/A	N/A
Netherlands^	100–250	1.2	0.85
Sweden^	100	1.2	0.9
UK^	100	Various	0.914
USA^	200	0.915	0.81

^SIMULEX modelling performed for these requirements

* Requirements sourced from: Australian Standards (2001); Interministry Circular (2000); RABT (2002); MTPW (2004); SNRA (2000); The Highways Agency (1999); NFPA (2004); NFPA (2006).

4 MODELLING OF ROAD TUNNEL EGRESS

4.1 *Description of SIMULEX*

The emergency exiting analysis was done using the computer program SIMULEX (Integrated Environment Systems Ltd., 1998) that models the emergency exiting of people from large complex geometries to a point of safety. SIMULEX allows the user to create a 3-D model of a building by using a number of CAD-designed floor plans, connected by escape passages or stairways. To do this the program assigns a body dimension, position, angle of orientation, occupant type, and a walking speed to each person. The

simulation of escape movement includes distance mapping, way finding, overtaking, route deviation, response time, and adjustments to individual speeds due to the proximity of crowd members. The program's algorithms for the movement of individuals are based on real-life data and predict realistic people flow rates.

4.2 *Population mix and walking speeds*

The commuters in the simulations consist of 50% male, 40% female and 10% children. Each commuter type has a body size and normal walking speed. The new versions of SIMULEX offer two commuter mixes comprised of Western countries or people from Asia, who differ in body size. However, the average walking speed for both types is 1.225 m/s. In the simulations performed in this study, people from Western countries have been used corresponding to the countries modelled. The data used is summarized in Table 3 below:

Table 3. Parameters of "commuters" in the SIMULEX* Model.

	Commuter type		
	Male	Female	Children
Average speed	1.35 m/s	1.15 m/s	0.9 m/s
Shoulder breadth	540 mm	480 mm	420 mm
Body depth	320 mm	280 mm	240 mm

* For additional information on SIMULEX modelling of Road Tunnel egress, refer to Li (2001) and Bendelius (2002).

4.3 *Tunnel occupancies*

To minimise the number of variables that can affect the results of the SIMULEX modelling, one set of vehicle fleet parameters was used to determine the tunnel's occupancy loading for all scenarios. In case of tunnel congestion, traffic density of 165 PCU/km/lane was used and 1.167 PCU/vehicle. The average traffic density is 141 vehicles/km/lane. To determine the number of vehicles per lane, this figure is multiplied by the length of road tunnel section (1.5 times the cross-passage spacing). The tunnel occupancies were derived by using fleet ratios and average number of people per vehicle as in Table 4.

Table 4. Fleet ratio and Average number of Passengers per vehicle.

	Fleet ratio %	Average Passengers/Vehicle No.
Car	85.7	2.5
LCV	9.5	2
HCV	4.8	45

A random distribution of 2, 3 and 4 people per passenger vehicle was used in the model, equating to an average of 2.5 passengers/vehicle. The number of occupants used in the egress modelling for 1, 2 and 3 lane tunnels are summarised in Table 5 below. The values in brackets next to each country indicate the distance between cross passages.

Table 5. Summary of number of occupants used in the egress analyses.

	Number of people evacuating a tunnel section		
	1-Lane	2-Lanes	3-Lanes
Australia (120 m)	115	229	343
France (200 m)	191	381	572
Netherlands (100 m)	95	191	286
Netherlands (250 m)	238	476	715
Sweden (100 m)	95	191	286
UK (100 m)	95	191	286
USA (200 m)	191	381	572

Most guidelines suggest that road tunnel egress provisions need to be assessed based on the tunnel length, the type of tunnel (uni-directional or bi-directional), number of lanes, and the traffic density. The focus for this study is based on long, twin tube, (uni-directional only) urban vehicle tunnels, with traffic congestion resulting in highest occupant loadings putting a greater demand on the tunnel emergency egress facilities.

4.4 *Egress analyses of a long, twin tube, uni-directional urban tunnels*

SIMULEX models were created representing the egress provision required by the guidelines for long, dual tube, uni-directional urban road tunnels in Australia, France, the Netherlands (100 m and 250 m distances), Sweden, UK and USA. The models were created using the following assumptions/parameters:

- Fire located next to a cross-passage, making escape into this passage impossible.
- Passengers exit in both directions using the closest unobstructed cross-passage. Due to symmetry, only egress from one side of the incident was required to be modelled, resulting in a model length of 1.5 times the cross-passage spacing
- Congested tunnel (maximum occupancy).
- No deluge system in operation (Australia only).
- 1, 2 and 3 lane tunnel configurations.

Typical tunnel layouts and egress passage geometry used in the model, and a typical egress simulation output layout showing positioning of people in front of an egress passage are shown in Figures 1, 2 & 3 below:

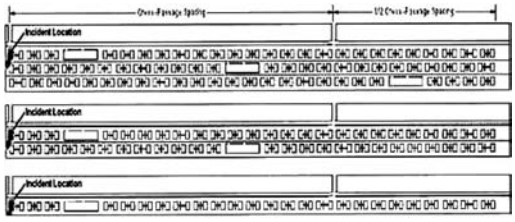


Figure 1. SIMULEX model layout for 1, 2 and 3 lane tunnels.

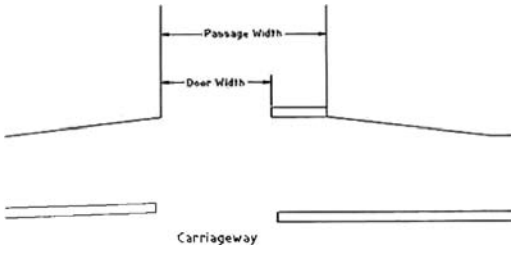


Figure 2. SIMULEX model cross-passage doorway layout.

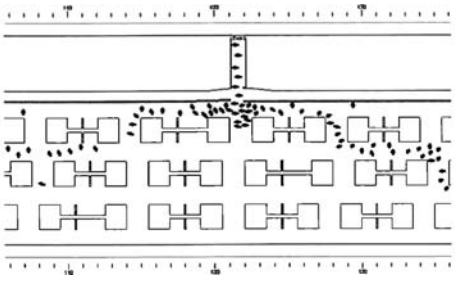


Figure 3. Screen shot of SIMULEX simulation, cross-passage close-up for an Australian 3-lane tunnel.

5 SIMULATION RESULTS

Egress times predicted by SIMULEX for each scenario modelled are summarized in Table 6 below:

Table 6. Summary of simulated egress times (min:seconds).

	Simulated Tunnel Egress Times (min:sec)		
	1-Lane	2-Lanes	3-Lanes
Australia (120)	3:12	3:55	5:00
France (200 m)	5:01	5:05	6:10
Netherlands (100 m)	2:36	3:20	4:50
Netherlands (250 m)	6:14	8:25	11:50
Sweden (100 m)	2:35	3:15	4:40
UK (100 m)	2:35	3:15	4:35
USA (200 m)	5:06	6:55	9:30

The actual progress of the egress during evacuation as predicted by the model for 1, 2 and 3 lane tunnels are shown in Figures 4, 5 & 6 below. The figures indicate the percentage of evacuees that are yet to evacuate the tunnel at any point in time during evacuation. The vertical line indicates the time when evacuation is expected to be complete in an Australian tunnel, and can be used to predict the percentage of people yet to evacuate tunnels designed in accordance with French, US or Netherlands (250 m) guidelines. Australian tunnel design was assumed as a reference point in this comparison.

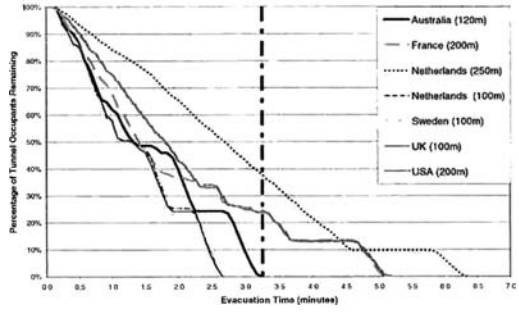


Figure 4. Egress results for 1-lane twin tube, urban road tunnels.

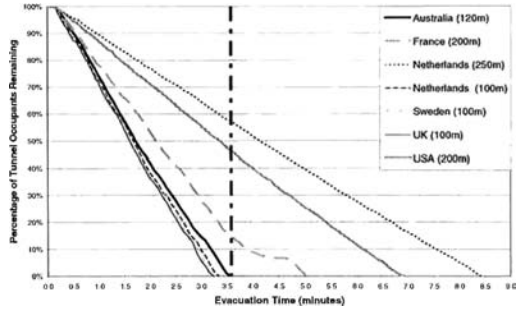


Figure 5. Egress results for 2-lane twin tube, urban road tunnels.

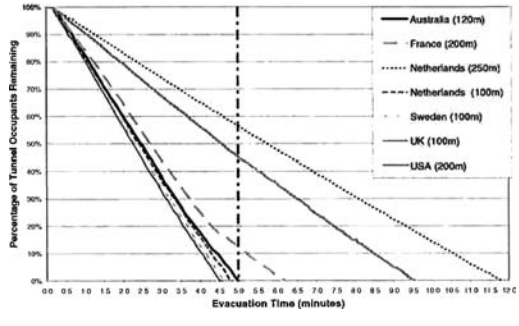


Figure 6. Egress results for 3-lane twin tube, urban road tunnels.

6 SUMMARY

The frequency of the egress passages has an impact on the occupants egress times and safe evacuation and the rapid implementation of fire fighting activities by the fire brigade to extinguish and control fires, therefore protecting and saving life and property. However, currently there is no uniform position on safe distances between egress passages in road tunnels internationally.

Internationally accepted guidelines such as PIARC, NFPA, EU Directive, and AFAC recommend varying egress/cross passage distances. In addition, various countries around the world have developed and adopted their own national guidelines that define the minimum safety provisions applicable to new tunnels, including maximum distance between egress points and, in some cases, the minimum passage and door widths.

SIMULEX models were created with egress provisions for long, dual tube, uni-directional urban road tunnels in Australia, France, the Netherlands (100 m and 250 m distances), Sweden, UK and USA in accordance with the applicable guidelines. The modelling results showed that the UK, Sweden and Netherlands (100 m passages) would achieve slightly better egress times than Australian tunnels, with France, Netherlands (250 m) and US expected to have longer egress times. The egress times ranged from 2 min 35 sec (for egress distances of 100 m) to 11 min 50 sec (for egress distances of 250 m).

7 OTHER PARAMETERS AFFECTING EGRESS

7.1 *General*

In addition to the frequency and size of egress points, there are other components that are critical for safe evacuation of tunnel occupants such as:

- traffic density and occupant loading
- allowance of congested traffic conditions
- occupants reaction (delay) time (greatly dependent on incident detection and advisory provisions)
- walking speed of occupants
- fire size and growth, fuel type, smoke production
- capacity and type of tunnel ventilation system (longitudinal, transverse, semi-transverse)
- smoke management systems (smoke ducts)
- tunnel detection and communication provisions
- fire protection systems (such as deluge)
- adopted emergency rescue scenarios

These components either help to directly shorten the evacuation time or prolong the time available for evacuation within a tenable environment inside tunnels. There are varying views on each component within the international tunnel engineering communities, and further research is required to determine acceptable values.

7.2 *Egress provisions and occupant loads*

Emergency egress provisions in road tunnels vary between countries, as do the occupancy loads. Australia and Japan install deluge systems that have a potential to improve the tenability inside tunnels, and can provide additional property protection. However, Australian tunnels have comparable egress provisions with European countries, but differ from Japanese tunnels.

In addition, new rail tunnels incorporate egress passages at a distance of not greater than 244 m as recommended by the NFPA 130, even though the occupancy level is expected to be a lot higher, (up to 1600 people for an 8 car train) and the egress time can take up to 2.5 hours if all goes well. Expected occupancy levels for the applications discussed are summarized in Table 7 below:

Table 7. Summary of expected occupancy levels.

	Number of people evacuating a tunnel section		
	1-Lane	2-Lanes	3-Lanes
Australia (120 m)	115	229	343
France (200 m)	191	381	572
Netherlands (100 m)	95	191	286
Netherlands (250 m)	238	476	715
Sweden (100 m)	95	191	286
UK (100 m)	95	191	286
USA (200 m)	191	381	572
Japan (700–800)	667	1333	2000
NFPA 130* (244 m)	1600	N/A	N/A

* Applicable to rail tunnels only

7.3 *Occupant reaction time and walking speeds*

The response times of tunnel occupants are highly unpredictable and there are no set values applicable to tunnel environments. Some test data is available and further tests and studies are being undertaken to research human behaviour during emergency evacuation from tunnel environments. Currently PIARC suggests delay times between 2 to 5 minutes. Most guidelines and studies suggest that the first 5–10 minutes after a fire incident are the most critical for safe evacuation, therefore shorter delay times are very critical for safe evacuation.

Occupant walking speeds also vary between various guidelines and the feedback from real tunnel evacuations and tests. Some of the recommended values are summarized in Table 8 below:

Table 8. Summary of recommended occupant walking speeds.

Values in m/s				
PIARC	NFPA 502	SFPE	SIMULEX	Japan
1–1.5	1	1.19–1.25	1.225	1.2–1.7

7.4 *Fire size and smoke production rates*

Fire size, fire growth and the smoke production rates are detrimental to the tenable environment during tunnel evacuation. Various guidelines offer different values. Comparison of current and recommended fire sizes are summarized in Table 9 below:

Table 9. Comparison of recommended fire sizes.

Type of vehicle	PIARC (MW)	NFPA502 (MW)	AFAC (MW)	France (MW)	Ingason (MW)
small car	2.5	5	2.5	–	5
large car	5	5	5	–	5
2–3 cars	8	–	8	8	10
van	15	–	15	15	20
bus	20	20	20	–	30
lorry	20–30	20–30	20–30	30	50
HGV	100–120	–	100–120	–	70–150
petrol tanker	–	100	100–120	200	200+

In addition, latest tunnel fire test results (Ingason, 2006) suggest adoption of increased fire sizes and faster fire growth values, reaching a maximum fire size within 10 minutes. These increases will also lead to new fire smoke production rates that are yet to be determined and will affect tenability inside tunnels.

Using "t-squared" fire growth is the most accepted description of the rate of heat release of accidental open flaming fires and adopted for tunnel fires. The general equation is as follows:

$$Q = \alpha t^2$$

Where: Q = fire hear release rate [kW]
α = coefficient of growth
t = time [s]

Current and future proposed fire growth rates are summarized in Table 10 below:

8 RECOMMENDATIONS

More research and field studies are being performed and new data is emerging on topics related to fire emergency within a tunnel environment such as:

- expected vehicle density and occupancy rates within a tunnel, including traffic control
- human behaviour
- impact of fire detection and communication systems on the occupants reaction (delay) time
- acceptable walking speed
- fuel type, smoke production, fire size and fire growth rates
- fire and life safety provisions including tunnel ventilation, smoke management (smoke exhaust ducts) and water suppression systems
- emergency operation procedures

The outcomes of the latest research results need to be analysed collectively by the worldwide tunnel engineering communities and authorities that have jurisdiction over setting of guidelines for road tunnel designs. As a consequence, the current guidelines and design practices adopted by various countries may need to be reviewed and updated subject to the outcomes of the latest research findings. Collective agreement on the design parameters, or at least an agreed design approach, within the tunnelling communities and project approval authorities is critical in order to guide tunnel designers in delivering safe and sustainable road tunnel projects in the future.

REFERENCES

Appendix No. 2 to interministry circular no. 2000-63 of 25 August 2000 relating to the safety of tunnels in the national highways network. *Technical Instruction Relating to Safety Measures in New Road Tunnels (Design and Operation)*, 2000.

Australian Standards, 2001. *AS1428.1 Design for Access and Mobility, Part 1: General Requirements*.

Australasian Fire Authorities Council, 2001. *Fire Safety Guidelines for Road Tunnels*.

Bendelius, A.G., Li, S.K., Kennedy W.D. & Harvey N. 2002. Simulation of Escape from Road Tunnels Using

Table 10. Comparison of recommended fire growth rates.

Fire growth	NFPA92B α	UK (Hall, 2006) α	MW	s	Ingason, 2006 MW/min	α
Slow	0.0029	0.0223	8	600	–	–
Medium	0.012	0.0833	30	600	–	–
Fast	0.0478	0.2778	100	600	10 for HRR $\leq$ MW	0.2778
Ultrafast	0.188	0.5556	200	600	20 for HRR $\leq$ MW	0.5556

SIMULEX, *International Conference Tunnel Safety and ventilation. Graz. Austria, April 2002*.

European Parliament, 2004. Directive 2004/54/EC of the European Parliament and of the Council, *Official Journal of the European Union, 2004*.

Hall, R.C, 2006. Ventilation during road tunnel emergencies, *PPR140, TRL Limited, August 2006.*

Ingason, H. 2006. Design fires in tunnels, *Second International Symposium, Lausanne, May 2006.*

Integrated Environmental Solutions, Ltd. 1998. *Simulex Users Manual*.

ITA, 2002. Who are you designing your tunnel for? *Journal of Tunneling and Underground Space Technology, 2002*.

Li, S.K., Kennedy W.D. & Harvey N. 2001. Simulations of Escape from Road and Rail Tunnels Using SIMULEX, *Safety in Road and Rail Tunnels, Fourth International Conference, Madrid, Spain, April 2001*.

Ministry of Transport, Public Works and Water Management, 2004. *Securities Directive Part C – Basic Measures*.

National Fire Protection Association (NFPA), 2004. *NFPA502 Standard for Road Tunnels, Bridges, and Other Limited Access Highways, 2004 Edition.*

National Fire Protection Association (NFPA), 2006. *NFPA101 Life Safety Code, 2006 Edition.*

Offfice of the Deputy Prime Minister, 2000. *The building Regulations 2000, Part B: Fire Safety*.

PIARC, 1999. *Fire and smoke Control in Road Tunnels, Report 05.05.B.*

PIARC, 2007. *Systems and Equipment for Fire and Smoke Control in Road Tunnels*. Not published yet, due 2007.

Roads and Transport Research Association, Federal Ministry of Traffic (RABT), 2002. *Guidelines of equipment and operation of road tunnels*.

SFPE, 2002. *The SFPE Handbook of Fire Protection Engineering, Third Edition*.

Swedish National Road Administration (SNRA), 2000. *Common Ring Road Building Specification.*

The Highways Agency, 1999. *Design Manual for Roads and Bridges, Volume 2 Highway Structure Design (substructures and special structures) materials, Section 2: Special Structures, Part 9, Design of Road Tunnels*.

This page intentionally left blank

Section 9
Historical underground construction; maintenance and reconstruction of underground constructions

This page intentionally left blank

Underground Space – the 4th Dimension of Metropolises – Barták, Hrdina, Romancov & Zlámal (eds)
© 2007 Taylor & Francis Group, London, ISBN 978-0-415-40807-3

Geotechnical recent issues in relation to past mining activities at urban area of historical mining towns in Slovakia

V. Bauer
Technical university of Košice, Department Mining & Geotechnics, Slovakia

E. Sombathy
Mining society, Banská Štiavnica, Slovakia

M. Stavnikovič
Technical university of Košice, Department Mining & Geotechnics, Slovakia

ABSTRACT: At the Slovak territory there are several historical mining towns with extensive underground spaces and construction systems. Nowadays, in aftercare and restoration mining stage, have these abandoned working and spaces systems oft unique character, but also with undesirable geotechnical risk and impact to surrounding in each individual towns.

After several years ago these geotechnical impacts makes itself also as a damages on the surface buildings and objects. First of all in old historical interesting gold and silver mining town Banská Štiavnica, that is except as well the cultural heritage of UNESCO town, they may to be survey some surface geotechnical changes and some destruction. In many case are being this changes straight bellow in the middle of the town near by residential area.

The contribution deals about the in underground developing geotechnical impacts and some new geotechnics situation, there are as a result of groundwater move effect as well as the various tectonic destroy. The geotechnics and environment issues could be considered as a main problems resulting from extraction of minerals in deepness more than 500 m under town. At present has town number thousand solid content of unknown opened underground spaces, there are constantly dangerous for living environment. Therefore the article deals also about the geotechnics methods there could be acceptable by problems solution from geotechnical point of view.

1 INTRODUCTIONS

The Slovakia has a long metal mining history, but at present time with the exception of two metal mines operated by Mining companies Siderit Nižná Slaná,Ltd. and Slovenská Banská spoločnost', Banská Hodruša, Ltd., there are hardly any metal mines still in operation. However a few years ago were on the all territory many that time economically important underground operated metal mines. In most cases they were localities with yearly extraction performance of industry minerals more than 1 Million tons, for example the mining fields in Rudňany and Slovinky on the east part of the country. Except above mentioned two most undergound mines in the region of the present Slovakia they were also the another mines with early very extensive mining activities. In this context they are scores of the time mentioned the oldest mining cities Banská Štiavnica, Kremnica and Špania Dolina, which are situated in the middle part of country, and that also were very closely connected with occurrence of ore deposits as both gold and silver. Alikes to Spiš-Gemer metalic ore-fields with many important rich in copper mines production, with the beginning of mining in 15th century, also Banská Štiavnica silver-gold ore field has belong among 13th and 18th century with its both gold and silver production to the richest in Europe. In a similar manner is to be mention the unique opal deposit and mine Dubnik, that is located in the middle of northen part of Slansky mountains. The beginning of noble opal mining might reach up to 16th century, what at present time shows numerous destroyed and collapsed underground and open pit mine areas.

Despite of all hereby stated facts is significant highlighted, that with the expection of Bansko-Štiavnicko-Hodrušský ore field there is not exist on the present any mining activities on the places, which were once upon in previous time so well-knowed. As it was discussed

above on the all oldest mining localities and also on the all till then operated mines, were aproximetly since of 1998 year the all mining activities stopped and the mines were fully closed in stages.

About present time period its began very strong consider respecting to underground mining spaces utilisation for so called non-mining purposes. The main task was to solve problems with stability of opened underground spaces, because non each of operated mines were closed according to technical requirement. Namely, the all reclamation after finishing or terminating of a mining activity belongs to responsibilities of a organization, to which a mining claim is registered. The reclamation itself is not permitted by a district mining office, but by a county office, division of allotments, agriculture and forest management. The all connecting activities with restoration and aftercare works in Slovakia it has to supply the main state institution, which has the financial purely for the mines in closure phase. However today is an increasing tendency to stipulate such provision for new projects.

At present time is considerable number of old and abandoned mine workings all over the country, that could have need more financial support with regards to the elimination of environmental impacts in connection with geospace and underground water. There is a considerable number of old and abandoned (orphaned) mine workings all over the country, and some of them cause quite substantial environmental impacts, especially in connection with surface run-off or water from underground workings. The Mining Directorate has for more than 15 years managed projects aimed at mitigation of the most severe negative cases. This work has mainly been financed by the Ministry of the Environment. Similar must to be to evaluate the all activity, associated with exploitation waste disposal within waste dumps, tailings, underground spaces and nature rock masses structures, is assumed as mining activity, and for its performance a mining license and a permission by the district mining office, is demanded.

On more mining localities of Slovak territory, e.g. Banská Štiavnica, Hodruša, Kremnica, Špania Dolina, Smolník, Rudňany, Gelnica and next old mining towns, at last 10 years was indicated negative demonstration of Mining activities on surface. This dangerous stage follows from:

- mining methods development
- long term underground exploitation
- unknown mining spaces and objects
- opened and abandoned spaces, which are not signate in any mining maps (there are the object 13th–16th century)
- geomorphological conditions
- progression of building plan in towns
- localization of surface objects by former operating mines.

2 GEOTECHNICAL REQUIREMENTS BY AFTERCARE MINING MANAGEMENT

In case of the termination of old mines, that they are near by settled zones is crucial to evaluate the all geotechnical aspects of abandoned underground spaces, first of all their condition of stability. The above mentioned polymetallic minerals and ore deposit districts at Slovakia territory have formerly belong to the most important localities for the gold, silver, copper and semi-precious stone underground mining. The mining of gold and silver-bearing minerals has been running across several centuries there. New geological exploration and mining works started at 50th years of the last century. Expect in old semi-precious stone opal/ hyalite at the deposit Dubník, on which the mining activities were closed in 1922 year, it went on the mining production by another mines till end–of nineties. In these years were the all polymetallic ores deposits at the territory of Slovakia over definitely closed including of their relatively modern plant processing.

Number of data and corresponding information related to the history of mining, exploration activities, mining technologies, the mineral processing plants, eventually another with mining coupled activities are scattered in separate records room and other institutes. Thus ways they are these data searched and processed uniformly for the subsequent utilisation for detailed studies and for the help to the state and municipial bodies. In Slovakia does these works the institution – Geological Survey of Slovak Republic, which represents an independent contributory organisation of the Ministry of the Environment of Slovak Republic.This institute, as a ministerial scientific research institute, besides its main goals focused to the geological research and exploration, deals also with geotechnical conditions of the territory, mainly for purposes of land use planning and aftercare mining monitoring. By one of his main goal is also the research into geological structures suitable for final waste storages into suitable natural rocks and underground spaces. The institute safeguards of obligations following from the Law of National Council of Slovak Republic No. 52/1988 of the Law Code on geological works and Slovak Geological Office in the wording of the Law of National Council of Slovak Republic No. 497/1991 of the Law Code and from the Law of National Council of Slovak Republic No. 44/1988 of the Law Code on the protection and utilisation of mineral resources, in wording of the Law of National Council of Slovak Republic No. 498/1991 of the Law Code on registers administration, management of exploration territories, administration of attests on exclusive deposits, administration of exclusive deposits resources and balance sources of mineral raw materials, management of register of old mining works, gathering, administration

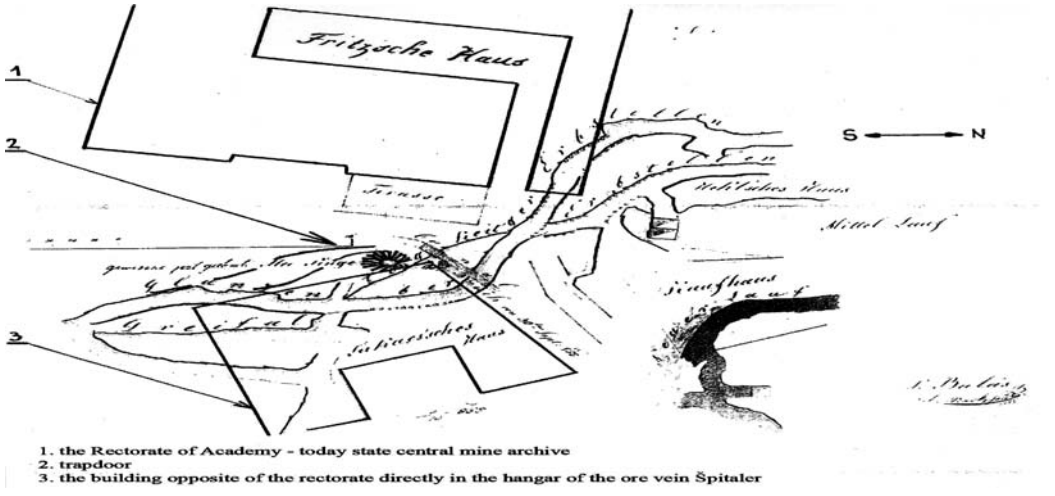


Figure 1. Historical map detail of collapsed mining area in part of old mining town Banská Štiavnica.

and making available of geological works results. In large measurement they are the activities of institute intent on protection and sustainable usage of rock environment and ground waters.

From abandoned underground spaces reemploying point of view is very necessary by evaluation concerning spaces to solve many of geotechnical and old mining technological issues. For the effectual solving of problems is to be go from searching and collecting of records indication at mining area, which are related to the watched mining district out. The same way is needed to have to disposal the database of geographic information from the old underground, in order to be completed the field data from the exploration of terminate mining.

By analyse of all condition of rock massive stability into old exploitation area including opened and abandoned underground spaces it must to be proceed with the respectable **methodology for obtaining of relevant information and** data primarily acquired from various sources. The periods of historical mining and dressing of ores, geological exploration, modern mining and dressing of ores and the period of mine workings closure and reclamation of areas affected by mining lasting up to now will be differentiated between one another.

In many parts of Slovakia underground cavities – corridors, tunnels and mining blocks, created by mining exist under surface areas that are now populated. This has come about because mine maps were not always available, for instance due to uncontrolled mining activities, the loss of mining documents – especially as a result of the not quite well assembling and the fact that some old mines were simply not mapped. Provided the underground mining structure is sufficiently stable, i.e. it is located deep enough with adequate pillar dimensions and provided there is no freshwater inflow into any regions located in different geological formation, then such old mine workings do not pose any danger to the earth's surface. If, however, the overlying rock is too weak or the pillar size is too small, any villages, roads or other structure located above the underground cavities are acutely endangered. This is particularly true for old mine workings or shafts in rock, in which there is an inflow of freshwater and the same time an outflow of brine. To protect urban areas threatened with collapse, large-scale redevelopment work using boreholes for mine filling is necessary to stabilize the underground. However, in order to efficiently position the needed filler boreholes, it is necessary to know accurate details of the underground mining structure. That is not usually possible to access these old structure, the information required can be gained only from exploration boreholes. Implicitly are being also any different techniques how to find the underground open space to identify its. By one of such method is a sonar tool usage to measure the all surrounding underground cavities. One different possible to search the opened spaces in underground after the mines activities is e.g. tomographic geophysical measurement. Namely, scores of the time just then, if its go to be about cases on former mining district nearby small cities damages of surface, that are caused by breakdown of subterranean cavities of mine, which e.g. had been exploited from the 19th century until fiftieth years. In these cases it is needed verified the hazards for surface areas by tomographic method. This measurement technique benefit

the statement building, roads and other public facilities being not endangered by effects of former mining activities.

By all above presented methods it is needful to understand very well the both geotechnical and also hydrogeological conditions at evaluated settlement areas. These requirements are respond to next utilization of abandoned underground spaces in extenso. It depends, whether opening spaces have to be construct for underground waste management or must to be flooded. In second mentioned case will to be needed in closed mines to propose such safety measures, which will help to lose problems with the drainage of minewater in abandoned tunnels (Fig. 1).

3 ENVIRONMENTAL INFLUENCES OF MINES FLOODING

The example of flooding mine in Rudňany at east Slovakia shows to important aspects of environmental part of technical issue solution. Within the scope of the technical part the solution of research works was concentrated first of all on creating the model for judging the overall hydrogeological and geotechnical situation, as well as on modelling some technological underground systems of the Rudňany mine, mainly the system of ventilation and pumping the underground mine waters. A part of the solution at the same time was judging the technical measures of flooding the mine in the relation to the safety requirements of the surface situation and from the point of view of the environmental protection, but also in the relation to the economical evaluation of the realisation of some technical–technological activities underground as well as on the surface.

The closure mine Rudňany was provided by a gradual flooding of individual mining levels. This solution it give not possibilities for the eventually secondary utilisation of abandoned mine spaces. With regard to the existing and fading away mining in above mentioned mine, but also from the point of view of adopted and agreed intention to liquidate the mine by flooding, by the management of the plant in Rudňany was decided to flood the mine in three stages. Individual stages of flooding supposed the total excluding the mine activities on the levels discussed and the following conditions.

The solution of the closure mine by flooding way was aimed at judging and re-evaluating all the aspects, factors, and influences of flooding, first of all from the point of view of the supposed flow and movement of underground water, but also from the point of view of the existing tectonic-geological structures, within the relation to the past as well as existing mining activity. The result of the mining activity at the deposit is a vast extent of mine openings of the whole ore field, which consists of very branched system of mine openings, underground spatial objects and mining blocs on all the underground levels of the mine. The yardage at disposal of these spaces nowadays, mainly in case of mined out exploitation blocks, is difficult to identify, as in the past caving and cut-and-fill technologies of mining were employed. The actual volume potential of existing system of underground spaces of collecting underground water is only supposed and quantified with a certain estimate. The total volume of the free space includes all the open spaces in the eastern and western part of the mine.

The aim of the study was to judge the consequences of flooding active levels of the mine and re-evaluate the sequence of flooding on already stopped levels. The study at the same time draws attention to technical measures and details of flooding, which will affect the geo environment of the mine and ecological components of the life environment on the surface. From the point of view of environmental judging the consequences of flooding the mine were evaluated the decisive factors connected with the underground water level or its flow in the whole space of the mine, as well as with the quality of these waters. When judging the fluctuation of the underground water level it was come out from the idea that the underground of the mine represents a connected system of tanks in which exists the all-directional water circulation. The predicted movements of the underground water were judged in the relation to the precipitation and the subsequent inflow of waters to the underground of the mine. At the same time the static level of flooding of mine on the Rochus tunnel level was determined and the possibility of mixing underground waters with flowing-in surface waters on the basis of the hydrological balance was re-evaluated. The substantial change in the chemist of flowing-out mine and underground waters and its influence on the environmental surrounding was not confirmed even in case of liquidation of oil substances as the residuals after mining technological processes. The influence of the water chemise acting on the hydro technical objects underground was not evaluated as these objects are not supposed to be built.

As grounded was shown the real possibility of weakening tectonically fractured zones by the effect of water flow and forming the area of undermining, caving belts and deformations of the surface mainly around shafts – Mier and 5 RP II. The supposed surface deformations of the terrain were confined by isolines of cavings in the exposed areas of the discussed mining space. The study re-evaluates the influence of the caving areas on important social and ecological objects in the built-on sections of the surface from the point of view of possible permanent movements. The assumption for correct technical solution of flooding the mine was the re-evaluation of the ventilation system on the basis of newly formed situation and the design

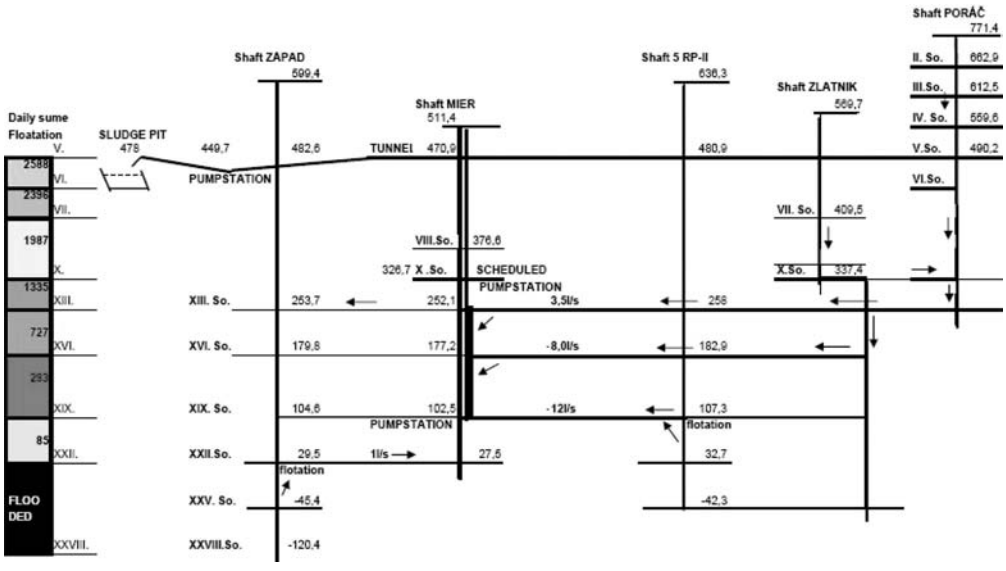


Figure 2. Preparation and building of shaft schema and drainage system mine Rudňany.

of ventilation objects for safeguarding the required regime of ventilation of abandoned and active working places above the 19th level. The study has shown the need of working out the updated ventilation balance as at the flooding a substantial change of the ventilation system is formed. For the system of pumping mine waters in the study there is proposed a pumping station on the 10th level of the Mier shaft. The proposed technical measures are economically judged on the basis of investment demand of the realisation of technical measures and required kinds of works on the basis of the supposed budget. The ecological and mine damage are in the study solved independently. The study analyses negative influences of the process of flooding the Rudňany mine and define possible consequences of these influences, mainly in the relation of the surface subsidence. At the same time proposes concrete technical measures and recommendations to prevent undesirable influences of flooding from the point of view of endangerment of the life environment in all its components (Fig. 2).

4 UNDERMINING OF HISTORICAL CENTERS IN OLD MINING TOWNS

Undermining influences has showed in full extenso to in conditions of gold – silver ore deposits district Banská Štiavnica – Hodruša. Most developed vein structure on deposit was Špitaler vein ore body, which was appeared to surface over the center of town Banská Štiavnica. Mining in 11th–15th century have not left any negative impacts on surface, with except heard quarks which have destroyed all buildings objects of Glanzenberg. In small depth under surface was mining activities directly under building plan of towns and villages in above mentioned ore districts. From surface negative impact are nowadays critical just those mining areas – without disposal mining maps (Fig. 2).

At last 10 years after finishing of extraction in old mining towns, which were mentioned, was 6 serious subsidence process of surface into mining spaces. In most cases handled it about local point depressions over some vertical mining objects as raise and shaft, which where insufficiently supplied by closing mining process. In one individual case in 1995 was large extend in crush about old mine spaces near by Maria shaft on vein Grüner and surface depression was in extend 10×30 meters. This cave-in was just 80 meters from building plan of residential house. Last 30 years was just one case of cave-in on surface of results in mining in 90th years. It was in year 1998 during drift of raise KT-221 on second deposit level of Teresia vein. In mentioned case was surface depression in extending 40×5 meters to depth 15 meters. After destruction of old mining areas in to this raise were outflow of fill materials into this raise (Fig. 3).

Cave-in was decline more and more in this reason was destroyed tourist way, which was just 1 meter from previous cave-in. Reason of building water-supply in town Banská Štiavnica, what is 17 years after cave-in the raise must be solved the effects of this event. In the last time period we can mention cave-in the town street in year 1973 in another place 10 meters far from tunnel

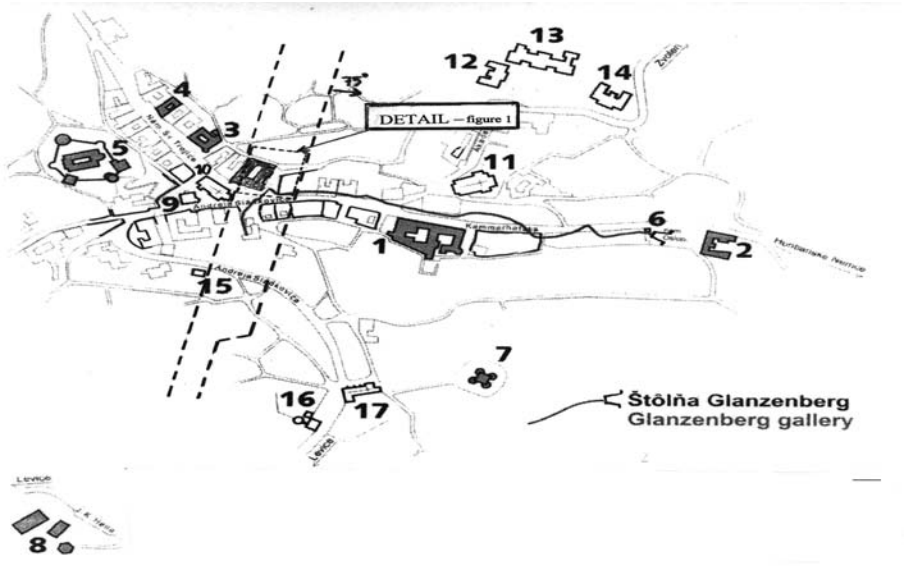


Figure 3. The process of ore vein Špitaler and the mining in depth till 30 m from the surface cross the city center of Báňská Štiavnica. Glazenberg country's gallery copies the main street (Kammerhofská) in length 450 m and in depth 3 m near portal till the depth 34 m in the crossing with sequence corridors.

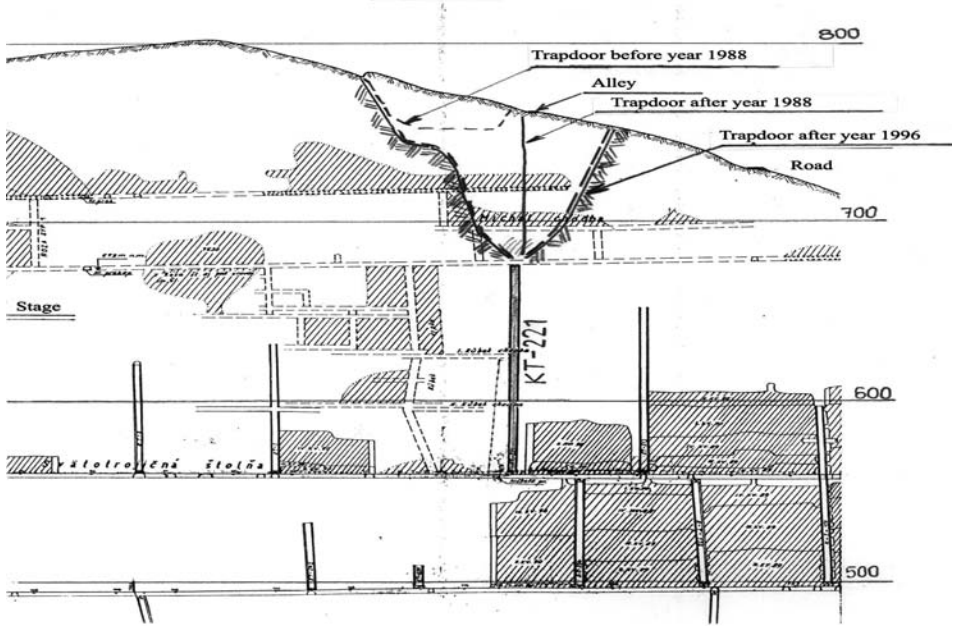


Figure 4. Situation of trapdoor shaft KT-221.

collar Glanzenberg, which was 9 meters under ground. This was solved by inbuilt TH segments of reinforces and concrete rafter of 5 meters long line and filling the surface slot with gravel. From this period since to year 1991 was tunnel not monitored. The tunnel Glanzenberg was first time reconstructed in year 1992. Since this is under consideration general rebuilding of tunnel Glanzenberg. To general repair of tunnel come

in year 2001, when it was reinforced with stone furring. In year 2001 was tunnel opened for visitors in framework with Slovak Mining Museum. Similar in year 2006 was rebuild the shaft Kaufhaus. Here bay where secured the two most critical object directly in the center of the town Banská Štiavnica (Fig. 4)

5 CONCLUSION

In the paper described issues impacts of subsidies in historical centers of old mining towns at Slovakia, will be needed to solve in particularly details. Results from facts in article is visible that after finishing the mining activities will take for some decade as far as the effect of the mining on surface will be eliminated. Favorable solve for all mining districts at Slovakia could be combination of looking for new utilization of old mining spaces and therewith possibility their monitoring respectively reconstructions. It shows that after care mining and closure mine could be one new study field. Till now has no connection with praxis and also haven't sufficient technical support. Therefore we must assume that many in last time realized technical projects could be after some time as inapt.

REFERENCES

Čech, J., Bauer, V. 2004. A computerized evaluation of mining project. (*MPES 2004, Wroclaw, Current Contents*), pp. 625–629, Amsterdam. Publishers B.V.

Bauer, V., 2005. Mineral policies and land use planing in Slovakia. Mining and Sustainable Development, *World Mining Congress, SUB Theme 1: Environment impact of Mining. Geological Survey and National Geoscience Database of IRAN,* (*Current Contents*), Teheran, pp. 149–160.

Bauer, V. Nielsen, K. 2005. Mineral Policies and Land Use Planning in two Central European and two Nordic Countries with a Long Metal Mining History. *Aachen International Mining Symposia* , SDIMI, (*Current Contents*), ISBN 3 –7739-5994-X, Aachen, pp. 577–599.

This page intentionally left blank

Underground Space – the 4th Dimension of Metropolises – Barták, Hrdina, Romancov & Zlámal (eds)
© 2007 Taylor & Francis Group, London, ISBN 978-0-415-40807-3

Results of the excavation works in upgrading the Frejus railway tunnel

P. Grasso, M. Pescara, F. Valdemarin & G. Beccaria
Geodata S.p.A., Turin, Italy

ABSTRACT: In reference to the paper presented to the ITA WTC 2005, concerning the design of the upgrading of the Frejus railway tunnel, this paper reports the excavation activities, the problems faced during the execution of works and the main results achieved to date. The upgrading works in the Frejus tunnel, followed on site by Geodata since 2003, according to the principle of flexible design and construction, are performed maintaining the international rail traffic on one single track, with thus significant constraints on the worksite logistics and safety. Keeping under monitoring the stress-deformation response of the tunnel's structures, the benching under the first track and the excavation of the new niches on the same side of the tunnel have been recently concluded. For effective management of the various construction phases an innovative Web-GIS application has been set-up to centralize all the geological, construction and monitoring data in order to facilitate their interpretation in real-time so as to drive the design optimizations.

1 INTRODUCTION

The Frejus Tunnel, bored between 1857 and 1871, connects Bardonecchia (I) to Modane (F), over the length of 13636 m (6791 m on the Italian side).

The tunnel is double track, with a maximum overburden of 1600 m, and an inclination varying from 1‰ to 30‰; the maximum height a.s.l. is 1296 m at the Border Line. The lining is in masonry, mainly made of stone blocks at the sidewalls and bricks at the crown; the lining thickness varies from 80 cm at the sidewalls to 45 cm at the crown.

The upgrading activities are part of the overall works to empower the historical Turin-Modane line managed by the railway administrations of Italy (RFI) and France (RFF), to allow the transportation of particular trains and to improve the safety endowments of the whole system.

In particular, the ongoing works include:

- adjustment to B1 gauge (Italians side);
- implementation of a more advanced system for managing the train circulation;
- upgrading of the safety system according to the new RFI guidelines for existing tunnels.

With respect to the new shape, it will be obtained by lowering the current rail plane by 60–70 cm and re-adjusting the two tracks in plan. As regards the system's adjustment, the new necessary apparatuses will be placed inside new or adapted niches.



Figure 1. The Italian historical portal of the Frejus Tunnel during benching of the even track.

2 OVERVIEW OF THE DESIGN PHASES

A detailed overview of the design can be found in Grasso et al. (ITA WTC 2005) and hence only some essential information is given below.

2.1 *The geology*

The Frejus tunnel is excavated in the formation of the calceschists of the "Serie Piemontese" (Schistes lustrés), which have been assembled in wide plicative structures.

Table 1. Representative geomechanical parameters of a section and used for the numerical analysis.

E_d	$\sigma_c \approx \sigma_{cm}$				
[GPa]	[MPa]	$m_b(=m_i)$	$s(=s_i)$	m_r	s_r
10	30	10	1	1.017	$8.1 \cdot 10^{-4}$

E_d = deformability modulus;
$\sigma_c \approx \sigma_{cm}$ = compressive strength of the rock mass;
m_b,s, m_r,s_r = constants of the Hoek-Brown failure criterion.

From the geologic-geomechanical point of view the calcschists show a remarkable variability (from almost massive to foliated) essentially due to tectonization, with a tendency of creeping behaviour.

The geomechanical characterization was developed on the basis of various in situ and laboratory tests and confirmed by back-analysis.

Table 1 shows the values of the main parameters derived and used for the numerical analysis.

For the in situ stress, a deficit of the vertical stress was verified, and the values of the k_0 (horiz./vert. stress ratio) quite variable, generally comprised between 0.7 and 1.3.

2.2 *Constraints of the site*

The need to maintain a well defined "respect zone" to guarantee safe exploitation of the tunnel on one track conditioned all the design and later on the construction activities, with sever limitations to the space available for the machinery. For most of the time the activities are undergoing in such conditions because only for few hours each day divided in 2 "windows" a complete interruption is foreseen.

2.3 *The actual tunnel conditions*

The tunnel lining in itself can be considered as still in quite a good condition. Anyway, the presence of a cracks located in the crown and a generally high level of stress in the blocks must be pointed out with an asymmetric distribution inside the arch. Moreover, the inspections of the lining's foundations revealed poor bearing conditions.

The back-analysis calculations, done with the code FLAC, reproduced the actual conditions of stress and strain inside the structure, which can be summarized as characterized by:

- asymmetry of loads;
- high stress values;
- tendency of the structure to converge at the sidewalls with consequent high compression stresses at the intrados of the crown, justifying the existing crack at the crown.

2.4 *The design solutions*

Starting from the results of the above mentioned studies, further numerical analyses were performed to evaluate the effects of the excavation on the existing tunnel structure. Such calculations allowed to define the targets to be reached through consolidation works which should permit the excavation to be done in safe conditions. The specific objectives are:

a. to contrast the lining convergence trend aggravating the compression at the crown, and thus limiting further weakening of the structure;
b. to prevent settlement of the structure due to potential sliding of loose materials underneath the foundation during bench excavation;
c. to completely support the arch in the zones where it will be partially demolished to create the new niches or in particular, delicate sections;
d. to support punctually the masonry arch in correspondence of the portal of any niche.

Hence, the design solution foresaw:

- filling of void at the extrados to re-establish the contact with the surrounding rock mass;
- installing rock bolts at the side walls to contrast the convergence;
- consolidating the foundations where needed to prevent potential settlements.
- to reinforce the whole arch with rock bolts when the niches should be excavated.

3 THE RESULTS OF THE FIRST HALF OF THE WORK

3.1 *The consolidation works*

The consolidation works, prior to every excavation, strictly followed the design, consuming in the period of 2003–2005 the following quantities of materials:

- 60.000 meters of CT-Bolt anchors,
- 9.600 meters of self-drilling bolts;
- 8.950 meters of Swellex Mn24;
- 3.250 tons of dry product injected corresponding to 4000 m^3 of grout mixture.

In accordance with the design philosophy based on a flexible approach, the choice was to achieve a generalized strengthening of the overall arch by making it collaborating with the surrounding rock mass. In the mean while, in collaboration with the Engineer and the Client, a systematic check of some particular conditions were made during the site operation in order to identify any special weak points.

One of these weaknesses was an almost continuous longitudinal crack located exactly at the top of the crown, which proved to be extending for more than 3 km on the Italian side. In October 2004 an unforeseen fall of a block of masonry occurred at Ch. 88 + 030,

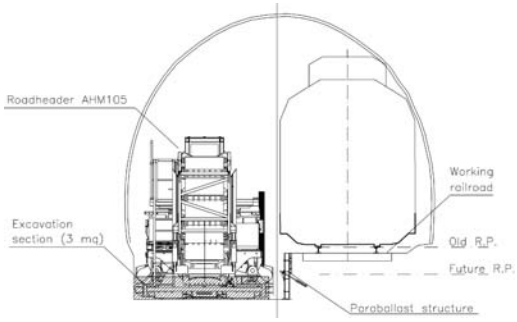


Figure 2. Geometry of the excavation phase.

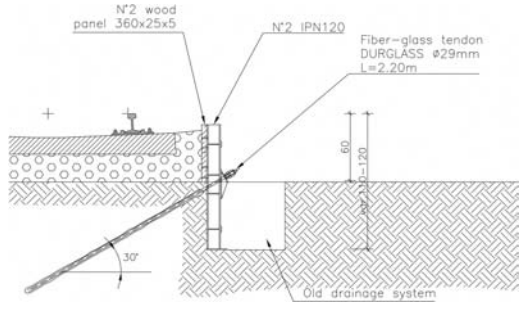


Figure 3. The "paraballast" in good rock, constituted by a continuous structure in wood anchored punctually to the rock by fiber-glass tendons connected to vertical steel beams.

just in correspondence of the crack, and such event, which caused the temporary closure of the railway line, led to the decision to integrate the interventions along an extension of the crack for about 2650 m. It is also probable that no major problem occurred because the basic consolidation work was already done, and thus the section was already partially strengthened.

The integrative works, which forced to postpone the benching activity, consisted of:

- one structural shell, 3 m wide, 8 cm thick, made of shotcrete reinforced with steel mesh (ϕ8 mm 10×10 cm), fixed to the masonry with ϕ18 mm L = 60 cm steel nails (pattern of $0.4\,\text{m} \times 0.5\,\text{m}$);
- complete grouting of the voids located in the crown and at sidewalls extrados with an expansive, light-weight, grouting mixture;
- bolting with CT-Bolt (M22 L = 3 m) in a pattern of $1.3\,\text{m} \times 1.5\,\text{m}$, pre-tensioned to 10 kN, to anchor the new structural shell also to the rock mass.

3.2 *The benching excavation*

Ending the consolidation works, the benching excavation started on the 6th of December 2005 using a Voest-Alpine AHM105 road-header advancing from the Border towards the Italian portal.

This benching operation involves:

- removing all the existing rails and ballasts;
- installing a so-called "paraballast" in between the two rails in order to guarantee the safety of the line in operation (see Figure 3).

Due to scheduling constraints, the benching operation had to be done as fast as possible, through a refinement of the normal driving procedure for the road-header. Thus, the following excavation steps were followed, which could be adopted also because the excavation face in reality was only 0.7 m high and 3.5 m wide (see Figure 2 & 4):

- "forward step": it consists of sinking the head in the front for a depth of $10 \div 20$ cm, with the arm of cutter laterally extended for the maximum width of the foreseen cross-section to be dug;



Figure 4. Road-header in action.

- "cutting step": it is the phase of the real digging, conducted by lateral movement of the cutterhead.

Moreover, in order to create the space for positioning a new central drainage pipe running below the rail level the transversal excavation profile was created with a 2% slope towards the axis of the tunnel.

The particular excavation face geometry and the original way to operate the machine, combined with the need to respect the gauge, forced to integrate the on-board instrumentation with a special monitoring of the road-header's position to reach a better precision of digging and minimize the over-excavations, with the following elements:

- laser system for the continuous excavation level control;
- systematic manual check of the height of excavation using the fixed pins anchored to the lining.

The bench excavation works on the even rail were completed on the 20th of August 2006.

From the point of view of production, the results of the excavation were better in the straight part (more than 6 km), where the benching was constantly driven in compact rocks, than those in the two long curved

Table 2. Main excavation parameters for Frejus road-header.

Parameter	Value	Units
Total excavated volume	27810	bank m^3
Effective net cutting time	49,36	%
Average net advance per hour	10,92	m/h
Average net cutting rate	45,98	bank m^3/h
Av. Spec. pick consumption	0,08	pick/bank m^3

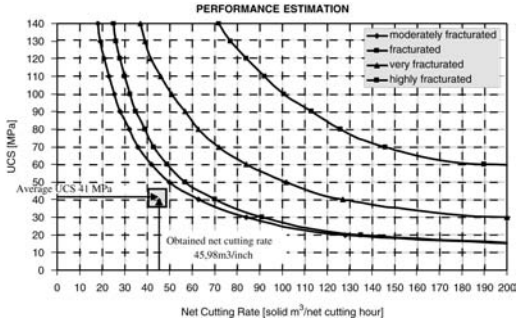


Figure 5. Indicative prediction diagram for NCT (low cutting speed).

sections where some excessive over-excavation were locally observed.

The reduced excavation section of about 3 m^2, permitted a high advance rate (maximum 190 m/day), despite the heavy limitations imposed by the track under exploitation. In fact, the critical activity of the benching was not the digging but the mucking, realized daily using railway wagons during the only 4 hours of total availability of the tunnel.

All the excavation parameters were recorded on a daily basis for analysis; the main parameters are summarised in the Table 2 above.

The comparison of these data with the available literature shows that:

- the net cutting rate (NCR) obtained compared with the results of the VAB studies (Peter Kogler, 2005), indicates that the performance is lower than what could be expected, considering the presence of a "fractured" or "moderately fractured" rock and an average value for the uniaxial compressive strength of 41 MPa.
- the specific peak consumption was slightly higher than the mean reference values given by a CAI value (characteristic abrasivity index) of the rock equal to 2,3 in present case.

The main reasons for this under-target performance (see Figure 5 & 6) were due to the reduced size of the cutting front and partly to the already-mentioned constraints.

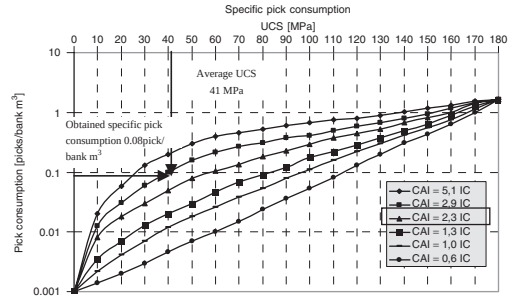


Figure 6. Indicative prediction diagram for specific pick consumption.

For the benching of the odd track, there will be no possibility to further optimise road-header digging, and great effort should be put on reducing the mucking time by, for example, starting excavation from the portal in order to have direct, continuous access to the machine with heavy trucks.

3.3 *The excavation of new niches*

The excavation of the new niches started in November 2004 and ended for the even track side at the end of June 2006.

The particular working conditions required:

- to use equipments not interfering with the track under exploitation;
- to minimize the disturbance to the portion of lining not interested by the digging.

These conditions and the constraints of the time schedule, demanded for a careful and even difficult research of the best excavation method, considering the prohibition to use a D&B technique.

The chosen alternative was a pre-cutting with multidisk saws coupled with a robotized demolisher.

Anyhow, it must be pointed out that this technique showed its limits (production around 2 m3/day), tied up also by the quite high strength in the direction of excavation, which was systematically perpendicular to the schistosity, and by the reduced space available for the manoeuvre.

New excavation techniques have already been tested to increase the productivity and accelerate the excavation of the remaining 51 new niches.

Of particular interest was the first test in Europe of the new CFI (Controlled Foam Injection) technique, which consists of injecting foam at high pressure in a drilled hole in the front, to cause a controlled fracturing of the rock, with a target of 1,5m^3/h of demolished rock. The tests however revealed the low efficiency of the CFI in a fractured-layered rock because of the escape of the foam.

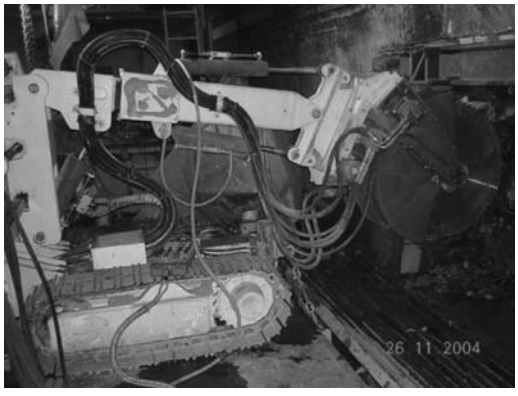


Figure 7. Multi-disk saw at work.

4 MONITORING DURING CONSTRUCTION

The interventions needed for the consolidation of the tunnel structure, for the niches' excavation and for the benching of the tunnel itself justify monitoring starting from the very first stage of the works, in order to guarantee the structural integrity during all the processes or to assure the timely application of pre-defined countermeasures in case of risks.

4.1 *The monitoring plan*

With reference to the targets of the design interventions (see Sec. 2.4), the monitoring scheme during the excavation activities was designed to:

a. quantify the tendency of lining convergence;
b. verify the settlements of the structurs foundations;
c&d. verify the effects induced onto the tunnel lining by the excavation of the new niches;
a&b. verify the effect of the vibrations of the road-header digging on the tunnel structures.

The monitoring system, based on a hierarchical system and divided in three levels, includes:

- the instruments and the topographic targets;
- the data acquisition units;
- the data centralization, management and distribution system (GIS application).

4.2 *The monitoring sections*

In order to achieve the above mentioned targets, two monitoring schemes were used: stress-deformation monitoring and vibration monitoring.

Regarding the stress-deformation monitoring three section-types were applied:

- *Current Section* (SC) spaced every 50 m with only optical reflectors;
- *Special Section* (SP), located along problematic zones (n.10 in total), consisting of five optical reflectors, plus four tangential pressure cells;
- *Niche Section* (SN) in correspondence of the new bigger niches, constituted by a wire extensometer installed to measure the lining settlement immediately above the niche excavation profile.

In the presence of cracks of the masonry in the crown, an electrical rod extensometer was added. In total, a huge number of instruments have been employed: more than 300 optical targets, 45 pressure cells, 5 wire extensomeres, 3 rod crackmeters, 2 laser distometers and 1 load cell on anchors.

Regarding vibrations, coupled with the already mentioned sections, a vibrometrical monitoring was applied during bench excavation: up to four moving sections (SV) that followed constantly the road-header which could potentially produce dangerous vibrations to the lining structure.

4.3 *The acquisition of monitoring data*

All the convergence data (SC & SP sections) and the stress data in masonry (SP sections) were manually acquired in accordance with the advance of the road-header.

Moreover, in order to avoid any problem, especially regarding the most critical points where high deformations and settlement could occur, a real-time monitoring was put in place; such continuous monitoring was applied in two situations:

- in correspondence of the new niches;
- for SV sections where the instruments were equipped with a GSM system to transfer data remotely.

4.4 *The GIS application*

Independently from the typology of the sensor, all the monitoring data (recorded in continuous with data-logger or taken by traditional methods), converged towards an unique management & distribution system, based upon a GIS-Web platform (see Figure 8).

The system allowed real-time monitoring data management and the automatic activation of alarm procedures if over-passing of predefined thresholds occurs. The link in the GIS system of the monitoring measurements with the design data and tunnel survey data, allowed to identify and to understand the instrumentally recorded phenomena and to bring them back to their correct physical meaning.

Thanks to the GIS-Web platform all the monitoring measurements are distributed in real time (with a protected Internet login) to the Contractor, the Client, the Resident Engineer and the Designer, facilitating rapid decision and activation of the counter-measures.

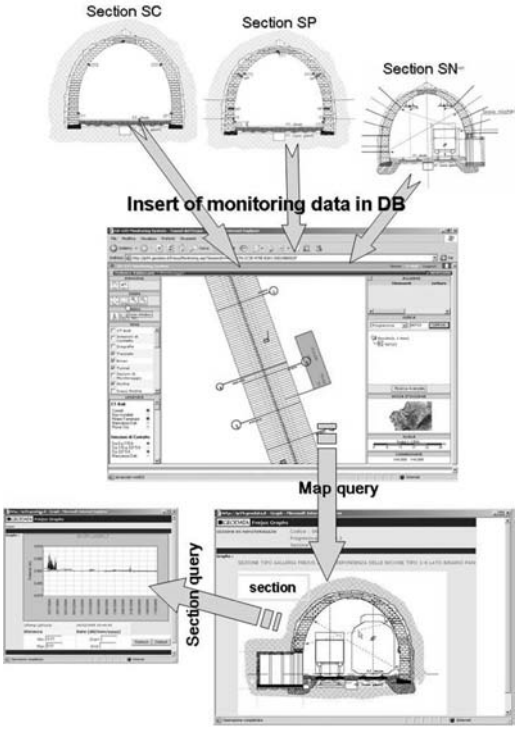


Figure 8. The monitoring with the GIS-Web application.

4.5 *The results*

The results of the stress-deformation monitoring implied very little movements of the tunnel structures during excavation phases. The measured convergences have been compared with the attention and alarm thresholds pre-defined at the design phase.

The maximum topographic recorded convergence was 5,3 mm while the maximum recorded settlement was 7,3 mm, without the evidence of any new damages or cracks.

All the installed wire extensometers on the portal of the niches did not register significant deformations.

Regarding the vibration monitoring, the results in terms of instantaneous speed PVS (Peak Vector Sum) have been compared with attention and alarm limits prudently defined at 8.0 and 12 mm/s. Maximum PVS value recorded during excavation was 15.0 mm at one single section. Also in this case no major effects were found on the structures.

5 CONCLUSIONS

Following the presentation of this challenging project in terms of design (Grasso et al., 2005), the present paper illustrated the first results of the works on site, which are at the half of the schedule.

The main points to be underlined are:

- the need to approach this kind of structure step by step, in order to better investigate, understand it and find the best solutions to assure and/or increase the general stability;
- the importance of the constraints of working inside a tunnel under exploitation;
- the great benefits of a real-time monitoring system, which helps to reduce the presence of personnel inside the tunnel and permits an efficient understanding of the response of the tunnel structure to the bench and niche excavations;
- the importance of the continuous presence on site during the works of a design & construction team able to face and to solve specific and critical problems that could arise.

ACKNOWLEDGMENTS

The authors thank for the availability of the data and the support activities the responsibles of Frejus Scarl of the Temporary Association of Enterprises constituted by CLF SpA –as leader, AR.FER Srl, GEFER SpA, SALCEF SpA, PASOLINI VCB Srl, RTS S.To:, VALDITERRA SpA, as mandator.

A special thank to L.Goffi for pictures, A.Zanichelli (CLF SpA) for contributions and S.Xu (Geodata SpA) for paper review.

BIBLIOGRAPHY

AFTES Groupe de Travail n. 14 (1983): "*Les travaux d'entretien et de réparation. Recommandations sur les travaux d'entretien et de réparation*" - Texte provisoire.

Beau J.R., Cabanius J., Courtecuisse G., Fourmaintraux D., Gesta P., Levy M., Néraud C., Panet M., Péra J., Tincelin E., Vouille G. (1980): "*Tunnel du Fréjus: les mesures géotechniques effectuées sur le chantier français et leur application pour la détermination et l'adaptation du soutènement provisoire*" – Revue Française de Géotechnique, n.12, Août 1980.

Geodata (1998): SITAF – *Traforo autostradale del Frejus, tratto italiano. Interventi di verifica delle condizioni di stabilità del traforo autostradale del Frejus lato Italia fra le progr. 4.900 m e 6.100 m – Monitoraggio, prove ed indagini in sito, prove di laboratorio*.

Grasso P., Pescara M., Valdemarin F. (2005) "*Consolidation and excavation works for the upgrading of Frejus Tunnel*" *ITA-AITES W.T. Congr. Istambul, Turkey 7–12 May 2005.* Balkema, Rotterdam.

Underground Space – the 4th Dimension of Metropolises – Barták, Hrdina, Romancov & Zlámal (eds)
© 2007 Taylor & Francis Group, London, ISBN 978-0-415-40807-3

Monitoring and evaluation after repair and reinforcement of damaged 3-lane Freeway Tunnel located within fault influenced zone

Jia-Song Hou
China Engineering Consultants, Inc. (CECI), Taiwan

Dar-Jen Tseng & Yeou-Herng Lee
Taiwan Area National Expressway Engineering Bureau (TANEEB), Taiwan

ABSTRACT: The Chungliao Tunnel is a twin-tube, 3-lane freeway tunnel located in southern Taiwan having a length of about 1800 m. The tunnel was completed and opened for traffic in February 2000, but after four years of operation, it was evident from the cracks of inner lining walls, the settlement of pavement and the increased flow of drained water, that the tunnel structure conditions were worsening possibly due to the severe earthquake that struck Taiwan in September 1999. Henceforth, it became a priority to (1) rehabilitate the pavement to meet the requirements for driving smoothness, (2) replace the main drain under the pavement and (3) reinforce the tunnel foundation. Furthermore, a detailed monitoring plan would have to be executed to verify the effectiveness of the repair efforts. The scope of the monitoring work covered the measurement of groundwater, ground settlement, etc., while inside the tunnel, monitoring focused on tunnel deformation, profile clearance and crack on pavement and side walls. This paper reviews the data measured from monitoring and further evaluates the cause-effect relationship between the fault and Chungliao tunnel. The results of one year of continuous monitoring and the final report of assessment of measured data are also discussed to determine the next step and whether or not future rehabilitation measures are required.

1 INTRODUCTION

The north portal section of the twin-tube, 3-lane Chungliao Freeway Tunnel features different mudstone and sandstone materials and a heavily sheared fault area. The tunnel is more than 1800 meters long and its dimensions include an excavation width of around 16 meters and excavation height of around 12.5 meters. Because of the wind and rain, the mudstone material is easy-to-erode and the topography of the area is a local representative landmark of the natural landscape of southern Taiwan.

On September 21st, 1999, around two months before tunnel construction was finished, a severe earthquake struck Taiwan. The quake, with its epicenter located in central Taiwan, brought about some damage to the Chungliao Tunnel, but it did not affect the tunnel's forthcoming opening to traffic in February 2000. However, after four years of operation, cracks of inner concrete lining walls, settlement of pavement and

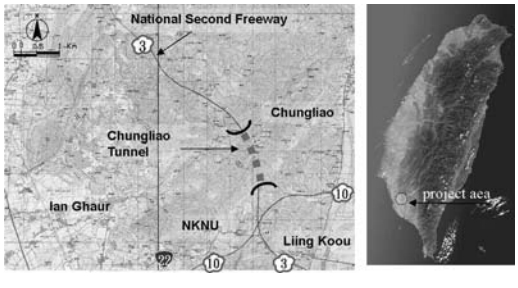


Figure 1. Location of tunnel Chungliao, Taiwan.



Photo 1. Landscape of mudstone topography.

increased flow of drained water became worse and seriously impeded the traffic functions of the freeway. In response, a rehabilitation plan was proposed by the Client, Taiwan Area National Expressway Engineering Bureau (TANEEB). Details of the repair works and the monitoring and evaluation report will be described in the following sections.

2 GEOLOGICAL CONDITIONS OF NORTH PORTAL OF CHUNGLIAO TUNNEL

2.1 *Strata and tectonics*

Based on the drilling results and field mapping, excavation at the beginning of the tunnel from North to South mainly goes through mudstone and sandstone. All rocks are seriously fractured resulting from tectonic events and highly weathered down to varying depths beneath the surface. The fault, which is a thrust fault located at the north portal, represents the tectonic border between mudstone (Pliocene) lying underneath and sandstone (Miocene) above. This fault is marked by fracture zones and mylonites dipping steeply to the south. Also, conjugated and associated fracture zones and gouge were found reaching far into the tunneling area as well as in the northern direction into the mudstone area.

2.2 *Hydrological and hydrogeological conditions*

The precipitation records show one peak of main rainfall. The main period lasts from the beginning of June to the end of August. The maximum value is frequently around 1083 mm in July and the dry season lasts for 9 months with the average precipitation of 20 mm per month.

3 LAYOUT OF TUNNEL STRUCTURE AND DAMAGE RECORDS

3.1 *Layout of tunnel structure*

According to the characteristics of topography and geological conditions, different design concepts were applied to the structure and the north portal sections were divided into 4 different structure sections, including cut & cover (without overburden section), prelining support (excavation along asymmetric slope),

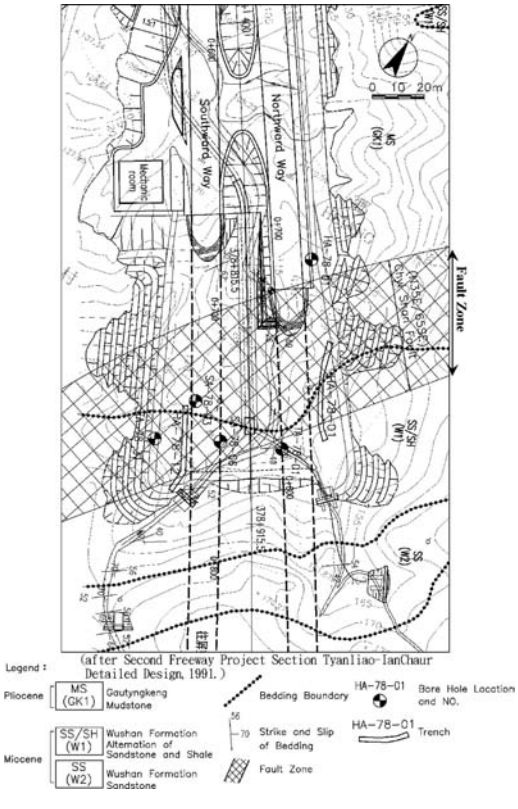


Figure 2. Geological map for north portal of Chungliao Tunnel.

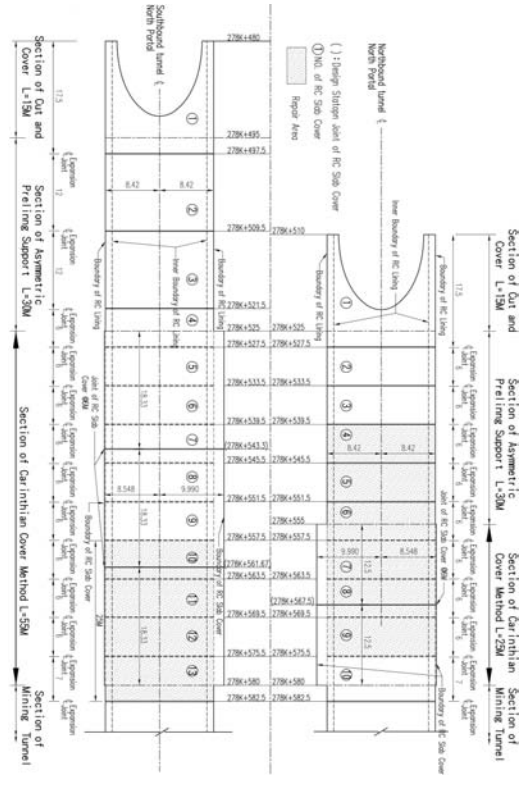


Figure 3. Plain view of structure layout at north portal section.

mining with concrete slab cover (reducing precut earth work), and normal mining tunnel sections (with enough and sound overburden).

In addition, when considering the possible ground movement due to strong earthquake, the concept of flexible concrete linings was applied by installing joints every 6 meters in order to restrain possible damage to a limited damaged area and be able to repair those sections easily in the future.

3.2 *Damage records of tunnel structure*

After four years of operation and the severe earthquake that occurred in 1999, the cracks of inner lining walls, the settlement of pavement and the increased flow of drained water were discovered and seriously impeding the traffic functions of the freeway. Hence, after surface mapping inside the tunnel, the major damage phenomena, including settlement and cavity on road pavement, cracks along inner lining walls and sidewalks, and their locations at both the northbound and southbound tunnels near the north portal were sketched as shown in Figure 5.

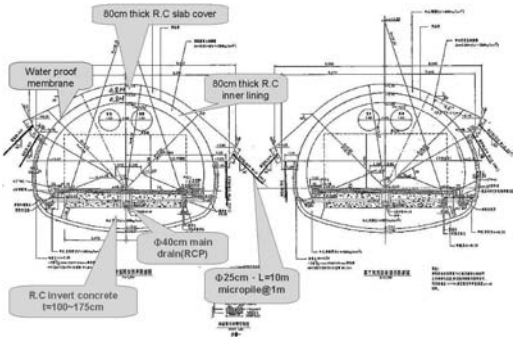


Figure 4. Typical Cross sections of concrete slab cover tunnel (so called Carinthian Cover method).

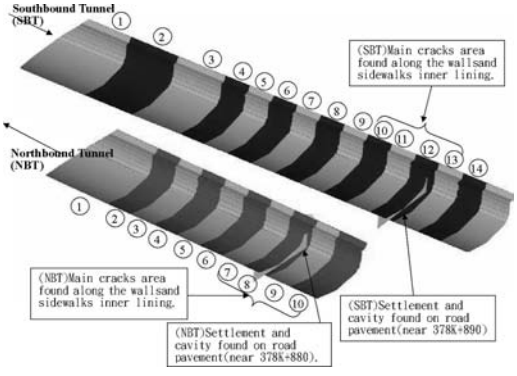


Figure 5. Sketch map of types of damage and location.

4 EXECUTION OF REHABILITATION WORKS AND MONITORING PLAN

Since the Chungliao Tunnel is an important access of the southern freeway system plus a scenic area for tourists, all repair works had to be finished based on a strict time schedule in order to reduce the traffic impact and inconvenience to drivers.

4.1 *Execution of rehabilitation works*

Due to the obvious settlement of pavement and increased flow of drained water, it became a priority to rehabilitate the pavement so that it would meet the driving smoothness requirements, and also minimize the impact during shutdown of the 3-lane freeway for replacing the main drain under the pavement and reinforcing the tunnel foundation. The repair works were executed for both the northbound and southbound tunnels in different stages. The major rehabilitation procedures are described as follows.

4.1.1 *The first stage-northbound tunnel*

(1) Investigation of cavity behind sidewalls and below invert by geophysical survey and core drilling.
(2) Open cut of pavement, removal of backfilled materials above concrete invert.
(3) Installation of 8 grouting pipes along the invert where expansion joint was damaged and grouting with cement.
(4) Replacement of main drainage system (RCP) with HDPE pipe.
(5) Backfilled with 245 kgf/cm^2 concrete instead of aggregates and finished with pavement.

4.1.2 *The second stage-southbound tunnel*

(1) Same as steps (1) ~ (4) for Northbound.
(2) Backfilled with 140 kgf/cm^2 concrete instead of aggregates and finished with pavement.

4.2 *Execution of Monitoring Plan*

The Monitoring Plan has to not only consider whether the effectiveness of rehabilitation works are being achieved, but also, as noted by the Client, whether these damages were caused only by the water problem,

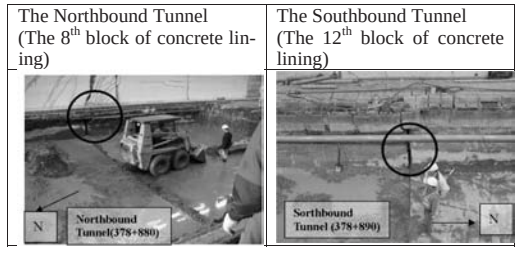


Photo 2. Opening at invert expansion joint for both tubes.

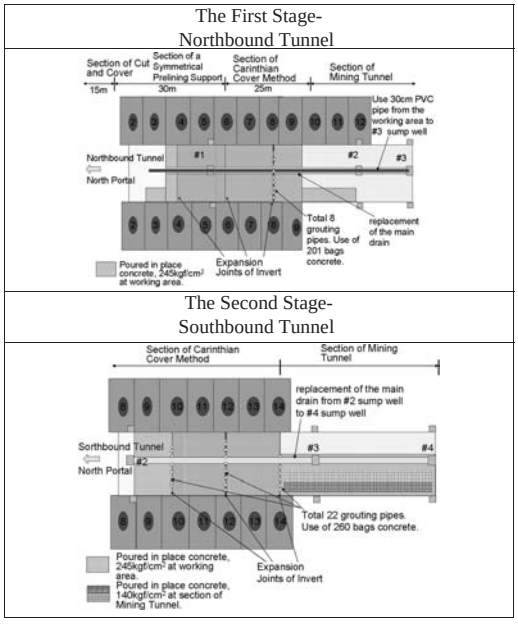


Figure 6. Sketch of major rehabilitation works for both tubes.

or also by the activity of the fault influence zone where Chungliao Tunnel is located.

Thus, a detailed monitoring plan was proposed to be executed to verify the effectiveness of the repair efforts. The monitoring scope covers the measurement of groundwater, ground settlement and surface subsidence, etc., while inside the tunnel, monitoring focused on tunnel deformation, profile clearance and crack on pavement and side walls of concrete lining (Table 1).

Besides this, an additional 7 subsidence measuring points were installed far ahead of the north portal of Chungliao Tunnel in order to check the stability of bench mark (Figure 7).

5 EVALUATION OF MONITORING DATA AND ASSESSMENT OF TUNNEL SAFETY

5.1 *Evaluation of monitoring data after rehabilitation works*

Based on one-year measurements, a summary of the acquired data is given as follows:

5.1.1 *Observation well for groundwater level*

It shows that groundwater level is discontinued because of obstruction by fault gouge.

Table 1. Summary of engineering consideration for monitoring layout.

Item	Objectives
Observation well for groundwater level	Measurement of water level for Up-thrust plane (well no. N-4, N-5, S-7), fault zone (well no. N-2), down-thrust plane (well no. S-1) in order to evaluate the possible change of water level and repairing effectiveness after replacement of main drain pipes.
Inclinometer for ground movement	Monitoring for 5 slope area of southbound tunnel (S-2, S-4), northbound tunnel (N-1, N-4) and upslope above tunnel portal (N-5) in order to evaluate the possible influence of groundwater to slope stability. Besides this, according to the slope moving direction and quantity, the stability of surrounding ground body of tunnel can be verified.
Subsurface settlement points observed well for ground movement	Measurement of the possible movement at different ground elevation (S-3 installed on southbound tunnel, N-3 on northbound tunnel) in order to monitor the influence of groundwater lowering down and the stability of surrounding ground body of tunnel also can be verified.
Subsidence measuring (Surface settlement) points	Focusing on the location of invert opening, 5 Subsidence measuring points (N-6, N-7, N-8, S-6, S-7) were installed to monitor the possible settlement above tunnel crown and surface condition. Also monitor the influence of groundwater lowering down and evaluating the stability of surrounding ground body of tunnel.
Crack measuring meter (Crack gauge)	Mainly installed on the side wall of concrete lining, especially where cracks were found and backfilled. The measured data can be evaluated and compared with other measurement for surface settlement, subsurface inclined and vertical movement.
Tunnel profile clearance and convergence measurement (Reflector prism survey)	The possible influenced blocks of concrete lining were installed with 5 sets of reflector prism. Profile clearance and convergence survey were executed periodically and also were compared with other monitoring data in order to evaluate the influence of groundwater lowering down and the stability of surrounding ground body of tunnel.

(1) Groundwater level, located at hanging wall of fault, almost maintains stable between the tunnel crown and invert.
(2) Groundwater level, located at foot wall of fault and within the fault zone, keeps dropping down and out of measurement because exceeding the depth of observation well (Figure 8).

5.1.2 *Inclinometer for ground movement*
No obvious records related to ground movement.

5.1.3 *Subsurface settlement points observed well for ground movement*
Records show there are differential movements at the depths of 10, 20, 30 meters below ground surface. The possible cause might be the re-organization of softened body around the invert which has slightly deformed with uneven settlement due to the grouting effect. No evidence related to the fault is shown (Figure 9).

5.1.4 *Subsidence measuring point*
Some dropdown settlement records were proved to be caused by construction activity on the surface but some other settlement needs more comparison and evaluation with other monitoring data (not consistent with other monitoring data).

5.1.5 *Crack measuring meter of tunnel walls*
Obvious cracks were recorded mainly on the sidewalk surface along concrete lining blocks No. 8 (Northbound) and Nos. 11 & 12 (Southbound). Only one

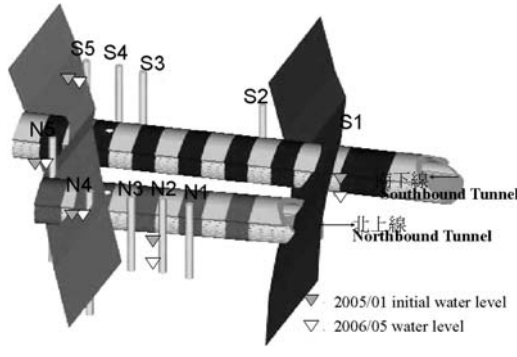


Figure 8. Groundwater level along the tunnel.

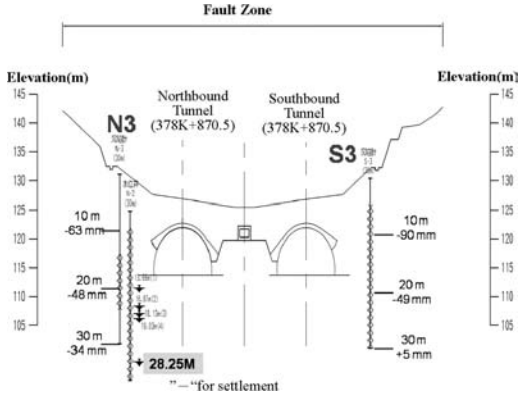


Figure 9. Sketch of measurements for subsurface settlement points observed well.

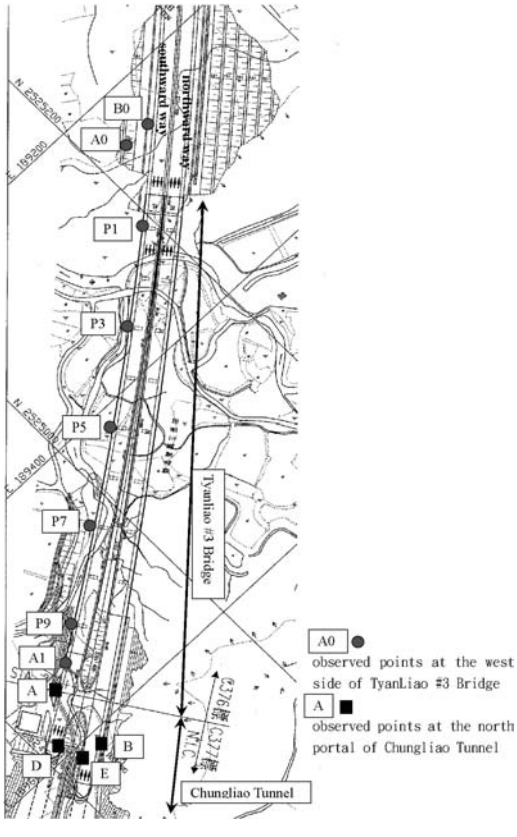


Figure 7. Layout of subsidence measuring points.

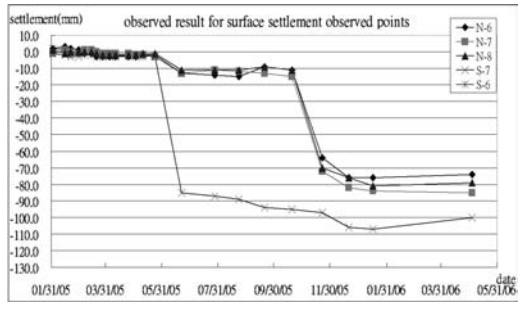


Figure 10. Deformed curve for surface settlement.

obvious crack found on the surface of side wall on concrete lining block No. 11 (Northbound) (Figure 10).

5.1.6 *Tunnel Profile Clearance & Convergence measurement*

The periodical measurement of Tunnel Profile Clearance and Convergence showed that the deformation problem of tunnel structure was not critical.

However, it was evaluated that the whole tunnel structure tilted slightly toward the southeastern direction after grouting below the tunnel invert. This was caused by the differential stiffness of grouted body while the rock mass might have stabilized when some of the muddy area became dry with no more differential settlement occurring.

5.2 *Assessment of tunnel safety*

After examining all measured data, the most problematic sections for both tubes of the tunnel are at the border of changing strata between sandstone and mudstone. It was realized that improvement of the tunnel foundation by grouting especially at sections 378K + 880(NBT) and 378K + 890(SBT) was essential owing to the cavities under the invert of the tunnel.

All the abnormal phenomena, including subsurface settlement, surface subsidence, and cracks measured on concrete lining and sidewalks, and deformation of tunnel profile clearance, had not been proved to be related to the activity of fault. In order to evaluate tunnel stability, a possible softened ground model was developed by senior geologists based on monitoring data and surface mapping. And it was concluded that broken main drain pipes provided leaking water to the bottom of the tunnel through cracks on expansion joint of the tunnel invert. The leaking water made ground beneath the tunnel invert a very soft muddy foundation.

Because grouting works only can be executed through two expansion joints of invert, the quality and effect of grouting work can not be fully assured. It also takes time for the soft ground beneath the tunnel invert to stabilize after cutting off leaking water. However, from the monitoring data, the tunnel structure at this stage is still in sound condition (Figure 11).

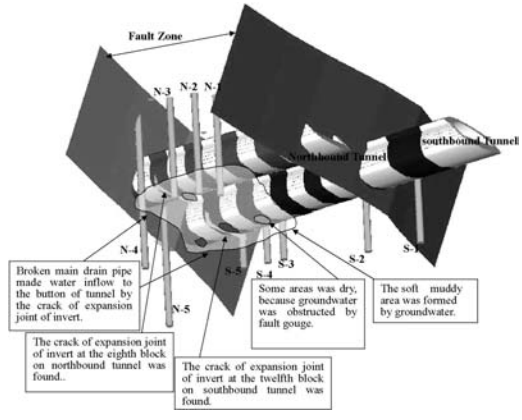


Figure 11. Possible softened ground under the invert for both tubes.

6 CONCLUSION

Using extension joints for every 6 meters in tunnel alignment has been proved to be very effective to reduce possible structure damage caused by strong earthquake. However, a broken main drain with fractured fault zone materials still caused severe deformation of the northern portal section of Chungliao Tunnel. In turns, after four-year operation, a thorough repair work was required and executed.

During the rehabilitation work, the replacement of the main drain pipes indeed cut off leaking water, while at the same time, it seems very difficult to grout the whole weak ground beneath the tunnel invert. But we did manage to partially fill the cavity and consolidate the ground. Later on, a one-year monitoring program has proven the tunnel structure to be stable, but uneven deformation still can not completely be avoided. Despite this unusual behavior and phenomena, the tunnels structure is still safe. It might, hopefully, takes several years for the soft ground beneath the tunnel invert to regain full stability. Hence, further continuous monitoring has been proposed. And, further ground improvement would be recommended if severe tunnel deformations are observed in the future.

REFERENCES

CECI, 2006, Final Report of Assessment of Measured Data and Engineering Evaluation for Chungliao Tunnel (Revised 2nd Ed.), July 2006.

CECI, 2005, Supervision Report of Rehabilitations Works for Chungliao Tunnel (Revised Ed.), April 2005.

CECI, 1992, Design Report for Kaoshiung-Pingtung Section of Second Freeway in Southern Taiwan, November 1992.

Underground Space – the 4th Dimension of Metropolises – Barták, Hrdina, Romancov & Zlámal (eds)
© 2007 Taylor & Francis Group, London, ISBN 978-0-415-40807-3

Environmentally friendly subway construction in the overcrowded city of Tokyo

K. Irie
Tokyo Metro Co., Ltd.

S. Nishibayashi
Metro Development Co., Ltd.

ABSTRACT: In Tokyo, Japan's capital city, construction of Subway Line 13 is about to reach a peak of activity. This subway line is the last that will be built by the former Teito Rapid Transit Authority (now Tokyo Metro), a Japanese government-affiliated corporation that had built subway lines in the metropolitan area since 1941. Various aspects of this project involve sophisticated technologies. Some are perfections of those developed while the Tokyo Metro was still called Teito Rapid Transit Authority. Above all, this project is wrestling with issues that will inevitably continue to arise in subway construction. These include global warming and resource recycling as part of the general requirement to reduce environmental impacts. This paper describes our efforts to address these issues.

1 OBJECTIVE OF SUBWAY LINE 13

Subway Line 13 will connect three major Tokyo sub-centers, Ikebukuro, Shinjuku, and Shibuya. The plan includes a route connecting Ikebukuro and Shibuya that is separate from the existing Ikebukuro-Shibuya section of the JR Yamanote Line. The main objective is to eliminate congestion at major terminals and to alleviate commuting congestion to points away from Ikebukuro and Shibuya.

The Subway Line 13 route, which is as shown in Fig. 1, has a total construction length of 8.9 km. Connecting at Ikebukuro Station, Tokyo Metro, Tobu Railway, and Seibu Railway operate to the west of Ikebukuro. The Tokyu Toyoko Line provides service southward from the other terminal, Shibuya Station. Together with Subway Line 13, the railways mentioned above will provide through train operation by mutual entry to stations at the ends of the line. When Subway Line 13 opens, a railway axis will be completed over a wide area, from southwestern Saitama Prefecture, through the metropolitan centers, and on to Yokohama in Kanagawa Prefecture.

Much of this route is constructed directly under Loop 5, a road with the greatest traffic congestion in Tokyo. Conversion from automobile traffic to the use of the subway, which will be promoted, is expected to contribute to eliminating road congestion as well as reducing the environmental burden imposed by transportation.



Figure 1. Subway Line 13 route map.

2 ROUTE AND GEOLOGICAL FEATURES

Lined on both sides with high-rise residential and office buildings, Loop 5 runs through the commercial area of Shinjuku, Japan's largest bustling quarter. Therefore, during the work, various difficulties will be encountered, such as the need to avoid worsening the surrounding environment with noise and vibration, and the substantial restrictions imposed on the scope and time allowed for using the road.

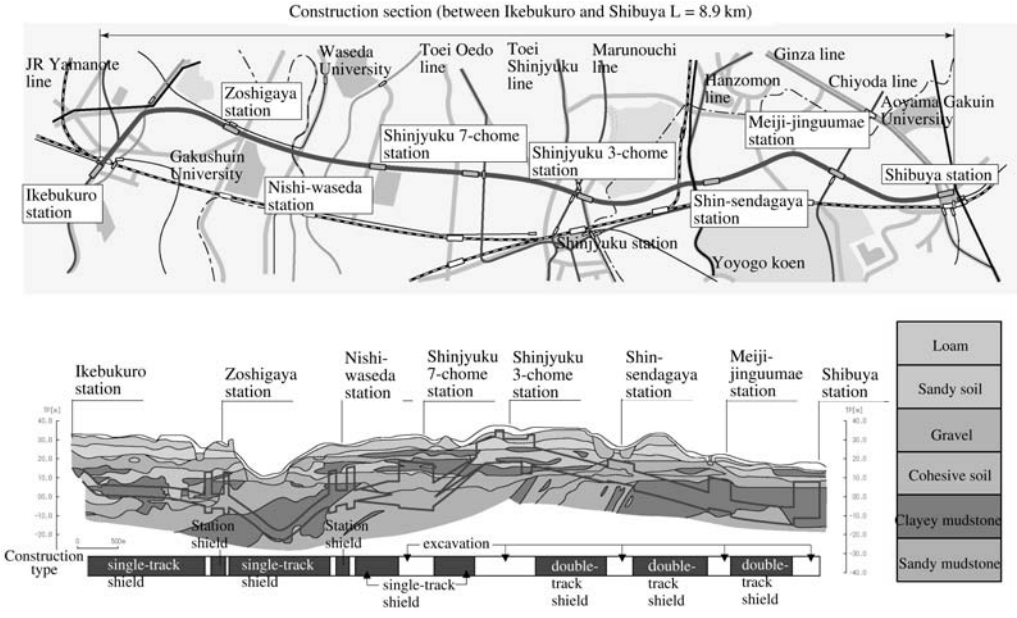


Figure 2. Plan view and geological profile of sections of Subway Line 13.

Horizontal and longitudinal alignments are as shown in Fig. 2. The smallest radius is 180 meters between Ikebukuro and Zoshigaya Stations, the steepest grade is 4.0% between Shinjuku 7-chome and Shinjuku 3-chome Stations, the deepest excavation point is 39 meters below the ground surface at Shinjuku 7-chome Station, and the greatest excavation width is 36 meters at Shibuya Station.

The geographical features of this section, shown in Fig. 2, include a plateau of the Quaternary Pleistocene of the Cenozoic era and a lowland or plateau-dissecting valley filled with sedimentation, which is located 35 to 10 meters above sea level. The plateau has volcanic ash clayey soil and terrace gravel, below which the Kazusa group, which is the foundation of this area, is distributed. In the lowland area, are an alluvial layer of deposited clayey soil and below which the Kazusa group distributed.

Groundwater is shielded against the terrace gravel layer and the Tokyo formation by low-permeability clayey soil, and free water is distributed in each layer. The lowest Kazusa group has a high head due to the existence of artesian water.

3 OUTLINE OF THE WORK

This construction work, which intersects nine existing subway lines, must deal with large infrastructure under the road, including electric power, communications, water supply and sewerage facilities. In this sense, this is a typical large-scale urban civil engineering project that has to be implemented while protecting existing facilities.

The subway line has seven stations along its course. One section with five stations that extends 1.9 km was constructed by the cut-and-cover method. Where station excavation was associated with a large amount of groundwater, a continuous underground wall was used for earth retaining to prevent adverse effects on the surrounding environment. The shield method was employed for the remaining two stations, whose excavation depth was greater. The total length of tunnels connecting these stations was 7.0 km. This was divided into seven sections, each constructed by the shield method.

The slurry shield method and high-density slurry shield method were used for the shield work, to enable recycling the soil discharged from the excavation process, to meet the geological conditions, and to protect neighboring structures.

4 MEASURES ADOPTED TO REDUCE THE ENVIRONMENTAL BURDEN

Subway construction exerts a considerable impact on the environment and requires a huge amount of materials, including concrete, steel, wood, sand, and water. These conditions exist in all stages of excavation. The work includes transporting excavated soil; quarrying, transporting, and refilling with sand in the cut-and-cover method; and shield excavation, transport of excavated soil in the tunnel, and road transport



Photo 1. The electric telescopic clamshell.

in the shield method. In the case of Subway Line 13, the total volume of excavated soil will be as much as 1,600,000 m^3, of which the cut-and-cover method will account for about 1,100,000 m^3, and the shield work will account for about 500,000 m^3. This amount will increase to about 1,700,000 m^3 when the volume of excavated soil for continuous retaining walls, and other work is added to the total.

As subway construction exerts a heavy environmental burden, the following measures were put into practice to reduce the impact as much as possible.

4.1 *Cut-and-cover method*

4.1.1 *Work vehicles*

The 4-ton trucks and dump trucks used for material and equipment transport during the work run on diesel fuel. As this fuel emits PM (particulate matter) during operation, work vehicles with a PM reduction unit were used.

In addition, for 2-ton trucks, compressed natural gas vehicles (CNG vehicles) were introduced. These vehicles are environmentally superior to gasoline-fueled vehicles due to their reduced noise and extremely low emission of black exhaust PM or NOX.

4.1.2 *Excavation machinery*

In the large-scale cut-and-cover work for subway construction, mechanized excavation is to a depth of about 20 meters below the road deck surface. The machine (called a telescopic clamshell) used for this excavation normally uses diesel fuel. However, in order to eliminate exhaust gas and to reduce the surrounding noise, the world's first electric excavation machine (Photo 1) operating on electric power was developed and introduced.

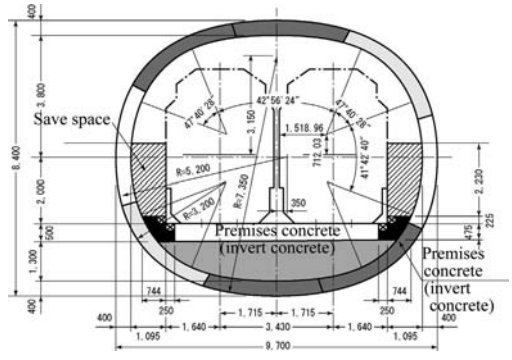


Figure 3. Standard section of composite circular tunnel.

Table 1. Area comparison table.

	Excavated sectional area	Tunnel space sectional area
Circular[A] (φ 9.7 m)	73.90 m^2	46.95 m^2
Composite circular [B] (W9.7 m × H8.4 m)	67.30 m^2	46.05 m^2
B÷A	0.91	0.98

For the same purpose, an electric-drive-type backhoe was selected for excavating and loading soil.

In this way, the PM in the exhaust gas can be reduced by 79% and nitrogen oxides by 24%. It is also estimated that carbon dioxide (CO_2) emissions considered responsible for global warming can be reduced by about 4,800 tons.

4.2 *Shield method*

4.2.1 *Reducing sectional area of shield tunnel*

For the double-track shield tunnel for Line 13 near Shibuya Station, we were able to reduce the volumes of excavated soil and invert concrete by eliminating unnecessary spaces in the upper and lower portions of the tunnel while securing the functions needed in a railway tunnel. We did this by adopting a composite circular section (non-circular section). (See Figure 3.)

The special feature of this type of section is that the cross-section of the tunnel interior space (the space minus the sectional area for concrete, invert, etc.) is nearly equivalent to that provided by a circular section. The composite circular section is formed by combining the radii of several curves.

As shown in Table 1, the interior cross-sectional area of the tunnel, including the maintenance space, can be nearly the same as that provided by a circular section, but the overall sectional area becomes about 10% less than that of a circular section. Invert concrete that has to be placed in unnecessary space can be reduced by about 40%.

Table 2. Environmental load reduction effect through reduction of the tunnel section.

	Circular tunnel	Composite circular tunnel
Real space of the tunnel	100	98.1
Volumes of excavated soil	100	91.1
Volumes of segment concrete	100	93.8
Volumes of invert concrete	100	60.0

Reducing the tunnel section leads not only to less excavation, but also to less use of such materials as segment material (concrete) and invert concrete supporting the subway tracks. As shown in Table 2, this can greatly contribute to effective reduction of the environmental burden.

4.2.2 *Recycling soil discharged in shield work*

The slurry shield and high-density slurry shield methods were used for this work.

In both methods, discharged high-density slurry (the slurry in the case of the slurry shield method) contains a large amount of water. Accordingly, it is designated as industrial waste and subject to legal regulations imposed on its handling. The percentage recycled is a low 45.3%. The material in high-density slurry ‘or slurry) is a substance existing in nature, which means it can only be recycled after it is dewatered.

- Recycling of slurry in slurry shield method
  Tokyo Metro has recycled slurry in the slurry shield method (specific gravity 1.3 to 1.4) by processing it into fluidized soil for refilling in the cut-and-cover method and invert material for the shield tunnel. It was decided that similar slurry recycling by processing it into fluidized soil could be used in the slurry shield method in the Subway Line 13 construction.
  The amount of slurry to be processed into fluidized soil for recycling for refilling in the cut-and-cover method and for tunnel invert material in the Subway Line 13 work is shown in Table 3 below.
- Recycling of high-density slurry in high-density slurry shield method
  The high-density slurry in this method has low water content – 50% to 80%. It is difficult to transport on the road without using special transport vehicles. In addition, the legal determination of whether or not this type of slurry is industrial waste is made at a “time point when the generated excavated material is discharged from the system separating it into soil and water.” Accordingly, we decided to improve and discharge high-density slurry in the rear base, which forms an integrated system with the shield. Improved high-density slurry is to be recycled for reclamation in Tokyo seaside commercial areas and elsewhere.

Table 3. Slurry recycling amounts.

Volumes of slurry	Recycling item	Recycling amounts (m^3)
131,000 m^3	Fluidized soil for refilling in the cut-and-cover method	135,000
	Invert material	26,000
	Total	161,000

Table 4. Volume of landfill embankment material recycled.

Volumes of high-density slurry (m^3)	The volume of high-density slurry recycled (m^3)
334,000	418,000

For improvement, research and development work was done on methods that could be used for physical dewatering for separation of slurry into water and soil according to the idea that the excavated soil could be returned to its natural state. Although practical implementation has proved to be possible, the improvement system is large in scale and the space needed at the rear base is difficult to secure in this project. In addition, improvement that fits in with the shield excavation process is difficult. For these reasons, we adopted the stabilization method described below in which additives are used.

a) Method using plaster neutral solidifying material
   This is a method using water absorption and solidification achieved by adding and mixing plaster-based neutral solidifying material into high-density slurry.
b) Method using sludge incineration ash
   This is a method using water absorption and improvement by adding PS ash from used paper manufacturing.
   Considering the environmental impact of the additives, a requirement was set so that the pH value of the improved soil remains in a neutral range and the soil will not be returned to slurry after improvement (solidification).
   The volume of high-density slurry recycled in the high-density slurry shield method is as shown in Table 4.
   As an example, the method using plaster neutral solidification material is introduced.

- Method using the plaster neutral solidification material
  In this method, high-density slurry discharged to the rear base by a conveyor belt is fed into a mixer.

Table 5. Mixing of plaster neutral solidification material and the cone index of the improved soil.

Additive mixing			Cone index of the improved soil	
Plaster neutral solidification material	Polymer cohesion material	Improvement time	In 2 hours	In 24 hours
86 kg/m^3	1 kg/m^3	60 s/batch	480∼500 KN/m^2	630∼670 KN/m^2

While adjusting mixer rotation speed and stirring, the neutral solidifying materials are added sequentially for instant improvement of soil (the specified strength appears in about five minutes). In this case, the neutral solidifying material and a batch-type 2-axis mixer for stirring are parts of a system used to achieve uniform quality.

The additive mixing rate and the cone index of this method are shown in Table 5.

This improvement technology can be applied for all work in which slurry with high water content must be handled. There is actually an example, in which slurry accumulated in marshes was improved then and there, and the improved soil was used to build a road to resurrect a park beautifully. We believe this technology to be applicable in many fields in view of the importance now placed on environmental protection.

5 SUMMARY

Compared with automobiles and buses as well as other forms of rail transportation, subways, which emit the lowest levels of CO_2 and impose the smallest environmental burden, are viewed very favorably in terms of prevention of global warming.

However, subway construction requires huge amounts of materials such as concrete and sand as well as large construction machinery and many work vehicles. In addition, the quarrying of huge amounts of materials damages mountains, and the utilities required to transport these materials as well as the operation of construction machinery over extended periods of time all exert a considerable impact on the environment. With an eye toward minimizing the use of materials taken from nature and the impact on the environment during the work period, we took up the challenge of recycling resources and reducing the environmental burden imposed by excavation machinery.

The construction work is still under way and we have just begun implementing the measures adopted to reduce the environmental burden. Today, prevention of global warming and resource recycling are unavoidable issues in construction work. We realize that we must continue to engage in research and development to effectively deal with environmental protection issues.

This page intentionally left blank

Underground Space – the 4th Dimension of Metropolises – Barták, Hrdina, Romancov & Zlámal (eds)
© 2007 Taylor & Francis Group, London, ISBN 978-0-415-40807-3

Reliability assessment, repair, and replacement of historic water tunnels and their contribution to California's sustainability

J. Kaneshiro[1], F. Kintzer[1], M.L. Piek[1] & R. Yoshimura[1]
[1]*Parsons*

D. Van Horsen[2], G. Korbin[3] & K. Lovelie[4]
[2] *Southern California Edison,* [3] *Consultant,* [4] *Shotcrete Technologies*

J. Carfrae[5], R. McManus[6] & C. Ovalle[7]
[5] *City of Pasadena Department of Water and Power,* [6] *Pacific Gas and Electric,* [7] *Metropolitan Water District of Southern California*

ABSTRACT: From the largest private and public water and power supply utility companies in the world to the smaller municipal water and power agencies and irrigation districts to the oldest water district in California, operations and maintenance of water tunnels has been an important factor and vital link in California's infrastructure. Michael O'Shaughnessy (San Francisco Hetch Hetchy Water Supply System), William Mulholland (Los Angeles Department of Water and Power and Metropolitan Water District of Southern California's Colorado River Aqueduct), John Eastwood (Southern California Edison Big Creek Hydroelectric Project) along with many late 19th and early to mid 20th century pioneers, visionaries, ordinary and extra-ordinary people built large and small water supply, irrigation and hydroelectric tunnels, which have supplied environmentally friendly- water supply and electricity, and uninterrupted service to customers for a burgeoning population and economy. This paper discusses case histories and lessons learned providing enlightenment in the reliability assessment of existing structural conditions of tunnels, repair, and replacement of historic and vital water tunnel projects in California.

1 INTRODUCTION

1.1 *Water tunnels and California sustainability*

California is blessed with natural resources and divided into 11 geomorphic provinces as shown in Figure 1. The Sierra Nevada mountain range, the largest mountain province, and several other major mountain ranges, require crossing with tunnels to feed water to the fertile valleys and major metropolitan areas. Spurred by unprecedented growth and opportunity after the gold rush, agriculture, the post industrial society of World War I, World War II, Cold War, and development of the transistor and the silicon chip, California has grown to be the world's 8th largest economy. The planning, maintenance, operations, and construction of water supply and energy projects (including the conveyance tunnels) since the founding of California has managed to keep pace with suburban growth, baby boomers, and the high technology sector in the information age.

By today's standards, construction of these historic water tunnels was relatively primitive (50 to 100 years before smooth wall blasting, automated equipment,



Figure 1. Geomorphic provinces of California.

Table 1. Partial List: Summary of significant or historical water tunnels in California by agency.

Tunnel name	Length (km)	Ave. bore (m)	Approx. completion date
California State Department of Water Resources			
Angeles	11.5	10.1	1970
Castaic Dam Diversion	1.5	6.7–9.1	1970
Porter	7.7	7.4	1970
San Bernardino	6.1	5.5	1971
City of Los Angeles Department of Water and Power			
Elizabeth	8.2	4.6	1913
Red Rock	3.5	3.9	1913
Elsmere	0.6	4.1	1913
Mono Craters	18.2	4.2	1939
Owens River Power	18.2	3.7	1931
Stone Canyon Bypass1	1.3	2.9	1952
East Bay municipal utility district			
Claremont	5.5	3.3	1929
San Pablo	4.1	3	1920
Metropolitan Water District of Southern California			
Coachella	29.5	5.8	1939
Eagle Mountain	9.8	5.5	1939
Iron Mountain	12.2	5.8	1939
San Jacinto	20.9	5.9	1939
Sierra Madre	2	3.9	1939
Valverde	9.8	11.6	1939
Whipple Mountain	9.8	5.8	1939
Pacific gas & electric			
Big Bend	4.8		1908
Cresta	6.4	5.8–7.9	1949
Poe	10	5.8	1957
Rock Creek	10.4	5.8–7.6	1950
Pasadena Department of Water and Power			
Azusa	9.2	1.5	1876–1933
Devil's Gate	1.2	1.2	1890's
Eaton Canyon No. 1–3	0.5	1.2	1888–1895
San Francisco Public Utilities Commission			
Canyon Power	17.7	4.3	1965
Cherry Power	2	2.7	1960
Crystal Springs Bypass	5.2	3.4	1968
Coast Range-Telsa	40.2	5	1934
Coast Range-Irvington	5.6	5	1934
Foothill	25.4	4.6	1929
Stone Dam Tunnel 1	0.24	1.8	1867
Moccasin Power	1.6	5.3	1925
Mountain	30.3	4.1	1925
Sacramento Municipal Utility District			
Camino	8.1	4.4	1961
Jaybird	6.4	4.3	1960
White Rock	7.9	7.3	1964
Southern California Edison			
Kern River #1	12.8	2.4	1906
Kern River #3	19.2	2.4	1912
Borel Flowline No. 1, 1-1/2, 2, 3	0.6	3.6	1905
Big Creek No. 1–8	34.9	3.1–7.2	1911–1950
Ward Tunnel	20.5	4.5	1925
Mammoth Tunnel	12	6.0	1960
Eastwood Diversion, Power, & Tailrace	5.2	6.0	1987
United States Bureau of Reclamation			
Pacheco	8.4	4.1	1982
Santa Clara	1.6	3.6	1984

TBM's, etc.) using mule, drill and blast "spiders", hand mining methods, timber supports, Ford's Model T's, and brute force. For the most part these tunnels have provided uninterrupted service from 50 to over 100 years, but nevertheless, environmental impacts, deterioration of rock and liner conditions, maintenance and repair, and occasional emergency outages have occurred.

1.2 *Some significant water tunnels in California*

Table 1 summarizes some of the significant and historical water tunnels in California by agency/project. From a new world standard, these tunnels are considered to be historical and seminal in contributing to the sustainability of California as a powerhouse economy in both innovation and education.

2 PIONEERS, ENGINEERS, LEADERS

2.1 *William Mulholland, 1855–1935*

Mulholland was born in Belfast, Ireland and came to the USA at the age of 15, first as a sailor, lumberer, dry goods clerk, miner, and finally as a ditch digger for the Los Angeles Department of Water and Power (LADWP). As a self taught engineer, he would ultimately rise to chief engineer, and is credited for bringing Owens Valley water to Southern California. The Owens Valley water project was politically charged for water rights, required over 5000 men (pioneers themselves), and included 164 tunnels (69 km); the entire aqueduct extending 362 km without a pump in the system. In 1913, when the project was completed and water arrived in Los Angeles, Mulholland's famous speech was: "There it is, take it." He also conceived the Colorado River Aqueduct (completed in 1941), which provides the majority of Southern California's imported surface water.

2.2 *John Eastwood, 1857–1924*

Eastwood was born in Minnesota and educated as a civil engineer. He began his career in the Pacific Northwest as a railroad engineer, but soon moved to Fresno, California where he designed flumes for the timber industry. It was during this work that he first began to study the hydroelectric potential of the San Joaquin



Figure 2. Mulholland, Eastwood, O'Shaughnessy.

River (Redinger, 1998) (Figure 1, E). After a short period as Fresno's City Engineer, and Chief Engineer for the San Joaquin Electric Company, he worked as a consulting engineer for Pacific Power and Light Company (PPL). It was in this last position that he surveyed stream flows and elevations of the San Joaquin River, designing the largest hydroelectric (1100 MW) project conceived by one man. This system of water storage dams linked with tunnels became known as the Big Creek Project with construction rivaling the Panama Canal. Tragically, Eastwood never participated in the construction of his project. In 1910, he was forced to sell his stock in PPL to pay his assessment for construction of Big Creek as was required by all PPL stockholders. Eastwood then began a long career in dam design, creating a unique reinforced concrete multiple-arch design that is well suited to remote sites.

In 1987, to honor the designer of Big Creek, Southern California Edison named their underground 200-MW pumped storage plant the John S. Eastwood Powerhouse.

2.3 *Michael M. O'Shaughnessy, 1864–1934*

O'Shaughnessy graduated from the Royal University of Dublin, Ireland, and arrived in San Francisco in 1885. He worked on Alpine dam in Marin County and later was chief engineer of the Southern California Mountain Water Company in San Diego. In 1912 he was appointed City Engineer for the City of San Francisco's Hetch Hetchy project (SFPUC, 2005) (Figure 1 E & F). The project was constructed between 1914 and 1937, and included over 100 km of tunnels. The dam spanning Hetch Hetchy valley provides his namesake.

Like the Owens Valley water, Hetch Hetchy water was also politically charged, and the damming of Hetch Hetchy valley was opposed by the highly esteemed environmentalist, John Muir. The Raker Act signed in 1913 by President Woodrow Wilson secured the rights to build Hetch Hetchy dam. O'Shaughnessy was a man of action at the Senate debate on the Raker Act.

2.4 *Other Pioneers, Politicians and Engineers*

There are numerous other significant pioneers who contributed to providing water to grow and sustain a thirsty and energy needy California. These leaders included men like William B. Matthews, Joseph B. Lippincott, Fred Eaton, Willie Chalfant, Harvey A. Van Norman and many others too numerous to mention (Nadeau, 1997; Reisner, 1993). A few others of note are discussed below.

Frank Weymouth was the Metropolitan Water District's first general manager and chief engineer from 1929 to 1941. He designed and constructed Mulholland's conception of the Colorado River Aqueduct (including the San Jacinto tunnel) at the height of the great depression.

Tunneling's role in the sustainability of California would not be complete without mentioning the Federal, U.S. Bureau of Reclamation's Central Valley Project (CVP) and the State Water Project (SWP). The CVP began in 1935 and continued into the 1980's with significant tunnels being the Pacheco and Santa Clara tunnels. There are many politicians and individuals who tirelessly worked for the SWP and cooperation with the CVP, including former US Secretary of Defense Caspar Weinberger when he was a California Assemblyman (Thomas, 2006). Several engineers who deserve mentioning include W.H. Hall beginning in 1873, E. Hyatt in 1931, A. D. Edmonston in 1950, and H. O. Banks in 1956 who were State Engineers who took part in SWP; and R.B. Marshall in 1919 of the U.S. Geological Survey was the first to conceive of SWP. The SWP significant underground works include the Angeles, Porter, San Bernardino, and Tehachapi tunnels and the underground hydroelectric plant at Oroville Dam.

There are also countless environmental pioneers that helped provide balance between California's population growth and the earth's sustainability starting with John Muir and the Sierra Club, David Gaines of the Mono Lakes Committee, and Tim Such of Friends of the Earth (SFPUC, 2005; Nadeau 1997).

3 CITY OF LOS ANGELES DEPARTMENT OF WATER AND POWER (LADWP)

The First Los Angeles Aqueduct has 164 tunnels totaling 83 km. The Second Los Angeles Aqueduct has 4 tunnels, totaling 1.9 km.

3.1 *Owens Valley Water Tunnels*

These tunnels located in the Eastern Sierra Nevada and Great Basin provinces (Figure 1, E & G) were part of LA's First aqueduct. World record advance rates were achieved on their tunnels, and in 1908 a soft-rock world record for advance of 323 m in a single month was set on the 3.5 km Red Rock tunnel. In 1910, on the 8.2 km Elizabeth tunnel, hard-rock a world record advance rate of 184 m in a single month was set.

To ensure continued operation in the 21st Century, maintenance inspections are performed annually. Repairs are scheduled during these outages based on the previous year's inspection. While the repairs are done in one section by the Construction and Maintenance Group, inspections are performed by the Engineering Group in another section. Once the tunnel is back in operation, the Engineering and Construction groups meet to discuss the following year's repair schedule (Miller et al., 2006).

Typically, relining with shotcrete is used to repair spalls and cracks. Removal and replacement of old concrete walls and floors that have buckled or cracked is sometimes needed. These areas are generally limited to small sections only. Tunnel shutdowns are usually scheduled during periods of low demand, and shutdowns range from 2 months or less during a wet year to 5 months during a dry year.

LADWP uses a special mix of shotcrete to reline the tunnels. On the Elsmere portion of the First Aqueduct, the shotcrete has proven to be dense enough to prevent seepage of naturally occurring crude oil into the tunnel. In some cases if the tunnel section allows, robotic shotcrete arms are used.

3.2 *Stone Canyon projects*

Stone Canyon dam, tunnel and pipeline facilities, located in the Santa Monica Mountains of the Transverse Range (Figure 1, I) were constructed in the 1920's, expanded in the 1950's, and expanded again and repaired in 2000's. The latest expansion was implemented to meet new EPA and California drinking water regulations, which mandated the filtration and disinfection of potable water supplies subject to surface water runoff (Bentwood, et al., 2006).

Bypass Tunnel No. 1 was completed in the 1950's. Inspection revealed the mortar lining was severely deteriorated (Anbessaw, 2005). After high water pressure cleaning, a new 13 to 38 mm shotcrete liner was placed over the 1340 m long by 1.7 m diameter horseshoe tunnel. Troublesome water leaks are panned using formation drain tubes. The work was completed in a round the clock operation in 19 days, 2 days ahead of planned shutdown schedule.

Bypass Tunnel No. 2, consisting of 870 m of 3 m average bore diameter was completed in 2006. The project provided for operations and maintenance flexibility and redundancy in addition to meeting new drinking water standards.

3.3 *Mono Crater's Water Tunnels*

The Mono Craters Tunnel, located in Great Basin province (Figure 1, G) was constructed in 1939. This tunnel is 18.2 km long and connects the Mono Basin to the Owens River Valley. Excavation of the west portal was started in September 1934. The Mono Craters Tunnel was watered up in 1940.

Inspections of the tunnel are scheduled every 3 to 5 years, requiring a shutdown of just a few days. Given confined space and air flow requirements caution is required for entry. Naturally occurring carbon dioxide gases in the area are monitored during inspections. Past inspections indicate that the tunnel is in good condition. These inspections indicate minor mineral deposits, cracks, root growth, some shifting of joints and rough portions of invert. Groundwater inflow into the tunnel is about 25 m^3/minute (417 l/sec) all year round (Miller et al., 2006).

4 METROPOLITAN WATER DISTRICT OF SOUTHERN CALIFORNIA (MWD)

MWD was incorporated in 1928 to provide water for Southern California. One of the two main surface water supplies comes through the Colorado River Aqueduct (CRA) which consists of 29 tunnels totaling 148 km, including most significantly, the 21-km long San Jacinto Tunnel, the 12.1 km long Iron Mountain Tunnel, 29.5 km Coachella Tunnel.

4.1 *San Jacinto Tunnel*

This tunnel is part of the San Jacinto Mountains (Figure 1, I) where extremely large groundwater inflows, usually associated with faults, were experienced during tunnel construction. The San Jacinto Tunnel (Anon. 1940; Thompson, 1966) was constructed by conventional drill and blast excavation from about 1935 to 1939. The 6-m ($\pm$) excavated diameter by 20,983 m long tunnel was constructed predominantly in granitic rocks with some zones of metamorphic rocks (mica schists, quartzites, and crystalline limestones).

The MWD Historical Record (Anon. 1940) indicates that during tunneling, four major faults and about 20 minor faults or fractures were encountered. There were 8 to 10 instances when peak flows of about 1,000 liter/second and associated peak water pressures of 41 bars were experienced with common pressures on the order of 10 to 25 bars. The maximum flow measured from all tunnel headings was about 2,500 liters/second. Tunnel construction records indicate about 190 hm^3(155,000 acre-ft) of water was drained through the tunnel from the surrounding rock. Groundwater that originally fed springs located as much as 11 km from the tunnel was lowered following tunnel construction. The Historical Record further indicates that the large quantities of inflow were associated with sudden surges of flow when tunneling through (impermeable) fault zones, usually major faults, which held back compartments of groundwater under high head. This was especially noteworthy with one

particular major fault, the Goetz fault. However, it should be noted that when crossing another major fault, the Mclnnes fault, the Historical Record indicates:

…Water originally percolating through the fracture zone on either side of the gouge . . . had been drained by the tunnel advancing from both sides. There were many indications that the water had been previously present, yet the quantities remaining at the time of penetration were relatively small. . . . Through the center of the fault the inflow was less than 100 gpm [6.3 l/sec]. *. . . drainage had occurred, perhaps largely through the water course . . ., six months before the Mclnnes fault was reached.*

It appears from examining the Historical Record that the Goetz fault and the Mclnnes fault are two fault zones, which form the boundaries of a groundwater compartment. Large quantities of water were not encountered along the Mclnnes fault because when tunneling through the Goetz fault large quantities of water were drained off from interconnected joints and fractures. It should be noted that grouting was performed as they approached the Goetz fault from the west, while when approaching from the east grouting was not performed because the water had largely drained to the west.

Thompson (1966) indicates another contributing factor or alternate explanation to higher flows when tunneling from the east.

…it was that water occurred in open interconnected fractures and joints in the hanging (northeast) wall of the northwest-striking faults. Out in the hanging wall the rock became increasingly tight away from the actual zone of shearing. When tunnel headings approached northwest-striking and easterly-dipping faults from the east, water under high pressure was generally developed at some distance away from the fault plane in hard but somewhat fractured rock. As the heading neared the fault the open fractures were numerous and volume of inflow increased. Normally by the time the footwall was reached, where gouge and crushed material was present, the hydrostatic head had generally been reduced to the extent that little difficulty was encountered in driving through the soft, faulted material characteristic of the actual planes of slippage. Conversely, when headings were being excavated from the southwest side of the northeasterly-dipping faults, (through their footwalls) large flows of water under very high pressures were freed instantaneously, resulting in strong surges that carried large quantities of broken rock, sand and clay gouge in the tunnel.

A decade later, major repair efforts to grout leaks in the liner were performed in 1947, and repairs to the floor were performed in 1952. To this day there are leaks in the San Jacinto tunnel; two of the leaks are known as the car wash zone and the high-pressure jet (Howser). The San Jacinto Tunnel construction experience is an extreme example of groundwater inflow into tunnels. Many of the tunnels constructed in the past had problematic groundwater inflows (100 to 200 l/sec typically and sometimes more). These tunnels crossed similar water bearing fault traps during construction and the inflows often can be a long term maintenance concern.

A major shutdown of the CRA is required in order to inspect the conveyance system. The inspection frequency for the entire CRA is once every 10 years or longer, with a typical shutdown period of three weeks. Recent inspections occurred in November 2002 (Beikake and Bell, 2003) and January 2005. MWD used a 4 category anomaly rating system for ranking damage, defects, or distress to the liner, with 1 requiring immediate attention, 2 repair be made in the next years inspection, 3 repair be made in two ears, to 4 not likely to be adversely impacted, but monitor for degradation in future inspections. Most fell in the category 3 or 4 anomalies. During the 2005 shutdown, crack monitoring gauges were placed at various tunnel cracks in San Jacinto and Iron Mountain tunnels to provide data on crack propagation behavior. The cracks will be visually inspected for changes in crack growth during the next CRA shutdown (possibly in 2007).

5 SOUTHERN CALIFORNIA EDISON (SCE)

SCE has over 100 km of tunnels, all located in the Sierra Nevada province, including the Kern River and Big Creek projects. SCE inspects their tunnels every 5 years with an average shutdown time of 1 week. Damaged areas and needed repairs are identified and are included in future operation budgets. Because of the long service history of SCE's tunnels a large archive exists that is used for long term trending of damage and repair monitoring.

5.1 *Big Creek No. 2*

Hydropower development of the San Joaquin River region, located in the south-central Sierra (east of Fresno, Figure 1), was begun by Eastwood (Redinger, 1998). Surveys, independently conducted with a string of pack mules, were done from 1896–1899 and again in 1902. By 1910, planning of the "Initial Development" of Big Creek, soon to be known as "The Hardest Working Water in the World", had begun. Development continued throughout the 1920's, the 1950's, and the late 1980's. Table 1 shows a listing of the primary tunnels in SCE's Big Creek system.

Big Creek No. 2 is 6,632 m long by 4 m nominal diameter and was accessed during construction by 9 adits and 2 portals. The project was built in 1912 by drill and blast methods (60 years prior to smooth

wall blasting techniques). The tunnel varies from 4.3 m wide by 4.9 m high horseshoe shaped tunnel cross section to completely enclosed 3.4 m by 3.4 m (ID) arched concrete cross section.

Problems with this tunnel began during construction as it is constructed through highly jointed rock, and some sections suffer from low cover. Consequently, 11 concrete support arches were installed. Many leaks to the surface as well as caveins and reactivation of a landslide have resulted in several repair efforts including reinforced concrete walls and floors, shotcrete, and complete lining of some sections with welded steel pipe.

Leaks to the surface continue to the present. Since 2003, visual inspections, ground penetrating radar (GPR) investigations, underground and surface mapping, and water tracing surveys have identified several leak locations (Willowstick, 2006). SCE is evaluating several repair options including steel liners and stage grouting with reinforced shotcrete.

5.2 *Kern River No. 1*

In the early 1900's the Edison Electric Company (precursor to Southern California Edison) undertook construction of a hydroelectric generation project utilizing the waters of the Kern River. The site is located approximately 190 km north of Los Angeles in the foothills of the southern Sierra Nevada (Figure 1, E). In February 1903, excavation of 19 tunnels that would ultimately form a continuous 12.9 km conduit flowline transporting up to 11.6 cubic meter per second of water from the dam and intake structure at Democrat Hot Springs to the powerhouse were started. The tunnels were advanced by conventional drill and blast methods using air drills.

The tunnels were designed as 2.7 m by 2.7 m rough cross section followed by the placement of a non-reinforced concrete lining to create a 2.4 m wide by 2.3 m high rectangular open channel with a 15 cm high natural rock wall above the concrete wall and a natural rock crown. At several locations a shallow rise unreinforced concrete arch cap with a shallow arch was installed to support areas of poor rock. There are 551 locations where a concrete cap was installed, in various lengths, with a total of amount of concrete cap of about 4,900 m.

During the 98 years that the tunnel system has been in service, there have been eight significant failures of capped sections that blocked the tunnel flow and caused a total outage until the area could be cleared and repairs completed. Other repairs have varied from as little as the removal of fallen material and returning the tunnel to service, to very large efforts involving rock bolting of continuous steel plates on the walls and cap with secondary grouting. The latest such cap failure occurred in July 2002. The full width of a 3.7 m long section of cap with approximately 3.7 cubic yards of rock fell into the tunnel, blocking the conduit and causing an overflow of water that cascaded down and across the highway 800 feet below. A detailed engineering, geological, and geophysical (GPR) survey of the conditions of the tunnel and geological features was performed. This survey was completed in early 2003 and the rehabilitation measures proposed included installation of rock bolts and shotcrete and repair or complete replacement of concrete walls. In tunnel 19, several alternatives were considered including replacement with a new tunnel. The final solution was to install a new thin reinforced concrete structural lining with cellular grout over the existing concrete cap (Fallesen et al., 2006).

6 SAN FRANCISCO PUBLIC UTILITIES COMMISION (SFPUC)

SFPUC has over 125 km of tunnel constructed for the San Francisco Bay Area's water supply from 1867 to present. The Hetch Hetchy system spans from the north central Sierra Nevada through the Central Valley to the Coast Range geomorphic provinces (Figure 1, E-F-B). Rehabilitation and reliability upgrades to the Hetch Hetchy system include tunnels, some of which are described below.

6.1 *Mountain Tunnels*

Located in the foothills of the Sierra Nevada, this 30.8 km tunnel by 3 m diameter tunnel was put into operation in 1925. Since 1925, there have been 11 inspections, 4 for the full length and 7 for a partial length. Even though the condition of the tunnel has continually degraded, there is no indication that any repairs have been made. Deterioration of the tunnel has resulted in increased head loss and a decrease in system capacity. Due to concern of future tunnel collapse and further restriction of flow, a future repair program is being implemented. As the storage capacity within the Bay Area is limited, the outage duration for tunnel repairs is severely limited. To minimize shutdowns, sub-aqueous ROV inspections may be used. Typically, the low demand period is from November to March and planned outages are normally scheduled in that timeframe.

It is speculated that changes in the operation of the Moccasin Powerhouse have led to increased deterioration of the Mountain Tunnel. Since about 1987, the powerhouse has been operated as a peaking plant resulting in large flow changes on a daily basis and causing tunnel pressure fluctuations and surges upon filling and emptying the tunnel.

Possible repair scenarios consider conventional shotcrete and rock bolts installed in less than 3 month outages over a 5 to 8 year period.

6.2 *Coast Range tunnels*

The Coast Range tunnels are divided into the Telsa-Alameda and the Irvington segments. The Telsa to Alameda segment is 40.2 km long by 5 m diameter average bore, and includes two portals and five access shafts used during construction. Early use of shotcrete (1 m thick) was implemented by Engineer Carl Rankin in 1930 to control squeezing ground here on the Telsa-Alameda segment and later on the San Jacinto tunnel (Proctor, 1998). The Irvington segment is 5.6 km long by 5 m diameter.

6.2.1 *Thomas Shaft*

Thomas Shaft, one of the five construction shafts for the Telsa-Alameda segment, is founded in weak sandstone and about 2 m wide by 5.5 long by 107 m deep, lined with 25 cm thick concrete liner with weep holes to full depth. Reinforced concrete struts were installed at regular intervals. In the early 1990's, Lawrence Livermore Laboratory required a water tap into the Coast Range tunnel for some site expansion improvements (ESA, 1990). Prior to the improvements, inspection, condition assessments, and shaft loading analysis were made. Previous borings and construction records from 1926 to 1927 were reviewed and the concrete cored and tested. In general, the shaft was found to be in good condition. Loose concrete was scaled, wrapped, and/or repaired, and struts replaced where required. The tap was done through a massive concrete bulkhead from an adit connected to the aqueduct. Controversy arose over the safety of taping into the bulkhead. Consequently, an extensive grouting program was employed prior to tapping.

6.2.2 *Irvington Tunnel*

Irvington Tunnel has not been inspected in about 40 years. There are no operational alternatives if it is taken out of service; it is a bottleneck. In the event of its failure, Hetch Hetchy water would not reach the San Francisco Bay Area. It is bounded on each side by the Hayward and Calaveras faults, so the reliability of the system is of concern. The length of the tunnel does not make it amenable to ROV inspections. Because the condition of the existing Irvington Tunnel is unknown, it is not possible to determine whether or not a new Irvington Tunnel is required. However, adding a new tunnel provides additional seismic reliability. Planning and engineering are underway for a new parallel tunnel.

7 PACIFIC GAS AND ELECTRIC (PG&E)

PG&E has over 200 km of tunnels in its extensive hydroelectric system located primarily in the Sierra Nevada Mountains. When possible, tunnels are evaluated in a watered condition using head loss, seepage, and discharge of debris as key indicators of condition. Remotely operated vehicles (ROVs) are increasingly used to inspect watered tunnels where their use makes economic sense.

Tunnels are not unwatered on a regular schedule for inspection. Unwatering is avoided unless evaluation criteria suggest a problem, ROV inspection is impractical because of tunnel length, or the tunnel must be unwatered anyway for project maintenance.

7.1 *Drum Tunnels*

There are a number of relatively short, small-diameter tunnels on PG&E's Drum hydro canal system in the central Sierra Nevada east of Sacramento (Figure 1, E). Many of these tunnels are quite old, having been built during the 19th Century as part of a system to bring water to the mining districts in the area. The tunnels take the canal lines under low ridges of granitic and metamorphic rock. In poor ground conditions timber sets were placed and unreinforced concrete liner was later installed, encasing the sets. Because the tunnels are part of a canal system with open channel flow, the timber sets did not remain submerged and eventually rotted.

During the last two decades several sinkholes formed above the lined sections of some tunnels. Inspections during outages for canal maintenance also revealed occasional cracked liners, the rotted timbers, and voids above the crowns of the liners. A systematic program was initiated to characterize the conditions of the tunnels, prioritize them for repairs and then design and construct these repairs.

In addition to visual inspection and sounding the liner with a hammer, the main tool for evaluating liner condition is to drill many small diameter (25 to 50 mm) holes through the liner with a pneumatic hammer. The thickness and condition of the liner, size of void and geologic condition can then be evaluated. Early on in this process large diameter cored holes and geophysical methods (primarily ground penetrating radar) were also tried, but the small diameter holes were found to economically yield the most useful information.

Cracked liner sections with evident bulges or offsets were reinforced or replaced. Repairs that significantly decrease the tunnel cross section cannot be used because the reduction in flow can affect canal freeboard upstream.

Many liner crown sections appear to be in good condition yet are only 75 mm thick. Void spaces above the crown are common. It is not apparent whether these voids were present from the time of construction because of the concrete placement methods in use at that time, or whether they formed during the subsequent decades of operation.

PG&E is in the process of backfilling all void areas with grout. This will eliminate the possibility of flowing water enlarging the voids or collapse of the ground

onto the thin liner. Because of the short duration of the annual outages (one to two weeks), only 100 m long sections of tunnel are backfilled at one time.

The thin unreinforced crown sections are not credited with any structural capacity to support the grout forces. Temporary tunnel supports are installed prior to grout placement. The small tunnel size (about 1 m wide by 2 m high) creates a logistical problem because men, equipment, and material must still have access through the sets and spreader beams. A maximum grout pressure of 0.7 bar is specified. This pressure is found to be sufficient back fill the voids as long as grout holes and grout relief holes are closely spaced and the grouting equipment is closely monitored.

8 CITY OF PASADENA

8.1 *Azusa Conduit*

The Azusa Conduit is a 9.3-km-long water tunnel and box culvert structure in the San Gabriel Mountains in the Transverse Range (I, Figure 1). It conveys water by gravity feed from San Gabriel Dam along the shore of Morris Reservoir to the south abutment of Morris Dam and from there to a forebay where the water drops 100 m through a penstock to a hydroelectric power plant. Much of the conduit was completed in the 1890's by P.G. and E. with various segments consisting of hard rock tunnel, redwood stave flume, or steel pipe armored with native rock and mortar. In the mid-1930's when Morris Dam was built, the old flume and steel pipe was abandoned, most of the conduit was upgraded with concrete encasement, and at least one tunnel section was rerouted deeper into the hillside to avoid deformation and damage caused by a deep-seated creeping landslide.

Much of the downstream half of the conduit alignment below Morris Dam lies high on the side of precipitously steep canyon walls. This portion has been damaged repeatedly by shallow-based rock and debris slides. The landslides and erosion have damaged tunnel access openings, damaged tunnel linings requiring interior repairs and rerouting with new tunnels, and cleaning out of debris. There are several inverted siphons that have had to be cleared of debris and replaced or repaired in the last 20 years. Some segments of the alignment remain very difficult to inspect due to steep topography, unstable slopes, forest cover, and inverted siphons that are obstructed or have impaired ability to drain.

The frequency of conduit condition inspections decreased over the years and overall operational reliability has been good. In 2006, the first complete exterior inspection in several decades was performed. This inspection was undertaken due to estimated water losses greater than 10%, increasing incidence of animal incursions and debris blockages of the tunnel, and greater emphasis on water conservation. The exterior inspection was carried out in two phases: Phase 1 backpacking on foot (5 days) and Phase 2 by boat timed to coincide with the high reservoir water level in the spring for the middle section of the alignment (2 days). All known access points that could be safely reached were inspected, photographed, and plotted on base maps. Coordinates were measured at key locations using a hand-held GPS unit and video recordings were made using a hard-disk camcorder. All hatch covers that could be moved were unlocked and opened, viewed internally to the extent that could be done by looking into the opening, and photographed with a digital camera. Several access points that had not been previously identified were discovered in the field. Findings were plotted aerial ortho-photographic base photos flown and compiled specifically for the project. Preliminary recommendations for repair under consideration for cost versus benefit evaluation include sealing identified point leakages, upgrading flume segments where cover is inadequate, repairing access hatches and ports that have been damaged, overgrown, or buried, armoring or buttressing sections that remain vulnerable to future rockslides, constructing better access to drain an inverted siphon, and performing internal inspections as required.

9 SACRAMENTO MUNICIPAL UTILITY DISTRICT (SMUD)

SMUD has about 38.5 km of tunnels located in the central Sierra Nevada Mountains for hydroelectric generation (Rummel, 2006). Water rights for power and consumptive use are retained by the SMUD and the City of Sacramento, respectively. The most significant tunnels were completed in the 1960's as shown in Table 1. Frequency of inspection is about every 5 years or greater. The tunnels were constructed horseshoe shape by conventional drill and blast in metamorphic and granitic rocks and are predominantly unlined. Those portions that are lined are typically fully lined as a concrete horseshoe with some portions of shotcrete and rock bolts. The Jaybird tunnel was extensively contact grouted to reduce and stop leakage to one of the original construction adits. The Loon Lake shaft and tunnel was grouted to minimize and stop leakage into the underground powerhouse.

10 EAST BAY MUNICIPAL UTILITY DISTRICT

EBMUD, located in Oakland, services the eastern communities of the San Francisco Bay (Figure 1, B). The 5.5 km long Claremont tunnel crosses the active

Hayward fault and is under distress. To provide redundancy and allow for repair of the existing tunnel, EBMUD constructed a 146 m access adit and a 479 m by pass tunnel for reliability and uninterrupted service in a major earthquake event (Caufield et al., 2005).

11 MARIN MUNICIPAL WATER DISTRICT

MMWD, located in Marin, is the oldest municipal water district (non private) in California, having received its charter in 1912. MMWD has eight reservoirs and many pipelines and tunnels, constructed from 1872 to 1982. Bon Tempe reservoir has an intake tunnel constructed in the 1950's (Figure 1, B). The 350 m by 2.5 m diameter tunnel constructed in sandstone housed a smaller diameter intake pipe, which was subject to damage by collapsed and dry rotted timber (ESA, 1992). In general the rock conditions were good, and all the timber was removed and replaced with a shotcrete liner and a new access shaft was added for better and safer maintenance service of the intake valves.

12 CONCLUSIONS

This paper has provided a sampling of tunneling's role in maintaining the sustainability of California as a leading social and economic power in the world today. Early planners and engineers built these tunnels to last. Water tunnels have had an extended service life afforded by the natural environment of being underground combined with the legacy of following generations to perform reliability assessments (inspection and analysis), repairs (maintenance), and replacements, when and where required. Although just one part in the grand scheme of water supply projects, tunnels have played a vital role in providing continuous service to Californians.

REFERENCES

Anbessaw, A. 2005. Stone Canyon inlet tunnel rehabilitation project. City of Los Angeles Department of Water and Power, Water Resources Business Unit, Southern District Aqueduct, prepared for Water Operating Division. Nov 1–18.

Anonymous. 1940. *Metropolitan Water District of Southern California Historical Record of San Jacinto Tunnels, Specification No. 3, Schedule No. 1.* Banning, California, June 30, 64–69 and 7 figures.

Beikake, M. and Bell, R. 2003. Draft CRA – Conveyance reliability investigation, Program part 2, Compilation tunnel inspection report, Lake Havasu to Lake Mathews, October, 2002, January 2003, and February 2003 shutdowns. Metropolitan Water District of Southern California.

Bentwood, R., Baunelos, R., Liu, P., Pierson, R., Kaneshiro, J., White, C., and Van Ryzin, J. 2006. Lower Stone Canyon Bypass Line No. 2, Los Angeles, California, lessons learned from reservoir bottom and tunnel pipeline, design and construction. *Proceedings of American Society of Civil Engineers Pipeline Conference, Chicago, Illinois.*

Caufield, R.J., Kieffer, D.S., Tsztoo, D., and Cain, B. 2005. Seismic Upgrades of the Claremont Tunnel. *Proceedings of the Rapid Excavation and Tunneling Conference, Seattle.* Chapter 68. Denver: Society of Mining Engineers.

City of Los Angeles, Board of Public Service Commissioners. 1916. *Complete report on construction of the Los Angeles Aqueduct, with introductory historical sketch, illustrated with maps, drawings, and photographs.* Los Angeles: Department of Public Service of the City of Los Angeles.

ESA [Earth Sciences Associates.]. 1990. Geotechnical investigation for water tank at Site 300 and facilities at Thomas shaft. For University of California, Lawrence Livermore National Laboratory.

ESA [Earth Sciences Associates]. 1992. Bon Tempe Tunnel Support Conditions Survey. Marin Municipal Water District.

Fallesen, T., Van Horsen, D., Piek, M., and Kaneshiro, J. 2006. Case History: Rebirth of a successful tunnel installation, Kern River # 1 hydro tunnel, Kern River, California. *North American Tunneling Conference 2006. Chicago, Illinois*. Rotterdam: Balkema.

Hannaford, M. 2006. San Francisco Public Utilities Commission. Personal Communication.

Howser, H., California's Gold # 804 – Mt. San Jacinto, Huell Howser Productions, video.

Korbin, G.E. 2005. Draft report Hetch Hetchy Tunnel Repair Assessment, Approach and Planning Level Estimates May 12. Appendix D of the SFPUC-WSIP July 29, 2005, facility sizing report, revised draft.

Kress, F. 2006. Personal Communication, former geologist with DWR during construction of SWP.

Macias, M. 2006. Harvey O. Banks DWR Director 1956–1961. DWR News/People DWR 50th Anniversary.

Miller, J., Cordova, F., and Rodrigues, C. 2006. Los Angeles Department of Water and Power. Personal communication.

Nadeau, R. 1997. *The Water Seekers.* 4th edition. Santa Barbara, CA: Crest Publishers.

Pierson, R. 2004. Stone Canyon Inlet Tunnel Restoration, Interdepartmental Correspondence, City of LA DWP, to G. Coufal. Nov. 29.

Proctor, R.V. and White, T.L. 1977. 3rd edition. *Rock Tunneling with Steel Supports.* Youngstown, OH: Commercial Shearing.

Proctor, R.J. 1992. Overview of tunneling in Southern California. In Pipkin, B.W. and Proctor, R.J. *Engineering Geology Practice in Southern California.* Special Publication No. 4, Association of Engineering Geologists, Southern California Section. Star Publishing Company.

Proctor, R.J. 1998. A Chronicle of California Tunnel Incidents. *Environmental & Engineering Geoscience.* Spring, Volume IV, No. 1. Joint publication of the Association of Engineering Geologists and the Geological Society of America.

Redinger, D.H. 1998. The Story of Big Creek, Revised Edition, Tucson, AZ: Ironwood Press, Hong Kong: Palace Press.

Reisner, M. 1993. *Cadillac Desert: The American West and Its Disappearing Water,* Revised Edition.

Rummel, G. 2006. Sacramento Municipal Utility District. Personal Communication September 25.
Thomas, T. 2006. The birth of DWR. DWR News/People.
Thompson, T.F. 1966. San Jacinto Tunnel. In Lung, R. and Proctor, R., eds. *Engineering Geology in Southern California, Association of Engineering Geologist publication,* 104–107
SFPUC [San Francisco Public Utilities Commission]. 2005. *San Francisco Water and Power: A history of the Municipal Water Department & Hetch Hetchy System.* San Francisco: SFPUC Communications.
Willowstick Technologies, LLC. 2006. Aquatrack geophysical investigation, leak location and delineation survey, report on Big Creek Tunnel # 2 for Southern California Edison.

WEBSITES

http://wsoweb.ladwp.com / Aqueduct / historyoflaa / world-records.htm City of LA DWP Website on history of LA Aqueduct
http://www.ldeo.columbia.edu/~martins/hydro/case_studies/cadillac_desert.htm Public Broadcasting System web site for TV series for Cadillac Desert
http://www.wplives.com/frc/pge/index.html Provides description of PG and E's Stairway of Power
http://www.calgold.com/ calgold/ Default.asp?Series=800&Show=76 California's Gold #804 – Mt. San Jacinto video
http://www.publicaffairs.water.ca.gov/swp/history_swp.cfm California State DWR website, history of water development and the SWP

Underground Space – the 4th Dimension of Metropolises – Barták, Hrdina, Romancov & Zlámal (eds)
© 2007 Taylor & Francis Group, London, ISBN 978-0-415-40807-3

Study on maintenance planning for tunnels by risk management system

S. Konishi
Railway Technical Research Institute, Tokyo, Japan

K. Kuribayashi
East Japan Railway Company, Tokyo, Japan

K. Sudou
Tokyo Metro Company, Tokyo, Japan

K. Kamemura, M. Hori & C. Hatakenaka
Taisei Corporation, Tokyo, Japan

ABSTRACT: This paper presents a planning method of maintenance strategy for railway tunnels in Japan. The method adopted in the case study aims to find an optimal maintenance strategy to minimize the expected "Total Cost", which includes costs and risks. In the formulation, the probabilistic state vector consisting of deterioration ranks defines the state of structures. The proposed new planning method is able to indicate the optimal repair timing considering each characteristic of lines. The new approach of tunnel management will provide rational and reliable maintenance for aged railway tunnels.

1 INTRODUCTION

There are thousands of tunnels for railways, highways, and aqueducts for electric power plants in Japan. The total length of them exceeds 10,000 km. Some of them are aged and deteriorated, thus repairs are needed. In addition, a number of defective tunnels will increase drastically in the near future. These tunnels should be maintained properly to be functional more efficiently than ever as it is essential because of social and economical circumstances of Japan. Cost reduction together with maintaining the required level of safety and reliability is a prerequisite for the maintenance. In view of such aspects, we have studied on a planning method for the maintenance of railway tunnels with a risk management technique.

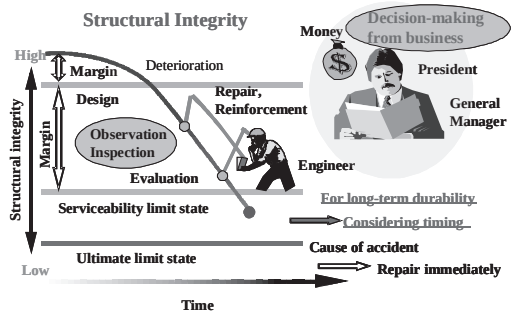


Figure 1. General relationship between maintenance and its structural integrity.

2 RISK MANAGEMENT SYSTEM

2.1 *Risk management for maintenance of structures*

Figure 1 shows a general relationship between the maintenance of a structure and its structural integrity. The vertical axis shows the structural integrity while the horizontal axis indicates time. Figure 1 shows a serviceability limit state and an ultimate limit state. The former signifies the limit state that the structure cannot be serviceable. The latter indicates the limit state that the structure is going to collapse.

Normally structural integrity is designed to be of a higher degree than that of serviceability limit state. Moreover, substantial structural integrity is higher than that of the design stage. Then, the structural integrity is gradually lost as time goes after commencement of operations. A structure engineer in charge of maintenance must understand existing structural conditions through periodic observations and inspections, and then he must consider a need of repair or an alternative measure to deal with substantial condition.

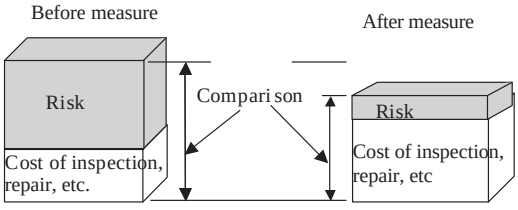


Figure 2. A concept of risk of a structure and management for maintenance.

As the structural integrity was discovered to be inferior to the serviceability limit state, an immediate repair should be made. However, as the degree of structural integrity is higher than the serviceability limit state, appropriate measures to cope with unsatisfactory conditions may be carried out until such time that the structural integrity further reduced to the serviceability limit state. Due consideration are essential in terms of an economical point of view for the following:

1. When will it be repaired? How will it be repaired?
2. Will it be repaired diligently, before the structural integrity degraded into a serious condition?
3. Will a large-scale repair be needed? When the structural integrity degraded into a serious condition?

In the case of an explanatory material, which is a common index between engineers and administrative managers, will be need. It is considered that risk management and asset management are one of the methods in preparing materials.

On a practical planning, many plans regarding inspection method, timing and scale of repair should be taken into account. In either risk management or asset management, the degree and extent of risk and a total cost required should be estimated quantitatively. Throughout the process of material preparation and comparative plans, an optimal plan among them should be selected for application.

The risk is a factor, which gets business worsens due to accidents and disasters. Total cost means the sum of the expenses, which consists of risk converted into money and cost for maintenance, such as inspection and repair. Risk management and asset management will prepare a material source where a total cost and annual risk are described. A manager in charge will make a decision by himself or in coordination with other responsible engineers in some occasions based on the type and quality of material.

2.2 *Procedure for risk management*

The risk management system is one of the methods controlling the risk and minimizing the probable effect caused thereby. It is a characteristic of the risk management to convert the risk into a quantitative loss,

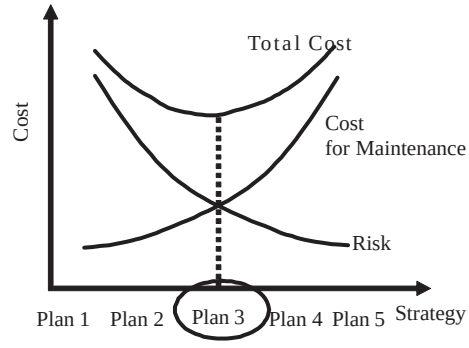


Figure 3. A concept of risk management for maintenance.

for example money, and to deal with quantitatively. In the report, the risk is formulated into Equation 1.

Provisos
Event Probability (P): Probability, which a supposed phenomenon happens
Importance (C): The amount of damage when the phenomenon happens

The method adopted in the case study aims to find an optimal maintenance strategy to minimize the expected "Total Cost", which includes costs and risks shown in Fig. 3.

In case of the investigation, it is important to keep the indispensable safety and reliance due to correctly quantify risks.

A procedure for preparation of a maintenance plan by the risk management is as follows:

1. Draft Preparation (Alternative plans for a period of inspection, method, method of countermeasure, timing of countermeasure, etc.
2. Modeling special qualities of the structure.
3. Extracting risks (With an event tree and scenario)
4. Evaluating for the probability of the risk (With the results of inspection, prediction of deterioration and other factors)
5. Evaluating importance of results (with an event tree and scenario.)
6. Evaluating risks
7. Comparison with the results from (1) stage to (6) stage of each plan

3 CASE STUDIES

3.1 *Subject model*

In the case study, optimal timing of repair was investigated for two imaginary tunnels, based on existing

Table 1. Component of model tunnels.

Item	Route A (A main line)	Route B (A local line)
Location	The old lines	The old lines
Number of trains	20 number/hour	1 number/hour
Length of a route	14 km	65 km
Average number of passengers	65 people/car	12 people/car
Compose of coaches	16 m a six-car train	16 m a three-car train
Length of a tunnel	1008.8 m	1008.8 m
Ground condition	Uniform	Uniform
Proceeds	40 billion yen/year	3.8 billion yen/year

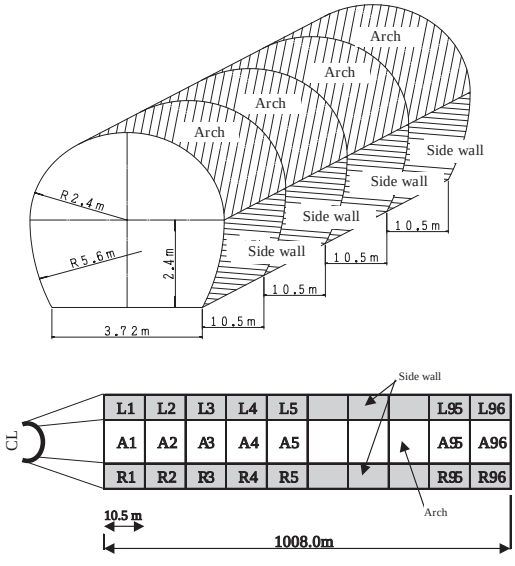


Figure 4. Modeling of tunnel.

data of various actual tunnels applying the above-mentioned method. One is located in a mainline and another is located in a local line as shown in Table 1.

The tunnels are assumed 30 year old. An actual tunnel has various unfavorable problems, for example leakage, deformation, deterioration of material, etc. However, to simplify the problems, only spalling of concrete blocks from tunnel lining was investigated in the case study. We assumed that the size of a concrete block is about 50 cm*50 cm*50 cm. For consideration, we divided a tunnel into many elements as shown in Fig. 4, and finally summed up the results of each element.

3.2 *Calculation of event probability*

A probability of spalling is estimated with a structural integrity classification of tunnel lining (Table 2) applied by many railway companies, because the probability of spalling depends on a condition of a structure. In the case study, the probability of spalling is estimated by previous inspection data assuming that the probability is constant in a similar rank of the integrity classification, as shown in Table 3.

Since tunnel linings are deteriorated due to various causes, the characteristic of deteriorations cannot be necessarily clarified. Accordingly, we assumed that the laws of probability dominate the deteriorating condition of the structure lead by regular inspections is dominated by the laws of probability, and evaluated the characteristic of it. When it is assumed that the state of the structure at time t_n depends on only the state of the structure at time t_{n-1}, (Markov chain), a transfer matrix, which indicates the possibility of the deteriorating progress due to data of past inspections, can be created for the state set up separately, (i.e. ranks from S to AA). Table 4 shows an example of the transfer matrix. The rank of the integrity on a lateral axis shows the condition of one year and it on a vertical axis means the state of the next year. For example, the matrix transfers the state of an element, which is rank S in a year, to the state, which 92.3% of it is rank S and 7.7% is rank C in the next year.

In the report, the transfer matrix was made by inspection data for the previous 30 years of a certain tunnel. In another word, values of the result are for only the tunnel, and other estimation is necessary as for another tunnel.

Figure 5 shows an estimated deterioration curve calculated by the transfer matrix. It indicates the distribution of annual ranks in the structural integrity classification.

In the deteriorating process of a tunnel is modelled by Markov chain. However, if deterioration could be estimated quantitatively due to progress of studying on a mechanism of lining deterioration, the estimation become accurate than it in the report. Next, calculation is made for each element of the tunnel as shown in Fig. 4, and sums the results; and a probability of spalling in the future is calculated.

3.3 *Calculation of importance and risk of event*

When listing facts use either the style tag List signs or the style tag List numbers.

The importance of the event and the damage by spalling cannot be classified easily, because various situations are supposed, for example, “only spalling with no damage”, “hit on a train”, “break signal facilities”, “hit on a person”, etc. However, if the events are verified neither too much nor too little, the amount of damage due to the event cannot be supposed. Moreover, if probability of event and of damage is analyzed enough, the amount of damage due to the event cannot be supposed. Then, with an event tree, we selected all

Table 2. Structural integrity classification of railway structure.

Classification	Influence on driving safety	Deformation	Measure
AA	Danger	Serious	In no time
A1	Danger in time	Progress of deformation and deterioration of performance	Immediately
A2	Danger in future	Apprehension about deterioration of performance when deformation is progressing	In case of need
B	Become rank A when unfavourable state is progressing	Become rank A when unfavourable state is progressing	Observation
C	No problem in the present	Minor deformation	Inspect some point
S	No problem	Nothing	

Table 3. An example of assuming probability of spalling.

Examples of assuming probability of spalling
AA: 3.3%/year*place
A1: 0.33%/year*place
B : *****
An example:
1. Grounds for a probability of spalling in case of rank AA
2. Assuming that four fifth of the spallings happen in case of rank AA
3. Assuming that total length of parts of the rank AA in the railway tunnel is about 300 m
4. Divide into arch and sidewall each 10.5 m
((12/4/300)*(10/3) = 3.3%

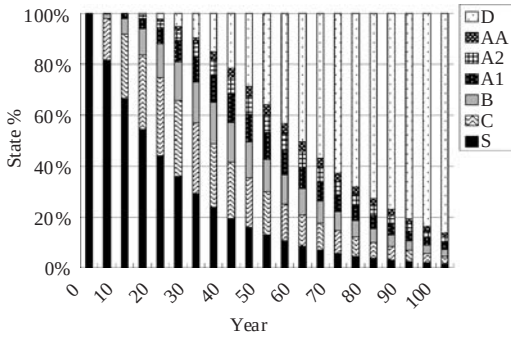


Figure 5. Estimated deterioration curve calculated by transfer matrix.

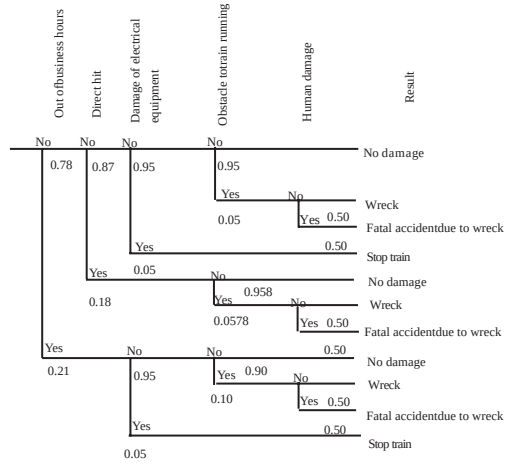


Figure 6. An example of an event tree.

Table 4. An example of transfer matrix.

N / N+1	S	C	B	A2	A1	AA
S	0.923					
C	0.077	0.998				
B		0.002	0.935			
A2			0.065	0.986		
A1				0.014	0.959	
AA					0.041	1

unfavourable problems due to spalling, and calculated its probability and the amount of the loss.

Next, multiplying the results, we estimated the risk A (predicted loss) due to spalling.

Figure 6 shows an example of an event tree. The event tree is the method picking out all unfavourable problems as follows: set the starting phenomenon on the left end, draw considerable choices in sequence and branch to lead many results. A probability of change is given to each factor changing a phenomenon, and the probability of the phenomenon due to plural factors is connected with the lost cost due to the phenomenon.

Throughout multiplying the risk A by probability of spalling, an annual risk was calculated (Fig. 6).

Incidentally, values themselves in Table 3, 4 and Figure 3 are not important, because the values were led

Probability	A sum of money (million yen)	Risk A (million yen)	Business loss (hour)	Human loss[*3] (%)	Material loss (million yen)
0.62	40		6		
0.02	510	8.34	19		400
0.02	1,000	16.27	19	0.05	400
0.03	120	4.17	12		100
0.10	50	4.76	6		
0.00[*1]	510	1.36	19		400
0.00[*2]	1,000	2.66	19	0.05	400
0.18	40	6.61	6		
0.01	510	5.07	19		400
0.01	1,000	9.89	19	0.05	400
0.01	70	0.75	12		100

[*1], [*2]: Round down 0.0024 to 0.00

[*3]: Multiply probability of the deceased per coach by a number of passengers per coach and human losses per the deceased.

by a limited data including some assumption. Please refer only to the procedure.

3.4 *Comparative investigation (repair timing)*

In this case study, the difference of risk and a total cost due to various repair timing were investigated. Five plans, which are shown in Table 5, were compared with each other to determine optimal repair timing in proportion to the degree of structural integrity evaluated by regular inspections.

No remedy has been considered for Plan #1. Plan #2 requires a measure (b) in the case of rank A1 and up. A measure (a) is applicable to Plan #3 in the case of rank A2 and up, and a measure (b) is taken in the case of rank 1 and up. The measure (a) is an injection. The measure (b) added a back filling in an emergency to the measure (a).

Figure 7 shows cumulative total costs of the main line. Figure 8 is annual risks of the main line. In view of the foregoing figures, the alternative 5 (the measure (c) taken) is the best among others as shown in Fig. 8 for busy lines if only a decrease in annual risk considered.

However, in the case of 50 years, a cumulative total cost of the plan 4 is the minimum, as shown in Fig. 7.

The risk under the plan 4 is not so extensive to compare with that of the plan 5; the plan 4 can be determined appropriate in general view. The repair cost required for the plan 5 from earlier stage becomes expensive. Where repairs are made on a late timing under the plans 1, 2 and 3 respectively, a higher risk is highly anticipated.

Figure 9 shows a cumulative total cost required for inactive local lines while Fig. 10 shows risk variation anticipated in each year.

Table 5. Each plan for repair timing.

Item	State	Plan#1	Plan#2	Plan#3	Plan#4	Plan#5
Repair timing	S	No	No	No	No	No
	C	No	No	No	No	Measure a
	B	No	No	No	Measure a	Measure a
	A2	No	No	Measure a	Measure a	Measure a
	A1	No	Measure b	Measure b	Measure b	Measure b
	AA	No	Measure b	Measure b	Measure b	Measure b

Measure a: Injection.
Measure b: Added a backfilling in an emergency to the measure (a).

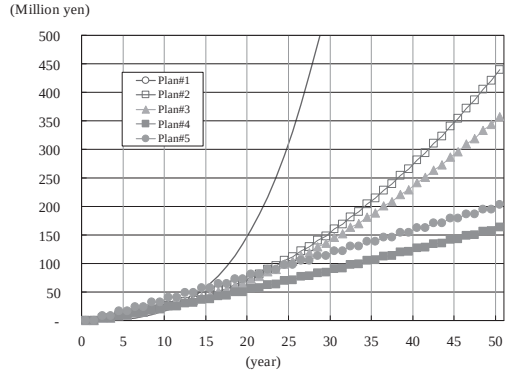


Figure 7. A cumulative total costs of the main line.

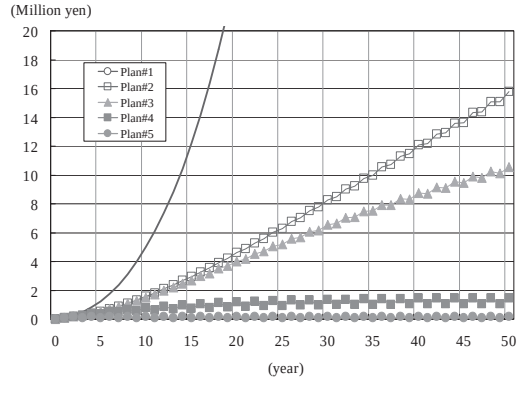


Figure 8. Annual risks of the main line.

For tunnels of inactive local line in terms of 50-year service, it is apparent that the plan 4 is the most appropriate, however, in terms of 20-year service, the plan 3 is another appropriate plan.

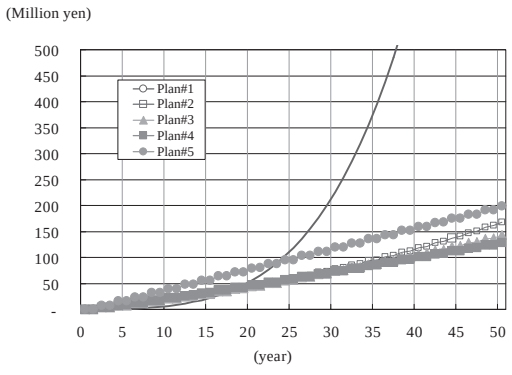


Figure 9. A cumulative total costs of the local line.

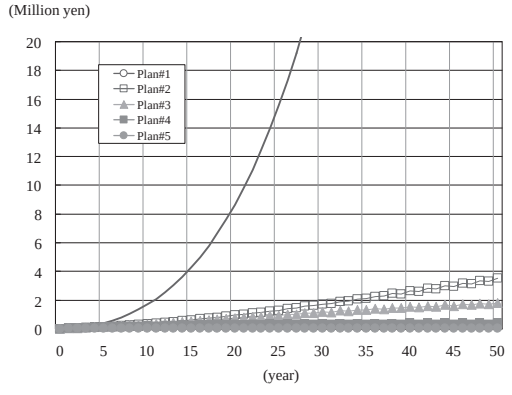


Figure 10. Annual risks of the local line.

4 CONCLUSIONS

We have established a model case based on the concrete results of inspections and repairs, and made a study on a substantial procedure to plan for the tunnel maintenance with the risk management technique. We pay attention to reduce an additional work by applying various data obtained through routine work. We evaluated each plan to compare annual risks and total costs of plans with different repair timings. It is conceivable that we can offer a concrete image of risk management to give examples.

We would like to collect more examples to solve the above-mentioned problems, and improve the accuracy of the method for future application.

REFERENCE

Konishi, S. and Kamemura, K. 2004. Application Method of Risk Management to Tunnel Maintenance, Tunnels and Underground, Japan Tunnelling Association., Vo35, pp.49–56.(In Japanese)

Underground Space – the 4th Dimension of Metropolises – Barták, Hrdina, Romancov & Zlámal (eds)
© 2007 Taylor & Francis Group, London, ISBN 978-0-415-40807-3

Reconstruction of the Jablunkov tunnels

J. Korejčík & J. Růžička
Metroprojekt Praha, Prague, The Czech Republic

ABSTRACT: Reconstruction of two parallel single-rail tunnel tubes had to be designed, as part of the Third Railway Corridor Modernisation Project, in the Czech Republic-Slovakian border section of the corridor. The client wished the old tunnel lining to be replaced and the tunnel clearance enlarged in both tunnel tubes. In view of operational and technical calculations, the authors of the design proved that a single-rail operation mode will be acceptable during the reconstruction period; they designed a new solution, which is based on reconstruction of one tunnel tube only, which is to be rebuilt into a double-rail tunnel with a total length of 612 m. The design reasonably utilises the existing tunnel as an initial excavation sequence, which also allows the part of the rock mass which got loosened after the tunnel destruction during World War II to be improved in advance. In addition, at the time of the top heading excavation, the tunnel will be used for removal of muck by rail. After the new tunnel is put into operation, the old single-rail tunnel tube will be closed.

1 INTRODUCTION

The Jablunkov tunnels are found near the municipality of Mosty u Jablunkova, in the Moravian-Silesian region, in the north-eastern corner of the Czech Republic. The state border with Poland and Slovakia is close to this place. The tunnels were built under a mountain pass lying at the altitude of 552 m above sea level. The pass is hammed in between the crests of the Moravian-Silesian Beskydy Mountains and the massif of the Silesian and Slovakian Beskydy Mountains. The divide between the Black Sea and the Baltic Sea runs along the pass. This location has always represented a connecting line between the northern Moravian industrial region with its coal mining and steel production centre, the city of Ostrava, and north-western Slovakia with its strategic centre, the city of Žilina, which is linked to the capital of Slovakia, Bratislava, from the south and to the industrial centre of eastern Slovakia, the city of Košice, from the east. Despite the splitting of former Czechoslovakia on 1st January 1993, the intensity of traffic on this railway line remains unchanged, today already within the European Union.

The 100-year service life of a pair of single-rail tunnel tubes which were built stepwise to allow the railway to overcome the pass is slowly drawing to the end. The decision to reconstruct the Jablunkov tunnels was given a boost by the fact that the line is part of the railway corridors being developed.

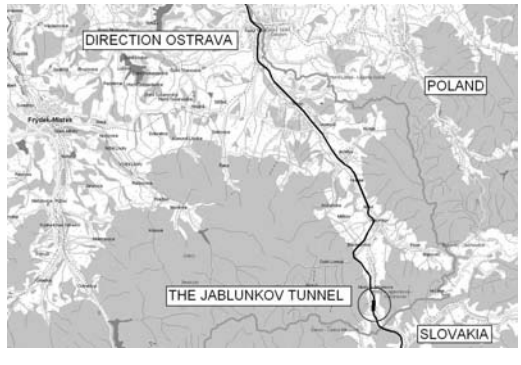


Figure 1. Location of the Jablunkov tunnel.

2 HISTORY OF THE JABLUNKOV TUNNELS

The Jablunkov I (Kalchberg) tunnel was built in 1870 as part of the Košice – Bohumín single-track line, which linked the Ostrava region in northern Moravia with the Košice region in eastern Slovakia. The second track in the Èadca – Jablunkov section was built, in the effort to accelerate and make the operation of the line more financially effective as long ago as 1898, however, without the tunnel. The Jablunkov II tunnel was opened as late as 1917. This construction began

in 1914 using the then modern standard Austrian Tunnelling Method (the Modified English Method) for the entire length of the tunnel. The tunnel was built using Beskydy sandstone from a nearby quarry.

The area of the Jablunkov Pass became the most unsuitable in terms of the vertical alignment of the track; initially, the 16‰ uphill gradient required additional pushing locomotives. In the beginning, coal transport from Ostrava represented nearly 90% of the transport; the transport of grain, rape, fruits, cattle, wood, gravel, ore and other materials started later.

At the beginning of the World War II in1939, charges were set off in both tunnels causing a daylight collapse. A secondary road leading above the tunnel also sank down. The cavity was backfilled and the damaged lining renewed in 1940.

The following years saw the completion of the doubling and electrification of the entire length of the track. The tunnels were partially reconstructed several times, the last time in 1999. Some sections were re-built and some were provided with an invert. Apart from this, drainage boreholes, re-pointing of the masonry and grouting, both into and behind the lining, were carried out. Water collecting drains were installed between some of the tunnel blocks to evacuate water from the external face of the lining. In 1971, the trackbed in the tunnel was replaced by a system with sleepers embedded in concrete. This system, however, had not acquitted itself well. For that reason it was replaced by traditional wooden-sleepers and ballast trackbed in 1987.

3 GEOLOGICAL AND HYDROGEOLOGICAL CONDITIONS

The bedrock in the north-western part of the area of operations is part of a Cretaceous Silesian unit consisting mainly of the Istebné Sand layers. In the south-eastern and eastern part of the location, the Pre-Quaternary bedrock is formed by Palaeogene Krosněny Member of the Silesian Unit, which means flysch-type alternation of calcareous sandstone and mudstone. Mudstone intercalated with sandstone prevails in the southern part of the location. The interface between the Istebné and Krosněny Members is faulted; the fault passes along the saddle, approximately in parallel to the tunnel centre line.

Due to the terrain configuration, there are several streams flowing down the surrounding slopes to the area of the mountain pass and supplying the area of the tunnel cover with water. The entire length of the tunnel tubes lies in the Palaeogene bedrock consisting chiefly of mudstone with irregular occurrence of clay layers and isolated sandstone intercalations. The cover is an about 2 m to 6 m thick layer of clayey loam, clay, made ground and sand with rock fragments, which is always saturated down to the interface with the Palaeogene bedrock. This means that the tunnel tube is completely submerged under the water table. The water penetrates to this level along faults in the environment which is otherwise little permeable or impermeable. The locations where water seeps to the tunnel structure depth correspond partially with the locations of surface watercourses, or with terrain depressions where long-standing accumulation of surface water occurs. The intensity of seepage follows the intensity of local rainfall with a certain delay.

4 DESCRIPTION OF CURRENT CONDITION

The Jablunkov I tunnel is 606.58 m long. The length of the Jablunkov II tunnel is 608.20 m. Both single-rail tunnels are straight in the ground plan. They are of the summit type, with a maximum gradient of 8.1‰. The overburden thickness reaches 24 m. The clearance height and width of the tunnel tube amount approximately to 6 m and 5.5 m respectively. The safety recesses are provided on both sides of the tunnel, alternately at about 50 m spacing. The portal blocks of the tunnel, including the front walls and wing walls, are made of the Beskydy sandstone, the same as the tunnel tubes.

The tunnel drainage is provided by hand-placed rubble behind the outer surface of the lining. The water is directed from the drains transversally to the main 400 mm-diameter tunnel drainage duct built in the centre of the tunnel bottom. The longitudinal gradient of the duct declines toward both portals. The waterproofing system consists of cement screed spread on the outer surface of the masonry lining, which is covered with corrugated steel sheets. The waterproof covering of the reconstructed sections was provided by asphaltic boards.

The Jablunkov tunnels are electrified; the design speed for the given section is 80 km per hour. The clearance envelope does not comply with the requirements for an electrified track.

5 DEVELOPMENT AND RECONSTRUCTION OF THE TUNNELS

The Jablunkov tunnels are parts of the railway corridor III Cheb – Plzeň – Prague – Česká Třebová – Ostrava – the state border with the SR. In particular they lie in the Dětmarovice – Mosty u Jablunkova – the Slovakian state border section, which is important for the connection of the transit corridor II Warsaw – Vienna with the Slovak Republic. The tunnels will be reconstructed in the framework of the construction lot "Optimisation of the SR state border – Mosty u Jablunkova – Bystřice nad Olší track section". The design documentation for issuance of the zoning and planning decision for this construction lot has been approved and the work on

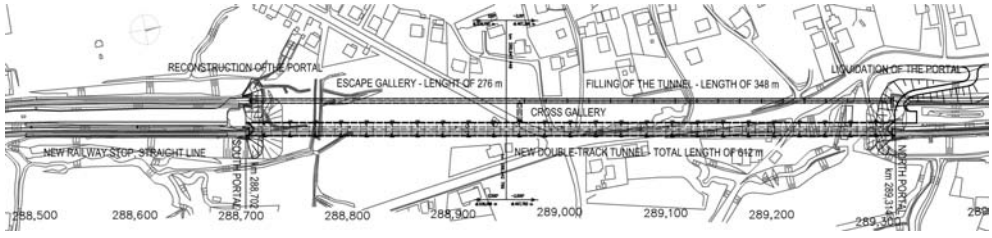


Figure 2. Tunnel layout.

the final design is in progress. The tunnel construction is expected to start in 2008 at the very earliest. The optimisation of this section even places increased demands on the Jablunkov tunnels. The design speed will be increased there to 120–140 km/hour for traditional trains, and to 140–160 km/hour for trains with tilting bodies. The vertical alignment must be modified and the tunnel cross-section enlarged. The overall reconstruction is necessary also because of the unsatisfactory structural condition of the tunnels.

The original solution which was under consideration in the regional planning and technical study assumed that both tunnels would be reconstructed to form a pair of new single-rail tunnels. The liners would have to be removed, then the profile of each tunnel tube enlarged and new liners erected. METROPROJEKT Praha, a. s., the designer, submitted a new solution where the Jablunkov II tunnel was enlarged and relined to form a double-rail tunnel. The Jablunkov I tunnel was proposed to be closed once this tunnel has been brought into service. However, a non-standard requirement for excavation of an escape gallery for the new double-track tunnel was imposed by the Fire Rescue Service of the Moravian-Silesian region during the comments-negotiation period. The client eventually accepted the requirement. According to the redesigned layout, only a part of the single-track tunnel will be closed and the remaining part plus a newly built cross passage will be utilised as the escape gallery.

The advantage of this new solution is, among others, the savings in the time required for the reconstruction of the tunnels, therefore also a shorter time for closing traffic, which will be required only for one track; the problem of staggered closing of the tunnels is thus removed. An economic assessment of the two variants, including associated structures, was carried out with a conclusion that the new solution is nearly by CZK 90 million cheaper. This saving is sufficient to cover the costs of closing the abandoned tunnel and the increased cost of the work on the preportal sections. The extension of the free space at the portals will render better conditions for the development of access roads for emergency vehicles. Owing to the existence of A straight section of the double-rail track in front of the southern portal of the new tunnel, it is possible to develop a new intermediate station Mosty u Jablunkova, which will replace the current intermediate station, which is inadequate because of its position in a curved track section. Another benefit of the new solution is a possibility of utilising a portion of the muck of the current tunnel for the backfill of the tunnel section that is to be closed. This material will be deposited on an intermediate stockpile near the portal, thus the transportation cost will be minimised.

6 THE TUNNEL PROFILE ENLARGEMENT TECHNIQUE

The newly designed Jablunkov double-rail tunnel is 612 m long; it is provided with an escape gallery. The track centre distance is 4 m; the horizontal tunnel alignment is straight. The axis of the new tunnel is shifted toward the other (single-rail) tunnel tube, to a distance of 4 m from the old single-rail tunnel. Regarding the gradient, the tunnel is of a summit type with an uphill and downhill gradient of 2.00‰. The inner radius of the tunnel vault is 5.7 m. There are safety recesses on either side of the tunnel at intervals of 24 m. Because of the rock environment consisting mainly of very weak and squeezing prone mudstone, the invert will be provided along the entire length of the tunnel.

6.1 *The mined tunnel section*

The excavation of the 588 m long mined section of the tunnel will be divided into three phases. The first phase will comprise the excavation of the entire length of the top heading together with the installation of the primary shotcrete support. In this phase, the existing single-rail tunnel will be utilised as the initial partial excavation of the bench. The muck from the top heading can be transported by railway wagons via the old single-rail tunnel up to the final dump. The second phase will comprise stepwise demolition of a major part of the old tunnel structure. It will be carried out concurrently with the excavation of the remaining part of new tunnel profile, while the external side wall of the existing tunnel will be incorporated into the primary lining of the new double-rail tunnel. Subsequently the whole profile will be provided with primary shotcrete support. The closed intermediate

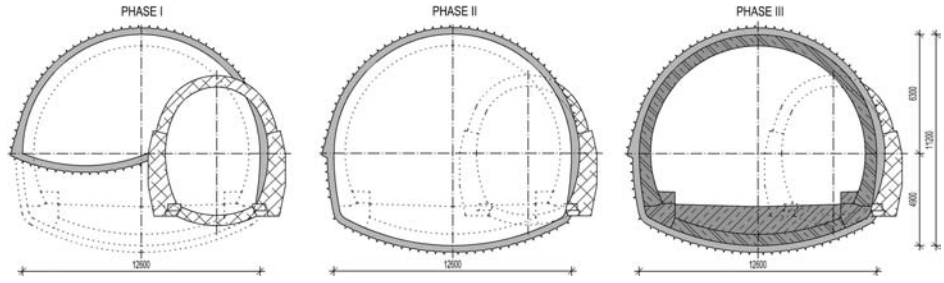


Figure 3. Driven technology of the tunnel.

waterproofing system will be installed and the final tunnel liner cast in the third phase.

The New Austrian Tunnelling Method is designed for the excavation. Application of the drill-and-blast technique is expected for partial operations. Mainly for the demolition of the existing tunnel lining. Weaker mudstone zones will be disintegrated mechanically using tunnel excavators. The excavation will be divided using a horizontal sequence of the headings. The size of the partial excavation faces is sufficient for the operation of high-performance tunnelling equipment. There is an assumption based on the geotechnical survey that the excavation in the mined sections will be categorised as support classes 3, 4 and 5. The theoretical excavated cross-section area ranges from 116.1 m^2 to 129.9 m^2. The primary support consists of C 16/20 sprayed concrete with welded mesh, lattice girders, rock bolts and forepoles. The thickness of the primary lining ranges from 150 mm to 350 mm, depending on the excavation support class. The mined portals are supported a 12 m long pre-support canopy.

The final lining of the mined tunnel, which is provided with an invert, will be constructed in two phases, using a travelling form. The invert will be cast first, the casting of the vault with side walls will follow. The length of the casting blocks is 12 m. The final liner is designed to be made from cast-in-situ reinforced concrete of C 25/30 grade; the thickness ranges from 400 to 600, depending on the excavation support class encountered. It was calculated for the ground water head, therefore there is no need for maintaining a permanent drainage system behind the outer surface of the lining. The concrete reinforcement consists of lattice arches, welded mesh and strap pieces if needed. Tied-up reinforcement is used for the invert, whose thickness is the same as the thickness of the lining. The gap between the invert and gravel ballast is filled with non-structural concrete. The intermediate waterproofing system is designed to be of a closed type, which means that it covers the entire tunnel circumference and no permanent longitudinal toe drainage is necessary. This system, in contrast with an unclosed system of the umbrella type, prevents a long-term impact on the natural regime of ground water in the vicinity of the tunnel. The draining of the tunnel interior is provided by the central drainage duct (a PE pipe 400 mm in diameter), which carries water to both portals. This duct is located in the centre of the tunnel profile, under the trackbed; it is embedded in porous concrete.

Walkways are provided on both sides of the tunnel; steel handrails are fastened to the tunnel lining. The lines of the handrails are broken at the safety recesses. A multi-way PE cable duct is embedded in each pavement. The cable duct is cut by manholes containing outlets for electrical equipment. In addition, there is a dry fire main embedded in one pavement (a 110 mm-diameter PE pipeline), which is fed with water from shafts built in front of the portals.

The numbers of all tunnel blocks, safety recesses and escape routes and their distance from the closest portal or escape gallery will be marked in the tunnel. There are oblique guide-strips interconnecting the neighbouring safety recesses designed with the aim of facilitating safe movement and search for a shelter in the tunnel. The marking will be painted on the internal surface of the final lining. Sign tables will be imprinted into the concrete surface during the casting.

6.2 *Cut-and-cover sections*

Both cut-and-cover entrance sections are designed at a length of 12 m, which corresponds to the length of the portal tunnel block. The sides of the open cuts will be stabilised by shotcrete reinforced with welded mesh. The portal wall of the construction trenches will have additional support in the form of anchoring.

The final lining of the cut-and-cover tunnel sections will be erected after the casting of the mined tunnel blocks has been finished. The same travelling formwork is planned to be used for both the mined and cut-and-cover sections of the tunnel; formwork for moulding of the outer surface will be added in the cut-and-cover sections. The cut-and-cover portal sections which are provided with the invert will be cast using C 25/30 water retaining concrete. The front ends of these sections are slanted and provided with flanges preventing rainwater from spilling over the edge.



Figure 4. Placement of the new double-track tunnel.

The thickness of the lining as well as the invert is 600 mm. Tied-up reinforcement is designed.

The design of the new portals is simple in terms of the style; the slant copies the surface of the grassed over terrain. Their incorporation into the surrounding landscape is very natural and unforced. Access roads will lead to both portals within the framework of the fire protection system. They will terminate at mustering areas provided for fire rescue service equipment and emergency vehicles.

7 CONSTRUCTION OF THE ESCAPE GALLERY AND CLOSURE OF A PART OF THE TUNNEL

All modifications of the existing single-rail Jablunkov I tunnel will be carried out only after the new double-rail tunnel has been commissioned. The beginning of the 276 m long escape gallery is at a safety recess found approximately in the middle of the double-rail tunnel. The escape route leads through the newly built 18 m long cross passage to the unused single-rail tunnel and ends at the southern portal of this tunnel.

The horseshoe shaped profile of the cross passage will be excavated using the NATM, with the primary support consisting of C 16/20 sprayed concrete, mesh, rock bolts and lattice arches. An 8 m long canopy tube pre-support will be installed from both sides of the cross passage.

The main reinforcing elements of the C 25/30 reinforced concrete final lining and invert will be transverse lattice girders and mesh. The vault and side-wall lining is 200 mm thick, while the maximum thickness of the invert is 500 mm. The casting of the final lining of the cross passage is expected in two phases, i.e. casting of the floor and of the vault and side walls. The closed waterproofing system designed is the same as that designed for the tunnel.

A 16.5 m long air-lock chamber will be installed in the cross passage. It is separated from the tunnel by a 2.2 m wide fire resistant door, and from the escape gallery by a steel door with the same dimension. The air lock is positively pressurised by a forced ventilation system independent of the escape gallery ventilation system to prevent smoke entry from the tunnel to the escape gallery.

Regarding the part of the Jablunkov I single-rail tunnel which will be utilised as the escape gallery, the first operation will be the removal of the ballast and proper treatment of the tunnel lining surface. The following phase will comprise installation of a closed waterproofing membrane system and construction of the 350 mm thick C 25/30 final lining. Travelling formwork will be used for casting of the 123 m long tunnel. The escape gallery will be terminated by a concrete bulkhead with a door passable only in the direction of escape.

The interior of the northern part of the single-rail tunnel will be thoroughly filled mostly with the muck from the new tunnel excavation, which will be temporarily stored in an intermediate stockpile. The remaining part of the cross section will be filled with cinder concrete, section by section. The space which will be developed when the process of the cinder concrete setting and shrinkage has been over will be filled by grouting. The drainage effect of the currently existing tunnels will be significantly reduced owing to the grouting and waterproofing membrane; the water table should return to the natural long-standing level.

The final action will be the demolition of the northern portal, including the skew wing walls, and final finishes of the slopes and sowing grass seed. The southern portal with a sign “Kalchberg 1870” will be rehabilitated and maintained as a technical monument for future generations.

8 CONCLUSION

The design expects that the tunnel profile will be enlarged even in adverse geological conditions. It reasonably takes advantage of the possibility to utilise the existing tunnel to serve as the initial partial excavation, which, at the same time, allows transportation of muck from the top heading excavation by rail to direct deposition in other parts of the construction lot in question where new backfill is to be carried out. In addition, this solution allows relocation of the Jablunkov – Mostly intermediate station to a place meeting operational requirements. At last but not least, the design allows deployment of high-performance excavation equipment, thus cutting the construction time. The application of the closed waterproofing system means that the hand-placed rubble drainage behind the tunnel lining can be eliminated. The favourable effect on the natural hydrological regime in the tunnel overburden is obvious.

This page intentionally left blank

Underground Space – the 4th Dimension of Metropolises – Barták, Hrdina, Romancov & Zlámal (eds)
© 2007 Taylor & Francis Group, London, ISBN 978-0-415-40807-3

Upgrading old masonry interceptor sewers to modern sewerage standards

Cezary Madryas, Arkadiusz Szot & Leszek Wysocki
Wroław University of Technology

ABSTRACT: A short history of brick interceptor sewers, surveys of sewer technical condition and analyses of its deterioration and ways of upgrading old masonry interceptor sewers to modern environmental standards and mechanical loads are presented. Both difficulties and benefits of such upgrading are considered. Most of the rehabilitation technologies used in Poland are described in detail in included case studies.

1 INTRODUCTION

A considerable part of the sanitary drainage network in Polish cities is well past its 50-year design service life and the boundary conditions formerly adopted when designing sewers and the associated facilities are much different from the conditions in which the structures serve today. This is especially true of brick sewers built at the turn of the 19th and 20th centuries. In Poland the first comprehensive sewage system design was developed for Gdańsk by the German engineer Friedrich Webe. The project was completed in 1871. But the historical development of sewerage systems in Polish cities should be mainly associated with the engineer William Lindley who designed the basic layout of a water supply and sewage system for Warsaw and his son Sir William Heerlein Lindley, DEng. who implemented the project. Sir William Heerlein Lindley's projects carried out in Poland include designs and their implementations as well as expert opinions relating to the provision of Łódź (1907–1909), Lvov (1909), Radom (1912) and Włocławek (1910–1914) with water supply and sewage systems [5]. Sewerage networks in the Western Territories (incorporated into Poland after WWII), e.g. in Wrocław, developed in a similar way whereas those in the Polish territory formerly under Austrian rule (e.g. in Cracow) developed somewhat differently.

Despite the exceptionally fine workmanship, the sewers are increasingly often damaged due to changed chemical, biological and mechanical loads and the passage of time. This often leads to failures of other structures, e.g. street surface cave-ins and the subsidence of buildings. The external factors causing damage to interceptor sewers are usually stochastic processes which are difficult to define. Predicting changes in their intensity over time is even more illusory than in the case of factors stemming from the sewer service function. Factors adversely affecting sewers include: mechanical (static and dynamic) loads, the chemical aggressiveness of the soil, biological aggressiveness (destructive action of bacteria, tree roots, etc.), the adverse effect of other structures (especially when they fail structurally or are under construction) as well as the effects of warfare, terrorist acts, disasters (e.g. floods) and seismic and paraseismic movements of the surrounding ground.

Surveys of sewers have been conducted by the Department of Urban Engineering of the Institute of Civil Engineering at Wrocław University of Technology since 1968. From the beginning of the 1990s the Department has also been designing trenchless reconstructions of brick sewers.

2 RANGE OF BRICK INTERCEPTOR SEWER INVESTIGATIONS

Sewers can be investigated by means of television cameras (closed circuit television) or by personnel working inside them. CCTV is mainly used in inaccessible non-walkthrough sewerage systems, but sometimes also in large-size interceptor sewers. In the authors' opinion, for all sewers CCTV investigations should be treated as merely tentative. The data acquired from such investigations provide only a qualitative picture of the damage without any quantitative parameters such as the width and depth of cracks or the depth of corroded concrete or mortar zones. By means of CCTV one cannot determine the actual strength or structural parameters and so no static strength analysis can be made. It is often the case, however, that the results CCTV examinations are considered as conclusive and a method of renovating the sewer is selected on their basis or even worse, they are used to dimension the liners. Therefore sewers, especially walkthrough interceptors, should be investigated from the inside and the investigations should include: a technical condition survey with

photographic documentation of characteristic damage (this corresponds to CCTV examinations), determination of the morphology of cracks and the depth of their penetration and determination of the depth of corroded mortar and brick zones; pull-off strength tests performed on the sewer's inside surface; taking samples of structural materials for laboratory tests, including chemical analyses of the composition of the structural materials (to determine the type of corrosion) and determination of their strength parameters; taking sewage, soil and groundwater samples to determine their chemical composition and aggressiveness towards the sewer structure; examination of the ground outside the sewer for voids, an analysis of the actual overburden loading; geodetic surveys of the grade line cross section and fall; geotechnical surveys.

Only on the basis of the data provided by such a wide range of investigations one can formulate a proper rehabilitation programme for the structure, which may cover: protection against the aggressive action of groundwaters, soil and sewage (it is particularly difficult to protect the sewer's outer surface), sealing the structure, strengthening the structure, correcting the grade line, filling in voids in the surrounding ground.

In some cases it may become necessary to replace the interceptor sewer.

3 TECHNOLOGIES OF RECONSTRUCTING BRICK INTERCEPTOR SEWERS

In Poland most of the brick interceptor sewers and associated facilities are in need of repair, which is made difficult by their location – sewers, manholes, connecting chambers and other accessories are situated under roadways. This was not a problem in the past when closing a street or two to traffic did not imply so great disturbance to the latter as today. Considering the congestion in cities and their transport inefficiency, sewerage system repairs are done now using almost exclusively trenchless technologies or techniques which limit excavations to minimum.

The shape, dimensions, technical condition and the current loading of interceptor sewers (including brick ones) usually make it necessary to strengthen their structure (reconstruction) which in Poland is usually done using trolining, short relining or the (close-fit) hardened sleeve technology.

Trolining consists in pulling a two-layered polyethylene sleeve into a sewer under repair. The sleeve's outer layer (preliner) is separated from its inner layer (inliner) by spacers whereby an empty space is created between the two layers. Once the sleeve is inserted, the empty space is filled with special injection compound. Spacer height is adjusted to a given sewer structure. In practice, 10, 13, 17 or 19 mm spacers are used. A modification of this technology consists in making a self-supporting reinforced concrete structure between the polyethylene sleeves, instead of injecting the compound. In this case, the preliner prevents sulphates from penetrating from the sewer structure to the reinforced concrete structure and the inliner provides insulation from the inside. Since the reinforced concrete structure carries loads its dimensions and reinforcement must be adequate to safely carry all the external loads. This modification has all the advantages of the trolining technology.

Short relining consists in inserting modules made (to order) of polyester resins and glass fibre, whose shape adjusts itself to the cross-sectional shape of the sewer under repair. This is very important in the case of brick interceptor sewers since they often have atypical cross-sectional dimensions. Liners made of other materials, e.g. PEHD, are used in sewers circular in cross section.

Through the insertion of a self-supporting lining the hardened sleeve technology allows one to increase the sewer's load-bearing capacity. The linings are made of synthetic fabric impregnated with resin. 'Soft' lining is introduced into a sewer using water column hydrostatic pressure or compressed air. Once inserted into the sewer and pressed against its inner surface, the lining is subjected to thermal (UV radiation) hardening treatment. The lining's load-bearing capacity, which depends on its thickness and fabric and resin parameters, is determined through a static strength analysis.

4 STATIC STRENGTH ANALYSIS

In order to reconstruct brick sewers one must introduce a load-bearing liner into them. Since there are no relevant Polish standards, usually the loads specified by German guidelines ATVA 127 [1] are used in static strength analyses. The authors do such calculations using the finite element method as implemented in COSMOS/M, making assumptions as for brickwork structures [2, 8, 9]. Because of the cross-sectional geometry and load symmetry only halves of the structure, for which the boundary conditions on the axis of symmetry ensure the symmetry of the solution, are considered. Segments of unit length along the sewer's axis are analysed. Systems are modelled by shell elements SHELL 4 with six degrees of freedom at each node. Figure 1 shows exemplary results of static strength computations of a GRP liner for reconstructing an oval brick interceptor sewer. The computations were performed for a 135×90 mm liner and the space between the liner and the sewer wall was filled with an injected compound with compressive strength not less than 5 MPa.

For the assumed liner wall thickness of 25 mm and an undeformable injected compound the following results were obtained:
displacement: the total short-term horizontal contraction in cross-sectional area is $2 \times 1.1 = 2.2$ cm which

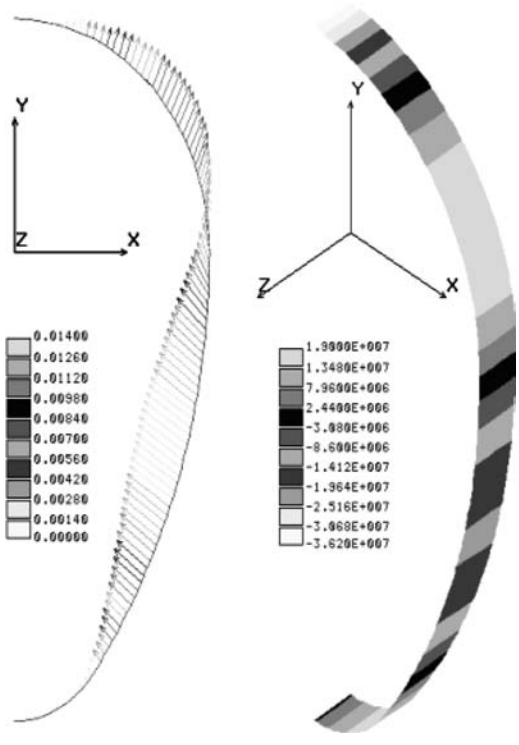


Figure 1. Exemplary calculation results for GRP liner: a – total displacement [m], b – normal circumferential stress [Pa].

amounts to $2.2/90 \times 100\% = 2.4\%$ and the long-term contraction is $2.4 \times 1.6 = 3.8\% < f_{perm} = 6\%$, maximum stress 36.2 MPa.

Special skills are required to design (determine the load-bearing capacity of) close-fit liners. Such liners are highly sensitive to cross-sectional geometric imperfections and on-site installation conditions. The former problem has been much investigated in the Institute of Civil Engineering at Wrocław University of Technology, which led to a PhD dissertation [10] whose selected results were published internationally [6].

5 CASE STUDIES

5.1 *Interceptor sewer in Pułaskiego Street in Wrocław*

Combined sewage interceptor Podwale was built in the second half of the 18th century. It runs in the embankment of the moat which encircles the southern side of the historic city centre. The sewer with a rather uncommon cross-sectional shape of an elevated circle (1.41×1.57 m) carries 500–1100 litres (even more during heavy rains) of sewage per second.



Figure 2. Fracture in interceptor sewer crown with structural displacement and brick loss in walls.

The interceptor sewer was constructed from two layers of brick, with meticulous care typical for sewers built in those times. Cement mortar was used as the binder. The interceptor's invert is 6.0 m underground. Its inspection manholes were also built from bricks and covered with cast iron plates. Because of its long service, the heavy war damage, the very poor quality of post-war repairs, the big change in traffic structure and intensity and the destructive action of roots of the old trees growing there the interceptor sewer had to undergo reconstruction. Pipes with a DN diameter of 1300 mm, made of epoxy resins with GRP fibres, were used as liners in the over 2 km long sewer section which first underwent reconstruction. The space between the old interceptor sewer and the new pipe was filled in stages with lightweight concrete introduced into sections not longer than 3–6 m to prevent the inner pipe from buckling under the pressure of the filler. In order to ensure continuous sewage collection along the interceptor sections undergoing rehabilitation, a floating pipeline made of PEHD was laid in the moat. All the works were supervised by a conservation officer.

The reconstruction went smoothly until May 2001 when during work on the last section of the interceptor sewer in the vicinity of the 1st of May Square it was found that the interceptor was fractured in the crown for a distance of about 25 m (the fracture was as much as 50 mm wide) and deformed to a degree hazardous to both the personnel working inside and the traffic on the roadway situated above the interceptor. In addition, it was found that the mortar in the brickwork joints had been washed out and weakened, the walls were damaged (missing bricks) and the invert was covered with an about 90 mm thick deposit of consolidated sludge.

The most dangerous damage to the interceptor sewer structure is shown in fig. 2.

In that situation reconstruction work was stopped and a temporary support structure for the interceptor was to be immediately designed to prevent it from

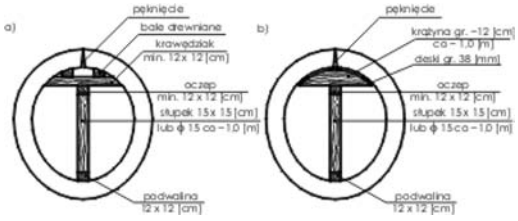


Figure 3. Scheme of temporary protection for interceptor structure. (fracture, wooden beams, square-sawn timber min. 12×12 [cm], capping beam min. 12×12 [cm], 15×15 [cm] post or ϕ 15 at every $\sim$1.0 m, 12×12 [cm] ground beam, $\sim$12 [cm] thick arch centre, 38 mm thick planks).

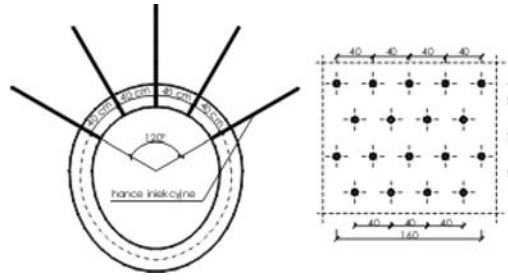


Figure 4. Location of anchors strengthening ground over interceptor sewer (injection lances).

collapsing until further repair work procedures were developed. The present authors were commissioned, via the Institute of Civil Engineering at Wrocław University of Technology, to prepare an expert opinion and to develop technical solutions.

The authors ordered a temporary support structure, consisting of wooden beams or arch centres and supports (wooden or steel posts with adjustable height), to be immediately made. A scheme of the protection is shown in fig. 3.

Before designing permanent protections for the interceptor (after the temporary protections had been constructed) the interceptor structure [4] and the surrounding ground [3] were examined to determine the causes of the damage. In situ investigations, laboratory analyses and calculations showed that the bad condition of the mortar and the bricks was the result of: the long action of sulphate corrosion (the sulphate content in brick amounted to 0.8 % and in mortar to 1.0–1.2%) due to the production of hydrogen sulphide following the decomposition of the organic matter deposited in the invert, the big change in traffic structure and loading in comparison with the 19th century design assumptions, loosening of the ground surrounding the interceptor sewer, in both the floor layer and above the interceptor.

Having analysed the condition of the interceptor and its surroundings and the results of the examinations, we concluded that personnel could work inside the interceptor after closing the street to traffic. Consequently, work was initially conducted only at night. First cavities in mortar and the fracture in the crown were filled in order to strengthen and seal the interceptor structure prior to petrifying (through injection) the surrounding ground to improve the foundation conditions and create a soil-cement vault which by taking over the traffic loading would make it possible to remove the temporary supports and finish relining.

Depending on the results of soil surveys, the subsoil was to be strengthened to a depth of 0.3 m along a distance of about 26 m and to a depth of 0.8 m along a distance of 41 m. The job was done from inside the interceptor by injecting cement slurry (with a predetermined composition) to bind loose sands and to obtain at least a medium subgrade compaction ($I_D \geq 0.5$) after cementation. Semiliquid fractions in local lens of soft-plastic aggradate mud were forced out by the injected cement suspension. It was recommended to perform injection using ϕ 30–40 mm lances (sealed in the interceptor structure) driven into the subsoil at every 1.0 m to a depth of about 20 cm greater than that of the injected zone. The tolerance of lance location in the cross section was set at $\pm 15°$. Slanting boreholes were to be shifted by about 0.5 m relative to the grid of vertical boreholes. Because of the bad condition of the interceptor, boreholes through its wall were drilled nonpercussively using diamond bits and small boring rigs. In total, in accordance with the adopted assumptions, there were to be: in the less deep (0.50 m) injection zone – 50 slanting boreholes and 25 vertical boreholes, with a total length of 37.5 m, which required 75 drillings 50–65 mm in diameter through the interceptor wall, with a total length of 18.75 m; in the deeper (1.0 m) injection zone – 80 slanting boreholes and 40 vertical boreholes, with a total length of 120.0 m, which required 120 drillings 50–65 mm in diameter through the interceptor wall, with a total length of 30.0 m.

Cement suspension with c/w = 1.0–2.0 (the optimum ratio was to be experimentally determined through trial injections) was to be injected. Pump delivery was adjusted to obtain a possibly low injection pressure of $0.1\,\text{MPa} < p < 0.3\,\text{MPa}$ for the set c/w ratio. The amount of cement slurry per borehole was determined on the basis of previous experience at: $0.08 < V < 0.25\,\text{m}^3$ for 0.50 m long boreholes, $0.10 < V < 0.35\,\text{m}^3$ for 1.0 m long boreholes.

The soil-cement vault was to be created along a 30.0 m long section after at least two weeks from the date of completion of subsoil petrification. The 'injection anchor' method was proposed for creating a load-bearing zone over the fractured crown of the interceptor. Such anchors were to be made on a grid with a mesh size of 0.40×0.40 m and shifted neighbouring rows. The location of anchors in the interceptor cross



Figure 5. Installation of liner.

section and a part of the layout of anchors are shown in fig. 4.

Boreholes in the interceptor structure, for introducing injection anchors into the ground, were to be drilled nonpercussively, similarly as boreholes in the floor layer. Their diameter was suitable for inserting steel pipes 0.5″ in diameter and 0.8 long into the ground. After sealing the boreholes cement slurry with an expanding agent (its amount was set in consultation with the manufacturer) was injected. Injection was conducted at very low pump delivery whereby pressure was reduced to $p < 0.3$ MPa. The amount of cement slurry with $c/w = 1.5$–2.0 was set at $0.20\ m^3$ per borehole (the amount was to be verified through on-site trials). Injections were done in the system: every other row and every other borehole in a row. In total, there were to be 6 anchors per borehole, which meant that at the assumed borehole spacing along the vault length of 30 m, 180 anchors had to be made. The temporary protections were to be disassembled two weeks after the completion of vault strengthening work. Only then the interceptor cross section could be calibrated in order to insert a liner into the sewer (fig. 5).

The described damage and the additional work enabling further safe reconstruction (using the relining technique) of the interceptor sewer show how important it is to precisely determine the condition of a sewer structure prior to repair work, especially when repairs are to be done by people working inside the underground structure and when the safety of the users of the streets situated above the sewer is to be ensured.

5.2 *Interceptor sewer in Kazimierza Wielkiego Street in Wrocław*

In July 2005 a part of the road surface of a major traffic artery in Wrocław caved in which made it necessary to close down one traffic lane in the street.

It was surmised that the cause of the damage was the bad condition of the interceptor sewer running under the street. Thus, as it is often the case in sewerage systems, invisible damage to the sewer resulted in visible



Figure 6. Examples of damages of the sewer channel. a. view of inside of interceptor sewer and fracture in its crown. b. view of damage to inside of brick inspection chamber.

damage to another structure – the street pavement. The present authors were commissioned, via the Institute of Civil Engineering at Wrocław University of Technology, to investigate the structures and to design their repairs.

The standard procedure applied in this case consisted in immediately carrying out a survey of the damage and a static strength analysis and determining the causes of the damage and ways of repairing it. The investigations covered the following structures: a reinforced concrete chamber built in the 1970s during the rebuilding of the city's transport system, a brick inspection chamber built at the beginning of the 20th century during the construction of the interceptor sewer, the oval brick interceptor sewer with dimensions $h \times b = 1700 \times 1200$ mm and a wall thickness of 250 mm.

The in situ investigations showed at fig. 6a: 3–7 mm wide fracture in the interceptor's crown, penetrating through its thickness and running along it for at least 55 m; longitudinal cracks in both walls at a height of about 500 mm above the invert, running for about 35 m; weakened mortar in brickwork joints to a depth of about 35 mm in the crown and to about 20 mm in the other part of the interceptor; weakened brick to a depth of about 15 mm; an about 0.14 thick sludge deposit extending from about 20 m from the reinforced concrete chamber to the end of the surveyed section; leaks between the sewers and the chamber; large caverns in the ground around the reinforced concrete chamber; two holes in the brick sewer and a hole 50 mm in diameter in the reinforced concrete chamber; serious damage to the brick inspection chamber: wall fractures with shifts (fig. 6b).

The in situ investigations were supplemented with laboratory tests of the interceptor structural materials' parameters and a static strength analysis of the interceptor structure. It was found that the technical condition of the interceptor sewer along a length of 75.03 m posed a serious construction disaster hazard.

Symptoms of exceeded limit load-bearing capacity, in the form of cracks in the invert channel and in the crown, were found. The cracks were the result of a considerable increase in load relative to the design load and deterioration of the interceptor structural materials due to corrosion processes.

Considering the local conditions, characterized by high traffic intensity, the City Road and Transport Authority gave permission to temporarily close to traffic only one of the three traffic lanes of the south-bound roadway. In practice, this meant that all the construction works, except for reconstruction of the street surface, were to be done using trenchless technologies. Short relining was chosen as most suitable for the reconstruction of the interceptor sewer in the local conditions. Made to order oval GRP modules with 1000×1500 mm inner dimensions were used for this purpose [11]. The short relining technology did not necessitate stopping the flow of sewage and building a sewage pumping installation and made it possible to carry out the works in a very short time. According to the static strength calculations, the liner had to be 27 mm thick.

Similarly as in the case of the Podwale Street interceptor sewer, extensive caverns in the ground around the reinforced concrete chamber had to be filled since they were the direct cause of the fracture and subsidence of the roadway structure. The caverns were filled using the jet grouting technique.

6 CONCLUSIONS

1. Because of their age and changed service conditions most of the brick sewers in Poland need repairs.
2. The brick sewers can be upgraded to current standards provided they are reconstructed.
3. In the case of streets with heavy traffic, sewers should be reconstructed using trenchless technologies.
4. The large number of existing trenchless technologies allows one to select a proper trenchless technology for any interceptor sewer under the present mechanical, chemical and biological loads.
5. The use of trenchless technologies, consisting in the insertion of a self-supporting liner into an interceptor sewer, upgrades the structural parameters of the sewer to its current service conditions.
6. The reconstruction of interceptor sewers should be accompanied by surveys of the surrounding ground and its reconstruction if it has been damaged by sewage exfiltrating and groundwater infiltrating for many years through leaks in the sewers.

REFERENCES

[1] ATV A 127 Richtline fur die statische Berechnung von Entwasserungsknalen und-leitungen.

[2] Bull J.W., Computational modelling of masonry, brickwork structures. Glasgow 2001.

[3] Expert opinion on soil under Podwale interceptor sewer from overflow chamber at St. Anthony footbridge to 1st of May Square (in Polish). Study by Novotech Company, Wrocław, 2001.

[4] Madryas C., Wysocki L., Surveys of and expert opinion on Podwale combined sewage interceptor in Wrocław at location of fracture in crown and repair design (in Polish), series SPR report no. 47/2001. Institute of Civil Engineering at Wrocław University of Technology, Wrocław, 2001.

[5] Madryas C., Kolonka A., Wysocki L., Sewer structures (in Polish), Wrocław University of Technology Press, Wrocław, 2002, p.377.

[6] Madryas C., Szot A., Structural sensitivity of circular sewer liners to geometrical imperfections, Tunnelling and Underground Space Technology, 2003, vol. 18, no. 4, pp. 421–434.

[7] Madryas C., Szot A., Wysocki L., Expert opinion on interceptor sewer in Kazimierza Wielkiego Street in Wrocław (in Polish), Institute of Civil Engineering at Wrocław University of Technology, series SPR 59/2004 report, Wrocław, 2004.

[8] Polish Standard PN-87/B-03002 Masonry structures. Static calculations and design (in Polish).

[9] Szołomicki J.P., Static strength analysis and computer modelling of masonry structures (in Polish), PhD dissertation, Wrocław, 1997.

[10] Szot A., Load-bearing capacity of sewer pipelines strengthened with continuous liners (in Polish), PhD dissertation, Institute of Civil Engineering at Wrocław University of Technology, series PRE report, Wrocław, 2002.

[11] Szot A., Wysocki L., Working construction design of interceptor sewer renovation (in Polish), Institute of Civil Engineering at Wrocław University of Technology, Wrocław, 2004.

[12] Part of this research was made possible by funding awarded as part of professorial grants to Prof. Cezary Madryas by the Foundation for Polish Science.

Underground Space – the 4th Dimension of Metropolises – Barták, Hrdina, Romancov & Zlámal (eds)
© 2007 Taylor & Francis Group, London, ISBN 978-0-415-40807-3

The old railway tunnel of Mainz – A design and construction concept for the expansion of two approx. 150 year old tunnels in urban areas

Th. Marcher, G. Braun & F. Jiricny
ILF Consulting Engineers, Rum/Innsbruck, Austria

ABSTRACT: In the City of Mainz, Germany, the railway runs through two approximately 150-year-old tunnels to reach the main station. To update the railway line to European High-speed Railway Standards, the German Railway (DB) decided to expand and reconstruct the tunnels with larger cross sections. The two tunnels, approx. 660 and 290 m long and separated by an approx. 290 m long cut, are located within a very attractive urban area, beneath historical and new multi-floor buildings and hotels with shallow overburden. The underground mainly consists of Tertiary sands and clays, with limestone deposits. The old tunnel masonry and the backfill behind are contaminated due to environmental aspects. This paper presents the design and construction concept of this project under conditions of particularly shallow overburden with sensitive, built-up areas. To protect the buildings at the surface against damaging deformations measures like "push up" injections in the underground or pile walls for deformation limitation are foreseen. The different building protection measures and deformation limiting measures will be presented.

1 INTRODUCTION

Because of the sensitive project conditions the main issue is a design concept which covers all surrounding conditions with respect to the stability of the tunnel tube during excavation and with respect to consistent deformations of the surface. Therefore, the first part of this paper describes three-dimensional FE-calculations which show the varying ground and load-bearing behaviour when simulating various excavation methods (full face versus heading/bench excavation). Stress redistribution due to the relevant excavation procedure will strongly influence the deformations and the load transfer ahead of the excavation face. As a result of the numerical study an optimized excavation concept will be provided which minimizes any additional load on the old masonry tunnel and avoids damaging settlements at the built-up areas. In the second part, emphasis is placed on the construction concept with respect to shallow overburden and a limited time frame of 3 years for realization of the project.

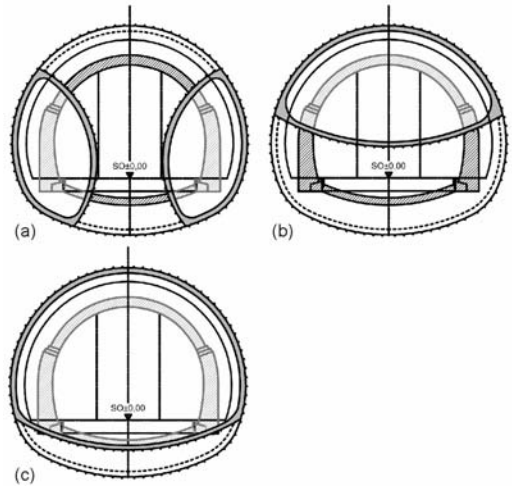


Figure 1. Excavations concepts.

2 EXCAVATION CONCEPTS

During the conceptual design phase various excavation sequences have been discussed. Three of the concepts are illustrated in Figure 1.

The first one considers a "side-drift excavation" followed by the excavation of the core (Figure 1a). The second one assumes a "temporary top heading invert" bedded on backfill to be provided within the area of the old tunnel (Figure 1b). The third concept assumes a "heading/bench excavation" with a quick invert closure, i.e. a full bench excavation is followed by the final invert excavation in a max. distance of 20 m (Figure 1c).

3 ADDITIONAL EXCAVATION MEASURES

Due to the particularly shallow overburden with sensitive built-up areas additional measures like "push-up" injections in the underground to compensate settlements directly above the excavation and installation of pile-walls parallel to the tunnel axis to limit deformations of buildings next to the tunnel axis are required.

4 GEOLOGY

The general stratigraphy comprises artificial fill material of various thickness underlain by tertiary sediments consisting of clay/silt layers, occasionally with silty sand and gravel lenses as well as limestone deposits.

The groundwater level is generally located below the invert.

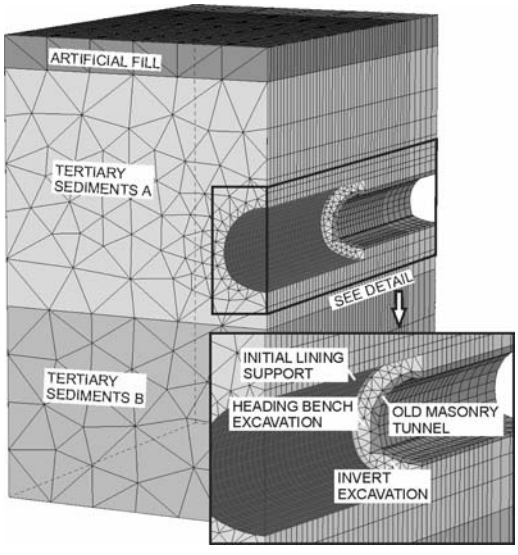


Figure 2. 3D FE-model of excavation concept 1a.

5 NUMERICAL ANALYSIS

5.1 *Tunnel geometry*

The old tunnel built as a "horse-shoe shaped tunnel" approx. 150 years ago was constructed according to the "Old German Tunnel Method". The tunnel has a min. height of approx. 6.5 m and a width of approx. 7.5 m. The tunnel masonry walls have a thickness of 0.6–0.7 m above the crown and increase to 0.8–1.0 m at the abutments. A flat invert arch has been built (approx. 1.5 m below line level). The equivalent tunnel area is 44 m^2.

The new cross section is typical for a single-track train tunnel in Germany. The height is approx. 7.5 m and the width approx. 11 m. The invert arch will probably be approx. 3 m below top of rail. The equivalent tunnel area will be 74 m^2, resulting in a theoretical tunnel diameter of approx. 5 m.

5.2 *FE-model*

The 3D Finite Element program "Plaxis 3D Tunnel" is used for the calculations, Brinkgreve et al. (200l). Because the geometry is symmetric, only half the boundary problem needs to be considered. The circumferential boundaries are restrained in both x and y directions. The ground surface is free to move, the bottom of the model is fully fixed. The dimensions of the FE mesh are chosen in such a way that the impact of the cavity on the edges of the FE mesh has subsided. The length of the model depends strongly on the excavation method and has to be evaluated depending on the relevant excavation phases in longitudinal direction. The ground is modeled with 15-noded wedge elements using the Hardening Soil model. This constitutive model is an advanced model for simulating shear hardening and compression hardening independently of each other. The stiffness is formulated stress-dependent and a distinction is made between first loading and un-/reloading, see Schanz (1998).

The tunnel masonry wall is also modeled with continuum elements using the Mohr-Coulomb model to simulate the masonry behavior. Beam elements are used to model the new shotcrete lining. Rock bolts, steel ribs and steel spiles are not included in the numerial calculations. No support ahead of face is considered.

The final lining is not taken into account as it will be installed after the lining deformations of the initial support have subsided.

5.3 *Calculation sequences*

A "step-by-step" tunneling sequence is applied using the phased analysis option available in the FE program used. The in-situ stress state is followed by the simulation of the excavation of the old tunnel. Next, compensation grouting is simulated using volumetric strains in the FE soil clusters.

Finally the individual excavation phases for heading, bench and invert each with separate application of "young/mature" shotcrete are considered.

5.4 *Ground and material properties*

The properties of the various formations are based on the site investigations carried out and summarized in table 1.

The stiffness parameters are listed for a reference stress of $\sigma_{ref} = 100\,kN/m^2$. A unit weight of

Table 1. Ground and material properties.

	Strength		Stiffness		
	c [kN/m^2]	φ [°]	E_{50}/E_{ur} [MN/m^2]	m [–]	ν_{ur} [–]
Artificial fill	0	27.5	100/–	–	0.3
Tertiary sed. A	20	20.0	25/75	0.5	0.2
Tertiary sed. B	20	20.0	40/120	0.5	0.2
Fill material tunnel	0	37.5	50/150	0.5	0.2

$\gamma = 19$ kN/m^3 is assumed. The initial stress conditions in the ground are defined by the overburden (20 m used for the present calculation section), by the unit weight and by the coefficient of lateral earth pressure at rest $K_0 = 0.5$.

In order to model time-dependent behavior of shotcrete (creep and hardening) two stiffnesses of the shotcrete lining are taken into account, i.e. John et al. (2003). For a short time after tunnel lining installation "young" shotcrete with E = 7500 MN/m^2 is used. For a long-term period "mature" shotcrete with E = 15000 MN/m^2 is applied. This change of lining properties is activated 3–5 round lengths behind the face, which corresponds to a shotcrete age of approx. 2–3 days.

The old tunnel masonry is characterized by an elastic module of 5000 MN/m^2, a Poisson ratio of $\nu = 0.1$, a unit weight of 22.5 kN/m^3 and a cohesion of 4 MN/m^2 (assuming zero for the friction angle φ). The compressive strength which results from this approach fits well to test results. Tensile strength is eliminated by a "tension-cut-off" criteria.

5.5 *Numerical results*

5.5.1 *Stress arching*

Every excavation state implies a change of the stresses and strains around the tunnel. Especially intermediate construction stages are subject to the greatest amount of stress as the disturbance is not yet fully supported by the lining. Generally the pre-existing stresses in the rock mass will be deviated by the tunnel excavation and will be channeled around the tunnel. This redistribution of stresses takes place as (see Figure 3):

(a) arching effect around the tunnel
(b) arching effect along the tunnel axis
(c) Dome effect in front of the tunnel

Arching effects around the tunnel (Figure 3a) are already mobilized due to the excavation of the old tunnel. The widening of the old tunnel increases this effect. The dome effect in front of the new tunnel is affected by the existing old tunnel. The resulting mean effective stresses around the new tunnel lining will

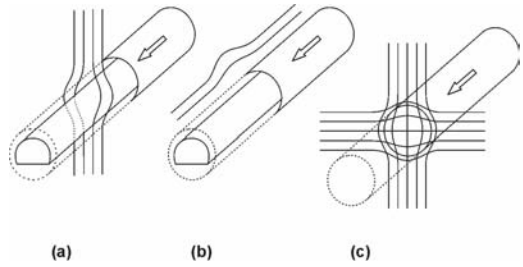


Figure 3. Stress arching effects.

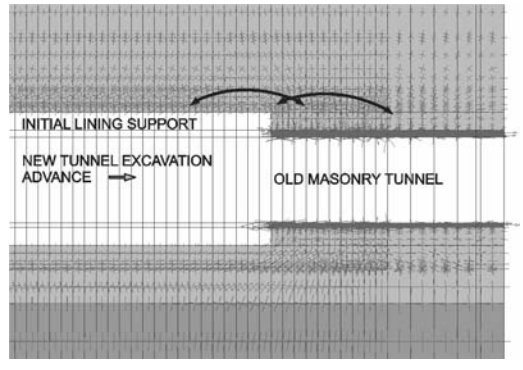


Figure 4. Arching effects along the tunnel axis.

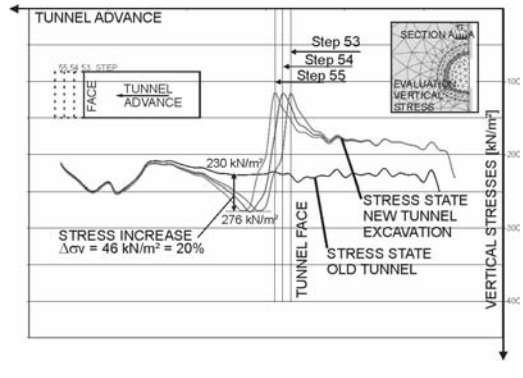


Figure 5. Vertical stress analysis along the tunnel.

be pronounced when considering the option with the "quick invert closure".

Essential for the present tunnel design is the analysis of the arching effect along the tunnel axis (see Figure 4). As evaluated in Figure 5, the old tunnel will be additionally loaded by 20% of the existing vertical load due to the longitudinal stress arching when widening the tunnel. At the same time the horizontal stresses remain almost unchanged (Figure 6).

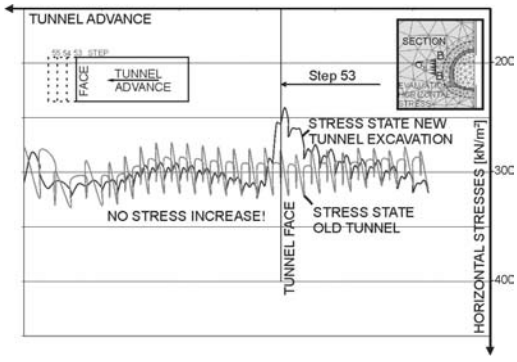


Figure 6. Horizontal stress analysis along the tunnel.

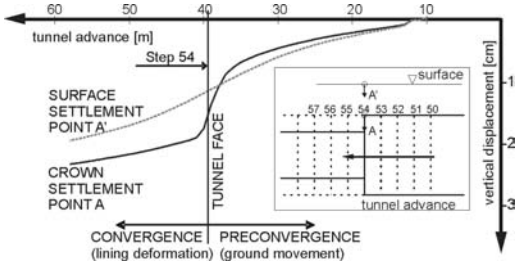


Figure 7. Vertical displacements at the tunnel face.

5.5.2 *Settlement behavior*

Figure 6 indicates that reduced settlements are achieved by the quick invert closure according to concept (1c).

5.5.3 *Bearing capacity of the shotcrete lining*

The calculations indicate that, following concept (1c), a shotcrete lining thickness of 25 cm is adequate for design. In contrast to this concept the side drift walls (concept 1a) and the temporary top heeding invert (concept 1b) are to be executed on a inhomogeneous bedding (partly masonry wall/backfill material and natural ground). High bending moments and shear forces require a strengthening of the shotcrete lining.

5.5.4 *Resulting loads on the old tunnel lining*

The numerical calculations indicate that due to longitudinal stress arching, a vertical stress increase of approx. 20% will develop. The "compensation grouting" procedure will also result in a vertical stress increase of additionally 20%.

Therefore the old tunnel masonry wall has to be improved by application of a shotcrete lining of minimum 10 cm thickness or alternatively by temporary steel girders before excavating the new tunnel.

5.6 *Summary of numerical results*

The most important results of the present study are summarized in Table 2.

Table 2. Summary of vertical displacements.

	Concept 1a [mm]	Concept 1b [mm]	Concept 1c [mm]
Crown settlement:			
Partial excavation	38	44	9
Full excavation	42	53	10
Surface settlement:	55	60	29

It shows that the settlement at the crown is reduced to 30% when applying a "quick invert closure" compared to the other options (concept with sequential excavations acc. to Figure 1a, 1b).

6 CONSTRUCTION CONCEPT

6.1 *Evaluation of the excavation and support concept*

With respect to the reported results of numerical analysis and with respect to other project conditions, namely

- unknown history of stress and strain of the tunnel lining, tunnel backfill and surrounding underground
- shallow overburden
- underpassing of historical and new multi-floor buildings and hotels
- small construction site areas available
- transportation of materials mainly by railway
- project realization time frame of 3 years, given by the owner
- a limitation of the settlements in the tunnel and at the surface
- a sufficient early strength of the shotcrete
- an increase of the bearing capacity of the old tunnel lining,

the usability of the 3 discussed concepts

1. "side drift concept"
2. temporary top heading invert, bedded on an artificial backfill
3. "heading/bench excavation" with a quick invert closure

has been evaluated. The first concept was eliminated because of its assumed construction time and an "unclear stability/settlement situation" at the side drift crown when cutting the temporary side drift wall (see figure 1a). The second concept was eliminated because of the additional masses for the artificial backfill and an "unclear stability/settlement situation" in the invert arch between the old tunnel lining and the artificial backfill (see figure 1b). Therefore the further design was based on the third concept.

With respect to the dimension of the unsupported excavation area and to safety aspects during

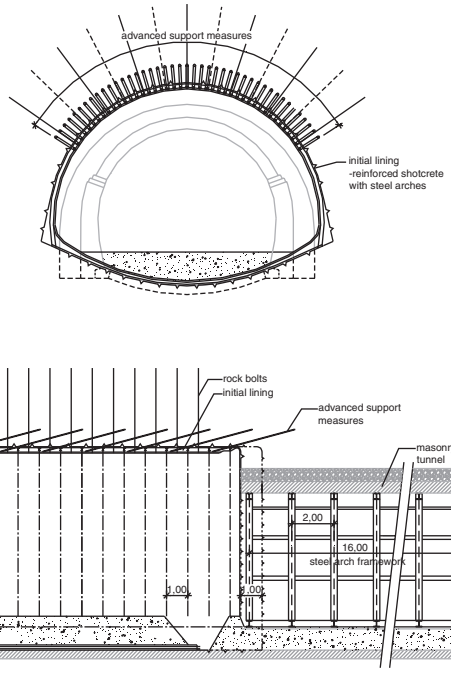


Figure 8. Excavation and support.

construction, the excavation cross section of the third concept was divided into two segments. One segment, the profile, with a temporary invert arch at the level of the existing invert and the other, the final invert (reference is made to Figure 8).

6.2 *Excavation and support*

With respect to these conditions 6 excavation and support types have been designed. All excavation and support types have a 30-cm thick reinforced shotcrete lining with steel arches and rock bolts. The difference between the excavation and support types are the advanced support measures, ranging from no advanced support measures to mortar spiles, steel liner plates and canopy pipes. The advanced support measures mainly serve to limit the excavation volume.

The existing old tunnel lining is generally supported by a steel arch framework construction, with force-closed connection to the lining. The framework is shifted in segments, ahead of the excavation and support procedure. In special tunnel areas such as the area where the surface settlement is limited by "push-up" underground injections, the lining of the old tunnel is stabilized by an additional reinforced shotcrete lining (see above).

The backfill of the old tunnel lining, consisting of small rock blocks, stones, gravel, etc., is stabilized by cement grouting to increase its stability.

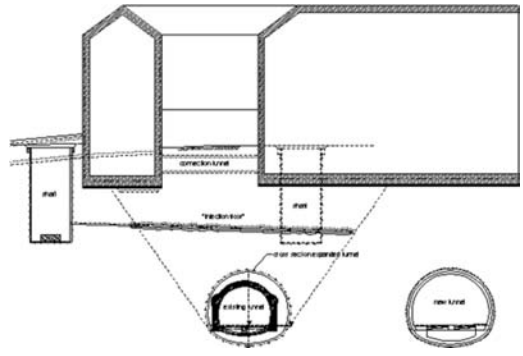


Figure 9. Push-up injection.

The sequence of tunnel excavation is generally designed in the following way:

Saw cuts in the masonry of the old tunnel lining – cut down of the masonry – excavation of backfill and underground – installation of support measures.

A typical excavation and support type is shown in Figure 8. Numerous geotechnical measurements, measuring the deformation of the tunnel lining, the settlement of the surface and the underground behaviour accompanying the excavation and support.

6.3 *Underpassing of buildings*

Because of the shallow overburden of the new tunnel (min. 11 m) and sensitive built-up areas at the surface in some areas (a multifloor hotel partly connected to and built on a historical Roman building) and in addition to the "low deformation" excavation and support concept, auxiliary measures have to be designed for limiting the impact of the excavation and support on the buildings. As reported, several measures have been foreseen. To protect the mentioned hotel and the adjacent buildings, a "push-up" injection is foreseen to control and to limit the settlements. For this the underground beneath the buildings is stabilized with a cement grouted "injection floor", located halfway between tunnel crown and foundation of the building (reference is made to Figure 9). If the buildings settle during the tunnel excavation, they can be pushed up to their original level by additional injections in the "injection floor". This operation can be done several times. The impact on the buildings and the success of the measure will be monitored by horizontal inclinometers in the underground, located between the "injection floor" and the foundation of the building, and with water level measurements in the buildings.

6.4 *Final lining*

The final lining of the tunnel is designed as a watertight reinforced concrete lining. The thickness of the

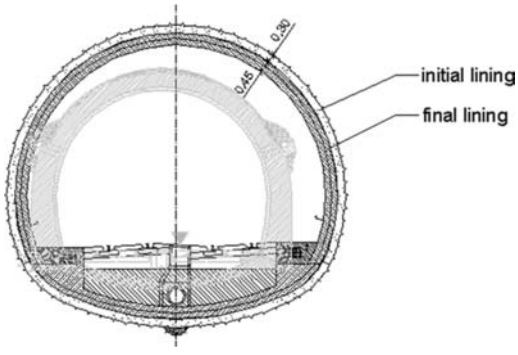


Figure 10. Tunnel cross section with final lining (inside: the existing tunnel).

lining is assumed to be 45 cm. The tunnel cross section is shown in Figure 10. The lengths of the final lining concrete blocks are mainly 9.20 m for equipment reasons. The joints are sealed with tapes.

7 ECONOMIC AFFECTS

The overall project costs are estimated at approximately 52 million €. The total construction costs for the tunnels will be approximately 33 million €. These costs include approximately 3 million € for additional measures to limit the tunnelling effects on the surface. In order not to exceed the project time frame, the 660-m long tunnel has to be driven from both sides.

Compared with the chosen and adapted construction concept "heading/bench excavation" with a "quick invert closure" (costs = 100%) the costs of the "side drift concept" would be approximately 120% and the costs of the temporary top heading invert, bedded on an artificial backfill concept would be approximately 110%.

8 CONCLUSIONS

For the renovation of the "Old Mainz Tunnel" and enlargement of the cross section, and taking into consideration the shallow overburden and sensitive built-up areas at the surface, a careful and comprehensive design was elaborated. With respect to the numerous and various project conditions three construction concepts have been verified and discussed with the Client and his experts.

1. "side drift concept"
2. temporary top heading invert, bedded on an artificial backfill
3. "heading/bench excavation" with a quick invert closure

As discussed above, the three concepts were analyzed by means of numerical simulations in order to get an idea of the interdependence of excavated tunnel, surrounding underground and surface impact. Based on this analysis, the construction concept No. 3 was chosen and designed in detail. Additional measures to protected the built-up areas have been designed, too. The tunnel works were tendered in the autumn of 2006. The start of the construction work is scheduled for March 2007.

REFERENCES

Brinkgreve, R.B.J. & Vermeer P.A. 2001. *User Manual for PLAXIS 3D-Tunnel, Finite Element Code for Soil and Rock Analysis.*

John, M. & Mattle, B. 2003. *Factors of shotcrete lining design*, T&T International.

Schanz, T. 1998. *Zur Modellierung des mechanischen Verhaltens von Reibungsmaterialien,* Mitteilungsheft Uni Stuttgart, Heft 45.

Underground Space – the 4th Dimension of Metropolises – Barták, Hrdina, Romancov & Zlámal (eds)
© 2007 Taylor & Francis Group, London, ISBN 978-0-415-40807-3

Analytical investigation of damaged tunnel linings by the action of excessive earth pressure

H.Mashimo
Public Works Research Institute, Tsukuba, Japan

ABSTRACT: The objective of this paper is to clarify the mechanism of the failure of tunnel concrete lining by the action of excessive earth pressure and establish the method to estimate the direction and magnitude of earth pressure acting on tunnel concrete lining. In this study, field inspection was carried out at two existing road tunnels, which have suffered serious damages on concrete lining, and numerical analysis using two-dimensional FEM, which can take account of development of cracks, was carried out. The results showed that failure patterns of concrete lining obtained from numerical analysis gave the good agreement with those of actual tunnels and the direction and magnitude of earth pressure assumed to act on the damaged concrete lining were obtained.

1 INTRODUCTION

In Japan, there are some existing road tunnels in service that have suffered serious damage such as compression or shear failure on their concrete lining by the action of excessive earth pressure. For these damaged tunnels, some kind of countermeasures such as rock-bolting, inner lining, backfill grouting etc. were adopted to rehabilitate the damaged concrete lining. In order to adopt appropriate countermeasures against the damaged tunnel, it is important to clarify the cause of failure and evaluate the direction and magnitude of the load acting on the concrete lining. However, the mechanism of the failure of concrete lining by the action of excessive earth pressure has not been clarified yet and establishment of the method to evaluate the load acting on the concrete lining is necessary to select the countermeasure most suitable for the condition of damaged tunnel.

In the first part of this paper, field inspection on two existing damaged road tunnels was carried out and an overview of damaged tunnel concrete lining with compression failure at crown or shear failure at invert concrete lining was provided.

In the second, in order to clarify the mechanism of the failure of these damaged tunnels and estimate the direction and magnitude of earth pressure acting on the damaged concrete lining, numerical analysis using two-dimensional FEM, which can take account of development of cracks, was carried out. Furthermore, numerical analysis results were compared with the field inspection results and the mechanism of the failure of concrete lining by the action of excessive earth pressure was discussed.

2 OUTLINE OF DAMAGED TUNNELS

In order to investigate the state of the deformation of existing tunnels, field inspection on the concrete lining surface was carried out at Tunnel A and Tunnel B.

2.1 *Description and inspection of Tunnel A*

Figure 1 shows the state of the deformation occurred in tunnel lining and geotechnical profile of Tunnel A. Tunnel A with a total length of 2,376 m was constructed by steel and logging method about 30 years ago. Tunnel A has a horseshoe shape with a width of 9.7 m and a height of 8.0 m. Its support structure consists of concrete lining with a thickness of 60 cm.

In Tunnel A, passing-through tensile cracks at the shoulders and compressive failure at the crown due to bending moment were observed at the section with a distance of 800 m from portal. The sling that suspended the ceiling boards showed buckling phenomena due to the upheaval of ceiling board. There was void between the ground and concrete lining around the crown. Figure 2 shows the detail of the compressive failure occurred at the crown. The ground at tunnel site and its vicinity, where the tunnel deformation occurred, appeared to be composed of mudstone with the uniaxial compressive strength of approximately 40 N/mm^2. The overburden height at the section where deformation occurred is 320 m.

2.2 *Description and inspection of Tunnel B*

Figure 3 shows the state of the deformation occurred in tunnel lining and geotechnical profile of tunnel B.

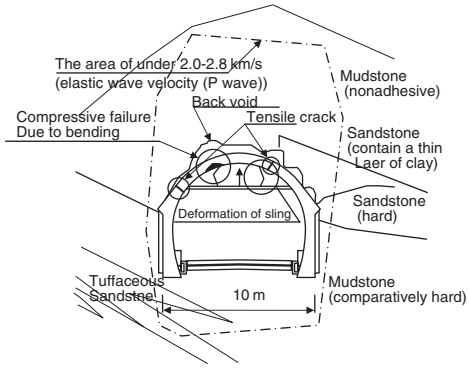


Figure 1. Deformation and geotechnical profile of Tunnel A.

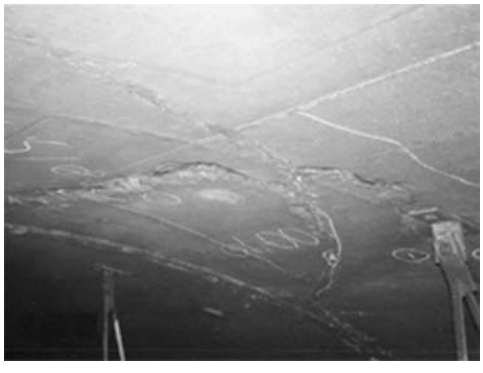


Figure 2. Detail of failure occurred at tunnel crown in Tunnel A.

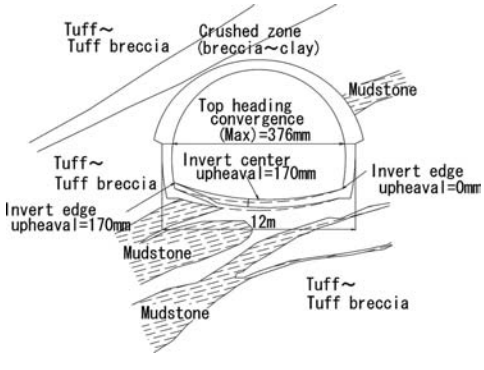


Figure 3. Deformation and geotechnical profile of Tunnel B.

Tunnel B with a total length of 1,013 m was constructed by steel and logging method about 15 years ago. Tunnel B has a horseshoe shape with a width of 11.3 m and a height of 8.9 m, and its support structure consists of concrete lining with a thickness of 60 cm.



Figure 4. Detail of failure occurred at junction between tunnel invert and sidewall foot in Tunnel B.

In Tunnel B, an upheaval of road surface was observed at the middle of the tunnel after about 10 years had passed since the completion of construction of tunnel. Therefore, the state of invert concrete lining was investigated by taking off the road bed material. As a result, it was found that shear failure had occurred at the junction between the invert and sidewall foot and an upheaval with a height of 170 mm had occurred at the invert center. In addition, the top heading arch convergence of 376 mm was obtained by measurement on the inner tunnel space, though no slippage at the construction junction between the top heading arch and sidewall was observed. Figure 4 shows the detail of failure occurred at the junction between the invert and sidewall foot. The ground at tunnel site and its vicinity, where the tunnel deformation occurred, appeared to be composed of mudstone and tuff with the uniaxial compressive strength of 8.4 N/mm^2 and 11.6 N/mm^2, respectively. The overburden height at the section where deformation occurred is 120 m.

3 ESTIMATION OF FAILURE MECHANISM OF DAMAGED TUNNELS

3.1 *Outline of the analysis*

For the purpose of clarifying the mechanism of the failure of damaged tunnels and estimating the direction and magnitude of earth pressure acting on concrete lining, FEM analysis considering the occurrence and development of cracks was carried out. In this analysis, nonlinear finite element method was used and modified Newton-Raphson method was adopted for the solution of nonlinear equations. Plane-stress elements for material and Kupfer's failure criterion were adopted (Mashimo et al. 2004).

Figure 5 shows the stress-strain relation in compression and tension adopted in the analysis. The curve in compression was modified as quadric curve

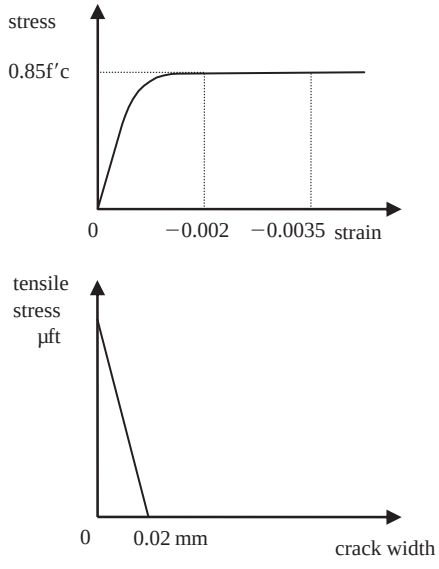


Figure 5. Stress-strain relation adopted in analysis.

until strain reached the ultimate compressive strain $-3{,}500 \times 10^{-6}$. No stiffness decrease was defined after that. The curve in tension was regulated by tensile-softening curve. The tensile strength f_t was calculated on the basis of compressive strength f'_c as $f_t = 0.23 f'^{2/3}_c$. Allowable crack width and ratio of residual strength μ in concrete was set as 0.02 mm and 1.0, respectively. The interaction between tunnel lining and ground was modeled by a series of spring support outside the tunnel lining, which were assumed to resist only compression and had zero stiffness when subjected to tension. The coefficient k of subgrade reaction was obtained from the following Eq.(1):

$$k = 1/0.3\alpha E(B/0.3)^{-3/4} \quad (1)$$

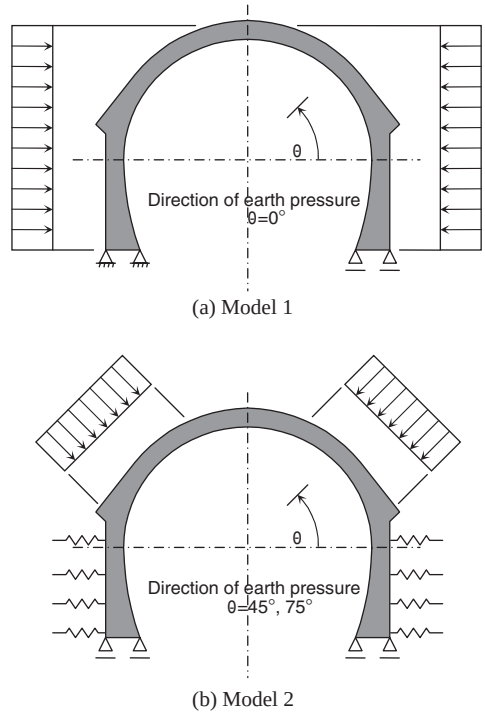
where α = correction factor(=0.4); E = Young's modulus of ground; B = tunnel height.

The mechanical properties of tunnel lining adopted in the FEM analysis are listed in Table 1.

Figure 6 shows the outline of analysis model of Tunnel A. In the calculation of Tunnel A, for the purpose of estimating the direction and magnitude of earth pressure acting on the concrete lining, two kinds of load condition and the arrangement of subgrade springs were adopted. In model 1, earth pressure acted on the concrete lining throughout the whole top heading arch and sidewall in the horizontal direction and there was no subgrade spring outside the concrete lining because void was found behind the crown. In model 2, earth pressure acted on the concrete lining throughout the top heading arch partially in the direction at an angle of 45 or 75 degree from the horizontal and the sidewall

Table 1. Mechanical properties adopted in analysis.

Item	
Design compressive strength: σ'_{ck} [N/mm^2]	18
Compressive strength of concrete: f'_c [N/mm^2]	18
Tensile strength of concrete: f_t[N/mm^2]	1.579
Fracture energy of concrete: G_f [N/m]	1.579
Poisson's ratio of concrete : ν	0.2
Initial elastic modulus of concrete [kN/mm^2]	22
Modulus of subgrade spring [MN/m^3]	4.3 (TunnelA) 96 (TunnelB)



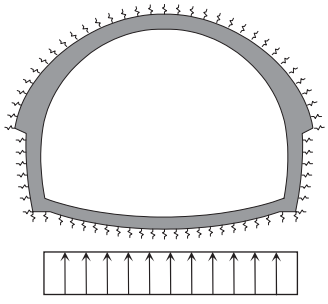
(a) Model 1

(b) Model 2

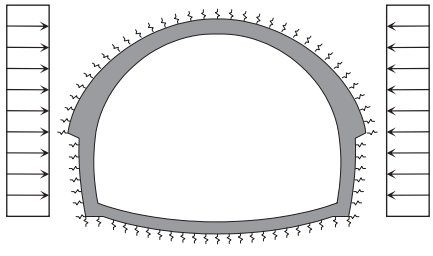
Figure 6. Outline of analysis model of Tunnel A.

was supported by subgrade springs. In the calculation, attention was given to tensile cracks at the shoulders and the compressive failure at the crown due to bending moment to evaluate the validity of analysis on the deformation of concrete lining.

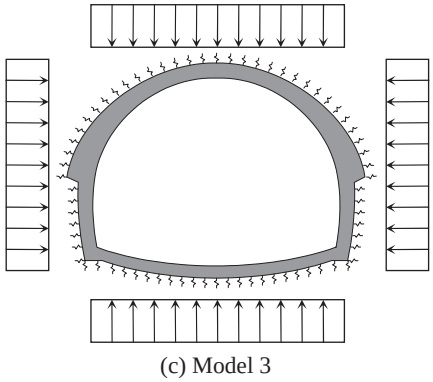
Figure 7 shows the outline of analysis model of Tunnel B. In the calculation of Tunnel B, whole concrete lining with invert was supported by subgrade springs. Construction joint between the top heading arch and sidewall was modeled by interface elements, which consisted of spring element in the normal and tangential direction. Four kinds of load conditions were adopted to estimate the direction and magnitude



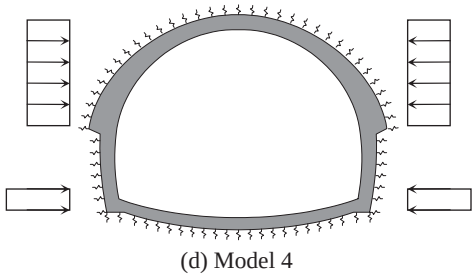
(a) Model 1



(b) Model 2

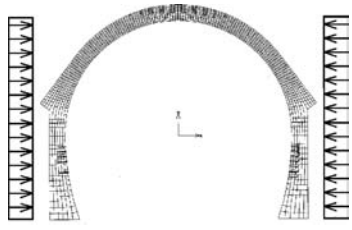


(c) Model 3

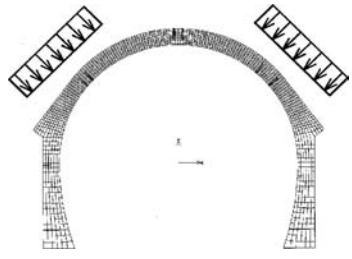


(d) Model 4

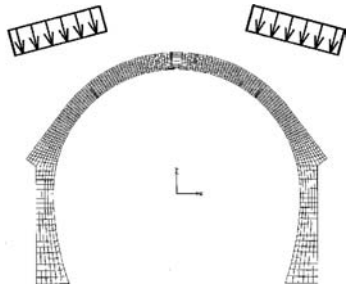
Figure 7. Outline of analysis model of Tunnel B.



(a) Model 1 θ = 0°



(b) Model 2 θ = 45°



(c) Model 2 θ = 75°

Figure 8. State of cracks obtained by analysis on Tunnel A.

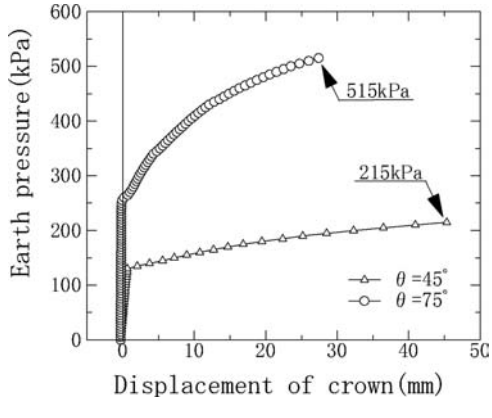


Figure 9. Earth pressure-displacement curve.

of earth pressure acting on concrete lining. In model 1, earth pressure acted on the invert in the vertical direction. In model 2, earth pressure acted on the concrete lining throughout the top heading arch and sidewall in the horizontal direction. In model 3, earth pressure acted on the concrete lining throughout the top heading arch in both the vertical and horizontal direction, sidewall in the horizontal direction and invert in the vertical direction. In model 4, earth pressure acted on the concrete lining throughout the whole top heading arch in the horizontal direction and the sidewall foot partially in the horizontal direction. In this model, the magnitude of earth pressure acting on the sidewall was assumed to be far larger than that acting on the top heading arch. In the calculation of every model, attention was given to the shear failure occurred at the joint between the invert and sidewall foot.

3.2 *Estimation of earth pressure acting on concrete lining*

Figure 8 shows the state of the cracks obtained by numerical analysis on Tunnel A. It can be seen that in the analysis model 1, tensile cracks occurred at the inside of the sidewall and at the outside of the crown. The compressive strains occurred at the inside of the crown showed a value above $3{,}000\mu$ and it was assumed that compressive failure occurred at the crown. However, tensile cracks at the shoulders did not occur. On the other hand, in model 2, tensile cracks occurred at the inside of the shoulders and at the outside of the crown in both cases of $\theta = 45°$ and 75°. The compressive strain occurred at the inside of the crown also showed a value grater than the ultimate compressive strain of $-3{,}500 \times 10^{-6}$ and it was assumed that compressive failure occurred at the crown in both cases. Therefore, it can be assumed that model 2 is more suitable than model 1 for simulating the state of deformation occurred in tunnel A. This means that deformation of Tunnel A was not induced by earth pressure acting on the concrete lining in the horizontal direction, but in the slanting direction.

Figure 9 shows the relationship between tunnel displacement at crown and earth pressure acting on concrete lining obtained numerical analysis using model 2 on Tunnel A. Tensile cracks occurred at the inside of the shoulders when the earth pressure reached approximately 130 kPa and 250 kPa in the case of $\theta = 45°$ and 75°, respectively, and shortly afterward tensile cracks occurred at the outside of the crown. When the earth pressure reached 515 kPa and 215 kPa in the case of $\theta = 45°$ and 75°, respectively, the strain of the inside of the crown exceeded the ultimate compressive strain and it was assumed that compressive failure occurred at these earth pressure values. The overburden height corresponding to these earth pressure values were calculated at approximately 9 m and 20 m by using the

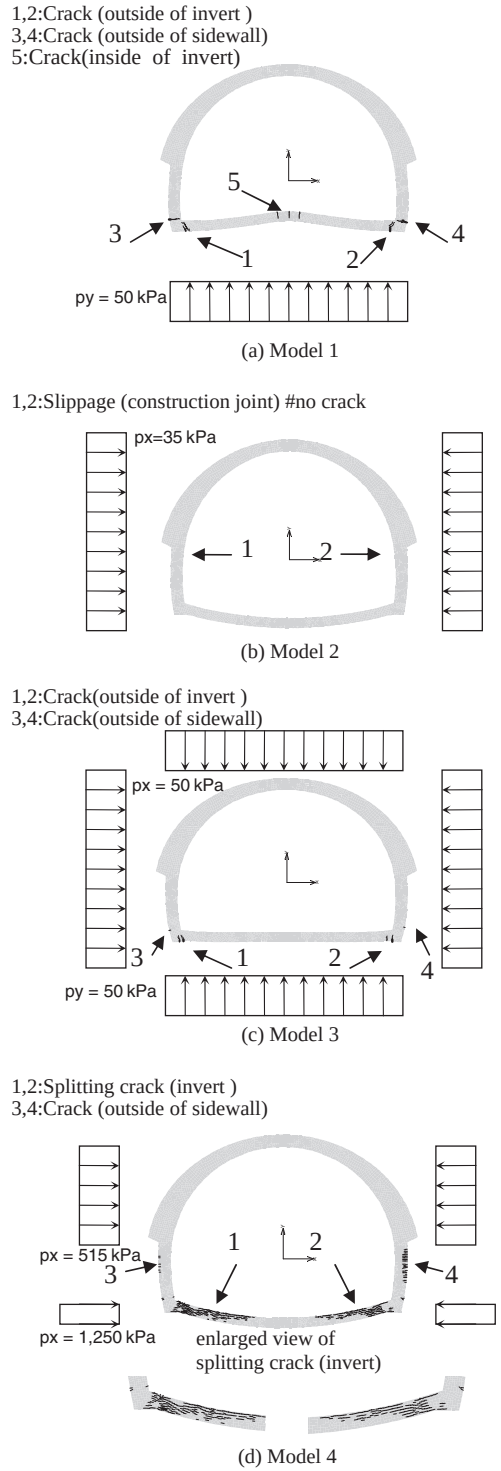


Figure 10. State of cracks obtained by analysis on Tunnel B.

unit weight of ground mass $\gamma = 25\,\mathrm{kN/m^3}$. Overburden height of 9 m in the case of $\theta = 45^\circ$ is almost the same height of loosened area estimated from the elastic wave velocity distribution of the ground.

Figure 10 shows the state of the cracks obtained by numerical analysis on Tunnel B. In model 1, tensile cracks occurred at the inside of the invert center and at the outside of the invert edge and sidewall foot when the earth pressure acting on the invert reached 50 kPa. In model 2, slippage at the construction joint between the top heading arch and sidewall occurred when the earth pressure acting on the concrete lining in the horizontal direction reached 35 kPa, though no tensile crack occurred. In model 3, tensile cracks occurred at the outside of the invert edge and sidewall foot when the earth pressure acting on the concrete lining in both the horizontal and vertical direction reached 50 kPa. In model 4, tensile cracks occurred at the outside of the sidewall and splitting cracks occurred at the invert edge, when the earth pressure acting on the top heading arch and sidewall foot in the horizontal direction reached 515 kpa and 12,500 kPa, respectively. Therefore we can conclude that shear failure occurred at the junction between the invert and sidewall was induced by excessive earth pressure acting on the tunnel sidewall foot in addition to that on the top heading arch in the horizontal direction. However, the earth pressure of 12,500 kPa acting on the sidewall foot is far larger than the overburden earth pressure of 3,000 kPa obtained by using the unit weight of ground mass $\gamma = 25\,\mathrm{kN/m^3}$.

4 CONCLUSION

In this study, field inspection on the damaged tunnels and numerical analysis using FEM were carried out to clarify the mechanism of the failure of concrete lining by the action of excessive earth pressure. The main conclusions obtained from the study are as follows.

(1) Excessive earth pressure acting on tunnel lining could induce compressive failure at tunnel crown or shear failure at junction between sidewall and invert
(2) FEM analysis considering the occurrence and development of cracks is effective in estimating the failure mechanism of damaged tunnel concrete lining by the action of excessive earth pressure.

REFERENCE

Mashimo,H.,Isago,N&Kitani,T. 2004. Numerical approach for design of tunnel concrete lining considering effect of fiber reinforcements, Tunnelling and Underground Space Technology, Vol.19, No.4–5: 454–455.

Underground Space – the 4th Dimension of Metropolises – Barták, Hrdina, Romancov & Zlámal (eds)
© 2007 Taylor & Francis Group, London, ISBN 978-0-415-40807-3

Historical damages of tunnels in Japan and case studies of damaged railway tunnels in the Mid Niigata Prefecture Earthquakes

M. Shimizu, T. Suzuki & S. Kato
East Japan Railway Company, Tokyo, Japan

Y. Kojima & K. Yashiro
Railway Technical Research Institute, Tokyo, Japan

T. Asakura
Kyoto University, Kyoto, Japan

ABSTRACT: Since mountain tunnels are mainly surrounded by stable ground, its displacement upon seismicity is less, therefore, they are structures less susceptible to seismic damage. However, many railway mountain tunnels have suffered damage from the 1923 Kanto Earthquake to the 2004 Mid Niigata Prefecture Earthquakes. This paper shows an outline of the historical damage of mountain tunnels in Japan and result of case studies of damage to mountain tunnels. This paper also shows classification of damage patterns and conditions of damage based on the result of the case studies, and refers estimated causes of damage of the tunnels in the 2004 Mid Niigata Prefecture Earthquakes.

1 INTRODUCTION

Since mountain tunnels are mainly surrounded by stable ground, its displacement upon seismicity is less, therefore, they are structures less susceptible to seismic damage to compare with other structures such as bridges and foundations. (Fig. 1) However, earthquake-resistant tunnels are highly noted since the 2004 Mid Niigata Prefecture Earthquakes occurred. Upon the foregoing earthquake, some tunnels located at disaster area were heavily damaged and have been impediment to reopening of Shinkansen and conventional lines. Especially, a concrete lining of the Uonuma Tunnel of the Jyoetsu Shinkansen located adjacent to the epicenter was heavily damaged and two-month time required for restoration.

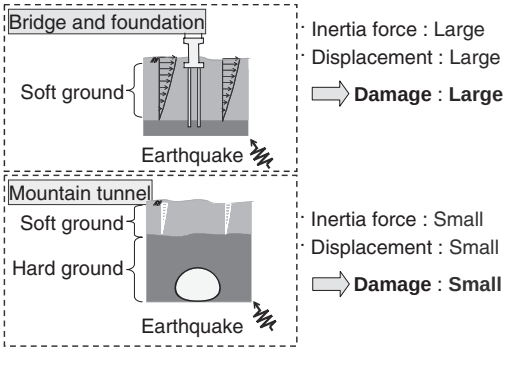


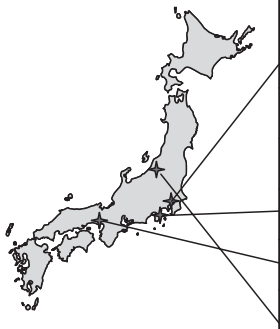
Figure 1. Difference of behavior during earthquake between bridges and foundations and mountain tunnels.

Owing to the progress of construction technology, more and more railway structures are being constructed by the tunneling method, and even tunnels need to have sufficient earthquake resistance. In this paper, we introduce case studies on the historical damage of mountain tunnels, an outline and assumed causes of damage by the foregoing earthquake.

2 HISTORICAL DAMAGE OF MOUNTAIN TUNNELS BY EARTHQUAKE

2.1 *Outline of damage*

Figure 2 summarizes the large-scale earthquakes which caused damage to mountain tunnels of railway in Japan. There are four major earthquakes: the 1923 Kanto Earthquake, the 1978 Izu-Oshima-kinkai Earthquake, the 1995 Hyogoken-nanbu Earthquake and the 2004 Mid Niigata Prefecture Earthquakes. The outline of damage of mountain tunnels will be respectively described below.



Year, Name	Magni -tude	Seismic intensity	Tunnel performance
1923 Kanto	7.9	6	Damage to 93 tunnels 25 tunnels required reinforce
1930 Kita-Izu	7.3	6	Very severe damage to 1 tunnel by a slide of the fault
1948 Fukui	7.1	6	Damage to 2 tunnels 1 tunnel required reinforce
1978 Izu-Oshima-kinkai	7.0	5	Damage to 9 tunnels 2 tunnels required reinforce
1995 Hyogoken-nanbu	7.2	7	Damage to 7 tunnels 5 tunnels required reinforce
2004 Mid Niigata Pref.	6.8	7	Damage to 24 tunnels 5 tunnels required reinforce

Figure 2. Historical damage of mountain tunnels by earthquake in Japan.

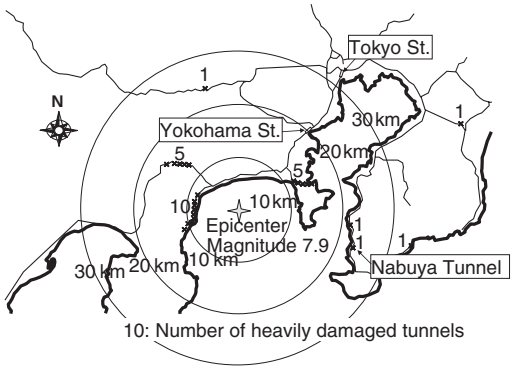


Figure 3. Distribution of heavily damaged railway tunnels upon the Kanto Earthquake.



Figure 4. Collapse of the Nabuya Tunnel.

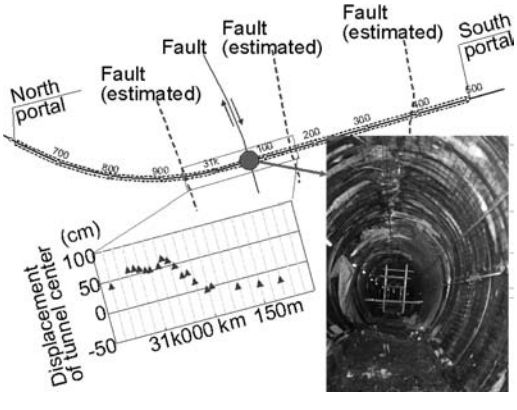


Figure 5. Damage of the Inatori Tunnel.

2.2 *The 1923 Kanto Earthquake*

The 1923 Kanto Earthquake is the earthquake, which caused the largest damage to mountain tunnels. There were 149 railway tunnels located within a range of a 120-km radius area from the epicenter at the time, and 93 tunnels among them were damaged to be reinforced; and 25 tunnels to be reconstructed due to collapse of linings. As an example of the heavily damaged tunnels, Figure 4 shows collapse of the Nabuya Tunnel. It is conceivable that a slide of an earthquake fault or a landslide caused the ground move to the tunnel and destructed a tunnel lining.

2.3 *The 1978 Izu-Oshima-kinkai Earthquake*

Upon the 1978 Izu-Oshima-kinkai Earthquake, nine railway tunnels suffered from damage. The largest damage is that of the Inatori Tunnel. (Fig. 5) A fault crossing the tunnel slid upon the earthquake, a lining of the tunnel collapsed and the track alignment longitudinally displaced. A relative displacement of the fault was 70-cm horizontally and 20-cm vertically according to the results of surveying.

2.4 *The 1995 Hyogoken-nanbu Earthquake*

Upon the 1995 Hyogoken-nanbu Earthquake, seven tunnels among 43 railway mountain tunnels located within a disaster area suffered serious damage, and five tunnels required repair and reinforcement. Figure 6 shows a distribution of heavily damaged railway

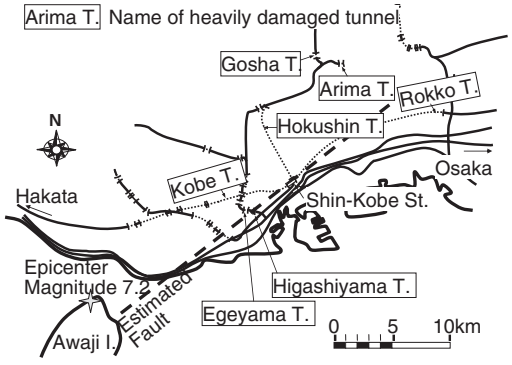


Figure 6. Distribution of heavily damaged railway tunnels upon the Hyogoken-nanbu Earthquake.

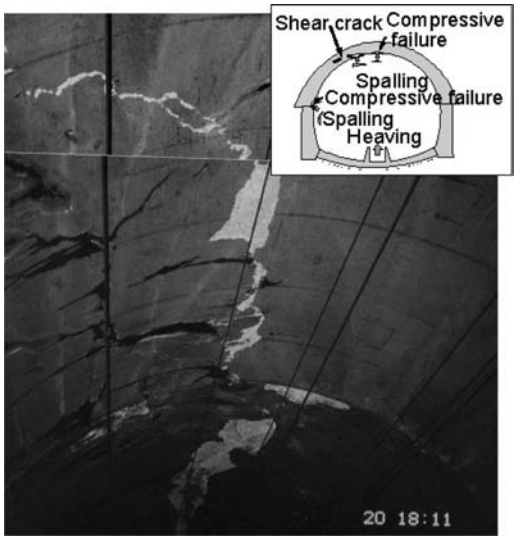


Figure 7. Damage of the Rokko Tunnel.

tunnels. As a typical example, Figure 7 shows the damaged conditions observed at the Rokko Tunnel. Several damage patterns observed at various locations are superimposed in one figure. Typical damage was of compressive and shear failures at the arch of a lining and compressive failures with spalling at joints between the arch and sidewall. Figure 8 shows a longitudinal profile and damaged locations of the Rokko Tunnel. Almost all the damaged locations coincide with faults or fractured zones.

2.5 *The 2004 Mid Niigata Prefecture Earthquakes*

On October 23, 2004, a large earthquake of magnitude 6.8 occurred at latitude 37°17′ N. and longitude 138°52′ E., depth 13-km of Niigata prefecture in

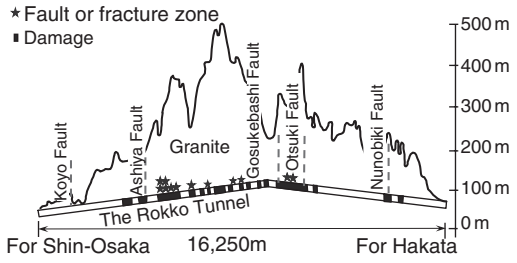


Figure 8. Longitudinal profile and damaged locations of the Rokko Tunnel.

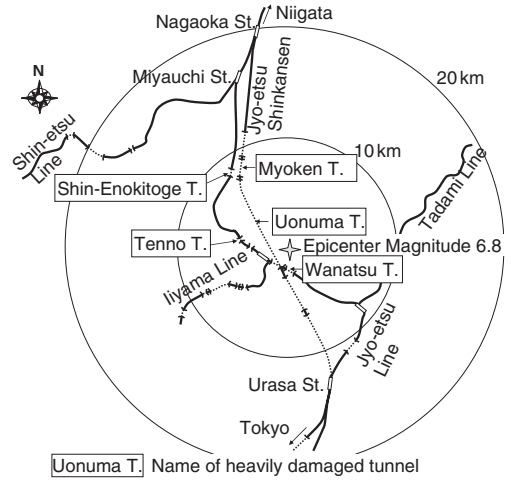


Figure 9. Distribution of heavily damaged railway tunnels upon the Mid Niigata Prefecture Earthquakes.

Japan. Due to this earthquake, a running Shinkansen train derailed and some mountain tunnels suffered from severe damage. Twenty-four railway tunnels had serious damage, and five tunnels (the Uonuma, Myoken, Wanatsu, Tenno and Shin-Enokitoge) required repair and reinforcement of linings. Figure 9 shows distribution of heavily damaged railway tunnels. It is obvious that heavily damaged tunnels concentrated at a limited area of approximately within a 10-km radius area from the epicenter. The most heavily damaged tunnel was the Uonuma Tunnel, which runs nearby the epicenter. The Uonuma Tunnel is a long railway tunnel driven in Neogene's mudstone with a length of 8,625-m. There were three heavily damaged sections in this tunnel. (Fig. 10).

Figure 11 shows a damage situation of the most heavily damaged section. A concrete lining was broken to fall off to a track. The largest concrete block amounted to approximately 2 m^2 (5ton). Other observed damage consisted of reduction of a tunnel diameter, heaving of a roadbed concrete and cracking of an invert. This is the largest disaster among the

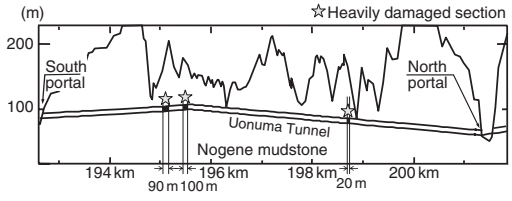


Figure 10. Longitudinal profile and damaged locations of the Uonuma Tunnel.

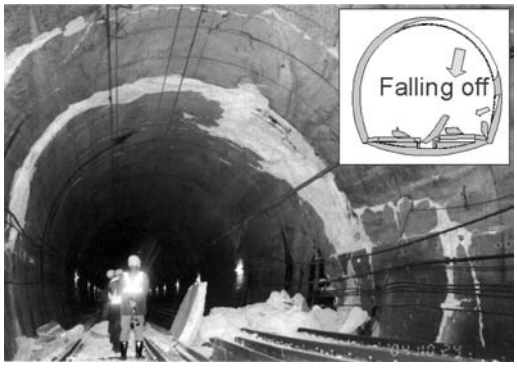


Figure 11. Damage of the Uonuma Tunnel.

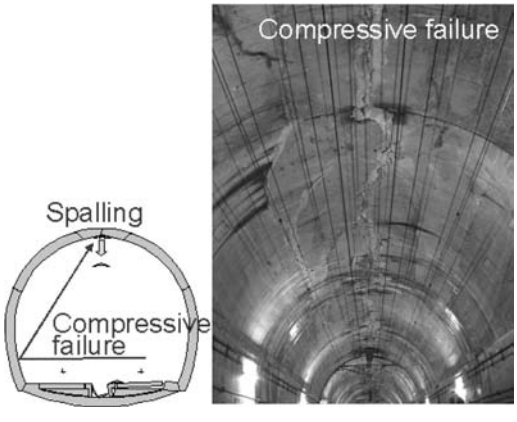


Figure 12. Damage of the Myoken Tunnel.

Shinkansen tunnels after inauguration. The locations were restored by rock bolting, removal of the concrete by breakers, shotcreting, and reinforcement by mortal precast boards; however it became a critical path and took two months until reopening. There was another damage of the Myoken Tunnel of the Jyoetsu Shinkansen. This tunnel had a compressive failure at a crown (Fig. 12) and an invert also heaved like the Uonuma Tunnel. At the Wanatsu Tunnel of the conventional line, there was a compressive failure at



Figure 13. Damage of the Wanatsu Tunnel.

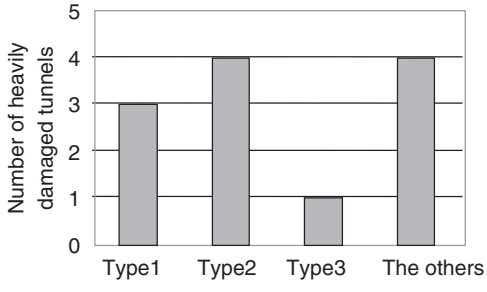


Figure 14. Number of damaged tunnel (respective types).

a crown and large brocks fell off a lining and steel supports of the tunnel were exposed. (Fig. 13) At the Tenno and Shin-Enoki Tunnel, bedrock collapsed and slid above the tunnel and cracks occurred on a lining.

3 CLASSIFICATION OF DAMAGE PATTERNS

Figure 14 shows result of classified damage patterns on the 1978 Izu-Oshima-kinkai Earthquake, the 1995 Hyogoken-nanbu Earthquake and the 2004 Mid Niigata Prefecture Earthquakes, for which various valuable information and data remained. In addition, we classified the damage patterns into three types as shown in Figure 15.

Type 1: Damage of shallow depth tunnels

There are many examples of damaged tunnels in the Type 1. In general, shallow depth tunnels are likely to suffer from earthquake, as they often constructed in the loose ground where a seismic activity is amplified and the ground deforms largely. Cracks in the arch of the lining are characteristic of this type. It is conceivable that tunnels deform like shearing deformation by

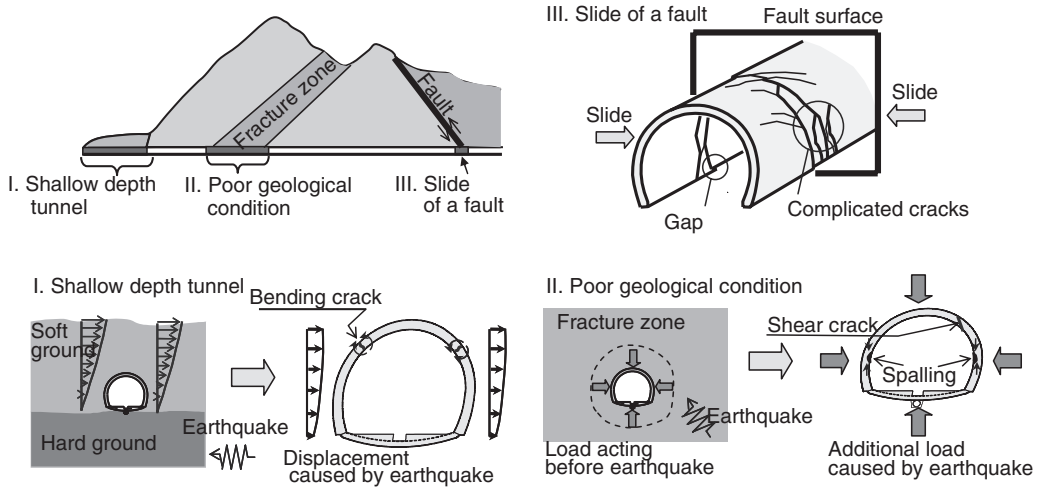


Figure 15. Classification of damage patterns.

displacement of the earthquake and cracks occur at a shoulder part of an arch by bending moment.

Type 2: Damage of tunnels of poor geological condition

This type is visible on tunnels in the soft ground like a fractured zone, sometimes on tunnels of large earth covering. In the fractured zone, the ground is generally soft and displacement in an earthquake becomes large. Furthermore, there have been other loads acting on the lining like loosening earth pressure and plastic earth pressure in the fractured zone before an earthquake. In such a case, the load acting on a lining becomes large and damage by the earthquake tends to be severe.

Type 3: Damage of tunnels by a slide of a fault

Type 3 is a type that an earthquake fault is crossing a tunnel. A slide of the earthquake fault makes various stress such as shear stress, tensile stress and compressive stress on a lining and cause complicated cracks like shear cracks and cracks in round slices.

4 CONDITIONS OF DAMAGE

From such case studies, it is evident that even mountain tunnels suffered damage by an earthquake. Susceptible conditions under which tunnels suffered from damage are provided that:

1. A great magnitude of an earthquake
2. Tunnels located adjacent to an epicenter or an earthquake fault.

Figure 16 shows relation of distance from an earthquake fault, magnitude of an earthquake and number of heavily damaged tunnels. From this figure, we find

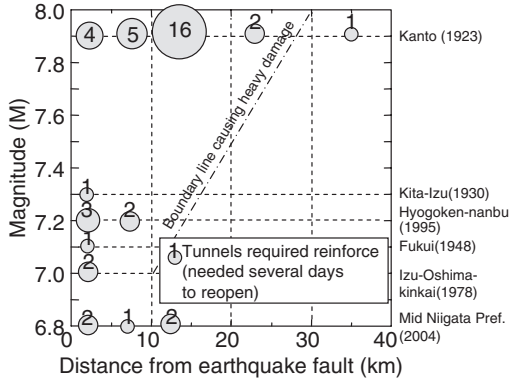


Figure 16. Relation of distance from an earthquake fault, magnitude of an earthquake and number of heavily damaged tunnels.

that a risk of earthquake damage becomes large under on the condition of both 1 and 2. Roughly speaking, tunnels suffered numerous damages at areas within 10 km from an earthquake fault in the case of M7, and areas within 30 km in the case of M8. Figure 17 shows relation between a distance from an earthquake fault and a percentage of damaged tunnels. From this figure, we find that damage that requires reinforcement occurred within 10 km from an earthquake fault. However, these figures have entirely not considered the conditions proper to tunnels such as the ground adjacent to the tunnel and a tunnel structure. It is conceivable that tunnels tend to suffer from an earthquake under,

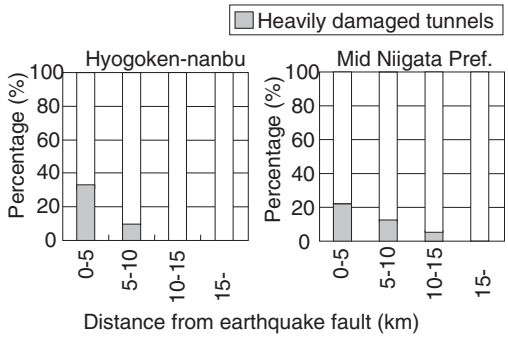


Figure 17. Relation between a distance from an earthquake fault and a percentage of heavily damaged tunnels.

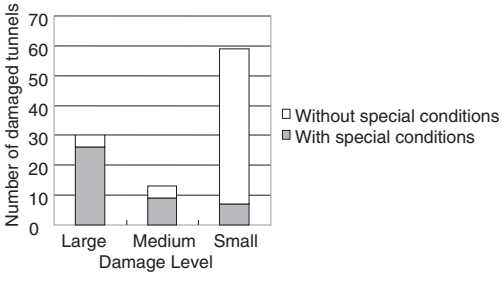


Figure 18. Number of damaged tunnels which have the special conditions (The Kanto Earthquake and Izu-Oshima-kinkai Earthquake).

3. tunnels have special conditions such as;

   a. shallow depth tunnels
   b. poor geological condition
   c. slide of an earthquake fault crossing the tunnel
   d. structural defects of a tunnel lining

Figure 18 shows number of damaged tunnels which have the special conditions. Many of heavily damaged tunnels have some special conditions. Therefore, we can conclude that a risk of earthquake damage becomes large under condition of both 1 and 2, and a level of damage becomes large under condition 3.

5 CAUSES OF DAMAGE OF THE UONUMA TUNNEL

In this chapter, we introduce the causes of damages of the Uonuma Tunnel, which suffered the heaviest damage in the Mid Niigata Prefecture Earthquakes. First of all, this tunnel was within 1-km from an epicenter and an earthquake motion was extremely strong. Secondly, the ground of this area is Neogene's mudstone and relatively soft. We surveyed a geological characteristic and a situation behind a tunnel lining by boring at the heaviest damaged section to find the following

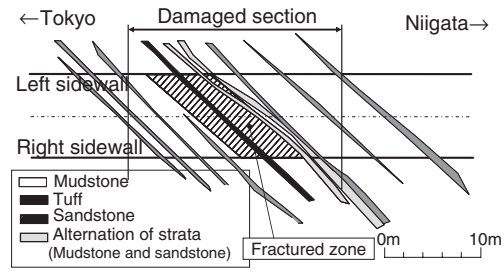


Figure 19. Geological characteristic of the damaged section of the Uonuma Tunnel (a ground plan).

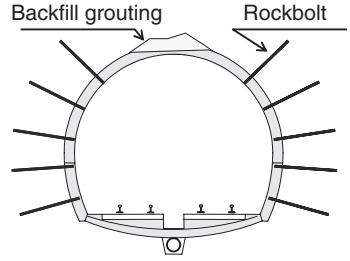


Figure 20. Fundamental countermeasures.

two facts. First, the ground of the damaged section had lower strength than that of neighboring sections, secondly there were voids behind the tunnel lining at an arch and the tunnel tends to deform largely. It is conceivable that the Uonuma Tunnel suffered large damage, because this tunnel was located adjacent to an epicenter, earthquake motion was extremely strong and there was void behind the tunnel lining.

6 COUNTERMEASURES AGAINST EARTHQUAKE OF TUNNELS

We are now planning the countermeasures against earthquake damage. Figure 20 shows countermeasures for existing tunnels. Backfill-grouting to a void behind linings and rockbolting to prevent spalling are fundamental countermeasures. For newly constructed tunnels, we adopt countermeasures to linings themselves. We use fiber reinforced concrete to improve ductility and performance of unti-spalling of linings.

7 CONCLUSIONS

In this paper we showed an outline of the historical damage of mountain tunnels in Japan and result of case studies of damage to mountain tunnels. We also showed classification of damage patterns and conditions of damage based on the result of the case studies.

However, there are many unknown factors on the damaging mechanism of tunnels under an earthquake. It is very important to establish the way to evaluate earthquake resistance of tunnels. We are planning model tests and numerical analyses to evaluate deformation behavior of tunnels under an earthquake and we are going to use the outcome for maintenance of railway tunnels.

REFERENCES

Asakura, T. & Sato, Y. 1996. Damage to mountain tunnels in hazard area, *Special issue of soils and foundations*, pp.301–310, Tokyo: Japanese geotechnical society.

Asakura, T. et al. 1998. Study on earthquake damage to tunnels and reinforcement of portals, *Quarterly report of RTRI*, vol.39, No.1, pp.17–21, Tokyo: Railway technical research institute

Asakura, T. et al. 2001. Damage to mountain tunnels by earthquake and its mechanism, *Modern tunneling science and technology; Proc. IS-Kyoto 2001*.

Shimizu, M. et al. 2005. Damages of railway tunnels by the Mid Niigata Prefecture Earthquakes, *Tunnels and underground*, vol.36, No.5, pp.421–428, Tokyo: Japan tunneling association

Yoshikawa, K. 1981. Investigations about past earthquake disasters of railway tunnels, *Quarterly report of RTRI*, vol.22, No.3, pp.103–107, Tokyo: Railway technical research institute

This page intentionally left blank

Underground Space – the 4th Dimension of Metropolises – Barták, Hrdina, Romancov & Zlámal (eds)
© 2007 Taylor & Francis Group, London, ISBN 978-0-415-40807-3

Close underpass of ancient tunnels: Methodology and results

Achille Sorlini
Geodata S.p.A., Turin, Italy

Guido Amoretti & Fabrizio Zannoni
"Pietro Micca e dell'assedio di Torino 1706" Civic Museum, Turin, Italy

ABSTRACT: Turin's countermine tunnels represent one of the most famous and extensive underground systems ever realized. *The Citadel*, a fortress built by Francesco Paciotto for the Duke of Savoy in the mid 1500's, saved the city from its enemies on several occasions. The alignment of the new automatic metro (VAL System) line 1 interacts with the ancient tunnel system for at least 1 km. Consequently, subway design was subjected to preservation of the historical underground tunnel network monument. To preserve the historical network, before metro subway excavation, the ancient defensive tunnels were consolidated by filling with sand sacks and grouted. Continuous monitoring of TBM parameters was accomplished for control of settlements. Removal of the tunnel consolidation filling material showed that the defensive tunnels had not been damaged by excavation of the new subway tunnel.

1 INTRODUCTION

The alignment of Line 1 of the new Turin metro (G.T.T. S.p.A., Gruppo Torinese Trasporti is the Metro owner) shared an extent of 1 km with the ancient tunnel system called countermine galleries.

The Citadel, the Turin fortress and its underground network, saved several times the city from its enemies. So the Italian Department of Arts strongly protects these ancient tunnels for their historical value. As a consequence, engineers had to give great consideration to avoid damage to subterranean monument.



Figure 1. Ancient map of *Cittadella* fortress.

2 THE CITADEL COUNTERMINE SYSTEM

2.1 *Historical introduction*

Turin's countermine galleries represent one of the most famous and extensive underground defense system ever realized. It is still existing and accessible. Duke Emanuele Filiberto of Savoy built the pentagonal Cittadella in the 1500s, following the style of modern forehead bastion – the *trace italienne* – invented at the beginning of the same century.

Tunnel construction started in 1572. The underground system was combined with surface fortifications to protect the city using a new, unknown strategy. Between the 1600s and 1700s surface and underground fortification were extended, reaching their maximum extension and efficiency. As a consequence, when French troops attacked the city in 1706, they were defeated.

The defensive network was organized in five large areas, corresponding to the five bastions of the fortress. Each of them had two main galleries placed one above the other, the shallowest between 6–7 m from the surface; the deepest at 12–14 m (just above the water table). The sectors were connected by the magistral gallery: it was the longest tunnel, about 2500 m long around the city. From the above tunnels many smaller branches were driven with small rooms at their end to blast mines below approaching enemies.

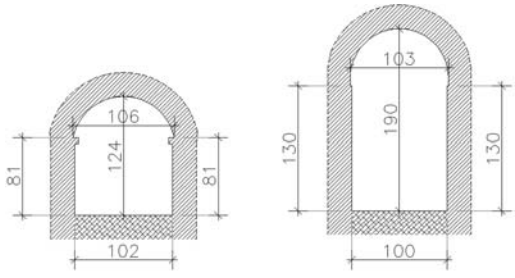


Figure 2. *Cittadella*'s type tunnels.

Around 1850, the city began an uncontrolled expansion which caused the demolition of the surface fortress. Tunnels survived, but they were filled with rubble and waste. New buildings cut connections or destroyed some parts of the network. During the second world war, many parts were reopened and used as air raid shelters. In the 1950s the construction of new buildings in bombed areas brought to the rediscovery of same of tunnels and at the beginning of 1960s the city established the Civic Museum in order to preserve and to recover the ancient galleries.

2.2 *Local geology*

Turin's soil is an alluvial deposit of gravel and sands with local presence of silt (<5%). The alluvial deposit also contains cobbles and rarely 1 m^3 blocks.

Natural cementation of soil varies from low to high. Permeability is at about 10–1 cm/s. Water level is between 15 and 20 m from surface, deeper than the underground network.

2.3 *Old tunnel features*

Ancient tunnel were manually excavated between the second half of 1500s and the end of 1700s. Excavation took advantage of soil cementation for cavity stability. Brick lining and semicircular vaults assured good air circulation and cleaning of galleries, they weren't put in place for support. Most parts of the tunnels have a 1.20 m width and a 1.80 m height; in the working area some lateral branches have a 1.40 m height only.

3 INTERFERENCES

3.1 *Spatial interference*

The Line 1 crosses down the Citadel underground network in the area between the XVIII Dicembre station and the new Porta Susa Metro – Railway station. The low level galleries and the lateral mine branches radial plan increase the number of crossings with the new metro alignment. The distance at the crossings between the crown of the new metro tunnel and the floor of the ancient tunnels is often at only 1.0–1.5 m. The

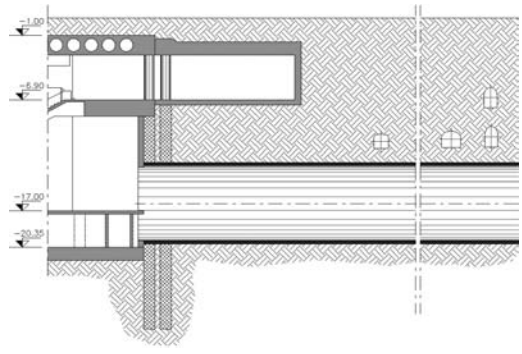


Figure 3. *A longitudinal section along the line: XVIII* December *station on the left, small ancient tunnels on the right.*

diaphragms of XVIII Dicembre station were planned very closed, less than 0.5 m from the historical brick lining of the ancient tunnels.

3.2 *Construction interaction*

Construction interaction with underground network were:

- Excavation and lining of main metro tunnel with TBM EPBS with close underpass of ancient galleries (1.0 m);
- Excavation and concrete filling of XVIII December station diaphragms with hydromill and bentonite slurry;
- Soil drilling and grouting with fluid concrete and chemical products along in/out approaches of TBM to station;
- Ventilation shaft n.11 construction with micropiles and waterproofing grouting.

4 METHODOLOGY TO PRESERVE TUNNELS

4.1 *Underground surveys*

A detailed survey was necessary to plan Line 1 and to locate the works of arts as well. That was accomplished during design. Actually old surveys and documents of the ancient tunnels were available, but they didn't fit to design needs to avoid interaction and to reduce damage risks. Therefore between 1999 and 2000 high quality underground surveys were carried out, some times with help of speleologists, where ancient tunnels were no longer easily accessible.

4.2 *Design criteria*

Aim of preventive protection works was to avoid damages to ancient structures, most of which open to public access from a civic museum.

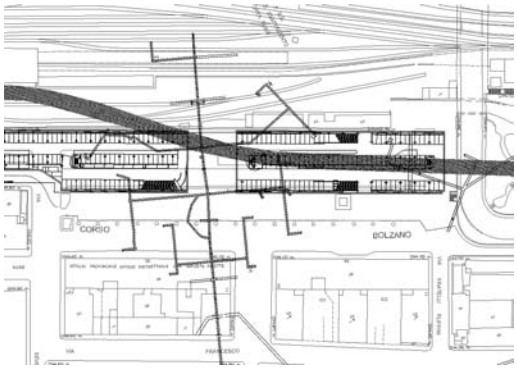


Figure 4. Result of detailed survey: underground network between an underground parking lot and the metro tunnel.

Two risks were considered:

– Soil slab subsidence between metro excavations and galleries pavement (between 5 and 1 m) with soil collapse up to city surface;
– Accidental filling from grouting from surface, not easily removable with consequent loss of gallery section.

Both of these problems were solved by filling systematically the *Cittadella*'s tunnels in the areas where the subway excavation could induce a collapse and where grouting was to take place close to ancient linings.

The filling was carried out with the following elements:

– contrast concrete slab between gallery piers;
– sand sacks and polystyrene blocks to tunnel cap inside a plastic membrane;
– stoppage grouting with cellular concrete.

Filled parts were closed with brick walls. Clinometers to measure settlements were installed inside the filling.

Concrete slab had the purpose of avoiding convergence between piers and of reinforcing tunnel foundations. Filling had to avoid that grouting and chemical or bentonite slurries could enter the tunnel cavity, preferring a designed removable filling, rather than an uncontrolled one.

4.3 *Construction phases*

Works took place in summer 2002. Tunnel filling was driven with manual techniques with some problems of ventilation and accessibility for their small size and positioning. It was necessary to build a new access shaft from surface and to prepare descent adequately to assure safety and rescue for workers.

All operations were supervised by archaeologists, who surveyed filled tunnels and took pictures of different phases. More than 250 m of ancient galleries were filled.



Figure 5. Plastic membrane and sand sacks inside the smallest tunnel.



Figure 6. Grouting of filled tunnels.

4.4 *EPBS excavation control and settlement monitoring*

Underground and surface subsidence measurements, together with TBM excavation monitoring gave evidence of the good results in the preservation of the ancient tunnels. No appreciable settlements were recorded; surface subsidence was of only 2–3 mm.

5 RESULTS

5.1 *Filling removal*

Filling removal operations and tunnel cleaning were carried out one year after TBM underpass and took some months to complete. Closure walls were destroyed and sand sack filling removed with manual tools and instruments. Slab demolition followed and the protective plastic membrane was detached from the

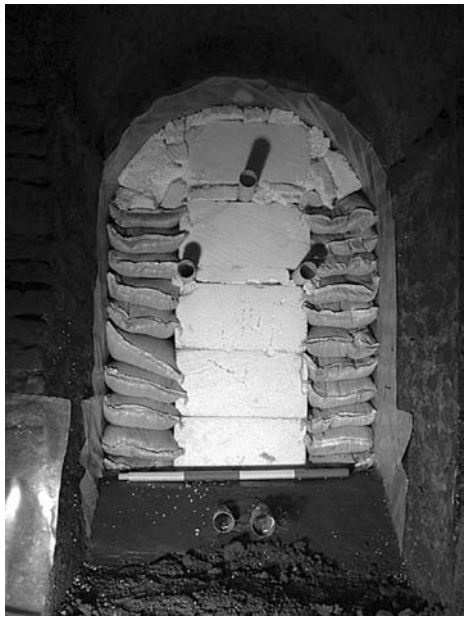


Figure 7. Final filling with polystyrene blocks and injection pipes. The bar is 1 m length.

brick lining. Archaeologists closely monitored each operations.

5.2 *Damage assessment*

Filling removal permitted to survey tunnel conditions. It became very clear that protective works avoided all damages to tunnels, to be caused by TBM excavation: design criteria proved to be correct.

Construction of the metro line had the following effects:

- no structural damage to lining from close TBM underpass or from diaphragm excavation;
- no underground or surface subsidence;
- no collapse;
- accidental drilling was recorded only in two single points of brick vault ;
- local bentonite slurry and concrete infiltration between plastic sheet and lining;
- high permeability chemical patina between plastic sheet and lining.

5.3 *Repair and cleaning*

Cleaning and repairing operations followed the completion of removal works. Brushes and low pressure water jets were the principal tools. Small specialized contractors made few lining reparations.

A new access shaft was kept permanently open and given to the museum in order to improve natural ventilation of the underground network.



Figure 8. Stoppage and filling removed; no damages to brick lining.



Figure 9. Bentonite patina below protection sheet before its removal.

6 CONCLUSION

Design methodology and choices proved to be appropriate to protect the ancient structures and to reduce risks of subsidence and collapse that could have involved buildings above ground level.

The Citadel tunnels were given back the civic museum and today are again open to visitors.

Underground Space – the 4th Dimension of Metropolises – Barták, Hrdina, Romancov & Zlámal (eds)
© 2007 Taylor & Francis Group, London, ISBN 978-0-415-40807-3

Advanced methods for tunnel assessment

Govind R. Sulibhavi,
Project Engineer, Maryland Transit Administration

William A. Parks, P. E
Chief, Maryland Transit Administration

ABSTRACT: There are numerous tunnels in the country, predominantly in Transit Sector, which needs periodic Inspection, Maintenance for safety and system preservation. Many Transit agencies operate round the clock, which limits the time for assessment. Budgets constraints reduced staff, commercial and environmental pressure to improve the performance of existing tunnels becomes difficult. We need to develop a comprehensive and standard rationale for tunnel assessment, which shall be feasible with time constraints. Present assessment methods are manually intensive, involving cross-referencing of the data, inspecting the tunnels during off-peak hours and recording the data. Maryland Transit Administration (USA) experienced similar problems and decided to utilize the "Three Dimensional Scanning" for tunnel assessment. The paper will describe the present tunnel assessment methods and compare to the evolution of "Three Dimensional Scanning" process as it currently stands and look at the future and where we think this effort will lead.

1 INTRODUCTION

1.1 *Maryland Transit Administration*

The Maryland Transit Administration is a Transit division of the Maryland Department of Transportation providing transportation in various modes. These modes are as follows:

- Metro System – Baltimore Metro System is in operations since 1983 with fourteen (14) Stations
- Bus – Operates more than fifty (50) routes throughout Maryland since 1973. It was known as Baltimore Transit Company (1935 – 1970)
- Light Rail – Baltimore Light Rail System is in operation since 1992 with 32 Stations
- MARC – Maryland Rail Commuter
- Freight – Various Freight Lines in Maryland.

1.2 *Baltimore Metro System*

The Baltimore Metro System operates along a 15.5 Miles (24.8 Km) long route between Downtown Baltimore and Owings Mills in Northwest Suburbs with fourteen (14) stations serving the communities along the line. Part of the Metro System is underground with eight (8) stations and the rest is at- grade and on Aerial Structures. See Map 1. The paper shall discuss the assessment methods deployed for the tunnel portion of Metro System.

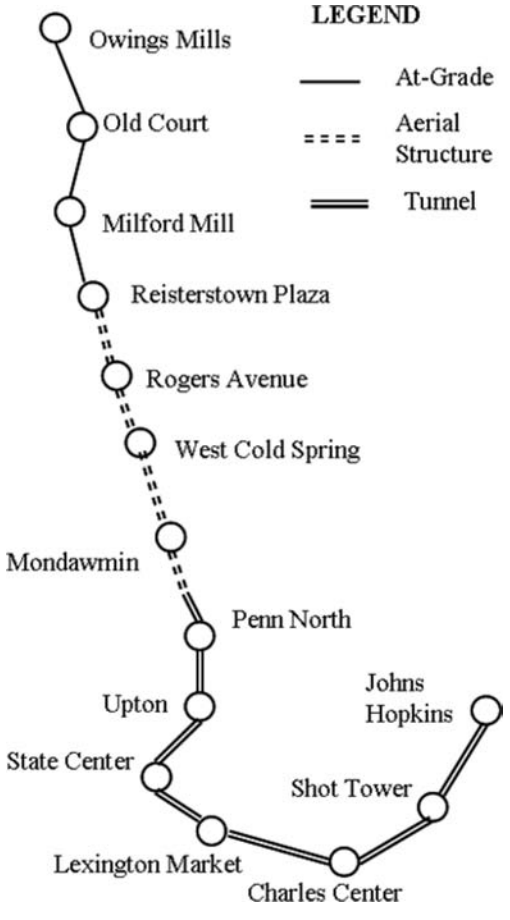
2 STRUCTURES ASSESSMENTS

2.1 *Tunnel assessment*

Maryland Transit Administration performs inspection of all the structures once every two (2) years and Tunnels (Underground Metro System) once every five (5) years for Safety and System Preservation. Based upon the Inspection findings, contract documents are prepared and rehabilitation is done. The Metro system Operates from Monday thru Sunday seven days a week. It becomes difficult to get "Track Access". Additionally the due to confined space in the tunnels, inspections cannot be performed during the operation of Metro System. So Maryland Transit Administration System was in search of "Drive through Tunnel Inspection System" which would benefit the Agency. In the process we contacted Takenaka Corporation, Japan, Ensco, Inc., Springfield, Virginia, US and Subterra Company, Germany. Due to various limitations it was not feasible for the mentioned companies to perform the required services. Then we initiated a pilot study to utilize Three Dimensional Laser scanning for Tunnel Inspection for approximately 183 meter (600 feet) of Tunnel Liner with a local Consulting Engineering Company by name Greenman Pedersen Inc.

2.2 *Application of 3D laser scanning*

Maryland Transit Administration/Consultant utilized a Leica Geosystems Three dimensional Scanner for



Map 1. Baltimore Metro System.

the study. Adequate three dimensional images of the tunnel liner were collected to perform the visual inspection entirely in the office. It was evident as seen in Figure 1, that significant detail is visible.

The image shows the artificial-color image that the scanner creates as a result of the various intensity of the reflected laser light. The 3D scanner captures up to 1,000,000 3D points in 15 minutes, in a rectangular grid – up to 1000×1000. In addition to an X, Y and Z coordinate; each point is also recorded with the previously mentioned intensity value. The value is based upon a number of surface and distance factors. To record approximately 183 meters (600±feet) of single track tunnel used for this pilot project, nine scan setups were required. Later, in the office, the separate scans are "joined" together and registered to a known coordinate system. The resultant "point-cloud" then becomes a virtual model of the tunnel, from which a variety of information can be obtained.



Figure 1. High resolution scan 1000×1000 Grid.

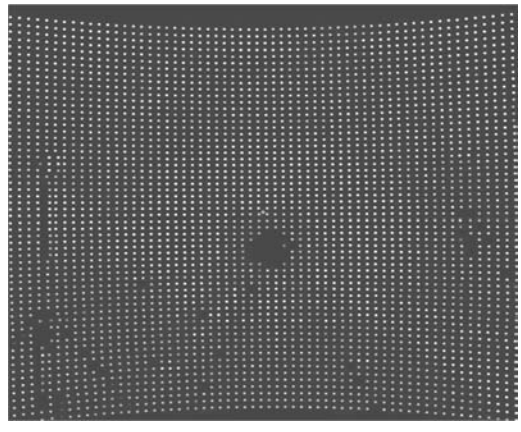


Figure 2. Low resolution scan 60×60 Grid.

2.3 *Data collection method*

To illustrate the orientation and distribution of scanner's grid collection system, an additional scan was collected from the setup. The scan consists of a 60×60 grid matrix. Figure 2 shows the result of the scan. It appears like a flat wall, except for the color of the scan points. Comparing this figure to the previous figure, there are some indications of the scan colors and tunnel liner.

In a scan if fewer points are used, the visibility of the image quickly breaks down. Interestingly, if same scan is viewed without the benefit of perspective (and at a slightly different angle) quite a different picture emerges.

In Figure 3 it is possible to clearly see the tunnel liner shape in the near scan points, but not so easily, as the distance from the scanner increases.

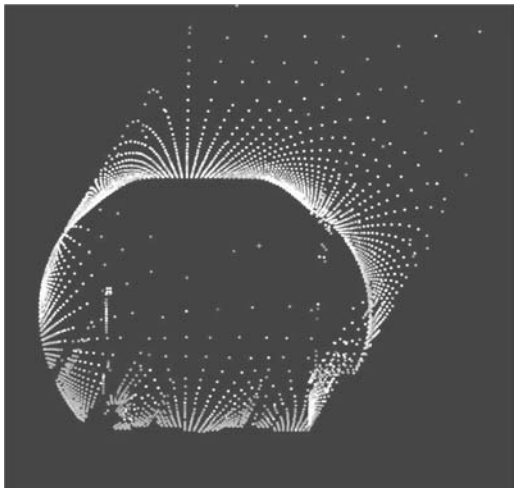


Figure 3. Low resolution scan.

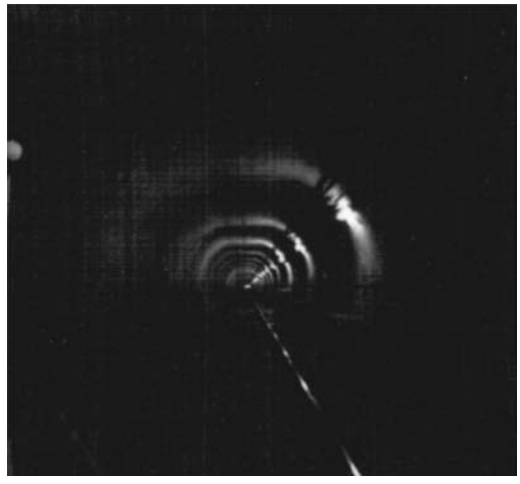


Figure 4. Tunnel image from scanner view finder.

The point dispersal pattern also affects the level of detail that can be seen in dense scans. As the distance from the scanner increases, so does the space between scan points. Due to the geometry of the tunnel, there is no way to avoid this phenomenon.

Additionally, even where there is a dense scan, as one zooms in for a closer look, the spacing between the points becomes visible and the visibility of the image degrades. The effect is similar to what happens to images of aerial or satellite photographs. From a certain distance, the images look highly detailed, but as you zoom in to a certain point, those images also begin to degrade. All of this is not to say that scanning is not a viable tool, but clearly points out that it is important to keep the expectations within the range of capability of not only the scanning technology, but also to the reality of the limitations that the geometry of tunnels will force upon you. Nor does this preclude the possibility of scanning a tunnel at a high level of detail. However, to do so would require far more scans than would be practical or cost effective, for that matter. One very significant benefit of the scanner is that the data that it collects is not affected by available light. Figure 4 shows the image used by the scan operator to align the scanner. As it can be seen the tunnel is extremely dark. Contrast this with the figure 1, the ability of this system has no a trivial benefit. However, this also brings up an other point. The scanner image, with its intensity driven display, while highly visible, may clearly display something, but interpreting what, will require further analysis. The current inspectors can look at the wall in true colors, and tell the type of defect that they are seeing, based in a large part to their past experience. Reading the false-color image from the scanner in a similar manner will take some time to develop. Furthermore, it is as equally possible that defects invisible to the naked eye will be detectable in the scan, and that other areas with markings that look like defects, will actually be simply some discoloration caused by variations in the intensity because of some surface condition that is unrelated to any defect.

2.4 *Extraction of collected data*

Having a fully registered model of the tunnel, in the form of a point-cloud, additional information can be extracted. Few tools come with the scanner where many different tasks can be performed. However, it is not designed for performing drafting.

Recognizing this, additional tools are also available to access the scanned data within the two most popular CAD software used in the transportation industry – Micro Station and AutoCAD. The software's are, CloudWorx, which allows for quick and efficient display and extraction of the scanned data within the CAD platforms. For this project, we primarily used one feature of the tool which allowed the placement of poly-lines and polygons whose vertices are automatically snapped to 3D points within the scan. This made it very easy for the CAD operator to draft outlines of the defects that were true 3D representations of the defect areas. Figure 5 shows a portion of the tunnel after creating these 3D graphics.

It was understood that the actual shape of the tunnel liner, in cross section form, could also be useful for defect analysis to show any deformation. However, with DTM software it is easily understood. Bentley's In Rail software (a rail design package, which also runs with both Micro Station and AutoCAD) has a tool for tunnel surface analysis. The standard DTM was utilized for un-rolling the tunnel data and re-rolling it for display. The way it works is to describe the geometry of the "ideal" or typical tunnel section. Once this

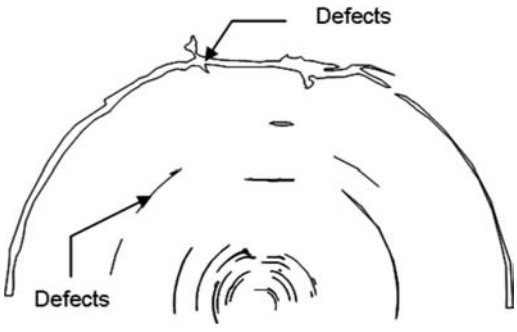


Figure 5. CAD drawing showing defects in view.

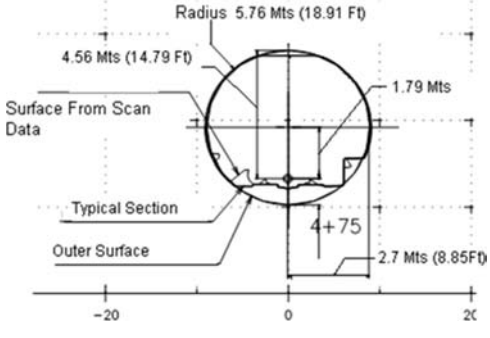


Figure 6. CAD Drawing Tunnel Cross section.

is created, we input the tunnel horizontal and vertical alignments into In Rail along with an ASCII form of the points from the scanned data. Triangulations of surfaces are performed to plot the tunnel cross sections. Figure 6 is an example of one of the cross sections.

In the figure, from the scan, we see indications of the safety walkway, the rails, the third rail with its protective cover, a 3" water line, a triplet run of electrical conduit, and at the center of the ceiling, an antenna wire. The cross sections can be compared in the future for any changes, and can also be compared to the original typical section. Then any deviation can be marked for further investigation back in the field. At this point, we had everything we needed to create drawing that could be used as documents for a repair contract. Utilizing In Rail plan and profile sheets were developed.

2.5 *Interpretation of spatial data*

To create plan sheets, would only require Micro Station and AutoCAD for their drafting capabilities – but to create a profile view would require some additional design software. The initial requirement was to display a left or right side of a tunnel aligned with the plan view of the top of the tunnel, as viewed from below. We also needed to display, in the profile view, the graphics of the defect areas.

- In Rail DTM's have a very powerful feature – and its ability to place points and lines in the DTM that are not used as surface points. Points (also known as random points) which represent discrete locations on the surface of the DTM. At times it is difficult to establish relationships between points.
- Break lines represent lines along changes in the slope of surfaces. Some break lines are very subtle while others are very obvious.

There are other types of data in many DTM's, but are irrelevant to this topic. Both of these sited data types would be used as surface points and would effect how a DTM displays contours and other data. For this task, although the tunnel surface is a DTM to In Rail, it is a special type, and currently only supports points. Since we need to represent linear objects, we used the traditional DTM tools and since some of the sidewall defects violated the 3D rules, if used as part of a surface, we decided to store them in a DTM as "exclude from triangulation" objects. Using In Rail's terminology, every object in a DTM is a feature. Features can be individual points, groups of points, linear elements and groups of linear elements. Every feature must have a unique name. Every feature must have one or more styles. A style is defined in In Rail as display characteristics for CAD elements. You can define a different style for plan, profile and cross section display and there are separate configurations for linear objects, point objects and text objects.

Additionally, it can assign a description to a feature and a "parent" – both of these are the text fields that can be filled with useful text information which can later be used as annotation labels or extracted into a report.

For this project, we created styles for each defect type, and as we stored each element, we gave them a simple generic name – Area 1, Area 2, etc. In the future, it may be possible to use more descriptive names, which will also include the defect type. As used in the profile, we can instruct In Rail to display these "features" on a profile by projecting the points to the profile, and to limit the display to only those features to the right of the centerline or the left of the centerline, as needed. For ease of use, we also wanted to display the scans on the drawings. This proved to be problematic and may eventually be dropped from the process. Since the drawings are not in "true coordinates" and it cannot easily manipulate the location and orientation of the display of the scan points, it was necessary to use images created from plots of the scans. Also, as the density of the scan increases, the software optimizes the display by thinning the number of points it will display (or plot) which limits how much of the scan can be plotted to a single image. Figure 7 displays one of the sheets created in this manner.

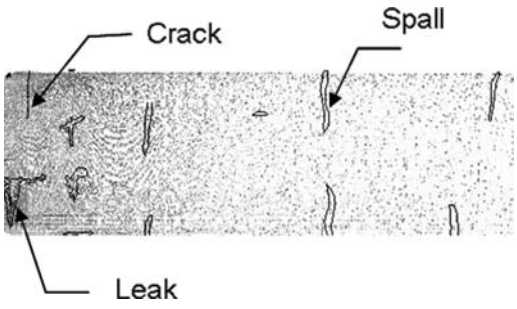


Figure 7. CAD drawing showing tunnel defect.

Table 1. Minimum clearance report.

Clearance alignment	Baseline station	Baseline elevation	Offset point		
			Northing	Easting	Elevation
Area 01	6+54.43	101.77	5005.93	5058.53	114.85
Area 02	5+87.51	102.49	4994.93	5125.45	115.40
Area 03	5+73.39	102.62	4995.91	5139.57	116.31
Area 04	5+64.39	102.70	4991.51	5148.57	109.13
Area 05	6+79.08	101.48	4991.36	5033.89	108.00
Area 06	5+87.85	102.49	5006.93	5125.11	114.79
Area 07	5+64.33	102.70	5003.59	5148.63	116.89
Area 08	5+47.36	102.84	5005.89	5165.59	116.03
Area 09	6+82.72	101.44	4996.52	5030.24	115.49
Area 10	6+58.50	101.72	4999.46	5054.46	116.02
Area 11	6+48.68	101.83	4998.64	5064.28	116.16
Area 12	6+54.14	101.77	4993.97	5058.82	114.15
Area 13	6+49.13	101.83	4991.49	5063.83	107.80
Area 14	6+80.97	101.46	5008.76	5031.99	110.86
Area 15	6+06.32	102.30	4991.85	5106.64	111.20
Area 16	6+03.82	102.33	4991.44	5109.14	109.51
Area 17	5+98.15	102.39	4991.44	5114.82	109.37
Area 18	5+64.75	102.70	4992.06	5148.21	111.82

3 DETAILED REPORTS – SUMMARY

3.1 *Utilization of digital terrain model*

With all of our pilot project defects stored in the DTM, we can now take advantage of the Reporting tools provided with In Rail. In Rail uses an XML (Extensible Markup Language) based system for reporting and translating design data of other software packages. After reviewing the various options for the report tools, we opted to use a clearance report. This allows us to generate a report which relates to the defects, to the alignment, reporting on a relative location to the alignment.

There are two clearance report templates provided with In Rail, a minimum clearance and a general clearance report. The general clearance report creates a table that is grouped by defect feature name includes a listing of every survey point of the feature, including its Northing, Easting Elevation, Station and Horizontal Offset.

Table 2. Defect location report.

Tunnel defect designation	Liner centerline station	O'Clock	Description	Length	Area
Area 01	6+54.43	1.13	Leak	1.38	0.07
Area 02	5+87.51	10.41	Leak	12.29	0.00
Area 03	5+73.39	10.58	Leak	4.3	0.62
Area 04	5+64.39	9.07	Spall	22.82	3.73
Area 05	6+79.08	9.08	Crack	15.41	0.00
Area 06	5+87.85	1.29	Leak	18.94	1.63
Area 07	5+64.33	12.39	Spall	23.13	0.00
Area 08	5+47.36	1.11	Leak	15.94	0.00
Area 09	6+82.72	11.07	Spall	6.59	0.71
Area 10	6+58.50	11.45	Spall	2.64	0.36
Area 11	6+48.68	11.34	Crack	7.71	0.86
Area 12	6+54.14	10.29	Crack	3.23	0.00
Area 13	6+49.13	9.01	Crack	20.44	0.33
Area 14	6+80.97	2.13	Leak	0.78	0.01
Area 15	6+06.32	9.38	Leak	3.17	0.1
Area 16	6+03.82	9.16	Crack	9.08	0.00
Area 17	5+98.15	9.13	Leak	2.46	0.07
Area 18	6+54.43	1.13	Leak	1.38	0.07

The intended use for these reports would be to enable someone to read the data on the report, and from it, to locate a particular defect within the tunnel. The current method of identifying a defect is by the use of a station value and a clock value. The clock value is defined using the standard surveying practice of looking up-station). taken from the hour hand positions on a clock face. Directly overhead would be 12 O' clock at halfway to accomplish this we first had to add a new column to the report. point of the tunnel on the left side would be 9 O' clock and on the right side, 3 O'clock. (Left and right are All In Rail XML reports are created XML file plus an XSL File. After research, we determined that data needed was in column. The modified In Rail report is displayed in Table 1.

Our research into XML and XSL transformations indicated that we would be unable to calculate the clock value with the tools. Additional processing would need to occur to complete the final tables. With In Rail's XML report tools, the report can be saved as an HTML file, which then can be opened in Excel and saved as an Excel File. The final step was to turn pairs of numbers into an angle that could be converted to the clock position. After combining the data from XML report, the finished report is displayed in Table 2.

3.2 *Research and future refinements*

Scanning is one of the powerful tools to perform three dimensional scanning for tunnels where a higher than normal level of details is required and where access

to the area is difficult, restricted or hazardous. With the experience, it is time to further refine the process and utilize the Scanners for the best possible manner. Until enough experience has been developed in use of three dimensional scanners for Tunnel assessment one may anticipate the following research for future refinements:

1. Inspectors to continue perform the initial field identifications of defects and label them in field and record them with digital camera. This approach is similar to one currently employed for identifying wetlands and trees.
2. The scanning team/Inspectors to revisit the tunnel to identify the details of the scan data.
3. Develop features representing each defect, identifying them by their defect type.
4. Compare the Summary reports developed with field data and the scanner data.
5. Repeat the process until one feels comfortable identifying the scanned image to field defects.

4 CONCLUSION

The "Three Dimensional Laser Scanning" can be successfully be used as one of the tool in the system of Tunnel assessment and maintenance. It offers fast, accurate and detailed information. As the advantage of this technology becomes recognized in the market place, this form of comprehensive data collection will become beneficial on the tunnel assessment. It is important that the limitations of technology be understood and the research be developed. Incorporating this new technology requires innovative procedures, methodologies and techniques. If the three dimensional laser scanning can be utilized to its fullest extent in appropriate way, substantial saving may be realized in terms of time and budget. Although the technology has been available for some time, and has been utilized by agencies for performing Tunnel Inspections, but "To date, there is neither a manual nor formal procedure developed for Tunnel Assessment" utilizing the "Three Dimensional Laser Scanning" technology. It shall be imperative for an Institution or an Agency to develop a manual for "Tunnel assessment" utilizing the "Three Dimensional Laser Scanner". Once the manual is developed it shall benefit the Transit Agencies with tunnels around the world.

REFERENCES

Biddiscombe P. & Gomes-Leal P., *3D Laser Scan Tunnel inspections keep Expressway infrastructure Project on Schedule* Trimble, Ohio USA

Langer D., Mettenleiter M., Hartl F. & Frohlich C., Imaging Ladar for 3-D Surveying and CAD Modeling of Real-World Environment *The International Journal of Robotics Research* Vol. 19, No.11, November 2000

Carmicheal B., Thayer O., Herbert S. & Osborn. An integrated mapping and object recognition system. *Proc. American Nuclear society 8th International Topical Meeting on Robotics and Remote Systems, Session 19 –Vision Systems*, Pittsburgh, PA, USA

Rheault C. & Sulibhavi G. 3D Laser Scanning as Applied to Subway Tunnel Inspection *TRB 84th Annual Meeting, Poster Session*, 2004.Washington DC, USA

Herbert M. & Krotkov E. 3-D Measurements from laser radars: How good are they? *Image and Vision Computing* pp. 170–178

Johnson A. *Spin Images: A representation for 3-D Surface matching*. Ph.D thesis, The Robotics Institute, Carnegie Mellon University, Pittsburgh, PA, USA

Huber D. & Herbert M. A new approach to 3-D terrain mapping. *Proc. IEEE/RSJ International Conference on Intelligent Robots and Systems*, Kyongju, Korea

Bowen, R. *Digital Mapping in 3-D, A revolutionary approach to construction and document procedures* Structural Engineer January 2005

Underground Space – the 4th Dimension of Metropolises – Barták, Hrdina, Romancov & Zlámal (eds)
© 2007 Taylor & Francis Group, London, ISBN 978-0-415-40807-3

"Lokve" tunnel rehabilitation – experiences and applied solutions

Z.Tomanović
Faculty of Civil Engineering, Podgorica, Montenegro

ABSTRACT: Building of the tunnel "Lokve", of the length 1117 m, on the trunk road Berane – Rožaje (Montenegro) was finished in 1972. Invert arch, which had been anticipated by the design, was not built. During the first five years of exploitation, abutment approach was 50 cm at several places. At the aim of preventing support dislocation RC struts were placed in the level of foundation of supporting concrete structure for twice, on each 4 m in about 2/3 tunnel length. At this moment support displacements are less, with some raise of road surface and they are located in the section of length approximately 70 m in the middle of the tunnel. In this moment, the basic problem is water inflow in the tunnel through no-fines concrete course, at the length of approximately 400 m with the west tunnel portal. In this paper you can see repair solutions for two particular tunnel sections and work experiences during the rehabilitation.

1 INSTRUCTIONS

Excavation of the tunnel "Lokve" in the period as of 1968 to1971 on the trunk road Berane – Rozaje, was conducted in very hard working conditions. With strong lateral pressures and frequent jets out of the rock in calotte in a form of high wedge shaped "chimneys", water inflow caused great problems during construction works, due to which works were stopped in certain periods. Tunnel lining was made of massive concrete, about 70–150 cm thick. Concrete was made of river unscreened aggregate and insufficient amount of cement compared to the quantities of cement used today. Difficult and complex working environment was the reason why temporary wooden support and plank were not removed from many places between lining and rock mass. Due to a primitive manner of building in concrete, calotte part was not filled in well and therefore now there are caverns between lining and rock. Invert arch, anticipated by the design, was not built. The tunnel was open to traffic in 1971.

During the first five years of exploitation, due to strong rock lateral pressures, abutment approach was 50 cm at several places. For the purpose of preventing horizontal dislocation of support, AB struts were built in twice at the level of foundation of supporting concrete structure (on each 4 m in about 2/3 tunnel length). From 1994 to 1998 (as of the time of beginning of geodetic measurements) support dislocations were reduced and accompanied by lifting of the road surface and were located in the middle part of the tunnel as of $0 + 400$ ch. to $0 + 470$ ch. In this part, struts at the contact point with lining foundation are broken and lifted for about 10 cm. At this section, traffic profile is a bit reduced due to arching ribs which were built at the course of construction because of a strong rock pressures.

Apart from this, water inflow in calotte and spring line represents a significant problem in terms of traffic security and maintenance of electrical installations in the tunnel. Water inflow is particularly expressed at the length of about 400 m along the west tunnel portal, where water sprouts in jets (most frequently sprouting in lining working joints), or appears in a form of leak and dripping from calotte onto the traffic road, or it leaks down spring line, which in winter time causes formation of thick ice layers and icicles.

Works on rehabilitation of the tunnel were conducted in the period 2001–2003.

2 DESCRIPTION OF REHABILITATION MEASURES

Rehabilitation of concrete lining of the tunnel is designed to be conducted with four different types of rehabilitation measures. In the part of lining with relatively good concrete quality, but with water inflow into the tunnel, planned is to set a polyethilene membrane protected with a shotcrete layer $d = 4–6$ cm (TIP-I).

In the part between ch. $0 + 45$ to $0 + 400$ anticipated is a non-construction rehabilitation of lining by putting a 3 cm shotcrete layer (TYPE-II).

For the section from ch. 400–470 m, where abutments are still approaching to a certain extent, planned is to put 20–25 cm of shotcrete, doubly reinforced,

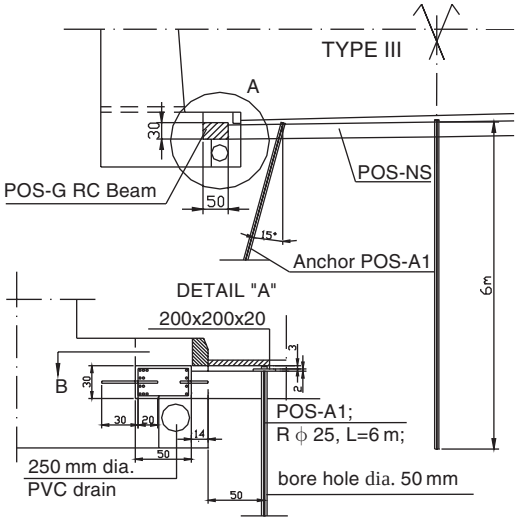


Figure 1. Lining rehabilitation TYPE III, RC struts under pavement.

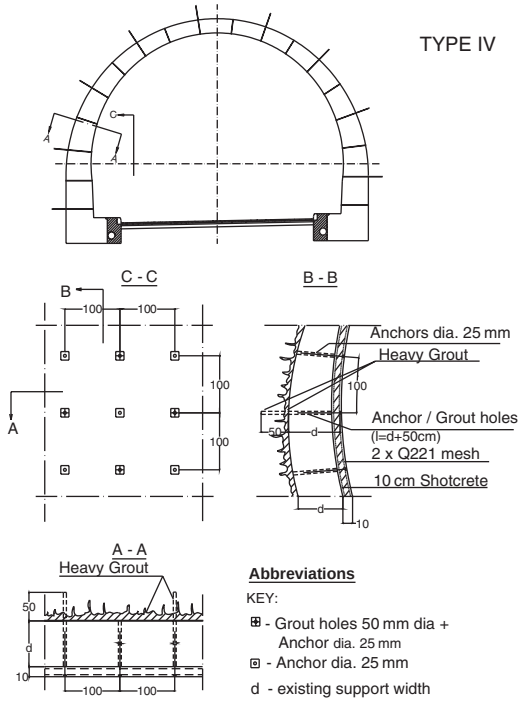


Figure 2. Lining rehabilitation TYPE IV.

between the present arched concrete ribs and anchors 2–3ϕR19/m^2 (60 cm length), as a connector between old and new concrete. Support reinforced in such a way with horizontal struts placed in the same altitude as abutment, makes a closed frame in a shape of timbered horseshoe with a purpose to accept rock mass lateral pressures, which in this zone caused horizontal approach of abutment lining for about 50 cm (TYPE-III, Figure 1).

In the part of the tunnel of ch. 0+750 up to ch. 1+117 (tunnel end) planned is a contact grouting with cement grout and setting of a 10 cm thick shotcrete layer, doubly reinforced and connected with the present lining by anchors: dia 25 mm, one piese/m^2, length 70 cm (TYPE-IV; Figure 2).

Apart from rehabilitation of the tunnel lining, planned is construction of main drainage pipes dia. 250 mm, on both sides of the tunnel, with manholes on each 20 m. Main drainage pipes serve for evacuation of water collected behind the membrane, local drainage systems, horizontal drainage boreholes, and for collection of potential water from the traffic road. Rehabilitation of the traffic road is limited to local repairs of bearing bitumenous layer and to setting of a new wearing course on the total tunnel length.

The design also anticipated total replacement of worn out electrical installations and tunnel illumination, video cameras setting on the tunnel portal zones, SOS stations with fire extinguishing equipment setting (on each 150 m on the left and right sides of the tunnel), automatic fire reporting, visual sign works for cessation of traffic in case of fire, or in the case of concentration of poisonous gasses in the tunnel above the allowed level.

2.1 *Description of the tunnel lining as of ch. 400–470 m (TYPE – III)*

Previously placed AB struts under the traffic road in this part of the tunnel are totally out of function. Namely, AB cleats which conveyed load from abutment to strut were broken (on the place of designed longitudinal beam POS-G). Breakage occurred on inclined planes which indicate that breakage occurred due to shear forces. Planes on which breakage occurred are partly spaced off, even for 10 centimeters.

This rehabilitation anticipates construction of longitudinal beam along with the present lining abutment (POS-G) and replacement of 11 broken AB strut beams. Newly designed struts (POS-NS) are dimensioned in such a way that they can convey twice as much of axial forces compared to the present ones. At the event of shaping of struts cross-section, a small free space between the traffic road and drainage pipes on both sides of the tunnel had a dominant role (see the details – Figure 2). Strut cross section of h/b = 30/70 cm could be placed in that free space. The problem of buckling of a slender present element was

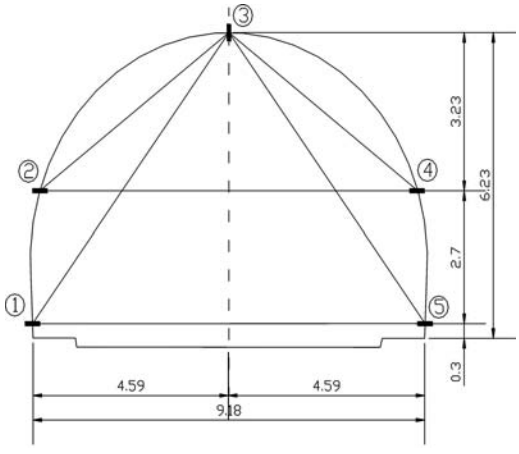


Figure 3. Convergence measurement cross section.

resolved with application of passive rock anchors by which the strut is fixed to a rock. Anchors need to eliminate the problem of vibration of strut arising due to frequent passing of the trucks, which was the cause of breakage of a certain number of struts on other sections of the tunnel.

This part of the tunnel is equipped with five measuring profiles for control of lining convergence during construction works, and for later monitoring in the course of exploitation (Figure 3).

2.2 *Description of rehabilitation of tunnel lining as of ch. 750–1117 m (TYPE – IV)*

Water inflow into the tunnel is mostly present as of ch. 750 m up to ch. 1+117 m and represents a significant problem from the point of view of traffic security. Concrete lining of the tunnel is on the surface greatly degraded, with many places in which ice caved caverns 5–20 cm deep. Concrete quality in regard with solidity is very weak and within the range as of 10–15 MPa on surface zones (thickness of lining in the spring line and abutment in this part of the tunnel is up to 1.5 m). On bad sections concrete can be dug without any special difficulties, with a pick and a jumper. A long-term influence of water and frost made concrete porous (washed cement filling), so that at the times of biggest inflow of underground water, it penetrates into the tunnel as a sprout, leak or dropping on almost complete tunnel lining surface.

Having in mind the fact that at the course of construction many caverns were left behind the lining as well as hardwood timber, which in the meantime putrefied, that water degraded concrete along total volume by constant flow into the tunnel, particularly on the surface (in combination with ice), rehabilitation solution anticipated contact grouting as a protection of the present concrete on the external side and setting of a 10 cm thick shotcrete on the inner side of lining – see Figure 2. The aim was to do conservation of degraded thick concrete layer of the present lining and fill it in, that is, stop further water inflow.

Apart from grouting the contact between lining and rock, purpose of positioning and number of boreholes was to do grouting of concrete lining. At the course of conducting grouting works, this proved to be very efficient. Namely, first grouting cycle (on a significant lining surface) at relatively low grout pressures of 1-2 bars, was actually reduced to grouting of lining itself. Only after the break of several hours and having grout in lining get hard, contact grouting could be initiated.

Attempt to determine rock permeability, that is, quantity of water penetration behind the lining, in order to determine density of grouting mass, at the course of designing, did not give any usable results. Namely, about ten tests of pumping water through borehole made in the lining, deep up to 1.0 m in the rock, gave the results which varied from almost impervious area to the situation where 15 minutes after pumping it was not possible to increase pressure with usage of water of about 100l per minute.

Composition of grout, along with preliminary lab tests, was defined during conducting construction works, depending on the tunnel zone. Water-cement factor ranged from $w/c = 0.7$ to $w/c = 0.5$, with supplement of accelerator of 1–1.5% (applied liquid ingunit – ADING Skoplje). Time of grout setting controlled by standard Vikat's needle, ranged from 45 to 90 min for $w/c \leq 0.55$, and it depended a great deal on small variations of additives quantity.

Interesting is to mention that Contractor tried to conduct grouting by applying packer of external diameter of 32 mm (designed 50 mm), but this was not feasible since it was necessary to decrease water-cement factor under 0.6, with accelerator added in a small percentage. By increasing diameter of packer to 48 mm, this problem was overcome. Best results were obtained by application of grout pumping only through one packer.

Accelerators in grout significantly contribute to plugging of the grouting hose on the branches for packers supply. By dislocating the hose from one packer to the others, the results were much better compared to simultaneous pumping into two or more packers. Grouting on the length of about 300 m of the tunnel length gave very good results; water inflow was reduced to several places only, where water will be accepted on local drainage system and taken to a main drainage pipe. On the remaining 100 m of the tunnel (from ch. 1000 to 1117) results of grouting were a bit worse.

Before putting any layer of shotcrete, lining surface is purified by sand blasting. Attempt to clean lining

by water jet under the pressure of 10 bars did not give desired results, especially in calotte where taken into account should be old and warn out cables under high electrical stress. Mentioned should be that works on rehabilitation were conducted during regular traffic operations, and therefore the existing illumination had to be preserved. Conducting construction works and works on replacement of electrical installations and illumination required a lot of efforts and work to keep minimal illumination of the tunnel on. Conducting works at the course of shuttle traffic caused additional costs of displacement of installations and significant time losses during project realization.

3 MONITORING

At the part of the tunnel where grouting is conducted, and at the part where during the so far exploitation significant abutment dislocation occurred, set was the system of iron pivots-bench marks for measurement of lining dislocation at the course of rehabilitation and at the course of future monitoring. Measurement profiles were set on each 50 m along the tunnel and were equipped with five bench mark out of which two in spring line and one in calotte of the tunnel as shown in Figure 3.

For convergence measuring used is the device with invar band and comparator with preciseness of 0.01 mm. Dislocations registered at the course of 6 months did not exceed 0.1 mm, which equals repetitiousness of results of the device used of 0.05 mm.

Measurement program defines measurement time intervals, directions of measuring, position of instruments at measuring and intervals for gauging of the device, so that all measurements are conducted in the same way. Convergence measurements organized in this way caused interruption of traffic, and therefore during construction works they were conducted once a month, with occasional control measurements of horizontal support dislocation only (direction 1-5, Figure 3).

4 CONCLUSION

Tunnel “Lokve” was built on hydro-geologically unfavourable location. Apart from that, tunnel lining was not made according to project documentation, that is, without invert arch. Major reason for rehabilitation of the tunnel “Lokve”, pointed out several times during 30 years of exploitation, refers actually to these two reasons. Law brand of concrete built in the tunnel lining can satisfy the bearing capacity, but in regard with durability, it represents a significant deficiency in the tunnel, especially for the tunnels placed in the geological area with a lot of water and tunnels on high altitude, especially having in mind icing in winter time.

Grouting with cement grout, applied in the tunnel “Lokve”, with immense water inflow and porous concrete tunnel lining, almost eliminated water inflow into the tunnel on the treated sections. According to the experience referring to grouting in this tunnel, time of grout setting needs to be reduced under 90 min by adding accelerator and adequate water-cement factor. Relatively short setting time needs a very organized work without any interruption in work and preparation of smaller quantities of grout.

Due to the previously mentioned, success of grouting, as a method of rehabilitation, significantly depends on how well organized Contractor is and how experienced are the workers. Also, presence of specialized Surveillance and permanent correction of content of grouting mass, depending on condition of lining, amount of water, caverns between the lining and rock mass have a significant role in achieving good grouting results.

REFERENCES

Main design of rehabilitation of the tunnel “Lokve”, 2001. Raughton International, Southampton, UK, in cooperation with “Univerzing” Bijelo Polje, Ministry of Maritime Affairs of the Government of Montenegro.

R.W. Henn, 1996. *Practical Guide to Grouting of Underground Structure.* American Society of Civ. Eng. New York.

B. Kujundzic, V.F. Demin, L.F. Fusov. 1984. *Instructions for consolidated grouting of rock masses in hydro-technical construction works*, Instit. “J. Cerni” Beograd, Instit. “B.E. Vedenejev” St. Petersburg.

Underground Space – the 4th Dimension of Metropolises – Barták, Hrdina, Romancov & Zlámal (eds)
© 2007 Taylor & Francis Group, London, ISBN 978-0-415-40807-3

The ring method application to the Prague Metro construction

Petr Vozarik
Metrostav, Prague, The Czech Republic

ABSTRACT: The construction of the first historic line of the Prague Metro started at the end of the 1960s. Czech construction companies lacked experience in projects of similar extent in an urban environment. This was why the experience, mainly for the construction of running tunnels, was sought abroad. The period of searching for suitable techniques and equipment was eventually terminated by a political decision. The basic technology and materials had to be taken over from the construction of the Moscow and Leningrad (today's Petrograd) metro tunnels. Czech technicians, representatives of the designer, employer and constractor, did not acquiesce in the relatively outdone and ineffective excavation technique and outdated design of the tunnels and stations. The ring method using cast-iron and, above all, reinforced concrete segments was improved and a very good technical level and effectiveness of the performance were achieved by the Czech teams during the course of several years. Their endeavour culminated by the development of the Prague-type three-vault station design lined with reinforced concrete segments, running tunnels with reinforced concrete segmental lining, development of new mining equipment, and improvement of the given mining technique. The modified ring method was applied to construction of tens of stations and kilometres of running tunnels.

1 INTRODUCTION

The Prague underground has won the reputation of an indispensable, high-quality and high-capacity means of transport. The underground has provided Prague inhabitants and visitors with a cutting edge public transport system – and a cornerstone of the city public transport. Almost 54 kilometres of lines with 53 stations are in operation today, joining the outskirts of the city through the city centre.

Major part of the 90 km-long single-track driven tunnels built between 1970 and the end of the century have been constructed by the ring method.

It is curious that 1968, the time of political liberalization, brought not only the touches of the freedom of speech and artistic freedom but also the formation of the Prague ring method, which became the major underground tunnel construction technology for the following more than 20 years.

Professor Mencl has defined this method as a tunnel construction technology for such ground types, where the stope stability is sufficient for construction of fixed lining. Its typical features include the use of blasting or machine extraction of the attack path of up to 1–1.5 metres and the installation of ring lining of panels in tunnels of 5.1 metre diameter or more (line tunnels) up to 7.8–7.9 metres (station tunnels). The lining was immediately engaged with the rock through filling grouting. The boring process was performed in short attacks and, typically, as full-face boring in order to enable installation of permanent prefabricated lining in the stope with minimum or no face support measures.

Most tunnels for underground in Prague are excavated in grounds, which provide 1 m attack stope stability of 1 hour through 1 month at maximum. The ground is a Paleozoic Ordovician complex of deposits containing mostly weak clay or silty shale or siltite, sometimes even very strong quartz rock. However, this whole complex is folded and damaged by a system of longitudinal and transversal dislocations.

2 THE RING METHOD USE ON THE FIRST UNDERGROUND LINE "C"

Six months after the government decreed the construction of the underground in 1967, the planning, investment and contracting organizations began to work on new basic technical and technological projects for the new C line. Six months later, the fundamental design solutions and technologies for boring the line tunnels by the ring method were prepared. The contractors' approaches to handling the technology varied. They stemmed from particular geological conditions on their sections of construction and also from their existing experience with tunnelling excavation or mining.

Vodní stavby (later Metrostav), the main contractor, took over the construction of the section involving soft roof, containing chiefly sandy sediments. The 5.1 metre diameter tunnels were excavated with the ring method by means of non-mechanical shields delivered by then Soviet Union. After Russian specialists trained the Czech operators, the technology was mastered to such extent, which permitted monthly advances of about 70–100 m as early as 1971. Another contractor, Vojenské stavby, was working on sections with rigid rocky roof. They used Soviet erectors for ring method boring with the aid of blasting. The monthly advance paths between 33 and 50 meters achieved with Russian-delivered cast iron lining were not impressive. However, with operators' training and collecting experience, this was deemed a fair result.

Yet another contractor, Výstavby kamenouhelných dolů (now the Division 5 of the Metrostav company), having their mining experience, decided to adopt their own technical solution. In the liberal political climate, they aimed to use their experience with construction of underground lines in West European countries. Their technical team has taken up the ring method as the fundamental technique as well. They used reinforced concrete panel lining of 5.2 m diameter by inland manufacturers.

Implementation of the proposed technology involved the most difficult step: developing a usable tunnel boring machine set. While the Soviet-made erectors were moving on skids, the current set, developed by Czech companies, used a different transport mechanism. Its two platforms were moving on track fixed to the tunnel lining at the height of the tunnel axis. The 10.3 metre self-driven two-part machine platform comprised a swivel-based panel segment unloader, extensible and suspended platforms, 2 tonne hoist and shotcreting equipment. Another self-driven 5.3 m-long platform carried 6 and 1.7 tonne hoists for materials handling within the tunnel.

Contrary to the Soviet-made erector, this set had substantial advantages in its motion variability and the free space at the bottom of the face. The latter permitted the use of mechanical equipment: drills and high-capacity transport vehicles, in some cases railless transport.

However, a Salzgiter shoveller with a 400-litre bucket combined with self-dumping railcars were used in the line tunnels of the IC line between the Kačerov and Budějovická and Pankrác – Pražského povstání stations. With this equipment, over 2,400 metres of line tunnels with monthly advances of 70–80 metres have been driven. The promising development of this technology and related equipment was terminated by the political situation of 1970's. Further advancements in the Prague-type ring method were based on Soviet directives and materials.

3 DEVELOPMENT OF THE RING METHOD IN OTHER UNDERGROUND LINES

Full development of technologies, which had been first adopted from the Moscow and Saint Petersburg underground constructions, took place in construction of the basic triangle comprising the A and B lines built between 1972 and 1985.

The expertise of construction and planning engineers was focused on upgrading the technologies and the machine equipment. At the end of the given period, the erectors and non-mechanical shields were fitted with supply equipment by Czech and Western manufacturers. This improved the quality of operation but did not eliminate fundamental drawbacks of obsolete boring machine sets. Heavy stationary equipment of the deposition sections ruled out almost any backward movement away from the face. Combined with the limited bottom space, they were an insurmountable hurdle to modernization of boring and loading and prevented the use of high-capacity loaders. The only substantial upgrade consisted in development of prefabricated lining with flat bottom.

The non-mechanical shields were deployed in A and IIC lines due to construction in greater depths and in more resistant rock. However, an assessment of the practice eventually showed that the technique is beneficial only in those segments where the rocky ground suitable for shield-tunnelling comprises more than 20% of the tunnel length.

The ring method using erectors with reinforced concrete panels for lining became the most widespread and best-proven technique for construction of Prague underground lines. Because of the method's simplicity and safety, the driving teams favoured its universal use in rocky ground containing low or medium strength shale, the stability of which permitted attacks between 1 and 2 metres. However, it disrupted the relationship between the massif and the face conditions. Despite the introduction of the streamline method, the average monthly advance paths did not exceed 70 metres.

Substantial increase in performance of the ring method was only possible through using a non-destructive breaking boring machine set. Throughout the underground construction, these machines were deployed in two instances. First, the Soviet-made TSČB-3 boring machine sets were used on the A line for excavation under Vltava river and the Staré Město quarter. The whole machine set was designed to drill rock of up to 80 MPa strength. Its full-face cutting head of 5.8 m diameter was protected by a hydraulic driven shield. Behind the shield, a device for construction of 60 cm-thick lining of pressed concrete was mounted.

Despite adaptations of the machine set, effective operation with regard to Prague area conditions has not been achieved. Therefore, two machine sets were

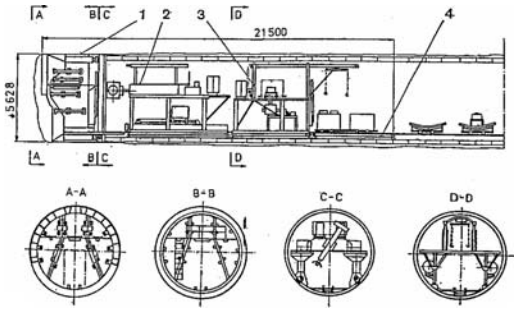


Figure 1. Soviet tunnel machine set KM 34. 1 – non-mechanical shield ŠČN-1; 2 – lining-laying machine; 3 – grouting platform TN 16; 4 – swerving platform.

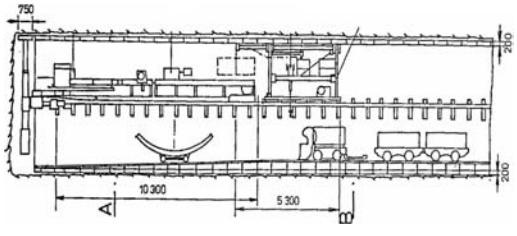


Figure 2. Mechanism of the ring method VKD-RS 218 for line C.

not used further, after drilling a total of 2.2 km length of tunnel.

Another machine set for excavation under geological conditions of Prague was planned and developed at the suggestion of Metrostav, the underground main contractor. This was a shield machine set with a milling tool. The machine set has driven the extension of the B line of 1,530 metres with average monthly advance path of 71 metres.

While we want to make a complex assessment of the ring method, we must not disregard the excavation under the Vltava river. The passage under a river bed has always been a demanding task both for the designer and the contractor. While the first river crossing on the A line was driven with a mechanical shield experiencing numerous difficulties tackled with consolidation grouting, the B and C line crossings were built with the conventional ring method using erectors for fitting the tubbing lining. In all these instances, advance headings have been driven to obtain precise data on geological and hydrogeological conditions. Best results were achieved in the passage of the C line. Its heading was driven with a non-destructive Alpine-50 milling tool and the subsequent ring method boring was troublefree with advance paths exceeding 50 m.

4 CONCLUSION

Upon the construction of the Prague underground, the ring method became the standard technology for excavation of both line tunnels and driven three-bay station tunnels. It turned out that specialist predictions and decisions based on results achieved between 1965 and 1969 were correct and viable. After all, this method has been used for more than 20 years to excavate tens of kilometres of line tunnels and kilometres of station tunnels. Despite the limiting conditions of the imported and obsolete machinery and materials, remarkable results were achieved. Sadly, though, the promising development of domestic equipment used for the first C line could not continue further.

For the last time, the ring method was used to large extent for line and station tunnels of the B-line final sections in 1980's and 1990's. However, the IVB line and last extensions of the C line to Severní město quarter make full use of the state-of-the-art NATM (New Austrian Tunnelling Method) with shotcrete lining and cast-in-place concrete.

REFERENCE

Vozarik, P. 1997. Technological method of tunnels driving on the line IVB of the Prague metro. *Underground constructions PS* '97: 208–212

This page intentionally left blank

Underground Space – the 4th Dimension of Metropolises – Barták, Hrdina, Romancov & Zlámal (eds)
© 2007 Taylor & Francis Group, London, ISBN 978-0-415-40807-3

Value preservation of underground infrastructure through focused conceptional planning

N. Winkler
Civil Engineer TU (MSc), Amberg Engineering Ltd., Regensdorf, Switzerland

A.W. Ackermann
Civil Engineer FH (BSc), Amberg Engineering Ltd., Regensdorf, Switzerland

ABSTRACT: Tunnels have a high economic value. Owners of tunnel infrastructure all have one goal in common: to maintain operational safety, serviceability and structural safety of their tunnels as economically as possible over the long term. To achieve these goals, a condition assessment is inevitable in order to focus the process of value preservation. The data collection is supported by modern digital technologies such as laser scanning and digital mapping software. Yet, the data are not only to be administered, but must flow into a long-term maintenance and value preservation concept. The core question arises as to how the acquisition and further processing of data should be linked in order to plan future actions and costs required to maintain tunnel safety and availability. This paper points out some key questions concerning value preservation concepts for tunnels and details the challenges for conceptional planning.

1 INTRODUCTION

The basis for the economic operation of transportation infrastructure is the long-term availability of the system. Specifically, negative consequences would result for the operator and the user, as well as for the economy and the environment, if the system or parts of it had to be unexpectedly removed from service due to the loss of safety or serviceability, even for a short period of time.

For road infrastructure, the closure of road sections would lead to delays and detours for the users, and thus to a greater environmental impact. In the case of unexpected closures, the operator will be faced with higher investments in order to refurbish his facilities.

In the case of rail infrastructure, interruptions in service result in high costs due to the irregularities of the schedule and/or the implementation of a shuttle service for passengers. Freight transport will also be affected. Refurbishment costs for railways, as in the case of roads, will increase accordingly.

These two examples involving critical transport infrastructure demonstrate the value of the facilities and the importance of preserving this value over the long term.

Civil structures, and especially underground facilities or tunnels, are key elements of road and railway networks worldwide. But underground structures are also utilized in supply and waste infrastructure, energy production, distribution infrastructure as well as military facilities.

Owners of all these types of infrastructure have one goal in common, namely to preserve the value of their facilities with the lowest possible financial burden over the long term by maintaining operational safety, serviceability and structural safety.

One of the most important boundary conditions of a value preservation concept is the accurate knowledge of the condition of the tunnels.

2 CONDITION ASSESSMENT OF TUNNELS

Only detailed knowledge of a tunnel's condition yields the basis for a focused management process to determine all necessary measures for structural value preservation.

Knowledge about the tunnel state is obtained in two steps. The first step – documenting the condition – consists of the comprehensive collection of technical data that concern the properties, characteristics and condition of the tunnel:

- Construction materials and their properties
- Geometry and profile of the cavity
- Installations for operation and clearance envelope
- Damage and deficiencies

Additional data and indications should be collected concerning the factors that could cause and influence the condition (subsequently called influence factors), such as:

- Construction method and tunnel age
- Geology and geologically induced forces
- Hydrogeology and chemistry of the groundwater
- Climatic conditions
- Rolling stock and operation types

A tunnel specialist can then carry out the evaluation and interpretation of the data in a second step to support assessment of the tunnel condition.

The condition assessment may indicate the necessity of various preservation measures and activities. National standards of different countries utilize highly varying terminology for tasks involving structural preservation and maintenance, whereby all standards basically express the same content: preservation is divided into surveying measures and maintenance measures.

Surveying measures are subdivided into inspections, visual and control measurements, as well as functional and material tests. Maintenance measures are subdivided into preventative maintenance, corrective maintenance and renewal measures.

Surveying measures serve both as the initial documentation of the condition, and as continuous or periodic documentation of the condition development.

Nowadays the tunnel engineer disposes over numerous computer-aided tools for carrying out the survey activities and data analysis.

3 MONITORING AND INSPECTION TECHNOLOGIES

IT developments have given the engineer opportunities to accomplish and evaluate measurements, inspections, tests, etc. faster and more efficiently by means of high-tech equipment and modern software solutions.

The digital tunnel scanner GRP 5000, for instance, which is capable of supplying both continuous profile measurements and a visual gray-scale image of the cavity surface, is the basis for further investigations such as clearance profile analyses and tunnel inspections.

The inspection software TunnelMap is a tool that allows a tunnel inspection to be carried out through digital data collection and analysis. Besides a graphical display (Fig. 1), the software also generates a statistical analysis of construction materials, operational equipment and damage. It exports the data into other software such as CAD for drawings (i.e. tunnel maps) and spreadsheets for the further processing of statistics.

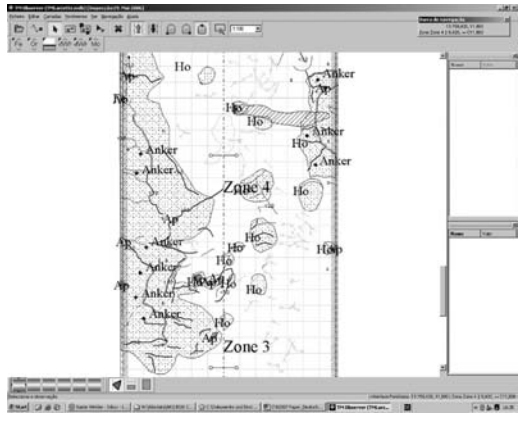


Figure 1. Example of a tunnel map generated with the TunnelMap software.

The link of these two technologies, which were developed within the Amberg Group, is the most efficient overall solution in the field of tunnel surveying:

Importing the gray-scale images recorded by GRP 5000 scanners into TunnelMap software has the decisive advantage of reducing inspection time in the tunnel to a minimum. For safety reasons, the inspections typically have to be carried out when the tunnel is closed to traffic (and with the catenary system turned off in railway tunnels), which often is only possible during night shifts. This process is accordingly time consuming and expensive. Higher efficiency is made possible by carrying out a pre-inspection in the office using the scanned image as background image for TunnelMap. The tunnel model, materials, installations and damage that have been input into the software prior to the field inspection must only be checked, corrected or supplemented during inspection in the tunnel.

Survey data collected and analyzed through these technologies constitute the basis for the condition interpretation and assessment by the tunnel engineer.

It is current practice that an experienced engineer assesses the state of a tunnel and plans the further measures. Naturally, this assessment is subjective, and thus various procedures are possible.

Current research and development projects address the topic of possible further processing of tunnel data. The goal is to help the engineer execute the condition assessment and plan economic value preservation concepts. The influence of subjectivity has to be reduced without relieving the engineer from responsibility.

4 DEVELOPMENT OF A MAINTENANCE MANAGEMENT TOOL

Several past and current research projects worldwide concern the topic of condition assessment and

(structural) maintenance concepts for tunnels. Some of the research projects conducted in Europe include:

- Instructions 779–10, UIC-Codex
- Guide de l'inspection du génie civil des tunnels routiers, CETU, France
- Tunconstruct, EU research project
- Prognosis model, SBB, Switzerland

Various manuals already contain basic concepts and recommendations for inspections and maintenance of tunnels. They represent a comprehensive collection of experience that helps the engineer analyze damage and the causes of damage. Thus, they represent a reference or support for determining the right maintenance measures.

Current research projects have set the goal of developing a comprehensive software solution that utilizes digital condition data and automatically:

- carries out the condition assessment,
- determines the life-cycle costs of a tunnel,
- defines the optimal maintenance intervals and
- recommends the most economic maintenance strategy.

Some projects also consider the question as to which issues have to be dealt with in the design phase of a new tunnel in order to optimize the costs during the operation and maintenance phase. However, this paper only treats the value preservation of existing tunnels.

A management tool shall be made available for the responsible owner of tunnels, which gives a quick and simple overview of the necessary investments to be made. The tool shall also make a statement concerning the optimal time intervals and the priority of the interventions.

In other words: How much money has to be invested in which tunnel and when, in order to obtain a 100% availability of the infrastructure? This core question is the object of a prognosis model that will be integrated into the inspection software TunnelMap.

5 PROGNOSIS MODEL

The prognosis model is the first step when developing a comprehensive software solution to support implementation of a value preservation concept. The objective of the prognosis model is to support the operator in determining the most economic maintenance strategy with regards to maintaining operational safety and serviceability. A maintenance strategy is the combination of various preventative maintenance, corrective maintenance and renewal measures.

After complete data acquisition regarding the damage and deficiencies of all tunnels on a network, the automatic condition assessment has to be calibrated and adjusted based on experience. The assessment is reasonable to define in accordance with the extent of damage in each zone. For the sake of simplicity, the classification can be carried out independently of the geometric position of the damage.

The result is the classification of each tunnel zone (typical zone length 10 m) into a condition class (mark). A possible definition of condition classes is as follows:

- 1 . . . Good
- 2 . . . Sufficient
- 3 . . . Insufficient
- 4 . . . Severe

Frequently, combinations of several damage types and deficiencies occur in the same zone. This situation is challenging with regards to the calculation of costs due to possible maintenance synergies.

It must be decided whether to apply maintenance measures to the whole zone for the sake of simplicity, or only to consider the effective damage area. This decision can again vary in accordance with the type of damage, and thus economic considerations have to be taken into account.

Furthermore, it has to be defined as to which standard of maintenance measures (preventative or corrective maintenance or renewal) is going to be applied to the different condition classes 2 to 4. In zones with a classification of 4, corrective maintenance or renewal measures must certainly be carried out. In zones with a classification of 2, preventative maintenance measures may be sufficient. This simple consideration leads to the question of how to define the effect of a measure. What shall be achieved with the measure? It is possible to define the maintenance goal as varying periods of operational time without the necessity of interventions, e.g. from 5 to 50 years? If so, this goal already has to be considered in the choice of the measures. In the end, the economic efficiency will be decisive, i.e. the relation between the overall maintenance costs and the period of time without the necessity of investments after the intervention.

Another important component of the prognosis model is the cost caused by the choice of construction measures. The maintenance measures, which correspond with a condition class (marks 2, 3 and 4) and with a damage type, have to be listed in a construction cost matrix. Examples of damage types include deformations, cavities, cracks, water inflow, joints, corrosion, etc.

It is important to consider, whether the costs should always be related to each m^2 of refurbished tunnel surface, even if the damage type is punctual, linear or planar. This question mainly has to be asked when cracks are considered. In order to obtain an order of magnitude for the construction costs, it is helpful to consult already realized refurbishment projects.

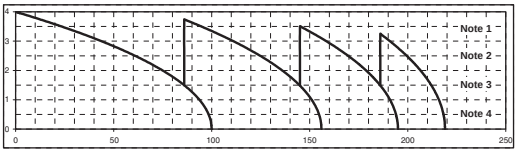


Figure 2. Visualization of an ageing curve by means of root functions.

The definition of the different cost components is also a very important aspect for the model. Do the costs only consider the construction works, or must the design and the construction management also be taken into account in this phase? How can the usually high costs for the site equipment be calculated? How can synergies be achieved that are able to reduce costs? These questions have to be clearly defined during the elaboration of the model concept.

All the above described considerations for the prognosis model are based on the actual state of a tunnel structure. When a necessary measure has to be postponed due to its lower priority, the condition of the tunnel can change because of the ageing of the structure.

Since the ageing curve and the damage development of a tunnel depend on different influence factors such as use, stresses, geology, cross-section, temperature etc., it is difficult to predict the ageing of a structure. For visualization purposes, it can be approximated by a root function (Fig. 2). It is hardly possible to make quantitative statements concerning the remaining service life or the expected costs. The latest possible intervention time is defined by the worst condition class.

Thus, such a prognosis model is conceptualized as an assessment system, which is based on the actual condition of the tunnels and which supports the operator in his choice of the most economic maintenance strategy, i.e. the right combination of maintenance measures. It is related to all the tunnels in a network of an operator and thus, does not make any statement concerning a specific tunnel. It only allows the emphasis of certain actions to be taken within the network. It is the basis upon which the owner can elaborate finance plans and intervention schedules.

Numerous factors and questions that influence the maintenance concept of a specific tunnel are being considered in the prognosis model as simplifying assumptions. These issues have to be further examined in current and future projects.

6 CHALLENGES FOR A MAINTENANCE MANAGEMENT TOOL

The goal of developing a computer aided management tool for a comprehensive value preservation concept makes it necessary to consider as many tangible influence factors as possible.

In order to obtain a detailed finance plan and intervention schedule, it is absolutely necessary to elaborate the maintenance concept for a specific tunnel, because the influence factors vary strongly in different tunnels.

One of the most important topics is the damage evolution and the interdependent ageing properties of a tunnel.

6.1 *Ageing curves of tunnels*

The ageing curves in many projects and publications represent only a qualitative visualization of the value consumption of an infrastructure (Fig. 2). This value consumption is related to the calculated depreciation period, at the lapse of which the construction costs are amortized. For reasons of amortization calculations, even a linear curve is sufficient. But these curves do not tell anything about the influences for instance of the geology, how long it takes that a zone moves from one condition class to a worse, or how long a zone remains in class 1 after refurbishment.

Thus, the numerical modelling of ageing curves certainly should be a subject-matter for further research activities. It should be related to specific tunnels or even – if necessary – to specific tunnel zones, and should also consider the factors listed in chapter 2, which cause and influence the damage. Of course, complete archive documents and existing damage documentation will be useful. For specific phenomena such as the corrosion of steel, the development of damage can be described by chemical-physical models.

By means of specific ageing curves it would be possible to predict – based on the actual condition – to which prolongation of the remaining service life a certain maintenance measure would lead to. Furthermore, the definition of the right intervention time would thus be possible.

But first, some questions arise concerning the factors that cause and influence damage.

6.2 *Influence factors of damage*

Without the evaluation of the precise geometric position of damage, only simplified statements can be made that serve as a means for the specification of priorities (which zones of a tunnel or network have to be maintained first?). For a detailed maintenance concept, this procedure is insufficient.

Different geometric positions of the same damage could lead to different condition assessments and thus to the necessity of different maintenance measures. Considering the geometric position therefore allows a more accurate calculation of maintenance costs. A leaking point in the tunnel crown for instance is more dangerous than in the side wall, a longitudinal crack more dangerous than a radial crack.

Thus, the appearance of several different damage types in one zone will also be taken into account. It is not necessary to treat the whole zone with the measure according to the worst damage, but only the corresponding area. Overlying damages can be dealt with in this way, which can have a different effect on the condition assessment. However, in these cases it is important to consider not only the geometric position of damages, but also their extent. In this context, the damage extent is not only important as a threshold for the classification of the zone, but also for the detailed calculation of the maintenance costs.

Another important influence factor is the construction material of the tunnel lining. A crack is more likely a sign of a weak point when appearing in reinforced shotcrete than when a similar crack appears in brick masonry. It would therefore be advantageous to model the influence of the construction material on the damage development.

The influence factors shown in the non-exhaustive list in chapter 2 are part of a complex interaction system. The combination of different causes can lead to new types of damage, which alone would not occur. For example, the combination of sprayed concrete and water containing sulfates leads to damage of the concrete, whereas the individual factors would not have the same damage potential without the influence of the other. It is therefore sensible to simulate the damage development for typical combinations of damage causes.

Planning maintenance measures for tunnel structures, those damages and deficiencies also play an important role, which are not immediately visible and require a special survey. The tunnel profile e.g. can only be monitored by measurement, and the tunnel drainage must be checked by function tests. The condition of the tunnel invert could for example be investigated using georadar measurements. Future research must therefore determine how these types of damage can flow into the automatic assessment and maintenance concept.

Besides the influences that are relevant for damage, there are also a series of topics related to the costs.

6.3 *Cost-relevant factors*

Like construction costs, maintenance costs of infrastructure consist of several components, whereby the most important are the following:

- Engineering fees for design, supervision etc.
- Construction works
- Site equipment and cleanup
- In-house services of the operator/owner
- Sales losses of the operator

Hence, it can only serve as decision aid for the choice of the best strategy if only the construction costs are considered. The detailed finance plan for maintenance is not possible without taking the other partial costs into account. The following considerations are decisive for the maintenance concept:

1. How can synergies be used when maintaining different zones/tunnels? Is it possible to install equipment in just one area for maintenance works in two tunnels? Is it reasonable to shift maintenance of a zone/tunnel temporally, in order to work more efficiently simultaneously to other nearby zones/tunnels?
2. Combination of structural and operational maintenance: Is it possible to execute structural maintenance during the same operational closures, in which maintenance for lighting, ventilation, tracks, catenary etc. is carried out?
3. Logistics: Can the construction yard be reached from the road network? How long does transport between the construction yard and the jobsite take? Must the transport be road or rail bound?
4. Working shifts: Can works be conducted during day shifts or only during night shifts? How long are operational closures? How long is the effective shift, how long are preparation and cleaning works before daily reopening?
5. How rising construction prices should be considered when planning maintenance measures long in advance?
6. Combination of economic and technical requirements: Is the construction of a new tunnel tube and the subsequent refurbishment of the old tunnel reasonable with regards to new safety requirements?

The evaluation of such very specific questions as well as the assessment of influence factors such as those mentioned in this chapter represent a challenge for any maintenance management tool, and is a possible subject for future research project.

7 CONCLUSION

In this paper, the topic of value preservation of tunnel infrastructure though focused maintenance planning is addressed. Modern digital technologies help the tunnel engineer incorporate and evaluate all relevant facts and data, such as:

- Condition and ageing of tunnel structure
- Influence factors of damage and deficiencies
- Measures and cost-relevant factors

On this basis, the condition assessment can be carried through.

By means of a prognosis model, a maintenance strategy for tunnel networks can be elaborated. The prognosis model serves as decision aid for the evaluation of necessary action and yields rough estimates of construction costs and time requirements.

The maintenance planning of specific tunnels requires detailed studies based on the prognosis model, which point out particular measures and detailed costs.

Comprehensive software solutions that shall support the engineer in this task are being developed worldwide. This paper discusses concrete questions and challenges for the development of a maintenance management tool from the standpoint of a tunnel engineer.

However, the engineer's experience and responsibility must remain in the foreground in order to verify the plausibility of the software results.

REFERENCES

Ackermann, A.W. 2004. Methodik der Zustandserfassung von Hohlraumbauten. *Rock Engineering: Theory and Practice*: 345–348. Essen: Verlag Glückauf GmbH.

Ackermann, A.W. & Modetta, F. 2005. Tunnel refurbishment under railway operations. *Underground Space Use: Analysis of the Past and Lessons for the Future* Volume 1: 613–618. Rotterdam: Balkema Publishers.

Underground Space – the 4th Dimension of Metropolises – Barták, Hrdina, Romancov & Zlámal (eds)
© 2007 Taylor & Francis Group, London, ISBN 978-0-415-40807-3

Diagnosis and repair of a subway tunnel 75 years old

T. Yamamoto & S. Matsukawa
Tokyo Metro Co., Ltd, Tokyo, Japan

ABSTRACT: More than 75 years have passed since the Suehirocho Station to Asakusa Station section of the Ginza Subway Line began service as the first subway in Japan. This section of the line has a box-section tunnel with a steel-framed reinforced concrete structure. Daily inspections and necessary repairs have been made. We recently conducted a detailed inspection, made predictions of the progress of deterioration, and performed structural analysis to ensure prolonged, safe use of the tunnel. This paper reports on the specific management and maintenance methods used in these activities.

1 INTRODUCTION

The Ginza Subway Line, specifically the section from Ueno Station to Asakusa Station, was opened for service in 1927 as the first subway in Japan. Since then, daily inspections and necessary repairs have been made for maintenance.

We have conducted detailed inspections, made predictions of the progress of deterioration, and conducted structural analysis, evaluation, and reviews of countermeasure methods according to JSCE Standard Specifications for Concrete Structures – 2001 "Maintenance." Our objectives were to evaluate overall present and future soundness in order to establish a maintenance policy for the future and to ensure prolonged safe use of the tunnel.

2 OVERVIEW OF THE TUNNEL

2.1 *Tunnel structure*

The Suehirocho Station to Asakusa Station section (3.3 km) of the Ginza Line covered by this inspection is a box-section tunnel of steel-framed reinforced concrete constructed while referring to the subway construction technologies in Berlin and New York in those days. (Photograph 1, Figure 1).

The overburden depth of this tunnel section ranges from 2 to 5 m.

2.2 *Tunnel design*

Reference documents from the time of tunnel design describe the allowable stress design method that was employed. The allowable compressive stress due to bending of concrete was specified at 3.5 N/mm^2, which suggests that the concrete used was expected to offer strength about one half that expected today. On the other hand, the allowable stress of steel was 120 N/mm^2, which is roughly equivalent to the present standard.

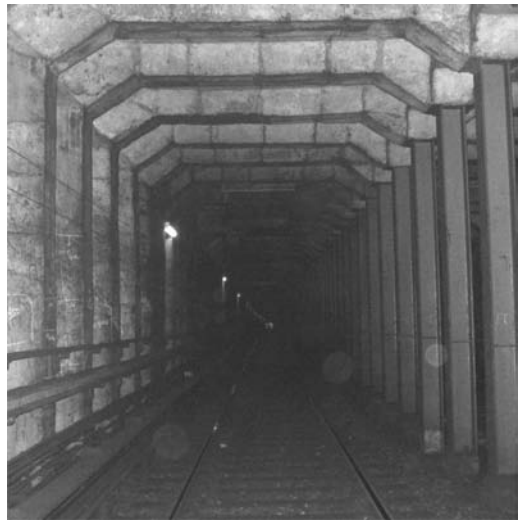


Photo 1. Current interior state of the tunnel.

We also found that the design road traffic load was substantially smaller than the current standard value.

2.3 *Materials used*

The cement used was Portland cement, with a mixing ratio of 1:2:4 (the volume ratio of cement: sand: aggregate).

For reinforcement, 13 mm and 16 mm plain round steel bars were used. The bar spacing and the concrete

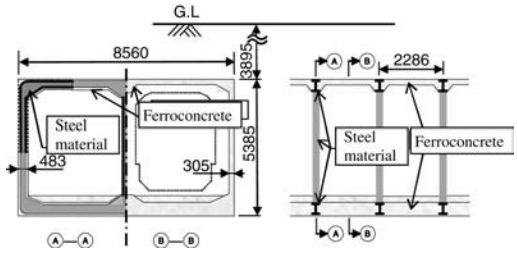


Figure 1. Tunnel structure.

Table 1. Inspection items and No. of inspection points.

Inspection items	No. of inspection points
Visual and hammering checks	12 points
Compressive strength test of concrete	105 pieces
Tensile strength test of reinforcement	9 pieces
Measurement of carbonated thickness of concrete	261 points
Measurement of concrete cover on embedded bars	261 points
Inspection of corrosion of reinforcement	17 points
Inspection of corrosion of steel frame	5 points
Measurement of water content of concrete	24 points
Estimate of concrete mix proportion	5 pieces at 5 points
Inspection for water leakage	Whole section
Component analysis of leaking water	3 points
Humidity and temperature measurement in tunnel	20 points
Vibration measurement of tunnel ceiling	1 point

cover were 100 to 150 mm and 50 to 75 mm, respectively, which were nearly equivalent to present design levels.

2.4 *Construction*

The tunnel in this section was constructed by the cut-and-cover method with concurrent road decking. Namely, steel frames were lined first at a given interval, followed by placement of reinforced concrete slabs between them.

As the tunnel was built below the groundwater level, an asphalt waterproofing layer was provided over the periphery of the tunnel structure.

3 INSPECTIONS

3.1 *Inspection items*

Table 1 shows the principal inspection items and the number of inspection points.

3.2 *Result of visual and hammering checks*

Deformation observed in the section included cracks, looseness, honeycomb, water leakage. There was no rust fluid indicating corrosion of reinforcement. The crack widths were about 0.1 to 0.3 mm

None of these deformation elements differed significantly from those cited in inspection results 15 years ago.

3.3 *Strength tests*

Concrete compressive strength was measured by a core-sampling test. In spite of a downward trend in strength in parts of the section, the average strength was 21.2 N/mm^2, and the measured values exceeded the estimated design standard strength of 10 N/mm^2 in all locations. No strength deterioration was observed from the inspection results 15 years ago.

The tensile strength of steel frames and reinforcement was also found to be sufficient.

3.4 *Measurement of carbonated thickness and concrete cover on embedded bars*

The carbonated thickness was measured by the drilling method while the concrete cover on embedded bars was determined by the electromagnetic induction method. The averaged carbonated thickness was 18 mm, and the averaged concrete cover was 43 mm.

Carbonated thickness data is distributed within an approximate range of 2 mm to 40 mm, with certain data exceeding 100 mm in a part of section. The concrete cover data is distributed within an approximate range of 20 mm to 70 mm.

3.5 *Inspection for corrosion of reinforcement*

We inspected for corrosion of reinforcement according to the self-potential method and by directly viewing the covering concrete that was partially chipped. The results showed that, in spite of the more than 75 years that had elapsed since construction, there was almost no corrosion proceeding in most locations. The condition was actually, “no corrosion” to “slight rust spots.” However, in certain locations there were signs of water leakage inside the tunnel, and some thin loose rust was detected in a few spots. (Photo 2).

Generally, it is said that corrosion of reinforcement proceeds when the carbonated thickness exceeds the depth of reinforcement. However, in the section inspected, there were many location points where corrosion was limited in spite of propagation of carbonation.

3.6 *Measurement of water content of concrete*

In this context, concrete water content, which influences reinforcement corrosion speed, was measured



Sound portion (no corrosion)



Leakage points (minor defect)

Photo 2. Corrosion state of reinforcing bar.

by using an electric resistance moisture meter. The results indicated that the concrete was considerably dry with both the surface and internal water content being extremely low; about 1–2% and about 0–1% respectively.

In other words, the tunnel was almost free of corrosion because of limited water supply in spite of propagation of carbonation beyond the reinforcement position.

The concrete had remained in a dry condition because there was naturally no rainfall inside the tunnel and because of the firm waterproofing layer provided at the time of construction.

However, around the points showing leaking of water, the internal water content was high at 5% or more at the source of the leak, and at the wet surface area below the source. It could be confirmed that corrosion of reinforcement there had proceeded because of the water supply.

3.7 *Vibration measurement of tunnel ceiling and verification of fatigue*

This tunnel has a small overburden depth and carries a load on the road surface that is larger than that at a time of design. The vibration of the tunnel ceiling was measured with a laser Doppler vibrometer (Fig. 2) to check for possible adverse affects from the repeated road traffic load on the tunnel.

The result shows that the maximum value of displacement (half amplitude) was extremely low at 0.075 mm.

Fatigue verification conducted to confirm this proved that the fatigue was not at a level that would cause fatigue failure within the service period.

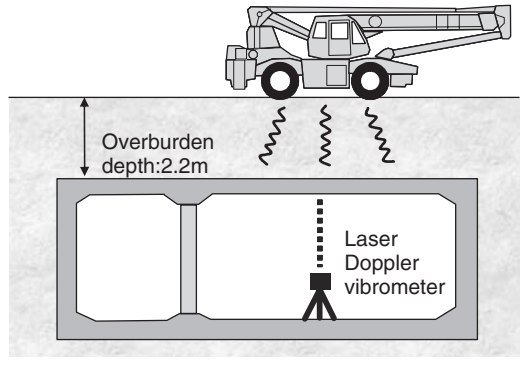


Figure 2. Conceptual view of vibration measurement of the tunnel upper portion using a laser Doppler vibrometer.

4 STRUCTURAL ANALYSIS

4.1 *Purpose of analysis*

A considerable number of years have passed since this tunnel was constructed, and environmental conditions have changed. In addition, the original design calculation sheets have been lost. Therefore, structural analysis was implemented using current load conditions and material physical values to assess the existing proof stress.

4.2 *Analytical model*

A two-dimensional frame linear analysis with a good track record was adopted as the analytical model. For analysis and verification we used a three-dimensional solid model that is an assembly of hexahedron solid

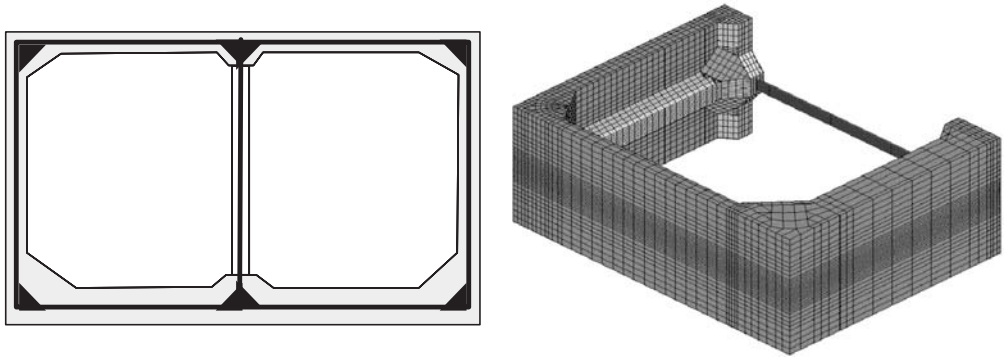


Figure 3. Analytical model.

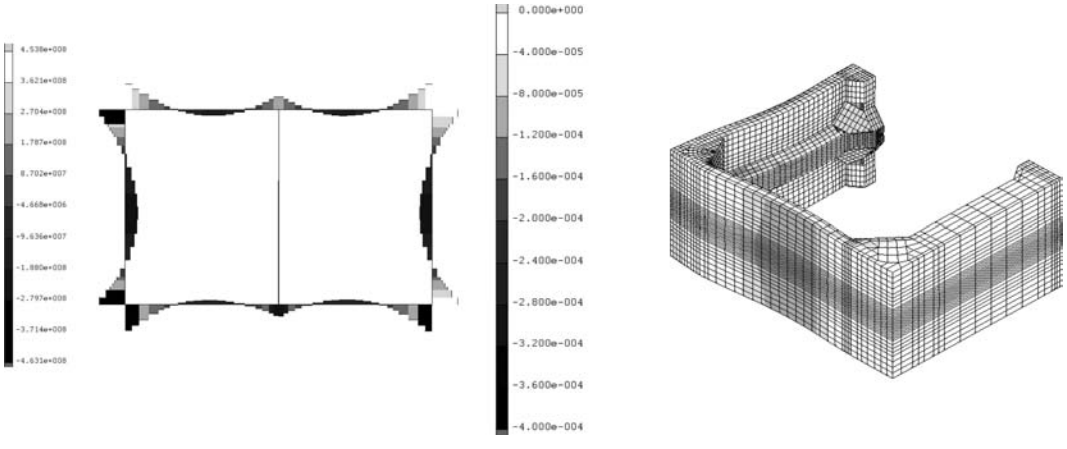


Figure 4. Typical analytical output results.

elements, to faithfully reproduce the complicated structure of steel-framed reinforced concrete.

Examples of the analytical model and output results are shown in Figs. 3 and 4, respectively.

In the actual field, partial loss or honeycomb were also observed in the covering concrete, which meant that the three-dimensional-model analysis involved an assumed case of loss or rigidity deterioration in a part of these concrete elements.

The results of the test implemented this time were used for property values, such as the material strength, etc. in analysis and verification.

4.3 *Results of analysis and verification*

In the two- and three-dimensional analyses, the response values I_{R_d} for flexural strength, axial strength, and shear strength were below the design strength I_{L_d}. The verification result from a three-dimensional model analysis was approximately $I_{R_d}/I_{L_d} = 0.3$ to 0.6, which proves sufficient allowance in strength.

The strength allowance could also be confirmed for cases in which the concrete element was partially lost.

5 PREDICTION OF THE PROGRESS OF DETERIORATION

5.1 *Purpose of prediction*

Judging from the in-situ inspection and test results, the principal deterioration mechanism of this tunnel was presumed to be carbonation. Therefore, we first predicted progress of carbonation. In this section where the concrete moisture content is low, however, it was presumed that the corrosion speed of reinforcement would be extremely low if there was no water leakage even when carbonation had progressed. Therefore, using the water content determined from the in-situ inspection, the time period from onset of carbonation at the reinforcement position up to occurrence of cracking caused by reinforcement corrosion was predicted.

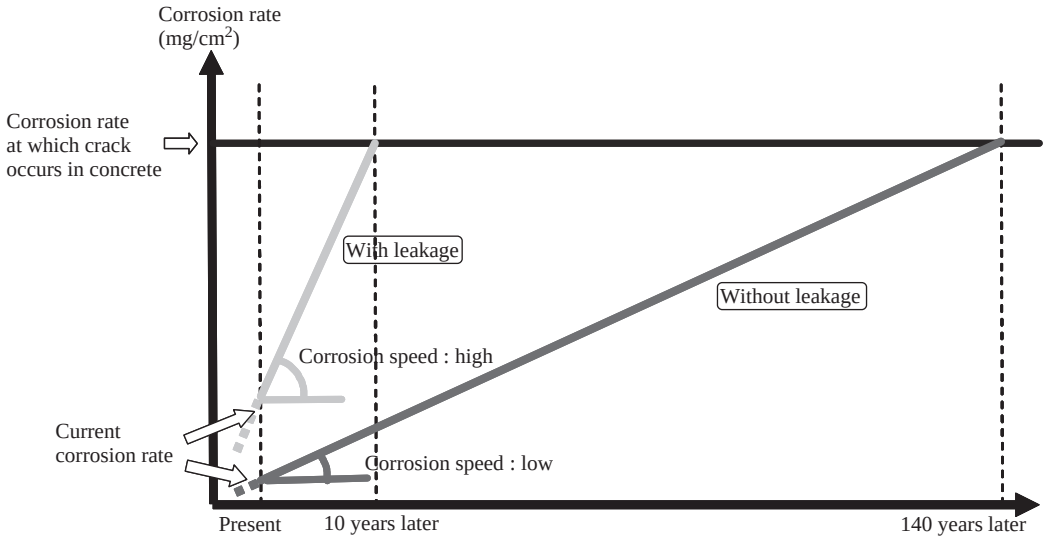


Figure 5. Conceptual view of predicting the timing of crack occurrence due to corrosion of reinforcement bar.

5.2 *Prediction of the progress of carbonation*

The progress of deterioration was predicted by using the following equation:

$Y = b\sqrt{t}$

Y: Carbonated thickness (mm)
t: Carbonation period (years)
b: Carbonation speed factor (mm/$\sqrt{t}$ year)

The carbonation speed factor "b" was determined by the actual measurement of carbonated thickness by drilling. The average carbonation speed factor "b" of all samples was 2.1; as compared with the average of 2.3 on the tunnel side. The average at the ceiling was as low as 1.5.

When viewed as the average between stations, deterioration progress could be predicted not to reach the reinforcement position in the five decades to come, that is, even 130 years after construction. Note, however, that in some locations where carbonation had progressed considerably, it was predicted that carbonation had already reached the reinforcement position or would reach it in the near future.

5.3 *Prediction of time of crack occurrence due to reinforcement corrosion*

Judging from the prediction average, carbonation may not reach the reinforcement position for a long period in the future. However, individual measurements indicate variances, and speed of reinforcement corrosion may vary greatly depending on the concrete moisture content.

Though there only a few research examples are now available, we did refer to cases that exist in order to predict the crack occurrence timing due to reinforcement corrosion by carbonation. This was done to obtain one set of judgment data to determine whether or not countermeasures would be necessary at present.

Prediction involved calculation of the corrosion speed from the concrete moisture content and calculation of the period up to occurrence of cracks by setting the corrosion amount at which cracks appear and the current corrosion amount.

The prediction results were as follows: the period up to occurrence of cracks is 140 to 200 years, provided there is no water leakage. It was predicted that, if water leakage occurs, cracks could be expected in about ten years. (Fig. 5)

6 EVALUATION

Firstly, in regard to load bearing capacity, visual inspection, structural analysis, and vibration measurement yielded sufficiently satisfactory results because there were no adverse effects from external forces such as overload or fatigue.

Fine cracks observed during inspection were judged to be predominantly due to drying shrinkage rather than insufficient bearing capacity or time-course deterioration.

As regards durability, various inspection results indicated that deterioration was mainly due to carbonation, not the effects of salt damage, alkali-aggregate reaction, or chemical corrosion.

In almost all locations, the existing deterioration progress due to carbonation had not yet reached the stage of starting reinforcement corrosion. In addition, as the deterioration progress prediction indicates, it could be confirmed that, in locations without water leakage, the possibility of reinforcement corrosion and thus crack occurrence would be small even 140 years from now.

7 COUNTERMEASURES

It was determined from the above results that the tunnel in its present state does not require any reinforcement to recover or enhance load-bearing capacity or rigidity. Countermeasures against deterioration for the entire tunnel were also judged to be unnecessary. Since cracks or loose portions were observed near localized water leakage, however, maintenance and repair work, including leak repair and recovery of those sections will be implemented without fail.

Research is still in progress in the fields in which analysis and inspection were conducted. For this reason and because each category of data contained unconfirmed elements, we decided to continue regular monitoring to follow the diagnostic results over a long period of time.

8 CONCLUSION

This inspection and diagnosis has proved that the tunnel, which was built over 75 years ago, can remain in service in sound condition if adequate maintenance is performed.

This fact is due to the implementation of the best design, construction, and maintenance work possible under past conditions by our forerunner railway civil engineers.

In a position to maintain an important property serving as social infrastructure, we will continue to perform the tasks required to ensure effective maintenance.

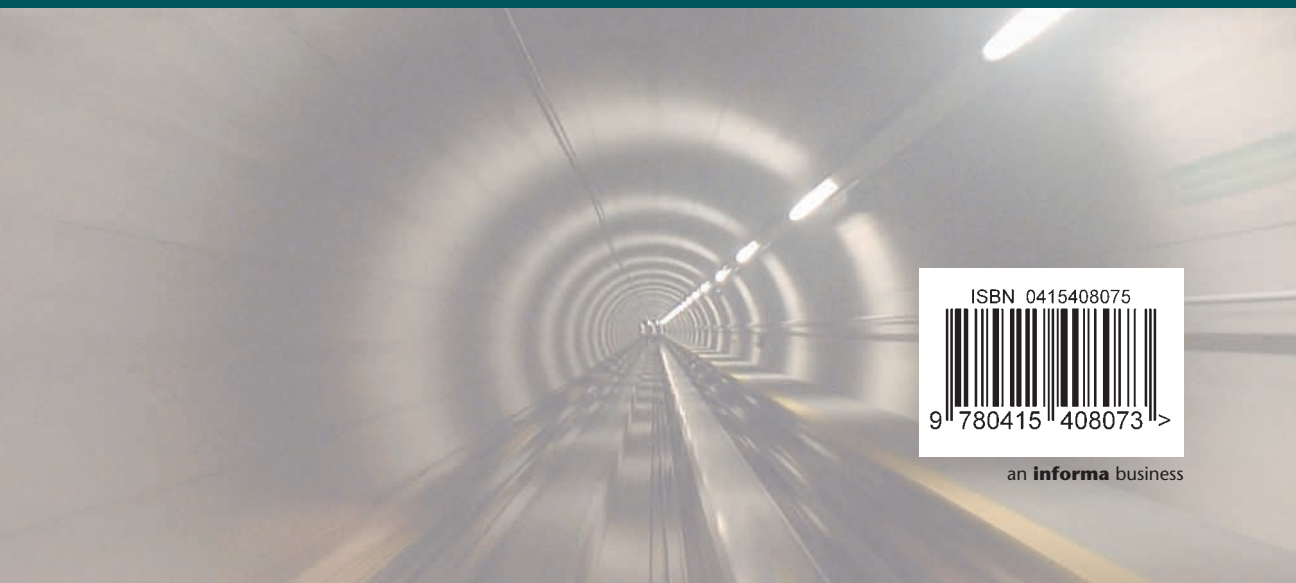
ACKNOWLEDGEMENTS

We would like to express our deepest gratitude for the kind guidance and cooperation extended by Professor Uomoto and Professor Kato of Tokyo University, Professor Futaba of Tokyo University of Technology, Professor Okui of Saitama University, Professor Koyama of the Regional Geo-Environment Institute, the staff of the Railway Technical Research Institute, the staff of Uomoto Laboratory, and all others who contributed to the inspection and diagnosis.

The so-called fourth dimension of a metropolis is the underground space beneath a city which typically includes structures such as tunnels, which facilitate transport, as well as providing gas, water and other supplies. Underground space may also be utilised for living, working and recreational facilities and provide storage for industrial materials.

Underground Space – the 4th Dimension of Metropolises focusses on underground city design and planning of subterranean constructions; geotechnical survey and improvement of ground mass; research, development and design of underground constructions in built-up areas; urban tunnelling, both conventional and mechanized, and its monitoring; underground constructions executed from the surface in built-up areas; concrete in underground construction; distribution and management of risks and accidents during tunnelling; tunnel equipment; fire and operational safety; and historical underground constructions.

Underground Space – the 4th Dimension of Metropolises reviews the state-of-the-art in tunnelling, discusses current tunnelling research and presents expectations for future development. This collection of papers will be invaluable to researchers, scientists, engineers and professionals working in tunnelling.



ISBN 0415408075
9 780415 408073 >
an **informa** business